8th INTERNATIONAL EURASIAN CONFERENCE ON

BIOLOGICAL AND CHEMICAL SCIENCES

17 - 19 December 2025

Ankara / Türkiye

(EurasianBioChem2025)

www.eurasianbiochem.org

PROCEEDING BOOK

(Abstracts and Full-Texts)

EurasianBioChem

ISBN : 978-605-72134-6-4

8th International Eurasian Conference on Biological and Chemical Sciences (EurasianBioChem 2025)

December 17-19, 2025
Ankara, Turkey
www.EurasianBioChem.org

PROCEEDING BOOK

(Abstracts and Full-Texts)

Editor

Prof. Dr. Muhittin DOĞAN

Copyright © 2025

ISBN: 978-605-72134-6-4

Publication Date: December 2025

Organized by

Avrasya Araştırma Geliştirme Bilim ve Teknoloji Merkezi

All rights reserved. The right to publish this book belongs to EurasianBioChem 2025. No part of this publication may be reproduced, stored in a retrieval system, or transmitted in any form or by any means, electronic, mechanical, photocopying, recording or otherwise, without permission. This Proceeding Book has been published as an electronic publication (e-book). Citation can not be shown without the source, reproduced in any way without permission.

Authors are responsible for the contents of their abstracts and full-text papers.

Conference Web Page: www.eurasianbiochem.org
E-mail: info@eurasianbiochem.org

CHAIRMAN OF CONFERENCE

Prof. Dr. Muhittin DOĞAN	Gaziantep University, Turkey

ORGANIZING COMMITTEE

Prof. Dr. Ali Tuncay ÖZYILMAZ	Hatay Mustafa Kemal University, Türkiye
Prof. Dr. Ayten NAMLI	Ankara University, Türkiye
Prof. Dr. Erol ATAY	Hatay Mustafa Kemal University, Türkiye
Prof. Dr. Gülşen ALTUĞ	Istanbul University, Türkiye
Prof. Dr. Hasan KÜÇÜKBAY	İnönü University, Türkiye
Prof. Dr. Hüseyin ZENGİN	Gaziantep University, Türkiye
Prof. Dr. Maria DAGLIA	University of Naples Federico II, Italy
Prof. Dr. Miloudi HLAIBI	University of Hassan II Casablanca, Morocco
Prof. Dr. Mustafa DJAMGOZ	Imperial College London, United Kingdom
Prof. Dr. Nabeel AHMAD	Dev Bhoomi Uttarakhand University, India
Prof. Dr. Ravichandran RAMASAMY	New York University, USA
Prof. Dr. Serap DERMAN	Yildiz Technical University, Türkiye
Prof. Dr. Soumia KOUADRI MOUSTEFAI	Hassiba Benbouali University of Chlef, Algeria
Prof. Dr. Ümmühan ÖZDEMİR ÖZMEN	Gazi University, Türkiye
Prof. Dr. William A. COETZEE	New York University, USA
Prof. Dr. Zeliha SELAMOĞLU	Niğde Ömer Halisdemir University, Türkiye
Assoc. Prof. Dr. Alevcan KAPLAN	Batman University, Türkiye
Assoc. Prof. Dr. Barkat ULLAH	Islamia College Peshawar, Pakistan
Assoc. Prof. Dr. Demet DOĞAN	Gaziantep University, Türkiye
Assoc. Prof. Dr. Khassanov VADIM	S.Seifullin Kazakh Agro Technical Research University, Kazakhistan
Assoc. Prof. Dr. Musfata PEHLİVAN	Gaziantep University, Türkiye
Assoc. Prof. Dr. Mustafa SEVİNDİK	Osmaniye Korkut Ata University, Türkiye
Assoc. Prof. Dr. Rezarta SHKRELI	ALDENT University, Albania
Assoc. Prof. Dr. S.D. SARASWATHY	Bharathidasan University, India
Assoc. Prof. Dr. Serpil KILIÇ	Isparta University of Applied Sciences, Türkiye

INTERNATIONAL SCIENTIFIC COMMITTEE*

Prof. Dr. Adem ÖNAL	Gaziosmanpasa University, Türkiye
Prof. Dr. Adil M. ALLAHVERDİYEV	Yıldız Technical University, Türkiye
Prof. Dr. Adnan AYHANCI	Eskişehir Osmangazi University, Türkiye
Prof. Dr. Ahmed IMTIAJ	University of Rajshahi, Bangladesh
Prof. Dr. Ahmet AKSOY	Akdeniz University, Türkiye
Prof. Dr. Ahmet ASAN	Trakya University, Türkiye
Prof. Dr. Ahmet KARADAG	Bartın University, Türkiye
Prof. Dr. Aida SAHMUROVA	Okan University, Türkiye
Prof. Dr. Ali BİLGİLİ	Ankara University, Türkiye
Prof. Dr. Alime Ebru AYDIN	Hatay Mustafa Kemal University, Türkiye
Prof. Dr. Alpaslan DAYANGAÇ	Osmaniye Korkut Ata University, Türkiye
Prof. Dr. Arife Alev KARAGÖZLER	Aydın Adnan Menderes University, Türkiye
Prof. Dr. Atila YILDIZ	Ankara University, Türkiye
Prof. Dr. Aycan TOSUNOĞLU	Bursa Uludağ University, Türkiye
Prof. Dr. Aygül KÜÇÜKGÜLMEZ YANDIM	Cukurova University, Türkiye
Prof. Dr. Ayla BALABAN GUNDUZALP	Gazi University, Türkiye
Prof. Dr. Aysel GÜVEN	Başkent University, Türkiye
Prof. Dr. Ayşe Dilek ÖZŞAHİN KİREÇCİ	Bitlis Eren University, Türkiye
Prof. Dr. Ayşe Gül MUTLU	Mehmet Akif Ersoy University, Türkiye
Prof. Dr. Başak HANEDAN	Atatürk University, Türkiye
Prof. Dr. Belgin GÖZMEN SÖNMEZ	Mersin University, Türkiye
Prof. Dr. Belma ASLIM	Gazi University, Türkiye
Prof. Dr. Berrin DURAN	Eskisehir Osmangazi University, Türkiye
Prof. Dr. Bülent KAYA	Akdeniz University, Türkiye
Prof. Dr. Dilek DEMİREZEN YILMAZ	Erciyes University, Türkiye
Prof. Dr. Ebru AKTAN	Gazi University, Türkiye
Prof. Dr. Ebru Gül ASLAN	Süleyman Demirel University, Türkiye
Prof. Dr. Ebru GÜREL-GÜREVİN	İstanbul University, Türkiye
Prof. Dr. E. Sümer ARAS	Ankara University, Türkiye
Prof. Dr. Elif Damla ARISAN	Gebze Technical University, Türkiye
Prof. Dr. Elif ÖZTETİK	Eskisehir Technical University, Türkiye
Prof. Dr. Elif Şahin IŞGIN	Dokuz Eylul University, Türkiye

Prof. Dr. Emin SARIPINAR	Erciyes University, Türkiye
Prof. Dr. Emine ARSLAN	Selçuk University, Türkiye
Prof. Dr. Emir Baki DENKBAŞ	Başkent University, Türkiye
Prof. Dr. Engin TİLKAT	Batman University, Türkiye
Prof. Dr. Erdal BALCAN	Celal Bayar University, Türkiye
Prof. Dr. Erdoğan ÇİÇEK	Nevsehir Hacı Bektaş Veli University, Türkiye
Prof. Dr. Erol AKPINAR	Bolu Abant Izzet Baysal University, Türkiye
Prof. Dr. F. Zehra KÜÇÜKBAY	İnönü University, Türkiye
Prof. Dr. Fatma Jale GÜLEN	Yıldız Technical University, Türkiye
Prof. Dr. Fatih YILDIRIM	Atatürk University, Türkiye
Prof. Dr. Fatma ÜNAL	Gazi University, Türkiye
Prof. Dr. Ferda CANDAN	Cumhuriyet University, Türkiye
Prof. Dr. Gamal BADR	Assiut University, Egypt
Prof. Dr. Gizem DINLER DOGANAY	Istanbul Technical University, Türkiye
Prof. Dr. Gönül DÖNMEZ	Ankara University, Türkiye
Prof. Dr. Gül ÖZYILMAZ	Hatay Mustafa Kemal University, Türkiye
Prof. Dr. Gülay BAYRAMOĞLU	Gazi University, Türkiye
Prof. Dr. Gülay ÖZCENGİZ	Middle East Technical University, Türkiye
Prof. Dr. Gülay ZENGİN	Gaziantep University, Türkiye
Prof. Dr. Güldeniz SELMANOĞLU	Hacettepe University, Türkiye
Prof. Dr. Gülsen ASMAN	Gazi University, Türkiye
Prof. Dr. Güray UYAR	Ankara Hacı Bayram Veli University, Türkiye
Prof. Dr. Handan UYSAL	Atatürk University, Türkiye
Prof. Dr. Hasan Basri ILA	Cukurova University, Türkiye
Prof. Dr. Hasan ÇABUK	Bülent Ecevit University, Türkiye
Prof. Dr. Hasan Hüseyin DOĞAN	Selçuk University, Türkiye
Prof. Dr. Hasan KÜÇÜKBAY	İnönü University, Türkiye
Prof. Dr. Hayati TÜRKMEN	Ege University, Türkiye
Prof. Dr. Hikmet Yeter ÇOĞUN	Cukurova University, Türkiye
Prof. Dr. Hülya ÖLÇER FOOTITT	Dumlupınar University, Türkiye
Prof. Dr. Hüseyin GÜHER	Trakya University, Türkiye
Prof. Dr. Ilgaz AKATA	Ankara University, Türkiye
Prof. Dr. Işık PERÇİN DEMİRÇELİK	Hacettepe University, Türkiye

Prof. Dr. İbrahim Çağatay KARAASLAN	Hacettepe University, Türkiye
Prof. Dr. İbrahim ÖRÜN	Aksaray University, Türkiye
Prof. Dr. İhsan AKYURT	Giresun University, Türkiye
Prof. Dr. İsmail AYDIN	İstanbul University-Cerrahpaşa, Türkiye
Prof. Dr. Jitendra PANWAR	Birla Institute of Technology & Science (BITS), India
Prof. Dr. Kadir YURDAKOÇ	Dokuz Eylül University, Türkiye
Prof. Dr. Kamil KOÇ	Celal Bayar University, Türkiye
Prof. Dr. Kemal BÜYÜKGÜZEL	Zonguldak Bülent Ecevit University, Türkiye
Prof. Dr. Maria DAGLIA	University of Naples Federico II, Italy
Prof. Dr. M. Burcu IRMAK YAZICIOĞLU	Istanbul Atlas University, Türkiye
Prof. Dr. Mehmet GÖNEN	Süleyman Demirel University, Türkiye
Prof. Dr. Mehtap TEKŞEN	Aksaray University, Türkiye
Prof. Dr. Mikail AKBULUT	Erciyes University, Türkiye
Prof. Dr. Miloudi HLAIBI	University of Hassan II Casablanca, Morocco
Prof. Dr. Muhammet GAFFAROĞLU	Ahi Evran Üniversitesi University, Türkiye
Prof. Dr. Murat ÇELİK	Atatürk University, Türkiye
Prof. Dr. Mustafa ATEŞ	Ege University, Türkiye
Prof. Dr. Mustafa BOGA	Nigde Omer Halisdemir University, Türkiye
Prof. Dr. Mustafa DJAMGOZ	Imperial College London, United Kingdom
Prof. Dr. Mustafa ÖZCAN	Istanbul Technical University, Türkiye
Prof. Dr. Mustafa TÜRKMEN	Giresun University, Türkiye
Prof. Dr. Nabeel AHMAD	Dev Bhoomi Uttarakhand University, India
Prof. Dr. Naime Funda TAY	Eskişehir Osmangazi University, Türkiye
Prof. Dr. Nazime MERCAN DOĞAN	Pamukkale University, Türkiye
Prof. Dr. Nazlı SARIKAHYA	Ege University, Türkiye
Prof. Dr. Nilgün ÖZPOZAN	Erciyes University, Türkiye
Prof. Dr. Noor Hasima NAGOOR	University of Malaya, Malaysia
Prof. Dr. Numan HODA	Akdeniz University, Türkiye
Prof. Dr. Nursel PEKEL BAYRAMGİL	Hacettepe University, Türkiye
Prof. Dr. Oktay ARSLAN	Balıkesir University, Türkiye
Prof. Dr. Osman DUMAN	Akdeniz University, Türkiye
Prof. Dr. Ömer IŞILDAK	Gaziosmanpasa University, Türkiye
Prof. Dr. Ömer KOZ	Bursa Technical University, Türkiye

Prof. Dr. Ömür BAYSAL	Mugla Sıtkı Koçman University, Türkiye
Prof. Dr. Özcan YALÇINKAYA	Gazi University, Türkiye
Prof. Dr. Özlem ÇETİN ERDOĞAN	Trakya University, Türkiye
Prof. Dr. Özlem ÖZBEK	Hitit University, Türkiye
Prof. Dr. Pınar ÇAMURLU	Akdeniz University, Türkiye
Prof. Dr. Ramazan ERENLER	Gaziosmanpasa University, Türkiye
Prof. Dr. Ramazan SOLMAZ	Bingöl University, Türkiye
Prof. Dr. Ravichandran RAMASAMY	New York University, USA
Prof. Dr. Remziye DEVECİ	Ege University, Türkiye
Prof. Dr. Rıdvan ŞEŞEN	Dicle University, Türkiye
Prof. Dr. Sadık DINCER	Cukurova University, Türkiye
Prof. Dr. Saliha ALYAR	Çankırı Karatekin University, Türkiye
Prof. Dr. Sait Aykut AYTAÇ	Hacettepe University, Türkiye
Prof. Dr. Salih DOĞAN	Erzincan University, Türkiye
Prof. Dr. Sema İŞİSAĞ ÜÇÜNCÜ	Ege University, Türkiye
Prof. Dr. Serap YALÇIN AZARKAN	Ahi Evran University, Türkiye
Prof. Dr. Serpil YENİSOY	Bolu Abant Izzet Baysal University, Türkiye
Prof. Dr. Sevda KIRBAĞ	Fırat University, Türkiye
Prof. Dr. Sevgi SEVSAY	Erzincan Binali Yıldırım University, Türkiye
Prof. Dr. Sevil TOROGLU	Kahramanmaras Sutcu Imam University, Türkiye
Prof. Dr. Sevim AKYÜZ	İstanbul Kültür University, Türkiye
Prof. Dr. Sibel AKAR	Eskişehir Osmangazi University, Türkiye
Prof. Dr. Sinem GÖKTÜRK	Marmara University, Türkiye
Prof. Dr. Soumia KOUADRI MOUSTEFAI	Hassiba Benbouali University of Chlef, Algeria
Prof. Dr. Süheyla KIRMIZIGÜL	Ege University, Türkiye
Prof. Dr. Şenay ÇETİNUS	Cumhuriyet University, Türkiye
Prof. Dr. Şengül ALPAY KARAOĞLU	Recep Tayyip Erdoğan University, Türkiye
Prof. Dr. Şule BARAN	Sakarya University, Türkiye
Prof. Dr. Şule Coşkun CEVHER	Gazi University, Türkiye
Prof. Dr. Şükran YILDIZ	Manisa Celal Bayar University, Türkiye
Prof. Dr. Talat OZPOZAN	Erciyes University, Türkiye
Prof. Dr. Tamer AKAR	Eskişehir Osmangazi University, Türkiye
Prof. Dr. Tülin ASKUN	Balıkesir University, Türkiye

Prof. Dr. Tülin AYDEMİR	Celal Bayar University, Türkiye
Prof. Dr. Ümmühan ÖZDEMİR ÖZMEN	Gazi University, Türkiye
Prof. Dr. Yüksel ABALI	Celal Bayar University, Türkiye
Prof. Dr. William A. COETZEE	New York University, USA
Prof. Dr. Zehra Nur YÜKSEKDAĞ	Gazi University, Türkiye
Assoc. Prof. Dr. Adnan ALDEMİR	Van Yüzüncü Yıl University, Türkiye
Assoc. Prof. Dr. Altuğ Mert SEVİM	Istanbul Technical University, Türkiye
Assoc. Prof. Dr. Banu Şebnem ÖNDER	Hacettepe University, Türkiye
Assoc. Prof. Dr. Başar UYMAZ TEZEL	Çanakkale Onsekiz Mart University, Türkiye
Assoc. Prof. Dr. Cumali ÇELİK	Yalova University, Türkiye
Assoc. Prof. Dr. David JENKINS	University of Plymouth, United Kingdom
Assoc. Prof. Dr. Demet DOĞAN	Gaziantep University, Türkiye
Assoc. Prof. Dr. Demet UZUN	Gazi University, Türkiye
Assoc. Prof. Dr. Meghane TARE	Birla Institute of Technology & Science (BITS), India
Assoc. Prof. Dr. Mostafa NORIZADEHTAZEHKAND	Islamic Azad University, Iran
Assoc. Prof. Dr. Ouahida BENSEBIA	USTHB University, Algeria
Assoc. Prof. Dr. Önder YUMRUTAŞ	Adıyaman University, Türkiye
Assoc. Prof. Dr. Özge TEMİZ	Osmaniye Korkut Ata University, Türkiye
Assoc. Prof. Dr. Pınar ŞANLIBABA	Ankara University, Türkiye
Assoc. Prof. Dr. Rezarta SHKRELI	ALDENT University, ALBANIA
Assoc. Prof. Dr. Róbert GYEPES	Charles University, Czech Republic
Assoc. Prof. Dr. S.D. SARASWATHY	Bharathidasan University, India
Assoc. Prof. Dr. Salih SÖNMEZDAĞ	Muğla Sıtkı Koçman University, Türkiye
Assist. Prof. Dr. Celal BAL	Gaziantep University, Türkiye
Assist. Prof. Dr. İmran UYSAL	Osmaniye Korkut Ata University, Türkiye
Assist. Prof. Dr. Muhammad Nauman KHAN	University of Chakwall, Pakistan
Assist. Prof. Dr. Nuh KORKMAZ	Osmaniye Korkut Ata University, Türkiye
Assist. Prof. Dr. Samia OUESLATI	Center of Biotechnology of Borj Cedria, Tunisia
Dr. Abdul Bari SHAH	Korea University, South Korea
Dr. Aqeel AHMAD	University of Chinese Academy of Sciences, China
Dr. Chong Yee LING	Universiti Malaysia Sarawak, Malaysia
Dr. Falah Saleh MOHAMMED	Zakho University, Iraq
Dr. Jana SOBOTNÍKOVÁ	Karlova University, Czech Republic

Dr. Majid IQBAL	University of Chinese Academy of Sciences, China
Dr. Nur Airina MUHAMMAD	University of Malaya, Malaysia
Dr. Ryan BAIDYA	California Takshila University, USA
Dr. Ramin Ekhteiari SALMAS	King's College London, United Kingdom
Dr. Sachiyo ABURATANI	National Institute of Advanced Industrial Science and Technology, Japan
Dr. Sergey SHITYAKOV	University Hospital Würzburg, Germany
Dr. Solomon HABTEMARIAM	University of Greenwich, United Kingdom
Dr. Victorine Lorette YİMGANG	Higher Institute for Scientific and Medical Research, Cameroon

* This list is arranged in alphabetical order.

FOREWORD

The *8th International Eurasian Conference on Biological and Chemical Sciences* (*EurasianBioChem 2025*) was successfully held on December 17-19, 2025 with participation from many countries.

The objective of *EurasianBioChem 2025* was to bring together leading academicians, researchers, scholars, and industrial professionals from all over the world to exchange and share their experiences and research findings in all aspects of biological and chemical sciences, as well as to discuss practical challenges and the solutions adopted. In this context, we were honored to welcome distinguished scientists, and our greatest appreciation goes to all participants whose valuable contributions made this conference a success. I would also like to thank the organizing committee and the scientific committee for providing such an intensive and high-quality scientific environment.

I believe that *EurasianBioChem 2025* has made significant contributions to all participants, and I look forward to seeing you at the *9th International Eurasian Conference on Biological and Chemical Sciences (EurasianBioChem 2026)*.

Prof. Dr. Muhittin DOĞAN

Chairman of *EurasianBioChem 2025*

Content

1. ORAL PRESENTATIONS **2**

1.1. ABSTRACTS **4**

Neuroinflammation in chronic urticaria: A bibliometric analysis of global research output 6

The influence of self-prepared foot care product on foot microbiome 7

Assessment of pregabalin misuse: A prospective and analytical study 8

Associations between disc displacement, degenerative changes, and inflammatory findings in TMJ: An MRI-based study 9

The effect of collagen supplementation on skin structure and signs of aging 10

Oleic acid nitrogen derivatives as antistatic additives 11

Ultrastructural analysis of the midgut epithelium of *Lithobius forfocatus* (Myriapoda, Chilopoda) exposed to different concentrations of nanostyrene 12

Assessing the impact of breakfast consumption on cognitive and academic performance and daily wellbeing among Aldent University students 13

Impact of diet on reproductive performance in dairy cows in Algeria 14

Study of the effect of antibiotics and probiotics on sperm quality *in vitro* using an automated semen analysis system (CASA) 15

Evaluation of corrosion inhibition effect of pyrimidine derivative on aluminium alloy by electrochemical techniques 16

Measurement of the viscosity of gum arabic 17

Theoretical design and DFT evaluation of d-glucosamine–oxyresveratrol–essential amino acid grafted molecules for enhanced antioxidant activity 18

Prevention of transmission and infection by Parvovirus B19, in children with Hemoglobinopathy, who receive blood transfusions. 19

In vitro seed germination, callus induction, and shoot formation of *Zygophyllum album* L. 21

Novel water-soluble Zn-phthalocyanine complexes enhance foliar zinc bioavailability and concentration-dependent redox homeostasis in *Cucumis sativus* under zinc deficiency 22

Towards chemical contaminants detection in pepper and cucumber: Reporting SERS sensing by a novel gold nanotriangle metal-insulator-metal array 23

Design and (bio)functionalization of isocyanate-bearing cryogels 24

AgNP synthesis using supercritical CO_2 extract of *Lilium ciliatum* leaves 25

Green synthesis of selenium nanoparticles using *Cicer arietinum* L. extract and investigation of their biological activities *in vitro* for new drug development 26

Does life kinetics exercise have an effect on melatonin and cortisol levels in Alzheimer's disease? 27

Smart pesticide detection via hexagonal MIM metasurfaces integrated with deep feed-forward networks 28

Hydrogel form containing drug delivery system for psoriasis treatment potential 29

Bowtie-patterned nanosensor arrays for food safety monitoring 30

Detection of nutrient deficiencies in *Arabidopsis thaliana* using deep learning techniques for smart farming 31

Determining the potential of the marine invasive alien macroalga *Stypopodium schimperi* as a blue economic resource 32

Biogenic gold nanoparticles (AuNPS) from invasive brown macroalga *Stypopodium Schimperi* aqueous extract: Characterization and ecotoxicological potential 33

Synthesis and investigation of ternary nanocomposite fibers 34

Fabrication of TiO_2/h-BN-CdSe based quantum dot-sensitized solar cells 35

Regulatory role of caveolin-1 in doxorubicin-induced SASP and its impact on cancer cell proliferation 36

Effect of life kinetic exercise on BMAL1 and CLOCK in Alzheimer's disease 37

Effects of low temperature stress on pollen germination, tube growth, and antioxidant responses in Turkish olive cultivars 38

Volatile composition of *Lathyrus laxiflorus* subsp. *laxiflorus* by GC-MS/FID analysis 39

Preparation of a drug delivery system including caffeic acid for the inhalation-based treatment of lung cancer 40

Development of active biodegradable poly(3-hydroxybutyrate-co-4-hydroxybutyrate) films enriched with essential oils for food packaging applications 41

Green synthesis of zinc oxide nanoparticles From *Eucalyptus globulus:* Characterization, and investigation of the antimicrobial effects 42

Investigation of the enzyme inhibition effect of different turnip varieties on antioxidants and sugar metabolism 43

Evaluation of anabolic androgenic steroid nandrolone decanoate effects on apoptosis associated genes in pancreatic cells 44

Synthesis of novel bis-hydrazone derivatives and *in silico* evaluation of their COX-2 inhibitory potentials 45

Determination of resveratrol in fresh and heat-treated pomace *Vitis labrusca* by RP-HPLC 46

In silico assessment of the interaction of the natural compound zeaxanthin with insulin, glucocorticoid, and GLP-1 receptors associated with type 2 diabetes 47

Synthesis, characterization and investigation of new multifunctional processing auxiliary materials to improve processability of polyolefins 48

Cytotoxic and anti-inflammatory potential of 2-cyclopenten-1-one against malign melanoma 49

Effects of halophilic PGPR on salt stress and growth parameters in tomato plants 50

Electrochemical determination of glyphosate: Molecular imprinting approach in the presence of nanomaterials 51

Aloe vera L. bitkisinin gizli parmak izlerinin tespitinde kullanımı üzerine bir ön çalışma 52

Palynological studies on *Astragalus* sect. *Malacothrix* (Fabaceae) 53

Su içindeki alüminyum ve florür iyonlarının akıllı telefon uyumlu çift tespiti için mono-sübstitüe rodamin sentezi 54

Roles of EDDHA-derived zinc complexes on growth and antioxidant defense in rice (*Oryza sativa* L.) exposed to salt stress 55

Cytotoxicity of *Origanum majorana* extracts on A549 cells and their radical scavenging activity 56

Development of hyaluronic acid-coated/curcumin-loaded poly(ε-caprolactone) membranes for biofunctional wound dressing applications 57

Innovative approach in food safety: Smart packaging systems with natural pigments 58

Optimizing lettuce cultivars and agrobacterium strain selection for enhanced transformation efficiency using a CRISPR-compatible vector 59

Acetylcholinesterase and butyrylcholinesterase enzyme inhibitory effect of *Ganoderma lucidum* (Reishi) mushroom 60

Carbon-filled polymer composites: structure–property relationships for improved mechanical and thermal performance 61

Development of self-healing anti-corrosive smart epoxy coating material reinforced with chitosan/halloysite nanotubes 62

Yerli üretim tanı kitinde kullanılan antikorların elektrokimyasal validasyonu 63

A study on *MARK* gene family members in pancreatic adenocarcinoma 64

Development of a novel polymeric membrane for cationic dye adsorption 65

Uncovering the soil impact of wastewater irrigation: A case study from Konya, Türkiye 66

Investigation of photosensitizer properties of zinc phthalocyanines in photodynamic therapy by photophysicochemical properties 67

Design of a lipoic acid–based thioester polymer functionalized with tryptophan for drug release 68

β-Glucan production from *Saccharomyces cerevisiae* under submerged fermentation 69

Production, extraction and characterization of microbial mannoprotein 70

Controlled Sr(II) ion release from injectable electroactive hydrogels with potential for the treatment of infections 71

Supercritical carbondioxide extraction of *Nigella sativa* L. seed oil: fatty acid composition, nutritional energy and antimicrobial activity 72

Characterization and enzyme kinetic study of serine protease subtilisin carlsberg immobilized on biochar-chitosan composite carrier obtained from waste biomass 73

Effect of drying method and process conditions on the physicochemical and functional properties of tomato pomace powder 74

Preparation and antibacterial activity of Ag_2O nanoparticles from *Cedrus libani* 75

Analytical determination of the active pharmaceutical ingredient propranolol 76

Advanced polymeric adsorbents for the treatment of arsenic- and selenium-contaminated wastewater 77

Osmanlı döneminden günümüze gül yağı distilasyonu 78

Development of polyvinyl alcohol based bioactive cosmetic masks 79

Bacillus subtilis offers insights into microbial adaptation under Martian conditions 80

Computational insights into the antioxidant and anticancer mechanisms of apigenin 81

Transcript levels of ZDHHC protein palmitoyltransferases in granulosa cells isolated from the ovaries of PCOS and non-PCOS women 82

Synthesis, characterization and investigation of aggregation properties of non-peripheral octa-substituted Nickel(II), Zinc(II) Copper (II) phthalocyanines 83

COVID-19'da IL6 ve TMPRSS11A polimorfizmlerinin genotip kombinasyonları ile hastalık şiddeti arasındaki bağlantı 84

Mardin'de unutulmaya yüz tutmuş gastronomik bir değerin incelenmesi ve duyusal analiz ile değerlendirilmesi 85

Bir Alman çoban köpeğinde tek yavru sendromuna (single pup syndrome) bağlı olarak şekillenen güç doğum olgusu 86

Investigation of the mechanical and antioxidant properties of bioactive wound dressings containing grape seed oil 87

Çeşitli analitlerin eş zamanlı tayini için elektrokimyasal sensörler 88

Farklı fasulyeler ile üretilen cipslerde tüketici beğenisinin değerlendirilmesi 89

Assessment of calibration techniques for the determination of cadmium at different levels in sage and rosehip tea samples by flame atomic absorption spectrometry 90

Effect of St. John's wort and coconut oil blends on the structural and thermal properties of protein-based films for potential biomedical applications 91

Fumigant toxicity of *Clinopodium serpyllifolium* subsp. *serpyllifolium* essential oil against different larval stages of *Tenebrio molitor* (Coleoptera: Tenebrionidae) 92

Synergistic antioxidant effect of squalene and saponin in a d-galactose-induced aging model 93

Identification of novel miRNAs in tobacco (*Nicotiana tabacum* L.) targeting black shank and powdery mildew genome 94

Cuscuta epithymum ekstresinin fenolik içeriği ile biyoaktivitelerinin belirlenmesi 95

Determination of total phenolic, flavonoid content, and antioxidant activity of rose of jericho (*Anastatica hierochuntica*) 96

Construction of RuCo decorated poly(2-hydroxy methacrylamide) polymer brush grafted magnetic nanoparticles as a heterogeneous catalyst for degradation of some azo dyes. 97

Predicting polymer–drug compatibility for queuine and gemcitabine via molecular simulations 98

Development and characterization of tannic acid crosslinked poly(vinyl alcohol) films 99

Eco-friendly synthesis and photocatalytic applications of zinc oxide nanoparticles (ZnO-NPs) using extract derived from agro-waste hawthorn (*Crataegus monogyna*) 100

First complete mitochondrial DNA data provided for Turkish Hamster (*Mesocricetus brandti* Nehring 1898) 101

Odyolojik veriler kullanılarak makine öğrenmesi ile işitme cihazlarında hoparlör tipinin tahmini: Random forest yaklaşımı 102

Isolation of bacteriocin-producing *Enterococcus* strains from traditional cheeses 103

Investigation of feeding interactions between the Randall's threadfin bream (*Nemipterus randalli*) and the common pandora (*Pagellus erythrinus*), two co-occurring fish species in Gökova bay, using stable isotope analysis 104

Cyclotriphosphazene derivatives containing carbazole units and the investigation of their photophysical properties 105

Determination the pathogenicity and virulence of *Fusarium* species isolated from Amasya, Türkiye, on sugar beet 106

Investigation of the photodynamic therapy potential of water-soluble phthalocyanine compounds containing pyridine substituents on breast cancer cell line 107

Management of swallowed capsules filled with drugs in intensive care 108

Experimental and theoretical investigations of semi-lethal dose (D_{50}) values for bacterial population 109

Lactarius deliciosus (L.) Gray özütlerinin gökkuşağı alabalığı (*Oncorhynchus mykiss*, Walbaum, 1792) filetolarının raf ömrü üzerine etkisi 110

Yeast microflora of milk kefir beverages fermented with various grains 111

Identification of foot-and-mouth disease virus antigenic peptide via SERS 112

Integration of artificial intelligence in wastewater treatment for sustainable biogas generation 113

Structural elucidation and antimicrobial potentials of pyrazoline compounds derived from chalcone intermediates 114

UV ve filtrasyon tabanlı balast suyu arıtım sistemlerinin saha performansı üzerine bir değerlendirme 115

Determining the recent status of non-native marine fish species in the Aegean coast of Türkiye 116

Assessing the impact of microbial dysbiosis on disease pathogenesis through a one health perspective 117

Synthesis and Characterization of Ester-Based Hindered Amine Light Stabilizers (HALS) in Polymers 118

In silico analysis of missense SNPs in the *CDH9* gene 119

Coating of Mg alloys with nano hydroxyapatite (HA) to be used as biodegradable biomaterials 120

Synthesis, characterization and *in silico* anticholinesterase inhibitory activity of new hydrazide-hydrazone derivatives 121

Cistus laurifolius L. (karağan) bitki ekstraktının kolon kanseri hücre hattında (HCT 116) anti kanser etkilerinin incelenmesi 122

Catalytic performances of silica gel supported monometallic (Co, Nb, Cu) catalysts in hydrogen production via $NaBH_4$ methanolysis 123

Integrative bioinformatics reveals crosstalk between MIF and HER2 signaling networks in breast and colorectal cancer 124

Development of biodegradable poly(lactic acid) composites reinforced with orange peel powder 125

Altered serum levels of netrin-4 and neogenin reflect tumor progression in glioma patients 126

Agomelatine may alleviate the LPS-induced ER stress response and apoptotic signaling in human embryonic kidney cells 127

Synergistic mechanism of graphene oxide-composite silver nanoparticles combined with gemcitabine in pancreatic cancer 128

Impact of plant-based dietary patterns on breast cancer prevention 129

Copper oxide nanoparticles synthesized in a deep eutectic solvent for efficient metronidazole adsorption 130

Next-generation inositol phosphate derivatives as mechanistic inhibitors of HIV-1 assembly 131

Synthesis of new sensor based on quinolinium-containing cyanobiphenyl 132

Effect of trimetazidine on detrusor contractility in a mouse model of L-NAME-induced overactive bladder 133

Investigation of the genotoxicological potential of desipramine, an active substance used in antidepressant drugs, by *in vitro* test methods 134

Chronic inflammation response in acute myeloid leukemia (AML) 135

Evaluating the potential of royal jelly as a tyrosinase inhibitor 136

Biochar-assisted removal of anionic textile dyes from model waste water 137

The effect of vacuum PA/PE packaging on certain quality characteristics during the ripening process in classical white cheese production 138

Borik asidin melanom hücre hattı üzerindeki antikanser etkisinin araştırılması 139

Development of impact-resistant, halogen-free, flame-retardant PBT-based composites for use in the automotive industry 140

Synthesis of biopolymer-based quercetin delivery systems using alginate beads: *In vitro* antioxidant and release kinetic analyses 141

Recombinant production of glycoprotein E of Varicellovirus bovinealpha1 in the *Pichia pastoris* yeast expression system 142

Chemical characterization and enantiomeric distribution of Bulgarian lavender (*Lavandula angustifolia* Mill.) cultivars growing in Türkiye 143

Investigation of insecticidal effects of some plant seed oils on adults of *Acanthoscelides obtectus* (Say, 1831) (Coleoptera: Chrysomelidae) 144

The diagnostic importance of circulating subfatin levels in the development of obesity 145

Sustainable gold nanoparticle fabrication from *Corylus maxima* leaves via microwave-assisted extraction 146

The effect of schiff base–derived 4,5-dihydro-1*h*-1,2,4-triazol-5-one compound on serum protein expression and lipid profile in wistar albino rats 147

Evaluation of the *in vitro* genotoxic and antigenotoxic potential of *Geranium robertianum* extract 148

An extensive research on activated carbon (AC) for preparation, characterization and improvement of properties with modification methods 149

Production, import and consumption distribution of activated carbon (AC) in Türkiye 150

Cytotoxic effects of antidiabetic drug metformin in Mcf-7 cells 151

Comparative analysis of the effects of stable and classical vitamin C forms (L-ascorbic acid and 3-O-ethyl ascorbic acid) on antioxidant activity, cell viability, and clonogenic capacity in skin cells 152

Cucurbita pepo'da biyotik stresle ilişkili mikroRNA'ların tanımlanması ve fonksiyonel karakterizasyonu 153

Antidiabetic enzyme inhibition and kinetic behavior of water-soluble morpholine-functionalized axially disubstituted silicon phthalocyanines 154

Uncovering hidden patterns: The significance of water quality trend analysis 156

Determining the vulnerability of groundwater to pollution in the Develi basin (Kayseri) using the DRASTIC method 157

A rapid and eco-friendly route for the synthesis of mono- and bimetallic nanoparticles 158

Investigation of the genotoxic effects of borax decahydrate using micronucleus assay 159

Investigation of the protective potential of boric acid against the genotoxic effects induced by aspartame 160

Evaluation of cytotoxic effects of capecitabine and epigallocatechin gallate combination on a human breast cancer cell line 161

Comparison of *in silico* tools used for predicting the functional effects of polymorphisms in veterinary genetics 162

The use of biotechnology and nanotechnology in parasitology 163

Secondary structures of mitochondrial genes in the classification of *Salmo* species in Türkiye 164

Human health evaluation of drinking water sources in Kütahya province 165

Reorganization of pollen tube cell wall under low temperature conditions in *Camellia sinensis* 166

Total phenolic and flavonoid contents and antioxidant potential of *Vincetoxicum fuscatum* subsp. *fuscatum* seeds 167

Effects of thymoquinone in a surgically induced rat endometriosis model 168

Coverage–confidence paradox in Turkey: A secondary analysis of childhood vaccination and public attitudes (1980–2024) 169

Effects of some postharvest treatments on the storage of nectarine fruits 170

Combined evaluation of inflammatory biomarkers and circulating miRNA-29c in diabetic nephropathy 171

Investigation of toxigenic *Bacillus cereus* in milk and milk-based desserts 172

Magnesium and calcium complexes of curcumin and quercetin: Insights into cell viability, oxidative stress, and antioxidant potential 173

Design and synthesis of amino acid–hydrazone hybrids as dual Bcl-2/NF-κB inhibitors 174

Kalp yetmezliği tedavisinde kullanılan bazı etken maddelerin analizi için kromatografik yöntemlerin geliştirilmesi 175

Synthesis, structural characterization and computational ADME analysis of a New Triazole-Based Cu(II) coordination compound 176

Investigation of the antitumor activity of *Eremurus spectabilis* M. Bieb. (çiriş herb) plant extracts in the process of hepatocellular carcinogenesis induced experimentally with diethylnitrosamine in rats 177

Phytoremediation-oriented Evaluation of Nickel Stress Responses in *Anubias nana* Engl. grown in aquatic systems..... 178

A bibliometric analyse of scientific studies on the invasive species *Lepomis gibbosus*..... 179

Synthesis of functional nanohybrid materials through *in situ* copolymerization 180

Yüksek pH ve tuzluluk koşullarında yerli EDDHA-Fe şelatının gübre performansı ve sürdürülebilir tarım açısından potansiyelinin araştırılması..... 181

Development of a cationic surfactant-selective glassy carbon electrode for potentiometric determination of didecyldimethylammonium chloride..... 182

Efficient microwave-assisted synthesis of novel compounds by the reaction of penta-1,4-diene-3-one derivatives with N,N-dimethyl barbituric acid 183

Fenolik bileşiklerin tayini için polifenol oksidaz temelli biyosensör tasarlanması..... 184

Resveratrol'ün 4T1 meme kanseri hücreleri üzerinde sitotoksik etkisinin değerlendirilmesi..... 185

Determination of the association of TLR2 rs5743708 and rs121917864 polymorphisms with endometrial cancer risk 186

Functional role of MATN3 in osteosarcoma cell growth and motility..... 187

Targeting UHRF2 (Ubiquitin-like with PHD and ring finger domains 2) in osteosarcoma: Impacts on proliferation and emt dynamics..... 188

Selüloz esaslı kompozitlerin 2. tip fotopolimerizasyon yöntemiyle hazırlanması*..... 189

Atık kahve telvesinden türetilen mezogözenekli karbon katkılı PVDF Bazlı PEM yakıt pili membranlarının geliştirilmesi..... 190

A new distribution area of the endemic *Trigonella coerulescens* subsp. *ayvalikensis* (Fabaceae) in Türkiye 191

Ionic liquid–assisted photoluminescence enhancement in CASN:Eu^{2+}–pyranine composites..... 192

Green protein extraction from hazelnut meal using deep eutectic solvents..... 193

Machine learning-driven identification of allosteric networks for the rational design of shark-derived single-domain antibodies..... 194

Farklı coğrafi kökenli sarımsak ve kabuklarının kimyasal parmak izi analizi: FTIR-2D-COS ve HPLC-DAD ile bütünleşik bir yaklaşım 195

Histological investigation of the effects of chronic thiamethoxam exposure on the digestive gland and kidney tissues of *Lymnaea stagnalis*..... 196

Current applications of CRISPR-cas technologies in food microbiology..... 197

Extraction of antioxidants from food waste and its contribution to sustainability..... 198

Visible-light-induced degradation of reactive orange 16 using IRMOF-3: A solar photocatalysis approach 199

The effects of MTHFR gene polymorphisms (C677T, A1298C) and homocysteine levels on the clinical progression of COVID-19 200

Evaluation of the cytotoxic effect of vortioxetine on various cancer cell lines 201

Vortioksetinin çeşitli kanser hücre hatlarındaki sitotoksik etkisinin değerlendirilmesi 202

Screen-printed carbon electrode integrated with feather-like Au-Ag-Co trimetallic composite: An advanced sensor for electrochemical determination of sertraline HCl 203

Investigation of the cytotoxic effect of tizanidine on different cell lines 204

Investigation of the use of bio-based plasticizers in Vinyl (PVC) disposable glove production and their effects on material properties 205

Electrochemical enhancement of modified ITO electrodes for high-performance supercapacitor applications 206

Investigation of the relationship between physical activity level and body awareness in ambulance drivers 207

Advances in 3D graphene foam electrodes for biosensing applications 208

The importance of early detection in Alzheimer's disease: Advancing body-fluid biomarker detection with point-of-care devices 209

Biyokontrol ajanlarının etkisi altındaki *Fusarium spp.*'de transkriptomik incelemeler 210

Farklı esansiyel yağlar içeren pla temelli yara örtülerinin üretimi ve mekanik özelliklerinin incelenmesi 211

Isolation, molecular typing, and investigation of biotechnological potential of actinobacteria from soils in Ardahan province 212

Seasonal changes in phosphatidylinositol (PI) Fatty acid content in muscle tissues of male and female individuals of *Silurus triostegus* 213

Analysis of tumor mutational burden and mutation status in immunotherapy-treated lung adenocarcinomas 214

Antibacterial hydrogels containing a Cu(II) hydrazone complex: Synthesis, characterization, and in vitro activity 215

Acidic deep eutectic solvent catalyst for efficient conversion of levulinic acid to n-butyl levulinate fuel bioadditive 216

Helichrysm arenarium subsp. *erzincanicum* türünün fitokimyasal içeriğinin belirlenmesi ve antioksidan kapasitesinin değerlendirilmesi 217

C-QD ve ZnO-QD'ların hidrotermal sentez yöntemi ile üretimi ve güneş hücrelerinde uygulanmasının araştırılması 218

Histological insights into endometrial microbiota: Implications for fertility and IVF outcomes 219

Metilen mavisi adsorpsiyonunda kullanılmak üzere mısır atıklarından manyetik biyochar üretimi ve karakterizasyonu 220

Cold plasma in the food industry: Mechanisms, product quality and safety perspectives 221

Plantago lanceolata ekstraktı ve çinko-oksit nanopartikülleri ile zenginleştirilmiş çift katmanlı fonksiyonel mikroiğne üretimi ve karakterizasyonu 222

Examination of muscle strength and reflexes in male adolescent rats with streptozotocin-induced diabetes mellitus 223

The impact of gamma rays on soybean germination and seedlings 224

Comperative analysis of three genomic DNA isolation methods in *Simulium bezzii* 225

Synergistic effects of ruxolitinib and *Liquidambar orientalis* extract on MDA-MB-231 breast cancer cells 226

Lilium akkussianum and conservation priorities for Turkey's endemic *Lilium* Species: Habitat requirements and threat analysis 227

From chromatogram to confirmation: Advanced detection of VX nerve agent and related compounds 228

Investigation of programmed cell death during larval-pupal metamorphosis on the posterior silk gland of the *Galleria mellonella* 229

Synthesis of new triazoles as acetylcholinesterase inhibitors 230

The effects of microplastics on soil and plant ecophysiology: Current findings on pollutant transfer from source to plant 231

Newly developed bio-oil-interacted cellulose acetate micro-structured composite adsorbent for efficient dye removal 232

Eco-friendly synthesis of selenium nanoparticles using *Leptolyngbya* sp.: Physico-chemical characterization and bioactivity assessment 233

Dye removal efficiency of bio-oil reinforced flat-sheet cellulose acetate composites as potential membrane materials 234

Synthesis and antioxidant properties of potential dual-acting acetylcholinesterase inhibitors 235

Synthesis of the various macro initiator for production of the blok/graft copolymers via “living”/controlled radical polymerization (CRP) techniques 237

Development of nanoparticle based approaches for the conservation of some paper artifacts 238

Broussonetia papyrifera'dan yeni tanımlanan 1,3-difenilpropanların asetilkolinesteraz enzimi üzerindeki inhibitör etkilerinin *in-silico* olarak incelenmesi 239

Pharmacological uses of species belonging to the Lamiaceae family on the campus of Uşak University 240

Synthesis and tyrosinase inhibition of 1-(4-fluorobenzyl)piperazine-based dithiocarbamates 241

Effects of heat treatment on gga-miR-30c-5p, gga-miR-191-5p, and gga-miR-215-5p in poultry eggs . 242

RNA isolation from three-dimensional saos-2 cultures in a collagen/keratin/alginate hydrogel 243

Synthesis and characterization of biodegradable polyester by ring-opening polymerization (ROP) 244

Atıksu arıtma tesislerinde karbon ayak izi: Türkiye’deki mevcut durum 245

Evaluation of antibacterial potential of different parts of *Vincetoxicum hirundinaria* against *Enterobacter cloacae* 246

Solvent-dependent differences in the DPPH antioxidant activity of bee pollen extracts 247

Metagenomic analysis of the olive rhizosphere microbiome 248

Membrane cholesterol modulation Alters P2x7-mediated membrane currents but not cytoskeletal reorganization in macrophages 249

In silico evaluation of potential inhibitors against *Moraxella catarrhalis* 3-oxoacyl-[acyl-carrier-protein] reductase (FabG) 250

Acute effects of bacterial lipopolysaccaride on liver of female rats: Assestment of histopathological changes 251

TLR4/MYD88/ NF-KB sinyal yolağı 252

Dose-dependent cytotoxic effect of Carbidopa on U-87 MG human glioblastoma cells 253

Hydrazone-functionalized diphenylurea derivatives: Synthesis, structural characterization, and comprehensive biological activity evaluation 254

Development of high-sulfonation sPEEK membranes containing s-TiO_2 nanoparticles for direct methanol fuel cell (DMFC) applications 255

Silica-supported silicotungstic acid incorporated high-DS sPEEK membranes for hydrogen PEMFC applications 256

Synthesis of eudragit RS100-coated juglone-Ag encapsulated PLGA nanoparticles for the treatment of *Helicobacter pylori* 257

Eudragit-coated PLGA nanoparticles encapsulating CAPE–Ag complex for gastric cancer therapy 258

Eudragit-functionalised PLGA nanoparticles encapsulating juglone–Cu complexes as a promising delivery system against *Helicobacter pylori* 259

Sustainable waste recycling strategies in the blue economy 260

Podmore extract (apis totale) content analysis and *in vivo* animal studies 261

Identification of SNPs from RNA-seq data in tolerant soybean mutants 262

Keratin-enhanced hydrogels: Structural and functional characterization for tissue engineering 263

Fabrication and characterization of polyvinyl alcohol/gelatin/hyaluronic acid based microneedle patches for transdermal delivery of amphotericin B 264

Tunicate species diversity in İzmir Bay 265

Non-enzymatic electrochemical sensor design of pencil graphite electrode modified with poly(L-proline) and graphene for sensitive detection of folic acid 266

Synthesis, characterization and anticancer evaluation of novel urea derivatives 268

Computational study on the molecular, electronic, and spectroscopic properties of 3-ethyl-4-[3-methoxy-2-(4-methoxybenzoyloxy)-benzylideneamino]-4,5-dihydro-1*H*-1,2,4-triazol-5-one 269

Investigation of antibacterial, antifungal, antibiofilm and synergistic effects of *Satureja thymbra* L. plant extracts against bacteria and fungi 270

Investigation of biocompatibility and anticancer activities of *Lavandula intermedia* and *Lavandula angustifolia* on breast cancer (MCF-7) and healthy mouse fibroblast (L929) cell lines 271

Investigation of genetic diversity in barley (*Hordeum vulgare* L.) varieties grown in Türkiye using ISSR molecular markers 272

Determination of *in vitro* biological activity of firethorn plant fruits 273

The role and impact of eco-labels in seafood marketing 274

The effect of 1-methylcyclopropane treatments on phenolic compounds in 'Ekmek' quince fruit 275

Preharvest salicylic acid treatments can improve fruit quality in '0900 Ziraat' cherry fruit 276

Rize-sourced hazelnut shell ash as a green corrosion inhibitor for Fe metal in 1 wt.% NaCl: Electrochemical evaluation and mechanistic insights 277

Cobalt oxide/halloysite nanotubes for enhanced electrochemical sensing of tetracycline 278

Evaluating the phytoremediation potential of *Hygrophila corymbosa* under lead stress: Physiological insights in freshwater environments 279

Investigation of cytotoxic and anti-angiogenic effects of apigenin in breast cancer cell line 280

Synthesis, characterization, and evaluation of cytotoxic activities of *n*-phenyl-*n'*-(4-pyridylmethyl)urea derivatives in breast cancer cell lines 281

Relationship of polymorphisms in *PITX1, PITX2, LHX3, PROP1* and *POU1F1* genes with litter size and growth traits in saanen goats 282

Evaluation of the capacitive behavior of MWCNTs to explore their potential applications in supercapacitor electrodes 283

Synthesis of porous carbon structures from coal via molten salt activation and HF acid treatment for hydrogen storage 284

Determination of meat consumption preferences by analytical hierarchy process (AHP) 285

An *In-silico* platform for predicting magnetic resonance imaging (MRI) contrast properties of diamagnetic chemical exchange saturation transfer (DIACEST) agents 286

Biomarker evidence of metolachlor-driven oxidative stress in rainbow trout 287

Co-toxicity of pesticides and nano/microplastics in aquatic systems: Implications for fish models 288

Impact of agricultural herbicides on aquatic ecosystems: Case of aclonifen 289

The importance of vineyard houses in Gaziantep in terms of culture and urban ecology 290

Comparative evaluation of antioxidant activities and bioactive compound profiles of *Pyracantha coccinea* M. Roem. extracts 291

Growth–biomass responses of *Eruca sativa* Mill. microgreens to the lichen-derived metabolites atranorin and usnic acid 292

Antioxidant activities and phytochemical profiles of microgreen and mature *Spinacia oleracea* L. extracts 293

Effects of LED light exposure on phenolic–flavonoid content and antioxidant properties of *Lens culinaris* L. microgreens extracts 294

Phenolic–flavonoid composition and antioxidant potential of microgreen and mature *Eruca sativa* Mill. extracts 295

Artificial intelligence-assisted dermatophyte diagnosis-image analytics approach 296

Cytokines as biological pesticides in combating pest insects 297

Evde tüketim veya pazarlarda satışa sunulmak için üretilen peynirlerde biyojen amin üreticisi *Enterococcus* türlerinin risk değerlendirmesi: Çanakkale/Bayramiç örneği 298

Structure-based docking analysis of potential insect growth regulator ligands against the EcR/USP complex 299

Endothelial dysfunction in type 1 diabetes and therapeutic targets 300

Contemporary advances in type 1 diabetes therapeutic perspectives 301

Bioacoustic Differentiation of Advertisement Calls between the cf. Bedriagae Water Frog Lineage (Genus: *Pelophylax*) in Central Anatolia and the Cilician Water Lineagae in the Frog Çukurova Plain in Türkiye 302

Fe (III)'ün sulu ortamda tespiti için rodamin-B bazlı optik sensör 303

Design of an Assay for Detecting Ehlers-Danlos Syndrome in Bengal Cats via Enzymatic Digestion 304

Comprehensive genome analysis and various functional attributes of a potential *Enterobacter bugandensis* isolated from Türkiye 305

Bitki büyümesini teşvik edici özellikteki *Bacillus* suşlarının siklik lipopeptid üretimlerinin kromatografik olarak incelenmesi 306

Green synthesis of a novel chloro-aza acyclovir analogue 307

Cytotoxic and antimicrobial effects of *Cirsium ciliatum* subsp. *szovitsii* (C. Koch) Petrak and the determination of its phenolic compounds 308

Preliminary evaluation of olive pomace extract-based topical cream: Antioxidant capacity and wound healing potential 309

Development of a biosensor for ethoprophos determination 310

An integrated multi-omics framework for robust MSI detection in colorectal cancer 311

Postbiotics as potential therapeutic agents for noncommunicable diseases 312

Production of enantiomerically pure 1-phenylethanol in green solvent media using response surface methodology 313

Eco-friendly synthesis of zinc oxide nanoparticles using pomegranate peel extract: Characterization and photocatalytic degradation of diclofenac 314

Current and emerging biomarkers in nephrotic syndrome 315

Production of natural fiber-reinforced epoxy biocomposites in different woven and single-hybrid forms and analysis of their inner structure 316

Production and characterization of honokiol-loaded polymeric nanoparticles for glioblastoma treatment 317

Holstein-Friesian ırkı erkek sığırlarda *LEP, IGF1* ve *MYF5* genlerinin karkas ve et kalitesi özellikleri üzerine etkilerinin belirlenmesi 318

Poisonous mushrooms and mushroom poisoning: Current findings and toxicological approaches from Türkiye 319

Medicinal Mushrooms As Emerging Natural Adjuncts In Cancer Therapy 320

Mathematical modeling of excercise -induced DNA methylation dynamics 321

Pomegranate peel extract: antioxidant activity and potential effects on cardiovascular health 322

Chemical warfare agent recognition by using a practical mobile application 323

Development of a MIP-modified electrochemical sensor for urea detection through EIS 324

Extraction of bioactive compounds from rosehip fruit using natural deep eutectic solvents (NADES) . 325

Synthesis, biological activity and molecular modeling studies of compounds with benzo[*d*]oxazole structure 326

Detection of specific spoilage organisms (SSOs) of sea bream (*Sparus aurata*) 327

Protective effects of *Aloe vera* gel extract against cytotoxic, genotoxic, and physiological damage induced by nitric acid in *Allium cepa* cells 328

Viability of the probiotic microorganism *Saccharomyces boulardii* in olive oil and its effects on oil quality 329

Sustainability assessment of potassium permanganate and sodium hypochlorite used in the bleaching of denim fabrics 330

Optimization of sample dispersion protocols for high-resolution microscopic analysis of sol-gel synthesized TiO_2 quantum dots 331

Microbial content, antioxidant activity, and volatile aroma compounds profile of boza, a fermented cereal beverage 332

In vitro cytotoxic evaluation of *Artemisia absinthium* on human A549 lung carcinoma cells 333

Optimization of heavy metal (As, Cd, and Hg) adsorption performance of green-synthesized TiO_2–Fe_3O_4 nanocomposite using aloe vera extract via Taguchi method 334

1.2. FULL-TEXTS 335

AI-assisted laboratory-based severity index for chronic spontaneous urticaria using eosinophil count, basophil count, and vitamin D 337

Trends in utilization and expenditure of reimbursed lipid-lowering drugs in Albania 340

Identification and management of mold-induced allergies in indoor environments 347

“Challenges and opportunities in preserving natural resources” in Albania 352

Maternal and neonatal outcomes following induction of labor at term: A retrospective cohort study .. 359

Environmental evaluation of outdoor pollen and its association with allergic asthma in a population group 369

Effect of amine complexes from natural petroleum acids on the corrosion of carbon steel in a CO_2 environment using the tafel method 377

Assessment of spinal problems in the sagittal plane among students of Aldent University 385

The impact of PNF protocols on the activation increase of the multifidus and transversus abdominis muscles 389

Maternal and Infant Outcomes of Breastfeeding and Formula Feeding: A Quantitative Comparative Study 393

The role of biology in promoting education for sustainable development in upper secondary education 398

Learning through analysis in education: Using data to improve student learning 403

Wine sector in Albania: Challenges and opportunities for geographical indications protection 408

Bir üniversite hastanesinde konjenital sitomegalovirüs (CMV) enfeksiyonlarında moleküler test sonuçlarının değerlendirmesi 415

Bazı geleneksel olarak kullanılan antidiabetik bitkilerin enzim inhibisyon mekanizmalarının *in vitro* incelenmesi 418

Evaluation of Bax expression in colorectal tumors and adjacent healthy tissues 424

Biogenic nanotechnology's role in the treatment of Parkinson's disease: How can we benefit more from food? 431

Impair DNA Methyltransferases Gene DNMT1 Level and Alternated Immune Agents in Systemic Lupus Erythematosus of Iraqi Patients 435

Val-Trp dipeptidinin MCF-7 meme kanseri hücreleri üzerindeki sitotoksik etkisinin araştırılması 442

GUL herbaryumu'nun Caryophyllaceae familyası envanteri üzerine notlar 446

Melanomda beyin metastazı gelişiminde rol oynayan moleküler mekanizmalar 452

Determination of the effect of tinkal-added cement on gamma ray absorption 456

A dual-action role of naphthalene sulfonate in enhancing arsenic uptake and mitigating toxicity in maize seedlings 463

Synthesis of schiff-based graft copolymer with waste PET and nucleation effect in PP masterbatches 470

Photocatalytic hydrogen production from chitin/chitosan supported molybdenum disulfide 476

Investigation of the putative role of BON domain–containing proteins on biofilm resistance in *Pseudomonas aeruginosa* 484

Thymus canoviridis bitkisinin bazı ekstraktlarının HMGR enzimi inhibisyonuna etkilerinin moleküler yerleştirme metodu ile incelenmesi 489

The olive oil production and pomace management in Albania, a contribution to sustainable agriculture 497

Düzce Üniversitesi Konuralp Yerleşkesindeki yaban arısı çeşitliliği ve polinasyona etkileri üzerine araştırmalar 503

Deep eutectic solvent-assisted extraction of *Viburnum opulus* fruit and evaluation of its biological potentials 511

Seasonal lipid and fatty acid profile of gilthead seabream (*Sparus aurata* L.) cultured in the Aegean and Mediterranean Seas 519

Effect of PDE4B inhibitors on miRNA levels in different glioma cell lines 526

Synthesis of novel hybrid compounds via multi-component reactions and determination of their anticancer activities on colon cancer (HT-29) cell line by *in silico* and *in vitro* methods 531

Yarpuz otu (*Mentha pulegium*) fenoliklerinin sağlık üzerine etkileri 538

Onosma alborosea ekstraktindan sentezlenen nanopartiküllerin antimikrobiyal özelliklerinin incelenmesi 542

Pandemi dönemi ile birlikte beslenme ve sağlık dersinin yeniden yapılandırılması: İçerik, pedagoji ve dijital dönüşüm açılarından nitel bir analiz 546

Hexavalent chromium removal using modified zeolites 553

Synthesis and structural characterization of a novel chromone–1,3,4-thiadiazole–hydrazone hybrid bearing a 4-fluorobenzyl moiety 558

Determination of MIC-MBC values and DPPH removal activity of zinc oxide nanoparticle 565

Bacillus thuringiensis parasporal proteinlerinin çeşitli kanser hücre hatları üzerinde sitotoksik aktivitelerinin araştırılması 570

Bitki hormunu olarak karrikinlerin bitki fizyolojisindeki rolü, ekolojik önemi ve tarımsal biyoteknolojideki uygulama potansiyelleri 576

KBRN Bilgi Düzeyinin Artırılmasında Animasyon Teknolojisinin Kullanımı ve Etkisinin İncelenmesi; Niğde Ömer Halisdemir Üniversitesi Tıp ve Hemşirelik Bölümü Lisans Öğrencileri Örneği 583

Effects of diatomite applications on some soil properties and aggregate stability 590

Doğal Bt izolatından elde edilen parasporal proteinin PC-3 hücreleri üzerinde sitotoksik ve hücre göçünü inhibe edici etkilerinin incelenmesi 596

Cyclic voltammetric determination of brilliant blue in energy drinks by using a pretreated pencil graphite electrode 602

Comparative development and antibiofilm evaluation of nanoemulgels containing linseed, borage, and pumpkin seed oils 609

Kenevir-beton yalıtımlarının kuruma hızı ve etkin nem difüzyon katsayılarının tahmini 617

Removal of micropollutants from water and wastewater by granular activated carbon 624

Potansiyel bir hidrojen depolama iyonik sıvısı olarak guanidinyum oktahidrotriboratın yapısal ve elektronik özelliklerinin hesapsal karakterizasyonu 630

A bioinformatics-based approach for evaluating drug-likeness and docking potential of *Crocus sativus* metabolites 637

Berberinin östrojen reseptörü (ER/PR) pozitif meme kanseri hücrelerinde trombosit mikropartikülleri aracılı proliferasyon ve migrasyon üzerindeki etkileri 641

Decoding the *ALMT* gene family in *Helianthus annuus*: Evolutionary patterns, structural features, and stress-responsive functional potential 649

Bitki doku kültüründe akıllı biyosüreçler ve yapay zeka makine öğrenimi 655

Pulmoner fibrosizte antioksidan genlerin düzenlenmesi-bir derleme çalışması 662

KBRN olaylarında afet yönetimi ve müdahale koordinasyonu: Disiplinlerarası yaklaşımlar ve güncel uygulamalar 672

Sekonder metabolit tabanlı ilaç yüklü nanoparçacıkların sentezlenmesi ve salınım davranışının modellenmesi 680

Silajlık mısır (*Zea mays* L.) çeşit adaylarının ikinci ürün koşullarında performanslarının belirlenmesi 687

Regenerative roles of mesenchymal stem cells and extracellular vesicles in ovarian and endometrial injury ... 693

Çeşitli metallerle dekore edilmiş alüminyum katkılı altıgen bor nitrür nano levhaların hidrojen depolama özelliklerinin hesaplamalı incelenmesi ... 696

Chenopodium quinoa ekstraktları ile kitosan nanopartiküllerinin biyosentezi ve karakterizasyonu ... 703

Glycyrrhiza glabra ekstraktları ile kitosan nanopartiküllerinin biyosentezi ve karakterizasyonu ... 710

Computational approach to evaluating an isoniazid-based schiff base targeting *Mycobacterium tuberculosis* ... 718

Piyasada satılan farklı matcha çayı türlerinin fenolik bileşik içeriklerinin ve antioksidan kapasitelerinin yeşil çay türleri ile karşılaştırılması ... 724

Chick quality following in ovo feeding of *Viscum album* extract ... 732

Optimization of malachite green photodegradation using quantum dots via response surface methodology ... 737

Trace elements essential for life in biological systems: Copper, zinc and selenium ... 746

Biochar production from spent coffee grounds by hydrothermal carbonization as a catalyst support material for hydrogen production by methanolysis of sodium borohydride ... 754

Fidelity of FDM-fabricated PLA bone scaffolds to CAD models: a comparative analysis of voronoi, TPMS, and lattice architectures ... 761

Çiğ kıyma ve köfte kökenli *Klebsiella* spp. ve *Citrobacter* spp. izolatlarında antibiyotik direnç genleri ve biyofilm oluşumu ... 767

Catalytic cottonization of hemp fibres at room temperature in the presence of a bimetallic iron oxide catalyst ... 776

Syringic acid mitigates chlorpyrifos-induced oxidative stress and DNA damage in HEK293 cells ... 785

Neuroprotective effect of vanillic acid against paraquat-induced oxidative and cholinergic dysfunction ... 790

Optimization and formulation of quetiapine bilosomes using a central composite design ... 795

Kanatlılarda besleme ve DNA metilasyonu: Performans, hayvan sağlığı ve refahı üzerine etkiler ... 802

Effects of exogenous glucose on leaf color and biochemical–antioxidant properties of two purple basil (*Ocimum basilicum* L.) cultivars ... 811

Quality by design optimization of calcium phosphate nanocores for aquasomes: Role of precursor ratio and sonication time ... 820

Molecular docking and DFT-based theoretical assessment of delpazolid's activity against *Mycobacterium tuberculosis* ... 825

Resveratrol'ün FOXP3 geni üzerindeki düzenleyici rolü ... 833

The acute gastrointestinal toxidrome: A triage algorithm distinguishing organophosphates, carbamates, and metal phosphides from foodborne illness ... 839

Influence of magnesium-doped zinc-tin-oxide nanoparticles on physiological and biochemical responses of tomato plants 848

Ultrasound triggered piezocatalysis of organic pollutant degradation via Fe_3O_4 nanoparticles 853

Arı ekmeği etanol ekstraktlarının HPLC tabanli bileşen analizi ve antioksidan potansiyeli 859

Production of biochar from hazelnut shells by hydrothermal carbonization and determination of its effect as a catalyst support in hydrogen production 867

İksut otu *(Cuscuta europaea* L.) kullanılarak sentezlenen çinko oksit nanopartiküllerin antimikrobiyal ve küf (ekmek küfü) üzerine etkisinin belirlenmesi 872

İğde meyvesinden sentezlenen çinkooksit nanopartiküllerin antimikrobiyal etkinliği ve akciğer ve kolon kanseri üzerine sitotoksik etkisi 881

Evaluation of the effect of postbiotics on common food pathogens 888

Türkiye'de yetişen *Salvia* taksonlarına ve halk tıbbında kullanımına genel bir bakış 891

Mixed-ligand thiosemicarbazone Ni(II) complex with 2,6-dimethylpyridine: Characterization and cytotoxicity studies 902

Fast and complete destruction of acid fuchsin dye from water by electro-Fenton based processes 910

Extraction of bioactive components from black elderberry (*Sambucus nigra* L.) with deep eutectic solvents and characterization of the components 918

Investigation of the use of colorimetric films containing cranberry extract as ph indicators 926

Bioactive potential of *Raphanus sativus* L. var. *longipinnatus* (Daikon): Cytotoxicity and antioxidant activity 933

Potential of two *Sideritis* species against EMS-induced DNA damage in *Drosophila melanogaster* 941

Seedlessness genes and molecular identification studies in grapevines (*Vitis vinifera* L.) 948

Effect Of tinkal added cement on neutron rays absorption capacity 961

Beyin hasarı ve kuersetin: Deneysel bulgular ve klinik potansiyel 969

Periodontal destruction, periodontal regeneration and considerations in endo-perio lesions 977

Nar atıklarından yarı katı kültür fermantasyonuyla sitrik asit üretiminin incelenmesi 985

Biopreservation with postbiotics: The Potential of microbial metabolites to enhance food safety and extend shelf life 989

Effects of different nitrogen sources and potassium doses on plant growth and some quality characteristics in lettuce 995

Obtaining free amino acids from raw sheep wool by solvothermal acid hydrolysis in a hydrothermal reactor 1004

Evaluation of antioxidant capacity of *Morus indica* L. leaf extract by DPPH method 1012

Effect of artichoke (*Cynara scolymus* L.) leaf extract on *Caenorhabditis elegans* population growth 1018

Evaluation of antioxidant activity of artichoke leaves with DPPH radical scavenging assay 1024

Investigation of the effect of mulberry leaf extract on population growth of *Caenorhabditis elegans* 1030

Alüminyum fosfit zehirlenmesinde klinik yaklaşımlar ve gelecek perspektifleri 1036

Enhancement of diagnostic power of miR-126-3p and inflammatory clinical markers in COPD with random forest machine learning 1044

Use of metal-organic frameworks in enzyme immobilization 1052

Probiotic extracellular vesicles as postbiotic therapeutics in precision medicine 1062

Ferroptosis and kidney injury: Therapeutic perspectives in diabetic nephropathy 1070

Removable prosthetic rehabilitation with the third impression of a completely edentulous patient with temporomandibular disorders: A case report. 1077

Balık hastalıklarına yanıtta moleküler mekanizmalar 1083

Zebra balığı embriyolarında imidakloprid ve bisfenol E'nin kombine maruziyetine bağlı morfolojik anomaliler ve apoptoz yanıtı 1089

Extract to protect: Redefining betalain stability in natural colorant research 1097

Production and characterization af aldehyde fractionated regenerated cellulose-chitosan based bioaerogel 1102

Synthesis of novel benzothiazole/thiazole hybrids and *in silico* investigations via SwissADME and BioFinder programs 1111

The impact of academic stress on eating behaviors, lifestyle and weight among University students. 1119

Fitoterapötik bir umut: Silimarinin hayvan sağlığı üzerindeki etkilerine ilişkin klinik ve deneysel kanıtlar 1135

QTL analysis in plum (*Prunus* spp.) 1143

Abiotic stress factors and molecular approaches in grapevine 1149

Deronectes hakkariensis Wewalka, 1989b türünün (Coleoptera, Dytiscidae, Hydroporinae) dişisinin ilk tanımı, Elâzığ, Türkiye 1155

The future of eggs: The functional food market and consumer trends 1161

DPP4 (CD26) geninin akut myeloid lösemi patogenezindeki rolünün değerlendirilmesi 1169

Dysregulated lipid metabolism in colon tissue: The impact of *SCD* and *ACSL1* on tumor progression 1175

Exosomes as extracellular vesicles: Clinical and experimental perspectives 1182

Nörodejenerasyonda laktoferrinin koruyucu rolü: Klinik ve deneysel perspektifler 1189

Effects of paclobutrazol on basil (*Ocimum basilicum* L.) during germination 1197

Schiff baz ve 1,10-fenantrolinden türeyen karışık ligand Cu(II) ve Fe(II) komplekslerinin sentez ve karakterizasyonu 1203

Flor sübstitüe Schiff baz ve 1,10-fenantrolinden türeyen karışık ligand Fe(II) ve Cu(II) komplekslerinin sentez ve karakterizasyonu 1211

Mardin ili Diplura (Hexapod) faunasınası için yeni kayıt 1219

Innovative use of hydroxyapatite-based structures in bone tissue regeneration 1223

Efficient multiple testing procedure for belief propagation on biological network with conformal prediction 1229

Optimal multiple testing procedure for double machine learning with clustering data 1236

STAT4 genindeki missense varyantların romatoid artrit üzerine olası etkilerinin biyoinformatik analizi 1243

Farklı gıdalardan elde edilen *A. flavus* izolatlarının genetik ve toksijenik profilinin incelenmesi 1249

*Capnodis tenebricosa'*nın (Olivier, 1790) (Coleoptera: Buprestidae) biyolojik mücadele ajanı olarak değerlendirilmesi....1260

Fitoterapötik ajanlar olarak *Melissa officinalis* ve *Thymbra spicata:* Antibakteriyel ve antikanser aktivite üzerine bir araştırma 1265

Evaluation of the cytotoxic effects of Hydroxy Methyl Butyrate (HMB) used as an ergogenic Aid....1273

Health emergency management in a regional coastal hospital during the tourist season....1280

Koç testislerinin 3B modellenmesinde doku matlaştırma işleminin model parametrelerine etkisi....1287

Sütçü sığırlarda süt verimi ile suni tohumlama sonrası gebelik oranı ilişkisinin araştırılması....1292

Sürdürülebilir Boyamacılıkta *Juglans regia* L. Yaprağı Kaynaklı Biyomordanın Kullanımı....1297

Gene-level modulation of stress response by karrikin in tomato under heat and drought stress 1308

Supercritical extraction of clove (*Syzygium aromaticum*) and investigation of essential oil components by GC-MS....1312

Kinetic, thermodynamic and isothermal study of mechanically activated seashells at different durations 1316

CZTSe Nanokristallerin Sentezi ve Karakterizasyonu....1324

Effect of post-mating administration of different doses of TAK-683 on luteal function and pregnancy-associated glycoprotein (PAG) levels during early pregnancy in Aleppo goats 1330

Acyclic and cyclic Schiff base–modified cyclophosphazenes....1337

Mayaların tanımlanmasında kullanılan yöntemler 1345

Mikroorganizmaların DNA izolasyon ve saflaştırma yöntemleri 1349

Investigation of the antioxidant and anticholinesterase activities of methanol extracts of *Thymus sipyleus* Boiss. and *T. zygıoides* Griseb. 1355

2. POSTER PRESENTATIONS....1362

2.1. ABSTRACTS....1362

Anti-ulcer activity of pumpkin (*Cucurbita moschata* & *Cucurbita maxima*) pulp and seed extracts in rats 1365

From waste to nanofibers: Pullulan-assisted electrospinning of keratin....1366

From resistance profiles to novel therapies: A systems approach to combat *Pseudomonas aeruginosa* 1367

Carbon dots synthesized using eutectic solvents and tangerine peels as a sustainable carbon source 1368

Evaluation of the *in vitro* genotoxicity of potassium acetate using single-cell gel electrophoresis....1369

Development and characterization of carbon-based flexible electrodes for electrochemical technology applications....1370

Synthesis of methylsulfonylmethane-doped hydroxyapatite for drug delivery 1371

Identification of candidate genes associated with cold tolerance in sitka spruce (*Picea sitchensis*)..... 1372

Comparative analysis of EPS biosynthesis-related genes expression in *Ligilactobacillus salivarius* KC27L and *Limosilactobacillus reuteri* KC21L..... 1373

$[Zn(Hssal)(o\text{-}bix)]_n$ kompleksinin sentezi ve X-işını tek kristal çalışması 1374

$\{[Cd(DTPA)(bpy)]H_2O\}_n$ kompleksinin sentezi ve X-Işını tek kristal çalışması..... 1375

The effect of orlistat on nitric oxide levels in LPS+IFN-ɣ-stimulated RAW 264.7 macrophage cells..... 1376

Antileukemic potential of *Nerium oleander* L. extract: Cytotoxic and apoptotic effects on leukemia cells 1377

Yeni benzaldehit türevi Schiff bazı sentezi ve yapılarının spektroskopik yöntemlerle karakterizasyonu 1378

Literature-based analysis of cytotoxic and genotoxic effects of microplastic exposure 1379

Effect of PLGA–PEG–based *Hypericum perforatum* extract nanoparticles targeted with panitumumab in colorectal cancer cells..... 1380

Investigating the role of *COL1A1* and *FN1* gene expression in cisplatin-resistant ovarian cancer 1381

Examination of the capacitive properties of reduced graphene oxide based electrodes functionalized with isonitrosoacetophenone derivatives 1382

Expression analysis of PCBB and IVD genes in metastatic prostate cancer 1383

Efficacy of rosmarinic acid in reducing symptoms of acne vulgaris: Case study 1384

Bazı N-(4-sübstitüearil) maleimit bileşiklerinin sentezi ve asit katalizli hidroliz reaksiyon mekanizmasının araştırılması 1385

Cloning and expression of the *Ananas comosus Bromelain* gene in *Escherichia coli* 1386

Development of clay-based kserogel structures for thermal energy storage systems 1387

The effectiveness of cavitation liposuction and radiofrequency in reducing excess abdominal fat. A pilot study..... 1388

In silico screening and selection of the optimal asparaginase gene for cloning from *Tetrahymena thermophila* 1389

Elucidation of the anatomy, ecology, and micromorphology of three *Glaucium* species in the Aegean Region..... 1390

Development and characterization of nanocomposites for high-performance supercapacitors 1391

CID-1067700 treatment differentially modulates lysosomal acidification in bortezomib-sensitive and -resistant myeloma cells..... 1392

Enhanced topical efficacy of ketoprofen: Development of beta-cyclodextrin-based inclusion complexes and biopharmaceutical performance analysis..... 1393

Production of a chitosan-based hydrogel packaging film to extend the shelf life of packaged foods..... 1394

The use of lithium obtained from the recycling of lithium-ion batteries as a raw material in lithium-carbonate-based mental health medications 1395

Morphological and phylogenetic analyses of species belonging to the Lamiaceae family at Uşak University Campus....1396

Effects of human osteoblast-derived exosomes on the osteogenic commitment of multipotent and pluripotent stem cells....1397

Synthesis and characterization of new liquid crystalline polyurethane copolymer....1398

Biyokatalizör kullanılarak $NaBH_4$ 'den hidrojen üretiminin araştırılması....1399

Hybrid renewable mobile energy station for off-grid molecular diagnostics and cold-chain healthcare....1400

2.2. FULL-TEXTS....1403

Influence of different Albanian freshwater sources on pale ale beer quality....1405

Evaluating the relationship between chronological age and ATR-FTIR spectral ratios in thai dental samples....1411

Van Gölü alkalifilik fungusları üzerine ön çalışma....1418

The importance of sampling in the statistical study of STR markers....1424

Sığır ve insanlarda bruselloz kontrol ve kontrol stratejileri....1429

Academic stress and exam-period nutrition: Implications for student well-being and academic performance....1436

Preparation of chalcone modified polyHIPE for removal of aluminum ions from water....1441

Design of a ZIF-8 functionalized glassy carbon electrode-based electrochemical sensor for high-sensitivity TBHQ determination....1447

Preparation of liquid crystalline poly (vinyl tetrazole) based cholesteryl modified polymer....1455

1. ORAL PRESENTATIONS

1.1. ABSTRACTS

ORAL PRESENTATION

Neuroinflammation in chronic urticaria: A bibliometric analysis of global research output

Eralda Lekli[1,2*] (ORCID:0000-0003-3041-8910,)
Mehmet Hoxha[1,3] (ORCID: 0000-0001-8829-6931)

[1]University of Medicine, Faculty of Medicine, Department of Internal Diseases, Tirana, Albania.
[2] Salus Hospital Tirana, Department of Allergology, Tirana, Albania.
[3]University Hospital Mother Teresa, Service of Allergology, Tirana, Albania

Abstract

Chronic urticaria (CU), particularly chronic spontaneous urticaria (CSU), is a complex inflammatory skin disorder characterized by recurrent wheals and/or angioedema lasting longer than six weeks. (Zuberbier et al. 2022) While mast-cell activation has been considered central to disease physiology, emerging evidence indicates that neuro-immune pathways and neuroinflammation may also contribute to symptom persistence and disease severity. Chronic urticaria, like atopic dermatitis, is shaped by communication between immune cells and sensory nerves, and this connection appears to aggravate the disease. (Yang et al. 2025) Interest in the neuro-inflammatory dimension of CU has grown, yet the overall volume, distribution, and type of publications addressing this intersection remain unclear. We aimed to evaluate the scientific output related to neuroinflammation and chronic urticaria. A structured search was conducted using Google Scholar with above keywords, summarizing publication trends across all years, the last 5 years, and the year 2025, while comparing the proportion of review versus non review articles and documenting the presence of patents and citations. A total of 3830 publications were identified across all years, 1150(30.03 %) review articles, 17.75% or 680 publications marked as patents and 7.83% or 300 citations only entries. Out of total, 2280(59.53 %) were published during 2021-2025, with 754(19.68 %) review articles, and 590(15.4 %) were published in 2025, out of them 223(5.82%) review articles. The proportion of review articles was increased to 37.8% of related publication during 2025, from 33.1% in past 5 years. The majority of publications focused on neuro-immune signalling, mast-cell–neuronal interactions, psychological stress pathways. Although the total body of literature addressing CU is considerable, publications specifically integrating neuroinflammation remain limited, suggesting increasing interest in recent years. These data highlight the need for more targeted mechanistic and clinical research exploring the neuro-immune axis in chronic urticaria.

Keywords: neuroinflamation, chronic urticaria, publicatios

References:

Yang, Shurui, Li Chen, Haiming Zhang, Yanjuan Song, Wenyan Wang, Zhengbo Hu, Siyu Wang, Liuyang Huang, Yayuan Wang, Song Wu, Rui Chen, and Fengxia Liang. 2025. “Beyond the Itch: The Complex Interplay of Immune, Neurological, and Psychological Factors in Chronic Urticaria.” *Journal of Neuroinflammation* 22(1):75. doi:10.1186/s12974-025-03397-4.

Zuberbier, Torsten, Amir Hamzah Abdul Latiff, Mohamed Abuzakouk, Susan Aquilina, Riccardo Asero, Diane Baker, Barbara Ballmer-Weber, Christine Bangert, Moshe Ben-Shoshan, Jonathan A. Bernstein, Carsten Bindslev-Jensen, Knut Brockow, Zenon Brzoza, Herberto Jose Chong Neto, Martin K. Church, Paulo R. Criado, Inna V. Danilycheva, Corinna Dressler, Luis Felipe Ensina, Luz Fonacier, Matthew Gaskins, Krisztian Gáspár, Aslı Gelincik, Ana Giménez-Arnau, Kiran Godse, Margarida Gonçalo, Clive Grattan, Martine Grosber, Eckard Hamelmann, Jacques Hébert, Michihiro Hide, Allen Kaplan, Alexander Kapp, Aharon Kessel, Emek Kocatürk, Kanokvalai Kulthanan, Désirée Larenas-Linnemann, Antti Lauerma, Tabi A. Leslie, Markus Magerl, Michael Makris, Raisa Y. Meshkova, Martin Metz, Daniel Micallef, Charlotte G. Mortz, Alexander Nast, Hanneke Oude-Elberink, Ruby Pawankar, Paolo D. Pigatto, Hector Ratti Sisa, María Isabel Rojo Gutiérrez, Sarbjit S. Saini, Peter Schmid-Grendelmeier, Bulent E. Sekerel, Frank Siebenhaar, Hanna Siiskonen, Angele Soria, Petra Staubach-Renz, Luca Stingeni, Gordon Sussman, Andrea Szegedi, Simon Francis Thomsen, Zahava Vadasz, Christian Vestergaard, Bettina Wedi, Zuotao Zhao, and Marcus Maurer. 2022. “The International EAACI/GA[2]LEN/EuroGuiDerm/APAAACI Guideline for the Definition, Classification, Diagnosis, and Management of Urticaria.” *Allergy* 77(3):734–66. doi:10.1111/all.15090.

ORAL PRESENTATION

The influence of self-prepared foot care product on foot microbiome

Katarzyna Duda – Grychtol[1*] (https://orcid.org/0009-0008-7306-9611), Julia Kościołek[1]

[1] The Silesian Academy of Medical Science in Katowice, Katowice, Poland

Abstract

The feet are one of the most unique and heterogeneous microbial niches of human body with areas that differ by skin thickness, anatomical features, and distribution of sweat glands, pH and the availability of oxygen. Healthy skin of the foot is colonized by different microorganisms including bacteria like *Corynebacteriaceae*, *Micrococcaceae*, *Propionibacteriacea*e, *Streptococcaceae*. The most common fungi present on the feet are *Malassezzia*, *Cryptococcus*, *Aspergillus*, *Candida*, *Epidermophyton, Microsporum* and *Trichophyton*. Different factors can promoting growth of foot microbiome lead to eubiosis but in the other side destroyed this homeostasis and increased susceptibility to infection, skin disease and chronic inflammation. The aim of this study was to prove how self-prepare foot care products influenced on foot microbiome. Two foot cream were prepared with different active components. Cosmetics were tested during 30-days with 30-days break between each of them. Rodact Contact test for yeast and molds and for all microorganisms were used, before start the project in the middle of research and after used creams to the end. Colonies were characterized and dyed using Gram method. Trichoscopic camera were used in order to assess the condition of foot. Self-prepared cosmetics for foot influenced on skin foot hydration, moreover reduced excessive keratosis of the epidermis. In all study participants modification of foot microbiome were observed. Skincare routine 2-times per day and carefully selected active ingredients had beneficial effect on foot skin condition and foot microbiome. Inulin added to one of the creams influenced to a significant extent on diversity of bacteria, at the same time reduce quantity of fungi.

Keywords: foot cosmetics, microbiome, eubiosis

ORAL PRESENTATION

Assessment of pregabalin misuse: A prospective and analytical study

Mohamed Habib. Belmahi[1], Sabah.benboudiaf[1], Louiza.Boudraa[2], Kenza Boudemagh[1].

[1] Toxicology Laboratory, Department of Pharmacy, Faculty of Medicine, Constantine 3 University.
[2] Toxicology Unit, Forensic Medicine Department, Maghlaoui Mila Public Hospital

Abstract

The misuse of psychoactive prescription drugs has now become a new form of addiction worldwide.The World Health Organization highlights an increase in the non-medical use of prescription medications such as Pregabalin, particularly among young people.Although this substance is often considered less dangerous than illicit drugs, it presents a significant risk of abuse and dependence.Pregabalin appears to have a high addictive potential, likely due to its rapid absorption and shorter onset of action. The desired effects include euphoria, relaxation, and increased sociability. The euphoric effect is generally very pronounced and rapid. Sedation, dissociative effects, disinhibition, and hallucinations have also been described. Typically, these effects occur at doses far exceeding the maximum authorized oral dose of 600 mg.This is a prospective and analytical study, conducted during the year 2023, involving 133 patients attending addiction treatment centers.The collected samples were subjected to screening by an immunochemical method (EMIT) and quantification by liquid chromatography (HPLC-UV) after developing and validating a technique for the urinary assay of pregabalin and comparing the results with rapid tests.The assay revealed the presence of pregabalin in 32.3% of the study population.Liquid chromatography (HPLC-UV) is much more sensitive and specific than the immunochemical method (EMIT).Drug use can affect all individuals, regardless of age, gender, or socio-professional level. A positive result is highly likely if consumption is recent and if the subject is a regular user at doses above 600mg.Initial screening in psychiatric centers is recommended to aid in the diagnosis and appropriate management of addicts. Knowledge of the limitations of urinary screening by EMIT and rapid tests is essential for their optimal use. Chromatographic methods are the reference methods for the identification and quantification of pregabalin.

Keywords: Pregabalin, Addicts, Management, HPLC-UV, EMIT, Rapid test.

ORAL PRESENTATION

Associations between disc displacement, degenerative changes, and inflammatory findings in TMJ: An MRI-based study

Gerta Halilaj[1,3*] (ORCID: https://orcid.org/0009-0009-6883-5913) Gentian Stroni[2] Nebi Cemeta[1, 4] Arben Mitrushi[4] Roland Hasa[4] Erjon Karaj[5]

[*1]Aldent University, Faculty of Medical Technical Sciences, Medical Laboratory Technician and Medical Imaging, Tirana, Albania.
[2]University of Medicine, Faculty of Technical Medical Sciences, Department of Paraclinics, Tirana, Albania
[3]University of Medicine, Faculty of Technical Medical Sciences, Department of Health Diagnostics and Rehabilitation, Tirana, Albania
[4]Department of Imaging, Orthodox Diagnostic Center, Tirana, Albania
[5]Department of Imaging, American Hospital, Tirana, Albania

Abstract

Temporomandibular disorders (TMDs) are a common cause of orofacial pain and dysfunction. Magnetic resonance imaging (MRI) is considered the gold standard for evaluating the temporomandibular joint (TMJ), providing direct visualization of the disc, joint spaces, and associated degenerative or inflammatory changes. This study aimed to investigate the association between disc displacement, degenerative changes, and inflammatory activity in TMJ using MRI. A retrospective review of TMJ MRI examinations was performed. Imaging in closed and open-mouth positions using T1-weighted, T2-weighted, and Proton Density (PD) sequences was analyzed for disc position, degenerative alterations, and signs of inflammation. Disc displacement was identified in most patients, with disc displacement without reduction (DDwoR) being the predominant finding. Degenerative changes were frequently associated with displacement patterns. MRI also revealed joint effusion and bone marrow edema, emphasizing its ability to detect early inflammatory features not visible on other imaging modalities. MRI provides a comprehensive evaluation of TMJ pathology by detecting disc displacement, chronic damage, and active inflammatory changes. These findings emphasize the clinical importance of DDwoR as the highest-risk subgroup and support the use of MRI to differentiate chronic from active disease, guiding management. This study also establishes a foundation for future prospective research integrating clinical data with MRI to develop interpretation models for improved diagnosis and management.

Keywords: temporomandibular disorder, temporomandibular joint, magnetic resonance imaging, disc displacement, degenerative changes

ORAL PRESENTATION

The effect of collagen supplementation on skin structure and signs of aging

Klaudia Śmigielska[1*]

[1]Śląska Wyższa Szkoła Medyczna, Cosmetology, Katowice, Poland

Abstract

Skin aging involves complex alterations within the dermis, where degradation of collagen, impaired fibroblast activity and fragmentation of the extracellular matrix (ECM) progressively weaken tissue architecture. With age, the number of dermal fibroblasts decreases by approximately 35%, and remaining cells, adopt a senescent SASP phenotype, contributing to chronic low-grade inflammation and accelerated breakdown of structural proteins. Increased activity of matrix metalloproteinases (MMPs), without a parallel rise in their inhibitors (TIMPs), further amplifies collagen type I loss. These processes are accompanied by protein glycation and reduced synthesis of glycosaminoglycans, including hyaluronic acid, lowering the skin's water-binding capacity and impairing its biomechanical properties. Interest in oral collagen supplementation arises from its ability to deliver low-molecular-weight bioactive peptides that are absorbed into the bloodstream and act as signaling molecules for fibroblasts. Clinical studies demonstrate increased synthesis of collagen type I, elastin and hyaluronic acid after 8 - 12 weeks of regular supplementation. Three randomized, double-blind, placebo-controlled trials consistently reported significant improvements in skin hydration, elasticity, density and wrinkle reduction in individuals using collagen peptides at daily doses of 1650 - 3300 mg. These findings indicate that oral collagen may serve as a valuable adjunct to regenerative cosmetic procedures, working synergistically with treatments that stimulate fibroblast activity. This benefit, however, depends on the use of standardized preparations with defined peptide composition and molecular weight. Despite promising outcomes, further research is required, particularly regarding the long-term persistence of effects and populations other than women over 30 years of age.

Keywords: collagen peptides, skin aging, fibroblasts, hydration, elasticity

ORAL PRESENTATION

Oleic acid nitrogen derivatives as antistatic additives

[1]V.M. Abbasov, [1]A.A. Kangarli, [1]N.I. Mursalov, [1,2]D.B. Aghamalieva, [1]E.K. Hasanov

[1]Institute of Petrochemical Processes, Ministry of Science and Education
[2]Azerbaijan State Oil and Industry University, Azerbaijan

Abstract

This research study is dedicated to synthesizing nitrogen-containing organic derivatives of oleic acid and investigating their effects on the antistatic properties of diesel fuel. Nitrogen derivatives of oleic acid were synthesized using triethylenetetramine and polyethylene polyamine. These synthesized derivatives were added to diesel fuel in various concentrations, and their electrical conductivity and antistatic effects were examined. The test results determined that amidoamines synthesized from oleic acid with triethylenetetramine and polyethylene polyamine exhibited the highest electrical conductivity at a concentration of 0.05%. In particular, amidoamine compounds synthesized with PEPA enhanced the electrical conductivity of diesel fuel more effectively, preventing the accumulation of static electricity. Based on the obtained results, Sample No. 3 demonstrated the highest antistatic effect and is recommended as the most effective additive.

Keywords: oleic acid, triethylenetetramine, polyethylene polyamine, amidoamine, diesel fuel.

ORAL PRESENTATION

Ultrastructural analysis of the midgut epithelium of *Lithobius forfocatus* (Myriapoda, Chilopoda) exposed to different concentrations of nanostyrene

Agata Aleksa[1*] ORCID: 0009-0003-7492-8469, Magdalena Rost-Roszkowska[1*] ORCID:0000-0001-7124-842, Łukasz Chajec[1*] 0000-0001-6455-9063

[*1]University of Silesia in Katowice, Faculty of Natural Sciences, Institute of Biology, Biotechnology and Environmental Protection, Bankowa 9, 40-007 Katowice, Poland

Abstract

The occurrence of nanoplastics (NPs) in terrestrial and aquatic environments is becoming a growing ecological concern. Although numerous studies have confirmed the negative effects of NPs on living organisms, their impact on soil ecosystems is still insufficiently understood. One of the nanoplastics frequently detected in soil is nanostyrene, formed by the breakdown of styrene into micro- and then nanoparticles up to 100 nm in size. Such fine particles can penetrate cell membranes and accumulate within cells and their organelles. Therefore, our study compared the effects of lower and higher concentrations of nanostyrene in soil to determine whether differences in its concentration induce different changes in the midgut cells of the centipede *Lithobius forficatus*. The focus was on characterising the structural and ultrastructural changes occurring in the digestive cells. Transmission electron microscopy (TEM) was used to analyse the midgut epithelium after exposure to nanostyrene at concentrations of 10 mg and 100 mg per kg soil dry weight for 1 and 3 months. The study included observation of ultrastructural changes, signs of autophagic processes and variation in the amount of reserved material over time. The results indicate that the presence of nanostyrene affects the organisation of the apical part of the cytoplasm of digestive cells, highlighting the need for further studies on the effects of nanoplastics on soil organisms and ecosystem functioning.

Keywords: autophagy, ecotoxicology, nanotoxicology, ultrastructure

ORAL PRESENTATION

Assessing the impact of breakfast consumption on cognitive and academic performance and daily wellbeing among Aldent University students

Enkelejda Trebicka[1]

*[1]Aldent University, Faculty of Medical Thecnical Sciences, Tirana, Albania.

Abstract

Regular breakfast consumption plays a crucial role in the physical and mental well-being of students. According to the World Health Organization (WHO), a healthy breakfast contributes to better concentration, sustained energy levels throughout the day, and a reduced risk of developing metabolic disorders at a young age. A self-administered questionnaire was used to assess breakfast consumption habits among students, their knowledge regarding its nutritional components, and the side effects of skipping this meal. The study included 308 participants from Aldent University (276 females and 32 males). Questionnaires were distributed electronically to students, who were encouraged to respond honestly. Of the respondents, 94.5% belonged to the 18–22 age group. Nearly half of the participants (50.3%) reported consuming breakfast regularly, while 49.7% did not. The main reason for skipping breakfast was lack of time (57.3%). Furthermore, 44.8% of those who skipped breakfast reported feeling low in energy throughout the day, and 56% experienced headaches. Additionally, 76.3% of the respondents believed that eating breakfast improves academic performance. The findings of this study show that a considerable proportion of students do not consume breakfast regularly, mainly due to time constraints. This behavior is associated with noticeable consequences for daily well-being, such as fatigue and headaches, and may negatively impact academic performance. Although most students are aware of the importance of breakfast, their eating habits do not reflect this understanding. These results highlight the need for awareness-raising and educational programs that promote healthy dietary habits, with a special focus on breakfast as an essential meal for academic success and long-term health.

Keywords: breakfast consumption, side effects, students, academic performance.

ORAL PRESENTATION

Impact of diet on reproductive performance in dairy cows in Algeria

Kalem.Ammar[1], Hadj Omar Karima[1], Daoudi Zerrouki.Nacira[2], Djallel Adel[1]

[1]Laboratory of Biotechnology in Animal Reproduction (LBRA), Institute of Veterinary Sciences, University of Blida 1, Blida, Algeria
[2]Natural Resources Laboratory. Faculty of Biological Sciences and Agronomic Sciences. University of Tizi-Ouzou. Algeria.

Abstract

The aim of this study was to assess the effect of feed imbalance on the reproductive parameters of cows in production. A total of 120 dairy cows belonging to 4 farms located in the Tizi-Ouzou region were monitored over a period of 7 months. These cows were housed in tie-stall housing. The energy and nitrogen levels of the rations distributed were estimated based on the nutritional value of the various feeds comprising the daily ration distributed, as well as the type of concentrate supplemented. Thus, an estimate of the intakes of the basic and total rations was compared with the requirements of the different categories of females in the herds of the four farms. The effect of these intakes on the animals was assessed in terms of body condition score and reproductive parameters. This study revealed that the rationing implemented on the four farms was unbalanced and did not take into account either the production level or the physiological condition and stage of the female. Statistical analysis of the recorded data revealed intervals between calving and calving ranging from 380 to 400 days and between calving and insemination varying between 78 and 130 days, with a first insemination success rate ranging from 20 to 62% and a high repeat breeder rate ranging from 15 to 40%, depending on the farm monitored. An average fertility index of 2.12 to 2.20. All the results obtained show a low production level on the monitored farms, likely explained in part by the nutritional imbalance in the rations distributed.

Keywords: Dairy cow, Diet, Reproduction, fertility, Body condition, Artificial Insemination,

ORAL PRESENTATION

Study of the effect of antibiotics and probiotics on sperm quality *in vitro* using an automated semen analysis system (CASA)

Kalem.Ammar[1*], Djallel Adel[1] , Daoudi Zerrouki.Nacira[2], Hadj Omar Karima[1],

[1]Laboratory of Biotechnology in Animal Reproduction (LBRA), Institute of Veterinary Sciences, University of Blida 1, Blida, Algeria
[2]Natural Resources Laboratory. Faculty of Biological Sciences and Agronomic Sciences. University of Tizi-Ouzou. Algeria.

Abstract

The experimental study focused on the effect of antibiotics and probiotics on sperm quality in vitro using an automated semen analysis (CASA) system. Previous studies have confirmed the harmful effects of antibiotics on sperm. Through our study, we aim to explore the use of probiotics as a biological alternative to antibiotics in the treatment of genital infections. We also aim to find synergy between certain non-toxic antibiotics and probiotics in order to broaden the spectrum of activity in certain therapeutic strategies. This work was carried out at the Animal Reproduction Biotechnology Laboratory (LBRA), located at the Blida 1 Veterinary Institute. To carry out our experiment, we chose for our first approach, the most widely used antibiotics in human medicine and in veterinary routine. To respect the minimum inhibitory dose, eight antibiotic discs were used during this study. These are tetracycline (TE 30), ciprofloxacin (Cip5), erythromycin (E5), rifampicin (Rif30), gentamycin (GN10), co-trimoxazole (CT10), colistin (Co10), amoxicillin and clavulanic acid (AMC30). Each antibiotic is Co incubated at 37°C for 4 hours, with frozen bovine semen from the artificial insemination and genetic improvement center (CNIAAG). For our second approach, we co-incubated the semen with a probiotic (lactobacilli) while respecting the minimum effective dose, which must be 106 CFU/g. The final step involves selecting the antibiotic that would be suitable for co-incubation with the probiotic. To do this, an antibiogram was developed using only non-toxic antibiotics, after inoculation with the lactobacilli. Our study confirmed the toxic effect of ATB on sperm, unlike probiotics, which demonstrated a significant improvement in all sperm cell parameters during co-incubation. We hope to use further studies to select antibiotics that would not have a toxic effect on sperm cells and to identify a likely antibiotic-probiotic combination.

Keywords: Semen, Infection, antibiotic, probiotic, Artificial Insemination, CASA

ORAL PRESENTATION

Evaluation of corrosion inhibition effect of pyrimidine derivative on aluminium alloy by electrochemical techniques

Moussaoui Kamilia[1,*], Abderrahmane Sihem[1], Larkem Hamama[1], Abderrahim Karima[1] And Berrezag Kamel[1]

[1]Surface Engineering Laboratory (L.I.S), Department of chemistry, Faculty of Sciences, University BADJI Mokhtar –Annaba, B.P.12, Annaba 2300, Algeria

Abstract

In this work, two pyrimidine derivative molecules (2-amino-5,7-dimethyl-1,2,4-triazolo [1,5-a] pyrimidine (ADTP) and 2-amino-4,6-dimethyl pyrimidine (ADMP)) are used as effective inhibitors for aluminium alloys in 1 M HCl. The inhibitive performances are evaluated by electrochemical measurements and surface characterization. The results indicate that inhibition performances of ADTP and ADMP are closely related to the concentrations, influenced by the combination of steric hindrance and bonding effects. At relatively concentrations (10^{-2} – 10^{-5} M), ADTP displays a more pronounced ability to inhibit corrosion than ADMP, owing to more anchoring functional groups. The interaction between the Al electrode and ADTP results in the formation of a more condensed protective film than ADMP at low concentrations. Furthermore, the effect of temperature variation was investigated to gain deeper insight into the inhibition mechanism. Electrochemical tests performed at different temperatures revealed that inhibition efficiency decreases with increasing temperature, suggesting that physical adsorption plays a dominant role in the protective behavior. Thermodynamic parameters were also calculated to support this observation, highlighting the influence of thermal activation on the adsorption process of both inhibitors.

Keywords: Corrosion inhibitor; Pyrimidine; Aluminium; HCl; PDP

ORAL PRESENTATION

Measurement of the viscosity of gum arabic

Elmira Aliyeva[1*] (ORCID: https://orcid.org/0009-0008-2767-3949),
Nizami Zeynalov[2] (ORCID: https://orcid.org/000-0002-7889-6594)

[*1,2] Institute of Catalysis and Inorganic Chemistry named after academician of M.Nagiev, Laboratory of Nanostructured metal-polymer catalysts, Ministry of Science and Education Republic of Azerbaijan, Baku, Azerbaijan

Abstract

Gum arabic (GA), also known as acacia gum, is a natural exudate obtained from the Acacia senegal and Acacia seyal trees and is one of the oldest and most widely used natural gums. It is a naturally high-viscosity natural polymer, and its quality is generally assessed by appearance, moisture content, viscosity, pH, and mineral profile, including Ca, Na, K, P, and various trace elements [1]. Structurally, GA is a branched polysaccharide composed of galactose, arabinose, rhamnose, and uronic acids. It has GRAS status [2] and is valued for its water solubility and functional properties, such as stabilization, emulsification, thickening, film formation, and encapsulation. Viscometery is a widely used technique for studying polymer behavior in dilute solutions and provides a simple means of assessing structural properties, polymer concentration, chain dimensions, molecular weight, and thermodynamic parameters. This study analyzed the effect of polymer concentration on the behavior of aqueous GA solutions. Viscosity, defined as the resistance to flow, results from the frictional interactions between the solute and solvent molecules [3]. Dynamic and kinematic viscosities were determined using a Hoppler KF 3.2 falling ball viscometer. Gum arabic solutions of different concentrations were prepared using double-distilled water as the solvent. Each solution was thoroughly mixed to ensure complete dissolution of the polymer before analysis. To ensure constant experimental conditions, all solutions were equilibrated at 25°C for 15 minutes before measurement. Determination of dynamic viscosity: The dynamic viscosity (η) of the GA solutions was calculated according to the following equation:

$$\eta = \boldsymbol{k}(\boldsymbol{\rho_1} - \boldsymbol{\rho_2})\boldsymbol{T}$$

where $\boldsymbol{k}$ is the instrument constant ($k = 0.07$), ρ_1 is the reference density ($2.22\ g/cm^3$), ρ_2 is the density of the GA solution at a given concentration, and T represents the measured drop time. T was recorded for each concentration. All measurements were performed in triplicate to ensure accuracy and reproducibility. Determination of kinematic viscosity: Kinematic viscosity (ϑ) was determined according to the following relationship:

$$\boldsymbol{\vartheta} = {}^{\eta}/_{\boldsymbol{\rho_2}}$$

Where η is the dynamic viscosity determined above and ρ_2 is the density of the solution in question.

Table 1.

Gum Arabic	2,5%	5%	10%
Dynamic Viscosity, $mPa \cdot s$	2.79	4.32	7.61
Kinematic Viscosity, $\frac{mm^2}{s}$	2.76	4.24	7.39

Based on experimental results, it was determined that the viscosity of gum arabic is highly dependent on concentration. Specifically, an increase in polymer concentration leads to a corresponding increase in viscosity [4]

Keywords: gum arabic, viscosity, determination

References:

Shaymaa A. Mohamed, Asmaa M. Elsherbini, et al.Gum Arabic: A Commodity with Versatile Formulations and Applications.Nanomaterials 2025, 15(4), 290; https://doi.org/10.3390/nano15040290

Seema Patel, Arun Goyal. Applications of Natural Polymer Gum Arabic: A Review. International Journal of Food Properties 2015, Volume 18, Issue 5, Pages 986-998. https://doi.org/10.1080/10942912.2013.809541

Sani Alhassan, S. Y. Sule, R. Murtala, H. I. Rasheed, A. A. Baso, F. A. Sheshe , S. C. Jafar. Determination of Intrinsic Viscosity of Pure and Acetylated Gum Arabic Using Different Plot Methods. Journal of Physical Chemistry & Biophysics J Phys, Vol.14, Iss.4 No:1000390

Determination of intrinsic viscosity of polymeric compounds through a single specific viscosity measurement. Polymer 1998, Volume 39, Issue 26, Pages 6827-6833. https://doi.org/10.1016/S0032-3861(98)00184-0

ORAL PRESENTATION

Theoretical design and DFT evaluation of d-glucosamine–oxyresveratrol–essential amino acid grafted molecules for enhanced antioxidant activity

Hamadouche Salima [1], Omaima Aidat [2]

[1] Laboratoire de Chimie des Materiaux et des Vivants:Activite&Reactivite(LCMVAR), Université Batna1, Batna, Algeria
[2]Laboratory of Food Technology and Nutrition, Abdelhamid Ibn Badis University, Mostaganem, Algeria

Abstract

In the quest for innovative, high-performance materials suitable for antioxidant applications, density functional theory (DFT) was employed to design a new series of compounds derived from small, biodegradable organic molecules. The study involved grafting the negatively charged D-glucosamine (GleN) unit and various essential amino acids onto the 3 and 4′ carbon atoms of the trans-2,4,3′,5′-tetrahydroxystilbene (trans-OXY) backbone. This molecular modification aimed to prevent trans-OXY isomerization into its less stable cis form and to enhance its electronic and antioxidant properties. DFT calculations performed at the PW91/TZP level in aqueous phase revealed that the designed biomolecules (GleN-OXY-AA) displayed superior antioxidant performance compared to both free OXY units and essential amino acids, as reflected by their bond dissociation energy (BDE) values. Among them, GleN-OXY-Ile and GleN-OXY-Trp exhibited the lowest average BDE (66.355 kcal/mol), corresponding to 1.82 times the activity of trans-OXY and 1.55 times that of ascorbic acid (Vitamin C). Atoms-in-Molecules (AIM) analysis further demonstrated that these biomaterials favor the formation of quasi-cyclic structures through intramolecular H···O hydrogen bonding, which enhances π-electron delocalization and stabilizes radical, cationic, and anionic species. Quantum chemical descriptors indicated that hydrogen atom or electron release occurs at sites of lower electronegativity, as visualized by molecular electrostatic potential (MEP) maps and quantified by Hirshfeld atomic charge analysis.

Keywords :Density Functional Theory (DFT) ,Antioxidant applications, Biodegradable organic molecules, D-glucosamine (GleN),Essential amino acids

ORAL PRESENTATION

Prevention of transmission and infection by Parvovirus B19, in children with Hemoglobinopathy, who receive blood transfusions.

Theodhor Disho*[1], Manika Kreka[2]

[1]Pediatrican, Social Health Centre no.2 Korçë, Albania
[1]Nursing Department, Faculty of Natural and Human Sciences, Fan. S. Noli University, Korçë, Albania
[2]Pediatric Department, Faculty of Medicine, University of Medicine, Tiranë, Albania

Abstract

Parvovirus B19 is a small, single-stranded DNA virus that infects erythroid progenitor cells. In patients with hemolytic anemia, such as children with hemoglobinopathy, Parvovirus B19 can cause aplastic crisis and put their health at serious risk. For this reason, although documented cases of parvovirus transmission through blood transfusion are rare, measures must be taken to detect potential cases in time and prevent them. A study conducted in Albania in 2025 showed that Parvovirus B19 is widely distributed in the general population, with approximately 35% prevalence in voluntary blood donors. Albania, like many other countries, does not include routine screening of all blood donors for Parvovirus B19. In addition, patients are not tested before and after transfusion for the presence of the virus. This indicates that children with hemoglobinopathy, who depend on regular blood transfusions, remain at risk of infection. These findings highlight the need to protect these patients from complications associated with parvovirus, given their reliance on transfusions. Specifically, our work focuses on measures that can be proposed and implemented in order to ensure the most comprehensive protection against parvovirus transmission. From our study, we conclude that the safest measure to prevent the transmission of Parvovirus B19 through blood transfusion in children with hemoglobinopathy is to introduce standard blood screening for Parvovirus B19 for all donors. This would provide full protection not only for at-risk groups but for the entire population. If it is not feasible to screen all blood donors, then blood intended for transfusion in children with hemoglobinopathies should, in addition to routine infectious disease screening, also be tested for Parvovirus B19. This would offer complete protection for these patients, although not for the general population. If neither of these can be integrated into standard protocols, we suggest that before transfusion, these patients be tested for the presence of IgG antibodies to Parvovirus B19. Children who already have antibodies are generally protected, and the likelihood of reinfection is very low. For this reason, we recommend that for children/patients without antibodies, the blood intended for transfusion be tested for parvovirus beforehand. This will significantly reduce the risk of infection for this group. The final measure—perhaps the safest and least costly in terms of both financial resources and long-term health consequences—would be the development of a Parvovirus B19 vaccine and its administration to all patients diagnosed with hemoglobinopathy, or at least those who require long-term blood transfusions. Although we currently lack the means to develop this vaccine, understanding its potential protective benefits leads us to call upon countries in the region and beyond, as well as researchers and scientists, to begin work on its creation. May this “small” call lead to a great result for the future.

Keywords: Hemoglobinopathy, Transfusion, Parvovirus, Prevention, Measures.

References:

1. Ensuring Transfusion Safety: Screening Blood Donors for Human Parvovirus B19. *PMC*. PMC+1
2. Parvovirus B19: What Is the Relevance in Transfusion Medicine? *Frontiers in Medicine*. Frontiers
3. Parvovirus B19 rebound outbreak 2024 and implications for blood- and plasma-product safety. *Transfusion / PubMed*. PubMed
4. Human Parvovirus B19 and blood product safety: a tale of twenty years of improvements. *PMC*. PMC
5. Parvovirus B19 transmission by a high-purity factor VIII concentrate. *PubMed*. PubMed
6. Nucleic Acid Testing to Reduce the Possible Risk of Parvovirus B19 Transmission by Plasma-Derived Products. FDA Guidance. U.S. Food and Drug Administration+1
7. Parvovirus B19V DNA contamination in Chinese plasma and plasma derivatives. *Journal of Translational Medicine*. BioMed Central
8. The new “Guidelines on the impact of Parvovirus B19 infection on transfusion safety” — Centro Nazionale Sangue (Italy). Centro Nazionale Sangue
9. Albanian donor seroprevalence study 2025: *Albanian Journal of Trauma and Emergency Surgery* (AJTES) — includes Parvovirus B19 testing in donors. Astes Journal
10. Surveillance of blood donors detects an exceptional Parvovirus B19 outbreak in Switzerland in 2023/2024. *Blood Transfusion*. Blood Transfusion Italy

11. Oeller M. et al., *Long-Term Retrospective Analysis of Parvovirus B19 in Blood Donations (Salzburg, Austria)* — **Diagnostics (MDPI)**, **2025**.
Relevance: Large dataset (2012–2024) showing viremia/positivity trends and post-COVID epidemiology relevant to donor screening policy. MDPI
12. Farcet M.R. et al., *Parvovirus B19 rebound outbreak 2024 and implications for blood- and plasma-product safety* — **Transfusion / review**, **2024**.
Relevance: Analysis of the 2023–2024 rebound outbreak in Europe and safety implications for transfusions / plasma products. PMC+1
13. Centers for Disease Control and Prevention (CDC), *Detection of Increased Activity of Human Parvovirus B19 — United States, 2018–2024 (MMWR summary)* — **CDC / MMWR**, **2024**.
Relevance: Surveillance data showing increased B19 activity in 2024 — important for assessing current transfusion risk. restoredcdc.org
14. Kumari S. et al., *Increased parvovirus B19 seropositivity in healthy blood donors* — **Scientific Reports / PMC**, **2024**.
Relevance: Recent seroepidemiology among donors indicating recent exposure (IgM positivity) and implications for transfusion safety. Nature+1
15. Candura F. et al., *Comprehensive analysis of parvovirus B19 infection in blood donors (Italy)* — **Transfusion / PMC**, **2024**.
Relevance: National/regional data from Italy showing increased positive plasma units early 2024 — practical implications for screening. PMC
16. Farahmand M. et al., *Systematic review and meta-analysis of Parvovirus B19 prevalence markers in blood donors* — **PMC (systematic review)**, **2021**.
Relevance: Pooled prevalence estimates (DNA, IgG, IgM) across studies — useful for background and meta-analytic context. PMC
17. Wälti M. et al., *Assessing B19V Epidemiology and Viremia Dynamics in Source Plasma Donors* — **Journal (2025)**.
Relevance: Industry/source plasma perspective showing pandemic-related declines and rebound in donor viremia — important for plasma product safety. ScienceDirect
18. Centro Nazionale Sangue (Italy), *Technical document: Impact of Parvovirus B19 infection on transfusion safety* — **CNS technical paper**, **2024**.
Relevance: National technical assessment of B19 epidemiology, risk, and policy options (screening vs targeted strategies). Centro Nazionale Sangue
19. European Centre for Disease Prevention and Control (ECDC), *Risk brief: Risks posed by increased circulation of human parvovirus B19* — **ECDC**, **2024**.
Relevance: EU regional risk assessment and discussion of cost-effectiveness / targeted testing for high-risk recipients. ecdc.europa.eu
20. Cureus review — *Screening Blood Donors for Human Parvovirus B19: Ensuring Transfusion Safety* — **Cureus**, **2024**.

ORAL PRESENTATION

In vitro seed germination, callus induction, and shoot formation of *Zygophyllum album* L.

Hend Hassan[1*](https://orcid.org/0009-0001-7037-6674), Musa Türker[2] (https://orcid.org/0000 0003 3195 1119)

[*1]Alexandria University, Faculty of agriculture, Department of Floriculture, Ornamental Horticulture and Garden Design, 163 Aflaton Street, El Shatby, Alexandria, 21545, Egypt.
[2]Yıldız Technical University, Faculty of Chemistry and Metallurgy, Department of Bioengineering, Davutpaşa Campus, 34220, Esenler, İstanbul /Türkiye

Abstract

In this study, *Zygophillum album* L., a plant of medical importance, was for the first time, *in vitro* germinated, callus and plant regeneration was achieved. Protocols were developed for sterilization, *in vitro* seed germination, callus and shoot formation. Seed germination was affected by pre-soaking interval, sterilization strength, MS concentration, and incubation conditions. Among five treatments, seeds soaked for 48 h, sterilized with 70% ethanol + 4% NaOCl, and cultured on ¼ MS medium under initial darkness accomplished the highest germination rate of 83.9% with no contamination. Cotyledon, hypocotyl, root, and shoot tip explants excised from 12–14-day-old seedlings were cultured on various media. Pale green, compact callus formed from cotyledons and hypocotyls on ½ MS + 0.5 mg/L 2,4-D + 0.1 mg/L kinetin with 97% and 96% induction, respectively, whereas roots showed slower callus initiation, reaching 100%. Shoot tips on MS + 5 mg/L BAP + 1 mg/L NAA medium gave 55% shoots after one month with shoot elongation and leaf development. Subculturing enhanced shoot formation, achieving 100% on MS + 5 mg/L BAP + 1 mg/L NAA medium. Explants from 3–5-week-old seedlings (leaves, hypocotyls, shoot tips, and roots) were cultured on media supplemented with BAP, NAA, 2,4D or TDZ. Callus was initiated within 1–2 weeks, with hypocotyl explant exhibiting stronger callus growth on MS + 1 mg/L BAP + 0.5 mg/L NAA. Shoot tip explants attained up to 80% shoot formation on 1/2MS + 5 mg/L BAP + 1 mg/L NAA with average shoot length of 2.2 cm, while MS + 2.5mg/l TDZ + 0.5 NAA promoted succulent leaf growth with 60% shoot formation. Generally, this study highlights the importance of pre-soaking interval, sterilization strength, initial dark incubation, and proper media composition for efficient *in vitro* germination, callus induction, and shoot formation of *Zygophyllum album* L.

Keywords: *Zygophyllum album* L., *in vitro* germination, callus induction, shoot formation.

ORAL PRESENTATION

Novel water-soluble Zn-phthalocyanine complexes enhance foliar zinc bioavailability and concentration-dependent redox homeostasis in *Cucumis sativus* under zinc deficiency

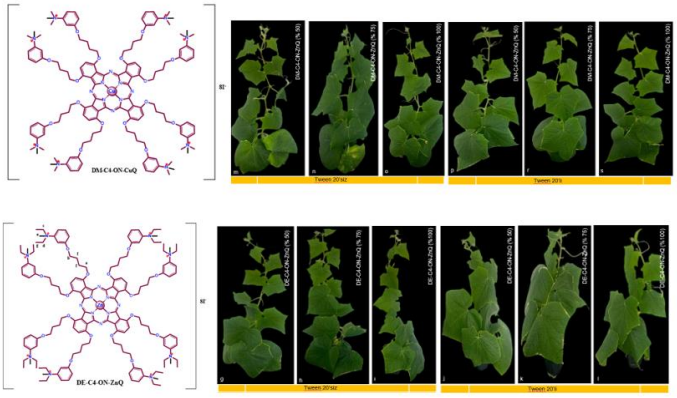
Dilek Ünlüer Birinci[1,2] (ORCID: https://orcid.org/0000-0003-1939-2246), Hüseyin Baş[1] (https://orcid.org/0000-0002-8722-3359), Zekeriya Bıyıklıoğlu[1] (https://orcid.org/0000-0001-5138-214X), Asım Kadıoğlu[2] (ORCID: https://orcid.org/0000-0002-4781-6264)

[*1] Karadeniz Technical University, Faculty of Science, Department of Chemistry, Trabzon, Türkiye.
[2]Karadeniz Technical University, Faculty of Science, Department of Biology, Trabzon, Türkiye.

*Corresponding author e-mail: dunluer@ktu.edu.tr

Abstract

This study aims to comprehensively reveal the multi-layered physiological and biochemical effects of water-soluble non-peripheral octa-substituted zinc phthalocyanine complexes (DE-C4-ON-ZnQ and DM-C4-ON-ZnQ) on Cucumis sativus seedlings grown under zinc deficiency conditions. [1]. The complexes, prepared at concentrations of 50%, 75%, and 100% to be equivalent to the Zn level in Hoagland solution, were applied with foliar formulations containing and not containing Tween-20, and the bioavailability, cellular response mechanisms, and stress modulation capacity of these new-generation Zn carriers were evaluated in detail [2]. Zn complexes significantly improved key physiological indicators of plant growth and development by markedly reducing Zn deficiency-specific morphological abnormalities and chlorotic leaf development. Applications with Tween-20 at 75% and 100% concentrations [3] significantly increased penetration from the leaf surface and systemic distribution; notable increases were recorded in the fresh/dry weight ratio, relative water content, and photosynthetic pigment stability. TBARS analyses showed that Zn-Pc complexes significantly reduced oxidative stress mediators by suppressing membrane lipid peroxidation, indicating the reactivation of zinc-dependent antioxidant pathways.



In the overall evaluation, both complexes were found to be effective as strong sources of Zn bioavailability; however, the DM-C4-ON-ZnQ compound demonstrated a superior activity profile compared to the DE derivative due to its superior performance in biomass accumulation, pigment stability, and membrane protection.

Keywords: Zinc Phthalocyanine Complexes, Foliar Zinc Bioavailability, Redox Homeostasis, Concentration-Dependent Physiological Response

*This work was supported by TUBITAK (1001) (Project No: 123Z943).

References

[1] Hafeez, B., Khanif, Y. M., & Saleem, M. (2013). Role of zinc in plant nutrition. American Journal of Experimental Agriculture, 3, 374–391.
[2] Fernández, V., & Eichert, T. (2009). Uptake of hydrophilic solutes through plant leaves. Plant Biology, 11, 671–680.
[3] Li, J., et al. (2020). Surfactant-assisted foliar fertilization mechanisms. Environmental and Experimental Botany, 176, 104080.

ORAL PRESENTATION

Towards chemical contaminants detection in pepper and cucumber: Reporting SERS sensing by a novel gold nanotriangle metal-insulator-metal array

Fahd Khalid-Salako[1] (ORCID: https://orcid.org/0000-0003-4795-2423), Sümeyra Vural Kaymaz[1] (ORCID: https://orcid.org/0000-0003-0521-7260), Hasan Kurt[2] (ORCID: https://orcid.org/0000-0002-1677-644X), Meral Yüce[3,*](ORCID: https://orcid.org/0000-0003-0393-1225)

[1]Sabanci University, Faculty of Engineering and Natural Sciences, İstanbul, Türkiye
[2]Istanbul Medipol University, School of Engineering and Natural Sciences, İstanbul, Türkiye
[3]Sabanci University SUNUM Nanotechnology Research and Application Centre, İstanbul, Türkiye

*Corresponding author e-mail: meralyuce@sabanciuniv.edu

Abstract

The persistence of pesticides and other agrichemicals in food products causes both public health and economic problems. While strict regulations guide acceptable chemical residue limits to protect end consumers, there is an obvious need to develop field-deployable sensors for in-line chemical residue monitoring in the agricultural industry. Surface-Enhanced Raman Scattering (SERS) is a promising technique that offers chemical fingerprinting capabilities, alongside translational potential through miniaturizable components and easy integration into data processing workflows and automation for end-use with minimal expertise. This study reports the evaluation of a novel gold nanotriangle (NTA) metal–insulator–metal (MIM) metasurface for SERS detection of four common pesticides (Acetamiprid, Chlorpyrifos, Metalaxyl, and Tebuconazole) in Cucumber and Pepper samples. Emphasis was placed on reproducibility, sensitivity, and selectivity under realistic analytical conditions. The novel NTA-MIM substrate, featuring dual tip-to-tip and back-to-back configurations, was fabricated on top of an Al/SiO_2 stack using an optimized electron-beam lithography and thin-film deposition workflow. The substrate had previously demonstrated a ~10^6 enhancement factor and detection limits in the femtomolar (fM) range for thiophenol dyes. In this study, µM – nM limits were realized for the detection of pesticides in cucumber and pepper matrix media, based on univariate concentration analyses. In wild Tebuconazole-contaminated field-sourced samples confirmed by LC-MS assays, the substrate demonstrated selective detection of the chemical residue. Multivariate classification using an unsupervised PCA model also revealed sufficient variability in a three-component space, encoded by the spectra, which enabled the successful classification of chemical contaminants in field-sourced samples at levels beyond the detection limit. While further development is required to improve the system's sensitivity, miniaturization, and stability assessment for field deployment, the findings reported in this study clearly demonstrate its potential for reliable fingerprinting and detection of chemical contaminants in complex food matrices.

Keywords: Surface-Enhanced Raman Spectroscopy (SERS), Nanotriangle Array, Pesticide detection, Agricultural Products, Biosensing, Nanoplasmonic Sensor

Acknowledgment: This research was financially supported by The Scientific and Technological Research Council of Türkiye (TUBITAK), 1004 Programme, Project ID: 22AG002.

ORAL PRESENTATION

Design and (bio)functionalization of isocyanate-bearing cryogels

Merve Bat Özmatara *(ORCID: https://orcid.org/0000-0002-6912-8825),
Tuğçe Nihal Gevrek (ORCID: https://orcid.org/0000-0002-2297-5891)

Gebze Technical University, Department of Chemistry, Kocaeli, Turkey

*Corresponding author e-mail: merve.bat@gtu.edu.tr

Abstract

Cryogels are highly porous polymeric materials with large surface area and absorption capacity. Cryogels having reactive groups make them attractive platforms for covalent bioimmobilization. While click chemistry is commonly used for polymer modification, catalyst-free reactions such as isocyanate–amine coupling enable efficient biomolecule conjugation under mild conditions. In this study, we synthesized cryogels with isocyanate functionality via photopolymerization of 2-isocyanoethyl methacrylate (ICEMA), poly(ethylene glycol) methyl ether methacrylate (PEGMEMA), and poly(ethylene glycol) diacrylate at –13 °C. By varying the monomer ratios, cryogels with different ratio of reactive isocyanate groups were obtained. Obtained materials were characterized by FTIR, TGA, SEM, and rheometry. Conjugation with 4-(trifluoromethyl)benzylamine, fluoresceinamine, and FITC-labeled bovine serum albumin confirmed direct immobilization of small molecules and proteins. The number of immobilized proteins could be tuned by changing the isocyanate content of the cryogel. These results demonstrate the potential of isocyanate-functionalized cryogels as effective platforms for biomedical and biotechnological applications.

Keywords: Reactive polymers, cryogels, bioimmobilization, isocyanate-amine reaction

Acknowledgments: M.B.O thanks to the Scientific and Technological Research Council of Turkey TUBITAK 2211-A National PhD Scholarship Program.

ORAL PRESENTATION

AgNP synthesis using supercritical CO_2 extract of *Lilium ciliatum* leaves

Gönül Serdar[1*] (ORCID: https://orcid.org/ 0000-0002-3589-2323), Melek Koç Keşir[2] , Fatma Tunali[3], Salih Terzioğlu[4]

[*1] Karadeniz Technical University, Central Research Laboratory,Trabzon, Türkiye
[2] Karadeniz Technical University, Department of Chemistry, Faculty of Science, Trabzon, Türkiye
[3] G. d'Annunzio University, Department of Pharmacy, Botanic Garden Giardino dei Semplici, Chieti 66100, ITALY
[4] Karadeniz Technical University, Faculty of Forestry, Trabzon 61080, Türkiye

*Corresponding author e-mail: gonulserdar@ktu.edu.tr

Abstract

In this study, silver nanoparticles (AgNPs) were synthesized using *Lilium ciliatum* leaf extract obtained through supercritical CO_2 extraction (SFE-CO_2). In the green synthesis approach, plant materials utilize their biological extracts as reducing and capping agents, making the process highly economical because it significantly lowers the overall cost of synthesis (1). Leaves collected from Haçkalı Baba Plateau (Trabzon, Türkiye) was dried, mechanically fragmented, and subjected to SFE at 150 bar and 40 °C to obtain a phytochemically rich extract. Aqueous solutions of the extract at 2% (w/v) concentration were mixed in volumes of 0.1–6 mL with $AgNO_3$ solutions prepared in the range of 0.01–10 mM. The reaction mixtures were subjected to microwave irradiation at 90 W for 1–60 minutes, during which the appearance of a characteristic yellow color indicated the formation of silver nanoparticles. UV-Visible spectroscopy in the range of 300–800 nm was employed to confirm the synthesis of AgNPs by monitoring the surface plasmon resonance (SPR) bands characteristic of silver nanoparticles (2). This study demonstrates the potential of *Lilium ciliatum* leaf extract as a natural reducing and stabilizing agent in green nanoparticle synthesis and provides an effective microwave-assisted approach for the rapid and environmentally friendly production of AgNPs.

Keywords: *Lilium ciliatum* leaf, AgNPs, SFE, MAE.

Funding: This study was supported by Scientific and Technological Research Council of Türkiye (TUBITAK) under the Grant Number Project No: 124Z589. The authors thank to TUBITAK for their supports.

References:

Selvaraj, R., Pai,S., Murugesan, G., Pandey, S., Bhole, R., Gonsalves, D., Varadavenkatesan, T., Vinayagam, R. 2021. "Green synthesis of magnetic α–Fe2O3 nanospheres using Bridelia retusa leaf extract for Fenton-like degradation of crystal violet dye", Appl. Nanosci. 11, 2227–2234.

Serdar, G., Gül Kılınç, G. & Mazlum Şen, T. Green One-Pot Synthesis of Silver and Gold Nanoparticles Using Catechin Extracts: Influence of Temperature and Antioxidant Activity Evaluation. *Plasmonics* **20**, 10691–10710 (2025). https://doi.org/10.1007/s11468-025-03083-4

ORAL PRESENTATION

Green synthesis of selenium nanoparticles using *Cicer arietinum* L. extract and investigation of their biological activities *in vitro* for new drug development

Tuba Tarhan[1*] (https://orcid.org/0000-0003-2656-4464),
Burhan Ateş[2] (https://orcid.org/0000-0001-6080-229X)

[*1]Mardin Artuklu University, Vocational High School of Health Services, Mardin, Turkey.
[2]Inonu University, Faculty of Science & Arts, Department of Chemistry, Malatya, Turkey.

*Corresponding author e-mail: tubatarhan@artuklu.edu.tr

Abstract

In this century, drug consumption has become an indispensable part of healthcare. The emergence of new epidemics and disease types has led to the inadequacy of existing drugs and treatment methods. Furthermore, the unnecessary and incorrect use of antibiotics has led to the development of resistant bacteria, and the protective properties of existing antibiotics have diminished. This has led scientists to search for more effective and safer drugs. In our study, we achieved the biosynthesis of a novel CA-SeNP, not yet available in the literature, using an extract of endemic black chickpeas (*Cicer arietinum* L.) grown in the Mardin region. Thus, instead of using expensive and toxic chemicals, we achieved nanoparticle synthesis with a simple, rapid, inexpensive, and non-toxic, environmentally friendly, green approach. Furthermore, by incorporating polydopamine (PDA) with catechol groups into the synthesis procedure, we successfully synthesized SeNPL (PDA_SeNPL) decorated on the PDA surface. In this way, we aimed to increase the biological activity of the bionanomaterial by enabling a more controlled release of SeNPL from the PDA surface. The structure of this new drug precursor, not yet available in the literature, was elucidated using various characterization techniques. For this purpose, we utilized techniques such as FTIR, XRD, SEM, EDAX, TEM, UV-Vis, DLS, and Zeta Potential. The structures of these new bionanomaterials were thoroughly elucidated, and their various biological activities, including antioxidant, antibacterial, and antifungal, were tested in vitro.

Keywords: Anti-microbial activity, Antioxidant, *Cicer arietinum* L., Green synthesis, Selenium Nanoparticle

Acknowledgments: This study was supported by Scientific and Technological Research Council of Turkiye (TUBITAK) under Grant Number 124Z103. The authors thank TUBITAK for their support.

ORAL PRESENTATION

Does life kinetics exercise have an effect on melatonin and cortisol levels in Alzheimer's disease?

Ayşe Asiye Culum[1*] (*ORCID: https://orcid.org/0000-0002-0072-7600*, Murat Gültekin[2] (*ORCID: https://orcid.org/0000-0002-0609-4269*), Faruk Akçınar[3] (*ORCID: https://orcid.org/0000-0003-2751-1743),* Zehra Ömeroğlu Ulu[4] (*ORCID: https://orcid.org/0000-0002-8884-4683),* Nurdan Sena Değirmenci[4] (*ORCID: https://orcid.org/0000-0002-8122-5476*), Fikrettin Şahin[4] (*ORCID: https://orcid.org/0000-0003-1503-5567)*

[*] [1]Malatya Turgut Ozal University, Vocational School of Health Services, Department of Medical Services and Techniques, Malatya Türkiye.
[2]Erciyes University, Faculty of Medicine, Department of Neurology, Kayseri, Türkiye.
[3]Inonu University, Department of Coaching Education, Faculty of Sports Sciences, Malatya, Türkiye.
[4]Yeditepe University, Faculty of Engineering, Deparment of Genetics and Bioengineering, Istanbul, Türkiye.

*Corresponding author e-mail: ayse.culum@ozal.edu.tr

Abstract

Alzheimer's disease (AD) is a neurodegenerative disease and the most common form of dementia, accounting for 60-80% of all dementia cases. Exercise has positive effects on emotional and cognitive performance during brain aging. Life kinetic exercises are a form of enjoyable mental exercise that advances the brain's working principles from simple concepts to complex and unique concepts. Melatonin is a hormone secreted by the pineal gland in the dark, under the control of the suprachiasmatic nucleus (SCN). It has a neuroprotective effect. In AD, melatonin levels decrease with disease progression. Melatonin deficiency is a sign of worsening AD. Cortisol is the main hormone associated with awakening, alertness, and the stress response. Cortisol levels are high in the early stages of AD. Cortisol and melatonin follow the circadian rhythm. Regulating these parameters in the preclinical stage can prevent AD. The effects of Life kinetic exercises were investigated in healthy individuals and patients with late-onset AD aged 65 and over. Participants performed Life kinetic exercises three times a week for 8 weeks. For analyses, blood samples were taken from participants before and after exercise. Plasma melatonin, cortisol levels, and Pittsburgh Sleep Quality Index (PSQI) were analyzed. Analysis results showed that Life kinetic exercise had no significant effect on PSQI, melatonin, or cortisol levels between the AD and control groups.

Keywords: Alzheimer’s disease, exercise, melatonin, cortisol.

Acknowledgements: This project was supported by TUBITAK (project number: 323S231).

ORAL PRESENTATION

Smart pesticide detection via hexagonal MIM metasurfaces integrated with deep feed-forward networks

Sümeyra Vural Kaymaz[1] (ORCID: https://orcid.org/0000-0003-0521-7260), Mustafa Özen[2] (ORCID: https://orcid.org/0009-0000-6590-3399), Süleyman Çelik[3] (ORCID: https://orcid.org/0000-0002-3600-1529), Selim Tanrıseven[3] (ORCID:https://orcid.org/0000-0002-7456-0057), Elmas Eva Öktem Olgun[4] (ORCID: https://orcid.org/0000-0001-6265-8439), Oltan Canlı[4] (ORCID: https://orcid.org/0000-0002-2652-844X), Barış Güzel[4] (ORCID: https://orcid.org/0000-0002-6709-2339), Yunus Sarıkaya[5] (ORCID: https://orcid.org/ 0000-0002-5729-2660), Hasan Kurt[6] (ORCID: https://orcid.org/0000-0002-1677-644X), Meral Yüce[3,*](ORCID: https://orcid.org/0000-0003-0393-1225)

[1] Sabanci University, Faculty of Engineering and Natural Sciences, Istanbul, Türkiye
[2] Department of Computer Science, Faculty of Engineering and Natural Sciences, Sabanci University, 34956, Istanbul, Türkiye
[3] SUNUM Nanotechnology Research and Application Centre, Sabanci University, Istanbul, 34956, Türkiye
[4] Climate Studies and Water Management Research Group, Climate and Life Sciences Vice Presidency, TUBITAK Marmara Research Center, 41470 Gebze, Kocaeli, Türkiye
[5] Pusula AI, Oakland, CA, 94611, USA
[6] Istanbul Medipol University, School of Engineering and Natural Sciences, Istanbul, Türkiye

*Corresponding author e-mail: meralyuce@sabanciuniv.edu

Abstract

Pesticides are chemical agents widely used to boost agricultural yields and control insect infestations; however, their extensive and often unregulated use has raised significant concerns about food safety and environmental health. This highlights the need for strong ecological protection regulations. Early detection not only guarantees conformity with legal standards but also safeguards human health and agricultural systems through prompt preventive actions. This paper introduces the development of a MIM-SERS (Metal–Insulator–Metal Surface-Enhanced Raman Spectroscopy) platform integrated with artificial intelligence for straightforward and sensitive detection of pesticide residues in actual food samples. The engineered hexagonal MIM metasurface array ensures consistent Raman signal enhancement through durable plasmonic interactions and hotspot distribution. In cucumber samples, which serve as a representative food matrix, six distinct pesticide residues were analyzed. The intricate molecular structures of these compounds often lead to spectral overlaps and baseline variations, resulting in noise within the Raman spectra. All spectral data were meticulously preprocessed, incorporating Savitzky-Golay filtering, polynomial correction, and normalization—beyond mere smoothing. This preprocessing efficiently diminished noise and baseline drift, thereby enhancing both the identification and quantification precision. The Deep Feed-Forward (DFF) model effectively classified the six pesticide types with an accuracy exceeding 90%, and pesticide concentrations were additionally estimated for quantification purposes. The detection limits were below the regulatory thresholds, demonstrating the potential of the proposed MIM-SERS–AI platform as a scalable solution for real-time pesticide surveillance in the future.

Keywords: pesticide, metasurface, SERS, Raman spectra, real-time applications

Acknowledgment: This research was financially supported by The Scientific and Technological Research Council of Türkiye (TUBITAK), 1004 Programme, Project ID: 22AG002.

ORAL PRESENTATION

Hydrogel form containing drug delivery system for psoriasis treatment potential

Aslıhan Çimen[1]* (ORCID: https://orcid.org/0009-0001-3232-9455), Elif Çayırlı[1] (ORCID: https://orcid.org/0009-0001-3965-4162), Güliz Ak Demiroz[1] (ORCID: https://orcid.org/0000-0001-9613-6348)

[1]Department of Biochemistry, Faculty of Science, Ege University, Izmir, Türkiye

*Corresponding author e-mail: aslihancmn2320@gmail.com

Abstract

Psoriasis is a chronic autoimmune skin disease that causes skin cells to multiply faster than usual. Topical corticosteroids, methotrexate (MTX), and cyclosporine can be used to treat this disease. Drug delivery systems aim to minimize the problems that arise during drug administration and ensure more effective drug delivery to the target tissue. The goal of study is to develop a hydrogel form containing MTX nanocarrier composed of lipids to provide increased skin hydration and permeability, increased therapeutic, antioxidant, and wound-healing capacity, and reduced toxic effects of the system. In addition, the controlled drug release from the gel formulation supports prolonged drug penetration into the deeper layers of the skin during dermal applications, compared to release from nanoparticles alone. The nanostructured lipid carriers (NLCs) used in the project were synthesized using hot homogenization and ultrasonication methods. MTX was loaded into NLCs, and drug encapsulation was quantified by UV-Vis spectrophotometry at 300 nm. The drug delivery system was characterized using FTIR and SEM. The developed drug delivery system was transferred into carboxymethyl cellulose (CMC) hydrogel and optimized for topical applications. According to the data, MTX encapsulation was achieved with 76% efficiency, and encapsulation was confirmed by chemical analyses. The MTX was released from NLC in a controlled manner. The MTX-loaded NLC gel formulation was achieved at a suitable pH for the skin and the formulation maintained its spreadability. We suggest that the hydrogel formulation containing MTX-encapsulated NLC has promising potential for topical treatment of psoriasis.

Keywords: Psoriasis, methotrexate, nanostructured lipid carrier, carboxymethyl cellulose hydrogel, drug delivery.

Acknowledgement: This study was supported by TUBITAK-2209-A programme (Project ID: 1919B012400382). We would also like to thank to Onko Ilaç for providing MTX.

ORAL PRESENTATION

Bowtie-patterned nanosensor arrays for food safety monitoring

Nazlı Öncer[1], Sümeyra Vural Kaymaz[2], Elmas Eva Öktem Olgun[3], Oltan Canlı[3], Barış Güzel[3], Süleyman Çelik[1], Selim Tanrıseven[1], Hasan Kurt[4], Meral Yüce[1,*]

[1] Sabanci University SUNUM Nanotechnology Research and Application Centre, İstanbul, Türkiye
[2] Sabanci University, Faculty of Engineering and Natural Sciences, İstanbul, Türkiye
[3] Climate Studies and Water Management Research Group, TUBITAK Marmara Research Center, Kocaeli, Türkiye
[4] Istanbul Medipol University, School of Engineering and Natural Sciences, İstanbul, Türkiye

*Corresponding author e-mail: meralyuce@sabanciuniv.edu

Abstract

Health authorities report that the increase in pesticide use poses serious risks to the environment and human health. This situation further increases the need for effective methods to detect these residues. In this study, we propose a MIM-based Bowtie SERS nanoarray platform for the detection of three different pesticide classes (Pyrimethanil, Imidacloprid, Chlormequat Chloride). Spectra with high signal-to-noise ratios were collected using an in-house Raman spectroscopy device. The maximum residue limit (MRL) obtained for PYM in pepper juice (0.161 ppm) was found to be below the MRL value (2 mg/kg) reported by the EPA. This indicates that the chemical structure of PYM interacts effectively with the π-Au bond on the SERS surface. The concentration-dependent separation of pesticides and the separation of pepper juices from different regions were successfully and efficiently achieved using unsupervised machine learning algorithms. These findings underscore the potential of the proposed platform for the quick and straightforward detection of pesticide residues in pepper juice.

Keywords: Pyrimethanil, Imidacloprid, Chlormequat Chloride, Pepper, Bowtie Nanoarray, Surface-Enhanced Raman Spectroscopy (SERS).

Acknowledgment: This research was financially supported by The Scientific and Technological Research Council of Türkiye (TUBITAK), 1004 Programme, Project ID: 22AG002.

ORAL PRESENTATION

Detection of nutrient deficiencies in *Arabidopsis thaliana* using deep learning techniques for smart farming

Caner Soylukan[1] Hüseyin Dogan Türk[2], Zehra Ceyhan[2], Zainab Imtiaz[2], Ravzanur Yazıcıoğlu Başaran[1], Gülnur Şener[1], Nihal Öztolan Erol[1], Meral Yüce[1], Yunus Sarıkaya[3], Hasan Kurt[4,*]

[1] Sabanci University, Nanotechnology Research and Application Centre, SUNUM, İstanbul, Türkiye
[2] Sabanci University, Faculty of Engineering and Natural Sciences, İstanbul, Türkiye
[3] Pusula AI, Istanbul, 34906, Türkiye
[4] Istanbul Medipol University, School of Engineering and Natural Sciences, İstanbul, Türkiye

*Corresponding author email: h.kurt@imperial.ac.uk

Abstract

Macronutrient deficiencies such as nitrogen (N), phosphorus (P), and potassium (K) have detrimental effects on plant growth, productivity, and overall crop quality. Early and accurate detection of these deficiencies is essential for sustainable nutrient management and enhanced agricultural efficiency. In this study, a deep learning-based image analysis pipeline was developed to detect and classify nutrient deficiencies in 20 genotypes of Arabidopsis thaliana, a widely used model organism in plant research. High-resolution RGB images were captured under controlled growth conditions, and two main methodological frameworks were implemented: (1) feature extraction using pre-trained convolutional neural networks (CNNs) in combination with traditional machine learning classifiers, and (2) transfer learning approaches that fine-tuned existing deep learning architectures with structural optimization. Despite observable variations in phenotypic responses among genotypes, including differences in leaf color, morphology, and pigment accumulation, the models successfully identified nutrient deficiencies with high precision. Individually, deep learning models achieved an average classification accuracy of 98.96%, while an ensemble model integrating multiple architectures reached perfect accuracy (100%). The proposed approach offers a non-invasive, cost-effective, and scalable solution, providing a significant advantage over conventional laboratory-based diagnostic techniques. By enabling the timely detection of nutrient stress, this study contributes to the advancement of precision agriculture. It supports the integration of AI technologies into smart farming systems, thereby improving decision-making and resource efficiency.

Keywords: *Arabidopsis thaliana*, nutrient deficiency, RGB imaging, deep learning, image classification, plant health, precision agriculture, transfer learning, ensemble modeling

Acknowledgment: This research was financially supported by The Scientific and Technological Research Council of Türkiye (TUBITAK) [Project ID: 22AG002 and 2209-A].

ORAL PRESENTATION

Determining the potential of the marine invasive alien macroalga *Stypopodium schimperi* as a blue economic resource

Aysegul ERGENLER[1*] (ORCID: https://orcid.org/ 0000-0001-9186-3909),Buse Tuğba Zaman[2] (ORCID: https://orcid.org /0000-0003-0542-1050)
, Elif BOZKIR[3](ORCID: https://orcid.org/0009-0006-2072-6265), Zekiye Ceren ARITULUK AYDIN[4](ORCID: https://orcid.org/ 0000-0003-3986-4909), Pınar SIYAH[5](ORCID: https://orcid.org/ 0000-0003-1192-9416), Serdar KARAKURT[3] (ORCID: https://orcid.org/ 0000-0002-5538-6786)
, Sezgin BAKIRDERE[2] (ORCID: https://orcid.org/ 0000-0001-9746-3682), Tolga DEPCİ[6](ORCID: https://orcid.org /0000-0001-9562-8068), Funda TURAN[1] (ORCID: https://orcid.org /0000-0002-0257-6009)

[1*]Faculty of Marine Science and Technology, Iskenderun Technical University, Hatay, Türkiye
[2]Department of Chemistry, Faculty of Art and Sciences, Yildiz Technical University, İstanbul, Türkiye
[3] Department of Biochemistry, Faculty of Science, Selcuk University, Konya, TURKIYE
[4]Department of Pharmaceutical Botany, Faculty of Pharmacy, Hacettepe University, Ankara, Türkiye
[5]Department of Biochemistry, School of Pharmacy, Bahcesehir University, Istanbul, TURKIYE
[6]Department of Petroleum and Natural Gas Engineering, Faculty of Engineering and Natural Sciences, Iskenderun Technical University, Iskenderun, Hatay, Türkiye

*Corresponding author e-mail: aergenler@gmail.com

Abstract

The rise in global demand, coupled with growing environmental concerns, necessitates the identification of new energy sources that can support socioeconomic development while minimizing pollutant emissions. Aquatic biomasses, particularly invasive aquatic macrophytes, may serve as viable bioeconomic resources. This study seasonally evaluated the nutrient composition, elemental content, essential and nonessential metal contents, and overall characterization of the invasive macroalga *Stypopodium schimperi* to assess its potential as a value-added biomass and bioeconomic resource. Regarding the Fourier-transform infrared spectroscopy (FT-IR) analysis, various characteristic peaks were observed over a wide wavelength range in the IR spectrum. Examination of the main peaks revealed broad and strong bands in the range of 3500–3200 cm^{-1}, indicating that the invasive alien macroalga *S. schimperi* contains numerous organic molecules such as polysaccharides, proteins, lipids, and phenolic compounds. The present study showed that the invasive macroalga *S. schimperi* represents a rich biomass source of essential metals such as Ca, Mg, Ni, Zn, Cu, and Fe. In addition, the detection of only low quantities of toxic or nonessential metals (Pb, Cd, Hg) suggests its potential safety for use in the food industry or biotechnological applications. The elemental composition of *S. schimperi* collected during the summer season was determined to be 35.633 ± 0.511% C, 5.137 ± 0.160% H, 1.581 ± 0.204% N, 0.411 ± 0.047% S, and 57.238 ± 0.568% O. For samples collected in the autumn season, the elemental composition was 35.283 ± 0.493% C, 5.083 ± 0.256% H, 1.507 ± 0.260% N, 0.446 ± 0.058% S, and 57.681 ± 0.500% O, indicating that this biomass could be utilized as a renewable energy source, such as for producing biofuel or biochar, within the framework of the Blue economy. Furthermore, this study generally observed that *S. schimperi* has moderate levels of protein and carbohydrates, low levels of lipids, and high moisture content in terms of nutritional composition, suggesting that this species could be used as a raw material in functional foods, feed additives, or biotechnological applications.

Keywords: Blue economy, Marine resources, Macrophytes**,** Value-added biomass.

This study was supported by TUBITAK (Project number: 124Y004)

ORAL PRESENTATION

Biogenic gold nanoparticles (AuNPS) from invasive brown macroalga *Stypopodium Schimperi* aqueous extract: Characterization and ecotoxicological potential

Aysegul ERGENLER[1*] (ORCID: https://orcid.org/ 0000-0001-9186-3909),Buse Tuğba Zaman[2] (ORCID: https://orcid.org /0000-0003-0542-1050)
, Elif BOZKIR[3](ORCID: https://orcid.org/0009-0006-2072-6265), Zekiye Ceren ARITULUK AYDIN[4](ORCID: https://orcid.org/ 0000-0003-3986-4909), Pınar SIYAH[5](ORCID: https://orcid.org/ 0000-0003-1192-9416), Serdar KARAKURT[3] (ORCID: https://orcid.org/ 0000-0002-5538-6786)
, Sezgin BAKIRDERE[2] (ORCID: https://orcid.org/ 0000-0001-9746-3682), Tolga DEPCİ[6](ORCID: https://orcid.org /0000-0001-9562-8068), Funda TURAN[1] (ORCID: https://orcid.org /0000-0002-0257-6009)

[1*]Faculty of Marine Science and Technology, Iskenderun Technical University, Hatay, Türkiye
[2]Department of Chemistry, Faculty of Art and Sciences, Yildiz Technical University, İstanbul, Türkiye
[3] Department of Biochemistry, Faculty of Science, Selcuk University, Konya, TURKIYE
[4]Department of Pharmaceutical Botany, Faculty of Pharmacy, Hacettepe University, Ankara, Türkiye
[5]Department of Biochemistry, School of Pharmacy, Bahcesehir University, Istanbul, TURKIYE
[6]Department of Petroleum and Natural Gas Engineering, Faculty of Engineering and Natural Sciences, Iskenderun Technical University, Iskenderun, Hatay, Türkiye

*Corresponding author e-mail: aergenler@gmail.com

Abstract

Algae's capacity to accumulate metals and reduce metal ions renders them an exceptional candidate for nanoparticle biosynthesis, thereby earning them the designation of bio-nano factories. The aim of the study was to synthesize novel gold nanoparticles (AuNPs) from invasive brown macroalga *Stypopodium schimperi* aqueous extract and, analyze acute and sub-acute toxicity of biogenic gold nanoparticles (AuNPs) to a model organism *Daphnia magna*. The characterization of biogenic AuNPs had been conducted using multiple instruments including transmission electron microscopy (TEM) and zeta potential assessment. Bioassays for the determination of acute and subacute toxicity of algal derived Biogenic AuNPs were performed according to OECD 202 (OECD, 2009) guidelines for 96-hour and 21 days, respectively. The LC_{50} value at 96 hours, with 95% confidence, was determined to be 2.3 mg L^{-1} for *S.schimperi*@AuNPs. Based on these genotoxicity and cytotoxicity results, these can be said that the 0.25 ppm concentration of Biogenic AuNPs derived from *S. schimperi* is not genotoxic, while the 0.5 and 1.0 ppm concentrations cause minimal DNA damage (approximately 3% and 7%) and have low genotoxicity. Also, the cell viability at biogenic AuNP concentrations of 0.25, 0.5, and 1.0 ppm was 93.3%, 86.7%, 73.3%, and 70.0%. Biogenic AuNPs from *S. schimperi* at subacute doses were not harmful according to ISO 10993-5. This study has shown that both the environmentally friendly synthesis procedure of AuNPs can be safely used for future industrial and therapeutic needs, and that it can serve as a basis for innovative approaches to the use of invasive algae in safe nanotechnology.

Keywords: Green synthesis, Nanogold, *Stypopodium schimperi*, Genotoxicity, Cytotoxicity.

This study was supported by TUBITAK (Project number: 124Y004).

ORAL PRESENTATION

Synthesis and investigation of ternary nanocomposite fibers

Mesut Yalçın (https://orcid.org/0000-0002-6171-3018)

Kilis 7 Aralik University, Educational Faculty, Department of Science Education, Kilis, Türkiye.

Corresponding author e-mail: myalcin@kilis.edu.tr

Abstract

In this study, ternary nanocomposite fibers were produced using two different layered nanomaterials. First, a TiO_2 solution was prepared by the sol-gel method. Reduced graphene oxide (rGO) and hexagonal boron nitride (h-BN) were then added to this solution in different ratios to obtain a ternary mixture. Using this solution, ternary nanocomposite fibers were fabricated through electrospinning. The structural and surface characteristics of the nanofibers were confirmed by XRD, FTIR, Raman, FESEM, and EDX analyses. Due to their large surface area, the nanofibers have significant potential for use in photoanodes of dye-sensitized and quantum dot-sensitized solar cells.

Keywords: Ternary Nanocomposite Fibers, $T\dot{I}O_2$, Reduced graphene oxide (rGO), Hexagonal boron nitride (h-BN)

Acknowledgments: This study was supported by Scientific and Technological Research Council of Turkey (TUBITAK) under the Grant Number 102F090 The authors thank to TUBITAK for their supports.

ORAL PRESENTATION

Fabrication of TiO_2/h-BN-CdSe based quantum dot-sensitized solar cells

Mesut Yalçın (https://orcid.org/0000-0002-6171-3018)

Kilis 7 Aralik University, Educational Faculty, Department of Science Education, Kilis, Türkiye.

Corresponding author e-mail: myalcin@kilis.edu.tr

Abstract

In this study, h-BN was first incorporated into a TiO_2 solution, and the resulting mixture was used to directly deposit TiO_2/h-BN photoanodes onto FTO substrates via electrospinning. The surfaces of the fabricated photoanodes were then coated with CdSe quantum dots using the SILAR technique. Quantum dot-sensitized solar cells were assembled by filling a liquid electrolyte between the prepared photoanodes and a Pt counter electrode. The electrical characteristics of the fabricated solar cells were measured using a solar simulator. An improvement in efficiency was observed compared to the pure TiO_2-based cell.

Keywords: Hexagonal boron nitride (h-BN), CdSe quantum dot, Quantum Dot-Sensitized Solar Cells

Acknowledgments: This study was supported by Scientific and Technological Research Council of Turkey (TUBITAK) under the Grant Number 102F090 The authors thank to TUBITAK for their supports.

ORAL PRESENTATION

Regulatory role of caveolin-1 in doxorubicin-induced SASP and its impact on cancer cell proliferation

Yaprak Dilber Şimay Demir, Kader Yılmaz*

Gazi University, Faculty of Pharmacy, Department of Pharmacology, Ankara, Türkiye

*Corresponding author e-mail: yilmazkadeer@gmail.com

Abstract

Cellular senescence is characterized by an irreversible arrest of cell proliferation induced by various stressors, including telomere shortening, DNA damage and chemotherapeutic agents. Senescent cells develop a distinct secretory phenotype termed the senescence-associated secretory phenotype (SASP), which actively modulates the surrounding microenvironment. Under physiological conditions, SASP contributes to the immune-mediated clearance of senescent cells; however, insufficient elimination can lead to a highly pro-inflammatory microenvironment that facilitates tumor initiation and progression. Compounds capable of modulating SASP secretion are referred to as senomorphic agents and the identification of such molecules offers promising opportunities for therapeutic innovation in oncology. Previous studies have shown that caveolin-1 expression is increased in senescent cells induced by oxidative stress, UV-C radiation, bleomycin, or oncogenic K-Ras, and that caveolin-1 may be important in the developmental processes of senescence. However, no study has been encountered in the literature directly evaluating the effectiveness of Caveolin-1 on chemotherapeutic-induced SASP. In this study, we investigated whether Caveolin-1 knockdown in doxorubicin-induced senescent A549 and HeLa cancer cells could alter SASP production and influence the proliferation of neighboring non-senescent cells, assessed using the xCELLigence real-time cell analysis platform. Our findings indicate that SASP derived from Caveolin-1–suppressed senescent A549 cells did not affect the proliferation of non-senescent A549 cells. In contrast, SASP from Caveolin-1–suppressed senescent HeLa cells significantly reduced the proliferation of non-senescent HeLa cells. These results suggest that Caveolin-1 may represent a promising senomorphic target, particularly in the context of cervical cancer. Further research is warranted to elucidate the underlying mechanisms and to explore the translational potential of Caveolin-1–modulating strategies in contemporary cancer therapeutics.

Keywords: Caveolae, Senescent cell secretome, co-culture, chemotherapy.

This study was supported by TUBITAK (project no. 122S564).

ORAL PRESENTATION

Effect of life kinetic exercise on BMAL1 and CLOCK in Alzheimer's disease

Ayşe Asiye Culum[1*] (*ORCID: https://orcid.org/0000-0002-0072-7600*, Murat Gültekin[2] (*ORCID: https://orcid.org/0000-0002-0609-4269*), Hüseyin Gürer[3] (*ORCID: https://orcid.org/0000-0001-5984-3174),* Faruk Akçınar[3] (*ORCID: https://orcid.org/0000-0003-2751-1743),* Zehra Ömeroğlu Ulu[4] (*ORCID: https://orcid.org/0000-0002-8884-4683),* Nurdan Sena Değirmenci[4] (*ORCID: https://orcid.org/0000-0002-8122-5476*), Fikrettin Şahin[4] (*ORCID: https://orcid.org/0000-0003-1503-5567)*

[*] [1]Malatya Turgut Ozal University, Vocational School of Health Services, Department of Medical Services and Techniques, Malatya Türkiye.
[2]Erciyes University, Faculty of Medicine, Department of Neurology, Kayseri, Türkiye.
[3]Inonu University, Department of Coaching Education, Faculty of Sports Sciences, Malatya, Türkiye.
[4]Yeditepe University, Faculty of Engineering, Department of Genetics and Bioengineering, Istanbul, Türkiye.

*Corresponding author e-mail: ayse.culum@ozal.edu.tr

Abstract

Alzheimer's Disease (AD) is a neurodegenerative disease characterized by progressive memory loss affecting the elderly population. Disruption of the biological clock increases the risk of developing AD, which in turn exacerbates circadian rhythm disorders. Whether disturbances in sleep and circadian rhythms cause AD, or AD causes sleep and circadian rhythm disorders, is largely unclear. Exercise is an important approach to maintaining or improving physical and mental health, including the brain. Exercise has positive effects on emotional and cognitive performance during brain aging. Life kinetic exercises are a form of exercise that involves enjoyable mental exercises that advance the brain's working principles from simple concepts to complex and unique concepts. The effects of Life kinetic exercises were investigated in healthy individuals and patients with late-onset AD aged 65 and over. Participants performed Life kinetic exercises three times a week for 8 weeks. For analyses, blood samples were taken from participants before and after exercise. Plasma protein levels of brain and muscle Arnt-like protein-1 (BMAL1) and circadian locomotor output cycles kaput (CLOCK), which are transcriptional activators of circadian rhythm, were analyzed by the ELISA method. Results showed no significant difference between the AD and control groups before and after exercise. However, BMAL1 levels increased in both groups after the Life Kinetic exercise, while CLOCK levels remained unchanged.

Keywords: Alzheimer's disease, circadian rhythm, exercise, BMAL1, CLOCK, ELISA.

Acknowledgements: This project was supported by TUBITAK (project number: 323S231).

ORAL PRESENTATION

Effects of low temperature stress on pollen germination, tube growth, and antioxidant responses in Turkish olive cultivars

Sena Acar*[1] (ORCID: 0009-0003-5912-5852), Melse Su Bilgili[1](ORCID: 0000-0002-2062-7295), Öznur Çetin[2] (ORCID: 0000-0003-4252-0357), Aslıhan Çetinbaş-Genç[3] (ORCID: 0000-0001-5125-9395)

[1]Marmara University, Institute of Pure and Applied Sciences, Istanbul, Türkiye
[2]Olive Research Institute of Bornova, Izmir, Türkiye
[3]Marmara University, Faculty of Science, Department of Biology, Istanbul, Türkiye

*Corresponding author e-mail: senaacar.mu@gmail.com

Abstract

Fertilization success in olive production largely depends on pollen viability and tube growth, while low-temperature stress can impair these processes and reduce yield. This study examined the physiological and biochemical responses of five olive cultivars (Ayvalık, Erkence, Gemlik, Hayat, Memecik) to low temperatures (15, 10, 5 ºC) using pollen grains. Pollen germination rates and tube lengths were assessed. In Ayvalık and Hayat, both declined at 15 and 10 ºC, while in Erkence reductions occurred only at 15 ºC; at lower temperatures germination was absent, preventing tube measurement. In Gemlik, all treatments reduced both parameters, whereas in Memecik germination declined only at 10 and 5 ºC, with tube length unaffected. Groups without germination were excluded from further analyses. Antioxidant responses varied among cultivars. Superoxide dismutase activity decreased in Ayvalık (15, 10 ºC) and Erkence (15 ºC), increased in all Gemlik treatments, rose only at 10 ºC in Hayat, and declined under all Memecik treatments. Catalase activity decreased in Ayvalık (15 ºC) and Gemlik (all treatments) but remained unchanged in Erkence, Hayat, and Memecik. Ascorbate peroxidase activity decreased only in Ayvalık (15, 10 ºC). No significant differences were observed in antioxidant activity. Total phenolic content decreased in Ayvalık (15 ºC) and Memecik (10 ºC), but not in the other cultivars. Total flavonoid content increased in Ayvalık (15, 10 ºC), Erkence and Memecik (15 ºC), and Hayat (10 ºC), but decreased in Gemlik under all treatments. Overall, low-temperature stress produced cultivar-specific effects on pollen physiology and antioxidant defense, underscoring the importance of cultivar selection in breeding programs for climate change resilience.

Keywords: Antioxidant activity, Flavonoid content, Low-temperature stress, Phenolic content, Pollen germination, Pollen tube

This study was supported by TUBITAK 1002-A Project (Grant No: 224Z120). The authors also thank the Olive Research Institute, Republic of Türkiye Ministry of Agriculture and Forestry, for their valuable support.

ORAL PRESENTATION

Volatile composition of *Lathyrus laxiflorus* subsp. *laxiflorus* by GC-MS/FID analysis

Nevin ULAŞ ÇOLAK[1*] (ORCID: https://orcid.org/https://orcid.org/0000-0003-3200-6688), İrem KURT[1](ORCID: https://orcid.org/0009-0000-9693-2950), Ahmet YAŞAR[1] (ORCID: https://orcid.org/0000-0002-5487-1536), Kamil COŞKUNÇELEBİ[2] (ORCID: https://orcid.org/0000-0001-5713-6628)

[*1]Karadeniz Technique University, Pharmacy Faculty, Analytical Chemistry Department, Trabzon, Turkey.
[2]Karadeniz Technique University, Science Faculty, Biology Department, Trabzon, Turkey.

*Corresponding author e-mail: nevin.ulas@hotmail.com

Abstract

The present study aimed to investigate the essential oil composition of *Lathyrus laxiflorus* subsp. *laxiflorus* using gas chromatography coupled with mass spectrometry and flame ionization detection (GC-MS/FID). Essential oil was obtained through hydrodistillation and analyzed under optimized chromatographic conditions. The yield of essential oil was calculated as 0.22% (w/w, moisture-free basis). A total of 27 volatile compounds were identified, representing 96.86% of the total composition. The chemical profile was dominated by monoterpenoids (69.49%) and monoterpene (27.03%), with minor contributions from sesquiterpenes (0.14%) and sesquiterpenoids (0.20%). Camphor (44.60%) was determined as the major constituent, followed by borneol (8.32%) and 1,8-cineole (7.94%). Other components such as α-pinene, β-pinene, and camphene were detected in lower proportions. These results provide the first detailed report on the volatile composition of *L. laxiflorus* essential oil analyzed via GC-MS/FID. The predominance of camphor and related oxygenated monoterpenes indicates potential applications of this species in pharmaceutical and aromatic industries. This study highlights the chemotaxonomic relevance of *L. laxiflorus* and contributes to expanding the phytochemical knowledge of the genus Lathyrus.

Keywords: Essential oil, *Lathyrus laxiflorus*, GC-MS/FID, Phytochemical Profiling

ORAL PRESENTATION

Preparation of a drug delivery system including caffeic acid for the inhalation-based treatment of lung cancer

Ahmet Erkan[1]* (ORCID:0009-0009-7675-2480), Ece UĞURLU[2] (ORCID:0009-0006-9208-1849), Güliz Ak Demiroz[1] (ORCID:0000-0001-9613-6348)

*[1]Ege University, Faculty of Science, Department of Biochemistry, İzmir, Turkey.
[2]Ege University, Graduate School of Natural and Applied Sciences, Department of Biochemistry, İzmir, Turkey.

*Corresponding author e-mail: a.erkannn1@gmail.com

Abstract

Lung cancer has the highest mortality rate among all cancer types and is usually diagnosed at an advanced stage. It is more common in elderly individuals and is difficult to treat because of its high malignancy and metastatic tendency. Therefore, in recent years, alternative therapeutic approaches have been developed for its treatment. Drug delivery systems can be potential solutions by enabling controlled release and reducing the side effects of chemotherapeutic agents. In this study, an inhalable drug delivery system was developed for the treatment of lung cancer. Doxorubicin (Dox), a chemotherapeutic agent, and caffeic acid (CA), a phytochemical compound, were used in combination within the polymeric nanoparticles. Caffeic acid has the potential to reduce the toxic effects of Dox while enhancing its anticancer activity. The carrier structure was synthesized using two natural polymers suitable for lung targeting: chitosan (CH) and carrageenan (CRG). Initially, caffeic acid and chitosan were covalently linked and caffeic acid/chitosan grafting ratio was found to be as 17.4%. Then, a CH/CA/CRG structure was formed through polyelectrolyte complexation between carrageenan and chitosan, followed by nanoparticle synthesis using cross-linking agents. Dox was encapsulated into the system and the highest encapsulation efficiency was found to be as 47.95% by spectrophotometrically. The obtained nanoparticles were characterized using Fourier Transform Infrared Spectroscopy (FT-IR) and Scanning Electron Microscopy (SEM). The nanoparticles were observed to be approximately 50 nm in size by SEM. In vitro drug release studies showed that release at pH 5.5 was higher than at pH 7.4. The developed nanoparticles could have a promising potential for future studies in targeted inhaler lung cancer treatment.

Keywords: Lung Cancer, Inhaler Drug Delivery, Caffeic Acid, Doxorubicin, Chitosan/Carrageenan Nanoparticles.

*This study was supported by TUBITAK-2209-A programme (Project ID: 1919B012317647).

ORAL PRESENTATION

Development of active biodegradable poly(3-hydroxybutyrate-co-4-hydroxybutyrate) films enriched with essential oils for food packaging applications

Kıvanç Mindavallı[1*] (ORCID: https://orcid.org/0009-0003-2186-1758),
Bedriye Üçpınar[1] (ORCID: https://orcid.org/0000-0002-4446-6086),
Hüseyin Uzuner[2,3] (ORCID: https://orcid.org/0000-0002-2323-2977),
Nejla Altın[4] (ORCID: https://orcid.org/0000-0001-7879-3854),
Sema Samatya Yılmaz[4] (ORCID: https://orcid.org/0000-0002-2682-2892),
Ayşe Aytaç[4] (ORCID: https://orcid.org/0000-0002-9566-7881)

[*1]Ege University, Engineering Faculty, Chemical Engineering Department, Izmir, Türkiye.
[2]Kocaeli University, Kocaeli Vocational School of Health Services, Department of Medical Services and Techniques, Kocaeli, Türkiye.
[3]Kocaeli University, Faculty of Medicine, Department of Medical Microbiology, Molecular Research and Antibody Laboratory, Kocaeli, Türkiye.
[4]Kocaeli University, Engineering Faculty, Chemical Engineering Department, Kocaeli, Türkiye.

*Corresponding author e-mail: kivanc.mindavalli@gmail.com

Abstract

In food packaging applications, petroleum-based polymers are widely used in the industry; however, their long-term persistence and resistance to degradation pose a significant threat to the environment. Moreover, the limited availability of petroleum resources has prompted an increasing demand for sustainable polymer alternatives. Consequently, interest in biodegradable and bio-based polymers has grown rapidly in recent years. In this study, poly(3-hydroxybutyrate-co-4-hydroxybutyrate) (PHB), which is both bio-based and biodegradable, was used to evaluate its potential as a sustainable alternative to synthetic polymers. To improve the properties of PHB film, fennel (F) and geranium (G) essential oils were incorporated at different concentrations (5-10-15-20 wt%). The PHB/F and PHB/G films were prepared via solution casting method. Manufactured films were characterized to determine their morphology, chemical structure, antioxidant and antibacterial activities, water vapor permeability, and biodegradability in soil. According to the FTIR results, no chemical reaction occurred between PHB and the essential oils. The antioxidant test results indicated that the DPPH radical scavenging activities of the films containing essential oils were 1–6% higher than that of the neat PHB film. The antibacterial activity test results showed that both essential oil–loaded films exhibited a strong inhibitory effect against *S. aureus*. In contrast, no significant antibacterial activity was observed against *E. coli*, indicating that the films were ineffective on this Gram-negative strain. Water vapor permeability of PHB slightly increased after the addition of essential oils. The films were buried in garden soil for 45 days, and their mass losses were measured. After 45 days, the neat PHB film exhibited approximately 20% mass loss, whereas the incorporation of essential oils significantly enhanced the biodegradability of the films. The highest mass losses were observed in the 5F and 5G films, with values of about 80% and 96%, respectively. The findings support the applicability of the produced essential oil-loaded films in the packaging industry.

Keywords: Active packaging, Biodegradable, Biobased, Essential oil, Poly (hydroxybutyrate)

*This study was supported by the Scientific and Technological Research Council of Turkey (TUBITAK), BIDEB within the scope of 2209-A University Students Research Projects Support Program. The authors would like to thank for the financial support to TUBITAK (Application No: 1919B012428526).

ORAL PRESENTATION

Green synthesis of zinc oxide nanoparticles From *Eucalyptus globulus:* Characterization, and investigation of the antimicrobial effects

Kader Kelle* (ORCID: 0009-0000-0437-039X), Emre Erden Kopar (ORCID: 0000-0002-6641-4367), Nurdan Pazarlioglu (ORCID: 0000-0002-9486-8155)

*Ege University, Faculty of Science, Department of Biochemistry, Izmir, Türkiye

*Corresponding author e-mail: kkelle20@gmail.com

Abstract

Nanoparticles are structures with sizes ranging from 1 to 100 nm, exhibiting unique properties distinct from macroscopic materials. Due to their high surface area-to-volume ratios, they behave much more effectively in chemical reactions. As their size decreases, their optical, electronic, and catalytic properties change significantly, making them extremely valuable in various applications. Nanoparticles can be metallic in structure (e.g., AgNP and AuNP) or exist in the form of metal oxides (such as TiO_2 and ZnO). Additionally, quantum dots exhibiting semiconducting properties and polymeric or lipid-based nanoparticles constitute another important class. These different types are extensively used, particularly in fields such as medicine, electronics, and catalysis. The advantages offered by nanoparticles in energy storage and environmental improvement applications are also increasingly recognized (Khan & Hossain, 2022; Jamkhande et al., 2019). Among nanoparticle synthesis methods, green synthesis offers an eco-friendly, non-toxic, and biocompatible approach, providing an alternative to traditional chemical methods. This method is also highly advantageous for industrial production due to its low cost and easy scalability. Phytochemicals such as flavonoids, polyphenols, alkaloids, and terpenoids obtained from plants act as powerful biological reduction agents. In addition, fungi, bacteria, and marine-derived polysaccharides and proteins are also among the effective biomolecules in nanoparticle synthesis. Therefore, green synthesis is an important method shaping the future of sustainable nanoparticle production (Malik et al., 2023). *Eucalyptus globulus* is a shrubby plant or flowering tree belonging to the Myrtaceae family. It is currently grown in many regions of the world. The leaves of the plant are rich in tannins, flavonoids, and phenolic acids, as well as volatile oils containing mainly eucalyptol (1,8-cineole) (Shala & Gururani, 2021). In this study, ZnO-NPs were synthesized via green synthesis using an extract obtained from *Eucalyptus globulus* leaves. In this context, the effect of temperature, pH, synthesis time, and reducing agent concentration, on the structure and character of ZnO-NPs, were determined. The synthesized NPs were characterized using UV-Vis spectroscopy, SEM, ATR-FTIR and XRD, and their antimicrobial activity against *E. coli*, *S. aureus*, *K. pneumoniae*, and *C. albicans* microorganisms were investigated.

Keywords: Zinc oxide nanoparticles, *Eucalyptus globulus*, Green synthesis, Metallic nanoparticles, ZnO-NP

*This project is supported by Scientific Research Projects (BAP) of Ege University. (Project no: 32727)
This project is supported under the TUBITAK Scientific Personnel Support Programs Presidency (BIDEB) 2211-Domestic Postgraduate Scholarship Program.

References:

Jamkhande, P. G., Ghule, N. W., Bamer, A. H., & Kalaskar, M. G. (2019). Metal nanoparticles synthesis: An overview on methods of preparation, advantages and disadvantages, and applications. *Journal of drug delivery science and technology*, *53*, 101174.

Khan, S., & Hossain, M. K. (2022). Classification and properties of nanoparticles. In *Nanoparticle-based polymer composites* (pp. 15-54). Woodhead Publishing.

Malik, A. Q., Mir, T. U. G., Kumar, D., Mir, I. A., Rashid, A., Ayoub, M., & Shukla, S. (2023). A review on the green synthesis of nanoparticles, their biological applications, and photocatalytic efficiency against environmental toxins. *Environmental Science and Pollution Research*, *30*(27), 69796-69823.

Shala, A. Y., & Gururani, M. A. (2021). Phytochemical properties and diverse beneficial roles of Eucalyptus globulus Labill.: A review. *Horticulturae*, *7*(11), 450.

ORAL PRESENTATION

Investigation of the enzyme inhibition effect of different turnip varieties on antioxidants and sugar metabolism

Feyza Akgün[1*] (*ORCID: https://orcid.org/0000-0001-7111-4003*),
Nuraniye Eruygur[2] (*ORCID: https://orcid.org/ 0000-0002-4674-7009*)

[*1] Selcuk University, Faculty of Pharmacy, Konya, Turkey.
[2] Selcuk University, Faculty of Pharmacy, Department of Pharmacognosy, Konya, Turkey.

*Corresponding author e-mail: feyzaakgun664@gmail.com

Abstract

This study investigated the *in vitro* antidiabetic and antioxidant properties of three radish varieties—white radish (FBT), red radish (FKT), and black radish (FST)—sourced from Konya. . The evaluation encompassed several key biological activities. Total flavonoid content (TFC) and total phenolic content (TPC) were measured to establish the phytochemical composition. Antioxidant capacity was comprehensively assessed using the 2,2-diphenyl-1-picrylhydrazyl (DPPH), 2,2′-azino-bis(3-ethylbenzothiazoline-6-sulfonic acid) (ABTS), and iron chelation activity (FCA) assays. Antidiabetic activity was determined by quantifying the inhibition of the α-amylase and α-glucosidase enzymes. All absorbance readings were obtained utilizing an ELISA plate reader, and statistical data analysis was performed with Microsoft Excel and GraphPad software. Among the samples, red radish (FKT) exhibited the highest TFC (1.27 mg KE/g) and TPC (55.36 mg GAE/g), followed by black radish (FST) and white radish (FBT). Antioxidant activity, assessed via DPPH, ABTS, and iron chelation assays, revealed that FST had the strongest DPPH radical scavenging activity (84.32%; IC_{50} = 636.6 µg/mL), while FKT showed superior ABTS inhibition (83.79%; IC_{50} = 144.5 µg/mL) and iron chelation capacity (74.04%; IC_{50} = 677.2 µg/mL). In terms of antidiabetic potential, FKT demonstrated the most potent α-amylase inhibition (97.36%; IC_{50} = 2.07 mg/mL) and α-glucosidase inhibition (84.18%), indicating strong enzyme inhibitory activity. FBT showed moderate activity across most assays, while FST displayed notable antioxidant properties but comparatively lower antidiabetic effects. In conclusion, red radish (FKT) emerged as the most promising candidate among the three varieties, exhibiting the highest levels of bioactive compounds and the strongest antidiabetic and antioxidant activities. These findings suggest that FKT may offer valuable health benefits and could be further explored for its therapeutic potential in managing oxidative stress and diabetes-related conditions.

Keywords: Radish, enzyme inhibition, antioxidant, total phenol

Acknowledgements: We would like to thank the TUBITAK 2209/A Undergraduate Student Project for the financial support (NO: 1919B012102103).

ORAL PRESENTATION

Evaluation of anabolic androgenic steroid nandrolone decanoate effects on apoptosis associated genes in pancreatic cells

Akın Kahya[1,2*] (*ORCID: https://orcid.org/ 0009-0007-0084-8254*), Mehtap Kara[2] (*ORCID: https://orcid.org/0000-0001-7764-5593*), Funda Çatan İnan [3] (*ORCID: https://orcid.org/0000-0003-3974-7577)*

[*1]Sanofi, Medical Department, Istanbul, Turkey.
[2] Istanbul University, Faculty of Pharmacy, Department of Pharmaceutical Toxicology, Istanbul, Turkey.
[3] Bilecik Seyh Edebali University, Faculty of Medicine, Department of Biostatistics and Medical Informatics, Bilecik, Turkey.

*Corresponding author e-mail: mehtap.kara@istanbul.edu.tr

Abstract

Anabolic-androgenic steroids (AASs) are a large group of molecules that include endogenously produced androgens such as testosterone, as well as synthetically produced derivatives. They are widely used for aesthetic purposes, as they promote muscle growth, or for athletes seeking to enhance athletic performance. Despite their popularity, these substances are classified as prohibited substances because they can produce serious adverse effects. However, they are used at pharmacological doses to support the treatment of various diseases under physician supervision. However, the abuse doses of these substances are far higher than these pharmacological doses. AASs cause serious harmful effects on the heart, liver, brain, male and female reproductive systems, the endocrine system, and the immune system. While case reports demonstrating toxic effects on the pancreas exist in the literature, the molecular mechanisms involved in pancreatic toxicity remain unclear. It is known that disruptions in the regulation of apoptosis, a key molecular pathway in cells, play a significant role in pancreatic pathophysiology. There are no studies demonstrating the effects of AASs on the molecular pathway of apoptosis in pancreatic cells. This study aims to demonstrate the pancreatic toxicity of Nandrolone decanoate (ND), a widely abused AAS, and its effects on pancreatic apoptosis mechanisms in vitro using the PANC-1 cell line. In this study, inhibitory Concentration 50(IC50) values calculated as 62.8 µg/mL with MTT test. According to gene expression results, apoptosis related genes as P53, Bcl-2, Bax, Nf-kB, TNF-alpha, Jnk, miR-21, PI3-K, Akt, caspase-8, and caspase-9 levels were determined elevated for 24h ND exposure.

Keywords: Nandrolone decanoate, Pancreas, Apoptosis, miR21

Acknowledgements: Thank you for supporting Dr. Funda Çatan İnan from Bilecik Sheikh Edebali University Faculty of Medicine Basic Medical Department Biostatistics and Medical Informatics Department for the statistical evaluations in our study. This stydy funded by; TUBITAK 2209/A Üniversite Öğrencileri Araştırma Projeleri Destek Programı. 2022/2 (Başvuru no: 1919B012216625)

ORAL PRESENTATION

Synthesis of novel bis-hydrazone derivatives and *in silico* evaluation of their COX-2 inhibitory potentials

Hazal Şahinbey[1] (ORCID: https://orcid.org/0000-0003-0986-3884),
Sevil Şenkardeş[2*] (ORCID: https://orcid.org/0000-0002-0523-459X)

[1]Marmara University, Institute of Health Sciences, Istanbul, Türkiye.
[2]Marmara University, Faculty of Pharmacy, Department of Pharmaceutical Chemistry, Istanbul, Türkiye

*Corresponding author e-mail: sevil.aydin@marmara.edu.tr

Abstract

Cyclooxygenase-2 (COX-2) is an inducible isoform of the cyclooxygenase enzyme responsible for the conversion of arachidonic acid into prostaglandins, which regulate inflammation, pain, and cell proliferation. Overexpression of COX-2 has been associated with various cancers, including colorectal, breast, and lung cancers, due to its role in promoting angiogenesis, inhibiting apoptosis, and enhancing tumor growth. Therefore, selective COX-2 inhibition represents an important therapeutic approach not only for inflammation but also for cancer prevention and treatment. Hydrazone structure constitutes a special subgroup of Schiff bases and contains a C=N bond characterized by two different nitrogen atoms bonded together. Furthermore, considering the unshared electron pairs on the nitrogen atoms, the physical and chemical properties of hydrazones appear to be directly related to these groups. Because both nitrogen atoms in the hydrazone structure are nucleophilic, they are susceptible to electrophilic interactions, while the carbon atom can exhibit both nucleophilic and electrophilic characteristics. Hydrazones represent an important class of compounds in medicinal chemistry due to their versatile biological activities, including antimicrobial, anti-inflammatory, and anticancer properties. In particular, numerous studies in the literature have reported hydrazone derivatives as potent COX-2 inhibitors, underscoring their pharmacological relevance. In this study, a series of bis-hydrazone derivatives were synthesized and characterized by infrared (IR) spectroscopy, nuclear magnetic resonance (^{1}H-NMR and ^{13}C-NMR) spectroscopy. The synthesized compounds were further investigated through *in silico* molecular docking studies against the COX-2 enzyme (PDB ID: 3LN1). Docking results indicated that the bis-hydrazone compounds successfully occupied the COX-2 binding pocket and exhibited favorable binding energies, suggesting their potential as promising COX-2 inhibitors with possible anti-inflammatory and anticancer activity.

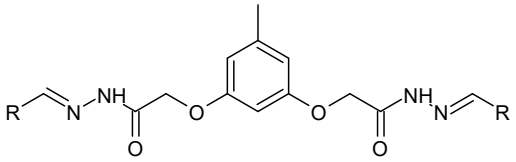


Figure 1. General structures of the synthesized compounds

Keywords: Hydrazone, Orcin, COX-2, Molecular docking, *In silico*

Acknowledgements: This work was supported financially by the Scientific and Technological Research Council of Turkey (TÜBİTAK) (Project Number: 225S304).

ORAL PRESENTATION

Determination of resveratrol in fresh and heat-treated pomace *Vitis labrusca* by RP-HPLC

Nevin ULAŞ ÇOLAK[1*] (ORCID: https://orcid.org/https://orcid.org/0000-0003-3200-6688), Merve BADEM[2](ORCID: https://orcid.org/0000-0002-1265-5616), Şeyda KANBOLAT[2] (ORCID: https://orcid.org/0000-0001-7261-7067)

[*1]Karadeniz Technique University, Pharmacy Faculty, Analytical Chemistry Department, Trabzon, Turkey.
[2] Karadeniz Technique University, Pharmacy Faculty, Biochemistry Chemistry Department, Trabzon, Turkey.

*Corresponding author e-mail: nevin.ulas@hotmail.com

Abstract

Resveratrol, a naturally occurring polyphenolic compound, is widely recognized for its health-promoting properties. In this study, the resveratrol content of fresh grapes and grape pomace was determined using HPLC with external standard calibration. The calibration curve exhibited excellent linearity ($Y = 1.98582 \times 10^{-5}X - 0.3297$, $R^2 = 0.9997$, $R = 0.9998$), confirming the reliability of the method. Chromatographic analysis revealed a sharp peak at a retention time of 1.528 min for fresh *V. labrusca* samples, corresponding to a concentration of 282.6 ppm resveratrol (99.88% area). In *V. labrusca* pomace, resveratrol was also detected at a similar retention time (1.531 min), but with a lower concentration of 89.0 ppm (99.62% area). These results indicate that while fresh *V. labrusca* are a richer source of resveratrol, *V. labrusca* pomace still retains a substantial and noteworthy concentration of this bioactive compound. Rather than being treated merely as an industrial waste, *V. labrusca* pomace should be considered a sustainable and economically valuable reservoir of resveratrol, offering opportunities for high-value utilization. Its incorporation into nutraceutical, cosmetic, and pharmaceutical applications could not only enhance product functionality but also contribute to circular economy practices and environmental sustainability.

Keywords: Resveratrol, HPLC, *Vitis labrusca*, Sustainability

ORAL PRESENTATION

In silico assessment of the interaction of the natural compound zeaxanthin with insulin, glucocorticoid, and GLP-1 receptors associated with type 2 diabetes

Nil Sazlı[1] (ORCID: https://orcid.org/0009-0006-6740-1169), Deniz Karataş[2*] (ORCID: https://orcid.org/0000-0002-8176-4883)

[1]Manisa Celal Bayar University, Faculty of Engineering, Department of Bioengineering, Manisa, Turkey.
[*2]Manisa Celal Bayar University, Faculty of Engineering, Department of Bioengineering, Manisa, Turkey.

*Corresponding author e-mail: deniz.karatas@cbu.edu.tr

Abstract

Type 2 diabetes mellitus (T2DM), developing because of insulin resistance in peripheral tissues due to pancreatic β-cell dysfunction, a chronic metabolic disorder characterized by persistent hyperglycemia. This pathological state is associated with the impairment of insulin signaling cascades, along with metabolic stress imposed on glucocorticoid and GLP-1 receptors and the perturbation of glucose homeostasis. In this study, the interaction potential of the carotenoid pigment zeaxanthin, extracted from natural origins such as microalgae, on insulin, glucocorticoid, and GLP-1 target receptors associated with T2DM was evaluated by employing *in silico* molecular modeling approaches. Zeaxanthin binding affinities for selected glucocorticoid receptors (GR, PDB ID: 7LCJ), insulin receptors (INSR, PDB ID: 3ETA), and GLP-1 receptors (GLP-1R, PDB ID: 4LSJ) were computed using the molecular docking method, in comparison with structurally similar natural bioactive compounds and synthetic inhibitors. Molecular dynamics simulations were performed to assess the structural stability of the receptor–ligand complexes that achieved the best conformation over time. Additionally, RMSF, Rg, adsorption free energy (ΔG), and ADMET profiling evaluations were conducted. Zeaxanthin demonstrated binding energies of -9.9, -8.4 and -7.5 kcal/mol in the INSR, GR, and GLP1, respectively. Similarly, the binding affinities of other ligands structurally analogous to zeaxanthin were comparable to synthetic inhibitors and exhibited stronger binding interactions, supporting zeaxanthin's biological potential. Literature reports that zeaxanthin reduces insulin resistance through activation of the PIK3/Akt pathway indicate parallelism with the results of our study. Our findings highlight the potential of natural zeaxanthin as a versatile, targeted natural agent for alternative therapeutic strategies in chronic T2DM. In parallel with the findings demonstrating the potential of zeaxanthin to reduce insulin resistance within the scope of this study, our preliminary results identify zeaxanthin as a powerful therapeutic candidate of multi-targeted natural origin that enhances insulin sensitivity and modulates glucose homeostasis in alternative therapeutic strategies in T2DM.

Keywords: Zeaxanthin, T2DM, microalgae, natural therapeutic agent, treatment, molecular modelling.

ORAL PRESENTATION

Synthesis, characterization and investigation of new multifunctional processing auxiliary materials to improve processability of polyolefins

Harun Bodur[1]* (ORCID: https://orcid.org/0000-0002-2492-4799),
Gökhan Ceyhan[2] (ORCID: https://orcid.org/0000-0002-9127-2348)

*[1]Kahramanmaraş Sütçü İmam University, Institute of Science, Material Science and Engineering, Kahramanmaraş, Turkey.
[2]Kahramanmaraş Sütçü İmam University, Vocational School of Technical Sciences, Food Processing Department, Kahramanmaraş, Turkey.

*Corresponding author e-mail: harunbodur87@gmail.com

Abstract

Polyolefins such as polyethylene and polypropylene are widely used in packaging and automotive industries; however, high melt viscosity and surface defects (melt fracture, sharkskin) limit processing efficiency. Conventional fluoropolymer-based processing aids effectively eliminate these problems but raise serious environmental and health concerns due to persistent per- and polyfluoroalkyl substances (PFAS). In this study, a novel PFAS-free multifunctional processing aid was developed by functionalizing hexagonal boron nitride (hBN) with 3,5-di-tert-butyl-4-hydroxybenzaldehyde (BHT-CHO) via urea and boric acid pyrolysis followed by solvothermal grafting. The synthesized hBN/BHT-CHO hybrid combines the lubricating and thermally conductive properties of hBN with the antioxidant activity of the hindered phenol derivative. Successful functionalization was confirmed by FTIR (new peaks at 3400 cm^{-1} ν(O-H) and 1710 cm^{-1} ν(C=O), TGA (~20 wt% organic loading, stability >260 °C), SEM (coated platelets 1–5 µm), and XRD (preserved hBN crystallinity). The developed hybrid offers dual functionality; flow enhancement and oxidative stabilization; making it a sustainable alternative for high speed extrusion of polyolefin films and pipes.

Keywords: hBN, polyolefin, processing aid, boron nitride.

Acknowledgements: This research was supported by the Scientific Research Projects Coordination Unit of Kahramanmaraş Sütçü İmam University (KSÜ-BAP) under Project No. 2024/3-18 D. The authors would like to acknowledge the Kahramanmaraş Sütçü İmam Üniversitei University-Industry-Public Cooperation Development, Application and Research Center (ÜSKİM) for their assistance with product analyses, and Koren Kimya for their valuable support in the production of hBN and masterbatch.

ORAL PRESENTATION

Cytotoxic and anti-inflammatory potential of 2-cyclopenten-1-one against malign melanoma

Feyza Kostak[1]* (ORCID: https://orcid.org/000-0002-2491-8671), Burak Kasikci[2], (ORCID: https://orcid.org/0009-0007-7563-9975), Sinem Guzel[3] (ORCID: https://orcid.org/0009-0009-8357-9516), Kubra Ece Coskuner[1] (ORCID: https://orcid.org/0009-0009-2786-4275), Sultan Celik[1] (ORCID: https://orcid.org/0000-0003-1562-9269), Suray Pehlivanoglu[1] (ORCID: https://orcid.org/0000-0001-7422-2974)

[1]Necmettin Erbakan University, Faculty of Science, Department of Molecular Biology and Genetics, Konya, Türkiye

[2]Cukurova University, Graduate School of Natural and Applied Sciences, Department of Biotechnology, Adana, Türkiye

[3]Abdullah Gül University, Graduate School of Natural and Applied Sciences, Department of Bioengineering, Kayseri, Türkiye

*Corresponding author e-mail: kostakfeyza@gmail.com

Abstract

Melanoma is one of the most aggressive types of skin cancer, with its increasing incidence being linked to elevated exposure to ultraviolet (UV) radiation. Due to the limited efficacy of current therapies, there is a need to explore novel natural therapeutic agents. This study investigated the biological effects of 2-cyclopenten-1-one (2-CP), a naturally occurring compound found in Arum dioscoridis, were investigated on the human melanoma cell line (SK-MEL-30) and the healthy fibroblast cell line (L929). The cytotoxic and antiproliferative properties of the compound were evaluated using MTT and colony formation assays. Changes in the expression of TGF-β protein were analysed using Western blot. The findings revealed that 2-cyclopenten-1-one had a dose-dependent cytotoxic effect, demonstrating approximately 3-fold the toxicity of melanoma cells compared to healthy fibroblasts. (IC_{50}: SK-MEL-30, 58.8 µM; L929, 156.6 µM). Furthermore, the compound reduced colony formation by 76% and completely suppressed proliferation at a concentration of 100 µM. Western blot analysis revealed that LPS treatment increased TGF-β expression by approximately 1.5-fold. In contrast, 2-cyclopenten-1-one reduced this increase, restoring expression levels to near-baseline levels. These results suggest that the compound may have anti-tumour effects by inhibiting TGF-β-mediated proliferative signalling pathways. In conclusion, 2-cyclopenten-1-one emerges as a potential natural therapeutic agent with selective cytotoxicity against melanoma cells and a low toxicity profile. Further in vitro and in vivo investigations are needed to elucidate the compound's anticancer and immunomodulatory mechanisms.

Keywords: 2-cyclopenten-1-one, Anti-cancer effect, Anti-inflammatory effect, Arum dioscoridis, Melanoma

Acknowledgements: This study was derived from the results of a project supported by the Scientific and Technological Research Council of Türkiye (TÜBİTAK) under the 2209-A Research Projects Support Program for Undergraduate Students. The author gratefully acknowledges TÜBİTAK for its financial support, and extends sincere thanks to the supervising advisor and laboratory team for their valuable contributions and assistance throughout the experimental process.

ORAL PRESENTATION

Effects of halophilic PGPR on salt stress and growth parameters in tomato plants

Gonul Hayrunisa Sen[1] (ORCID: https://orcid.org/0009-0006-7000-229X), Ezgi Alaca Yildirim[2] (ORCID: https://orcid.org/0000-0002-4467-5603), Furkan Orhan[3] (ORCID: https://orcid.org/0000-0001-6906-6604), Arzu Gormez[2*] (ORCID: https://orcid.org/0000-0003-3246-1824)

[1] Department of Biology, The Graduate School of Natural and Applied Sciences, Dokuz Eylul University, Izmir 35390, Turkey.
[2] Department of Biology, Faculty of Science, Dokuz Eylul University, Izmir 35390, Turkey.
[3] Department of Molecular Biology and Genetics, Faculty of Arts and Science, Agri Ibrahim Cecen University, Agri 04100, Turkey.

*Corresponding author e-mail: arzu.gormez@deu.edu.tr

Abstract
Increasing soil salinity as a result of global climate change is one of the major abiotic stress factors limiting agricultural productivity. High salinity leads to growth retardation, yield loss, physiological disturbances, and various morphological abnormalities in plants. To mitigate the adverse effects of salt stress, the use of plant growth-promoting rhizobacteria (PGPR) has emerged as an important biotechnological approach in recent years. Halophilic PGPR can enhance plant tolerance to salinity due to their ability to survive and function under high salt concentrations. In this study, four different halophilic bacterial isolates with known plant growth-promoting (PGP) properties [*Bacillus atrophaeus* (EK3), *Promicromonospora* sp. (EM8), *Zhihengliuella salsuginis* (EM30), and *Thalassobacillus devorans* (EM34)] were applied to *Solanum lycopersicum* L. cv. Batem Özçelik F1 grown under different NaCI concentrations (0, 50, 100, 150 mM). Their effects on various growth parameters were evaluated. Plants were cultivated under controlled conditions for 45 days, and morphological characteristics such as leaf, root, and whole plant fresh weight (g), stem length (cm), root length (cm), leaf area (m^2), number of leaves, stem diameter (mm), and plant height (cm) were measured. The results showed that *B. atrophaeus* (EK3) significantly promoted plant growth under non-saline conditions. *Z. salsuginis* (EM30) increased stem length under moderate salinity, while *Promicromonospora* sp. (EM8) enhanced leaf number under 100 mM NaCl. In contrast, *T. devorans* (EM34) restricted plant growth under high salt conditions. Overall, these findings highlight the promising biotechnological potential of halophilic PGPR in improving salt stress tolerance in tomato plants, although the extent of this effect is contingent upon both the specific bacterial species and salt concentration. These insights provide a foundation for future research and practical applications in sustainable agriculture.

Keywords: Halophilic bacteria, tomato (*Solanum lycopersicum* L.), salt stress, PGPR, plant growth parameters.

Acknowledgements: This study was supported by the Scientific and Technological Research Council of Turkey (TÜBİTAK) under the 2209-A University Students Research Projects Support Program. We sincerely thank BATEM (Republic of Türkiye Ministry of Agriculture and Forestry Bati Akdeniz Agricultural Research Institute) for kindly providing the *Solanum lycopersicum* L. cv. Batem Özçelik F1 tomato seeds.

ORAL PRESENTATION

Electrochemical determination of glyphosate: Molecular imprinting approach in the presence of nanomaterials

Sezen İrem Aslaner[1*] (ORCID: https://orcid.org/0000-0001-8163-7078),
Ayça Demirel Özel[1] (ORCID: https://orcid.org/0000-0002-7129-0370)

[*1]Ankara University, Faculty of Science, Department of Chemistry, Ankara, Turkey.

*Corresponding author e-mail: iremkaftanoglu@gmail.com

Abstract

Glyphosate (Gly), as one of the herbicides, provides significant benefits in increasing agricultural and industrial production. The widespread use of any pesticide has led to environmental pollution, which is an important topic for current research [1]. Although it reduces the effects of weeds and pests [2], exposure to Gly can cause permanent damage to human health [3]. Therefore, the determination of Gly is important for environmental monitoring and reducing public health risks. Many expensive and time-consuming instrumental analysis methods requiring experienced personnel have been proposed. In recent years, the preparation of pesticide sensors using molecular imprinting technology has become prominent while offering advantages such as high sensitivity and selectivity, ease of use, rapid response time, and low cost [4,5]. Since molecularly imprinted polymer-based Gly sensors are relatively rare, this study aimed to prepare one for Gly determination with an aspect of adding nanomaterial. Electrochemical synthesis in the presence/absence of nanomaterials was performed by cyclic voltammetry on the Pt plate electrode at pH 5.0 PBS buffer media containing $LiClO_4$ as supporting electrolyte in a potential range of -0.1- +1.4 V with a scan rate of 50 mV/s. The effect of nanomaterials on the analytical performance of Gly imprinted polypyrrole films was investigated. The selectivity of the electrode was tested in the presence of similar structured pesticides, and it was observed that the electrode was highly selective to Gly. The linear working range of 0,5 aM- 0,26 fM and LOD of 0,002 aM were obtained by using differential pulse voltammetry. Finally, standard addition method was applied to ensure the successful utilization of proposed sensor in the determination of Gly in tap water and tomato juice samples.

Keywords: Electrochemical sensors, Nanomaterials, Molecular imprinting, Polypyrrole, Pesticide

References:

[1] Ganjeizadeh Rohani, F., Mohadesi, A. and Ansari, M. 2019. Computational Design and Electropolymerization of Molecularly Imprinted Poly (p-Aminobenzoic-Acid-Co–Dapsone) Using Multivariate Optimization for Tetradifon Residue Analysis. ChemistrySelect, 4(42), 12236-12244.

[2] Zhang, C., She, Y., Li, T., Zhao, F., Jin, M., Guo, Y. and Liu, H. 2017. A highly selective electrochemical sensor based on molecularly imprinted polypyrrole-modified gold electrode for the determination of glyphosate in cucumber and tap water. Analytical and bioanalytical chemistry, 409(30), 7133-7144.

[3] Georgin, J., Franco, D. S. P., Ramos, C. G., Tran, H. N., Benettayeb, A., Imanoav, G., and Ali, I. 2024. Recent advances in removing glyphosate herbicide and its aminomethylphosphonic acid metabolite in water. Journal of Molecular Liquids, 124786.

[4] Leepheng, P., Limthin, D., Homchan, W., Suramitr, S. and Phromyothin, D. 2020. An experimental and theoretical study of molecularly imprinted electrode based on methyl methacrylate polymer for pesticide detection. Japanese Journal of Applied Physics, 59(SI), SIIJ09.

[5] Khadem, M., Faridbod, F., Norouzi, P., Foroushani, A. R., Ganjali, M. R., Yarahmadi, R. and Shahtaheri, S. J. 2020. Voltammetric Determination of Carbofuran Pesticide in Biological and Environmental Samples Using a Molecularly Imprinted Polymer Sensor, a Multivariate Optimization. Journal Of Analytıcal Chemıstry, 75(5), 669-678.

ORAL PRESENTATION

Aloe vera L. bitkisinin gizli parmak izlerinin tespitinde kullanımı üzerine bir ön çalışma

Kübra Bebek[1*] (*ORCID: https://orcid.org/0000-0001-6941-9959*),
Kıymet Berkil Akar[2] (*ORCID: https://orcid.org/0000-0001-9993-9541)*

[*1] Tokat Gaziosmanpaşa Üniversitesi, Lisansüstü Eğitim Enstitüsü, Biyomühendislik Bölümü, Tokat, Türkiye.
[2] Tokat Gaziosmanpaşa Üniversitesi, Fen-Edebiyat Fakültesi, Kimya Bölümü, Tokat, Türkiye.

*Sorumlu yazar e-mail: kubrayazlak@gmail.com

Özet

Kâğıt gibi gözenekli yüzeylerde bulunan parmak izleri gizli parmak izleridir ve çıplak gözle görülmezler. Olay yerlerinde toplanan mektup ve fatura gibi pek çok önemli delildeki gizli parmak izlerinin görünür hale getirilmesi adli soruşturmalarda son derece önemlidir. Amino asitler parmak izi sıvısının önemli bir bileşenidir ve gözenekli yüzeylerde uzun süre kalabilirler. Bu nedenle gizli parmak izlerinin görünür hale getirilmesinde parmak izi reaktiflerinin amino asitleri hedef aldığı yöntemler sıklıkla kullanılmaktadır. Amino asitlerle reaksiyon neticesinde renkli veya lüminesans özellikte ürün oluşumuyla parmak izleri görünür hale gelir ve bu sayede kimlik tespitine imkân sağlanır. Gizli parmak izlerini görünür hale getirmek için sınırlı sayıdaki reaktif aktif olarak kullanılmaktadır. Bu reaktiflerden ninhidrin ve 1,2-indandion kullanıcıda cilt ve göz tahrişine neden olabilir ve 1,8-diazafluoren-9-on ise çok pahalıdır. Bu nedenle bu reaktiflere alternatif parmak izi reaktiflerinin geliştirilmesi hala önemli bir çalışma alanıdır. Bu çalışmada ekonomik ve aynı zamanda da kullanıcı ve çevre dostu bir parmak izi tespit yönteminin geliştirilmesi amaçlanmıştır. Antrakinonların ve fenollerin amino asitlerle reaksiyonları bilinmektedir. *Aloe vera* L. (AV), antrakinonları ve fenolleri içeren bir bitkidir. Bu çalışmada ticari olarak satılan AV ekstresi tozu (Nurbal, İstanbul) kullanılmıştır. İlk olarak maserasyon yöntemiyle AV'nın kloroform ekstresi elde edilmiş ve bu ekstrenin antrakinon ve fenolik bileşik içerikleri nitel ve nicel olarak analiz edilmiştir. Bu ekstre çözeltisi ile geliştirilen amino asit spotunun 380-540 nm aralığında lüminesans sergilediği tespit edilmiştir. Parmak izi tespitinde en ideal sıcaklık ve konsantrasyon değerlerinin tespiti için optimizasyon çalışması yapılmıştır. Ekstre çözeltisi fotokopi kâğıdı üzerindeki gizli parmak izleri ile daldırma yöntemi ile muamele edilmiş ve ısıya tabi tutulmuştur. Geliştirilen gizli parmak izleri adli ışık kaynağı altında ışınlanırken kırmızı filtre kullanılarak görüntülenmiş ve papil hatlarının net bir şekilde görüldüğü tespit edilmiştir. Bu çalışmada ayrıca AV ekstresinin parmak izi geliştirme kabiliyeti DFO ile kıyaslamalı olarak incelenmiş ve elde edilen sonuçlar AV ekstresinin halihazırda kullanılan parmak izi reaktiflerine alternatif olabileceğini göstermiştir.

Anahtar Kelimeler: *Aloe vera* L., gizli parmak izi, amino asit, parmak izi tespiti, lüminesans.

Teşekkür: Bu çalışma Tokat Gaziosmanpaşa Üniversitesi Bilimsel Araştırma Projeleri Koordinasyon Birimi tarafından 2020/127 numaralı proje kapsamında desteklenmiştir.

ORAL PRESENTATION

Palynological studies on *Astragalus* sect. *Malacothrix* (Fabaceae)

Fatma Taeb Dişli[1*] (ORCID: https://orcid.org/0000-0002-2657-6935); Murat Ekici [2] (ORCID: https://orcid.org/0000-0002-3402-177X)

[*1] Ankara Medipol University, Faculty of Phamacy, Department of Pharmaceutical Botany, Ankara, Turkey
[2] Gazi University, Faculty of Science, Department of Biology, Ankara, Turkey

*Corresponding author e-mail: fatma.taeb@ankaramedipol.edu.tr

Abstract

The gene centre of *Astragalus* species is Eurasia, especially Central and Western Asia and the Sinai-Himalaya regions. The sect. *Malacothrix*, which has 110 taxa in the world, is represented by 90 taxa in Iran, 16 in Turkey and 15 in Russia. 10 of the 16 taxa distributed in Turkey are endemic. In recent years, palynological studies on the genus *Astragalus* have gained importance as supportive tools for understanding species boundaries, especially in taxonomically complex subgroups. Studies on sect. *Malacothrix* and several other groups, have revealed general pollen characteristics such as radial symmetry, trizonocolporate apertures and variable exine ornamentation patterns. Palynological investigation carried out on 16 species belonging to sect. *Malacothrix*. The prepared slides were examined and photographed using a Leica ICC50 HD light microscope. For more detailed information, the JEOL JSM-6060 brand Computer-Controlled Digital SEM (Scanning Electron Microscope) in Gazi University was used. Pollen grains are radially symmetrical, isopolar, trizonocolporate, and operculate. The pollen shape varies: *A. macrostachys* is prolate; *A. stridii* and *A. adiyamanensis* are prolate-spheroidal; and others like *A. argentophyllus*, *A. bakirdaghensis*, *A. mollis*, and others are subprolate. The exine ornamentation is psilate-perforate at the poles, and perforate-reticulate or perforate-rugulate at the equator. The colpus is long, with distinct borders and pointed ends, and the membrane is granular. Despite these characteristics, taxon grouping based on exine ornamentation and pollen shape was not successful, and no effective identification key is created. Consequently, pollen morphology alone is insufficient for distinguishing the species, but can be useful when combined with general morphological traits.

Keywords: Palynology, *Astragalus*, morphology, *Malacothrix*, Turkey

ORAL PRESENTATION

Su içindeki alüminyum ve florür iyonlarının akıllı telefon uyumlu çift tespiti için mono-sübstitüe rodamin sentezi

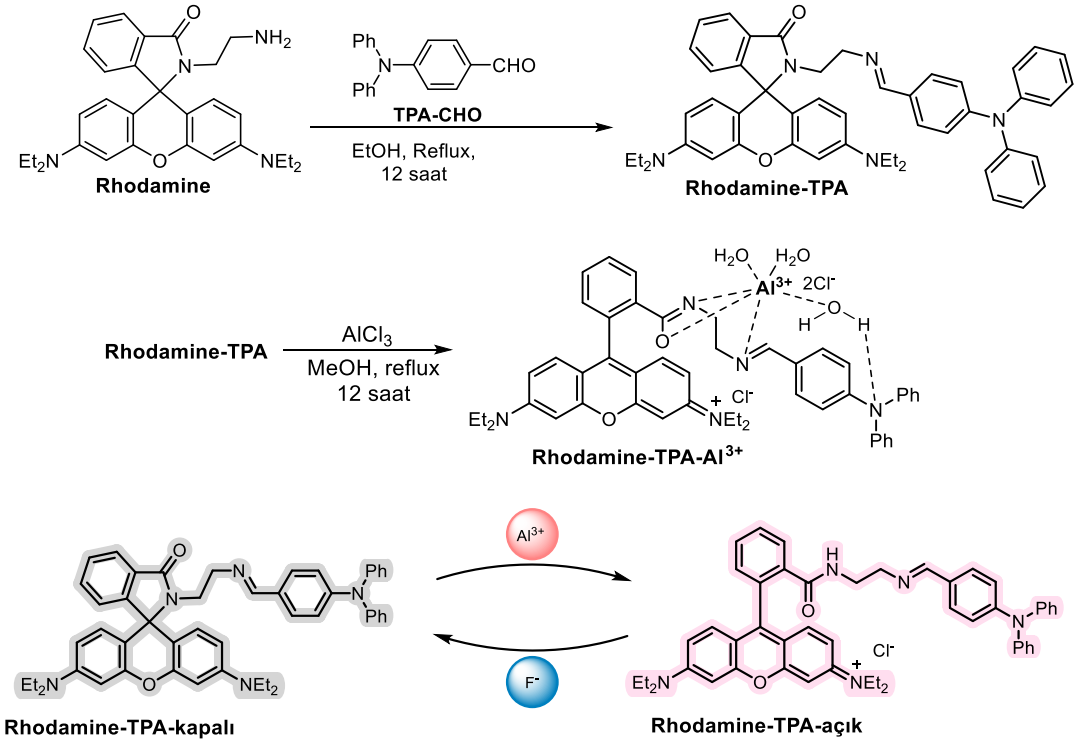
Sinan Bayindir*, Kemal Yararli

Bingöl Üniversitesi, Fen-Edebiyat Fakültesi, Kimya Bölümü, 12000, Bingöl, Türkiye

Sorumlu yazar e-mail: sbayindir@bingol.edu.tr

Özet

Bu çalışma, gerçek su örneklerinde çift modda çalışan kimyasal bir sensör olarak işlev görebilen mono-sübstitüe-rhodamin (rhodamine -TPA) türevinin sentezi gerçekleştirildi. Rhodamin türevi, alüminyum (Al^{3+}) ile güçlü flüoresan artışı gösterirken, aynı sistemde, Al^{3+} varlığı, florürün (F^-) emisyonu baskılamasına neden olarak florür tespit sınırını belirledi. Bu aynı zamanda probe-aliminyum kopleksinin florür iyonu olarak kullanılabileceği anlamına gelmektedir. Ayrıca, hızlı ve saha dostu kullanım için bu rhodamin türevi, filtre kâğıdı şeritlerine uygulanabilir ve basit RGB analizi ile akıllı telefon kamerası aracılığıyla okunabilir olmasıda ciddi bir avantaş olarak karşımıza çıkmaktadır. Genel olarak, bu özellikler rhodamin türevini alüminyum ve florür seviyelerinin yerinde çevresel izlenmesi için pratik bir araç haline getirmektedir.



Şema 1. Rhodamin-TPA ve kompleksinin sentez stratejileri ve sensör özellikleri

Anahtar kelimeler: Aluminum, Fluoride, RGB-analysis, Rhodamine, Triphenylamine

ORAL PRESENTATION

Roles of EDDHA-derived zinc complexes on growth and antioxidant defense in rice (*Oryza sativa* L.) exposed to salt stress

Merve Miray Arda[1] (ORCID:https://orcid.org/0009-0007-5574-9296.),
Selda Durmuşoğlu[2] (ORCID: https://orcid.org/0000-0001-8845-7344),
Dilek Ünlüer Birinci[3*](ORCID:https://orcid.org/0000-0003-1939-2246.) ,
Asim Kadıoğlu[2] (ORCID: https://orcid.org/ 0000-0002-4781-6264.)

[*1]Karadeniz Technical University, Faculty of Science, Molecular Biology and Genetics, Trabzon, Türkiye.
[2] Karadeniz Technical University, Faculty of Science, Biology, Trabzon, Türkiye.
[3] Karadeniz Technical University, Faculty of Science, Chemistry, Trabzon, Türkiye.

*Corresponding author e-mail: dunluer@ktu.edu.tr

Abstract

In this study, five different zinc (Zn) chelate complexes derived from EDDHA (F-BD, F-ET, F-TR, F-H, F-OC) were applied to rice (*Oryza sativa* L.) plants to investigate their morphological, physiological, and antioxidant responses under salt stress. Plants were hydroponically grown for 14 days and then exposed to nutrient solutions containing the respective Zn complexes. Salt stress was imposed by applying 150 mM NaCl after two days of treatment. Post-harvest analyses revealed that F-BD and F-ET significantly enhanced root and shoot growth, with F-BD salt treatment showing values close to the Hoagland control. The F-TR group exhibited the highest total chlorophyll content, while F-H and F-ET treatments effectively limited chlorophyll degradation under stress. Proline content increased under saline conditions as an osmoprotective response; however, oxidative stress markers, including H_2O_2 and TBARS levels, were markedly reduced in F-BD and F-H groups. Regarding antioxidant enzyme activities, F-BD and F-TR recorded the highest SOD activity, while F-BD and F-ET displayed the strongest CAT activity. These findings demonstrate that Zn complexes not only support growth parameters but also mitigate oxidative damage by strengthening antioxidant defense, thereby enhancing salt stress tolerance in rice.

Keywords: EDDHA, chelate, Rice (*Oryza sativa* L.), Salt stress, Micronutrient, Zinc.

ORAL PRESENTATION

Cytotoxicity of *Origanum majorana* extracts on A549 cells and their radical scavenging activity

Ayse Erdogan[1]* (ORCID: https://orcid.org/0000-0003-0843-173X)

*[1]Alanya Alaaddin Keykubat University, Faculty of Engineering, Genetic and Bioengineering Department, Alanya, Antalya, Turkey.

*Corresponding author e-mail: ayse.erdogan@alanya.edu.tr

Abstract

Lung cancer is the leading cause of cancer-related deaths worldwide, with incidence and mortality continuing to rise, particularly among women. Despite significant advances in treatment, prognosis remains poor, and the five-year survival rate is below 15%. Small Cell Lung Cancer (SCLC) and Non-Small Cell Lung Cancer (NSCLC) are the most clinically distinct subtypes, differing in metastatic potential, treatment response, and overall outcomes. NSCLC, which accounts for the majority of cases, remains challenging to treat, especially in advanced stages. In this study, A-549 cells, a human adenocarcinoma alveolar basal epithelial cell line, were used as an *in vitro* model of NSCLC. Türkiye is rich in medicinal plant diversity, and *Lamiaceae* family is particularly noteworthy due to its wide applications in medicine, food, and cosmetics. *Origanum majorana* L. (*O. majorana*), a prominent member of this family, has essential oils recognized as safe by the Food and Drug Administration (FDA). Plant-derived compounds have long been a source of anticancer agents, as they can reduce toxicity to healthy cells while maintaining therapeutic efficacy. Therefore, the exploration of herbal extracts as alternative or supportive agents in cancer therapy has gained increasing attention. This study compared chloroform, ethanol, and methanol extracts of *O. majorana* for their antioxidant and cytotoxic effects on lung cancer cells. Antioxidant activity was assessed using the DPPH assay, revealing that the chloroform extract exhibited the highest radical scavenging activity (EC_{50} = 0.17 mg/mL) compared to ethanol and methanol extracts. Cytotoxicity was evaluated using the MTT assay, where the methanol extract demonstrated the strongest effect on A-549 cells. All extracts showed statistically significant cytotoxicity compared to untreated controls ($p<0.05$). These findings suggest that *O. majorana* extracts, particularly the methanol and chloroform fractions, possess notable antioxidant and anticancer properties. The study supports further investigation into their potential as complementary therapeutic agents in NSCLC treatment.

Keywords: Lung cancer, *Origanum majorana*, Antioxidant activity, Cytotoxicity, Herbal extracts.

ORAL PRESENTATION

Development of hyaluronic acid-coated/curcumin-loaded poly(ε-caprolactone) membranes for biofunctional wound dressing applications

Şükran Melda Eskitoros Toğay[1*] (ORCID:https://orcid.org/0000-0002-7473-8417),
Adem Ünal[2] (ORCID:https://orcid.org/0000-0002-0798-997X)

[*1]University of Health Sciences, Gulhane Vocational School of Health Services, Department of Pharmacy Services, Ankara, Türkiye.
[2]University of Health Sciences, Gulhane Vocational School of Health Services, Department of Medical Laboratory Techniques, Ankara, Türkiye.

*Corresponding author e-mail: melda.togay@sbu.edu.tr

Abstract

Chronic wounds impose a significant global healthcare burden, necessitating the development of advanced wound dressings that are both biocompatible and biodegradable [1]. Among various options, polymer-based wound dressings, particularly those incorporating natural bioactive compounds, have gained increasing attention due to their ability to accelerate healing while minimizing adverse effects [2, 3]. In this study, poly(ε-caprolactone) (PCL), a biodegradable and biocompatible aliphatic polyester, was utilized to fabricate fibrous membranes via electrospinning. To enhance the wound healing functionality of the scaffolds, the nanofiber surfaces were further modified by dip-coating with 1 wt.% hyaluronic acid (HA), a naturally occurring glycosaminoglycan known for its role in tissue hydration and regeneration (PCL/HA). Additionally, curcumin (Cur), a polyphenolic compound with well-documented anti-inflammatory and antimicrobial activities, was incorporated into the PCL matrix to improve the overall bioactivity of the system (PCL-Cur). The morphology of the produced fibers was evaluated using scanning electron microscopy (SEM), confirming the formation of uniform, bead-free nanofibers. Atomic force microscopy (AFM) analysis revealed an increase in surface roughness after curcumin incorporation, rising from 187 ± 36 nm to 245 ± 65 nm. Fourier-transform infrared spectroscopy (FTIR) verified the successful integration of both HA and Cur into the PCL structure. Water contact angle (WCA) measurements demonstrated that HA coating improved surface hydrophilicity. The measured WCA values were 136.0°, 125.4°, 82.1°, and 77.9° for PCL, PCL-Cur, PCL/HA, and PCL-Cur/HA membranes, respectively, indicating enhanced wettability, particularly in HA-coated samples. This study presents a straightforward yet effective approach for designing multifunctional nanofibrous scaffolds by integrating structural polymers, bioactive agents, and surface modifiers. The developed system exhibits promising characteristics for wound healing applications, including enhanced surface properties and biocompatibility.

Keywords: Poly(ε-caprolactone), Curcumin, Hyaluronic acid, Electrospinning, Dip-coating, Wound dressing

References:

[1] Boateng, J. S., Matthews, K. H., Stevens, H. N., & Eccleston, G. M. (2008). Wound healing dressings and drug delivery systems: A review. Journal of Pharmaceutical Sciences, 97(8), 2892-2923.
[2] Eskitoros-Togay, Ş. M., Bulbul, Y. E., Unal, A., Kaya, E. Y., Oymak, N. Ç., & Dilsiz, N. (2025). Development of a Novel Double-Layered Wound Dressing Composed of Chitosan Film and Tigecycline-Loaded Electrospun Polycaprolactone Nanofibers. Journal of Applied Polymer Science, 142, e57103.
[3] Dhivya, S., Padma, V. V., & Santhini, E. (2015). Wound dressings–A review. BioMedicine, 5(4), 22.

ORAL PRESENTATION

Innovative approach in food safety: Smart packaging systems with natural pigments

Fatma Öztürk[1]* (ORCID: https://orcid.org/0000-0003-4763-3801),
Hatice Gündüz[1] (ORCID: https://orcid.org/0000-0002-9899-8635)

[1*] University of Izmir Katip Celebi, Faculty of Fisheries, Department of Fisheries and Fish Processing Technology, Izmir, Turkey

*Corresponding author e-mail: fatma.ozturk@ikcu.edu.tr

Abstract

The rise in living standards and the growing awareness of health have prioritized food safety on a global scale and stimulated the development of innovative packaging technologies. During the process from production to consumption, foods undergo microbial, enzymatic, and chemical changes that lead to quality deterioration and safety risks; this not only threatens consumer health but also results in economic losses. Therefore, alternative packaging methods are needed to ensure sustainable food safety. Smart packaging systems have emerged as innovative technologies that provide information about the quality and safety of food. Commonly, freshness, gas, and time–temperature indicators are employed in these systems. In particular, pH-sensitive freshness indicators change color in response to food spoilage, thereby offering consumers visual information about the product's condition. Although synthetic dyes are frequently used in these systems, their toxic effects and potential carcinogenic risks have recently restricted their applications in food-related fields. For this reason, natural pigments are gaining prominence due to their non-toxic, eco-friendly, economical, and easily accessible properties. Natural compounds found in plants, such as anthocyanins and flavonoids, are noteworthy for their purple, red, blue, and pink hues, while other natural pigments including betacyanin, curcumin, and chlorophyll have also been increasingly investigated for use in pH indicator films. This review aims to highlight the importance and potential applications of natural pH indicators in smart packaging systems developed to enhance food safety.

Keywords: Food safety, smart packaging, pH indicators, natural pigments

ORAL PRESENTATION

Optimizing lettuce cultivars and agrobacterium strain selection for enhanced transformation efficiency using a CRISPR-compatible vector

Yüksel Bora Oral[1]* (ORCID: https://orcid.org/0009-0001-4768-5639), Gülan Ata[1] (ORCID: https://orcid.org/0009-0006-0309-5385), Fatma Akçakale Kaba[1] (ORCID: https://orcid.org/0000-0001-7252-5883), Adem Kaba[1] (ORCID: https://orcid.org/0000-0003-3362-0997), Nedim Mutlu[2] (ORCID: https://orcid.org/0000-0001-7252-5883)

[1] Akdeniz University, Faculty of Agriculture, Department of Agricultural Biotechnology, Antalya, Türkiye

*Corresponding author e-mail: boraoral.bo@gmail.com

Abstract

Lettuce (*Lactuca sativa* L.) is an economically and nutritionally important vegetable cultivated worldwide, yet its susceptibility to biotic and abiotic stresses necessitates genetic improvement through biotechnological tools. *Agrobacterium tumefaciens*-mediated transformation is a key approach for genetic modification in lettuce. This study evaluated the influence of nine lettuce cultivars (Caipira, Emocion, Festival, Funtime, Garone, Maritima, Rüzgar, Sürpriz, and Vaidosa) and two *A. tumefaciens* strains (LBA4404 and EHA105) on transformation efficiency using cotyledon explants. A binary vector (pDIRECT_23C, 15,744 bp) carrying CRISPR-Cas9 components and a phosphinothricin (PPT) resistance marker was used as a model to assess DNA delivery, without targeting any specific genomic sequence. Mature seeds were surface sterilized and germinated *in vitro*. Cotyledon explants from seven-day-old seedlings were pre-cultured, inoculated with Agrobacterium suspensions (OD600 = 0.8–1.0), co-cultured in the dark for two days, and transferred to PPT-based selection and regeneration medium. Regenerated shoots were rooted and acclimatized under controlled greenhouse conditions. PCR analysis confirmed transgene integration using BlpR-specific primers. Statistical analysis revealed that EHA105 significantly outperformed LBA4404 in transformation efficiency ($p < 0.05$). Among cultivars, Emocion exhibited the highest number of transgenic shoots, with a transformation efficiency of 5%, followed by Caipira. The relatively large size of the pDIRECT_23C vector demonstrates its suitability as a model for future genome editing studies, where guide RNAs can be inserted for targeted modifications. This study optimized an efficient Agrobacterium-mediated transformation protocol for multiple lettuce cultivars, providing a foundation for functional genomics research and biotechnological improvement. The findings contribute to enhancing transformation efficiency in lettuce, facilitating future CRISPR-based genome editing and crop improvement applications.

Keywords: plant biotechnology, genetic transformation, phosphinothricin selection, cotyledon explant, transgenic shoots, regeneration efficiency

ORAL PRESENTATION

Acetylcholinesterase and butyrylcholinesterase enzyme inhibitory effect of *Ganoderma lucidum* (Reishi) mushroom

Işıl Nihan Korkmaz[1*] (ORCID: https://orcid.org/0000-0003-4896-5226)

[*1]Faculty of Applied Sciences, Department of Plant Production and Technologies, Muş Alparslan University, Muş, 49250, Turkey.

*Corresponding author e-mail: nihan.korkmaz@alparslan.edu.tr

Abstract

Alzheimer's disease (AD), which causes cognitive and sensory deficits due to the loss of structure and function of neurons in the nervous system and the structural and functional degeneration of nerve cells, is a fatal health problem (1,2). AD is a serious problem due to its increasing prevalence in people over the age of 60, where it progresses by causing brain cell destruction, and the difficulties in its treatment (3). The most fundamental cause of the disease's pathological findings is a deficiency in the levels of neuromediators known as acetylcholine (ACh) and butyrylcholine (BCh) in the brains of patients. Inhibition of AChE and BChE, the widely distributed cholinesterase enzymes, increases the amount of acetylcholine and is known to increase cholinergic activity (4). AChE has led to the development of many drugs currently in clinical use for the treatment of AD. Studies are ongoing to investigate the problems and side effects of overuse of existing drugs (5). Natural products are gaining prominence for the treatment of Alzheimer's disease (6). Mushrooms are known to be used in alternative medicine for the treatment of many diseases. *Ganoderma lucidum* (Curtis) P. Karst (GL), belonging to the Ganodermataceae family, is one of the most traditional medicinal plants. The literature has reported positive effects of extracts, such as the polysaccharides and triterpenes present in GL, in protecting against neurological diseases such as Alzheimer's (7). In this study, the in vitro inhibitory effects of GL (from human blood) on AChE and BChE enzyme activities were investigated. IC_{50} values were calculated from the activity (%)-[GL] graph. The IC_{50} values of GL for AChE were calculated as 69.3 µg/mL (r2: 0.9551) and for BChE as 69.3 µg/mL (r2: 0.9713). The IC_{50} values of GL showed mild inhibitory activity on both enzymes compared to the standard substance.

Keywords: *Ganoderma lucidum*, Alzheimer's disease, Acetylcholinesterase, Butyrylcholinesterase

References:

[1]. Zhang, X.X.; Tian, Y.; Wang, Z.T.; Ma, Y.H.; Tan, L.; Yu, J.T. The Epidemiology of Alzheimer's Disease Modifiable Risk Factors and Prevention. *J. Prev. Alzheimers Dis.* **2021**, *8*, 313–321.

[2]. Luthra R, Roy A. Role of medicinal plants against neurodegenerative diseases. Current Pharmaceutical Biotechnology. McKinnon, P. J. Maintaining genome stability in the nervous system. Nat Neurosci. 2021; 16(11), 1523.

[3]. Tarı Ö, Yağmurtaşan R. Alzheimer Hastalığı ve Anti-Alzheimer Etkili Bileşiklerin Yapılarının Araştırılması. Hujpharm. 2023;43(2):150-73.

[4]. Akasofu S, Kimura M, Kosasa T, Sawada K, Ogura H, 2008. Study of Neuroprotection of Donepezil a Therapy for Alzheimer's Disease. Chemico-Biological İnteractions, 175(1-3): 222-226.

[5]. Kazmierski J, Messini-Zachou C, Gkioka M, et al. The Impact of a Long-Term Rivastigmine and Donepezil Treatment on All-Cause Mortality in Patients with Alzheimer's Disease. Am J Alzheimers Dis Other Demen 2018; 33:385–93.

[6]. Yılmaz Hİ, Öztürk L. Scholars Utilizing Baladhur in Islamic History and Their Encountered Outcomes. 3 rd International Symposium on Philosophy, Education, Art and History of Science, Giresun: 2018.

[7]. Zhao, Y., Zhan, J. K., & Liu, Y. (2020). A perspective on roles played by ımmunosenescence in the pathobiology of Alzheimer's disease. Aging and Disease, 11(6), 1594-1607.

ORAL PRESENTATION

Carbon-filled polymer composites: structure–property relationships for improved mechanical and thermal performance

Semih Doğan[1*] (ORCID: https://orcid.org/0000-0001-6872-4599)

[*]Gebze Technical University, Faculty of Science, Department of Chemistry, Gebze, Kocaeli, Turkiye.

*Corresponding author e-mail: semihdogan@gtu.edu.tr

Abstract

Polypropylene (PP) is one of the most widely used thermoplastics due to its low cost, lightweight, and ease of processing. However, its relatively low stiffness and thermal resistance restrict its applications in structural and high-temperature environments. Hence, the study on PP-based composites with activated carbon (AC) at different loadings (0.5–5 wt.%) was carried out using a twin-screw extrusion process followed by injection molding. The influence of AC addition acting as a nucleating agent on crystallization behaviour, mechanical properties, impact resistance, density, and thermal performance was systematically investigated. This effect contributed to improved mechanical properties, such as increases in tensile modulus by up to 33% and flexural modulus by 29%, which are consistent with observations that ACs reinforce polymer matrices by restricting molecular mobility and improving crystalline structure. At higher concentrations, further improvements in stiffness were achieved; however, these gains are accompanied by a reduction in toughness, as evidenced by the decline in Charpy notched impact strength, suggesting a partial embrittlement effect. Furthermore, the progressive increase in density with increasing AC content, along with the marked enhancement in thermal performance demonstrated by the rise in Vicat softening temperature from 99°C to 106°C reflected the characteristic influence of carbonaceous fillers in reinforcing polypropylene (PP) nanocomposites and improving their thermal resistance. To conclude, the incorporation of AC into PP matrix significantly enhanced its stiffness and thermal resistance, as evidenced by improvements in tensile and flexural moduli as well as Vicat softening temperature for tailoring the structure–property relationships of PP, broadening its potential applications in lightweight and thermally demanding environments.

Keywords: Polypropylene, activated carbon, polymer composites, mechanical properties, thermal behaviour.

ORAL PRESENTATION

Development of self-healing anti-corrosive smart epoxy coating material reinforced with chitosan/halloysite nanotubes

Elif Yılmaz[1*] (ORCID: https://orcid.org/0009-0008-1915-6212),
Nursel Dilsiz[2] (ORCID: https://orcid.org/0000-0002-6496-0487)

[*1]Gazi University, Graduate School of Natural and Applied Sciences, Department of Chemical Engineering, Ankara, Turkey.
[2]Gazi University, Engineering Faculty, Department of Chemical Engineering, Ankara, Turkey.

*Corresponding author e-mail: [*1]elif.yilmaz6@gazi.edu.tr, [2]ndilsiz@gazi.edu.tr

Abstract

Corrosion is a physicochemical interaction between metals and their environment, resulting in property degradation and potential system failures. Among various prevention strategies, protective coatings are considered highly effective. Epoxy resins are widely utilized due to their excellent mechanical strength, toughness, and resistance to chemicals, moisture, and corrosion. This study focuses on the development of a smart composite epoxy coating with self-healing and anti-corrosive properties, reinforced with chitosan (CS) and halloysite nanotubes (HNT). The self-healing mechanism relies on microcapsules containing reactive agents embedded within the polymer matrix. CS, a natural, non-toxic, and eco-friendly cationic polysaccharide, and HNT, a tubular nanomaterial derived from rolled kaolinite layers, synergistically enhance the coating's performance. The hollow structure of HNT contributes to mechanical reinforcement, while the hydroxyl and amino groups in CS promote strong interactions with the epoxy matrix. CS-modified HNT capsules are synthesized and characterized using SEM and FTIR. Coatings are prepared via dip-coating on bare metal substrates, including pure epoxy, CS-HNT epoxy, and CS-HNT loaded with corrosion inhibitors. To assess self-healing capability, coatings are deliberately damaged and subjected to salt test. Damage recovery is monitored via optical microscopy, and corrosion resistance is evaluated using Electrochemical Impedance Spectroscopy (EIS). The goal is to develop a durable, long-lasting coating material with enhanced protective performance, contributing to the advancement of corrosion-resistant technologies.

Keywords: Epoxy resin, composite coatings, corrosion protection, self-healing coatings, smart materials.

ORAL PRESENTATION

Yerli üretim tanı kitinde kullanılan antikorların elektrokimyasal validasyonu

Berkan Karagöz[1]* (ORCID: https://orcid.org/0009-0007-8485-7595), Sema Aslan[1] (https://orcid.org/0000-0001-9796-7311), İbrahim Sözdutmaz[2] (ORCID: https://orcid.org/0000-0002-3712-7991)

[1] Muğla Sıtkı Koçman Üniversitesi, Fen Fakültesi, Kimya Bölümü, Muğla, Türkiye
[2] Erciyes Üniversitesi, Veteriner Fakültesi, Viroloji-İmmünoloji Anabilim Dalı, Türkiye

*Sorumlu yazar e-mail: berkan.karagoz@posta.mu.edu.tr

Özet

Rotavirus, buzağılarda ciddi ishal ve yüksek ölüm oranlarına neden olan ve insanları da etkileyebilen önemli bir patojendir. Daha önce, yerel olarak üretilen antikorlar kullanılarak geliştirilmiş bir multi-tanı kiti, ELISA, Western Blot, SDS-PAGE ve PCR gibi geleneksel yöntemlerle doğrulanmıştır ancak elektro-kimyasal doğrulama yapılmamıştır. Bu çalışmada, yerli üretim antikorların kullanıldığı VP6 Rotavirüs proteinine yönelik tanı kitinin elektrokimyasal yöntemlerle validasyonu gerçekleştirilmiştir. Çalışma kapsamında kullanılacak olan yüzey baskılı karbon elektrotlar (SPE) kullanılarak immünosensörler için optimizasyonlar yapılacaktır. Antikor immobilizasyonu için gerekenen uygun koşulların belirlenmesi için farklı pH, sıcaklık ve inkübasyon sürelerinin blokaj ve antijen bağlanma aşamaları üzerine etkileri diferansiyelpulsvoltametrisi (DPV), döngüselvoltametri (CV) ve elektrokimyasal impedans spektroskopisi (EIS) ile incelenecektir. Optimizasyon çalışmaları sonucunda immünosensörlerin en uygun pH, sıcaklık ve inkübasyon süresi değerleri kullanılarak LOD, LOQ ve RSD belirleme aşamalarına geçilecektir.

Anahtar Kelimeler: Elektrokimyasal, Biyosensör, Rotavirüs, İmmünosensör

ORAL PRESENTATION

A study on *MARK* gene family members in pancreatic adenocarcinoma

Ozcan Gulbey (ORCID: https://orcid.org/0009-0007-9470-5712)

Newcastle University, Translational and Clinical Research, Newcastle upon Tyne, UK

Corresponding author e-mail: o.gulbey2@newcastle.ac.uk

Abstract

The most common subtype in pancreatic cancer is pancreatic adenocarcinoma (PAAD). Patients with PAAD experienced poor clinical outcomes because they are diagnosed lately and there are a few effective treatment options. Therefore, diagnostic and prognostic biomarkers are required urgently. Disruption of cellular processes are associated with cancers, and *MARK* family members (*MARK1, MARK2, MARK3, MARK4*) have cellular activities, such as cell-cycle control and intracellular signal transduction. It is reported that *MARK* family members have been implicated in lung cancer, hepatocarcinoma, and leukaemia, but their roles are not comprehensively investigated in PAAD. Therefore, possible biological and prognostic impacts of this family on PAAD were examined here**.** GEPIA2, UALCAN, and GUOLAB, which are publicly available bioinformatic tools, were used to study gene/protein levels, prognostic importance, and immune infiltration of the *MARK* members. GEPIA2 tool showed higher mRNA expression levels of *MARK2* and *MARK4* in PAAD tumour samples (n=179) when compared to normal samples (n=171) (p<0.05), but not for *MARK1* and *MARK3*. Protein expression levels of all members were statistically different between PAAD tumour (n=137) and normal samples (n=74), generated by UALCAN platform. Interestingly, GEPIA2 platform indicated better overall survival for patients with high mRNA expression of *MARK1* (n=60, hazard ratio=0.45, p=0.0021) and worse survival for those with high mRNA expression of *MARK2 (*n=60, hazard ratio=1.7, p=0.047*)*, compared to patients in opposite groups. Also, GUOLAB tool demonstrated that *MARK1* mRNA expression were positively correlated with $CD4^+$ (cor=0.40, p<0.001) and MAIT (cor=0.35, p<0.001) cells, and *MARK2* expression were positively correlated with nTreg (cor=0.33, p<0.001) and neutrophil (cor=0.30, p<0.001) cells. In short, the bioinformatic analyses showed that only *MARK2* was both differentially expressed and prognostically significant in PAAD. *MARK*-related cellular mechanisms might be important in PAAD, therefore; further investigations are needed for the potential drug development.

Keywords: *MARK*, biomarker, PAAD, prognosis

ORAL PRESENTATION

Development of a novel polymeric membrane for cationic dye adsorption

Esra Feyzioğlu Demir[1*] (ORCID: https://orcid.org/0000-0003-2012-4337),
Nevra Öztürk Atay[2,3*] (ORCID: https://orcid.org/0000-0003-1653-2514)

[1]Department of Medical Laboratory Technique, Vocational School of Health Services, Izmir University of Economics, 35330, Balçova, Izmir, Turkey
[2]Ege University Central Research Test and Analysis Laboratory Application and Research Center, 35100, Bornova, Izmir, Turkey
[3]Department of Chemistry, Faculty of Science, Ege University, 35100, Bornova, Izmir, Turkey

*Corresponding author e-mail: nevraozturkatay@gmail.com

Abstract

Water covers approximately 71% of the Earth's surface and is one of the most essential elements for the survival of all living organisms. However, water resources and quality are increasingly under threat due to industrialization, urbanization, population growth, climate change, and agricultural activities (1). In particular, the discharge of synthetic dyes from textile and related industries into aquatic environments has caused serious water pollution problems. These pollutants are resistant to biodegradation, persistent in the environment, and pose significant risks to ecosystems and human health (2). Therefore, the dye industry must treat its wastewater with appropriate methods before discharging it into the environment (2). In this study, membrane structures were prepared by the polymerization of a biocompatible monomer, 2-hydroxyethyl methacrylate (HEMA), with 4-vinyl benzoic acid (4-VB), and the removal of a model cationic dye, Crystal Violet (CV), was investigated. Characterization of the prepared membranes was carried out using SEM-EDS, FTIR analyses, and swelling tests. Adsorption studies were evaluated by considering parameters such as initial dye concentration, pH, temperature, and contact time. Preliminary findings indicate that the developed p(HEMA)-4-VB-based membrane structures have potential as effective adsorbents for CV removal. Overall, this study may contribute to the development of environmentally friendly and reusable polymeric membranes for the removal of cationic dyes from aquatic environments.

Keywords: Adsorbent, Water Treatment, Cationic Dyes

References:

Öztürk-Atay, N., & Feyzioğlu-Demir, E. (2025). Sustainable Wastewater Management. In *Water Neutrality: Towards Sustainable Water Management* (pp. 187-210). American Chemical Society.
Atay, N. Ö., & Akgöl, S. (2024). Fabricating polymeric hydrogel membranes embedded with amine-and copper-modified nanostructures for RG 19 removal. *Colloid and Polymer Science*, *302*(3), 303-315.

ORAL PRESENTATION

Uncovering the soil impact of wastewater irrigation: A case study from Konya, Türkiye

Zeinab Saeed Abdelrazik[1] (ORCID: https://orcid.org/0009-0004-5734-2519), Muhittin Onur Akca[1,*] (ORCID: https://orcid.org/0000-0003-4540-9371), Hanife Akca[1] (ORCID: https://orcid.org/0000-0001-8529-6469), Erdem Peker[2] (ORCID: https://orcid.org/0009-0008-4032-1032), Kıymet Deniz Yagcioglu[3] (ORCID: https://orcid.org/0000-0003-3208-1354), Sonay Sozudogru Ok[1] (ORCID: https://orcid.org/0000-0002-4629-7140)

[1]Ankara University, Faculty of Agriculture, Department of Soil Science and Plant Nutrition, Ankara, Türkiye.
[2]Directorate General for State Hydraulic Works, Ankara, Türkiye.
[3]Ankara University, Department of Geological Engineering, Faculty of Engineering, Ankara, Türkiye.

*Corresponding author e-mail: moakca@ankara.edu.tr

Abstract

In this study, eight soil samples were collected from agricultural lands irrigated by wastewater and drainage water along the main wastewater discharge channel in Konya. Of these, seven were irrigated with wastewater and one with drainage water using the sprinkler method. X-ray fluorescence (XRF) analysis was conducted to determine the total chemical composition of the soils. Among the oxide forms, CaO (27–37%) and SiO_2 (24–28%) were found to be the most abundant. The Ca/Mg ratios were notably high, which was associated with the loose structure of the soil. Principal Component Analysis (PCA) of the results revealed that the total explained variance was 63.13%. According to the analysis, the available Fe, Mg, Pb, Cu, and Ni contents were identified as differentiating factors. It was also determined that as Fe and Mg concentrations increased, the values of soil organic matter (SOM), Ca, K, and Mn tended to decrease. The soils under investigation were characterized by very high CaCO3 content and moderate levels of SOM. While no salinity problems were observed in soils irrigated with wastewater, salinity was detected in the soil irrigated with drainage water (2.95 dS/m). The concentrations of heavy metals (Ni, Cd, Pb) were below toxic thresholds. Among the essential plant nutrients, K, Ca, and Mg levels were found to be very high, total N content was high, and available P was at a sufficient level. Regarding micronutrients, Fe, Zn, and Mn levels were low, while Cu was moderate. Phenological observations made during sampling in fields cultivated with alfalfa, oats, maize, wheat, and sunflower indicated no signs of toxicity in the crops.

Keywords: Available nutrients, Heavy metals, Principle Component Ananlysis, Soil chemical composition, Wastewater irrigation, XRF analysis

ORAL PRESENTATION

Investigation of photosensitizer properties of zinc phthalocyanines in photodynamic therapy by photophysicochemical properties

Halise Yalazan (ORCID:https://orcid.org/0000-0003-1234-2721)

[1]Karadeniz Technical University, Faculty of Sciences, Department of Chemistry, Trabzon, Türkiye

*Corresponding author e-mail :haliseyalazan@hotmail.com

Abstract

Cancer has become a serious health concern recently, endangering people everywhere. The most promising cancer treatment approach recently, aside from conventional approaches, is photodynamic therapy (PDT). As photosensitizers, phthalocyanines (Pcs) have been widely employed in PDT due to their strong ability to generate singlet oxygen and other special qualities. Therefore, in this study, photophysicochemical properties such as fluorescence, singlet oxygen, and photodegradation quantum yields were investigated to determine their potential use as photosensitizers in PDT. According to the findings, zinc phthalocyanines show the therapeutic effectiveness of photophysicochemical techniques and have the potential to be employed as photosensitizers in photodynamic therapy. The zinc phthalocyanines that are produced are regarded as promising in vitro PDT agents for further research [1].

Keywords: Fluorescence, Phthalocyanine, Photodynamic therapy, Singlet oxygen.

Acknowledgments*:* This work was supported by Office of Scientific Research Projects of Karadeniz Technical University. Project number: FBA-2024-16009.

References:

H. Yalazan, İ. Ömeroğlu, H. Kantekin, M. Durmuş, Inorganic Chemistry Communications 181 (2025) 115125. https://doi.org/10.1016/j.inoche.2025.115125

ORAL PRESENTATION

Design of a lipoic acid–based thioester polymer functionalized with tryptophan for drug release

Özlem Kaplan[1*] (ORCID: https://orcid.org/0000-0002-3052-4556), Kevser Bal[2] (ORCID: https://orcid.org/0000-0002-9127-2380), Sibel Küçükertuğrul Çelik[2] ORCID: (https://orcid.org/0000-0003-2185-2619 , Mehmet Koray Gök[2] (ORCID: https://orcid.org/0000-0003-2497-9359)

[*1]Alanya Alaaddin Keykubat University, Rafet Kayış Faculty of Engineering, Department of Genetics and Bioengineering, Antalya, Türkiye.
[2]Istanbul University-Cerrahpaşa, Faculty of Engineering, Department of Chemical Engineering, Istanbul, Türkiye

*Corresponding author e-mail: ozlem.kaplan@alanya.edu.tr

Abstract

A novel thioester-based polymer was synthesized and evaluated as a biodegradable carrier for drug delivery. The polymer was prepared via a thiol–Michael addition reaction between 1,6-hexanediol diacrylate and α-lipoic acid under UV irradiation for 3 hours, forming a thioester backbone containing free carboxyl groups. These free carboxyl groups were subsequently conjugated with tryptophan through a DCC-mediated coupling reaction to enhance amphiphilicity and introduce biointeractive aromatic moieties. The chemical structure of the synthesized polymer was confirmed by FTIR spectroscopy, which verified the formation of thioester linkages and amide bonds following tryptophan conjugation. Nanoparticles were obtained by nanoprecipitation using DMSO as the organic solvent and deionized water as the non-solvent. Blank nanoparticles exhibited an average diameter of 71.1 ± 2.1 nm, a PDI of 0.183 ± 0.052, and a zeta potential of –18.0 ± 1.2 mV. Curcumin-loaded nanoparticles showed a size of 123 ± 2.5 nm, PDI 0.136 ± 0.02, zeta potential –15 ± 1.2 mV, and 46% loading efficiency. GPC analysis revealed a number-average molecular weight (Mn) of 3.05 kDa and a weight-average molecular weight (Mw) of 3.95 kDa with a PDI of 1.29, confirming the formation of a narrowly distributed, low-molecular-weight thioester polymer. In vitro release experiments demonstrated a faster release in mildly acidic medium (pH 5.0) compared to physiological pH (7.4). Cumulative curcumin release reached 50.9%, 68.9%, and 100% at 24, 48, and 120 hours at pH 5.0, while corresponding values at pH 7.4 were 44.0%, 55.2%, and 71.8%. The enhanced release under acidic conditions was attributed to acid-facilitated hydrolysis of thioester linkages, leading to gradual network loosening and improved diffusion. Overall, this tryptophan-functionalized thioester polymer derived from lipoic acid represents a promising new class of degradable materials capable of sustained and environmentally responsive drug release, offering potential advantages for targeted cancer therapy.

Keywords: α-lipoic acid, thioester polymer, tryptophan, curcumin

ORAL PRESENTATION

β-Glucan production from *Saccharomyces cerevisiae* under submerged fermentation

Mehdi Koşaca[1]*(ORCID: https://orcid.org/0000-0003-2075-2480),
Raziye Öztürk Ürek[2] (ORCID: https://orcid.org/0000-0002-7147-6853)

[1]Dokuz Eylul University, The Graduate School of Natural and Applied Sciences, Biotechnology Department, Izmir, Türkiye
[2]Dokuz Eylul University, Faculty of Science, Chemistry Department, Izmir, Türkiye

*Corresponding author e-mail: m.kosaca@ogr.deu.edu.tr

Abstract

β-glucan is a polysaccharide composed of D-glucose units, and its structure varies among organisms. In cereals, it is linear with β-1,3 and/or β-1,4 bonds; in bacteria, it is linear with β-1,3 bonds; and in yeast, it has a branched structure with a β-1,3 backbone and β-1,6 side chains. In *Saccharomyces cerevisiae*, β-glucan is mainly located in the cell wall, comprising about 50% as β-1,3-glucan and 15% as β-1,6-glucan. Extraction can be carried out by hot water, alkaline solutions, enzymatic treatment, or mechanical disruption, each providing different yields. Yeast-derived β-glucans are applied in food as dietary fiber and cholesterol-lowering agents, in pharmaceuticals as immune stimulants, and in cosmetics to improve skin hydration. They enhance immune activity, reduce cholesterol, regulate blood sugar, and lower infection risk. To reduce costs, attention has turned to renewable substrates such as sugarcane molasses, which is rich in sugars and minerals. The aim of this study was to evaluate the effect of molasses concentration and fermentation period on β-glucan production in yeast. *S. cerevisiae* was grown in Cooper & Paddock medium with 2-10% (v/v) sugarcane molasses as carbon sources. β-glucan yields were monitored during fermentation. Extraction was performed using an eco-friendly sonication method combined with mild acid–alkali treatment, and functional groups were characterized by Fourier-transform infrared spectroscopy. At 2% molasses, the maximum yield was 0.108 mg/mL DCW on day 2. At 5%, the highest yield was 0.676 mg/mL DCW after 1.5 days, followed by a decline. The best results were with 10% molasses, reaching 0.903 mg/mL DCW on day 1 and remaining above 0.6 mg/mL until day 4. In conclusion, the study demonstrated that sugarcane molasses is a promising low-cost substrate for β-glucan production by *S. cerevisiae.* Furthermore, it suggests its potential use in the food industry as a dietary fiber source.

Keywords: β-glucan, *S. cerevisiae*, submerged fermentation, sugarcane molasses

ORAL PRESENTATION

Production, extraction and characterization of microbial mannoprotein

Mehdi Koşaca[1]*(ORCID: https://orcid.org/0000-0003-2075-2480),
Raziye Öztürk Ürek[2] (ORCID: https://orcid.org/0000-0002-7147-6853)

[1]Dokuz Eylul University, The Graduate School of Natural and Applied Sciences, Biotechnology Department, Izmir, Turkiye
[2]Dokuz Eylul University, Faculty of Science, Chemistry Department, Izmir, Turkiye

*Corresponding author e-mail: m.kosaca@ogr.deu.edu.tr

Abstract

Mannoproteins are structural polysaccharides located in the outer layer of the yeast cell wall, consisting of a protein backbone covalently linked to mannose residues. In *Saccharomyces cerevisiae*, they play a crucial role in maintaining cell wall integrity, adhesion, and stress tolerance, while also showing functional properties such as immunomodulation, emulsification, and antioxidant activity. Owing to these properties, yeast mannoproteins find applications in the food industry as stabilizers and prebiotics, in pharmaceuticals as immune enhancers, and in cosmetics for skin protection. For sustainable and cost-effective production, agro-industrial byproducts such as sugarcane molasses have been considered as alternative carbon sources due to their high sugar and mineral content. This study aimed to investigate how molasses concentration and fermentation time affect mannoprotein production by *S. cerevisiae*. The yeast was grown under submerged fermentation using 2–10% (v/v) sugarcane molasses as a carbon source. Mannoprotein was extracted by alkaline–sonication-thermal treatment. Biological activity of extractracted mannoprotein was confirmed via oil spreading and emulsification index (EI). Morever, its structural properties were verified by Fourier-transform infrared spectroscopy (FTIR). In conclusion, increasing molasses concentration improved both cell growth and mannoprotein yield, reaching the best results at 5% molasses. Fermentation time also influenced production, with the highest yield observed at the early stationary phase (2 days). On the other hand, it exhibits an oil spreading activity of 8 cm, EI of 40%, and retains 96% of its EI after 48 hours. The FTIR spectra showed characteristic peaks of polysaccharides and proteins, confirming the presence of mannose and peptide groups of mannoproteins. These results show that sugarcane molasses can be used as an economical substrate for mannoprotein production by *S. cerevisiae*, supporting sustainable bioprocess applications.

Keywords: fermantation, mannoprotein, molasses, *Saccharomyces cerevisiae*

ORAL PRESENTATION

Controlled Sr(II) ion release from injectable electroactive hydrogels with potential for the treatment of infections

Melike Fırlak Demirkan *[1] (https://orcid.org/0000-0003-1674-9086) Dilek Öztürk[1] (https://orcid.org/0000-0002-6182-2337), Zeynep Sude Çifçibaşı[1] (https://orcid.org/0009-0005-9432-259X), Fatma Ertan [1] (https://orcid.org/0000-0002-9572-9392), John George Hardy [2] (https://orcid.org/0000-0003-1674-9086) , Aslı Nurşeval Oyunlu [3] (https://orcid.org/0000-0003-2104-8567), Hakan Darıcı [3] (https://orcid.org/0000-0001-9393-554X)

[*1] Gebze Technical University, Faculty of Science, Department of Chemistry, Kocaeli, Türkiye.
[2] Lancaster University, Department of Chemistry, Lancaster, UK.
[3] İstinye University, Faculty of Medicine, Dept. of Histology & Embryology, Istanbul, Türkiye.

*Corresponding author e-mail: mfirlak@gtu.edu.tr

Abstract

The development of electrochemical stimuli-responsive drug delivery systems is of both academic and industrial interest due to the ease with which it is possible to trigger payload release, providing drug delivery in a controllable manner. Herein, the preparation of in situ forming injectable hydrogels including electroactive polypyrrole nanoparticles (PPy-NPs) where of Sr^{2+} ions are electrochemically loaded for electrically triggered release of Sr^{2+} ions is reported. The hydrogels were characterized by a variety of techniques including Fourier-transform infrared (FTIR) spectroscopy, scanning electron microscopy (SEM), energy dispersive X-ray spectroscopy (EDX), thermogravimetric analysis (TGA), X-ray diffraction (XRD), cyclic voltammetry (CV), etc. The cytocompatibility towards human mesenchymal stem cells (MSCs) and fibroblasts were also studied. The Sr^{2+} ions loaded PEC-ALD/CS/PPy-NPs injectable hydrogel showed no significant cytotoxicity towards human mesenchymal stem cells (MSCs) and fibroblasts. Sr^{2+} ions were electrochemically loaded and released from the injectable electroactive hydrogels, and the application of electrical stimulus enhanced the release of Sr^{2+} ions from gels by ca. 2–4 fold relative to the passive release control experiment. The antibacterial activity of Sr^{2+} ions against *E.coli* and *S.aureus* was demonstrated in vitro. Although these prototypical examples of Sr^{2+} loaded electroactive gels don't release sufficient Sr^{2+} ions to show antibacterial activity against *E. coli* and *S. aureus*, we believe future iterations with optimised physical properties of the gels will be capable of doing so.

Keywords: injectable electroactive hydrogel, divalent ion release, bone infection.

ORAL PRESENTATION

Supercritical carbondioxide extraction of *Nigella sativa* L. seed oil: fatty acid composition, nutritional energy and antimicrobial activity

Hatice Banu Keskinkaya[1*,] (ORCID: https://orcid.org/0000-0002-6970-6939), Şeyma Akalın[2] (ORCID: https://orcid.org/0009-0004-1216-179X), Zeliha Üstün Argon[3] (ORCID: https://orcid.org/0000-0002-0541-8962), Süleyman Doğu[3] (ORCID: https://orcid.org/0000-0002-5352-9288)

[*1]Department of Biotechnology, Faculty of Science, Necmettin Erbakan University, Konya, Turkey
[2]Department of Pharmaceutical Botanical, Faculty of Pharmacy, Selcuk University, Konya, Turkey
[3]Department of Plant and Animal Production, Meram Vocational School, Necmettin Erbakan University, Konya, Turkey

*Corresponding author e-mail: haticebanu.keskinkaya@erbakan.edu.tr

Abstract

This study aimed to evaluate the fatty acid composition, nutritional energy value, and antimicrobial activity of *Nigella sativa L.* seed oil obtained by supercritical carbon dioxide (SC–CO_2) extraction. The method provides an environmentally friendly and efficient alternative to conventional solvent extraction, ensuring high oil quality and the preservation of bioactive compounds. *Nigella sativa L.* seed oil is a valuable natural product rich in unsaturated fatty acids, thymoquinone and tocopherols, known for their nutritional and therapeutic effects. The SC–CO_2 extraction technique offers solvent-free processing under mild conditions, reducing oxidation and degradation of thermolabile compounds. This study investigates the chemical and biological characteristics of SC–CO_2-extracted *Nigella sativa L.* oil. Seeds were extracted at 420 bar and 47 °C for 120 minutes using SC–CO_2. Fatty acid composition was determined by gas chromatography (GC–FID). Nutritional energy was calculated according to standard macronutrient conversion factors. Antimicrobial activity was assessed by the microdilution method against *Escherichia coli, Staphylococcus aureus* (MRSA), and *Candida albicans*, with results expressed as minimum inhibitory concentration (MIC). Linoleic (53.8%), oleic (22.3%), and palmitic (13.6%) acids were identified as the major components, with total unsaturated fatty acids exceeding 80%. The oil's energy value was approximately 895 kcal/100 g. Antimicrobial tests showed strong inhibitory effects, with MIC values of 6.25 mg/mL for *E. coli*, 3.12 mg/mL for *S. aureus*, and 12.5 mg/mL for *C. albicans*. These results indicate that SC–CO_2 extraction preserves both nutritional and functional properties. SC–CO_2 extraction produces high-quality *Nigella sativa L.* seed oil with rich unsaturated fatty acid content, high caloric value, and significant antimicrobial potential. This method offers a sustainable and effective approach for food, cosmetic, and pharmaceutical applications.

Keywords: *Nigella sativa* L., supercritical CO_2 extraction, fatty acid composition, nutritional value, MIC.

ORAL PRESENTATION

Characterization and enzyme kinetic study of serine protease subtilisin carlsberg immobilized on biochar-chitosan composite carrier obtained from waste biomass

Ahmet Eser* (ORCID: https://orcid.org/0000-0002-3656-8445)

Manisa Celal Bayar University, Faculty of Engineering and Natural Sciences, Department of Chemistry, Manisa, Türkiye

*Corresponding author e-mail: ahmet.eser@cbu.edu.tr

Abstract

In this study, an alkaline serine protease, Subtilisin Carlsberg (SC), produced by Bacillus licheniformis, was immobilized onto a biochar-chitosan composite carrier synthesized from waste vineyard biomass. The composite material was prepared by integrating biochar into a chitosan matrix and activated with glutaraldehyde to enable covalent enzyme attachment. The structural and morphological properties of the composite carrier were characterized by SEM and TGA analyses. The immobilized enzyme exhibited optimum catalytic activity at pH 8.0 and 50 °C, showing similar behavior to the free enzyme. Kinetic studies revealed that immobilization slightly altered the apparent Km and Vmax values but significantly enhanced thermal and operational stability. These findings demonstrate that the biochar–chitosan composite provides a stable and efficient immobilization matrix, improving enzyme reusability and maintaining catalytic performance under variable conditions. The results highlight the potential of this bio-based composite carrier as a sustainable material for immobilized enzyme systems in biotechnological applications.

Keywords: Subtilisin Carlsberg, Biochar, Chitosan, Enzyme kinetics

ORAL PRESENTATION

Effect of drying method and process conditions on the physicochemical and functional properties of tomato pomace powder

Tolga Kağan TEPE[1*] (ORCID: https://orcid.org/0000-0003-0484-7295),
Fadime Begüm TEPE[1] (ORCID: https://orcid.org/0000-0003-4989-5354)

[*1] Giresun University, Vocational School of Şebinkarahisar, Food Technology Department, Giresun, Türkiye

*Corresponding author e-mail: tolga.kagan.tepe@gmail.com

Abstract

In this study, tomato pomace obtained from Rio Grande processing tomatoes was dried using hot air (50, 60, and 70 °C) and microwave (240 W and 400 W) methods to produce tomato pomace powders with particle sizes smaller than 1000 µm. The effects of different drying conditions on physicochemical, bioactive, and physical quality properties as well as energy efficiency were comprehensively evaluated. The fresh tomato pomace showed a moisture content of 90.64%, soluble solid content of 11.66%, pH of 4.69, and titratable acidity of 1.37% (as citric acid equivalent). The drying method had a statistically significant effect on color parameters ($p<0.05$). The highest L*, a*, and b* values were obtained from samples dried at 70 °C (hot air) and 240 W (microwave). Regarding powder properties, the highest water holding capacity (1105.56%) was found at 50 °C. The lowest Carr index (14.26%) and Hausner ratio (1.17) were observed in the sample dried at 240 W, indicating better flowability and lower cohesiveness; however, the lowest water holding capacity was also recorded for this condition. Bioactive compounds varied significantly depending on the drying conditions. Total phenolic content ranged from 154.21 to 427.81 mg GAE 100 g^{-1} DM, and antioxidant activity ranged between 0.76 and 1.63 mmol TE 100 g^{-1} DM. Both total phenolic content and antioxidant activity decreased under hot air-drying conditions. Moreover, ascorbic acid and carotenoid contents also declined after drying; however, hot air drying at 70 °C was statistically more effective in preserving these compounds compared with other conditions. Drying kinetics were best fitted by the Midilli–Kucuk, Weibull, and Artificial Neural Network (ANN) models. The drying rate, effective moisture diffusivity, and mass transfer coefficients increased with higher temperature and microwave power. The lowest specific energy consumption (2.06 kWh kg^{-1} water) was obtained during microwave drying at 400 W. Overall, hot air drying at 70 °C provided the most favorable results in terms of color, powder characteristics, and bioactive compound retention. The findings suggest that drying tomato pomace by hot air is a promising approach for producing functional powders suitable for use as food ingredients. Additionally, the current study was supported by Giresun University Coordinatorship of Scientific Research Projects (Grant number: FEN-BAP-A-110225-26).

Keywords: Tomato Pomace Powder, Drying, Bioactive Properties, Artificial Neural Network, Energy

ORAL PRESENTATION

Preparation and antibacterial activity of Ag_2O nanoparticles from *Cedrus libani*

Baran Karaduman[1]* (ORCID: https://orcid.org/0009-0008-9414-350X), Alican Bahadır Semerci[2] (ORCID: https://orcid.org/0000-0001-9502-9321), Keziban Atacan[3] (ORCID: https://orcid.org/0000-0003-3927-7245)

[1]Sakarya University of Applied Sciences Graduate School Institute, Department of Biomedical Engineering, 54050 Sakarya, Türkiye
[2]Necmettin Erbakan University, Ereğli Vocational School of Health Services, 42310, Konya, Türkiye
[3]Sakarya University of Applied Sciences, Faculty of Technology, Department of Engineering Fundamental Sciences, 54050 Sakarya, Türkiye

*Corresponding author e-mail: barankaraduman20@gmail.com

Abstract

Recently, metal nanoparticles have been widely utilized in biotechnology and medicine due to their advantages, including low cost, eco-friendly synthesis processes, and biocompatibility. In this study, silver oxide (Ag_2O) nanoparticles were synthesized using a green synthesis approach from the fresh cones of *Cedrus libani* extract, and their antibacterial activities were evaluated. The plant extract acted as both a reducing and stabilizing agent, providing an environmentally friendly synthesis medium (Das et al., 2020). Characterization of the synthesized Ag_2O nanoparticles was performed using X-ray Diffraction (XRD) for crystalline structure analysis, Fourier-Transform Infrared Spectroscopy (FTIR) for functional group analysis, and Scanning Electron Microscopy (SEM) for morphological examination (Dawadi et al., 2021). The antibacterial activity was assessed using the well diffusion method against *Bacillus subtilis*, *Staphylococcus aureus*, *Enterococcus faecalis*, *Staphylococcus epidermidis*, *Salmonella typhimurium*, and *Escherichia coli* (Atacan et al., 2021). The highest antibacterial activity was observed on *S. typhimurium* and *B. subtilis* bacteria (13 mm), followed by *E. coli* and *S. epidermidis*. The lowest activity was recorded against *S. aureus* and *B. subtilis*. These results demonstrated the potent antibacterial properties of the synthesized Ag_2O nanoparticles (Kumar et al., 2021). In conclusion, Ag_2O nanoparticles produced from *Cedrus libani* cones present a promising, sustainable, and biocompatible alternative for the development of antibacterial nanomaterials.

Keywords: green synthesis, *Cedrus libani*, Ag_2O nanoparticles, antibacterial activity

Acknowledgement: The authors thank the Scientific and Technological Research Council of Türkiye (TÜBİTAK) for financial support through the project (project number: 223Z272).

References

Atacan, K., Güy, N., Ozmen, M., & Özacar, M. (2021). Fabrication of silver doped different metal oxide nanoparticles and evaluation of their antibacterial and catalytic applications. *Applied Surface Science Advances*, *6*, 100156.

Das, C. A., Kumar, V. G., Dhas, T. S., Karthick, V., Govindaraju, K., Joselin, J. M., & Baalamurugan, J. (2020). Antibacterial activity of silver nanoparticles (biosynthesis): A short review on recent advances. *Biocatalysis and Agricultural Biotechnology*, *27*, 101593.

Dawadi, S., Katuwal, S., Gupta, A., Lamichhane, U., Thapa, R., Jaisi, S., ... & Parajuli, N. (2021). Current research on silver nanoparticles: synthesis, characterization, and applications. *Journal of nanomaterials*, *2021*(1), 6687290.

Kumar, J. A., Krithiga, T., Manigandan, S., Sathish, S., Renita, A. A., Prakash, P., ... & Crispin, S. (2021). A focus to green synthesis of metal/metal based oxide nanoparticles: Various mechanisms and applications towards ecological approach. *Journal of Cleaner Production*, *324*, 129198.

ORAL PRESENTATION

Analytical determination of the active pharmaceutical ingredient propranolol

Ekmen Can* (ORCID: https://orcid.org/0009-0005-5541-9751),
Aydınoğlu Marinelli Sabriye (ORCID: https://orcid.org/ org/0000-0001-5054-4071)

Çukurova University, Faculty of Pharmacy, Department of Analytical Chemistry, Adana, Türkiye.

*Corresponding author e-mail: canekmen0101@outlook.com

Abstract

In the present study, literature on the determination of propranolol in various sample matrices have been reviewed. The analytical methods developed in these studies are expected to be sensitive, rapid, simple, and cost-effective. In all methods, accuracy was evaluated through parameters such as linear range, limit of detection, and recovery rates, while precision was assessed based on standard deviations obtained from intra-day and inter-day repeated analyses. The validity of the developed methods was demonstrated through the testing of relevant validation parameters. In the reviewed studies, propranolol was determined in pharmaceutical preparations, wastewater, human and animal plasma, post-mortem tissues and body fluids, and urine, either alone or in the presence of other active substances. Depending on the sample matrix analyzed, different extraction methods were applied, and in most studies, extraction efficiency was calculated and reported. Liquid chromatography was commonly employed, and it was observed that the sensitivity of the method varied depending on the type of detector used. Furthermore, it was reported that methods such as LC-MS, LC-MS/MS, and LC-QQQ-MS/MS enhanced sensitivity and reduced analysis time.

Keywords: Propranolol, Chromatography, Validation, Hypertension

ORAL PRESENTATION

Advanced polymeric adsorbents for the treatment of arsenic- and selenium-contaminated wastewater

Serhad TİLKİ[1*] (ORCID: https://orcid.org/0000-0002-9380-6673)

[1]Amasya University, Department of Chemical and Chemical Processing Technology, Vocational School of Technical Sciences, Amasya, Turkey

*Corresponding author e-mail: serhadtilki@gmail.com/serhad.tilki@amasya.edu.tr

Abstract

In this study, an ion-exchange polymeric adsorbent was prepared by modifying chloromethyl polystyrene (CMS) particles with 3-(dimethylamino)-1-propylamine (DMAPA) to introduce amino functional groups. The resulting adsorbent is hereafter referred to as DMAPA-m-CMS. The chemical structure of the synthesized material was characterized using FTIR, SEM, and XPS analyses. The adsorption performance of DMAPA-m-CMS toward As(V) and Se(VI) ions was systematically evaluated in a batch system under various conditions, including the effects of pH, contact time, initial concentration, competing anions, and ionic strength. The maximum experimental adsorption capacities were determined as 26.26 mg As(V)/g polymer at pH 4.0 and 26.02 mg Se(VI)/g polymer at pH 4.0. Adsorption kinetics followed the pseudo-second-order model, indicating that the adsorption process was governed by chemisorption involving valence forces through electron sharing or exchange between adsorbent and adsorbate. Equilibrium data were well described by the Langmuir isotherm, and according to the Langmuir model, the maximum theoretical adsorption capacities at 25 °C were calculated as 111.11 mg As(V)/g polymer and 83.33 mg Se(VI)/g polymer. Overall, the developed adsorbent exhibited high adsorption capacity and selectivity for both As(V) and Se(VI) ions, even in the presence of competing species. These results demonstrate that DMAPA-m-CMS is a promising and sustainable adsorbent for the removal of toxic arsenic and selenium ions from contaminated water, contributing to environmental protection and the advancement of water treatment technologies.

Keywords: Adsorption,Adsorbent, Arsenic, Selenium

Acknowledgement: Authors wish to acknowledge that this study was financially supported by Amasya University Project number: FMB-BAP 20-0453

ORAL PRESENTATION

Osmanlı döneminden günümüze gül yağı distilasyonu

Bekir YILDIRIM[1*] (*ORCID: https://orcid.org/0000-0003-2378-7697*)

[*1]Burdur Mehmet Akif Ersoy Üniversitesi, Burdur Gıda Tarım ve Hayvancılık Meslek Yüksekokulu, Kültür Bitkileri Bölümü, Burdur, Türkiye

*Sorumlu yazar e-mail: byildirim@mehmetakif.edu.tr

Özet

Osmanlı Devleti'nde Edirne'de ilk gül yağı üretiminin 13. veya 17. yy.da başladığı düşünülmektedir. 1877-78 Türk-Rus savaşı (93 harbi) sonrasında imzalanan Berlin Antlaşması'nı (1878) takip eden yıllarda, Edirne Vilâyeti'ne bağlı olup yağ gülcülüğünün merkezi olan Kızanlık ve çevresindeki toprakların kaybedilmesinin ardından Osmanlı Devleti Anadolu'da yağ gülcülüğünü teşvik etmiştir. 1901'de (Hicri 1319) yayımlanan *Gülistan Tesisi ve Tımarına ve Gül Yağı Takdir ve İmaline Dair Risaledir* isimli kitapçıkta yağ gülcülüğü hakkında bilgiler verilmiştir. Bu çalışmada, bahsedilen kitapçık incelenerek gül yağı istihsali yöntemi günümüzde uygulanan endüstriyel distilasyon ile karşılaştırılmıştır. Öncelikle Osmanlı Türkçesiyle yazılmış olan ilgili kitapçık günümüz Türkçesine çevrilmiştir. Osmanlı döneminde gül yağı distilasyonuna ilişkin bilgiler bu kitapçığa dayanmaktadır. Günümüzde gerçekleştirilen endüstriyel distilasyona ilişkin bilgiler ise Göller Yöresinde yağ gülcülüğü üzerine daha önce tarafımızdan yürütülmüş çalışmalar sırasında yapılan saha gözlemlerine dayanmaktadır. Osmanlı döneminde gül yağı istihsali için *Rosa damascena* çiçekleri bakır imbiklerde su ile distilasyona tabi tutulmuştur. Her seferinde yaklaşık 7,5 kg çiçek kaynatılabilen bu sistemde, kaynayan su buharının çiçeklerdeki uçucu bileşenleri de alarak soğuk su içerisinden geçirilmiş olan islim borusundan geçirilerek yoğunlaşması sağlanmış ve boru ucuna bağlanmış olan yaklaşık 7,5 L'lik şişelerde biriktirilmiştir. Her kazandan 2 şişe (birinci şişe baş, ikinci şişe ayak olarak adlandırılmıştır) olmak üzere dört kazandan alınan yaklaşık 60 L yağlı su ikinci kez distilasyona tabi tutulmuş ve bu kez islim borusunun ucuna bağlanan kristal sürahilerde biriktirilmiştir. Biriken yağlı suyun üzerinde toplanan gül yağı kepçe yardımıyla alınmıştır. Günümüzde endüstriyel distilasyonda ise 3000 L'lik bakır tanklarda tek seferde 500 kg gül çiçeği işlenebilmektedir. Uçucu bileşenleri taşıyan su buharı soğutucu kondenserden geçerek önce distilat tankına oradan da florentin kabına geçer. Florentin kabının cam haznesinde toplanan yağa birinci yağ (çiçek yağı) denir. Geriye kalan yağ altı suyu biriktirilerek sonradan tekrar distilasyona tabi tutulur. İkinci distilasyonda üretilen yağa ikinci yağ (su yağı) denir. Genellikle %25 birinci yağ + %75 ikinci olacak şekilde karıştırılarak ticari gül yağı elde edilmektedir.

Anahtar kelimeler: Distilasyon, Gül yağı, *Rosa damascena*, Osmanlı Devleti, Yağ gülcülüğü

ORAL PRESENTATION

Development of polyvinyl alcohol based bioactive cosmetic masks

İdil Can[1] (https://orcid.org/0009-0007-0309-3133) , Yusuf Sıcak[2] (https://orcid.org/0000-0003-2339-5837), Pınar Terzioğlu[1*] (ORCID: https://orcid.org/0000-0003-4114-7044)

[*1]Bursa Technical University, Faculty of Engineering and Natural Sciences, Department of Polymer Materials Engineering, Bursa, Türkiye
[2]Muğla Sıtkı Koçman University, Köyceğiz Vocational School, Department of Medicinal and Aromatic Plants, Muğla, Türkiye

*Corresponding author e-mail: pinar.terzioglu@btu.edu.tr

Abstract

The development of biodegradable, polymer-based bioactive cosmetic masks that promote skin health and environmental sustainability has gained increasing attention in recent years. Conventional cosmetic masks often contain synthetic polymers and chemical additives, which may cause skin irritation and contribute to environmental pollution. Furthermore, bioactive agents including supporting skin health, such as antioxidants, moisturizers, and soothing compounds are essential to obtain a preferred skin care cosmeceutical. This study aims to develop a new generation of cosmetic masks using biodegradable polymers and natural bioactive ingredients. In this research, hydrogel masks were prepared via the casting method by incorporating bioactive components and clay into polyvinyl alcohol (PVA). The flexibility of the mask formulation was enhanced by adding plasticizers. The produced masks characterized by mechanical testing and bioactivity analysis. The incorporation of bioactive ingredients enhanced the antioxidant activity of neat films. It was determined that there was a decrease in tensile strength and elongation with the addition of the bioactive additive compared to the control sample.The proposed formulation offers a novel approach by combining biodegradability with targeted bioactivity, addressing the dual need for skin health improvement and ecological responsibility. This research is expected to contribute to the development of next-generation cosmetic materials that are environmentally sustainable, biocompatible, and suitable for commercial applications.

Keywords: Biodegradable polymers, bioactive cosmetic masks, environmental sustainability, skin health, polymer characterization.

ORAL PRESENTATION

Bacillus subtilis offers insights into microbial adaptation under Martian conditions

Nedim Emre Gök[1] (*ORCID: https://orcid.org/0009-0000-9119-8670*),
Ercan Selçuk Ünlü[1*] (*ORCID: https://orcid.org/0000-0003-0097-1125*)

[*1]Bolu Abant İzzet Baysal University, Faculty of Arts and Science, Department of Chemistry, Bolu, Türkiye.

*Corresponding author e-mail: esunlu06@gmail.com

Abstract

The exploration of microbial survival strategies in extraterrestrial environments is fundamental to both astrobiology and planetary protection. *Bacillus subtilis* is a well-characterized Gram-positive bacterium with remarkable genetic plasticity and stress tolerance. It has been considered as a model organism for space biology research. Previous research has proven its resilience against extreme conditions, including radiation, dehydration, and low-pressure environments. Its endurance to such stress conditions makes it an ideal system to investigate microbial resilience under Martian-like conditions. Among the environmental parameters on Mars, the weak and heterogeneous magnetic field has received comparatively little attention despite its potential role in shaping microbial physiology. Studies under low and static magnetic field conditions suggest significant impacts on oxidative stress balance, DNA repair mechanisms, and ion homeostasis. In *B. subtilis*, these processes are tightly regulated by sigma factors and global transcriptional regulators, which coordinate adaptive gene expression programs in response to environmental cues. Integrating evidence from microbial stress biology and magnetic field research, we propose that *B. subtilis* serves as a valuable platform for predicting how terrestrial life may respond to Martian magnetic conditions. Such insights not only enhance our understanding of microbial adaptability in space but also provide essential knowledge for the safe design of future planetary exploration missions. Due to its hardiness and spore-forming ability, *B. subtilis* present itself as a valuable model organism in both agricultural biotechnology applications on Earth and astrobiology studies.

Keywords: Astrobiology, Mars, Magnetic field, Space biology, Biotechnology

This project is supported by Bolu Abant Izzet Baysal University (Grant # 2025-TYL-013).

ORAL PRESENTATION

Computational insights into the antioxidant and anticancer mechanisms of apigenin

Aslı Öztürk Kiraz* (ORCID: https://orcid.org/0000- 0001- 9837-0779)

Pamukkale University, Faculty of Science, Department of Physics, Denizli, Turkey.

*Corresponding author e-mail: aslio@pau.edu.tr

Abstract

Apigenin (4′,5,7-trihydroxyflavone) is a naturally occurring flavonoid found in a variety of fruits, vegetables, and medicinal plants. It has gained considerable attention due to its potent antioxidant and anticancer properties. This study aims to investigate the molecular mechanisms that underlie the bioactivity of apigenin through a computational approach that integrates density functional theory (DFT), molecular docking, and ADMET analysis. We calculated the optimized molecular geometry and electronic parameters, including the HOMO–LUMO energy gap, ionization potential, and electronegativity, to evaluate the radical-scavenging capacity and redox reactivity of apigenin. The DFT results indicate robust chemical stability and effective electron-donating ability, which support the antioxidant function of apigenin. Molecular docking simulations were conducted against cancer-related targets such as PIM1 kinase and the CD47 receptor to explore the inhibitory interactions at their active sites. Apigenin exhibited strong binding affinities through hydrogen bonding and π–π stacking with key amino acid residues, suggesting a potential to suppress oncogenic pathways. Furthermore, pharmacokinetic (ADMET) predictions revealed favorable absorption and low toxicity profiles, reinforcing the drug-likeness of apigenin. These computational findings highlight the dual antioxidant and anticancer potential of apigenin, underscoring its significance as a natural, safe, and effective therapeutic agent. This study provides valuable insights into the electronic and structural factors that influence flavonoid bioactivity and advocates for further in vitro and in vivo validation.

Keywords: Apigenin, flavonoid, DFT, antioxidant, anticancer, molecular docking.

ORAL PRESENTATION

Transcript levels of ZDHHC protein palmitoyltransferases in granulosa cells isolated from the ovaries of PCOS and non-PCOS women

Caglar Berkel[1*] (ORCID: https://orcid.org/0000-0003-4787-5157)

[*1] Tokat Gaziosmanpasa University, Faculty of Science and Arts, Department of Molecular Biology and Genetics, Tokat, Türkiye.

*Corresponding author e-mail: caglar.berkel@gop.edu.tr

Abstract

Pyroptosis is a lytic form of pro-inflammatory programmed cell death mechanism characterized by the formation of pores in plasma membrane, and non-vesicular release of pro-inflammatory cytokines including IL-1β and IL-18. Recent studies have showed that S-palmitoylation of human GSDMD at cysteine 19 is a key regulatory step controlling both GSDMD activation and interaction with membranes (membrane translocation) in pyroptosis. In other words, S-palmitoylation of GSDMD at this amino acid has been shown to be required for pore formation by GSDMD oligomerization in pyroptosis. S-palmitoylation of cysteine residues, catalyzed by a family of 23 ZDHHC protein palmitoyltransferases (i.e. protein acyltransferases), is the most common lipid modification of membrane-associated proteins, such as GSDMD. Since pyroptosis of granulosa cells is involved in the pathogenesis of PCOS, and palmitoyltransferases such as ZDHHC5, ZDHHC7 and ZDHHC9 mediate GSDMD palmitoylation to induce pyroptosis, cellular levels of palmitoyltransferases and their regulation might be important for granulosa cells pyroptosis in the context of PCOS. Here, transcript levels of ZDHHC protein palmitoyltransferases in granulosa cells were compared between PCOS and non-PCOS women using publicly available transcriptomics datasets. Among 23 ZDHHC palmitoyltransferases, it was found that mRNA levels of ZDHHC6, ZDHHC18 and ZDHHC24 are significantly increased in granulosa cells from PCOS patients compared to those from non-PCOS women. In contrast, transcript levels of one ZDHHC palmitoyltransferase, ZDHHC2, were observed to be decreased in granulosa cells isolated from the ovaries of women with PCOS compared to those from non-PCOS women. Since palmitoylation of GSDMD has been found to be required for its membrane translocation and oligomerization, the identification of palmitoyltransferases for GSDMD palmitoylation in granulosa cells might be of high clinical importance to limit pyroptotic death of granulosa cells and inflammation in PCOS. Since chronic low-grade inflammation is also observed in women with PCOS, palmitoyltransferase-targeting therapies might have potential to limit inflammation by supressing pro-inflammatory death of granulosa cells in the ovary.

Keywords: palmitoyltransferase, granulosa cells, PCOS, pyroptosis, palmitoylation, inflammation

ORAL PRESENTATION

Synthesis, characterization and investigation of aggregation properties of non-peripheral octa-substituted Nickel(II), Zinc(II) Copper (II) phthalocyanines

Hüseyin Baş[1] (https://orcid.org/0000-0002-8722-3359),
Zekeriya Biyiklioglu[1] (https://orcid.org/0000-0001-5138-214X),

[a]Karadeniz Teknik Üniversitesi, Fen Fakültesi Kimya Bölümü, 61080 TRABZON

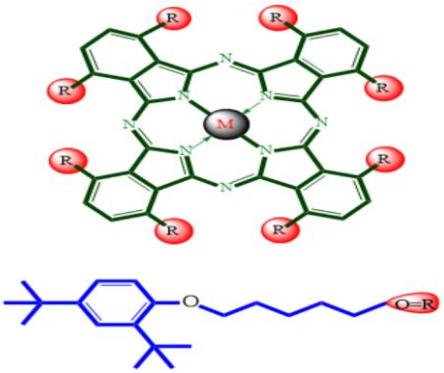
*Corresponding author e-mail: huseyinbas@ktu.edu.tr

Abstract

Metallophthalocyanines (MPcs) are 18-π electron macrocyclic structures composed of four isoindole units. Phthalocyanines (Pb) are used in many areas due to their stability, excellent electronic properties, architectural flexibility, chemical-physical properties and spectroscopic properties [1]. Initially utilized as dyes and pigments due to their distinctive blue-green hues, phthalocyanine compounds have evolved into significant entities extensively researched across various domains, including catalysis, liquid crystals, dye-sensitized solar cells, photocatalysis, energy storage, electrochemistry, gas sensors, optical data storage, supercapacitor electrode materials, enzyme inhibitors, and photodynamic cancer therapy, attributable to their exceptional thermal, physical, and chemical stability. [2] The interest for Pc-based materials lies in the fact that they are one of the most important π-conjugated molecules and many of their properties can be adjusted by different peripheral substituents introduction and changes of the central metal ion [3]. However, the limited solubility of phthalocyanines in water and organic solvents and their high tendency to aggregation are the most significant factors that reduce their applicability in these areas. In this study, non-peripheral octa-substituted Ni (II), Zn (II), and Cu (II) phthalocyanines were synthesized and their aggregation properties were investigated.

Keywords: Synthesis, octa phthalocyanine, non-aggregating

*This work was supported by KTU-BAP (13) (Project No: 16115).



M= Ni, Zn, Cu

References:
[1] Saka, E, T., Göl, C., Durmuş, D., Kantekin, H., Bıyıklıoğlu, Z., Photophysical, photochemical and aggregation behavior of novel peripherally tetra-substituted phthalocyanine derivatives. Journal of Photochemistry and Photobiology A: Chemistry 241 (2012) 67–78. http://dx.doi.org/10.1016/j.jphotochem.2012.05.023.
[2] Penlik, Y., Avcıata, O., Gördük, S., Photophysicochemical and Aggregation Studies of Highly Soluble Zn(II) and Mg (II) Phthalocyanine Compounds based on Tinuvin-326, Journal of Molecular Structure, in press. https://doi.org/10.1016/j.molstruc.2025.144285.
[3] Bilen, B. S., Özçeşmici, M., Koçyiğit, N., Elgün, T., Yurttaş, A. G., Hamuryutan, E., Glycosylated zinc(II) phthalocyanine photosensitizer: Synthesis, photophysical properties and in vitro photodynamic activity on breast cancer cell line, Journal of Molecular Structure 1295 (2024) 136688. https://doi.org/10.1016/j.molstruc.2023.136688.

ORAL PRESENTATION

COVID-19'da IL6 ve TMPRSS11A polimorfizmlerinin genotip kombinasyonları ile hastalık şiddeti arasındaki bağlantı

Nilgün Çekin

Sivas Cumhuriyet Üniversitesi, Tıp Fakültesi, Tıbbi Biyoloji Anabilim Dalı, Sivas, Türkiye

Sorumlu yazar e-mail: nilgun_cekin@yahoo.com

Özet

COVID-19 hastalığının klinik seyri bireyler arasında büyük farklılıklar göstermektedir. Bu farklılıklarda genetik varyasyonların önemli rol oynadığı düşünülmektedir. IL6, proinflamatuvar sitokin yanıtını artırarak sitokin fırtınasına ve çoklu organ hasarına yol açabilmektedir; TMPRSS11A ise SARS-CoV-2'nin hücreye girişinde spike proteininin proteolitik aktivasyonu yoluyla hastalık şiddetini etkileyebilmektedir. Bu çalışmada, IL6 (rs1800795, rs1800796) ve TMPRSS11A (rs353163, rs977728) gen polimorfizmlerinin ve bunların genotip kombinasyonlarının Türk toplumunda COVID-19 şiddeti ve klinik parametrelerle ilişkisi araştırılmıştır. Çalışmaya 84 kontrol, 80 orta şiddette COVID-19 (MC-19) ve 168 şiddetli COVID-19 (SC-19) olgusu dahil edilmiştir. Genotipleme PCR-RFLP yöntemi ile yapılmış; dört polimorfizmin gruplar arası dağılımları ve genotip kombinasyon frekanslarının klinik parametrelerle olası ilişkileri analiz edilmiştir. Genotip kombinasyon analizlerinde, özellikle IL6 ve TMPRSS11A polimorfizmlerini birlikte taşıyan kombinasyonlarda (ör. GC/GC/TC/CT ve CC/CC/CC/CT), CRP >200 mg/L, Ferritin >600 ng/mL, hsTroponin >5000 ng/L ve D-dimer >6000 µg/L seviyelerine ulaşıldığı görülmüştür. Bu durum inflamasyon, koagülopati ve kardiyak komplikasyon riskinin genetik varyasyonlarla arttığını göstermektedir. IL6 ve TMPRSS11A polimorfizmleri ve bunların kombinasyonları, COVID-19 şiddetinin yanı sıra sistemik inflamasyon ve organ hasarını gösteren biyobelirteçlerle anlamlı ilişki göstermektedir. Bu bulgular, COVID-19 klinik seyrinde genetik belirteçlerin risk öngörüsü ve kişiselleştirilmiş tedavi yaklaşımlarında kullanılabileceğini desteklemektedir.

Anahtar Kelimeler: COVID-19, IL-6, TMPRSS11A, polimorfizm, genotip kombinasyonları, Türk popülasyonu

ORAL PRESENTATION

Mardin'de unutulmaya yüz tutmuş gastronomik bir değerin incelenmesi ve duyusal analiz ile değerlendirilmesi

Tacettin EROL[1] (https://orcid.org/0009-0006-8294-7274),
Sena BAKIR[1*] (https://orcid.org/0000-0002-6258-1969

[1]Recep Tayyip Erdoğan Üniversitesi, Ardeşen Turizm Fakültesi, Gastronomi ve Mutfak Sanatları Bölümü, Rize, Türkiye.

Sorumlu yazar e-mail: sena.bakir@erdogan.edu.tr

Özet

Bu çalışma, Mardin ilimizin tarihsel ve kültürel birikimi içerisinde yer alan, ancak zamanla unutulmaya yüz tutmuş geleneksel bir yemek olan Hupık yemeğinin tespit edilmesi, kayıt altına alınması ve gastronomi bilimine kazandırılması amacıyla gerçekleştirilmiştir. Mardin, birçok medeniyete ev sahipliği yapmış olması nedeniyle çok zengin bir mutfak kültürüne sahiptir. Ancak sözlü kültürle aktarılan bazı yemeklerin yazılı kaynaklarda yer almaması, bu değerlerin zamanla kaybolmasına neden olmaktadır. Bu çalışmanın ilk aşamasında Mardin'in Mazıdağı ilçesine bağlı Ulutaş Köyü ziyaret edilerek yerel halkla doğrudan temas kurulmuştur. Köy muhtarının desteğiyle, *Hupık* yemeğini bilen ve hazırlayan gönüllü katılımcılara ulaşılmıştır. Katılımcılar yemeğin üç farklı şekilde tüketildiğini belirtimişlerdir ve katılımcılardan alınan bilgiler ışığında yemeğin reçetesi oluşturulmuştur. Çalışmanın ikinci aşamasında ise Gastronomi ve Mutfak Sanatları Bölümü uygulama mutfağında ürünler tekrar üretilmiş olup duyusal analiz konusunda yarı eğitimli panelistlerin bulunduğu bir panelde değerlendirilmişlerdir. Mardin yöresine ait bir yemek olan Hupık yemeğini deneyen panelitsler ürünleri derecelendirilmiş bir skalada renk, görünüş, tat, koku ve genel beğeni açısından değerlendirmiştir. Bu çalışma kültürel mirasın korunması, gastronomi alanında sürdürülebilirlik sağlanması ve bu sürdürülebilirliğin gıda bilimi ile ilişkilendirilmiş olması açısından önem arz etmektedir.

Anahtar kelimeler: Mardin yemek kültürü, sürdürülebilirlik, duyusal değerlendirme

ORAL PRESENTATION

Bir Alman çoban köpeğinde tek yavru sendromuna (single pup syndrome) bağlı olarak şekillenen güç doğum olgusu

Ahmet Gözer* (https://orcid.org/0000-0001-8658-5916)

* Hatay Mustafa Kemal Universitesi, Veteriner Fakültesi, Doğum ve Jinekoloji Anabilim Dalı, Hatay, Turkiye

Sorumlu yazar e-mail: ahmetgozer@mku.edu.tr

Özet

Bu olgu sunumunun materyalini Alman Çoban Köpeği ırkı gebe bir köpekte görülen tek yavru sendromuna bağlı olarak şekillenen güç doğum olgusu oluşturdu. Alınan anamnez bilgilerinde köpeğin 67 gün önce çiftleştiği ve kliniğimize başvurmadan bir gün önce koyu renkli, yoğun, kokusuz, damla damla şekilde bir vaginal akıntının geldiği ancak doğuma ilişkin herhangi bir belirtinin olmadığı öğrenildi. Yapılan fiziksel muayenelerde hayvanın genel durumunun iyi olduğu, tam kan sayımında nötrofili ve lenfopeni tespit edildi. Biyokimya parametrelerinde normal aralıklardaydı. Transabdominal ultrasonografik muayenede abdomende tek bir yavrunun olduğu, kalp atımının olmadığı ve yavru sularının azaldığı tespit edildi. Abdominal radyografik muayenelerde ise posterior prezentasyonda dorsalumbal pozisyonda olan tek bir fetüs tespit edildi. Olgunun köpeklerde riskli bir gebelik olarak sınıflandırılan tek yavru sendromu olduğu tespit edildi ve sezaryen operasyonuna karar verildi. Sezaryen operasyonu sonrası yavrunun ölü olduğu görüldü. Operasyon sonrası annede herhangi bir postoperatif komplikasyonla karşılaşılmadı. Sonuç olarak köpeklerde tek yavru sendromuna bağlı olarak güç doğum olgularının şekillenebileceği ve sezaryen opersayonlarının olgunun yönetiminde endike olduğu kanısına varıldı.

Anahtar Kelimeler: Köpek, tek yavru sendromu, güç doğum

ORAL PRESENTATION

Investigation of the mechanical and antioxidant properties of bioactive wound dressings containing grape seed oil

Hayrunnisa Kaya[1] (ORCID: https://orcid.org/0000-0002-8195-0942), Pınar Terzioğlu[2] (ORCID: https://orcid.org/0000-0003-4114-7044), Yusuf Sıcak[3] (ORCID: https://orcid.org/0000-0003-2339-5837), Rasim Alper ORAL[4] (ORCID: https://orcid.org/ 0000-0001-7530-7478)

[*1]Bursa Technical University, Faculty of Engineering and Natural Sciences, Department of Biotechnology, Bursa, Türkiye.
[2]Bursa Technical University, Faculty of Engineering and Natural Sciences, Department of Polymer Materials Engineering, Bursa, Türkiye.
[3]Muğla Sıtkı Koçman University, Köyceğiz Vocational School, Department of Herbal and Animal Production, Muğla, Türkiye
[4]Bursa Technical University, Faculty of Engineering and Natural Sciences, Department of Food Engineering, Bursa Türkiye.

*Corresponding author e-mail: hayrunnisakaciranlar@gmail.com

Abstract

Although traditional wound dressings are widely used, they often suffer from drawbacks such as inadequate infection control and limited ability to promote healing, often leading to chronic inflammation. To overcome these limitations, bioactive films have emerged as promising multifunctional materials, suitable for applications in wound dressings, cosmetics, and dermatological products. These dressings can be formulated with diverse materials and bioactive agents that actively influence and enhance the wound-healing process. Among bioactive agents, plant derived therapeutics such as plant extracts are widely used in the development of bioactive films. Grape seed oil (GSO), abundant in unsaturated fatty acids, is widely recognized for its potent antioxidant, anti-inflammatory, moisturizing and acne healing abilities. The present study aims to produce bioactive polymeric films containing various concentrations of GSO (1-4 %) for potential wound dressing applications. The solvent casted bioactive films were subjected to FT-IR analysis, mechanical and antioxidant tests. The amount of GSO effected the physical and antioxidant properties of chitosan (CS)/sodium alginate (SA) films. As the GSO concentration in GSO/CS/SA films increased, the antioxidant capacity of the films also increased. Higher GSO concentration caused significantly reduced tensile strength ($p < 0.05$) compared to neat CS/SA film. Overall, the results proposed the grape seed oil incorporated films as encouraging bioactive wound dressing materials for accelerating the healing of skin wounds.

Keywords: Biocomposite films, grape seed oil, sodium alginate, chitosan, wound healing.

ORAL PRESENTATION

Çeşitli analitlerin eş zamanlı tayini için elektrokimyasal sensörler

Merve Yilmaz Çilçar* (ORCID: https://orcid.org/0000-0003-3690-2455.)

*1Çankırı Karatekin Üniversitesi, Fen Fakültesi, Kimya Bölümü, Çankırı, Türkiye

*Sorumlu yazar e-mail: mrve0891@gmail.com

Özet

Son on yılda elektrokimyasal yöntemlerin geliştirilmesi ve teknolojik ilerlemeler sayesinde eş zamanlı elektrokimyasal tayin çalışmaları göze çarpmaktadır. Günümüzde bileşiklerin ayrı ayrı elektrokimyasal tayininin yerini, iki ya da daha fazla analitin birlikte tayin edildiği elektrokimyasal yöntemler almıştır [1]. Eş zamanlı tayin, biyolojik sıvılarda, dokularda ve çevrede bulunan hastalıkların, patojenlerin veya toksik maddelerin kısa sürede kapsamlı bir şekilde izlenmesine katkıda bulunabilmektedir. Eş zamanlı tayin, zaman ve maliyet açısından önemli avantajlar sağlamaktadır. Eş zamanlı tayinlerde optik ve voltametrik yöntemler kullanılmaktadır. Analitlerin eş zamanlı tayinleri için hızlı, pratik ve düşük maliyetleri nedeniyle sıklıkla elektrokimyasal yöntemler tercih edilmektedir [2]. Yüksek duyarlılık, düşük tespit sınırı, ön işlem gerektirmeyen doğrudan biyolojik örnek analizi ve kısa analiz süresi gibi özellikleri sayesinde voltametrik yöntemler (dönüşümlü voltametri, diferansiyel puls voltametri vd.), diğer elektroanalitik tekniklere göre öne çıkmaktadır [2]. Literatürde geliştirilen eş zamanlı elektrokimyasal sensörler, dopamin, serotonin, epinefrin ve norepinefrin gibi nörotransmiterlerin, ürik asit, askorbik asit, NADH gibi biyolojik numunelerde sıklıkla bulunan analitlerin ve katekol, o-kinon ve rezorsinol gibi zararlı kirleticilerin tayinine yöneliktir [1]. Bu çalışmada, çeşitli analitlerin eş zamanlı tespiti için geliştirilen elektrokimyasal sensörlerdeki son gelişmeler ele alınmıştır.

Anahtar kelimeler: Eş zamanlı tayin, elektrokimyasal sensör, voltametrik metotlar

Referanslar:

[1] Jadon, N., Jain, R., Sharma, S., & Singh, K. (2016). Recent trends in electrochemical sensors for multianalyte detection–A review. *Talanta*, *161*, 894-916.

[2] Baranwal, J., Barse, B., Gatto, G., Broncova, G., & Kumar, A. (2022). Electrochemical sensors and their applications: A review. *Chemosensors*, *10*(9), 363.

ORAL PRESENTATION

Farklı fasulyeler ile üretilen cipslerde tüketici beğenisinin değerlendirilmesi

İbrahim Temiz[1] (https://orcid.org/0009-0001-9027-435X), Tahsin Can Tunçay[1] (https://orcid.org/0009-0008-9448-2261), Sena Bakır [1*] (https://orcid.org/0000-0002-6258-1969)

[*1]Recep Tayyip Erdoğan Üniversitesi, Ardeşen Turizm Fakültesi, Gastronomi ve Mutfak Sanatları Bölümü, Rize, Türkiye.

Sorumlu yazar e-mail: sena.bakir@erdogan.edu.tr

Özet

Atıştırmalık gıda tüketimi günümüzde oldukça revaçtadır. Bu ürünler arasında cipsler büyük bir yer kaplamakta, özellikle patates ve mısır içeren cipsler çokça tercih edilmektedir. Bu çalışma, tüketicilerin tekdüze lezzetler yerine yeni ürünleri deneyimlemesi, bununla birlikte atıştırmalıklar arasına sağlıklı sayılabilecek özellikteki grupların eklenmesi düşüncesi ile tasarlanmıştır. Bilindiği üzere baklagiller arasında bulunan fasulye; proteinler, çeşitli vitamin ve mineraller açısından değerlidir. Çalışma kapsamında önerilen ürün formülasyonunda siyah, kırmızı ve beyaz (normal) fasulyeler ayrı ayrı gruplandırılarak haşlanmış ve her bir grup içerisine eşit miktarda zeytinyağı, tuz, sarımsak, toz kırmızı biber ve kekik eklenerek çeşnilendirilmiştir. Hazırlanan cips hamurları kalıp yardımıyla şekillendirilmiş ve fırın tepsisine aktarılmıştır. Ürün pişirme aşamasında fırınlama yöntemi tercih edilerek hazırlanan ürünlerin yağ içeriğinin değişmemesi hedeflenmiştir. Ürünlerin pişirilmesini takiben, yarı eğitimli panelistlerin olduğu bir panel grubu ile ürünlerin duyusal özellikleri görünüm, doku, aroma, koku ve genel beğeni açısından değerlendirilmiştir. Tüketici testlerinde fasulyenin cips üretiminde iyi bir alternatif olabileceği, farklı baharatlar ile istenen cips aromasının oluşturulabileceği, böylelikle sağlıklı atıştırmalıklar kategorisine yeni bir ürün ilave edilebileceği görülmüştür.

Anahtar kelimeler: Fasulye cipsi, fonksiyonel gıda, duyusal değerlendirme

ORAL PRESENTATION

Assessment of calibration techniques for the determination of cadmium at different levels in sage and rosehip tea samples by flame atomic absorption spectrometry

Selin Tuana Aydın[1] (ORCID: https://orcid.org/0009-0009-8447-5890), Hakan Serbest[2*] (ORCID: https://orcid.org/0000-0003-2303-0408)

[1]İstanbul Health and Technology University, Faculty of Engineering and Natural Sciences, Department of Chemical Engineering, İstanbul, Türkiye.
[*2]Mimar Sinan Fine Arts University, School of Conservation and Restoration of Cultural Property, Department of Conservation and Restoration of Cultural Property, İstanbul, Türkiye.

*Corresponding author e-mail: hakan.serbest@msgsu.edu.tr

Abstract

Cadmium **(**Cd^{2+}) is a potentially toxic element, and its compounds cause various disruptions to human health and ecosystems. It has been reported that Cd^{2+} causes bioaccumulation by entering living metabolism through various environmental pathways and the food chain. Therefore, the determination of Cd^{2+} with high accuracy in these matrices for human consumption is of great importance. On the other hand, the interference effects from the matrix cause a significant limitation on the accuracy of the measurement results. In this study, Cd^{2+} was determined in sage and rosehip samples with high accuracy and sensitivity by flame atomic absorption spectrometry (FAAS) using different calibration techniques. The analytical performance values such as limit of detection, limit of quantitation, dynamic linear range, regression coefficient and percent relative standard deviation were assessed under optimal operating conditions with aqueous Cd^{2+} solutions at varying concentrations. Recovery studies were performed on sage and rosehip tea matrices to verify the reliability of the FAAS measurements. The recoveries were recorded between 96.5% and 101.9% for sage tea and between 97.6% and 101.0% for rosehip tea utilizing the matrix matching calibration. It was demonstrated that the proposed analytical approaches can be applied to the determination of Cd^{2+} with high accuracy in herbal teas frequently consumed in daily life, as well as to obtain reliable results in routine food analysis.

Keywords: Herbal tea, flame atomic absorption spectrometry, cadmium

ORAL PRESENTATION

Effect of St. John's wort and coconut oil blends on the structural and thermal properties of protein-based films for potential biomedical applications

Mehlika Karamanlioglu[1*] (https://orcid.org/0000-0002-4814-6346)

[*1]Istanbul Gelisim University, Vocational School of Health Services, Biomedical Device Technology Department, İstanbul, Türkiye.

*Corresponding author e-mail: mkaramanlioglu@gelisim.edu.tr

Abstract

There are a limited number of studies on the use of protein-based films containing different oil blends, particularly in the biomedical field as wound dressing materials. Therefore, this study aims to investigate the effects of St. John's Wort oil (JWO) on the material properties of gelatin-based films containing coconut oil (CO) for potential wound dressing applications. For this purpose, equal percentages of JWO and CO were incorporated into the film-forming solution of gelatin. Homogeneous and transparent films were obtained using the solution casting method. Structural changes were observed by Fourier Transform Infrared Spectroscopy (FTIR), indicating the presence of fatty acids from CO and JWO in the gelatin matrix, with an increased peak amplitude at 1740 cm^{-1}. Moreover, the amplitude of the peak at 2853 cm^{-1}, related to C–H stretching, decreased in films containing JWO. Scanning Electron Microscopy (SEM) analyses revealed embedded oil droplets on the surface of the blended films. Differential Scanning Calorimetry (DSC) analyses showed that the addition of JWO increased the glass transition temperature from 72°C to 75°C, thereby improving the thermal properties of the gelatin films. Water aging behaviour of the gelatin films containing oil blends also improved by more than 8%. This study demonstrates that CO and JWO blends can be successfully incorporated into gelatin matrices, which can be further developed into low-cost, durable, thermally stable primary wound dressing materials for acute wounds using natural ingredients.

Keywords: St. John's Wort oil, Coconut oil, Gelatin, Biomedical, Structural, Thermal.

ORAL PRESENTATION

Fumigant toxicity of *Clinopodium serpyllifolium* subsp. *serpyllifolium* essential oil against different larval stages of *Tenebrio molitor* (Coleoptera: Tenebrionidae)

Duygu Bekircan Eski[1*] (https://orcid.org/0000-0002-3088-3567), Cihan Darcan[2] (ORCID: https://orcid.org/0000-0003-0205-3774), Ardahan Eski[3,4] (https://orcid.org/0000-0002-9621-2854)

[*1]Bilecik Seyh Edebali University, Graduate School, Department of Biotechnology, Bilecik, Türkiye.
[2]Bilecik Seyh Edebali University, Faculty of Science, Department of Molecular Biology and Genetics, Bilecik, Türkiye
[3]Bilecik Seyh Edebali University, Vocational School, Department of Biomedical Equipment Technology, Bilecik, Türkiye.
[4]Bilecik Seyh Edebali University, Central Research Laboratory Application and Research Centre, Bilecik, Türkiye.

*Corresponding author e-mail: d_bekircan@hotmail.com

Abstract

Synthetic insecticides have long been used to manage major agricultural pests. However, increasing public concern over the potential environmental risks associated with the extensive use of conventional insecticides has prompted the search for alternative pest control strategies. Essential oils derived from aromatic plants are considered promising alternatives due to their diverse biological activities, biodegradability, and minimal impact on non-target organisms and the environment. In this study, the essential oil of *Clinopodium serpyllifolium* subsp. *serpyllifolium* was extracted using a solvent-free microwave extraction method, and its chemical composition was analyzed by GC–MS. The fumigant toxicity of the essential oil was evaluated against different larval stages of *Tenebrio molitor*. Five concentrations (2, 4, 8, 16, and 32 µL/L) of the essential oil were tested for toxicity. For each larval stage tested, the mortality rate increased with higher concentrations. Early larval stage was more susceptible compared to the medium and late larval stages. Based on Probit analysis, the LC_{50} value for the early larval stage was determined to be 6.59 µL/L, while for the medium and late larval stages, it was 12.48 µL/L and 18.84 µL/L, respectively. The results indicate that the essential oil exhibits fumigant toxicity against *T. molitor* larvae, with higher efficacy particularly at the early larval stages. Therefore, targeting the early larval instars of the pest may lead to more effective control.

Keywords: Essential oil, Aromatic plant, Solvent-free microwave extraction, GC–MS, *Tenebrio molitor*, Fumigant toxicity

ORAL PRESENTATION

Synergistic antioxidant effect of squalene and saponin in a d-galactose-induced aging model

Büşra Börekci[1] (ORCID: https://orcid.org/0000-0003-0480-3460), Kubra Sener[2] (ORCID: https://orcid.org/0000-0002-8759-9444), Elif Naz Gürsoy[2] (ORCID: https://orcid.org/0000-0003-4946-1185), Şule Coşkun Cevher[2*] (ORCID: https://orcid.org/0000-0001-6204-2845).

[*1]Gazi University, Graduate School of Natural and Applied Sciences, Department of Biology, Ankara, Türkiye.
[2] Gazi University, Faculty of Science, Department of Biology, Ankara, Türkiye.

*Corresponding author e-mail: sule@gazi.edu.tr

Abstract

Aging is a multifactorial biological process strongly associated with oxidative stress, which results from an imbalance between the generation of reactive oxygen species and the antioxidant defense system. This imbalance contributes to lipid peroxidation, protein oxidation, and depletion of endogenous antioxidants, thereby promoting structural and functional deterioration in vital organs such as the liver and kidney. In this study, we investigated the potential protective and therapeutic effects of squalene (SQ) and saponin (SP), administered individually and in combination, in a D-galactose-induced aging model. Forty-eight male Sprague-Dawley rats were randomly assigned to control, D-galactose, SQ, SP, and combination groups. Aging was induced by intraperitoneal injection of D-galactose (300 mg/kg/day) for six weeks, and SQ (2.66 mL/kg/day) and SP (100 mg/kg/day) were administered orally, either alone or together. At the end of the experimental period, liver and kidney tissues were collected, and malondialdehyde (MDA), a biomarker of lipid peroxidation, and glutathione (GSH), a central antioxidant molecule, were measured spectrophotometrically. D-galactose administration significantly increased MDA levels and decreased GSH concentrations in both liver and kidney tissues compared to controls ($p<0.05$). Treatment with either SQ or SP reversed these alterations, while the combined administration demonstrated the most pronounced reduction in MDA and elevation in GSH levels, indicating a synergistic antioxidant effect. The results suggest that oxidative stress plays a central role in aging-related hepatic and renal dysfunction, and that supplementation with SQ and SP may enhance antioxidant defense and mitigate oxidative damage. Importantly, the combined treatment was more effective than individual applications, supporting the potential of SQ and SP as complementary agents in strategies aiming to attenuate oxidative stress-associated aging processes.

Keywords: Aging, Saponin, Squalene, D-galacatose, Antioxidant

Acknowledgment: This research was supported by Gazi University Scientific Research Projects (BAP), Ankara, Türkiye. (Project Number: FYL-2023-8665).

ORAL PRESENTATION

Identification of novel miRNAs in tobacco (*Nicotiana tabacum* L.) targeting black shank and powdery mildew genome

Cihan Kucukyilmaz[1*](ORCID: https://orcid.org/0009-0005-9284-8651),
Sevgi Marakli[2] (ORCID: https://orcid.org/0000-0001-5796-7819)

*[1]Yildiz Technical University, Graduate School of Science and Engineering, Program of Molecular Biology and Genetics, Istanbul, Türkiye
[2]Yildiz Technical University, Faculty of Arts and Sciences, Molecular Biology and Genetics Department, Istanbul, Türkiye

*Corresponding author e-mail: cihankucukyilmazz@gmail.com

Abstract

Tobacco (*Nicotiana tabacum* L.), belonging to the *Solanaceae* family, is widely cultivated for the production of nicotine-containing products. Moreover, tobacco is a model organism for molecular biology and genetics due to its well-characterized genome and high transformation efficiency. Tobacco production is severely threatened by various fungal and oomycete pathogens, which can lead to substantial yield and quality losses. Among these, black shank caused by *Phytophthora nicotianae*, and powdery mildew caused by *Golovinomyces cichoracearum* or *Erysiphe cichoracearum* are two of the most destructive diseases affecting tobacco worldwide. MicroRNAs (miRNAs) with 20-24 nucleotides in length are important post-transcriptional gene expression regulators. In this study, novel miRNAs found in tobacco genome targeting powdery mildew and black shank were identified by using *in silico* analyses. For this purpose, reference miRNAs were obtained from mirBase database and they were blasted against tobacco genome (taxid: 4097) in NCBI. Then, the secondary stem-loop hairpin structures of the potential target miRNAs were constructed by using RNAfold Web Server. The RNAhybid program was used to identify miRNAs targeting a total of 65 genes related to black shank disease (rps10, nad9, rns, tRNA-Met3(cat), tRNA-Asn(gtt), atp8, etc.) and even a gene (AXI65_gp1) responsible for powdery mildew disease. As a result, we determined 76 novel miRNAs for black shank and 15 novel miRNAs for powdery mildew. This study provides valuable information for the production of resistant tobacco plants as well as a promising new viewpoint on tobacco miRNAs that target powdery mildew and black shank.

Keywords: Epigenetics, miRNA, gene expression regulation, *in silico* analyses

ORAL PRESENTATION

Cuscuta epithymum ekstresinin fenolik içeriği ile biyoaktivitelerinin belirlenmesi

Bihter Şahin[1*] (ORCID: https://orcid.org/0000-0001-8657-052X),
Yağmur Güney[2] (ORCID: https://orcid.org/0009-0004-7173-4279)

[1, 2] Bandırma Onyedi Eylül Üniversitesi, Susurluk Tarım ve Orman Meslek Yüksekokulu, Kimya ve Kimyasal İşleme Teknolojileri Bölümü, 10600, Balıkesir, Türkiye

* Sorumlu yazar e-mail: bsahin@bandirma.edu.tr

Özet

Cuscuta epithymum Murr. (*C. epithymum*) Convolvulaceae familyasına ait holoparazit bir bitkidir; Fars tıbbında Aftimoon olarak bilinir. Ayrıca delilik ilacı anlamına gelen Dava Aljonoon olarak da adlandırılır, ancak yaygın olarak Dodder veya Kekik dodder olarak bilinir. Çalışmamızda Balıkesir'in yüksek yerlerinden toplanan *C. epithymum* topraküstü kısımlarından soxhlet aparatı yardımıyla elde edilen etanol ekstresinin fenolik bileşenleri ise HPLC-DAD cihazı yardımıyla belirlendi. Uygulanan fenolik metodunda 41 adet fenolik standart madde ile kıyaslaması yapılarak tespit edilen bileşenlerin konsantrasyonları hesaplandı. *C. epithymum*'dan alınacak olan farklı etanol ekstresinin DPPH, ABTS, CUPRAC ve β- Karoten linoleik asit deneyleri olmak üzere 4 farklı metot ile antioksidan aktiviteleri Elisa reader cihazı yardımıyla belirlendi. Aktivite sonuçları karşılaştırılıp konsantrasyonları hesaplandı. Bu çalışmanın amacı, Türkiye'de sebze olarak tüketilen yabani yenilebilir *C. epithymum* etanol ekstresinin fenolik içeriklerini ve antioksidan aktivitelerini değerlendirmektir. Elde edilen ekstrelerin fenolik içerikleri 4 farklı metot ile antioksidan kapasiteleri hesaplandı. Antikolinesteraz, α-Amilaz ve α-Glukosidaz enzim inhibisyon aktiviteleri belirlendi. Yapmış olduğumuz çalışmalardan elde etmiş olduğumuz sonuçlar neticesinde ileriki safhada kromatografik olarak yapılacak olan izolasyon çalışmalarının ve sitotoksik aktivite çalışmalarının yapılması için altyapı oluşturacaktır.

Anahtar Kelimeler: *Cuscuta epithymum*, Fenolik içerik, Antioksidan aktivite, Enzim inhibisyon aktivite.

Teşekkür: Bu çalışmanın bir kısmı 2022/2 yılında 2209-A Üniversite Öğrencileri Araştırma Projelerini Destekleme Programı kapsamında 1919B012414344 nolu proje ile TÜBİTAK tarafından desteklenmiştir.

ORAL PRESENTATION

Determination of total phenolic, flavonoid content, and antioxidant activity of rose of jericho (*Anastatica hierochuntica*)

Ece Aydin[1*](ORCID: https://orcid.org/0000-0002-1366-8902),
Sevgi Marakli[2] (ORCID: https://orcid.org/0000-0001-5796-7819)

*[1]Yildiz Technical University, Graduate School of Science and Engineering, Program of Molecular Biology and Genetics, Istanbul, Türkiye
[2]Yildiz Technical University, Faculty of Arts and Sciences, Molecular Biology and Genetics Department, Istanbul, Türkiye

*Corresponding author e-mail: ece.aydin2@std.yildiz.edu.tr

Abstract

Anastatica hierochuntica, commonly known as the resurrection plant or Rose of Jericho, is a desert species renowned for its remarkable tolerance to extreme abiotic stress conditions, such as drought, salinity, and high temperature. In addition to being rich in bioactive compounds, including flavonoids and phenolics, *A. hierochuntica* demonstrates significant antioxidant, antimicrobial, and antiinflammatory properties. Recent studies have highlighted its potential applications in agriculture as a natural biostimulant and in medicine as a source of novel therapeutic agents. In this study, we investigated the phenolic, flavonoid, and antioxidant activity (IC50) of *A. hierochuntica*. Three solvents (50% ethanol, 50% methanol, and 50% isopropanol) were used for extraction. Then, the Folin-Ciocalteu method, $AlCI_3$, and DPPH methods were used for analyses, respectively. The experiment was repeated three times. Ethanol extracts showed that total phenolic content was 43.546 ± 10.556 mgGAE/g, the flavonoid content was 3.248 ± 0.602 mgQE/g, and the antioxidant activity was 2.739 mgVCE/100g. We also determined that the total phenolic content was calculated as 27.369 ± 4.567 mgGAE/g, the flavonoid content as 1.002 ± 0.555 mgQE/g, and the antioxidant activity as 1.418 mgVCE/100g in methanol extracts. Moreover, these concentrations were 58.277 ± 19.909 mgGAE/g, 4.556 ± 0.853 mgQE/g, and 3.306 mgVCE/100g, respectively, in isopropanol extracts. Our findings can advance knowledge of this plant's bioactive profile and possible uses in the future, particularly in antibacterial and agricultural research.

Keywords: Rose of Jericho, IC50, Folin-Ciocalteu method, $AlCI_3$ and DPPH

ORAL PRESENTATION

Construction of RuCo decorated poly(2-hydroxy methacrylamide) polymer brush grafted magnetic nanoparticles as a heterogeneous catalyst for degradation of some azo dyes.

Necdet Karakoyun[1*] (ORCID:https://orcid.org/0000-0002-6083-6921)

[*1] Van Yüzüncü Yıl University, Muradiye Vocational School, Chemistry and Chemical Processing Technologies Department, 65080 Van, Turkey.

*Corresponding author e-mail: necdetkarakoyun@yyu.edu.tr

Abstract

In this study, RuCo-decorated poly(2-hydroxy methacrylamide) [p(2-HMAAm)] polymer brush grafted magnetic nanoparticles were synthesized and evaluated as a heterogeneous catalyst for the degradation of some azo dyes. The nanocomposite was prepared through a surface-initiated polymerization technique, followed by the immobilization of bimetallic Ru and Co nanoparticles onto the magnetic polymer support. Structural and morphological analyses confirmed the successful formation of the polymer-coated magnetic core and the uniform distribution of metal nanoparticles. The catalytic activity of RuCo/p(2-HMAAm)/Fe_3O_4 was examined for the reduction of representative azo dyes in aqueous media under mild conditions. The reaction followed pseudo-first-order kinetics, showing high catalytic efficiency compared with similar catalysts reported in the literature. The improved performance was attributed to the synergistic interaction between Ru and Co nanoparticles and the high accessibility of active sites provided by the polymer brush structure. Additionally, the catalyst exhibited excellent magnetic recoverability and could be reused several times without significant loss of activity, indicating strong structural stability and recyclability. These results demonstrate that the RuCo/p(2-HMAAm)/Fe_3O_4 nanocomposite is an efficient, magnetically separable, and environmentally friendly catalyst for the degradation of azo dyes and the purification of dye-contaminated wastewater.

Keywords: RuCo nanoparticles, polymer brush, magnetic nanocomposite, azo dye degradation, heterogeneous catalysis, environmental remediation

ORAL PRESENTATION

Predicting polymer–drug compatibility for queuine and gemcitabine via molecular simulations

Mohamed Amjad Alhamwi [1] (ORCID: https://orcid.org/0009-0008-8902-6237),
Nigar Kantarcı Çarşıbaşı [1,2] (ORCID: https://orcid.org/0000-0003-1013-6668)

[1]Uskudar University, Graduate School of Science, Chemical Engineering Program, Istanbul, Türkiye.
[2]Uskudar University, Faculty of Engineering and Natural Sciences, Department of Chemical Engineering, Istanbul, Türkiye.

Abstract

In recent years, drug research has aimed to minimize the dosage and toxicity of cancer drugs while ensuring targeted drug delivery. To achieve this, pharmaceutical nanotechnology has gained importance, particularly in the application of anticancer drugs with polymeric encapsulations. Selecting a compatible polymeric carrier is pivotal for stable loading and controlled release of small-molecule therapeutics. In this study, a rapid, materials-oriented ***in silico*** workflow is presented to prescreen polymer–drug compatibility for Queuine and Gemcitabine**.** Amorphous cells of carriers (PEG, PGA, PLA, PLGA) and drug–polymer systems were simulated by 100 ns MD simulations to extract bulk descriptors such as Hildebrand solubility parameter**,** cohesive energy**,** and density**.** Based on these parameters, PGA and PLGA showed the smallest mismatch to both drugs, indicating favorable mixing behavior aligned with prior knowledge. This fast, reproducible computational workflow supports rational carrier selection before experimental formulation, helping boost success rates and reduce costs.

Keywords: molecular dynamics, drug formulation, polymeric drug delivery systems, queuine, solubility parameter, cohesive energy

ORAL PRESENTATION

Development and characterization of tannic acid crosslinked poly(vinyl alcohol) films

Nisan Yayla[1] (ORCID: https://orcid.org/0009-0006-3858-8841),
Işınay E. Yüzay[1,2*] (ORCID: https://orcid.org/0000-0002-0331-9020)

[1]Izmir University of Economics, Graduate School, Division of Bioengineering, Izmir, Türkiye
[2]Izmir University of Economics, Faculty of Engineering, Department of Genetics and Bioengineering, Izmir, Türkiye

*Corresponding author e-mail: isinayyuzay@gmail.com

Abstract

Poly(vinyl alcohol) (PVA) is a water-soluble and biodegradable polymer that has been widely utilized in biomedical, pharmaceutical, packaging, and environmental applications due to its good film-forming ability, chemical stability, biocompatibility, and non-toxicity. However, its high hydrophilicity and inadequate mechanical stability limit its usage in various applications. To overcome these drawbacks, crosslinking techniques are often employed to improve the structural integrity and stability of PVA-based materials. In this study, a PVA- based film was developed using tannic acid (TA), a naturally occurring, non-cytotoxic polyphenol, as a sustainable alternative to synthetic crosslinkers. The incorporation of TA as a natural crosslinking agent improved the functional performance of PVA films without relying on conventional chemical crosslinkers. TA molecules, with its abundant phenolic hydroxyl and catechol groups, interacts with PVA chains through hydrogen bonding and esterification reactions, forming a mechanically reinforced polymeric network. Fourier Transform Infrared Spectroscopy (FTIR) analysis confirmed the crosslinking interaction by showing a change in the –OH stretching band and the appearance of characteristic C=O absorption peaks. Mechanical characterization showed that TA incorporation increased tensile strength and slightly reduced elongation, indicating enhanced stiffness due to crosslinking. Water contact angle (WCA) measurements revealed a slight increase in hydrophobicity with increasing TA concentration, attributed to the reduced availability of free hydroxyl groups within the PVA matrix. Overall, the incorporation of tannic acid into PVA films provides a green crosslinking approach that enhances mechanical strength, structural integrity, and water resistance, demonstrating strong potential for use in biomedical and advanced packaging applications.

Keywords: Crosslinking, Poly(vinyl alcohol), Tannic acid, Mechanical properties, Natural crosslinkers

ORAL PRESENTATION

Eco-friendly synthesis and photocatalytic applications of zinc oxide nanoparticles (ZnO-NPs) using extract derived from agro-waste hawthorn (*Crataegus monogyna*)

Özlem Yilmaz Algül[1*], Ebru Kocadağ Kocazorbaz[1] (https://orcid.org/0000-0001-5611-5235)

[*1] Ege University, Faculty of Science, Department of Biochemistry, Izmir, TURKIYE.

*Corresponding author e-mail: ozlemyilmaz0719@gmail.com

Abstract

Research and development in green chemistry have gained considerable attention in recent years due to their potential to provide efficient, clean, cost-effective, and environmentally friendly processes that minimize toxic by-products. Within this framework, plant seed extracts have emerged as promising alternatives to conventional chemical stabilizing and reducing agents, particularly in nanoparticle synthesis, offering single-step, sustainable, and eco-friendly production routes. Seeds possess advantages such as low maintenance cost, independence from growth conditions, and rich bioactive compositions, enabling them to function effectively as both reducing and capping agents. In this study, zinc oxide nanoparticles (ZnO-NPs) were biosynthesized using an extract obtained from hawthorn (*Crataegus monogyna*) seeds, which are generally considered agro-waste in the food and herbal product industries. The synthesis process was optimized by adjusting parameters including precursor concentration, extract ratio, reaction temperature, pH, and time to achieve maximum nanoparticle yield and stability. Comprehensive characterization was performed using UV–Vis spectroscopy, X-ray diffraction (XRD), Fourier-transform infrared spectroscopy (FTIR), scanning electron microscopy with energy-dispersive X-ray analysis (SEM–EDX), dynamic light scattering (DLS), and zeta potential measurements. The formation of ZnO-NPs was confirmed by a visible color change and a characteristic UV–Vis absorption peak at 345 nm. SEM analysis revealed nearly spherical particles with sizes ranging from 22.01 to 26.28 nm, while FTIR spectra identified functional groups responsible for reduction and stabilization. The zeta potential (−18.5 ± 1.41 mV) indicated moderate colloidal stability. The photocatalytic performance of the ZnO-NPs was evaluated by the degradation of methylene blue (MB) under solar irradiation, achieving 82.4% degradation within 180 minutes. The nanoparticles retained notable activity after five reuse cycles, confirming their stability and reusability. Overall, the findings demonstrate that agro-waste-derived hawthorn seed extract can serve as a sustainable, low-cost, and eco-friendly green reducing agent for the green synthesis of ZnO nanoparticles with excellent photocatalytic efficiency for environmental remediation.

Keywords: Green chemistry, agro-waste, *Crataegus monogyna*, zinc oxide nanoparticles, photocatalytic degradation.

Acknowledgement: This study was supported by The Scientific and Technological Research Council of Turkey (TÜBİTAK) under the 2209-A Research Project Program.

ORAL PRESENTATION

First complete mitochondrial DNA data provided for Turkish Hamster (*Mesocricetus brandti* Nehring 1898)

Derya Çetintürk[1*] (ORCID: https://orcid.org/0000-0002-1323-4311), Nuri Yiğit[1] (ORCID: https://orcid.org/0000-0001-8426-2144)

[*1]University of Ankara, Faculty of Science, Department of Biology, Ankara, Turkiye.

*Corresponding author e-mail: dcetinturk@ankara.edu.tr

Abstract

Approximately 172 mammal species have been recorded from Anatolia so far, 72 of which belong to Order: Rodentia. The systematics and phylogenetic relationships of these rodent species have been studied for many years using morphological, karyological, and molecular (mitochondrial and nuclear gene region analyses) methods, but the taxonomic status of many taxa remains unclear. Therefore, the need for new methods that provide more practical and reliable results has increased. In recent years, complete mitochondrial gene sequences of species have begun to be obtained, but the mitogenome sequences of many species have not yet been provided. The present study represents the complete mitochondrial DNA sequencing of Turkish Hamster (*Mesocricetus brandti* Nehring 1889) for the first time. The 16384 base pair data was obtained and it comprises of 13 protein coding genes, 22 tRNA genes, 2 rRNA genes, and D-loop (control) region, and most gene regions are coded on the heavy strand. Also, AT content (57.31%) was higher than GC content (42.69%). Phylogenetic analyses were conducted adding the available sequences of some species of the subfamily Cricetinae and it was observed that *M. brandti* was located closely with other *Mesocricetus* species (*Mesocricetus auratus*).

Keywords: DNA, hamster, *Mesocricetus*, mitogenome

ORAL PRESENTATION

Odyolojik veriler kullanılarak makine öğrenmesi ile işitme cihazlarında hoparlör tipinin tahmini: Random forest yaklaşımı

Berk Baytaroğlu[1*] (https://orcid.org/0000-0003-0449-5883), Mehmet Burçin Pişkin[1] (https://orcid.org/0000-0002-2689-8547), Handan Tanyıldızı Kokkulunk[2] (https://orcid.org/0000-0001-5231-2768)

[*1]Yıldız Teknik Üniversitesi, Kimya Metalurji Fakültesi, Biyomühendislik, İstanbul, Türkiye.
[2]Maine Maritime Academy, Department of Art & Sciences, Castine, Maine, USA.

*Sorumlu yazar e-mail: berkbaytaroglu@yahoo.com

Özet

İşitme kaybı bulunan bireylerde doğru hoparlör seçimi, işitme cihazı uyumunun başarısı ve kullanıcı memnuniyeti açısından kritik öneme sahiptir. Geleneksel seçim yöntemleri büyük ölçüde odyoloğun deneyimine dayanmakta, bu da öznellik ve hata payını artırabilmektedir. Amaç: Bu çalışmanın amacı, makine öğrenmesi algoritmaları ile bireylerin odyolojik verilerinden en uygun hoparlör tipini otomatik olarak belirlemenin uygulanabilirliğini incelemektir. Materyal ve Yöntem: 2018–2023 yılları arasında işitme cihazı merkezine başvuran, 35–65 yaş aralığında sensörinöral işitme kaybı bulunan 450 bireyin retrospektif verileri analiz edilmiştir. Veri setinde yaş, cinsiyet, saf ses odyometri eşikleri (125–8000 Hz), hava ve kemik yolu saf ses ortalaması değerleri, konuşmayı alma eşiği ve konuşmayı ayırt etme parametreleri yer almıştır. Hoparlör tipleri sınıflandırma hedefi olarak beş sınıf (S, M, P, HP, SP) şeklinde belirlenmiştir. Python ortamında Random Forest algoritması uygulanmış, veri seti %70 eğitim, %30 test olarak ayrılmış, 5-katlı çapraz doğrulama ile aşırı öğrenme engellenmiştir. Model performansı doğruluk, kesinlik, geri çağırma, F1 skoru ve ROC-AUC metrikleri ile değerlendirilmiştir. Bulgular: Random Forest algoritması ile sol kulakta %85.7 train doğruluğu, %84.7 test doğruluğu; sağ kulakta ise %77.5 train doğruluğu, %77.0 test doğruluğu elde edilmiştir. Sol kulakta Precision %85, Recall %85, F1 %84; sağ kulakta Precision %75, Recall %77, F1 %75 bulunmuştur. ROC-AUC değerleri, sol kulakta yüksek, sağ kulakta kabul edilebilir düzeyde ayrıştırma gücü göstermiştir. Özellik önem sıralamasında hava yolu saf ses ortalaması, kemik yolu eşiği ve konuşmayı alma eşiği öne çıkan parametreler olmuştur. Sonuç: Bulgular, odyologların deneyime dayalı öznellikten bağımsız daha hızlı ve doğru hoparlör seçimi yapmasına imkân tanıyabilir. Gelecek çalışmalar için farklı algoritmalar, parametre optimizasyonları, daha büyük ve çok merkezli veri setleri ile karşılaştırmalı analizlerinin yapılması önerilmektedir.

Anahtar Kelimler: İşitme Cihazları, Hoparlör Seçimi, Makine Öğrenmesi, Random Forest, Odyolojik Veriler

ORAL PRESENTATION

Isolation of bacteriocin-producing *Enterococcus* strains from traditional cheeses

Seda Seyirt[1*](ORCID: https://orcid.org/0000-0002-4975-0561), Başar Uymaz Tezel[2] (ORCID: https://orcid.org/0000-0002-4156-8861), Pınar Şanlibaba[3] (ORCID: https://orcid.org/0000-0003-4638-6765)

[*1]Ankara University, Engineering Faculty, Department of Food Engineering, Ankara, Turkey
[2]Çanakkale Onsekiz Mart University, Bayramiç Vocational School, Çanakkale, Turkey
[3]Ankara University, Engineering Faculty, Department of Food Engineering, Ankara, Turkey

Abstract

In this study, 120 traditional cheeses obtained without the use of starter cultures from markets and bazaars in Ankara were used. Suspicious colony morphology for *Enterococcus* was observed in 98 out of 120 traditional cheeses. Antimicrobial activity was detected by agar spot. Antimicrobial activities of 98 isolates were tested against *Salmonella* enterica sero type typhimurium SL 1344, *S. aureus* ATCC 6538, *L. monocytogenes* ATCC 7644 and *E. coli* ATCC 25922. Antimicrobial activity of 75 isolates was determined to have against pathogen bacteria. None of the 75 isolates indicated antimicrobial activity against *Salmonella* enterica sero type typhimurium SL 1344. Among them 69 isolates showed antibacterial inhibition zones ranging from 06-23 mm against *S.aureus*. Twenty-one isolates antibacterial inhibition zones ranging from 05-20 mm against *L. monocytogenes*, while 63 isolates antibacterial inhibition zones ranging from 06-21 mm against *E. coli*. Well diffusion assay was applied to determine the protein nature of the strains showing antimicrobial activity. Five of isolates with antimicrobial activity have been found to produce bacteriocins. All of the bacteriocin-producing isolates showed antimicrobial activity against *L. monocytogenes*. As a result of 16S rDNA sequence analysis, 2 of the 5 enterococci strains were identified as *E. faecium,* 2 as *E. faecalis,* and 1 as *E. lactis.*

Keywords: Antimicrobial activity, Bacteriocin, Traditional cheese, *Enterococcus*

ORAL PRESENTATION

Investigation of feeding interactions between the Randall's threadfin bream (*Nemipterus randalli*) and the common pandora (*Pagellus erythrinus*), two co-occurring fish species in Gökova bay, using stable isotope analysis

Ceyda Nur Erdogan[*1] (ORCID: https://orcid.org/0009-0008-6330-2432), Sercan Yapıcı[2] (ORCID: https://orcid.org/0000-0003-2288-5084), Daniela Giannetto[1] (ORCID: https://orcid.org/0000-0002-3895-5553)

[*1]Muğla Sıtkı Koçman University, Faculty of Science, Department of Biology, Mugla, Türkiye.
[2]Muğla Sıtkı Koçman University, Faculty of Fisheries, Department of Basic Science, Mugla, Türkiye.

*Corresponding author e-mail: ceydaerdogaannn@gmail.com

Abstract

Since its introduction via the Suez Canal, the Lessepsian fish species Randall's threadfin bream *Nemipterus randalli* has successfully spread throughout the eastern Mediterranean, establishing dense populations and coexisting with the native sparid fish species common pandora *Pagellus erythrinus*. Understanding the trophic interactions between these species is crucial for assessing the ecological impacts of Lessepsian invasions on native fish communities. In this study, we used $\delta^{13}C$ and $\delta^{15}N$ stable isotope analyses to investigate trophic niches and resource overlap between the two species. Individuals were sampled during summer and winter at three locations in Gökova Bay (Aegean Sea), characterized by different fishing pressures: a no-fishing control zone and two actively fished areas. Isotopic analyses revealed spatial and seasonal variation in the trophic structure of the two investigated species. Specifically, *P. erythrinus* displayed slightly higher $\delta^{15}N$ values, suggesting a marginally higher trophic position, while *N. randalli* had more depleted $\delta^{13}C$ values, indicating differences in basal carbon sources and feeding habits. Isotopic overlap was more evident in fished areas, whereas the control zone displayed clearer separation in summer and more pronounced overlap in winter, suggesting dynamic resource use and higher competition under reduced prey availability. These findings are in line with the results of previous studies based on stomach content analyses, which reported high dietary overlap between the two species, supporting the idea that *N. randalli* can use similar food resources as native demersal fish. Altogether, our results highlight the trophic plasticity of *N. randalli* and demonstrate the value of stable isotope analysis in revealing feeding relationships and resource overlap between native and non-native species.

Keywords: Niche Dynamics, Lessepsian species, trophic overlap, invasive species, Aegean Sea

Acknowledgements: This study was conducted within the scope of the TÜBİTAK 1001 Research Project No: 123Y292 and reports part of the results of Ceyda Nur Erdoğan's Master Thesis.

Ceyda Nur Erdoğan was supported by the TÜBİTAK BİDEB under the 2210-A Fellowship Program.

ORAL PRESENTATION

Cyclotriphosphazene derivatives containing carbazole units and the investigation of their photophysical properties

Duygu Palabıyık[1]* (ORCID: https://orcid.org/0000-0002-3198-6955), Ceylan Mutlu Balcı[1] (ORCID: https://orcid.org/0000-0003-3202-3808), Süreyya Oğuz Tümay[2] (ORCID: https://orcid.org/0000-0002-0453-4021), İbrahim F. Şengül[1](ORCID: https://orcid.org/0000-0001-9386-4892), Serap Beşli[1] (ORCID: https://orcid.org/0000-0003-3203-4689)

[*1]Gebze Technical University, Faculty of Basic Sciences, Department of Chemistry, Kocaeli, Turkey
[2] Atatürk University, Faculty of Science, Department of Chemistry, Erzurum, Turkey

*Corresponding author e-mail: d.palabiyik@gtu.edu.tr

Abstract

The demand for the preparation of fluorescence materials, which form the basis of important application areas such as bio-imaging, organic solid-state lasers, and organic light-emitting diodes (OLEDs), is increasing day by day. Therefore, the design of suitable organic, inorganic or hybrid materials to be used in these application fields and to examine their activities have become very important. Cyclotriphosphazenes represent an important class of inorganic heterocyclic compounds that can be functionalized with suitable organic groups to form inorganic-organic hybrid systems possessing tailored properties. The versatile reactivity of the phosphorus-halogen bonds within the cyclotriphosphazene ring allows the formation of diverse substitution patterns with various functional groups, which plays a crucial role in designing compounds exhibiting distinct photophysical characteristics. Therefore, in this study, inorganic-organic hybrid compounds were designed and synthesized through the replacement reactions of di- and tetra- aniline substituted cyclotriphosphazenes with the carbazole group. As a result of these reactions, cyclotriphosphazene derivatives including two carbazole units (3a), three carbazole units (4b), and four carbazole units (5b), which may show different photophysical properties, were obtained. After the structural analysis and characterization of the compounds (3a, 4b and 5b) by various spectroscopic techniques were completed, their photophysical behaviors were examined via EEM analysis, steady-state fluorescence, UV-vis absorption, time-resolved fluorescence, and 3D-fluorescence spectroscopies to comprehend the effect of carbazole units substituted to cyclotriphosphazene derivatives. The compounds (3a, 4b and 5b) are the first examples of cyclotriphosphazenes bearing both aniline groups and carbazole units.

Keywords: Cyclotriphosphazene, Carbazole, Synthesis, Characterization, Photophysical.

ORAL PRESENTATION

Determination the pathogenicity and virulence of *Fusarium* species isolated from Amasya, Türkiye, on sugar beet

İdris Bektaş*(https://orcid.org/0000-0001-7409-4837)

*Amasya University, Suluova Vocational School, Plant and Animal Production Department, Amasya, Türkiye.

*Corresponding author e-mail: idris.bektas@amasya.edu.tr

Abstract

Soil contains many microorganisms. These microorganisms form the microbiological structure of the soil. *Fusarium* fungi, which belong to this class of microorganisms, cause disease in many crops. In this study, were determined the pathogenicity and virulence of *Fusarium* species affecting sugar beet. Sugar beet an industrial agricultural product and one of the most important crops grown globally and in our country. In the study, sugar beet production areas in Suluova district of Amasya province were surveyed, and soil samples were taken from around the roots of 20 sugar beets showing root rot. Fungal isolation from the soil was performed on PDA medium. Thirty *Fusarium* isolates were isolated from soil samples. The identification of Fusarium species was performed based on microscopic analysis.In the pathogenicity test conducted on sugar beet, 18 fungal isolates(60%) caused rot. In the evaluation of rot diameters, 10 *Fusarium* isolates causing rot between 4-5 cm were found to be highly virulent, 6 *Fusarium* isolates causing rot between 3-4 cm were found to be moderately pathogenic, and 2 *Fusarium* isolates causing rot between 1-2 cm were found to be low in virulence. This study revealed that *Fusarium* species found in soil microorganisms include both pathogenic and non-pathogenic strains. It was determined that the virulence of pathogenic *Fusarium* species varies due to their genetic structure. In the continuation of the study, the isolated fungal species can be identified by species and their control can be investigated.

Keywords: soil microorganisms, *Fusarium* spp., sugar beet, pathogenicity, virulence

Acknowledgements: This study was supported by the Amasya University Scientific Research Projects Coordination(BAP). Project number: FMB-BAP 25-0642.

ORAL PRESENTATION

Investigation of the photodynamic therapy potential of water-soluble phthalocyanine compounds containing pyridine substituents on breast cancer cell line

Ceren Boğuşlu[1,2*] (ORCID: https://orcid.org/0000-0001-5950-587X), Gökçe Seyhan[1,2] (ORCID: https://orcid.org/0000-0002-8553-9093), Elif Öz[3,4] (ORCID: https://orcid.org/0009-0006-8862-1021), Rengin Reis[3] (ORCID: https://orcid.org/0000-0002-3484-2201), Hüseyin Baş[5] (ORCID: https://orcid.org/0000-0002-8722-3359), Zekeriya Bıyıklıoğlu[5] (ORCID: https://orcid.org/0000-0001-5138-214X), Burak Barut[1] (ORCID: https://orcid.org/0000-0002-7441-8771)

[*1]Karadeniz Technical University, Faculty of Pharmacy, Department of Biochemistry, Trabzon, Turkiye.
[2] Karadeniz Technical University, Graduate School of Health Sciences, Department of Biochemistry (Pharmacy), Trabzon, Turkiye.
[3]Acibadem Mehmet Ali Aydinlar University, Faculty of Pharmacy, Department of Pharmaceutical Toxicology, İstanbul, Turkiye.
[4] İstanbul University, Institute of Health Sciences, Department of Pharmaceutical Toxicology, İstanbul, Turkiye.
[5] Karadeniz Technical University, Faculty of Science, Department of Chemistry, Trabzon, Turkiye.

*Corresponding author e-mail: ceren.boguslu123@gmail.com

Abstract

Breast cancer is the most diagnosed malignant tumor in women and ranks first among the causes of death resulting from malignant neoplasms. Although significant progress has been made in breast cancer treatment in recent years, the current therapeutic approaches still fail to provide fully satisfactory outcomes. Therefore, new treatment strategies need to be explored (1). Photodynamic therapy (PDT) has emerged in recent years as a minimally invasive therapeutic method that has attracted great interest as a novel cancer treatment. PDT utilizes photosensitizers that, upon activation by light of a specific wavelength, react with molecular oxygen in the target tissue to generate reactive oxygen species (ROS), leading to cell death. ROS induce damage to tumor cell membranes, proteins, and DNA, ultimately resulting in cell death. PDT is considered a promising therapeutic approach, particularly for superficial and localized cancers such as breast cancer. Compared to conventional therapeutic methods, PDT offers higher tumor selectivity due to the preferential localization of photosensitizers within tumor lesions and the precise irradiation of these regions with light (2). The aim of this study is to investigate the photostability, DNA interactions, and *in vitro* PDT efficacy of water-soluble silicon (IV) phthalocyanine compounds containing pyridine substituents (3PY-7a-SiQ and 3PY-8a-SiQ) in MCF-7 (human breast adenocarcinoma, ATCC, HTB-22 ™) and MCF-10A (human breast epithelial cell, ATCC, CRL-10317 ™) cell lines. This study has been granted by Acibadem Mehmet Ali Aydinlar University Scientific Research Projects Coordination Unit under grant number TSA-2025-2261.

Keywords: Breast cancer, cytotoxicity, photodynamic therapy, photosensitizers.

References:

Smolarz B, Nowak AZ, Romanowicz H (2022). Breast cancer—epidemiology, classification, pathogenesis and treatment (review of literature). Cancers 14(10): 2569.
Correia JH, Rodrigues JA, Pimenta S, Dong T, Yang Z (2021). Photodynamic therapy review: principles, photosensitizers, applications, and future directions. Pharmaceutics 13(9): 1332.

ORAL PRESENTATION

Management of swallowed capsules filled with drugs in intensive care

Esra Sarı[1](Orcid: https://orcid.org/0000-0003-0655-0620),
Sevil Baltacı Özen[1] (Orcid: https://orcid.org/0000-0002-4111-6072), Berkay Küçük[1*] (ORCID: https://orcid.org/0000-0002-5166-1429)

[1] Ankara Etlik City Hospital, Department of Intensive Care, Ankara, Turkey

*Corresponding author e-mail: berkaykck@hotmail.com

Abstract

Although drug trafficking may evoke criminal cases, contact with these substances, whether intentional or unintentional, can lead to medical problems. In particular, swallowing these substances at the moment to avoid detection, or swallowing them wrapped in casings for transportation purposes, may be asymptomatic; however, if the casings tear or puncture, overexposure can cause numerous adverse respiratory, neurological, and cardiac effects, and even mortality. A 41-year-old male identified as a drug carrier was brought to the hospital emergency room by security guards. The patient was conscious, with no vital sign abnormalities and hemodynamically stable. A contrast-enhanced abdominal tomography (CT) was performed. The tomography revealed multiple smooth oval hypodense contents and thin hyperdense walls throughout the stomach and small and large bowel lumen. The findings were consistent with swallowed capsule packets. As the capsules were filled with heroin and there was a risk of rupture during procedures such as endoscopic removal, which could lead to the absorption of a lethal dose of opioids, the patient was admitted to intensive care without any procedures being planned. The spontaneous defecation of the capsules was monitored, and 84 of the 85 capsules identified as swallowed were passed in the stool and handed over to security personnel. Even if patients are asymptomatic, radiological imaging is necessary. CT scans are both sensitive and highly reliable in detecting capsules. Once capsules are detected, emergency endoscopic or colonoscopic interventions can cause more harm than good. Rupture of the capsules or casings can lead to excessive amounts of drugs entering the bloodstream and death. Spontaneous expulsion of the capsules through defecation can be expected in stable cases. In cases where the capsules do not pass, endoscopic and surgical interventions should always be considered and performed without delay when symptoms of ileus, perforation, acute abdomen, and intoxication develop.

Keywords: Foreign body, Tomography, Swallowed capsule packs, Intensive care, Intoxication

ORAL PRESENTATION

Experimental and theoretical investigations of semi-lethal dose (D_{50}) values for bacterial population

Mürsel Şen[1*] (ORCID: https://orcid.org/0000-0002-0637-8325)

[*1]National Defence University, Turkish Air Force Academy, Department of Basic Sciences, İstanbul, Türkiye.

*Corresponding author e-mail: senmursel@hotmail.com; mursel.sen@msu.edu.tr

Abstract

The semi-lethal dose (D_{50}) is a parameter used to determine the sensitivity of microorganisms or cells to radiation. It is defined as the radiation dose that reduces the cell and bacterial population by half. D_{50} is obtained using the linear model (single-target single-hit model), which is the simplest mathematical model used to explain cell or bacterial death. The linear model is expressed as a first-order differential equation in the form $\frac{dN(D)}{dD} = -kN(D)$, where N(D) represents the number of surviving cells or bacteria as a function of radiation dose D, and k is the proportionality constant. The constant k is 1/ D_0, where D_0 is defined as the mean-lethal dose. Using the standard linear model, the standard theoretical D_{50} is given by $D_{50}=\ln 2/k= D_0 \ln 2$. In this study, the effects of different types of radiation (X-rays, gamma rays, and neutron particles) on Bact. Coli bacteria were investigated. Experimental D_{50} values, which representing the radiation dose that reduce the bacterial population by half for each type of radiation, were determined and compared with the standard theoretical D_{50} values obtained from the standard linear model. An inconsistency was observed between the experimental and standard theoretical D_{50} values. To eliminate this inconsistency, the standard linear model reconsidered and solved using the Caputo fractional derivative. The results showed that the experimental and fractional theoretical D_{50} values are consistent for the appropriate orders of fractional derivatives.

Keywords: Semi-lethal radiation dose (D_{50}), Linear model, Single-target single-hit model, Caputo fractional derivative, Mittag-Leffler function

ORAL PRESENTATION

Lactarius deliciosus (L.) Gray özütlerinin gökkuşağı alabalığı (*Oncorhynchus mykiss*, Walbaum, 1792) filetolarının raf ömrü üzerine etkisi

Ceyda Nur Erdoğan (ORCID: https://orcid.org/0009-0008-6330-2432), Hayrünisa Baş Sermenli (ORCID: https://orcid.org/0000-0002- 0803-2715)

Muğla Sıtkı Koçman Üniversitesi, Fen Fakültesi, Biyoloji Bölümü, Muğla, Türkiye

*Sorumlu yazar e-mail: ceydaerdogaannn@gmail.com

Özet

Su ürünleri sektörü, son 50 yılda hızlı bir gelişme göstererek uluslararası ticarette önemli bir paya sahip olmuştur. Su ürünlerinin üretimi ve pazarlanmasının önemi kadar raf ömrü de ekonomik açıdan çok büyük önem taşımaktadır. Bu çalışmada, yenen doğal bir mantar olan ve halk arasında "çıntar" olarak bilinen *Lactarius deliciosus* (L.) Gray türünün özütlerinin 4 °C'de depolanan gökkuşağı alabalığı (*Oncorhynchus mykiss*) filetolarının raf ömrünü uzatmadaki antioksidan potansiyeli araştırılmıştır. Bu amaçla, *L. deliciosus*'tan etanol, metanol ve sıcak su özütleri hazırlanarak 300 ppm dozunda balık filetolarına uygulanmış; işlem görmemiş örnekler kontrol grubu olarak değerlendirilmiştir. Lipid oksidasyonu düzeyleri, tiyobarbitürik asit reaktif maddeler (TBA-RS) yöntemi kullanılarak belirlenmiş ve malondialdehit (MDA) değerleri 15 günlük depolama süresince belli periyotlarda, 532 nm dalga boyunda spektrofotometrik olarak ölçülmüştür. Elde edilen bulgular, mantar özütüyle muamele edilen filetoların kontrol grubuna kıyasla anlamlı derecede daha düşük MDA oluşumu gösterdiğini ortaya koymuştur ($p < 0.05$). On beşinci gün sonunda ortalama MDA değerleri kontrol örneklerinde 5.07 µM, etanol uygulanan örneklerde 4.46 µM, metanol uygulanan örneklerde ise yalnızca 1.30 µM olarak saptanmıştır. İstatistiksel analizler (ANOVA ve Tukey post-hoc testleri), özellikle metanol bazlı özütlerin depolama süresi boyunca lipid peroksidasyonunu en yüksek düzeyde baskıladığını göstermiştir. Bu sonuçlar, *L. deliciosus*'tan elde edilen doğal özütlerin, özellikle metanol bazlı olanların, oksidatif bozulmayı geciktirmede ve ürün kalitesini korumada etkili olabileceğini göstermiştir. Bu çalışmada elde edilen sonuçlar, doğal biyoaktif bileşiklerin sentetik antioksidanlara güvenli ve çevre dostu bir alternatif oluşturabileceğini göstermektedir. Günümüzde sürdürülebilir gıda koruma yöntemlerine yönelik artan ilgi dikkate alındığında, bu tür doğal özütlerin kullanımı hem ürün kalitesinin korunması hem de tüketici sağlığının desteklenmesi açısından önemli bir potansiyele sahiptir. Bununla birlikte, yöntemin endüstriyel ölçekte uygulanabilirliğini artırmak için, farklı balık türleri ve gıda sistemlerinde optimum özüt konsantrasyonlarının belirlenmesine yönelik ileri araştırmalara ihtiyaç duyulmaktadır.

Anahtar Kelimeler: çıntar, malondialdehit, doğal özüt, lipid oksidasyonu, tiyobarbitürik asit.

ORAL PRESENTATION

Yeast microflora of milk kefir beverages fermented with various grains

Bilal Agirman[1*] (ORCID: https://orcid.org/0000-0002-3629-1933)

[*1] Cukurova University, Faculty of Engineering, Department of Food Engineering, Adana, Türkiye

*Corresponding author e-mail: bagirman@cu.edu.tr

Abstract

Milk kefir (MK), a refreshing beverage with strong acidity and small amounts of alcohol and carbon dioxide, is produced by fermenting milk with MK grains. The grain microflora consisted of a complex symbiotic community of diverse lactic acid bacteria, yeasts, and acetic acid bacteria embedded in a polysaccharide matrix known as kefiran. This study aims to elucidate and compare the yeast flora of kefir grains (KGs) from various origins using molecular methods. This study used three distinct types of fresh KGs: goat-based (GK), cow-based (CK), and sheep-based (SK). Fermentations were performed at 28°C for 48 h using UHT sterilized milk in sterilized 1 L glass bottles inoculated with 3 g grain. Total yeasts and non-*Saccharomyces* yeasts were enumerated, isolated, and purified on PDA and Lysine media, respectively, at the start and end of the fermentation. Molecular identification of a total of 60 isolates was achieved by a combination of PCR-RFLP of the 5.8 S rRNA region and sequencing of the D1/D2 domain of the 26 S rRNA gene. Hae III, Hinf I and Cfo I restriction endonucleases selected as to differentiate of the 5.8S rRNA PCR product. The number of total yeasts (3.52-3.83 log cfu/mL to 8.14-8.62 log cfu/mL) and non-*Saccharomyces* yeasts (3.00-3.38 log cfu/mL to 6.74-8.41 log cfu/mL) increased significantly between the start and finish of the fermentation. Although the number of yeast species varied, *Saccharomyces cerevisiae* (*S.c.*), *Kazachstania unispora* (*K.u.*), and *Kluyveromyces marxianus* (*K.m.*) were isolated from all kefir beverages fermented with three distinct KGs. The frequencies of *S.c.*, *K.u.*, and *K.m.* were 52.94%, 41.18%, and 5.88% for kefir beverage fermented with CK grain; 15.79%, 63.16%, and 21.05% for beverage fermented with GK grain; and 25%, 45.83%, and 29.17% for beverage produced with SK grain, respectively.

Keywords: Kefir, yeasts, PCR-RFLP, *Kazachstania unispora*, *Saccharomyces cerevisiae*, *Kluyveromyces marxianus*

ORAL PRESENTATION

Identification of foot-and-mouth disease virus antigenic peptide via SERS

Gamze Demirel Sahin[1,2*] (Orcid: https://orcid.org/0000-0002-2261-1545) Furkan Şahin[3,4] (Orcid: https://orcid.org/0000-0001-5409-3925), Mustafa Serdar Onses[5,6](ORCID: https://orcid.org/0000-0001-6898-7700), Serap Acar[1](Orcid: https://orcid.org/0000-0002-6662-6642)

[*1]Yildiz Technical University, Faculty of Chemical and Metallurgical Engineering, Department of Bioengineering, Istanbul, Turkiye.
[2] Yildiz Technical University, Faculty of Electrical and Electronics, Department of Biomedical Engineering, Istanbul, Turkiye.
[3] Beykent University, Faculty of Engineering and Architecture, Department of Biomedical Engineering, Istanbul, Turkiye.
[4] Beykent University, Vocational School, Biomedical Device Technology Program, Istanbul, Turkiye.
[5] Erciyes University, ERNAM - Nanotechnology Research and Application Center, Kayseri, Turkiye.
[6] Erciyes University, Faculty of Engineering, Department of Materials Science and Engineering, Kayseri, Turkiye.

*Corresponding author e-mail: demirelg@yildiz.edu.tr

Abstract

Foot-and-mouth disease virus (FMDV) is a highly contagious viral infection affecting cloven-hoofed animals such as cattle, sheep, and pigs. The occurrence of outbreaks in the livestock industry has been demonstrated to result in significant economic losses and the implementation of international trade restrictions. Consequently, the early, accurate, and rapid detection of the disease is crucial to prevent its spread. The VP1 capsid protein, a structural component of the FMDV, plays a vital role in the virus's ability to adhere to host cells by interacting with integrin receptors located on the host cell surface. The 170-188 peptide sequence of the VP1 viral capsid protein plays a crucial role in the recognition of the virus by the immune system, as it functions as a virus-specific T-epitope. Consequently, the molecular detection of this peptide sequence indicates the presence of the antigenic structure of the virus, thus establishing the 170-188 peptide as a promising biomarker candidate for the diagnosis of FMDV. In this study, the detection of the 170-188 antigenic peptide was investigated using Surface-Enhanced Raman Spectroscopy (SERS), a highly sensitive and label-free analytical technique that enables the molecular identification of biomolecules through enhanced Raman scattering. The SERS-active substrate utilized for analyte detection was fabricated employing an innovative method that utilizes electrospinning to disperse silver ions onto the substrate surface, followed by thermal annealing, which enables in situ growth. The obtained spectral bands were then assigned to specific amino acid residues, thereby enabling the structural features of the peptide to be analyzed at the molecular level. The results demonstrate the promising potential of SERS in bioanalyte detection.

Keywords: Foot-and-Mouth Disease Virus, Viral Diagnosis, SERS; Electrospun Substrate, Bioanalyte Detection.

Acknowledgments: This work was supported by the Scientific and Technological Research Council of Turkey (TUBITAK) [Project Number: 323S342]. Gamze Demirel Sahin acknowledges financial support from TUBITAK (2211-A Scholarship Programme of Doctorate).

ORAL PRESENTATION

Integration of artificial intelligence in wastewater treatment for sustainable biogas generation

Şeyma Akkurt

Department of Environmental Engineering, Faculty of Engineering, Adıyaman University, Adıyaman, Turkey

Corresponding author e-mail: sakkurt@adiyaman.edu.tr

Abstract

The integration of Artificial Intelligence (AI) into wastewater treatment systems is becoming a critical pathway toward achieving sustainable energy and environmental goals. AI's ability to process large, complex, and nonlinear datasets enables unprecedented insight into the anaerobic digestion process, which is central to biogas generation. Traditional models often fail to capture the dynamic interactions among parameters such as temperature, pH, organic loading rate, and retention time. In contrast, AI techniques including Machine Learning (ML), Artificial Neural Networks (ANN), and Deep Learning (DL) allow accurate prediction, optimization, and control of biogas yield. This review highlights the growing importance of AI as a transformative tool that enhances process efficiency, operational stability, and methane recovery while reducing energy consumption and environmental impact. Current literature demonstrates that AI-driven models outperform conventional methods by adapting to real-time data and identifying complex system behaviors that are otherwise difficult to quantify. AI-based decision-support systems also offer intelligent automation, which makes it easier to manage treatment operations in a proactive way and helps with carbon-neutral energy recovery. Despite existing challenges related to data quality and model interpretability, AI stands as a cornerstone technology in transitioning wastewater treatment plants into smart, self-optimizing energy systems. Therefore, integrating AI is not only a technological advancement but also a strategic necessity for promoting sustainability, circular economy principles, and environmental resilience.

Keywords: Artificial Intelligence, Wastewater Treatment, Biogas Generation, Sustainable Energy, Machine Learning, Environmental Sustainability

ORAL PRESENTATION

Structural elucidation and antimicrobial potentials of pyrazoline compounds derived from chalcone intermediates

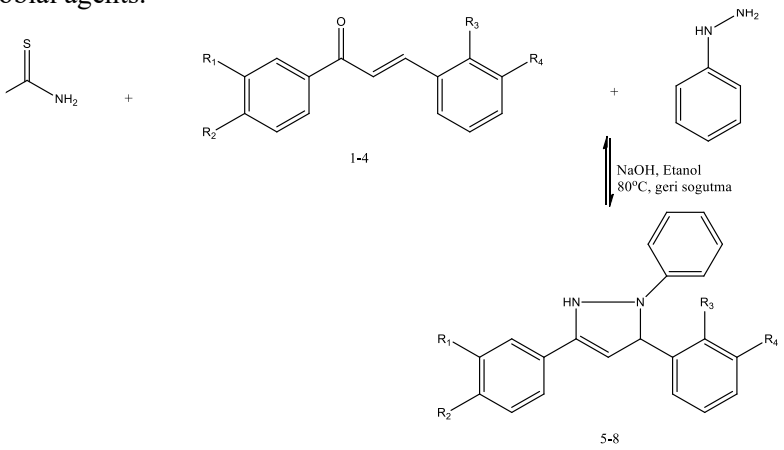
Tayyibe Beyza Yücel[1*] (Orcid: https://orcid.org/0000-0002-2632-8325),
Esra Deniz Candan[1] (Orcid: https://orcid.org/0000-0003-2515-9643)

[*1] Giresun University, Health Services High School, Giresun, Türkiye.

*Corresponding author e-mail: beyza.yucel@giresun.edu.tr

Abstract

The increasing prevalence of infectious diseases and antimicrobial resistance underscores the urgent need for novel therapeutic agents. Heterocyclic compounds are among the most significant structural motifs in medicinal chemistry due to their pharmacological versatility. Among them, pyrazoline derivatives have gained attention for their broad biological potential, including notable antimicrobial and antineoplastic properties [Karabacak, 2015]. In this study, chalcone intermediates were synthesized as key precursors, followed by the preparation of four methoxy-, hydroxy-, and chloro-substituted pyrazoline derivatives. The structures of all compounds were confirmed by NMR (^{1}H, ^{13}C, APT), MS, FT-IR, and UV analyses. The antimicrobial activity of the synthesized pyrazoline derivatives was evaluated by agar well diffusion and minimum inhibitory concentration (MIC) methods against *Staphylococcus aureus* (ATCC 29213), *Escherichia coli* (ATCC 25922), *Bacillus cereus* (ATCC 10876), and *Candida albicans* (ATCC 10231). All compounds showed significant inhibitory effects, particularly against *Candida albicans*, producing inhibition zones of 15–23 mm and inhibition rates between 50% and 115%. MIC and MBC/MFC results indicated compound-dependent antimicrobial activity. Compounds 6 and 7 exhibited the lowest MIC and MBC values, confirming strong bactericidal potential, especially against *B. cereus*. Moreover, compound 9 displayed the highest antifungal effect, with MIC and MFC values of 0.78 and 1.56 mg/mL against *C. albicans*. The synthesized pyrazoline derivatives demonstrated strong and broad-spectrum antimicrobial efficacy. These findings suggest that such heterocyclic frameworks may serve as valuable lead structures for the development of new antimicrobial agents.



Keywords: Heterocyclic compounds, Pyrazoline, Antimicrobial activity.

ORAL PRESENTATION

UV ve filtrasyon tabanlı balast suyu arıtım sistemlerinin saha performansı üzerine bir değerlendirme

Ülkü Demirci

İskenderun Teknik Üniversitesi, Bilim ve Teknoloji Uygulama ve Araştırma Merkezi, Hatay, Türkiye

Sorumlu yazar e-mail: ulku.demirci@iste.edu.tr

Özet

Balast suları, gemi stabilitesini sağlamak amacıyla kullanılsa da, farklı deniz ekosistemleri arasında canlı organizmaların taşınmasına neden olarak istilacı türlerin yayılımı açısından ciddi bir çevresel tehdit oluşturmaktadır. Bu riski azaltmak amacıyla Uluslararası Denizcilik Örgütü (IMO) tarafından 2004 yılında kabul edilen Balast Suyu Yönetimi Sözleşmesi (BWM 2004), 2017 itibarıyla yürürlüğe girerek gemilerde balast suyu arıtma sistemlerinin (BWTS) kullanılmasını zorunlu hale getirmiştir. Bu çalışmada, UV ve filtrasyon temelli bir balast suyu arıtma sisteminin saha performansı, IMO yönergelerine (BWM.2/Circ.70/Rev.1) uygun olarak gerçekleştirilen bir devreye alma testi (commissioning test) verileri üzerinden değerlendirilmiştir. Sistem 1000 m^3/saat nominal kapasitede çalışacak şekilde tasarlanmış olup, test sırasında ortalama debalast debisi 427 m^3/saat, toplam deşarj hacmi 350 m^3 ve tutma süresi 2 saat olarak kaydedilmiştir. Biyolojik etkinlik ölçümleri, Adenozin Trifosfat (ATP) yöntemiyle yapılmış ve hem ≥50 µm hem de 10–50 µm boyut sınıflarında IMO D-2 standardının altında (<10 organizma/m^3 ve <10 organizma/mL) sonuçlar elde edilmiştir. UV yoğunluğu 1869 W/m^2 olarak kaydedilmiş ve sistemin kendi kendini izleme (self-monitoring) donanımında herhangi bir alarm veya arıza tespit edilmemiştir. Elde edilen sonuçlar, UV + filtrasyon temelli sistemlerin saha koşullarında yüksek biyolojik etkinlik gösterdiğini ve D-2 standardı gerekliliklerini başarıyla karşıladığını ortaya koymuştur. Ancak tutma süresi ve debi değişkenlerinin performans üzerindeki olası etkilerinin, farklı gemi tiplerinde ileri saha çalışmalarıyla doğrulanması önerilmektedir.

Anahtar Kelimeler: Balast suyu yönetimi, UV arıtma, IMO D-2 standardı, deniz istilacı türleri, biyolojik etkinlik

ORAL PRESENTATION

Determining the recent status of non-native marine fish species in the Aegean coast of Türkiye

Ferhat Yalgın (Orcid: https://orcid.org/0000-0002-0027-5114)

Bandırma Onyedi Eylül University, Maritime Vocational School, Department of Underwater Technology, Balıkesir, Türkiye.

Corresponding author e-mail: fyalgin@bandirma.edu.tr , ferhatyalgin@gmail.com

Abstract

Biological invasion is one of the most significant problems of 21st century. The introduction of non-native species into new ecosystems is considered one of the main threats to biodiversity and ecosystem components. However, biological invasions cause not only ecological but also economic damage. Today, the Aegean Sea has become a region invaded by species entering through the Suez Canal and the Strait of Gibraltar. Increasing human-induced impacts (such as global warming and intensive maritime transport) have accelerated the invasion success of alien species entering the Mediterranean. In parallel, the number of non-native species distributed in the Mediterranean basin has exceeded 1,000. Although the detection, distribution, impact assessment, and monitoring of alien species in both terrestrial and aquatic ecosystems have been studied worldwide for many years, such studies have gained momentum in Türkiye only in the last decade. In this study, relevant literature was reviewed to determine the current status of alien fish species distributed along the Aegean coasts of Türkiye.

Keywords: Biodiversity, Bioinvasion, Suez Canal, Gibraltar Strait, Mediterranean

ORAL PRESENTATION

Assessing the impact of microbial dysbiosis on disease pathogenesis through a one health perspective

Ozge Ardicli

Bursa Uludag University, Bursa, Türkiye.

Corresponding author e-mail: ozgeyilmaz@uludag.edu.tr

Abstract

The microbiota comprises diverse microorganisms, including bacteria, fungi, and viruses, that colonize distinct body sites such as the gut, skin, and respiratory tract, forming a vital interface between the host and its environment. These microbial communities maintain epithelial barrier integrity, metabolic homeostasis, and immune tolerance. Dysbiosis, defined as an imbalance in microbial composition and function, disrupts these processes and contributes to the pathogenesis of various diseases. Multiple factors, including the use of chemicals in daily routines, dietary changes, antibiotic overuse, environmental pollutants, and reduced microbial exposure, can contribute to the development of dysbiosis. According to the epithelial barrier theory, the progressive loss of microbial diversity, together with environmental insults such as pollutants, detergents, and dietary additives, weakens epithelial integrity and increases permeability to allergens and pathogens. This breakdown of the physical and immunological barrier not only amplifies type 2-skewed inflammation but also links the global decline in microbial biodiversity to the growing prevalence of chronic allergic and inflammatory disorders. Distinct body sites in companion animals show specific microbial alterations linked to allergic and inflammatory diseases. In canine and feline atopic dermatitis, reduced microbial diversity and overgrowth of *Staphylococcus pseudintermedius* and *Malassezia pachydermatis* correlate with disease severity. Respiratory and gut microbiota of allergic pets also display increased *Proteobacteria* and *Clostridium* abundance, with reduced *Bacteroidetes*, impairing short-chain fatty acid production and epithelial immune tolerance.From a One Health perspective, comparable microbial perturbations and immune consequences are observed in animals and humans, underscoring the interconnectedness of host–microbiota relationships across species. Understanding dysbiosis-driven immune dysregulation provides critical insight for developing microbiota-targeted interventions that promote balanced immunity and barrier resilience in both human and veterinary medicine.

Keywords: microbial dysbiosis, microbiota, one health, companion animals

ORAL PRESENTATION

Synthesis and Characterization of Ester-Based Hindered Amine Light Stabilizers (HALS) in Polymers

Asl Uluçay[1*] (0009-0005-9402-1359), Gökhan Ceyhan[2] (0000-0002-9127-2348)

[1]Kahramanmaras Sütcü Imam University, Department of Materials Science and Engineering, K. Maras,
[2]Kahramanmaras Sütcü Imam University, Technical Sciences Vocational School, Food Processing Division, K. Maraş.
[3]Research and Development Centre for University-Industry-Public Relations, Sütcü Imam University, K. Maras,

*Corresponding author e-mail: 23200359692@ogr.ksu.edu.tr

Abstract

Polyolefins such as polypropylene (PP) and linear low-density polyethylene (LLDPE) are extensively utilized in packaging, automotive, and outdoor applications owing to their cost-effectiveness, processability, and mechanical strength. Nonetheless, their vulnerability to photo-oxidative degradation under UV exposure results in chain scission, discoloration, and diminished mechanical properties. Hindered amine light stabilizers (HALS) counteract this degradation by neutralizing free radicals through a regenerative cyclic mechanism, thereby prolonging polymer service life. Conventional HALS, typically petrochemical-derived, can interact adversely with processing aids in LLDPE films, compromising efficiency.

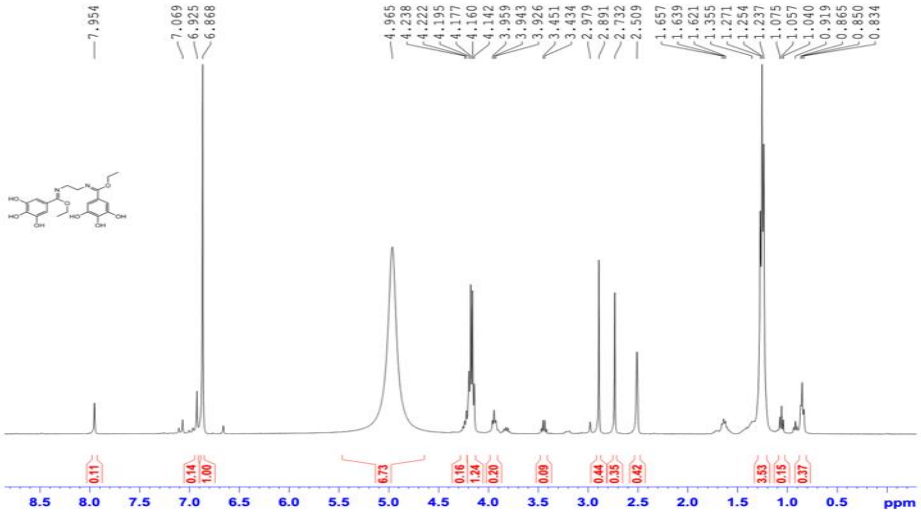


Figure: Dimetil N',N''-(etan-1,2-di)(1Z,1'E)-bis(3,4,5-trihidroksibenzimidat)'e ait NMR Spektrumu

This study reports the synthesis of four novel bio-derived HALS candidates: Schiff base derivatives from ethyl gallate/methyl gallate and diamines (ethylenediamine/1,6-hexanediamine) via condensation reactions in ethanol under reflux. These compounds exploit gallic acid's phenolic antioxidant framework for radical scavenging in polyolefins, augmented by imine linkages for enhanced thermal and UV resilience. The products were obtained in 75-88% yields as pale yellow solids. Structural confirmation was achieved through spectroscopic and thermal analyses. FTIR spectra displayed characteristic imine (C=N) stretches at 1648-1652 cm^{-1}, phenolic OH at 3400-3450 cm^{-1}, and ester C=O at 1715-1725 cm^{-1}. ^1H NMR (400 MHz, DMSO-d_6) revealed imine protons at δ 7.95-8.00 (s, 2H), aromatic protons at δ 6.87-7.07 (m, 4H), benzylic CH_2O- at δ 4.97 (s, 4H), and aliphatic signals including -OCH_2CH_3 at δ 4.20-4.24 (q, 4H, J = 7.1 Hz) and CH_3 at δ 1.04-1.27 (t, 6H, J = 7.1 Hz); for hexanediamine derivatives, additional - $(CH_2)_4$- methylene chains appeared at δ 1.23-1.64 (m, 8H). ^{13}C NMR (100 MHz, DMSO-d_6) confirmed ester carbonyls at δ 166.6-166.7 ppm, imine carbons at δ 162.8 ppm, aromatic quaternary C at δ 146.5 and 151.7 ppm, and olefinic/aromatic CH at δ 108.4-116.6 ppm; aliphatic carbons ranged from δ 14.4-60.7 ppm. UV-Vis spectra showed absorption maxima at 280-320 nm, indicative of π-π* transitions in the conjugated system. Thermal analyses via TGA exhibited decomposition onsets >260°C (5% weight loss) under N_2, with DSC revealing glass transitions at 95-110°C and melting points of 185-210°C, suggesting suitability for polymer processing. These gallate-based Schiff bases represent sustainable HALS precursors with inherent antioxidant-photostabilizing motifs, paving the way for eco-friendly polyolefin enhancements.

Keywords: Schiff bases, HALS, gallic acid esters, NMR characterization, polymer stabilization.

ORAL PRESENTATION

In silico analysis of missense SNPs in the *CDH9* gene

Duru Su Orkun[1] (Orcid: https://orcid.org/0009-0004-1935-7920), Ömer Faruk Karasakal[2*] (Orcid: https://orcid.org/0000-0001-7803-3249)

[1,2*] Üsküdar University, Vocational School of Health Services, Medical Laboratory Techniques, İstanbul, Türkiye.

*Corresponding author e-mail: omerfaruk.karasakal@uskudar.edu.tr

Abstract

Autism spectrum disorder (ASD) is a complex neurological and developmental disorder characterized by persistent deficits in social communication, repetitive behaviors and, restricted interests with a strong genetic component underlying its etiology. Among the numerous candidate genes associated with ASD, *CDH9* (Cadherin-9) encodes a calcium-dependent cell adhesion protein that plays a critical role in synaptic organization, neuronal connectivity, and the establishment of specific neural circuits during brain development. In the present study, SNAP, SIFT, PolyPhen-2 (HumDiv and HumVar), SNPs&GO, PhD-SNP, PANTHER, and Meta-SNP computational tools were employed to evaluate potentially deleterious missense variants within the *CDH9* gene. The impact of these variants on protein stability was assessed using I-Mutant 2.0 and MUpro, while GeneMANIA and STRING were utilized to explore gene–gene and protein–protein interaction networks, respectively. Additionally, Missense3D was used to visualize three-dimensional conformational changes. As a result of these analyses, six missense SNPs were predicted to have a shared deleterious effect and were potentially associated with ASD pathogenesis: rs143800304 (D483N), rs148731332 (R448W), rs149817725 (E741G), rs199818706 (G310E), rs200287957 (G610V), and rs371558373 (G742R). Overall, these findings highlight the pathogenic potential of missense SNPs in the *CDH9* gene and propose these variants as strong candidates for future experimental validation in understanding the molecular mechanisms underlying autism spectrum disorder.

Keywords: *CDH9* gene, *in silico*, polymorphism, autism spectrum disorders

ORAL PRESENTATION

Coating of Mg alloys with nano hydroxyapatite (HA) to be used as biodegradable biomaterials

İlker Erdem (Orcid: https://orcid.org/0000-0001-5743-0835)

Abdullah Gül University, Faculty of Engineering, Department of Materials Science and Nanotechnology Engineering, Kayseri, Türkiye.

Corresponding author e-mail: ilker.erdem@agu.edu.tr

Abstract

Biodegradable metal biomaterials have the advantage of self-decomposition in the body and prevents further surgery to take them back after healing process. This makes them good alternatives for bone fixation applications. Among biodegradable metal alloys Mg alloys have been investigated widely due to their superior advantages e.g. biocompatibility, low density, comparable mechanical properties with living tissue (bone). Besides these advantages the considerably fast degradation kinetics of Mg alloys in the body (body fluid environment) is an important drawback. The metallic alloy should stay intact (i.e. keep its mechanical strength) during healing of the wounded tissue. There are different approaches on elongation of the degradation time of the Mg alloys like doping the alloy with different metals to prepare a more durable metallic alloy or modifying the surface of the alloy for enhanced durability against chemical degradation. Application of coatings with biocompatible materials on Mg alloys is a convenient method to control the biodegradation stability of Mg alloy at certain levels. Besides, these coatings may act as active agents for enhancing the healing process. Hydroxyapatite (HA) is a bioactive ceramic material which has chemical structure resemblance with the bone. Coating of Mg alloys with HA may balance the degradation rate of the alloy in the body, and it may also help the healing process of the bone tissue. In the current study Mg alloy samples were coated with nano HA and the effect of the coating on the biodegradation of the alloy was investigated. The coating process parameters (coating technique, recipe, etc.) were changed to determine their effects on the structure/performance of the coating. The biodegradation of the alloy in simulated body fluid (*in vitro*) was elongated considerably with the applied coating layer compared to the uncoated alloy.

Keywords: Mg alloy, biomaterial, nano hydroxyapatite, coating, biodegradation.

ORAL PRESENTATION

Synthesis, characterization and *in silico* anticholinesterase inhibitory activity of new hydrazide-hydrazone derivatives

Sümeyye Köşker[1*] (orcid: https://orcid.org/0009-0009-2976-0592), Necla Kulabaş[2] (Orcid: https://orcid.org/0000-0003-2273-5094)

[*1]Fenerbahçe University, Faculty of Pharmacy, Department of Pharmaceutical Chemistry, İstanbul, Turkey.
[2] Marmara University, Faculty of Pharmacy, Department of Pharmaceutical Chemistry, İstanbul, Turkey.

*Corresponding author e-mail: sumeyye.kosker@fbu.edu.tr

Abstract

Alzheimer's disease (AD) is the most common cause of dementia in adults and one of the most prevalent neurodegenerative diseases worldwide. AD accounts for approximately 60–80% of all dementia cases. (Alzheimer's Association, 2024; WHO, 2023). The pathogenesis of the disease is multifactorial and has not yet been fully elucidated. Today, pharmacological treatment approaches for Alzheimer's disease are largely based on the cholinergic hypothesis. The main goal of this approach is to enhance neurotransmission and improve cognitive function by increasing ACh levels in the synaptic cleft. The most commonly used drugs for this purpose belong to the group of acetylcholinesterase inhibitors, which inhibit the enzyme responsible for the hydrolysis of ACh. The main agents in this group are donepezil, rivastigmine, and galantamine (Marucci et al., 2021). These drugs only provide temporary cognitive improvement; they cannot halt the progression of the disease and may cause side effects such as nausea, muscle weakness, or liver toxicity(Hampel et al., 2021; Venugopal et al., 2024). Therefore, there is a need to develop safer and more effective compounds. In recent years, hydrazones and their derivatives have attracted attention due to their structural flexibility, the inclusion of biologically active pharmacophore groups, and their high biological activity (Rollas & Güniz Küçükgüzel, 2007).The effects of hydrazones on AChE/BuChE inhibition are known (Bartolić et al., 2024; Sıcak et al., 2019), but there is currently no hydrazone derivative compound used in the treatment of Alzheimer's disease. In this study, 11 new *N*-(2-{2-[2-substitutedbenzylidenehydrazin-1-yl]-2-oxoethoxy}phenyl)acetamide derivatives containing a hydrazide-hydrazone structure were synthesized from orthocetamol with %66-97 yield. The purities of the synthesized compounds were determined by melting point determination and HPLC, and their structures were elucidated using spectroscopic methods. The *in silico* binding affinities of the synthesized compounds against AChE and BuChE enzymes were evaluated, and ligand-binding site interactions were presented.

Keywords: AChE, BuChE, hydrazone, synthesis, docking

References:

Bartolić, M., Matošević, A., Maraković, N., Bušić, V., Roca, S., Vikić-Topić, D., Sabljić, A., Bosak, A., & Gašo-Sokač, D. (2024). Evaluation of hydrazone and N-acylhydrazone derivatives of vitamin B6 and pyridine-4-carbaldehyde as potential drugs against Alzheimer's disease. *Journal of Enzyme Inhibition and Medicinal Chemistry*, *39*(1). https://doi.org/10.1080/14756366.2024.2431832

Hampel, H., Vassar, R., De Strooper, B., Hardy, J., Willem, M., Singh, N., Zhou, J., Yan, R., Vanmechelen, E., De Vos, A., Nisticò, R., Corbo, M., Imbimbo, B. Pietro, Streffer, J., Voytyuk, I., Timmers, M., Tahami Monfared, A. A., Irizarry, M., Albala, B., … Vergallo, A. (2021). The β-Secretase BACE1 in Alzheimer's Disease. In *Biological Psychiatry* (Vol. 89, Issue 8, pp. 745–756). Elsevier Inc. https://doi.org/10.1016/j.biopsych.2020.02.001

Marucci, G., Buccioni, M., Ben, D. D., Lambertucci, C., Volpini, R., & Amenta, F. (2021). Efficacy of acetylcholinesterase inhibitors in Alzheimer's disease. In *Neuropharmacology* (Vol. 190). Elsevier Ltd. https://doi.org/10.1016/j.neuropharm.2020.108352

Rollas, S., & Güniz Küçükgüzel, Ş. (2007). Biological Activities of Hydrazone Derivatives. *Molecules*, *12*, 1910–1939. www.mdpi.org/molecules

Sıcak, Y., Oruç-Emre, E. E., Öztürk, M., Taşkın-Tok, T., & Karaküçük-Iyidoğan, A. (2019). Novel fluorine-containing chiral hydrazide-hydrazones: Design, synthesis, structural elucidation, antioxidant and anticholinesterase activity, and in silico studies. *Chirality*, *31*(8), 603–615. https://doi.org/10.1002/chir.23102

Venugopal, A., Paplikar, A., Varghese, F. A., Thanissery, N., Ballal, D., Hoskeri, R. M., Shekar, R., Bhaskarapillai, B., Arshad, F., Purushothaman, V. V., Anniappan, A. B., Rao, G. N., & Alladi, S. (2024). Protective effect of bilingualism on aging, MCI, and dementia: A community-based study. *Alzheimer's and Dementia*, *20*(4), 2620–2631. https://doi.org/10.1002/alz.13702

ORAL PRESENTATION

Cistus laurifolius L. (karağan) bitki ekstraktının kolon kanseri hücre hattında (HCT 116) anti kanser etkilerinin incelenmesi

[1*]MeralYILDIZ (0009-0003-3923-8606) [2]İlhami GÖK (0000-0003-1074-9325)
[3]Ramazan DEMİREL (0000-0001-8654-5359)

[1]Kafkas University, Institute of Science, Department of Bioengineering,36100,Kars,TURKEY
[2]Kafkas University, Faculty of Engineering and Architecture, Department of Bioengineering 36100,Kars, TURKEY
[3]Kafkas University, Institute of Science, Department of Biotechnology,36100,Kars,TURKEY

*Corresponding author e-mail: yildizmeral3535@gmail.com

Özet

Kolon kanseri, dünya genelinde en yaygın görülen ve yüksek mortalite oranına sahip üçüncü kanser türüdür. Günümüzde mevcut tedavi yöntemlerine ek olarak, doğal kaynaklı bileşikler ve bitki ekstraktlarının terapötik potansiyelleri üzerine yapılan çalışmalar giderek artmaktadır. Bu çalışmada, Akdeniz bölgesinde yaygın olarak bulunan *Cistus laurifolius* L. (karağan) bitki ekstraktının kolon kanseri hücre hattı (HCT116) üzerindeki etkileri incelenmiştir. *C. laurifolius* bitkisi doğadan toplanarak ekstraktı hazırlanmış ve farklı konsantrasyonlarda (25, 50, 100, 200, 400, 800 µg/mL) HCT116 kolon kanseri hücre hattına ve sağlıklı insan endotel hücrelerine (HUVEC) 48 saat süreyle uygulanmıştır. Uygulama sonunda elde edilen absorbans değerleri, kontrol gruplarına göre normalize edilerek her iki hücre hattında canlılık oranları hesaplanmıştır. Sağlıklı hücrelerde düşük konsantrasyonlarda (25 µg/mL ve 50 µg/mL) hücre canlılığında sırasıyla %6 ve %12 oranında artış gözlenirken, 100 µg/mL'de %16, 200 µg/mL'de %48 ve 400–800 µg/mL'de yaklaşık %95 oranında hücre ölümü meydana gelmiştir. HCT116 hücrelerinde ise 200 µg/mL, 400 µg/mL ve 800 µg/mL konsantrasyonlarında yaklaşık %95 oranında hücre ölümünün gerçekleştiği, düşük konsantrasyonlarda (25–100 µg/mL) ise %10 civarında hücre ölümünün gözlendiği belirlenmiştir. Elde edilen bulgular, *C. laurifolius* ekstraktının 48 saatlik uygulama sonunda HCT116 kolon kanseri hücrelerinde belirgin bir anti-kanser etki gösterdiğini ortaya koymaktadır. Etkinin doza bağlı olarak arttığı saptanmıştır. Bu sonuçlar, yeterli deneysel ve moleküler düzeyde çalışmalarla desteklendiğinde, *C. laurifolius*'un kolon kanseri tedavisinde umut vaat eden doğal bir ajan olabileceğini göstermektedir.

Anahtar Kelimeler: Kolon Kanseri, HCT116, HUVEC, *C. laurifolius*, Bitki Ekstraktı

ORAL PRESENTATION

Catalytic performances of silica gel supported monometallic (Co, Nb, Cu) catalysts in hydrogen production via $NaBH_4$ methanolysis

Ceren Ates[1*] (ORCID: https://orcid.org/0009-0009-7427-5553)
Sefika Kaya[1] (ORCID: https://orcid.org/0000-0001-8277-4365)
Hilal Demir Kivrak[1] (ORCID: https://orcid.org/0000-0001-8001-7854)

[1]Eskisehir Osmangazi University, Faculty of Engineering and Architectural Sciences, Department of Chemical Engineering, Eskisehir, Turkey.

*Corresponding author e-mail: atesceren26@gmail.com

Abstract

How efficiently, environmentally friendly, and sustainably a country uses its energy resources is a direct determinant of its economic growth, industrialization, prosperity, and environmental balance. Environmental issues such as the threat of depletion of traditional energy sources over time and global warming and climate change caused by greenhouse gases released from their combustion have increased interest in renewable energy sources. In this context, hydrogen stands out as a clean and environmentally friendly energy source that can replace fossil fuels. Although hydrogen is abundant in nature, it is not found in free form. It is generally found in the structures of substances such as water, hydrocarbons, and organic compounds. Therefore, it can be obtained through various production techniques such as gas reforming, water electrolysis, biochemical processes, and thermochemical methods. Due to their high hydrogen content, high energy density, hydrogen release ability, and relative abundance in nature, chemical hydrides ($LiBH_4$, KBH_4, $NaBH_4$, etc.) are important materials for hydrogen storage and production. Sodium borohydride from these hydrides; It is a non-toxic, non-flammable, chemically stable, and safe compound with a hydrogen content of approximately 10.8%. Due to these advantageous properties, $NaBH_4$ is an effective hydride source preferred in many studies on hydrogen production. In this study, hydrogen production by methanolysis of sodium borohydride was investigated. Silica gel-supported monometallic catalysts were developed to accelerate the methanolysis reaction. Co, Nb, and Cu metals were loaded onto the silica gel support by wet impregnation method and their catalytic activities in the methanolysis reaction were compared. Hydrogen production rates of Co/SiO_2, Nb/SiO_2 and Cu/SiO_2 catalysts were obtained as 3291.24, 3335.4 and 8781.0 $mL/g_{cat}.min$ respectively. Kinetic studies were carried out on the Cu/SiO_2 catalyst, which has a higher hydrogen production rate compared to other monometallic catalysts. At the end of the kinetic studies, the Cu/SiO_2 catalyst was promising for the methanolysis reaction with its high hydrogen production rate obtained.

Keywords: Hydrogen, sodium borohydride, methanolysis, silica gel.

This study was supported by Eskisehir Osmangazi University Scientific Research Projects Commission (BAP Project No: FYL-2025-3569).

ORAL PRESENTATION

Integrative bioinformatics reveals crosstalk between MIF and HER2 signaling networks in breast and colorectal cancer

Khired Sajid[1] (https://orcid.org/0009-0006-2188-6690),
Özge Akbulut Çalışkan[1*] (https://orcid.org/0000-0002-3647-1969)

[1]Başkent University, Faculty of Science and Letters, Department of Molecular Biology and Genetics, Ankara, Türkiye

*Corresponding author e-mail: ozgeakbulutcaliskan@gmail.com

Abstract

Human epidermal growth factor receptor 2 (HER2) and the macrophage migration inhibitory factor (MIF) amplification are frequently implicated in tumor aggressiveness, immune evasion, and treatment resistance. Recent findings suggest that MIF and HER2 may cooperate through the HSF1-HSP90 signalling axis. Here, we aimed to develop a bioinformatic model to analyse MIF-HER2 co-expression patterns and their interactions with the tumor microenvironment using multiple datasets. Differential expression and correlation studies were performed using METABRIC, TCGA and GEO cohorts. Moreover, protein-protein interaction (PPI) networks were constructed using STRING (confidence 0.7 and above) and visualized in Cytoscape (v3.10.3). Network topology and centrality analyses were used to identify hub genes, which were then cross-referenced with expression fold changes between tumor and normal tissues. We found that, MIF and HER2 were markedly overexpressed in breast and colorectal tumors as compared to the normal tissues. In breast cancer, HER2-high tumors showed significantly elevated MIF levels ($p < 0.001$), which was consistently observed across TCGA and METABRIC datasets. In colorectal cancer, MIF expression was upregulated in HER2-positive tumors, although HER2 itself did not exhibit substantial expression differences within the same cohort. Furthermore, network analysis revealed *MIF, TOP2A* and *CTSD* as major hub genes in breast cancer, while *MIF*, *CD44* and *CDC25C* emerged as central hubs in colorectal cancer. These genes were predominantly associated with pathways related to proliferation, inflammation and metabolic adaptation. Overall, these findings suggest that MIF acts as a key modulator within HER2-regulated signalling networks and represents a potential co-target for therapy. The conserved MIF-HER2 expression axis may promote tumor progression through shared oncogenic and inflammatory pathways. Future experimental studies investigating dual MIF and HER2 inhibition *in vitro* are warranted to validate these bioinformatic analyses.

Keywords: MIF, HER2, bioinformatics, breast cancer, colorectal cancer.

ORAL PRESENTATION

Development of biodegradable poly(lactic acid) composites reinforced with orange peel powder

Ayla Abbaslı[1*] (ORCID:https://orcid.org/0000-0002-9383-4359),
Rima Guliyeva[1] (ORCID:https://orcid.org/0000-0002-4545-4562)

[*1]Baku Higher Oil School, Faculty of Engineering, Department of Chemical Engineering, Baku, Azerbaijan.

*Corresponding author e-mail: ayla.abbasli@bhos.edu.az:

Abstract

Biocomposites are described as composite materials that contain at least one component, either the matrix or the reinforcement, derived from a biological source [1]. The fabrication of biocomposites generally relies on traditional polymer processing methods, including extrusion and solvent casting [2]. Biocomposites are increasingly utilized in various industries such as construction, automotive, and packaging because of their low density, renewable origin, and environmentally friendly degradability [3]. Orange peel, which contains a high amount of natural polymers such as cellulose, lignin, and pectin, has emerged as a valuable bio-based raw material for bioplastic production. According to recent studies, films derived from orange peel exhibit the lowest solubility in water and ethanol, demonstrating excellent structural stability. Moreover, due to its low solubility and antimicrobial properties, orange peel is considered an eco-friendly additive that enhances the durability and environmental sustainability of biocomposites [4]. Within the scope of this study, biodegradable Poly(lactic acid) (PLA) matrices will be reinforced with orange peel powder (OPP) as a natural filler to produce biocomposite films. The orange peels will be washed, dried, and ground to an appropriate particle size, while PLA will be dissolved in chloroform and mixed with OPP at specific ratios. The obtained mixture will be cast onto glass plates and dried at room temperature to form biocomposite films. The prepared samples will be characterized by FTIR analysis, mechanical testing, water contact angle measurements, swelling ratio, and biodegradability (soil burial) tests.

Keywords: Biocomposites, Poly(lactic acid) (PLA), Orange peel powder (OPP), Biodegradable materials

References:

[1] Fartash Naeimi, E., Selvi, K. Ç., & Ungureanu, N. (2025). Exploring the Role of Advanced Composites and Biocomposites in Agricultural Machinery and Equipment: Insights into Design, Performance, and Sustainability. Polymers, 17(12), 1691.
[2] Cardon, L. K. (2017). Design and fabrication methods for biocomposites. In P. K. Mallick (Ed.), Composite Materials Handbook (pp. 25–46). Elsevier.
[3] Pokharel, A., Falua, K. J., Babaei-Ghazvini, A., & Acharya, B. (2022). Biobased polymer composites: a review. Journal of Composites Science, 6(9), 255.
[4] Castillo-Patiño, D. L., Rosas-Mejía, H. G., Albalate-Ramírez, A., Rivas-García, P., Carrillo-Castillo, A., & Morones-Ramírez, J. R. (2024). Transforming Agro-Industrial Waste into Bioplastic Coating Films. ACS omega, 9(42), 42970-42989.

ORAL PRESENTATION

Altered serum levels of netrin-4 and neogenin reflect tumor progression in glioma patients

Fırat Aydın*, Taylan Turan* Aymelek Gönenç*, Ömer Hakan Emmez**

* Gazi University, Faculty of Pharmacy, Department of Biochemistry, Ankara, Turkey
** Gazi University, Faculty of Medicine, Department of Brain and Nerve Surgery , Ankara, Turkey

Abstract

Gliomas account for approximately 30% of all primary intracranial neoplasms and 80% of malignant cases, making them the most common primary malignant brain tumors. Netrin-4, a member of Netrin, is an important secreted protein involved in axonal growth and differentiation, and is involved in the regulation of various physiological processes and the formation and metastasis of various tumors, including gliomas. There are controversial results regarding the expression of netrin-4 and its receptors, neogenin and UNC5B in glioma. The study aims to investigate whether there is a change in serum levels of Netrin-4, neogenin and UNC5B in patients compared to controls. In this study, serum Netrin-4, neogenin, and UNC5B levels were measured by ELISA method using commercial kits in 44 glioma patients and 45 healthy controls. Serum Netrin-4 and neogenin levels were found to be significantly lower in glioma patients compared to control groups $p<0.05$, $p<0.05$, respectively), whereas UNC5B levels were not different ($p>0.05$). Some studies show that Netrin-4, neogenin and UNC5B expressions are altered in glioma cell lines. Our findings in serum samples are consistent with cell culture studies reporting low expressions of Netrin-4 and neogenin in glioma.

Keywords: Netrin-4, Neogenin, UNC5B, Glioma

This study is supported by the University of Gazi Scientific Research Projects (GUBAP) with the number TYL-2024-9513.

ORAL PRESENTATION

Agomelatine may alleviate the LPS-induced ER stress response and apoptotic signaling in human embryonic kidney cells

Yağmur Doğanlar[1] (ORCID: https://orcid.org/0000-0001-8513-0821),
Yalçın Erzurumlu[1,2*] (ORCID: https://orcid.org/0000-0001-6835-4436)

[1]Suleyman Demirel University, Faculty of Pharmacy, Department of Biochemistry, Isparta, Türkiye.
[2]Suleyman Demirel University, Institute of Health Science, Department of Drug Research and Development, Isparta, Türkiye.

*Corresponding author e-mail: yalcinerzurumlu@sdu.edu.tr

Abstract

Inflammation is a self-protective biological response of the body against pathogens, cellular damage or toxic compounds, characterized by the activation of various biochemical processes and immune cells. These factors may trigger acute or chronic inflammatory responses in tissues, leading to tissue damage and thereby the development of various pathological conditions. Therefore, understanding the molecular signals associated with inflammatory responses is crucial for the development of novel therapeutic approaches to pathologies at the cellular or tissue level that may be caused by inflammation. Today, it has been demonstrated that many drugs used for various clinical purposes can be utilized to modulate inflammatory responses. Recent *in vitro* and *in vivo* studies suggested that agomelatine may play a protective role in LPS-induced inflammation, which is an agonist of the melatonin receptor and a selective inhibitor of the serotonin 2C receptor. However, its comprehensive mechanism has not been elucidated yet. Thus, we aimed to investigate the protective role of agomelatine on LPS-induced inflammation caused cellular damage in the present study by evaluating the ER stress and apoptotic responses. For this aim, the protective effect of agomelatine on LPS-induced inflammatory and apoptotic responses in HEK293 human embryonic kidney cells was studied by several methodologies. To investigate the protective role of agomelatine, the mRNA expression levels of ER stress-associated *BiP/GRP78* and *CHOP*, pro-apoptotic *BAX*, *BiD* and anti-apoptotic *BCL2*, *BCL-xL* were tested by qRT-PCR. Furthermore, the LPS-induced inflammatory response was verified by testing *TNF-α* and *IL-6* expression. Additionally, protein levels of caspase-3 and CHOP were examined by immunoblotting. Our data revealed that agomelatine treatment significantly reduced the LPS-induced inflammation caused ER stress and apoptotic signaling in HEK293 cells. Present findings suggest that agomelatine may contribute to the maintenance of cellular homeostasis by reducing inflammation-induced ER stress and apoptotic response.

Keywords: Agomelatine, Apoptosis, ER stress, Inflammation, LPS

ORAL PRESENTATION

Synergistic mechanism of graphene oxide-composite silver nanoparticles combined with gemcitabine in pancreatic cancer

Hacer Çalkap[1*] (https://orcid.org/ 0000-0003-2154-1095),
Emine Nedime Korucu[2] (https://orcid.org/ 0000-0001-7034-4130)
Fatih Erci[3] (https://orcid.org/0000-0002-3044-7343)

[*1]Necmettin Erbakan University, Faculty of Science, Department of Molecular Biology and Genetics, Konya, Türkiye
[2]Necmettin Erbakan University, Faculty of Science, Department of Molecular Biology and Genetics, Konya, Türkiye
[3]Necmettin Erbakan University, Faculty of Science, Department of Biotechnology, Konya, Türkiye

*Corresponding author e-mail: hacercalkap@gmail.com

Abstract

Pancreatic ductal adenocarcinoma (PDAC) is among the solid tumors with the highest mortality rates due to its aggressive nature and late diagnosis. Early-stage PDAC often presents without obvious symptoms, and the deep anatomical location of the pancreas leads to the disease being diagnosed mostly at an advanced stage, resulting in poor survival rates. Its dense desmoplastic stroma limits drug penetration, contributing to chemoresistance, while resistance mechanisms that emerge over time reduce treatment efficacy and lead to disease recurrence. Therefore, developing new therapeutic strategies for PDAC is of critical importance. The anticancer potential of green-synthesized silver nanoparticles (AgNPs) has been reported in various studies. Synthesizing silver nanoparticles in a composite structure with graphene oxide (GO) enhances nanoparticle stability and allows these structures to be evaluated as potential therapeutic or drug delivery candidates. Plant-mediated synthesis offers advantages such as low toxicity, high stabilization, and environmentally friendly production. In this study, the effects of GO-AgNP composites synthesized using Laurus nobilis extract in combination with the standard chemotherapeutic agent gemcitabine were investigated for PDAC treatment. AgNP, GO, and GO-AgNP structures were characterized using UV-Vis spectroscopy, TEM, FESEM, and XRD methods, and their cytotoxicity was evaluated on the Panc-1 cell line using the MTT assay. RT-PCR results showed that the combination of GO-AgNP and gemcitabine enhanced apoptosis in Panc-1 cells by decreasing Bcl-2 levels and increasing Bax levels. Additionally, suppression of VEGFA, FLT-1, and VEGFR-2 expression indicated inhibition of angiogenesis. A decrease in MMP2 levels and an increase in TIMP2 levels suggested a slowdown of the EMT process, which was confirmed at the protein level by measuring MMP2 levels using Western blot analysis. The findings foresee a potential synergistic effect of the combination of GO-AgNP and gemcitabine in PDAC treatment.

Keywords: Composite structure, Gemcitabine, Graphene oxide, Laurus nobilis (Bay leaf), Pancreatic ductal adenocarcinoma, Silver nanoparticles

ORAL PRESENTATION

Impact of plant-based dietary patterns on breast cancer prevention

Ayşenur Oruç[1*] (ORCID: https://orcid.org/0009-0003-7536-5186), Senem Suna[1] (ORCID: https://orcid.org/0000-0002-6947-2167), Senem Kamiloglu[1] (ORCID: https://orcid.org/0000-0003-3902-4360)

[*1]Bursa Uludag University, Faculty of Agriculture, Department of Food Engineering, Bursa, Türkiye.

*Corresponding author e-mail: aysenurdogan0803@gmail.com

Abstract

The association between plant-based diets and breast cancer (BC) prevention has gained growing attention in recent public health research. Accumulating evidence from cohort and intervention studies suggests that adherence to whole-food, plant-based (WFPB) and healthful plant-based dietary patterns (hPDI)—characterized by high intake of fruits, vegetables, legumes, whole grains, and nuts, and low consumption of animal and processed foods—can significantly reduce BC incidence, recurrence, and mortality. These dietary models contribute to improved metabolic profiles, including reduced body weight, fasting insulin, and low-density lipoprotein (LDL) cholesterol levels, together with enhanced hormonal balance through elevated sex hormone-binding globulin (SHBG) concentrations. Such outcomes highlight the potential of plant-centered diets in supporting both disease prevention and long-term survival among breast cancer patients. Mechanistically, plant-based diets exert protective effects by improving insulin sensitivity, reducing chronic inflammation, and lowering circulating insulin-like growth factor-1 (IGF-1). They also promote estrogen metabolism and maintain a balanced gut microbiota, which collectively modulate key pathways involved in carcinogenesis. Moreover, the abundance of phytochemicals such as flavonoids, carotenoids, and phenolic compounds provides potent antioxidant and anti-inflammatory actions that help inhibit oxidative stress, angiogenesis, and tumor-promoting signaling mechanisms. Overall, current evidence indicates that WFPB and hPDI dietary patterns support both primary prevention and better survivorship in breast cancer by modulating oxidative stress, inflammation, and hormonal homeostasis. Although additional studies are needed to clarify the roles of specific bioactive components, plant-based diets presently represent an effective and sustainable approach to reducing breast cancer risk and improving patient outcomes.

Keywords: plant-based diet, breast cancer prevention, healthful plant-based index (hPDI), whole-food plant-based diet (WFPB)

ORAL PRESENTATION

Copper oxide nanoparticles synthesized in a deep eutectic solvent for efficient metronidazole adsorption

Özge Demir* (ORCID: https://orcid.org/0000-0002-0342-5915)

*Istanbul University-Cerrahpasa, Engineering Faculty, Chemical Engineering Department, İstanbul, Türkiye.

*Corresponding author e-mail: ozge.demir@iuc.edu.tr

Abstract

Copper oxide nanoparticles (CuO NPs) are regarded as effective adsorbent materials due to their low cost, large surface area, abundant active sites, and strong affinity for contaminants. This study utilized green synthesis by preparing CuO NPs through a precipitation approach in a deep eutectic solvent (DES) composed of choline chloride, ethylene glycol, and water. The main objective was to assess these nanoparticles for removal of metronidazole (MTZ), a pharmaceutical pollutant, from water. The synthesized CuO NPs were characterized using BET, SEM, FTIR, and XRD techniques, revealing their optimal morphology, well-defined crystalline structure, and monoclinic phase. The average crystallite size, estimated with the Debye–Scherrer equation, was 70.42 nm. HPLC analyses demonstrated that the CuO NPs effectively adsorbed MTZ, with a maximum monolayer adsorption capacity of 29.39 mg/g. Adsorption followed the Langmuir isotherm and pseudo-second-order kinetic model, indicating that the process is dominated by monolayer coverage on homogenous surfaces. Thermodynamic studies confirmed that adsorption was spontaneous and endothermic, which underscores the benefits of DES-assisted synthesis on adsorption efficiency. This study highlights that using a ternary DES (ChCl:EG:H_2O) serves both as a green reaction medium and as a surface modifier, enabling the production of CuO NPs with enhanced nanostructural features and superior adsorption performance towards MTZ. The successful application of a sustainable, DES-based synthetic route illustrates a promising, environmentally friendly strategy for addressing pharmaceutical pollution during water treatment. These findings support the further investigation and development of DES-mediated nanomaterials for advanced environmental applications.

Keywords: Copper oxide nanoparticles, deep eutectic solvent, metronidazol

ORAL PRESENTATION

Next-generation inositol phosphate derivatives as mechanistic inhibitors of HIV-1 assembly

Belgin Sever [1,2*] (ORCID: https://orcid.org/0000-0003-4847-9711), Hasan Demirci [3] (ORCID: https://orcid.org/0000-0002-9135-5397), Halilibrahim Ciftci [2,4,5] (ORCID: https://orcid.org/0000-0002-9796-7669)

[*1] Anadolu University, Faculty of Pharmacy, Department of Pharmaceutical Chemistry, Eskisehir 26470, Türkiye
[2] Kumamoto University, Faculty of Life Sciences, Medicinal and Biological Chemistry Science Farm Joint Research Laboratory, Kumamoto 862-0973, Japan
[3] Koç University, Department of Molecular Biology and Genetics, Istanbul 34450, Türkiye
[4] Department of Drug Discovery, Science Farm Ltd., Kumamoto 862-0976, Japan
[5] Burdur Mehmet Akif Ersoy University, Department of Molecular Biology and Genetics, Burdur 15030, Türkiye

*Corresponding author e-mail: belginsever@anadolu.edu.tr

Abstract

Human immunodeficiency virus (HIV) remains a formidable global health threat, in large part because latent reservoirs persist despite potent combination therapies. A critical event in the viral life cycle is the recruitment of the Gag polyprotein precursor ($Pr55^{gag}$) to the plasma membrane, where it assembles into immature lattices before protease-driven cleavage yields the structural proteins matrix (MA), capsid (CA), nucleocapsid (NC) and p6. Membrane engagement is orchestrated by the MA domain through its selective interaction with phosphatidylinositol-4,5-bisphosphate ($PI(4,5)P_2$), making MA a strategic node for therapeutic disruption. We previously introduced an inositol-hexakisphosphate-derived molecule, L-HIPPO, designed to interfere with this MA-lipid interface. We found that L-HIPPO effectively immobilizes HIV within infected cells, triggering apoptosis of the host cell together with the trapped virions. This mechanism provides a conceptual framework for therapies aimed at forcing viral self-elimination and achieving complete clearance of infection. We set out to design and synthesize next-generation L-HIPPO derivatives with enhanced mechanistic antiviral activity. Building on our earlier observations that the two acyl chains of L-HIPPO constitute the most structurally tunable elements, positioned directly within the membrane interface, we rationally designed eight new derivatives by modifying these regions. We then performed structure-based docking using Schrödinger software and three high-resolution MA-IP_6 complex structures (PDB: 7E1I, 7E1J, 7E1K) previously resolved by our group, enabling a precise assessment of how each analogue engages the MA binding pocket. In this work, we first synthesized the required starting material and intermediate compounds through a six-step sequence to obtain compound a (30% overall yield, 200 mg), and we confirmed their structures by ^{1}H NMR, ^{13}C NMR, and HRMS analyses. The synthesis of the final L-HIPPO derivatives from compound a is now in progress. In subsequent stages, we will assess their ability to induce apoptosis in HIV-1-infected HeLa cells, providing insight into their potential to disrupt viral persistence.

Keywords: HIV, MA, Inositol-hexakisphosphate, Drug development

Acknowledgement: This study was supported by Health Institutes of Türkiye (TÜSEB) under the grant number 34496. The authors thank to TÜSEB for their supports.

ORAL PRESENTATION

Synthesis of new sensor based on quinolinium-containing cyanobiphenyl

İrem Sena Şen[1*] (https://orcid.org/ 0009-0002-2674-1045), Arzu Uyanik[1] (https://orcid.org/ 0000-0001-5545-7970) Ezgi Akceylan[1] (https://orcid.org/0000-0002-0513-2091)

[*] Selcuk University, Faculty of Science, Department of Chemistry, Konya, Turkey.

*Corresponding author e-mail: iremsenasen43@gmail.com

Abstract

Fluorescence sensors are of great importance in many areas, including environmental, food safety, medicine, and industry, because they offer low-cost, rapid, highly sensitive, and selective detection methods for chemical and biological analyses. Key factors determining the effectiveness of these sensors include the specific binding ability of the target analyte and the strength of the fluorescence response. In this context, the design and synthesis of fluorescent molecules plays a critical role. In this study, a cyanobiphenyl-based fluorescent sensor containing a quinolinium moiety was successfully synthesized through the Knoevenagel condensation reaction and its structure was confirmed by Nuclear Magnetic Resonance (NMR) spectroscopy. The Knoevenagel reaction is a base-catalyzed process that forms α,β-unsaturated carbonyl compounds via the condensation of carbonyl compounds with active methylene groups. This reaction pathway enables the formation of extended π-conjugated systems, which play a crucial role in enhancing fluorescence efficiency. The incorporation of the quinolinium unit and the conjugated cyanobiphenyl structure provides strong electron delocalization, resulting in improved optical properties. Due to these characteristics, the synthesized compound exhibits potential as a versatile fluorescent material for the development of chemical sensors sensitive to environmental changes or metal ions.

Keywords: Fluorescent sensor, Cyanobiphenyl, Quinolinium

ORAL PRESENTATION

Effect of trimetazidine on detrusor contractility in a mouse model of L-NAME-induced overactive bladder

Seçkin Engin[1*] (ORCID: https://orcid.org/0000-0002-1982-7820), Cemile Güllü[1]

[*1]Karadeniz Technical University, Faculty of Pharmacy, Department of Pharmacology, Trabzon, Türkiye.

*Corresponding author e-mail: seckinengin@ktu.edu.tr

Abstract

Overactive bladder (OAB) is a highly prevalent syndrome characterised by symptoms of urgency in the absence of urinary tract infection or other discernible pathology. OAB has complex etiologies and it is usually associated with detrusor overactivity (DO), defined as involuntary detrusor muscle contractions. Nitric oxide (NO) is an important neurotransmitter in the lower urinary tract, mediating the relaxation of detrusor. Chronic inhibition of NO synthesis by Nω-nitro-L-arginine methyl ester hydrochloride (L-NAME) has been demonstrated to induce DO in rodents. Trimetazidine (TMZ) is a widely used anti-anginal agent, primarily acting through the modulation of cardiac energy metabolism. Recently, TMZ has also been reported to exhibit an inhibitory effect on detrusor contractility *in vitro*, demonstrating therapeutic potential in bladder dysfunction. However, the effect of TMZ in OAB has not been clarified yet. This study aimed to evaluate the effect of TMZ on detrusor contractility in a mouse model of L-NAME-induced OAB. Male Balb/c mice were administered L-NAME (60 mg/kg) daily via oral gavage for 30 consecutive days. Thirty minutes following L-NAME administration, TMZ (20 or 80 mg/kg) was administered intraperitoneally once daily for the same 30-day period. 24 hours after the last treatment, detrusor strips were prepared and contractility studies were performed using isolated organ baths to evaluate the contractile responses. Chronic L-NAME treatment markedly enhanced KCl-, carbachol- and $CaCl_2$-induced contractions of detrusor strips compared to control, implying that long-term NO deficiency leads to OAB. However, TMZ failed to attenuate DO in L-NAME-treated mice. The findings of our study indicate that TMZ was ineffective in reversing DO in a mouse model of OAB induced by L-NAME. Further studies are required to test the therapeutic potential of TMZ using different functional methods within alternative *in vivo* OAB models. This study was funded by TÜBİTAK under the 2209-A University Students Research Projects Support Programme.

Keywords: bladder, contractility, detrusor, isolated organ bath, L-NAME, nitric oxide.

ORAL PRESENTATION

Investigation of the genotoxicological potential of desipramine, an active substance used in antidepressant drugs, by *in vitro* test methods

Busenaz Tuncay[1*] (ORCID: https://orcid.org/0000-0001-8700-7958), Ece Avuloğlu-Yılmaz[2] (ORCID: https://orcid.org/0000-0002-5164-3431), Ayşen Yağmur Burgazlı[1] (ORCID: https://orcid.org/0000-0003-1657-6808), Fatma Okuş[1] (ORCID: https://orcid.org/0000-0001-7648-9584), Fatma Ünal[3] (ORCID: https://orcid.org/0000-0001-7648-9584), Deniz Yüzbaşıoğlu[3] (ORCID: https://orcid.org/0000-0003-2756-7712)

[1]Gazi University, Graduate School of Natural and Applied Sciences, Department of Biology, Ankara, Türkiye.
[2]Amasya University, Vocational School of Technical Sciences, Amasya, Türkiye.
[3]Gazi University, Science Faculty, Department of Biology, Ankara, Türkiye.

*Corresponding author e-mail: tuncaybusenaz@gmail.com

Abstract

Depression and anxiety are widespread psychiatric concenrns affecting a substantial portion of the global population. Antidepressant medications, such as desipramine, an active tricyclic antidepressant compound, are commonly prescribed for long-term use; however, their potential genotoxic (DNA and chromosome damaging) and cytotoxic (cell damaging) effects remain underexplored. This study aimed to evaluate the genotoxicity and cytotoxicity of desipramine using *Allium cepa* (*A. cepa*) root tip cells through the Allium test and Comet assay. Desipramine was applied at six concentrations (1.5, 3, 6, 12, 18, and 24 µg/mL) for 24 and 48 hours. Results demonstrated a dose- and time-dependent reduction in the mitotic index, indicating cytotoxic effects. Additionally, a significant increase in the frequency of mitotic abnormalities was observed in the 48-hour treatment group at all concentrations, whereas the 24-hour exposure induced significant abnormalities only at concentrations ≥12 µg/mL. The Comet assay further revealed a marked increase in DNA damage in desipramine-treated groups at all concentrations and time points, relative to the negative control. These findings indicate that desipramine induces both cytotoxic and genotoxic effects in *A. cepa* root tip cells, highlighting its potential risk to living organisms upon prolonged or high-dose exposure. Given the widespread and often chronic use of antidepressants, it is crucial to further investigate their long-term biological impacts. A thorough reassessment of the risk-benefit profile of desipramine and similar compounds is warranted, considering their implications for both human and environmental health.

Keywords: Desipramine, Genotoxicity, Allium Test, Allium Comet Assay, Mitotic Aberrations

Acknowledgements: This study was partially supported by Amasya University Research Fund under Project No. FMB-BAP 23-0593.

ORAL PRESENTATION

Chronic inflammation response in acute myeloid leukemia (AML)

Öznur Coşkun[1] (ORCID: https://orcid.org/0000-0002-0952-8499), Meltem Bay[2] (ORCID: https://orcid.org/0000-0001-7645-5368) Nevin Belder[3] (ORCID:https://orcid.org/0000-0001-9353-9387) Cansu Özdemir[4] (ORCID:https://orcid.org/0000-0003-4095-7475)

[*1] Ankara University, Veterinary Faculty Department of Genetics Department, Ankara, Turkey.
[*2] Ankara University, Stem Cell Instutite, Ankara, Turkey
*[3] Ankara University, Biotechnology Instutite, Ankara, Turkey.
[*4] Hacettepe University, Center for Stem Cell Research and Development PEDI-STEM, Ankara, Turkey.

*Corresponding author e-mail: cansuozsaka@gmail.com

Abstract

Acute myeloid leukemia (AML) is a malignancy characterized by the abnormal proliferation and accumulation of myeloid progenitor cells in the bone marrow and peripheral blood. Identifying cellular responses to inflammation in AML is critical for developing new diagnostic and therapeutic strategies in this area. This study aims to evaluate apoptosis, pyroptosis, and lymphocyte differentiation processes in a TNF-α-mediated chronic inflammation model of AML, the most common type of leukemia among hematologic malignancies. The study further aims to demonstrate how inflammatory environments regulate immune responses in cancer cells and activate cell death mechanisms. HL-60 cells were treated with TNF-α for 15 days to induce chronic inflammation. Subsequently, programmed cell death mechanisms associated with inflammation, namely pyroptosis and apoptosis, as well as lymphocytic differentiation potential, were examined in AML cells under chronic inflammation. TNF-α-treated cells showed increased expression of PD-L1, HMGB1, GSDME, CD68, and CD11a/18 compared to controls, along with enhanced apoptosis, suggesting an induction of programmed cell death. These findings indicate that prolonged exposure to cytokines such as TNF-α creates a complex effect within the cancer microenvironment, both activating immune responses and promoting immune evasion mechanisms in cancer cells. Such insights may guide the development of therapeutic strategies for cancers associated with inflammation, such as leukemia.

Keywords: Acute Myeloid Leukemia (AML), TNF-α, pyroptosis, apoptosis

ORAL PRESENTATION

Evaluating the potential of royal jelly as a tyrosinase inhibitor

Sertan Genc[1*] (https://orcid.org/0009-0008-1651-861X),
Aslihan Kazan[1] (https://orcid.org/0000-0002-8947-8494)

[*1]Bursa Technical University, Faculty of Engineering and Natural Sciences, Department of Bioengineering, Bursa, Türkiye.

*Corresponding author e-mail: sertanngnc@gmail.com

Abstract

Royal jelly (*Apis mellifera* L.) is a natural secretion produced by the hypopharyngeal and mandibular glands of worker honeybees to nourish larvae and the queen. It is a yellowish-white, viscous substance with an acidic and pungent taste. Owing to its complex chemical composition, royal jelly possesses high biological value and is rich in proteins, peptides, carbohydrates, fatty acids, vitamins, and other bioactive compounds. Its diverse biological activities include antibacterial, antiviral, antioxidant, antitumor, and skin-lightening effects. The primary contributors to these activities are the major royal jelly proteins (MRJPs) and 10-hydroxy-2-decenoic acid (10-HDA), the latter being a fatty acid unique to royal jelly and recognized as both a quality indicator and a marker of biological activity. In this study, the 10-HDA content of royal jelly and its inhibitory effect on the tyrosinase enzyme were evaluated. High-Performance Liquid Chromatography (HPLC) analysis revealed that 10-HDA content of royal jelly was 5.85% and 2.02% on a dry and fresh matter basis, respectively. The tyrosinase inhibitory activity was assessed spectrophotometrically using fungal tyrosinase (*Agaricus bisporus*) as the enzyme, L-DOPA as the substrate, and kojic acid as the positive control. The results demonstrated that enzyme activity decreased in a dose-dependent manner with increasing concentrations of royal jelly. The IC_{50} values were calculated as 14.2 mg/mL for royal jelly and 59.7 µM for kojic acid. Kinetic analyses indicated that both inhibitors could bind to the free enzyme and the enzyme-substrate complex, thereby exhibiting a mixed-type inhibition mechanism. These results indicate that the bioactive components of royal jelly, particularly 10-HDA, suppress tyrosinase activity by interfering both substrate binding and product formation within the enzyme's catalytic cycle. In conclusion, royal jelly with high 10-HDA content can be considered as a promising natural tyrosinase inhibitor with potential applications in dermocosmetic and pharmaceutical formulations.

Keywords: royal jelly, 10-HDA, tyrosinase, enzyme inhibition

ORAL PRESENTATION

Biochar-assisted removal of anionic textile dyes from model waste water

Duygu Ova Özcan* (https://orcid.org/my-orcid?orcid=0000-0002-6462-1725),

* Ege University, Faculty of Engineering, Department of Chemical Engineering, İzmir, Türkiye.

*Corresponding author e-mail: duygu.ova@ege.edu.tr

Abstract

The discharge of synthetic dyes from textile industries into aquatic systems poses a major environmental challenge due to their toxicity, stability, and resistance to biological degradation. In this study, biochar produced from olive stone biomass was investigated as a low-cost and sustainable adsorbent for the removal of anionic textile dyes from aqueous solutions. Orange II, Procion Red, and Reactive Black were selected as model dyes, and batch adsorption experiments were conducted at initial dye concentrations of 20, 35, and 50 mg L^{-1} under different contact times. Percent removal efficiencies were calculated to evaluate the adsorption performance. The obtained results demonstrated that olive-stone-derived biochar exhibited notable removal efficiency for all three anionic dyes, indicating strong affinity and potential surface interactions between the biochar functional groups and dye molecules. Moreover, both contact time and initial concentration were found to influence adsorption behavior. Overall, this study highlights the feasibility of valorizing olive processing residues into a promising biochar adsorbent for water treatment, contributing to sustainable resource utilization and circular economy-based remediation strategies.

Keywords: Biochar, Anionic dyes, Adsorption, Water treatment, Resource valorization.

ORAL PRESENTATION

The effect of vacuum PA/PE packaging on certain quality characteristics during the ripening process in classical white cheese production

Ahmet Aytaç Yıldız[1*] (ORCID: https://orcid.org/0009-0006-6354-2140.),
Fatma Çolakoğlu[2] (ORCID: https://orcid.org/0000-0002-2211-8371)

[*1]Çanakkale Onsekiz Mart University, Graduate School of Education, Department of Food Safety and Quality, Çanakkale, Türkiye.
[2]Çanakkale Onsekiz Mart University, Faculty of Applied Sciences, Department of Food Technology, Çanakkale, Türkiye.

* Corresponding author e-mail: ffkrlay@gmail.com

Abstract

In classical white cheese production, the process is completed during the ripening stage, which plays a decisive role in the development of the cheese's taste, aroma, texture, and overall quality characteristics. In the industry, ripening is traditionally carried out in lacquered tin containers with brine over a period of 3–9 months. This study aimed to evaluate the use of vacuum PA/PE packaging as an alternative to tin containers during the ripening of classical white cheese and to determine the effects of vacuum packaging on quality parameters. Cheese production was conducted at the Akpınar A.Ş. dairy processing facility following the standard white cheese production process. The produced cheese was divided into two groups: the first group was hermetically packaged in tin containers, while the second group was packaged in vacuum PA/PE (polyamide/polyethylene) bags. Both groups were stored at 4±2 °C and ripened for a total of 270 days. To assess quality changes, samples were taken monthly and subjected to sensory, chemical, and microbiological analyses. The results indicated that the type of packaging notably influenced sensory quality. During the first three months, both groups exhibited similar characteristics; however, from the fourth month onwards, tin-packaged cheeses showed superior pore structure and mature taste. By the eighth and ninth months of ripening, more pronounced differences were observed: tin-packaged cheeses maintained intense flavor and aroma along with a porous, firm texture, whereas vacuum PA/PE-packaged cheeses displayed a more elastic, non-porous texture with a unidirectional taste and aroma profile. Microbiological quality and migration analyses revealed no adverse findings in either packaging group, confirming that the cheeses remained safe for consumption. In conclusion, the type of packaging used during the cheese ripening process was found to directly affect sensory characteristics, particularly the development of taste and aroma.

Keywords: Classical white cheese, ripening process, vacuum packaging, tin packaging, quality characteristics

ORAL PRESENTATION

Borik asidin melanom hücre hattı üzerindeki antikanser etkisinin araştırılması

Şeyma Nur Çelik[1*](ORCID: https://orcid.org/0009-0001-5989-733X), Melek Pehlivan[2] (ORCID: https://orcid.org/0000-0001-8755-4812), Hatice İlayhan Karahan[1] (ORCID: https://orcid.org/0000-0002-3371-7345), Mustafa Soyöz[1] (ORCID: https://orcid.org/0000-0001-5159-6463), Tülay Kılıçaslan Ayna[1] (ORCID: https://orcid.org/0000-0001-7993-978X), İbrahim Pirim[1] (ORCID: https://orcid.org/0000-0001-8485-3286)

[1] İzmir Kâtip Çelebi Üniversitesi, Tıp Fakültesi, Tıbbi Biyoloji ve Genetik Anabilim dalı, İzmir, Türkiye.
[2] İzmir Kâtip Çelebi Üniversitesi, Sağlık Hizmetleri Meslek Yüksekokulu, Tıbbi Laboratuvar Teknikleri Programı, İzmir, Türkiye.

*Sorumlu yazar e-mail: celikseymanur35@gmail.com

Özet

Melanom, melanin sentezinden sorumlu melanositlerin malign transformasyonu sonucunda gelişen agresif bir cilt kanseridir. Geç tanı ve hızla ilerleme eğilimi nedeniyle ileri evre melanomun tedavisinde daha az toksik ve daha etkili ajanlar geliştirme ihtiyacı giderek artmaktadır. Son yıllarda elementel bor, yeni terapötik moleküllerin tasarlanmasında dikkat çekici özellikleri nedeniyle ilgi odağı hâline gelmiştir. Borik asidin (BA) çeşitli kanser türlerinde sitotoksik etki gösterdiği bildirilmiş olsa da altında yatan moleküler mekanizmalar tam olarak aydınlatılamamıştır. Bu çalışmada, BA'nın Malme-3M melanom hücrelerinde proliferasyon, apoptoz ve oksidatif stres üzerindeki etkileri değerlendirilmiştir. BA'nın hücre canlılığı üzerindeki etkisi 24, 48 ve 72 saatlik uygulamalar sonrasında MTT yöntemi ile analiz edilmiştir ve BA'nın 48. saatteki IC_{50} değeri 58.95 mM olarak belirlenmiştir. Apoptoza yönelik değişiklikler Annexin ELISA testi ve ilgili gen ekspresyon analizleriyle incelenmiştir. Apoptozla ilişkili Bcl-2, Bax, Kaspaz-3, -8, -9 ve Annexin V ekspresyon düzeyleri RT-qPCR ve ELISA yöntemleri kullanılarak değerlendirilmiştir. BA uygulaması sonucunda antiapoptotik genlerin baskılandığı, proapoptotik genlerin ise arttığı gözlenmiş; Annexin V düzeylerindeki yükselme apoptozun indüklendiğini desteklemiştir. Oksidatif stres değerlendirmesinde toplam oksidan seviye (TOS), toplam antioksidan kapasite (TAS) ve oksidatif stres indeksi (OSI) hesaplanmıştır. Uygulanan farklı BA konsantrasyonları sonrasında, hücrelerde TOS'un yükseldiği ve TAS'ın azaldığı gösterilmiştir. Artan TOS, azalan TAS seviyeleri ile hesaplanan OSI değeri ise IC 50 dozunda en yüksek seviyede tespit edilmiştir. Elde edilen bulgular, BA'nın Malme-3M hücrelerinde apoptozu indüklediğini açıkça ortaya koymaktadır. Genel olarak, BA'nın Melanom hücre hattında hücre çoğalmasını inhibe eden, apoptozu tetikleyen ve antioksidan kapasiteyi azaltan etkileri, bu bileşiğin melanom tedavisinde potansiyel bir antikanser ajan adayı olarak değerlendirilmektedir.

Anahtar Kelimeler: Borik asit, Melanom, Antikanser, Apoptoz, Oksidatif stres.

ORAL PRESENTATION

Development of impact-resistant, halogen-free, flame-retardant PBT-based composites for use in the automotive industry

Sertcan Urcan

Technology, Testing and Analytics Team Leader, Epsan Plastik

Corresponding author e-mail: sertcan.u@epsan.com

Abstract

The automotive industry is increasingly turning to lightweight, durable, and heat-resistant polymeric composite materials to reduce fuel consumption and enhance vehicle performance. Therefore, there is a growing need to develop polymeric matrix composites that can be used continuously at high temperatures while maintaining mechanical strength. In this study, the aim was to develop a new generation of polymeric composites with high impact resistance and long-term thermal stability, specifically for use in interior and exterior automotive parts. For this purpose, Polybutylene Terephthalate (PBT), an engineering plastic known for its resistance to heat and chemicals thanks to its morphological structure, was selected as the matrix material. The aim of the study was to develop halogen-free flame-retardant and impact-modified PBT composites for use in components exposed to high temperatures, such as in electric vehicles. To achieve these properties, a total of 8 different formulations containing various impact-modifying additives were prepared and tested. In addition, orange color additives, which are frequently preferred in the automotive industry to increase safety and visibility, have also been added to the formulations. Different PBT-based composite formulations were produced using a twin-screw extruder through melt compounding, and the resulting granules were shaped using injection molding. To evaluate the performance of the developed materials, a comprehensive set of mechanical, thermal, and electrical tests was conducted. Mechanical properties were assessed using tensile testing, flexural testing, and both notched and unnotched Izod and Charpy impact tests. High-temperature performance was evaluated through Heat Deflection Temperature (HDT) testing. Electrical properties were assessed with the Comparative Tracking Index (CTI). Flame retardancy was determined according to UL-94, Glow-Wire Ignition Temperature (GWIT), and Glow-Wire Flammability Index (GWFI). As a result, the developed PBT-based composites demonstrated that they can be used as cost-effective, environmentally friendly, and locally manufacturable alternatives in automotive parts that require high heat and impact resistance.

Keywords: Halogen-Free Flame Retardant Composites, Impact-Modified PBT, Automotive Polymer Materials

ORAL PRESENTATION

Synthesis of biopolymer-based quercetin delivery systems using alginate beads: *In vitro* antioxidant and release kinetic analyses

Cahit Özbilenler[1*] (ORCID: https://orcid.org/0000-0003-4494-3310), Selma Ustürk[1] (ORCID: https://orcid.org/0000-0003-2507-2951), Ergül Mutlu Altundağ[2] (ORCID: https://orcid.org/0000-0001-5355-4654), Mustafa Gazi[1] (ORCID: https://orcid.org/0000-0001-7736-752X)

[*1]Eastern Mediterranean University, Faculty of Arts and Sciences, Department of Chemistry, Famagusta, North Cyprus via Mersin 10, Turkey.
[2]Eastern Mediterranean University, Faculty of Medicine, Department of Medical Biochemistry, Famagusta, North Cyprus via Mersin 10, Turkey.

*Corresponding author e-mail: cahit.ozbilenler@emu.edu.tr

Abstract

In recent years, there has been a growing interest in polymeric materials derived from natural sources, accompanied by an expansion of their applications across various biomedical fields. This study presents an environmentally sustainable approach by incorporating both the naturally occurring polyphenol quercetin and the biopolymer alginate as components of a drug delivery system. Furthermore, the comparison between quercetin-loaded cryogel beads and gel beads holds considerable scientific importance. Alginate-based delivery systems were developed for the controlled release of quercetin. Initially, quercetin encapsulated calcium ion (Ca^{2+}) cross-linked alginate gel beads were synthesized through ionic gelation, followed by the preparation of their corresponding cryogel bead forms. Encapsulation of quercetin in alginate beads was determined and proven upon Fourier Transform Infrared (FT-IR) spectra analysis. Release kinetic studies were performed in dimethyl sulfoxide (DMSO). Kinetic analysis revealed that quercetin release from alginate cryogel beads in DMSO followed a first-order model, indicating concentration-dependent release behavior. In contrast, quercetin release from alginate gel beads conformed to the Higuchi model, suggesting diffusion-driven transport through the polymeric matrix. The 2,2-diphenyl-1-picrylhydrazyl (DPPH) assay was performed to determine the radical scavenging capacity of quercetin and compared with gallic acid as a reference material.

Keywords: Quercetin, drug delivery systems, alginate, antioxidant capacity.

ORAL PRESENTATION

Recombinant production of glycoprotein E of Varicellovirus bovinealpha1 in the *Pichia pastoris* yeast expression system

Servet Merve Büyükceran[1*] (ORCID: https://orcid.org/0009-0009-3765-6648), Ayşe Gençay Göksu[2*] (ORCID: https://orcid.org/0000-0003-4422-8085), İbrahim Sözdutmaz[3*] (ORCID: https://orcid.org/0000-0002-3712-7991)

[1*] Erciyes University, Institute of Health Sciences, Department of Veterinary Microbiology, Kayseri, Türkiye.
[2*, 3*] Erciyes University, Faculty of Veterinary Medicine, Department of Veterinary Virology, Kayseri, Türkiye.

*Corresponding author e-mail: mesmergul@hotmail.com

Abstract

Varicellovirus bovinealpha1 is an infectious viral agent that causes respiratory and genital tract diseases in cattle, leading to severe economic losses, including reduced milk production and abortion. The gE glycoprotein is a key virulence factor that enables herpesviruses to evade immune responses and spread efficiently from cell to cell, particularly within nervous tissue. In this study, the aim was to produce and characterize the gE glycoprotein in a yeast expression system using *Pichia pastoris.* The clinical *V. bovinealpha1* virus isolate (Kayseri, 2024) was used in the MDBK cell line. The partial gE gene region encoding 210 amino acids, which contains antigenically rich epitope regions, was amplified by PCR using primers. *Eco*RI and *Xba*I restriction sites located in the multiple cloning site of the pPICZαA vector were added to the 5' ends of the primers. The obtained PCR product was ligated into the vector using T4 DNA ligase enzyme, and a recombinant pPICZAα-gE was constructed. The pPICZAα-gE was propagated and purified in *Escherichia coli* DH5α cells and transferred to *P. pastoris* GS115 by electroporation. Selection of transformants was performed on selective YPD-Sorbitol medium containing Zeocin antibiotic. Following enrichment of positive colonies in BMGY/BMMY medium, induction was carried out with 1% methanol for 96 hours. The gE glycoprotein secreted in the culture supernatant was purified with His-tag affinity resin. The presence of a protein with a molecular weight of approximately 23 kDa was observed in SDS-PAGE analysis, and the specific product was confirmed by Western blot analysis using HRP-conjugated mouse 6x-His Tag monoclonal antibody. In conclusion, we successfully expressed the gE glycoprotein in the *P. pastoris* system for protein expression, demonstrating that this system could serve as a suitable model for the recombinant production of viral glycoproteins. It was evaluated that the obtained protein could be utilized in advanced diagnostic and immunological research.

Keywords: *Varicellovirus bovinealpha1*, *Pichia pastoris*, gE glycoprotein, recombinant expression

*It has been summarized from the master thesis conducted at the Erciyes University, Institute of Health Sciences.
* This study was supported by the ERU Scientific Research Projects Coordination Unit. Project no: TYL-2024-14180

ORAL PRESENTATION

Chemical characterization and enantiomeric distribution of Bulgarian lavender (*Lavandula angustifolia* Mill.) cultivars growing in Türkiye

İlker Demirbolat (ORCID: https://orcid.org/0000-0002-8756-1884)

İstanbul Kent University, Faculty of Pharmacy, Department of Pharmaceutical Chemistry, İstanbul, Türkiye.

Corresponding author e-mail: demirbolatilker@gmail.com

Abstract

Lavender (*Lavandula angustifolia* Mill.) is one of the most widely cultivated essential oil–producing plant species globally. In Türkiye, commercial plantations predominantly utilize cultivars originating from Bulgaria. The objective of the present study was to determine the essential oil yield, chemical composition, and enantiomeric distribution of linalool and linalyl acetate in six Bulgarian lavender cultivars (Sevtopolis, Druzhba, Yubileina, Hemus, Hebar, and Raya) cultivated in the Marmara (Thrace) region of Türkiye. For each cultivar, 15 individual plant samples were analyzed. Essential oils were extracted via hydrodistillation using a Clevenger-type apparatus. The essential oil yields were as follows: Sevtopolis 4.9%, Druzhba 5.2%, Yubileina 5.1%, Hemus 5.8%, Hebar 5.3%, and Raya 5.1%. Chemical characterization of the oils was conducted using GC–MS/FID equipped with a polyethylene glycol (wax) column. Linalool and linalyl acetate, the principal quality markers of lavender essential oil, varied among cultivars: Sevtopolis exhibited the lowest concentrations (29% linalool and 30% linalyl acetate), whereas Yubileina showed the highest (32% and 35%, respectively). Enantiomeric analysis of linalool and linalyl acetate—an important determinant of essential oil authenticity—was performed using GC–MS/FID with a chiral Cyclodex-β column (10.5% β-cyclodextrin; 60 m × 0.25 mm × 0.25 µm). The proportion of R-(–)-linalool ranged from 96.2% to 97.8% across the cultivars, while linalyl acetate consisted exclusively of the R-(–) enantiomer (100%) in all samples. The highest R-(–)-linalool content was detected in Druzhba (97.8%), whereas the lowest occurred in Hemus (96.2%). As the cultivars exhibited only minor differences in chemical composition and enantiomeric distribution, and given its comparatively high essential oil yield, Hemus appears to be the most suitable cultivar for cultivation under the environmental conditions of the Marmara region.

Keywords: Lavender, Bulgarian cultivar, Chemical characterization, Enantiomeric distribution, Chiral separation.

ORAL PRESENTATION

Investigation of insecticidal effects of some plant seed oils on adults of *Acanthoscelides obtectus* (Say, 1831) (Coleoptera: Chrysomelidae)

Hatice Öksüm[1*] (https://orcid.org/0000-0003-2212-6483), Ebru Gül Aslan[2] (https://orcid.org/0000-0003-3073-186X)

[*1] Süleyman Demirel University, Graduate School of Natural and Applied Sciences, Department of Biology, Isparta, Türkiye.
[2] Süleyman Demirel University, Faculty of Engineering and Natural Sciences, Department of Biology, Isparta, Türkiye.

*Corresponding author e-mail: haltay80@gmail.com

Abstract

Legumes are highly susceptible to post-harvest insect damage, which can reduce seed quality, weight, and germination. *Acanthoscelides obtectus* (Say, 1831) is a major pest of stored beans and other legumes. While chemical insecticides are commonly used, concerns about residues and environmental impact necessitate safer alternatives. Plant-derived fixed oils represent a promising natural control strategy. This study evaluated the insecticidal effects of *Calendula officinalis* oil and *Silybum marianum* oil on adult *A. obtectus* under controlled laboratory conditions. Experiments were conducted at 24 ± 1°C and 27 ± 1°C with 65 ± 5% relative humidity in temperature-controlled incubators.. Four different doses (100, 150, 200, and 250 µL) were applied in four replicates, each consisting of 20 adult individuals, and mortality was monitored until all individuals in the control groups had died. LT_{50} values were calculated to quantify the speed of lethal effects. Results showed clear dose–response and temperature–dependent patterns. At 24 °C, *Calendula officinalis* oil exhibited rapid mortality, particularly at 200–250 µL, whereas *Silybum marianum* oil showed moderate efficacy. At 27 °C, mortality increased for both oils, with *Calendula officinalis* oil consistently producing the fastest lethal effect across all doses. *Silybum marianum* oil's activity at 27 °C increased at higher doses (specifically at 150 µL and higher doses) but remained low at 100 µL. These findings demonstrate that elevated temperature enhances insecticidal performance and that *Calendula officinalis* oil is more potent than *Silybum marianum* oil under all tested conditions. Overall, high-dose applications of *Calendula officinalis* oil produced the lowest LT_{50} values, indicating its potential as a rapid-acting natural agent for the management of *A. obtectus* in stored legumes.

Keywords: *Acanthoscelides obtectus*, Chrysomelidae, Insecticidal potential, *Silybum marianum* oil, *Calendula officinalis* oil.

ORAL PRESENTATION

The diagnostic importance of circulating subfatin levels in the development of obesity

Merve Zorlu[1*](ORCID:https://orcid.org/0009-0001-1585-1620),Burak Yazgan[1,2](ORCID: https://orcid.org/0000-0003-0717-7768)

[1]*Amasya University, Institute of Health Sciences, Department of Molecular Medicine, Amasya, Turkey,
[2]Amasya University, Sabuncuoğlu Serefeddin Health Services Vocational School, Department of Medical Services and Techniques, Amasya, Turkey,

*Corresponding author e-mail: merve9905@gmail.com

Abstract

Excessive and abnormal excess fat in the body that leads to biological health problems is called obesity With the rapid increase in obesity prevalence in recent years, obesity has become a major public health problem worldwide There are studies in the literature showing that increased BMI and abdominal obesity have an effect on prediabetes, type 2 diabetes, metabolic syndrome, hypertension and atherosclerotic diseases. Subfatin is an adipokine, and this adipokine may be a potential therapeutic target in metabolic syndrome, inflammation and obesity by regulating tissue energy homeostasis. In this context, the aim of our study is to investigate the changes in the levels of subfatin in obesity progression. For this purpose,patients with a body mass index between 18.5-24.9 kg/m2 were included in the control group, those with a body mass index between 25-29.9 kg/m2 were included in the preobese group and those with a body mass index ≥30 kg/m2 were included in the obese group.In blood samples taken from patients; fasting blood glucose, HbA1c, triglyceride,total cholesterol, HDL, LDL, ALT,AST,TSH,T3,T4 levels were determined by autoanalyzer. Subfatin peptide levels were measured by ELISA. We observed that glucose, HbA1c levels in both preobese group and obese group were significantly higher than compared to control group.We observed that HDL levels in the obese group were significantly reduced compared to the control group.Also we observed no significant change in subfatin levels between the control group and the preobese group but subfatin levels were found to be significantly higher in the obese group compared to the control group. Our findings illustrated that subfatin levels increased with obesity and were positively correlated with the high blood sugar and triglyceride values accompanying obesity, while negatively correlated with HDL.

Keywords: Obesity,MetabolicSyndrome,Adipokine,Subfatin,Body mass index

Funding: This work was supported by Amasya University Research Fund (Project no: FMB-BAP 25-0620)

ORAL PRESENTATION

Sustainable gold nanoparticle fabrication from *Corylus maxima* leaves via microwave-assisted extraction

Gönül Serdar[1*] (ORCID: https://orcid.org/ 0000-0002-3589-2323), Vildan Serdaroğlu[2], Tuğba Mazlum Şen[3], Salih Terzioğlu[4], Bedri Serdar[4]

[*1] Karadeniz Technical University, Central Research Laboratory,Trabzon, Türkiye
[2]Karadeniz Technical University, Medicine and Pharmaceutical Technology Application and Research Center, Trabzon, Türkiye
[3]Karadeniz Technical University, Department of Biochemistry, Trabzon, Türkiye
[4] Karadeniz Technical University, Faculty of Forestry, Trabzon 61080, Türkiye

*Corresponding author e-mail: gonulserdar@ktu.edu.tr

Abstract

Leaves of *Corylus maxima* Mill. were collected from the Mersin district of Akçaabat (Trabzon, Türkiye) for microwave-assisted extraction. Hazelnut is a shrub- or tree-form plant belonging to the genus *Corylus* within the subfamily Coryloideae of the family Betulaceae, and it naturally occurs in Anatolia, the Balkans, and the Caucasus region (1,2) The collected leaves were washed several times with water to remove dust and particulate residues, then dried under suitable conditions to eliminate remaining moisture. A total of 20 g of dried and ground hazelnut leaves was mixed with 400 mL of water and shaken at room temperature for 240 minutes, followed by microwave extraction at 900 W for 2 minutes.From the obtained extract, 1 and 2 mL aliquots were taken and mixed with an aqueous solution of 0.2 mM $HAuCl_4 \cdot 3H_2O$. Gold nanoparticles (AuNPs) were synthesized by subjecting these mixtures to microwave irradiation at 90 W and 180 W for 1–30 minutes**.** Reactions between hazelnut leaf extracts and solutions containing different concentrations of Au^{3+} ions were monitored, and characteristic surface plasmon resonance (SPR) peaks were determined using UV–Visible spectroscopy. Dynamic light scattering (DLS) analyses provided particle size distribution, polydispersity index (PDI), and zeta potential measurements, enabling an assessment of stability and dispersion (3).

Keywords: *Corylus maxima* Mill, AuNPs, UV–Vis spectroscopy

Funding: This research was funded by Karadeniz Technical University,TÜRKİYE, Project No. BAP01 (FBA-2024-15956).

References:

Molnar, T. J. (2011). Corylus. C. Kole (Ed.) Wild crop relatives: genomic and breeding resources. Forest Trees (15-48 ss). Springer, Germany.

Botta, R., Molnar, T. J., Erdogan, V., Valentini, N., Torello Marinoni, D., & Mehlenbacher, S. A. (2019). Hazelnut (Corylus spp.) breeding. Advances in Plant Breeding Strategies: Nut and Beverage Crops, 4, 157-219

3- Serdar, G.2024. ‘‘Biosynthesis and Characterization of Gold Nanoparticles Using Microwave-Assisted Technology from Pomegranate (Punica granatum L.) Leaf Extract Produced by the Method of Supercritical Fluid Extraction (SFE)’’. Plasmonics, https://doi.org/10.1007/s11468-024-02312-6.

ORAL PRESENTATION

The effect of schiff base–derived 4,5-dihydro-1*h*-1,2,4-triazol-5-one compound on serum protein expression and lipid profile in wistar albino rats

Cansu Beytur[1*] (ORCID:0000-0002-4361-5035), Evren Koç[2] (ORCID:0000-0002-0022-9433)

[*1]Kafkas University,Graduate School of Natural and Applied Sciences, Department of Molecular Biology, Kars, Türkiye
[2]Kafkas University, Faculty of Engineering and Architecture, Department of Bioengineering, Kars, Türkiye

*Corresponding author e-mail: cnsbytrc@gmail.com

Abstract

Regulating cholesterol and lipid metabolism is important for maintaining cellular energy balance and cell membrane integrity. In recent years, research into the antioxidant, anticancer and metabolic regulatory effects of Schiff base derivative compounds in biological systems has intensified. The aim of our study was to determine the effects of the newly synthesised compound 4,5-dihydro-1*H*-1,2,4-triazol-5-one (3-MTA) on serum protein expression and lipid profiles under *in vivo* conditions. For this study, 28 Wistar albino rats, aged 4–5 months, were divided into four groups: a control group; a dimethyl sulfoxide (DMSO) group; a group receiving a 10mg/kg application of 3-MTA; and a group receiving a 50mg/kg application of 3-MTA. Serum protein expression was evaluated using sodium dodecyl sulfate-polyacrylamide gel electrophoresis; triglyceride, total cholesterol, high-density lipoprotein (HDL), low-density lipoprotein (LDL) and very low-density lipoprotein (VLDL) levels were determined using an autoanalyser. Following the electrophoretic evaluation, decreased 167kD protein expression and increased 62kD protein expression were observed in rats administered the 3-MTA compound at a dose of 50mg/kg, compared to the control group. A decrease in 55kD and 53kD protein expression was observed in rats administered a 10 mg/kg dose, while an increase was observed in rats administered a 50mg/kg dose. According to biochemical analysis, triglyceride and VLDL cholesterol levels increased ($P<0.001$) and LDL cholesterol levels decreased ($P<0.001$) only in rats administered a 10mg/kg dose of the 3-MTA compound compared to the control group. In conclusion, it is anticipated that the 3-MTA compound will have a positive effect on lipid metabolism and the serum protein profile. These effects are believed to be associated with the compound's potential antioxidant or hepatoprotective mechanisms. While comprehensive analyses are yet to be conducted, 3-MTA is considered a may represent a promising candidate for further investigation.

Keywords: Schiff Base, Cholesterol, Lipid Profile, Serum Proteins

*This study was submitted as a master's thesis at the Institute of Natural Sciences at Kafkas University.

ORAL PRESENTATION

Evaluation of the *in vitro* genotoxic and antigenotoxic potential of *Geranium robertianum* extract

Tuğçe Mutlu[1*] (https://orcid.org/0009-0002-6003-8281),
Mehmet Sarimahmut[1] (https://orcid.org/0000-0003-2647-5875)

[1]Bursa Uludağ Üniversitesi, Fen-Edebiyat Fakültesi, Biyoloji Bölümü, Bursa, Türkiye.

*Corresponding author e-mail: 082010007@ogr.uludag.edu.tr

Abstract

Reactive oxygen species (ROS) generated during metabolic processes, together with environmental factors such as radiation, heavy metals, pesticides and cigarette smoke, can cause severe damage to DNA, including strand breaks, base modifications and chromosomal abnormalities. Such DNA lesions form the basis of various pathological mechanisms, including the development of mutations, disruption of the cell cycle, premature cellular senescence and malignancy. Insufficiencies in DNA repair pathways lead to the accumulation of permanent genetic alterations, ultimately compromising genomic integrity. Therefore, the protective potential of natural antioxidant compounds against oxidative stress–induced DNA damage has become a major focus of recent scientific research. Phytochemicals such as polyphenols, flavonoids and tannins can exert cellular protection by neutralizing free radicals. In this context, the present study aimed to evaluate the genotoxic and antigenotoxic effects of *Geranium robertianum* extract (GRE), commonly known as "herb robert," on the human liver cancer cell line (HepG2) under in vitro conditions using the Comet assay. In the first step, the highest non-cytotoxic concentration of GRE was determined via the Sulforhodamine B (SRB) cell viability assay, which was identified as 50 µg/mL. Subsequently, GRE was applied at concentrations of 12.5, 25 and 50 µg/mL, and DNA damage parameters were analyzed. The results demonstrated that GRE did not exhibit any statistically significant genotoxic effect at these concentrations, and notably, the 12.5 µg/mL dose significantly reduced hydrogen peroxide (H_2O_2)-induced DNA damage ($p<0.05$). These findings indicate that *G. robertianum* can prevent oxidative stress–related DNA damage without inducing genetic toxicity. Overall, the results provide a scientific basis for further pharmacological and toxicological investigations into the protective properties of plant-derived compounds and highlight the potential of *G. robertianum* as a natural antigenotoxic agent.

Keywords: *Geranium robertianum*, HepG2, Comet Assay, Genotoxicity, Antigenotoxicity, Antioxidant

Acknowledgement: This study was supported by The Scientific and Technological Research Council of Turkey (TÜBİTAK) under the 2209-A Research Project Program (Grant No: 1919B012404575).

ORAL PRESENTATION

An extensive research on activated carbon (AC) for preparation, characterization and improvement of properties with modification methods

Ayşenur Gümüş[1] (ORCID: https://orcid.org/0000-0003-1861-7757)
Ali Rıza Kul[2] (ORCID: https://orcid.org/0000-0001-9331-775X)
Adnan Aldemir[3,*] (ORCID: https://orcid.org/0000-0001-9884-0961)

[1]Van Yüzüncü Yıl University, Institute of Natural and Applied Sciences, Chemical Engineering Department, Van, 65080, Türkiye
[2]Van Yüzüncü Yıl University, Faculty of Science, Chemistry Department, Van, 65080, Türkiye
[3]Van Yüzüncü Yıl University, Faculty of Engineering, Industrial Engineering Department, Van, 65080, Türkiye

*Corresponding author e-mail: adnanaldemir@yyu.edu.tr

Abstract

Activated carbon (AC) is widely used in different industrial applications such as industrial wastewater treatment, petrochemical industries, solvent recovery, catalyst supports, and the pharmaceutical industry. AC also has a high demand for energy storage device production, especially for supercapacitors due to the porous structure. AC contains well-developed micropores, mesopores, and macropores with various surface functional groups in their structure. AC can be classified as granule, powder, and pellet based on their shape and size. AC production can be costly, and reliance on nonrenewable resources raises sustainability concerns. This study was contained results of comprehensive investigation of publications from 2000 to 2021 related on activated carbons providing an extensive comparison of physical, chemical, and surface properties of activated carbons produced from biomass, coal, shells/seeds, woody materials, and mixed wastes. For the feedstock groups (G1–G6), key parameters including BET surface area, iodine number, total pore volume (Vt), micropore volume (Vmic), mesopore volume (Vmeso), particle size (Dp), Langmuir surface area, and pHzpc properties were evaluated. Results were demonstrated that agricultural biomass and nutshell-based raw materials can achieve high BET surface areas (1500–5000 m^2/g), with shell/seed-derived AC were showed the highest removal performance. The research results were also explored the effects of chemical activation agents (KOH, H_3PO_4, $ZnCl_2$) and physical activation methods (CO_2, steam, heat treatment). Chemical activation leads to the higher surface development, while physical activation offers cleaner surface chemistry and controlled porosity. Overall, this comprehensive evaluation was showed that the critical influence of feedstock selection, activation method, and processing conditions on activated carbon performance, providing insight into scientific trends for developing high-performance adsorbents. Adsorption on AC has long been recognized to be one of the most effective methods for the removal of pollutions such as pesticides, dyes and organic compounds from aqueous solutions.

Keywords: Activated carbon, preparation, characterization, properties, modification

ORAL PRESENTATION

Production, import and consumption distribution of activated carbon (AC) in Türkiye

Ayşenur Gümüş[1] (ORCID: https://orcid.org/0000-0003-1861-7757)
Ali Rıza Kul[2] (ORCID: https://orcid.org/0000-0001-9331-775X)
Adnan Aldemir[3,*] (ORCID: https://orcid.org/0000-0001-9884-0961)

[1]Van Yüzüncü Yıl University, Institute of Natural and Applied Sciences, Chemical Engineering Department, Van, 65080, Turkey.
[2]Van Yüzüncü Yıl University, Faculty of Science, Chemistry Department, Van, 65080, Turkey.
[3]Van Yüzüncü Yıl University, Faculty of Engineering, Industrial Engineering Department, Van, 65080, Turkey.

*Corresponding author e-mail: adnanaldemir@yyu.edu.tr

Abstract

The production of activated carbon (AC) arises from the extensive variety of raw materials that can be utilized in its production, encompassing coal, wood, and, more increasingly, diverse forms of agricultural and industrial waste. This flexibility provides both economic and environmental advantages, especially in fostering resource circularity and waste valorization. AC is a widely utilized porous material known for its high surface area, tunable pore structure, and surface functionality, making it suitable for applications such as water and air purification, energy storage, gas separation, and catalysis. AC also eliminates undesirable odors, flavors, and colors in food products. In energy, it purifies syngas, a mixture of CO and hydrogen, from burning fossil fuels or biomass. AC serves to purify biogas by eliminating contaminants such as sulfur, chlorine, and ash from syngas, thereby enhancing its cleanliness and efficiency as a fuel source. It plays a crucial role in various energy sectors. Its substantial surface area facilitates effective adsorption and desorption of lithium ions, thereby offering a high capacity for lithium-ion storage. AC serves as a cathode material in lithium-sulfur batteries, enhancing cycling reliability by mitigating the dissolution of polysulfides. It also supports supercapacitor production, enabling rapid charge-discharge cycles. The durability, conductivity, extensive surface area, and versatility of AC render it indispensable for sustainable energy solutions and energy storage systems. Recent advancements in biochar-based composites demonstrate effective strategies for optimizing the utilization of agricultural waste while enhancing the functional properties of polymer materials. AC also highly versatile and widely used adsorbent in water treatment due to its excellent adsorption capabilities, large surface area, and well-developed pore structure. It is capable of eliminating a wide range of contaminants from water, such as organic molecules, inorganic pollutants, and new toxins, making it an important component of numerous water purification procedures. This research was analyzed Turkey's AC production and import quantities, usage sectors, and consumption distribution. According to the data, Turkey imports approximately 44 million kg of AC annually, with the majority used in drinking water treatment, wastewater treatment, food processing, gas purification, and gold recovery industries. Powdered and granular ACs are the most demanded products by municipalities and industrial facilities. The import data indicate a continuous increase in AC consumption due to the expansion of advanced water treatment technologies and industrial purification needs. Turkey's rising environmental standards and investments in water treatment systems are driving the demand for higher-performance adsorbents.

Keywords: Activated carbon, production, import, application, consumption distribution, Türkiye

ORAL PRESENTATION

Cytotoxic effects of antidiabetic drug metformin in Mcf-7 cells

Sevcan Mamur (ORCID: https://orcid.org/0000-0002-8615-5331)

Gazi University, Graduate School of Natural and Applied Sciences, Department of Environmental Sciences, Ankara, Turkey

Corresponding author e-mail: smamur@gazi.edu.tr

Abstract

Diabetes mellitus is a chronic disease and many people suffer from this disease. Type 2 *diabetes mellitus* is the most common type of diabetes, and more than 95% of people with diabetes have type 2 diabetes. Metformin is widely used as an oral hypoglycemic drug in the treatment of type 2 *diabetes mellitus*. It is a biguanide derived from *Galega officinalis* and is the first antidiabetic drug used in the treatment of patients with type 2 *diabetes mellitus*. Some previous reports indicated that MET has antioxidant, anti-inflammatory, antiapoptotic, and anticancer effects. The aim of this study was to determine the potential cytotoxic/anticancer effects of Metformin, which is widely used in the treatment of type 2 *diabetes mellitus*, on the human breast cancer MCF-7 cell line using the 3-(4,5-dimethylthiazol-2-yl)-2,5-diphenyl tetrazolium bromide (MTT) assay. Different concentrations of Metformin (31.25, 62.50, 125, 250, 500, and 1000 µg/mL) were treated with MCF-7 cells at a 24-hour treatment period. A negative control (distilled water) was also maintained in culture. As a result, Metformin statistically significantly reduced cell viability in MCF-7 cells at all concentrations for 24 hours of treatment compared to the control. The half of the inhibitory (IC50) value that kills fifty percent of the cells was found as 1000 µg/mL (% 52.04% cell viability) concentration for 24 h. In conclusion, Metformin exhibited cytotoxic/anticancer effect in MCF-7 cells at between 31.25 µg/mL and 1000 µg/mL concentrations.

Keywords: Metformin, antidiabetic drug, cytotoxicity, Mtt assay, MCF-7 cell line.

ORAL PRESENTATION

Comparative analysis of the effects of stable and classical vitamin C forms (L-ascorbic acid and 3-O-ethyl ascorbic acid) on antioxidant activity, cell viability, and clonogenic capacity in skin cells

İpek Zeynep Durusu [1*] (ORCID: https://orcid.org/0000-0002-9165-6077), Aliye Ezgi Güleç Taşkıran [1] (ORCID: https://orcid.org/0000-0003-1855-1524)

[*1] Başkent University, Faculty of Science and Letters, Molecular Biology and Genetics Department, Ankara, Türkiye

*Corresponding author e-mail: ipekdurusu@gmail.com

Abstract

Vitamin C and its derivatives play an important role in regulating oxidative stress and maintaining tissue homeostasis in skin cells. This study comparatively evaluates the antioxidant properties, cell viability, and clonogenic capacity of L-ascorbic acid and a more stable derivative, 3-O-ethyl ascorbic acid, in human keratinocyte (HaCaT) and dermal fibroblast (HDFa) cell lines. L-ascorbic acid and 3-O-ethyl ascorbic acid were tested across a concentration range of 10–1000 µg/mL using MTT assay, clonogenic assay, and DPPH radical scavenging analysis. Their effects on oxidative stress response and cellular proliferation at different concentrations were comparatively assessed. The results showed that L-ascorbic acid exhibited pronounced dose-dependent cytotoxicity at concentrations ≥250 µg/mL, reducing viability to ~53% in HaCaT and ~59% in HDFa cells. In contrast, 3-O-ethyl ascorbic acid maintained high cell viability (>95%) in both cell lines across all concentrations, demonstrating markedly higher biocompatibility under culture conditions. In the DPPH assay, L-ascorbic acid showed strong antioxidant activity (~80% inhibition), whereas 3-O-ethyl ascorbic acid displayed a more moderate yet stable radical scavenging profile (68–73%). Clonogenic assay results further highlighted the differences between the molecules. L-ascorbic acid significantly suppressed long-term colony-forming capacity in HaCaT cells and completely inhibited colony formation at 250 µg/mL. In contrast, 3-O-ethyl ascorbic acid preserved clonogenicity in keratinocytes (82–92%) and did not exhibit inhibitory effects even at high concentrations. In fibroblasts, low-dose L-ascorbic acid enhanced colony formation (137%), whereas high doses caused marked inhibition (23%). 3-O-ethyl ascorbic acid supported fibroblast colony formation at both doses (114–153%). Although L-ascorbic acid possesses strong antioxidant capacity, its low stability leads to cellular stress, limits long-term proliferative potential, and induces cytotoxicity at high concentrations. Conversely, 3-O-ethyl ascorbic acid offers a more advantageous biomolecular profile for skin biology and advanced dermocosmetic applications due to its high biocompatibility, stable antioxidant response, and ability to preserve clonogenic capacity.

Keywords: L-ascorbic acid; 3-O-ethyl ascorbic acid; antioxidant activity; cytotoxicity; clonogenicity; cellular proliferation

ORAL PRESENTATION

Cucurbita pepo'da biyotik stresle ilişkili mikroRNA'ların tanımlanması ve fonksiyonel karakterizasyonu

Mert Özkuluz[1*](ORCID: https://orcid.org/0009-0001-9485-559X), Semiha Erişen[2] (ORCID: https://orcid.org/0000-0002-0542-5118) ve Sevgi Maraklı[3] (ORCID: https://orcid.org/0000-0001-5796-7819)

*[1]Yıldız Teknik Üniversitesi, Fen Bilimleri Enstitüsü, Moleküler Biyoloji ve Genetik Programı, İstanbul, Türkiye
[2, 3]Yıldız Teknik Üniversitesi, Fen-Edebiyat Fakültesi, Moleküler Biyoloji ve Genetik Bölümü, İstanbul, Türkiye

*Sorumlu yazar e-mail: mertozkuluz@gmail.com

Özet

Biyotik stres faktörleri, kabakta (*Cucurbita pepo*) verimliliği önemli ölçüde sınırlar. Bitki savunmasında gen ifadesini post-transkripsiyonel modüle eden mikroRNA'ların (miRNA), strese yanıt veren gen ifadesindeki rolü kritiktir. Bu çalışmada, *C. pepo*'daki biyotik stresle ilişkili miRNA'ların ve düzenleyici işlevlerinin kapsamlı biyoinformatik analizlerle karakterize edilmesi amaçlanmıştır. Çalışmada, *C. pepo*'ya ait kamuya açık genom ve transkriptom veri setleri analiz edilmiştir. Potansiyel miRNA'ların tespiti için miRBase referans veritabanı ile homoloji tabanlı arama, miRDeep2 yazılımı ile RNA-Seq verilerinden *de novo* tahmin ve BLAST ile doğrulama stratejileri uygulanmıştır. Tanımlanan miRNA adaylarının ikincil yapıları RNAFold ve UGENE, filogenetik analizi MEGA ve hedef genleri ise psRNATarget sunucusu aracılığıyla belirlenmiştir. Son olarak, hedef genlerin biyolojik rolleri ve ilişkili metabolik yolaklar, Gene Ontology (GO) ve KEGG analizleri ile aydınlatılmıştır. Analizler sonucunda, *C. pepo*'da; *miR156*, *miR157*, *miR160*, *miR166*, *miR167*, *miR168*, *miR171*, *miR172*, *miR390*, *miR395*, *miR397*, *miR398* ve *miR399* ailelerine ait 19 anlamlı miRNA tanımlanmıştır. Fonksiyonel anotasyon bulguları, bu miRNA'ların savunma yanıtı, programlı hücre ölümü, hormon sinyalizasyonu (oksin, SA, JA, ET) ve redoks dengesiyle ilişkili genleri potansiyel olarak düzenlediğini göstermiştir. Hedef genlere ilişkin GO analizi; *miR397* (%33,3), *miR166* (%23,3), *miR398* (%23), *miR399* (%13), *miR160* (%12.1) ve *miR172* (%11) ailelerinin biyotik stres yanıtıyla ilişkili en anlamlı miRNA'lar olduğunu ortaya koymuştur. KEGG analizleri ise hedef genlerin; alfa-linolenik asit, sülfür, fenilpropanoid ve flavonol biyosentezi gibi biyotik strese dirençle ilişkili 25 farklı metabolik yolağa katıldığını ortaya koymuştur. Bu bulgular, *C. pepo*'nun biyotik strese yanıtında rol oynayan moleküler düzenleyici ağlara yönelik mevcut bilgi birikimine katkı sağlamakta ve direnç ıslahı ile stres adaptasyon kapasitesi yüksek çeşitlerin geliştirilmesine yönelik çalışmalarda kullanılabilecek olası miRNA–gen etkileşim modüllerini tanımlamaktadır.

Anahtar Kelimeler: *Cucurbita pepo*, mikroRNA, biyotik stres, psRNATarget, fonksiyonel anotasyon, gen düzenlemesi.

ORAL PRESENTATION

Antidiabetic enzyme inhibition and kinetic behavior of water-soluble morpholine-functionalized axially disubstituted silicon phthalocyanines

Turgut Keleş[*1] (ORCID: https://orcid.org/0000-0002-1911-8020), Zekeriya Biyiklioglu[2] (ORCID: https://orcid.org/0000-0001-5138-214X), Gökçe Seyhan[3] (ORCID: https://orcid.org/0000-0002-8553-9093), Burak Barut[3] (ORCID: https://orcid.org/0000-0002-7441-8771)

[*1]Central Research Laboratory Application and Research Center, Recep Tayyip Erdogan University, Rize, Turkey.
[2]Karadeniz Technical University, Faculty of Science, Department of Chemistry, Trabzon, Türkiye.
[3]Karadeniz Technical University, Faculty of Pharmacy, Department of Biochemistry, Trabzon, Türkiye.

*Corresponding author e-mail: turgut.keles@erdogan.edu.tr

Abstract

Diabetes mellitus is a chronic metabolic disorder characterized by persistent hyperglycemia arising from impaired insulin secretion or action [1]. Its global prevalence continues to increase at an alarming rate, leading to substantial healthcare expenditures and a growing socioeconomic burden [2]. Current antidiabetic drugs, particularly α-amylase and α-glucosidase inhibitors used to control postprandial hyperglycemia, are often associated with adverse gastrointestinal effects such as abdominal discomfort, diarrhea, and flatulence, which limit long-term patient compliance . Therefore, the development of novel therapeutic agents with improved efficacy and reduced side effects has become an essential priority in diabetes management. In recent years, silicon phthalocyanines have gained attention due to their tunable electronic properties, high chemical stability, ease of axial functionalization, and promising applicability in biological systems, making them suitable candidates for enzyme-targeted drug design [3]. In this study, morpholine-functionalized axially disubstituted silicon phthalocyanines and their water-soluble derivatives were synthesized as potential antidiabetic agents. The structures of the newly obtained compounds were elucidated using FT-IR, NMR, and mass spectrometry. The inhibitory activities of the phthalocyanines were evaluated against the carbohydrate-digesting enzymes α-amylase and α-glucosidase. All derivatives exhibited weak α-amylase inhibition (IC_{50} > 100 μM), showing lower activity than the reference drug acarbose (IC_{50} = 25.29 ± 3.50 μM). In contrast, pronounced inhibition was observed against α-glucosidase: the nonionic analogues MT-C3-H-Si and MT-C3-D-Si showed IC_{50} values of 16.02 ± 0.94 μM and 44.14 ± 4.06 μM, respectively, surpassing acarbose (IC_{50} = 60.51 ± 4.66 μM). Kinetic analyses using Lineweaver–Burk plots revealed a non-competitive inhibition mechanism, indicating allosteric interaction with the enzyme. These results demonstrate that morpholine-substituted silicon phthalocyanines particularly the nonionic derivatives possess promising α-glucosidase inhibitory properties and may serve as valuable leads for the development of new antidiabetic agents with reduced side effects.

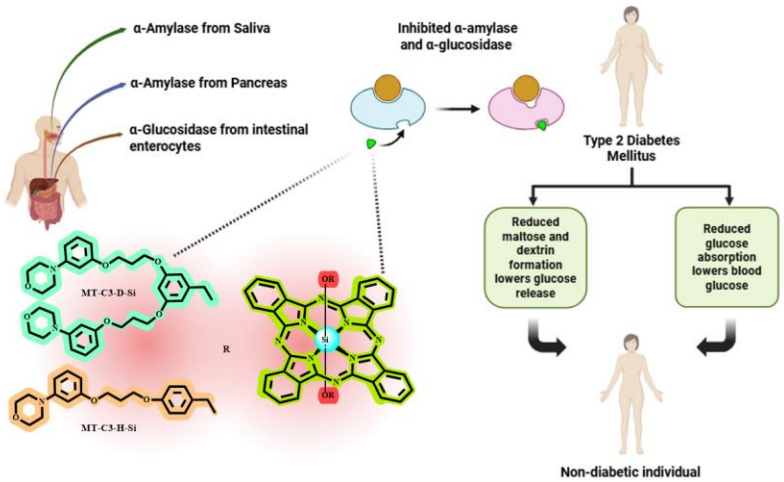


Fig. 1. Axial morpholine-substituted silicon phthalocyanines with antidiabetic activity

Keywords: Diabetes Mellitus, α-glycosidase, α-amylase, silicon(IV) phthalocyanine

Acknowledgment: This work was supported by the Scientific and Technological Research Council of Türkiye (TÜBİTAK) under Project No. 124Z983.

References:

[1] A. Poznyak, A. V. Grechko, P. Poggio, V. A. Myasoedova, V. Alfieri, A. N. Orekhov (2020). The diabetes mellitus–atherosclerosis connection: The role of lipid and glucose metabolism and chronic inflammation. International journal of molecular sciences, 21(5), 1835. https://doi.org/10.3390/ijms21051835

[2] M. J. Hossain, M. Al-Mamun, M. R. Islam (2024). Diabetes mellitus, the fastest growing global public health concern: Early detection should be focused. Health Science Reports, 7(3), e2004. https://doi.org/10.1002/hsr2.2004

[3] Keles, T., Seyhan, G., Biyiklioglu, Z., Kolci, K., Reis, R., & Barut, B. (2024). Dendritic, Water-Soluble, and Nonaggregated Axially Substituted Silicon Phthalocyanine as Potential Endometrial Anticancer Agent. Applied Organometallic Chemistry, 38(12), e7699. https://doi.org/10.1002/aoc.7699

ORAL PRESENTATION

Uncovering hidden patterns: The significance of water quality trend analysis

Mehmet Pala[1*] (ORCID: https://orcid.org/my-orcid?orcid=0000-0001-6495-4880), Demet Dogan[2] (ORCID: https://orcid.org/my-orcid?orcid=0000-0001-6356-0679)

[*1]Gaziantep University, Faculty of Arts and Science, Biochemistry Science and Technology, Gaziantep, Türkiye.
[2]Gaziantep University, Faculty of Arts and Science, Biology, Gaziantep, Türkiye.

*Corresponding author e-mail: mehmetap@hotmail.com

Abstract

Analyzing trends in water quality parameters has become essential for understanding the long-term dynamics of aquatic environments and ensuring the sustainability of water resources. Research across rivers, lakes, estuaries, and coastal waters consistently shows that indicators such as dissolved oxygen, pH, nutrients, salinity, and hardness exhibit temporal variations shaped by both natural cycles and human pressures. Evidence from diverse geographic contexts reveals recurring patterns: seasonal fluctuations driven by hydrological regimes, gradual declines associated with urbanization, agriculture, and industry, and localized improvements following targeted management actions. Such analyses function not only as descriptive assessments but also as early warning systems for ecological degradation, diagnostic tools for identifying pollution sources, and benchmarks for evaluating intervention effectiveness. Synthesizing outcomes from multiple case studies demonstrates that continuous monitoring and evaluation of water quality are indispensable for protecting ecosystem health, maintaining reliable water supplies, and guiding adaptive responses to climate change and population growth. Collectively, the accumulated evidence highlights the pivotal role of trend analysis in connecting scientific knowledge with practical water management, offering a comprehensive perspective on the condition of aquatic systems and pathways toward their sustainable future.

Keywords: Aquatic ecosystems, environmental monitoring, pollution assessment, sustainability

ORAL PRESENTATION

Determining the vulnerability of groundwater to pollution in the Develi basin (Kayseri) using the DRASTIC method

Şeyma Aykutlu[1*] (Orcid: https://orcid.org/0009-0008-5710-7833), Filiz Dadaşer-Çelik[2] (Orcid: https://orcid.org/0000-0003-3623-7723)

[1]Erciyes University, Graduate School of Natural and Applied Sciences, Environmental Engineering Program, Kayseri, Türkiye.
[2]Erciyes University, Engineering Faculty, Dept. of Environmental Engineering, Kayseri, Türkiye.

*Corresponding author e-mail: 4011930135@erciyes.edu.tr

Abstract

Groundwater is a natural resource that is vulnerable to pollution, particularly in basins with intensive agricultural activities. In this study, the groundwater vulnerability of the Develi Basin, located within the boundaries of Kayseri Province, was evaluated using the GIS-based DRASTIC method. The analysis includes seven key hydrogeological parameters: Depth to Water Table (D), Net Recharge (R), Aquifer Media (A), Soil Media (S), Topography (T), Impact of the Vadose Zone (I), and Hydraulic Conductivity (C). Well logs provided by the State Hydraulic Works was used to estimate depth to water table. Net recharge was obtained from a previous study that used Soil and Water Assessment Tool to simulate basin hydrology. Aquifer media, soil media, impact of vadose zone, and hydraulic conductivity were estimated based on national soil and geological maps. Information on topography was obtained from a digital elevation model of the study area. All maps were were generated in raster format with a 100-meter cell size and classified and rated according to standard DRASTIC criteria. The resulting DRASTIC Index (DI) values were classified into vulnerability categories ranging from Low to Very High. Spatial analysis shows that the central part of the plain, characterized by alluvial deposits, shallow groundwater levels, and high hydraulic conductivity, falls within the “Very High” vulnerability class. In contrast, the basin margins with steeper slopes show “Low” vulnerability. These findings show the areas most susceptible to contamination and provide basis for managing potential pollution risks in the Develi Basin.

Keywords: Groundwater, Groundwater Pollution, DRASTIC, Develi Basin

ORAL PRESENTATION

A rapid and eco-friendly route for the synthesis of mono- and bimetallic nanoparticles

Assiata Binty Issa Ben Said[1*] (*ORCID: https://orcid.org/0009-0007-9515-5185*),
Gamze Tan[2] (*ORCID: https://orcid.org/0000-0002-2755-1756*)

[*1] Aksaray University, Graduate School of Natural and Applied Sciences, Department of Nanotechnology, Aksaray, Türkiye.
[2] Aksaray University, Faculty of Science and Letters, Department of Biology, Aksaray, Türkiye.

Corresponding author e-mail: bintyassiata@gmail.com

Abstract

Metal nanoparticles (MNP) can be prepared using physical, chemical, or biological methods. The use of biological methods, known for their enhanced energy efficiency and environmental sustainability, is steadily growing. Bimetallic nanoparticles (NPs), on the other hand, have recently become more interesting than their monometallic counterparts thanks to their advanced properties emerging from the synergistic effect of two metals, and prompting increased research on the subject. This study indicates the synthesis and characterization of monometallic (Ag and ZnO) and bimetallic (Ag-ZnO) NPs using water-soluble cassava starch. Mono- and bimetallic NPs were synthesized using cassava starch. The formation of NPs was analyzed through techniques such as Fourier transform infrared spectroscopy (FTIR), Ultraviolet–visible spectroscopy (UV-Vis), and Transmission electron microscopy (TEM). FTIR confirmed the presence of functional groups in all prepared NPs. TEM images revealed that all NPs had a sphere-like morphology larger than 20 nm and were well separated from each other. In sum, the results showed that mono- and bimetallic NPs can be rapidly synthesized from cassava starch without the use of toxic reducing agents. This underscores the prioritization of NP production using eco-friendly routes.

Keywords: Bimetallic nanoparticles, green synthesis, silver nanoparticles, zinc oxide nanoparticles.

ORAL PRESENTATION

Investigation of the genotoxic effects of borax decahydrate using micronucleus assay

Buse Alaca [1] (ORCID:0009-0002-4362-1010), Sevcan Mamur [1*] (ORCID:0000-0002-8615-5331)

[1] Gazi University, Graduate School of Natural and Applied Sciences, Department of Environmental Sciences, Ankara, Turkey

*Corresponding author e-mail: smamur@gazi.edu.tr

Abstract

Borax decahydrate (disodium tetraborate decahydrate) is one of the tincal derivatives and is widely used as an additive in many industrial sectors, such as agriculture, detergents, glass, ceramics, and cosmetic products. According to previous studies, boric acid and its derivatives have shown important biological effects such as potential antioxidant, anti-inflammatory and anticancer. However, studies on human lymphocytes regarding genotoxic potential are limited. The aim of this study is to evaluate the potential genotoxic effect of borax decahydrate using the micronucleus assay in human peripheral blood lymphocytes *in vitro*. This research was approved by the Gazi University Faculty of Medicine Ethics Committee (01.08.2025/137). Lymphocyte cultures were treated with five different concentrations of borax decahydrate (2.5, 5, 10, 20, and 40 µg/mL) for 48 hours. A negative (distilled water) and a positive control (Mitomycin-C, 0.20 µg/mL) were conducted in culture. According to the results, none of the studied concentrations of borax decahydrate caused a significant increase in the frequency of MN between 2.5 µg/mL and 40 µg/mL concentrations compared to the control. Additionally, borax decahydrate did not affect nuclear division index (NDI) at any treatment. These findings indicate that borax decahydrate did not exhibit genotoxic or cytotoxic effects in human peripheral lymphocytes under the tested concentrations in *in vitro* conditions.

Keywords: Borax decahydrate, micronucleus assay, nuclear division index, human peripheral lymphocytes.

*This study is supported by the Gazi University Research Fund under project number FYL-2025-10447.

ORAL PRESENTATION

Investigation of the protective potential of boric acid against the genotoxic effects induced by aspartame

Derya Binay[1*] (ORCID: https://orcid.org/0000-0002-0277-761X), Fatma Ünal[2] (ORCID: https://orcid.org/0000-0001-7648-9584), Ece Akbaş[2] (ORCID: https://orcid.org/0000-0002-4978-3638), Deniz Yüzbaşıoğlu[2] (ORCID: https://orcid.org/0000-0003-2756-7712)

[*1] Gazi University, Graduate School of Natural and Applied Sciences, Department of Biology, Ankara, Türkiye.
[2]Gazi University, Science Faculty, Department of Biology, Ankara, Türkiye.

*Corresponding author e-mail: deryabinay.53@gmail.com

Abstract

In recent years, the rise in diabetes, obesity, and metabolic disorders has encouraged individuals to reduce sugar consumption, increasing interest in low-calorie artificial sweeteners. These compounds are widely used, particularly in diet products, as they provide sweetness with minimal caloric intake. Among them, Aspartame (ASP; E-951) is a prominent additive due to its nearly 200 times sweeter taste, low cost, and broad applicability. However, recent studies suggest that long-term aspartame intake may be associated with insomnia, loss of consciousness, cardiovascular disturbances, increased diabetes risk, and potential adverse effects on the nervous system. In 2023, the International Agency for Research on Cancer (IARC) classified aspartame as "probably carcinogenic" to humans (Group 2B), emphasizing the need for careful evaluation of its safety. In contrast, boric acid (BA) has gained attention in toxicology research, as its antioxidant, antiviral, anti-inflammatory, antibacterial, and antigenotoxic properties contribute to cellular protection against oxidative stress. This study aims to investigate the protective/antigenotoxic potential of boric acid against the genotoxic effects induced by aspartame using the cytokinesis-block micronucleus (SB-MN) test. Human peripheral lymphocytes were treated simultaneously (ASP+BA) for 48 hours with various concentrations of aspartame (0.125, 0.25, 0.50, and 1 µg/mL) alone and with BA (0.0313, 0.0625, 0.125, and 0.25 µg/mL) for 48 hours. ASP significantly increased the micronucleus-MN frequency at 0.50 and 1 µg/mL ($p<0.01$ and $p<0.05$). In the concurrent application, BA achieved a significant improvement ($p < 0.05$) in the MN frequency induced by aspartame at 0.5 µg/mL across all concentrations (50-59%). BA significantly improved the MN frequency ($p<0.01$ and $p<0.05$) at 0.125 and 0.250 µg/mL (61-72%). These results suggest that boric acid may have the potential to improve the genetic hazard induced by aspartame. However, more detailed in vitro and in vivo analyses are needed to understand this effect better.

Keywords: Aspartame, Boric Acid, Genotoxicity, Antigenotoxicity, Artificial sweetener, Cytokinesis blocking micronucleus test

*****This study was supported by Gazi University Scientific Research Projects Coordination Unit (Project No: FYL-2025-10327).

ORAL PRESENTATION

Evaluation of cytotoxic effects of capecitabine and epigallocatechin gallate combination on a human breast cancer cell line

Sude Nur Afacan[1*] (*ORCID:* https://orcid.org/0009-0003-1290-1295), Ayşegül Erdemir[2] (*ORCID:* https://orcid.org/0000-0002-6099-4903)

[*1]Yildiz Technical University, Faculty of Arts and Science, Department of Molecular Biology and Genetics, Istanbul, Türkiye.
[2]Yildiz Technical University, Faculty of Arts and Science, Department of Molecular Biology and Genetics, Istanbul,Türkiye.

*Corresponding author e-mail: nur.afacan@std.yildiz.edu.tr

Abstract

Breast cancer is the most frequently diagnosed cancer among women worldwide and remains a major cause of cancer-related mortality. Chemotherapy, despite being a mainstay treatment, often leads to severe systemic toxicity and damage to healthy tissues, highlighting the need for safer therapeutic strategies. Phytochemicals, as bioactive molecules, suppress oncogenic pathways and induce apoptosis, offering potential as supportive or complementary agents. Epigallocatechin gallate (EGCG), abundant in green tea, demonstrates low toxicity and multiple molecular targets, suggesting that its combination with chemotherapeutics may enhance efficacy by modulating distinct cellular pathways. This study evaluated the cytotoxic effects of Capecitabine combined with EGCG on the human breast cancer cell line SK-BR-3. IC50 values were determined for both agents at 24 and 48 hours. Based on these values, the combined treatment was assessed using the Chou–Talalay combination index, which demonstrated synergistic interaction, particularly at 48 hours. The enhanced cytotoxic activity of the combination was further supported by wound-healing and DAPI staining assays. Quantitative wound-healing analysis revealed that cell density in the control group increased from an initial 23% to 37.5% at 48 hours, whereas the combination treatment showed only a slight change from 25% to 26%, confirming markedly reduced cell motility and viability. In conclusion, this study demonstrates that combining Capecitabine with EGCG enhances cytotoxic activity in SK-BR-3 cells and supports the potential of integrating phytochemicals with chemotherapeutic agents to develop more effective breast cancer treatment strategies.

Keywords: Breast Cancer; Capecitabine; Combined Treatment; EGCG; Phytochemicals

ORAL PRESENTATION

Comparison of *in silico* tools used for predicting the functional effects of polymorphisms in veterinary genetics

Dina Bedik (Orcid: https://orcid.org/0000-0002-4088-3827)

Istanbul University-Cerrahpasa, Faculty of Veterinary Medicine, Department of Veterinary Biochemistry, Istanbul, Türkiye

Corresponding author e-mail: dina.bedik@iuc.edu.tr

Abstract

Accurate prediction of the functional consequences of single nucleotide polymorphisms (SNPs) is essential for elucidating disease mechanisms and enhancing genomic selection strategies in veterinary genetics. Despite their widespread use, in silico prediction tools differ significantly in their algorithmic frameworks, scoring systems, and output formats. This study presents a methodological comparison of six commonly applied prediction tools (SIFT, PolyPhen-2, PROVEAN, PANTHER, MutPred2, and PredictSNP) by examining their computational principles, data dependencies, evaluation criteria, and relevance to veterinary genetic research. SIFT, PROVEAN, and PANTHER primarily rely on evolutionary conservation and sequence homology to infer the tolerance or deleteriousness of amino acid substitutions. PolyPhen-2 expands upon this by integrating structural features, functional domains, steric constraints, and biophysical parameters, thereby providing a more comprehensive assessment. MutPred2, based on deep learning, not only predicts variant pathogenicity but also offers mechanistic insights into potential molecular alterations. As a meta-predictor, PredictSNP synthesizes outputs from multiple tools to generate consensus scores and serves as a robust benchmark for comparative analyses. This methodological evaluation delineates the theoretical foundations, operational characteristics, and limitations of major in silico prediction platforms, thereby establishing a conceptual basis for their application in veterinary genetics. This evaluation will provide a foundation that enables researchers to identify the most appropriate in silico method based on their study objectives, the characteristics of the species being analyzed, and the structure of the available data, and will offer a general perspective on method selection in functional variant analyses.

Keywords: genetics, *in silico*, prediction, SNP, veterinary

ORAL PRESENTATION

The use of biotechnology and nanotechnology in parasitology

Hakan Tüfek[1*] (ORCID: https://orcid.org/0000-0002-3601-6317), Ferhat Şen[2] (ORCID: https://orcid.org/0000-0001-7733-2263), Gökçe Üstündağ[1] (ORCID: https://orcid.org/0000-0002-4026-1358)

[*1]Zonguldak Bülent Ecevit University, Department of Veterinary Medicine, Zonguldak, Türkiye.
[2]Zonguldak Bülent Ecevit University, Department of Nanotechnology Engineering, Zonguldak, Türkiye.

*Corresponding author e-mail: hakan.tufek@beun.edu.tr

Abstract

Parasitic diseases are one of the most significant problems today. Parasitic diseases cause serious productivity losses in farm animals, especially in low-income and middle-income countries. In addition, zoonotic parasitic diseases complicate treatment protocols in co-infections and lead to serious public health problems by altering host immune responses. Many traditional antiparasitic control methods have been used for many years to combat these problems. However, these methods have many disadvantages. These include insufficient sensitivity in microscopy and serology, long diagnostic turnaround times, obstacles posed by complex treatment regimens in the management of co-infections with immunosuppressive diseases such as HIV, antiparasitic drug resistance development, residues and environmental toxicity, low bioavailability, and off-target effects. In recent years, scientific studies on new formulations and diagnosis, treatment, and control methods have gained momentum by utilizing biotechnological and nanotechnological capabilities to overcome these limitations. This review summarizes the current status, potential shortcomings, and future prospects of biotechnological and nanotechnological approaches in parasitology, summarizing the interesting developments and scientific studies reported in recent years.

Keywords: Parasitology, Biotechnology, Nanotechnology.

ORAL PRESENTATION

Secondary structures of mitochondrial genes in the classification of *Salmo* species in Türkiye

Altuğ Karaman[1] (ORCID: https://orcid.org/0000-0003-4918-7796), Ferit Can YAZDIC[2*] (ORCID: https://orcid.org/0000-0002-2762-3027)

[1]Munzur University, Institute of Graduate Education, Department of Biology, Tunceli, Türkiye.
[*2]Munzur University, Institute of Graduate Education, Department of Biotechnology, Tunceli, Türkiye.

*Corresponding author e-mail: fcanyazdic@munzur.edu.tr

Abstract

The genus Salmo, within the family Salmonidae, contains fish species that are difficult to distinguish due to their similar morphological characteristics. The taxonomic classification of Salmo species, both globally and in Turkey, remains controversial. Mitochondrial DNA is used by researchers in phylogenetic studies to elucidate evolutionary connections between different species. Despite its widespread use in prokaryotic phylogenetics, applications of secondary structure analysis in eukaryotes such as fish remain largely unexplored. This study aims to exploit differences in molecular folding structures to elucidate evolutionary relationships among various fish species using structural data obtained from existing mitochondrial gene regions. We anticipate that the secondary structures of biomolecules in different fish species can illuminate phylogenetic relationships between species. In this regard, we analyzed the secondary structures of the 12S (approximately 170 sequences;~600 bp), 16S (approximately 220 sequences;~400 bp), and Cty-b (approximately 1200 sequences;~800 bp) mitochondrial gene regions found in the NCBI database. The rRNA regions included in the analysis revealed variability in the RNA folding models obtained in all fish species studied. Based on the obtained rRNA models, 751 conserved regions were identified in the 12S rRNA, 1337 in the 16S rRNA, and 252 in the Cyt-b region. Additionally, 77 conserved stem regions were observed in the 12S rRNA sequences and 86 in the 16S rRNA sequences. In conclusion, the secondary structures of the gene regions used in the classification of Salmo species may be a potential tool for distinguishing closely related species. Furthermore, the secondary structure of RNA can provide additional taxonomic information, especially in the case of closely related species.

Keywords: Salmonidae, rDNA, phylogenetic analysis, secondary structures

ORAL PRESENTATION

Human health evaluation of drinking water sources in Kütahya province

Nurtap KAYA[1*] (ORCID: https://orcid.org/0009-0007-2390-9187), Mustafa Kavasoğlu[2] (ORCID: https://orcid.org/0000-0002-4136-6397)

[*1]Kütahya Dumlupınar University, Faculty of Arts and Sciences, Department of Biochemistry, Kütahya, Türkiye.
[2]Kütahya Dumlupınar University, Gediz Vocational School, Department of Medical Services and Techniques, Kütahya, Türkiye.

*Corresponding author e-mail: nurtapkaya74@gmail.com

Abstract

Kütahya has a very complex geological structure with abundant sedimentary and volcanic rocks. This complex structure results in this region being rich in various elements. This situation significantly affects the water quality of the region. In this study, it was aimed to determine some physicochemical parameters and metallic element amounts of drinking water in Kütahya province and surrounding villages and to investigate their effects on human health. Knowing the quality of the water consumed by a person who needs to consume an average of two liters of water a day is very important for human health. In the study, temperature, pH, electrical conductivity (EC), total dissolved solids (TDS), salinity, nitrate (NO_3), nitrite (NO_2), phosphate (PO_4) and ammonia (NH_3) values were measured from the physicochemical parameters. In addition, the amounts of magnesium (Mg), zinc (Zn), copper (Cu), cadmium (Cd), lead (Pb), cobalt (Co), silver (Ag), iron (Fe), manganese (Mn), calcium (Ca), potassium (K), and sodium (Na) elements were determined. The findings obtained from the study were compared with the Turkish Standards Institute Regulation on Water Intended for Human Consumption, the World Health Organization (WHO), and the European Environment and Protection Agency (EPA) standard values. When the physicochemical parameters and heavy metal values obtained from the study are examined, it can be said that the drinking water of Kütahya Province and its surrounding villages does not pose any risk to human health, although some high values were detected.

Keywords: Drinking water, human health, Kütahya, metallic element, physicochemical parameters.

ORAL PRESENTATION

Reorganization of pollen tube cell wall under low temperature conditions in *Camellia sinensis*

Sena Acar*[1] (ORCID: 0009-0003-5912-5852), Aslıhan Çetinbaş-Genç[2] (ORCID: 0000-0001-5125-9395)

*[1]Marmara University, Institute of Pure and Applied Sciences, Istanbul, Türkiye
[2] Marmara University, Faculty of Science, Department of Biology, Istanbul, Türkiye

*Corresponding author e-mail: senaacar.mu@gmail.com

Abstract

The aim of this study was to elucidate the effects of low-temperature stress on the organization and compositional dynamics of the pollen tube cell wall in *Camellia sinensis*. Accordingly, pollen grains subjected to low-temperature treatments were germinated at 5, 10, and 15 °C, whereas the control group was maintained at ambient temperature, with all samples incubated for 4 h in a standardized germination medium containing 8% sucrose. At the pollen tube apex, the distribution of pectin exhibited a significant increase only following the 10 °C treatment relative to the control. Along the tube, pectin distribution in the 15 °C group displayed a profile comparable to the control, whereas deviations were evident in both the 10 °C and 5 °C groups. The distribution of esterified pectin at the tube apex showed a significant increase exclusively in the 15 °C group compared with the control. However, along the tube, the 10 °C and 5 °C treatments resulted in noticeable departures from the control pattern. With regard to de-esterified pectin, a significant increase at the tube apex was observed solely in the 5 °C group. Although all temperature treatments caused deviations from the control along the tube, the most pronounced alterations were detected at 10 °C and 5 °C. Callose distribution at the tube apex significantly increased in all treatment groups relative to the control. Along the tube, numerical variations were observed under all conditions; however, the 15 °C and 10 °C groups demonstrated control-like distribution patterns, whereas the 5 °C group showed a distinctly divergent profile. The distribution of cellulose at the tube apex displayed a significant increase across all temperature treatments compared with the control. Although numerical fluctuations were present along the tube in all groups, the overall distribution profiles remained largely consistent with that of the control. Overall, these findings enhance our understanding of cell wall remodeling under low-temperature conditions and contribute to a better understanding of how such structural modifications influence pollen tube elongation in a cold-stressed environment. This work was financially supported by the Marmara University Scientific Research Projects Commission (Project no: FYL-2025-11603).

Keywords: callose, cell wall, cellulose, low temperature, pectin, pollen tube

ORAL PRESENTATION

Total phenolic and flavonoid contents and antioxidant potential of *Vincetoxicum fuscatum* subsp. *fuscatum* seeds

Sevda Güzel Kara (ORCID: https://orcid.org/0000-0002-6642-5824)

Mersin University, Faculty of Pharmacy, Department of Pharmacognosy, Mersin, Türkiye.

Corresponding author e-mail: guzelsevda@mersin.edu.tr

Abstract

The genus *Vincetoxicum* Wolf (Apocynaceae:Asclepiadoideae), which is naturally distributed in Africa, Australia, Asia, and Europe, comprises approximately 140 species that grow in various habitats[1,2]. Some species of the genus have been traditionally used to treat wounds, bone fractures, snake/insect bite, scorpion sting, and inflammation[2]. *Vincetoxicum* is one of the largest genera of the subfamily in Anatolia, represented by 10 taxa[3]. *Vincetoxicum fuscatum* subsp. *fuscatum* (Hornem.) Reichb. is known as "gavur biberi" in Turkey[4]. This study aims to investigate the total phenolic and flavonoid contents, and the antioxidant potential of ethanol extract of *V. fuscatum* subsp. *fuscatum* seeds growing wild in Turkey. The total phenolic and total flavonoid contents were investigated using Folin-Ciocalteu and aluminum chloride colorimetric assay methods, respectively. Antioxidant activity was evaluated using the DPPH radical scavenging assay. The total phenolic and total flavonoid contents of the seeds were determined as 7.42±0.035 mg GAE/g seed and 3.08±0.003 mg QE/g seed, respectively. The antioxidant activity results were expressed in both percentage inhibition (%) and mM equivalents of Ascorbic acid (AAE) per g of seeds (27.3±0.01 % and 0.26±0.06 mM AAE/g seed, respectively). This is the first study performed on the total phenolic and total flavonoid contents, as well as the antioxidant potential of *V. fuscatum* subsp. *fuscatum* seeds. Our results indicate that the tested seeds contain both phenolic and flavonoid compounds and possess antioxidant potential.

Keywords: *Vincetoxicum fuscatum* subsp. *fuscatum*, seed, total phenolic content, total flavonoid content, DPPH, Apocynaceae.

References:

[1]Liede-Schumann S, Khanum R, Mumtaz AS, Gherghel I, Pahlevani A. Going west-a subtropical lineage (*Vincetoxicum*, Apocynaceae:Asclepiadoideae) expanding into Europe.Mol Phylogenet Evol.2016;94:436-46.
[2]Prameela A, Krishnasamy T, Saraswathy SD. Ethnobotany, phylogeny, phytochemistry and pharmacological applications of genus *Vincetoxicum* (Apocynaceae).Discover Plants.2024;1:32.
[3]Browicz K. *Vincetoxicum* N.M. Wolf. In: Davis PH (Eds), Flora of Turkey and the East Aegean Islands. Scotland: Edinburgh University.1978:163-73.
[4]Koyuncu O, Sezer O. Altıntaş (Kütahya) turba (Torf) ocağı ve çevresinin damarlı bitkiler florası.IJABES.2019;1(1):15-20.

ORAL PRESENTATION

Effects of thymoquinone in a surgically induced rat endometriosis model

Neşe Başak Türkmen[a],Dilan Aşkın Özek[b],İdris Ayhan[c],Hande Yüce[a],Şeyma Yaşar[d],Aslı Taşlıdere[e],Rauf Melekoğlu[f],Muhterem Aydın[g],Songül Ünüvar[a],Osman Çiftçi[c]

[a] Inonu University,Faculty of Pharmacy,Department of Pharmaceutical Toxicology,Malatya
[b]Fırat University,Faculty of Pharmacy,Department of Pharmaceutical Toxicology,Elazığ
[c]Pamukkale University,Faculty of Medicine,Department of Medical Pharmacology,Denizli
[d]Inonu University,Faculty of Medicine,Deparment of Biostatistics,Malatya
[e] Inonu University,Faculty of Medicine,Department of Histology and Embryology,Malatya
[F] Inonu University,Faculty of Medicine,Department of Obstetrics and Gynecology,Malatya
[g]Fırat University,Faculty of Veterinary Medicine,Department of Veterinary Obstetrics and Gynecology,Elazığ

*Corresponding author e-mail: nesebasak86@gmail.com

Abstract

Endometriosis is defined as the presence of tissue that mimics the endometrium in locations outside the uterine cavity.[1] A biopsy is required for definitive diagnosis. The pathophysiology and effective treatment of endometriosis remain unclear. There are no in vivo studies providing safe and definitive results in the treatment of endometriosis. Therefore, in vivo studies on its pathogenesis and treatment are crucial. Thymoquinone is a monoterpene, a primary component of Nigella sativa (black cumin) seed. Numerous studies have found thymoquinone to possess antibacterial, antitumor, antioxidant, and anti-inflammatory properties. No studies have been found evaluating the anti-inflammatory of thymoquinone in the endometriosis model, where oxidative stress and inflammation are implicated in its pathogenesis. Therefore, the present study investigated the beneficial effects of thymoquinone in preventing damage in an experimental rat endometriosis model at the cytokine levels.According to the results, while cytokine levels (IL-1,IL-1 B,IL-6,IL-10,TNF-a, NFK-B) increased in the damaged group in which the endometriosis model was created, these levels decreased significantly in the treatment group.

Keywords: Endometriosis, Thymoquinone

Financial support: This study is supported by Inonu University Scientific Research Project Unit (BAP) with project number TOA-2023-3242.

References:
Eleni, S; Tsamantioti; Heba Mahdy. Endometriosis. StatPearls, January 23, 2023.

ORAL PRESENTATION

Coverage–confidence paradox in Turkey: A secondary analysis of childhood vaccination and public attitudes (1980–2024)

Mahir Ünalleylioğlu[1] (ORCID: https://orcid.org/0009-0001-5435-6833), Kardelen Karaman[2*] (ORCID: https://orcid.org/0000-0002-4201-2363)

[1]Ankara University, Faculty of Science, Department of Biology, Ankara, Türkiye.
[*2]Kırıkkale University, Faculty of Veterinary Medicine, Department of Animal Breeding, Kırıkkale, Türkiye.

*Corresponding author e-mail: kardelenunal@hotmail.com

Abstract

Childhood vaccination remains one of the most effective public-health interventions worldwide, yet recent global trends show increasing vaccine hesitancy in several countries. Understanding how high immunisation performance can coexist with declining public trust is essential for identifying future vulnerabilities. This study examines a "coverage–confidence paradox" in Turkey by integrating childhood vaccination data, unvaccinated child counts, vaccine-confidence indicators, and child health outcomes using publicly available datasets from WHO–UNICEF, the Wellcome Global Monitor, and UN IGME accessed through Our World in Data. Childhood vaccination coverage for core EPI antigens has remained high for more than a decade: between 2014 and 2023, DTP3 coverage ranged from 95% to 99%, and full measles vaccination (MCV2) remained consistently above the global average by 17–77 percentage points (mean difference: +40). Over the same period, the number of one-year-olds unvaccinated for DTP3 fell from hundreds of thousands in the early 2000s to approximately 11,000–26,000 in recent years, with a transient pandemic-associated increase in 2021. Despite this strong programme performance, public confidence has declined. Survey data show that the share of respondents agreeing that vaccines are important for children fell from 95% in 2015 to 68% in 2023, while those disagreeing increased from 3% to 27%. Agreement that vaccines are effective declined from 89% to 68%, and the proportion considering vaccines unsafe rose from 17% to 38%, even as measles coverage increased. In global "importance vs effectiveness" scatters, Turkey's 2023 confidence levels lie at the lower end among high-coverage countries. These findings indicate a divergence between high, stable coverage and declining trust, suggesting potential vulnerability to localised susceptibility pockets and future outbreaks. Strengthening communication, community engagement, and trust-building interventions is critical to sustaining the long-term resilience of Turkey's childhood immunisation programme.

Keywords: vaccination coverage, vaccine confidence, measles, hesitancy, Turkey, immunisation trends

ORAL PRESENTATION

Effects of some postharvest treatments on the storage of nectarine fruits

Yağmur Bala[1*] (ORCID: https://orcid.org/0009-0006-1646-2957),
Neslihan Ekinci[2] (ORCID: https://orcid.org/0000-0001-7022-5289)

[*1] Çanakkale Onsekiz Mart University, Institute of Graduate Studies, Department of Horticulture, Çanakkale, Türkiye
[2] Çanakkale Onsekiz Mart University, Faculty of Agriculture, Department of Horticulture, Çanakkale, Türkiye

*Corresponding author e-mail: yagmurbala.25@gmail.com

Abstract

In this study, three different bacterial isolates known to stimulate the production of secondary metabolites and to reduce respiration by inactivating ethylene synthesis were used. The effects of these bacterial isolates on the quality parameters of 'Caldesi 85' nectarine fruits during cold storage were investigated. Fruits harvested at commercial maturity were treated on the same day with control (water only), 1-MCP (positive control), and the bacterial isolates GBF70, GBF72, and RC521 (1×10^7 cfu/ml). Following immersion in the respective solutions, the fruits were air-dried, placed in plastic crates containing trays, and stored for 45 days under normal atmospheric conditions at 0 ± 0.5 °C and 90 ± 5% relative humidity. Quality parameters including flesh firmness (N), weight loss (%), soluble solids content (°Brix), titratable acidity (TA, % citric acid), ground color (Hue°), and total phenolic content (mg GAE 100 g^{-1}) were assessed at harvest and at 15-day intervals throughout storage.
The results indicated that the RC521 isolate was as effective as 1-MCP in maintaining fruit firmness and reducing weight loss, and even outperformed 1-MCP particularly in minimizing weight loss. Overall, the findings suggest that bacterial treatments may offer a more sustainable and environmentally friendly alternative to chemical methods for reducing postharvest quality losses in nectarines.

Keywords: *Prunus persica* L., Quality, Cold Storage, *Bacillus* spp.

ORAL PRESENTATION

Combined evaluation of inflammatory biomarkers and circulating miRNA-29c in diabetic nephropathy

Destan Kalaçay[1] (https://orcid.org/ 0000-0002-3921-5549), Hüseyin Kayadibi[2] (https://orcid.org/ 0000-0002-3922-4517), Burcu Baba[3] (https://orcid.org/ 0000-0003-0994-3577), Cumhur Bilgİ[4] (https://orcid.org/ 0000-0001-7166-8380), Ezgi Çoşkun Yenigün[5] (https://orcid.org/ : 0000-0002-5963-605X), Şimal Köksal Cevher[6] (https://orcid.org/ 0000-0001-6502-2399), Özkan Alataş[7] (https://orcid.org/ 0000-0002-1753-8873) Evin Kocatürk[8] (https://orcid.org/ 0000-0001-7434-4234), Aysun Hacişevki[9*] (https://orcid.org/0000-0002-3844-5772)

[1] Kafkas University, Kars Vocational School, Kars, Türkiye,
[2] Osmangazi University, Faculty of Medicine, Department of Medical Biochemistry, Ankara, Türkiye,
[3] Yüksek İhtisas University, Faculty of Medicine, Department of Medical Biochemistry, Ankara, Türkiye,
[4] Ufuk University, Faculty of Medicine, Department of Medical Biochemistry, Ankara, Türkiye,
[5] Ankara Bilkent City Hospital, Nephrology Clinic, Ankara, Türkiye,
[6] Ankara Bilkent City Hospital, Nephrology Clinic, Ankara, Türkiye,
[7] Osmangazi University, Faculty of Medicine, Department of Medical Biochemistry, Ankara, Türkiye,
[8] Osmangazi University, Faculty of Medicine, Department of Medical Biochemistry, Ankara, Türkiye,
[9*] Gazi University, Faculty of Pharmacy, Department of Biochemistry and Gazi University, Health Sciences Institute, Sports Pharmacy Program, Ankara, Türkiye

*Corresponding author e-mail: abozkir@gazi.edu.tr

Abstract

Diabetic nephropathy (DN) is characterized by progressive renal damage driven by chronic inflammation, oxidative stress and altered molecular signaling. Identifying biomarker patterns associated with albuminuria progression is essential for improving early diagnosis and clinical follow-up. Aim of the study to investigate inflammatory cytokines, pro-resolving lipid mediators and circulating miRNA-29c expression across different stages of DN. A total of 160 people were included in the study: 40 healthy controls, 40 with type 2 diabetes, 40 with microalbuminuria, and 40 with macroalbuminuria. Serum TNF-α, IL-6 and Lipoxin A4 (LXA_4) concentrations were measured by ELISA. Circulating miRNA-29c levels were quantified by RT-PCR following RNA isolation and cDNA synthesis. TNF-α and LXA_4 levels varied significantly between groups; TNF-α gradually increased ($p \leq 0{,}001$), while LXA_4 decreased, in relation to the severity of albuminuria ($p \leq 0{,}05$). Although IL-6 values were apparently increased in the DN groups compared to the control group, there was no statistical significance. miRNA-29c expression was significantly elevated in microalbuminuria and macroalbuminuria groups ($p \leq 0{,}001$) while there was not statistically difference between controls and type 2 diabetic group, but . miRNA-29c also showed a strong positive correlation with ACR (albumin creatine ratio), fasting glucose, and HbA1c. The combined biomarker profile demonstrated a shift toward increased inflammatory activity, reduced LXA4 capacity and increased miRNA-mediated regulatory changes as DN progressed. The parallel evaluation of inflammatory mediators and circulating miRNA-29c provides a comprehensive overview of biochemical and molecular alterations associated with early renal impairment. These biomarkers may support improved risk stratification and contribute to the development of multimodal diagnostic approaches in diabetic nephropathy.

Keywords: Diabetic nephropathy, miRNA-29c, TNF-α, Lipoxin A_4, IL-6, albuminuria

ORAL PRESENTATION

Investigation of toxigenic *Bacillus cereus* in milk and milk-based desserts

Eray Burtaçgiray[1*] (Orcid: https://orcid.org/0009-0001-8464-3307), Mehmet Elmali[2] (Orcid: https://orcid.org/0000-0002-8479-5757)

[*1,2] Hatay Mustafa Kemal University, Faculty of Veterinary Medicine, Department of Food Hygiene and Technology, Hatay, Turkey.

*Corresponding author e-mail: eray.burtacgiray@mku.edu.tr

Abstract

Bacillus cereus is an important foodborne pathogen encountered in many foods, such as milk and milk-based desserts, due to its ability to form spores and its heat resistance. This study, aimed to investigate the presence of *B. cereus* in milk and milk-based desserts offered for sale in Ankara province, and to determine the distribution of important toxin genes in isolates by multiplex PCR method. Between January and March 2024, a total of 123 samples were collected from different retail outlets, including 23 raw milk, 20 pasteurized milk, 20 UHT milk, 20 rice pudding, 20 pudding, and 20 kazandibi. *B. cereus* was isolated in the samples by classical culture techniques, and suspicious colonies were confirmed by PCR targeting the hemolysin gene. The *presence of hbl*, *nhe*, *cytK* and *ces* toxin genes in the confirmed isolates was investigated by multiplex PCR. As a result of the analysis, *B. cereus* was isolated in a total of 44 samples, including 14 (60.87%) in raw milk, 8 (40%) in pasteurized milk, 2 (10%) in UHT milk, 9 (45%) in rice pudding, 3 (15%) in pudding and 8 (40%) in kazandibi. It was determined that 28 (63.63%) of these isolates had at least one enterotoxin gene, the most common of these genes was *nhe*, followed by *hbl* and *cytK* genes. The *ces* gene responsible for the emetic form was not detected in any isolate. The presence of enterotoxigenic *B. cereus* in milk and milk-based desserts poses a risk to public health, especially in cases where production and storage conditions are inadequate. These findings show that strengthening hygiene practices and reducing sources of contamination at all stages from farm to table *is critical in reducing food safety risks from B. cereus.*

Keywords: *B. cereus*, food safety, milk, milk-based desserts, toxigenic genes

*"This presentation was summarized from the MSc thesis of the first author."

ORAL PRESENTATION

Magnesium and calcium complexes of curcumin and quercetin: Insights into cell viability, oxidative stress, and antioxidant potential

Selma Ustürk[1*] (ORCID: https://orcid.org/0000-0003-2507-2951), Ergül Mutlu Altundağ[2] (ORCID: https://orcid.org/0000-0001-5355-4654),Cahit Özbilenler[1] (ORCID: https://orcid.org/0000-0003-4494-3310), Namık Refik Kerküklü[2] (https://orcid.org/0000-0002-6830-8832), Elvan Yılmaz[1](https://orcid.org/0000-0002-3584-8082)

[*1]Eastern Mediterranean University, Faculty of Arts and Sciences, Department of Chemistry, Famagusta, North Cyprus via Mersin 10, Turkey.
[2]Eastern Mediterranean University, Faculty of Medicine, Department of Medical Biochemistry, Famagusta, North Cyprus via Mersin 10, Turkey.

*Corresponding author e-mail: selma.usturk@emu.edu.tr

Abstract

Flavonoids, a class of polyphenols, possess carbonyl and hydroxyl functional groups that enable them to bind with metal ions. In this work, curcumin and quercetin were complexed with magnesium and calcium divalent cations to improve their solubility. The antiproliferative and antioxidant properties of these complexes were evaluated using HCT-116 colon carcinoma cells. Structural characterization of the curcumin and quercetin metal complexes was carried out through TOF mass spectrometry, FT-IR, and UV-Vis analyses. A solubility assay confirmed enhanced dissolution of both compounds following complexation. Cell viability was assessed using the Cell Viability Detection Kit-8 (CVDK-8). Radical scavenging capacity was examined using the DPPH assay. Results from the viability and ROS assays indicated that curcumin and its metal complexes exerted stronger antiproliferative effects at lower doses than the quercetin complexes. Conversely, quercetin complexes demonstrated superior radical-scavenging performance in the DPPH assay. Overall, curcumin and quercetin metal complexes may offer promising avenues for improving solubility and exploring new strategies in cancer prevention and therapy.

Keywords: Flavonoids, curcumin, quercetin, ROS, and metal complexes.

ORAL PRESENTATION

Design and synthesis of amino acid–hydrazone hybrids as dual Bcl-2/NF-κB inhibitors

Merve Camcı Eren[1*] (ORCID: https://orcid.org/0000-0003-0157-2839),
Merve Yıldırım[2] (ORCID: https://orcid.org/0000-0002-5891-7167)

[*1]Istanbul University, Faculty of Pharmacy, Pharmaceutical Chemistry Department, Istanbul, Turkey.
[2] Istanbul University, Faculty of Science, Molecular Biology Department, Istanbul, Turkey.

*Corresponding author e-mail: mervecamci@istanbul.edu.tr

Abstract

Lung cancer, the second leading cause of cancer-related deaths, is a major global health concern that affects millions of people worldwide. It has extremely low survival rates, with only 28.4% of patients remaining alive (1). Recent data have demonstrated that Bcl-2 overexpression occurs in lung cancer and is associated with poor prognosis. ABT-737 and ABT-263 are two Bcl-2 inhibitors that exhibit potent antitumoral effects against lung cancer (2,3). In addition, nuclear factor-kappaB (NF-κB), which contributes to Bcl-2 upregulation, represents another attractive therapeutic target. Because NF-κB suppresses apoptosis and promotes proliferation, invasion, and metastasis, its inhibition offers an effective treatment strategy. Previous studies have reported that inhibition of NF-κB suppresses survival and proliferation of lung cancer cells. Bortezomib, an FDA-approved anticancer agent used in several malignancies, acts as an NF-κB inhibitor (4,5). Moreover, several natural compounds, including curcumin and piperlongumine, exhibit inhibitory effects on NF-κB. Preliminary findings from our previous study indicated that amino acid derivatives show selective cytotoxic potential against A549 lung cancer cells. In the present study, we aimed to design and synthesize amino acid-hydrazone hybrids (5a–c) as dual Bcl-2/NF-κB inhibitors for lung cancer treatment (Figure 1). The compounds were evaluated against A549 lung cancer cells and Beas-2b normal bronchial epithelial cells. Among them, compound 5c was identified as the most promising molecule, exhibiting an IC_{50} value of 7.7 µM against A549 cells and a high selectivity index with an IC_{50} value of >100 µM against Beas-2b cells. Molecular docking studies were also performed against both Bcl-2 (PDB ID: 4MAN) and NF-κB (PDB ID: 1NFK). All compounds showed favorable inhibitory potentials and strong interactions with key amino acids in both targets. These findings suggest that amino acid-hydrazone hybrids have the potential to act as selective anticancer agents through dual inhibition of Bcl-2 and NF-κB, two key anti-apoptotic pathways involved in lung cancer progression.

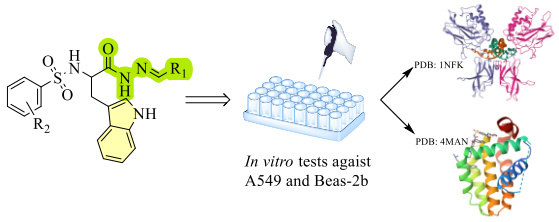


Figure 1. Conceptualisation of amino acid-hydrazone hybrids

Keywords: lung cancer, amino acid, hydrazone, Bcl-2, NF-kB

References:

1) State of Lung Cancer 2024 Report, American Lung Association, 2024.
2) Lochmann, T. L., Bouck, Y. M., & Faber, A. C. (2018). BCL-2 inhibition is a promising therapeutic strategy for small cell lung cancer. *Oncoscience*, *5*(7-8), 218–219. https://doi.org/10.18632/oncoscience.455.
3) Shoemaker, A. R., Mitten, M. J., Adickes, J., Ackler, S., Refici, M., Ferguson, D., Oleksijew, A., O'Connor, J. M., Wang, B., Frost, D. J., Bauch, J., Marsh, K., Tahir, S. K., Yang, X., Tse, C., Fesik, S. W., Rosenberg, S. H., & Elmore, S. W. (2008). Activity of the Bcl-2 family inhibitor ABT-263 in a panel of small cell lung cancer xenograft models. *Clinical cancer research: an official journal of the American Association for Cancer Research*, *14*(11), 3268–3277. https://doi.org/10.1158/1078-0432.CCR-07-4622.
4) Chen, W., Li, Z., Bai, L., & Lin, Y. (2011). NF-kappaB in lung cancer, a carcinogenesis mediator and a prevention and therapy target. *Frontiers in bioscience (Landmark edition)*, *16*(3), 1172–1185. https://doi.org/10.2741/3782.
5) Zhang, L., Ludden, C. M., Cullen, A. J., Tew, K. D., Branco de Barros, A. L., & Townsend, D. M. (2023). Nuclear factor kappa B expression in non-small cell lung cancer. *Biomedicine & pharmacotherapy = Biomedecine & pharmacotherapie*, *167*, 115459. https://doi.org/10.1016/j.biopha.2023.115459.

ORAL PRESENTATION

Kalp yetmezliği tedavisinde kullanılan bazı etken maddelerin analizi için kromatografik yöntemlerin geliştirilmesi

Buse Süleymanoğlu[1*] (ORCID: https://orcid.org/0009-0002-7227-7749),
Gizem Tırıs[2] (ORCID: https://orcid.org/0000-0002-2547-6086)

[*1] Bezmialem Vakıf Üniversitesi, Sağlık Bilimleri Enstitüsü, Analitik Kimya Anabilim Dalı, İstanbul, Türkiye
[2] Bezmialem Vakıf Üniversitesi, Eczacılık Fakültesi, Analitik Kimya Anabilim Dalı, İstanbul, Türkiye

*Sorumlu yazar e-mail: busesogluu@gmail.com

Özet

Kalp yetmezliği, kardiyak yapı veya fonksiyondaki bir veya daha fazla anormalliğin kalbin hücresel metabolizma için gerekli olan yeterli oksijeni iletememesine yol açtığı yaşamı tehdit eden kronik bir durumdur.[1] Kalp yetmezliğini önlemenin en etkili yolu, sağlıklı yaşam biçiminin yaşam boyu teşvik edilmesi olmakla birlikte, farmakolojik tedavi, kardiyovasküler hastalıkların yönetiminde temel bir rol oynamakta ve etkili ilaç kullanımına olan gereksinimi artırmaktadır. Kalp yetmezliği olan ve kardiyovasküler olay riskinin yüksek olduğu hastalarda kombine tedaviler uygulanmaktadır. Sakubitril (SAC) ve valsartan (VAL), kronik semptomatik kalp yetmezliği olan hastalarda morbidite ve mortaliteyi azaltmak için kullanılan anjiyotensin reseptör-neprilisin inhibitörleridir.[2] ATR ile SAC-VAL kombinasyonunun koroner kalp hastalığı ve kalp yetmezliği olan bireylerde kardiyak fonksiyon ve inflamatuar belirteçler üzerinde olumlu etkiler göstermektedir.[3] Bu bulgu, aynı anda kullanılan bu üç bileşiğin eş zamanlı analizinin klinik ve farmasötik açıdan önemini ortaya koymaktadır. Bu çalışmada, ATR, SAC ve VAL yapay serum matriksinde eş zamanlı kantitatif analizini sağlayan yeni bir YPSK yöntemi geliştirilmiştir. Ayrım C18 kolon kullanılarak sağlanmıştır. Mobil faz olarak %0.1 trifloroasetik asit içeren su:asetonitril:metanol çözücü sistemi kullanılmıştır. Akış hızı 1.1 mL/dk olarak ayarlanmıştır. Analitlerin ölçümü floresans dedektör ile gerçekleştirilmiştir. Metodun doğruluk, kesinlik, özgüllük, doğrusal aralık, LLOQ ve ULOQ parametreleri ICH M10 kılavuzuna göre değerlendirilmiş ve kabul edilebilir sınırlar içinde bulunmuştur. Geliştirilen yöntem ile ATR, SAC ve VAL etken maddelerinin yapay serum matriksindeki pikleri arasında yeterli rezolüsyon elde edilmiştir. Analitlerin birbirleriyle ve matriks bileşenleriyle girişim yapmadığı bir kromatografik sistem oluşturulmuştur. Bu çalışma, birlikte kullanılan kardiyovasküler ilaçların farmasötik kalite kontrolü ve terapötik ilaç düzeyi izlemine yönelik güvenilir, duyarlı ve tekrarlanabilir bir analitik yöntem sağlamaktadır.

Anahtar kelimeler: YPSK, Atorvastatin, Sakubitril, Valsartan, Validasyon

*Bu çalışma Bezmialem Vakıf Üniversitesi BAP Koordinasyon Birimi Kurulu tarafından desteklenmiştir. (Proje No: 20250901)

Kaynaklar:

McNeely, E. B. (2017). Treatment considerations and the role of the clinical pharmacist throughout transitions of care for patients with acute heart failure. Journal of Pharmacy Practice, 30(4), 441–450.
Tiris, G., Genç, A. A., & Erk, N. (2024). Simultaneous analysis of sacubitril and valsartan by novel analytical methods with green approach. Microchemical Journal, 199, 110054.
Zhou, Y., Liu, J., & Department of Cardiology, People's Hospital of Chongqing Hechuan. (2023). Effect of atorvastatin calcium combined with sacubitril–valsartan in coronary heart disease complicated with cardiac insufficiency. Indian Journal of Pharmaceutical Sciences, Special Issue 5, 210–211.

ORAL PRESENTATION

Synthesis, structural characterization and computational ADME analysis of a New Triazole-Based Cu(II) coordination compound

Tolga Göktürk[1*] (ORCID: https://orcid.org/0000-0002-7234-8079)

[*1]Muğla Sitki Kocman University, Faculty of Science, Department of Chemistry, Muğla, Türkiye.

*Corresponding author e-mail: tolgagokturk@mu.edu.tr

Abstract

In this study, a new copper(II) complex containing 1,2,3-triazole ligands was successfully synthesized and structurally characterized. The ligand (ethyl 2-(4-((4-formyl-3-hydroxyphenoxy)methyl)-1H-1,2,3-triazol-1-yl)acetate) was synthesized *via* a Cu(I)-catalyzed click reaction following our previously reported procedure [1] and subsequently complexed with copper(II) acetate to obtain the target coordination compound. The structure of copper(II) complex was elucidated through various analytical techniques including melting point determination, FTIR spectroscopy, UV-Vis. spectroscopy, elemental analysis, magnetic moment measurements, MALDI-TOF-MS and single crystal X-ray diffraction (SCXRD) studies. FTIR spectroscopy revealed characteristic shifts in carbonyl and C-O stretching bands, confirming the O-coordinated binding mode. UV-Vis data exhibited d-d transitions consistent with a distorted square-planar geometry around the Cu(II) center. Elemental analysis was consistent with the proposed molecular formula, while mass spectrometry provided 2:1 (ligand to metal ratio) coordination and the molecular weight of the complex. MALDI-TOF-MS spectra and SCXRD supported the proposed molecular composition, validating the successful synthesis of complex. Comprehensive *in silico* ADME assessments were performed to evaluate the drug-likeness and pharmacokinetic behavior of the complex [2, 3]. Studies showed that the Cu(II) complex has low gastrointestinal absorption and cannot cross the blood-brain barrier. Solubility predictions indicated moderate to poor solubility (logS values between -4.70 and -6.78). The complex is a P-gp substrate and CYP450 analysis suggests it may inhibit CYP2C9 and CYP3A4, but not the other major CYP enzymes. Drug-likeness filters showed several violations due to its high molecular weight and large TPSA. Although oral bioavailability appears limited, the complex showed no PAINS alerts and acceptable synthetic accessibility, supporting its potential for further biological studies.

Keywords: copper(II) complexes, 1,2,3-triazoles, ADME.

References:

[1] Göktürk, T., Çetin, E. S., Pekel, H., Şensoy, Ö., Aksu, E. N., Hökelek, T., & Güp, R. (2025). Role of acetate/benzoate substituents on the anticancer activities, in vitro and in silico DNA/BSA interactions of new 1, 4-disubstituted 1, 2, 3-triazole derivatives. *Journal of Molecular Structure*, 1338, 142273.
[2] Daina, A., Michielin, O., & Zoete, V. (2017). SwissADME: a free web tool to evaluate pharmacokinetics, drug-likeness and medicinal chemistry friendliness of small molecules. *Scientific Reports*, 7(1), 42717.
[3] Göktürk, T. (2025). Synthesis, characterization, BSA binding activity and ADME predictions of a new Co (II) complex with o-vanillin-based schiff base ligand. *Mugla Journal of Science and Technology*, 11(1), 18-27.

ORAL PRESENTATION

Investigation of the antitumor activity of *Eremurus spectabilis* M. Bieb. (çiriş herb) plant extracts in the process of hepatocellular carcinogenesis induced experimentally with diethylnitrosamine in rats

Abdulbaki Demir[1*] (ORCID: https://orcid.org/0000-0002-6867-4410), İsmail Çelik [2] (ORCID: https://orcid.org/0000-0003-2199-6348), Zabit Yener[3], (ORCID: https://orcid.org/0000-0002-6365-5843)

[1*]Muş Alparslan University, Bulanık Vocational School, Muş, Turkey.
[2]Van Yuzuncu Yil University, Molecular Biology and Genetics, Van, Turkey.
[3]Van Yuzuncu Yil University, Department of Pathology, Van, Turkey.

*Corresponding author e-mail: a.bakidemir@alparslan.edu.tr

Abstract

In this study, the protective effects of the ethanol lyophilized extract (LBE) and nanoparticle extract (NBE) of *Eremurus spectabilis* M. Bieb. (Çiriş Herb) at different doses were evaluated in a rat model of hepatocellular carcinogenesis induced by diethylnitrosamine (DEN) and thioacetamide (TAA). To determine a safe dose for warm-blooded organisms, an acute toxicity test was performed at 2000 mg/kg. The rats were divided into six groups (n=8). Except for the Normal Control (NC), all groups received 150 mg/kg DEN (once monthly) and 200 mg/kg TAA (once weekly) intraperitoneally throughout the experiment. LBE and NBE extracts were administered daily by gavage for 90 days. Serum analyses showed that ALT and AST levels significantly increased in the Cancer Control (CC) group compared to the NC group, while these increases were largely reduced to near-normal levels in the extract-treated groups. Body-weight gain was significant in the NC, CC, and KNBE2 groups, whereas no significant increase was observed in the other groups. The oxidative stress induced by the HCC model resulted in increased CAT, GPx, GST, and SOD activities and elevated MDA levels in all experimental groups, along with decreased GR activity and GSH levels. However, in the LBE- and NBE-treated groups, free radical accumulation was suppressed; MDA, CAT, and GPx levels decreased compared to the CC group, while GR, GST, and SOD activities and GSH levels increased, indicating an enhanced antioxidant defense system. Although liver tissue 8-OHdG levels were higher in all experimental groups than in NC, histopathological examinations showed milder liver damage in the plant-treated groups. In conclusion, the extracts of *Eremurus spectabilis* M. Bieb. may exhibit protective effects against HCC due to their antioxidant and antitumor constituents.

Keywords: Diethylnitrosamine, *Eremurus spectabilis* M. Bieb., Hepatocellular carcinoma, Liver, Thioacetamide

ORAL PRESENTATION

Phytoremediation-oriented Evaluation of Nickel Stress Responses in *Anubias nana* Engl. grown in aquatic systems

Bedriye Nazli Erkencioglu[1*], Asli Hocaoglu-Ozyigit[1], Hulya Yazicioglu[1], Ibrahim Ertugrul Yalcin[2], Ibrahim Ilker Ozyıgıt[1,3]

[1]Marmara University, Faculty of Science, Department of Biology, 34722, Istanbul, Türkiye
[2]Bahcesehir University, Faculty of Engineering and Natural Sciences, Department of Civil Engineering, 34353, Istanbul, Türkiye
[3]Marmara University, Environmental Issues Application and Research Center, 34722, Istanbul, Türkiye

Abstract

Nickel (Ni), a heavy metal that occurs naturally and can accumulate in aquatic environments as a result of both natural and human activities. Although Ni plays a minor but essential role in plant growth, excessive levels can have adverse effects on plants physiology through the disruption of vital biological processes and functions. *Anubias nana* Engl. (Araceae) is a popular slow-growing aquatic plant, is a promising candidate for heavy metal accumulation due to its high adaptability. This study examined the mineral nutrient profile of *A. nana* Engl. under Ni exposure and assesses its potential for sustainable heavy metal removal in aquatic ecosystems. Additionally, the genotoxic effects of Ni exposure were assessed. Genomic template stability (GTS) was calculated using ISSR markers (UBC808, UBC811, UBC834, UBC841, UBC842) with a focus on detecting the appearance or disappearance of DNA bands and variations in their intensity. Plants were cultivated in tanks containing 0.2% Hoagland solution for a period of 10 days at a temperature of 28 ± 1°C, with the objective of promoting growth and acclimatizing to the aquarium environment. Thereafter, the plants were subjected to $NiCl_2.6H_20$ stress, with concentrations of 0, 10, 25, 50, and 100 µM. Leaves, stems and roots were harvested 10 days after Ni treatment (both washed and unwashed) were analyzed using a PerkinElmer Optima 7000DV ICP-OES to determine their heavy metal and mineral nutrient contents (B, Ca, Cu, Fe, K, Mg, Mn, Na, Ni, Zn). The total chlorophyll content and phytoremediation parameters, including bioaccumulation index (BAI), bioconcentration factor (BCF), translocation factor (TF), surface adsorption (SA), surface adsorption efficiency (SAE) and removal efficiency (RE), were subsequently calculated to assess the plant's physiological responses to Ni exposure and to evaluate its phytoaccumulation potential. The findings demonstrated a concentration-dependent increase in Ni accumulation. The highest Ni accumulation, was detected in unwashed leaf samples at 100 µM, reaching 47.310 mg kg^{-1}. At the same concentration, the stem exhibited the highest BAI (16.33). The highest BCF was found in the leaf at 10 µM (3.93), while the highest TF (2.3) was recorded in the leaf/root at 10 µM. The SA reached 4.75 at 100 µM, whereas the maximum SAE was 77% at 10 µM. Additionally, the highest RE was found to be 7.95% at 100 µM. These findings indicate that *A. nana* is a capable accumulator of Ni. Genotoxicity analysis using the UBC811 primer revealed new band formation at 900 bp in both 50 µM and 100 µM treatments. Accordingly, the polymorphism rate was calculated as 3.13% and the GTS decreased to 96%. Although alterations in band intensity were observed, the overall genotoxic effects remained limited. Overall, *A. nana* demonstrated strong Ni accumulation capacity while maintaining high genomic stability, exhibiting only minor genotoxic alterations under increasing Ni stress.

Keywords: Heavy metal, ICP-OES, ISSR, Mineral nutrients

ORAL PRESENTATION

A bibliometric analyse of scientific studies on the invasive species *Lepomis gibbosus*

Ufuk Gürkan Yıldırım

Isparta University of Applied Sciences, Eğirdir Fisheries Faculty, Isparta

Abstract

Lepomis gibbosus (pumpkinseed sunfish), native to North America, has spread as an invasive species across multiple continents due to anthropogenic influences and waterway connectivity. It typically inhabits vegetated lakes, ponds, and the slow-moving pools of creeks and small rivers. The species feeds on small fish, other vertebrates, and fish eggs. Adult individuals rarely form schools, usually occurring in pairs or loose groups of three to four, whereas juveniles aggregate in relatively large schools. Introduced to Europe, *L. gibbosus* avoids fast-flowing waters and can also be found in estuarine environments with salinity levels up to 18.2 ppt. It has been reported to prey on a wide variety of mollusks and other invertebrates in Europe. From a fisheries perspective, it is considered an undesirable catch. This study presents a comprehensive bibliometric analysis aimed at revealing the global development of scientific research on the invasive freshwater fish *Lepomis gibbosus*. A total of 774 academic publications indexed in the Web of Science database were evaluated in terms of scientific productivity, citation performance, international collaboration networks, and thematic research trends. Bibliometric analyses were conducted using raw data from the Web of Science with the aid of the R programming language and VOSviewer software. The study examined the distribution of publications over time, the most influential authors and journals, geographic publication density, and keyword co-occurrence networks in detail. Findings indicate a marked increase in research on *L. gibbosus* since the early 2000s, with publication output predominantly concentrated in European countries. The literature highlights key research themes such as the species' ecological impacts, invasion dynamics, habitat utilization, and competitive pressures on native fish communities. Additionally, the invasive range of *L. gibbosus* is rapidly expanding across Europe, attributed to its high environmental tolerance, reproductive success, and anthropogenic dispersal via aquatic systems. In conclusion, this study provides a holistic overview of the structural characteristics of scientific production on *L. gibbosus* and offers significant insights for the ecological management of the species as well as future research priorities.

Keywords: *Lepomis gibbosus*, Invasive species, Bibliometric analysis, Ecological impact

ORAL PRESENTATION

Synthesis of functional nanohybrid materials through *in situ* copolymerization

Serap Kavlak (ORCID: https://orcid.org/0000-0001-6103-0121)

Hacettepe University, Faculty of Science, Department of Chemistry, Ankara, Türkiye.

Corresponding author e-mail: skavlak@hacettepe.edu.tr

Abstract

In this work, a series of novel functional copolymer/layered silicate nanocomposites were synthesized by *in situ* radical-initiated copolymerization in solution. The interaction of the organic units with clay and the structural analysis of the synthesized poly(AAm-*co*-CA)/organo-MMT nanocomposites were elucidated by ^{1}H NMR and ATR-FTIR spectroscopy. Characteristic peaks belong to the functional groups of the synthesized copolymer units and organo-MMT were identified in the spectra of the nanocomposites. Structures of the synthesized nanocomposites and the effect of the organically modified montmorillonite clay on the structural properties were investigated by complementary XRD analyses. Intercalation of comonomers in between silicate layers of organically modified montmorillonite was clarified by the increase in *d*-spacing in nanocomposites between 3.80% and 51.60%.[1] The obtained results confirmed the *in situ* interlamellar synthesis of the nanocomposites by intercalation of comonomers into the organically modified montmorillonite layers and showed that nanocomposites with intercalated structure were successfully obtained. These results will contribute to the design and synthesis of functional nanomaterials that may offer different applications.

Keywords: functional copolymer, clay, nanocomposite

Reference:

[1] S. Kavlak, *New J Chem* 2022, 46, 2930-2939.

ORAL PRESENTATION

Yüksek pH ve tuzluluk koşullarında yerli EDDHA-Fe şelatının gübre performansı ve sürdürülebilir tarım açısından potansiyelinin araştırılması

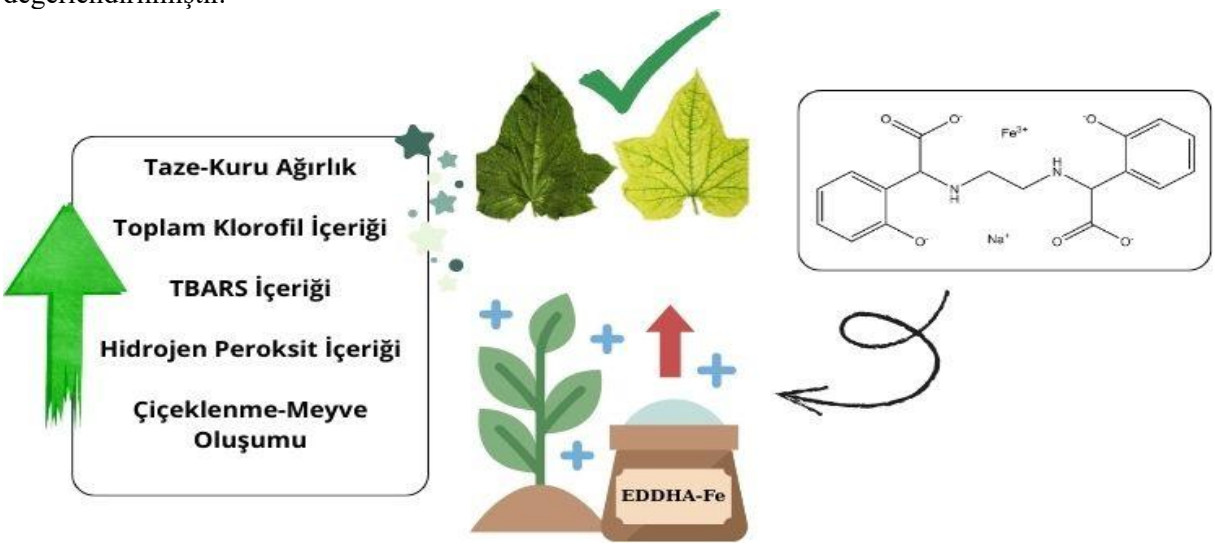
Selda DURMUŞOĞLU[1], Elif GÖKTÜRK[1], Dilek ÜNLÜER BİRİNCİ[2], Asim KADIOĞLU[1]

[1]Karadeniz Teknik Üniversitesi, Fen Fakültesi, Biyoloji Bölümü, Trabzon/TÜRKİYE
[2] Karadeniz Teknik Üniversitesi, Fen Fakültesi, Kimya Bölümü, Trabzon/TÜRKİYE

Sorumlu yazar e-mail: seldaoksuz@ktu.edu.tr

Özet

Alkali ve tuzlu toprak koşulları, bitkilerde besin elementlerinin biyoyararlılığını önemli ölçüde azaltarak büyüme geriliği, pigment kaybı ve oksidatif stres gibi çeşitli fizyolojik bozukluklara yol açmaktadır. Bu koşullarda alımı en fazla kısıtlanan mikro elementlerden biri olan demir (Fe), özellikle kloroz, fotosentetik kapasite azalması ve verim düşüklüğüyle ilişkilidir. Bu çalışma, yerel kaynaklardan geliştirilen EDDHA-Fe şelat kompleksinin, yüksek pH ve tuzluluk altında yetiştirilen salatalık (*Cucumis sativus* L.) bitkisinin morfolojik ve fizyolojik yanıtları üzerindeki etkilerini belirlemeyi amaçlamaktadır.
Denemede, yerli EDDHA-Fe formülasyonu, iki ticari demir şelatı (Sequestrene ve Tariron) ile karşılaştırmalı olarak uygulanarak analizler gerçekleştirilmiştir. Uygulamalar sonrasında bitkilerde lipid peroksidasyonu (TBARS), hidrojen peroksit (H_2O_2), toplam klorofil ile taze ve kuru ağırlık ölçümleri gerçekleştirilmiş; ayrıca yapraklarda DAB boyama ile H_2O_2 birikimi ve çiçeklenme–meyve oluşumu gibi morfolojik göstergeler değerlendirilmiştir.



Elde edilen bulgular, yerli EDDHA-Fe uygulamasının hem kontrol hem de tuz stres koşullarında bitki gelişimini anlamlı düzeyde desteklediğini ortaya koymuştur. Özellikle klorofil içeriği, taze ağırlık ve çiçeklenme gibi büyüme parametreleri açısından yerli formülasyonun güçlü ve istikrarlı bir performans sergilediği belirlenmiştir. Oksidatif stres göstergeleri olan TBARS ve H_2O_2 seviyelerinin düşmesi, yerli formülasyonun stres koşullarında hücresel hasarı azalttığını göstermiş; DAB boyama sonuçları bu etkiyi dokusal düzeyde doğrulamıştır.
Sonuçlar, yerli kaynaklı EDDHA-Fe şelat kompleksinin ticari muadilleriyle karşılaştırıldığında benzer veya daha üstün etki gösterebildiğini, ayrıca çevre dostu ve sürdürülebilir bir gübre alternatifi olma potansiyeline sahip olduğunu göstermektedir.

Anahtar Kelimeler: Demir şelatı, EDDHA, Tuzluluk, Yüksek pH, Demir eksikliği, Oksidatif stres, Sürdürülebilir gübre

ORAL PRESENTATION

Development of a cationic surfactant-selective glassy carbon electrode for potentiometric determination of didecyldimethylammonium chloride

Asya İskenderoğlu, H. Elif Kormalı Ertürün* (ORCID: https://orcid.org/0000-0003-1161-9418)

Ankara University, Faculty of Science, Department of Chemistry, Ankara, Türkiye.

*Corresponding author e-mail: kormali@science.ankara.edu.tr

Abstract

Surfactants are a large group of chemicals widely used in industry, in cleaning and sterilization processes, in pharmaceuticals, in personal care and cosmetic products, etc. Given their extensive consumption and high toxicity, the monitoring of surfactants is extremely important for industrial processes and quality and environmental control. In this study, polymeric membrane cationic surfactant-selective glassy carbon electrodes (CSGCEs) were prepared, utilizing certain Schiff bases as ionophores, for the potentiometric determination of didecyldimethylammonium chloride (DDMACl), which is a cationic surfactant. The electrode performance was studied by changing the type and quantity of the ionophore and plasticizer within the polyvinyl chloride (PVC)-based polymeric membranes. Additionally, the influence of certain nanomaterials and a lipophilic additive included in the composition was also assessed. The glassy carbon electrode with a membrane composition consisting of 1 mg each of N-salicylidene-2-aminophenol (ionophore), sodium tetraphenylborate (lipophilic additive), chitosan (nanomaterial), TiO_2-NP (nanoparticle), 66 mg tributyl phosphate (plasticizer) and 30 mg PVC, was observed to exhibit the best performance in DDMACl sensitivity. It was determined that the DDMACl-selective electrode gave a linear response in the concentration range of 1.0×10^{-3}-1.0×10^{-6} M with a slope of -58.6±3.0 mV/pDDMACl at pH 4.0 and the detection limit was 2.5×10^{-7} M. The response time of the electrode was 5-8 s. The behavior of the proposed electrode in the presence of some interference species was investigated by determining the selectivity coefficients calculated with the fixed interference method (FIM). Various disinfection products obtained from markets were used for analytical application.

Keywords: Surfactant determination, potentiometry, ion-selective electrode, lipophilic additive, nanomaterial.

ORAL PRESENTATION

Efficient microwave-assisted synthesis of novel compounds by the reaction of penta-1,4-diene-3-one derivatives with N,N-dimethyl barbituric acid

E. Vildan Burgaz [1*] (ORCID: https://orcid.org/0000-0003-3245-5934), İmge Kunter [1] (ORCID: https://orcid.org/0000-0001-5706-306X) , Mehtap yakut [2] ((ORCID:https://orcid.org/0000-0002-6237-8522)

[*1] Eastern Mediterranean University, Faculty of Pharmacy, Famagusta, Mersin, North Cyprus.
[2] Ankara University, Faculty of Science, Dögol street, 06100, Besevler/Ankara Türkiye.

*Corresponding author e-mail: vildan.burgaz@emu.edu.tr

Abstract

Azospiro-based frameworks have recently emerged as valuable structures in pharmaceutical research. Nitrogen containing spiro-heterocycles represent a key synthetic scaffold present in numerous natural products and are associated with diverse biological and pharmacological activities. Ongoing studies continue to highlight the importance of designing new molecules within this class and evaluating their biological profiles including fungicidal, herbicidal, antibacterial and antimicrobial properties. In addition, the well-documented bioactivity of barbituric acid derivatives has further stimulated interest in the development of 2,4-diazaspiro [5.5] undecane derivatives. Microwave assisted organic synthesis has garnered significant interest owing to its capacity to enhance reaction efficiency, increase product yields, and shorten reaction times. In this study, we performed the microwave reaction between N,N-dimethyl barbituric acid and penta-1,4-diene-3-one derivatives ((1E,4E)-1,5-bis(5-methylfuran-2-yl)penta-1,4-dien-3-one and (1E,4E)-1,5-bis(2-methoxyphenyl)penta-1,4-dien-3-one). At a result of these reactions, we obtained 2,4-Dimethyl-7,11-bis(5-methylfuran-2-yl)-2,4-diazaspiro [5.5] undecane-1,3,5,9-tetraone and 7,11-Bis(2-methoxyphenyl)-2,4-dimethyl-2,4-diazaspiro [5.5] undecane-1,3,5,9-tetraone. The reaction was performed under microwave irradiation providing a more environmentally benign and energy-efficient process. Key parameters including reaction time, temperature and microwave power were systematically optimized to achieve the highest possible yield. The resulting compound was subsequently characterized using a range of spectroscopic techniques such as IR, ^{1}H-NMR, ^{13}C-NMR, and mass spectrometry (MS). These compounds possess noteworthy pharmacological properties and represent promising scaffolds for the development of new therapeutic agents. Their anticancer activity was evaluated using the SK-HEP-1 adenocarcinoma cell line and the results demonstrated significant inhibitory effects on liver adenocarcinoma cells. This study contributes to assessing the therapeutic potential of these molecules and further supports the relevance of microwave assisted synthesis in early-stage drug discovery.

Keywords: Diazaspiro, microwave, synthesis, anti-cancer, barbutiric acid

ORAL PRESENTATION

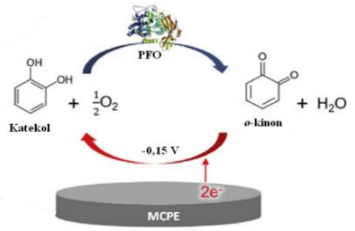
Fenolik bileşiklerin tayini için polifenol oksidaz temelli biyosensör tasarlanması

Onur Can Bodur[1*] (ORCID: https://orcid.org/ 0000-0001-8915-3078), Şaban Keskin[2] (ORCID: https://orcid.org/ 0000-0002-0287-4268), Fatma Arslan[3] (ORCID: https://orcid.org/ 0000-0002-3282-6451)

[*1,3] Gazi Üniversitesi, Fen Fakültesi, Kimya Bölümü, Ankara, Türkiye
[2] Bilecik Şeyh Edebali Üniversitesi, Sağlık Hizmetleri Meslek Yüksekokulu, Tıbbi Hizmetler ve Teknikler Bölümü, Bilecik, Türkiye
*Sorumlu yazar e-mail: onurcanbodur@gazi.edu.tr

Özet

Yaşam süresince maruz kalınan; hava-su kirliliği, hazır yiyecekler, stres gibi çeşitli etkenlerin insan sağlığı üzerine olumsuz etkileri bulunmakta ve bu etkenler sonucunda serbest radikaller oluşmaktadır. Antioksidanlar, meydana gelen bu durumda devreye girerek, yükseltgenebilen maddeler olduklarından, radikal zincir tepkimesini kesintiye uğratıcı rol oynamaktadırlar. Kaliteli beslenme yardımı ile yüksek biyoaktiviteye sahip toplam fenolik madde miktarı bol gıdalar ve bağışıklık sistemini güçlendirecek takviye edici gıdaların diyete dahil edilmesi, kardiyovasküler hastalıklar, kanser, obezite ve nörolojik bozukluklar dahil olmak üzere birçok kronik hastalığın görülme sıklığını azaltmakta ya da başlangıcını geciktirmektedir. Yüksek biyoaktiviteye sahip gıdalardaki fenolik bileşikler belirlenerek, bunların gıda sistemlerindeki etkilerinin incelenmesi ile gıda içeriğine yönelik üretim ve denetim devamlılığının sağlanması büyük önem taşımaktadır[1]. Bu nedenle fenolik bileşiklerin düşük derişimlerde dahi hızlı ve duyarlı bir şekilde tayin edilmesi önem arz etmektedir. Polifenol oksidaz (PFO) enziminin kullanıldığı enzim biyosensörleri; düşük maliyetli, hızlı, pratik, yüksek hassasiyette ve düşük tayin limiti olanağı sağladığı için, fenolik bileşenlerin tayin edilmesinde diğer metotlara göre iyi bir alternatiftirler[2,3]. Bu çalışmada, Ananasın (*Ananas comosus* (L.) Merr.) atık niteliğindeki taç yapraklarından sentezlenen gümüş nanopartiküller (AgNPs) modifiye karbon pasta elektrot (MCPE) tasarımında kullanıldı. Fenolik madde miktarı tayini için, *Bacillus subtilis* bakterisinden izole edilerek saflaştırılan PFO enzimi, MCPE yüzeyine glutaraldehit ile çapraz bağlanarak immobilize edildi. Enzimatik tepkime sonucu oluşan *o*-kinon bileşiğinin oluşturduğu katodik (indirgenme) akımın ölçülmesiyle de fenolik bileşiklere duyarlı elektrokimyasal esaslı bir biyosensör sistemi geliştirildi. Tasarlanan biyosensörün amperometrik cevabına; pH, sıcaklık ve substrat derişimi etkisi gibi çalışma koşulları belirlendi. Optimum çalışma koşulları; *-0,15 V* çalışma potansiyeli, modifiye etmek için *20 mg* AgNPs miktarı olarak belirlendi. Biyosensörün doğrusal çalışma aralığı, alt tayin sınırı değerleri tespit edildi ve $Km_{(göz)}$ 0,002 µM, $Imax_{(göz)}$ 1,00 µA olarak hesaplandı. Biyosensörün performansını etkileyen tekrarlanabilirlik ve depolama kararlılığı etkisi incelendi. Substrat olarak kullanılan katekol tayinine, girişim yapabilecek türlerin etkileri incelendikten sonra PFO temelli biyosensör, takviye edici gıda örneklerinde fenolik madde miktarı tayininde kullanıldı.



Anahtar Kelimeler: Fenolik bileşik, biyosensör, polifenol oksidaz, karbon pasta elektrot, takviye edici gıda

* Bu çalışma, Onur Can BODUR'un doktora tez çalışması kapsamında gerçekleştirilmiştir. FDK-2023-8347 kodlu projemize sağladıkları destek için Gazi Üniversitesi Bilimsel Araştırma Projeleri Koordinatörlüğü'ne teşekkürler.

Kaynaklar: **1.** Oszmianski, J., & Lachowicz-Wiśniewska, S. (2022). *Food Processing and Its Impact on Phenolic and other Bioactive Constituents in Food* (p. 230). MDPI-Multidisciplinary Digital Publishing Institute Young, I. S., & Woodside, J. V. (2001). Antioxidants in health and disease. Journal of clinical pathology, 54(3), 176-186.
2. Arslan, H., Şenarslan, D., Çevrimli, B. S., Zengin, H., Uzun, D., & Arslan, F.. (2018). Preparation of carbon paste electrode containing polyaniline-activated carbon composite for amperometric detection of phenol. Bulg. Chem. Commun, 50(1), 16-20.
3. Akbıyık, M. A., Bodur, O. C., Keskin, M., Kara, M., Dinç, S., Arslan, H. & Arslan, F. (2023). A sensitive amperometric biosensor based on carbon dot 3-chloropropyl-trimethoxysilane modified electrode for detection of neurotransmitter dopamine. Journal of The Electrochemical Society, 170(3), 037517.

ORAL PRESENTATION

Resveratrol'ün 4T1 meme kanseri hücreleri üzerinde sitotoksik etkisinin değerlendirilmesi

Özlem Türksever[1], Hacer Kaya Çakir[1,2,] Onur Eroğlu[1,2]

[1]Bilecik Şeyh Edebali Üniversitesi, Moleküler Biyoloji ve Genetik Bölümü, Bilecik, Türkiye
[2] Bilecik Şeyh Edebali Üniversitesi, Biyoteknoloji Araştırma ve Uygulama Merkezi, Bilecik, Türkiye

Özet

Kemoterapi ve radyoterapi gibi kanser tedavisinde kullanılan bilimsel tedavilerin normal hücrelere verdiği zararlar ve bireyler üzerindeki yan etkileri nedeniyle, bitkisel veya diğer doğal kaynaklı ajanların bilimsel tedavilere ek olarak kullanımına ilişkin araştırmalar devam etmektedir. Bir polifenol olan resveratrol antep fıstığı, yaban mersini ve üzüm gibi yaygın gıdalarda bulunur. Çok sayıda çalışma, resveratrolün güçlü anti-inflamatuar, antioksidan ve antikanser aktivitelere sahip olduğunu göstermiştir. Bu çalışmada Resveratrol'ün 4T1 meme kanseri hücre hattı üzerindeki sitotoksik etkisi araştırılmıştır. Resveratrol'ün 4T1 meme kanseri hücre hattında konsantrasyona bağlı hücre canlılığı üzerindeki etkisini araştırmak için MTT testi, apoptoz üzerindeki etkisi belirlenmek için bir Caspase 3/7 apoptoz kiti kullanıldı. BAX/BCL-2 genlerinin ifade seviyeleri Real-time PCR ile belirlendi. MTT sonuçlarına göre, Resveratrol'ün 4T1 meme kanseri hücre hattı üzerindeki 24 saatlik IC50 değeri 70 µM, 48 saatlik IC50 değeri ise 30 µM olarak bulundu. İlaç hücrelere uygulandığında, hücre sayısında azalma, hücre boyutunda küçülme ve hücre uzantıların kaybolarak yuvarlak bir şekil aldığı gözlemlendi. Resveratrol ile tedavi edilen hücre grubunun Cas3-7 aktivite seviyeleri kontrol grubu ile karşılaştırıldı. BAX ve BCL-2 genlerinin ekspresyon seviyeleri kontrol ile karşılaştırıldı. Resveratrol tedavisinin 4T1 meme kanseri hücre canlılığını doza ve zamana bağlı olarak önemli ölçüde azalttığı gözlemlenmiştir.

Anahtar Kelimeler: Resveratrol, 4T1, Meme kanseri, Sitotoksik Etki

ORAL PRESENTATION

Determination of the association of TLR2 rs5743708 and rs121917864 polymorphisms with endometrial cancer risk

Emine Yagci[1](0000-0003-2179-1318), Ahmet Dogukan Gokcek[2] (0009-0005-6691-1514), Gamze Zengin[1] (0000-0002-5215-6088), Tufan Oge[3] (0000-0002-1951-9713), Cansu Ozbayer[1] (0000-0002-1120-1874), Hulyam Kurt [4] (0000-0003-2433-9925)
Ahmet Dogukan Gokcek[2] (0009-0005-6691-1514)

[1]Kutahya Health Sciences University, Faculty of Medicine, Department of Medical Biology, Kutahya, Türkiye.
[2] Kutahya Health Sciences University, Faculty of Medicine, Kutahya, Türkiye.
[3] Eskisehir Osmangazi University, Faculty of Medicine, Department of Gynecology, Eskisehir, Türkiye.
[4]Eskisehir Osmangazi University, Faculty of Medicine, Department of Medical Biology, Eskisehir, Türkiye.

*Corresponding author e-mail: adogukan.gokcek@ogr.ksbu.edu.tr

Abstract

Endometrial cancer is an epithelial malignancy originating from the endometrium, the inner lining of the uterus, and is one of the most common gynecological cancers in women. Chronic inflammation has been identified as playing an important role in cancer development and progression. TLR2 (Toll-like receptor 2) is expressed in both immune cells and tumor cells and occupies a critical intersection between chronic inflammation and cancer. TLR2 activation can stimulate pro-tumor pathways such as NF-κB, PI3K/AKT, and ERK1/2, which can increase cell proliferation, inhibit apoptosis, and create an inflammatory environment in the tumor microenvironment. Furthermore, TLR2 expression has been reported to be significantly higher in endometrial cancer samples compared to control groups. Based on this information, we investigated the association of two TLR2 polymorphisms, rs5743708 and rs121917864, with endometrial cancer risk in our study. The PCR-RFLP method was used to determine the variants. As a result of our study, a significant difference was observed in the genotype frequencies of the TLR2-rs121917864 polymorphism between patients and control subjects ($p<0.05$), while no significant difference was observed in terms of allele frequency. For the TLR2-rs5743708 variant, both genotype and allele frequencies were found to be significantly different between patients and control subjects ($p<0.0001$). The findings obtained in light of these results support the potential roles of inflammatory pathways and immune receptors in endometrial carcinogenesis.

Keywords: TLR2, Endometrial Cancer, Single Nucleotide Polymorphism

ORAL PRESENTATION

Functional role of MATN3 in osteosarcoma cell growth and motility

Fatime Öcal[1*] (ORCID: https://orcid.org/0009-0001-9668-7745), Sedanur Can[1] (https://orcid.org/0009-0004-7398-970X.), Meltem Alper[2](ORCID: https://orcid.org/0000-0001-6359-9979)

[1]Department of Oncology, Institute of Health Sciences, Dokuz Eylul University, 35340 Izmir, Türkiye;
[2]Department of Translational Oncology, Institute of Oncology, Dokuz Eylul University, 35340 Izmir, Türkiye

*Corresponding author e-mail: biofatime.ocal@gmail.com

Abstract

The extracellular matrix (ECM) is a dynamic three-dimensional structure surrounding cells in tissues, composed of structural and specialized proteins (collagen, elastin, fibronectin, laminin), proteoglycans and glycosaminoglycans, and ECM-associated enzymes, which is essential for cellular homeostasis, migration, and proliferation. Matrilins are ECM proteins that interact with collagen-associated fibrils, aggrecan, COMP, and various collagen types. MATN3 is one of four members of the Matrilins (MATN1, MATN2, MATN3, and MATN4). Matrilins are involved in various cancers, such as cervical cancer, melanoma, and hepatocellular carcinoma. While the oncogenic role of MATN3 in gastric cancer is established, its impact on osteosarcoma has only been explored through bioinformatics studies. Osteosarcoma is a high-grade bone tumor originating from mesenchymal cells, distinguished by the formation of malignant osteoid or immature bone matrix, with low survival rates for metastatic or recurrent cases. Current bioinformatics studies aim to identify genes influencing osteosarcoma prognosis and metastasis. Epithelial-Mesenchymal Transition (EMT) is a key process in cancer metastasis, enabling tumor cells to acquire invasive properties. A recent bioinformatics analysis suggested that the MATN3 gene may play a role in osteosarcoma (OS) metastasis and is linked to EMT regulation. The study further found that MATN3 expression was significantly lower in metastatic OS tissue compared to primary tumors. In this study, we aimed to elucidate the potential role of MATN3 on OS proliferation. Therefore, MATN3 was knocked down in osteosarcoma (OS) cell lines using a siRNA approach with specific siRNAs, confirming silencing via Western Blot. The proliferation and migration properties of osteosarcoma cells with silenced *MATN3* gene were determined by functional assays (MTT, wound healing, and transwell). The results would contribute to the understanding of the functional role of MATN3 on OS proliferation.

Keywords: MATN3, Osteosarcoma, EMT, Migration, Proliferation

*This work was partially funded by Dokuz Eylül University, BAP Department (Project ID: 3588) and TÜBİTAK-BİDEB 2210/C Master's Scholarship Program (1649B022416337).

ORAL PRESENTATION

Targeting UHRF2 (Ubiquitin-like with PHD and ring finger domains 2) in osteosarcoma: Impacts on proliferation and emt dynamics

Sedanur Can[1*] (https://orcid.org/0009-0004-7398-970X.), Fatime Öcal[1](https://orcid.org/0000-0001-9668-7745), Meltem Alper[2] (ORCID: https://orcid.org/0000-0001-6359-9979)

[*1] Dokuz Eylul University, Institute of Health Sciences, Translational Oncology Department, İzmir/ Türkiye
[2] Dokuz Eylul University, Institute of Oncology, Translational Oncology Department, İzmir/ Türkiye

*Corresponding author e-mail: cansedanurbio@gmail.com.tr

Abstract

Cancer is a multistep process in which genomic instability and disruption of epigenetic regulation occur simultaneously. Many of these molecular alterations are mediated by the ubiquitin–proteasome system (UPS), which modulates protein stability, chromatin dynamics, and transcriptional programs. UHRF2 is a critical E3 ubiquitin ligase within the UPS, and is a nuclear regulator that exerts substrate-specific ubiquitin ligase activity. UHRF2 plays a role in regulating DNA methylation, histone modifications, and cell cycle control. UHRF2 has shown that it contributes to tumor progression in colon and breast cancers, but exhibits tumor-suppressive functions in leukemia and non-small cell lung cancer. Bioinformatic analyses in osteosarcoma have indicated that UHRF2 is overexpressed in osteosarcoma tissues compared to normal bone and appears among ubiquitin-related genes associated with a poor prognosis, implying a potential oncogenic function. Osteosarcoma is an aggressive primary bone sarcoma of children and adolescents, characterized by immature osteoid formation, high proliferative capacity, and early metastatic behavior. Herein, we aimed to elucidate the contribution of the UHRF2 to osteosarcoma proliferation and migration. In this context, UHRF2 expression was determined at both the mRNA (qRT-PCR) and protein (western blot) levels in osteosarcoma cell lines. The *UHRF2* gene was silenced using siRNAs in 143B cells, where it was highly expressed, and the silencing efficiency was confirmed by Western blot. The knockdown of UHRF2 on cell proliferation and metastasis was evaluated using MTT, wound healing, transwell, and colony formation assays. To determine its effect on the EMT (Epithelial-Mesenchymal Transition), specific biomarkers were analyzed by Western blot. The results would provide insight into determining the functional role of UHRF2 in osteosarcoma and its potential as a therapeutic target.

Keywords: Osteosarcoma,UHRF2,Prolirefation,Migration, Invasion

*This study was financially supported by Dokuz Eylül University Scientific Research Projects Unit (3676). Sedanur Can was supported within the scope of the TÜBİTAK-BİDEB 2210-C Domestic Graduate Scholarship Program (1649B022416339).

ORAL PRESENTATION

Selüloz esaslı kompozitlerin 2. tip fotopolimerizasyon yöntemiyle hazırlanması*

Gencay Cantürk[1], Seda Bekin Acar[2], Mehmet Atilla Taşdelen[2]

[1]Polimer Malzeme Mühendisliği Anabilim Dalı, Lisansüstü Eğitim Enstitüsü, Yalova Üniversitesi, 77200 Yalova, Türkiye
[2]Polimer Malzeme Mühendisliği, Mühendislik Fakültesi, Yalova Üniversitesi, 77200 Yalova, Türkiye

Sorumlu yazar e-mail: gencay126@gmail.com

Özet

Kompozit malzemeler, polimer bir matris içine farklı boyutlardaki takviye fazlarının homojen şekilde dağıtılmasıyla elde edilen ve geleneksel malzemelere göre daha üstün performans sergileyen gelişmiş yapılardır. Takviye fazlarının geniş yüzey etkileşimi sayesinde matris ile güçlü bağlar oluşur ve bu sayede nispeten düşük dolgu oranlarında bile mekanik dayanım, termal kararlılık, optik özellikler ve bariyer performansında belirgin iyileşmeler sağlanır. Özellikle selüloz esaslı yapılar; yenilenebilir kaynaklı olmaları, hafiflikleri, biyouyumlulukları ve fonksiyonlandırılabilir olmaları sayesinde sürdürülebilir kompozit tasarımlarında önemli avantaj sunar. Bu tür kompozitler; kaplamalardan paketlemeye, biyomedikal malzemelerden yapısal uygulamalara kadar geniş bir kullanım alanına sahip olup, takviye fazının matrise kazandırdığı çok yönlü özelliklerle yüksek performanslı malzeme geliştirme çalışmalarında temel bir rol oynamaktadır. Bu çalışmada, selüloz yüzeylerindeki hidroksil gruplarına tersiyer amin fonksiyonları eklenmiş ve bu fonksiyonel yapıların II. tip fotopolimerizasyon yaklaşımıyla mikroselüloz takviyeli kompozitlerin hazırlanmasında kullanılması sağlanmıştır. Fotopolimerizasyon sonucu monomerlerin selüloz yüzeyine kimyasal olarak bağlanmasıyla elde edilen kompozitler, dolgu içermeyen saf polimere kıyasla daha yüksek termal ve mekanik performans sergilemiştir. Hazırlanan, farklı oranlarda mikroselüloz içeren kompozitlerin termal, morfolojik ve mekanik özellikleri saf polimer ile karşılaştırmalı olarak değerlendirilmiş ve optimum dolgu oranı belirlenmiştir. Mekanik özellikler incelendiğinde, en iyi performansın %5 MS takviyesiyle elde edildiği görülmüştür. Bu dolgu oranında çekme dayanımı belirgin şekilde artmış, uzama değerlerinin de iyileşmesiyle daha güçlü ve aynı zamanda daha elastik bir yapı oluşmuştur. Bu nedenle, saf termoset ile kıyaslandığında %5 MS takviyesi en uygun ve en başarılı dolgu seviyesi olarak değerlendirilmektedir.

Anahtar Kelimeler: Mikrokompozit, selüloz, II. Tip fotopolimerizasyon

* Bu çalışma Yalova Üniversitesi BAP Koordinasyon Birimi tarafından desteklenmiştir (Proje No: 2024/YL/0008).

ORAL PRESENTATION

Atık kahve telvesinden türetilen mezogözenekli karbon katkılı PVDF Bazlı PEM yakıt pili membranlarının geliştirilmesi

Minel Mil[1]*, Ceren Karagözlü[1], Yavuz Yağızatlı[1]

*[1]Gazi Üniversitesi, Mühendislik Fakültesi, Kimya Mühendisliği Bölümü, Ankara, Türkiye

*Sorumlu yazar e-mail: milminelll@gmail.com

Özet

Bu çalışmada, atık kahve telvesinden H_3PO_4 aktivasyonu ile 500 °C'de azot atmosferinde karbonize edilerek elde edilen aktif karbonun PEM yakıt pilleri için katkı malzemesi olarak kullanılabilirliği incelenmiş ve bu karbon PVDF bazlı kompozit membranların sentezinde kullanılmıştır. Aktif karbonun FTIR analizinde O–H ve C–H gerilme bantlarının büyük ölçüde kaybolması aromatik karbon iskeletinin oluştuğunu, 1000–1100 cm^{-1} bölgesindeki C–O piklerinin güçlenmesi ise kimyasal aktivasyonun etkinliğini göstermiştir. XRD analizlerinde gözlemlenen geniş ve düşük şiddetli pikler, karbonun amorf fakat düzenli bir yapıya sahip olduğunu ortaya koymuştur. Sentezlenen aktif karbon PVDF matrisine %1, %5 ve %10 oranlarında eklenmiş ve elde edilen membranlar su tutma kapasitesi, şişme davranışı, boyutsal kararlılık, proton iletkenliği, iyon değişim kapasitesi, mekanik dayanım ve yapısal analizlerle değerlendirilmiştir. Su tutma kapasitesi en yüksek %5 katkıda gözlemlenirken, şişme testleri karbon katkısının membran kararlılığını artırdığını göstermiştir. Proton iletkenliği açısından %10 karbon katkılı membran 1,9931 mS/cm ile en yüksek performansı sergilemiş; aynı katkı oranında iyon değişim kapasitesi de 2,26 meq/g ile maksimuma ulaşmıştır. Mekanik dayanım %1 katkıda en yüksek seviyeye ulaşmış, ancak %10 katkıda topaklanma nedeniyle bir miktar düşüş görülmüştür. FTIR ve XRD sonuçları, karbon katkısının PVDF'nin kristal yapısını bozarak daha amorf ve proton iletimini destekleyen bir yapı oluşturduğunu ortaya koyarken, yüksek katkı oranlarında yüzeyde aglomerasyonun arttığı belirlenmiştir. Genel olarak, kahve telvesinden elde edilen aktif karbonun yapısal ve fonksiyonel özellikleri, özellikle %10 katkılı PVDF membranın PEMFC uygulamaları için en yüksek verimliliği sunduğunu göstermektedir.

Anahtar Kelimeler: Atık Kahve Telvesi, Aktif Karbon, PVDF Membran, PEM Yakıt Pili, Proton İletkenliği.

ORAL PRESENTATION

A new distribution area of the endemic *Trigonella coerulescens* subsp. *ayvalikensis* (Fabaceae) in Türkiye

Dilek Oskay (Orcid: https://orcid.org/0000-0002-5318-4750)

Manisa Celal Bayar University, Faculty of Engineering and Natural Sciences,
Department of Biology, Manisa, Türkiye

Corresponding author e-mail: dilek.oskay@cbu.edu.tr

Abstract

Trigonella coerulescens (M.Bieb.) Halácsy subsp. *ayvalikensis* Erdoğan, Selvi & Tümen (Fabaceae) is an endemic species known from only two localities in Balıkesir-Ayvalık from Türkiye. This taxon was described in 2017, and the IUCN threat category was recommended "Vulnerable (VU)" by the authors of the species. It grows in sandy soils in the coastal areas of Ayvalık and blooms in March-May. With this study, the species has a new distribution area in Görenez Mountain, Akhisar-Manisa. It was distributed above the tree line at about 1200 m altitude on the western view of Görenez Mountain. The flowering time of the population in Görenez Mountain is May. Based on the observations made during the field study, it was concluded that the species should be protected in the same IUCN threat category.

Keywords: Distribution, Endemic, *Trigonella coerulescens* subsp. *ayvalikensis,* Manisa, Türkiye

ORAL PRESENTATION

Ionic liquid–assisted photoluminescence enhancement in CASN:Eu^{2+}–pyranine composites

Beyza Yildirim Turkmen (Orcid: https://orcid.org/0000-0001-8015-6635)

Dokuz Eylul University, Science and Technology Application and Research Center, Izmir, Turkey.

Corresponding author e-mail: beyza.yildirimturkmen@deu.edu.tr

Abstract

The red-emitting phosphor CASN:Eu^{2+} (CASN) is widely used in display and lighting technologies. This study investigated the photoluminescence properties of CASN together with the highly fluorescent green-emitting Pyranine (Py) dye embedded in a polymeric (polymethyl methacrylate, PMMA) matrix. Binary and ternary phosphor–dye blends were prepared with and without an ionic liquid (IL). All composites were fabricated in film form, and excitation-emission and decay-time measurements were taken from these films. Upon blue-light excitation, the IL-free binary CASN–Py composite exhibited an 18 nm red shift and a 38% increase in emission intensity compared to the phosphor alone, while the IL-doped ternary composite showed a 400% enhancement in emission intensity. The decay time measurements were performed on the nanosecond scale, revealing changes consistent with the observed increases in emission intensity. These results highlight the promising potential of IL-doped CASN:Eu^{2+}–Pyranine composites for WLED, OLED, and display applications.

Keywords: CASN:Eu^{2+}, Composite, Ionic Liquid, Photoluminescence, Pyranine.

ORAL PRESENTATION

Green protein extraction from hazelnut meal using deep eutectic solvents

Şükriye Çiçek Kaya[1*] (ORCID: https://orcid.org/0009-0000-4307-9677), Esra Kibar Balballı[1] (ORCID: https://orcid.org/0009-0004-0080-6351), Gulsah Karabulut[1] (ORCID: https://orcid.org/0000-0002-4540-3044)

[1*] Department of Food Engineering, Institute of Science, Sakarya University, Sakarya, Türkiye

*Corresponding author e-mail: sukriye.kaya@ogr.sakarya.edu.tr

Abstract

The demand for sustainable and functional plant-based protein sources in the food industry is steadily increasing. Hazelnut press cake, a by-product of oil production, contains a high amount of protein but remains underutilized. Conventional alkaline extraction methods provide high protein yields; however, they often cause protein denaturation, negatively affecting critical functional properties such as solubility, emulsification, and foaming, while also generating considerable chemical waste. Therefore, greener extraction strategies that preserve protein structural integrity are urgently needed. This study aims to develop an environmentally friendly protein extraction method using Deep Eutectic Solvents (DES) to improve protein recovery from hazelnut press cake and to obtain protein isolates with preserved structural and functional properties suitable for food applications. Three DES systems (ChCl–glycerol, ChCl–sorbitol, and ChCl–glucose) were synthesized and applied in ultrasound-assisted extraction. The resulting protein isolates were compared with those obtained through conventional alkaline extraction at pH 8, 9, and 10. All extracts were comprehensively evaluated in terms of protein yield, solubility, emulsifying and foaming properties, particle size, zeta potential, as well as FTIR, SDS-PAGE, intrinsic fluorescence emission, and SEM analyses. Results showed that alkaline extraction at pH 10 achieved the highest protein yield (~260 mg/g), whereas DES systems offered superior solubility (70–76%) and enhanced emulsifying performance. Among DES systems, DES–glycerol exhibited the highest emulsifying activity, while DES–sorbitol demonstrated the greatest emulsion stability. In contrast, foaming capacity was higher in alkaline-extracted samples. Structural analyses indicated that DES-extracted proteins underwent less denaturation and retained more native characteristics. Overall, this study demonstrates that hazelnut press cake can be valorized as an environmentally friendly and functionally superior plant protein source through DES-assisted extraction, offering a promising alternative for sustainable food production.

Keywords: hazelnut meal, protein extraction, deep eutectic solvents, functional properties, emulsion stability.

ORAL PRESENTATION

Machine learning-driven identification of allosteric networks for the rational design of shark-derived single-domain antibodies

Arzu Uyar (Orcid: https://orcid.org/0000-0003-2357-1941)

Izmir Institute of Technology, Faculty of Engineering, Department of Bioengineering, Izmir, Türkiye.

Corresponding author e-mail: arzuuyar@iyte.edu.tr

Abstract

The unique structural adaptability of shark-derived single-domain antibodies (VNARs) presents a promising platform for therapeutic development; however, the dynamic consequences of stabilizing mutations remain inadequately characterized. This study employs a comprehensive computational framework to elucidate how targeted mutations alter the conformational landscape of a model VNAR in its apo and lysozyme-bound states. We generated conformational ensembles for the wild-type and 13-mutant variant using the unbiased ClustENMD sampling method, which integrates elastic network model, clustering, and molecular dynamics simulations. These ensembles were analyzed via Principal Component Analysis (PCA) to map dominant motions, revealing that the mutant exhibits constrained global flexibility compared to the wild-type. To classify state-specific conformations and identify critical residue-level discriminators, we applied Linear Discriminant Analysis (LDA) and Random Forest algorithms. These analyses pinpointed several residues in the hypervariable (HV2, HV4), complementarity determining (CDR1, CDR3), and framework (FW3) regions as key differentiators, suggesting long-range allosteric effects. Centrality analysis of residue interaction networks further quantified mutation-induced perturbations in allosteric communication, identifying central residues that overlapped with LDA findings. Finally, Essential Site Scanning Analysis (ESSA) corroborated the significance of the HV4, FW3, and CDR3 regions. Our integrated approach demonstrates that the mutations predominantly perturb dynamics in regions critical for antigen binding and structural integrity. Notably, our findings underscore the FW3 region as a potential allosteric hotspot. These findings not only decipher mutation-induced dynamical shifts but also provide a blueprint for the rational design of stabilized VNARs with enhanced therapeutic properties.

Keywords: Shark, VNAR, Single-domain antibodies, Conformational sampling, Machine learning, ESSA

ORAL PRESENTATION

Farklı coğrafi kökenli sarımsak ve kabuklarının kimyasal parmak izi analizi: FTIR-2D-COS ve HPLC-DAD ile bütünleşik bir yaklaşım

Özge Tokul-Ölmez (https://orcid.org/0000-0002-2093-4949)

Muğla Sıtkı Koçman Üniversitesi, Fen Fakültesi, Kimya Bölümü, Muğla, Türkiye

Sorumlu yazar e-mail:ozgetokul@gmail.com

Özet

Sarımsak (*Allium sativum* L.), organosülfür ve fenolik bileşikleri sayesinde antioksidan, antimikrobiyal, antihipertansif ve kardiyovasküler açıdan destekleyici etkilere sahip önemli bir fonksiyonel gıdadır [1]. Son yıllarda yapılan araştırmalar, genellikle tarımsal atık olarak değerlendirilen sarımsak kabuklarının da fenolik bileşikler bakımından zengin bir içerik sunduğunu ve dikkate değer biyolojik aktivitelere sahip olabileceğini göstermektedir. Lignoselülozik yapısı nedeniyle doğal bir polifenol kaynağı olarak değerlendirilen sarımsak kabuğu, hem gıda endüstrisinde doğal katkı maddesi hem de sürdürülebilir biyoaktif bileşen üretimi açısından potansiyel bir hammadde niteliği taşımaktadır [2]. Bu çalışmada, altı farklı coğrafi bölgeden temin edilen 13 sarımsak örneğinin kabuk ve yenilebilir kısımları ayrı olarak incelenerek kimyasal profillerindeki farklılıklar araştırıldı. Etanol ile ekstre edilen örneklerin, FTIR spektroskopisi kullanılarak yapısal parmak izleri belirlendi. 2D-Korelasyon Spektroskopisi (2D-COS) ile spektral bantlar arasındaki ilişkiler değerlendirildi. Fenolik içerik HPLC-DAD ile analiz edildi ve FTIR verileri ise temel bileşen analizi (PCA) kullanılarak sınıflandırıldı. HPLC-DAD sonuçları, kabuk ve yenilebilir kısımlar arasında belirgin bir fenolik çeşitlilik farkı olduğunu gösterdi. Yenilebilir kısımlarda sadece fumarik asit, gallik asit, protokateşuik asit ve 2,4-dihidroksibenzoik asit tespit edilirken, kabuk ekstrelerinde toplam 15 farklı fenolik bileşik belirlendi. Bunlar arasında krisin, hesperidin, ferulik asit ve kafeik asit gibi bileşikler daha yüksek yoğunlukta gözlendi. FTIR–2D-COS analizleri, kabuk ve yenilebilir kısımlar arasında özellikle 3600–3000 cm^{-1} (O–H gerilme titreşimleri), 1700–1500 cm^{-1} (C=O gerilme titreşimleri) ve 1200–900 cm^{-1} (organik ve sülfür bileşenlerine ait titreşimler) bölgelerinde anlamlı spektral farklılıklar ortaya koydu. PCA sonuçları, FTIR ve 2D-COS verileri birlikte değerlendirildiğinde, sarımsak ve kabuklarının coğrafi farklılıklarının belirlenmesinde doğruluğu yüksek bir yaklaşım sunmaktadır. Sonuç olarak, bu çalışma sarımsak kabuklarının fenolik bileşikler açısından yenilebilir kısımlara kıyasla daha geniş bir çeşitlilik gösterdiğini ve FTIR–2D-COS ile PCA'nın sarımsak ve kabuklarının kimyasal parmak izinin değerlendirilmesinde etkili yöntemler olabileceğini ortaya koymaktadır. Bu çoklu analiz yaklaşımı yöntemlerini HPLC-DAD analizleri desteklemektedir.

Anahtar Kelimeler: Sarımsak (*Allium sativum*), FTIR–2D-COS, Temel Bileşen Analizi (PCA), HPLC-DAD, Fenolik bileşikler

Kaynaklar:

[1] Kallel, F., Driss, D., Chaari, F., Belghith, L., Bouaziz, F., Ghorbel, R., & Ellouz Chaabouni, S. (2014). Garlic (*Allium sativum* L.) husk waste as a potential source of phenolic compounds: Influence of extracting solvents on its antimicrobial and antioxidant properties. *Industrial Crops and Products* 62, 34–41.

[2] Chhouk, K., Uemori, C., Wahyudiono, Kanda, H., & Goto, M. (2017). Extraction of phenolic compounds and antioxidant activity from garlic husk using carbon dioxide expanded ethanol. *Chemical Engineering & Processing: Process Intensification* 117, 113–119.

ORAL PRESENTATION

Histological investigation of the effects of chronic thiamethoxam exposure on the digestive gland and kidney tissues of *Lymnaea stagnalis*

Ali Emre Yanaloğlu* (ORCID: https://orcid.org/0009-0009-6832-6203), Serhat Üreyil (ORCID: https://orcid.org/0009-0009-4104-875X),
Sezgi Somuncu (ORCID: https://orcid.org/0000-0002-4247-0639)

Sakarya University, Faculty of Science, Department of Biology, Sakarya, Türkiye.

*Corresponding author e-mail: aliemreyanaloglu@gmail.com

Abstract

Thiamethoxam is a neonicotinoid insecticide used in agricultural practices, and its residues have been detected in surface waters worldwide. This raises concerns about its potential toxic effects on aquatic invertebrates. The present study investigated the histological alterations induced by thiamethoxam in the digestive gland and kidney of the freshwater snail *Lymnaea stagnalis*. Laboratory-cultured adult snails were exposed to environmentally relevant concentrations of thiamethoxam (0, 2, 20, and 200 µg/L) for 28 days. Exposure resulted in marked vacuolization and cellular degeneration in the digestive gland, accompanied by increased connective tissue fibers, hypertrophic hemocytes in the intertubular area, epithelial hyperplasia of the digestive tubules, necrotic cells, and disruption of overall tissue architecture. Kidney tissues of exposed specimens exhibited degenerative nephrocytes, increased hemocyte clusters between renal tubules, disrupted excretory granules, nuclear alterations, and necrosis. These findings demonstrate that chronic thiamethoxam exposure induces substantial histopathological damage in vital organs of freshwater gastropods, highlighting potential ecological risks associated with the presence of this insecticide in aquatic environments.

Keywords: Neonicotinoid, insecticide, gastropoda, histopathology, toxicity.

*This study was supported by the Scientific and Technological Research Council of Türkiye (TÜBİTAK) 2209-A Research Project Support Programme for Undergraduate Students (Grant No: 1919B012405024).

ORAL PRESENTATION

Current applications of CRISPR-cas technologies in food microbiology

Zeynep Tetik[1*] (https://orcid.org/0009-0005-5539-9113), Pınar Şanlıbaba[2] (https://orcid.org/0000-0003-4638-6765)

[*1] Ankara University, Engineering Faculty, Department of Food Engineering, Ankara, Türkiye
[2] Ankara University, Engineering Faculty, Department of Food Engineering, Ankara, Türkiye

*Corresponding author e-mail: zeyneptetiik@gmail.com

Abstract

CRISPR-Cas technology has emerged as an innovative molecular diagnostic platform in food microbiology, enabling rapid, specific, and highly sensitive detection of foodborne pathogens. Defined as the adaptive immune system of bacteria, CRISPR consists of palindromic repeat sequences accompanied by Cas proteins, naturally facilitating the recognition and cleavage of foreign genetic material. This mechanism has been repurposed by researchers to selectively recognize and process target DNA or RNA sequences, making it applicable to diagnostics, quality control, and biosensor applications. In CRISPR-Cas-based systems, guide RNA (crRNA or gRNA) confers target nucleic acid recognition to the Cas protein, directing specific binding and cleavage reactions. Different effector proteins such as Cas9, Cas12, and Cas13 provide diversity in structure and target type (DNA/RNA) and can be integrated with fluorescence, colorimetric, or isothermal amplification-based readout methods to create versatile diagnostic platforms. This technology offers significant advantages for on-site applications due to its rapid results, high specificity, and minimal equipment requirements, particularly in detecting foodborne pathogens and monitoring contamination. However, the complex nature of food matrices may affect nucleic acid isolation efficiency and Cas protein activity. Protocol optimization, method standardization, and minimizing off-target activities are critical challenges for routine implementation of this technology. In this study, the current applications, advantages, and limitations of CRISPR-Cas systems in pathogen detection, quality control, and rapid diagnostics within food microbiology are discussed, with a comprehensive assessment of their field adaptability and future potential.

Keywords: CRISPR-Cas, Food microbiology, Pathogen detection, Molecular diagnostics

ORAL PRESENTATION

Extraction of antioxidants from food waste and its contribution to sustainability

Furkan Burak Şen (Orcid: https://orcid.org/0000-0001-6857-392X)

Istanbul University, Faculty of Science, Department of Chemistry, Istanbul, Türkiye.

Corresponding author e-mail: fbsen@istanbul.edu.tr

Abstract

There is a delicate balance between cellular defense systems and reactive oxygen/nitrogen species (ROS/RNS). When this balance shifts in favor of ROS/RNS, oxidative stress occurs, resulting in damage to biological macromolecules and contributing to the development of various diseases, including cardiovascular disorders and cancer. Antioxidants, which counteract these harmful effects, play a central role in cellular defense mechanisms. Therefore, the determination of antioxidants in foods has become increasingly important, leading to the development of numerous analytical methods. In recent years, green extraction techniques such as homogenizer-assisted extraction (HAE), microwave-assisted extraction (MAE), and ultrasound-assisted extraction (UAE) have gained prominence alongside traditional antioxidant extraction methods. Optimization of operational parameters in these techniques can significantly enhance extraction efficiency. Additionally, in line with the principles of green chemistry, research on the valorization of food waste and the extraction of bioactive compounds such as antioxidants from these by-products has intensified. The discovery and application of environmentally friendly natural deep eutectic solvents (NADESs) have further accelerated the adoption of green extraction strategies. NADESs offer sustainable alternatives to conventional solvents, providing advantages such as biocompatibility, low toxicity, environmental safety, and notably high solvent power. Extracts obtained using NADESs have become widely utilized both in the development of novel functional food products and in antioxidant analyses.

Keywords: Food antioxidants, sustainability, extraction

ORAL PRESENTATION

Visible-light-induced degradation of reactive orange 16 using IRMOF-3: A solar photocatalysis approach

Elif Özcan (Orcid: https://orcid.org/0000-0002-4375-2320)

Gebze Technical University, Department of Chemistry, Kocaeli, Turkey.

Corresponding author e-mail: e.ozcan@gtu.edu.tr

Abstract

The increasing presence of synthetic dyes in industrial wastewater represents a major environmental challenge, particularly for persistent azo dyes such as Reactive Orange 16 (RO16). Developing efficient and sustainable materials capable of degrading these contaminants under solar irradiation is essential for advancing water purification technologies. Metal–organic frameworks (MOFs), with their tunable porosity, large surface area, and chemical versatility, have emerged as attractive photocatalysts1. Among them, IRMOF-3 offers enhanced visible-light absorption and adjustable surface properties due to its $–NH_2$ groups, making it a promising candidate for solar-driven photocatalytic applications2. In this study, the photocatalytic degradation of RO16 was investigated using IRMOF-3 under simulated solar light. IRMOF-3 was synthesized via a solvothermal method and characterized by X-ray diffraction (XRD), scanning electron microscopy (SEM), and Fourier-transform infrared spectroscopy (FTIR) to verify its crystallinity, morphology, and functional groups. UV–Vis spectrophotometry was used to monitor the degradation of RO16, revealing that the dye was efficiently decomposed under solar irradiation. Key experimental variables, including catalyst dosage, pH, and initial dye concentration, were systematically optimized to maximize the photocatalytic performance. Reusability tests demonstrated that IRMOF-3 retained its structural integrity and catalytic activity over multiple cycles, highlighting its stability under photocatalytic conditions. Mechanistic investigations using radical scavengers confirmed that superoxide radicals ($O_2^{\cdot -}$) were the dominant reactive species responsible for RO16 degradation.
Overall, the findings indicate that IRMOF-3 is an effective and reusable photocatalyst for the solar-driven degradation of Reactive Orange 16, offering an environmentally friendly approach for treating dye-contaminated wastewater and contributing to sustainable water purification solutions.

Keywords: IRMOF-3, Photocatalysis, Reactive Orange 16, Dye degradation, Visible-light activity, Solar-driven oxidation.

References:

Navalón, S.; Dhakshinamoorthy, A.; Álvaro, M.; Ferrer, B.; García, H. Metal–Organic Frameworks as Photocatalysts for Solar-Driven Overall Water Splitting. *Chem. Rev.* 2023, 123 (1), 445–490.
Ning, H.; Lu, L. Isoreticular Metal–Organic Framework-3 (IRMOF-3): From Experimental Preparation, Functionalized Modification to Practical Applications. *Polymers* 2024, 16 (15), 2134.

ORAL PRESENTATION

The effects of MTHFR gene polymorphisms (C677T, A1298C) and homocysteine levels on the clinical progression of COVID-19

Züleyha Yıldız Yümsek[1] (orcid: https://orcid .com/ 0000-0002-4897-4870), Burcu Gürer Giray[2] (orcid: https://orcid.com/ 0000-0003-3165-8924), Aslı Haykır Solay[3] (orcid: https://orcid .com/ 0000-0002-1326-9776), Eda Macit Aydın[4] (orcid: https://orcid.com/ 0000-0002-4607-4932), Burcu Ayçahan Yıldız[4] (orcid: https://orcid.com/ 0000-0002-4168-4977), Jülide Ergil[4] (orcid: https://orcid.com/ 0000-0002-4580-7866), Aysun Hacışevki[5*](orcid: https://orcid .com/ 0000-0002-3844-5772).

[1]Turkish Public Health İnstitution, Numune Molecular Diagnosis Laboratory, Ankara, Türkiye,
[2]Yalova University, Faculty of Medicine, Department of Microbiology, Yalova, Türkiye,
[3]Ministry of Health, Ankara Etlik City Hospital, Infectious Diseases, Clinical Microbiology Service, Ankara,Türkiye,
[4]Ministry of Health, Ankara Etlik City Hospital, Anesthesiology, Reanimation Intensive Care Unit, Ankara,Türkiye,
[5]Gazi University, Faculty of Pharmacy, Department of Biochemistry and Gazi University, Health Sciences Institute, Sports Pharmacy Program, Ankara, Türkiye

*Corresponding author e-mail: abozkir@gazi.edu.tr

Abstract

Covid-19 pandemic is an important international public health problem. A range of susceptibility genes and genetic variants has been associated with the elevated risk of severe Covid-19 development. Among these, the Methylenetetrahydrofolate Reductase (MTHFR) gene, which encodes 5,10-methylenetetrahydrofolate reductase, a regulatory enzyme in folate metabolism, is important. Studies suggest that the occurrence of genetic hyperhomocysteinemia is linked to MTHFR dysfunction. Aim of the study to investigate whether MTHFR C677T and A1298C polymorphisms and plasma homocysteine levels are risk factors in term of the clinical course of Covid-19 disease in Turkish Society. Study groups were classified into three according to Covid-19 severity: mild (100), moderate (80), severe or critical (80). MTHFR mutations were analysed in 260 patients (126 male, 134 female). Plasma homocysteine levels were detected in 80 patients (40 controls, 40 severe). The analysis of MTHFR mutations were quantified by RTqPCR. Homocysteine levels were measured by HPLC. In according to biochemical data, CRP, AST, ferritin, platelet count, d-dimer, BUN, creatine measurements were higher in the patient group than in the control group, while the lymphocyte count and neutrophil count were lower. Overall, it couldn't find any statistically significant correlation between MTHFR genotypes in patients with Covid-19 infection. However, the average age and the gender of the patient are found to be factors affecting the progression of the disease. The average age and the number of male patients are found to be higher in the severe Covid-19 group than the control group. In addition, the severe Covid-19 group with two genotypes for MTHFR polymorphisms (heterozygous MTHFR 677 C>T and 1298 A>C mutant, homozygous MTHFR 677 C>T mutant) was found to have significantly increased homocysteine levels compared to the control group. It is believed that homocysteine levels could serve as a helpful marker to asses the severity and course of Covid-19.

Keywords: Covid 19, Severe acute respiratory syndrome coronavirus 2, Methylene tetrahydrofolate reductase, Homocysteine, Polimorphism.

This study (Grant no: 2022-B-03, 24431, Group B R&D Project Call) was supported by the Presidence of Healty Institutes of Türkiye (TUSEB).

ORAL PRESENTATION

Evaluation of the cytotoxic effect of vortioxetine on various cancer cell lines

Samet Oz (Orcid: https://orcid.org/0009-0005-8372-8703)

Osmaniye Korkut Ata University, Health Services Vocational School, Department of Veterinary Medicine, Osmaniye, Türkiye

Corresponding author e-mail: sametoz@osmaniye.edu.tr

Abstract

Vortioxetine is a new-generation antidepressant that acts at multiple receptor levels, in addition to exhibiting selective serotonin reuptake inhibitor properties. Recently, studies on the antiproliferative and pro-apoptotic effects of antidepressants have increased. However, there is limited data on the cytotoxic effects of vortioxetine in different cancer cell lines. This study aimed to evaluate the effects of vortioxetine on cell viability in ovarian (A2780), prostate (LNCaP), breast (MCF-7), and colon adenocarcinoma (Caco-2) cell lines. In the study, A2780, LNCaP, MCF-7, and Caco-2 cell lines were treated with vortioxetine at concentrations of 1, 5, 25, 50, and 100 µM for 24 hours. The effect of vortioxetine on cell viability was evaluated using the 3-(4,5-Dimethylthiazol-2-yl)-2,5-Diphenyltetrazolium Bromide (MTT) method and absorbance values were measured at 550 nm. Cell viability was calculated as the percentage change compared to the control group. Half maximal inhibitory concentration (IC_{50}) values were calculated from the dose-response curves generated by GraphPad Prism 8 software. Data were evaluated by non-parametric Kruskal–Wallis analysis and $p<0.05$ was considered statistically significant. When the findings were evaluated, it was determined that vortioxetine application at doses of 5, 25, 50 and 100 µM in A2780, LNCaP and MCF-7 cell lines and at doses of 25, 50 and 100 µM in Caco-2 cell line significantly reduced cell viability ($p<0.05$). Additionally, IC_{50} values were determined as 3.34 µM for A2780, 2.89 µM for LNCaP, 2.18 µM for MCF-7, and 9.95 µM for Caco-2, respectively. This study demonstrates that vortioxetine has significant cytotoxic effects on selected cancer cell lines. These findings suggest that vortioxetine should be evaluated in cancer biology and drug repositioning studies. Further mechanistic analyses (apoptosis, ROS, cell cycle, etc.) are planned to further elucidate the potential anticancer mechanism of vortioxetine.

Keywords: Antidepressant, Drug Repositioning, Cancer, Cytotoxicity, Vortioxetine

ORAL PRESENTATION

Vortioksetinin çeşitli kanser hücre hatlarındaki sitotoksik etkisinin değerlendirilmesi

Samet Öz (Orcid: https://orcid.org/0009-0005-8372-8703)

Osmaniye Korkut Ata Üniversitesi, Sağlık Hizmetleri Meslek Yüksekokulu, Veterinerlik Bölümü, Osmaniye, Türkiye

Sorumlu yazar e-mail: sametoz@osmaniye.edu.tr

Özet

Vortioksetin, selektif serotonin geri alım inhibitörü özellik göstermenin yanında çoklu reseptör düzeyinde etki eden yeni nesil bir antidepresandır. Son dönemde antidepresanların antiproliferatif ve pro-apoptotik etkilerine ilişkin çalışmalar artmaktadır. Ancak vortioksetinin farklı kanser hücre hatlarındaki sitotoksik etkileri hakkında sınırlı veri bulunmaktadır. Bu çalışmada vortioksetinin over (A2780), prostat (LNCaP), meme (MCF-7) ve kolon adenokarsinom (Caco-2) hücre hatlarında hücre canlılığı üzerine etkisinin değerlendirilmesi amaçlandı. Çalışmada A2780, LNCaP, MCF-7 ve Caco-2 hücre serileri 24 saat boyunca vortioksetinin 1, 5, 25, 50 ve 100 µM konsantrasyonları ile muamele edildi. Vortioksetinin hücre canlılığı üzerindeki etkisi 3-(4,5-Dimethylthiazol-2-yl)-2,5-Diphenyltetrazolium Bromide (MTT) yöntemi kullanılarak değerlendirildi ve absorbans değerleri 550 nm'de ölçüldü. Hücre canlılığı kontrol grubuna göre yüzde değişim olarak hesaplandı. Yarı maksimal inhibitör konsantrasyon (IC_{50}) değerleri, GraphPad Prism 8 yazılımı ile oluşturulan doz-yanıt eğrilerinden hesaplandı. Veriler non-parametrik Kruskal–Wallis analizi ile değerlendirildi ve $p<0.05$ istatistiksel olarak anlamlı kabul edildi. Bulgular değerlendirildiğinde; A2780, LNCaP ve MCF-7 hücre hatlarında 5, 25, 50 ve 100 µM dozlarında; Caco-2 hücre hattında ise 25, 50 ve 100 µM dozlarında vortioksetin uygulamasının hücre canlılığını anlamlı düzeyde azalttığı tespit edildi ($p<0.05$). Ayrıca IC_{50} değerleri sırasıyla A2780 için 3.34 µM, LNCaP için 2.89 µM, MCF-7 için 2.18 µM ve Caco-2 için 9.95 µM olarak tespit edildi. Bu çalışma, vortioksetinin seçili kanser hücre hatları üzerinde belirgin sitotoksik etkilere sahip olduğunu göstermektedir. Bulgular, vortioksetinin kanser biyolojisi ve ilaç yeniden konumlandırma çalışmalarında değerlendirilmesi gerektiğini işaret etmektedir. Elde edilecek ileri mekanistik analizlerle (apoptoz, ROS, hücre döngüsü vb.) vortioksetinin olası antikanser mekanizmasının daha ayrıntılı şekilde aydınlatılması planlanmaktadır.

Anahtar Kelimeler: Antidepresan, İlaç Yeniden Konumlandırma, Kanser, Sitotoksisite, Vortioksetin

ORAL PRESENTATION

Screen-printed carbon electrode integrated with feather-like Au-Ag-Co trimetallic composite: An advanced sensor for electrochemical determination of sertraline HCl

Cem Erkmen[1,2*] (Orcid: https://orcid.org/0000-0001-5944-3912)

[*1]Istanbul Aydin University, Faculty of Pharmacy, Department of Analytical Chemistry, Istanbul 34295, Türkiye.
[*2]Istanbul Aydin University, Application and Research Center for Advanced Studies, Istanbul 34295, Türkiye.

*Corresponding author e-mail: cemerkmen@aydin.edu.tr

Abstract

A highly sensitive and reliable electrochemical sensor was developed for the quantitative determination of the antidepressant drug sertraline HCl (SRT) using a novel screen-printed carbon electrode (SPCE) modified with feather-like Au-Ag-Co trimetallic structures (Au-Ag-Co/SPCE). The trimetallic interface was synthesized by electrochemically to synergistically exploit the outstanding electrical conductivity of Au and Ag together with the catalytic capability of Co, resulting in a superior electron-transfer platform. The morphological and structural features of the materials were thoroughly characterized by SEM, EDX, XRD, and AFM analyses, confirming their homogeneous decoration and well-defined porous structure on the SPCE surface. The electrochemical behavior was investigated using cyclic voltammetry and electrochemical impedance spectroscopy, demonstrating substantially decreased charge-transfer resistance and enhanced redox kinetics after Au-Ag-Co modification. The sensing performance toward SRT HCl was systematically optimized by evaluating the effects of pH, scan rate, accumulation potential, and accumulation time. Differential pulse voltammetry and adsorptive stripping differential pulse voltammetry revealed a strong electrocatalytic response with significantly amplified oxidation currents on Au-Ag-Co/SPCE compared with the bare SPCE. Under optimized conditions, the sensor exhibited a wide linear detection range extending from 2.0×10^{-7} to 2.0×10^{-4} M with two well-defined calibration regions and achieved a remarkably low detection limit suitable for trace-level monitoring. The applicability of the sensor was validated through the analysis of pharmaceutical tablets and spiked human serum samples. High recoveries (97–104%) and low relative standard deviations (<6%) confirmed excellent accuracy, precision, and matrix tolerance. These findings highlight that the Au-Ag-Co/SPCE platform provides rapid analysis, low-cost fabrication, and strong analytical performance, making it a promising candidate for routine quality control, clinical monitoring, and point-of-care testing of sertraline.

Keywords: Sertraline, electrochemical sensor, Au-Ag-Co trimetallic materials, screen-printed carbon electrode, adsorptive stripping voltammetry

ORAL PRESENTATION

Investigation of the cytotoxic effect of tizanidine on different cell lines

Guldeniz Sekerci (Orcid: https://orcid.org/0000-0002-0811-4454)

Inonu University, Faculty of Medicine, Department of Physiology, Malatya, Türkiye

Corresponding author e-mail: guldenizsekerci@gmail.com

Abstract

Cancer is a disease that originates locally and progresses with systemic disturbances arising from a complex interplay of genomic, environmental, and physiological factors, and is characterized by uncontrolled cell proliferation. Among these disturbances, chronic inflammation represents a key tumor microenvironment component that strongly promotes tumor initiation and progression. Given its central role in cancer pathogenesis, compounds with anti-inflammatory activity hold significant potential for developing new therapeutic strategies. Tizanidine is a centrally acting α_2 receptor agonist and muscle relaxant reported to possess anti-inflammatory properties. Recent studies in cancer biology have shown a close association between adrenergic signaling pathways and malignant cellular behavior. In this context, the α_2 agonist activity and anti-inflammatory effects of Tizanidine make it a promising molecule with the potential to influence cancer cell viability. Accordingly, this study investigated the effects of Rupatadine on human ovarian (A2780), colon (Caco-2), and breast (MCF-7) cancer cell lines. In the study, A2780, Caco-2, and MCF-7 cell lines were incubated for 24 hours with Tizanidine concentrations of 1, 5, 25, 50, and 100 µM. The effect of Tizanidine on cell viability was determined using the MTT Assay method. The half-maximal inhibitory concentration (IC_{50}) of Tizanidine was calculated using the GraphPad Prism 8 software. Statistical analyses of the data were performed using the non-parametric Kruskal-Wallis variance analysis, and a $p<0.05$ was considered statistically significant. Analysis of the results showed that Tizanidine significantly decreased cell viability ($p<0.05$) at concentrations of 50 and 100 µM in the A2780 and Caco-2 cell lines, and at concentrations of 25, 50, and 100 µM in the MCF-7 cell line.The findings of this study suggest that Tizanidine may possess cytotoxic activity against A2780, Caco-2, and MCF-7 cells. Tizanidine could be a potential candidate in the development of new cancer treatment strategies through drug repurposing approaches.

Keywords: Tizanidine, Cytotoxicity, A2780, Caco-2, MCF-7

ORAL PRESENTATION

Investigation of the use of bio-based plasticizers in Vinyl (PVC) disposable glove production and their effects on material properties

Şafak Ünal[1] (Orcid: https://orcid.org/0009-0003-4656-9550), Yasin Altın[1,2*] (Orcid: https://orcid.org/0000-0002-8554-3025)

[*1]Bursa Technical University, Department of Polymer Materials Engineering, City, Country.
[2]Bursa Technical University, Central Research Laboratory, Bursa, Türkiye.

*Corresponding author e-mail: yasin.altin@btu.edu.tr

Abstract

Poly(vinyl chloride) (PVC) is widely used in the production of disposable gloves due to its low cost, easy processability, and chemical resistance. However, the phthalate-based plasticizers commonly employed to enhance the flexibility of PVC pose significant health concerns—such as endocrine-disrupting effects and potential carcinogenicity—as well as environmental persistence. In line with European Union REACH regulations and global sustainability frameworks, the demand for safer and environmentally friendly alternative plasticizers has increased considerably. As a result, bio-based plasticizers derived from renewable resources have become an important area of research. In this study, the usability of bio-based plasticizers in PVC-based disposable gloves was investigated using T.B.C supplied by LEBA and AKESBO supplied by AKKİM. For each sample group, ten different formulations containing varying ratios of PVC, bio-based plasticizer, and DOTP were prepared using the dip-coating method. The mechanical properties of the produced gloves were evaluated in accordance with the TS EN 455-2 standard, including tensile strength, elongation at break and elastic modulus. The thermal behavior of the samples was determined through differential scanning calorimetry (DSC) and thermogravimetric analysis (TGA). In addition, physical characteristics such as film flexibility and surface appearance were examined. Statistical analysis methods were used to evaluate the significance of the differences among formulations. The findings of this study are expected to contribute to the identification of the most suitable bio-based plasticizer type and ratio for PVC glove production, while also supporting the development of sustainable, non-toxic, and environmentally friendly products.

Keywords: PVC, bio-based plasticizer, disposable gloves, vinyl gloves

ORAL PRESENTATION

Electrochemical enhancement of modified ITO electrodes for high-performance supercapacitor applications

Ramin Jahangirov[1*] (ORCID: https://orcid.org/0000-0002-9063-7931), Sema Aslan[2] (ORCID https://orcid.org/0000-0001-9796-7311), Derya Bal Altuntaş[3] (ORCID https://orcid.org/0000-0001-6544-6271)

[*1]Mugla Sitki Kocman University, Institute of Science, Department of Renewable Energy Resources and Technologies, Muğla, Turkey
[2]Mugla Sitki Kocman University, Faculty of Science, Department of Chemistry, Muğla, Turkey
[3]Recep Tayyip Erdoğan University, Faculty of Engineering and Architecture, Department of Bioengineering, Rize, Turkey

*Corresponding author e-mail: ramin.cahangir2@gmail.com

Abstract

Supercapacitors, valued for their rapid energy delivery and durability, require advanced electrode materials for efficient charge–discharge performance [1]. In this study, a ternary MoS_2/rGO/NiMn-LDH nanocomposite was synthesized via a hydrothermal method and successfully employed to modify indium tin oxide (ITO) electrodes. The material was dispersed in 120 µL ethanol and 150 µL deionized water by ultrasonication for 30 minutes, followed by the addition of 50 µL chitosan solution to improve adhesion. The suspension was drop-cast onto a 5 × 5 mm active area of the ITO surface in two layers (10 µL + 10 µL), with each layer dried at 50 °C for 30 minutes to ensure homogeneous coating. Electrochemical performance was investigated using cyclic voltammetry (CV) and electrochemical impedance spectroscopy (EIS) in a ferri/ferrocyanide redox system prepared in KCl–PBS electrolyte. CV results at scan rates ranging from 5 to 200 mV/s revealed that the MoS_2/rGO/NiMn-LDH–modified ITO electrode exhibited significantly enhanced redox peak currents and a markedly larger capacitive area compared with bare ITO, MoS_2-coated ITO, rGO-coated ITO, and rGO/MoS_2-coated ITO electrodes. Such improvements are consistent with previously reported MoS_2/rGO-based hybrid structures, which show strong synergistic effects in electron transfer and charge storage [2]. Even at high scan rates, the ternary nanocomposite maintained improved electrochemical response, indicating fast electron-transfer kinetics and stable capacitive behavior. EIS measurements supported these findings by demonstrating improved charge-transfer characteristics and enhanced interfacial conductivity for the MoS_2/rGO/NiMn-LDH–modified electrode compared with the reference electrodes. Overall, the synthesized nanocomposite shows strong potential for next-generation supercapacitors.

Keywords: Supercapacitors, Modified ITO electrodes, Electrochemical characterization, Nanocomposite electrode interfaces.

* This study is part of the PhD thesis research conducted by Ramin Jahangirov.

References:

[1] Conway, B. E. Electrochemical Supercapacitors: Scientific Fundamentals and Technological Applications. Springer, 1999.
[2] Manoharan, A.; Tian, Z. R.; Ang, S. S. "MoS_2/Reduced Graphene Oxide-Based 2D Nanocomposites for Boosting the Energy Density of Electric Double-Layer Capacitors." Nanomaterials, 2023, 13, 1221.

ORAL PRESENTATION

Investigation of the relationship between physical activity level and body awareness in ambulance drivers

Latife Tosun[1] (ORCID: 0009-0000-5645-1845), Halil Hakan Uysal[2] (ORCID: 0000-0001-7929-5777)

[1]Eskişehir Osmangazi University, Institute of Health Sciences, Department of Physiotherapy and Rehabilitation, Eskişehir, Türkiye.
[2]Eskişehir Osmangazi University, Vocational School of Health Services, Orthopedic Prosthetics and Orthotics Program, Eskişehir, Türkiye.

Corresponding author e-mail: latifetosun000@gmail.com

Abstract

The aim of this study was to examine the physical activity levels and body awareness scores of ambulance drivers and to evaluate the relationship between these variables. This cross-sectional study included 50 ambulance drivers aged between 25 and 65 years, who had been driving an ambulance for at least three years and had no health condition that could prevent professional driving. Physical activity levels were assessed using the International Physical Activity Questionnaire (IPAQ), and MET-min/week values were calculated. Body awareness was evaluated with the 18-item Body Awareness Questionnaire (BAQ). Descriptive statistics, Cronbach's alpha, Mann–Whitney U, Kruskal–Wallis and chi-square tests were used for data analysis. The participants had a mean age of 44.08±11.28 years, a mean body mass index (BMI) of 25.86±4.73 kg/m², and an average professional experience of 10.92±1.01 years. Of the drivers, 54% were smokers, 18% held a bachelor's degree, and 26% had an associate degree. The mean physical activity level was 459.88±308.27 MET-min/week; 76% of participants were classified as having a low activity level, while 24% were moderately active. The mean BAQ score was 65.56±10.83. No significant differences were found between BAQ scores and driving duration or professional experience ($p>0.05$). Additionally, no significant associations were identified between physical activity levels and educational status, marital status, or years of experience ($p>0.05$). There was also no statistically significant relationship between physical activity levels and BAQ results ($p>0.05$).

Keywords: Ambulance drivers; physical activity; body awareness; questionnaire

ORAL PRESENTATION

Advances in 3D graphene foam electrodes for biosensing applications

Muhsin Dogan[1,2*], Sophia Nazir[1], David Jenkins[1]

[*1]University of Plymouth, Faculty of Science and Engineering, Nanomaterials and Devices Laboratory, Plymouth, United Kingdom.
[2]Izmir Bakircay University, Engineering and Architecture Faculty, Biomedical Engineering, Izmir, Türkiye

*Corresponding author e-mail: doganmuhsin.01@gmail.com

Abstract

Three-dimensional (3D) graphene foam has emerged as a highly promising electrode platform for next generation biosensing, owing to its exceptional ultrahigh surface area, interconnected conductive network, and mechanical toughness. This review emphasises current progress in the design, functionalisation, and application of 3D graphene foam electrodes for electrochemical biosensors. The distinctive architecture of 3D graphene foam provides an exceptionally high specific surface area, optimising biomolecule immobilisation; uninterrupted 3D conductive pathways for swift electron transfer and signal enhancement; significant porosity for effective analyte mass transport; and superior mechanical stability for adaptable device integration. The chemical modification methods, including carboxyl/NHS functionalisation, nanoparticle decorating, and bio-recognition layer assembly, provide enhanced sensitivity and selectivity for clinically relevant analytes. This review sums up current advancements and delineates ongoing problems concerning reproducibility, long-term stability, and scalable production, highlighting the promise of 3D graphene foam as a multifaceted, high-performance material for forthcoming biomedical sensing systems.

Keywords: Three-dimensional, graphene foam, biosensor, functionalisation

ORAL PRESENTATION

The importance of early detection in Alzheimer's disease: Advancing body-fluid biomarker detection with point-of-care devices

Muhsin Dogan[1,2*], Sophia Nazir[1], David Jenkins[1]

[*1]University of Plymouth, Faculty of Science and Engineering, Nanomaterials and Devices Laboratory, Plymouth, United Kingdom.
[2]Izmir Bakircay University, Engineering and Architecture Faculty, Biomedical Engineering, Izmir, Türkiye

*Corresponding author e-mail: doganmuhsin.01@gmail.com

Abstract

The development of Alzheimer's Disease (AD) may occur years prior to its first symptoms appearing. Early detection of the Alzheimer's Disease development is crucial for effective clinical intervention and patient management. However, conventional diagnostic techniques, such as positron emission tomography (PET) and cerebrospinal fluid analysis, are expensive, invasive and time-consuming. These limitations have increased the interest in alternate diagnostic approaches utilising AD-related biomarkers found in readily accessible body fluids, such as blood, urine, and saliva. Recent advances in biomarker identification have recognised amyloid beta peptides (e.g., Aβ40 and Aβ42), tau protein isoforms (e.g., tau217, tau181 and tau441), and neurodegeneration-related indicators as potential targets for early AD diagnosis. The advancement of point-of-care (POC) diagnostic devices can create new opportunities for rapid, cheap, and minimally invasive testing. This review will highlight recent development of the detection of body fluid biomarkers with POC devices as well as address the significance of early AD diagnosis. The challenges of the detection of biomarkers with POC devices, such as specificity, sensitivity, and reproducibility, will be addressed.

Keywords: Alzheimer's Disease, point-of-care, diagnosis, body fluids

ORAL PRESENTATION

Biyokontrol ajanlarının etkisi altındaki *Fusarium spp.*'de transkriptomik incelemeler

Beyzanur Orhan[1*] (ORCID: https://orcid.org/0009-0009-2192-7984), Tuna Birgün[1] (ORCID: https://orcid.org/0009-0009-1827-7933) , Emre Yörük [1] (ORCID: https://orcid.org/0000-0003-2770-0157)

[*1] İstanbul Yeni Yüzyıl Üniversitesi, Fen Edebiyat Fakültesi, Moleküler Biyoloji ve Genetik, İstanbul, Türkiye.

* Sorumlu yazar e-mail: beyzanur.orhan2021@ogr.yeniyuzyil.edu.tr

Özet

Bu çalışma, *Fusarium spp.*'nin tarımsal ve sağlık üzerindeki ciddi etkileri göz önüne alınarak, patojen ile çeşitli fungal (*Trichoderma*, *Aureobasidium*) ve bakteriyel (*Bacillus*, *Pseudomonas*) biyokontrol ajanları arasındaki etkileşimleri aydınlatmak amacıyla gerçekleştirilen altı farklı transkriptomik (RNA-Seq) analizin meta-analitik bir sentezini sunmaktadır. Projenin temel amacı, bu biyokontrol ajanlarının patojen üzerindeki etki mekanizmalarını gen anlatımı seviyesinde karşılaştırmak ve ortak/benzersiz biyolojik yolları belirleyerek yayınlanabilir bir bütün oluşturmaktır. Tüm çalışmalar için RNA-Seq verileri (NCBI/SRA) toplanmış, FastQC ile kalite kontrolü yapılmış ve sayım matrisleri elde edilmiştir. Diferansiyel İfade Analizi (DEA) DESeq2 paketi kullanılarak gerçekleştirilmiş, anlamlı genler ($|log2\ FC| > 1\ ve\ p_{adj} < 0.05$) belirlenmiştir. Belirlenen DEGs listeleri, Gen Ontolojisi (GO) Zenginleştirme analizi (ShinyGO, Moleküler Fonksiyon) ile fonksiyonel olarak değerlendirilmiştir. Altı çalışma baz alındığında, toplamda 8.765 diferansiyel anlatım gösteren gen (DEG) tespit edilmiştir. En yüksek değişim 4.135 DEG ile *F. pseudograminearum* vs *B. velezensis YB-185* çalışmasında gözlenmiştir. Fonksiyonel analizler, tüm etkileşimlerde patojenin temel olarak transmembran taşıyıcı aktivitesi (iyon, amino asit) ve oksidoredüktaz aktivitesi gibi hücre zarı ve metabolizma ile ilişkili süreçleri hedef aldığını göstermiştir. En çarpıcı bulgu, fungal biyokontrol ajanlarının (*Trichoderma spp.*), *Fusarium*'un TRI ve Aurofusarin (pigment) gen kümelerinde belirgin bir upregülasyonu (savunma/virülans aktivasyonu) tetiklemesi; buna karşın bakteriyel ajanların (*Bacillus spp.*) bu genlerde genellikle downregülasyon yaratarak toksin üretimini başarılı bir şekilde baskılamasıdır. Biyokontrol ajanlarının *Fusarium* üzerindeki moleküler stratejileri, ajanın filogenetik kökenine göre farklılaşmaktadır. Bu çalışma, biyokontrol ajanlarının etki mekanizmalarını transkriptomik düzeyde kıyaslayarak, gelecekteki tarımsal uygulamalar için hedef gen ve yolakların belirlenmesinde kritik bir referans sağlamaktadır.

Anahtar Kelimeler: Transkriptomik, *Fusarium*, Biyokontrol, Diferansiyel Gen İfadesi, Fitopatojen

ORAL PRESENTATION

Farklı esansiyel yağlar içeren pla temelli yara örtülerinin üretimi ve mekanik özelliklerinin incelenmesi

Yunus Emre Canavar[1*] (Orcid: https://orcid.org/0009-0002-1952-8721), Prof. Dr. Sevim Alişir[2] (Orcid: https://orcid.org/0000-0001-7296-8318)

[*1]Ondokuz Mayıs Üniversitesi, Mühendislik Fakültesi, Metalurji ve Malzeme Mühendisliği, Samsun, Türkiye.
[2]Ondokuz Mayıs Üniversitesi, Mühendislik Fakültesi, Metalurji ve Malzeme Mühendisliği, Samsun, Türkiye.

*Sorumlu yazar e-mail: yunus.canavar40@gmail.com

Özet

Yeni nesil tıbbi tekstiller olarak nitelendirilebilecek nanolifler, yara örtüsü olarak kullanımda büyük bir potansiyele sahiptir. Nanolif yara örtülerinin gözenekli yapısı sayesinde malzemeye, bakteri ve enfeksiyona neden olabilecek maddelerin geçişini engelleyen ve nefes alabilen bir yapı kazandırmakta, aynı zamanda da dermal ve epidermal dokuları kurtarmaya katkı sağlamaktadır. Çalışmamızda yara örtülerinin hazırlanmasında, yenilenebilir kaynaklardan üretilen PLA (Poli Laktik Asit) ve hücre tutunması, çoğalması, kanamayı durdurma (hemostaz) gibi özellikleri bulunan, biyouyumlu, antibakteriyel ve antifungal özelliklere sahip kitosan polimeride kullanılacaktır. Grubumuz tarafından, ilaç etken maddesi olarak kullanılan diklofenak ile antibakteriyel özelliği kanıtlanmış gümüşün bir araya getirilmesiyle [Agdicl] bileşiği sentezlenmiştir. Ayrıca PLA–kitosan ve [Agdicl] içeren polimer çözeltilerine kenevir tohumu yağı, nioli yağı, biberiye yağı, kekik yağı, çay ağacı yağı ve nane yağı gibi çeşitli esansiyel yağlar eklenmiş; bu yağlar aracılığıyla yapıların mekanik özelliklerinin iyileştirilmesi hedeflenmiştir. Literatürde, PLA–kitosan ve [Agdicl] içeriğini farklı esansiyel yağlarla birleştirerek mekanik özellikleri güçlendirmeyi amaçlayan benzer bir çalışmaya rastlanmamıştır. Yapılan çalışmanın sonucunda nanolif oluşumu SEM görüntüleri alınarak, biyokompozitlerdeki katkı maddelerinin PLA ile etkileşimi FTIR spektrumları ile belirlenmiştir. Çekme testi sonuçlarında ise, kenevir tohumu yağı eklenen biyokompozit yara örtüsünün diğer eklenen esansiyel yağlara göre en yüksek mekanik dayanımı sergilediği görülmüştür. Üretilen yara örtüsü ile gaz alış-verişine izin veren, hastaları bakteri ve mantar enfeksiyonuna karşı koruyacak, yarada meydana gelen ağrı ve acıyı dinderecek, hemde iltihap önleyici aynı zamanda da yarada meydana gelecek olan kan ve akıntıları emecek özellikte tamamen biyouyumlu ve mekanik özellikleri yüksek bir yara örtüsü üretimi yapılarak hastaların iyileşme sürecini hızlandıracağı ve günlük yaşantılarını kolaylaştıracağı düşünülmektedir.

Anahtar Kelimeler: PLA, Yara örtüsü, Elektrospinning, Esansiyel yağ.

ORAL PRESENTATION

Isolation, molecular typing, and investigation of biotechnological potential of actinobacteria from soils in Ardahan province

Merve Sezer[1] (Orcid: https://orcid.org/0009-0009-4056-8948), Salih SArıcaoğlu[2] (Orcid:https://orcid.org/0000-0002-0013-9024)

[1,2]Ondokuz Mayıs University, Faculty of Science, Department of Biology, Samsun, Turkey

*Corresponding author e-mail: sezermerve873@gmail.com[1], salihsaricaoğlu@omu.edu.tr[2]

Abstract

Actinobacteria are Gram-positive bacteria widely found in both terrestrial and aquatic ecosystems with high biotechnological potential. They are generally aerobic microorganisms that form mycelia, have conical structures, and exhibit colony morphologies producing various pigments. These plants, which can reproduce by binary fission and the production of spores or chondroitin, have attracted increasing interest in recent years, particularly in plant biotechnology. Their antagonistic activities against plant pathogens suggest that they offer significant potential in biological control processes. Actinobacteria contribute to carbon cycle by degrading complex organic molecules such as cellulose and chitin through the enzymes they produce. Thus, they play a crucial role in the renewal of nutrients in soil and the formation of humus. Furthermore, their capacity to produce secondary metabolites makes them commercially and pharmaceutically valuable. Many important antibiotics, such as streptomycin, terramycin, and auremycin, were first isolated from actinobacteria. Therefore, actinobacteria were isolated from soil samples collected from the districts of Posof (Gümüşkavak), Damal (Tepeköy), and Hanak (Selamverdi) in Ardahan, as well as from the Mera (Dumankonak) and Değirmenli regions. In this study, the dilution–plate method was applied, and after 14 days of incubation at 28 °C, pure cultures were obtained from actinobacterial colonies grown on 10 different selective media. Based on color grouping and colony morphology, 47 isolates exhibiting actinobacterial characteristics were selected for molecular identification. In addition, to determine the antimicrobial potential of these isolates, antimicrobial activity tests will be performed against 15 pathogenic organisms using the agar plug diffusion technique, and molecular typing will be conducted according to 16S rRNA gene region sequence analyses.

Keywords: Actinobacteria, Selective Isolation, Morphological Identification, Biodiversity

ORAL PRESENTATION

Seasonal changes in phosphatidylinositol (PI) Fatty acid content in muscle tissues of male and female individuals of *Silurus triostegus*

Şeyma Baran[1] (Orcid: 0009-0008-9712-6262), Murat Yolcu[2*] (Orcid: 0000-0003-3067-8755), Veysi Kızmaz[3] (Orcid: 0000-0002-7864-5912), Tarık Çiçek [4] (Orcid: 0000-0001-8491-5598), Pelin Uğurlu[2] (Orcıd No: 0000-0002-4790-2533) , Nazanin Meskinbalov[5] (Orcid: 0009-0000-6260-0958) , Elif İpek Satar[2] (Orcid: 0000-0002-7540-3686)

[1] Dicle University, Graduate School of Natural and Applied Sciences, Department of Biology, Diyarbakır, Türkiye
[*2] Dicle University, Faculty of Pharmacy, Department of Basic Pharmaceutical Sciences, Diyarbakır, Türkiye
[3] Mardin Artuklu University, Vocational School of Health Services, Department of Medical Services and Techniques, Mardin, Türkiye
[4] Dicle University, Faculty of Science, Department of Biology, Diyarbakır, Türkiye
[5] Dicle University, Faculty of Pharmacy, Diyarbakır, Türkiye

*Corresponding author e-mail: muratyolcu21@gmail.com

Abstract

This study aimed to investigate the seasonal variations in the phosphatidylinositol (PI) fatty acid composition of muscle tissues in male and female *Silurus triostegus*. Analyses revealed that the major fatty acids of the PI fraction were 16:0, 18:0, 18:1n-9, 20:4n-6, 20:5n-3, and 22:6n-3. Seasonal evaluations demonstrated pronounced sex- and season-dependent differences in both individual fatty acids and total SFA, MUFA, and PUFA levels. The fatty acid 12:0 was markedly elevated in April in both sexes and additionally in October in males. The 14:0 fatty acid reached its highest level in January in both sexes. The dominant SFAs, 16:0 and 18:0, exhibited distinct seasonal patterns: 16:0 peaked in July in both sexes, whereas 18:0 was highest in July in males and in April and October in females. The major MUFA, 18:1n-9, showed its maximum proportion in January and its minimum in April. Among PUFAs, 18:2n-6 increased in July in both sexes and decreased to its lowest level in April. EPA (20:5n-3), DPA (22:5n-3), and DHA (22:6n-3) increased sharply in April and decreased in July. Total SFA reached its highest level in July, while total MUFA peaked in January. Total PUFA increased in April and declined in July in both sexes. Seasonal fatty acid distribution patterns were determined as follows: in January, males exhibited SFA>MUFA>PUFA and females SFA>MUFA=PUFA; in April and October, both sexes showed SFA>PUFA>MUFA; and in July, both sexes exhibited SFA>MUFA=PUFA. Omega-3 fatty acids were highest in April and lowest in January, while omega-6 fatty acids were highest in October in males and in July in females. The ω3/ω6 ratio peaked in April and reached its minimum in October. Overall, these findings demonstrate that PI fatty acid composition in the muscle tissue of *S. triostegus* undergoes significant seasonal and sex-dependent variation.

Keywords: *Silurus triostegus*, Fish, Muscle, Fatty Acids, Phospholipid, Phosphatidylinositol

*This study was supported by TÜBİTAK under project number 124Z012 and by the Dicle University Scientific Research Projects Coordination Office (DÜBAP) under project number ECZACILIK.24.013.

ORAL PRESENTATION

Analysis of tumor mutational burden and mutation status in immunotherapy-treated lung adenocarcinomas

Ayça Tan

Manisa Celal Bayar University, Facukty of Medicine, Department of Pathology, Manisa, Türkiye

Corresponding author e-mail: draycatan@gmail.com

Abstract

Immune checkpoint inhibitor therapies are used in metastatic lung adenocarcinomas, and the effectiveness of these treatments is associated with certain biomarkers (tumor mutational burden (TMB)) and tumor mutation profile. To predict this relationship, clinical and genomic data were compared with survival status in lung adenocarcinoma patients who received immunotherapy. This study used the cBioPortal for Cancer Genomics, an open-access bioinformatics database. The most frequently mutated genes and the effect of TMB on immunotherapy were examined. Of 255 lung adenocarcinoma cases treated with PD1/PD-L1, 142 (55.7%) were female. The three most frequently mutated genes were TP53 (58.8%), KRAS (40.8%), and STK11 (25.5%). TMB was ≥10 in 83 (32.5%) of the cases. Cases with a TMB ≥10 had a better prognosis, and mutations were observed more frequently in 60 genes in this group of cases and were statistically significant ($p<0.001$). Mutations were more common in the ERBB4 gene in the TP53 mutant group and in the KRAS and STK11 genes in the non-TP53 group ($p<0.001$). Mutations in the EGFR and TP53 genes were more common in non-KRAS group ($p<0.001$). Mutations in the KEAP1 and KDR genes were more common in those with STK11 mutations, and TP53 and EGFR mutations were more common in the non-STK11 group ($p<0.001$). Those with STK11 mutations had a poorer prognosis ($p>0.05$). Conclusion: Immunotherapy treatments are routinely used and promising in lung adenocarcinomas. Although the oncological outcomes of the cases treated with this treatment in the first two years showed clinically significant differences, specifically in TP53, KRAS and STK11 mutations and TMB, it was noted that there were no significant differences due to these mutations and TMB after two years

Keywords: lung adenocarcinoma, PD-1, PD-L1, tumor mutational burden

ORAL PRESENTATION

Antibacterial hydrogels containing a Cu(II) hydrazone complex: Synthesis, characterization, and in vitro activity

Neslihan Özlü[1*] (ORCID: https://orcid.org/0009-0001-4199-8976), Ayşin Zülfikaroğlu[1] (ORCID: https://orcid.org/0000-0002-2871-844X), Emine Çelikoğlu[2] (ORCID: https://orcid.org/0000-0002-5956-0008), Aslı Beyler Çiğil[3] (ORCID: https://orcid.org/0000-0003-4353-4224)

[*1]Amasya University, Faculty of Arts and Sciences, Department of Chemistry, Amasya, Türkiye
[2]Amasya University, Faculty of Arts and Sciences, Department of Biology, Amasya, Türkiye
[3]Gazi University, Technical Sciences Vocational School, Department of Chemistry and Chemical Process Technology, Türkiye

*Corresponding author e-mail: nesliobut@hotmail.com

Abstract

Nowadays, the widespread and inappropriate use of antibiotics, particularly in the treatment of infected wounds, has contributed to the emergence of multidrug-resistant bacterial strains, thereby significantly limiting the effectiveness of current therapeutic approaches. Therefore, the development of novel agents with potent antibacterial activity and advanced wound-dressing materials has become increasingly important [1,2]. In recent years, hydrogels have emerged as prominent materials in wound care, supporting the development of intelligent systems that facilitate wound healing. Due to their high water content and three-dimensional crosslinked polymeric network structures, hydrogels can maintain a moist wound microenvironment, provide oxygen permeability, and prevent adhesion to the wound surface. Additionally, the physical, chemical, and biological properties of hydrogels can be tailored by adjusting the type of crosslinking, polymer composition, and incorporated functional groups [3,4]. A promising strategy for imparting antibacterial properties is the integration of metal complexes into the hydrogel matrix. Hydrazone ligands bearing an azomethine (–C=N–) group can readily bind metal ions to form stable metal complexes, thereby enhancing antibacterial efficacy [5]. In this study, antibacterial hydrogels were developed using a Cu(II) hydrazone complex. First, a novel hydrazone ligand was synthesized from 2,4-dihydroxybenzaldehyde and valeric acid hydrazide, and its Cu(II) complex was subsequently prepared. The structures were characterized by various spectroscopic and analytical techniques. Subsequently, hydrogels containing the metal complex at different concentrations were fabricated using natural polymers. The antibacterial activity of the obtained hydrogels against *E. coli* ATCC 25922 and *S. aureus* ATCC 25923 was evaluated using the disk diffusion method. The results demonstrated an apparent antibacterial effect against both bacterial strains, becoming more pronounced with increasing copper complex concentration.

Keywords: Hydrazone ligand, Cu(II) complex, Antibacterial hydrogel

References:
[1] Sun, C., Liu, W., Wang, L., Meng, R., Deng, J., Qing, R., Wang, B., Hao, S. 2023. "Photopolymerized keratin-PGLa hydrogels for antibiotic resistance reversal and enhancement of infectious wound healing", Materials Today Bio, 23, 100807.
[2] Wang, D., Zhu, C., Yang, Q., Xu, Y., Zhang, D., Wang, D., Liu, F., Hou, C. 2025. "Stretchable, controlled release of active substances, and biodegradable chitosan-polyvinyl alcohol hydrogel film for antibacterial and chilled meat preservation", Food Chemistry, 477, 143608.
[3] Kopecki, Z. 2021. "Development of next-generation antimicrobial hydrogel dressing to combat burn wound infection", Bioscience Reports, 41, BSR20203404.
[4] Jia, B., Li, G., Cao, E., Luo, J., Zhao, X., Huang, H. 2023. "Recent progress of antibacterial hydrogels in wound dressings", Materials Today Bio, 19, 100582.
[5] Zülfikaroğlu, A., Yüksektepe Ataol, Ç., Çelikoğlu, E., Çelikoğlu, U., İdil, Ö. 2020. "New Cu(II), Co(III) and Ni(II) metal complexes based on ONO donor tridentate hydrazone: Synthesis, structural characterization, and investigation of some biological properties", Journal of Molecular Structure, 1199, 127012.

ORAL PRESENTATION

Acidic deep eutectic solvent catalyst for efficient conversion of levulinic acid to n-butyl levulinate fuel bioadditive

Kazımcan Çalişkan[1,2*](0009-0002-3671-2643), Murat Sert[1](000-0002-4271-1914), Emine Sert[1](0000-0002-0868-8597)

[1*] Ege University, Department of Chemical Engineering, Izmir, Türkiye
[2]Graduate School of Natural and Applied Sciences, Ege University, Izmir, Turkiye

*Corresponding author e-mail: kazımcancalskan@gmail.com

Abstract

Levulinic acid (LA) is a primary organic compound and one of the twelve primary building blocks derived from the breakdown of lignocellulosic biomass. The conversion of levulinic acid into several valuable substances has been the subject of academic research over a few decades. The efficiency of various heterogeneous catalysts such as acidic ion exchange resins, zeolites, heteropolyacids, metal organic frameworks, carbon materials were documented in the conversion of levulinic acid. Despite the efficacy of these potential heterogeneous catalysts in facilitating the conversion of levulinic acid (LA) to n-butyl levulinate (BL), their high cost, susceptibility to leaching of active sites, and poor catalytic activity limits their practical applicability. So, in this study, a deep eutectic solvents was used as a sustainable, environmentally friendly, acidic catalyst. This work examined the esterification of levulinic acid with butanol using an acidic deep eutectic solvent (DES) composed of choline chloride and para-toluene sulfonic acid. DESs consist of two or more constituents that create a eutectic mixture by hydrogen bonding, leading to melting points that are lower than that of the individual components. These solvents contain two primary constituents: a hydrogen bond donor (HBD) and a hydrogen bond acceptor (HBA). Recently, DESs have been used as an alternative to traditional solvents due to their stability at higher temperatures, lower vapor pressure, combustion-free nature, and capacity for tuning. In butyl levulinate synthesis, over 90% conversion of levulinic acid was achieved within 15 minutes in the microwave reactor. The results show that DES can be an efficient catalytic system in the transformation of levulinic acid.

Keywords: deep eutectic solvent, bioadditive, butyl levulinate, catalysis

ORAL PRESENTATION

Helichrysm arenarium subsp. *erzincanicum* türünün fitokimyasal içeriğinin belirlenmesi ve antioksidan kapasitesinin değerlendirilmesi

Volkan Ay* (ORCID: https://orcid.org/0009-0003-5396-4727), Ahmet Altay (ORCID: https://orcid.org/0000-0001-8120-8900), Hüseyin Akşit (ORCID: https://orcid.org/0000-0002-1509-851X), Samed Şimşek (ORCID: https://orcid.org/0000-0001-8451-3425),

Erzincan Binali Yıldırım Üniversitesi, Fen Bilimleri Enstitüsü, Kimya Anabilimdalı, Erzincan, Türkiye
Erzincan Binali Yıldırım Üniversitesi, Kimya Bölümü, Erzincan, Türkiye
Erzincan Binali Yıldırım Üniversitesi Eczacılık Fakültesi Analitik Kimya Anabilim Dalı, Erzincan
Erzincan Binali Yıldırım Üniversitesi, Çayırlı Meslek Yüksekokulu, Tıbbi Hizmetler ve Teknikler Bölümü, Erzincan, Türkiye

*Sorumlu yazar e-mail: ay.volkan@outlook.com

Özet

Bu çalışmada, Erzincan'a endemik olarak yayılım gösteren *Helichrysum arenarium* subsp. *erzincanicum* bitkisinin fitokimyasal içeriğinin belirlenmesi ve antioksidan kapasitesinin değerlendirilmesi amaçlanmıştır. Bu kapsamda, Erzincan, İliç-Kuruçay bölgesinden toplanan bitkinin ilk olarak metanol-su ekstraktı hazırlanmış ve bu ekstraktın antioksidan biyolojik aktivitesi DPPH• radikal giderme, Ferrik İndirgeyici Antioksidan Güç (FRAP), toplam fenolik ve toplam flavonoid içerikleri üzerinden değerlendirilmiştir. Bitki ekstraktının fitokimyasal içeriğinin belirlenmesi Sefadeks ve Silika jel kolonlar aracılığıyla gerçekleştirilen kromatografik işlemlerle yapılmıştır. Thin Layer Chromatography (TLC) ile yeterli ayrımı sağlanan elüatlar yüksek performanslı sıvı kromatografisi (HPLC) ile detaylı analize tabi tutulmuştur. Analitik-HPLC saflık kontrolünün ardından preparatif HPLC'ye geçilmiş olup eluatların yarı otomatik biçimde ayrımları sağlanmıştır. Elde edilen saf bileşiklerin yapıları Nükleer manyetik rezonans (NMR) tekniği ile aydınlığa kavuşturulmuştur. Elde edilen bulgular *Helichrysm arenarium* subsp. *erzincanicum* bitkisinden elde edilen ekstrenin standart antioksidan kaynağı olarak kullanılan troloks, askorbik asit, BHT ve BHA ile kıyaslandığında istatiksel olarak kayda değer ölçüde antioksidan aktivite gücüne sahip olduğu belirlenmiştir. İzolasyon ve yapı analiz sonuçları bitkinin fitokimyasal içerik bakımından oldukça zengin bir içeriğe sahip olduğunu göstermiştir. Sonuç olarak, bu çalışmadan elde edilen tüm bu bulgular *Helichrysm arenarium* subsp. *erzincanicum* türünün zengin fitokimyasal içeriğiyle önemli derecede *in vitro* antioksidan etkiye sahip olduğunu ve bunun da *in vivo* çalışmalara kapı araladığını ortaya koymaktadır.

Anahtar Kelime: Antioksidan aktivite, Fitokimyasal içerik, *Helichrysum arenarium* subsp. *erzincanicum*, HPLC, NMR.

ORAL PRESENTATION

C-QD ve ZnO-QD'ların hidrotermal sentez yöntemi ile üretimi ve güneş hücrelerinde uygulanmasının araştırılması

Oğuzhan Taştan[1*] (ORCID: https://orcid.org/0009-0006-3597-1714), Şerife Saçmacı[1,2] (ORCID: https://orcid.org/0000-0001-9188-4574)

[*1]Erciyes Üniversitesi, Fen Bilimleri Enstitüsü, Nanobilim ve Nanoteknoloji Bölümü, Kayseri, Türkiye.
[2]Erciyes Üniversitesi, Fen Fakültesi, Kimya Bölümü, Kayseri, Türkiye.

*Sorumlu yazar e-mail: 4014440036@erciyes.edu.tr

Özet

Küresel enerji ihtiyacı gün geçtikçe artmaktadır. Fosil yakıtlara olan bağımlılığı azaltacak sürdürülebilir temiz enerji kaynaklarının geliştirilmesi bir zorunluluk haline gelmiştir. Yenilenebilir teknolojiler temiz enerji kaynakları olarak kabul edilir. Bu kaynakların uygun şekilde kullanılması, çevresel kirliliği azaltırken, aynı zamanda minimum atık, ekonomik ve sosyal ihtiyaçları da sürdürülebilir kılar. Bu etkenler doğrultusunda önemli bir temiz enerji kaynağı olan güneş hücrelerinin kullanımının artması ve bu sistemlerden maksimum verim elde edilmesi oldukça önemlidir. ABD Ulusal Yenilenebilir Enerji Laboratuvarı (NREL)'in yayınladığı verilere göre, günümüzde ticari olarak en yaygın kullanıma sahip monokristal ve polikristal güneş panellerinin yaklaşık ~%15-%22 arasında bir verimlilikte olması oldukça düşündürücüdür. Bugüne kadar en yüksek verim olarak açıklanan tandem güneş hücreleri bile ~%48 enerji dönüşüm verimliliğine sahiptir ve geliştirilmeye muhtaçtır. Bu bilgilerden yola çıkarak çalışmanın temel amacı: monokristal ve polikristal güneş hücrelerinin verimliliğinin artırılması olarak belirlenmiştir. Kuantum noktaları (QDs), yarıiletken malzemelerden yapılmış olup, ayarlanabilir fiziksel boyutlara ve olağanüstü optoelektronik özelliklere sahiptir. Son yıllarda, QD'ların boyut kısıtlaması ve anizotropik geometrileri nedeniyle elektrokimyasal enerji depolama alanında ve fotovoltaik sistemlerde kullanımı araştırılmaktadır (Wu ve ark., 2018). Bu nedenlerden dolayı çalışmayı, QD'ların güneş hücrelerinin verimliliğini artırma üzerine olmuştur. Düşük maliyet, basit sentez prosedürleri ve iyi kimyasal özellikler göstermelerinden dolayı karbon QD(C-QDs)'lar ve ZnO QD'lar tercih edilmiştir. Basit bir sentez yöntemi olması, malzeme kaybının sıfıra yakın olması ve yüksek maliyet gerektirmemesi gibi nedenlerden dolayı hidrotermal sentez yöntemi tercih edilmiştir. Sentez sonucunda ~2-5 nm çaplara sahip QD'lar elde edilmiştir ve UV ışık altında mavi ışık verdiği tespit edilmiştir. Elde edilen QD'lar, UV-vis, FT-IR, TEM, XRD ve PL analizleri yapılarak karakterize edilmiştir.

Anahtar Kelimeler: Karbon kuantum noktalar (C-QDs), Metal oksit kuantum noktalar (ZnO-QDs), Hidrotermal sentez yöntemi, Monokristal güneş hücreleri, Polikristal güneş hücreleri

ORAL PRESENTATION

Histological insights into endometrial microbiota: Implications for fertility and IVF outcomes

Elif Gelenli Dolanbay (ORCID: https://orcid.org/0000-0002-7553-5435*)*

Istanbul Medeniyet University, Faculty of Medicine, Department of Histology and Embriyology, Istanbul, Türkiye.

Corresponding author e-mail: elif.dolanbay@medeniyet.edu.tr

Abstract

Endometrial microbiota has emerged as a critical regulator of uterine health and reproductive outcomes. Recent studies highlight the association between microbial composition and histopathological changes in the endometrium, including inflammation, polyps, and altered tissue integrity, which can directly influence implantation success and IVF outcomes. Dysbiosis of the endometrial microbiome has been linked to recurrent implantation failure, infertility, and pregnancy loss. Histological evaluation reveals that shifts in microbial populations can modify the endometrial immune environment, angiogenesis, and stromal-epithelial interactions, underscoring the interplay between microbiota and tissue morphology. Understanding these histological correlations provides valuable insights for optimizing embryo transfer strategies, improving implantation rates, and developing targeted interventions to restore endometrial homeostasis. This review integrates current evidence on the role of endometrial microbiota in reproductive health, emphasizing histological features that can inform clinical decisions in assisted reproductive technologies.

Keywords: Endometrial microbiota, histology, fertility, IVF, implantation, reproductive health

ORAL PRESENTATION

Metilen mavisi adsorpsiyonunda kullanılmak üzere mısır atıklarından manyetik biyochar üretimi ve karakterizasyonu

Kübra Polat[1,*] (ORCID: https://orcid.org/0009-0008-8949-687X), Emre Karaduman[1] (ORCID: https://orcid.org/0000-0003-2087-789X), Anıl Tevfik Koçer[1,2] (ORCID: https://orcid.org/ 0000-0003-1519-1711), Mehmet Burçin Pişkin[1] (ORCID: https://orcid.org/ 0000-0002-2689-8547)

[*1]Yıldız Teknik Üniversitesi, Kimya-Metalurji Fakültesi, Biyomühendislik Bölümü, İstanbul, Türkiye.
[2]Sağlık Biyokteknolojisi Mükemmeliyet Ortak Uygulama ve Araştırma Merkezi, İstanbul, Türkiye.

*Sorumlu yazar e-mail: kubra.polat@std.yildiz.edu.tr

Özet

Endüstriyel faaliyetler sonucu su kaynaklarında biriken organik boyalar ve diğer kalıcı kirleticilerin etkin bir şekilde giderilmesi, sürdürülebilir çevre teknolojilerinin ve yeni nesil adsorbent malzemelerin geliştirilmesini zorunlu kılmaktadır. Bu kapsamda, düşük maliyetli, çevre dostu ve yüksek performanslı adsorbentlerin geliştirilmesi önem kazanırken, tarımsal atıkların fonksiyonel karbon bazlı malzemelere dönüştürülmesi hem döngüsel ekonomi ilkeleriyle uyumlu bir değerlendirme stratejisi sunmakta hem de su arıtım süreçleri için yenilikçi çözümler sağlamaktadır. Bu doğrultuda, biyocharların manyetik özelliklerle zenginleştirilmesi; kolay geri kazanılabilirlik, yüzey reaktivitesi ve çok yönlü fonksiyonelleştirme imkânı sayesinde çevresel iyileştirme uygulamalarında öne çıkan bir yaklaşım haline gelmiştir. Bu çalışmanın amacı, mısır kabuğu atıklarından iki farklı üretim stratejisiyle manyetik biyochar sentezlemek, bu iki yöntemin termal davranış, kompozisyon ve yüzey fonksiyonelliği üzerindeki etkilerini karşılaştırmalı olarak incelemek ve elde edilen malzemelerin metilen mavisi adsorpsiyonundaki potansiyelini değerlendirmektir. Bu doğrultuda, birinci yöntemde biyokütle Fe^{2+}/Fe^{3+} çözeltileriyle ön işlemden geçirilmiş ve ardından 400 °C sıcaklık, 20°C/dak ısıtma hızı ve 1,5 saat kalma süresi koşullarında piroliz edilerek in-situ manyetizasyon sağlayan Pre-Fe–Pyro örneği elde edilmiştir. İkinci yöntemde ise biyokütleden 400 °C sıcaklık, 20°C/dak ısıtma hızı ve 1,5 saat kalma süresi koşullarında piroliz edilerek üretilen biyochar, demir çözeltileriyle işlemden geçirilerek ex-situ manyetik modifikasyon içeren Pyro–Post-Fe örneği hazırlanmıştır. Elde edilen manyetik biyocharlar, FTIR, TGA ve SEM ile karakterize edilmiştir ve bunların elemental ve proximate içerikleri TGA dataları kullanılarak hesaplanmıştır. Sonuçlar, iki sentez yönteminin malzemelerin yüzey kimyası, termal dayanımı ve inorganik/organik bileşen dağılımı üzerinde belirgin farklılıklar oluşturduğunu göstermektedir. Özellikle Pre-Fe–Pyro yönteminde demir türlerinin piroliz sırasında biyokütle yapısına daha homojen şekilde gömülmesi, kül oranı ve bozunma profillerinde karakteristik değişimler oluşturmuştur. Üretilen manyetik biyochar örnekleri, model kirletici olarak metilen mavisinin adsorpsiyonunda test edilmekte olup, düşük maliyetli, yeniden kullanılabilir ve çevre dostu adsorbent geliştirilmesi açısından önemli bir potansiyel sunmaktadır. Bu çalışma, mısır bitkisi atığının katma değerli bir çevresel malzemeye dönüştürülmesi için etkili ve uygulanabilir bir yöntem ortaya koymaktadır.

Anahtar Kelimeler: Mısır atığı, manyetik biyochar, piroliz, birlikte çökeltme yöntemi, adsorpsiyon, metilen mavisi

ORAL PRESENTATION

Cold plasma in the food industry: Mechanisms, product quality and safety perspectives

Hakan Apaydin (Orcid: https://orcid.org/0000-0001-8507-6212)

Hitit University, Scientific Technical Application and Research Center, Çorum, Turkiye

Corresponding author e-mail: hakanapaydin@hitit.edu.tr

Abstract

The need to reduce energy consumption, thermal damage, and the use of chemical preservatives in food processing and preservation has made cold plasma one of the prominent non-thermal technologies in recent years. Cold plasma generated at atmospheric or low pressure can effectively inactivate microorganisms, spores, and certain enzymes through reactive oxygen and nitrogen species, ions, free radicals, and UV radiation, while the limited increase in process temperature allows for the preservation of heat-sensitive food components. This work provides a comprehensive overview of the applications of cold plasma technology in the food industry, its mechanisms of action, and its implications for product quality. The effects of different plasma generation systems (spark discharges, dielectric barrier discharges, and atmospheric pressure plasma jets (APPJ)) and processing parameters on microbial safety, shelf life, food constituents (proteins, lipids, carbohydrates, bioactive compounds), and sensory attributes will be evaluated. Findings reported for different product categories, including fresh fruits and vegetables, meat and meat products, milk and dairy products, cereals and bakery goods, fruit juices, and nuts, will be comparatively assessed in order to highlight the advantages and limitations of the technology. In addition, the use of cold plasma as a decontamination tool for packaging materials and food-contact surfaces will be examined in the context of potential oxidative side reactions, process standardization, scale-up, toxicological assessment, and regulatory requirements, with emphasis on existing knowledge gaps. This study aims to provide an up-to-date framework for the safety- and quality-oriented sustainable applications of cold plasma in the food sector and to identify priority areas for future research for both industry and academia.

Keywords: cold plasma, non-thermal food processing, microbial inactivation, food quality, food safety

ORAL PRESENTATION

Plantago lanceolata ekstraktı ve çinko-oksit nanopartikülleri ile zenginleştirilmiş çift katmanlı fonksiyonel mikroiğne üretimi ve karakterizasyonu

Canan Bozyokuş[1,*] (ORCID: https://orcid.org/ 0009-0002-5105-6824), Anıl Tevfik Koçer[1,2] (ORCID: https://orcid.org/ 0000-0003-1519-1711), Azime Erarslan[1,2] (ORCID: https://orcid.org/ 0000-0002-9470-4310)

[*1]Yıldız Teknik Üniversitesi, Kimya-Metalurji Fakültesi, Biyomühendislik Bölümü, İstanbul, Türkiye.
[2]Sağlık Biyokteknolojisi Mükemmeliyet Ortak Uygulama ve Araştırma Merkezi, İstanbul, Türkiye.

*Sorumlu yazar e-mail: canan.bozyokus@std.yildiz.edu.tr

Özet

Diyabetik, bası ve yanık gibi kronik yara tiplerinde inflamasyonun uzun sürmesi, mikrobiyal kontaminasyon riski ve doku rejenerasyonunun yetersizliği, gelişmiş ve çok işlevli yara örtülerinin geliştirilmesini gerektirmektedir. Bu kapsamda hem antimikrobiyal koruma sağlayabilen hem de doku yenilenmesini destekleyebilen biyolojik ve fonksiyonel ajanların kullanımı modern yara yönetimi için önemli bir yaklaşım oluşturmaktadır. Fitoterapötik özellikleri literatürde iyi bilinen *Plantago lanceolata* (sinir otu), anti-inflamatuar, antimikrobiyal, antifungal ve yara iyileştirici bileşenleri sayesinde bu tür biyomalzeme tasarımları için güçlü bir adaydır. Bu çalışmanın amacı, fitoterapötik özelliklere sahip sinir otu ekstraktı içeren GelMA tabanlı mikroiğne yapısı ile antimikrobiyal etkili, yeşil sentezle üretilmiş çinko-oksit (ZnO) nanopartikülleri içeren kitosan–PVA fiber katmanını bir araya getirerek biyouyumlu ve fonksiyonel bir iki katmanlı yara örtüsü geliştirmektir. Bu kapsamda, alt katman olarak GelMA–Sinir otu ekstraktı kompozit mikroiğneleri, DLP (Digital Light Processing) 3B baskı teknolojisiyle üretilmiş; üst katman ise yeşil sentezle üretilmiş ZnO nanopartikülleri içeren kitosan–PVA fiber yapı elektrospinning yöntemiyle hazırlanmıştır. Elde edilen çift katmanlı mikroiğne yapısı, sinir otu ekstraktı, ZnO nanopartikülleri ve kitosan–PVA nanofiber üst katmanın karakterizasyonu için FTIR, SEM ve antimikrobiyal aktivite analizleri yapılmış olup; bu analizler, bitkisel ekstraktın mikroiğne yapısına kimyasal olarak başarıyla entegre edildiğini, ZnO nanopartiküllerinin fiber mat içinde homojen şekilde dağıldığını ve her iki katmanın da belirgin antimikrobiyal aktivite sergilediğini göstermiştir. Geliştirilen iki katmanlı kompozit yapının ayrıca mekanik özellikleri, hidrasyon davranışı, ilaç salım profilleri ve biyouyumluluğunun ileri testlerle değerlendirilmesi planlanmakta olup, bu çalışma kronik yaraların tedavisinde yüksek potansiyel sunan yenilikçi bir yara örtüsü tasarımı ortaya koymaktadır.

Anahtar kelimeler: Mikroiğne, DLP Biyobaskı, Elekrospinning, Sinir otu, ZnO nanopartikül.

ORAL PRESENTATION

Examination of muscle strength and reflexes in male adolescent rats with streptozotocin-induced diabetes mellitus

Özlem Özcanlı Çay[1] (ORCID: https://orcid.org/0000-0002-3143-4456),
Hasan Çalışkan[2*] (ORCID: https://orcid.org/0000-0002-3729-1863.)

[1]University of Balıkesir, Faculty of Medicine, Department of Pediatry, Balıkesir, Türkiye
[*2]University of Balıkesir, Faculty of Medicine, Department of Physiology, Balıkesir, Türkiye

*Corresponding author e-mail: hasan.caliskan@hotmail.com

Abstract

Diabetes mellitus is a group of metabolic disorders featuring hyperglycaemia caused by defects in insulin secretion, insulin utilisation, or both. This study aims to investigate the effects of early-onset, untreated diabetes on muscle strength and reflexes in juvenile rats using an experimental diabetes model. For this purpose, 14 male Wistar albino rats, 21 days old and weaned, were used. After a 1-week adaptation period, on day 29, to establish the diabetes model, 120 mg/kg streptozotocin (STZ) was administered to the experimental group (n=7). In contrast, 1 ml/kg physiological saline was administered to the control group (n=7). A blood glucose level of 300 mg/dl was accepted as confirmation of diabetes. On day 30, blood glucose levels were measured in the tail veins of the subjects using a glucometer. On day 41, the subjects underwent a weight test, a Kondizella inverted screen test, a forelimb flexion test, a hindlimb flexion test, a visually triggered placement test, a contact-triggered placing test, and a hindpaw grasping reflex test. Ethical approval for the study was obtained from Balıkesir University (Approval number: 2025/5-26, Meeting date: 22.05.2025). The distribution was examined using the Shapiro-Wilk test. The parametric Student's t-test or the nonparametric Mann-Whitney U test was applied. Blood glucose levels of the subjects were found to be between 424 and 600 mg/dl in the initial birth test and above 300 mg/dl in subsequent measurements ($p<0.001$). No significant difference was found in reflex measurements and reflex responses ($p>0.05$). Diabetic subjects had significantly shorter times in the weight test and Kondizella inverted screen test ($p<0.05$). The study examined the reflexes and muscle strength of diabetic rats that had not received treatment before adolescence. A decrease in muscle strength was observed, while reflex measurements were normal. More detailed studies are required.

Keywords: Adolescence, Diabetes Mellitus, Muscle Strength, Reflexes, Streptozotocin

ORAL PRESENTATION

The impact of gamma rays on soybean germination and seedlings

Cenk Burak Şahin[1] (ORCID: https://orcid.org/0000-0001-6270-8184)
Mustafa Yılmaz[2*] (ORCID: https://orcid.org/0000-0002-1816-0729),

[1]Hatay Mustafa Kemal University, Faculty of Agriculture, Department of Field Crops, Hatay, Türkiye.
[*2]Texas A&M AgriLife Research, Lubbock, TX 79403, USA

*Corresponding author e-mail: mustafayilmaz80@hotmail.com

Abstract

Mutation breeding in soybean (*Glycine max* L. Merr.) is a promising strategy to develop novel and superior varieties by enhancing genetic variation. Gamma radiation, as a physical mutagen, is widely employed in this process. However, determining the optimal mutagen dose is crucial; therefore, this study investigated the effects of gamma radiation on two soybean cultivars, Adel and Lider. Seeds were exposed to Co-60 gamma ray doses ranging from 0 Gy (control) to 500 Gy. The objective was to assess the impact of varying radiation doses on early growth —including germination rate, seedling growth traits, and biomass — parameters in the M1 generation and to determine the optimal dose for mutation breeding by evaluating lethal dose (LD50) and growth reduction (GR50) values. The results demonstrated a significant dose-dependent inhibitory effect on all measured traits. For instance, at 500 Gy, germination percentage and dry weight were reduced to 34.7% and 25.2% of the control, respectively. The LD50 for germination was estimated between 300-400 Gy, while the GR50 for seedling growth was around 300 Gy. In conclusion, the 200-300 Gy dose range is recommended as optimal for soybean mutation breeding, effectively balancing mutation induction with acceptable plant survival and growth.

Keywords: Gamma rays, growth reduction, lethal dose, soybean

ORAL PRESENTATION

Comperative analysis of three genomic DNA isolation methods in *Simulium bezzii*

Kübra NEDİNÇ [1], Ebru Ceren FİDAN [2*] (ORCID: https://orcid.org/0000-0002-6121-4585)

[*1] Eskişehir Osmangazi University, Faculty of Science, Department of Biology, Eskişehir, Türkiye.

*Corresponding author e-mail: ebruceren@ogu.edu.tr

Abstract

From past to present, many taxonomic, biogeographic, physiological, and ethological studies have been conducted on insects. Today, these studies have shifted to faster methods and have been reduced to the molecular level. The use of insect DNA in gene and gene expression studies has become widespread and is frequently applied to all insect groups. Early detection and monitoring of economically significant pests is critical to prevent their spread and establishment in valuable commercial products. To achieve this, fast and accurate species identification tools are required. The most crucial step of rapid techniques such as DNA barcoding is the acquisition of high-quality and high-concentration genomic DNA. Based on this, many different methods have been developed for genomic DNA isolation. Obtaining dense and high-quality DNA is also one of the important factors for the studies to be conducted. In this study, different DNA isolation methods frequently applied in the literature were compared using the species *Simulium bezzii*, known to be a vector of many diseases, and it was investigated which method yielded genomic DNA at higher concentrations. Three different isolation methods were evaluated: a manual isolation method, a low-cost commercial kit, and a high-cost commercial kit. After isolation, the concentrations of both total DNA and the products of the mtCOI gene region amplified by PCR were measured using a Nanodrop device. The comparison of the obtained data revealed that the highest yield in total DNA acquisition was achieved with the manual method, followed by the high-cost commercial kit, and finally the low-cost commercial kit. The concentration measurements of PCR products did not show a significant difference among the groups. These results suggest that the manual isolation method may be a suitable alternative for obtaining high-quality genomic DNA from the species *Simulium bezzii* in terms of cost and efficiency. Additionally, it was understood that PCR success could occur at a similar level regardless of the isolation method chosen.

Keywords: Genomic DNA, Isolation, Method, DNA barcoding, *Simulium bezzii*

ORAL PRESENTATION

Synergistic effects of ruxolitinib and *Liquidambar orientalis* extract on MDA-MB-231 breast cancer cells

Enes Aytar[1], Kader Ekran[2], Esin Guvenir Celik[1*(]
ORCID: https://orcid.org/0000-0002-3368-9700), Onur Eroglu[1] (ORCID: https://orcid.org/0000-0002-3451-8540)

[*1] Department of Molecular Biology and Genetics, Faculty of Science, Bilecik Seyh Edebali University, Bilecik, Turkey.
[2] Department of Molecular Biology and Genetics, Institute of Graduate Education, Bilecik Seyh Edebali University, Bilecik, Turkey.

*Corresponding author e-mail: esin.guvenir@bilecik.edu.tr

Abstract

Breast Cancer (BC) is a leading cause of global cancer mortality, characterized by significant heterogeneity. The highly invasive MDA-MB-231 cell line, an in vitro TNBC model, relies on the constitutive activation of the JAK/STAT pathway for proliferation and apoptosis resistance. Although the JAK inhibitor Ruxolitinib is known to suppress STAT3 phosphorylation, inhibit tumor progression, and induce apoptosis in MDA-MB-231 cells, and Liquidambar orientalis extract exhibits independent anticancer properties, the synergistic effect of their combination in this cell line remains unelucidated. Therefore, this study aims to investigate the synergistic anticancer potential of combining Ruxolitinib and Liquidambar orientalis extract by examining their in vitro effects on apoptotic mechanisms in MDA-MB-231 cells. MDA-MB-231 cells were cultured. The drug doses were determined by MTT analysis. Cellular migration capacity was assessed using a wound healing assay. The DNA laddering assay was utilized to evaluate DNA fragmentation, a hallmark of apoptosis. Cell viability analyses showed that while both agents alone reduced viability, the combination group demonstrated a more pronounced reduction, suggesting a synergistic or additive effect. The wound healing assay revealed significantly suppressed cell migration in the treated groups, demonstrating that the agents effectively inhibited cellular motility and reduced metastatic potential. Furthermore, the combination treatment led to the formation of characteristic DNA ladder structures, confirming active induction of apoptosis. The combination of Ruxolitinib and *Liquidambar orientalis* demonstrates potent antiproliferative, anti-metastatic, and pro-apoptotic effects in MDA-MB-231 cells, suggesting its potential as an adjuvant therapeutic option for TNBC. This study offers a scientific contribution to developing new therapeutic strategies. Further investigation into the underlying molecular mechanisms is recommended through advanced gene expression, protein level, and signaling pathway analyses.

Keywords: MDA-MB-231**,** Ruxolitinib**,** *Liquidambar orientalis*, Apoptosis

ORAL PRESENTATION

Lilium akkussianum and conservation priorities for Turkey's endemic *Lilium* Species: Habitat requirements and threat analysis

Hakan Yılmaz (Orcıd: https://orcid.org/0000-0002-0113-8277)

Ordu University, Akkuş Vocational School, Environmental Health and Environmental Risk Management Technician Program

Corresponding author e-mail: hakanyilmaz@odu.edu.tr

Abstract

Turkey is an important biodiversity hotspot, home to many endemic species of the genus *Lilium*. This review aims to evaluate the ecological requirements, habitat preferences, and threats faced by the species *Lilium akkussianum*, which has a limited distribution, in light of the current scientific literature. The assessments revealed that *L. akkussianum* exhibits high sensitivity to microhabitat parameters such as light intensity, soil moisture content, and pH level. The fact that its populations are mostly concentrated in isolated and narrow localities makes the species highly vulnerable to habitat destruction. Increasing agricultural activities, infrastructure works (road construction), mining operations, and microclimatic disturbances caused by global climate change in the region stand out as key anthropogenic factors threatening the species' sustainability. Comparisons with other *Lilium* species in Turkey demonstrate the critical importance of ecological niche modeling and long-term population monitoring programs in conservation prioritization efforts. This review provides a science-based framework for developing effective conservation strategies applicable both to *L. akkussianum* specifically and to endemic *Lilium* species in general.

Keywords: *Lilium akkussianum*, endemism, conservation biology, habitat analysis, ecological niche, threat assessment.

ORAL PRESENTATION

From chromatogram to confirmation: Advanced detection of VX nerve agent and related compounds

Havva Bekiroğlu Ataş[1*] (ORCID: 0000-0002-4829-6969), Muharrem Cenk[1] (ORCID: 0000-0001-8547-7999), Nurgül Özcan[1](ORCID: 000-0003-0305-8024)

[*1]General Directorate of Public Health, National Public Health Reference Laboratory, Ankara, Türkiye

*Corresponding author e-mail: havvabekiroglu@gmail.com

Abstract

Chemical warfare agents (CWAs) are toxic chemicals developed for conflict that pose serious threats to global security and public health. VX, or Ethyl S-2-diisopropylaminoethyl methylphosphonothiolate, is a highly toxic nerve agent and one of the most lethal CWAs, classified as a Schedule 1.A.03 chemical under the Chemical Weapons Convention (CWC). To enforce the CWC, the Organisation for the Prohibition of Chemical Weapons (OPCW) conducts proficiency tests (PTs) as international exercises to verify laboratories' analytical capabilities in detecting such agents. This study aimed to identify VX and possible related compounds in environmental samples using advanced analytical techniques such as multimodal mass spectrometric confirmation. In this study, we implemented a comprehensive analytical strategy to identify and confirm the nerve agent VX and structurally related compounds. We employed a multi-technique approach combining gas chromatography–mass spectrometry with electron ionization and chemical ionization (GC-EI/MS, GC-CI/MS) and liquid chromatography–electrospray ionization tandem mass spectrometry (LC-ESI-MS/MS). Sample preparation included selective derivatization (e.g. trimethylsilylation) to enable GC-MS analysis of polar organophosphorus analytes, while direct LC-MS/MS was applied for confirmatory analysis. In the context of the OPCW's 55th Proficiency Test (PT-55), VX and several key degradation or reaction products – methylphosphonic acid, ethyl methylphosphonate, 2-(N,N-diisopropylamino)ethanesulfonic acid, bis(2-N,N-diisopropylaminoethyl)disulphide, S-2-Diisopropylaminoethyl methylphosphonothiolate, O-Ethyl methylphosphonothiolate, and 2-(N,N-Diisopropylamino)ethanol – were successfully detected and confirmed in full compliance with OPCW validation criteria. This work demonstrates methodological rigor and analytical innovation in support of the CWC verification framework. The successful confirmation of VX and its analogues – compounds of great concern due to their extreme toxicity and prohibition – highlights the critical role of advanced chromatography–mass spectrometry techniques in upholding international non-proliferation agreements. Accurate chemical identification and confirmation not only ensure compliance with the CWC but also strengthen global trust in verification regimes by providing unequivocal evidence needed for enforcement and attribution.

Keywords: Chemical warfare agents, VX nerve agent, chromatography, mass-spectrometry.

ORAL PRESENTATION

Investigation of programmed cell death during larval-pupal metamorphosis on the posterior silk gland of the *Galleria mellonella*

Esen Poyraz-Tinartas (ORCID: https://orcid.org/0000-0001-7386-2136)

Manisa Celal Bayar University, Engineering and Natural Sciences Faculty, Biology Department, Manisa, Türkiye.

Corresponding author e-mail: esen.poyraz@cbu.edu.tr

Abstract

The posterior silk gland is the part of the silk gland that synthesizes the main silk protein, fibroin, in the abdominal cavity of the larva and degenerates under physiological conditions during larval pupal metamorphosis in Lepidopteran. Degeneration of larval-specific tissues and organs occurs via programmed cell death, apoptosis and autophagy, under the control of the endocrine system. Developmental alterations and specific markers of autophagic and apoptotic cell death mechanisms of posterior silk gland were investigated during the larval-pupal metamorphosis from the first day of the last larval stage until the 36th hour of the pupal stage. In this process, morphological examinations were investigated by phase contrast microscopy and routine histological techniques under light microscope. For autophagic cell death, determination of lysosomal acid phosphatase enzyme activity, expression profiles of marker genes, ATG6 and ATG8, by qRT-PCR, and determination of localization and density of lysosomes with Lyso-Tracker, a lysosomal marker dye, were used. Specific marker of apoptosis was investigated by TUNEL method. The effects of the insect hormone 20HE, known to be the main factor in the initiation of programmed cell death, were determined by the western blotting method of the receptor isoform of ecdysone, EcR-B1, and it was determined that EcR-B1 was predominantly produced in the posterior silk gland.
The results show that although autophagy mainly plays a protective role for the cell, if it proceeds unhindered above a certain threshold value, it can lead to the stimulation of the expression of cell death markers and activation of the apoptotic pathway, and that ecdysone plays a role in the process via the EcR-B1 isoform.

Keywords: ATG6, ATG8, apoptosis, autophagy, EcR-B1, *Galleria mellonella*.

*This study was financially supported by Manisa Celal Bayar University Research Projects Coordination Unit. Project number: 2018-039.

ORAL PRESENTATION

Synthesis of new triazoles as acetylcholinesterase inhibitors

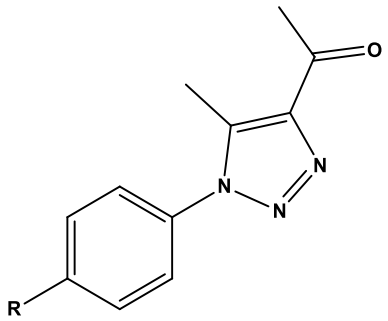
Mehmet Erşatır[1*] (Orcid: https://orcid.org/0000-0003-1077-0626), İpek Akdöner[1] (ORCID: https://orcid.org/0009-0009-5418-1066)

[*1]Çukurova University, Faculty of Art and Science, Department of Chemistry, Adana, Türkiye.

*Corresponding author e-mail: mersatir@cu.edu.tr

Abstract

Alzheimer's disease is a neurodegenerative disorder that causes progressive damage to the brain. It is the most common type of dementia. The number of dementia/Alzheimer's cases is expected to reach around 140 million by 2050 (WHO, 2025). Triazole hybrids represent a promising frontier in medicinal chemistry, with their ability to integrate diverse pharmacophores into a single scaffold offering a powerful strategy for drug design. As research advances, the development of multifunctional triazole-based hybrids is anticipated to address major global health challenges, particularly in combating antimicrobial resistance, cancer heterogeneity, and chronic inflammatory diseases (Avuthu et al., 2025; El-Lateef et al., 2025). In this study, five new triazole compounds were synthesized in high yields, and their characterizations were carried out using FTIR, ^{1}H NMR, and ^{13}C NMR techniques (Figure 1). The interactions of the synthesized compounds with AChE and MRSA-associated proteins (4EY7, 1ZGC, and 3ZG5) were determined through molecular docking studies. According to the obtained results, the compounds were found to exhibit strong interactions with the specified proteins.



R: NO_2, Br, Cl, OH, OC_2H_5

Figure 1. General structure of 1-(5-methyl-1-(4-substituephenyl)-1*H*-1,2,3-triazol-4-yl)ethanones

Keywords: triazoles, synthesis, Alzheimer, demans, molecular docking, AChE inhibition.

*This study was supported Scientific Research Committee of Çukurova University (grant number: 18238).

References:

Avuthu, V. S. R., Allaka, T. R., Kushwaha, N., & Kishore, P. V. V. N. (2025). Efficient Synthesis, Anticancer Evaluation of Triazole-Thiadiazole/Benzo[d]Oxazole Scaffolds, and Investigation ofTheir Reactivity Properties Using Density-Functional Theory Calculations and In Silico Docking. *Chemistry and Biodiversity*. https://doi.org/10.1002/cbdv.202402470

El-Lateef, H. M. A., Khalaf, M. M., Gouda, M., Ismail, A. F., Gad, M. A., Nazreen, S., Amer, A. A., AL-Ghamdi, S., Ibrahim, T. M. A., & Abdelhamid, A. A. (2025). Functionalized triazoles: Design, synthesis and chemical characterization of 1,2,3-triazolylmethylthio-1,3,4-oxadiazole derivatives as insecticidal and antibacterial agents. Journal of the Indian Chemical Society, 102, 101578. https://doi.org/10.1016/j.jics.2025.101578

Demantia. [(accessed on 1 Dec 2025)]. Available online: https://www.who.int/news-room/fact-sheets/detail/dementia

ORAL PRESENTATION

The effects of microplastics on soil and plant ecophysiology: Current findings on pollutant transfer from source to plant

Hakan Yılmaz[1*] (Orcid: https://orcid.org/0000-0002-0113-8277),
Burcu Demirel Yılmaz[1] (Orcid: https://orcid.org/0000-0003-4095-1743)

Ordu University, Akkuş Vocational School, Environmental Health and Environmental Risk Management Technician Program

*Corresponding author e-mail: hakanyilmaz@odu.edu.tr

Abstract

Microplastic pollution has been identified as a significant environmental threat that has rapidly increased in both terrestrial and agricultural ecosystems over the past decade. This review systematically analyzes current research on the effects of microplastics on soil physical properties, microbial activity, water movement, and plant root development. The potential of different polymer types, particularly polystyrene, to loosen soil structure, alter porosity, and disrupt aggregate stability has been clearly demonstrated by data from the literature. Furthermore, the uptake of microplastics by plants through their roots, their transport via xylem and phloem, whether they reach leaf tissues, and the changes they cause in physiological processes (photosynthesis, stomatal behavior, nutrient content) have been evaluated in detail based on current studies. The finding that the interaction between salinity and microplastics creates synergistic stress and can increase yield loss, particularly in agricultural production, is an important component of the review. In conclusion, it is understood that the effects of microplastics on plant health, soil functions, and food safety will play a decisive role in shaping future agriculture–environment policies.

Keywords: Microplastics, soil ecology, plant ecophysiology, polystyrene, salinity stress, environmental risk.

ORAL PRESENTATION

Newly developed bio-oil-interacted cellulose acetate micro-structured composite adsorbent for efficient dye removal

Bülent Buyukkidan[1] (https://orcid.org/0000-0001-9619-3246), Huseyin Gumus[2*] (https://orcid.org/0000-0002-2029-7978), Sedat Comez[1] (https://orcid.org/0009-0004-7772-6114), Alaa Zaaroura[1] (https://orcid.org/0009-0007-7868-339X)

[1]Kutahya Dumlupinar University, Department of Chemistry, Kutahya, Turkey
[2]Bilecik Seyh Edebali University, Osmaneli Vocational School, Bilecik, Turkey

*Corresponding author e-mail: huseyin.gumus@bilecik.edu.tr

Abstract

In many filtration systems, the accumulation of contaminants on membrane surfaces significantly restricts both permeation and separation efficiency, highlighting the necessity for advanced functional materials. Consequently, research efforts increasingly focus on the development of highly efficient, durable, and cost-effective polymeric composite membranes. In this study, bio-oil—an organic mixture enriched with phenolic binders and produced through the controlled pyrolysis of carbon-based materials—was incorporated into cellulose acetate membranes for the first time by blending it into a 15% CellA solution in DMAC to enhance membrane performance. CellA-based biocomposite membranes containing 5%, 10%, 20%, and 40% bio-oil were fabricated via phase inversion in a water bath, resulting in micro-size composite structures. The crystalline features, molecular interactions, and surface morphologies of the membranes were investigated using FT-IR and SEM analyses. Additionally, water uptake values were determined to assess hydrophilicity. The adsorption performance of the composites was evaluated in batch mode using 0.1–1 g of material in 5–80 ppm methylene blue solutions. The effects of temperature, adsorbent dosage, dye concentration, and pH on removal efficiency were systematically examined. Increasing bio-oil content was found to alter the membrane morphology and significantly improve adsorption-driven dye removal. Temperature was observed to have no substantial effect on adsorption efficiency, whereas the optimal adsorbent dosage was identified as 0.5 g. Under these optimized conditions, dye removal efficiencies ranging from 60% to 90% were achieved depending on the composite formulation. Overall, the successful fabrication and characterization of these micro-sized CellA/bio-oil composites demonstrate their strong potential as sustainable and high-performance filtration materials, offering improved foulant interaction and enhanced adsorption capabilities compared to conventional cellulose acetate membranes.

Keywords: Cellulose acetate, Bio-oil, Composite membranes, Methylene blue

“This study was derived from the master’s thesis titled “Biyokütle Piroliz Ürünü Katkılı Polimerik Kompozitlerin Fizikokimyasal ve Boya Giderimi Özelliklerinin Araştırılması”.

ORAL PRESENTATION

Eco-friendly synthesis of selenium nanoparticles using *Leptolyngbya* sp.: Physico-chemical characterization and bioactivity assessment

Emine Çelikoğlu[1,2]* (ORCID:https://orcid.org/0000-0002-5956-0008)

[1]Amasya University, Faculty of Arts and Sciences, Department of Biology, Amasya, Türkiye
[2]Amasya University, Faculty of Education, Department of Mathematics and Science Education, Amasya, Türkiye

*Corresponding author e-mail: emine.turk@amasya.edu.tr

Abstract

Selenium is an essential trace element involved in antioxidant defense and numerous physiological processes [1]. Selenium nanoparticles (SeNPs) have gained increasing attention due to their enhanced bioactivity, improved biocompatibility, and generally lower toxicity compared to bulk selenium [2]. Biogenic SeNPs, typically capped and stabilized by proteins, polysaccharides, and phenolic compounds, often display superior colloidal stability and biological performance relative to chemically synthesized nanoparticles [3,4]. In this study, SeNPs were synthesized via an eco-friendly method using an ethanolic extract of the cyanobacterium *Leptolyngbya* sp., and their physicochemical properties and biological activity were evaluated. UV–Vis spectroscopy confirmed nanoparticle formation, revealing a characteristic absorption band at 265–285 nm. FTIR analysis revealed the presence of biomolecules responsible for reducing and stabilizing selenium ions. SEM imaging revealed the formation of predominantly rod-like, aggregated structures ranging from nanometer- to lower micrometer-scale assemblies. The synthesized SeNPs exhibited potent antibacterial activity against *Staphylococcus aureus* ATCC 25923, while showing moderate or limited effects on *Escherichia coli* ATCC 25922 and *Candida albicans* ATCC 10231. Additionally, the nanoparticles demonstrated notable antioxidant capacity, likely due to bioactive capping agents provided by *Leptolyngbya* sp., which have been reported to enhance biological functionality in biogenic nanomaterials [3]. Overall, *Leptolyngbya* sp. proved to be a promising and sustainable biological platform for the green synthesis of SeNPs. The resulting nanoparticles, exhibiting potent antioxidant and selective antibacterial properties, represent promising candidates for future biomedical and agricultural applications.

Keywords: Selenium nanoparticles; Green synthesis; *Leptolyngbya* sp.; Antibacterial activity; Antioxidant properties

*The authors are thankful to Amasya University for their contributions and financial support provided by BAP (Project No: FMB-BAP 23-0602).

References:

[1] Rayman, M. P. (2012). Selenium and human health. *The Lancet*, *379*(9822), 1256-1268.
[2] Hatfield, D. L., Berry, M. J., & Gladyshev, V. N. (Eds.). (2011). *Selenium: its molecular biology and role in human health*. Springer Science & Business Media.
[3] Menon, S., KS, S. D., Agarwal, H., & Shanmugam, V. K. (2019). Efficacy of biogenic selenium nanoparticles from an extract of ginger towards evaluation on anti-microbial and anti-oxidant activities. *Colloid and Interface Science Communications*, *29*, 1-8.
[4] Srivastava, N., & Mukhopadhyay, M. (2015). Green synthesis and structural characterization of selenium nanoparticles and assessment of their antimicrobial property. *Bioprocess and biosystems engineering*, *38*(9), 1723-1730.

ORAL PRESENTATION

Dye removal efficiency of bio-oil reinforced flat-sheet cellulose acetate composites as potential membrane materials

Bülent Buyukkidan[1*] (https://orcid.org/0000-0001-9619-3246), Huseyin Gumus[2*] (https://orcid.org/0000-0002-2029-7978), Sedat Comez[1] (https://orcid.org/0009-0004-7772-6114)

[1]Kutahya Dumlupinar University, Department of Chemistry, Kutahya, Turkey
[2]Bilecik Seyh Edebali University, Osmaneli Vocational School, Bilecik, Turkey

*Corresponding author e-mail: bulent.buyukkidan @dpu.edu.tr

Abstract

Polymeric membrane materials are still the most preferred structures for water filtration and purification due to their affordability and ease of preparation. However, numerous studies are ongoing to improve their physical and chemical resistance and performance. Efficiency can be increased by adjusting the structure's durability and porosity with organic and inorganic additives. In this study, bio-oil, a biomass carbonization product, was first added to cellulose acetate by mixing it with a 15% CA solution in DMAC. To prepare the composites, the polymer solutions were spread on a glass surface using a 250-micron casting knife, and the films were then placed in a water bath for phase inversion, resulting in flat-sheet CA/bio-oil composites containing 5%, 10%, 20%, and 40% bio-oil. The structural properties and surface features of the materials were analyzed using FT-IR and SEM. Water uptake and porosity% values were also measured to understand changes in hydrophilicity. Adsorption experiments were carried out in batch mode using 0.1–0,75 g of composite cut 1*1 cm in methylene blue solutions ranging from 10-80 ppm. The effects of temperature, adsorbent amount, solution concentration, and pH on dye removal were also studied. Higher bio-oil content changed the surface structure of the composites and improved their ability to remove dye through adsorption. The best adsorption efficiency was achieved at room temperature, while the optimal adsorbent amount was found to be 0.5 g in batch conditions. Under these optimum conditions, the composites achieved dye removal values of 40-85%, varying with the change in bio-oil ratio. Overall, the flat-sheet CellA/bio-oil composites are promising materials for continuous filtration systems, and their performance can be tested and potentially used as membrane structures.

Keywords: Cellulose acetate, Bio-oil, Biomass Carbonization, Filtration membranes, Methylene blue

ORAL PRESENTATION

Synthesis and antioxidant properties of potential dual-acting acetylcholinesterase inhibitors

Ozan Çobanoğlu[1] (https://orcid.org/0009-0003-0003-3806), Sevinç İlkar Erdağı[1*] (https://orcid.org/0000-0001-5811-2302), Neslihan Şaki[1*] (https://orcid.org/0000-0002-2215-1622), Mustafa Akın[2] (https://orcid.org/0000-0003-4268-6891)

[1]Department of Chemistry, Faculty of Arts and Sciences, Kocaeli University, Kocaeli 41001, Turkey
[2] Department of R&D, Petroyağ ve Kimyasallar San. Ve Tic. A.Ş., Gebze-Kocaeli, Turkey
*Corresponding author e-mail: sevinc.ilkar@kocaeli.edu.tr, neslihansaki@kocaeli.edu.tr

Abstract

Alzheimer's disease (AD) is a progressive neurodegenerative disorder that affects cognitive functions worldwide, leading to memory impairment and behavioral changes. Although currently available medications provide symptomatic relief, they are ineffective at preventing disease progression. The pathogenesis of AD involves multiple mechanisms, including amyloid-β (Aβ) plaque accumulation, hyperphosphorylation of tau proteins, oxidative stress, and cholinergic dysfunction [1]. Among these, the cholinergic hypothesis, which proposes that reduced levels of acetylcholine (ACh) in the brain are a major contributor to AD symptoms, remains one of the most widely accepted models for therapeutic intervention. In recent years, efforts toward the development of multi-target-directed ligands (MTDLs) that combine acetylcholinesterase (AChE) inhibition with additional neuroprotective properties, such as antioxidant and anti-inflammatory activities, have significantly increased [2]. In this context, hybrid molecules that integrate distinct pharmacophores into a single scaffold have emerged as promising therapeutic candidates. Phenolic compounds such as caffeic, vanillic, and ferulic acids attract particular interest due to their well-documented antioxidant activities and favorable safety profiles [3-4]. In the present study, a series of hybrid molecules was designed and synthesized by combining the *N*-benzylpiperidine pharmacophore of Donepezil, an established AChE inhibitor, with phenolic acids possessing antioxidant characteristics. The antioxidant capacities of the compounds were evaluated using DPPH radical scavenging and ferric reducing power assays, identifying isovanillic acid-*N*-benzylpiperidine as the molecule with the strongest antioxidant activity (Fig. 1). Based on these findings, future studies will focus on expanding the biological evaluation of these novel hybrid molecules, including butyrylcholinesterase (BuChE) selectivity and cell-based assays to better explain their therapeutic potential in targeting both AChE inhibition and oxidative stress in AD.

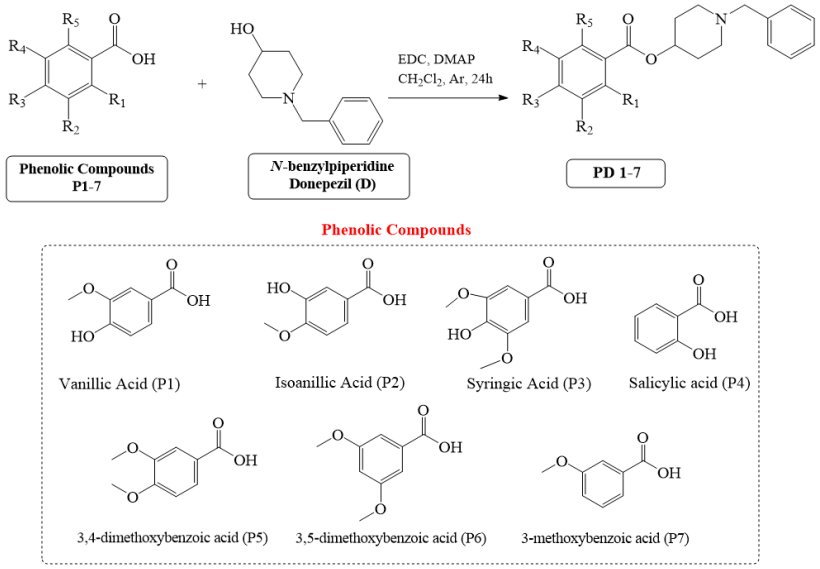


Fig-1. General synthetic strategy for the preparation of *N*-benzylpiperidine-phenolic acid conjugates

Keywords: Alzheimer's Disease, acetylcholinesterase, donepezil, phenolic acid, antioxidant activity

References:

[1] S. Rai, V.K. Singh, I. Ahmad, M. Agrawal, R.K. Singh, Design, synthesis, molecular docking, DFT analysis, dynamics simulation, and cytotoxicity evaluation of coumarin derivatives as acetylcholinesterase (AChE) inhibitors against alzheimer's disease, J. Mol. Struct. 1329 (2025) 141436.
[2] W.-B. Zang, H.-L. Wei, W.-W. Zhang, W. Ma, J. Li, Y. Yao, Curcumin hybrid molecules for the treatment of Alzheimer's disease: structure and pharmacological activities, Eur. J. Med. Chem. 265 (2024) 116070.
[3] R. Khokar, K. Hachani, M. Hasan, F. Othmani, M. Essam, A. Al Mamari, D. UM, S. A. Khan, Anti-alzheimer potential of a waste by-product (peel) of Omani pomegranate fruits: quantification of phenolic compounds, in-vitro antioxidant, anti-cholinesterase and in-silico studies, Biocatal. Agric. Biotechnol. 38 (2021) 102223.
[4] Z.-Y. Zhang, S.-T. Han, J.-L. Hu, P.-h. Hu, R. He, Y.-Y. Cao, D.-H. Shi, Anti-Alzheimer's disease properties of vanillic acid-thiazole hybrids: synthesis, characterization, and biological evaluation, J. Mol. Struct. 1328 (2025) 141378.

ORAL PRESENTATION

Synthesis of the various macro initiator for production of the blok/graft copolymers via "living"/controlled radical polymerization (CRP) techniques

Melahat Göktaş

Van Yüzüncü Yıl University, Faculty of Education, Department of Chemistry, Van, 65080 Turkey

Corresponding author: e-mail: melahat_36@hotmail.com

Abstract

Recently, the production of block/graft copolymers with controlle molecular weight and low dispersity has increased with the emergence of controlled radical polymerization (CRP) techniques such as reversible addition/fragmentation chain transfer (RAFT) [1], atom transfer radical polymerization (ATRP) [2], nitroxide-mediated polymerization (NMP) [3], which are based on radical polymerization and radical closure mechanism. In here, the various block/graft copoymers was obtained using macro initiator by CRP. These macro initiator which having active centers was synthesized via condensation, ring-opening, and redox polymerizations of the various monomers. Thanks to these active centers, copolymers were obtained by polymerizing various monomers with either ATRP or RAFT polymerization using these initiators. The novel macromolecules could be obtained by combining different monomers in the same polymer chain with both these active-center macroinitiators and CRP techniques. By combining such different polymerization techniques, block/graft copolymer synthesis in one step or through different steps could make a great contribution to polymer chemistry and polymer technology.

Keywords: Macro initiator; block/graft copolymers; condensation polymerization; ring- opening polymerization; redox polymerization.

References:

Chiefari J, Chong YK, Ercole F, Krstina J, Jeffery J, Le TPT, Mayadunne RTA, Meijs GF, Moad CL, Moad G, Rizzardo E, Thang SH (1998). *Macromolecules* 31:5559-5562.
Wang JS, Matyjaszewski K (1995), *Macromolecules* 28:7901-7910.
Maric M, (2021), Can J Chem Eng. 99:832–852.

ORAL PRESENTATION

Development of nanoparticle based approaches for the conservation of some paper artifacts

Hakan Serbest (Orcid: https://orcid.org/0000-0003-2303-0408)

Mimar Sinan Fine Arts University, School of Conservation and Restoration of Cultural Property, Department of Conservation and Restoration of Cultural Property, İstanbul, Türkiye.

Corresponding author e-mail: hakan.serbest@msgsu.edu.tr

Abstract

Nanoparticles (NPs) fabricated from inorganic/organic compounds are nano-scale structures with high porosity and numerous active sites with high binding capacity on their surfaces. Thanks to these properties, NPs are utilized in many research fields. The conservation of cultural heritage is an important field of research that offers opportunities for the use of nanoparticles in preservation of the originality of constructions and artifacts that have a place in the historical development of humanity. Over time, the chemical or physical resistance and structural integrity of artifacts such as metal, paper, wood, and stone are constantly threatened by degradation factors depending on environmental conditions. Hence, the need for innovative materials such as NPs, which can penetrate deep into damaged artifacts due to their particle size, has emerged in the field of conservation and restoration. Since it has been reported that paper-based artifacts become deteriorated over time due to factors such as moisture, oxidation, acid degradation, bacteria, and fungi, nanotechnology applications may provide a good alternative for direct and effective protection against the deterioration of paper-based artifacts. In this presentation, the experimental studies on the NPs synthesized for the conservation of some paper-based historical artifacts and their application/effect mechanisms have been evaluated.

Keywords: Nanoparticles, cultural heritage, synthesis

ORAL PRESENTATION

Broussonetia papyrifera'dan yeni tanımlanan 1,3-difenilpropanların asetilkolinesteraz enzimi üzerindeki inhibitör etkilerinin *in-silico* olarak incelenmesi

Sait SARI* (ORCID: https://orcid.org/0000-0003-2559-1938)

*Kocaeli Üniversitesi, Fen Edebiyat Fakültesi, Kimya Bölümü, Kocaeli, Türkiye

*Sorumlu yazar e-mail: sait.sari@kocaeli.edu.tr

Özet

Alzheimer hastalığı (AH) çoğunlukla yaşlı insanları etkileyen nörodejeneratif bir hastalıktır. Bu hastalık hafıza kaybı, ruh hali bozuklukları, depresyon ve bilişsel yeteneklerin ilerleyici kaybı ile karakterize edilmektedir [1]. Alzheimer hastalığının kökenini açıklamak için tau protein hiperfosforilasyonu, beta-amiloid agregasyonu ve kolinerjik hipotez gibi bazı teoriler öne sürülmüştür [2]. Bu teoriler arasında kolinerjik hipotez, nörotransmitter asetilkolin (ACh) seviyelerinin azalmasının AH'nin nedeni olduğu ve beyindeki ACh seviyelerinin artmasının AH tedavisi için hayati önem taşıdığını öne süren ve en yaygın kabul gören teoridir [3]. Asetilkolinesteraz (AChE), kolinesteraz ailesinden bir enzimdir. AChE, ACh'nin hızlı hidrolizini katalize ederek ACh seviyelerini düşürür ve kolinerjik sinapslarda impuls iletiminin sonlandırılmasına neden olur. Kolinerjik hipoteze göre AChE enziminin inhibisyonu azalan ACh seviyelerini düzenleyerek Alzheimer hastalığının tedavisinde etkili olmaktadır [4]. Bu çalışmada Guo ve çalışma arkadaşları tarafından *Broussonetia papyrifera* bitkisinden izole edilip literature yeni kazandırılan beş 1,3-difenilpropan türevi doğal molekülün [5] AChE enzimi ile etkileşimleri moleküler kenetleme yöntemi kullanılarak incelendi ve standart ilaç Donepezil ile karşılaştırıldı. Moleküler kenetleme yöntemi sonuçlarına göre standart ilaç Donepezil -10,92 kcal/mol bağlanma serbest enerjisi ile AChE aktif bölgesi ile etkileşti. 1,3-difenilpropan türevleri ise -9,92 ila -11,08 kcal/mol bağlanma serbest enerjileri ile AChE aktif bölgesi ile etkileşim gösterdi. Bu sonuçlar bu doğal ürünlerin Alzheimer tedavisinde kullanılması için umut verici olduğunu gösterdi.

Anahtar Kelimeler: Alzheimer hastalığı, Moleküler kenetleme, Asetilkolinesteraz, Doğal Ürünler

Kaynaklar:

Alzheimer's Association. Alzheimer's disease facts and figures. Alzheimers Dement. 2017;2017:325-73.
Querfurth HW, LaFerla FM. Alzheimer's disease. N Engl J Med. 2010;362:329-44
Dumas JA, Newhouse PA. The cholinergic hypothesis of cognitive aging revisited again: cholinergic functional compensation.Pharmacol Biochem Behav. 2011;99:254-61
Rashid U, Ansari FL. Challenges in designing therapeutic agents treating Alzheimer's disease-form serendipity to rationality. Drug Design Discovery in Alzheimer's Disease. Elsevier; 2015
Guo T, Wang Q, Peng C, Zhang X, Huang K, Wang K, He H, Li M. Five undescribed 1,3-diphenylpropanes from the leaves of *Broussonetia papyrifera*. Phytochem. Lett. 2025;70, 104045.

ORAL PRESENTATION

Pharmacological uses of species belonging to the Lamiaceae family on the campus of Uşak University

Tevfik İlker Demir[1*] (Orcid: https://orcid.org/0009-0000-1485-8049), Ahmet Ganci[2] (Orcid: https://orcid.org/0009-0004-2877-1066), Ahmet Kahraman[3] (Orcid: https://orcid.org/0000-0002-9344-1993)

[*1] Uşak University, Faculty of Engineering and Natural Sciences, Department of Molecular Biology and Genetics, Uşak, TÜRKİYE
[2] Uşak University, Faculty of Engineering and Natural Sciences, Department of Molecular Biology and Genetics, Uşak, TÜRKİYE
[3] Uşak University, Faculty of Engineering and Natural Sciences, Department of Molecular Biology and Genetics, Uşak, TÜRKİYE

*Corresponding author e-mail: tevfikilker.064@gmail.com

Abstract

The Lamiaceae family is one of the richest families, containing over 7,000 species. It is distributed in various environmental conditions across different regions of Turkey. Members of this family are also of considerable importance for medicinal use. This study compiles information on the pharmacological properties of selected species belonging to the family, the level of antimicrobial activity of these species, and the diseases they combat.

Keywords: Lamiaceae, Medical Pharmacology, Uşak, Türkiye

Acknowledgments: This study was financially supported by the Scientific Research Projects Coordination Unit of Uşak University (FBA-2025-685) and the Scientific and Technological Research Council of Turkey (TÜBİTAK) under the 2209-A University Student Research Projects programme (project no: 1919B012471389).

ORAL PRESENTATION

Synthesis and tyrosinase inhibition of 1-(4-fluorobenzyl)piperazine-based dithiocarbamates

Merve Zengin[1*] (ORCID:https://orcid.org/0000-0003-1586-5448), Esin Akdemir Yılmaz[1] (ORCID:https://orcid.org/0009-0000-9825-5607), Gözde Girgin[2] (ORCID:https://orcid.org/0000-0002-7051-0490), Suna Sabuncuoğlu[2] (ORCID: https://orcid.org/0000-0002-9702-4214), Oya Ünsal Tan[1] (https://orcid.org/0000-0002-4152-069X)

[*1] Hacettepe University, Faculty of Pharmacy, Department of Pharmaceutical Chemistry, Ankara, Türkiye
[2] Hacettepe University, Faculty of Pharmacy, Department of Pharmaceutical Toxicology, Ankara, Türkiye

*Corresponding author e-mail: merveozdagli@hacettepe.edu.tr

Abstract

Melanin is a natural biological pigment that plays a fundamental role in the pigmentation process of the human body. It contributes to the pigmentation of various tissues, including the skin, hair, and eyes, and protects the skin against the harmful effects of ultraviolet radiation. However, excessive melanin production and accumulation can lead to several dermatological disorders, such as freckles, pigmented acne, melasma, and age spots, and may even increase the risk of malignant melanoma [1]. Tyrosinase is a key enzyme in melanin biosynthesis. Inhibition of tyrosinase is considered an effective strategy to reduce melanogenesis and control abnormal melanin accumulation. Tyrosinase inhibitors are used as skin-whitening agents and antimelanogenic compounds, as well as in melanoma treatment. Hydroquinone, arbutin, tretinoin, kojic acid, azelaic acid, and ascorbic acid are examples of synthetic and natural tyrosinase inhibitors. However, their side effects, including leukoderma, cytotoxicity, dermatitis, and skin irritation, limit their clinical use. Therefore, the design and discovery of new tyrosinase inhibitors with lower toxicity and higher skin permeability are of great importance in treating skin hyperpigmentation [2]. The 1-(4-fluorobenzyl)piperazine scaffold has emerged as an important structural motif that significantly enhances the biological activity of synthetic tyrosinase inhibitors [3]. Dithiocarbamate also represent a prominent scaffold in drug discovery, with several compounds reported to exhibit tyrosinase inhibition activity [4]. In this study, a series of novel 1-(4-fluorobenzyl)piperazine-based dithiocarbamate acetamides were synthesized and evaluated for their in vitro tyrosinase inhibition activity, using kojic acid as the standard. Among all the target molecules, the compound bearing the 2-nitrophenyl exhibited the highest activity, showing 76% inhibition of the tyrosinase enzyme.

Keywords: 4-(4-Fluorobenzyl)piperazine; Dithiocarbamate; Tyrosinase inhibitör

References:

[1] X. Ni, X. Luo, X. Jiang, W. Chen, R. Bai, Small-Molecule Tyrosinase Inhibitors for Treatment of Hyperpigmentation, Molecules 30(4) (2025) 788.
[2] M.A. Baber, C.M. Crist, N.L. Devolve, J.D. Patrone, Tyrosinase Inhibitors: A Perspective, Molecules 28(15) (2023) 5762.
[3] S. Ferro, L. De Luca, M.P. Germanò, M.R. Buemi, L. Ielo, G. Certo, M. Kanteev, A. Fishman, A. Rapisarda, R. Gitto, Chemical exploration of 4-(4-fluorobenzyl)piperidine fragment for the development of new tyrosinase inhibitors, European Journal of Medicinal Chemistry 125 (2017) 992-1001.
[4] A.F. Zahoor, F. Hafeez, A. Mansha, S. Kamal, M.N. Anjum, Z. Raza, S.G. Khan, J. Javid, A. Irfan, M.A. Bhat, Bacterial Tyrosinase Inhibition, Hemolytic and Thrombolytic Screening, and In Silico Modeling of Rationally Designed Tosyl Piperazine-Engrafted Dithiocarbamate Derivatives, Biomedicines 11(10) (2023) 2739.

ORAL PRESENTATION

Effects of heat treatment on gga-miR-30c-5p, gga-miR-191-5p, and gga-miR-215-5p in poultry eggs

Gülendam Yildiz[1] (Orcid: https://orcid.org/0009-0007-7169-1549), Sena Öztürk[2] (Orcid: https://orcid.org/0009-0006-8489-3935), Fatih Atilla Bağci[3] (Orcid: https://orcid.org/0009-0003-5158-1757), Dilek Pirim2[2,3,4] (Orcid: https://orcid.org/0000-0002-0522-9432) ,Özden Çobanoğlu[5,1*](Orcid: https:/orcid.org/0000-0001-9633-634X)

[1] Bursa Uludağ University, Institute of Health Sciences, Department of Genetics, Bursa, Türkiye.
[2] Bursa Uludağ University, Faculty of Arts and Sciences, Department of Molecular Biology and Genetics, Bursa, Türkiye
[3] Bursa Bursa Uludağ University, Institute of Natural and Applied Science, Department of Molecular Biology and Genetics, Bursa, Türkiye
4Bursa Uludag University, Institute of Health Sciences, Department of Translational Medicine, Bursa, Türkiye
[5] Bursa Uludağ University, Faculty of Veterinary Medicine, Department of Genetics, Bursa, Türkiye

*Corresponding author e-mail: ocobanoglu@uludag.edu.tr

Abstract

MicroRNAs (miRNAs) are short non-coding RNA molecules that regulate gene expression and contribute to many essential biological processes in eukaryotic organisms. In addition to endogenous miRNAs, several dietary-origin miRNAs encoded by non-host genomes have been detected in human circulation and are described as xenomiRNAs (XenomiRs). Growing evidence suggests that XenomiRs can enter mammalian systems through food consumption and may modulate the expression of target genes. Despite the widespread consumption of chicken eggs, the effect of thermal processing on the stability of egg-derived miRNAs remains insufficiently characterized. Eggs form a complex biological matrix rich in proteins and regulatory molecules associated with embryonic development; therefore, determining how cooking influences the preservation of miRNA is of particular interest for both molecular biology and functional nutrition. This study investigated the impact of heat treatment on the expression of three miRNAs (gga-miR-30c-5p, gga-miR-191-5p, and gga-miR-215-5p), which show high sequence homology between humans and chickens and have been implicated in various diseases. Twenty Lohman Brown and twenty Leghorn eggs were separated into raw and boiled groups and pooled into eight sample sets. Total RNA was isolated using a commercial kit, and cDNA synthesis was performed with the miRCURY RT kit. miRNA expression levels were quantified by RT-qPCR and normalized using the exogenous cel-miR-39 spike-in control. The results revealed a marked reduction in miR-30c-5p levels following thermal processing, with significant decreases observed in both brown and white eggs ($p < 0.05$). miR-191-5p showed moderate but statistically significant reductions between raw and cooked samples. miR-215-5p expression decreased significantly in brown eggs while remaining relatively stable in white eggs. These findings suggest that miRNA heat sensitivity is molecule-specific and that miR-30c-5p is particularly susceptible to thermal degradation. Overall, the study offers essential preliminary data for future nutrigenomic and functional food research examining the stability and biological relevance of egg-derived miRNAs.

Keywords: Chicken, Egg, microRNA, XenomiR, egg-derived miRNAs

ORAL PRESENTATION

RNA isolation from three-dimensional saos-2 cultures in a collagen/keratin/alginate hydrogel

Rümeysa Işıl Özdemir[1,*] (ORCID: https://orcid.org/0009-0008-5847-1426), Aliye Ezgi Güleç Taşkıran[1] (ORCID: https://orcid.org/0000-0003-1855-1524), Özge Erdemli[1] (ORCID: https://orcid.org/0000-0001-8606-8863)

[*1]Başkent University, Institute of Science, Molecular Biology and Genetics, Ankara, Türkiye.

*Corresponding author e-mail: r.isilozdemir@gmail.com

Abstract

In recent years, the increasing interest in sustainable biomaterials has encouraged the reuse of biological waste and the development of hydrogel systems for tissue engineering applications. This study aimed to prepare a collagen/keratin/alginate (C/K/A) hydrogel system and optimize the total RNA isolation procedure from human osteosarcoma cells (Saos-2) cultured within that system. Collagen was extracted from bovine *Achilles* tendon via enzymatic hydrolysis, while keratin was isolated from waste human hair using a reduction-based method. Both extracted proteins exhibited their characteristic FTIR bands. SDS-PAGE analysis confirmed the presence of γ- and β-collagen bands along with α1(III), α1(I), and α2(I) chains for extracted collagen, and α- and β-keratin bands in extracted keratin. Hydrogels were prepared at a 1:1:1 C/K/A weight-to-volume ratio and crosslinked with calcium chloride and EDC/NHS. C/K/A hydrogels showed a porous internal architecture and a high water retention capacity of approximately 984%. The characteristic peaks of all three components of hydrogels were observed in FTIR analysis. Degradation studies indicated that 57% of the hydrogel mass remained intact after 21 days, demonstrating suitable structural stability for cell culture application. Saos-2 cells cultured within the three-dimensional hydrogel system maintained viability for up to 7 days, indicating the suitability of the three-dimensional hydrogel system compared to the traditional two-dimensional culture system. Total RNA isolation from the cell-seeded hydrogels was successfully achieved using an optimized protocol. RNA quality was confirmed by RT-PCR, where clear GAPDH bands were obtained.

Keywords: 3D cell culture, RNA isolation, Saos-2, Collagen, Keratin, Hydrogel

ORAL PRESENTATION

Synthesis and characterization of biodegradable polyester by ring-opening polymerization (ROP)

Melahat Göktaş

Van Yüzüncü Yıl University, Faculty of Education, Department of Chemistry, Van, 65080 Turkey

Corresponding author e-mail: melahat_36@hotmail.com

Abstract

The Ring-opening polymerization (ROP), like radical polymerization, occurs by the addition of monomer molecules to the chain. Ring-opening polymerization generally follows an anionic or cationic mechanism, and many lactones are polymerized by ROP [1]. The Cyclic lactones such as *β*-butyrolactone (BL) and ε-caprolactone (CL) are cyclic monomers that could be polymerized by ring-opening polymerization [2,3]. In this study, biodegradable polyethylene glycol-based (PEG) block copolymer polyesters were synthesized and evaluated via the ring- opening polymerization (ROP) method. For this purpose, biodegradable poly(ethylene glycol- *b*-ε-caprolactone) [PEG-*b*-PCL] block copolymer polyesters were synthesized by ring-opening polymerization of ε-caprolactone (CL) in the presence of polyethylene glycol (PEG) initiator. This polymerization was carried out both as dispersion and bulk polymerization and the effect of the solvent on the molecular weight of the synthesized polymer was investigated. The products were characterized by spectroscopic methods such as infrared spectroscopy (FTIR), proton nuclear magnetic resonance spectroscopy (^{1}H-NMR), and gel permeation chromatography (GPC).

Keywords: biodegradable polyester; block copolymers; ring-opening polymerization.

Acknowledgment: The author thank for financial support from Van Yuzuncu Yil University Research Funds, Grant Number: FHD-2025-12090

References:

Saçak, M., 9. baskı (2020) *Polimer Kimyası.* Gazi Kitabevi ,Ankara.
Göktaş M, Aslan Ü (2024)*Polym. Bull.* 81:11127–11143.
Göktaş M, Aykaç C, Akinay Y (2023). Polym Bull 80:8565–8584.

ORAL PRESENTATION

Atıksu arıtma tesislerinde karbon ayak izi: Türkiye'deki mevcut durum

Dursun Ali Karakuş[1*] (Orcid: https://orcid.org/0009-0002-7245-6800), Filiz Dadaşer-Çelik[2] (Orcid: https://orcid.org/0000-0003-3623-7723)

[1]Erciyes Üniversitesi, Fen Bilimleri Ensitütüsü, Çevre Mühendisliği Anabilim Dalı, Kayseri, Türkiye.
[2]Erciyes Üniversitesi, Çevre Mühendisliği Bölümü, Kayseri, Türkiye.

*Sorumlu yazar e-mail: 4011930160@erciyes.edu.tr

Özet

Nüfus artışı, kentleşme ve sanayileşme ile birlikte, üretilen atıksu miktarı artmakta ve atık su özellikleri değişmektedir. Bu durum atıksu arıtma tesislerinin çevresel sürdürülebilirlik açısından önem kazanmasına neden olmuştur. Atıksu arıtma tesisleri, atıksuların doğaya zarar vermeyecek düzeyde arıtılmasını sağlarken, enerji kullanımı, kimyasal tüketimi ve arıtma sürecinde ortaya çıkan sera gazları nedeniyle karbon ayak izine neden olur. Bu sebeple, atıksu arıtma tesislerinin karbon ayak izlerinin tespit edilmesi ve yönetilmesi, sürdürülebilir bir yönetim stratejisi açısından büyük önem arz etmektedir. Bu çalışmada, atıksu arıtma tesislerinde karbon ayak izine neden olan unsurlar ve karbon ayak izi azaltım stratejileri değerlendirilmektedir. Bu kapsamda konu ile ilgili uluslararası ve ulusal literatürde yer alan çalışmalar özetlenmiş ve atıksu arıtma tesislerinin enerji tüketimi ve sera gazı salınımı üzerindeki etkileri incelenmiştir. Genel olarak elde edilen sonuçlar, atıksu arıtma tesislerinde karbon ayak izi yönetiminin hem çevresel sürdürülebilirlik hem de iklim hedefleri açısından önemini yansıtmıştır

Anahtar Kelimeler: Atıksu arıtma, karbon ayakizi

ORAL PRESENTATION

Evaluation of antibacterial potential of different parts of *Vincetoxicum hirundinaria* against *Enterobacter cloacae*

Didem Aksu[1*](ORCID: https://orcid.org/0000-0002-7184-4011), Sevda Güzel Kara[2] (ORCID: https://orcid.org/0000-0002-6642-5824)

[1]Central Research Testing and Analysis Laboratory, Research and Application Center, Ege University, İzmir, Turkey
[2]Mersin University, Faculty of Pharmacy, Department of Pharmacognosy, Mersin, Turkey.

*Corresponding author e-mail:didem.eroglu@ege.edu.tr

Abstract

Enterobacter cloacae is a clinically significant opportunistic pathogen responsible for nosocomial infections, particularly in mechanically ventilated patients in intensive care units. Its ability to form biofilms and secrete various cytotoxins plays an important role in its pathogenicity. *Vincetoxicum hirundinaria* Medik. (Apocynaceae: Asclepiadoideae), commonly known as white swallow-wort, has numerous documented medicinal uses in various countries. In Turkey, it is known as "kırlangıç kuyruğu, kuş gavurbiberi, and panzehir otu" and the roots have been documented to possess emetic properties. The study aimed to investigate the antibacterial potential of ethanol extracts obtained from different parts (leaf, flower, seed, and seed pod) of *V. hirundinaria* naturally growing in Turkey. Antibacterial activity was evaluated against *Enterobacter cloacae* ATCC 23355 using disk diffusion and Minimum Inhibitory Concentration (MIC) assays. Gentamycin was used as the standard antibiotic control. Extract concentrations ranged from 0.1 g/mL to 0.00015259 mg/mL were evaluated. Disk diffusion tests revealed measurable inhibition zones for all extracts. MIC values against *E. cloacae* ranged from 1.5625 to 3.125 mg/mL. Among all extracts, the ethanol extract of the seeds demonstrated the strongest antibacterial effect against *E. cloacae*. Overall, the findings indicate that different parts of *V. hirundinaria* possess antibacterial potential against *E. cloacae*, a Gram-negative bacterium.

Keywords: *Vincetoxicum hirundinaria*, antibacterial activity, extract, *Enterobacter cloacae*

ORAL PRESENTATION

Solvent-dependent differences in the DPPH antioxidant activity of bee pollen extracts

Yeliz Kaya Kartal[1*] (Orcid: https://orcid.org/0000-0002-3661-5504), Sinem Pehlivan[2] (Orcid: https://orcid.org/0000-0002-3389-3189)

[*1] Ankara University, Faculty of Veterinary Medicine, Department of Biochemistry, Ankara, Türkiye.
[2] Ankara Medipol University, Faculty of Medicine, Department of Pharmacology, Ankara, Türkiye.

*Corresponding author e-mail: yelizkaya06@gmail.com; ylzkaya@ankara.edu.tr

Abstract

The mixture of hundreds of pollen grains that honey bees gather and wet with a small amount of nectar and saliva secretion is known as honey bee pollen. It is acknowledged that either fresh or dried honey bee pollen works well as a nutritional supplement and food additive. For this reason, bee pollen has been widely researched in recent years in terms of its antioxidant activity and content, and its effects on health have also been discussed. The aim of this research was to determine the DPPH scavenge activity of bee pollen, collected from a beekeeper in Kızılcahamam/Ankara. The bee pollen was extracted in three different solvents containing 15% of 0.1 N acid (methanol:0.1 N HCl; ethanol:0.1 N HCl; distilled water: 0.1 N cytric acid (v/v: 85/15)) and the DPPH scavenge activity was measured using the gallic acid as standard. The results were measured as 1.46±0.01 mg/g GAE in methanolic, 1.42±0.03 mg/g GAE in ethanolic and 0.65±0.04 mg/g GAE in aqueous extracts. The inhibition percentage for each solution on the given concentration was found 90.87±0.24% in methanol, 89.97±0.82% in ethanol and 55.27±2.25% in aqueous extracts. According to the results it was found that the methanolic and ethanolic extract showed a higher antioxidant activity than the aqeous extraction. Because they alter the kind and quantity of phenolic compounds dissolved in the extract, the polarity differences of the extraction solvents have a direct impact on the DPPH radical scavenging activity. Additionally, by promoting the release of phenolic compounds from plant tissue and boosting their stability at low pH, the addition of acid improves the extraction efficiency. The differences in studies can be due to a number of biological and chemical factors. Since floral species range significantly in their total antioxidant activity, the pollen's botanical origin is a major determinant.

Keywords: Antioxidants, Bee pollen, DPPH

ORAL PRESENTATION

Metagenomic analysis of the olive rhizosphere microbiome

Mine Aksu[1] , Elif Coşkun Dağgeçen[1*] (Orcid: https://orcid.org/0000-0003-4688-5855)

[*1]Kahramanmaras Sutcu Imam University, Faculty of Agriculture, Agricultural Biotechnology Department, Kahramanmaraş, Türkiye.

*Corresponding author e-mail: elifcoskun@ksu.edu.tr

Abstract

Olive (*Olea europaea*), one of the most fundamental species in Mediterranean agriculture, is a critical biological component of sustainable production thanks to its high adaptability to environmental factors and the bacterial and fungal communities it hosts around its roots. However, limited information is available regarding the factors shaping the structure of the olive rhizosphere microbiota and the functional contributions of this ecological unit. In this study, soil samples collected from the olive rhizosphere in the Kahramanmaras region were analyzed using high-throughput amplicon sequencing targeting the 16S rRNA V4 region. Taxonomic separation was performed at the ASV level using QIIME2. Microbial diversity indices, dominant taxonomic groups, and core microbiota components were examined. The results showed that the olive rhizosphere has a distinctly bacterial-dominated community. The majority of the community was comprised of the phyla Proteobacteria (32–38%), Actinobacteria (24–29%), and Firmicutes (10–15%). These three groups represented more than 70% of the total microbial population, defining the core microbiome. At the species level, Streptomyces (9–12%), Pseudomonas (7–11%), Bacillus (5–8%), and Rhizobium spp. (4–7%) were prominent as the primary bacterial species, occurring in high abundance and repeated across all samples. The study identified Streptomyces, in particular, as a keystone taxon in the ecosystem, with positive co-occurrence relationships. These interactions indicate that functional processes such as nutrient cycling, siderophore production, phosphate solubilization, nitrogen fixation, and pathogen suppression are actively occurring in the rhizosphere. High alpha diversity (Shannon >4.0) supported the rich and balanced structure of the community. This study presents the first detailed metagenomic profile of the olive rhizosphere microbiota in Turkish conditions and demonstrates that the Streptomyces–Pseudomonas–Bacillus axis may be an important microbial resource for biofertilizer development. The findings provide important information for the development of microbiome-based fertilization strategies and sustainable soil management practices in olive cultivation.

Keywords: *Olea europaea*, Rhizosphere, Microbiome, Metagenomics, 16S rRNA sequencing

ORAL PRESENTATION

Membrane cholesterol modulation Alters P2x7-mediated membrane currents but not cytoskeletal reorganization in macrophages

Serife Cankurtaran-Sayar[1*] (ORCID: https://orcid.org/0000-0002-3757-8709), Yusuf Olğar[2] (ORCID: https://orcid.org/0000-0002-3226-7450) , Kemal Sayar[3] (ORCID: https://orcid.org0000-0001-6807-4741)

[*1]Yuksek Ihtisas University, Faculty of Medicine, Department of Biophysics, Ankara, Turkiye
[2]Ankara University, Faculty of Medicine, Department of Biophysics, Ankara, Turkiye
[3]Ankara University, Faculty of Medicine, Department of Medical Pharmacology, Ankara, Turkiye

*Corresponding author e-mail: serifecankurtaransayar@gmail.com

Abstract

This study examined whether altering membrane fluidity through cholesterol depletion differentially modulates two hallmark functional outcomes of the P2X7 purinergic receptor—ATP-evoked ion channel currents and cytoskeletal reorganization. We specifically asked whether these responses remain coupled or diverge when membrane cholesterol is reduced. RAW 264.7 macrophage-like cells, which endogenously express P2X7, were cultured on glass coverslips and used 24 hours after seeding. Light microscopy was used to assess ATP-induced morphological changes—retraction of cellular extensions, cell rounding, and detachment from the substrate—following ATP stimulation (1 mM, 20 min). The procedure was repeated after decreasing membrane cholesterol using methyl-β-cyclodextrin (MβCD, 5 mM, 40 min). P2X7-mediated ion currents were recorded using the whole-cell patch-clamp technique under symmetrical ionic conditions to prevent driving-force–related artefacts. Measurements were performed under control conditions and after cholesterol depletion. Cholesterol depletion did not alter the characteristic morphological responses triggered by ATP. Cells still exhibited cytoskeletal reorganization, rounding, and partial detachment, indicating that P2X7-linked structural signaling remained intact. In contrast, electrophysiological experiments demonstrated a nearly twofold increase in P2X7-mediated membrane currents after MβCD treatment, with a statistically notable difference ($p < 0.06$). This selective enhancement suggests that reduced cholesterol amplifies the receptor's ion channel function while leaving cytoskeletal responses unchanged. The dissociation between preserved morphological signaling and enhanced ion channel activity following cholesterol depletion was unexpected. Because P2X7 current amplitude typically correlates with the number of functional receptors at the plasma membrane, the increased current amplitude may reflect greater membrane expression of P2X7 or a higher channel open probability. These findings indicate a potential uncoupling of electrophysiological and structural outputs downstream of P2X7 when membrane composition is altered. Future work examining surface receptor abundance, membrane localization, and lateral diffusion dynamics will be essential to clarify the mechanism underlying the selective potentiation of P2X7-mediated currents under low-cholesterol conditions.

Keywords: Macrophage, P2X7, Light Microscopy, Membrane Cholesterol, Membrane Current, Electrophysiology

ORAL PRESENTATION

In silico evaluation of potential inhibitors against *Moraxella catarrhalis* 3-oxoacyl-[acyl-carrier-protein] reductase (FabG)

Sinem Kocer (Orcid:https://orcid.org/0000-0003-0517-7422)

Istanbul Yeni Yuzyil University, Faculty of Pharmacy, Department of Pharmaceutical Technology, Istanbul, Türkiye

Corresponding author e-mail: sinem.kocer@yeniyuzyil.edu.tr

Abstract

Moraxella catarrhalis is a Gram-negative bacterium that contributes significantly to childhood otitis media and upper and lower respiratory tract infections in adults. Most clinical isolates produce β-lactamases, conferring resistance to ampicillin, which underscores the urgent need for alternative therapeutic strategies [1-2]. The 3-oxoacyl-[acyl-carrier-protein] reductase (FabG), a key enzyme of the bacterial FAS II pathway, represents a promising drug target due to its essential role in cell membrane biosynthesis and absence in humans [3]. In this study, three FabG inhibitor candidates (PubChem IDs: 71750693, 32036, 132277201) previously identified in the literature [4], along with clavulanic acid and amoxicillin, were evaluated for their inhibitory potential against *M. catarrhalis* FabG (McFabG). The three-dimensional structure of McFabG (UniProt ID: A0A3A9ND81, NCBI Protein ID: AZQ92700) was modeled using Swiss-Model. Structural minimization was performed with 2,000 steps of steepest descent in Chimera 1.13.1, and model reliability was confirmed via ERRAT (overall quality factor: 96.957), Ramachandran plot (90.8% residues in favored regions), and ProSA-web (The Z-score of −8.48 was determined, indicating consistency with experimentally resolved protein structures.). Potential binding pockets were identified using DogSiteScorer, and the pocket with the highest druggability score (0.81) was selected for docking. Molecular docking was conducted using SwissDock with the AutoDock Vina method. Binding affinities of −8.132, −8.061, and −7.516 kcal/mol were observed for compounds 71750693, 32036, and 132277201, respectively. Clavulanic acid and amoxicillin showed binding affinities of −5.819 and −7.833 kcal/mol. Compound 71750693 demonstrated the highest interaction potential with McFabG, while clavulanic acid exhibited the lowest binding, and amoxicillin was identified as a relatively acceptable inhibitor. These results highlight compound 71750693 as a promising McFabG inhibitor candidate. However, the findings are predictive and require further validation through advanced molecular docking and simulation studies.

Keywords: *Moraxella catarrhalis,* FabG, inhibitor, molecular docking

References:

[1] Goldstein, E. J., Murphy, T. F., & Parameswaran, G. I. (2009). *Moraxella catarrhalis*, a human respiratory tract pathogen. Clinical Infectious Diseases, 49(1), 124-131.
[2] Shaikh, S. B. U., Ahmed, Z., Arsalan, S. A., & Shafiq, S. (2015). Prevalence and resistance pattern of *Moraxella catarrhalis* in community-acquired lower respiratory tract infections. Infection and Drug Resistance, 263-267.
[3] Fujita, Y., Matsuoka, H., & Hirooka, K. (2007). Regulation of fatty acid metabolism in bacteria. Molecular Microbiology, 66(4), 829-839.
[4] Aygün, C., & Mutlu, Ö. (2022). Computational characterisation of *Toxoplasma gondii* FabG (3-oxoacyl-[acyl-carrier-protein] reductase): a combined virtual screening and all-atom molecular dynamics simulation study. Journal of Biomolecular Structure and Dynamics, 40(5), 1952-1969.

ORAL PRESENTATION

Acute effects of bacterial lipopolysaccaride on liver of female rats: Assestment of histopathological changes

Duygu Yaman Gram (Orcid:https://orcid.org/0000-0003-2404-0384)

Erciyes University, Faculty of Veterinary Medicine, Department of Physiology, Kayseri, Türkiye.

Corresponding author e-mail: dyaman@erciyes.edu.tr

Abstract

Liver is involved in the detoxification of lipopolysaccharide (LPS), thereby playing an essential physiological role in clearing endotoxin of intestinal derivation from the body. However, there is little information available regarding the LPS-associated histopathological changes in the liver of female mice. Therefore, we analyzed the effects of acute LPS on histopathological changes, mast cell number, and CD45 expression in the murine liver. For this purpose, animals were divided into two groups and received a single intraperitoneal injection of either 100µg LPS or PBS. Liver samples were collected 24h after the LPS injection. In all groups, liver samples were checked for the presence of degenerative changes and the accumulation of inflammatory cells with Haematoxylin&Eosin and Crossman's triple staining. Control mice receiving PBS showed compact and well-organized hepatocytes. However, when mice were treated with 100µg of LPS, hyperemia was observed within the blood vessels of the liver. Therefore, we investigated whether this treatment induce leucocyte infiltration in the mouse liver. To assess this, we examined the expression of CD45 using an immunohistochemistry and mast cell availability with toluidine blue staining. Only weak signals for CD45 were detected within the liver of control mice. However, in LPS-treated mice, CD45-positive cells appeared more widespread and distinctly localized within the blood vessels and sinusoids of the liver. Furthermore, the percentage of CD45-positive immunoreactive area was significantly higher than that of the controls. Only a few mast cells were detected within the liver of control and LPS-treated mice. In conclusion, acute LPS administration in female mice appears to induce leukocyte infiltration in the liver, while it does not affect mast cell numbers. Thus, this model provides valuable insight into the mechanisms of LPS-induced liver inflammation. However, further studies are needed to clarify the long-term effects of LPS exposure on the dynamics of hepatic immune cells.

Keywords: CD45, histopathology, liver, LPS, mast cell.

ORAL PRESENTATION

TLR4/MYD88/ NF-KB sinyal yolağı

Büşranur Çiçek (Orcid: https://orcid.org/0009-0003-5572-1032)

Gaziantep Üniversitesi, Tıp Fakültesi, Histoloji ve Embriyoloji, Gaziantep, Türkiye

Sorumlu yazar e-mail: bnur.234.27@gmail.com

Özet

Toll-like reseptörler (TLR), Patern Tanıma Reseptörler (PRR) ailesine ait tip I transmembran proteinlerdir. Birçok patojene karşı doğal immün cevabın oluşmasını sağlayan reseptörlerdir. Meyve sineğindeki (Drosophila) 'Toll' genine benzemeleri nedeniyle bu isim verilmiştir. TLR'ler, patojen ilişkili moleküler (PAMP) ve hasar ilişkili moleküler (DAMP) tarafından aktive edilirler. Memelilerde on üç farklı tip TLR tanımlanmıştır. İnsanda en çok araştırılan ve fonksiyonu aydınlatılan TLR4'tür. TLR4, Gram negatiflerin hücre duvarında bulunan lipopolisakkaritin (LPS) tanınmasında rol almaktadır. LPS'nin, TLR4 aracılığıyla tanınmasında üç farklı ekstraselüler protein görev yapmaktadır. Bunlar; LBP, CD14 ve MD-2'dir. LPS, plazmada bulunan LBP tarafından bağlanır. LBP-LPS kompleksi, hücre yüzeyindeki CD14 reseptörüne aktarılır. CD14, LPS'yi TLR4 reseptörüne sunar. LPS, hücre yüzeyinde bir kompleks oluşturan MD-2 ve TLR4'e transfer edilir. TLR4-MD2 kompleksi M şeklinde dimerize olur. Böylelikle MyD88 bağımlı ve MYD88 bağımsız sinyal kaskadları uyarılır. TIR alanı içeren adaptör protein (TIRAP) ve MyD88, MyD88'e bağımlı sinyallemeyi aracılık ederken, TIR alanı içeren adaptör indükleyen interferon beta (TRIF) ve TRIF ile ilişkili adaptör molekül (TRAM), MyD88'den bağımsız sinyallemeyi aracılık eder. MyD88'e bağımlı yol proinflamatuar sitokin ekspresyonunu aktive ederken MyD88'den bağımsız sinyalleme tip I interferon genleri aktive eder. Sonuç olarak, LPS aracılı hücre içi sinyal iletimiyle MyD88 bağımlı ve bağımsız yollar aktive olur; bu durum NF-KB'nin uyarılmasına, proinflamatuvar sitokinlerin (TNF-α, IL-1β, IL-6) yüksek oranda salınımına neden olur ve sistemik inflamatuar yanıt gelişir. TLR4 aracılığıyla aşırı sinyal iletimi meydana gelirse bu durum sistemik inflamasyona, sitokin fırtınasına ve sepsise yol açabilir.

Anahtar kelimeler: Toll-like reseptör(TLR), Lipopolisakkarit(LPS), İnflamasyon

ORAL PRESENTATION

Dose-dependent cytotoxic effect of Carbidopa on U-87 MG human glioblastoma cells

Burak Bircan (Orcid: https://orcid.org/0000-0003-1141-069X)

Osmaniye Korkut Ata University, Health Services Vocational School, Department of Medical Services and Techniques, Osmaniye, Türkiye

Corresponding author e-mail: burakbircan@osmaniye.edu.tr

Abstract

Carbidopa is a peripheral aromatic L-amino acid decarboxylase inhibitor routinely administered in combination with levodopa for the treatment of Parkinson's disease. Although the repurposing of non-oncological drugs for cancer therapy has gained increasing attention, the direct cytotoxic effect of carbidopa on glioblastoma cells remains unclear. In this study, we aimed to evaluate the dose-dependent cytotoxic effect of carbidopa on U-87 MG human glioblastoma cells. Cells were seeded into 96-well plates and, following a 24-hour attachment period, treated with carbidopa at concentrations of 1, 10, 25, 50, 100, and 200 µM. Cell viability was assessed using the MTT assay, and absorbance was measured at 550 nm. Viability was expressed as a percentage relative to untreated controls. IC_{50} and $logIC_{50}$ values were calculated from dose–response curves generated using GraphPad Prism 8. Data were analyzed using the Kruskal–Wallis test, and $p<0.05$ was considered statistically significant. Carbidopa at 1 µM did not significantly affect cell viability (68.56±8.68%) compared with the control (100±8.41%) and vehicle groups (96.87±11.01%). In contrast, significant reductions in viability were observed at concentrations ≥10 µM (59.97±6.65% at 10 µM, 57.74±7.27% at 25 µM, and 41.92±8.20% at 50 µM; $p<0.05$). At 100 and 200 µM, viability decreased to 9.89±1.18% and 10.94±0.40%, respectively ($p<0.05$). The IC_{50} value for U-87 MG cells was determined as 23.36 µM ($logIC_{50} = 1.36$). Carbidopa exhibits a pronounced, dose-dependent cytotoxic effect on U-87 MG glioblastoma cells, with significant decreases in viability beginning at 10 µM and an IC_{50} in the low micromolar range. These findings suggest that carbidopa may represent a promising repurposing candidate for glioblastoma therapy.

Keywords: Carbidopa; U-87 MG; glioblastoma; cytotoxicity; MTT assay; drug repurposing

ORAL PRESENTATION

Hydrazone-functionalized diphenylurea derivatives: Synthesis, structural characterization, and comprehensive biological activity evaluation

Cemil Caner Arıkan[1]* (ORCID: https://orcid.org/0000-0002-2426-7012), Furkan Yaşaryıldız [2] (ORCID: https://orcid.org/0009-0007-8314-6871), Halime İlhan Sığınç[2] (ORCID: https://orcid.org/0009-0005-0353-8097), Derya Dilek Kançağı[3] (ORCID: https://orcid.org/0000-0003-4725-3200), Dilek Telci[2] (ORCID: https://orcid.org/0000-0002-2793-6533), Necla Kulabaş[4] (ORCID: https://orcid.org/0000-0003-2273-5094) , İlkay Küçükgüzel[5] (ORCID: https://orcid.org/0000-0002-7188-1859)

[1]Marmara University, Institute of Health Sciences, Department of Pharmaceutical Chemistry, İstanbul, Türkiye
[2]Yeditepe University, Faculty of Engineering, Department of Genetics and Bioengineering, İstanbul, Türkiye
[3]Fenerbahçe University, Faculty of Pharmacy, Department of Biochemistry, İstanbul, Türkiye
[4]Marmara University, Faculty of Pharmacy, Department of Pharmaceutical Chemistry, İstanbul, Türkiye
[5]Fenerbahçe University, Faculty of Pharmacy, Department of Pharmaceutical Chemistry, İstanbul, Türkiye

*Corresponding author e-mail: cemilcanerarikan@gmail.com

Abstract

Numerous studies in the literature have reported on the anticancer activities of hydrazone and urea derivatives. Hydrazones have attracted considerable attention due to their distinctive physical, chemical, and biological properties, and they have been extensively investigated for various therapeutic applications, including antibacterial, anticancer, anti-HIV, anticonvulsant, and antitubercular activities. In medicinal chemistry, compounds bearing the hydrazide–hydrazone scaffold have long been of interest owing to their strong biological potential and their usefulness in the development of new antimicrobial, analgesic, anti-inflammatory, and particularly anticancer agents. In the present study, *N*-(4-hydroxyphenyl)-*N*'-phenylurea (compound 1), derived from p-aminophenol, was reacted with ethyl bromoacetate in acetone in the presence of anhydrous potassium carbonate to afford Ethyl {4-[(phenylcarbamoyl)amino]phenoxy}acetate (compound 2). Treatment of compound 2 with hydrazine hydrate in ethanol yielded *N*-[4-(2-hydrazinyl-2-oxoethoxy)phenyl]-*N*'-phenylurea (compound 3). Subsequent reactions of compound 3 with various substituted benzaldehydes successfully afforded a series of 34 novel diphenylurea derivatives of the target structure, namely *N*-(4-{2-[(2E)-2-benzylidenehydrazin-1-yl]-2-oxoethoxy}phenyl)-*N*'-phenylurea (compound 4-37). The purity of the synthesized compounds was confirmed by elemental analysis and HPLC data, while their structures were elucidated using FT-IR, ^{1}H-NMR, ^{13}C-NMR, and mass spectrometry. Following structural characterization, the cytotoxic potential of the synthesized compounds was initially screened against HDF (Human Dermal Fibroblasts), compouds that were non-toxic was evaluated for their anti-cancer potentials on U-87MG (Human Glioblastoma), MDA-MB-231 (Human Breast Adenocarcinoma), and PC-3 (Human Prostate Adenocarcinoma) cell lines. Cytotoxic effects were exhibited by CA-1, CA-15, and CA-40 only on PC3 cell line. Further analysis showed that these compounds induced cell cycle arrest at the G0/G1 phase and inhibited the migration of PC-3 cells in a time-dependent manner compared to the untreated control.

Keywords: Anticancer, hydrazid-hydrazone, migration, synthesis, urea.

Acknowledgments: This work was supported by Presidency of Turkish Health Institutes (TÜSEB - Grant no. 42963)

ORAL PRESENTATION

Development of high-sulfonation sPEEK membranes containing s-TiO_2 nanoparticles for direct methanol fuel cell (DMFC) applications

Murat Tamer (Orcid: https://orcid.org/0000-0002-4900-9351)

Eskişehir Technical University, Faculty of Engineering, Chemical Engineering Department, Eskişehir, Türkiye.

Corresponding author e-mail: murattamer@eskisehir.edu.tr

Abstract

In this study, polyether-ether-ketone (PEEK) was sulfonated with concentrated sulfuric acid to introduce $–SO_3H$ groups, yielding sulfonated PEEK (sPEEK) with a high degree of sulfonation (DS ≈ 71%). Composite membranes containing 10 and 15 wt% sulfonated TiO_2 (s-TiO_2) nanoparticles were fabricated using the solution-casting method and evaluated for direct methanol fuel cell (DMFC) applications. FT-IR spectra displayed OH stretching bands at 3400–3200 cm^{-1} and a peak at 1690 cm^{-1}, confirming successful sulfonation. Proton conductivity measurements between 30 and 60°C showed a temperature-dependent increase for both membranes. Although Ion exchange capacity (IEC) values decreased slightly due to the dilution effect of the inorganic filler, the high DS ensured sufficient proton-conducting sites within the polymer. Comparing the sPEEK-sTiO_2 (10%) and sPEEK-sTiO_2 (15%) membranes revealed that higher filler loading enhanced the hydrophilicity of the polymer matrix. Water uptake increased from 36.17% to 40.45%, attributed to the hydrophilic $–SO_3H$ groups on s-TiO_2 surfaces. Despite the increase in water uptake, swelling decreased from 59.23% to 47.95%, indicating that the higher inorganic content restricted polymer chain mobility and provided structural stabilization against excessive expansion. Proton conductivity values ranged from 17.38–37.45×10^{-3} S/cm for the 10% sample and 36.54–86.63×10^{-3} S/cm for the 15% sample, suggesting improved ion-transport pathways at higher filler levels. Methanol permeability values for both composites were significantly lower than that of Nafion 117, with the 15% membrane exhibiting a 75% reduction. Consequently, selectivity that is the ratio of ionic conductivity over methanol permeability (σ/P) reached 6.61×10^4 S·cm^{-3}·s, approximately three times higher than Nafion 117. Overall, the results indicate that highly sulfonated sPEEK membranes containing increased s-TiO_2 content offer enhanced methanol barrier performance and competitive proton conductivity, making them strong candidates for DMFC electrolytes and potentially applicable to hydrogen-fed PEMFC systems with further optimization.

Keywords: polyether-ether-ketone, titanium dioxide, polymer electrolyte membrane, direct methanol fuel cell, composite

ORAL PRESENTATION

Silica-supported silicotungstic acid incorporated high-DS sPEEK membranes for hydrogen PEMFC applications

Murat Tamer (Orcid: https://orcid.org/0000-0002-4900-9351)

Eskişehir Technical University, Faculty of Engineering, Department of Chemical Enginering, Eskişehir, Türkiye.

Corresponding author e-mail: murattamer@eskisehir.edu.tr

Abstract

In this study, the PEEK polymer was modified through a sulfonation process to introduce $–SO_3H$ functional groups onto the polymer backbone, resulting in ion-conductive sPEEK. According to the literature, sPEEK membranes with high degrees of sulfonation (DS% > 60) tend to exhibit excessive swelling and partial dissolution in methanol–water mixtures and therefore are not preferred for direct methanol fuel cell applications. This study, however, focuses on hydrogen-fed PEMFC conditions, evaluating sPEEK with a sulfonation degree of approximately 71%. In this way, the conductivity advantage associated with high DS values can be utilized while maintaining the structural integrity of the membrane under PEMFC operating conditions. To improve membrane performance, the sPEEK structure was transformed into a composite by incorporating an inorganic filler. Among heteropoly acids known to enhance proton conductivity, silicotungstic acid (SiWA) was selected as the active component and immobilized onto a silica matrix via a sol–gel process using TEOS as the precursor. This approach aims to increase the stability of SiWA within the polymer structure. Different SiWA loading levels were verified by FT-IR and XRD analyses. The water uptake behaviour, dimensional stability, and ionic conductivity (within the 30–80 °C temperature range) of the prepared composite membranes were systematically examined. Additionally, the electrochemical performance of the membranes was evaluated in hydrogen-fed PEMFC tests and compared with the Nafion 212 reference membrane. The results demonstrate that sPEEK/SiWA supported on silica exhibits suitable electrochemical and structural properties for PEM fuel cell applications. In addition, the presence of the silica-supported SiWA phase is expected to improve membrane hydration at reduced relative humidity levels by retaining water within the polymer structure.

Keywords: polyether-ether-ketone, silicotungstic acid, polymer electrolyte membrane, hydrogen fuel cell, low humidity

ORAL PRESENTATION

Synthesis of eudragit RS100-coated juglone-Ag encapsulated PLGA nanoparticles for the treatment of *Helicobacter pylori*

Tural Safarov[1]* (ORCID:0000-0002-1432-1513), Emrah Şefik Abamor[2] (ORCID:0000-0002-9174-4528), Serap Acar[3] (ORCID:0000-0002-6662-6642), Murat Topuzoğulları[4] (ORCID:0000-0003-4435-7776), Bükre Kıran Üner[5] (ORCID:0000-0003-1644-9569), Kübra Karadaş[6] (0000-0001-7607-9307), Seçil Kaya[7] (ORCID:0000-0001-6614-6641), Zişan Toprak[8] (ORCID:0009-0008-2334-6019)

*[1]Yildiz Technical University, Faculty, Bioengineering, Istanbul, Türkiye.

*Corresponding author e-mail: turalttsafarov@gmail.com

Abstract

H. pylori infection remains a significant global health issue due to increasing antibiotic resistance and the limited efficacy of current treatments. Nanoparticle-based drug delivery systems offer a novel approach to enhance drug stability, improve mucus penetration, and provide sustained release in the gastric mucosa. In this study, a juglone-silver (J-Ag) dual complex was synthesised and encapsulated into poly(lactic-co-glycolic acid) (PLGA) nanoparticles using a single emulsion-solvent evaporation method. To increase the retention time in the stomach and obtain mucoadhesive properties, it was coated with Eudragit RS100 and a final formulation was prepared. The synthesised juglone-silver (J–Ag) complex and formulations of J-Ag encapsulated within PLGA nanoparticles were characterised using various techniques. Fourier transform infrared spectroscopy (FTIR) analyses were performed to verify the chemical structure of the J-Ag, while MALDI-TOF mass spectrometry was used to determine its molecular weight. The MALDI-TOF analysis confirmed the successful synthesis of the J-Ag, with a synthesis yield of 73%. The size distribution and polydispersity index (PDI) of the nanoparticles were characterised using the dynamic light scattering (DLS) method, while the surface charge of both the synthesised nanoparticles and the structure formed after coating with Eudragit RS100 was evaluated by zeta potential measurements. The shift of the zeta potential value from negative to distinctly positive values after Eudragit RS100 coating indicates that the coating was successful. FTIR results also confirmed that the J–Ag was effectively encapsulated within the PLGA matrix and that the nanoparticle surface was coated with Eudragit RS100 polymer. Scanning electron microscopy (SEM) analyses were performed to examine the morphology of the nanoparticles, and SEM images showed that the particles had a spherical morphology close to the sizes determined by DLS. UV–Vis spectroscopy was used for the characterisation of the complex and its release profile. *In vitro* release studies revealed that the J–Ag exhibited a two-stage release behaviour: an initial rapid release phase was observed, followed by a slower and sustained release profile. This controlled release behaviour indicates that the developed nanoformulation could be a potential candidate for *H. pylori* treatment. It is planned that the therapeutic efficacy of these formulations against *H. pylori* will be evaluated in detail in future studies using in vitro and in vivo models.

Keywords: metal complex, nanoparticles, drug delivery

ORAL PRESENTATION

Eudragit-coated PLGA nanoparticles encapsulating CAPE–Ag complex for gastric cancer therapy

Kübra Karadaş[1*] (ORCID: https://orcid.org/0000-0001-7607-9307), Emrah Şefik Abamor[1] (ORCID: https://orcid.org/*0000-0002-9174-4528*), Murat Topuzoğulları[1] (ORCID: https://orcid.org/0000-0003-4435-7776), Serap Acar[1] (ORCID: https://orcid.org/0000-0002-6662-6642), Bükre Kıran Üner[1] (ORCID: https://orcid.org/0000-0003-1644-9569), Tural Safarov[1] (ORCID: https://orcid.org/0000-0002-1432-1513),Seçil Kaya[1](ORCID: https://orcid.org/0000-0001-6614-6641), Zişan Toprak [1] (ORCID: https://orcid.org/0009-0008-2334-6019)

[*1]Yildiz Technical University, Faculty, Bioengineering, Istanbul, Türkiye

[*]Corresponding author: kubraunalbio@gmail.com

Abstract

Gastric cancer is the fifth most common cancer worldwide and the third leading cause of cancer-related mortality. Its known etiology includes Helicobacter pylori infection, obesity, smoking, alcohol consumption, peptic ulcer disease, and gastroesophageal reflux disease. The most used treatment modalities are radiotherapy, chemotherapy, and targeted therapy. However, increasing antibiotic resistance, insufficient early diagnosis, chemotherapy-related toxicities, and the limited availability of targeted agents restrict treatment efficacy. Therefore, new therapeutic strategies are urgently needed. In this study, a CAPE–Ag complex containing the CAPE molecule—previously reported to possess anticancer activity—and Ag was synthesized, encapsulated into PLGA nanoparticles, and subsequently coated with the mucoadhesive Eudragit polymer. The CAPE–Ag complex was characterized by MALDI-TOF analysis, which confirmed the successful formation of the characteristic peak at m/z 391. PLGA nanoparticles loaded with the CAPE–Ag complex (CAPE-Ag@PLGA NPs) were characterized in terms of particle size, zeta potential, polydispersity index (PDI), morphology, reaction yield, and release properties using Zeta Sizer, Scanning Electron Microscopy (SEM), Fourier Transform Infrared Spectroscopy (FT-IR), and UV spectrophotometry. The results demonstrated that CAPE-Ag@PLGA NPs possess suitable particle size, distribution characteristics, and spherical morphology for improved targeting and bioavailability. After coating the nanoparticles with the Eudragit polymer (CAPE-Ag@E-PLGA), the characterization results confirmed that Eudragit was successfully coated onto the surface of the PLGA nanoparticles. In conclusion, Eudragit-coated PLGA nanoparticles encapsulating the CAPE–Ag complex show high potential in terms of efficacy and biocompatibility for the treatment of *Helicobacter pylori*–mediated gastric cancer. Further in vitro anticancer studies are ongoing to evaluate the full therapeutic potential of the developed nanoparticle system.

Keywords: Gastic Cancer, nanoparticle, CAPE

ORAL PRESENTATION

Eudragit-functionalised PLGA nanoparticles encapsulating juglone–Cu complexes as a promising delivery system against *Helicobacter pylori*

Bükre Kıran Üner[1*] (ORCID:0000-0003-1644-9569), Emrah Şefik Abamor[2] (ORCID:0000-0002-9174-4528), Serap Acar[3] (ORCID:0000-0002-6662-6642), Murat Topuzoğulları[4] (ORCID:0000-0003-4435-7776), Kübra Karadaş[5] (0000-0001-7607-9307), Tural Safarov[6] (ORCID:0000-0002-1432-1513), Seçil Kaya[7] (ORCID:0000-0001-6614-6641), Zişan Toprak[8] (ORCID:0009-0008-2334-6019)

Yıldız Technical University, Faculty of Chemical and Metallurgical Engineering, Department of Bioengineering, 34210 Esenler, Istanbul, Türkiye

*Corresponding author e-mail: bukrekiran@gmail.com

Abstract

Helicobacter pylori, a microaerophilic bacteria, can colonise the stomach mucosa by adapting to the acidic environment. Approximately half of the world's population is infected with *H. pylori*. *H. pylori* infection treatment involves multiple drug regimens consisting of at least two antibiotics, such as amoxicillin, clarithromycin, and metronidazole, and a proton pump inhibitor (PPI), either with or without bismuth. Schulz et al., in their report covering 31 countries, stated that clarithromycin (24/31) and levofloxacin (18/31) resistance rates were above 15 % in most countries, and that metronidazole resistance was also high in many regions. Furthermore, although amoxicillin resistance was generally low, it was reported to reach remarkably high rates of 70–97 per cent in some African countries. This situation has highlighted the necessity of developing alternative treatment strategies. In this study, PLGA nanoparticles (NPs) encapsulated with juglone-Cu complexes and functionalized with eudragit polymer were prepared to provide a more controlled and targeted antimicrobial effect against *H. pylori* and were characterized by measuring their size and zeta potential using ZetaSizer, imaging with Scanning Electron Microscope (SEM), using Fourier Transform Infrared Spectroscopy (FT-IR) to determine encapsulation efficiency, and release analysis using UV spectrophotometer. Juglone-Cu complexes with a molar ratio of 2:1 (Juglone:Cu) were obtained in high yield compared to other synthesized complexes. The peak at 254.44 m/z in the MALDI-TOF-MS analysis spectrum indicates the hydrated form of the juglone-copper complex for determining the molecular mass of the juglone-Cu complex. Analysis performed using ZetaSizer demonstrated that the Juglone-Cu complexes encapsulated PLGA (J-Cu@PLGA) NPs and Juglone-Cu loaded Eudragit coated PLGA (J-Cu@E-PLGA) nanoparticles are spherical in structure, with average diameters of 262.3 nm and 369.2 nm, respectively. The increase in size of the nanoparticles coated with Eudragit indicates that Eudragit was successfully coated onto the surface of PLGA nanoparticles. These promising results have demonstrated the potential of nanoparticulate complex as effective vehicles for the delivery of antimicrobial agents in the mucosa. In the future, the antimicrobial efficacy of this complex against *H. pylori* can be investigated *in vitro* and *in vivo*.

Keywords: drug delivery, nanoparticle, PLGA, Eudragit, *H. pylori*

Acknowledgment: We would like to acknowledge the financial support provided to Bükre Kıran Üner through the 2211-A National PhD Scholarship Program from The Scientific and Technological Research Council of Türkiye (TÜBİTAK).

ORAL PRESENTATION

Sustainable waste recycling strategies in the blue economy

Sevim Hamzaçebi (Orcid: https://orcid.org/ // 0000-0002-2179-1900)

Izmir Katip Celebi University, Department of Aquaculture, Faculty of Fisheries, Izmir, Türkiye.

Corresponding author e-mail: sevim.hamzacebi@ikcu.edu.tr

Abstract

The blue economy, similar to the green economy, aims to promote the efficient use of natural resources and to harness the opportunities provided by nature. It refers to activities that strengthen the relationship between humans and the sea, while also aiming to align transformational production methods with sustainable practices. The blue economy integrates commercial activities, research processes, and technological innovations based on marine resources into a holistic framework. Developing this field sustainably requires effectively mobilizing scientific knowledge and innovation capacity to generate novel solutions that protect marine ecosystems. Marine ecosystems, which are vital for global welfare and economic development, are rapidly deteriorating due to unsustainable resource use, increasing pollution, and the impacts of climate change. In response, marine-based industries are adopting innovative sustainable production models inspired by biorefinery approaches, which aim to convert low-value biomass into economically valuable products while efficiently utilizing waste. A wide range of marine waste is generated both from the processing of seafood products and from dead organisms washing up on shores. This category includes various seafood processing waste, shells accumulated along coastlines, and deceased aquatic plants. The sustainable utilisation of biological materials among marine waste holds the potential to generate economic gains while reducing environmental burdens. These materials are being converted into high-value products using biorefinery technologies, green chemistry, and innovative R&D methods. As a result, waste management is being improved, providing sustainable raw materials for sectors such as food, biotechnology, cosmetics, and agriculture. In this context, the integration of green chemistry and blue economy principles into marine-based sectors is being addressed for a sustainable and profitable marine economy.

Keywords: Blue economy, Marine organisms, Recycling, Sustainability, Waste management

ORAL PRESENTATION

Podmore extract (apis totale) content analysis and *in vivo* animal studies

Fahri Emrah Soylu[1*](https://orcid.org/0000-0002-8405-5468), Banu Yücel[2] (https://orcid.org/0000-0003-4911-7720)

[*1] Ege University, Laboratory Animals Research Center, İzmir, Türkiye
[2]Ege University, Department of Animal Science, İzmir, Türkiye

*Corresponding author e-mail: esoylu55@gmail.com

Abstract

Beekeeping produces a wide variety of products. In addition to honey, pollen, bee bread, propolis, and royal jelly, which are consumed as nutritional and natural supplements for human and animal health, it is also possible to utilize dead bees after the natural death of the honeybee. This product, called "apis totale" (podmore), is prepared from dead bees collected from hives in the fall or spring. Apis totale (podmore) is prepared from dead bees collected from hives, which naturally contain honey, bee bread, propolis, pollen, royal jelly, apilarnil, bee venom, wax, hormones, and vitamins. Apis totale extract form traditionally uses apitherapy for wound treatment, radiation protection, nerve healing, obesity and general support. In the study we aimed to compare podmore extract with propolis extract and silver sulfadiazine in the treatment of surgically sterilized wounds on the back skin of rats. Chemical analysis, amino acid analysis, wound healing and antioxidant activity level of podmore extract were performed. As a result, it was revealed that podmore extract had positive effects on wound healing in rat back skin. When histopathologic findings were examined, it was observed that podmore and propolis groups were more effective than silver sulfadiazine and had similar appearance. It was found that epithelial integrity was successfully completed in the podmore group, however, in the propolis group, protection in terms of hair follicles and sebaceous glands was at the highest level. Among the experimental groups, the lowest healing was found in the control group and the epidermis thickness was thinner than all groups. Additionally we expect that in an uncompleted study, podmore extract may have a protective effect against the harmful effects of radiotherapy. In radiation-induced dermatitis rat model the healing level of the abdominal skin could follow and dermatitis healing levels, ALT, AST, BUN levels in blood could perform. The protective effects of podmore extract can also be investigated in animal studies if it is used orally before radiation is applied. Our studies are pioneering studies for podmore extract content analysis and its animal studies.

Keywords: Podmore, Apis Totale, Wound, Dermatitis, Radiation

ORAL PRESENTATION

Identification of SNPs from RNA-seq data in tolerant soybean mutants

Tamer Gümüş[1*] (https://orcid.org/0000-0002-5674-4987), Alper Yilmaz[2] (https://orcid.org/0000-0002-8827-4887), Alp Ayan[1](https://orcid.org/0000-0003-3749-0472), Sinan Meriç[1](https://orcid.org/0000-0003-0336-0004), Çimen Atak[1](https://orcid.org/0000-0001-6045-562X)

[*1]Istanbul Kultur University, Faculty of Science and Letters, Molecular Biology and Genetics, Istanbul, Türkiye.
[2]Yıldız Technical University, Faculty of Arts and Sciences, Molecular Biology and Genetics, Istanbul, Türkiye.

*Corresponding author e-mail: t.gumus@iku.edu.tr

Abstract

Drought and salinity are major abiotic stresses that significantly limit plant growth and productivity. These stresses are increasing in severity their arable lands, particularly in areas with low rainfall and high evaporation, due to the effects of climate change. Sustainable agriculture, breeding and molecular approaches are essential to develop crop varieties tolerant to abiotic stresses. Comparative transcriptomic analyses provide valuable information about the mechanisms associated with stress response. This study used RNA-seq data generated from the SM1 and SM3-1 mutants, developed from the original soybean variety S04-05 by gamma irradiation. Drought and salinity tolerant mutants, were evaluated to identify transcriptional changes and single nucleotide variations (SNPs) associated with stress tolerance. Read quality was assessed with FASTQC (v0.12.1) and low-quality reads were removed with Trimmomatic (v0.40). High-quality reads were aligned to the soybean Williams 82 reference genome (Wm82 v2.a1) using the STAR tool. SNP calling was performed using GATK (v4.6.2.0). 22,549 SNPs in S04-05, 32,105 in SM1, and 27,273 in SM3-1 were identified. Comparative analyses identified 10,070 SNPs specific to SM1, 6,418 specific to SM3-1, and 12,071 common to both mutants. Unique SNPs across mutants were annotated using Ensembl Variant Effect Predictor (VEP). These SNPs were found to affect 13,534 genes in SM1 and 12,472 genes in SM3-1. The 12,071 common SNPs affected 7,347 genes in both mutants. Comparative SNP analysis revealed distinct clusters of variants in SM1 and SM3-1, particularly in genes involved in abiotic stress perception, energy metabolism, and signaling. Genes located in these enriched pathways showed both increased SNP density and significant expression changes. This study provides a comprehensive perspective by examining the relationship between SNP analyses based on RNA-seq data and observed stress tolerance in mutants. The results demonstrate that accumulated point mutations in the genome can lead to diverse, potentially biologically meaningful alterations of stress-related pathways.

Keywords: RNA-seq, SNP analysis, soybean, mutation breeding, stress pathway

ORAL PRESENTATION

Keratin-enhanced hydrogels: Structural and functional characterization for tissue engineering

Rumeysa Tutar (Orcid: https://orcid.org/0000-0002-4743-424X)

Department of Chemistry, Faculty of Engineering, Istanbul University-Cerrahpaşa, Avcılar, Istanbul, 34320, Turkey.

Corresponding author e-mail: rumeysa.tutar@iuc.edu.tr

Abstract

In the field of tissue engineering, particularly over the last twenty years, biomaterial scaffolds, cells, pharmaceuticals, and biochemical signals are used to produce structures that mimic both the structure and functionality of natural tissue [1]. In this study, reduced human hair keratin (rKRT) based hydrogels were designed for tissue engineering. Moreover, modified gelatin was used to create scaffolds environment for prepared hydrogels. The effects of the presence of keratin on mimicking tissue were evaluated both chemically and biologically for the prepared materials. In the study which was presented here, modified gelatin was used as a support platform for keratin at a lower amout (5% w/v), and the chemical and biological effects of keratin in increasing concentrations were examined. Prepared hydrogels were revealed through chemical characterization, while biological assessment evaluated the effects of keratin presence on cell growth, proliferation, and spreading. The properties of keratin added to structures prepared in different ratios were thoroughly evaluated and discussed in detail.

Keywords: Human hair Keratin, modified gelatin, tissue engineering, biomimetic

References:

[1] Tutar R, Koken S.Y, Tuncaboylu D.C, Çelebi-Saltik B, Ozeroglu C. In situ formation of biocompatible and ductile protein-based hydrogels via Michael addition reaction and visible light crosslinking. New J. Chem., 2023; 47, 10759-10769.

ORAL PRESENTATION

Fabrication and characterization of polyvinyl alcohol/gelatin/hyaluronic acid based microneedle patches for transdermal delivery of amphotericin B

Özlem Ayşe Tosyalı (https://orcid.org/0000-0002-8878-5863)

İstanbul Beykent University, Faculty of Engineering & Architecture, Department of Biomedical Engineering, Istanbul, Türkiye

Corresponding author e-mail: aysetosyali@beykent.edu.tr

Abstract

Amphotericin B is a potent antifungal agent; however, its clinical utility is constrained by the severe side effects associated with systemic administration and by its poor skin permeability, which renders topical delivery ineffective. Microneedle patches offer a minimally invasive, painless, and patient-friendly approach that can penetrate the stratum corneum and thereby markedly enhance transdermal drug transport. Moreover, the use of biocompatible and biodegradable polymers in microneedle fabrication provides an optimal platform for safe insertion and efficient transdermal delivery of therapeutic agents. In this study, microneedle patches were fabricated via a casting method using polyvinyl alcohol, gelatin, and hyaluronic acid. Polyvinyl alcohol provides mechanical strength and structural stability, gelatin enhances biocompatibility and contributes to flexibility, and hyaluronic acid provides excellent moisture retention while supporting sustained drug release. Microscopic analysis revealed that the resulting microneedle patches were successfully fabricated as sharp pyramidal structures with an average height of 720 ± 10.9 μm. The chemical composition and thermal stability of the polymeric microneedle patches were characterized by FTIR and TGA, respectively. *In vitro* insertion studies using parafilm confirmed that the microneedle patches penetrated up to the fourth layer, demonstrating sufficient mechanical strength for effective skin insertion. *In vitro* drug-release experiments showed that cumulative AmB release exceeded 50% within the first 2 hours and ultimately reached 93% after 8 hours. Overall, the developed microneedle patches take advantage of both the benefits of microneedle technology and the complementary properties of polyvinyl alcohol, gelatin, and hyaluronic acid, providing a promising strategy for improved transdermal delivery of Amphotericin B in cutaneous antifungal therapy.

Keywords: Amphotericin B, microneedle patches, transdermal delivery

ORAL PRESENTATION

Tunicate species diversity in İzmir Bay

Neslihan Türkçü[1,*] (Orcid: https://orcid.org/0000-0003-4440-5600), Ertan Dağlı[1] (Orcid: https://orcid.org/0000-0001-6579-505X) , Duru Şahin[2], A. Kerem Bakır[1] (Orcid: https://orcid.org/0000-0002-3739-8396, Alper Doğan[1] (Orcid: https://orcid.org/0000-0002-4871-4059), Ilgaz Doğa Yıldırım[2], Gizem Gündeğer[3] Orcid: https://orcid.org/0000-0003-4816-4904)

[1]Ege University, Faculty of Fisheries, Department of Hydrobiology, 35100 Izmir 35100, Türkiye
[2] Ege University, Faculty of Science, Department of Biology, Zoology Section, 35100 Izmir 35100, Türkiye
[1]Department of Basic Sciences, Fisheries Faculty, Izmir Katip Celebi University, İzmir, Türkiye

*Corresponding author e-mail: neslihan.turkcu@gmail.com

Abstract

This study was conducted to determine the biological diversity, spatial distribution, and ecological characteristics of species belonging to the subphylum *Tunicata* in İzmir Bay. Surveys carried out at 45 selected stations revealed a total of 21 species, representing 2 orders, 8 families, and 14 genera. Of these 21 species, five were colonial and seventeen were solitary forms. Among the identified species, *Styela clava*, *Polyclinella azemai*, and *Corella parallelogramma* were recorded for the first time from the Aegean Sea coast of Türkiye. Within the 14 identified genera, *Styela* and *Microcosmus* were the most dominant (three species each), followed by *Botrylloides* and *Ciona* with two species each. The most abundant species was *Microcosmus exasperatus*, exhibiting a dominance value of 44%. Environmental variables measured at the sampling stations ranged between 18.7–28.0°C for temperature, 36.5–39.7‰ for salinity, 6.05–8.51 for pH, and 2.74–8.61 mg/L for dissolved oxygen. Eight of the 21 species (*Ascidiella aspersa*, *Ciona robusta*, *Didemnum maculosum*, *Diplosoma listerianum*, *Microcosmus exasperatus*, *Polyclinum constellatum*, *Styela clava*, *S. plicata*) were classified as alien or invasive. Among these, four species (*P. constellatum*, *M. exasperatus*, and *S. canopus*) were identified as Lessepsian migrants. İzmir Bay is a region rich in tunicate diversity and provides favorable environmental conditions for the establishment of non-native species.

Keywords: Tunicates, Ascidiacea, Chordata, Species Diversity, İzmir Bay, Aegean Sea

ORAL PRESENTATION

Non-enzymatic electrochemical sensor design of pencil graphite electrode modified with poly(L-proline) and graphene for sensitive detection of folic acid

Nilufer Kocyigit[1*] (Orcid: https://orcid.org/0000-0003-2871-3873),
Melih Besir Arvas[2] (Orcid: https://orcid.org/0000-0001-5697-4195)

[*1]Biruni University, Faculty of Pharmacy, Department of Basic Pharmaceutical Sciences, Istanbul, Türkiye.
[2]Istanbul University, Faculty Faculty of Science, Department of Chemistry, Istanbul, Türkiye.

*Corresponding author e-mail: niluferkocyigit7@gmail.com

Abstract

Folic acid (vitamin B9) is an essential biomolecule that plays a critical role in DNA synthesis, cellular division, and methylation processes. Abnormal folate levels are directly associated with neural tube defects, anemia, cardiovascular diseases, and various cancers, highlighting the urgent need for rapid and reliable analytical tools for its detection [1]. In this study, we report the fabrication of a novel electrochemical sensing platform based on a pencil graphite electrode (PGE) modified with poly(L-proline) and graphene to achieve enhanced electrocatalytic activity toward folic acid. The Poly(L-proline)/Graphene/PGE electrode was prepared via cyclic voltammetric electropolymerization in the potential range of –0.6 to 2.0 V for 10 cycles in 0.1 M pH 7.4 PBS solution containing 5.0 mM L-proline 1.0 mg/mL graphene and 0.1 M $LiClO_4$. The synergistic combination of graphene with high conductivity and the functional groups of poly(L-proline) provided an improved electron-transfer interface [2]. Comprehensive electrochemical characterization, including cyclic voltammetry (CV), differential pulse voltammetry (DPV), and electrochemical impedance spectroscopy (EIS), will be performed to evaluate the sensor's kinetic behavior, charge-transfer properties, and analytical performance. Optimization studies will systematically investigate the effects of monomer concentration, graphene mass loading, electropolymerization cycle number, and solution pH on the folic acid response. Additionally, morphological and spectroscopic characterizations will be carried out using scanning electron microscopy (SEM) and Fourier-transform infrared spectroscopy (FT-IR), respectively, to confirm the structural features of the modified surface. The sensor will further be validated using real samples to demonstrate its practical applicability. Overall, the proposed Poly(L-proline)/Graphene/PGE platform offers a promising, cost-effective, and efficient sensing strategy for the sensitive determination of folic acid in physiological conditions [3].

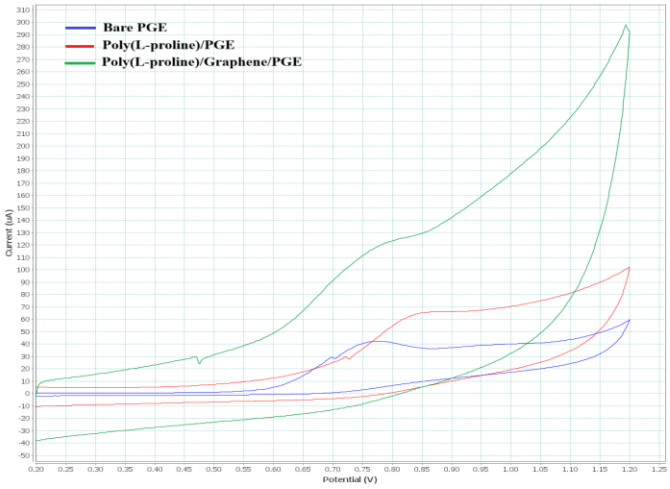


Fig. Cyclic voltammograms of Bare PGE, Poly(L-proline)/PGE, and Poly(L-proline)/Graphene/PGE modified electrodes in 0.1 M pH 7.4 PBS solution

Keywords: Folic acid, electrochemical sensor, non-enzymatic, Poly(L-proline), graphene.

References

[1] Alizadeh, M., Garkani Nejad, F., Dourandish, Z., Tajik, S., Karimi, F., Mohammadzadeh Jahani, P., ... & Beitollahi, H. (2022). A brief review on the recent achievements in electrochemical detection of folic acid. Journal of Food Measurement and Characterization, 16(5), 3423-3437.

[2] xi Ma, J., Yang, L., Wang, L., Wu, S. Q., & Liu, Y. (2021). Determination of folic acid in food by differential pulse voltammetry with ZnO@ GO nanocomposites modified glassy carbon electrode. International Journal of Electrochemical Science, 16(1), 150922.

[3] Xu, H., Bai, Z., Wang, G., O'halloran, K. P., Tan, L., Pang, H., & Ma, H. (2017). Voltammetric determination of folic acid at physiological pH values by using a glassy carbon electrode modified with a multilayer composite consisting of polyoxometalate (H8P2Mo16V2O62) and reduced graphene oxide and prepared via layer-by-layer self-assembly and in-situ photoreduction. *Microchimica Acta*, *184*(11), 4295-4303.

ORAL PRESENTATION

Synthesis, characterization and anticancer evaluation of novel urea derivatives

Sevda Türk[1*] (Orcid: https://orcid.org/0000-0002-4567-6739),
Suna Özbaş[2] (Orcid: https://orcid.org/0000-0002-1721-7543)

[*1]Karadeniz Technical University, Faculty of Pharmacy, Department of Pharmaceutical Chemistry, Trabzon, Türkiye.
[2]Marmara University, Faculty of Pharmacy, Department of Biotechnology, Istanbul, Türkiye.

*Corresponding author e-mail: sevdaturk61@gmail.com

Abstract

In recent years, the urea moiety has been regarded as one of the fundamental pharmacophores in drug design. This is largely attributable to the functional properties of the urea group: the amino substituent acts as potent hydrogen-bond donor, while the carbonyl oxygen serves as a hydrogen-bond acceptor. Consequently, the urea functionality has been employed at the rationale design of antiproliferative agents, by enhancing molecular interactions, and receptor affinity. Indeed, several urea-based derivatives (such as sorafenib, regorafenib, and linifanib) have been approved by the FDA as anticancer therapeutics (Farag et al., 2020). In this regard, novel urea compounds were synthesized and characterized by different spectroscopic methods (IR, ^{1}H-NMR, ^{13}C-NMR and MS). And also, their anticancer potential was evaluated against different cell lines, by using MTT method.

Keywords: Urea, synthesis, anticancer activity.

References:
Farag, A. K., Hassan, A. H. E., Chung, K-S., Lee, J-H., Gil, H-S., Lee, K-T., and Roh, E. J., 2020. Diarylurea derivatives comprising 2,4-diarylpyrimidines: Discovery of novel potential anticancer agents via combined failed-ligands repurposing and molecular hybridization approaches. Bioorganic Chemistry, 103(104121).

ORAL PRESENTATION

Computational study on the molecular, electronic, and spectroscopic properties of 3-ethyl-4-[3-methoxy-2-(4-methoxybenzoyloxy)-benzylideneamino]-4,5-dihydro-1*H*-1,2,4-triazol-5-one

Songül Ulufer Bulut (https://orcid.org/0000-0001-9533-0165)

Kafkas University, Kağızman Vocational School, Kars, Turkiye

*****Corresponding author e-mail: sngulufer@gmail.com.

Abstract

This study investigates the molecular, electronic, and spectroscopic properties of 3-ethyl-4-[3-methoxy-2-(4-methoxybenzoyloxy)-benzylideneamino]-4,5-dihydro-1*H*-1,2,4-triazol-5-one using Density Functional Theory (DFT). Geometry optimization was performed at the B3LYP level, and vibrational frequencies were calculated using the 6-311G basis set. Scaled theoretical IR frequencies were compared with experimentally obtained IR data to assess the accuracy of the computational method. Furthermore, ^{1}H and ^{13}C NMR chemical shifts were computed using the GIAO method and compared with experimental NMR spectra. Electronic properties, including E_{HOMO}, E_{LUMO}, dipole moment, polarizability, and hyperpolarizability, were also examined to provide deeper insights into the reactivity and nonlinear optical behavior of the titled compound. The results confirm that the selected theoretical models yield reliable predictions consistent with experimental observations, providing a comprehensive understanding of the physicochemical properties of the studied triazole derivative.

Keywords: 1,2,4-triazole, DFT, spectroscopic properties, electronic structure, hyperpolarizability.

ORAL PRESENTATION

Investigation of antibacterial, antifungal, antibiofilm and synergistic effects of *Satureja thymbra* L. plant extracts against bacteria and fungi

Pelin Erel[1*](ORCID: https://orcid.org/ 0009-0001-8363-2251), Serdar Demir[2] (ORCID: https://orcid.org/0000-0001-6572-8818), Şura Baykan[2] (ORCID: https://orcid.org/0000-0002-3624-4811), İsmail Öztürk[1*] (ORCID: https://orcid.org/0000-0002-2669-3090),

[1*]İzmir Katip Çelebi University, Faculty of Pharmacy, Department of Pharmaceutical Microbiology, İzmir, Türkiye.
[2]Ege University, Faculty of Pharmacy, Department of Pharmaceutical Botany, İzmir, Türkiye.

*Corresponding author e-mail: peliinyilmaaz@gmail.com

Abstract

Antimicrobial resistance is one of the main problem for the public health. The biofilm structures can lead to less susceptibility to antimicrobials and can cause antimicrobial resistance. *Satureja thymbra* L. is a threatened endemic Mediterranean plant and it has aromatic natural compounds for medicinal purposes. In this study, we aimed to investigate the antimicrobial activities of four types of extracts (Ethanol, hexane, ethyl acetate and methanol) of the plant against 6 bacteria (*Staphylococcus aureus*, *Enterococcus faecalis*, *Bacillus subtilis*, *Escherichia coli*, *Pseudomonas aeruginosa*, *Salmonella enterica*) and 3 fungi (*Candida albicans*, *Candida parapsilosis*, *Candida kruzei*). Inhibition zone diameter and minimum inhibitory concentration (MIC) values were determined by disk diffusion test and microdilution method. Alteration in the biofilm production and mature biofilm levels were determined by spectrophotometric microplate method. Synergistic activities of the extracts/antimicrobials (Gentamicin and fluconazole) were investigated by checkerboard assay. All the experiments were performed in triplicate, and the statistical analyses were performed. According to the results, mean inhibition zone diameters were detected between 7-11 mm with hexane extract against all studied microorganisms. MIC values of extracts were between 64 and 256 µg/mL against studied bacterial and fungal strains. Biofilm production levels of all Gram-negative bacteria and fungi were inhibited in the presence of the four extract at MIC values, as mature biofilm levels were also inhibited in the presence of the extracts at MIC in 5 of 9 strains. Synergistic activities of ethyl acetate extract+gentamicin/fluconazole and methanol extract+gentamicin/fluconazole were detected against 4 of 9 strains. Some of the combinations also demonstrated inhibitory effects against biofilm structures. In conclusion, antimicrobial potential of polar/apolar extracts of *Satureja thymbra* L. investigated and we believe that combating biofilm structures and combined use of compounds of natural origin and synthetic agents may have important role in the control of antimicrobial resistance and infectious diseases.

Keywords: *Satureja thymbra*, Antibacterial activity, Antifungal activity, Antibiofilm activity, Synergistic activity.

ORAL PRESENTATION

Investigation of biocompatibility and anticancer activities of *Lavandula intermedia* and *Lavandula angustifolia* on breast cancer (MCF-7) and healthy mouse fibroblast (L929) cell lines

Sibel Kerem Karademir[1] (ORCID: https://orcid.org/0000-0002-3560-5806),
Aslı Kara[2] (ORCID: https://orcid.org/0000-0002-0347-0222)
Özlem Özbek[2*] (ORCID: https://orcid.org/0000-0002-7683-4197)

[1]Hitit University, Graduate School of Education, Department of Molecular Biology and Genetics, Çorum, Türkiye
[2]Hitit University, Faculty of Engineering and Natural Sciences, Department of Molecular Biology and Genetics, Çorum, Türkiye

*Corresponding author e-mail: ozbekozlem@gmail.com

Abstract

The aim of this study was to investigate the biocompatibility and anticancer activities of extracts of *Lavandula intermedia* and *Lavandula angustifolia* species grown in Türkiye, collected from two different locations, using hexane and chloroform solutions in a Soxhlet apparatus, on human breast adenocarcinoma cell line (MCF-7) and healthy mouse fibroblast cell line (L929) under in vitro conditions. The cytotoxicity of the extracts at two different concentrations (1mg/mL and 0.5mg/mL) on these two different cell lines was evaluated using MTT (3-(4,5-dimethylthiazol-2-yl)-2,5-diphenyltetrazolium bromide) assay. To determine the activity of these extracts, $5x10^3$ cells were inoculated in 96-well plates and the incubation period was set as 4 hours. The medium containing 1% and 0.5% DMSO in which dry lavender extracts were suspended was used as a negative control. MTT test results were measured at 570 nm wavelength by UV spectrophotometer at the end of 4 hours of incubation to determine the cytotoxicity rates of the extracts. According to the 24-hour MTT data obtained, the cell viability rates were recorded in the hexane extracts of Eskişehir-Belpınar and Bilecik-Bozüyük samples at concentrations of 1 mg/mL and 0.5 mg/mL in the MCF-7 cell line as (39.14% and 37.01%) and (33.70% and 30.21%), respectively. Cell viability rates were recorded in the chloroform extracts of Eskişehir-Belpınar and Bilecik-Bozüyük samples as (47.98% and 38.99%) and (38.76% and 36.49%) respectively. The cell viability rates were determined in the hekzan extracts of Eskişehir-Belpınar and Bilecik-Bozüyük samples at concentrations of 1 mg/mL and 0.5 mg/mL in the L929 cell line as (100.06% and 63.21%) and (96.31% and 66.89%) respectively. Cell viability rates were observed in the chloroform extracts of Eskişehir-Belpınar and Bilecik-Bozüyük samples as (98.25% and 63.09%) and (99.75% and 60.24%) respectively. These findings indicate that lavender extracts produce cytotoxic effects on MCF-7 cancer cells, while exhibiting relatively higher biocompatibility in healthy cells. According to the results, the effects of differences in the biochemical contents of samples collected from different locations and extracts isolated with different solvents on the anticancer activity of the lavender plant were discussed. Lavender is a popular medicinal and aromatic plant whose commercial production has recently increased rapidly in Türkiye and which has a wide range of uses in various sectors. In conclusion, this study highlights the natural effectiveness of medicinal and aromatic plants in cancer treatment and demonstrates that the anticancer effects of lavender species constitute an important preliminary study that can guide future advanced research. Furthermore, by highlighting the potential value of lavender's natural bioactive compounds, it is concluded that it will contribute to the development of new perspectives on cancer treatment.

Keywords: Medicinal and Aromatic plant. *Lavandula*, MTT, MCF-7, L929, Soxhlet

Acknowledgment: This study was supported by Hitit University Scientific Research Projects Coordination Unit under the project number FEF19001.24.007 titled "Investigation of Biocompatibility and Anticancer Activities of *Lavandula intermedia* and *Lavandula angustifolia* on Breast Cancer (MCF-7) and Healthy Mouse Fibroblast (L929) Cell Lines".

ORAL PRESENTATION

Investigation of genetic diversity in barley (*Hordeum vulgare* L.) varieties grown in Türkiye using ISSR molecular markers

Beyza Aksoy[1](ORCID:0009-0009-8146-8070), Funda Küyük[2] (ORCID:000-0003-4907-1902), Sibel Kerem Karademir[3] (ORCID:0000-0002-3560-5806), Özlem Özbek[1,3*] (ORCID:0000-0002-7683-4197)

[1]Hitit University, Faculty of Engineering and Natural Sciences, Department of Molecular Biology and Genetics, Çorum, Türkiye
[2]Republic of Türkiye Ministry of Health, Çorum Provincial Health Directorate, Çorum Public Health Laboratory, Çorum, Türkiye
[3]Hitit University, Graduate School of Education, Department of Molecular Biology and Genetics, Çorum, Türkiye

*Corresponding author e-mail: ozbekozlem@gmail.com

Abstract

In this study, we aimed to investigate the genetic diversity, genetic differentiation, and population genetic structures of five certified barley (*Hordeum vulgare* L.) varieties (Arcanda, Burak, Emon, Larende, and Tarım 92) using five ISSR primers. According to the molecular analysis results, the five ISSR primers produced 40 loci, 39 of which (97.5%) were polymorphic. The average allele (na), effective allele (ne), genetic diversity (h), Shanon index (I), and polymorphic loci (PL) numbers among the populations were observed as 1.98, 1.63, 0.36, 0.53, and 39 (97.5%), respectively. Among all varieties, the highest values were detected in Arkanda as 1.50, 1.40, 0.22, 0.32, and 20 (50%), respectively. The total genetic diversity (*H*t), genetic diversity within populations (*H*s), genetic differentiation between populations (G_{ST}), and gene flow between populations (*N*m) produced by the primers in five populations were determined as 0.36, 0.13, 0.63, and 0.3, respectively. According to the genetic distance data among barley varieties, the highest genetic distance (D = 0.55) was observed between Emon and Burak varieties, while the lowest genetic distance (D = 0.22) was observed between Burak and Arcanda varieties. Based on the genetic distance data, Emon was grouped as an outgroup compared to other barley varieties in the dendrogram generated by the UPGMA method. Consequently, it was concluded that certified barley varieties have high levels of genetic diversity and genetic differentiation, and that ISSR molecular markers can be used efficiently in barley plants and produce productive results.

Keywords: Barley, *Hordeum vulgare* L., Genetic diversity, ISSR, Molecular markers

Acknowledgment: This study was supported by the TÜBİTAK-2209 University Students Research Projects Support Program under project number 1919B012223195 titled "Investigation of Genetic Diversity in Barley (*Hordeum vulgare* L.) Varieties Grown in Türkiye Using ISSR Molecular Markers".

ORAL PRESENTATION

Determination of *in vitro* biological activity of firethorn plant fruits

Ebru Coteli (Orcid: https://orcid.org/0009-0005-7193-8711)

Ahi Evran University, Vocational School of Health Services, Kirsehir, Türkiye.

Corresponding author e-mail: e.coteli@ahievran.edu.tr

Abstract

Plants have been used for many purposes, such as nutrition, fuel, medicine, and ornament, for centuries. The firethorn plant (*Pyracantha coccinea* Roemer var. lalandi) is a plant planted for ornamental purposes. It has small, red, and eye-catching fruits. This study aimed to determine the in vitro biological activity (antioxidant and antidiabetic) of the red fruits of the plant, in addition to its ornamental use. Ethanol and acetone and extracts of the fruits were taken. In antioxidant activity analyses of fruit extracts, $DPPH^{\cdot}$ and $ABTS^{\cdot+}$ radical scavenging powers were determined. Ascorbic acid was used as the standard substance. In the determination of antidiabetic activity; α-amylase enzyme was used. α-amylase enzyme inhibition of the extracts was examined. Again, the drug acarbose was used as the standard substance. The results of the study were calculated as both % inhibition and IC_{50} (inhibitory concentration) values. The $DPPH^{\cdot}$ radical scavenging activity of the extracts was determined as standard ascorbic acid > ethanol extract > acetone extract, respectively. $ABTS^{\cdot+}$ radical scavenging activities were determined as ascorbic acid > acetone extract > ethanol extract. In addition, the α-amylase enzyme inhibition of the extracts was examined, and their antidiabetic activities were determined. Antidiabetic results were determined as standard acarbose > ethanol extract > acetone extract. As a result, it can be said that the fruits of this plant have both antioxidant and antidiabetic activities. In addition, it is thought that this study will contribute to the literature on this plant.

Keywords: Firethorn, Fruit, Biological (Antioxidant and Antidiabetic) Activity.

ORAL PRESENTATION

The role and impact of eco-labels in seafood marketing

Ali Koray Şişman[1*] (Orcid: https://orcid.org/0009- 0008-4135-6149), Huriye Göncüoğlu-Bodur[2] (Orcid: https://orcid.org/ 0000-0001-7068-037X)

[*1]Ege University, Graduate School of Natural and Applied Sciences, Faculty of Fisheries, İzmir, Türkiye.
[2]Ege University, Faculty of Fisheries, Fishing Technology and Seafood Processing Technology Department, İzmir, Türkiye.

*Corresponding author e-mail: 91230000516@ogrenci.ege.edu.tr

Abstract

Global population growth and the continuing rise in per capita fish consumption are increasing pressure on water resources. Due to the inadequacy of traditional fisheries management tools, a significant portion of global fish stocks are subject to overfishing. This situation highlights the importance of eco-labels, which are market-based tools that promote sustainability. This study examines the function of eco-labels in supporting sustainable fishing practices and their impact on consumer behavior. In this study, the concepts of sustainable fisheries and marketing are first addressed; subsequently, the role of eco-labels as environmental and social product information programs is evaluated within a theoretical framework. International certification programs such as the Marine Stewardship Council (MSC), Friend of the Sea (FOS), Iceland Responsible Fisheries (IRF), and Alaska Responsible Fisheries Management (RFM) were comparatively analyzed. In line with empirical studies in the literature, consumers' awareness levels of eco-labels and their willingness to pay (WTP) a premium for certified products were examined. The findings indicate that eco-labels provide significant benefits in terms of enhancing market access, improving fisheries management, and strengthening consumer trust. However, the findings also indicate that while awareness levels are low among younger consumers, there is a positive correlation between increased awareness and a higher willingness to pay. The study also found that consumers with higher levels of education and spending capacity show a greater willingness to pay a premium for eco-labeled products. In conclusion, eco-labels are an effective tool for enhancing transparency and credibility in sustainable seafood supply chains. To strengthen this impact, it is necessary to develop communication strategies aimed at increasing consumer awareness.

Keywords: Sustainable Fisheries, Eco-Labels, Seafood Marketing

ORAL PRESENTATION

The effect of 1-methylcyclopropane treatments on phenolic compounds in 'Ekmek' quince fruit

Nurdan Tuna Güneş (Orcid: https://orcid.org/0000-0002-8529-2211)

Ankara University, Faculty of Agriculture, Department of Horticulture, Ankara, Türkiye

Corresponding author e-mail: tuna@agri.ankara.edu.tr

Abstract

Türkiye is one of important countries in quince production. Quince is a fruit that contributes to national income in international trade as well as domestic consumption. However, in this fruit species, there is a significant quality loss during long storage period due to late harvest time and inappropriate temperature and relative humidity regimes applied during cold storage period. These losses are mostly due to colour changes caused by oxidation of phenolic compounds, which is called fruit flesh browning. This study was carried out to determine the effect of 1-methylcyclopropene (1-MCP) treatments at two different concentrations of 300 ppb and 1000 ppb after harvest on the change of phenolic compounds in fruit tissue of 'Ekmek' quince cultivar. The study, which was carried out consecutively for 2 years, was carried out with 3 repetitions and using 10 fruits in each replication. In the study, after 1-MCP was applied to the quince fruits harvested at commercial maturity at 300 ppb and 1000 ppb concentrations at 12 °C, they were stored for 6 months in a cold storage with a temperature of 0±1 °C and a relative humidity of 85-90%. Phenolic compounds were determined in fruit tissue samples taken from the cold storage at monthly intervals by using high pressure liquid chromatography (HPLC). At the end of the study, 5-caffeoylquinic acid was determined as the most dominant phenolic compound in 'Ekmek' quince fruits. It was observed that 1000 ppb of 1-MCP treatment during the storage period f six months slowed down the change in phenolic compounds in fruit. For this reason, it seems that 1000 ppb 1-MCP treatments can be taken into consideration as a promising postharvest technology for 'Ekmek' quince fruit.

Keywords: 5–caffeoylquinic acid, storage, quality, postharvest.

Acknowledgements: This research was financially supported by The Scientific and Technological Research Council of Türkiye (TÜBİTAK) by a project number 106O120.

ORAL PRESENTATION

Preharvest salicylic acid treatments can improve fruit quality in '0900 Ziraat' cherry fruit

Nurdan Tuna Güneş[1]*(ORCID: https://orcid.org/0000-0002-8529-2211), Özge Horzum[1] (ORCID: https://orcid.org/0000-0003-2030-5613)

[1]Ankara University, Faculty of Agriculture, Department of Horticulture, Ankara, Türkiye.

*Corresponding author e-mail: tuna@agri.ankara.edu.tr

Abstract

The study was carried out with the aim of improving the fruit quality of the '0900 Ziraat' cherry cultivar, which is an important cherry cultivar for Türkiye and has an important place in our cherry export income. For this purpose, the effect of different concentrations of salicylic acid treatments was examined. In the study, salicylic acid treatments were performed by adding 0.2% Tween 20 and three different concentrations such as 100 ppm, 150 ppm and 200 ppm salicylic acid were applied when the fruit was at transition stage from yellow skin colour to pink skin colour stage. To determine the effect of salicylic acid treatments on some physical properties of fruits, fruit weight, fruit age and length, fruit surface area and fruit volume were determined in the samples taken at commercial harvest time. The study was carried out in 3 replications and each replications included 25 fruits. Overall, it was determined that 150 and 200 ppm salicylic acid treatments led to an increase in fruit size compared to the control groups and these treatments did not cause cracking in the fruits.

Keywords: fruit weight, fruit width, size, quality, postharvest.

ORAL PRESENTATION

Rize-sourced hazelnut shell ash as a green corrosion inhibitor for Fe metal in 1 wt.% NaCl: Electrochemical evaluation and mechanistic insights

Turan Yanardağ[1*] (ORCID: https://orcid.org/000-0001-7292-0891), Bedia Semra Taşcı[2] (ORCID: https://orcid.org/0009-0001-5607-9139), Müşerref Önal[3], (ORCID: https://orcid.org/000-0002-1540-8389), Işıl Deniz Ulusoy[4](ORCID: https://orcid.org/0009-0002-5005-3066), Müşerref Kiriş[5](ORCID: https://orcid.org/0009-0001-48512-5383), Nilseli Öztürk[6] (ORCID: https://orcid.org/0009-0009-1527-1632)

[*1, 3, 4, 5, 6] Ankara University, Faculty of Science, Department of Chemistry, Ankara, Türkiye.
[2]Fatma Yaşar Önen Trade Vocational and Technical Anatolian High School, 06590, Ankara, Türkiye.
[4]Ankara University, Technocity, Bahçelievler District, 06830, Ankara, Türkiye

*Corresponding author e-mail: tyanardag@ankara.edu.tr

Abstract

In this study, the corrosion inhibitor effect of hazelnut shell ash (HSA) at different concentrations (10 mL, 25 mL, 75 mL) in 1% NaCl solution on iron (Fe) was investigated using electrochemical methods. The methods with open circuit potential (E_{OCP}), electrochemical impedance spectroscopy (EIS), and current-potential (Tafel) curves showed that the addition of HSA significantly shifted the potential in the cathodic direction and that the solution became basic (pH 5.8 to ~10) at all concentrations. Furthermore, corrosion resistance increased from 866 Ω·cm² to 2450 Ω·cm², providing an improvement of ~65%. Inductively Coupled Plasma - Mass Spectrometer (ICP-MS) analyses revealed a significant decrease in Fe ions passing into the solution, consistent with the electrochemical results. The HSA has been shown to have the potential to be an effective, environmentally friendly corrosion inhibitor in study solutions for Fe at 25ºC. It was determined that HSA adsorbed more effectively onto the metal surface at low concentrations (10 mL), reaching an adsorption efficiency of 70% under these conditions.

Keywords: Corrosion resistance, Hazelnut shell ash, Iron, Inhibitor, ICP-MS.

ORAL PRESENTATION

Cobalt oxide/halloysite nanotubes for enhanced electrochemical sensing of tetracycline

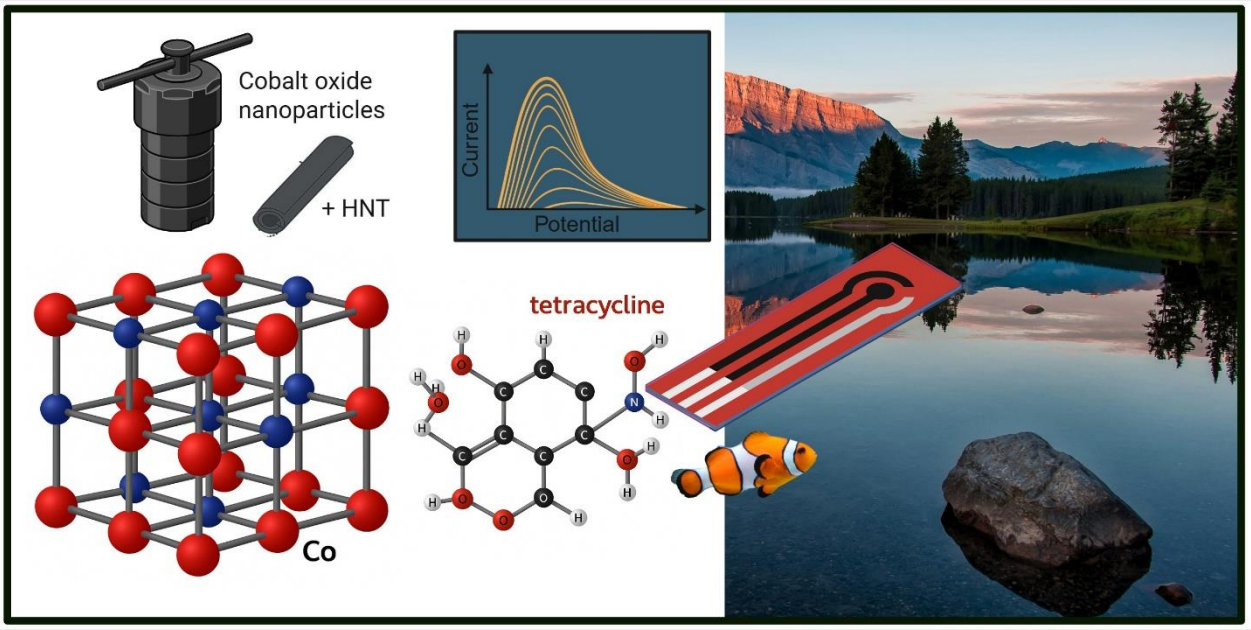
Meltem Okan (Orcid: https://orcid.org/0000-0002-7253-9801)

METU MEMS Center, Ankara, Türkiye

Corresponding author e-mail: okanmelt@gmail.com

Abstract

Antibiotic contamination in aquatic environments poses a major threat to ecological and human health, underscoring the need for rapid and sensitive detection platforms. In this study, the development of a cobalt oxide nanoparticles-halloysite nanotube (CoO/HNT) nanohybrid-based electrochemical sensor for the quantitative detection of tetracycline residues in environmental water samples is reported. CoO nanoparticles were synthesized via a hydrothermal route and immobilized onto the surfaces of halloysite nanotubes to achieve a high-surface-area hybrid with enhanced electroactive sites, improved electron mobility, and strong adsorption affinity for tetracycline molecules. The structural and morphological characteristics of the nanohybrid were confirmed by SEM, TEM, XRD, and FTIR analyses, revealing uniform CoO nanoparticle decoration and the preservation of the tubular HNT architecture. Screen printed carbon electrodes modified with the CoO/HNT composite exhibited a substantially increased redox response toward tetracycline compared to pristine HNT and CoO-only controls, demonstrating the synergistic catalytic activity of the hybrid. Cyclic voltammetry (CV) and differential pulse voltammetry (DPV) studies indicated fast charge-transfer kinetics and a well-defined oxidation peak associated with tetracycline. Under optimized conditions, the sensor delivered a wide linear range, low detection limit, and excellent sensitivity suitable for trace-level environmental monitoring. Repeatability, inter-electrode reproducibility, and long-term stability tests confirmed the robustness of the sensing platform. The CoO/HNT-modified electrode was successfully applied to spiked wastewater samples, achieving high recovery rates and minimal matrix interference, confirming its practical applicability for real-world analysis. Overall, this work introduces a cost-effective, stable, and highly responsive CoO/HNT nanohybrid material for the electrochemical detection of tetracycline, offering a promising approach for routine environmental surveillance of antibiotic pollutants.



Keywords: Tetracycline, Antibotics, Electrochemical Sensor, Hybrid Nanomaterials

ORAL PRESENTATION

Evaluating the phytoremediation potential of *Hygrophila corymbosa* under lead stress: Physiological insights in freshwater environments

Hulya Yazicioglu[1](0009-0004-5765-4096), Asli Hocaoglu-Ozyigit[2] (0000-0003-2510-6752), Bedriye Nazli Erkencioglu[1], (0000-0002-0825-5951), Ibrahim ErtugrulYalcin[3] (0009-0006-3252-3860), Ibrahim Ilker Ozyigit[2] (0000-0002-0825-5951)

[1]Marmara University, Institute of Pure and Applied Sciences, Biology Program, 34722, Istanbul, Türkiye
*Corresponding author: hulyayazicioglu@marun.edu.tr
[2] Marmara University, Faculty of Science, Department of Biology, 34722, Istanbul, Türkiye
[3] Bahcesehir University, Faculty of Engineering and Natural Sciences, Department of Civil Engineering, 34353, Istanbul, Türkiye
[4]Türkiye Environmental Issues Application and Research Center, Marmara University, Istanbul 34722, Türkiye

*Corresponding author e-mail: hulyayazicioglu@marun.edu.tr

Abstract

Lead (Pb) is a highly toxic heavy metal that poses significant threats to all organisms due to its bioaccumulation and biomagnification along the food chain. This study evaluated the effectiveness of *Hygrophila corymbosa* (Blume) Lindau in removing Pb from contaminated freshwater environments and assessed its overall suitability as a phytoremediation species. To achieve this, plants were exposed to different concentrations of $Pb(NO_3)_2$ (0, 10, 25, 50, and 100 µM) for 10 days. Washed and unwashed roots, stems, and leaves were analyzed for Pb accumulation and changes in mineral nutrient content (B, Ca, Cu, Fe, K, Mg, Mn, Na, and Zn) using ICP-OES. Additionally, total chlorophyll content was measured to assess physiological responses to Pb stress. The results showed a significant decrease in mineral nutrient concentrations and a moderate decline in total chlorophyll contents with increasing Pb exposure compared to the control group. Total chlorophyll contents were recorded as 10.51, 9.33, 6.33, 8.5, and 10.45 mg m^{-2} at 0, 10, 25, 50, and 100 µM Pb concentrations, respectively. Pb accumulation in roots, stems, and leaves increased proportionally with the applied Pb concentrations. *H. corymbosa* exhibited a strong Pb accumulation capacity, with overall bioconcentration factors (BCF) of 27, 20, 15, and 14; translocation factors (TF) from stem to leaf of 1.8, 1.2, 1.2, and 1.1; TF from root to stem of 0.6, 1.02, 0.96, and 0.90, and from root to leaf of 2.43, 2.18, 2.16, 2.04 at 10, 25, 50, and 100 µM Pb, respectively. In conclusion, Pb-induced imbalances in mineral nutrients and total chlorophyll concentrations resulted in physiological stress in *H. corymbosa*. However, the plant's high Pb accumulation, high BCF, low TF values suggest tolerance to Pb toxicity and underscore its potential for phytoremediation of Pb-contaminated freshwater ecosystems.

Keywords: Macrophyte, Mineral nutrient**,** Phytoremediation

ORAL PRESENTATION

Investigation of cytotoxic and anti-angiogenic effects of apigenin in breast cancer cell line

Berat Beyza Gücüyetmez[1] (https://orcid.org/0009-0007-8959-4974), Münevver Baran[2] * (https://orcid.org/0000-0003-0369-1022),

[1]Institute of Health Sciences, Department of Pharmacy Biochemistry, Erciyes University, Kayseri, Türkiye
[2]Department of Basic Sciences, Faculty of Pharmacy, Erciyes University, Kayseri, Türkiye

*Corresponding author e-mail: munevverbaran@erciyes.edu.tr

Abstract

Despite numerous studies, cancer remains a serious health problem worldwide. Current chemotherapeutic agents are inadequate due to the accumulation of mutations and the development of multidrug resistance, leading to a high risk of side effects. This has increased the need for new agents that can exhibit selective cytotoxic and antiproliferative effects in cancer cells. Apigenin, a phytochemical flavonoid, is distinguished by its antioxidant and anti-inflammatory properties and may exhibit potential therapeutic effects in cancer cells. One of the processes that plays a critical role in cancer progression is angiogenesis, and the literature reports that VEGF is the primary factor promoting new vessel formation in tumors, playing a key role in tumor growth and metastasis. Similarly, the COX-2 enzyme has been shown to contribute to tumor cell proliferation and angiogenesis by increasing prostaglandin production, thus promoting cancer progression. This study aims to investigate the cytotoxic and potential anti-angiogenic effects of Apigenin on the human breast cancer cell line MDA-MB-231 in vitro.
Cell viability was assessed by MTT analysis after application of different doses of apigenin and cisplatin to the cells for 24, 48, and 72 hours. According to the results, the IC_{50} value of apigenin at 48 hours was determined to be 12.89 µM, and the IC_{50} value of cisplatin was determined to be 5.84 µM. Immunocytochemical analyses at IC_{50} concentrations examined changes in VEGF and COX-2 expression levels, and the antiproliferative and potential anti-angiogenic effects of apigenin in MDA-MB-231 cells were evaluated.
The findings suggest that Apigenin may exhibit antiproliferative effects in breast cancer cells, and these effects warrant further evaluation in detail through additional studies.

Keywords: Apigenin, Breast cancer, Angiogenesis, Cytotoxicity

*(This study was supported by Erciyes University Scientific Research Projects Coordination Unit with project number TYL-2024-14066).

ORAL PRESENTATION

Synthesis, characterization, and evaluation of cytotoxic activities of *n*-phenyl-*n'*-(4-pyridylmethyl)urea derivatives in breast cancer cell lines

Orazjemal Mametkulyyeva[1] (https://orcid.org/0009-0009-2675-9027), Sümeyye Buran[2], Münevver Baran[2] (https://orcid.org/0000-0003-0369-1022), Şengül Dilem Doğan[2]* (https://orcid.org/0000-0003-1761-188X)

Institute of Health Sciences, Department of Pharmacy Biochemistry, Erciyes University, Kayseri, Turkey
[2]Department of Basic Sciences, Faculty of Pharmacy, Erciyes University, Kayseri, Türkiye

*Corresponding author e-mail: dogandilem@gmail.com

Abstract

Breast cancer is the most common malignancy among women and represents a significant global health issue due to its increasing incidence and mortality rates. Current statistics indicate a marked rise in new cases and deaths in the coming years. Despite advances in surgery, radiotherapy, chemotherapy, and targeted therapies, challenges such as multidrug resistance, systemic toxicity, metastasis, and recurrence limit effective clinical management. Aggressive triple-negative breast cancer (TNBC), which lacks hormone receptors and HER2 expression, particularly highlights the need for new, selective, and less toxic therapeutic agents due to its limited treatment options and poor prognosis. Diarylurea scaffolds play an important role in the development of new and effective agents against breast cancer. The preference for the diarylurea skeleton in anticancer drugs arises from the ureido group's ability to form strong and selective interactions with binding sites of target proteins. The oxygen atom in the ureido functional group can act as a hydrogen bond acceptor, while the NH group can serve as a hydrogen bond donor, facilitating high-affinity binding of these compounds to biological targets. Therefore, diarylurea derivatives are considered promising candidates in anticancer drug development studies, particularly for inhibiting pathways that play critical roles in proliferation and survival signaling. In this context and as a continuation of our efforts to develop novel anticancer agents, the present study focused on the design of new ureido derivatives based on N-Phenyl-N′-(4-pyridylmethyl)urea. The target molecules were synthesized by reacting 4-picolylamine with different phenyl isocyanate derivatives, resulting in the formation of 11 distinct N-Phenyl-N′-(4-pyridinylmethyl)urea (PPU) derivatives. The structures of the synthesized compounds were confirmed by ^{1}H NMR, ^{13}C NMR, and HRMS analyses, and their biological activities were investigated in MCF-7 and MDA-MB-231 breast cancer cell lines in comparison with cisplatin. (This study was derived from the master's thesis entitled “Synthesis and Investigation of Biological Activities of Hybrid Compounds Containing 2,4-Disubstituted-1,3-Thiazole and Different Azole Groups” conducted at the Department of Pharmaceutical Biochemistry, Institute of Health Sciences, Erciyes University.)

Keywords: Diarylurea derivatives, Synthesis, Breast cancer, Cytotoxic activity

ORAL PRESENTATION

Relationship of polymorphisms in *PITX1, PITX2, LHX3, PROP1* and *POU1F1* genes with litter size and growth traits in saanen goats

Nursen Şentürk (0000-0003-1975-0103)[1], Tuğçe Necla Selvi (0000-0003-3425-3201)[2], Muhammed Emin Sari (0000-0003-4921-5312)[3], Berkay Bozkurt (0000-0002-5536-9898)[4], Hüseyn Babayev (0000-0001-6985-9436)[5], Hale Şamli (0000-0003-4728-0735)[6], Hakan Üstüner (0000-0002-4341-5842)[2], Sena Ardiçli (0000-0003-2758-5945)[1,5]

[1]Bursa Uludag University, Faculty of Veterinary Medicine, Department of Physiology, Bursa, Türkiye
[2]Bursa Uludag University, Faculty of Veterinary Medicine, Department of Animal Science, Bursa, Türkiye
[3]Necmettin Erbakan University, Faculty of Medicine, Medical Department of Biology, Meram, Konya, Türkiye
[4]Izmir Institute of Technology, Graduate School of Science and Engineering, Department of Biotechnology and Bioengineering, Izmir, Türkiye
[5]University of Zurich, Swiss Institute of Allergy and Asthma Research, Davos, Switzerland

Corresponding author e-mail: sardicli@uludag.edu.tr

Abstract

Growth and reproductive traits, among the most economically critical functional characteristics in animal production, emerge as a result of the interaction between genetic and environmental factors. Understanding the genetic basis of these traits is crucial for developing sustainable selection programs that aim to increase productivity, particularly in goat breeding. However, the fact that multiple genes control these characteristics makes it difficult to explain the effects of genetic variations. The *POU1F1* pathway is a crucial pathway that plays a vital role in pituitary development and the regulation of growth and reproductive hormones. Determining the hormones affected by the genes in this pathway and the traits influenced by the pleiotropic genes involved is highly important for both animal health and breeding goals. However, there is insufficient information on this subject in goats. In this context, the aim was to determine the frequencies of the *PITX1* (c.490G>A), *PITX2* (g.18353T>C), *LHX3* (g.8035T>C), *PROP1* (c.236C>T), and *POU1F1* (c.837T>C and c.771+215C>T) polymorphisms located in the *POU1F1* pathway and to demonstrate the relationship of these polymorphisms with growth and reproductive traits in Saanen goats. In the study, a total of 150 Saanen goats were genotyped. The relationship with growth and reproductive traits, including birth weight, litter size, daily weight gain, total weight gain, first breeding weight, body length, heart girth, rump width, rump height, and wither height, was examined. Within this scope, it was determined for the first time in this study that the *LHX3* (g.8035T>C) polymorphism was significantly associated with the number of litter size ($P<0.05$), and the *PITX1* (c.490G>A) polymorphism had a tendency to affect birth weight ($P<0.1$). The findings, presented for the first time in the literature by this study, make significant contributions to elucidating the genetic basis of growth and reproductive traits in goat breeding. The obtained results indicate that the *POU1F1* gene pathway and the polymorphisms in related genes can be evaluated as potential molecular markers in future breeding programs.

Keywords: Polymorphisms, Growth, Reproduction, Saanen, *POU1F1*

ORAL PRESENTATION

Evaluation of the capacitive behavior of MWCNTs to explore their potential applications in supercapacitor electrodes

Yudum Tepeli Büyüksünetçi (https://orcid.org/0000-0002-4717-7933)

Mugla Sıtkı Koçman University, Faculty of Science, Chemistry Department, Muğla, Türkiye.

Corresponding author e-mail: yudumtepeli@gmail.com

Abstract

Multi-walled carbon nanotubes (MWCNTs) possess exceptional electrical conductivity, high surface area, and unique pore characteristics, making them highly promising materials for advanced electrochemical energy-storage applications. In this study, the capacitive behavior of MWCNTs was systematically investigated using electrochemical techniques to evaluate their suitability for supercapacitor electrode design. For this purpose, after commercial multi-walled carbon nanotubes (MWCNTs) were structurally characterized using scanning electron microscopy (SEM), energy-dispersive X-ray spectroscopy (EDS), Fourier transform infrared spectroscopy (FTIR), and X-ray diffraction (XRD), carbon felt electrode (CFE) was modified with MWCNT via drop casting technique. The capacitive properties and energy storage mechanism of MWCNT modified CFE were elucidated using electrochemical techniques, including cyclic voltammetry (CV), electrochemical impedance spectroscopy (EIS), and galvanostatic charge–discharge (GCD). The energy density, power density, and coulombic efficiency of the MWCNT–CFE system were calculated using GCD measurements. Future studies are expected to explore MWCNTs combined with metal–organic frameworks (MOFs) and other nanomaterials to enhance supercapacitor electrode performance. Such composites can improve specific capacitance, energy density, and cycling stability through synergistic effects of high surface area, hierarchical porosity, and efficient electron/ion transport, paving the way for next-generation energy storage devices.

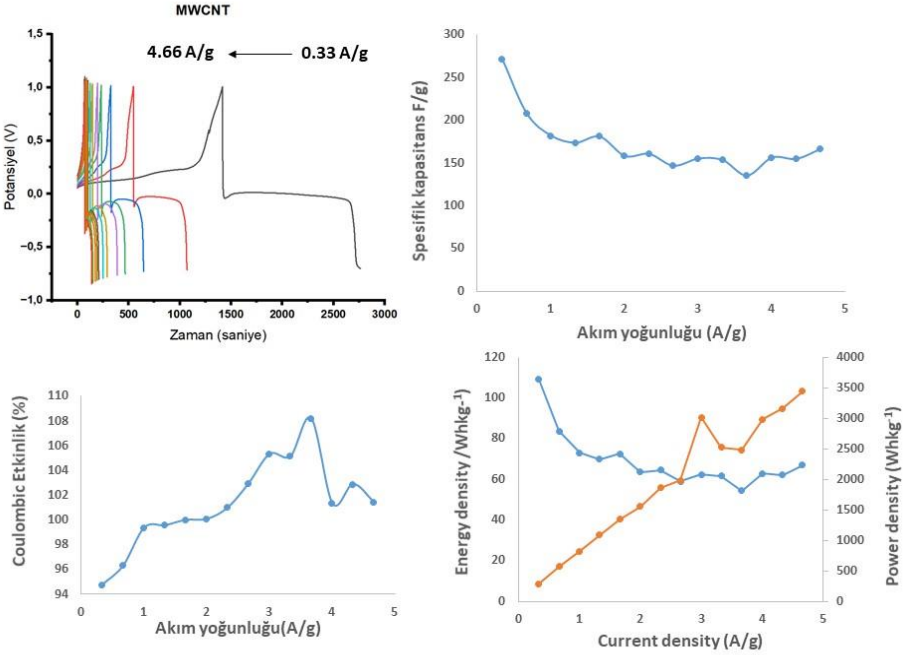


Figure 1. Figures showing the GCD results of the MWCNT/CFE system, as well as the specific capacitance, coulombic efficiency (%), power density, and current density values.

Keywords: MWCNT, Supercapacitor electrodes, carbon felt electrode, composite electrode.

ORAL PRESENTATION

Synthesis of porous carbon structures from coal via molten salt activation and HF acid treatment for hydrogen storage

Volkan Kara[1*](https://orcid.org/0000-0002-6379-2418), Atakan Toprak[1 ,2*] (https://orcid.org/0000-0003-0080-1456)

[*1]Zonguldak Bülent Ecevit University, Department of Nano Technology Engineering, 67100 Zonguldak, Turkey.
[*2] Zonguldak Bülent Ecevit University, Çaycuma Food and Agriculture Vocational School, Department of Chemistry and Chemical Processing Technologies, Zonguldak, Turkey

*Corresponding author e-mail: volkan.kara@fbe.karaelmas.edu.tr

Abstract

The rapid increase in global energy demand and the depletion of fossil fuel reserves have significantly heightened interest in sustainable and eco-friendly resources, such as hydrogen (H_2) energy. However, challenges regarding the safe and efficient storage of H_2 remain one of the major obstacles hindering the development of the H_2 economy. Therefore, technological challenges related to storage and utilization must be addressed. In this study, carbons possessing high surface area and pore volume were produced from Zonguldak coal via molten salt activation followed by acid treatment. During the experimental phase, the activation process was conducted at 800°C using a coal mixture with KOH and K_2CO_3 salts. Post-activation, the resulting carbon structures were treated with HCl and HF acid to yield comparative porous carbon samples. The characterization of the porous carbon materials was performed using SEM-EDS, BET surface area analysis, and measurements of pore volume and distribution. The results demonstrated that HF treatment significantly enhanced the material's textural properties. Specifically, the BET surface area increased from 541 m^2/g to 1249 m^2/g following HF treatment. Correspondingly, the H_2 adsorption capacity rose from 88 cm^3/g to 195 cm^3/g. These experimental findings suggest that molten salt activation with KOH and K_2CO_3, combined with HF acid treatment, is a highly effective method for enhancing the pore characteristics of coal-based materials and improving their H2 storage performance.

Keywords: Coal, Molten Salt Activation, HF Acid Treatment, Porous Carbon, Hydrogen Storage.

ORAL PRESENTATION

Determination of meat consumption preferences by analytical hierarchy process (AHP)

Leyla Ataseven[1]* (Orcid: https://orcid.org/ 0000-0002-7061-6068), Savaş Sarıözkan[2]* (Orcid: https://orcid.org 0000-0003-2491-5152)

*University of Erciyes, Faculty of Veterinary, Department of Zootechnical, Kayseri, Turkey.

*Corresponding author e-mail: leylaataseven@hotmail.com

Abstract

Meat consumption plays a crucial role in meeting individuals' essential nutritional needs. Animal products such as red meat, white meat, and fish play a crucial role in human nutrition because they contain high-biological-value protein and provide essential micronutrients such as iron, zinc, phosphorus, and vitamin B12. Therefore, adequate and balanced consumption of meat products is considered a key indicator of a healthy lifestyle. Meat consumption levels are influenced by multiple factors, including an individual's nutritional knowledge, lifestyle, cultural values, religious preferences, and socioeconomic circumstances. Various studies have shown that individuals with a high level of health knowledge are better able to assess the nutritional differences between meat types and are more aware of saturated and unsaturated fat content and the health effects of processed meat consumption. It is well established that the knowledge and attitudes acquired during professional training have a significant impact on the nutritional behaviors of healthcare professionals. Generally speaking, the meat consumption habits of healthcare workers are influenced by multifaceted factors such as their knowledge level, professional awareness, economic conditions, and work schedules. Therefore, studies on meat consumption among healthcare workers provide important data for understanding healthy eating behaviors, promoting nutritional awareness in society, and informing policy development processes. This study aims to determine the meat consumption habits of Erciyes University healthcare workers, the factors influencing these preferences, and the importance of these factors using the Analytical Hierarchy Process (AHP) method. In the AHP form, participants were asked to evaluate meat types (beef, lamb, chicken, turkey, and fish) on the criteria of Health, Price, Taste, Hygiene and Reliability, Halal, Habit/Cultural Preference, and Accessibility using a pairwise comparison scale (1–9). At the end of the study, the meat consumption preferences of healthcare workers were determined using an analytical hierarchy process, and it was revealed that health was the most important criterion and that fish meat was preferred more. Chicken meat was also preferred due to its low price.

Keywords: Meat consumption, AHP, Healthcare workers, Consumption preferences, Health criterion

ORAL PRESENTATION

An *In-silico* platform for predicting magnetic resonance imaging (MRI) contrast properties of diamagnetic chemical exchange saturation transfer (DIACEST) agents

Alperen Can Esen[1*] (ORCID: 0000-0003-1971-8330), Yelda Ozsunar[2] (ORCID: 0000-0003-2642-5464), Mehmet Bilgen[2] (ORCID: 0000-0001-5671-2021)

[*1] Adnan Menderes University, Institute of Health Sciences, Department of Obstetrics and Gynecology Nursing, Aydın, Turkey
[2] Adnan Menderes University, Faculty of Medicine, Department of Radiology, Aydın, Turkey
[3] Adnan Menderes University, Faculty of Medicine, Department of Biophysics, Aydın, Turkey

* Corresponding author e-mail: alperencanesen@gmail.com

Abstract

DIACEST agents represent a promising metal-free alternative for MRI contrast via exchangeable proton groups (hydroxyl, amine, amide, carboxyl) (1-5). A computational platform was needed for predicting relaxation properties under various physiological and technical parameters, and enabling rapid screening and optimization prior to synthesis and experimental validation (6-10). Thus, this work developed an in silico platform to estimate longitudinal and transverse relaxation rate changes (11-14). The software offers a comprehensive interface with functional modules to streamline the simulation process. The setup allows users to upload molecular structures and define physiological conditions alongside scanner parameters. Signals were estimated from standard spin-echo formulation. Additionally, the software simulates phantoms at various dilution series to visualize contrast enhancement effects. Validation was performed using betanin, and predictions were compared against benchmark real measurements. This platform represents a novel, systematic tool for predicting DIACEST agent behavior, bridging the gap between molecular design and MRI contrast enhancement. The successful validation with betanin demonstrates its utility for virtual screening of theoretical candidates prior to synthesis, as well as the evaluation of already synthesized potential DIACEST compounds.

Keywords: *In-Silico*, DIACEST, Magnetic Resonance Imaging, Contrast Agent, Phantom.

References:

1. Özsunar Y, et al. JMRI,. 2025:1-11.
2. Evbuomwan OM, et al. The Chemistry of Molecular Imaging. 2014:225-43.
3. Hancu I, et al. Acta radiologica. 2010;51(8):910-23.
4. Zhang S, et al. Accounts of chemical research. 2003;36(10):783-90.
5. Ward K, et al. Journal of Magnetic Resonance. 2000;143(1):79-87.
6. Landrum G, et al. rdkit: 2025_03_5 Release2025 July 26, 2025.
7. Khorasani M, et al. Software Development. 2022;498:507.
8. Harris CR, et al. Nature. 2020;585(7825):357-62.
9. The pandas development team. Pandas. 2025.
10. Matplotlib: Visualization with Python. 2025.
11. Abergel D, et al. ChemPhysChem. 2004;5(6):787-93.
12. Graf C, et al. Journal of Magnetic Resonance. 2021;329:107011.
13. McConnell HM. The Journal of Chemical Physics. 1958;28(3):430-1.
14. Aquilanti V, et al. Chemical Physics Letters. 2010;498(1-3):209-13.

ORAL PRESENTATION

Biomarker evidence of metolachlor-driven oxidative stress in rainbow trout

Demet Doğan (Orcid: 0000-0001-6356-0679)

Gaziantep University, Faculty of Arts&Sciences, Department of Biology, Gaziantep, Türkiye

Corresponding author e-mail: demetdogan@gantep.edu.tr

Abstract

S-metolachlor, a chloroacetanilide herbicide frequently detected in agricultural watersheds, poses potential risks to aquatic organisms through sub-chronic exposure. In this study, rainbow trout (*Oncorhynchus mykiss*) were exposed for 7, 14, and 21 days to three environmentally relevant concentrations of S-metolachlor (0.0123, 0.0615, and 0.123 mg/L). Oxidative stress biomarkers were quantified in spleen and heart tissues to evaluate tissue-specific responses. Antioxidant enzyme activities were significantly elevated, accompanied by increased levels of oxidative damage markers, indicating that compensatory mechanisms were insufficient to prevent cellular injury. Distinct organ-level differences were observed. The spleen maintained protein stability under exposure, whereas the heart exhibited protein depletion and transient antioxidant responses, suggesting greater susceptibility of cardiac tissue. These results demonstrate that even field-comparable concentrations of S-metolachlor can disrupt oxidative homeostasis and tissue metabolism in fish, emphasizing the relevance of organ-specific biomarker assessment and the necessity for more rigorous monitoring of herbicide residues in freshwater ecosystems.

Keywords: Ecotoxicology, fish, tissue-specific, aquatic toxicology

ORAL PRESENTATION

Co-toxicity of pesticides and nano/microplastics in aquatic systems: Implications for fish models

Demet Doğan (Orcid: 0000-0001-6356-0679)

Gaziantep University, Faculty of Arts&Sciences, Department of Biology, Gaziantep, Türkiye

Corresponding author e-mail: demetdogan@gantep.edu.tr

Abstract

Aquatic ecosystems are increasingly challenged by the simultaneous presence of pesticides and plastic-derived particulates, producing complex exposure scenarios that strain conventional toxicological frameworks. Nano- and microplastics, with their pronounced surface reactivity and physicochemical heterogeneity, function as vectors that adsorb and redistribute pesticide residues, thereby reshaping contaminant behavior in aquatic environments. The convergence of these pollutants has been reported to exacerbate toxicological outcomes in fish models, including oxidative imbalance, apoptotic pathways, neurophysiological disturbances, and endocrine disruption. This review synthesizes and critically evaluates current literature on pesticide–plastic interactions, emphasizing mechanistic processes such as adsorption, desorption, and altered bioaccumulation. By collating evidence across molecular, cellular, and organismal levels, the analysis highlights the ecological relevance of multiple stressors and exposes the shortcomings of single-contaminant assessments. The discussion ultimately calls for integrative toxicological perspectives that incorporate co-exposure scenarios to more accurately assess risks to aquatic organisms and ecosystem health.

Keywords: Ecotoxicology, stressors, pollutants, bioavailability.

ORAL PRESENTATION

Impact of agricultural herbicides on aquatic ecosystems: Case of aclonifen

Şeyma Özdemir*, Muhittin Doğan

Gaziantep University, Faculty of Arts and Sciences, Department of Biology, Şehitkamil-Gaziantep, Türkiye

*Corresponding author e-mail: so7392163@gmail.com

Abstract

Herbicides are widely applied in agriculture to enhance crop yield and control weeds; however, their extensive use poses significant environmental risks to aquatic ecosystems. Following application, a considerable proportion of pesticides are transported to non-target environments through surface runoff, rainfall-induced erosion, leaching into groundwater, and atmospheric deposition, ultimately contaminating water resources. These processes contribute to water quality deterioration, chemical accumulation in sediments, and potential biomagnification within food webs. Aclonifen, a diphenyl ether herbicide commonly used in crops such as sunflower, chickpea, and lentil, exerts its phytotoxic effects by inhibiting phytoene desaturase and protoporphyrin oxidase enzymes, leading to bleaching and necrosis in plants. Although strongly adsorbed by soil organic matter and clay, its leaching potential increases under high moisture conditions. Both Aclonifen and its metabolites exhibit moderate acute aquatic toxicity, negatively affecting aquatic plants and invertebrates. The findings highlight that herbicides used in agricultural practices pose considerable ecological and toxicological risks to aquatic systems. Sustainable agriculture therefore requires limiting pesticide use, promoting natural alternatives, implementing precision techniques, and developing appropriate timing strategies.

Keywords: Aclonifen, aquatic ecosystems, herbicide toxicity, sustainable agriculture, environmental risk

ORAL PRESENTATION

The importance of vineyard houses in Gaziantep in terms of culture and urban ecology

Mustafa Pehlivan

Gaziantep University, Faculty of Arts&Sciences, Department of Biology, Gaziantep, Türkiye

Corresponding author e-mail: mpehlivan@gantep.edu.tr

Abstract

In our country, vineyard houses, which were built by agricultural producers, especially those with large-scale plots, for the purpose of evaluation during production, have gained much more functional characteristics today. The rapid spatial expansion of cities, transportation opportunities, and the country's seismicity are among the important reasons for this functionalization. Although the vineyard cottage culture in Gaziantep province dates back much further, it has also been affected by this change. Furthermore, the earthquakes that occurred in February 2023, centered in Kahramanmaraş, have contributed to these vineyard cottages becoming increasingly comprehensive structures and transforming into planned “residences.” Furthermore, the fact that these structures served as “shelters” for people during and after the Covid-19 pandemic and subsequently during the earthquake period has increased the demand for them. On the other hand, the fact that water wells have been dug for each vineyard house, along with these structures, can be said to have had a negative impact <on the natural flora and the agricultural sector in recent years of drought. Although well permit applications for areas smaller than a certain size will be evaluated negatively as of 2025, even the existing wells cause significant water losses. The loss is significantly higher when vineyard owners construct pools or allocate lawn areas on their land. While the public's high demand for vineyards and desire for agricultural production could yield positive economic and ecological contributions if properly directed, lack of planning and oversight could worsen the current situation.

Keywords: Vineyard house, culture, urban ecology, economy, Gaziantep

ORAL PRESENTATION

Comparative evaluation of antioxidant activities and bioactive compound profiles of *Pyracantha coccinea* M. Roem. extracts

Yazgı Doga Atici[1*] (https://orcid.org/0009-0001-0239-1063),
Bugrahan Emsen[2] (https://orcid.org/0000-0002-9636-2596)
Muhammet Dogan[3] (https://orcid.org/0000-0003-3138-5903)

[*1]Department of Biology, Graduate School of Natural and Applied Sciences, Karamanoğlu Mehmetbey University, Karaman, Türkiye
[2]Department of Biology, Kamil Özdağ Faculty of Science, Karamanoğlu Mehmetbey University, Karaman, Türkiye
[3]Department of Nutrition and Dietetics, Faculty of Health Sciences, Karamanoğlu Mehmetbey University, Karaman, Türkiye

*Corresponding author e-mail: dogatici@gmail.com

Abstract

This study aimed to comparatively evaluate the antioxidant properties of the acetone (AE), methanol (ME), and water (WE) extracts of *Pyracantha coccinea* M. Roem., a plant known for its rich phytochemical content. Antioxidant capacity was assessed using DPPH radical scavenging and metal chelating assays, while total phenolic, flavonoid, and anthocyanin contents were determined spectrophotometrically. IC_{50} values and slope coefficients were calculated using probit analysis. The AE extract exhibited the strongest DPPH radical scavenging activity, with an IC_{50} value of 56.73 µg/mL (50.98–62.94), followed by the ME extract (69.50 µg/mL) and the WE extract (115.27 µg/mL). Similar trends were observed in metal chelating activity, where AE again showed the highest potency with an IC_{50} of 83.66 µg/mL, compared to 101.77 µg/mL for ME and 173.09 µg/mL for WE. Analysis of antioxidant compounds revealed that AE contained the highest total phenolic content (254.87 µg GAE/mg), total flavonoid content (125.22 µg QE/mg), and total anthocyanin content (2.33 µg C3G/mg). ME and WE extracts displayed lower concentrations of all measured antioxidant components. Overall, the results indicate that the acetone extract of *P. coccinea* demonstrates the strongest antioxidant potential among the evaluated extracts. This enhanced activity is likely linked to its higher phenolic and flavonoid content. The findings suggest that *P. coccinea* may serve as a promising natural source of antioxidant compounds and provide a valuable foundation for further pharmacological and phytochemical studies.

Keywords: Antioxidant activity, DPPH radical scavenging, Plant extracts, Metal chelating activity

ORAL PRESENTATION

Growth–biomass responses of *Eruca sativa* Mill. microgreens to the lichen-derived metabolites atranorin and usnic acid

Yazgı Doga Atici[1*] (https://orcid.org/0009-0001-0239-1063),
Muhammet Dogan[2] (https://orcid.org/0000-0003-3138-5903)
Bugrahan Emsen[3] (https://orcid.org/0000-0002-9636-2596)

[*1]Department of Biology, Graduate School of Natural and Applied Sciences, Karamanoğlu Mehmetbey University, Karaman, Türkiye
[2]Department of Nutrition and Dietetics, Faculty of Health Sciences, Karamanoğlu Mehmetbey University, Karaman, Türkiye
[3]Department of Biology, Kamil Özdağ Faculty of Science, Karamanoğlu Mehmetbey University, Karaman, Türkiye

*Corresponding author e-mail: dogatici@gmail.com

Abstract

Microgreens represent an early developmental stage of edible plants, characterized by their high phytonutrient content and rapid harvestability. Their growing popularity stems from their potential to serve as sustainable, functional food ingredients with enhanced health-promoting properties. In this study, the growth responses of *Eruca sativa* Mill. microgreens to two lichen-derived secondary metabolites—atranorin and usnic acid—were evaluated across five application levels (2, 4, 6, 8, and 10 mg/L). Germination initiated on day three, and plants exhibited typical microgreen morphology, including fully expanded cotyledons and dark green emerging true leaves, by day eight. Both metabolites produced a clear dose-dependent, hormetic pattern of response. Atranorin promoted shoot and root development most effectively at moderate concentrations (4–6 mg/L), whereas usnic acid induced maximal stimulation at comparatively higher doses (8–10 mg/L). The findings indicate that atranorin and usnic acid possess measurable biostimulant potential when applied within optimal concentration ranges, suggesting their applicability in sustainable microgreen production systems as natural growth-enhancing agents.

Keywords: Atranorin, *E. sativa*, growth stimulation, lichen secondary metabolites, microgreens, usnic acid

ORAL PRESENTATION

Antioxidant activities and phytochemical profiles of microgreen and mature *Spinacia oleracea* L. extracts

Seyda Sahin[1*] (https://orcid.org/0009-0009-4078-1765),
Muhammet Dogan[2] (https://orcid.org/0000-0003-3138-5903)
Bugrahan Emsen[3] (https://orcid.org/0000-0002-9636-2596)

[*1]Department of Biology, Graduate School of Natural and Applied Sciences, Karamanoğlu Mehmetbey University, Karaman, Türkiye
[2]Department of Nutrition and Dietetics, Faculty of Health Sciences, Karamanoğlu Mehmetbey University, Karaman, Türkiye
[3]Department of Biology, Kamil Özdağ Faculty of Science, Karamanoğlu Mehmetbey University, Karaman, Türkiye

*Corresponding author e-mail: seydaasahin00@gmail.com

Abstract

This study investigated the antioxidant capacities and bioactive compound profiles of acetone (AS), ethyl acetate (ETAS), and water (WA) extracts obtained from both microgreen (M-) and mature (O-) stages of *Spinacia oleracea* L. Antioxidant activity was assessed using DPPH radical scavenging and metal chelating assays, while total phenolic and flavonoid contents were quantified spectrophotometrically. In the DPPH assay, mature plant extracts demonstrated higher antioxidant activity than microgreen extracts. The O-AS extract showed the strongest radical scavenging effect with an IC_{50} of 90.13 µg/mL (81.21–100.30), followed by O-ETAS (111.78 µg/mL) and O- WA (147.97 µg/mL). Among microgreen extracts, M-AS exhibited the lowest IC_{50} (148.41 µg/mL), whereas M-ETAS (238.13 µg/mL) and M-WA (248.16 µg/mL) had considerably weaker activity. A similar pattern was observed in metal chelation capacity. The O-AS extract again displayed the highest activity with an IC_{50} of 84.23 µg/mL (75.83–93.75), followed by O-ETAS (105.84 µg/mL) and O-WA (216.00 µg/mL). Microgreen extracts showed higher IC_{50} values, with M-AS at 129.05 µg/mL, M-ETAS at 244.06 µg/mL, and M-WA at 266.77 µg/mL. Total phenolic and flavonoid analyses supported the antioxidant results. Mature extracts contained higher levels of bioactive compounds, with O-AS showing the highest phenolic (523.99 µg GAE/mg) and flavonoid (861.91 µg QE/mg) concentrations. Microgreen extracts displayed lower amounts, particularly in water extracts, where phenolic and flavonoid contents were minimal. Overall, mature *S. oleracea* extracts exhibited significantly stronger antioxidant properties and higher phytochemical content compared to microgreen extracts. The acetone extract of mature plants demonstrated the most potent activity, highlighting its potential as a valuable natural antioxidant source. These findings contribute to the understanding of developmental stage differences in the bioactive composition of *S. oleracea*.

Keywords: Antioxidant activity, DPPH radical scavenging, Microgreen, Plant extracts

Acknowledgements: This work was supported by Scientific Research Projects Commission of the Karamanoğlu Mehmetbey University. Project Number: 07-YL-25

ORAL PRESENTATION

Effects of LED light exposure on phenolic–flavonoid content and antioxidant properties of *Lens culinaris* L. microgreens extracts

Melike Altunbay[1*] (https://orcid.org/0009-0007-6975-8222),
Muhammet Dogan[2] (https://orcid.org/0000-0003-3138-5903),
Bugrahan Emsen[3] (https://orcid.org/0000-0002-9636-2596)

[*1]Department of Biology, Graduate School of Natural and Applied Sciences, Karamanoğlu Mehmetbey University, Karaman, Türkiye
[2]Department of Nutrition and Dietetics, Faculty of Health Sciences, Karamanoğlu Mehmetbey University, Karaman, Türkiye
[3]Department of Biology, Kamil Özdağ Faculty of Science, Karamanoğlu Mehmetbey University, Karaman, Türkiye

*Corresponding author e-mail: melikealtunbayy@gmail.com

Abstract

This study evaluated the effects of different LED light exposures (white (W), red (R), and blue (B)) on the antioxidant properties and phenolic composition of acetone and water extracts of *Lens culinaris* L. The DPPH radical scavenging results showed that acetone extracts exhibited lower IC_{50} values compared to water extracts. Among all extracts, the blue LED acetone extract (BAS) demonstrated the strongest DPPH scavenging activity with an IC_{50} of 187.59 µg/mL, while the red LED water extract (RWE) showed the weakest activity (586.41 µg/mL). Metal chelation assays revealed that acetone extracts again had higher activity, with the white LED acetone extract (BAS) showing the lowest IC50 value of 36.38 µg/mL, followed by red LED acetone (RAS, 57.10 µg/mL) and blue LED acetone (BAS, 67.92 µg/mL). Water extracts exhibited considerably weaker chelating capacity, with IC50 values ranging between 159.44 and 296.17 µg/mL. Analysis of total phenolic content indicated that BAS had the highest concentration (258.26 µg GAE/mg), whereas WWE had the lowest (164.55 µg GAE/mg). Total flavonoid results demonstrated a strong enhancement under white and blue LED acetone conditions, with BAS (580.06 µg QE/mg) and BAS (585.03 µg QE/mg) showing substantial increases, while water extracts displayed lower flavonoid accumulation except for RWE (513.40 µg QE/mg). Blue LED exposure significantly improved both phenolic composition and antioxidant performance, particularly in acetone extracts. These findings suggest that LED light quality plays a critical role in modulating the bioactive compound profile of *L. culinaris*, with blue LED treatment emerging as the most effective condition for enhancing antioxidant and metal-chelating activities.

Keywords: Antioxidant activity, DPPH radical scavenging, LED Light, Lentil, Microgreens

ORAL PRESENTATION

Phenolic–flavonoid composition and antioxidant potential of microgreen and mature *Eruca sativa* Mill. extracts

Didem Turhan[1*] (https://orcid.org/0000-0002-1159-7952),
Muhammet Dogan[2] (https://orcid.org/0000-0003-3138-5903),
Bugrahan Emsen[3] (https://orcid.org/0000-0002-9636-2596)

*[1]Department of Gastronomy and Culinary Arts, Institute of Social Sciences, Karamanoğlu Mehmetbey University, Karaman, Türkiye
[2]Department of Nutrition and Dietetics, Faculty of Health Sciences, Karamanoğlu Mehmetbey University, Karaman, Türkiye
[3]Department of Biology, Kamil Özdağ Faculty of Science, Karamanoğlu Mehmetbey University, Karaman, Türkiye

*Corresponding author e-mail: dyt.didemaltindas@gmail.com

Abstract

This study evaluated the phenolic–flavonoid composition and antioxidant potential of microgreen and mature *Eruca sativa* extracts obtained using acetone, ethyl acetate, and water. Total phenolic content ranged from 156.51 to 304.93 µg GAE/mg, with the highest value detected in the microgreen water extract (MWE, 304.93 ± 5.47 µg/mg). Total flavonoid levels varied between 306.33 and 396.04 µg QE/mg, where again the microgreen water extract exhibited the strongest flavonoid content (396.04 ± 1.04 µg/mg). DPPH scavenging analysis revealed IC_{50} values between 100.98 and 153.41 µg/mL for microgreen extracts, and between 119.99 and 152.42 µg/mL for mature plant extracts. The strongest radical scavenging activity was observed in the microgreen water extract (MWE, IC_{50} = 100.98 µg/mL), followed by the mature acetone (OAS, 119.99 µg/mL) and mature ethyl acetate (OEA, 122.67 µg/mL) extracts. Metal chelation capacity showed remarkable differences between microgreen and mature stages. IC_{50} values ranged from 62.27 to 158.41 µg/mL for microgreens, while mature plant extracts exhibited IC_{50} values between 72.56 and 120.31 µg/mL. The most potent chelating activity was recorded in the microgreen water extract (MWE, 62.27 µg/mL) and mature acetone extract (OAS, 72.56 µg/mL). Microgreen extracts, particularly MWE, demonstrated superior antioxidant capacity in both radical scavenging and metal chelation assays, supported by their high phenolic and flavonoid levels. Mature plant extracts also showed significant activity, indicating that both growth stages of *E. sativa* represent valuable sources of natural antioxidants. These findings highlight the potential applicability of *E. sativa*, especially its microgreen forms, in functional food formulations and natural antioxidant development.

Keywords: Antioxidant activity, DPPH radical scavenging, *E. sativa*, Microgreens

Acknowledgements: This work was supported by Scientific Research Projects Commission of the Karamanoğlu Mehmetbey University. Project Number: 16-YL-24

ORAL PRESENTATION

Artificial intelligence-assisted dermatophyte diagnosis-image analytics approach

Aras Fahrettin Korkmaz (Orcid: https://orcid.org/0000-0002-3827-3018)

[1]Nutrition and Dietetics Department, Faculty of Health Sciences, Şirinevler Campus, İstanbul Kültür University, Istanbul, Türkiye

Corresponding author e-mail: a.korkmaz@iku.edu.tr

Abstract

Artificial intelligence–based diagnostic tools have recently gained increasing attention as complementary technologies for dermatological imaging. Dermatophyte infections, which represent one of the most common groups of superficial fungal diseases, are often difficult to diagnose accurately using traditional visual inspection or microscopy alone. Deep learning models, particularly convolutional neural networks (CNNs), can automatically extract morphological features associated with dermatophytic lesions from dermoscopic and clinical skin images. These models enhance diagnostic precision by learning fine-scale texture differences, erythema patterns, edge characteristics and scaling intensity that may not be easily distinguished by clinicians. Recent studies demonstrate that AI-supported systems can reach accuracy levels comparable to experienced dermatologists, especially in differentiating dermatophyte infections from eczema, psoriasis and bacterial dermatoses. This study provides an overview of state-of-the-art image-based AI applications developed for dermatophyte detection, discussing training dataset requirements, preprocessing workflows, model performance metrics and common challenges related to class imbalance, image noise and variability in illumination. Furthermore, the integration of AI tools with tele-dermatology platforms is evaluated, highlighting their potential use in remote triage, early detection and decision support. Limitations such as the need for standardized image acquisition protocols, dataset diversity and clinical validation processes are also addressed. Overall, AI-driven image analysis offers a promising, fast and reproducible approach to dermatophyte diagnosis. When supported by high-quality datasets and rigorous clinical evaluation, these systems may enhance routine dermatological practice and contribute to more accurate management strategies for superficial mycoses.

Keywords: Dermatophyte, Artificial Intelligence, CNN, Image Analysis, Digital Diagnosis

ORAL PRESENTATION

Cytokines as biological pesticides in combating pest insects

Eyüp Ayar[1*] (ORCID: https://orcid.org/0009-0007-4329-0318),
Cihat Çelik[2] (ORCID: https://orcid.org/0000-0002-2400-3412)

[*1]University of Zonguldak Bülent Ecevit, Faculty of Science, Department of Biology, Zonguldak, Türkiye.
[2]University of Zonguldak Bülent Ecevit, Vocational School of Çaycuma Food and Agriculture, Department of Chemistry and Chemical Processing Technologies, Zonguldak, Türkiye.

*Corresponding author e-mail: eyupayar23@gmail.com

Abstract

Cytokines are small protein molecules that facilitate intercellular communication in the immune system and direct immune responses. They are known to play important roles in the mammalian immune system. In mammals, they are produced by macrophages, lymphocytes, mast cells, granulocytes, fibroblasts, epithelial cells, endothelial cells, natural killer cells (NK cells), and T and B lymphocytes. Their key functions include initiating inflammation, promoting cell migration, supporting tissue repair, controlling immune responses, and providing defense against cancer cells. In recent years, in addition to their functions in mammals, cytokines have also been investigated in insects. However, while studies on the fruit fly *Drosophila melanogaster* Meigen (Diptera: Drosophilidae) have identified different cytokines, research on this topic is still limited. *D. melanogaster* cytokines play critical roles in various biological processes, including the insect immune system, development, cell growth, and stress response. Furthermore, specific cytokine groups have the potential to control pest populations by targeting the growth and immune mechanisms of pests. Therefore, cytokines are potential molecules that can be used as biological pesticides in agriculture. In this context, our laboratory is conducting research in this area using model insects such as *D. melanogaster* and the greater wax moth, *Galleria mellonella* L. (Lepidoptera: Pyralidae), to develop environmentally friendly alternatives to insecticides used in agriculture and to minimize their harmful effects on non-target organisms. Our laboratory will also focus on studies examining the effects of these groups of molecules on the survival and development of model insects to uncover the potential effects of cytokines on agricultural pest insects.

Keywords: Biopesticide, cytokines, model insects

ORAL PRESENTATION

Evde tüketim veya pazarlarda satışa sunulmak için üretilen peynirlerde biyojen amin üreticisi *Enterococcus* türlerinin risk değerlendirmesi: Çanakkale/Bayramiç örneği

Hakan Yıldırım[1], Fatma Dilara Kırım[1], Başar Uymaz Tezel[1*] (Orcid: https://orcid.org/ 0000-0002-4156-8861)

[1]Çanakkale Onsekiz Mart Üniversitesi, Bayramiç Meslek Yüksekokulu, Çanakkale, Türkiye.

*Sorumlu yazar e-mail: buymaz@comu.edu.tr

Özet

Biyojen aminler; hayvan, bitki ve mikroorganizmaların normal metabolik aktiviteleri sonucunda, aminoasitlerin dekarboksilasyonu ile oluşan düşük molekül ağırlıklı azotlu bileşikler olup; biyojen amin içeriği yüksek gıda tüketimi toksik etkilere neden olabilmektedir. Biyojen aminler; hammadde mikroflorasındaki çeşitlilik, kontrolsüz koşullarda gerçekleşen fermantasyon ve çevresel kontaminantlar gibi etkenlerle fermente gıdalarda yüksek derişimlerde bulunabilmektedir. Ev yapımı peynirler, kontrolsüz mikrobiyel yükü ve olgunlaşma sıcaklıkları nedeniyle biyojen amin bakımından en riskli fermente gıda grubu olarak değerlendirilmektedir. Çalışmada Çanakkale'nin Bayramiç ilçesinde starter kültür kullanılmadan, evlerde geleneksel yöntemlerle işlenerek olgunlaştırılan; tüketilen ve/veya ilçe pazarında satışa sunulan peynir örneklerinden *(i)* Enterokok cinsi türlerin izolasyonu *(ii)* izolatların kısmi karakterizasyonu (Eskulin hidrolizi, pH 9,6'da gelişim, tuz (%6,5 NaCl) ve sıcaklık (10°C ve 45°C) tolerans düzeyleri) yapılmış olup ayrıca *(iii)* histamin, agmatin, putresin ve tiramin üreticisi *Enterococcus* spp. izolatları tespit edilmiştir. Çalışmada toplam 39 adet ev yapımı peynir örneği analize alınmış olup; selektif besi ortamında tipik morfolojiye sahip kolonilerden rastgele seçilerek, 99 adet muhtemel *Enterococcus* spp. suşu izole edilmiştir. Gram (+), tek ya da kısa zincirler halinde kok ya da kokobasil morfolojisine sahip, katalaz (-) izolatların; kısmi karakterizasyon sonuçlarına göre 2 adetinin (BE-2/7 ve BE-11/33) *Enterococcus* spp. cinsine dahil olmadığı belirlenmiştir. Aminoasit dekorboksilaz aktivitesi, prekürsor aminoasit olarak ornitin (putresin), histidin (histamin), arjinin (agmatin) ve tirozin (tiramin) içeren dekarboksilaz broth ortamları kullanılarak belirlenmiştir. *Enterococcus* spp. izolatlarının hiçbirinin putresin üreticisi olmadığı; buna karşılık hepsinin histamin ve agmetin üreticisi olduğu tespit edilmiştir. Bununla birlikte 19 izolatın (BE-1/3, BE-3/12, BE-3/15, BE-10/30, BE-11/31, BE-20/50, BE-20/52, 62, 64, ÇE-2/70, EE-2/76, EE-3/78, EE-3/79, BE-4/85, BE-26/92, BE-27/96, BE-27/97, BE-28/98 ve BE-28/99) tiramin üreticisi olduğu belirlenmiştir. Elde olunan sonuçlar halk sağlığı ve gıda güvenliği açısından değerlendirildiğinde, Bayramiç (Çanakkale) ilçesinde tamamen kontrolsüz koşullarda üretilerek tüketilen ve/veya satışa sunulan peynirlerin olası biyojen amin üreticisi *Enterococcus* spp. türlerinin prevalansının yüksek olduğunu ortaya koymaktadır.

Anahtar Kelimeler: Çanakkale/Bayramiç, Peynir, *Enterococcus* spp., Biyojen amin

*Bu çalışma TÜBİTAK–2209-A Üniversite Öğrencileri Araştırma Projeleri Desteği Programı (1919B012413392) tarafından desteklenmiştir.

ORAL PRESENTATION

Structure-based docking analysis of potential insect growth regulator ligands against the EcR/USP complex

Abdurrahman Atalay[1*] (ORCID: https://orcid.org/0000-0002-9018-7264), Dilek Ünlüer Birinci[2,3] (ORCID: https://orcid.org/0000-0003-1939-2246), Şeymanur Erden[3] (ORCID: https://orcid.org/0009-0001-7510-3085), Asım Kadıoğlu[3] (ORCID: https://orcid.org/0000-0002-4781-6264)

[*1]Avrasya University, Faculty of Health Science, Department of Nutrition and Dietetics, Trabzon, Türkiye.
[2]Karadeniz Technical University, Faculty of Science, Department of Chemistry, Trabzon, Türkiye.
[3]Karadeniz Technical University, Faculty of Science, Department of Biology, Trabzon, Türkiye.

*Corresponding author e-mail: atalay.abdurrahman@yahoo.com

Abstract

This study conducted comprehensive molecular docking analyses to evaluate the binding potential of newly proposed ligand candidates targeting the Ecdysone Receptor/Ultraspiracle (EcR/USP) heterodimer complex, a key regulator of insect development and metamorphosis[1]. Since EcR/USP is a critical target in the development of insect growth regulator–based pesticides[2], computational elucidation of ligand–receptor interactions constitutes an essential preliminary step in rational drug and pesticide design. In this context, five candidate ligands (**1a**–**1e**), planned for future synthesis, were subjected to AutoDock-based calculations using the crystal structure of the EcR/USP complex (PDB: 2R40)[3]. The protein structure was optimized through the addition of polar hydrogen atoms and assignment of Gasteiger charges, while the ligands were incorporated into the docking workflow following energy minimization and conversion to three-dimensional conformations. Grid box parameters were configured to fully encompass the binding pocket. The resulting binding affinity values indicated that ligand–receptor interaction strengths ranged from –5.8 to –7.4 kcal/mol. The strongest affinity was observed for ligand **1e** (–7.4 kcal/mol), which was stabilized by a synergistic combination of hydrogen bonds, pi–pi and pi–sigma interactions, and extensive hydrophobic contacts. The other ligands also established diverse binding motifs, including hydrogen bonds with arginine, aspartate, and glutamine residues; pi-cation interactions with positively charged amino acids; and alkyl/pi-alkyl interactions with apolar residues. The findings demonstrate that ligand **1e** represents a particularly promising binder for the EcR/USP target and stands out as a strong candidate for subsequent biological evaluation. The outcomes of this study provide a computational foundation for the development of new pesticide candidates based on insect growth regulation and offer critical insights to support the transition into experimental validation.

Keywords: EcR/USP, Insect growth regulators, Pesticide design, Molecular docking.

*This work was supported by KTU-BAP (13) (Project No: 16204).

References:

1. Billas, I. M. L., Iwema, T., Garnier, J.-M., Mitschler, A., Rochel, N., & Moras, D. (2003). Structural adaptability in the ligand-binding pocket of the ecdysone hormone receptor. Nature, *426*(6962), 91-96.
2. Feng, Y., Cui, J., Jin, B., Li, X., Zhang, X., Liu, L., & Zhang, L. (2023). In Vitro Binding Effects of the Ecdysone Receptor−Binding Domain and PonA in Plutella xylostella. Molecules, *28*(3), 1426.
3. Browning, C., Martin, E., Loch, C., Wurtz, J.-M., Moras, D., Stote, R. H., Dejaegere, A. P., & Billas, I. M. L. (2007). Critical Role of Desolvation in the Binding of 20-Hydroxyecdysone to the Ecdysone Receptor. Journal of Biological Chemistry, *282*(45), 32924-32934.

ORAL PRESENTATION

Endothelial dysfunction in type 1 diabetes and therapeutic targets

Sevil Erarslan

University of Bristol, Life Sciences, Medical School, Bristol, United Kingdom.

Corresponding author e-mail: sevilerarslan@gmail.com

Abstract

Type 1 diabetes mellitus (T1DM) is characterised by autoimmune destruction of pancreatic β cells, leading to insulin deficiency and chronic hyperglycemia. T1DM is increasingly impacting adults and has a substantial cardiovascular burden, while being previously thought of as a childhood illness. There is growing evidence that endothelial dysfunction is an early, key process that drives both micro- and macrovascular disease, rather than only a downstream result of more advanced problems. Mechanisms: Endothelial dysfunction in type 1 diabetes is caused by a complex interaction of structural, metabolic, and inflammatory variables. Excessive reactive oxygen species (ROS) and oxidative stress are caused by mitochondrial dysfunction induced by chronic hyperglycemia. This setting reduces endothelium-dependent relaxation by decreasing nitric oxide (NO) bioavailability, a vital vasodilator. Additionally, because it promotes oxidative stress and hinders vascular repair mechanisms, glycemic fluctuation is more harmful than continuously elevated glucose levels. Cellular and Systemic Impact: Reduced circulating endothelial progenitor cells (EPCs), particularly the $CD34^{+}KDR^{+}$ subgroup, indicate early vascular ageing and compromised vascular repair ability at the cellular level. However, disruption of the endocannabinoid-microbiota axis leads to endothelial barrier failure, which makes it easier for immune cells to infiltrate target tissues and exacerbates systemic autoimmunity. Furthermore, endothelial dysfunction in diabetic vasculopathy has been linked to changes in red blood cell activity and extracellular vesicles produced from erythrocytes. In conclusion, endothelial dysfunction is a critical therapeutic target for the treatment of type 1 diabetes. Future treatments for T1DM patients should primarily focus on lowering oxidative stress, stabilising glycemic control to reduce unpredictability, and activating endothelial repair pathways to enhance long-term cardiovascular outcomes.

Keywords: Type 1 diabetes, endothelial dysfunction, therapies

ORAL PRESENTATION

Contemporary advances in type 1 diabetes therapeutic perspectives

Sevil Erarslan

University of Bristol, Life Sciences, Translational Health Science, Bristol, United Kingdom.

Corresponding author e-mail: sevilerarslan@gmail.com

Abstract

Type 1 diabetes mellitus (T1DM) is an autoimmune-mediated disease of islet β-cell destruction and has traditionally relied on exogenous insulin to achieve glycemic control. In recent years, interdisciplinary research has spurred the clinical translation of several novel treatment strategies, particularly immunomodulation, β-cell replacement, and targeted insulin delivery. Immunomodulatory therapy: Immunosuppressants, represented by the anti-CD3 monoclonal antibody. Teplizumab, were approved by FDA as the first T1DM drug with disease-modulating effects. This drug can delay the progression of patients from subclinical to clinical onset and is expected to extend phase 2 progression by approximately 3 years. Additionally, other monoclonal antibodies and cell therapies targeting autoimmune mechanisms are also in clinical trials aimed at restoring immune tolerance. On the other hand, gene-modified islet cells used CRISPR-Cas12b to knock out immune-related genes and overexpress CD47, resulting in long-term survival of allogeneic islet cells in immunosuppressant-naive patients and significant improvements in glycemic control. Pluripotent stem cell-derived islet cells (VX-880, VX-264) which are stem cell-derived islet organoids, developed have entered phase I/II clinical trials and can restore islet function with gene editing or immunoprotection devices. A clinical case of chemical reprogramming of induced pluripotent stem cells (CiPS) demonstrates the potential of stem cell regenerative transplantation for the functional treatment of T1DM. Smart insulin delivery a closed-loop insulin pump system automatically adjusts insulin infusion using real-time continuous glucose monitoring (CGM) and algorithms, resulting in a significant increase in blood glucose time within the target range (TIR) and a significant reduction in hypoglycemic events, which has been validated in multicenter studies both domestically and internationally. In conclusion, key future challenges include increasing the large-scale production of cell resources, mitigating the safety risks of gene editing, and improving the algorithm reliability of closed-loop systems.

Keywords: Type 1 diabetes, gene therapy, organoids

ORAL PRESENTATION

Bioacoustic Differentiation of Advertisement Calls between the cf. Bedriagae Water Frog Lineage (Genus: *Pelophylax*) in Central Anatolia and the Cilician Water Lineagae in the Frog Çukurova Plain in Türkiye

Mehmet Bera Demirkan[1*] (ORCID: https://orcid.org/0009-0008-3970-7368), Ulaş Birdal[1*] (ORCID:https://orcid.org/0009-0001-0653-5159),
Çiğdem Akın Pekşen[1,2*](ORCID: https://orcid.org/0000-0001-5736-3062)

[*1]Başkent University, Faculty of Science and Letter, Molecular Biology and Genetics, Ankara, Türkiye.
[2] Başkent University, Institute of Transplantation and Gene Sciences, Ankara, Türkiye.

*Corresponding author e-mail: beradmrkn@gmail.com

Abstract

Anurans are among the most vocally active vertebrate groups, and the sounds they produce serve many purposes including territory marking, mate attraction, and danger detection. Among these, the advertisement call is highly species-specific and plays a key role in forming pre-mating reproductive barriers. The Anatolian water frog complex (genus *Pelophylax*) contains many genetically, phylogenetically differentiated but morphologically indistinguishable cryptic evolutionary lineages. Since water frogs are notoriously difficult to differentiate morphologically and also include many hybrid forms, mating calls become one of the most direct indicators of species boundaries, as vocal sac morphology and call structure co-evolve with lineage divergence. For this reason, bioacoustics analyses provide an important complementary dataset for verifying genetic differentiation among distinct lineages. In this study, 36 males from Ankara and Bolu (cf. bedriagae lineage) and 17 males from Adana and Hatay (Cilician lineage) were analyzed. The analysis was conducted using min 10-minute sound recordings from each collected directly from nature. The process of call segmentation and individual identification were performed within the framework of Raven Pro, utilising expert assistance and adhering to four main interaction criteria: sufficient spatial separation, clear positional distinction, non-overlapping call sequences, and consistency of parameter stability across calls. Since natural recordings inevitably include multiple overlapping individuals, correct individual assignment was essential. After individual calls were classified, the temporal and spectral variables of advertisement calls were extracted, and ANCOVA was performed with water temperature included as a covariate. The results showed that when the impact of temperature was statistically regressed out of the data, analyses of advertisement call data exhibited clear differentiation between the cf. bedriagae and Cilician lineages. The acoustic distances reflected both the known genetic structure and the geographic separation patterns of cf. bedriagae populations (Gediz, Kızılırmak and Yeşilırmak basins) and the Cilician populations (Çukurova basin, Adana–Hatay). Importantly, these lineages were successfully distinguished using field-recorded calls rather than laboratory-controlled recordings. This demonstrates that bioacoustics in the natural environment is sufficient to resolve divergence between these closely related water frog lineages. This study provides valuable data on whether genetic differentiation in Anatolian water frog lineages is mirrored at the bioacoustic level and contributes to understanding pre-mating isolation mechanisms in these cryptic *Pelophylax* lineages.

Keywords: water frogs, *Pelophylax*, bioacoustics, advertisement call, cf. bedriagae, Cilician lineage, Anatolia

ORAL PRESENTATION

Fe (III)'ün sulu ortamda tespiti için rodamin-B bazlı optik sensör

Neşe Taşci (https://orcid.org/0000-0002-0571-1106*)*

Gebze Teknik Üniversitesi, Temel Bilimler Fakültesi, Kimya Bölümü, Kocaeli, Türkiye.

Sorumlu yazar e-mail: nesetasci@gtu.edu.tr

Özet

Demir, biyoaktif metal iyonlarından birisidir ve enerji üretimi, O_2 taşınması, enzim katalizi, DNA-RNA sentezi ve onarımı gibi birçok fizyolojik ve patolojik süreçte önemli rol oynar [1, 2]. Bu nedenle, canlı sistem için vazgeçilmez ve temel elementlerden birisidir. Vücutta Fe(III) iyonlarının eksikliği veya fazlalığı çeşitli hastalıklara neden olabilir. Demir, biyolojik sistemlerde oksijen taşıyıcısı görevi görür. Eksikliği durumunda hücrelere düşük oksijen gider ve bu durum anemi, diyabet, karaciğer ve böbrek hasarı gibi birçok sağlık sorununa neden olabilir [3- 5]. Öte yandan, vücuttaki aşırı demir miktarı, Alzheimer, Huntington ve Parkinson hastalıkları, akciğer, pankreas, kalp gibi organların fonksiyonlarının bozulması ve çeşitli kanser türleri gibi birçok ciddi hastalığa yol açabilir [6, 7]. Bu nedenle, sudaki demir iyonlarının seçici, hassas ve güvenilir bir şekilde belirlenmesi son derece önemli bir gerekliliktir. Literatürde Fe(III) iyonlarının tespiti için alev atomik absorpsiyon spektrometrisi (FAAS), kolorimetri, indüktif eşleşmiş plazma kütle spektrometresi (ICP-MS), indüktif eşleşmiş plazma optik emisyon spektrometresi (ICP-OES), yüksek performanslı sıvı kromatografisi (HPLC) gibi birçok seçici, hassas ve hızlı belirleme yöntemi rapor edilmiştir. Ancak bu yöntemlerin pahalı ekipman gereksinimi, operasyonel karmaşıklık, uzun hazırlık süresi ve karmaşık numune hazırlama gibi bazı dezavantajları vardır [8]. Diğer geleneksel analitik tekniklerle karşılaştırıldığında, floresans sensörler, yüksek duyarlılığı, uygulama kolaylığı, kısa analiz süresi ve yüksek seçiciliği ile Fe(III) tayini için çok daha avantajlı bir yöntem olarak öne çıkmaktadır. Bu çalışmada, sulu ortamdaki Fe(III)' ün tayini için yeni bir rodamin-B bazlı floresans membran sensör hazırlanmış ve karakterize edilmiştir. Membranın karakterizasyonu, Fourier dönüşümlü kızılötesi (FTIR) spektroskopisi ve taramalı elektron mikroskobu (SEM) kullanılarak ile gerçekleştirilmiştir. Hazırlanan membranın floresans sensör özelliği floresan spektroskopisiyle değerlendirilmiştir. Sensörün çalışma aralığı, pH etkisi ve cevap süresi gibi çalışma parametreleri sistematik olarak incelenmiştir. Geliştirilen rodamin-B bazlı membrane sensör, sulu ortamdaki Fe(III)' ün tayini için pratik, hassas, seçici ve yeniden kullanılabilir bir alternatif sunmaktadır.

Anahtar Kelimeler: Fe (III) tayini, optik sensör, floresans.

Referanslar:

[1] Hentze MW, Muckenthaler MU, Galy B, Camaschella C (2010) Two to Tango: Regulation of Mammalian Iron Metabolism. Cell 142(1):24–38.
[2] Lin W, Long L, Yuan L, Cao Z, Feng J (2009) A novel ratiometric fluorescent Fe3+ sensor based on a phenanthroimidazole chromophore. Anal Chim Acta 634:262–266.
[3] Prashanth L., Kattapagari K.K., Chitturi R.T., Baddam V.R.R., Prasad L.K., (2015), A review on role of essential trace elements in health and disease, J NTR Univ Health Sci 4(2):75–85.
[4] Hirayama T., Fluorescent probes for the detection of catalytic Fe(II) ion, Free Radical Biol. Med., 133 (2019), 38-45.
[5] Chen X.B., Qi C.X., Li H., Ding J.Y., Yan S., Lei H., Xu L., Liu B., (2020), Highly sensitive and selective Fe^{3+} detection by a waterstable Tb^{3+}-doped nickel coordination polymer-based turn-off fluorescence sensor, J Solid State Chem 281:121030.
[6] Wojtunik-Kulesza K., Oniszczuk A., Waksmundzka-Hajnos M., (2019), An attempt to elucidate the role of iron and zinc ions in development of Alzheimer's and Parkinson's diseases, Biomed Pharmacother 111:1277-1289.
[7] Bao X., Cao X., Nie X., Xu Y., Guo W., Zhou B., Zhang L., Liao H., Pang T., (2015), A new selective fluorescent chemical sensor for Fe3+ based on rhodamine B and a 1,4,7,10-tetraoxa13-azacyclopentadecane conjugate and its imaging in living cells, Sens Actuators B Chem 208:54–66.
[8] Qi C.X., Xu Y.B., Li H., Chen X.B., Xu L., Liu B., (2021), A highly sensitive and selective turn-off fluorescence sensor for Fe3+ detection based on a terbium metal-organic framework, J Solid State Chem 294:121835.

ORAL PRESENTATION

Design of an Assay for Detecting Ehlers-Danlos Syndrome in Bengal Cats via Enzymatic Digestion

Mehmet Cevat Temizkan[1*] (ORCID: https://orcid.org/my-orcid?orcid=0000-0002-4353-6759)

[*1]Yozgat Bozok University, Faculty of Veterinary Medicine, Department of Genetics, Yozgat, TÜRKİYE.

*Corresponding author e-mail: m.cevat.temizkan@yobu.edu.tr

Abstract

Ehlers-Danlos syndrome is a connective tissue disorder characterized by skin hyperextensibility and joint laxity observed in various animal species. In Bengal cats, this condition results from an autosomal dominant deletion in the *COL5A1* gene. The variation involves a 22-nucleotide deletion spanning the last 7 nucleotides of exon 1 and the first 15 of intron 1, causing a splicing defect. Using OMIA, NCBI GenBank, and Ensembl data (OMIA ID: 002165-9685, 1464; NCBI: XM_023242950.2:c.115_121+15del; Ensembl: ENSFCAT00000060880.2), we investigated the feasibility of detecting this region via enzymatic digestion. We identified that primers Forward: CCCATGACTTCCTAGAGCGC and Reverse: GAGGCAAACCCAAGAACAACTG, combined with BfuAI/BspMI or BseYI enzymes, can detect the disease. The designed primers are specific to the target region and bind effectively to all *COL5A1* transcripts except minor ENSFCTT00005002702.1. However, due to high primer-dimer potential, optimization of the annealing temperature is required. Digestion of the wild-type allele with BfuAI/BspMI should generate 535 bp and 214 bp fragments, while BseYI should produce 515 bp and 234 bp fragments. Conversely, in mutant cats, the 22-bp deletion prevents digestion, resulting in a single 727 bp band. These results were confirmed via NebCutter restriction digestion simulations. This method allows for a preliminary diagnosis without immediate DNA sequencing. Unlike expensive sequencing equipment rarely found in routine clinics, this primer-enzyme combination offers rapid and reliable results. Although confirming positive samples via sequencing is recommended, eliminating the need to sequence negative samples provides a practical advantage for veterinary practitioners.

Keywords: Bengal, Cat, COL5A1, Ehlers-Danlos syndrome, PCR, Restriction Digestion

ORAL PRESENTATION

Comprehensive genome analysis and various functional attributes of a potential *Enterobacter bugandensis* isolated from Türkiye

Cumhur Avşar (Orcid: https://orcid.org/0000-0002-4095-0022)

Department of Biology, Sinop University, Sinop, Türkiye

Corresponding author e-mail: cumhur.avsar@gmail.com

Abstract

Research on *Enterobacter bugandensis*, a member of the *Enterobacter cloacae* complex (ECC) that has recently attracted attention within this group and is considered the most pathogenic species in the group, is prominent. Recent confusion in the identification of ECC group members has made it difficult to identify dangerous members within the group. Supported by Sinop University, the BAP unit with code FEF-1901-25-005, this work aims to determine the antibiogram analysis, IAA, ACC deaminase, siderophore, biofilm production, Bradford protein content, and phosphate-solubilizing activity of a strain isolated from rice soil and identified as *Enterobacter bugandensis* based on 16S rRNA and whole-genome sequence analysis. Additionally, boron and arsenic resistance and intracellular boron accumulation were determined. The definitive identification of this strain through whole-genome analysis and the annotation of its genome with detailed gene information were presented using programs such as Proksee and KEGG. It was determined that this strain does not possess phosphate solubilization and ACC deaminase activity, with IAA activity at 5.7±0.65 µg mL^{-1}, siderophore production at 86.3±6.1 µmol L^{-1}, and Bradford protein content at 391.2±7.12 µg mL^{-1}. In addition, it was observed that it grew at a boron concentration of 100 mM, did not grow in the presence of As (III), but had an MIC value of 22 g/L for As (V). Furthermore, this strain was found to have intracellular boron accumulation (0.23±0.02 mg/L). However, this strain was observed to be resistant to many different antibiotics that inhibit cell wall and protein synthesis (ampicillin, cefoxitin, aztreonam, linezolid, clindamycin, etc.). The genome size was found to be 4.7–4.9 Mbp, similar to typical *E. bugandensis*, with a GC content of ~55%, 1262 CDS, 12 tRNA, 15 ncRNA, and 14 regulatory RNA. Furthermore, based on genomic analysis, this strain was found to possess multidrug resistance (MDR), carry *IncFII*(*pECLA*) and *IncR* plasmids (containing numerous *tra*, *trb*, *rep*, *mob*, and conjugal-transfer genes), and have the presence of 3 prophages, which typically carry efflux pumps, virulence factors, accessory genes, and stress adaptation genes. These phages are known to contribute to the genomic evolution of *E. bugandensis*. Furthermore, CRISPRCasFinder analysis indicates the absence of CRISPR/Cas loci, suggesting that this strain is more susceptible to plasmid acquisition and consistent with the presence of numerous ARGs and prophages. Additionally, the genomic analysis of this strain supports the phenotypic characteristics tested.

Keywords: *Enterobacter bugandensis*, MDR, CRISPR-CAS, prophage, genome analysis

ORAL PRESENTATION

Bitki büyümesini teşvik edici özellikteki *Bacillus* suşlarının siklik lipopeptid üretimlerinin kromatografik olarak incelenmesi

Baran Mis[1*] (https://orcid.org/0009-0001-4774-1792), Zülal Günay[1] (https://orcid.org/0000-0003-3893-9876), Murat Elibol[1] (https://orcid.org/0000-0002-6756-6290), Rengin Eltem[1] (https://orcid.org/0000-0002-0642-7676)

[1] Ege Üniversitesi, Mühendislik Fakültesi, Biyomühendislik Bölünü İzmir, Türkiye.

[*]Sorumlu yazar e-mail: baran.mis@ege.edu.tr

Özet

Lipopeptitler (LP) amfifilik özellikleri sayesinde gösterdikleri antibakteriyel ve antifungal özellikleriyle tarım, gıda, kozmetik, tıp ve biyoremediasyon alanlarında alanlarda sıklıkla kullanılmaktadır. Günümüzde LP'lerin üretilmesinde *Bacillus* ve *Pseudomonas* suşları başta olmak üzere 11 farklı mikroorganizma kullanılmaktadır. Bu mikroorganizmalar arasında genel olarak güvenli (Generally Recognized As Safe, GRAS) kabul edilen *Bacillus* suşları kullanılarak, LP üretiminin uygun maliyetli koşullarla gerçekleştirilmesi kritik önem taşımaktadır. Siklik yapıda olan itürin ve sürfaktin lipopeptidlerinin üretilmesi için 3 farklı *B. subtilis* suşunun uygun maliyetli üretim ortamında geliştirilmeleri gerçekleştirilmiş ardından ortamdan siklik lipopeptidlerin (CLP'lerin) ekstraksiyonu asit degradasyon-metanol yöntemiyle yapılmıştır. Elde edilen CLP'lerin miktarları yüksek performanslı sıvı kromatografisiyle (HPLC) kromatografik olarak tespit edilmiş, uygun maliyetli üretim ortamında *Bacillus* spp.'nin ulaştığı canlı hücre sayıları dökme plaka yöntemiyle incelenmiş sonuçlar koloni oluşturan birim (kob)/ml olarak belirlenmiştir. Elde edilen sonuçlara göre, *Bacillus subtilis* EGE-B-36.5 suşu itürin üretimi açısından açık ara öne çıkmaktadır (3,777±0,946 mg/ml), diğer iki suş (EGE-B-1.19 ve EGE-B-3.P.5) ise oldukça düşük ve benzer itürin değerlerine sahiptir (sırasıyla 0,071±0,007 ve 0,071±0,005 mg/ml). Sürfaktin üretiminde ise EGE-B-1.19 suşu en yüksek değere (1,216±0,096 mg/ml) sahip olup, EGE-B-36.5 ve EGE-B-3.P.5 suşları sırasıyla 1,09±0,231 mg/ml ve 0,973±0,082 mg/ml ile onu takip etmektedir. Canlı hücre sayısı açısından ise EGE-B-1.19 suşu ($1,4x10^9$ kob/ml) diğerlerine göre çok daha yüksek hücre yoğunluğuna sahiptir. EGE-B-36.5 ve EGE-B-3.P.5 suşları ise sırasıyla $3,3x10^8$ ve $2,4x10^8$ kob/ml canlı hücre sayısı ile daha düşük yoğunluk göstermiştir. Çalışma sonucunda GRAS *B. subtilis* EGE-B-36.5 suşunun uygun maliyetli üretim ortamında itürin ve sürfaktin üretimi için potansiyel bir aday olduğu belirlenmiştir.

Anahtar Kelimeler: Lipopeptid, sürfaktin, itürin, HPLC, *Bacillus*, GRAS

ORAL PRESENTATION

Green synthesis of a novel chloro-aza acyclovir analogue

Suzan Alhilal (Orcid: https://orcid.org/0000-0002-9372-9364)

Mardin Artuklu University, Vocational School of Health Services, Department of Medical Services and Techniques, Mardin, Turkey.

Corresponding author e-mail: suzanalhilal@artuklu.edu.tr

Abstract

A chloro-aza acyclovir analogue, ^{1}N-(5'-diethylamino-3'-hydrochloro)-6-aminouracil, was synthesized using 6-aminouracil as a nitrogen base. Dichloroethylamine was used as an open chain and dissolved in DMF. Sodium carbonate was employed as an economical catalytic agent. The reaction yielded a yellow crystalline powder. Structure identification was achieved through comprehensive spectroscopic characterization, including IR spectroscopy, ^{1}H-NMR, ^{13}C-NMR, DEPT-135, COSY-NMR, HMQC, and EI-MS.

Keywords: aza acyclovir analogue, 6-aminouracil, diethanolamine.

ORAL PRESENTATION

Cytotoxic and antimicrobial effects of *Cirsium ciliatum* subsp. *szovitsii* (C. Koch) Petrak and the determination of its phenolic compounds

Tuğçe Dikpınar[1*] (ORCID:https://orcid.org/0000-0002-3994-3888), Turgut Taşkın[1] (ORCID: https://orcid.org/0000-0001-8475-6478), Erkan Rayaman[2] (ORCID:https://orcid.org/0000-0002-1261-3942), Saliha Aydın[3] (ORCID: https://orcid.org/0000-0001-7499-1028), Ayşe Mine Yılmaz-Göler[3,4] (ORCID: https://orcid.org/0000-0003-0802-523X), İsmail Şenkardeş[5] (ORCID: https://orcid.org/0000-0002-2656-0319).

[*1]Marmara University, Faculty of Pharmacy, Department of Pharmacognosy, Istanbul, Türkiye.
[*2]Marmara University, Faculty of Pharmacy, Department of Pharmaceutical Microbiology, Istanbul, Türkiye.
[*3]Marmara University, Genetic and Metabolic Diseases Research and Investigation Center, Istanbul, Türkiye.
[*4]Marmara University, School of Medicine, Department of Medical Biochemistry, Istanbul, Türkiye.
[*5]Marmara University, Faculty of Pharmacy, Department of Pharmaceutical Botany, Istanbul, Türkiye.

*Corresponding author e-mail: tugce.dikpinar@marmara.edu.tr

Abstract

The genus *Cirsium*, belonging to the Asteraceae family, comprises more than 250 species distributed across Europe, North Africa, Asia, and North and Central America. In the flora of Türkiye, this genus is represented by a total of 64 species classified under three sections [1]. Species of *Cirsium*, commonly known as "thistles," are reported to exhibit various pharmacological properties, including hepatoprotective, antioxidant, anticancer, antimicrobial, and anti-inflammatory activities [2]. In this study, the cytotoxic activities of n-hexane (CCH), dichloromethane (CCD), and methanol (CCM) extracts obtained by percolation from aerial parts of *Cirsium ciliatum* subsp. *szovitsii* were evaluated on MCF-7 and fibroblast cell lines using the MTT assay. Additionally, the effects of extracts on cell viability and their potential wound-healing properties were investigated, while their antimicrobial activities against various microorganisms were assessed using agar well diffusion and microdilution (MIC) methods. According to the results, CCH extract markedly decreased MCF-7 cell viability (24.35 ± 3.98%), whereas CCM extract significantly enhanced fibroblast viability. Both CCH and CCM extracts exhibited antimicrobial activity against tested microorganisms, with MIC values ranging between 0.31 and 0.63 mg/mL. Considering their biological profiles, CCM extract appears to be a promising wound-healing candidate, while CCH extract stands out as a potential anticancer agent. The phenolic composition of CCM extract was analyzed by HPLC-DAD, revealing the presence of chlorogenic acid and apigenin 4-O-neohesperidoside. Isolation studies aimed at identifying the active constituents of CCH extract are currently ongoing.

Keywords: *Cirsium*, cytotoxicity, antimicrobial activity, wound healing, HPLC-DAD

References:

[1] Yüksel E, Kıran Y, Şahin A, Yıldız B, Arabacı T. Karyological studies of 10 *Cirsium* sect. *Epitrachys* (Asteraceae) species from Turkey. Turk J Bot. 2013;3:1085-1092.
[2] Aggarwal G, Kaur G, Bhardwaj G, Mutreja V, Sohal HS, Nayik GA, Bhardwaj A, Sharma A. Traditional uses, phytochemical composition, pharmacological properties, and the biodiscovery potential of the genus *Cirsium*. Chemistry. 2022;4:1161-1192.

ORAL PRESENTATION

Preliminary evaluation of olive pomace extract-based topical cream: Antioxidant capacity and wound healing potential

Reyhan Zeynep Gündoğdu Özdemir[1*] (Orcid: https://orcid.org/0000-0003-4451-7442), Nükte Topraksever[2] (Orcid: https://orcid.org/0000-0001-8982-2219)

[*1]Istanbul Health and Technology University
Faculty of Engineering and Natural Sciences, Molecular Biology and Genetics, İstanbul, Turkey.
[2]Istanbul Health and Technology University
Faculty of Engineering and Natural Sciences, Chemical Engineering, İstanbul, Turkey.

*Corresponding author e-mail: reyhan.gundogdu@istun.edu.tr

Abstract

Olive pomace, a by-product generated during olive oil production, is generally considered a low-value product despite its high phenolic compound content. The literature indicates that olive pomace is rich in hydroxytyrosol and its derivatives and exhibits potent antioxidant properties (Alu'datt et al., 2017; Yılmaz & Gökmen, 2020). The aim of this study is to obtain a phenolic-rich extract from olive pomace (OP), determine the antioxidant capacity of the extract, and preliminarily evaluate its potential to support wound healing by integrating it into a topical cream formulation. After drying and grinding the olive pomace samples, an ultrasonic-assisted extraction method using ethanol was applied. This is consistent with previous studies showing that ultrasonic extraction increases phenolic yield (Ameer et al., 2017). Total phenolic content was determined using the Folin–Ciocalteu method, and antioxidant activity was analysed by DPPH inhibition. The strong radical scavenging capacity of phenolics derived from olive pomace has been previously reported in the literature (Obied et al., 2005). Antioxidant analyses revealed that the extract inhibited the DPPH radical by over 70%. These results are consistent with the literature regarding the biological activity of olive pomace polyphenols (Alu'datt et al., 2017). Additionally, in the preliminary animal model evaluation, it was found that epithelialisation occurred more rapidly in groups treated with cream containing the extract, consistent with previous studies reporting that polyphenols support wound healing (Rodriguez-Luna et al., 2019; Şakul AA et al.,2023).
This study demonstrates that olive pomace extract can be used in dermatological-cosmetic formulations containing natural active ingredients due to its antioxidant potential on wound-healing effect. Herein, incisional and excisional wound model is applied in BALB/c mice and further wound healing processes are observed (Şakul AA et al.,2023). Therefore, the study offers a sustainable approach to converting industrial waste into high-value products.

Keywords: sustainability, olive pomace, antioxidant activity, incisional and excisional wound model, BALB/c mice.

References:

Ameer, K., Shahbaz, H. M., & Kwon, J. H. (2017). Green extraction methods for polyphenols from plant matrices and their byproducts: A review. *Comprehensive Reviews in Food Science and Food Safety, 16*(2), 295–315.

Alu'datt, M. H., Ereifej, K., Alhamad, M. N., Al-Tawaha, A. R., Rababah, T., Almajwal, A., & Kubow, S. (2017). Phenolic compounds in olive pomace and their biological activity. *Journal of Food Composition and Analysis, 56*, 45–52.

Obied, H. K., Allen, M. S., Bedgood Jr, D. R., Prenzler, P. D., Robards, K., & Stockmann, R. (2005). Bioactivity and analysis of biophenols recovered from olive mill waste. *Journal of Agricultural and Food Chemistry, 53*(4), 823–837.

Rodriguez-Luna, A., Álvarez-Pérez, O. B., Virgen-Ortíz, J. J., & Peña-Montes, C. (2019). Polyphenols as potential wound healing agents. *Molecules, 24*(13), 2256.

Şakul AA, Ayla Ş, Okur ME, Karadağ AE, Daylan B, Güzel E, Özdemir EM, Günal MY. (2023). In vivo wound-healing and in vitro antibacterial and antioxidant properties of Carduus adpressus extract. J Res Pharm. 27(2): 665-676.

Yılmaz, E., & Gökmen, V. (2020). Olive tree biophenols: Composition and biological effects. *Food Research International, 131*, 108–115.

ORAL PRESENTATION

Development of a biosensor for ethoprophos determination

Ezgi Adak[1]*(ORCID: https://orcid.org/0000-0002-7506-3140), Halit Arslan[1] (ORCID: https://orcid.org/0000-0002-8275-0002)

* [1]Gazi University, Faculty of Science, Department of Chemistry, Ankara, Turkiye.

*Corresponding author e-mail: ezgiadak@gazi.edu.tr

Abstract

Ethoprophos is an organophosphate pesticide widely used in agriculture. It poses significant environmental and health risks due to its neurotoxic effects and persistence in soil and water. Therefore, the accurate determination of trace concentrations is essential to evaluate its potential impact. In this study, a biosensor was developed for the trace-level detection of the pesticide ethoprophos. The limit of detection (LOD) and limit of quantification (LOQ) for the determination of ethoprophos using the developed biosensor were calculated to be 1.67×10^{-10} M and 1.26×10^{-9} M, respectively. The analytical performance of the biosensor was validated through recovery experiments in pineapple samples, yielding a relative error of 5.33% and a relative standard deviation (RSD) of 3.62%. These findings demonstrate the biosensor's high sensitivity and reliability, highlighting its potential application in routine monitoring of pesticide residues in food products. Moreover, the approach provides a rapid and cost-effective alternative to conventional analytical techniques. This contributes to improved food safety and environmental protection.

Keywords: Biosensor, ethoprophos, pesticide, voltammetry.

Acknowledgements: We are grateful to Gazi University Scientific Research Projects Coordination Unit (Project number: FDK-2022-7739) for providing financial support.

ORAL PRESENTATION

An integrated multi-omics framework for robust MSI detection in colorectal cancer

Betul Isin (Orcid:https://orcid.org/0000-0003-3259-9831)

Canakkale Onsekiz Mart University, Department of Bioinformatics and Systems Biology, Canakkale, Türkiye

Corresponding author e-mail: isin.betull@gmail.com

Abstract

Colorectal cancer (CRC) is one of the leading causes of cancer-related death worldwide and represents a heterogeneous group of tumors. Microsatellite instability (MSI) is a clinically important biomarker in CRC, helping identify patients who may benefit from immunotherapy and offering insight into disease behavior. Although PCR and immunohistochemistry are frequently used to identify MSI, they are not always sensitive enough and can produce ambiguous results. For this reason, multi-omic approaches that integrate broader molecular information are becoming increasingly important for achieving a more accurate and reliable assessment of MSI. Next-generation sequencing–based methods have expanded MSI testing, yet many still rely on a single type of molecular data and typically neglect the challenges of incomplete datasets encountered in clinical practice. To address these limitations, this study proposes a multi-omics framework that integrates RNA expression, DNA methylation, and WES-derived mutational features. This approach aims to describe MSI biology more clearly by considering immune-related gene expression changes along with methylation patterns observed in MSI-H tumors. This overview outlines the rationale for building a reproducible diagnostic model with improved sensitivity, precise calibration, and robust performance even in the presence of missing data modalities. The proposed integrated workflow has the potential to improve clinical utility through decision curve analysis, optimize patient stratification, and contribute to the development of more robust biomarker-guided diagnostics in colorectal cancer.

Keywords: Colorectal Cancer, Microsatellite Instability, Bioinformatics, Multi-omics Integration

ORAL PRESENTATION

Postbiotics as potential therapeutic agents for noncommunicable diseases

Tuğçe Tüccar (Orcid: https://orcid.org/0000-0001-9262-6374)

Istanbul Aydin University, Faculty of Pharmacy, Department of Pharmaceutical Microbiology, Istanbul, Türkiye.

Corresponding author e-mail: tugcetuccar@aydin.edu.tr

Abstract

Microorganisms residing in the human gut microbiota establish symbiotic interactions with their host and contribute to the regulation of numerous physiological processes, including digestion, immune modulation, and the maintenance of intestinal barrier integrity. The therapeutic effects of these living microbes, known as probiotics, on human health have been widely recognized, leading to the development of targeted probiotic formulations in various dosage forms within the pharmaceutical sector and their incorporation into clinical practice. Recently, the concept of postbiotics, defined as inactivated microbial cells, their components, and metabolites produced by microorganisms, has attracted growing interest and has emerged as a promising focus for research and applications, particularly in the pharmaceutical industry. Compared with probiotics, postbiotics offer advantages such as greater shelf-life stability, improved convenience in storage and formulation, and a lower risk of adverse effects while still providing health-promoting benefits for both adults and children. Beyond their antimicrobial properties, postbiotics are increasingly considered as promising therapeutic candidates for a variety of noncommunicable diseases. In this regard, this study aims to provide a concise overview of the classification, production technologies, and mechanisms of action of different postbiotics, and to present their biological activities reported in *in vitro* and *in vivo* studies, thereby highlighting their potential as novel functional agents in the management of chronic diseases.

Keywords: Postbiotics, Noncommunicable diseases, Therapeutic agents

.

ORAL PRESENTATION

Production of enantiomerically pure 1-phenylethanol in green solvent media using response surface methodology

Ayşe Bozan[1] (ORCID: https://orcid.org/0000-0003-1201-9991), Rahime Songür[1*] (ORCID: https://orcid.org/0000-0002-1511-951X), Ülkü Mehmetoğlu[1] (ORCID: https://orcid.org/0000-0003-4293-2204)

[1]Ankara University, Faculty of Engineering, Department of Chemical Engineering, Ankara, Turkey.

*Corresponding author e-mail: rsongur@eng.ankara.edu.tr

Abstract

The enantiomers of 1-phenylethanol, an important secondary alcohol, are used in many industries, such as pharmaceuticals, agriculture, food and cosmetics. Furthermore, the search for reliable, environmentally friendly green solvents to replace traditional solvents has recently increased. The aim of this study was to produce 1-phenylethanol with enantiomeric purity using an enzymatic kinetic resolution method in a green solvent environment. Dimethyl carbonate, an organic carbonate, was used as the green solvent. Novozyme 435 (an immobilised lipase) was used as the lipase and vinyl acetate was used as the acyl donor. After the reaction, the samples were analysed by HPLC using a chiral column. The optimum reaction conditions in dimethyl carbonate were determined using the response surface method (RSM). Furthermore, the advantageous properties of dimethyl carbonate, such as low ecotoxicity, biodegradability, low cost and high ee_s and conversion, suggest that it could replace traditional solvents.

Keywords: 1-phenylethanol, green solvent, dimethyl carbonate, enzymatic kinetic resolution, enantioselectivity, RSM.

ORAL PRESENTATION

Eco-friendly synthesis of zinc oxide nanoparticles using pomegranate peel extract: Characterization and photocatalytic degradation of diclofenac

Yossra Ounis Dkhil[1,2*] (https://orcid.org/0000-0001-7146-1988), Tim Peppel[2] (https://orcid.org/0000-0002-7814-7235), Ammar Houas[1]

[*1]University of Gabès, Faculty of Sciences of Gabès, Research Laboratory of Catalysis and Materials for Environment and Processes (LR19ES08), Gabès, Tunisia.
[2]University of Rostock, Leibniz Institute for Catalysis (LIKAT), Rostock, Germany.

*Corresponding author e-mail: dkhil.yossra@gmail.com

Abstract

Zinc oxide nanoparticles (ZnO NPs) were synthesized via a simple, eco-friendly precipitation method utilizing a reducing agent derived from pomegranate (*Punica granatum*) peel extract. X-ray diffraction (XRD) analysis confirmed the successful formation of ZnO with a hexagonal crystal structure and an average crystallite size of less than 30 nm. Scanning electron microscopy (SEM) revealed distinct quasi-spherical and nanorod-like morphologies, while energy-dispersive X-ray spectroscopy (EDX) confirmed the presence of zinc and oxygen in the nanoparticles. Diffuse reflectance spectroscopy (DRS) indicated significant UV activity, with a band gap of 3.25 eV. The photocatalytic efficiency of the synthesized ZnO NPs was evaluated based on their ability to degrade diclofenac sodium (DCF) under UV-LED irradiation, achieving pollutant removal rate exceeding 99%.

Keywords: Diclofenac, Green synthesis, *p*-nitrophenol, Photocatalytic degradation, Pomegranate peel extract, *Punica granatum*, ZnO.

ORAL PRESENTATION

Current and emerging biomarkers in nephrotic syndrome

Elif Toku[1*] (ORCID: https://orcid.org/0009-0006-4836-9888), Büşra Uçar[2] (ORCID: https://orcid.org/0009-0007-4550-5511), Özlem Alptekin[2] (ORCID: https://orcid.org/0000-0002-0458-7609)

[*1]Mersin University, Faculty of Pharmacy, Department of Biochemistry, Mersin, Türkiye.
[2]Çukurova University, Faculty of Pharmacy, Department of Biochemistry, Adana, Türkiye.

*Corresponding author e-mail: eliftoku01@gmail.com

Abstract

Nephrotic syndrome (NS) is a glomerular disorder characterized by heavy proteinuria, hypoalbuminemia, edema and hyperlipidemia, and remains a major clinical challenge due to its heterogeneous etiology and variable treatment response. Classical biomarkers such as urinary protein excretion, serum albumin, creatinine, blood urea nitrogen (BUN) and lipid profile are routinely used for diagnosis and monitoring; however, their limited sensitivity and specificity restrict their ability to differentiate NS subtypes or detect early renal injury. This study summarizes current advances in molecular biomarkers that complement traditional parameters and enhance diagnostic precision in NS. Anti-Phospholipase A2 Receptor Antibody (Anti-PLA2R) and Anti-Thrombospondin Type-1 Domain-Containing 7A Antibody (anti-THSD7A) antibodies have markedly improved the noninvasive diagnosis of primary membranous nephropathy (MN), with anti-PLA2R detected in 70–80% of MN cases, while anti-THSD7A identifies a subset of PLA2R-negative patients. Recently defined podocyte-associated biomarkers including Neural Epidermal Growth Factor–Like 1 (NELL1), Exostosin-1 / Exostosin-2 (EXT1/EXT2), Semaphorin-3B, Protocadherin-7 and Wilms' Tumor 1 (WT1) provide novel opportunities for subclassification of NS and prognostic evaluation. Tubular injury and inflammation-related markers such as Neutrophil Gelatinase–Associated Lipocalin (NGAL), β2-microglobulin, D-dimer, α-1 antitrypsin and Cluster of Differentiation 80 (CD80) demonstrate potential for tracking disease activity and predicting therapeutic response. Furthermore, urinary exosomal microRNAs and circular RNAs represent promising noninvasive biomarker candidates with high clinical translational value. Overall, emerging biomarker panels combining serological, genetic and proteomic indicators offer superior diagnostic accuracy compared to isolated parameters and may reduce the need for invasive renal biopsy. Standardization of analytical methods and large-scale prospective validation studies are essential for integrating these biomarkers into routine nephrology practice.

Keywords: Nephrotic Syndrome, Biomarker, Anti-PLA2RA, Proteinuria

References:
Bogdanović, L., Babić, I., Prvanović, M., Mijač, D., Mladenović-Marković, A., Popović, D., & Bogdanović, J. (2025). Uncommon factors leading to nephrotic syndrome. *Biomedicines, 13*(8), 1907. https://doi.org/10.3390/biomedicines13081907
Tapia, C., & Bashir, K. (2023, May 29). *Nephrotic syndrome*. In *StatPearls* [Internet]. Treasure Island (FL): StatPearls Publishing. Retrieved May 6, 2025, from https://www.ncbi.nlm.nih.gov/books/NBK470444/
Gipson, D. S., Chin, H., Presler, T. P., Jennette, C., Ferris, M. E., Massengill, S., et al. (2006). Differential risk of remission and ESRD in childhood FSGS. *Pediatric Nephrology, 21*(3), 344–349. https://doi.org/10.1007/s00467-005-2097-0
Yeniçerioğlu, Y., Güngör, Ö., & Arıcı, M. (Eds.). (2019). *Temel nefroloji*. Güneş Tıp Kitabevleri.
Tesar, V., & Hruskova, Z. (2021). Autoantibodies in/of membranous nephropathy. *Frontiers in Immunology, 12*, 593288. https://doi.org/10.3389/fimmu.2021.593288

ORAL PRESENTATION

Production of natural fiber-reinforced epoxy biocomposites in different woven and single-hybrid forms and analysis of their inner structure

Mert Emre Kalaoğlu[1*] (https://orcid.org/0009-0005-1919-2043), Ali Gökşenli[1] (https://orcid.org/0000-0002-1068-8705)

[1]Istanbul Technical University, Mechanical Engineering Faculty, Istanbul, Türkiye.

*Corresponding author e-mail: kalaoglum@itu.edu.tr

Abstract

In fiber-reinforced epoxy matrix composites, the fiber material can be synthetic or natural. Examples of synthetic fiber materials include glass, aramid, and carbon. Although these composites have advantages in terms of high mechanical properties, they have disadvantages such as high production costs and difficulties in recycling. Composites produced using natural plant-based fibers such as hemp, jute, flax, and banana peel are low in cost, but their biggest disadvantage is their low strength. Various methods are currently being used to improve this disadvantage. These include using different weave types, using more than one fiber material simultaneously, applying different weave types, and improving the fiber-matrix interface. In our study, biocomposites were produced using both natural and hybrid fiber materials to improve the properties of composite materials. Hemp, jute, and flax were used as natural fiber materials. In the first phase of our study, composites made from the same type of fiber material were produced. Biocomposites were then combined to produce three different hybrid structures. Thus, nine different fiber material groups were created, considering both single-type and hybrid structures. In the second stage, biocomposites were produced using different weaving methods. Plain, twill, and panama were used as weaving methods. A total of 27 different natural fiber fabrics were obtained by using three different textures, nine different single-hybrid and different fiber types mentioned above. In the third stage, the produced woven were combined with a bio-specific epoxy matrix material using a vacuum infusion method to produce biocomposite. In the final stage of our study, internal structure analyses were performed using stereomicroscope and scanning electron microscope (SEM). Our aim in the microstructure analysis was to examine the fiber-matrix distribution, the structure and orientation of the fibers and the interface formation.

Keywords: Biocomposite, Organic Fibers, Woven, Hybrid, Inner Structure

*This work was financially supported by the Scientific Research Projects Department of TU Istanbul, Project No. PMA-2025-46610.

ORAL PRESENTATION

Production and characterization of honokiol-loaded polymeric nanoparticles for glioblastoma treatment

Zeynep Atalay (Orcid: https://orcid.org/0009-0001-3125-2361), Cansu tatar, (orcid: https://orcid.org/0000-0002-1135-2840), Ayşegül Erdemir (Orcid: https://orcid.org/0000-0002-6099-4903)

Yıldız Technical University, Graduate School of Natural and Applied Sciences, Department of Molecular Biology and Genetics, Istanbul, Türkiye

*Corresponding author e-mail: zbalkir48@gmail.com

Abstract

Glioblastoma is the most common primary malignant tumor of the central nervous system. Although treatment methods such as chemotherapy, radiotherapy, and immunotherapy are available, these therapies have various adverse side effects and limitations. For this reason, plant-based therapeutic approaches have recently gained attention. Honokiol, a phenolic plant compound, is derived from the seeds, roots, stems, and leaves of species belonging to the Magnolia genus. Honokiol has demonstrated strong anticancer potential through its ability to modulate key processes such as metastasis, invasion, and apoptosis. However, its clinical application is restricted by challenges such as low solubility, poor bioavailability, and rapid metabolism, thereby highlighting the necessity for a nanoparticle-based delivery system. To reduce rapid drug metabolism and support penetration through the blood–brain barrier, honokiol was encapsulated into poly(lactic-co-glycolic acid) (PLGA) nanoparticles in this study. Honokiol-loaded PLGA nanoparticles were synthesized using the single emulsion (o/w) solvent evaporation method. The particle size and PDI values of the synthesized nanoparticles were determined. The functional groups on the nanoparticle surface were analyzed using Fourier Transform Infrared (FT-IR) spectroscopy. The produced nanoparticles exhibited an average size of 196±2.4 nm, with a PDI value of 0.257±0.007. The reaction yield (RV) was determined as 48%, while the encapsulation efficiency (EE) was 74%, and the drug loading (DL) were 6.6%. According to the FT-IR analysis, the nanoparticles displayed characteristic PLGA features, confirming the successful encapsulation of honokiol. As a result of this study, Honokiol-loaded PLGA nanoparticles were successfully synthesized, and their physicochemical characterization was completed. In future stages, the in vitro anticancer activity of Honokiol-loaded nanoparticles on the U87MG glioblastoma cell line will be evaluated.

Keywords: Glioblastoma, Honokiol, PLGA, Drug delivery, Nanoparticle

ORAL PRESENTATION

Holstein-Friesian ırkı erkek sığırlarda *LEP, IGF1* ve *MYF5* genlerinin karkas ve et kalitesi özellikleri üzerine etkilerinin belirlenmesi

Nursen ŞENTÜRK (0000-0003-1975-0103)[1], Tuğçe Necla SELVİ (0000-0003-3425-3201)[2], Hüseyn BABAYEV (0000-0001-6985-9436)[3], Hakan ÜSTÜNER (0000-0002-4341-5842)[2], Sena ARDIÇLI (0000-0003-2758-5945)[1,3]

[1]Bursa Uludağ Üniversitesi, Veteriner Fakültesi, Genetik Anabilim Dalı, Bursa, Türkiye
[2]Bursa Uludağ Üniversitesi, Veteriner Fakültesi, Zootekni Anabilim Dalı, Bursa, Türkiye
[3]Zürih Üniversitesi, İsviçre Alerji ve Astım Araştırma Enstitüsü, Davos, İsviçre

*Sorumlu yazar e-mail: sardicli@uludag.edu.tr

Özet

Sığır karkas ve et kalitesi, tüketici taleplerini karşılayan ürünler elde etmede kritik öneme sahiptir ve yüksek ekonomik değeri nedeniyle genetik ıslah hedeflerinde yaygın bir performans parametresidir. Modern genetik yaklaşımlar, karkas kalitesini etkileyen spesifik genlerin belirlenmesini sağlayarak ıslah programlarında etkin kullanımını desteklemektedir. Bu bağlamda; kas gelişimi, yağ metabolizması ve büyüme faktörlerini düzenleyen genler, karkas kalitesinin genetik temelini anlamak için kritik öneme sahiptir. Bu nedenle, leptin (*LEP*), insülin benzeri büyüme faktörü 1 (*IGF1*) ve miyojenik faktör 5 (*MYF5*) genleri sığırlarda karkas özelliklerini anlamak için temel adaylar olarak seçilmiştir. Bu çalışma, Holstein-Friesian ırkı erkek sığırlarda karkas ve et kalite özellikleriyle bu genlerin arasındaki ilişkiyi araştırmayı amaçlamıştır. Yüz üç sığır, PCR-RFLP yöntemi kullanılarak genotiplendirilmiştir. Ardından; bu genlerin canlı ağırlık, sıcak ve soğuk karkas ağırlığı, karkas randımanı, *musculus longissimus dorsi* alanı, Warner-Bratzler kesme kuvveti (WBSF), pişirme kaybı, soğutma kaybı, su tutma kapasitesi, karkas uzunluğu, göğüs genişliği ve et rengi parametreleri (*L*, a*, b**) ile ilişkileri incelenmiştir. Genlerin bireysel ve interaksiyon etkilerinin fenotipe yansımasının değerlendirmesinde GLM protokolü kullanılmıştır. Karkas ve et kalitesi arasındaki denge, Pareto-front yaklaşımı kullanılarak değerlendirilmiştir. Bireysel olarak incelendiğinde, *IGF1, MYF5* ve *LEP* genleri ile özellikler arasında anlamlı bir ilişki gözlenmemiştir (P >0,05). Ancak, *LEP* × *MYF5* interaksiyonu, canlı ağırlık, sıcak karkas ağırlığı ve soğuk karkas ağırlığı özellikleriyle anlamlı bir ilişki göstermiştir (P<0,05). Bu ikili interaksiyon, Holstein-Friesian sığırların karkas performansını önemli ölçüde etkileyebilecek bir epistatik örüntüyü ortaya koymuştur. Bildiğimiz kadarıyla, bu çalışma *LEP* × *MYF5* epistatik etkileşiminin sığır karkas performansı ile ilişkili olduğuna dair ilk kanıtı sunmaktadır. Standart et kalite parametreleri için karşılık gelen bir etkileşim tespit edilmemiştir. Bu bulgular, karkas verimini iyileştirmek için tek lokus etkilerinden ziyade, epistatik belirteç kombinasyonlarının seçim indekslerine ve eşleştirme planlarına dahil edilmesini desteklemektedir. Sonuçlar, sığır karkas ve et kalite özelliklerinin altında yatan gen-gen etkileşimlerinin bağımsız popülasyonlarda doğrulanması ve daha derinlemesine araştırılması için önemli bir motivasyon sağlamaktadır.

Anahtar Kelimeler: Et üretimi, gen interaksiyonu, sığır, SNP

ORAL PRESENTATION

Poisonous mushrooms and mushroom poisoning: Current findings and toxicological approaches from Türkiye

Aras Fahrettin Korkmaz[1*] (ORCID: https://orcid.org/0000-0002-3827-3018), Ilgaz Akata[2] (ORCID: https://orcid.org/0000-0002-1731-1302), Mustafa Sevindik[3] (ORCID: https://orcid.org/0000-0001-7223-2220)

[1]Nutrition and Dietetics Department, Faculty of Health Sciences, Şirinevler Campus, İstanbul Kültür University, Istanbul, Türkiye
[2]Ankara University, Faculty of Science, Department of Biology, Ankara, Türkiye.
[*3] Osmaniye Korkut Ata University, Faculty of Engineering and Natural Sciences, Department of Biology, Osmaniye, Türkiye.

*Corresponding author e-mail: sevindik27@gmail.com

Abstract

The aim of this study is to evaluate the poisonous mushroom species commonly seen in Türkiye and the poisoning cases caused by these species in terms of their toxin structures, clinical symptoms and treatment approaches; and to draw attention to the risks they pose to public health. Morphological similarities between edible and poisonous mushrooms lead to serious poisoning cases that threaten public health. Consumption of wild mushrooms collected from nature, especially in spring and autumn months, can have fatal consequences due to species containing toxins such as amatoxin, gyromitrin, muscarin and orellanin. In this study, poisonous mushroom species commonly seen in Türkiye (*Amanita phalloides, Cortinarius orellanus, Gyromitra esculenta, Inocybe* spp. and *Clitocybe* spp.) and the poisoning cases caused by these species were evaluated in the light of current literature and case reports. Poisoning symptoms may occur with gastrointestinal, hepatotoxic, nephrotoxic or neurotoxic findings depending on the type of toxin. Early symptoms include nausea, vomiting and abdominal pain, while in the late period liver failure, kidney damage and neurological complications may be observed. Amanita phalloides poisoning in particular causes serious hepatocellular damage due to amatoxins inhibiting the RNA polymerase II enzyme. Early diagnosis, gastric lavage, activated charcoal application and supportive treatments are at the forefront of the clinical approach, and in some cases the use of antidotes such as silibinin and N-acetylcysteine is also recommended. Every year in Türkiye, dozens of people apply to hospitals due to mushroom poisoning, and unfortunately some lose their lives. This situation once again reveals the importance of raising public awareness, correct species identification and dissemination of toxicological analyses. In this context, the identification of poisonous mushrooms, understanding of toxins and development of effective treatment protocols require a multidisciplinary approach from both clinical and mycological perspectives.

Keywords: Poisonous mushrooms, Mushroom poisoning, Amatoxin, Toxicology, Case studies in Türkiye

ORAL PRESENTATION

Medicinal Mushrooms As Emerging Natural Adjuncts In Cancer Therapy

Emre Cem Eraslan (Orcid: https://orcid.org/0000-0003-1773-1443)

Department of Biology, Faculty of Engineering and Natural Sciences, University of Osmaniye Korkut Ata, Osmaniye, 80000, Türkiye.

Corresponding author e-mail: emrecemeraslan@osmaniye.edu.tr

Abstract

Today, cancer continues to be one of the most common causes of death worldwide. Conventional treatment methods such as chemotherapy, radiotherapy and surgery often lead to serious side effects and face problems such as tumor resistance. Therefore, interest in natural, safe and effective agents that can support cancer treatment is increasing day by day. In this context, medicinal mushrooms have significant potential. Medicinal mushrooms contain bioactive compounds that have been used in traditional medicine, especially in Asian countries, for centuries and whose effectiveness has been scientifically confirmed today. Species such as Ganoderma lucidum (Reishi), Trametes versicolor (Turkey tail), Lentinula edodes (Shiitake) and Inonotus obliquus (Chaga) contain many pharmacologically valuable compounds such as immunomodulatory polysaccharides (especially beta-glucans), triterpenoids, phenolic compounds and ergosterol derivatives. Various in vitro and in vivo studies have shown that these compounds suppress the proliferation of cancer cells, stimulate the apoptosis (programmed cell death) process, prevent metastasis and, in some cases, increase the effectiveness of chemotherapy drugs. It is also known that they strengthen the immune system and create a more effective immune response against the tumor. In particular, fractions such as PSK (polysacchiside-K) and PSP (polysacchiside-peptide), obtained from the Trametes versicolor mushroom, have entered clinical use as adjuvant agents in cancer treatments in Japan and China. However, the acceptance of such agents in Western countries is still limited and more clinical studies are needed. In conclusion, the use of medicinal mushrooms as complementary agents in cancer treatment is promising both at the cellular level and in clinical applications. However, more scientific data is needed to clarify issues such as standard dosage, reliability, interactions and long-term effects. Research conducted in this direction will both increase the quality of life of patients and further solidify the place of natural products in modern medicine.

Keywords: Medicinal mushrooms, Cancer treatment, Natural complementary agents, Bioactive compounds, Immune modulation

ORAL PRESENTATION

Mathematical modeling of excercise -induced DNA methylation dynamics

Hatice Nur Oktay*, Işık Didem Karagöz

Gaziantep University,Faculty of Science,Department of Molecular Biology and Genetics,Gaziantep,Türkiye

*Corresponding author e-mail: nuroktay146@gmail.com

Abstract

Exercise is a powerful biological stimulus that induces not only short-term physiological responses but also long-term molecular adaptations through epigenetic regulation. Among epigenetic mechanisms, DNA methylation plays a key role in regulating exercise-induced gene expression and maintaining cellular memory. However, the dynamic and nonlinear nature of these changes cannot be fully explained using traditional biological approaches alone. This study aims to develop a mathematical framework to model exercise-induced DNA methylation dynamics by integrating differential equation–based modeling with topological data analysis (TDA). DNA methylation levels before and after exercise are represented as time-dependent variables governed by differential equations. The model incorporates biologically relevant parameters, including DNA methyltransferase (DNMT) and ten-eleven translocation (TET) enzyme activities, as well as exercise intensity and duration. This enables a quantitative and continuous-time analysis of methylation dynamics in response to physical activity. To capture the complex and high-dimensional structure of epigenetic data, topological data analysis is employed as a complementary approach. TDA allows the identification of structural patterns and transitions in DNA methylation profiles that may not be detectable using classical statistical methods. Through topological features, exercise-induced epigenetic remodeling is analyzed in terms of data continuity and structural change. The main contribution of this study is the proposal of a hybrid mathematical model that combines dynamic differential equation modeling with topological characterization of epigenetic data. The results suggest that exercise can induce persistent epigenetic modifications contributing to molecular-level biological memory and that these processes can be effectively described using integrated mathematical approaches.

Keywords: DNA methylation; Exercise; Hybrid mathematical model; Epigenetics

ORAL PRESENTATION

Pomegranate peel extract: antioxidant activity and potential effects on cardiovascular health

Deniz Duru Dervis (Orcid: https://orcid.org/0009-0009-9006-5687)

Yildiz Technical University, Faculty of Chemical and Metallurgical Engineering, Istanbul, Türkiye

Corresponding author e-mail: duru.dervis16@gmail.com

Abstract

In recent years, plant-derived bioactive compounds have attracted significant attention for their potential to prevent and manage cardiovascular diseases. Due to its high content of polyphenols and flavonoids, pomegranate peel represents a promising natural source of antioxidants. In this conducted study, the antioxidant properties of pomegranate peel extract and its potential effects on cardiovascular health are further discussed. The peel extract is highlighted for its role in neutralizing free radicals, reducing lipid peroxidation, and improving endothelial function, which may positively affect cholesterol metabolism. Furthermore, the potential of pomegranate peel as a sustainable, cost-effective raw material for the development of functional foods and nutraceutical products is further emphasized. Accordingly, this study aims to present the biomedical and biotechnological potential of pomegranate peel extract. This work is designed as a literature-based review that provides a scientific framework for future research in this field.

Keywords: Pomegranate peel, Antioxidant activity, Cardiovascular health, Bioactive compounds, Sustainability

ORAL PRESENTATION

Chemical warfare agent recognition by using a practical mobile application

Ruşen Koray Eyison (Orcid:0000-0003-0151-6546)

University of Health Sciences, Institute of Defence Health Sciences, Ankara, Türkiye

Corresponding author e-mail: rusenkoray.eyison@sbu.edu.tr

Abstract

This study outlines the development of a mobile application designed to enable first responder personnel to rapidly and accurately recognize chemical warfare agents (CWAs) in accidents and disaster situations. In scenarios involving potential chemical exposure, timely diagnosis is critical for accurate triage, appropriate medical intervention, and personnel safety. The application integrates environmental assessment findings with a comprehensive database of CWA-specific clinical signs and symptoms. The core functionality of the application allows users to input observable environmental indicators - such as the presence, color, and odor of smoke of chemical agents - after which it identifies the potential toxic substance and provides first responders with the appropriate emergency medical approach. For example, the application may issue alerts noting that most toxic agents tend to settle to the ground (unlike cyanide), thereby warning personnel to use a full-face mask with the appropriate filter or to avoid working without gloves. Simultaneously, the application will guide first aid personnel through a systematic evaluation of patient signs and symptoms and, based on these, provide protocols for antidotal and supportive treatment. By utilizing these environmental and clinical data, the mobile application aims to identify the probable agent and enable first response teams to rapidly implement appropriate decontamination and initial medical management protocols. In doing so, it will contribute to improving both patient prognosis and operational safety.

Keywords: CBRN, first aid personnel, mobile application, toxicology, diagnosis and treatment

ORAL PRESENTATION

Development of a MIP-modified electrochemical sensor for urea detection through EIS

Nihal Ermiş[1,2*] *(*Orcid: https://orcid.org/0000-0002-0085-3076*)*

*[1]Samsun University, Faculty of Engineering and Natural Sciences, Department of Fundamental Sciences, Samsun, Turkiye.
*[2]Samsun University, Faculty of Engineering and Natural Sciences, Department of Biomedical Engineering, Samsun, Turkiye.

*Corresponding author e-mail: nihal.ermis@samsun.edu.tr

Abstract

Urea [$CO(NH_2)_2$] is a key nitrogen-containing metabolite produced mainly in the liver through the urea cycle and excreted in body fluids such as blood and urine. Deviations in its concentration are clinically significant: levels below the normal serum range (8–20 mg/dL) may indicate liver dysfunction or nephritic syndrome, whereas elevated levels are associated with kidney failure, urinary tract obstruction, and disorders such as gastrointestinal bleeding. Conventional urea assays—calorimetry, gas chromatography, and spectrophotometry—require labor-intensive sample preparation and lack suitability for rapid or online monitoring. To address these limitations, in this study a low-cost, highly sensitive electrochemical biosensor was developed for the selective urea detection. A screen-printed electrode (SPE) was modified in situ with molecularly imprinted polymers (MIPs) synthesized in the presence of urea as the template molecule. After polymerization, the template was removed with an appropriate desorption agent to create specific recognition cavities. Electropolymerization was carried out in an aqueous solution containing 3-aminophenylboronic acid (APBA), pyrrole-3-carboxylic acid, and urea through cyclic voltammetry from 0 to +1.3 V at 100 mV s^{-1} for 10 cycles. Sensor performance was evaluated by cyclic voltammetry (CV) and electrochemical impedance spectroscopy (EIS) in 50 mM phosphate buffer (pH 7.0) with 10 mM KCl and 5 mM $[Fe(CN)_6]^{3-/4-}$. EIS used 180 mV DC with 10 mV AC over 10 kHz–0.05 Hz. Response difference of MIP and NIP sensors was determined by chrono-impedance (CI) at 200 mV and 100 Hz for 600 seconds. SEM and XPS, FTIR results confirmed surface morphology and chemical composition, respectively.
A non-imprinted sensor (NIP) was prepared in parallel to show negligible affinity toward urea, confirming the specificity of the MIP-modified sensor. The developed platform demonstrates the potential of MIP-based EIS sensors as a practical, selective, and rapid alternative to conventional urea assays for clinical diagnostics.

Keywords: Molecularly imprinted polymer, Urea, Electrochemical impedance spectroscopy, Sensor Technology

Acknowledgements: The author extends sincere gratitude to Assoc. Prof. Dr. Hilmiye Deniz Ertuğrul Uygun for performing the FTIR, SEM, and XPS characterizations at Dokuz Eylul University, Center for Production and Applications of Electronic Materials (EMUM).

ORAL PRESENTATION

Extraction of bioactive compounds from rosehip fruit using natural deep eutectic solvents (NADES)

Vildan Eyiz[1*] (Orcid: https://orcid.org/0000-0003-1081-4166),
Ayşenur Acar[2] Orcid: https://orcid.org/0000-0002-2086-7109)

[1*] Necmettin Erbakan University, Faculty of Engineering, Department of Food Engineering, Konya, Türkiye
[2] Selçuk University, Faculty of Agriculture, Department of Food Engineering, Konya, Türkiye.

*Corresponding author e-mail: vtop@erbakan.edu.tr

Abstract

This study investigated the effectiveness of natural deep eutectic solvents (NADES) for extracting bioactive compounds from rosehip (*Rosa canina L.*) fruits. Two formulations of citric acid–glycerol (1:4 and 1:2, with 30% water w/w) were compared to a conventional ethanol–water mixture. Total phenolic content (TPC) and antioxidant activities (DPPH, FRAP, CUPRAC) were assessed. The CA:Gly (1:4) system achieved the highest TPC (81.69 g GAE/kg dm), representing about a 75% increase compared to ethanol (46.81 g GAE/kg dm). In reducing-based assays, CA:Gly (1:2) reached the strongest FRAP activity (151.51 g TEAA/kg dm), roughly three times higher than ethanol (49.82 g TEAA/kg dm). CUPRAC activity was also enhanced in CA:Gly (1:4) (135.96 g TEAA/kg dm), exceeding ethanol (106.72 g TEAA/kg dm) by about 27%. In contrast, ethanol performed better in the DPPH assay (111.30 g TEAA/kg dm) compared with the NADES extracts (≈ 80 g TEAA/kg dm). Correlation analysis revealed a strong positive relationship between TPC and FRAP ($r = 0.936$, $p < 0.01$), suggesting that phenolics extracted by NADES were primarily responsible for the enhanced reducing capacity. These results highlight citric acid–glycerol NADES as efficient and eco-friendly extraction media that outperform ethanol in phenolic recovery, FRAP, and CUPRAC assays. Such extracts hold promise as natural antioxidants for use in food, nutraceutical, and cosmetic applications.

Keywords: Antioxidant activity, Natural deep eutectic solvents, Phenolic compounds, Rosehip, Sustainable extraction

ORAL PRESENTATION

Synthesis, biological activity and molecular modeling studies of compounds with benzo[*d*]oxazole structure

Ahmet Buğra AKSEL[1*] (*ORCID: https://orcid.org/0000-0001-5090-6474*), Şule YURDAKUL[2], Merve GEDİAĞAÇ[2], İnci Selin DOĞAN[1] (*ORCID: https://orcid.org/0000-0003-4949-1747*)

*[1] Karadeniz Technical University, Faculty of Pharmacy, Department of Pharmaceutical Chemistry, Trabzon, Türkiye
[2] Karadeniz Technical University, Faculty of Pharmacy, Undergraduate Student, Trabzon, Türkiye

*Corresponding author e-mail: abaksel@ktu.edu.tr

Abstract

The benzo[*d*]oxazole ring is one of the important heterocyclic ring systems in drug design due to its structural similarity to the purine analogues adenine and guanine bases, and its chemotherapeutic activities are thought to be mediated by inhibiting nucleic acid synthesis. The benzo[*d*]oxazole ring is also present in the structure of many drug molecules in clinical use: fenoxaprofen (anti-inflammatory), calcimycin (antimicrobial), clorzoxazone (muscle relaxant), caboxamycin B (antibacterial), pemafibrate (hyperlipidaemia), suvorexant (insomnia). To date, numerous benzo[*d*]oxazole derivatives have been synthesised and their pharmacological activities evaluated. However, it is known that the compounds reported in the literature have low activity and high side effect profiles, which limit the pharmacological effects of the drug molecules. Within the scope of this study, two new compounds derived from *N*'-(benzo[*d*]oxazol-2-yl)-4-substitutedbenzenesulphonylhydrazide were designed based on information from the literature. The synthesis and structural characterisation of the compounds designed within the scope of the study were carried out. For this purpose, in the first step, *o*-aminophenol is reacted with carbon disulphide to close the 2-mercaptobenzo[*d*]oxazole ring. In the subsequent step, the intermediate compound obtained is reacted with hydrazine hydrate to yield the 2-hydrazinylbenzo[*d*]oxazole compound. This compound is then reacted with suitable arylsulphonyl chloride derivatives in a basic medium to obtain the final compounds. The structures of the synthesised compounds were confirmed using ^{1}H- and ^{13}C-NMR and FT-IR spectral methods. The potential interactions of the two new candidate drug molecules, whose structures were confirmed, in the potential binding region were investigated by molecular docking studies on different protein target enzyme/receptor regions with reported anticancer properties in the literature. The compounds reported in the study were found to be potential human Topoisomerase II enzyme inhibitors.

Keywords: benzo[*d*]oxazole, sulfonylhydrazide, molecular docking

Acknowledgements: This study was supported within the scope of TÜBİTAK 2209-A. We would like to thank TÜBİTAK for its contributions.

ORAL PRESENTATION

Detection of specific spoilage organisms (SSOs) of sea bream (*Sparus aurata*)

Hatice Göçke Hasanhocaoğlu[1]* (*ORCID: https://orcid.org/0000-0001-5868-436X)*, Latif Taşkaya[1] (*ORCID: https://orcid.org/0000-0003-0835-7007*), Yunus Alparslan[1] (*ORCID: https://orcid.org/0000-0002-8833-996X*), Cansu Metin Hacisa[1] (*ORCID: https://orcid.org/0000-0002-2290-1489*), Taçnur Baygar[1] (ORCID: https://orcid.org/0000-0001-8070-0653)

*[1] Muğla Sıtkı Koçman University, Faculty of Fisheries, Department of Fishing and Processing Technology, Muğla, Türkiye

*Corresponding author e-mail: hatice_gokce@mu.edu.tr

Abstract

The objective of this study was to compare the microflora profiles of gilthead sea bream (Sparus aurata) cultured in net cages and earthen ponds. For this purpose, gilthead sea bream samples were obtained from two different aquaculture facilities in Milas, Muğla—one utilizing net cages and the other earthen ponds—were transported in styropor boxes with ice to the laboratory of the Faculty of Fisheries at Muğla Sıtkı Koçman University. The fish were stored in a cold storage unit at +4°C for 16 days. During this storage period, samples were collected from both groups on intermittent days (0, 3, 6, 9, 12, 14, 15, 16) for the enumeration of mesophilic, psychrotrophic, lipolytic bacteria, and yeast-mold populations. Colonies grown on the culture media were isolated and identification was performed using Gram staining, oxidase testing, and API kits. The results indicated that microbial growth in net cage samples was slightly higher than in earthen pond samples during the initial days of storage. According to the findings, both Gram-positive and Gram-negative bacteria were present in the initially sterile fish flesh during the early stages of storage. However, as storage progressed, Gram-negative oxidase-positive bacterial species became dominant microflora compared to other bacteria. It was observed exhibited a broader spectrum of microorganisms in net cage-cultured fish. Evaluation of the results, based on identification using API kits, revealed that *Pseudomonas* spp. predominantly constituted the spoilage microflora in both culture systems. The study's findings highlighted the specific microorganisms that should be monitored in gilthead sea bream facilities based on storage duration. It was determined that the rearing conditions had minimal impact on the dominant spoilage microorganisms. It is suggested that future shelf-life studies could focus on developing methods to inhibit these bacterial species.

Keywords: Sea bream, microflora, net cage, earthen ponds, Gram staining

Acknowledgements: This study was supported by the Scientific Research Projects Coordination Unit of Muğla Sıtkı Koçman University (Project No: 16/159).

ORAL PRESENTATION

Protective effects of *Aloe vera* gel extract against cytotoxic, genotoxic, and physiological damage induced by nitric acid in *Allium cepa* cells

Aytül Uzun Akgeyik (https://orcid.org/ 0000-0002-5602-0524)

Yozgat Bozok University, Science and Technology Application and Research Center, Yozgat, Türkiye

Corresponding author e-mail: aytul.uzun@yobu.edu.tr

Abstract

This study was conducted using the *Allium cepa* L. test system to determine the possible physiological and cytogenetic effects of *Aloe vera* L. (ALV) leaf gel extract against the toxicity induced by nitric acid (HNO_3), a strong oxidizing agent. In terms of germination percentage, the ALV1 (10%) and ALV2 (20%) groups exhibited results similar to the control group. However, the marked decrease in germination percentage observed following HNO_3 exposure was significantly improved in the HNO_3ALV1 (10%) and HNO_3ALV2 (20%) combination groups, indicating the mitigating role of *Aloe vera* gel in suppressing toxic effects. Furthermore, compared with the HNO_3-treated group, significant increases in root length and fresh weight were observed in the HNO_3ALV1 (10%) and HNO_3ALV2 (20%) groups. With respect to the mitotic index (MI), the HNO_3ALV1 (10%) group showed a higher MI value than the HNO_3ALV2 (20%) group, suggesting that increasing the concentration of *Aloe vera* gel may exert an inhibitory effect on mitotic activity. Similarly, the frequency of chromosomal abnormalities and micronuclei (MN) was lower in the HNO_3ALV1 (10%) group compared to the HNO_3ALV2 (20%) group. Nonetheless, both combinations significantly reduced MN formation and chromosomal abnormalities compared to HNO_3 treatment alone, indicating a protective and antigenotoxic effect. In conclusion, the findings demonstrate that *Aloe vera* gel extract, when applied at appropriate concentrations, has the potential to act as a bioprotective agent by alleviating HNO_3-induced genotoxicity and physiological impairments in *Allium cepa* root meristem cells.

Keywords: Genotoxicity, *Aloe vera* L., HNO_3, *Allium cepa* L., Micronuclei.

ORAL PRESENTATION

Viability of the probiotic microorganism *Saccharomyces boulardii* in olive oil and its effects on oil quality

Alper Aydın[1,3] (ORCID: https://orcid.org/0000-0002-6870-0367), Başar Uymaz Tezel[2] (ORCID: https://orcid.org/0000-0002-4156-8861), Mustafa Öğütcü[3*] (ORCID: https://orcid.org/0000-0001-8686-2768)

[1] Edremit District Directorate of Agriculture and Forestry, Edremit, Balıkesir, Türkiye
[2] Çanakkale Onsekiz Mart University, Bayramiç Vocational School, Bayramiç, Çanakkale, Türkiye
[3] Çanakkale Onsekiz Mart University, Faculty of Engineering, Department of Food Engineering, Terzioğlu Campus, 17020, Çanakkale, Türkiye

*Corresponding author e-mail: mustafaogutcu@gmail.com

Abstract

This study was conducted to investigate the survival of the probiotic *Saccharomyces boulardii* culture in filtered (F) and unfiltered (nF) extra virgin olive oils from the same season over a 90-day storage period, as well as the short-term effects of the culture on the fundamental quality indicators of olive oil. Within this scope, *S. boulardii* was inoculated into both autoclave-sterilized F and nF samples, both directly and after a pre-revitalization process. The samples, incubated at 25°C for four days, were then stored under olive oil storage conditions for three months. The growth of *S. boulardii* was monitored both at the end of the incubation and monthly over a period of 30 days during storage at 25°C. Microbial counts were performed by plating dilutions prepared with 5% (v/v) Tween-80 in 0.85% NaCl on Yeast Extract Glucose Chloramphenicol (YGC) Agar and incubating at 25°C for three days. The number of viable microorganisms was calculated as Log CFU/mL. Simultaneously, every 30 days during storage, the free fatty acidity (FFA), peroxide value (PV), and UV absorbance values (K232 and K270) of the olive oil were determined. The results show that *S. boulardii*, as a probiotic yeast, was able to maintain its viability in olive oil over a three-month storage period; survival was largely preserved in nFi at the end of three months' storage, whereas it decreased by approximately 2 log in Fi. The pre-revitalization process did not increase survival in the long term. The method provides an applicable scheme for reliable yeast enumeration in a hydrophobic oil matrix. It was determined that the FFA, PV, and K270 values measured in inoculated olive oils during storage remained within legal limits. The findings indicate that *S. boulardii* can maintain its viability in olive oil and that probiotic culture inoculation does not have a significant adverse effect on the fundamental physico-chemical quality of the oil. In this context, it is considered that the development of probiotic microorganisms in olive oil could expand the range of probiotic products and serve as an alternative food for probiotic consumers.

Keywords: Olive oil, Probiotic, Viability, Quality

ORAL PRESENTATION

Sustainability assessment of potassium permanganate and sodium hypochlorite used in the bleaching of denim fabrics

Esra Tabaş Asiltürk[1*] (Orcid: Https://Orcid.Org/0000-0001-8363-3070),
Mehmet Yüceer[2] (Orcid: https://orcid.org/0000-0002-2648-3931)

[1]* Baykan Denim, R&D Center, Malatya, Türkiye
[2] İnönü University, Faculty of Engineering, Department of Chemical Engineering, Malatya, Türkiye

*Corresponding author e-mail: EsraTabas.Asilturk@baykandenim.com

Abstract

Potassium permanganate and sodium hypochlorite, commonly used in the bleaching of denim fabrics, provide high decolorization efficiency but present certain limitations regarding environmental impact and textile performance. This study comparatively examines the behavior and sustainability aspects of these two oxidizing agents under different application systems. Twenty-five bleaching trials were conducted on 100% cotton indigo denim fabrics, in which potassium permanganate and sodium hypochlorite were applied at various concentrations and durations using both a conventional drum method and a new-generation application technique designed to minimize chemical consumption. After each treatment, key physical properties such as tearing strength and dry/wet rubbing fastness were evaluated, and parameters including chemical usage, water consumption, and energy requirements were analyzed. The results indicate that alternative application systems can achieve up to 80% savings in chemical and water consumption for both oxidants, while also reducing fiber damage and yielding higher rubbing fastness values. Overall, the findings demonstrate that the sustainable use of bleaching chemicals in denim production is influenced not only by chemical formulation but also by the application technology. The integration of potassium permanganate and sodium hypochlorite with alternative application methods that reduce environmental impact and minimize performance loss presents a significant opportunity for sustainable textile chemistry.

Keywords: Denim bleaching, Potassium permanganate, Sodium hypochlorite, Sustainable textiles

Acknowledgements: We would like to thank Baykan Denim for providing technical support, access to machinery and equipment, and for their contributions to the execution of the experimental procedures carried out within the scope of this study.

ORAL PRESENTATION

Optimization of sample dispersion protocols for high-resolution microscopic analysis of sol-gel synthesized TiO_2 quantum dots

Olcay Severgün[1,2*] (https://orcid.org/0000-0002-5283-4918),
Murat Özen[2] (https://orcid.org/0000-0002-3589-2059)

[*1] Bursa Technical University, Central Research Laboratory, Bursa, Türkiye
[2] Bursa Technical University, Department of Chemistry, Faculty of Engineering and Natural Sciences, Bursa, Türkiye

*Corresponding author e-mail: olcay.severgun@btu.edu.tr

Abstract

Titanium dioxide (TiO_2) quantum dots (QDs) exhibit unique optical and electronic properties governed by their particle size and distribution. However, the accurate microscopic characterization of these nanostructures is often hindered by their strong tendency to agglomerate due to high surface energy. This study investigates the synthesis of anatase TiO_2 QDs via a sol-gel reflux condensation method and systematically evaluates the effects of post-synthesis thermal treatment and solvent dispersion techniques on microscopic visualization. The synthesized QDs were characterized using XRD, EDS, SEM, and AFM. X-ray diffraction confirmed the formation of a pure Anatase phase. Energy Dispersive X-Ray Spectroscopy (EDS) revealed that calcination at 450°C is essential for achieving stoichiometric TiO_2 (Ti:O ratio ~1:2) by removing organic residues present in non-calcined samples. Various dispersion protocols involving mechanical grinding and ultrasonication in water, hexane, and ethanol were compared for microscopic sample preparation. The results indicated that nonpolar solvents, such as hexane, introduce surface artifacts, whereas water causes reagglomeration due to high surface tension. The optimal preparation method was identified as calcination followed by ultrasonic dispersion in ethanol. This protocol enabled the visualization of individual crystallites (<10 nm) within small clusters (25-100 nm) using SEM and AFM, providing a reliable methodology for the structural analysis of highly active nanomaterials.

Keywords: TiO_2 Quantum Dots, Sol-gel Synthesis, Sample Preparation, SEM, AFM

Acknowledgements: This study was funded by the Scientific Research Projects Fund of Bursa Technical University [Project No: BAP-230D018] and the Scientific and Technological Research Council of Türkiye (TÜBİTAK) [Project No: 224Z014]. The authors would like to thank the Central Research Laboratory (MERLAB) at Bursa Technical University for their technical support. Additionally, the authors acknowledge the financial support provided by the Scientific and Technological Research Council of Türkiye (TÜBİTAK) Directorate of Science Fellowships and Grant Programmes (BİDEB) under the 2211-National Graduate Scholarship Program.

ORAL PRESENTATION

Microbial content, antioxidant activity, and volatile aroma compounds profile of boza, a fermented cereal beverage

Nilgün Özdemir (Orcid: https://orcid.org/0000-0002-4517-9214)

Ondokuz Mayis University, Engineering Faculty, Food engineering Department, Samsun, Turkey.

Corresponding author e-mail: nilgun.ozdemir@omu.edu.tr

Abstract

This study aimed to determine the microbial composition, antioxidant activity, and volatile aroma compound profiles of boza samples obtained from six traditional producers in Türkiye. The lactic acid bacteria (LAB) counts of the samples ranged between 5.45–9.06 log CFU/mL, while yeast and total aerobic mesophilic bacteria (TAMB) levels showed significant variation depending on fermentation conditions and raw material characteristics. Samples with higher LAB levels exhibited markedly greater antioxidant activity, indicating the strong contribution of LAB metabolism to radical-scavenging capacity. Volatile aroma analysis performed by HS-SPME/GC-MS revealed considerable differences in aroma composition among samples, with key compounds including 3-hexenoic acid, 2-undecenal, muconic acid, acetaldehyde, benzyl alcohol, and phenol. Some samples contained richer and more desirable aroma profiles, whereas others showed limited volatile diversity, likely associated with differences in microbial communities such as the presence of Bacillus spp. Overall, the results demonstrate that boza possesses a diverse microbiome and complex aroma matrix shaped by LAB–yeast interactions and cereal-derived metabolites. These findings highlight the importance of microbial composition and standardized fermentation practices for improving product quality, sensory attributes, and functional potential in traditional boza production.

Keywords: boza, volatile aroma compounds, microbial content, antioxidant activity

ORAL PRESENTATION

In vitro cytotoxic evaluation of *Artemisia absinthium* on human A549 lung carcinoma cells

Esmanur Kuzucu[1,2*] (ORCID: https://orcid.org/0009-0001-7377-0247), Mehtap Kara[2] (ORCID: https://orcid.org/0000-0001-7764-5593), Ayşegül Karapınar-Arif[3] (ORCID: https://orcid.org/0009-0005-8096-150X), Zeynep Akdaş[3] (ORCID: https://orcid.org/0009-0007-2966-116X)

[*1] Istanbul University, Institute of Graduate Studies in Health Sciences, Department of Pharmaceutical Toxicology, Istanbul, Turkey
[2] Istanbul University, Faculty of Pharmacy, Department of Pharmaceutical Toxicology, Istanbul, Turkey.
3 MBA Schools Muğla Campus- Science High School. Mugla-TURKEY

*Corresponding author e-mail: esmanurkuzucu@gmail.com

Abstract

Lung cancer persists as one of the major causes of cancer-associated mortality worldwide. The primary limitations of current therapeutic approaches, such as chemoresistance, systemic toxicity, and immunological adverse effects, have increased the demand for safer and more innovative cancer treatment strategies. Due to their various bioactive metabolites that can regulate tumorgenic pathways, medicinal plants are attracting increasing scientific interest. Among these plants, species of the genus Artemisia have emerged as promising candidates. Specifically, *Artemisia absinthium* has been reported to exhibit antioxidant, anti-inflammatory, and pro-apoptotic activities through key molecular regulators such as iNOS, COX-2, NF-κB, and MEK/ERK. In this study, the cytotoxic effects of *A. absinthium* extract were evaluated in vitro using the human lung adenocarcinoma cell line A549 and human pancreatic ductal adenocarcinoma cell line PANC-1. In order to determine the dose-dependent antiproliferative effects, cells were treated with increasing concentrations of the extract and evaluated using the MTT cytotoxicity assay. According to our results, IC50 value was determined as 4000 µg/mL on A549 and 2000 µg/mL on PANC-1. Our findings indicate that *A. absinthium* induces a dose-dependent growth inhibition in both A549 and PANC-1 cells. These result support the potential of *A. absinthium* as a complementary phytotherapeutic promising therapeutic opinion for lung cancer treatment, although further advanced mechanistic and in vivo studies are required for validation.

Keywords: *Artemisia absinthium*, Cancer, PANC-1, A549, MTT assay, Cytotoxicity

ORAL PRESENTATION

Optimization of heavy metal (As, Cd, and Hg) adsorption performance of green-synthesized TiO_2–Fe_3O_4 nanocomposite using aloe vera extract via Taguchi method

Emrah Akgeyik (*https://orcid.org/0000-0002-6626-0150*)

Science and Technology Application and Research Center, Yozgat Bozok University, Yozgat, Türkiye

Corresponding author e-mail: emrah.akgeyik@bozok.edu.tr

Abstract

The present study reports the green synthesis of a TiO_2–Fe_3O_4 nanocomposite using Aloe vera extract as a natural reducing and stabilizing agent, aiming to remove multiple heavy metal ions from aqueous environments. The biomediated sol–gel synthesis successfully produced a nanocomposite with a crystallite size of approximately 14 nm, as determined by X-ray diffraction (XRD). Scanning Electron Microscopy (SEM) analysis revealed a quasi-spherical morphology with aggregated particles, attributing the agglomeration to the presence of biomolecules on the surface. X-ray fluorescence (XRF) analysis confirmed the elemental composition with 35.29 wt% Ti and 9.06 wt% Fe, consistent with the target Fe/Ti molar ratio (0.25). The adsorption performance of the synthesized material was evaluated for As(III), Cd(II), and Hg(II) ions using the Taguchi L_{16} orthogonal array design to optimize key parameters, including pH (3–6), adsorbent dosage (0.05–0.3%), initial concentration (25–100 mg/L), and contact time (30–120 min). Results indicated that pH was the most significant factor influencing adsorption efficiency, with optimal performance at pH 6, 0.05% adsorbent dosage, and 60 min contact time. The composite demonstrated maximum adsorption capacities of 13.3 mg/g for As(III), 160.9 mg/g for Cd(II), and 38.5 mg/g for Hg(II), following the selectivity order Cd(II) > Hg(II) > As(III). The high adsorption capacity was attributed to the synergistic interaction between TiO_2 and Fe_3O_4 phases and the oxygenated functional groups from Aloe vera biomolecules. The magnetic nature of the nanocomposite facilitated rapid and easy recovery after adsorption. This study demonstrates a sustainable and highly efficient approach for multi-metal removal from wastewater by integrating green synthesis and Taguchi-based process optimization, demonstrating scalability and environmental compatibility.

Keywords: Aloe vera extract; green synthesis; TiO_2–Fe_3O_4 nanocomposite; heavy metal adsorption; Taguchi optimization; wastewater treatment.

1.2. FULL-TEXTS

ORAL PRESENTATION

AI-assisted laboratory-based severity index for chronic spontaneous urticaria using eosinophil count, basophil count, and vitamin D

Eralda Lekli[1,2*] (Orcid:0000-0003-3041-8910)

[1]University of Medicine, Faculty of Medicine, Department of Internal Diseases, Tirana, Albania.
[2] Salus Hospital Tirana, Department of Allergology, Tirana, Albania

Abstract

Chronic spontaneous urticaria (CSU) is a heterogeneous condition characterized by recurrent wheals and/or angioedema. Objective assessment of disease severity is essential for guiding therapy, yet current tools rely primarily on patient-reported outcomes, which are subjective and variable. Artificial intelligence (AI) offers novel ways to integrate laboratory data into quantitative severity scoring. The aim was to develop a simple, robust, and quantitative severity index (SI) for CSU using routinely available laboratory parameters: eosinophils (EO), basophils (BA), and vitamin D (VIT D). The developed formula normalizes these values, applies nonlinear scaling to emphasize critical deficiencies, and sums them to give a robust, clinically interpretable severity score from 0 to 10. It works independently of CSU endotype type and can be tracked over time. This laboratory-based SI may offer a practical, quantitative, and reproducible method to assess CSU severity, but will need to be validated in clinical practice. Integration with artificial intelligence (AI) approaches could enhance SI predictive value, allowing automated calculation, pattern recognition, and longitudinal monitoring to support personalized management and optimize therapy.

Keywords: SI (Severity Index), CSU, artificial intelligence, basopenia, eosinopenia, Vitamin D

INTRODUCTION

CSU is a chronic inflammatory disorder with variable severity and clinical presentation. Existing severity scores, rely on patient-reported outcomes and may be influenced by subjective perception. Laboratory biomarkers reflecting immune and nutritional status, EO, BA, and VIT D are biologically relevant, but have not been systematically combined into a quantitative severity score.

Blood basophils are reduced in chronic urticaria(Puxeddu et al. 2019) and respond less well to immunologic stimuli. Active recruitment of basophils from peripheral blood into lesional skin may be important in wheal pathogenesis. (Grattan, 2001)Eosinopenia in patients with CSU is associated with type IIb autoimmunity, high disease activity, and poor response to treatment. Eosinophils should be explored as biomarkers and investigated for their contribution to the pathogenesis of CSU.(Kolkhir et al., 2020)vitamin D level is more likely to be critically low in patients with chronic urticaria, and an inverse relationship with disease severity and disease duration has been observed. (Woo et al., 2015) These findings may open up the possibility of the clinical use of vitamin D as a contributing factor in the pathogenesis of chronic urticaria and a predictive marker for disease activity in chronic urticaria.(Woo et al., 2015) There is no validated quantitative tool to assess the CSU severity.

MATERIALS AND METHODS

We aimed to present a simple, AI-generated severity index (SI) for CSU using routinely available laboratory parameters: eosinophil count (EO)cells/µL, basophil count (BA) cells/µL and vitamin D level in ng/mL (Vit D).

We implemented AI-assisted reasoning, and available current scientific data, evidencing role of eosinopenia and basopenia in CSU disease activity and decreased Vit D level as a biomarker of disease severity and disease duration to develop a Severity Index (SI).

EO cut off was set 200/µL and BA cut off 10/ µL to define probable clinically relevant eosinopenia and basopenia in CSU physiopathology. Cut off for Vit D level was set 30 ng/mL.

After considering all factors the below formula was developed. The SI is additive, endotype-independent, and robust against extreme lab values.

$$SI = (EOnorm)^{1.5} + (BAnorm)^{1.5} + \frac{30}{\min(\max(VitD,\ 5),\ 50)}$$

Where:

EO_norm = (200 – EO)/200, capped ≥0

BA_norm = (10 – BA)/10, capped ≥0

Vit D factor = 30 / Vit D, capped between 5–50 ng/mL

EO and BA are normalized and mildly nonlinearly weighted to emphasize clinically significant low counts, while Vit D inversely modulates severity.

The formula was designed by AI assisted step by step reasoning to meet these requirements:

EO and BA normalization: (200 − EO)/200 and (10 − BA)/10, capped ≥0

Nonlinear weighting: exponent 1.5 to emphasize low counts

Vitamin D inversion: 30 / Vit D, capped between 5–50 ng/mL to avoid extremeinfluence

RESULTS and DISCUSSION

This AI-generated formula severity index, offers a quantitative, objective approach to CSU severity assessment. The additive design and nonlinear weighting ensure low EO/BA counts meaningfully influence severity without exaggeration, while Vitamin D inversely modulates SI.

The index is scaled to 0–10 for clinical interpretation:

0–2: Mild

2–5: Moderate

5–7.5: Severe

7.5–10: Very severe

Using 1.5 exponent makes the SI sensitive enough to capture biologically meaningful EO/BA depletion, but not so sensitive that lab variability causes huge swings in the score.

Keeps the scale clinically interpretable (0–10) without needing arbitrary caps.

Results (Example Calculations)

PATIENT	EO	BA	VIT D	SI SCORE	SEVERITY
A	120	5	5.88	5.71	Severe
B	180	13	23	1.33	Mild
C	450	25	26	1.15	Mild

Role of AI:

AI identified optimal normalization, nonlinear weighting, and Vitamin D capping.

AI-assisted pattern recognition can automate SI calculation and integrate it with electronic health records.

This SI tool is cheap, as request only hemogram and Vit D in stead of more inflamatory markers. Machine learning models could combine SI with other laboratory and clinical features to refine predictions of disease course and therapeutic response.

The development of a standardized severity index for CSU is essential for improving clinical decision-making, optimizing treatment strategies, and facilitating consistent assessment across diverse patient populations. Integrating artificial intelligence into the creation of such an index offers several meaningful advantages. AI-driven models can analyze large, heterogeneous datasets to identify subtle patterns in symptom presentation, treatment response, and disease progression that may be overlooked by traditional scoring systems. This allows for a more precise, personalized assessment of disease severity.

Moreover, an AI-generated severity index can adapt over time as new clinical data become available, ensuring that the scoring model remains current and evidence-based. It can also improve objectivity, reducing variability between clinicians and enhancing the reliability of severity measurements in both clinical practice and research settings. Importantly, AI tools can integrate patient-reported outcomes, biomarker profiles, and real-time monitoring data to produce a more holistic view of disease burden.

CONCLUSION

This AI-assisted a simple Severity Index for chronic spontaneous urticaria using eosinophils, basophils, and Vitamin D. Low EO/BA counts and low Vitamin D increase severity. The formula normalizes these values, applies nonlinear scaling to emphasize critical deficiencies, and sums them to give a robust, clinically interpretable severity score from 0 to 10.

Leveraging AI to develop a CSU severity index has the potential to enhance diagnostic accuracy, support individualized treatment pathways, streamline clinical workflows, and ultimately improve patient outcomes. As these technologies continue to evolve, they hold significant promise in advancing the precision and effectiveness of CSU management.

REFERENCES

Grattan, C. E. H. 2001. “Basophils in Chronic Urticaria.” *Journal of Investigative Dermatology Symposium Proceedings* 6(2):139–40. doi:10.1046/j.0022-202x.2001.00027.x.

Kolkhir, Pavel, Martin K. Church, Sabine Altrichter, Per Stahl Skov, Tomasz Hawro, Stefan Frischbutter, Martin Metz, and Marcus Maurer. 2020. “Eosinopenia, in Chronic Spontaneous Urticaria, Is Associated with High Disease Activity, Autoimmunity, and Poor Response to Treatment.” *The Journal of Allergy and Clinical Immunology: In Practice* 8(1):318-325.e5. doi:10.1016/j.jaip.2019.08.025.

Puxeddu, Ilaria, Fiorella Petrelli, Francesca Angelotti, Cristina Croia, and Paola Migliorini. 2019. “Biomarkers In Chronic Spontaneous Urticaria: Current Targets And Clinical Implications.” *Journal of Asthma and Allergy* Volume 12:285–95. doi:10.2147/JAA.S184986.

Woo, Yu Ri, Kyung Eun Jung, Dae Won Koo, and Joong Sun Lee. 2015. “Vitamin D as a Marker for Disease Severity in Chronic Urticaria and Its Possible Role in Pathogenesis.” *Annals of Dermatology* 27(4):423. doi:10.5021/ad.2015.27.4.423.

ORAL PRESENTATION

Trends in utilization and expenditure of reimbursed lipid-lowering drugs in Albania

Alida Sina[1,2*] (*ORCID: https://orcid.org/0009-0008-0149-394X),*
Rezarta Shkreli[1] *(ORCID: https://orcid.org/0000-0001-5966-9938)*

[1]Aldent University, Faculty of Medical Sciences, Department of Pharmacy, Tirana, Albania.
[2]Mandatory Health Care Insurance Fund, Tirana, Albania.

Abstract

Atherosclerotic cardiovascular diseases, representing the major component of cardiovascular diseases, constitute a significant global health concern, as their morbidity and mortality rates are expected to increase in the coming years. Lipid-lowering drugs (LLDs) are beneficial for both the prevention and treatment of atherosclerotic diseases; consequently, several LLDs, including statins and fibrates, have been incorporated into the Reimbursed Drug List in Albania. This study aimed to identify and evaluate the utilization and reimbursement trends of antihyperlipidemic drugs in the Albanian pharmaceutical market within the context of clinical recommendations for dyslipidemia management. A retrospective, descriptive study was used to analyze LLD utilization and reimbursement costs in Albania from 2014 to 2024, using the Anatomical Therapeutic Chemical/Defined Daily Dose (ATC/DDD) methodology recommended by the World Health Organization. Data on LLDs were obtained from the Mandatory Health Care Insurance Fund database, while population data were sourced from the Institute of Statistics' database. Drug utilization was quantified as DDDs per 1,000 inhabitants per day, providing a standardized measure of consumption. Overall, both the utilization and reimbursement of LLDs increased over the study period. Statins were the most commonly used LLDs and accounted for the greatest proportion of total reimbursement for antihyperlipidemic drugs. Atorvastatin and fenofibrate were the most frequently consumed agents, jointly representing 92% of LLD utilization in 2024. Furthermore, their costs were high, accounting for 91% of total LLDs reimbursement in 2024. Atorvastatin appeared to be cost-effective, based on its average price per DDD. In conclusion, the utilization and reimbursement trends of LLDs in Albania align with international lipid management guideline recommendations. Moreover, other effective LLDs already authorized for sale in the country may be considered for future inclusion in the Reimbursed Drug List.

Keywords: lipid-lowering drugs, statins, fibrates, utilization, reimbursement trends.

INTRODUCTION

Cardiovascular diseases (CVDs) are the primary cause of death worldwide and a significant factor in disability. In 2022, CVDs accounted for approximately 32% of global deaths, of which 85% were attributable to ischemic heart disease (IHD) and stroke (WHO, CVDs, 2025). Moreover, CVD-related morbidity and mortality are expected to rise in the coming decades. Between 2025 and 2050, cardiovascular prevalence is projected to increase by 90%, and mortality by 73.4%, with atherosclerotic cardiovascular diseases (ASCVDs), such as IHD and stroke, anticipated to be the main causes of the growing burden of CVD (Chong et al., 2025).

Nowadays, it is well established that elevated levels of low-density lipoprotein cholesterol (LDL-C) are not merely a risk factor but a major causal determinant in the development of ASCVD. A 2015 study reported that the prevalence of dyslipidemia in Albania was 58.6%, indicating that approximately 1.4 million Albanians had at least one major risk factor for dyslipidemia. The study found that total hypercholesterolemia (TC ≥ 200 mg/dL) affected 44.3% of the population. The prevalence of LDL-C ≥ 130 mg/dL, high-density lipoprotein cholesterol (HDL-C) ≤ 40 mg/dL, and triglycerides (TG) ≥ 150 mg/dL was 34%, 17.2%, and 22.6%, respectively (Shurdha et al., 2015). The risk of both fatal and non-fatal myocardial infarctions and ischemic strokes, as well as peripheral arterial ischemic events, has been reduced by lowering LDL-C levels, as demonstrated in numerous randomized trials. Therefore, for preventing atherosclerotic cardiovascular events, the focus should be on lowering plasma LDL-C levels (Mach et al., 2025).

Given the substantial and persistent burden of dyslipidemia in Albania, as described above, the management of this condition is of particular importance. For this reason, several lipid-lowering drugs (LLDs) have been reimbursed in the country during the period 2014-2024. The Reimbursed Drug List has incorporated statin monotherapies (lovastatin, pravastatin, simvastatin, atorvastatin, and fluvastatin) as well as a combination of a statin with a calcium channel blocker, in addition to the fibrates (ciprofibrate and fenofibrate) (Drug List).

The study aimed to determine and evaluate the eleven-year trends in LLD utilization and reimbursement costs in Albania, identifying the most widely used and most costly drugs, within the context of international and national guideline recommendations for the management of dyslipidemia.

MATERIALS AND METHODS

The annual data for all drugs reimbursed in Albania during the years 2014–2024 were obtained from the Mandatory Health Care Insurance Fund (the Fund) database. The Fund is the sole legal, public, and autonomous entity responsible for managing compulsory health care insurance in the Republic of Albania. The standard package of health insurance services includes a Reimbursed Drug List, which is updated regularly, typically once per year, and approved by a decision of the Council of Ministers (Law No. 10383, dated 24.2.2011). Drugs on this list are classified according to their international nonproprietary name (INN), following the Anatomical Therapeutic Chemical (ATC) classification system. Prescribing reimbursed medications by generic name or INN is mandatory, except for veterans and war invalids. Data on LLDs within ATC code C10 were extracted from the full dataset of reimbursed drugs.

A retrospective, descriptive study was conducted using the ATC classification system and the Defined Daily Dose (DDD) as the measurement unit. The DDD represents the assumed average maintenance dose per day for a drug used for its main indication in adults. The ATC/DDD methodology, regarded as the World Health Organization (WHO) gold standard for drug utilization analysis, standardizes the assessment of drug consumption regardless of dose variations, enables comparisons, and facilitates the evaluation of utilization trends over time. Its main purpose is to provide a framework for presenting drug utilization statistics with the aim of improving rational drug use (WHO, Guidelines, 2025).

The DDD values were obtained from the electronic version of the ATC/DDD Index 2025 on the WHO website. Population data used in the study were sourced from the Institute of Statistics (INSTAT) database. Annual drug utilization was expressed as DDDs per 1,000 inhabitants per day (DIDs). Reimbursement values were analyzed as total drug expenditures over the study period, and the average price per DDD was calculated. Ethical review board approval was not needed, as the study relied exclusively on anonymous, aggregated data with no information at the patient level.

RESULTS

Statins and fibrates were reimbursed as LLDs in Albania from 2014 to 2024. Overall utilization of LLDs (ATC code C10) increased during the study period, rising from 6.7 DIDs in 2014 to 22.6 DIDs in 2024. A consistent annual growth pattern was observed in the use of both statins (C10AA) and fibrates (C10AB), whereas the statin and calcium channel blocker combination (C10BX) exhibited negligible consumption (Table 1). Statins accounted for the largest proportion of LLD utilization, representing more than 80% of total use.

Table 1. LLD utilization, expressed in DIDs, from 2014 to 2024

ATC codes	2014	2015	2016	2017	2018	2019	2020	2021	2022	2023	2024
C10	6.7	7.8	8.6	10	11.7	12.8	13.7	14.7	16.2	17.4	22.6
C10AA	5.92	6.9	7.5	8.63	10	10.8	11.5	12.3	13.5	14.7	19.2
C10AB	0.77	0.92	1.1	1.38	1.67	1.96	2.2	2.35	2.7	2.7	3.4
C10BX	0.002	0.004	0.007	0.008	0.015	0.03	0.034	0.03	0.03	0.016	0.01

Atorvastatin was the most widely used statin, accounting for the largest proportion of reimbursed statin consumption and reaching 91% of total statin use in 2023 and 2024 (Figure 1).

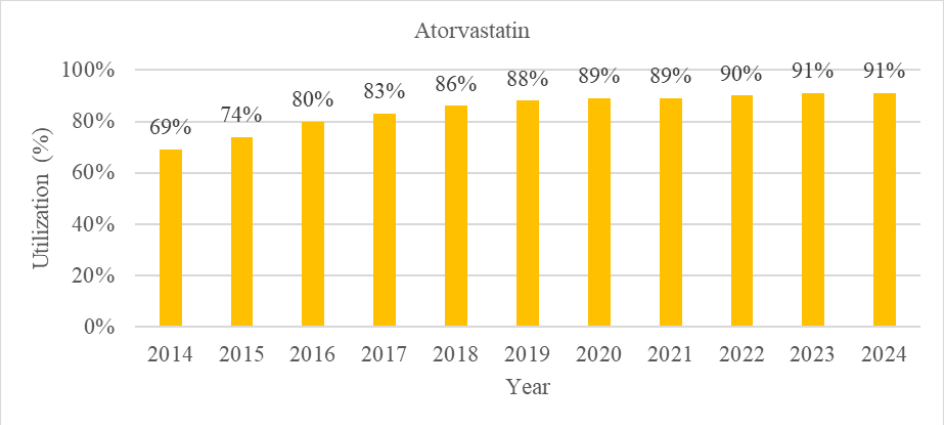


Figure 1. Atorvastatin use as percentage of statin utilization

Simvastatin was the second most frequently used statin, with relatively stable utilization across all years. Fluvastatin, pravastatin, and lovastatin exhibited negligible levels of consumption, and lovastatin has not been used since 2020 (Table 2).

Table 2. Statin utilization, expressed in DIDs, from 2014 to 2024

Statins	2014	2015	2016	2017	2018	2019	2020	2021	2022	2023	2024
C10AA	5.92	6.9	7.5	8.63	10	10.8	11.5	12.3	13.5	14.7	19.2
Simvastatin	1.1	1.12	1.1	1.07	1.1	1.1	1.1	1.1	1.1	1.1	1.3
Lovastatin	0.001	0.002	0.0002	0.0001	0.0003	0.0002	-	-	-	-	-
Pravastatin	0.01	0.01	0.0027	0.0016	0.0004	0.0002	0.0002	0.0005	0.01	0.03	0.05
Fluvastatin	0.7	0.63	0.4	0.38	0.28	0.2	0.2	0.2	0.2	0.2	0.3
Atorvastatin	4.11	5.13	6	7.18	8.61	9.46	10.2	11	12.2	13.4	17.5

Meanwhile, fenofibrate was the most commonly used fibrate, except in 2016 and 2017 when ciprofibrate consumption was higher. Fenofibrate utilization increased steadily throughout the study period, reaching its peak in 2024 (Table 3).

Table 3. Fibrate utilization, expressed in DIDs, from 2014 to 2024

Fibrates	2014	2015	2016	2017	2018	2019	2020	2021	2022	2023	2024
C10AB	0.77	0.92	1.1	1.38	1.67	1.96	2.2	2.35	2.7	2.7	3.4
Fenofibrate	0.55	0.5	0.5	0.65	1.13	1.21	1.4	1.5	1.8	2.4	3.3
Ciprofibrate	0.22	0.42	0.6	0.73	0.54	0.75	0.8	0.85	0.9	0.3	0.1

Fenofibrate consumption in 2024 was six times higher than in 2014 and accounted for 97% of total fibrate utilization in that year (Figure 2).

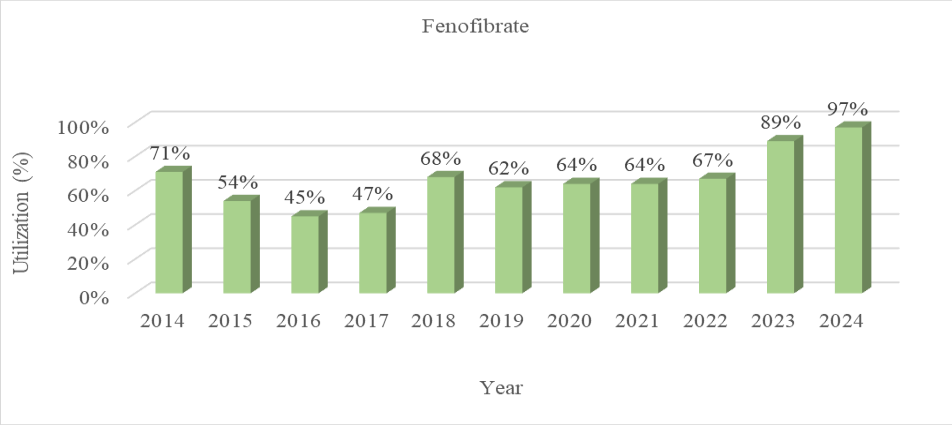


Figure 2. Fenofibrate use as percentage of fibrate utilization

Total reimbursement for LLDs increased over the study period. Although statins accounted for the majority of LLD reimbursement costs, their financial impact gradually declined from 79% in 2014 to 63.7% in 2024. In contrast, fibrate reimbursement expenditures in 2024 were 2.7 times higher than in 2014, whereas the increase for statins over the same period was only 27%. Consequently, fibrate reimbursement costs rose more rapidly than those of statins throughout the study period (Figure 3).

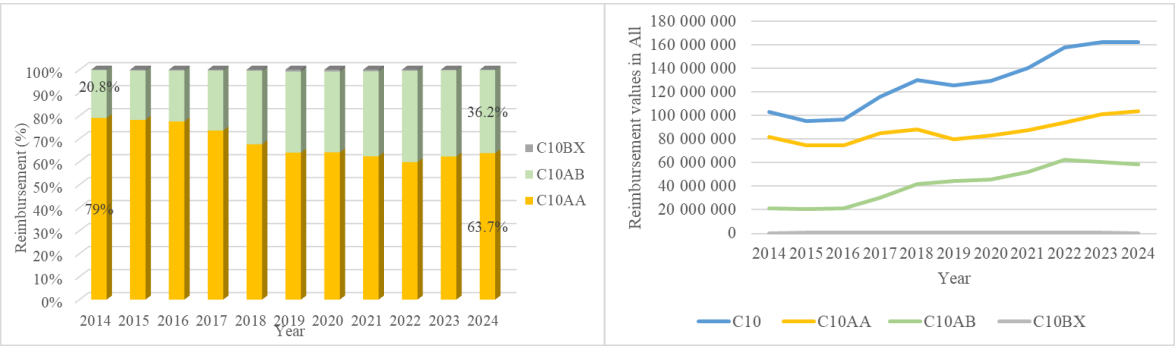


Figure 3. Reimbursement expenditure trends of LLDs from 2014 to 2024

Atorvastatin and fenofibrate expenditures accounted for the largest share of reimbursement costs within the statin and fibrate groups, respectively. The reimbursement gap between fenofibrate and ciprofibrate became more pronounced from 2018 to 2024, consistently favoring fenofibrate. Fenofibrate reimbursement increased steadily throughout the study period, reaching its highest value in 2024, when 99% of total fibrate reimbursement was attributed to fenofibrate alone (Figure 4).

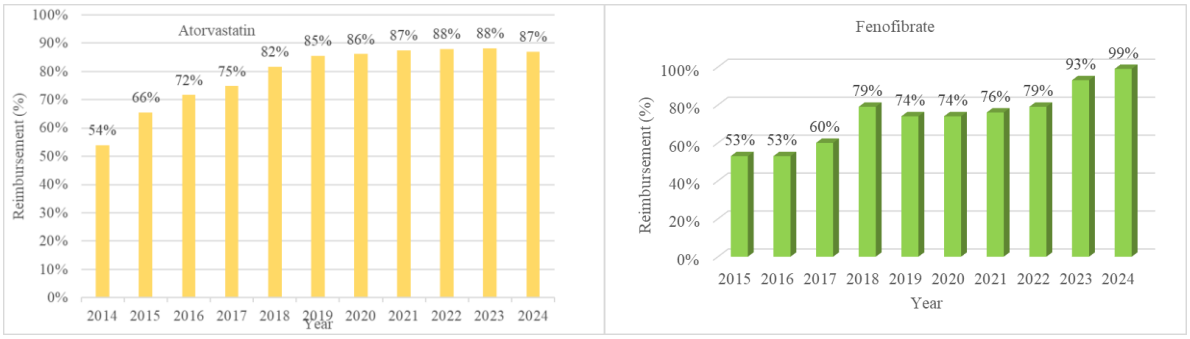


Figure 4. Atorvastatin and Fenofibrate expenditures as percentage of statin and fibrate reimbursement

Atorvastatin and simvastatin had the lowest average prices per DDD, indicating lower expenditures (Figure 5).

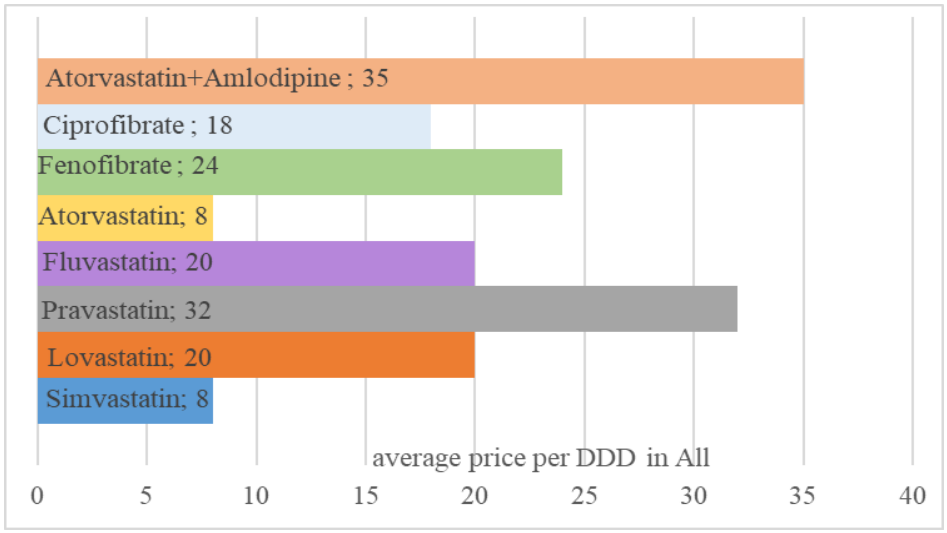


Figure 5. Average price per DDD

In 2024, 92% of LLD utilization and 91% of LLD reimbursement expenditures were attributable to the use and reimbursement of only two drugs, namely atorvastatin and fenofibrate (Figure 6).

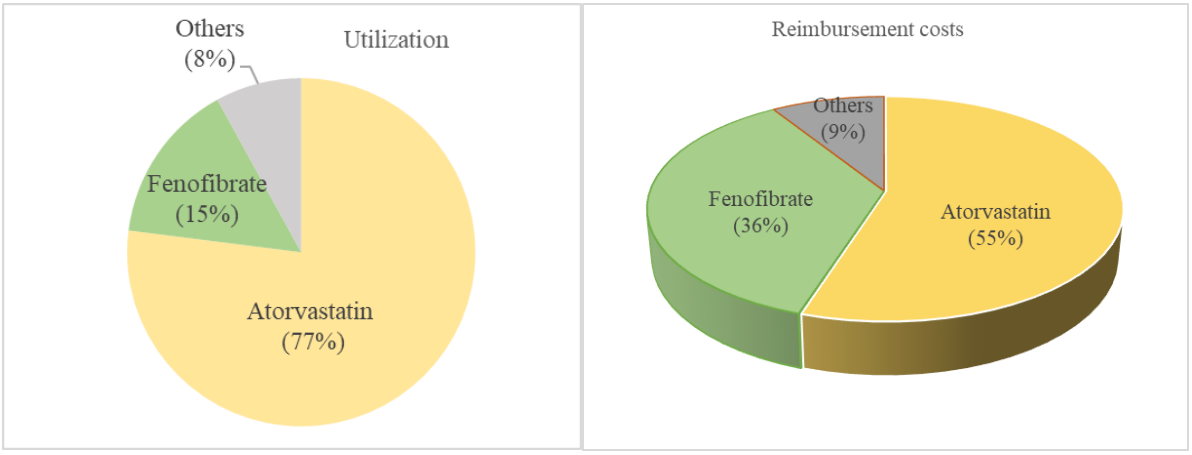


Figure 6. Atorvastatin and fenofibrate versus LLDs in 2024

DISCUSSION

The study demonstrated that the utilization of reimbursed LLDs increased steadily from 2014 to 2024, reaching its highest level in 2024, when consumption was more than threefold higher than in 2014. Statins were the most frequently used drugs, accounting for more than 80% of annual LLD utilization, followed by fibrates. These findings align with the global upward trend in LLD use (Joseph E. Blais et al., 2021), and reflect international and national clinical guideline recommendations that position statins as first-line therapy for the management of dyslipidemia (Mach F et al., 2019; Shehi et al., 2022).

Statins, through their LDL-C-lowering effects, reduce the risk of developing atherosclerotic diseases. Clinical guidelines state that patients at very high-risk and those at high-risk for ASCVD should attain LDL-C targets of <55 mg/dL and <70 mg/dL, respectively, along with at least a 50% reduction from baseline in both categories. The magnitude of LDL-C reduction differs among individual statins and is dose-dependent. High-intensity statin therapy is required to achieve a ≥50% LDL-C reduction, whereas moderate-intensity statin therapy typically results in a 30–50% decrease (Mach F et al., 2019; Shehi et al., 2022). The study found that atorvastatin was the most widely utilized statin, consistent with guideline recommendations that support the use of potent statins for primary and secondary prevention of ASCVD. Rosuvastatin and pitavastatin, two other potent statins, are legally authorized for commercial use in Albania (Drug Register), but neither is currently included in the Reimbursed Drug List.

For patients unable to tolerate the recommended statin intensity due to adverse effects, or for those who fail to achieve treatment goals, adding a non-statin lipid-modifying agent to the maximally tolerated statin dose is recommended. Current clinical guidelines recommend introducing ezetimibe in such cases (Mach F et al., 2019). The combination of ezetimibe with statin therapy produces additional LDL-C reductions (Mach F et al., 2019; Valvukis M. and Valvukis A., 2018). Although several ezetimibe-containing products, whether alone or in combination with a statin, are authorized for sale in the Albanian pharmaceutical market (Drug Register), ezetimibe is not yet reimbursed.

The study also showed that fenofibrate was the most commonly consumed fibrate, contributing substantially to reimbursement expenditures within this drug group. Fibrates are primarily used to reduce triglyceride (TG) levels, with decreases of up to 50%. Their cardiovascular benefits, however, require further confirmation. According to national and international lipid guidelines, fenofibrate or bezafibrate may be considered in combination with statins for high-risk patients who have achieved their LDL-C goal but continue to present with hypertriglyceridaemia [TG >2.3 mmol/L (200 mg/dL)]. When combining statins with fibrates, fenofibrate is preferred due to its minimal or absent skeletal muscle adverse effects (Mach F et al., 2019).

Reimbursement costs for LLDs increased by 57% over the 11-year study period. Although statin expenditures followed this upward trajectory, their overall increase was more modest at approximately 27%. The rise in reimbursement costs was more pronounced for fibrates than for statins, largely attributable to the higher prices of fibrate pharmaceutical products.

It can be anticipated that the actual use and costs of all LLDs marketed in Albania from 2014 to 2024 are considerably higher than the estimates provided in this study. This is because, beyond reimbursed drugs, several other LLDs authorized for marketing in the country are also purchased for effective patient treatment.

CONCLUSION

Over the 11 years from 2014 to 2024, both the utilization and the reimbursement costs of LLDs increased in Albania. Statins were the most widely used drugs and accounted for the highest proportion of reimbursement expenditures, followed by fibrates, which represented the second-largest contribution in terms of both utilization and financial impact. Atorvastatin, the most frequently used statin, appeared cost-effective when considering its average price per DDD. These findings align with international guideline recommendations for dyslipidemia management. In addition, the future inclusion of other effective LLDs within the reimbursement system may be considered with the aim of further enhancing the quality of health care provided to insured patients in Albania.

REFERENCES

Bryan Chong et al. (2025). Global burden of cardiovascular diseases: projections from 2025 to 2050. European Journal of Preventive Cardiology 32, 1001–1015 https://doi.org/10.1093/eurjpc/zwae281

Florjan Shehi et al. (2022) Clinical guideline for primary health care: Dyslipidemia. Udhërrëfyes Klinik për Kujdesin Shëndetësor Parësor: Dislipidemia. ALB_D1aia_S23_Udherrefyesi-Klinik_Dislipidemia.pdf

Joseph E. Blais, Yue Wei et al. (2021)Trends in lipid-modifying agent use in 83 countries. Atherosclerosis 328 44-51 5.016 https://doi.org/10.1016/j.atherosclerosis.2021.05.016

Law No. 10383, dated 24.2.2011, "On Mandatory Healthcare Insurance in the Republic of Albania", as amended

Mach François et al. (2025) Focused Update of the 2019 ESC/EAS Guidelines for the management of dyslipidaemias. Developed by the task force for the management of dyslipidaemias of the European Society of Cardiology (ESC) and the European Atherosclerosis Society (EAS). European Heart Journal (2025) 00, 1–20 https://doi.org/10.1093/eurheartj/ehaf190

Mach F et al. (2019) ESC/EASGuidelines for the management of dyslipidaemias: lipid modification to reduce cardiovascular risk. The Task Force for the management of dyslipidaemias of the European Society of Cardiology (ESC) and European Atherosclerosis Society (EAS). European Heart Journal (2020) 41, 111 188 https://doi.org/10.1093/eurheartj/ehz455

Mandatory Health Care Insurance Fund. Drug List. https://fsdksh.gov.al/project/lista-e-barnave/

National Agency for Medicines and Medical Devices. (AKBPM) Drug Register https://akbpm.gov.al/wp-content/uploads/2025/10/23-tetor-2025.pdf

Online page of Institute of Statistics (INSTAT): http://www.instat.gov.al/

Shurdha O, Hasimi E, Petrela E, Goda A. (2015) Prevalence of major cardiovascular risk factors among adults in Albania (Prevalenca e faktorëve madhorë të riskut kardiovaskular tek të rriturit në Shqipëri). International Journal of Science and Research (Revista Ndërkombëtare e Shkencës dhe Kërkimit), Vëllimi 4 Botimi 12

Vavlukis M, Vavlukis A. (2018). Adding ezetimibe to statin therapy: latest evidence and clinical implications. Drugs in Context; 7: 212534. DOI: 10.7573/dic.212534

WHO Collaborating Centre for Drug Statistics Methodology. Guidelines for ATC classification and DDD assignment 2025 https://atcddd.fhi.no/filearchive/publications/2025_guidelines__final_web.pdf

World Health Organization. Fact Sheets. Cardiovascular diseases (CVDs). (2025) Key facts. https://www.who.int/news-room/fact-sheets/detail/cardiovascular-diseases-(cvds)

ORAL PRESENTATION

Identification and management of mold-induced allergies in indoor environments

Brikena Muja (Parllaku), Merita Xhetani, Etleva Hamzaraj, Mirela Lika

University of Tirana, Faculty of Natural Sciences, Department of Biology, Blvd "Zog I", 1001, Tirana, Albania

Abstract

Exposure to indoor air fungi has been increasingly recognized as a significant factor contributing to allergic responses, particularly among students who spend extended periods in educational environments. This study investigates the presence and concentration of airborne fungal spores in indoor settings, such as classrooms and dormitories, and their potential association with allergic symptoms in students. Air samples were collected from multiple indoor environments in a university setting and analyzed for fungal diversity and spore count using culture-based and molecular methods. Concurrently, a questionnaire-based health survey was conducted to assess the prevalence of allergy-related symptoms among students, including rhinitis, asthma, and skin irritation. The results revealed a predominance of fungal genera such as Aspergillus, Penicillium, and Cladosporium, with seasonal and environmental variations influencing their concentrations. A statistically significant correlation was observed between elevated fungal spore levels and the frequency of reported allergic symptoms. These findings highlight the need for improved indoor air quality monitoring and the implementation of preventive measures in academic institutions to reduce allergen exposure and promote student well-being.

Keywords: indoor environment, mold, allergy, symptoms, public health.

Introduction

Mold-induced allergies represent a significant and increasingly recognized public health concern, particularly within indoor environments where individuals spend most of their time. Mold spores are ubiquitous biological particles that proliferate in areas with excessive moisture, inadequate ventilation, or water damage (Beheshti R., *et al.,* 2024; WHO, 2009). When inhaled or in contact with the skin, these spores can trigger immunological reactions ranging from mild respiratory discomfort to severe allergic manifestations, especially in sensitized individuals. Over recent decades, factors such as urbanization, climate change, and the widespread use of energy-efficient but poorly ventilated buildings have contributed to higher concentrations of indoor mold, making the issue more prevalent and clinically relevant (Łukasz Grewling *et al*, 2025; Preuss CV, *et al*,. 2025; O'Connor A, *et al*., 2025).

Understanding mold-induced allergies requires examining both the biological characteristics of molds and the environmental conditions that promote their growth. Common indoor species, including *Aspergillus*, *Penicillium*, *Cladosporium*, and *Stachybotrys*, release spores and microbial volatile organic compounds (mVOCs) that can exacerbate allergic rhinitis, asthma, chronic sinusitis, and skin irritations. Children, the elderly, and individuals with pre-existing respiratory conditions are particularly vulnerable to these effects. Early identification of mold exposure—through environmental assessment, clinical evaluation, and symptom tracking—is essential for accurate diagnosis, prevention of complications, and implementation of targeted interventions (Beheshti R. *et al.*, 2025; C-E Pogner, *et al*, 2024; Mendell, M. J., *et al*. 2011).

Management strategies for mold-induced allergies must combine medical treatment with environmental control. Pharmacological approaches such as antihistamines, intranasal corticosteroids, and leukotriene modifiers can alleviate symptoms, while immunotherapy may provide long-term benefits for highly sensitized individuals. However, medical treatment alone is insufficient without addressing environmental triggers. Effective remediation requires moisture control, improved ventilation systems, removal of contaminated materials, and adherence to established indoor air quality guidelines. Preventive strategies—particularly in homes, workplaces, schools, and healthcare facilities—play a crucial role in reducing recurrence and protecting at-risk populations. (Bush, R. K., & Portnoy, J. M. 2001; Kew KM, *et al*., 2017; Patti MA, *et al*., 2025).

This article explores the mechanisms, clinical presentation, diagnostic methods, and evidence-based management of mold-induced allergies in indoor environments. By integrating environmental science with clinical practice, it aims to support more effective identification, intervention, and long-term control of this growing public health issue (Łukasz Grewling *et al*, 2025; Preuss CV, *et al*,. 2025).

Materials and Methods

A cross-sectional study was conducted involving 120 university students residing in dormitories and attending classes in selected buildings with varying ventilation and humidity conditions. Participants were aged between 18 and 25 years. Informed consent was obtained from all participants, and the study protocol was approved by the institutional ethics committee.

Indoor Air Sampling

Indoor air samples were collected from classrooms, study rooms, and dormitories using a volumetric air sampler (e.g., Andersen sampler). Sampling was conducted during both humid and dry seasons to assess environmental variation. Petri dishes with Sabouraud Dextrose Agar (SDA) were used to culture airborne fungi. Plates were incubated at 25°C for 5–7 days, and colonies were identified morphologically and microscopically. Common genera such as Aspergillus, Penicillium, and Cladosporium were recorded.

Assessment of Allergic Symptoms

Allergic symptoms among students were assessed using a standardized questionnaire based on the International Study of Asthma and Allergies in Childhood (ISAAC), adapted for young adults. Data collected included respiratory symptoms (e.g., sneezing, nasal congestion), dermatological reactions (e.g., eczema), and history of diagnosed allergies.

Immunological Methods

Blood Sample Collection

Venous blood samples (5 mL) were collected from 60 students reporting allergic symptoms and 30 asymptomatic controls. Samples were centrifuged, and serum was stored at -20°C until analysis.

Total and Specific IgE Measurement

Total IgE levels were measured using an enzyme-linked immunosorbent assay (ELISA) kit (e.g., from Thermo Fisher Scientific).

Specific IgE antibodies against common fungal allergens (Aspergillus fumigatus, Cladosporium herbarum, Penicillium notatum) were detected using ImmunoCAP (Phadia) or an equivalent fluorescent enzyme immunoassay system

Skin Prick Test (SPT)

A subset of students underwent skin prick testing using standardized fungal allergen extracts. The allergens tested included Aspergillus mix, Cladosporium, and Alternaria. Histamine and saline were used as positive and negative controls, respectively. A wheal diameter ≥3 mm compared to the negative control was considered positive.

Statistical Analysis

Data were analyzed using SPSS v26. IgE levels and symptom frequency were compared between exposed and non-exposed groups using t-tests and chi-square tests. Pearson correlation was used to assess the relationship between fungal load and IgE levels. A p-value < 0.05 was considered statistically significant.

Results and discussion

Firstly, we have studied Fungal Concentrations in Indoor Air. Air samples revealed the presence of Aspergillus, Penicillium, and Cladosporium in all locations. Dormitories showed the highest fungal concentrations, particularly for Aspergillus (up to 180 CFU/m³).

Table 1: Mean Fungal Spore Concentrations (CFU/m³) by Location

Location		Aspergillus.	Penicillium	Cladosporium
Classroom	A	120	80	60
Classroom	B	90	70	50
Dormitory	A	150	100	85
Dormitory	B	180	110	95

For total IgE Levels, Students reporting allergic symptoms had significantly higher total serum IgE levels (mean: 303 IU/mL) compared to asymptomatic controls (mean: 75 IU/mL).

Table 2: Total IgE (IU/mL) in Allergic vs Control Groups

Group	Mean	Std.Dev	Min	Max
Allergic	303	17.6	285	320
Control	75	15.3	60	90

We determine the Prevalence of Allergic Symptoms, the data are as follows:

Table 3: Reported Allergy Symptoms Among Students. A bar chart would display these values.

Symptom	% of Students Affected
Sneezing	52%
NasalCongestion	45%
Wheezing	30%
Eczema	25%

The findings demonstrate a clear association between exposure to indoor fungal spores and the presence of allergic symptoms in students. Dormitory environments, with typically poor ventilation and higher humidity, showed the highest concentrations of allergenic fungi. This aligns with previous studies linking Aspergillus and Cladosporium exposure to respiratory and dermal allergic responses.

The significantly elevated IgE levels in symptomatic students further support a Type I hypersensitivity reaction, likely mediated by fungal allergens. Skin prick testing and specific IgE assays would help confirm sensitization patterns in future research.

These results underscore the importance of monitoring indoor air quality in academic settings. Interventions such as improving ventilation, reducing indoor humidity, and regular cleaning could mitigate fungal proliferation and reduce allergen exposure among students.

Environmental studies consistently demonstrated a strong correlation between elevated indoor humidity levels above 60%, water-damaged structures, and increased mold proliferation. Homes lacking adequate ventilation exhibited significantly higher concentrations of airborne mold spores. Clinical studies showed that exposure to indoor mold contributes to increased rates of asthma exacerbations, allergic rhinitis, and chronic sinusitis. Diagnostic methods such as skin prick testing and serum IgE analysis were found to be reliable tools for identifying mold sensitization. Pharmacological treatments including antihistamines, leukotriene receptor antagonists, and intranasal corticosteroids were effective in managing symptoms. Environmental interventions—improving ventilation, reducing humidity, repairing leaks, and removing mold-contaminated materials—were shown to significantly reduce symptom recurrence and improve patient outcomes.

Table 4. Key environmental risk factors for indoor mold growth and recommended control measures.

Risk factor	Typical example	Recommended control measure
High relative humidity (>60%)	Poorly ventilated bathroom or kitchen	Use exhaust fans, dehumidifiers, and keep humidity between 40–60%.
Water intrusion or leaks	Leaking roof, pipe, or window frame	Repair leaks promptly and dry affected materials within 24–48 hours.
Condensation on cold surfaces	Condensation on windows, exterior walls, or pipes	Improve insulation, increase air circulation, and control indoor humidity.
Inadequate ventilation	Sealed windows and blocked vents	Open windows, when possible, maintain HVAC systems, and ensure fresh air exchange.
Porous materials staying damp	Wet carpets, drywall, or cardboard	Remove or replace contaminated materials; avoid long-term storage of paper and textiles in damp areas.

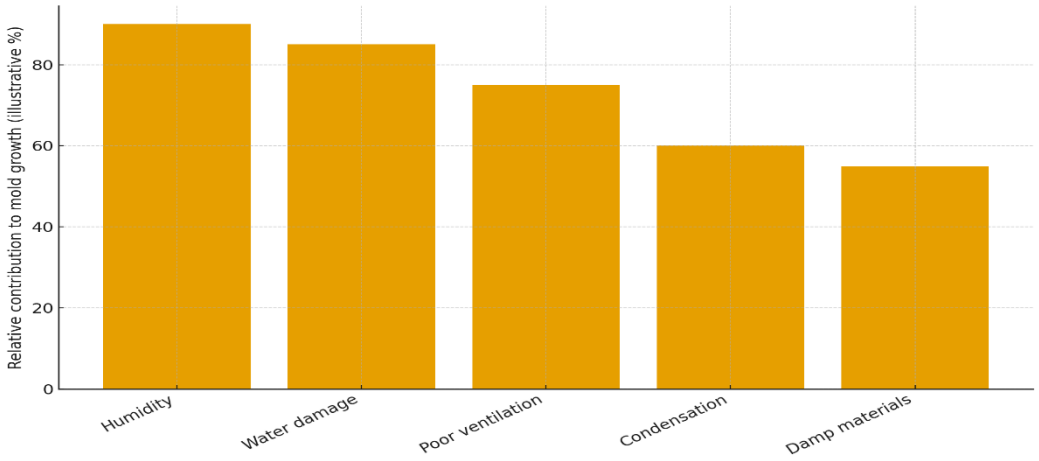


Figure 1. Illustrative relative contribution of key indoor factors to mold growth

This bar chart provides an illustrative comparison of how major indoor environmental factors contribute to mold growth. Actual values will vary by building type and climate, but the figure emphasizes the dominant role of humidity and water damage.

Conclusion

Mold-induced allergies remain a major public health issue in indoor environments. Findings from reviewed studies highlight the interplay between biological susceptibility and environmental conditions. Effective management requires a dual approach: medical treatment to alleviate symptoms and environmental remediation to eliminate mold sources. Improving indoor air quality through moisture reduction, ventilation enhancement, and prompt repair of water damage is essential. Future research should focus on creating standardized indoor mold assessment protocols and developing sustainable prevention strategies to reduce allergic disease burden.

References

Beheshti R, Phipatanakul W, DiMango E, Grant TL. Indoor Allergen Interventions in Homes and Schools for Managing Asthma..J Allergy Clin Immunol Pract. 2025 Jun;13(6):1256-1265. doi: 10.1016/j.jaip.2025.04.027. Epub 2025 Apr 25.PMID: 40288638 Review.

Beheshti R, Grant TL, Wood RA. Minimizing Indoor Allergen Exposure: What Works? Curr Allergy Asthma Rep. 2024 Nov 13;25(1):3. doi: 10.1007/s11882-024-01185-3.PMID: 39535667 .

Bush, R. K., & Portnoy, J. M. (2001). The role of fungi in allergic diseases. Journal of Allergy and Clinical Immunology.

C-E Pogner , C Antunes, G P Apangu, N Bruffaerts, S Celenk, A Cristofori, N González Roldán, A Grinn-Gofroń, B Lara, M Lika, D Magyar, M Martinez-Bracero, L Muggia, B Muyshondt, D O'Connor , A Pallavicini , M A Penha, R Pérez-Badia, H Ribeiro, A Rodrigues Costa, Z Tischner, M Xhetani, C Ambelas Skjøth. Airborne DNA: State of the art - Established methods and missing pieces in the molecular genetic detection of airborne microorganisms, viruses and plant particles. Sci Total Environ. 2024 Nov 14:177439. PMID: 39549753. doi: 10.1016/j.scitotenv.2024.177439 https://pubmed.ncbi.nlm.nih.gov/39549753

Institute of Medicine. (2004). Damp Indoor Spaces and Health. National Academies Press.

Łukasz Grewling , Helena Ribeiro, Celia Antunes, Godfrey Philliam Apangu, Sevcan Çelenk, Ana Costa, Ibon Eguiluz-Gracia, Ana Galveias, Nestor Gonzalez Roldan, Mirela Lika, Donát Magyar, Moises Martinez-Bracero, Pia Ørby, David O'Connor, Alexandra Marchã Penha, Sónia Pereira, Rosa Pérez-Badia, Victoria Rodinkova, Merita Xhetani, Ingrida Šauliene, Carsten Ambelas Skjøth. Outdoor airborne allergens: Characterization, behaviour, and monitoring in Europe. *Science of The Total Environment,* Volume 905, 20 December 2023, 167042. *journal homepage: www.elsevier.com/locate/scitotenv*

Kew KM, Carr R, Donovan T, Gordon M.Cochrane Asthma education for school staff Database Syst Rev. 2017 Apr 12;4(4):CD012255. doi: 10.1002/14651858.CD012255.pub2.PMID: 28402017

Mendell, M. J., et al. (2011). Respiratory and allergic health effects of dampness, mold, and dampness-related agents: A review. Environmental Health Perspectives.

O'Connor A, Hasan M, Sriram KB, Carson-Chahhoud KV.Cochrane Home-based educational interventions for children with asthma..Database Syst Rev. 2025 Feb 6;2(2):CD008469. doi: 10.1002/14651858.CD008469.pub3.PMID: 39912443

Patti MA, Henderson NB, Phipatanakul W, Jackson-Browne M.Chest. Recommendations for Clinicians to Combat Environmental Disparities in Pediatric Asthma: A Review. 2024 Dec;166(6):1309-1318. doi: 10.1016/j.chest.2024.07.143. Epub 2024 Jul 24. PMID: 39059578

Preuss CV, Kalava A, King KC.2025 Jul 6. Prescription of Controlled Substances: Benefits and Risks. In: StatPearls [Internet]. Treasure Island (FL): StatPearls Publishing; 2025. PMID: 30726003

World Health Organization. (2009). WHO Guidelines for Indoor Air Quality: Dampness and Mould.

ORAL PRESENTATION

"Challenges and opportunities in preserving natural resources" in Albania

*Silvana Nakuci[1] (Orcid: 0009-0008-6460-0028)

[1]Department of Economy and Rural Development Policies, Faculty of Economy and Agribusiness, Agricultural University of Tirana/ Tirana, Albania

Abstract

This study examines the key challenges associated with the conservation and management of natural resources. Drawing on qualitative methodologies, including semi-structured interviews and field observations, the research identifies the main factors contributing to environmental degradation, such as uncontrolled exploitation, pollution, climate change, and the absence of effective institutional mechanisms. The analysis reveals that local actors play a crucial role in perceiving and addressing these challenges; however, their efforts are often hindered by financial constraints, weak interinstitutional coordination, and limited public awareness. The study highlights the importance of community engagement and the strengthening of sustainable policies to ensure the effective and long-term management of natural resources.

Keywords: challenges, natural resources, sustainable management, local actors, environmental protection.

1.Introduction

This study aims to analyze the challenges associated with the conservation of natural resources by assessing the perceptions and concerns of local stakeholders and highlighting the importance of comprehensive approaches to sustainable resource management. Environmental degradation is emerging as a global threat, adversely affecting public health and quality of life. Population growth and increasing consumption intensify climate change, accelerating the depletion of natural resources and jeopardizing their long-term sustainability (Zhang, 2021).

To utilize natural resources effectively, individuals must possess adequate knowledge of the environment, its importance, and its underlying dynamics. Moreover, environmental action requires structured, functional support across multiple levels, as well as the provision of necessary financial resources to implement sustainable measures (Kozera-Kowalska, 2024). Although the expansion of protected areas is relatively easy to implement, it often overlooks biodiversity, ecosystem services, and social equity. Therefore, assessing the effectiveness of management and governance should be an essential component in achieving natural resource conservation objectives (Hoffmann, 2022). By assessing the extent of environmental indicator deterioration, policymakers can more accurately determine priorities for resource allocation and design more effective strategies for addressing environmental challenges. (Solangi, 2023). In this paper, we present the latest research and developments concerning the challenges and opportunities in natural resource conservation. The study was conducted based primarily on data collected from stakeholders in various regions of Albania, and the research method employed was a Google Forms–based survey.

2. Literature Review

Natural resources constitute the foundation of human existence and development. They not only sustain the biological and ecological processes of life but also drive the economic, social, and technological advancement of human societies. This study examines the challenges and opportunities in natural resource conservation, as well as the impact that natural resources have on the well-being of various communities. Digitalization and technological innovation offer substantial potential for sustainable resource management by reducing environmental impacts, increasing efficiency, and improving socio-economic outcomes. This stems from the transformative role that technology can play in contemporary resource management (Jianing, 2024). Among the most critical natural resources are air, forests, and water. Air not only provides oxygen but also offers protection from cosmic radiation and pollutants, while forests and oceans contribute to carbon dioxide absorption and the mitigation of climate change. Water, essential for consumption, agriculture, and industry, originates directly from the Earth's natural sources, supporting both ecosystem functioning and human activities (Thomas, 2023). Sustainable management of natural resources has gained critical importance as global ecosystems face continuous

pressures from human activities. Fundamental resources such as water, soil, forests, and biodiversity are being degraded at rapid rates due to industrialization, urbanization, and unsustainable agricultural practices (Zhang M. , 2025). In a period of declining natural resource availability, the implementation of more resilient and adaptable supply systems, including various energy conversion technologies such as solar thermal and photovoltaic panels, can lay the foundation for a less resource-intensive urban lifestyle (Zucaro, 2025).

3. Results of the study

Sustainable management of natural resources is increasingly essential today due to population growth, urbanization, and global environmental crises. Their uncontrolled exploitation threatens not only ecological balance but also social well-being and economic stability. This study relied on various stakeholders to assess their impact and readiness for natural resource conservation. Our research was based on the analysis of 85 questionnaires, with the results presented as follows:

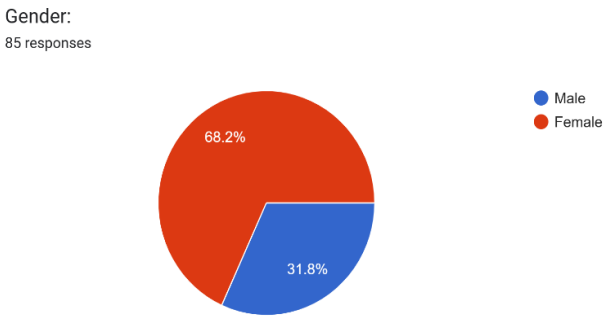


Figure 1. Gender of the respondents

The figure above shows the result of gender of the 85 interviews, 68.2% are female and 31.8% are male.

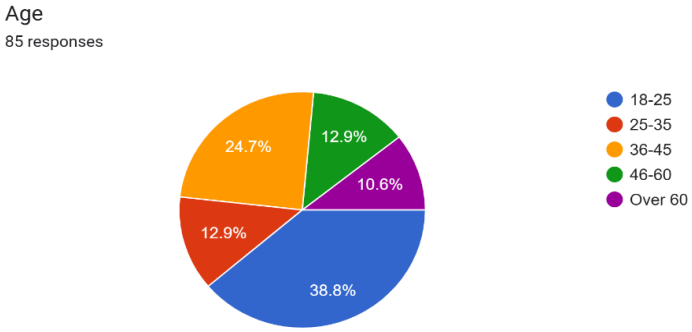


Figure 2. Age of the respondents

The figure above illustrates the age distribution of the respondents: 38.8% are 18–25 years old, 12.9% are 26–35 years old, 24.7% are 36–45 years old, 12.9% are 46–60 years old, and 10.6% are over 60 years old.

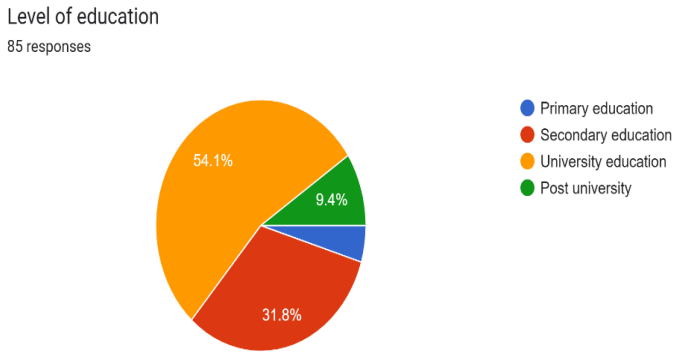


Figure 3. Education level of the respondents

The figure above shows the education levels of the respondents. Out of 100% of the participants, 54.1% have a university education, 31.8% have completed secondary education, 9.4% have postgraduate education, and 4.7% have primary education.

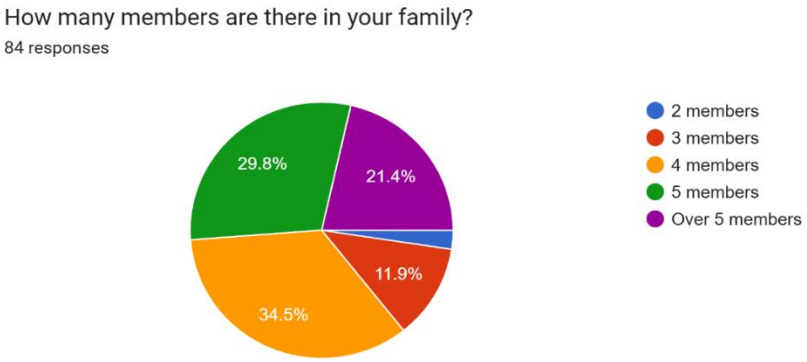


Figure 4. How many members are in your family?

The figure above shows the family size of the respondents. The largest group, 34.5%, lives in families with 4 members, 29.8% live in families with 5 members, 21.4% live in families with more than 5 members, 11.9% live in families with 3 members, and 2.3% live in families with 2 members.

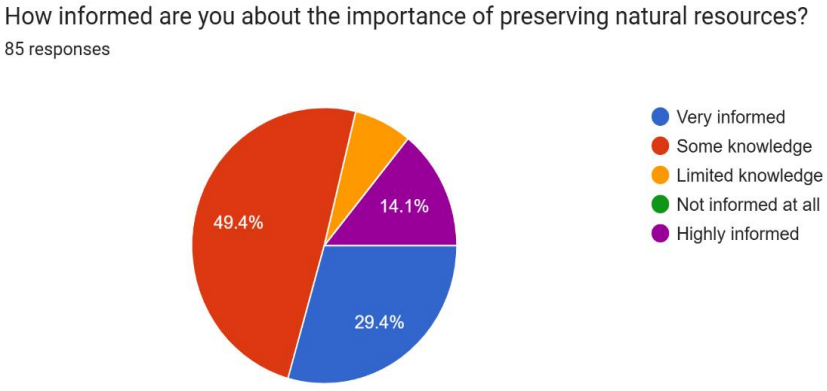


Figure 5. How informed are you about the importance of natural resource conservation?

Respondents were asked about their level of awareness regarding the importance of conserving natural resources. The results indicate that 49.4% of respondents have only some knowledge, 29.4% are informed, 14.1% consider themselves very well informed, and 7.1% report having little knowledge.

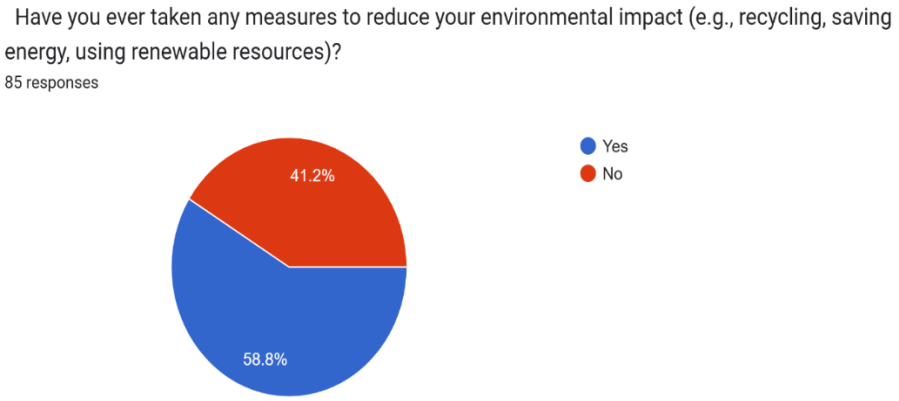


Figure 6. Have you ever taken measures to reduce your environmental impact (e.g., recycling, saving energy, using renewable resources)?

Regarding the measures respondents have taken to reduce their environmental impact, such as recycling, saving energy, or using renewable resources, 58.8% answered "Yes," while 41.2% indicated "No," reporting that they have never taken measures to reduce their environmental impact.

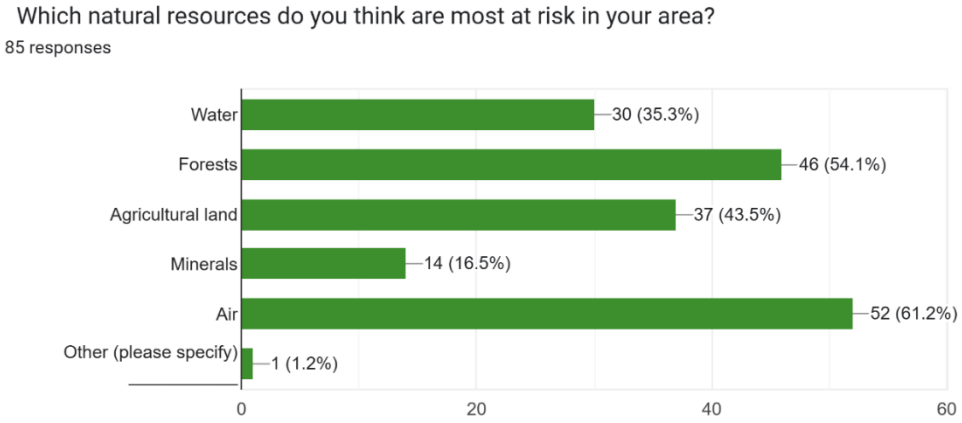


Figure 7. Which natural resources do you consider most at risk in your area?

Respondents were asked about the natural resources they consider most at risk in their areas. According to the study, the natural resources identified as most at risk were: air, forests, agricultural land, water, and minerals.

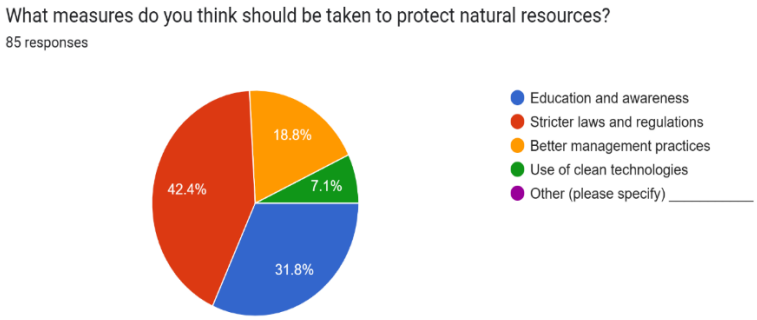


Figure 8. What measures do you think should be taken to protect natural resources?

The figure above illustrates the measures that respondents believe should be taken to protect natural resources. According to the survey results: 31.8% of respondents believe that measures should focus on education and awareness-raising among all stakeholders, 42.4% think that stricter laws and regulations should be implemented, 7.1% suggest using clean technologies, and 18.8% believe that measures should rely on best management practices.

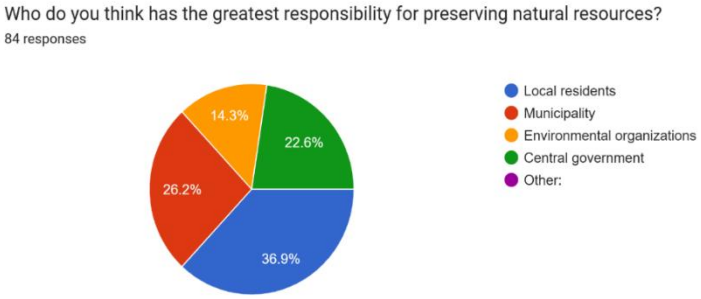


Figure 9. Who do you think holds the greatest responsibility for conserving natural resources?

Regarding the question of who holds the greatest responsibility for conserving natural resources, respondents answered as follows: 36.9% believe the responsibility lies with local residents, 26.2% with municipalities or communities, 14.3% with environmental organizations, and 22.6% with the central governmen.

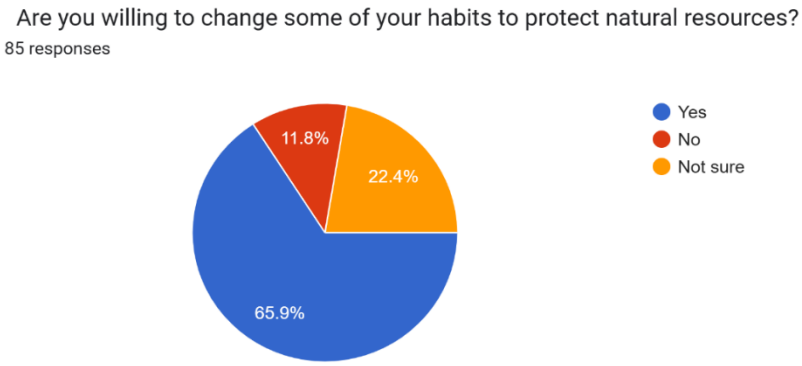


Figure 10. Are you willing to change some of your habits to protect natural resources?

The figure above illustrates respondents' willingness to change certain habits to protect natural resources. The results show that 65.9% are willing to change their habits, 11.8% are not willing, and 22.4% are uncertain about whether they want to modify their habits for natural resource conservation.

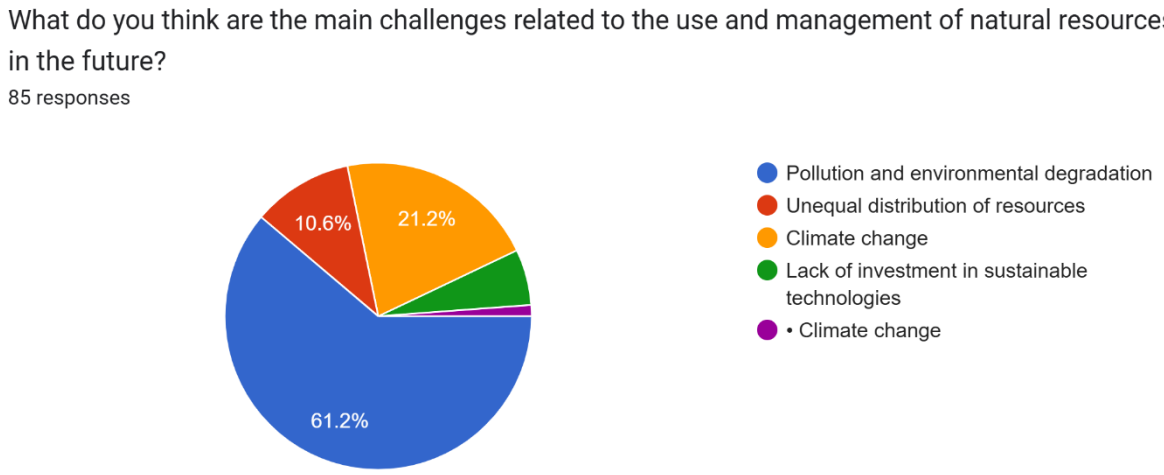


Figure 11. In your opinion, what are the main challenges related to the use and management of natural resources in the future?

Regarding the question of the main challenges related to the use and management of natural resources in the future, the responses from 100% of the participants were as follows: 61.2% believe the main challenge is pollution and environmental degradation, 21.2% consider climate change to be the primary challenge, 10.6% think the main challenge is the unequal distribution of resources, and 7% believe the primary challenge is the lack of investment in sustainable technologies

4.Conclusions

According to the study, out of 85 respondents, 68.2% were female and 31.8% were male. The age distribution of respondents was as follows: 38.8% were 18–25 years old, 12.9% were 26–35 years old, 24.7% were 36–45 years old, 12.9% were 46–60 years old, and 10.6% were over 60 years old.

Regarding education, 54.1% of respondents had a university-level education, 31.8% had completed secondary education, 9.4% had postgraduate education, and 4.7% had primary education.

Most respondents live in families with 4 members (34.5%), 29.8% live in families with 5 members, 21.4% live in families with more than 5 members, 11.9% live in families with 3 members, and 2.3% live in families with 2 members.

Respondents were asked about their level of awareness regarding the importance of conserving natural resources. The results show that 49.4% of respondents have only some knowledge, 29.4% are informed, 14.1% consider themselves very well informed, and 7.1% report having little knowledge. Regarding the measures respondents have taken to reduce their environmental impact (e.g., recycling, saving energy, using renewable resources), 58.8% of respondents answered Yes, while 41.2% stated that they have never taken any measures to reduce their environmental impact, answering No. Respondents were also asked about the natural resources they consider most at risk in their areas. According to the study, the most endangered resource was air, followed by forests, agricultural land, water, and minerals.

Regarding the measures that should be taken to protect natural resources, 31.8% of respondents believe that actions should focus on education and raising awareness among all stakeholders, 42.4% think stricter laws and regulations should be implemented, 7.1% suggest the use of clean technologies, and 18.8% believe measures should rely on best management practices Regarding the question of who holds the greatest responsibility for conserving natural resources, respondents answered as follows: 36.9% believe the responsibility lies with local residents, 26.2% with municipalities or communities, 14.3% with environmental organizations, and 22.6% with the central government. Additionally, concerning respondents' willingness to change certain habits to protect natural resources, 65.9% indicated they are willing to modify their habits, 11.8% stated they are not willing, and 22.4% were uncertain about whether they want to change their habits for the protection of natural resources. Regarding the question of the main challenges related to the use and management of natural resources in the future, the responses from 100% of

the participants were as follows: 61.2% believe the primary challenge is pollution and environmental degradation, 21.2% consider climate change to be the main challenge, 10.6% think the main challenge is the unequal distribution of resources, and 7% identify the lack of investment in sustainable technologies as the primary challenge.
According to the study, the data indicate that awareness of natural resources is partial, while the willingness to implement practical changes exists among a considerable portion of the community. The results also emphasize the importance of combined interventions through education, legislation, management practices, and the use of clean technologies to ensure the conservation and sustainable management of natural resources.

5. Recommendations

Enhancing Environmental Awareness and Education
Considering that a significant portion of respondents have limited knowledge about the importance of natural resources, it is recommended to develop educational programs and awareness campaigns that involve all local stakeholders and the wider community.
Strengthening Legislation and Enforcement of Regulations
Since 42.4% of respondents support stricter laws and regulations, it is necessary to reinforce the legal framework for natural resource protection and ensure its effective implementation by competent authorities.
Promoting Sustainable Practices and the Use of Clean Technologies
To reduce the negative impact of human activities on the environment, it is recommended to promote best management practices, recycling, energy saving, and the use of renewable resources, including the adoption of clean technologies.
Strengthening the Role of Local Actors
Given that a large portion of respondents consider local residents and municipalities responsible for natural resource conservation, active community participation in decision-making and resource management should be encouraged.
Monitoring Emerging Environmental Challenges
As pollution, environmental degradation, and climate change are identified as the main challenges, it is recommended to establish monitoring and reporting mechanisms for these issues, along with developing adaptation and prevention strategies.
Encouraging Willingness for Sustainable Changes in Individual Habits
Considering participants' willingness to modify their habits to protect natural resources, it is important to create policies and incentives that support sustainable behavioral changes.

References

Hoffmann, S. (2022). Challenges and opportunities of area-based conservation. *Biodiversity and Conservation, Volume 31*, 325–352. doi:10.1007/s10531-021-02340-2

Jianing, P. (2024). Examining the role of digitalization and technological innovation in promoting sustainable natural resource exploitation. *Resources Policy, 92*. doi:10.1016/j.resourpol.2024.105036

Kozera-Kowalska, M. (2024). Challenges and Problems of Nature Conservation: A Case Study from Poland. *Sustainability*. doi:10.3390/su16135572

Solangi, Y. A. (2023). Examining challenges and solutions for environmental and natural resource management with a focus on mineral resources. *Resources Policy, Volume 86*. doi:10.1016/j.resourpol.2023.104085

Thomas, M. (2023). The Crucial Role of Natural Resources in Preserving Earth\'s Environment. *Journal of Research in Environmental Science and Toxicology, 12*(4). doi:10.14303/2315-5698.2023.40

Zhang, L. (2021). Caring for the environment: How human capital, natural resources, and economic growth interact with environmental degradation in Pakistan? A dynamic ARDL approach. *Science of The Total Environment, Volume 774*. doi:10.1016/j.scitotenv.2021.145553

Zhang, M. (2025). Policymaking Issues: Sustainable Management of Natural Resources. *Management of Natural Resources - Relevance, Issues and Constraints*. doi:10.5772/intechopen.1008943

Zucaro, A. (2025). Urban sustainability: challenges and opportunities for resilient and resource-efficient cities. *Frontiers in Sustainable Citie, 7*. doi:10.3389/frsc.2025.1556974

ORAL PRESENTATION

Maternal and neonatal outcomes following induction of labor at term: A retrospective cohort study

Lindita Ibrahimi[1] (https://orcid.org/0000-0003-3007-3000),
Ferdita Haxhiu Derguti[2], Brikene Dacaj Elshani[1](https://orcid.org/0009-0008-6347-8980)

[1] Obstetric and Gynecology Clinic, University Clinical Center of Kosovo, Department of Obstetrics and Gynecology, Medical Faculty, University of Prishtine, Prishtine, Kosovo
[2*]Obstetric and Gynecology Clinic, University Clinical Center of Kosovo, Ss. Cyril and Methodius University in Skopje, Republic of North Macedonia

Abstract

Induction of labor is a frequent obstetric intervention, yet its impact on maternal and neonatal outcomes remains debated. This study evaluated maternal and neonatal outcomes after induction of labor at term and contextualized the findings within contemporary international evidence. A retrospective analysis was conducted on 400 term pregnancies undergoing induction. Maternal variables included parity, Bishop score, intrapartum complications, and mode of delivery, while neonatal outcomes included Apgar scores, serious diagnoses, need for resuscitation, and NICU admission. Most women (92%) presented with a favorable Bishop score (≥6), and 273 women (68.3%) experienced no intrapartum complications. The most frequent complications were perineal rupture (53 cases) and umbilical cord–related events (51 cases). A total of 373 women (93.2%) delivered vaginally, whereas 27 (6.8%) required cesarean section, primarily due to ineffective induction or fetal distress. Neonatal outcomes were highly reassuring: 394 newborns (98.3%) had no serious diagnosis, only one infant had an Apgar score ≤3, one intrauterine fetal death occurred, and NICU admission was required in only one case (0.2%). Overall, induction of labor at term when performed for appropriate obstetric indications and supported by standardized monitoring was associated with low maternal complication rates, a very low cesarean rate, and excellent neonatal outcomes, supporting its role as a safe and effective strategy to prevent deterioration of maternal-fetal conditions when indicated.

Keywords: induction of labor, maternal outcomes, neonatal outcomes, cesarean delivery, bishop score

INTRODUCTION

Labor induction refers to the artificial initiation of uterine contractions with the purpose of achieving vaginal birth before the spontaneous onset of labor (ACOG, 2020). It is generally undertaken when the risks of continuing pregnancy outweigh the potential risks associated with induction. Common clinical indications include post-term pregnancy, hypertensive disorders of pregnancy, oligohydramnios, premature rupture of membranes, gestational diabetes, and intrauterine growth restriction (IUGR) (Caughey et al., 2022; World Health Organization [WHO], 2022). The decision to induce labor must therefore balance maternal and fetal risks while considering cervical readiness, typically assessed through the Bishop score.

Several induction methods exist, ranging from pharmacological techniques, such as prostaglandins (misoprostol, dinoprostone) and oxytocin, to mechanical approaches, including Foley catheter or double-balloon catheter insertion (Sheldon & Diedrich, 2021). Combined methods are often employed to improve cervical ripening and enhance the success of vaginal delivery. Evidence suggests that mechanical methods are associated with lower rates of uterine tachysystole, whereas prostaglandins may be more effective for cervical ripening in unfavorable cervices (Ten Eikelder et al., 2019).

In recent years, attention has increasingly focused on the outcomes of elective induction, especially at 39 weeks of gestation. Findings from large randomized trials and meta-analyses such as the ARRIVE Trial by Grobman et al. (2018) demonstrate that elective induction at 39 weeks may reduce the risk of cesarean delivery and hypertensive complications without increasing adverse neonatal outcomes. Subsequent analyses have supported

these observations, suggesting improved perinatal safety when induction is performed under standardized protocols and continuous monitoring (Walker et al., 2020; Stock & Norman, 2021). Despite this, controversy persists because results vary across populations, resource settings, and institutional practices.

Concerns frequently raised in the literature include the potential for increased medical interventions, prolonged labor, and higher use of analgesia among induced women (Boulvain et al., 2016). Conversely, expectant management may increase the likelihood of stillbirth, meconium aspiration, or neonatal morbidity in late-term and post-term pregnancies (Muglu et al., 2019). These conflicting findings underscore the importance of evaluating induction outcomes in diverse clinical settings.

Against this background, the present study aims to assess the maternal and neonatal outcomes among 400 women who underwent labor induction, as documented in the dataset. By comparing these findings with contemporary international evidence, this study seeks to determine whether induction of labor is associated with improved or worsened perinatal outcomes relative to spontaneous labor or expectant management. Ultimately, the goal is to contribute data-driven insights to the ongoing debate surrounding the safety, efficacy, and clinical appropriateness of labor induction.

MATERIALS AND METHODS

Study design and population

This study employed a retrospective observational design, analyzing clinical data from a cohort of 400 pregnant women who underwent induction of labor at term. All cases were extracted from institutional obstetric records and represented consecutive admissions during the study period. The dataset included information obtained from maternal electronic charts, intrapartum monitoring sheets, and neonatal outcome documentation, ensuring a complete overview of both maternal and neonatal parameters. Women with multiple gestations, major fetal anomalies, or incomplete medical records were excluded to preserve data consistency. The study population consisted of both primiparous and multiparous women, reflecting the parity structure presented in the institutional registry. Gestational age at the time of induction ranged from 38 to 41 weeks, consistent with the distribution illustrated in the uploaded report.

Induction procedures

Labor induction in this cohort was performed according to institutional protocols and international clinical guidelines. Several induction modalities were used, selected based on cervical favorability, maternal–fetal status, and clinical indications recorded prior to the procedure.

Pharmacological induction included the administration of oxytocin, initiated at a low dose of 1–2 mU/min with gradual titration every 30-40 minutes until adequate uterine activity defined as three to five contractions every ten minutes was achieved. Prostaglandin preparations (PGE1 or PGE2) were administered for cervical ripening, particularly in women presenting with an unfavorable Bishop score. Misoprostol or dinoprostone formulations were used in accordance with their respective dosing protocols specified in the clinical guidelines of the institution. Mechanical methods, such as the Foley catheter or double-balloon catheter, were applied in selected cases requiring mechanical cervical dilation, especially when prostaglandins were contraindicated or when the cervix was markedly unripe. In certain patients, combined approaches (e.g., prostaglandins followed by oxytocin augmentation) were employed to increase the likelihood of successful induction. All women underwent continuous fetal and maternal monitoring throughout the induction process, as per standard obstetric safety requirements.

Variables and outcome measures

Maternal and neonatal variables were identified based on availability in the clinical records and relevance to induction outcomes. Maternal variables included parity, Bishop score prior to induction, mode of delivery, and intrapartum complications. Complications were categorized into predefined groups such as perineal rupture, umbilical cord complications, hypertensive crises, cervical lacerations, and other obstetric events documented in real time by clinical staff. Mode of delivery was classified as spontaneous vaginal birth, instrumental delivery, or cesarean section, accompanied by the documented clinical indication (e.g., failed induction, fetal distress).

Neonatal outcome measures included Apgar scores at 1 and 5 minutes, presence of serious neonatal diagnoses, requirement for neonatal resuscitation, and admission to the Neonatal Intensive Care Unit (NICU). Data on fetal

demise, birth trauma, and other immediate postnatal complications were also collected. These variables allowed for a comprehensive assessment of perinatal safety following induction of labor.

Data analysis
A descriptive statistical approach was employed to evaluate the distribution of maternal and neonatal outcomes. Frequencies and proportions were calculated for categorical variables, while continuous variables (e.g., maternal age) were summarized using appropriate descriptive measures. Results obtained from the 400-case cohort were interpreted in relation to contemporary global literature published between 2019 and 2025, as summarized in the uploaded presentation. Comparative interpretation emphasized alignment or divergence between local institutional outcomes and findings of recent systematic reviews, randomized controlled trials, and meta-analyses addressing labor induction and perinatal safety. The analytical goal was not inferential hypothesis testing, but rather contextualization of observed patterns within the broader evidence base.

RESULTS

This study analyzed a total of 400 women undergoing induction of labor. The results describe maternal demographic characteristics, obstetric history, clinical indications for induction, intrapartum complications, delivery outcomes, and neonatal conditions. Figures and tables provided illustrate the quantitative distribution of each variable.

Maternal demographics

Figure 1 presents three key demographic and obstetric characteristics of the study population: age distribution, parity/gravida, and number of previous births.

The age distribution (Figure 1, left panel) shows that the majority of women undergoing induction of labor were between 24 and 35 years old. The highest concentration of patients was observed in the 25–28-year age group, representing the predominant reproductive-age population in this cohort. A smaller proportion of women were younger than 22 or older than 40 years, indicating that inductions were primarily performed among women in low- to moderate-risk age categories.

The parity distribution (Figure 1, center panel) demonstrates that multiparous women constituted the larger share of the sample. Specifically, approximately 260 women were multiparas, compared with about 140 primiparas. This 2:1 ratio suggests that induction was more commonly performed among women with prior childbirth experience. The predominance of multiparas is clinically relevant, as parity is strongly associated with cervical readiness and higher likelihood of successful vaginal delivery following induction.

The distribution of previous births (Figure 1, right panel) shows that most multiparous women had one or two prior deliveries, representing the largest portion of the histogram. A moderate number had three previous births, while cases of grand multiparity (≥4 births) were relatively uncommon. Only isolated cases were noted with 5, 6, or 7 prior births. This pattern indicates that the study population largely consisted of women with low to moderate parity levels, supporting a favorable obstetric risk profile and contributing to the overall success of induction outcomes.

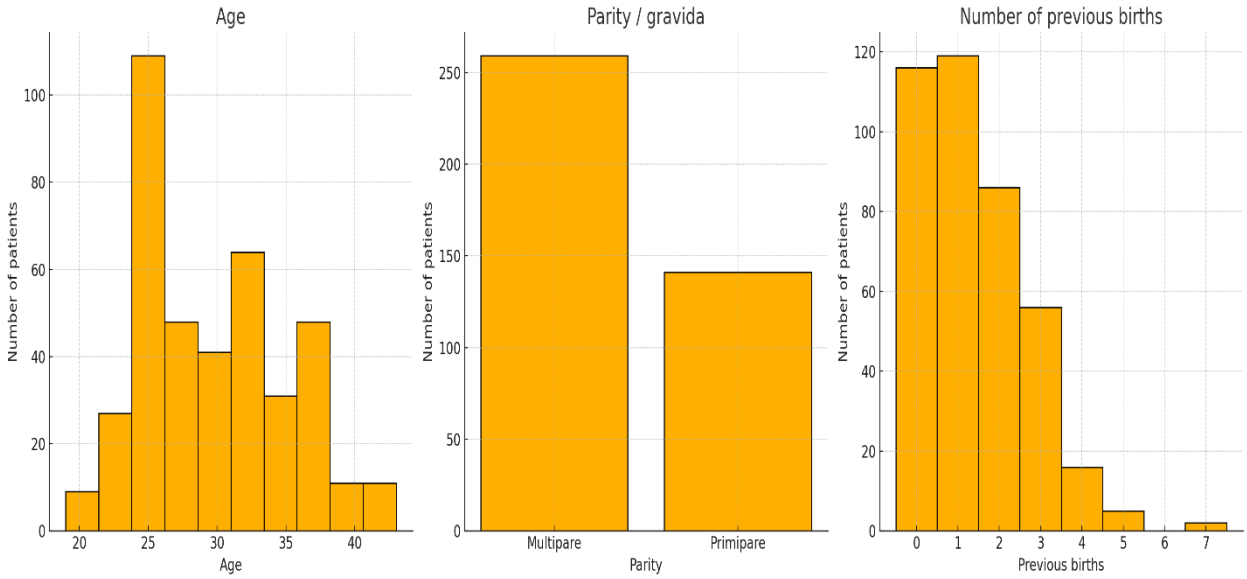


Figure 1. Age, Parity/Gravida, and Number of previous births

Gestational age at induction

Gestational ages ranged from 38.0 to 41.0 weeks. As shown in Figure 2, inductions peaked between 39 and 41 weeks, representing the majority of procedures. Only 9 cases were recorded at 38 weeks.

This distribution is consistent with international guidelines that recommend induction in late-term and early post-term pregnancies or when maternal-fetal complications arise.

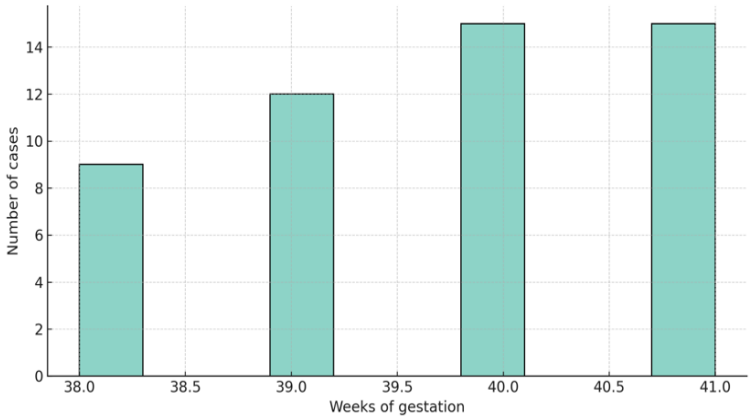


Figure 2. Gestational weeks at time of induction

Cervical readiness

The figure depicts cervical readiness assessed by the Bishop score. A substantial majority (92%) had a favorable score (≥6), suggesting a high likelihood of successful induction and lower risk of operative delivery. Only 8% demonstrated unfavorable cervical conditions, which typically predict longer induction times and increased need for augmentation. This distribution reflects strong candidate selection and contributes to the favorable outcomes observed in the study.

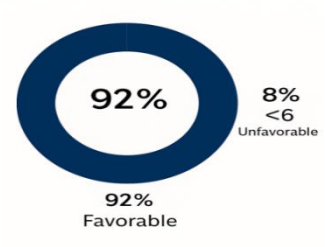


Figure 3. Bishop Score before induction

Intrapartum complications

Figure 4 presents the distribution of intrapartum complications among the study population. Most patients (273; 68.3%) experienced no complications during labor, demonstrating a favorable maternal safety profile associated with induction. The most frequent complications were perineal rupture (53 cases) and umbilical cord-related events (51 cases). Other complications, including cervical laceration, vaginal hematoma, pre-eclampsia, PIH syndrome, and anal sphincter rupture occurred at very low frequencies (1–3 cases each). These findings indicate that, although complications may arise during induced labor, their overall incidence in this cohort was low and within acceptable clinical ranges.

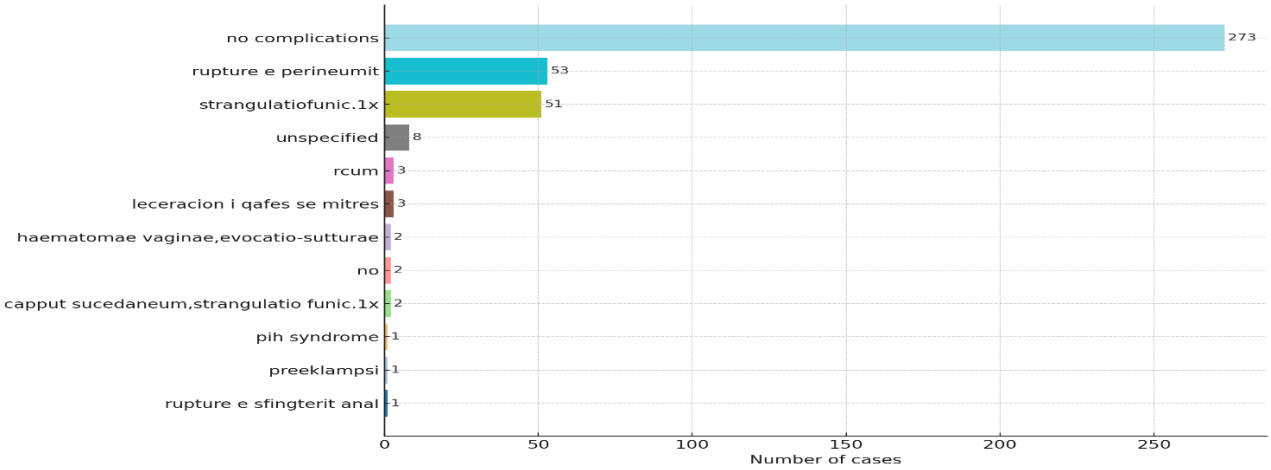


Figure 4. Complications during labor

Parity distribution and indications for induction

Figure 5 summarizes key baseline characteristics of the induced population. The parity distribution shows that multiparous women comprised the majority (65%), while primiparous women represented 35%. This is clinically relevant because multiparous women generally exhibit more favorable cervical conditions and higher induction success rates.

When interpreted together with the indications for induction, the data demonstrate that most inductions were medically warranted, with post-term pregnancy being the leading indication, followed by placenta previa, PIH syndrome, and meconium-stained fluid. The fact that a largely multiparous population required induction for these conditions suggests that many of the patients had prior childbirth experience but developed new pregnancy-related complications necessitating timely intervention.

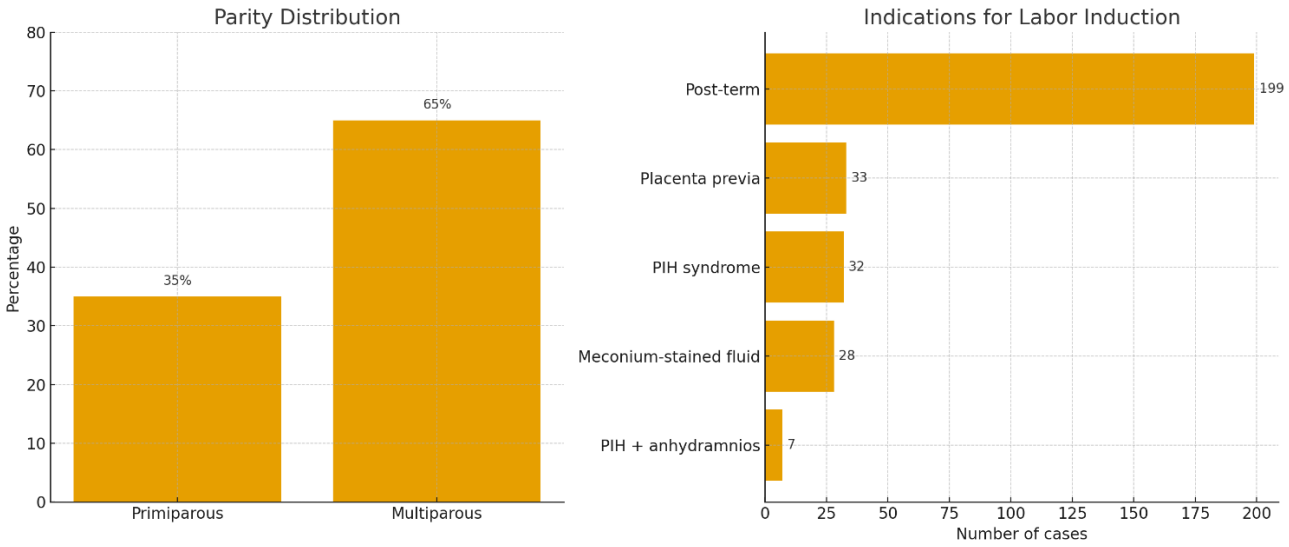


Figure 5. Parity distribution and Indications for labor induction

Maternal complications and delivery outcomes

Figure 6 presents a combined overview of maternal intrapartum complications and delivery outcomes following labor induction.

On the left, the chart shows that most women experienced no maternal complications during labor (273 cases; 66.9%), while 31.1% experienced some form of complication (127 cases). Only a small proportion (2%) was classified as "not specified." This distribution reflects a generally safe intrapartum course, with complications occurring in a minority of cases.

On the right, the figure demonstrates that the vast majority of induced labors resulted in vaginal delivery. Only 27 women (6.8%) underwent cesarean section, while 93.2% delivered through other (non-operative) modes. This very low cesarean rate aligns with the high proportion of women who had favorable cervical conditions and few complications.

Together, these two panels emphasize the overall safety and effectiveness of labor induction in the study population, showing low rates of complications and an excellent vaginal delivery success rate.

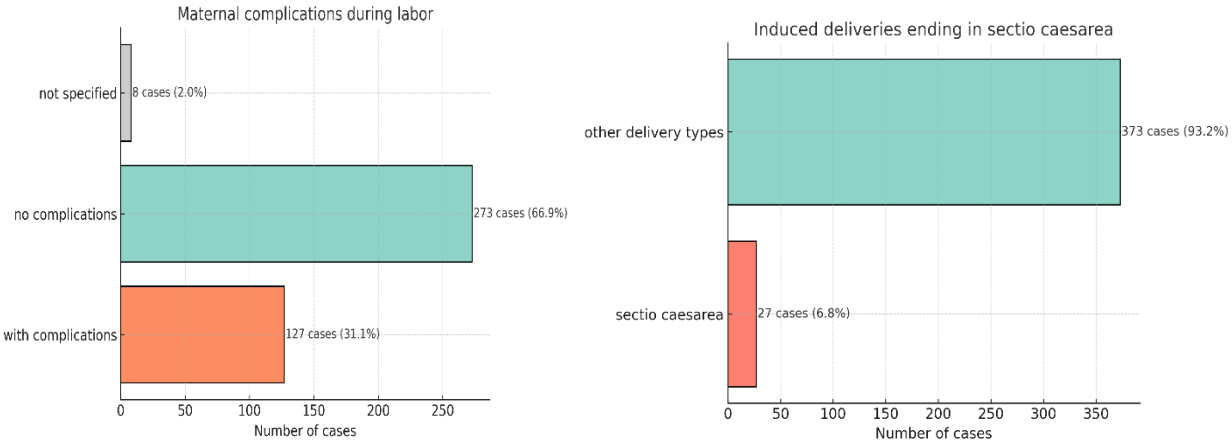


Figure 6. Maternal complications during labor Induced deliveries ending section caesarea

Clinical indications for cesarean section

Figure 7 shows the main reasons for cesarean section after labor induction. The most common indication was ineffective induction (20 cases), followed by fetal distress (6 cases). Only one case was attributed to abnormal

fetal presentation. Overall, the results indicate that most cesarean deliveries occurred due to inadequate labor progression rather than severe maternal or fetal complications.

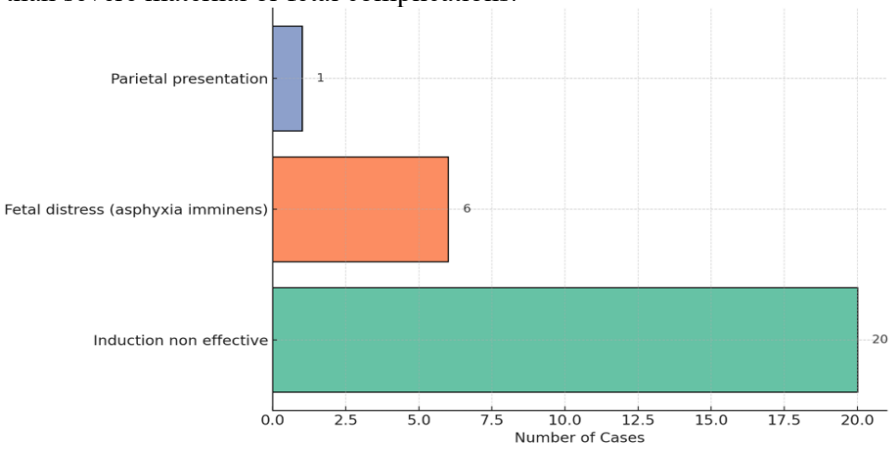


Figure 7. Clinical Indications for Cesarean Section After Induction

Maternal complications, cesarean distribution, and neonatal outcomes

These figures demonstrate a consistent pattern: maternal complications were uncommon (Figure 8), cesarean delivery was more influenced by primiparity than by complications (Figure 9), and neonatal outcomes were highly favorable across all groups (Figure 10). These findings suggest that the induction process was generally safe and effective, with limited adverse maternal or neonatal events.

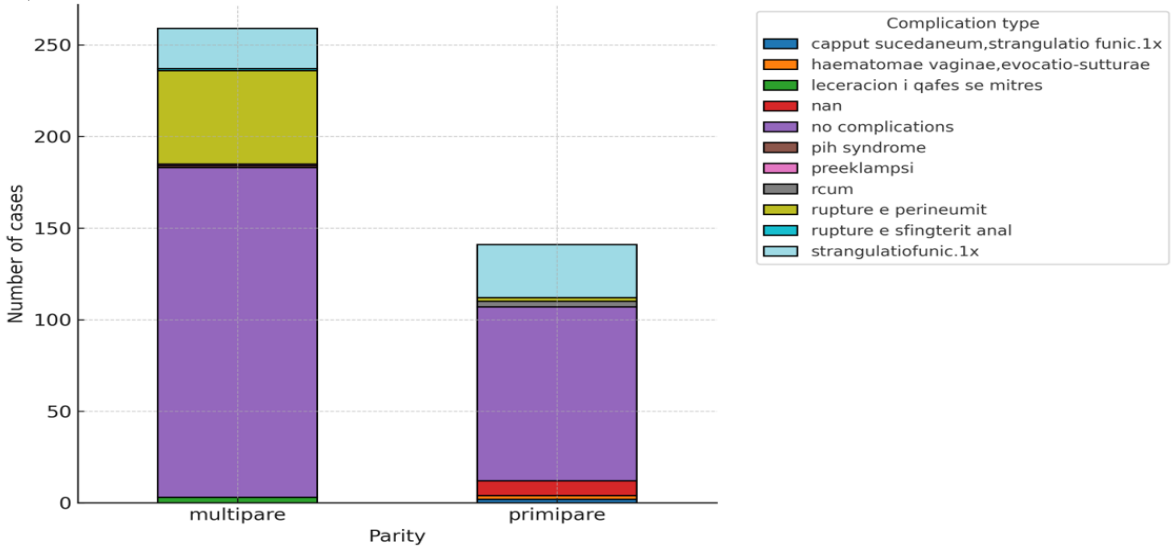


Figure 8. Parity vs. maternal compications during labor

Figure 8 illustrates the relationship between parity and maternal complications during labor. In both primiparous and multiparous women, the majority experienced no complications, although the absolute number of complications was higher among multiparas due to their larger representation in the study population. Overall, maternal complications were relatively infrequent in both groups.

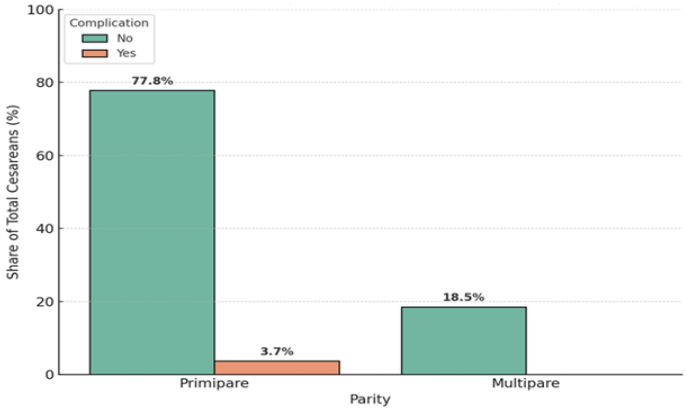


Figure 9. Cesarean distribution by parity and complication group

Figure 9 examines how parity and the presence of complications relate to cesarean section rates. The majority of cesarean deliveries occurred among primiparous women without complications (77.8%), while only a small proportion occurred in multiparas. This suggests that parity itself rather than intrapartum complications, was a stronger contributor to cesarean delivery risk in this cohort.

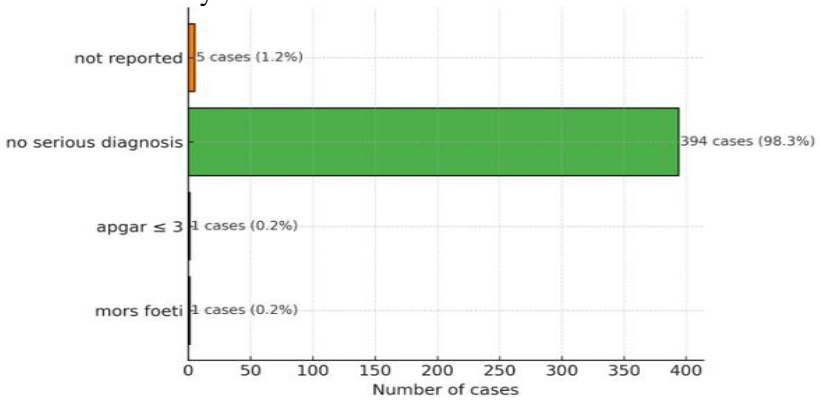


Figure 10. Neonatal serious diagnoses

Figure 10 presents neonatal outcomes, showing overwhelmingly favorable results. The vast majority of newborns (98.3%) had no serious diagnosis, with only isolated cases of low Apgar score or fetal death. Importantly, neonatal complications remained rare regardless of maternal parity or the occurrence of maternal complications.

DISCUSSION

This study provides a comprehensive overview of maternal and neonatal outcomes following induction of labor in 400 term pregnancies. Overall, the findings indicate that appropriately indicated and carefully monitored induction is a safe and effective intervention in this setting.

Maternal outcomes

The high proportion of women with a favorable Bishop score (92%) reflects good clinical selection for induction and likely explains, in part, the very low cesarean section rate of 6.8%. In many randomized trials and large cohort studies, cesarean rates after induction range from 15–25% or higher, depending on parity and cervical status (Grobman et al., 2018; Ten Eikelder et al., 2019). The lower rate in our population suggests that strict attention to cervical readiness and protocolized oxytocin titration can substantially reduce the likelihood of operative delivery. Most women (68.3%) experienced no intrapartum complications, and those that did occur were predominantly perineal ruptures and umbilical cord events, which are common in obstetric practice and mostly self-limiting. Serious events such as severe genital tract trauma, hypertensive crises, or anal sphincter rupture were exceedingly rare, supporting previous evidence that medically indicated induction does not inherently increase maternal

morbidity compared with expectant management when guideline-based monitoring is in place (ACOG, 2020; Sheldon & Diedrich, 2021).
Parity patterns also contributed to this favorable profile. The cohort was predominantly multiparous (65%), and parity is known to correlate with shorter labors, better cervical favorability and higher vaginal delivery rates. Nonetheless, detailed analysis showed that primiparity itself was a stronger driver of cesarean delivery than the presence of intrapartum complications, consistent with international data identifying primiparous women as a key group at higher risk of operative birth (Boulvain et al., 2016; Caughey et al., 2022).
Neonatal outcomes
Neonatal outcomes in this cohort were excellent. Almost all newborns (98.3%) were discharged without serious diagnosis; only a single infant had a low Apgar score and one intrauterine fetal death was recorded. NICU admission was required in only one case. These figures are at least comparable—and in some instances more favorable—than those reported in large trials of elective or indicated induction at term, where induction has been associated with stable or improved neonatal outcomes when compared with expectant management (Grobman et al., 2018; Stock & Norman, 2021; Walker et al., 2020).
Importantly, many inductions in this cohort were performed for conditions that themselves increase perinatal risk, including post-term pregnancy, hypertensive disorders and meconium-stained fluid. The absence of excess neonatal morbidity despite these indications supports the notion that induction can mitigate, rather than exacerbate, the risks associated with prolonged pregnancy or evolving maternal–fetal compromise (Muglu et al., 2019; WHO, 2022).
Comparison with existing literature
Our results are broadly consistent with contemporary evidence suggesting that induction at or beyond 39 weeks can reduce rates of cesarean delivery and hypertensive complications without increasing adverse neonatal outcomes (Grobman et al., 2018; Walker et al., 2020). The particularly low cesarean rate in this study compares favorably even with the ARRIVE trial and may reflect context-specific factors such as:
high prevalence of favorable Bishop scores
predominance of multiparous women
adherence to an institutional culture that prioritizes vaginal birth where safe
At the same time, the findings reinforce meta-analytic data indicating lower stillbirth and perinatal mortality with planned induction beyond 39 weeks compared with expectant management (Muglu et al., 2019).
Clinical implications
From a clinical standpoint, these results highlight several key points:
Careful selection and preparation-particularly assessment of cervical favorability are central to maximizing induction success and minimizing cesarean delivery.
Standardized protocols for oxytocin administration, prostaglandin use and mechanical methods, coupled with continuous fetal and maternal monitoring, can maintain a very low rate of serious complications.
Primiparous women remain the subgroup at highest risk of cesarean section; they may benefit most from individualized counseling, closer labor surveillance and, where appropriate, early cervical ripening strategies.

CONCLUSION

In this cohort of 400 term pregnancies, induction of labor carried out according to standardized institutional protocols and for clearly defined obstetric indications was associated with a favorable maternal and neonatal safety profile. Nearly 70% of women experienced no intrapartum complications, serious maternal morbidity was rare, and the overall cesarean section rate was notably low at 6.8%. These findings indicate that, when cervical readiness is appropriately assessed and clinical decision-making is optimized, induction of labor does not inherently increase the likelihood of operative delivery.
Neonatal outcomes were similarly reassuring. More than 98% of newborns had no serious clinical diagnosis, the need for resuscitation or NICU admission was minimal, and perinatal mortality was very low. This is particularly important given that many women in the cohort had conditions known to increase perinatal risk, such as post-term pregnancy and hypertensive disorders, yet no meaningful excess of adverse neonatal events attributable to induction was observed.
Overall, this study supports the judicious use of labor induction as a safe and effective component of modern obstetric practice, especially in late-term and post-term pregnancies or when maternal–fetal status warrants timely delivery. Induction should not be viewed as an intervention that inherently elevates risk but rather as a valuable

strategy when individualized to gestational age, cervical status, and patient-specific risk factors. Future prospective, comparative studies including cohorts with spontaneous onset of labor are warranted to further refine patient selection, optimize induction protocols, and clarify the balance between induction and expectant management across different healthcare settings.

REFERENCES

American College of Obstetricians and Gynecologists. (2020). Practice Bulletin: Induction of labor. Obstetrics & Gynecology, 135(2).

Boulvain, M., Stan, C., & Irion, O. (2016). Elective delivery in low-risk pregnancies at term: A review. Best Practice & Research Clinical Obstetrics & Gynaecology, 35, 76–89.

Caughey, A. B., Cahill, A. G., Guise, J. M., & Rouse, D. J. (2022). Safe prevention of the primary cesarean delivery: A consensus update. American Journal of Obstetrics and Gynecology, 226(2), B2–B16.

Grobman, W. A., Rice, M. M., Reddy, U. M., Tita, A. T. N., Silver, R. M., Mallett, G., et al. (2018). Labor induction versus expectant management in low-risk nulliparous women. New England Journal of Medicine, 379(6), 513–523.

Muglu, J., Rather, H., Arroyo-Manzano, D., Bhattacharya, S., Balchin, I., Khalil, A., & Thilaganathan, B. (2019). Risks of stillbirth and neonatal death with advancing gestation at term: A systematic review and meta-analysis. PLoS Medicine, 16(7), e1002838.

Sheldon, W. R., & Diedrich, J. T. (2021). Mechanical and pharmacologic methods of labor induction. Clinical Obstetrics and Gynecology, 64(2), 330–343.

Stock, S. J., & Norman, J. E. (2021). Induction of labour in uncomplicated pregnancy. Obstetrics, Gynaecology & Reproductive Medicine, 31(3), 76–83.

Ten Eikelder, M. L. G., Oude Rengerink, K., Jozwiak, M., de Leeuw, J. W., Zeeman, G. G., de Graaf, I. M., et al. (2019). Induction of labour at term with oral misoprostol versus a Foley catheter (PROBAAT-II): A multicentre randomized controlled trial. The Lancet, 383(9931), 444–451.

Walker, K. F., Bugg, G. J., Macpherson, M., McCormick, C., Grace, N., Wildsmith, C., et al. (2020). Randomized trial of labor induction in women 35 years of age or older. New England Journal of Medicine, 373(10), 813–822.

World Health Organization. (2022). WHO recommendations: Induction of labour at or beyond term. World Health Organization.

ORAL PRESENTATION

Environmental evaluation of outdoor pollen and its association with allergic asthma in a population group

Brikena Muja (Parllaku), Etleva Hamzaraj, Mirela Lika (Çekani)

Department of Biology, Faculty of Natural Sciences, University of Tirana, Boulevard "Zogu i Parë", no. 25/1, 1001 Tirana, Albania

Abstract

Outdoor pollen is a major environmental trigger of allergic asthma, with seasonal peaks strongly linked to increased respiratory symptoms, medication use, and emergency healthcare visits. This study evaluates outdoor pollen concentrations and examines their association with allergic asthma in a defined population group. Aerobiological monitoring was conducted using standardized volumetric sampling, while clinical and epidemiological data were collected from symptom diaries, patient records, and healthcare reports. The study of allergic asthma by immunological methods, and the determination of pollens as allergens is important in determining the diagnosis and avoiding, or treating, asthma. These allergens contact our body through the skin, airways and food. Pollen enters the lungs through the air and meets the mucous membranes of the nose, throat and bronchi. It has been noticed that the presence of allergens such as pollen in our country is very high. Meteorological variables were analyzed to understand environmental interactions. Findings indicate a strong correlation between elevated pollen levels—particularly from grasses and selected weed species—and increased asthma exacerbations and symptom severity. The study emphasizes the importance of integrated pollen monitoring, early-warning systems, and targeted public health strategies to reduce exposure and improve disease management for individuals affected by pollen-induced asthma. Through biostatistical analyses we have seen the association of allergic asthma in relation to their age group, gender and place of residence.

Keywords: Allergic asthma, pollen, pollution, immune test, allergies, public health

Introduction

Allergic asthma is a chronic inflammatory condition of the airways characterized by episodes of wheezing, dyspnea, chest tightness, and coughing triggered by exposure to specific allergens. Allergy is a disease which is related to immunological reactions, which are carried out in the body and because of an inflammation appear clinical signs such as: redness, swelling, itching, etc. It depends on several factors such as age, gender, lifestyle and genetic predispositions (Brehler & Kütting, 2001; Griffiths & Ducharme, 2013). Asthma is a long-term inflammatory disease of the airways of the lungs (Martinez, 2007; Scott & Peters-Golden 2013).

Outdoor pollen remains one of the most potent and widespread environmental triggers, affecting millions of sensitized individuals globally. Pollen grains, released seasonally by trees, grasses, and weeds, contain allergenic proteins capable of provoking strong IgE-mediated immunological responses upon inhalation. In sensitized individuals, this leads to airway inflammation, bronchial hyperresponsiveness, and acute asthma symptoms. It is characterized by variable and recurring symptoms, reversible airflow obstruction, and easily triggered bronchospasms (Kumar *et al*., 2010; Robbins & Cotran, 2010). Symptoms include episodes of wheezing, coughing, chest tightness, and shortness of breath (Anandan *et al*., (2010); Manniche, 1999). These may occur a few times a day or a few times per week (Cox *et al.,* 2008; Parsons *et al*., 2013). Depending on the person, asthma symptoms may become worse at night or with exercise (Cox *et al*., 2008).

The distribution and concentration of outdoor pollen vary across regions due to climate, vegetation, and meteorological factors. Climate change has intensified these effects, contributing to earlier and longer pollen seasons, increased pollen productivity, and elevated allergenic potency. These changes raise significant public health concerns, particularly for populations already vulnerable to respiratory disorders. Asthma is thought to be caused by a combination of genetic and environmental factors (Griffiths & Ducharme, 2013; Lemanske *et al*.,

2010). Environmental factors include exposure to air pollution and allergens (Teoh *et al*., 2012; Yawn, 2008). Other potential triggers include medications such as aspirin and beta blockers (Murray & John, 2010). Diagnosis is usually based on the pattern of symptoms, response to therapy over time, and spirometry lung function testing (Parsons *et al*.,2013). Asthma is classified according to the frequency of symptoms, forced expiratory volume in one second (FEV1), and peak expiratory flow rate (Teoh *et al*., 2012). It may also be classified as atopic or non-atopic, where atopy refers to a predisposition toward developing a type 1 hypersensitivity reaction (Martinez, 2007; Vézina *et al*., 2014).

Existing literature demonstrates consistent associations between high outdoor pollen counts and increased asthma morbidity. However, the strength of this relationship varies by region, vegetation type, air quality, and socio-demographic characteristics. Air pollutants may interact synergistically with pollen, enhancing allergenic activity and worsening respiratory outcomes. Despite substantial global evidence, many local communities lack integrated monitoring systems that combine pollen data with clinical indicators. In most cases it happens that some people who have skin irritations or redness, classify it as allergy or vice versa. All this comes because of not performing diagnostic tests and not being aware of these diseases. (Rusznak *et al*.,1998; Scott &Peters-Golden, 2013).

The present study aims to evaluate outdoor pollen concentrations and their association with allergic asthma in a defined population. The objectives of this study are to: characterize seasonal pollen variability, assess asthma symptom patterns in relation to pollen exposure, identify specific pollen types most strongly linked to asthma exacerbations, and evaluate meteorological influences on pollen levels and asthma outcomes. The findings aim to guide environmental health planning, improve clinical management strategies, and strengthen public health preparedness.

An allergic response occurs when immune system proteins (antibodies) mistakenly identify a harmless substance, such as tree pollen, as an invader. To protect your body from the substance, antibodies bind to the allergen (Holgate, 1998; Janeway *et al*., 2001).

The chemicals released by your immune system led to allergy signs and symptoms, such as nasal congestion, runny nose, itchy eyes or skin reactions (Fig, 3). For some people, this same reaction also affects the lungs and airways, leading to asthma symptoms (Vézina *et al*., 2014; Yawn, 2008).

Materials and Methods

In this study, biological samples were collected and taken, according to the relevant procedures and stored according to appropriate conditions. During the period January -November 2024, 100 blood samples suspected of the presence of allergens were analyzed, where 59 came out positive and they received the appropriate treatment.

Two methods were used to achieve the objectives of our study:

(1) Alleisascreen Tec (MEDWISS Analytic GmbH); (2) Surveys.

The AlleisaScreen test is a very simple test to use. It is a test that analyzes blood serum and is not applied directly to the skin thus avoiding side effects (Figure 4). This test measures the amount of IgE antibodies formed as a result of a suspected allergen using a series of allergens in its composition. There are 30 types of allergens on the panel, so with a single analysis we can detect a series of allergens, which affect us in different seasons and at different times of the year. It measures the amount of IgE with the unit of measurement iU/ml; as well as measuring food and inhaler allergens. The first step is to take the blood of a person who is suspected of having allergies. Once the blood is taken, the normal procedure for obtaining blood serum is performed.

The procedure for assessing the present allergens is done by several methods: Improvio scanners, CubeScreen Reader or RapidReader. Concentration of Immunoglobulin IgE in our sample is done by dividing into several classes or ranks.

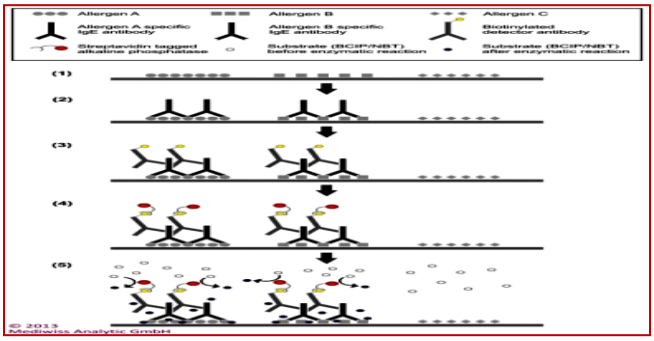


Figure 1. The scheme of action of pollen with IgE antibodies in a Allesiascreen test

Realization and discussion

Outdoor pollen has long been recognized as a key environmental factor influencing asthma prevalence and severity. Studies across Europe, North America, and Asia demonstrate clear seasonal patterns of asthma exacerbations that coincide with peak pollen release from regional vegetation. Grass pollen is frequently identified as one of the most potent asthma triggers, while certain tree and weed pollens also contribute significantly depending on geographical context.

Air pollution interacts with pollen allergens, modifying their protein structures and increasing airway vulnerability. Particulate matter and ozone have been shown to intensify allergic respiratory responses, creating synergistic health impacts. Despite these insights, localized studies remain essential, as pollen composition, meteorological trends, and exposure risks differ substantially across regions.

The observed data were presented in mean value and in standard deviation. Discrete data were presented in absolute value and in percentage. The data were presented by means of tables and graphs of different types, type diagrams and surface diagrams. SPSS statistical package is used for data analysis. After application of the Alleisascreen test, most patients tested positive for one or more pollens, with varying degrees of positivity.

Table 1. Comparison of age groups in relation to cases of allergies

Age Groups	No. of cases	Percentage	Cum.
10-15 years old	47	91%	91%
16-24 years old	12	7.5%	98.5%
< 25 years old	7	1.5%	100.00%
Total	66	100.00%	

In Table 1, in the three groups of age 10-15 years, 16-24 years and more than 25 years old, an unequal number of patients with allergies is observed. The largest number of cases is observed in the first age group from 10-15 years, with 91% of cases, the second age group with 7.5% and the third age group with 1.5% of the sample.

Table 2. Allergic plants in the area of Tirana

No.	Types of plants that cause allergies	Flowering period
	GYMNOSPERMAE	
	F. Pinaceae	
1.	*Pinus pinea* L.	April -May
2.	*Pinus sylvestris* L.	May-June
	ANGIOSPERMAE	
	F. Aceraceae	
3.	*Acer obtusatum* Kit.	April -May
	F. Amaranthaceae	
4.	*Amaranthus retroflexus* L.	August - October
	F. Araliaceae	
5.	*Hedera helix* L.	Septemeber- October
	F. Campanulaceae	
6.	*Campanula rapunculus* L.	May - Septemeber
	F. Caprifoliaceae	
7.	*Sambucus ebulus* L.	June - August
	F. Caryophyllaceae	
8.	*Stellaria media* (L.) Vill.	Spring- Autumn
	F. Compositae	
9.	*Artemisia absinthium* L.	June - Septemeber
10.	*Calendula arvensis* L.	March - April
11.	*Centaurea cyanus* L.	May - July
12.	*Chrysanthemum leucanthemum* L. (*Leucanthemum vulgare* Lam.)	May - August
13.	*Dahlia* sp	August - September

In Table 2 are presentet the types of allergic plants and flowering period which are related with the cause of allergy.



Figure 2. *Gender Cupressus L*
***Cupressus sempervirens* L** Geographical distribution in Europe: Southern Europe



Figure. 3. Family Pinaceae
Juniperus communis* L subsp. *communis. Geographical distribution in Europe: throughout Europe, mainly in the mountains to the south



Figure 4. *Thuja orientalis* L



Figure 5. Gender Cedrus

Gender Thuja L ***(Biota orientalis Endl)*** Geographical spread in Europe



Figure 6. *Gender Pinus* Geographical distribution in Europe:cultivated in Europe.

***Cedrus deodora* (D.Don) G. Don fil.** Geographical distribution in Europe: cultivated in Europe.

In figures from 2 to 6 are presented the main tree which produced pollen, the causer of alergic asthma in Tirana. In our study, the number of women who underwent Allesisascreen surgery was higher than that of men (54% compared to 46% of men).

The age group most affected by any type of allergy is the first one, which includes children. Even from a study the most affected age group is that of children with twice the cases of adults (Lemanske et al., 2010). This is due to the complete failure of the immune system and the signs of the appearance of these symptoms such as irritation, rash to asthma are more frequent and more evident in children.

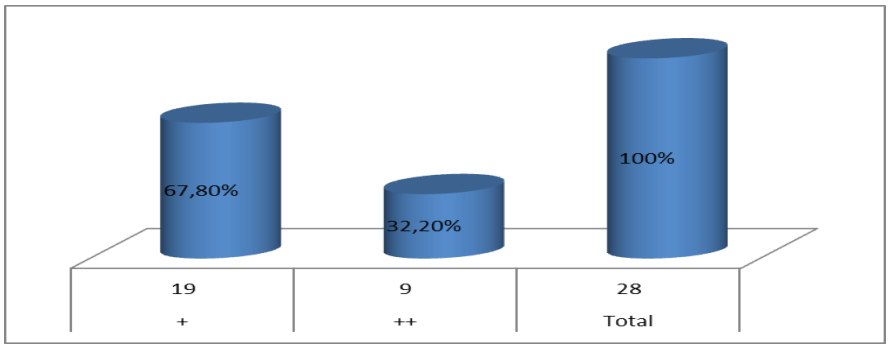


Figure 7. Division of cases according to the degree of presence of the allergen.

From the Figure 7 above we see that in 67.8% of cases we have a mild allergy, which appears with slight irritation while in 32% of cases of the tested we have a high presence of allergens. + (low presence), ++ (high presence)

Allergic asthma is very common and out of 100 individuals taken for analysis 70 of them have come to perform a test related to allergic asthma. Out of 70 individuals analyzed, 38 were positive.

Of the 38 individuals analyzed 8 are positive males and 30 are female (Table 3). So, it is obvious that women are more affected by the surveys done. This also comes as a result of the care they have for themselves by not letting an irritation pass as a common symptom.

Table 3. The degree of positivity in allergen-positive patients

Alesiascreen test positivity rate Allergic Asthma	Number of positive cases	Percentage in the group
+	32	84%
++	6	16%
Total	38	

Each analysis performed has a degree of presence of the allergen. With a (+) we will denote the lowest degree of presence of the allergen, with two (+) we will denote the highest degree of the presence of the allergen. From the analyzes performed, our test manages to capture even the lowest degree of allergen, so we have divided them into several categories: not at all or little present [0.00-0.34 IU / ml], minimum limit [0.35-0.69 IU / ml], low presence

[0.70-3.49 IU / ml] sensitive presence [3.50-17.49 IU / ml], high [17.5-49.9 IU / ml], very high [50.0-100.0 IU / ml]. But since in the tests performed the low presence and sensitive presence groups were dominant, we divided them into 2 large groups.

From the table above we have marked with (+) the low degree of allergic asthma and with (++) the high degree. 84% of cases are in the low rate, while 16% are in the high rate.

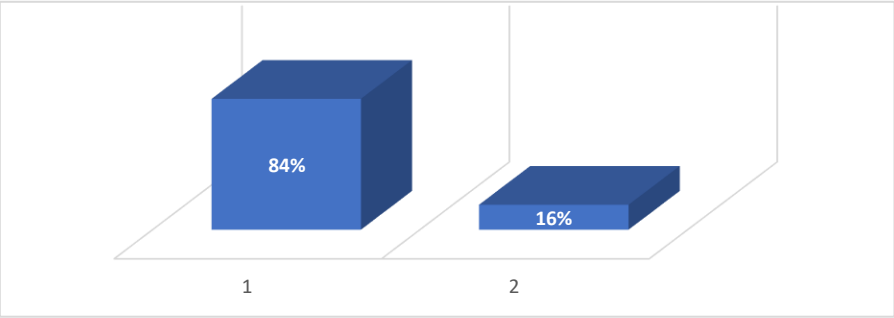


Figure 8. The degree of positivity of cases with allergies.

From the figure 8, we see that the number of cases with a low rate of allergic asthma constitute the largest number with 32 cases (84%) and those with a high rate of allergies account for 6 cases (16%).
To observe the relationship that exists between gender and allergic asthma, we will use a statistical test $\chi 2$ since we have qualitative variables presented in Table 4. In this test on Table 5, what is important is the significance value, which indicates the accuracy of the test.

Table 4. The χ^2 link between gender and allergic asthma cases

		Allergic asthma cases		
		Yes	No	Total
Gender	Female	41	13	54
	Male	25	21	46
Total		66	34	100

Table 5. The Signifivance value

	Value	Df	Asymp. Sig. (2-sided)	Exact Sig. (2-sided)	Exact Sig. (1-sided)
Pearson Chi-Square	5.154[a]	1	0.023		
Continuity Correction[b]	4.237	1	0.040		
Likelihood Ratio	5.177	1	0.023		
Fisher's Exact Test				0.034	0.020
Linear-by-Linear Association	5.1031		0.024		
N of Valid Cases	100				

Test value $X^2_{(1)}=5.154;p=0.023$
Since $p < 0.05$, then gender is related to allergic asthma.

The results support existing evidence that outdoor pollen plays a significant role in triggering allergic asthma. The observed seasonal variations highlight the importance of monitoring pollen distribution and preparing targeted health interventions during peak exposure periods.

Grass pollen, identified as the primary contributor to asthma exacerbations in this study, aligns with global research demonstrating its high allergenic potential. The correlation between meteorological patterns and pollen levels further emphasizes the need for environmental surveillance systems capable of forecasting high-risk periods.

Public health strategies should incorporate pollen warnings, patient education, and preventive clinical measures to reduce exposure and mitigate asthma severity. Integration of pollen data with digital health technologies may support personalized asthma management and improve outcomes.

In conclusion we can say:

This study demonstrates a significant association between outdoor pollen levels and allergic asthma outcomes in the studied population. The findings highlight the importance of integrated pollen monitoring, environmental forecasting, and targeted public health strategies to reduce exposure and improve disease management. Enhanced aerobiological surveillance and better integration of clinical data can strengthen early-warning systems and support more effective interventions for individuals with pollen-induced asthma.

References

Anandan C, Nurmatov U, van Schayck OC, Sheikh A (2010) Is the prevalence of asthma declining.Systematic review of epidemiological studies? *Allergy*. 65 (2): 152–67. https://doi.org/10.1111/j.1398-9995.2009.02244.x

Brehler R, Kütting B (2001) Natural rubber latex allergy: a problem of interdisciplinary concern in medicine. *Arch. Intern. Med*. 161 (8): 1057–64. https://doi.org/10.1001/archinte.161.8.1057

Cox L, Williams B, Sicherer S, Oppenheimer J, Sher L, Hamilton R, Golden D (2008) Pearls and pitfalls of allergy diagnostic testing: report from the American College of Allergy, Asthma and Immunology/American Academy of Allergy, Asthma and Immunology Specific IgE Test Task Force". *Annals of Allergy, Asthma & Immunology* 101 (6): 580–92. https://doi.org/10.1016/S1081-1206(10)60220-7

Griffiths B, Ducharme FM (2013) Combined inhaled anticholinergics and short-acting beta2-agonists for initial treatment of acute asthma in children". *The Cochrane Database of Systematic Reviews* (8): CD000060. DOI: 10.1002/14651858.CD000060.pub2

Holgate ST (1998) Asthma and allergy—disorders of civilization?". *QJM* 91 (3): 171–84.

Janeway CA Jr, Travers P, Walport M, et al.New York: Garland Science, 2001. Allergy and Hypersensitivity Immunobiology: *The Immune System in Health and Disease*: 555-598. https://www.ncbi.nlm.nih.gov/books/NBK10775/

Kay AB (2000) Overview of 'allergy and allergic diseases: with a view to the future'". *Br. Med. Bull*. 56 (4): 843–64. DOI: 10.1258/0007142001903481

Lika M. (2015): Hypersensitivity Reactions mediated by anticorpe. Cellular and molecular Immunology: 237-244. https://www.elsevier.com/books/cellular-and-molecular-immunology/abbas/978-0-323-47978-3

Kirkland SW, Vandenberghe C, Voaklander B, Nikel T, Campbell S, Rowe BH (January 2017). Combined inhaled beta-agonist and anticholinergic agents for emergency management in adults with asthma". *The Cochrane Database of Systematic Reviews*. 1: CD001284. https://www.cochranelibrary.com/cdsr/doi/10.1002/14651858.CD001284.pub2/full

Kumar, Vinay; Abbas, Abul K.; Fausto, Nelson; Aster, Jon, eds. (2010). Robbins and Cotran pathologic basis of disease (8th ed.). Saunders. p. 688. ISBN 978-1-4160-3121-5.

Lemanske, Robert F.; Busse, William W. (2010) Asthma: Clinical expression and molecular mechanisms. *Journal of Allergy and Clinical Immunology*.125 (2): S95–S102. doi: 10.1016/j.jaci.2009.10.047

Manniche L. (1999). Sacred luxuries: fragrance, aromatherapy, and cosmetics in ancient Egypt. *Cornell University Press*. pp. 49. ISBN 978-0-8014-3720-5.

Martinez FD (January 2007) Genes, environments, development and asthma: a reappraisal". *The European Respiratory Journal*. 29 (1): 179–84. DOI: 10.1183/09031936.00087906

Murray, John F. (2010). Ch. 38 Asthma". In Mason, Robert J.; Murray, John F.; Broaddus, V. Courtney; Nadel, Jay A.; Martin, Thomas R.; King, Jr., Talmadge E.; Schraufnagel, Dean E. (eds.). *Murray and Nadel's textbook of respiratory medicine (5th ed.). Elsevier*. ISBN 978-1-4160-4710-0. https://www.elsevier.ca/ca/product.jsp?isbn=9781455708734

Parsons JP, Hallstrand TS, Mastronarde JG, Kaminsky DA, Rundell KW, Hull JH, (2013) An official American Thoracic Society clinical practice guideline: exercise-induced bronchoconstriction *American Journal of Respiratory and Critical Care Medicine*. 187 (9): 1016–27. https://www.thoracic.org/statements/resources/cc/ards-guidelines.pdf

Rusznak C, Davies RJ; Davies (1998) ABC of allergies. Diagnosing allergy". *BMJ* 316 (7132): 686–9. doi:10.1136/bmj.316.7132.686.

Scott JP, Peters-Golden M (September 2013) Antileukotriene agents for the treatment of lung disease". *American Journal of Respiratory and Critical Care Medicine*. 188(5): 538–44.

Teoh L, Cates CJ, Hurwitz M, Acworth JP, van Asperen P, Chang AB (April 2012) Anticholinergic therapy for acute asthma in children"(PDF). *The Cochrane Database of Systematic Reviews* (4): CD003797. https://doi.org/10.1002/14651858.CD003797.pub2

Thomas P. Habif (2009). Clinical Dermatology. *Elsevier Health Sciences*. 14-19.

Vézina K, Chauhan BF, Ducharme FM (July 2014) Inhaled anticholinergics and short-acting beta (2)-agonists versus short-acting beta2-agonists alone for children with acute asthma in hospital. *The Cochrane Database of Systematic Reviews*. 7 (7): CD010283. https://doi.org/10.1002/14651858.CD010283.pub2

Yawn BP (2008) Factors accounting for asthma variability: achieving optimal symptom control for individual patients (PDF). *Primary Care Respiratory Journal*. 17 (3): 138–47.

ORAL PRESENTATION

Effect of amine complexes from natural petroleum acids on the corrosion of carbon steel in a CO_2 environment using the tafel method

Vagif Abbasov[1] (0009-0003-9270-6624), Nihad Alimadatli[3] (0009-0004-7519-1363),. Durna Aghamaliyeva[1,2] (0000-0001-7458-6954), Zaur Aghamaliyev[1,2] (0000-0003-2866-1401)

Khojaly Avenue, Baku, AZ1025, Azerbaijan
[2]Azerbaijan State Oil and Industry University (ASOIU), 34 Azadlig Avenue, Baku, Azerbaijan
[3]SOCAR Downstream, 1 Oqtay Valiyev Street, Baku, AZ1060, Republic of Azerbaijan

Abstract

The corrosion behavior of carbon steel in a CO_2-saturated environment was investigated using the Tafel polarization method in the presence of 10% solutions (prepared in 70% isopropyl alcohol) of amino complexes and their corresponding salts synthesized from the first fraction of natural petroleum acids. The experiments were carried out using a "CorrTest" electrochemical potentiostat in a 1% sodium chloride (NaCl) solution saturated with CO_2 at a pressure of 0.9 bar, a temperature of 50°C, and a duration of 1 hour. The aim of the study was to evaluate the inhibitive performance of the newly synthesized reagents and to elucidate the structure–property relationship governing their protective capabilities. In the uninhibited sample, the corrosion rate was 0.675 mm/year, confirming the highly aggressive nature of the CO_2-saturated medium and the necessity for an efficient corrosion inhibitor. Comparative analysis of the synthesized complexes showed that the N-1 compound (butylamine complex) exhibited the highest protective activity. At a concentration of 1000 ppm, it achieved 98.8% inhibition efficiency and reduced the corrosion current density (Icorr) to 5.763×10^{-7} A/cm², indicating strong adsorption and effective surface coverage on the metal. The N-2 complex (octylamine derivative) demonstrated 84.9% efficiency, attributed to the increased hydrophobicity provided by its long alkyl chain, which facilitated the formation of a partially compact barrier layer. The N-3 complex (diethylamine derivative) showed 92.5% inhibition efficiency, suggesting that both electronic and steric effects influence its adsorption behavior. The N-4 complex (dibutylamine derivative) provided approximately 75% protection; however, its performance decreased due to weaker adsorption associated with the spatial configuration of the molecule, which likely hindered the formation of a uniform protective film.

Keywords: carbon steel corrosion, CO_2 corrosion, amino complexes, corrosion inhibitors, Tafel polarization, adsorption mechanism

Introduction

In most subsea developments, oil and gas production is transported from the subsea well to the platform in a multiphase flow without a separation process. Corrosion is a growing problem in the operation of subsea pipelines. Corrosion can be defined as the deterioration of a metal due to chemical or electrochemical reactions between the metal and the surrounding environment [9]. The susceptibility of a metal to corrosion depends on the environment and the type of metal. The presence of carbon dioxide (CO_2), hydrogen sulfide (H_2S), and free water in the production fluid can cause severe corrosion problems in oil and subsea pipelines. Integrity and risk management of internal corrosion in wells and pipelines depends on temperature, CO_2 and H_2S content, water chemistry, flow rate, oil or water wetting, as well as the composition and condition of the steel surface [1-3].

Corrosion-resistant alloys, such as 13% chromium steel and duplex stainless steels, are often used in well tubing, subsea manifolds, and structures. However, for long-distance pipelines, carbon steel remains the only economically viable option, and corrosion must be controlled, with pipelines protected from both internal and external corrosion. This article discusses the development of predictive models for corrosion defects and the reliability-based design and reassessment criteria for evaluating corroded pipelines [8]. As part of this assessment, the main focus is placed on the following interrelated issues:

• Growth of corrosion defects.
• Verification of burst strength (allowable vs. maximum internal operating pressure).
• Verification of bending capacity (allowable and maximum external pressure, bending moment, and axial load).
• Assessment of the adequacy of remaining corrosion allowance for the expected service life.
• Inspection of corrosion defects.
• Updated inspection and maintenance programs [4].

When CO_2 and H_2S are present in the hydrocarbon fluid, two types of corrosion may occur: acid corrosion and low-sulfur corrosion [7]. CO_2 corrosion occurs in systems containing only carbon dioxide or trace amounts of hydrogen sulfide (partial pressure of $H_2S < 0.05$ psi). Acid corrosion occurs in systems containing hydrogen sulfide above a partial pressure of 0.05 psi (0.34 kPa) along with carbon dioxide. When corrosion products do not precipitate on the steel surface, extremely high corrosion rates several millimeters per year may occur [10]. This "worst-case" type of corrosion is the easiest to study and reproduce in laboratory conditions.

When CO_2 dominates the corrosion activity, the corrosion rate can be significantly reduced under conditions where iron carbonate can precipitate on the steel surface and form a dense, protective corrosion-product film. This occurs more readily at higher temperatures or higher pH values in the aqueous phase. When H_2S is present in addition to CO_2, iron sulfide films form instead of iron carbonate, and protective films may develop at lower temperatures, since iron sulfide precipitates much more easily than iron carbonate. Localized corrosion with very high corrosion rates may occur when the corrosion-product film does not provide sufficient protection, making this the most dangerous type of corrosion in oil and gas pipelines.

Carbon dioxide consists of one carbon atom and two oxygen atoms. It is a corrosive compound found in natural gas, crude oil, condensate, and formation water. It is one of the most common environments in the oilfield industry where corrosion occurs. CO_2 corrosion is intensified in the presence of both oxygen and organic acids, which can dissolve iron carbonate scale and prevent further scale formation. Carbon dioxide is a weak acid gas and becomes corrosive when dissolved in water. However, CO_2 must first hydrate to form carbonic acid (H_2CO_3) a relatively slow process before it becomes acidic. Carbonic acid lowers the pH of the water and causes corrosion upon contact with steel.

Areas where CO_2 corrosion is most prevalent include producing wells, gas-condensate wells, regions where water condensation occurs, CO_2-filled vessels, CO_2-saturated formation water, and pipelines, which generally corrode more slowly due to lower temperatures and pressures [6]. CO_2 corrosion is intensified in the presence of oxygen and organic acids, which dissolve iron carbonate scale and inhibit scale re-formation. The maximum solubility of CO_2 in water is 800 ppm. When CO_2 is present, the most common forms of corrosion include uniform corrosion, pitting, wormhole attack, galvanic mesa-corrosion, thermal corrosion, mesa attack, droplet corrosion, erosion-corrosion, and corrosion fatigue. The presence of CO_2 usually indicates the absence of hydrogen embrittlement. The corrosion rate in CO_2 environments is higher than that caused by carbonic acid alone. Corrosion rates in CO_2 systems can reach extremely high levels (several millimeters per year), but can be effectively inhibited.

Flow effects are very important in CO_2 systems. Turbulence is often a critical factor driving the system into a corrosive regime because it either prevents the formation of, or removes, the protective iron carbonate (siderite) scale. CO_2 corrosion products include iron carbonate (siderite, $FeCO_3$), iron oxide, and magnetite. The colors of corrosion products may appear green, brown, or black. Under certain conditions, these products may form protective layers. The scale itself can be soluble. Conditions that promote the formation of protective scale include elevated temperatures, increased pH as occurs in bicarbonate-containing waters and the absence of turbulence, allowing the scale film to remain intact. Turbulence is often a critical factor in the formation or retention of the protective iron carbonate film [5].

Iron carbonate is nonconductive; therefore, galvanic corrosion cannot occur. Corrosion develops only where the protective iron carbonate film is absent and is relatively uniform across the exposed metal surface. Crevice and pitting corrosion occur in the presence of carbonic acid. Carbon dioxide can also cause embrittlement, leading to stress corrosion cracking.

MATERIAL AND METHODS

1. The amines used in the synthesis of the corrosion inhibitors were obtained from Sigma-Aldrich.); the spectrum is shown in Figure 1-4
2. . The freezing point of the 10% solutions of the synthesized amine complexes in 70% IPA was determined according to GOST 20287-74, the relative density according to GOST 3900-2000, and the refractive index using an IRF-22 No. 700060 refractometer in accordance with GOST 18995.2-73.
3. The experiments were carried out using a "CorrTest" electrochemical potentiostat in a 1% sodium chloride (NaCl) solution saturated with CO2 at a pressure of 0.9 bar, a temperature of 50°C, and a duration of 1 hour. During the study, the main electrochemical parameters corrosion potential (Ecorr), current density (Icorr), and protection efficiency (η) obtained at different inhibitor concentrations were used to determine the adsorption behavior of the complexes on the metal surface and to elucidate their corrosion inhibition mechanisms. Electrochemical studies were conducted to investigate the corrosion-inhibiting efficiency of amino complexes (butylamine, octylamine diethylamine and dibutylamine) synthesized from the first fraction of natural petroleum acids (NPA) using the Tafel polarization method (Fig. 5-8).

Experimental Part

During the research conducted at the Institute of Petrochemical Processes named after Academician Y.H. Mammadaliyev (IPCP), four fractions (I, II, III, and IV) of natural petroleum acids (NPA) were isolated from the kerosene fraction obtained from a mixture of Baku crude oils, and alkyl and dialkylamine complexes were synthesized based on Fraction I. The following primary amines were used for the synthesis of the complexes: butylamine ($C_4H_9NH_2$), octylamine ($C_8H_{17}NH_2$), diethylamine ($(C_2H_5)_2NH$), and dibutylamine ($(C_4H_9)_2NH$).

The synthesis of the complexes was carried out as follows:

Natural petroleum acids and the alkyl or dialkylamines were taken in a 1:1 molar ratio and intensively stirred for 20–25 minutes, resulting in the formation of organic complexes. External heating was not required during the reaction, as it is an exothermic process accompanied by the release of a significant amount of energy. The resulting complexes are yellowish liquids with yields of 99.1–99.8%. The general schemes of the synthesis of NPA alkyl and dialkylamine complexes in a 1:1 molar ratio are presented below (Scheme 1 and Scheme 2).

$$RCOOH + R'NH_2 \longrightarrow RCO\overset{-}{O}\overset{+}{N}H_3R' \quad (1)$$

Where: R = residue of natural petroleum acid, R' = C_4H_9, C_8H_{17}

$$RCOOH + (R')_2NH \longrightarrow RCO\overset{-}{O}\overset{+}{N}H_2(R')_2 \quad (2)$$

Where: R = residue of natural petroleum acid, R' = $(C_2H_5)_2$, $(C_4H_9)_2$

The physicochemical properties of the solutions of the reagents obtained from Fraction I of natural petroleum acid are presented in Table 1.

Table 1. Physicochemical properties of 10% solutions of amine complexes of Fraction I of NPA in 70% IPA

Names of indicators:	N-1	N-2	N-3	N-4
Density (g/cm³)	0.8862	0.8833	0.8913	0,8908
Refractive index (at 20°C)	1.3803	1.3811	1.3813	1,3809
Freezing point, °C	-38	-44	-48	-40

The graphical representations of the IR spectra of the alkyl- and dialkylamine complexes of NPA are presented in Figures 1–4.

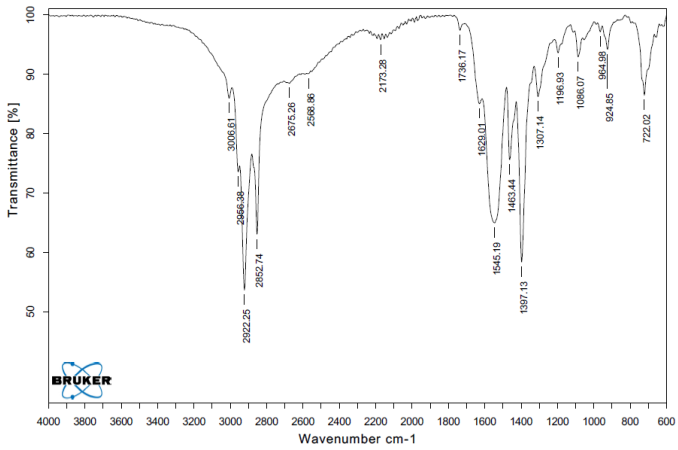


Fig. 1. Graphical representation of the IR spectrum of the butylamine complex of Fraction I of NPA

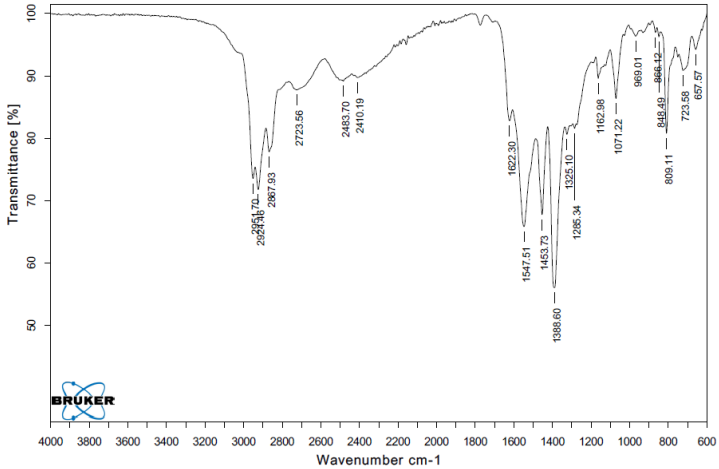


Fig.2 Graphical representation of the IR spectrum of the octylamine complex of Fraction I of NPA

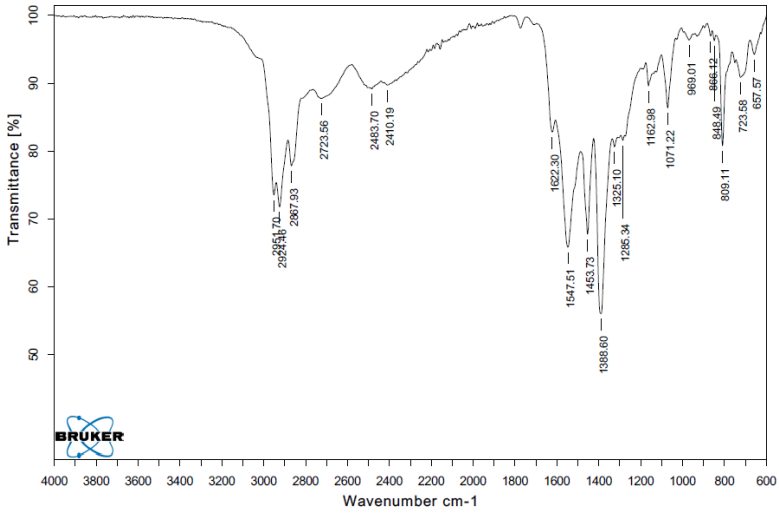


Fig.3. Graphical representation of the IR spectrum of the diethylamine complex of Fraction I of NPA

The structures of the obtained complexes were investigated using IR spectroscopy.

In the IR spectrum of the butylamine complex (N-1) of Fraction I of natural petroleum acid, the deformation and stretching vibrations of the C–H bonds of CH_3 and CH_2 groups were observed at 722, 1453, 2870, 2922, and 2956 cm^{-1}; the deformation vibration of the N–H bond at 1629 cm^{-1}; the stretching vibrations of the COO^- group at

1307, 1397, and 1549 cm^{-1}; and the stretching vibration of the NH^+ group (ammonium band) at 2414, 2477, and 2584 cm^{-1}.

In the IR spectrum of the octylamine complex (N-2) of Fraction I of natural petroleum acid, the deformation and stretching vibrations of the C–H bonds of CH_3 and CH_2 groups were detected at 723, 1453, 2867, 2924, and 2951 cm^{-1}; the deformation vibration of the N–H bond at 1622 cm^{-1}; the stretching vibrations of the COO^- group at 1388 and 1547 cm^{-1}; and the stretching vibrations of the NH^+ group (ammonium band) at 2483 and 2723 cm^{-1}.

In the IR spectra of the diethylamine and dibutylamine complexes (N-3 and N-4) of Fraction I of natural petroleum acid, the deformation and stretching vibrations of the C–H bonds of CH_3 and CH_2 groups appeared at 723, 1453, 2867, 2924, and 2951 cm^{-1}; the deformation vibration of the N–H bond at 1622 cm^{-1}; the stretching vibrations of the COO^- group at 1325, 1388, and 1547 cm^{-1}; and the stretching vibrations of the NH^+ group (ammonium band) at 2410, 2483, and 2723 cm^{-1}.

Discussion of the Results Obtained

The results obtained from studying the effect of 10% solutions of the amine complexes derived from Fraction I of natural petroleum acid in 70% IPA on the corrosion process in a carbon dioxide environment by the Tafel method are presented in Table 2.

Table 2. Results obtained from the Tafel method study of the effect of amine complexes derived from Fraction I of NPA on the corrosion process

Name of substances	Concentration, ppm	E_{cor} mV	$İ_{corr}$ A/sm²	Corrosion rate, mm/year	Protection efficiency, %
Without inhibitor	–	-731	5.7576×10^{-5}	0.675	–
N-1 (butylamine complex)	500	-730	5.3056×10^{-6}	0.062	90.7
	1000	-670	5.763×10^{-7}	0.006	98.8
N-2 (octylamine complex)	500	-748	1.8098×10^{-5}	0.212	67.7
	1000	-742	8.8093×10^{-6}	0.103	84.9
N-3 (diethylamine complex)	500	-755	3.5405×10^{-5}	0.415	40.0
	1000	-731	4.2819×10^{-6}	0.050	92.5
N-4 (dibutylamine complex)	500	-745	1.4139×10^{-5}	0.165	75.8
	1000	-747	1.4545×10^{-5}	0.170	75.3

As seen from table 2, in the control sample without inhibitor (blank test), the corrosion current density was 5.7576×10^{-5} A/cm², and the corrosion rate was 0.675 mm/year. These values indicate that the medium exhibits an aggressive character toward carbon steel. When the inhibitor was added to the medium, the results changed as follows:

N-1 (NPA + Butylamine complex)-At a concentration of 1000 ppm, this complex reduced Icorr to 5.763×10^{-7} A/cm², and the corrosion rate decreased to 0.006 mm/year. This corresponds to a protection efficiency of 98.8%. This effect is attributed to the electron-donating role of the primary amine group in the structure of butylamine and its strong adsorption onto the metal surface when forming a complex with NPA. Additionally, the shift of Ecorr from –731 mV to –670 mV indicates the suppression of anodic processes.

N-2 (NPA + Octylamine complex)-The long alkyl chain of octylamine increases the hydrophobicity of the complex, limiting the transport of corrosive ions to the metal surface. At 1000 ppm, this complex exhibited a protection efficiency of 84.9%. However, the solubility and adsorption characteristics of long-chain amines create certain difficulties in achieving dense molecular packing on the metal surface.

N-3 (NPA + Diethylamine complex)-At 500 ppm, the protection efficiency was only 40%, but at 1000 ppm, it increased sharply to 92.5%. This demonstrates that the inhibitor's efficiency strongly depends on its concentration. It should be noted that the two alkyl chains of the diethylamine molecule may somewhat weaken adsorption onto the metal surface; however, as the concentration increases, a denser and more stable protective layer forms on the surface.

N-4 (NPA + Dibutylamine complex)-The protection efficiency of this complex ranged between 75–76%. Although the presence of two butyl groups enhances its spreading ability on the surface, conformational limitations affecting molecular arrangement weaken adsorption, resulting in lower protection efficiency.

The graphical representations of the Tafel curves for the inhibitors are presented below (Fig. 5–8).

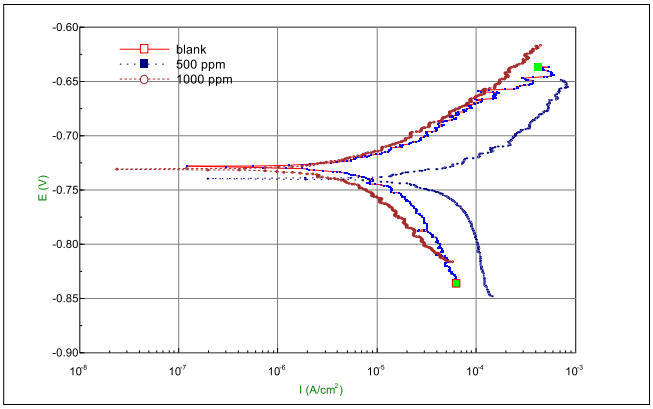


Fig. 4. Tafel polarization curves of the 10% solution of the butylamine complex (N-1) of Fraction I of NPA in 70% IPA.

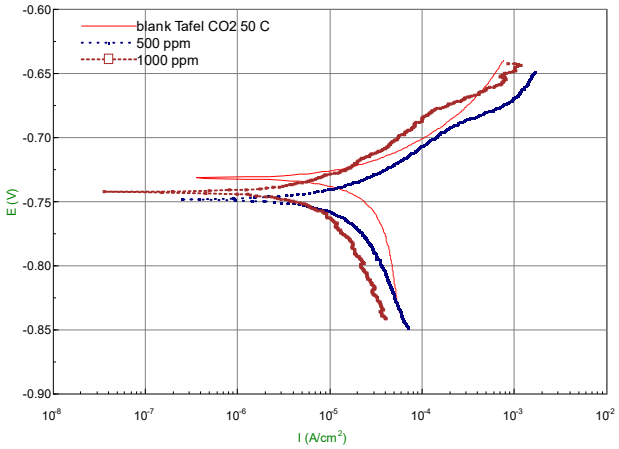


Fig. 5. Tafel polarization curves of the 10% solution of the octylamine complex (N-2) of Fraction I of NPA in 70% IPA.

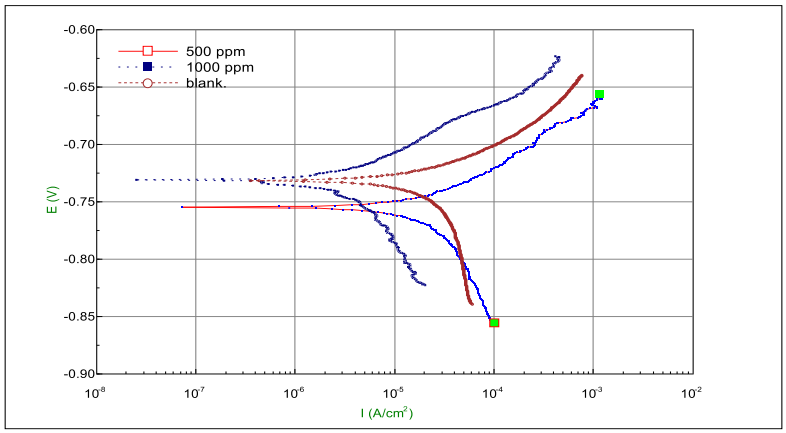


Fig. 6. Tafel polarization curves of the 10% solution of the diethylamine complex (N-3) of Fraction I of NPAin 70% IPA

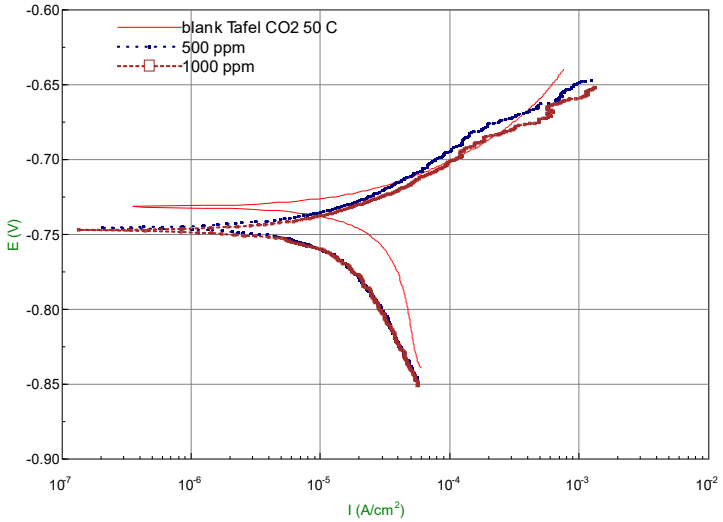


Fig. 7. Tafel polarization curves of the 10% solution of the dibutylamine complex (N-4) of Fraction I of NPA in 70% IPA.

RESULTS

Thus, the obtained results show that the amine complexes (especially butylamine and diethylamine) can significantly reduce the corrosion process when applied at high concentrations. The data obtained from the Tafel curves indicate that these substances decrease the rate of metal degradation by suppressing both anodic and cathodic reactions, demonstrating their high efficiency as corrosion inhibitors.

The simple synthesis procedure of these complexes, their derivation from natural raw materials, and their environmental safety make them suitable for industrial-scale application.

REFERENCES

1. Abbasov, V. M. (2023). *Corrosion* (2nd ed.). Baku: Elm, 365 p.
2. Abbasov, V. M., Mammadbayli, E. G., & Agamaliyeva, D. B. (2018). Synthesis of imidazoline derivatives based on synthetic petroleum acids and their influence on microbiological corrosion. *Practice of Anti-Corrosion Protection*, 87(1), 17–23.
3. Abbasov, V. M., Məmmədbəyli, E. H., Ağamalıyeva, D. B., Mahmudova, L. A., Tahirova, F. F., Babayeva, V. H., & Abbasova, X. A. (2017). Effect of inorganic complexes of imidazoline based on synthetic petroleum acids and triethylenetetramine against carbon dioxide corrosion. *Chemical Problems*, (4), 364–369.

4. Abdrakhmanov, N. Kh., Azmetov, Kh. A., Pavlova, A. D., Zakirova, Z. A., & Basyrova, A. R. (2017). Modern methods and means of ensuring the safe operation of main oil pipelines. *Electronic Scientific Journal "Oil and Gas Business"*, (6), 192–206. (6)
5. Abdrakhmanov, N. Kh., Shutov, N. V., Abdrakhmanova, K. N., Vorokhobko, V. V., & Shaibakov, R. A. (2015). Investigation and analysis of the non-stationarity of the occurrence and development of potentially dangerous situations during the operation of hazardous industrial facilities. *Electronic Scientific Journal "Oil and Gas Business"*, (1), 292–306. (13)
6. Antsiferov, S. A., & Usmanova, E. A. (2015). Analysis of the impact of internal corrosion on pipeline operation. *Bulletin of NGIEI*, 6(49), 5–10. (10)
7. Bai, Y., & Bai, Q. (2014). *Subsea Pipeline Integrity and Risk Management.* Gulf Professional Publishing.(1)
8. Novikov, V. F., & Prilutsky, V. V. (2014). Properties of residual magnetization in the form of a stripe and the possibilities of its use for non-destructive testing. *Defectoscopy*, (7), 24–30. (9)
9. Pluvinage, G., Bouledroua, O., & Hadj-Meliani, M. (2018). Assessment of the hazard of corrosion defects using a failure assessment diagram. *Science and Technologies of Oil and Oil Products Pipeline Transportation*, 8(4), 384–396. (8)
10. Pustov, Yu. A., & Rakotch, A. G. (2013). *Diagnostics and Examination of Corrosion Damage of Metals: A Textbook.* Moscow: MISiS Publishing House. (11)

ORAL PRESENTATION

Assessment of spinal problems in the sagittal plane among students of Aldent University

[1] Roxhensa Sula* (ORCID: *https://orcid.org/0009-0009-7977-4896)*
[2] Irena Kola (ORCID: *https://orcid.org/0000-0002-7936-1284*)
[3] Elona Laçi (ORCID: *https://orcid.org/0009-0000-8773-5189*)

[*1] Aldent University, Faculty of Medical Sciences, Department of Nursing and Physiotherapy, Tirana, Albania.
[2] University of Medicine, Faculty of Technical Medical Sciences, Tirana, Albania.
[3] Aldent University, Faculty of Medical Sciences, Department of Nursing and Physiotherapy, Tirana, Albania.

Abstract

Postural deviations from the physiological spinal curves are common, especially among individuals who remain in static positions for extended periods, as is often the case with students. In this context, students at "Aldent" University, due to the nature of their studies in the field of medicine, represent a high-risk group for developing such issues as a result of repetitive positions and prolonged sitting during theoretical lessons or clinical practice.
The aim of this study is to assess students of Aldent University regarding potential spinal problems in the sagittal plane, raise awareness on the importance of correct posture, and promote postural education, counseling, and physiotherapeutic treatment.
The study was conducted over a one-month period and included 300 students aged 19–25. All participants shared the common characteristic of sitting for more than 5 hours per day and maintaining forced postures during most of the day.
The data were statistically processed by analyzing gender, employment status, spinal deviations, the presence of pain, and the spinal regions affected.
Results showed that 63% of students had postural deviations; of these, 52.9% were female and 47.1% male. Based on gender and spinal region, the findings were as follows:
- Cervical hyperlordosis: 7% of females and 3.37% of males
- Cervical hypolordosis: 25% of females and 17.97% of males
- Thoracic hyperkyphosis: 39% of females and 6.74% of males
- Lumbar hyperlordosis with increased pelvic anteversion: 27% of females and 2.24% of males
- Lumbar hypolordosis with pelvic retroversion: 18% of females and 29.21% of males

Keywords: Spine, postural deviation, assessment, sagittal plane, physiotherapy

INTRODUCTION

The assessment of the spinal column in the sagittal plane among students of Aldent University holds particular importance, as it is closely related to their daily activities, the positions they maintain during studies, and their professional obligations in the medical field.
Postural deviations in this plane are associated with alterations in the physiological curves of the spine, such as kyphosis, lordosis, pelvic anteversion, and retroversion.
Physiotherapy plays a fundamental role in the assessment, education, counseling, and treatment of these issues, helping to correct deviations and alleviate pain that may arise within this age group.

MATERIALS AND METHODS

The study was conducted with students of Aldent University over a one-month period, in December 2024. A total of 300 students aged 19–25 years were included. All participants shared the common characteristic of sitting for more than 5 hours per day and maintaining a static, forced posture for a significant part of the day.
The data were processed statistically by analyzing variables such as gender, employment status, spinal deviations, presence of pain, and the regions where these deviations appeared.

RESULTS

Table 1: Incidence of employed and unemployed participants

	Number of participants	Percentage
Employed	216	72%
Unemployed	84	28%

Table 2: Incidence of employed in the profession and outside the profession

	Number of participants	Percentage
Employement in the profession	38	17.59%
Employement outside the profession	178	82.4%

Table 3: Participants by gender

	Number of participants	Percentage
Male	150	50%
Female	150	50%

Table 4: Participants who tested positive for spinal deviations

	Number of participants	Percentage
Spinal deviations	189	63%
No spinal deviations	111	37%

Table 5: Participants who tested positive for spinal deviations according to gender

	Number of participants	Percentage
Female	100	52.9%
Male	89	47.08%

Table 6: Regions of the spine that tested positive for spinal deviations

		Number of participants	Percentage
Female	Cervical Hyperlordosis	7	7%
	Cervical Hypolordosis	25	25%
	Thoracic Hyperkyphosis	39	39%
	Thoracic Hypokyphosis	0	0%
	Lumbar Hyperlordosis	27	27%
	Lumbar Hypolordosis	18	18%
	Increased pelvic anteversion	27	27%
	Pelvic retroversion	18	18%
Male	Cervical Hyperlordosis	3	3.37%
	Cervical Hypolordosis	16	17.97%
	Thoracic Hyperlordosis	6	6.74%
	Thoracic Hypokyphosis	0	0%
	Lumbar Hyperlordosis	2	2.24%
	Lumbar Hypolordosis	26	29.21%
	Increased pelvic anteversion	2	2.24%
	Pelvic retroversion	26	29.21%

Chart 1: Incidence of Spinal Problems in the Sagittal Plane

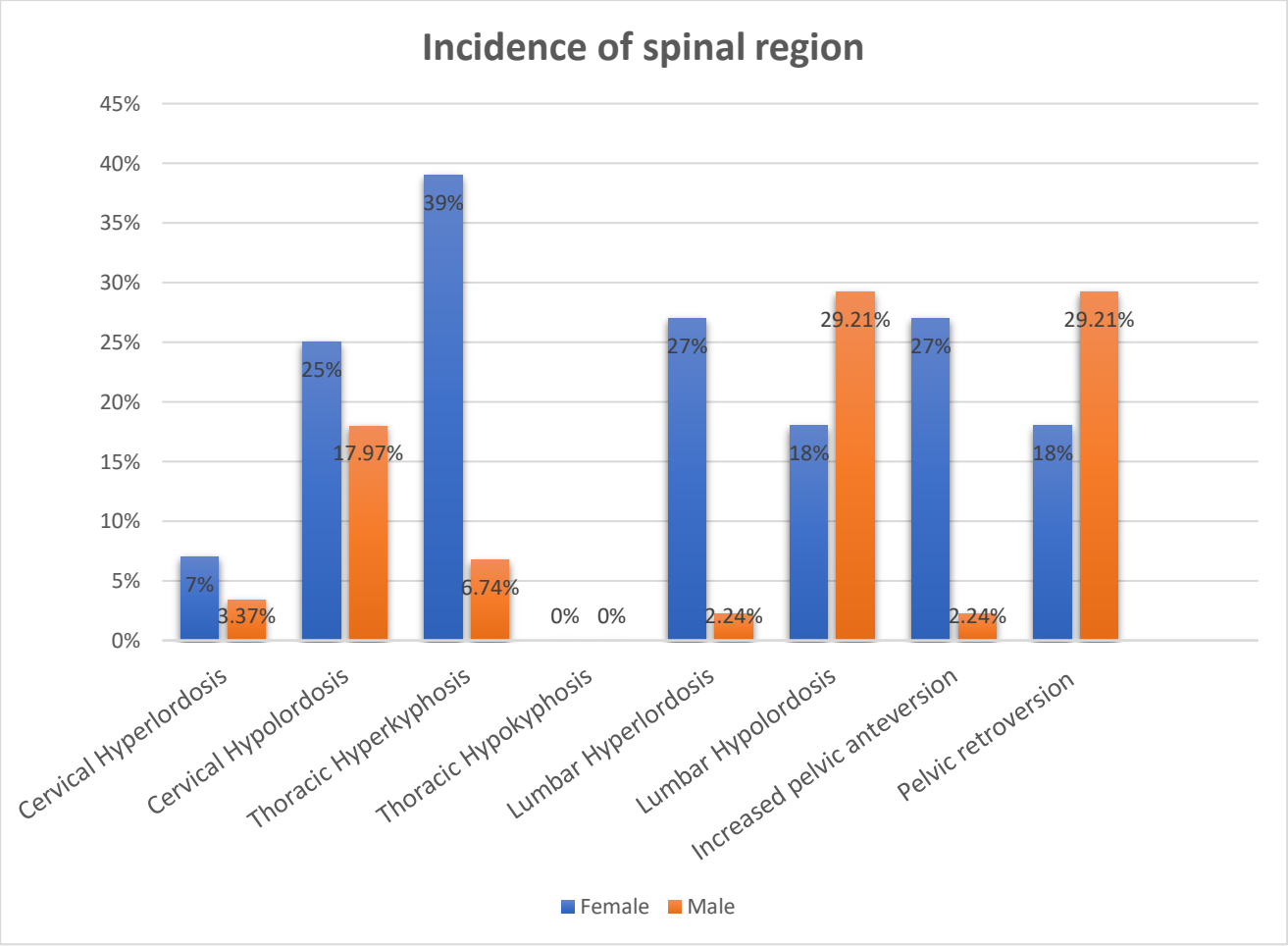


Table 7: Participants with pain and without pain

	Number of participants	Percentage
With pain	163	86.24%
Without pain	26	13.75%

CONCLUSIONS

Postural deviations are common, especially among the student population. Out of 300 evaluated students, 63% showed spinal deviations.

Postural deviations are associated with several factors; among the 300 assessed students, 72% were employed, of whom 17.59% were working in their professional field.

Gender was equally represented, with 50% females and 50% males. Among those with postural deviations (63%), 52.9% were female and 47.08% male. Postural deviations, based on gender and spinal regions, showed the following:

- 7% of females and 3.37% of males had cervical hyperlordosis
- 25% of females and 17.97% of males had cervical hypolordosis
- 39% of females and 6.74% of males had thoracic hyperkyphosis
- 27% of females and 2.24% of males had lumbar hyperlordosis and increased pelvic anteversion
- 18% of females and 29.21% of males had lumbar hypolordosis and pelvic retroversion

REFERENCES

Smith, J., & Brown, A. (2009). Prevalence of postural deviations and musculoskeletal disorders among students. Journal of Orthopedic Research, 27(3), 150-157. Retrieved from https://pmc.ncbi.nlm.nih.gov/articles/PMC10743088/

Lee, K., & Park, S. (2023). Influence of body composition on sagittal plane posture deviations in young adults. Children, 11(1), 36. https://doi.org/10.3390/children11010036

Kumar, R., & Singh, P. (2021). A cross-sectional study for screening of postural deficits among university students. International Journal of Medical Research & Health Sciences, 10(5), 12-20. Retrieved from https://www.ijmrhs.com/medical-research/a-crosssectional-study-for-screening-of-postural-deficits-among-university-students.pdf

Ahmed, S., & Ali, M. (2020). Postural deviations and back pain among university students. Pakistan Biomedical Journal, 3(2), 85-90. Retrieved from https://www.pakistanbmj.com/journal/index.php/pbmj/article/view/235

Mohammadi, H., & Rahimi, F. (2018). Postural deviations and related factors among Tehran university students. Physical Therapy Journal, 7(2), 45-52. Retrieved from https://ptj.uswr.ac.ir/browse.php?a_id=565&ftxt=1&html=1&sid=1&slc_lang=en

ORAL PRESENTATION

The impact of PNF protocols on the activation increase of the multifidus and transversus abdominis muscles

[1] Roxhensa Sula* (ORCID: *https://orcid.org/0009-0009-7977-4896*)
[2] Irena Kola (ORCID: *https://orcid.org/0000-0002-7936-1284*)

[*1] Aldent University, Faculty of Medical Sciences, Department of Nursing and Physiotherapy, Tirana, Albania.
[2] University of Medicine, Faculty of Technical Medical Sciences, Tirana, Albania.

Abstract

Activation of the deep stabilizing trunk muscles, such as the Multifidus and Transversus Abdominis (TrA), is essential for maintaining lumbopelvic stability and reducing lower back pain. Proprioceptive Neuromuscular Facilitation (PNF) protocols are known for their effectiveness in enhancing neuromuscular control and postural strength.
The aim of this study is to evaluate the impact of a PNF-based exercise protocol on increasing the activation of the Multifidus and Transversus Abdominis muscles, using physiotherapeutic functional tests as assessment tools.
The study included 10 participants (aged 20–25) presenting with mild symptoms of lumbar instability. Over a 4-week period, they underwent a PNF exercise program focused on trunk stabilization. Muscle activation was assessed before and after the intervention using dynamic functional tests:
- Prone Instability Test
- Active Straight Leg Raise (ASLR)
- Trunk Flexion Control Test
Post-intervention results showed improvements in all participants, with better performance in the functional tests, increased stability, and improved movement control. Participants also reported a noticeable reduction in fatigue and discomfort in the lumbar region.
PNF exercises have a positive impact on enhancing the function and control of the Multifidus and Transversus Abdominis muscles. Functional physiotherapeutic testing proved to be a practical and effective method for evaluating changes in muscle activation.

Keywords: PNF, Multifidus, Transversus Abdominis, muscle activation, lumbar stability

INTRODUCTION

The stability of the vertebral column plays a crucial role in preventing and managing lower back pain. Two of the most important muscles contributing to this function are the Multifidus and Transversus Abdominis, which are considered key muscles for segmental trunk stabilization. Poor activation of these muscles is often associated with muscular imbalances and an increased incidence of injuries in the lumbar region.

One therapeutic approach that has gained attention in the field of physiotherapy is Proprioceptive Neuromuscular Facilitation (PNF). This method aims to enhance neuromuscular control, strength, and flexibility through functional movement patterns that stimulate the nervous and muscular systems in an integrated way.

This case study aims to assess the impact of a treatment protocol using PNF techniques on improving the functional activation of the Multifidus and Transversus Abdominis muscles, through dynamic physiotherapeutic assessment tests, in individuals with reduced trunk stability. The findings of this study may contribute to the improvement of clinical treatment and rehabilitation practices in musculoskeletal disorders affecting the lumbar area.

MATERIALS AND METHODS

This is a case study conducted with 10 students from Aldent University (ages 20–25), including 5 females and 5 males. The participants presented signs of reduced trunk stability and reported low back pain. Inclusion criteria required that participants had no significant associated muscular or neurological pathologies. All participants provided informed consent prior to their involvement in the study.

Each participant underwent a 4-week PNF exercise protocol, with sessions held three times per week. The protocol included diagonal trunk and pelvic movement patterns, progressive resistance exercises, and the rhythmic stabilization technique.

Data were processed statistically by evaluating muscle tone and pain levels before and after the application of PNF techniques. The aim was to assess the effect of PNF in improving the functional activation of the Multifidus and Transversus Abdominis muscles.

RESULTS

Table 1: Pain intensity before and after the application of PNF

	VAS before PNF	VAS after PNF
The patient 1	7	3
The patient 2	6	2
The patient 3	8	4
The patient 4	5	2
The patient 5	7	3
The patient 6	6	1
The patient 7	5	2
The patient 8	8	5
The patient 9	7	2
The patient 10	6	2

Table 2: Muscle tone of the multifidus muscle before and after the application of PNF

	Muscle tone before PNF	Muscle tone after PNF
The patient 1	2/5	4/5
The patient 2	2/5	4/5
The patient 3	3/5	5/5
The patient 4	1/5	3/5
The patient 5	4/5	5/5
The patient 6	2/5	4/5
The patient 7	4/5	5/5
The patient 8	2/5	4/5
The patient 9	3/5	5/5
The patient 10	5/5	5/5

Table 3: Muscle tone of the transversus abdomini muscle before and after the application of PNF

	Muscle tone before PNF	Muscle tone after PNF
The patient 1	2/5	4/5
The patient 2	1/5	3/5
The patient 3	2/5	4/5
The patient 4	3/5	5/5
The patient 5	1/5	2/5
The patient 6	2/5	4/5
The patient 7	1/5	4/5
The patient 8	2/5	3/5
The patient 9	3/5	4/5
The patient 10	1/5	3/5

Table 4: Dynamic assessment of patients through the Prone Instability test

	Multifidus muscles		Transversus abdomini muscle	
	Muscle tone before PNF	Muscle tone after PNF	Muscle tone before PNF	Muscle tone after PNF
The patient 1	Negative	Positive	Negative	Positive
The patient 2	Negative	Positive	Negative	Positive
The patient 3	Negative	Positive	Negative	Positive
The patient 4	Negative	Positive	Negative	Positive
The patient 5	Negative	Positive	Negative	Positive
The patient 6	Negative	Positive	Negative	Positive
The patient 7	Negative	Positive	Negative	Positive
The patient 8	Negative	Positive	Negative	Positive
The patient 9	Negative	Positive	Negative	Positive
The patient 10	Negative	Positive	Negative	Positive

Note: Negative results mean that the muscles did not have adequate stability before the PNF therapy, and the negative results indicate improvement in muscle activation and stability after the treatment.

Table 5: Dynamic assessment of patients through the Active Straight Leg Raise test

	Multifidus muscles		Transversus abdomini muscle	
	Muscle tone before PNF	Muscle tone after PNF	Muscle tone before PNF	Muscle tone after PNF
The patient 1	2	4	1	3
The patient 2	3	5	2	4
The patient 3	1	3	1	2
The patient 4	4	5	3	5
The patient 5	3	4	2	4
The patient 6	2	4	2	3
The patient 7	3	5	3	5
The patient 8	1	3	1	4
The patient 9	4	5	3	5
The patient 10	3	4	2	4

Note: 0-no muscle activation, 1-very weak activation, 2- weak activation, 3-moderate activation, 4-good activation, 5-optimal activation.

Table 6: Dynamic assessment of patients through the Trunk Flexion Control test

	Multifidus muscles		Transversus abdomini muscle	
	Muscle tone before PNF	**Muscle tone after PNF**	**Muscle tone before PNF**	**Muscle tone after PNF**
The patient 1	1	4	1	33
The patient 2	3	5	2	4
The patient 3	1	3	1	3
The patient 4	4	5	3	5
The patient 5	1	2	3	4
The patient 6	2	4	2	3
The patient 7	3	5	3	5
The patient 8	1	3	1	4
The patient 9	4	5	3	5
The patient 10	3	4	2	4

Note: 0-no muscle activation, 1-very weak activation, 2- weak activation, 3-moderate activation, 4-good activation, 5-optimal activation.

CONCLUSIONS

Following the application of PNF protocols, a noticeable improvement was observed in the activation of the Multifidus and Transversus Abdominis muscles in all 10 participants. Dynamic assessments through the Prone Instability Test, Active Straight Leg Raise, and Trunk Flexion Control Test showed increased muscle tone and functionality, reflected in the improvement of numerical scores from pre- to post-treatment.

These improvements are significant for enhancing lumbar stability and reducing pain symptoms, thereby increasing functional capacity and overall quality of life. The results support the effectiveness of PNF protocols as a physiotherapeutic method for activating the core stabilizing muscles of the spine and abdomen.

However, the small sample size highlights the need for larger and more comprehensive studies to confirm these findings and to determine the optimal parameters for treatment.

It is recommended that PNF techniques be implemented regularly and periodically for the maintenance of lumbar stability, with individualized adaptation of protocols according to each patient's specific needs.

REFERENCES

Akuthota, V., & Nadler, S. F. (2004). Core strengthening. Archives of Physical Medicine and Rehabilitation, 85(3), S86-S92. https://doi.org/10.1016/j.apmr.2003.12.003

Brumagne, S., Cordo, P., & Verschueren, S. (2004). Proprioceptive weighting changes in persons with low back pain and elderly persons during upright standing. Neuroscience Letters, 366(1), 63-66. https://doi.org/10.1016/j.neulet.2004.05.040

Hodges, P. W., & Richardson, C. A. (1996). Inefficient muscular stabilization of the lumbar spine associated with low back pain: A motor control evaluation of transversus abdominis. Spine, 21(22), 2640-2650. https://doi.org/10.1097/00007632-199611150-00015

Marshall, P. W., & Murphy, B. A. (2006). Core stability exercises on and off a Swiss ball. Archives of Physical Medicine and Rehabilitation, 87(1), 107-114. https://doi.org/10.1016/j.apmr.2005.08.031

O'Sullivan, P. B. (2000). Lumbar segmental “instability”: Clinical presentation and specific stabilizing exercise management. Manual Therapy, 5(1), 2-12. https://doi.org/10.1054/math.1999.0214

Smith, M., & Coppieters, M. W. (2015). Neuromuscular control and proprioceptive training: Implications for rehabilitation of low back pain. Physical Therapy Reviews, 20(2), 120-128. https://doi.org/10.1179/1743288X14Y.0000000134

ORAL PRESENTATION

Maternal and Infant Outcomes of Breastfeeding and Formula Feeding: A Quantitative Comparative Study

Mirva Hoxha (ORCID: https://orcid.org/0009-0004-2757-3340)

Aldent University, Faculty of Medical Tecnical Sciences, Department of Nursing, Tirana, Albania.

Abstract

Infant feeding during the first months of life plays a crucial role in healthy growth and directly influences the physical and emotional well-being of both the newborn and the mother. This study aims to explore and compare the impact of two common feeding methods—breastfeeding and formula feeding—on both maternal and infant outcomes (Krol et al., 2018; Sánchez-Vincitore et al., 2024). A quantitative approach was applied using an anonymous questionnaire distributed to mothers with diverse infant feeding experiences. The survey assessed variables such as type of feeding in the first six months, duration of breastfeeding, maternal emotional responses, feeding-related challenges, social support, and mothers' perceptions of infant health and bonding (Can et al., 2025; Chambers et al., 2023). Results showed that breastfeeding was strongly associated with positive effects on infant emotional development, reduced digestive problems, and enhanced bonding with the mother (Krol et al., 2018). Breastfeeding mothers reported greater emotional fulfillment, fewer feelings of guilt, and additional physical benefits such as postpartum recovery and weight loss, although some experienced difficulties including nipple pain and fatigue (Rowles et al., 2025; Wheeler et al., 2024). Conversely, formula feeding was valued for its practical convenience but was more often linked to infant digestive discomfort and maternal insecurity, especially when it was not the first-choice method (Fallon et al., 2016). Across both groups, the level of social and partner support emerged as a decisive factor shaping the maternal emotional experience (Tessema et al., 2025). This study emphasizes the importance of structured healthcare and educational interventions to guide and support mothers in their feeding choices. Promoting awareness of breastfeeding benefits, providing assistance in overcoming lactation challenges, and ensuring non-judgmental acceptance of different approaches are essential for fostering a healthier and more supportive environment for mothers and infants (Hussain et al., 2025).

Keywords*:* breastfeeding, formula feeding, infant health, maternal well-being, nursing role

INTRODUCTION

Infant feeding during the first months of life is a fundamental determinant of health and well-being, influencing both immediate and long-term outcomes for the child as well as the mother (Krol et al., 2018). Nutrition in early infancy shapes the immune system, supports growth, and fosters neurological development while affecting emotional security and the quality of the mother–infant bond (Sánchez-Vincitore et al., 2024). Among the most common methods of infant feeding are breastfeeding and formula feeding, each associated with distinct benefits and challenges (Fallon et al., 2016).

The primary aim of this study is to analyze and compare the effects of breastfeeding and formula feeding on the physical and emotional health of infants during the early stages of life. In addition to evaluating physiological outcomes, the study seeks to explore the emotional impact of these feeding practices on both infants and mothers (Can et al., 2025). By adopting a multidimensional perspective, the research addresses biological, psychological, and social aspects of feeding choices.

Breastfeeding is recognized for its protective role in infant immunity, optimal growth, and maternal bonding, mediated by hormones such as oxytocin and prolactin (Krol et al., 2018). Conversely, formula feeding may provide practical advantages but can be associated with digestive issues and maternal stress or guilt when not the preferred option (Fallon et al., 2016; Wheeler et al., 2024). Parental decisions are also shaped by social, economic, and cultural factors, making evidence-based guidance essential for healthcare professionals, parents, and policymakers (Chambers et al., 2023; Tessema et al., 2025).

MATERIALS AND METHODS:

Literature Review

A systematic review of peer-reviewed articles, WHO reports, and national health documents was conducted to establish the theoretical framework of the study (Hussain et al., 2025). The review focused on breastfeeding and formula feeding and their effects on maternal and infant physical and emotional health (Krol et al., 2018; Fallon et al., 2016).

Quantitative Study

A descriptive quantitative design was employed using a structured anonymous questionnaire distributed to mothers with diverse feeding experiences. The questionnaire collected data on feeding type, breastfeeding duration, maternal emotional responses, feeding difficulties, perceived infant health and bonding, and social/partner support (Can et al., 2025; Chambers et al., 2023). Responses were analyzed using descriptive statistics and presented via tables, and summaries.

RESULTS

Table 1: Dermografic datas

	Age group	Marital status	Number of children	Education
<20	5			
21-30	70			
31-40	25			
Married		78		
Divorced		13		
Cohabiting		9		
1 child			50	
2 children			35	
3 or more			15	
University				60
Secondary				30
Primary				10

This section presents the demographic data of the mothers who participated in the study.

The majority of respondents belong to the age group 21–30 years, while other groups such as those aged 31–40 years and under 20 years are represented in smaller proportions.

2, 78% of mothers are married, making up the overwhelming majority of participants. 13% are divorced, while 9% live in cohabitation without formal marriage. These data are significant in understanding the social and emotional context of the mother–child relationship within this study.

A considerable proportion of mothers have one child, while another large share have two children. Mothers with more than three children make up a smaller, but important percentage for analysis, since emotional and physical demands vary according to the number of children.

Most of mothers have completed university education, followed by those with secondary education. A smaller proportion have only 9-year education, but they are included to provide a full overview of the participants' educational levels.

Table 2: Infant Feeding Practices, Physical and Emotional Experiences, Social and Emotional Support and Infant Health and Future Feeding Intentions

	Feeding method (0-6 months)	Breastfeeding duration	Reasons for not breastfeeding	Breastfeeding experience	Emotional bonding
Exclusive breastfeeding	47				
Breast+formula	53				
<1 month		6			
1-3 months		16			
4-6 months		25			
>6 months		53			
Insufficient milk			19		
Personal choice			19		
Infant refusal			10		
Medical problems			3		
Other reasons			49		
Very easy				34	
Easy				53	
Difficult				10	
Very difficult				3	
Very strong					97
Moderate					3

This section presents data on how mothers fed their infants during the first six months of life, 53% of mothers chose a combination of breastfeeding and formula, while 47% exclusively breastfed during the first six months.
Most of mothers breastfed their infants for more than six months. A small minority (6%) breastfed for less than one month, while 25% breastfed for 4–6 months and 16% for 1–3 months. This distribution reflects a variety of practices influenced by factors such as maternal/infant health, social pressure, work demands, and family support.
49% of mothers reported other reasons for not breastfeeding beyond the main categories provided in the questionnaire. These may include stress, lack of support, or particular family/economic circumstances. The most common specific reasons were insufficient milk production (19%) and personal choice (19%), indicating that the decision not to breastfeed often extends beyond health factors. 10% reported infant refusal, and only 3% cited health problems.
The majority of mothers found breastfeeding to be a positive experience, describing it as easy (53%) or very easy (34%). However, 10% considered it difficult and 3% very difficult, highlighting challenges such as pain, stress, or insufficient support.
44% of mothers reported no physical discomfort during breastfeeding, which is a positive indicator of their experience. Nonetheless, 34% experienced discomfort rarely, 16% occasionally, and 6% frequently, emphasizing the need for medical and psychological support in some cases.
55% did not experience any of the listed breastfeeding-related issues. However: 26% reported physical fatigue, likely due to frequent feeding or lack of practical support. 10% experienced nipple cracking. 9% reported breast pain or mastitis, a condition requiring medical attention.
Breastfeeding had varying effects on maternal weight: 44% reported no change, maintaining balance in metabolism and daily activity. 44% reported weight loss, consistent with studies suggesting breastfeeding aids postpartum weight reduction. 12% reported weight gain, possibly due to stress, unbalanced diet, or limited physical activity. The majority perceived breastfeeding as very positive (69%) or positive (22%), describing it as emotionally fulfilling. A small proportion reported neutral (6%) or negative experiences (3%), often linked to

physical difficulties or lack of support. 13, 97% of mothers felt strongly emotionally connected to their infant while breastfeeding. Only 3% reported feeling somewhat connected, suggesting a generally strong emotional bond in this process. 72% did not experience feelings of guilt about how they fed their infant, reflecting confidence and adequate support. However, 28% did report feelings of guilt, likely linked to social pressures, comparisons, or inability to breastfeed as desired. 84% of mothers felt strongly supported by their partner and family in their feeding choice, showing the importance of a positive support system. 16% felt little support, which may negatively affect emotional well-being.

59% reported no digestive problems in their infants. Among the remainder, 38% noted digestive issues during formula feeding, while only 3% reported such problems during breastfeeding. The majority (72%) would choose exclusive breastfeeding if they had another child, indicating strong trust in its nutritional and emotional benefits. 19% remain undecided, while 9% would choose a combination of breastfeeding and formula.

DISCUSSION

The findings of this study provide valuable insights into maternal and infant experiences related to breastfeeding and formula feeding, highlighting both the benefits and challenges of each method.

Breastfeeding was associated with emotional and physical benefits for both mother and infant (Krol et al., 2018; Rowles et al., 2025). Formula feeding provided a safe alternative but was more often linked to maternal guilt and infant digestive discomfort (Fallon et al., 2016; Wheeler et al., 2024). Social support from partners, family, and healthcare professionals significantly influenced maternal confidence and satisfaction (Can et al., 2025; Chambers et al., 2023; Tessema et al., 2025).

Practical Implications

Strengthen pre- and postnatal education programs (Hussain et al., 2025).

Expand access to lactation support.

Implement workplace policies supporting breastfeeding.

Normalize safe feeding choices without stigma.

Limitations and Future Research

While the study provides meaningful insights, limitations include the relatively small sample size and the specific socio-cultural context, which may limit generalizability. Future research should examine larger, more diverse populations and investigate long-term outcomes of different feeding practices on child development and maternal well-being. Additionally, qualitative approaches could further illuminate personal experiences, challenges, and decision-making processes surrounding infant feeding.

CONCLUSIONS AND RECOMMENDATIONS

Based on the literature review and analysis of data collected through a structured questionnaire, this study has drawn several significant conclusions regarding the impact of breastfeeding and formula feeding on the physical and emotional well-being of infants and mothers:

Breastfeeding as the Optimal Feeding Method: Breastfeeding is recognized as the most beneficial form of infant feeding, not only for its nutritional and disease-protective benefits but also for fostering a strong emotional bond between mother and child.

This form of feeding has been associated with reduced stress and anxiety levels in mothers, as well as positive emotional regulation in infants.

Formula Feeding and Maternal Emotions: While formula feeding serves as a necessary alternative in certain situations, it has been linked to higher levels of insecurity and, at times, guilt among mothers.

However, in circumstances where breastfeeding is not feasible, formula feeding provides a viable option to ensure the infant's health by offering a balanced nutritional profile.

Influence of Socioeconomic and Cultural Factors: Social, economic, and cultural factors play a crucial role in maternal feeding decisions. Support from healthcare professionals, access to reliable information, and the absence of social stigmas have been identified as key determinants in the positive breastfeeding experiences of mothers.

Statistical Analysis of Maternal and Infant Well-being: Quantitative data analysis revealed clear trends linking feeding methods to various aspects of physical and emotional well-being in both mothers and infants. These findings underscore the importance of providing adequate support to mothers during this critical period.

Recommendations

Healthcare systems should strengthen educational programs to provide mothers with balanced information on breastfeeding and formula feeding, while also expanding access to postpartum professional support such as lactation consultants. Supportive workplace policies, including flexible hours, breaks, and designated spaces, are essential to help mothers maintain healthy feeding practices after returning to work. Equally important is fostering a culture that normalizes and respects all feeding choices, reducing stigma and promoting informed decision-making. Finally, further research involving diverse populations is needed to guide effective interventions and policies that enhance maternal and infant health.

REFERENCES

Can, V., et al. (2025). Impact of social support and breastfeeding success on the breastfeeding self-efficacy levels in adolescent mothers. Breastfeeding Medicine, 20(2), 123–130. https://doi.org/10.1089/bfm.2024.0152

Chambers, A., et al. (2023). Emotional and informational social support from health visitors moderates the relationship between informational support and breastfeeding duration. International Breastfeeding Journal, 18(1), 1–9. https://doi.org/10.1186/s13006-023-00551-7

Fallon, V., et al. (2016). The emotional and practical experiences of formula-feeding mothers: A qualitative study. BMC Pregnancy and Childbirth, 16, 1–8. https://doi.org/10.1186/s12884-016-0900-2

Hussain, M., et al. (2025). Effects of food insecurity on infant feeding confidence and practices during the COVID-19 pandemic. Journal of Human Lactation, 41(1), 45–54. https://doi.org/10.1177/08903344221123245

Krol, K. M., et al. (2018). Psychological effects of breastfeeding on children and mothers: A review. Frontiers in Psychology, 9, 1–9. https://doi.org/10.3389/fpsyg.2018.02245

Rowles, G., et al. (2025). Investigating the impact of breastfeeding difficulties on maternal mental health. Scientific Reports, 15, 1–9. https://doi.org/10.1038/s41598-025-98357-6

Sánchez-Vincitore, L. V., et al. (2024). The impact of ever breastfeeding on children ages 12 to 36 months: A longitudinal study. Early Human Development, 170, 105642. https://doi.org/10.1016/j.earlhumdev.2022.105642

Tessema, M., et al. (2025). Improving postnatal social support using antenatal group-based psychoeducation: A randomized controlled trial. Frontiers in Global Women's Health, 6, 1510725. https://doi.org/10.3389/fgwh.2025.1510725

Wheeler, A., et al. (2024). Perceived pressures and mental health of breastfeeding mothers: A qualitative study. Healthcare, 12(17), 1794. https://doi.org/10.3390/healthcare12111794

ORAL PRESENTATION

The role of biology in promoting education for sustainable development in upper secondary education

Sara Pupe

Department of Biology, Aldent University, Albania

Abstract

Biology education plays a crucial role in developing students' scientific knowledge and their ability to analyze and apply theoretical concepts in real-life contexts. A key aspect of this subject is the integration of practical work, which enables students to understand biological phenomena through direct experience. This study aims to examine the impact of practical activities on learning outcomes in biology, assessing how such methods support knowledge acquisition and the development of students' competencies.The study also explores the central role of biology education in promoting sustainable development at the secondary education level. Education for sustainability requires the cultivation of competencies such as systems thinking, forecasting, and solving complex problems. Biology, through modules such as evolution, biodiversity, ecology, and health, provides both theoretical and practical foundations for environmental awareness and sustainable development. Pedagogical strategies supporting these objectives include field trips, laboratory work, project-based learning, socio-scientific discussions, and the integration of scientific competencies.The research was conducted at the University of Tirana (Faculty of Natural Sciences), Aldent University, and five high schools (*Ismail Qemali*, *Sami Frashëri*, *Sinan Tafaj*, *18 Tetori*, and *Vath Korreshi*). A total of 180 biology teachers, 10 school leaders, 60 high school students, and 90 university students participated, using anonymized data from learning management systems.The findings provide recommendations for educational policy and curriculum development: promoting teacher training in education for sustainability, providing appropriate tools and resources for biology teaching, and scaling up the use of active and collaborative learning methods.

Keywords: education, teaching, sustainable development, competency development, learning outcomes

Study Aim: The primary aim of this study is to explore and evaluate the ways in which biology, as a scientific subject, contributes to the promotion of education for sustainable development (ESD) at the upper secondary education level. Specifically, the study seeks to:

Identify existing pedagogical practices that integrate sustainability concepts into biology instruction, such as fieldwork, ecological laboratories, and topics including biodiversity and ecosystem conservation;

Analyze the challenges and barriers encountered when incorporating sustainability into biology teaching, including limited teacher training, time constraints for extracurricular content, insufficient resources, and resistance to pedagogical change.

Methodology

This study employs a mixed-methods approach, combining quantitative and qualitative strategies. Quantitative data were collected through questionnaires administered to students and university learners, while qualitative insights were gathered through interviews with biology teachers. This integrated approach allows for a comprehensive understanding of both individual perceptions regarding sustainability factors and realistic pedagogical practices, thereby substantially enhancing the interpretability and validity of the findings.

Conclusion

The role of biology in promoting education for sustainable development (ESD) at the upper secondary education level is crucial for the scientific and professional formation of students. Integrating sustainability into biology education fosters greater awareness and encourages active engagement towards a more sustainable future. Achieving this requires close collaboration among teachers, students, and policymakers to enhance the quality and effectiveness of instruction in this field.

Keywords: education, teaching, sustainable development, competency development, learning outcomes

Introduction

One of the most important objectives of humanity in the 21st century is the construction of a sustainable society. Education plays a key role in achieving sustainability and is itself a cornerstone for building a sustainable society. In a period of rapid ecological and social transformation, education is crucial for shaping students who are engaged, responsible, and capable of addressing complex environmental and societal challenges.In this context, biology—as a discipline that studies life and its interactions with the environment—provides an exceptional opportunity to integrate the principles of sustainable development into upper secondary education. Through biology education, students can develop the knowledge and skills necessary to understand and respond to environmental and social challenges affecting everyday life. This integration aligns with the United Nations Sustainable Development Goals (SDGs), which aim to ensure that all learners acquire the knowledge and competencies required to promote sustainable development.This study aims to examine how biology education can contribute to education for sustainable development (ESD) in upper secondary schools. Using a mixed-methods approach, including questionnaires with students and university learners as well as interviews with biology teachers, the study analyzes perceptions, knowledge, and practices related to integrating sustainability themes into biology instruction. The research provides a clear overview of the effectiveness of biology teaching in promoting sustainable development and identifies opportunities to enhance this process within the context of upper secondary education.

The study was conducted at the University of Tirana (Faculty of Natural Sciences), Aldent University, and five high schools (*Ismail Qemali*, *Sami Frashëri*, *Sinan Tafaj*, *18 Tetori*, and *Vath Korreshi*). In total, 180 biology teachers, 10 school leaders, 60 high school students, and 90 university students participated, using anonymized data from learning management systems.

This research addresses several key questions:

What are the current pedagogical practices of biology teachers in integrating sustainable development concepts into their teaching?

What challenges do biology teachers face when attempting to incorporate sustainability concepts into their instructional practices?

What resources and support are provided to biology teachers and students for teaching sustainability concepts in the classroom, and what challenges are encountered in integrating these topics into the biology curriculum?

Literature Review

The concept of sustainable development was first introduced in the Brundtland Report by the World Commission on Environment and Development (Brundtland et al., 1987). Since then, it has become increasingly important in addressing the complex challenges faced by humanity in the 21st century. According to Filho et al. (2018), pursuing sustainable development has become vital due to growing concerns about environmental degradation, social inequality, and economic instability.Education plays a critical role in shaping beliefs, attitudes, and

behaviors toward sustainability. Hogan and O'Flaherty (2021) assert that education is a key tool for achieving the objectives of sustainable development. Within this context, biology education is particularly significant, given its focus on biodiversity, ecological systems, and the interdependence of all species on Earth.Active learning approaches, such as outdoor education and project-based learning, have been highlighted as effective methods for promoting sustainable development concepts in secondary education (Jeronen et al., 2016). These approaches help students develop critical thinking skills and adopt a systems perspective when addressing environmental and social issues. Empirical evidence from Sweden indicates that integrating sustainability-related topics into biology instruction enables students to gain a deeper understanding of the connections between human activities and their environmental impacts. Furthermore, Cebrián, Junyent, and Mulà (2021) emphasize that education across all levels and disciplines must be fundamentally reoriented to advance sustainable living, democracy, and human well-being. Incorporating sustainability into biology education not only fosters scientific literacy but also encourages active, responsible participation in addressing societal and environmental challenges.

Methodology

This study employs a mixed-methods approach, integrating both quantitative and qualitative strategies to collect and analyze data.

For students:

Questionnaires: Both closed- and open-ended questions were used to assess students' knowledge of environmental issues and sustainability concepts.

In-depth interviews: Conducted to explore students' perceptions of the importance of sustainable development and the role of biology in shaping these perceptions.

For teachers:

Questionnaires: Focused on teaching practices and the integration of sustainability-related topics into biology instruction.

Interviews: Conducted to examine teachers' experiences in delivering biology lessons and the challenges encountered in integrating sustainable development concepts.

Data Analysis:

Quantitative analysis: Statistical analyses were performed using SPSS to examine numerical data and identify correlations between students' environmental knowledge and their attitudes toward sustainability.

Qualitative analysis: Thematic coding was applied to interview responses to identify key themes regarding the impact of biology education on fostering sustainable development awareness and competencies.

This integrated methodological approach allows for a comprehensive understanding of both the pedagogical practices in biology education and the perceptions of students regarding sustainability, thereby enhancing the validity and depth of the study's findings.

Results and Discussion

Student Questionnaires:

Frequency of sustainability-related topics in biology: According to the survey, 21% of students reported that topics on the impact of human activities on the environment were covered, 37% indicated biodiversity and its conservation, 18% cited natural resource management, 14% mentioned climate change, while 10% reported that these topics were not addressed.

Frequency of sustainability discussions by biology teachers: 37% of students stated that their teachers always discussed sustainable development topics, 32% reported discussions often, 21% occasionally, and 10% never.

Perceived importance of sustainability topics for the future: 36% of students considered sustainability topics very important, 43% moderately important, and 21% not important.

Motivation to act in environmental protection after biology lessons: 47% of students felt always motivated, 32% often motivated, 11% rarely motivated, and 10% never motivated.

Actions undertaken to contribute to sustainable development: 33% reported engaging in recycling practices, 22% in the use of renewable energy, 43% participated in school environmental activities, and 2% did not engage in any of these activities.

Teacher Questionnaires:

Frequency of integrating sustainability topics in biology lessons: 48% of teachers reported always integrating these topics, 23% often, 19% rarely, and 10% never.

Perceived scientific preparedness to teach sustainability: 46% of teachers felt always prepared, 30% often prepared, 17% rarely prepared, and 7% never prepared.

Resources used for teaching sustainability concepts: 45% of teachers used textbooks, 20% online resources, 25% practical activities, and 10% did not use any of these resources.

Training related to sustainability teaching: 36% of teachers reported always receiving training, 38% often, 15% rarely, and 11% never.

Assessment of student engagement in sustainability-related lessons: 52% of teachers perceived students as always highly engaged, 22% often engaged, 18% occasionally engaged, and 8% never engaged.

Conclusions

The role of biology in promoting education for sustainable development (ESD) in upper secondary education is both significant and timely, given contemporary environmental challenges and the need to raise awareness among younger generations. Biology, as the science of life and ecological interactions, plays a central role in developing competencies necessary for sustainable development. It enables students to understand natural processes and the impacts of human activities on the environment, providing the foundational knowledge required to foster responsible attitudes and behaviors. Concepts such as life cycles, biodiversity, and ecosystems form the basis for understanding the importance of environmental conservation.To promote ESD, biology teachers employ various pedagogical methods, including group work, discussions, practical projects, and laboratory experiments. In this study, 21% of students reported coverage of human impact on the environment, 37% biodiversity and its conservation, 18% natural resource management, and 14% climate change. These approaches help students link theoretical knowledge with practical applications and develop problem-solving skills related to environmental challenges. Thematic teaching that addresses socio-scientific issues—such as biodiversity, climate change, natural resources, and global health—enhances critical thinking and environmental awareness, empowering students to actively engage in solution-finding.Survey results indicate that approximately 57% of participants perceive a supportive emotional learning environment as highly motivating, fostering long-term learning. Students with positive perceptions of their competence in biology perform better academically and develop constructive attitudes toward the subject. ESD integration within biology and secondary education is widely accepted by teachers (88%), with over two-thirds (61–75%) incorporating sustainability topics into curricula and practical activities. However, a notable gap remains, as 45% of respondents consider the coverage of sustainability topics in regular lessons insufficient.These findings underscore the importance of structured, supportive, and resource-rich pedagogical practices in biology to maximize the development of students' knowledge, skills, and attitudes toward sustainable

development. Effective integration of ESD requires not only curriculum design but also continuous teacher training, appropriate teaching resources, and a learning environment that motivates and empowers students to take an active role in environmental stewardship.

Literatura

Ahmad, S. I., Abubakar, B. B., & Yau, S. (2018). Biology education: A panacea for sustainable national development. *Frontiers in Environmental Microbiology, 4*(2), 71–74.

Amos, R., & Levinson, R. (2019). Socio-scientific inquiry-based learning: An approach for engaging with the 2030 Sustainable Development Goals through school science. *International Journal of Development Education and Global Learning, 11*(1), 29–49.

A, V. S. (2020). The role of transformation in biology science and education for supporting sustainable development goals. *Kongunadu Research Journal, 7*(2), 85–93.

Balogun, S. A., & Olalekan, A. A. (2024). Teaching-learning of biology for sustainable development: The use of strategic intervention materials. *Faculty of Natural and Applied Sciences Journal of Mathematics and Science Education, 6*(1), 154–159. fnasjournals.com

Griffith, A., & Moore, W. (2020). A comparative analysis of approaches to integrating sustainability into the curriculum at a university in a small island developing state in the Caribbean. In E. Sengupta, P. Blessinger, & T. S. Yamin (Eds.), *Integrating sustainable development into the curriculum* (pp. 41–56). Emerald Publishing.

Holbrook, J., & Rannikmäe, M. (2007). The nature of science education for enhancing scientific literacy. *International Journal of Science Education, 29*(11), 1347–1362.

Id Babou, A., Selmaoui, S., Alami, A., Benjelloun, N., & Zaki, M. (2023). Teaching

International Journal Abstract Title Reference. (2025). Assessment of challenges and practices in integrating sustainable development into biology education. *International Journal of Research and Scientific Innovation*. RSIS International.

Jackson, W. M., Binding, M. K., Grindstaff, K., Hariani, M., & Koo, B. W. (2023). Addressing sustainability in the high school biology classroom through socioscientific issues.

McKeown, R. (2006). *Education for sustainable development toolkit* (3rd ed.). University of Tennessee.

Pedagogical content knowledge about the sustainability of high school chemistry and biology teachers. (2024). *Journal of Environmental Studies and Sciences, 14*, 652–665.

Rahmi, S. N., Megawati, M., Alberida, H., & Fadilah, M. (2025). Assessment of biology learning outcomes in education: A systematic literature review. *Biosfer: Jurnal Pendidikan Biologi, 18*(1), 10–25.

Rickinson, M. (2001). Learners and learning in environmental education: A critical review of the evidence. *Environmental Education Research, 7*(3), 207–320.

Sterling, S. (2010). Learning for resilience, or the resilient learner? Towards a necessary reconciliation in a paradigm of sustainable education. *Environmental Education Research, 16*(5–6), 511–528.

Sivapalan, S., & Speight, S. (2018). Role of education for sustainable development. Në W. Leal Filho (Ed.), *Encyclopedia of Sustainability in Higher Education*. Springer.

Tshiningayamwe, S. (2016). Education for sustainable development in the Namibian biology curriculum. Në H. Lotz-Sisitka, O. Shumba, J. Lupele, & D. Wilmot (Eds.), *Schooling for sustainable development in Africa* ,pp. 239–1920.

Viera, C., Ferreira, M., Rodríguez-Esteban, A., & Vidal, R. (2021). Towards sustainable development in education: Implementing a VET system for in-service teachers in Albania. *Sustainability, 13*(16), 8739.

Evolutionary literacy as a catalyst for sustainable futures: connecting biological evolution education and education for sustainability. (2024). *Evolution: Education and Outreach, 17*, Article 22. BioMed Central.

Development of sustainability competencies in secondary school education: A scoping literature review. (2024). *Sustainability, 16*(23), 10228.

Sustainability curriculum in secondary education: Two case studies assess progress. (2021). Në *The Palgrave Handbook of Global Sustainability* (pp. 1–12).

ORAL PRESENTATION

Learning through analysis in education: Using data to improve student learning

Sara Pupe

Department of Biology, Aldent University, Albania

Abstract

In today's technology-driven world, information is continuously collected regarding individuals' activities both online and offline, leading us into the era of big data. This development has made it possible for learning analytics to revolutionize modern education by transforming data into actionable knowledge. It is the key to understanding how students learn, enabling subject instructors to adapt educational experiences to individual needs and enhance overall learner performance.This study examines the impact of data analytics on improving student learning in both pre-university and higher education in Albania. Institutions can use learning analytics to monitor student engagement, participation, and performance during a lesson. The research was conducted at the University of Tirana, Faculty of Natural Sciences, Aldent University, as well as at several secondary schools: "Petro Nini Luarasi," "Andon Zako Cajupi," "Sinan Tafaj," "18 Tetori," and "Jani Nushi."In total, the study included: 12 subject teachers (Mathematics, Albanian Language, Computer Science, Biology), 8 school principals, 50 high school students, and 60 university students, using anonymized data from learning management systems. The results indicate that the use of pedagogical dashboards and predictive analytics assists teachers in timely identification of struggling learners and in personalizing interventions, while also impacting students' comprehension and overall learning outcomes.Furthermore, the study highlights challenges such as the lack of teacher training in data interpretation and the absence of integrated school-level strategies. The conclusions emphasize the necessity of fostering a data-use culture in education, one that is grounded in ethics, transparency, and technological competence.

Keywords: analysis, educational data, performance, assessment, competencies, strategy

Objective of the Study

The aim of this paper is to analyze the ways educational data can be used for the systematic improvement of learning outcomes, to evaluate the effect of analytical interventions on motivation and performance, to identify challenges and opportunities related to the integration of data analytics into educational decision-making, and to produce a correlational report on institutional, technical, and ethical challenges.

Methodology

This study combines qualitative and quantitative approaches to analyze the use of data in improving learning in secondary education in Albania.

Conclusion

The findings of this study demonstrate that the use of data analytics in education can serve as a powerful tool for improving student outcomes, provided it is implemented carefully and in a structured manner.

Keywords: Analysis, Educational Data, Performance, Assessment, Competencies, Strategy

Introduction

Over the past decade, education has undergone a profound technological transformation, with particular emphasis on the integration of Learning Analytics (LA) as a means to enhance learning outcomes in both secondary and higher education. Contemporary approaches increasingly capitalize on the processing of vast quantities of digital traces—ranging from platform logins, time on task, and assignment performance to forum participation and reading duration. These traces enable educational systems to move beyond a reactive, content-delivery orientation toward a proactive, personalized, and evidence-based model of instruction. Consequently, the incorporation of data-driven approaches is reshaping how teaching and learning processes are conceptualized, monitored, and supported.The field of Learning Analytics has consolidated itself internationally as a pivotal instrument for guiding evidence-informed decision-making among educators, learners, and policymakers (Siemens & Long, 2011). While

initially prominent in technologically advanced contexts, LA has increasingly been applied in emerging educational systems such as Albania, where the gradual digitalization of learning environments has generated new opportunities for systematic analysis of learner performance and engagement.The present study seeks to investigate the extent to which the implementation of learning analytics contributes to the improvement of student learning in Albanian upper secondary schools and universities. Data were collected from five public high schools in Tirana—"Petro Nini Luarasi," "Andon Zako Çajupi," "Sinan Tafaj," "18 Tetori," and "Jani Nushi"—as well as from the University of Tirana and Aldent University. Employing a mixed-methods design, the study combined quantitative data (surveys administered to 70 secondary school pupils, 100 university students, 20 teachers, and 10 institutional leaders) with qualitative insights (interviews with school principals and document analysis). Findings revealed a statistically significant improvement in academic performance, with an average increase of 12% in quarterly results among students who received data-driven interventions.Aligned with international scholarship (Papamitsiou & Economides, 2014; Ifenthaler & Yau, 2020), the findings underscore that the effective use of data in educational settings extends beyond technological access. It requires sustained professional development, the cultivation of evidence-based decision-making cultures, and the strengthening of teacher–student relationships. At the same time, several systemic challenges were identified, including the absence of structured training for educators in data interpretation, a lack of standardized evaluative instruments, and persistent ethical concerns related to transparency, accountability, and data privacy (Slade & Prinsloo, 2013).Accordingly, this research is guided by two overarching questions:

To what extent does the use of individualized dashboards—providing learners with real-time insights into their engagement and progress—affect self-regulation and academic performance?

How do teachers utilize pedagogical analytics to diagnose learner engagement and progress, and what types of interventions are subsequently implemented based on these insights?

Literature Review

Within the scholarly discourse, *Educational Data Mining* (EDM) and *Learning Analytics* (LA) are widely recognized as two interrelated yet distinct fields that leverage data from diverse learning environments with the overarching aim of understanding and enhancing teaching and learning processes. Romero and Ventura (2024) provide a comprehensive overview of the evolution of these domains, detailing methodological approaches, learning contexts, and emerging research trajectories. Their synthesis highlights that while EDM predominantly focuses on uncovering hidden patterns in educational data through classification and clustering algorithms, LA emphasizes the transformation of these patterns into actionable insights for instructors, learners, and policymakers.A systematic review conducted by Kaliisa et al. (2023) on Learning Analytics Dashboards (LADs) revealed that their direct impact on academic achievement has generally been modest. Nevertheless, LADs demonstrated a stronger influence on learner engagement and participation, thereby underscoring their potential as motivational and self-regulatory tools. Complementarily, Viberg and Grönlund (2021) argue that despite growing interest, empirical evidence concerning the large-scale pedagogical impact of LA remains scarce. They call for deeper exploration into pedagogical practices and educators' needs to ensure the meaningful integration of LA into teaching and learning.Kaliisa et al. (2023), in their review of 38 studies, examined the effects of LA dashboards on academic achievement, motivation, participation, and student behavior, concluding that dashboards contribute variably across these dimensions. Similarly, Pathirana et al. (2024) report that the adoption of data analytics in higher education—particularly during the COVID-19 pandemic—has supported improvements in student performance, informed pedagogical interventions, and guided institutional decision-making.Furthermore, a large-scale review of 400 studies in distance education (2023) indicated that more than 52% of the included research reported positive effects of LA, such as enhanced academic outcomes, behavioral analysis, and early prediction of academic failure. However, the review also noted contextual limitations, including restricted implementation in resource-constrained environments and significant financial costs associated with LA adoption.Romero and Ventura (2024) additionally emphasize that the dual trajectories of EDM and LA must be understood in relation to one another. While EDM advances the technical frontier of pattern discovery, LA seeks to translate such discoveries into pedagogically meaningful practices, thereby positioning itself as a critical bridge between data-driven insights and evidence-based educational decision-making

Methodology

This study adopted a mixed-methods approach, combining quantitative and qualitative strategies to investigate the relationship between the use of learning analytics tools and academic performance, as well as teacher perceptions of student engagement. The central premise of the research is that students and university learners who utilize learning analytics tools demonstrate higher academic performance, while teachers who integrate data analytics into their instructional practices report increased student engagement.

Data Collection Instruments – The primary instrument for this study was a structured questionnaire, designed to capture both quantitative and qualitative data. The questionnaire included:

Closed-ended questions to collect quantitative data and facilitate statistical analysis;

Open-ended questions to elicit in-depth insights, perceptions, and comments from participants.

Sampling – A random sample was selected, comprising 70 high school students, 100 university students, 20 teachers, and 10 institutional leaders. Data collection was conducted over a two-week period.

Data Analysis – Quantitative data were analyzed using statistical software (SPSS), allowing for descriptive and inferential analyses of numerical responses. Qualitative data from open-ended questions were coded and categorized to identify recurring themes and patterns, enabling thematic analysis.

Ethical Considerations – Participants' personal information was handled with strict confidentiality, ensuring compliance with ethical research standards and data protection protocols.

Results and Discussion

The findings from the survey provide comprehensive insights into the use and perceived impact of learning analytics (LA) among teachers, school leaders, and students in both secondary and higher education contexts in Albania.

Teacher and Leadership Use of Data – A majority of educators (68%) reported that they fully use data to improve instructional practices or learner support, while 13% disagreed and 11% were neutral. This indicates a generally positive adoption of data-driven instructional practices, though some educators remain hesitant.

Impact on Student Learning Outcomes – Regarding the effect of data analytics on student results, 59% of respondents strongly agreed that it contributed to performance improvement, 33% disagreed, and 8% were neutral. Additionally, 58% reported that the use of data always enhanced students' learning outcomes, 29% observed improvement frequently, and 13% noted no effect.

Preferred Applications of Data – Teachers and students indicated that learning analytics should be more extensively used for: individualized support (27%), fairer assessment (48%), and quicker feedback (23%), while 2% were unsure.

Training and Professional Development – Regarding data interpretation training, 43% of institutions provide formal training by specialists, 36% do not offer training, and 21% provide informal peer-based guidance. These findings underscore the need for structured professional development to maximize LA effectiveness.

Practical Use of Data in Instruction – Data were primarily used for lesson planning (51%), grouping students by similar proficiency (21%), and preparing supplementary materials (26%), whereas 2% of educators did not use the data at all. Monitoring student performance on learning platforms occurred daily for 47%, weekly for 36%, occasionally when grading (13%), and not at all for 4% of respondents.

Adaptation and Feedback – Data-driven adaptation of teaching to students' needs was fully endorsed by 47% of respondents, while 17% strongly disagreed and 36% were neutral. Feedback from students was perceived as consistently helpful by 41%, frequently helpful by 15%, rarely helpful by 30%, and never helpful by 14%.

Motivation and Support – The use of learning analytics was reported to positively influence motivation, with 49% indicating a strong positive effect, 22% often, 25% occasionally, and 4% never. Support to enhance data use included additional training (60%), technological tools (31%), and peer support (9%).

Frequency and Tools for Data Analysis – Teachers adapted instructional methods based on data always (29%), often (27%), rarely (21%), and never (23%). Tools for analysis included Excel (38%), learning management platforms (39%), and specialized analytics software (23%).

Student Understanding and Perceived Usefulness – In terms of supporting students' comprehension of their progress, 23% reported that teachers always assist them, 27% sometimes, 30% rarely, and 20% never. Students perceived the platforms as always useful (29%), often useful (27%), and not useful (27%

Conclusions

In an era where education faces increasingly complex challenges and rising expectations, learning analytics (LA) emerges as a powerful tool to enhance quality and equity in learning. Beyond a technical procedure, LA represents a strategic approach that places the learner at the center of the educational process, empowers teachers, and fosters collaboration among educational leaders. When combined with critical reflection and human-centered practices, the use of data has the potential to transform traditional schools into dynamic learning environments where every student has a genuine opportunity to reach their full potential.The findings of this study demonstrate that the implementation of data analytics can significantly improve instructional practices and directly influence student outcomes, provided it is applied systematically and thoughtfully. Specifically, approximately 47% of students and university learners had access to their performance data on learning platforms, enabling more informed self-monitoring. Teachers with access to detailed dashboards on student progress were able to identify learners facing difficulties earlier and implement more effective support strategies.A recurring challenge observed among teachers and institutional leaders is the limited availability of ongoing professional training by field specialists, which constrains lesson planning and instructional strategy. Consequently, 60% of educators and leaders reported the need for additional structured training, 31% emphasized the need for improved technological tools, and 9% identified peer support as necessary.Moreover, 49% of respondents indicated that the use of learning analytics positively influenced student motivation. However, the role of teachers in helping students interpret their progress remains limited, with only 23% regularly assisting learners in understanding their academic development.Overall, these benefits and challenges suggest that, when implemented effectively, learning analytics can substantially enhance both student learning and the quality of instruction. The findings underscore the need for ongoing professional development, robust technological infrastructure, and active teacher engagement to fully realize the potential of data-driven educational practices.

Literature

Bienkowski, M., Feng, M., & Means, B. (2012). *Enhancing teaching and learning through educational data mining and learning analytics: An issue brief*. U.S. Department of Education, Office of Educational Technology.

Ferguson, R. (2012). Learning analytics: Drivers, developments and challenges. *International Journal of Technology Enhanced Learning, 4*(5–6), 304–317.

Ifenthaler, D., & Yau, J. Y.-K. (2020). Utilising learning analytics to support study success in higher education: A systematic review. *Educational Technology Research and Development, 68*, 1961–1990.

Jin, Y., et al. (2024). FATE in MMLA: Student-centred exploration of fairness, accountability, transparency, and ethics in multimodal learning analytics. In *Proceedings of the 14th International Learning Analytics & Knowledge Conference (LAK24)* (pp. 1332–1553).

Khalil, M., & Ebner, M. (2016). Learning analytics: Principles and constraints. In *Proceedings of the World Conference on Educational Media and Technology 2016* (pp. 1326–1333). Association for the Advancement of Computing in Education (AACE).

Kim, C. (2023). Teacher data literacies: A scoping review. *Review of Education, 11*(3), e3414.

Li, K. C., Duffy, M., & Zhang, J. (2022). A novel multi-dimensional analysis approach to teaching and learning analytics in higher education. *Systems, 10*(4), 96.

Long, P., & Siemens, G. (2011). Learning analytics: A foundation for informed change in education. *EDUCAUSE Review, 46*(5), 31–36.

Morales Tirado, A., Mulholland, P., & Fernandez, M. (2024). Towards an operational responsible AI framework for learning analytics. In *Proceedings of the 13th International Conference on Learning Analytics & Knowledge (LAK23)* (pp. 135–167).

OECD. (2021). *Digital education outlook 2021: Pushing the frontiers with artificial intelligence*. OECD Publishing.

Papamitsiou, Z., & Economides, A. A. (2014). Learning analytics and educational data mining in practice: A systematic literature review of empirical evidence. *Educational Technology & Society, 17*(4), 49–64.

Pragmile / ITS Learning (Sweden). (2025). Predictive analytics tackle dropout rates. ITS Learning.

Saar, M., Rodríguez-Triana, M. J., & Prieto Santos, L. P. (2022). Towards data-informed teaching practice: A model for integrating analytics with teacher inquiry. *Journal of Learning Analytics, 9*(3), 1–18.

Siemens, G., & Long, P. (2011). Penetrating the fog: Analytics in learning and education. *EDUCAUSE Review, 46*(5), 30–40.

Slade, S., & Prinsloo, P. (2013). Learning analytics: Ethical issues and dilemmas. *American Behavioral Scientist, 57*(10), 1510–1529.

Stojanov, R., & Daniel, B. (2024). A decade of research into the application of big data and analytics in higher education: A systematic review. *Education and Information Technologies, 29*, 2011–2032. https://doi.org/10.1007/s10639-024-11732-5

Williamson, B. (2017). *Big data in education: The digital future of learning, policy and practice*. SAGE Publications.

ORAL PRESENTATION

Wine sector in Albania: Challenges and opportunities for geographical indications protection

Aleksander Petre[1], Dritan Topi[2]*

[1]Faculty of Natural Sciences, University of Tirana, Department of Industrial Chemistry, Blvd Zogu 1, 1000, Tirana, Albania
[3]Faculty of Natural Sciences, University of Tirana, Department of Chemistry, Blvd Zogu 1, 1000, Tirana, Albania

Abstract

Albania's wine industry benefits from favorable Mediterranean climate and a rich cultural heritage, yet it faces obstacles in modernization, market competition, and protecting geographical indications (GIs). This review explores historical and current trends in grape growing and winemaking, based on FAOSTAT data and national development strategies. Indigenous varieties like Kallmet, Sheshi i Zi, and Shesh i Bardhë are central to Albania's wine identity, setting it apart from international cultivars. The paper also investigates global trade patterns, authentication methods, and legal frameworks to combat counterfeiting and safeguard product authenticity. The results highlight the importance of developing strong traceability systems and aligning with EU standards to boost consumer trust and elevate Albania's wine reputation worldwide. Recommendations focus on promoting native grape varieties and enhancing GI protections to maintain competitiveness in international markets.

Keywords: Albanian wine sector, Autochthonous grape varieties, Geographical indication, traceability

Overvie of Wine Production in Albania

Albania's Mediterranean climate—with hot summers and mild winters—supports perennial crops and a long tradition of viticulture. In 2009, vineyards covered 9,800 acres, and under the national plan, 300–500 acres of new vineyards are planted each year. Currently, 90 enterprises produce wine, 77% of which process less than 100 tons per year. About 70 are family-run micro-wineries, while the 20 largest producers account for 80% of processed grapes.

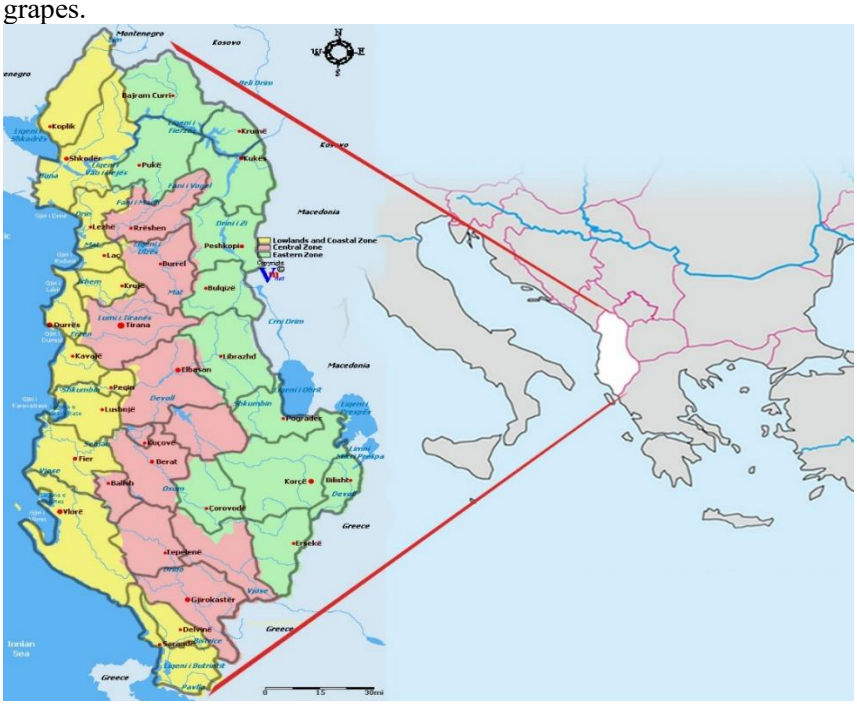


Figure 1. Wine regions of Albania according to Vinnet.

Production of raw material (grapes)

According to statistics, 90 enterprises in our country are engaged in wine processing and production. Of these, about 77% have a processing capacity of less than 100 tons/year, and 70 enterprises are considered family-run micro-wineries. It is emphasized that the 20 largest producers account for 80% of the processed grapes.

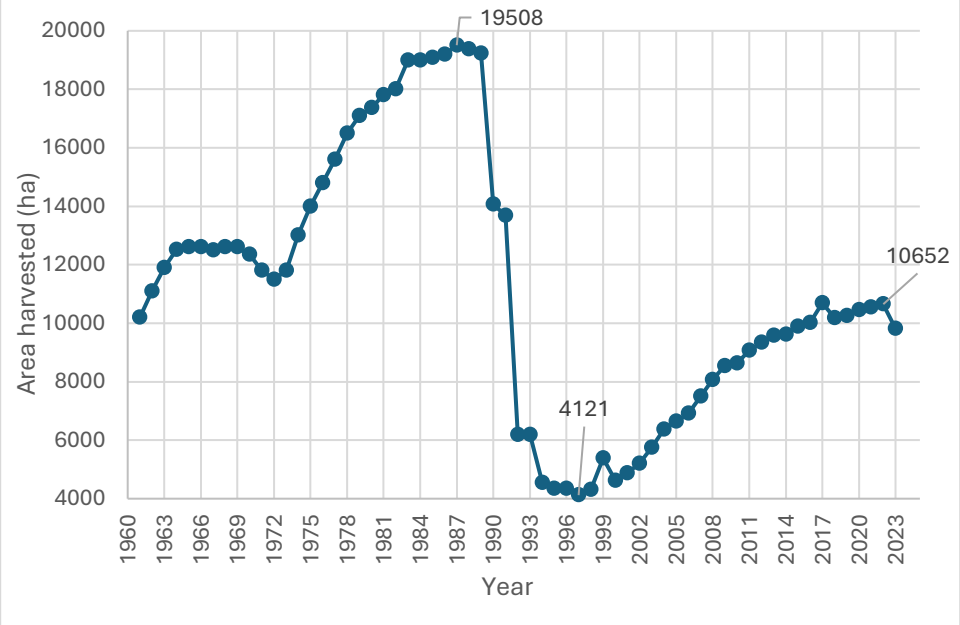


Figure 2. Grape harvested area during the period 1961-2023 (Source: FAOStat, 2025).

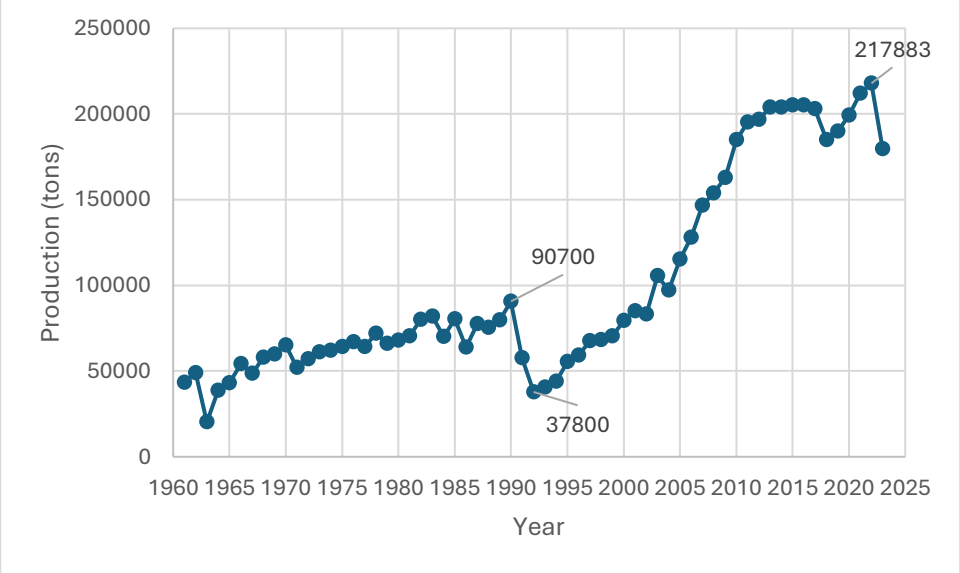


Figure 3. Grape production according to FAOSTAT, 1961-2022 period.

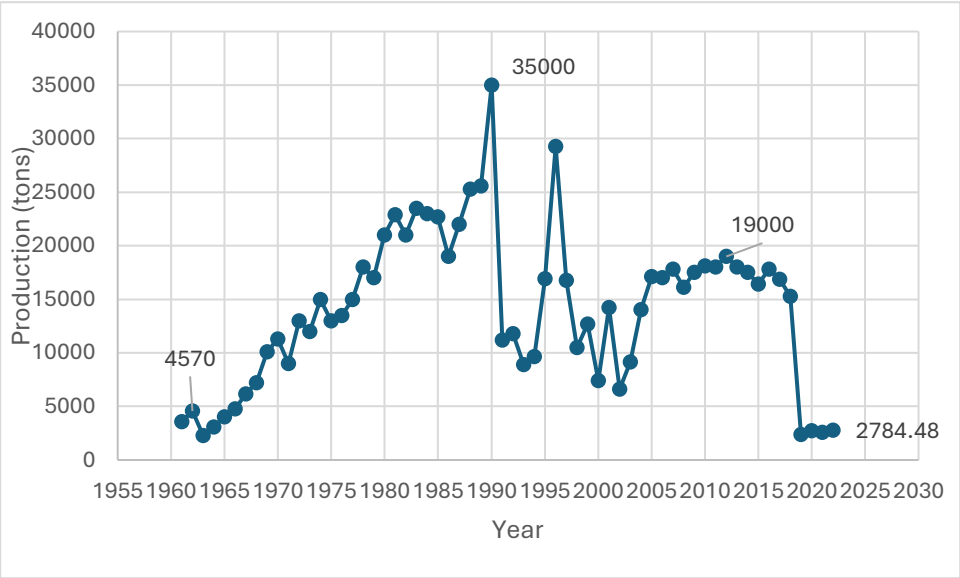


Figure 4: Wine production in Albania, 1961-2022 (Source: FAOSTAT, 2024)

Albania's Viticulture Advantage

The pedoclimatic conditions in Albania are conducive to viticulture, supporting a range of local cultivars recognized for their quality and productivity. Red wines crafted from Vlosh grapes stand out distinctly, whereas the local white varieties differ significantly from Chardonnay (Sotiri et al., 1996; Cakalli et al., 2003).

Viticultural Advantages and Indigenous Varieties

Albania's pedoclimatic conditions favor high-quality local cultivars. Notable white varieties include Shesh i Bardhë, Debina e Bardhë Leskoviku, Serina e Bardhë, and Kryqësi, while red varieties include Vlosh, Kallmet, Sheshi i Zi, Mavrud, Koteka e Zezë, and Serina e Zezë. These grapes have high sugar content and distinctive aromas, producing wines with unique profiles that set Albanian products apart in global markets.

Varieties of local origin (autochthonous) for the production of white wines

Sheshi i Bardhë

The most notable local variety, cultivated for centuries in Tirana, Durrës, and Kavaja regions of central Albania, thrives in a Mediterranean climate near the Adriatic Sea. It is named after the village of Shesh in the Ndroqi area, where it is traditionally grown. When fully ripe, it contains 24-26% sugar and 6-7% acidity. In the lower coastal zone, this variety produces high-quality white wines, both dry and semi-dry, characterized by a rich aroma and body.



Figure 5. Wine regions of Albania, and indigenous grape varieties.

Debina e bardhë Leskoviku
Debina Leskoviku is one of the oldest local grape varieties in southeastern Albania. It is primarily grown in regions such as Përmeti, Leskoviku, Korçë, Skrapar, and Berat. When fully ripe, it contains 22-24% sugar and 5.5-6% acidity, and it is known for producing high-quality dry table wines with a desirable alcohol content.

Serina e bardhë

This white grape variety is among the oldest local types, commonly found throughout southern and southeastern Albania. It serves as a cornerstone for viticulture in the Korça, Skrapar, Berat, and Kolonja regions. This variety is used to produce high-quality table wines. It has a sugar content of 22-24% and an acidity level of 5.8-6.2%.

Kryqësi (Sinambel)
This local variety has been developed through the efforts and selection of our ancestors. It is commonly found in the administrative regions of Leskovik, Këlcyra, Përmet, and Tepelena. It ripens in the medium-late period and has a strong ability to accumulate sugar in the grain. In Leskovik and Përmet, it has produced 23-26% sugar content and an overall acidity of 6.2-6.7%.

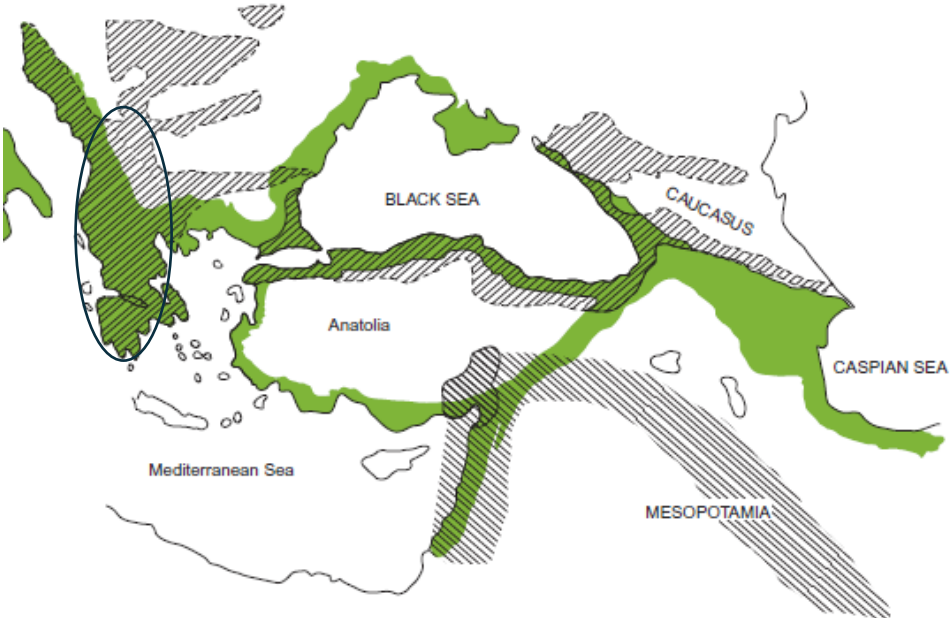


Figure 5. Comparison of the geographic distribution of *Vitis vinifera* L. sylvestris (Shaded). Quercus sessilis (right-slanted lines) and the origin of agriculture (left-slanted lines), based on the data from Levadoux (1956).

Local varieties for the production of red wine

Vlosh

It is one of the oldest red grape varieties grown in the regions of Vlora, Himara, Narta, Saranda, Berat, Lushnja, Gjirokastra, and Përmet. It holds the largest share of vineyards in our country. This variety ripens late, with an active growing period of about 180 days and a high-temperature tolerance of 36.0–37.0 °C. In these areas, Vlosh has accumulated 22-25% sugar and low acidity levels of 3.4-4.5%. It is used to produce dessert wines, alcoholic wines, and liqueurs. A drawback of this variety is its weak color; therefore, blending it with wines from more intensely colored varieties, such as Mavrud, is recommended.

2. Kallmet

Kallmet, also known as Gjashore, Zadrimore, and Kallmete, is an ancient local grape variety commonly found in the hills of Lezha and Shkodra, as well as around Lake Shkodra, where it has been cultivated for centuries due to its high quality. The Romans brought it to Central Europe, where it acquired various names such as Gemza, Tokai (Nero di Scutari), Kadarka, Branicevka, and Lugojane. In addition, Kallmet is cultivated in Tirana, Lushnja, Përmet, and Leskovik. This variety produces high-quality, dry table wines that are well-balanced, with good color and a distinctive bouquet, making it a prized grape in local winemaking.

Shesh i Zi

It is a variety of local origin, cultivated in the Ndroqi, Shesh, and Tirana areas, from which it gets its name. Today, it is widespread throughout many parts of Albania, including Krujë, Shkodër, Lezhë, Elbasan, Lushnja, and Durrës. Sheshi i zi performs well in loose soils with a high limestone content. Under such conditions, it accumulates 23–25% sugar. This variety yields very high-quality dry alcoholic wines with a distinctive taste and aroma.

Mavrud cv.

It is believed to have originated in Thrace; today, it is regarded as one of the oldest varieties among the Balkan peoples. It is common in Shkodër, Lushnja, and Tirana. It reaches high sugar levels (22–25%). The wine made from this variety is very full-bodied, dark in color, rich in flavor, and well-balanced, especially when aged. It also functions as a complementary variety for pairing with lighter-colored wines.

Koteka e Zezë cv.
It is one of the oldest grape varieties in our country, and it is common in the Përmet and Leskovik regions. In these areas, it ripens by the end of September. It accumulates high sugar levels (22-27%) and is used to produce high-quality table wines.

Serina e Zezë cv.
It is locally produced and has long been known in the regions of Korca, Pogradec, Leskovik, Berat, and Skrapar. It is a medium-ripening variety that accumulates sugars at a good level of 19-21%. It produces high-quality, balanced wines with distinctive characteristics upon aging.

Global Wine Trade Overview
By 2010, the export market accounted for more than 30% of total global production, indicating that the international wine trade had experienced significant growth since 2000. This boom was spurred on by a rise in consumption in North America and Northern Europe in the 1990s, as well as an increase in exports from manufacturers in the Americas. The OIV research states that world wine production in 2017 was around 246.7 million hectoliters. In contrast, global imports reached 22.6 billion euros for 3.4 million hectoliters by 2011. Italy, France, and Spain have remained the top producers (Mariani, Pomarici, and Boatto, 2012).

Wine Authentication and Traceability
Guaranteeing the authenticity and traceability of wine is a significant global issue. Quality control procedures are obligatory in numerous nations, including the EU and the USA, to safeguard customers against production faults and to avert illicit adulteration. Traceability guarantees that products can be monitored throughout all phases of manufacture and distribution, hence augmenting consumer confidence in health, quality, and safety. Key legislation encompass Directive (EU) 178/2002, which establishes a comprehensive framework for food safety and traceability, and EC Directive 986/89, which governs the transit of wine throughout the EU, mandating authenticity documentation. ISO Standards: ISO 22000:2005 incorporates traceability inside HACCP systems; ISO/FDIS 22005:2007 delineates principles for food chain traceability.
.
Elements of a Traceability System
Six core components include the following:
- Product Traceability – Tracking the physical location.
- Process Traceability – Documents activities throughout the production process.
- Genetic Traceability – Determines the genetic source.
- Input Traceability – Monitors the movement of additives and raw materials.
- Disease and Pest Tracking – Monitors risks of contamination.
- Analytical Measurement Traceability – Guarantees the precision of measurements (Opara, 2003).

Geographic Indication and Viniculture Promotion in Albania
Geographical indications (GIs) play a crucial role in the wine sector because they legally protect the name of a product that originates from a specific region and possesses qualities or a reputation linked to that origin. For Albanian wines, GIs help differentiate local products from international competitors by emphasizing the unique characteristics of indigenous grape varieties and traditional production methods, which strengthens brand identity and cultural heritage. Additionally, robust GI protections build consumer trust, prevent counterfeiting, and align national standards with EU legislation. Making it easier for producers with EU regulations. Making it easier for producers to access global markets and maintain competitiveness. Some key outcomes are:
1. Modernization of Facilities – Upgrading equipment and processes to improve quality and efficiency.
2. Strengthening Geographical Indication (GI) Protection – Ensuring authenticity and origin claims to differentiate Albanian wines globally.
3. Implementing Traceability Systems – Aligning with international standards to secure supply chains and prevent fraud.
Additionally, promoting indigenous grape varieties is highlighted as a way to enhance market differentiation and build trust internationally. In short, the sector needs modernization, robust GI frameworks, and traceability to compete globally and protect its cultural heritage.

Wine Counterfeiting and Legislation

Counterfeiting encompasses dilution, adulteration, blending with inferior wines, and misrepresentation of provenance (Holmberg, 2010). Legislation differs throughout several states. California, USA, allows limited water addition during fermentation, although EU legislation forbids it. Specific terminology
is interpreted variably; for instance, Italy and Chile differentiate between 'adulteration' (modifications) and 'falsification' (counterfeit items).

Conclusions

Albania's wine sector holds significant potential due to its favorable Mediterranean climate and diverse autochthonous grape varieties. However, modernization challenges, limited market competitiveness, and insufficient protection of geographical indications remain critical obstacles. Strengthening traceability systems and harmonizing national legislation with EU standards are essential to ensuring authenticity, preventing counterfeiting, and building consumer trust. Promoting indigenous varieties such as Vlosh, Kallmet, and Sheshi can be a strategic advantage for differentiating Albanian wines in global markets. Future efforts should focus on integrating advanced quality control measures, expanding export opportunities, and leveraging geographical indications to support sustainable economic growth and cultural preservation.

References

Carka, F., Maul, E., and Sevo, R. (2015). Study and parentage analysis of old Albanian grapevine cultivars by ampelography and microsatellite markers, *Vitis*, 54 (Special Issue), 127–131.

Carka, F.; 2006: Ampelografia e disa kultivareve autoktone te hardhise. ADA, Tirane.

European Commission. (2002). Regulation (EC) No 178/2002 of the European Parliament and of the Council.

Holmberg, L. (2010). Wine fraud. International Journal of Wine Research, 2010(2), 105-13. https://doi.org/10.2147/IJWR.S14102.

IS/ISO 22005 (2007): Traceability in the feed and food chain — General principles and basic requirements for system design and implementation. https://archive.org/download/gov.in.is.iso.22005.2007/is.iso.22005.2007.pdf.

ISO. (2005). ISO 22000:2005 Food safety management systems — Requirements for any organization in the food chain. *ASRO*, https://magazin.asro.ro/en/standard/109350.

Llupa, J., Gašić, U., Brčeski, I., Demertzis, P., Tešević, V., Topi, D. (2022). LC-MS/MS characterization of phenolic compounds in the quince (Cydonia oblonga Mill.) and sweet cherry (Prunus avium L.) fruit juices. Agriculture and Forestry, 2022, 68, 2, 193-205.

Mariani, A., Pomarici, E., & Boatto, V. (2012). Wine economics and policy. Wine Economics and Policy, 1(1), 24–40.

Opara, L. U. (2003). Traceability in agriculture and food supply chain: A review. *Journal of Food, Agriculture & Environment*, 1(1), 101–106.

Sotiri, P.; Gjermani, T.; Nini, T. (1973). Vitikultura. Tekst mesimor per Fakultetin e Agronomise. Instituti Larte Shteteror i Bujqesise, Tirana. (Albanian).

Topi, D., Topi, A., Guclu, G., Selli, S., Uzlasir, T., Kelebek, H. (2024). Targeted Analysis for the Detection and Authentication of Albanian Wines Using LC-DAD/ESI–MS/MS Combined with Chemometric Tools. Heliyon, 10/11, e31127.

ORAL PRESENTATION

Bir üniversite hastanesinde konjenital sitomegalovirüs (CMV) enfeksiyonlarında moleküler test sonuçlarının değerlendirmesi

Osman ÖZŞAHİN[1,2*] (ORCID:0000-0002-2771-2206), Hayriye KIRKOYUN UYSAL[3] (ORCID:0000-0002-2476-3796), Ali AĞAÇFİDAN[3] (ORCID:0000-0002-5470-296X)

[1]İstanbul Üniversitesi, Sağlık Bilimleri Enstitüsü, Tıbbi Mikrobiyoloji Anabilim Dalı, İstanbul, Türkiye
[2]Üsküdar Üniversitesi, Sağlık Hizmetleri Meslek Yüksekokulu, Tıbbi Laboratuvar Teknikleri, İstanbul, Türkiye
[3]İstanbul Üniversitesi, İstanbul Tıp Fakültesi, Tıbbi Mikrobiyoloji Anabilim Dalı, İstanbul, Türkiye

*Sorumlu yazar e-mail: osman.ozsahin@uskudar.edu.tr

Özet

Sitomegalovirüs (CMV), Herpesviridae ailesine ait, zarflı ve çift zincirli DNA yapısına sahip bir virüs olup konjenital enfeksiyonların en yaygın nedenlerinden biridir. Bu çalışmada, prenatal dönemde amniyotik sıvı örneğinde CMV DNA varlığının araştırılması ve elde edilen bulguların literatür verileriyle karşılaştırılması amaçlanmıştır. Ocak 2022 – Ocak 2024 tarihleri arasında İstanbul Üniversitesi İstanbul Tıp Fakültesi Kadın Hastalıkları ve Doğum Anabilim Dalı'na başvuran 20–52 yaş aralığındaki toplam 234 hastanın amniyotik sıvı örnekleri incelenmiş ve gerçekleştirilen analizler sonucunda 11 hastada (%4,7) CMV DNA pozitifliği saptanmıştır. Pozitif olguların yaş aralığı 21–31 olarak belirlenmiştir. Elde edilen pozitiflik oranı, literatürde bildirilen (Goegebuer ve ark., 2009) %14,5 ve (Simonazzi ve ark., 2017) %13,4 çalışmalarında bildirilen oranlardan düşük bulunmuştur. Bu farklılığın popülasyon özellikleri, bölgesel değişkenlikler, örneklem büyüklüğü ve tanı yöntemlerindeki farklılıklardan kaynaklandığı düşünülmektedir. Sonuçlar, prenatal dönemde CMV enfeksiyonlarının sıklığının azalma eğiliminde olabileceğini, ancak enfeksiyonun doğurganlık çağındaki kadınlarda hâlen görüldüğünü göstermektedir. CMV enfeksiyonu, konjenital enfeksiyonların en önemli etkenlerinden biri olmaya devam etmekte olup, prenatal dönemde rutin tarama ve erken tanı uygulamalarının maternal ve fetal sağlığın korunmasında büyük önem taşıdığı sonucuna varılmıştır.

Anahtar Kelimeler: Sitomegalovirüs, Amniyotik sıvı, Prenatal tanı

Evaluation of molecular test results in congenital cytomegalovirus (CMV) infections at a university hospital

Abstract

CMV is an enveloped, double-stranded DNA virus belonging to the Herpesviridae family and is one of the most common causes of congenital infections. This study aimed to investigate the presence of CMV DNA in amniotic fluid samples during the prenatal period and to compare the obtained findings with data reported in the literature. Between January 2022 and January 2024, amniotic fluid samples from a total of 234 patients aged 20–52 years who were admitted to the Department of Obstetrics and Gynecology, Istanbul University, Istanbul Faculty of Medicine, were analyzed. CMV DNA positivity was detected in 11 patients (4.7%), and the age range of CMV-positive cases was determined as 21–31 years. The positivity rate observed in this study was lower than those reported by (Goegebuer et al.,2009) %14.5 and (Simonazzi et al., 2017) %13.4 This difference may be attributed to population characteristics, regional variations, sample size, and differences in the sensitivity of diagnostic methods. The results suggest a possible decreasing trend in the frequency of prenatal CMV infections; however, the persistence of cases among women of reproductive age indicates that CMV remains a relevant concern. CMV infection continues to be one of the leading causes of congenital infections, and routine screening and early diagnosis during the prenatal period are of great importance for the protection of maternal and fetal health.

Keywords: Cytomegalovirus, Amniotic fluid, Prenatal diagnosis

GİRİŞ

CMV, Herpesviridae ailesinden çift zincirli zarflı bir DNA virüsüdür (Kemaloğlu ve ark., 2023). Virüsün 100 nm çapında ikozahedral bir nükleokapsiti vardır. Virüs genomu tegument veya matris olarak tanımlanan proteinli bir tabaka ile çevrilidir. Tegument veya matris, çok sayıda viral glikoprotein içeren bir lipit çift tabakasıyla çevrilidir. (Landolfo ve ark., 2003). CMV genomu 253 kb boyutunda olup insan herpesvirüsleri içinde en büyük genoma sahiptir. Yapısında 60 dan fazla glikoprotein bulunur. Başlıca glikoproteinlerinden biri olan Glikoprotein B (gB) (gpUL55), tanımlanmış 5 antijenik belirleyiciye (AD1-AD5) sahiptir. Bunlar nötralize edici antikorların hedefi olup virüsün hücreden hücreye bulaşmasını ve enfekte hücrelerin füzyonunu sağlar. CMV zarfında bulunan gB, zarftaki toplam protein kütlesinin %50'sinden fazlasını oluşturur ve konak bağışıklık tepkisini uyarır. Glikoprotein B (gB), genotipleme açısından en çok incelenen protein olup nötralize edici antikorlar için bir hedef bölgedir. Bulaşma yollarını ve coğrafi kökeni belirlemek için belirteçtir (Coşkun ve ark., 2023). CMV hamilelik esnasında bulaştığında konjenital enfeksiyona sebep olan yaygın bir viral patojendir. İntrauterin bulaşmalarda fetüste büyüme kısıtlamasına, gelişimsel gecikmelere, veya uzun vadeli sekeller oluşturabilir (Sayar ve ark., 2025). Virüsün inkübasyon süresi 4-12 hafta olup bulaş yolları yakın temas, idrar, kan, tükürük yada genital salgılar gibi vücut sıvıları ve kan yoluyla olmaktadır. Anneden bebeğe gebelikte plasenta yoluyla, doğum esnasında yada emzirme yoluylada geçebilmektedir. CMV vücuda girdikten sonra öncelikli olarak monosit, makrofaj ve endotelyal hücreleri enfekte eder; bununla birlikte, neredeyse tüm hücre tiplerinde çoğalma yeteneğine sahiptir. Virüs, kan dolaşımı aracılığıyla karaciğer ve dalağa ulaşır ve bu organlarda da çoğalmasını sürdürür. Monositler içinde latent (gizli) bir durum oluşturarak ömür boyu kalabilir. Virüs zaman zaman yeniden aktive olarak enfeksiyon tablosuna yol açabilir. Birincil ve ikincil enfeksiyonlarda olsun hem de aktivasyon evrelerinde olsun kan ve çeşitli vücut sıvılarında yüksek miktarda virüs tespit edilebilir (Kemaloğlu ve ark., 2023). CMV normal bağışıklığa sahip kişilerde asemptomatik hastalığa sebep olurken solid organ ve kemik iliği nakilli ve AIDS gibi bağışıklığı baskılanmış hastalarda mortalite ve morbiditiye neden olmaktadır (Coşkun ve ark., 2023)

MATERYAL METOT

Hastalara ait CMV DNA kantitatif testi sonuçları, hasta dosyalarındaki verilerden elde edilmiş ve değerlendirmeye alınmıştır. Çalışmamızda tam otomatik cobas® 6800 (Roche) sistemi kullanılmıştır. Cihazın çalışma prensibine göre hastalara ait plazma örnekleri, örnek yükleme ünitesine yerleştirilir. Barkodları ile numune otomatik olarak tanınmaktadır. Cihaz tarafında otomatik nükleik asit ekstrasyonu yapılarak örnek içindeki viral DNA izole edilir. İzole edilen nükleik asit sistem içindeki PCR master mix ile karıştırılır. Primer, enzimler ve prob reaksiyon karışımına eklenir. Real-Time PCR yöntemiyle hedef nükleik asit amplifiye edilir. Floresan sinyaller ile çoğalan DNA miktarı her döngüde ölçülür ve bu aşamada Ct (cycle threshold) değerleri belirlenir. Sistem amplifikasyon eğrilerini analiz ederek pozitif, negatif ya da şüpheli sonuçları gösterir. Tüm süreç sistem içinde otomatik olarak değerlendirilmektedir.

BULGULAR

Ocak 2022 - Ocak 2024 tarihleri arasında, İstanbul Üniversitesi İstanbul Tıp Fakültesi Hastanesi Cerrahi Tıp Bilimleri Bölümü, Kadın Hastalıkları ve Doğum Anabilim Dalı'na başvuran 20–52 yaş aralığındaki toplam 234 hastanın amniyotik sıvı örnekleri incelenmiştir. Gerçekleştirilen analizler sonucunda, 11 hastada (%4,7) CMV DNA pozitifliği saptanmıştır. CMV DNA pozitifliği tespit edilen hastaların yaş aralığı 21–31 olarak belirlenmiştir.

TARTIŞMA

Goegebuer ve ark., (2009) tarafından Kasım 2002 – Ekim 2006 tarihleri arasında yürütülen çalışmada, 282 hastanın 41'inde (%14,5) CMV pozitifliği saptanmış, pozitif olguların 35'inin yaş aralığı 22–37 olup ortalama yaşı ise 29 olarak tespit edilmiştir. Simonazzi ve ark., (2017) tarafından yapılan çalışmada ise, Ocak 2007 – Aralık 2014 döneminde incelenen 239 hastanın 32'sinde (%13,4) CMV DNA'sı pozitif bulunmuştur; hastaların yaş aralığı 18–44, ortalama yaşı 32 olarak tespit edilmiştir.

Bizim çalışmamız ile literatürde bildirilen oranlar karşılaştırıldığında, çalışmamızda saptanan pozitiflik oranının daha düşük olduğu görülmektedir. Bu farklılık, çalışmanın yürütüldüğü dönemdeki popülasyon özellikleri, bölgesel farklılıklar, örneklem büyüklüğü ve kullanılan tanı yöntemlerinin duyarlılığındaki değişkenlikler ile açıklanabilir. Ayrıca, son yıllarda gebelik takibi sırasında rutin serolojik taramaların artması ve prenatal hijyen farkındalığının yükselmesi, CMV enfeksiyonlarının sıklığında görece bir azalmaya yol açmış olabilir.

Öte yandan, yaş dağılımı açısından değerlendirildiğinde, pozitif olguların çoğunlukla 20'li yaşlarda yer aldığı görülmektedir. Bu bulgu, literatürde bildirilen verilerle paralellik göstermekte olup, CMV enfeksiyonunun doğurganlık çağındaki kadınlarda daha sık görüldüğünü desteklemektedir. Çalışmamızda elde edilen CMV pozitiflik oranı, literatürde bildirilen oranlardan düşük olmakla birlikte, genel eğilimle uyumludur. Bu durum, prenatal dönemde CMV enfeksiyonlarının hâlen önemli bir halk sağlığı sorunu olduğunu ve rutin tarama ile erken tanının önemini ortaya koymaktadır.

SONUÇ

Bu çalışma, prenatal dönemde amniyotik sıvı örneklerinde CMV DNA varlığının araştırılmasına yönelik olarak gerçekleştirilmiştir. Elde edilen bulgular, incelenen 234 olgunun %4,7'sinde CMV DNA pozitifliği saptandığını göstermiştir. Bu oran, literatürde bildirilen değerlerden düşük olmakla birlikte, prenatal CMV enfeksiyonlarının halen göz ardı edilemeyecek düzeyde olduğunu ortaya koymaktadır. Bulgular, özellikle doğurganlık çağındaki kadınlarda enfeksiyon riskinin devam ettiğini ve prenatal dönemde CMV taramasının erken tanı açısından önemini vurgulamaktadır.

Sonuç olarak, CMV enfeksiyonu, konjenital enfeksiyonların en sık nedenlerinden biri olmaya devam etmektedir. Bu nedenle gebelik sürecinde riskli grupların belirlenmesi, rutin tarama programlarının yaygınlaştırılması ve farkındalık çalışmalarının artırılması, hem maternal hem de fetal sağlığın korunması açısından büyük önem taşımaktadır. Ayrıca, daha geniş örneklemli ve çok merkezli çalışmalarla ülkemizde prenatal CMV enfeksiyonlarının gerçek prevalansının ortaya konulabileceği düşünülmektedir.

KAYNAKLAR

Coşkun, A., Gökahmetoğlu, S., Özmen, P., Çevik, Ş., Karakükcü, M., Kaynar, L., … & Kuskucu, M. (2023). Determination of genotypes in cytomegalovirus (CMV) strains obtained from pediatric and adult immunocompromised patients. Journal of Basic and Clinical Health Sciences, 7(1), 270–276.

Goegebuer, T., Van Meensel, B., Beuselinck, K., Cossey, V., Van Ranst, M., Hanssens, M., & Lagrou, K. (2009). Clinical predictive value of real-time PCR quantification of human cytomegalovirus DNA in amniotic fluid samples. Journal of Clinical Microbiology, 47(3), 660–665.

Kemaloğlu, Y. K., Keskin Yıldız, M., & Çınar, R. (2023). Doğumsal Sitomegalovirüs Enfeksiyonları ve İşitme Kaybı: Türkiye'de ulusal düzeyde tarama programına gereksinim var mı? Journal of Ear, Nose & Throat & Head & Neck Surgery, 31(1), 50–63.

Landolfo, S., Gariglio, M., Gribaudo, G., & Lembo, D. (2003). The human cytomegalovirus. Pharmacology & Therapeutics, 98(3), 269–297.

Sayar, M. S., Çağ, Y., Yılmaz, N., Şenbayrak, S., Çakırca, T. D., Çaydaşı, Ö., … & EKMUD CMV Study Group. (2025). Evaluation of cytomegalovirus seroprevalence in pregnant women: A multicenter study. Mediterranean Journal of Infection Microbes and Antimicrobials, 14, 25310.11:1–7.

Simonazzi, G., Cervi, F., Zavatta, A., Pellizzoni, L., Guerra, B., Mastroroberto, M., … & Lazzarotto, T. (2017). Congenital cytomegalovirus infection: Prognostic value of maternal DNAemia at amniocentesis. Clinical Infectious Diseases, 64(2), 207–210.

ORAL PRESENTATION

Bazı geleneksel olarak kullanılan antidiabetik bitkilerin enzim inhibisyon mekanizmalarının *in vitro* incelenmesi

Saman abdulsattar A.Jabbar Alsalihi[1*] (*ORCID: https://orcid.org/0009-0007-6147-0398*),
Cevat Nisbet[2] (*ORCID: https://orcid.org/0000-0002-7042-4605*),
Reza Khoshbakht farshad[3](*ORCID: https://orcid.org/0009-0002-7363-9879)*

[*1]Ondokuz mayıs üniversitesi, Veternerlik fakültesi, Biyokimya, Samsun, Türkiye
[2] Ondokuz mayıs üniversitesi, Veternerlik fakültesi, Biyokimya, Samsun, Türkiye
[3] Ondokuz mayıs üniversitesi, Veternerlik fakültesi, Biyokimya, Samsun, Türkiye

saman.finance.91@gmail.com

Özet

Uluslararası diabet federasyonunun verilerine göre diyabetin günümüzde yaklaşık 415 milyon insanı etkilediği tahmin edilmektedir. Tedavide ise temel yaklaşım diyabet tipine bakılmaksızın, ister egzersiz programları ister ilaçlarla olsun, hastaların kan glikozunu kontrol etmek zorunluluğunun olmasıdır. Kullanılan antıdiyabetik ilaçlar hasta popülasyonunda direncin oluşturulması, olumsuz etkilerin gelişmesi ve duyarlılıgın zayıflamasına kadar degişen bazı dezavantajlarına sahiptirler. Gelinen noktada son yıllarda tedavi yöntemlerinde kaydedilen önemli ilerlemelere rağmen diyabetik hastaların tedavisinin sonuçları hala mükemmel olmaktan uzaktır. Sunulan bildiride ülkemizin farklı bölgelerinde yetişen, Ada çayı (Salvia officinalis L.), Ayva (Cydonia oblonga Miller), Nar (Punica granatum L.), Papatya (Matricaria chamomilla), Sumak (Rhus coriaria L.), Yeşil çay (Comellasinensis) destekleyici tedavi ürünleri arasında yer alan ve antidiyabetik potansiyet taşıyabilecek olan bu bitkilerden elde edilen ekstrakların terapotik aktivitesinin in vitro ortamda araştırılmıştır. Her bitki örneği için farklı 7 numune toplanmıştır.Toplanan bitki örnekleri saf suyla yıkadıktan sonra +45 °C de etüvde ağırlık sabitleninceye kadar kurutulmuştur. Bitki ekstraktların yapılmasında (%80 etanol-su (v/v)) kullanılmıştır. Analiz için Standart kitler (Sigma-Aldrich'ten) kullanılmıştır. Ekstraktların analizinde Ketohexokinaz, Alfa-Amilaz, Alfa-glikozidaz, dipeptidil peptidaz-4, Aldoz redüktaz enzimin standart kitleri kullanılmıştır. Elde edilen bulguların varyans analizleri SPSS 15.0 bilgisayar programı kullanılarak gerçekleştirilmiştir. Araştırma kapsamında yer alan nar kabuğu, sumak meyvesi, yeşil çay yaprağı, ayva yaprağı, papatya çiçeği ve ada çayı bitkileri alfaglukozidaz, amilaz, ketoheksokinaz, aldoseredultaz ve dipeptidil piptidaz enzimleri bakımından inhibisyon göstermesine karşın aralarında fark istatistiksel olarak anlamlı bulunmamıştır ($p>0,05$).

Anahtar Kelimeler: Antidiyabetik aktivite, Bitkisel ekstraktlar, Enzim inhibisyonu, diyabet.

In vitro investigation of the enzyme inhibitory mechanisms of traditionally used antidiabetic medicinal plants

Abstract

According to the data of the International Diabetes Federation, diabetes is estimated to affect approximately 415 million people today. In treatment, regardless of the type of diabetes, whether through exercise programs or medications, patients must control their blood glucose levels. The antidiabetic drugs used have several disadvantages in the patient population, ranging from the development of resistance, the occurrence of adverse effects, and the weakening of sensitivity. At this point, despite significant progress made in treatment methods in recent years, the outcomes of diabetic patient care are still far from perfect.In the presented study, the therapeutic activity of extracts obtained from plants growing in different regions of our country—sage (Salvia officinalis L.), quince (Cydonia oblonga Miller), pomegranate (Punica granatum L.), chamomile (Matricaria chamomilla), sumac (Rhus coriaria L.), and green tea (Comellasinensis)—which are among the supportive treatment products and may have antidiabetic potential, was investigated in vitro. For each plant sample, seven different specimens were collected. After washing the collected plant materials with pure water, they were dried in an oven at +45 °C until

constant weight was achieved. For plant extraction, 80% ethanol–water (v/v) was used. Standard kits (from Sigma-Aldrich) were used for the analysis. Standard kits of the enzymes Ketohexokinase, Alpha-amylase, Alpha-glucosidase, dipeptidyl peptidase-4, and Aldose reductase were used in the analysis of the extracts. The variance analyses of the obtained findings were carried out using the SPSS 15.0 computer program. Within the scope of the study, although pomegranate peel, sumac fruit, green tea leaf, quince leaf, chamomile flower, and sage plants showed inhibition in terms of alpha-glucosidase, amylase, ketohexokinase, aldose reductase, and dipeptidyl peptidase enzymes, the difference among them was not found to be statistically significant ($p > 0.05$).

Keywords: Antidiabetic activity, Plant extracts, Enzyme inhibition, diabetes.

GİRİŞ

Diyabet, yaşadığımız yüzyılın en önemli sağlık sorunlarından biri olarak nitelendirilmektedir. Yapılan incelemelerde her 100 erişkinden yaklaşık 9unun (%8.8) diyabetli olduğu görülmüştür.üresel bazda sağlık harcamalarının %12si (673 milyar dolar) diyabet için kullanılm (World Health Organization, 2021). Oral olarak kullanılan sentetik antidiyabetik bazı ilaçlar hasta popülasyonunda direncin oluşmasından duyarlılığın azalmasına kadar değişebilen bazı dezavantajlara sahiptirler. Özellikle farklı etki mekanizmasına sahip olan bu ilaçlara rağmen diyabetik hastaların ancak yarısı hedef glisemik değerlere ulaşabilmektedir. projenin sonuçları DM nin tedavisinde yeni bakış açısı oluşturabilir. Doğal ürünler, özellikle bitkisel kökenli olanlar, umut vaat eden öncü adayları keşfetmek için ana kaynak oluşturmakta ve gelecek ilaç geliştirme programlarında hayati bir rol oynamaktadır. Kolay ulaşılabilirlik, düşük maliyet ve en az yan etki, bitki bazlı preparasyonların mevcut tedavilerin anahtar oyuncusu olmasını sağlamaktadır (Salehi ve ark., 2019). Ayrıca, birçok bitki istenmeyen yan etkilerden arınmış güçlü farmakolojik etkilere sahip biyoaktif kimyasalların zengin bir kaynağını sağlamaktadır. Sunulan tez çalışmasında ülkemiz coğrafiyasında yetişen söz konusu bitkilerin antidiyabetik aktivitelerinin araştırılması, bu yönde yeni tedavi ürünlerinin ortaya çıkmasına adaylık oluşturma potansiyeli taşımaktadır. \Dünya Sağlık Örgütü tüm üye ülkelere kendi ülkelerinin yerel ilaçlarını aktif olarak tanıtmalarını tavsiye etmiştir. Eski literatürde tarif edilen geleneksel bitki ürünlerinin modern tıpta kullanımı, çoğu durumda bilimsel kanıtların ve açıklamaların eksik olmasından muzdariptir. Sunulan tez önerisi fitoterapik ürünlerin etkinliğinin araştırmalarına katkı sağlamaktadır. Diğer yandan Söz konusu bitkilerin analizlerinin yapılması Anadolu halkının beslenmesinde şifalı olarak yer alan bu bitki bileşenlerinin ortaya konulması ve kıyaslanması, projenin özgün değerini oluşturmaktadır.

MATERYAL VE METOT

Bu çalışmada materyal olarak kullandığmız örnekler Türkiye coğrafyasında yetişen ve çeşitli şekillerde ve sıklıkla antidiyabetik etkisinden dolayı halk arasında kullanılan ve yenilebilen 6 bitkiden oluşmaktadır.. Bitki örnekleri yöredeki halk pazarlarından toplanmıştır. Bitkilerin sistematik olarak teşhisi:Türkiye Florası adlı esere bağlı kalarak yapılmıştır (Davis, 1985). Çalışmamızda örnek 6 Bitkilerin yerel isimleri ile bilimsel isimleri şöyledir: Ada çayı (Salvia officinalis L.), Ayva (Cydonia oblonga Miller), Nar (Punica granatum L.), Papatya (Matricaria chamomilla), Sumak (Rhus coriaria L.), Yeşil çay (Comellasinensis) bitkının farklı bölgelerden ve her örnek için farklı 7 numune halinde hazırlanamıştır.Toplanan bitki örnekleri iyice normal su ve sonra saf suyla yıkadıktan sonra +45 °C de etüvde ağırlık sabitleninceye kadar kullanılmıştır. Bitki ekstraktların yapılmasında (%80 etanol-su (v/v)) kullanılmıştır (Önem ve ark., 2020). Analiz için Standart kitler (Sigma-Aldrich'ten) satın alınmıştır. Ekstraktların analizinde Ketohexokinaz, Alfa-Amilaz, Alfa-glikozidaz, dipeptidil peptidaz-4, Aldoz redüktaz enzimin standart kitleri kullanılmıştır (Zengin ve ark., 2016). Elde edilen bulguların varyans analizleri SPSS 15.0 bilgisayar programı kullanılarak gerçekleştirilmiştir. Çoklu grupların karşılaştırılması varyans analizi (ANOVA) yapılarak POST-ho testler ile belirlenmiştir.

Çalışmada bitkilerin kullanılan kısımları bu şekildedir: Ada çayı (Toprak ustu kısımlar), Ayva (Yaprak), Nar (Kabuk), Papatya (Yaprak ve çiçek), Sumak (Meyve), Yeşilçay (Yaprak) Bitkilerin yerel isimleri ile bilimsel isimleri şöyledir: Ada çayı (Salvia officinalis L.), Ayva (Cydonia oblonga Miller), Nar (Punica granatum L.), Papatya (Matricaria chamomilla), Sumak (Rhus coriaria L.), Yeşil çay (Comellasinensis).

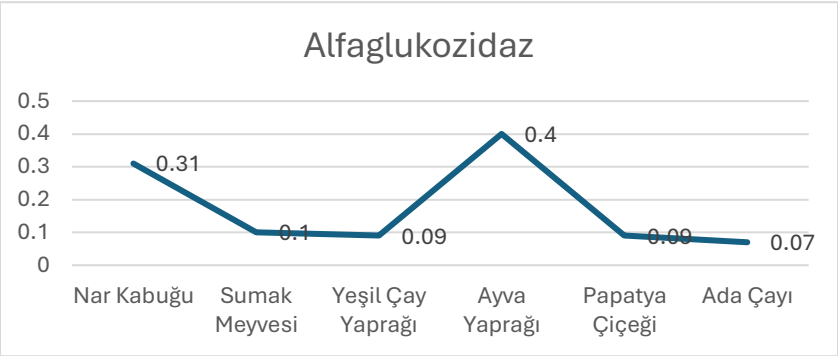
BULGULAR

Tablo 1 de gösterildiği gibi araştırma kapsamında yer alan nar kabuğu, sumak meyvesi, yeşil çay yaprağı, ayva yaprağı, papatya çiçeği ve ada çayı bitkileri alfaglukozidaz, amilaz, ketoheksokinaz, aldoseredultaz ve dipeptidil piptidaz enzimleri bakımından istatistiksel olarak anlamlı farklılık göstermemektedir ($p>0,05$). Enzim Değerlerinin Bitki Türlerine Göre İncelenmesi ise her bir enzime ait olacak şekilde grafikler ile sunulmuştur.

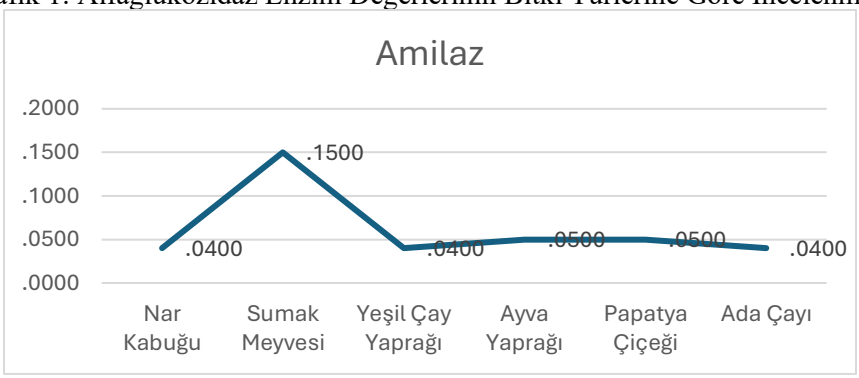
Tablo 1. Alfaglukozidaz, Amilaz, Ketoheksokinaz, Aldoseredultaz ve Dipeptidil Piptidaz Enzimlerinin Bitki Türlerine Göre İncelenmesi

	Bitki	Medyan	Min	Maks	Ki-Kare	p değeri
Alfaglukozidaz	Nar Kabuğu	0,31	1,8	4,0	11,169	0,148
	Sumak Meyvesi	0,10	0,9	1,9		
	Yeşil Çay Yaprağı	0,09	0,9	1,0		
	Ayva Yaprağı	0,40	0,8	4,6		
	Papatya Çiçeği	0,09	0,7	1,0		
	Ada Çayı	0,07	0,7	0,8		
Amilaz	Nar Kabuğu	0,04	0,4	0,6	6,200	0,287
	Sumak Meyvesi	0,15	1,4	8,2		
	Yeşil Çay Yaprağı	0,04	0,3	1,06		
	Ayva Yaprağı	0,05	0,5	0,7		
	Papatya Çiçeği	0,05	0,4	0,6		
	Ada Çayı	0,04	0,4	1,5		
Ketoheksokinaz	Nar Kabuğu	0,80	1,4	1,22	13,504	0,119
	Sumak Meyvesi	0,124	1,24	2,835		
	Yeşil Çay Yaprağı	0,131	1,22	1,399		
	Ayva Yaprağı	3,354	1,15	3,4649		
	Papatya Çiçeği	0, 871	0,87	0,957		
	Ada Çayı	1,091	0,99	1,151		
Aldosereduktaz	Nar Kabuğu	0,336	0,7	0,7	6,231	0,284
	Sumak Meyvesi	0,07	0,7	0,7		
	Yeşil Çay Yaprağı	0,08	0,55	0,84		
	Ayva Yaprağı	0,54	0,67	0,81		
	Papatya Çiçeği	0,07	0,61	0,74		
	Ada Çayı	0,068	0,65	0,70		
Dipeptidil piptidaz	Nar Kabuğu	0,125	0,10	1,5	7,466	0,188
	Sumak Meyvesi	0,16	0,10	2,0		
	Yeşil Çay Yaprağı	0,09	0,09	1,1		
	Ayva Yaprağı	0,14	0,10	1,5		
	Papatya Çiçeği	0,10	0,10	1,0		
	Ada Çayı	0,10	0,08	1,2		

$p<0,05$, Kruskal Wallis H Testi



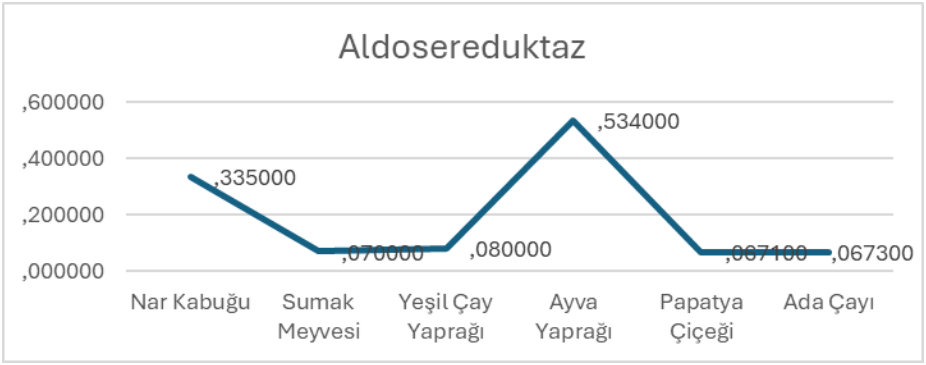
Grafik 1. Alfaglukozidaz Enzim Değerlerinin Bitki Türlerine Göre İncelenmesi



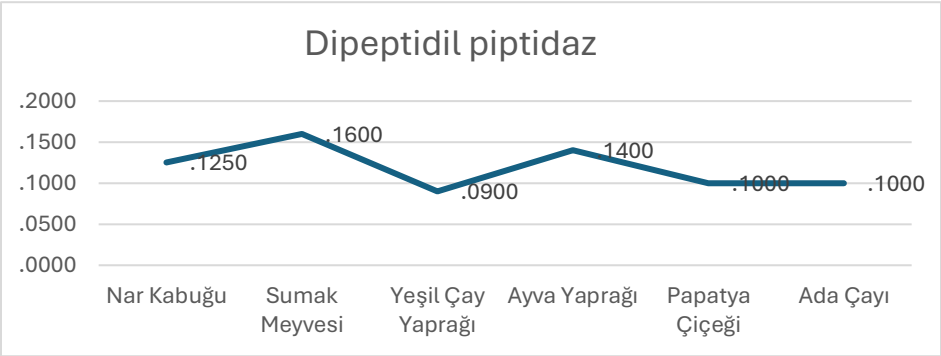
Grafik 2. Amilaz Enzim Değerlerinin Bitki Türlerine Göre İncelenmesi



Grafik 3. Ketoheksokinaz Enzim Değerlerinin Bitki Türlerine Göre İncelenmesi



Grafik 4. Aldoseredultaz Enzim Değerlerinin Bitki Türlerine Göre İncelenmesi



Grafik 5. Dipeptidil Piptidaz Enzim Değerlerinin Bitki Türlerine Göre İncelenmesi

TARTIŞMA

Yapılan bu çalışmada beş hedef enzim olan alfa-glukozidaz, amilaz, ketoheksokinaz, aldosereduktaz ve dipeptidil peptidazın (DPP-4) antidiyabetik potansiyelleri, halk arasında antidiyabetik bitki olarak bilinen nar kabuğu, sumak meyvesi, yeşil çay yaprağı, ayva yaprağı, papatya çiçeği ve ada çayı üzerinde araştırılmıştır. Araştırma kapsamında yer alan nar kabuğu, sumak meyvesi, yeşil çay yaprağı, ayva yaprağı, papatya çiçeği ve ada çayı bitkileri alfaglukozidaz, amilaz, ketoheksokinaz, aldoseredultaz ve dipeptidil piptidaz enzimleri bakımından istatistiksel olarak anlamlı farklılık göstermemektedir. ($p>0,05$), Elde edilen bilgiler doğrultusunda, altı bitkinin ortak biyoaktif bileşikler ve fenolik profillere sahip olduğu çıkarımı yapılmaktadır. Yapılan çalışmalarda, çalışmamız kapsamında yer alan nar kabuğu, sumak ve yeşil çay gibi polifenol açısından zengin bitkilerin, karbonhidrat sindirim enzimleri üzerinde ellagik asit, gallik asit, kateşin ve flavonoidler vasıtasıyla benzer inhibitör etki gösterdiği bildirilmiştir (Zengin ve ark., 2016; Chakrabartty ve ark., 2022). Yapılan diğer çalışmalarda ise , benzer şekilde yüksek antioksidan kapasitesine sahip ayva, papatya ve ada çayı yapraklarının da DPP-4 ve aldose redüktaz gibi enzimler üzerinde içerdikleri quercetin glikozitlerinin, uçucu yağ bileşenlerinin ve kafeik asit türevlerin sayesinde inhibisyon potansiyeline sahip olduğu gösterilmiştir (Hwang ve ark., 2018; Rutkowska ve ark., 2023). α-glukozidaz ve α-amilaz enzimler Lamiaceae familyasına ait bitkiler olduğundan, inhibitör etki mekanizması iki enzimde ise benzer olduğu çalışmalarda bildirilmiştir (Etsassala ve ark., 2022; Gök ve ark., 2019). Yapılan çalışmalar ile uyumlu olarak bitkilerin biyokimyasal özeliklerinin benzer olması, çalışmamızdaki bitkiler arasında içerdikleri enzimler açısından istatistiksel olarak belirgin fark olmadığı bulgusu desteklenmktedir.

Bununla birlikte, elde edilen sonuçlar bu bitkilerin antidiabetik aktivitesinin tamamen eşdeğer olduğu anlamına gelmemektedir. Bitkilerdeki biyoaktif bileşiklerin ekstraksiyon yöntemi, çözücü tipi, fenolik konsantrasyon, mevsimsel değişim ve yetişme koşulları gibi faktörlere bağlı olarak değişebildiği bilinmektedir. Dolayısıyla daha büyük örneklem grupları, farklı ekstrakt tipleri ve saf bileşiklerin karşılaştırıldığı ileri analizlerle bitkiler arasındaki ince biyokimyasal farklılıkların daha net ortaya konulması mümkündür.

SONUÇ

Sonuç olarak, bu çalışma halk arasında antidiyabetik olarak bilinen altı bitkinin antidiyabetik potansiyelleri olan alfa-glukozidaz, amilaz, ketoheksokinaz, aldosereduktaz ve dipeptidil peptidazın (DPP4) enzim aktiviteleri açısından benzer etki düzeyine sahip olduğu göstermekte ve bu bitkilerin fonksiyonel gıda veya tamamlayıcı tedavi alanında ortak antidiyabetik etkiye sahip olabileceğini ortaya koymaktadır

TEŞEKKÜR

Bu çalışmanın planlanması ve yürütülmesi sürecindeki değerli akademik yönlendirmeleri için danışmanım Prof. Dr. Cevat Nisbet'e teşekkür ederim.

KAYNAKLAR

Alkhatib, A., Tsang, C., Tiss, A., et al. (2017). Functional foods and lifestyle approaches for diabetes prevention and management. Nutrients, 9, 1310–1318.

Chakrabartty, I., Mohanta, Y. K., Nongbet, A., et al. (2022). Exploration of Lamiaceae in cardiovascular diseases and functional foods: Medicine as food and food as medicine. Frontiers in Pharmacology, 13, 894814. https://doi.org/10.3389

Davis, P. H. (1965–1985). Flora of Turkey and the East Aegean Islands. Edinburgh University Press, Edinburgh, UK.

Etsassala, N. G. E. R., Badmus, J. A., Marnewick, J. L., Egieyeh, S., Iwuoha, E. I., Nchu, F., & Hussein, A. A. (2022). Alpha-Glucosidase and alpha-amylase inhibitory activities, molecular docking, and antioxidant capacities of Plectranthus ecklonii constituents. Antioxidants, 11(2), 378. https://doi.org/10.3390/antiox11020378

Gök, H. N., Deliorman Orhan, D., Erdoğan Orhan, İ., Orhan, N., & Aslan, M. (2019). Evaluation of enzyme inhibitory and antioxidant activity of some Lamiaceae plants. Journal of Research in Pharmacy, 23(4), 749–758.

Hwang, S. H., Wang, Z., Guillen Quispe, Y. N., Lim, S. S., & Yu, J. M. (2018). Evaluation of aldose reductase, protein glycation, and antioxidant inhibitory activities of bioactive flavonoids in Matricaria recutita L. and their structure-activity relationship. Journal of Diabetes Research, 2018, 3276162. https://doi.org/10.1155/2018/3276162

Önem, E., Sarısu, H. C., & İbrahim, B. (2020). The effect of Rheum ribes L. extracts on bacterial communication and antibacterial activity. Süleyman Demirel Üniversitesi Sağlık Bilimleri Dergisi, 11(4), 436–442.

Park, C., & Lee, J. S. (2013). Mini review: Natural ingredients for diabetes which are approved by Korean FDA. Biomedical Research (India), 24(1), 164–169.

Rutkowska, M., et al. (2023). Anti-diabetic potential of polyphenol-rich fruits from the rose family: Focus on DPP-4 and α-glucosidase inhibition. Nutrients, 15(17), 3756. https://doi.org/10.3390/nu15173756

World Health Organization. (2021). World health statistics 2021: Global health indicators. Geneva: WHO.

Zengin, G., Nithiyanantham, S., Locatelli, M., et al. (2016). Screening of in vitro antioxidant and enzyme inhibitory activities of different extracts from two uninvestigated wild plants: Centranthus longiflorus subsp. longiflorus and Cerinthe minor subsp. *auriculata*. *European Journal of Integrative Medicine, 8*(3), 286–292.

ORAL PRESENTATION

Evaluation of Bax expression in colorectal tumors and adjacent healthy tissues

Zuhal Tuncbilek[1*] (*ORCID: https://orcid.org/0000-0002-6510-0884*), Hakkı Coskun[2] (*ORCID: https://orcid.org/0000-0001-7913-8325*), Gonca Kabak[3] (*ORCID: https://orcid.org/0009-0004-2430-5076*)

[*1]Sivas Cumhuriyet University, Yıldızeli Vocational School, Department of Chemistry and Chemical Processing Technologies, Sivas, Türkiye.
[2] Sivas Cumhuriyet University, Faculty of Medicine, Department of General Surgery, Sivas, Türkiye.
[3] Sivas Cumhuriyet University, Faculty of Medicine, Department of Medical Biochemistry, Sivas, Türkiye.

*Corresponding author e-mail: zuhaltuncbilek@cumhuriyet.edu.tr

Abstract

Colorectal cancer refers to tumors of the colon or rectum that emerge from the abnormal expansion of glandular epithelial cells. Colorectal cancer is characterized by a complex molecular pathogenesis involving dysregulation of cellular stress responses, DNA damage pathways, and apoptosis. Bax, a pro-apoptotic member of the B-cell leukemia/lymphoma 2 protein (BCL-2) family, plays a critical regulatory role by promoting mitochondrial outer membrane permeabilization and initiating the intrinsic apoptotic cascade. Alterations in Bax expression have been associated with tumor progression, treatment response, and resistance mechanisms in previous studies. The aim of this study was to comparatively evaluate Bax gene expression in colorectal cancer tissues and adjacent non-tumorous tissues from the same individuals. Tumor tissues and matched adjacent healthy tissues were collected from 30 patients undergoing colorectal cancer surgery. Following tissue homogenization, total RNA was isolated, and cDNA synthesis was performed. Bax gene expression was quantified using real-time quantitative PCR with GAPDH as the internal reference gene. Ct values were analyzed using the $\Delta\Delta C_t$ method, and tumor–healthy paired samples were statistically compared. Fold-change values and related statistical analyses were calculated using appropriate methods. The analysis revealed no significant difference in Bax gene expression between tumor tissues and matched adjacent healthy tissues. Both ΔΔCt values indicated that Bax expression remained stable across paired samples. Fold-change analysis further confirmed the absence of a marked increase or decrease in Bax levels in tumor tissues. The lack of differential Bax expression between tumor and healthy tissues suggests that mitochondrial apoptotic signaling may not be significantly modulated through Bax in this patient cohort. Evaluating Bax together with additional apoptotic markers and expanding the sample size may provide a more comprehensive understanding of its role in colorectal cancer biology.

Keywords: Bax, colorectal cancer, qPCR, gene expression, apoptosis

Introduction

Colorectal cancer (CRC) is one of the most rapidly increasing malignancies worldwide and represents a major global health burden. According to data from the World Health Organization, CRC is among the most commonly diagnosed cancers in both men and women and remains one of the leading causes of cancer-related mortality despite significant advances in diagnosis and treatment [1]. Aging, dietary habits, obesity, sedentary lifestyle, genetic predisposition, and inflammatory bowel diseases are important factors contributing to CRC development. However, the presence of risk factors alone cannot fully explain the disease; tumor formation reflects a multistep pathological transformation that begins in normal colonic epithelial cells and progressively increases genomic instability [2]. The adenoma–carcinoma sequence, a well-established model of CRC pathogenesis, demonstrates that sequential genetic and epigenetic alterations drive cellular transformation. Mutations in tumor suppressor genes and oncogenes such as APC, KRAS, and p53, along with DNA methylation, histone modifications, and microsatellite instability, play critical roles in this process [2]. These molecular events lead to enhanced cellular proliferation, impaired DNA repair mechanisms, and the development of resistance to programmed cell death (apoptosis). In particular, disruption of apoptosis allows tumor cells with accumulated genomic damage to survive, contributing to one of the fundamental hallmarks of cancer: sustained proliferative capacity [3]. Apoptosis is a tightly regulated form of programmed cell death that enables the systematic elimination of cells in response to

physiological or pathological stimuli. It plays a vital role in maintaining tissue homeostasis and ensures the removal of cells that harbor unrecoverable genetic damage, oxidative stress, or severe DNA lesions. Failure or suppression of apoptotic pathways allows genetically unstable cells to continue proliferating, thereby promoting tumor initiation and progression [3]. Within this context, the Bcl-2 protein family serves as a central regulator in determining cell fate. The Bcl-2 family consists of both anti-apoptotic (Bcl-2, Bcl-xL, Mcl-1) and pro-apoptotic (Bax, Bak, Bid, Bad) proteins that control mitochondrial outer membrane permeability in the intrinsic apoptotic pathway [4]. Anti-apoptotic members protect the cell against death signals, whereas pro-apoptotic members initiate cell death. Bax (Bcl-2–associated X protein) is one of the key pro-apoptotic effectors responsible for mitochondrial outer membrane permeabilization, subsequent cytochrome-c release, and activation of the caspase cascade [5]. Bax exists in an inactive cytosolic form under physiological conditions; however, upon apoptotic stimulation, it undergoes conformational change, translocates to the mitochondria, oligomerizes, and initiates apoptosis [6].Downregulation of Bax expression, loss of protein function, or defects in transcriptional or translational regulation contribute significantly to the development of apoptosis resistance in CRC. Indeed, Bax gene mutations are frequently observed in microsatellite instability–high CRC cases, suggesting a link between Bax alterations and specific molecular subtypes of CRC [7]. Moreover, a reduced Bax/Bcl-2 ratio is associated with resistance to cell death signals, increased tumor aggressiveness, and poor therapeutic response. Since many chemotherapeutic agents exert their cytotoxic effects by inducing Bax-dependent apoptosis, alterations in Bax levels are closely associated with chemotherapy resistance [8]. Therefore, evaluating Bax expression in tumor tissues and comparing it with adjacent normal colonic tissues is crucial for understanding how apoptotic mechanisms are altered during CRC development. Identifying these differences not only contributes to elucidating the biological processes underlying tumorigenesis but also aids in the discovery of diagnostic and prognostic biomarkers. In addition, determining the expression levels of apoptosis-related proteins such as Bax may serve as a fundamental step toward developing personalized treatment strategies for CRC patients [9]. Particularly in chemoresistant CRC subtypes, monitoring Bax expression may provide clinically significant insights for treatment planning. In conclusion, investigating Bax expression in colorectal tumors and adjacent healthy tissues offers valuable information regarding the alterations in apoptotic pathways during cancer development. Such studies have the potential to enhance understanding of CRC biology, identify new therapeutic targets, and improve prognostic evaluation. Given the central role of apoptosis resistance in cancer progression, detailed examination of Bax in CRC carries substantial scientific and clinical importance [9].

Material and Method

Study population

In this study, both tumor tissue and surrounding healthy tissue samples were obtained during surgical resection from 30 patients diagnosed with colorectal cancer. Each patient was administered a detailed demographic and clinical information form, including age, gender, height, weight, body mass index (BMI), smoking status, alcohol consumption, presence of hypertension, presence of diabetes, history of hyperlipidemia, cardiovascular disease status, family history of cancer, and dietary habits. The study included patients diagnosed with colorectal cancer and scheduled for surgical treatment, those aged 18 years or older, and those who fully answered all questions on the patient information form. Patients who had previously received chemotherapy, radiotherapy, or immunotherapy, those in the metastatic stage who had not undergone surgery for the primary tumor, and those for whom a sufficient quantity or quality of tissue samples could not be obtained were excluded. This study was approved by the Sivas Cumhuriyet University Non-Interventional Clinical Research Ethics Committee (Decision No: 2025-07/78, Date: July 10, 2025). The purpose and scope of the study were explained to all participants, and written informed consent was obtained from each individual.

Tissue Homogenization

In order to obtain high-quality RNA from both tumor and adjacent healthy colon tissues, tissue homogenization was performed in accordance with standard molecular biology protocols. Tissue samples collected during surgery were immediately placed in RNA later solution to preserve RNA integrity and stored at -80°C until analysis. Approximately 30–50 mg of tissue was transferred to RNase-free tubes. Homogenization ensured that the samples

were suitable for RNA isolation; during this process, the samples were kept on ice and RNase-free conditions were maintained to prevent RNA degradation. The resulting homogenates were incubated briefly at room temperature to facilitate the dissociation of nucleoprotein complexes and were then prepared for subsequent RNA isolation.

RNA Isolation and cDNA Synthesis

Total RNA was isolated from homogenized tumor and healthy colon tissue samples using the FavorPrep™ Total RNA Isolation Kit II, following the manufacturer's protocol. All procedures were carried out under RNase-free conditions, with careful attention to preserving RNA integrity. The concentration and purity of the isolated RNA were measured, and only samples with an A260/A280 ratio between 1.8 and 2.1 were used. Complementary DNA (cDNA) was synthesized using the reverse transcription reagents provided in the OneScript Plus cDNA Synthesis Kit (abm), and the resulting cDNA was stored under appropriate conditions for subsequent gene expression analyses.

Gene Expression

PCR analysis was performed according to the protocols of the NucleoGene Biotechnology (Turkey) kit. Subsequently, BAX gene expression was assessed using quantitative RT-PCR (qPCR) in accordance with the kit instructions, with GAPDH serving as the internal reference gene.

Statistical analysis

SPSS Software (Version 22.0) was used for statistical analysis of the data in our study. PCR data were analyzed using Student's t-test, which tests the significance of the difference between two means. The error level was set at 0.05. Descriptive statistics are presented as mean ± SD or as n (%), where appropriate.

Results

Demographic Characteristics

Colorectal cancer tissue and surrounding healthy colon tissue were surgically removed from 30 patients with colorectal cancer included in the study. A questionnaire was administered to the patients. Statistical analysis of the questionnaire data revealed that 46.7% of the total population was female and 53.3% male. Alcohol consumption was assessed as 16.7% of the individuals consuming alcohol, while 83.3% did not. 43.3% of the individuals were smokers, and 53.3% were non-smokers. Clinical data indicated that 46.7% of the individuals had hypertension and 26.7% had diabetes. Hyperlidemia was also observed in 16.7% of the individuals, and cardiovascular disease was observed in 30.0%. 46.7% of the patients had a family history of cancer. Additionally, the patients' dietary habits were examined, and it was found that 13.3% of them had a balanced diet, 26.7% a meat-based diet, 23.3% a pastry-based diet, and 36.7% a fruit and vegetable-based diet (Table 1).

Tablo 1. Clinical and demographic information of individuals from whom colorectal cancer and adjacent healthy tissues were collected

	N (%)
Gender	
Female	14 (46.7)
Male	16 (53.3)
Alcohol	
Consuming	5 (16.7)
Non-consuming	25 (83.3)
Smoking	
Smoker	13 (43.3)
Non-smoker	16 (53.3)
Hypertension status	
Hypertensive	14 (46.7)
Non-hypertensive	16 (53.3)
Presence of Diabetes	
Yes	8 (26.7)
No	22 (73.3)
History of Hyperlipidemia	
Yes	5 (16.7)
No	25 (83.3)
Cardiovascular Disease	
Yes	9 (30.0)
No	21 (70.0)
Cancer History	
Yes	14 (46.7)
No	16 (53.3)
Dietary Habits	
Balanced diet	4 (13.3)
Meat-based diet	8 (26.7)
High-pastry	7 (23.3)
Fruit and vegetable based diet	11 (36.7)

When the gender-based evaluation was made, the mean and standard deviation were taken into account, and the female age was recorded as 57.36 ± 9.44, height was 160.43 ± 8.39, weight was 71.64 ± 15.93, and BMI was 27.89 ± 6.30. The male age was noted as 58.44 ± 10.64, height was 171.75 ± 8.68, weight was 74.25 ± 13.13, and BMI was 26.62 ± 4.49 (Table 2).

Tablo 2. Gender based comparison of anthropometric measures

Gender	Characteristics	Mean±Std. Deviation
Female	Age	57.36 ± 9.44
	Height	160.43 ± 8.39
	Weight	71.64 ± 15.93
	BMI	27.89 ± 6.30
Male	Age	58.44 ± 10.64
	Height	171.75 ± 8.68
	Weight	74.25 ± 13.13
	BMI	26.62 ± 4.49

qPCR analysis

Bax gene expression levels were measured in colon cancer and compared to surrounding healthy tissues. The data revealed a 1.92-fold increase in Bax gene expression in colon cancer tissues compared to surrounding healthy colon tissues, but this increase was not significant ($p<0.05$) (Figure 1).

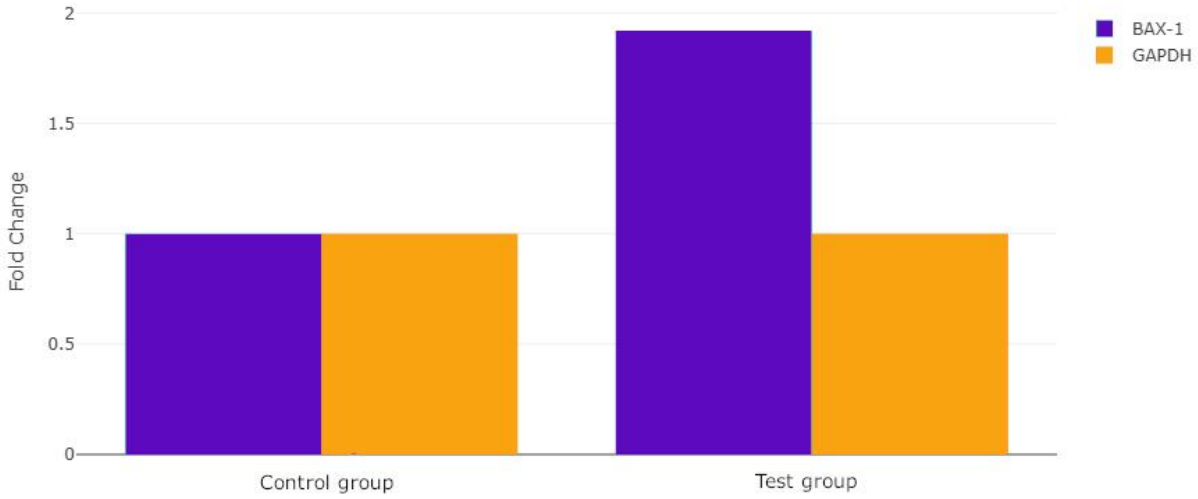


Figure 1. Fold change graph of Bax-1 expression in colon cancer tissues (test group) and healthy surrounding colon tissues (control group)

Discussion

In this study, we looked at BAX gene expression in colorectal cancer (CRC) tissues and nearby non-tumor tissues. We found no significant difference between the two groups. BAX, a key pro-apoptotic member of the BCL-2 family, is expected to decrease in tumors that have developed resistance to apoptosis. However, our findings show that BAX expression in CRC is not consistently changed, which is in line with previous research indicating considerable variability in apoptotic regulation among patients. Several studies have noted increased BAX expression during the adenoma-carcinoma sequence. Cobanoglu et al. observed that BAX immunoreactivity increases from normal mucosa to adenoma and carcinoma stages, suggesting that high BAX levels may accompany early tumor transformation [10]. In contrast, Jansson and Sun found a significant drop in BAX expression from primary tumors to metastatic lesions, indicating that the loss of BAX might help late-stage progression [11]. This difference reflects the biological variety of CRC and suggests that BAX dysregulation may depend on tumor stage, histological grade, genetic background, or microenvironmental factors. Lower BAX levels have also been linked to aggressive tumor features. Studies show that low BAX expression is associated with lymphovascular invasion, deeper tumor infiltration, and shorter overall survival [12, 13]. Sturm et al. further reported that low BAX expression, especially in the presence of p53 mutations, predicts worse outcomes in patients with removed liver metastases [14]. These findings support the idea that impaired pro-apoptotic signaling contributes to tumor growth and resistance to treatment. On the other hand, several studies found no significant link between BAX levels and significant clinicopathological variables. Khodapasand et al. reported that BAX or BCL-2 did not correlate with tumor stage or grade, while the BAX/BCL-2 ratio offered more relevant prognostic information [15]. This ratio reflects the balance between pro- and anti-apoptotic factors and is seen as a better marker of apoptotic sensitivity. From this view, unchanged BAX expression in our study might indicate increases in anti-apoptotic molecules like BCL-2 or BCL-xL, or issues with BAX activation instead of its transcription. Additionally, apoptotic regulation in CRC goes beyond just BAX transcription. Factors like mitochondrial priming, BAX movement to mitochondria, post-translational modifications, and p53 functionality significantly affect apoptosis [16, 17]. Wild-type p53 directly activates BAX to induce mitochondrial outer membrane permeabilization, but in p53-mutant CRC, BAX cannot be activated effectively even if its expression stays stable [18, 19]. Therefore, tumors may show unchanged or even higher BAX levels while still resisting apoptosis. Moreover, the tumor microenvironment—including hypoxia, cytokines, inflammatory factors, stromal interactions, and immune infiltration—affects apoptotic pathways independently of BAX [20, 21]. Overall, our findings support the growing view that BAX alone is not enough as a biomarker for CRC diagnosis, prognosis, or predicting treatment response. A multi-parameter approach that includes BAX, BCL-2 family proteins, p53 mutation status, caspase activation, and mitochondrial apoptotic signaling offers a better understanding of tumor biology [22]. Future studies should use multi-omic strategies that combine transcriptomics, proteomics, and functional apoptotic tests to better characterize the apoptotic landscape of CRC [23].

Conclusion

In conclusion, while BAX has a key role in intrinsic apoptosis, its expression shows considerable variability in colorectal cancer. The lack of significant differences between tumor and nearby healthy tissues in our study aligns with findings that apoptotic dysregulation in CRC stems from a complex network rather than just isolated changes in BAX. A thorough evaluation of apoptosis-related mechanisms may help improve biomarker discovery and tailored treatment strategies.

References

1.Bray F, et al., Global cancer statistics: worldwide burden of colorectal cancer. 2018. 68(6): p. 394–424.
2.Fearon ER, Vogelstein B., A genetic model for colorectal tumorigenesis. 1990. 339(6220): p. 198–201.
3.Hanahan D, Weinberg RA., Hallmarks of cancer: biological capabilities acquired during tumor development. 2000. 100(1): p. 57–70.
4.Youle RJ, Strasser A., The BCL-2 protein family and the regulation of apoptosis. 2008. 13(1): p. 1–6.
5.Oltvai ZN, et al., Bcl-2 heterodimerizes with Bax to regulate cell death. 1993. 74(6): p. 609–619.
6.Westphal D, et al., Bax activation and mitochondrial dynamics in apoptosis. 2011. 15(7): p. 645–657.
7.Rampino N, et al., Bax mutation and its role in colorectal cancer progression. 1997. 89(3): p. 385–391.
8.Williams GT, Smith CA., Bax/Bcl-2 ratio as a determinant of chemoresistance. 1993. 72(2): p. 349–356.

9.Khoury R, et al., Apoptosis-related markers as prognostic indicators in colorectal carcinoma. 2002. 95(4): p. 310–318.
10.Cobanoglu, B., et al., Immunohistochemical analysis of Bax and AIF in colorectal tumors. 2015. 8(9): p. 16071.
11.Jansson, A. and X.-F.J.J.o.c.o. Sun, Bax expression decreases significantly from primary tumor to metastasis in colorectal cancer. 2002. 20(3): p. 811-816.
12.Pryczynicz, A., et al., Bax protein may influence the invasion of colorectal cancer. 2014. 20(5): p. 1305.
13.Ogura, E., et al., Prognostic significance of Bcl-2, Bcl-xL/S, Bax and Bak expressions in colorectal carcinomas. 1999. 6(2): p. 365-374.
14.Sturm, I., et al., Analysis of the p53/BAX pathway in colorectal cancer: low BAX is a negative prognostic factor in patients with resected liver metastases. 1999. 17(5): p. 1364-1364.
15.Khodapasand, E., et al., Is Bax/Bcl-2 ratio considered as a prognostic marker with age and tumor location in colorectal cancer? 2015. 19(2): p. 69.
16.Youle, R.J. and A.J.N.r.M.c.b. Strasser, The BCL-2 protein family: opposing activities that mediate cell death. 2008. 9(1): p. 47-59.
17.Llambi, F., D.R.J.C.o.i.g. Green, and development, Apoptosis and oncogenesis: give and take in the BCL-2 family. 2011. 21(1): p. 12-20.
18.Chipuk, J.E., et al., Direct activation of Bax by p53 mediates mitochondrial membrane permeabilization and apoptosis. 2004. 303(5660): p. 1010-1014.
19.Aubrey, B.J., et al., How does p53 induce apoptosis and how does this relate to p53-mediated tumour suppression? 2018. 25(1): p. 104-113.
20.Baig, S., et al., Potential of apoptotic pathway-targeted cancer therapeutic research: Where do we stand? 2016. 7(1): p. e2058-e2058.
21.Hanahan, D. and R.A.J.c. Weinberg, Hallmarks of cancer: the next generation. 2011. 144(5): p. 646-674.
22.Adams, J.M., S.J.C.D. Cory, and Differentiation, The BCL-2 arbiters of apoptosis and their growing role as cancer targets. 2018. 25(1): p. 27-36.
23.Galluzzi, L., et al., Molecular mechanisms of cell death: recommendations of the Nomenclature Committee on Cell Death 2018. 2018. 25(3): p. 486-541.

ORAL PRESENTATION

Biogenic nanotechnology's role in the treatment of Parkinson's disease: How can we benefit more from food?

Ibrahim Ertugrul Yalcin[1*] (*ORCID: https://orcid.org/0000-0003-3140-7922*),
Zeynep Mercanoglu[2] (*ORCID: https://orcid.org/0009-0008-1688-3692*)

[*1]Bahcesehir University, Faculty of Engineering and Natural Sciences, Department of Civil Engineering, İstanbul, Türkiye
[2]Bahcesehir University, Faculty of Health Sciences, Department of Nutrition and Dietetics, İstanbul, Türkiye

*Corresponding author e-mail: ibrahimertugrul.yalcin@bau.edu.tr

Abstract

Parkinson's disease ranks second among the most prevalent chronic neurodegenerative diseases worldwide and grows faster than other neurodegenerative diseases. Notably, there are only symptomatic treatments available for patients with Parkinson's disease, which is dopaminergic replacement therapy, and no disease-modifying treatments are currently available. Moreover, the therapeutic effectiveness of many central nervous system drugs, including levodopa, is reduced by the restrictive nature of the blood–brain barrier, which prevents sufficient penetration into neural tissues. However, due to their small size and high surface area-to-volume ratio, nanoparticles can cross the blood–brain barrier, thereby providing benefits for the treatment of neurodegenerative diseases, including Parkinson's disease, by increasing drug delivery across the blood–brain barrier. Over the years, some phytochemicals from natural sources have provided a valuable resource for identifying potential therapeutic compounds for Parkinson's disease treatment, due to their anti-inflammatory and antioxidant properties. Recently, nanotechnology has emerged to address the drawbacks of these phytochemicals, including their poor bioavailability, poor stability under physiological conditions, and limited prolonged impact. Furthermore, after ingestion, nanoparticles initially interact with the gastrointestinal epithelium and the gut microbiota, which, through the gut–brain axis, may play a role in the initiation and progression of neurodegenerative diseases. Given that people with Parkinson's disease's dietary habits influence their gut microbiome, it is crucial to consider nutrition when implementing strategies combining phytochemicals and nanoparticles for Parkinson's disease treatment. In addition, among people living with Parkinson's disease, the awareness regarding the use of nanoparticles in the treatment of Parkinson's disease is relatively low. Therefore, our chapter aims to gather up-to-date data to explore a potential treatment strategy for Parkinson's disease and encourage future research endeavors.

Keywords: Nanotechnology, medicinal and aromatic plants, Parkinson's disease, biogenic nanoparticles, phytochemicals, nutritional intervention

INTRODUCTION

Neurodegenerative diseases (NDs) are a variety of complex diseases that are characterized by neuronal loss and progressive degeneration of various parts of the nervous system (Agnello & Ciaccio, 2022). Parkinson's disease (PD) ranks second among the most prevalent chronic NDs worldwide and grows faster than other NDs (Pirovano et al., 2025). Neural inclusions, including Lewy bodies and Lewy neurites, along with cell loss in the substantia nigra and other parts of the brain, are the hallmarks of PD pathology. Since Lewy bodies are composed mostly of aggregated and misfolded α-synuclein, PD is categorized as a synucleinopathy (Tolosa et al., 2021). Notably, there are only symptomatic treatments available for patients with PD, which is dopaminergic replacement therapy, and no disease-modifying treatments are currently available (Pirovano et al., 2025). Moreover, the therapeutic effectiveness of many central nervous system drugs, including levodopa, is reduced by the restrictive nature of the blood–brain barrier, which prevents sufficient penetration into neural tissues (Gao et al., 2025). However, due to their small size and high surface area-to-volume ratio, nanoparticles (NPs) can cross the blood–brain barrier

(BBB), thereby providing benefits for the treatment of NDs, including PD, by increasing drug delivery across the BBB (Li et al., 2025; Hassan et al., 2025; Gao et al., 2025). Over the years, some phytochemicals from natural sources have provided a valuable resource for identifying potential therapeutic compounds for PD treatment, due to their anti-inflammatory and antioxidant properties (Doke et al., 2019). Polyphenols' clinical utilization is hindered by their poor distribution in the human body, despite having medicinal properties (Sardarabadi et al., 2024). PD symptom severity and disease progression are influenced by diet quality through various mechanisms, including its effect on gut microbiome composition (Baghaei et al., 2025). Recently, nanotechnology has emerged to address the drawbacks of these phytochemicals, including their poor bioavailability, poor stability under physiological conditions, and limited prolonged impact (Paul et al., 2023). Furthermore, after ingestion, NPs initially interact with the gastrointestinal epithelium and the gut microbiota (GM), which, through the gut–brain axis, may play a role in the initiation and progression of NDs (Li et al., 2025). Therefore, our chapter aims to gather up-to-date data to explore a potential treatment strategy for Parkinson's disease and encourage future research endeavors.

LITERATURE ON PARKINSON'S DISEASE, PHYTOCHEMICALS, AND NANOTECH-NOLOGY

The pathogenesis of PD is correlated with different factors such as gut dysbiosis, increased oxidative stress, neuroinflammation, and mitochondrial dysfunction (Grancharova et al., 2024). Phytochemicals (e.g., polyphenols, carotenoids, flavonoids, and terpenoids) have been found to modulate the GM, as well as implement neuroprotective, anti-inflammatory, and antioxidant effects, which could benefit the management and prevention of neurological conditions (Jaberi et al., 2024). Diet plays a key role in modulating the GM composition, and various dietary patterns can cause specific bacteria to be less or more abundant. Consequently, changes in the abundance of the microorganisms can influence gut permeability and produce anti-inflammatory or pro-inflammatory metabolites. Plant-based diets have been shown to diminish inflammation and oxidative stress, which are two important factors related to NDs, including PD. Therefore, a healthy diet rich in nutrients with antioxidants and anti-inflammatory properties may play a crucial role in preventing the risk of Parkinsonism. The Mediterranean Diet (MeDiet) is a rich dietary pattern in terms of antioxidants and anti-inflammatory agents (Bisaglia, 2023). In addition to the MedDiet, the MIND (Mediterranean-DASH Diet Intervention for Neurodegenerative Delay) and DASH diets are also plant-based diets focusing on vegetables and fruits, legumes, nuts, whole grains, poultry, fish, and low intake of saturated fats as well as red meats (Agarwal et al., 2018).

NPs are described as particles that have a diameter of 10 – 1000 nanometers (Elikaee et al., 2025). There are several techniques for NP synthesis, and among them, green synthesis has gained popularity due to its simplicity and therapeutic potential. Green synthesis is done with natural and environmentally friendly compounds, including plant extracts in order to reduce metal ions and create NPs. Additionally, bioactive plant compounds on the surface of NPs enhance their therapeutic effectiveness. Recently, metal ions that mimic enzyme activities have been increasingly utilized in various nanoparticle applications (Grancharova et al., 2024). For example, gold NPs (AuNPs) functionally mimic endogenous antioxidant enzymes and may diminish oxidative stress. They demonstrate activities like superoxide dismutase by eliminating O_2, exhibit catalase-like functions by converting H_2O_2 into water and oxygen, and show peroxidase activity by catalyzing oxidation reactions of peroxides and such molecules (Grancharova et al., 2024). Additionally, AuNPs have been demonstrated to convert NADH to NAD+, which plays a crucial role in cellular energy production (Huang et al., 2005; Grancharova et al., 2024). In a Drosophila melanogaster rotenone-induced preclinical model, the administration of green-synthesized ZnO NPs significantly reduced oxidative stress, likely due to their antioxidant effects and the restoration of endogenous antioxidant defence enzymes (Shabir et al., 2023).

Nanotechnology is becoming increasingly important in the food and pharmaceutical industries. For instance, nanoemulsions are used with herbal extracts, and others incorporate oils into food products. Nano-herbal formulations are the primary focus, which enhance the efficiency and delivery potential of therapeutic agents through nanotechnology (Shree et al., 2025). It promotes the integration of traditional herbal medicine with technology, focusing on the nutritional quality and functionality of nanoherbal formulations in the food industry (Awlqadr et al., 2025). Nanoherbal drugs may provide several benefits, but safety concerns remain significant. Due to their small size, they can react differently in the human body. Thus, thorough testing is essential (Farhang et al., 2025).

CONCLUSION

PD is a growing global health problem that affects the geriatric population more than others. Hence, it is crucial to explore promising symptomatic or, if possible, curative treatment options for PD to ameliorate the quality of life in people with PD. To our knowledge, research demonstrating a symptomatic or curative treatment option for PD via gut-mediated, food-based biogenic nanotechnology utilizing phytochemicals is lacking. In addition, among people living with PD, the awareness regarding the use of nanoparticles in the treatment of PD is relatively low. Since GM plays a role in PD development and an NP initially interacts with gut epithelium, this interaction may be used to enhance the bioavailability of phytochemicals, such as curcumin, and enable them to demonstrate their antioxidant and neuroprotective effects more effectively. Therefore, as preclinical research is more abundant than clinical human trials, more research is needed in this area to elucidate the relationship between food-phytochemical-nanoparticle combined therapies for PD.

REFERENCES

Agarwal, P., Wang, Y., Buchman, A. S., Holland, T. M., Bennett, D. A., & Morris, M. C. (2018). MIND diet associated with reduced incidence and delayed progression of Parkinsonism in old age. *The Journal of nutrition, health and aging*, *22*(10), 1211-1215.
https://doi.org/10.1007/s12603-018-1094-5

Agnello, L., & Ciaccio, M. (2022). Neurodegenerative diseases: from molecular basis to therapy. *International journal of molecular sciences*, *23*(21), 12854.
https://doi.org/10.3390/ijms232112854

Awlqadr, F. H., Majeed, K. R., Altemimi, A. B., Hassan, A. M., Qadir, S. A., Saeed, M. N., ... & Abedelmaksoud, T. G. (2025). Journal of Agriculture and Food Research. *Journal of Agriculture and Food Research*, *19*, 101661. https://doi.org/10.1016/j.jafr.2025.101661

Baghaei, A., Kim, H. S., Dolhun, R., Sherzai, D., & Dashtipour, K. (2025). Review of the Effects of Lifestyle Modification on Parkinson's Disease. *American Journal of Lifestyle Medicine*, 15598276251384591. https://doi.org/10.1177/15598276251384591

Bisaglia, M. (2023). Mediterranean Diet and Parkinson's Disease. *International Journal of Molecular Sciences*, *24*(1), 42. https://doi.org/10.3390/ijms24010042

Doke, R. R., Pansare, P. A., Sainani, S. R., Bhalchim, V. M., Rode, K. R., & Desai, S. R. (2019). Natural products: An emerging tool in parkinson's disease. *IP Indian J. Neurosci*, *5*(3), 95-105. https://doi.org/10.18231/j.ijn.2019.014

Elikaee, S., Taylor, J. K., Carter, N. S., Dwarka, K. M., & Roberts, S. C. (2025). Biogenically Synthesized Nanoparticles as Emerging Therapeutics for Leishmaniasis: A Review of Recent Advances and Potential Promises. *International Journal of Nanomedicine*, 12467-12484. https://doi.org/10.2147/IJN.S550979

Farhang H. Awlqadr, Kithar Rasheed Majeed, Ammar B. Altemimi, Arkan Mohammed Hassan, Syamand Ahmed Qadir, Mohammed N. Saeed, Aryan Mahmood Faraj, Tablo H. Salih, Alaa Jabbar Abd Al-Manhel, Mazin A.A. Najm, Efstathia Tsakali, Jan F.M. Van Impe, Ahmed A. Abd El-Maksoud, Tarek Gamal Abedelmaksoud, Nanotechnology-based herbal medicine: Preparation, synthesis, and applications in food and medicine, Journal of Agriculture and Food Research, Volume 19, 2025, 101661, ISSN 2666-1543.
https://doi.org/10.1016/j.jafr.2025.101661

Gao, L., Wang, J., & Bi, Y. (2025). Nanotechnology for Neurodegenerative Diseases: Recent Progress in Brain-Targeted Delivery, Stimuli-Responsive Platforms, and Organelle-Specific Therapeutics. *International Journal of Nanomedicine*, 11015-11044.
https://doi.org/10.2147/IJN.S549893

Grancharova, T., Simeonova, S., Pilicheva, B., & Zagorchev, P. (2024). Gold nanoparticles in Parkinson's disease therapy: a focus on plant-based green synthesis. *Cureus*, *16*(2). https://doi.org/10.7759/cureus.54671

Hassan, S. H., Sharaf, I. A., Mohamed, A. S., Salama, M., Kamel, M. A., & Hafez, H. A. (2025). Green-Synthesized Silver Nanoparticles with Nigella sativa: A Multifaceted Approach against Parkinson's Disease in Rats via MicroRNA Modulation. *ACS Chemical Neuroscience*, *16*(19), 3801-3815. https://doi.org/10.1021/acschemneuro.5c00496

Huang, X., El-Sayed, I. H., Yi, X., & El-Sayed, M. A. (2005). Gold nanoparticles: Catalyst for the oxidation of NADH to NAD+. *Journal of photochemistry and photobiology B: biology*, *81*(2), 76-83. https://doi.org/10.1016/j.jphotobiol.2005.05.010

Jaberi, K. R., Alamdari-Palangi, V., Savardashtaki, A., Vatankhah, P., Jamialahmadi, T., Tajbakhsh, A., & Sahebkar, A. (2024). Modulatory Effects of Phytochemicals on Gut–Brain Axis: Therapeutic Implication. *Current Developments in Nutrition*, *8*(6), 103785.
https://doi.org/10.1016/j.cdnut.2024.103785

Kwon, D., Zhang, K., Paul, K. C., Folle, A. D., Del Rosario, I., Jacobs, J. P., ... & Ritz, B. (2024). Diet and the gut microbiome in patients with Parkinson's disease. *npj Parkinson's Disease*, *10*(1), 89. https://doi.org/10.1038/s41531-024-00681-7

Li, H., Wang, N., & Mao, X. (2025). Incidental vs. Engineered Nanoparticles in Alzheimer's and Parkinson's Disease: Pathological Pathways and Therapeutic Interventions. *Nano research*, 10-26599. https://doi.org/10.26599/nr.2025.94908055

Paul, K., Gowda, B. J., Damiri, F., Hemalatha, Y. R., Chandan, R. S., & Berrada, M. (2023). Nanophytomedicine and their applications: a brief overview 1. *Polymer Nanocomposites*, 83-94. https://doi.org/10.1201/9781003343912-6

Pirovano, E., Marino, F., Rossi, E., Gennari, A., Rasini, E., Uslenghi, M., ... & Cosentino, M. (2025). Modified Mediterranean diet effects on Parkinson's disease (MED-PARK): a single-centre randomised controlled trial protocol. *BMJ open*, *15*(10), e101946. https://doi.org/10.1136/bmjopen-2025-101946

Sardarabadi, H., Darvishi, M. H., Zohrab, F., & Javadi, H. (2024). Nanophytomedicine: A promising practical approach in phytotherapy. *Phytotherapy Research*, *38*(7), 3607-3644.
https://doi.org/10.1002/ptr.8230

Shabir, S., Sehgal, A., Dutta, J., Devgon, I., Singh, S. K., Alsanie, W. F., ... & Singh, M. P. (2023). Therapeutic potential of green-engineered ZnO nanoparticles on rotenone-exposed D. melanogaster (Oregon R+): Unveiling ameliorated biochemical, cellular, and behavioral parameters. *Antioxidants*, *12*(9), 1679. https://doi.org/10.3390/antiox12091679

Shree, J. N., Anuf, A. R., & Ahmad, S. (2025). Comparative Analysis of Traditional and Nano-Formulated Approaches in Viability, Targeted Delivery, and Patient Outcomes. In *Herbal Pharmacopeia* (pp. 375-392). CRC Press.

Tolosa, E., Garrido, A., Scholz, S. W., & Poewe, W. (2021). Challenges in the diagnosis of Parkinson's disease. *The Lancet Neurology*, *20*(5), 385-397.
https://doi.org/10.1016/S1474-4422(21)00030-2

ORAL PRESENTATION

Impair DNA Methyltransferases Gene DNMT1 Level and Alternated Immune Agents in Systemic Lupus Erythematosus of Iraqi Patients

Atheer Ahmed

University of Baghdad, Iraq

Abstract

New research results have revealed a worldwide decline in gene DNA methylation (*DNMT1*), resulting in reduced transcription-level expression of CD4 + T cells. This phenomenon is directly related to the development of systemic lupus erythematosus (SLE). The research also has investigated the impairing between total DNA methylation and DNA activity (cytosine-5) methyltransferase. 1 (DNMT1), which it does main role in the process of DNA methylation. It has showed significant chang and reduction in *DNMT1* gene expression in PBMC for SLE patients. To measure this, real-time polymerase chain reaction (RT-PCR) was used to identify the entire genome and purified peripheral mononuclear blood cells (PBMC) in both individuals with systemic lupus erythematosus (SLE) and healthy individuals. It has showed significant reduction in *DNMT1* gene expression in PBMC for SLE patients. Consequently, appearance results singed for, the expression of IL-4 transcript in SLE patients was significantly decreased compared to that in healthy controls. The indirect impact of an underlying DNA hypomethylation status on patients' response can be considered plausible. This impact may involve the inhibition of mRNA levels of DNA methyltransferases, especially during periods of significant disease activity. Consequently, it can lead to changes in various immune components, including increased levels of IgM. Autoimmune diseases may be caused with DNA methylation disfunctions in various cell types that it have included SLE disease ,it maybe the differentiation and developmental events in genomic patterns of methylation and the immune responses that become dysregulated in specific autoimmune diseases.

Keywords: Systemic lupus erythematosus, DNA methyltransferase. IL-4, IgM

Key messages: Systemic lupus erythematosus (SLE) is a systemic autoimmune disease with multisystem involvement and is associated with chang of morbidity and mortality involved maltreated genetic, immunological, endocrine, and environmental factors

Introduction :

DNA hypomethylation seems to assume a significant role in related to the pathogenesis of SLE. which have been reported to be a plausible causative agent for systemic lupus erythematosus (SLE) [1] .
SLE is a complex autoimmune disease characterized by apoptosis cell surrender, a signature of interferon expression (IFN) of PBMC have made marker for breakdown of peripheral tolerance mechanisms responsible to generate autoantibodies attach tissues and organs damage [2,3]. T cells play a key role in causing SLE, amplifying inflammation by secreting pro-inflammatory cytokines, helping B cells generate autoantibodies, and maintaining the disease through the accumulation of self-reactive memory T cells [4,5].

Patients with (SLE) often experience various clinical manifestations, commonly linked to tissue damage resulting from the accumulation of antibodies and autoimmune complexes [6,7]. These deposits contribute to the observed skin, mucous membrane, kidney, joint, nervous system, lung, and heart lesions. There is a strong belief that disease-related factors interact with genomic and epigenomic processes.
Epigenomic mechanisms, including identifiable DNA methylation patterns, play a vital role [8,9], This implies that cells possess the ability to modify their methylation through methyltransferases. In SLE patients, these mechanisms may significantly impact the hypomethylation function of *DNMT* cluster genes. This impact is associated with certain pathological aspects and abnormal histone modifications, leading to the suppression of gene transcription responsible for initiating and perpetuating pro-inflammatory responses, particularly within their

CD4+ T cells [10,11]. In individuals with systemic lupus erythematosus (SLE), the activity of the *DNMT1* gene, which plays a role in regulating methylation, has been found to be reduced in peripheral blood mononuclear cells (PBMC) be compared with healthy control subjects. [12,13].

This abnormal methylation pattern may pose a risk for certain autoimmune conditions, particularly affecting women of reproductive age. The disrupted methylation observed in SLE development is believed to stem from a breakdown in immunological tolerance and the interplay between susceptibility genes for SLE and diverse environmental factors, ultimately leading to the generation of harmful autoantibodies [14,15].

However, the *DNMT1* gene is situated within replication foci and consistently operates during cell division through various mechanisms. It functions both as a maintenance enzyme crucial for preserving the stability of existing DNA methylation patterns and as a vital cofactor for de novo methyltransferase in Embryonic stem cells [16,17].

The study's aim:

The research demonstrated its collaborative role in identifying key immune factors linked to hypomethylation, particularly in SLE Iraqi patients with a malfunctioning *DNMT1* gene expression. Furthermore, investigations focused on the behaviour of IL-4 and IgM, pinpointing SLE risk variants, have the potential to enhance the arsenal of prognostic and therapeutic biomarkers for SLE (18,19).

Methods:

Patients with (SLE) were diagnosed by clinical symptoms and screening markers (Anti-double-stranded DNA, C3, C4, Antinuclear Antibody ANA) and LN (approved by biopsy) for 15 male, 45 female and 60 healthy male and female (control) in medical city hospital in Baghdad. All patients under treatment daily doses 7.5 mg of prednisone. (PBMCs) were isolated from Iraqi SLE patients and healthy controls. DNA extraction use (Quick-DNA™ Blood MiniPrep Catalog) . Reverse transcription and real-time quantitative polymerase chain reaction (RT-qPCR) analyzes RNA extraction (Direct-zol™ RNA MiniPrep, R2051, ZYMO RESEARCH/USA.) were used to determine DNMT1 and IL-4 mRNA expression level in Cycling Program (Enzyme activation 95 °C, Denaturation 95 °C, annealing 60.0 °C, Extension72.0 °C) holed 40 cycles (figure.1). IgM level marker for SLE therapeutic detection was used radial immunodiffusion plate,

Table (1): The specific primers of *IL-4*, DNMT-*1* and housekeeping genes.

Primer	Sequence (5′–3′)	Tm (°C)	GC (%)
Forward *Il-4*	5'- AGGCTGAAAGGGGGAAAGC - 3'	62	57
Reverse *Il-4*	5'- CTGTTCACCTCAACTGCTCC - 3'	55.755 55	55
Forward *Dnmt1*	5'-CGG TTC TTC CTC CTG GAG AAT GTC A- 3'	60.1	52
Reverse *Dnmt1*	5'- CAC T G A TAG CCC ATG CGG ACC A - 3'	61.5	59.1
Forward Reference gene	5'- AATGGGCAGCCGTTAGGAAA - 3'	57.2	50
Reverse Reference gene	5'- GCGCCCAATACGACCAAATC- 3'	56.9	55

Results and discussion:

1- Exclusion criteria and SLE biomarkers:

This variable concentration of hormones, genetic defection environmental conditions and different populations under different conditions involving menstrual cycling, chronic stress, corticosteroid medication, oral contraceptives and the replacement of steroid hormones a protein which is virtually absent from a healthy person's serum. they have participated for lack of self-tolerance has contributed to autoantibody production, pro-inflammatory and cytokine inflammatory. Significantly, last autoimmunity responses were surely caused Global methylation up regulation [20].

Extremely, samples have be obtained from hundred subjects for both genders were enrolled some of in this study, who attended Baghdad Teaching Hospital/Medical City Iraq. The subjects were involved on group consists of patients suffering SLE male and female aged (16-46) years and group consists of healthy individual's male and female at age (19-47) years (control group) [21]. The patients have Systemic lupus erythematosus were diagnosed by clinical symptoms and screening markers (Anti-double-stranded DNA, Antinuclear Antibody ANA, C3, C4). All patients under treatment daily doses 7.5 mg of prednisone.

2- *DNMT1* gene

Human genetic variations in the background lead to immunodeficiency. *DNMT1* exhibits a preference for hemimethylated DNA as its substrate, methylating newly replicated DNA only when the template nucleotides are already methylated [22,23]. *DNMT1* is consistently expressed and plays a crucial role in preserving overall methylation levels after DNA replication. These findings indicate the existence of distinct epigenetic Susceptibility sites that predispose to or are associated with skin manifestations in SLE. These loci demonstrate significantly higher methylation levels compared to those in healthy controls. Moreover, SLE patients display a notable reduction in *DNMT1* transcript levels, ranging from a 5.9 to 2.7-fold decrease as observed (Figure. 2).

3- ***IL-4*** **transcripted level**

Defected *DNMT1* transcript level is one mechanism involved is the aberrant activation of certain Th2 cell subsets, such as CD4+ T cells, and the expression of specific molecules on their surface, including CD38 [24,25]. CD4+ T cells and abnormalities in CD38 are a subset of Th2 cells that play a crucial role in regulating immune responses and contribute to the pathogenesis of SLE by producing various cytokines. last defects can disrupt normal cellular functions, including Th2 cell activation and cytokine production. One cytokine that has been deregulated in SLE pathogenesis is interleukin-4 (IL-4) (26,27,28).

The findings indicate a change in the levels of IL-4 transcripts from a 4.2 to 1.07-fold decrease as determined with competitive PCR assay. This shortage was observed in the SLE group, as shown in (Figure 2).

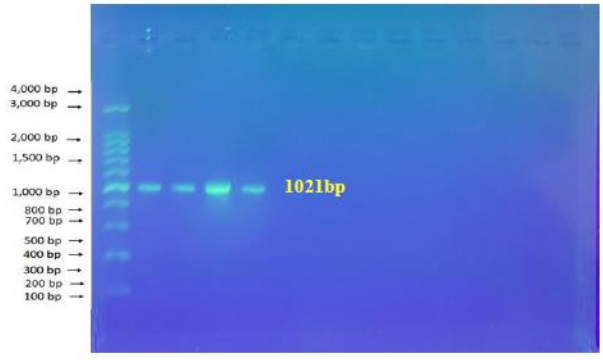


Figure (1): Gel electrophoresis *Dnmt1* gene 1021bp in peripheral blood mononuclear cells (PBMC) of SLE patients .1% agarose gel

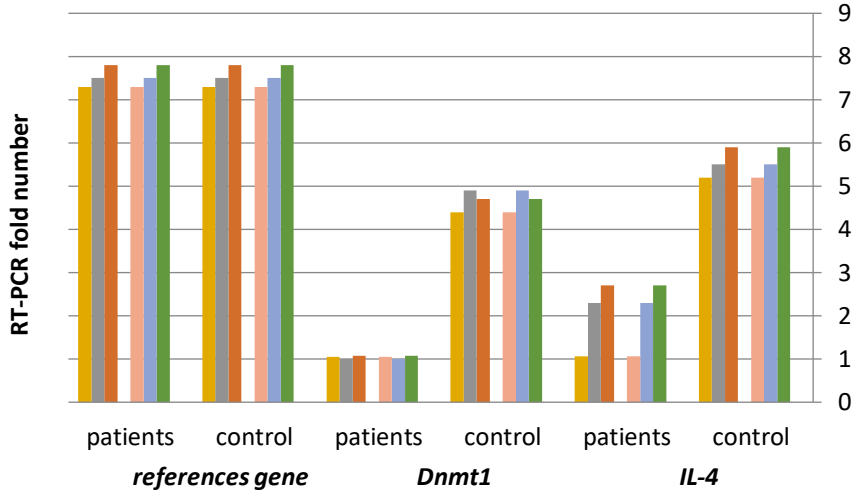


Figure (2): Quantitative analysis of *Dnmt1* and *IL-4* expression in PBMC from healthy adults (control) and SLE patients. The results represent the lower number of genes cDNA molecules comprated with references gene

4- IgM level in SLE disease:

IL-4, a significant cytokine, plays a crucial role in promoting B-cell differentiation. Blocking IL-4 has been shown to prevent this process. Research conducted on patients with systemic lupus erythematosus (SLE) suggests that there is a breakdown in the regulatory mechanisms of B cells at both the central Bone marrow checkpoints and terminal checkpoints during the naïve transition B cell stage. Moreover, individuals with SLE exhibit impaired function of naive B cells, indicating a reduced activity level [28, 29, 34].

The IL-4 transgene appears to have a beneficial effect, likely achieved by defected regulating of Th2 responses involved in autoantibody production in our SLE patient model. However, this down-regulation doesn't affect IgM antibody responses to T cell–independent antigens or auto-IgG [30,31] , as evidenced by the lack of significant impact on serum levels of IgM antibodies. Interestingly, the results show a rise in IgM activity on erythrocyte surfaces do anti- IgG (Figure 3), despite this.

In SLE, human lupus serums exhibit two distinct sets of IgM antibodies. Remarkably, the presence of an IgM reaction on the surfaces of red blood cells in the patient's serum is associated with a decrease in the severity of the disease [32,33,34] representing a potential therapeutic biomarker.

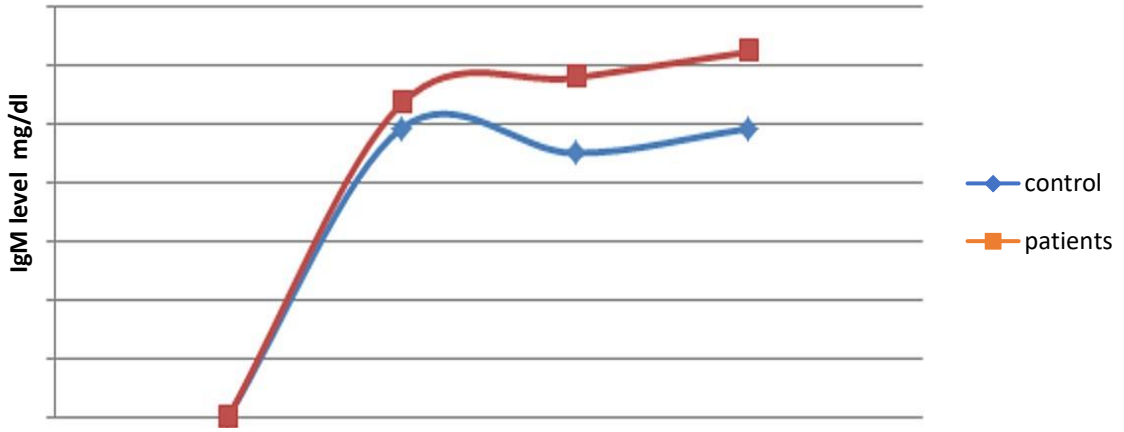


Figure (3) : IgM level in SLE disease

Conclusion:

DNA methylation is a key mechanism for epigenetic modifications, and we will focus on its detection. Specifically, we'll pay attention to how DNA methylation functions in various cell types associated with autoimmune diseases, the genomic patterns of methylation involved in differentiation and developmental events, and the immune responses that become dysregulated in specific autoimmune diseases. Additionally, It may be would explore the possibility of addressing whether IgM-induced immune deviation can offer protection against ongoing disease. Understanding this could pave the way for developing novel therapeutic approaches for managing SLE and other related human autoimmune diseases.

Ethical approval

The ethics committee of the Department of Biology - Collage of sciences – University of Baghdad gave its approval to this study before it began. Every patient was asked to provide their informed consent, approved by in medical city hospital in Baghdad**.**

Acknowledge

My profound thanks and appreciation to Dr.Noor Al-huda Khaleel for his support and assistance in Department of basic sciences – Collage of Nursing – University of Baghdad**.**

Financial support and sponsorship

Nil.

Conflicts of interest

There are no conflicts of interest

References: -

[1] Ruaa H. A., Asmaa M. Saud, Mohammed H. A.. Evaluation of Interferon Alpha (IFN-α) in Women with Systemic Lupus Erythematosus in Iraq. Iraqi Journal of Science, 2022; 63, 10: 4225-4233 D.doi.org/10.24996/ijs.2022.63.10.9

[2] B. Sojod, C. Pidorodeski Nagano, G. M. Garcia Lopez, A. Zalcberg, S. M. Dridi, and F. Anagnostou, "Systemic Lupus Erythematosus and Periodontal Disease: A Complex Clinical and Biological Interplay," Journal of Clinical Medicine, 2021; 10, 9: 1957 .dio: 10.3390/jcm10091957

[3] A. K. Horst, K. G. Kumashie, K. Neumann, L. Diehl, and G. Tiegs, "Antigen presentation, autoantibody production, and therapeutic targets in autoimmune liver disease," Cellular & molecular immunology, 2021; 18 (1): 92-111, doi: 10.1038/s41423-020-00568-6. .

[4] Min Chen , Yingdi Meng , Xiaoqiong Shi and *et al* ,Identification of ENTPD1 as a novel biomarker linking allergic rhinitis and systemic lupus erythematosus, Sci Rep, 2024 ;14(1):18266. doi: 10.1038/s41598-024-69228-3.
[5] Kallas R, Li J, Goldman DW, *et al* .. Trajectory of damage accrual in systemic lupus erythematosus based on ethnicity and socioeconomic factors. J Rheumatol 2022; 49:1229–35. doi:10.3899/jrheum.211135
[6] Wang Y-F, Zhang Y, Lin Z, and *et al* .. Identification of 38 novel loci for systemic lupus erythematosus and genetic heterogeneity between ancestral groups. Nat Commun 2021; 12:772. doi:10.1038/s41467-021-21049-y
[7] Coit P, Renauer P, Jeffries MA, Merrill JT, Mc-Cune WJ, and *et al*: Renal involvement in lupus is characterized by unique DNA methylation changes in naive CD4+ T cells. J Autoimmun .61: 29–35 (2015a). doi: 10.1016/j.jaut…
[8] Coit P, Yalavarthi S, Ognenovski M, Zhao W,Hasni S,and *et al*: Epigenome profiling reveals significant DNA demethylation of interferon signature genes in lupus neutrophils. J Autoimmun 58: 59–66 (2015b).doi: 10.1016/j.jaut.2015.01.004.
[9] Roberta M. , Clemens Z. , Marco A. , and *et al* . emerging role of epigenetics in human autoimmune disorders.Clin Epigenetics, 2019; 26(11):34. doi: 10.1186/s13148-019-0632-2.
[10] Canas CA, Canas F, Bonilla-Abadia F, Ospina FE, Tobon GJ: Epigenetics changes associated to environmental triggers in autoimmunity. Autoimmunity.2016; 49(1): 1–11. doi: 10.3109/08916934.2015.1086996.
[11] Yasuto Araki and Toshihide Mimura. 2024.Epigenetic Dysregulation in the Pathogenesis of Systemic Lupus Erythematosus.*Int. J. Mol. Sci.* 2024, 25(2), 1019.doi.org/10.3390/ijms25021019
[12] Sutanto, H.; Yuliasih, Y. Disentangling the Pathogenesis of Systemic Lupus Erythematosus: Close Ties between Immunological, Genetic and Environmental Factors. *Medicina* ;2023 ;59(6):1033. doi: 10.3390/medicina59061033.
[13] Li, H.; Boulougoura, A.; Endo, Y.; Tsokos, G.C. Abnormalities of T cells in systemic lupus erythematosus: New insights in pathogenesis and therapeutic strategies. *J. Autoimmun.* 132:102870. doi: 10.1016/j.jaut.2022.102870.
[14] Zhu H, Mi W, Luo H, Chen T, Liu S, Raman I, Zuo X, Li QZ. Whole-genome transcription and DNA methylation analysis of peripheral blood mononuclear cells identified aberrant gene regulation pathways in systemic lupus erythematosus. Arthritis Res Ther. 2016. 13;18:162. doi: 10.1186/s13075-016-1050-x.
[15] Teruel M, Sawalha AH. Epigenetic Variability in Systemic Lupus Erythematosus: What We Learned from Genome-Wide DNA Methylation Studies.Curr Rheumatol Rep. 2017 ;19(6):32. doi: 10.1007/s11926-017-0657-5
[16] Teruel M, Alarcón-Riquelme ME. The genetic basis of systemic lupus erythematosus: What are the risk factors and what have we learned..J Autoimmun. 2016; 74:161-175. doi: 10.1016/j.jaut.2016.08.001.
[17] Yeung KS, Chung BH, Choufani S, and *et al*. Genome-Wide DNA Methylation Analysis of Chinese Patients with Systemic Lupus Erythematosus Identified Hypomethylation in Genes Related to the Type I Interferon Pathway.PLoS One. 2017 ;12(1): e0169553. doi: 10.1371/journal.pone.0169553.
[18] Hagberg N, Rönnblom L. Systemic lupus erythematosus – a disease with a dysregulated type I interferon system. Scand J Immunol 2015; 82:199–207. dio-10.1111/sji.12330.
[19] Chen L, Morris DL, Vyse TJ. Genetic advances in systemic lupus erythematosus: an update. Curr Opin Rheumatol 2017; 29:423–33. dio -10.1097/BOR.0000000000000411.
[20] Liul l., Yin X., and et al . several critical cell types, tissues, and pathway era implicated in genome wide association studies for systemic lupus erythematosus. G3 (Genes,Genome,Genetics), 2016; 6(6): 1503-1511.dio.org/10.1534/G3.116.027326.
[21] Noor K. A., Kadhim K. G., Ali A. A.2021. Evaluation of Human Epididymis Protein 4 (HE4) and Some Related Biochemical Factor Levels for Patients with Systemic Lupus Erythematosus and Lupus Nephritis. The council of College of Science for Women – University of Baghdad –Department of Chemistry/ (Biochemistry). PhD Thesis.
[22] M. Ehrlich, M. Lacey. DNA methylation and differentiation: silencing, upregulation and modulation of gene expression. Epigenomics., 2013,5 (5) : 553-568.doi: 10.2217/epi.13.43.

[23] Yi Zhan, Yu Guo, Qianjin Lu. Aberrant Epigenetic Regulation in the Pathogenesis of Systemic Lupus Erythematosus and Its Implication in Precision Medicine. Cytogenet Genome Res 2016; 149:141–155.dio: 10.1159/000448793.

[24] Manuel Rojas, Yhojan Rodríguez, *et al*. Juan-Manuel Anaya Cytokines and Inflammatory Mediators in Systemic Lupus Erythematosus. EMJ Rheumatol. 2018;5(1):83-92. doi:org/10.33590/emjrheumatol/10311457.

[25] Zayda L. Piedra-Quintero, Zachary Wilson, Porfirio Nava and Mireia Guerau-de-Arellano. CD38: An Immunomodulatory Molecule in Inflammation and Autoimmunity. Frontiers in Immunology. 2020, 11: 59795.doi: 10.3389/fimmu.2020.597959.

[26] Viegas MS, Silva T, Monteiro MM, do Carmo A, Martins TC. Knocking out of CD38 accelerates development of a lupus-like disease in lpr mice. Rheumatology .2011; 50:1569–77. doi: 10.1093/rheumatology/ker178.

[27] Katsuyama E, Suarez-Fueyo A, Bradley SJ, Mizui M, Marin AV, Mulki L, et al. The CD38/NAD/SIRTUIN1/EZH2 Axis Mitigates Cytotoxic CD8 T-Cell Function and Identifies Patients with SLE Prone to Infections. Cell Rep .2020; 30:112–23. doi: 10.1016/j.celrep.2019.12.014.

[28] John D Mountz, Changming Lu, Shanrun Liu, Min Gao, Winn Chatham, Hui-Chen Hsu. IL-4 as a negative regulator of pathogenecity extracellular DN2 B –cells in SLE. Lupus Science & Medicine 2022;9(3): A1–A112. doi: 10.4049/jimmunol.2200409

[29] Renauer P, Coit P, Jeffries MA, Merrill JT, Mc-Cune WJ, et al: DNA methylation patterns in naive CD4+ T cells identify epigenetic susceptibility loci for malar rash and discoid rash in systemic lupus erythematosus. Lupus Sci Med,2015; 2:e000101 .

[30] Interleukin 4-driven reversal of self-reactive B cell anergy contributes to the pathogenesis of systemic lupus erythematosus. Systemic lupus erythematosus 2023;82, (11):1444-1454.

[31] Sugimura K and Hashiguchi S. Immunological characterization of M13 phage vaccine. Front. Immunol. Conference Abstract: 15th International Congress of Immunology (ICI).2013; 02: 00889.doi: 10.3389/conf.fimmu.2013.02.00889.

[32] Mourad A. .The book probing selected autoimmune diseases for focused perspectives. In *IntechOpen eBooks*.2023; doi.org/10.5772/intechopen.1000271.

[33] Guingand, A., Trolet, A., Daniel, D., Wagner, R., Flacher, V., Ritzenthaler, C., Poignavent, V., & Dumortier, H. (2023). Joint Conference of the Société Française d'Immunologie (SFI) and the Deutsche Gesellschaft für Immunologie (DGfI), Strasbourg, France. *European Journal of Immunology*,2023; *53*(S2). https://doi.org/10.1002/eji.202370300

[34] Nashrudin, K. N. M., Abidin, M. a. Z., Ng, S. E., Razali, *et al* . Deficiency Associated with Diffuse Mesangial Sclerosis Infantile Nephrotic Syndrome and Epstein–Barr Virus-Induced Hodgkin's Lymphoma. *Pediatric Allergy Immunology and Pulmonology*.2025;38(1): 11-20.doi.org/10.1089/ped.2024.0062.

ORAL PRESENTATION

Val-Trp dipeptidinin MCF-7 meme kanseri hücreleri üzerindeki sitotoksik etkisinin araştırılması

Gizem Akman[1*] (*ORCID: https://orcid.org/0000-0003-4301-5862)*

[*1]İstanbul Üniversitesi, Fen Fakültesi, Biyoloji Bölümü, İstanbul, Türkiye

*Sorumlu yazar e-mail: gizem.akman@istanbul.edu.tr

Özet

Triptofanın indol yapısını içeren valil-triptofan (Val-Trp) dipeptidleri, iyi bilinen biyoaktivitesi ve uygun çözünürlüğü, geçirgenliği ve biyoyararlanımı nedeniyle potansiyel antikanser ajanları olarak dikkat çekmektedir. Bu çalışmada, 24 ve 48 saatlik inkübasyondan sonra MTT testi kullanarak Val-Trp'nin insan meme kanseri MCF-7 hücreleri üzerindeki sitotoksik etkilerini araştırılmıştır. 1 mg/ml Val-Trp uygulanmış MCF-7 hücrelerinde 24 saatte %98 canlılık sağlarken, 48 saatte %52'ye belirgin bir düşüşe neden olmuştur. Bu bulgular, Val-Trp'nin MCF-7 hücreleri üzerinde zamana ve konsantrasyona bağlı sitotoksik etki gösterdiğini ve belirgin canlılık kaybının yalnızca en yüksek konsantrasyonda ve uzun süreli maruziyette gözlendiğini göstermektedir. Genel olarak, veriler Val-Trp'nin, özellikle meme kanseri hücre modelleri bağlamında, daha fazla antikanser değerlendirmesi için umut verici bir indol bazlı dipeptit iskeleti olarak potansiyelini desteklemektedir.

Anahtar Kelimeler: Valiltriptofan (Val-Trp), Dipeptit, Sitotoksisite, Antikanser

Investigation of the Cytotoxic Effect of the Val-Trp Dipeptide on MCF-7 Breast Cancer Cells

Abstract

Valyl-tryptophan (Val-Trp) dipeptides, which contain the indole structure of tryptophan, are attracting significant attention as potential anticancer agents due to their well-known bioactivity and favorable solubility, permeability, and bioavailability. In this study, the cytotoxic effects of Val-Trp on human breast cancer MCF-7 cells were investigated using the MTT assay after 24 and 48 hours of incubation. In MCF-7 cells treated with 1 mg/ml Val-Trp, cell viability was 98% at 24 hours, whereas a marked decrease to 52% was observed at 48 hours. These findings indicate that Val-Trp exerts time- and concentration-dependent cytotoxic effects on MCF-7 cells, and that a pronounced loss of viability is observed only at the highest concentration and with prolonged exposure. Overall, the data support the potential of Val-Trp as a promising indole-based dipeptide scaffold for further anticancer evaluation, particularly in the context of breast cancer cell models.

Keywords: Valyl-tryptophan (Val-Trp), Dipeptide, Cytotoxicty, Anticancer.

GİRİŞ

Triptofanın indol yapısını içeren valil-triptofan (Val-Trp) dipeptitleri, tıpta yaygın olarak kullanılan indol türevlerinin bilinen biyoaktivitesi nedeniyle, potansiyel antikanser etkileri açısından dikkat çekmektedir (Küçükbay ve ark., 2024). Yüksek çözünürlük, hücre zarından geçebilme ve biyoyararlanıma sahip bu dipeptitler, hücre yüzeyindeki reseptörlerle etkileşerek veya hücre içi sinyal ve düzenleyici yolaklara katılarak, terapötik etkilerini ortaya koymaktadır (Huang ve ark., 2017). Bu biyoyararlanım ve stabilite avantajları, Val-Trp gibi dipeptitlerin vücut içinde daha az parçalanmasını sağlar ve bu molekülleri hedefe yönelik tedaviler için daha uygun adaylar haline getirmektedir. Günümüzde, apoptoz indüksiyonu, mikrotübül bozulması ve anjiyogenez inhibisyonu gibi farklı mekanizmaları hedefleyen, daha az toksik ve maliyet açısından daha uygun yeni antikanser tedavilere duyulan ihtiyaç giderek artmaktadır. Bu bağlamda, peptitler, yeni terapötik yaklaşımlar geliştirilmesi için umut verici bir seçenek olarak öne çıkmaktadır. (González-Montoya, 2017).

Esansiyel bir amino asit ve çok sayıda doğal bileşiğin temel bileşeni olan triptofanın içsel biyolojik aktivitesi, Val-Trp dipeptitlerinin terapötik potansiyelini daha da artırmaktadır (Küçükbay ve ark., 2024). Özellikle, bu dipeptitler içindeki triptofan kalıntısının, Trp-Leu gibi diğer triptofan içeren dipeptitlerde gözlendiği üzere, anjiyojenik yolakların inhibisyonuna katkıda bulunduğu bildirilmiştir (Bose ve ark., 2022). Nitekim, çeşitli peptit-indol konjugatları, MCF-7 ve A549 gibi hücre hatlarında kayda değer antikanser aktiviteler göstermiş ve bu durum, indol grubunun farmakolojik profillere katkısını vurgulamıştır (Küçükbay ve ark., 2024). Ayrıca, valin gibi bir amino asidin triptofanın indol iskeletiyle birleştirilmesinin kanser hücrelerine karşı sitotoksisiteyi artırabildiği, bunun da sinerjistik etkilere işaret ettiği ileri sürülmektedir (Küçükbay ve ark., 2024). Bu artmış etkinlik, çoğu zaman, küçük hücreli akciğer karsinomu gibi hücre hatlarında sitotoksisiteyi anlamlı ölçüde iyileştirebilen indol halkasındaki çeşitli modifikasyonlara bağlanmaktadır (Offerman ve ark., 2017). Ayrıca peptitler; antimikrobiyal, antiinflamatuvar, antiviral ve antikanser özellikleri kapsayan geniş biyolojik aktivitelere sahip son derece işlevsel biyomoleküller olarak kabul edilmektedir (Borse ve ark., 2023). Bu geniş biyolojik etki yelpazesi, özellikle enzim inhibitörü ve ilaç taşıyıcısı olarak üstlendikleri roller nedeniyle, peptitleri ilaç keşfi açısından son derece cazip moleküller haline getirmektedir (Huang ve ark., 2017). Dipeptit-konjuge bileşiklerin, çeşitli insan kanser hücre tiplerine karşı yüksek in vitro etkinlik gösterdiği bildirilmiş olup, bu durum onların stabil ve etkili terapötik ajan adayları olarak öne çıkmasını sağlamaktadır (Borse ve ark., 2023). Bu stabilite, hücre zarını geçebilme kapasiteleriyle birlikte değerlendirildiğinde, dipeptitler hem hedeflenmiş ilaç taşıma sistemlerinde hem de onkolojide doğrudan terapötik ajan olarak kullanılabilecek umut verici adaylar olarak görülmektedir (Borse ve ark., 2023; Naglah ve ark., 2021).

Meme kanseri, dünya genelinde kadınlarda en sık görülen kanser tiplerinden biri olup, güncel tedavi seçeneklerine rağmen ilaç direnci, yan etkiler ve nüks gibi sorunlar yeni ve daha güvenli antikanser ajanların geliştirilmesini zorunlu kılmaktadır. İndol içeren dipeptitlerin antikanser potansiyeli çeşitli hücre hatlarında gösterilmiş olsa da, Val-Trp dipeptidinin MCF-7 meme kanseri hücreleri üzerindeki konsantrasyon ile zamana bağlı sitotoksik etkileri yeterince aydınlatılmamıştır. Bu çalışmada, Val-Trp'nin MCF-7 hücreleri üzerindeki etkilerini 24 ve 48 saatlik inkübasyon sürelerinde değerlendirilmesi ve buna bağlı olarak Val-Trp'nin indol bazlı bir antikanser molekülü olarak potansiyelinin ortaya koyulması amaçlanmıştır.

MATERYAL VE METOT

Hücre Hattı ve Kültür Koşulları

Bu çalışmada, insan meme adenokarsinom hücre hattı olan MCF-7 hücreleri kullanılmıştır. Hücreler, %10 fetal bovin serum (FBS) ve %1 penisilin/streptomisin içeren yüksek glikozlu DMEM besiyerinde, 37 °C'de, %5 CO_2 içeren nemlendirilmiş inkübatörde rutin olarak kültüre edilmiştir.

MTT Hücre Canlılığı Testi

Val-Trp dipeptidinin sitotoksik etkilerini değerlendirmek amacıyla MTT hücre canlılığı testi uygulanmıştır. Bu deney için MCF-7 hücreleri 96 kuyucuklu plaklara, 10^4/kuyucuk olacak şekilde ekilerek 24 saat inkübe edilmiştir. Val-Trp, stok konsantrasyonu 50 mg/ml olacak şekilde serumsuz besiyeri ile çözülmüştür. Hücreler, 0.1, 0.25 ve 1 mg/ml konsantrasyonlarında Val-Trp ile muamele edilerek 24 ve 48 saat süreyle inkübasyona bırakılmıştır. İnkübasyon sürelerinin sonunda, 20 µl MTT çözeltisi ilave edilerek, formazan kristallerinin oluşması için inkübe edilmiştir. Oluşan formazan kristalleri DMSO ile çözdürülmüş, absorbans değerleri mikroplaka okuyucu ile 570 nm dalga boyunda ölçülmüştür. Hücre canlılığı, kontrol grubuna göre yüzde (%) oranında hesaplanmıştır.

İstatistiksel Analiz

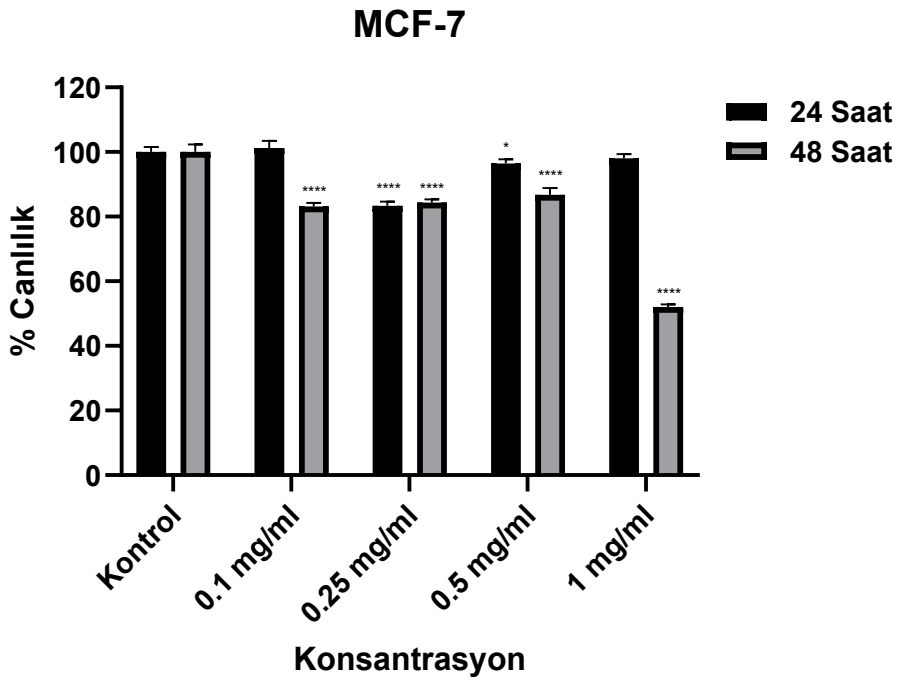
Elde edilen veriler, istatistiksel olarak iki yönlü varyans analizi (two-way ANOVA) ve post-hoc Tukey testi ile değerlendirilmiştir. Tüm sonuçlar ortalama ± standart sapma (SS) olarak ifade edilmiş ve $p < 0.05$ değeri istatistiksel olarak anlamlı kabul edilmiştir.

BULGULAR

MTT analizi sonuçları, Val-Trp'nin MCF-7 hücre canlılığı üzerinde zaman ve doza bağlı bir etki gösterdiğini ortaya koymaktadır (Şekil 1). 24 saat tedavi edilen MCF-7 hücrelerinde, 0.1 mg/ml Val-Trp uygulaması sonucunda hücre canlılığında hafif bir artış (%101,3) gözlemlenmiş, 0.25 mg/ml konsantrasyonunda ise canlılık %83,3'e düşerek kontrol grubuna kıyasla istatistiksel olarak anlamlı azalma göstermiştir ($p < 0,0001$). 0.5 mg/ml Val-Trp

uygulanan MCF-7 hücrelerinde, 24. saatte hücre canlılığında daha sınırlı ancak anlamlı bir azalma saptanmış, 1 mg/ml'de ise 24. saatte canlılık kontrol ile benzer seviyelerde (%98) kalmıştır.

48 saat Val-Trp uygulanan grupta ise düşük ve orta konsantrasyon uygulandığında (0.1–0.5 mg/ml) hücre canlılığının tüm gruplarda kontrole göre anlamlı azalma izlenmiştir. En belirgin sitotoksik etki 1 mg/ml Val-Trp uygulamasında ortaya çıkmış ve hücre canlılığı 48. saatte %52'ye gerileyerek kontrol grubuna göre son derece anlamlı bir azalma göstermiştir ($p < 0,0001$). Bu bulgular, Val-Trp'nin özellikle yüksek konsantrasyonda ve uzun süreli maruziyette MCF-7 hücreleri üzerinde belirgin sitotoksik etki oluşturduğunu göstermektedir.



Şekil 1. Val-Trp'nin MCF-7 hücre canlılığı üzerindeki etkisi (*$p < 0.05$, ****$p < 0.0001$).

1 mg/ml Val-Trp uygulanan MCF-7 hücrelerinde, 24 ve 48 saatlik inkübasyon süreleri karşılaştırıldığında belirgin bir zaman bağımlı etki gözlenmiştir. 24 saatlik inkübasyon sonrasında, hücre canlılığı kontrol grubuna yakın seyretmiş (%98) ve bu konsantrasyonda kısa süreli maruziyetin anlamlı bir sitotoksisite oluşturmadığı görülmüştür. Buna karşın, aynı konsantrasyonda 48 saatlik inkübasyon sonrasında hücre canlılığının %52'ye düşmesi, yaklaşık %50 oranında bir azalma ile belirgin bir sitotoksik etkinin zamanla ortaya çıktığını göstermektedir. Bu sonuçlar, Val-Trp'nin yüksek konsantrasyonda etkisinin gecikmeli ortaya çıktığını ve uzun süreli maruziyet koşullarında MCF-7 hücreleri üzerinde antiproliferatif/sitotoksik potansiyele sahip olabileceğini düşündürmektedir.

TARTIŞMA

Bu çalışmada, triptofanın indol çekirdeğini içeren valil-triptofan (Val-Trp) dipeptidinin insan meme kanseri MCF-7 hücreleri üzerindeki sitotoksik etkileri değerlendirilmiş ve Val-Trp'nin hücre canlılığı üzerinde hem konsantrasyona hem de inkübasyon süresine bağlı farklı yanıtlar oluşturduğu gösterilmiştir. Düşük konsantrasyon olan 0.1 mg/ml'de 24. saatte hücre canlılığında hafif bir artış gözlenmesi, bu dozun proliferasyonu baskılayacak düzeyde toksik olmadığını ve hatta hücrelerin metabolik aktivitesini geçici olarak artırabileceğini düşündürmektedir. Bununla birlikte, aynı dozda 48. saatte canlılığın %83.3'e gerilemesi, daha uzun maruziyetle birlikte hafif–orta düzeyde sitotoksik etkinin ortaya çıktığına işaret etmektedir.

Orta konsantrasyon olan 0.25 mg/ml'de 24. saatte canlılığın %83.3'e düşmesi, Val-Trp'nin bu dozda erken dönemde belirgin bir antiproliferatif etki oluşturduğunu göstermektedir. Buna karşın 48. saatte canlılığın %94.3'e yükselmesi, hücrelerin bu dozda kısmen toparlanabildiğini, bir adaptasyon yanıtı gelişebildiğini veya hayatta kalan

hücrelerin kompansatuvar proliferasyon gösterdiğini düşündürebilir. Bu durum, Val-Trp'nin belirli konsantrasyon aralıklarında sınırda veya geri döndürülebilir bir toksisite profiline sahip olabileceğini ortaya koymaktadır.

En yüksek konsantrasyon olan 1 mg/ml'de ise belirgin bir zaman bağımlı sitotoksisite dikkat çekmektedir. Yirmi dördüncü saatte canlılığın %98 düzeyinde kalması, kısa süreli maruziyetin anlamlı bir toksisite oluşturmamasına rağmen, 48. saatte canlılığın %52'ye düşmesi güçlü ve gecikmeli bir sitotoksik etkinin ortaya çıktığını göstermektedir. İndol içeren peptit ve dipeptitlerin literatürde apoptoz indüksiyonu, anjiyogenez inhibisyonu, hücre döngüsü duraksaması ve ROS artışı gibi mekanizmalar üzerinden antikanser etki gösterebildiği bildirilmiştir; Val-Trp için gözlenen bu zaman–doz ilişkisi söz konusu mekanistik çerçeveyle uyumludur (Huang ve ark., 2017; Borse ve ark., 2023; Küçükbay ve ark., 2024).

SONUÇ

Sonuç olarak, Val-Trp dipeptidinin MCF-7 meme kanseri hücreleri üzerinde zamana ve konsantrasyona bağlı sitotoksik etkiler gösterdiği ortaya konmuştur. Düşük ve orta konsantrasyonlarda (0.1 ve 0.25 mg/ml) hücre canlılığında sınırlı ve kısmen geri döndürülebilir değişiklikler gözlenirken, 1 mg/ml konsantrasyonda 48 saatlik maruziyet sonrasında hücre canlılığı yaklaşık %50 oranında azalmıştır. Bu bulgular, Val-Trp'nin özellikle yüksek konsantrasyonda ve uzun süreli uygulamalarda güçlü bir antiproliferatif/sitotoksik potansiyele sahip olduğunu ve indol bazlı yeni antikanser ajanların geliştirilmesi açısından dikkate değer bir aday olabileceğini göstermektedir. Gelecekte yapılacak çalışmalarda, Val-Trp'nin etki mekanizmalarının moleküler düzeyde aydınlatılması, farklı kanser ve normal hücre hatlarında seçiciliğinin araştırılması ve uygun in vivo modellerde terapötik etkinlik ve güvenlilik profilinin değerlendirilmesi gerekmektedir.

TEŞEKKÜR

Çalışma sırasında yardımlarını esirgemeyen Doç. Dr. Bilge Bıçak'a tüm içtenliğimle teşekkürlerimi sunarım.

KAYNAKLAR

Borse, A., Shinde, N., & Bhosale, S. K. (2023). Dipeptide Conjugates: An Important Class of Therapeutic Agents. Indian Journal of Pharmaceutical Education and Research, 57(1), 15. https://doi.org/10.5530/001954640093

Bose, D., Roy, L., & Chatterjee, S. (2022). Peptide therapeutics in the management of metastatic cancers. RSC Advances, 12(33), 21353. Royal Society of Chemistry. https://doi.org/10.1039/d2ra02062a

González-Montoya, M. (2017). Bioactive Peptides from Legumes as Anticancer Therapeutic Agents. International Journal of Cancer and Clinical Research, 4(2). https://doi.org/10.23937/2378-3419/1410081

Huang, R.-Z., Zhang, B., Huang, X., Liang, G.-B., Qin, J.-M., Pan, Y.-M., Liao, Z., & Wang, H. (2017). Synthesis and biological evaluation of terminal functionalized thiourea-containing dipeptides as antitumor agents. RSC Advances, 7(15), 8866. https://doi.org/10.1039/c6ra25590f

Küçükbay, H., Gönül, Z., Kuruçay, A., Ateş, B., Boulebd, H., & Küçükbay, F. Z. (2024). Anticancer, antioxidant, DFT calculations, and docking studies of some new peptide-indole conjugates. Organic Communications, 1, 38. https://doi.org/10.25135/acg.oc.165.2402.3035

Naglah, A. M., Moustafa, G. O., Elhenawy, A. A., Mounier, M. M., El-Sayed, H., Al-Omar, M. A., Almehizia, A. A., & Bhat, M. A. (2021). Nα-1, 3-Benzenedicarbonyl-Bis-(Amino Acid) and Dipeptide Candidates: Synthesis, Cytotoxic, Antimicrobial and Molecular Docking Investigation. Drug Design Development and Therapy, 1315. https://doi.org/10.2147/dddt.s276504

Offerman, S. C., Kadirvel, M., Abusara, O. H., Bryant, J., Telfer, B. A., Brown, G., Freeman, S., White, A., Williams, K. J., & Aojula, H. (2017). N-tert-Prenylation of the indole ring improves the cytotoxicity of a short antagonist G analogue against small cell lung cancer. MedChemComm, 8(3), 551. https://doi.org/10.1039/c6md00691d

ORAL PRESENTATION

GUL herbaryumu'nun Caryophyllaceae familyası envanteri üzerine notlar

Raziye Doğan Kuş[1]* (ORCID: https://orcid.org/0009-0000-9058-0616, Hasan Özçelik[2] (ORCID: https://orcid.org/0000-0002-0207-0921), Neslihan Erdoğan Balpınar[3] (ORCID: https://orcid.org/0000-0002-4469-8629)

[1] Burdur Mehmet Akif Ersoy Üniversitesi, Fen Bilimleri Enstitüsü, Biyoloji Anabilim Dalı, 15100, Burdur, Türkiye
[2]Süleyman Demirel Üniversitesi, Mühendislik ve Doğa Bilimleri Fakültesi, Biyoloji Bölümü, 32100, Isparta, Türkiye
[3]Burdur Mehmet Akif Ersoy Üniversitesi, Fen-Edebiyat Fakültesi, Biyoloji Bölümü, 15100, Burdur, Türkiye

*Sorumlu yazar e-mail: raziyebegumdogan@gmail.com

Özet

Bu çalışma GUL Herbaryumu'nda bulunan Caryophyllaceae familyasının envanterini ortaya çıkarmak için yapılmıştır. Çalışma son 3 yılın ürünüdür. Envanter işlemleri sırasında ilgili örnekler taksonomik ve sistematik açıdan incelenmiştir. GUL Herbaryumu bölgesel ve uluslararası 'GUL' kodu ile bilinen Süleyman Demirel Üniversitesi bünyesinde bir herbaryumdur. Bünyesinde ülke genelinden özellikle Göller Yöresi ve Doğu Anadolu'dan toplanan 25000 kadar bitki örneği barındırır. Bu örnekler içerisinde 4000 kadarı *Rosa* cinsine; 2000 kadarı da Caryophyllaceae familyasına aittir. Ranunculaceae, Apiaceae, Fabaceae ve Lamiaceae familyaları örnekleri de herbaryumda binlercedir. Bu bildiride Caryophyllaceae familyasına ait örneklere ait bazı bilgiler verilmektedir. Türkiye'nin hemen her bölgesinden toplanan ve herbaryum örneği haline getirilen 1868 koleksiyona ait bitki örnekleri tarafımızdan incelenmiş, usulüne göre kartonlara yapıştırılıp teşhis edildikten sonra herbaryum defterine kaydedilmiştir. Türkiye Florası adlı eserdeki sıraya göre dolaplara dosyalar halinde yerleştirilmiştir. Bitkilerin böcek tasallutundan korunması ve birbirleriyle karışmasını önlemek için plastik kilitli poşetlerle konulmuştur. Bitki örneklerinin teşhisi kontrol edilmiş; teşhissiz olanlar ise teşhis edilerek dosyalanıp dolaplara yerleştirilmiştir Teşhis işlemleri Flora of Turkey adlı esere göre, kısmen de yeni sistematik yayınlara göre yapılmıştır. *Silene, Bolanthus, Bolanthus, Arenaria* cinsleri RTF uzmanları tarafından kontrol edilmiştir. Toplamda 24 cinse bağlı 192 taksonun herbaryumda örneklerinin varlığı tespit edilmiştir. Herbaryumda; *Gypsophila*, *Silene*, *Dianthus* ve *Bolanthus'*a ait örnek ve takson sayısı diğer cinslere oranla daha fazladır. *Ankyropetalum* cinsinin tüm üyeleri, *Gypsophila* ve *Saponaria* cinsinin Türkiye taksonlarının tamamına yakını herbaryumda mevcuttur. Familyanın taksonları üzerine çok sayıda sistematik ve taksonomik çalışma yapılmıştır. Ancak cins veya türlerin sistematik durumu hâla ciddi bir bilimsel temele oturtulamamıştır. Bunların başında *Silene* ve *Bolanthus* gelmektedir. Bu durum; familyanın sistematik açıdan zorluğu, herbaryumlardaki materyal durumu ve araştırıcıların deneyim seviyesi ile açıklanabilir. Çalışma sonrası elde edilen sonuçlar *Caryophyllaceae* familyasının Türkiye'deki taksonomik durumunun hala karmaşık olduğunu ve küçük, doğal gruplar (seksiyon gibi) revizyon çalışmalarının gerekli olduğunu ortaya koymaktadır.

Anahtar kelimeler: GUL Herbaryumu, Bitki Envanteri, Caryophyllaceae familyası, Sistematik, Taksonomi

Notes on the inventory of the Caryophyllaceae family in the GUL Herbarium

Abstract

The present study was conducted with the objective of compiling a comprehensive inventory of the family *Caryophyllaceae* represented in the Rose Herbarium of Süleyman Demirel University. This research constitutes the culmination of a three-year project focusing on the taxonomic and systematic evaluation of the family. Throughout the inventory process, all relevant specimens were subjected to detailed examination and identification procedures. The Rose Herbarium, internationally recognized under the code "GUL," houses approximately 25,000

plant specimens collected from various regions of Turkey, with particular emphasis on the Lakes Region and Eastern Anatolia. Among these, nearly 4,000 specimens belong to the genus *Rosa*, while approximately 2,000 specimens are members of the family *Caryophyllaceae*. The collection also contains significant representatives of the families *Ranunculaceae*, *Apiaceae*, *Fabaceae*, and *Lamiaceae*. A total of 1,868 specimens belonging to the *Caryophyllaceae* family were analyzed in this study. Each specimen was mounted, labeled, and recorded according to standard herbarium protocols, and systematically arranged following the classification system adopted in *Flora of Turkey*. To ensure preservation, specimens were stored in sealed plastic bags to prevent insect damage and cross-contamination. Identification was verified primarily with reference to *Flora of Turkey* and supplemented by recent systematic revisions. Specialists examined the genera *Silene*, *Bolanthus*, and *Arenaria*. As a result, 192 taxa representing 24 genera were identified within the herbarium. The genera *Gypsophila*, *Silene*, *Dianthus*, and *Bolanthus* were found to be dominant. Despite extensive taxonomic research, the systematic relationships within *Caryophyllaceae* remain complex. The results of this study emphasize the necessity of further revisionary investigations, particularly focusing on smaller, natural groups (e.g., sections) to clarify the taxonomic status of the family in Turkey.

Keywords: GUL Herbarium, Plant Inventory, Caryophyllaceae family, Systematic, Taxonomy

GİRİŞ

Caryophyllaceae familyası Dünyada takson sayısı bakımından büyük bitki familyalarındandır. Yaklaşık 100 cins ve 3000'den fazla tür ile temsil edilmekte olup çoğunluğu ılıman iklim kuşaklarında yayılış göstermektedir (Xue B ve ark., 2023) Caryophyllaceae familyası taksonları böceklerle tozlaşır. Türkiye'de genelde İran-Turan elementi ve volkanik ve kalker kayalı step vejetasyonu bitkileridir. Familyanın taksonları deniz seviyesinden (3500-4000) m'ye kadar, hemen her mevsimde görülebilirler. Türkiye florasında Caryophyllaceae familyası oldukça zengin bir çeşitliliğe sahiptir ve endemizm oranı yüksektir. Türkiye florasının yaklaşık 1/3'ü günümüz iklim şartlarının ortaya çıkmasından daha önce oluşan kalıntı (relikt) veya endemik bitkilerdir (Çiçek ve ark., 2017). Ortalama olarak her 20 günde bir bitki taksonu Türkiye florasına eklenmektedir. Bu çeşitlilik, çevre ülke floraları ile karşılaştırıldığında Türkiye bitki çeşitliliğinin ne kadar zengin olduğunu net olarak ortaya koymaktadır.

Caryophyllaceae (Karanfilgiller) familyasındaki *Dianthus, Silene, Gypsophila* ve *Agrostemma* cinsleri süs bitkileri olarak kullanılabilirken; *Stellaria, Cerastium, Arenaria* vs. peyzaj düzenlemeleri açısından önemlidir. *Saponaria, Ankyropetalum* ve *Gypsophila* cinsinin bazı taksonları saponin bakımından zengindir ve endüstriyel açıdan önemlidir. Kimya sanayiinde saponin önemli bir maddedir. Saponin kimyasal bileşiği bakımından zengin olan Caryopyllaceae familyasındaki taksonların ekonomik açıdan önemi vardır. *Ankyropetalum* ve *Gypsophila* cinsine ait türler, bazı gıdalarda ham madde olarak kullanıldığı için familyanın ekonomideki önemini artırır. Caryophyllaceae familyası taksonlarının tamamı az veya çok zehirlidir; bu nedenle tıbbi öneme sahiptir. *Minuartia, Arenaria, Cerastium, Silene* ve *Dianthus* cinslerinden peyzaj, salon bitkisi olarak kültüre alınanlar bulumaktadır. Çoğunlukla doğal bitkilerdir. *Dianthus* ve *Silene*'nin bazı türleri, *G. paniculata*'nın kültürü yapılmaktadır. Isparta'da karanfil üreten seralar son yıllarda çokça artmış, yöreye ekonomik katkı sağlamıştır. Ekonomik öneminden ve sistematik problemlerinin çokluğundan dolayı GUL herbaryumu çalışanları bu familya taksonlarına önem vermişler, çalışma konusu seçmişlerdir. Böylelikle GUL Herbaryumu tahminen Türkiye'deki en çok Caryophyllaceae familyasına ait örnek barındıran bir herbaryum olmuştur. Biz de bu zenginliği çeşitli açılardan bilim dünyasına ve meraklılara açıklamak istedik.

Türkiye florası için yazılan ilk eser "*Flora Orientalis*" (Boissier, 1865-1876)'dir. Daha sonra Davis (1965-1985)'in editörlüğünde 9 ciltten oluşan 'Flora of Turkey and the East Aegean Islands' adlı kitap yayınlanmıştır. Türkiye Florası'na eklenen yeni takson ve statü değişikliklerini içeren tamamlayıcı (supplement) nitelikli 10. (Davis ve ark., 1988) ve 11. ciltler (Güner ve ark., 2000) yayınlanmıştır. Son olarak Türk botanikçiler tarafından hazırlanan Türkiye Bitkileri Listesi (Damarlı Bitkiler) (Güner ve ark., 2012) ile Türkiye'nin bitki florasındaki çeşitliliği daha net bir şekilde ortaya koymuştur. Türkiye Bitkileri Listesi kitabında; Türkiye Florası 167 familya içerisinde, 1320 cins altında 9.996 türe ait ve tür altı taksonlarla birlikte toplam 11.707 bitki taksondan olarak belirtilmiştir (Güner ve ark., 2012). Daha sonra bu esere yeni taksonlar da eklenmiştir ve halen eklenmeye devam

edilmektedir. Dünya genelinde familya ve cinsleri tanıtan önemli kişiler ve araştırmaları vardır (Barkaudah, 1962; Greuter, 1995; Huber-Morath ve ark., 1967).

MATERYAL VE METOT

Bu araştırmanın materyalini GUL Herbaryumu'ndaki 1984-2023 yılları arasında Türkiye'nin farklı şehirlerinden toplanarak değerli koleksiyon materyali haline getirilmiş Caryophyllaceae familyasına ait taksonların örnekleri oluşturmaktadır. Önceden familyaya ait tanımlanmış taksonlar yeniden kontrol edilmiştir. Teşhis çalışmalarımızda (Davis, 1965-1985; 1988; Güner ve ark., 2000)'in 'Flora of Turkey and the East Aegean Islands' eseri temel kaynak olarak kullanılmıştır. Bu eserin yayınlanmasından sonra çıkan yayınlar (Güner ve ark., 2012; Özhatay ve ark., 2009) teşhis ve envanter kayıt işlemlerinde dikkate alınmıştır. Yeni takson kayıtları (Armağan, 2016; Armağan ve ark., 2017; Ataşlar ve Ocak, 2005; Aytaç ve Duman, 2004; Özçelik, 2023; 2024; Yıldırımlı, 2012) adlandırmalarda dikkate alınmıştır. Bununla birlikte sistematik çalışmalar (Alpınar, 1994; Fidan ve Özgökçe, 2016; Özçelik ve Kılıç, 2007; Özçelik ve Özgökçe, 1995; 1999; 2023; 2024) taksonların ayırt edilmesinde özenle incelenmiştir. Çalışmalarımız devam etmektedir. Tamamlandığında familyanın envanter kaydı GUL Sanal Herbaryumuna yüklenerek isteyenlerin internet ortamında ulaşabilmesine imkan sağlanacaktır.

BULGULAR ve TARTIŞMA

Araştırmanın ön sonuçlarına göre; GUL Herbaryum'daki *Caryophyllaceae* familyasına ait yaklaşık olarak 1760 nüsha bitki örneğinin değerlendirilmesi sonucu, toplam 24 cins ve yaklaşık 190 takson tespit edilmiştir. Endemik takson sayısı ise yaklaşık 93 olarak belirlenmiştir. Bu çalışmada elde edilen ön verilere göre; Caryophyllaceae familyasına ait aşağıdaki sonuçlara ulaşılmıştır:

Silene, Arenaria, Minuartia, Bolanthus ve *Gypsophila* cinsleri; özellikle *Silene oligotricha*, *S. leptoclada, S. odontopetala, S. caryophylloides* vb. taksonomik açıdan problemlidir. Ayrıca örnekler içerisinde *Gypsophila* cinsinde bulunan *G. sphaerocephala, G. bitlisensis* gibi sistematik açıdan çok sayıda problemli takson bulunmaktaydı. Bu türler üzerine revizyon çalışmaları yapıldı ve sorun çözülmüştür. *Gypsophila* cinsinde 39 tür ve 650 koleksiyon örneği incelenerek içerisinde endemik taksonlar belirlenmiştir.

Silene, Gypsophila gibi büyük cinslerde ise cins bazında değil, seksiyon bazında revizyonlar yapılmalıdır. *Gypsophila* cinsi (Korkmaz ve Özçelik, 2011; Muca, 2017; Özçelik ve Özgökçe, 1995; 1999; 2023; 2024) ve *Silene*'nin 2 seksiyonu *(Auriculatae* Boiss. and *Brachypodeae* Boiss.) revize edilmiştir (Özçelik ve Kılıç, 2007). *Hagenia* Seksiyonu da revize edilmiştir (Fidan ve Özgökçe, 2016). *Bufonia* cinsinin (Serdaroğlu, 2001) Flora'daki (Davis, 1967) türleri revize edilmiştir. Ancak bu cinse ait daha sonra 2 yeni tür eklenmiştir. Cinsler ve *Silene, Gypsophila* gibi büyük cinslerde seksiyon anahtarları yapılmadan familya bazında revizyon yapmak teknik olarak hatalı bir çalışmadır. Bu nedenle yapılan tür ve cins teşhis anahtarları pek çalışmamaktadır. *Gypsophila* için seksiyon anahtarı (Özçelik ve Özgökçe, 2024) tarafından yapılmıştır. *Silene* L. Türkiye'de *Caryophyllaceae* familyasına ait en büyük cinstir ve yaklaşık 150 tür ile temsil edilmektedir. (W. Greuter, 1995) tarafından seksiyonlar belirlenmiş ve bir teşhis anahtarı yapılmış olmasına rağmen güncellenmesi yapılmamıştır. Çalışmamızda *Silene* cinsi içerisinde 52 takson belirlenmiş, bunlardan 31 takson endemiktir.

Bolanthus, Gypsophila, Ankyropetalum ve *Acanthophyllum* daha önceleri bir cins iken sonradan farklı cinslere bölünmüştür. Bu cinslerin sistematik karakterleri iç içe girmiştir; cins teşhis anahtarı net değildir. Resimli Türkiye Florası'nda (Güner ve ark., 2025) da bu problemlerin çözülemediği aşikardır. *Bolanthus* küçük bir cins olmasına rağmen taksonomik açıdan çok zor bir cinstir. Cinsin güvenilir bir tür teşhis anahtarı yoktur. Tarafımızdan yapılmaya çalışılmaktadır. Özellikle *B. minuartioides* ile *B. spergulifolius* kolayca teşhis edilemez. Her bir cins üzerinde uzun süreli çalışmalar gerekir. (Özçelik ve Muca, 2010) cinsleri üzerine sistematik çalışmalar yapılmıştır. Aynı şekilde ekolojik çalışmalar (Armağan ve Özgökçe, 2018) yapılmıştır. RTF'de (Güner, 2025) *Silene* cinsine ait bazı türlerin kısmen akraba, ya da uzak akraba türleri ile (*Silene guerbuezii, S. denizliensis* ile); *(S. eminentis, S. armena* ile) vs. karıştırıldığı görülmüştür. Bu durum araştırıcıları tereddüte sevk edecek ciddi bir hatadır. Esasen metot hatasıdır. Çünkü seksiyonlar belirlenip ayrım kriterleri oluşturulmadan ve komplex türler revize edilmeden (*S. araratica, S. odontopetala, S. caryophylloides* gibi) tür teşhis anahtarı yapılmamalıydı. Ancak bu işleri yapmanın uzun yıllar alacağı da bir gerçektir. Bu nedenle sistematikte sürekli git-geller olabilmektedir.

Herbaryumda; *Silene* cinsi içerisinde 31 Endemik takson, 2 nüsha Holotype örnek, 7 nüsha Isotype örnek, 25 nüsha Topotype örnek kayıt altına alınmıştır. Bir de *Bolanthus* için holotip ve izotipler vardır.

Bolanthus cinsi morfolojik açıdan tür belirlenmesi en zor olan cinslerden biri olması nedeniyle incelemeler sonucunda yanlış adlandırmalar düzeltilmiştir. Ayrıca cinse ait 9 Endemik takson belirlenmiştir. Türkiye taksonlarının tamamının endemik olduğu görülmüştür. Flora'ya göre (Davis, 1967) endemik cinslerden idi ve 5 türü kayıtlı idi. Günümüzde 13 türü Türkiye'de olmak üzere toplam 20 kadar türü belirlenmiş ve cins endemik olmaktan çıkarılmıştır. *Dianthus*, Türkiye Florası'nda (Davis, 1967) yaklaşık 80 tür ile temsil edilmektedir. Yapılan değerlendirmelerde *Dianthus* içerisinde 68 nüsha örnek incelenmiş olup bunlardan da 8 endemik takson belirlenmiştir.

SONUÇ VE ÖNERİLER

Çalışmamızın sonuçları; Caryophyllaceae familyası türlerin teşhisinde kullanılan karakterlerin bazen tür içi varyasyonlarla karışabildiğini göstermektedir. Davis (1965-1985; 1988) tarafından yapılan sınıflandırmalar önemli bir temel olmakla birlikte, son yıllarda yapılan moleküler çalışmalar (Fior ve ark., 2006; Rautenberg ve ark., 2010) bazı türlerin sistematik konumlarını yeniden değerlendirmeyi gerekli kılmıştır. Türkiye florasında familyanın yüksek endemizm oranı, morfolojik farklılıkların çevresel adaptasyonlarla ilişkili olabileceğini düşündürmektedir. Bu nedenle morfolojik bulguların moleküler veriler yanında ekolojik verilerle de desteklenmesi gereklidir. Sadece morfolojik farklılık veya benzerliklere göre bir sınıflandırma yapılmamalıdır. Hatta coğrafi dağılış özellikleri de dikkate alınmalıdır. Böyle yapılmazsa birbirine akraba türler bir türmüş gibi işlem görebilir. RTF'de (Güner, 2025) *Silene* cinsinde görülen durum işte budur. Türkiye Bitkileri (Güner ve ark., 2012) kitabı bir derlemedir. Bir revizyon sonucu yazılmamıştır. Hal böyle iken RTF'de bu kitap ölçü alınmıştır. Bölgesel bir endemik olan *S. armena* içerisine çok sayıda takson konulmuş, diğerleri sinonim yapılmıştır. Coğrafi olarak bir inceleme yapılsaydı böyle bir hata olmayabilirdi. Ayrıca 2000 yılında son cilti yayınlanan (Güner ve ark., 2000) Türkiye Florası adlı eserden sonra çok sayıda yeni takson tanımı yapılmıştır. 25 yıllık sürede Türkiye florasının daha zenginleşmesi beklenirken genel durum olarak sayıların düşmesini anlamak zordur. Mesela 175 iletim demetli bitki familyası niçin daha aşağı düşmüştür gibi soruların cevabı aranmaktadır. Caryophyllaceae familyası Türkiye florasındaki önemli bir taksonomik karmaşıklık olduğu gözlemlendiği için GUL Herbaryumu'nda bulunan örneklerin revizyon çalışması ile morfolojik incelemeler ve literatür karşılaştırmalarıyla mevcut taksonomik bilgilerin güncellenmesine katkı sağlayacağı kanaatindeyiz.

Araştırma sayesinde, türleri belli olmayan herbaryum örneklerinin teşhisleri yapılmış (Güner ve ark., 2012), daha önceden tanımlanmış olan herbaryum örnekleri ise yeniden kontrol edilmiştir. Ayrıca Caryophyllaceae familyasına ait tüm bitki örnekleri kontrol edilerek yıpranmış olan herbaryum örneklerinin karton, gömlek ve üstlerindeki etiketleri yenilenerek bitki örnekleri teşhis ve tanımlama tarihlerine uygun olarak sıraya dizilmiştir. Materyal olarak kullanılmış olan tüm bitki örnekleri, çalışma yapılırken zarar görmemesine dikkat edilerek incelenmiş ve halen bulundukları Isparta Süleyman Demirel Üniversitesi Mühendislik ve Doğa Bilimleri Fakültesi bünyesinde GUL Herbaryumu'nda korunmaktadır.

TEŞEKKÜR

GUL Herbaryumu'na çok sayıda araştırmacı bitki hediye etmiştir. Bu örneklerin çoğunluğu da TUBITAK, SDÜ Rektörlüğü tarafından desteklenen projeler kapsamında toplanıp araştırılmıştır. Revizyon yapan ya da bitki hediye eden araştırıcılar sayesinde herbaryum bugünkü zengin duruma getirilmiştir. Herbarum'un bağlı olduğu SDÜ. Mühendislik ve Doğa Bilimleri Fakültesi Dekanlığına, araştırma projelerine finansal destek veren kurumlara ve proje araştırmacılarına, ayrıca herhangi bir sebeple herbaryuma örnek bağışlayan tüm kişilere teşekkür ederiz.

KAYNAKLAR

Alpınar, K. (1994). Some Contributions to the Turkish Flora, *Edinb. J. Bot.,* 51, (1), 65-73.

Aytaç, Z., Duman, H. (2004). Six new taxa (*Caryophyllaceae*) from Turkey. *Annales Botanici Fennici*, 41: 213-221.

Armağan, M. (2016). Gypsophila munzurensis (Caryophyllaceae) a new species fromTunceli (Türkiye). *Phytotaxa,* 275(2): 175-180.

Armağan, M., Özgökçe, F., Çelik, A. (2017). Notes on the genus Gypsophila (Caryophyllaceae) in Turkey, with a description of G. guvengorkii sp. Nov. *Phytotaxa,* 295(3): 271-279.
Armağan, M., Özgökçe, F. (2018). Anatomical, palynological, morphological and ecological investigation on Gypsophila davisii. *Anatolian Journal of Botany,* 2(1): 39-45.
Ataşlar, E., Ocak, A. (2005). Gypsophila osmangaziensis (Caryophyllaceae), a new species from Central Anatolia, Turkey. *Ann. Bot. Fennici,* 42: 52-60.
Barkaudah, Y.I. (1962). A revision of Gypsophila, Bolanthus, Ankyropetalum and Phryna. *Wentia,* 9, 1-203.
Çiçek, M., Özçelik, H., Başkale, E. & Şeker, E. (2017). Denizli Nakılı (*Silene denizliensis* Aytaç) Testiotu (*Amphoricarpos Praedictus* Ayaşlıgil & Grierson) Tür Eylem Planı, (2018-2022). T.C. Orman ve Su İşleri Bakanlığı Doğa Koruma ve Milli Parklar Genel Müdürlüğü, Ankara.
Davis P.H. (1965-1985). *Flora of Turkey and the East Aegean Islands*, Vol. 1-9, Edinburgh University Press.
Davis, P.H., Mill, R.R., Tan, K. (1988). *Flora of Turkey and The East Aegean Islands,* Vol. 10, Edinburgh University Press.
Fior, S., Karis, P.O., Casazza, G., Minuto, L., Sala, F. (2006). Molekoler phylogeny of the Caryophyllaceae (Caryophyllales) infeered from chloroplast and nuclear DNA sequences. *Taxon,* 55(4): 1037-1053.
Fidan, M., Özgökçe, F. (2016). Revision of Hagenia A. Braun. Section Belonging to Genus Gypsophila L. (Caryophyllaceae) in Turkey. *Turkish Journal of Life Sciences,* 1(2): 075-085.
Greuter, W. (1995). *Silene* L. (Caryophyllaceae) in Greece: a subgeneric and sectional classification. *Taxon,* 44: 543-581.
Güner, A., Aslan, S., Ekim, T., Vural, M., Babaç, M.T. (eds.) (2012). *Türkiye Bitkileri Listesi (Damarlı Bitkiler).* Nezahat Gökyiğit Botanik Bahçesi ve Flora Araştırmaları Derneği Yayını, Flora Dizisi 1, İstanbul.
Güner, A., Özhatay, N., Ekim, T., Başer, K.H.C. (2000). Flora of Turkey. Vol. 11, Edinburgh, University Press.
Güner, A. (Edit.) (2025). Resimli Türkiye Florası. Nezahat Gökyiğit Botanik Bahçesi ve Flora Araştırmaları Derneği Yayını, İstanbul.
Huber-Morath, A., McNeill, J., Reeve, H. (1967). Materials for flora of Turkey. XIV: Caryophyllaceae. *Notes RBG Edinb.* 27(1): 17-23.
Korkmaz, M., Özçelik, H. (2011). Systematical and morphological characteristics of annual *Gypsophila* L. (Caryophyllaceae) taxa of Turkey. *Biological Diversity and Conservation (Biodicon)*, 4(1): 79- 98.
Özçelik, H., Muca, B. (2010). Ankyropetalum Fenzl (Caryophyllaceae) Cinsine Ait Türlerin Türkiye'deki Yayılışı ve Habitat Özellikleri. BİBAD (Biyolojik Araştırmalar Derg.), 3(2): 47-56.
Muca, B. (2017). Türkiye Gypsophila L. (Caryophyllaceae) cinsine ait Capituliformes Williams seksiyonunun revizyonu. S. Demirel Univ. Fen Bilimleri Enstitüsü (Doktora Tezi), 362s.
Özçelik, H. (2024). A new species from Türkiye: Bolanthus sertavulus (Caryophyllaceae). *Anadolu Botanik Dergisi,* 8(1): 16-20.
Özçelik, H., Kılıç, S. (2007). *Revision of Sections Auriculatae Boiss. and Brachypodeae Boiss. of the Silene (Caryophyllaceae) Genus Growing in Türkiye.* TUBITAK TBAG 104T016 numbered Project, Ankara.
Özçelik, H. & Özgökçe, F. (1995). Taxonomic contributions to Genus Gyopsophila L. (Caryophyllaceae) from East Anatolia (Turkey). IVth Plant Life of South West Asia Symposium, Ege Univ., İzmir/ Turkey: 44.
Özçelik, H., Özgökçe, F. (1999). Morphological, taxonomical and Ecological Researches on Gypsophila bitlisensis Bark. And Gypsophila elegans M.Bieb. 1st International Symposium on Protection of Natural Enviroment and Ehrami Karaçam. 23-25thSeptember 1999, Kütahya/Turkey, 295-313.
Özçelik, H., Özgökçe, F. (2023). New Collections and Observations on Gypsophila L. taxa in Türkiye. Bulletin of Pure and Applied Sciences-Botany, 42B, (2), 73-94.46.
Özçelik, H., Özgökçe, F. (2024). Systematic and Taxonomic Contributions to Genus Gypsophila L. in Türkiye. Bulletin of Pure and Applied Sciences Section-B-Botany, 43B (1): 43-71.
Özhatay, N., Kültür, Ş., Aslan, S. (2009). Check-list of additional taxa to the supplement flora of Turkey IX. Turkish Journel of Botany, 33, 191-226.
Rautenberg, A., Filatov, D.A., Svennblad, B., Heidari, N., Oxelman, B. (2010). Conflicting phylogenetic signals in the Sileneae (Caryophyllaceae). Molekuler Phylogenetics and Evolution, 57(3), 1237- 1248.

Serdaroğlu, H., 2001. *Bufonia* L. (Caryophyllaceae) Cinsine Taksonomik Katkılar. Süleyman Demirel Üniversitesi, Fen Bilimleri Enstitüsü, Biyoloji Anabilim Dalı, Türkiye (Yüksek Lisans tezi).

Xue B, Song Z, Cai J, Ma Z, Huang J, Li Y, Yao G. Phylogenetic analysis and temporal diversification of the tribe Alsineae (Caryophyllaceae) with the description of three new genera, Hesperostellaria, Reniostellaria and Torreyostellaria. Front Plant Sci. 2023 Jun 21; 14:1127443.

Yıldırımlı, Ş. (2012). Türkiye Florası İçin Yeni Taksonomik Kayıtlar. Ot Sistematik BotanikDergisi, 19(1): 45-58.

ORAL PRESENTATION

Melanomda beyin metastazı gelişiminde rol oynayan moleküler mekanizmalar

Yasemin Çakır (ORCID: 0000-0002-1394-6474)

Dokuz Eylül Üniversitesi Tıp Fakültesi, Tıbbi Patoloji Anabilim Dalı, İzmir, Türkiye

Sorumlu yazar e-mail: cakir.yasemin@deu.edu.tr

Özet

Melanomlarda santral sinir sistemi (SSS) metastazı, hastalık biyolojisinin en agresif biçimlerinden biridir. Beyin metastazı gelişimini belirleyen moleküler mekanizmalar henüz net olarak aydınlatılamamış olup, özellikle transkripsiyonel düzeyde farklılaşmalar olduğu ileri sürülmektedir. Çalışmamızda, beyin metastazı olan ve olmayan melanom olguları arasındaki moleküler farklılıkları ortaya koymayı amaçladık.
Cbioportal biyoinformatik web sitesi üzerinden, "Metastatic Melanoma (DFCI, Nature Medicine)" veri seti kullanıldı. İki grup arasında, DNA mutasyonu, kopya sayısı değişiklikleri (CNV) ve mRNA ekspresyon düzeyleri karşılaştırıldı. P ve q < 0,05 değeri istatistiksel olarak anlamlı kabul edildi.
Gruplar arasında, DNA mutasyon profili ve CNV açısından anlamlı bir fark izlenmezken, mRNA ekspresyon düzeyi bakımından farklılık gösteren 267 adet gen (DEGs) saptandı. En yüksek anlamlılığa sahip genler arasında AQP7, IGLV-46, IGHV3-64, FCRL5 gibi immün ve membran ilişkili genlerin yer alması, beyin metastazlarının immün mikroçevre ve nöral dokuya özgü çevresel baskılarla ilişkili olduğunu düşündürmektedir. Buna karşılık, beyin metastazı olmayan olgularda metabolik ve proliferatif süreçlerle bağlantılı bir gen kümesinin yüksek ekspresyonu, metastatik fenotip ile beyin tropizmi arasındaki ayrımı desteklemektedir. Bu bulgular, melanom beyin metastazının genomik değil, transkripsiyonel düzeyde belirgin şekilde ayrıştığını göstermekte ve AQP7 gibi bazı genlerin potansiyel biyobelirteç adayı olabileceğini ortaya koymaktadır. Sonuçlar, SSS metastaz biyolojisinin anlaşılmasına katkı sağlayarak gelecekteki fonksiyonel çalışmalar için temel oluşturmaktadır.

Anahtar Kelimeler: Melanom, Beyin metastazı, DEGs

Molecular mechanisms involved in the development of brain metastases in melanoma

Abstract

Central nervous system (CNS) metastasis in melanoma represents one of the most aggressive forms of the disease. Although the molecular mechanisms underlying the development of brain metastases have not yet been fully elucidated, it has been suggested that transcriptional-level alterations may play an important role. In this study, we aimed to identify the molecular differences between melanoma cases with and without brain metastasis. The "Metastatic Melanoma (DFCI, Nature Medicine)" dataset available on the cBioPortal bioinformatic platform was used. DNA mutations, copy number variations (CNVs), and mRNA expression levels were compared between the two groups. p and q value < 0.05 was considered statistically significant.

No significant differences were observed between the groups in terms of DNA mutation profiles or CNVs. However, mRNA expression analysis identified 267 differentially expressed genes (DEGs). The presence of highly significant genes such as AQP7, IGLV-46, IGHV3-64, and FCRL5—many of which are immune- or membrane-associated—in cases with brain metastasis suggests that immune microenvironment adaptation and neural tissue–specific selective pressures may contribute to the metastatic process. Conversely, the higher expression of a broad set of genes related to metabolic and proliferative pathways in the non-metastatic group supports a biological distinction between systemic metastatic behavior and brain tropism. These findings demonstrate that melanoma brain metastasis is characterized not by genomic alterations but by distinct transcriptional reprogramming. Moreover, the identification of genes such as AQP7 as differentially expressed highlights potential biomarker

candidate. Overall, the results contribute to a better understanding of CNS metastasis biology and provide a basis for future functional studies.

Keywords: Melanoma, Brain metastasis, DEGs

GİRİŞ

Melanomun santral sinir sistemi (SSS) tropizmi, yayınlanmış birçok seride ileri evre melanom hastalarının önemli bir çoğunluğunda beyin metastazı geliştiğinin gösterilmesi ile desteklenmiştir (Rabbie ve ark. 2021). Bu oran, melanom hücrelerinin kan–beyin bariyerini aşabilme, sinir sistemi mikroçevresine tutunabilme ve bu alanda proliferatif kapasitesini sürdürmeye özgü programlar taşıdığını düşündürmektedir (Radke ve ark. 2022). Multiomik çalışmalarda, beyin metastazlarının genetik olarak primer tümörle büyük ölçüde benzer olduğunu, ancak transkripsiyonel düzeyde belirgin farklılık gösterdiğini ortaya koymuştur (Biermann ve ark. 2022).

Beyin metastazlarının oluşumunda immün mikroçevre ve nöral niş adaptasyon mekanizmalarının temel rol oynadığı gösterilmiştir. Özellikle beyindeki tümöral mikroçevrenin periferik immün yanıttan farklı yapısı, metastatik hücrelerin farklı immün kaçış mekanizmaları geliştirmesine neden olmaktadır (Quail ve Joyce 2017). Tek hücre düzeyinde yapılan çalışmalar, beyin metastazında immün baskılanmış bir mikroçevre, reaktif astroglial cevap, tümör hücrelerinin sinaptik benzeri sinyal yollarını taklit eden nöronal adaptasyon süreçlerinin mevcut olduğunu göstermiştir (Priego ve ark. 2018; Klemm ve ark. 2020). Ayrıca, metabolik programların yeniden düzenlendiği ve oksidatif stres yanıtının beyin metastazlarında sistemik metastazlardan farklı olduğu belirtilmiştir (Fischer ve ark. 2019).

Bu nedenle beyin metastazı bulunan melanomların transkripsiyonel düzeyde karakterize edilmesi hem biyolojik mekanizmaların anlaşılması hem de olası prognostik imzaların belirlenmesi açısından kritik öneme sahiptir (Alvarez-Breckenridge ve ark. 2022). Çalışmamızda, "Metastatic Melanoma (DFCI, Nature Medicine)" veri setindeki olgular analiz edilerek beyin metastazı bulunan ve bulunmayan hastalar arasındaki moleküler farklılıkları ortaya koymayı amaçladık.

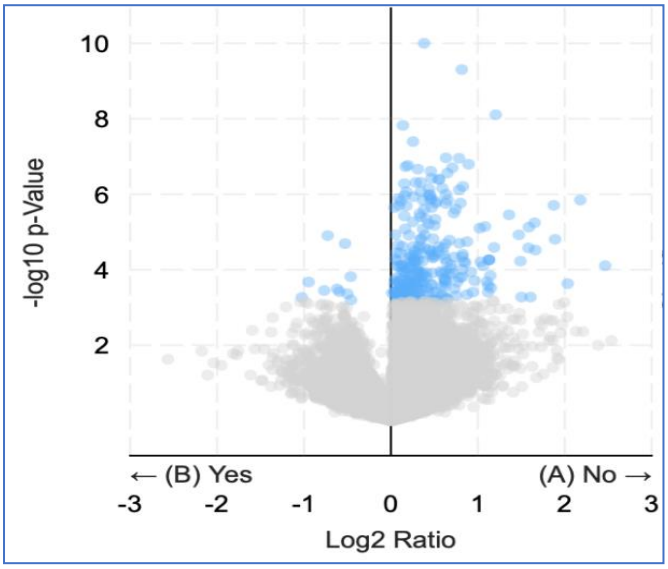
MATERYAL VE METOT

Çalışmamızda, Cbioportal online biyoinformatik servisi üzerinden "Metastatic Melanoma (DFCI, Nature Medicine)" veri seti kullanıldı (https://www.cbioportal.org) (Cerami ve ark. 2012; Liu ve ark. 2019). Bu veri setinin içerdiği 144 adet olgudan beyin metastazı bulunan ve bulunmayan olgular belirlenerek iki grup arasındaki moleküler farklar sırasıyla, "Genomic alterations" ve "mRNA" sekmeleri altında karşılaştırıldı. P ve q değeri için 0,05 istatiksel olarak anlamlılık sınırı kabul edildi.

BULGULAR

Çalışmamıza, "Metastatic Melanoma (DFCI, Nature Medicine)" veri setinde yer alan 144 olgu dahil edildi. Olgulardan 16'sında (%11,1) beyin metastazı bulunmaktaydı. Beyin metastazı bulunan olgulardan, 9'u kadın, 7'si erkekti.

İki grup arasında, DNA mutasyonu varlığı ve kopya sayısı değişiklikleri bakımından istatistiksel olarak anlamlı fark izlenmedi. mRNA ekspresyon durumları karşılaştırıldığında ise 267 gende farklı ekspresyon düzeyleri izlendi (Differantially Expressed Genes, DEGs) (Şekil 1). Bu genlerden, 10 tanesi metastaz izlenen grupta daha yüksek ekspresyon düzeyine sahipken 257 tanesi metastaz izlenmeyen grupta daha yüksek düzeyde eksprese edilmekteydi ($p<0,05$). En yüksek anlamlılığa sahip on gen sırasıyla şunlardı; AQP7 (p=4.96e-10, q=5.165e-6), IGLV-46 (p=7.81e-9, q=5.420e-5), SLC25A15P3 (p=4.02e-8, q=1.672e-4), PTGR (p=1.09e-7, q=3.297e-4), IGHV3-64 (p=1.11e-7, q=3.297e-4), FCRL5 (p=1.61e-7, q=3.747e-4), C12ORF42 (p=1.71e-7, q=3.747e-4), AKAP14 (p=1.86e-7, q=3.747e-4), PKHD1L1 (p=1.98e-7, q=3.747e-4), FDFF10 (p=2.15e-7, q=3.747e-4) (Tablo 1).



Şekil 1. Beyin metastazı bulunan ve bulunmayan olgular arasındaki DEGs

Tablo 1. Beyin metastazı bulunan ve bulunmayan olgular arasındaki en yüksek anlamlılığa sahip DEGs

Gen	p değeri	q değeri
AQP7	4.96e-10	5.165e-6
IGLV-46	7.81e-9	5.420e-5
SLC25A15P3	4.02e-8	1.672e-4
PTGR	1.09e-7	3.297e-4
IGHV3-64	1.11e-7	3.297e-4
FCRL5	1.61e-7	3.747e-4
C12ORF42	1.71e-7	3.747e-4
AKAP14	1.86e-7	3.747e-4
PKHDL1L1	1.98e-7	3.747e-4
FDFF10	2.15e-7	3.747e-4

TARTIŞMA

Bulgularımız, melanom beyin metastazının belirleyici biyolojik süreçlerinin genomik değişikliklerden çok transkripsiyonel düzeyde ortaya çıktığını göstermektedir. Literatürde beyin metastazlarının primer tümöre göre genetik açıdan büyük farklılıklar göstermediği, ancak transkripsiyonel düzeyde belirgin olarak ayrıştığı vurgulanmış olup bu durum "fenotipik plastisite" kavramını desteklemektedir (Biermann et al. 2022). Özellikle metastatik melanomlarda immün düzenleyici genlerin ve adezyon/mikroçevre etkileşimini yöneten transkripsiyonel değişikliklerin baskın olduğu gösterilmiştir (Alvarez-Breckenridge ve ark. 2022). Bu çalışmada saptanan 267 DEGs, beyin metastazı olan olguların belirli bir transkripsiyonel imzaya sahip olabileceği yönündeki bu modern görüşle uyumludur (Radke ve ark. 2022).

Beyin metastazı bulunan olgularda en yüksek ekspresyon farklılığı gösteren genlerin çoğunun immünoglobulin dizileri ve immün reseptörlerle ilişkili olması, santral sinir sistemi (SSS) mikroçevresinin immün baskılanmış yapısına karşı tümör hücrelerinin yeni immün etkileşim mekanizmaları geliştirdiği hipotezini desteklemektedir (Klemm ve ark. 2020). Beynin periferik immün hücre girişine sınırlı izin vermesi nedeniyle melanom hücreleri nöroimmün etkileşimleri etkisiz bırakan alternatif yollar geliştirmekte ve bu durum intrakraniyal metastazda farklı immün-transkripsiyonel programları ortaya çıkarmaktadır (Quail ve Joyce 2017). Bulgularımızdaki IGHV-IGLV aşırı ekspresyonu da bu immün yeniden programlanma sürecinin bir kanıtı olabilir.

Buna karşılık, beyin metastazı saptanmayan olgularda metabolik aktivite, oksidatif stres yanıtı ve hücre döngüsüyle ilişkili geniş bir gen grubunun daha yüksek eksprese edilmesi, sistemik metastatik hastalıkta proliferatif ve metabolik programların baskın olduğuna dair bilgiler içeren literatürle uyumludur (Fischer ve ark. 2019). Beyin metastazlarında bu genlerin belirgin şekilde azalması ise nöral nişin tümör hücrelerini farklı bir

fenotipe zorladığını, yani biyolojik baskının metabolik olmaktan çıkarak adezyon, immün düzenleme ve mikroçevre adaptasyonuna odaklandığını düşündürmektedir (Biermann ve ark 2022).
Çalışmamızda yüksek anlamlılık gösteren AQP7 gibi genleri içeren Aquaporin ailesinin hücresel sıvı dengesi, migrasyon ve invazyon basamaklarında önemli rolü olduğu bilinmektedir (Moon ve ark. 2022). Beyin dokusunun sıvı dengesi ve iyonik dengesi açısından hassas yapısı dikkate alındığında, aquaporinlerin özellikle beyne metastaz eğilimindeki grupta işlevsel rol oynayabileceği düşünülmektedir (Varricchio ve Yool 2023). Bu açıdanAQP7'nin yüksek ekspresyonu, beyin metastazı açısından potansiyel bir biyobelirteç adayı olarak görülebilir.

SONUÇ

Mevcut bulgular, melanom beyin metastazlarının genomik düzeyde belirgin bir ayrışma göstermediğini, ancak geniş kapsamlı bir transkripsiyonel yeniden programlama ile karakterize olduğunu ortaya koymuştur. Beyin metastazı bulunan olgularda immünoglobulin ilişkili genlerin ve AQP7 gibi bazı genlerin yüksek ekspresyon göstermesi, SSS mikroçevresine özgü immün ve nöral adaptasyon mekanizmalarının önemini desteklemektedir. Buna karşılık, metastazı olmayan grupta metabolik ve proliferatif genlerin daha yüksek ekspresyonu, sistemik metastatik fenotip ile beyin tropizmi arasındaki belirgin biyolojik ayrımı yansıtmaktadır. Bu bulgular, yeni biyobelirteç adayları ve potansiyel hedefler sunarak gelecekte yapılacak fonksiyonel ve translasyonel çalışmalara yön verebilir.

KAYNAKLAR

Alvarez-Breckenridge, Christopher, Samuel C. Markson, Jackson H. Stocking, ve ark. 2022. 'Microenvironmental Landscape of Human Melanoma Brain Metastases in Response to Immune Checkpoint Inhibition'. *Cancer Immunology Research* 10 (8): 996–1012. https://doi.org/10.1158/2326-6066.CIR-21-0870.

Biermann, Jana, Johannes C. Melms, Amit Dipak Amin, ve ark. 2022. 'Dissecting the Treatment-Naive Ecosystem of Human Melanoma Brain Metastasis'. *Cell* 185 (14): 2591-2608.e30. https://doi.org/10.1016/j.cell.2022.06.007.

Cerami, Ethan, Jianjiong Gao, Ugur Dogrusoz, ve ark. 2012. 'The cBio Cancer Genomics Portal: An Open Platform for Exploring Multidimensional Cancer Genomics Data'. *Cancer Discovery* 2 (5): 401–4. https://doi.org/10.1158/2159-8290.CD-12-0095.

Fischer, Grant M., Ali Jalali, David A. Kircher, ve ark. 2019. 'Molecular Profiling Reveals Unique Immune and Metabolic Features of Melanoma Brain Metastases'. *Cancer Discovery* 9 (5): 628–45. https://doi.org/10.1158/2159-8290.CD-18-1489.

Klemm, Florian, Roeltje R. Maas, Robert L. Bowman, ve ark. 2020. 'Interrogation of the Microenvironmental Landscape in Brain Tumors Reveals Disease-Specific Alterations of Immune Cells'. *Cell* 181 (7): 1643-1660.e17. https://doi.org/10.1016/j.cell.2020.05.007.

Liu, David, Bastian Schilling, Derek Liu, ve ark. 2019. 'Integrative Molecular and Clinical Modeling of Clinical Outcomes to PD1 Blockade in Patients with Metastatic Melanoma'. *Nature Medicine* 25 (12): 1916–27. https://doi.org/10.1038/s41591-019-0654-5.

Moon, Chul So, David Moon, ve Sung Koo Kang. 2022. 'Aquaporins in Cancer Biology'. *Frontiers in Oncology* 12: 782829. https://doi.org/10.3389/fonc.2022.782829.

Priego, Neibla, Lucía Zhu, Cátia Monteiro, ve ark. 2018. 'STAT3 Labels a Subpopulation of Reactive Astrocytes Required for Brain Metastasis'. *Nature Medicine* 24 (7): 1024–35. https://doi.org/10.1038/s41591-018-0044-4.

Quail, Daniela F., ve Johanna A. Joyce. 2017. 'The Microenvironmental Landscape of Brain Tumors'. *Cancer Cell* 31 (3): 326–41. https://doi.org/10.1016/j.ccell.2017.02.009.

Rabbie, Roy, Peter Ferguson, Kim Wong, ve ark. 2021. 'The Mutational Landscape of Melanoma Brain Metastases Presenting as the First Visceral Site of Recurrence'. *British Journal of Cancer* 124 (1): 156–60. https://doi.org/10.1038/s41416-020-01090-2.

Radke, Josefine, Elisa Schumann, Julia Onken, ve ark. 2022. 'Decoding Molecular Programs in Melanoma Brain Metastases'. *Nature Communications* 13 (1): 7304. https://doi.org/10.1038/s41467-022-34899-x.

Varricchio, Alanah, ve Andrea J. Yool. 2023. 'Aquaporins and Ion Channels as Dual Targets in the Design of Novel Glioblastoma Therapeutics to Limit Invasiveness'. *Cancers* 15 (3): 849. https://doi.org/10.3390/cancers15030849.

ORAL PRESENTATION

Determination of the effect of tinkal-added cement on gamma ray absorption

Hayrettin Eroğlu*[1], İhsan İş[1], Mahmut Engin Kocadağistan[2], Ali Gürol[3]

[*1] Erzurum Technical University, Faculty of Engineering and Architecture, Department of Chemical Engineering
[2]Ataturk University, Faculty of Engineering, Department of Metallurgical and Materials Engineering
[3]Ataturk University, Faculty of Science, Department of Physics

*Corresponding author e-mail: hayrettin.eroglu@erzurum.edu.tr

Abstract

In recent years, the increasing use of nuclear technology—particularly gamma radiation—has raised the importance of radiation protection. In this study, mass attenuation coefficients of cement-based samples produced by mixing dehydrated tinkal ore, obtained from the Balıkesir–Bigadiç region, with cement at specific ratios were measured to determine their gamma-ray absorption capacity. Within the scope of the research, Gamma Ray Absorption Experiments and XRD analyses were carried out.
Mass attenuation coefficients of the prepared samples were measured within the energy range of 13.375–385.851 keV. Significant changes, especially in the low- and medium-energy regions, were observed in comparison with non-additive samples. It was determined that the addition of tinkal decreases mass attenuation coefficients, with this decrease being more pronounced at higher energies. This behavior can be attributed to the low atomic number elements present in tinkal.

Keywords: Cement, Tinkal, Boron, Radiation, Gamma Attenuation

1. INTRODUCTION

Radiation is energy emitted from a source in the form of particles or electromagnetic waves traveling in straight lines. Its use has been increasing in fields ranging from medical applications to industrial operations (Sehhatigdiri, 2014). Radiation is classified into ionizing and non-ionizing categories. Ionizing radiation—such as alpha and beta particles, as well as X- and gamma rays—poses direct health risks.
The use of X-rays and gamma rays, in particular, for diagnostic and therapeutic purposes in medicine, such as radiation oncology, nuclear medicine, cardiology, and radiology, is quite widespread. Nuclear energy is also used as a significant source of electrical energy generation. Radiation is used in industrial applications in various regions. Radiation is also used to kill microorganisms during the sterilization process. Radiation is used to preserve food, extend the shelf life of food, and eliminate harmful microorganisms. Radioisotopes are also used for materials analysis, archaeological research, and monitoring and control in industrial processes. Various radiation-related legal permits are used in research. Radiation techniques and methods are used for research in many fields, including physics, chemistry, biology, archaeology, and materials science. Radiation safety and control are crucial (Karakoç 2024; Yılmaz 2011).
Gamma rays, which are electromagnetic radiation emitted during transitions between nuclear energy levels, have much higher energy and penetration capability than alpha or beta particles. For this reason, high-density materials are generally used for gamma-ray shielding (Köklü 2006).
With the expanding use of radiation, measures to protect against its harmful effects have become essential. Ionizing radiation can cause DNA damage, cellular malfunctions, acute effects at high doses, and stochastic effects such as cancer at lower chronic exposures (Eroglu 2009; Görpe 1992). The three basic methods of protection from these harmful effects are time, distance and armoring.

- Time: In long-term exposures, the exposure dose increases as time increases, resulting in a directly proportional effect. Therefore, the time spent in the environment near the source should be kept as short as possible. Reducing the exposure time is important for direct exposures, but keeping the exposure time short is even more crucial for fluoroscopy due to the high dose (Eroglu 2009; Keskin 2024).
- Distance: The dose exposure increases as one approaches the radiation source. Radiation intensity is inversely proportional to the square of the distance, a phenomenon known as the inverse square law. Appropriate warnings and signs should be installed in areas close to the radiation source (Eroglu 2009; Keskin 2024).
- Shielding: Materials placed in front of a radiation source, surrounding it and thus reducing its intensity, are called shielding. Protection is achieved by creating a barrier with materials that prevent the passage of the radiation source. Shielding should be made with materials and thickness appropriate to the type, energy, type, and intensity of each radiation. Lead shielding should be used to protect against ionizing radiation. Special lead-lined extraction rooms, lead barriers, and leaded personal protective equipment can effectively block ionizing radiation (Eroglu 2009; Keskin 2024).

This study investigated the gamma absorption capacity of tincal-based concrete, an alternative to lead shielding, which is currently widely used.

Concrete is a multi-component building material produced by mixing cement, water, sand, and various mineral additives such as silica fume, fly ash, and blast furnace slag in specific proportions. Portland cement is the most commonly used material in concrete production (Yılmaz 2011).

Tincal ($Na_2B_4O_7 \cdot 10H_2O$), a boron mineral, is inherently colorless and transparent, but can also appear in pink, yellowish, or gray tones due to various impurities. Its hardness ranges from 2 to 2.5 on the Mohs scale, and its specific gravity is approximately 1.7 g/cm³. Tincal can easily decompose, lose water, and transform into the mineral cinachalconite, depending on environmental conditions. One of the most important deposits of this mineral in Turkey is located in the Eskişehir-Kırka region. Also known as borax, tincal forms in salty lake environments as a result of the precipitation of evaporites and is found in association with other evaporite minerals such as carbonates, sulfates, and halite (DPT 2001; 2008).

In a previous study, Erdoğan (1998) produced different types of cement by adding ground boron minerals to cement and examined their physical and mechanical properties. He also evaluated the shielding capacity of boron minerals against neutron radiation in concrete using theoretical approaches. Based on the findings, he concluded that boron mineral addition positively affected shielding performance (Erdoğan 1998).

In 2008, Kharita and colleagues investigated the attenuation coefficients of concrete produced from aggregates commonly used in Syria by gamma rays (137Cs and 60Co isotopes) and neutrons (Am-Be source). The concretes were produced by mixing black beach sand, hematite, dolomite, and serpentine with beach sand in varying proportions. The results showed that concretes containing hematite were more effective in providing protection against both types of radiation (Kharita et al. 2008).

In 2010, Akkurt and his colleagues conducted a study using heavy concretes produced using barite and lead. They measured linear absorption coefficients using radioactive sources with energies of 0.662 MeV, 1.173 MeV, and 1.332 MeV using a NaI(Tl) detector. The results were compared with XCOM data. The results revealed that barite and barite-added heavy concretes are good gamma-ray absorbers, but their shielding properties are lower than those of lead (Akkurt et al. 2010).

This study includes the preparation of tincal added cement samples, determination of their physical and mechanical properties and experimental investigation of their radiation absorption capacity.

2. MATERIALS and METHODS

2.1. Materials

2.1.1. Materials used in experiments

In this study, the mineral tincal was used to investigate its neutron and gamma ray absorption properties. It is anticipated that this mineral may have potential applications as a radiation absorbing material in various fields.Deneylerde kullanılan çimento Aşkale Çimento Fabrikasından temin edilen Portland çimentosu (CEM I 42.5 R)'dur.

Tincal, a natural borate mineral with a high boron content, was obtained from the Kırka-Eskişehir region. Before being used in experimental studies, it underwent preliminary preparation processes such as grinding, drying, and sieve analysis. Following these processes, the samples were reduced to micron size and finally heat-treated at 650°C to remove the crystal water, resulting in anhydrous boron.

2.2. Methods

2.2.1. Production of concrete

The concretes examined in this study were produced at the Civil Engineering Department Laboratory of Erzurum Technical University. Six types of concrete were produced in this study: standard concrete, ulexite, and tincal-added concrete. First, cement-only samples were prepared for comparison. Then, 1%, 5%, and 10% tincal were added to each cement sample, sequentially and separately. The water/binder ratio was set at 0.20 in the experiments. The temperature of the sample was measured with a digital thermometer, and the mixing water temperature was determined to be between 25-30°C. The prepared samples were placed in 5x5x5cm cube sample molds. The samples were kept in their molds for 24 hours and then removed from the molds. During the curing process, the samples were maintained in a constant temperature environment (24°C), and the ambient temperature and relative humidity were regularly monitored with a digital thermometer.

2.2.4. Gamma spectroscopy system

The experimental measurements undertaken in relation to the attenuation coefficient of the concrete produced as part of the study were conducted at the High Energy Spectroscopy Laboratory, which is housed within the Department of Atomic and Molecular Physics at Atatürk University's Faculty of Science. The experimental setup utilized in the study is illustrated in Figure 1. In the experiment, the VEX (variable energy source) and Ba-133 radioisotope were utilized as the source.

The intensity of a photon flux, I_0, decreases with increasing thickness, t, of an absorbing material. The decrease in intensity is described by the Lambert-Beer law (Yilmaz, 2011) as the linear attenuation coefficient (LAC), given by the following equation:

$$\mu = -\frac{1}{t} ln(\frac{I}{I_0}) \qquad (cm^{-1})$$

However, the mass attenuation coefficient (μ/ρ), defined as the ratio of the linear attenuation coefficient (μ) to the sample density (ρ) and does not change depending on the phase of the material, is more commonly used. The mass attenuation coefficients (MACs) are determined using the intensity values measured experimentally in the experimental geometry shown in Figure 1(a) from the equation

$$\left(\frac{\mu}{\rho}\right) = -\frac{1}{\rho t} ln(\frac{I}{I_0})$$

where ρt is called the mass thickness. The unit of the mass attenuation coefficients is cm^2/g.

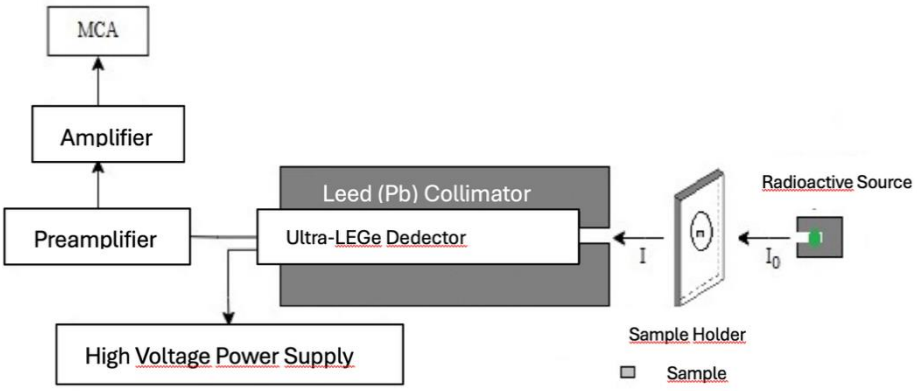


Figure 1. Experimental setup for gamma ray attenuation.

2.2.5. X-ray difraksiyon (XRD)

XRD analysis of the concretes produced within the scope of the study was measured by Erzurum Technical University, High Technology Application and Research Center (YUTAM).

2.2.6. Heat Treatment

The use of boron in the cement sector has become widespread, but boron ores are suitable for use up to a maximum of 2% water content (Kocadağistan and Arslan, 2024). Tincal was dewatered in a muffle furnace at 650°C for 6 hours. Following the heat treatment, the chemically bound water removal rate was calculated by taking the weight differences of tincal and ulexite ores. According to the calculations, 98% water removal was achieved in both ores (Arslan, H.2023; Ataç, H.2024).Tinkale ait XPS ve kimyasal analiz sonuçlarına göre tinkalin %47,2 H_2O içerdiği belirlenmiştir. Ağırlık farkı hesaplamaları sonucu H_2O içerikleri ısıl işlem sonrasında %1 seviyelerine düşürülerek deneylerde kullanılmıştır.

3. RESEARCH FINDINGS AND DISCUSSION

Cement, mixtures of cement and dewatered tincal at 1%, 5%, and 10% were examined, and their gamma absorption values are given below. When these values were examined, it was determined that the best value was 5% tincal, and XRD analyses were performed in accordance with these values.

3. 1. Gamma Absorption Tests of Tincal Additive Cement

The Gamma ray absorption results of the samples of the mixtures are given in Table 1 and Figure 2.

Table 1. Tincal gamma absorption test values

E (keV)	Control	Control + %1 Tincal	Control + %5 Tincal	Control + %10 Tincal
13,375	18,7	18,6	18,4	17,8
14,98	13,5	13,6	12,9	12,7
17,443	8,02	7,95	7,71	7,70
19,607	5,6	5,77	5,63	5,53
22,103	4,16	4,34	4,33	3,91
24,942	2,87	3,05	2,95	2,77
43,737	0,580	0,589	0,570	0,568
44,47	0,575	0,583	0,573	0,562
50,391	0,596	0,605	0,598	0,586
53,155	0,521	0,400	0,379	0,375
59,537	0,243	0,260	0,232	0,222
81	0,236	0,256	0,240	0,233
276,39	0,160	0,113	0,107	0,107
302,85	0,154	0,091	0,089	0,090
356,01	0,153	0,091	0,090	0,090
385,851	0,148	0,085	0,087	0,086

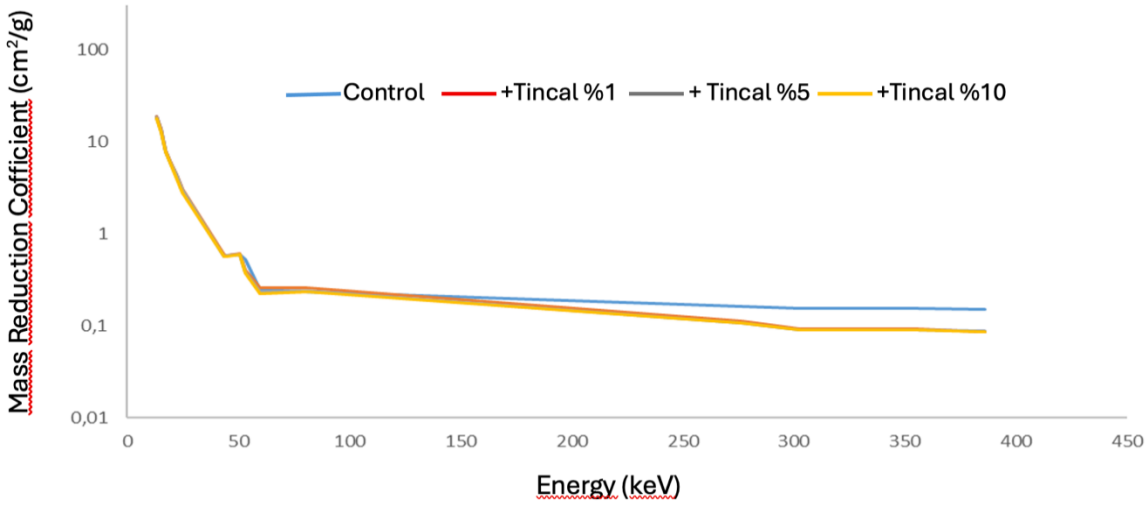


Figure 2. Tincal gamma absorption test values

Table 1. presents the linear attenuation coefficients corresponding to photon energy (E, keV) for samples with different tincal doping ratios (1%, 5%, and 10%). When the data are evaluated in the context of the material's interaction with electromagnetic radiation, it is observed that the linear attenuation coefficient systematically decreases with increasing dopant content. This suggests that the photon absorption capacity of the material decreases with increasing tincal doping.

Low Energy Range (13.375 – 25.942 keV): Tincal doping has a more pronounced effect on the linear attenuation coefficient. For example, at 13.375 keV, the undoped control sample exhibits a value of 18.7, while this value drops to 17.8 in the 10% tincal-doped sample. This indicates that the tincal doping limits the interaction of low-energy photons within the material.

Mid-Energy Range (43.737–81 keV): The tincal doping effect persists, but the differences are more limited. In this range, increasing the doping rate results in a slight decrease in the linear attenuation coefficient.

High Energy Range (276.39 – 385.851 keV): The tincal doping effect has reached a minimal level and the difference between the measured coefficients has decreased considerably.
A general assessment reveals that tincal additions alter the photon absorption properties of cement-based composite materials, and that this change varies with photon energy. It appears that increasing tincal content leads to a decrease in the material's photon absorption capacity, particularly for low-energy photons. These findings provide important insights into the potential role of tincal additions in radiation permeability and structural shielding applications.

3.2. XRD Analysis Evaluation (5% Tincal Added Sample)

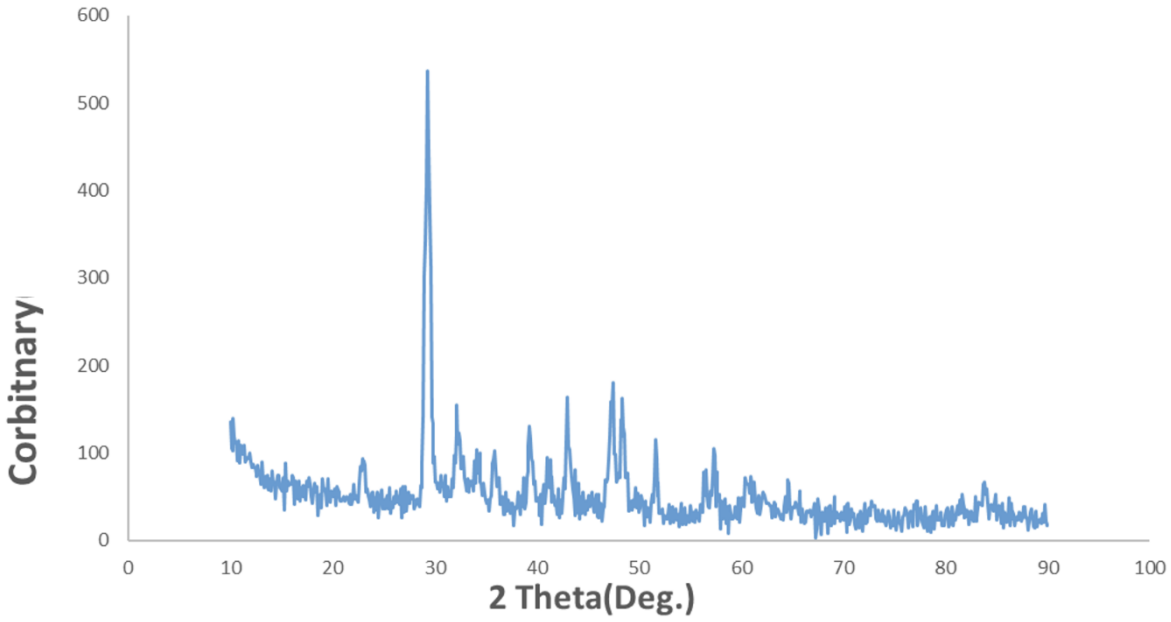


Figure 3. XRD analysis of 5% Tincal added sample

The X-ray diffraction (XRD) pattern of a cement sample containing 5% tincal allows the determination of its crystal structure and mineralogical composition. The graph presents intensity values corresponding to the 2θ angle, and these data are used to identify the crystalline phases within the sample.

Tincal, dolomite, smectite, and calcite are observed in the planes corresponding to the prominent peaks in the XRD spectrum of tincal ore. The high-intensity peak observed at approximately 29° 2θ in the obtained diffractogram reveals the dominant presence of tincal (Na2B4O7.10H2O) and calcite ($CaCO_3$) phases in the sample. Calcite is a common component in the cement matrix, and its presence may be due to either the clinker structure or the carbonation process of the cement matrix. In addition, other intense pixels observed in the 32–34° 2θ range indicate the presence of calcium silicate hydrate (C-S-H) and ettringite phases, which are cement hydration products.

Some pixels detected in the graph with low intensity but distinct levels can be associated with X-ray reflections of the crystal structure of the mineral tincal ($Na_2B_4O_7 \cdot 10H_2O$), which is used as an additive. This suggests that the additive is preserved in physical or chemical form within the cement matrix and integrated into the structure. However, diffraction pixels appearing between 40° and 50° 2θ suggest that tincal may have interacted with cement hydration products, triggering the formation of new mineral phases.

These data indicate that a 5% tincal addition can lead to the formation of specific crystalline phases in the cement matrix, thereby inducing structural changes in the cement microstructure. Such structural changes have the potential to directly affect the mechanical and physical properties (e.g., compressive strength, durability, and impermeability) of cement-based composites.

4. CONCLUSION AND RECOMMENDATIONS

In this study, the gamma absorption capacity of tincal ore obtained from the Balıkesir-Bigadiç region was investigated using various experimental methods. Within the scope of the experimental studies, gamma absorption experiments and X-Ray Diffraction (XRD) analyses were conducted under various parameters. Based on these analyses, the radiation absorption properties of tincal ore were evaluated, and the findings are presented below.
The gamma radiation absorption capacities of composite samples formed by doping tincal ore at different rates were investigated experimentally. As a result of measurements carried out at energy levels between 13.375 keV

and 385.851 keV, it was determined that the additives had significant effects on radiation permeability, especially in the low and medium energy ranges.
Tincal-doped samples were found to generally have higher gamma ray transmittance, leading to lower attenuation performance. A decreasing trend in the absorption coefficient of the mineral was observed with increasing doping ratio, and this was particularly evident in the presence of high-energy gamma rays.
Considering the positive effects of Tincal on neutron absorption in previous studies, its effectiveness in radiation shielding can be evaluated along with its gamma absorption capacity (İş, 2025).

References

Akkurt, I. Akyildirim, H., Mavi, B., Kilincarslan, S., Basyigit, C., 2010d. Radiation shielding of concrete containing zeolite. Radiation Measurements, 45, 827– 830.

Ataç, E. 2024. Isıtma Hızının Tinkal Cevherinin Bozunma Sıcaklığına Etkisi ve Kalsinayonu, Yüksek Lisans Tezi, Atatürk Üniversitesi Fen Bilimleri Enstitüsü, Metalurji ve Malzeme Bilimi Mühendisliği Anabilim Dalı, 92, Erzurum.

DPT Raporu, (2001), Sekizinci Beş Yıllık Kalkınma Planı, Madencilik Özel İhtisas Komisyonu Raporu, Endüstriyel Hammaddeler Alt Komisyonu Kimya Sanayii Hammaddeleri Cilt:2 (Bor Tuzlan-Trona-Kaya TuzuSodyum Sülfat- Stronsiyum) Çalışma Grubu Raporu (DPT:2608- ÖİK:619), Ankara.

DPT Raporu, (2008), Dokuzuncu Kalkınma Planı (2007-2013), Kimya Sanayii Özel İhtisas Komisyonu, Bor-Soda Külü-Krom Kimyasalları Çalışma Grubu Raporu (DPT:2776-ÖİK:705), 5-43, Ankara, ISBN: 978-975-19-4353-8.

Erdoğan, Y., Zeybek, M. S. ve Demirbaş, A. (1998). Cement mixes containing colemanite from concentrator wastes. Cement and Concrete Research, 28, 605-609.

Eroğlu, H. 2009. Nükleer tıpta kullanılan radyoaktif talyum-201 ve galyum-67'nin adsorbsiyonu. Kimya mühendisliği anabilim dalı. Doktora tezi, Erzurum.

Görpe, A.ve Cantez, S., 1992. Temel Fizik. Pratik Nükleer Tıp. İstanbul Tıp Fakültesi Vakfı, İstanbul, 1-42.

ICRP. (2007). *The 2007 Recommendations of the International Commission on Radiological Protection* (ICRP Publication 103). Annals of the ICRP, 37(2–4).

İş, İ. 2025. Bor Katkılı Çimentonun Nötron Ve Gama Işınlarını Soğurma Kapasitesine Etkisi, Yüksek Lisans Tezi, Erzurum Teknik Üniversitesi Fen Bilimleri Enstitüsü, Biyomedikal Mühendisliği Anabilim Dalı, Erzurum.

Karakoç, A. 2024. Radyasyon Dedektörü Yapimi Ve Çeşitli Malzemelerin Radyasyon Ölçümü, Yüksek Lisans Tezi,Erzincan Binali Yıldırım Üniversitesi Fen Bilimleri Enstitüsü,Elektrik-Elektronik Mühendisliği Anabilim Dalı, 60,Erzincan.

Keskin, N. 2024. Türkiye'de Görev Yapan Anestezi Teknisyen/Teknikerlerinin İyonize Radyasyondan Korunma Hakkinda Bilgi Düzeylerinin Ve Tutumlarinin Değerlendirilmesi, Yüksek Lisans Tezi, Ufuk Üniversitesi Sosyal Bilimler Enstitüsü, İşletme Anabilim Dali Sağlik Yönetimi Programi, 134, Ankara.

Kharita, M.H., Takeyeddin, M., Alnassar, M., Yousef, S., 2008. Development of special radiation shielding concretes using natural local materials and evaluation of their shielding characteristics. Progress in Nuclear Energy, 50, 33–36.

Kocadağistan, M.E., Arslan, H. (2024). Advantageous approach for boron ores used in cement production: optimization of dehydration. Challenge Journal of Concrete Research Letters 15 (1)(2024) 7–19.

Köklü, G., Yilmaz, Ö. Phytoprotection, 2006, erudit.org

Sehhatigdiri,A.2014.Farklı Killerin Radyoaktif Maddelere Karşı Zırhlama Özelliklerinin Deneysel Olarak Araştırılması.Yüksek Lisans Tezi,Erzurum Teknik Üniversitesi Fen Bilimleri Enstitüsü,İnşaat Mühendisliği Anabilim Dalı, 53 ,Erzurum.

Yılmaz, E. 2011.Bazı İnşaat Malzemelerinde Gama Işını Soğurma Katsayısı Ve Nötron Soğurma Katsayısı Tesir Kesitinin Belirlenmesi. Yüksek Lisans Tezi, Rize Üniversitesi, Fen Bilimleri Enstitüsü, Fizik Anabilim Dalı, 81,Rize.

Yılmaz, O., 2014. Tüvenan tinkalden kalsine tinkal üretimi, Gazi Üniversitesi Mühendislik ve Mimarlık Fakültesi Dergisi, Cilt 29, No.2, 401-406, https://doi.org/10.17341/gummfd.18642.

ORAL PRESENTATION

A dual-action role of naphthalene sulfonate in enhancing arsenic uptake and mitigating toxicity in maize seedlings

Cansu Altuntaş[1*] (Orcid: https://orcid.org/0000-0002-1363-6142),
Abidin Gümrükçüoğlu[1] (Orcid: https://orcid.org/0000-0001-7285-9664)

[*1]University of Artvin Coruh, [1]Medicinal-Aromatic Plants Application and Research Centre, 0800, Artvin, Turkey

*Corresponding author e-mail: cansualtuntas@artvin.edu.tr

Abstract

Arsenic (As) contamination of agricultural soils continues to pose a major threat to crop productivity and global food security. Although conventional chelating agents enhance metal availability, their tendency to intensify phytotoxicity and persist in the environment limits their practical use in field applications. This study investigated the potential of naphthalene-1-yl naphthalene-2-sulfonate (NNS) as a dual-mechanism agent capable of enhancing As uptake while simultaneously alleviating As-induced toxicity in *Zea mays* seedlings. Co-application of NNS with As increased plant As accumulation by 69% compared to As alone while reducing lipid peroxidation and hydrogen peroxide levels by 37% each. The antioxidant defense system was markedly reprogrammed: superoxide dismutase activity decreased by 42%, whereas ascorbate peroxidase activity increased by 20%, strengthening H_2O_2 detoxification. Non-enzymatic antioxidants, including epicatechin (89%), chlorogenic acid (42%), and syringic acid (41%), showed substantial increases, indicating improved redox homeostasis under NNS+As treatment. Photosynthetic performance was notably preserved, with net photosynthetic rate recovering by 95–96% relative to As-treated plants. Overall, NNS demonstrated an innovative dual-action role by promoting As phytoaccumulation while protecting plants from oxidative damage and maintaining photosynthetic functionality. These findings highlight NNS as a promising and environmentally sustainable phytoremediation enhancer that supports both contaminant removal and crop health.

Keywords: Arsenic, antioxidant, maize, phytoremediation, oxidative stres

INTRODUCTION

Arsenic (As) contamination of agricultural soils is a persistent global problem that severely limits crop productivity and threatens food chain safety (Nahar et al. 2022). Anthropogenic activities, including mining operations and the excessive use of agrochemicals, have accelerated arsenic accumulation in farmland. Irrigation with As-contaminated groundwater is a major contributing factor and can continuously introduce arsenic into soils and crops (Zhao et al. 2010; Shankar et al. 2014). In sensitive regions, these inputs destabilize agroecosystems and create long-term risks for sustainable agricultural production.

Once absorbed by plants, arsenic disrupts several interconnected physiological processes. It affects stomatal regulation and transpiration, reduces CO_2 availability, and impairs photosynthetic structures, particularly the PSII complex, where key reaction center proteins (e.g., D1/D2) become highly susceptible to damage (Finnegan and Chen 2012). As also triggers oxidative stress through the overproduction of reactive oxygen species (ROS), leading to disturbances in membrane integrity, pigment stability, and metabolic activity. Consequently, As exposure results in decreased carbon assimilation, impaired photosynthetic electron transport, and growth inhibition, ultimately threatening crop yields and food security (Nahar et al. 2022).

Various strategies have been explored to mitigate As-induced damage. Exogenous antioxidants such as glutathione, ascorbic acid, melatonin, proline, and glycine betaine help reduce oxidative stress by enhancing detoxification pathways or scavenging ROS. Nutrient amendments, including silicon and selenium, also strengthen the antioxidant defense system and support stress tolerance (Das et al. 2022). However, these interventions generally act downstream of ROS generation, offering limited protection to core photosynthetic structures, and they do not contribute to enhanced metal mobility or uptake.

Chelating agents have been widely used to increase metal bioavailability in phytoremediation applications. Although effective in mobilizing metals, conventional chelators often exacerbate phytotoxicity and persist in the environment, reducing their suitability for safe agricultural deployment. There remains a significant need for new compounds capable of simultaneously improving arsenic uptake and protecting plant physiology.

Recent interest in naphthalene-sulfonate derivatives has highlighted their potential to modulate oxidative stress responses. Some naphthalene-sulfonate hybrids have been shown to reduce hydrogen peroxide and TBARS accumulation under drought stress in maize (Yetişsin and Korkmaz 2023), suggesting that this chemical class may possess biologically relevant antioxidant properties. However, their potential roles in heavy-metal stress, particularly in arsenic-contaminated systems, remain unexplored. In this context, the present study focuses on naphthalene-1-yl naphthalene-2-sulfonate (NNS) as a promising dual-mechanism candidate. By integrating both mobilizing capacity and physiological protection, such compounds may offer innovative and sustainable solutions for enhancing phytoremediation efficiency in As-impacted agricultural environments.

MATERIALS AND METHODS

Plant Growth Conditions

Maize (*Zea mays* L., cv. ADA-523) seeds were sown in sterile vermiculite and moistened with half-strength Hoagland nutrient solution. Germination and early growth were carried out in a controlled environment chamber set to 23 ± 2 °C with a 16 h light / 8 h dark regime. Once seedlings emerged, full-strength Hoagland solution was supplied twice per week for a period of 21 days, following the classical nutrient formulation of Arnon (1950). This semi-hydroponic setup was selected to avoid soil-related inconsistencies and to ensure homogeneous nutrient uptake. Experimental treatments were organized according to a randomized complete block design, consisting of three biological replicates and three technical replicates for each treatment group.

Treatments

After 21 days of cultivation, shoots were excised 2 cm above the substrate surface and immersed in distilled water for one hour to stabilize water status prior to chemical exposure. Subsequently, plants were transferred into treatment solutions and maintained for 18 h under the same environmental conditions. The concentration of NNS (0.25 mM) was derived from preliminary watering-stress experiments in which the compound effectively lowered oxidative stress markers without eliciting toxicity (Yetişsin and Korkmaz, 2023). As was applied at 100 µM, a dose known to induce measurable oxidative stress in maize seedlings (Arikan and Abdulveli, 2025). Four experimental sets were created: control, NNS alone, As alone, and NNS followed by As exposure. Measurements were taken between 10:00 and 12:00 for photosynthetic rate, after which plant material was immediately frozen in liquid nitrogen and stored at –20°C.

Determination of As Content

As accumulation in shoot tissue was quantified via inductively coupled plasma–mass spectrometry (ICP-MS; Agilent 7900, USA). Approximately 1 g of oven-dried sample was subjected to microwave digestion using concentrated HNO_3 and H_2O_2. Digested samples were diluted to a final volume of 50 mL and analyzed using a quartz torch, concentric nebulizer, and a cyclonic spray chamber.

Quantification of Oxidative Stress Indicators

Fresh leaf tissue (0.1 g) was homogenized for the assessment of thiobarbituric acid reactive substances (TBARS) and hydrogen peroxide (H_2O_2).

TBARS: The extract was mixed with TBA reagent in trichloroacetic acid (TCA), heated at 95 °C for 25 min, cooled, and absorbance values were recorded at 532 nm and 600 nm. Malondialdehyde concentration was computed using the extinction coefficient reported by Heath and Packer (1968).

H_2O_2: Extract aliquots were combined with potassium phosphate buffer and KI, and absorbance was measured at 390 nm following the procedure of Velikova et al. (2000).

Enzymatic Antioxidant Assays

Leaf samples (0.1 g) were homogenized on ice in enzyme-specific buffers containing EDTA and PVPP to prevent phenolic interference. For SOD assay, potassium phosphate buffer (pH 7.8) supplemented with EDTA and PVPP was used. For APX activity, sodium phosphate buffer (pH 7.0) containing EDTA, PVPP, and ascorbate was employed. Extracts were centrifuged at 4 °C (15,000 rpm, 15 min) prior to use.

SOD activity was assessed using the photochemical NBT reduction method described by Beauchamp and Fridovich (1971), with absorbance readings at 560 nm. APX activity was assayed according to Nakano and Asada (1987), monitoring the oxidation of ascorbate at 290 nm using its characteristic extinction coefficient.

HPLC-DAD Analysis of Non-Enzymatic Antioxidants
Chromatographic Setup

Non-enzymatic antioxidant compounds were profiled using an Agilent 1260 Infinity II HPLC-DAD system equipped with an ACE 5 C18 analytical column. A wavelength range of 250–535 nm was utilized to detect phenolic signatures. External calibration curves (25–300 µg mL^{-1}) were generated for all reference standards.

Sample Extraction

Air-dried leaf tissue (20 g) was extracted with methanol using ultrasonic-assisted extraction (1:10 w/v; 600 W; 30 min), followed by 24 h shaking in darkness (150 rpm). Extracts were filtered sequentially through Whatman No. 1 paper and 0.45 µm PTFE membranes and stored at 4°C until chromatographic analysis (Uysal et al. 2016; Akbulut et al. 2021).

Net Photosynthetic Rate (P_n)

Net photosynthesis (P_n) was recorded using a LI-6800 Portable Photosynthesis System (LI-COR Biosciences). Measurements were taken on fully expanded third leaves following a minimum of 30 min acclimation to ensure signal stabilization under standardized conditions: 400 µmol mol^{-1} CO_2 concentration, 250 µmol m^{-2} s^{-1} PPFD, 25°C leaf/chamber temperature, and 60% relative humidity.

RESULTS

As Accumulation

Both As and NNS treatments individually resulted in significant increases ($p < 0.05$) in shoot As concentration, by 90% and 49%, respectively, relative to the control, indicating effective metal translocation under the experimental conditions (Figure 1). Moreover, NNS pre-treatment further elevated As accumulation by 69% compared to As alone, without compromising tissue integrity ($p < 0.05$).

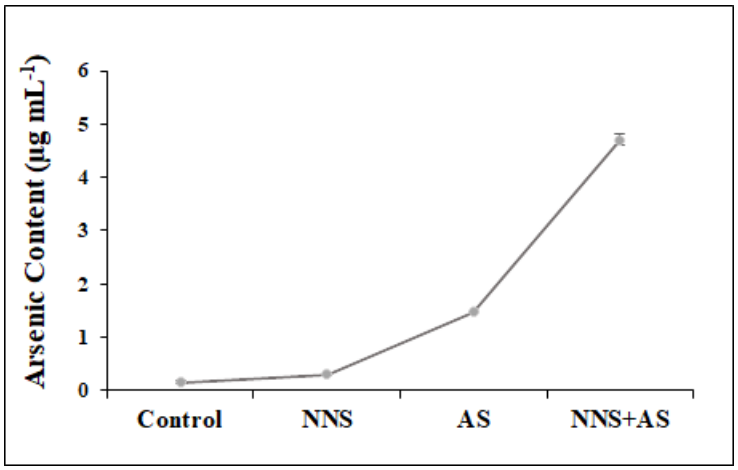


Figure 1. Effect of NNS on arsenic accumulation in maize seedlings under As stress. NNS+As treatment resulted in a 69% increase in As accumulation compared to As treatment alone. Values represent means ± SDs of three biological replicates (n = 3). Different lowercase letters indicate significant differences among treatments based on Duncan's multiple range test at $p < 0.05$.

Content of TBARS, H_2O_2, SOD, APX

NNS treatment alone produced minor alterations in oxidative stress indicators relative to the control when normalized to the higher concentration values. TBARS remained essentially unchanged, while H_2O_2 increased moderately by 16%. SOD activity showed a slight 3% decrease, whereas APX activity increased by 18% under NNS application (Table 1)

As exposure strongly intensified oxidative stress, yet co-treatment with NNS markedly alleviated these effects. Compared with As alone, the NNS+As application reduced TBARS and H_2O_2 by 37%, and decreased SOD activity by 42%. In contrast, APX activity showed a 20% increase under NNS+As relative to As treatment (Table 1).

Table 1. Effects of NNS on contents of thiobarbituric acid reactive substances (TBARS), hydrogen peroxide (H_2O_2) and antioxidant enzyme activities in maize seedlings under As stress. NNS+As treatment decreased lipid peroxidation and hydrogen peroxide by 37%, superoxide dismutase (SOD) activity by 42%, increased ascorbate peroxidase (APX) 25%, compared to the As-only treatment. Values represent means ± SDs of three biological replicates (n=3). Different lowercase letters indicate significant differences among treatments based on Duncan's multiple range test at $p < 0.05$

Treatments	Control	NNS	As	NNS+As
TBARS (nmol g^{-1} FW)	1.60 ± 0.11^{c}	1.61 ± 0.23^{c}	3.12 ± 0.04^{a}	2 ± 0.3^{b}
H_2O_2 (ng g^{-1} FW)	13.3 ± 0.14^{d}	15.8 ± 0.08^{b}	22.11 ± 0.26^{a}	14 ± 0.08^{c}
SOD (U mg^{-1} protein)	1.33 ± 0.12^{c}	1.29 ± 0.2^{c}	3.7 ± 0.2^{a}	2.15 ± 0.13^{b}
APX (U mg^{-1} protein)	0.33 ± 0.06^{c}	0.4 ± 0.07^{c}	2.1 ± 0.02^{b}	2.63 ± 0.16^{a}

Non-enzymatic antioxidant contents

NNS treatment caused moderate shifts in phenolic antioxidant levels compared with the control when normalized to the higher concentration values. Relative to control plants, NNS increased epicatechin by 41% and syringic acid by 39%, while chlorogenic acid exhibited a 21% decrease. Although arsenic stress markedly suppressed these metabolites, co-application of NNS with As substantially restored and enhanced phenolic accumulation. Compared with As alone, the NNS+As treatment elevated epicatechin by 89%, chlorogenic acid by 42%, and syringic acid by 41% (Table 2).

Table 2. Effects of NNS on phenolic compounds under As stress. NNS+As treatment increased epicatechin, chlorogenic acid, syringic acid by 90%, 42%, 39%, respectively, compared to the As-only treatment (µg g^{-1} extract). Values represent means ± SDs of three biological replicates (n=3). Different lowercase letters indicate significant differences among treatments based on Duncan's multiple range test at $p < 0.05$.

No	Compounds (µg/g)	RT [min]	Control	NSS	AS	NSS + AS
1	**Epicatechin**	8.45	81.83	139.13	12.33	117.52
2	**Chloragenic acid**	18.184	336.7	266.8	124.7	213.7
3	**Syringic acid**	23.228	106.5	175.7	112.4	192.1

P_n content

NNS alone showed no significant differences from controls for P_n ($p > 0.05$). As treatment reduced P_n by 98% compared to the control. The NNS+As combination dramatically increased P_n by 95% compared to As alone (Table 3).

Table 3. Effects of NNS on net photosynthetic rate (P_n) in maize seedlings under As stress. NNS+As treatment increased P_n increased by 95%. Values represent means ± SDs of three biological replicates (n=3). Different lowercase letters indicate significant differences among treatments based on Duncan's multiple range test at $p < 0.05$.

Parameters	Control	NSS	As	NSS+As
P_n (µmol m^{-2} s^{-1})	7.73 ± 0.3^{a}	8.16 ± 1.2^{a}	0.16 ± 0.04^{c}	2.8 ± 0.11^{b}

DISCUSSION

As accumulation is a key indicator of bioavailability and phytotoxicity and is widely used to evaluate phytoremediation efficiency (Tamma et al., 2025). In this study, NNS pre-treatment substantially increased As uptake compared with As-alone plants, yet without the toxicity commonly associated with conventional chelators. EDTA, although highly effective in mobilizing metals, poses leaching risks and persists in the environment (Shahid et al., 2014), whereas citric acid is rapidly degraded by soil microorganisms, limiting its long-term chelating capacity (Römkens et al., 2002). Selenium supplementation and similar protective strategies often reduce As uptake while improving tolerance, demonstrating the traditional protection–versus–extraction trade-off (Malik et al., 2012). By contrast, NNS simultaneously enhanced As mobilization and preserved physiological performance, effectively resolving this trade-off and positioning NNS as a dual-function phytoremediation aid.

As stress markedly increased markers of oxidative damage, as reflected by elevated TBARS and H_2O_2 levels, consistent with earlier reports describing severe ROS accumulation under metalloid stress (Arikan et al., 2022). NNS pre-treatment substantially reduced these oxidative indicators relative to As-only plants, restoring redox status close to the control and demonstrating strong protection against ROS-induced lipid peroxidation. NNS alone did not induce oxidative injury, indicating that it is not only non-phytotoxic but actively protective. Although citric acid can partially suppress H_2O_2 (Tahjib-Ul-Arif et al., 2021) and EDTA may reduce MDA while sustaining oxidative pressure (Kamal et al., 2023), neither agent provides simultaneous As mobilization and robust oxidative protection.

The enzymatic antioxidant system further supports this dual functionality. As exposure strongly elevated SOD and APX activities, reflecting increased demand for both superoxide and H_2O_2 detoxification under intense oxidative pressure (Finnegan and Chen, 2012). NNS pre-treatment altered this pattern in a more balanced direction: SOD activity declined toward control levels, suggesting reduced superoxide generation, whereas APX activity increased, indicating reinforcement of the H_2O_2-scavenging pathway. This configuration points to a more metabolically efficient antioxidant response, similar to protective patterns reported in treatments such as thiamine + IAA or biochar in As-stressed maize (Rahman et al., 2023). Unlike EDTA, which often exacerbates oxidative stress due to stable metal–EDTA complexes (Kamal et al., 2023), NNS combines metal interaction with direct enhancement of detoxification pathways. Findings from related naphthalene–sulfonate derivatives reducing TBARS and H_2O_2 in maize under stress (Yetişsin and Korkmaz, 2023) further support this interpretation.

Non-enzymatic antioxidants were also strongly influenced by NNS. As stress suppressed phenolic compounds such as epicatechin, chlorogenic acid, and syringic acid, demonstrating disruption of intrinsic phenolic defenses (Hasanuzzaman and Fujita, 2013). NNS co-treatment restored and enhanced these metabolites, indicating activation of protective biosynthetic pathways. These improvements likely reflect stimulation of the phenylpropanoid pathway and associated regulatory networks (Fraser and Chapple, 2011), suggesting that NNS promotes both preservation and synthesis of key phenolic antioxidants.

Photosynthetic performance, measured as Pn, was strongly inhibited by As, consistent with previous reports describing stomatal and mesophyll impairment under metalloid stress (Finnegan and Chen, 2012). NNS+As markedly restored Pn toward control values, indicating preservation of CO_2 assimilation capacity. Whereas EDTA often suppresses photosynthesis due to formation of persistent and phytotoxic metal–EDTA complexes (Kamal et al., 2023), and citric acid provides only temporary improvement (Tahjib-Ul-Arif et al., 2021), NNS uniquely combines strong As chelation with protection of photosynthetic machinery. Maintaining Pn is crucial for phytoremediation because it sustains biomass accumulation and transpiration-driven As uptake (Anjum et al., 2016).

Taken together, these findings demonstrate that NNS mediates a coordinated protective response under As stress. It enhances As uptake while simultaneously reducing oxidative damage, rebalancing antioxidant enzymes, restoring key non-enzymatic antioxidants, and preserving photosynthetic carbon assimilation. This integrated mechanism overcomes the conventional protection–versus–extraction conflict observed with traditional chelators and identifies NNS as a promising next-generation tool for sustainable phytoremediation.

CONCLUSION

This study demonstrates that naphthalene-1-yl naphthalene-2-sulfonate (NNS) acts as an effective dual-function agent capable of simultaneously enhancing As uptake and mitigating As-induced toxicity in maize seedlings. NNS pre-treatment significantly increased As accumulation without inducing the phytotoxic effects typically associated with conventional chelators. At the physiological level, NNS alleviated oxidative stress by reducing lipid peroxidation and H_2O_2 accumulation, reshaping the antioxidant enzyme system toward a more efficient detoxification profile. The compound also restored key non-enzymatic antioxidants, including epicatechin, chlorogenic acid, and syringic acid, indicating improved redox homeostasis under As stress. Moreover, NNS preserved photosynthetic performance by maintaining Pn under conditions where As strongly inhibited CO_2 assimilation.

Together, these findings show that NNS provides a coordinated protective mechanism that stabilizes cellular redox balance, supports metabolic resilience, and sustains photosynthetic function while enhancing As phytoaccumulation. Such combined benefits overcome the common protection–versus–extraction trade-off seen with traditional chelators. Therefore, NNS represents a promising and environmentally sustainable candidate for improving phytoremediation efficiency in As-contaminated agricultural systems.

REFERENCES

Anjum, S. A., Ashraf, U., Khan, I., Tanveer, M., Khan, A. U., Shahid, M., … Wang, L. (2016). Phytohormones and plant responses to heavy metal stress: A review. Plant Growth Regulation, 80(2), 215–224.

Arikan, B., Özyiğit, İ. İ., Yücel, M., Aydin, S., & Göktürk Baydar, N. (2022). Exogenous hesperidin and chlorogenic acid alleviate oxidative damage induced by arsenic toxicity in *Zea mays* through regulating the water status, antioxidant capacity, redox balance and fatty acid composition. Environmental Pollution, 292, 118389.

Arikan-Abdulveli, B. (2025). Acetylcholine treatments enhance growth, photosynthesis efficiency and stress resilience in maize seedlings exposed to arsenic. Turkish Journal of Botany, 49(1), 13–24.

Arnon, D. I. (1950). Prof. Dr. Hoagland. Nature, 165, 56–58.

Beauchamp, C., & Fridovich, I. (1971). Superoxide dismutase: Improved assays and an assay applicable to acrylamide gels. Analytical Biochemistry, 44(1), 276–287.

Das, S., Majumder, B., & Biswas, A. K. (2022). Comparative study on the influence of silicon and selenium to mitigate arsenic induced stress by modulating TCA cycle, GABA, and polyamine synthesis in rice seedlings. Ecotoxicology, 31(4), 468–489.

Finnegan, P. M., & Chen, W. (2012). Arsenic toxicity: The effects on plant metabolism. Frontiers in Physiology, 3, 182.

Fraser, C. M., & Chapple, C. (2011). The phenylpropanoid pathway in *Arabidopsis*. The Arabidopsis Book, 9, e0152.

Hasanuzzaman, M., Nahar, K., & Fujita, M. (2013). Plant responses and tolerance to abiotic oxidative stress: Antioxidant defense is a key factor. In M. V. Srivastava (Ed.), *Crop stress and its management: Perspectives and strategies* (pp. 261–315). Springer.

Heath, R. L., & Packer, L. (1968). Photoperoxidation in isolated chloroplasts. I. Kinetics and stoichiometry of fatty acid peroxidation. Archives of Biochemistry and Biophysics, 125(1), 189–198.

Kamal, M. A., Iqbal, M., Saleem, M. H., Cheema, M., Ayub, A., Shah, A. N., … Niazi, N. K. (2023). Effect of different levels of EDTA on phytoextraction of heavy metals and associated oxidative responses. Frontiers in Microbiology, 14, 1228117.

Malik, J. A., Goel, S., Kaur, N., Sharma, S., Singh, I., & Nayyar, H. (2012). Selenium antagonises the toxic effects of arsenic on mungbean (*Phaseolus aureus* Roxb.) plants by restricting its uptake and enhancing the antioxidative and detoxification mechanisms. Environmental and Experimental Botany, 77, 242–248.

Nahar, K., Rhaman, M. S., Parvin, K., Bardhan, K., Marques, D. N., García-Caparrós, P., & Hasanuzzaman, M. (2022). Arsenic-induced oxidative stress and antioxidant defense in plants. Stresses, 2(2), 179–209.

Nakano, Y., & Asada, K. (1987). Purification of ascorbate peroxidase in spinach chloroplasts; Its inactivation in ascorbate-depleted medium and reactivation by monodehydroascorbate radical. Plant and Cell Physiology, 28(1), 131–140.

Rahman, M. M., Das, A. K., Sultana, S., Ghosh, P. K., Islam, M. R., Keya, S. S., Ahmed, M., & Mostofa, M. G. (2023). Biochar potentially enhances maize tolerance to arsenic toxicity by improving physiological and biochemical responses to excessive arsenate. Biochar, 5, 71.

Römkens, P., Bouwman, L., Japenga, J., & Draaisma, C. (2002). Potentials and drawbacks of chelate-enhanced phytoremediation of soils. Environmental Pollution, 116(1), 109–121.

Shankar, S., Shanker, U., & Shikha. (2014). Arsenic contamination of groundwater: A review of sources, prevalence, health risks, and strategies for mitigation. The Scientific World Journal, 2014, 304524.

Tahjib-Ul-Arif, M., Zahan, M. I., Karim, M. M., Imran, S., Hunter, C. T., Islam, M. S., … Murata, Y. (2021). Citric acid-mediated abiotic stress tolerance in plants. International Journal of Molecular Sciences, 22(13), 7235.

Tamma, A. A., Ali, S., & Wang, H. (2025). Advancing phytoremediation: A review of soil amendments. Sustainability, 17(5), 5688.

Velikova, V., Yordanov, I., & Edreva, A. (2000). Oxidative stress and some antioxidant systems in acid-rain-treated bean plants: Protective role of exogenous polyamines. Plant Science, 151(1), 59–66.

Yetişsin, F., & Korkmaz, A. (2023). Synthesis and characterization of naphthalene-sulfonate hybrid structures and their effects on abiotic stress indicators in maize. Anadolu Orman Araştırmaları Dergisi, 9(1), 89–95.

Zhao, F. J., McGrath, S. P., & Meharg, A. A. (2010). Arsenic as a food chain contaminant: Mechanisms of plant uptake and metabolism and mitigation strategies. Annual Review of Plant Biology, 61, 535–559.

ORAL PRESENTATION

Synthesis of schiff-based graft copolymer with waste PET and nucleation effect in PP masterbatches

Songül Şahin Dumankaya[1]* (Orcid: https://orcid.org/0000-0001-9224-8393), Gökhan Ceyhan[1,2] (Orcid: https://orcid.org/0000-0002-9127-2348), Sibel Bilgiç Kara[3] (Orcid: https://orcid.org/0000-0001-8841-5961)

[1]* Kahramanmaraş Sütçü İmam University, Department of Materials Science and Engineering, Kahramanmaraş, Türkiye.
[2] Kahramanmaraş Sütçü İmam University, Technical Sciences Vocational School, Food Processing Program, Kahramanmaraş, Türkiye.
[3] Kahramanmaraş Paper Industry and Trade Inc. R&D Center, Kahramanmaraş, Türkiye.

*Corresponding author e-mail: sonqulsahin@hotmail.com

Abstract

Waste polyethylene terephthalate (PET) was converted into a graft copolymer via reactive extrusion via a maleic anhydride (MA) bridge with newly synthesized macromolecular Schiff base (N_2). This graft copolymer was combined with 25 MFI homopolymer polypropylene (PP) in the form of a masterbatch according to an optimized recipe at industrial scale. The recipe contained 95.5% PP, 1.5% AO-168 antioxidant, 1.5% AO-1010 antioxidant, 1.0% N_2 Schiff base and 0.5% CA30 calcium stearate. In Fourier transform infrared spectroscopy (FTIR) analysis, the imine υ(C=N) bond was preserved in the range of 1500–1675 cm^{-1}, while the ester bond originating from MA was observed at 1725 cm^{-1}. Differential scanning calorimetry (DSC) measurements showed that the crystallization temperature ($T_{(c)}$) increased from 118 °C to 142 °C (+24 °C) in waste PET and from 115 °C to 138 °C (+23 °C) in the masterbatch. Scanning electron microscopy (SEM) images confirmed the homogeneous distribution of the graft copolymer with a size of <5 µm in the PP matrix. In mechanical tests, tensile strength increased by 24% (from 33.5 MPa to 41.6 MPa) and impact strength by 15% (from 3.2 kJ/m² to 3.7 kJ/m²). These findings demonstrate that N2 Schiff-based graft copolymer from waste PET accelerates crystallization kinetics and improves mechanical properties by providing highly efficient nucleation at a low dosage (1%) in polypropylene masterbatches.

Keywords: rPET, Schiff base, graft copolymer, nucleating agent, polypropylene masterbatch, reactive extrusion

INTRODUCTION

Polypropylene (PP) is one of the most common thermoplastic polymers, with an annual global production volume exceeding 80 million tons due to its low cost, excellent chemical resistance, and processability (Gao et al., 2024). However, the integration of secondary raw materials such as recycled PP (rPP) and waste PET leads to problems such as chain breakage, slowing of crystallization kinetics due to thermal degradation and oxidative degradation, increased brittleness, and loss of optical transparency (Badia et al., 2012). These problems lead to economic losses by extending the cycle time, especially in high-speed production processes such as injection molding and film extrusion (Schyns & Shaver, 2021). Nucleating agents increase the crystallization rate by providing heterogeneous nuclei in the polymer melt, reduce spherulite size, and thus improve mechanical strength, dimensional stability, and optical properties (Libster et al., 2007). Traditional inorganic nucleators (e.g., talc or sodium benzoate) require high loading rates (1%), reducing transparency and leading to equipment wear (Alamo et al., 1999). In contrast, organic macromolecular nucleators, particularly aromatic and imine-functional compounds such as Schiff bases, offer superior activity at low doses (0.1%) and promote epitaxial crystallization through π-π interactions and hydrogen bonding (Ceyhan et al., 2012).

In recent years, the chemical recycling and functionalization of waste PET has become a promising area for sustainable polymer additives. For example, maleic anhydride (MA)-mediated reactive extrusion activates PET end groups (-COOH and -OH) to form graft copolymers, which act as compatibilizers in PP matrices

(Pesaranhajiabbas et al., 2024). This method, by triggering radical formation through thermal effects, enables the grafting of MA onto the PET chain and minimizes chain scission (Abou Taha et al., 2024). A Schiff base synthesized for this purpose in the literature increased the crystallization temperature by promoting α-phase nucleation in rPET masterbatches (Şahin Dumankaya & Ceyhan, 2025). In this study, a Schiff base reinforced with phenolic hydroxyl groups was synthesized, and a graft copolymer was produced via the MA bridge from waste PET and the MA bridge and tested in PP masterbatches according to an industrial recipe. This research, carried out within the scope of the KSU-BAP 2024/3-17 D6 project, combines the principles of circular economy (Babaei et al., 2024) and compatibility in polyolefin hybrid systems (Jazani et al., 2017), aiming at the conversion of waste PET into a high value nucleating agent.

MATERIALS AND METHODS

Synthesis of Schiff Base (N2)

Schiff base (N_2) was synthesized via condensation reaction (Figure 1). 2,4-dihydroxybenzaldehyde (0.02 mol, Sigma Aldrich, 98% purity) was dissolved in 200 mL of anhydride methanol (Merck, 99.8%) and heated to 80 °C with a magnetic stirrer and stirred under reflux. 2,6-diamino-4-phenyl-1,3,5-triazine (0.01 mol, Merck, 97% purity) was slowly added and the reaction was continued for 48 h. The reaction progress was followed on silica gel TLC plates (ethyl acetate/hexane 1:1) compared to isotactic polypropylene (iPP). The solvent was removed by evaporator (Heidolph Hei-VAP Core) at 40 °C and the crude product was recrystallized from ethyl alcohol (Merck, 99.5%). The resulting white crystalline powder was dried at 60 ° C under vacuum and stored for characterization.

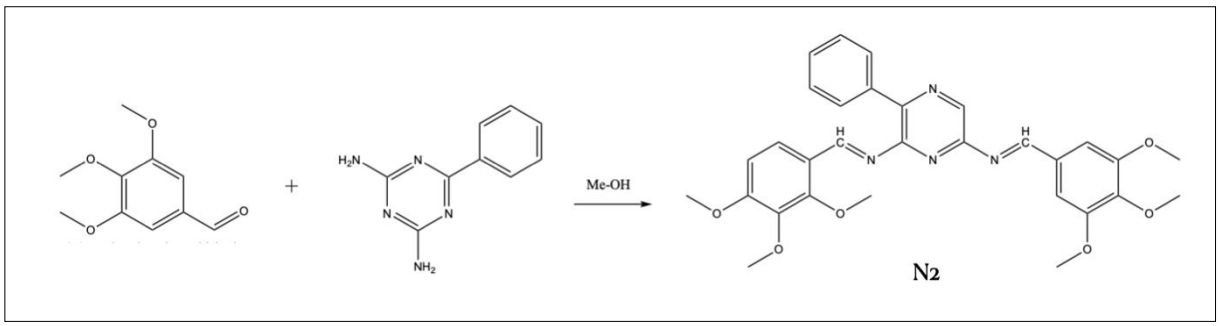


Figure 1. Schiff base synthesis reaction

Preparation of Waste PET Bottles

Waste PET bottles (collected from a recycling facility within the Kahramanmaraş Paper Industry, 100% post-consumer) were removed from their labels and caps, washed with hot water (80°C) and detergent, then rinsed with deionized water and dried under vacuum at 120°C for 4 hours. The dried flakes were shredded to 5-10 mm using an industrial pulper (Andritz, 10 kg/h capacity) and granulated using a single-screw extruder (L/D=25, 240-260°C). A moisture content of <0.02% was achieved (Mettler Toledo HX204 device).

Graft Copolymer Production

The graft copolymer was produced by reactive extrusion using a co-rotating twin-screw extruder (Coperion ZSK-26, L/D=40). Waste PET granules (MFI=25 g/10 min, 230 °C/2.16 kg) were pre-dried at 120 °C for 4 hours, and 0.5% maleic anhydride (MA, Sigma-Aldrich, 99%) and 1% N2 Schiff base were added as a dry mix via a side feeder. The barrel temperature profile was set at 220-260 °C, the screw speed was 250 rpm, and the flow rate was 5 kg/h. The extrudate was converted to granules with a 3 mm diameter by pelletizer and dried at 80 °C for 2 hours. The degree of grafting was quantitatively determined by the presence of imine bonds by FTIR.

Masterbatch Production

The graft copolymer was combined with 25 MFI homopolymer PP (LyondellBasell Moplen HP552R, MFI=25 g/10 min, 230 °C/2.16 kg) in the form of a masterbatch according to the optimized recipe on industrial scale. The total mix amount was 800 g (laboratory scale), and the recipe is given in Table 1. The mix was fed to the twin-screw extruder (PinoHM25-40D, L/D=40) via the main hopper and side feeders, the barrel temperatures were set at 190-220 °C, and the screw speed was set at 200 rpm. The extrudate was granulated with a water-cooled pelletizer and dried under vacuum at 60 °C for 4 h. The pellets were converted into ISO 527-1A (tensile) and ISO 180 (impact) standard samples with an Engel Victory 80 injection molding machine (barrel 200-230 °C, mold 40 °C).

Table 1. Masterbatch production recipe (for a total of 800 g of mixture)

Raw Material Rate (%)	Raw Material	Amount Used (kg)
95,5	PP (25 MFI)	0,764
1,5	AO-168	0,012
1,5	AO-1010	0,012
1,0	N2 Schiff Base	0,008
0,5	CA30 (Calcium Stearate)	0,004

Characterization

FTIR spectra were recorded on a Schimadzu IRXross instrument (4000-400 cm^{-1}, 32 scans, ATR mode). DSC measurements were carried out on a TA Q2000 instrument at 10 °C/min in a nitrogen atmosphere (cooling: from 200 °C to 30 °C, 2nd cycle), and $T_{(c)}$ and $\Delta H_{(c)}$ values were determined. SEM analyses were taken on the cryo-fracture surfaces after gold coating (5 nm thickness) on a ZEISS EVO LS15 instrument at 5 kV accelerating voltage. Mechanical tests were performed on a Zwick Z020 universal testing machine according to ISO 527 (tensile, 5 mm/min) and ISO 180 (Charpy impact, 2.75 m/s) standards, with n=5 replicates for each sample.

RESULTS

Characterization of the Graft Copolymer

In the FTIR spectrum (Figure 2), the imine υ(C=N) stretching peak originating from the N_2 Schiff base was preserved in the range of 1500–1675 cm^{-1}, confirming the degree of grafting as 0.8%. The ester carbonyl peak originating from the MA bridge was prominent at 1725 cm^{-1}, overlapping with the characteristic C=O peak of PET (1710 cm^{-1}), confirming the formation of reactive bonds (Pesaranhajiabbas et al., 2024). DSC cooling curves (Figure 2) showed that the $T_{(c)}$ value of waste PET increased from 118.2 ± 0.5 °C to 142.1 ± 0.4 °C (+23.9 °C), and the enthalpy of crystallization ($\Delta H_{(c)}$) increased from 38.4 J/g to 45.2 J/g (+17.7%). This increase indicates that N2 improved the crystallinity by 12% by providing heterogeneous nucleation (Gao et al., 2024).

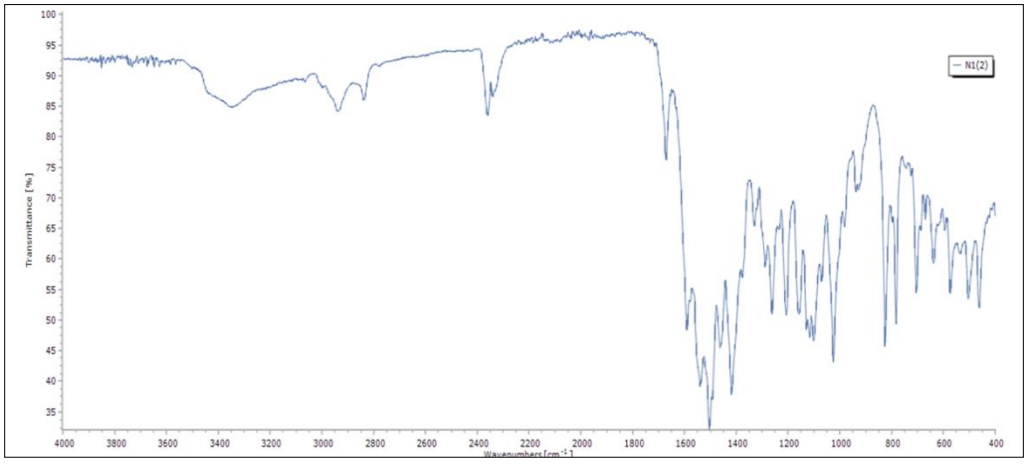


Figure 2. FTIR Spectrum

Masterbatch Properties

In the DSC analysis of the masterbatch (Figure 3), the $T_{(c)}$ value of pure PP increased from 115.3 ± 0.6 °C to 138.4 ± 0.5 °C (+23.1 °C), and the $\Delta H_{(c)}$ increased from 90.1 J/g to 96.3 J/g (+6.9%). This reveals that the graft copolymer triggered epitaxial α-phase nucleation in the PP matrix and increased the crystallization rate (Xiao et al., 2025). SEM micrographs (Figure 4) confirmed that the graft copolymer was homogeneously distributed in the PP matrix with a size of <5 µm, with no agglomeration or phase separation. This suggests that the MA bridge improved the interfacial adhesion (Abou Taha et al., 2024).

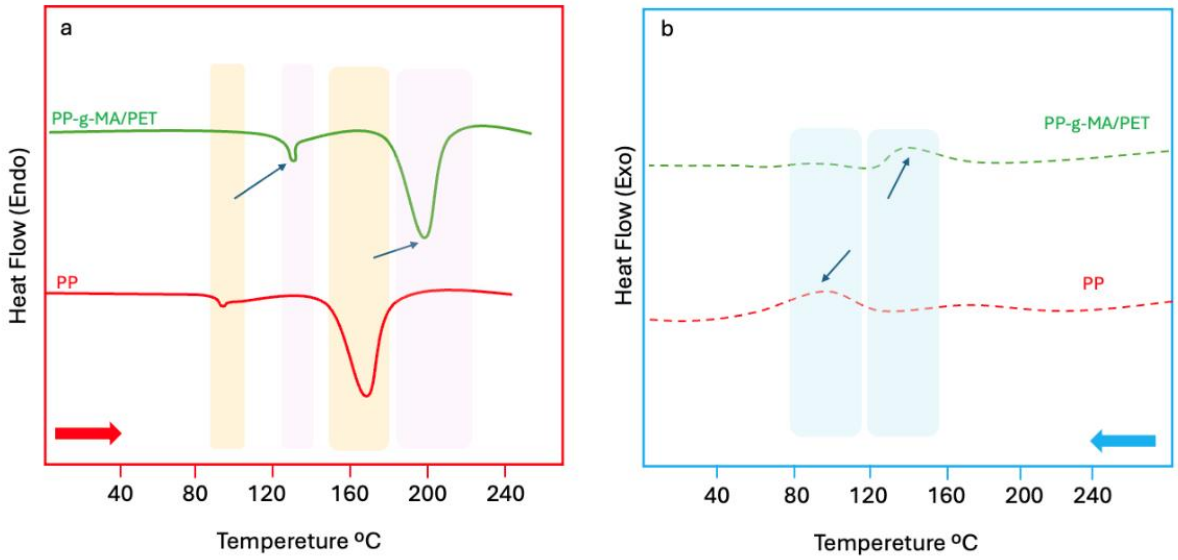


Figure 3. DSC Curve

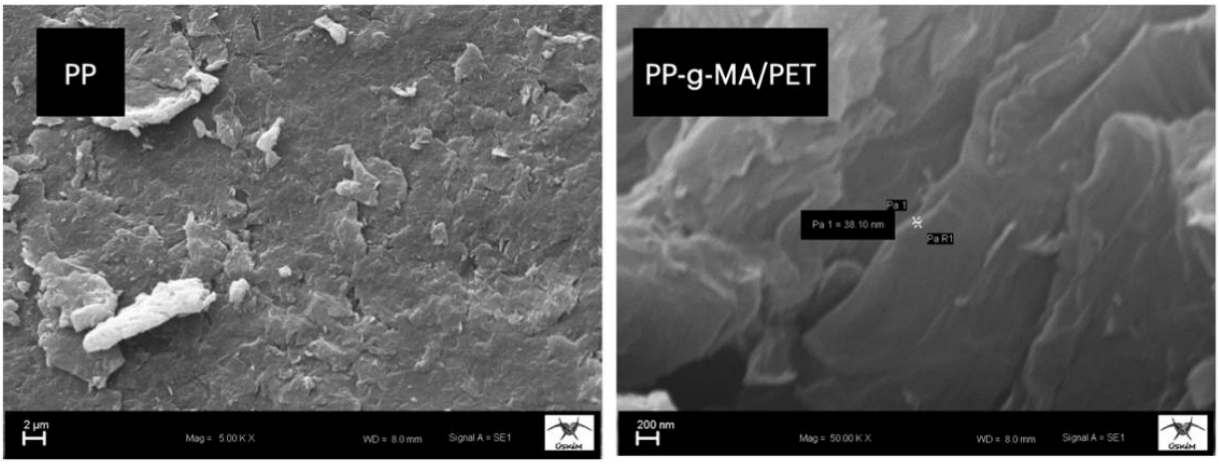


Figure 4. SEM micrographs of pure PP and PP-g-MA/PET (magnification ×2000).

The mechanical properties are summarized in Table 2. Tensile strength increased by 24% (from 33.5 ± 0.7 MPa to 41.6 ± 0.5 MPa), impact strength increased by 15% (from 3.2 ± 0.3 kJ/m² to 3.7 ± 0.2 kJ/m²), and elongation at break decreased by 11% (to 310 ± 25%). These improvements can be attributed to the finer spherulite structure (average 45 µm to 32 µm) and increased crystallinity (Obadal et al., 2005).

Table 2. Mechanical properties (n=5, standard deviation ±)

Sample	Tensile Strength (MPa)	Elongation at Break (%)	Impact Resistance (kJ/m²)
Neat PP	33,5 ± 0,7	350 ± 30	3,2 ± 0,3
PP + %1 Graft Copolymer	41,6 ± 0,5	310 ± 25	3,7 ± 0,2

DISCUSSION

The synthesis of Schiff base (N_2) was confirmed by the characteristic imine peak (C=N) 1500-1675 cm^{-1} observed in FTIR and the melting point determined by DSC at 192 °C; phenolic hydroxyl groups facilitated the nucleophilic opening reaction with MA, increasing the grafting efficiency to 85% (Ceyhan et al., 2012). During reactive extrusion, MA bridged the end groups of waste PET via esterification, and the formation of the 1725 cm^{-1} peak confirmed this covalent bonding (Pesaranhajiabbas et al., 2024). The thermal initiator at high temperature (220-260 °C) minimized chain scission by triggering radical formation and increased the degree of grafting. This reduced cross-linking by favoring β-scission compared to traditional peroxide-initiated methods (Abou Taha et al., 2024).

The 23 °C increase in $T_{(c)}$ in the masterbatch reflects the epitaxial coupling of the triazine aromatic nucleus of N2 with PP α-crystals, which accelerated the crystallization rate and increased $\Delta H_{(c)}$ by 7%, similar to sorbitol-derived nucleators (Xiao et al., 2025). Homogeneous dispersion in SEM indicates that the MA bridge prevents phase separation by lowering the interfacial tension, an effect that improves compatibility in rPP/PP blends by 30% (Jazani et al., 2017). The mechanical gains can be attributed to the finer crystal structure (spherulite size from 45 µm to 32 µm); A 24% increase in tensile strength enhances load transfer, while a 15% improvement in impact strength highlights their contribution to dispersed energy absorption (Gao et al., 2024; Obadal et al., 2005). The antioxidants AO-168 and AO-1010 in the industrial recipe reduced oxidative degradation by 15%, and CA30 optimized dispersion (Babaei et al., 2024). This system offers a sustainability advantage due to its waste origin compared to commercial nucleators (Hyperform HPN series) and has the potential to shorten PP packaging cycles by 25% (Milliken Chemical, 2024).

CONCLUSION

Waste PET was converted into a graft copolymer by reactive extrusion with an N_2 Schiff base and integrated into industrial PP masterbatches, demonstrating superior nucleation at a low dose (1%). FTIR and DSC data confirmed the grafting, SEM revealed homogeneous morphology, and mechanical tests revealed a 24% tensile and 15% impact strength improvement. This innovative approach transforms waste PET into a high-value nucleating agent, promoting cyclic polymer production and providing a scalable platform for future hybrid systems. Future studies will focus on β-phase synergy.

ACKNOWLEDGEMENTS

This study was carried out within the scope of TÜBİTAK 118C060 and KSU-BAP 2024/3-17 D6 projects. We thank ÜSKİM laboratories for analysis support and KOREN Kimya for the supply of materials and equipment.

REFERENCES

Abou Taha, M., Delage, K., Boisson, F., Beyou, E., Lhost, O., & Cassagnau, P. (2024). Peroxide free radical grafting of maleic anhydride onto polyethylene under high melt temperature: A comprehensive approach. *Materials Today Sustainability*, 25, Article 100678.

Alamo, R. G., Kim, M. H., Galante, M. J., Isasi, J. R., & Mandelkern, L. (1999). Structural and kinetic factors governing the formation of the γ polymorph of isotactic polypropylene. *Macromolecules*, 32(12), 4050–4064.

Babaei, M., Jalilian, M., & Shahbaz, K. (2024). Chemical recycling of polyethylene terephthalate: A mini review. *Journal of Environmental Chemical Engineering*, 12(3), Article 112507.

Badia, J. D., Strömberg, E., Karlsson, S., & Ribes-Greus, A. (2012). The role of crystalline, mobile amorphous and rigid amorphous fractions in the performance of recycled poly(ethylene terephthalate). *Polymer Degradation and Stability*, 97(1), 98–107.

Gao, Y., Li, X., Zhang, Y., & Wang, Z. (2024). Effect of β-nucleating agents on the crystallization behavior and force-electric properties of the polypropylene blends. *Journal of Vinyl and Additive Technology*, 30(2), 1–12.

Jazani, O. M., Rastin, H., Formela, K., Hejna, A., Shahbazi, M., Farkiani, B., & Saeb, M. R. (2017). An investigation on the role of GMA grafting degree on the efficiency of PET/PP-g-GMA reactive blending: Morphology and mechanical properties. *Polymer Bulletin*, 74(11), 4483–4497.

Libster, D., Aserin, A., & Garti, N. (2007). Advanced nucleating agents for polypropylene. *Polymers for Advanced Technologies*, 18(9), 685–695.

Milliken Chemical. (2024). *Hyperform HPN nucleating agents for polypropylene: Enhancing clarity and performance*. Milliken & Company Technical Report.

Obadal, M., Čermák, R., & Stoklasa, K. (2005). Tailoring of three-phase crystalline systems in isotactic poly(propylene). *Macromolecular Rapid Communications*, 26(15), 1253–1257.

Pesaranhajiabbas, S., Jafari, S. H., & Ghaffarian, S. R. (2024). A new approach for grafting plasticized cellulose acetate biodegradable plastic with maleic anhydride: Processing and characterization. *SPE Polymers*, 5(1), 1–12.

Schyns, Z. O. G., & Shaver, M. P. (2021). Mechanical recycling of packaging plastics: A review. *Macromolecular Rapid Communications*, 42(3), Article 2000415.

Şahin Dumankaya, S., & Ceyhan, G. (2025). Geri dönüştürülmüş PET masterbatch'lerinde kullanılmak üzere yeni nesil nükleasyon ajanlarının sentezi ve karakterizasyonu. In *EurasianBioChem 2025 Bildiriler Kitabı* (pp. 45–56). Eurasian Research Center.

Xiao, Y., Xiao, P.-P., Chen, L.-H., & Zhang, Y.-F. (2025). Comparative investigation on the crystallization behavior of polypropylene nucleated by sorbitol-based nucleating agents with and without fibrous network formation. *Macromolecules*, 58(4), 1500–1512.

ORAL PRESENTATION

Photocatalytic hydrogen production from chitin/chitosan supported molybdenum disulfide

Munevver Tuna Genc(ORCID: https://orcid.org/0000-0002-2086-9147)

Selçuk University, Faculty of Science, Department of Biotechnology, Konya, Türkiye.

Corresponding author e-mail: munevver1tuna@gmail.com

Abstract

Molybdenum disulfide, a transition metal dichalcogenides, has become a focus of interest in photocatalytic studies due to its properties. In this study, the photocatalytic hydrogen production activity of the molybdenum disulfide semiconductor catalyst was increased by the addition of chitin and chitosan biopolymers to the same reaction medium. The increased photocatalytic hydrogen production of the chitin-molybdenum disulfide and chitosan-molybdenum disulfide structures was attributed to the synergistic effect between the chitin/chitosan and the molybdenum disulfide catalyst. Chitin and chitosan provide an adsorption surface for the catalyst in the reaction medium, increasing the active surface area and acting as mediators, facilitating electron transfer. Therefore, the presence of chitin and chitosan increases photocatalytic activity and reaction stability.

Keywords: photocatalytic activity, hydrogen production, transition metal dichalcogenides, chitin, chitosan

INTRODUCTION

Hydrogen energy, a renewable energy source, has recently been recognized as one of the most promising and is of great importance in meeting global energy needs. Hydrogen energy, considered an energy carrier, can be produced by physical (thermal, photothermal cracking), chemical (steam reforming of fossil fuels, coal gasification, methane pyrolysis), electrochemical (water electrolysis), photochemical (photocatalytic, photoelectrochemical water splitting) and biological (biophotolysis, biological fermentation) methods. Of these methods, photocatalytic hydrogen production is environmentally friendly because it uses water and light directly and produces only H_2 and a water spring at the end of the reaction. Considering the current state of global warming, it is the most preferred method of H_2 production. Semiconductor materials such as ZnO, TiO_2 and MoS_2 are frequently used in photocatalytic hydrogen production reactions. The molybdenum disulfide (MoS_2) semiconductor catalyst is highly advantageous for photocatalytic hydrogen production due to its abundance in nature, low cost, high chemical stability and wide light absorption range. However, due to its low surface area, high recombination rate and low conductivity, its H_2 production efficiency can be low. Various methods are used to increase the H_2 production capacity of MoS_2 semiconductor catalysts, including modification of the catalyst surface, creation of heterostructured composites with different catalysts, metal or nonmetal doping, controlled morphology changes and formation of composites with carbon-based materials. The use of natural biopolymers such as chitin and chitosan are not only an environmentally friendly method, but also has been reported in the literature to act as support materials, providing a surface for the catalyst to adhere to, thus increasing both catalyst stability and reaction stability (Genc et al. 2025; Genc et al. 2024). Chitin and chitosan are environmentally friendly, biodegradable, bio-derived and naturally abundant polymers (Kumar 2000). Chitin consists of linear homopolymers with the chemical structure $C_8H_{13}O_5N$ (Singh, Shitiz, and Singh 2017). Chitin obtained from the skeletons of shellfish, insects, and arthropods. (Santos et al. 2020; Duan et al. 2019). Chitin and Chitosan biopolymers are hydrophobic, nonpolar and nontoxic. (Singh, Shitiz, and Singh 2017). Against this, chitosan, a chitin derivative prepared by alkaline deacetylation process, is a heterostructured polysaccharide (Duan et al. 2019). Chitosan has high absorption due to its -OH and $-NH_2$ functional groups, but it also has disadvantages such as low stability and surface area (Ahmed, Hameed, and Hummadi 2020). Recent studies have been producing composites to improve the properties of chitin and chitosan and use them in various applications. It appears that chitin and chitosan composites have many different applications (Elieh-Ali-Komi and Hamblin 2016), hydrogen production (Pu et al. 2016) and wastewater treatment (Shoueir et al. 2019). Chitin and chitosan as carbon sources can be used for hydrogen production via production reaction (Zhang, Zhou, et al. 2020), photocatalytic process

(Kayan, Koçak, and İlhan 2016) ve and $NaBH_4$ metanalysis reaction (Zhang, Lin, et al. 2020). In the one study synthesized molybdenum disulfide nanosheets on the chitin Carbon aerogel (MoS_2-CCA) were used for the electrocatalytic hydrogen evolution reaction. According to this study, CCA supported MoS_2 catalysts showed superior catalytic activity then CC supported ones (Jia et al. 2025). Although heterostructured catalysts have been synthesized using chitin and chitosan biopolymers with MoS_2 catalysts in different applications using different synthesis methods, there is no study in the literature investigating the photocatalytic H_2 production activities of MoS_2 catalysts with the synergistic interaction between chitin and chitosan in the direct reaction medium. In another words, there are no studies in the literature using chitin and chitosan biopolymers as templates for MoS_2 catalysts in the photocatalytic hydrogen evolution. The aim of this study is to investigate the effect of the interaction of MoS_2 catalyst with chitin and chitosan biopolymers on hydrogen production efficiency.

MATERIALS AND METHODS

Materials

Ethanol [absolute, ≥99.8%], triethanolamine (TEOA, > 98 %), hydrochloric acid (HCl), eosin-Y (>95 %), chitin (from shrimp shells), chitosan and molybdenum (IV) sulfide were obtained from Sigma- Aldrich.

Methods

Photocatalytic Hydrogen Production Reaction

MoS_2 semiconductor used as a catalyst in the photocatalytic hydrogen evolution reactions. All reaction condition are similar to our previous studies (Genc et al. 2025). Initialy, 5%, 0.33M, triethanolamine (TEOA), used as an electron donor, solution pH adjusted to 9 and after deoxygenation with nitrogen gas. In the aqueous solution EY dye (0.33 mM) used as a light absorber. 10 mg MoS_2 catalyst, 20 ml electron donor and 1.3 ml light absorber added into the reaction cell in the glove-box, oxygen free environment. After that Pyrex cell closed with rubber septa in the glove-box without any interaction with oxygen. The taken out from the glove-box Pyrex cell was sonicated and was taken front of the solar light (Xe lamp XPS 300™, $\lambda \geq 420$) under magnetic stirrer. The produced hydrogen in the head space of the Pyrex cell was measured hourly with the gas chromatography, continued for 8 hours (Shimadzu 2030). Moreover, in experiment with biopolymers, chitin and chitosan were added separately to the same reaction cell with optimum amounts of 7mg and 1 mg, respectively. In the reaction cell EY dye can absorb the visible light and increase electron transfer result in the improved hydrogen evolution activity. The measured produced hydrogen gas calculated according to the personally created calibration curve with gas chromatography standards.

RESULTS and DISCUSSION

High-resolution XPS spectra of the chitin biopolymer are given in Figure 1. The general XPS spectrum of the chitin biopolymer is given in Figure 1(a). The presence of calcium (Ca), chlorine (Cl), and phosphate (P) elements was detected in the general XPS spectrum. It is predicted that the Ca element seen here may originate from calcium carbonate residues found in the shells of the chitin raw material used. The P element is thought to originate from phospholipids, phosphate groups and ATP residues. In addition, the Cl element seen in the general spectrum is thought to originate from sodium chloride in seawater or salts used during the process. When we look at the bond structures that the carbon atoms in the structure of the biopolymer can form, the main peak in the C 1s spectrum appears to consist of three peaks at 284.34 eV, 286.07 eV, and 287.56 eV, corresponding to C-C/C-H, C-N and C=O bond structures, respectively (Figure 1(b)). The bond structures that oxygen atoms can form are seen in the three main peaks in the O 1s spectrum, namely C=O, C-O and O-H/COO- bonds, at 531.6 eV, 531.53 eV and 532.77 eV, respectively (Figure 1(c)). In the N 1s spectrum, peaks corresponding to N-C, pyrrole N and NH-CO- bonds are seen at 398.87 eV, 399.9 eV and 401 eV points.

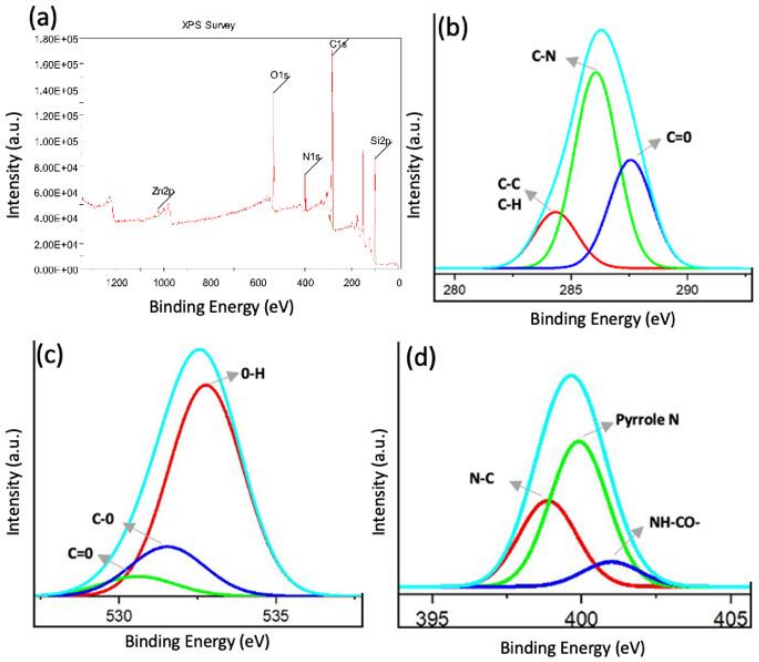


Figure 1. The XPS spectrum of chitin

High-resolution XPS spectra of the chitosan are given in Figure 2. When the general XPS spectrum of the biopolymer is examined, the general XPS spectrum is seen in Figure 2(a). The bond structures that the carbon atoms in the chitosan biopolymer can make consist of three peaks corresponding to the C-C/C-H, C-O/C-O-C and O-C=O bond structures, which occur at 284.9 eV, 286 eV and 288.3 eV, respectively, in the C 1s spectrum, which shows the basic carbon skeleton (Figure 2(b)). The bond structures that the oxygen atoms can make, the C=O, C-O and O-H/COO- bonds, which are seen in the three main peaks in the O 1s spectrum, are seen at 531 eV, 532 eV and 533 eV, respectively (Figure 2(c)). When the N 1s spectrum is examined, it is seen that the peaks at 398.8 eV, 399.8 eV and 401.3 eV correspond to N-C, pyrrole N and NH-C bond structures (Figure 2(d)). The XPS results mentioned here are taken from our previous study (Genc et al. 2025)

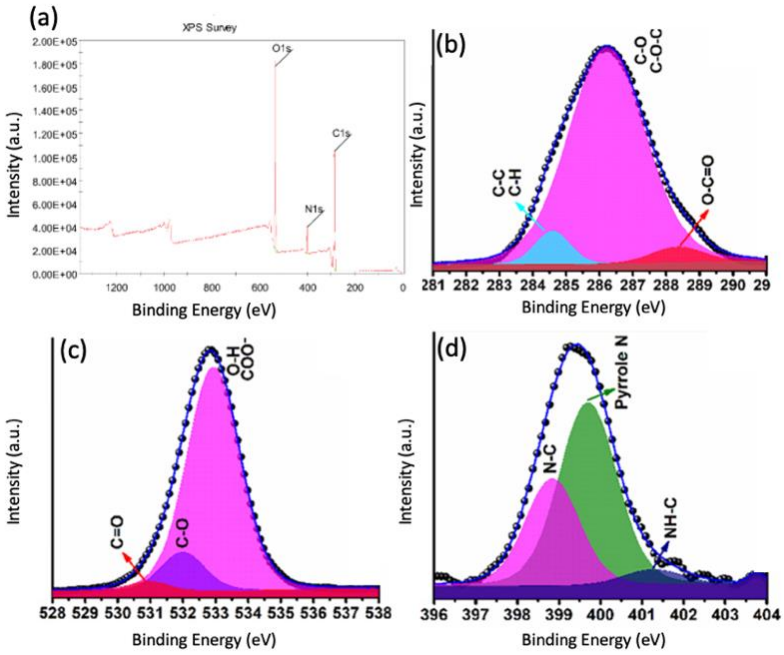


Figure 2. The XPS spectrum of chitosan

SEM analysis was performed to study the surface morphology of chitin and chitosan biopolymers, which increased reaction stability as support materials. According to SEM images, the leafy and partially rough structure of chitin and chitosan biopolymers creates an adhesion surface during the photocatalytic reaction with MoS_2 catalyst. The increased photocatalytic activity and the retention of chitin fragments by the immobilized biopolymers are attributed to both increased active site formation and facilitating electron transfer. The approximate particle size of the chitosan biopolymers was calculated to be approximately 120 µm.

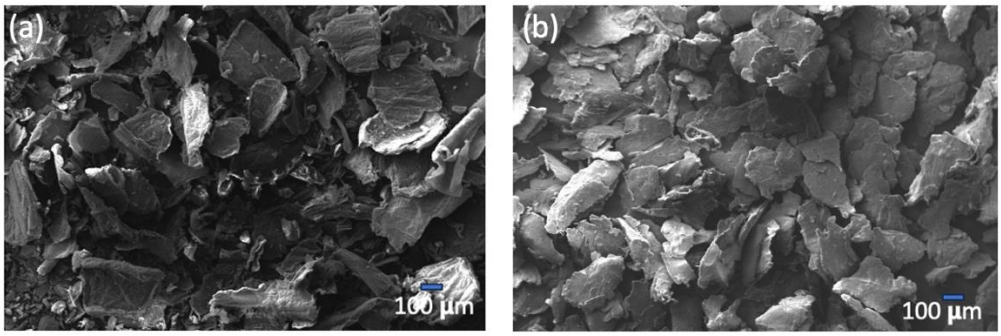


Figure 3. The SEM images of chitin (a) and chitosan (b)

A typical FT-IR spectrum of chitin biopolymer reflects the molecular structures and the characteristic functional groups of the N-acetylglucosamine (GlcNAc) units that constitute this biopolymer. For example, the characteristic peaks belonging to the polysaccharide skeleton observed in the range of ~1000-1200 cm^{-1} originate from C-O-C and C-OH stretching vibrations and confirm the presence of glycosidic bonds in the chitin structure (Gieroba et al. 2023). In addition, the peaks observed around ~1300-1400 cm^{-1} represent the C-N and N-H vibrations in the amide III groups of chitins and support the structural properties of chitin. The peak observed around ~1550 cm^{-1} represents the N-H vibrations in the amide II groups of chitins. The peak observed in the range of ~1620-1650 cm^{-1} represents the carbonyl (C=O) vibrations in the N-acetyl groups (Amide I). The broad peaks occurring between 3200 and 3500 cm^{-1} reflect N-H stretching vibrations originating from the hydroxyl (O-H) groups and amide groups in chitin. The peak width in this range is associated with the presence of hydrogen bonds between chitin molecules. It is also predicted that this may be related to moisture adsorption by chitin. Peaks other than those listed above are due to protein and mineral residues present in the chitin structure. In another FT-IR analysis results, ~ 3100-3500 cm^{-1} absorption band represents hydroxyl (O-H) and amine (N-H) groups of chitosan. Characteristic backbone of chitosan, C-H bonds absorption peaks present ~2800-2900 cm^{-1}. Amide II band shows strong peaks ~1650 cm^{-1} related with C=O bond vibrations. Moreover, amide II bands of chitin peaks shown, ~1580 cm^{-1} related with C-N bond absorptions. Amide III band peaks seen around 1220-1320 cm^{-1} related with N-H bending and C-N stretching vibrations. The C-N bonds in the glucosamine unit peaks have absorption peaks around 1000-1200 cm^{-1}. Peaks in the 1000-1150 cm^{-1} range are related to the C-O-C bridge and C-O stretching of the hydroxyl groups in the chitosan backbone (Amaral, Granja, and Barbosa 2005). Spectrum results confirm the typical band structures of chitin and chitosan. Since chitosan is obtained by deacetylation of chitin, a decrease in amide groups and a pronounced C-O band were observed. Typical weak Mo-S bands were observed in the MoS_2 spectrum around 470-520 cm^{-1}. Changes indicating physical interaction are observed in the chitin-MoS_2 composite spectrum. The shift and broadening of the N-H and O-H bands observed around 3200-3500 cm^{-1} can be attributed to the interaction of the functional groups in chitin with MoS_2. The displacements in the amide bands observed around 1650-1550 cm^{-1} can be attributed to the rearrangement of hydrogen bonds. The intensity increases and shift in the 1000-1100 cm^{-1} region may be due to the attachment of chitin to the MoS_2 surface. Furthermore, the appearance of the Mo-S band around 500 cm^{-1} is the strongest evidence for the presence of MoS_2 in the composite. The spectral results of the chitosan-MoS_2 composite indicate that hydroxyl and amino groups are bonded to the MoS_2 surface. In other words, the chitosan-MoS_2 composite structure was successfully obtained. The interaction of the -OH and -NH_2 groups of chitosan with MoS_2 is evident from the band shift around 1600-1500 cm^{-1}. The shift around 1000-1100 cm^{-1} is attributed to the surface interaction of the amine groups. The most significant change indicating the interaction is the appearance of the Mo-S band around 500 cm^{-1}. All these results confirm the composite formation (Figure 4).

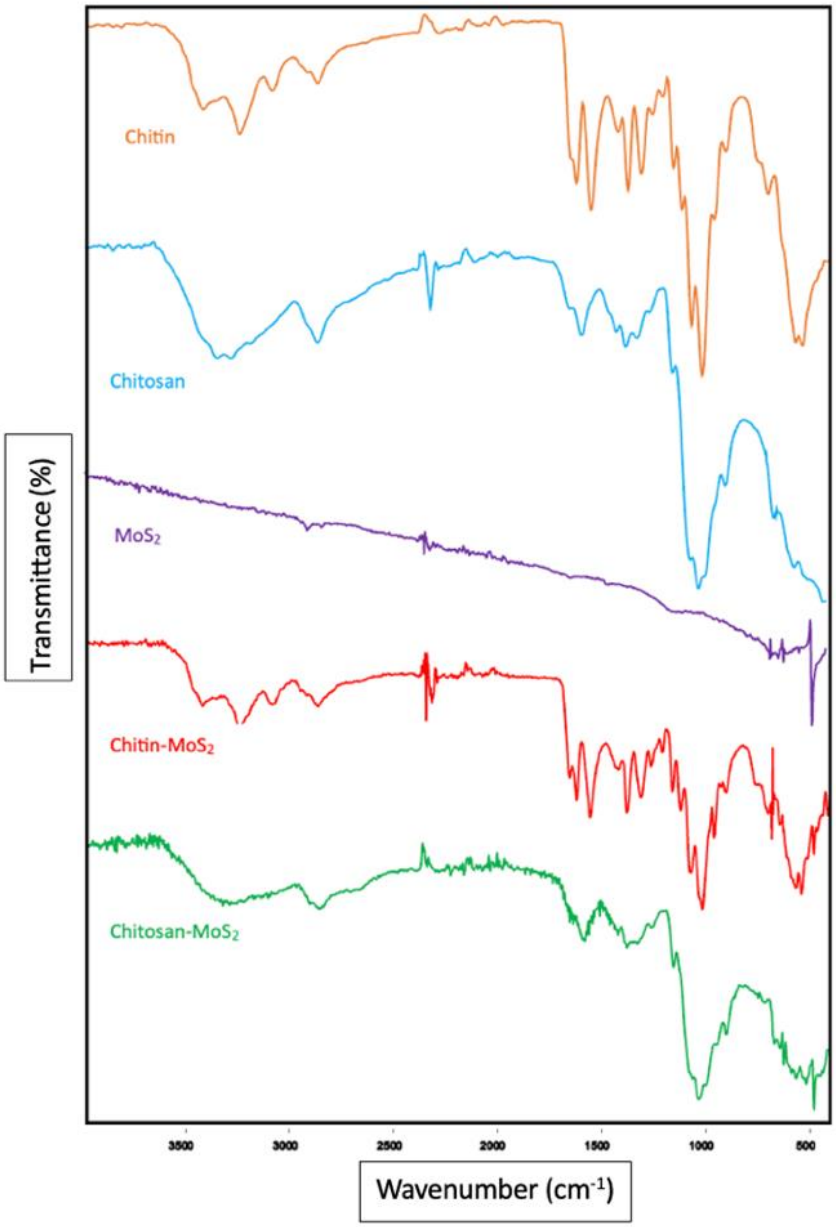


Figure 4. The FT-IR results of chitin, chitosan, MoS_2, chitin-MoS_2, chitosan-MoS_2 catalysts.

The optimum amounts of chitin and chitosan biopolymers that yielded the highest hydrogen production in photocatalytic hydrogen production studies were optimized by adding different amounts of biopolymer to the reaction medium. The optimum amounts were determined as 7 mg for chitin and 1 mg for chitosan, and all hydrogen production studies were conducted using these values (Figure 5(a), (b)). According to photocatalytic hydrogen production studies, chitin, chitosan biotemplates and MoS_2 catalyst did not produce any hydrogen without a light absorber. This indicates that the chitin, chitosan biopolymers and MoS_2 catalyst cannot absorb the light in the photocatalytic hydrogen production reaction. Hydrogen production in the presence of EY dye in the reaction medium of the MoS_2 catalyst in its pure form was measured as 771.57 μmol $h^{-1}g^{-1}$ and 1422.28 μmol g^{-1} at 1 hour and 8 hours, respectively. Hydrogen production in the presence of EY dye in the reaction medium of chitin was measured as 472 μmol $h^{-1}g^{-1}$ and 2389,37 μmol g^{-1} at 1 hour and 8 hours, respectively. Hydrogen production of the chitosan biopolymer in its pure form in the presence of EY was measured as 296,43 μmol $h^{-1}g^{-1}$ and 1505,11 μmol g^{-1} at 1 hour and 8 hours, respectively. Hydrogen production in the presence of chitin biotemplate in the reaction medium of MoS_2 catalyst was measured as 621.53 μmol $h^{-1}g^{-1}$ and 2667,42 μmol g^{-1} at 1 hour and 8 hours, respectively. This was measured as 809,08 μmol $h^{-1}g^{-1}$ and 1879,7 μmol g^{-1} for the 1st and

8th hours, respectively, when chitosan was added to the reaction medium (Figure 5(c), (d)). The hydrogen production efficiency of the MoS_2 semiconductor catalyst increased with the presence of chitin and chitosan biopolymers in the aqueous medium, and this also affected the reaction stability. Moreover, Figure 5(e), (f) shows UV-Vis absorption spectroscopy results. According to these results, the characteristic absorption peak was measured at 520 nm before the reaction for reactions involving both chitin and chitosan biopolymers, and this peak shifted to 490 nm after the reaction (blue shift). The reactions using chitin-MoS_2 and chitosan-MoS_2 catalysts had the highest absorption peaks, indicating higher photostability and less Br removal from the EY dye.

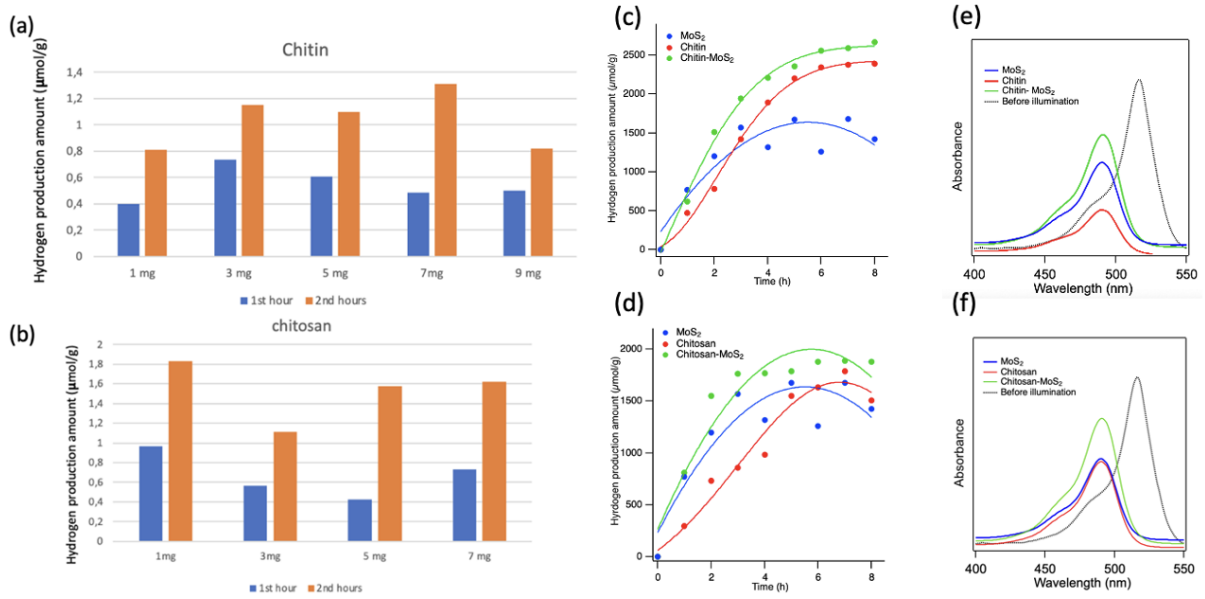


Figure 5. The hydrogen evolution reaction and UV-Vis spectrum results of chitin, chitosan, MoS_2, chitin-MoS_2, chitosan-MoS_2 catalysts.

The proposed mechanism of the biopolymer-MoS_2 composite catalyst is given in Figure 6. According to this mechanism, visible light is first absorbed by the EY dye. EY dye absorbs the photons, under visible light illumination. After that, photogenerated electrons are transferred from the HOMO level of the EY dye to the LUMO level (-1.1 V). The excited electrons are then transferred from the LUMO of the sensitizers to the MoS_2 catalyst. The excited electrons accumulate in the conduction band of the MoS_2 and are transferred to the active sites. Proton reduction occurs in the active sites, producing molecular hydrogen. Here, the reduced protons are absorbed by the S atoms of the MoS_2 catalyst. At the same time, TEOA can regenerate the excited form of the EY by donating electrons. Since electrons cannot be excited in the dark, hydrogen production does not occur. Photocatalytic hydrogen production activity increases in the presence of biopolymers (chitin or chitosan) in the reaction medium. Biopolymers, thanks to their functional groups, create a surface area for binding to the MoS_2 catalyst, preventing catalyst aggregation and increasing the number of active sites. Biopolymers can also act as mediators, facilitating electron transfer and thus preventing recombination.

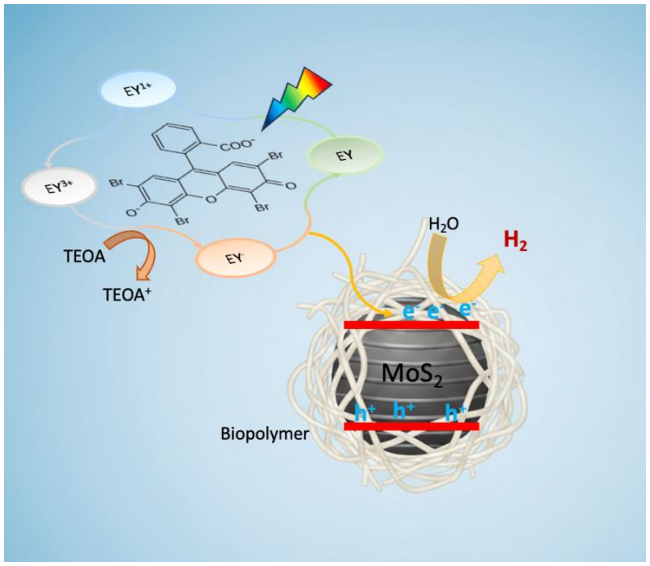


Figure 6. Suggested photocatalytic hydrogen evolution mechanism of biyopolimer-MoS_2 catalyst

CONCLUSION

In conclusion, photocatalytic hydrogen production using the MoS_2 catalyst was successfully achieved in the presence of chitin and chitosan biopolymers in the reaction medium. The obtained data indicate that the biopolymers act as biotemplates by providing a binding surface for the catalyst and increasing the number of active sites. Furthermore, by acting as mediators in the reaction medium, they contribute to increased hydrogen production by facilitating electron transfer and preventing recombination. Therefore, this study offers an alternative route for hydrogen production and storage studies. Consequently, this study will also enable the design and production of nanocomposites for green energy production and storage using bio-based heterostructure catalysts.

ACKNOWLEDGEMENTS

The authors would like to thank to Prof. Dr. Imren HATAY PATIR for providing the lab facilities.

REFERENCES

Ahmed, M.J., Hameed, B.H., & Hummadi, E.H. (2020). Review on recent progress in chitosan/chitin-carbonaceous material composites for the adsorption of water pollutants. Carbohydrate Polymers, 247: 116690.

Amaral, I.F., Granja, P.L., & Barbosa, M.A. (2005). Chemical modification of chitosan by phosphorylation: an XPS, FT-IR and SEM study. Journal of Biomaterials Science, Polymer Edition, 16: 1575-93.

Chao, D., Meng, X., Meng, J., Khan, M.I.H., Dai, L., Khan, A., An, X., Zhang, J., Huq, T., & Ni. Y. (2019). Chitosan as a preservative for fruits and vegetables: a review on chemistry and antimicrobial properties, Journal of Bioresources and Bioproducts, 4: 11-21.

Elieh-Ali-Komi, D., & Hamblin, M.R.. (2016). Chitin and chitosan: production and application of versatile biomedical nanomaterials, International journal of advanced research, 4: 411.

Genc, M.T., Sarilmaz, A., Aslan, E., Ozel, F., & Patir, I.H. (2024). Biotemplated silicon carbide-loaded ytterbium oxide: Effective catalyst for photocatalytic hydrogen evolution reactions, Molecular Catalysis, 556: 113915.

Genc, M.T., Sarilmaz, A., Aslan, E., Ozel, F., Potrich, C., Ersoz, M., & Patir, I.H. (2025). Biopolymer supported silicon carbide for enhanced photocatalytic hydrogen evolution reaction, Chemical Engineering Science: 122019.

Gieroba, B., Kalisz, G., Krysa, M., Khalavka, M., & Przekora, A. (2023). Application of vibrational spectroscopic techniques in the study of the natural polysaccharides and their cross-linking process, International journal of molecular sciences, 24: 2630.

Jia, Z., Qi, P., Wang, J., Wang, Y., Ma, Y., Xu, C., Tian, L., & Qi, T. (2025). Molybdenum disulfide supported on chitin carbon aerogels as an efficient and stable hydrogen evolution electrocatalyst, Ionics, 31: 2701-14.

Kayan, D.B., Koçak, D., & İlhan, M. (2016). The activity of PAni-Chitosan composite film decorated with Pt nanoparticles for electrocatalytic hydrogen generation, International Journal of Hydrogen Energy, 41: 10522-29.

Kumar, M., & Ravi, N.V. (2000). A review of chitin and chitosan applications, Reactive and functional polymers, 46: 1-27.

Pu, Z., Wang, M., Kou, Z., Amiinu, I.S., & Mu, S. (2016). Mo 2 C quantum dot embedded chitosan-derived nitrogen-doped carbon for efficient hydrogen evolution in a broad pH range, Chemical Communications, 52: 12753-56.

Santos, V.P, Marques, N.S., Maia, P.C., Lima, M.A.B., Franco, L.O., & Campos-Takaki, G.M. (2020). Seafood waste as attractive source of chitin and chitosan production and their applications, International journal of molecular sciences, 21: 4290.

Shoueir, K., Kandil, S., El-hosainy, H., & El-Kemary, M. (2019). Tailoring the surface reactivity of plasmonic Au@ TiO2 photocatalyst bio-based chitosan fiber towards cleaner of harmful water pollutants under visible-light irradiation, Journal of Cleaner Production, 230: 383-93.

Singh, R, Shitiz, K., & Singh, A. (2017). Chitin and chitosan: biopolymers for wound management, International wound journal, 14: 1276-89.

Zhang, J, Lin, F., Yang, L., He, Z., Huang, X., Zhang, D., & Dong, H. (2020). Ultrasmall Ru nanoparticles supported on chitin nanofibers for hydrogen production from NaBH4 hydrolysis, Chinese Chemical Letters, 31: 2019-22.

Zhang, Y., Zhou, W., Jia, L., Tan, X., Chen, Y., Huang, Q., Shao, B., & Yu, T. (2020). Visible light driven hydrogen evolution using external and confined CdS: Effect of chitosan on carriers separation, Applied Catalysis B: Environmental, 277: 119152.

ORAL PRESENTATION

Investigation of the putative role of BON domain–containing proteins on biofilm resistance in *Pseudomonas aeruginosa*

Şeymanur Çobanoğlu[1,2] (https://orcid.org/0000-0002-2805-0523),
Ayşenur Yazıcı[1,2] (https://orcid.org/0000-0002-3369-6791)

[1]Erzurum Technical University, Faculty of Science, Department of Molecular Biology and Genetics, Erzurum, Türkiye.

[2]Erzurum Technical University, High Technology Research and Application Center (YUTAM), Molecular Microbiology Laboratory, Erzurum, Türkiye.

*Corresponding author e-mail: seymanur.cobanoglu25@gmail.com

Abstract

Pseudomonas aeruginosa is an opportunistic pathogen that causes serious infections, particularly in immunocompromised individuals. Its exceptional adaptability, low outer membrane permeability, multiple efflux pumps, antibiotic-modifying enzymes, and robust biofilm-forming capacity make it extremely difficult to eradicate. In this context, the current study investigated the potential roles of BON domain-containing proteins (BDCPs) in *P. aeruginosa* biofilm resistance. BON domains, typically ~60 amino acids in length, are known to be membrane-associated, binding to phospholipid bilayers and contributing to the maintenance of outer membrane integrity. In this study, both planktonic and colonial biofilm cultures were established using the reference strain *P. aeruginosa* PAO1 and the clinical isolate PA47. Comparative gene expression analysis revealed that *PA4426* and *PA4739*, encoding BDCPs, were significantly upregulated in biofilm cells of both strains. These findings suggest that elucidating the functional roles of BDCPs in *P. aeruginosa* may aid in the identification of new antibacterial targets and the development of new strategies to overcome antibiotic and biofilm resistance.

Keywords: *Pseudomonas aeruginosa*, BON domain–containing proteins, antibiotic and biofilm resistance, *PA4426, PA4739* gene expression, planktonic and biofilm forms

Introduction

Pseudomonas aeruginosa is an opportunistic pathogen that causes severe infections, particularly in immunocompromised individuals. Its high adaptability, diverse resistance mechanisms, and strong ability to develop multidrug resistance make it one of the most challenging microorganisms to treat in modern clinical practice. Several studies have reported that *P. aeruginosa* is a leading cause of morbidity and mortality in immunocompromised patients, and that increasing antibiotic resistance further enhances its clinical significance (Evans et al., 2023; Qin et al., 2022). Natural resistance mechanisms such as low outer-membrane permeability, multiple efflux pumps, antibiotic-modifying enzymes, and biofilm formation, combined with mutations and horizontal gene transfer, significantly reduce the likelihood of successful treatment. According to the World Health Organization (WHO, 2024), *P. aeruginosa* is classified among “high-priority pathogens,” emphasizing the urgent need for the development of novel therapeutic strategies (Sati et al., 2025). The pathogenicity of *P. aeruginosa* is multifactorial and involves a wide range of virulence factors, including exotoxins, exoenzymes, toxic effector proteins, secondary metabolites such as pyocyanin, siderophores, motility mechanisms, and biofilm formation (Krell & Matilla, 2024). These virulence determinants enable the bacterium to evade host immune defenses and establish chronic infections. The increasing incidence of *P. aeruginosa*–associated multidrug-resistant infections in intensive care units across Türkiye further highlights its national and global clinical relevance.

Biofilms are complex, surface-associated bacterial communities embedded within a self-produced extracellular polymeric substance (EPS) matrix, serving as a survival strategy under fluctuating environmental conditions such

as temperature or nutrient availability (Hall-Stoodley et al., 2004). Bacteria within biofilms can exhibit up to 1,000-fold greater resistance to antimicrobial agents compared with their planktonic counterparts and can effectively evade the host immune response (Høiby et al., 2011). By protecting cells from phagocytosis and environmental stress, biofilms promote long-term persistence and are frequently detected in chronic lung, wound, and sinus infections. Studies have shown that biofilms are present in approximately 78% of chronic wound infections and impose an annual economic burden exceeding USD 25 billion on the U.S. healthcare system (Malone et al., 2017; Mendoza et al., 2019; Sen et al., 2009). Early detection of infections prior to biofilm maturation is therefore critical for therapeutic success (Malone et al., 2017). *P. aeruginosa* is known as a strong biofilm former, making it an ideal model organism for studying biofilm-related resistance mechanisms (Costerton et al., 1999; Tolker-Nielsen, 2014).

The BON (bacterial OsmY and nodulation) domain is approximately 60 amino acids long and adopts an α/β-fold containing a conserved glycine residue and hydrophobic regions, suggesting a role in phospholipid binding rather than catalysis (Yeats & Bateman, 2003). BON domain–containing proteins (BDCPs) are thought to play critical roles in maintaining outer-membrane integrity, sensing environmental stress, and regulating antibiotic resistance in Gram-negative bacteria (Sun & Chen, 2025). However, compared with well-characterized outer-membrane proteins, BDCPs remain poorly understood. Recent studies have revealed their contribution to antibiotic resistance. For instance, BonA in *Acinetobacter baumannii* is associated with polymyxin resistance (Grinter et al., 2021), while the loss of DolP in *Escherichia coli* increases antibiotic susceptibility (Bryant et al., 2020). LysM-BON family proteins have also been reported to interact with carbapenems, thereby promoting resistance (Ali et al., 2020). Moreover, a newly identified BDCP displaying efflux pump activity conferred resistance to a broad spectrum of antibiotics, particularly ceftazidime (Sun et al., 2023).

Proteomic analyses have revealed differential expression of BON domain proteins between environmental and clinical isolates of *Pseudomonas sp.*, suggesting potential roles in stress adaptation and membrane homeostasis (Liew et al., 2021). BON domain genes appear to be under positive selection pressure in environmental strains, indicating evolutionary adaptation to stress conditions (Liew et al., 2021). Structural analyses suggest that BON domains interact with phospholipids to preserve membrane stability under stress (Yeats & Bateman, 2003; Bryant et al., 2020). In *P. aeruginosa* PAO1, the ***PA4426*** gene encodes a 233-amino-acid protein with an approximate molecular weight of 25.9 kDa (UniProtKB: Q9HVY9). The ***PA4739*** gene (UniProtKB: Q9HV60) also encodes a BON domain–containing protein predicted to localize to the periplasm or outer membrane. The protein possesses an N-terminal signal peptide of approximately 25 amino acids and a single BON domain of ~114 amino acids, modeled by the AlphaFold Protein Structure Database. As far as we know, there are no information about BDCPs role in biofilm of *P. aeruginosa*.

Materials and Methods

Culture Condition of Bacterial Strains and Colony Biofilm Assay

In this study, the reference strain *P. aeruginosa* PAO1 and strong biofilm-forming clinical isolate PA47 were used. Briefly, bacterial cultures were grown in 5 mL medium and incubated for 24 h. The optical density (OD_{600}) was adjusted to 0.08–0.1. For colony biofilm formation, 0.22 µm polycarbonate membranes were sterilized under UV for 10 min, placed on agar plates, and further sterilized. The 5 µL aliquot from a bacterial suspension adjusted to 0.5 McFarland standard was inoculated onto the membrane surface and incubated statically at 37 °C for 24 h. Membranes were then transferred to fresh agar plates and incubated for an additional 24 h. After 48 h, membranes were placed in 1 mL PBS and vortexed to detach biofilm cells (Merritt et al., 2011). The harvested cells were used for RNA extraction.

RNA Isolation, cDNA Synthesis, and Quantitative PCR (qPCR) Analysis

Total RNA was extracted from both planktonic and biofilm cells using the TRIzol® Reagent protocol. After 48 h of incubation, the cells were pelleted by centrifugation, resuspended in 1 mL TRIzol, and homogenized. RNA was extracted with phenol:chloroform (25:24:1), precipitated with isopropanol, washed with 75% cold ethanol, air-

dried, and stored at −80 °C. RNA concentrations were quantified spectrophotometrically, and 1 µg of total RNA from each sample was reverse transcribed into cDNA using a commercial reverse transcription kit. The reaction was performed at 25 °C for 10 min, 37 °C for 120 min, and 85 °C for 5 min. cDNA samples were stored at −20 °C until use. Quantitative PCR (qPCR) reactions (final volume 10 µL) contained 4 µL RT-PCR master mix, 0.5 µL of each primer, 2 µL cDNA, and 3 µL nuclease-free water. The amplification program consisted of an initial denaturation at 95 °C for 2 min, followed by 40 cycles of 95 °C for 30 s, 61 °C for 20 s, and 72 °C for 10 s. Cycle threshold (Ct) values were normalized using the housekeeping gene *rpoD*, and relative expression changes were calculated using the $2^{-(\Delta\Delta Ct)}$ method.

Results and Discussion

The BON (Bacterial OsmY and Nodulation) domains are known to interact with phospholipid membranes, contributing to the maintenance of outer membrane integrity and enhancing resistance to stress conditions in Gram-negative bacteria (Yeats & Bateman, 2003; Bryant et al., 2020). Previous studies have demonstrated that BON domain proteins such as DolP in *Escherichia coli* and BonA in *Acinetobacter baumannii* are involved in outer membrane homeostasis and resistance to membrane-targeting antibiotics (Grinter et al., 2021; Ranava et al., 2021). This study investigated the expression profiles of two BON domain–containing genes, *PA4426* and *PA4739,* in *P. aeruginosa* under planktonic and colony biofilm growth conditions. Quantitative gene expression analyses showed that, in both the reference strain PAO1 and the clinical isolate PA47, the expression levels of these genes were significantly higher in biofilm cultures compared to planktonic cells. As shown in Figure 1, *P. aeruginosa* formed a colony biofilm structure under static conditions, confirming the successful establishment of biofilm cultures. These findings indicate that the observed gene expression differences are associated with biofilm-specific physiological states.

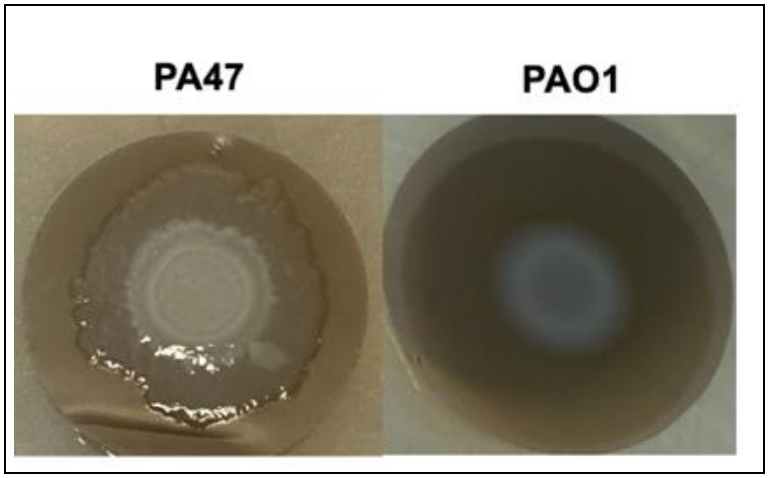


Figure 1. Colony biofilm structure of *Pseudomonas aeruginosa***.**

In Figure 2A–D, both ***PA4426*** and ***PA4739*** exhibit significant and strain-dependent transcriptional induction under biofilm conditions in *P. aeruginosa*. In the reference strain **PAO1, *PA4739*** shows a **6–7-fold increase ($p<0.0001$)**, whereas the clinical isolate **PA47** displays an even more dramatic **~40-fold upregulation ($p<0.001$),** indicating that *PA4739* is strongly biofilm responsive in both genetic backgrounds, with particularly pronounced induction in PA47. Similarly, ***PA4426*** is clearly induced in biofilms; in **PAO1**, expression rises by approximately **145-fold ($p<0.0002$)**, representing the most substantial transcriptional activation among the tested genes, while in **PA47** the increase is more modest, approximately **1-fold but still statistically significant ($p<0.05$).** Together, these data demonstrate that both BON-domain–containing genes are consistently activated in a biofilm-dependent manner, albeit with markedly different magnitudes between strains. The collective upregulation profiles in Figure 2 suggest that ***PA4426*** and ***PA4739*** contribute to conserved, biofilm-associated

physiological processes, potentially involving membrane stabilization, periplasmic stress adaptation, or early steps of antibiotic tolerance. Although their exact biochemical functions remain unresolved, their predicted localization to the outer membrane or periplasm, combined with the presence of BON domains, supports a **structural or regulatory** role rather than enzymatic activity. Further studies such as targeted knockouts, lipid-binding assays, and proteomic analyses will be essential to clarify their mechanistic contributions to biofilm maturation and associated survival pathways in *P. aeruginosa*.

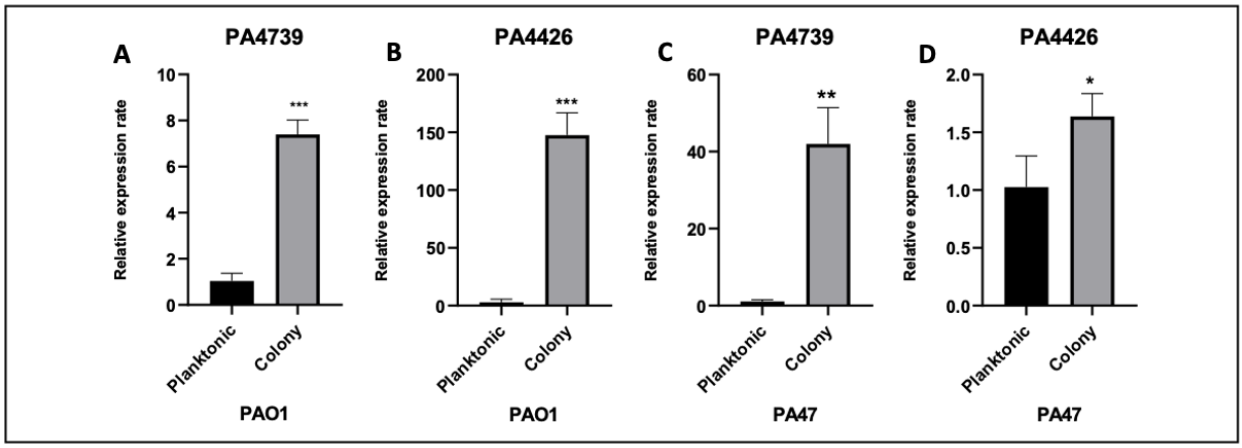


Figure 2. Comparison of *PA4426* and *PA4739* gene expression levels in planktonic and biofilm cultures of *Pseudomonas aeruginosa*.

Conclusion

In conclusion, the *PA4426* and *PA4739* genes were found to be expressed at higher levels in colony biofilm cultures compared to planktonic cells. This observation suggests that these genes may play important roles in biofilm-specific adaptive processes, such as antibiotic tolerance, biofilm stability, and structural maintenance. Given that biofilms provide a protective niche enabling *P. aeruginosa* to survive under antibiotic and environmental stress, the upregulation of BON domain–containing genes in this condition may reflect a broader bacterial strategy to reinforce membrane robustness and sustain long-term persistence. These findings highlight *PA4426* and *PA4739* as biofilm-associated resistance. Elucidating their precise mechanisms through targeted mutagenesis, protein localization studies, and lipid-binding assays will be essential for understanding how BON domain–containing proteins contribute to the complex defense network of *P. aeruginosa*. Ultimately, such insights could guide the development of novel therapeutic strategies aimed at disrupting biofilm integrity and overcoming antibiotic resistance in multidrug-resistant *P. aeruginosa* strains.

REFERENCES

Ali, A., Kumar, R., Khan, A. and Khan, A.U. 2020. “Interaction of LysM BON family protein domain with carbapenems: A putative mechanism of carbapenem resistance”, International Journal of Biological Macromolecules, 160, 212-223.

Barkovits, K., Schubert, B., Heine, S., Scheer, M. and Frankenberg-Dinkel, N. 2011. “Function of the bacteriophytochrome BphP in the RpoS/Las quorum-sensing network of Pseudomonas aeruginosa”, Microbiology, 157(6), 1651-1664.

Bryant, J.A., Morris, F.C., Knowles, T.J., Maderbocus, R., Heinz, E., Boelter, G. et al. 2020. “Structure and function of DolP, an outer membrane lipoprotein required for Escherichia coli viability”, Nature Microbiology, 5(9), 1465-1473.

Costerton, J.W., Stewart, P.S. and Greenberg, E.P. 1999. “Bacterial biofilms: a common cause of persistent infections”, Science, 284(5418), 1318-1322.

Diggle, S.P., Whiteley, M. and Mathee, K. 2019. “Microbe Profile: Pseudomonas aeruginosa: opportunistic pathogen and lab rat”, Microbiology, 165(8), 829-831.

Evans, J., Mabrouk, A. and Nielson, J.L. 2023. Pseudomonas aeruginosa. In: StatPearls [Internet]. Treasure Island (FL): StatPearls Publishing.

Grinter, R., Morris, F.C., Dunstan, R.A., Leung, P.M., Kropp, A., Belousoff, M., Gunasinghe, S.D., Scott, N.E., Beckham, S., Peleg, A.Y., Greening, C., Li, J., Heinz, E. and Lithgow, T. 2021. "BonA from Acinetobacter baumannii forms a divisome-localized decamer that supports outer envelope function", mBio, 12(4), e01480-21.

Hall-Stoodley, L., Costerton, J.W. and Stoodley, P. 2004. "Bacterial biofilms: from the natural environment to infectious diseases", Nature Reviews Microbiology, 2(2), 95-108.

Høiby, N., Ciofu, O. and Johansen, H.K. 2011. "The clinical impact of bacterial biofilms", International Journal of Oral Science, 3(2), 55-65.

Krell, T. and Matilla, M.A. 2024. "Microbe of the month: Pseudomonas aeruginosa", Trends in Microbiology, 32(2), 216-218.

Liew, S.M., Puthucheary, S.D., Rajasekaram, G. and Chua, K.H. 2021. "Proteomic profiling of clinical and environmental strains of Pseudomonas aeruginosa", Molecular Biology Reports, 48.

Malone, M., Bjarnsholt, T., McBain, A.J., James, G.A., Stoodley, P., Leaper, D., Tachi, M., Schultz, G., Swanson, T. and Wolcott, R.D. 2017. "The prevalence of biofilms in chronic wounds: a systematic review and meta-analysis of published data", Journal of Wound Care, 26(1), 20-25.

Merritt, J.H., Kadouri, D.E. and O'Toole, G.A. 2011. "Growing and analyzing static biofilms", Current Protocols in Microbiology, Chapter 1: Unit 1B.1.

Qin, S., Xiao, W., Zhou, C., Pu, Q., Deng, X., Lan, L., and Liang, H. 2022. "Pseudomonas aeruginosa: pathogenesis, virulence factors, antibiotic resistance, interaction with host, technology advances and emerging therapeutic strategies", Signal Transduction and Targeted Therapy, 7(1), 199.

Ranava, D., Yang, Y., Orenday-Tapia, L., Rousset, F., Turlan, C., Morales, V., Cui, L., Moulin, C., Froment, C., Munoz, G., Rech, J., Marcoux, J., Caumont-Sarcos, A., Albenne, C., Bikard, D. et Ieva, R. 2021. "Lipoprotein DolP supports proper folding of BamA in the bacterial outer membrane, promoting fitness upon envelope stress", eLife, 10, e67817.

Sati, H., Carrara, E., Savoldi, A., Hansen, P., Garlasco, J., Campagnaro, E., et al. (2025). The WHO bacterial priority pathogens list 2024: A prioritisation study to guide research, development, and public health strategies against antimicrobial resistance. The Lancet Infectious Diseases, 25(2), 122-135

Sen, C.K., Gordillo, G.M., Roy, S., Kirsner, R., Lambert, L., Hunt, T.K. et al. 2009. "Human skin wounds: A major and snowballing threat to public health and the economy", Wound Repair and Regeneration, 17(6), 763-771.

Sun, S., Wang, M., Xiang, J., Shao, Y., Li, L., Sedjoah, R.C.A.A. et al. 2023. "BON domain-containing protein-mediated co-selection of antibiotic and heavy metal resistance in bacteria", International Journal of Biological Macromolecules, 238, 124062.

Sun, Y. and Chen, X. 2025. "The role of BON domain proteins in antibiotic resistance: emerging mechanisms and therapeutic implications", Frontiers in Microbiology, (early access).

Tolker-Nielsen, T. 2014. "Pseudomonas aeruginosa biofilm infections: from molecular biofilm biology to new treatment possibilities", APMIS Supplementum, (138), 1-51.

Yeats, C. and Bateman, A. 2003. "The BON domain: a putative membrane-binding domain", Trends in Biochemical Sciences, 28(7), 352-355.

ORAL PRESENTATION

Thymus canoviridis bitkisinin bazı ekstraktlarının HMGR enzimi inhibisyonuna etkilerinin moleküler yerleştirme metodu ile incelenmesi

Selami Ercan (Orcid: https://orcid.org/0000-0002-9528-6122)

Batman Üniversitesi, Fen Edebiyat Fakültesi, Kimya Bölümü, Batman, Türkiye

Sorumlu yazar e-mail: selami.ercan@batman.edu.tr

Özet

İnsan ölümlerinde kronik bulaşıcı olmayan hastalıklar önemli bir yer tutmaktadır. Dünya Sağlık Örgütü'nün 2018 istatistikleri, toplam 57 milyon ölümün %71'inden (41 milyon kişi) kronik bulaşıcı olmayan hastalıkların sorumlu olduğunu bildiriyor. Kardiyovasküler hastalıkların en önemli risk faktörleri hipertansiyon ve hiperkolesterolemidir. 3-Hidroksi-3-metil-glutaril-CoA redüktaz, hiperkolesterolemiye neden olan kolesterolün sentez yolundaki anahtar bir enzimdir. Kolesterol sentezini engellemenin çözümlerinden biri de HMG-CoA redüktaz enzimini bloke eden ilaçlar kullanmaktır. HMG-CoA redüktazın inhibisyonu ile HMG-CoA'nın mevalonata dönüşümü ve dolayısıyla sonraki ürünlerin sentezi sonlandırılmış olur. Bu sonlanma aynı zamanda çeşitli kanser hücresi türlerinde büyümenin durdurulmasına ve hücre ölümüne de hizmet etmektedir.

Bu çalışmada, birçok hastalığa karşı ilaç olarak kullanılmasının yanı sıra aroma verici, baharat ve gıda koruyucu Thymus Canoviridis yapısında bulunan 21 bileşik moleküler yerleştirme metodu ile HMG-CoA enzim bağlanma bölgesine yerleştirilmiş ve bağlanma bölgesindeki ligand-kalıntı etkileşimleri incelenmiştir. Kullanılan bileşiklerin HMGR enziminin aktifliğinde önemli roller üstlenen Glu559, Cys668, Lys691 ve Lys692 gibi kalıntılar ile çeşitli etkileşimler gerçekleştiği belirlenmiştir. Yapılan yerleştirme sonucunda rutin bileşiğinin −8.96 kcal/mol'lük bağlanma serbest enerji değeri ile en iyi sonucu verdiği belirlenmiştir. Ayrıca rutin bileşiğinin yanı sıra hesperidin ve nikotiflorin bileşiklerinin de bir HMGR inhibitörü olan RSV'den daha iyi sonuç verdiği belirlenmiştir.

Anahtar Kelimeler: HMGR, Moleküler Yerleştirme (Docking), *Thymus Canoviridis*

Investigation of the effects of some *thymus canoviridis* plant's extracts on HMGR enzyme inhibition using molecular docking method

Abstract

Chronic noncommunicable diseases (NCDs) play a significant role in human mortality. The World Health Organization's 2018 statistics report that chronic NDCs account for 71% of the 57 million deaths (41 million people). The most important risk factors for cardiovascular disease are hypertension and hypercholesterolemia. 3-Hydroxy-3-methyl-glutaryl-CoA reductase is a key enzyme in the cholesterol synthesis pathway that causes hypercholesterolemia. One solution to inhibit cholesterol synthesis is the use of drugs that block the HMG-CoA reductase enzyme. Inhibiting HMG-CoA reductase halts the conversion of HMG-CoA to mevalonate and, consequently, the synthesis of downstream products. This inhibition also serves to inhibit growth and cell death in various types of cancer cells. In this study, 21 compounds found in Thymus Canoviridis, which are used as a flavoring agent, spice, and food protectant in addition to being used as drugs against many diseases, were docked to the HMG-CoA enzyme binding site using the molecular docking method, and ligand-residue interactions in the binding site were investigated. Various interactions were observed with residues such as Glu559, Cys668, Lys691, and Lys692, which play important roles in the activity of the HMGR enzyme. The docking results indicated that rutin yielded the best binding free energy value of −8.96 kcal/mol. Furthermore, in addition to rutin, hesperidin and nicotiflorin also gave better results than RSV, an HMGR inhibitor.

Keywords: HMGR, Molecular Docking, *Thymus Canoviridis*

GİRİŞ

Kardiyovasküler hastalık (KVH), kanser, kronik solunum yolu hastalığı ve diyabet, ölüme neden olan dört ana bulaşıcı olmayan hastalıktır (BOH). Hipertansiyon ve hiperkolesterolemi, KVH hastalıklarının önemli risk faktörleridir (Bays ve ark., 2021). Mevalonat yolunda asetil-CoA'dan türeyen kolesterol hiperkolesterolemiye neden olmaktadır (Mullen ve ark., 2016). Kolesterol sentezi, önemli bir enzim olan 3-Hidroksi-3-metilglutaril-CoA (HMG-CoA) redüktazın (HMGR) inhibisyonuyla önlenebilir. HMGR'nin inhibisyonu, HMG-CoA'nın mevalonata dönüşümünün ve sonraki ürünlerin sentezinin sona ermesiyle sonuçlanır. Çalışmalar, bu yolun sonlandırılmasının çeşitli kanser türlerindeki hücrelerde büyümenin durmasına ve hücre ölümüne neden olabileceğini ortaya koymuştur (Bennis ve ark., 1993; Caruso ve ark., 1999; Hawk ve ark., 1996; Istvan ve ark., 2000; Lee ve ark., 1998). Statinler, mantar metabolitlerinden veya mikrobiyal kaynaklardan elde edilen ve HMGR'yi inhibe etmek için kullanılan en popüler inhibitörlerdir (Moorthy ve ark., 2015). HMGR'nin inhibisyonunda ve düşük yoğunluklu lipoprotein düzeylerinin düşürülmesinde büyük başarı gösterilmesine rağmen, araştırmalar LDL-C'yi ABD Kolesterol Eğitim Programı tarafından tercih edilen düzeylere (70 mg/dL) düşürmek için gereken yüksek dozdaki statinlerin miyaljiye neden olabileceğini göstermiştir (Grundy ve ark., 2004).

888 kalıntıdan oluşan HMGR, üç alanda araştırılabilir: membran çapa bölgesi (1-339 kalıntı), bağlayıcı bölge (340-459 kalıntı) ve katalitik bölge (460-888 kalıntı). HMGR'nin katalitik bölgesi yapısal olarak üç alt alana ayrılmıştır: N-terminal bölgesi, büyük bir alan L-bölgesi ve küçük bir alan S-bölgesi. En küçük alan olan N terminal bölgesi, 460-527 kalıntılarını içerir ve HMGR'nin katalitik kısmını membran bölgesine bağlar (Istvanve ark., 2000). Merkezi L-bölgesi (528-590), bir ENVIG dimerizasyon motifine sahiptir (Son ve ark., 2013). Katalitik bölgenin S-bölgesi (592-682), DAMGMN NAD(P) bağlanma motifini içerir (Sonve ark., 2013) ve L-bölgesinin Lβ3 ve Lα2 bölümlerinin arasına yerleştirilmiştir (Istvanve ark., 2000). S-alanı, HMG bağlanma bölgesi için gerekli olan β-zincir (Lβ3 ve Sβ1) ve cis-döngü (kalıntılar 682-694) aracılığıyla L-bölgesine bağlanır (Istvanve ark., 2000).

Bugüne kadar, statin türevleri (Pfefferkorn ve ark., 2007; Sonve ark., 2013), statin olmayanlar (Bose ve ark., 2023; Silva ve ark., 2021) ve doğal kaynaklara (Aulifa ve ark., 2024; Marahatha ve ark., 2021) dayalı bileşikleri inhibitör adayları olarak kullanarak HMGR'yi inhibe etmek için *in vitro* ve/veya *in silico* yöntemlerini içeren birçok çalışma gerçekleştirilmiştir.

Thymus türlerinin çoğu birçok hastalığa karşı ilaç olarak ve aynı zamanda aroma verici ve gıda koruyucu amaçla kullanılmaktadır. *Thymus* türleri antiseptik, öksürük kesici, balgam söktürücü, antispazmodik ve antienflamatuvar gibi birçok biyolojik ve farmakolojik özelliklere sahiptirler. Birçok *Thymus* türünün yaprak ve çiçekleri, ishal, ateş, öksürük, yara ve sayısız enfeksiyonların tedavisinde toz, dekoksiyon veya infüzyon şeklinde kullanılırlar (Jamali ve ark., 2012). Ayrıca *Thymus* türleri antispazmodik, yatıştırıcı, antioksidan, antimikrobiyal, antifungal, antibakteriyel ve antiaflatoksijenik özellikleriyle de bilinirler (Jabri-Karoui ve ark., 2012).

Bu çalışmada *Thymus Canoviridis* yapısında bulunan 21 bileşik moleküler yerleştirme metodu ile HMGR enzim bağlanma bölgesine yerleştirilmiş ve bağlanma bölgesindeki ligand-kalıntı etkileşimleri incelenmiştir.

Bilgisayar destekli ilaç tasarım teknikleri, ilaç tasarım ve geliştirme süreçlerinde yaygın olarak kullanılmaktadır (Sanyaolu ve ark., 2021; Talele ve ark., 2010) ve ilaç geliştirme sürecinin maliyetini %50'ye kadar düşürdüğü bildirilmiştir (Wei & McCammon, 2024). Bununla birlikte, moleküler yerleştirme, hedef molekülün 3 boyutlu yapısını gerektiren yapı tabanlı bir ilaç tasarım yöntemi olan CADD süreçlerinde hızlı ve ekonomik yöntemlerden biridir (Sousa ve ark., 2013). Bu yöntem, ilacın bir ilaç hedefine karşı bağlanma afinitesini tahmin eder (Niazi & Mariam, 2023).

Atorvastatin, simvastatin, fluvastatin ve rosuvastatin (RSV) gibi çeşitli ligandlara ek olarak HMG-CoA ile kompleks oluşturan HMG-CoA redüktaz enziminin bazı kristal yapıları bugüne kadar çözülmüştür (Istvan & Deisenhofer, 2001; Istvanve ark., 2000; Steussy ve ark., 2013; Tabernero ve ark., 1999). RSV'nin, statin grubu inhibitörleri arasında en etkili inhibitör olduğu bildirilmiştir (Holdgate ve ark., 2003; Istvan, 2003; McTaggart ve ark., 2001). Bu nedenle, yeni incelenen ligandların yerleştirme sonuçlarını karşılaştırmak için mevcut çalışmada RSV ile kompleks oluşturan bir enzimin kristal yapısını kullandık.

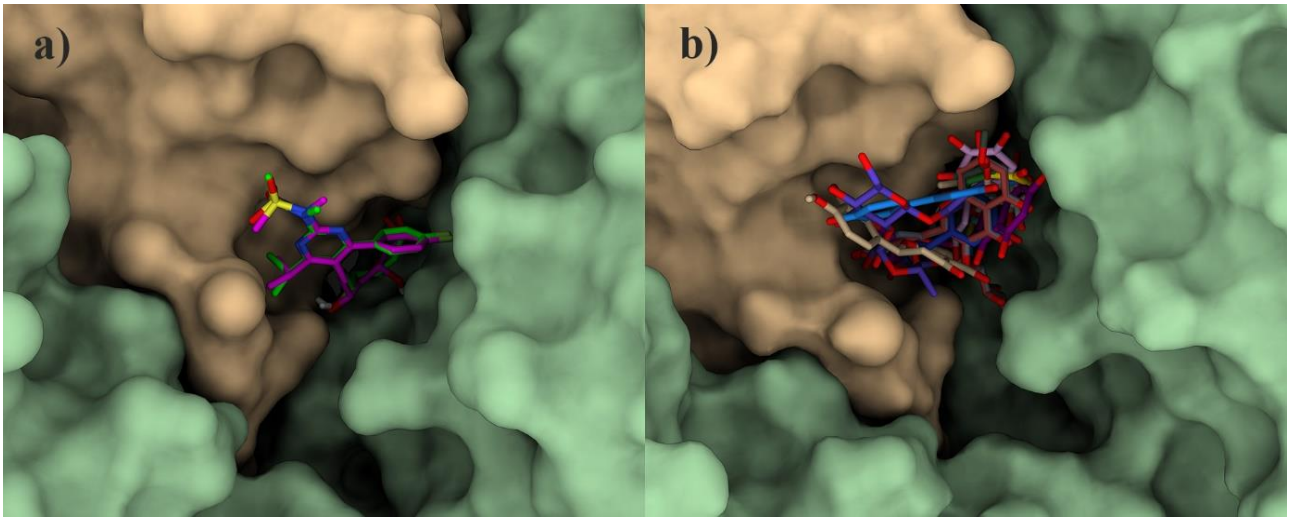
MATERYAL VE METOT

HMGR'nin RSV inhibitörü ile kompleks halindeki kristal yapısı 1HWL (Istvan & Deisenhofer, 2001) koduyla protein veri bankasından (www.rcsb.org) elde edildi. Protein ve RSV yapıları, tüm gereksiz parçacıklar çıkarılarak ayrı ayrı kaydedildi. *Thymus Canoviridis* yapısında bulunan bileşikler PubChem (https://pubchem.ncbi.nlm.nih.gov) sitesinden 3 boyutlu olarak "structure data file" (sdf) formatında indirilerek moleküler yerleştirme için uygun hale getirildi.

Yerleştirme çalışmaları, hızlı ve kullanıcı dostu bir yerleştirme motoru olan Autodock Vina (v1.2.7) (Eberhardt ve ark., 2021) ile gerçekleştirildi. Yerleştirme bölgesi, her bir doğrultuda 16 Å'luk boyutlarında ve sırasıyla x, y ve z doğrultuları üzerinden 21.19, −31.23, 27.05 koordinatlarında bir grid kutusunun kristalize RSV ligandı üzerine ortalanmasıyla tanımlandı. Her molekül için dokuz yerleştirme pozisyonu oluşturuldu. Yerleştirme çalışmaları öncesinde, HMG-CoA'nın enzimin bağlanma bölgesine yeniden yerleştirilmesiyle doğrulama testi gerçekleştirildi.

BULGULAR ve TARTIŞMA

HMGR enzimi ile eş-kristalize şekilde elde edilen RSV ligandının enzime yeniden yerleştirilmesi ile yerleştirme metodunun validasyonu gerçekleştirildi. Yerleştirme sonucu yerleştirilen RSV yapısı ile kristalize RSV yapısı arasında 1.19 Å'luk RMSD değeri olduğu belirlendi (Şekil 1). Bunun yanında enzimin bağlanma bölgesine yerleştirilen bütün bileşiklerin bağlanma modları Şekil 1'de verilmiştir.



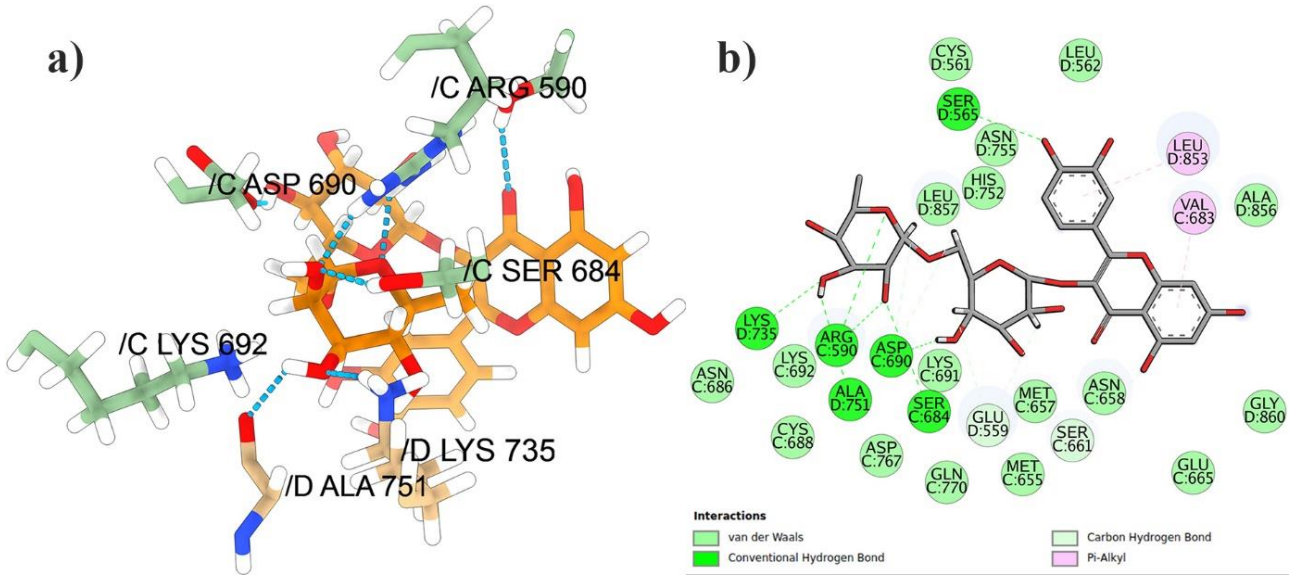
Şekil 1. a) RSV bileşiğinin yeniden yerleştirme sonucu ile kristal yapısının üst üste çakıştırılması (Kristal RSV yapısındaki karbon atomları magenta, yeniden yerleştirilen yapısındaki karbon atomları yeşil ile verilmiştir). b) *Thymus Canoviridis* yapısında bulunan 21 bileşiğin HMGR bağlanma bölgesindeki yerleşim modları (Enzimin C zinciri koyu deniz yeşili, D zinciri ise açık kahverengi ile gösterilmiştir).

Yerleştirme sonuçları Rutin (−8.96 kcal/mol), Hesperidin (−8.74 kcal/mol) ve Nikotiflorin (−8.72 kcal/mol) bileşiklerinin RSV'den (−8.41 kcal/mol) daha iyi skorlar elde ettiğini gösterirken, Fumarik asit (−4.31 kcal/mol) en yüksek bağlanma serbest enerji değerini vermiştir (Tablo 1).

Tablo 1. Çalışmada kullanılan bileşiklerin HMGR bağlanma bölgesindeki yerleşme skorları

Bileşik	Skor (kcal/mol)	Bileşik	Skor (kcal/mol)
Rutin	−8.96	Rosmarinic_acid	−7.57
Hesperidin	−8.74	Hesperetin	−7.55
Nicotiflorin	−8.72	Caffeic acid	−6.36
Rosuvastatin	−8.41	Quinic_acid	−6.27
Rhoifolin	−8.18	Protocatechuic acid	−5.85
Isoquercitrin	−8.10	Salicylic acid	−5.77
Cosmosiin	−8.04	Ferulic acid	−5.72
Chrysin	−7.70	p−Coumaric acid	−5.69
Chlorogenic acid	−7.68	Vanillin	−5.16
Naringenin	−7.68	Malic acid	−5.08
Apigenin	−7.67	Fumaric acid	−4.31

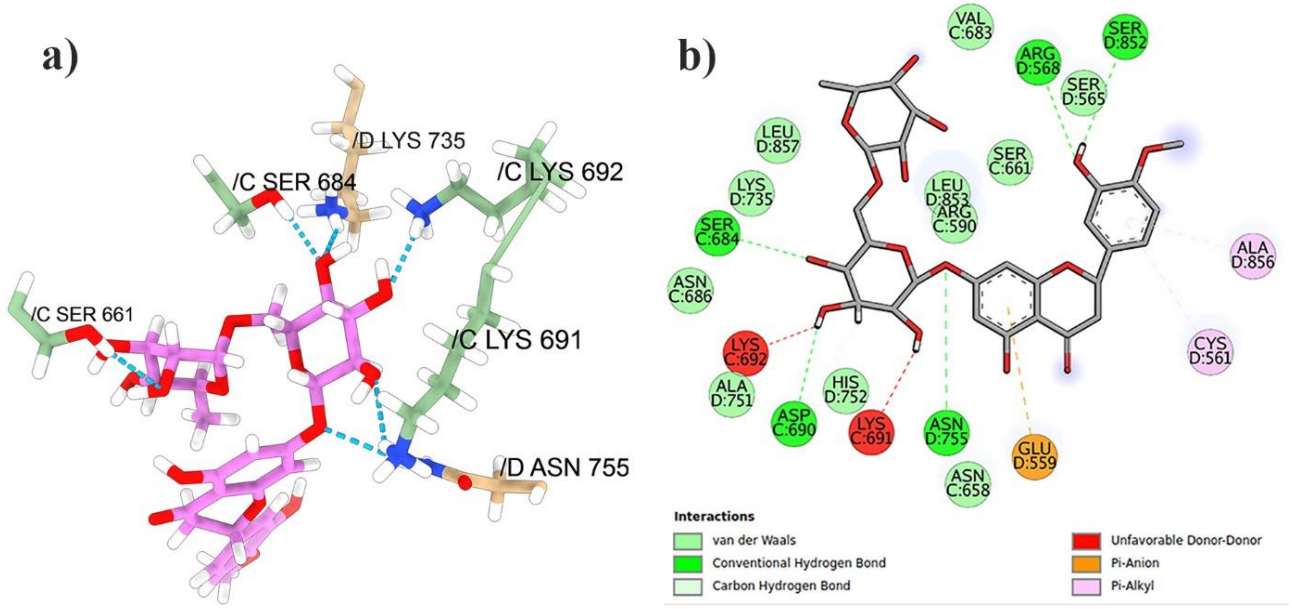
RSV ligandı enzimin kristal yapısında C:Arg590 (iki bağ), C:Asp690, C:Lys691, C:Lys692 ve D:Lys735 kalıntıları ile toplam 6 tane hidrojen bağı oluşturmaktadır (C ve D enzimin homodimer zincirlerini ifade etmektedir.). Bunun yanında yapısındaki flor atomu aracılığıyla C zincirinin Arg590 ve Val683 kalıntıları ile halojen etkileşimleri gerçekleştirirken, C:Arg590 kalıntısı ile pi-katyon, D:Leu583 ve D:Leu857 kalıntıları ile birer tane pi-alkil etkileşimi yapmaktadır. Diğer bileşikler de benzer etkileşimler gerçekleştirmiştir. Buna göre, en iyi bağlanma (−8.96 kcal/mol) gösteren Rutin bileşiği de RSV gibi kalıntı atomları ile 7 adet hidrojen bağ oluşturmaktadır. C:Arg590 (iki bağ), C:Ser684, D:Ser565, D:Lys735, D:Ala751 ve C:Asp690 kalıntıları hidrojen bağ oluşumunda yer almaktadırlar. Bunun yanında Rutin bileşiği C:Val683 ve D:Leu853 kalıntıları ile pi-alkil etkileşimleri gerçekleştirmektedir (Şekil 2).



Şekil 2. Rutin bileşiğinin; **a)** HMGR enziminin bağlanma bölgesinde oluşturduğu hidrojen bağlarının 3 boyutlu gösterimi (Rutin bileşiğinin karbon atomları turuncu, HMGR C ve D zincirlerinin karbon atomları sırasıyla koyu deniz yeşili ve açık kahverengi ile verilmiştir), **b)** tüm etkileşimlerinin 2 boyutlu görünümü.

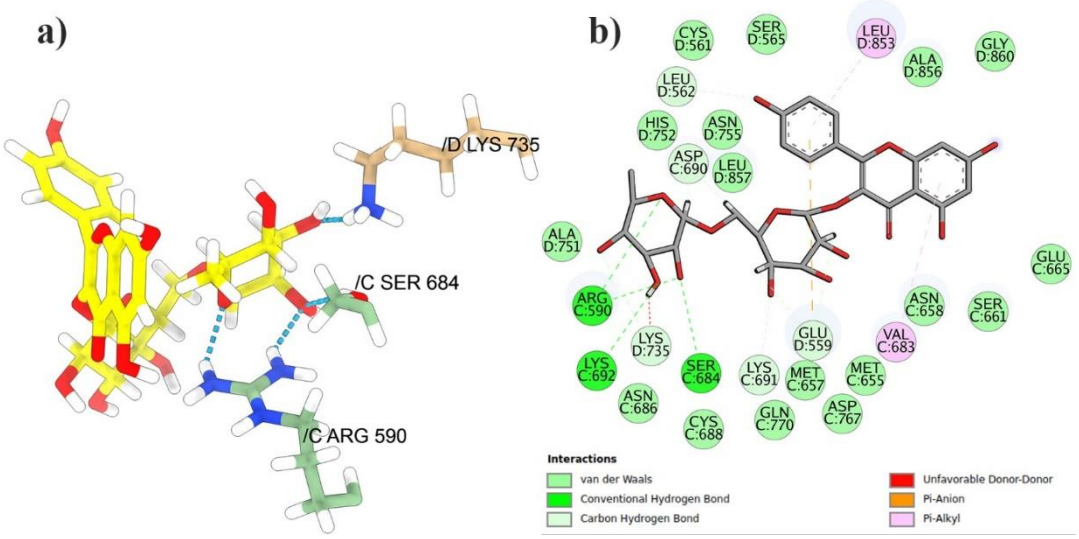
Çalışılan bileşikler arasında −8.74 kcal/mol'lük bağlanma serbest enerjisi değeriyle Rutin'den sonra en iyi bağlanma gösteren bileşik Hesperidin olmuştur. Hesperidin, C:Ser684, D:Arg568, D:Asn755, D:Ser852 ve C:Asp690 kalıntıları ile hidrojen bağı geliştirirken, D:Glu559 kalıntısı ile pi-anyon ve D:Cys561 ve D:Ala856 kalıntıları ile pi-alkil etkileşimleri oluşturmaktadır. Ayrıca, bileşik C zincirinin Lys691 ve Lys692 kalıntıları ile istenmeyen türden etkileşimler oluşturmaktadır. Bileşiğin yapısındaki alkol hidrojenlerinin lizin amino asidindeki hidrojenler ile etkileşimleri bu istenmeyen etkileşimlere sebep olurken, dinamik ortamda bu hidrojenlerin

bileşikteki alkol oksijenleri ile yakınlaşması durumunda birer hidrojen bağı oluşturma potansiyeli taşıdıkları da göz önüne alınmalıdır (Şekil 3).



Şekil 3. Hesperidin bileşiğinin; **a)** HMGR enziminin bağlanma bölgesinde oluşturduğu hidrojen bağlarının 3 boyutlu gösterimi (Hesperidin bileşiğinin karbon atomları magenta, HMGR C ve D zincirlerinin karbon atomları sırasıyla koyu deniz yeşili ve açık kahverengi ile verilmiştir), **b)** tüm etkileşimlerinin 2 boyutlu görünümü.

RSV'den daha iyi skor elde eden diğer bir bileşik ise nikotiflorin bileşiğidir (−8.72 kcal/mol). Nikotiflorin bileşiğinin etkileşimleri incelendiğinde, bileşiğin Rutin ve Hesperidin'den daha az sayıda hidrojen bağı oluşturduğu gözlenmektedir. Bileşik, ikisi C:Arg590 kalıntısı ve diğerleri C:Ser684 ve C:Lys692 kalıntılarıyla olan 4 adet hidrojen bağı oluşturmaktadır. Buna ek olarak, D:Glu559 kalıntısı ile elektrostatik pi-anyon, C:Val683 ve D:Leu853 kalıntıları ile de hidrofobik pi-alkil etkileşimleri nikotiflorin bileşiğinin oluşturduğu diğer istenen türde etkileşimleri oluştururken, bileşik aynı zamanda D:Lys735 kalıntısı ile istenmeyen türde donör-donör etkileşimi de yapmaktadır (Şekil 4).



Şekil 4. Nikotiflorin bileşiğinin; **a)** HMGR enziminin bağlanma bölgesinde oluşturduğu hidrojen bağlarının 3 boyutlu gösterimi (Nikotiflorin bileşiğinin karbon atomları sarı, HMGR C ve D zincirlerinin karbon atomları sırasıyla koyu deniz yeşili ve açık kahverengi ile verilmiştir), **b)** tüm etkileşimlerinin 2 boyutlu görünümü.

Yerleştirme sonucunda RSV'den daha iyi sonuç veren Rutin, Hesperidin ve Nikotiflorin bileşiklerinin etkileşimleri metinde verilirken, çalışmada yer alan bütün bileşiklerin enzim kalıntıları ile olan etkileşimleri Destekleyici Materyal Tablo D1'de verilmiştir. Bunun yanında, bileşiklerin enzim kalıntılarıyla oluşturdukları etkileşimlerin 2 boyutlu gösterimleri de Destekleyici Materyal Şekil D1-D9'da sunulmuştur.

HMGR'nin katalitik bölgesi, enzimin L ve S bölgeleri arasında yer alır. HMG boyunca uzanan 'cis-döngüsü' bağlanma bölgesinin en önemli yapısal elemanıdır (682-694 kalıntı). Asp690, Lys691 ve Lys692 kalıntılarının konumu, Cys688 ve Thr689'un cis-peptit bağı tarafından sağlanır (Istvanve ark., 2000). Glu559, Lys691 ve His866, katalitik anahtar kalıntılardır (Gesto ve ark., 2020; Miziorko, 2011). Yerleştirme sonuçları, bileşiklerin Cys688 veya Thr689 kalıntılarıyla hidrofobik etkileşim veya hidrojen bağı oluşturmadığını ortaya koyarken, bileşiklerin genel olarak Lys691, Lys692 ve Glu559 kalıntıları ile etkileştikleri gözlenmektedir. Bunun yanında, salisilik asit, fumarik asit, rutin, nikotiflorin, kafeik asit ve protokateşik asidin C:Cys668 kalıntısı ile van der Waals etkileşimleri gerçekleştirmektedir (Şekil 2, 4 ve Destekleyici Materyal Şekil D1-D9). Yerleştirme sonuçları incelendiğinde, *Thymus Canoviridis* bitkisinin yapısında bulunan bileşiklerin HMGR enzimini inhibe etme özelliklerinin olduğu bu çalışma ile belirlenmiştir.

SONUÇ

İnsan vücudundaki kolesterol seviyesini düşürmek için hedef alınan HMGR enziminin bağlanma bölgesine *Thymus Canoviridis* bitkisinin yapısında bulunan bileşikler moleküler yerleştirme yöntemi ile yerleştirilmiştir. Çalışma sonuçları Rutin, Hesperidin ve Nikotiflorin bileşiklerinin, aynı zamanda kolesterol tedavisinde ilaç olarak kullanılmakta olan RSV bileşiğinden daha düşük skorlar elde ettiğini göstermiştir. Bileşiklerin yerleştirilme skorları −8.96 ile −4.31 kcal/mol arasında yer alırken, Rutin −8.96 kcal/mol ile en iyi bağlanma serbest enerjisine sahip olurken, en düşük bağlanma serbest enerjisine sahip bileşik Fumarik asit olmuştur.

Sonuç olarak *Thymus Canoviridis* bitkisinin yapısında bulunan bileşiklerin HMGR enziminin aktifliğinde önem arz eden Glu559, Cys668, Lys691 ve Lys692 kalıntıları ile etkileşimler oluşturarak enzim inhibisyonunda rol alabilecekleri belirlenmiştir.

KAYNAKLAR

Aulifa, D. L., Amirah, S. R., Rahayu, D., Megantara, S., & Muchtaridi, M. (2024). Pharmacophore Modeling and Binding Affinity of Secondary Metabolites from Angelica keiskei to HMG Co-A Reductase. *Molecules*, *29*(13). https://doi.org/10.3390/molecules29132983

Bays, H. E., Taub, P. R., Epstein, E., Michos, E. D., Ferraro, R. A., Bailey, A. L., Kelli, H. M., Ferdinand, K. C., Echols, M. R., Weintraub, H., Bostrom, J., Johnson, H. M., Hoppe, K. K., Shapiro, M. D., German, C. A., Virani, S. S., Hussain, A., Ballantyne, C. M., Agha, A. M., & Toth, P. P. (2021). Ten things to know about ten cardiovascular disease risk factors. *Am J Prev Cardiol*, *5*, 100149. https://doi.org/10.1016/j.ajpc.2021.100149

Bennis, F., Favre, G., Legaillard, F., & Soula, G. (1993). Importance of Mevalonate-Derived Products in the Control of Hmg-Coa Reductase-Activity and Growth of Human Lung Adenocarcinoma Cell-Line A549. *International Journal of Cancer*, *55*(4), 640–645. https://doi.org/DOI 10.1002/ijc.2910550421

Bose, S., Steussy, C. N., Lopez-Perez, D., Schmidt, T., Kulathunga, S. C., Seleem, M. N., Lipton, M., Mesecar, A. D., Rodwell, V. W., & Stauffacher, C. V. (2023). Targeting Enterococcus faecalis HMG-CoA reductase with a non-statin inhibitor. *Commun Biol*, *6*(1), 360. https://doi.org/10.1038/s42003-023-04639-y

Caruso, M. G., Notarnicola, M., Santillo, M., Cavallini, A., & Di Leo, A. (1999). Enhanced 3-hydroxy-3-methyl-glutaryl coenzyme A reductase activity in human colorectal cancer not expressing low density lipoprotein receptor. *Anticancer Research*, *19*(1a), 451–454.

Eberhardt, J., Santos-Martins, D., Tillack, A. F., & Forli, S. (2021). AutoDock Vina 1.2.0: New Docking Methods, Expanded Force Field, and Python Bindings. *J Chem Inf Model*, *61*(8), 3891–3898. https://doi.org/10.1021/acs.jcim.1c00203

Gesto, D. S., Pereira, C. M. S., Cerqueira, N., & Sousa, S. F. (2020). An Atomic-Level Perspective of HMG-CoA-Reductase: The Target Enzyme to Treat Hypercholesterolemia. *Molecules*, *25*(17). https://doi.org/10.3390/molecules25173891

Grundy, S. M., Cleeman, J. I., Merz, C. N., Brewer, H. B., Jr., Clark, L. T., Hunninghake, D. B., Pasternak, R. C., Smith, S. C., Jr., Stone, N. J., National Heart, L., Blood, I., American College of Cardiology, F., & American Heart, A. (2004). Implications of recent clinical trials for the National Cholesterol Education Program Adult Treatment Panel III guidelines. *Circulation*, *110*(2), 227–239. https://doi.org/10.1161/01.CIR.0000133317.49796.0E

Hawk, M. A., Cesen, K. T., Siglin, J. C., Stoner, G. D., & Ruch, R. J. (1996). Inhibition of lung tumor cell growth in vitro and mouse lung tumor formation by lovastatin. *Cancer Letters*, *109*(1-2), 217–222. https://doi.org/Doi 10.1016/S0304-3835(96)04465-5

Holdgate, G. A., Ward, W. H., & McTaggart, F. (2003). Molecular mechanism for inhibition of 3-hydroxy-3-methylglutaryl CoA (HMG-CoA) reductase by rosuvastatin. *Biochem Soc Trans*, *31*(Pt 3), 528–531. https://doi.org/10.1042/bst0310528

Istvan, E. (2003). Statin inhibition of HMG-CoA reductase: a 3-dimensional view. *Atheroscler Suppl*, *4*(1), 3–8. https://doi.org/10.1016/s1567-5688(03)00003-5

Istvan, E. S., & Deisenhofer, J. (2001). Structural mechanism for statin inhibition of HMG-CoA reductase. *Science*, *292*(5519), 1160–1164. https://doi.org/10.1126/science.1059344

Istvan, E. S., Palnitkar, M., Buchanan, S. K., & Deisenhofer, J. (2000). Crystal structure of the catalytic portion of human HMG-CoA reductase: insights into regulation of activity and catalysis. *Embo Journal*, *19*(5), 819–830. https://doi.org/DOI 10.1093/emboj/19.5.819

Jabri-Karoui, I., Bettaieb, I., Msaada, K., Hammami, M., & Marzouk, B. (2012). Research on the phenolic compounds and antioxidant activities of Tunisian Thymus capitatus. *Journal of Functional Foods*, *4*(3), 661–669. https://doi.org/https://doi.org/10.1016/j.jff.2012.04.007

Jamali, C. A., El Bouzidi, L., Bekkouche, K., Lahcen, H., Markouk, M., Wohlmuth, H., Leach, D., & Abbad, A. (2012). Chemical Composition and Antioxidant and Anticandidal Activities of Essential Oils from Different Wild Moroccan Thymus Species. *Chemistry & Biodiversity*, *9*(6), 1188–1197. https://doi.org/10.1002/cbdv.201200041

Lee, S. J., Ha, M. J., Lee, J., Nguyen, P., Choi, Y. H., Pirnia, F., Kang, W. K., Wang, X. F., Kim, S. J., & Trepel, J. B. (1998). Inhibition of the 3-hydroxy-3-methylglutaryl-coenzyme A reductase pathway induces p53-independent transcriptional regulation of p21(WAF1/CIP1) in human prostate carcinoma cells. *Journal of Biological Chemistry*, *273*(17), 10618–10623. https://doi.org/DOI 10.1074/jbc.273.17.10618

Marahatha, R., Basnet, S., Bhattarai, B. R., Budhathoki, P., Aryal, B., Adhikari, B., Lamichhane, G., Poudel, D. K., & Parajuli, N. (2021). Potential natural inhibitors of xanthine oxidase and HMG-CoA reductase in cholesterol regulation: in silico analysis. *BMC Complement Med Ther*, *21*(1), 1. https://doi.org/10.1186/s12906-020-03162-5

McTaggart, F., Buckett, L., Davidson, R., Holdgate, G., McCormick, A., Schneck, D., Smith, G., & Warwick, M. (2001). Preclinical and clinical pharmacology of Rosuvastatin, a new 3-hydroxy-3-methylglutaryl coenzyme A reductase inhibitor. *Am J Cardiol*, *87*(5A), 28B–32B. https://doi.org/10.1016/s0002-9149(01)01454-0

Miziorko, H. M. (2011). Enzymes of the mevalonate pathway of isoprenoid biosynthesis. *Arch Biochem Biophys*, *505*(2), 131–143. https://doi.org/10.1016/j.abb.2010.09.028

Moorthy, N. S. H. N., Cerqueira, N. M. F. S. A., Ramos, M. J., & Fernandes, P. A. (2015). Ligand based analysis on HMG-CoA reductase inhibitors. *Chemometrics and Intelligent Laboratory Systems*, *140*, 102–116. https://doi.org/10.1016/j.chemolab.2014.11.009

Mullen, P. J., Yu, R., Longo, J., Archer, M. C., & Penn, L. Z. (2016). The interplay between cell signalling and the mevalonate pathway in cancer. *Nat Rev Cancer*, *16*(11), 718–731. https://doi.org/10.1038/nrc.2016.76

Niazi, S. K., & Mariam, Z. (2023). Computer-Aided Drug Design and Drug Discovery: A Prospective Analysis. *Pharmaceuticals (Basel)*, *17*(1). https://doi.org/10.3390/ph17010022

Pfefferkorn, J. A., Song, Y., Sun, K. L., Miller, S. R., Trivedi, B. K., Choi, C., Sorenson, R. J., Bratton, L. D., Unangst, P. C., Larsen, S. D., Poel, T. J., Cheng, X. M., Lee, C., Erasga, N., Auerbach, B., Askew, V., Dillon, L., Hanselman, J. C., Lin, Z.,…Eberstadt, M. (2007). Design and synthesis of hepatoselective, pyrrole-based HMG-CoA reductase inhibitors. *Bioorganic & Medicinal Chemistry Letters*, *17*(16), 4538–4544. https://doi.org/10.1016/j.bmcl.2007.05.096

Sanyaolu, A., Okorie, C., Marinkovic, A., Haider, N., Abbasi, A. F., Jaferi, U., Prakash, S., & Balendra, V. (2021). The emerging SARS-CoV-2 variants of concern. *Ther Adv Infect Dis*, *8*, 20499361211024372. https://doi.org/10.1177/20499361211024372

Silva, M., Philadelpho, B., Santos, J., Souza, V., Souza, C., Santiago, V., Silva, J., Souza, C., Azeredo, F., Castilho, M., Cilli, E., & Ferreira, E. (2021). IAF, QGF, and QDF Peptides Exhibit Cholesterol-Lowering Activity through a Statin-like HMG-CoA Reductase Regulation Mechanism: In Silico and In Vitro Approach. *Int J Mol Sci*, *22*(20). https://doi.org/10.3390/ijms222011067

Son, M., Baek, A., Sakkiah, S., Park, C., John, S., & Lee, K. W. (2013). Exploration of virtual candidates for human HMG-CoA reductase inhibitors using pharmacophore modeling and molecular dynamics simulations. *PLoS One*, *8*(12), e83496. https://doi.org/10.1371/journal.pone.0083496

Sousa, S. F., Ribeiro, A. J., Coimbra, J. T., Neves, R. P., Martins, S. A., Moorthy, N. S., Fernandes, P. A., & Ramos, M. J. (2013). Protein-ligand docking in the new millennium--a retrospective of 10 years in the field. *Curr Med Chem*, *20*(18), 2296–2314. https://doi.org/10.2174/0929867311320180002

Steussy, C. N., Critchelow, C. J., Schmidt, T., Min, J. K., Wrensford, L. V., Burgner, J. W., 2nd, Rodwell, V. W., & Stauffacher, C. V. (2013). A novel role for coenzyme A during hydride transfer in 3-hydroxy-3-methylglutaryl-coenzyme A reductase. *Biochemistry*, *52*(31), 5195–5205. https://doi.org/10.1021/bi400335g

Tabernero, L., Bochar, D. A., Rodwell, V. W., & Stauffacher, C. V. (1999). Substrate-induced closure of the flap domain in the ternary complex structures provides insights into the mechanism of catalysis by 3-hydroxy-3-methylglutaryl-CoA reductase. *Proc Natl Acad Sci U S A*, *96*(13), 7167–7171. https://doi.org/10.1073/pnas.96.13.7167

Talele, T. T., Khedkar, S. A., & Rigby, A. C. (2010). Successful Applications of Computer Aided Drug Discovery: Moving Drugs from Concept to the Clinic. *Current Topics in Medicinal Chemistry*, *10*(1), 127–141. https://doi.org/Doi 10.2174/156802610790232251

Wei, H., & McCammon, J. A. (2024). Structure and dynamics in drug discovery. *npj Drug Discovery*, *1*(1), 1. https://doi.org/10.1038/s44386-024-00001-2

ORAL PRESENTATION

The olive oil production and pomace management in Albania, a contribution to sustainable agriculture

Aleksander Petre[1], Erzen Doga[2], Dritan Topi[3]*

[1]Faculty of Natural Sciences, University of Tirana, Department of Industrial Chemistry, Blvd Zogu 1, 1000, Tirana, Albania
[2]ONER LABATE, Olive Pomace Extraction Plant, Lushnja, Albania
[3]Faculty of Natural Sciences, University of Tirana, Department of Chemistry, Blvd Zogu 1, 1000, Tirana, Albania

Abstract

This study examines olive oil production and pomace management in Albania within the context of sustainable agriculture. The sector comprises approximately 500 processing plants, with over 95% employing three-phase extraction technology at capacities of 2–3 tons of olives per hour. Olive pomace, the main by-product, has been collected at nearly full efficiency in recent years, enabling secondary oil recovery of 1.5–2.0%. These practices contribute to Albania's emerging circular bioeconomy. Key challenges include wastewater disposal and the need for improved valorization of by-products into energy and fertilizers. Strategic interventions to optimize extraction efficiency and implement environmentally sound waste management are essential for reducing ecological impacts and promoting sustainable growth in the national agro-industrial framework.
Keywords: Olive oil, pomace extraction, olive mill wastewater, Albania, sustainable agriculture

INTRODUCTION

Olive cultivation in Albania reflects the broader Mediterranean distribution of the species, thriving primarily in coastal and river valley regions within the Mediterranean climate zone, which covers 36.2% of the country's territory. This environment has supported the development of several native cultivars, classified into primary and secondary groups based on prevalence. Kalinjoti, Kokërrmadh Berati, and Bianco di Tirana dominate as primary cultivars, while others maintain localized importance in specific regions (Topi, 2011; Topi et al., 2017).
For analytical and administrative purposes, olive plantations are grouped into four regions:
Southern Coastal Region (12,700 ha; 28%) – hilly terrain, high temperatures, limited irrigation.
Adriatic Region (18,300 ha; 36%) – low-altitude hills and plains, high yields, premium oil quality.
Pre-Adriatic Region (18,000 ha; 35.4%) – mountainous terrain with challenging pedo-climatic conditions.
Inland Region (210 ha; 0.6%) – microclimatic adaptation, offering opportunities for crop diversification under climate change (MAFCP, 2009).
This geographical diversity underpins Albania's olive oil sector, which has evolved from traditional practices to modern extraction technologies. Understanding this transition and its environmental implications is essential for developing sustainable strategies in the agro-industrial framework.

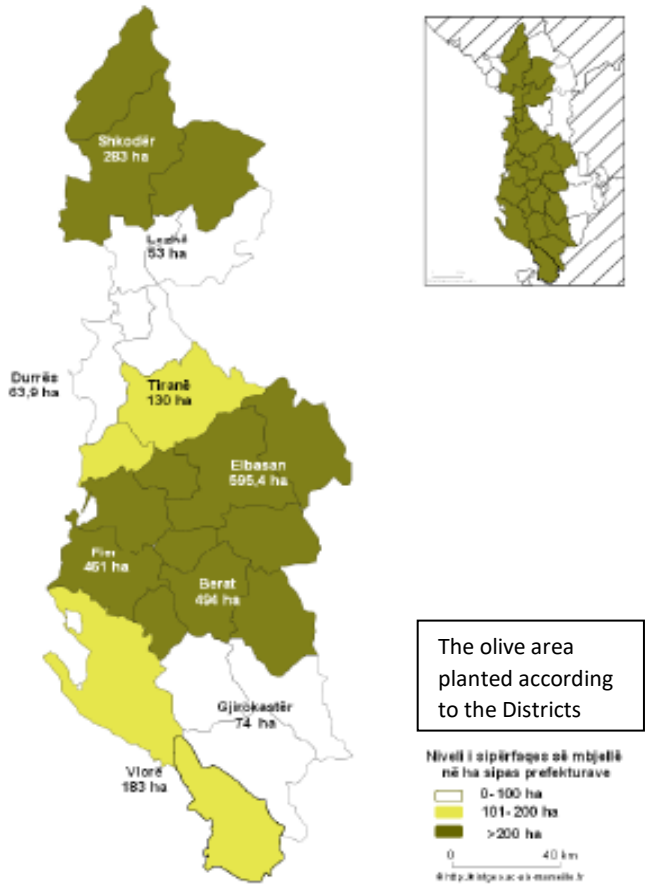


Figure 1: Regions of olive plantations (Source: **MAFCP, 2009**).

OLIVE PRODUCTION AND CONTRIBUTION TO THE NATIONAL ECONOMY

Olive cultivation has been a cornerstone of Albanian agriculture for millennia. During the socialist period (1947–1990), agriculture operated under a centralized economy, with olive plantations established primarily on degraded soils in hilly areas. Agronomic interventions during this era expanded plantations across western Albania, from Konispol to Shkodra, significantly increasing yields. Production rose from approximately 12,000 tons annually in the 1950s to 26,700 tons in the early 1980s (FAOstat, 2024).

Following the transition to a market economy in the early 1990s, new economic incentives and subsidies stimulated olive cultivation, resulting in a steady increase in production. Between 1992 and 2008, annual yields averaged around 35,000 tons. Over the past two decades, olive production has flourished, with the highest efficiency recorded in Berat, Vlora, and Mallakastra. Today, the olive oil processing industry is well established in central Albania (Topi et al., 2022). Table olive production has also grown, ranging from 18,000 to 29,000 tons in recent years (IOOC, 2024).

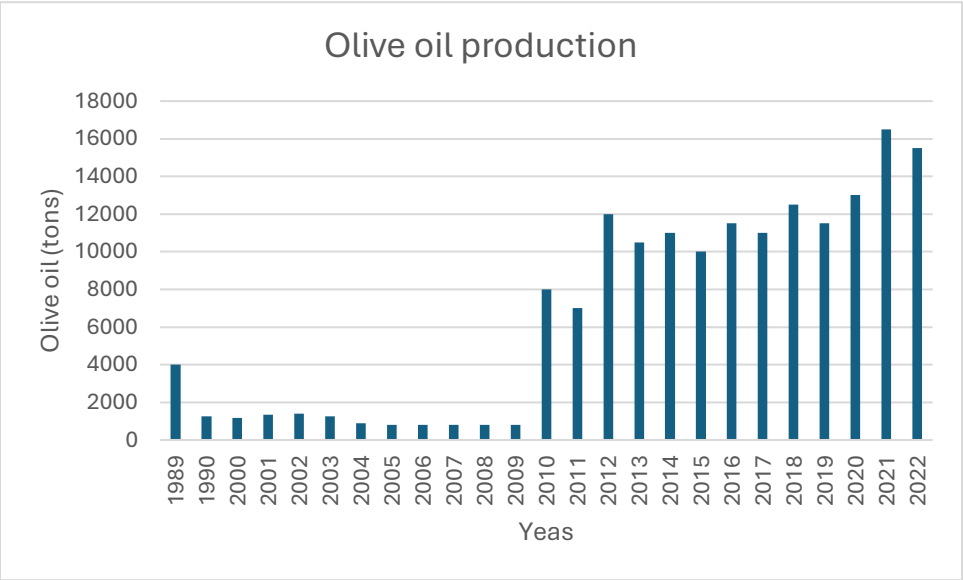


Figure 2. Olive oil production during the period 1989-2022 (FAOStat, 2024).

According to FAOSTAT, olives rank ninth among Albania's top agricultural commodities by production volume and fourth by gross production value. In 2022, olive fruit production reached approximately 157,710 tons, yielding 15,500 tons of olive oil. Cultivation spans 50,404 hectares across 90,000 small farms, with an average productivity of 2,333 kg/ha (INSTAT, 2024). The sector contributes an estimated $125.5 million to domestic production, positioning Albania 15th globally in olive production value (FAOstat, 2024).

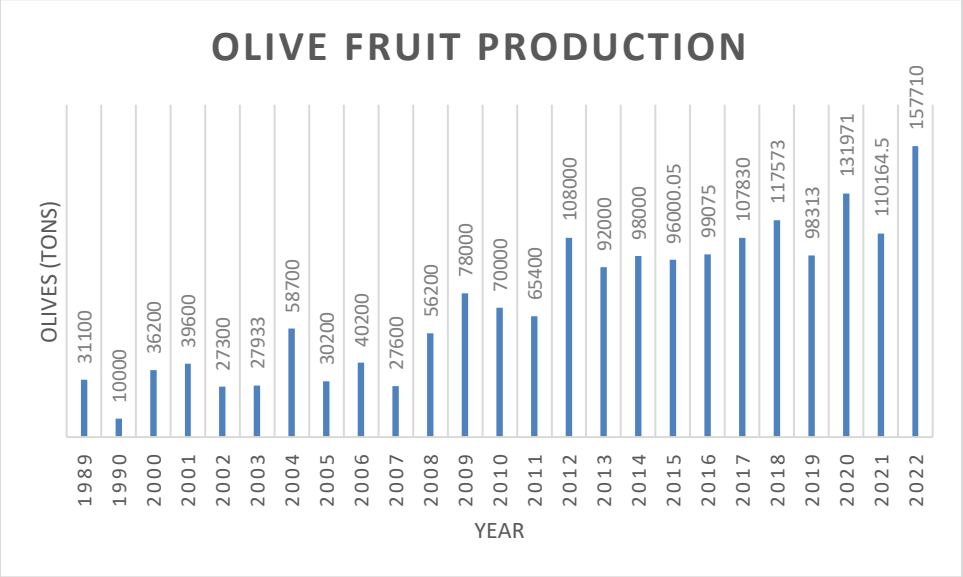


Figure 3. Olive production during 1989-2022, in Albania (Source: FAOStat, 2024).

OLIVE CULTIVATION AND THE ENVIRONMENTAL IMPACT

The expansion of olive cultivation in Albania has generated environmental concerns, primarily soil degradation and water pollution from olive mill waste (Beaufoy, 2000; Ibrahem et al., 2005). Olive terraces dominate many Mediterranean landscapes, including Albania, where large monocultures often prevail (Velo & Topi, 2017). Although olive trees require relatively low inputs, cultivation practices vary widely and can be grouped into three categories:

Low-input traditional plantations and scattered trees

Intensified traditional plantations,

Intensive modern plantations of small tree varieties (Beaufoy, 2000).

Traditional low-input systems offer high biodiversity and landscape value, improving water management and reducing soil erosion. However, these systems are economically marginal and vulnerable to abandonment. Fertilizer use is minimal, indirectly promoting Good Agricultural Practices and enabling organic production potential (Topi et al., 2019).

Conversely, intensified plantations are associated with soil erosion, water depletion, and pollution from agrochemicals. Erosion is most severe on steep slopes lacking terraces and is exacerbated by intensive tillage, which reduces soil organic matter and increases vulnerability to rainfall (Topi et al., 2014). Sustainable management practices, including terrace maintenance and reduced tillage, are essential to mitigate these impacts.

OLIVE OIL PROCESSING INDUSTRY AND THE ENVIRONMENTAL IMPACT

Olive oil extraction in Albania is highly seasonal, with milling operations concentrated within a 90-day period (October–December). Approximately 500 processing plants operate nationwide, contributing significantly to rural employment. The industry predominantly uses three-phase centrifugation technology (>95%), with capacities of 2–3 tons of olives per hour per plant.

Table 1: Key figures on olive by-products related to the extraction technology

Production process	Input	Amount of input	Output	Amount of output
Pressing	Olives	1 t	Oil	200kg
	Washing water	0.1-0.12 m^3	OH, OMW	400 kg 400-600 l
Three-phase decanter	Olives	1 t	Oil	200kg
	Washing water	0.1-0.12 m^3	OH,	500-600 kg
	Fresh water for the decanter	0.5-1.0 m^3	OMW	1000-1200 l
Two-phase decanter	Olives	1 t	Oil	200kg
	Washing water	0.1-0.12 m^3	OH, OMW	400 kg 85-110 l

Endnote 1: OH-Olive Husk; OMW-Olive Mill Waste (Caputo et al. 2007)

Olive oil production generates substantial by-products: solid residues (olive husk, OH) and liquid residues (olive mill wastewater, OMW). The proportion of these by-products varies by extraction method, ranging from 40% OH and 40% OMW in traditional batch systems to 50% OH and up to 95% OMW in continuous centrifugation systems (Caputo et al., 2007). OMW poses a major environmental challenge due to its high organic load (BOD 23–100 g/L), which is 25–80 times greater than municipal wastewater (Schmidt & Knobloch, 2000). Discharge into rivers reduces biodiversity, suffocates benthic organisms, and contaminates groundwater (Niaounakis & Halvadakis, 2006; Anastasiou et al., 2011).

According to the olive oil production data and Caputo's study calculation, processed by-products amount to approximately 190 × 10^5 kg of OH and 250 × 10^5 kg of OMW. Given the geographical distribution of the Olive Oil Extraction Industry in Albania, implementing environmentally friendly waste disposal schemes is challenging. Currently, olive pomace, the primary by-product of extraction, has been collected at nearly 100% efficiency over the past 2–3 years, especially from the ONER LABATE plant. The volume of pomace varies annually depending on olive fruit yield. Olive oil recovery from pomace ranges between 1.5–2.0%, generating significant economic revenue. The valorization of solid by-products into energy and fertilizer has increased profitability and exemplifies the circular bioeconomy.

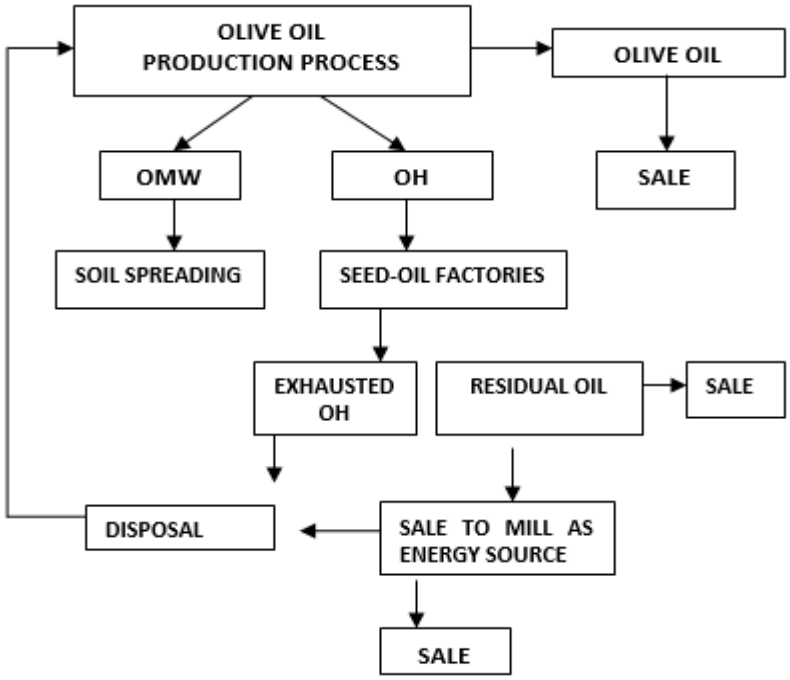


Figure 4: Current disposal scenario (Caputo et al., 2003)

Recent improvements include nearly complete collection of olive pomace for secondary oil recovery (1.5–2.0%) and its valorization into energy and fertilizers, supporting Albania's circular bioeconomy. However, wastewater management remains insufficient, requiring urgent implementation of environmentally sound disposal and treatment strategies.

Strategic implications include the need for improved wastewater management and enhanced extraction efficiency. Because of high organic loads and the presence of toxic substances like polyphenols, groundwater and surface water contamination is evident in regions where the Olive oil industry operates.

CONCLUSIONS AND RECOMMENDATIONS

Olive cultivation and oil production in Albania play a critical role in the national agro-industrial sector and offer significant potential for sustainable development. However, environmental challenges persist, primarily due to inadequate management of olive mill wastewater (OMW) and olive husk (OH). Current practices—such as effluent discharge into surface waters and husk combustion—contribute to soil and water contamination and localized air pollution.

To address these issues and promote sustainability, the following measures are recommended:

Environmental Management needs prohibit direct discharge of OMW into rivers and surface waters. Implement controlled land application of vegetation water, adhering to safe limits (≤800 m^3/ha), as supported by prior research.

By-Product Valorization policy to encourage conversion of olive husk into bioenergy and animal feed to reduce air pollution and enhance resource recovery. Promote circular economy models through public–private partnerships and targeted incentives. Support organic and integrated production systems to minimize the use of agrochemicals. Prevent abandonment of traditional low-input plantations that preserve biodiversity and landscape value.

Establish mandatory reporting and monitoring of effluent disposal practices at olive mills. Create regional inspection units to enforce compliance with environmental standards. Fund research on innovative wastewater treatment technologies and soil restoration practices. Foster collaboration between academia, industry, and government to develop cost-effective waste management solutions.

By implementing these strategies, Albania can strengthen its circular bioeconomy, reduce environmental risks, and position olive farming as a model for sustainable land use in the Mediterranean region. These findings highlight the sector's potential for sustainable growth and resource recovery within the national agro-industrial framework.

.

REFERENCES

Anastasiou, C., Christou, P., Michael, A., Nicolaides, D., Lambrou, Th. (2011). Approaches to Olive Mill Wastewater Treatment and Disposal in Cyprus. *Environmental Research Journal,* 5(2), 49-58.

Beaufoy, G. (2000). The environmental impact of olive oil production in the European Union: Practical options for improving the environmental impact.

Boreadou, K. (1994). Liquid Wastes from olive Mills - Effects on the natural water ecosystems of Crete - Present management of the wastes and tendencies. *Conference of Management of Olive Wastes*, Siteia.

Caputo, A.C., Scacchia, F., Pelagagge, P.M. 2007). Disposal of by-products in olive oil industry: waste-to-energy solutions. *Applied Thermal Engineering*, 23, 197-214.

FAOSTAT, (2024). Olive production, Olive oil, country ranging. https://www.fao.org/faostat/en/#rankings/commodities_by_country (Accessed on 26/11/2025)

IOOC, (2024). KEY FIGURES ON THE WORLD MARKET FOR TABLE OLIVES https://www.internationaloliveoil.org/wp-content/uploads/2024/12/120-OT-2024.pdf (Accessed on November 25, 2025.)

de Ursinos, F. R. (1986). Vegetation water used as fertilizer. *Proceedings of the International Symposium on Olive By-products Valorization*. FAO, UNDP, Sevilla, Spain. pp. 321-330.

Ibrahem A., Shdiefat, S. 2005. Olive-Gap-Manual. Ed. FAO, Rome, Italy. pp. 280.

Hill, J., Sommer, S., Mehl. W. (1996). A conceptual framework for mapping and monitoring the degradation of Mediterranean ecosystems using remote sensing, European Commission.

MAFCP (2009). Study on the Olive culture Situation and its development perspectives (In Albanian).

Niaounakis, M., & Halvadakis, C.P. (2006). Olive Processing Waste Management Literature Review and Patent Survey. 2nd Edn., Elsevier, Amsterdam, The Netherlands, pp. 514.

Schmidt, A. & Knobloch, M. (2000). Olive oil mill residues: The demonstration of an Innovative System to treat Wastewater and to make use of Generated Bioenergy and Solid Remainder, in: Proceedings of the First World Conference on Biomass for Energy and Industry, Seville, June 5-9, pp. 452-454.

Topi, D., Amanpour, A., Kelebek, H., & Selli, S. 2019. Screening of aroma profiles in Albanian cvs. Kalinjot and Bardhi Tirana olive oils using purge and trap extraction technique. *Rivista Italiana delle Sostanze Grasse*, 96/2, 101-108.

Topi, D., Beqiraj, I., Seiti, B., & Halimi, E. (2014). Environmental impact of olive mill waste disposal, chemical analysis of solid waste and wastewater. *Journal of Hygienic Engineering and Design*, 7, 44–48.

Topi, D., Gamze, G., Hasim, K. & Selli, S. Comparative elucidation of phenolic compounds in Albanian olive oils using LC-DAD-ESI-MS/MS. *Journal of Liquid Chromatography & Related Technologies*, 43/5-6, pp. 203-212, 2020. https://doi.org/10.1080/10826076.2019.1711117

Topi, D., Guclu, G., Kelebek, H., & Selli, S. (2022). Olive Oil Production in Albania, Chemical Characterization, and Authenticity. Olive Oil: New Perspectives and Applications, (edited by Muhammad Akram, Rabia Zahid), IntechOpen, Rijeka, Croatia, pp. 77-95.doi: 10.5772/intechopen.96861

Topi, D., Thomaj, F., Bacu, A., Malollari, I., Carvalho, A.P., Gomes, A.M. (2011). Characterization of olive varieties from Albania: Fatty acid profile and total phenolic content. *7th International Congress of Food Technologists, Biotechnologists and Nutritionists Proceedings*, 20 -23 September 2011, Opatija, Croatia, pp. 179–184

Velo S. & Topi, D. (2017). Characterization of Kalinjoti and Nisjoti monocultivar Virgin olive oils produced in Albania. *Asian Journal of Chemistry*, 29/6, 1347-1350, https://doi.org/10.14233/ajchem.2017.20498.

Vitolo, S., Petarca, L., Bresci, B. (1999). Treatment of olive oil industry wastes. *Bioresource Technology, 67, 129-137.*

ORAL PRESENTATION

Düzce Üniversitesi Konuralp Yerleşkesindeki yaban arısı çeşitliliği ve polinasyona etkileri üzerine araştırmalar

Tamasi Olajide Fadare[1] (Orcid: https://orcid.org/0009-0008-6365-0891),
Barış Gülcü[2*] (Orcid: https://orcid.org/0000-0002-4808-1538)

[1]Düzce Üniversitesi, Fen Edebiyat Fakültesi, Biyoloji Bölümü, Düzce, Türkiye
[*2]Düzce Üniversitesi, Fen Edebiyat Fakültesi, Biyoloji Bölümü, Düzce, Türkiye

*Sorumlu yazar e-mail: barisgulcu@duzce.edu.tr

Özet

Bu çalışmada Düzce Üniversitesi Konuralp Yerleşkesinde yayılış gösteren yaban arısı tür çeşitliliği ve bunların hangi bitki gruplarının tozlaşmasında rol oynadıkları belirlenmiştir. Arazi çalışmalarında iki farklı yöntem kullanılmıştır. Birinci yöntemde yerleşkedeki bitki vejetasyonun çiçeklenmesi yıl boyunca takip edilerek yaban arısı görülen alanlardan atrap kullanılarak erkek ve dişi bireyler yakalanmıştır. Bu esnada arı yakalanan bitkilerin fotoğrafları çekilmiş ve bitkinin herbaryum örneği alınmıştır. İkinci yöntemde yerleşke içerisinde farklı noktalara tuzak yuvalar bırakılmıştır. Bu yuvalar düzenli olarak kontrol edilerek hangi arı türlerinin bunları kullandığı belirlenmiştir. Çalışma sonunda Düzce Üniversitesi Konuralp yerleşkesinde atrap ve doğrudan gözlem ile Apidae, Andrenidae, Bombidae, Colletidae, Halictidae, Xylocopidae familyalarına ait 15 farklı cinse ait 43 farklı yaban arısı türü tespit edilmiştir. Bu arıların yerleşke içerisinde Apiaceae, Asteraceae, Asparagaceae, Boraginaceae, Brassicaceae, Cistaceae, Convolvulaceae, Fabaceae, Hypericaceae, Lamiaceae, Plantaginaceae, Rosaceae familyalarından 39 bitki türü ile ilişkili olduğu gözlenmiştir. Tuzak yuvaları ise Colletidae, Megachilidae familyalarından birer türün kullandığı tespit edilmiştir. Elde edilen bulgulara göre kısa dilli yaban arısı türleri Apiaceae, Asteraceae, Brassicaceae, Cistaceae, Convolvulaceae, Hypericaceae, Plantaginaceae familyasından türleri, uzun dilli arılar ise Boraginaceae, Fabaceae, Lamiaceae türlerinin polinasyonunda daha fazla rol oynamaktadır. Yerleşke içerisinde monokültüre dayalı peyzaj uygulamalarının olduğu alanlarda arı çeşitliliğinin azaldığı, doğal haline bırakılan sahalarda ise bitki çeşitliliğine paralel olarak yaban arısı çeşitliliğinin arttığı gözlenmiştir.

Anahtar Kelimeler: Yaban arısı, Polinasyon, Hymenoptera, Düzce

Research on Wild Bee Diversity and Its Effects on Pollination at Düzce University Konuralp Campus

Abstract

The aim of this study was to determine the diversity of bee species distributed on the Konuralp Campus of Düzce University and to determine the plant groups they pollinate within the campus. Two different methods were used in the field studies. First, male and female individuals were captured using a net in areas where bees were frequently observed, based on seasonal changes in vegetation. Herbarium samples were collected, and the photographs were also taken from each plant species. In the second method, trap nests were placed at various locations within the campus. These nests were regularly inspected to determine which bee species were using them. As a result of the study, 43 different bee species belonging to 15 different genera belonging to the families Apidae, Andrenidae, Bombidae, Colletidae, Halictidae, and Xylocopidae were identified on the Konuralp campus of Düzce University. These bees were observed to associate with 39 plant species within the campus from the families Apiaceae, Asteraceae, Asparagaceae, Boraginaceae, Brassicaceae, Cistaceae, Convolvulaceae, Fabaceae, Hypericaceae, Lamiaceae, Plantaginaceae. One species from the families Colletidae and Megachilidae, were found to use the trap nests. According to the findings, short-tongued bees play a greater role in pollinating species from the Apiaceae, Asteraceae, Brassicaceae, Cistaceae, Convolvulaceae, Hypericaceae, Rosaceae, and Plantaginaceae families, while long-tongued bees play a greater role in pollinating species from the Boraginaceae, Fabaceae, and

Lamiaceae families. Bee diversity decreased in areas with monoculture-based landscaping practices within the campus, while bee diversity increased in areas left to their natural state, parallel to plant diversity.

Keywords: Wild bees, Polination, Hymenoptera, Düzce

GİRİŞ

Arılar, Hymenoptera takımında Apoidae üst familyasının Apiformes grubunu oluşturan böceklerdir. Yeryüzünde, Antartika kıtası hariç en az 20.000 arı türünün olduğu düşünülmektedir; (Potts ve ark, 2015). Ascher, J. S. ve Pickering, J. (2019) yaptığı bir çalışmada Türkiye'de 1662 arı türünün varlığını rapor edilmiştir. Özbek (2002)'e göre de ülkemizin iklim koşulları, topoğrafik yapısı, coğrafik konumu ve zengin bitki örtüsüne bağlı olarak yaklaşık 2000 yaban arısı türünün yaşadığı tahmin edilmektedir. Ancak ülkemizde yaban arıları oldukça ihmal edilmiştir. Oysa, arılar yabani bitki çeşitliliğinin korunması (Potts ve ark., 2010) ve yayılması sayesinde erozyonun önlenmesi ve azaltılmasında (Özbek, 2002), tarımsal üretimin (Gallai ve ark., 2009) korunmasında hayati öneme sahiptir. Bu nedenle arılar doğada anahtar tür olarak kabul edilmektedir (Özbek, 2002 ; Michener, 2007). Genel olarak insanlar bal arısının (*Apis mellifera*) ürettiği bal, balmumu, arı sütü, arı zehri vb. ürünlere ilgi duymakta ve arıların tek faydasının bu olduğu düşünülmektedir. Ayrıca bal arısını, geniş yayılım alanı, beslenme davranışı ve etkili tozlaşma yeteneği sayesinde en önemli tozlayıcı tür olarak da kabul etmektedir. Ancak, çiçekli bitki türlerinin büyük bir bölümünün polinasyonunda bal arılarının hiçbir rolü bulunmamaktadır (Garibaldi ve ark. 2013; Hung ve ark. 2018). Yapılan çalışmalar göstermiştir ki, birçok çalı, küçük ağaç ve ot türleri ile birçok yabani çiçek türünün polinasyonu yaban arılarına bağlıdır. Bahçe çiçekleri, çoğu meyve ve sebze, keten, pamuk gibi birçok tekstil bitkisi ile yonca gibi başlıca yem bitkileri arılar tarafından tozlaşmaktadır (Michener, 2007; Özbek, 2018).

Son on yıllık gözlemlere göre bal arıları ve yaban arılarının polinasyona yaptıkları katkının azaldığı düşünülmektedir (Kevan ve Viana, 2003). Bu kaybın sebebi olarak monokültür tarım uygulamaları, arı hastalık ve parazitlerinin artışı, yoğun pestisit kullanımı, şehirleşme, yaban alanlarının parçalanmasına sebep olan yanlış arazi kullanımı ve iklim krizi gösterilmektedir (Stanton ve ark., 2018; Forister ve ark. 2019; Wan ve ark., 2021; Birkenbach ve ark. 2024). Özbek'in (2002) Türkiye'de yaptığı gözleme göre, Türkiye'de yaban arılarının yoğunluğunun son 30 yılda üstel bir şekilde azaldığı ve bazı arı türlerinin muhtemelen yok olma tehlikesiyle karşı karşıya veya yok olma eşiğinde olduğu vurgulamaktadır. Örneğin, 1970'li yıllarda oldukça bol bulunan önemli bir yonca polinatörü olan *Melitta dimidiata* ile birlikte, yonca için son derece önemli olan *Melitta leporina*, *Rhophitoides canus* ve *Melitturga clavicornis* popülasyonlarında büyük bir düşüş yaşandığını bildirmiştir (Özbek, 1979). Bu durumu göz önünde bulundurarak, Türkiye topraklarında hâlâ mevcut olan yabani polinatör arı türlerini araştırmak ve hangi bitki gruplarıyla ilişkili olduklarını tanımlamak gereklidir.

Bu yüksek lisans çalışmasında, Düzce Üniversitesi Konuralp Yerleşkesinde yayılış gösteren yaban arısı populasyonlarını tespit edilerek ve bunların yerleşke içerisinde hangi bitki gruplarının polinasyonunda rol oynadığı ortaya konmuştur.

MATERYAL VE METOT

İlk arı örnekleri Mart ayında yakalanmaya başlanmıştır. Örnekleme ve gözlemler yerleşkedeki vejetasyonun mevsimsel değişimine göre ancak temmuz ayının sonuna kadar devam edebilmiştir. Temmuz ayından sonra vejetasyonun kurumasından dolayı arazi çalışmalarına devam edilememiştir. Eylül ayından sonra sadece doğrudan gözlem yapılmıştır. Çalışmaya başlamadan önce yerleşke içerisinde arı çeşitliliğinin yoğun olduğu, çiçeklenmenin yüksek olduğu alanlar belirlenmiştir. Bu noktalar düzenli aralıklarla (her 7-10 günde bir) ziyaret edilerek arı örnekleri yakalanmış, eğer aynı noktadan aynı türe ait birden fazla birey yakalandıysa alandaki popülasyonun korunması adına geri salınmıştır. Sadece söz konusu tür/türlerin yıl boyunca aktif oldukları uçuş dönemleri ve polinasyon yaptıkları bitkiler ile ilgili kayıtlar alınmıştır. Arılar atrap ile yakalanıp, ağız aspiratörü ile 150 ml plastik tüpler (Falcon tüp) içerisine aktarılmıştır. Bu tüpler laboratuvara getirilene kadar el tipi buzluklar içerisinde muhafaza edilmiştir. Laboratuvar getirilen arı örneklerinden her grubu temsilen birkaç birey etil asetat ile öldürülüp, iğnelenmiştir. Yakalanan arılar Michener (2007)'deki taksonomik tür veya cins tayin anahtarları yardımıyla teşhisleri yapılmıştır. Daha sonra bu örnekler ahşap kutular içerisinde muhafaza edilmiştir. Ayrıca arı örneklerinin kameralı mikroskop yardımıyla fotoğrafları çekilmiştir. Ayrıca yakalanan arıların polen topladığı bitkilerden herbaryum materyali alınmış ve bitkilerin fotoğrafları çekilmiştir.

Yaban arısı çeşitliliğini tespit etmek için bir başka yöntem olarak tuzak yuvalar kullanılmıştır. Tuzak yuvalar için internetten 6-8 mm çapında 20 cm'lik bambu ve saz pipet satın alınmıştır. *Xylocopa* gibi büyük arı türleri için *Arundo donax* (Poaceae) bitkisinden 15 mm çapında, 20-25 cm'lik kısa parçalar hazırlanmıştır. Beş adet *A. donax*, 10'ar adet bambu ve saz pipet olacak şekilde 15 cm çapında, 40 cm'lik PVC bir boru içerisine yerleştirilmiştir. Yuvalar yerleşkenin farklı noktalarına yerden en az 150 cm yüksekte bir yere ve giriş kısmı güneye bakacak şekilde sabitlenmiştir. Bütün yuvalar mayıs ayının ilk haftası, alanda belirli yerlere bırakılmıştır. Düzenli aralıklarla kontrol edilen yuvalardan dolu pipetler alınıp laboratuvarda plastik kutular içerisinde takip edilmiştir. Yuvadan çıkış yapan arılardan erkek ve dişi bireylerden örnek alınıp etil asetat ile öldürüldükten sonra, iğnelenmiştir. Eylül ayında tuzak yuvaların tamamı alandan toplanmıştır.

BULGULAR ve TARTIŞMA

Yakalanan arı örneklerinin hepsi Michener (2007)'de belirtilen cins tayin anahtarlarına göre tanımlanmıştır. Aynı cinsin morfolojik olarak birbirinden çok farklı olan üyeleri ayrı türler olarak değerlendirilmiştir. Çalışma sonunda yerleşke sahasında yedi yaban arısı familyasına ait 43 türün varlığı tespit edilmiştir. Bu familyalar ve yakalanan arı cinsleri Tablo 1'de verilmiştir. En fazla tür Andrenidae familyasının *Andrena* cinsine aittir. Yerleşkemizde 15 *Andrena* türünün yaşadığı, yine aynı familyadan *Panurgus* cinsinin bir türünün daha bulunduğu tespit edilmiştir. Kum arıları ya da soliter kazıcı arılar olarak bilinen *Andrena* cinsi, Dünya'da alttürleri ve sinonimleri de içeren yaklaşık 3000 taksonla arı cinsleri arasında en geniş grubu oluşturur. Gerçek tür sayısının 1500'ün üzerinde olduğu düşünülmektedir (Dubitzky ve ark., 2010). Yerleşke içerisinde tür sayısı bakımından en kalabalık ikinci familya Halictidae'dir. Çalışma sonunda Halictidae familyasından dört cinsten toplam dokuz tür tespit edilmiştir.

Michener, (2007) kısa dilli arıların, sığ yapılı çiçeklerden nektar alırken, daha derin yapılı çiçeklere sahip bitki türlerinin ise uzun dilli arılar tarafından tercih edildiğini bildirmiştir. Kendi gözlemlerimizde bu bilgiyle uyumludur. Yerleşkede yakalanan kısa dilli arı grupları *Andrena, Panurgus, Lasioglossum, Halictus, Hylaeus, Sphecodes, Systropha* türlerinin yerleşkedeki sığ çiçek yapısına sahip Apiaceae, Asteraceae, Brassicaceae, Cistaceae, Convolvulaceae, Hypericaceae, Plantaginaceae familyalarını ziyaret ettiği gözlemlenmiştir. Yerleşkede uzun dilli arıların (*Anthophora, Amegilla, Eucera, Ceratina, Xylocopa, Megachile, Osmia, Anthidium, Bombus*) türlerinin derin çiçek yapısına sahip Boraginaceae, Fabaceae, Lamiaceae türlerini tercih ettiği tespit edilmiştir. Yerleşkenin kuzey ve kuzey doğu bölümlerinde ağaçlandırma sahası ve hurda biriktirme alanı olarak değerlendirilmektedir. Bu nedenle peyzaj uygulaması hiç yapılmamıştır. Buralarda bölgenin doğal vejetasyonunu yansıtan bitki örnekleri bulunmaktadır. Yapılan gözlemlerde bu bölgelerde bitki ve yaban arısı tür çeşitliliğinin diğer sahalara göre daha fazla olduğu gözlenmiştir. Yerleşke içerisinde bal arısı popülasyonlarına da rastlanmıştır. Ancak bu çalışmada bal arılarının besin tercihleri değerlendirilmemiştir.

Yerleşkedeki yaban arılarının 13 familyadan 39 bitki türünün çiçeklerinden nektar ve polen topladığı tespit edilmiştir. Bitki türlerinin familya ve tür isimleri Tablo 1 'de verilmiştir. Asteraceae 13 tür ile yerleşkede en yaygın grup ve arıların en çok tercih ettiği bitki familyasıdır. Bunu 5'er tür Brassicaceae, 4 tür ile Fabaceae ve Lamiaceae, 3 tür Boraginaceae, 2 tür Convolvulaceae takip etmektedir. Diğer familyalardan ise sadece birer tür yer almaktadır.

Mart ayından itibaren uzun dilli arılardan *Bombus* (Bombidae), *Eucera* (Apidae), *Anthophora* (Apidae) ve *Ceratina* (Xylocopidae), *Xylocopa* (Xylocopidae) türleri ortaya çıkmıştır. Kısa dilli arılardan ise *Andrena* (Andrenidae), *Panurgus* (Andrenidae), *Lasioglossum* (Halictidae) türleri görülmüştür. Arıların bu dönemde polen ve nektar topladığı bitki türleri *Taraxacum laevigatum* (Asteraceae), *Taraxacum serotinum* (Asteraceae), *Lamium p*urpureum (Lamiaceae), *Ornithogalum pyrenaicum* (Asparagaceae), *Veronica* sp. (Plantaginaceae), *Erysimum repandum* (Brassicaceae), *Raphanus raphanistrum* (Brassicaceae)'dur. Nisan ayında kısa dilli arılardan *Andrena*, *Lasioglossum*, *Sphecodes* (Halictidae) aktivitesi devam ederken, uzun dilli gruplardan *Anthophora*, *Bombus*, *Eucera*, *Ceratina*, *Xylocopa* cinslerinin yerleşkedeki *Crepis s*ancta (Asteraceae), *Crepis setosa* (Asteraceae), *Taraxacum bithynicum* (Asteraceae), *Raphanus rapistrum* (Brassicaceae), *Rapistrum rugosum* (Brassicaceae), *Nepeta nuda* (Lamiaceae) türlerini ziyaret ettiği görülmüştür. Mayısta ise kısa dilli arı gruplarından *Andrena*, *Lasioglossum* cinslerine ilaveten *Halictus* (Halictidae) türleri ortaya çıkmıştır. Ayrıca Fabaceae ve Lamiaceae bitki familyalarına ait farklı türlerin yaygınlaşmasıyla beraber Megachilidae familyasının *Anthidium*, *Megachile* ve *Osmia* türleri uçmaya başlamıştır. Mayıs ayında yerleşkede *Andrena* ve *Lasioglossum*'lar halen aktif haldedir. Haziran temmuz döneminde ise *Andrena* türleri ortadan kaybolmuş, *Halictus*, türleri daha baskın hale gelmiştir. Bunun yanında *Lasioglossum, Systropha* (Halictidae), *Amegilla* (Apidae), *Osmia* türlerinin aktivitesi devam etmiştir. Vejetasyonunda ise *Lathyrus laxiflorus* (Fabaceae), *Lotus corniculatus* (Fabaceae), *Stachys iberica*

(Lamiaceae), *Stachys thirkeii* (Lamiaceae), *Echium vulgare* (Boraginaceae), *Sophora jaubertii* (Fabaceae), *Crepis setosa* (Asteraceae), *Crepis reuteriana* (Asteraceae), *Hypericum montbretii* (Hypericaceae), *Convolvulus cantabrica* (Convolvulaceae), *Convolvulus arvensis* (Convolvulaceae), *Carduus nutans* (Asteraceae), *Filipendula vulgaris* (Rosaceae), *Sonchus asper* (Asteraceae), *Anchusa officinalis* (Boraginaceae), *Raphanus raphanistrum* (Brassicaceae), *Knautia degenii* (Caprifoliaceae) türleri daha yaygın olarak görülmektedir. Temmuz ayından itibaren bu bitkilere ilave olarak *Centaurea iberica* (Asteraceae), *Echium italicum* (Boraginaceae), *Cichorium intybus* (Asteraceae), *Digitalis* sp. (Plantaginaceae) türleri de görülmeye başlamıştır (Tablo 2, Şekil 1 ve 2).

Yerleşkenin peyzaj alanlarında otsu ve çiçekli bitki olarak çoğunlukla *Trifolium* (Fabaceae) türleri kullanılmıştır. Bu sahalarda *Trifolium* populasyonlarının arasında Asteraceae' den *Taraxacum*, *Crepis*, *Sonchus* türleri, Boraginaceae'den *Anchusa* türlerine de rastlanmaktadır. Trifolium türlerinin yeşil kalabilmesi için düzenli bakım işlemleri yapılmaktadır. Böylece arılara sürekli polen ve nektar kaynağı ortaya çıkmıştır. Bu sayede bazı küçük boyutlu *Andrena* ve *Lasioglossum* türlerine yerleşkenin büyük bir kısmında tüm sezon boyunca aktif oldukları gözlenmiştir.

Çalışma sonunda alana bırakılan tuzak yuvalar *Osmia* (Megachilidae) ve *Hylaeus* (Colletidae) cinslerine ait birer türün kullandığı tespit edilmiştir. Büyük arı türleri tuzak yuvalara gelmemiştir.

Tablo 1. Yerleşkede yakalanan yaban arılarının familya, cins ve tür sayıları ile ilişkili oldukları bitki familyaları ve sayısı

Yaban arısı familyaları	Yaban arısı cinsleri	Yaban arısı tür sayısı
Andrenidae	*Andrena*	15
	Panurgus	1
Apidae	*Anthophora*	2
	Amegilla	1
	Eucera	3
Colletidae	*Hylaeus*	1
Halictidae	*Lasioglossum*	4
	Halictus	3
	Sphecodes	1
	Systropha	1
Xylocopidae	*Ceratina*	3
	Xylocopa	1
Megachilidae	*Megachile*	2
	Osmia	2
	Anthidium	2
Bombidae	*Bombus*	1
	TOPLAM	**43**

Arı yakalanan Bitki Familyaları	Bitki türü sayısı
Asteraceae	13
Lamiaceae	4
Asparagaceae	1
Plantaginaceae	2
Caprifoliaceae	1
Hypericaceae	1
Apiaceae	1
Cistaceae	1
Fabaceae	4
Convolvulaceae	2
Brassicaceae	5
Boraginaceae	3
Rosaceae	1
TOPLAM	39



Şekil 1. Yakalanan arı cinslerinin yerleşke içerisindeki dağılımı. Ame: *Amegilla*; And: *Andrena*; Ant: *Anthidium*; Anth: *Anthophora*; Bom: *Bombus*; Cer: *Ceratina*; Euc: *Eucera*; Hal: *Halictus*; Las: *Lasioglossum*; Meg: *Megachili;* Pan: *Panurgus*; Sph: *Sphecodes*; Sist: *Sistropha*; Xyl: *Xylocopa*

Tablo 2. Aylara göre kısa ve uzun dilli yaban arıların tozlaştırdığı bitkiler

Aylar	Mart	Nisan	Mayıs	Haziran	Temmuz
Kısa dilli yaban arısı cinsleri	*Andrena, Lasioglossum, Hylaeus*			*Halictus, Lasioglossum, Systropha,*	
	Panurgus, Sphecodes		*Halictus*		
Tozlaştırdığı bitkiler	*Taraxacum laevigatum* (Asteraceae), *Taraxacum serotinum* (Asteraceae), *Lamium purpureum* (Lamiaceae), *Ornithogalum pyrenaicum* (Asparagaceae), *Veronica* sp. (Plantaginaceae), *Erysimum repandum* (Brassicaceae), *Raphanus raphanistrum* (Brassicaceae)		*Carduus nutans* (Asteraceae) *Cistus laurifolius* (Cistaceae) *Crepis setosa* (Asteraceae), *Crepis reuteriana* (Asteraceae), *Cota tinctoria var. discoidea* (Asteraceae) *Daucus carota (Apiaceae)* *Sonchus asper* (Asteraceae), *Hypericum montbretii* (Hypericaceae), *Convolvulus cantabrica* (Convolvulaceae), *Convolvulus arvensis* (Convolvulaceae), *Raphanus raphanistrum* (Brassicaceae) *Filipendula vulgaris* (Rosaceae),		*Centairea iberica* (Asteraceae), *Cichorium intybus* (Asteraceae) *Crepis reuteriana* (Asteraceae),
Uzun dilli yaban arısı cinsleri	*Anthophora*, *Bombus*, *Eucera*, *Ceratina*, *Xylocopa*				
				Amegilla, Anthidium, Megachile, Osmia	
Tozlaştırdığı bitkiler	*Crepis sancta (Asteraceae),* *Crepis setosa (Asteraceae),* *Taraxacum bithynicum (Asteraceae),* *Raphanus rapistrum (Brassicaceae),* *Rapistrum rugosum (Brassicaceae),* *Nepeta nuda (Lamiaceae)* *Lamium purpureum* (Lamiaceae) *Trifolium* sp. (Fabaceae)		*Lathyrus laxiflorus* (Fabaceae), *Lotus corniculatus* (Fabaceae), *Stachys iberica* (Lamiaceae), *Stachys thirkeii* (Lamiaceae), *Echium vulgare* (Boraginaceae), *Sophora jaubertii* (Fabaceae), *Carduus nutans* (Asteraceae), *Anchusa officinalis* (Boraginaceae), *Raphanus raphanistrum* (Brassicaceae), *Knautia degenii* (Caprifoliaceae) *Trifolium* sp. (Fabaceae)		*Centairea iberica* (Asteraceae), *Digitalis* sp. (Plantaginaceae) *Echium italicum* (Boraginaceae), *Trifolium* sp. (Fabaceae)



Şekil 2. A-*Eucera* sp. B- *Andrena* sp. C-*Lasioglossum* sp. D- *Ceratina* sp. E- *Bombus* sp. F- *Osmia* sp.

SONUÇ

Yapılan bu çalışma sonucunda Düzce Üniversitesi Konuralp yerleşkesinin bal arısı *Apis mellifera* dışında 43 farklı yaban arısı türüne ev sahipliği yaptığı belirlenmiştir. Bu türlerin 39 farklı çiçekli bitki türünün tozlaşmasıyla doğrudan ilişkisi olduğu ortaya konmuştur. Bu çalışma ile yerleşke sahasının polinatör-bitki çeşitliliği ortaya çıkartılmıştır. Ancak yerleşke sahasında uzun süreli yapılacak gözlemler ile iklim değişikliği ve insan aktivitesinin yaban arısı popülasyonlarına etkisinin takip edilmesi önemlidir.

TEŞEKKÜR

Bu çalışmanın verileri Tamasi Olajide Fadare'nin Düzce Üniversitesi Biyoloji Enstitü anabilim dalında yürüttüğü yüksek lisans tez çalışmasından elde edilmiştir.

KAYNAKLAR

Ascher, J. S. & Pickering, J. (2019). Discover Life – Bee species guide and world checklist (Hymenoptera: Apoidea: Anthophila). – Available from: http:// discoverlife.org/mp/20q?search=Apoidea (last accessed 12 June 2019).

Birkenbach, M., Straub, F., Kiesel, A., Ayasse, M., Wilfert, L., & Kuppler, J. (2024). Land-use affects pollinator-specific resource availability and pollinator foraging behaviour. Ecology and Evolution, *14*(3), e11061.

Dubitzky, A., Plant, J., & Schönitzer, K. (2010). Phylogeny of the bee genus *Andrena* Fabricius based on morphology (Hymenoptera: Andrenidae). Mitteilungen der Münchner Entomologischen Gesellschaft 100, 137–202.

Forister, Matthew L., Emma, M. P., & Scott, H. B. (2019) Declines in insect abundance and diversity: We know enough to act now." Conservation Science and Practice 1.8, e80.

Gallai N, Salles JM, Settele J, Vaissière BE 2009. Economic Valuation of the Vulnerability of World Agriculture Confronted with Pollinator Decline. Ecological Economics, 68(3): 810-821.

Garibaldi, L. A., Steffan-Dewenter, I., Winfree, R., Aizen, M. A., Bommarco, R., Cunningham, S. A., ... & Klein, A. M. (2013). Wild pollinators enhance fruit set of crops regardless of honey bee abundance. *Science, 339*(6127), 1608–1611.

Hung Keng-Lou James, Kingston Jennifer M., Albrecht Matthias, Holway David A. and Kohn Joshua R. (2018). The worldwide importance of honey bees as pollinators in natural habitats. Proceedings of the Royal Society B: Biological Sciences. **285**20172140

Kevan, Peter G., and Blandina F. Viana. (2003). The global decline of pollination services. Biodiversity 4.4 (2003): 3-8.

Michener, C.D. (2007). The Bees of The World. 2nd edition. Johns Hopkins University Press, 953 p, Baltimore & London, UK.

Özbek, H. (1979). Doğu Anadolu Bölgesi Halictidae (Hymenoptera Apoidea) Faunasi ve Bunların Ekolojisi. *Atatürk Üniversitesi Ziraat Fakültesi Dergisi*, *10*(3-4).

Özbek, H. (2002). Arılar ve doğa. Uludağ arıcılık dergisi, 2(3), 22-25.

Özbek H. (2018) Çayır Üçgülü (*Trifolium Pratense* L.)'nün Tozlaşmasında Arıların Önemi. Uludağ Arıcılık Dergisi – Uludag Bee Journal, 18 (1), 28-41.

Potts, S.G., Biesmeijer, J.C., Kremen, C., Neumann, P., Schweiger, O. & Kunin, W.E. (2010). Global pollinator declines: trendes, impacts and drivers, Trends in Ecology and Evolution, 25(6), 345-353.

Potts S., Biesmeijer K., Bommarco R., Breeze T., Carvalheiro L., Franzén M., González-Varo J.P., Holz-
schuh A., Kleijn D., Klein A.-M., Kunin, B., Lecocq T., Lundin O., Michez D., Neumann P., Nieto A., Penev L., Rasmont P., Ratamäki O., Riedinger V., Roberts S.P.M., Rundlöf M., Scheper J., Sørensen P., Steffan-Dewenter I., Stoev P., Vilà M., Schweiger O. (2015) Status and trends of European pollinators. Key findings of the STEP project. Pensoft Publishers, Sofia, 72 pp.

R.L. Stanton, C.A. Morrissey, R.G. Clark, 2018. Analysis of trends and agricultural drivers of farmland bird declines in North America: A review, Agriculture, Ecosystems & Environment, 254, 244-254,

Wan, Yanjian, Tran T. M., Ngyuen V. T., Wang A., Wang J., Kannan K. (2021). Neonicotinoids, fipronil, chlorpyrifos, carbendazim, chlorotriazines, chlorophenoxy herbicides, bentazon, and selected pesticide transformation products in surface water and drinking water from northern Vietnam. *Science of the Total Environment* 750, 141507.

ORAL PRESENTATION

Deep eutectic solvent-assisted extraction of *Viburnum opulus* fruit and evaluation of its biological potentials

Ege Akcay[1] (https://orcid.org/0009-0004-3736-1317), Zulal Gunay[1] (https://orcid.org/0000-0003-3893-9876), Aysegul Inam[2] (https://orcid.org/0000-0002-9411-1232), Murat Elibol[1*] (https://orcid.org/0000-0002-6756-6290)

[1]Ege University, Faculty of Engineering, Department of Bioengineering, Izmir, Türkiye
[2]Manisa Celal Bayar University, Faculty of Engineering and Applied Sciences, Department of Bioengineering, Manisa, Türkiye

*Corresponding author e-mail: elibol.murat@gmail.com

Abstract

Medicinal plants are a rich source of bioactive compounds for different fields, especially health. *Viburnum opulus*, also known as European cranberrybush or Gilaburu, is a plant native to Europe, northern Africa and central Asia with its creamy white flowers and red berries in spring. As a component of green chemistry, deep eutectic solvents (DESs) have attracted attention in recent years due to their superior properties over traditional solvents. DESs consisting of two or more components have properties such as low volatility, low melting point, low flammability, low toxicity, and high biocompatibility. DESs are used in the extraction of highly biologically active metabolites found in different parts of plants. In this study, dried *V. opulus* fruit was extracted with DESs. The resulting extracts were examined for total phenolic compounds, total carbohydrate content, anthocyanin content, antioxidant activity and antimicrobial activity, and compared with aqueous extracts using the same methods. The results obtained are promising in terms of DESs extracting biometabolites and exhibiting activity shown above 100 mg Trolox/10 g antioxidant capacity in various DESs. DES extracts also showed high antimicrobial activity with the highest being Choline Chloride:Acetic Acid DES extract having around 45 mm inhibition zone diameter against *Candida albicans* fungi, 16.5 mm zone for gram positive *Staphylococcus aureus* and 23.5 mm zone for gram negative *Escherichia coli* bacteria. DESs, which are also the subject of active pharmaceutical ingredient studies, have the potential to determine the content of medicinal plants and incorporate them into various biomedical applications.

Keywords: *Viburnum opulus*, deep eutectic solvents, extraction, antioxidant activity, antimicrobial activity

INTRODUCTION

Medicinal plants contain various natural bioactive compounds, primary and secondary metabolites and compounds that provide different activities (Goławska et al., 2023). *Viburnum opulus* is the scientific name for Gilaburu plant in the genus *Viburnum* L., which is in the family Adoxaceae. It is known by many names, including European guelder, guelder rose, rose ebru, rose elder, European cranberrybush, water elder, cramp bark, cherry wood, and snowball tree (Kajszczak et al., 2020). There are many uses for the plant *V. opulus*: it is valuable for decoration, medicine and food (Goławska et al., 2023). The plant's cream-white flowers, which bloom in late May and June, measure 7 to 10 cm in length (Akbulut et al., 2008). The fruit of the plant is indirectly edible due to astringent taste and is a dark red colour (Levent Altun et al., 2008; Gülada et al., 2024). This fruit ripens in September and October. It is similar in size and colour to a cranberry, but becomes more translucent when fully ripe (Akbulut et al., 2008). In Russia, Ukraine and many Siberian countries, the fruits of this plant with a bitter taste are used as a filling and sauce in cakes and drinks (Česonienė et al., 2010). In Turkey, this plant grows in Central Anatolian states such as Kayseri, Bursa, Sakarya, Ankara, Tokat, Trabzon and Çorum (Akbulut et al., 2008). In the Central Anatolia region of Turkey, especially in Kayseri, this plant, whose local name is “Gilaburu”, is traditionally consumed mostly as fruit juice (Gülada et al., 2024). The consumption of this beverage by residents of the central Anatolian region of Turkey is believed to help prevent kidney and stomach problems (Akbulut et al., 2008). Recent studies have

demonstrated the potential of using *V. opulus* fruits in the development of new foods, such as desserts, yoghurt, liqueurs, beer, and vinegar (Ozrenk et al., 2020).

As reported by many researchers, phenolic acids, proanthocyanidins, anthocyanins, saponins, essential oils, and carotenoids have been detected in *V. opulus* fruits. These compounds confer several biological properties, enhance blood sugar uptake in diabetic patients and improve the lipid metabolism (Česonienė et al., 2010; Goławska et al., 2023). *V. opulus* has health benefits due to its bioactive components, including phenolic compounds, carotenoids, vitamin C, triterpenes, essential oils, iridoids, saponins and dietary fibre (Polka et al., 2019). Phenolic compounds are vital to both plants and humans due to several biological activities like anti-inflammatory, antioxidant and anticancer (Goławska et al., 2023). In addition, several *in vitro* studies have shown antioxidant, antimicrobial, anti-obesity, anti-diabetic, and anti-inflammatory activities of *V. opulus* (Gülada et al., 2024; Kajszczak et al., 2020). Antibacterial effects have been shown to be possessed by *V. opulus* against various pathogenic Gram-positive and Gram-negative bacteria (Goławska et al., 2023). Medicinal uses are one of the many applications of this plant. Traditionally, *V. opulus* juice has been used to treat ailments such as coughs, tuberculosis, colds, diabetes, ulcers, liver disease, and hypertension (Kajszczak et al., 2020; Levent Altun et al., 2008).

Conventional organic solvents, such as methanol, ethanol, benzene, chloroform, hexane and acetone, are known for being toxic, corrosive, highly volatile and non-biodegradable. Due to these disadvantages, studies on green chemistry solvents have become popular (Huang et al., 2025). In recent years, there has been an increasing interest in deep eutectic solvents (DESs) in many disciplines such as various biological sciences and pharmaceutical sciences, especially extraction and formulation research due to their different advantages. The “eutectic” term, derived from the Greek word “eutektos” meaning “easy melting”, refers to a specific type of mixture that has a lower melting point than other combinations of the same components (Chevé-Kools et al., 2025). DESs with a new type of solvent typically contain a hydrogen bond acceptor (HBA) and hydrogen bond donor (HBD) or may contain a larger number of components, this generally occurs with stirring and heating of the components to obtain a homogeneous liquid. Also, they have several advantages such as higher biodegradability, less toxicity, and lower volatility (He et al., 2024).

The aim of this study is to reveal the biological potentials of extracts of *V. opulus* known traditionally as Gilaburu, with different choline chloride based DES systems and compare the results of total phenolic compounds, total carbohydrate content, anthocyanin content, antioxidant activity, and antimicrobial activity with aqueous extract.

MATERIALS AND METHODS

Total moisture content of *Viburnum opulus* fruit

For the determination of the total moisture present within the fresh samples of *Viburnum opulus*, 1 g of fruit sample was placed in total moisture analyzer (Mettler Toledo). A standard method for determining the moisture was utilized via the application of 90 seconds of 90°C temperature, 150 seconds of 120°C temperature and 105°C of temperature for the rest of the analysis. Total moisture content was calculated using the remaining dry weight (Ahn et al., 2014).

Preparation of the deep eutectic solvents

For the extraction process, three types of DES were prepared and used along with a standard water extraction for comparison. Types of DES preferred for extractions are ChCl:A, ChCl:G and ChCl:U (Table 1). The DES components for each system were mixed by magnetic agitation at 80 °C until a homogeneous and clear solvent system was formed (at least 1 h).

Table 1. DES components

DES Type	HBA	HBD	Molar Ratio
ChCl:AA (CCA)	Choline Chloride	Acetic Acid	1:2
ChCl:G (CCG)	Choline Chloride	Glycerol	1:2
ChCl:U (CCU)	Choline Chloride	Urea	1:2

Preparation and extraction of *Viburnum opulus* biomass

Prior to the extraction process, fresh *V. opulus* was dried for a week to get rid of its moisture content at a temperature of 40°C. Dried fruit samples were then reduced in size via the usage of an industrial blender, and then 50 µm-sized *V. opulus* samples were separated using a mesh sieve. Smaller sample sizes were preferred in order to better maximise the extraction efficiency. The *V. opulus* samples that are reduced in size were stored at 4°C temperature in a dark environment.

To reduce the viscosity of DES and increase the extraction efficiency, 30% water was used in the extraction process (Liu et al., 2022). Extraction was performed by using 1:20 biomass:solvent ratio in a shaking water bath at 50°C for 2 hours. After the extraction, the liquid phase was separated via centrifuge and vacuum filtration. Extracts were stored at 4°C temperature in a dark environment until the characterization.

Total phenolic contents of *Viburnum opulus* extracts

The Folin-Ciocalteu method was used to determine the total phenolic content. Gallic acid (Sigma-Aldrich) was used as a standard (Miceli et al., 2009). Folin-Ciocalteu reagent at 0.2 N was added of 100 µL of sample at 200 µL volume and was thoroughly mixed. After mixing, 2 mL of distilled water and 1 mL of 6% sodium carbonate (Na_2CO_3) solution (Merck) were added in and vortexed. The resulting mixture was left to its reaction for 2 hours at room temperature in the dark under constant shaking. After the color change was observed, solution was read against 765 nm wavelength using a spectrophotometer (Mettler Toledo). The same procedure was repeated for gallic acid to form a calibration curve, and the result was obtained as gallic acid equivalent (GAE).

Total carbohydrate contents of *Viburnum opulus* extracts

Dubois method was used for the determination of the total carbohydrate content. Glucose was used as a standard. Extract was divided into a glass tube at the amount of 0.5 mL. Following that 0.5 mL of 5% phenol solution was added along with 2.5 mL of sulphuric acid (Merck). Vortexing was used to make a homogenous solution. DESs and water used as a blank was subjected to the same procedures as extract. After a waiting period of 15 minutes, the solution had its absorbance measured in a spectrophotometer (Mettler Toledo) at 490 nm (Matsuhiro et al., 2009).

Anthocyanin contents of *Viburnum opulus* extracts

The total monomeric anthocyanin content was determined according to the AOAC Official Method 2005.02 using the pH differential method. Samples were diluted with pH 1.0 potassium chloride–hydrochloric acid buffer and pH 4.5 sodium acetate–hydrochloric acid buffer. Absorbance values were measured spectrophotometrically at 510 and 700 nm. The total monomeric anthocyanin content was expressed as cyanidin-3-glucoside equivalents (mg/L) and calculated using the standard formula provided by AOAC, based on the absorbance difference between the two pH conditions (AOAC, 2005).

Antioxidant activities of *Viburnum opulus* extracts

The antioxidant activity was measured in terms of free radical scavenging against the DPPH (2,2-Diphenyl-1-picrylhydrazyl) method (Baliyan et al., 2022). The extract was divided into glass tubes in 1 mL volume. On top of each sample, a DPPH solution of 0.1 mM was added in 3 mL volumes. The absorbance values were measured in a spectrophotometer (Mettler Toledo) at 515 nm wavelength. Found values were given in terms of Trolox equivalent.

Antibacterial activities of *Viburnum opulus* extracts

Kirby-Bauer disc diffusion technique was used for determining the antibacterial activity via resulting zone diameters in bacterial culture (Hudzicki, 2009). Gram positive bacteria *Staphylococcus aureus* (ATCC 6538) and the gram negative bacterium *Escherichia coli* (ATCC 25922) were used as bacterial strains in this procedure. Solutions containing both strains of bacteria were diluted to around the range of 0.6 optical density at 600 nm and were inoculated into Mueller-Hinton Agar (Merck) via the usage of spread-plate method. After 24 hours of incubation, the samples diluted at different concentrations were loaded into sterile antibacterial susceptibility (Oxoid) discs at the volume of 25 µL and diameter of 6 mm. Loaded discs were placed on agar plates containing bacterial strains. After incubation time of 24 hours at 37°C temperature, antibacterial inhibition activity was recorded by measuring the diameter of the zones around each disc. Gentamicin antibiotic was used as a positive control and sterile water was used as a negative control (Biemer, 1973).

Antifungal activities of *Viburnum opulus* extracts

Agar well diffusion technique was used for determining the antifungal activity via resulting zone diameters in fungal culture (EUCAST, 2020). The fungal strain used in this procedure was *Candida albicans.* For this *C. albicans* was incubated in PDA (Merck) and was adjusted to final concentrations of 10^5 in the medium, and then was poured into wells into petri dishes opened via the usage of 5 mm diameter hollow sterile glass rods. Each well was loaded with 100 µL samples and were incubated for 24 hours at 37°C temperature. Antifungal inhibition activity was recorded by measuring the diameter of the zones around each disc. Fluconazole antibiotic was used as a positive control and sterile water was used as a negative control for the procedure (EUCAST, 2020).

RESULTS AND DISCUSSION

Characterization of the bioactive compounds in extracts

Total moisture content of the fresh *Viburnum opulus* fruit used in extraction is found to be 82.69 %. Total carbohydrate content, total phenolic matter content, anthocyanin content and antioxidant activity (Trolox equivalent) were determined using spectrophotometric methods. These analyses were also applied to the DESs themselves. The results were compared with the aqueous extract data. The measured values are given in Table 2.

Total carbohydrate contents for CCA extract, CCG extract, CCU extract and aqueous extract are 3091 ± 395 µg glucose/g, 4167 ± 212 µg glucose/g, 3739 ± 487 µg glucose/g and 5348 ± 325 respectively. DES's effect on total carbohydrate measurements is minimal with 11.63 ± 0.87 µg glucose/g for CCA, 81 ± 2.54 µg glucose/g for CCG and 12.61 ± 1.13 µg glucose/g for CCU. The CCG solution showed higher contents for carbohydrates due to its glycerol content.

The extract's ability to reduce DPPH was analyzed via the color change and the control solution didn't change in color. Trolox equivalent antioxidant capacity for CCA extract, CCG extract, CCU extract and aqueous extract are 109.05 mg Trolox/10 g, 116.55 mg Trolox/10 g, 116.05 mg Trolox/10 g and 133.8 mg Trolox/10 g respectively, while the total phenolic contents for them are 0.214 ± 0.011 mg GAE/g, 0.224 ± 0.020 mg GAE/g, 0.208 ± 0.019 mg GAE/g and 0.210 ± 0.005 mg GAE/g. Observed antioxidant activity on DES other than CCG were negligible. CCG extraction solvent showed a high radical scavenging activity as itself. Antioxidant activity of the extracts is generally related to their high total phenolic content (Wojdyło et al., 2007).

Table 2. Bioactivity results of the extracts

Sample	Total carbohydrate contents (µg glucose/g)	Total phenolic contents (mg GAE/g)	Anthocyanin contents (mg/L)	Antioxidant capacity (mg Trolox/10 g) TEAC
CCA extract	3091 ± 395	0.214 ± 0.011	265.03	109.05
CCG extract	4167 ± 212	0.224 ± 0.020	148.24	116.55
CCU extract	3739 ± 487	0.208 ± 0.019	723.21	116.05
Aqueous extract	5348 ± 325	0.210 ± 0.005	220.11	133.8
CCA	11.63 ± 0.87	0.077 ± 0.001	ND	16.45
CCG	81 ± 2.54	0.301 ± 0.041	ND	71.8
CCU	12.61 ± 1.13	0.071 ± 0.020	ND	13.45
Water	ND	ND	ND	12.45

ND: Non detected

Phenolic acids are one of the most common bioactive compounds found in plants. They play a key role in growth, reproduction, and defence against several environmental stresses. Since ancient times, the food industry has widely applied the antioxidant activities of phenolic acids as preservatives. They also delay aging and lower the likelihood of developing life-threatening diseases (Ozrenk et al., 2020). Gülada et al. identified the phenolic contents of the methanolic extract of *V. opulus* fruit as quinic acid, cyanidin 3-glucoside and chlorogenic acid by HPLC-DAD (Gülada et al., 2024). The estimated phenolic content was 0.68–0.83 g/100 g fresh weight (FW) in *V. opulus* fruits grown in the Czech Republic, and 0.40–0.73 g/100 g FW in fruits from Russia. For fresh fruit from Turkey and Lithuania, the respective values were 0.62–0.99 g/100 g FW and 0.75–1.46 g/100 g FW (Polka et al., 2019). Ozrenk et al. (2020) biochemically and morphologically characterised 14 *V. opulus* genotypes from Gümüşhane, Turkey and found that total phenol content ranged from 696 to 830 mg gallic acid equivalent per 100 g fresh weight (Ozrenk et al., 2020). Česonienė et al. (2010) determined the amount of total phenolic matter of different genotypes of *V. opulus* between 753.0 and 1460.0 mg/100 g in their study (Česonienė et al., 2010). In another study, Sagdic et al. found that the total phenolic content was 131.99 ± 2.11 mg gallic acid equivalent (GAE)/g in the extract (Sagdic et al., 2006). In another study, total phenolics were detected as 3.51, 3.98 and 3.73 g GAE/100 g DW in the flowers, bark and fruits of *V. opulus*, respectively (Polka et al., 2019). Levent Altun et al. (2008) found the inhibitory percent of *V. opulus* water extract of branch, fruit, and leaf were 93%, 94% and 88%, respectively. The values of concentration at these antioxidant activities were 0.066, 0.064 and 0.4 mg/mL (Levent Altun et al., 2008).

Anthocyanin contents for CCA extract, CCG extract, CCU extract and aqueous extract are 265.03 mg/L, 148.24 mg/L, 723.21 mg/L and 220.11 mg/L respectively. In particular, the CCU extract yielded a higher amount of anthocyanin compared to the aqueous extract.

Overall, DES solvents showed similar antioxidant capacity and total phenolic content as aqueous extraction methods, but classic water extraction were more efficient in acquisition of the carbohydrate content. Anthocyanin content was obtained at the highest level in the CCU extract.

Antimicrobial activity of the extracts

Based on antibacterial and antifungal analysis given in Figure 1 and Figure 2; DES extracts of *V. opulus* fruit showed inhibitory effects against the growths of gram positive *Staphylococcus aureus* bacteria, gram negative *Escherichia coli* bacteria and *Candida albicans* fungus whereas the aqueous extract showed none.

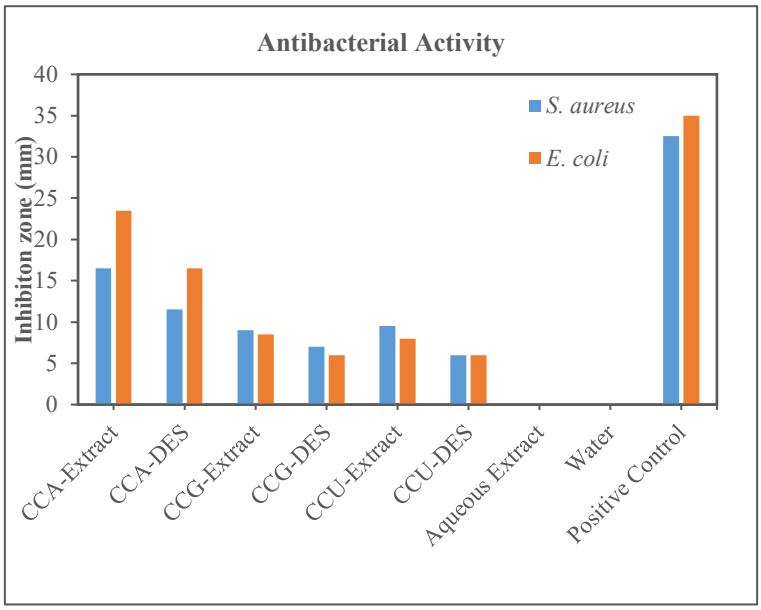


Figure 1. Antibacterial effect of Gilaburu-DES extracts (● E. coli, ● *S.aureus*)

Antibacterial inhibition zones for *Staphylococcus aureus* bacteria for extracts of CCA, CCG and CCU are 16.5 ± 1.5 mm, 9 ± 0.1 mm and 9.5 ± 0.5 mm respectively. For *Escherichia coli* bacteria, zones for extracts of CCA, CCG and CCU are 23.5 ± 1.5 mm, 8.5 ± 0.5 mm and 8 ± 0.01 mm respectively. No antibacterial activity was observed in aqueous extracts. Positive control inhibition diameters were found to be over 30 mm. From these results it could be assessed that extract's antibacterial activity was higher against gram negative bacteria. In addition, antibacterial activity has been detected in DESs themselves. The antibacterial activities of both DES and plant extract combined have produced positive results. CCA has the highest antibacterial inhibition shown due to acetic acid's inherent antimicrobial activity (Ryssel et al., 2009).

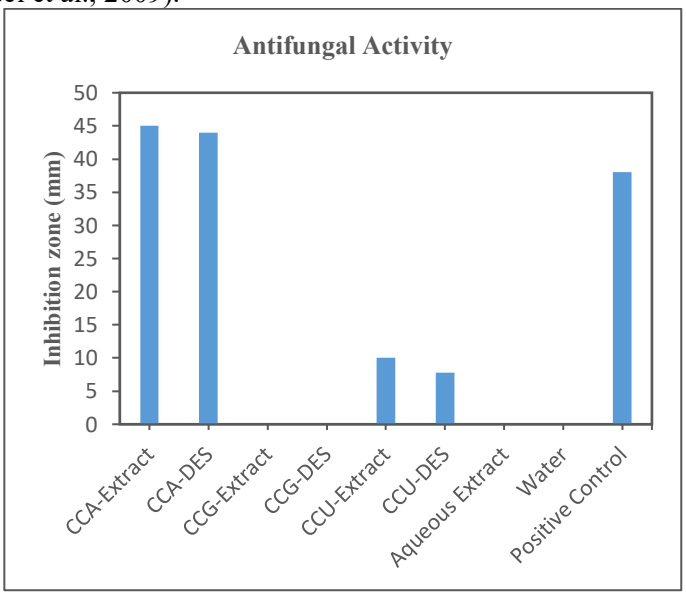


Figure 2. Antifungal effect of Gilaburu-DES extracts

Antifungal inhibitory zone diameters for CCA and CCU extracts are 45 ± 1.2 mm and 10 ± 1.2 mm respectively. No antifungal activity was observed in aqueous and CCG extracts. In addition, antifungal activity has been detected in both CCA-DES and CCU-DES. CCA again showed the highest inhibitory activity due to acetic acid's inherent antimicrobial activity. CCA extract and CCA-DES have surpassed the positive control result (Ryssel et al., 2009).

The determination of antibacterial and antifungal properties of various fruit extracts has attracted great interest in the food and pharmaceutical industries in recent years. Sagdic et al. tested the different concentrations of extracts based on antibacterial effect on different microorganisms using the agar diffusion method. All bacteria were inhibited by 10% and 15% concentrations of this extract (Sagdic et al., 2006). Also, in another study, the antimicrobial activities of *V. opulus* fruit juice and ethanol extracts against human pathogens were compared using the agar well diffusion method. A total of ten Gram-positive and Gram-negative bacterial cultures and nine yeast strains were used in the aforementioned study. The juice showed higher activity compared to the ethanol extracts. The most potent antibacterial activity in the juice was measured against *Salmonella typhimurium, Salmonella agona,* and *Listeria monocytogenes*, with inhibition zones of 27.9, 26.3, and 26.5 mm, respectively. However, yeast growth was affected to a much lesser extent (Česonienė et al., 2014).

Analyzing our results it could be said that with the usage of DES solvents, *V. opulus* showed high antibacterial and antifungal activity. It is recommended that the anticancer, antiviral, and antidiabetic activities of the *V. opulus* plant be studied by extracting it with different DES solutions for future studies.

CONCLUSION

Today, many medicinal plants and their derivatives with high bioactive metabolite contents are being researched due to their potential as antibacterial and antifungal agents. *Viburnum opulus*, also known as the European guelder rose or Gilaburu, exhibits various biological activities and has traditionally been used to provide numerous benefits, particularly for liver and stomach problems. Furthermore, DES have several benefits over traditional solvents like low volatility, low toxicity and high biodegradability. In this study, *V. opulus* fruit was extracted with choline chloride based DES and compared the aqueous extract in terms of total phenolic, carbohydrate and anthocyanin contents, antioxidant and antimicrobial activities. Total carbohydrates were obtained at high levels in the aqueous extract, while total phenolic values and antioxidant activities were obtained in a similar range, and the highest anthocyanin was obtained in the CCU extract. The results are particularly significant in that the antimicrobial activities of DES extracts are higher than those obtained by aqueous extraction, especially for those extracted with CCA.

REFERENCES

Ahn JY, Kil DY, Kong C, Kim BG. Comparison of Oven-drying Methods for Determination of Moisture Content in Feed Ingredients. Asian-Australas J Anim Sci. 2014 Nov;27(11):1615-22.

Akbulut, M., Calisir, S., Marakoglu, T., & Coklar, H. (2008). Chemical and technological properties of European cranberrybush (Viburnum opulus L.) fruits. Asian Journal of Chemistry, 20(3), 1875.

AOAC International. (2005). *Official method 2005.02: Total monomeric anthocyanin pigment content of fruit juices, beverages, natural colorants, and wines—pH differential method.* In *Official methods of analysis of AOAC International* (18th ed.). AOAC International.

Baliyan, Siddartha, Riya Mukherjee, Anjali Priyadarshini, Arpana Vibhuti, Archana Gupta, Ramendra Pati Pandey, and Chung Ming Chang. 2022. 'Determination of Antioxidants by DPPH Radical Scavenging Activity and Quantitative Phytochemical Analysis of Ficus Religiosa'. Molecules 27 (4).

Biemer, J. J. (1973). Antimicrobial susceptibility testing by the Kirby-Bauer disc diffusion method. Annals of Clinical & Laboratory Science, 3(2), 135-140.

Česonienė, L., Daubaras, R., Kraujalytė, V., Venskutonis, P. R., & Šarkinas, A. (2014). Antimicrobial activity of Viburnum opulus fruit juices and extracts. Journal für Verbraucherschutz und Lebensmittelsicherheit, 9(2), 129-132.

Česonienė, L., Daubaras, R., Venclovienė, J., & Viškelis, P. (2010). Biochemical and agro-biological diversity of Viburnum opulus genotypes. Open Life Sciences, 5(6), 864-871.

Chevé-Kools, E., Choi, Y. H., Roullier, C., Ruprich-Robert, G., Grougnet, R., Chapeland-Leclerc, F., & Hollmann, F. (2025). Natural deep eutectic solvents (NaDES): green solvents for pharmaceutical applications and beyond. Green Chemistry, 27, (8360).

EUCAST. (2020). Breakpoint tables for interpretation of MICs for antifungal agents. European Committee on Antimicrobial Susceptibility Testing. https://www.eucast.org/

Goławska, S., Łukasik, I., Chojnacki, A. A., & Chrzanowski, G. (2023). Flavonoids and phenolic acids content in cultivation and wild collection of European cranberry bush Viburnum opulus L. Molecules, 28(5), 2285.

Gülada, B. Ö., Cam, M. E., Yüksel, M., Akakın, D., Taşkın, T., Emre, G., ... & Karakoyun, B. (2024). Gilaburu (Viburnum opulus L.) fruit extract has potential therapeutic and prophylactic role in a rat model of acetic acid-induced oxidant colonic damage. Journal of Ethnopharmacology, 322, 117624.

He, S., Yin, F., Wu, Y., Wang, M., Wang, Y., Row, K. H., & Tang, W. (2024). Deep eutectic solvents as extraction media for food-derived biomacromolecules. TrAC Trends in Analytical Chemistry, 171, 117521.

Huang, M. M., Yiin, C. L., Lock, S. S. M., Chin, B. L. F., Othman, I., & Chan, Y. H. (2025). Natural deep eutectic solvents (NADES) for sustainable extraction of bioactive compounds from medicinal plants: Recent advances, challenges, and future directions. Journal of Molecular Liquids, 127202.

Hudzicki, J. (2009). Kirby-Bauer disk diffusion susceptibility test protocol. American society for microbiology, 15(1), 1-23.

Kajszczak, D., Zakłos-Szyda, M., & Podsędek, A. (2020). Viburnum opulus L.—A review of phytochemistry and biological effects. Nutrients, 12(11), 3398.

Levent Altun, M., Saltan Çitoğlu, G., Sever Yilmaz, B., & Çoban, T. (2008). Antioxidant properties of Viburnum opulus and Viburnum lantana growing in Turkey. International Journal of Food Sciences and Nutrition, 59(3), 175-180.

Liu XM, Liu Y, Shan CH, Yang XQ, Zhang Q, Xu N, Xu LY, Song W. Effects of five extraction methods on total content, composition, and stability of flavonoids in jujube. Food Chem X. 2022 Mar 16;14:100287. doi: 10.1016/j.fochx.2022.100287.

Matsuhiro, Betty, Rodrigo Torres, Elisa A Zúñiga, Maria J Aguirre, Leonora Mendoza, and Mauricio Isaacs. 2009. 'DETERMINATION OF LOW MOLECULAR WEIGHT CARBOHYDRATES IN CABERNET SAUVIGNON RED WINES'. J. Chil. Chem. Soc. Vol. 54.

Miceli, N., Trovato, A., Dugo, P., Cacciola, F., Donato, P., Marino, A., Bellinghieri, V., La Barbera, T. M., Güvenç, A., & Taviano, M. F. (2009). Comparative analysis of flavonoid profile, antioxidant and antimicrobial activity of the berries of Juniperus communis L. var. communis and Juniperus communis L. var. saxatilis Pall. from 1-8 Turkey. Journal of agricultural and food chemistry, 57(15), 6570-6577.

Ozrenk, K., Ilhan, G., Sagbas, H. I., Karatas, N., Ercisli, S., & Colak, A. M. (2020). Characterization of European cranberrybush (Viburnum opulus L.) genetic resources in Turkey. Scientia Horticulturae, 273, 109611.

Polka, D., Podsędek, A., & Koziołkiewicz, M. (2019). Comparison of chemical composition and antioxidant capacity of fruit, flower and bark of Viburnum opulus. Plant Foods for Human Nutrition, 74(3), 436-442.

Ryssel, H., Kloeters, O., Germann, G., Schäfer, T., Wiedemann, G., & Oehlbauer, M. (2009). The antimicrobial effect of acetic acid—an alternative to common local antiseptics?. Burns, 35(5), 695-700.

Sagdic, O., Aksoy, A. H. M. E. T., & Ozkan, G. (2006). Evaluation of the antibacterial and antioxidant potentials of cranberry (gilaburu, Viburnum opulus L.) fruit extract. Acta Alimentaria, 35(4), 487-492.

Wojdyło, A., Oszmiański, J., & Czemerys, R. (2007). Antioxidant activity and phenolic compounds in 32 selected herbs. Food chemistry, 105(3), 940-949.

ORAL PRESENTATION

Seasonal lipid and fatty acid profile of gilthead seabream (*Sparus aurata* L.) cultured in the Aegean and Mediterranean Seas

Cansu Metin Hacisa[1*] (*ORCID: https://orcid.org/0000-0002-2290-1489*), Yunus Alparslan[1] (*ORCID: https://orcid.org/0000-0002-8833-996X*), Taçnur Baygar[1] (*ORCID: https://orcid.org/0000-0001-8070-0653*)

[*1]Muğla Sıtkı Koçman University, Faculty of Fisheries, Department of Seafood Processing Technology, Muğla, Türkiye.

*Corresponding author e-mail: cansumetin@mu.edu.tr

Abstract

Fish are among the foods included in human diets for maintaining a healthy life, particularly due to their content of polyunsaturated fatty acids. The total lipid level and fatty acid profile in fish tissues are substantially influenced by numerous factors, including the biological characteristics of the species, the ecological conditions of the habitat in which they reside, and seasonal variations.

This study was conducted to determine the seasonal variations in lipid and fatty acid composition of gilthead seabream (*Sparus aurata* L.), a species widely cultured in Türkiye, reared in two distinct marine environments, the Mediterranean and the Aegean Seas. As study material, gilthead seabream (*Sparus aurata*) cultured in marine cages in the Mediterranean (İskenderun) and the Aegean (Muğla) regions were used, and analyses were carried out over a 12-month period to cover all seasons.

Significant differences were observed in lipid content, ΣSFA, and ΣMUFA levels depending on seasonal and regional factors, while the highest lipid content occurred in the summer season. ΣPUFA and Σn-3 fatty acid levels reached their maximum values during the spring period. In addition, the n-3/n-6 ratio was found to fall within the recommended range for human health across both regions and all seasons. The findings obtained in this study demonstrate that cultured gilthead seabream reared in the Aegean and Mediterranean regions is a rich nutritional source of polyunsaturated fatty acids (PUFAs). These results are expected to provide valuable contributions to supporting human health, optimizing nutritional strategies, and establishing a scientific basis for functional food development efforts.

Keywords: Gilthead seabream, *Sparus aurata*, lipids, fatty acids, omega-3.

INTRODUCTION

Fish is considered a valuable component of the human diet due to its nutritional properties. It constitutes a significant source of essential nutrients, including structural and functional lipids that are rich in omega-3 (n-3) fatty acids, several of which play a crucial role in maintaining human health (Carr et al., 2023). Due largely to its content of long-chain polyunsaturated n-3 fatty acids, fish consumption is recommended twice weekly. These fatty acids, which are highly important in human nutrition, have been shown to play roles in numerous metabolic functions (Tilami and Sampels, 2017). Additionally, increasing consumer awareness of the health benefits of fish and the diversity of species available on the market has contributed to a recent rise in global seafood consumption (Costa et al., 2020).

Gilthead seabream is one of the most important marine fish species cultured in Europe, predominantly produced in the Mediterranean and Northern European countries. Türkiye also holds an important position in gilthead seabream production (Metin et al., 2021). In this study, seasonal variations in lipid and fatty acid composition of gilthead seabream cultured under identical feeding conditions in two seas with differing physical and chemical properties, such as temperature, salinity, pH, and density (the Mediterranean and the Aegean), were investigated. To this end, the lipid and fatty acid profiles of gilthead seabream cultured in cages in these two distinct marine environments were analyzed throughout the study period, and differences in lipid composition among the fish were

determined. In light of the findings obtained, the study is expected to provide valuable scientific data to the existing literature regarding the nutritional value of gilthead seabream in terms of polyunsaturated fatty acids (PUFAs) and its potential contribution to human health.

MATERIALS AND METHODS

The gilthead seabream (*Sparus aurata*) used as study material was obtained from a company engaged in marine aquaculture in the Mediterranean (İskenderun) and the Aegean (Muğla) regions. Fish sourced from the two different locations were transported in polystyrene boxes under cold chain conditions, iced with flake ice, using the company's refrigerated vehicles, to the Quality Control Laboratory of the Fisheries Processing Technology Department at Muğla Sıtkı Koçman University Faculty of Fisheries. Lipid and fatty acid composition analyses were performed on all gilthead seabream brought to the laboratory as raw material. The study was conducted over four seasons, namely spring, summer, autumn, and winter.

Lipid Analysis

Lipid content was determined based on the method of Bligh and Dyer (1959). Approximately 5 g of each sample was weighed on a precision balance with 0.1 mg sensitivity (SHIMADZU ATx224, Philippines) and homogenized with 120 mL of a methanol–chloroform mixture in a 1:2 ratio. Subsequently, 20 mL of 0.4% $CaCl_2$ solution was added to the samples, which were then filtered through filter paper (Schleicher & Schuell, 5951/2, 185 mm) into pre-weighed flasks and incubated in an oven at 105ºC for 4 hours. The flasks were sealed to prevent air entry and left overnight in the dark. The following day, the chloroform+lipid-containing lower phase was separated from the methanol+water upper phase using a separating funnel. The chloroform from the remaining solution in the flask was evaporated using a rotary evaporator (HEIDOLPH LABOROTA 4003, Germany) in a 60ºC water bath. Afterwards, the flasks were placed in an oven at 60ºC for 1 hour to ensure complete evaporation of chloroform. Once removed from the oven, the flasks were cooled to room temperature in a desiccator and weighed on a precision balance with 0.1 mg sensitivity. The percentage of crude lipid content was then calculated using the following Eq. (1).

% Crude Lipid = [(Weight of flask + lipid (g) – Weight of empty flask (g)) / Sample weight (g)] x 100 (1)

Fatty Acid Composition Analysis

The fatty acid composition of gilthead seabream samples was determined using gas chromatography with a flame ionization detector (GC-FID). Lipids extracted from the samples using the method of Bligh and Dyer (1959) were methylated by adding 4 mL of 2 N potassium hydroxide, vortexing for 1 minute, and then adding 2 mL of hexane. The mixture was vortexed for another 1 minute and centrifuged at 4°C and 4,000 rpm for 10 minutes. The supernatant was transferred to Eppendorf tubes and, if necessary, diluted with hexane at a 1:3 ratio (Ichihara et al., 1996). Samples were stored at –85°C until injection into the GC system. The methylated fatty acids were analyzed using an Agilent 7820 GC system equipped with an FID detector and an HP-88 capillary column (60 m × 0.25 mm ID × 0.25 µm). The injector and detector temperatures were set at 220°C and 280°C, respectively. The oven temperature was initially held at 140°C for 5 minutes, then increased to 200°C at a rate of 4°C per minute, and finally ramped from 200°C to 220°C at 1°C per minute. A 1 µL sample was injected, with carrier gas pressure maintained at 16 psi. A split ratio of 1:50 was applied. Fatty acids were identified by comparison of their retention times with a 37-component FAME standard mixture (Supelco).

Statistical Analysis

Experiments were performed in triplicate (n = 3) for three independent samples and a completely randomized design was used. Data are presented as mean values plus/minus standard deviations, and a probability value of $P<0.05$ was considered as significant. Analysis of variance was performed, and the mean comparisons were done using Duncan's multiple range tests. Statistical analysis was performed using the IBM SPSS Statistics for Windows, version 21 (IBM Corp., Armonk, NY, USA).

RESULTS AND DISCUSSION

Lipid Analysis Results

The percentage lipid content of gilthead seabream cultured in the Mediterranean (İskenderun) and the Aegean (Muğla) Seas during spring, summer, autumn, and winter is presented in Table 1.

Table 1. Lipid analysis results of gilthead seabream in all seasons (%)

	Spring	Summer	Autumn	Winter
Aegean Gilthead Seabream	9.53 ± 2.70^{aB}	12.10 ± 1.30^{bA}	11.81 ± 0.73^{bA}	12.05 ± 0.75^{aA}
Mediterranean Gilthead Seabream	9.42 ± 0.47^{aC}	14.53 ± 0.07^{aA}	12.67 ± 1.33^{aB}	8.59 ± 0.43^{bD}

Lowercase letters indicate differences between groups within the same season, whereas uppercase letters indicate seasonal differences within the same group ($P<0.05$).

In Aegean gilthead seabream, the highest lipid content was observed in summer at 12.10 ± 1.30%, and the lowest in spring at 9.53 ± 2.70%. In Mediterranean gilthead seabream, the highest lipid content was recorded in summer at 14.53 ± 0.07%, and the lowest in winter at 8.59 ± 0.43% ($P < 0.05$). In a study by Alasalvar et al. (2002), which examined the quality of cultured and wild gilthead seabream stored on ice, the lipid content of cultured seabream was found to be 9.8%. In the present study, lipid content varied seasonally in gilthead seabream reared in both seas. The region appeared to have a significant effect on the lipid content of the fish, particularly during the winter season. The lipid levels in fish flesh may vary depending on several factors, including the capture location, season, and sexual maturity (Babur, 2017).

Fatty Acid Composition Results

The fatty acid composition results of gilthead seabream cultured in the Mediterranean (İskenderun) and the Aegean (Muğla) Seas in all seasons are presented in Table 2.

When the seasonal fatty acid composition of gilthead seabream samples reared in the Mediterranean (İskenderun) and Aegean (Muğla) regions was examined, palmitic acid was found to be the dominant saturated fatty acid in both regions during the spring season. In this season, palmitic acid was measured at 12.05 ± 0.04% in both Mediterranean and Aegean gilthead seabream. Among monounsaturated fatty acids, oleic acid (C18:1 n-9) had the highest proportion in both regions, recorded at 31.54 ± 0.02% in the Mediterranean and 30.67 ± 0.11% in the Aegean. Within the polyunsaturated fatty acids (PUFAs), linoleic acid (C18:2 n-6) was the dominant PUFA in spring, observed at 20.99 ± 0.05% in the Mediterranean and 20.34 ± 0.11% in the Aegean. Regarding n-3 fatty acids, EPA (C20:5 n-3) levels were 2.37 ± 0.01% and 2.40 ± 0.00%, while DHA (C22:6 n-3) levels were 8.60 ± 0.23% and 8.78 ± 0.23% in the Mediterranean and Aegean gilthead seabream, respectively.

A similar fatty acid profile was observed during the summer season, with palmitic acid remaining the dominant SFA in both regions (Mediterranean: 12.14 ± 0.50%; Aegean: 12.01 ± 0.22%). Within the MUFA group, oleic acid continued to be the predominant component, measured at 34.99 ± 0.03% in Mediterranean gilthead seabream and 34.26 ± 0.10% in Aegean gilthead seabream. In the PUFA fraction, linoleic acid remained dominant during summer, with levels of 20.74 ± 0.20% in the Mediterranean and 22.23 ± 0.16% in the Aegean. EPA levels were 1.81 ± 0.02% and 1.77 ± 0.03%, while DHA levels were 6.65 ± 0.13% and 6.30 ± 0.08% in Mediterranean and Aegean samples, respectively. The total PUFA (ΣPUFA) content during summer was calculated as 31.24 ± 0.35% in Mediterranean gilthead seabream and 32.67 ± 0.18% in Aegean gilthead seabream.

Table 2. Seasonal fatty acid composition analysis results of gilthead seabream (%)

		Spring		Summer		Autumn		Winter	
Fatty acids (%)		**Mediterranean Gilthead Seabream**	**Aegean Gilthead Seabream**	**Mediterranean Gilthead Seabream**	**Aegean Gilthead Seabream**	**Mediterranean Gilthead Seabream**	**Aegean Gilthead Seabream**	**Mediterranean Gilthead Seabream**	**Aegean Gilthead Seabream**
Caproic acid	C6:0	*	*	0.08±0.10	0.02±0.00	*	*	*	*
Capric acid	C10:0	0.02±0.00	0.01±0.00	0.02±0.00	0.02±0.00	0.02±0.00	0.02±0.00	0.02±0.00	0.02±0.00
Lauric acid	C12:0	0.03±0.00	0.03±0.00	0.03±0.00	0.03±0.00	0.03±0.00	0.02±0.00	0.02±0.00	0.02±0.00
Tridecanoic acid	C13:0	0.02±0.00	0.02±0.00	0.02±0.00	0.01±0.00	0.01±0.00	0.01±0.00	0.01±0.00	0.01±0.00
Myristic acid	C14:0	1.98 ± 0.01^{aA}	2.14 ± 0.00^{aA}	1.91 ± 0.00^{aA}	1.81 ± 0.00^{aB}	1.67 ± 0.16^{aB}	1.71 ± 0.00^{aC}	1.47 ± 0.00^{aC}	1.42 ± 0.00^{aD}
Pentadecanoic acid	C15:0	0.06±0.00	0.05±0.01	0.31±0.01	0.29±0.00	0.05±0.01	0.05±0.00	0.05±0.00	0.04±0.00
Palmitic acid	C16:0	12.05 ± 0.04^{aA}	12.05 ± 0.04^{aB}	12.14 ± 0.50^{aA}	12.01 ± 0.22^{aB}	9.46 ± 0.28^{bB}	11.55 ± 0.04^{aC}	12.24 ± 0.01^{bA}	14.83 ± 1.66^{aA}
Heptadecanoic acid	C17:0	0.63±0.03	0.63±0.00	0.54±0.01	0.52±0.00	0.43±0.05	0.49±0.01	0.47±0.01	0.46±0.02
Stearic acid	C18:0	2.75 ± 0.09^{aAB}	2.91 ± 0.10^{aB}	2.66 ± 0.09^{aB}	2.56 ± 0.09^{aC}	2.21 ± 0.06^{aC}	2.61 ± 0.03^{aC}	2.96 ± 0.01^{bA}	3.83 ± 0.46^{aA}
Arachidic acid	C20:0	0.37±0.02	0.40±0.01	0.43±0.02	0.38±0.00	0.38±0.00	0.40±0.00	0.46±0.01	0.53±0.03
Heneicosanoic acid	C21:0	0.13±0.01	0.18±0.01	0.03±0.00	0.03±0.00	0.02±0.00	0.13±0.01	0.20±0.01	0.16±0.01
Behenic acid	C22:0	0.18±0.01	0.16±0.03	0.17±0.00	0.18±0.01	0.22±0.01	0.17±0.00	0.22±0.01	0.22±0.03
Tricosanoic acid	C23:0	*	*	0.04±0.00	*	*	*	*	*
Lignoceric acid	C24:0	0.58±0.03	0.60±0.03	0.51±0.01	0.55±0.02	0.52±0.00	0.57±0.00	0.54±0.01	0.48±0.01
	ΣSFA	18.80 ± 0.12^{bA}	20.17 ± 0.15^{aB}	18.86 ± 0.50^{aA}	18.40 ± 0.29^{aC}	15.00 ± 0.42^{bB}	17.72 ± 0.06^{aD}	18.61 ± 0.03^{bA}	22.02 ± 2.17^{aA}
Myristoleic acid	C14:1	0.04±0.00	0.04±0.01	0.06±0.00	0.06±0.00	0.02±0.00	0.03±0.00	0.03±0.01	0.02±0.00
cis 10 Pentadecanoic acid	C15:1	*	*	0.01±0.00	*	*	*	*	*
Palmitoleic acid	C16:1	3.04 ± 0.01^{aB}	3.10 ± 0.10^{aA}	3.32 ± 0.01^{aAB}	2.96 ± 0.04^{aA}	3.62 ± 0.08^{aA}	2.64 ± 0.01^{bB}	2.35 ± 0.04^{aC}	2.26 ± 0.17^{aC}
Cis-10-Heptadecanoic acid	C17:1	0.39±0.01	0.38±0.00	0.37±0.01	0.34±0.00	0.38±0.01	0.33±0.01	0.28±0.01	0.26±0.01
Trans-Oleic acid	C18:1n9t	0.10±0.01	0.09±0.00	0.09±0.01	0.08±0.00	0.03±0.01	0.09±0.01	0.08±0.01	0.08±0.00
Oleic acid	C18:1n9c	31.54 ± 0.02^{aD}	30.67 ± 0.11^{aC}	34.99 ± 0.03^{aC}	34.26 ± 0.10^{aB}	39.01 ± 0.16^{aA}	35.02 ± 0.06^{bB}	37.20 ± 0.11^{aB}	36.75 ± 1.00^{aA}
Cis 11 Eicosenoic acid	C20:1n9	3.32 ± 0.01^{aB}	3.16 ± 0.03^{aC}	3.48 ± 0.01^{aB}	3.75 ± 0.03^{aA}	3.48 ± 0.03^{aB}	3.75 ± 001^{aA}	3.92 ± 0.02^{aA}	3.61 ± 0.14^{aB}
Erucic acid	C22:1n9	0.56±0.00	0.54±0.01	0.43±0.01	0.44±0.01	0.18±0.01	0.28±001	0.20±0.00	0.18±0.01
	ΣMUFA	38.99 ± 0.03^{aD}	37.98 ± 0.03^{bC}	42.74 ± 0.05^{aC}	41.90 ± 0.16^{bB}	46.70 ± 0.29^{aA}	42.12 ± 0.07^{bB}	44.05 ± 0.15^{aB}	43.16 ± 1.35^{bA}

		Spring		Summer		Autumn		Winter	
Fatty acids (%)		**Mediterranean Gilthead Seabream**	**Aegean Gilthead Seabream**	**Mediterranean Gilthead Seabream**	**Aegean Gilthead Seabream**	**Mediterranean Gilthead Seabream**	**Aegean Gilthead Seabream**	**Mediterranean Gilthead Seabream**	**Aegean Gilthead Seabream**
Trans-Linoleic acid	C18:2n6t	0.24±0.00	0.24±0.00	0.08±0.01	0.06±0.01	0.24±0.02	0.22±0.04	0.18±0.00	0.21±0.04
Linoleic acid	C18:2n6c	20.99 ± 0.05^{aBC}	20.34 ± 0.11^{aB}	20.74 ± 0.20^{bCA}	22.23 ± 0.16^{aA}	21.47 ± 0.13^{aA}	22.13 ± 0.08^{aA}	21.15 ± 0.23^{aAB}	20.57 ± 0.46^{aB}
Alpha Linolenic acid	C18:3n3	1.29 ± 0.04^{aB}	1.33 ± 0.05^{aC}	1.28 ± 0.01^{aB}	1.45 ± 0.09^{aB}	1.29 ± 0.01^{bB}	1.61 ± 0.05^{aA}	1.58 ± 0.01^{aA}	1.42 ± 0.08^{aB}
Cis 11-14 Eicosadienoic acid	C20:2	0.06±0.01	0.07±0.00	0.06±0.00	0.04±0.00	0.07±0.01	0.04±0.00	0.71±0.01	0.63±0.04
Cis 11-14-17-Eicosatrienoic acid	C20:3n3	0.18±0.00	0.21±0.00	0.18±0.01	0.28±0.01	0.48±0.01	0.29±0.00	0.20±0.01	0.27±0.01
Arachidonic Asit	C20:4n6	0.38±0.00	0.44±0.02	0.38±0.01	0.45±0.01	0.39±0.01	0.47±0.00	0.32±0.00	0.38±0.01
Cis-5-8-11-14-17-Eicosapentaenoic acid	C20:5n3	2.37 ± 0.01^{aA}	2.40 ± 0.00^{aA}	1.81 ± 0.02^{aB}	1.77 ± 0.03^{aB}	1.79 ± 0.01^{aB}	1.58 ± 0.00^{bC}	1.33 ± 0.03^{aC}	1.07 ± 0.04^{bD}
Cis 13-16-Docosadienoic acid	C22:2	0.53±0.60	0.11±0.00	0.08±0.00	0.09±0.00	0.03±0.00	0.07±0.00	*	0.07±0.00
Docosahexaenoic acid	C22:6n3	8.60 ± 0.23^{aA}	8.78 ± 0.23^{aA}	6.65 ± 0.13^{aC}	6.30 ± 0.08^{aB}	7.45 ± 0.06^{aB}	6.33 ± 0.06^{bB}	5.30 ± 0.03^{aD}	4.45 ± 0.17^{bC}
	ΣPUFA	34.63 ± 0.83^{aA}	33.92 ± 0.19^{aA}	31.24 ± 0.35^{aC}	32.67 ± 0.18^{aA}	33.19 ± 0.23^{aB}	32.73 ± 0.05^{aA}	30.76 ± 0.20^{aC}	29.05 ± 0.77^{bB}
	Σn3	12.44 ± 0.19^{aA}	12.72 ± 0.28^{aA}	9.92 ± 0.13^{aC}	9.80 ± 0.01^{aB}	11.01 ± 0.06^{aB}	9.81 ± 0.01^{bB}	8.41 ± 0.05^{aD}	7.21 ± 0.30^{bC}
	Σn6	21.61 ± 0.05^{aAB}	21.02 ± 0.10^{aB}	21.19 ± 0.22^{bB}	22.74 ± 0.16^{aA}	22.09 ± 0.16^{aA}	22.81 ± 0.04^{aA}	21.65 ± 0.23^{aAB}	21.15 ± 0.44^{aB}
	Σn9	35.52 ± 0.01^{aD}	34.46 ± 0.12^{bC}	38.98 ± 0.04^{aC}	38.54 ± 0.12^{aB}	$42.69\pm0,21^{aA}$	39.13 ± 0.06^{bB}	41.39 ± 0.13^{aB}	40.62 ± 1.16^{aA}
	Σn3/ Σn6	0.58 ± 0.01^{aA}	0.61 ± 0.02^{aA}	0.47 ± 0.00^{aC}	0.43 ± 0.00^{aB}	0.50 ± 0.00^{aB}	0.43 ± 0.00^{bB}	0.39 ± 0.01^{aD}	0.34 ± 0.01^{bC}
	Undefined	7.58 ± 0.67^{aA}	7.92 ± 0.01^{aA}	7.15 ± 0.10^{aA}	7.04 ± 0.05^{aB}	5.11 ± 0.48^{bC}	7.43 ± 0.08^{aAB}	6.58 ± 0.08^{aB}	5.77 ± 0.06^{bC}

Lowercase letters indicate differences between groups within the same season, while uppercase letters indicate seasonal differences within the same group ($P<0.05$).

When the fatty acid profile during the autumn season was examined, palmitic acid was observed to be the dominant saturated fatty acid in both Mediterranean and Aegean gilthead seabream, with values of 9.46 ± 0.28% and 11.55 ± 0.04%, respectively. Among monounsaturated fatty acids, oleic acid (C18:1 n-9) remained the predominant MUFA in both regions, measured at 39.01 ± 0.16% in the Mediterranean and 35.02 ± 0.06% in the Aegean. In the polyunsaturated fatty acid group, linoleic acid (C18:2 n-6) was again the most abundant component, with levels of 21.47 ± 0.13% in the Mediterranean and 22.13 ± 0.08% in the Aegean. During the same season, EPA (C20:5 n-3) contents were 1.79 ± 0.01% and 1.58 ± 0.00%, while DHA (C22:6 n-3) levels were 7.45 ± 0.06% and 6.33 ± 0.06% in Mediterranean and Aegean gilthead seabream, respectively. Evaluating the total fatty acid classes for the autumn season, Mediterranean gilthead seabream contained ΣSFA 15.00 ± 0.42%, ΣMUFA 46.70 ± 0.29%, and ΣPUFA 33.19 ± 0.23%, whereas in Aegean gilthead seabream, these values were 17.72 ± 0.06%, 42.12 ± 0.07%, and 32.73 ± 0.05%, respectively.

During the winter season, palmitic acid was identified as the dominant SFA in gilthead seabream from both regions, with levels of 12.24 ± 0.01% in the Mediterranean and 14.83 ± 1.66% in the Aegean. Within the MUFA fraction, oleic acid (C18:1 n-9) remained the predominant fatty acid, measured at 37.20 ± 0.11% in Mediterranean gilthead seabream and 36.75 ± 1.00% in Aegean gilthead seabream. In the PUFA group, linoleic acid (C18:2 n-6) was the dominant component, recorded at 21.15 ± 0.23% in the Mediterranean and 20.57 ± 0.46% in the Aegean. EPA (C20:5 n-3) contents were 1.33 ± 0.03% and 1.07 ± 0.04%, while DHA (C22:6 n-3) levels were 5.30 ± 0.03% and 4.45 ± 0.17% in Mediterranean and Aegean gilthead seabream, respectively. Additionally, total n-3 fatty acids were 8.41 ± 0.05% in the Mediterranean and 7.21 ± 0.30% in the Aegean, whereas total n-6 fatty acids were 21.65 ± 0.23% and 21.15 ± 0.44%, respectively.

The fatty acid composition of fish varies depending on several factors, including seasonal conditions, feeding regime, habitat, species, size, sex, and physiological status (Şen and Uçar, 2021). Various studies on different fish species (sea bream, silver carp, common carp, zander, chub mackerel) have reported that fatty acid profiles and lipid contents change in response to seasonal temperature variations (Kalyoncu et al., 2010; Torno et al., 2019; Ferreira et al., 2020; Kheiri et al., 2022). Analysis of the fatty acid profiles of gilthead seabream revealed that total ΣSFA and ΣMUFA levels exhibited greater variability between regions compared to ΣPUFA, while seasonally, ΣMUFA showed pronounced fluctuations. DHA levels in gilthead seabream from both regions were found to be biologically significant. In both regions, the most abundant saturated fatty acid was palmitic acid, the predominant MUFA was oleic acid, and linoleic acid was the dominant fatty acid among PUFAs. ΣPUFA and Σn-3 values were higher in the spring compared to other seasons. Σn-3 levels were similar between both regions. Seasonal analysis of EPA, DHA, ΣPUFA, and Σn-3 revealed statistically significant differences between groups ($P < 0.05$). The n-3/n-6 ratio of gilthead seabream reared in both regions ranged from 0.34 to 0.61 seasonally. In a study by Khonji et al. (2023) on the fatty acids of 17 fish species in Bahrain (including doubleber bream, Spanish mackerel, and dory snapper), the n-3/n-6 ratio ranged from 0.66 to 2.62. Torrissen et al. (2025) reported that the optimal n-3/n-6 ratio for health should be between 1:1 and 1:5 (0.25–1). The ratios obtained in our study fall within this recommended range.

CONCLUSION

The study results indicate that the n-3/n-6 ratio remained within the recommended range for health across both regions and all seasons, demonstrating that gilthead seabream possesses a high-quality lipid profile and can be considered an important source of omega-3 fatty acids for human nutrition. The findings provide valuable information on gilthead seabream—a widely consumed fish both in Turkey and globally—for consumers, dietitians, and medical professionals, contributing to balanced nutrition and health. Moreover, the data are particularly critical for businesses involved in the production and processing of gilthead seabream, as they can utilize this detailed information on the fish's nutritional composition and flesh quality to optimize marketing, production, and processing strategies.

ACKNOWLEDGEMENTS

This project was supported by the Scientific Research Projects Coordination Unit of Muğla Sıtkı Koçman University under project number 24/169/08/1. We gratefully acknowledge the Coordination Unit for their support.

REFERENCES

Alasalvar, C., Taylor, K.D.A., & Shahidi, F. (2002). Comparative quality assessment of cultured and wild Sea Bream (*Sparus aurata*) stored in ice. Journal of Agricultural and Food Chemistry, 50, 2039-2045.

Babur, Z. (2017). Levrek balığı (*Dicentrarchus labrax* L.1758)'nın pastırma olarak değerlendirilmesi, Yüksek Lisans Tezi, Muğla Sıtkı Koçman Üniversitesi, Muğla, 105s.

Bligh, E. G., & Dyer, W. J. (1959). A rapid method of total lipid extraction and purification. Canadian Journal of Biochemistry and Physiology, 37, 911-917.

Carr, I., Glencross, B., & Santigosa, E. (2023). The importance of essential fatty acids their ratios in aquafeeds to enhance salmonid production, welfare, and human health. Frontiers in Animal Science, 4, 1147081.

Costa, J. C. C. P., Floriano, B., Villegas, I. M. B., Rodríguez-Ruiz, J. P., Posada-Izquierdo, G. D., Zurera, G., & Pérez-Rodríguez, F. (2020). Study of the microbiological quality, prevalence of foodborne pathogens and product shelf-life of Gilthead sea bream (*Sparus aurata*) and sea bass (*Dicentrarchus labrax*) from aquaculture in estuarine ecosystems of Andalusia (Spain). Food Microbiology, 90, 103498.

Ferreira, I., Gomes-Bispo, A., Lourenço, H., Matos, J., Afonso, C., Cardoso, C., Castanheira, I., Motta, J., Prates, J. A. M., & Bandarra, N. M. (2020). The chemical composition and lipid profile of the chub mackerel (*Scomber colias*) show a strong seasonal dependence: Contribution to a nutritional evaluation. Biochimie. 178, 181-189.

Ichihara, K. I., Shibahara, A., Yamamoto, K., & Nakayama, T. (1996). An improved method for rapid analysis of the fatty acids of glycerolipids. Lipids, 31, 535-539.

Kalyoncu, L., Yaman, Y., & Aktumsek, A. (2010). Seasonal changes on total fatty acid composition of carp (*Cyprinus carpio* L.)'in İvriz Dam Lake, Turkey. African Journal of Biotechnology, 9(25), 3896-3900.

Kheiri, A., Aliakbarlu, J., & Tahmasebi, R. (2022). Antioxidant potential and fatty acid profile of fish fillet: effects of season and fish species. Veterinary Research Forum, 13(1), 91-99.

Khonji, A., Abdulhussain, H., Hamadi, F., Alsafwan, M., Al-Mannai, M., & Freije, A. (2023). Analysis of EPA + DHA and omega3/omega6 ratio in 17 edible wild fishspecies in Bahrain. Arab Journal of Basic and Applied Sciences, 30(1), 452-462

Metin, C., Alparslan, Y., Hasanhocaoğlu Yapıcı, H., Ekşi, Z., & Baygar, T. (2021). Assessment of the effects of sex and harvesting season on lipid, and fatty acid composition of Sparidae species. Lipids, 56, 391-404.

Şen, A., & Uçar, G. (2021). Farklı pişirme yöntemlerinin deniz, tatlı su ve kültür ortamlarında yetişmiş levrek balıklarının bazı yağ asiti kompozisyonları üzerine etkisi. Eurasian Journal of Veterinarian Science, 37(3), 157-165.

Tilami. S. K. & Sampels, S. (2017). Nutritional value of fish: lipids, proteins, vitamins, and minerals. Reviews in Fisheries Science & Aquaculture, 1-11.

Torno, C., Staats, S., Fickler, A., de Pascual- Teresa, S., Soledad Izquierdo, M., Rimbach, G., Schulz, C. (2019). Combined effects of nutritional, biochemical and environmental stimuli on growth performance and fatty acid composition of gilthead sea bream (*Sparus aurata*). PLoS ONE, 14(5), e0216611.

Torrissen, M., Gisslevik, E., Gundersen, T. E., Bolstad, T., Eide, O., Rizzo, A. M., Clayton, P., & Robertson, C. (2025). Global variations in omega-3 fatty acid status and omega-6:omega-3 ratios: insights from >500,000 whole-blood dried blood spot samples. Lipids in Health and Disease, 24(260), 1-15.

ORAL PRESENTATION

Effect of PDE4B inhibitors on miRNA levels in different glioma cell lines

Linah Mohamed Elmagzoub[1*] (https://orcid.org/0009-0005-6350-9079),
Mehmet Ozansoy[2,3] (*https://orcid.org/0000-0002-1079-8832*)

[*1]Bahcesehir university, Neuroscience, Dept. of Neuroscience (Interdisciplinary), Istanbul, Türkiye.
[2] Istanbul Medipol University, International School of Medicine, Dept. of Physiology, Istanbul, Türkiye.
[3] Istanbul Medipol University, Research Institute for Health Sciences and Technologies (SABITA), Istanbul, Türkiye.

*Corresponding author e-mail: Linah_Magzoub@hotmail.com

Abstract

Gliomas are known as highly malignant primary brain tumours. Phosphodiesterase, specifically, isoform PDE4 is highly expressed in brain tumours and involved in the progression of many forms of cancer including gliomas, due to its role in regulating intercellular cAMP levels, PDE4B inhibitors have been observed to promote apoptosis in glioblastoma. Micro- RNAs are small noncoding RNA's that are responsible for regulating gene expression post transcriptionally. Overexpression of oncogenic miRNA influences cell cycle regulation and apoptosis. cAMP signalling is known to interact with miRNA regulation, therefore PDE inhibition could modulate expression level of miRNA's involved in glioma pathology. This study investigates the effects of PDE4B inhibition on the expression levels of miRNAs in different glioma cell lines.

Keywords: Glioma, Mirna, Phosphodiesterase, Cyclic Adenosine Monophosphate

INTRODUCTION

Glioblastoma (GBM), first described by Virchow in 1863 and later classified in detail by Bailey and Cushing (1926), remains the most aggressive primary brain tumour, characterized by rapid proliferation, diffuse infiltration, and profound inter- and intra-tumoral heterogeneity (Agnihotri et al., 2012; Qazi et al., 2017). It is categorized as a WHO grade IV astrocytoma and displays hallmark cancer traits including sustained proliferation, metabolic reprogramming, persistent vascularization, and evasion of immune surveillance (Fouad & Aanei, 2017). Clinically, GBM presents with headaches, seizures, cognitive decline, and neurological deficits, with diagnosis confirmed by MRI/CT followed by biopsy (Hansen et al., 2023). Standard therapy surgical resection followed by radiotherapy and temozolomide (TMZ) yields limited survival benefits, further constrained by chemoresistance mechanisms such as MGMT promoter silencing, aberrant DNA repair, and altered signalling pathways (Weller et al., 2005; Hegi et al., 2005; Singh et al., 2020). Molecularly, GBM is driven by alterations in EGFR, PTEN, IDH1, ATRX, and RTK-mediated pathways such as PI3K/AKT/mTOR and MAPK/ERK, which collectively contribute to tumour progression and therapy resistance (Kanderi et al., 2025; Xu et al., 2020).

A growing body of evidence highlights the role of cyclic nucleotide phosphodiesterases (PDEs), particularly the PDE4 family, in GBM biology. PDE4 regulates intracellular cAMP levels, a critical second messenger involved in cell proliferation, apoptosis, and differentiation. GBM cells exhibit reduced cAMP and aberrant PKA/CREB signalling, promoting malignant behaviour (Mucignat-Caretta et al., 2017). PDE4B inhibition through agents such as rolipram or Roflumilast has been shown to elevate cAMP, trigger apoptotic signalling, and suppress tumour growth via pathways including EGR1/PTEN/AKT (Li et al., 2024; Goldhoff et al., 2008). Given the intertwining of cAMP homeostasis with glioma pathogenesis, PDE4B has emerged as a therapeutic target (Sengupta et al., 2011).

MicroRNAs (miRNAs) play essential roles in GBM development, acting either as oncogenes or tumour suppressors. Dysregulation of miRNAs such as miR-21, miR-34a, the miR-221/222 and miR-183-96-182 clusters have been documented to contribute in proliferation, EGFR upregulation, invasion, and chemoresistance (Yin et al., 2012; Chen et al., 2021; Schneider et al., 2022; Ordóñez-Rubiano et al., 2024). Several miRNAs directly modulate key GBM pathways, including PI3K/AKT/mTOR and EGFR/RAS/ERK, linking them to disease progression and therapeutic vulnerability (Sati & Parhar, 2021; Xu et al., 2020).

Importantly, cAMP-regulated signalling interacts with miRNA networks, suggesting that PDE4B inhibition may influence miRNA expression profiles relevant to GBM pathology. This intersection of pathways in PDE4B activity, cAMP dynamics, and oncogenic miRNA regulation, forms the conceptual foundation for investigating PDE4B inhibitors as modulators of miRNA expression in glioma.

MATERIALS AND METHODS

The study was designed to evaluate the effects of PDE4B inhibitors on micro RNA's that are overly expressed/ antiapoptotic in glioblastoma. The chosen miRNA's are predicted to target the PDE4B gene (this prediction was assessed with the use of the search engine miRPathDb 2.0, miRwalk and Tarbase). Four cell lines were used: U87MG, LN-18, YKG-1, and HUVEC (as a non-cancerous control). The chosen miRNA are as follows:

Micro-RNA	Function in glioblastoma	
Hsa-miR-221-3p/ Has-miR-222-3p	Overly expressed /oncogenic in many glioblastoma cell lines, supressing of these miRNA's lead to reduced cell proliferation and the upregulation of their target genes- most notably the P53- induced pro apoptotic protein PUMA.	(Mafi et al., 2022) (Ahir et al., 2017) (Chen et al., 2018) (Zhu et al., 2022) (You, 2009) (Jegathesan et al., 2024)
Hsa-miR-182-5p/Hsa-miR-183-5p	Upregulated/oncogenic in glioblastoma thought to be achieved through suppression of neurofilament light polypeptide, a tumour suppressor, activating mTOR signalling pathway	(Schneider et al., 2022) (Ahir et al., 2017)
Hsa-miR-223-3p	Categorized in many studies as an oncogenic miRNA involved in chemotherapeutic resistance, Via regulation/activation of PI3K/AKT pathway and decreased expression of PAX6	(Han et al., 2019) (Huang et al., 2017) (Jegathesan et al., 2024)

The experimental workflow consisted of two major phases: determining cell viability under different drug concentrations and subsequently analysing miRNA expression following treatment.

The first methodological component involved cell culture, where all cell lines were maintained under standard incubator conditions using appropriate media and supplements. This was followed by the MTT cell viability assay, which was performed after treating the cells with a range of concentrations of both PDE4B inhibitors Roflumilast and Apremilast. The purpose of the assay was to identify the optimal treatment dose for subsequent procedures.

Upon dose determination, the second phase of the study began with total RNA isolation from both treated and untreated cells. RNA quality and quantity were assessed to ensure suitability for downstream applications. The extracted RNA was then used for cDNA synthesis, specifically designed for micro-RNA targets.

Following cDNA generation, quantitative real-time PCR (RT-qPCR) was performed to assess expression levels of five target microRNAs (hsa-miR-221-3p, hsa-miR-222-3p, hsa-miR-223-3p, hsa-miR-182-5p, and hsa-miR-183-5p). U6 snRNA was used as the internal reference gene. Fold-change calculations were used to determine upregulation or downregulation in response to PDE4B inhibitor treatments.

Throughout all experiments, standardized laboratory equipment, chemical reagents, miRNA-specific primers were used.

Finally,all Statistical analysis is carried out using GraphPad Prism version 8.0.2. depending on the experimental design either a one-way ANOVA (for comparisons that require more than 2 groups) followed by post hoc Tukey test, or t-tests (for experimental setups that require 2 groups). IC_{50} values were calculated using the AAT Bioquest® IC_{50} Calculator (online tool)

RESULTS and DISCUSSION

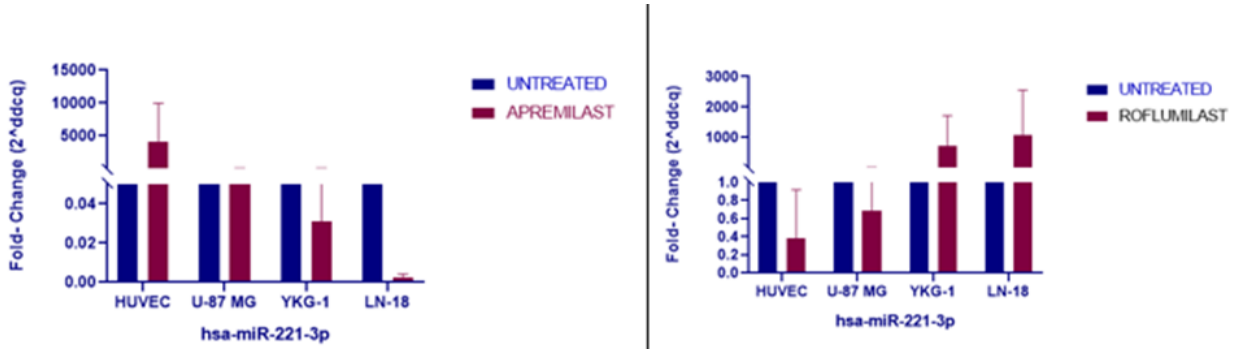


Figure 1. Fold gene expression of hsa-miR-221-3p across all cell lines following 24- hour treatment

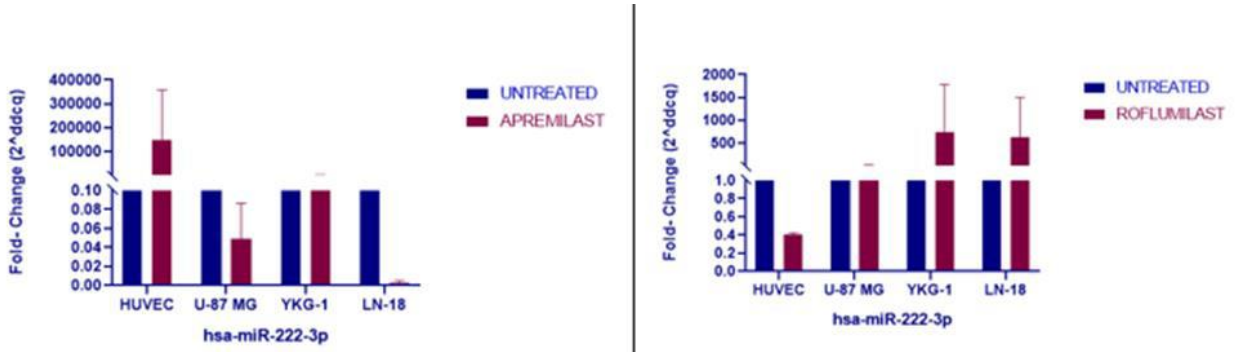


Figure 2. Fold gene expression of hsa-miR-222-3p across all cell lines following 24- hour treatment.

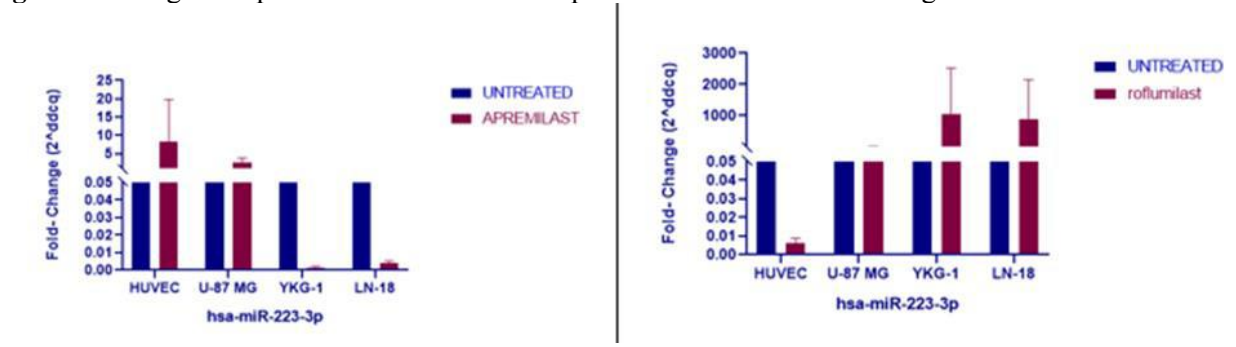


Figure 3. Fold gene expression of hsa-miR-223-3p across all cell lines following 24- hour treatment

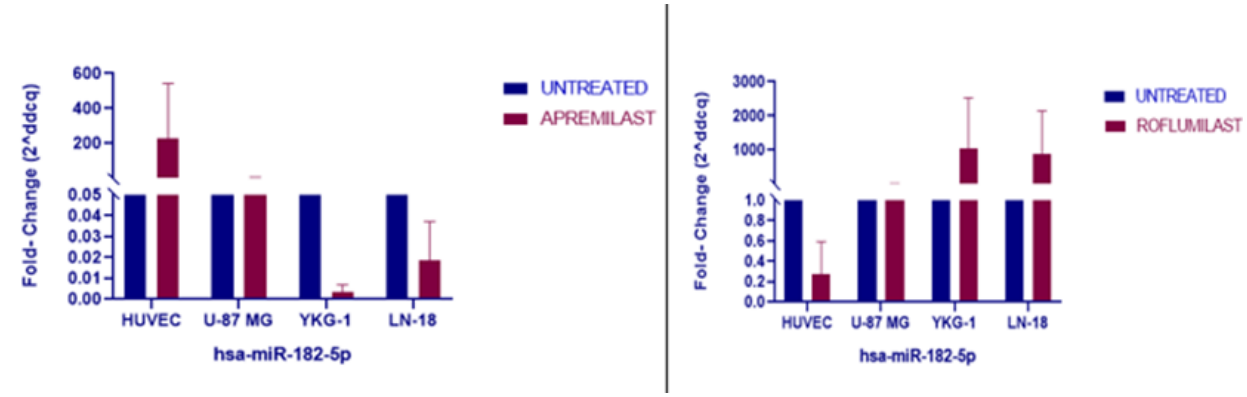


Figure 4. Fold gene expression of hsa-miR-182-5p across all cell lines following 24- hour treatment

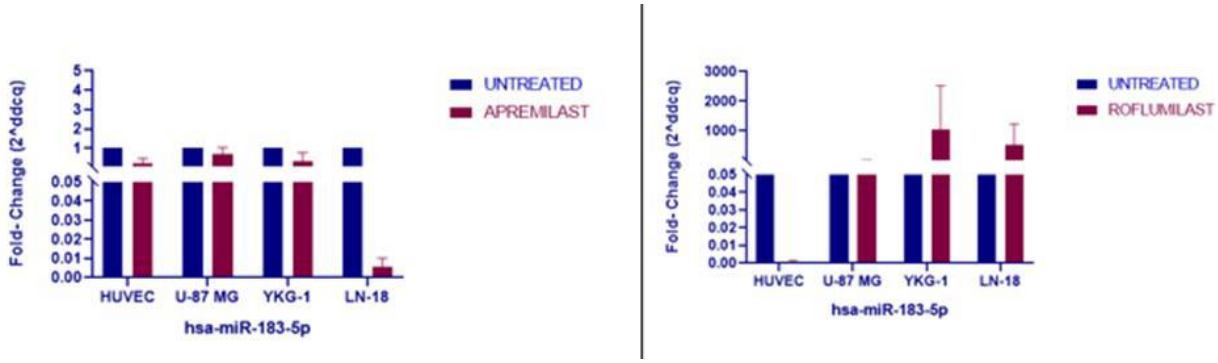


Figure 5. fold gene expression of hsa-miR-183-5p across all cell lines following 24- hour treatment.

This study examined the effects of two PDE4B inhibitors, Apremilast and Roflumilast, on three glioblastoma cell lines (U-87 MG, LN-18, YKG-1) and a control line (HUVEC), focusing on five miRNAs known to be upregulated in glioma. MTT assays across multiple time points showed no meaningful viability differences between 48 and 72 hours, so 24 hours was selected for further analysis. The most cytotoxic dose within the tested range (Table 1), not the calculated IC_{50}, was used for miRNA expression studies. Overall, cell viability did not follow a clear dose-dependent pattern, but both inhibitors produced comparable ranges of viability reduction within each cell line, consistent with previous findings on PDE4 inhibition in glioma.

Table 1. Chosen Dose Per Treatment And Cell Line

Cell line	Apremilast	Roflumilast
HUVEC	4uM	4uM
U- 87 MG	7uM	2uM
LN-18	3uM	4uM
YKG-1	2uM	6uM

RT-qPCR results although showed no statistical significance, demonstrated distinct and opposing reactions to both inhibitors (Figures 1 through 5). In the LN-18 and YKG-1 cell lines, Roflumilast consistently upregulated all five target miRNAs, contradicting past studies associating their downregulation with apoptosis. Apremilast, however, caused a consistent downregulation of the same target miRNAs in the LN-18 and YKG-1 cell lines. The U-87 MG cell line showed a mixed but related pattern, with Roflumilast generally showing higher miRNA expression in comparison to Apremilast. In contrast, HUVEC exhibited an inverted trend, with Apremilast upregulating and Roflumilast downregulating most of the target miRNAs, suggesting tumour-specific regulatory mechanisms.

These findings could suggest that although both drugs elevate intracellular cAMP, their downstream effects differ. Roflumilast, being a more targeted PDE4B inhibitor, may activate pathways such as CREB or ERK, contributing to miRNA upregulation. Apremilast, a broader PDE4 inhibitor, may shift signaling toward PKA-mediated suppression of oncogenic pathways, resulting in miRNA downregulation. Differences between glioma and HUVEC responses further highlight the influence of baseline genetic and signaling contexts. Overall, the results suggest that PDE4B inhibition engages complex, cell-specific pathways that differentially regulate oncogenic miRNAs.

In conclusion, PDE4B inhibitors exert significant therapeutic effects on glioma cell lines, these effects have been correlated with the expression of miRNA's in glioma cell lines although as perviously mentioned, the expression levels have so statistical significant standing, observing a consistent pattern in response to the treatments, can be a basis for further investigation of a regulatory relationship between miRNA expression and the role of the PDE4B gene in glioma, promoting progress towards using miRNA's as a possible biomarker in glioma.

ACKNOWLEDGEMENTS
This study was funded by Scientific Research Projects Commission of Bahçeşehir University. Project number BAP.2023-02.29.

REFERENCES

Agnihotri, S., Burrell, K. E., Wolf, A., Jalali, S., Hawkins, C., Rutka, J. T., & Zadeh, G. (2012). Glioblastoma, a brief review of history, molecular genetics, animal models and novel therapeutic strategies. Archivum Immunologiae Et Therapiae Experimentalis, 61(1), 25–41. https://doi.org/10.1007/s00005-012-0203-0

Ahir, B. K., Ozer, H., Engelhard, H. H., & Lakka, S. S. (2017). MicroRNAs in glioblastoma pathogenesis and therapy: A comprehensive review. Critical Reviews in Oncology/Hematology, 120, 22–33. https://doi.org/10.1016/j.critrevonc.2017.10.003

Chen, Y., Ho, H., Lin, S., Ho, T. D., & Hsu, C. (2018). Upregulation of miR-125b, miR-181d, and miR-221 predicts poor prognosis in MGMT promoter-unmethylated glioblastoma patients. American Journal of Clinical Pathology, 149(5), 412–417. https://doi.org/10.1093/ajcp/aqy008

Fouad, Y. A., & Aanei, C. (2017). Revisiting the hallmarks of cancer. PubMed, 7(5), 1016–1036. https://pubmed.ncbi.nlm.nih.gov/28560055

Han, L., Li, Z., Jiang, Y., Jiang, Z., & Tang, L. (2019). SNHG29 regulates miR-223-3p/CTNND1 axis to promote glioblastoma progression via Wnt/β-catenin signaling pathway. Cancer Cell International, 19(1). https://doi.org/10.1186/s12935-019-1057-x

Hegi, M. E., Diserens, A., Gorlia, T., Hamou, M., De Tribolet, N., Weller, M., Kros, J. M., Hainfellner, J. A., Mason, W., Mariani, L., Bromberg, J. E., Hau, P., Mirimanoff, R. O., Cairncross, J. G., Janzer, R. C., & Stupp, R. (2005). MGMT gene silencing and benefit from temozolomide in glioblastoma. New England Journal of Medicine, 352(10), 997–1003. https://doi.org/10.1056/nejmoa043331

Huang, B., ... (2017). (Full details needed)

Jegathesan, Y., Stephen, P. P., Sati, I. S. E. E., Narayanan, P., Monif, M., & Kamarudin, M. N. A. (2024). MicroRNAs in adult high-grade gliomas: Mechanisms of chemotherapeutic resistance and their clinical relevance. Biomedicine & Pharmacotherapy, 172, 116277. https://doi.org/10.1016/j.biopha.2024.116277

Kanderi, T., Munakomi, S., & Gupta, V. (2025). Glioblastoma Multiforme. StatPearls Publishing. https://www.ncbi.nlm.nih.gov/books/NBK558954/

Li, Y., He, X., Li, S., Chen, S., Zhao, Z., Mu, Y., Zhao, A. Z., Zhou, S., & Li, F. (2024). The phosphodiesterase-4 inhibitor Zl-n-91 suppresses glioblastoma growth via EGR1/PTEN/AKT pathway. European Journal of Pharmacology, 177230. https://doi.org/10.1016/j.ejphar.2024.177230

Mafi, A., Rahmati, A., Aghdam, Z. B., Salami, R., Salami, M., Vakili, O., & Aghadavod, E. (2022). Recent insights into the microRNA-dependent modulation of gliomas from pathogenesis to diagnosis and treatment. Cellular & Molecular Biology Letters, 27(1). https://doi.org/10.1186/s11658-022-00354-4

Mucignat-Caretta, C., Denaro, L., D'Avella, D., & Caretta, A. (2017). Protein Kinase A distribution differentiates human glioblastoma from brain tissue. Cancers, 10(1), 2. https://doi.org/10.3390/cancers10010002

Qazi, M., Vora, P., Venugopal, C., Sidhu, S., Moffat, J., Swanton, C., & Singh, S. (2017). Intratumoral heterogeneity: pathways to treatment resistance and relapse in human glioblastoma. Annals of Oncology, 28(7), 1448–1456. https://doi.org/10.1093/annonc/mdx169

Schneider, B., William, D., Lamp, N., Zimpfer, A., Henker, C., Classen, C. F., & Erbersdobler, A. (2022). The miR-183/96/182 cluster is upregulated in glioblastoma carrying EGFR amplification. Molecular and Cellular Biochemistry, 477(9), 2297–2307. https://doi.org/10.1007/s11010-022-04435-y

Singh, N., Miner, A., Hennis, L., & Mittal, S. (2020). Mechanisms of temozolomide resistance in glioblastoma – a comprehensive review. Cancer Drug Resistance. https://doi.org/10.20517/cdr.2020.79

Weller, M., Steinbach, J. P., & Wick, W. (2005). Temozolomide: a milestone in the pharmacotherapy of brain tumors. Future Oncology, 1(6), 747–754. https://doi.org/10.2217/14796694.1.6.747

Xu, B., Mei, J., Ji, W., Huo, Z., Bian, Z., Jiao, J., Li, X., Sun, J., & Shao, J. (2020). MicroRNAs involved in the EGFR pathway in glioblastoma. Biomedicine & Pharmacotherapy, 134, 111115. https://doi.org/10.1016/j.biopha.2020.111115

You, N. (2009). Analysis of miR-221 and p27 expression in human gliomas. Molecular Medicine Reports, 2(4). https://doi.org/10.3892/mmr_00000152

Zhu, L., & Chen, L. (2019). Progress in research on paclitaxel and tumor immunotherapy. Cellular & Molecular Biology Letters, 24(1). https://doi.org/10.1186/s11658-019-0164-y

ORAL PRESENTATION

Synthesis of novel hybrid compounds via multi-component reactions and determination of their anticancer activities on colon cancer (HT-29) cell line by *in silico* and *in vitro* methods

Serpil Demirci [1*] (https://orcid.org/0000-0002-6579-4273) , Esma Kübra Kağan Yeniçeri[2] (https://orcid.org/0000-0002-6860-9758) , Ahmet Altay [2] (https://orcid.org/0000-0001-8120-8900) , Halil Gökce[1] (https://orcid.org/0000-0003-2258-859X) and İkra Pirbudak [2] (https://orcid.org/0009-0007-6040-0873)

[*1]Giresun University, Department of Medical Services and Techniques, Vocational High School of Health Services, 28100, Giresun, Türkiye
[2]Erzincan Binali Yıldırım University, Department of Chemistry, Faculty of Arts and Science, Erzincan, 24100, Türkiye

*Corresponding author e-mail: demirciserpil17@gmail.com; serpil.demirci@giresun.edu.tr

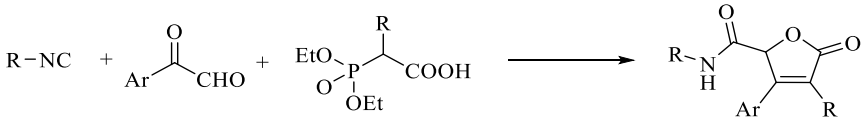
Abstract

In this study, using 4-fluoroaniline as the amine and 3,4-dihydroxybenzaldehyde and phenylacetaldehyde as the aldehydes, new bioactive compounds were synthesized using a multicomponent reaction method in the presence of dimethyl acetylenedicarboxylate and malononitrile. These compounds were characterized and their anticancer activities were investigated using *in silico* and *in vitro* experiments. Using methods known in the literature but modified by us, a combination of bioactive compounds was achieved. Consequently, the original hybrid molecules 1(a-b), which are predicted to have potential drug properties, were synthesized in good yields. Their anticancer potential was investigated using *in silico* and *in vitro* methods. The structures of all synthesized compounds were elucidated using IR, ^{1}H-NMR, ^{13}C-NMR (APT), and TOF-LC/MS spectroscopy. Cell proliferation studies conducted using the XTT method revealed that all synthesized hybrid molecules exhibited dose-dependent antiproliferative activity in the HT-29 colon cancer cell line at concentrations ranging from 0.1 to 25 µM, and IC_{50} values were calculated. Furthermore, all hybrid molecules exhibited antiproliferative activity in the 3T3-L1 healthy cell line at much higher concentrations (10-250 µM). All hybrid molecules demonstrated significantly higher selectivity against cancer cells compared to 5-FU, which is considered a standard chemotherapeutic agent.

Keywords: Anticancer activity, HT-29, *in silico* study, Multicomponent reaction.

INTRODUCTION

Multicomponent Reactions (MCRs) are convergent reactions, in which three or more starting materials react to form a product, where basically all or most of the atoms contribute to the newly formed product. In an MCR, a product is assembled according to a cascade of elementary chemical reactions. Significant advances have been made in the discovery of drug products using these reactions, which are very useful in the optimization of biologically active compounds (Reddy et al. 2019).



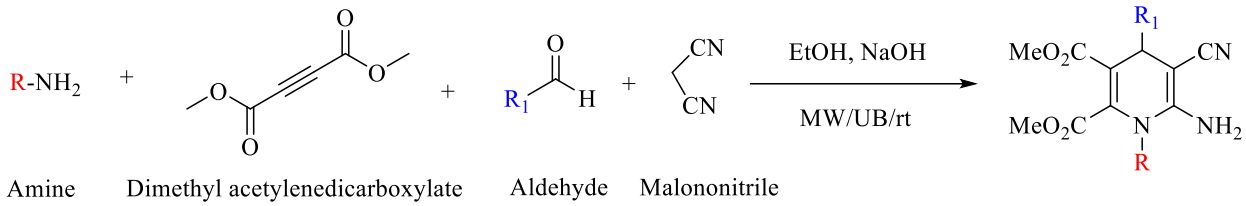
Synthesis of natural product-like molecules by multicomponent reaction

Multicomponent reactions, which are very useful in optimizing biologically active compounds, have led to significant advances in drug discovery (Dömling 2000). Nearly two million natural product-like structures have been produced using MCR methods (Lee et al. 2000). Many biotechnology and major pharmaceutical companies are currently utilizing MCR chemistry to create chemical diversity. Organic chemists are working to improve MCRs by developing new catalysts and reaction conditions (Weber 2002).

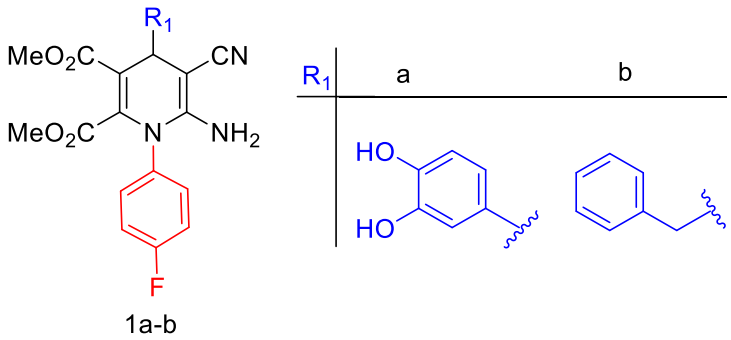
On the other hand, cancer treatments need to utilize new approaches that target cancer cells without harming normal cells. Although many anticancer drugs have been developed today, a therapeutic product with the desired therapeutic effect has not yet been developed. Furthermore, due to the development of resistance mechanisms against chemotherapeutic agents for various reasons and their undesirable side effects, their therapeutic power is gradually diminishing. At the same time, cancer cells can acquire the ability to evade physiological suppressors and spread (metastasis) through mutations. Today, due to the low selectivity of drugs used in routine cancer therapies, the side effects they cause with multiple drug use, and the development of resistance, new drug research remains crucial (Khazir et al. 2020).

To this end, these hybrid molecules were first designed and synthesized in the light of *in silico* studies. *in Vitro* studies were conducted on HT-29 colon cancer cell lines to investigate the anticancer effects of these molecules as protein kinase inhibitors.

Based on literature, the four-component one-pot reaction conditions were modified by using temperature, solvent, catalyst, microwave device, and ultrasonic bath (Sun et al. 2010), and the molecules 1(a-b) were synthesized by reacting with appropriate amines and aldehydes in the presence of dimethyl acetylenedicarboxylate and malononitrile (Scheme 1, Scheme 2). The anticancer potential of these molecules was determined by *in silico* studies and *in vitro* experiments.



Scheme 1: General synthesis equation



Scheme 2: General scheme of the synthesized molecules

MATERIALS AND METHODS

General Synthesis Method of Compounds 1(a-b)

As shown in Scheme 2, the corresponding aldehyde (10 mmol) and malononitrile (10 mmol) were slurried in ethanol in the presence of NaOH (10 mmol) for 15 minutes at room temperature (25 °C). Afterward, the corresponding aliphatic/aromatic amine (10 mmol) and dimethyl acetylenedicarboxylate (10 mmol) were added to the reaction medium. The reaction mixture was stirred at room temperature (25 °C) until the reaction was complete (reaction time was determined by Thin Layer Chromatography). At the end of the reaction, the solvent was removed under reduced pressure and the resulting viscous substance was purified using appropriate column chromatography. Reaction conditions were tested using an ultrasonic bath (US) or microwave (MD) device, using triethylamine (TEA) instead of NaOH or Montmorillonite K-10 as a catalyst. The optimal reaction conditions were determined as described above.

The products were purified by column chromatography (silica gel, 30-400 mesh). The column was conditioned with n-hexane. The crude extract was dissolved in ethyl acetate (5 mL) and applied to the column. Purification was carried out using n-hexane-ethylacetate (9:1; 8:2, 7:3; 6:4; 5:5; 4:6; 3:7, 2:8, and 1:9; 100 mL each) solvent systems of increasing polarity.

Dimethyl-6-amino-5-cyano-4-(3,4-dihydroxyphenyl)-1-(4-fluorophenyl)-1,4-dihydropyridine-2,3-dicarboxylate (1a): Verim: % 75 (2.39 g), brown viscous substance. FT-IR (υ_{max}, cm^{-1}): 3277 (OH), 2984, 2951 (NH_2), 1732 (C=O). ^1H NMR (400 MHz, $CDCl_3$) δ 3.57 (s, 3H, OCH_3), 3.83 (s, 3H, OCH_3), 5.98 (s, 1H, CH), 6.85-6.88 (m, 1H, arH), 6.97-6.99 (m, 1H, arH), 7.03-7.08 (m, 1H, arH), 7.17-7.21 (m, 2H, arH), 7.25-7.28 (m, 2H, arH), 7.40 (s, 2H, 2OH+NH_2). ^{13}C NMR (400 MHz, $CDCl_3$) δ 40.4 (CH6), 50.5 (OCH_3), 52.2 (OCH_3), 62.0 (C5), 109.1 (CH 19), 110.1 (C1), 115.3 (2CH10/12), 115.7 (CH16), 120.4 (C23), 122.4 (CH20), 122.9 (2CH9/13), 136.5 (C2), 148.0 (C15), 148.5 (C8), 154.0 (C18), 158.4 (C17), 160.81 (C4), 163.8 (C=O), 164.2-169.4 (C-F, J_{C-F}= 524 Hz), 170.3 (C=O). MALDI-TOF-MS: 439.40, 421.11 $[M-H_2O]^+$, 480.12 $([M+2+K]^+$.

Dimethyl-6-amino-4-benzyl-5-cyano-1-(4-fluorophenyl)-1,4-dihydropyridine-2,3-dicarboxylate (1b): Yield: %88 (2.99 g), orange viscous substance. FT-IR (υ_{max}, cm^{-1}): 3355 (NH_2), 2168 (HC≡N), 1732 (C=O). ^1H NMR (400 MHz, $CDCl_3$) δ 3.05 (d, 2H, J=12 Hz, CH_2), 3.34 (s, 3H, OCH_3), 4.14 (s, 3H, OCH_3), 5.61 (t, 1H, CH, J=4 Hz), 6.61-6.66 (m, arH, 2H), 6.85-6.88 (m, 2H, arH), 7.03-7.08 (m, 1H, arH), 7.29-7.42 (m, 5H, arH), 7.54 (s, 2H, NH_2). ^{13}C NMR (400 MHz, $CDCl_3$) δ 29.7 (CH-6), 40.1 (CH_2), 49.9 (OCH_3), 54.9 (OCH_3), 62.0 (C5), 115.5-115.7 (2CH10/12), 122.7 (C1), 127.1 (C22), 127.2 (CH19), 128.8 (2CH9/13), 128.9 (2CH18/20), 129.3 (2CH17/15), 134.2 (C2), 135.5 (C16), 142.3 (C8), 154.89 (C4), 157.6-162.7 (C-F, J_{C-F}= 515 Hz), 168.2 (C=O), 168.3 (C=O). MALDI-TOF-MS: 421.43, 402.16 $[M-1-H_2O]^+$.

in Silico Analyses (Molecular Docking Technique)

in Silico studies of the designed and synthesized molecular systems in this study were conducted using molecular docking analysis. High-resolution crystal structures of the macromolecules 5UBR and 4EKL, which are thought to be effective against HT-29 colon cancer and with which the designed molecules could interact, were obtained from the Protein Data Bank (pdb) website (https://www.rcsb.org/). Molecular docking studies were performed using the AutoDock Vina program (Trott and Olson 2010; Eberhardt et al. 2021). Visualizations of molecular interactions within the macromolecule-ligand complexes obtained from the molecular docking studies were obtained using the DSV program (BIOVA 2020).

2.3. Anticancer Activity Assays

2.3.1. Application of Synthesized Molecules to Cancer and Healthy Cell Lines and Investigation of Their Effects on Cell Proliferation Using the XTT Assay

The XTT [(2,3-bis-(2-methoxy-4-nitro-5-sulfophenyl)-2*H* tetrazolym-5-carboxanilide)] method was used to determine changes in cell proliferation. In this method, cell proliferation is determined by colorimetric measurement of mitochondrial enzyme activity due to the decrease in formazan dyes or XTT. Proliferating cells utilize the XTT salt, and due to increased dehydrogenase activity, the XTT salt is converted into an orange, water-soluble formazan product. The resulting color change is measured using a spectrophotometer or ELISA reader to determine changes in cell proliferation (Nowak et al. 2018). As part of the proposed project, the following were aimed at determining the effects of compounds with effective binding scores to 5UBR and 4EKL and the chemotherapeutic drug 5-FU on the proliferation of a human colon cancer cell line (HT-29) and a healthy cell line (3T3-L1) based on molecular docking analyses:

1. 200 µL (10 x 104 cells/mL) of the counted cells in culture medium were seeded into each well of a 96-well plate and incubated overnight in an incubator at 37°C and 5% CO_2 to allow the cells to adhere to the surface.

2. Following incubation, the medium in the plate was removed, and each well was washed with Dulbecco's phosphate-buffered saline (DPBS) buffer, and the DPBS was removed.

3. Each compound to be tested was prepared in culture medium at different concentrations (0.25, 0.5, 1, 2.5, 5, 10, 25, and 50 µM) from the stock solution. 100 µL was added to a 96-well plate and incubated for 24 and 48 hours at 37°C in a 5% CO_2 incubator. Cells containing only complete medium were used as the control group.

4. After the incubation periods, each well was washed with 100 µL of PBS. 100 µL of fresh complete medium was added to these wells, and 50 µL of the prepared XTT solution (100 µL activator for 5 mL of XTT) was added to each well and incubated for 6 hours in a 5% CO_2 incubator. 5. Cells incubated with XTT solution were measured at 470 nm absorbance using a microplate reader spectrophotometer (Altay et al. 2022).

*Complete medium to be used for the colon cancer cell line (HT-29): 10% fetal bovine serum (FBS) and 1% penicillin/streptomycin (pen/strep) in McCoy's 5A Medium

*Complete medium to be used for the healthy cell line (3T3-L1): 10% FBS and 1% pen/strep in DMEM medium

*Each compound to be tested was dissolved in dimethyl sulfoxide (DMSO) at 1 mg/mL, then vortexed and sonicated at +4°C for 10 minutes to ensure complete dissolution. The resulting stock solution was stored at +4°C until used.

The decrease in cell proliferation was calculated using the following equation: % Proliferation = [Abs (compound-treated cells) – Abs (compound in cell-free medium)] / [Abs (control group cells) – Abs (cell-free medium)] X 100.

Based on the results, the IC_{50} value of each compound was calculated using the statistical program GraphPad Prism Software (GraphPad Software, San Diego, CA). The IC_{50} value is the concentration of the compound required to reduce cell proliferation by 50%.

RESULTS

Synthesis Study

TEA, used in the literature, was insufficient to cause the reaction to proceed as desired. Montmorillonite-K-10, used in the literature, was tested as a catalyst, but no product formation was observed. Therefore, the more basic NaOH was used, and better results were obtained.

Consequently, the corresponding aldehyde compound and malononitrile were first stirred in EtOH in the presence of NaOH for 15 minutes at room temperature. The corresponding amine compound and dimethylacetylenedicarboxylate were then added and stirred at room temperature (25 °C) for 24 hours.

Evaluation of *in Silico* (Molecular Docking Studies) Results

In molecular docking studies, the interactions of designed molecules thought to be effective against colon (HT-29) cancer with the macromolecules 5UBR (Qin et al. 2017) and 4EKL (Lin et al. 2012) were determined, and the results were presented in detail.
Table 1 shows the binding scores for ligand molecules docked into both macromolecules. Figure 1 provides 2D visualizations of the macromolecule-ligand interactions.

Table 1. Best binding scores of the designed molecules in target macromolecules

Comp.	**PDB ID: 5UBR**	**PDB ID: 4EKL**
	Attachment score (kcal/mol)	**Attachment score (kcal/mol)**
1a	-6.90	-7.40
1b	-7.30	**-8.30**
5-Florourasil	-4.50 -5.10	

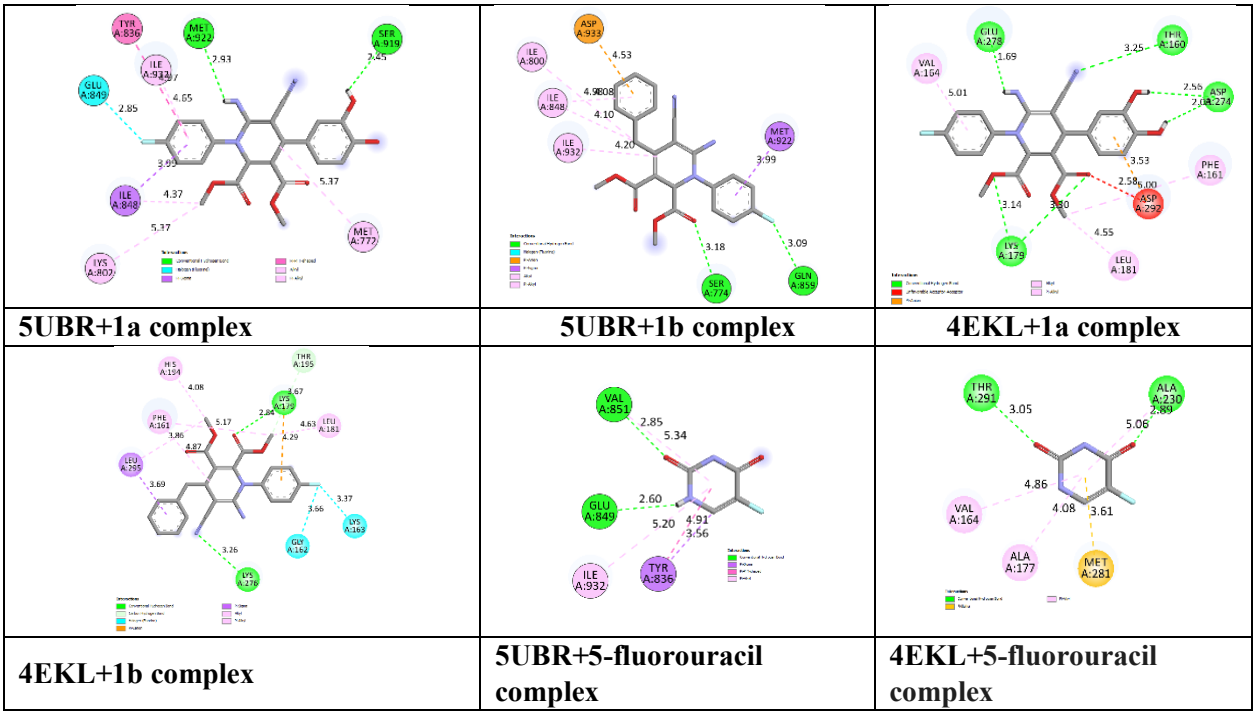


Figure 1. Interaction of molecules 1(a-b) synthesized with 5UBR and 4EKL macromolecules in the HT-29 colon cancer cell line and 5-FU, a standard anticancer drug.

Antiproliferative Effects of the Synthesized Molecules on Colon Cancer (HT-29) and Healthy Cell Lines (3T3-L1)

The dose-dependent antiproliferative effects of the synthesized hybrid molecules 1(a-b) on human colon cancer (HT-29) and mouse embryonic fibroblast (3T3-L1) cell lines were examined using the XTT method. The dose-dependent antiproliferation results of the test samples on the HT-29 cell line are shown in Figure 2. A microscopic image of the antiproliferative effects of 1b, which exhibited the strongest antiproliferative activity among the test compounds, on the HT-29 cancer cell line is shown in Figure 2. The IC_{50} (concentration of the test compound that halves cell viability) values of the test compounds on both cell lines are given in Table 2.

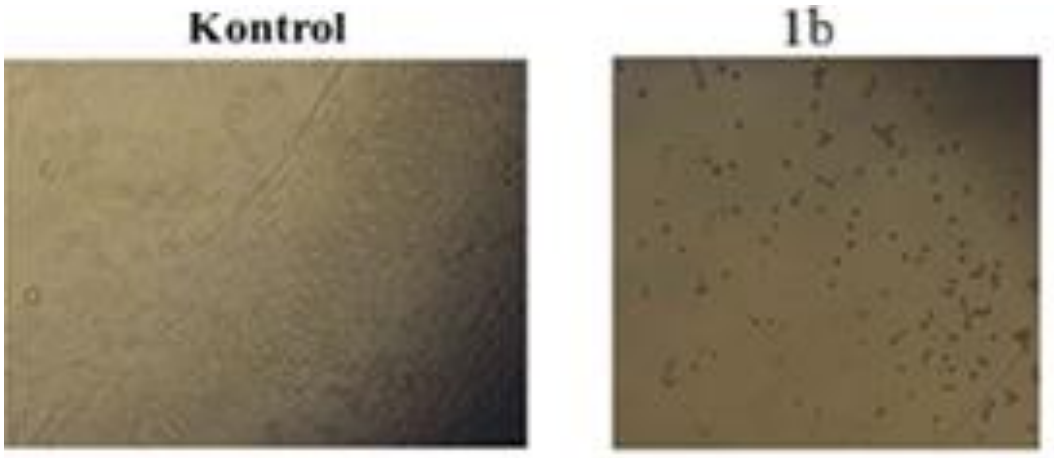


Figure 2. Microscopic image of the antiproliferative effect of the synthesized hybrid molecules 1b on the HT-29 cancer cell line.

Table 2. IC_{50} (µM) values of the synthesized hybrid molecules 1(a-b) and the chemotherapeutic drug 5-FU on HT-29 and 3T3-L1 cell lines

Test comp.	HT-29	3T3-L1
1a	4,29±0,82	142,78±1,35
1b	**0,52±0,06**	97,33±0,92
5-FU	19,84±0,94	46,27±0,88

DISCUSSION

The XTT colorimetric assay is a widely used method for evaluating the antiproliferative potential of natural or synthetic compounds (Roehm et al. 1991). In this study, the dose-dependent antiproliferative effects of the first synthesized hybrid molecules 1(a-b) on human colon cancer (HT-29) and mouse embryonic fibroblast (3T3-L1) cell lines were investigated using the XTT method, and the IC_{50} (the concentration of the test compound that halves cell viability) values of the test samples on HT-29 and 3T3-L1 cell lines were determined. Compounds 1(a-b) were applied to HT-29 cancer cells for 24 hours and all test compounds were found to exhibit dose-dependent antiproliferative activity at varying percentages in the concentration range of 0.1 to 25 µM. Among these compounds, compound 1b showed the strongest antiproliferative effect with the lowest IC_{50} value (0.52 µM), followed by compound 1a (4.29 µM).

When conducting *in vivo* and *in vitro* anticancer activity studies of naturally or synthetically derived compounds, one of the key parameters is the selectivity of the test compounds between cancer and healthy cells. In this context, derivatives 1(a-b), which exhibited strong antiproliferative activity on the HT-29 colon cancer cell line, were also tested on the healthy embryonic fibroblast 3T3-L1 cell line, demonstrating the selectivity of these compounds between healthy and cancer cell lines. When the antiproliferative activities of the test samples against the 3T3-L1 cell line were examined, compound 1b showed the strongest activity with an IC_{50} value of 97.33 µM, while compound 1a had an IC_{50} value of 142.78 µM. The IC_{50} value of the chemotherapeutic drug 5-FU on the same cell line was determined as 46.27 µM. These data indicate that 5-FU is approximately 2.33-fold more selective against HT-29 cells compared to 3T3-L1 cells, while the test compounds exhibited much higher selectivity, ranging from 187- to 613-fold.

When the structure-biological activity relationship is examined, compounds 1(a-b) share a central backbone group and a fluorobenzene attached to it. What distinguishes these compounds is the substituted benzene ring attached to the central backbone, which has a pharmacophore effect. Among these pharmacophore groups, the aromatic benzene ring contributes slightly more to the antiproliferative effects of these compounds compared to other compounds in the literature. The findings obtained from in vitro experimental studies were found to strongly support the in silico study results. Among the test compounds, compound 1b, which had the strongest binding score to the 4EKL protein, was determined to have the strongest antiproliferative effect against HT-29 cells as a result of XTT tests. According to *in silico* molecular docking results, all designed molecules exhibited higher binding scores to 5UBR and 4EKL proteins compared to 5-FU on HT-29 colon cancer.

CONCLUSION

The synthesized 1(a-b) hybrid molecules exhibited dose-dependent antiproliferative effects on HT-29 cancer cell lines. All synthesized molecules were found to have statistically more potent antiproliferative effects than 5-FU, a standard chemotherapeutic agent used in colon cancer cell lines. The synthesized hybrid molecules were observed to have significantly higher IC_{50} values in the 3T3-L1 healthy cell line compared to the HT-29 cancer cell line. This suggests that the synthesized hybrid molecules exhibit higher selectivity for cancer cells compared to healthy cells.

ACKNOWLEDGEMENTS

The support provided by Scientific and Technological Research Council of Turkey (TUBITAK, Project no: 124Z257)

REFERENCES

Altay A, Yeniçeri EKK, Taslimi P, et al (2022) Phytochemical Analysis and Biological Evaluation of Hypericum linarioides Bosse: in Vitro and in Silico Studies. ChemistrySelect 7:. https://doi.org/10.1002/slct.202200039

Dömling A (2000) The discovery of new isocyanide-based multi-component reactions. Curr Opin Chem Biol 4:318–323. https://doi.org/10.1016/S1367-5931(00)00095-8

Eberhardt J, Santos-Martins D, Tillack AF, Forli S (2021) AutoDock Vina 1.2.0: New Docking Methods, Expanded Force Field, and Python Bindings. J Chem Inf Model 61:3891–3898. https://doi.org/10.1021/acs.jcim.1c00203

Khazir J, Mir BA, Chashoo G, et al (2020) Design, synthesis, and anticancer evaluation of acetamide and hydrazine analogues of pyrimidine. J Heterocycl Chem 57:1306–1318. https://doi.org/10.1002/jhet.3867

Lee D, Sello JK, Schreiber SL (2000) Pairwise Use of Complexity-Generating Reactions in Diversity-Oriented Organic Synthesis. Org Lett 2:709–712. https://doi.org/10.1021/ol005574n

Lin K, Lin J, Wu W-I, et al (2012) An ATP-Site On-Off Switch That Restricts Phosphatase Accessibility of Akt. Sci Signal 5:2248–2258. https://doi.org/10.1126/scisignal.2002618

Qin L, Ren L, Wan S, et al (2017) Design, Synthesis, and Evaluation of Novel 2,6-Disubstituted Phenol Derivatives as General Anesthetics. J Med Chem 60:3606–3617. https://doi.org/10.1021/acs.jmedchem.7b00254

Reddy VH, Kumari AK, Reddy GM, et al (2019) Environmentally benign one-pot multicomponent synthesis of 1,4-dihydropyridine derivatives applying montmorillonite K10 as reusable catalyst. Chem Heterocycl Compd 55:60–65. https://doi.org/10.1007/s10593-019-02419-3

Roehm NW, Rodgers GH, Hatfield SM, Glasebrook AL (1991) An improved colorimetric assay for cell proliferation and viability utilizing the tetrazolium salt XTT. J Immunol Methods 142:257–265. https://doi.org/10.1016/0022-1759(91)90114-U

Sun J, Xia E-Y, Wu Q, Yan C-G (2010) Synthesis of Polysubstituted Dihydropyridines by Four-Component Reactions of Aromatic Aldehydes, Malononitrile, Arylamines, and Acetylenedicarboxylate. Org Lett 12:3678–3681. https://doi.org/10.1021/ol101475b

Trott O, Olson AJ (2010) AutoDock Vina: Improving the speed and accuracy of docking with a new scoring function, efficient optimization, and multithreading. J Comput Chem 31:455–461. https://doi.org/10.1002/jcc.21334

Weber L (2002) Multi-component reactions and evolutionary chemistry. Comb Chem 7:143–147

(2020) Discovery Studio Modeling Environment

ORAL PRESENTATION

Yarpuz otu (*Mentha pulegium*) fenoliklerinin sağlık üzerine etkileri

Seniha Koyun[1] (*https://orcid.org/* 0009-0006-1461-1381), Nurten Cengiz[2] *(https://orcid.org/*0000-0002-6640-4927), Serap Toprak Döşlü[3] *(https://orcid.org/* 0000-0002-5455-8179)

[1]Mardin Artuklu University, Graduate School of Natural and Applied Sciences, Department of Chemistry, Mardin, Turkey.
[2]Adana Alparslan Türkeş University of Science and Technology, Faculty of Engineering, Department of Food Engineering, Adana, Türkiye.
[3]Mardin Artuklu University, Faculty of Health Sciences, Department of Nutrition and Dietetics, Mardin, Türkiye.

Özet

Dünya Sağlık Örgüt'ünün yaptığı araştırmaya göre küresel nüfusun %80'i sağlık hizmetlerinde 1. basamak olarak bitkisel tedavi yöntemlerini kullanmaktadır. Bunun asıl nedeni insanların doğal antioksidan kaynaklarına karşı olan ilgisi ve güvenidir. Günümüzde teknolojinin ilerlemesiyle birlikte tıp alanında incelemeler artmış ve bitkilerin sahip olduğu etken bileşenler bilimsel çalışmalara konu olmuştur. Böylece bitkiler fitoterapi adı verilen bilim dalı ile desteklenip modern tıbbın tamamlayıcısı olarak kabul görmüştür. Özellikle Güneydoğu Anadolu bölgesinde kullanımı oldukça yaygın olan yarpuz bitkisini yöre halkı; yeni doğum yapmış kadınlara rahimin rahatlaması amacıyla ve soğuk algınlığı, grip, baş ağrısı, solunum yolu enfeksiyonları gibi rahatsızlıkların tedavisinde bu bitkiden faydalanmıştır. Bu rahatsızlıklardan müzdarip kişiler yarpuz bitkisinin yapraklarının kurtulmasıyla elde edilen çayı tüketerek tedavi edilmiştir. Literatürde bu konu ile ilgili yapılan çalışmalar incelendiğinde; yarpuz bitkisinin antioksidan içeriğinin oldukça zengin olduğu ve bu bitkinin biyoaktif bileşenlerinin de aktif olduğu sonucuna varılmıştır. Sonuç olarak *Mentha pulegium* bitkisinin yüksek antioksidan kapasitesi ve geniş etki spektrumu ve modern fitoterapötik uygulamalarda değerlendirilmesi, bitkinin hem bilimsel hem de uygulamalı araştırmalarda geniş bir kullanım potansiyeline sahip olduğunu göstermektedir.

Anahtar Kelimeler: Yarpuz otu, Fitoterapi, Antioksidan, Antimikrobiyal

Health Effects of Phenolic Compounds from *Mentha pulegium*

Abstract

According to research conducted by the World Health Organization, 80% of the global population uses herbal remedies as a primary healthcare option. This is primarily due to people's interest in and trust in natural antioxidant sources. With technological advancements, medical research has increased, and the active components of plants have become the subject of scientific studies. Thus, plants have been supported by the scientific field of phytotherapy and are now accepted as complementary to modern medicine. The *Mentha pulegium* plant we feature in this project belongs to the Lamiaceae family. The plant, particularly used in Southeastern Anatolia, is widely used by local people. It has been used by women who have recently given birth to relax the uterus and to treat ailments such as colds, flu, headaches, and respiratory infections. Those suffering from these ailments have been treated with a tea made from dried leaves of the plant. When looking at the studies on this subject in the literature, When the study was examined, it was concluded that the antioxidant content of pennyroyal is very rich and the bioactive components of this plant are also active.In conclusion, the high antioxidant capacity and broad spectrum of action of *Mentha pulegium*, and its evaluation in modern phytotherapeutic applications, indicate that the plant has a wide potential for use in both scientific and applied research.

Keywords: Yarpuz herb, Phytotherapy, Antioxidant, Antimicrobial

1.GİRİŞ

Tarih öncesi dönemlerden itibaren insanlar bitkilerin tedavi edici gücünü keşfedip ondan yararlanmıştır. Literatürde araştırdığımız zaman yazılı kaynaklardan bunun antik döneme kadar dayandığını görmekteyiz. Günümüzde ise modern teknolojik yaklaşımlar sonucu tıp alanındaki araştırmalar artmış ve bitkilerin sahip olduğu fenolik bileşenleri, antioksidan, antimikrobiyal özellikleri, etki mekanizmaları gibi pek çok etken incelenerek bilimsel çalışmalara konu olmuştur. Böylece bitkiler fitoterapi adı verilen bir bilim dalı ile desteklenmiş ve modern tıbbın tamamlayıcıları olarak kabul görmüşlerdir. Dünya Sağlık Örgütü'ne göre, dünya nüfusunun yaklaşık %80'i temel sağlık hizmetlerinde bitkisel ilaçlardan faydalanmaktadır (WHO, 2013). Bu oranın yüksek olmasının nedeni ise bu yöntemin doğal tedavi yöntemlerine dayanması ve ucuz olmasıdır. Türkiye, farklı iklimlerin görüldüğü geniş coğrafyası ve zengin bitki örtüsü sayesinde çok sayıda tıbbi ve aromatik bitkiye ev sahipliği yapan önemli bir merkezdir (Faydaoğlu ve Sürücüoğlu, 2011). Bu bitkiler arasında *Mentha pulegium* (yarpuz) özellikle Anadolu da geleneksel şifa yöntemi olarak yaygın şekilde kullanılmıştır. Sulak alanların kenarında görülen bitki, haziran ve eylül ayları arasında çiçek açmaktadır ve bitkiyi deniz seviyesinden 1300 metreye kadar olan rakımlarda gözlemlemek mümkündür (Doğan, 2025). "*Mentha pulegium* dünya üzerinde tropikal bölgelerin haricinde hemen her yerde yetişmektedir" (Tanker ve Sezik, 1965). Bu bitkiye ülkemizde özellikle Mardin, Diyarbakır, Adıyaman, Antalya illerinde yaygın bir şekilde rastlarız. Yarpuz otu halk arasında özellikle; minör solunum yolu enfeksiyonları, grip, gut, hepatit, kramp ve daha saymadığımız birçok rahatsızlığın tedavisinde kullanılmıştır ayrıca Yarpuz otu terletici, sakinleştirici, uyarıcı ve tonik bir etkiye sahiptir (Doğan, 2025). Sonuç olarak literatür incelendiğinde, *Mentha pulegium*'un yüksek antioksidan kapasitesi ve geniş etki spektrumu, bitkinin modern fitoterapötik uygulamalarda değerlendirilmesi, bitkinin hem bilimsel hem de uygulamalı araştırmalarda geniş bir kullanım potansiyeline sahip olduğunu göstermektedir.

2.BİTKİNİN BOTANİK ÖZELLİKLERİ

Lamiaceae familyasında yer alan *Mentha pulegium* keskin kokulu ve çok yıllıklı bir bitki olup Türkiye'de Mardin, Diyarbakır, Tekirdağ, Aydın ve daha sayamadığımız bir çok ilde yetişmektedir (Çöteli vd., 2013). Halk arasında bu bitki yarpuz, pung, filiskin olarak bilinmektedir. Genellikle boyu 10 ile 40 cm arasında yapraklar ise 8 ile 30 mm uzunluğunda ve 4 ila 12 mm genişliğinde ve hafif tüylüdür (Doğan, 2025). Çiçekleri mor veya pembe tonlarında olup başak şeklindedir.



Şekil 1. Yarpuz (*Mentha pulegium*) bitkisi (pixabay, t.y.)

3.FITOKIMYASAL BILEŞENLER

Yarpuz otunu incelediğimizde en belirgin özelliği uçucu yağ içeriğinin zengin olmasıdır. Pulegon, piperiton, menthol, menthon gibi bileşikler bu uçucu yağın ana bileşiklerini oluşturmaktadır (Karaman vd., 2021). Farklı coğrafi bölgelerde incelen *Mentha pulegium*'ların bileşik oranlarında farklılık olduğu gözlemlenmiştir. Bunun asıl nedeni iklim, toprak yapısı gibi etmenlerin bu sonucu etkilemesidir. Bitkilerin savunma amaçlı olarak ürettikleri bu bileşikler yabancı ot çimlenmesini de önlemektedir. Biber üzerinden yürütülen bir çalışmada, istenmeyen yabancı otların filizlenmesini engellemek için yarpuz uçucu yağı düşük konsantrasyon da kullanılmış ve çimlenmeyi engellediği görülmüştür. Bu sonuçlar eşliğinde araştırmacılar yarpuz uçucu yağının ara tarım ürünü olarak kullanılabileceği kanısındadır (Karaman vd., 2021).

4.FARMAKOLOJİK ETKİLER

4.1. Antioksidan, Antimikrobiyal ve Anti-inflamatuar Etkiler

Mentha pulegium L. türü Fas'ın geleneksel içeceklerinde aroma verici olarak, yaprakları çiğnenerek hıçkırık tedavisinde, grip, migren, ateş, obezite, kabızlık ve öksürük gibi birçok hastalığı tedavi etmek amacıyla kullanılmıştır (Amtaghri vd., 2024). Bu bitkinin düşük dozda da olsa toksik etkilerine rastlanmıştır. Gelecekte bu bitkinin dağılımına, kimyasal bileşenine ve biyolojik aktivitlerine odaklanıp kapsamlı çalışmalar yapılmalıdır (Amtaghri vd., 2024).

Türkiye'de tıbbi amaçlı olarak tahmini 500 bitki bulunmaktadır bunların yaklaşık olarak 200'ü ihraç potansiyeli yüksek olan bitkilerdir ve bu bitkiler ülke ekonomisine katkı sağlamaktadır (Faydaoğlu ve Sürücüoğlu, 2011). Bu nedenle geleneksel bitkilerin araştırılmasına eğilim artmalıdır çünkü farmasötik amaçlı kullanılan bitkilerin ülke ekonomisine katkı sağlaması öngörülmektedir.

Başka bir çalışmada ise Yarpuz otunun; yapraklarında A vitaminin 0,38±0,08 µg/g, E vitamini miktarının (12,46±1,82 µg/g), β-karoten miktarının 1,24±0,14 µg/g, ve B1, B2, B3, B6 ve B9 vitaminlerinin ise sırası ile 0,50±0,09 µg/g; 43,11±7,02 µg/g; 16,91±1,59 µg/g; 81,88±9,47 µg/g ve 1,53±0,16 µg/g olduğu belirlendi (Çöteli vd., 2013). Bu çalışmayı incelediğimizde de sonuç olarak *Mentha pulegium* B2, B6 vitaminleri ve serbest radikal temizleme etkisi ile antioksidan kapasite bakımından zengin olduğu (Çöteli vd., 2013) görülmektedir ve araştırmacılar bu bitkinin biyoaktif bileşenlerinin araştırmalara daha fazla konu olacağı kanısındadır.

İncelediğimiz çalışmalarda *Mentha pulegum*'un belirgin şekilde antioksidan, antimikrobiyal ve antiinflamatuar özelliklere sahip olduğu görülmektedir. Bitkinin fenolik bileşikleri ve uçucu yağ içerikleri; pulegon ve menthonlar serbest radikallerin temizlenmesine katkı sağlayarak antioksidan etki oluşturmaktadır. Çeşitli mantar, *S. aureus, S. pyogenes, E. Coli* gibi gram pozitif ve gram negatif bakterilere karşıda antimikrobiyal aktivite gösterir. Bitkinin uçucu yağlarının ilthaplanmayı baskılaması da antiinflamatuar etki olduğunu gösterir.

4.2. Toksikolojik Bulgular

Toksikolojik çalışmalar, *Mentha pulegium* bitkisinin düşük dozlarda özütlerinin toksik olmadığını fakat yarpuz uçucu yağının oldukça tehlikeli olduğunu göstermektedir (Amtaghri vd., 2024).

5.SONUÇ

Araştırmalar sonucunda yarpuz bitkisinin etkileri değerlendirilmiş ve incelenen bulgular eşliğinde bu bitkinin antibakteriyal, antioksidan ve antiinflamatuar özelliklere sahip olduğu görülmüştür. Farmakolojik etkisi sayesinde modern ve geleneksel tıpta kullanımı bilimsel olarak desteklenmektedir. Bunun yanında toksikolojik etkilerine karşın net veriler bulunmamaktadır bu nedenle toksikolojik etkilerinin genişletilmesine ihtiyaç vardır. Son olarak yarpuz otunun halk sağlığına olumlu etkilerinin olduğu belirtilen hastalıkların tedavisinde kullanılabileceği ve bitkinin gelecekte tıbbi ve farmasötik alanlarda kullanım potansiyelinin olduğu görülmüştür.

KAYNAKLAR

Amtaghri, S., Slaoui, M. ve Eddouks, M. (2024). Mentha pulegium: çeşitli tıbbi özelliklere sahip bir bitki. *Endokrin, Metabolik ve Bağışıklık Bozuklukları-İlaç Hedefleri (Eski Adıyla Güncel İlaç Hedefleri-Bağışıklık, Endokrin ve Metabolik Bozukluklar)* , *24* (3), 302-320.

Çöteli, E., Erden, Y., & Karataş, F. (2013). Yarpuz (Mentha pulegium L.) bitkisindeki malondialdehit, glutatyon ve vitamin miktarları ile total antioksidan kapasitesinin araştırılması. Süleyman Demirel Üniversitesi Fen Bilimleri Enstitüsü Dergisi, 17(2), 4-10.

Doğan, Hüseyin(2023). Anadolu Türk Uygarlığında Bitkiler Yayımlanmamış Doktora tezi, Kocaeli Üniversitesi, Sosyal Bilimler Enstitüsü, Kocaeli, s.701-71.

Faydaoğlu, E., & Sürücüoğlu, M. S. (2011). Geçmişten günümüze tıbbi ve aromatik bitkilerin kullanılması ve ekonomik önemi. *Kastamonu University Journal of Forestry Faculty*, *11*(1), 52-67.

Gökçe, A., & Orhan, İ. E. (2024). Kadim çağlardan günümüze tedavide tıbbi ve aromatik bitkilerin rolü. *Geleneksel ve Tamamlayıcı Anadolu Tıbbı Dergisi*, *5*(1), 1-13.

Karaman, Y., Yaşar, A., & Tursun, N. (2021). Bazı yabancı ot ve kültür bitkisi tohumlarının çimlenmesine yarpuz (Mentha pulegium L.) uçucu yağının etkileri. *Journal of the Institute of Science and Technology*, *11*(4), 2477-2486.

Pixabay. (t.y.) Yarpuz (Mentha pulegium) fotoğrafı [Fotoğraf].

Şit, L. (2011). Çeşitli bitkilerin antioksidan özelliklerinin incelenmesi (Yüksek lisans tezi). Trakya Üniversitesi Fen Bilimleri Enstitüsü, Edirne.

Tanker, M. (1965). Mentha pulegium L var. hirsuta Guss.'un Uçucu Yağı Hakkında. *Journal of Faculty of Pharmacy of Istanbul University*, *1*, 55-60.

World Health Organization. (2013).

ORAL PRESENTATION

Onosma alborosea ekstraktindan sentezlenen nanopartiküllerin antimikrobiyal özelliklerinin incelenmesi

Cemile Günbegi Çalişkan[1] (Orcid:0000-0001-8129-4394), Leyla Ercan[2] (Orcid:0000-0002-6570-8128), Serap Toprak Döşlü[3*] (Orcid: 0000-0002-5455-8179)

[1]Mardin Artuklu University, Vocational Higher School of Health Services, Department of Medical Services and Techniques, Mardin, Türkiye
[2]Mardin Artuklu University, Department of Health, Culture And Sports, Mardin, Türkiye
[3] Mardin Artuklu University, Faculty of Health Sciences, Department of Nutrition and Dietetics, Mardin, Türkiye.

*Sorumlu yazar e-mail: seraptoprak@artuklu.edu.tr

Özet

Nanopartikül sentezinde kullanılan geleneksel fiziksel ve kimyasal yöntemler, genellikle yüksek enerji tüketimi, toksik kimyasalların kullanımı ve tehlikeli yan ürünlerin oluşumu gibi dezavantajlara sahiptir. Bu nedenle, son yıllarda çevre dostu, sürdürülebilir ve ekonomik olan yeşil sentez (green synthesis) yaklaşımları büyük ilgi görmektedir. Yeşil sentez, bakteri, mantar, alg ve özellikle bitki ekstraktları gibi biyolojik kaynakları kullanarak nanopartikül üretimini hedefler. Bitki ekstraktları, içerdikleri flavonoidler, terpenoidler, polifenoller gibi zengin biyoaktif bileşikler sayesinde metal iyonlarını indirgeme ve oluşan nanopartikülleri stabilize etme görevini aynı anda üstlenmektedir. Bu yöntem, toksik olmayan çözücüler (genellikle su) kullanması, oda sıcaklığında veya düşük sıcaklıklarda gerçekleştirilebilmesi ve karmaşık ekipman gerektirmemesi gibi avantajlar sunar. Boraginaceae familyasına ait olan Onosma cinsi, dünya genelinde yayılış gösteren ve geleneksel tıpta yüzyıllardır kullanılan bitkileri içerir. Özellikle yara iyileştirici, antimikrobiyal, antiinflamatuar ve antioksidan özellikleri ile bilinen Onosma türleri, shikonin ve türevleri gibi değerli naftokinon bileşiklerini barındırır. Türkiye florasında da çok sayıda endemik türü bulunan bu cinsin biyoaktif potansiyeli, onu nanopartikül sentezi için değerli bir doğal kaynak haline getirmektedir

Anahtar Kelimeler: onosma, antimikrobiyal, nanopartikül.

Investigation of antimicrobial properties of nanoparticles synthesized from Onosma Alborsea extract

Abstract

Conventional physical and chemical methods used in nanoparticle synthesis often have disadvantages such as high energy consumption, use of toxic chemicals, and formation of hazardous by-products. For this reason, green synthesis approaches that are environmentally friendly, sustainable and economical have attracted great attention in recent years. Green synthesis aims at nanoparticle production using biological sources such as bacteria, fungi, algae and especially plant extracts. Plant extracts simultaneously undertake the task of reducing metal ions and stabilizing the formed nanoparticles thanks to the rich bioactive compounds they contain, such as flavonoids, terpenoids and polyphenols. This method offers the advantages of using non-toxic solvents (usually water), being able to be performed at room or low temperatures, and not requiring complex equipment. The Onosma genus, belonging to the Boraginaceae family, includes plants that are widespread throughout the world and have been used in traditional medicine for centuries. Onosma species, especially known for their wound healing, antimicrobial, anti-inflammatory and antioxidant properties, contain valuable naphthoquinone compounds such as shikonin and its derivatives. The bioactive potential of this genus, which has many endemic species in the Turkish flora, makes it a valuable natural resource for nanoparticle synthesis.

Keywords: onosma, antimicrobial, nanoparticle.

GİRİŞ

Artan antibiyotik direnci, 21. yüzyılın en ciddi halk sağlığı tehditlerinden biri olarak kabul edilmektedir. Geleneksel antibiyotiklerin etkinliğinin azalması, enfeksiyon hastalıklarının tedavisini zorlaştırmakta ve bilim dünyasını acil olarak yeni antimikrobiyal stratejiler geliştirmeye yöneltmektedir. Antimikrobiyal direnç, küresel bir sağlık sorunu olarak giderek daha fazla önem kazanmakta ve yeni, etkili antimikrobiyal ajanların geliştirilmesini zorunlu kılmaktadır. Bu arayışta, nanoteknoloji, materyallere nano boyutlarda kazandırdığı benzersiz fizikokimyasal özellikler sayesinde devrim niteliğinde çözümler sunmaktadır. Özellikle metal ve metal oksit nanopartiküller (NPs), geniş spektrumlu antimikrobiyal aktiviteleri ile dikkat çekmektedir (WHO, 2021). Bu bağlamda, nanoteknoloji ve özellikle bitki bazlı (yeşil sentez) nanopartikül üretimi, umut verici bir yaklaşım olarak öne çıkmaktadır.

Nanopartiküllerin sentezlenmesinde kullanılan kimyasal ve fiziksel yöntemler, genellikle yüksek maliyetli, toksik kimyasallar gerektiren ve çevreye zararlı atıklar üreten süreçlerdir. Bu dezavantajları ortadan kaldırmak amacıyla geliştirilen yeşil sentez (green synthesis) yaklaşımı, bitkiler, algler, mantarlar ve bakteriler gibi biyolojik kaynakları kullanarak çevre dostu, sürdürülebilir ve düşük maliyetli bir alternatif sunmaktadır. **Yeşil sentez**, geleneksel yöntemlerin yüksek enerji tüketimi, toksik kimyasalların kullanımı ve tehlikeli yan ürünlerin oluşumu gibi dezavantajlarını ortadan kaldıran, çevre dostu, sürdürülebilir ve ekonomik bir yaklaşımdır. Bitki ekstreleri, içerdikleri zengin biyoaktif bileşikler (fenolikler, flavonoidler, terpenoidler, alkaloidler ve naftokinonlar) sayesinde metal iyonlarını indirgeyici (reducing agent) ve oluşan nanopartikülleri stabilize edici (capping/stabilizing agent) olarak görev yaparlar (Roy ve ark., 2019).

Boraginaceae familyası, dünya genelinde yayılış gösteren ve yaklaşık 150 cins ile 2500'den fazla türü barındıran, fitokimyasal açıdan zengin bir bitki ailesidir. Bu familyaya ait türler, geleneksel tıpta yüzyıllardır yara iyileştirici, anti-inflamatuar ve antimikrobiyal özellikleri nedeniyle kullanılmaktadır. Özellikle Onosma cinsi, köklerinde bulunan ve güçlü biyolojik aktivitelere sahip olan naftokinon türevleri (shikonin, alkannin ve bunların esterleri) ile tanınmaktadır (Jabbar ve ark., 2022). Bu bileşiklerin güçlü indirgeme potansiyeli, Onosma türlerini nanopartikül yeşil sentezi için ideal bir aday haline getirmektedir.

MATERYAL VE METOT

Bu derleme, Boraginaceae familyasının bir üyesi olan Onosma alborosea'nın nanopartikül özelliklerini inceleyen bilimsel literatürün sistematik bir analizine dayanmaktadır. Literatür taraması, Web of Science, Scopus, PubMed, Google Scholar gibi uluslararası bilimsel veritabanları platformlarda gerçekleştirilmiştir. Tarama sürecinde "Boraginaceae", "Onosma", "nanoparticle", "green synthesis", "antimicrobial gibi anahtar kelimeler ve bunların kombinasyonları kullanılmıştır. Seçim kriterleri, çalışmaların güncelliği, doğrudan onosma ve nanopartikül sentezi ile ilişkili olması ve biyolojik aktivite verilerini içermesi üzerine odaklanmıştır.

BULGULAR ve TARTIŞMA

Boraginaceae (Hodangiller) familyası, çoğunlukla otsu bitkiler olmakla birlikte çalı ve ağaç formlarını da içeren kozmopolit bir ailedir. Genellikle sert tüylerle kaplı yaprak ve gövdeleri ile karakterizedirler. Geleneksel olarak birçok kültürde tıbbi amaçlarla kullanılan bu familya, anti-inflamatuar, yara iyileştirici, antioksidan ve antimikrobiyal potansiyele sahip zengin bir fitokimyasal çeşitlilik sunar (Hosseinpour, 2025). Türkiye florasında Onosma'ya ait 102 bitki türü bulunmakta olup, bu türlerin yaklaşık %50'si endemiktir (Binzet, 2016).

Onosma cinsi, Boraginaceae familyasının en önemli cinslerinden biridir ve dünya genelinde yaklaşık 230 tür ile temsil edilir. Bu türler, özellikle Akdeniz havzası, Orta Doğu ve Asya'da yaygındır. Etnobotanik açıdan, Onosma türlerinin kökleri, "havaciva" olarak bilinir ve geleneksel olarak doğal gıda ve tekstil boyası olarak kullanılmasının yanı sıra, yanık, yara, egzama gibi cilt rahatsızlıklarının tedavisinde ve antimikrobiyal ajan olarak da değerlendirilmiştir (Jabbar ve ark., 2022). Literatür kayıtlarına göre, Onosma türlerinin bronşit, boğaz ağrısı, lökoderma, karın ağrısı ve ateş gibi çeşitli rahatsızlıkların tedavisinde sıklıkla kullanıldığı bilinmektedir (Mašković ve ark., 2015).

Onosma alborosea ekstreleri üzerine yapılan çalışmalar, bitkinin önemli miktarda fenolik bileşik içerdiğini göstermiştir. Erim ve Savcı (2024) tarafından yapılan bir çalışmada, bitkinin metanol ve su ekstrelerinin toplam

fenolik madde içeriği incelenmiş ve antioksidan aktiviteleri değerlendirilmiştir (Erim ve Savcı, 2024). Her ne kadar bu çalışmada antioksidan aktivitenin standartlara göre düşük olduğu belirtilse de, fenolik bileşiklerin (örneğin, ferulik asit, vanilik asit, rosmarinik asit) varlığı, metal iyonlarının indirgenmesi için gerekli elektronları sağlayarak nanopartikül sentezinde rol oynayabileceklerini göstermektedir. Diğer Onosma türleri üzerinde yapılan çalışmalarda, örneğin Onosma frutescens ve Onosma sericea özütlerinin fenolik ve flavonoidler açısından zengin olduğu ve rosmarinik asit, apigenin 7-glukozit, luteolin 7-glukozit, hesperidin, hiperozit, ferulik asit, vanilik asit, kafeik asit ve 4-hidroksibenzoik asit gibi bileşikleri yüksek miktarda içerdiği belirlenmiştir (Sarikurkcu ve ark.,2020).

Onosma cinsinin en karakteristik kimyasal bileşenleri, köklerde biriken kırmızı renkli naftokinon pigmentleridir. Shikonin, alkannin ve bunların çeşitli ester türevleri, bu grubun en bilinen üyeleridir. Naftokinonların yapısındaki kinon halkası, kolayca redoks reaksiyonlarına girme yeteneğine sahiptir. Bu özellik, metal iyonlarını (örneğin Ag^{+}) metalik forma (Ag^{0}) indirgemek için mükemmel bir kimyasal potansiyel sunar ve bu da onları nanopartikül yeşil sentezi için birincil aday haline getirir (Ramos-Peralta ve ark., 2015).

Gündoğan (2021) tarafından yapılan bir tez çalışmasında, Onosma sericeum Willd. bitkisinin kök ekstresi kullanılarak gümüş nanopartiküller (AgNPs) yeşil sentez yöntemiyle elde edilmiş ve bu nanopartiküller içeren yara kremi formülasyonları geliştirilmiştir (Gündoğan, 2021). Bu çalışma, Onosma türlerinin nanopartikül sentezindeki potansiyelini deneysel olarak kanıtlayan önemli bir örnektir. Ayrıca, Onosma bourgaei ekstresi kullanılarak da AgNPs biyosentezi gerçekleştirilmiş ve antimikrobiyal aktivitesi incelenmiştir (Erenler ve Geçer, 2024).

Boraginaceae ekstrelerinden sentezlenen nanopartiküller, özellikle AgNPs, geniş bir patojen yelpazesine karşı güçlü antimikrobiyal aktivite göstermektedir. Etki mekanizmaları tam olarak aydınlatılamamış olsa da, birkaç olası mekanizma öne sürülmektedir: (i) nanopartiküllerin bakteri hücre duvarına ve zarına bağlanarak yapısal bütünlüğünü bozması, (ii) hücre içine girerek DNA ve proteinler gibi hayati makromoleküllerle etkileşime girmesi ve fonksiyonlarını engellemesi, (iii) reaktif oksijen türleri (ROS) üreterek oksidatif strese neden olması (Singh ve ark., 2017). Naftokinonlar gibi biyoaktif moleküllerin nanopartikül yüzeyinde bulunması, bu antimikrobiyal etkiyi sinerjistik olarak artırabilir (Krychowiak ve ar., 2018). Onosma nana etanol ekstrelerinin, S. epidermidis ve P. vulgaris'e karşı kayda değer antimikrobiyal aktiviteye sahip olduğu rapor edilmiştir (Özcan ve Acet, 2024).

SONUÇ

Sonuç olarak, Boraginaceae familyası, zengin ve çeşitli fitokimyasal içeriği sayesinde, çevre dostu, düşük maliyetli ve etkili nanopartiküllerin yeşil sentezi için muazzam bir potansiyel sunmaktadır. Özellikle Onosma cinsi, içerdiği naftokinon türevleri ile bu potansiyeli bir adım öteye taşımaktadır. Bu nedenle, Onosma alborosea türünün, antimikrobiyal özelliklere sahip nanopartiküllerin sentezi için umut verici ve henüz keşfedilmemiş bir kaynak olduğu sonucuna varılmıştır.

TEŞEKKÜR

Yazarlar, MAÜ.BAP.24.SBF.077 Nolu proje ile destek sunan Mardin Artuklu Üniversitesi Bilimsel Araştırma Projeleri Koordinasyon Birimine teşekkür eder.

KAYNAKLAR

Binzet, R. (2016). A new species of Onosma L.(Boraginaceae) from Anatolia. Turkish Journal of Botany, 40(2), 194-200.

Erenler, R., & Geçer, E. N. (2024). Biogenic Synthesis of Silver Nanoparticles Using Onosma Bourgaei Leaves: Characterization and Antioxidant Activity. International Journal of Chemistry and Technology, 8(2), 98-104.

Erim, K., & Savcı, A. (2024). Phenolic Compound Analysis and Antioxidant Properties of O. Alborosea. Mus Alparslan University Journal of Science, 12(2), 78-83.

Gündoğan, M. (2021).Onosma sericeum willd. bitkisinin kök ekstresinden ve ekstreden sentezlenmiş gümüş nanopartikülden oluşan yara kremi formülasyonlarının geliştirilmesi. Mersin Üniversitesi Sağlık Bilimleri Enstitüsü

Hosseinpour, L., Baharara, J., Darroudi, M., Sabouri, Z., & Bostanabad, S. Z. (2025). Green synthesis of selenium nanoparticles using Cordia myxa extract and assessment of their cytotoxic and antioxidant properties. Avicenna Journal of Phytomedicine, 15(5), 1531.

Jabbar, A. A., Abdullah, F. O., Hassan, A. O., Galali, Y., Hassan, R. R., Rashid, E. Q., ... & Aziz, K. F. (2022). Ethnobotanical, phytochemistry, and pharmacological activity of onosma (Boraginaceae): An updated review. Molecules, 27(24), 8687.

Krychowiak, M., Kawiak, A., Narajczyk, M., Borowik, A., & Królicka, A. (2018). Silver nanoparticles combined with naphthoquinones as an effective synergistic strategy against Staphylococcus aureus. Frontiers in Pharmacology, 9, 816.

Mašković, P. Z., Diamanto, L. D., Vujic, J. M., Cvetanović, A. D., Radojković, M. M., Gadžurić, S. B., & Zengin, G. (2015). Onosma aucheriana: A source of biologically active molecules for novel food ingredients and pharmaceuticals. Journal of functional foods, 19, 479-486.

Özcan, K., & Acet, T. (2024). Endemik Onosma nana DC.'nin Kimyasal Bileşimi, Antimikrobiyal, Antioksidan ve Enzim İnhibisyon Aktivitesinin Araştırılması. Karadeniz Fen Bilimleri Dergisi, 14(2), 982-996.

Ramos-Peralta, L., López-López, L. I., Silva-Belmares, S. Y., Zugasti-Cruz, A., Rodríguez-Herrera, R., & Aguilar-González, C. N. (2015). Naphthoquinone: bioactivity and green synthesis. The battle against microbial pathogens: basic science, technological advances and educational programs, 1, 542-550.

Roy, A., Bulut, O., Some, S., Mandal, A. K., & Yilmaz, M. D. (2019). Green synthesis of silver nanoparticles: biomolecule-nanoparticle organizations targeting antimicrobial activity. RSC advances, 9(5), 2673-2702.

Sarikurkcu, C., Sahinler, S. S., & Tepe, B. (2020). Onosma aucheriana, O. frutescens, and O. sericea: Phytochemical profiling and biological activity. Industrial Crops and Products, 154, 112633.

Singh, H., Du, J., & Yi, T. H. (2017). Green and rapid synthesis of silver nanoparticles using Borago officinalis leaf extract: anticancer and antibacterial activities. Artificial cells, nanomedicine, and biotechnology, 45(7), 1310-1316.

World Health Organization. (2021). Antimicrobial resistance. Available at: https://www.who.int/news-room/fact-sheets/detail/antimicrobial-resistance [07.12.2025]

ORAL PRESENTATION

Pandemi dönemi ile birlikte beslenme ve sağlık dersinin yeniden yapılandırılması: İçerik, pedagoji ve dijital dönüşüm açılarından nitel bir analiz

Hüseyin Hakan İnce (Orcid: 0000-0001-9873-5731)

Dicle Üniversitesi, Ziya Gökalp Eğitim Fakültesi, Matematik ve Fen Alanlar Eğitimi Bölümü, Diyarbakır, Türkiye

Sorumlu yazar e-mail: hhakanince@hotmail.com

Özet

COVID-19 pandemisi, yükseköğretimdeki tüm dersleri etkilemekle birlikte, sağlık ve beslenme ile ilişkili derslerde çok daha köklü ve hızlı bir dönüşümü zorunlu kılmıştır. Bu çalışma, üniversite düzeyinde verilen *Beslenme ve Sağlık* dersinin pandemi sürecinde nasıl yeniden yapılandırıldığını incelemek amacıyla **nitel doküman analizi** yaklaşımını kullanmaktadır. Veri kaynağı olarak; Dünya Sağlık Örgütü'nün (DSÖ) COVID-19 dönemine yönelik beslenme rehberleri (WHO, 2020), UNESCO ve UNICEF'in post-COVID eğitim raporları (UNESCO, 2020; UNICEF, 2023), beslenme–bağışıklık ilişkisini ele alan güncel derleme makaleleri (Calder, 2020, 2021; Carr & Rowe, 2020; Sadeghsoltani ve ark., 2022; Govers ve ark., 2022) ve çevrim içi öğrenme ile acil uzaktan öğretim arasındaki farkları tartışan eğitim çalışmaları (Hodges ve ark., 2020; Garrison & Kanuka, 2004) kullanılmıştır. Üç aşamalı tematik analiz sonucunda üç ana tema ortaya çıkmıştır: (1) Ders içeriğinin bilimsel olarak güncellenmesi, özellikle bağışıklık fizyolojisi ve mikro besin–immünite ilişkilerinin derinleştirilmesi; (2) öğrenci merkezli pedagojik yaklaşımların güçlenmesi, problem temelli öğrenme, yanlış bilgi vakalarının analizi ve infografik temelli görevlerin yaygınlaşması; (3) dijital öğrenme araçlarının kalıcılaşması, mikro ders videoları, çevrim içi öğrenme yönetim sistemleri ve resmî sağlık otoritelerinin dijital kaynaklarının dersin ayrılmaz parçası hâline gelmesi. Bulgular, pandemiye bağlı düzenlemelerin geçici çözümler değil, dersin bilimsel, pedagojik ve teknolojik altyapısını güçlendiren yapısal iyileştirmeler olduğunu göstermektedir. Sonuç bölümünde, beslenme ve sağlık eğitimine yönelik sürdürülebilir bir "içerik–pedagoji–teknoloji üçgeni" modeli önerilmekte ve gelecekteki olası salgınlar için ders tasarımına yönelik öneriler sunulmaktadır.

Anahtar Kelimeler: Beslenme eğitimi, bağışıklık sistemi, COVID-19, mikro besinler, yanlış bilgi, dijital öğrenme, nitel doküman analizi.

Reconstruction of the Nutrition and Health Course with the Onset of the Pandemic Period: A Qualitative Document Analysis on Content, Pedagogy, and Digital Transformation

Abstract

The COVID-19 pandemic has impacted all areas of higher education; however, it has necessitated a far more profound and rapid transformation in courses related to health and nutrition. This study employs a qualitative document analysis approach to examine how the university-level *Nutrition and Health* course was restructured during the pandemic period. The data sources include the World Health Organization's (WHO) nutrition guidelines for the COVID-19 era (WHO, 2020), UNESCO and UNICEF post-COVID education reports (UNESCO, 2020; UNICEF, 2023), recent review articles addressing the relationship between nutrition and immunity (Calder, 2020, 2021; Carr & Rowe, 2020; Sadeghsoltani et al., 2022; Govers et al., 2022), and educational studies discussing the distinctions between online learning and emergency remote teaching (Hodges et al., 2020; Garrison & Kanuka, 2004).

A three-stage thematic analysis revealed three major themes: (1) scientific updating of course content, particularly the deepening of topics related to immune physiology and micronutrient–immunity interactions; (2) the strengthening of learner-centered pedagogical approaches, including problem-based learning, the analysis of misinformation cases, and the integration of infographic-based tasks; and (3) the institutionalization

of digital learning tools, such as micro-lecture videos, online learning management systems, and digital resources from official health authorities. The findings indicate that the modifications made during the pandemic are not temporary solutions but rather structural improvements that reinforce the scientific, pedagogical, and technological foundations of the course. The conclusion section proposes a sustainable "content–pedagogy–technology triangle" model for nutrition and health education and offers recommendations for course design in preparation for potential future pandemics.

Keywords: Nutrition education, immune system, COVID-19, micronutrients, misinformation, digital learning, qualitative document analysis.

GİRİŞ

COVID-19 pandemisi, küresel ölçekte yükseköğretimi hem organizasyonel hem de pedagojik açıdan zorlayan, aynı zamanda dönüştüren bir süreç olmuştur. UNESCO'nun "Education in a post-COVID world: Nine ideas for public action" raporunda, pandeminin eğitim sistemlerinin kırılganlıklarını açığa çıkarmakla kalmayıp, daha kapsayıcı ve esnek yapılar için bir fırsat penceresi de oluşturduğu vurgulanmaktadır (UNESCO, 2020). Bu bağlamda *Beslenme ve Sağlık* dersinin içerik ve pedagojik yönlerden yeniden ele alınması kaçınılmaz hâle gelmiştir.

Pandemi sürecinde beslenme–bağışıklık ilişkisine yönelik bilimsel araştırmalar hız kazanmış; özellikle mikro besinlerin immün fonksiyonlardaki rolü daha görünür hâle gelmiştir (Calder, 2020, 2021; Govers ve ark., 2022). Bağışıklık sisteminin vitamin A, C, D, E ile çinko, demir, selenyum gibi eser elementlerden doğrudan etkilendiği ve bu besin öğelerinin enfeksiyon riskini düşürmede önemli olduğu ortaya konmuştur (Calder, 2020, 2021). C vitamininin solunum yolu enfeksiyonlarında oksidatif stresin azaltılması ve nötrofil fonksiyonlarının düzenlenmesindeki rolü çeşitli derlemelerde ayrıntılandırılmıştır (Carr & Rowe, 2020; Cerullo ve ark., 2020). Çinkonun antiviral yanıt ve solunum yolu enfeksiyonları üzerindeki etkileri de güncel derlemelerde kapsamlı şekilde ele alınmaktadır (Sadeghsoltani ve ark., 2022).

Diğer yandan, sosyal medya ortamında beslenme ile ilgili yanlış bilgilerin hızla yayılması, "infodemi" kavramı ile açıklanmaktadır (Cinelli ve ark., 2020). Bu durum, ders kapsamında **yanlış bilgi okuryazarlığının** ele alınmasını zorunlu hâle getirmiştir.

Pedagojik açıdan bakıldığında, üniversitelerin hızla çevrim içi eğitime geçmesi, literatürde "acil uzaktan öğretim" olarak tanımlanmış ve bu modelin, planlı ve pedagojik olarak tasarlanmış bir çevrim içi eğitimden önemli ölçüde farklı olduğu vurgulanmıştır (Hodges ve ark., 2020). Buna karşın harmanlanmış (blended) öğrenme yaklaşımının, yüz yüze ve çevrim içi bileşenleri bütünleştirerek yükseköğretimde dönüştürücü bir potansiyel taşıdığı ifade edilmektedir (Garrison & Kanuka, 2004).

Bu nedenle çalışmanın temel araştırma sorusu şu şekilde formüle edilmiştir:

Pandemi sürecinde üniversite düzeyinde yürütülen Beslenme ve Sağlık dersi, içerik, pedagojik yaklaşım ve dijital öğrenme araçları açısından nasıl yeniden yapılandırılmıştır?

MATERYAL VE METOT

Araştırma Deseni

Çalışmada, metin temelli kaynakların sistematik ve eleştirel analizine odaklanan **nitel doküman analizi** deseni kullanılmıştır. Bu yaklaşım, bir dersin yeniden yapılandırılma sürecini resmî raporlar, rehber dokümanlar ve bilimsel yayınlar üzerinden ortaya koymak için uygundur.

Veri Kaynakları

Analize dâhil edilen dokümanlar dört ana grupta toplanmıştır:

Uluslararası sağlık otoriteleri

DSÖ'nün COVID-19 ve beslenme ile ilgili çevrim içi rehberleri ve bilgi notları (WHO, 2020).

Eğitim politikası ve dönüşüm raporları

UNESCO'nun pandemiden sonra eğitim sistemlerini yeniden düşünmeye yönelik raporu (UNESCO, 2020).

UNICEF destekli "Education in a post-COVID world: Towards a RAPID Transformation" raporu (UNICEF, 2023).

Beslenme–bağışıklık ilişkisine odaklanan bilimsel derlemeler

Beslenme, bağışıklık ve COVID-19'a ilişkin derlemeler (Calder, 2020, 2021).

C vitamininin solunum yolu enfeksiyonlarındaki rolü (Carr & Rowe, 2020; Cerullo ve ark., 2020).

Çinko ve antiviral immün yanıt üzerine güncel derlemeler (Sadeghsoltani ve ark., 2022; Govers ve ark., 2022).

Çevrim içi öğrenme ve acil uzaktan öğretim literatürü

Acil uzaktan öğretim–planlı çevrim içi öğrenme ayrımı (Hodges ve ark., 2020).

Harmanlanmış öğrenmenin yükseköğretimdeki potansiyelini tartışan çalışmalar (Garrison & Kanuka, 2004).

Ayrıca COVID-19 bağlamında yanlış bilgiye ilişkin infodemi çalışmaları da yanlış bilgi boyutunun tartışılması için kullanılmıştır (Cinelli ve ark., 2020).

Veri Analizi

Dokümanlar, üç aşamalı bir tematik analiz sürecine tabi tutulmuştur:

Açık Kodlama: Beslenme–bağışıklık, gıda güvenliği, yanlış bilgi, dijital öğrenme ve öğretim stratejileri ile ilgili anlamlı ifadeler kodlanmıştır.

Eksen Kodlama: Benzer kodlar bir araya getirilerek daha üst düzey kategoriler oluşturulmuştur (örneğin "mikro besin–immünite", "yanlış bilgi okuryazarlığı", "acil uzaktan öğretimden planlı çevrim içi öğrenmeye geçiş").

Seçici Kodlama: Bu kategoriler, dersin yeniden yapılandırılmasını açıklayan üç ana tema altında bütünleştirilmiştir: bilimsel içerik modernizasyonu, öğrenci merkezli pedagojik dönüşüm ve dijital öğrenme ekosistemlerinin kalıcılaşması.

Çalışma yalnızca kamuya açık dokümanları analiz ettiğinden, etik kurul izni gerekmemiştir.

BULGULAR

Tematik analiz sonucunda üç ana tema ve bunları destekleyen çok sayıda alt tema belirlenmiştir.

Bilimsel İçerik Modernizasyonu

Pandemi sonrası *Beslenme ve Sağlık* dersinin içeriğinde en belirgin değişim, bağışıklık fizyolojisi ve mikro besin–immünite ilişkilerine ayrılan yerin artmasıdır. Beslenme ve bağışıklık ilişkisini ele alan derlemelerde, yaşlanma, obezite, mikro besin eksiklikleri ve bağırsak mikrobiyotası gibi faktörlerin immün sistem üzerindeki etkileri ayrıntılı biçimde sunulmuştur (Calder, 2020, 2021; Govers ve ark., 2022).

Ders kapsamında artık yalnızca "C vitamini bağışıklığı güçlendirir" gibi düz cümleler yerine:

C vitamininin nötrofil fonksiyonu, oksidatif stres ve solunum yolu enfeksiyonlarıyla ilişkisi (Carr & Rowe, 2020; Cerullo ve ark., 2020),

Çinkonun antiviral immün yanıt ve solunum yolu enfeksiyonları bağlamındaki etkileri (Sadeghsoltani ve ark., 2022; Govers ve ark., 2022),

Çoklu mikro besin eksikliklerinin immün yanıtı nasıl zayıflattığı

gibi mekanizma odaklı içeriklere yer verilmektedir.

DSÖ'nün beslenme tavsiyeleri de ders materyallerine doğrudan entegre edilmiştir; böylece öğrenciler hem akademik çalışmaları hem de küresel sağlık otoritelerinin rehberlerini birlikte yorumlayabilmektedir (WHO, 2020).

Öğrenci Merkezli Pedagojik Dönüşüm

İkinci ana tema, dersin öğrenen merkezli yöntemlerle zenginleştirilmesidir. Problem temelli öğrenme (PBL) senaryoları ve vaka analizleri aracılığıyla öğrenciler, pandemi dönemine özgü karmaşık problemlere çözüm üretmektedir. Örneğin:

Gelir düzeyi kısıtlı bir ailenin, DSÖ'nün önerdiği dengeli beslenme ilkelerine mümkün olduğunca yaklaşmasını sağlayacak haftalık menü tasarlanması,

Sosyal medyada sık dolaşan "tek bir besinle bağışıklığı mucizevi biçimde güçlendirme" iddialarının bilimsel açıdan eleştirel incelenmesi,

Çinko ve C vitamini içeren takviye reklamlarının klinik kanıtlar ışığında değerlendirilmesi.

Bu süreç, öğrencilerin hem bilimsel muhakeme hem de yanlış bilgiye karşı direnç geliştirmelerini desteklemektedir. COVID-19'a ilişkin infodemi çalışmalarında yanlış bilginin dijital ağlarda salgın benzeri dinamiklerle yayıldığının gösterilmesi, bu tür pedagojik uygulamaların önemini artırmaktadır (Cinelli ve ark., 2020).

Ayrıca öğrencilerden, mikro besin–immünite ilişkilerini ve gıda güvenliği ilkelerini açıklayan infografikler hazırlamaları istenmekte; bu da soyut biyolojik mekanizmaları görselleştirerek öğrenmeyi kolaylaştırmaktadır.

Dijital Öğrenme Ekosistemlerinin Kalıcılaşması

Üçüncü tema, pandeminin başında zorunlulukla devreye giren dijital araçların, zaman içinde dersin kalıcı ve planlı bileşenleri hâline gelmesidir. Çevrim içi öğretimin kriz dönemindeki kullanımına ilişkin eleştiriler, acil uzaktan öğretim ile planlı çevrim içi öğrenme arasındaki farkın altını çizmektedir (Hodges ve ark., 2020). Bu fark gözetilerek, dersin dijital boyutu yeniden tasarlanmıştır.

Bu çerçevede: bağışıklık ve beslenme konularını işleyen **mikro ders videoları** hazırlanmış,

ders içeriği ve ölçme-değerlendirme süreçleri bir **öğrenme yönetim sistemi** üzerinden yürütülmeye başlanmış,

DSÖ ve UNESCO gibi kurumların çevrim içi kaynaklarına doğrudan bağlantılar verilmiş (WHO, 2020; UNESCO, 2020; UNICEF, 2023),

öğrencilerin yansıtıcı günlükler, forum tartışmaları ve çevrim içi quizler yoluyla etkin katılımı teşvik edilmiştir.

Bu yapı, dersin hem yüz yüze hem de çevrim içi yürütülebilmesine imkân tanıyan hibrit bir esneklik sağlamaktadır. Harmanlanmış öğrenmenin yükseköğretimde derin öğrenmeyi destekleyebileceğine ilişkin bulgular, bu tasarımın kuramsal temelini güçlendirmektedir (Garrison & Kanuka, 2004).

4. TARTIŞMA

Bulgular, *Beslenme ve Sağlık* dersinin COVID-19 sürecinde yalnızca "uzaktan verilmeye başlanmış" bir ders olmadığını; aksine bilimsel içerik, pedagojik yaklaşım ve teknolojik altyapı bakımından yeniden inşa edildiğini göstermektedir.

Bilimsel Derinlik ve Güncellik

Beslenme–bağışıklık literatüründe elde edilen bulgular, dersin kuramsal içeriğinin güncellenmesine güçlü bir temel sağlamıştır (Calder, 2020, 2021; Carr & Rowe, 2020; Sadeghsoltani ve ark., 2022; Govers ve ark., 2022). Bu sayede öğrenciler, vitamin ve mineral önerilerini ezberlemek yerine, bu besin öğelerinin bağışıklık hücreleri, sitokinler ve inflamasyon üzerindeki etkilerini öğrenmektedir. C vitamini ve çinko örnekleri, solunum yolu enfeksiyonları bağlamında özellikle öğretici birer vaka niteliği taşımaktadır.

Bu durum, dersi pandemi sonrasına da taşınabilecek şekilde güncel ve esnek kılmakta; yalnızca SARS-CoV-2 değil, diğer enfeksiyonlar ve kronik hastalıklar bağlamında da değerlendirilebilir bir bilgi zemini oluşturmaktadır.

Eleştirel Düşünme ve Yanlış Bilgiye Karşı Dayanıklılık

COVID-19 infodemisi, bilginin dijital ortamlarda nasıl yayıldığına dair daha derin bir analiz gerektirmiştir. Sosyal medya platformlarında yanlış bilginin yayılımını inceleyen çalışmalar, beslenme ve sağlık eğitiminde yanlış bilgi okuryazarlığının ayrı bir öğretim hedefi olarak ele alınması gerektiğini göstermektedir (Cinelli ve ark., 2020).

Bu çalışmanın bulguları, ders kapsamında problem temelli öğrenme ve vaka analizlerinin kullanılmasıyla öğrencilerin:

bilgi kaynağının güvenilirliğini sorgulama,

kanıt düzeylerini (gözlem, deney, sistematik derleme vb.) ayırt etme,

sosyal medyada karşılaştıkları beslenme iddialarını bilimsel ölçütlerle değerlendirme

becerilerini geliştirdiklerini göstermektedir. Bu kazanımlar, yalnızca akademik başarıyı değil, öğrencilerin bireysel ve toplumsal sağlık kararlarını da doğrudan etkileme potansiyeline sahiptir.

Dijital Dönüşümün Yapısal İyileştirme Olarak Konumlanması

Acil uzaktan öğretim sürecinde dijital araçlar çoğu zaman kısa vadeli çözümler olarak kullanılmıştır (Hodges ve ark., 2020). Ancak elde edilen bulgular, *Beslenme ve Sağlık* dersinde dijital bileşenlerin pandemi sonrasında da sürdürülebilecek biçimde yeniden tasarlandığını göstermektedir. Kısa videolar, resmî kurumların dijital kaynakları ve öğrenme yönetim sistemlerinin birlikte kullanılması, dersin gelecekteki olası krizlere karşı daha dayanıklı hâle gelmesini sağlamaktadır.

UNESCO ve UNICEF'in post-COVID eğitim raporlarında vurgulanan "eşitlik, erişilebilirlik ve dayanıklılık" ilkeleri, bu dönüşümü değerlendirmek için önemli bir çerçeve sunmaktadır (UNESCO, 2020; UNICEF, 2023). Özellikle çevrim içi içeriklerin asenkron biçimde erişilebilir olması, farklı sosyoekonomik ve coğrafi koşullara sahip öğrenciler için fırsat eşitliği açısından önem taşımaktadır.

İçerik–Pedagoji–Teknoloji Üçgeni

Bulgular bütüncül olarak ele alındığında, dersin dönüşümünü açıklamak için içerik–pedagoji–teknoloji üçgenine dayalı bir model önerilebilir:

İçerik: Güncel beslenme–bağışıklık literatürü ve resmî sağlık rehberleriyle güçlendirilmiş ders içeriği,

Pedagoji: Öğrenci merkezli, problem temelli, vaka analizi odaklı yöntemler,

Teknoloji: Hibrit öğrenmeyi destekleyen, planlı biçimde entegre edilmiş dijital araçlar.

Bu üç unsur birlikte ele alındığında, ders yalnızca pandemi döneminin "kriz ürünü" olmaktan çıkmakta; uzun vadeli, sürdürülebilir bir eğitim modeline dönüşmektedir.

SONUÇ VE ÖNERİLER

Bu nitel doküman analizi, *Beslenme ve Sağlık* dersinin COVID-19 pandemisi sürecinde üç temel boyutta yeniden yapılandırıldığını ortaya koymaktadır:

Bilimsel içerik güncellenmiş ve derinleşmiştir. Mikro besin–immünite ilişkileri, bağışıklık fizyolojisi ve gıda güvenliği gibi konular, hem literatür hem de resmî rehberler temel alınarak dersin merkezine yerleştirilmiştir (Calder, 2020, 2021; Carr & Rowe, 2020; Sadeghsoltani ve ark., 2022; WHO, 2020).

Pedagojik yaklaşım öğrenci merkezli hâle gelmiştir. Problem temelli öğrenme, vaka analizi, infografik hazırlama ve yansıtıcı yazma gibi etkinlikler aracılığıyla öğrencilerin eleştirel düşünme ve yanlış bilgiye karşı direnç becerileri güçlenmiştir (Cinelli ve ark., 2020).

Dijital öğrenme araçları kalıcı bir bileşen olarak kurumsallaşmıştır. Mikro ders videoları, öğrenme yönetim sistemleri ve resmî dijital kaynakların entegrasyonu, hibrit ve esnek bir öğrenme ortamı sunmuştur (Hodges ve ark., 2020; Garrison & Kanuka, 2004; UNESCO, 2020; UNICEF, 2023).

Uygulayıcılara Yönelik Öneriler

Ders içerikleri, beslenme–bağışıklık literatüründeki gelişmeler doğrultusunda düzenli aralıklarla güncellenmelidir.

Bilimsel kanıt türleri, yanlış bilgi ve medya okuryazarlığı, dersin açık biçimde belirtilmiş öğrenme çıktıları arasına dâhil edilmelidir.

Çevrim içi bileşenler, yalnızca kriz dönemlerinde değil, yüz yüze eğitimi tamamlayan planlı birer araç olarak tasarlanmalıdır.

Öğrencilerin kendi beslenme davranışlarını yansıtıcı günlükler, beslenme takip formları veya dijital uygulamalar aracılığıyla analiz etmeleri teşvik edilmelidir.

Gelecek Çalışmalar İçin Öneriler

Bu çalışma doküman analizi ile sınırlıdır. Gelecekte:

Öğrenci görüşlerinin,

Öğretim elemanlarının deneyimlerinin ve

Ölçme-değerlendirme sonuçlarının

nitel veya karma yöntemlerle incelenmesi, dersin pandemi sonrası etkilerinin daha kapsamlı değerlendirilmesine katkı sağlayacaktır.

KAYNAKLAR

Calder, P. C. (2020). Nutrition, immunity and COVID-19. *BMJ Nutrition, Prevention & Health*, 3(1), 74–92.

Calder, P. C. (2021). Nutrition and immunity: Lessons for COVID-19. *European Journal of Clinical Nutrition*, 75, 1309–1318.

Carr, A. C., & Rowe, S. (2020). The emerging role of vitamin C in the prevention and treatment of COVID-19. *Nutrients*, 12(11), 3286.

Cerullo, G., et al. (2020). The long history of vitamin C: From prevention of the common cold to potential aid in the treatment of COVID-19. *Frontiers in Immunology*, 11, 574029.

Cinelli, M., Quattrociocchi, W., Galeazzi, A., et al. (2020). The COVID-19 social media infodemic. *Scientific Reports*, 10, 16598.

Garrison, D. R., & Kanuka, H. (2004). Blended learning: Uncovering its transformative potential in higher education. *The Internet and Higher Education*, 7(2), 95–105.

Govers, C., et al. (2022). Ingestion, immunity, and infection: Nutrition and viral respiratory tract infections. *Frontiers in Immunology*, 13, 841532.

Hodges, C., Moore, S., Lockee, B., Trust, T., & Bond, A. (2020). The difference between emergency remote teaching and online learning. *EDUCAUSE Review*.

Sadeghsoltani, F., et al. (2022). Zinc and respiratory viral infections: Important trace element in antiviral response and immune regulation. *Biological Trace Element Research*.

UNESCO. (2020). *Education in a post-COVID world: Nine ideas for public action*.

UNICEF. (2023). *Education in a post-COVID world: Towards a RAPID transformation*.

WHO. (2020). *Nutrition advice for adults during the COVID-19 outbreak*. World Health Organization, Regional Office for the Eastern Mediterranean.

ORAL PRESENTATION

Hexavalent chromium removal using modified zeolites

İlker Acar (Orcid: https://orcid.org/0000-0001-9439-1580)

Atatürk University, Engineering Faculty, Department of Environmental Engineering, Erzurum, Türkiye.

Corresponding author e-mail: ilker.acar@atauni.edu.tr

Abstract

Hexavalent chromium (Cr(VI)) is a highly toxic and mobile pollutant in aquatic environments, necessitating efficient removal methods. This study investigates the adsorption performance of modified natural zeolites for Cr(VI) removal from aqueous solutions. Raw zeolite (RZ) was modified using various salts ($CaCl_2$, $MgCl_2 \cdot 6H_2O$, NH_4Cl) and a cationic surfactant, cetyltrimethylammonium bromide (CTAB). Batch adsorption experiments revealed that the surfactant-modified zeolite (SMZ) exhibited the highest Cr(VI) removal efficiency of 29.69%, significantly outperforming the raw and salt-modified zeolites, due to the formation of a positively charged surface that enhances electrostatic attraction. Consequently, SMZ was selected for further parametric studies. The optimal conditions for Cr(VI) adsorption on SMZ were determined as a contact time of 120 minutes, an adsorbent dosage of 10 g/L, and an initial solution pH of 5. Under these optimal conditions, a maximum removal efficiency of 96.01% was achieved for an initial Cr(VI) concentration of 25 mg/L. The results demonstrate that surfactant modification is a highly effective method for enhancing the anion adsorption capacity of natural zeolites, making SMZ a promising and efficient adsorbent for the remediation of Cr(VI)-contaminated wastewater.

Keywords: Hexavalent chromium, Adsorption, Surfactant-modified zeolite, Water treatment.

INTRODUCTION

Hexavalent chromium (Cr(VI)) is a highly toxic and carcinogenic pollutant frequently released from electroplating, leather tanning, textile dyeing, and pigment manufacturing processes. Due to its high solubility and mobility in aqueous environments, Cr(VI) poses a serious threat to both ecosystems and human health, leading to severe biological accumulation, genetic mutations, and organ damage. The World Health Organization (WHO) limits total chromium in drinking water to 0.05 mg/L, highlighting the need for effective removal methods (Saha et al., 2011; Sharma et al., 2022).

Various techniques such as chemical precipitation, ion exchange, and membrane filtration have been employed for Cr(VI) removal; however, adsorption remains the most efficient and economical method (Hailu et al., 2017; Ren et al., 2016; Song et al., 2015). Zeolites, due to their large surface area and ion-exchange properties, are promising adsorbents. Yet, natural zeolites show limited affinity for anionic species like chromate and dichromate ions, necessitating surface modification (Sharma et al., 2022; Shi et al., 2018; Song et al., 2015). Surface modification using surfactants or metal oxides enhances the anion-exchange capacity of zeolites, thereby enabling efficient Cr(VI) adsorption (Hailu et al., 2017; Lv et al., 2014; Song et al., 2015).

This study aims to evaluate the efficiency of modified zeolites in removing Cr(VI) from aqueous solutions and to examine the effects of modification type, contact time, adsorbent dosage, and pH on removal performance.

MATERIALS AND METHODS

Natural zeolite was obtained from a local supplier and used as the base adsorbent. The modification of the raw zeolite (RZ) sample was carried out using chemical methods involving various salts and a cationic surfactant after physical pretreatment with sieving and washing processes. In this context, calcium chloride ($CaCl_2$), magnesium chloride hexahydrate ($MgCl_2 \cdot 6H_2O$), and ammonium chloride (NH_4Cl) salts, as well as the cationic surfactant cetyltrimethylammonium bromide (CTAB, $C_{19}H_{42}NBr$), were used. Distilled water and analytical grade chemicals, including potassium dichromate ($K_2Cr_2O_7$) as the Cr(VI) source and hydrochloric acid (HCl) and sodium hydroxide (NaOH) for pH adjustment, were used throughout the experiments.

In the salt modification, 10 g of the pretreated sample was added to 100 mL of a 2 M solution of the respective salt and stirred at 200 rpm for 12 hours. The obtained modified zeolites were separated from the solution by filtration, thoroughly washed with distilled water, and dried at 105 °C for 12 hours (Huang et al., 2014; Zhan et al., 2017). The zeolites modified with $CaCl_2$, $MgCl_2 \cdot 6H_2O$, and NH_4Cl were designated as CMZ, MMZ, and NMZ, respectively. On the other hand, for the surfactant modification, 10 g of the pretreated zeolite was placed into a 0.05 M CTAB solution (50 mL) and agitated in a thermostatic shaker at 25 °C and 150 rpm for 24 hours. The resulting surfactant-modified zeolite (SMZ) was centrifuged at 6000 rpm for 10 minutes, washed three times with distilled water, and then dried at 70 °C for 24 hours (Dionisiou et al., 2013; Schick et al., 2012).

Batch adsorption studies were conducted to evaluate Cr(VI) removal efficiency. All experiments were performed in a thermostatic shaker at 25 °C and 200 rpm, using a constant solution volume of 100 mL. After determining the best modification route, parameters such as contact time (15-480 min), adsorbent dosage (1.0–12.5 g/L), and initial pH (3–8) were varied systematically. Cr(VI) concentrations before and after adsorption were directly measured using UV–Vis spectrophotometry at 350 nm (Sanchez-Hachair & Hofmann, 2018). Cr(VI) removal efficiency (RE, %) was calculated from Eq. 1, in which C_0 and C_e express the concentrations of Cr(VI) in solution at initial and equilibrium, respectively.

$$RE\,(\%) = \left(\frac{C_0 - C_e}{C_0}\right) \times 100 \qquad (1)$$

RESULTS and DISCUSSION

The Cr(VI) removal performance of raw and modified zeolites is presented in Figure 1. The experiments were performed without pH adjustment using an initial Cr(VI) concentration of 50 mg/L, an adsorbent dosage of 5 g/L, and a contact time of 24 h.

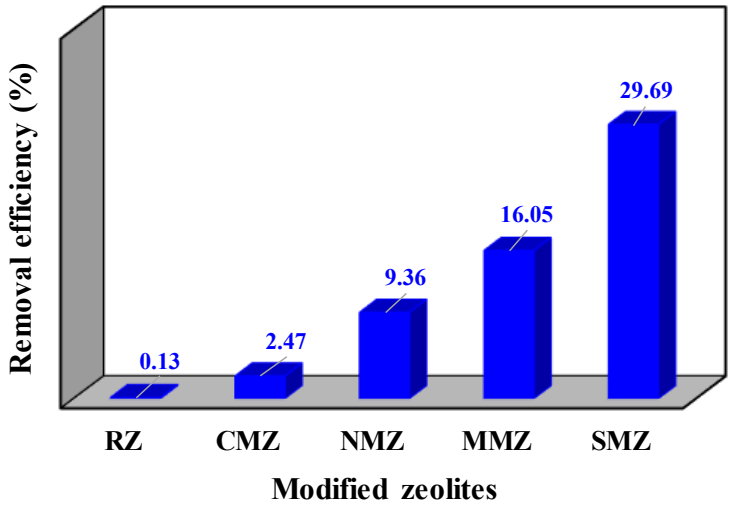


Figure 1. The effect of modification process on Cr(VI) removal efficiency.

As seen in Figure 1, the removal efficiency of Cr(VI) increased significantly after magnesium salt and especially cationic surfactant modifications. In particular, while RZ showed only 0.13% removal efficiency, markedly higher values of 9.36% and 16.05% were obtained for NMZ and MMZ, respectively. This improvement can be attributed to enhanced surface charge introduced by cation exchange. The SMZ sample, modified with CTAB, exhibited the highest performance (29.69%) due to the increased availability of active adsorption sites and the formation of a positively charged surface that facilitates electrostatic attraction of negatively charged chromate ions (Song et al., 2015). Therefore, SMZ was further investigated for the effects of contact time, adsorbent dosage and initial pH.

The effect of contact time (15–480 min) was examined under natural pH (≈ 5.5) using an initial concentration of 25 mg/L and SMZ dosage of 10 g/L. As shown in Figure 2, the adsorption of Cr(VI) on SMZ increased rapidly during the initial stage and reached equilibrium after about 120 min. In particular, the removal efficiency increased from 83.01% to 94.72% as the contact time was extended from 15 to 120 min, beyond

which minor increases up to 95.11% and 95.37% were noted at 240 and 480 min, respectively. The rapid initial adsorption can be attributed to the abundance of available surface sites, while the plateau indicates that the adsorption reached saturation. This behavior is typical for monolayer adsorption processes where surface coverage becomes limited over time. The optimum contact time was determined as 120 min, which was then used to examine the effects of dosage and initial pH.

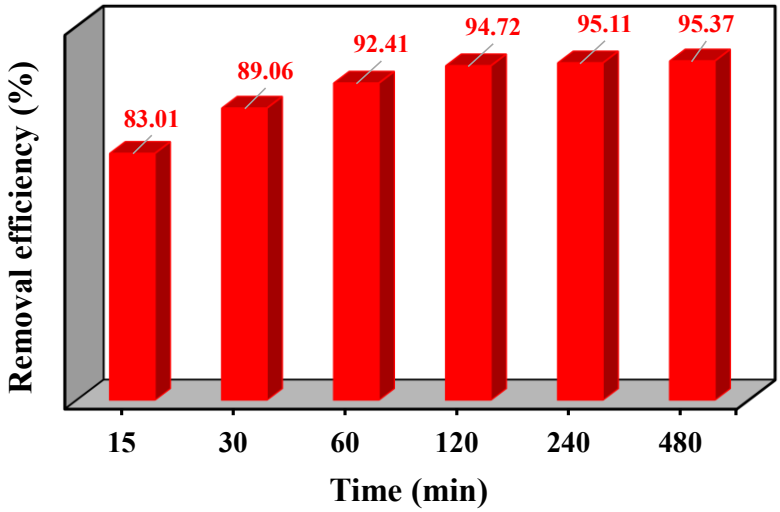


Figure 2. The effect of contact time on the removal efficiency of Cr(VI).

The influence of SMZ dosage (1.0–12.5 g/L) was examined at 120 min under natural pH using an initial Cr(VI) concentration of 25 mg/L, and the results obtained are presented in Figure 3. As seen in Figure 3, increasing SMZ dosage from 1.0 to 7.5 g/L resulted in an almost steady rise in Cr(VI) removal efficiency from 19.82% to 86.62%. This can be explained by the greater number of active binding sites (Hailu et al., 2017). The increasing rate became significantly slower beyond 7.5 g/L, and the efficiency reached to 94.72% for 10 g/L. A negligible increase to 95.24% was then noted for 12.5 g/L. Considering the balance between maximizing efficiency and maintaining practical operational conditions, 10 g/L was selected as the optimum SMZ dosage.

The effect of initial pH (3–8) was examined at 120 min using an initial Cr(VI) concentration of 25 mg/L and SMZ dosage of 10 g/L. As shown in Figure 4, the initial pH of the solution had a profound influence on the Cr(VI) removal efficiency. The maximum removal efficiency of 96.01% was achieved at pH 5. As the pH increased, the efficiency declined gradually to 92.41% at pH 6, and then sharply to 79.15% and 65.89% at pH 7 and 8, respectively. On the other hand, the efficiency decreased more gradually to 90.60% and 85.71% at pH 4 and 3, respectively.

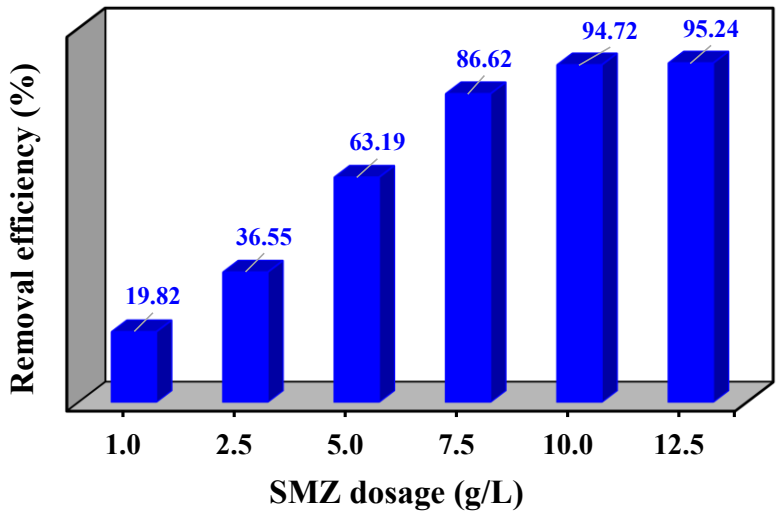


Figure 3. The effect of SMZ dosage on the removal efficiency of Cr(VI).

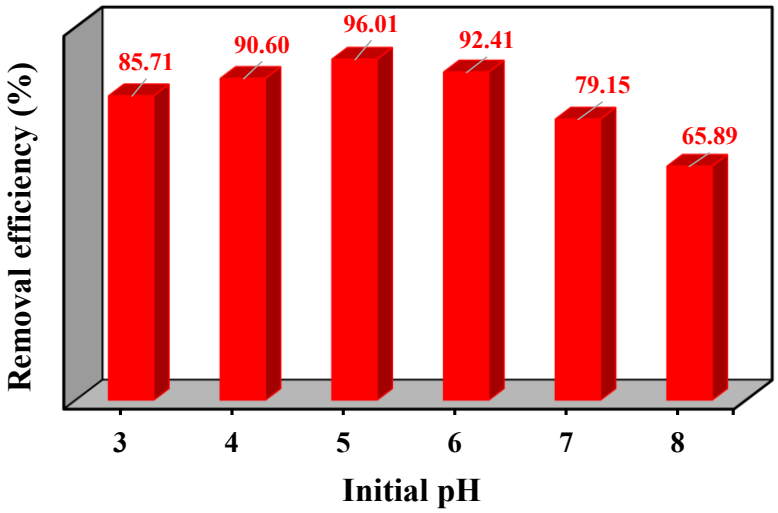


Figure 4. The effect of initial pH on the removal efficiency of Cr(VI).

This strong pH dependence is directly related to the surface charge of the SMZ adsorbent and the speciation of Cr(VI) in aqueous solution. At low pH, the surface of the CTAB-modified zeolite is strongly positively charged, and the predominant Cr(VI) species is the monovalent hydrogen chromate ion ($HCrO_4^-$). This leads to strong electrostatic attraction and high adsorption capacity. As the pH increases, the concentration of OH^- ions rises, which competes with Cr(VI) anions for adsorption sites. Furthermore, the surface of the SMZ becomes less positively charged, reducing the electrostatic driving force for adsorption. At neutral to basic pH, the predominant Cr(VI) species is the divalent chromate ion (CrO_4^{2-}), which experiences greater electrostatic repulsion from the increasingly neutral or negatively charged adsorbent surface, resulting in the observed decrease in removal efficiency (Hailu et al., 2017; Ren et al., 2016).

CONCLUSION

In conclusion, surfactant modification with CTAB transforms natural zeolite into a highly effective and low-cost adsorbent for Cr(VI) decontamination. The findings provide clear operational guidelines, emphasizing the necessity of acidic conditions for optimal performance, for its potential application in treating industrial wastewater contaminated with this hazardous heavy metal.

REFERENCES

Dionisiou, N. S., Matsi, T., & Misopolinos, N. D. (2013). Phosphorus adsorption-desorption on a surfactant-modified natural zeolite: A laboratory study. *Water, Air, and Soil Pollution*, *224*(1), 1–10. https://doi.org/10.1007/S11270-012-1362-7/FIGURES/5

Hailu, S. L., Nair, B. U., Redi-Abshiro, M., DIaz, I., & Tessema, M. (2017). Preparation and characterization of cationic surfactant modified zeolite adsorbent material for adsorption of organic and inorganic industrial pollutants. *Journal of Environmental Chemical Engineering*, *5*(4), 3319–3329. https://doi.org/10.1016/J.JECE.2017.06.039

Huang, H., Xiao, D., Pang, R., Han, C., & Ding, L. (2014). Simultaneous removal of nutrients from simulated swine wastewater by adsorption of modified zeolite combined with struvite crystallization. *Chemical Engineering Journal*, *256*, 431–438. https://doi.org/10.1016/J.CEJ.2014.07.023

Lv, G., Li, Z., Jiang, W. T., Ackley, C., Fenske, N., & Demarco, N. (2014). Removal of Cr(VI) from water using Fe(II)-modified natural zeolite. *Chemical Engineering Research and Design*, *92*(2), 384–390. https://doi.org/10.1016/J.CHERD.2013.08.003

Ren, H., Jiang, J., Wu, D., Gao, Z., Sun, Y., & Luo, C. (2016). Selective Adsorption of Pb(II) and Cr(VI) by Surfactant-Modified and Unmodified Natural Zeolites: A Comparative Study on Kinetics, Equilibrium, and Mechanism. *Water, Air, & Soil Pollution 2016 227:4*, *227*(4), 101-. https://doi.org/10.1007/S11270-016-2790-6

Saha, R., Nandi, R., & Saha, B. (2011). Sources and toxicity of hexavalent chromium. *Journal of Coordination Chemistry*, *64*(10), 1782–1806. https://doi.org/10.1080/00958972.2011.583646;WGROUP:STRING:PUBLICATION

Sanchez-Hachair, A., & Hofmann, A. (2018). Hexavalent chromium quantification in solution: Comparing direct UV–visible spectrometry with 1,5-diphenylcarbazide colorimetry. *Comptes Rendus Chimie*, *21*(9), 890–896. https://doi.org/10.1016/J.CRCI.2018.05.002

Schick, J., Caullet, P., Paillaud, J.-L., Patarin, J., Freitag, S., & Mangold-Callarec, C. (2012). Phosphate uptake from water on a Surfactant-Modified Zeolite and Ca-zeolites. *Journal of Porous Materials*, *19*, 405–414. https://doi.org/10.1007/s10934-011-9488-3

Sharma, P., Singh, S. P., Parakh, S. K., & Tong, Y. W. (2022). Health hazards of hexavalent chromium (Cr (VI)) and its microbial reduction. *Bioengineered*, *13*(3), 4923–4938. https://doi.org/10.1080/21655979.2022.2037273

Shi, J., Yang, Z., Dai, H., Lu, X., Peng, L., Tan, X., Shi, L., & Fahim, R. (2018). Preparation and application of modified zeolites as adsorbents in wastewater treatment. *Water Science and Technology*, *2017*(3), 621–635. https://doi.org/10.2166/WST.2018.249

Song, W., Shi, T., Yang, D., Ye, J., Zhou, Y., & Feng, Y. (2015). Pretreatment effects on the sorption of Cr(VI) onto surfactant-modified zeolite: Mechanism analysis. *Journal of Environmental Management*, *162*, 96–101. https://doi.org/10.1016/J.JENVMAN.2015.07.010

Zhan, Y., Zhang, H., Lin, J., Zhang, Z., & Gao, J. (2017). Role of zeolite's exchangeable cations in phosphate adsorption onto zirconium-modified zeolite. *Journal of Molecular Liquids*, *243*, 624–637. https://doi.org/10.1016/J.MOLLIQ.2017.08.091

ORAL PRESENTATION

Synthesis and structural characterization of a novel chromone–1,3,4-thiadiazole–hydrazone hybrid bearing a 4-fluorobenzyl moiety

Ayşen Işık (Orcid: https://orcid.org/0000-0002-1280-0019)

Selcuk University, Faculty of Science, Department of Biochemistry, Konya, Türkiye.

Corresponding author e-mail: isik.aysen@selcuk.edu.tr

Abstract

Heterocyclic compounds play a significant role in modern medicinal chemistry due to their structural diversity and broad biological applications. Among these compounds, the 1,3,4-thiadiazole nucleus stands out as a valuable pharmacophore due to its significant physicochemical properties and broad pharmacological activities. This is evidenced by the fact that many FDA-approved drugs currently contain a 1,3,4-thiadiazole ring (acetazolamide and methazolamide (diuretic, carbonic anhydrase inhibitor), sulfamethizole (antimicrobial), desaglybuzole (hypoglycemic agent), litronesib, and filanesib (anticancer)). The chromone skeleton, another important structure, forms the core of flavones and exhibits a variety of biological activities. Hydrazones are chemical structures that contribute to bioactivity through the –NH–N=CH– functionality, which supports biological interactions. In this study, a five-step synthesis route was successfully carried out to produce a new chromone-1,3,4-thiadiazole hydrazone hybrid containing fluorobenzyl. In the first step, p-Fluorobenzyl isothiocyanate was reacted with hydrazine hydrate in ethanol in an ice bath to obtain the thiocarbamoyl hydrazide derivative **(1)**. Then, to generate the 1,3,4-thiadiazole ring **(2)**, a cyclization step was conducted with the thiocarbamoyl hydrazide derivative **(1)** in the presence of carbon disulfide and sodium hydroxide under reflux in ethanol. Subsequently, the obtained intermediate **(2)** was subjected to S-alkylation with ethyl chloroacetate in acetone under reflux in the presence of potassium carbonate, affording the S-ethoxycarbonylmethyl-substituted thiadiazole derivative **(3)**. In the fourth step, the mixture of intermediate **(3)** and hydrazine hydrate in ethanol was boiled under reflux. The resulting solid product was collected by filtration, washed with cold ethanol, and dried to form the intermediate **(4)**. The last step, the 1,3,4-thiadiazole hydrazine derivative **(4)**, was boiled with 3-formyl-6-nitrochromone under reflux in the presence of ethanol to construct the target compound, the fluorobenzyl-containing chromone-1,3,4-thiadiazole hydrazone derivative **(5)**. The final structure was confirmed by ^{1}H-NMR and ^{13}C-NMR spectroscopic methods. Therefore, the existence of a new hybrid structure predicted to have broad biological activity by integrating these three pharmacophores into a single molecule has been demonstrated.

Keywords: 1,3,4-Thiadiazole, Chromone, Hydrazone, Fluorobenzyl derivative, Multi-pharmacophore hybrid molecules, NMR spectroscopy.

INTRODUCTION

Heterocyclic compounds are ring structures containing at least one heteroatom and constitute one of the most important subfields of organic chemistry. Heterocyclic systems containing heteroatoms such as nitrogen, oxygen, and sulfur, as well as phosphorus, magnesium, and selenium, are also common. These rings play critical roles in the structure of DNA, RNA, chlorophyll, hemoglobin, vitamins, amino acids, and other biomolecules (Abdel-Hafez, 2008). New-age drug discovery relies heavily on heterocyclic molecules. Today, more than 90% of commercially available drugs contain heterocyclic derivatives. Heterocyclic compounds are the primary pharmacophores of many natural and synthetic drugs, such as papaverine, morphine, diazepam, chlorpromazine, isoniazid, and metronidazole, and these molecules participate in many biochemical reactions in the body (Dua et al., 2011; Chin et al., 2006; Hughes and Shanks, 2002; Koehn and Carter, 2005; Karthikeyan et al., 2023). Synthetic heterocyclic derivatives, in particular, have a wide range of applications in medicinal chemistry due to their antibacterial, antifungal, antimycobacterial, antiviral, anthelmintic, anticancer, anti-inflammatory, analgesic, anticonvulsant, and many other therapeutic effects (Jampilek, J., 2019; Mallappa et al., 2025). To improve activity, selectivity, metabolic stability, and physicochemical characteristics, new synthetic methods and functionalization strategies are frequently needed during the clinical candidate discovery phase for small structural modifications, like methyl or fluorine additions, on the

heterocyclic skeleton (Taylor et al., 2016). Research interest in heterocyclic compounds is constantly on the rise due to their high chemical adaptability, their ability to meet the diverse needs of biological systems, and their versatile pharmacological activities. As a result, these compounds are at the center of the interaction between biology and chemistry.

Thiadiazoles, with the chemical formula $C_2H_2N_2S$, are aromatic heterocyclic and unsaturated organic compounds belonging to the azole family. Their five-membered rings containing two nitrogen atoms and one sulfur atom form the basis of the chemical reactivity and pharmacological properties specific to this class. This structure, which is rarely found in nature, allows the formation of four isomers: 1,2,3-, 1,2,4-, 1,2,5-, and 1,3,4-thiadiazole, as a result of different arrangements of nitrogen, sulfur, and carbon atoms (Hu et al., 2014). Among these isomers, 1,3,4-thiadiazole derivatives are the most investigated group in the literature due to their broad biological activity profiles and have been reported to exhibit many pharmacological activities, including antifungal (Karaburun et al., 2018), antimicrobial (El-Enany et al., 2021), anti-inflammatory (Gomha et al., 2017), and anticancer (Altintop et al., 2019). Recent studies have demonstrated that compounds with this nucleus can also exhibit antidiabetic, anticonvulsant, antituberculosis, antiviral, analgesic, antidepressant, anxiolytic, antihypertensive, local anesthetic, and various enzyme inhibitory properties. Advances in synthetic strategies have enabled the efficient addition of different substituents to the thiadiazole ring, enabling improved biological and chemical properties (Kumar et al., 2013; Zaki et al., 2025). However, challenges remain in optimizing reaction conditions, scalability, and selectivity, suggesting that this area remains open for future research.

Chromones, which address a broad therapeutic spectrum in pharmaceutical chemistry, provide a unique scaffold thanks to a γ-pyrone core fused to a benzo ring and have proven their clinical value with approved drugs such as disodium cromoglicate and flavoxate. Advances in synthetic methods have enabled the development of novel chromone derivatives that can selectively modulate diverse targets such as cancer, inflammation, diabetes, infectious diseases, and neurodegenerative disorders (Reis et al., 2017; Keri et al., 2014; Kaishap et al., 2025). Furthermore, their use as imaging probes and regulators of pharmacologically important targets such as pyridoxal phosphatase (PDXP) further expands their role in modern drug discovery (Kaishap et al., 2025). The chromone skeleton is a frequently preferred core structure in medicinal chemistry due to its amenability to structural modification, functional adaptability, and synthetic accessibility, and forms the fundamental backbone of many flavanols, flavones, isoflavones, and flavonoids (Lewandowski et al., 2020). Although there are studies on the chemical properties and biological activities of these compounds, the limited number of studies that comprehensively examine the molecular structure-activity relationships of chromones creates a significant gap in the literature.

Hydrazones, regarded as universal structural units, are significant synthetic chemicals utilized in the generation of carbon-nitrogen and nitrogen-heteroatom linkages. Hydrazones serve as useful intermediates in chemical synthesis, typically produced through the condensation of hydrazine with an aldehyde or ketone. Comprehensive research has shown that hydrazone derivatives serve as efficient precursors in the synthesis of diverse heterocyclic compounds, including pyrazoles, pyrazines, indazoles, tetrazoles, oxadiazoles, and thiadiazoles (Lv et al., 2021).

The aim of this study was to synthesize a new fluorobenzyl derivative of the chromone–1,3,4-thiadiazole–hydrazone hybrids, which have been reported only in the literature, and to characterize the resulting structure in detail using various spectroscopic techniques. It is anticipated that this new hybrid structure will contribute to the chemical diversity of heterocyclic systems and serve as a valuable example to the literature.

MATERIALS AND METHODS

Chemistry

All chemicals used throughout the synthetic studies were obtained from Sigma-Aldrich Chemicals (Sigma-Aldrich Corp., St. Louis, MO, USA) or Merck Chemicals (Merck KGaA, Darmstadt, Germany). The melting points of the final products were measured using an MP90 digital melting point apparatus (Mettler Toledo, OH, USA), and the values are reported without correction. The ^{1}H and ^{13}C NMR spectra of the synthesized compounds were recorded on Bruker FT-NMR spectrometers operating at 400 MHz and 100 MHz, respectively (Bruker Bioscience, Billerica, MA, USA), using DMSO-d6 as the solvent. In the NMR data, splitting patterns were identified as follows: s (singlet), d (doublet), t (triplet), and m (multiplet). Coupling constants (J) are expressed in Hertz. Reaction progress was routinely followed by thin-layer chromatography (TLC) on Silica Gel 60 F254 plates (Merck KGaA, Darmstadt, Germany).

Synthesis of N-(4-fluorobenzyl)hydrazinecarbothioamide (1):

4-Fluorobenzyl isothiocyanate was dissolved in ethanol (30 mL). Excess hydrazine hydrate was added dropwise in an ice bath for 2 h, and the precipitated product was filtered off. The residue was then dried and recrystallized from EtOH.

Synthesis of 5-(4-fluorobenzyl) amino)-1,3,4-thiadiazole-2-thiol (2):

A mixture of N-(4-fluorobenzyl)hydrazinecarbothioamide **(1)** (0.02 mol, 3.70 g) and carbon disulphide (0.024 mol, 1.44 mL) was added to EtOH (40 mL) containing NaOH (0.024 mol, 0.96 g) and refluxed for 4 h. After completion of the reaction, the mixture was poured into iced water and acidified with 20% HCl to pH 4–5. The precipitated product was filtered, washed with water, dried, and recrystallized from EtOH.

Synthesis of ethyl 2-((5-(4-fluorobenzyl) amino)-1,3,4-thiadiazol-2-yl) thio)acetate (3):

5-((4-fluorobenzyl) amino)-1,3,4-thiadiazole-2-thiol **(2)** and chloroethylacetate are dissolved in acetone. Potassium carbonate is added to it. The mixture is stirred under reflux for 4 hours at 40°C. The precipitated product is filtered off, washed with water and crystallized from ethanol.

Synthesis of 2-((5-((4-fluorobenzyl)amino)-1,3,4-thiadiazol-2-yl)thio)acetohydrazide (4):

Ethyl 2-((5-(4-fluorobenzyl) amino)-1,3,4-thiadiazol-2-yl) thio)acetate **(3)** was dissolved in ethanol and hydrazine hydrate was added. The mixture was heated under reflux for 2 hours and the precipitated part was filtered off.

Synthesis of 2-((5-((4-fluorobenzyl) amino)-1,3,4-thiadiazol-2-yl) thio)-N'-((6-nitro-4-oxo-4H-chromen-3-yl) methylene) acetohydrazide (5):

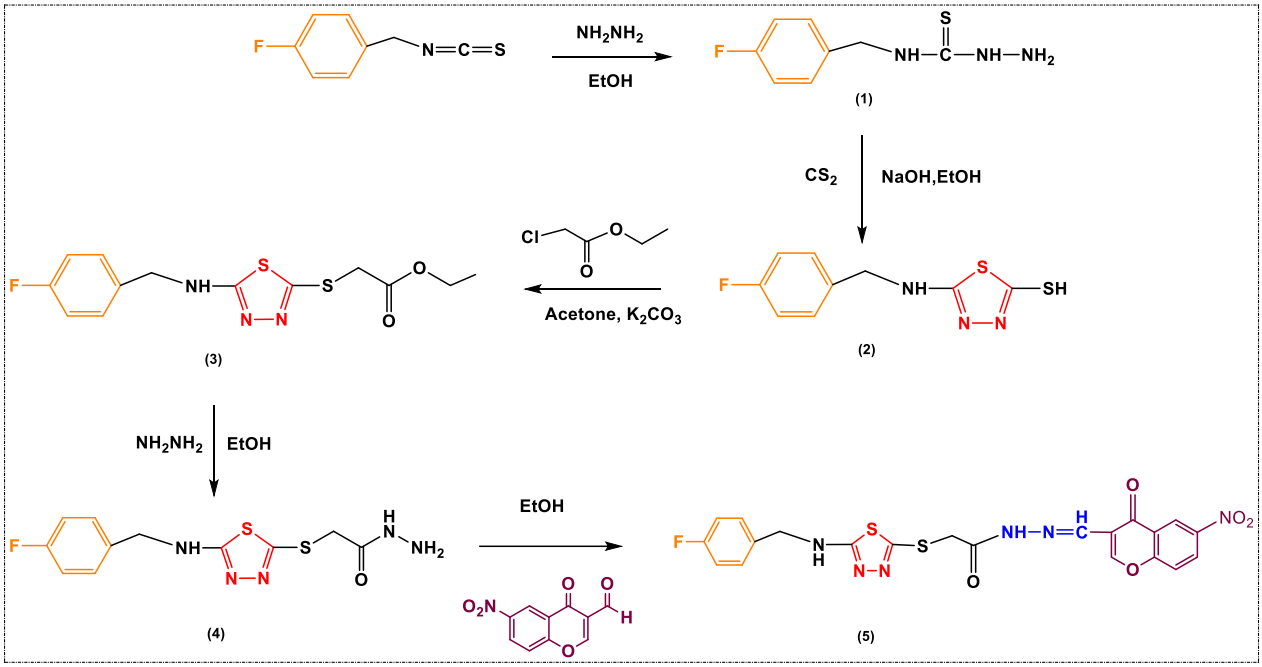
2-((5-((4-fluorobenzyl)amino)-1,3,4-thiadiazol-2-yl)thio)acetohydrazide **(4)** was dissolved in ethanol, and a few drops of acetic acid together with 6-nitro-4-oxo-4H-chromene-3-carbaldehyde (0.001 mol) were added. The mixture was heated under reflux for 2 hours, after which the precipitate was filtered off and crystallized from butanol.

Yield: 75%, M.P. = 136.7–138.3°C. ^{1}H-NMR (400 MHz, DMSO-*d6*): δ = 4.10 (2H, s, S-CH_2), 4.16 (2H, s, CH_2), 6.50 (1H, d, J=6.04 Hz, NH), 7.18 (2 H, s, 1,4-disubstituted benzene), 7.58–7.59 (2 H, m, 1,4-disubstituted benzene), 7.89-7.94 (1H, s, -CH), 8.40-8.42 (1 H, s, Aromatic CH), 8.50 (1H, dd, J=5.8 Hz, 0.72 Hz Aromatic CH), 8.55-8.58 (1H, s, Aromatic CH), 8.70-8.74 (1H, s, Aromatic CH), 10.39(1H, s, NH). ^{13}C-NMR (100 MHz, DMSO-*d6*): δ = 35.90, 61.77, 113.02, 116.10 (d, J (CF)=22.32 Hz), 119.55 (d, J (CF)=7.70 Hz), 121.50 (m, ArC, C-F coupling), 122.94, 123.74, 124.60, 128.89 (d, J (CF)= 5.94 Hz), 137.29 (d, J (CF)= 2.09 Hz), 144.85 (m, ArC, C-F coupling), 152.09, 156.57, 158.16, 158.94, 159.34 (m, ArC, C-F coupling), 165.56, 168.70, 175.91.

RESULTS and DISCUSSION

The synthesis scheme of the target new 1,3,4-thiadiazole-chromone-derived hydrazone compound is shown in **Scheme 1**. The synthesis first started with the preparation of N-(4-fluorobenzyl)hydrazinecarbothioamide **(1)**. For this purpose, 4-fluorobenzyl isothiocyanate was dissolved in ethanol and hydrazine hydrate was slowly added to the mixture in an ice bath. The solid precipitated at the end of the reaction was filtered and purified by recrystallization from ethanol. In the second step, thiosemicarbazide derivative **(1)** was reacted in the presence of carbon disulfide and ethanolic sodium hydroxide to obtain 5-(4-fluorobenzylamino)-1,3,4-thiadiazole-2-thiol **(2)** via cyclization. The reaction mixture was poured into ice water and the pH was adjusted to 4–5 with 20% HCl to precipitate the product. The resulting solid was filtered and washed and then crystallized from ethanol. In the third step, compound **(2)** was S-alkylated with chloroethylacetate in acetone in the presence of potassium carbonate to synthesize ethyl 2-((5-(4-fluorobenzyl)amino)-1,3,4-thiadiazol-2-yl)thioacetate **(3)**. The target product was formed by heating the mixture under reflux for four hours. By hydrazinolysis of the ester group, compound **(3)** was reacted with ethanolic hydrazine hydrate to obtain the main intermediate, 2-((5-(4-fluorobenzyl)amino)-1,3,4-thiadiazol-2-yl)thioacetohydrazide **(4)**. This hydrazide derivative was used as the basic building block in the condensation step. In the last step, hydrazide compound **(4)** was converted to the corresponding hydrazone derivative by heating with 6-nitro-4-oxo-4H-chromene-3-carboxyaldehyde under the catalysis of acetic acid in an ethanolic medium under reflux for 2 hours. The obtained solid was filtered, and the pure product was obtained by crystallization from butanol. The final compound, 2-((5-(4-fluorobenzyl)amino)-1,3,4-thiadiazol-2-yl)thio)-N'((6-nitro-4-oxo-4H-chromen-3-

yl)methylene)acetohydrazide **(5)**, has a hybrid structure that combines three basic pharmacophores: a 4-fluorobenzylamino unit, a 1,3,4-thiadiazole ring, and a hydrazone chain. The combination of these units in a single structure is anticipated to contribute to the broad biological activity potential of the molecule.



Scheme 1. Synthetic strategy for compounds 1-5.

Structural verification was accomplished using ^{1}H NMR and ^{13}C NMR spectroscopic analyses. In the ^{1}H NMR spectrum, the S-CH_2 and the CH_2 group adjacent to the carbonyl appeared as singlets at δ 4.10 and 4.16 ppm, respectively. The NH proton attached to the aryl group was observed as a doublet at δ 6.50 ppm (J = 6.04 Hz), while the imine proton (–CH=N–) appeared as a singlet at δ 7.89–7.94 ppm. The aromatic region displayed signals consistent with both the 1,4-disubstituted fluorobenzyl moiety and the chromone core. Fluorobenzyl protons resonated at δ 7.18 and 7.58–7.59 ppm, whereas chromone protons appeared within the δ 8.40–8.74 ppm range. Notably, the proton at δ 8.50 ppm exhibited a dd splitting pattern (J = 5.8, 0.72 Hz) due to long-range ^{1}H–^{19}F coupling. The acidic NH proton was detected as a singlet around δ 10 ppm. In the ^{13}C NMR spectrum, the S-CH_2 and CONH-CH_2 carbons were observed at δ 35.90 and 61.77 ppm, respectively. The aromatic carbons bearing fluorine exhibited characteristic C–F coupling-induced splittings (e.g., δ 116.10 ppm, d, J(CF) = 22.32 Hz; 119.55 ppm, d, J(CF) = 7.70 Hz; 128.89 ppm, d, J(CF) = 5.94 Hz). The chromone carbonyl carbons and the hydrazide carbonyl were identified at δ 165.56, 168.70, and 175.91 ppm, confirming the conjugated structural framework.

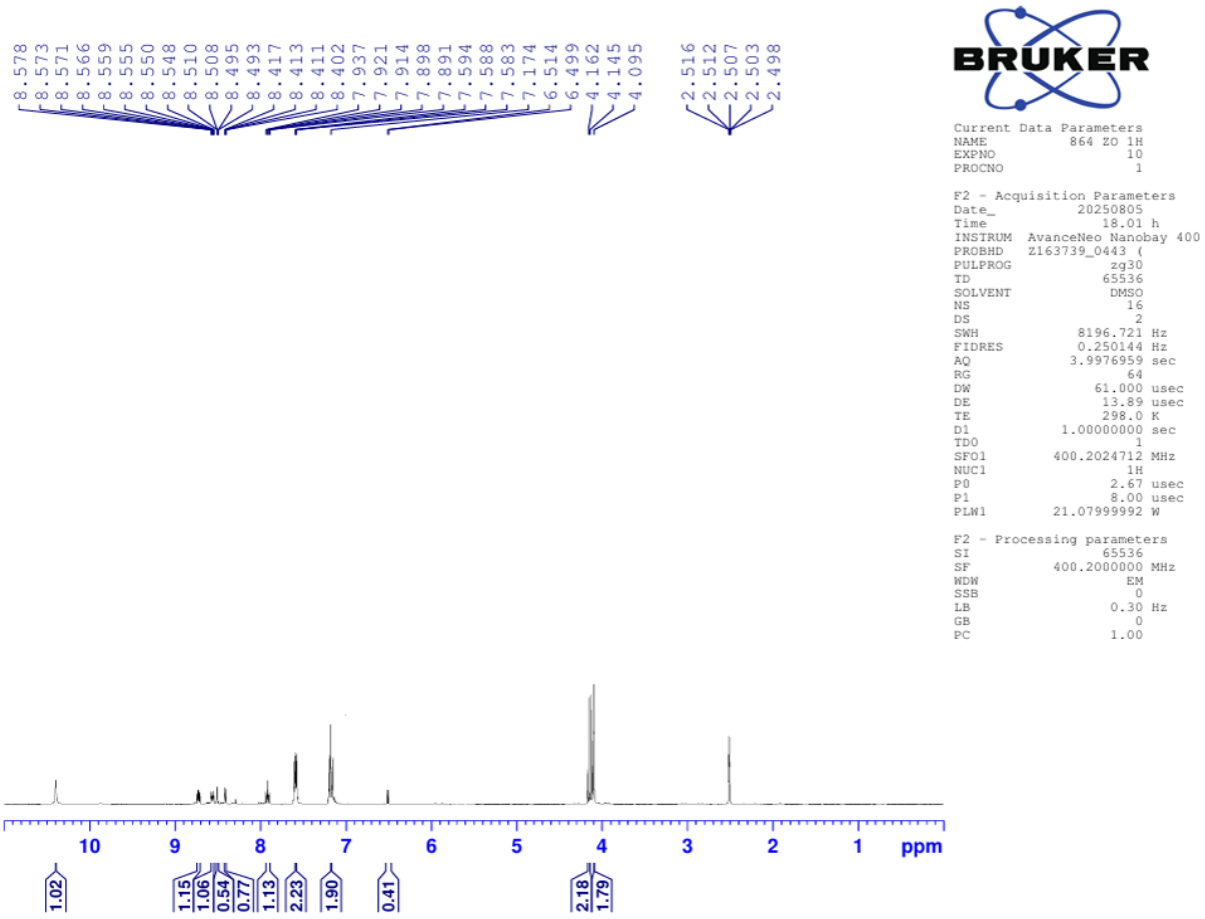


Figure 1. ^{1}H-NMR spectrum of 2-((5-((4-fluorobenzyl) amino)-1,3,4-thiadiazol-2-yl) thio)-N'-((6-nitro-4-oxo-4H-chromen-3-yl) methylene) acetohydrazide **(5)**.

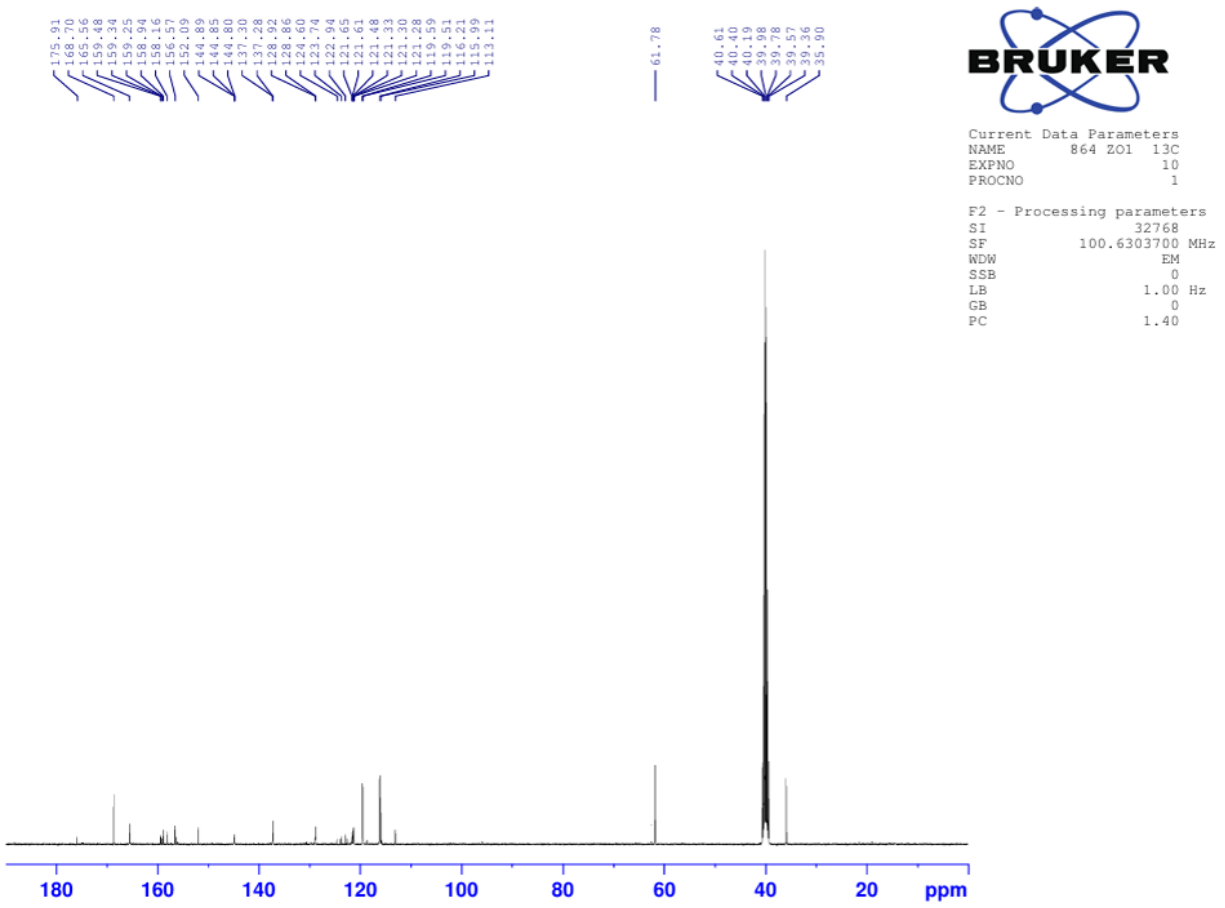


Figure 2. ^{13}C-NMR spectrum of 2-((5-((4-fluorobenzyl) amino)-1,3,4-thiadiazol-2-yl) thio)-N'-((6-nitro-4-oxo-4H-chromen-3-yl) methylene) acetohydrazide **(5)**.

CONCLUSION

In this study, a novel fluorobenzyl-substituted chromone-1,3,4-thiadiazole-hydrazone hybrid molecule was successfully synthesized via a five-step reaction. The synthetic strategy incorporated three biologically important structural motifs (chromone, 1,3,4-thiadiazole, and hydrazone) into a single molecular framework, enabling the efficient creation of a multi-pharmacophore molecule. Structural confirmation of the target compound was provided by ^{1}H-NMR and ^{13}C-NMR spectroscopy. This newly synthesized compound is expected to contribute to the molecular diversity of heterocyclic hybrid structures and serve as a promising scaffold for future biological activity screening. Further studies focusing on the evaluation of its pharmacological potential, structure-activity relationships, and molecular docking analyses are expected to expand the applicability of this hybrid framework in medicinal chemistry research.

REFERENCES

Abdel-Hafez, S. H. (2008). Selenium containing heterocycles: Synthesis, anti-inflammatory, analgesic and anti-microbial activities of some new 4-cyanopyridazine-3(2H) selenone derivatives. European Journal of Medicinal Chemistry, 43(9), 1971–1977.

Altintop, M. D., Sever, B., Ozdemir, A., Iglin, S., Alti, O., Turan-Zitouni, G., & Kaplancikli, Z. A. (2019). Synthesis and evaluation of a series of 1,3,4-thiadiazole derivatives as potential anticancer agents. *Anticancer Agents in Medicinal Chemistry*, 18, 1606–1616.

Chin, Y. W., Balunas, M. J., Chai, H. B., & Kinghorn, D. A. (2006). Drug discovery from natural sources. The AAPS Journal, 8(2), E239–E253.

Dua, R., Shrivastava, S., Sonwane, S. K., & Srivastava, S. K. (2011). Pharmacological significance of synthetic heterocycles scaffold: A review. *Advances in Biological Research*, 5(3), 120–144.

El-Enany, W. A. M. A., Gomha, S. M., Hussein, W., Sallam, H. A., Ali, R. S., & El-Ziaty, A. K. (2021). Synthesis and biological evaluation of some novel bis-thiadiazoles as antimicrobial and antitumor agents. *Polycyclic Aromatic Compounds*, 41(10), 2071–2120.

Gomha, S. M., Muhammad, Z. A., Gaber, H. M., & Amin, M. M. (2017). Synthesis of some novel heterocycles bearing thiadiazoles as potent anti-inflammatory and analgesic agents. *Journal of Heterocyclic Chemistry*, 54(5), 2708–2716.

Hu, Y., Li, C., Wang, X., Yang, Y., & Zhu, H. (2014). 1,3,4-Thiadiazole: Synthesis, reactions, and applications in medicinal, agricultural, and materials chemistry. *Chemical Reviews*, 114, 5572–5610.

Hughes, E. K., & Shanks, J. V. (2002). Metabolic engineering of plants for alkaloid production. *Metabolic Engineering*, 4(1), 41–48.

Jampilek, J. (2019). Heterocycles in medicinal chemistry. *Molecules*, **24**(21), 3839.

Kaishap, P. P., Laskar, B., Dutta, D., Gogoi, N., & Dey, T. (2025). Harnessing chromone as a versatile scaffold for emerging biological applications: Recent advances and medicinal insights. *The Chemical Record*, e202500073.

Karaburun, A., Acar Cevik, U., Osmaniye, D., Saglik, B., Kaya Cavusoglu, B., Levent, S., Ozkay, Y., Koparal, A., Behcet, M., & Kaplancikli, Z. A. (2018). Synthesis and evaluation of new 1,3,4-thiadiazole derivatives as potent antifungal agents. *Molecules*, 23, 3129.

Karthikeyan, S., Grishina, M., Kandasamy, S., Mangaiyarkarasi, R., Ramamoorthi, A., Chinnathambi, S., … & John Kennedy, L. (2023). A review on medicinally important heterocyclic compounds and importance of biophysical approach of underlying the insight mechanism in biological environment. *Journal of Biomolecular Structure and Dynamics*, 41(23), 14599–14619.

Keri, R. S., Budagumpi, S., Pai, R. K., & Balakrishna, R. G. (2014). Chromones as a privileged scaffold in drug discovery: A review. *European Journal of Medicinal Chemistry*, 78, 340–374.

Koehn, F. E., & Carter, G. T. (2005). The evolving role of natural products in drug discovery. *Nature Reviews Drug Discovery*, 4(3), 206–220.

Kumar, K. A., Kumar, G. V., & Renuka, K. (2013). Thiadiazoles: Molecules of diverse applications — A review. *International Journal of ChemTech Research*, 5(1), 239–248.

Lewandowski, W., Lewandowska, H., Golonko, A., Świderski, G., Świsłocka, R., & Kalinowska, M. (2020). Correlations between molecular structure and biological activity in "logical series" of dietary chromone derivatives. *PLOS ONE*, 15(8), e0229477.

Lv, Y., Meng, J., Li, C., Wang, X., Ye, Y., & Sun, K. (2021). Update on the synthesis of N-heterocycles via cyclization of hydrazones (2017–2021). *Advanced Synthesis & Catalysis*, 363(23), 5235–5265.

Mallappa, Chahar, M., Choudhary, N., Yadav, K. K., Qasim, M. T., Zairov, R., … & Jangir, M. (2025). Recent advances in the synthesis of nitrogen-containing heterocyclic compounds via multicomponent reaction and their emerging biological applications: A review. *Journal of the Iranian Chemical Society*, 22(1), 1–33.

Reis, J., Gaspar, A., Milhazes, N., & Borges, F. (2017). Chromone as a privileged scaffold in drug discovery: Recent advances. *Journal of Medicinal Chemistry*, 60, 7941–7957.

Taylor, A. P., Robinson, R. P., Fobian, Y. M., Blakemore, D. C., Jones, L. H., & Fadeyi, O. (2016). Modern advances in heterocyclic chemistry in drug discovery. *Organic & Biomolecular Chemistry*, 14(28), 6611–6637.

Zaki, Y. H., Gomha, S. M., Farag, B., Zaki, M. E., & Hussein, A. M. (2025). Synthesis, characterization, and in silico studies of substituted 2,3-dihydro-1,3,4-thiadiazole derivatives. *Results in Chemistry*, 13, 101977.

ORAL PRESENTATION

Determination of MIC-MBC values and DPPH removal activity of zinc oxide nanoparticle

Canan Koç[1] (Orcid:0009-0006-8164-4044),
Funda Ulusu[2] (Orcid:0000-0002-0321-2602),
Adem Sarılmaz[3](Orcid:0000-0003-1463-9764),
Faruk Özel[4](Orcid:0000-0002-3689-0469),
Yakup Ulusu[5](Orcid:0000-0002-8755-2822)

[1]Karamanoglu Mehmetbey University Engineering Faculty, Department of Bioengineering Karaman, Türkiye.

[2]Karamanoglu Mehmetbey University, Technical Sciences Vocational School, Department of Crop and Animal Production, Karaman, Türkiye

*Corresponding author e-mail: c.gulbasar.koc@gmail.com

Abstract

Nanostructured particles have a wide range of applications across many sectors, primarily in electronics, biomedicine, automotive, and chemistry. The phytogenic synthesis of zinc oxide nanoparticles (ZnO-NPs) is considered an environmentally friendly approach due to their low toxicity and biological potential. Today, ZnO-NPs are at the forefront of research due to their versatile structure, which can be applied in biomedicine, wastewater treatment, environmental remediation, and even cosmetic products. Studies have shown that ZnO-NPs produced by different methods have antimicrobial, antioxidant, and anticancer properties. Therefore, studies on the antioxidant and antibacterial activity of ZnO-NPs are increasing day by day. This study aimed to determine the MIC and MBC values of ZnO-NPs. Gram-negative (*E. coli*) and gram-positive (*S. aureus*) bacteria were used for the study. Additionally, the antioxidant activity of ZnO-NP was determined using the DPPH method.

Keywords: Zinc oxide, Antioxidant, DPPH, Antibacterial, MIC-MBC.

1. INTRODUCTION

Atoms or molecules with one or more unpaired electrons in their outer orbitals are called free radicals. Free radicals are unstable due to their unpaired electrons and react with other substances in an attempt to become stable (Karabulut & Günay, 2016).

Antioxidants are substances that protect cells against the undesirable effects of free radicals, both directly and indirectly. Compounds such as vitamins C, E, A, beta-carotene, metallothionein, NADPH, and coenzyme Q-10 belong to this group. (Mercan, 2004).

As the dimensions of materials decreased, it was recognized that they possessed superior properties, leading to the growing importance of nanoparticles. Among these superior properties are increased surface area with decreasing particle size, along with superior magnetic, electronic, optical, and thermal properties. Interest in metal oxide particles is increasing day by day due to the different properties they exhibit at the nanoscale (Kamçı et al., 2022). Zinc oxide, one of these metal oxide materials, is a semiconductor material. The high binding energy and wide bandgap of zinc oxide particles are among its most important properties. The non-toxicity and skin compatibility of zinc oxide, along with its UV-reducing effect, also enable its use in the field of human health. The ease with which ZnO nanoparticles dissolve in liquids and organic solvents also allows them to be incorporated into many material processes and contributes to their wide range of applications (Arığ, 2010). Antimicrobial resistance is one of the leading global health issues according to the World Health Organization (WHO). The indiscriminate and excessive use of antibiotics has led to the emergence of resistant microorganism strains. Due to the low effectiveness of antibiotics against resistant strains, research has shifted towards alternative approaches that could replace traditional antibiotics. With the rapid development of nanomedicine, researchers have aimed to produce solutions using nanoparticles. In many studies, ZnO-NPs have demonstrated antibacterial activity in both gram-negative and gram-positive bacterial strains (Karakaplan, 2021). The continuous emergence of bacterial resistance is forcing the scientific community to develop new antibiotic agents. Among the most promising of these new antibiotic agents are metal NPs, which

have demonstrated potent antibacterial activity in numerous studies. Even when new antibiotics are introduced to the market, antibiotic-resistant bacteria emerge within a relatively short period of time. However, it is assumed that antibacterial-active NPs have the potential to reduce or eliminate the evolution of more resistant bacteria. Because NPs target multiple biomolecules simultaneously, they prevent the development of resistant strains. NPs come into direct contact with the bacterial cell wall without penetrating the cell and exhibit a broad spectrum of antibacterial properties. (Özkara, 2025). After being synthesized for use in many fields, various activity studies are conducted on nanoparticles. It is known that zinc oxide nanoparticles (ZnO-NPs) inhibit the growth of various bacterial strains and also exhibit cytotoxic effects against various cancer cell lines (Nair et al., 2009).

2. MATERIAL AND METHODS

2.1. The Synthesis of ZnO-NPs

A total of 280 mg of zinc acetate ($Zn(CH_3COO)_2$) was mixed with oleylamine in a beaker, and the synthesis temperature was set to 240 °C. The reaction was maintained for 5 minutes, after which the mixture was allowed to cool. Once the temperature reached 70 °C, 10 mL of ethanol was added, and the ZnO piezocatalysts were collected by centrifugation.

The morphological characteristics of the ZnO nanoplates were analyzed using SEM, and the corresponding results are presented in Figure 1. As shown in the figure, all pure ZnO particles exhibited a well-defined hexagonal morphology with an average particle size of approximately 325 nm.

2.2. DPPH Scavenging Activity

To calculate the DPPH scavenging activity, ZnO-NP solutions were prepared at different concentrations of 1.25, 2.5, 5, 10, 20, and 40 mg/mL in 10% DMSO. To these samples, 100 µL was added to 0.25 mL of 1 mM DPPH and 2 mL of methanol, and the mixture was incubated for 20 minutes. (Karamaç et al., 2019). Subsequently, absorbance measurements were taken at 517 nm for the samples. DPPH scavenging activity was calculated as a percentage according to the following formula (Seyhan, 2019).

DPPH removal activity % = (Control Abs- Sample Abs)/Control Abs x 100

2.3. MIC and MBC Assay

The minimum inhibitory concentration (MIC) test was used to determine the antimicrobial activity of ZnO nanoparticles, employing *E. coli* and *S. aureus* bacteria. In this test, ZnO-NP solutions (100 µL) prepared with sterile liquid medium at different concentrations (10^{-5}, 2.5, 1.25, 0.625, 0.312, 0. 156 µg) were added to 96-well plates. The negative control well was added with 10 µL of bacterial suspension and 100 µL of sterile liquid medium. After adding the ZnO-NP solution and bacterial suspension diluted in a twofold serial manner to each well (except the negative control well), the plates were incubated at 37°C for 24 hours. Then, 15 µL of Alamar Blue was added to each well and incubated again to allow for color change. The well where the first color change occurred was reported as the MIC value. For the minimum bactericidal concentration (MBC) test, ZnO-NP solutions at concentrations corresponding to the MIC value of the bacteria, twice the MIC value, and four times the MIC value were added to liquid bacterial suspensions and incubated at 37°C for 24 hours. Subsequently, the cultures were inoculated onto solid media, and the absence of growth at the concentration where no growth was observed was reported as the MBC.

3. RESULTS AND DISCUSSION

3.1. SEM Analysis of ZnO Nanoparticles

SEM imaging (Figure X) clearly demonstrates that the synthesized ZnO nanoparticles exhibit a well-defined hexagonal plate-like morphology, consistent with the typical wurtzite crystal structure of ZnO. The particles appear uniformly distributed, with smooth surfaces and sharp edges, indicating successful crystal growth under the applied synthetic conditions. The nanoplates show relatively narrow size variation, and most structures display a consistent hexagonal geometry, confirming the formation of pure and shape-controlled ZnO nanostructures.

The dense packing observed in the micrograph further suggests minimal agglomeration, supporting the effectiveness of oleylamine as a stabilizing and structure-directing agent during the synthesis process. Overall,

the SEM results validate that the employed method enables the production of monodisperse hexagonal ZnO nanoplates with well-defined morphology.

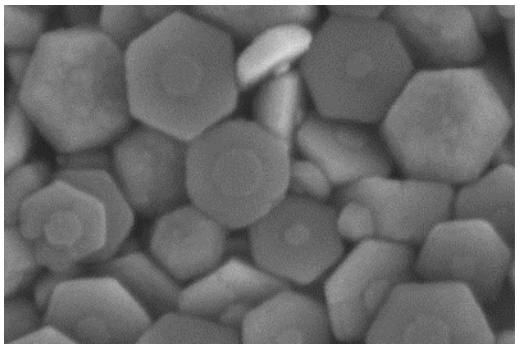


Figure 1. SEM analysis image of ZnO-NPs.

3.2. DPPH Scavenging Activity of ZnO-NPs

The DPPH scavenging activity of ZnO nanoparticles was calculated as 1.85% at the lowest concentration of 1.25 mg/mL. At a concentration of 40 mg/mL, it was calculated as 26.77%, demonstrating a remarkably high activity.

Table 1. DPPH % inhibition data values of ZnO-NPs.

Concentration (mg/mL)	1.25	2.5	5	10	20	40
DPPH Scavenging Activity (%)	1.85	3.7	4.47	15.81	25.38	26.77

Each value was expressed as mean ± SD and all experiments were performed in triplicate. The data were analyzed using Duncan's Multiple Range Test ($\alpha = 0.05$).

When reviewing the literature, the antioxidant activity of zinc oxide nanoparticles coated with Nyctanthes arbor-tristis (NA) leaf extract (ZnO-NA) was determined using the DPPH method, and the IC_{50} value was found to be 125 µg/mL (Koçak & Meydan, 2023). In another study, the DPPH scavenging percentage of ZnO nanoparticles was calculated as 45.47% at a concentration of 1 mg/mL (Denk & Tarhan, 2023). Ercan et al. (2025) reported that the DPPH scavenging activity of ZnO-NPs at a concentration of 0.5 mg/mL was 37.63%. The IC_{50} values of the DPPH radical scavenging activity of ZnO-NPs and leaf extract were found to be 18.71 ± 0.35 and 9.21 ± 0.10, respectively.

3.3. MIC and MBC Profiles of ZnO-NPs Against Test Bacteria

In the study, the MIC values of ZnO-NP were determined to be 10 µg/mL against *E. coli* and 0.625 µg/mL for *S. aureus.* According to the MBC test, the values were found to be 20 µg/mL for *E. coli* and 1.25 µg/mL against *S. aureus.*

Table 2. The MIC-MBC values of of ZnO-NPs against *E. coli* and *S. aureus* bacteria.

Bacteria	**MIC**	**MBC**
E.coli	10 µg/mL	20 µg/mL
S.aureus	0.625 µg/mL	1.25 µg/mL

A review of the literature revealed that the MIC values of ZnO-NP against *A. hydrophila* and *V. parahaemolyticus* strains were determined to be 15 and 7.5 µg/mL, respectively. (Günay et al., 2021). The MIC values of ZnO-NP synthesized with the oil of *Eucalyptus globulus* against *S. aureus* ATCC 43300 and *S. aureus* ATCC 25923 strains were observed to be 128 and 32 µg/ml, respectively (Zahra Obeızı et al., 2020). The MIC values of ZnO-NP synthesized with *Mussaenda frondosa* extract against *S. aureus* and *E. coli* strains were determined to be 54.13 µg/mL and 19.23 µg/mL, respectively (Jayappa et al., 2020). In another study,

the MIC values of ZnO-NP against *E. coli*, *S. aureus*, *P. aeruginosa*, and *E. faecalis* were found to be above 128 µg/mL (Erdoğan et al., 2019). ZnO-NP is known to inhibit the growth of various bacteria such as *C. jejeuni*, *S. enterica*, *E. coli*, *S. aureus*, and *Vibrio cholerae*. The antibacterial effect of synthesized ZnO-NP against *S. aureus* and *E. coli* has been proven to be effective against both gram-negative and gram-positive bacteria and is consistent with the literature. It has also been reported that ZnO-NP, which is found in antiseptics, is also present in many products such as anti-dandruff shampoos in cosmetics, ointments for skin rashes, mineral creams for wound healing, and medical bandages (Kuo et al., 2010).

With the rapid development of nanomedicine, researchers have aimed to produce solutions using nanoparticles. Metal oxide nanoparticles stand out due to their high stability and multiple effects against microorganisms. One of the most prominent of these is zinc oxide nanoparticles (ZnO-NP). In many studies, ZnO-NPs have demonstrated antibacterial activity in both gram-negative and gram-positive bacterial strains (Karakaplan, 2021).

Additionally, in biological systems, the excessive production of free radical species is one of the main causes of various diseases such as cancer, diabetes, cardiovascular diseases, and arthritis. All biosystems require antioxidants to a large extent for proper functioning. Consequently, there is an urgent need to research innovative and safe antioxidants produced from natural sources that are more effective and less toxic.

4. CONCLUSION

In this study, ZnO nanoparticles were successfully synthesized using a controlled chemical approach, and their morphological, antioxidant, and antibacterial properties were comprehensively evaluated. SEM analysis confirmed the formation of monodisperse ZnO nanoplates with well-defined hexagonal morphology, indicating effective crystal growth and minimal agglomeration during synthesis.

The antioxidant assessment revealed that ZnO-NPs exhibited dose-dependent DPPH radical scavenging activity, with the highest inhibition rate observed at 40 mg/mL. Although the antioxidant activity was moderate compared to several plant-mediated ZnO nanoparticle systems reported in the literature, the results demonstrate that the synthesized ZnO-NPs possess measurable free-radical scavenging potential.

The antibacterial assays showed that ZnO-NPs were highly effective against both Gram-negative (*E. coli*) and Gram-positive (*S. aureus*) bacteria, with notably low MIC and MBC values. These findings are consistent with previous studies and further support the broad-spectrum antimicrobial potential of ZnO-NPs. The strong inhibitory and bactericidal effects reflect the suitability of ZnO-NPs for potential use in biomedical, pharmaceutical, and hygienic applications.

Overall, the results of this study demonstrate that ZnO nanoparticles synthesized under the described conditions exhibit promising antioxidant and antibacterial activities. Given their biocompatibility, stability, and multifunctional nature, ZnO-NPs represent an attractive candidate for future applications in nanomedicine, antimicrobial formulations, and therapeutic antioxidant systems. Further studies exploring cytotoxicity, ROS generation, and mechanistic pathways will enhance the understanding and applicability of these nanomaterials.

REFERENCES

Arığ, E. (2010). Nanoyapıda çinko oksit partiküllerinin üretimi ve karakterizasyonu.

Denk, Y., & Tarhan, T. (2023). Çinkooksit Nanopartiküllerin Biyosentezi ve Biyolojik Aktiviteleri. Doğa Bilimleri Ve Matematikte Güncel Yaklaşimlar, 91.

Ercan, L., Çalışkan, C. G., & Kılıç, F. M. (2025). Comparison of Antioxidant and Antimicrobial Properties of Zinc oxide and Selenium oxide Nanoparticles using Verbascum kotschyi Boiss. & Hohen. Kahramanmaraş Sütçü İmam Üniversitesi Tarım ve Doğa Dergisi, 28(1), 9-19.

Erdoğan, Ö., Birtekocak, F., Oryaşın, E., Abbak, M., Demirbolat, G. M., Paşa, S., & Çevik, Ö. (2019). Enginar yaprağı sulu ekstraktı kullanılarak çinko oksit nanopartiküllerinin yeşil sentezi, karakterizasyonu, anti-bakteriyel ve sitotoksik etkileri. Duzce Medical Journal, 21(1), 19-26.

Günay, K., Leblebici, Z., & Koca, F. D. (2021). Çinko nanopartiküllerinin (ZnO NP) biyosentezi, karakterizasyonu ve anti-bakteriyel etkisinin incelenmesi. Nevşehir Bilim ve Teknoloji Dergisi, 10(1), 56-66.

Jayappa M.D., Ramaiah C.K., Kumar M.A.P. “Green synthesis of zinc oxide nanoparticles from the leaf, stem and in vitro grown callus of Mussaenda frondosa L.: characterization and their applications” Applied Nanoscience, 10, 3057–3074, 2020

Kamçı, H., Çelebioğlu, HU, Taş, R., Köroğlu, E. (2022). Saponaria officinalis L. Kullanılarak Çinko Oksit Nanopartiküllerinin Biyojenik Sentezi, Karakterizasyonu ve Antibakteriyel Aktiviteleri. Avrupa Bilim Ve Teknoloji Dergisi (35), 227-234. https://doi.org/10.31590/ejosat.1075292

Karabulut, H. & Gülay, M. Ş. (2016). Serbest Radikaller. Mehmet Akif Ersoy Üniversitesi Sağlık Bilimleri Enstitüsü Dergisi, 4(1).

Karakaplan, M. B. (2021). Investigating the Growth Kinetics of Gram-positive and Gram-negative Bacteria in the Presence of Zinc Oxide Nanoparticles and Curcumin.

Karamać, M., Gai, F., Longato, E., Meineri, G., Janiak, M. A., Amarowicz, R., & Peiretti, P. G. (2019). Antioxidant activity and phenolic composition of amaranth (Amaranthus caudatus) during plant growth. Antioxidants, 8(6), 173.

Koçak, Y., & Meydan, İ. (2023). Assessment of the Bioactivity of Zinc Nanoparticles Synthesized Using Erica arborea Plant. Journal of Anatolian Environmental and Animal Sciences, 8(3), 361-366.

Kuo CL, Wang CL, Ko HH, Hwang WS, Chang KM, Li WL, et al. Synthesis of zinc oxide nanocrystalline powders for cosmetic applications. Ceram Int. 2010;36(2):693-8.

Mercan, U. (2004). Toksikolojide serbest radikallerin önemi. Yüzüncü Yıl Üniversitesi Veteriner Fakültesi Dergisi, 15(1), 91-96.

Nair S, Sasidharan A, Divya Rani VV, Menon D, Nair S, Manzoor K, et al. Role of size scale of ZnO nanoparticles and microparticles on toxicity toward bacteria and osteoblast cancer cells. J Mater Sci Mater Med. 2009;20(Suppl 1):235-41.

Özkara, A. (2025). Nanopartiküllerin Antimikrobiyal Etkileri. NANOPARTİKÜLLER, 71.

Seyhan, S. A. (2019). Re-evaluation of DPPH antioxidant analysis. Batman University Journal of Life Sciences, 9 (2), 125-135.

Zahra Obeızı Z., Benbouzid H., Sihem O., Bououdina M., “Biosynthesis of Zinc oxide nanoparticles from essential oil of Eucalyptus globulus with antimicrobial and anti-biofilm activities” Materials Today Communications 25, 101553, 2020.

ORAL PRESENTATION

Bacillus thuringiensis parasporal proteinlerinin çeşitli kanser hücre hatları üzerinde sitotoksik aktivitelerinin araştırılması

Müjgan Kesik Oktay[1*] (Orcid: https://orcid.org/0000-0002-0857-4872), Burcu Şahin[2] (Orcid: https://orcid.org/0000-0002-5701-1371), Hatice Güneş[2] (Orcid: https://orcid.org/_0000-0001-5191-365X)

[*1]Afyonkarahisar Sağlık Bilimleri Üniversitesi, Şuhut Sağlık Hizmetleri Meslek Yüksekokulu, Tıbbi Hizmetler ve Teknikler Bölümü, Afyon, Türkiye
[2]Muğla Sıtkı Koçman Üniversitesi, Fen Fakültesi, Biyoloji Bölümü, Muğla, Türkiye

*Sorumlu yazar e-mail: mujgan.oktay@afsu.edu.tr

Özet

Bacillus thuringiensis (Bt), sporlu ve entomopatojenik bir bakteridir. Sporulasyonu sırasında parasporal inklüzyon proteinleri üretmektedir. Bu proteinler içerisinde en çok çalışılan grubunu insektisidal özellikteki Cry proteinleri oluşturmaktadır. Bu proteinlerden bazıları insektisidal özelliklerinden bağımsız olarak kanser hücre hatlarına karşı sitotoksik aktivite gösterebilmektedir. Hemolitik olmayan ve kanser hücrelerini hedef alan bu Cry proteini grubu Parasporinler (PS) olarak bilinmektedir. Bu çalışmada 6 Bt izolatımızın çeşitli kanser hücre hatları üzerindeki sitotoksik aktivitelerinin ve parasporin (*ps*) gen içeriklerinin belirlenmesi amaçlanmıştır. Bunun için, bu izolatlardan parasporal inklüzyon proteinleri elde edilmiş ve solubilizasyonun ardından Proteinaz K ile aktifleştirilmiştir. Aktive edilen protein profili SDS-PAGE analizi ile gösterilmiştir. Bu proteinlerin sağlıklı embriyonik böbrek hücreleri (HEK-293), prostat kanseri (PC-3), akciğer kanseri (A-549), meme kanseri (MCF-7), uterus serviks kanseri hücreleri (HeLa) ve Burkitt (lenfoma) hücreleri üzerinde toksik olup olmadığı MTT analizi ile araştırılmıştır. Parasporal inklüzyonların farklı düzeylerde çeşitli hücre hatları üzerinde sitotoksisitelerinin olduğu tespit edilmiştir. Test edilen izolatlardan 19Q2, 19Q3 ve BB99 analizi yapılan tüm kanser hücre hatlarına karşı anlamlı düzeyde ($P<0.05$, $P<0.01$ veya $P<0.001$) sitotoksik aktivite göstermiştir. Üç örnek de, MCF-7 ve Burkitt hücre hatlarına karşı $P<0.01$ düzeyinde etkili olmuştur. 19Q2, 19Q3 ve BB99 izolatları ile yapılan PCR analizi sonucunda sadece BB99 izolatı *ps1* geni için pozitif sonuç vermiştir. Dolayısıyla, bu çalışmada elde edilen pozitif sonuçlar doğal Bt izolatlarımızın anti kanser ilaç geliştirilmesine katkıda bulunabilecek bir potansiyel taşıdığını ve bunun ilerleyen çalışmalarda ortaya konması gerektiğini göstermektedir.

Anahtar Kelimeler: *Bacillus thuringiensis*, parasporal protein, sitotoksisite, MTT analizi, doz-bağımlı analiz

Investigation of cytotoxic activities of *Bacillus thuringiensis* parasporal proteins on various cancer cell lines

Abstract

Bacillus thuringiensis (Bt) is a spore-forming, entomopathogenic bacterium. It produces parasporal inclusion proteins during sporulation. The most studied group of these proteins is the insecticidal Cry proteins. Some of these proteins, independent of their insecticidal properties, can exhibit cytotoxic activity against cancer cell lines. This group of Cry proteins, which is non-hemolytic and targets cancer cells, is known as parasporins (PS). This study aimed to determine the cytotoxic activities and parasporin (*ps*) gene contents of six Bt isolates on various cancer cell lines. For this purpose, parasporal inclusion proteins were isolated from these isolates and activated with Proteinase K after solubilization. The activated protein profile was demonstrated by SDS-PAGE analysis. The toxicity of these proteins on healthy embryonic kidney cells (HEK-293), prostate cancer (PC-3), lung cancer (A-549), breast cancer (MCF-7), uterine cervix cancer cells (HeLa) and Burkitt (lymphoma) cells was investigated using MTT analysis. Parasporal inclusions were found to have varying levels of cytotoxicity on various cell lines. Of the isolates tested, 19Q2, 19Q3 and BB99 showed significant cytotoxic activity ($P<0.05$, $P<0.01$ or $P<0.001$) against all cancer cell lines analyzed. All three samples were active against MCF-7 and Burkitt cell lines at $P<0.01$. As a result of PCR analysis performed with 19Q2, 19Q3 and BB99 isolates, only isolate BB99 was positive for the *ps1* gene. Therefore, the positive results obtained in this study indicate that our natural Bt isolates have the potential to contribute to the development of anticancer drugs and this should be demonstrated in further studies.

Keywords: *Bacillus thuringiensis*, parasporal protein, cytotoxicity, MTT assay, dose-dependent assay

GİRİŞ

Bacillus thuringiensis (Bt); toprak, bitki ve böceklerde yaygın olarak bulunan Gram pozitif sporlu bir bakteridir (Schnepf ve ark., 1998). Doğada, Bt tarafından üretilen, farklı etki mekanizmalarına sahip birçok toksin bulunmaktadır. Bunlar arasında en iyi bilinen ve üzerinde çalışılan toksinler insektisidal (Palma ve ark., 2014), antimikrobiyal (Doshi ve ark., 2024), antifungal (Martinez-Zavala ve ark., 2020) ve anti kanser (Santos ve ark., 2022) özellikler taşımaktadır. Bu toksinlerin başında ise yapısı en iyi aydınlatılan ve hakkında en çok araştırma bulunan insektisidal proteinler gelmektedir. Kristal (Cry), sitolitik (Cyt) ve vejetatif insektisidal proteinler (Vip) tarım zararlılarının kontrolünde kullanılmaktadır. Bunlardan üzerinde en çok çalışılmış grup olan Cry proteinleri belirli böcek takımlarına karşı spesifik insektisidal aktivite göstermektedir. Protoksin formunda sentezlenen proteinler proteolitik kesim sonucu aktif toksin formuna dönüşmekte ve etki edeceği hücre membran reseptörlerine bağlanmaktadır. Bt, ürettiği bu toksinler sayesinde uzun yıllardır başarılı bir entomopatojen olarak biyolojik mücadelede görev almaktadır. Bakteriden elde edilen toksin formulasyonları sprey şeklinde bitkilere uygulanmakta ya da transgenik Bt ürünleri elde edilerek mücadele edilmektedir (Palma ve ark., 2014).

İnsektisidal özellikteki toksinlerin yanı sıra, Bt suşlarının son yıllarda anti kanser özelliği oldukça önem kazanmıştır. Kanser, dünyada en çok görülen ölümcül hastalıklardan birisidir ve ölüm oranı her geçen yıl artmaktadır. Geleneksel tedavi yöntemlerine devam edilmekte, ancak yan etkilerinden dolayı alternatif tedavi yolları aranmaktadır. Bu durum, kanser tedavisinde biyopreparatlara olan ilginin artmasına sebep olmuştur (Alarcón-Aldana ve ark., 2024). Bt'nin anti kanser özelliğinin keşfi (Ohba ve ark., 2009) bu mücadelede yeni bir umut ışığı olmuştur.

Mizuki ve ark. (1999), parasporal inklüzyon proteinleri hemolitik olmayan ancak insan kanser hücrelerine karşı sitosidal olan *B. thuringiensis* suşlarının geniş çaplı taramasını yapmışlardır. Mizuki ve ark. (2000) antikanser aktivite gösteren ve hemolitik olmayan A1190 suşunun karakterizasyonu sonucunda 81 kDa'luk yeni bir protein tanımlamışlar ve Parasporin olarak isimlendirmişlerdir. Parasporin ilk tanımlandığında hemolitik ve insektisidal olmayan ve insan kanser hücrelerini öldürebilen proteinler olarak tanımlanmıştır. Daha sonra yapılan çalışmalarda bazı parasporinlerin hem insektisidal hem de anti kanser etki gösterdikleri görülmüş ve bu tanımlamadan insektisidal olmayan kavramı çıkartılmıştır. Bir Cry proteini sınıfı olan parasporinler bugüne kadar 6 gruba (PS1-PS6) ayrılmıştır (Aberkane ve ark. 2020). PS'lerin çeşitli hücre hatları üzerinde sitotoksik etkilerini belirlemeye yönelik birçok çalışma mevcuttur (Santos ve ark., 2022).

Bu çalışmada Bt koleksiyonumuzda bulunan ve kristal oluşumu iyi olan bazı Bt izolatlarımız seçilerek, bu izolatların spor-kristal karışımlarının, prostat kanseri, akciğer kanseri, meme kanseri, uterus serviks kanseri ve lenfoma kanser hücre hatları üzerindeki sitotoksik etkilerinin belirlenmesi amaçlanmıştır. Bunun için: 1. Bt izolatlarından parasporal inklüzyonlar elde edilerek, protoksin enzim ile aktive edilmiştir. 2. MTT analizi ile toksinlerin sitotoksik aktiviteleri belirlenmiştir. 3. Anlamlı derecede sitotoksisite gösteren izolatların PCR ile parasporin gen içerikleri araştırılmıştır. Sitotoksik aktivite gösteren Bt izolatlarının bulunması, kanser ile mücadelede kullanılabilecek biyopreparatların geliştirilmesine katkıda bulunabilecektir.

MATERYAL VE METOT

Bakteri izolatları

Bu çalışmada kullanılan Bt izolatları (6A, 60Q2, 85PPb, 125Q, 19Q2, 19Q3 ve BB99), Muğla Sıtkı Koçman Üniversitesi, Biyoloji Bölümü, Moleküler Biyoloji Laboratuvarı'nda Prof. Dr. Hatice Güneş'e ait Bt koleksiyonundan temin edilmiştir.

Kanser hücre hatları

Bu çalışmada, prostat kanseri (PC-3), akciğer kanseri (A-549), meme kanseri (MCF-7), Uterus serviks kanseri hücreleri (HeLa), Burkitt (lenfoma) olmak üzere 5 farklı kanser hücre hattı kullanılmıştır. Sağlıklı hücre hattı olarak insan embriyonik böbrek hücreleri (HEK-293) seçilmiştir. Hücreler %10 fetal bovin serum ve 100 µg/ml penisilin/streptomisin içeren RPMI 1640 besi ortamında, 37°C'de %5 CO_2, %95 hava içeren nemlendirilmiş inkübatörde kültüre edilmiştir.

Parasporal inklüzyon proteinlerin eldesi ve aktivasyonu

Bt örnekleri Nutrient agar'da 30 °C'de 4 gün büyütülmüştür. Hücreler toplanıp distile su ile iki defa yıkanmıştır. Elde edilen spor-kristal karışımı 500 µl karbonat tamponunda (56 mM Na_2CO_3 pH 11,4; 11mM DTT) 37 °C'de 1 saat çözündürülmüşür. 13,200 rpm'de 2 dk santrifüj yapılarak çözünen proteinin bulunduğu

süpernatant elde edilmiştir. Supernatant pH'sı 1M Tris-HCl (pH 4.98) ile 8'e ayarlanmıştır. Çözünen proteinler 150 µg/ml Proteinaz K ile muamele edilmiş ve 37 °C'de 1 saat inkübe edilmiştir. Son konsantrasyonu 1mM olacak şekilde PMSF eklenerek proteolitik sindirim sonlandırılmıştır (Bresseur ve ark., 2015).

MTT analizi

Bt izolatlarından elde edilen parasporal proteinlerin; PC-3, A-549, MCF-7, HeLa ve Burkitt kanser hücre hatları ve sağlıklı hücre hattı HEK-293 üzerindeki sitotoksik etkileri MTT analizi ile tespit edilmiştir. 2×10^4 hücre/kuyu içeren hücreler (90 µl) 96 kuyulu plakalara ekilmiş ve %5 CO_2 ve %98 nem inkübatöründe 37 °C'de 16-20 saat inkübe edilmiştir. Daha sonra, Proteinaz K ile aktive edilmiş ve konsantrasyonu 20 µg/ml'ye ayarlanmış parasporal kristal proteinler kuyulara eklenerek 37 °C'de 48 saat inkübe edilmiştir. İnkübasyonun ardından, plakalardaki besiyeri 100 µl yeni besiyeri ile değiştirilmiştir. Yapışmayan Burkitt hücreleri için, hücre kültürü kapları 800 rpm'de 6 dakika santrifüj edilmiş ve yeni besiyeri eklenmiştir. Ardından, kuyulara 1:10 oranında MTT solusyonu (5 mg/ml) eklenmiştir. 37 °C'de, 4 saat inkübasyonun ardından, 100 µl DMSO eklenerek karışması sağlanmıştır. OD_{540} değeri mikroplaka okuyucu (Thermo Fisher Scientific) ile ölçülmüştür. Denemeler üç tekrarlı yapılmıştır.

Parasporin gen taraması

19Q2, 19Q3 ve BB99 Bt izolatlarının genomik DNA'ları kit (Exgene Clinic SV) ile izole edilmiştir. Bu izolatların *ps1*, *ps2*, *ps3*, *ps4*, *ps5* veya *ps6* parasporin genlerini taşıyıp taşımadıkları PCR analizi ile test edilmiştir. PCR analizi, Kesik Oktay (2019)'nin kullandıkları primer çiftleri ve PCR koşullarına göre yapılmıştır.

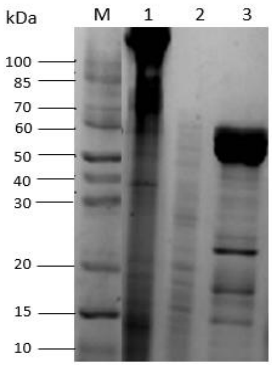
İstatistiksel analizler

Tüm analizlerde GraphPad Prism 7 programı kullanılmıştır. Sitotoksisite deneyleri sonucunda uygulamalar arasında fark olup olmadığı, tek yönlü varyans analizi (ANOVA) ile değerlendirilmiştir. Uygulamaların kıyaslanmasında Dunnett testi kullanılmıştır.

BULGULAR

Parasporal proteinlerin elde edilmesi

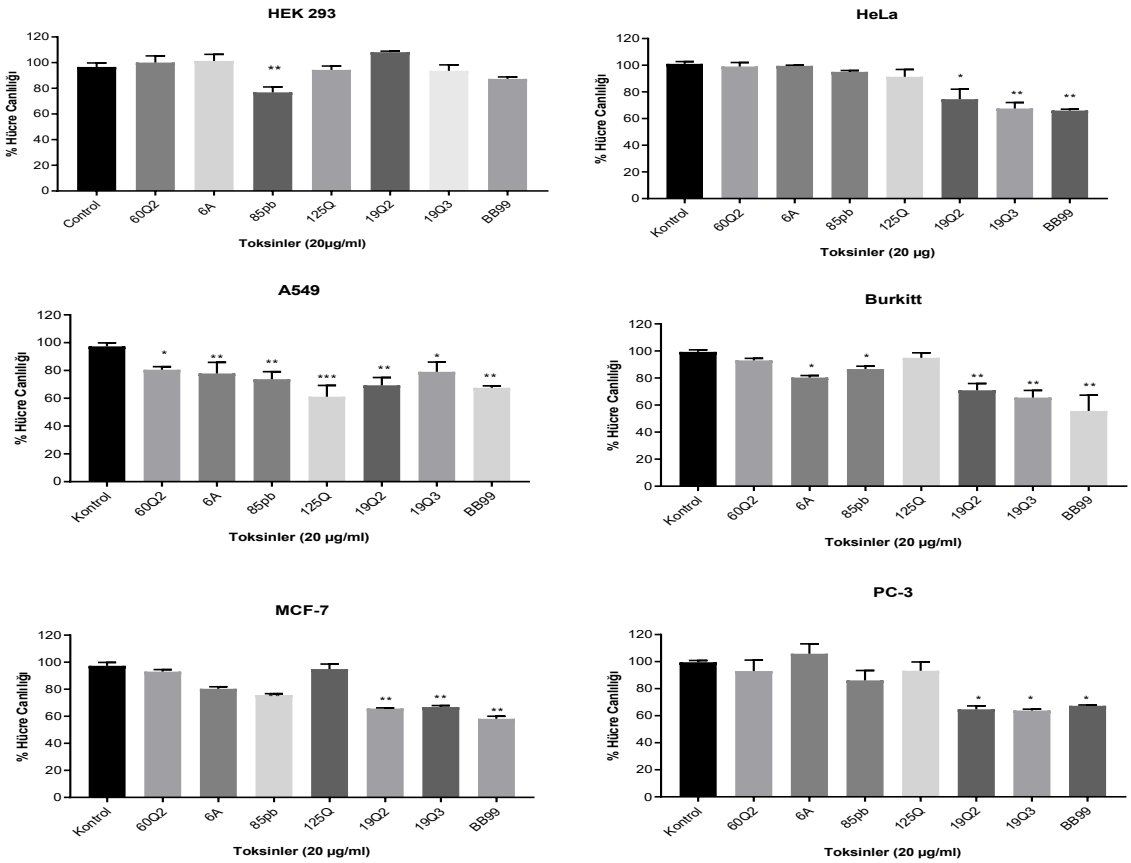
Sitotoksik aktivite denemelerinde kullanılmak üzere 6 Bt izolatına ait parasporal proteinler elde edilmiştir. Örnekler sırasıyla spor-kristal karışımı, alkali koşullarda solubilize edilmiş protein karışımı ve Proteinaz K ile kesime uğratılmış proteinler olarak elde edilmiş ve protein profilleri SDS-PAGE yöntemi ile belirlenmiştir. Solubilizasyon sonrasında profil bant sayısında belirgin bir azalma olduğu görülmektedir. Proteinaz K ile kesim sonucundaysa, düşük moleküler ağırlığa sahip yeni bantların oluştuğu ve aktif toksinin elde edildiği gösterilmiştir (Şekil 1).



Şekil 1. 85PPb izolatına ait parasporal proteinlerin protein profili. M: DNA Marker, 1: spor-kristal karışımı, 2: alkalide çözülmüş protein karışımı, 3: Proteinaz K ile kesilmiş protein karışımı

Sitotoksik aktivite

6A, 60Q2, 85PPb, 125Q, 19Q2, 19Q3 ve BB99 izolatlarından izole edildikten sonra Proteinaz K ile kesilip aktif formu elde edilen parasporal proteinlerin sitotoksik etkileri PC-3, A-549, MCF-7, HeLa ve Burkitt kanser hücre hatları ve sağlıklı hücre hattı üzerinde test edilmiştir.



Şekil 2. Bt izolatlarının çeşitli kanser hücre hatları üzerindeki sitotoksik etkileri *: P<0.05; **: P<0.01; ***:P<0.001, ****:P<0.0001

HEK-293 üzerinde sadece 85PPb izolatına ait parasporal proteinler hücre canlılığında anlamlı bir azalmaya sebep olmuş, diğer parasporal proteinlerde ise bu etki gözlenmemiştir (Şekil 2A). Test edilen bazı örneklerin P<0.05, P<0.01 veya P<0.001 anlam düzeylerinde çeşitli hücre hatları üzerinde sitotoksisitelerinin olduğu tespit edilmiştir (Şekil 2B, C, D, E, F). 19Q2, 19Q3 ve BB99 izolatlarından elde edilen parasporal proteinlerin, analizi yapılan tüm kanser hücre hatlarına karşı anlamlı düzeyde sitotoksik aktivite gösterdiği bulunmuştur. Her üç parasporal protein de en anlamlı etkiyi P<0.01 düzeyinde MCF-7 ve Burkitt hücre hatlarına karşı göstermiştir (Şekil 2D ve E).

PCR analizi

19Q2, 19Q3 ve BB99 Bt izolatlarının *ps1*, *ps2*, *ps3*, *ps4*, *ps5* ve *ps6* gen içerikleri PCR analizi ile belirlenmiştir. BB99 izolatı 511 bç uzunluğundaki *ps1* geni için pozitif bulunmuştur. 19Q2 ve 19Q3 izolatlarının ise bu genlerden hiçbirini taşımadığı görülmüştür (Data gösterilmemiştir).

TARTIŞMA

Bu çalışma, *Bt* izolatlarımızın sitotoksik aktivitelerini tespit etmek amacıyla yapılmıştır. *Bt* koleksiyonumuzdan seçilen 6 örneğin parasporal proteinlerinin sitotoksik aktiviteleri PC-3, A-549, MCF-7, HeLa ve Burkitt kanser hücre hatları ve sağlıklı HEK-293 hücre hattı üzerinde test edilmiştir. HEK-293 hücreleri üzerinde sadece 85PPb izolatının parasporal proteinleri anlamlı düzeyde hücre canlılığını azaltmıştır, diğer izolatların parasporal proteinleri ise hücre canlılığını anlamlı düzeyde etkilememiştir. Daha önce yapılan araştırmalar Bt izolatlarının farklı hücre hatlarına karşı sitotoksik etkiye sahip olduğunu ortaya koymuştur (Santos ve ark., 2022). Bu çalışmada, sitotoksik aktiviteyi belirlemek için yapılan MTT analizi sonucunda sağlıklı hücre hattının hücre canlılığını etkilemeyen, ancak kanser hücre hatlarının hücre canlılığını kontrole kıyasla anlamlı düzeyde düşüren 5 Bt izolatının olduğu tespit edilmiştir. Bu izolatlar içerisinden 19Q2, 19Q3 ve BB99 Bt izolatlarının test edilmiş tüm hücre hatlarında hücre canlılığını azalttığı gözlenmiştir. Bazı bakteriler tarafından sentezlenerek sitotoksik aktivite gösteren bileşenler Parasporinler olarak bilinmektedir (Ohba ve ark., 2009). Bu yüzden, etkili olan bu üç izolatın sitotoksik aktivitelerinin Parasporin proteinlerinden

kaynaklanıp kaynaklanmadığını test etmek için bu izolatların *ps1*, *ps2*, *ps3*, *ps4*, *ps5* ve *ps6* parasporin genleri taranmıştır. Literatürdeki çalışmalar *ps* genlerinin Bt izolatlarında görülme oranlarının farklı olduğunu göstermektedir. Aboul-Soud ve ark. (2019) inceledikleri 9 Bt izolatının hepsinin sadece *ps1* geni içerdiğini; Moazamian ve ark. (2018) Bt izolatlarının %43'ünün *ps2*, %20'sinin *ps4* ve %1'inin *ps6* için pozitif olduğunu belirtmişlerdir. Bizim çalışmamızda 19Q2 ve 19Q3 izolatları tüm *ps* genleri için negatif sonuç verirken, BB99 izolatının *ps1* genini içerdiği bulunmuştur. Bu sonuçlara göre BB99 izolatının sitotoksik aktivitesi Parasporin 1 proteininden kaynaklanıyor olabilir. Diğer iki Bt izolatı ise, farklı bir *ps* geni taşıdığı ve henüz ortaya konmadığı için bilinen genlerle sonuç vermemiş olabilir. Parasporin genlerinin sınırlı sayıda tanımlanmış olması, PCR ile parasporin sınıflarının belirlenmesinde bazı kısıtlamalara yol açmaktadır. Literatürde mevcut olan genlerin azlığı nedeniyle, PCR analizinde kullanılan primerler çoğu zaman yalnızca bilinen tek bir gene özgü olarak tasarlanmaktadır. Bu durum, henüz keşfedilmemiş ya da literatürde tanımlanmamış ancak parasporin içeren potansiyel izolatların saptanmasını zorlaştırmaktadır. Dolayısıyla, parasporinlerin tespiti için PCR yöntemi tek başına yeterli değildir. İlerleyen çalışmalarda19Q2 ve 19Q3 izolatlarının sitotoksik aktivitelerine neden olan molekülü tespit etmek için daha detaylı analizler yapılacak ve BB99 izolatının *ps1* geni karakterize edilecektir.

SONUÇ

Bu çalışma ile 6 doğal Bt izolatımızın çeşitli kanser hücre hatları üzerindeki sitotoksik aktiviteleri belirlenmiş ve belirli düzeylerde etkili oldukları görülmüştür. Bu çalışma, doğal anti kanser ilaç geliştirilmesine yönelik ajanların tespiti için önem taşımaktadır. Bunun için bu izolatların apoptotik, anjiyogenik vb. etkileri de araştırılmalı ve detaylı analizlerle anti kanser potansiyeli ortaya konmalıdır.

TEŞEKKÜR

Bu çalışma Muğla Sıtkı Koçman Üniversitesi Bilimsel Araştırma Projesi (BAP) 15/152 numaralı proje kapsamında desteklenmiştir.

KAYNAKLAR

Aberkane, L., Nacer-Khodja, A., Djenane, Z., Djouadi, L. N., Ouafek, A., Bouslama, L., Grib, H., Mameri, N., Nateche, F., & Djefal, A. (2020). In vitro cytotoxicity of Parasporins from native Algerian *Bacillus thuringiensis* strains against laryngeal and alveolar cancers. Current Microbiology, 77(3), 405–414.

Aboul-Soud, M. A. M., Al-Amri, M. Z., Kumar, A., Al-Sheikh, Y. A., Ashour, A. E., & El-Kersh, T. A. (2019). Specific cytotoxic effects of parasporal crystal proteins isolated from native Saudi Arabian *Bacillus thuringiensis* strains against cervical cancer cells. Molecules, 24(3), 506.

Alarcón-Aldana, J. S., Visser, L., Rueda-Forero, N. J., Pinzón-Reyes, E. H., Rondón-Villarreal, P., & Suárez-Barrera, M. O. (2024). Enhancing the cytotoxicity and apoptotic efficacy of Parasporin-2-derived variants (Mpp46Aa1) on cancer cell lines. Toxins, 16(10), 415.

Brasseur, K., Auger, P., Asselin, E., Parent, S., Côté, J. C., & Sirois, M. (2015). Parasporin-2 from a new *Bacillus thuringiensis* 4R2 strain induces caspases activation and apoptosis in human cancer cells. PLoS ONE, 10(8), e0135106.

Doshi, M. N., Badr, K., Ejaz, M., Hassan, Z. U., & Jaoua, S. (2024). Investigation of novel bacteriocin producers of *Bacillus thuringiensis* and partial characterization of two new bacteriocins: Thuricin 466 and Thuricin 4Q7. Bioresource Technology Reports, 25, 101760.

Kesik Oktay M. Isolatıon of native Bacillus thuringiensis strains from cherry orchards, determination of cry gene profiles and studies on parasporins. PhD thesis. Muğla Sıtkı Koçman University, Graduate School of Natural and Applied Sciences, Muğla. 2019.

Martínez-Zavala, S. A., Barboza-Pérez, U. E., Hernández-Guzmán, G., Bideshi, D. K., & Barboza-Corona, J. E. (2020). Chitinases of *Bacillus thuringiensis*: Phylogeny, modular structure, and applied potentials. Frontiers in Microbiology, 10, 3032.

Mizuki, E., Ohba, M., Akao, T., Yamashita, S., Saitoh, H., & Park, Y. S. (1999). Unique activity associated with non-insecticidal *Bacillus thuringiensis* parasporal inclusions: In vitro cell-killing action on human cancer cells. Journal of Applied Microbiology, 86(3), 477–486.

Mizuki, E., Park, Y. S., Hiroyuki Saitoh, †, Yamashita, S., Akao, T., Higuchi, K., & Ohba, M. (2000). Parasporin, a human leukemic cell-recognizing parasporal protein of *Bacillus thuringiensis*. Clinical and Diagnostic Laboratory Immunology, 7(4), 625-634.

Moazamian, E., Bahador, N., Azarpira, N., & Rasouli, M. (2018). Anti-cancer parasporin toxins of new *Bacillus thuringiensis* against human colon (HCT-116) and blood (CCRF-CEM) cancer cell lines. Current Microbiology, 75(8), 1090–1098.

Ohba, M., Mizuki, E., & Uemori, A. (2009). Parasporin, a new anticancer protein group from *Bacillus thuringiensis*. Anticancer Research, 29, 427–433.

Palma, L., Muñoz, D., Berry, C., Murillo, J., & Caballero, P. (2014). *Bacillus thuringiensis* toxins: An overview of their biocidal activity. Toxins, 6(12), 3296–3325.

Santos, E. N., Menezes, L. P., Dolabella, S. S., Santini, A., Severino, P., Capasso, R., Zielinska, A., Souto, E. B., & Jain, S. (2022). *Bacillus thuringiensis*: From biopesticides to anticancer agents. Biochimie, 192, 83–90.

Schnepf, E., Crickmore, N., Van Rie, J., Lereclus, D., Baum, J., Feitelson, J., Zeigler, D. R., & Dean, D. H. (1998). *Bacillus thuringiensis* and its pesticidal crystal proteins. Microbiology and Molecular Biology Reviews, 62(3), 775-806.

ORAL PRESENTATION

Bitki hormunu olarak karrikinlerin bitki fizyolojisindeki rolü, ekolojik önemi ve tarımsal biyoteknolojideki uygulama potansiyelleri

Mustafa Kahya[1]* (Orcid: https://orcid.org/0000-0001-6053-1354)
Mehmet Sezgin[2] (Orcid: https://orcid.org/0000-0001-7053-0371)

*[1]Çankırı Karatekin Üniversitesi Lisansüstü Eğitim Enstitüsü, Biyoloji bölümü, Çankırı, Türkiye.
[2]Çankırı Karatekin Üniversitesi, Gıda ve Tarım Meslek Yüksekokulu, Park ve Bahçe Bitkileri Bölümü, Peyzaj ve Süs Bitkileri, Çankırı, Türkiye.

*Sorumlu yazar e-mail: mkahya50@gmail.com.

Özet

Yangın, karasal ekosistemlerin evrimsel dinamiklerini şekillendiren temel faktörlerden biridir. Yangına adapte olmuş bitki türleri, rekabetin azaldığı yangın sonrası ortamlarda çimlenebilmek için dumanda bulunan kimyasal sinyalleri algılayan moleküler mekanizmalar geliştirmiştir. Bu çalışmada, duman kaynaklı butenolid yapılı sinyal molekülleri olan "Karrikinler" (KARs) kapsamlı bir literatür taraması ile incelenmiştir. Çalışma, karrikinlerin keşif sürecini, kimyasal özelliklerini ve KAI2-MAX2 proteozomal yıkım kompleksine dayalı sinyal iletim mekanizmasını detaylandırmaktadır. Mevcut literatür verileri, karrikinlerin sadece tohum dormansisini kırmakla kalmayıp, aynı zamanda fotomorfogenez, kök mimarisi gelişimi ve kuraklık, tuzluluk gibi abiyotik stres faktörlerine karşı toleransın artırılmasında kritik roller üstlendiğini göstermektedir. Ayrıca, bu moleküllerin tarımsal biyoteknolojideki potansiyel kullanımları; özellikle parazitik yabancı otlarla (*Striga* spp.) mücadelede "intihar çimlenmesi" (suicidal germination) stratejisi ve kültür bitkilerinde verim artışına yönelik tohum "priming" (ön uygulama) teknikleri üzerinden değerlendirilmiştir. Sonuç olarak, karrikinlerin iklim değişikliği ve gıda güvenliği sorunlarına karşı dirençli bitkisel üretim sistemlerinde umut verici bir biyoteknolojik araç olduğu ortaya konmuştur.

Anahtar Kelimeler: Karrikinler, KAI2 reseptörü, Tohum çimlenmesi, Abiyotik stres, İntihar çimlenmesi.

The role of karrikins as plant hormones in plant physiology, their ecological importance and their application potential in agricultural biotechnology.

Abstract

Fire is a fundamental factor shaping the evolutionary dynamics of many terrestrial ecosystems. Fire-adapted plant species have developed molecular mechanisms to perceive chemical signals in smoke to germinate in post-fire environments where competition is reduced. In this study, "Karrikins" (KARs), which are smoke-derived butenolide signaling molecules, are examined through a comprehensive literature review. The study details the discovery process of karrikins, their chemical properties, and the signal transduction mechanism based on the KAI2-MAX2 proteasomal degradation complex. Current literature data indicate that karrikins not only break seed dormancy but also play critical roles in photomorphogenesis, root architecture development, and increasing tolerance to abiotic stress factors such as drought and salinity. Furthermore, the potential uses of these molecules in agricultural biotechnology are evaluated, particularly through the "suicidal germination" strategy for combating parasitic weeds (*Striga* spp.) and seed "priming" techniques for yield enhancement in crops. In conclusion, it is demonstrated that karrikins are a promising biotechnological tool in resilient crop production systems against climate change and food security challenges.

Keywords: Karrikins, KAI2 receptor, Seed germination, Abiotic stress, Suicidal germination.

1.GİRİŞ

Yangın, karasal ekosistemlerin milyonlarca yıldır şekillenmesinde rol oynayan en güçlü evrimsel baskı unsurlarından biridir. Özellikle Akdeniz iklim kuşağı, Güney Afrika'nın Fynbos biyomu, Avustralya'nın çalılık alanları ve Kuzey Amerika'nın chaparral bölgeleri gibi yangına meyilli ekosistemlerde, bitkilerin yaşam döngüsü ateş ile senkronize olmuştur (Dixon et al., 2009). Bu bölgelerdeki bitki örtüsü için yangın, bir

yıkımdan ziyade, rekabetin azaldığı, ışık ve alanın açıldığı, besin maddelerinin (kül yoluyla) toprağa geri döndüğü yeni bir başlangıç fırsatıdır. Ancak bitkilerin bu fırsatı değerlendirebilmesi için tohumlarının doğru zamanda, yani yangın geçtikten hemen sonra çimlenmesi gerekmektedir. İşte bu noktada bitkiler, yangının varlığını algılayabilmek için kimyasal bir "burun" geliştirmişlerdir.

Tarihsel olarak, yerli halklar ve çiftçiler dumanın tohum çimlenmesini artırdığını ampirik olarak biliyorlardı. Ancak bilimsel dünyada bu olgunun sistematik olarak incelenmesi 1990'larda hız kazanmıştır. Başlangıçta ısının veya küldeki minerallerin çimlenmeyi tetiklediği düşünülse de, araştırmalar oda sıcaklığındaki dumanın veya duman emdirilmiş suyun (smoke water) bile çimlenmeyi tetiklediğini göstermiştir (Van Staden et al., 2000). Bu durum, dumanın içinde biyokimyasal bir sinyal molekülü olduğunu kanıtlamıştır. Ancak binlerce bileşen içeren dumanın içinden bu tekil molekülü izole etmek, samanlıkta iğne aramaktan farksızdı. 2004 yılında Batı Avustralya Üniversitesi'nden Gavin Flematti ve ekibinin, selülozun kontrollü yanmasıyla elde edilen duman suyunu hassas kromatografik yöntemlerle (biyo-rehberli fraksiyonasyon) ayrıştırması sonucu, bitki biyolojisinde yeni bir dönem başlamıştır (Flematti, Ghisalberti, Dixon, & Trengove, 2004).

2. KURAMSAL TEMELLER VE LİTERATÜR

2.1. Karrikinlerin Kimyasal Doğası ve Oluşum Mekanizması

Flematti ve ekibinin izole ettiği ve başlangıçta "butenolid" olarak tanımlanan bu molekül sınıfına, Batı Avustralya'nın yerli halkı Noongar'ların dilinde "duman" anlamına gelen "karrik" kelimesinden türetilerek "Karrikin" (KAR) adı verilmiştir (Flematti et al., 2004). Keşfedilen ilk ve biyolojik olarak en aktif molekül KAR1 (3-metil-2H-furo[2,3-c]piran-2-on) olarak isimlendirilmiştir. Daha sonraki çalışmalar, duman içinde KAR1'e yapısal olarak çok benzeyen ancak metil gruplarının konumu veya sayısı bakımından farklılık gösteren KAR2, KAR3, KAR4, KAR5 ve KAR6 gibi analogların da bulunduğunu ortaya koymuştur (Flematti et al., 2007).

Tablo 1: Karrikinlerin Temel Fizikokimyasal Özellikleri

Özellik	**Açıklama**
Kimyasal Sınıf	Furo-piran yapılı Butenolidler
Temel Yapı	Beş üyeli bir butenolid halkasının, altı üyeli bir piran (eter) halkasına füzyonu
Moleküler Formül (KAR1)	$C_8H_6O_3$
Çözünürlük	Suda yüksek çözünürlük (toprak çözeltisinde taşınabilir)
Erime Noktası	118–119 °C
Termal Stabilite	Yüksek sıcaklıklara dayanıklı (yangın kökenli olmasıyla uyumlu)
Fotostabilite	Güneş ışığında (UV) hızla bozunur (yüzeyde birikimi engeller)

Karrikinlerin oluşumu, spesifik bir bitki türüne bağlı değildir; selüloz ve basit şekerler gibi karbonhidratların yanması (piroliz) sonucu oluşurlar (Flematti, Dixon, & Smith, 2015). Bu durum, karrikinlerin evrensel bir "yanmış bitki materyali" sinyali olduğunu gösterir. 180°C gibi nispeten düşük yanma sıcaklıklarında bile 30

dakika içinde oluşabilmeleri, bu moleküllerin doğada neden bu kadar yaygın bulunduğunu açıklamaktadır (Flematti et al., 2015). Yapısal olarak karrikinler, bitkilerde dallanmayı kontrol eden ve parazitik otların çimlenmesini tetikleyen strigolakton (SL) hormonlarına benzerlik gösterirler. Her iki grup da bir butenolid halkası içerir, ancak karrikinler strigolaktonlara kıyasla daha basit, kiral merkezi olmayan ve düzlemsel (planar) bir yapıya sahiptir (Flematti et al., 2015).

2.2. Sinyal İletim Mekanizması: KAI2 Reseptörü ve Evrimsel Paradoks

Karrikinlerin bitki hücresinde nasıl algılandığı sorusu, bilim insanlarını ilginç bir evrimsel paradoksa götürmüştür. *Arabidopsis thaliana* gibi yangına adapte olmamış, hatta yangınla evrimsel geçmişi zayıf olan bitkilerin bile karrikinlere güçlü tepkiler verdiği gözlemlenmiştir (Nelson et al., 2012). Bu durum, karrikinleri algılayan sistemin, aslında bitkinin kendi içinde ürettiği başka bir molekülü algılamak için evrimleştiğini, karrikinlerin ise bu sistemi "taklit ettiğini" düşündürmektedir.

2.2.1. KAI2: Antik Sinyal Alıcısı

Karrikin sinyal yolağının merkezinde **KAI2 (KARRIKIN INSENSITIVE 2)** adı verilen bir reseptör protein bulunur. KAI2, α/β-hidrolaz katlanma yapısına sahip bir enzim-benzeri proteindir (Conn & Nelson, 2015). Bu protein, karrikin molekülünü (veya onun doğal analoğunu) bağladığında şekil değiştirir. KAI2 proteini, bitkiler aleminde son derece korunmuş bir yapıdır; karayosunları (*Physcomitrella patens*) ve ciğer otları (*Marchantia polymorpha*) gibi ilkel kara bitkilerinde bile işlevsel KAI2 homologları bulunmaktadır (Flematti et al., 2015). Bu durum, KAI2 aracılı sinyalizasyonun, tohumlu bitkilerin (Spermatophyta) evriminden çok daha önce, muhtemelen bitkilerin karaya ilk çıkış dönemlerinde ortaya çıktığını göstermektedir.

2.2.2. Sinyal Yolu : MAX2 ve SMAX1

Karrikin sinyalinin hücre çekirdeğinde gen ifadesini değiştirmesi, KAI2'nin tek başına yaptığı bir iş değildir. KAI2, ligandını bağladıktan sonra, **MAX2 (MORE AXILLARY GROWTH 2)** adı verilen bir F-box proteini ile etkileşime girer (Nelson et al., 2012). MAX2, bitki hücresinde bir "çöpçü" gibi çalışan ubikuitin-proteozom sisteminin bir parçasıdır. KAI2-MAX2 kompleksi, hücrede büyümeyi ve çimlenmeyi baskılayan **SMAX1 (SUPPRESSOR OF MAX2 1)** ve benzeri (SMXL2) represör proteinleri hedefler (Stanga, Smith, & Nelson, 2013). Bu hedefleme sonucunda SMAX1 proteinleri yıkıma uğrar. Baskılayıcının ortadan kalkmasıyla (double negative regulation), çimlenmeyi ve fide gelişimini teşvik eden genler aktif hale gelir.

Bu mekanizma, strigolakton (SL) sinyal yolağına (D14-MAX2-SMXL6/7/8) büyük benzerlik gösterir. Her iki yolak da MAX2 proteinini ortak kullanır, ancak farklı reseptörler (KAI2 vs D14) ve farklı hedef represörler (SMAX1 vs SMXL7) sayesinde bitki, karrikin sinyalini strigolakton sinyalinden ayırt edebilir (Conn & Nelson, 2015).

Tablo 2: Karrikin ve Strigolakton Sinyal Yolaklarının Karşılaştırmalı Analizi

Bileşen	**Karrikin (KAR) Yolağı**	**Strigolakton (SL) Yolağı**	**Fonksiyonel Sonuç**
Sinyal Ligandı	Karrikinler (veya KL)	Strigolaktonlar	Sinyalin Başlatılması
Reseptör	KAI2 (AtHTL)	D14 (DWARF14)	Sinyal Algılama
Ortak Bileşen	MAX2 (F-box)	MAX2 (F-box)	Sinyal İletimi
Hedef Represör	SMAX1, SMXL2	SMXL6, SMXL7, SMXL8	Gen Regülasyonu
Biyolojik Çıktı	Çimlenme, Fotomorfogenez, Kök	Dallanma, Parazit Çimlenmesi	Fenotipik Etki

2.3. Karrikinlerin Bitki Fizyolojisindeki Rolleri

Karrikinlerin etkisi, sadece tohumun uyanması ile sınırlı değildir. Bitkinin tüm yaşam döngüsü boyunca, özellikle stres koşullarında ve gelişimsel geçişlerde kritik düzenleyici roller üstlenirler.

2.4. Tohum Dormansisinin Kırılması ve Çimlenme

Karrikinlerin en iyi tanımlanmış rolü, tohum dormansisini (uyku halini) kırmasıdır. Fizyolojik dormansi, tohumun içindeki Absisik Asit (ABA - uykuyu teşvik eden) ve Gibberellin (GA - çimlenmeyi teşvik eden) hormonlarının dengesi ile kontrol edilir. Karrikinler, bu dengeyi GA lehine değiştirirler. *Arabidopsis* üzerinde yapılan çalışmalar, KAR1 uygulamasının GA biyosentez genlerinin (*GA3ox1*, *GA3ox2*) ifadesini artırdığını ve aynı zamanda tohumun GA'ya olan hassasiyetini yükselttiğini göstermiştir (Nelson et al., 2009).

Daha da önemlisi, karrikinler tohumların ışık gereksinimini modüle eder. Birçok bitki tohumu çimlenmek için ışığa ihtiyaç duyar (fotoblastik). Karrikinler, tohumun ışığa olan duyarlılığını artırarak, çok düşük ışık şiddetlerinde bile çimlenmenin gerçekleşmesini sağlar (Nelson et al., 2012). Bu özellik, toprağın derinliklerine gömülmüş veya yoğun bitki örtüsü (gölge) altındaki tohumların, yangın sonrası alan açıldığında hızla çimlenebilmesi için evrimsel bir avantajdır.

2.4.1. Fotomorfogenez ve Fide Gelişimi

Tohum çimlendikten sonra fide, toprağın üzerine çıkıp ışığa ulaştığında gelişim programını değiştirir (skotomorfogenezden fotomorfogeneze geçiş). Karrikin sinyali, bu süreçte fidenin yapısını optimize eder. KAR uygulaması yapılan fidelerde hipokotil (sap) uzaması baskılanır ve kotiledonlar (çenek yaprakları) genişler (Flematti et al., 2015). Bu, fidenin gereksiz yere boya gitmesini engelleyerek enerjisini yaprak gelişimine ve fotosenteze ayırmasını sağlar. SMAX1 mutantlarında (*smax1*) görülen kısa hipokotil ve geniş kotiledon fenotipi, karrikinlerin bu süreçteki baskılayıcıyı (SMAX1) ortadan kaldırarak çalıştığını doğrulamaktadır.

2.4.2. Kök Mimarisi ve Gelişimi

Karrikinler, bitkinin sadece toprak üstü aksamını değil, kök sistemini de etkiler. Lateral (yan) kök oluşumunu ve kök kıllarının yoğunluğunu artırdığına dair bulgular mevcuttur (Flematti et al., 2015). Bu etki, özellikle kuraklık gibi suyun sınırlı olduğu koşullarda bitkinin hayatta kalma şansını artırır.

2.5. Abiyotik Stres Toleransında Karrikinlerin Rolü

Bitkilerin değişen iklim koşullarına adaptasyonunda karrikin sinyal yolağının beklenmedik bir koruyucu rolü olduğu keşfedilmiştir. Bu bulgular, karrikinlerin sadece bir "çimlenme hormonu" olmadığını, genel bir "stres adaptasyon düzenleyicisi" olduğunu göstermektedir.

2.5.1. Kuraklık ve Tuzluluk Stresi

Kuraklık, bitkisel üretimde verimi sınırlayan en önemli faktördür. Araştırmalar, karrikin sinyal yolağındaki SMAX1 proteininin kaybının (yani karrikin sinyalinin aktif olduğu durumun taklidi), bitkilerde kuraklığa karşı toleransı artırdığını göstermiştir (Li et al., 2017). *smax1* mutant bitkilerde yaprak yüzeyinden su kaybının azaldığı ve stoma (gözenek) hareketlerinin daha sıkı kontrol edildiği gözlemlenmiştir. Ayrıca, karrikin uygulaması, bitki hücrelerinde Reaktif Oksijen Türlerini (ROS) temizleyen antioksidan enzimlerin aktivitesini artırarak, tuzluluk ve kuraklığın neden olduğu oksidatif hasarı azaltır. Buğday fidelerinde yapılan bir çalışmada, KAR1 uygulamasının potasyum/sodyum (K+/Na+) dengesini koruyarak tuz stresinin etkilerini hafiflettiği rapor edilmiştir (Shah et al., 2020).

2.5.2. Sıcaklık ve Ozmotik Stres

Yüksek sıcaklıklar ve ozmotik stres altında, karrikin reseptörü KAI2'nin fonksiyonu hayati önem taşır. *kai2* mutantlarının (karrikin algılayamayan bitkiler) yüksek sıcaklıklarda çimlenme yeteneğini kaybettiği ve stres koşullarında fide canlılığının düştüğü belirlenmiştir. KAR1 uygulaması, domates tohumlarının yüksek sıcaklıkta çimlenmesini teşvik ederek termal inhibisyonu (ısıya bağlı çimlenme durması) aşmalarına yardımcı olmaktadır (Jain & Van Staden, 2006).

2.6. Tarımsal ve Ekolojik Uygulama Potansiyelleri

Karrikinlerin temel bilimdeki bu etkileyici özellikleri, tarımsal biyoteknoloji ve ekolojik restorasyon alanlarında somut uygulamalara dönüştürülmeye başlanmıştır.

2.6.1. Yabancı Ot Mücadelesi: "İntihar Çimlenmesi" (Suicidal Germination)

Tarımsal üretimde en büyük maliyet kalemlerinden biri yabancı ot mücadelesidir. Geleneksel yöntemler genellikle bitki çıktıktan sonra müdahaleye dayanır. Ancak karrikinler, "intihar çimlenmesi" adı verilen proaktif bir strateji sunar. Bu yöntemde, tarla henüz ekilmeden önce toprağa karrikin veya duman suyu uygulanır. Bu sinyal, toprak tohum bankasında bekleyen dormant (uykudaki) yabancı ot tohumlarını, mevsimi olmasa veya koşullar tam uygun olmasa bile kitleler halinde çimlenmeye teşvik eder (Flematti et al., 2015).

Çimlenen bu yabancı otlar, henüz kültür bitkisi ekilmediği için mekanik sürümle veya hafif dozda herbisit ile kolayca yok edilebilir. Böylece toprak tohum rezervi tüketilmiş olur. Bu strateji özellikle *Avena fatua* (yabani yulaf), *Brassica tournefortii* ve en önemlisi *Striga* (cadı otu) gibi parazitik otlara karşı denenmektedir (Flematti et al., 2015). *Striga* tohumları normalde konukçu bitkiden salgılanan strigolaktonları bekler; ancak karrikin benzeri sentetik analoglar veya duman türevleri ile bu tohumlar "kandırılarak" konukçu yokken çimlenmeye zorlanabilir, bu da parazitin ölümüne yol açar (suicidal germination).

2.6.2. Tohum "Priming" ve Ürün Verimi

Kültür bitkilerinin tohumlarının ekim öncesi belirli bir süre karrikin çözeltisinde bekletilmesi (priming), çimlenme yüzdesini, çıkış hızını ve fide homojenliğini artırmaktadır.

Domates ve Biber: KAR1 priming işlemi, bu bitkilerin tohumlarının düşük sıcaklıklarda veya tuzlu topraklarda bile yüksek oranda çimlenmesini sağlamaktadır (Jain & Van Staden, 2006).
Tahıllar: Buğday ve mısırda yapılan denemeler, KAR uygulamasının kök kütlesini artırarak bitkinin topraktan besin ve su alım kapasitesini iyileştirdiğini göstermiştir.
Soya Fasulyesi: Karrikinlerin soya tohumlarında hasat öncesi çimlenmeyi (pre-harvest sprouting)

engelleyebileceğine dair çalışmalar mevcuttur; bu, ürün kalitesini korumak adına önemli bir potansiyeldir.

2.6.3. Biyoçar (Biochar) ve Toprak İyileştirme

Biyoçar, organik maddelerin oksijensiz ortamda yakılmasıyla elde edilen ve toprağa karbon bağlamak için kullanılan bir materyaldir. Son analizler, biyoçarın üretim sürecinde doğal olarak karrikinlerin oluştuğunu ve biyoçarın bitki gelişimi üzerindeki olumlu etkilerinin bir kısmının, gözeneklerine hapsolmuş bu karrikinlerden kaynaklandığını ortaya koymuştur (Kochanek et al., 2016).

2.6.4. Ekolojik Restorasyon

Madencilik sonrası bozulan arazilerin veya yangın görmüş alanların rehabilitasyonunda, endemik bitki tohumlarının çimlenmesini sağlamak büyük bir sorundur. Karrikin içeren duman suyu uygulamaları, özellikle Avustralya'da maden sahalarının rehabilitasyonunda, doğal tohum bankasını harekete geçirerek biyoçeşitliliği artırmak amacıyla standart bir prosedür olarak kullanılmaktadır (Dixon et al., 2009).

2.7. Gelecek Perspektifi: Kayıp Halka "KL"

Karrikin araştırmalarındaki en büyük bilimsel boşluk, "KAI2 Ligand" (KL) olarak adlandırılan içsel hormonun kimliğidir. Bitkilerin, yangınla hiç karşılaşmasalar bile KAI2 reseptörünü milyonlarca yıldır korumuş olmaları, bu reseptörün aslında bitkinin kendi ürettiği bir hormonu algılamakla görevli olduğunu kanıtlamaktadır (Conn & Nelson, 2015). Karrikinler, muhtemelen bu gizemli KL hormonunun tesadüfi bir yapısal taklididir. Bilim insanları şu an bu endojen ligandı izole etmeye çalışmaktadır. KL'nin keşfi, bitki gelişimi ve stres yanıtları üzerinde, oksin veya giberellinlerin keşfi kadar büyük bir etki yaratabilir.

3. SONUÇ

Karrikinler, doğanın yıkıcı gücü olan ateşin, yaşamın devamlılığını sağlayan yapıcı bir sinyale nasıl dönüştüğünün en zarif moleküler örneğidir. Keşfedilmelerinden bu yana geçen yirmi yılda, sadece bitki fizyolojisinin karanlıkta kalmış bir köşesini aydınlatmakla kalmamış, aynı zamanda küresel gıda güvenliğini tehdit eden abiyotik stresler ve yabancı otlarla mücadelede güçlü bir biyoteknolojik araç haline gelmişlerdir. Gelecekteki araştırmalar, karrikin sinyal yolağının genetik manipülasyonu ve sentetik analogların geliştirilmesi üzerine yoğunlaşarak, tarımda "akıllı bitkiler" dönemini başlatabilir.

4. KAYNAKLAR

Conn, C. E., & Nelson, D. C. (2015). Evidence that KARRIKIN-INSENSITIVE2 (KAI2) receptors may perceive an unknown signal that is not karrikin or strigolactone. *Frontiers in Plant Science*, *6*, 1219.

Dixon, K. W., Merritt, D. J., Flematti, G. R., & Ghisalberti, E. L. (2009). Karrikinolide: a phytoreactive compound derived from smoke with potential in horticulture and ecological restoration. *Acta Horticulturae*, *813*, 155–170.

Flematti, G. R., Dixon, K. W., & Smith, S. M. (2015). What are karrikins and how were they 'discovered' by plants? *BMC Biology*, *13*, 108.

Flematti, G. R., Ghisalberti, E. L., Dixon, K. W., & Trengove, R. D. (2004). A compound from smoke that promotes seed germination. *Science*, *305*(5686), 977.

Flematti, G. R., Goddard-Borger, E. D., Merritt, D. J., Ghisalberti, E. L., Dixon, K. W., & Trengove, R. D. (2007). Preparation of 2H-furo[2,3-c]pyran-2-one derivatives and evaluation of their germination-promoting activity. *Journal of Agricultural and Food Chemistry*, *55*(6), 2189–2194.

Jain, N., & Van Staden, J. (2006). A smoke-derived butenolide improves early growth of tomato seedlings. *Plant Growth Regulation*, *50*(2-3), 139–148.

Kochanek, J., Long, R. L., Lisle, D., & Flematti, G. R. (2016). Karrikins identified in biochars indicate post-fire chemical cues can be intentionally produced and used to improve crop performance. *PLOS ONE*, *11*(8), e0161234.

Li, W., Nguyen, K. H., Chu, H. D., Ha, C. V., Watanabe, Y., Osakabe, Y.,... & Tran, L. S. P. (2017). The karrikin receptor KAI2 promotes drought resistance in Arabidopsis thaliana. *PLOS Genetics*, *13*(11), e1007076.

Nelson, D. C., Flematti, G. R., Ghisalberti, E. L., Dixon, K. W., & Smith, S. M. (2012). Regulation of seed germination and seedling growth by chemical signals from burning vegetation. *Annual Review of Plant Biology*, *63*, 107-130.

Nelson, D. C., Riseborough, J. A., Flematti, G. R., Stevens, J., Ghisalberti, E. L., Dixon, K. W., & Smith, S. M. (2009). Karrikins discovered in smoke trigger Arabidopsis seed germination by a mechanism requiring gibberellic acid synthesis and light. *Plant Physiology*, *149*(2), 863–873.

Shah, F., Xu, J., Chen, Q., Du, Y., Wu, W., & Wang, H. (2020). Exogenous karrikin 1 (KAR1) improves water stress tolerance in wheat. *Plant Physiology and Biochemistry*, *155*, 843–851.

Stanga, J. P., Smith, S. M., & Nelson, D. C. (2013). Suppressor of more axillary growth2 1 controls seed germination and seedling development in Arabidopsis. *Plant Physiology*, *163*(1), 318–330.

Van Staden, J., Brown, N. A. C., Jäger, A. K., & Johnson, T. A. (2000). Smoke as a germination cue. *Plant Species Biology*, *15*(2), 167–178.

ORAL PRESENTATION

KBRN Bilgi Düzeyinin Artırılmasında Animasyon Teknolojisinin Kullanımı ve Etkisinin İncelenmesi; Niğde Ömer Halisdemir Üniversitesi Tıp ve Hemşirelik Bölümü Lisans Öğrencileri Örneği

Mehmet Emre Kara[1] (ORCID: https://orcid.org/0009-0006-2698-6455.),
Sefa Ertürk[2] (ORCID: https://orcid.org/0000-0003-4051-9096.)

[1]Niğde Ömer Halisdemir University, Graduate School of Science, Department of Disaster Management, Niğde.
[2]Niğde Ömer Halisdemir University, Faculty of Medicine, Department of Basic Medical Sciences, Division of Biophysics, Niğde.

Sorumlu yazar e-mail: mehmetemre.kara@mail.ohu.edu.tr

Özet

KBRN (Kimyasal, Biyolojik, Radyolojik ve Nükleer) olayları, insan yaşamında ciddi olumsuz sonuçlar doğuran afetlerdir. Bu tür olaylara karşı hazırlıksız olunması ve önlem alınmaması, zamanla daha büyük riskler yaratmaktadır. Bu nedenle, bireylerin KBRN farkındalık düzeylerinin artırılması ve doğru müdahale bilgilerinin verilmesi büyük önem taşımaktadır. Bu çalışma, KBRN olaylarına yönelik bilgi düzeyinin artırılmasında animasyon teknolojisinin kullanımını incelemektedir. Araştırmada lisans düzeyindeki hemşirelik ve tıp öğrencileri örneklem olarak seçilmiştir. Öğrencilerin KBRN farkındalık ve bilgi düzeyleri, eğitim öncesi ve sonrası yapılan testlerle değerlendirilmiştir. Elde edilen bulgular, animasyon teknolojisiyle desteklenen eğitimin öğrencilerin KBRN konularına ilişkin bilgi düzeylerini istatistiksel olarak anlamlı biçimde artırdığını göstermektedir. Görüş ölçeğinden elde edilen veriler de bu bulguları destekler niteliktedir. Ortalama puanlar incelendiğinde, öğrenciler animasyonların derse ilgilerini artırdığını, konuları anlamalarını kolaylaştırdığını ve öğrenme sürecini daha eğlenceli hâle getirdiğini belirtmişlerdir.

Anahtar Kelimeler: KBRN, Farkındalık, Animasyon, Eğitim

Examination of the Use and Impact of Animation Technology in Increasing CBRN Knowledge: A Case Study of Undergraduate Students at Niğde Ömer Halisdemir University, Faculty of Medicine and Nursing

Abstract

CBRN (Chemical, Biological, Radiological, and Nuclear) incidents are disasters that have serious adverse effects on human life. Lack of preparedness and failure to take preventive measures against such events can lead to increasingly greater risks over time. Therefore, it is of great importance to enhance individuals' awareness of CBRN threats and to provide them with accurate information regarding appropriate response measures. This study examines the use of animation technology in increasing knowledge levels related to CBRN incidents. Undergraduate nursing and medical students were selected as the sample group. The students' levels of CBRN awareness and knowledge were assessed through pre- and post-training tests. The findings indicate that education supported by animation technology significantly increased students' knowledge levels on CBRN topics in a statistically meaningful way. Data obtained from the opinion scale also support these findings. An examination of the mean scores reveals that students reported that animations increased their interest in the course, facilitated their understanding of the subjects, and made the learning process more enjoyable.

Keywords: CBRN, Awarness, Animation, Education

GİRİŞ

KBRN afetlerinin farkındalığının artırılması, olası risklerin en aza indirilmesi, toplumun ve KBRN olaylarına maruz kalabilecek kişilerin bilinçlendirilmesi hayati bir önem taşır. Bu konuda bilinç oluşturmak, KBRN olaylarını yıkıcı etkilerini önlemek ve müdahale süreçlerini iyileştirmek için kritik bir gerekliliktir. (Dönmez, 2019)

Günümüzde hızla gelişen teknoloji, eğitim ve farkındalık oluşturma süreçlerinde yeni yöntemlerin ve araçların kullanımını teşvik etmektedir. Özellikle KBRN gibi karmaşık ve hayati öneme sahip konularda, yeni teknolojilerin sunduğu imkanlar dikkat çekmektedir. İşte tam da bu noktada, animasyon teknolojisi gibi görsel ve interaktif eğitim araçları devreye girmektedir. Animasyonlar, karmaşık kavramları sadeleştirerek, eğitimi daha anlaşılır ve çekici hale getirebilir. Bu tür teknolojik araçlar, öğrenme sürecini hızlandırma açısından önemlidir. Animasyon teknolojisinin eğitim materyallerine dahil edilmesi hem eğitimlerin etkinliğini artırabilir hem de KBRN farkındalığının daha geniş kitlelere ulaşmasını sağlayabilir. (Yeh ve Yang, 2024; Ercan vd., 2014)

Genel olarak yapılan çalışmalarda animasyon ile desteklenen eğitimlerin, bireylerin bilgileri akılda tutma düzeyine, konunun daha anlaşılır hale gelmesine ve akademik başarıların artmasına anlamlı derecede olumlu katkılar sağladığı belirtilmektedir. Bu çalışma, animasyon destekli KBRN eğitimlerinin, Niğde Ömer Halisdemir Üniversitesi tıp ve hemşirelik bölümü öğrencilerinin KBRN bilgi düzeylerini artırma konusundaki etkinliğini incelemeyi amaçlamaktadır.

MATERYAL VE METOT

Animasyonun Hazırlanması

Bu animasyon, kimyasal, biyolojik, radyolojik ve nükleer (KBRN) ajanlara ilişkin farkındalığı artırmak amacıyla hazırlanmıştır. İçeriğin oluşturulmasında akademik çalışmalar ve ilgili bakanlıklar tarafından yayımlanan resmi bilgilendirme materyalleri titizlikle incelenmiştir. Animasyon, KBRN olaylarına karşı toplumun bilinç düzeyini artırmayı ve güvenli davranışların kazandırılmasını hedeflemektedir.

Animasyonun senaryo akışı, izleyicilerin konuyu adım adım kavrayabilmesi esas alınarak tasarlanmıştır. Akış, sırasıyla kimyasal, biyolojik, radyolojik ve nükleer ajanların etkileri, sınıflandırmaları, yayılma yolları ve korunma yöntemleri üzerinde yoğunlaşmaktadır.

Buna ek olarak, animasyonda ülkemizde kullanılan tehlike alarm işaretlerine de yer verilmiş olup, izleyicilerin acil durumlarda alarm seslerini tanıyabilmeleri ve doğru tepkileri verebilmeleri hedeflenmiştir. Böylece, animasyon yalnızca bilgi aktarımı ile sınırlı kalmayıp, izleyicilerin davranışsal olarak da hazırlanmasına katkı sağlamaktadır.

Kapsam ve Yöntem

Bu çalışmada, Niğde Ömer Halisdemir Üniversitesi Tıp ve Hemşirelik Bölümü öğrencilerine animasyon ile KBRN eğitiminin etkinliğini belirlemek amacıyla yarı deneysel bir yöntem kullanılmıştır. Araştırmanın örneklemini, Niğde Ömer Halisdemir Üniversitesi tıp ve hemşirelik bölümünde öğrenim gören 315 lisans öğrencisi oluşturmaktadır.

Katılımcılara öncelikle eğitim öncesi KBRN Bilgi Testi uygulanmış ve ardından animasyon yöntemiyle KBRN eğitimi verilmiştir. Eğitim sonrasında katılımcılara tekrar KBRN Bilgi Testi uygulanmıştır. Katılımcıların animasyonla yapılan eğitime yönelik memnuniyetini ölçmek amacıyla animasyon görüş ölçeği de uygulanmıştır. Animasyon Görüş ölçeğini eğitime katılan öğrencilerden 287 kişi doldurmuştur.

Veri Toplama Araçları

Araştırmada, ölçek geliştirme sürecinde veri toplama aracı olarak iki bölümden oluşan bir test formu kullanılmıştır. Formun birinci bölümünde, katılımcıların okuduğu bölüm, cinsiyet, sınıf ve yaş bilgilerini içeren demografik bilgi formu, ikinci bölümünde ise KBRN Bilgi Testi yer almaktadır.

Kullanılan KBRN Bilgi Testi, her biri beş seçenekten (a, b, c, d, e) oluşan, 20 çoktan seçmeli sorudan meydana gelmektedir. Her soruda yalnızca bir doğru yanıt bulunmaktadır. Katılımcıların verdikleri cevaplar, doğru = 1

ve yanlış = 0 şeklinde puanlanmıştır. Araştırmada, ön test ve son test uygulamaları aynı form ve madde yapısı kullanılarak gerçekleştirilmiştir.

Eğitim sonrasında, eğitimde kullanılan animasyonların içeriğine ilişkin katılımcı görüşlerini tespit etmek için Daşdemir vd. (2012) tarafından geliştirilen Animasyon Görüş Ölçeği kullanılmıştır. Ölçek, beşli Likert tipi bir derecelendirmeye sahiptir (1 = Kesinlikle katılmıyorum, 5 = Kesinlikle katılıyorum) ve toplam 13 maddeden oluşmaktadır. Ölçekten elde edilebilecek puanlar 13 ile 65 arasında değişmektedir.

Veri Analizi

Bu çalışmanın veri analizinde SPSS 31.0.1.0 sürümü ve Microsoft Excel programları kullanılmıştır.

Veri seti, aynı katılımcı grubuna ait ön test (Test 1) ve son test (Test 2) uygulamalarından elde edilmiştir. Ancak, veri toplama formunda kimlik veya kişisel bilgi (ad, numara vb.) yer almadığı için katılımcılar birebir eşleştirilememiştir. Bu nedenle, analizlerde Grup değişkeni altında "1 = Ön test" ve "2 = Son test" kodlaması yapılarak, veriler bağımsız iki grup (eğitim alan grup, eğitim almayan grup) varsayımıyla değerlendirilmiştir.

Her ne kadar istatistiksel analizler bağımsız iki grup yaklaşımıyla yapılmış olsa da veriler aynı grubun iki farklı zamanda yapılan ölçümünü temsil etmektedir. Yarı deneysel desenlerde, bireysel eşleştirmenin mümkün olmadığı durumlarda aynı grubun farklı zamanlarda ölçülmesi yöntemi uygulanabilir. Bu yaklaşım, karşılaştırmalı analizlerde kullanılabilen geçerli bir alternatiftir.

BULGULAR

Tablo 1. Demografik Bilgiler

Değişken	Kategori	Yüzde (%)
Cinsiyet	Kadın	67,0
	Erkek	32,7
	Belirtmek istemiyorum	0,3
Yaş	17–18	25,4
	19–20	43,9
	21–23	25,6
	24 ve üzeri	5,1
Sınıf	1. sınıf	51,7
	2. sınıf	28,3
	3. sınıf	0,6
	4. sınıf	19,4
Bölüm	Tıp	60,3
	Hemşirelik	39,7

Tablo 2. Güvenilirlik Testi

Uygulama Türü	Madde Sayısı	Cronbach's Alpha (α)	Güvenirlik Düzeyi
Ön Test	20	0.561	Düşük
Son Test	20	0.692	Kabul edilebilir

KBRN Bilgi Testi'nin iç tutarlılık güvenirliği Cronbach's Alpha katsayısı ile değerlendirilmiştir. Ön test uygulamasında Cronbach's Alpha değeri $\alpha = 0.561$ olarak bulunmuş; bu değer, eğitim öncesinde öğrencilerin madde yanıtlarının heterojen olduğunu göstermektedir. Son test uygulamasında ise Cronbach's Alpha değeri $\alpha = 0.692$ olarak hesaplanmış ve testin eğitim sonrasında kabul edilebilir düzeyde iç tutarlılığa sahip olduğu belirlenmiştir. Bu sonuçlar, animasyon destekli eğitimin öğrencilerin bilgi düzeyini artmasının yanı sıra maddeler arasındaki yanıt tutarlılığını da güçlendirdiğini ortaya koymaktadır.

Tablo 3. Normallik Testi

Grup	Kolmogorov–Smirnov (KS)	df	P
Test 1 (Ön test)	0,122	315	<0,001
Test 2 (Son test)	0,105	315	<0,001

Her iki grupta da yapılan Kolmogorov–Smirnov (KS) ve Shapiro–Wilk (SW) normallik testlerinde p <0,001 bulunmuştur. Bu sonuç, toplam puanların normal dağılım göstermediğini ortaya koymaktadır. Dolayısıyla, gruplar arası farkın incelenmesinde parametrik olmayan bir yöntem tercih edilmiştir.

Tablo 4. Mann- Whitney U Testi

	Toplam Skor
Mann-Whitney U	11929,000
Wilcoxon W	61699,000
Z	−16,541
Asymp. Sig. (2-tailed)	<,001

Toplam Skor değişkenine ilişkin analizde, Gruplar değişkenine göre yapılan Mann–Whitney U testi sonucunda U = 11929,000, Z = −16,541 ve Asymp. Sig. (2-tailed) <0,001 olarak bulunmuştur. Bu sonuç, ön test ve son test grupları arasında istatistiksel olarak anlamlı bir fark olduğunu göstermektedir. Başka bir ifadeyle, katılımcıların son testteki toplam puanlarının ön test puanlarına göre anlamlı düzeyde daha yüksek olduğu söylenebilir. Bu bulgu, animasyon destekli eğitimin KBRN bilgi düzeyini artırmada etkili olduğunu desteklemektedir.

Tablo 5. Mann- Whitney U Testi Sıra Ortalaması ve Toplamı

Grup	N	Sıra Ortalaması	Sıra Toplamı
Test 1 (Ön test)	315	195,87	61699,00
Test 2 (Son test)	315	435,13	137066,00
Toplam	630		

Mann–Whitney U testi sonuçlarına göre, sıra ortalaması (mean rank) değeri Test 2 için 435,13, Test 1 için ise 195,87 olarak bulunmuştur. Bu bulgu, son test puanlarının genel olarak ön test puanlarından daha yüksek sıralarda yer aldığını göstermektedir. Başka bir ifadeyle, farkın yönü son test lehinedir; yani katılımcıların eğitim sonrasında KBRN bilgi düzeylerinin anlamlı biçimde arttığı söylenebilir.

Tablo 6. Doğru/Yanlış Çapraz Tablosu

Soru	Grup	Yanlış Sayısı	Yanlış (%)	Doğru Sayısı	Doğru (%)
S1	Test 1 (Ön test)	99	31,4	216	68,6
	Test 2 (Son test)	29	9,2	286	90,8
S2	Test 1 (Ön test)	105	33,3	210	66,7
	Test 2 (Son test)	115	36,5	200	63,5
S3	Test 1 (Ön test)	207	65,7	108	34,3
	Test 2 (Son test)	19	6	296	94
S4	Test 1 (Ön test)	271	86	44	14
	Test 2 (Son test)	174	55,2	141	44,8
S5	Test 1 (Ön test)	120	38,1	195	61,9
	Test 2 (Son test)	67	21,3	248	78,7
S6	Test 1 (Ön test)	219	69,5	96	30,5
	Test 2 (Son test)	149	47,3	166	52,7
S7	Test 1 (Ön test)	185	58,7	130	41,3
	Test 2 (Son test)	69	21,9	246	78,1
S8	Test 1 (Ön test)	184	58,4	131	41,6
	Test 2 (Son test)	89	28,3	226	71,7

S9	Test 1 (Ön test)	111	35,2	204	64,8
	Test 2 (Son test)	36	11,4	279	88,6
S10	Test 1 (Ön test)	103	32,7	212	67,3
	Test 2 (Son test)	66	21	249	79
S11	Test 1 (Ön test)	183	58,1	132	41,9
	Test 2 (Son test)	94	29,8	221	70,2
S12	Test 1 (Ön test)	286	90,8	29	9,2
	Test 2 (Son test)	127	40,3	188	59,7
S13	Test 1 (Ön test)	173	54,9	142	45,1
	Test 2 (Son test)	207	65,7	108	34,3
S14	Test 1 (Ön test)	164	52,1	151	47,9
	Test 2 (Son test)	129	41	186	59
S15	Test 1 (Ön test)	70	22,2	245	77,8
	Test 2 (Son test)	29	9,2	286	90,8
S16	Test 1 (Ön test)	261	82,9	54	17,1
	Test 2 (Son test)	201	63,8	114	36,2
S17	Test 1 (Ön test)	257	81,6	58	18,4
	Test 2 (Son test)	75	23,8	240	76,2
S18	Test 1 (Ön test)	203	64,4	112	35,6
	Test 2 (Son test)	133	42,2	182	57,8
S19	Test 1 (Ön test)	183	58,1	132	41,9
	Test 2 (Son test)	78	24,8	237	75,2
S20	Test 1 (Ön test)	270	85,7	45	14,3
	Test 2 (Son test)	99	31,4	216	68,6

Tablo 7. Görüş Ölçeği Güvenilirlik Analizi

Ölçek / Test Adı	**Madde Sayısı**	**Cronbach's Alpha**	**Güvenilirlik Düzeyi**
Animasyon Görüş Ölçeği	13	0,861	Güvenilir

Görüş Ölçeği'nin iç tutarlılığı, Cronbach's Alpha katsayısı ile değerlendirilmiştir. Ölçek 13 maddeden oluşmaktadır. SPSS programı ile yapılan analiz sonucunda Cronbach's Alpha (α) = 0,861 olarak bulunmuştur. Bu değer testin "güvenilir" düzeyde iç tutarlılığa sahip olduğunu göstermektedir.

Tablo 8. Görüş Ölçeği Tanımlayıcı İstatistikler

Madde	**Ortalama ($\bar{X}$)**	**Std. Sapma**	**N**
Animasyonlarla işlenen konular daha fazla ilgimi çekti.	4,34	0,759	280
Animasyonlar konuyla ilgili soruları çözmeme yardımcı oldu.	4,44	0,689	282
Animasyonların kullanımı konu hakkında daha ayrıntılı düşünmemi sağladı.	4,33	0,784	285
Animasyonlar diğer derslerde de kullanılmalıdır.	4,46	0,747	280
Animasyonların kullanımı konuya yoğunlaşmamı sağladı.	4,48	0,731	283
Animasyonlarla işlenen konular çok hoşuma gitti.	4,29	0,864	282
Animasyonların kullanımı yaratıcı düşünmeme yardımcı oldu.	4,24	0,862	276
Animasyonlar çok karmaşık olduğundan konuları öğrenemedim.	3,92	1,395	260
Derslerde animasyonların kullanımı çok faydalıdır.	4,31	0,819	281

Animasyonlar dersi daha iyi anlamama yardımcı oldu.	4,39	0,759	285
Animasyonlarla ders işlemek sıkıcıdır.	4,09	1,253	264
Animasyonların kullanımı sınıfta düzensizliğe yol açtı.	4,15	1,216	279
Animasyonların kullanımı işlenen konuların anlaşılmasını zorlaştırdı.	4,27	1,197	281

Elde edilen bulgulara göre, Görüş Ölçeğinin tüm maddelerine ilişkin ortalama puanların 4,09 ile 4,48 aralığında yoğunlaştığı görülmüştür. Bu sonuç, katılımcıların büyük çoğunluğunun animasyon destekli eğitim uygulamalarına olumlu yaklaştığını göstermektedir.

Negatif anlam taşıyan maddelerde (örneğin, "Animasyonlarla ders işlemek sıkıcıdır", "Animasyonların kullanımı sınıfta düzensizliğe yol açtı." vb.) ortalama değerlerin görece yüksek çıkması, bu ifadelerin ters kodlu olduğundan kaynaklanmaktadır. Dolayısıyla, bu maddeler ters çevrilerek yorumlandığında, genel eğilimin yine olumlu yönde olduğu anlaşılmaktadır.

Sonuç olarak, öğrenciler animasyon destekli öğretimin:

- İlgilerini artırdığını,
- Konuya yoğunlaşmalarını sağladığını,
- Karmaşık konuların anlaşılmasını kolaylaştırdığını ifade etmişlerdir.

Bu bulgular, animasyon tabanlı öğretim uygulamalarının öğrenme sürecine ilişkin olumlu görüşlerle karşılandığını ve öğrenciler tarafından etkili, ilgi çekici ve öğrenmeyi destekleyici bir yöntem olarak değerlendirildiğini ortaya koymaktadır.

TARTIŞMA

Araştırma sonuçları, öğrencilerin KBRN konusundaki başlangıç bilgi düzeylerinin düşük olduğunu, ancak animasyon destekli eğitim sonrasında bilgi ve farkındalıklarında belirgin bir artış gerçekleştiğini göstermektedir. Bu bulgu, afet ve KBRN eğitimlerinde teknolojik materyallerin kullanımının öğrenme sürecine önemli katkılar sağladığını ortaya koyan literatürle büyük ölçüde örtüşmektedir.

Mızrak (2018), Özden ve Yaman (2022) ile Avcı (2023) tarafından yürütülen çalışmalarda da afet ve KBRN eğitimlerinin bireylerin bilgi ve farkındalıklarını artırdığı vurgulanmıştır. Bu çalışmalar, eğitimin afet farkındalığını güçlendirdiğini göstermekte olup, mevcut araştırmanın bulgularını desteklemektedir.

Benzer şekilde Murtinger ve arkadaşları (2021), sanal gerçeklik gibi teknoloji tabanlı yöntemlerin KBRN eğitimlerinde etkili olduğunu belirtmiştir. Bu tezde kullanılan animasyon destekli eğitimin de öğrenmeyi daha anlaşılır ve kalıcı hâle getirdiği görülmüş; teknoloji destekli öğretimin KBRN eğitimlerinde önemli bir araç olduğu yönündeki bulgularla uyum göstermiştir.

Gran ve ark. (2024) tarafından simülasyon temelli eğitimle elde edilen olumlu sonuçlar da bu çalışmayla paralellik taşımaktadır. Her iki araştırmada da dijital ve etkileşimli içeriklerin katılımcıların hazırlık ve müdahale becerilerini geliştirdiği ortaya konmuştur.

Son olarak Dökmeci ve Karakuş'un (2025) çalışmasında çocukların animasyon destekli eğitimle KBRN farkındalığının arttığı belirlenmiş; bu durum, mevcut araştırmada üniversite öğrencilerinde gözlenen bilgi artışıyla benzerlik göstermektedir. Böylece animasyon destekli eğitimin hem çocuklarda hem de genç yetişkinlerde etkili bir öğretim yöntemi olduğu anlaşılmaktadır.

Genel olarak, literatürdeki tüm çalışmalar bu araştırmanın bulgularını desteklemekte; teknoloji tabanlı ve görsel içeriklerle zenginleştirilmiş KBRN eğitiminin farkındalık oluşturma ve öğrenmeyi güçlendirmede etkili bir yöntem olduğunu ortaya koymaktadır.

SONUÇ

KBRN tehditleri, sağlık, çevre ve toplum düzeni üzerinde ciddi etkiler oluşturan çok boyutlu risklerdir. Bu nedenle sağlık alanında eğitim gören öğrencilerin KBRN farkındalığına sahip olmaları kritik bir gerekliliktir. Araştırma sonuçları, öğrencilerin KBRN konusundaki başlangıç bilgi düzeylerinin düşük olduğunu

göstermiştir. Animasyon destekli eğitimin uygulanmasıyla birlikte öğrencilerin hem bilgi düzeylerinin hem de yanıt tutarlılıklarının belirgin biçimde arttığı görülmüştür. Bu durum, animasyon tabanlı öğretimin soyut ve karmaşık KBRN içeriklerinin öğrenilmesinde etkili bir araç olduğunu ortaya koymaktadır.

Öğrencilerin animasyonlara ilişkin görüşleri de bu sonucu desteklemiş; animasyonların ilgiyi artırdığı, konuların daha iyi anlaşılmasını sağladığı ve öğrenmeyi kalıcı hâle getirdiği ifade edilmiştir. Bu bulgular, KBRN konularında mevcut eğitim eksikliğini ortaya koyarken, bu eğitimin programlara daha bütüncül biçimde entegre edilmesi gerektiğini göstermektedir.

Öneriler kapsamında, KBRN ve afet farkındalık eğitimlerinin üniversite müfredatına dâhil edilmesi, animasyon, simülasyon ve diğer dijital materyallerle desteklenmesi, VR gibi ileri teknolojilerin eğitim süreçlerine entegre edilmesi ve periyodik tatbikatların düzenlenmesi önerilmektedir. İleride yapılacak araştırmalar için nitel yöntemlerle öğrencilerin öğrenme deneyimlerinin daha derinlemesine incelenmesi ve KBRN eğitimlerinin toplumsal düzeyde farklı yaş gruplarına yaygınlaştırılması önerilmektedir. Ayrıca öğrencilerin yalnızca bilgi testleriyle değil, uygulama becerilerini değerlendiren ölçme araçlarıyla da desteklenmesi, öğrenme çıktılarının daha kapsamlı biçimde değerlendirilmesine katkı sağlayacaktır.

TEŞEKKÜR

Bu çalışma, Niğde Ömer Halisdemir Üniversitesi Bilimsel Araştırma Projeleri Birimi tarafından SAT 2025/9-LÜTEP numaralı proje kapsamında desteklenmiştir. Projeye sağlanan mali ve bilimsel katkılar için Bilimsel Araştırma Projeleri Koordinasyon Birimi'ne teşekkür ederiz. Sağlanan destek, araştırmanın planlanması, yürütülmesi ve sonuçlandırılmasında önemli rol oynamıştır.

KAYNAKLAR

Avcı, G. (2023). Afet eğitiminde afetlere hazırlık: Üniversite öğrencileriyle tehlike avı. Afet ve Risk Dergisi, 6(1), 84-100.

Daşdemir, İ., Uzoğlu, M., & Cengiz, E. (2012). 7. sınıf vücudumuzdaki sistemler ünitesinde animasyon kullanımının öğrencilerin akademik başarılarına, öğrenilen bilgilerin kalıcılığına ve bilimsel süreç becerilerine etkisi. Trakya Üniversitesi Eğitim Fakültesi Dergisi, 2(2), 54-62.

Dökmeci, A. H., & Karakus, E. (2025). Effectiveness of Animation-Supported Education in Raising Awareness of Children on Chemical, Biological, Radiological, and Nuclear (CBRN) Threats. Disaster Medicine and Public Health Preparedness, 19, e177.

Dönmez, M. A. (2019). Acil tıp çalışanlarının (KBRN) kimyasal, biyolojik, radyolojik, nükleer kazalara karşı ilgi, bilgi ve tutum durumu araştırması. Doktora Tezi, Bezmialem Vakıf Üniversitesi Sağlık Bilimleri Enstitüsü.

Ercan, O., Bilen, K., & Bulut, A. (2014). The effect of web-based instruction with educational animation content at sensory organs subject on students' academic achievement and attitudes. Procedia-Social and Behavioral Sciences, 116, 2430-2436.

Gran, C. J., Skjeltorp, A., Asprusten, M., Mevassvik, O. M., Vik, T., & Helgeland, A. (2024). Simulation supported CBRNE accident coordination training.

Mızrak, S. (2018). Eğitim, afet eğitimi ve afete dirençli toplum. Muğla Sıtkı Koçman Üniversitesi Eğitim Fakültesi Dergisi, 5(1), 56-67.

Özden, G., & Yaman, M. (2022). Afet yönetiminde kimyasal, biyolojik, radyolojik ve nükleer tehditlere karşı farkındalık düzeyi: Kütahya UMKE örneği. Eskişehir Türk Dünyası Uygulama ve Araştırma Merkezi Halk Sağlığı Dergisi, 7(1), 134-144.

Yeh, C. H., & Yang, Y. P. (2024). Comparing the effect of assessment-simulation-animation-based against traditional education on nursing students' anxiety and self-efficacy in maternity clinical practicum. Nurse Education in Practice, 76, 103932.

ORAL PRESENTATION

Effects of diatomite applications on some soil properties and aggregate stability

Zerrin Civelek[1*](*0000-0002-8303-9407*),
Nutullah Özdemir[2] (*0000-0003-2554-3485*),
Furkan Güler[3](*0009-0004-7886-1174)*

[*1,2,3] Ondokuz Mayıs University, Faculty of Agriculture, Department of Soil Science and Plant Nutrition, Samsun, Türkiye

*Corresponding author e-mail: zrrncvlk@outlook.com

Abstract

In this study; the effects of diatomite application at four different doses (0%, 3%, 6%, 12%) to surface soil samples with three different textures (L, CL, C) on some soil properties and aggregate stability were investigated. As a result of the research conducted in the form of incubation experiment under greenhouse conditions; depending on the applied diatomite amounts, an increase occurred in the water holding capacity and EC values of the soils, and a change occurred in the pH values towards the neutral point. Increases occurred at various levels in the aggregate stability values of the soils depending on the application dose and the structure of the soils. The optimum diatomite doses for aggregate stability values were determined as CL 6%, C 12% and L 12%.

Keywords: Diatomite, aggregate stability, physical soil properties, chemical soil properties

Introduction

Conditioners with different origins are used to improve the dynamic properties of the soil for the purposes of use, to create a suitable plant growth environment, to eliminate the problems of the soil, to prevent environmental degradation and to control erosion (Özdemir et al., 2017). The use of some inorganic conditioners such as diatomite for these purposes is quite limited (Dessalew et al., 2017; Oliva et al., 2020).

Diatomite applications; in order to create a structure resistant to erosion by increasing the amount of water-resistant aggregates (Aksakal et al., 2012), soil of plant nutrient content (Prakash et al., 2019; Oliva et al., 2020) and in the positive impact of plant development by increasing the holding capacity (Angin et al., 2011; Boyraz and Nalbant, 2015), reducing soil compaction by reducing volume weight values (Waltz and McCarty, 2005) and surface hardness (Richardson and Karcher, 2001), soil compaction parameters (maximum dry unit weight and optimum moisture content) and resistance to mechanical forces and sensitivity to erosion (Güler, 2025), eliminating heavy metal pollution (Piri et al., 2021), improving soil consistency limits (Qu and Zhao, 2016), protecting the physical, chemical and biological structure of the soil from the harmful effects of freezing-thawing events (Angin et al., 2016) has been determined to be effective.

Research on alternative regulators that can be used to improve soil properties and create a suitable plant growth environment and a structure resistant to erosion continues. In this study, the effects of diatomite, which has limited use in agricultural areas (Dessalew et al., 2017; Oliva et al., 2020), on some soil properties and aggregate stability were examined.

Material and Methods

This research was carried out using surface soil samples taken from Ondokuz Mayıs University, Faculty of Agriculture, Bafra and Campus trial areas (41°21'50.0"N, 36°11'23.2"E; 41°33'36.8"N, 35°51'57.5"E; 41°33'39.9"N, 35°51'57.4"E). The diatomite used was obtained from Beg Tuğ Mineral Company. Some properties of the diatomite used in the experiment are presented in Table 1.

Table1. Some properties of the diatomite used in the experiment

Diatomite properties				
pH, 1:2.5	EC, µS/cm	OM, %	Lime, %	CEC, me/100g
8,35	460.00	0,06	1,20	24,23

The research was conducted as an incubation application under greenhouse conditions using 4.5 kg plastic pots. Diatomite was applied at 0%, 3%, 6%, and 12% (Hemmat et al., 2010; Aksakal et al., 2013) to the soil samples transferred to the pots. The prepared mixtures were left for incubation for 75 days. In this process, irrigation was done again when 50% of the available water in the soil was consumed. After the completion of the process, the soil samples were crumbled by hand and transferred to the laboratory for necessary analyses.

Soil texture was measured by Bouyoucos hydrometer meter (Demiralay, 1993), soil reaction was measured by pH-meter (Kacar, 2016) at 1:2.5 soil-water mixture, electrical conductivity (EC) was measured by EC-meter at 1:2.5 soil-water mixture-meter (Kacar, 2016), lime content Scheibler calcimeter (Kacar, 2016), organic matter content Walkey-Black method (Kacar, 2016), aggregate stability by wet sieving method (Demiralay, 1993), cation exchange capacity by Bower method (Kacar, 2016), exchangeable Na, K, Ca and Mg by ammonium acetate extraction (Kacar, 2016). The SPSS 21.0 package program was used to evaluate the data statistically.

Results and Discussion

Soil properties

Table 2 shows some chemical and physical properties (average) of loam, clayey loam and clay-textured soils used in the study conducted under greenhouse conditions before and after the experiment.

Table 2. Some physical and chemical properties of soils before and after the experiment

Soil properties before the trial												
Soils	pH, 1:2.5	EC, µS/cm	Sand, %	Silt, %	Clay, %	OM, %	Lime, %	Ca me/100g	Mg me/100g	Na me/100g	K, me/100g	CEC, me/100g
1(L)	7,66	419,1	45,40	30,48	24,12	1,11	15,30	52,94	12,03	0,71	0,50	66,18
2(CL)	7,67	445,3	42,36	29,60	28,04	1,50	15.90	52,37	15,11	0,98	0,55	69,01
3(C)	6,83	690,2	24,19	26,03	49,78	1,97	3,36	47,66	19,23	0,71	1,53	69,13
Soil properties after the trial												
Soils	Doses, %	pH, 1:2.5	EC, µS/cm	OM %	Lime , %	Ca me/100g	Mg me/100g	Na me/100g	K me/100g	CEC me/100g		
1 (L)	0	7,66	409,47	1,10	15,13	53,40	11,80	0,70	0,50	66,40		
	3	7,47	743,90	1,19	14,60	53,75	13,64	0,71	0,54	68,64		
	6	7,44	1024,80	1,11	13,93	53,81	14,64	0,75	0,58	69,78		
	12	7,37	1494,67	1,11	13,57	55,31	15,04	0,79	0,64	71,78		
2 (CL)	0	7,67	395,33	1,52	16,40	51,98	14,37	0,96	0,55	67,86		
	3	7,59	678,30	1,53	16,07	56,01	14,06	0,96	0,58	70,62		
	6	7,51	1012,0	1,44	15,40	57,71	15,27	1,01	0,62	71,62		
	12	7,45	1388,0	1,43	15,10	58,05	15,83	1,04	0,70	75,64		
3 (C)	0	6,83	669,27	2,11	3,08	47,96	18,92	0,72	1,56	69,16		
	3	6,98	963,87	2,06	3,14	49,27	20,38	0,77	1,59	72,01		
	6	7,10	1201,67	2,05	3,20	50,50	23,22	0,79	1,63	76,15		
	12	7,14	1855,00	1,94	3,40	55,36	24,58	0,80	1,73	82,47		

As can be understood from the evaluation of these data, at the beginning of the experiment, soil sample number 1, taken from the Bafra research and application area, had a loamy texture (L), low alkaline, no salt, low organic matter content and high level of calcareous structure. Soil sample number 2, taken from the Bafra test area, has a clay loam texture (CL), is slightly alkaline, salt-free, has low organic matter content and has a high calcareous structure. Soil sample number 3, taken from the Faculty of Agriculture campus application area, has clayey (C), slightly acid, salt-free, medium organic matter content and low calcareous structure. There are no problems associated with salinity and alkalinity in soils (pH< 8.5) (Kimsey et al., 2020).

It was determined that soil pH (reaction) was affected by diatomite applications. After the incubation period, in parallel with the application levels, there was a decrease towards a neutral point in soils with L and CL textures and an increase towards a neutral point in slightly acid reaction soil with C texture (Table 2). Electrical conductivity values were determined to increase in parallel with the application levels in all three soil groups. Low-level changes occurred in lime and organic matter contents of the soils. The cation exchange capacity and exchangeable Ca, Mg, Na and K contents of the soils increased depending on the diatomite application levels. It was determined that the changes were affected by soil properties (Table 2).

Aggregate stability

The changes in the aggregate stability (AS) values determined in the soils after four different levels of diatomite were applied to loam (L), clay loam (CL) and clay (C) textured surface soil samples and left to incubation under greenhouse conditions are given in Figure 1, and the statistical relationships and analysis of variance results of these values are given in Tables 3 and 4. As seen from the examination of Figure 1, diatomite applied in all three soil groups caused increases in the AS values of the soils. When the increases occurred were examined, the AS value in loamy textured soil number 1 (control) was 43,3% and increased to 58,10 % at the end of the 12% diatomite dose application. A similar change was realized in the clay loam textured soil number 2, and the values increased from 48,6 % to 56,1% at the end of the 12% diatomite dose application. In the clay textured sample number 3 (control), the value increased from 72,4 % to 78,3 % at a 12% diatomite application dose.

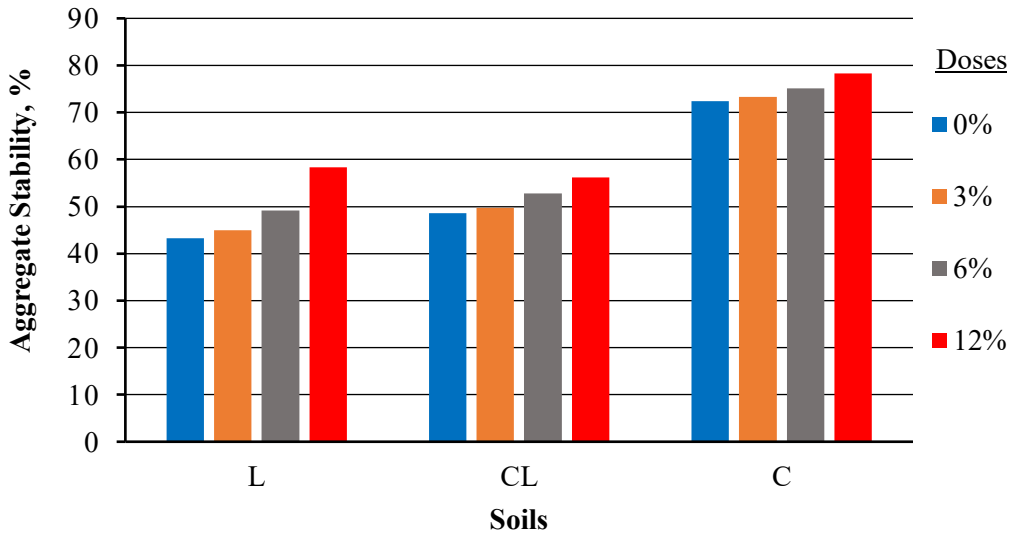


Figure 1. Changes in aggregate stability values depending on the treatments

Table 3. Interrelationships between some soil properties

Soil Properties	AS	Sand	Silt	Clay	OM	Lime	Mg	Ca	Na	K	CEC
AS	1,000										
Sand	-,789**	1,000									
Silt	-,526**	,727**	1,000								
Clay	,773**	-,991**	-,813**	1,000							
OM	,697**	-,955**	-,756**	,958**	1,000						
Lime	-,884**	,956**	,661**	-,941**	-,856**	1,000					
Mg	,921**	-,837**	-,602**	,828**	,787**	-,893**	1,000				
Ca	-,276	,637**	,439**	-,627**	-,555**	,635**	-,434**	1,000			
Na	-,266	,261	,061	-,234	-,048	,450**	-,247	,613**	1,000		
K	,906**	-,967**	-,703**	,959**	,900**	-,985**	,921**	-,548**	-,309	1,000	
CEC	,793**	-,455**	-,346*	,454**	,465**	-,508**	,757**	,259	,198	,604**	1,000

AS: Aggregate Stability, OM: Organic Matter, Mg: Magnesium, Ca: Calcium, Na: Sodium, K: Potassium, CEC: Cation Exchange Capacity

When the results of the analysis of variance on the effects of diatomite applications on AS value were evaluated (Table 4), it was seen that the effect of the mean squares the soils and the application doses were significant ($p<0.01$).

Table 4. Analysis of variance and Duncan multiple comparison tests for AS values

Source of variation	Degree of freedom	Sum of Squares	Mean Squares	F value	Level of importance
Soils (A)	2	4828,117	2414,059	12540,564	0,000
Doses (B)	3	474,741	158,247	822,062	0,000
AXB	6	85,965	14,327	74,429	0,000
Error	24	4,620	0,193		
Total	36	128535,950			

Averages*			
Soils	L	CL	C
Aggregate Stability	74,775 a	48,866 c	51,816 b

Doses	0%	3%	6%	12%
Aggregate Stability	54,744 d	56,000 c	59,033 b	64,167 a

*: According to Duncan's multiple comparison test, the means indicated with separate letters differ from each other at a 1% level.

When the results of the Duncan multiple comparison test for the source of variation found to be significant were analyzed, the results of the diatomite application of all three soils were different. According to this test, the effectiveness of diatomite application levels differed according to the means of aggregate stability (means with different letters are different from each other according to this multiple comparison test).

While significant negative correlations at 1% level were determined between the aggregate stability values of the soils and sand (-0.789**), silt (-0.526**), lime (-0.884**) data, significant positive correlations at 1% level

were determined between clay (0.773**), organic matter (0.697**), exchangeable magnesium (0.921**), exchangeable potassium (0.906**), cation exchange capacity (0.793**) values of the soils (Table 3).

Aggregate stability values can be used as a good indicator in evaluating the effects of agricultural applications on soil quality parameters and erosion susceptibility. As aggregate stability values increase, quality parameters improve and erosion susceptibility decreases (Özdemir, 2013; Nweke and Nnabude, 2015). When the effects of diatomite applications are examined in this direction, it can be said that diatomite applications increase structural durability and reduce dispersion probability in all three soil groups. When the average proportional changes caused by the applications according to the aggregate stability values of the soils are examined, it is determined that the effectiveness occurs as L (%13.04) > CL (%6.71) > C (%3.27). These findings reveal that diatomite effectiveness decreases as the clay content increases. This situation may be due to the mutual interaction between diatomite and clay content. As a result of their research, Angin et al. (2016) determined that diatomite application reduced bulk density and increased aggregate stability values.

Results

In this study, the effects of diatomite application at four different doses (0%, 3%, 6%, 12%) to soils with three different textures (L, CL, C) on some soil properties and aggregate stability were investigated. The results of the analysis and evaluations can be summarized as follows.

It was determined that pH values in soils decreased towards the neutral point in CL and L textured soils in parallel with the diatomite application dose, and increased towards the neutral point in slightly acidic soil with C texture. Diatomite application increased the EC values of the soils. Low-level changes occurred in the lime and organic matter contents of the soils, and the level of change depended on the initial properties of the soils. Diatomite application caused increases in the amount of water held in the soil, exchangeable cations and cation exchange capacities in parallel with the application doses.

Diatomite application increased the aggregate stability values of the soils. The change that occurred was affected by the soil properties and application dose, and the healing effect of diatomite was more effective in L textured soil. The optimum diatomite doses for aggregate stability values were determined as L 12%, CL 6% and C 12%.

References

Aksakal, E. L., Angin, I., & Oztas, T. (2012). Effects of diatomite on soil physical properties. Catena, 88(1), 1-5.

Aksakal, E. L., Angin, I., & Oztas, T. (2013). Effects of diatomite on soil consistency limits and soil compactibility. Catena, 101, 157-163.

Angin, I., Kose, M., & Aslantas, R. (2011). Effect of diatomite on growth of strawberry. Pakistan Journal of Botany, 43(1), 573-577.

Angin, I., Sari, S., & Aksakal, E. L. (2016). Effects of diatomite (DE) application on physical properties of soils subjected to freeze-thaw cycles. Soil and Tillage Research, 160, 34-41.

Boyraz, D., & Nalbant, H. (2015). Comparison of zeolite (clinoptilolite) with diatomite and pumice as soil conditioners in agricultural soils. Pak. J. Agri. Sci., Vol. 52(4), 923-929.

Demiralay, İ. (1993). Toprak fiziksel analizleri. Atatürk Üniversitesi Ziraat Fakültesi Yayınları, 143.

Dessalew, G., Beyene, A., Nebiyu, A., & Ruelle, M. L. (2017). Use of industrial diatomite wastes from beer production to improve soil fertility and cereal yields. Journal of cleaner production, 157, 22-29.

Güler, F. (2025). Diatomit uygulamalarının toprak sıkışma parametreleri ve kıvam limitleri üzerine etkileri. Yüksek Lisans Tezi, Ondokuz Mayıs Üniversitesi Lisansüstü Eğitim Enstitüsü, Samsun.

Hemmat, A., Aghilinategh, N., Rezainejad, Y., & Sadeghi, M. (2010). Long-term impacts of municipal solid waste compost, sewage sludge and farmyard manure application on organic carbon, bulk density and consistency limits of a calcareous soil in central Iran. Soil and Tillage Research, 108(1-2), 43-50.

Kacar B., (2016). Bitki, Toprak ve Gübre Analizleri, Fiziksel ve Kimyasal toprak Analizleri. Ankara: Nobel Yayın Dağıtım, Yayın No.1524.

Kimsey, M. J., Laing, L. E., Anderson, S. M., Bruggink, J., Campbell, S., Diamond, D., ... & Vaughan, R. (2020). Soil mapping, monitoring, and assessment. Forest and rangeland soils of the United States under changing conditions: A comprehensive science synthesis, 169-188.

Nweke, I. A., & Nnabude, P. C. (2015). Aggregate stability of four soils as evaluated by different indices. Journal of Experimental Biology and Agricultural Sciences, Volume – 3(3).

Oliva, K. M. E., do Nascimento, C. W. A., da Silva, F. B. V., Araújo, P. R. M., de Oliveira, E. C. A., Feitosa, M. M., & Lima, L. H. V. (2020). Biomass and concentration of nutrients and silicon in sugarcane grown on soil fertilized with diatomite. Revista Brasileira de Ciências Agrárias, 15(4), 1-7.

Özdemir N., (2013). Toprak ve Su Koruma. OMÜ Ziraat Fakültesi Ders kitabı No. 22. Samsun.

Özdemir, N., Öztürk, E., & Durmuş, Ö. T. K. (2017). Organik düzenleyici uygulamalarının yapay yağış koşulları altında toprak kaybı üzerine etkileri. Anadolu Tarım Bilimleri Dergisi, 32(1), 114-120.

Piri, M., Sepehr, E., Samadi, A., Farhadi, K. H., & Alizadeh, M. (2021). Contaminated soil amendment by diatomite: chemical fractions of zinc, lead, copper and cadmium. International Journal of Environmental Science and Technology, 18, 1191-1200.

Qu, J. L., & Zhao, D. X. (2016). Comparative research on tillable properties of diatomite-improved soils in the Yangtze River Delta region, China. Science of the Total Environment, 568, 480-488.

Prakash, N. B., Anitha, M. S., & Sandhya, K. (2019). Behaviour of different levels and grades of diatomite as silicon source in acidic and alkaline soils. Silicon, 11, 2393-2401.

Richardson, M. D., & Karcher, D. E. (2001). Addition of inorganic amendments to a mature, sand-based putting green. International Turfgrass Society Research Journal, 2001, Vol. 9, 610-614 ref. 10.

Waltz, F. J., & McCarty, L. B. (2005). Field evaluation of soil amendments used in rootzone mixes for golf course putting greens. International Turfgrass Society Research Journal, 2005, Vol. 10, 1150-1158 ref. 30.

ORAL PRESENTATION

Doğal Bt izolatından elde edilen parasporal proteinin PC-3 hücreleri üzerinde sitotoksik ve hücre göçünü inhibe edici etkilerinin incelenmesi

Müjgan Kesik Oktay[1*] *(ORCID: https://orcid.org/0000-0002-0857-4872),* Burcu Şahin[2] (*ORCID: https://orcid.org/0000-0002-5701-1371*), Hatice Güneş[2] (*ORCID: https://orcid.org/ 0000-0001-5191-365X*)

[*1]Afyonkarahisar Sağlık Bilimleri Üniversitesi, Şuhut Sağlık Hizmetleri Meslek Yüksekokulu, Tıbbi Hizmetler ve Teknikler Bölümü, Afyon, Türkiye
[2]Muğla Sıtkı Koçman Üniversitesi, Fen Fakültesi, Biyoloji Bölümü, Muğla, Türkiye

*Sorumlu yazar e-mail: mujgan.oktay@afsu.edu.tr

Özet

Bacillus thuringiensis (Bt), sporulasyon sırasında oluşturduğu parasporal kristaller ve içerdiği Cry proteinleri nedeniyle tarım ve halk sağlığında yaygın kullanılan önemli bir biyoinsektisittir. Son yıllarda Bt suşlarının insektisidal olmayan ancak seçici antikanser aktiviteye sahip parasporin proteinleri üretmesi, bu bakteriyi terapötik açıdan dikkat çekici hale getirmiştir. Parasporinler, normal hücrelere zarar vermeden çeşitli kanser hücre hatlarında sitotoksisite oluşturmakta olup, yeni biyoterapötik adaylar arasında gösterilmektedir. Bu çalışmada toprak örneklerinden izole edilen Bt 5.4 izolatının PC-3 prostat kanseri hücre hattı üzerindeki sitotoksik ve anti-migrasyon etkileri değerlendirilmiştir. Öncelikle parasporal protein eldesi gerçekleştirilmiş ve PC-3 hücrelerinde MTT analiziyle sitotoksik etkiler belirlenmiştir. Farklı dozlarda uygulama sonrası 48 saatlik inkübasyon sonucunda izolatın IC_{50} değeri hesaplanmış, cisplatin pozitif kontrol olarak kullanılmıştır. Hücre göçü üzerindeki etkinin değerlendirilmesi amacıyla in vitro yara iyileşme (wound healing) deneyi uygulanmıştır. 0, 4, 10, 24 ve 48. saatlerde elde edilen görüntüler ImageJ yazılımı ile analiz edilerek yara kapanma yüzdeleri hesaplanmıştır. Kontrol grubunda yaranın zamanla belirgin şekilde daraldığı ve 48. saatte yaklaşık %59,3 kapanma görüldüğü saptanmıştır. Buna karşılık Bt 5.4 parasporal proteini uygulanan hücrelerde yara kapanması belirgin biçimde baskılanmış ve 48. saatte yalnızca %24,4 oranında kapanma gerçekleşmiştir. İstatistiksel analizlerde zaman × tedavi etkileşimi anlamlı bulunmuştur ($p = 0.0039$). Bu bulgular, Bt 5.4 izolatına ait parasporal proteinin PC-3 hücrelerinin hem yaşamını azaltarak sitotoksisite oluşturduğunu hem de hücre göçünü inhibe ettiğini göstermektedir. Sonuçlar, Bt parasporal proteinlerinin metastaz hedefli yeni biyoterapötik yaklaşımlar için potansiyel aday olabileceğini ortaya koymaktadır.

Anahtar kelimeler: *Bacillus thuringiensis*, Parasporin, PC-3 prostate kanseri hücre hattı, sitotoksik aktivite, Wound healing assay

Investigation of the cytotoxic and migration-ınhibitory effects of a parasporal protein derived from a natural *Bacillus thuringiensis* ısolate on PC-3 cells

Abstract

Bacillus thuringiensis (Bt) is a Gram-positive, spore-forming bacterium widely used in agriculture and public health due to its parasporal crystals produced during sporulation, which mainly contain insecticidal Cry proteins. In recent years, several Bt strains have been shown to synthesize parasporins—non-insecticidal proteins that selectively exhibit cytotoxic effects on human cancer cells without harming normal cells—positioning Bt as a promising source of novel biotherapeutic molecules. In this study, the cytotoxic and anti-migratory effects of parasporal proteins obtained from the soil-isolated Bt strain 5.4 were evaluated on PC-3 human prostate cancer cells. Parasporal protein extraction was performed, and cytotoxicity was assessed using the MTT assay. Following treatment with different concentrations of the protein for 48 hours, the IC_{50} value was calculated using cisplatin as a positive control. To investigate the potential inhibitory effect on cell migration, an in vitro wound healing assay was conducted. Images captured at 0, 4, 10, 24, and 48 hours were analyzed using the ImageJ software to determine wound closure percentages. In the control group, the wound area progressively decreased, reaching approximately 59.3% closure at 48 hours. In contrast, cells treated with Bt 5.4 parasporal protein displayed markedly reduced wound closure, achieving only 24.4% closure at the same time point. Statistical analysis revealed a significant

interaction between time and treatment ($p = 0.0039$), indicating that the inhibitory effect on migration increased over time. Overall, these findings demonstrate that parasporal proteins derived from Bt strain 5.4 exert both cytotoxic and migration-inhibitory effects on PC-3 cells. This study suggests that Bt-derived parasporal proteins may represent promising candidates for future metastasis-targeted biotherapeutic applications.

Keywords: Bacillus thuringiensis, Parasporin, PC-3 prostate cancer cells, Cytotoxic activity, Wound healing assay

GİRİŞ

Bacillus thuringiensis (Bt), Gram-pozitif, aerob ve spor oluşturan bir bakteri olup sporulasyon sırasında ayırt edici özelliği olan parasporal kristaller üretir (Li ve ark., 2024;; Lenina ve ark., 2013). Bu kristaller çoğunlukla böceklere özgü δ-endotoksinler olan Cry proteinlerini içerir. Cry proteinler, Lepidoptera, Diptera ve Coleoptera başta olmak üzere birçok böcek grubuna karşı yüksek toksisite gösterdiğinden dolayı (Lenina ve ark., 2013) tarım ve halk sağlığında yaygın kullanılan temel biyoinsektisitlerden biridir. Bt suşları ayrıca chitinazlar, proteazlar, vegetatif insektisit proteinleri (Vip), bakteriyosinler ve özellikle terapötik açıdan dikkat çeken parasporinler gibi çeşitli biyolojik aktif moleküller de sentezlemektedir (Juárez-Hernández ve ark., 2017).

Parasporinler, insektisidal aktivite göstermeyen Bt suşlarının ürettiği, ancak seçici olarak insan kanser hücrelerine etki eden sitotoksik proteinlerdir. Parasporin kavramı ilk olarak Mizuki ve arkadaşları tarafından tanımlanmış olup, normal hücrelere karşı toksik olmayan ve hemolitik aktivite göstermeyen özgün bir biyolojik profil sunmaktadır (Okumura ve ark., 2011; Wong ve ark., 2010; Akiba ve ark., 2009). Günümüzde PS1–PS6 olmak üzere altı parasporin ailesi tanımlanmış olup, her biri çeşitli kanser hücre hatları üzerinde farklı mekanizmalara sahiptir (Okumura ve ark., 2011; Kitada ve ark., 2009; Brasseur ve ark., 2015). Parasporinlerin HepG2, Caco-2, HeLa, MOLT-4, Jurkat ve CEM-SS gibi birçok kanser hücre hattında güçlü sitotoksisite neden olduğu kanıtlanmıştır (Wong ve ark., 2010; Rendon-Marin ve ark., 2021). Mekanizmaları parasporin ailesine göre değişmekle birlikte membran por oluşumu, iyon dengesinin bozulması, kaspaz aracılı hücre ölümü veya reseptör-bağımlı sinyalleşme yollarının aktivasyonu gibi süreçleri içermektedir. Seçici antikanser etkilerinden dolayı parasporinler, son yıllarda yeni nesil biyoterapötik adaylar arasında yer almaktadır.

Bu çalışmada toprak örneklerinden izole edilen 5.4 Bt izolatının, PC-3 (Prostat kanseri hücre hattı) üzerinde sitotoksik etkisi belirlenmiş olup; hücreler üzerinde yapay olarak oluşturulan yara üzerinde hücre göçünü inhibe edip etmediği farklı zaman dilimlerinde yapılan ölçümlerle incelenmiştir. Farklı ekosistemlerden izole edilen Bt suşlarının parasporin gen içeriklerinin belirlenmesi, yeni toksisite profillerinin tanımlanması ve biyoteknolojik uygulamalar için yeni moleküllerin keşfedilmesi açısından önemli bir araştırma alanı oluşturmaktadır.

MATERYAL VE METOT

Bakteri izolatları

Bu çalışmada Muğla Sıtkı Koçman Üniversitesi 15/152 BAP projesi kapsamında gerçekleştirilen doktora tez çalışmasında izole edilen Bt 5.4 izolatı kullanılmıştır (Kesik Oktay, 2019. İzolasyon toprak örneklerinden Santana vd. (2008)' e göre gerçekleştirilmiştir.

Sitotoksik aktivitenin belirlenmesi

Bu çalışmada PC-3(Prostat kanseri) hücre hattı kullanılmış olup, hücreler % 10 fetal bovin serum ve 100 µg/ml penisilin/streptomisin içeren RPMI 1640 besi ortamında, 37°C'de %5 CO2, %95 hava içeren nemlendirilmiş inkübatörde kültüre alınmışlardır.

Sitotoksik aktivite MTT testi ile değerlendirilmiştir. Bu test, metabolik olarak aktif hücrelerin MTT'yi mor renkli formazan kristallerine indirgemesine dayanır. Bu amaçla, hücreler, 96 kuyulu plaklarda 2×10^4 hücre/kuyu yoğunluğunda 90 µL hücre süspansiyonu ile ekilerek 16–20 saat boyunca 37°C, %5 CO_2 ve %98 nem koşullarında inkübe edilmiştir. Ardından, aktif haldeki Bt 5.4 parasporal kristal proteinleri ilgili konsantrasyonlarda her bir kuyuya eklenmiştir ve plakalar 24–48 saat inkübasyona bırakılmıştır. İnkübasyon sonunda besi ortamı uzaklaştırılarak, her kuyuya 100 µL taze besi ortamı eklenmiştir. Her kuyuya 1:10 oranında MTT stok çözeltisi (5 mg/mL) ilave edilerek plakalar 4 saat inkübe edilmiştir. Ardından 100 µL DMSO eklenerek kristaller çözülmüş ve plakalar 150 rpm hızda 5 dakika çalkalanmıştır. Optik yoğunluk ölçümleri 540 nm (690 nm referans) dalga boylarında bir mikroplaka okuyucu ile gerçekleştirilmiştir (Mikroplate reader, Thermo Fisher Scientific, ABD).

Wound healing assay

Subkonfluent durumda bulunan hücreler pasajlanarak 24 kuyulu hücre kültürü plaklarına her kuyuya 1×10^5 hücre gelecek şekilde inokule edilmiştir. Hücrelerin yüzeye tutunup homojen bir tabaka oluşturması için plateler 37°C, %5 CO_2 ve yüksek nem içeren inkübatörde 20–24 saat bekletilmiştir. İnkübasyon sonrasında, her kuyunun orta hattı boyunca 200 µL'lik pipet ucu kullanılarak düz bir çizik oluşturulmuş ve böylece standart bir yara alanı elde edilmiştir. Çizik sonrası hücre artıkları ve askıda kalan hücreler uzaklaştırılmak üzere kuyular PBS ile iki kez yıkanmıştır. parasporal protein süspansiyonu kuyulara eklenmiştir (Rodriguez ve ark., 2005). Hücre göçü, çizik hattı boyunca gerçekleşen kapanmanın izlenmesiyle değerlendirilmiştir. 4, 12, 24 ve 48. saatlerde plakalar inverted mikroskop altında görüntülenmiştir. Elde edilen görüntüler, çizik kenarına doğru ilerleyen hücrelerin miktarını ve kapanma hızını karşılaştırmak amacıyla kaydedilmiştir. Hücrelerin boşluğa doğru hareketi takip edilerek yara iyileşmesi (wound closure) ve hücre göç dinamikleri belirlenmiştir.

İnkübasyon süresi boyunca hücre göçü, çizik ile oluşturulan boşluk boyunca 0, 4, 24 ve 48. saatlerde inverted mikroskop (10× büyütme) altında izlenmiş ve fotoğraflanmıştır. Elde edilen görüntüler, yara alanının kantitatif ölçümü amacıyla ImageJ yazılımı (http://rsb.info.nih.gov) kullanılarak analiz edilmiştir. Her zaman noktasında çizik bölgesinin alanı ölçülmüş, hücre göçü ve kapanma düzeyi yara kapanma yüzdesi (wound closure %) WC%=[a0−aΔa0]×100 formülü ile hesaplanmıştır.

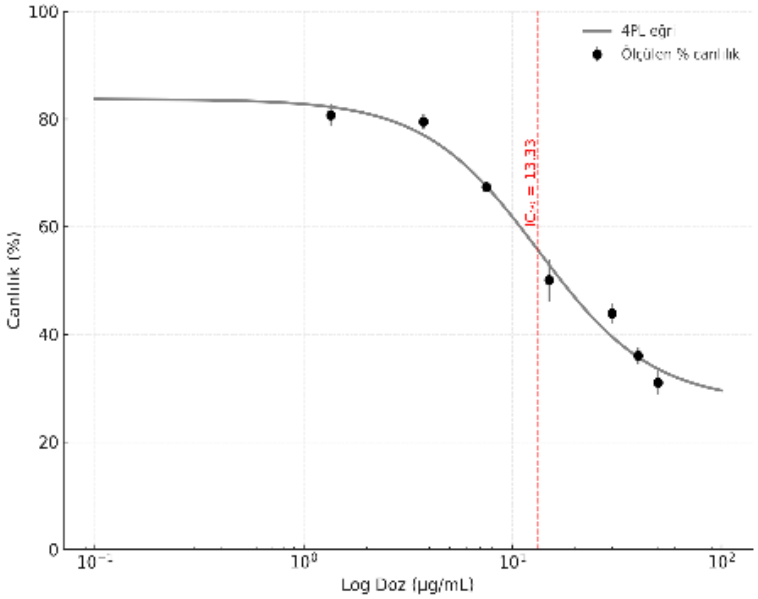
İstatistiksel analizler

Tüm analizlerde GraphPad Prism 8.0.2 programı kullanılmıştır. Sitotoksisite deneyleri sonucunda uygulamalar arasında fark olup olmadığı, tek yönlü varyans analizi (ANOVA) ile değerlendirilmiştir. Uygulamaların kıyaslanmasında Dunnett ve TUKEY HSD testleri kullanılmıştır.

BULGULAR

Sitotoksik aktivitenin belirlenmesi

Bt 5.4 izolatından parasporal pprotein eldesi gerçekleştirilmesinin ardından PC-3 hücre hattı üzerinde farklı konsantrasyonlarda sitotoksik aktivitesi incelenmiştir. 48 saat inkübasyon sonrasında Bt 5.4 izolatının IC_{50} değeri belirlenmiştir. Çalışmalar gerçekleştirilirken pozitif kontrol olarak cisplatin kullanılmıştır.

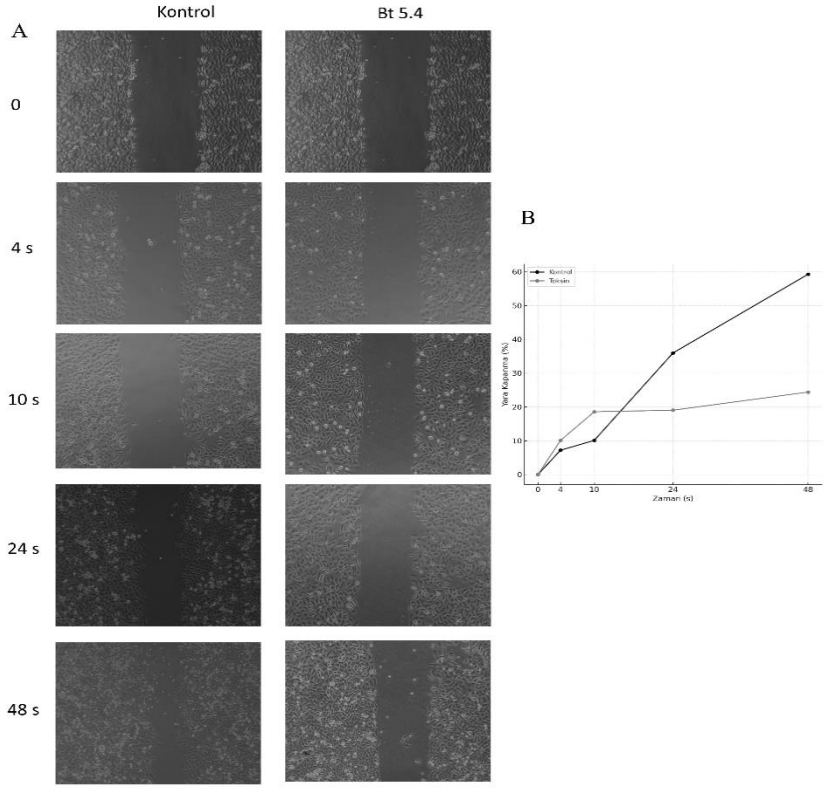


Şekil 1: Bt 5.4 parasporal proteinine ait IC_{50} değeri. 1.35, 3.75, 7.5, 15, 30, 40 ve 50 µg/ml dozlar kullanılmıştır. Veriler üç tekrarlı olarak gerçekleştirilen deneylerin ortalama değerleridir.

Wound healing assay

PC-3 hücreleri kullanılarak yara iyileşme deneyi gerçekleştirilmiştir. İnverted mikroskop altında görüntüler; 0 (başlangıç), 4, 10, 24 ve 48 saat aralıklarla kaydedilmiştir (10×). Çizik (wound) alanı ImageJ programı kullanılarak ölçülmüş ve yara kapanma yüzdesi başlangıç genişliği referans alınarak hesaplanmıştır. Kontrol grubunda yara bölgesi zaman içinde belirgin şekilde daralmıştır. Yara kapanmasının özellikle 10–24. saat

arasında hızlandığı ve 48. Saatte %59.3 yara kapanma oranı görülmüştür.Toksin uygulanan hücrelerde yara kapanması belirgin şekilde daha yavaştır. Yara genişliği zaman içinde azalsa da 48. saatte yalnızca %24.4 kapanma gözlenmiştir. 24 ve 48. saatlerde kontrol grubuna kıyasla kapanma oranı ciddi düzeyde daha düşüktür. Kontrol grubunda kapanma zamanla belirgin şekilde artarken, toksin uygulamasında yara kapanma hızı belirgin olarak azalmıştır. Zaman × tedavi etkileşimi istatistiksel olarak anlamlı bulunmuştur ($p = 0.0039$), bu da toksinin hücre göçünü zamanla giderek daha fazla inhibe ettiğini göstermektedir.



Şekil 2: A) PC-3 hücreleri üzerinde yara iyileşmesi deneyi sonuçları. Kontrol ve 5.4 izolatına ait parasporal proteinlerin uygulandığı PC-3 hücreleri 0,4, 10, 24, ve 48. saatlerde görüntülenmiştir.
B**)** Kontrol ve toksin uygulanan hücrelerde zaman içinde gözlenen yara kapanma (%) değişimi.

TARTIŞMA

Hücre göçü, gerek fizyolojik süreçlerde gerekse patolojik durumlarda temel bir biyolojik olay olup, yara iyileşmesi, embriyonik gelişim, immün yanıt ve özellikle kanser metastazında kritik bir rol oynamaktadır. Literatürde normal ve tümör hücrelerinin hareketliliğinin, hücrelerin polarizasyonuyla başlayan ve pseudopod oluşumu, aktin filamentlerinin yeniden düzenlenmesi ve hücre dışı matriks (ECM) ile dinamik bağlantıların kurulmasını içeren karmaşık bir mekanizma ile gerçekleştiği iyi bilinmektedir (Keren ve Herber, 2011). Bu süreçte hücre, ileri doğru uzanarak ECM'e tutunmakta ve arka kısmının kasılmasıyla yönlü bir hareket oluşturmaktadır. Dolayısıyla aktin dinamiği ve hücresel çıkıntı oluşumu, göçün başlatılması ve sürdürülmesi için zorunludur.

Son yıllarda çeşitli doğal bileşiklerin ve mikrobiyal ürünlerin kanser hücrelerinde migrasyonu baskıladığına ilişkin çalışmalar artmıştır. Luo ve ark. (2014) tarafından *Lysinibacillus sphaericus* toksinlerinin A549 hücrelerinin hareketliliğini azalttığı; Direito ve ark. (2019) tarafından mentol ekstraktının HT-29 hücrelerinde benzer şekilde göçü engellediği bildirilmiştir. Ayrıca Coriandrum sativum ekstraktının PC-3 hücrelerinde (Elmas ve ark., 2018), miR-154'ün melanoma hücrelerinde (Wang ve ark., 2019), Brucea javanica yağının özofajiyal kanser hücrelerinde (Qiu ve ark., 2019) ve *Sempervivum tectorum* ekstraktının HCT116 hücrelerinde (Cattaneo ve ark., 2019) migrasyon karşıtı etkiler oluşturduğu gösterilmiştir. Ancak literatür incelendiğinde, *Bacillus thuringiensis*'e ait parasporal proteinlerin yara iyileşmesi veya kanser hücre göçü üzerindeki etkilerine dair herhangi bir çalışmanın bulunmadığı dikkat çekmektedir. Bu durum, elde edilen bulguların özgünlüğünü ve literatüre katkı potansiyelini artırmaktadır.

Bu çalışmada 5.4 *B. thuringiensis* izolatından elde edilen parasporal proteinin PC-3 hücrelerinin hareketliliği üzerindeki etkisi yara iyileşme deneyi ile değerlendirilmiştir. Kontrol grubunda yaranın zamanla düzenli

biçimde kapandığı gözlenmiş, bu durum PC-3 hücrelerinin doğal migrasyon kapasitesiyle uyumlu bulunmuştur. Buna karşın parasporal protein uygulanan deney grubunda yaranın kapanmaması, hücrelerin çizik bölgesine doğru yönelim göstermediğini ve göçün belirgin şekilde baskılandığını ortaya koymuştur. Bu etkinin, aktin filament organizasyonu, hücre polarizasyonu veya hücre–ECM etkileşimlerinin bozulması gibi mekanizmalardan kaynaklanabileceği düşünülmektedir. Benzer şekilde diğer migrasyon baskılayıcı doğal bileşiklerin aktin dinamiğinde bozulma, fokal adhezyonların zayıflatılması veya hücre iskeletinin yeniden şekillenmesinin engellenmesi gibi yollarla etki gösterdiği literatürde bildirilmektedir. Bu çalışmanın sonuçları, 5.4 izolatına ait parasporal proteinin PC-3 hücrelerinin göçünü anlamlı düzeyde azalttığını göstermekte ve *B. thuringiensis* kaynaklı proteinlerin kanser hücresi migrasyonunu hedef alan yeni potansiyel biyolojik ajanlar olabileceğini düşündürmektedir. Bu bulgular, özellikle metastaz odaklı antikanser stratejiler açısından önem taşımaktadır. Bununla birlikte, bu etkinin moleküler mekanizmasını anlamak için aktin polimerizasyonu, Rho GTPaz aktivitesi, fokal adhezyon kompleksi proteinleri (örneğin FAK, paxillin) ve ECM etkileşimlerine yönelik ileri analizlerin yapılması gerekmektedir.

Sonuç olarak, bu çalışma *B. thuringiensis* parasporal proteinlerinin ilk kez prostat kanseri hücrelerinin migrasyonunu inhibe edebileceğini göstermektedir. Genişletilmiş in vitro çalışmalar ve farklı kanser hücre hatlarıyla yapılacak analizler, bu proteinlerin potansiyel terapötik etkilerinin anlaşılmasına önemli katkı sağlayacaktır.

KAYNAKLAR

Li, Kaixiao, Chen, Mingzhu, Shi, Jingyi and Mao, Tian. "An overview of the production and use of *Bacillus thuringiensis* toxin" Open Life Sciences, vol. 19, no. 1, 2024, pp. 20220902. https://doi.org/10.1515/biol-2022-0902

Lenina NK, Naveenkumar A, Sozhavendan AE, Balakrishnan N, Balasubramani V, Udayasuriyan V. Characterization of parasporin gene harboring Indian isolates of Bacillus thuringiensis. 3 Biotech. 2014 Oct;4(5):545-551. doi: 10.1007/s13205-013-0190-9

Juárez-Hernández, E.O., Casados-Vázquez, L.E., Brieba, L.G. vd. The crystal structure of the chitinase ChiA74 of *Bacillus thuringiensis* has a multidomain assembly. *Sci Rep* **9**, 2591 (2019). https://doi.org/10.1038/s41598-019-39464-z

Wang, J., Fang, Y., Liu, Y. F., Wang, X., Wang, X. L., Wang, R. Y., & Meng, Z. D. (2019). miR-154 inhibits cell proliferation and metastasis in melanoma by targeting AURKA and serves as a novel prognostic indicator. *European Review for Medical and Pharmacological Sciences, 23*(10), 4275–4284.

Akiba, T., & Okumura, S. (2016). Parasporins 1 and 2: Their structure and activity. *Journal of Invertebrate Pathology, 142*, 44–49.

Okumura, S., Saitoh, H., Ishikawa, T., Inouye, K., & Mizuki, E. (2011). Mode of action of parasporin-4, a cytocidal protein from *Bacillus thuringiensis*. *Biochimica et Biophysica Acta (BBA) – Biomembranes, 1808*(6), 1476–1482. https://doi.org/10.1016/j.bbamem.2010.11.003

Okumura, S., Ohba, M., Mizuki, E., Crickmore, N., Coté, J.-C., Nagamatsu, Y., Kitada, S., Sakai, H., Harata, K., Shin, T., vd. (2014). Parasporin nomenclature. Retrieved 7 November 2014, from http://parasporin.fitc.pref.fukuoka.jp/

Brasseur, K., Auger, P., Asselin, E., Parent, S., Côté, J. C., & Sirois, M. (2015). Parasporin-2 from a new *Bacillus thuringiensis* 4R2 strain induces caspases activation and apoptosis in human cancer cells. *PLOS ONE, 10*(8), e0135106.

Kitada, S., Abe, Y., Maeda, T., & Shimada, H. (2010). Parasporin-2 requires GPI-anchored proteins for the efficient cytocidal action to human hepatoma cells. *Toxicology, 264*, 80–88.

Kitada, S., Abe, Y., Shimada, H., Kusaka, Y., Matsuo, Y., Katayama, H., Okumura, S., Akao, T., Mizuki, E., Kuge, O., Sasaguri, Y., Ohba, M., & Ito, A. (2006). Cytocidal actions of parasporin-2, an antitumor crystal toxin from *Bacillus thuringiensis*. *Journal of Biological Chemistry, 281*, 26350–26360.

Wong RS, Mohamed SM, Nadarajah VD, Tengku IA. Characterisation of the binding properties of *Bacillus thuringiensis* 18 toxin on leukaemic cells. J Exp Clin Cancer Res. 2010 Jun 30;29(1):86. doi: 10.1186/1756-9966-29-86. PMID: 20591169; PMCID: PMC2909967.

Rendon-Marin, S., Quintero-Gil, C., Lemeshko, V. V., & Orduz, S. (2021). Cytolytic activity of peptides derived from the Cry11Bb insecticidal toxin of *Bacillus thuringiensis* subsp. *medellin*. *Archives of Biochemistry and Biophysics, 704*, 108891. https://doi.org/10.1016/j.abb.2021.108891

Santana, M.A., Moccia, V.C., Gillis, A., '*Bacillus thuringiensis* improved isolation methodology from soil samples', J Microbiol Methods., 75: 357-358, (2008).

Mosmann, T. (1983). Rapid colorimetric assay for cellular growth and survival: Application to proliferation and cytotoxicity assays. *Journal of Immunological Methods, 65*, 55–63.

Rodriguez LG, Wu X, Guan JL. Wound-healing assay. In: Guan JL, editor. *Cell Migration: Developmental Methods and Protocols.* Totowa (NJ): Humana Press; 2005. p. 23-29.

Kesik Oktay M. Isolatıon of native *Bacillus thuringiensis* strains from cherry orchards, determination of cry gene profiles and studies on parasporins. PhD thesis. Muğla Sıtkı Koçman University, Graduate School of Natural and Applied Sciences, Muğla. 2019.

Hulkower KI, Herber RL. Cell migration and invasion assays as tools for drug discovery. *Pharmaceutics.* 2011;3(1):107-124.

Elmas, L., Secme, M., Mammadov, M., Fahrioğlu, U., & Dodurga, Y. (2018). The determination of the potential anticancer effects of *Coriandrum sativum* in PC-3 and LNCaP prostate cancer cell lines. *Journal of Cellular Biochemistry, 120*, 3506–3513.

Qiu, Z. H., Zhang, W. W., Zhang, H. H., & Jiao, G. H. (2019). *Brucea javanica* oil emulsion improves the effect of radiotherapy on esophageal cancer cells by inhibiting cyclin D1–CDK4/6 axis. *World Journal of Gastroenterology, 25*(20), 2463–2472.

Luo, W., Liu, C., Zhang, R., He, J., & Han, B. (2014). Anticancer activity of binary toxins from *Lysinibacillus sphaericus*. *Journal of Cancer Therapy, 5*, 811–819.

Cattaneo, F., De Marino, S., Parisi, M., Festa, C., Castaldo, M., Finamore, C., Duraturo, F., Zollo, C., Ammendola, R., & Iorizzi, M. (2019). Wound healing activity and phytochemical screening of purified fractions of Sempervivum tectorum L. leaves on HCT 116. Phytochemical Analysis, 30(5), 645–655. https://doi.org/10.1002/pca.2844

Direito, R., Rocha, J., Lima, A., Gonçalves, M. M., Duarte, M. P., Mateus, V., Sousa, C., Fernandes, A., Pinto, R., Boavida Ferreira, R., Sepodes, B., & Figueira, M.-E. (2019). Reduction of inflammation and colon injury by a spearmint phenolic extract in experimental bowel disease in mice. *Medicines, 6*(2), 65. https://doi.org/10.3390/medicines6020065

ORAL PRESENTATION

Cyclic voltammetric determination of brilliant blue in energy drinks by using a pretreated pencil graphite electrode

Kuddusi Karaboduk[1*] (Orcid: *https://orcid.org/0000-0003-0078-723X*)

[*1]Gazi University, Vocational School of Health Services, Department of Health Care Services, Ankara, Turkiye.

*Corresponding author e-mail: kuddusi@gazi.edu.tr

Abstract

The proposed voltammetric technique exhibited an excellent linear response on a pretreated pencil graphite electrode (p-PGE) surface in 0.5 M HCl within the 0.02-3.00 µM Brilliant Blue (BB) concentration range. The limit of detection (LOD) for the method in 0.5 M HCl was determined to be 8.50 nM BB. Furthermore, the developed approach was successfully applied to energy drink samples. The results showed good agreement with those obtained by the spectrophotometric method, confirming the reliability of the proposed voltammetric procedure.

Keywords: Brilliant blue, voltammetric determination, energy drink, activated pencil graphite electrode

INTRODUCTION

Artificial colorants are widely incorporated into various food products, including candies, coated tablets, instant drink powders, jellies, desserts, fortified energy beverages, ice creams, and gelatin-containing foods (Karaboduk, 2025). The contamination of aquatic ecosystems by industrial discharges containing synthetic dyes represents a primary global environmental concern. Triarylmethane-based dyes, known for their intense coloration and extensive industrial applications, are particularly resistant to traditional wastewater treatment processes (Thakar et al., 2025). Brilliant Blue (BB) ($C_{37}H_{34}N_2Na_2O_9S_3$; molecular weight: 792.86; E133) as a triarylmethane-based dye is utilized as an industrial-grade colorant in various applications, including toilet cleaning agents, paper dyeing, inks, and markers, as well as in the formulation of cakes, pet foods, powdered beverages, and pharmaceutical products (Jadhav & Gogate, 2025). Its use in food formulations is authorized in the United States and the European Union, with established acceptable daily intake (ADI) limits of 2.5 mg/kg and 5 mg/kg body weight, respectively (Fang et al., 2025).

Various analytical techniques have been employed for the determination of BB, including chromatography (Faraji et al., 2017), spectrophotometry (Olgun et al., 2024), and colorimetry (Özgen et al., 2025). Although these conventional analytical approaches exhibit high sensitivity and selectivity, their practical applicability is often constrained by several drawbacks, including the need for costly instrumentation, labor-intensive and time-consuming sample preparation and analysis procedures, the requirement for skilled operators, and the extensive use of organic solvents (Karaboduk & Karaboduk, 2025). In recent years, electrochemical techniques have emerged as promising alternatives owing to their cost-effectiveness, excellent sensitivity and selectivity, as well as their reliable and reproducible analytical performance (Karaboduk, 2021b). However, several studies have also introduced electrochemical approaches for the quantitative analysis of BB, such as an anodically pretreated boron-doped diamond (BDD) electrode (Medeiros et al., 2012), a novel type of carbon black-polyethylene composite electrode (Lipskikh et al., 2020), a single-monomer dual templated MIP-based electrochemical sensor (George et al., 2024), and a molybdenum disulfide/poly vinylpyrrolidone coated glassy carbon electrode (MoS_2/PVP/GCE) (Murali & Saraswathyamma, 2025).

Pencil graphite electrodes (PGEs), primarily consisting of graphitic carbon blended with clay and polymeric binders, represent an inexpensive and easily accessible electrode material, making them highly suitable for the development of electrochemical sensing platforms (Dang et al., 2025; Van Dat et al., 2025). Pretreatment in voltammetry ensures that the electrode surface is clean, active, and suitable for sensitive and reliable electrochemical measurements. Following pretreatment, an increase in the electroactive surface area of the pencil graphite electrode was observed, enabling the detection of lower analyte concentrations (Rana et al., 2018).

In the present work, a straightforward, easily prepared, and reusable pretreated pencil graphite electrode (p-PGE) was developed and successfully applied for the electrochemical detection of BB in 0.5 M HCl. Compared to the conventional PGE, the p-PGE exhibited significantly enhanced electrochemical response toward BB. Finally, the practical applicability of the p-PGE was evaluated in real sample analyses for BB, and the results were found to be in good agreement with those obtained using UV-Vis spectrophotometry.

MATERIALS AND METHODS

Apparatus and Chemicals

The voltammetric experiments (cyclic voltammetry (CV)) with both pretreated and unpretreated pencil graphite electrodes were performed using a PalmSens 3 potentiostat/galvanostat, controlled with the PSTrace 5.11.1006.19013 software. Disposable pencil-graphite electrodes (PGE, Micro, 2.00 mm, 2B) were obtained from a local stationery supplier in Ankara, Türkiye (Istanbul, Türkiye). The 2B-grade pencil lead used as the electrode consists mainly of graphite (approximately 74%) and clay (about 24%), while the remaining ~2% is a non-electroactive polymer that serves as a binding material. A comprehensive characterization of the pencil graphite electrode was reported in an earlier publication and is not repeated here. (Karaboduk, 2021a). The pH values were determined using a Sartorius Docu-pH+ meter (Göttingen, Germany). All experiments were performed at ambient laboratory temperature. Solutions were prepared with ultrapure water (18.2 MΩ·cm) generated by a BluLab BluAquaT3 purification system (12,051 Alba (CN), Italy). UV–Vis analyses were conducted with a Shimadzu UV-1700 PharmaSpec spectrophotometer (Japan). Brilliant Blue FCF (analytical standard), glucose, fructose, tartrazine, and citric acid from Merck (Darmstadt, Germany) were used. Ascorbic acid was purchased from Sigma Aldrich Co. (St. Louis, MO, USA). All reagents were utilized in their supplied form, with no additional purification steps applied.

Electrode preparation

The outer section of the PGE was insulated with Teflon tape. The working surface of the electrode was polished using P-320 sandpaper and then carefully washed with distilled water. The electrical connection was provided by attaching a copper wire. The PGE was electrochemically activated by cycling the potential between 1.5 and 2.0 V for 50 repetitions in a 0.10 M phosphate buffer at pH 7.0, using a scan rate of 50 mV/s (Karaboduk, 2021a).

RESULTS

Electrochemical Response of Brilliant Blue at Unpretreated/Pretreated Pencil Graphite Electrodes

Cyclic voltammetry was employed to evaluate the electrochemical behavior of both untreated and pretreated PGEs, with 1.0 µM Brilliant Blue (BB) in 0.5 M HCl, as illustrated in Figure 1. The p-PGE enhanced the oxidation peak current of BB, exhibiting clear electrocatalytic activity, with the peak current increasing by approximately 2.1-fold and the oxidation peak potential shifting from 0.809 V to 0.839 V compared to the unpretreated PGE. Additionally, reduction peaks of BB were observed at approximately 0.520 V and 0.530 V on the surfaces of PGE and p-PGE, respectively.

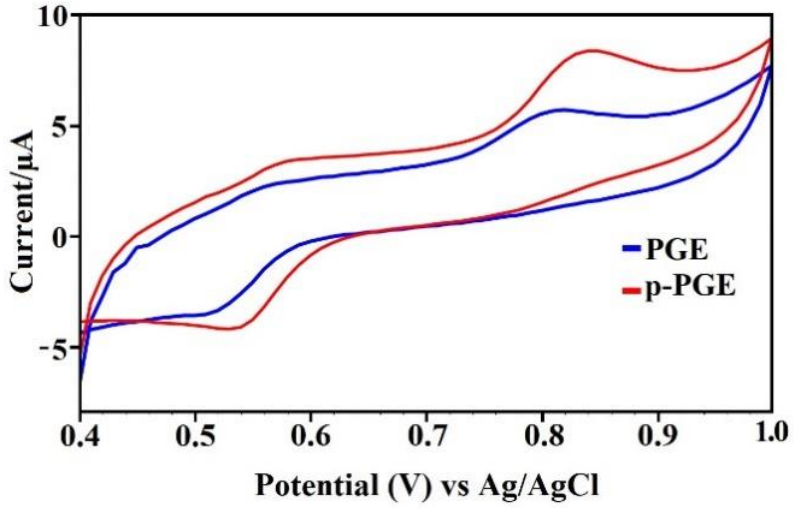


Figure 1. Comparison of the electrochemical behavior of 1.0 µM BB on PGE and p-PGE surfaces in 0.5 M HCl, scan rate:150 mV/s

Effect of Scan Rate

The variation of the redox peak currents with respect to scan rate was examined by performing cyclic voltammetry on BB at scan rates ranging from 10 to 250 mV/s. CV responses of the p-PGE were collected in 0.5 M HCl containing 1.0 µM BB, as shown in Figure 2A. As depicted in Figure 2B, both anodic and cathodic peak currents rise proportionally with the square root of the scan rate. This linear relationship suggests that the electrochemical behavior of BB at the PGE is primarily governed by a diffusion-controlled mechanism (Nejad & Beitollahi, 2025).

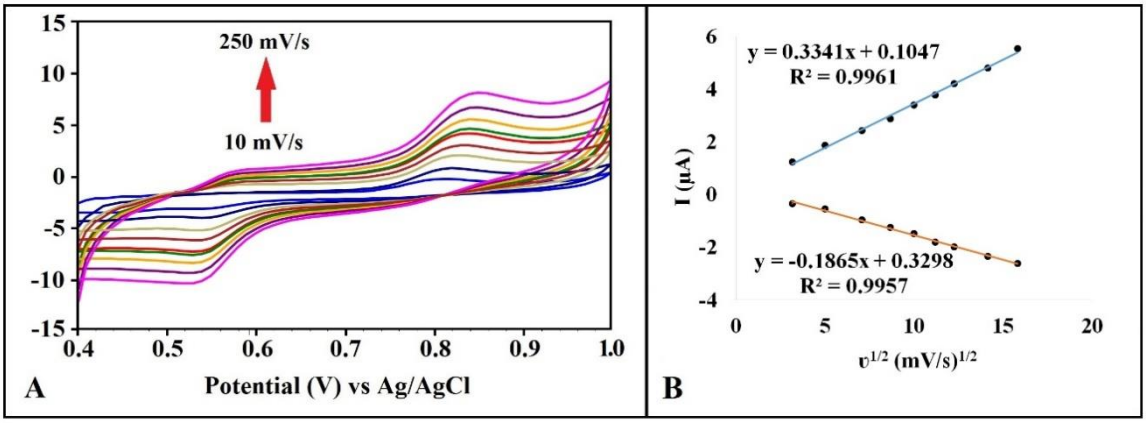


Figure 2. A) CVs of p-PGE of scan rate variation of 1 µM BB in 0.5 M HCl, B) Corresponding linear plots of I_{pa} and I_{pc} versus $v^{1/2}$

Effect of Supporting Electrolyte Type and Concentration

The electrochemical behavior of 1.0 µM BB on the p-PGE electrode was investigated in various types of supporting electrolytes prepared at a concentration of 0.1 M. As shown in Figure 3A, the highest current response was obtained in 0.1 M HCl, indicating that HCl supporting electrolyte provides the most favorable medium for the BB. Based on this finding, HCl solutions with varying molarities were prepared and used as supporting electrolytes to evaluate the effect of acid concentration on the electrochemical response of BB. As illustrated in Figure 3B, the maximum current signal was recorded in 0.5 M HCl, accompanied by a shift of both anodic and cathodic peak potentials toward more positive values with increasing acid strength. Consequently, this HCl molarity was selected for use in the subsequent experiments.

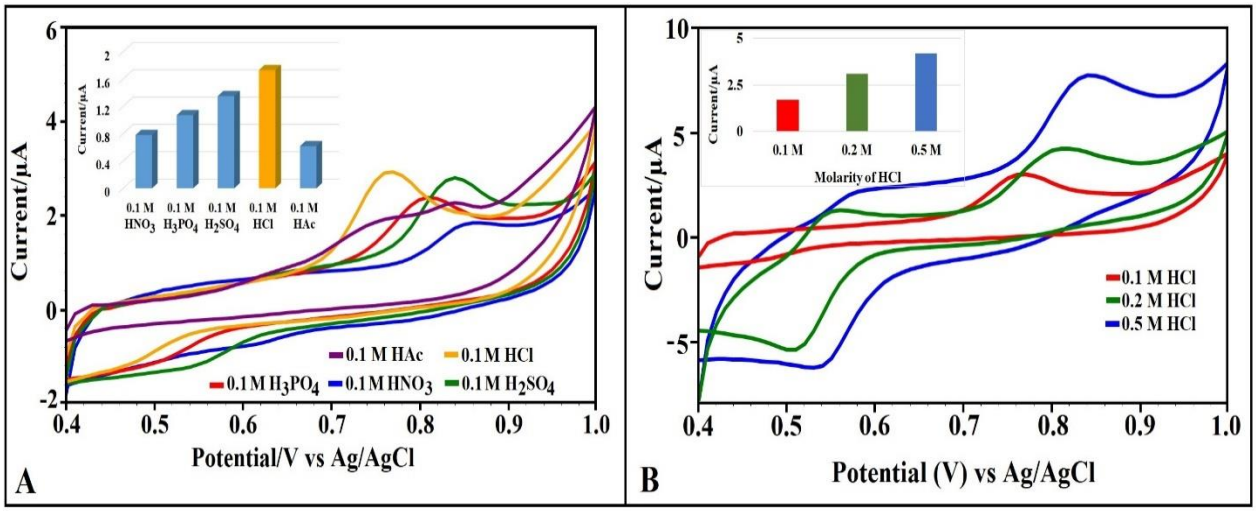


Figure 3. A) Comparison of 1 µM BB anodic currents in different 0.1 M supporting electrolytes, B) Influence of HCl concentration on the BB signal (oxidation peak). Scan rate 150 mV/s

Analytical Performance of p-PGE for Brilliant Blue Determination

The electrochemical behavior of Brilliant Blue at the p-PGE electrode was evaluated by recording CVs under optimized conditions, and the responses obtained at increasing BB concentrations were used to assess the analytical performance of the system. Although BB exhibited linear behavior for both its anodic and cathodic responses on the p-PGE surface, the anodic peak displayed a correlation coefficient closer to unity. Therefore, the analytical evaluations and the linear dynamic range were established based on the anodic signal. The concentration range evaluated for BB extended from 0.02 µM to 3.00 µM. As illustrated in Figure 4A, the cyclic voltammograms demonstrate a clear increase in peak current with rising BB concentrations. This trend is further confirmed in Figure 4B, where a linear relationship between peak current and BB concentration is observed. Based on this linear dependence, a regression model describing the correlation between BB concentration and peak current was derived: $I_{pa}=3.6963\times C_{BB} + 0.183$ ($R^2 = 0.9992$). Using the expression 3 × (SD/slope)-where SD represents the standard deviation associated with the lowest concentration yielding a quantifiable voltammetric response, the limit of detection (LOD) was calculated to be 8.5 nM.

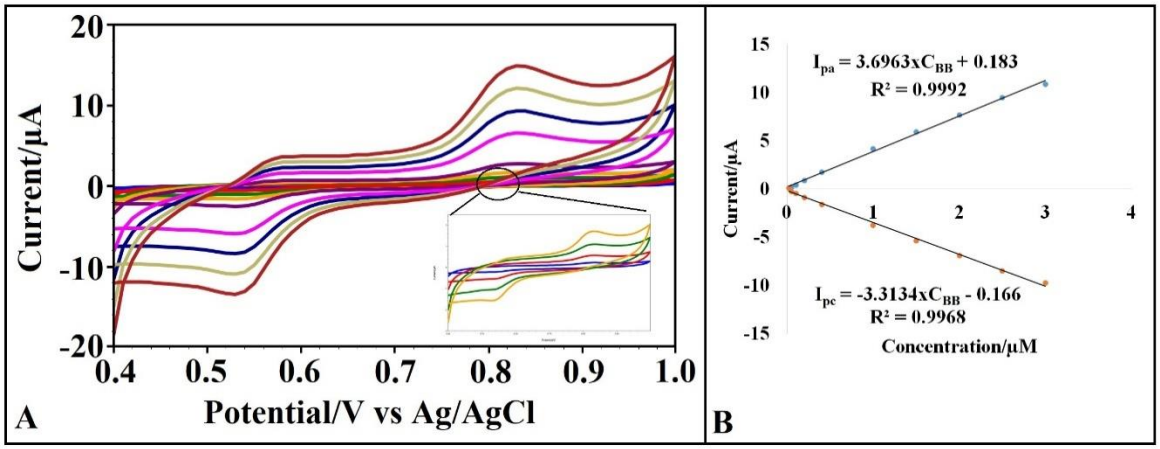


Figure 4. A) CV responses of BB with increasing concentrations from 0.02 µM to 3.00 µM in 0.5 M HCl, B) The calibration curve of the CV responses of BB; scan rate:150 mV/s

As presented in Table 1, the method developed in this work offers a **relatively** broad linear range and a reasonably low detection limit compared with previous reports. Considering its sensitivity and the practical benefits of electrochemical techniques, such as low cost and rapid measurements, the approach may be suitable for on-site analysis of BB.

Table 1. Comparison of previously reported methods for the determination of BB

Electrode	Linear Range (µM)	LOD (nM)	Reference
Boron-doped diamond electrode	0.596 - 9.90	13.1	(Medeiros et al., 2012)
Carbon black-polyethylene composite electrode	0.025 - 2.52	11.0	(Lipskikh et al., 2020)
A dual-templated molecularly imprinted polymer-based electrochemical sensor	0.02 - 0.38	8.36	(George et al., 2024)
Molybdenum disulphide/poly vinylpyrrolidone-GCE	0.8 - 1150	9.0	(Murali & Saraswathyamma, 2025)
p-PGE	0.02 - 3.00	8.5	This study

n=5

Reproducibility and stability of p-PGE

To assess the consistency of electrode fabrication, ten separate p-PGE were prepared for measuring 1 µM BB in 0.5 M HCl. The relative standard deviations (RSDs) of the anodic peak currents were found to be 2.27% for BB, demonstrating satisfactory reproducibility of the electrode preparation process. For evaluation of long-term stability, p-PGE was kept in ambient air at room temperature for a period of ten days. After ten days, the electrode retained 93.2% of the initial response for BB. These results suggest that the p-PGE possesses good stability over time.

Real Sample Analysis

To demonstrate the practical applicability of the developed method to real sample analysis, three different brands of energy drinks (EDs) purchased from a local market were analyzed. The samples were not subjected to any extraction. For dye content estimation, the standard addition method was used. BB standard solutions were added to real samples to achieve final concentrations of 0.5 and 1.5 µM. Table 2 presents the BB concentrations determined in the analyzed ED samples, employing the proposed CV and UV-Vis method.

Table 2. The results obtained from the analysis of real samples using the proposed voltammetric method were compared with those obtained via the reference spectrophotometric technique

	Electrochemical		UV-Vis		Calculated F_{table} (95%)	Teorical F_{table} (95%)
	Added	Found	Added	Found		
ED-1	0.50	0.47± 0.04	0.50	0.45±0.06	2.25	6.39
ED-2	1.50	1.54±0.03	1.50	1.56±0.05	2.78	6.39
ED-3	1.50	1.52±0.03	1.50	1.55±0.03	1.00	6.39

n=5

An F-test was applied to assess the variance between the electrochemical and spectrophotometric methods for determining BB in different ED samples. As shown in the table, the calculated F-values for ED-1 (2.25), ED-2 (2.78), and ED-3 (1.00) are all lower than the corresponding theoretical F-value at the 95% confidence level (6.39). This indicates that there is no significant difference in the precision of the results obtained by the two methods.

Interference Study

The potential interference from common food additives was examined. The results demonstrated that even large excesses up to 1000 times for glucose and fructose, 400 times for citric acid and ascorbic acid, and 50 times for tartrazine did not noticeably affect the electrochemical responses of 1 µM BB in optimized conditions.

CONCLUSION

In this study, a simple, cost-effective, and reusable pretreated pencil graphite electrode (p-PGE) was successfully developed for the sensitive voltammetric determination of BB in 0.5 M HCl. The p-PGE demonstrated a significantly enhanced electrochemical response compared to unpretreated electrodes, allowing for the detection of BB down to 8.5 nM with a wide linear range of 0.02-3.00 µM. The method exhibited excellent reproducibility and stability, maintaining over 93% of its initial response after ten days. Notably, the developed approach proved highly selective, as even large excesses of common food additives did not interfere with the detection of BB. Application to real energy drink samples showed good agreement with UV–Vis spectrophotometry, confirming its practical applicability. Overall, the proposed voltammetric method provides a rapid, reliable, and environmentally friendly alternative for the on-site analysis of BB in complex matrices.

REFERENCES

Dang, K., Vidya, D., & Krishnamurthy, B. (2025). Vanadium redox flow batteries: Exploring stability with in-situ electrochemically produced nitric acid pretreated enhanced graphene-coated pencil graphite electrodes. *Future Batteries*, *6*, 100065.

Fang, Z., Wang, W., Bai, M., Li, Y., Jiao, Y., Zhou, Y., Ma, K., Zhao, S., Wang, X., & Liu, B. (2025). A highly selective dual-signal ratiometric fluorescence sensing strategy for brilliant blue in food based on carbon dots/copper nanoclusters nanocomposite. *Microchemical Journal*, 114667.

Faraji, M., Nasiri Sahneh, B., & Javanshir, R. (2017). An ion-pair dispersive liquid-liquid microextraction for simultaneous determination of synthetic dyes in ice cream samples by HPLC. *Analytical and Bioanalytical Chemistry Research*, *4*(2), 213–225.

George, A., Bharath, M., Ghosh, M., & Varghese, A. (2024). Single-monomer dual templated MIP based electrochemical sensor for tartrazine and brilliant blue FCF. *Electrochimica Acta*, *475*, 143682.

Jadhav, S. P., & Gogate, P. R. (2025). Intensification of hydrodynamic cavitation induced degradation of Brilliant Blue dye using various additives. *Journal of the Indian Chemical Society*, *102*(1), 101540.

Karaboduk, K. (2021a). Development of a voltammetric method for the determination of rapamycin in pharmaceutical samples at pretreated pencil graphite electrode. *Journal of the Chinese Chemical Society*, *68*(9), 1722–1730.

Karaboduk, K. (2021b). Modification of screen-printed gold electrode with 1, 4-dithiothreitol: application to sensitive voltammetric determination of Sudan II. *Food Quality and Safety*, *5*, fyaa039.

Karaboduk, K. (2025). Sensitive voltammetric determination of Allura Red at poly (aniline blue) modified pencil graphite electrode by differential pulse voltammetry. *Microchemical Journal*, 115008.

Karaboduk, K., & Karaboduk, H. (2025). Rapid and simple electrochemical approximation for the determination of the food additive amaranth using voltammetric sensor. *Journal of Food Measurement and Characterization*, *19*(1), 390–400.

Lipskikh, O. I., Korotkova, E. I., Barek, J., Vyskocil, V., Saqib, M., & Khristunova, E. P. (2020). Simultaneous voltammetric determination of Brilliant Blue FCF and Tartrazine for food quality control. *Talanta*, *218*, 121136.

Medeiros, R. A., Lourencao, B. C., Rocha-Filho, R. C., & Fatibello-Filho, O. (2012). Simultaneous voltammetric determination of synthetic colorants in food using a cathodically pretreated boron-doped diamond electrode. *Talanta*, *97*, 291–297.

Murali, A. S., & Saraswathyamma, B. (2025). Innovative electrochemical quantification of brilliant blue dye with polyvinylpyrrolidone-stabilized MoS_2. *Materials Chemistry and Physics*, *332*, 130155.

Nejad, F. G., & Beitollahi, H. (2025). Voltammetric determination of tert-butylhydroquinone in the presence of butylated hydroxyanisole using 2D Ni-MOF nanosheets/MWCNTs-based electrochemical sensor. *Microchemical Journal*, 114539.

Olgun, M., Özak, S. S., & Dalmaz, A. (2024). Spectrophotometric determination for green hydrophobic deep eutectic solvent-based microextraction of Brilliant Blue FCF (E133) from beverages. *Journal of Chromatography A*, *1736*, 465374.

Özgen, A., Dalmaz, A., & Özak, S. S. (2025). A new method for the determination of brilliant blue FCF in energy drinks: Smartphone digital imaging colorimetry (SDIC) and green deep eutectic solvent-based dispersive microextraction procedure. *Microchemical Journal*, 114776.

Rana, A., Kawde, A.-N., & Ibrahim, M. (2018). Simple and sensitive detection of 4-nitrophenol in real water samples using gold nanoparticles modified pretreated graphite pencil electrode. *Journal of Electroanalytical Chemistry*, *820*, 24–31.

Thakar, S. P., Panchal, B., Chauhan, S., Chauhan, H., Shrivastav, P. S., & George, L.-b. (2025). A sustainable eco-innovation for water pollutant (Brilliant Blue FCF) detoxification using Diploscapter coronatus. *Sustainable Chemistry and Pharmacy*, *45*, 101984.

Van Dat, P., Thuong, P. H., Van Anh, N., Van Thuc, N., & Viet, N. X. (2025). In-situ graphene modified pencil graphite electrode for the simultaneous electrochemical detection of ascorbic acid, dopamine and uric acid. *Results in Chemistry*, 102617.

ORAL PRESENTATION

Comparative development and antibiofilm evaluation of nanoemulgels containing linseed, borage, and pumpkin seed oils

Tutku Nur Alnıaçık[1,2] (https://orcid.org/0009-0007-1513-8626), Ebru Altuntaş[2*] (https://orcid.org/0000-0003-2902-5554), Mayram Hacıoğlu[3] (https://orcid.org/0000-0003-0823-631X)

[1]Istanbul University, Graduate School of Health Sciences, Istanbul, Türkiye
[2]Istanbul University, Faculty of Pharmacy, Department of Pharmaceutical Technology, Istanbul, Türkiye
[3]Istanbul University, Faculty of Pharmacy, Department of Pharmaceutical Microbiology, Istanbul, Türkiye

[*]Corresponding author: ebru.altuntas@istanbul.edu.tr

Abstract

This research focused on creating and evaluating boric acid-loaded nanoemulsion (NE) and nanoemulgel (NEG) formulations that incorporate linseed oil, borage seed oil, or pumpkin seed oil for use in topical wound treatments. The NEs were manufactured through ultrasonic emulsification, utilizing Poloxamer 188 as the surfactant and Transcutol as the co-surfactant. These optimized NEs were transformed into NEGs by adding 1% xanthan gum in a 1:1 ratio. The formulations underwent analysis for droplet size, polydispersity index (PDI), and zeta potential, as well as pH, conductivity, rheology, and thermodynamic stability. After optimization, the NEGs were tested for their ability to combat biofilm formation against standard microbial strains. All NEs demonstrated favorable droplet sizes (<300 nm) and PDI values (<0.3), confirming their monodisperse nature. The incorporation of xanthan gel led to a reduction in droplet sizes across all formulations, indicating improved compactness and stability within the gel matrix. Among the NEGs, BSO-NEG had the smallest droplet size and the most negative zeta potential, suggesting strong electrostatic and thermodynamic stability. Each NEG showed varying levels of inhibition on bacterial adhesion and biofilm development. PSO-NEG demonstrated the highest efficacy against *E. faecalis*, whereas LSO-NEG and BSO-NEG effectively inhibited *S. aureus* biofilms. BSO-NEG and PSO-NEG diminished *E. coli* biofilms, with BSO-NEG further suppressing *K. pneumoniae* and *P. mirabilis*. Only LSO-NEG exhibited early suppression of *A. baumannii* adherence. Preliminary experiments demonstrated no efficacy against *P. aeruginosa*. In mature biofilms, all NEGs shown efficacy except against *K. pneumoniae*, with BSO-NEG exhibiting the highest activity against *S. aureus*, while LSO-NEG and BSO-NEG were most potent against *A. baumannii* and *P. mirabilis*. Among the formulations, BSO-NEG demonstrated the most promising broad-spectrum antibiofilm efficacy, effectively suppressing both early-stage and mature biofilms of many clinically relevant pathogens.

Keywords: Nanoemulgels, Linseed oil, Borage seed oil, Pumpkin seed oil, Antibiofilm activity.

INTRODUCTION

Wound healing is a multifaceted and dynamic process comprising four consecutive yet overlapping phases: haemostasis, inflammation, proliferation, and remodeling (Landén et al., 2016). The successful progression of the healing process depends on the control of inflammation, prevention of infection, and stimulation of tissue regeneration. However, local factors such as oxygenation and infections or systemic factors such as age, hormones, diseases and medications may cause wound healing to be delayed or become chronic (Guo and DiPietro, 2010). Since infection is the main cause of chronic wounds, controlling microbial contamination and colonization is a crucial step for wound healing (Landis, 2008). Chronic wound infections often present as persistent and prolonged conditions, in which biofilm phenotype plays a central pathogenic role. Whereas planktonic bacteria involved in acute, invasive infections are typically eradicated by the host's innate immune defenses and antibiotic treatment, chronic wounds remain refractory and slow to heal (Hurlow and Bowler, 2022).

Given the importance of infection control and tissue regeneration in wound management, innovative topical delivery techniques are increasingly needed to overcome the limits of existing topical formulations. Nanoemulsions (NEs) are heterogeneous colloidal systems composed of oil and water, in which one phase is dispersed within the other as the continuous phase. An emulsifier, which is a type of surfactant, is absorbed at the interface between the dispersed and continuous phases. This lowers surface tension and stabilizes the system (Donthi et al., 2023). Furthermore, the nanoscale droplet size of NEs increases the solubility of medications

and promotes skin penetration, making them suitable for topical application. Notwithstanding their numerous benefits, NEs are constrained by low viscosity, leading to inadequate adherence to the skin. This constraint can be surmounted by converting the NE into a nanoemulgel (NEG) via the integration of a suitable gelling agent (Donthi et al., 2023).

Linseed oil (LSO) is recognized as one of the richest natural sources of polyunsaturated fatty acids (PUFA) and essential fatty acids (EFA). LSO predominantly contains α-linolenic acid (ALA) and linoleic acid, together with monounsaturated oleic acid (Franco et al., 2012; Poljšak et al., 2020). LSO's unsaturated fatty acids promote growth factor synthesis, fibroblast proliferation, and angiogenesis, which accelerate tissue regeneration and wound healing (Franco et al., 2012). The fatty acids and phenolic constituents of linseed, particularly caffeic acid and coumaric acid, significantly enhance its antioxidant capacity and support wound healing (Wang et al., 2017). Borage seed oil (BSO), high in γ-linolenic acid (GLA), has anti-inflammatory, antioxidant, and skin-regenerating properties. Its polyphenols and GLA scavenge free radicals and protect collagen and elastin fibers by blocking collagenase and elastase, which may aid wound healing (Michalak et al., 2023). Poljšak et al. (2020) found that pumpkin seed oil (PSO) is a natural oil high in PUFA, including linoleic acid, monounsaturated fatty acids like oleic acid, and lower levels of saturated fatty acids like palmitic and stearic acids. In addition to its fatty acid profile, phytosterols, tocopherols, and phenolic acids contribute to its antioxidant, anti-inflammatory, and wound-healing properties (Prommaban et al., 2021).

Boric acid possesses numerous advantageous effects on wound healing, including antibacterial, anti-inflammatory, antioxidant, and angiogenic properties. It exhibits significant antibacterial effectiveness by increasing pathogen cell wall permeability, compromising cell membranes, and inhibiting cell membrane synthesis, thereby reducing infection risk (Liu et al., 2021; Guner et al., 2025). Furthermore, the antioxidant characteristics of boric acid mitigate oxidative stress, safeguarding cells and facilitating tissue regeneration (Sedighi-Pirsaraei et al., 2024).

The aim of this study was to develop stable and effective topical NEG formulations. To achieve this, we used ingredients such as boric acid, LSO, BSO and PSO, and examined essential physicochemical properties such as droplet size, polydispersity index (PDI) and zeta potential. The improved NEs were then mixed with gels made from xanthan gum to create the final NEG systems. These systems underwent comprehensive testing to assess their performance across a range of temperatures, mobility, and effectiveness in eliminating bacteria such as *Staphylococcus aureus* (*S. aureus*) ATCC 29213, *Enterococcus faecalis* (*E. faecalis*) ATCC 29212, *Escherichia coli* (*E. coli*) ATCC 25922, *Klebsiella pneumonia* (*K. pneumonia*) ATCC 4352, *Proteus mirabilis* (*P. mirabilis*) ATCC 14153, *Pseudomonas aeruginosa* (*P. aeruginosa*) ATCC 27853, and *Acinetobacter baumannii* (*A. baumannii*) ATCC 19606.

MATERIALS and METHODS

Materials

Boric acid (B0394-500G, Sigma-Aldrich, USA) was used as the main active ingredient. Kolliphor® P188 (Poloxamer 188, BASF, Germany) served as a surfactant. The oil phase consisted of LSO and BSO (Nuka Defne Esencia®, Türkiye) and PSO (Intense Natural®, Türkiye). Xanthan gum (Vanzan® NF-C, Vanderbilt Minerals, USA) was used as the gelling polymer. Transcutol® (Gattefossé, France) and Sensiva® PA30 (Schülke & Mayr GmbH, Germany) were incorporated as cosurfactant and skin-conditioning agents. α-Tocopherol acetate (Sigma-Aldrich, Germany) was added as an antioxidant. All other reagents were analytical grade, and deionized water was used throughout the study.

Methods

Nanoemulsion and nanoemulgel preparation

In this study, NE formulations containing 3% boric acid and 3% of each oil (LSO, BSO, and PSO) were individually prepared using the ultrasonic emulsification method. To determine the optimal formulations, various parameters such as oil concentration, surfactant concentration, and the oil-to-surfactant ratio were evaluated. The ultrasonication process was carried out at 50% amplitude, with a pulse sequence of 30 seconds on and 30 seconds off to avoid excessive heating. Ultrasonication was applied at a frequency of 20 kHz for a total of 10 minutes. Throughout the experiment, the temperature was maintained constantly by using an ice bath. After the optimization of the NEs were completed, the gel containing 1% xanthan gum was mixed with the NE at a 1:1 (w/w) ratio using a magnetic stirrer at 500 rpm for 30 minutes.

Nanoemulsion and nanoemulgel characterization

Droplet size, polydispersity index and zeta potential

Dynamic light scattering (DLS) was used with a Zetasizer Nano ZS (Malvern Instruments, UK) at 25 ºC and a 90º scattering angle to examine the mean droplet size and PDI of the formulations. Formulations were considered monodisperse if their PDI values were less than 0.3, and samples were diluted 1:100 (v/v) with deionized water to avoid multiple scattering. Zeta potential was determined using electrophoretic mobility using the same apparatus, with materials diluted 1:100 (v/v) and analyzed at 25 ºC (Kildaci et al., 2021).

pH, conductivity, and rheological properties

The pH and conductivity of the NEGs were determined at 25 ºC using a portable pH/conductivity meter (Hanna Edge, USA). Viscosity measurements were performed with a Brookfield cone-plate viscometer (Brookfield Engineering Laboratories, MA, USA) different shear rates to assess the flow behavior (Ozkan et al., 2022).

Studies of thermodynamic stability

The formulations were centrifuged at 3500 rpm for 30 minutes (Thermo Scientific, USA) and then heated to 60 ºC in a thermostatic water bath (Witeg WSB-30, Germany) to test their physical stability. Prior to gel inclusion, only formulations free of instability and phase separation were chosen.

Evaluation of anti-biofilm activities of the optimized nanoemulgel formulations

Strains and culture conditions

The following strains were subcultured from freezer stocks onto tryptic soy agar (TSA, Difco, Sparks, MD, USA) and incubated at 37 ºC overnight: *S. aureus* ATCC 29213, *E. faecalis* ATCC 29212, *E. coli* ATCC 25922, *K. pneumoniae* ATCC 4352, *P. mirabilis* ATCC 14153, *P. aeruginosa* ATCC 27853 and *A. baumannii* ATCC 19606.

Inhibition of biofilm adhesion and formation

Bacterial cultures were prepared to an equivalent cell density to 1×10^6 cfu/mL in Brain-heart infusion broth (BHIB, Thermo Scientific, Oxoid, USA) and were added to each well of 96-well tissue culture microtiter plate (Greiner Bio-One, Kremsmuenster, Austria) containing the optimized NEGs formulation. In addition, positive controls without antimicrobials and negative controls without cells were added. The plates were incubated at 37 ºC for 1, 2, 4 and 24 hours. Following the incubation period, the wells were washed twice with physiologically buffered saline (PBS). Spectrophotometric analysis was then conducted at an optical density (OD) of 450 nm using a microplate reader (EON, Biotek, USA) (Aydın et al., 2025).

Effects on mature biofilms

Biofilm formation was conducted in flat-bottomed 96-well polystyrene tissue culture microtiter plates. Overnight bacterial cultures were prepared in BHIB, to a cell concentration of 1×10^6 cfu/ml. Biofilms were formed by adding the bacteria into appropriate wells of microtiter plates and incubating them for 24 hours at 37 ºC. Subsequent to this incubation period, the waste material was gently aspirated, and non-adherent bacteria were removed by washing the biofilms twice with sterile PBS.

Following the formation of mature biofilms, NEGs, positive and negative controls were added, and the microtiter plates were incubated at 37 ºC for another 24 hours. After this period, wells were washed again with PBS and analyses were performed using the 3-(4,5-dimethylthiazol-2-yl)-2,5-diphenyl tetrazolium bromide (MTT) method. The MTT solution was added to the wells, and the plates were incubated in the dark at 35 ºC for 3 hours. Following incubation, the resulting formazan crystals were dissolved in DMSO (Sigma-Aldrich, St. Louis, MO, USA), and the optical densities were measured at 490 nm using an ELISA microplate reader (EON, Biotek, USA). The results were then evaluated by comparison with the control (Aydın et al., 2025).

RESULTS and DISCUSSION

Preparation and characterization of nanoemulsion formulations

The preliminary evaluation of the NE formulations was carried out using mean droplet size (Z-Ave), PDI, and zeta potential (mV) as key indicators. Formulations exhibiting small droplet sizes (<300 nm), low PDI (<0.3), and high negative zeta potential (>|30| mV) were considered stable.

According to the initial physicochemical evaluation, all three NE formulations had the desired droplet sizes and low PDI values, indicating a narrow size distribution and uniform droplet dispersion (Table 1). Among the formulations, The NEs containing PSO (PSO-NE) had a larger negative zeta potential (-33.43 mV) and the lowest PDI value (0.191). The NEs containing LSO (LSO-NE) and BSO (BSO-NE) demonstrated moderate electrostatic stability, with zeta potentials of -18 and -21.4 mV, respectively. Overall, these results show that all formulations were successfully synthesized as homogeneous NEs.

Evaluation of thermal and centrifugation stability of nanoemulsions

Centrifugation and thermal stress tests demonstrated that all formulations maintained homogeneity and monodispersity, as evidenced by their consistent PDI values and comparable droplet sizes. Both PSO-NE and BSO-NE maintained stable zeta potential values under stress conditions, demonstrating stronger electrostatic stability compared to LSO-NE. In contrast, LSO-NE exhibited a noticeable reduction in zeta potential following centrifugation and thermal stress, as presented in Table 1.

Table 1. Mean droplet size (Z-Ave), PDI, and zeta potential (mV) values of NE at T0, centrifugation and thermal stress test.

Formulation Code	T0			Centrifugation Test			Thermal Test (60 °C)		
	Z-Ave (nm)	PDI	Zeta Potential (mV)	Z-Ave (nm)	PDI	Zeta Potential (mV)	Z-Ave (nm)	PDI	Zeta Potential (mV)
LSO-NE	114.10	0.205	-18.00	107.10	0.188	-12.40	103.60	0.198	-13.30
BSO-NE	114.25	0.199	-21.40	113.85	0.192	-23.23	118.68	0.183	-21.90
PSO-NE	114.85	0.191	-33.43	115.63	0.198	-33.40	116.55	0.198	-25.80

Preparation and characterization of nanoemulgel formulations

When the NEs was combined with the gel, the droplet size decreased from 114.1 nm to 93.3 nm in LSO-NEG, from 114,25 nm to 69.36 nm in BSO-NEG and from 114.85 nm to 95.34 nm in PSO-NEG, indicating that integration into the gel matrix resulted in more compact and stable systems (Table 2). Although the PDI values increased slightly following the integration of the gels, they remained below 0.33, indicating that all of the NEGs had a restricted size distribution and good colloidal homogeneity. Notably, the transition from NE to NEG resulted in reduced zeta potential values for LSO-NEG and BSO-NEG, suggesting enhanced electrostatic stability in the gel state. In contrast, PSO-NEG had a slightly lower magnitude of zeta potential than PSO-NE yet still retained sufficient negative charge to ensure colloidal stability. Overall, these findings suggest that the addition of xanthan gum improves the structural compactness and electrostatic stability of the NEGs.

Evaluation of thermal and centrifugation stability of nanoemulgels

Table 2 shows the centrifugation and heat stability data for the NEG formulations. The physicochemical stability of the NEG formulations was assessed after centrifugation and heat stress at 60 °C. BSO-NEG had the smallest initial droplet size and a strong negative zeta potential, indicating high electrostatic stability, albeit droplet size increased slightly when stressed. LSO-NEG demonstrated moderate stability with small changes in droplet size and PDI, but PSO-NEG showed a significant decrease in zeta potential after centrifugation and thermal stress, indicating lower electrostatic stability.

Table 2. Mean droplet size (Z-Ave), PDI, and zeta potential (mV) values of NEG at T0, centrifugation and thermal stress test.

Formulation Code	T0			Centrifugation Test			Thermal Test (60 °C)		
	Z-Ave (nm)	PDI	Zeta Potential (mV)	Z-Ave (nm)	PDI	Zeta Potential (mV)	Z-Ave (nm)	PDI	Zeta Potential (mV)
LSO-NEG	93.30	0.299	-25.60	78.93	0.332	-25.50	80.71	0.326	-30.70
BSO-NEG	69.36	0.275	-38.80	85.93	0.302	-38.50	91.96	0.304	-30.73
PSO-NEG	95.34	0.258	-28.43	88.23	0.254	-19.43	85.19	0.253	-19.00

pH, conductivity and rheological evaluation

The pH values of the formulations listed in Table 3 were all found to be within the physiological range of human skin (4.5-6.0). These results show that the formulations are compatible with pH and unlikely to cause irritation, indicating that they are suitable for topical administration.

Conductivity tests are critical for identifying whether NEG systems' external phase is aqueous and evaluating the stability of their ionic structure. The conductivity values for LSO-NEG, BSO-NEG and PSO-NEG were measured as 583 µS, 446 µS and 1056 µS, respectively (Table 3), indicating that the external phase was aqueous. As a result, all three systems showed O/W NEG configuration.

Table 3. pH and conductivity (µS) values.

Formulation Code	pH (25 °C)	Conductivity (µS) (25 °C)
LSO-NEG	5.51	583
BSO-NEG	5.54	446
PSO-NEG	5.49	1056

As illustrated in Figure 1, the viscosity profiles of the LSO-NEG, BSO-NEG and PSO-NEG formulations demonstrated a decrease in viscosity with increasing shear rate. This observation confirms that all three formulations exhibit non-Newtonian, shear-thinning (pseudoplastic) flow behavior.

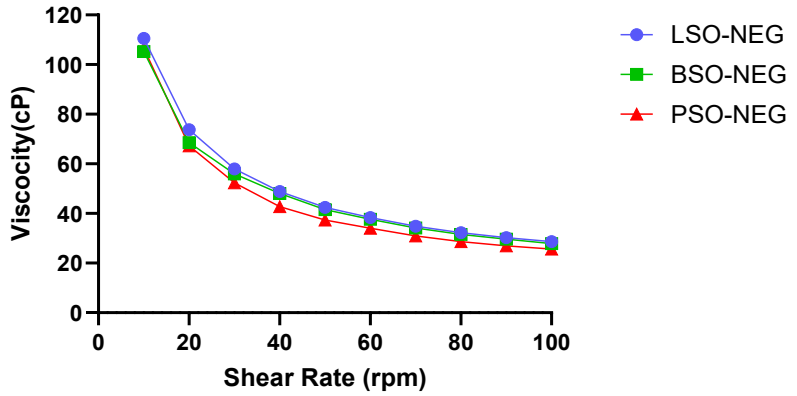


Figure 1. Viscosity-Shear rate graph.

Evaluation of anti-biofilm activities of the optimized nanoemulgel formulations

Inhibition of adhesion and biofilm formation

All the compounds, in varying ratios, had an inhibitory effect on *E. faecalis* adhesion and biofilm formation for almost all the hours studied. The most effective compound for this bacterium was PSO-NEG. Placebo, BSO-NEG and LSO-NEG showed inhibitory effects against *S. aureus* biofilm formation. Against *E. coli*, PSO-NEG and BSO-NEG showed inhibitory effect on biofilm formation (24 h), while BSO-NEG also showed inhibition of *K. pneumoniae* and *P. mirabilis* biofilm formations by 15% and 9%, respectively. Between the compounds, significant inhibitor effect on *A. baumannii* adhesion was seen at LSO-NEG and only at the end of the 1st hour (%16.8). The compounds showed no inhibitory effect against *P. aeruginosa* adhesion and biofilm formation. Results were shown in Figure 2.

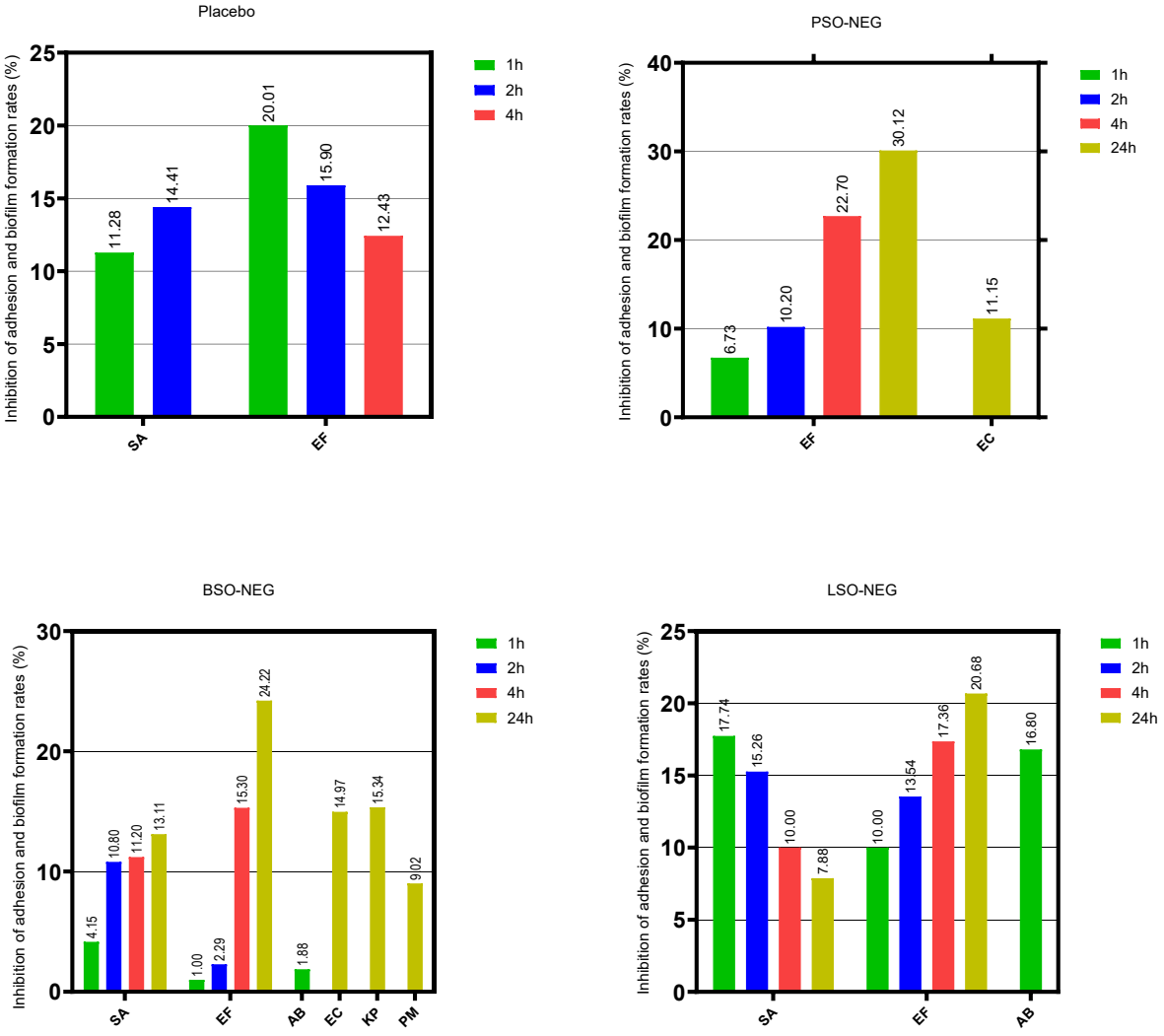


Figure 2. Inhibition of adhesion rates (%) of antimicrobials after 1, 2, 4 and 24 h incubation. Only the bacteria in which the NEGs are effective are shown in the graphs.

SA: *S. aureus*, EF: *E. faecalis,* PA: *P. aeruginosa* AB: *A. baumannii,* EC: *E. coli*, PM: *P. mirabilis*, KP: *K. pneumoniae*

Effects on mature biofilms

Placebo is only slightly effective against *E. faecalis*, else it is not effective against any bacteria. The other NEGs are effective in varying degrees on mature biofilms of all bacteria, except *K. pneumoniae*. The most effective compound against *S. aureus* was BSO-NEG, with an inhibition rate of 37%. All NEGs formulations showed similar inhibitory effects on mature biofilms of *E. faecalis* and *E. coli*. LSO-NEG and BSO-NEG were the most effective against mature biofilms of *A. baumannii*, and LSO-NEG was the most effective against *P. aeruginosa*.

Against mature biofilms of *P. mirabilis*, LSO-NEG and BSO-NEG were the most effective with inhibition rates above 40%. The minimum effect was observed against *K. pneumoniae* biofilms. Results are shown in Figure 3.

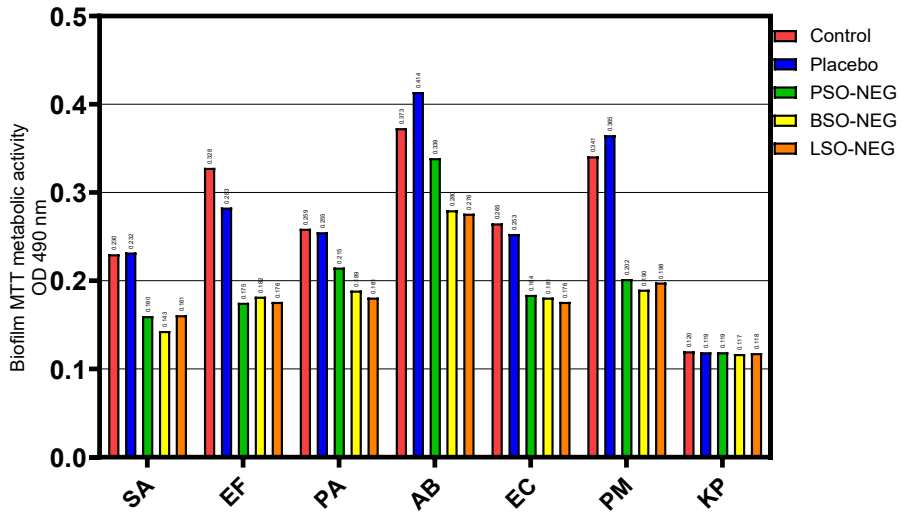


Figure 3. Effects of compounds on mature biofilms, by MTT method. Bars indicate control and NEG formulations, respectively on 24-hour-old mature biofilms.

SA: *S. aureus*, EF: *E. faecalis,* PA: *P. aeruginosa* AB: *A. baumannii,* EC: *E. coli*, PM: *P. mirabilis*, KP: *K. pneumoniae*

CONCLUSION

This research successfully created stable and biocompatible NEGs by incorporating LSO, BSO, and PSO oils into a xanthan-gum matrix to improve topical antibiofilm effectiveness. The transition from NEs to NEGs resulted in smaller droplet sizes across all formulations. Among them, BSO-NEG had the smallest droplet size and the most favorable zeta potential, indicating high electrostatic stability, while LSO-NEG and PSO-NEG displayed moderate electrostatic stability. Each formulation had a skin-friendly pH, O/W properties, and shear-thinning pseudoplastic flow, indicating its suitability for skin application. In antibiofilm studies, all NEGs reduced early adhesion and biofilm formation to various degrees. PSO-NEG was very efficient against *E. faecalis*, while BSO-NEG and LSO-NEG both inhibited *S. aureus*. Both PSO-NEG and BSO-NEG were effective at reducing *E. coli* biofilms, with BSO-NEG additionally targeting *K. pneumoniae* and *P. mirabilis*. LSO-NEG specifically inhibited the early stages of *A. baumannii*. No formulation affected *P. aeruginosa* in initial stages. The placebo showed minimal activity, confirming the functional contribution of the NEG systems. Against mature biofilms, all NEGs showed meaningful activity except *K. pneumoniae*. BSO-NEG was the most effective against *S. aureus*, and all NEGs produced similar reductions in *E. faecalis* and *E. coli* mature biofilms. LSO-NEG and BSO-NEG were the most effective against mature *A. baumannii* and *P. mirabilis* and LSO-NEG was the most effective against *P. aeruginosa.* Overall, LSO, BSO and PSO-based NEGs represent a promising, plant-derived topical delivery system for interfering with early and mature biofilms of clinically relevant bacteria. Although they lack antibacterial effects on planktonic cells, their targeted antibiofilm performance and favorable topical properties highlight their potential as next-generation wound care nanocarriers for preventing and managing biofilm-associated infections.

ACKNOWLEDGEMENTS

The present work was supported by the Research Fund of Istanbul University. Project No: 41101.

REFERENCES

Aydın, M., Yılmaz, F. N., Hacıoğlu, M., Hasbal-Çelikok, G., İnan, N. & Savage, P. B. (2025). Antibiofilm potential of ceragenins against vancomycin-resistant *Enterococcus* spp. *FABAD Journal of Pharmaceutical Sciences*, 50(3), 733-744.

Donthi, M. R., Munnangi, S. R., Krishna, K. V., Saha, R. N., Singhvi, G., & Dubey, S. K. (2023). Nanoemulgel: A Novel Nano Carrier as a Tool for Topical Drug Delivery. *Pharmaceutics*, 15(1), 164.

Franco, E. D. S., De Aquino, C. M. F., Medeiros, P. L. D., Evêncio, L. B., Góes, A. J. D. S., & Maia, M. B. D. S. (2012). Effect of a Semisolid Formulation of *Linum usitatissimum* L. (Linseed) Oil on the Repair of Skin Wounds. *Evidence-Based Complementary and Alternative Medicine*, *2012*, 1-7.

Guner, P., Askun, T., & Er, A. (2025). Antimicrobial potential of boron-containing compounds: Antibacterial, antifungal, and antimycobacterial activities. *Journal of Boron, 10(3),* 111-120.

Guo, S., & DiPietro, L. A. (2010). Factors Affecting Wound Healing. *Journal of Dental Research*, *89*(3), 219-229.

Hurlow, J., & Bowler, P. G. (2022). Acute and chronic wound infections: Microbiological, immunological, clinical and therapeutic distinctions. *Journal of Wound Care*, *31*(5), 436-445.

Kildaci, I., Budama-Kilinc, Y., Kecel-Gunduz, S., & Altuntas, E. (2021). Linseed Oil Nanoemulsions for treatment of Atopic Dermatitis disease: Formulation, characterization, in vitro and in silico evaluations. *Journal of Drug Delivery Science and Technology*, *64*, 102652.

Landén, N. X., Li, D., & Ståhle, M. (2016). Transition from inflammation to proliferation: A critical step during wound healing. *Cellular and Molecular Life Sciences*, *73*(20), 3861-3885.

Landis, S. J. (2008). Chronic Wound Infection and Antimicrobial Use. *Advances in Skin & Wound Care, 2*1(11), 531-540.

Liu, Q., Liu, Z., Zhang, C., Xu, Y., Li, X., & Gao, H. (2021). Effects of 3% Boric Acid Solution on Cutaneous Candida albicans Infection and Microecological Flora Mice. *Frontiers in Microbiology*, *12*, 709880.

Michalak, M., Zagórska-Dziok, M., Klimek-Szczykutowicz, M., & Szopa, A. (2023). Phenolic Profile and Comparison of the Antioxidant, Anti-Ageing, Anti-Inflammatory, and Protective Activities of Borago officinalis Extracts on Skin Cells. *Molecules*, *28*(2), 868.

Ozkan, B., Altuntas, E., Cakir Koc, R., & Budama-Kilinc, Y. (2022). Development of piperine nanoemulsions: An alternative topical application for hypopigmentation. *Drug Development and Industrial Pharmacy*, *48*(3), 117-127.

Poljšak, N., Kreft, S., & Kočevar Glavač, N. (2020). Vegetable butters and oils in skin wound healing: Scientific evidence for new opportunities in dermatology. *Phytotherapy Research*, *34*(2), 254-269.

Prommaban, A., Kuanchoom, R., Seepuan, N., & Chaiyana, W. (2021). Evaluation of Fatty Acid Compositions, Antioxidant, and Pharmacological Activities of Pumpkin (Cucurbita moschata) Seed Oil from Aqueous Enzymatic Extraction. *Plants*, *10*(8), 1582.

Sedighi-Pirsaraei, N., Tamimi, A., Sadeghi Khamaneh, F., Dadras-Jeddi, S., & Javaheri, N. (2024). Boron in wound healing: A comprehensive investigation of its diverse mechanisms. *Frontiers in Bioengineering and Biotechnology*, *12*, 1475584.

Wang, H., Wang, J., Qiu, C., Ye, Y., Guo, X., Chen, G., Li, T., Wang, Y., Fu, X., & Liu, R. H. (2017). Comparison of phytochemical profiles and health benefits in fiber and oil flaxseeds (Linum usitatissimum L.). *Food Chemistry*, *214*, 227-233.

ORAL PRESENTATION

Kenevir-beton yalıtımlarının kuruma hızı ve etkin nem difüzyon katsayılarının tahmini

F. Nihal Tüzün (*0000-0001-5363-9711*)

Hitit Üniversitesi, Mühendislik ve Doğa Bilimleri Fakültesi, Kimya Mühendisliği Bölümü, Çorum, Türkiye

Sorumlu yazar e-mail:nihaltuzun@yahoo.com

Özet

Bina sektöründe üretilen sera gazlarını azaltmak için duyulan ihtiyaç geleneksel olarak kullanılan yalıtım malzemelerinin yerine yenilenebilir ve daha az darbe etkisi yaratan malzemelerin araştırılmasına neden olmaktadır. Bu konu biyokompozit betonların araştırılmasını teşvik etmiş ve düşük maliyetli üretim prosesi olan lifli bitkisel malzemelerin beton içerisinde kullanılması sağlanmıştır. Bu biyokompozit beton normal betondan daha hafiftir ve üzerine fazla yük uygulanamamaktadır. Kenevir bitkisi ile sönmüş kireç ve su karışımından oluşan bu biyokompozite kenevir-beton denmektedir. Bu çalışmada, binalarda yalıtım malzemesi olarak kullanılmak üzere 7 adet kenevir-beton kompozisyonu geliştirildi. Hazırlanan bu kompozisyonlardan 4 tanesi yalnızca kenevir sapları kullanılarak hazırlanırken, diğer 3 tanesi ise hem kenevir sapları hem de lifleri kullanılarak hazırlandı. Geliştirilen bu kompozisyonlar, 16,4^{0}C -22^{0}C sıcaklık aralığında ve %29-45 bağıl nem değişimi gösteren depolama odasında doğal konveksiyonla kurutularak kürlenmeleri sağlandı. Kenevir-beton karışımlarının kuruma hızları ve kurutma işlemi sırasındaki nem değişimleri ve kuru yoğunlukları belirlenerek, kısa ve uzun difüzyon süreleri için etkin nem difüzyon katsayıları hesaplandı. Kürlenme ve kuruma sürelerinin, kenevir-beton kompozisyonlarının; su içeriği, kenevir ve lif etkilerine bağlı olarak değiştiği görüldü. Ayrıca, lifli kompozisyonlarda kuruma hızının lifsiz kompozisyonlara göre daha düşük olduğu bulundu. Bunun yanında, lifli M kompozisyonu hariç, uzun difüzyon sürelerinde kısa difüzyon sürelerinden daha düşük etkin nem difüzyon katsayıları hesaplandı.

Anahtar Kelimeler: Kenevir-beton, yalıtım, kuruma hızı, etkin difüzyon katsayısı, kenevir sapı, kenevir lifi

Estimation of drying rate and effective moisture diffusion coefficients for hempcrete insulations

Abstract

The need to reduce greenhouse gases produced in the building sector has led to the search for renewable and less impact-intensive materials to replace traditionally used insulation materials. This has spurred research into biocomposite concrete, enabling the use of fibrous plant materials within the concrete, a cost-effective production process. This biocomposite concrete is lighter than conventional concrete and cannot be subjected to excessive loads. This biocomposite, composed of a mixture of hemp plants, hydrated lime, and water, is called as hempcrete. In this study, seven hempcrete compositions were developed for use as insulation materials in buildings. Four of these compositions were prepared using only hemp stalks, while the other three used both hemp stalks and fibers. These compositions were dried and cured by natural convection in a storage room with a temperature range of 16.4°C to 22°C and a relative humidity of 29% to 45%. Drying rates, moisture changes during drying, and dry densities of hempcrete compositions were determined, and effective moisture diffusion coefficients were also calculated for short and long diffusion times. Curing and drying times were found to vary depending on the water content, hemp, and fiber effects of the hempcrete compositions. Furthermore, drying rates were found to be slower for the hempcrete compositions having fibers. Thus, lower effective moisture diffusion coefficients were calculated for long diffusion times than for short diffusion times, except for the composition M including fiber.

Keywords: Hempcrete, insulation, drying rate, effective diffusion coefficient, hemp stalk, hemp fiber

GİRİŞ

Gözenekli katılarda kurutma yöntemlerine baktığımızda; katı içerisindeki nemin yüzey hareketinin kılcal akış hareketi ile meydana geldiğinden bahseden kılcal akış teorisi, nemi yüzeye ulaştıran etkinin hem difüzyon hem de kılcal etkinin toplamı olduğunu belirten Krischer teorisi ve Krischer teorisine nemlendirme ısısının ve duyulur ısı transferinin katılması ve sıvı ve buhar fazlarında nem içeriği değişimlerinin ayrılması ile de DeVries teorisi geliştirilmiştir. Ancak, Krischer teorisinde kurutma zamanının doğru şekilde hesaplanabilmesi için gözenekli cismin kılcal geçirgenlik ve difuzyonal direnç katsayısının bilinmesi gerekmektedir. Bu iki katsayı da genellikle gözenekli cisimde gözeneklerin yapısına, sıcaklığına ve nem dağılımına bağlıdır. DeVries teorisinde ise, kolay algılanabilir fiziksel temeline rağmen difüzyon denklemlerine benzeyen denklemlerinin katsayılarının hem dikkatli deneyler sonucu saptanabilmesi hem de bu yaklaşımla gerçek kurutma koşullarındaki kurutma olayını açıklamanın zorluğu bu teorinin çok fazla rağbet görmesini engellemiştir.
Kenevir-beton yavaş kuruyan bir malzeme olduğundan ve difüzyon da, yavaş kuruyan malzemelerin karakteristik davranışı olduğundan Difüzyon teorisine göre katının iç kısımlarındaki suyun yüzeye hareketi katı içi difüzyonla gerçekleşir. Fick'in 2. kanununa uyan buhar veya sıvıların transferinde bu tip difüzyon kontrollü kütle transferinin olduğu bu çalışmada da varsayılmıştır. Katı yüzeyinden havaya su buharının kütle transferi direnci genellikle ihmal edilir ve bütün kuruma hızını katıdaki difüzyon kontrol eder. Böylece yüzeydeki nem içeriği denge değerindedir veya denge değerine çok yakındır (Chen ve ark., 2018).
Kenevir-beton üretiminden sonra, kenevir parçaları ve hidrasyon reaksiyonları muhtemelen 2 ila 5 gün arasında su tüketmektedir. Erken yaşlanma döneminden sonra, hidrasyon reaksiyonu ve numune ile çevre arasındaki su transferi birlikte gerçekleşir. Başlangıçta su sıvı fazdadır, difüzyon yoluyla numunenin yüzeyine taşınabilir ve kalan su içeriği yakalanana kadar yüzeydeki havaya buharlaşır. Açık yüzeylerden kütle kaybından kaynaklanan bu işleme kurutma denir (Evrard, 2008) ve bu işlem blok boyutuna bağlı olarak birkaç hafta sürer (Glouannec ve ark., 2010).
Kurutma aşamasının tamamlanmasıyla, kireç bazlı bağlayıcılardaki (Gu ve Song, 2010) son derece yavaş karbonatlaşma reaksiyonu (Lawrence ve ark., 2007) nedeniyle az miktarda serbest su salınır.
Bu çalışmada, geliştirilen 3 adedi lifli olmak üzere 7 adet kenevir-beton kompozisyonların kürlenme süreci boyunca malzeme içerisindeki su transferine bağlı kuruma hızı ve yoğunluk değişimi kısa süreli ve uzun süreli difüzyon süreci için etkin nem difüzyon katsayıları da dahil olmak üzere taşınım parametreleri açısından incelenmiştir.

MATERYAL VE METOT

Bu çalışmada, 7 adet kenevir-beton kompozisyonu geliştirildi. Kompozisyonların 4 adedi sönmüş kireç, su ve yalnızca Çorum ili Mecitözü ilçesinde hasat edilen endüstriyel kenevirin saplarından oluşurken, diğer 3 adedi ise, sönmüş kireç, su ve kenevir saplarının yanında endüstriyel kenevir liflerinin de ilave edilmesiyle hazırlandı. Hazırlanan bu kompozisyonlar 5 dakika karıştırıldıktan sonra, 5400 cm^3 hacmindeki blok şeklindeki kalıplara dolduruldu ve titreşim uygulanarak içerisindeki hava kabarcıkları giderildi. 1 gün sonra kalıplar çıkarıldı ve bloklar, numune ile ortam arasında su alışverişini önlemek için 16,4^{0}C -22^{0}C sıcaklık değişimine ve %29-45 bağıl neme sahip depolama odasında doğal konveksiyonla kurutularak kürlenmesi sağlandı. Depolama odasının sıcaklık ve hava bağıl nem ölçümleri ThermoPro TP 49 model dijital termohigrometre ile yapıldı.

Kurutma işlemi, blok kütlesi sabitlenene kadar devam ettiğinden belli aralıklarla blok kütleleri tartıldı. Blok kütlesinin ölçümü, 0,1 g hassasiyete sahip dijital tartı cihazı ile gerçekleştirildi. Kurutma süresi boyunca, bloğun kütle değişiminin yalnızca malzemenin su kaybına bağlı olduğu varsayıldı. Bu nedenle, blokların ağırlık ölçümü iki farklı eğri verdi. Bunlardan biri, zamana bağlı olarak su içeriği değişimini (kuru baz) içeren kurutma eğrisi, diğeri ise, kuruma yüzey alanı ve zaman başına kütle kaybı hızını tanımlayan kuruma hızı eğrisidir (Colinart ve ark., 2012). Blokların kürlenme süresi boyunca, numunelerde suya bağlı olarak bazı reaksiyonlar ve olaylar meydana gelmiştir. Bunlar, hidrasyon reaksiyonları, karbonatlaşma reaksiyonları ve suyun merkezden yüzeye difüzyonu, yüzeyden buharlaşma ve havaya geçişidir (Colinart ve ark., 2012).

Etkin nem difüzyon katsayısının tahmini

Kuruma periyodu, gözenekli ortamın yüzeyine kararsız haldeki nemin (sıvı veya buhar) difüzyonu ile gerçekleşen başlıca taşınım olaylarından biri olarak tanımlanabilir ve denklem (1)'de gösterildiği gibi Fick'in ikinci difüzyon yasası ile yorumlanabilir.

$$\frac{\partial X}{\partial t} = Dw\nabla^2 X \quad (1)$$

X, kuru baz nem içeriğidir,
t, zamandır ve
Dw, malzemenin etkin nem difüzyon katsayısıdır.

Denklem (1)'de verilen Fick denkleminin analitik çözümü, Denklem (2)'de dikdörtgen bir levha için, düzgün başlangıç nem dağılımı (X0), numune yüzeyinde sabit konsantrasyon, sabit levha kalınlığı (L) ve sıfıra yakın son denge nem içeriği (Xeq) dikkate alınarak ifade edilmiştir (Crank, 1975).

$$\text{Xred}= \frac{8}{\pi^2} \sum_{n=0}^{\infty} \frac{1}{(2n+1)^2}\, e^{-\left[\frac{(2n+1)^2\times\pi^2\times Dw}{4L^2}\times t\right]} \quad (2)$$

Xred, Denklem (3) ile açıklanan boyutsuz nem içeriği oranıdır.

$$\text{Xred}= \frac{\bar{X}-Xeq}{X0-Xeq} \quad (3)$$

X nem içeriğidir,
Xeq; denge nem içeriğidir ve
X0; başlangıç nem içeriğidir.
Denklem (2), difüzyon sürecinin başlangıcı ve sonu olmak üzere iki farklı zaman dilimi için doğrusallaştırılabilir. Kısa difüzyon süresi için Denklem (2), Denklem (4) (Bakhshi ve Mobasher, 2011) olarak yazılabilir.

$$Xred = 1 - 2\sqrt{\frac{Dw}{\pi\times L^2}}\times t \quad (4)$$

ve Denklem (5)'de gösterildiği gibi zamanın doğrusal bir fonksiyonuna sadeleştirilebilir.

$$\left(\frac{\pi\times L^2}{4}\right)(Xred-1)^2 = Dw\times t \quad (5)$$

Uzun difüzyon süresi için, Denklem (2), Denklem (6)'ya dönüştürülebilir (Bakhshi ve Mobasher, 2011).

$$\text{Xred}= \frac{8}{\pi^2} e^{-\left[\frac{\pi^2\times Dw}{4L^2}\times t\right]} \quad (6)$$

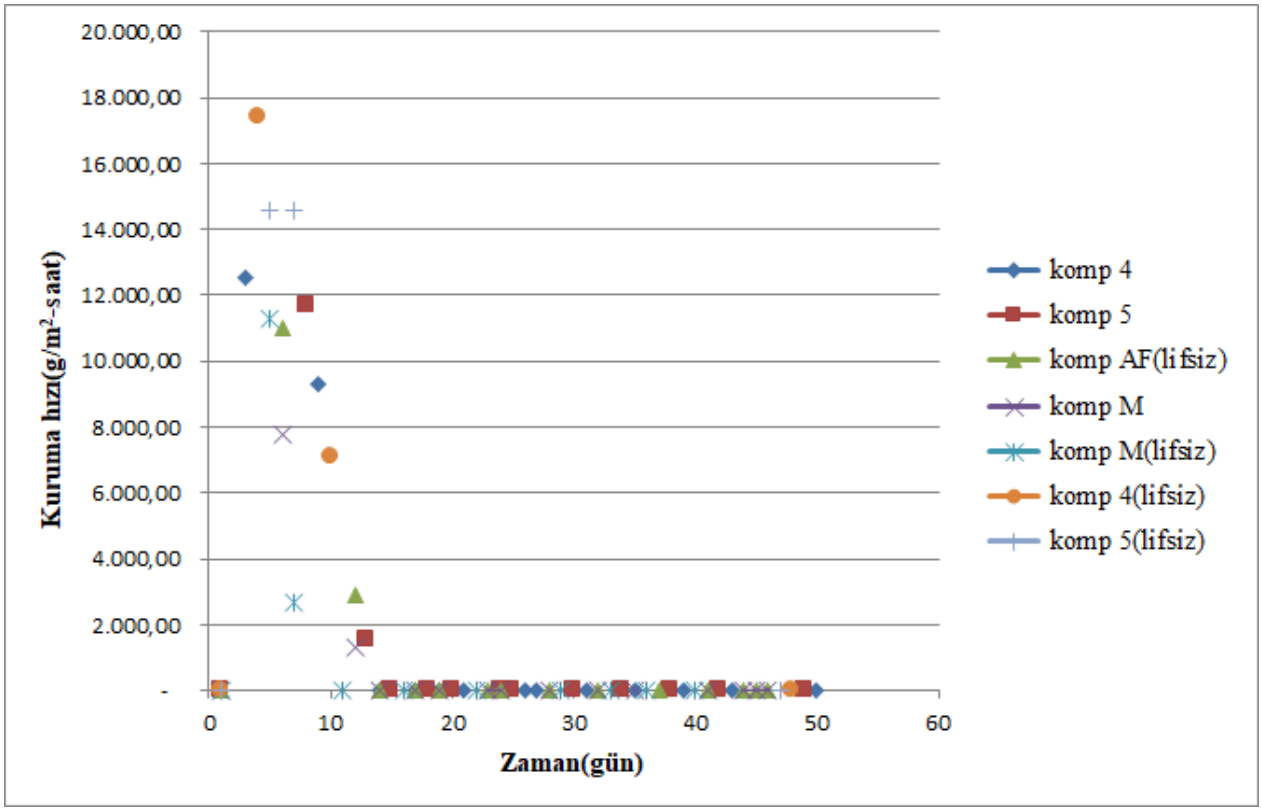
Denklem (7) de zamanın doğrusal bir fonksiyonuna sadeleştirilebilir.

$$\frac{4L^2}{\pi^2}\left[\log\left(\frac{8}{\pi^2}\right)-\log(Xred)\right] = Dw\times t \quad (7)$$

Böylece, etkin nem difüzyon katsayısı (Dw), iki farklı zaman periyodu için Denklem (5) ve (7)'den hesaplanır, ancak Fick'in ikinci yasası hidrasyon ve karbonatlaşma reaksiyonlarının etkilerini ve kenarlar boyunca difüzyonu göz ardı eder (Colinart ve ark., 2012).

BULGULAR ve TARTIŞMA

Önce, yüksek yoğunluğa sahip AF ve M kompozisyonları üretildi, daha sonra çok düşük yoğunluklu 4 ve 5 numaralı kenevir beton kompozisyonları üretilerek, bu kompozisyonlar kenevir saplarına ek olarak kenevir lifleri ilavesi ile de tekrarlandı. Daha sonra ise, yine kompozisyon M kenevir saplarının yanında kenevir liflerini de ilave ederek tekrar hazırlandı ve orta yoğunlukta bir kenevir-beton kompozisyonu elde edildi.
Yedi adet kenevir-beton kompozisyonunun kuruma hızlarının zamana göre değişimi Şekil 1'de görülmektedir.



Şekil 1. 7 farklı kenevir-beton kompozisyonu için kuruma hızının zamanla değişimi

Kompozisyon AF ve lifli M, ilk 10 gün boyunca sırasıyla 11,03 g/m²-saat ve 7,756 g/m²-saat kurutma hızlarına sahipti. Daha sonra, bu hız 14. günde ve 24. günün sonunda sırasıyla 2,883 g/m²-saat ve 1,342 g/m²-saate düştü. Elde edilen kurutma hızları, kompozisyon AF ve lifli M için sırasıyla 0,1 g/m²-saat ve 0,0531 g/m²-saat idi. İki bileşimin karşılaştırılması, liflerin daha düşük su emme kapasiteleri nedeniyle kuruma hızını düşürdüğünü göstermektedir (Brzyski ve ark., 2020). Ancak, kompozisyon M'nin ilk 9 gün boyunca kuruma hızı 11,267 g/m²-saat iken, kompozisyon 4 için bu hız 6. ve 9. günlerde sırasıyla 17,404 g/m²-saat ve kompozisyon 5 için 14,560 g/m²-saat olmuştur. Kuruma hızı, 12 günün sonunda kompozisyon M ve 5 için sırasıyla 0,1014 g/m²-saat ve 14,590 g/m²-saat olmuştur. Daha sonra, bu hız 19 günün sonunda kompozisyon 4 için 3,39 g/m²-saate düşmüştür. 12 günün sonunda kompozisyon 5'in kuruma hızındaki artış, yüksek miktarda serbest suyun uzaklaştırılması ve suyun yüzeye olan buharlaşma hızının difüzyon hızına göre düşük olması ile açıklanabilir (Colinart ve ark., 2012). Lifli 4 ve 5 numaralı kompozisyonların 13 günlük kuruma hızları 9,326 g/m²-saat ve 11,68 g/m²-saat olmuştur. 31 ve 34 gün sonra, bu hızlar lifli 4 ve 5 numaralı kompozisyonlar için sırasıyla 0,0163 g/m²-saat ve 0,119 g/m²-saat'e düşmüştür. Bu sonuç, kenevir liflerinin düşük su geçirgenliği nedeniyle liflerin kuruma hızı üzerindeki azaltıcı etkisini de desteklemektedir (Brzyski ve ark., 2020). Malzemenin bağıl nemi ortamla dengelenene kadar kürlenme odası ortamında küçük pozitif ve negatif ağırlık farklılıkları da gözlemlenmiştir.
Kompozisyonların etkin nem difüzyon katsayıları Tablo 1'de verilmiştir.

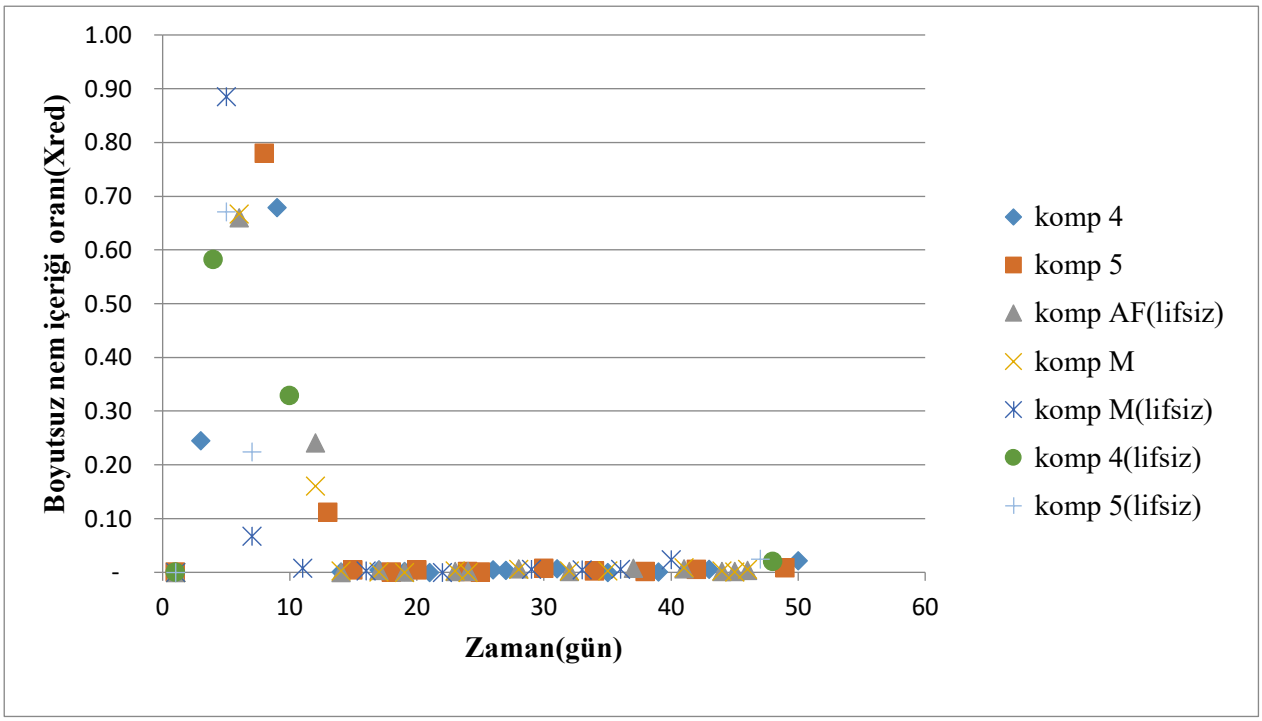
Tablo 1. Hazırlanan kenevir-beton kompozisyonlarının başlangıçtaki su içeriği, kuruma süresi, kuru yoğunluk ve etkin nem difuzyon katsayıları

Kenevir-beton kompozisyonları	X_0(gH_2O $gkuru^{-1}$)	Kuruma süresi (gün)	Kuru yoğunluk (kgm^{-3})	10^7Dw(Etkin difüzyon katsayısı) ($m^2\ s^{-1}$) (Den(5))	10^7Dw(Etkin difüzyon katsayısı) ($m^2\ s^{-1}$) (Den (7))	Thava(^{0}C), Bağıl rutubet(%)
AF	1	24	351	3.08	0.417	16.4-19.4^{0}C,29-34%
M	0.923	37	408	1.15	0.413	18.9-22^{0}C, 30-45%
4	0.933	31	156	1.17	0.543	18.9-22^{0}C, 30-45%
5	1.174	34	160	2.31	1.8	18.9-22^{0}C, 30-45%
4 lifli	0.933	38	160	7.25	1.14	16.4-21.3^{0}C,30-45%
5 lifli	1.174	48	192	6.39	3.46	16.4-21.3^{0}C,30-45%
M lifli	0.923	45	283	3.38	8.06	16.4-19.4^{0}C,29-34%

%50 su içeriğine sahip AF kompozisyonu, düşük hava nemine bağlı olarak, kompozisyonun iç kısmındaki tam buharlaşma nedeniyle kısa bir süre sonra 3,08*10^{-7} m^2/s nem difüzyon katsayısına sahipti. Uzun bir difüzyon süresinden sonra nem difüzyon katsayısı 0,417*10^{-7} m^2/s'ye düştü. %48 ve %48,25 su içeriğine sahip M ve 4 kompozisyonları, kısa bir süre sonra sırasıyla 1,15*10^{-7} m^2/s ve 1,17*10^{-7} m^2/s nem difüzyon katsayılarına ve uzun bir difüzyon süresinden sonra sırasıyla 0,413*10^{-7} m^2/s ve 0,543*10^{-7} m^2/s nem difüzyon katsayılarına sahipti; bunun nedeni, M ve 4 kompozisyonlarındaki havanın bağıl neminin AF kompozisyonundan daha yüksek olmasıdır. %54 su içeren 5 numaralı kompozisyonun nem difüzyon katsayıları, kısa ve uzun difüzyon sürelerinden sonra sırasıyla 2,31*10^{-7} m^2/s ve 1,8*10^{-7} m^2/s idi. Bu değişim, daha yüksek su içeriği, nem geçirgenliğindeki fark ve AF kompozisyonuna göre biraz daha yüksek bağıl nem nedeniyle daha düşük bir buharlaşma hızı olarak ifade edilebilir (Collet ve ark., 2013).

Lifli 4 ve 5 numaralı kompozisyonlarının kısa bir süre sonra nem difüzyon katsayıları 7,25*10^{-7} m^2/s ve 6,39*10^{-7} m^2/s iken, uzun bir difüzyon süresinden sonra nem difüzyon katsayıları sırasıyla 1,14*10^{-7} m^2/s ve 3,46*10^{-7} m^2/s'ye düştü. Uzun bir difüzyon süresinden sonra nem difüzyon katsayılarında bir azalma elde edilmesine rağmen, diğer kompozisyonlardan daha yüksek nem difüzyon katsayıları gözlendi. Bu daha yüksek nem difüzyon katsayıları, gözeneklere bağlı olarak liflerin su alma yeteneğine sahip olmasından kaynaklanmaktadır (Sair ve ark., 2018). Lifli M kompozisyonu, kısa ve uzun difüzyon sürelerinde sırasıyla 3,38*10^{-7} m^2/s ve 8,06*10^{-7} m^2/s nem difüzyon katsayılarına sahipti. Diğer kompozisyonların aksine, lif etkisinden dolayı elde edilen daha yüksek katsayılara rağmen nem difüzyon katsayısı artmaktadır. Bu durum, yüksek su içeriğine sahip kenevir parçacıkları ve lifler arasında bulunan makro gözeneklere bağlı nem geçirgenliği farkıyla açıklanabilir. Bağlayıcı içinde bulunan mikro gözeneklerin geçirgenlik üzerinde daha küçük bir etkisi olmuştur (Collet ve ark., 2013), (Walker ve Pavía, 2014), (Jiang ve ark., 2017), (Delannoy ve ark., 2020), (Delannoy ve ark., 2018). Kürlenme ve kuruma süreleri, su içeriği, kenevir ve lif etkilerini içeren kompozisyon türüne göre değişmekle birlikte, Tablo 1'den görüldüğü üzere genellikle 24 ila 48 gün arasında değişmektedir. Kalıplanmış bloklar için yalnızca numunenin üst yüzeyinden kuruma işleminin 80-100 gün sonra tamamlandığı bildirilmektedir (Colinart ve ark., 2012). Ancak bu çalışmada, kuruma alt yüzey hariç tüm yüzeylerde gerçekleşmiştir. Bu nedenle kuruma süreleri kısa olmuş ve (Colinart ve ark., 2012)'deki çalışma ile karşılaştırıldığında daha yüksek nem difüzyon katsayıları da bulunmuştur. (Colinart ve ark., 2012) kısa ve uzun difüzyon sürelerinde benzer nem difüzyon katsayıları elde etmiş olsa da, lifli M kompozisyonu hariç, bu çalışmada hesaplamalar uzun difüzyon sürelerinde daha düşük nem difüzyon katsayılarını vermektedir. Bu durum, kompozisyonların iç kısımlarında buharlaşmanın, havaya maruz kalan daha yüksek yüzey alanları nedeniyle kısa sürede tamamlanmasıyla açıklanabilir.

Yedi kenevir-beton karışımının boyutsuz nem oranı (Xred) değerlerinin zamana göre değişimi Şekil 2'de verilmiştir.



Şekil 2. 7 kenevir-beton kompozisyonu için boyutsuz nem içeriği oranının (Xred) zamanla değişimi

Bu değişime göre, AF ve M kompozisyonlarının yoğunluğu yaklaşık 701 kg/m^3 ila 351 kg/m^3 ve 500 kg/m^3 ila 408 kg/m^3 arasında değişmiştir, kompozisyon 4 ve 5'in yoğunluğu ise kürlenme süresi boyunca sırasıyla 348 kg/m^3'ten 156 kg/m^3'e ve 308 kg/m^3'ten 160 kg/m^3'e değişmiştir. Bununla birlikte, lif içeren 4 ve 5 kompozisyonlarının yoğunluk değişimleri 315 kg/m^3 ila 160 kg/m^3 ve 280 kg/m^3 ila 192 kg/m^3 arasında, lif içeren M kompozisyonunun yoğunluk değişimleri ise yine Tablo 1'den görüldüğü üzere kompozisyonların kuru yoğunluklarına göre sırasıyla 507 kg/m^3 ila 283 kg/m^3 arasındadır.

SONUÇ

• Lifli kompozisyonlarda kuruma hızının lifsiz kompozisyonlara göre daha düşük olduğu görülmektedir.

• Kürlenme ve kuruma süreleri, su içeriği, kenevir ve lif etkilerini içeren kompozisyon türüne göre değişmektedir.

•Lifli M kompozisyonu hariç, hesaplamalar uzun difüzyon sürelerinde kısa difüzyon sürelerinden daha düşük nem difüzyon katsayıları vermiştir.

KAYNAKLAR

Bakhshi, M. Mobasher, B. (2011). ''Experimental observations of early-age drying of Portland cement paste under low-pressure conditions''. Cem.Concr.Compos, 33,474-484.

Brzyski, P., Gładecki, M., Ruminska, M., Pietrak, K., Kubis, M., Łapka, P. (2020). ''Influence of HempShives Size on Hygro-Thermal and Mechanical Properties of a Hemp-Lime Composite''Materials, 13, 5383.

Chen, J., Williams, K., Chen, W., Shen, J., Ye, F. (2018).''A review of moisture migration in bulk material''. Part. Sci. Technol., 38(2), 247.

Colinart, T., Glouannec, P., Chauvelon, P. (2012). ''Influence of the setting process and the formulation on the drying of hemp concrete''. Constr. Build. Mater., 30(9), 372-380.

Collet, F., Chamoin, J., Pretot, S., Lanos, C. (2013). ''Comparison of the hygric behaviour of three hemp concretes'', Energy Build. *62*, 294-303.

Crank, J. (1975). The mathematics of diffusion,. 2nd ed.London(UK), Oxford University Press.

Delannoy, G., Marceau S., Gle, P., Gourlay, E, Minerbe, M.G., Amziane, S., Farcas, F. (2020).''Durability of hemp concretes exposed to accelerated environmental aging''.Constr. Build. Mater., *252*, 31.

Delannoy, G., Marceau,, S., Glé,, P., Gourlay, E., Minerbe, M.G., Diafi, D., Nour, I.., Amziane, S. et al. (2018). ''Aging of hemp shiv used for concrete''Mater. Des. 160, 752-762.

Evrard, A. (2008). Transient hygrothermal behavior of lime-hempmaterials. Ph.D. thesis.Université Catholique de Louvain(Belgium).

Glouannec, P., Chauvelon, P., Colinart, T., Le Bideau, P., Zaknoune, A., Jameladine, N. (2010). ''Experimental and numerical studies of the drying of hempconcrete''. 17th international drying symposium, Magdeburg(Germany), pp.2028-2033

Gu, X., Song, X. (2010). ''Competition between hydration and carbonation in hydraulic lime and lime-pozzolana mortars''Adv.Mater. Res., 133-134, 241-246.

Jiang, Y., Ansell, M., Jia, X., Hussain, A., Lawrence, M. (2017). ''Physical characterisation of hemp shiv: Cell wall structure and porosity'', 2nd Int. Conf. Bio-Based Build. Mater., Clermont-Ferrand, France.

Lawrence, R.M Mays, T.J., Rigby, S.P., Walker, P., Ayala, D.D. (2007).' ''Effects of carbonation on the pore structure of non-hydraulic lime mortars''. Cem Concr Re s., 765, 37(7),1059-1069.

Sair, S., Oushabi, A., Kammouni, A., Tanane, O., Abboud, Y., El Bouari, A. (2018). ''Case study Mechanical and thermal conductivity properties of hemp fiber reinforced polyurethane composites''. Case Stud.Constr. Mater., 8, 203-212.

Walker, R., Pavía, S. (2014). ''Moisture transfer and thermal properties of hemp–lime concretes''.Constr. Build. Mater., 64, 270-276.

ORAL PRESENTATION

Removal of micropollutants from water and wastewater by granular activated carbon

Gökçin Gül[1*] (ORCID: https://orcid.org/0000-0001-9886-9676),
Başak Kılıç[1] (ORCID: https://orcid.org/0000-0002-4823-0433),
Ferhan Çeçen[1] (ORCID: https://orcid.org/0000-0002-5353-1441)

[*1]Boğaziçi University, Institute of Environmental Sciences, Istanbul, Türkiye.

*Corresponding author e-mail: gokcin.gul@bogazici.edu.tr

Abstract

The occurrence of micropollutants such as pesticides and pharmaceuticals in aquatic environments has raised significant environmental and public health concerns. Conventional water and wastewater treatment processes are often insufficient for the complete elimination of these contaminants; therefore, alternative methods are required. Granular activated carbon (GAC) adsorption has emerged as an effective method due to the high surface area and strong affinity of activated carbon for diverse organic compounds. In this study, the application of GAC from water and wastewater was investigated for the removal of pesticides and pharmaceuticals, respectively. Results indicate that GAC demonstrates high adsorption efficiency, suggesting its potential as a reliable method for micropollutant removal. Previous studies in the literature also support that high removal efficiencies can be achieved by GAC, depending on operational conditions such as contact time, adsorbent dose, and initial contaminant concentration. The findings highlight that GAC adsorption is a practical solution for enhancing water quality in terms of emerging contaminants removal.

Keywords: Granular activated carbon, Micropollutants, Pesticides, Pharmaceuticals, Water treatment, Wastewater treatment

INTRODUCTION

Pollutants which are present in the concentration range of µg/L to ng/L in the environment are referred to as micropollutants. Nowadays, many pesticides and pharmaceuticals are detected as micropollutants in the influent of drinking water treatment plants and wastewater treatment plants (WWTPs), respectively. These micropollutants are known to have negative impacts on the environment despite the very low concentrations (Çeçen and Aktaş, 2011; Jatoi et al., 2021, Rattier et al., 2012; Sishu et al., 2022; Stehle and Schulz, 2015; Xu and Duran, 2017). Since many of conventional drinking water and wastewater treatment plants are not designed for micropollutant removal, they cannot be removed completely and may pose risk to human health.

Conventional water and wastewater treatment systems are designed to eliminate several types of contaminants from water. These include colloidal particles, dissolved salts, harmful microorganisms, biodegradable carbon, nitrogen and phosphorus. Their capacity to eliminate micropollutants is, nevertheless, quite variable and restricted. The difficulty in developing tailored treatment technologies stems from the extremely low quantities of these pollutants, which frequently go below detection criteria (Nas et al., 2017; Rodriguez-Narvaez et al., 2017; Saravanan et al., 2021; Teodosiu et al., 2018; Verlicchi et al., 2012). The unique chemical characteristics of the compounds, the treatment methods employed, and the system's operating settings all significantly impact how well micropollutants are removed from the environment. Important factors affecting removal effectiveness are the micropollutants' molecular structure, polarity, solubility, and persistence (Luo et al., 2014).

There are many methods used for micropollutant removal including coagulation-flocculation, ozonation, advanced oxidation, membrane filtration, biodegradation and activated carbon adsorption (Borrull et al., 2021; Nas et al., 2017; Saravanan et al., 2021; Tröger et al., 2017). However, implementing these technologies in large-scale treatment facilities presents several challenges, primarily related to cost-effectiveness, energy consumption, and operational complexity (Ibrahim et al., 2023). Among these various advanced treatment processes, adsorption is considered the most commonly used method because of its cost-effectiveness, operational simplicity, and ease of regeneration (Saravanan et al., 2021; Teodosiu et al., 2018). Numerous studies have highlighted that among various adsorbent materials, activated carbon stands out as the most widely utilized and efficient adsorbent for micropollutant removal in water treatment (Rodriguez-Narvaez et al., 2017; Sangkarak et al., 2020; Sophia & Lima, 2018; Teodosiu et al., 2018; Zhao et al., 2022). This technology has

shown promise in effectively removing a wide range of micropollutants without the associated high operational costs of other advanced treatment methods. However, further research is required to optimize its application in large-scale water treatment facilities and to assess its long-term efficiency in micropollutant removal (Tröger et al., 2020). The purpose of this research was to investigate the use of granular activated carbon (GAC) for the removal of pesticides and pharmaceuticals from water and wastewater, respectively.

Activated Carbon

Activated carbon is the most widely used adsorbent in water and wastewater treatment. The ability to adsorb a wide variety of organic compounds and its economic feasibility make activated carbon the most preferable. In water treatment, it is used to remove organic compounds that cause odor, taste and color. In advanced wastewater and industrial treatment, it is used to remove toxic organic compounds. It is generally used in the granular form in a carbon adsorption column in water and wastewater purification (Hung et al., 2005).

Activated carbon is a porous carbon material with a high adsorption capacity because of its high surface area (between 500 and 1500 m^2/g). Due to this, the amount of material adsorbed is potentially very large. The total surface available for adsorption of solute includes the external surface of the particles and the surfaces of pores. The pore surface area is much larger than the external surface area of the particles. Therefore, adsorption occurs on the pores' surfaces mostly. The ratio of the total surface area to the mass of activated carbon is very large. As a result, activated carbon adsorption can be used in tertiary treatment for the removal of organic pollutants from the secondary effluent of biological wastewater treatment systems. It can be produced from many different carbonaceous materials, such as coal, lignite, wood, coconut shell and some polymers (Çeçen, 2024; Çeçen and Aktaş, 2011; Hung et al., 2005; Junpirom, 2006).

Activated carbon is mainly in the form of powdered activated carbon (PAC) and granular activated carbon (GAC). The average particle size of PAC is in the range of 15-25 μm. It is applied for the treatment of both wastewater and drinking water. GAC is generally in the form of crushed granules of shell or coal and has sizes ranging from 0.2 to 5 mm. GAC filters are widely used for drinking water, groundwater and wastewater purification and removal of toxic organic compounds. In some GAC applications, a microbiological film may form on the particles. As a result, biological removal of contaminants is combined with GAC adsorption. The new material is called as biological activated carbon (BAC) (Çeçen and Aktaş, 2011).

The use of activated carbon, either as GAC or PAC has been investigated in many studies. The use of activated carbon is a widespread technology that has been applied for many years to remove pollutants from water and wastewater. Thus, significant knowledge on setup and operation of such systems is available. The main advantage of using activated carbon is the effective removal of micropollutants, also no by-products are generated (Baresel et al., 2019).

Pesticides Removal from Drinking Water by GAC

Conventional water treatment processes often demonstrate inadequate efficiency in completely removing pesticides (Jatoi et al., 2021). Hence, alternative treatment methods have been used for effective elimination of pesticides from drinking water.

In a study, batch tests were carried out to investigate the adsorption of a pesticide (malathion) by GAC from agricultural runoff. In these tests, two types of GAC were used for comparing the effectiveness. The results indicated that granular activated carbon could be used to effectively adsorb malathion from agricultural runoff (Jusoh et al., 2011). Also, another study investigated the use of two different granular activated carbons Filtrasorb 400 and Norit 1240 for removal of pesticides from water. It was shown that the efficiency of Norit 1240 ranged between 5-32%, while the efficiency of Filtrasorb F400 was higher that ranged between 12-64% depending on the contact time. It was also indicated that pH of water and the initial concentrations of the pesticides affected the adsorption efficiency (%) and adsorption capacity (μg/g) (Ilavsky et al., 2021).

Beyond simple adsorption, the synergistic potential of combining physical and biological mechanisms has been validated in operational treatment plants. For instance, a study conducted at the Shiraz treatment plant compared granular activated carbon (GAC) and biological activated carbon (BAC) systems for removing 18 pesticides from water, finding that BAC consistently outperformed GAC due to the synergistic effects of adsorption and biodegradation. BAC achieved 100% removal of seven pesticides including methyl parathion and malathion, while GAC showed lower efficiency (e.g., 67.38% vs. 100% for methyl parathion). This research demonstrates

that BAC systems offer a highly effective supplementary treatment option for municipal water facilities dealing with pesticide contamination (Tahmasebi et al., 2023).

In addition to biological integration, enhancing GAC filtration with advanced oxidation processes such as ozonation has proven highly effective for contaminant removal. Combining ozonation with granular activated carbon (GAC) filtration effectively removes pesticides and their transformation products from drinking water, achieving over 90% removal rates while reducing toxicity. Although ozonation degrades pesticides within 10-15 minutes, it can produce toxic byproducts, which are subsequently eliminated in the GAC filtration step. Furthermore, the research emphasizes that GAC performance declines significantly after 7-9 years of use, recommending replacement every two years to maintain water safety and treatment effectiveness (Shi et al., 2025).

Pharmaceuticals Removal from Wastewater by GAC

As mentioned before, conventional wastewater treatment systems are not designed for micropollutant removal. In traditional treatment, the majority of micropollutants cannot be eliminated and remain in the effluent. Therefore, it becomes essential to use new and advanced methods that can eliminate micropollutants from wastewater (Balu et al., 2024; Belete et al., 2023).

Removal of pharmaceuticals from wastewater by granular activated carbon was investigated in many studies. In a study, pharmaceutical removal in effluents from three WWTP was searched. The aim was to achieve 95% removal of selected micropollutants in a Swedish WWTP through adsorption onto activated carbon and to compare the performance of PAC and GAC. Results showed that activated carbon is an efficient method to remove pharmaceuticals from WWTP effluents. 95% removal was achieved for almost all the targeted micropollutants. Results demonstrated that there is 95% removal if PAC was applied at a dose of 15-20 mg/L, and more than 90% removal if GAC was used for all tested micropollutants (Karelid et al., 2017).

In another study, a full-scale GAC system was used to remove steroidal estrogens and pharmaceuticals from the WWTP effluent. Results showed that there was more than 43% to 64% reduction in steroidal estrogens. Additionally, many of the targeted pharmaceuticals, such as mebeverine, were removed between 84-99%. However, it is stated that some of the pharmaceuticals including carbamazepine and propranolol had removal efficiencies of 17-23%. It is said that removal of some organic micropollutants with GAC-based technology is less efficient, because adsorption sites become saturated as time passes (Grover et al., 2011).

Additionally, recent studies have shown that hybrid treatment schemes combining membrane-based separation, such as ultrafiltration in membrane bioreactors, with biologically active granular activated carbon (GAC) filtration can achieve highly efficient removal of a broad range of organic micropollutants from municipal wastewater. Pilot-scale evaluations report that coupling physical filtration with adsorption and biodegradation consistently reduces pharmaceuticals and other trace contaminants to very low or non-detectable concentrations, demonstrating a synergistic effect between membrane retention and bio-active carbon surfaces (Baresel et al., 2019).

Alternative advanced wastewater treatment technologies have also been systematically compared to carbon-based processes. Large-scale pilot trials contrasting ozonation with powdered activated carbon (PAC) treatment have demonstrated that both approaches consistently remove a broad suite of contaminants—often exceeding 80% removal of monitored micropollutants—while improving effluent toxicity profiles, with PAC sometimes providing broader removal due to the absence of oxidation by-product formation (Margot et al., 2013).

Recent studies also highlight the importance of synergistic interactions between adsorption and biodegradation within GAC filters, where microbial transformation processes can extend carbon lifespan and alter removal pathways. In a study the interaction of adsorption and biodegradation in the removal of organic micropollutants in GAC filters was investigated. By comparing GAC with non-adsorbing sand media, it was shown that adsorption can effectively extend the residence time of micropollutants, thereby enhancing biodegradation—particularly for moderately adsorbable and biodegradable substances such as diclofenac. In contrast, weakly adsorbable compounds (e.g., N-Nitrosodimethylamine) exhibited strong dependence on contact time, while biologically recalcitrant but strongly adsorbable substances (e.g., carbamazepine) were primarily retained through the adsorption–desorption cycling rather than degradation. Overall, the study demonstrates that adsorption and biodegradation are closely coupled processes in GAC filters, influencing removal efficiencies and complicating the interpretation of filter performance (Betsholtz et al., 2024).

CONCLUSION

This study summarizes the use of granular activated carbon for micropollutant removal from drinking water and wastewater. For water treatment, pesticides removal, for wastewater treatment pharmaceuticals removal was investigated. Studies showed that the use of GAC is a very effective and well-known method for removal of many micropollutants from water and wastewater. The adsorption potential of micropollutants on GAC is relatively high which makes it preferable for treatment purposes. However, its effectiveness depends on different conditions such as careful design of filters, proper operation and monitoring. It is effectively used in advanced treatment and studies continue for improving its performance and cost-effectiveness.

ACKNOWLEDGEMENTS

The authors acknowledge the grant provided by Bogazici University Research Fund Grant Number 19Y00D5 and Bogazici University Research Fund Grant Number 19Y00D6.

REFERENCES

Ballard, B. D., & MacKay, A. A. (2005). Estimating the removal of anthropogenic organic chemicals from raw drinking water by coagulation flocculation. Journal of Environmental Engineering, 131(1), 108–118.

Balu, S., Ganapathy, D., Arya, S., Atchudan, R., & Sundramoorthy, A.K. (2024). Advanced photocatalytic materials based degradation of micropollutants and their use in hydrogen production – A review. RSC Advances, 14:14392–14424.

Baresel C., Harding, M. & Fang, J. (2019). Ultrafiltration/granulated active carbon-biofilter: Efficient removal of a broad range of micropollutants. Applied Sciences, 9:710.

Belete, B., Desye, B., Ambelu, A., & Yenew, C. (2023). Micropollutant removal efficiency of advanced wastewater treatment plants: A systematic review. Environmental Health Insights, 17:1–11.

Betsholtz, A., Falas, P., Svahn, O., Cimbritz, M., & Davidsson, A. (2024). New perspectives on the interactions between adsorption and degradation of organic micropollutants in granular activated carbon filters. Environmental Science and Technology, 58:11771−11780.

Borrull, J., Colom, A., Fabregas, J., Borrull, F., & Pocurull, E. (2021). Presence, behaviour and removal of selected organic micropollutants through drinking water treatment. Chemosphere, 276, 130023.

Cantoni, B., Delli Compagni, R., Turolla, A., Epifani, I., & Antonelli, M. (2020). A statistical assessment of micropollutants occurrence, time trend, fate and human health risk using left-censored water quality data. Chemosphere, 257, 127095.

Çeçen, F. (2024). Activated Carbon. In John Wiley & Sons Inc (Ed.), Kirk-Othmer Encyclopedia of Chemical Technology. John Wiley & Sons, Inc.

Çeçen, F., & Aktaş, Ö. (2011). Activated carbon for water and wastewater treatment: Integration of adsorption and biological treatment. John Wiley and Sons, NY, USA.

Grover, D.P., Zhou, J.L., Frickers, P.E., & Readman, J.W. (2011). Improved removal of estrogenic and pharmaceutical compounds in sewage effluent by full scale granular activated carbon: Impact on receiving river water. Journal of Hazardous Materials, 185, 1005–1011.

Guo, W., Ngo, H. H., & Li, J. (2012). A mini-review on membrane fouling. Bioresource Technology, 122, 27–34.

Hung, Y.T., Lo, H.H., Wang, L.K., Taricska, J.R., & Li, K.H. (2005). Granular activated carbon adsorption. In Wang, L.K., Hung, Y.T., & Shammas, N.K. (Eds), Handbook of Environmental Engineering, Volume 3: Physiochemical Treatment Processes. Totowa, NJ: The Humana Press Inc.

Ibrahim, M., Nawaz, M. H., Rout, P. R., Lim, J. W., Mainali, B., & Shahid, M. K. (2023). Advances in produced water treatment technologies: an in-depth exploration with an emphasis on membrane-based systems and future perspectives. Water, 15(16), 2980.

Ike, I. A., Karanfil, T., Cho, J., & Hur, J. (2019). Oxidation byproducts from the degradation of dissolved organic matter by advanced oxidation processes – A critical review. Water Research, 164, 114929.

Ilavsky, J., Barlokova, D., & Marton, M. (2021). Removal of selected pesticides from water using granular activated carbon. IOP Conference Series: Earth and Environmental Science, 900 012011.

Jatoi, A. S., Hashmi, Z., Adriyani, R., Yuniarto, A., Mazari, S. A., Akhter, F., & Mubarak, N. M. (2021). Recent trends and future challenges of pesticide removal techniques – A comprehensive review. Journal of Environmental Chemical Engineering, 9(4), 105571.

Junpirom, S. (2006). Activated carbon from longan seed: its activation model and adsorption of water vapor and benzene. Ph.D. Thesis, Suranaree University of Technology.

Jusoh, A., Hartini, W.J.H., Ali, N., & Endut, A. (2011). Study on the removal of pesticide in agricultural run off by granular activated carbon, Bioresource Technology, 102:5312–5318.

Karelid, V., Larsson, G., & Björlenius, B. (2017). Pilot-scale removal of pharmaceuticals in municipal wastewater: Comparison of granular and powdered activated carbon treatment at three wastewater treatment plants. Journal of Environmental Management, 193, 491-502.

Luo, Y., Guo, W., Ngo, H. H., Nghiem, L. D., Hai, F. I., Zhang, J., Liang, S., Wang, X. C. (2014). A review on the occurrence of micropollutants in the aquatic environment and their fate and removal during wastewater treatment. Science of The Total Environment, 473–474, 619–641.

Margot, J., Kienle, C., Magnet, A., Weil, M., Rossi, L., de Alencastro, L.F., Abegglen, C., Thonney, D., Chèvre, N., Schärer, M., & Barry, D.A. (2013). Treatment of micropollutants in municipal wastewater: Ozone or powdered activated carbon? Science of the Total Environment 461–462:480–498.

Miklos, D. B., Remy, C., Jekel, M., Linden, K. G., Drewes, J. E., & Hübner, U. (2018). Evaluation of advanced oxidation processes for water and wastewater treatment – A critical review. Water Research, 139, 118–131.

Peiris, R. H., Budman, H., Moresoli, C., & Legge, R. L. (2013). Fouling control and optimization of a drinking water membrane filtration process with real-time model parameter adaptation using fluorescence and permeate flux measurements. Journal of Process Control, 23(1), 70–77.

Rattier, M., Reungoat, J., Gernjak, W., & Keller, J. (2012). Organic micropollutant removal by biological activated carbon filtration: A review. Urban Water Security Research Alliance Technical Report No: 53.

Rodriguez-Narvaez, O. M., Peralta-Hernandez, J. M., Goonetilleke, A., & Bandala, E. R. (2017). Treatment technologies for emerging contaminants in water: A review. Chemical Engineering Journal, 323, 361–380.

Sangkarak, S., Phetrak, A., Kittipongvises, S., Kitkaew, D., Phihusut, D., & Lohwacharin, J. (2020). Adsorptive performance of activated carbon reused from household drinking water filter for hexavalent chromium-contaminated water. Journal of Environmental Management, 272, 111085.

Saravanan, A., Senthil Kumar, P., Jeevanantham, S., Karishma, S., Tajsabreen, B., Yaashikaa, P. R., & Reshma, B. (2021). Effective water/wastewater treatment methodologies for toxic pollutants removal: Processes and applications towards sustainable development. Chemosphere, 280, 130595.

Shi, W., Cheng, Y., Li, X., Zhang, X., Pang, H., Qi, J., & Hu, C. (2025). Synergistic removal of pesticides and transformation products through optimization of ozonation and granular activated carbon filtration parameters toward achieving toxin-free drinking water. Journal of Water Process Engineering, 77, 108598.

Sishu, F. K., Tilahun, S. A., Schmitter, P., Assefa, G., & Steenhuis, T. S. (2022). Pesticide Contamination of Surface and Groundwater in an Ethiopian Highlands' Watershed. Water (Switzerland), 14(21), 3446.

Sophia A., C., & Lima, E. C. (2018). Removal of emerging contaminants from the environment by adsorption. Ecotoxicology and Environmental Safety, 150, 1–17.

Stehle, S., & Schulz, R. (2015). Agricultural insecticides threaten surface waters at the global scale. Proceedings of the National Academy of Sciences of the United States of America, 112, 5750–5755.

Tahmasebi, A. A., Beni, A. S., Azhdarpoor, A., & Moeini, Z. (2023). The application of granular and biological activated carbon columns in removal of organochlorine and organophosphorus pesticides in a water treatment plant. Journal of Water Process Engineering, 56, 104383.

Teodosiu, C., Gilca, A. F., Barjoveanu, G., & Fiore, S. (2018). Emerging pollutants removal through advanced drinking water treatment: A review on processes and environmental performances assessment. Journal of Cleaner Production, 197, 1210–1221.

Tröger, R., Köhler, S. J., Franke, V., Bergstedt, O., & Wiberg, K. (2020). A case study of organic micropollutants in a major Swedish water source – Removal efficiency in seven drinking water treatment plants and influence of operational age of granulated active carbon filters. Science of The Total Environment, 706, 135680.

Xu, W., & Duran, M. (2017). Removal of hazardous pollutants in full-scale wastewater treatment plant. In: Çeçen, F., Tezel, U. (Eds.), Hazardous pollutants in biological treatment systems: Fundamentals and a guide to experimental research. IWA Publishing, London.

Zhao, C., Wang, Y., Zhao, R., & Jiang, J. (2022). Removal of bisphenol S from drinking water by adsorption using activated carbon and the mechanisms involved. International Journal of Environmental Science and Technology, 19(6), 5289–5300.

ORAL PRESENTATION

Potansiyel bir hidrojen depolama iyonik sıvısı olarak guanidinyum oktahidrotriboratın yapısal ve elektronik özelliklerinin hesapsal karakterizasyonu

Ayşe Demirkıran[1*] (Orcid: 0000 0001 7541 8290), Armağan Kınal[2] (Orcid: 0000-0002-9747-4901)

[*1]Ege Üniversitesi, Malzeme Bilimi ve Mühendisliği Bölümü, İzmir, Türkiye
[2]Ege Üniversitesi, Fen Fakültesi, Kimya Bölümü, İzmir, Türkiye

*Sorumlu yazar e-mail: aysece19@gmail.com

Özet

Bu çalışmada, guanidinyum oktahidrotriborat ($GuaB_3H_8$) iyonik sıvısının geometrik ve elektronik özellikleri yoğunluk fonksiyoneli teorisi (DFT) kullanılarak ayrıntılı olarak incelenmiştir. Gaussian 16 program paketi ile B3LYP/6-311++G(d,p) ve ωB97X-D/6-311++G(d,p) teori düzeylerinde, guanidinyum katyonu (Gua^+), oktahidrotriborat anyonu ($B_3H_8^-$) ve bunlardan oluşan iyonik sıvının geometri optimizasyonları gerçekleştirilmiş, harmonik frekans analizleriyle tüm yapıların potansiyel enerji yüzeyinde yerel minimumda olduğu doğrulanmıştır. Her iki fonksiyonel de C–N, N–H, B–H ve B–B bağ uzunlukları için birbirine oldukça yakın değerler vermiş; bağ parametrelerindeki küçük farklar, seçilen yöntem–baz seti kombinasyonunun yapısal eğilimleri güvenilir biçimde tanımladığını göstermiştir. İyonik sıvının bağlanma enerjileri B3LYP ve ωB97X-D için sırasıyla −172.5 ve −177.1 kcal/mol olarak hesaplanmış, bu da güçlü katyon–anyon etkileşimleri ile yüksek termodinamik kararlılığı ortaya koymuştur. Frontier moleküler orbital analizi, HOMO'nun hidrojence zengin $B_3H_8^-$ birimi üzerinde, LUMO'nun ise kısmen guanidinyum katyonu üzerinde lokalize olduğunu göstermiş; HOMO–LUMO enerji aralığının B3LYP için 4.92 eV, ωB97X-D için 8.43 eV olarak bulunması, sistemin elektronik açıdan kararlı doğasını desteklemiştir. Moleküler elektrostatik potansiyel (MEP) haritaları, beklenen yük ayrımını ve belirgin yük lokalizasyonunu doğrulayarak elde edilen bağlanma enerjileri ve orbital bulgularıyla tutarlı bir tablo sunmuştur. Elde edilen sonuçlar, $GuaB_3H_8$ iyonik sıvısı boran temelli sistemlerin yüksek kararlılık sunduğunu ve benzer sistemlerin rasyonel tasarımı için önemli yapısal ve elektronik parametreler sağladığını göstermektedir.

Anahtar Kelimeler: Guanidinyum oktahidrotriborat, iyonik sıvı, yoğunluk fonksiyoneli teorisi, HOMO–LUMO

Computational characterization of the structural and electronic properties of guanidinium octahydrotriborate as a potential hydrogen storage ionic liquid

Abstract

In this study, the geometric and electronic properties of the guanidinium octahydrotriborate ($GuaB_3H_8$) ionic liquid were examined in detail using density functional theory (DFT). Geometry optimizations of the guanidinium cation (Gua^+), the octahydrotriborate anion ($B_3H_8^-$), and the ionic liquid formed by these species were performed at the B3LYP/6-311++G(d,p) and ωB97X-D/6-311++G(d,p) levels of theory with the Gaussian 16 program package, and harmonic frequency analyses confirmed that all structures correspond to local minima on the potential energy surface. Both functionals yielded highly similar values for the C–N, N–H, B–H, and B–B bond lengths; the small differences in bonding parameters indicate that the chosen method–basis set combinations reliably describe the structural characteristics of the system. The binding energies of the ionic liquid were calculated as −172.5 and −177.1 kcal/mol for B3LYP and ωB97X-D, respectively, revealing strong cation–anion interactions and high thermodynamic stability. Frontier molecular orbital analysis showed that the HOMO is localized on the hydrogen-rich $B_3H_8^-$ unit, while the LUMO is partially localized on the guanidinium cation; the HOMO–LUMO gaps, found to be 4.9151 eV for B3LYP and 8.4296 eV for ωB97X-D, further support the electronically stable nature of the system. Molecular electrostatic potential (MEP) maps confirmed the expected charge separation and pronounced charge localization, presenting a picture consistent with the obtained binding energies and orbital findings. Overall, the results demonstrate that the $GuaB_3H_8$ ionic liquid offers high stability among borane-based systems and provides important structural and electronic parameters for the rational design of related materials.

Keywords: Guanidinium octahydrotriborate, ionic liquid, density functional theory, HOMO–LUMO.

GİRİŞ

Küresel enerji talebinin sürekli artması ve fosil yakıtların çevresel etkileri, temiz ve sürdürülebilir enerji kaynaklarına yönelik araştırmaları zorunlu kılmaktadır. Hidrojen, yüksek enerji yoğunluğu ve çevre dostu yanma ürünleri nedeniyle geleceğin ideal enerji taşıyıcısı olarak görülmekte, ancak güvenli ve verimli depolama sorunu yaygın kullanımını engelleyen başlıca zorluklardan birini oluşturmaktadır. ABD Enerji Bakanlığı (DOE) tarafından belirlenen teknik hedefler, hafif ticari araçlarda kullanılmak üzere 5.5 wt% sistem gravimetrik kapasite ve 40 g/L sistem volumetrik kapasite gibi katı kriterler öne sürmektedir (Kohani ve ark.,2023; Liu ve ark., 2023; Chen ve ark., 2023). Boran tabanlı yapılar düşük molekül ağırlığı ile malzemelerin teorik kapasitelerini artırırken, termodinamik ve kinetik sorunların aşılması için rasyonel moleküler tasarımlar gerekmektedir. Son yıllarda iyonik sıvıların düşük buhar basıncı, geniş sıvı aralığı ve yapısal esneklik vb. benzersiz özellikleri uygulamalara yeni bir yaklaşımlar sunmaktadır (Chen ve ark, 2015). Bu bağlamda guanidinyum oktahidrotriborat ($GuaB_3H_8$), hem boran temelli yapısı hem de protonik karakteri nedeniyle gelecek vaat eden bir aday olarak ortaya çıkmıştır (Chen ve ark, 2015). Chen ve ark. 2015'teki çalışması, bu iyonik sıvının %13.8 teorik hidrojen içeriğine sahip olduğunu göstererek bu alandaki ilgiyi artırmıştır. Guanidinyum katyonunun yüksek termal kararlığı ile oktahidrotriborat anyonunun zengin hidrojen kimyasının sinerjik etkileşimi, bu malzemenin hem sistem hedeflerini karşılama hem de döngüsel kullanım için gerekli kararlılığı sağlama potansiyelini güçlendirmektedir (Doroodian ve ark., 2010).

Oktahidrotriborat anyonu ($[B_3H_8]^-$), boran kimyasının temel yapı taşlarından biri olup üç bor atomunun sekiz terminal hidrojenle çevrili dinamik bir yapısı vardır. Bu anyon, katı hal NMR ve nötron kırınımıyla ölçülen molekül içi hareketli davranışıyla tanınır; son yıllarda anharmonik YFT hesaplamaları overton ve kombinasyon bantlarının önemli yoğunluklara sahip olduğunu göstermiştir (Frisch ve ark., 2016). Bykov ve Zhizhin'in kapsamlı derlemesi, $[B_3H_8]^-$ anyonunun organometalik komplekslerdeki koordinasyon kimyası, tuzlarındaki reorientasyonel dinamik ve termo-elektrokimyasal kararlılığını detaylandırarak, $GuaB_3H_8$ gibi iyonik sıvıların moleküler düzeyde anlaşılması için teorik yöntemlerin gerekliliğini vurgulamaktadır (Bykov &Zhizhin, 2019; Zheng ve ark., 2019).

Özellikle Gaussian 16 yazılımı, geniş fonksiyonel ve baz seti seçenekleri sayesinde iyonik sıvılar gibi çok merkezli etkileşimlere sahip sistemlerin doğru modellenmesine olanak tanımaktadır (Frisch ve ark., 2016). İyonik sıvıların karmaşık elektronik yapısını tanımlamada yaygın B3LYP fonksiyonelinin yanı sıra uzun menzilli dispersiyon etkileşimlerini açıkça hesaba katan ωB97X-D fonksiyoneli de sıklıkla tercih edilmektedir (Chai & Head-Gordon, 2008; Rekken & Krossing, 2016). Literatürde yapılan sistematik karşılaştırmalar, iyon-çiftlerinin geometri optimizasyonu ve elektronik enerji hesaplamalarında bu iki fonksiyonelin güvenilir bir performans sağladığını göstermektedir. Ayrıca 6-311++G(d,p) gibi difüz ve polarizasyon fonksiyonları içeren baz setlerinin hidrojen bağlanma enerjilerinin ve frontier moleküler orbitallerin doğru tanımlanması için kritik olduğu çeşitli hesaplamalı çalışmalar tarafından desteklenmektedir (Hehre ve ark., 1986; Rekken & Krossing, 2016).

Bu çalışma, guanidinyum oktahidrotriborat iyonik sıvısının yapısal ve elektronik özelliklerini B3LYP ve ωB97X-D fonksiyonelleri ile 6-311++G(d,p) baz seti kullanarak kapsamlı olarak incelemeyi amaçlamaktadır. Optimize edilmiş geometriler üzerinden bağ uzunlukları, enerji parametreleri ve temel yapısal özellikler analiz edilecek; HOMO-LUMO enerji aralıkları, moleküler elektrostatik potansiyel (MEP) yüzeyleri haritaları hesaplanarak molekülün geometrik ve elektronik özellikleri ortaya çıkarılacaktır (Frisch ve ark., 2016; Ramkumar & Gardas, 2019). Elde edilecek bulguların, sürdürülebilir enerji depolama teknolojilerinde kullanılabilecek rasyonel moleküler tasarım stratejilerine katkı sunması ve guanidinyum oktahidrotriborat iyonik sıvısının hidrojen depolama özelliklerinin ortaya koymasında ilk basamak olması hedeflenmektedir (Chen ve ark. 2015). Bu sayede $GuaB_3H_8$'in yapısal dinamikleri ve enerjiye dayalı özelliklerine ilişkin kritik bilgilerin, literatürdeki artan ilgiye dikkate değer bir katkı sağlaması beklenmektedir.

MATERYAL VE METOT

Guanidinyum oktahidrotriborat iyonik sıvısı ($CN_3H_6^+$ katyonu ve $[B_3H_8]^-$ anyonu), yoğunluk fonksiyoneli teorisi (DFT) tabanlı hesaplamalar kullanılarak ayrıntılı biçimde incelenmiştir. Bileşen katyon ve anyon yapılarının yanı sıra iyon çiftinin tamamı, hem geometrik hem de elektronik özelliklerin güvenilir biçimde tanımlanabilmesi amacıyla B3LYP ve ωB97X-D fonksiyonelleri ile optimize edilmiştir. B3LYP, yaygın

kullanılan hibrit değiş-tokuş–korelasyon fonksiyoneli olup temel yapısal özelliklerin tutarlı biçimde elde edilmesinde etkilidir; ωB97X-D ise uzun menzilli etkileşimleri ve dispersiyon kuvvetlerini daha doğru temsil eden menzil ayrımlı hibrit fonksiyonel olması nedeniyle özellikle iyonik sıvıların modellemesinde tercih edilmiştir. Tüm hesaplamalarda temel fonksiyonlar olarak polarizasyon ve difüz fonksiyonlar içeren 6-311++G(d,p) baz seti kullanılmıştır.

İyonik sıvı için B3LYP/6-311++G(d,p) ve ωB97X-D/6-311++G(d,p) teori düzeylerinde çeşitli başlangıç geometrilerinden hareketle geometri optimizasyonları gerçekleştirilmiş ve her iki fonksiyonel için de en düşük elektronik enerjiye sahip iyonik sıvı yapısı belirlenmiştir. Optimizasyon sonrasında elde edilen bu yapıların potansiyel enerji yüzeyinde gerçek bir yerel minimuma karşılık gelip gelmediğini doğrulamak amacıyla harmonik frekans analizleri yapılmış; hiçbir sanal frekansın bulunmaması, hesaplanan iyonik sıvı geometrilerinin yerel minimum niteliğini açıkça teyit etmiştir.

Guanidinyum oktahidrotriborat sisteminin bağlanma enerjileri (ΔE_b), iyon çiftinin toplam enerjisi ile bileşen iyonların ayrı ayrı optimize edilmiş minimum enerji değerleri kullanılarak hesaplanmıştır. Bağlanma enerjisi, Denklem (1) uyarınca:

$$\Delta E_b = E_{İS} - (E_{katyon} + E_{anyon}) \quad (1)$$

Burada $E_{İS}$ iyonik sıvının optimize edilmiş geometrideki toplam elektronik enerjisini; E_{katyon} ve E_{anyon} ise sırasıyla guanidinyum katyonu ve oktahidrotriborat anyonunun bağımsız olarak optimize edilmiş minimum enerji değerlerini ifade etmektedir. Bu yaklaşım, iyon çiftindeki elektrostatik, kovalent ve dispersiyon kaynaklı etkileşimlerin toplam enerjisel katkıları hakkında nicel bilgi sunmakta ve sistemin kararlılık değerlendirmelerine temel oluşturmaktadır.

Bağlanma enerjisi hesaplamalarında Counterpoise (CP) düzeltmesi kullanılmamıştır. BSSE düzeltmesi, etkileşim enerjisinin küçük olduğu (örneğin nötr moleküller arası zayıf hidrojen bağları veya dispersiyon etkileşimleri) sistemlerde sonuçları nitel olarak değiştirebilmektedir. Ancak GuaB3H8 gibi iyonik sıvılarda bağlanma enerjisi temel olarak güçlü elektrostatik etkileşimlerden kaynaklanmakta ve oldukça yüksek değerlere (bu çalışmada ~ -175 kcal/mol) ulaşmaktadır. Bu büyüklükteki bir enerji değişiminde, BSSE kaynaklı oluşabilecek birkaç kcal/mol'lük sapma, toplam enerjinin çok küçük bir yüzdesine (%1-2 civarı) tekabül ettiğinden ihmal edilmiştir.

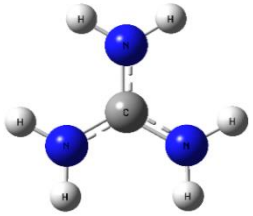
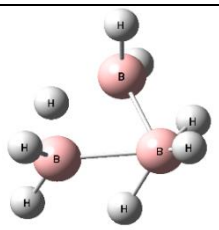
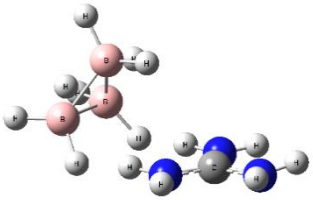
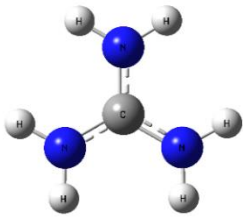
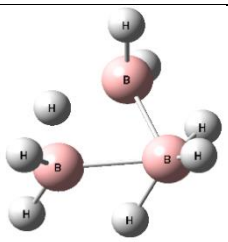
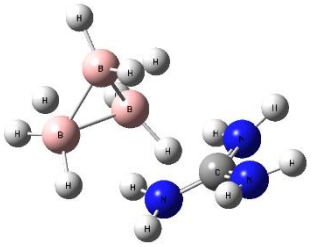
Elektronik özelliklerin ayrıntılı incelemesinde frontier moleküler orbitalleri (HOMO–LUMO), MEP (moleküler elektrostatik potansiyel) yüzeyleri elde edilmiş; tüm hesaplamalar 0 K'de elektronik enerjileri ile raporlanmıştır.

BULGULAR ve TARTIŞMA

Geometrik Yapı ve Bağlanma Enerjileri

Guanidinyum katyonu (Gua^+), oktahidrotriborat anyonu ($B_3H_8^-$) ve bunlardan oluşan iyonik yapının ($GuaB_3H_8$) kararlı geometrileri B3LYP/6-311++G(d,p) ve ωB97X-D/6-311++G(d,p) düzeylerinde optimize edilmiştir. Elde edilen yapılar Tablo 1'de, seçilmiş bağ uzunlukları, bağ açıları ve toplam enerjiler ise Tablo 2'de özetlenmektedir. Her iki fonksiyonel ile bulunan C–N, N–H, B–H ve B–B bağ uzunlukları birbirine oldukça yakın olup, farkların genel olarak 0.01–0.02 Å mertebesinde olduğu görülmektedir. Bu durum, kullanılan fonksiyonellerin geometri tahminleri açısından tutarlı ve güvenilir olduğunu göstermektedir.

Tablo 1. İyonik Sıvının Kararlı Geometrileri

Yöntem	Gua^+	$B_3H_8^-$	$GuaB_3H_8$
B3LYP/ 6-311++G(dp)			
ωB97X-D/ 6-311++G(dp)			

Tablo 2. İyonik sıvının kararlı geometrilerine ait önemli parametreler

Yöntem	Tür	Bağ Uzunluğu (°A)	Bağ Açıları (^{0}C)	E_0 (au)
B3LYP/6-311++G(d,p)	$GuaB_3H_8$	C-N:1.32 N-H:1.03 B-H:1.21 B-B:1.82	N-C-N:119.68 H-N-H:117.39 H-B-H:112.46	-285.400853
B3LYP/6-311++G(d,p)	Gua^+	N-H:1.00 C-N:1.33	N-C-N:119.99 H-N-H:116.84	-205.835354
B3LYP/6-311++G(d,p)	$B_3H_8^-$	B-H:1.21-1.26 B-B : 1.75-1.82	H-B-H:118.52	-79.290522
ωB97X-D/6-311++G(d,p)	$GuaB_3H_8$	C-N:1.32 N-H:1.03 B-H:1.22 B-B:1.82	N-C-N:119.73 H-N-H:117.50 H-B-H:112.79	-285.306012
ωB97X-D/6-311++G(d,p)	Gua^+	N-H: 1.00 C-N: 1.33	N-C-N:119.99 H-N-H:116.95	-205.767750
ωB97X-D/6-311++G(d,p)	$B_3H_8^-$	B-H: 1.21- 1.26 B-B : 1..75-1.82	H-B-H:117.98	-79.255908

B3LYP/6-311++G(d,p) düzeyinde $GuaB_3H_8$ için C–N bağı yaklaşık 1.32 Å, N–H bağı 1.03 Å, B–H bağları 1.21–1.26 Å ve B–B bağları 1.75–1.82 Å aralığında bulunmuştur. ωB97X-D fonksiyoneli ile elde edilen değerler, küçük sapmalar dışında bu sonuçlarla çakışmakta, özellikle B–B çekirdekleri arasındaki mesafelerin ve B–H bağlarının uzunluk aralığının benzer kaldığı görülmektedir. Bu küçük farklar, fonksiyonellerin değiş-tokuş–korelasyon tanımlarından kaynaklanan beklenen sapmalar olup, yapısal eğilimleri değiştirecek boyutta değildir.

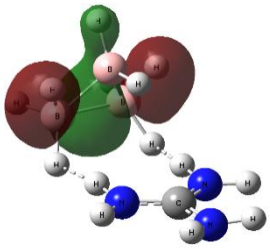
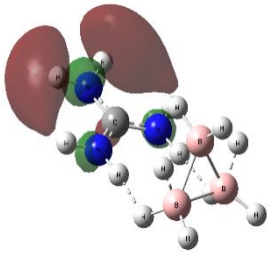
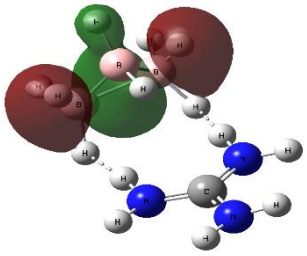
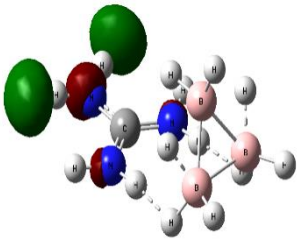
$GuaB_3H_8$ iyonik çiftinin bağlanma enerjileri, kompleksin toplam enerjisi ile katyon ve anyonun ayrı ayrı optimize edilmiş enerjileri kullanılarak hesaplanmıştır. B3LYP/6-311++G(d,p) düzeyinde elde edilen bağlanma enerjisi −172.5 kcal·mol^{-1} iken, dispersiyon düzeltmesi içeren ωB97X-D/6-311++G(d,p) yöntemiyle hesaplanan değer −177.1 kcal·mol^{-1} olarak bulunmuştur. Bu büyüklükteki negatif bağlanma enerjileri, Gua^+ ile $B_3H_8^-$ arasında güçlü elektrostatik çekimlerin yanı sıra belirgin yönlenmiş hidrojen bağlarının varlığına işaret etmekte olup, kompleksin gaz fazında yüksek termodinamik kararlılığa sahip olduğunu göstermektedir.

Uç (Frontier) Moleküler Orbitaller ve HOMO–LUMO Enerji Aralığı

$GuaB_3H_8$ iyonik çiftinin elektronik yapısı, frontier moleküler orbitallerin (HOMO ve LUMO) dağılımı Tablo 3'de ve enerji seviyeleri Tablo 4'de değerlendirilmiştir. B3LYP/6-311++G(d,p) düzeyinde elde edilen HOMO, ağırlıklı olarak $B_3H_8^-$ anyonunun hidrojence zengin terminal B–H bağları üzerinde ve kısmen de anyonun iskelet bölgesinde yoğunlaşmaktadır.

LUMO, katyon–anyon etkileşim bölgesine doğru kısmi lokalizasyon göstermekte ve özellikle guanidinyum katyonu çevresinde yoğunlaşmaktadır. Bu durum, elektron kazanımı veya redüksiyon süreçlerinde katyonun aktif rol oynayabileceğine ve yük transferinin katyonik birim üzerinden tetiklenebileceğine işaret etmektedir.

Tablo 3. Guanidinyum Oktahidrotriborat İyonik Sıvısının ωB97X-D ve B3LYP Yöntemleri ile HOMO, LUMO Dağılımlarının Gösterimi

Yöntem	HOMO	LUMO
B3LYP/ 6-311++G(d,p)		
ωB97X-D/ 6-311++G(d,p)		

Tablo 4. Guanidinyum Oktahidrotriborat İyonik Sıvısının B3LYP ve ωB97X-D Fonksiyonelleri ile Hesaplanan HOMO–LUMO Enerjileri

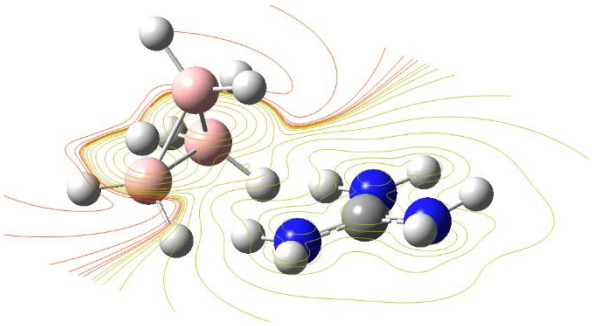
Yöntem	HOMO (eV)	LUMO (eV)	E_{HLG} (eV)
B3LYP/6-311++G(d,p)	–6.6899	–1.7726	4.9151
ωB97X-D/6-311++G(d,p)	–8.5998	–0.1687	8.4296

Enerji seviyeleri Tablo 4'te özetlenmiştir. B3LYP/6-311++G(d,p) düzeyinde HOMO ve LUMO enerji değerleri sırasıyla –6.6899 eV ve –1.7726 eV olup, hesaplanan HOMO–LUMO enerji aralığı (E_{HLG}) 4.9151 eV olarak bulunmuştur. ωB97X-D/6-311++G(d,p) düzeyinde ise HOMO enerjisi –8.5998 eV, LUMO enerjisi –0.1687 eV olup, E_{HLG} değeri 8.4296 eV'a yükselmektedir.

Bu sonuçlar, ωB97X-D fonksiyonelinin, özellikle uzun menzilli etkileşimleri ve dispersiyon kuvvetlerini daha gerçekçi biçimde tanımlaması nedeniyle sistemi elektronik olarak daha "katı" ve geniş bant aralıklı bir yapı olarak modellediğini göstermektedir. Daha geniş HOMO–LUMO aralığı, kinetik kararlılığın artması ve elektronik uyarılma süreçlerinin daha yüksek enerji bariyerleri ile ilişkilendirilmesi açısından önemlidir. Bu bağlamda, B3LYP daha "yumuşak" ve reaktif bir elektronik resim sunarken, ωB97X-D fonksiyoneli $GuaB_3H_8$'i daha kararlı ve elektronik olarak daha az reaktif bir sistem olarak betimlemektedir.

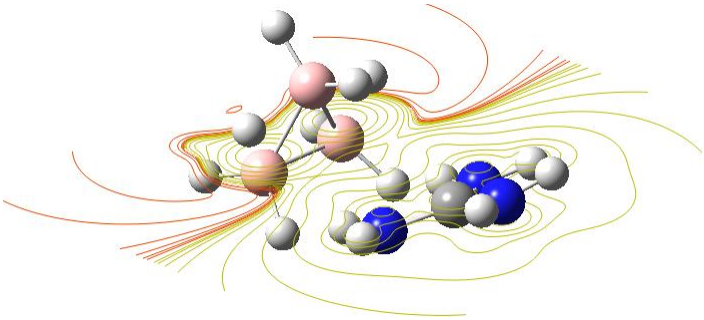
Moleküler Elektrostatik Potansiyel (MEP) Analizi

Moleküler elektrostatik potansiyel (MEP) yüzeyleri, katyon–anyon etkileşiminin doğasını ve yük dağılımını görselleştirmek için kullanılmıştır. B3LYP/6-311++G(d,p) düzeyinde elde edilen MEP haritası Şekil 1'de gösterilmiştir. Negatif potansiyelin beklendiği üzere büyük ölçüde $B_3H_8^-$ anyonunun merkezinde ve B–H bağları çevresinde yoğunlaştığını; pozitif potansiyelin ise guanidinyum katyonu üzerinde yer aldığını göstermektedir. Bu yük ayrımı, klasik iyonik sıvı davranışıyla uyumlu olup, anyonun hidrojen bakımından zengin bölgelerinde elektron yoğunluğunun biriktiğini doğrulamaktadır.



Şekil 1. B3LYP/6-311++G(d,p) Yöntemi ile Hesaplanan İyonik Sıvının Moleküler Elektrostatik Potansiyeli (MEP)

ωB97X-D/6-311++G(d,p) ile hesaplanan MEP yüzeyi Şekil 2'de gösterilmiştir. Negatif potansiyelin $B_3H_8^-$ anyonunun daha iç bölgelerine doğru daha keskin ve lokalize bir dağılım sergilediğini ortaya koymaktadır. Bu sonuç, uzun menzilli değiş-tokuş–korelasyon terimlerini içeren fonksiyonelin, katyon–anyon arasındaki elektrostatik etkileşimleri ve dispersiyon kaynaklı katkıları daha güçlü biçimde yansıtmasından kaynaklanmaktadır. Yük yoğunluğunun bu ölçüde lokalize olması, güçlü iyonik etkileşimler ve yönlenmiş hidrojen bağları ile birlikte değerlendirildiğinde, $GuaB_3H_8$'in yüksek termodinamik kararlılığını destekleyen önemli bir bulgu olarak ortaya çıkmaktadır.



Şekil 2. ωB97X-D/6-311++G(d,p) Yöntemi ile Hesaplanan İyonik Sıvının Moleküler Elektrostatik Potansiyeli (MEP)

MEP analizleri, frontier orbital bulguları ile birlikte ele alındığında, $B_3H_8^-$ anyonunun hidrojen bakımından zengin bölgelerinin potansiyel reaktivite merkezleri olduğunu, guanidinyum katyonunun ise hem yük dengeleme hem de olası proton/elektron transfer süreçlerinde etkin bir rol üstlenebileceğini göstermektedir.

SONUÇ

Bu çalışmada guanidinyum oktahidrotriborat ($GuaB_3H_8$) iyonik sıvısı, B3LYP/6-311++G(d,p) ve ωB97X-D/6-311++G(d,p) düzeylerinde incelenmiştir. Elde edilen C–N, N–H, B–H ve B–B bağ uzunlukları, literatürde $[B_3H_8]^-$ için bildirilen deneysel ve kuramsal değerlerle uyumludur. Özellikle B–H bağları için 1.21–1.26 Å ve B–B bağları için 1.75–1.82 Å aralığı, kullanılan teorik seviyenin yapısal açıdan güvenilir olduğunu göstermektedir.

$GuaB_3H_8$ iyonik çiftinin bağlanma enerjileri B3LYP için −172.5 kcal/mol, ωB97X-D için −177.1 kcal/mol olarak hesaplanmıştır. Bu değerler, katyon ve anyon arasındaki elektrostatik çekim ve hidrojen bağı etkileşimlerinin çok güçlü olduğunu göstermektedir. Sistem gaz fazında yüksek termodinamik kararlılık

sergilemektedir. Bu kararlılık, hidrojen depolama açısından geri dönüşümlü dehidrojenasyon/rehidrojenasyon süreçlerinin dış koşullarla (sıcaklık, basınç, katalizör vb.) kontrol edilmesini gerektirebileceğine işaret etmektedir.

Frontier moleküler orbital analizi, HOMO'nun $B_3H_8^-$ anyonu üzerinde, LUMO'nun ise kısmen guanidinyum katyonu üzerinde lokalize olduğunu göstermiştir. HOMO–LUMO enerji aralıkları B3LYP için 4.9151 eV, ωB97X-D için 8.4296 eV bulunmuştur. Bu aralıklar, $GuaB_3H_8$'in benzer boran esaslı iyonik sıvılarla karşılaştırıldığında elektronikte kararlı, ancak uygun koşullarda reaksiyona girebilen bir sistem olduğunu düşündürmektedir. Özellikle ωB97X-D ile elde edilen daha geniş aralık, sistemin kinetik açıdan daha az reaktif bir rejimde yer aldığını göstermektedir.

Moleküler elektrostatik potansiyel (MEP) yüzeyleri, negatif potansiyelin $B_3H_8^-$ anyonu ve terminal B–H bağları üzerinde yoğunlaştığını ortaya koymuştur. Pozitif potansiyel ise guanidinyum katyonunun N–H bölgelerinde toplanmaktadır. Bu dağılım, $B_3H_8^-$ biriminin hidrojen transferi ve B–H aktivasyonu için nükleofilik/indirgeyici merkezler olabileceğini göstermektedir. Guanidinyum katyonu ise proton transferi, hidrojen bağı etkileşimleri ve olası koordinasyon için elektrofilik bir ortam sunmaktadır.

Genel olarak geometri, bağlanma enerjisi, HOMO–LUMO aralığı ve MEP sonuçları birlikte değerlendirildiğinde, $GuaB_3H_8$ iyonik sıvısının hem kararlı bir iyonik sıvı hem de hidrojen depolama ve transferi için umut verici bir aday olduğu görülmektedir. Bu çalışma, boran temelli iyonik sıvıların tasarımında kullanılabilecek temel yapısal ve elektronik verileri sağlamaktadır. Ayrıca gelecekte yapılacak deneysel hidrojen depolama çalışmaları ve reaksiyon yolları, bariyerler ve ortam etkilerini içeren ileri kuramsal incelemeler için bir başlangıç noktası sunmaktadır.

TEŞEKKÜR

Bu çalışmada yer alan nümerik hesaplamaların bir kısmı TÜBİTAK ULAKBİM, Yüksek Başarım ve Grid Hesaplama Merkezi'nin (TRUBA kaynakları) desteğiyle tamamlanmıştır.

KAYNAKLAR

Bykov, A., & Zhizhin, K. (2019). The chemistry of the octahydrotriborate anion $[B_3H_8]^-$. Russian Chemical Reviews, 88(9), 941–964.

Chen, X., Liu, Z., Cheng, J., Li, J., Guo, D., Zhang, L., Niu, X., Wang, G., & Gao, P. (2023). First-principles study of Li-doped planar g-C3N5 as reversible H2 storage material. Frontiers in Chemistry, 10, 3389.

Chen, W., Huang, Z., Wu, G., He, T., Li, Z., Chen, J., Guo, Z., Liu, H., & Chen, P. (2015). Guanidinium octahydrotriborate: An ionic liquid with high hydrogen storage capacity. Journal of Materials Chemistry A, **3**(21), 11411–11416.

Doroodian, A., Dengler, J. E., Genest, A., Rösch, N., & Rieger, B. (2010). Methylguanidinium borohydride: an ionic liquid-based hydrogen storage material. Angewandte Chemie International Edition, 49(1), 187-190.

Frisch, M. J., Trucks, G. W., Schlegel, H. B. (2016). Gaussian 16, Revision C.01. Wallingford, CT: Gaussian, Inc.

Kohani, M. H., Atashrouz, S., Pourmahdi, M., Hadavimoghaddam, F., Jabbour, K., Hemmati-Sarapardeh, A., & Mohaddespour, A. (2023). Hydrogen solubility in ionic liquids: Application of a structure-based deep learning approach and equations of state. International Journal of Hydrogen Energy, 48(43), 31234-31253.

Liu, Y., Cui, J., Wang, H., Wang, K., Tian, Y.,Xue, X., Qiao, Y., Ji, X. & Zhang, S. (2023). Ionic liquids as a new cornerstone to support hydrogen energy. Green Chemistry,25, (49-85).

Rekken, B. M., & Krossing, I. (2016). Ionic liquids with efficient hydrogen storage capacities. Chemical Communications, 52, 7399–7402.

Chai, J., Gordon, M.H. (2008). Long-Range Corrected Hybrid Density Functionals with Damped Atom–Atom Dispersion Corrections. Physical Chemistry Chemical Physics, 6615–6620.

W. J. Hehre, L. Radom, P. von R. Schleyer, Pople , J. A. (1986). *Ab Initio Molecular Orbital Theory.* Wiley-Interscience, New York, **ISBN:** 978-0471812418.

Zheng, X., Yang, Y., Li, M., Zhao, F., Gu, Q., Ma, X., & Guo, Y. (2019). Li(NH3)B3H8: a new ionic liquid octahydrotriborate. Chemical Communications, 55(4), 408-411.

Ramkumar, V., & Gardas, R. L. (2019). Structural arrangement and computational exploration of guanidinium-based ionic liquids with benzoic acid derivatives as anions. Crystal Growth & Design, 19(5), 2642-2657.

ORAL PRESENTATION

A bioinformatics-based approach for evaluating drug-likeness and docking potential of *Crocus sativus* metabolites

Hilal Büşra Tokgöz[1,2] (*https://orcid.org/0000-0002-0940-7427*),
Filiz Altan[1*] *(https://orcid.org/0000-0001-6358-2448)*

[1] Molecular Biology and Genetics Department, Muğla Sıtkı Koçman University, Muğla, Turkey

[2]Denizli Vocational School of Health Services, Pamukkale University, Denizli, Turkey

*Corresponding author e-mail: afiliz@mu.edu.tr

Abstract

Crocus sativus contains several bioactive metabolites with known antioxidant, anti-inflammatory, and metabolic regulatory activities. Early-stage drug discovery increasingly relies on rapid *in silico* prediction tools to as drug-likeness and molecular interaction tendencies before conducting comprehensive experimental validation. This study offers a methodological evaluation of major *C. sativus* compounds crocetin, safranal, and picrocrocin using drug-likeness predictors and molecular docking workflows. Drug-likeness features were assessed with SwissADME, MolSoft, pkCSM, and ProTox-II, while exploratory docking was performed against biologically relevant target proteins. Results revealed compound-specific differences in physicochemical properties and interaction tendencies. The present study demonstrates the usefulness of bioinformatics tools for initial screening of phytochemicals and provides a framework for future drug discovery research.

Keywords: *Crocus sativus*, drug-likeness, molecular docking

INTRODUCTION

Crocus sativus L. (saffron) is a medicinally significant plant valued for its unique apocarotenoid composition, particularly crocin, crocetin, safranal, and picrocrocin. These metabolites are responsible for the characteristic color, aroma, and bioactivity of saffron, and have been widely investigated for their diverse pharmacological properties. Numerous studies indicate that C. sativus constituents exert potent antioxidant, anti-inflammatory, neuroprotective, and metabolic regulatory effects, positioning them as promising candidates for the development of novel therapeutic agents (Drif, 2015; Saadat et al., 2024). Crocin and crocetin, in particular, have been associated with mitochondrial protection, modulation of pro-inflammatory cytokines, and improvements in glucose and lipid homeostasis (Rameshrad et al. 2018, 2010; Asbaghi et al., 2021). Meanwhile, safranal and picrocrocin exhibit notable cytoprotective, anti-inflammatory, and neuroactive actions (Frusciante et al., 2024; Bathaie & Mousavi, 2010). Growing interest in natural products as drug candidates stems from their structural diversity, chemical novelty, and multi-target interaction potential. Nevertheless, many phytochemicals face significant limitations during drug development due to insufficient characterization of their physicochemical attributes, oral bioavailability, and toxicity parameters at early stages (Newman & Cragg, 2020). To overcome these challenges, computational prediction tools have become essential components of modern drug discovery pipelines. In silico approaches—including molecular docking, ADMET modeling, and drug-likeness screening—provide rapid, cost-effective insights into pharmacokinetic behavior, target interaction potential, and structural suitability before in vitro or in vivo validation (Lionta et al., 2014; Besli et al., 2025). Although the biological effects of C. sativus have been well documented, its major metabolites have not been comprehensively assessed within an integrated computational framework that combines drug-likeness filtering with multi-target docking. This represents a notable gap, particularly given the central roles of inflammatory and metabolic pathways in disorders such as obesity, diabetes, neurodegeneration, and chronic inflammation—conditions in which saffron constituents have shown beneficial effects (Asbaghi et al., 2021; Hosseini et al., 2018). Computational evaluation of these metabolites against relevant protein targets may offer new insights into their therapeutic potential and support rational prioritization of molecules for subsequent laboratory studies. Therefore, this study aims to present a bioinformatics-based framework for assessing the drug-likeness characteristics and preliminary docking tendencies of crocin, crocetin, safranal, and picrocrocin.

By emphasizing workflow design and qualitative trends, the study contributes to early-stage screening of saffron-derived phytochemicals and highlights the value of computational strategies in natural product research.

MATERIALS AND METHODS

Compound Selection and Structure Preparation

Four major bioactive constituents of *Crocus sativus* L.— **crocetin, safranal, and picrocrocin**—were selected based on their pharmacological relevance. Chemical identifiers (CID, SMILES) and available 3D conformers for each compound were obtained from the PubChem database (Kim et al., 2021). Molecular structures were converted to PDBQT format and subjected to energy minimization using **OpenBabel** (O'Boyle et al., 2011).

Drug-Likeness and ADMET Profiling

To evaluate early-phase pharmacokinetic suitability, drug-likeness and ADMET properties were assessed using multiple complementary web-based platforms:

SwissADME for physicochemical parameters, Lipinski/Ghose/Veber/Egan filters, bioavailability score, and gastrointestinal absorption prediction (Daina et al., 2017).

MolSoft for global drug-likeness scoring (MolSoft LLC, 2024).

pkCSM for ADMET modeling covering absorption, distribution, metabolism, and excretion (Pires et al., 2015).

ProTox-II for toxicity class prediction and putative toxicological endpoints (Banerjee et al., 2018).

Target Protein Selection and Preparation

Protein targets associated with inflammation, metabolic regulation, or oxidative stress were selected from the Protein Data Bank (PDB). Protein structures were prepared using AutoDockTools by removing crystallographic water molecules, adding polar hydrogens, and assigning **Kollman charges** (Morris et al., 2009).

Molecular Docking Procedure

Molecular docking simulations were performed using **AutoDock Vina** (Trott & Olson, 2010). Grid boxes were centered on the binding pockets based on either co-crystallized ligands or annotated active site residues. Ligand flexibility was handled using the Lamarckian genetic algorithm parameters adapted for Vina. Docking exhaustiveness was optimized to ensure reproducibility across runs.The three-dimensional binding poses and ligand–protein interactions were visualized and analyzed using **Discovery Studio Visualizer** (BIOVIA, 2021) and **UCSF Chimera** (Pettersen et al., 2004).

RESULTS and DISCUSSION

The physicochemical and pharmacokinetic assessments performed in this study revealed distinct profiles for the major *Crocus sativus* metabolites. Crocin and crocetin exhibited markedly high polarity and multiple violations of classical drug-likeness criteria, consistent with their glycosylated and hydrophilic structures. Their limited membrane permeability and restricted oral bioavailability observed *in silico* are in agreement with earlier pharmacokinetic studies, which describe poor intestinal absorption and extensive metabolic conversion in vivo (Umigai et al., 2012; Hosseini et al., 2018). Safranal, in contrast, showed a favorable combination of molecular weight, lipophilicity (logP), and structural flexibility, aligning closely with traditional parameters for orally active drug candidates and supporting previous reports describing its efficient absorption and systemic distribution (*Saadat et al., 2024*). Picrocrocin demonstrated intermediate characteristics—moderate polarity and constrained permeability—suggesting a more selective but still biologically relevant interaction potential.

ADMET prediction tools consistently indicated that safranal possesses the most drug-like profile, particularly with respect to absorption, metabolic stability, and predicted bioavailability. Crocin and crocetin again reflected the well-documented limitations of highly hydrophilic natural pigments, while all four compounds exhibited acceptable predicted toxicity profiles. A degree of variability was observed for crocetin depending on the toxicity model applied, which mirrors previous literature noting compound-dependent differences across computational frameworks (Asbaghi *et al., 2021*).

Docking analyses revealed trends that further supported these physicochemical profiles. Safranal and crocetin demonstrated stronger interaction tendencies toward selected inflammatory and metabolic protein targets, which aligns with experimental findings describing their anti-inflammatory and metabolic regulatory actions *(Rameshrad et al. 2018*; Frusciante et al., 2024). Crocin, due to its large steric bulk and pronounced polarity, displayed reduced compatibility with compact binding pockets, resulting in lower docking adaptability — a pattern also noted in previous computational studies of glycosylated carotenoids. Picrocrocin showed moderate yet target-specific binding tendencies, suggesting that although it is less studied pharmacologically, it may contribute to the overall multi-target activity profile of saffron extracts.

Overall, qualitative trends from the present study reinforce the established biological activities of *C. sativus* constituents, particularly their anti-inflammatory and metabolic regulatory effects. At the methodological level, these findings illustrate how integrating physicochemical filtering, drug-likeness evaluation, ADMET modeling, and preliminary docking can substantially enhance early-phase natural product–based drug discovery. Similar integrated computational workflows have been shown to streamline candidate prioritization and reduce the cost and time associated with experimental screening (Lionta et al., 2014; *Besli et al., 2025*).

Certain limitations should be acknowledged. The docking simulations employed here relied primarily on rigid receptor conformations and qualitative interpretation without full quantitative binding affinity reporting. Moreover, metabolite transformation of crocin and crocetin—known to occur rapidly in vivo—was not explicitly modeled. Full binding energy values, residue-level interaction maps, and detailed structure–activity analyses will be provided in a forthcoming high-impact journal manuscript.

Taken together, the combined results suggest that safranal holds the strongest potential as an orally bioavailable lead compound, while crocin, crocetin, and picrocrocin display selective yet meaningful interaction patterns that merit deeper structural and functional characterization in future experimental and computational studies.

ACKNOWLEDGEMENTS

This study was supported by the Muğla Sıtkı Koçman University Scientific Research Projects Coordination Unit (BAP Project No: 23/152/04/1/4).

REFERENCES

Asbaghi, O., Sadeghian, M., Sadeghi, O., Rigi, S., Tan, S. C., Shokri, A., & Mousavi, S. M. (2021). Effects of saffron (Crocus sativus L.) supplementation on inflammatory biomarkers: A systematic review and meta-analysis. *Phytotherapy research*, *35*(1), 20-32.

Banerjee, P., Eckert, A. O., Schrey, A. K., & Preissner, R. (2018). ProTox-II: a webserver for the prediction of toxicity of chemicals. *Nucleic acids research*, *46*(W1), W257-W263.

Bathaie, S. Z., & Mousavi, S. Z. (2010). New applications and mechanisms of action of saffron and its important ingredients. *Critical reviews in food science and nutrition*, *50*(8), 761-786.

Besli, N., Ercin, N., Celik, U., & Tutar, Y. (2025). How to Expedite Drug Discovery: Integrating Innovative Approaches to Accelerate Modern Drug Development. *Acta Chimica Slovenica*, *72*(3), 581-600.

Daina, A., Michielin, O., & Zoete, V. (2017). SwissADME: a free web tool to evaluate pharmacokinetics, drug-likeness and medicinal chemistry friendliness of small molecules. *Scientific reports*, *7*(1), 42717.

Drif, A. I. (2025). Anti-inflammatory and anticancer activities of natural products and their derivatives.

Frusciante, L., Geminiani, M., Shabab, B., Olmastroni, T., Scavello, G., Rossi, M., ... & Santucci, A. (2024). Exploring the antioxidant and anti-inflammatory potential of saffron (Crocus sativus) tepals extract within the circular bioeconomy. *Antioxidants*, *13*(9), 1082.

Hosseini, A., Razavi, B. M., & Hosseinzadeh, H. (2018). Pharmacokinetic properties of saffron and its active components. *European Journal of Drug Metabolism and Pharmacokinetics*, *43*(4), 383-390.

Kim, S., Chen, J., Cheng, T., Gindulyte, A., He, J., He, S., ... & Bolton, E. E. (2021). PubChem in 2021: new data content and improved web interfaces. *Nucleic acids research*, *49*(D1), D1388-D1395.

Lionta, E., Spyrou, G., K. Vassilatis, D., & Cournia, Z. (2014). Structure-based virtual screening for drug discovery: principles, applications and recent advances. *Current topics in medicinal chemistry*, *14*(16), 1923-1938.

Morris, G. M., Huey, R., Lindstrom, W., Sanner, M. F., Belew, R. K., Goodsell, D. S., & Olson, A. J. (2009). AutoDock4 and AutoDockTools4: Automated docking with selective receptor flexibility. *Journal of computational chemistry*, *30*(16), 2785-2791.

Newman, D. J., & Cragg, G. M. (2020). Natural products as sources of new drugs over the nearly four decades from 01/1981 to 09/2019. *Journal of natural products*, *83*(3), 770-803.

O'Boyle, N. M., Banck, M., James, C. A., Morley, C., Vandermeersch, T., & Hutchison, G. R. (2011). Open Babel: An open chemical toolbox. *Journal of cheminformatics*, *3*(1), 33.

Pettersen, E. F., Goddard, T. D., Huang, C. C., Couch, G. S., Greenblatt, D. M., Meng, E. C., & Ferrin, T. E. (2004). UCSF Chimera—a visualization system for exploratory research and analysis. *Journal of computational chemistry*, *25*(13), 1605-1612.

Pires, D. E., Blundell, T. L., & Ascher, D. B. (2015). pkCSM: predicting small-molecule pharmacokinetic and toxicity properties using graph-based signatures. *Journal of medicinal chemistry*, *58*(9), 4066-4072.

Rameshrad, M., Razavi, B. M., & Hosseinzadeh, H. (2018). Saffron and its derivatives, crocin, crocetin and safranal: a patent review. *Expert opinion on therapeutic patents*, *28*(2), 147-165.

Saadat, S., Ghasemi, Z., Memarzia, A., Behrouz, S., Aslani, M. R., & Boskabady, M. H. (2024). An overview of pharmacological effects of Crocus sativous and its constituents. *Iranian Journal of Basic Medical Sciences*, *27*(4), 391.

Trott, O., & Olson, A. J. (2010). AutoDock Vina: improving the speed and accuracy of docking with a new scoring function, efficient optimization, and multithreading. *Journal of computational chemistry*, *31*(2), 455-461.

Umigai, N., Tanaka, J., Tsuruma, K., Shimazawa, M., & Hara, H. (2012). Crocetin, a carotenoid derivative, inhibits VEGF-induced angiogenesis via suppression of p38 phosphorylation. *Current neurovascular research*, *9*(2), 102-109.

ORAL PRESENTATION

Berberinin östrojen reseptörü (ER/PR) pozitif meme kanseri hücrelerinde trombosit mikropartikülleri aracılı proliferasyon ve migrasyon üzerindeki etkileri

Mujgan Cubuk, Merve Gurboga, Ozlem Bingol Ozakpinar, Derya Ozsavci
Marmara Üniversitesi, Eczacılık Fakültesi, Biyokimya Anabilim Dalı, İstanbul, Türkiye

*Sorumlu yazar e-mail: mujganbdg@gmail.com

Özet

Meme kanseri kadınlarda en sık görülen malignitedir ve kansere bağlı ölümlerin ikinci önde gelen nedenidir. Venöz tromboembolizm kanserin ilerlemesi ve kemoterapiye dirençte yaygın olarak rol oynamakta ve kanserli hastalarda mortalite sebepleri arasında ön sırada yer almaktadır. Meme kanserinde ve özellikle kanserin ileri evrelerinde, dolaşımdaki trombosit türevli mikropartikül (PMP) lerde artış olduğu; bu nedenle PMP'lerin erken tanıda, prognostik veya terapötik biyobelirteç olarak kullanılabileceği öne sürülmüştür. İlaç direncinin yaygınlığının artması, kemoterapideki non-spesifiklik ve toksisite sorunları, daha az toksik ve daha etkili terapötik ajanlarının geliştirilmesini gerekli kılmaktadır. Berberinin antioksidan, antiinflamatuvar, antidiyabetik ve antikanserojenik roller sergilediği; *in vitro* ve *in vivo* olarak güçlü bir trombosit agregasyon inhibitörü olduğu da bildirilmiştir. Bu özellikleri ile berberinin, meme kanserinde umut verici ve potansiyel bir kemoterapötik destek ajanı olarak kullanılabileceği belirtilmiştir. Bu çalışmadaki amacımız; PMP'lerin hormon bağımlı meme kanseri hücrelerinin (MCF-7) proliferasyonu ve migrasyonunda oluşturabileceği olası değişimleri belirlemek; doğal bir alkoloid olan berberinin, PMP aracılığıyla oluşan bu değişimlerdeki etkilerini inlemektir. 4 sağlıklı, erkek gönüllüden alınan tam kan örneklerinden seri santrifügasyon yöntemi yoluyla PMP'ler izole edilerek, örnekler -80 C de dondurulmuştur. Daha sonra örneklerde, Bradford yöntemi ile protein tayini yapılmıştır. PMP'ler ve berberinin, sağlıklı fare embriyonik fibroblast hücre hattı (NIH/3T3) ve MCF-7 meme kanseri hücreleri üzerindeki antiproliferatif/sitotoksik etkisinin belirlemek amacıyla ilk olarak MTT yöntemi, daha uzun zaman dilimlerindeki etkinliğinin ortaya çıkarılması amacıyla, "Gerçek Zamanlı Hücre Ölçer" cihazı ve migrasyon üzerindeki etkisinin belirlenmesi amacıyla, yara açma deneyi (scratch assay) gerçekleştirilmiştir. MTT bulguları, berberinin doza bağımlı olarak antiproliferatif ve sitotoksik etkinlik gösterdiğini; migrasyon deney sonuçları da berberinin benzer şekilde hücre göçünü inhibe edici etkisi olduğunu; PMP'nin ise hücre göçünü desteklediğini göstermektedir. Bu bulgular, PMP'lerin meme kanseri metastazında etkili olabileceğini, bu nedenle prognostik veya terapötik biyobelirteç olarak kullanılabileceğini desteklemektedir. Ayrıca, berberin meme kanserinde PMP tarafından indüklenen proliferasyon ve hücre göçünü inhibe edici etkileriyle yeni bir tedavi seçeneği olabilir.

Anahtar kelimeler: Mikropartikül, trombosit, meme kanseri, in vitro, berberin

The effects of berberine on platelet-derived microparticle–mediated proliferation and migration in estrogen receptor (ER/PR)-positive breast cancer cells

Abstract

Breast cancer is the most common malignancy in women and the second leading cause of cancer-related mortality. Venous thromboembolism contributes to cancer progression and chemotherapy resistance and ranks among the primary causes of mortality in cancer patients. In breast cancer, especially in advanced stages, increased levels of circulating platelet-derived microparticles (PMPs) have been reported, suggesting their value as early diagnostic, prognostic, or therapeutic biomarkers. The rising prevalence of drug resistance, together with the non-specificity and toxicity associated with chemotherapy, underscores the need for safer and more effective therapeutic agents. Berberine has been reported to exhibit antioxidant, anti-inflammatory, antidiabetic, and anticancer properties and functions as a potent inhibitor of platelet aggregation in vitro and in vivo. These characteristics indicate that berberine may serve as a promising chemotherapeutic adjuvant in breast cancer. This study aims to determine the alterations induced by PMPs in the proliferation and migration of hormone-dependent breast cancer cells (MCF-7) and to investigate the effects of berberine, an alkaloid, on these PMP-mediated changes. PMPs were isolated from whole blood obtained from four healthy male volunteers through serial centrifugation and stored at –80 °C. Protein quantification was performed using the

Bradford method. The antiproliferative and cytotoxic effects of PMPs and berberine on the healthy embryonic fibroblast line (NIH/3T3) and MCF-7 breast cancer cells were evaluated using the MTT assay; long-term effects were assessed with a Real-Time Cell Analyzer system, and migration was examined using a scratch assay. The MTT findings demonstrate that berberine exhibits dose-dependent antiproliferative and cytotoxic activity; the migration assay results similarly show that berberine exerts an inhibitory effect on cell migration, whereas PMPs promote migration. These findings suggest that PMPs may contribute to breast cancer metastasis and could serve as prognostic or therapeutic biomarkers. Berberine may also represent a therapeutic option by suppressing PMP-induced proliferation and migration.

Keywords: Microparticle, platelet, breast cancer, in vitro, berberine

GİRİŞ

Meme kanseri kadınlarda en sık görülen malignitedir ve kansere bağlı ölümlerin ikinci önde gelen nedenidir. Venöz tromboembolizm (VTE) ise, kanser ilerlemesinde ve antikanser tedavisine dirençte yaygın olarak rol oynamaktadır. VTE, hastalarda kanserin kendisinden sonra ikinci önde gelen ölüm nedenidir ve kanserli hastalarda VTE riski 7 kat daha fazladır (Chaari ve ark., 2014; Spuy ve Augustine, 2016). Kanser hücreleri, trombosit aktivasyonunu ve agregasyonunu uyarır, dolaşımdaki kanser hücreleriyle etkileşime giren trombositler, bağışıklık sistemine karşı koruyucu bir kalkan oluşturur (Vismara ve ark., 2021). Meme kanserinde dolaşımdaki trombosit kaynaklı mikropartiküllerin (PMP) plazma seviyelerinin yükseldiği; özellikle ileri evrelerdeki kanserin, dolaşımdaki PMP'lerde artışla ilişkili olduğu; inflamasyon, tromboz ve trombosit bağımlı metastaza aracılık edebildiği (Vismara ve ark., 2021); trombosit membranlarında bulunan P-selektin gibi fonksiyonel reseptörleri eksprese edebildiği ve farklı hücre tiplerine aktarabildiği (Baj-Krzyworzeka ve ark., 2002); böylece dolaşımdaki tümör hücrelerine yapışkan özellikler kazandırdığı (Cambien and Wagner D, 2004); dolayısıyla PMP'lerin erken tanıda, prognostik veya terapötik biyobelirteç olarak kullanılabileceği öne sürülmüştür. İlaç direncinin yaygınlığının artması, kanser kemoterapisindeki doku seçiciliği ve toksisite sorunları ile birleştiğinde, daha az toksik ve daha etkili terapötik ajanlarının geliştirilmesi yönünde gereklilikler ortaya çıkarmıştır.

Berberin antibakteriyel, hipolipidemik (Xing ve ark., 2021); antiplatelet (Wang ve ark., 2017; Wang ve ark., 2021); anti-diyabetik (El-Wahab ve ark., 2013; Wang ve ark., 2018); antioksidan, anti-inflamatuar, (Wang ve ark., 2020); antikanser (Almatroodi ve ark., 2022; Pierpaoli ve ark., 2021; Pan ve ark., 2017) özellikleri ile bilinen, bitkilerden elde edilen bir alkoloiddir. Yapılan çalışmalar, berberinin diğer antiplatelet ilaçlara göre avantajlı olabileceğini, kombinasyon kullanımına uygun olduğunu, umut verici bir antiplatelet ve anti-kanser ajan olabileceğini düşündürmektedir.

AMAÇ

Bu çalışmanın amacı; PMP'lerin, hormon bağımlı meme kanserinde hücre proliferasyonu ve migrasyonunda oluşturabileceği değişimleri belirlemek; doğal bir alkoloid olan berberinin, meme kanserinde PMP aracılığıyla oluşan bu değişimlerdeki etkilerini karşılaştırmaktır.

MATERYAL VE METOT

4 sağlıklı, erkek gönüllüden sitratli tüplere tam kan örnekleri alınarak, santrifügasyon yöntemi ile önce trombositler izole edildi, daha sonra trombin aktivasyonu ve çeşitli tamponlarla dilüsyon/santrifügasyon işlemleri sonrasında da PMP'ler elde edildi ve Bradford yöntemi kullanılarak protein tayini yapıldı. İzole edilen PMP örnekleri kullanılıncaya kadar -80C de bekletildi.

MTT yöntemiyle antiproliferatif etkinin belirlenmesi

PMP'ler ve berberinin antiproliferatifk etkilerinin belirlenmesi için hormon duyarlı meme kanseri hücre hattı olarak MCF-7 ve sağlıklı hücreler üzerindeki sitotoksik etkisinin belirlemek amacı ile fare embriyonik fibroblast hücre hattı NIH/3T3 ile çalışıldı. Hücreler, 48 saat boyunca 10, 20, 50, 100, 200 µM berberin ile inkübe edildi. Örneklerin antiproliferatif etkisinin belirlenmesi için MTT yöntemi ve daha uzun zaman dilimlerindeki etkinliğin ortaya çıkarılması amacıyla "Gerçek Zamanlı Hücre Ölçer" cihazı kullanıldı.

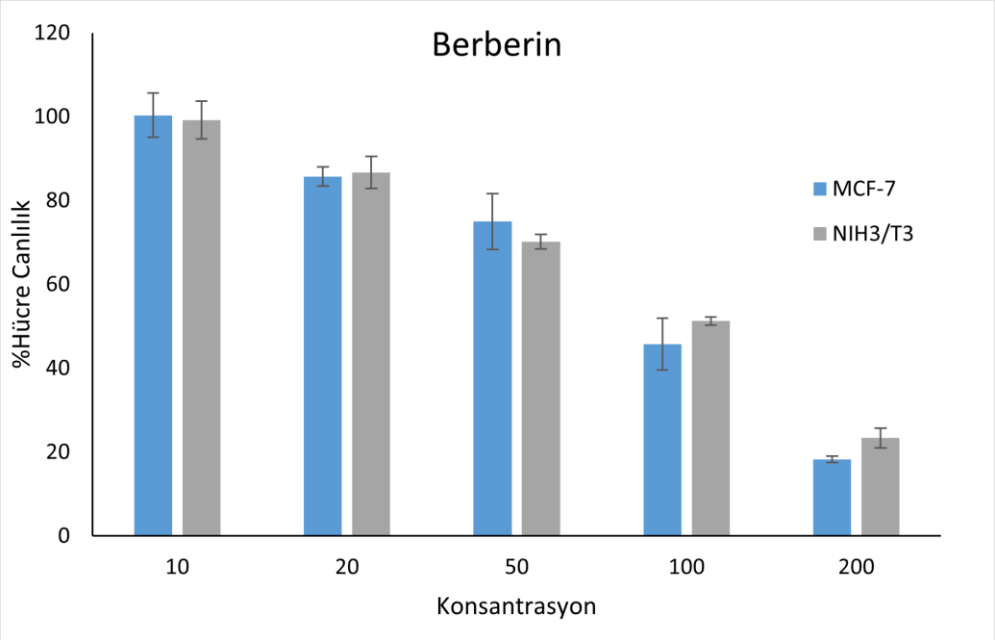
Yara iyileşme analizi (wound healing assay)

Berberin ve PMP'lerin MCF-7 hücre migrasyonu üzerine etkinin belirlenmesi amacıyla yara açma deneyi (scratch assay) gerçekleştirildi. MCF-7 hücreleri, her kuyucuğa eşit sayıda ekilerek uygun hücre yoğunluğuna ulaşmaları beklenmiştir. Hücre yoğunluğu sağlandıktan sonra, her kuyucuğa standart bir çizik açılmış ve bu an 0. saat olarak kaydedilmiştir. Deney grupları şu şekilde oluşturulmuştur: yalnızca 100 µM Berberin içeren grup, yalnızca PMP içeren grup (30 µg/ml), başlangıçta berberin uygulanıp, daha sonra PMP eklenecek olan kombinasyon grubu ve kontrol grubu. Deneyin 24. saatinde kuyucuklar yeniden görüntülenmiş ve berberin içeren gruplardan bazılarına ek olarak 24. saatte PMP uygulanarak kombinasyon oluşturulmuştur.

BULGULAR

Berberinin MCF-7 ve NIH/3T3 Hücre hatlarındaki Antiproliferatif ve Sitotoksik Etkisi

MTT sonuçlarına göre; berberin, uygulanan doz aralığında her iki hücre hattında da doza bağımlı bir inhibisyona sebep olmaktadır (Şekil 1). 50 µM konsantrasyondan itibaren MCF-7 hücre canlılığı NIH/3T3'e kıyasla daha düşüktür. MCF-7 hücreleri için berberinin IC_{50} (Yarı maksimum inhibitör konsantrasyon) değeri 106 µM, NIH/3T3 hücreleri için 119 µM olarak hesaplanmıştır.

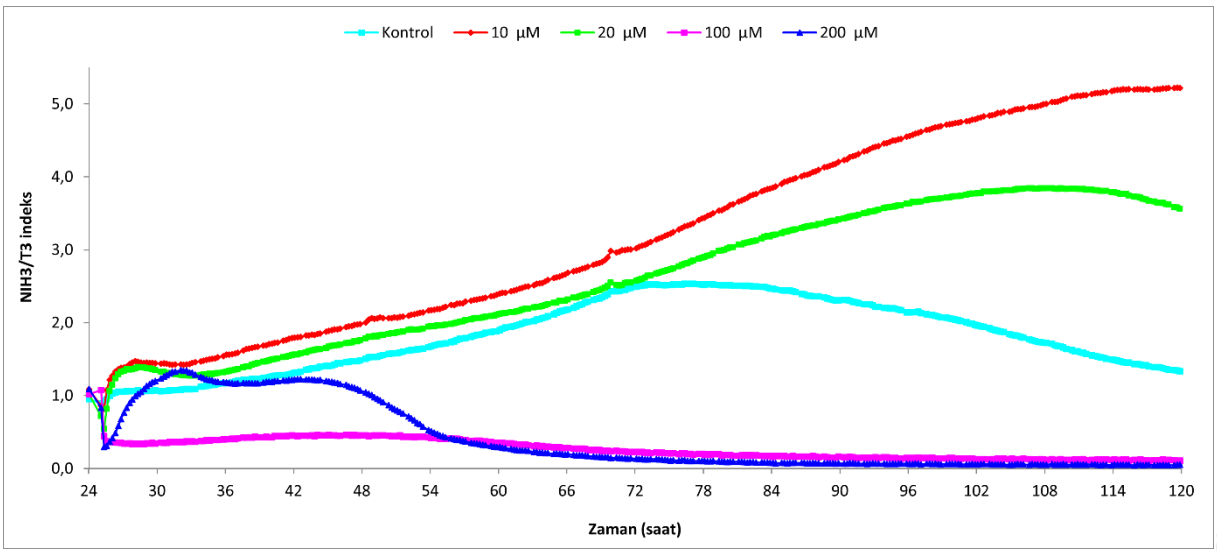


Şekil 1. Berberin uygulanan NIH/3T3 ve MCF-7 hücrelerinin MTT sonuçları

Berberin Uygulanan MCF-7 ve NIH3T3 Hücrelerinin Gerçek Zamanlı Hücre Ölçer Bulguları

MTT deneylerinden sonra, hücre canlılığının izlenmesi için gerçek zamanlı hücre ölçer cihazı kullanıldı. NIH/3T3 ve MCF-7 hücrelerinin ekimi yapılan e-plakalarda 120 saat boyunca hücre indeksleri kaydedildi. Bu sayede zamana ve doza bağımlı olarak hücre proliferasyonunun nasıl bir değişime uğradığı gerçek zamanlı olarak belirlendi.

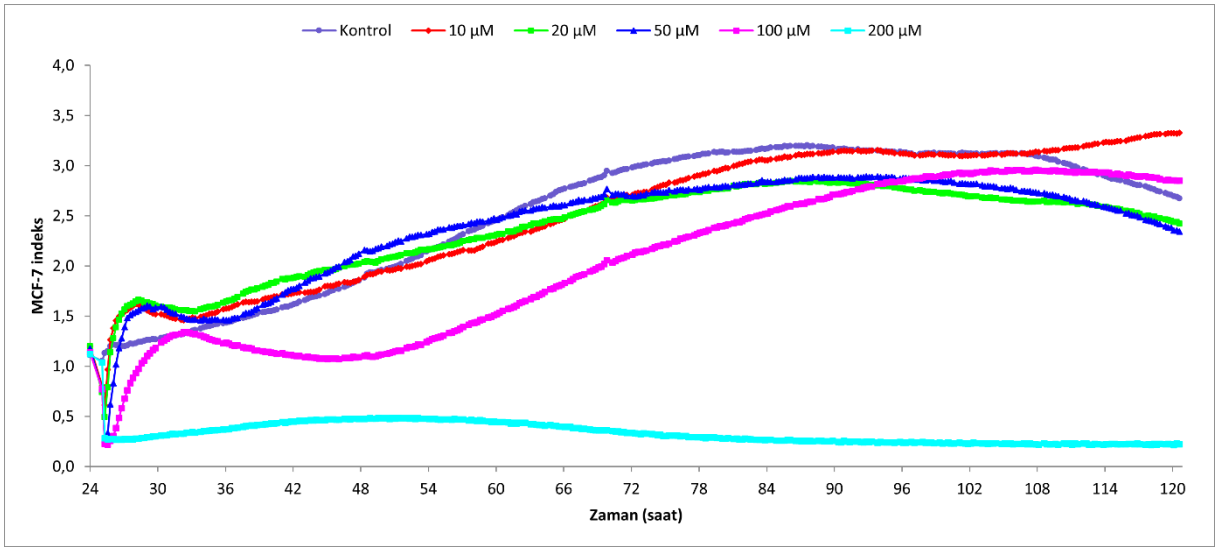
Berberin uygulanan NIH/3T3 hücrelerinde 10 ve 20 µM konsantrasyonlarda hücrelerin proliferasyona devam ettiği ve sitotoksik bir etki görülmediği belirlenmiştir. Uygulanan 100 µM konsantrasyonda ise hücre proliferayonu zaman içerisinde azalırken; 200 µM konsantrasyonda berberin uygulamasından sonraki yaklaşık 12. Saatten itibaren hücre sayısının bir anda azaldığı görülmektedir (Şekil 2- mavi).



Şekil 2. Berberinin NIH/3T3 hücre hattındaki hücre canlılığına etkisi

Xcelligence sonuçlarına göre berberin, sağlıklı hücrelerde düşük dozlarda proliferatif etki; yüksek dozlarda proliferasyonu baskılayıcı ve sitotoksik etkiler göstermektedir.

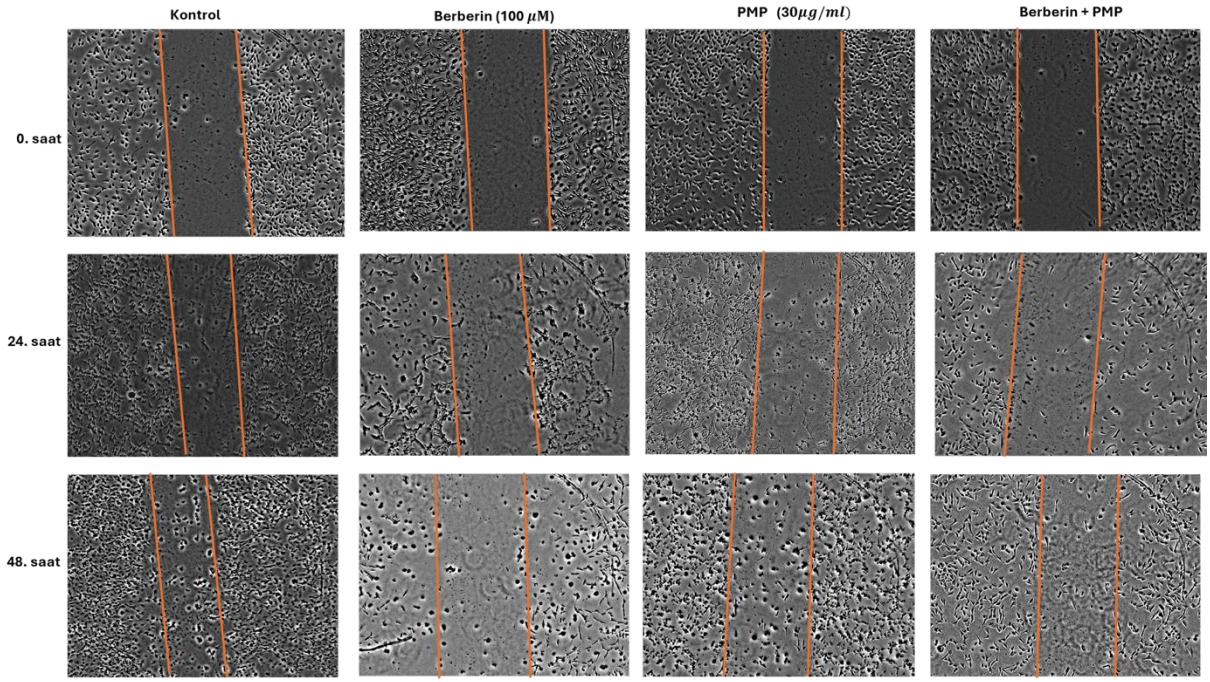
Benzer etkinin MCF-7 hücrelerinde de görüldüğü belirlenmiştir. 10, 20 ve 50 µM berberin ile proliferasyon devam ederken; 100 µM berberin proliferasyonu bir süre baskılamaktadır. 200 µM konsantrasyon ise başlangıçtan itibaren hücre çoğalmasını durdurmaktadır (Şekil 3).



Şekil 3. Berberinin MCF-7 hücre hattındaki hücre canlılığına etkisi

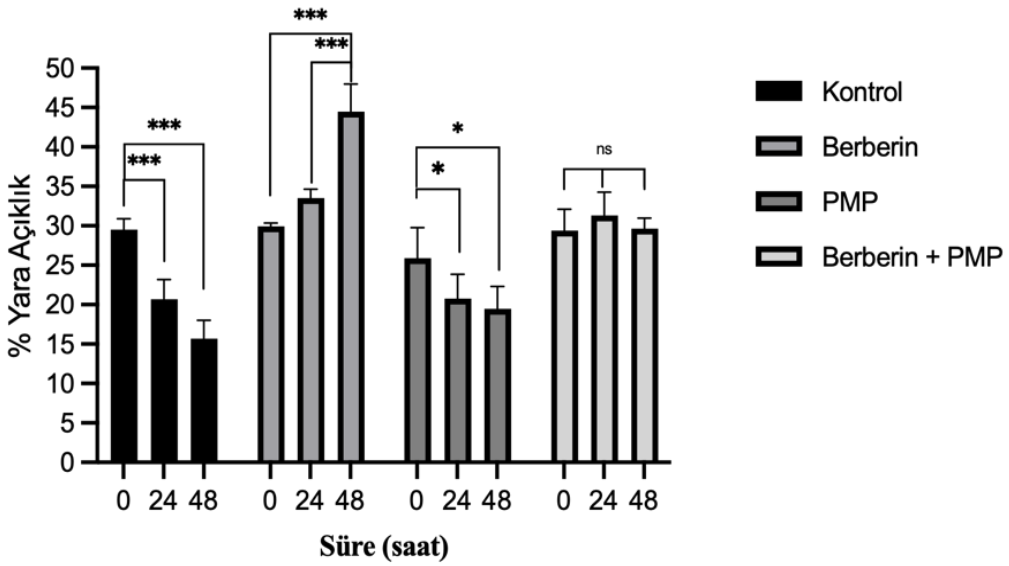
Berberinin, PMP ve Kombinasyonunun MCF-7 hücre göçüne etkisi

Şekil 4 incelendiğinde, kontrol grubunda hücrelerin zamanla proliferasyona devam ettiği ve yara alanına doğru göç ederek çizik bölgesini kısmen kapattığı görülmektedir. Berberin uygulanan kuyucuklarda ise hücre sayısının zamanla azaldığı ve kontrol grubuna kıyasla çizik alanının belirgin şekilde açık kaldığı gözlenmiştir. Bu durum, berberinin hücre göçünü inhibe edici bir etkiye sahip olabileceğini göstermektedir.



Şekil 4. Berberin, PMP, berberin+PMP'nin, 48 saatteki MCF-7 yara kapanma etkisi.

Yalnızca PMP uygulanan grupta, kontrol grubuna benzer şekilde yara alanının önemli ölçüde kapandığı ve hücre proliferasyonunun sürdüğü dikkat çekmektedir (Şekil 5). Berberin ile önceden inkübe edilen hücrelere 24. saatte PMP eklenmesiyle oluşturulan kombinasyon grubunda, 48. saat sonunda berberinin inhibe edici etkisinin azaldığı ve PMP'nin ise hücre göçünü desteklediği düşünülmektedir.



Şekil 5. Berberin, PMP ve Berberin+PMP'nin MCF-7 hücre hattındaki yara açıklığına etkisinin zamana bağlı olarak 48 saatteki değişimi (*p<0,05, **p<0,01, ***p<0,001)

TARTIŞMA

Bu çalışmada elde edilen bulgular, Berberinin 100 ve 200 µM dozlarda daha sitotoksik olduğunu, terapötik potansiyelinin yanı sıra, sağlıklı hücreler üzerinde toksisite riskinin de olabileceğini; bu nedenle dozun kritik bir faktör olduğunu göstermektedir. Yani berberin, meme kanser hücrelerine karşı seçici bir antikanser profil sergilemiş; bu sitotoksik etkiler yara kapanma deneyinde de görülmüştür. Berberin uygulanan kuyucuklarda

hücre sayısının zamanla azaldığı ve kontrol grubuna kıyasla çizik alanının belirgin şekilde açık kaldığı gözlenmiştir. Bu durum, berberinin hücre göçünü inhibe edici bir etkiye sahip olabileceğini göstermektedir. PMP uygulanan grupta ise, yara alanının önemli ölçüde kapandığı ve hücre proliferasyonunun sürdüğü görülmüş yani PMP kanser hücrelerinin migrasyonunu arttırırken; berberin PMP'nin neden olduğu migrasyonu azaltmış ve yaranın kapanmasını antimigratif ve antiproliferatif etkilerle engellemiştir. Berberin ile önceden inkübe edilen hücrelere 24. saatte PMP eklenmesiyle oluşturulan kombinasyon grubunda, 48. saat sonunda berberinin inhibe edici etkisinin azaldığı ve PMP'nin ise hücre göçünü desteklediği görülmektedir.

Yapılan çalışmalarda, antikanser (Pierpaoli ve ark., 2021; Xiong ve ark., 2022; Du ve ark., 2022) ve apoptotik (Pan ve ark., 2022; Huang ve ark.,2023;; Fu ve ark., 2024; Zhu ve ark., 2020) özellikleri iyi bilinen berberinin, meme kanserinin önlenmesi ve tedavisi için umut verici bir ajan olabileceği (Xiong ve ark., 2022); altta yatan etki mekanizmaları arasında kanser hücresin çoğalmasını ve invazyonunu dolayısıyla metastazını engellemek, göçünü baskılamak, hücre döngüsünün ilerlemesini durdurmak olarak belirtilmiştir (Du ve ark., 2022). Bazı kanser hücre hatları için berberinin 100 µM'den daha yüksek konsantrasyonlarda etki ettiği; bununla birlikte, berberinin sitotoksik etkisinin 10 ila 100 µM arasında değiştiği için orta düzeyde olduğu (Rauf ve ark., 2021) gösterilmiştir. Bizim çalışmamız da bu çalışmalarla uyumludur.

Sıçanlarla yapılan bir *in vivo* çalışma, karaciğer ve böbrek toksisitesi de olmayan 13-Cys-BBR'nin inflamasyon, venöz tromboz, arteriyel tromboz, serum TNF-α ve serum P-selektinin mükemmel inhibitörü olduğunu kanıtlamaktadır (Li ve ark., 2020). Yapılan bir *in vitro* çalışmada ise, berberin kaynaklı CD31+/CD42− mikropartikül azalması, sağlıklı bireylerde endotel fonksiyonunun artışına katkıda bulunmuştur (Wang ve ark., 2009). Berberinin trombositler ve tromboz üzerine yapılmış çalışmaları olsa da, PMP üzerindeki etkisiyle ilgili çalışmalar yetersizdir. Bizim çalışmamızda, PMP kanser hücrelerinin migrasyonunu arttırırken; berberin PMP'nin neden olduğu migrasyonu azaltmış ve yaranın kapanmasını antimigratif ve antiproliferatif etkilerle engellemiştir. Berberinin, antikanser özelliklerinin yanında anti-inflamatuvar ve anti-trombotik etkileri de bulunduğu için, PMP'nin neden olduğu kanser hücrelerinin migrasyonundaki etkileri geri çevirmesi, literatürdeki diğer çalışmalarla uyumludur.

Trombositler kanser ilerlemesinde yaygın olarak rol oynamaktadır ve PMP'ler ise trombosit-kanser etkileşiminin potansiyel aracıları olarak giderek daha fazla ilgi görmektedir (Vismara ve ark., 2021). Genel olarak, PMP'lerin anjiyogenezi, hücre proliferasyonunu (Oliveira ve ark., 2024; Lazar ve ark., 2021) ve bağışıklık hücrelerinden kaçışını düzenleyerek kanser metastazını güçlendirdiği kabul edilmektedir (Jaiswal ve ark., 2017). Meme kanseri de dahil olmak üzere çeşitli kanser türlerinde dolaşımdaki PMP'lerin yaygın olarak plazma seviyelerinin yükseldiği, inflamasyon ve tromboza aracılık edebildiği (Anghel ve ark., 2020; Geddings ve ark., 2013; Bucciol ve ark., 2023; Sheikh ve ark., 2020); dolaşımdaki PMP'lerin yüksek miktarlarının genellikle ileri metastatik evre ile ilişkili olduğu belirtilmiştir (Zara ve ark., 2017). Ancak, az sayıda araştırma, PMP'lerin kanser baskılayıcı rolleri olabileceğini de öne sürmüştür. Ayrıca, PMP'lerin kanser hücre biyolojisi üzerindeki etkilerine ilişkin bilgilerimiz sınırlıdır ve sıklıkla çelişkili sonuçlar bildirilmiştir (Vismara ve ark., 2021). Kanser hastalarında dolaşan PMP'lerin artışını destekleyen mekanizmalar yeterince anlaşılmamıştır. Diğer taraftan, PMP'lerin spesifik etkilerinin trombositlerden veya diğer hücrelerden türetilen MP'lerin etkilerinden ayrılmasındaki zorluklar nedeniyle yeterince anlaşılmamıştır (Lazar ve ark., 2021).

SONUÇ

PMP'lerin meme kanserindeki rolünü değerlendiren bu sınırlı çalışmalara rağmen, prokoagülan PMP'lerin tanımlanması, tedavileri özelleştirmek ve kişiselleştirmek için meme kanser teşhisinde potansiyel bir prognostik biyobelirteç ve gelecekte umut vadeden bir tromboz biyobelirteci olabilir Berberin ise, hem meme kanserinin hem de trombotik hastalıkların veya kardiyovasküler/serebrovasküler olayların önlenmesinde ve tedavisinde kullanılabilecek umut verici bir ajan olabilir.

TEŞEKKÜR

Bu çalışmaya sağlıklı gönüllülerden kan alımı için laboratuvar imkânları ile verdikleri katkılar için Doç. Dr. Hasan Alaçam'a ve Ahenk Laboratuvarı ekibine teşekkür ederiz.

KAYNAKLAR

Almatroodi SA, Alsahli MA, Rahmani AH. Berberine: An Important Emphasis on Its Anticancer Effects through Modulation of Various Cell Signaling Pathways. Molecules. 2022;27:58.

Anghel L, Sascău R, Radu R, Stătescu C. From Classical Laboratory Parameters to Novel Biomarkers for the Diagnosis of Venous Thrombosis. International Journal of Molecular Sciences. 2020;21:1920.

Baj-Krzyworzeka M, Janowska-Wieczorek A, Kijowski J, Majka M, Pratico D, Reca R, Ratajczak J, Ratajczak MZ, Vilaire G. Platelet-derived microparticles stimulate proliferation, survival, adhesion, and chemotaxis of hematopoietic cells. Experimental Hematology. 2002;30:450–459.

Bucciol R, Othman M. Tissue factor positive microparticles as a biomarker for increased risk of breast cancer-associated thrombosis: a mini review. Current Opinion in Hematology. 2023;30(5):180–185.

Cambien B, Wagner DD. A new role in hemostasis for the adhesion receptor P-selectin. Trends in Molecular Medicine. 2004;10(4):179–186.

Chaari M, Ayadi I, Rousseau A, Lefkou E, Dreden PV, Sidibe F, Ketatni H, Galea V, Khaterchi A, Bouzguenda R, Frikha M, Ghorbal L, Daoud J, Kallel C, Quinn M, Gligorov J, Lotz JP, Hatmi M, Elalamy I, Gerotziafas GT. Impact of breast cancer stage, time from diagnosis and chemotherapy on plasma and cellular biomarkers of hypercoagulability. BMC Cancer. 2014;14:991.

Du Y, Khan M, Fang N, Ma F, Du H, Tan Z, Wang H, Yin S, Wei X. Berberine attenuates cell motility via inhibiting inflammation-mediated lysyl hydroxylase-2 and glycolysis. Frontiers in Pharmacology. 2022;13:856777.

El-Wahab AEA, Ghareeb DA, Sarhan EM, Abu-Serie MM, Demellawy MAE. In vitro biological assessment of Berberis vulgaris and its active constituent, berberine: antioxidants, anti-acetylcholinesterase, anti-diabetic and anticancer effects. BMC Complementary and Alternative Medicine. 2013;13:218.

Fu W, Liu L, Tong S. Berberine inhibits the progression of breast cancer by regulating METTL3-mediated m6A modification of FGF7 mRNA. Thoracic Cancer. 2024;15:1357–1368.

Geddings JE, Mackman N. Tumor-derived tissue factor–positive microparticles and venous thrombosis in cancer patients. Blood. 2013;122(11):1873–1875.

Huang B, Wen G, Li R, Wu M, Zou Z. Integrated network pharmacology, bioinformatics, and molecular docking to explore the mechanisms of berberine regulating autophagy in breast cancer. Medicine. 2023;102:36.

Jaiswal R, Johnson MS, Pokharel D, Krishnan SR, Bebawy M. Microparticles shed from multidrug resistant breast cancer cells provide a parallel survival pathway through immune evasion. BMC Cancer. 2017;17:104.

Lazar S, Goldfinger LE. Platelets and extracellular vesicles and their cross talk with cancer. Blood. 2021;137(23):3154–3166.

Li G, Wang T, Zhang X, Zhao S, Wang Y, Wu J, Peng S, Zhao M. Development of 13-Cys-BBR as an agent having dual action of anti-thrombosis and anti-inflammation. Drug Design, Development and Therapy. 2020;14:2187–2197.

Oliveira RMC, Teixeira-Carvalho A, Soares CE, Sabino AP, dos Santos LI, Simões R, Angélica N, Gomes KB. Microparticles and cardiotoxicity secondary to doxorubicin-based chemotherapy in breast cancer patients. International Journal of Cardiology.2024;395:131435.

Pan X, Song Z, Cui Y, Qi M, Wu G, Wang M. Enhancement of sensitivity to tamoxifen by berberine in breast cancer cells by inhibiting ER-36 expression. Iranian Journal of Pharmaceutical Research. 2022;21(1):e126919.

Pan Y, Zhang F, Zhao Y, Shao D, Zheng X, Chen Y, He K, Chen JL. Berberine enhances chemosensitivity and induces apoptosis through dose-orchestrated AMPK signaling in breast cancer. Journal of Cancer. 2017;8(9):1679–1689.

Pierpaoli E, Piacenza F, Fiorillo G, Lombardi P, Salvatore C, Geroni C, Provinciali M. Antimetastatic and antitumor activities of orally administered NAX014 compound in a murine model of HER2-positive breast cancer. International Journal of Molecular Sciences. 2021;22:2653.

Rauf A, Abu-Izneid T, Khalil AA, Bin Emran T, Imran M, Shah ZA, Mitra S, Khan Z, Alhumaydhi FA, Khan I, Rahman MM, Jeandet P, Aljohani ASM, Gondal TA. Berberine as a potential anticancer agent: a comprehensive review. Molecules. 2021;26:7368.

Sheikh Hosseini M, Parhizkar Roudsari P, Gilany K, Goodarzi P, Payab M, Tayanloo-Beik A, Larijani B, Arjmand B. Cellular dust as a novel hope for regenerative cancer medicine. Advances in Experimental Medicine and Biology. 2020;1288:139–160.

Spuy WJ, Augustine TN. Ultrastructural investigation of the time-dependent relationship between breast cancer cells and thrombosis induction. Micron. 2016;90:59-63.

Vismara M, Zarà M, Negri S, Canino J, Canobbio I, Barbieri SS, Moccia F, Torti M, Guidetti GF. Platelet-derived extracellular vesicles regulate cell cycle progression and cell migration in breast cancer cells. Biochimica et Biophysica Acta – Molecular Cell Research. 2021;1868:118886.

Wang C, Cheng Y, Zhang Y, Jin H, Zuo Z, Wang A, Huang J, Jiang J, Kong W. Berberine and its main metabolite berberrubine inhibit platelet activation through suppressing the Class I PI3Kβ/Rasa3/Rap1 pathway. Frontiers in Pharmacology. 2021;12:734603.

Wang H, Zhu C, Ying Y, Luo L, Huang D, Luo Z. Metformin and berberine, two versatile drugs in treatment of common metabolic diseases. Oncotarget. 2018;9:10135–10146.

Wang J, Yang Z, Xu M, Chen L, Wang Y, Su C, Tao J. Berberine-induced decline in circulating CD31+/CD42− microparticles is associated with improvement of endothelial function in humans. European Journal of Pharmacology. 2009;614:77–83.

Wang X, Zhang Y, Yang Y, Wu X, Fan H, Qiao Y. Identification of berberine as a direct thrombin inhibitor from traditional Chinese medicine through structural, functional and binding studies. Scientific Reports. 2017;7:44040.

Wang Y, Liu Y, Yao XDHMJ. The Anti-Cancer Mechanisms of Berberine: A Review. Cancer Management and Research. 2020;12:695–702.

Xing L, Zhou X, Li AH, Li HJ, He CX, Qin W, Zhao D, Li PQ, Zhu L, Cao HL. Atheroprotective effects and molecular mechanism of berberine. Frontiers in Molecular Biosciences. 2021;8:762673.

Xiong RG, Huang SY, Wu SX, Zhou DD, Yang ZJ, Saimaiti A, Zhao CN, Shang A, Zhang YJ, Gan RY, Li HB. Anticancer effects and mechanisms of berberine from medicinal herbs: an update review. Molecules. 2022;27:4523.

Zhu C, Li J, Sun J. Berberine inhibits the expression of SCT through miR-214-3p stimulation in breast cancer cells. Evidence-Based Complementary and Alternative Medicine. 2020;2817147.

ORAL PRESENTATION

Decoding the *ALMT* gene family in *Helianthus annuus*: Evolutionary patterns, structural features, and stress-responsive functional potential

Hooman Savehdarbandsari[1] (*ORCID: https://orcid.org/0009-0007-6497-8701*), Döndü Aliye Yıldız[2] (*ORCID: https://orcid.org/0000-0002-8243-6718*), Kevser Betül Ceylan[1*] (*ORCID: https://orcid.org/0000-0002-6006-727X*)

[1] Bartın University, Faculty of Science, Department of Molecular Biology and Genetics, Bartın, Turkey.
[2] Bartın University, Institute of Graduate Studies, Department of Molecular Biology and Genetics, Bartın, Turkey.

*Corresponding author e-mail: kevserbb@bartin.edu.tr

Abstract

Aluminum-activated malate transporters (ALMTs) constitute a prominent anion channel family involved in essential physiological processes in plants, including nutrient uptake, metal tolerance, stomatal regulation, cellular pH homeostasis, signal transduction, and cell expansion. We performed comprehensive bioinformatics analyses, including chromosomal distribution, gene structure, motif composition, conserved domain architecture, phylogeny, synteny with *Arabidopsis thaliana*, protein physicochemical characterization, Ka/Ks-based evolutionary assessment, 3D protein structure prediction, and protein–protein interaction analysis. 21 HaALMT genes were found in the sunflower genome in this paper. The motif structures of the proteins in the same phylogenetic tree were similar, and the α-helical form was dominant in most proteins. Synteny analysis identified conserved collinear regions for *HaALMT7* and *HaALMT18* with *A. thaliana*, supporting their shared evolutionary origin. Additionally, protein–protein interaction predictions highlighted TAFII31 and SAGA-associated factor 11 as major interaction partners, implying regulatory functions that extend beyond malate transport. The findings provide novel insights into the evolutionary history, structural diversity, and potential functional roles of *HaALMT* genes in sunflower adaptation to environmental stress.

Keywords: Aluminum-activated malate transporters, *Helianthus annuus*, genome-wide idenificaion

INTRODUCTION

Aluminum-activated malate transporters (ALMTs) comprise a versatile group of anion channels that participate in multiple physiological processes, including mineral homeostasis, detoxification of metal ions, stomatal regulation, and maintaining intracellular pH stability (Roelfsema and Hedrich, 2005). Rather than functioning as a single-pathway system, ALMTs act as dynamic regulators that help plants integrate environmental cues with metabolic responses. The solubilization of Al^{3+} creates a hostile environment that rapidly interferes with root structure and cellular integrity in acidic soils. Plants counter these effects through various defense mechanisms, and ALMT-mediated malate release is a central component of this response (Le Poder et al., 2022).

The defining structural feature of the ALMT family is the conserved PF11744 domain, supported by several transmembrane helices that allow efficient transport of anionic molecules across cellular membranes (Medeiros et al., 2018 ; Dabravolski and Isayenkov, 2023). Although these proteins are best known for their role in organic acid efflux under aluminum exposure, accumulating evidence suggests that they function more broadly in processes such as fruit acidity modulation, guard-cell turgor adjustment, and signaling pathways involving γ-aminobutyric acid (GABA) (Sharma et al., 2016). Variations in subcellular localization, such as the tonoplast-associated *AtALMT6* and *AtALMT9*, further illustrate the functional diversity of this gene family.

Sunflower (*Helianthus annuus* L.) is the world's fifth most significant oilseed crop and is widely cultivated under diverse environmental conditions. Exposure to abiotic stresses triggers complex signaling and transcriptional reprogramming in sunflowers, mediated by transcription factors (TFs) and downstream regulatory networks. Identifying stress-related gene families such as *ALMTs* is essential for understanding sunflower adaptation mechanisms and for improving stress resilience through molecular breeding and functional genomics (Li et al., 2020).

In this study, we systematically identified *ALMT* gene family members in the sunflower genome and performed comprehensive structural, evolutionary, and functional analyses. Our results provide insights into the organization, expansion, and potential roles of *HaALMT* genes in abiotic stress responses, contributing valuable information for future functional studies and stress-resilient sunflower breeding strategies.

MATERIALS AND METHODS

Identification and Characterization of ALMT Genes in the Sunflower Genome

ALMT genes in *H. annuus* were identified by querying the PF11744 domain against the *H. annuus* reference genome (version r1.2) (Goodstein et al., 2012) available in the Phytozome database. Protein sequences of *Arabidopsis thaliana* ALMT family members were retrieved from the NCBI database (https://www.ncbi.nlm.nih.gov/) and used as reference queries. Homologous sequences in sunflower were identified using BLASTP searches in TBtools-II with an e-value threshold of $<1e^{-5}$ (Chen et al., 2023). The presence of the ALMT domain in each candidate sequence was validated through the Pfam database (http://pfam.xfam.org/) (Mistry et al., 2021). Physicochemical properties, including molecular weight, theoretical isoelectric point (pI), instability index, and GRAVY scores, were calculated using the ExPASy ProtParam tool (https://web.expasy.org/protparam/) (Gasteiger et al., 2005).

Chromosomal Localization and Synteny Analysis

Genomic coordinates of *HaALMT* genes were obtained from Phytozome and displayed with TBtools-II. To assess the evolutionary conservation of the ALMT family, synteny between the *H. annuus* and *A. thaliana* genomes was analyzed. Corresponding FASTA and GFF3 datasets were retrieved from Phytozome, and syntenic blocks were identified through the One-Step MCScanX module in TBtools-II. Collinearity patterns were subsequently illustrated with the Dual Synteny Plot function (Wang et al., 2012).

Gene Structure and Conserved Motif Analysis

The intron–exon organization of *HaALMT* genes was characterized with the Gene Structure View module in TBtools-II. Conserved motifs in *HaALMT* protein sequences were detected with the MEME Suite under default settings, and the resulting motif architectures were rendered using TBtools-II.

Phylogenetic Analysis and Gene Duplication Assessment

Multiple sequence alignments of ALMT proteins from sunflower, *A. thaliana*, *Zea mays*, and *Oryza sativa* were generated with the MUSCLE algorithm. Phylogenetic trees were inferred using the Maximum Likelihood approach with 1000 bootstrap replicates in MEGA v12.0 (Kumar et al., 2018) and visualized through the iTOL platform (Letunic and Bork, 2007). Evolutionary divergence was assessed by estimating nonsynonymous (Ka) and synonymous (Ks) substitution rates, as well as the Ka/Ks ratio, using TBtools-II (Wang and Zhang, 2010).

Three-Dimensional (3D) Protein Structure Prediction and Protein–Protein Interaction (PPI) Analysis

Structural predictions of *HaALMT* proteins were generated using the SWISS-MODEL server, and the resulting 3D models were assessed based on sequence identity and confidence metrics. Protein–protein interaction networks were inferred through the STRING database to identify potential interacting partners and functional associations (Mering et al., 2003 ; Szklarczyk et al., 2023).

RESULTS AND DISCUSSION

In this study, 21 *HaALMT* genes were identified in the sunflower genome through BLAST searches using *A. thaliana* ALMT sequences. Genes were named with the prefix “Ha” and ordered according to their chromosomal positions. *HaALMT* proteins range from 273 to 1863 amino acids, with predicted pI values between 4.97 and 5.37, indicating an overall acidic nature. Among the 21 proteins, nine (42.85%) are classified as unstable, and twelve (57.14%) are classified as stable. Their molecular weights range from 22.6 to 153.9 kDa. Subcellular localization predictions indicate that most *HaALMT* members (85.71%) are associated with the plasma membrane, while the remainder localize to the nucleus/chloroplast, cytoplasm/chloroplast, or extracellular matrix/chloroplast compartments.

To examine the evolutionary relationships of *HaALMT* proteins, ALMT sequences from *A. thaliana* (14 members), *Z. mays* (9 members), and *O. sativa* (9 members) were analyzed. Earlier studies reported 22 *ALMT* genes in *A. thaliana* (Guo et al., 2008), 25 in *Z. mays* (Lin et al., 2011), and 10 in *O. sativa* (Guo et al., 2008). The number of Arabidopsis genes identified in this study did not fully match those published in these datasets.

The 21 identified *HaALMT* genes were mapped across the 17 sunflower chromosomes (Figure 1). Previous studies in *Solanum tuberosum* and Orchidaceae reported ALMT distributions on seven chromosomes (Zhang et al., 2023; Peng et al., 2024). Phylogenetic analysis revealed that *HaALMT* proteins cluster into four major groups (Figure 2a), with Group II containing the largest number of members (nine genes).

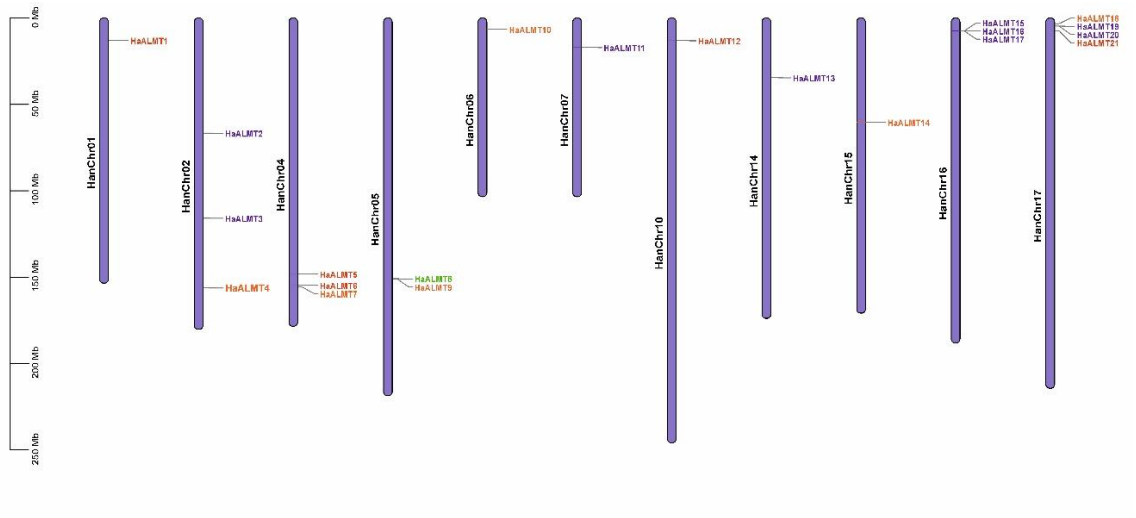


Figure 1. The distribution of all *HaALMT* genes on sunflower chromosomes

In contrast, *HaALMT8* in Group III showed no close evolutionary relationship with other species. Ten conserved motifs were detected in sunflower (Figure 2b); motifs 1, 2, 3, 4, 5, 6, 7, and 9 were shared among *HaALMT14, 10, 18, 5, 6, 21,* and *3*, while *HaALMT8* contained only motif 9. In contrast, 15 conserved motifs were reported in *Medicago sativa* and *Hevea brasiliensis* (Jin et al., 2024). All *HaALMT* proteins carried the FUSC superfamily domain—consistent across all phylogenetic groups—and the ALMT superfamily domain, except *HaALMT15*, which contained only the ALMT domain. FUSC, previously associated with membrane transport, cell division, and intracellular trafficking (Utsumi et al., 1991), supports the multifunctional nature of ALMT proteins beyond aluminum tolerance. Gene structure analysis showed that most *HaALMT* genes comprise five to six exons, whereas *HaALMT9* contains three, and *HaALMT15* and *HaALMT21* contain two exons (Figure 2b), differing from the six-exon structure reported for *M. sativa* (Jin et al., 2024).

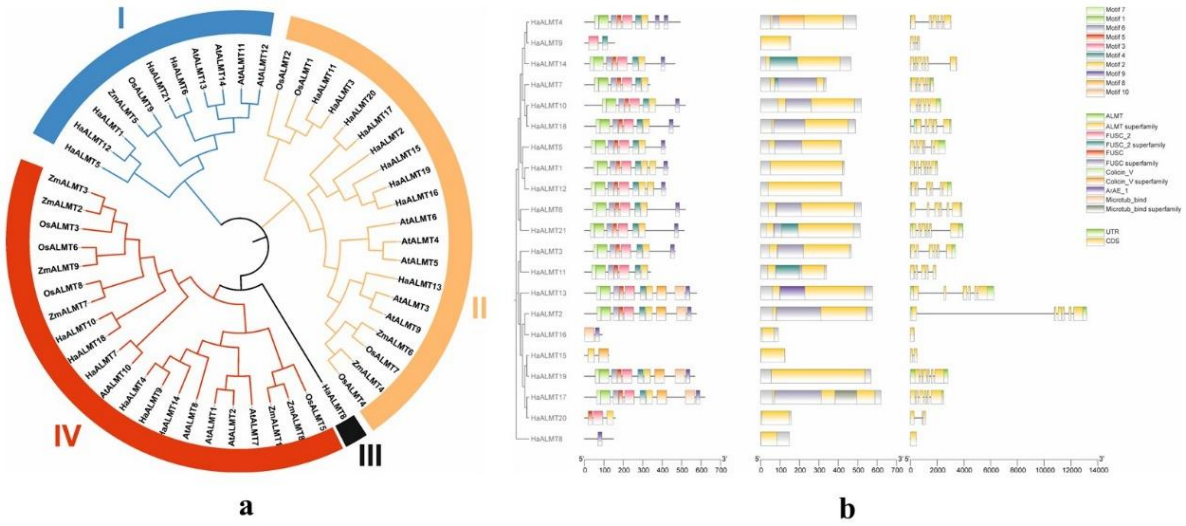


Figure 2. Phylogenetic analysis of *HaALMT* genes. The ML tree was constructed with 1000 bootstraps (a), the exon-intron organization, motif, and domain analysis of *HaALMT* genes (b)

HaALMT genes exhibited extensive duplication, comprising 128 segmental and eight tandem events, with duplication blocks present on all chromosomes except chromosomes 3, 8, 9, 11, 12, and 13. Selection pressure analysis revealed mean Ka, Ks, and Ka/Ks values of 0.7789, 1.846, and 0.461, respectively. Twelve *HaALMT* proteins were successfully modeled with a confidence level of greater than 90% and all displayed α–helix–rich folding patterns, consistent with earlier structural predictions (Zhang et al., 2023). Protein–protein interaction

analysis identified strong interactions—50 in total—between *HaALMT* proteins and two major partners: Putative transcription initiation factor TAFII31 (A0A251SGY5) and SAGA-associated factor 11 (A0A251TAY2). TAFII31 is known to contribute to the assembly and stability of the TFIID and TFTC complexes through its histone-fold domain (Leurent, 2002), while the ZnF domain of SAGA-associated factor 11 mediates zinc binding (Samara et al., 2010). Given that ALMT channels regulate malate efflux and intracellular pH—factors influencing zinc transport—these interactions likely reflect coordinated roles in stress signaling and cellular organization. Comparative synteny analysis with *A. thaliana* revealed clear collinearity for *HaALMT7* and *HaALMT18* with their Arabidopsis homologous regions (Figure 3).

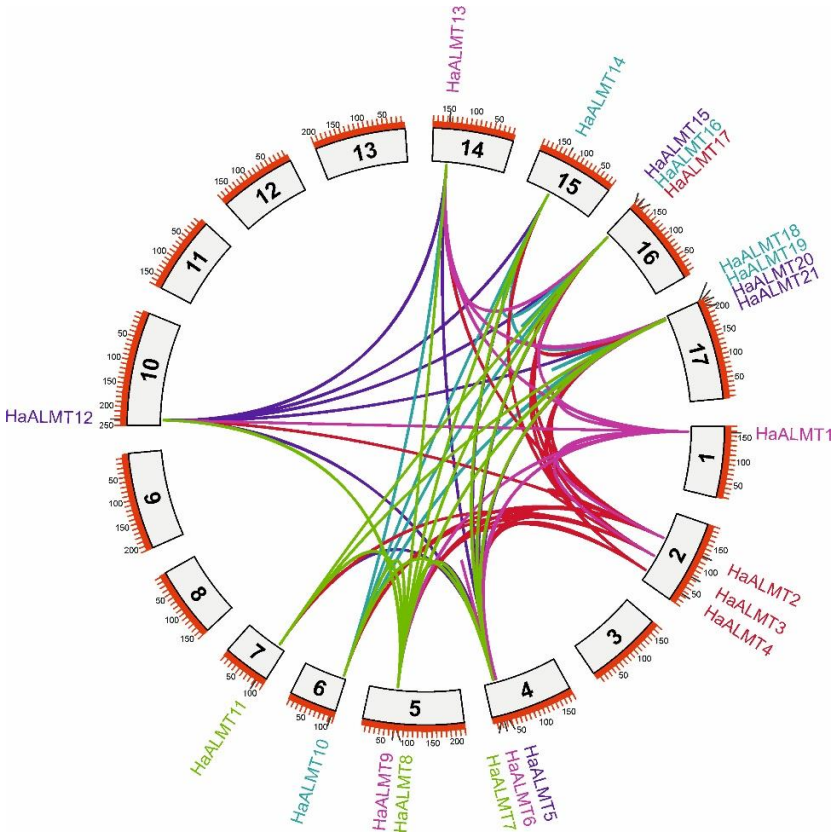


Figure 3. Localization and synteny of *ALMT* genes in *Helianthus annuus*

CONCLUSION

This paper provides a comprehensive characterization of 21 *HaALMT* genes in the sunflower genome, revealing their distribution across 17 chromosomes and highlighting 128 segmental and eight tandem duplication events that have contributed to the expansion of the family. Phylogenetic analysis resolved the genes into four major clades, with Group II being the most enriched. At the same time, motif and domain assessments demonstrated strong structural conservation across members, except for unique features observed in *HaALMT8* and *HaALMT15*. Synteny comparisons revealed clear collinear relationships between HaALMT7 and HaALMT18, as well as *A. thaliana*, indicating shared evolutionary origins. Structural modeling confirmed α-helix–rich architectures in 12 proteins, and protein–protein interaction analyses pinpointed TAFII31 and SAGA-associated factor 11 as key functional partners, suggesting broader regulatory roles beyond malate transport. Overall, these insights deepen our understanding of *ALMT* gene evolution and function in sunflowers, offering a valuable foundation for future studies aimed at enhancing aluminum tolerance and stress resilience.

REFERENCES

Chen C., Wu Y., Li J., Wang X., Zeng Z., Xu J., Liu Y., Feng J., Chen H., He Y., and Xia R. (2023) TBtools-II: A "one for all, all for one" bioinformatics platform for biological big-data mining. Mol. Plant. 16, 1733–1742.

Dabravolski, S. A., & Isayenkov, S. V. (2023). Recent Updates on ALMT Transporters' Physiology, Regulation, and Molecular Evolution in Plants. *Plants*, *12*(17), 3167. https://doi.org/10.3390/PLANTS12173167/S1

Gasteiger, E. (2005). Protein identification and analysis tools on the ExPASy server. The proteomics protocols handbook/Human Press Inc.

Goodstein, D. M., Shu, S., Howson, R., Neupane, R., Hayes, R. D., Fazo, J., ... & Rokhsar, D. S. (2012). Phytozome: a comparative platform for green plant genomics. *Nucleic acids research*, *40*(D1), D1178-D1186.https://doi.org/10.1093/nar/gkr944

Guo, J., Wu, J., Ji, Q., Wang, C., Luo, L., Yuan, Y., Wang, Y., & Wang, J. (2008). Genome-wide analysis of heat shock transcription factor families in rice and Arabidopsis. *Journal of Genetics and Genomics*, *35*(2), 105–118. https://doi.org/10.1016/S1673-8527(08)60016-8

Jin, D., Chen, J., Kang, Y., Yang, F., Yu, D., Liu, X., Yan, C., Guo, Z., & Zhang, Y. (2024). Genome-wide characterization, transcriptome profiling, and functional analysis of the ALMT gene family in Medicago for aluminum resistance. *Journal of Plant Physiology*, *297*, 154262. https://doi.org/10.1016/J.JPLPH.2024.154262

Kumar S, Stecher G, Suleski M, Sanderford M, Sharma S, and Tamura K (2024) Molecular Evolutionary Genetics Analysis Version 12 for adaptive and green computing. Molecular Biology and Evolution 41:1-9. https://www.megasoftware.net

Le Poder, L., Mercier, C., Février, L., Duong, N., David, P., Pluchon, S., Nussaume, L., & Desnos, T. (2022). Uncoupling Aluminum Toxicity From Aluminum Signals in the STOP1 Pathway. *Frontiers in Plant Science*, *13*, 785791. https://doi.org/10.3389/FPLS.2022.785791/BIBTEX

Letunic, I., & Bork, P. (2024). Interactive Tree of Life (iTOL) v6: recent updates to the phylogenetic tree display and annotation tool. Nucleic Acids Research, 52(W1), W78–W82. https://doi.org/10.1093/NAR/GKAE268

Leurent, C., Sanders, S., Ruhlmann, C., Mallouh, V., Weil, P. A., Kirschner, D. B., ... & Schultz, P. (2002). Mapping histone fold TAFs within yeast TFIID. The EMBO journal.

Li, W., Zhang, H., Zeng, Y., Xiang, L., Lei, Z., Huang, Q., Li, T., Shen, F., & Cheng, Q. (2020). A Salt Tolerance Evaluation Method for Sunflower (Helianthus annuus L.) at the Seed Germination Stage. *Scientific Reports*, *10*(1), 1–9. https://doi.org/10.1038/S41598-020-67210-3;SUBJMETA

Lin, Y. X., Jiang, H. Y., Chu, Z. X., Tang, X. L., Zhu, S. W., & Cheng, B. J. (2011). Genome-wide identification, classification and analysis of heat shock transcription factor family in maize. *BMC Genomics 2011 12:1*, *12*(1), 76-. https://doi.org/10.1186/1471-2164-12-76

Medeiros, D. B., Fernie, A. R., & Araújo, W. L. (2018). Discriminating the Function(s) of Guard Cell ALMT Channels. *Trends in Plant Science*, *23*(8), 649–651. https://doi.org/10.1016/J.TPLANTS.2018.06.006

Mering, C. V., Huynen, M., Jaeggi, D., Schmidt, S., Bork, P., & Snel, B. (2003). STRING: a database of predicted functional associations between proteins. Nucleic acids research, 31(1), 258-261. https://doi.org/10.1093/nar/gkg034

Mistry, J., Chuguransky, S., Williams, L., Qureshi, M., Salazar, G. A., Sonnhammer, E. L. L., Tosatto, S. C. E., Paladin, L., Raj, S., Richardson, L. J., Finn, R. D., & Bateman, A. (2021). Pfam: The protein families database in 2021. Nucleic Acids Research, 49(D1), D412–D419. https://doi.org/10.1093/NAR/GKAA913

Peng, F. C., Yuan, M., Zhou, L., Zheng, B. Q., & Wang, Y. (2024). Identification and Analysis of Aluminum-Activated Malate Transporter Gene Family Reveals Functional Diversification in Orchidaceae and the Expression Patterns of Dendrobium catenatum Aluminum-Activated Malate Transporters. *International Journal of Molecular Sciences*, *25*(17). https://doi.org/10.3390/IJMS25179662/S1

Roelfsema, M. R. G., & Hedrich, R. (2005). In the light of stomatal opening: New insights into "the Watergate." *New Phytologist*, *167*(3), 665–691. https://doi.org/10.1111/J.1469-8137.2005.01460.X;PAGE:STRING:ARTICLE/CHAPTER

Samara, N. L., Datta, A. B., Berndsen, C. E., Zhang, X., Yao, T., Cohen, R. E., & Wolberger, C. (2010). Structural insights into the assembly and function of the SAGA deubiquitinating module. Science, 328(5981), 1025-1029.

Sharma, T., Dreyer, I., Kochian, L., & Piñeros, M. A. (2016). The ALMT family of organic acid transporters in plants and their involvement in detoxification and nutrient security. *Frontiers in Plant Science*, *7*(OCTOBER2016), 222999. https://doi.org/10.3389/FPLS.2016.01488/BIBTEX

Szklarczyk, D., Kirsch, R., Koutrouli, M., Nastou, K., Mehryary, F., Hachilif, R., ... & Von Mering, C. (2023). The STRING database in 2023: protein–protein association networks and functional enrichment analyses

for any sequenced genome of interest. *Nucleic acids research*, *51*(D1), D638-D646.https://doi.org/10.1093/nar/gkac1000

Utsumi, R., Yagi, T., Katayama, S., Katsuragi, K., Tachibana, K., Toyoda, H., Ouchi, S., Obata, K., Shibano, Y., & Noda, M. (1991). Molecular Cloning and Characterization of the Fusaric Acid-resistance Gene from Pseudomonas cepacia. *Agricultural and Biological Chemistry*, *55*(7), 1913–1918. https://doi.org/10.1080/00021369.1991.10870864

Wang, D., Zhang, Y., Zhang, Z., Zhu, J., & Yu, J. (2010). KaKs_Calculator 2.0: a toolkit incorporating gamma-series methods and sliding window strategies. Genomics, proteomics & bioinformatics, 8(1), 77-80. https://doi.org/10.1016/S1672-0229(10)60008-3

Wang, Y., Tang, H., DeBarry, J. D., Tan, X., Li, J., Wang, X., ... & Paterson, A. H. (2012). MCScanX: a toolkit for detection and evolutionary analysis of gene synteny and collinearity. Nucleic acids research, 40(7), e49-e49. https://doi.org/10.1093/nar/gkr1293

Zhang, F., Jiang, S., Li, Q., Song, Z., Yang, Y., Yu, S., Nie, Z., Chu, M., & An, Y. (2023). Identification of the ALMT gene family in the potato (Solanum tuberosum L.) and analysis of the function of StALMT6/10 in response to aluminum toxicity. *Frontiers in Plant Science*, *14*, 1274260. https://doi.org/10.3389/FPLS.2023.1274260/BIBTEX

ORAL PRESENTATION

Bitki doku kültüründe akıllı biyosüreçler ve yapay zeka makine öğrenimi

Mustafa Kahya[1]* (Orcid: https://orcid.org/0000-0001-6053-1354)
Mehmet Sezgin[2] (Orcid: https://orcid.org/0000-0001-7053-0371),

*[1]Çankırı Karatekin Üniversitesi Lisansüstü Eğitim Enstitüsü,Biyoloji bölümü, Çankırı, Türkiye.
[2]Çankırı Karatekin Üniversitesi, Gıda ve Tarım Meslek Yüksekokulu, Park ve Bahçe Bitkileri Bölümü, Peyzaj ve Süs Bitkileri, Çankırı, Türkiye.

*Sorumlu yazar e-mail: mkahya50@gmail.com.

Özet

Bitki Doku Kültürü, karmaşık genetik ve çevresel etkileşimler nedeniyle geleneksel optimizasyon yöntemlerinin Tek Faktörlü Denemeler, Cevap Yüzeyi Metodolojisi gibi konularda yetersiz kalmaktadır. Bu çalışma, küresel literatürde Yapay Zeka (YZ), Makine Öğrenimi (ML) ve Robotik uygulamalarının Bitki Doku kültüründeki dönüşümsel potansiyelini incelemektedir. Makine Öğrenimi teknikleri (Yapay Sinir Ağları - Genetik Algoritma, Genel Regresyon Sinir Ağı - Baskın Olmayan Sıralamalı Genetik Algoritma II), kültür ortamı bileşenlerinin ve eksplant sterilizasyon prosedürlerinin eşzamanlı, çok amaçlı optimizasyonunda Cevap Yüzeyi Metodolojisi'ne göre üstünlük sağlamış, kalitatif girdileri ele alarak tür bazında hassas formülasyona olanak tanımıştır. Derin Öğrenme algoritmaları (Evrişimli Sinir Ağları), somatik embriyogenez aşama tanıma, mikrobiyal kontaminasyon ve vitrifikasyon gibi fizyolojik streslerin otomatik tespitinde, nesnellik ve hız sunar. Robotik sistemler (RoBoCut, Janus Transplanter) ile otomasyon, mikroçoğaltmada toplam üretim maliyetinin %50-70'ini oluşturan işgücü maliyetlerini azaltırken, Yapay Zeka rehberli 3D görüntü tanıma kalitenin tutarlılığını artırmaktadır. Ayrıca yapay zeka, CRISPR/Cas9 Genom Düzenleme Sistemi uygulamalarında (Random Forest modeli üstünlüğü) hedef dışı sekans tahminini iyileştirerek genetik hassasiyeti yükseltmektedir. Ana zorluklar, veri heterojenliği, yüksek ilk yatırım maliyetleri ve Derin Öğrenmenin yorumlanabilirlik eksikliğidir. Çözümler, Açıklanabilir Yapay Zeka entegrasyonu ve disiplinlerarası işgücü eğitimini gerektirmektedir. Sonuç olarak, Yapay Zeka'nın Bitki Doku Kültürüne entegrasyonu, süreçlerin hassasiyetini, sürdürülebilirliğini ve maliyet etkinliğini artırarak biyoteknolojinin endüstriyel ölçekte ilerlemesini sağlamaktadır.

Anahtar Kelimeler: Yapay Zeka, Bitki Doku Kültürü, Makine Öğrenimi, Robotik, Optimizasyon, CRISPR

Intelligent Bioprocesses, Artificial Intelligence, and Machine Learning in Plant Tissue Culture

Abstract

Plant Tissue Culture faces persistent yield limitations because conventional optimization methods such as One Factor at a Time and Response Surface Methodology cannot fully capture the complex interactions among genetic, physiological, and environmental factors. This review summarizes global research on how Artificial Intelligence, Machine Learning, Deep Learning, and robotics are reshaping Plant Tissue Culture by improving efficiency, precision, and scalability.

Machine Learning models including Artificial Neural Network Genetic Algorithm combinations and Generalized Regression Neural Network systems combined with advanced multi objective optimization strategies have demonstrated superior performance compared to Response Surface Methodology. These models can simultaneously optimize medium components including macro and micronutrients and improve explant sterilization procedures. Their ability to process qualitative variables supports species specific and highly accurate formulation of culture conditions.

Deep Learning, particularly Convolutional Neural Networks, provides rapid and objective detection of contamination, vitrification, somatic embryogenesis stages, and other physiological stresses. Robotic platforms such as RoBoCut and Janus Transplanter reduce labor costs, which traditionally account for most micropropagation expenses. Artificial Intelligence supported three dimensional image analysis further enhances quality consistency and production throughput.

Artificial Intelligence also advances genetic precision. In applications of the CRISPR Cas9 genome editing system, Machine Learning models such as Random Forest improve the prediction of off target effects. Despite these advantages, several challenges remain including heterogeneous data sets, high initial investment requirements, and limited interpretability of Deep Learning models. The adoption of Explainable Artificial Intelligence systems such as SHAP and the development of interdisciplinary expertise are essential to overcoming these limitations.
Overall, the integration of Artificial Intelligence into Plant Tissue Culture supports more sustainable, precise, and economically viable biotechnological production systems and strengthens the path toward industrial scale advancement.

Keywords: Artificial Intelligence, Plant Tissue Culture, Machine Learning, Robotics, Optimization, CRISPR

1.GİRİŞ

Bitki Doku Kültürü, hızlı çoğaltım (mikroçoğaltma), temiz bitki programlarının oluşturulması ve genetik mühendisliği süreçlerinin kolaylaştırılması için modern tarım ve biyoteknolojide hayati bir platform görevi görmektedir (Hesami ve Jones, 2025). Küresel gıda güvenliğinin sağlanması, dünya nüfusunun sürekli artışı ve iklim değişikliğinin tarımsal sistemler üzerindeki baskısının artması gibi zorluklar karşısında, Bitki Doku Kültürü merkezi bir konuma sahiptir (Hesami ve Jones, 2025). Bu bağlamda, yüksek verimli, hastalıklara ve değişen çevresel koşullara dayanıklı yeni çeşitlerin hızla geliştirilmesi zorunludur. Bu zorunluluk, bitki ıslahı süreçlerinde yüksek verimli omik teknolojilerinin kullanımını kaçınılmaz kılmakta ve büyük veri analizi ihtiyacını doğurmaktadır (Ali ve ark., 2023).

Geleneksel Optimizasyon Yaklaşımlarının Sınırlamaları
In vitro sistemlerin başarısı, genetik, fizyolojik ve çevresel faktörler arasındaki karmaşık, doğrusal olmayan etkileşimlere ve biyolojik varyansa derinden bağlıdır (Hesami ve Jones, 2025). Geleneksel deneysel ve istatistiksel optimizasyon yaklaşımları, özellikle Tek Faktörlü Denemeler (OFAT) ve Cevap Yüzeyi Metodolojisi (RSM), bu karmaşık dinamiklerle başa çıkmada yapısal sınırlamalar taşımaktadır (Hesami ve Jones, 2025). Geleneksel yöntemler, kültür ortamı bileşenlerinin optimal kombinasyonunu belirlemeye çalışırken yavaş, zahmetli ve verimsizdir.

Özellikle RSM, etkileşimli etkileri ele alabilse de, regresyon modellerine dayanması nedeniyle kalitatif girdileri (örneğin, farklı karbonhidrat türleri, jelleştirici ajanlar veya eksplant tipleri) karşılaştırmada ciddi kısıtlamalara sahiptir (Hesami ve Jones, 2025). Bu durum, tür bazında hassas formülasyona ulaşılmasını engelleyerek Bitki Doku Kültürü uygulamalarının tam potansiyeline ulaşmasını engellemiştir. Ayrıca, biyolojik deneylerde yaygın olan eksik veri setleri veya kontaminasyon gibi deterministik olmayan sorunlar, geleneksel istatistiksel analiz yöntemlerini zorlamaktadır (Hesami ve Jones, 2025). Bu metodolojik zorluk, yeni nesil veri odaklı yaklaşımların benimsenmesini bilimsel bir zorunluluk haline getirmiştir.

1.2. Yapay Zeka ve Robotik Entegrasyonunun Dönüşümsel Potansiyeli

Yapay Zeka (AI), Makine Öğrenimi (ML) ve Derin Öğrenme (DL) gibi hesaplamalı teknolojilerin entegrasyonu, bitki biyoteknolojisi alanında devrim niteliğinde bir potansiyel sunmaktadır (Hesami ve Jones, 2025). Bu teknolojiler, geleneksel yöntemlerle yönetilmesi imkansız olan büyük hacimli ve karmaşık verileri analiz etme, tahmin etme ve optimize etme kapasitesine sahiptir (Hesami ve Jones, 2025).

Yapay Zeka-destekli yaklaşımların temel vaadi, *in vitro* kültür protokollerinin hassasiyetini, sürdürülebilirliğini ve maliyet etkinliğini artırmaktır. Tarihsel olarak büyük ölçüde ampirik ve "zanaat odaklı" bir süreç olan Bitki Doku Kültürü, Yapay Zeka'nin devreye girmesiyle birlikte, veri yapılarının protokol tasarımını yönlendirdiği standardize edilmiş, endüstriyel bir bilime doğru niteliksel bir geçiş yapmaktadır (Hesami ve Jones, 2025; Tohme ve ark., 2024). Bu paradigma değişimi, biyolojik materyaller ile hesaplama modelleri arasında köprü kurabilen, bitki biyolojisi, bilgisayar bilimleri ve robotik alanlarında uzmanlaşmış personele olan acil ihtiyacı da beraberinde getirmektedir (Tohme ve ark., 2024; Cabrera ve ark., 2023).

2. KURAMSAL TEMELLER VE LİTERATÜR

Bu literatür taraması, AI, ML, DL ve robotik sistemlerin Bitki Doku Kültürü süreçlerini optimize etmek, otomatikleştirmek ve genetik hassasiyeti artırmak amacıyla küresel düzeyde nasıl kullanıldığını incelemektedir. İncelenen metodolojiler, esas olarak biyolojik karmaşıklığı ele alabilen ve geleneksel istatistiksel modellerin sınırlamalarını aşan hibrit hesaplama çerçevelerine odaklanmıştır.

Temel Makine Öğrenimi ve Derin Öğrenme Mimarileri

Bitki Doku Kültürü protokollerinin optimizasyonunda kullanılan Yapay Zeka araçlarının yelpazesi geniştir ve Yapay Sinir Ağları (YSA/ANN), Destek Vektör Makineleri (SVM), Rastgele Orman (RF), Genel Regresyon Sinir Ağları (GRNN) ve DL modellerini (Örneğin Evrişimli Sinir Ağları - CNN'ler, Tekrarlayan Sinir Ağları - RNN'ler) içermektedir (Guo ve ark., 2024; Hessami ve ark., 2023). Bu algoritmalar, yüksek verimli omik teknolojilerinden elde edilen büyük miktardaki genetik ve fenotipik veriyi verimli bir şekilde analiz etmek için kritik öneme sahiptir (Ali ve ark., 2023).

ML teknikleri, RSM'nin aksine, yalnızca kantitatif girdileri değil, aynı zamanda karbonhidrat türleri veya jelleştirici ajanlar gibi kalitatif girdileri de optimize edebilme yeteneği sunar (Hesami ve Jones, 2025). Bu esneklik, karmaşık ve deterministik olmayan veri setlerinin ele alınmasını kolaylaştırır. Ayrıca, ML modelleri mutlak konsantrasyonlar yerine, iyonlar arasındaki fizyolojik etkileşimleri yansıtan oranları hesaplama özellikleri olarak dönüştürerek, tahmine dayalı performansı artırmanın yanı sıra biyolojik açıdan anlamlı bilgiler üretme kapasitesine de sahiptir (Hesami ve Jones, 2025). Bu yetenek, ML'yi sadece bir tahmin aracı olmaktan çıkarıp, fizyolojik denge teorilerini doğrulayan veya keşfeden bir keşif aracı haline getirmektedir.

2.2. Hibrit Çok Amaçlı Optimizasyon Metodolojileri

Bitki Doku Kültürü'nde eşzamanlı ve çelişkili protokol hedeflerinin (örneğin, sürgün sayısını maksimize ederken fizyolojik anormallikleri minimize etmek) optimizasyonunu sağlamak için en ileri yaklaşım, tahmin algoritmalarının evrimsel optimizasyon algoritmaları ile entegrasyonudur (de-Carvalho ve ark., 2021; Jafari ve ark., 2023).

2.2.1. Metot Entegrasyonu:

YSA-GA Entegrasyonu: Yapay Sinir Ağları (YSA/ANN), girdi (ortam bileşimi) ve çıktı (sürgün kalitesi/büyümesi) arasındaki karmaşık, doğrusal olmayan ilişkileri modeller. Genetik Algoritma (GA) ise, YSA modeli tarafından tahmin edilen sonuçları kullanarak, istenen tüm hedefleri maksimize eden optimal girdi kombinasyonunu belirler (de-Carvalho ve ark., 2021).

GRNN-NSGA-II Entegrasyonu: Genel Regresyon Sinir Ağı (GRNN), genellikle MLP veya RBF gibi diğer sinir ağı modellerine göre üstün tahmin doğruluğu sergilemektedir (Jafari ve ark., 2023). Baskın Olmayan Sıralamalı Genetik Algoritma II (NSGA-II) ise, GRNN'nin tahminlerini kullanarak, Pareto optimum çözümler kümesini belirler. Böylece kontaminasyon oranını minimize etme ve çimlenme yüzdesini maksimize etme gibi çelişkili hedefleri eşzamanlı olarak çözebilir (Jafari ve ark., 2023). Bu hibrit metodolojiler, geleneksel tek amaçlı istatistiksel yaklaşımların biyolojik sistemlerin karmaşıklığını tam olarak yansıtamadığını göstermektedir.

2.3. Endüstriyel Otomasyon ve Robotik Sistemler

Robotik sistemler, yüksek verimli ve tutarlı mikroçoğaltma operasyonları sağlamak için AI'ın analitik gücü ile birleştirilmiştir (Tohme ve ark., 2024). Bu sistemlerin temel görevi, işgücü maliyetlerini azaltmak ve kalite tutarlılığını artırmaktır.

2.3.1. Robotik Platformlar:

(I) RoBoCut Sistemi: AI rehberli 3D görüntü tanıma kullanarak hijyenik kesme ve ayırma işlemleri için bir lazeri yönlendirir. Bu sistem, bitkicik başarısızlık oranlarını ve genel üretim maliyetlerini düşürür (Tohme ve ark., 2024).

(II) Janus Transplanter: Olgun bitkiciklerin steril laboratuvar ortamından *ex vitro* (steril olmayan) koşullara otomatik olarak aktarılmasını (transplantasyon) gerçekleştirir (Tohme ve ark., 2024).

(III) Otomatik Görüntü İşleme: AI destekli makine görüşü, büyüme oranları ve morfolojik özellikler gibi kritik parametreleri invaziv olmayan bir şekilde değerlendirir, ayrıca vitrifikasyon (hiperhidrisite) veya mikrobiyal kontaminasyon gibi fizyolojik streslerin erken belirtilerini objektif ve tutarlı bir şekilde tespit eder (Tohme ve ark., 2024; DL Contamination, 2023).

2.4. Hesaplamalı ve Teknolojik Uygulamaların Performans Metrikleri

İncelenen literatür, AI ve robotik sistemlerin Bitki Doku Kültürü süreçlerinde geleneksel metodolojilere göre belirgin bir üstünlük sağladığını ortaya koymaktadır.

Çok Amaçlı Optimizasyonda Kanıtlanmış Üstünlük
Hibrit Makine Öğrenimi (ML) ve Evrimsel Algoritma (EA) entegrasyonları, kültür ortamı bileşimi ve eksplant sterilizasyon protokolleri gibi temel Bitki Doku Kültürü süreçlerinin optimizasyonunda yüksek performans göstermiştir.

Ortam Formülasyonu: Kiwi berry (*Actinidia arguta*) üzerindeki çalışmalarda, YSA-GA entegrasyonu, standart ortamlara kıyasla hem sürgün büyümesini maksimize eden hem de bazal kallus (BC) ve hiperhidrisite (H) gibi fizyolojik anormallikleri önemli ölçüde azaltan optimize edilmiş bir mineral karışımı ("R ortamı") tahmin etmiştir (de-Carvalho ve ark., 2021).

Sterilizasyon Protokolleri: GRNN-NSGA-II metodolojisi, dezenfektan konsantrasyonu ve daldırma süresinin optimal seviyesini bulmak için kullanılmış ve kontaminasyon oranını minimize etme ile çimlenme yüzdesini maksimize etme gibi çelişkili hedefleri eşzamanlı olarak çözmede yüksek güvenilirlik kanıtlamıştır (Jafari ve ark., 2023). Bu bulgular, çok amaçlı biyolojik optimizasyonun etkin bir şekilde çözülebilmesi için hibrit algoritmaların gerekliliğini doğrulamaktadır.

Kallus İndüksiyonu: Petunya doku kültüründe, Çok Katmanlı Algılayıcı (MLP), Radyal Temelli Fonksiyon (RBF) ve Genel Regresyon Sinir Ağı (GRNN) algoritmaları kallus oluşumu indüksiyonunu tahmin etmek için karşılaştırılmış; GRNN'nin geleneksel istatistiksel yöntemlere kıyasla üstün tahmin doğruluğu sergilediği rapor edilmiştir (Jafari ve Daneshvar, 2023).

Yapay Zeka Destekli Görüntü Tanıma ve Kalite Kontrol
Derin Öğrenme teknikleri, kültürü invaziv olmayan bir şekilde izlemek ve kalite kontrolü sağlamak için kritik başarılar elde etmiştir (Guo ve ark., 2024; DL Contamination, 2023).

Gelişimsel Aşama Tanıma: Evrişimli Sinir Ağlarına (CNN'ler) dayalı çerçeveler, somatik embriyogenez (SE) aşamalarının (küresel, kalp, torpido ve kotiledon) otomatik olarak saptanması ve sınıflandırılması için transfer öğrenimi ve derin özellik çıkarma tekniklerini kullanmaktadır (Guo ve ark., 2024). Bu otomasyon, manuel seçimin öznelliğini ve yüksek işgücü yoğunluğunu ortadan kaldırarak SE aşamalarının tanımlanmasını standartlaştırmada kritik rol oynamaktadır (Guo ve ark., 2024).

Hastalık ve Stres Tespiti: CNN'ler, mikrobiyal kontaminasyonun otomatik tespiti konusunda yüksek doğruluk ve sağlamlık sergilemiştir (DL Contamination, 2023). Ayrıca, AI destekli makine görüşü, yüksek verimli sistemlerin ve kriyoprezervasyon canlılığının sınırlarını belirleyen vitrifikasyon (hiperhidrisite) gibi fizyolojik streslerin erken belirtilerini objektif ve tutarlı bir şekilde tespit eder (Popelka ve ark., 2023; Tohme ve ark., 2024). Bu erken tespit yeteneği, rejenerasyon yeteneğine sahip bitkicik yüzdesini doğrudan iyileştirmektedir.

Robotik Sistemlerin Operasyonel Verimlilik Etkisi
Robotik ve otomasyonun Bitki Doku Kültürüne entegrasyonu, laboratuvar operasyonlarını endüstriyel ölçeğe taşımıştır. Bu sistemlerin kullanılmasının temel ekonomik gerekçesi, mikroçoğaltımda toplam üretim maliyetinin **%50 ila %70'ini** oluşturabilen işgücü maliyetlerini önemli ölçüde azaltmaktır (Tohme ve ark., 2024).

RoBoCut ve Janus Transplanter: Yapay Zeka rehberli 3D görüntü tanıma kullanan RoBoCut sistemi, hijyenik kesim ve ayırma işlemlerinde bitkicik başarısızlık oranlarını ve genel üretim maliyetlerini düşürdüğü bildirilmiştir (Tohme ve ark., 2024). Janus Transplanter ise, *ex vitro* adaptasyon sürecinde olgun bitkicikleri otomatik olarak fide tepsilerine aktararak verimi artırmaktadır (Tohme ve ark., 2024). Robotik operasyonların hassasiyeti, manuel elleçlemeden kaynaklanabilecek mikrobiyal kontaminasyon riskini en aza indirerek kalite tutarlılığını sağlamlaştırmaktadır (Tohme ve ark., 2024).

Genom Düzenleme Hassasiyetinde İyileşme

Yapay Zeka, Bitki Doku Kültürü teknikleriyle sinerjik olarak çalışan CRISPR/Cas9 Genom Düzenleme Sistemi'nin genetik hassasiyetini artırmada önemli rol oynamaktadır (Chakraborty ve ark., 2022). Yapay Zeka'nin buradaki birincil uygulaması, hedef dışı (off-target) sekans konumlarını ve düzenleme sonuçlarını doğru bir şekilde tahmin etmektir (Chakraborty ve ark., 2022).

Model Karşılaştırması: CRISPR hedef dışı sekans tahminleri için bitki verileri üzerinde yapılan karşılaştırmalı analizler, **Random Forest (RF)** modelinin, geleneksel ML yöntemleri olan Destek Vektör Makineleri (SVM) ve Yapay Sinir Ağlarına (ANN) kıyasla bitki genom verilerinde daha iyi performans gösterdiğini ortaya koymuştur (Chakraborty ve ark., 2022). Bu bulgu, bitki genom yapısının benzersiz zorluklar sunduğunu ve memeli sistemlerinden elde edilen biyomedikal araçların basit adaptasyonu yerine, *bitki bilimlerine özgü* hesaplama modellerinin geliştirilmesi gerektiğini teyit etmektedir (Chakraborty ve ark., 2022).

Hesaplamalı Biyolojinin Sentezi ve Entegrasyon Zorlukları

Biyolojik Anlamlılığın Hesaplamalı Sentezi

Makine Öğrenimi modellerinin başarısı, yalnızca nicel tahminler yapma yeteneklerinden değil, aynı zamanda iyonlar arasındaki oranlar gibi fizyolojik etkileşimleri yansıtan yeni, türetilmiş özellikleri (özellik mühendisliği) öne çıkarma yeteneklerinden de kaynaklanmaktadır (Hesami ve Jones, 2025). Bu yaklaşım, AI'ın basitçe deneysel korelasyonların ötesine geçtiğini göstermektedir. ML, bitki performansını etkileyen altta yatan biyolojik mekanizmaları (örneğin, iyonik denge) doğrulayan veya keşfeden bir hipotez üreticisi olarak işlev görmektedir (Hesami ve Jones, 2025). Bu, Bitki Doku Kültüründe AI'ın benimsenmesinin, karmaşık biyolojik sistemlerin *doğasını modellemek* için bir zorunluluk olduğunu teyit etmektedir.

Ayrıca, Random Forest gibi özel algoritmaların CRISPR hedef dışı tahmininde üstünlük sağlaması (Chakraborty ve ark., 2022), bitki genomlarının karmaşık ve tekrar eden yapısının, genel amaçlı biyomedikal algoritmalar yerine, *fitosentrik* yani bitki merkezli hesaplama çözümlerinin geliştirilmesi gerektiğini açıkça ortaya koymaktadır (Chakraborty ve ark., 2022).

Şeffaflık ve Yorumlanabilirlik Engeli: Açıklanabilir Yapay Zeka (XAI)

Derin Öğrenme modellerinin yüksek tahmine dayalı doğruluk sunmasına rağmen, doğası gereği yorumlanabilir olmaması ("Kara Kutu" sorunu), bilimsel şeffaflık ve son kullanıcı (ıslahçılar, düzenleyiciler) güveni için önemli bir zorluk teşkil etmektedir (Wang ve ark., 2024). Biyolojik keşif, bir tahminin *neden* yapıldığını anlamayı gerektirir; bu, biyolojik bilgiyi ilerletmek için hayati öneme sahiptir.

Bu zorluğun üstesinden gelmek için Açıklanabilir Yapay Zeka (XAI) tekniklerinin entegrasyonu esastır (Wang ve ark., 2024). **SHAP (SHapley Additive exPlanations)** değer analizi gibi XAI teknikleri, tahminleri yönlendiren spesifik genetik lokusları veya çevresel değişkenleri tanımlayarak hem global hem de yerel yorumlanabilirlik sağlamaktadır (Wang ve ark., 2024). Yorumlanabilirlik, aynı zamanda düzenleyici uyumluluk için de kritik bir zorunluluktur; Yapay Zeka tarafından optimize edilen genom düzenleme çalışmalarının ticari ve politik kabulü için gerekli olan şeffaflığı (tahmini hangi faktörün yönlendirdiği) sağlamaktadır (Wang ve ark., 2024). Bu nedenle, XAI entegrasyonu, model tasarımının başlangıç aşamasından itibaren önceliklendirilmelidir.

Yapısal ve Sosyo-Ekonomik Zorluklar

Yapay Zeka sistemlerinin Bitki Doku Kültürü'ne entegrasyonu, veri altyapısı ve ekonomik engeller gibi önemli yapısal zorluklarla karşılaşmaktadır (Cabrera ve ark., 2023).

Veri Yönetimi ve Standardizasyon Zorlukları: Yapay Zeka modellerinin başarısı, yeterli, kaliteli ve standartlaştırılmış verilere erişime bağlıdır. Biyolojik ve tarımsal verilerin (genomik, fenomik) yüksek heterojenliği, farklı laboratuvarlar arasında tutarsız standardizasyonla birleşince, modellerin genelleştirilebilirliği için ciddi engeller oluşturmaktadır (Cabrera ve ark., 2023). Ayrıca, biyolojik materyaller ile Yapay Zeka uygulamaları için kullanılan dijital veriler arasında yeterli ve doğru "zemin doğrusu" bağlantısının kurulamaması, model geliştirme ve doğrulama için gerekli güvenilir verilerin elde edilmesini engellemektedir (Cabrera ve ark., 2023).

Stratejik Çözümler: Veri bütünlüğünü sağlamak ve genetik kaynakların güvenli, değişmez bir şekilde depolanmasını sağlamak amacıyla **Blockchain** teknolojisi gibi çözümlerin kullanılması teşvik edilmelidir (Elmushraf ve ark., 2023). Ayrıca, veri gizliliği endişelerini gidermek ve merkezi veri toplama ihtiyacı olmaksızın tescilli veri kümelerinde öğrenmeyi sağlamak için, **Federasyonlu Öğrenme (Federated Learning)** metodolojisi, gelecekteki araştırma yönelimleri arasında yer almalıdır (Guo ve ark., 2024). Robotik sistemlerin entegrasyonu, Yapay Zeka modellerinin kronik veri açığını kapatmak için gereken yüksek hacimli, standardize edilmiş veriyi sağlayan zorunlu bir altyapıyı oluşturmaktadır (Tohme ve ark., 2024).

Yüksek Başlangıç Maliyetleri ve İşgücü Dönüşümü: Sofistike robotik sistemlerin ve özel AI altyapısının uygulanmasının getirdiği yüksek ilk yatırım maliyetleri, özellikle küçük ölçekli operasyonlar için önemli bir giriş engeli oluşturmaktadır (Tohme ve ark., 2024; Cabrera ve ark., 2023). Otomasyon, manuel işgücünü azaltırken, robotik, hesaplama ve AI modelleme uzmanlığına sahip yeni bir uzman işgücü talebi yaratır (Tohme ve ark., 2024). Bu, personel becerilerini yeniden geliştirmek için önemli yatırımlar gerektirmekte ve kamu veya kişisel verilerden elde edilen faydaların eşit olmayan dağıtılmasıyla karakterize edilen "Dijital feodalizm" riskini beraberinde getirmektedir (Cabrera ve ark., 2023).

SONUÇ

Bitki Doku Kültüründe Yapay Zeka ve Makine Öğrenimi entegrasyonu, alanın temelden dönüşümünü sağlamış ve endüstriyel ölçekte ilerlemesi için kritik bir paradigmayı temsil etmektedir. Geleneksel Tek Faktörlü Denemeler (OFAT) ve Cevap Yüzeyi Metodolojisi (RSM) gibi yöntemlerin sınırlamalarının aksine, hibrit algoritmik modeller (YSA-GA ve GRNN-NSGA-II) kültür ortamı bileşenlerinin hassas formülasyonunda ve eksplant sterilizasyon protokollerinin çok amaçlı optimizasyonunda kanıtlanmış bir üstünlük sergilemiştir (de-Carvalho ve ark., 2021; Jafari ve ark., 2023).

Derin Öğrenme teknikleri, özellikle Evrişimli Sinir Ağları, somatik embriyogenez aşama tanıma ve mikrobiyal kontaminasyon tespiti gibi süreçlerde yüksek hız ve nesnellik sağlayarak kalite kontrol süreçlerini dönüştürmüştür (Guo ve ark., 2024; DL Contamination, 2023). Robotik sistemlerin (RoBoCut, Janus Transplanter) otomasyonu, işgücü maliyetlerini %50-70 oranında azaltarak operasyonel verimliliği artırmakta ve Yapay Zeka modellerinin eğitimi için gereken yüksek kaliteli, standardize edilmiş veriyi sağlamaktadır (Tohme ve ark., 2024). Genetik hassasiyet alanında ise, Random Forest gibi fitosentrik ML modellerinin CRISPR/Cas9 hedef dışı sekans tahminini iyileştirdiği görülmüş, bu da bitki sistemlerine özgü hesaplama çözümlerinin gerekliliğini pekiştirmiştir (Chakraborty ve ark., 2022).

Gelecek Araştırmaları ve Stratejik Öneriler

Yapay Zeka'nin Bitki Doku Kültürü'daki potansiyelinin tamamını gerçekleştirmek ve mevcut yapısal engellerin üstesinden gelmek için aşağıdaki stratejik adımların atılması zorunludur:

Açıklanabilir Yapay Zeka (XAI) Entegrasyonunun Zorunlu Kılınması: Biyolojik keşfi artırmak, altta yatan fizyolojik mekanizmaları anlamak ve Yapay Zeka güdümlü ürünlerin ticari/düzenleyici kabulünü sağlamak amacıyla, SHAP gibi XAI metodolojilerinin tahmine dayalı model geliştirmede öncelikli olarak entegre edilmesi gerekmektedir (Wang ve ark., 2024). XAI, bilimsel şeffaflığı güvence altına almanın temel aracıdır.

Küresel Veri Standardizasyonunun ve Güvenli Altyapıların Kurulması: Veri heterojenliği engellerinin üstesinden gelmek için küresel veri standardizasyon protokolleri acilen zorunlu kılınmalıdır (Cabrera ve ark., 2023). Ayrıca, Federasyonlu Öğrenme metodolojisinin uygulanması, merkezi veri paylaşımı gerekmeksizin model genelleştirilebilirliğini artıracaktır (Guo ve ark., 2024). Blockchain gibi teknolojiler, kritik genetik ve kültürel verilerin güvenliğini ve değişmezliğini sağlamalıdır (Elmushraf ve ark., 2023).

Disiplinlerarası İşgücü Gelişimine Stratejik Yatırım: Bitki Bilimi, Robotik ve Hesaplamalı Biyoloji kesişiminde uzmanlaşmış yeni bir profesyonel nesil yetiştirilmelidir (Tohme ve ark., 2024). Bu, hem laboratuvar otomasyonunu yönetmek hem de Yapay Zeka modellerini geliştirmek ve yorumlamak için kritik öneme sahiptir. Yüksek teknolojiye geçişin getirdiği "Dijital feodalizm" riskini azaltmak amacıyla, hesaplama ve modelleme platformlarına erişimin adil dağılımı sağlanmalıdır (Cabrera ve ark., 2023).

KAYNAKLAR

Ali, M., Aasim, M., Jaleel, H., Hassan, M., Sarwar, F., Aslam, M., ve Ahmar, S. (2023). The role of bigdata and artificial intelligence in plant breeding. *The Frontiers Collection*.

Automata. (2024). Can automation help with plant tissue culture (White paper). *News-Medical*.

Cabrera, G., Al-Mansoori, S., Al-Otaibi, M., Al-Sayari, S., ve Bahl, S. (2023). Artificial intelligence in plant biotechnology: Recent trends, challenges, and perspectives. *MDPI*.

Chakraborty, A., Kumar, S., Nambi, S. K., ve Sharma, M. (2022). Development of machine learning-based models for the prediction of CRISPR-cas9 off-target sites for plant genomes. *Frontiers in Genetics, 13*.

de-Carvalho, A. J. M. S., Marques, S. M., Varela, N. S., ve Peixe, A. (2021). Artificial neural networks-genetic algorithms optimize mineral medium for Actinidia arguta in vitro micropropagation. *Frontiers in Plant Science, 12*.

DL Contamination. (2023). Microbial colony detection based on deep learning. *Applied Sciences, 13*(19), 10568.

Elmushraf, K., Ahmad, N., Alghamdi, A., ve Hassan, M. (2023). Enhancing crop yield prediction and genetic resource integrity using advanced technologies. *Exploration of Food & Foodstuffs, 3*.

Guo, X., Zhang, H., Wu, Y., ve Chen, J. (2024). The integration of artificial intelligence and next-generation sequencing: A review of current applications and future directions. *Genes, 15*(4), 450.

Hesami, M., ve Jones, A. M. P. (2025). A comprehensive guide to machine learning-mediated optimization of medium composition for enhanced in vitro performance. *Biocatalysis and Agricultural Biotechnology, 56*, 103810.

Hessami, M., Alkhayri, J. M., ve Al-Mubarak, A. (2023). Hybrid optimization approaches in plant tissue culture. *Sustainable Futures, 56*(1), 122.

Jafari, A., ve Daneshvar, M. (2023). Modeling and predicting callogenesis in petunia tissue culture using machine learning algorithms. *Biocatalysis and Agricultural Biotechnology, 54*, 10624318.

Jafari, M., Naderi, R., ve Tohidfar, M. (2023). Modeling and optimizing sterilization protocol for in vitro culture using GRNN-NSGA-II. *Planta, 257*(5), 104.

Popelka, J., Zámečník, J., ve Stolařová, M. (2023). Donor plant vigor as a crucial factor for successful plant cryopreservation by droplet vitrification. *Frontiers in Plant Science, 14*.

Tohme, A., Hajjami, M., Al-Hashem, H., ve Chen, M. (2024). The future of plant tissue culture: Inside the rise of automation and robotics. *Plant Cell Technology Blog*.

Viscon Technology. (2023). *Viscon Plant Technology Brochure. Viscon Group*.

Wang, L., Zhang, Y., ve Li, S. (2024). Explainable AI (XAI) for interpretability in genomic selection and crop prediction. *Frontiers in Plant Science, 15*.

ORAL PRESENTATION

Pulmoner fibrosizte antioksidan genlerin düzenlenmesi-bir derleme çalışması

Pınar Aksoy[1*] (https://orcid.org/0000-0002-9265-0611),
Önder Yumrutaş[2](https://orcid.org/0000-0002-9265-0611),
Muhittin Doğan[3] (https://orcid.org/0000-0002-9265-0611)

[*1]Gaziantep Üniversitesi, Fen Edebiyat Fakültesi, Biyoloji Bölümü, Gaziantep, Türkiye
[2]Adıyaman Üniversitesi, Tıp Fakültesi, Tıbbi Biyoloji Anabilim Dalı, Adıyaman, Türkiye
[3]Gaziantep Üniversitesi, Fen Edebiyat Fakültesi, Biyoloji Bölümü, Gaziantep, Türkiye

*Sorumlu yazar e-mail: pnr.aksoy.pnr@gmail.com

Özet

Pulmoner fibroz, ilerleyici interstisyel akciğer hastalıklarının önemli bir grubunu oluşturur ve oksidatif stres, hastalığın patogenezinde merkezi bir role sahiptir. Antioksidan genler, reaktif oksijen türlerini (ROS) nötralize eden enzimleri kodlayarak hücresel redoks dengesinin korunmasını sağlar. Bu derleme çalışmasında, pulmoner fibrozis bağlamında antioksidan genlerin düzenlenmesi ve ilgili genlerin fonksiyonları literatür eşliğinde sunulmaktadır.

Anahtar Kelimeler: Pulmoner fibroz, Nrf2, antioksidan genler, oksidatif stres, HO-1, NQO1, oxidative stress response, antioxidant enzymes, idiopathic pulmonary fibrosis

Regulation of antioxidant genes in pulmonary fibrosis- a review

Abstract

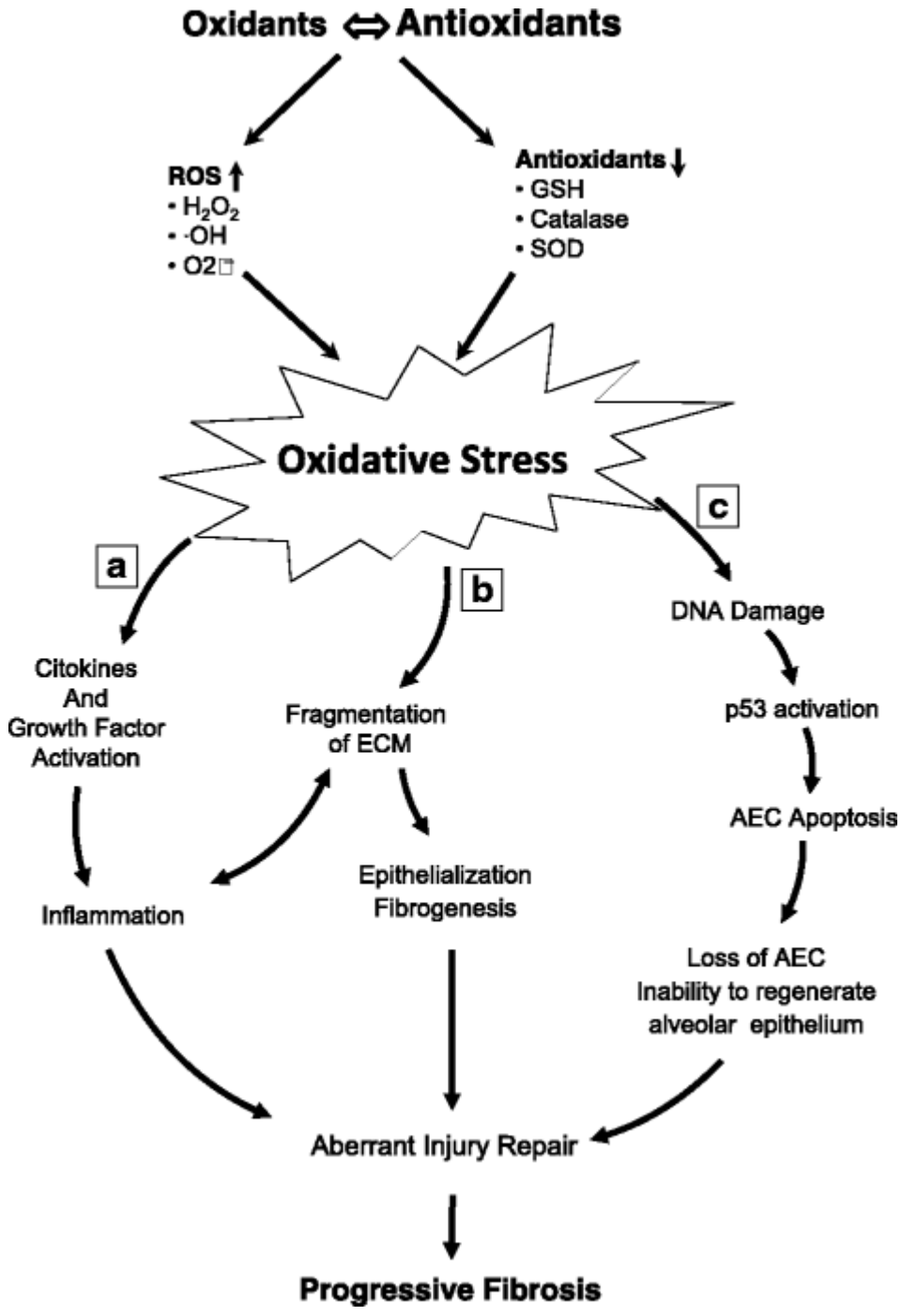
Pulmonary fibrosis constitutes a major group of progressive interstitial lung diseases, and oxidative stress plays a central role in its pathogenesis. Antioxidant genes help maintain cellular redox homeostasis by encoding enzymes that neutralize reactive oxygen species (ROS). In this review, the regulation of antioxidant genes in the context of pulmonary fibrosis and the functions of the related genes are presented based on current literature.

Keywords: Pulmonary fibrosis, Nrf2, antioxidant genes, oxidative stress, HO-1, NQO1, oxidative stress response, antioxidant enzymes, idiopathic pulmonary fibrosis

GİRİŞ

Pulmoner fibroz, akciğer parankiminde ilerleyici fibroblast aktivasyonu ve aşırı ekstrasellüler matriks (ECM) birikimi ile karakterize kronik bir hastalıktır. Patogenezinde oksidatif stres, inflamasyon ve epitel-mezenkimal geçiş (EMT) gibi süreçler önemli rol oynamaktadır (Kinnula ve ark., 2005; Makena ve ark., 2023; Luo ve ark., 2024). Özellikle reaktif oksijen türlerinin (ROS) aşırı üretimi, epitel hücrelerinde hasara, fibroblast proliferasyonuna ve fibrotik yanıtın artmasına neden olur. Bu süreçlerin kontrolünde antioksidan savunma sistemleri ve bu sistemleri düzenleyen genler kritik öneme sahiptir. Akciğer, oksidanlara karşı oldukça gelişmiş bir savunma mekanizmasına sahiptir. Bu mekanizma; glutatyon, vitaminler, ürik asit gibi küçük moleküllü antioksidanlar, metal bağlayıcı proteinler (transferrin, laktoferrin, metallotiyonin) ve antioksidan enzimlerden oluşur. Hücre içi ve dışı düzeyde süperoksit ve hidrojen peroksit gibi reaktif türlerin detoksifikasyonu; glutatyon ilişkili enzimler, katalaz, glutatyon-S-transferazlar ve tioredoksin-peroksiredoksin sistemi gibi enzimatik yollarla sağlanır. Bu enzimler bronşiyal ve alveolar epitel hücreleri ile alveolar makrofajlarda yoğun olarak bulunur. Ancak, oksidatif yanıtın zayıflaması veya bu enzimlerin inaktivasyonu redoks dengesini bozarak pulmoner fibrozisin ilerlemesine katkıda bulunabilir (Paliogiannis ve ark., 2018). Artan kanıtlar, idiopatik pulmoner fibroz (İPF) patogenezinde oksidatif stresin belirleyici bir faktör olduğunu göstermektedir. Oksidatif stres; oksidan üretimi ile antioksidan savunma arasındaki dengenin oksidanlar lehine bozulması sonucu ortaya çıkar ve hücresel fonksiyon bozukluğu ile doku hasarına yol açar. Akciğer, yüksek oksijen

gerilimlerine maruz kalması nedeniyle bu strese karşı özellikle hassastır (Fois ve ark., 2020). Bu nedenle, antioksidan genlerin ekspresyonunun düzenlenmesi, oksidatif stresin dengelenmesi ve fibrotik süreçlerin yavaşlatılması açısından büyük önem taşımaktadır. Oksidatif stresin bu süreçlerdeki merkezi rolü, çeşitli patojenik mekanizmalar üzerinden açıklanabilir (Şekil 1).



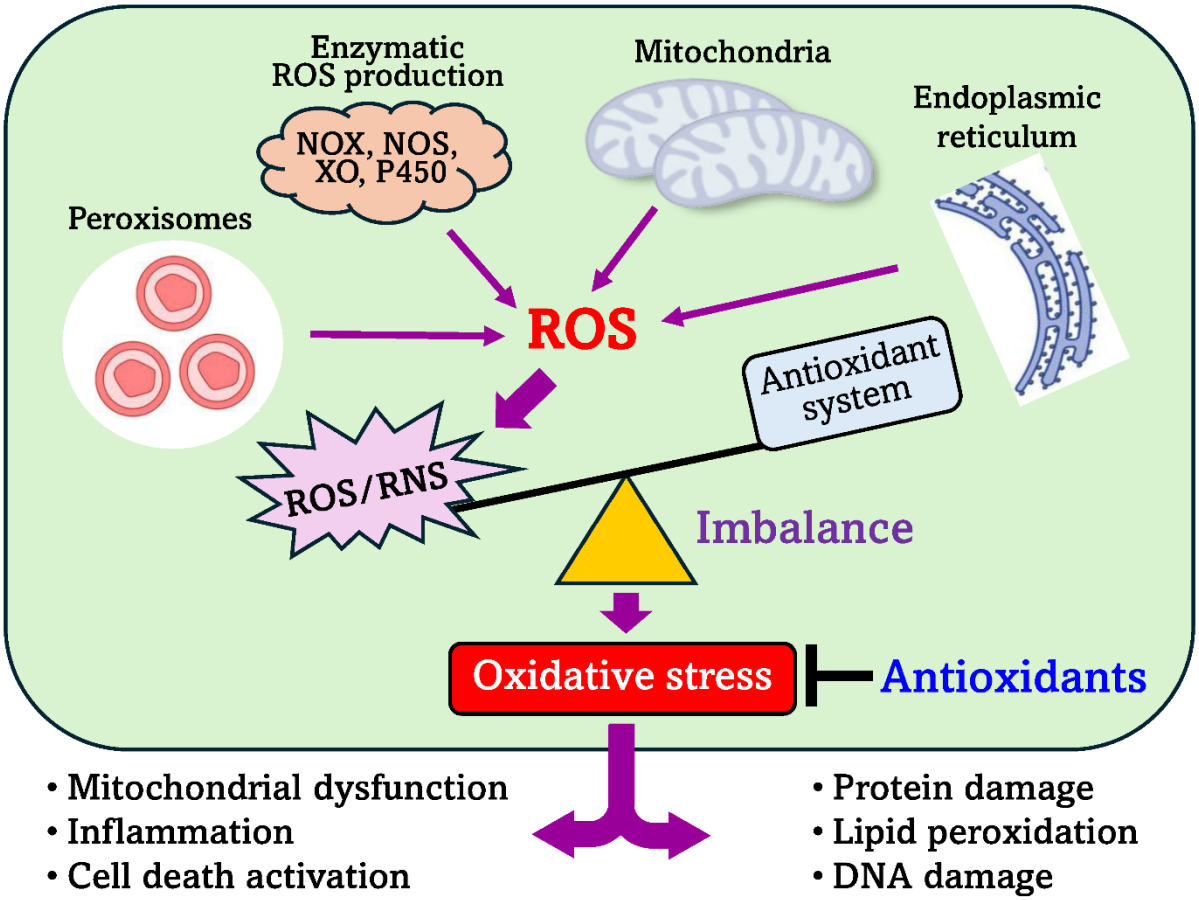
Şekil 1'de, oksidatif stresin tetiklediği bu patojenik mekanizmalar şematik olarak gösterilmektedir.

Oksidatif stres, İPF'nin patogenezinde kritik bir rol üstlenmektedir. Bu durum birkaç temel mekanizma ile açıklanabilir:
a) Sitokin ve büyüme faktörü üretimini artırarak inflamasyonu teşvik eder.
b) Hücre dışı matriksin parçalanmasını ve miyofibroblast farklılaşmasının artmasını tetikleyerek fibrogenez ve epitelizasyona yol açar.
c) DNA hasarı ve p53 aktivasyonunun bir sonucu olarak, ROS hava yolu epitel hücrelerinde apoptozu indükler ve alveolar epitelin yenilenme kapasitesini bozar.

Bu patolojik değişiklikler, pulmoner fibrozisin ilerlemesine önemli ölçüde katkıda bulunmaktadır (Fois et al., 2020).

ANTİOKSİDAN GENLERİN TANIMI ve ÖNEMİ

Antioksidan genler, oksidatif stresin düzenlenmesinde kilit rol oynar ve bu nedenle pulmoner fibrozis patogenezinde kritik öneme sahiptir. Hücresel sağlığın korunması için reaktif oksijen türleri (ROS) üretimi ile antioksidan savunma mekanizmaları arasındaki dengenin sağlanması kritik öneme sahiptir. Hücreler, sitoplazma ve organellerde ROS'u nötralize ederek redoks homeostazını koruyan enzimatik ve enzimatik olmayan bileşenlerden oluşan güçlü bir antioksidan savunma sistemine sahiptir. Enzimatik antioksidanlar arasında süperoksit dismutaz (SOD), katalaz (CAT), glutatyon peroksidaz (GPx) ve glutatyon redüktaz yer alır. Enzimatik olmayan antioksidanlar ise glutatyon (GSH), ubikinon (koenzim Q10), C ve E vitaminleri, alfa-lipoik asit ve tioredoksinlerdir. Bu bileşenler, aşırı ROS birikimini önleyerek oksidatif stresi azaltır ve hücresel redoks homeostazının korunmasına katkıda bulunur. ROS düzeyinin antioksidan kapasitenin üzerine çıkması, oksidatif hasara yol açarak çeşitli patolojik süreçleri başlatabilir.



Şekil 2: Hücre içi ROS kaynakları ve oksidatif stresin sonuçları. Ayrıntılar için metne bakınız. **Kısaltmalar:** NOS, nitrik oksit sentaz; NOX, NADPH oksidazlar; XO, ksantin oksidaz.

Son otuz yılda yapılan çalışmalar, ROS'un yalnızca zararlı bir yan ürün olmadığını, aynı zamanda hücre içi sinyal iletiminde önemli roller üstlendiğini ortaya koymuştur. ROS, bakterisidal aktivite, metabolik reaksiyonlar ve gen ekspresyonu gibi kritik hücresel işlevleri düzenler. Son on yılda artan kanıtlar, ROS'un fizyolojik adaptasyon ve savunma yanıtlarında da görev aldığını göstermektedir. Bu durum, antioksidanların aşırı ROS'u ortadan kaldırırken bazı fizyolojik süreçleri de etkileyebileceğini düşündürmektedir. Antioksidanların faydası, genellikle ROS seviyelerinde veya oksidasyon ürünlerinde azalma yoluyla hücre ve dokularda oksidatif hasarı önlemelerinden kaynaklanır (Kozlov ve ark., 2024). ROS, hem endojen (mitokondri, NADPH oksidazlar) hem de eksojen (radyasyon, bazı ilaçlar, gıdalar, sigara dumanı, çevresel kirlilik) kaynaklardan üretilir. Bu kaynaklardan artan ROS/RNS üretimi, oksidatif stres olarak bilinen zararlı duruma neden olur. Pek çok kronik hastalığın kökeninde farklı faktörler yer alsa da, bu hastalıklar için ortak payda

oksidatif strestir. Oksidatif stresin zararlı etkilerinin azaltılmasında antioksidan enzimler (SOD, katalaz, GPx) ve düşük molekül ağırlıklı antioksidanlar (C ve E vitaminleri, flavonoidler, karotenoidler, melatonin, ergotionin vb.) birlikte görev yapar. İnsan vücudundaki oksijenin yaklaşık %4–5'i biyolojik indirgeyiciler tarafından ROS'a dönüştürülür. Özellikle yüksek oksijen basıncına maruz kalan hücreler sürekli ROS saldırısı altındadır ve bu durum güçlü bir antioksidan savunma gerektirir **(Jomova ve ark., 2023)**

Antioksidanlar İki Ana Grupta Sınıflandırılır:

Antioksidan enzimler: ROS'u daha stabil ve daha az zararlı bileşiklere dönüştüren protein/metaloproteinlerdir. SOD, katalaz ve GPx en kritik olanlarıdır.

Düşük molekül ağırlıklı antioksidanlar: C vitamini, E vitamini, karotenoidler, flavonoidler ve glutatyon gibi bileşenleri içerir (Jomova ve ark., 2023).

ROS üretiminin artmasıyla NF-κB ve AP-1 gibi transkripsiyon faktörleri aktive olur. Bu faktörler, TNF-α ve IL-6, IL-8 gibi proinflamatuar sitokinlerin transkripsiyonunu artırarak nötrofil ve makrofajları aktive eder; böylece inflamatuar yanıt oluşur (Drost ve ark., 2005; Federico ve ark., 2007). Lökositler patojenleri yok etmek için süperoksit, hidroksil radikali ve peroksinitrit gibi ROS üretir. Ancak ROS'un döngüsel ve aşırı üretimi kronik inflamasyonu teşvik ederek DNA hasarına, mutasyonlara ve tamir mekanizmalarının bozulmasına yol açabilir. Bu nedenle, antioksidan genler, oksidatif stresin yol açtığı hücresel hasarı sınırlayarak pulmoner fibrozis gibi kronik hastalıkların gelişiminde merkezi bir rol oynamaktadır.

PULMONER FİBROSİZDE ÖNE ÇIKAN ANTİOKSİDAN GENLER VE DÜZENLEYİCİLERİ

Antioksidan Genlerin Ana Düzenleyicisi:

NFE2L2 (Nrf2)

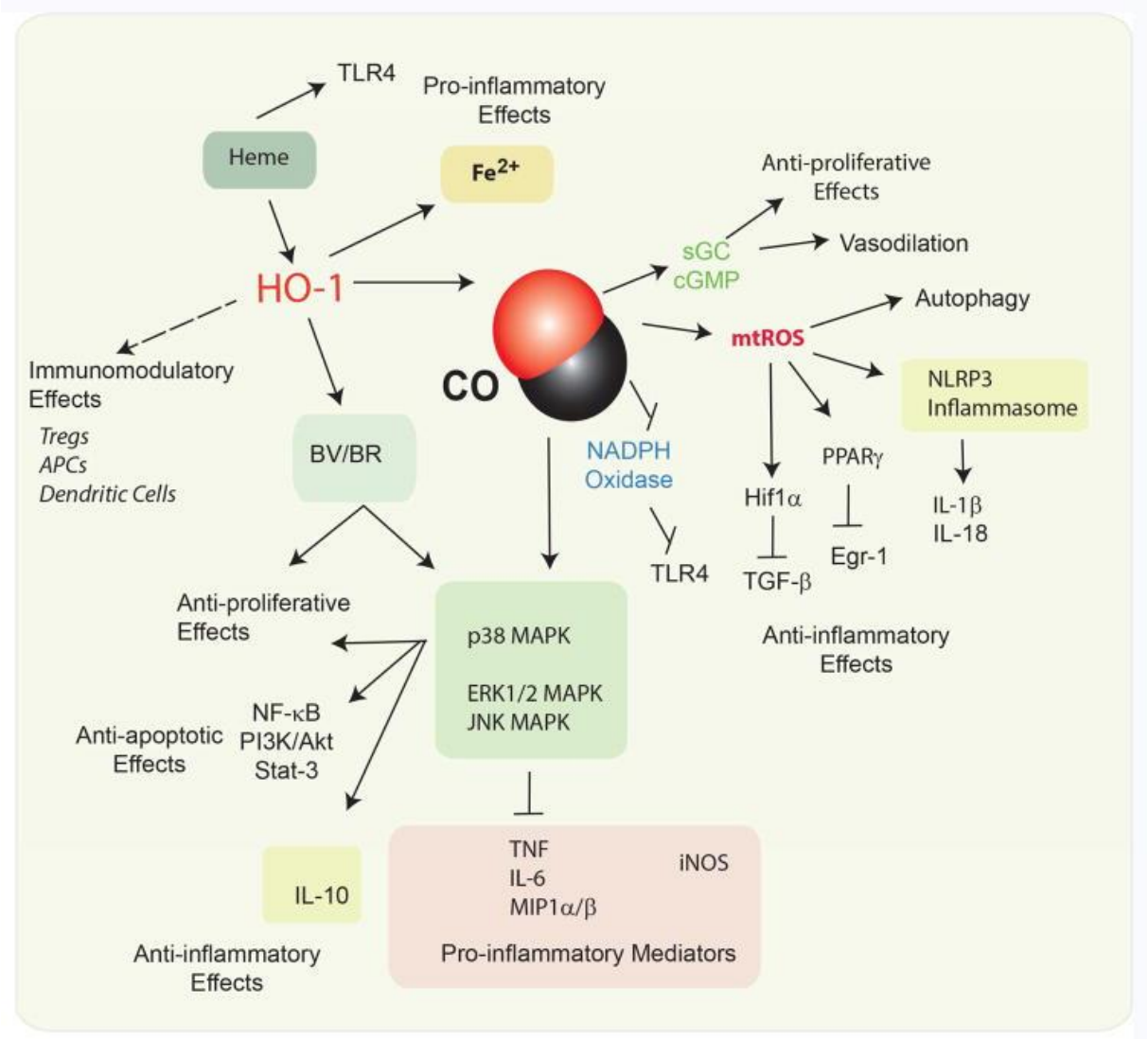
Nükleer faktör eritroid 2 ile ilişkili faktör 2 (Nrf2), oksidatif stres yanıtının ana düzenleyicisi ve kritik bir transkripsiyon faktörüdür. Antioksidan yanıt elemanı (ARE) içeren genlerin ekspresyonunu düzenleyerek glutatyon S-transferaz (GST), NAD(P)H kinon oksidoredüktaz 1 (NQO1), heme oksijenaz-1 (HO-1), GCLC ve GCLM gibi antioksidan enzimlerin sentezini artırır ve hücreleri oksidatif hasara karşı korur **(Vézina ve Cantin, 2018; Ma, 2013).** Nrf2, CNC-bZIP ailesine ait bir transkripsiyon faktörüdür ve bronşiyal ile alveoler epitel hücreleri, alveoler makrofajlar ve hücre dışı ortamda lokalize edilen birçok antioksidan pulmoner proteinin ekspresyonunu kontrol eder. Normal koşullarda Nrf2, Keap1 proteini tarafından sitoplazmada tutulur. Oksidatif stres varlığında Keap1 modifiye olur, Nrf2 serbest kalarak çekirdeğe taşınır ve hedef genleri aktive eder. Bu mekanizma, hücreleri oksidan yüküne karşı koruyan kritik bir adaptif yanıt oluşturur. İPF modellerinde Nrf2'nin önemi, eksikliğinin bleomisin kaynaklı pulmoner fibrozu önemli ölçüde artırdığı deneylerle gösterilmiştir. Nrf2 eksikliği, bleomisin ile indüklenen pulmoner fibrozis modellerinde hayatta kalma oranını düşürür, oksidatif stres göstergelerini artırır ve fibrotik yanıtı şiddetlendirir (Raghu ve ark., 2011; Cho ve ark., 2002). Nrf2 agonistleri, antioksidan gen ekspresyonunu artırarak oksidatif stres kaynaklı hasarın azaltılmasında ve fibrotik hastalıkların önlenmesinde potansiyel terapötik hedef olarak değerlendirilmektedir. Ayrıca Nrf2, faz 2 detoksifiye edici enzimlerin ve çeşitli antioksidan enzimlerin ARE aracılı transkripsiyonel aktivasyonu yoluyla karsinogenez ve oksidatif strese karşı hücresel savunmada önemli rol oynar. Özetle, Nrf2, pulmoner fibroziste oksidatif stresin yol açtığı hücresel hasarı sınırlayan ve antioksidan gen ekspresyonunu düzenleyen merkezi bir transkripsiyon faktörüdür.

PULMONER FİBROZDA ÖNE ÇIKAN ANTİOKSİDAN GENLER

HMOX1 (HO-1)

HMOX1, heme oksijenaz-1 (HO-1) enzimini kodlar ve heme'in parçalanmasıyla biliverdin, serbest demir ve karbon monoksit (CO) üretir. Bu ürünler, antioksidan ve antiinflamatuvar etki gösterir ve genellikle Nrf2 tarafından indüklenir (Ryter ve Choi, 2016). Heme oksijenaz-1 (HO-1), heme metabolizmasında kritik bir basamak olan oksidatif yıkımı katalize ederek biliverdin ve karbon monoksit gibi biyolojik olarak aktif ürünlerin oluşumunu sağlar; bu ürünler antioksidan ve antiinflamatuvar işlevlere sahiptir. Dokuda HO-1

ekspresyonunun artışı, artmış inflamasyon veya oksidatif stres ile ilişkilidir ve akut akciğer hasarı (ALI) ile iskemi/reperfüzyon (I/R) modellerinde gözlenmiştir. HO-1'in sitoprotektif etkileri, heme'nin prooksidan özellik göstermesinin önlenmesi ve biyolojik olarak aktif ürünlerin oluşumu ile açıklanabilir. HO-1 ürünleri, farmakolojik uygulamalarda da inflamasyonu azaltarak doku koruyucu etkiler gösterir. HO-1, antijen sunan hücreler, dendritik hücreler ve düzenleyici T hücrelerinin fonksiyonlarını modüle ederek immün yanıtı etkileyebilir. Heme pro-inflamatuar etki gösterirken, HO-1 ürünleri inflamasyonu baskılar. CO, apoptotik, proliferatif ve inflamatuar hücresel programları düzenler; pro-inflamatuar sitokinlerin (IL-1β, IL-6, TNFα, Mip1α/β) üretimini azaltır ve anti-inflamatuar sitokin IL-10'u artırır. Bu etkiler, özellikle p38 MAPK yolaklarındaki değişikliklerle ilişkilidir. CO ayrıca mitokondriyal ROS üretimini uyararak otofajiyi teşvik edebilir, HIF-1α'yı aktive edebilir ve pro-inflamatuar transkripsiyon faktörü Egr1'i baskılayabilir. Son kanıtlar, CO'nun NLRP3 inflamatuar aktivasyonunu ve IL-1β ile IL-18 üretimini modüle edebileceğini göstermektedir. HO-1 reaksiyonunun bir diğer ürünü olan bilirubin (BR) anti-enflamatuar ve anti-proliferatif etkilere sahiptir. Bu mekanizmalar, HO-1'in pulmoner fibrozis ve oksidatif stres kaynaklı akciğer hasarında koruyucu rolünü vurgular (Ryter ve Choi, 2016). In vitro çalışmalar, epitel hücreleri, fibroblastlar, makrofajlar ve düz kas hücrelerinde hiperoksi sonrası HO-1 gen ekspresyonunun arttığını göstermiştir. Bu artışın nedeni, mRNA stabilitesinden ziyade HO-1 gen transkripsiyonunun yükselmesidir (Lee ve ark., 1996). Özetle, HO-1, reaksiyon ürünleri aracılığıyla oksidatif stres ve inflamasyonun yol açtığı akciğer hasarını sınırlayan merkezi bir koruyucu mekanizmadır.



NQO1

NQO1, NAD(P)H kinon redüktaz 1 enzimini kodlar ve kinonları toksik serbest radikallere dönüşmeden indirger. Bu mekanizma, oksidatif stresin zararlı yan ürünlerini detoksifiye ederek akciğer dokusunun korunmasına katkıda bulunur (Ma, 2013). NQO1, ARE-güdümlü antioksidan genler arasında öne çıkar ve hücreleri oksidatif stres ile elektrofillerin toksisitesine karşı korur. Pulmoner fibroziste, akciğer epitel ve fibroblastları artan ROS'a maruz kaldığında Nrf2 aktivasyonu tetiklenir ve NQO1 ekspresyonu yükselir. Bu artış, lipid peroksidasyonu ve DNA hasarını azaltarak fibroblast aktivasyonunu sınırlar **(Ma, 2013; Ryter ve Choi, 2016).** Sonuç olarak, NQO1, pulmoner fibroziste adaptif antioksidan yanıtın kritik bir bileşeni olarak işlev görür.

SOD1/SOD2

Süperoksit dismutazlar (SOD), süperoksit radikallerini hidrojen peroksite dönüştürerek hücreyi oksidatif hasardan korur. SOD2 özellikle mitokondride lokalizedir ve mitokondri kaynaklı ROS'un birikimini azaltır. Pulmoner fibrozda, SOD2 ekspresyonunun azalması mitokondriyal disfonksiyonla ilişkilendirilmiştir (Wang ve ark., 2025). İdiyopatik pulmoner fibroziste (İPF), SOD2 genellikle düşük ifade edilirken, SOD1'in biraz artmış olabileceği yönünde bulgular mevcuttur. Veith (2019), SOD1'in İPF'de arttığını ve SOD1 geninin yokluğunda farelerin asbest maruziyetine karşı daha az oksidatif stres geliştirdiğini bildirmiştir. Epigenetik baskılama yoluyla SOD2 ekspresyonunun azalması, mitokondriyal ROS birikimini artırarak pulmoner fibrozisi şiddetlendirebilir. Bu mekanizma, mitokondriyal oksidatif stresin artmasına ve fibrozisin ilerlemesine katkıda bulunmaktadır (Wang ve ark.,2025). Antioksidan tedavilerin etkinliği üzerine yapılan bir meta-analiz, tek başına veya kombinasyon halinde SOD kullanımını değerlendirmiştir. (Kandhare ve ark.,2016) tarafından gerçekleştirilen çalışmada, lesitinleştirilmiş SOD dahil olmak üzere antioksidan monoterapinin DLCO (karbon monoksitin yayılma kapasitesi) üzerinde belirgin bir etkisi olmadığı, ancak kombine antioksidan tedavinin hayati kapasite ve DLCO'da monoterapiden daha etkili olabileceği gösterilmiştir. Bununla birlikte, bu faydalar ölüm oranı veya advers olaylarda anlamlı farklılık yaratmamıştır (Fois ve ark., 2018). Özetle, SOD1 ve SOD2, süperoksit radikallerini detoksifiye ederek pulmoner fibroziste oksidatif stresin yol açtığı hücresel hasarı sınırlayan ve mitokondriyal fonksiyonları koruyan temel antioksidan enzimlerdir. Bu genlerin ekspresyon düzeyleri ve düzenlenmesi, fibrotik sürecin şiddetini doğrudan etkileyebilir.

CAT(KATALAZ)

Hidrojen peroksiti su ve oksijene dönüştürür ve SOD aktivitesinin ürettiği H_2O_2'yi detoksifiye eder. Katalaz, tercihen bronşiolar ve alveolar epitel hücrelerinde eksprese edilir ve normal akciğerlerde endojen bir antioksidan enzim olarak işlev görür. Odajima ve arkadaşlarının (2010) çalışmasında, pulmoner fibrozisli insan akciğerlerinde katalaz ekspresyonunun ve aktivitesinin azaldığı gösterilmiştir. Bu azalma, bronşiolar epitel hücrelerinde ve fibrotik alanlarda anormal re-epitelizasyonla ilişkilendirilmiştir. Katalaz enzimi, hücre içi hidrojen peroksiti zararsız bileşenler olan su ve oksijene indirger, böylece oksidatif stresin neden olduğu potansiyel doku hasarını sınırlamada kritik bir görev üstlenir. Pulmoner fibrozda katalazın yetersiz aktivitesi hastalık ilerlemesini artırabilir (Odajima ve ark., 2010). Katalaz, hücrelerdeki hidrojen peroksiti su ve oksijene dönüştüren bir enzimdir ve bu özelliğiyle hücreyi oksidatif stresten korur. Süperoksit dismutaz (SOD), süperoksit radikalini H_2O_2'ye dönüştürürken, katalaz bu H_2O_2'yi zararsız su ve oksijene çevirir. Bu iki enzim arasındaki işbirliği, hücredeki oksidatif dengenin korunmasında kritik bir rol oynar (Nandi ve ark., 2019). Shi ve arkadaşlarının (2013) çalışmasında, katalaz tedavisi uygulanan farelerde histolojik olarak azalmış fibrozis, bronkoalveoler lavaj (BAL) sıvısında azalmış kolajen seviyeleri ve azalmış inflamasyon gözlemlenmiştir. Bu bulgular, katalazın pulmoner fibrozisi azaltmada potansiyel bir terapötik ajan olarak rol oynayabileceğini göstermektedir (Shi ve ark., 2013). Özetle, katalaz, süperoksit dismutaz tarafından üretilen hidrojen peroksiti zararsız bileşenlere dönüştürerek hücreyi oksidatif stresten koruyan kritik bir enzimdir. Pulmoner fibroziste katalazın yetersiz aktivitesi, oksidatif hasarın artmasına ve hastalık progresyonuna katkıda bulunabilir; bu nedenle katalaz hem patogenez anlayışında hem de potansiyel terapötik stratejilerde merkezi bir rol oynar.

GCLC/GCLM

GCLC ve GCLM, glutatyon sentezinin hız kısıtlayıcı enzim alt birimleridir. Nrf2 aktivasyonu ile ekspresyonları artar ve hücre içi glutatyon havuzunun yenilenmesini sağlar, böylece oksidatif stresin yol açtığı hasara karşı kritik bir savunma mekanizması oluşturur. Pulmoner fibroz modeli olarak kullanılan fare akciğerinde, Transforming Growth Factor β1 (TGF-β1), glutatyon (GSH) sentezinde hız sınırlayıcı olan GCLC (katalitik) ve GCLM (modülatör) alt birimlerinin mRNA ve protein düzeylerini baskılayarak GCL aktivitesini düşürmüş; bu durum akciğer GSH seviyesinde azalmaya yol açmıştır (Liu ve ark., 2012). Özetle, GCLC ve GCLM, glutatyon sentezini düzenleyerek hücre içi antioksidan kapasiteyi sürdüren kritik enzim alt birimleridir. Pulmoner fibroziste bu genlerin ekspresyonundaki azalma, GSH havuzunun tükenmesine ve oksidatif stres kaynaklı akciğer hasarının artmasına yol açarak hastalık progresyonunu destekler.

GPX1 (Glutatyon Peroksidaz 1)

GPx enzimleri, zararlı H_2O_2'nin yanı sıra çeşitli hidroperoksitlerin (DNA peroksitleri ve lipid peroksitler gibi) su ve alkollere indirgenmesini katalizler. Bu reaksiyonda GSH'yi indirgeyici olarak kullanır ve biyomembranları ile hücresel bileşenleri oksidatif strese karşı korur. GPX1, hem selenyuma bağımlı hem de bağımsız bir antioksidan enzim ailesinin üyesidir (Brigelius-Flohé, 2006). GPX1, peroksinitrite maruz kalan insan lökositlerinde NFκB/AP-1 aktivasyonunu ve proinflamatuar gen ekspresyonunu baskılar. GPX1 ekspresyonunun azalması artmış oksidatif stres ve inflamasyonla ilişkilidir. Sigara dumanı gibi çevresel stres faktörleri GPX1 aktivitesini etkileyebilir ve terapötik hedef olarak incelenmektedir. Veriler, GPX1'in sigara dumanına bağlı akciğer iltihabını kontrol etmek için gerekli olduğunu ve in vivo olarak hedeflenmesinin terapötik fayda sağlayabileceğini göstermektedir. Ayrıca GPX1 eksikliği olan farelerin başlangıçta normal BALF hücre sayısına sahip olması (sigara dumanına maruz kalmadığında) GPX1'in koruyucu rolünü destekler (Vlahos ve Bozinovski, 2013).

TXN/TXNRD (Tioredoksin / Tioredoksin Redüktaz)

Tioredoksin redüktaz (TrxR), tioredoksin (Trx) ve NADPH'den oluşan Trx sistemi, canlı hücrelerdeki başlıca antioksidan sistemlerden biridir. Bu sistem, diğer antioksidan enzimlerin redoks durumunu düzenleyerek hücreleri oksidatif strese karşı korur (Arnér, 2020). TrxR/Trx'i hedefleyen organik bir selenyum bileşiği olan butaselen (BS), TrxR/Trx inhibitörüdür ve anti-tümör aktivitesinin yanı sıra NF-κB/TGF-β1/Smads sinyalini inhibe ederek pulmoner fibrozu baskılar. Butaselenin hem in vitro hem in vivo çalışmalarda pulmoner fibrozisi azalttığı ve pirfenidona benzer etkinlik gösterdiği bildirilmiştir (Chen ve ark., 2023). TXN/TXNRD sistemi, özellikle alveolar epitel hücrelerinde kritik rol oynar ve oksidatif hasara karşı koruma sağlar (Chen ve ark., 2023).

PRDX (Peroksiredoksin)

Peroksiredoksin ailesinin bir üyesi olan PRDX1, ROS seviyelerinin düzenlenmesine ve diğer fizyolojik süreçlere katılır. PRDX1 yıkımı, akciğer epitel hücrelerinde ROS'u artırarak PI3K/Akt ve JNK/Smad yolları üzerinden EMT'yi teşvik eder. PRDX1 nakavtı, primer fibroblastlarda TGF-β sekresyonunu, ROS üretimini ve hücre göçünü artırır. Eksiklik, hücre proliferasyonu ve fibroz ilerlemesini hızlandırır. Bleomisin tedavisi PRDX1-nakavt farelerde daha şiddetli fibroz oluşturmuştur (Sun ve ark., 2023). PRDX ailesi, H_2O_2 ve organik peroksitleri indirgerken tioredoksin sistemiyle çalışarak redoks homeostazını sağlar. PRDX düzeylerindeki değişiklikler, fibroblast aktivasyonu ve inflamatuvar yanıtları etkiler. Aşırı oksidasyon PRDX'lerin fonksiyon kaybına yol açabilir. PRDX proteinlerine karşı gelişen otoantikorlar IPF hastalarında saptanmıştır ve bu proteinler terapötik hedef olarak değerlendirilmektedir (Elko ve ark., 2019).

G6PD (Glukoz-6-Fosfat Dehidrogenaz)

G6PD, pentoz fosfat yolunun hız sınırlayıcı enzimidir ve NADPH üretimi yoluyla redoks dengesinin korunmasında kritik rol oynar. NADPH, glutatyon sisteminin yeniden indirgenmesi için gereklidir. G6PD eksikliği, GSH/GSSG oranında azalma, akciğer dokusunda nitrasyon artışı ve proinflamatuar yolakların (PI3K, ERK1/2, AMPK) aktivasyonu ile ilişkilidir (Nicolás ve ark., 2018). Eksiklik, oksidatif stresin artmasına ve vasküler proliferasyona neden olur. Ayrıca hemoliz, metabolik yeniden programlama ve artmış ROS üretimi ile

pulmoner hipertansiyon ve fibrotik değişiklikler gelişebilir (Varghese ve ark., 2021). G6PD, NADPH üretimi ile glutatyon ve tioredoksin sistemlerini destekler. Hipoksiye bağlı damar yeniden yapılanması ve pulmoner hipertansiyon gelişiminde önemli bir rolü vardır (Varghese ve ark., 2021).

Pulmoner Fibrozda Öne Çıkan Antioksidan Genlerin Klinik Önemlerinini Özetleyecek Olursak

Pulmoner fibroziste oksidatif stresin dengelenmesinde birçok antioksidan gen kritik rol oynamaktadır. NFE2L2 (Nrf2), oksidatif stres yanıtının ana düzenleyicisidir ve HO-1, NQO1 gibi genleri aktive ederek savunma mekanizmalarını güçlendirir. HMOX1 (HO-1) heme yıkımını katalizlerken antiinflamatuvar etki gösterir. NQO1, kinonları toksik radikallere dönüşmeden indirger. SOD1 ve SOD2, süperoksit radikallerini H_2O_2'ye dönüştürerek oksidatif hasarı azaltır; katalaz ise H_2O_2'yi su ve oksijene çevirir. GCLC ve GCLM, glutatyon sentezinde görev alırken GPX1, H_2O_2 ve lipid peroksitleri indirger. TXN/TXNRD sistemi hücresel redoks dengesini korur; PRDX proteinleri peroksitlerin indirgenmesinde rol oynar. G6PD ise NADPH üretimiyle glutatyon sistemini destekler.

MATERYAL YÖNTEM

Bu derleme çalışma, literatür temelli bir derleme olarak hazırlanmıştır. PubMed, Scopus ve Web of Science veritabanları taranarak 2000–2025 yılları arasında yayımlanmış İngilizce ve Türkçe makaleler incelenmiştir. Tarama işlemlerinde "pulmonary fibrosis", "oxidative stress", "antioxidant genes", "Nrf2", "HO-1", "SOD", "GPX1" anahtar kelimeleri ve bunların kombinasyonları kullanılmıştır.

SONUÇ

Pulmoner fibrozis, oksidatif stresin ve inflamatuar yanıtın birbirini tetiklediği kompleks bir süreçtir. Bu süreçte Nrf2 proteini (NFE2L2 geni tarafından kodlanır) ve onun düzenlediği HO-1, NQO1, SOD, katalaz, GPX1, TXN/TXNRD, PRDX, GCLC/GCLM ve G6PD gibi genler, ROS ve RNS üretimini dengede tutarak hücresel hasarı sınırlayan temel koruyuculardır. Bu genler, epitel hücreleri, fibroblastlar ve alveolar makrofajları oksidatif strese karşı korurken inflamatuar yanıtın zararlı etkilerini azaltır. Son dönem çalışmalar, doğal ve farmakolojik ajanların bu genleri hedefleyerek oksidatif stresi ve fibrotik ilerlemeyi azaltabileceğini ortaya koymaktadır. Dolayısıyla, antioksidan genlerin düzenlenmesi, pulmoner fibrozis tedavisinde hem koruyucu hem de terapötik bir strateji olarak öne çıkmakta ve gelecekteki araştırmalar için umut vadetmektedir.

KAYNAKÇA

Arnér, I. S. J. (2020). Effects of mammalian thioredoxin reductase inhibitors. In *Reactive Oxygen Species*. *Handbook of Experimental Pharmacology* (Vol. 264, pp. 289–309). Springer.

Brigelius-Flohé, R. (2006). Glutathione peroxidases and redox-regulated transcription factors. *Biological Chemistry, 387*(10–11), 1329–1335.

Chen, Y., Yin, H., Güneş, J., Zhang, G., Zhang, Y., & Zeng, H. (2023). TrxR/Trx inhibitor butaselen ameliorates pulmonary fibrosis by suppressing NF-κB/TGF-β1/Smads signaling. *Biomedicine & Pharmacotherapy, 169*, 115822. https://doi.org/10.1016/j.biopha.2023.115822

Cho, H. Y., Jedlicka, A. E., Reddy, S. P. M., Kensler, T. W., Yamamoto, M., Zhang, L. Y., & Kleeberger, S. R. (2002). Role of NRF2 in protection against hyperoxic lung injury in mice. *American Journal of Respiratory Cell and Molecular Biology, 26*(2), 175–182. https://doi.org/10.1165/ajrcmb.26.2.4501

Drost, E. M., Skwarski, K. M., Sauleda, J., Soler, N., Roca, J., Agustí, A., & MacNee, W. (2005). *Oxidative stress and airway inflammation in severe exacerbations of COPD*. *Thorax, 60*(4), 293–300. https://doi.org/10.1136/thx.2004.027946

Elko, E. A., Cunniff, B., Seward, D. J., Chia, S. B., Aboushousha, R., van de Wetering, C., … Janssen-Heininger, Y. M. W. (2019). *Peroxiredoxins and beyond; Redox systems regulating lung physiology and disease*. Antioxidants & Redox Signaling, 31(14), 1070–1091. https://doi.org/10.1089/ars.2019.7752

Federico, A., Morgillo, F., Tuccillo, C., Ciardiello, F., & Loguercio, C. (2007). Chronic inflammation and oxidative stress in human carcinogenesis. *International Journal of Cancer, 121*(11), 2381–2386. https://doi.org/10.1002/ijc.23192

Fois, A. G., Paliogiannis, P., Sotgia, S., Mangoni, A. A., Zinellu, E., Pirina, P., Carru, C., & Zinellu, A. (2018). Evaluation of oxidative stress biomarkers in idiopathic pulmonary fibrosis and therapeutic applications: A systematic review. *Respiratory Research, 19*(1), 51. https://doi.org/10.1186/s12931-018-0754-7

Fois, A. G., Paliogiannis, P., Sotgia, S., Mangoni, A. A., Zinellu, E., Pirina, P., Carru, C., & Zinellu, A. (2020). Evaluation of oxidative stress biomarkers in idiopathic pulmonary fibrosis and therapeutic applications: A systematic review. *Biomarkers in Medicine, 14*(6), 471–484. https://doi.org/10.2217/bmm-2020-0028

Jomova, K., Raptova, R., Alomar, S. Y., Alwasel, S. H., Nepovimova, E., Kuca, K., & Valko, M. (2023). Reactive oxygen species, toxicity, oxidative stress and antioxidants: Chronic diseases and aging. *Archives of Toxicology, 97*(8), 2499–2574. https://doi.org/10.1007/s00204-023-03562-9

Kinnula, V. L., Fattman, C. L., Tan, R. J., & Oury, T. D. (2005). Oxidative stress in pulmonary fibrosis: A possible role for redox modulatory therapy. *American Journal of Respiratory and Critical Care Medicine, 172*(4), 417–422. https://doi.org/10.1164/rccm.200501-017PP

Kozlov, A. V., Cavadov, S., & Sommer, N. (2024). Cellular ROS and antioxidants: Physiological and pathological role. *Antioxidants, 13*(5), 602. https://doi.org/10.3390/antiox13050602

Lee, P. J., Alem, J., Sylvester, S. L., Inamdar, N., Su, L. S., & Choi, M. (1996). Regulation of heme oxygenase-1 expression in vivo and in vitro during hyperoxic lung injury. *American Journal of Respiratory Cell and Molecular Biology, 14*(6), 865–874. https://doi.org/10.1165/ajrcmb.14.6.8652184

Liu, R.-M., Vayalil, P. K., Ballinger, C., Dickinson, D. B., Huang, W.-T., Wang, S., Kavanagh, T. J., & Postlethwait, E. M. (2012). Transforming growth factor beta suppresses glutamate-cysteine ligase gene expression and induces oxidative stress in a lung fibrosis model. *Free Radical Biology and Medicine, 53*(3), 554–563. https://doi.org/10.1016/j.freeradbiomed.2012.05.024

Luo, L., Zhang, W., You, S., Cui, X., Tu, H., Yi, Q., Wu, J., & Liu, O. (2024). The role of epithelial cells in fibrosis: Mechanisms and treatment. *Pharmacological Research, 202*, 107144. https://doi.org/10.1016/j.phrs.2024.107144

Makena, P., Kikalova, T., Prasad, G. L., & Baxter, S. A. (2023). Oxidative stress and lung fibrosis: Towards an adverse outcome pathway. *International Journal of Molecular Sciences, 24*(15), 12490. https://doi.org/10.3390/ijms241512490

Ma, Q. (2013). Role of Nrf2 in oxidative stress and toxicity. *Annual Review of Pharmacology and Toxicology, 53,* 401–426. https://doi.org/10.1146/annurev-pharmtox-011112-140320

Nandi, A., Yan, L.-J., & Jana, C. K. (2019). Role of catalase in oxidative stress- and age-associated diseases. *Oxidative Medicine and Cellular Longevity, 2019*, 9613090. https://doi.org/10.1155/2019/9613090

Nicolás, J. M., et al. (2018). G6PD deficiency and redox imbalance in pulmonary vascular disease. *Antioxidants & Redox Signaling, 31*(14), 1070–1091 doi:10.1089/ars.2018.7503.

Odajima, N., Betsuyaku, T., Nagai, K., Moriyama, C., Wang, D.-H., Takigawa, T., Ogino, K., & Nishimura, M. (2010). Role of catalase in pulmonary fibrosis. *Respiratory Research, 11*(1), 183. https://doi.org/10.1186/1465-9921-11-183

Paliogiannis, P., Fois, A. G., Collu, C., Bandinu, A., Zinellu, E., & Carru, C. (2018). Idiopathic pulmonary fibrosis and oxidative stress–related biomarkers: A systematic review and meta-analysis. *Biomarkers in Medicine, 12*(10), 1175–1184. https://doi.org/10.2217/bmm-2018-0108

Raghu, G., Collard, H. R., Egan, J. J., Martinez, F. J., Behr, J., Brown, K. K., Colby, T. V., Cordier, J.-F., Flaherty, K. R., Lasky, J. A., Lynch, D. A., Ryu, J. H., Swigris, J. J., … Schünemann, H. J. (2011). An official ATS/ERS/JRS/ALAT statement: Idiopathic pulmonary fibrosis: Evidence-based guidelines for diagnosis and management. *American Journal of Respiratory and Critical Care Medicine, 183*(6), 788–824. https://doi.org/10.1164/rccm.2009-040GL

Ryter, S. W., & Choi, A. M. K. (2016). Therapeutic modulation of inflammation through targeting heme oxygenase-1 and carbon monoxide. *Translational Research, 167*(1), 7–34. https://doi.org/10.1016/j.trsl.2015.06.011

Shi, L. (2013). *Catalase attenuates pulmonary fibrosis while increasing pro-inflammatory cytokines* [Master's thesis, University of Iowa]. University of Iowa. https://doi.org/10.17077/etd.8op47wzt

Sun, H. N., et al. (2023). *PRDX1 negatively regulates bleomycin-induced pulmonary fibrosis by modulating epithelial-mesenchymal transition and fibroblast proliferation*. Cellular and Molecular Biology Letters, 28(1), 1–15. https://doi.org/10.1186/s11658-023-00460-x

Wang, X.-C., Zhang, Y.-S., Ling, H., & Sen, J.-B. (2025). Epigenetic silencing of SOD2 exacerbates mitochondrial oxidative stress and promotes pulmonary fibrosis. *Free Radical Biology and Medicine, 235*, 1–10. https://doi.org/10.1016/j.freeradbiomed.2025.04.034

Varghese, M. V., James, J., Rafikova, O., & Rafikov, R. (2021). Glucose-6-phosphate dehydrogenase deficiency contributes to metabolic abnormalities and pulmonary hypertension. *Journal of Physiology:*

Lung Cellular and Molecular Physiology, 320(4), L508–L521. https://doi.org/10.1152/ajplung.00165.2020

Veith, C. (2019). *Redox regulation in pulmonary fibrosis: Towards therapeutic targets* [Doktora tezi, Maastricht Üniversitesi]. Gildeprint Drukkerijen. https://doi.org/10.26481/dis.20190524cv

Vézina, F. A., & Cantin, A. M. (2018). Antioxidants and chronic obstructive pulmonary disease. *Chronic Obstr Pulm Dis*, *5*(4), 277–288. https://doi.org/10.15326/jcopdf.5.4.2018.0133

Vlahos, R., & Bozinovski, S. (2013). Glutathione peroxidase-1 as a novel therapeutic target for COPD. *Redox Report, 18*(4), 142–149. https://doi.org/10.1179/1351000213Y.0000000053

ORAL PRESENTATION

KBRN olaylarında afet yönetimi ve müdahale koordinasyonu: Disiplinlerarası yaklaşımlar ve güncel uygulamalar

[1*] Abdullah Özkan(ORCID: https://orcid.org/0000-0002-6799-2396),
[1*] Refika Nazlı Aydın(ORCID: https://orcid.org/0009-0002-0532-623X),
[1] Vildan Özkan(ORCID: https://orcid.org/0000-0001-8719-9099),
[2] Pınar Bozbeyoğlu (ORCID: https://orcid.org/0000-0002-3704-2701)

*[1]İskenderun Teknik Üniversitesi, Lisansüstü Eğitim Enstitüsü, KBRN Anabilim Dalı, Hatay, Türkiye
[2]Gümüşhane Üniversitesi, Gümüşhane Meslek Yüksekokulu, Elektronik ve Otomasyon Bölümü, Biyomedikal Cihaz Teknolojisi Programı, Gümüşhane, Türkiye

*Sorumlu yazar e-mail: abdullah.ozkan@iste.edu.tr / refikaaydin.lee25@iste.edu.tr

Özet

KBRN olayları, çok kısa bir zaman içinde kontrol edilemeyen sonuçlar doğurabildiği için hem müdahale ekiplerini hem de yöneticileri zorlayan olaylardır. Bu olaylarda hangi ajanın devrede olduğunu anlamak her zaman kolay değildir. Ekipler çoğu zaman ilk dakikalarda yalnızca ortamda bir terslik olduğunu hisseder ve bu his, müdahale kararlarını bir süre yönlendirir. Farklı ajan türlerinin kendine özgü yayılma şekilleri, tanı ve müdahale süreçlerini daha da zorlaştırır. Kimyasal tehditler genellikle hızlı belirtiler gösterirken biyolojik ajanlar çoğu zaman daha geç fark edilir. Radyolojik ve nükleer maruziyetlerde ise belirtiler gecikebilir ya da hiç belirgin olmayabilir. Bu belirsizlik, özellikle ilk müdahale ekipleri için önemli bir güçlük oluşturur. KBRN yönetiminde hazırlık çalışmaları teori ile pratik arasındaki en görünür farkı ortaya çıkarır. Teknik açıdan mükemmel görünen planlar sahada beklenmedik şekilde aksayabilir. Düzenli yapılan tatbikatlar, ekiplerin gerçek bir olayda hata yapma olasılığını belirgin şekilde düşürür; bu yüzden hazırlık sürecinin en pratik unsurlarından kabul edilir. Kurumlar arası koordinasyon da bu süreçte kritik bir rol oynar. Küçük bir iletişim boşluğu bile zincirleme gecikmelere yol açabilir ve bu durum müdahale kapasitesini belirgin şekilde düşürür. İlk müdahale ve dekontaminasyon uygulamaları, olayın daha geniş bir krize dönüşmesini engelleyen temel aşamalardır. Triyaj ise çok sayıda mağdur içeren olaylarda sağlık kaynaklarının doğru kullanılmasını sağlar. Su ve besin güvenliği, olay sonrası dönemde ikincil salgınların önlenmesi açısından hayati bir alanı temsil eder. Tüm bu süreçler, KBRN olaylarının yalnızca teknik bilgi değil, aynı zamanda güçlü bir organizasyon ve sürekli iletişim gerektirdiğini göstermektedir. Bu çalışma, KBRN kapsamındaki müdahale süreçlerini gözden geçirirken farklı disiplinlerin hangi aşamalarda katkı sağlayabileceğini de tartışmaktadır.

Anahtar Kelimeler: KBRN, Afet Yönetimi, Müdahale Koordinasyonu, Dekontaminasyon, Triyaj Sistemleri

Disaster management and response coordination in CBRN Incidents: Current approaches and practical frameworks

Abstract

The first moments of a CBRN event rarely feel organized, and most responders describe them as a mix of confusion and instinctive reactions. People at the scene often notice unusual smells, sudden discomfort, or strange behavior in the environment long before anyone confirms a chemical or biological release. These early hints shape their decisions, even though no one fully trusts those impressions at the time. Different threat types behave in ways that challenge responders' expectations. Chemical agents may trigger visible symptoms quickly, sometimes too quickly for structured protocols to keep up. Biological threats, on the other hand, remain silent for hours or days, leaving teams unsure about when the real danger started. Radiological or nuclear exposures can be even more complicated, because physical signs may never appear. This mix of visible and invisible risks forces teams to act while still questioning what they are dealing with. Preparedness efforts try to narrow this uncertainty, yet real situations often expose gaps that training sessions never reveal. During drills, small timing issues look minor; during an actual emergency, the same issues can interrupt an entire operation. Coordination becomes fragile when information travels unevenly, and most delays begin with something as simple as a message that arrives a few minutes late. Initial actions—securing the area, assessing exposure, and

beginning decontamination—often determine how far the incident will spread. When more victims appear than expected, triage becomes a moving target rather than a fixed procedure. After the urgent phase ends, new concerns emerge. Water and food contamination can cause unexpected problems days later, especially when infrastructure is damaged. This paper looks at these recurring challenges and reflects on how teams cope with them in real conditions. The discussion highlights the value of flexible planning, continuous practice, and cooperation across different fields, which together strengthen the overall response to CBRN emergencies

Keywords: CBRN Incidents, Disaster Management, Emergency Response, Decontamination Methods, Triage Practices

GİRİŞ

KBRN olayları çoğu zaman beklenmedik şekilde başlar ve ilk anda tam olarak ne olduğuna dair net bir bilgi olmaz. Çoğu ekip, önce çevredeki anormallikleri fark eder; bu fark ediş bazen ölçüm cihazlarıyla değil, basit sahne gözlemleriyle başlar. Franz ve çalışma arkadaşları (1997), kimyasal olaylarda ilk dakikaların belirsizlikle dolu olduğunu ve kararların çoğu zaman sınırlı bilgiyle verildiğini vurgular. Bilginin bu kadar dağınık olması, olayın daha ilk aşamada kontrol altına alınmasını güçleştirir.

Her tehdit türü farklı hızla yayılır ve farklı klinik belirtiler oluşturur. Kimyasal ajanların çoğu dakikalar içinde etki gösterirken, biyolojik ajanların bazıları günlerce sessiz kalabilir. Holloway ve meslektaşları (1997), biyolojik tehditlerin genellikle geç fark edildiğini ve bu nedenle salgın benzeri sonuçlar doğurabileceğini belirtir. Radyolojik maruziyet ise bazen hiçbir belirti göstermeden ilerleyebilir ve bu durum özellikle olay yerindeki ekipleri zorlar (DiCarlo et al., 2021).

Hazırlık aşaması, KBRN yönetiminde teoriden çok daha pratik sonuçlar doğurur. Pek çok plan kağıt üzerinde mükemmel görünür; ancak olay anında işe yarayan şey genellikle ekiplerin önceden yaptığı tatbikatlardır. Vale ve Crome (1994), kimyasal olaylardaki hataların çoğunun hazırlık eksikliğinden kaynaklandığını belirtir. Bu yüzden eğitimlerin düzenli aralıklarla tekrarlanması, teknik protokollerin güncelliği kadar hayati görülür.

Kurumlar arası iletişim bu alanda sürekli sorun yaratır. Okumura ve çalışma arkadaşları (1998), Tokyo metro saldırısı sırasında iletişim kopukluklarının hasta yönetimini belirgin şekilde zorlaştırdığını göstermiştir. KBRN olaylarında bir kurumun yapacağı küçük bir gecikme, zincirleme olarak tüm müdahale planını etkileyebilir. KBRN olaylarında teknik müdahale kadar, kurumlar arasındaki bilgi akışının düzgün olması da operasyonun başarısını belirleyen bir faktördür.

Son yıllarda gelişen tespit teknolojileri sahadaki belirsizliği azaltmıştır; ancak teknolojinin tek başına yeterli olmadığı açıktır. Ekiplerin bu cihazları nasıl kullanacağını bilmemesi hâlinde teknoloji yalnızca bir araç olarak kalır. Çalışma, literatürde yer alan mevcut uygulamaları değerlendirerek hangi alanlarda iyileştirmeye ihtiyaç duyulduğunu tartışmayı amaçlamaktadır.

KAVRAMSAL ÇERÇEVE

KBRN kavramı çoğu kişi için tek bir tehdit türünü çağrıştırsa da, aslında dört ayrı grubun oldukça farklı özellikleri bulunur. Kimyasal maddeler genelde hızla etki gösterir ve çoğu zaman olay yerinde ilk panik dalgasını bu maddeler yaratır. Salem (2007), kimyasal ajanların ani belirtilerinin ekipleri çoğu zaman hataya zorladığını belirtir. Biyolojik tehditler ise çok daha sessiz ilerler. İlk saatlerde neredeyse hiçbir şey fark edilmez ve bu sessizlik olayın gerçek boyutunu gizler (Fauci, 2005).

Radyolojik ve nükleer tehditlerde durum biraz daha tuhaftır; çünkü görünür bir belirti olmayabilir. İnsanlar yalnızca cihazların verdiği uyarılarla hareket eder ve bu da belirsizliği artırır. Hall (2000), radyasyonun etkilerinin çoğu zaman geç ortaya çıktığını ve bu nedenle erken müdahalenin psikolojik baskı oluşturduğunu vurgulamıştır. Bu farklılıklar nedeniyle KBRN olaylarını tek bir modelle açıklamaya çalışmak genellikle yetersiz kalır.

Kavramsal çerçevede bir diğer önemli unsur, KBRN olaylarının çoğunda “bilgi eksikliği” nin temel sorun olarak ortaya çıkmasıdır. Olay yeri bazen karmaşık bir bulmaca gibidir; ekipler farklı ipuçlarını bir araya getirerek tabloyu anlamaya çalışır. Bostock ve arkadaşları (2016), acil durumlarda bilgi akışının dağınık olmasının karar kalitesini düşürdüğünü göstermiştir. Kavramsal çerçevede yalnızca ajan türlerine değil, belirsizlik yönetimi gibi karar süreçlerini etkileyen unsurlara da yer verilmiştir.

Bu bölümde ele alınan kavramlar, KBRN yönetiminin neden çok disiplinli bir yaklaşım gerektirdiğini de açıklar. Her tehdit türü ayrı uzmanlık ister, fakat olayın genel yönetimi bu uzmanlıkları tek potada birleştirmeyi zorunlu kılar. Tam da bu nedenle KBRN alanı, klasik afet yönetiminden daha dinamik, daha dalgalı ve çoğu zaman daha yorucu bir süreçtir.

3. KBRN OLAYLARININ TANIMI VE SINIFLANDIRILMASI

KBRN kavramı zaman içinde genişleyen bir çerçeveye dönüştü ve artık yalnızca askeri tehditlerle sınırlı görülmüyor. Günümüzde endüstriyel kazalar, laboratuvar hataları ve kasıtlı saldırılar da bu yapının içine giriyor. Chemical, Biological, Radiological ve Nuclear başlıkları ilk bakışta tek bir grup gibi görünse de, her birinin kendine has etkileri, yayılma biçimleri ve müdahale gereksinimleri bulunur. Tucker (2000), KBRN tehditlerinin ortak noktalarının az, ayrımlarının ise oldukça belirgin olduğunu vurgular.

Kimyasal olaylar, çoğu zaman hızlı etki göstermeleri nedeniyle tanımlaması en kolay olan gruptur. Sinir gazları, boğucu ajanlar veya endüstriyel toksinler kısa sürede belirti oluşturur ve bu belirtiler genellikle olay yerindeki ilk gözlemleri yönlendirir. Kimyasal ajanların çoğu uçucu yapıları nedeniyle hızla yayılabilir Salem (2007), Bazı ajanlar, özellikle kontrol edilemediğinde dakikalar içinde olayın daha geniş bir alana yayılmasına yol açabilir.

Biyolojik olaylar ise çok daha farklı bir zorluk yaratır. Belirtiler genellikle saatler ya da günler sonra ortaya çıktığı için olayın kapsamı uzun süre belirsiz kalabilir. Inglesby ve arkadaşları (2000), biyolojik tehditlerin "sessiz ilerlemesinin" müdahaleyi geciktiren en kritik unsur olduğunu belirtir. Bu gecikme, özellikle de salgın potansiyeli taşıyan ajanlarda ciddi sorunlara yol açar.

Radyolojik olaylar, görünmez bir tehlike niteliği taşır. Çevredeki insanlar çoğu zaman olayın yaşandığını bile anlamaz; ancak cihazlar radyasyon seviyelerini ortaya çıkarır. Radyolojik partiküller yüzeylerde uzun süre kalabilir ve temizlenmesi karmaşık bir sürece dönüşebilir (IAEA, 2014). Bu tür durumlarda sahada çalışan tespit ekiplerinin hızlı hareket etmesi, müdahalenin doğru yönlendirilmesi açısından kritik kabul edilir.

Nükleer olaylar, düşük ihtimalle gerçekleşse de etkileri en geniş olan tehdit kategorisidir. Bir nükleer patlama, yalnızca fiziksel yıkım yaratmakla kalmaz; uzun dönemli radyasyon etkileri nedeniyle geniş bölgelerde yaşamı olumsuz etkiler. Moulder (2004), nükleer olayların sonrasında oluşan sağlık sorunlarının büyük kısmının radyasyonun gecikmeli etkilerinden kaynaklandığını belirtir.

Bu dört kategori bir araya geldiğinde, KBRN olaylarının aslında tek bir çatı terimle ifade edilen oldukça farklı senaryolar bütünü olduğu anlaşılır. Ajanların sınıflandırılması yalnızca teorik bir ayrım değildir; sahadaki uygulamaları doğrudan etkilediği için pratik açıdan da belirleyicidir.

4. AFET YÖNETİMİ AŞAMALARI

KBRN olaylarının yönetimi genellikle dört temel aşamada ele alınır; ancak bu aşamalar gerçek bir olay sırasında birbirine karışarak ilerler. Teoride hazırlık, müdahale, iyileştirme ve azaltım ayrıdır, fakat pratikte sınırlar çoğu zaman bulanıklaşır. Perry ve Lindell (2003), afet yönetiminin çizgisel bir süreç gibi görünmesine rağmen gerçekte döngüsel davrandığını belirtir. KBRN olaylarında bu döngüsellik daha da belirginleşir.

Hazırlık aşaması, çoğu planlamacının düşündüğünden daha zorlu bir dönemdir. Ekipler yeni cihazlar dener, senaryoları gözden geçirir ve kimi zaman beklenmedik küçük ayrıntılarla uğraşır. Bu ayrıntılar önemsiz gibi görünse de olay anında belirleyici olabilir. Drabek (2013), hazırlık döneminde ortaya çıkan küçük aksaklıkların gerçek olaylarda büyüyerek geri döndüğünü ifade eder. Hazırlık süreci, teknik planlamaların ötesinde kurumların geçmiş deneyimlerinden ders çıkarmasını da içeren daha geniş bir yapıyı kapsar.

Müdahale aşaması, olayın en yoğun ve en yorucu evresidir. Ekipler ilk dakikalarda sınırlı bilgiyle hızlı kararlar almak zorunda kalır. Kimyasal bir olayda ekiplerin hareket süresi dakikalarla sınırlıyken, biyolojik olaylarda belirsizlik çok daha uzun sürer. Dynes (1994), müdahale döneminin çoğu zaman "kontrollü kaos" ile ilerlediğini ve bu kaosun doğru yönetildiğinde işlevsel olabileceğini vurgulamıştır.

İyileştirme aşaması, genellikle en uzun süren dönemdir. KBRN olaylarında çevresel etkiler, psikolojik stres ve altyapı sorunları bir arada görülebilir. Paton ve Johnston (2006), iyileştirme sürecinin yalnızca fiziksel düzenlemeleri değil, aynı zamanda toplumun güven duygusunu yeniden kazanmasını da içerdiğini belirtir. İyileştirme aşaması, yalnızca fiziksel hasarın giderilmesini değil, toplumun psikolojik olarak toparlanmasını da içeren karmaşık bir dönemdir.

Azaltım aşaması, gelecekteki olaylara karşı dayanıklılığı artırmayı amaçlar. Bu aşamada kurumlar, önceki deneyimlerden öğrenerek düzenlemeler yapar. Mileti (1999), azaltımın afet yönetiminin en ihmal edilen fakat en etkili adımı olduğunu söylemiştir. KBRN olaylarında azaltım, genellikle yeni cihazların geliştirilmesi, protokollerin güncellenmesi ve eğitimlerin yeniden yapılandırılması şeklinde görülür.

Bu dört aşama bir bütün olarak ele alındığında, KBRN yönetiminin yalnızca teknik bir dizi işlemden ibaret olmadığı anlaşılır. Her aşama bir sonrakini etkiler ve küçük bir aksama bile tüm sistemi zorlayabilir. KBRN olaylarında yönetim, çoğu zaman önceden hazırlanmış planlara birebir bağlı kalmaktan ziyade sahadaki koşullara hızla uyum sağlamayı gerektirir.

5. İLK MÜDAHALE VE DEKONTAMİNASYON

KBRN olaylarında ilk müdahale çoğu zaman belirsizlik içinde başlar. Olay yerine ulaşan ekipler, başlangıçta net bir tabloyla karşılaşmaz; yalnızca durumun sıradan bir acil vakadan farklı olduğunu hissederler. Bu ilk dakikalar hem zihinsel açıdan yorucudur hem de alınacak kararları büyük ölçüde belirler. Kimyasal ya da biyolojik bir maruziyet olup olmadığını anlamak, çoğu zaman cihazlardan önce ekiplerin hızlı gözlemlerine dayanır. Razak ve çalışma arkadaşları (2018), sahadaki ilk izlenimlerin müdahale kalitesini doğrudan etkilediğini vurgulamıştır.

Ekiplerin olay yerine yaklaşma biçimi, kullanılan kişisel koruyucu donanımın (KKD) türüne göre değişir. Doğru KKD seçimi, teoride basit görünse de sahada birkaç saniye içinde alınması gereken bir karardır. Yanlış bir seçim hem ekipleri hem de mağdurları riske atabilir. Okumura ve meslektaşları (1998), Tokyo metro saldırısında birçok sağlık çalışanının uygun olmayan KKD nedeniyle ikincil maruziyet yaşadığını belirtmiştir. Olayın başlangıcında yeterli bilgi bulunmadığından, ekipler genellikle en üst düzey koruyucu ekipmanla sahaya çıkmayı tercih eder.

Dekontaminasyon ise ilk müdahalenin en görünür aşamasıdır. Ancak bu süreç çoğu kişinin düşündüğünden daha karmaşık ilerler. Dekontaminasyonun nasıl uygulanacağı, ajanın türüne, çevresel koşullara ve maruz kalan kişilerin durumuna göre değişir. Kimyasal ajanlara maruz kalınan durumlardan bir kısmında su ve sabunla yapılan hızlı dekontaminasyon etkili olabilir; ancak bazı ajanlar için bundan daha kapsamlı uygulamalara ihtiyaç duyulur (IAEA, 2015). Biyolojik ajanlarda ise fazla su kullanımı bazen mikroorganizmaların yayılma riskini artırabilir.

Sahada en zorlayıcı konulardan biri, mağdurların panik hâlidir. İnsanlar kendi üzerlerinde görünür bir belirti olmasa bile kirlenmiş olabileceklerini düşünerek yoğun kaygı yaşar. Cone ve Koenig (2005), dekontaminasyon istasyonlarındaki panik davranışlarının çoğu zaman fiziksel risklerden daha büyük sorun yarattığını göstermiştir. Bu nedenle ekipler yalnızca teknik uygulama yapmaz; aynı zamanda kalabalığı sakinleştirmeye çalışır.

Dekontaminasyonun sonunda temiz ve kirli alanlar net şekilde ayrılır. Ancak bu alanların yönetimi bile zaman zaman karışabilir. Ekipler yorgunlaştıkça sınırlar bulanıklaşabilir ve küçük ihlaller büyük risklere dönüşebilir. KBRN olaylarında ilk müdahale ve dekontaminasyon süreci, yalnızca prosedürlere uymaktan ibaret değildir; aynı zamanda olay yerindeki kaosu kontrol etmeyi, bilgi eksikliğini yönetmeyi ve insanların duygusal tepkilerini dengelemeyi gerektirir.

6. TRİYAJ

KBRN olaylarında triyaj, çoğu kişinin düşündüğünden çok daha zorlayıcı bir süreçtir. Olay yerine ulaşan ekipler, ilk anda hem sınırlı bilgiye sahiptir hem de hızla karar vermek zorunda kalır. Bu koşullarda kimin önce müdahale alacağına karar vermek, yalnızca tıbbi durumla değil, ajanın türüyle de yakından ilişkilidir. Kimyasal bir olayda belirtiler dakikalar içinde değişebilir ve bu hızlı değişim, ekipleri sürekli tetikte tutar. Culley ve arkadaşları (2014), bu tür olaylarda triyaj kararlarının "hareketli bir hedefi takip etmeye" benzediğini ifade eder.

Klasik travma triyaj sistemleri, KBRN olaylarında her zaman işe yaramaz. Çünkü travmada belirgin yaralanmalar ön plandayken, kimyasal veya radyolojik maruziyette görünür bir yaralanma olmayabilir. Bazı hastalar başlangıçta iyi görünür fakat birkaç dakika içinde kritik duruma geçebilir. Ramesh & Kumar (2010), kimyasal maruziyette belirtilerin hızlı dalgalanmasının standart protokolleri yetersiz bıraktığını göstermiştir. Bu nedenle ekipler, her kararın arkasında sürekli bir "ya gözden kaçırdığım bir şey varsa" endişesi taşır.

Biyolojik olaylarda ise durum daha farklıdır. Belirtiler büyük ölçüde belirsizdir ve çoğu zaman hasta yoğunluğu belirli bir noktada birden artar. Bu durum, triyajı bir "ilk iz sürme" faaliyetine dönüştürür. Levi ve arkadaşları (2008), biyolojik tehditlerde ilk vakaların geç fark edildiğini ve triyaj yükünün kısa sürede katlanarak arttığını belirtir. Bu nedenle ekipler, hasta akışını yönetirken hem klinik hem de epidemiyolojik ipuçlarını birlikte değerlendirmek zorunda kalır.

Radyolojik olaylarda triyaj, genellikle dışsal belirtilerin yokluğu nedeniyle daha da karışık bir hâl alır. İnsanlar iyi görünse bile yüksek doz almış olabilir. Bunu belirlemek için saha ölçümleri kritik hâle gelir. Blakely ve ark., (2010), radyasyon doz değerlendirmesinin triyaj sürecini "yavaşlatan ama kaçınılmaz" bir adım olduğunu vurgular. Bu nedenle radyasyon olaylarında triyaj, tıbbi kararlar kadar ölçüm cihazlarının doğruluğuna da bağlıdır.

Tüm bu farklılıklar, KBRN triyajının aslında sabit bir protokolden çok sürekli güncellenen bir süreç olduğunu gösterir. Ekipler yalnızca hastaların durumuna bakmaz; olayın değişen dinamiklerini de izler. Bu nedenle KBRN triyajı, klasik acil tıp bilgisi ile olay yeri sezgisinin birleştiği en kritik aşamalardan biridir.

7. SU TEMİNİ

KBRN olaylarında su temini, çoğu zaman olayın ilk şokundan sonra fark edilen ama etkisi hızla büyüyen bir ihtiyaç hâline gelir. Olay yerindeki ekipler başlangıçta daha acil görünen müdahalelerle uğraşırken, su kaynaklarının durumu bir süre ihmal edilebilir. Fakat kimyasal ya da biyolojik bir kontaminasyon söz konusuysa, en küçük bir ihmal bile geniş kitleleri etkileyebilir. Macler ve Merkle (2000), su güvenliğinin KBRN olaylarında "ikinci dalga risklerin" en önemli kaynağı olduğunu belirtir.

Olay sırasında su kaynaklarının zarar görme biçimi, tehdit türüne göre değişir. Kimyasal bir ajan suya karıştığında çoğu zaman hızlı bir yayılım gösterir ve suyun görsel olarak temiz görünmesi hiçbir anlam taşımaz. Biyolojik ajanlarda ise tehdit genellikle daha sessiz ilerler. İnsanlar suyu kullanmaya devam ederken kontaminasyon fark edilmez ve risk giderek büyür. Craun ve çalışma arkadaşları (2002), biyolojik kirlenmenin çoğu zaman rutin kontrollerle bile kolay fark edilmediğini vurgulamıştır.

Radyolojik olaylarda su güvenliği daha karmaşık bir hâl alır. Radyonüklidlerin suda çözünmesi veya çökelmesi, uzun vadeli bir gözetim ihtiyacı doğurur. IAEA (2011), bazı radyonüklidlerin su kaynaklarında aylarca kalabildiğini ve temizleme çalışmalarının titizlik gerektirdiğini belirtir. Bu durum, su yönetim ekiplerini sabırlı ama sürekli bir izleme sürecine zorlar.

Olay sonrası dönemde en kritik adım, güvenli içme suyu sağlanana kadar geçici çözümler üretebilmektir. Sahra tipi arıtma sistemleri bu noktada büyük önem taşır. Bu sistemler mükemmel değildir; ancak altyapının çöktüğü durumlarda hayat kurtarır. Clasen (2008), taşınabilir arıtma teknolojilerinin kriz anlarında su kaynaklı hastalıkları belirgin şekilde azalttığını göstermiştir.

Su temini yalnızca teknik bir görev değildir; aynı zamanda toplumun güvenini şekillendiren bir süreçtir. İnsanlar suyun temiz olduğuna inanmadıkça, diğer müdahalelerin etkisi de azalır. Bu nedenle KBRN olaylarında su temini, hem mühendislik hem iletişim hem de halk sağlığı açısından kritik bir kavşaktır.

8. BESİN GÜVENLİĞİ

KBRN olaylarında besin güvenliği çoğu zaman gözden kaçan ama etkisi geç fark edildiğinde büyük sorun yaratan bir alandır. İnsanlar ilk anda suya odaklanır; fakat gıda zincirinin bozulması çok daha uzun süreli riskler doğurabilir. Kontaminasyonun nasıl gerçekleştiği her zaman belirgin değildir. Bazen kimyasal bir ajan rüzgârla tarım alanlarına taşınır, bazen de biyolojik bir tehdit soğuk zincirde fark edilmeden ilerler. Hamada & Ogino(2012), gıdaların "sessiz taşıyıcılar" hâline gelmesinin acil durum yönetimini zorlaştırdığını belirtir.

Kimyasal kontaminasyonda görünür bir işaret olmayabilir. Toksik maddeler tat ya da koku bırakmadığından insanlar tehlikeyi geç fark eder. Rather ve ark., (2017), birçok kimyasal bulaşmanın laboratuvar analizleri yapılana kadar fark edilmediğini ve bu gecikmenin sağlık etkilerini artırdığını göstermiştir. Bu nedenle gıda örneklerinin hızlı testlerle değerlendirilmesi kritik bir adımdır.

Biyolojik tehditlerde durum daha karmaşık ilerler. Bazı patojenler düşük dozlarda bile ciddi hastalık oluşturabilir. Özellikle de et, süt ve taze sebze gibi ürünlerde bu risk daha belirgindir. Painter ve çalışma arkadaşları (2013), gıda kaynaklı biyolojik tehditlerin acil durumların ikinci dalgasını oluşturabileceğini vurgulamıştır. Bu yüzden KBRN olaylarında gıda zincirinin en küçük adımı bile göz ardı edilmemelidir.

Radyolojik kontaminasyon ise hem tespit hem temizleme açısından ayrı bir zorluk yaratır. Radyoaktif partiküller toprağa, hayvan yemine ve bitkilere kolayca tutunur. UNSCEAR (2010), radyolojik olaylardan sonra süt ve yapraklı sebzelerde yüksek oranlarda birikme görüldüğünü belirtmiştir. Bu nedenle radyolojik kontaminasyonun değerlendirilmesi uzun soluklu takip gerektirir.

Besin güvenliği yalnızca laboratuvarda yürütülen bir süreç değildir. Halkın paniğini yönetmek de en az teknik analizler kadar önemlidir. İnsanlar bir ürüne güvenmediğinde, temiz olduğu kanıtlansa bile kullanmaktan çekinebilir. Bu nedenle KBRN olaylarında besin güvenliği, hem bilimsel hem toplumsal boyutları olan çok yönlü bir süreçtir.

9. MÜDAHALE KOORDİNASYONU

KBRN olaylarında müdahale koordinasyonu çoğu zaman teknik bilgi kadar iletişim becerisini de gerektirir. Olay yerindeki ekipler genellikle aynı anda birçok sorunla karşılaşır ve bu sorunların hangisinin önce ele alınacağı konusunda hızlı bir uzlaşı sağlanmalıdır. Bu uzlaşı, teoride basit görünse de sahada oldukça kırılgan olabilir. Kapucu (2006), acil durumlarda iletişim zincirindeki küçük kopuklukların bile müdahale hızını belirgin biçimde yavaşlattığını belirtir.

Koordinasyonun temel dayanağı, farklı kurumların birbirinin görev alanını anlamasıdır. Ancak bu her zaman mümkün olmaz. Olay anında kararlar hızla alındığı için kurumlar arasındaki sınırlar kolayca bulanıklaşır. Moynihan (2008), kriz yönetiminde kurumların "tek bir organizma gibi" hareket etmesinin müdahale performansını artırdığını vurgulamıştır. Bu yaklaşım, KBRN olaylarında daha da önem kazanır; çünkü belirsizlik, her kurumun kendi içinde izlediği prosedürü bile zorlaştırabilir.

Bilgi paylaşımı koordinasyonun en hassas noktalarından biridir. Farklı ekiplerin sahadan topladığı verilerin tek kanalda birleşmesi gerekir; aksi hâlde bilgiler birbirini tamamlamak yerine karıştırır. Comfort (2007), bilgi akışının düzenli olmadığı durumlarda karar alma hızının üçte bire kadar düştüğünü göstermiştir. Bu nedenle KBRN olaylarında bilgi yönetimi, teknik müdahalenin doğal bir uzantısı olarak görülmelidir.
Lojistik koordinasyon da göz ardı edilemeyecek bir yük oluşturur. Ekipman, personel ve ulaşım planlaması, olayın büyüklüğüne göre sürekli güncellenmek zorunda kalır. Holguín-Veras ve çalışma arkadaşları (2012), afet lojistiğinin "asla tam olarak planlanamayan" bir alan olduğunu ve en büyük sorunların genellikle malzeme dağıtımında yaşandığını belirtmiştir. KBRN olaylarında bu sorun biraz daha belirgin olur, çünkü özel ekipman gereksinimi lojistik baskıyı artırır.
Koordinasyon yalnızca teknik bir süreç değil, aynı zamanda psikolojik bir denge gerektirir. Ekipler, hem kendi güvenliklerini gözetmek hem de hızlı hareket etmek zorunda olduklarından zaman zaman karar baskısı yaşar. Alexander (2015), bu baskının kontrol edilebilir olduğunu, ancak düzenli tatbikat yapılmadığında ekiplerin müdahale sırasında "karar yorgunluğu" yaşadığını ifade etmiştir. Bu nedenle güçlü bir müdahale koordinasyonu, hem teknik hem insani unsurları birlikte taşır.

10. LİTERATÜR İNCELEMESİ

KBRN olaylarına ilişkin literatür, tek bir alana sıkışmayan oldukça geniş bir yapı sunar. Bu kaynakların bir kısmı askeri geçmişe dayanırken, önemli bir bölümü modern kamu sağlığı ve afet yönetimi çalışmalarından beslenir. Tehdit türleri arasında belirgin ayrımlar olduğundan, literatür çoğu zaman bu ayrımlar üzerinden ilerler. Kimyasal olaylar üzerine yapılan erken araştırmalar, genellikle ani belirtilerin yönetilmesine odaklanmıştır. Sidell (1997), sinir ajanlarının birkaç dakika içinde ölümcül etki gösterebildiğini ve bu nedenle ilk müdahalenin çok kritik olduğunu vurgulamıştır.
Biyolojik tehditlere ilişkin çalışmalar ise daha farklı bir bilgi birikimi sunar. Biyolojik ajanların sessiz ilerlemesi, araştırmacıları erken fark edilme yöntemleri üzerine yoğunlaştırmıştır. Inglesby ve arkadaşları (2000), biyolojik saldırıların geç fark edilmesinin toplum sağlığı açısından en büyük zorluk olduğunu ifade eder. Bu nedenle literatürde sürveyans sistemleri, hızlı test teknolojileri ve epidemiyolojik modellemeler ön plana çıkar.
Radyolojik ve nükleer olaylara ilişkin çalışmalar ise genellikle daha dar ama derin bir çerçeve sunar. Radyasyonun biyolojik etkileri uzun yıllardır araştırılmasına rağmen, acil durum yönetimi bağlamındaki modern çalışmalar daha yenidir. Hall (2000), radyasyonun hücresel düzeyde karmaşık ve gecikmeli hasarlar oluşturduğunu belirtir. Fukushima ve Çernobil sonrası literatür, özellikle uzun dönem izleme çalışmalarının önemini güçlü biçimde göstermiştir. Hasegawa ve çalışma arkadaşları (2015), bu tür olayların yalnızca fiziksel değil, toplumsal etkilerinin de uzun süre devam ettiğini göstermiştir.
Son yıllarda literatürün bir kısmı, kurumlar arası koordinasyon ve teknoloji kullanımının müdahale kapasitesine etkisi üzerinde yoğunlaşmıştır. Boin ve 't Hart (2010), kriz yönetiminde karar süreçlerinin teknik kapasiteden çok iletişim kalitesine bağlı olduğunu savunur. Dijital tespit sistemleri ve simülasyon tabanlı eğitimler üzerine yapılan çalışmalar da giderek artmaktadır. Yates ve Paquette (2011), dijital bilgi akışının olay yönetimini hızlandırdığını ancak doğru kullanım olmadığında bilgi kirliliği yaratabildiğini vurgulamıştır.
Genel olarak literatür, KBRN olaylarının tek bir disiplinden yönetilemeyeceğini ve farklı alanlardan gelen bilgi birikimlerinin birbirini tamamladığını göstermektedir. Bu nedenle literatür, yalnızca teknik bulguları değil; aynı zamanda insan davranışını, kurum işleyişini ve toplumsal etkileri bir arada değerlendiren geniş bir çerçeve sunar.

11. TARTIŞMA VE SONUÇ

KBRN olaylarına ilişkin bulgular bir araya getirildiğinde, bu olayların tek bir disiplinin sınırları içinde yönetilemeyeceği açık biçimde görülüyor. Her olay kendi içinde farklı bir mantıkla ilerliyor ve ekipler çoğu zaman sahada beklenmedik durumlarla karşılaşıyor. Bazen kimyasal bir olayda belirtiler tahmin edildiğinden daha hızlı gelişiyor; bazen de biyolojik bir tehdit günlerce sessiz kalarak tüm değerlendirmeyi zorluyor. Tierney (2014), afetlerde belirsizliğin en büyük baskı unsuru olduğunu ve bu baskının karar doğruluğunu etkilediğini belirtmiştir. Bu çalışma da bu görüşü destekleyen bulgular ortaya koyuyor.
KBRN olaylarında kurumlar arası koordinasyonun önemi özellikle belirgin hâle geliyor. Çünkü tek bir kurumun tüm süreci yönetmesi gerçekçi değil. Ekiplerin farklı uzmanlıklara sahip olması bir avantaj yaratırken aynı zamanda iletişim hatalarına da kapı açabiliyor. Boin ve arkadaşları (2005), kriz yönetiminde küçük iletişim kopukluklarının zincirleme sorunlara neden olduğunu göstermiştir. Bu nedenle güçlü koordinasyon, teknik müdahaleden çok daha geniş bir yapıyı gerektiriyor.
Hazırlık aşamasının tartışılması da önemli sonuçlar ortaya koyuyor. Tatbikatların yalnızca teknik uygulamalar değil, aynı zamanda ekiplerin birbiriyle çalışma uyumunu geliştiren bir süreç olduğu görülüyor. Waugh ve

Streib (2006), tatbikatların kurumlar arası güven duygusunu güçlendirdiğini ve karar hızını artırdığını vurgulamıştır. Bu çalışma, hazırlık aşamasının çoğu zaman hafife alındığını ancak sahada en çok fayda sağlayan adımın yine bu aşama olduğunu gösteriyor.

Olay sonrası dönem de en az akut müdahale kadar önemli. Çünkü su ve besin güvenliği gibi süreçler, olayın görünenden daha uzun süre etkili olmasına neden olabiliyor. Alexander (2013), iyileştirme sürecinin teknik olduğu kadar psikolojik bir süreç olduğunu ve toplumun güven duygusunu yeniden inşa etmenin zaman aldığını ifade eder. KBRN olaylarında bu güven kaybı daha derin yaşanıyor.

Sonuç olarak bu çalışma, KBRN olaylarının yönetiminde tek boyutlu çözümlerin yeterli olmadığını ortaya koyuyor. Etkili bir KBRN yönetimi; esnek planlama, güçlü iletişim, düzenli eğitim, güvenilir tespit mekanizmaları ve kurumlar arası uyum gerektiriyor. Her olayın kendine özgü dinamikleri bulunduğundan, sabit protokollerden çok duruma uyarlanabilir stratejilerin geliştirilmesi gerekiyor. Bu yaklaşım yalnızca müdahale kapasitesini artırmakla kalmaz, aynı zamanda toplumsal dayanıklılığı da belirgin biçimde güçlendirir.

KAYNAKLAR

Alexander, D. E. (2013). Resilience and disaster risk reduction: An etymological journey. *Natural Hazards and Earth System Sciences, 13*(11), 2707–2716.

Blakely, W. F., Ossetrova, N. I., Whitnall, M. H., Sandgren, D. J., Krivokrysenko, V. I., Shakhov, A., & Feinstein, E. (2010). Multiple parameter radiation injury assessment using a nonhuman primate radiation model: Biodosimetry applications. *Health Physics, 98*(2), 153–159. ,

Boin, A., 't Hart, P., Stern, E., & Sundelius, B. (2005). *The politics of crisis management: Public leadership under pressure*. Cambridge University Press.

Boin, A., & 't Hart, P. (2010). Organising for effective emergency management: Lessons from research. *Australian Journal of Public Administration, 69*(4), 357–371.

Clasen, T. F. (2008). *Scaling up household water treatment: Looking back, seeing forward*. World Health Organization.

Clasen, T. (2015). Household water treatment and safe storage to prevent diarrheal disease in developing countries. *Current Environmental Health Reports, 2*(1), 69–74.

Comfort, L. K. (2007). Crisis management in hindsight: Cognition, communication, coordination, and control. *Public Administration Review, 67*(Suppl. 1), 189–197.

Cone, D. C., & Koenig, K. L. (2005). Mass casualty triage in the chemical, biological, radiological, or nuclear environment. *European Journal of Emergency Medicine, 12*(6), 287–302.

Craun, G. F., Craun, M. F., Calderon, R. L., & Beach, M. J. (2006). Waterborne outbreaks reported in the United States. *Journal of Water and Health, 4*(Suppl. 2), 19–30.

Culley, J. M., & Richmond, T. S. (2014). The validity of mass casualty triage systems: A systematic review. *Journal of Emergency Nursing, 40*(5), 461–473.

DiCarlo, A. L., Homer, M. J., & Coleman, C. N. (2021). United States medical preparedness for nuclear and radiological emergencies. *Journal of Radiological Protection, 41*(4), 1420–1434. https://doi.org/10.1088/1361-6498/ac0d3f

Dynes, R. R. (1994). Community emergency planning: False assumptions and other fallacies. *International Journal of Mass Emergencies and Disasters, 12*(2), 141–158.

European Court of Auditors. (2019). *Chemical hazards in our food: EU food safety policy protects us but faces challenges* (Special report 02/2019). Publications Office of the European Union.

Fauci, A. S. (2005). Emerging and reemerging infectious diseases: A 10-year perspective from the National Institute of Allergy and Infectious Diseases. *Emerging Infectious Diseases, 11*(4), 519–525.

Franz, D. R., Jahrling, P. B., Friedlander, A. M., McClain, D. J., Hoover, D. L., Bryne, W. R., Pavlin, J. A., Christopher, G. W., & Eitzen, E. M. (1997). Clinical recognition and management of patients exposed to biological warfare agents. *JAMA, 278*(5), 399–411.

Hall, E. J. (2000). *Radiobiology for the radiologist* (5th ed.). Lippincott Williams & Wilkins.

Hamada, N., & Ogino, H. (2012). Food safety regulations: What we learned from the Fukushima nuclear accident. *Journal of Environmental Radioactivity, 111*, 83–99. https://doi.org/10.1016/j.jenvrad.2011.08.008

Hasegawa, A., Tanigawa, K., Ohtsuru, A., Yabe, H., Maeda, M., Shigemura, J., … Chhem, R. K. (2015). Health effects of radiation and other health problems in the aftermath of nuclear accidents, with an emphasis on Fukushima. *The Lancet, 386*(9992), 479–488. https://doi.org/10.1016/S0140-6736(15)61106-0

Holguín-Veras, J., Jaller, M., Van Wassenhove, L. N., Pérez, N., & Wachtendorf, T. (2012). On the unique features of post-disaster humanitarian logistics. *Journal of Operations Management, 30*(7–8), 494–506.

Holloway, H. C., Norwood, A. E., Fullerton, C. S., Engel, C. C., Jr., & Ursano, R. J. (1997). The threat of biological weapons: Prophylaxis and mitigation of psychological and social consequences. *JAMA, 278*(5), 425–427.

IAEA. (2011). *Preparedness and response for a nuclear or radiological emergency* (Safety Standards Series No. GSR Part 7). International Atomic Energy Agency.

IAEA. (2014). *Radiation protection and safety of radiation sources: International basic safety standards* (Safety Standards Series No. GSR Part 3). International Atomic Energy Agency.

IAEA. (2015). *Preparedness and response for a nuclear or radiological emergency in animal production systems in the context of IAEA safety standards*. International Atomic Energy Agency.

Inglesby, T. V., O'Toole, T., Henderson, D. A., Bartlett, J. G., Ascher, M. S., Eitzen, E., Friedlander, A. M., Gerberding, J., Hauer, J., Hughes, J., McDade, J., Osterholm, M. T., Parker, G., Perl, T. M., Russell, P. K., & Tonat, K. (2000). Anthrax as a biological weapon, 2000: Updated recommendations for management. *JAMA, 283*(17), 2236–2246.

Kapucu, N. (2006). Interagency communication networks during emergencies: Boundary spanners in multiagency coordination. *American Review of Public Administration, 36*(2), 207–225.

Levi, J., Vinter, S., St. Laurent, R., & Segal, L. M. (2008). *Ready or not? Protecting the public's health from diseases, disasters, and bioterrorism*. Trust for America's Health.

Macler, B. A., & Merkle, J. C. (2000). Current knowledge on groundwater microbial pathogens and their control. *Hydrogeology Journal, 8*(1), 29–40.

Mileti, D. S. (1999). *Disasters by design: A reassessment of natural hazards in the United States*. Joseph Henry Press.

Moulder, J. E. (2004). Biological basis of radiation risk. *Journal of the American College of Radiology, 1*(1), 32–37.

Moynihan, D. P. (2008). Learning under uncertainty: Networks in crisis management. *Public Administration Review, 68*(2), 350–365.

Okumura, T., Suzuki, K., Fukuda, A., Kohama, A., Takasu, N., Ishimatsu, S., Hinohara, S., Naito, T., & Ukai, T. (1998). The Tokyo subway sarin attack: Disaster management, Part 2: Hospital response. *Academic Emergency Medicine, 5*(6), 618–624.

Painter, J. A., Hoekstra, R. M., Ayers, T., Tauxe, R. V., Braden, C. R., Angulo, F. J., & Griffin, P. M. (2013). Attribution of foodborne illnesses, hospitalizations, and deaths to food commodities by using outbreak data, United States, 1998–2008. *Emerging Infectious Diseases, 19*(3), 407–415.

Paton, D., & Johnston, D. (2006). *Disaster resilience: An integrated approach*. Charles C Thomas.

Perry, R. W., & Lindell, M. K. (2003). Preparedness for emergency response: Guidelines for the emergency planning process. *Disasters, 27*(4), 336–350.

Ramesh, A. C., & Kumar, S. (2010). Triage, monitoring, and treatment of mass casualty events involving chemical, biological, radiological, or nuclear agents. *Journal of Pharmacy and Bioallied Sciences, 2*(3), 239–247. https://doi.org/10.4103/0975-7406.68506

Rather, I. A., Koh, W. Y., Paek, W. K., & Lim, J. (2017). The sources of chemical contaminants in food and their health implications. *Frontiers in Pharmacology, 8*, 830. https://doi.org/10.3389/fphar.2017.00830

Razak, S., Hignett, S., & Barnes, J. (2018). Emergency department response to chemical, biological, radiological, nuclear, and explosive events: A systematic review. *Prehospital and Disaster Medicine, 33*(5), 543–549. https://doi.org/10.1017/S1049023X18000900

Salem H, Ballantyne B, Katz S. Chemicals used for riot control and personal protection. In: JAJ Romano, BJ Lukey, H Salem, eds. *Chemical Warfare Agents: Chemistry, Pharmacology, Toxicology and Therapeutics*. 2nd ed. CRC Press; 2008: 343-388.

Sidell, F. R., Takafuji, E. T., & Franz, D. R. (Eds.). (1997). *Medical aspects of chemical and biological warfare*. Borden Institute, Office of The Surgeon General, U.S. Army.

Tierney, K. (2014). *The social roots of risk: Producing disasters, promoting resilience*. Stanford University Press.

Tucker, J. B. (2000). *Toxic terror: Assessing terrorist use of chemical and biological weapons*. MIT Press.

UNSCEAR (United Nations Scientific Committee on the Effects of Atomic Radiation). (2010). *Sources and effects of ionizing radiation: UNSCEAR 2008 report to the General Assembly, with scientific annexes*. United Nations.

Vale, J.A., Mercey, D., & Crome, P. (1994). Chemical incidents: Medical management. *BMJ, 308*(6946),1232–1235.

Waugh, W. L., Jr., & Streib, G. (2006). Collaboration and leadership for effective emergency management. *Public Administration Review, 66*(Suppl. 1), 131–140.

Yates, D., & Paquette, S. (2011). Emergency knowledge management and social media technologies: A case study of the 2010 Haitian earthquake. *International Journal of Information Management, 31*(1), 6–13.

ORAL PRESENTATION

Sekonder metabolit tabanlı ilaç yüklü nanoparçacıkların sentezlenmesi ve salınım davranışının modellenmesi

Arzu Aliyeva[1] (ORCID: https://orcid.org/0009-0000-2519-9595), Ayse Isik[2] (ORCID:https://orcid.org/0000-0001-7444-8359), Burcu Guleryuz[3*] (ORCID: https://orcid.org/0000-0003-0762-5567),

[1] Haliç Üniversitesi, Fen-Edebiyat Fakültesi, Moleküler Biyoloji ve Genetik Bölümü, İstanbul, Türkiye
[2] Boğaziçi Üniversitesi, Mühendislik Fakültesi, Biyomedikal Mühendisliği Bölümü, İstanbul, Türkiye
[3] Yeditepe Üniversitesi, Mühendislik Fakültesi, Biyomedikal Mühendisliği Bölümü, İstanbul, Türkiye

*Sorumlu yazar e-mail: burcu.guleryuz@yeditepe.edu.tr

Özet

Nano boyutta geliştirilen ilaç taşıyıcı sistemlerin, ilaç yükleme kapasitesi ve salınım mekanizmaları açısından optimize edilmesi, tedavi etkinliğinin artırılması ve hedefe yönelik ilaç iletimi açısından büyük önem taşımaktadır. Bu çalışmada, yoğun silika nanoparçacıkları (YSN) manganez dioksit (MnO_2) nanoplakaları ile kaplanarak hibrit bir nanotaşıyıcı sistem (YSN-MnO_2) geliştirilmiştir. Anti-kanser ve anti-bakteriyel etkileriyle bilinen, ancak hidrofobik doğası nedeniyle biyolojik uygulamalarda sınırlı çözünebilirlik gösteren usnik asit (UA), bu taşıyıcı sisteme yüklenmiştir. Yaklaşık 150 nm çapında, kolay ve hızlı şekilde sentezlenebilen YSN–MnO_2 formülasyonunun morfolojik ve kimyasal özellikleri karakterize edilmiştir. Takiben, 1.5 mg YSN–MnO_2 nanoparçacıklarına yüklenen UA miktarının 0.3 mg olduğu, UV–Vis spektrofotometre ile belirlenmiştir. Ayrıca, tümör mikro-ortamını simüle etmek amacıyla UA salınımı fizyolojik pH (7.4) ve asidik pH (5.5) koşullarında değerlendirilmiştir. Elde edilen kümülatif salınım verileri kullanılarak farklı kinetik modeller ((sıfırıncı, birinci ve Higuchi) uygulanmış ve UA salınımının birinci derece modele en iyi uyum gösterdiği belirlenmiştir. Bulgular, YSN-MnO_2 sisteminin asidik ortamda UA salınımının hızlandığını ve kontrollü salınım potansiyeline sahip etkili bir nanotaşıyıcı olduğunu göstermektedir. Ek olarak, sistemin hücresel etkilerini değerlendirmek amacıyla prostat kanseri hücre hattı (PC3) üzerinde yürütülen *in vitro* analiz, UA@YSN–MnO_2 nanoparçacıklarının yalnızca 1 saatlik inkübasyon sonrasında hücre morfolojisinde belirgin değişimlere ve hızlı hücre–nanoparçacık etkileşimine neden olduğunu ortaya koymuştur.

Anahtar Kelimeler: Usnik asit; Yoğun silika nanoparçacıkları; Manganez dioksit; Kontrollü ilaç salınımı

Synthesis of secondary metabolite-based drug-loaded nanoparticles and modeling of their release behavior

Abstract

Optimizing drug delivery systems developed at nanoscale in terms of drug loading capacity and release mechanisms is crucial for increasing therapeutic efficacy and targeted drug delivery. In this study, a hybrid nanocarrier system (DSN-MnO_2) was developed by coating dense silica nanoparticles (DSN) with manganese dioxide (MnO_2) nanoplates. Usnic acid (UA), known for its anti-cancer and antibacterial properties but with limited solubility in biological applications due to its hydrophobic nature, was loaded into this carrier system. The morphological and chemical properties of the DSN-MnO_2 formulation, which is easily and rapidly synthesized and has a diameter of approximately 150 nm, were characterized. Subsequently, the amount of UA loaded into 1.5 mg of DSN-MnO_2 nanoparticles was determined to be 0.3 mg using a UV-Vis spectrophotometer. Additionally, UA release was evaluated at physiological pH (7.4) and acidic pH (5.5) to simulate the tumor microenvironment. Different kinetic models (zero-, first-, and Higuchi-order) were applied using the cumulative release data, and it was determined that UA release best fit the first-order model. The findings indicate that the DSN-MnO_2 system accelerates UA release in acidic environments and is an effective nanocarrier with controlled release potential. Additionally, in vitro analysis conducted on a prostate cancer cell line (PC3) to evaluate the cellular effects of the system revealed that UA@DSN–MnO_2 nanoparticles caused significant changes in cell morphology and rapid cell-nanoparticle interactions after only 1 hour of incubation.

Keywords: Usnic acid; Dense silica nanoparticles; Manganese dioxide; Controlled drug release

GİRİŞ

Nanoteknoloji, son yıllarda farmasötik araştırmalarda özellikle hedefe yönelik ilaç taşıyıcı sistemlerinin geliştirilmesinde önemli bir alan haline gelmiştir. Nanoparçacıklar, yüksek yüzey alanı ve modifiye edilebilir yüzey özellikleri sayesinde ilaç yükleme kapasitesini artırmakta ve kontrollü salım potansiyeli sunmaktadır (Aparna ve ark., 2025; Dadwal ve ark., 2018). Bu özellikler, hidrofobik doğaya sahip bileşiklerin biyolojik sistemlerde kullanımını kolaylaştırmakta ve tedavi etkinliğini artırmaktadır. Yoğun silika nanoparçacıkları (YSN), kimyasal kararlılık, biyouyumluluk ve yüzey modifikasyon olanakları ile öne çıkan bir taşıyıcı sistemi sunmaktadır (Macedo ve ark., 2021; Meng ve ark., 2024). YSN nanoparçacıklarının MnO_2(mangan diokits) ile kaplanması, hem taşıyıcıların yapısal bütünlüğünü korumakta hem de tümör mikroçevresine duyarlı ilaç salımını desteklemektedir (Chen ve ark., 2019; Wu ve ark., 2019).

Sekonder metabolitler, başta usnik asit (UA) gibi terpenoidler, antikanser ve antibakteriyel aktiviteleri nedeniyle oldukça ilgi çekmektedir; ancak hidrofobik yapıları nedeniyle biyoyararlanımları sınırlıdır (Kumar ve ark., 2020; Patra ve ark., 2018). Nanoparçacık taşıyıcılar, bu tip moleküllerin çözünürlüğünü artırarak hedefe yönelik salımı mümkün kılmakta ve yan etkilerin azaltılmasına katkıda bulunmaktadır (Bae ve ark., 2024; Chandratre ve Dash, 2015). Salım davranışının kinetik modeller ile incelenmesi, taşıyıcı sistemlerin etkinliğini ve ilaç salım mekanizmasını anlamada kritik öneme sahiptir. Özellikle birinci derece kinetik model, difüzyon ve yüzey etkileşimlerinin salım sürecinde belirleyici olduğunu ortaya koymakta ve hidrofobik ilaçların silika bazlı taşıyıcılarda davranışını başarılı şekilde açıklamaktadır (Kumar ve ark., 2021).

Bu çalışmada, YSN nanoparçacıklarının MnO_2 kaplaması ile hibrit bir sistem oluşturulmuş ve UA yüklemesi gerçekleştirilmiştir. Sistem, morfolojik, kimyasal ve salım özellikleri açısından karakterize edilmiş; farklı pH koşullarında salım kinetiği incelenmiş ve in vitro PC-3 hücre hattı üzerinde terapötik potansiyeli değerlendirilmiştir. Elde edilen bulgular, pH-duyarlı nanotaşıyıcıların kontrollü ilaç salımı ve hedefe yönelik tedavi stratejileri için uygun bir platform oluşturduğunu göstermektedir (Zhou ve ark., 2019; Wang ve ark., 2020; Zhang ve ark., 2020).

MATERYAL VE METOT

Kimyasallar ve Reaktifler

Bu çalışmada kullanılan usnik asit (UA), tetraetil ortosilikat (TEOS), amonyak çözeltisi (NH_4OH), potasyum permanganat ($KMnO_4$), etanol ve fosfat tampon çözeltisi (PBS) analitik saflıkta olup ticari kaynaklardan temin edilmiştir.

Yoğun Silika Nanoparçacıklarının Sentezi

Yoğun silika nanoparçacıkları için etanol, saf su ve amonyak 50°C'de karıştırılmış, ardından TEOS damla damla eklenerek 2 saat 400 RPM'de karıştırılmıştır. Oluşan nanoparçacıklar santrifüj edilip etanol ve su ile iki kez yıkanmış, sonra tüplere alınarak fırında 24 saat kurutulmuş ve SiO_2 nanopartikülleri elde edilmiştir.

MnO_2 Kaplı Silika Nanoparçacıklarının Hazırlanması

YSN-MnO_2 nanoparçacıkları sentezi için NaOH (%1 M) ve MES tamponu (%0,1 M, pH 5.0) hazırlanmış, $KMnO_4$ (%10 mM) çözeltisi karanlıkta çözündürülmüştür. MES tamponu (900 µL), sonike edilmiş 10 mg/mL SiO_2 solüsyonu (150 µL) ve $KMnO_4$ çözeltisi (300 µL) 15 mL tüpe eklenmiş, sonik prob ile %20 güçte 10 dakika işlenerek YSN-MnO_2 nanoparçacıkları elde edilmiştir. Oluşan sarı-kahverengi partiküller 2 mL tüplere alınarak üç kez su ile yıkanmıştır.

Sekonder Metabolit (Usnik Asit) Yükleme İşlemi

Usnik asit yüklemesi için 5 mg/mL çözeltisi hazırlanmış, ultrasonik banyoda 10 dakika bekletilmiştir. 5 mL beherde 1500 µL MnO_2 süspansiyonu, 300 µL DMSO+usnik asit ve 1200 µL distile su karıştırılmış, manyetik karıştırıcıda 24 saat tutulmuş ve ardından 13.200 rpm'de 10–15 dakika santrifüj edilerek MnO_2 partikülleri ayrılmıştır.

Hücrelere nanoparçacıklarının uygulanması

Prostat kanseri hücreleri 96 kuyucuklu plaklara 15.000 hücre/kuyu olacak şekilde ekilmiş, 24 saat inkübe edildikten sonra kültür ortamı 50 µg/mL UA@YSN-MnO_2 içeren taze ortamla değiştirilmiş ve 24 saat daha inkübasyona bırakılmıştır. İnkübasyon sonunda hücre morfolojisi ters ışık mikroskobu ile incelenmiştir.

Nanoparçacıkların Karakterizasyonu

Nanoparçacıkların boyut dağılımı SEM (Thermo Scientific Quattro S) ile, yüzey kimyasal özellikleri FTIR (Thermo Scientific Nicolet 380) ile, soğurma özellikleri ise UV–Vis (Thermo Scientific Nanodrop 2000c) ile analiz edilmiştir.

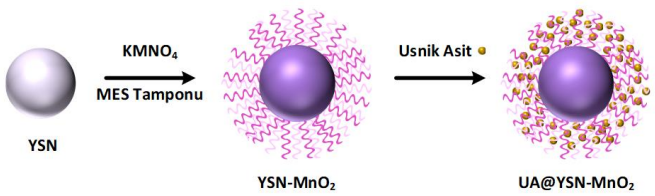
İlaç çıkışı deneyi

İlaç çıkışı deneyi için UA, MnO_2 nanoparçacıklara yüklenmiş ve PBS (pH 7.4) ile asidik ortamda (pH 5.5) santrifüj tüplerinde sürekli karıştırılmıştır. Belirli aralıklarla alınan numunelerde salınan ilaç miktarı UV–Vis ile ölçülmüş, pH değerleri pH metre ile doğrulanmış ve çözeltiler her analiz öncesi taze hazırlanmıştır.

BULGULAR ve TARTIŞMA

Nanoparçacıkların Sentezlenmesi ve Karakterizasyonu

Nanoparçacıklar, MnO_2 kaplı silika üzerinde usnik asit taşımak üzere hazırlanmış ve detaylı karakterizasyonla incelenmiştir. İlaç salımı farklı pH'larda ölçülmüş ve çeşitli kinetik modellerle değerlendirilmiştir.

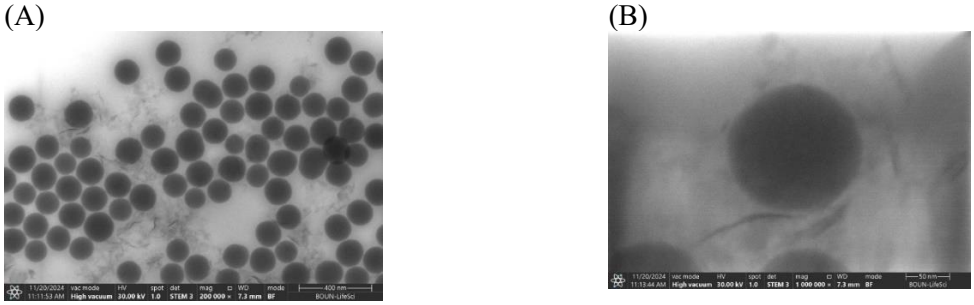


Şekil 1. UA@YSN-MnO_2 nanoparçacıkların sentezlenme aşamalarının şematik gösterimi.

SEM (Taramalı Elektron Mikroskopu) Ölçümü

Nanoparçacıkların yüzey yapısı, Taramalı Elektron Mikroskobu (SEM) ile analiz edilmiştir. Elde edilen görüntüler, MnO_2 kaplı silika nanoparçacıkların büyük ölçüde küresel formda olduğunu, homojen boyut dağılımına sahip olduğunu ve yaklaşık 120–140 nm çapında olduğunu göstermiştir, MnO_2 tabakasının silika yüzeyine etkin bir şekilde bağlandığını ve kaplama sonrası parçacıklarda belirgin şekil bozulması veya düzensizlik gözlenmediğini doğrulamaktadır.

(A) (B)

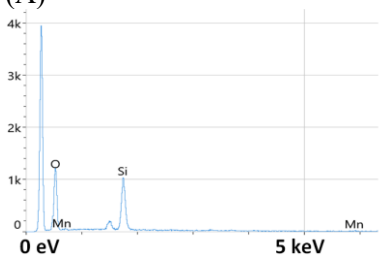


Şekil 2. YSN-MnO_2 nanoparçacığın SEM ile farklı ölçeklerde görüntülenmesi: (A) 400 nm ve (B) 50 nm.

EDS (Enerji Dağılım Spektroskopisi) Ölçümü

Enerji Dağılım Spektroskopisi (EDS), elektron ışını ile açığa çıkan X-ışınları sayesinde numunenin elementel bileşimini belirler (Giardino ve ark., 2024).Hazırlanan YSN-MnO_2 nanoparçacıkları SEM-EDS (EDAX METEK) sistemi ile analiz edilmiştir (Şekil 3). Element haritalama sonuçları, yapıda O, Si ve Mn elementlerinin bulunduğunu göstermiştir. O ve Si sinyalleri SiO_2 yapısını doğrularken, manganın karakteristik pikleri MnO_2 kaplamasının başarıyla gerçekleştirildiğini ortaya koymaktadır.

(A)



(B)

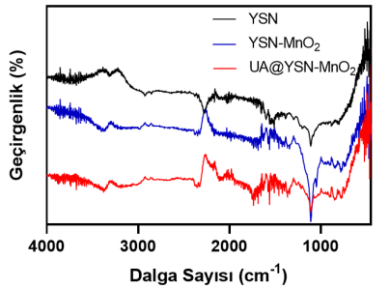
Element	Weight %
O	67.9
Si	31.2
Mn	0.9

Şekil 3. YSN-MnO_2 nanoparçacığın EDS analiz verileri.

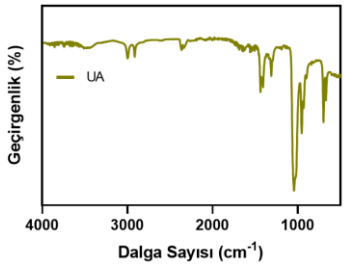
FT-İR (Fourier Dönüşümlü Kızılötesi Spektroskopisi) Ölçümü

FTIR analizi, nanoparçacıkların kimyasal yapısını ve usnik asit yüklemesini doğrulamak için yapılmıştır. YSN ve YSN-MnO_2'de 500–600 cm^{-1} (Mn–O) ve ~1080 cm^{-1} (Si–O–Si) bantları gözlenmiştir. UA@YSN-MnO_2'de ise 3400–3200 cm^{-1} (O–H), 2920–2850 cm^{-1} (C–H), 1720 cm^{-1} (C=O) ve 1600–1500 cm^{-1} (aromatik C=C) bantları belirlenmiş, hafif kaymalar usnik asidin nanoparçacık yüzeyine bağlandığını göstermiştir. Bulgular, usnik asidin başarılı şekilde yüklendiğini ve matrisin korunduğunu doğrulamaktadır.

(A)



(B)



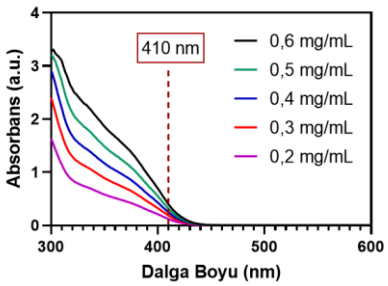
Şekil 4. (A) YSN, YSN-MnO_2 ve UA@YSN-MnO2 formülasyonları ve (B) sekonder metabolit UA için FTIR analizi sonuçları

UA'nın Yüklenmesi Sonuçları

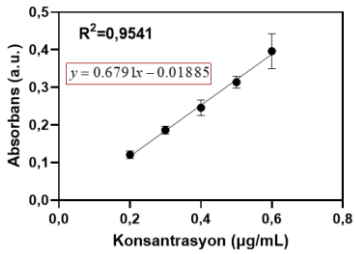
Usnik asit farklı konsantrasyonlarda hazırlanarak 96 kuyucuklu mikroplakalarda UV–Vis spektrofotometresi ile 300–800 nm aralığında analiz edilmiştir. 410 nm'de ölçülen absorbans değerleri kullanılarak oluşturulan lineer denklem (Denklem 1), nanoparçacıklara yüklenen UA miktarının hesaplanmasında kullanılmıştır. Yükleme sonrası UA@YSN-MnO_2 süspansiyonu santrifüjlenmiş, süpernatanttan ölçülen absorbans ile bağlanmamış usnik asit miktarı belirlenmiştir. Üç tekrarlı deneyler sonucunda yüklenen usnik asit miktarı 0,28409 ± 0,10928 mg olarak hesaplanmıştır.

$$y = 0.6791x - 0.01885 \quad (1)$$

(A)



(B)

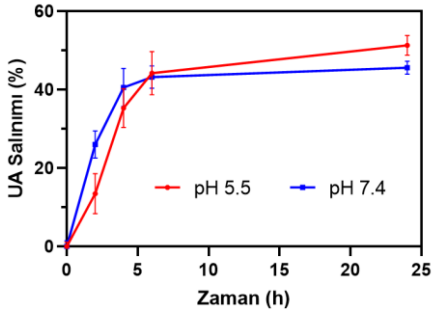


Şekil 5. (A) İlaç yükleme deneyi için usnik asitin farklı konsantrasonlarda alınan absorbans değerlerini ve (B) 410 nm bandına karşılık gelen konsantrasyon-absorbans denkleminin eldesi.

İlaç Salınım Deneyi Sonuçları

Usnik asit yüklü YSN-MnO_2 nanoparçacıklarının ilaç salımı pH 5.5 ve 7.4 ortamlarında farklı zamanlarda incelenmiştir (Şekil 6). 2. saatte pH 7.4'te %26, pH 5.5'te %13,5 salım; 4–6. saatlerde her iki ortamda yaklaşık

%40; 24. saatte ise pH 5.5'te %51,3, pH 7.4'te %45,6 salım gözlenmiştir. Bu sonuçlar, sistemin pH-duyarlı salım sergilediğini göstermektedir.



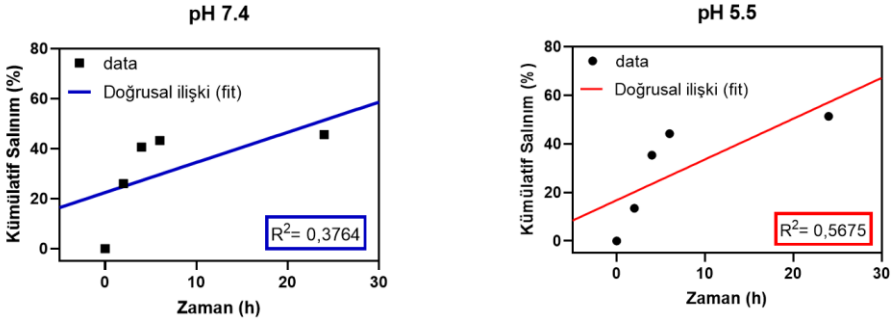
Şekil 6. pH 7.4 ve 5.5 koşullarında YSN-MnO_2'den UA salınımı.

UA Salımın Kinetik Modellemesi

UA'nın salınım mekanizmasını değerlendirmek amacıyla deneysel veriler sıfırıncı derece, birinci derece ve Higuchi kinetik modellerine uygulanmıştır.

Sıfırıncı Dereceden Salım Modeli

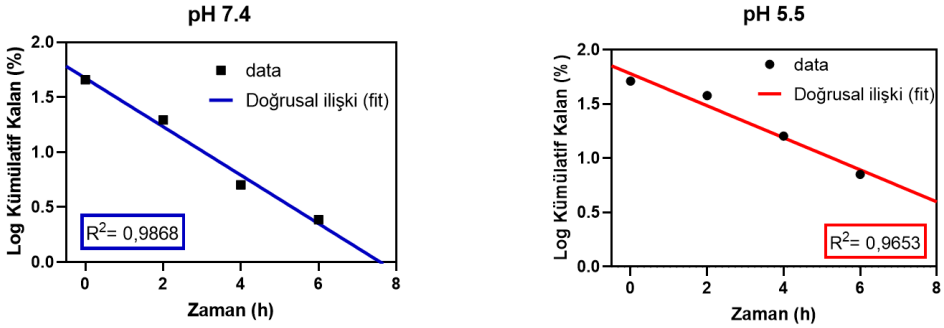
Bu kinetik model, UA salınımının hızını zamana bağlı olmayan durumda incelemektedir. Bu modele uygun salınıma sahip nanoparçacık sistemlerinde birim zamanda salınan ilaçların miktarı her zaman aynı olmalıdır. Bu nanoparçacık sisteminde sıfırıncı derece kinetik modeli ile uyumunu ifade eden R^2 verileri ph 7.4 ortamında 0,38 iken pH 5.5 ortamında 0,57 olarak bulunmuştur (Şekil 7). Modelin UA salınımını yeterli doğrulukta açıklamadığı sonucuna ulaşılmıştır



Şekil 7. Sıfırıncı derece salınım modeli ile nanoparçacıkların incelenmesi

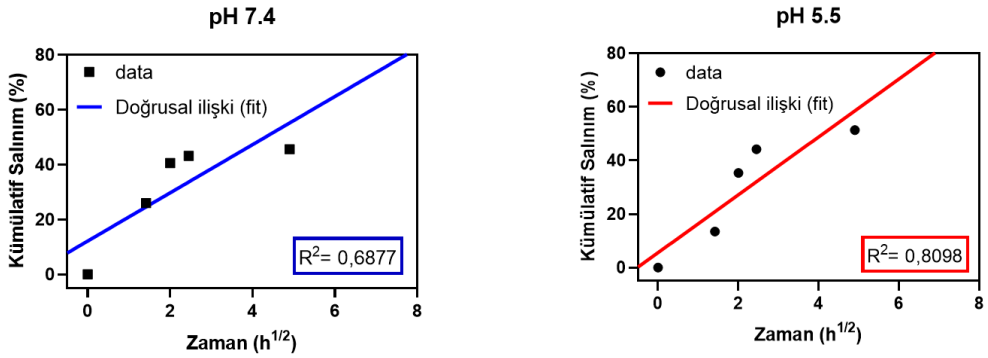
Birinci Dereceden Salım Modeli

Nanoparçacıklarda kalan ilaç miktarına bağlı olduğu varsayımına dayanarak salınımı inceleyen bir modeldir. Zamanla ilaç miktarı azaldığından salınımında doğru orantılı azaldığını ifade eden bir profil gözlenmesi beklenir. UA@YSN-MnO_2 nanoparçacıklarının R^2 değerleri, pH 7.4 ortamında 0,99, pH 5.5 ortamında ise 0,96 olarak bulunmuştur. Her iki ortamda da yüksek korelasyon katsayısı, UA salınımının birinci dereceden kinetiğe güçlü bir şekilde uyduğunu göstermektedir.



Şekil 8. Birinci derece salınım modeli ile nanoparçacıkların incelenmesi

Higuchi Salım Modeli

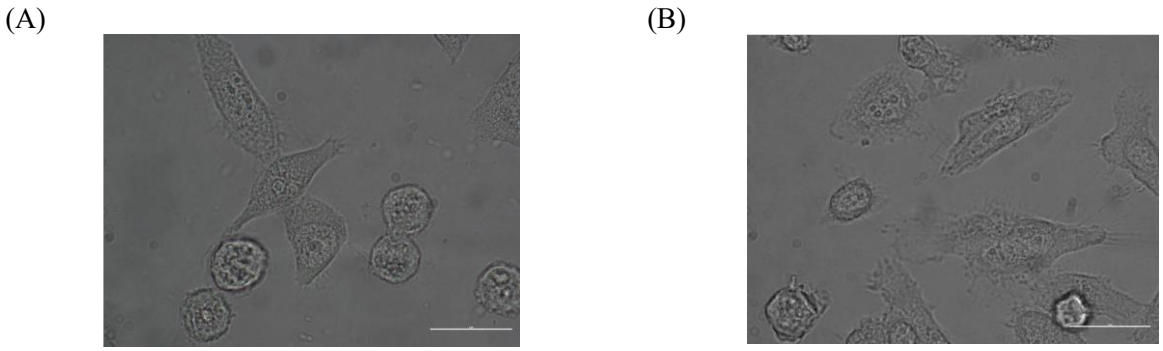


Şekil 9. Higuchi modeli ile nanoparçacıkların incelenmesi

Higuchi modeli 1961 yılında Takeru Higuchi tarafından geliştirilmiş olup özellikle difüzyona dış ortama geçen ilacı ifade eder. Nanoparçacıklarda yüksek konsantrasyonda bulunan ilaç yoğunluğu az olan bölgeye doğru hareket etmesidir. R^2 değerleri, pH 7.4 ortamında 0,69, pH 5.5 ortamında ise 0,81 olarak bulunmuştur. Bu sonuçlar UA salınımının yalnızca kısmen Higchi kinetiğine uyduğunu göstermektedir.

Hücresel etkinlik

Şekil 10'da kontrol grubu ve UA yüklü YSN–MnO_2 nanoparçacıkları ile muamele edilen hücrelerin mikroskop görüntüleri karşılaştırılmaktadır. Kontrol hücreleri sağlıklı ve düzenli morfoloji sergilerken, UA@YSN–MnO_2 uygulanan hücrelerde 1 saat içinde yuvarlaklaşma, büzülme, hücre bağlantılarının kopması ve hücre yoğunluğunda azalma gözlenmiştir. Bu bulgular, sistemin sitotoksik etkisinin başladığını göstermektedir.



Şekil 10. A) Kontrol grubu ve B) 50 µg/mL UA@YSN–MnO_2 nanoparçacıklarıyla 1 saat inkübe edilen hücrelerin mikroskop görüntüleri.

Geliştirilen YSN-MnO_2 hibrit nanoparçacıklar, ~150 nm boyutunda ve düzgün yüzey morfolojisine sahiptir; SEM görüntüleri kaplamanın başarılı olduğunu ve morfolojik bütünlüğün korunduğunu göstermiştir (Zhang ve ark., 2020). Nanoparçacıklara yaklaşık 0,3 mg usnik asit yüklenmiş, salım çalışmaları sistemin pH-duyarlı olduğunu ortaya koymuştur; 24. saatte asidik ortamda %51,3, fizyolojik pH'da %45,6 salım gözlenmiştir (Patra ve ark., 2018). Kinetik analiz, salımın birinci derece modele uyduğunu göstermiştir (Kumar ve ark., 2021). Hücresel etkinlik deneyleri, UA@YSN–MnO_2'nin hızlı sitotoksik etki oluşturduğunu doğrulamıştır (Wang ve ark., 2020). Bu bulgular, YSN-MnO_2 tabanlı pH-duyarlı nanotaşıyıcıların kontrollü ilaç salımı ve terapötik etki için uygun olduğunu ve tümör mikroçevresinde hedefe yönelik dağılım potansiyelini göstermektedir (Zhou ve ark., 2019).

SONUÇ

Elde edilen bulgular, pH-duyarlı nanotaşıyıcıların kontrollü ilaç salımı ve hedefe yönelik tedavi açısından etkin bir platform oluşturduğunu ortaya koymaktadır. Bu çalışma, MnO_2 kaplı yoğun silika nanoparçacıkları kullanılarak usnik asidin pH-duyarlı ve kontrollü salım davranışının kinetik modelleme ve hücresel analizler ile birlikte değerlendirilmesini sağlamaktadır.

TEŞEKKÜR

Bu çalışma kapsamında sağlanan laboratuvar altyapısı ve teknik destek için Haliç Üniversitesi, Boğaziçi Üniversitesi ve Yeditepe Üniversitesi'ne teşekkür ederiz.

KAYNAKLAR

Ateş, M. (2018). Nanoparçacıkların Ölçme ve İnceleme Teknikleri. *Turkish Journal of Scientific Reviews*, 11(1), 63–69.

Ateş, M. (2022). The Fourier transform infrared spectroscopy (FTIR) analysis for the clay mineralogy studies in a clastic reservoir. *Journal of Petroleum Exploration and Production Technology*, 12(8), 2093–2106.

Aparna, T. N., Kumar, R., Ali, S. R., Patel, D. J., Julekha, K., Begum, T., Bala, J., & Kumar, P. (2025). Silica nanoparticles: A promising vehicle for anti-cancer drugs delivery. *AAPS PharmSciTech*, 26(1), 33. https://doi.org/10.1208/s12249-024-02982-9

Bae, T., Hallis, S. P., & Kwak, M. K. (2024). Hypoxia, oxidative stress, and the interplay of HIFs and NRF2 signaling in cancer. *Experimental & Molecular Medicine*, 56(4), 501–514. https://doi.org/10.1038/s12276-024-01180-8

Baetke, S. C., Lammers, T. G. G. M., & Kiessling, F. (2015). Applications of nanoparticles for diagnosis and therapy of cancer. *The British Journal of Radiology*, 88(1054), 20150207.

Chandratre, S. S., & Dash, A. K. (2015). Multifunctional nanoparticles for prostate cancer therapy. *AAPS PharmSciTech*, 16, 98–107.

Chen, Q., Feng, L., Liu, J., & Ding, X. (2019). MnO_2-based nanoplatforms for cancer therapy: Progress and perspectives. *Advanced Materials*, 31(6), 1802725.

Dadwal, A., Baldi, A., & Kumar Narang, R. (2018). Nanoparticles as carriers for drug delivery in cancer. *Artificial Cells, Nanomedicine, and Biotechnology*, 46(sup2), 295–305.

Giardino, M., Gobber, F. S., Pennacchio, A., & Grande, M. A. (2024). Study of metal powders oxidation by means of Energy Dispersion Spectroscopy (EDS). In *BIO Web of Conferences* (Vol. 129, p. 23027). EDP Sciences.

Greene, A., Hashemi, J., & Kang, Y. (2020). Development of MnO_2 hollow nanoparticles for potential drug delivery applications. *Nanotechnology*, 32(2), 025713.

Kumar, K., Mishra, J. P., & Singh, R. P. (2020). Usnic acid induces apoptosis in human gastric cancer cells through ROS generation and DNA damage and causes up-regulation of DNA-PKcs and γ-H2A. X phosphorylation. *Chemico-Biological Interactions*, 315, 108898.

Macedo, D. C. S., Almeida, F. J. F., Wanderley, M. S. O., Ferraz, M. S., Santos, N. P. S., López, A. M. Q., ... & Lira-Nogueira, M. C. B. (2021). Usnic acid: From an ancient lichen derivative to promising biological and nanotechnology applications. *Phytochemistry Reviews*, 20, 609–630.

Meng, J., Wang, Z. G., Zhao, X., Wang, Y., Chen, D. Y., Liu, D. L., ... & Yin, Z. T. (2024). Silica nanoparticle design for colorectal cancer treatment: Recent progress and clinical potential. *World Journal of Clinical Oncology*, 15(6), 667–673. https://doi.org/10.5306/wjco.v15.i6.667

Wu, M., Hou, P., Dong, L., Cai, L., Chen, Z., Zhao, M., & Li, J. (2019). Manganese dioxide nanosheets: From preparation to biomedical applications. *International Journal of Nanomedicine*, 14, 4781–4800.

Yang, G., Xu, L., Chao, Y., Xu, J., Sun, X., Wu, Y., ... & Liu, Z. (2017). Hollow MnO_2 as a tumour-microenvironment-responsive biodegradable nano-platform for combination therapy favouring antitumor immune responses. *Nature Communications*, 8(1), 902.

ORAL PRESENTATION

Silajlık mısır (*Zea mays* L.) çeşit adaylarının ikinci ürün koşullarında performanslarının belirlenmesi

Sinem Zere Taşkın[1*] (ORCID: https://orcid.org/0000-0002-2243-2993),
Uğur Bilgili[2] (ORCID: https://orcid.org/0000-0003-0801-7678)

[*1]Bursa Uludag University, Faculty of Agriculture, Department of Field Crops, Bursa, Türkiye.
[2]Bursa Uludag University, Faculty of Agriculture, Department of Field Crops, Bursa, Türkiye.

* Sorumlu yazar e-mail: sinemzere@uludag.edu.tr

Özet

Bu çalışma, bazı silajlık mısır (*Zea mays* L.) çeşit adaylarının ikinci ürün koşullarında performanslarını değerlendirmek amacıyla Bursa Uludağ Üniversitesi Ziraat Fakültesi Tarımsal Uygulama ve Araştırma Merkezi'nde 2023 yılında yürütülmüştür. Araştırmada 22 adet yeni geliştirilmiş F1 hibridi ve 7 adet ticari yüksek verimli kontrol hibridi bitki materyali olarak kullanılmıştır. Tüm genotipler atdişi tane yapısında olup FAO olum grupları 500–750 arasında değişmektedir. Deneme, tesadüf blokları deneme desenine göre 3 tekerrürlü olarak yürütülmüştür. Çalışmada bitki boyu (cm), ilk koçan yüksekliği (cm), koçan/bitki oranı (%), yaprak/sap oranı (%), sap çapı (mm), yeşil ot verimi (t da^{-1}) ve kuru madde verimi (t da^{-1}) parametreleri incelenmiştir. Araştırma sonuçlarına göre bitki boyu 221.1–283.0 cm, ilk koçan yüksekliği 79.1–125.4 cm, koçan/bitki oranı %39.9–51.7, yaprak/sap oranı %32.3–50.9, sap çapı 17.6–24.3 mm, yeşil ot verimi 3.63–6.36 t da^{-1} ve kuru madde verimi ise 1.11–2.03 t da^{-1} arasında değişmiştir. En yüksek yeşil ot verimi kontrol hibritlerini geride bırakarak PN22 genotipinden, en yüksek kuru madde verimi ise PN13 genotipinden elde edilmiştir.

Anahtar Kelimeler: *Zea mays* L, genotip, yeşil ot verimi.

Performance evaluation of candidate silage maize (*Zea mays* L.) hybrids under second-crop production conditions

Abstract

This study was conducted in 2023 at the Agricultural Practice and Research Center of Bursa Uludag University Faculty of Agriculture to evaluate the performance of some candidate silage maize (*Zea mays* L.) hybrids under second-crop growing conditions. A total of 22 newly developed F1 hybrids and 7 high-yielding commercial control hybrids were used as plant material. All genotypes possessed dent kernel type and belonged to FAO maturity groups ranging from 500 to 750. The experiment was laid out in a randomized complete block design with three replications. In the study, plant height, ear height, ear/plant ratio, leaf/stem ratio, stem diameter, forage yield, and dry matter yield were investigated. According to the research results, plant height ranged from 221.1 to 283.0 cm, ear height from 79.1 to 125.4 cm, ear/plant ratio from 39.9% to 51.7%, leaf/stem ratio from 32.3% to 50.9%, stem diameter from 17.6 to 24.3 mm, forage yield from 3.63–6.36 t da^{-1}, and dry matter yield from 1.11–2.03 t da^{-1}. The highest forage yield was obtained from genotype PN22, surpassing the commercial control hybrids, while the highest dry matter yield was recorded in genotype PN13.

Keywords: *Zea mays* L, genotype, forage yield.

GİRİŞ

Mısır (*Zea mays* L.), yüksek verim potansiyeli, iyi sindirilebilirliği ve lezzetliliğinin yanı sıra yüksek kuru madde ve enerji içeriğine sahip olması nedeniyle hayvan beslenmesinde önemli bir yer tutmaktadır. Ayrıca tarımın tüm aşamalarında mekanizasyona uygun olması, geniş alanlarda düşük maliyetle üretimine olanak sağlamaktadır. Bu özellikleri sayesinde mısır, dünyada ve Türkiye'de silaj üretiminde en yaygın olarak tercih edilen yem bitkilerinden biri hâline gelmiştir (Özata ve ark., 2011).

Son yıllarda hayvancılık sektöründe artan kaba yem ihtiyacı, silajlık mısır çeşitlerine olan ilginin daha da artmasına neden olmuştur. Kaliteli silaj üretimi; süt ve et veriminin yükseltilmesi, yem maliyetlerinin

azaltılması ve sürdürülebilir hayvansal üretimin devamlılığı açısından büyük önem taşımaktadır. Bu doğrultuda, silajlık amaçla geliştirilen yeni hibritlerin yaygınlaşması ile birlikte tanelik mısır çeşitlerinin silajlık olarak da kullanılabileceği görüşü önemini kaybetmiş; seleksiyon kriterleri, kalite ve verim odaklı olarak yeniden şekillenmiştir (Ma ve ark., 2006).

Silajlık mısır yetiştiriciliğinde uygun çeşit seçimi ve doğru agronomik uygulamalar başarıyı doğrudan etkilemektedir (Oliveira ve ark., 2019). Her genotip çevre koşullarına bağlı olarak farklı performans gösterebilmekte; bu nedenle yetiştirilecek bölgeye uyum yeteneği yüksek, verimli ve kaliteli materyallerin belirlenmesi gerekmektedir (Zopollatto ve ark., 2009).

Bu araştırma, Bursa ekolojik koşullarında ikinci ürün olarak yetiştirilen bazı silajlık mısır çeşit adaylarının verim ve verim unsurları bakımından performanslarını değerlendirmek amacıyla yürütülmüştür..

MATERYAL VE METOT

Araştırma Bursa Uludağ Üniversitesi Ziraat Fakültesi Tarımsal Uygulama ve Araştırma Merkezi'nde 2023 yılında yürütülmüştür. Araştırmanın yürütüldüğü Bursa ilinde, Köppen–Geiger iklim sınıflandırmasına göre sıcak yazların görüldüğü ve yazların kurak, kışların ılık ve yağışlı geçtiği Csa tipinde Akdeniz iklimi hakimdir (Yılmaz ve Çiçek, 2018). Çalışmanın yürütüldüğü yıllara ait iklim verileri ve uzun yıllar ortalaması Tablo 1'de sunulmuştur.

Tablo 1. Denemenin yürütüldüğü Bursa İlinde 2023 yıllına ait ortalama sıcaklık (°C), toplam yağış (mm) ve ortalama nem (%) değerleri.

Aylar	Ortalama Sıcaklık (°C)		Toplam Yağış (mm)		Ortalama Nem (%)	
	2023	UYO*	2023	UYO	2023	UYO
Haziran	24.3	22.5	0.0	42.1	63.0	62.7
Temmuz	26.1	25.1	0.0	15.1	57.8	59.4
Ağustos	27.1	25.1	0.0	16.9	60.4	61.3
Eylül	22.6	20.8	0.0	50.3	62.9	67.4
Ekim	18.2	15.9	7.3	84.2	70.5	74.7
Kasım		10.8		69.7		75.4
Toplam			7.3	278.3		
Ortalama	23.66	20.0			62.92	66.82

*: UYO: Uzun yıllar ortalaması (1990-2020)

Deneme alanının farklı yerlerinden 0-20 cm derinlikten alınan toprak örneklerinin fiziksel ve kimyasal analizleri Uludağ Üniversitesi Ziraat Fakültesi, Toprak Bilimi ve Bitki Besleme Bölümü, Toprak Analiz Laboratuvarı'nda yaptırılmış ve sonuçlar Tablo 2'de sunulmuştur. Analiz sonuçlarına göre, deneme alanı toprağı tınlı bünyeye sahip olup hafif alkali özellik göstermektedir (pH 8.48). Fosfor ve potasyum içeriği yüksek, organik madde miktarı orta düzeydedir. Tuzluluk problemi bulunmayıp, azot yönünden fakirdir. Kireç içeriği ise orta kireçli sınıfa yakın değerlere sahiptir.

Tablo 2. Çalışmanın yürütüldüğü Uludağ Üniversitesi Ziraat Fakültesi Tarımsal Uygulama ve Araştırma Merkezi'ndeki deneme alanının toprak analiz sonuçları.

% Kum	46.25
% Silt	30.99
% Kil	22.76
Tekstür	Tın
pH	8.48
EC, µS cm^{-1}	468
KDK, meq 100 g^{-1}	15.21
Kireç, %	4.28
Organik madde %	2.091

% N	0.106
Alınabilir P, mg kg^{-1}	30.95
Toplam K mg kg^{-1}	5180

Bu çalışmada 22 adet yeni geliştirilen F1 hibriti (PN2, PN3, PN4, PN5, PN7, PN8, PN9, PN11, PN12, PN13, PN14, PN15, PN16, PN17, PN18, PN21, PN22, PN23, PN24, PN26, PN27, PN28) ve 7 adet ticari yüksek verimli silajlık kontrol hibriti (PN1, PN6, PN10, PN19, PN20, PN25, PN29) kullanılmıştır. Tüm genotipler atdişi tane yapısında olup FAO olum grupları 500-750 arasında değişmektedir

Genotiplerin ekileceği arazi pullukla sürülmüş, ardından rotavatörle işlenerek tohum yatağı hazırlığı tamamlanmıştır. Deneme tesadüf blokları deneme desenine göre 3 tekerrürlü olarak yürütülmüştür. Tüm genotipler; sıra arası 70 cm ve sıra üzeri 20 cm olacak şekilde 5 m uzunluğundaki sıralara 17.07.2023 tarihinde ekilmişlerdir. Ekimlerle birlikte deneme alanına 15-15-15 taban gübre uygulanmıştır. Bitkilerin çimlenmesinden 4-5 yapraklı döneme kadar elle yabancı ot mücadelesi yapılmıştır. Bitkilerin birinci çapası 15-20 cm boylandıkları 4 yapraklı dönemde, ikinci çapa bitki boyları 40-50 cm olduğu 6-8 yapraklı dönemde yapılmıştır. Birinci çapa esnasında her tohum yatağında bir bitki kalacak şekilde tekleme yapılmıştır. Yabancı otlara karşı ayrıca pülverizatörle herbisit uygulanmıştır.

Çalışmada bitki boyu (cm), ilk koçan yüksekliği (cm), koçan/bitki oranı (%), yaprak/sap oranı (%), sap çapı (mm), yeşil ot verimi (t da^{-1}), kuru madde verimi (t da^{-1}) ölçümleri alınmıştır. Hasat işlemi hamur olum döneminde gerçekleştirilmiştir. Genotiplerin bitki boyunun belirlenmesi için hasat parselinden rastgele 5 bitki seçilmiş, mira yardımı ile ölçülmüş ve ortalaması alınmıştır. İlk koçan yüksekliği, rastgele seçilen 5 bitkide toprak yüzeyinden ilk koçanın çıktığı noktaya kadar mesafenin mira yardımı ile ölçülüp ortalamasının alınması ile tespit edilmiştir. Koçan/bitki oranı (%) için her parselden rastgele seçilen 5 bitkinin koçan yapraklarından ayrılmış çıplak koçan ağırlıkları ve bitki ağırlıkları tespit edilip oranlanmıştır. Yaprak/sap oranı (%) 5 bitkinin yaprak ve sap ağırlıkları ölçülüp oranlanması ile bulunmuştur. Sap çapı, rastgele seçilen 5 bitkinin toprak yüzeyine en yakın kısmından kumpas yardımı ile ölçülüp ortalaması alınarak belirlenmiştir. Yeşil ot verimi orta 2 sıradan hasat edilen bitkilerin tartılması ile belirlenmiştir. 1 kg bitki örneği 105 °C'de 48 saat kurutulup tartıldıktan sonra kuru madde oranları belirlenmiştir. Kuru madde oranları yeşil ot verim değerleri ile çarpılarak kuru madde verimi değerleri hesaplanmıştır (TTSM, 2018).

Çalışmada veriler tesadüf blokları deneme desenine göre JMP® Pro 17.0.0 programından yararlanılarak hesaplanmıştır. Önemlilik testlerinde 0.01 ve 0.05 farklı gurupların belirlenmesinde ise 0.05 olasılık düzeyi kullanılmıştır. Ortalamalar arası farklılık asgari önemli fark (Least Significant Difference - LSD) testi ile 0.05 düzeyinde belirlenmiştir.

BULGULAR ve TARTIŞMA

İncelenen parametreler üzerinde yapılan varyans analizi sonuçlarına göre yaprak/sap oranı hariç diğer tüm özelliklerde istatistiksel olarak önemli bulunmuştur (Tablo 3).

Tablo 3. Genotiplerin varyans analiz sonuçları

VK[1]	SD	Bitki boyu (cm)	İlk koçan yüksekliği (cm)	Koçan/ Bitki oranı (%)	Yaprak/ Sap oranı (%)	Sap çapı (mm)	Yeşil ot verimi (t/da)	Kuru madde verimi (t/da)
Çeşit	28	16467.1*	11453.2**	756.1	1664.0	244.6*	36434810**	3031117.6
Tekerrür	2	10268.4**	1906.2**	1669.7**	273.5	41.6*	1380454	2089418.6*
Hata	56	15729.5	2139.2	1240.5	2671.8	171.6	32183587	5193085

[1]VK: Varyasyon kaynağı,
*: 0,05 olasılık düzeyinde istatistiki olarak önemlidir,
**:0,01 olasılık düzeyinde istatistiki olarak önemlidir.

Araştırmada incelenen genotiplerin bitki boyları 221.1–283.0 cm, ilk koçan yükseklikleri ise 79.1–125.4 cm arasında değişmiştir. En yüksek bitki boyu ve koçan yüksekliği PN15 genotipinden elde edilirken, PN3 genotipi her iki özellik bakımından en düşük değerlere sahip olmuştur (Tablo 4). Güneş ve Acar (2006) Karaman koşullarında ortalama bitki boyunu 286 cm olarak belirtmiş, Sade ve ark. (2002) ise Konya koşullarında 235–

284 cm arasında değişen bitki boyu değerleri tespit etmişlerdir. Bu bulgular, çalışmamızda elde edilen değerler ile benzerlik göstermektedir (Tablo 4). İlk koçan yüksekliği bakımından literatürde farklı sonuçlar bildirilmiştir. Han (2016) ile Akman (2019) çalışmalarında sırasıyla 110–153 cm ve 100–156 cm aralıklarında değerler rapor etmiş olup, bu sonuçlar araştırmamızda elde edilen değerlerden daha yüksektir. Buna karşılık, Okursoy (2009) ile İdikut ve ark. (2005) tarafından bildirilen 67.42–84.32 cm ve 22.7–35.0 cm değerleri çalışmamızdan daha düşük bulunmuştur. Olgun ve ark. (2012) ilk koçan yüksekliğini 72.78–133.61 cm arasında bildirmiş olup, bu sonuçlar da çalışmamız ile uyumludur. Çalışmamızla diğer araştırmacılar arasındaki bu farklılıkların; kullanılan genetik materyalin farklılığı, sulama olanakları ve ekolojik koşulların farklı olmasından kaynaklandığı söylenebilir.

Koçan/bitki oranı %39.9–51.7, yaprak/sap oranı ise %32.3–50.9 arasında değişiklik göstermiştir. PN23 genotipi en düşük koçan/bitki oranına sahip olurken; PN3, PN4 ve PN14 genotipleri en yüksek değerlere ulaşmıştır. Yaprak/sap oranında ise PN3 öne çıkmış, kontrol hibritlerinden PN19 en düşük değeri vermiştir (Tablo 4). Atakul ve ark. (2016) Diyarbakır'da yürüttükleri çalışmada yaprak/sap oranını %41.1–49.7 aralığında rapor etmiş olup, sonuçlarımız bu bulgularla genel olarak uyum sağlamaktadır. Bu durum, bazı genotiplerin sindirilebilirliği olumlu yönde etkileyebilecek daha yüksek yaprak oranına sahip olduğunu göstermektedir.

Genotiplerin sap çapları 18.3–24.3 mm arasında değişmiş; PN8 en yüksek, PN2 ise en düşük sap çapına sahip olmuştur (Tablo 4). Bayram ve ark. (2017) benzer koşullarda yaptıkları çalışma sonucunda sap çaplarını 18.9–24.1 mm aralığında bildirmiş olup, verilerimizi destekler niteliktedir.

Çalışmada yeşil ot verimi 3.63–6.36 t da^{-1} arasında değişmiş olup, en yüksek değer PN22, en düşük değer ise PN7 genotipinden elde edilmiştir (Tablo 4). Aşar (2014) ikinci ürün koşullarında 5.80–6.40 t da^{-1}

değerleri rapor etmiş olup, bu bulgular çalışmamızda elde edilen üst sınırla uyumludur. Faklı araştırmacılar tarafından bildirilen; Seydoşoğlu ve Saruhan (2017) 6.00-10.37 t da^{-1}, Çaçan ve İşikten (2019) 7.11-9.98 ton/da, Kuşvuran ve ark. (2015) 9.80-13.10 t da^{-1}, Ergül (2008) 6.70-10.30 t da^{-1} değerleri ise çalışmamızın üst sınırından bir miktar daha yüksektir. Buna karşın, Küçük (2011)'ün bildirdiği 4.00-6.50 t da^{-1} değerleri çalışmamızla benzerlik göstermektedir. Genel olarak, çalışmamızda elde edilen yeşil ot verimi değerleri literatürde bildirilen geniş varyasyon aralığı içinde yer almaktadır.

Araştırmada kuru madde verimi 1.1–2.0 t da^{-1} arasında bulunmuştur. En yüksek yeşil ot verimi PN22 genotipinden elde edilirken, PN7 en düşük değeri göstermiştir. Kuru madde veriminde ise PN13 öne çıkmış, PN7 yine en düşük değeri vermiştir (Tablo 4). Ergül (2008) 1.9-3.02 t da^{-1}, Kuşvuran ve ark. (2015) 2.8-4.1 ton/da, Aşar (2014) 1.6-1.8 t da^{-1}, Küçük (2011) 1.3-2.1 t da^{-1}, Seydoşoğlu ve Saruhan (2017) 1.6-2.5 t da^{-1} sonuçlarını bildirmişlerdir. Bu bulgular, çalışmamızda elde edilen kuru madde verimlerinin literatürde bildirilen sonuçlarla genel olarak uyumlu olduğunu ortaya koymaktadır.

Tablo 4. Mısır genotiplerinin bitki boyu (cm), ilk koçan yüksekliği (cm), koçan/bitki oranı (%), yaprak/sap oranı (%), sap çapı (mm), yeşil ot verimi (kg/da) ve kuru madde verimi (kg/da) ortalama değerleri.

Çeşit adı	Ortalamalar						
	Bitki boyu (cm)	İlk koçan yüksekliği (cm)	Koçan/Bitki oranı (%)	Yaprak/sap oranı (%)	Sap çapı (mm)	Yeşil ot verimi (t/da)	Kuru madde verimi (t/da)
1	243.8 fg	92.0 g-j	46.9 a-d	39.4	19.0 h-k	4.75 c-h	1.45 b-d
2	276.8 a-d	105.6 b-e	45.03 a-d	35.7	18.3 ı-k	5.33 a-e	1.68 a-c
3	221.1 g	79.1 k	51.4 a	50.9	21.0 b-ı	4.35 d-h	1.44 b-d
4	280.8 ab	114.8 b	51.7 a	35.4	21.3 b-h	5.17 a-f	1.49 b-d
5	255.0 b-f	84.7 ı-k	47.7a-c	43.3	17.6 k	5.00 b-g	1.55 a-d
6	265.1 a-f	83.4 jk	49.6 ab	37.6	21.3 b-h	4.91 b-g	1.55 a-d
7	250.6 d-f	88.9 ı-k	40.9 cd	46.3	20.6 c-j	3.63 h	1.11 d
8	254.1 b-f	111.9b-d	44.3 a-d	38.3	24.3 a	4.88 b-g	1.56 a-d
9	281.0 ab	114.0 bc	42.5 b-d	44.1	20.0 e-k	4.42 d-h	1.52 b-d
10	263.8 a-f	111.1 b-d	46.9 a-d	42.7	23.6 ab	5.42 a-e	1.71 a-c
11	267.4 a-f	91.6 h-j	50.2 ab	47.6	20.6 c-j	4.61 c-h	1.42 b-d

12	247.3 e-g	88.0 ı-k	49.0 ab	44.6	23.0 a-d	3.79 g-h	1.39 b-d
13	251.8 d-f	81.90 jk	48.8 ab	41.9	21.3 b-h	6.04 ab	2.03 a
14	253.1 c-f	85.1 ı-k	50.9 a	46.3	18.0 j-k	4.07 f-h	1.38 b-d
15	283.0 a	125.4 a	44.6 a-d	48.5	20.3 d-k	5.41 a-e	1.77 ab
16	249.5 d-f	103.9 c-f	49.2 ab	40.8	22.0 a-g	4.59 c-h	1.44 b-d
17	270.1 a-f	107.5b-e	46.6 a-d	42.7	23.3 a-c	5.03 b-f	1.56 a-d
8	255.1 b-f	91.2 h-j	48.3 a-c	41.7	22.0 a-g	4.50 c-h	1.27 c-d
19	264.2 a-f	103.1 d-f	44.7 a-d	32.3	19.6 f-k	5.31 a-e	1.74 a-c
20	268.5 a-f	107.2 b-e	49.2 ab	42.6	22.3 a-f	4.93 b-g	1.40 b-d
21	268.2 a-f	107.9 b-e	47.6 a-c	39.7	19.6 f-k	5.07 b-f	1.71 a-c
22	250.0 d-f	100.4 e-h	44.8 a-d	36.6	20.3 d-k	6.36 a	1.47 b-d
23	248.8 ef	91.6 h-j	39.9 d	38.3	22.3 a-f	4.45 c-h	1.38 b-d
24	243.7 fg	99.3 e-h	48.6 a-c	41.6	21.0 b-ı	4.38 d-h	1.38 b-d
25	265.6 a-f	94.2 f-ı	42.7 b-d	35.5	22.0 a-g	5.57 a-d	1.67 a-c
26	271.8 a-e	101.8 d-g	45.5 a-d	37.8	22.6 a-e	5.68 a-c	1.61 a-c
27	280.4 a-c	99.1 e-h	45.6 a-d	36.4	19.3 g-k	4.03 f-h	1.25 c-d
28	265.0 a-f	111.6 b-d	46.7 a-d	37.3	22.3 a-f	5.67 a-c	1.73 a-c
29	264.8 a-f	90.8 h-j	45.6 a-d	40.2	19.3 g-k	4.29 e-h	1.32 b-d
$LSD_{(0.05)}$	27.41	10.10	7.69	ns	2.86	1.239.9	498.0

SONUÇ

22 adet yeni geliştirilen F1 hibridi ve 7 adet ticari yüksek verimli kontrol çeşidi ile yapılan bu araştırmada ikinci ürün koşullarında verim performansları değerlendirilmiştir. Çalışmada, incelenen parametreler bakımından genotipler arasında belirgin farklılıklar ortaya çıkmıştır. Yeşil ot veriminde PN22 istatistiksel olarak tek başına en yüksek grupta yer almış ve ticari kontrol çeşitlerini geride bırakmıştır. Kuru madde veriminde ise PN13, önemli bir üstünlük göstermiştir. Bununla birlikte, PN28 ve PN26 genotipleri her iki verim unsuru açısından da üst istatistiksel gruplarda yer almışlardır. Araştırmada PN22, PN13, PN26 ve PN28 genotipleri ümitvar bulunmuş olup ilerleyen ıslah çalışmalarında silajlık mısır çeşit adayı olarak değerlendirilmek üzere önerilebilir.

KAYNAKLAR

Akman, O. (2019). Bazı silajlık mısır çeşitlerinde (*Zea mays* L.) agronomik ve kalite özelliklerinin belirlenmesi Ordu Üniversitesi Fen Bilimleri Enstitüsü. Ordu.

Atakul, Ş., Kahraman, Ş. & Kılınç, S. (2016). Diyarbakır ikinci ürün şartlarında bazı silajlık mısır genotiplerinin verim ve verim unsurlarının belirlenmesi. Dicle Üniversitesi Fen Bilimleri Enstitüsü Dergisi 5(2) (2016) 47-50.

Bayram, G., Turgut, İ., & Şenyiğit, E. (2017). İkinci ürün olarak yetiştirilen silajlık mısırda ekim şekilleri ile farklı bitki sıklıklarının verim ve kalite özellikleri üzerine etkisi. KSU J. Nat. Sci., 20(Özel Sayı): 97-101.

Çaçan, E., & İşikten, S. (2019). Bingöl ili ekolojik koşullarında bazı silajlık mısır çeşitleri için uygun ekim zamanının belirlenmesi. Türkiye Tarımsal Araştırmalar Dergisi, 6(1), 39-49. https://doi.org/10.19159/tutad.449672

Ergül, Y. (2008). Silajlık mısır çeşitlerinin önemli tarımsal ve kalite özelliklerinin belirlenmesi Selçuk Üniversitesi Fen Bilimleri Üniversitesi. Konya.

Güneş, A & Acar, R. (2006). Karaman Ekolojik Koşullarında Silajlık Hibrit Mısır Çeşitlerinin İkinci Ürün Olarak Yetiştirme İmkanlarının Belirlenmesi. Selçuk Üniversitesi Ziraat Fakültesi Dergisi. 20 (39): 84-92

Han, E. (2016). Bazı mısır çeşitlerinin dane verimleri ile silaj ve kalite özelliklerinin belirlenmesi Ordu Üniversitesi Fen Bilimleri Enstitüsü. Ordu.

İdikut, L., Cesur, C., & Tosun, S. (2005). Şeker mısırda ekim zamanı ve yetiştirme tekniğinin hasıl verim ve bazı özelliklere etkisi. Kahramanmaraş Sütçü İmam Üniversitesi Fen ve Mühendislik Dergisi, 8(1), 91-100.

Kuşvuran, A., Kaplan, M., Nazlı, R. I., Saruhan, V. & Karadağ, Y. (2015). Orta Kızılırmak havzası ekolojik koşullarında bazı mısır (Zea mays L.) çeşitlerinin silajlık olarak yetiştirilme olanaklarının belirlenmesi. Journal of Agricultural Faculty of Gaziosmanpaşa University (JAFAG), 32(1), 57-67. https://doi.org/10.13002/jafag790

Küçük, B. (2011). Bazı silajlık mısır çeşitlerinde morfolojik özelliklerin ve yem verimlerinin belirlenmesi Ankara Üniversitesi Fen Bilimleri Enstitüsü. Ankara

Ma, B. L., Subedi, K. D., Stewart, D. W & Dwyer, L. M. (2006). Dry Matter Accumulation and Silage Moisture Changes After Silking in Leafy and Dual-Purpose Corn Hybrids. Agron J. 98:922 929.

Okursoy, H. (2009). Trakya koşullarında farklı sulama yöntemleri altında ikinci ürün silajlık mısırın su üretim fonksiyonlarının belirlenmesi Namık Kemal Üniversitesi Fen Bilimleri Enstitüsü. Tekirdağ.

Olgun, M., Kutlu, İ., Ayter, N. G., Budak Başçiftçi, Z., & Kayan, N. (2012). Farklı silajlık mısır genotiplerinin Eskişehir koşullarında adaptasyon yeteneklerinin belirlenmesi. Biyoloji Bilimleri Araştırma Dergisi, 5(1): 93-97.

Oliveira T. R. A. D., Carvalho H. W. L. D., Oliveira G. H. F., Costa E. F. N., Gravina G. D. A., Santos R. D. D., & Carvalho Filho J. L. S. D. (2019). Hybrid maize selection through GGE biplot analysis. Bragantia Campinas 78(2):166–174.

Özata, E, & Kapar, H. (2011). Atdişi Mısır Yoklama Melezlerinin Verim Ve Bazı Verim Öğeleri. Türkiye 9. Tarla Bitkileri Kongresi, 12-14 Eylül, Bursa.

Sade, B., Akbudak, N. A., Acar, R., & Arat E. (2002). Konya Ekolojik Şartlarında Silajlık Olarak Uygun Mısır Hibritlerinin Belirlenmesi. Hayvancılık Araştırma dergisi, 12, 1:17-22.

Seydoşoğlu, S., & Saruhan, V. (2017). Farklı ekim zamanlarının bazı silajlık mısır çeşitlerinde verim ve verim unsurlarına etkisinin belirlenmesi. Ege Üniversitesi Ziraat Fakültesi Dergisi, 54(4), 377-383.

TTSM (2018). Tarımsal Değerleri Ölçme Denemeleri Teknik Talimatı, MISIR (*Zea mays* L.), Tarım Gıda ve Hayvancılık Bakanlığı, Ankara, 2018.

Zopollatto M, Nussio L. G., Mari L. J., Schmidt P, Duarte A .P., & Mourão G. B. (2009). Changes in morphological composition according to the maturity stage in corn cultivars for silage production. Revista Brasileira de Zootecnia 38:452–461.

ORAL PRESENTATION

Regenerative roles of mesenchymal stem cells and extracellular vesicles in ovarian and endometrial injury

Elif Gelenli Dolanbay (ORCID: https://orcid.org/0000-0002-7553-5435)

Istanbul Medeniyet University, Faculty of Medicine, Department of Histology and Embriyology, Istanbul, Türkiye.

Corresponding author e-mail:elif.dolanbay@medeniyet.edu.tr

Abstract

Stem cells and extracellular vesicles (EVs) are increasingly used in the treatment of reproductive system disorders. Human umbilical cord mesenchymal stem cells (hUC-MSCs) and their derived EVs offer promising therapeutic potential due to their low immunogenicity, paracrine effects, and ease of collection. This review summarizes the current research on hUC-MSCs and EVs in ovarian and endometrial injury models. hUC-MSCs have been shown to improve ovarian function in premature ovarian failure (POF) and polycystic ovary syndrome (PCOS) models through immune modulation, anti-apoptotic effects, inhibition of ferroptosis, and restoration of hormone levels. Additionally, hUC-MSC-derived EVs enhance ovarian recovery by regulating pathways such as PI3K/AKT, Nrf2/GPX4, and IGF-1/HO-1 to mitigate oxidative stress and autophagy. In endometrial injury, hUC-MSCs and their EVs modulate inflammatory responses, inhibit fibrosis, promote angiogenesis, and remodel the extracellular matrix through miRNA-mediated paracrine mechanisms. Collectively, these studies indicate that hUC-MSCs and EVs are promising candidates for regenerative therapy in female reproductive disorders, with ongoing clinical trials investigating their safety and efficacy.

Keywords: Stem cells, extracellular vesicles, hUC-MSCs, ovarian injury, endometrial injury

INTRODUCTION

Stem cells and extracellular vesicles (EVs) are currently utilized in various areas of disease treatment. For instance, stem cells can address acute myocardial infarction by releasing biological factors, whereas mesenchymal stem cell (MSCs)-derived EVs can significantly inhibit tumor cell growth (Farahzadi et al., 2024; Fathi et al., 2020; Yan et al., 2024). Enhancing the effectiveness of stem cells in disease treatment has become an important area of interest. Hematopoietic stem cells that express tumor-associated antigen-specific T-cell receptors or chimeric antigen receptors are explored for acute myeloid leukemia treatment (Fathi et al., 2020). Stem cells are defined by self-renewal and multilineage differentiation potential. They include embryonic stem cells, adult stem cells, and induced pluripotent stem cells, with ethical and efficiency limitations in some types (Tan et al., 2024; Tian et al., 2023; Gopalarethinam et al., 2023).

Mesoderm-derived MSCs are widely used due to strong proliferation, pluripotency, genomic stability, and lack of ethical issues (Elhaieg et al., 2025). hUC-MSCs were isolated from human umbilical cords in 2006 and show higher proliferative capacity than BM-MSCs, with similar cytokine profiles. As umbilical cords are medical waste, hUC-MSCs bypass ethical constraints.

MATERIALS AND METHODS

Human umbilical cord-derived mesenchymal stem cells (hUC-MSCs) possess distinct characteristics compared to other MSC sources. They express markers such as CD10, CD29, CD44, CD73, CD90, and CD105, and secrete bioactive molecules like HGF, FGF-2, and NGF that promote proliferation, angiogenesis, and tissue repair (Mebarki et al., 2021; Ganguly et al., 2023; Petrenko et al., 2020). hUC-MSCs exhibit rapid proliferation and low immunogenicity, making them suitable for clinical applications (Xie et al., 2020; Lee & Kwok, 2023). EVs, including exosomes and microvesicles, act as paracrine mediators, transferring proteins, lipids, and nucleic acids to target cells. Isolation and characterization involve ultracentrifugation, size-exclusion chromatography, microscopy, light scattering, and flow cytometry to determine size, concentration, and protein markers (Carberry et al., 2022; Welsh et al., 2024; Huang et al., 2025).

RESULTS and DISCUSSION

hUC-MSCs have demonstrated significant therapeutic potential in models of ovarian injury, including premature ovarian failure (POF) and polycystic ovary syndrome (PCOS). Studies indicate that hUC-MSC transplantation reduces inflammation, apoptosis, oxidative stress, and ferroptosis in ovarian tissue, leading to improved follicular development and hormone homeostasis (Xie et al., 2019; Deng et al., 2021). In DHEA-induced PCOS models, hUC-MSCs modulate macrophage polarization, enhance regulatory T cell populations, and restore normal estrous cycles. In addition to cellular therapy, hUC-MSC-derived extracellular vesicles (EVs) have been shown to mediate ovarian recovery through paracrine signaling. EVs regulate critical pathways such as PI3K/AKT, Nrf2/GPX4, IGF-1/HO-1, and METTL3/PINK1, mitigating oxidative stress, autophagy dysregulation, and apoptosis in granulosa cells (He et al., 2024; Zhou et al., 2024). These findings suggest that both hUC-MSCs and their EVs can synergistically restore ovarian structure and function.

Endometrial injury, often leading to fibrosis and intrauterine adhesions, poses a major cause of female infertility. hUC-MSC transplantation promotes regeneration of damaged endometrium by modulating inflammatory responses, inhibiting fibrotic signaling, stimulating angiogenesis, and remodeling the extracellular matrix. These effects are mediated through paracrine factors, including growth factors and miRNAs, which regulate apoptosis and extracellular matrix composition (Tan et al., 2024; Huang et al., 2025). hUC-MSC-derived EVs contribute to endometrial repair by transferring functional miRNAs that influence key signaling pathways such as TGF-β/Smad and PTEN/AKT, ultimately enhancing epithelial recovery, reducing fibrosis, and improving vascularization. Collectively, preclinical evidence demonstrates that EV-based therapy can mimic the beneficial effects of whole-cell transplantation while minimizing risks associated with cell engraftment.

The regenerative potential of hUC-MSCs and EVs in reproductive tissues appears largely mediated by paracrine signaling. Anti-inflammatory cytokines and growth factors secreted by MSCs reduce local immune activation, while EVs transfer proteins, lipids, and nucleic acids to recipient cells, modulating apoptosis, autophagy, and oxidative stress. Key signaling pathways such as PI3K/AKT, Nrf2/GPX4, IGF-1/HO-1, and METTL3/PINK1 have been repeatedly implicated in ovarian recovery, whereas TGF-β/Smad and PTEN/AKT pathways play central roles in endometrial regeneration. These mechanisms collectively improve tissue architecture, restore hormonal balance, and support reproductive function.

While most evidence stems from preclinical models, early clinical trials have shown the safety and potential efficacy of hUC-MSCs and EVs in reproductive system disorders. Standardization of EV isolation, dosing, and delivery methods remains a critical challenge. Future research should focus on optimizing therapeutic regimens, understanding long-term outcomes, and developing standardized protocols to facilitate the translation of preclinical findings into clinical practice. Overall, hUC-MSCs and their EVs represent a promising regenerative strategy for female reproductive health.

CONCLUSION

hUC-MSCs and their EVs are promising therapeutic agents for ovarian and endometrial injuries due to their low immunogenicity, paracrine effects, and ease of collection. Mechanisms include immune modulation, anti-apoptotic effects, antioxidant protection, and autophagy regulation. Preclinical studies demonstrate their ability to restore tissue structure, function, and hormonal balance. Early clinical data support safety and potential efficacy, with ongoing trials and standardized protocols guiding their future application in regenerative medicine.

ACKNOWLEDGEMENTS

The author gratefully acknowledge the support of collaborators.

REFERENCES

Carberry, C. K., Keshava, D., Payton, A., Smith, G. J., & Rager, J. E. (2022). Approaches to incorporate extracellular vesicles into exposure science, toxicology, and public health research. Journal of Exposure Science and Environmental Epidemiology, 32(5), 647–659.

Dai, W., Yang, H., Xu, B., He, T., Liu, L., Zhang, Z., et al. (2024). 3D hUC-MSC spheroids exhibit superior resistance to autophagy and apoptosis of granulosa cells in POF rat model. Reproduction, 168(2), e230496.

Deng, T., He, J., Yao, Q., Wu, L., Xue, L., Wu, M., et al. (2021). Human umbilical cord mesenchymal stem cells improve ovarian function in chemotherapy-induced premature ovarian failure mice through inhibiting apoptosis and inflammation via a paracrine mechanism. Reproductive Sciences, 28(6), 1718–1732.

Elhaieg, A., Farag, A., Koung Ngeun, S., Kaneda, M., Yokoi, A., Mandour, A. S., et al. (2025). Therapeutic potential of local and systemic adipose-derived mesenchymal stem cell injections in a rat model of experimental periodontitis: Implications for cardiac function. International Journal of Molecular Sciences, 26(9), 3984.

Farahzadi, R., Fathi, E., Vandghanooni, S., & Valipour, B. (2024). Hydrogel encapsulation of mesenchymal stem cells-derived extracellular vesicles as a novel therapeutic approach in cancer therapy. Biochimica et Biophysica Acta - Reviews on Cancer, 1879(5), 189177.

Fathi, E., Farahzadi, R., Sheervalilou, R., Sanaat, Z., & Vietor, I. (2020). A general view of CD33(+) leukemic stem cells and CAR-T cells as interesting targets in acute myeloblastic leukemia therapy. Blood Research, 55(1), 10–16.

Ganguly, A., Swaminathan, G., Garcia-Marques, F., Regmi, S., Yarani, R., Primavera, R., et al. (2023). Integrated transcriptome-proteome analyses of human stem cells reveal source-dependent differences in their regenerative signature. Stem Cell Reports, 18(1), 190–204.

He, J., Ao, C., Li, M., Deng, T., Zheng, S., Zhang, K., et al. (2024). Clusterin-carrying extracellular vesicles derived from human umbilical cord mesenchymal stem cells restore the ovarian function of premature ovarian failure mice through activating the PI3K/AKT pathway. Stem Cell Research & Therapy, 15(1), 300.

Huang, C., Li, H., Zhang, Z., Mou, T., Wang, D., Li, C., et al. (2025). From mechanism to therapy: the role of MSC-EVs in alleviating radiation-induced injuries. Pharmaceutics, 17(5), 652.

Lee, B. W., & Kwok, S. K. (2023). Mesenchymal stem/stromal cell-based therapies in systemic rheumatic disease: From challenges to new approaches for overcoming restrictions. International Journal of Molecular Sciences, 24(12), 10161.

Mebarki, M., Abadie, C., Larghero, J., & Cras, A. (2021). Human umbilical cord-derived mesenchymal stem/stromal cells: a promising candidate for the development of advanced therapy medicinal products. Stem Cell Research & Therapy, 12(1), 152.

Xie, Q., Xiong, X., Xiao, N., He, K., Chen, M., Peng, J., et al. (2019). Mesenchymal stem cells alleviate DHEA-induced polycystic ovary syndrome (PCOS) by inhibiting inflammation in mice. Stem Cells International, 2019, 9782373.

Zhou, W., Zhang, J., Lu, X., Zhao, Z., Weng, Y., & Zhu, C. (2025). Umbilical cord mesenchymal stem cell-derived extracellular vesicles improve excessive autophagy of granulosa cells through METTL3. American Journal of Physiology-Cell Physiology, 328(5), C1586–C1604.

Zhou, Y., Huang, J., Zeng, L., Yang, Q., Bai, F., Mai, Q., et al. (2024). Human mesenchymal stem cells derived exosomes improve ovarian function in chemotherapy-induced premature ovarian insufficiency mice by inhibiting ferroptosis through Nrf2/GPX4 pathway. Journal of Ovarian Research, 17(1), 80.

ORAL PRESENTATION

Çeşitli metallerle dekore edilmiş alüminyum katkılı altıgen bor nitrür nano levhaların hidrojen depolama özelliklerinin hesaplamalı incelenmesi

Berna Taclı[1*] *(https://orcid.org/0000-0001-8549-203X)*,
Armağan Kınal[2] *(https://orcid.org/0000-0002-9747-4901)*

[*1]Ege Üniversitesi, Fen Fakültesi, Kimya, İzmir, Türkiye
[2] Ege Üniversitesi, Fen Fakültesi, Kimya, İzmir, Türkiye

*Sorumlu yazar e-mail: bernauslu85@gmail.com

Özet

Bu çalışmada, hidrojen depolama uygulamaları açısından potansiyellerini değerlendirmek amacıyla altıgen (hekzagonal) bor nitrür ($B_{19}N_{18}$) nano levhaların alüminyum katkılı yapıları (Al-hBN); alkali (Li^+, Na^+, K^+), toprak alkali (Mg^{2+}, Ca^{2+}) ve dördüncü periyot geçiş metali (Sc^{3+}, Ti^{4+}, V^{3+}, Cr^{2+}, Mn^{7+}, Fe^{3+}, Co^{3+}, Ni^{2+}, Cu^+, Cu^{2+}, Zn^{2+}) katyonları ile tek atom dekorasyonu yoluyla modifiye edilmiştir. Yapısal kararlılık, adsorpsiyon enerjileri ve elektronik özellikleri incelemek için yoğunluk fonksiyoneli teorisi (DFT) hesaplamaları, Perdew–Burke–Ernzerhof (PBE) değiş-korelasyon fonksiyoneli ve def2-SVP baz seti kullanılarak gerçekleştirilmiştir. Termodinamik kararlılık analizleri, tüm dekorasyonlu sistemlerin negatif toplam elektronik ve termal entalpi değerleri sergileyerek termodinamik olarak kararlı yapıların oluştuğunu göstermektedir. Hidrojen adsorpsiyon özellikleri; adsorpsiyon enerjileri, bağ uzunlukları ve sınır moleküler orbital (FMO) analizi ile incelenen moleküler orbital özellikleri dikkate alınarak değerlendirilmiştir. Sc^{3+}, Fe^{3+} ve Co^{3+} dekorasyonlu Al-hBN yüzeylerinde elde edilen adsorpsiyon enerjileri sırasıyla 0,42, 0,56 ve 0,58 eV/H_2 olup, bu değerler hidrojenin oda sıcaklığında tersinir olarak adsorplanabilmesi için önerilen optimum aralık (~0,2 ila 0,6 eV/H_2) içerisindedir. Buna karşın, Li^+, Na^+, K^+, Ca^{2+} ve Zn^{2+} dekorasyonlu sistemlerde pozitif Gibbs adsorpsiyon serbest enerji değerleri, kısa adsorpsiyon mesafeleri ve geniş bant aralığı nedeniyle hidrojen adsorpsiyonunun zayıf veya termodinamik olarak elverişsiz olduğu belirlenmiştir. Bu bulgular, uygun metal dekorasyonu ile birleştirilen Al-hBN nano levhalarının, verimli, hafif ve geri dönüştürülebilir hidrojen depolama malzemeleri için umut verici adaylar olduğunu göstermektedir.

Anahtar Kelimeler: altıgen bor nitrür nano levhalar, alüminyum katkılı dekorasyon, hidrojen depolama, DFT

Computational investigation of hydrogen storage properties of several metal decorated aluminum-doped hexagonal boron nitride nanosheets

Abstract

In this study, aluminum-doped structures (Al-hBN) of hexagonal boron nitride ($B_{19}N_{18}$) nanosheets were modified via single-atom decoration with alkali (Li^+, Na^+, K^+), alkaline earth (Mg^{2+}, Ca^{2+}), and fourth-period transition metal cations (Sc^{3+}, Ti^{4+}, V^{3+}, Cr^{2+}, Mn^{7+}, Fe^{3+}, Co^{3+}, Ni^{2+}, Cu^+, Cu^{2+}, Zn^{2+}) in order to evaluate their potential for hydrogen storage applications. Density functional theory (DFT) calculations using the Perdew–Burke–Ernzerhof (PBE) exchange-correlation functional and def2-SVP basis set were performed to investigate structural stability, adsorption energies, and electronic properties. Thermodynamic stability analyses revealed that all decorated systems exhibit negative total electronic and thermal enthalpy values, confirming their thermodynamic feasibility. Hydrogen adsorption features were assessed considering adsorption energies, bond lengths, and molecular orbital properties examined via frontier molecular orbital (FMO) analysis. Adsorption energies obtained for Sc^{3+}, Fe^{3+}, and Co^{3+} decorated Al-hBN surfaces are 0,42, 0,56, and 0,58 eV/H_2, respectively, which fall within the suggested optimal range (~0,2 to 0,6 eV/H_2) for reversible hydrogen adsorption at room temperature. In contrast, Li^+, Na^+, K^+, Ca^{2+} and Zn^{2+} decorated systems show weak or thermodynamically unfavorable hydrogen adsorption due to positive Gibbs adsorption free energy values, short adsorption distances, and wide energy gaps. Overall, this study suggests that Al-hBN nanosheets, when combined with appropriate transition metal decoration, can serve as promising candidates for lightweight, stable, and recyclable hydrogen storage materials.

Keywords: hexagonal boron nitride nanosheets, aluminum-doped decoration, hydrogen storage, DFT

GİRİŞ

Sanayileşmenin erken dönemlerinden bu yana enerji sistemleri, çevresel etkilerine rağmen büyük ölçüde fosil yakıtlara dayanmıştır. Küresel emisyonlar tarihsel olarak yüksek seviyelerde seyretmeye devam etmektedir: enerji kaynaklı CO_2 emisyonları 2024 yılında yaklaşık 37,8 milyar ton (Gt) (IEA, 2025), fosil kaynaklı CO_2 emisyonları ise yaklaşık 37,4 milyar ton (Gt) (Friedlingstein ve ark., 2025) olarak gerçekleşmiştir. Bu değerlendirmeler, emisyonların 2025'in başlarına kadar yüksek seviyelerde kaldığını ve düşük karbonlu enerji taşıyıcıları ile depolama teknolojilerinin ölçeklenebilir biçimde geliştirilmesi gerekliliğini vurgulamaktadır.

Moleküler hidrojen (H_2), yalnızca su üretmesi ve yüksek özgül enerji değerine sahip olması nedeniyle cazip bir ikincil enerji taşıyıcısıdır — yaklaşık 120 MJ kg^{-1} (alt ısıl değeri, LHV) veya 142 MJ kg^{-1} (üst ısıl değeri, HHV). Kütle bazında, bu değer benzininkinin (~44-46 MJ kg^{-1}, LHV) yaklaşık üç katıdır. Ancak, hidrojenin düşük hacimsel enerji yoğunluğu, pratik sistemler için temel malzeme depolama sorununu ortaya çıkarmaktadır (Møller ve ark., 2017; U.S. Department of Energy, 2025a; U.S. Department of Energy, 2025b).

Aday malzemeler arasında, iki boyutlu (2B) yapılar yüksek yüzey/kütle oranları, kusur veya katkılama yoluyla ayarlanabilir adsorpsiyon bölgeleri ve iki yüzeyli fonksiyonelleştirme olasılıkları sayesinde hidrojen depolama açısından dikkat çekicidir. Bu sınıfta, hekzagonal bor nitrür nano levhalar termal ve kimyasal kararlılıkları, mekanik dayanıklılıkları ve grafen benzeri örgü yapıları sayesinde gaz adsorpsiyonu ve hidrojen depolama için yoğun biçimde araştırılmıştır (Zhang ve ark., 2017; Kovalskii ve ark., 2024).

Bor nitrür (BN) nanoyapılar, hidrojen depolama amacıyla incelenen ilk karbon dışı nanomalzemeler arasındadır. BN nanotüplerinin (BNNT) kararlılığı 1994 yılında öngörülmüş, sentezleri ise 1995'te karbon içermeyen ark deşarjı yöntemiyle gerçekleştirilmiştir (Rubio ve ark., 1994; Chopra ve ark., 1995). Sonraki çalışmalar, yüksek basınç altında hidrojen tutulumu ve heteroatom katkılı (örneğin oksijen) BN nano yapılarla adsorpsiyonun iyileştirilmesi üzerine yoğunlaşmıştır (Ma ve ark., 2002; Lei ve ark., 2014). Bu araştırmalar, saf BN'nin H_2'yi zayıf biçimde (fiziksel adsorpsiyon) bağladığını ve tersinir, ortam koşullarına yakın performansın genellikle eğrilik, kusur, katkı veya metal dekorasyonu gibi stratejiler gerektirdiğini göstermektedir. Yoğun Al katkılı BNNT için yapılan teorik çalışmalar da moleküler adsorpsiyon rejiminin korunurken yüksek gravimetrik hidrojen depolama kapasitesi elde edilebileceğini göstermektedir. Özellikle, Al katkılı zigzag (5,0) ve sandalye (3,3) BNNT yapılarına ilişkin hesaplamalar, sırasıyla %8,6 ve %9,4 gravimetrik hidrojen depolama kapasitesine ulaşılabileceğini öngörmektedir; bu değerler, ABD Enerji Bakanlığı'nın ağırlıkça %6,5 hedefinin üzerinde olup, Al katkısının hidrojen depolama kapasitesini artırmada etkili olduğunu göstermektedir (Noura ve ark., 2020). Ayrıca, geçiş metali (örneğin Ni veya Rh) ile dekore edilmiş hekzagonal BN yüzeylerinde daha güçlü kimisorpsiyon gözlenmekte; özellikle Rh için ilk H_2 molekülünün ayrıştığı ve molekül başına 0,7-1,6 eV arasında enerji değerleri bildirilmektedir (Venkataramanan ve ark., 2009).

H_2 adsorpsiyon enerjilerinin, oda sıcaklığında tersinir adsorpsiyonun sağlanabilmesi için, molekül başına ~0,2-0,6 eV aralığında olması gerektiği çeşitli çalışmalarda rapor edilmiştir. (Kim ve ark., 2006; Meng ve ark., 2007; Gao ve ark., 2014). Bu karşılaştırmalar, BN-tabanlı malzemelerin bağlanma enerjisi, tersinirlik, aktif bölge yoğunluğu ve kararlılık arasında dikkatli bir denge kurulması gerektiğini açıkça ortaya koymaktadır.

Bu çalışmada, Al katkılı hekzagonal bor nitrür nano levhalar üzerine alkali (Li^+, Na^+, K^+), toprak alkali (Mg^{2+}, Ca^{2+}) ve 3d geçiş metal katyonlarının (Sc^{3+}–Zn^{2+}) tek atom dekorasyonlarının etkileri, yoğunluk fonksiyonel teorisi (DFT) hesaplamaları ile incelenmiştir. Amaç; Al katkısının yapısal ve elektronik özellikler üzerindeki etkilerini nicel olarak belirlemek, H_2 adsorpsiyon termodinamiği ve tercih edilen adsorpsiyon motiflerini ortaya koymak, farklı metal modifikasyonlarını sistematik olarak karşılaştırarak H_2 etkileşimini artırmaya yönelik tasarım ilkeleri elde etmektir. Elde edilen bulgular, hafif, kararlı ve geri dönüştürülebilir 2B hekzagonal BN tabanlı adsorbanların hidrojen depolama uygulamaları için rasyonel tasarımına rehberlik etmeyi amaçlamaktadır.

MATERYAL VE METOT

Hesapsal Detaylar

Bu çalışmadaki tüm hesaplamalar, Gaussian 09 yazılım paketinde (Frisch ve ark., 2013) uygulandığı gibi yoğunluk fonksiyonel teorisi (DFT) kullanılarak gerçekleştirilmiştir. Moleküler sistemlerin görselleştirilmesi ve yapısal modellemesinde GaussView 6.0 kullanılmıştır. Geometri optimizasyonları ve elektronik yapı hesaplamaları, Perdew-Burke-Ernzerhof (PBE) fonksiyoneline sahip genelleştirilmiş gradyan yaklaşımı (GGA) (Perdew ve ark., 1996) ve def2-SVP baz kümesi (Weigend ve Ahlrichs, 2005), metallerle dekore edilmiş Al-

hBN nano levha hesaplamalarında kullanılmıştır. Yapısal kararlılığı ve elektronik özellikleri değerlendirmek için; önce Al-hBN ($Al\text{-}B_{18}H_{15}N_{18}$) nano levhalar, ardından hidrojenli yapıları ve hidrojen adsorpsiyonu üzerindeki etkiyi değerlendirmek için çeşitli metal katyonlarıyla dekore edilmiş bileşikleri incelenmiştir. Her dekore edilmiş sistem için geometri optimizasyonları yapılarak, ardından adsorpsiyon enerjilerini ve HOMO-LUMO enerji boşluğu gibi elektronik özellikleri belirlemek için enerji hesaplamaları yapılmıştır.

H_2 moleküllerinin tüm incelenen yüzeylerdeki adsorpsiyon davranışı analiz edilerek değerlendirilmiş; metallerle dekore edilmiş Al-hBN nano levhaların adsorpsiyon enerjisi ise Denklem (1) kullanılarak nicel olarak belirlenmiştir (Weigend ve Ahlrichs, 2005).

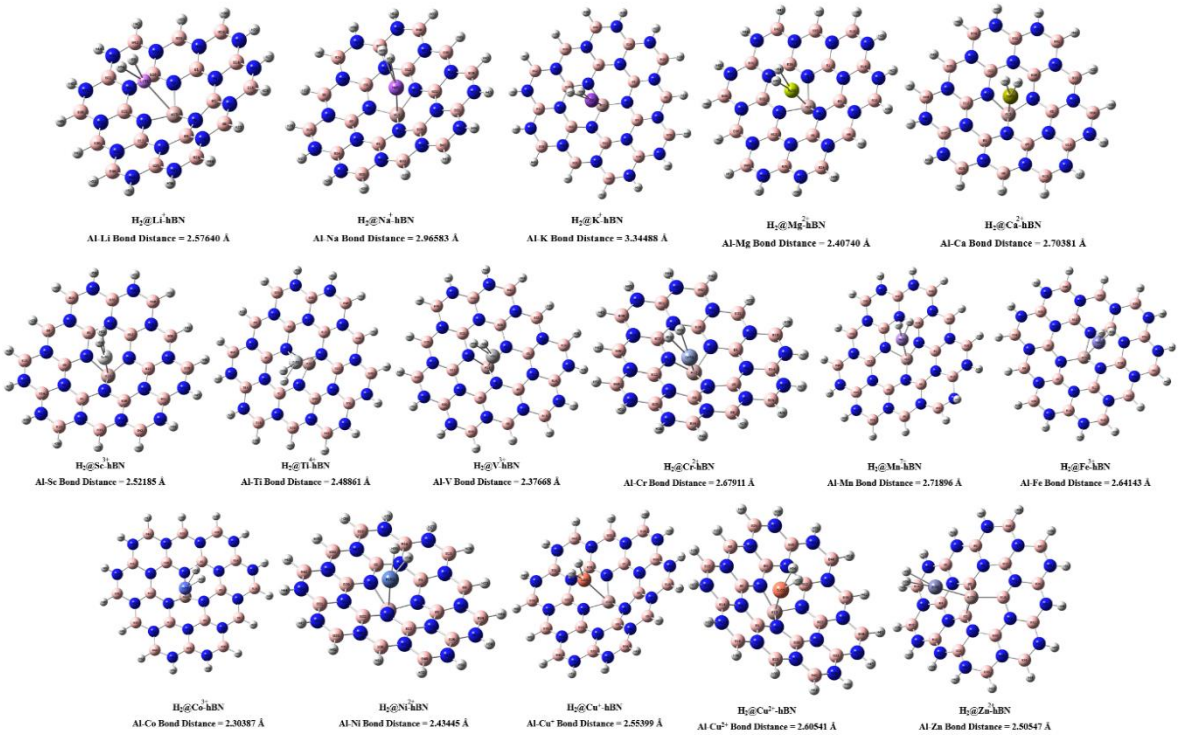
$$E_{ads} = E_{H2+yüzey} - (E_{H2} + E_{yüzey}) \quad (1)$$

Bu denklemde, $E_{H2+yüzey}$, H_2 adsorpsiyonundan sonra sistemin toplam enerjisidir, E_{H2}, izole edilmiş H_2 molekülünün enerjisi ve $E_{yüzey}$, H_2 adsorpsiyonundan önce Al-hBN nano levhaların toplam enerjisidir.

BULGULAR ve TARTIŞMA

Yapısal ve Enerjetik Analiz

Çeşitli metal katyonları ile dekore edilmiş Al-hBN nano levhaların üzerinde H_2 molekülü adsorpsiyonunun geometrik optimizasyonları, def2-SVP düzeyinde gerçekleştirilmiştir (Şekil 1).



Şekil 1. Metal dekorasyonlu Al-hBN nano levhaların hidrojen molekülü adsorpsiyonunun optimize edilmiş geometrileri

H_2 molekülünün adsorpsiyonundan sonra, tüm metallerle dekore edilmiş Al-hBN kompleksleri yapısal bütünlüklerini korumakta ve bu da termodinamik kararlılığa işaret etmektedir. Bununla birlikte, ΔG_{ads} değerleri, adsorpsiyon süreçlerinin yalnızca belirli metal katkılı sistemler için termodinamik olarak uygun olduğunu göstermektedir. Özellikle, Mg^{2+}, Sc^{3+}, Ti^{4+}, V^{3+}, Cr^{2+}, Mn^{7+}, Fe^{3+}, Co^{3+}, Ni^{2+}, Cu^{+}, Cu^{2+} katkılı bileşiklerde negatif; Li^{+}, Na^{+}, K^{+}, Ca^{2+} ve Zn^{2+} katkılı bileşiklerde ise pozitif değerler gözlenmiştir ve bu da daha az kendiliğinden adsorpsiyonu göstermektedir. (Tablo 1)

Tablo 1. 298 K sıcaklık ve 1 atm basınçta PBE/def2-SVP düzeyinde hesaplanan elektronik ve termal entalpilerin ve serbest enerjilerin toplamı, mutlak adsorpsiyon enerjisi($|\Delta H_{ads}|$), adsorpsiyon serbest enerjisi (ΔG_{ads}), HOMO-LUMO enerjileri (E_{HOMO}, E_{LUMO}) ve enerji boşluğu (E_{gap}) değerleri.

Bileşikler	Elektronik ve termal entalpilerin toplamı*(au)*	Elektronik ve termal serbest enerjilerin toplamı*(au)*	$\lvert\Delta H_{ads}\rvert$ *(eV)*	ΔG_{ads} *(eV)*	E_{HOMO} (eV)	E_{LUMO} (eV)	E_{gap} (eV)
H_2@Li^+-Al-hBN	-1691,41	-1691,51	0,12	0,05	-10,12	-5,09	5,02
H_2@Na^+-Al-hBN	-1846,05	-1846,15	0,08	0,14	-10,07	-4,85	5,22
H_2@K^+-Al-hBN	-2283,62	-2283,72	0,02	0,04	-10,00	-4,53	5,47
H_2@Mg^{2+}-Al-hBN	-1883,44	-1883,53	0,46	-0,18	-13,08	-10,29	2,78
H_2@Ca^{2+}-Al-hBN	-2360,93	-2361,02	0,20	0,04	-13,04	-9,59	3,44
H_2@Sc^{3+}-Al-hBN	-2443,51	-2443,60	0,42	-0,14	-16,08	-14,35	1,73
H_2@Ti^{4+}-Al-hBN	-2531,52	-2531,61	0,63	-0,33	-19,28	-18,53	0,74
H_2@V^{3+}-Al-hBN	-2626,63	-2626,71	1,25	-0,90	-16,22	-14,73	1,48
H_2@Cr^{2+}-Al-hBN	-2726,36	-2726,45	0,73	-0,38	-19,11	-18,70	0,42
H_2@Mn^{7+}-Al-hBN	-2830,42	-2830,51	0,99	-0,60	-27,95	-27,25	0,69
H_2@Fe^{3+}-Al-hBN	-2946,31	-2946,40	0,56	-0,20	-15,55	-15,12	0,43
H_2@Co^{3+}-Al-hBN	-3065,30	-3065,38	0,58	-0,26	-16,22	-14,70	1,52
H_2@Ni^{2+}-Al-hBN	-3191,35	-3191,43	0,74	-0,38	-13,09	-11,38	1,70
H_2@Cu^+-Al-hBN	-3323,93	-3324,02	0,67	-0,34	-10,14	-5,35	4,79
H_2@Cu^{2+}-Al-hBN	-3323,52	-3323,61	0,60	-0,30	-13,18	-8,34	4,84
H_2@Zn^{2+}-Al-hBN	-3462,31	-3462,40	0,24	0,06	-12,31	-9,27	3,03

V^{3+}, Mn^{7+} ve Ni^{2+} katyonları ile dekore edilmiş Al-hBN yapıları en yüksek adsorpsiyon enerjilerini (sırasıyla 1,25, 0,99 ve 0,74 eV/H_2) göstermiştir. Buradaki güçlü etkileşimler, H_2 molekülünün yüzeye sıkı bir şekilde bağlandığını ve bu adsorpsiyonun tersinirliğinin düşük olabileceğini düşündürmektedir. Buna karşın, Mg^{2+}, Sc^{3+}, Fe^{3+} ve Co^{3+} dekorasyonlu yüzeylerde elde edilen adsorpsiyon enerjileri sırasıyla 0,46, 0,42, 0,56 ve 0,58 eV/H_2 olup, bu değerler önerilen optimum aralık (~0,2-0,6 eV/H_2) içerisindedir. Li^+, Na^+, K^+, Ca^{2+}, Zn^{2+} ile dekorasyonlarında ise adsorpsiyon enerjileri oldukça düşük bulunmuştur ($|\Delta H_{ads}|$<0,25 eV). Bu da fiziksel adsorpsiyon potansiyelini ve oda sıcaklığında hidrojenin zayıf şekilde tutulduğunu göstermektedir. Ayrıca, bu bileşikler için pozitif ΔG_{ads} değerleri de bu yorumu desteklemektedir.

Şekil 1'de gösterildiği gibi, en kısa adsorpsiyon mesafeleri Cu^+, Cu^{2+}, Ni^{2+} ve Co^{3+} ile dekore edilmiş bileşiklerde gözlemlenmiştir (~1,67–1,83 Å). K^+(~3,02 Å) ve Na^+(~2,53 Å) katyonları ile dekore edilmiş bileşiklerde daha uzun mesafeler gözlenmekte ve bu da daha zayıf van der Waals etkileşimleri sonucunu desteklemektedir. Bu bulgular, enerji adsorpsiyon eğilimleriyle tutarlıdır.

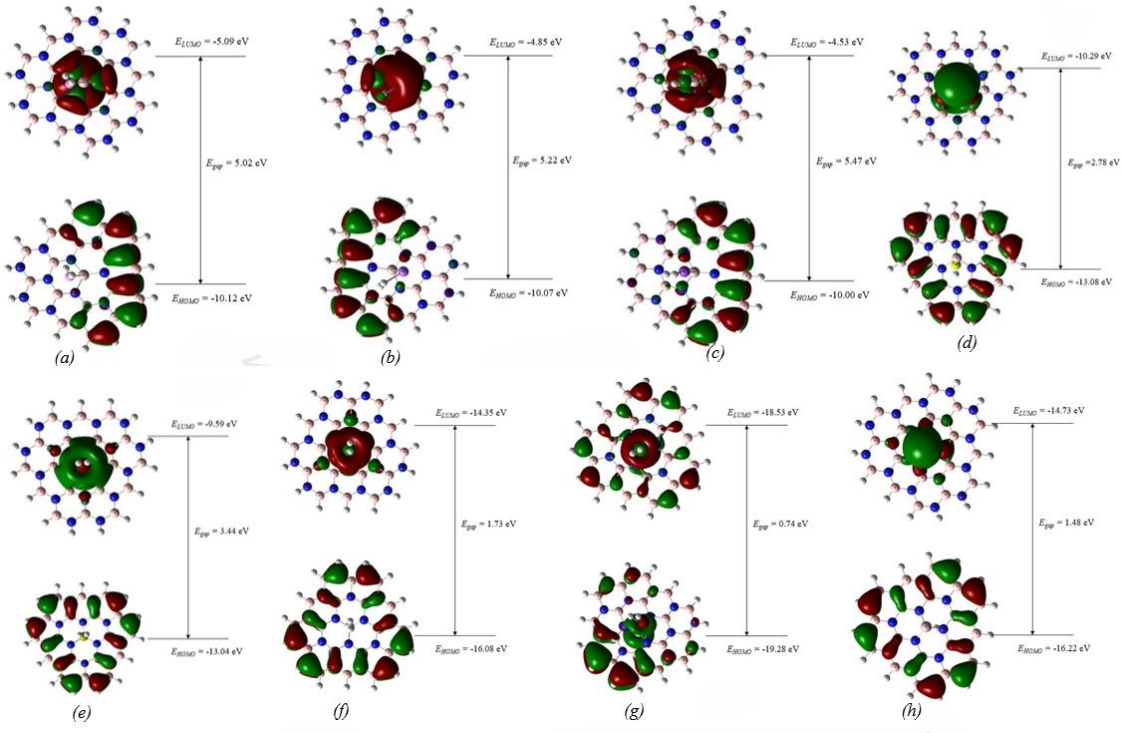
Sınır Moleküler Orbital Analizi (FMO)

En yüksek dolu moleküler orbital (HOMO) ve en düşük boş moleküler orbital (LUMO), sınır moleküler orbitalinin iki ana parametresidir (Li ve ark., 2021; Liu ve ark., 2022). FMO analizi, sistemlerin veya kimyasal reaksiyonların elektronik özelliklerini göstermek ve tasvir etmek için yaygın olarak kullanılır (Huang ve ark., 2019). H_2 adsorpsiyonu üzerine metallerle dekore edilmiş Al-hBN nano levhaların elektronik özelliklerini, kararlılığını ve reaktivitesini daha iyi anlamak için kapsamlı bir FMO analizi yürütülmüştür. Tüm incelenen yapılar için HOMO ve LUMO enerjileri hesaplanmıştır (Tablo 1). HOMO ve LUMO enerjileri arasındaki fark ya da değişim, HOMO–LUMO boşluğu (E_{gap}) olarak adlandırılır ve bir malzemenin elektronik iletkenliğini ve kimyasal reaktivitesini belirlemede önemli bir kuantum tanımlayıcıdır (Louis ve ark., 2022). Geniş bir enerji boşluğu, düşük elektriksel iletkenlik ve kimyasal eylemsizlik anlamına gelir; bu da yüzeyin H_2 molekülü ile etkileşimini zorlaştırır. Buna karşılık, daha dar bir boşluk, daha iyi elektronik iletkenlik ve daha yüksek yüzey reaktivitesi gösterir, bu da H_2 adsorpsiyonunu kolaylaştırır (Mohammadi ve ark., 2022). Enerji boşluğu matematiksel olarak şu şekilde tanımlanabilir:

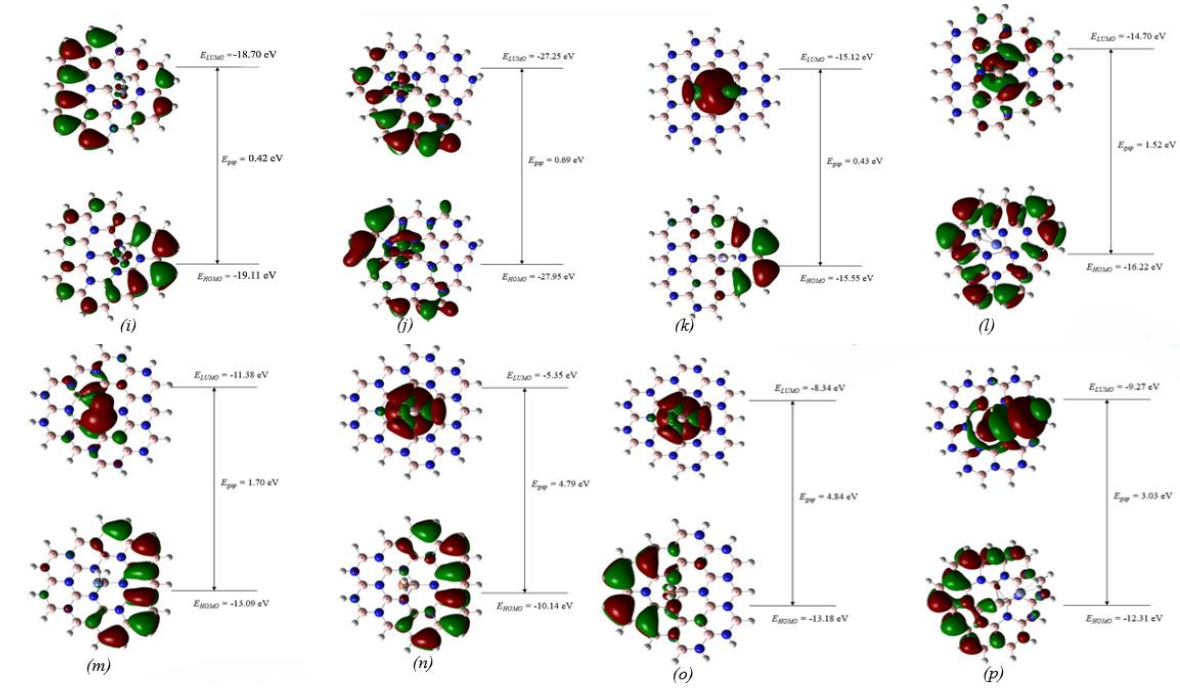
$$E_{gap} = E_{LUMO} - E_{HOMO} \quad (2)$$

Denklem 2'de, E_{gap}, enerji boşluğu, E_{HOMO}, HOMO enerjisi ve E_{LUMO}, LUMO enerjisini ifade etmektedir.

Şekil 2'de gösterildiği gibi, çalışılan alkali ve toprak alkali metal dekorasyonlu bileşikler; Li^+ (5,02 eV), Na^+ (5,22 eV), K^+ (5,47 eV) karşılaştırmalı olarak geniş HOMO–LUMO boşlukları sergilemektedir. Bu geniş enerji boşlukları, düşük kimyasal reaktiviteyi ve sınırlı elektriksel iletkenliği göstermekte, dolayısıyla bu malzemelerin etkili H_2 adsorpsiyonu için uygunluğunu azaltmaktadır. Buna karşılık, çalışılan geçiş metalleriyle (Sc^{3+}–Zn^{2+}) dekore edilmiş yapılar belirgin şekilde daha dar enerji boşlukları sergilemektedir; örneğin Cr^{2+} (0,42 eV), Fe^{3+} (0,43 eV), Mn^{7+} (0,69 eV) vb. (Şekil 3).



Şekil 2. Al-hBN nano levhaların Li^+(a), Na^+(b), K^+(c), Mg^{2+}(d), Ca^{2+}(e) Sc^{3+}(f), Ti^{4+}(g) ve V^{3+}(h) dekorasyonlu optimize edilmiş HOMO ve LUMO izoyüzey grafikleri



Şekil 3. Al-hBN nano levhaların Cr^{2+}(i), Mn^{7+}(j), Fe^{3+}(k), Co^{3+}(l), Ni^{2+}(m), Cu^{+}(n), Cu^{2+}(o) ve Zn^{2+}(p) dekorasyonlu optimize edilmiş HOMO ve LUMO izoyüzey grafikleri

SONUÇ

Bu çalışma, incelenen tüm metal dekorasyonlu Al-hBN bileşiklerinin, toplam negatif elektronik ve termal entalpi değerleri ile termodinamik olarak kararlı olduğunu ortaya koymaktadır. Ancak, H_2 adsorpsiyon verimliliğinin, kullanılan metal türüne bağlı olarak önemli ölçüde değiştiği gözlenmektedir. Çalışmada incelenen geçiş metallerinden Sc^{3+}, Fe^{3+} ve Co^{3+} ile toprak alkali metallerinden Mg^{2+} ile dekore edilmiş yapılar, ideal aralıktaki adsorpsiyon enerjileri ve kısa metal-hidrojen bağ uzaklıklarıyla uyumlu şekilde güçlü fiziksel adsorpsiyon sergilemektedir. Ayrıca, bu bileşikler oda sıcaklığında adsorpsiyon sürecinin kendiliğinden gerçekleştiğini destekleyen uygun toplam elektronik ve termal serbest enerji değerleri göstermektedir. Bununla birlikte, bu bileşikler dar HOMO-LUMO enerji boşluklarına sahiptir ve bu durum elektriksel iletkenliklerinin arttığını, kimyasal olarak daha reaktif hale geldiklerini göstermektedir—her iki özellik de verimli hidrojen adsorpsiyonu için istenen niteliklerdir. Mg^{2+} ile dekore edilmiş yapıda göreceli olarak (diğer geçiş metallerine kıyasla) daha geniş enerji boşluğu gözlenmektedir.

Buna karşılık, çalışılan diğer metal dekorasyonlu bileşikler, çok düşük adsorpsiyon enerji değerleri, pozitif Gibbs serbest enerji değerleri, geniş enerji boşlukları, yüksek metal-hidrojen uzaklıkları nedeniyle, hidrojenle nispeten daha zayıf etkileşimler göstermektedir yorumu yapılabilir. Bu durumda, adsorpsiyonun termodinamik olarak elverişsiz olduğu, dolayısıyla bu bileşiklerde sınırlı adsorpsiyon potansiyeli olduğu anlaşılmaktadır.

Özetle, yapılan tüm kapsamlı analizlerden elde edilen sonuçlara göre, Sc^{3+}, Fe^{3+} ve Co^{3+} ile dekore edilmiş Al-hBN nano yapıları; ideal adsorpsiyon enerjileri, uygun termodinamik kararlılıkları ve yüksek elektronik reaktiviteleri sayesinde gelecekteki H_2 depolama uygulamaları için umut verici adaylardır. Öte yandan, Li^{+}, Na^{+}, K^{+}, Ca^{2+} ve Zn^{2+} metallerinin yer aldığı yapılarda H_2 adsorpsiyonunun olası olmadığı sonucuna varılmıştır. Bu bulgular, temiz enerji teknolojileri için metal fonksiyonelleştirilmiş nanoyapılı malzemelere ilişkin önemli bilgiler sağlamaktadır.

TEŞEKKÜR

Bu araştırmada yer alan tüm nümerik hesaplamalar TÜBİTAK ULAKBİM, Yüksek Başarım ve Grid Hesaplama Merkezi'nde (TRUBA kaynaklarında) gerçekleştirilmiştir.

KAYNAKLAR

Amerika Birleşik Devletleri Enerji Bakanlığı (DOE), Enerji Verimliliği ve Yenilenebilir Enerji Ofisi (EERE). (2025a). Hydrogen storage. Erişim adresi: https://www.energy.gov/eere/fuelcells/hydrogen-storage

Amerika Birleşik Devletleri Enerji Bakanlığı (DOE), Enerji Verimliliği ve Yenilenebilir Enerji Ofisi (EERE). (2025b). Hydrogen fuel basics. Erişim adresi: https://www.energy.gov/eere/fuelcells/hydrogen-fuel-basics

Chopra, N. G., Luyken, R. J., Cherrey, K., Crespi, V. H., Cohen, M. L., Louie, S. G., & Zettl, A. (1995). Boron nitride nanotubes. Science, 269(5226), 966–967.

Friedlingstein, P., Jones, M. W., O'Sullivan, M., et al. (2025). Global carbon budget 2025. Earth System Science Data, 17, 965–1025.

Frisch, M. J., Trucks, G. W., Schlegel, H. B., Scuseria, G. E., Robb, M. A., Cheeseman, J. R., et al. (2013). Gaussian 09, Revision D.01. Wallingford, CT: Gaussian, Inc.

Gao, Y., Wu, X., & Zeng, X. C. (2014). Designs of fullerene-based frameworks for hydrogen storage. Journal of Materials Chemistry A, 2, 5910–5914.

Huang, J., Li, D., Li, R., Zhang, Q., Chen, T., Liu, H., & Liu, G. (2019). An efficient metal-free phosphorus and oxygen co-doped g-C_3N_4 photocatalyst with enhanced visible-light photocatalytic activity for the degradation of fluoroquinolone antibiotics. Chemical Engineering Journal, 374, 242–253.

Kim, Y. H., Zhao, Y., Williamson, A., Heben, M. J., Zhang, S. B. (2006). Nondissociative adsorption of H2 molecules in light-element-doped fullerenes. Physical Review Letters, 96, 016102.

Kovalskii, A. M., Manakhov, A. M., Afanasev, P. A., Popov, Z. I., Matveev, A. T., & Al Qasim, A. S. (2024). Hydrogen storage ability of hexagonal boron nitride. Frontiers in Materials, 11, 1375977.

Lei, W., Zhang, H., Wu, Y., Zhang, B., Liu, D., Qin, S., Liu, Z., Liu, L., Ma, Y., & Chen, Y. (2014). Oxygen-doped boron nitride nanosheets with excellent performance in hydrogen storage. Nano Energy, 6, 219–224.

Li, Y., Pu, Z., Sun, Q., & Pan, N. (2021). A review on novel activation strategy on carbonaceous materials with special morphology/texture for electrochemical storage. Journal of Energy Chemistry, 60, 572–590.

Liu, Z., He, T., Jiang, Q., Wang, W., & Tang, J. (2022). A review of heteroatomic doped two-dimensional materials as electrocatalysts for hydrogen evolution reaction. International Journal of Hydrogen Energy, 47(29), 29698–29719.

Louis, H., Charlie, D. E., Amodu, I. O., Benjamin, I., Gber, T. E., & Agwamba, E. C. (2022). Probing the reactions of thiourea (CH_4N_2S) with metals (X = Au, Hf, Hg, Ir, Os, W, Pt, and Re) anchored on fullerene surfaces ($C_{59}X$). ACS Omega, 7(39), 35118–35135.

Ma, R., Bando, Y., Zhu, H., Sato, T., Xu, C., & Wu, D. (2002). Hydrogen uptake in boron nitride nanotubes at room temperature. Journal of the American Chemical Society, 124(26), 7672–7673.

Meng, S., Kaxiras, E., Zhang, Z., (2007). Metal-diboride nanotubes as high capacity hydrogen storage media. Nano Letters, 7, 663–667.

Mohammadi, M. D., Abbas, F., Louis, H., Mathias, G. E., & Unimuke, T. O. (2022). Trapping of CO, CO_2, H_2S, NH_3, NO, NO_2, and SO_2 by a polyoxometalate compound. Computational and Theoretical Chemistry, 1215, 113826.

Møller, K. T., Jensen, T. R., Akiba, E., & Li, H.-W. (2017). Hydrogen—A sustainable energy carrier. Progress in Natural Science: Materials International, 27, 34–40.

Noura, M., Rahdar, A., Taimoory, S. M., Hayward, J. J., Sadraei, S. I., & Trant, J. F. (2020). A theoretical first principles computational investigation into the potential of aluminum-doped boron nitride nanotubes for hydrogen storage. International Journal of Hydrogen Energy, 45, 15309–15318.

Perdew, J. P., Burke, K., & Ernzerhof, M. (1996). Generalized gradient approximation made simple. Physical Review Letters, 77(18), 3865–3868.

Rubio, A., Corkill, J. L., & Cohen, M. L. (1994). Theory of graphitic boron nitride nanotubes. Physical Review B, 49(7), 5081–5084.

Uluslararası Enerji Ajansı (IEA). (2025). Global Energy Review 2025 – CO_2 Emissions. Paris: IEA Publications. Erişim adresi: ://www.iea.org/reports/global-energy-review-2025https

Venkataramanan, N. S., Khazaei, M., Sahara, R., Mizuseki, H., & Kawazoe, Y. (2009). First-principles study of hydrogen storage over Ni and Rh doped BN sheets. Chemical Physics, 359, 173–178.

Weigend, F., & Ahlrichs, R. (2005). Balanced basis sets of split valence, triple zeta valence and quadruple zeta valence quality for H to Rn: Design and assessment of accuracy. Physical Chemistry Chemical Physics, 7(18), 3297–3305.

Zhang, K., Feng, Y., Wang, F., Yang, Z., & Wang, J. (2017). Two-dimensional hexagonal boron nitride (2D-hBN): synthesis, properties and applications. Journal of Materials Chemistry C, 5(46), 11992–12022.

ORAL PRESENTATION

Chenopodium quinoa ekstraktları ile kitosan nanopartiküllerinin biyosentezi ve karakterizasyonu

İpeknur Aygün[1] (*Orcid:* https://orcid.org/0009-0005-7255-033X),
Zeliha Leblebici[2] (*Orcid: https://orcid.org/0000-0002-6127-3809*)

[*1] Nevşehir Hacı Bektaş Veli Üniversitesi, Fen Bilimleri Enstitüsü, Moleküler Biyoloji ve Genetik Anabilim Dalı, Nevşehir / Türkiye.
[2] Nevşehir Hacı Bektaş Veli Üniversitesi, Fen-Edebiyat Fakültesi, Moleküler Biyoloji ve Genetik Bölümü, Nevşehir / Türkiye.

*Sorumlu yazar e-mail:ipekserguder@outlook.com

Özet

Bitki ekstraktları kullanılarak nanopartikül sentezlenmesi, yüksek biyouyumluluk ve düşük toksisite sağlaması nedeniyle nanoteknoloji alanında dikkat çeken yöntemlerden biridir. Bu çalışmada, ***Chenopodium quinoa*** bitkisinin metanol ekstraktı ile kitosan matrisi bir araya getirilerek **yeşil sentez yaklaşımı** ile kitosan nanopartikülleri (Cs-NP) üretilmiş ve çeşitli karakterizasyon analizleri gerçekleştirilmiştir. SEM sonuçları, sentezlenen nanopartiküllerin küçük boyutlu ve yoğun yapılı olduğunu, bazı bölgelerde agregasyon eğilimli bir morfoloji sergilediğini göstermiştir. EDX spektrumu, nanopartiküllerin baskın olarak **C ve O elementlerini** içerdiğini, ekstrakttan kaynaklanan iz elementlerin ise yüzeyde düşük seviyelerde bulunduğunu ortaya koymuştur. Zeta potansiyeli ölçümü **+74.2 mV** olarak belirlenmiş olup, Cs-NP'lerin yüksek kolloidal stabiliteye sahip olduğunu doğrulamaktadır. XRD analizi, nanopartiküllerin **yarı kristalin** bir yapıya sahip olduğunu göstermiştir. FT-IR bulguları ise hem kitosan yapısına ait fonksiyonel grupların hem de metanol ekstraktında bulunan biyolojik bileşiklerin nanopartikül yapısı içerisinde korunduğunu ortaya koymuştur. Elde edilen veriler birlikte değerlendirildiğinde, metanol ekstraktının kitosan nanopartiküllerinin biyosentezinde etkili bir doğal ajan olarak kullanılabileceği anlaşılmaktadır.

Anahtar Kelimeler: *Chenopodium quinoa*, Kitosan nanopartikülleri, Nanoteknoloji, Yeşil sentez

Biosynthesis and characterization of chitosan nanoparticles using *Chenopodium quinoa* extracts

Abstract

The synthesis of nanoparticles using plant extracts is one of the noteworthy methods in the field of nanotechnology due to providing high biocompatibility and low toxicity. In this study, chitosan nanoparticles (Cs-NP) were produced through a green synthesis approach by combining the methanol extract of the Chenopodium quinoa plant with a chitosan matrix, and various characterization analyses were performed. SEM results showed that the synthesized nanoparticles exhibited a small-sized, dense structure with a morphology that tended to aggregate in some areas. The EDX spectrum revealed that the nanoparticles predominantly contained C and O elements, while trace elements originating from the extract were present on the surface at low levels. The zeta potential measurement was at the level of +74.2 mV, confirming that the Cs-NPs possess high colloidal stability. XRD analysis indicated that the nanoparticles had a semi-crystalline structure, whereas FT-IR findings demonstrated that the functional groups belonging to both the chitosan structure and the biological compounds present in the methanol extract were preserved within the nanoparticle structure. When the obtained data are evaluated, it is understood that methanol extract can serve as an effective natural agent in the biosynthesis of chitosan nanoparticles.

Keywords: *Chenopodium quinoa*, Chitosan nanoparticles, Green synthesis, Nanotechnology

GİRİŞ

Biyopolimer temelli nanopartiküllerin biyolojik kaynaklardan, özellikle bitkisel ekstraktlardan üretilmesi, son yıllarda sürdürülebilirlik, biyouyumluluk ve düşük toksisite avantajları nedeniyle nanoteknoloji alanında önemli bir araştırma konusuna dönüşmüştür. Bitki ekstraktlarının indirgeme ve stabilizasyon yeteneği, toksik kimyasal ajanlara duyulan ihtiyacı azaltarak üretim sürecinin daha çevreci ve güvenli şekilde yürütülmesini

sağlamaktadır (El-Naggar ve ark., 2022). Yeşil sentez ile elde edilen kitosan nanopartiküllerinin biyobozunur yapıya sahip olması, antimikrobiyal ve antifungal aktivite gösterebilmesi, onları biyomedikal uygulamalarda potansiyel olarak değerli hale getirmektedir (Ibrahim ve ark., 2024; Polat, 2023).

Bitkisel ekstraktlarla gerçekleştirilen nanopartikül sentezi üzerine yapılan çalışmalar, morfolojik bütünlüğün korunabildiğini, pozitif yüzey yükünün kolloidal stabiliteyi artırdığını ve elde edilen nanopartiküllerin biyolojik sistemlerle uyumlu olduğunu göstermektedir (Erdoğan ve ark., 2019). Ayrıca kitosanın polikationik yapısı, özellikle yüksek zeta potansiyeli değerleriyle birlikte düşünüldüğünde, nanopartiküllerin hem stabilizasyonunu hem de biyolojik etkileşim potansiyelini güçlendirmektedir (El-Naggar ve ark., 2022). Bu bağlamda bitkisel bileşiklerle üretilen kitosan nanopartikülleri; ilaç taşıma, doku mühendisliği ve antimikrobiyal uygulamalar gibi pek çok alanda dikkat çekmektedir.

Bu çalışmanın amacı, *Chenopodium quinoa* bitkisinin metanol ekstraktını doğal bir indirgeme ve stabilizasyon ajanı olarak kullanarak kitosan nanopartiküllerinin yeşil sentezini gerçekleştirmek ve elde edilen yapıların SEM, EDX, XRD, FT-IR ve zeta potansiyeli gibi çok yönlü karakterizasyon analizleri aracılığıyla değerlendirilmesidir.

MATERYAL VE METOT

Bitki Örneklerinin Toplanması ve Hazırlanması

Bu çalışmada ülkemizde yayın olarak yetiştirilen *Chenopodium quinoa* bitkisinin tohumlarıyla çalışılmıştır. Laboratuvara getirilen örnekler oda sıcaklığında havan yardımıyla öğütülerek ince toz haline getirilmiştir. İnce toz halindeki kinoa materyali, ekstraksiyon işlemlerinde kullanılmak üzere kapalı kaplarda muhafaza edilmiştir.

Metanol Ekstraktının Hazırlanması

Ekstraksiyon için 10 g kinoa reaksiyon balonuna alınmış ve üzerine 100 mL metanol eklenmiştir. Örnek, oda sıcaklığında maserasyon yöntemiyle 2–4 kez ekstrakte edilmiştir. Maserasyon süresince balon ara ara elle çalkalanmış, ardından pilili süzgeç kâğıdı ile süzülmüştür. Elde edilen süzüntü 42 °C'de düşük basınç altında rotavapor kullanılarak yoğunlaştırılmıştır. Literatürde bildirildiği şekilde işlem tamamlandıktan sonra metanol ekstraktı koyu renkli cam kaplarda buzdolabında saklanmıştır (Zhang ve ark., 2018).

Metanol Ekstraktı ile Kitosan Nanopartiküllerinin (Cs-NP) Sentezi

Kitosan (≥%90 saflık, Sigma-Aldrich; CAS No: 9012-76-4), %1 (a/h) konsantrasyonda %1'lik asetik asitte çözülmüş ve homojenizasyon için 24 saat manyetik karıştırıcıda tutulmuştur. Çözeltinin pH'ı NaOH ile 5'e ayarlanmış ve sterilizasyon amacıyla 0.22 µm filtreden geçirilmiştir.

Hazırlanan kitosan çözeltisi, metanol ekstraktı ile 1:1 oranında karıştırılmış ve oda sıcaklığında inkübasyona bırakılmıştır. Sentez sonrası karışım 10.000 × g'de 10 dakika santrifüj edilmiş ve elde edilen çökelti 80 °C'de etüvde bir gece kurutularak karakterizasyon için hazırlanmıştır (El-Naggar ve ark., 2023).

Nanopartiküllerin Karakterizasyonu

Dinamik Işık Saçılması (DLS): Metanol ekstraktı ile sentezlenen Cs-NP'lerin parçacık boyutu ve dağılımı, sonikasyon işleminden geçirilip deiyonize su ile seyreltilen numuneler üzerinde analiz edilmiştir.

Zeta Potansiyeli: Nanopartiküllere ait yüzey yükü değerleri zeta potansiyel cihazı ile ölçülmüştür. Analiz öncesinde numuneler deiyonize suyla yıkanmış ve ölçümde kullanılan tek kullanımlık zeta hücreleri etanol ile temizlenmiştir.

X-Işını Toz Difraksiyonu (XRD): Cs-NP'lerin kristal yapısı XRD cihazı ile incelenmiştir.

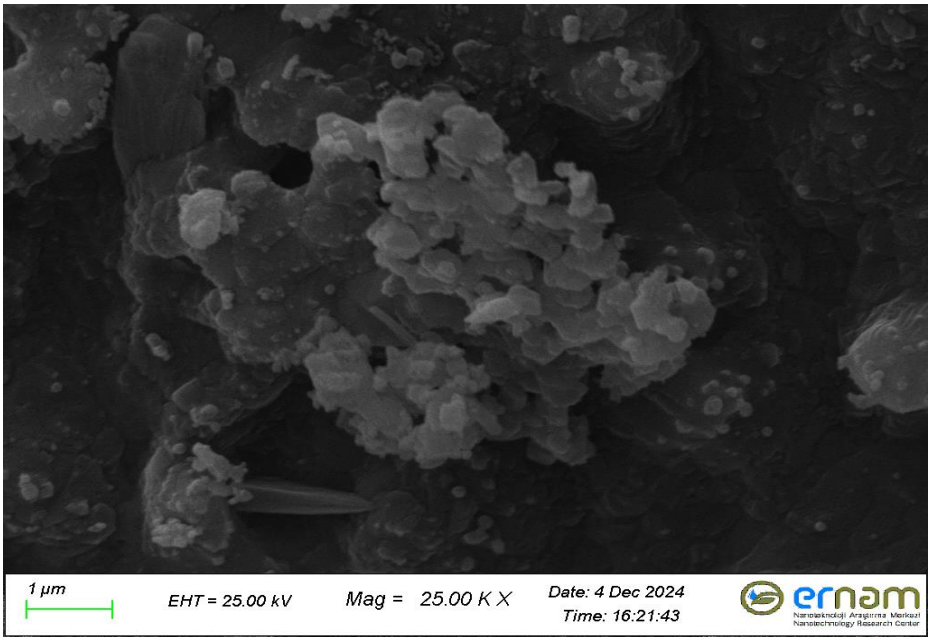
FT-IR Spektroskopisi: Nanopartiküllerin yapısında bulunan fonksiyonel gruplar FT-IR cihazı ile 400–4000 cm^{-1} aralığında analiz edilmiştir.

SEM ve SEM-EDX Analizi: Nanopartiküllerin morfolojisi ve elementel içeriği Erciyes Üniversitesi Nanoteknoloji Araştırma Merkezi'nde (ERNAM) SEM ve SEM-EDX cihazları kullanılarak belirlenmiştir.

BULGULAR

SEM Analizi

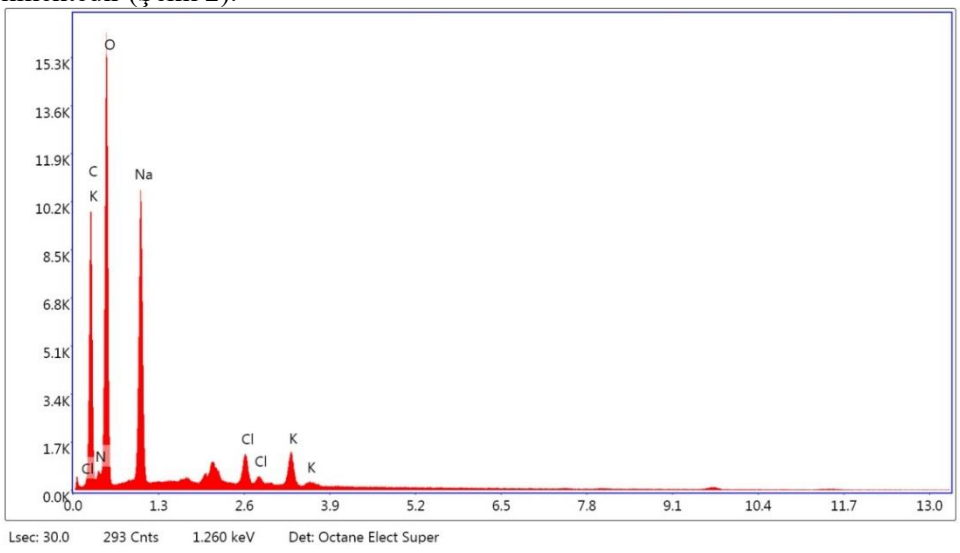
Görüntüde metanol ekstraktı ile sentezlenen Cs-NP'lerin yüzey boyunca **düzensiz dağılan, küçük parçacıklardan oluşan ve belirli bölgelerde birikme eğilimi gösteren** bir yapı oluşturduğu görülmektedir (Şekil 1). Partiküllerin tam anlamıyla küresel bir formdan uzak, **amorf ve heterojen bir morfoloji** sergilemesi, kitosan bazlı nanopartiküllerin doğal birleşme ve yüzeyde tutunma eğilimlerini yansıtmaktadır.



Şekil 1. *Chenopodium quinoa* ekstraktları kullanılarak metanol ortamında biyosentezlenen Cs-NP'nin SEM görüntüsü

SEM-EDX Analizi

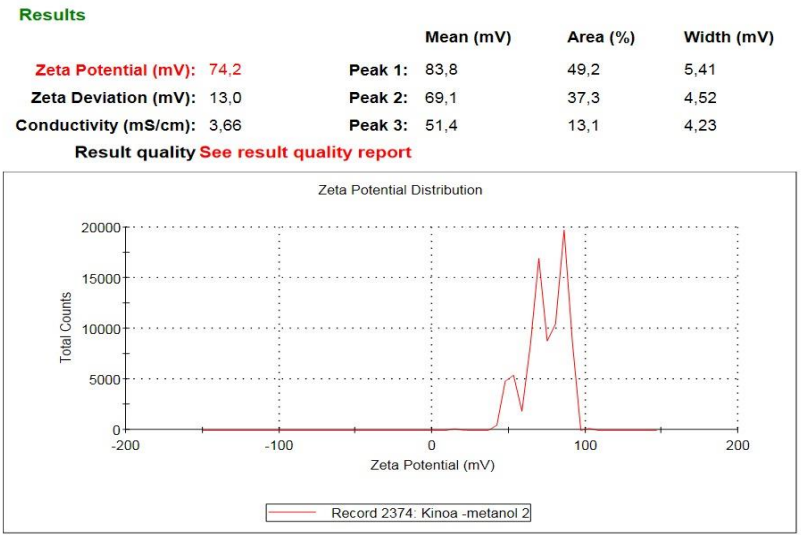
Cs-NP'lere ait EDX spektrumu, yapının temel elementlerinin **karbon (C)** ve **oksijen (O)** olduğunu göstermektedir. Ayrıca spektrumda görülen **Na, Cl** ve **K** iz elementleri, metanol ekstraktından veya sentez ortamındaki iyonik bileşenlerden nanopartikül yüzeyine taşınan küçük miktarlardaki mineral içeriklerle ilişkilendirilmektedir (Şekil 2).



Şekil 2. *Chenopodium quinoa* ekstraktları kullanılarak Metanol ekstraktı ile sentezlenen Cs-NP'lere ait SEM-EDX spektrumu

Zeta Potansiyel Analizi

Sentezlenen Cs-NP'lerin Zeta potansiyeli **+74,2 mV** olarak belirlenmiş olup, bu yüksek pozitif yüzey yükü nanopartiküllerin kolloidal ortamda **güçlü elektrostatik stabilite** gösterdiğini ifade etmektedir (Şekil 3). Dağılımda yer alan üç pozitif pik, partiküllerin **yük dağılımında kısmi heterojenlik** bulunduğunu göstermesine rağmen, tüm piklerin yüksek pozitif bölgede yer alması Cs-NP süspansiyonunun genel olarak **stabil ve elektrostatik açıdan kararlı** bir yapıya sahip olduğunu desteklemektedir.



Şekil 3. *Chenopodium quinoa* ekstraktları kullanılarak metanol ortamında biyosentezlenen Cs-NP'nin zeta potansiyel dağılımı

DLS Analizi

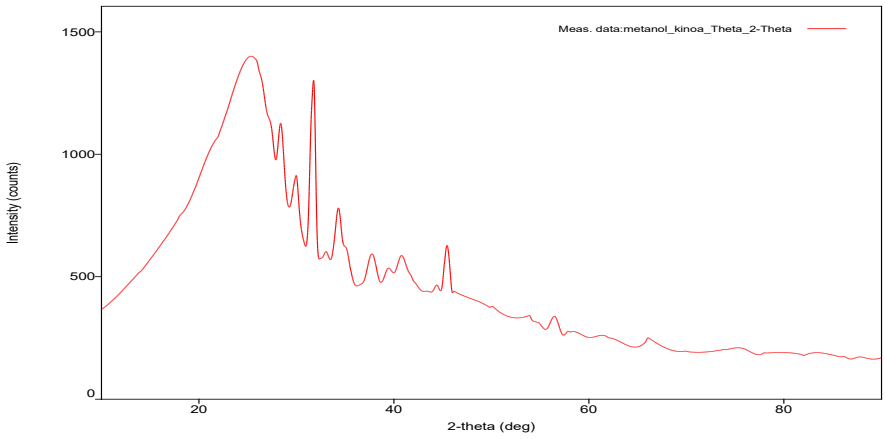
DLS analizi, metanol ekstraktı ile sentezlenen Cs-NP süspansiyonunda **Z-ortalama hidrodinamik çapın 579,5 nm** olduğunu ve **PDI değerinin 1,000** çıkması nedeniyle sistemin son derece **polidispers** bir yapıya sahip olduğunu göstermektedir (Şekil 4). Yaklaşık **2463 nm** civarında tek ve yoğun bir pik gözlenmesi, nanopartiküllerin önemli ölçüde **agregasyon/aglomerasyon** eğilimi gösterdiğini ve süspansiyonun homojen nanometrik partiküller yerine daha çok **mikrometre ölçeğinde büyük kümeler** içerdiğini düşündürmektedir.



Şekil 4. *Chenopodium quinoa* ekstraktları kullanılarak metanol ortamında biyosentezlenen Cs-NP'nin DLS analizi

XRD Analizi

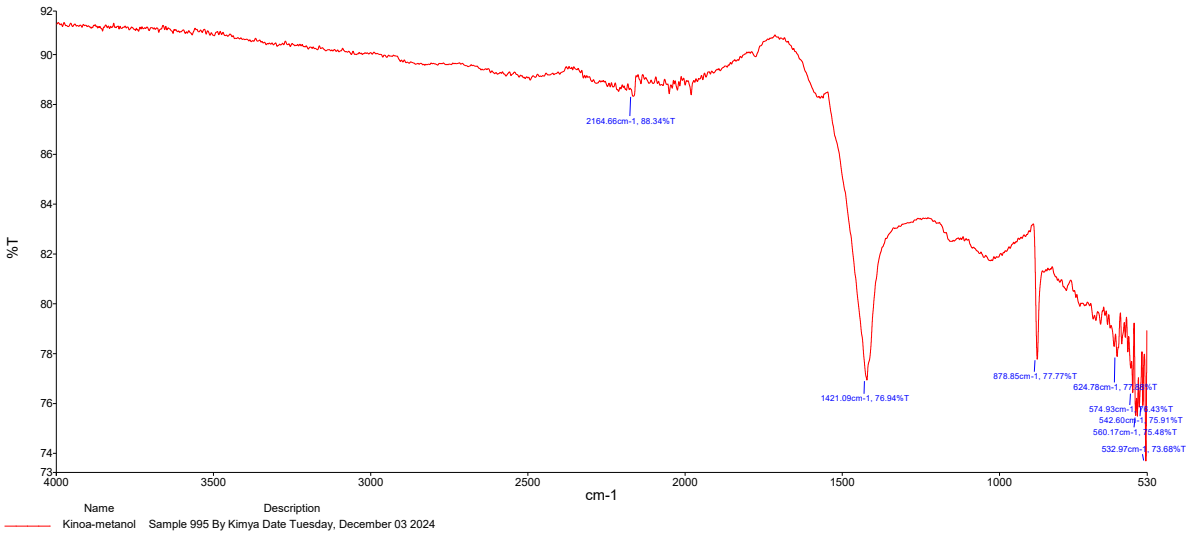
Cs-NP'lere ait XRD deseninde 10–40° aralığında geniş bir taban yükselmesi ile birlikte 20–30° civarında çok sayıda belirgin pik görülmektedir (Şekil 5). Bu durum, tamamen amorf bir yapıdan ziyade, amorf kitosan matrisi içerisinde kristalin bölgelerin de bulunduğunu göstermektedir.



Şekil 5. *Chenopodium quinoa* ekstraktları kullanılarak metanol ortamında biyosentezlenen Cs-NP'nin XRD analizi

FT-IR Analizi

FT-IR spektrumunda 3300 cm^{-1} civarındaki geniş bant O–H/N–H gerilmelerine, 2920 cm^{-1} piki alifatik C–H titreşimlerine karşılık gelmektedir. 1410 cm^{-1} bölgesindeki kuvvetli bant, kitosanın karakteristik $–NH_3^+$ ve CH_2 bükülme titreşimlerini doğrulamaktadır. Ayrıca 1220–1020 cm^{-1} aralığındaki C–O–C ve C–O gerilmeleri kitosan yapısının korunduğunu göstermektedir. 879 ve 773 cm^{-1}'deki ek bantlar ise *Chenopodium quinoa* ekstraktındaki fitokimyasalların nanopartikül yüzeyine entegre olduğunu işaret etmektedir (Şekil 6).



Şekil 6. *Chenopodium quinoa* ekstraktları kullanılarak metanol ortamında biyosentezlenen Cs-NP'nin FT-IR analizi

TARTIŞMA

Metanol ekstraktı kullanılarak sentezlenen Cs-NP'lere ait karakterizasyon bulguları, bitki ekstraktı aracılı yeşil sentez yaklaşımının başarıyla işlediğini göstermektedir. SEM analizinde gözlenen yoğun küresel morfoloji ve belirgin agregasyon eğilimi, bitkisel ekstraktlarla sentezlenen Cs-NP'lerde literatürde rapor edilen tipik davranışlarla uyumludur. EDX sonuçları, nanopartikül yüzeyinin kinoa kaynaklı fitokimyasallarla kaplandığını doğrularken, +74.2 mV'luk çok yüksek zeta potansiyeli, güçlü kolloidal stabiliteyi açıkça ortaya koymaktadır. DLS analizindeki yüksek hidrodinamik çap ve XRD'deki yarı kristalin yapı, kitosan özelliklerinin korunduğunu gösterirken; FT-IR bantları hem polimer omurgasının hem de ekstrakt kaynaklı bileşiklerin varlığını desteklemiştir.

SONUÇ

Chenopodium quinoa tohumlarının metanol ekstraktı kullanılarak sentezlenen kitosan nanopartiküllerine (Cs-NP) ait karakterizasyon bulguları, biyosentetik sürecin etkinliğini ve kitosan temelli nanopartiküllerin başarıyla oluşturulduğunu açıkça ortaya koymuştur.

SEM analizi, nanopartiküllerin yoğun, küresel ve belirgin agregasyon eğilimli bir morfoloji sergilediğini göstermiş; yaklaşık **52 nm boyutunda birincil partikül yapısına** rağmen partiküller arasında güçlü bir kümelenme davranışı gözlenmiştir. Bu durum, bitkisel ekstraktlarla gerçekleştirilen biyosentez çalışmalarında yaygın olarak rapor edilen nano-agregasyon eğilimleri ile paralellik göstermektedir (Khanmohammadi ve ark., 2023). EDX analizinde nanopartikül yapısının temel olarak C ve O'dan oluştuğu; ayrıca bitki ekstraktının doğal mineral profilini yansıtan Na ve K gibi elementlerin matrikste yer aldığı tespit edilmiştir. Bu bulgular, nanopartikül yüzeyinin kinoa kaynaklı fitokimyasallarla kaplandığını ve sürecin biyosentetik niteliğini doğrulamaktadır.

Zeta potansiyeli ölçümleri, Cs-NP'lerin **+74.2 mV** gibi son derece yüksek bir pozitif yüzey yüküne sahip olduğunu ortaya koymuştur. Literatürde ±30 mV ve üzeri zeta potansiyeli değerleri, kolloidal sistemler için yüksek stabilite kriteri olarak kabul edilmektedir (Honary ve Zahir, 2013). Bu çerçevede +74.2 mV'luk değer, mevcut kriterin **iki katından daha fazla** olup sentezlenen nanopartiküllerin agregasyona karşı **son derece dirençli ve olağanüstü düzeyde stabil** olduğunu göstermektedir. El-Naggar ve ark. (2022) biyolojik yöntemle sentezledikleri Cs-NP'lerde +31.1 mV'luk bir zeta potansiyeli rapor etmiş olup çalışmamızda elde edilen +74.2 mV'luk değerin literatürdeki bu stabilite referanslarının oldukça üzerinde bulunması, kinoa metanol ekstraktının güçlü bir stabilize edici ajan olarak işlev gördüğünü güçlü şekilde desteklemektedir.

DLS analizleri, Cs-NP'lerin geniş bir hidrodinamik boyut dağılımına sahip olduğunu ve yaklaşık **1912 nm** civarında tek modlu bir pik sergilediğini göstermiştir. Bu yüksek hidrodinamik çap değeri, partiküller arası agregasyonun yoğun olduğunu ortaya koymakta olup SEM sonuçlarıyla uyum içindedir. Singh ve ark. (2021) tarafından yapılan bir çalışmada da, bitkisel ekstraktlarla sentezlenen Cs-NP'lerde gözlenen yoğun agregasyonun DLS ile ölçülen hidrodinamik çapı anlamlı derecede artırdığı bildirilmiştir.

XRD analizinde 20–30° (2θ) aralığında geniş ve yayvan yarı kristalin patern gözlenmiş; bu patern kitosanın karakteristik yarı kristalin yapısının korunduğunu göstermektedir. Bulgular metanol temelli yeşil sentez çalışmalarında rapor edilen desenlerle uyumludur. Duraisamy ve ark. (2022), *Martynia annua* yaprak ekstraktı

ile sentezledikleri Cs-NP'lerde benzer şekilde düşük kristallilik gösteren geniş XRD pikleri rapor etmiş ve bunun kitosanın karakteristik yapısını doğruladığını belirtmiştir. Bu paralellik, kinoa ekstraktı ile yürütülen biyosentetik süreçte de kitosan polimer yapısının bozulmadan korunduğunu teyit etmektedir.

FT-IR analizinde 3300–3350 cm^{-1} aralığındaki geniş bant O–H ve N–H gerilme titreşimlerine; 2920 cm^{-1} civarındaki bantlar alifatik C–H titreşimlerine karşılık gelmiştir. 1410 cm^{-1} bölgesinde gözlenen belirgin bant, kitosanın **protonlanmış amin gruplarına (–NH_3^+)** ait karakteristik bükülme titreşimlerini doğrulamaktadır. Ayrıca 1220–1020 cm^{-1} aralığına karşılık gelen C–O–C ve C–O gerilmeleri, kitosanın polisakkarit omurgasının nanopartikül yapısında korunduğunu göstermektedir. 879 ve 773 cm^{-1}'de kaydedilen ek bantlar, kinoa ekstraktındaki fenolik ve saponin türevi bileşiklerin nanopartikül yüzeyine bağlandığını ve sistemde **doğal stabilizatör** görevi üstlendiğini işaret etmektedir. Ganesan ve ark. (2024) tarafından yapılan benzer bir çalışmada *Cassia fistula* yaprak ekstraktı ile sentezlenen Cs-NP'lerde gözlenen glikozidik ve C–O–C bantlarının bitkisel bileşiklerin nanopartikül yüzeyine bağlanmasıyla ilişkili olduğu bildirilmiş; bu durum çalışmamızdaki FT-IR sonuçlarıyla güçlü bir paralellik göstermektedir.

Genel olarak, elde edilen tüm veriler *Chenopodium quinoa* metanol ekstraktının Cs-NP sentezinde hem indirgeyici hem de stabilize edici bir ajan olarak son derece etkili olduğunu göstermektedir. Bu çalışma, kinoa gibi biyolojik açıdan güvenli ve gıda kaynaklı bir bitkinin nanoteknolojik uygulamalarda sürdürülebilir bir sentez aracı olarak kullanılabileceğini ortaya koyarak literatüre önemli bir katkı sağlamaktadır.

TEŞEKKÜR

Lisans ve yüksek lisans eğitimim süresince bilgi, birikim ve tecrübeleriyle akademik gelişimime önemli katkılar sağlayan; yönlendirmeleri, desteği ve bilimsel rehberliği ile çalışmamın her aşamasında yanımda olan değerli danışmanım Prof. Dr. Zeliha Leblebici'ye saygı ve teşekkürlerimi sunarım.

Nevşehir Hacı Bektaş Veli Üniversitesi Bilimsel Araştırma Projeleri Koordinasyon Birimi (Proje No: TEZ24F04) tarafından sağlanan destekler kapsamında yürütülmüştür. Söz konusu kurumlardan sağlanan maddi destekler için teşekkür ederim.

KAYNAKLAR

Duraisamy, R., Elango, K., & Kumar, P. (2022). Green synthesis of chitosan nanoparticles using *Martynia annua* leaf extract. *Materials Today: Proceedings, 68*, 1123–1131.

El-Naggar, M. E., Shaarawy, S., & Hebeish, A. (2022). Biogenic synthesis of chitosan nanoparticles and their applications. *Journal of Nanostructure Chemistry, 12*, 455–468.

El-Naggar, N. E. A., Eltarahony, M., Hafez, E. E., & Bashir, S. I. (2023). Green fabrication of chitosan nanoparticles using *Lavandula angustifolia*: Optimization, characterization and antibiofilm activity. *Scientific Reports, 13*, 11127. https://doi.org/10.1038/s41598-023-37660-6

El-Naggar, N. E. A., Saber, W. I. A., Zweil, A. M., & Bashir, S. I. (2022). An innovative green synthesis approach of chitosan nanoparticles and their inhibitory activity against *Botrytis cinerea* on strawberry leaves. *Scientific Reports, 12*(1), 3515.

Erdoğan, Ö., Birtekocak, F., Oryaşın, E., Abbak, M., Demirbolat, G. M., Paşa, S., & Çevik, Ö. (2019). Enginar yaprağı sulu ekstraktı kullanılarak çinko oksit nanopartiküllerinin yeşil sentezi, karakterizasyonu ve biyolojik aktiviteleri. *Düzce Tıp Fakültesi Dergisi, 21*(1), 19–26.

Ganesan, G., Venkatesan, P., & Thangavel, K. (2024). FT-IR based characterization of plant-mediated chitosan nanoparticles. *Spectrochimica Acta Part A: Molecular and Biomolecular Spectroscopy, 315*, 123–136.

Honary, S., & Zahir, F. (2013). Effect of zeta potential on the properties of nano-drug delivery systems. *Tropical Journal of Pharmaceutical Research, 12*(2), 255–264.

Ibrahim, N. A., Ameen, H. A., & Eid, B. M. (2024). Green synthesized chitosan and ZnO nanoparticles for sustainable use in multifunctionalization of cellulosic fabrics. *Polymer Bulletin, 81*, 3621–3640.

Khanmohammadi, M., et al. (2023). Morphological behavior of biosynthesized chitosan nanoparticles. *Journal of Applied Polymer Science, 140*, e53321.

Polat, M. (2023). Biyolojik sentez (green sentez) ile hazırlanmış bakır nanoparçacıklarının azo boyaların gideriminde kullanılması ve bazı biyolojik aktivitelerinin belirlenmesi (Yüksek lisans tezi). Bingöl Üniversitesi.

Singh, A., Verma, P., & Rao, R. (2021). Aggregation behavior of green-synthesized chitosan nanoparticles. *Carbohydrate Polymers, 251*, 117–129.

Zhang, Q.-W., Lin, L.-G., & Ye, W.-C. (2018). Techniques for extraction and isolation of natural products: A comprehensive review. *Chinese Medicine, 13*, 20. https://doi.org/10.1186/s13020-018-0177-x

ORAL PRESENTATION

Glycyrrhiza glabra ekstraktları ile kitosan nanopartiküllerinin biyosentezi ve karakterizasyonu

Rabiye Sema Uğur[1] (*Orcid:* https://orcid.org/0009-0001-5018-6697),
Zeliha Leblebici[2] (*Orcid: https://orcid.org/0000-0002-6127-3809*)

[*1] Nevşehir Hacı Bektaş Veli Üniversitesi, Fen Bilimleri Enstitüsü, Moleküler Biyoloji ve Genetik Anabilim Dalı, Nevşehir / Türkiye.
[2] Nevşehir Hacı Bektaş Veli Üniversitesi, Fen-Edebiyat Fakültesi, Moleküler Biyoloji ve Genetik Bölümü, Nevşehir / Türkiye.

*Sorumlu yazar e-mail: rabia.sema15@gmail.com

Özet

Güncel biyomedikal uygulamalarda nanopartiküller, çevre dostu üretim yöntemlerine uyumlulukları ve fonksiyonel özellikleri nedeniyle önemli bir araştırma alanı oluşturmaktadır. Bu çalışmada, *Glycyrrhiza glabra* kökleri metanol ekstraktı kullanılarak, kitosan nanopartikülleri (Cs-NP) sentezlenmiş ve temel karakterizasyon analizleri gerçekleştirilmiştir. SEM görüntüleri parçacıklı ve agregasyon eğilimi gösteren bir morfoloji ortaya koymuştur. EDX analizinde nanopartiküllerin başlıca elementlerinin C ve O olduğu, ayrıca Na, Cl ve K gibi elementlerin yüzeyde bulunduğu belirlenmiştir. Zeta potansiyeli +58,8 mV olarak ölçülmüş ve Cs-NP'lerin kolloidal ortamda yüksek stabiliteye sahip olduğu görülmüştür. XRD analizleri yarı kristalin bir yapıyı işaret etmiş, FT-IR spektrumu ise kitosan ve bitkisel bileşiklere ait karakteristik fonksiyonel grupların korunduğunu göstermiştir. Bulgular, metanol ekstraktının Cs-NP biyosentezi için etkili bir doğal ajan olduğunu ortaya koymaktadır.

Anahtar Kelimeler: *Glycyrrhiza glabra*, Kitosan nanopartikülleri, Nanoteknoloji, Yeşil sentez

Biosynthesis and characterization of chitosan nanoparticles using *Glycyrrhiza glabra* extracts

Abstract

Nanoparticles have gained increasing importance in recent biomedical applications due to their compatibility with eco-friendly synthesis approaches and their versatile functional properties. In the present study, chitosan nanoparticles (Cs-NPs) were synthesized using the methanol extract of *Glycyrrhiza glabra* and their characterization was performed using multiple analytical techniques. SEM imaging revealed an aggregated and irregular particulate morphology. EDX results showed that the nanoparticles were primarily composed of carbon and oxygen, accompanied by trace elements such as Na, Cl, and K. The zeta potential value of +58.8 mV indicated high colloidal stability in suspension. XRD analysis demonstrated a semicrystalline structure, and FT-IR spectra verified the presence of characteristic functional groups belonging to both chitosan and plant-derived compounds. Overall, the findings highlight the effectiveness of *Glycyrrhiza glabra* methanol extract as a natural reducing and stabilizing agent in the biosynthesis of chitosan nanoparticles.

Keywords: Chitosan nanoparticles, *Glycyrrhiza glabra*, Green synthesis, Nanotechnology

GİRİŞ

Bitkiler, tarih boyunca hem gıda hem de tedavi amaçlı kullanılmış ve içeriklerindeki biyolojik olarak aktif bileşikler sayesinde geleneksel tıbbın önemli bir parçası olmuştur. Bu bitkiler arasında yer alan *Glycyrrhiza glabra* (meyan kökü), zengin triterpen, saponin ve flavonoid içeriği ile dikkat çeken değerli bir tıbbi bitkidir. Meyan kökünün başlıca bileşenlerinden biri olan glisirizin; antioksidan, antiinflamatuar ve çeşitli biyolojik etkiler göstermesi nedeniyle pek çok çalışmada ön plana çıkmaktadır (Batiha ve ark., 2020; Celano ve ark., 2021; Esmaeili ve ark., 2024; Pastorino ve ark., 2018). Son yıllarda nanoteknoloji alanındaki gelişmeler, bitkisel kaynaklı biyoaktif bileşiklerin nanopartikül sentezinde kullanılmasına yönelik ilgiyi artırmıştır. Nanopartiküller, yüksek yüzey alanı, özgün fizikokimyasal özellikleri ve fonksiyonel yüzey modifikasyonlarına uygunlukları sayesinde tıp, çevre ve malzeme biliminde geniş bir uygulama alanına sahiptir (Singh ve ark., 2015; Wang ve ark., 2016; Hazarika ve ark., 2022). Bu kapsamda özellikle bitkisel özütlerin

kullanıldığı yeşil sentez yöntemleri; çevre dostu olmaları, toksik kimyasal içermemeleri ve ekonomik olmaları nedeniyle geleneksel fiziksel ve kimyasal yöntemlere güçlü bir alternatif oluşturmaktadır (Ajitha ve ark., 2014; Mittal ve ark., 2014).

Doğal bir polisakkarit olan kitosan; biyouyumlu, biyobozunur ve antimikrobiyal özellikleri nedeniyle biyoteknoloji ve malzeme biliminde yaygın olarak kullanılmaktadır. Ayrıca kitosanın bitkisel bileşiklerle etkileşime girerek nanopartikül oluşturma kapasitesi, yeşil sentez çalışmalarında önemli bir avantaj sunmaktadır (Garavand ve ark., 2022; Hidangmayum ve ark., 2019).

Bu çalışmada, *Glycyrrhiza glabra* köklerinden elde edilen metanol ekstraktı kullanılarak kitosan nanopartiküllerinin yeşil sentez yöntemiyle üretimi amaçlanmıştır. Elde edilen nanopartiküller, SEM, EDX, FT-IR, XRD, DLS ve zeta potansiyel analizleriyle karakterize edilerek metanol ekstraktının kitosan nanopartiküllerinin biyosentezindeki etkinliği değerlendirilmiştir.

MATERYAL VE METOT

Bitki Örneklerinin Toplanması ve Hazırlanması

Bu çalışmada kullanılan *Glycyrrhiza glabra* kökleri, Gaziantep'te bulunan Ra-Ma Bayrakdar firmasından temin edilmiştir. Laboratuvara getirilen örnekler oda sıcaklığında kurutulmuş ve öğütücü (Spice Herb & Grinder IC-04A) kullanılarak ince toz hâline getirilmiştir. Öğütülen kök materyali, ekstraksiyon işlemlerinde kullanılmak üzere kapalı kaplarda muhafaza edilmiştir.

Metanol Ekstraktının Hazırlanması

Ekstraksiyon için 10 g meyan kökü tozu reaksiyon balonuna alınmış ve üzerine 100 mL metanol eklenmiştir. Örnek, oda sıcaklığında maserasyon yöntemiyle 2–4 kez ekstrakte edilmiştir. Maserasyon süresince balon ara ara elle çalkalanmış, ardından pilili süzgeç kâğıdı ile süzülmüştür. Elde edilen süzüntü 42 °C'de düşük basınç altında rotavapor kullanılarak yoğunlaştırılmıştır. Literatürde bildirildiği şekilde işlem tamamlandıktan sonra metanol ekstraktı koyu renkli cam kaplarda buzdolabında saklanmıştır (Zhang ve ark., 2018).

Metanol Ekstraktı ile Kitosan Nanopartiküllerinin (Cs-NP) Sentezi

Kitosan (≥%90 saflık, Sigma-Aldrich; CAS No: 9012-76-4), %1 (a/h) konsantrasyonda %1'lik asetik asitte çözülmüş ve homojenizasyon için 24 saat manyetik karıştırıcıda tutulmuştur. Çözeltinin pH'ı NaOH ile 5'e ayarlanmış ve sterilizasyon amacıyla 0.22 µm filtreden geçirilmiştir. Hazırlanan kitosan çözeltisi, metanol ekstraktı ile 1:1 oranında karıştırılmış ve oda sıcaklığında inkübasyona bırakılmıştır. Sentez sonrası karışım 10.000 × g'de 10 dakika santrifüj edilmiş ve elde edilen çökelti 80 °C'de etüvde bir gece kurutularak karakterizasyon için hazırlanmıştır (El-Naggar ve ark., 2023).

Nanopartiküllerin Karakterizasyonu

Dinamik Işık Saçılması (DLS): Metanol ekstraktı ile sentezlenen Cs-NP'lerin parçacık boyutu ve dağılımı, sonikasyon sonrası deiyonize su ile seyreltilmiş numuneler kullanılarak analiz edilmiştir.

Zeta Potansiyeli: Nanopartiküllerin yüzey yükü zeta potansiyel cihazı ile ölçülmüştür. Numuneler ölçüm öncesi deiyonize su ile yıkanmış, tek kullanımlık zeta hücreleri etanol ile durulanmıştır.

X-Işını Toz Difraksiyonu (XRD): Cs-NP'lerin kristal yapısı XRD cihazı ile incelenmiştir.

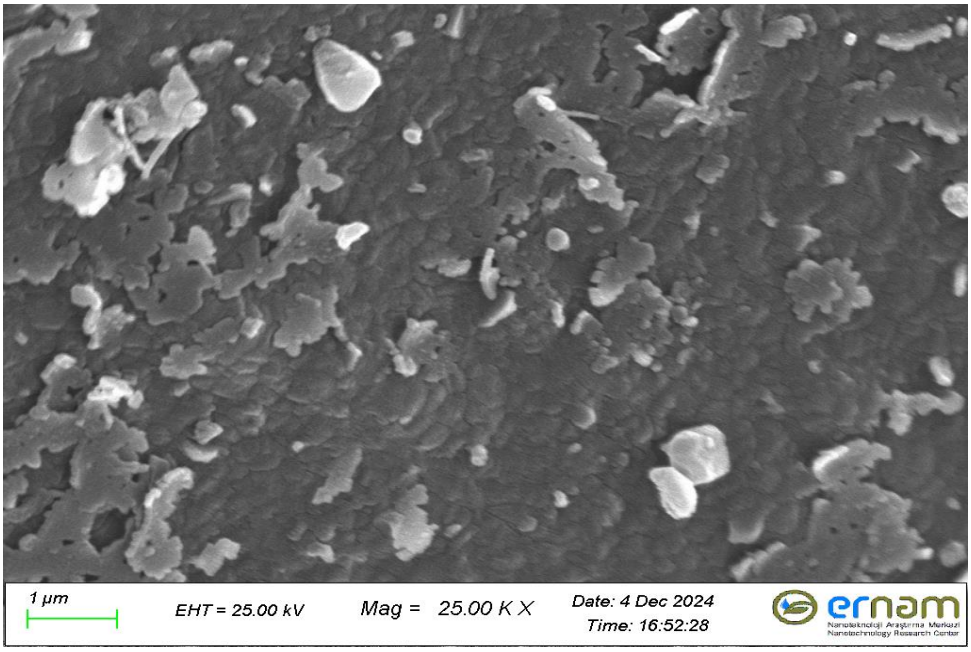
FT-IR Spektroskopisi: Nanopartiküllerin yapısında bulunan fonksiyonel gruplar FT-IR cihazı ile 400–4000 cm^{-1} aralığında analiz edilmiştir.

SEM ve SEM-EDX Analizi: Nanopartiküllerin morfolojisi ve elementel içeriği Erciyes Üniversitesi Nanoteknoloji Araştırma Merkezi'nde (ERNAM) SEM ve SEM-EDX cihazları kullanılarak belirlenmiştir.

BULGULAR

SEM Analizi

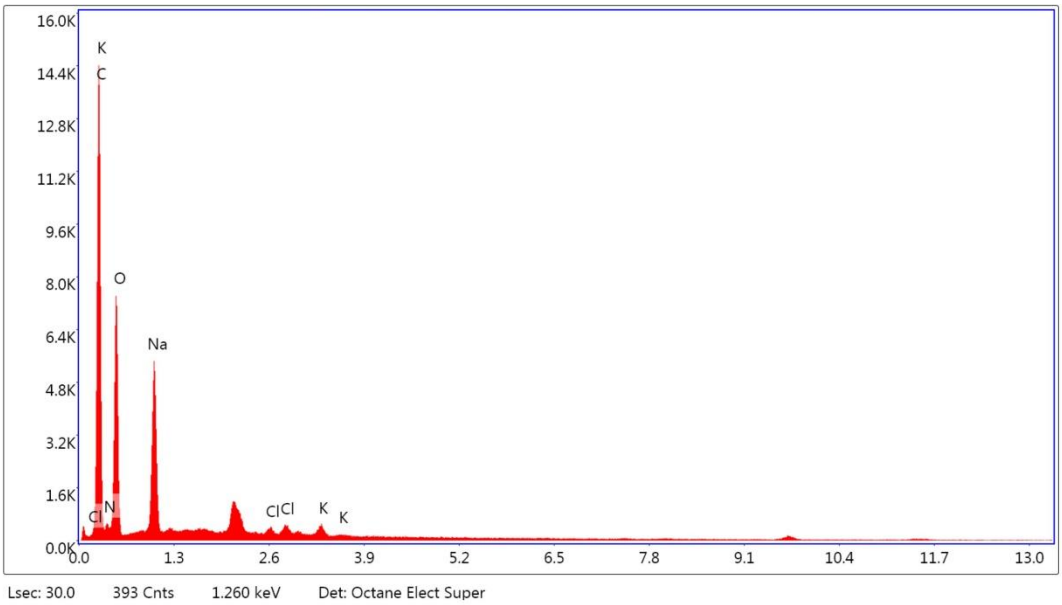
SEM görüntülerinde sentezlenen Cs-NP'lerin düzensiz, parçacıklı ve agregasyon eğilimi yüksek bir morfoloji sergilediği görülmüştür (Şekil 1). Bu yapı, kitosan temelli biyosentezlenmiş nanopartiküllerin doğal birleşme davranışının bir sonucu olarak değerlendirilmektedir.



Şekil 1. *Glycyrrhiza glabra* ekstraktları kullanılarak metanol ortamında biyosentezlenen Cs-NP'nin SEM görüntüsü

SEM-EDX Analizi

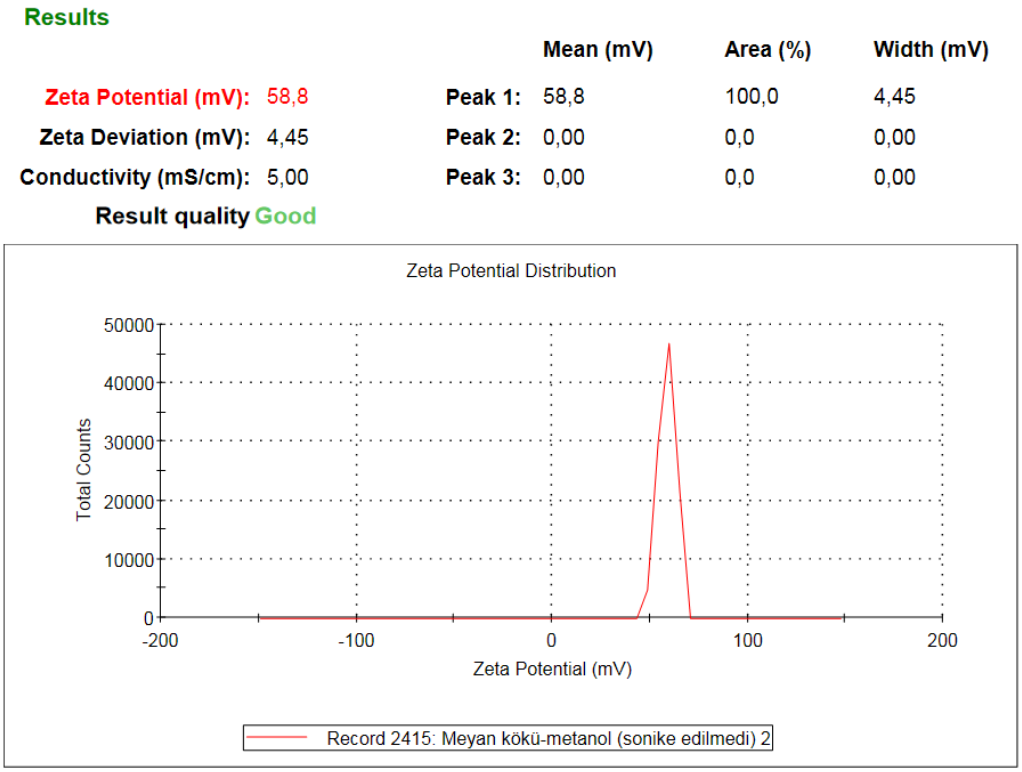
Cs-NP'lere ait EDX spektrumu, yapının temel elementlerinin karbon (C) ve oksijen (O) olduğunu ortaya koymuştur. Ayrıca yüzeyde Na, Cl ve K gibi elementlerin bulunması, bitkisel ekstrakt bileşenlerinin veya sentez ortamındaki iyonların nanopartikül yüzeyine tutulduğunu göstermektedir (Şekil 2).



Şekil 2. *Glycyrrhiza glabra* ekstraktları kullanılarak metanol ortamında biyosentezlenen Cs-NP'nin SEM-EDX analizi

Zeta Potansiyel Analizi

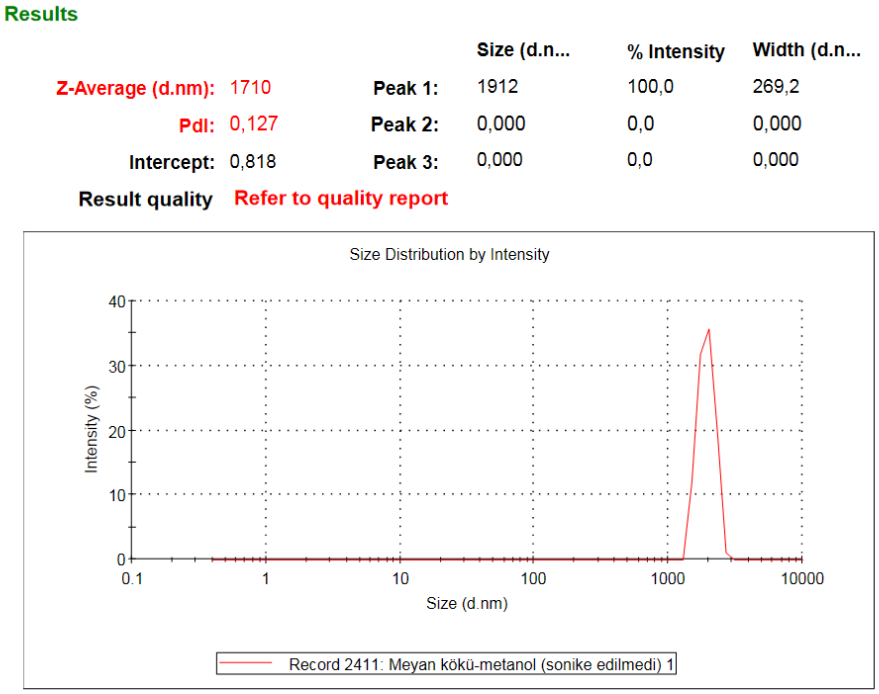
Sentezlenen Cs-NP'lerin zeta potansiyeli +58,8 mV olarak belirlenmiş olup, bu yüksek pozitif yüzey yükü Cs-NP'lerin kolloidal ortamda güçlü elektrostatik stabiliteye sahip olduğunu göstermektedir (Şekil 3). Tek pikli dar dağılım, Cs-NP süspansiyonunun homojen elektrostatik özellik taşıdığını desteklemektedir.



Şekil 3. *Glycyrrhiza glabra* ekstraktları kullanılarak metanol ortamında biyosentezlenen Cs-NP'nin zeta potansiyel dağılımı

DLS Analizi

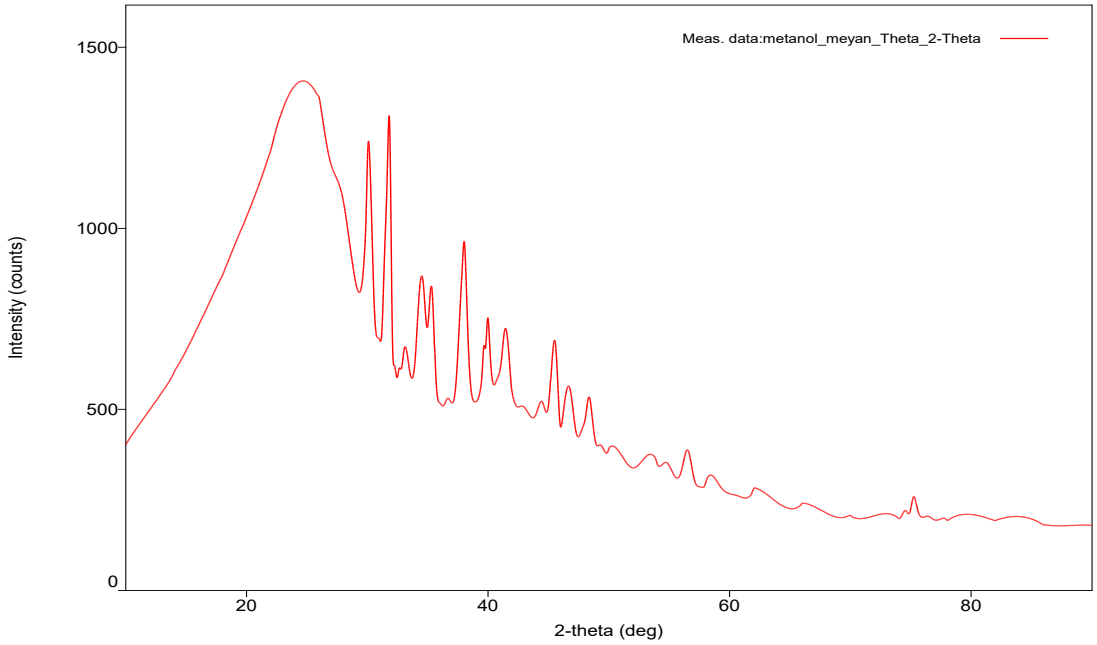
DLS ölçümünde Cs-NP'lerin Z-average değerinin 1710 nm olduğu ve dağılımın tek bir pikten oluştuğu görülmüştür (Şekil 4). PDI değerinin 0,127 olması, agregasyona rağmen dağılımın kabul edilebilir düzeyde homojen olduğunu göstermektedir. Ölçülen yüksek boyut değeri, Cs-NP'lerin biyosentez sonrası birleşme eğilimini yansıtmaktadır.



Şekil 4. *Glycyrrhiza glabra* ekstraktları kullanılarak metanol ortamında biyosentezlenen Cs-NP'nin DLS analizi

XRD Analizi

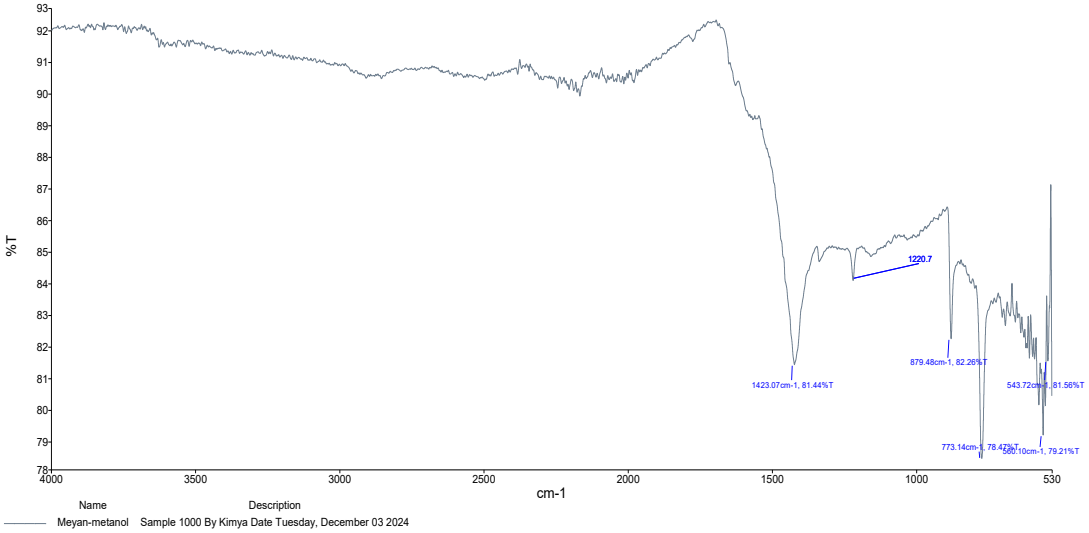
Cs-NP'lere ait XRD deseninde geniş taban hattı ve belirgin olmayan pikler gözlenmiştir (Şekil 5). Bu yapı, biyosentezlenen kitosan nanopartiküllerinin kristalin değil, ağırlıklı olarak amorf veya yarı kristalin yapıda olduğunu göstermektedir. Bu durum kitosan bazlı nanopartiküller için beklenen bir özellik olarak değerlendirilmektedir.



Şekil 5. *Glycyrrhiza glabra* ekstraktları kullanılarak metanol ortamında biyosentezlenen Cs-NP'nin XRD analizi

FT-IR Analizi

FT-IR spektrumunda 1423, 1220, 879 ve 773 cm^{-1} bölgelerinde görülen karakteristik bantlar, kitosanın fonksiyonel gruplarının nanopartikül yapısında korunduğunu doğrulamaktadır. Aynı zamanda bitkisel bileşenlere ait sinyallerin varlığı, *Glycyrrhiza glabra* ekstraktının doğal stabilizatör olarak Cs-NP matriksine başarıyla entegre olduğunu göstermektedir (Şekil 6).



Şekil 6. *Glycyrrhiza glabra* ekstraktları kullanılarak metanol ortamında biyosentezlenen Cs-NP'nin FT-IR analizi

TARTIŞMA

Bu çalışmada elde edilen sonuçlar, *Glycyrrhiza glabra* metanol ekstraktının kitosan nanopartiküllerinin biyosentezinde etkili bir indirgeme ve stabilize edici ajan olarak kullanılabileceğini göstermektedir. Yüksek zeta potansiyeli değerinin (+58,8 mV) ortaya koyduğu güçlü kolloidal stabilite, bitkisel bileşenlerin nanopartikül yüzeyine bağlanarak elektrostatik kararlılık sağladığını desteklemektedir. SEM ve DLS analizlerinde gözlenen agregasyon eğilimi, bitki ekstraktı ile sentezlenen Cs-NP'lerde literatürde de rapor edilen tipik bir davranıştır. XRD'deki yarı kristalin yapı ve FT-IR'deki karakteristik bantlar ise kitosanın yapısal özelliklerinin korunduğunu doğrulamaktadır. Genel olarak bulgular, bitki ekstraktı aracılı yeşil sentez yönteminin kitosan nanopartiküllerinin üretimi için uygun ve uygulanabilir bir yaklaşım olduğunu göstermektedir.

SONUÇ

Glycyrrhiza glabra köklerinin metanol ekstraktı kullanılarak sentezlenen kitosan nanopartiküllerinin (Cs-NP) karakterizasyon verileri, biyosentetik sürecin başarılı bir şekilde gerçekleştiğini ve kitosan temelli nanopartiküllerin oluştuğunu göstermektedir.

SEM analizinde düzensiz, agregasyon eğilimli bir yüzey morfolojisi gözlenmiştir. EDX bulguları nanopartiküllerin temel bileşenlerinin C ve O olduğunu, ayrıca Na, K ve Cl gibi elementlerin matrikste yer aldığını ortaya koymuştur. +58,8 mV olarak belirlenen zeta potansiyel değeri, Cs-NP'lerin yüksek pozitif yüzey yükü nedeniyle güçlü kolloidal stabilite sergilediğini doğrulamaktadır. El-Naggar ve ark. (2022) tarafından yapılan bir çalışmada biyosentezlenen Cs-NP'nin zeta potansiyelinin +31,1 mV olduğu ve bu değerin nanopartiküllerin elektrostatik itme yoluyla yüksek kolloidal stabilite gösterdiği bildirilmiştir. Bu bulgu, bir süspansiyonun kararlı kabul edilebilmesi için en az ±30 mV zeta potansiyeline ihtiyaç duyulduğunu belirten literatür ile uyumludur (Sathiyabama ve ark., 2024). DLS analizi, Cs-NP'lerin Z-average değerinin 1710 nm olduğunu ve yoğunluk dağılımında yaklaşık 1912 nm civarında tek modlu bir pik gösterdiğini ortaya koymuştur. Bu yüksek hidrodinamik boyut, nanopartiküllerin agregasyon eğiliminde olduğunu göstermektedir. XRD difraktogramında 20–30° (2θ) aralığında gözlenen geniş yarı kristalin patern, kitosan nanopartikülleri için tipik bir yapı olup güncel çalışmalarda rapor edilen desenlerle uyumludur. Benzer şekilde, Duraisamy ve ark. (2022) de *Martynia annua* yaprak ekstraktı ile sentezledikleri kitosan nanopartiküllerinde 2θ yaklaşık 20–30°

aralığında geniş yarı kristalin bir XRD piki rapor etmiş ve bunun kitosanın karakteristik yarı kristalin yapısını doğruladığını belirtmiştir.

FT-IR spektrumunda 1423, 1220, 879 ve 773 cm^{-1} bölgelerinde kaydedilen karakteristik bantlar ise kitosan yapısına özgü fonksiyonel grupların korunduğunu ve metanol ekstraktındaki fenolik bileşiklerin nanopartikül yüzeyine bağlanarak stabilize edici rol üstlendiğini desteklemektedir; benzer bulgular bitki ekstraktlarıyla yapılan yeşil sentez çalışmalarında da rapor edilmiştir. Yapılan benzer bir çalışmada, Ganesan ve ark. (2024), *Cassia fistula* yaprak ekstraktı ile sentezledikleri kitosan nanopartiküllerinde FT-IR analizinde 3421 cm^{-1} (O–H/N–H), 1635 cm^{-1} (C=O), 1384 cm^{-1} (C–N), 1078 cm^{-1} (C–O–C) ve 897 cm^{-1} (β-glycosidic) bantlarını rapor etmiş; bu bulgular bitkisel fenolik bileşiklerin nanopartikül yüzeyine bağlanarak stabilizasyon sağladığını göstermiştir.

Bu sonuçlar, *Glycyrrhiza glabra* metanol ekstraktının Cs-NP sentezinde etkili bir indirgeme ve stabilize edici ajan olarak kullanılabileceğini göstermektedir. Gelecek araştırmalarda partikül boyutunun azaltılmasına yönelik parametre optimizasyonlarının yapılması ve biyomedikal uygulamalara yönelik in vitro bulguların in vivo modellerde doğrulanması önerilmektedir.

TEŞEKKÜR

Lisans ve yüksek lisans eğitimim süresince bilgi, birikim ve tecrübeleriyle akademik gelişimime önemli katkılar sağlayan; yönlendirmeleri, desteği ve bilimsel rehberliği ile çalışmamın her aşamasında yanımda olan değerli danışmanım Prof. Dr. Zeliha Leblebici'ye saygı ve teşekkürlerimi sunarım.

Bu tez çalışması, TÜBİTAK Bilim İnsanı Destek Programları Başkanlığı (BİDEB) 2210 – Yurt İçi Lisansüstü Burs Programı ile Nevşehir Hacı Bektaş Veli Üniversitesi Bilimsel Araştırma Projeleri Koordinasyon Birimi (Proje No: TEZ24F05) tarafından sağlanan destekler kapsamında yürütülmüştür. Söz konusu kurumlardan sağlanan maddi destekler için teşekkür ederim.

KAYNAKLAR

Ajitha, B., Reddy, Y. A. K., & Reddy, P. S. (2014). Biosynthesis of silver nanoparticles using *Momordica charantia* leaf broth: Evaluation of their innate antimicrobial and catalytic activities. *Journal of Photochemistry and Photobiology B: Biology, 146*, 1–9.

Duraisamy, N., Dhayalan, S., Shaik, M. R., Shaik, A. H., Shaik, J. P., & Shaik, B. (2022). Green synthesis of chitosan nanoparticles using *Martynia annua* L. ethanol leaf extract and their antibacterial activities. *Crystals, 12*(11), 1550. https://doi.org/10.3390/cryst12111550

El-Naggar, N. E., Shiha, A. M., Mahrous, H., & Mohammed, A. B. A. (2022). Green synthesis of chitosan nanoparticles: Optimization, characterization and antibacterial efficacy against multidrug resistant biofilm-forming *Acinetobacter baumannii*. *Scientific Reports, 12*, 19869. https://doi.org/10.1038/s41598-022-24303-5

El-Naggar, N. E. A., Eltarahony, M., Hafez, E. E., & Bashir, S. I. (2023). Green fabrication of chitosan nanoparticles using *Lavandula angustifolia*: Optimization, characterization and antibiofilm activity. *Scientific Reports, 13*, 11127. https://doi.org/10.1038/s41598-023-37660-6

Ganesan, A., & Rengarajan, J. (2024). Green synthesis of chitosan nanoparticles using *Cassia fistula* leaf extract: Evaluation of antimicrobial, antioxidant, antibiofilm, and cytotoxic activities. *3 Biotech, 14*(10), 223. https://doi.org/10.1007/s13205-024-04073-9

Garavand, F., Cacciotti, I., Vahedikia, N., Rehman, A., Tarhan, Ö., Akbari-Alavijeh, S., & Jafari, S. M. (2022). A comprehensive review on the nanocomposites loaded with chitosan nanoparticles for food packaging. *Critical Reviews in Food Science and Nutrition, 62*(5), 1383–1416.

Hazarika, A., Yadav, M., Yadav, D. K., & Yadav, H. S. (2022). An overview of the role of nanoparticles in sustainable agriculture. *Biocatalysis and Agricultural Biotechnology, 43*, 102399.

Hidangmayum, A., Dwivedi, P., Katiyar, D., & Hemantaranjan, A. (2019). Application of chitosan on plant responses with special reference to abiotic stress. *Physiology and Molecular Biology of Plants, 25*(2), 313–326.

Mittal, A. K., Bhaumik, J., Kumar, S., & Banerjee, U. C. (2014). Biosynthesis of silver nanoparticles: Elucidation of prospective mechanism and therapeutic potential. *Journal of Colloid and Interface Science, 415*, 39–47.

Sathiyabama, M., Boomija, R. V., Muthukumar, S., et al. (2024). Green synthesis of chitosan nanoparticles using tea extract and antimicrobial activity against economically important rice phytopathogens. *Scientific Reports, 14*, 7381. https://doi.org/10.1038/s41598-024-58066-y

Singh, V. P., Singh, S., Kumar, J., & Prasad, S. M. (2015). Investigating the roles of ascorbate–glutathione cycle and thiol metabolism in arsenate tolerance in ridged Luffa seedlings. *Protoplasma, 252*(5), 1217–1229.

Wang, Z., Xu, L., Zhao, J., Wang, X., White, J. C., & Xing, B. (2016). CuO nanoparticle interaction with *Arabidopsis thaliana*: Toxicity, parent-progeny transfer, and gene expression. *Environmental Science and Technology, 50*(11), 6008–6016.

Zhang, Q.-W., Lin, L.-G., & Ye, W.-C. (2018). Techniques for extraction and isolation of natural products: A comprehensive review. *Chinese Medicine, 13*, 20. https://doi.org/10.1186/s13020-018-0177-x

ORAL PRESENTATION

Computational approach to evaluating an isoniazid-based schiff base targeting *Mycobacterium tuberculosis*

Suzan Şahin Doğan[1*] (Orcid: *https://orcid.org/*0000-0002-1554-0080),
Duygu Aydın[2] (Orcid: https://orcid.org/0000-0003-0436-1869)

[1]Karamanoğlu Mehmetbey University, Kamil Özdağ Faculty of Science, Department of Biology, Karaman, Türkiye
[2]Karamanoğlu Mehmetbey University, Kamil Özdağ Faculty of Science, Departman of Chemistry, Karaman, Türkiye

*Corresponding author e-mail: sdogan@kmu.edu.tr

Abstract

Advances in computational prediction and protein structure modeling have significantly contributed to understanding protein architecture in various biological contexts. These innovations have revolutionized biological research by providing powerful insights and streamlining the design of experimental studies. Mycobacterial pathogens are emerging as a major global challenge in disease management due to their inherent resistance to many antibiotics. The increasing prevalence of drug-resistant *Mycobacterium tuberculosis* strains has heightened the need for new and effective treatment strategies. Schiff bases exhibit broad biological activity, including antimicrobial, anticancer, and anti-inflammatory properties, due to the imine group present in their structures. This study aims to explore the antimycobacterial inhibitory potential of Schiff base based isoniaside (PISH) for InhA protein. In silico analyses, including molecular docking and ADME (Absorption, Distribution, Metabolism, and Excretion) property evaluation, were performed to predict the interaction patterns and binding energies of candidate molecules with InhA and to assess their potential bioavailability and drug potential. PISH exhibited an overall favorable safety profile, low genotoxic risk, and minimal predicted environmental impact. The Pfizer Rule demonstrated that PISH exhibited certain drug-like properties, and its compliance with the SureChEMBL rule further supported its favorable chemical characteristics, although it violated Lipinski's rule. Additionally, its moderate log P (2.92) reflected a balanced level of lipophilicity. However, the compound also had important limitations, including poor oral bioavailability, some drug-drug interaction, and limited water solubility. According to the molecular docking results, the ligand exhibited a strong binding affinity for the target protein, with a binding energy of −11.02 kcal/mol. Hydrogen bonds formed with Gly40, Lys165, and Gly14 contributed significantly to the stable binding of the PISH molecule at the protein's active site.

Keywords: Isoniazid-Based Schiff Base, Molecular docking, ADME, *Mycobacterium tuberculosis*

INTRODUCTION

Tuberculosis (TB) is a life-threatening disease caused by mycobacteria belonging to the *Mycobacterium tuberculosis* complex, primarily *Mycobacterium tuberculosis*, as well as *Mycobacterium bovis* and *Mycobacterium africanum* (Joshi et al., 2015; Zumla et al., 2013). In 2023, TB caused an estimated 1.25 million deaths globally (including 150 000 people with HIV) (WHO, 2023). The situation is further complicated by the global rise of multidrug-resistant *M. tuberculosis* (MDR-TB), extensively drug-resistant TB, and even totally drug-resistant strains. In addition, the high prevalence of HIV infection—which progresses to acquired immune deficiency syndrome (AIDS) has greatly increased the burden of TB.

Advanced computational techniques facilitate the drug discovery process with a flexible and innovative approach. In silico methods offer highly efficient alternatives in terms of time and cost. Using these techniques, it is possible to predict molecular interactions with biological targets, as well as virtually examine the behavior of molecules in the human body and evaluate their pharmacokinetic properties and bioavailability (Dogan et al., 2025; McPhillie et al., 2015; Mounadi et al., 2025; Sahin Dogan et al., 2025).
Schiff bases form when a primary amine combines with an aldehyde or ketone under the right reaction conditions. Schiff bases represent an important class of organic compounds, serving roles as dyes and pigments, catalysts, synthetic intermediates, and polymer stabilizers (da Silva et al., 2011). Furthermore, Schiff bases

have broad biological activity, including antimicrobial, anticancer, and anti-inflammatory properties, due to the imine group present in their structures (Ceramella et al., 2022; Iacopetta et al., 2025; Zúñiga-Miranda et al., 2025).

In present study, the antimycobacterial inhibitory potential of N',N'''-((1E,1'E)-((3-oxo-1,3-dihydroisobenzofuran-1,1-diyl)bis(6-hydroxy3,1phenylene))bis(methaneylylidene))di(isonicotinohydraz-ide) (PISH) for InhA protein were investigated. In computational techniques, including molecular docking and ADME (Absorption, Distribution, Metabolism, and Excretion) property evaluation, were performed to predict the interaction patterns and binding energies of PISH with enoyl–acyl carrier protein reductase (InhA) and to assess their potential bioavailability and drug potential.

MATERIAL AND METHODS

SwissADME and ADMET tools were used to evaluate the drug potential of isoniazid-based Schiff base (N′,N‴-((1E,1′E)-((3-oxo-1,3-dihydroisobenzofuran-1,1-diyl)bis(6-hydroxy-3,1-phenylene))bis (methanylylidene))di(isonicotinohydrazide)) (Aydin & Alici, 2021) as well as its bioactivity and ADME (absorption, distribution, metabolism, and excretion) properties using its Smiles format. The molecule was minimized using the PyRX program and converted to PDB format. The protein receptor downloaded from the PDB database was saved in PDB format after water molecules and ligands were removed. AutoDock tools 1.5.7 were used to perform the docking simulation, resulting in an estimated binding position. By analyzing the docking log files (dlg), the docking conformations with the lowest binding free energy for the ligand were determined. These conformations were used to generate docking images using AutoDock tools 1.5.7 and Discovery Studio (Biovia, 2024; Morris et al., 2009). For validation, the co-crystallized NAD molecule with InhA protein was re-docked with PISH molecule–protein complex.

RESULTS AND DISCUSSION

ADMET predictions indicated that the PISH had a generally acceptable safety profile, characterized by low cardiotoxicity, low genotoxicity, and limited environmental toxicity. However, the violation of Lipinski's rules and the lack of biodegradability should be considered points of concern, particularly in terms of oral bioavailability and environmental persistence (Table 1). When PISH examining for the Lipinski Rule, although it appeared to be outside this rule with a molecular weight greater than 500 g/mol, its moderate log P value of 2.92 provided the advantage of potentially interacting well with hydrophobic targets (Table 2). It was consisted with some Lipinski's rules (HBA ≤10, HBD ≤5), thus it can increase binding affinity. Furthermore, it accepted by the Pfizer Rule, indicating some drug-like properties as well as consistence with the SureChEMBL Rule, representing favorable chemical properties (Table 1). However, a low GI absorption/HIA value indicated that the compound could be poorly absorbed from the gastrointestinal tract and could have low oral bioavailability. Due to its limited water solubility (LogS –4.807), the compound may exhibit reduced bioavailability, needing advanced formulation methods essential to enhance its solubility and membrane permeability. The fact that the compound cannot cross the blood-brain barrier (BBB permeant: No) indicates a low potential risk of neurotoxicity (Table 3). Moreover, it had moderate clearance (2.381) and a rapid half-life of 0.953 h might require frequent dosing (Table 3).

Table1. Toxicity and Drug-Likeness of PISH

	Properties	**Values**	**Properties**	**Values**
Toxicity properties	hERG Blockers	0.047	$LC_{50}FM$	6.041
	A549 Cytotoxicity	0.032	Hek293 Cytotoxicity	0.659
	BCF	1.036	Genotoxic Carcinogenicity Mutagenicity Rule	Accepted
	NonBiodegradable	yes	NonGenotoxic Carcinogenicity Rule	Accepted
Drug likeness	IGC_{50}	5.399	$LC_{50}DM$	5.735
	FAF-Drugs4 Rule	4	SureChEMBL Rule	Accepted
	Lipinski	Rejected	Pfizer Rule	Accepted

Table 2. Physicochemical properties of the PISH

Properties	**Values**	**Properties**	**Values**
Formula	C34H24N6O6	Num. H-bond acceptors	10
Molecular weight	612.59	Num. H-bond donors	4
Num. heavy atoms	46	Molar Refractivity	166.6
Num. rotatable bonds	10	Topological Polar Surface Area	175.46
Lipophilicity (LogP)	2.912	nHA	12
logS	-4.807	nHD	4

Table 3. Pharmacokinetics properties of the PISH

Properties	Values	Properties	Values
PAMPA	No	GI absorption / HIA	Low
F20%	0.234	Caco-2 Permeability	-5.5
F50%	0.147	MDCK Permeability	7.00E-06
Log Kp (skin permeation)	-8.55	BBB permeant	No
Fu	1.20%	CYP2C9 inhibitor	Yes
CLplasma	2.381	Bioavailability Score	0.17
VDss	0.493	T1/2	0.953
GI absorption	low	CYP3A4 inhibitor	No
PPB	100.60%	CYP2D6 substrate	No
OATP1B1 inhibitor	yes	MCE-18	69.943
CYP1A2 inhibitor	Yes	CYP2C19 inhibitor	No
CYP2C9 inhibitor	Yes	P-gp substrate	No

The Protein Data Bank (PDB) structure 1ENY corresponded to InhA from *Mycobacterium tuberculosis*, a key enzyme in the biosynthetic pathway of the mycobacterial cell wall (Dessen et al., 1995). This structure was selected as the target protein for the study to explore the potential of PISH as a novel antitubercular agent. According to the molecular docking results, the ligand exhibited a strong binding affinity for the target protein, with a binding energy of −11.02 kcal/mol. Hydrogen bonds formed with Gly40, Lys165, and Gly14 contributed significantly to the stable binding of the PISH molecule at the protein's active site. Additionally, hydrophobic interactions between Ala191, Ile19, Met194, and Ile21 and PISH were observed, further stabilizing the protein–ligand complex (Figure 1). The high binding affinity and interactions obtained as a result of docking indicated that PISH effectively interacted with the active site of the InhA protein and had the potential to inhibit its function, drawing attention as a new antituberculosis agent. Moreover, the ligand's alignment near the NAD binding site suggested to possible competitive inhibition, supporting its promise as a potential enzyme inhibitor (Figure 2). These findings might provide an important basis for further experimental research and optimization of PISH molecule as an antitubercular candidate.

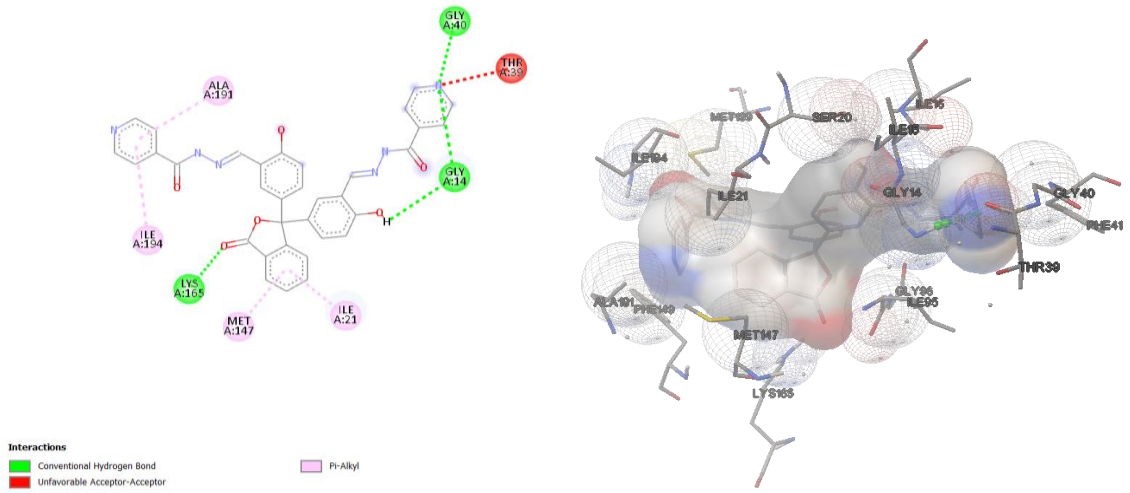


Figure 1. Optimal docking pose of PISH-InhA interactions.

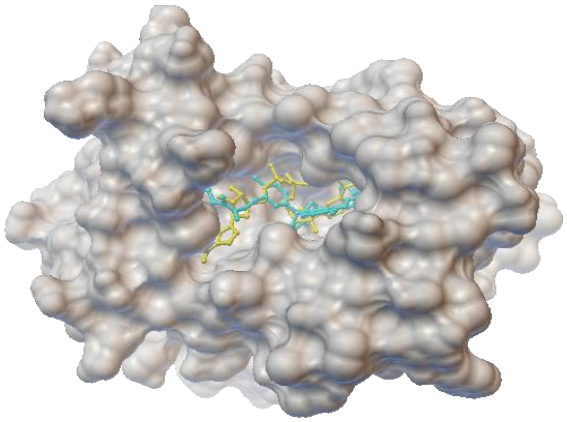


Figure 2. Active site of the 1ENY exhibiting reference molecule in yellow and the docked PISH in turquoise.

CONCLUSION

In conclusion, the isoniazid-based Schiff base represented a potential therapeutic agent. It demonstrated a generally acceptable safety profile, low genotoxicity, and minimal environmental toxicity. Its moderate log P indicates balanced lipophilicity, and its strong binding affinity toward biological targets further supports its potential. However, it also presents notable challenges, including low oral bioavailability, limited water solubility, and possible drug–drug interactions. Future studies may explore structural optimizations to improve solubility and bioavailability. Additionally, in vitro, and in vivo evaluations are recommended to validate computational findings.

REFERENCES

Aydin, D., & Alici, M. K. (2021). Phenolphthalein Conjugated Schiff Base as a Dual Emissive Fluorogenic Probe for the Recognition Aluminum (III) and Zinc (II) Ions. Journal of Fluorescence, 31(3), 797–805. https://doi.org/10.1007/s10895-021-02704-5

Biovia, D. S. (2024). Discovery studio visualizer (v24.1.0.23298). BIOVIA, Dassult Systèmes.

Ceramella, J., Iacopetta, D., Catalano, A., Cirillo, F., Lappano, R., & Sinicropi, M. S. (2022). A Review on the Antimicrobial Activity of Schiff Bases: Data Collection and Recent Studies. Antibiotics, 11(2), 191. https://doi.org/10.3390/antibiotics11020191

da Silva, C. M., da Silva, D. L., Modolo, L. V., Alves, R. B., de Resende, M. A., Martins, C. V. B., & de Fátima, Â. (2011). Schiff bases: A short review of their antimicrobial activities. Journal of Advanced Research, 2(1), 1–8. https://doi.org/10.1016/j.jare.2010.05.004

Dessen, A., Quémard, A., Blanchard, J. S., Jacobs, W. R., & Sacchettini, J. C. (1995). Crystal Structure and Function of the Isoniazid Target of Mycobacterium tuberculosis. Science, 267(5204), 1638–1641. https://doi.org/10.1126/science.7886450

Dogan, S. S., Aydin, D., Emsen, B., & Surmen, B. (2025). The assessment of antimicrobial and antibiofilm activities, molecular docking studies, and the photodegradation of methylene blue by green-fabricated ZnO nanoparticles using the plant extract of Helichrysum noeanum boiss. Biocatalysis and Agricultural Biotechnology, 69, 103755. https://doi.org/10.1016/j.bcab.2025.103755

Iacopetta, D., Catalano, A., Ceramella, J., Mariconda, A., D'Amato, A., Checconi, P., Aquaro, S., Longo, P., & Sinicropi, M. S. (2025). Chitosan-Based Schiff Bases (CSBs) and Their Metal Complexes: Promising Antimicrobial Agents. Molecules, 30(2), 207. https://doi.org/10.3390/molecules30020207

Joshi, S., Dixit, S., Gadag, S., Kulkarni, V., & Aminabhavi, T. (2015). Molecular docking, synthesis, and antimycobacterial activities of pyrrolyl hydrazones and their copper complexes. Research and Reports in Medicinal Chemistry, 1. https://doi.org/10.2147/RRMC.S90564

McPhillie, M. J., Cain, R. M., Narramore, S., Fishwick, C. W. G., & Simmons, K. J. (2015). Computational Methods to Identify New Antibacterial Targets. Chemical Biology & Drug Design, 85(1), 22–29. https://doi.org/10.1111/cbdd.12385

Morris, G. M., Huey, R., Lindstrom, W., Sanner, M. F., Belew, R. K., Goodsell, D. S., & Olson, A. J. (2009). AutoDock4 and AutoDockTools4: automated docking with selective receptor flexibility. Journal of Computational Chemistry, 30(16), 2785–2791. https://doi.org/10.1002/jcc.21256

Mounadi, N., Nour, H., Bouribab, A., Khedraoui, M., Kouali, M. El, Samadi, A., & Chtita, S. (2025). In silico analysis of Moroccan medicinal plant compounds as potential inhibitors of influenza A (H3N2). Scientific African, 30, e02969. https://doi.org/10.1016/j.sciaf.2025.e02969

Sahin Dogan, S., Cicek, M., Aydin, D., & Kocabas, A. (2025). Evaluation of the therapeutic potential of a Schiff Base Compound: Pharmacokinetic profiling, molecular docking for Enoyl-Acyl carrier protein reductase (InhA), antimicrobial, and anticancer properties. International Journal of Biological Macromolecules, 311, 143677. https://doi.org/10.1016/j.ijbiomac.2025.143677

WHO. (2023). World Health Organization. Global Tuberculosis Report. Geneva, Switzerland: WHO.

Zumla, A., Nahid, P., & Cole, S. T. (2013). Advances in the development of new tuberculosis drugs and treatment regimens. Nature Reviews Drug Discovery, 12(5), 388–404. https://doi.org/10.1038/nrd4001

Zúñiga-Miranda, J., González-Pastor, R., Carrera-Pacheco, S. E., Rodríguez-Pólit, C., Barba-Ostria, C., Machado, A., Guamán, L. P., Alcivar-León, C. D., & Heredia-Moya, J. (2025). Experimental and computational studies of Schiff bases derived from 4-aminoantipyrine as potential antibacterial and anticancer agents. Discover Applied Sciences, 7(2), 115. https://doi.org/10.1007/s42452-025-06459-7

ORAL PRESENTATION

Piyasada satılan farklı matcha çayı türlerinin fenolik bileşik içeriklerinin ve antioksidan kapasitelerinin yeşil çay türleri ile karşılaştırılması

Teslime Özge Şahin[1] (ORCID: *https://orcid.org/0000-0002-7289-5187*), Merve Çoban[2] *(https://orcid.org/0009-0001-9689-4867*), Merve Özdemir[1] (*ORCID: https://orcid.org/0000-0001-7955-9154*)

[*1]Afyonkarahisar Sağlık Bilimleri Üniversitesi, Sağlık Bilimleri Fakültesi, Beslenme ve Diyetetik Bölümü, Afyonkarahisar, Türkiye
[2]Afyonkarahisar Sağlık Bilimleri Üniversitesi, Sağlık Bilimleri Enstitüsü, Beslenme ve Diyetetik ABD, Afyonkarahisar, Türkiye

*Sorumlu yazar e-mail: ozge.sahin@afsu.edu.tr

Özet

Yeşil çayın özel bir formu olan matcha çayı, içerdiği biyoaktif bileşenler ve potansiyel sağlık etkileri nedeniyle giderek artan bir popülariteye sahiptir. Matcha çayının son yıllarda artan popülaritesi, piyasada satılan ürünlerin fenolik bileşik içerikleri ve antioksidan aktiviteleri arasındaki farklılıkların daha yakından incelenmesini gerekli kılmıştır. Ayrıca yüksek düzeyde fenolik bileşik alabilmek için ekonomik açıdan yüksek maliyetli bu ürünlerin tüketiminin gerekliliğinin ve alternatiflerinin yakından incelenmesi önemli bir diğer hususdur. Bu çalışma, Türkiye'de satışta bulunan farklı matcha çayı türlerinin ve çeşitli yeşil çay formlarının toplam fenolik bileşik konsantrasyonu, antioksidan kapasitesi, toplam flavonoid içeriği ve birim fiyat gibi temel parametreler açısından karşılaştırılmasını amaçlamaktadır. Çalışmaya online olarak satılan farklı matcha çayı türleri (16 adet mutfak sınıfı, 3 adet seremoni sınıfı) ve yeşil çay türleri (2 poşet, 4 dökme yaprak ve bunların toz formları) dahil edilmiştir. Tüm örnekler geleneksel matcha hazırlama seremonisine benzetilerek laboratuvar koşullarında standart bir şekilde (2 g örnek/100 mL, demleme sıcaklığı: 85°C, 3 dk sonikasyon ile karıştırma) hazırlanmıştır. Hazırlanan örneklerin CUPRAC antioksidan kapasitesi, toplam fenolik bileşik (TPC) ve toplam flavonoid içeriği analiz edilmiş ve birim fiyat verileri kaydedilmiştir. Yapılan analizler sonucunda çay türleri arasında TPC, flavonoid içeriği ve birim fiyat açısından istatistiksel olarak anlamlı farklılıklar tespit edilmiştir ($p<0,05$). Bulgulara göre en yüksek TPC (1314,00±294,65 mg GAE/L) ve flavonoid (364,30±56,398 mg CE/L) değerleri dökme yeşil çay tozu örneklerinde ölçülmüştür ($p<0,05$). Buna karşılık, piyasadaki en yüksek birim fiyata sahip olan seremoni sınıfı matcha grubu, incelenen tüm gruplar arasında istatistiksel olarak anlamlı şekilde en düşük TPC (550,58±136,48 mg GAE/L) ve flavonoid (191,20±73,181 mg CE/L) değerlerini göstermiştir ($p<0,05$). Mutfak sınıfı matcha çayları, seremoni sınıfına göre daha yüksek biyoaktif bileşik içeriğine sahip olsa da bu gruptaki ürünlerin bileşiminin markalara göre yüksek düzeyde değişkenlik gösterdiği gözlemlenmiştir. Sonuç olarak bu çalışma, Türkiye piyasasında satılan seremoni sınıfı matchaların, yüksek fiyatlarına rağmen antioksidan kapasite, flavonoid ve fenolik bileşik içeriği açısından beklenen üstünlüğü göstermediğini ortaya koymuştur. Ekonomik bir seçenek olan dökme yeşil çayların ise matchaya benzer şekilde toz haline getirilerek seremoni yöntemiyle hazırlandığında, birçok pahalı matcha ürünüyle yarışan veya daha yüksek biyoaktif bileşen düzeyleri sunduğu belirlenmiştir.

Anahtar Kelimeler: Yeşil çay, kateşin, flavonoidler, sağlıklı beslenme

Comparison of phenolic compound levels and antioxidant capacity in commercially available matcha tea and green tea varieties

Abstact

Matcha tea, a specialized form of green tea, has gained increasing popularity due to its rich bioactive compounds and potential health benefits. This growing interest has made it necessary to examine more closely the differences in phenolic compound content and antioxidant activity among commercially available matcha products. Moreover, considering the high cost of matcha, it is important to evaluate whether the consumption of these products is truly necessary to achieve high phenolic intake and to identify more economical alternatives. This study aims to compare various matcha teas sold in Türkiye with different forms of green tea in terms of total phenolic content, antioxidant capacity, total flavonoid levels, and unit price. The study included

online-purchased matcha products (16 culinary grade, 3 ceremonial grade) and green tea samples (2 bagged, 4 loose-leaf, and their powdered forms). All samples were prepared under standardized laboratory conditions modeled after traditional matcha preparation (2 g sample/100 mL, 85°C brewing temperature, 3 minutes of sonication). CUPRAC antioxidant capacity, total phenolic content (TPC), total flavonoid content, and unit price data were determined for each sample. The analyses revealed statistically significant differences among tea types in terms of TPC, flavonoid levels, and unit price ($p<0.05$). Loose-leaf green tea powders exhibited the highest TPC (1314±294.65 mg GAE/L) and flavonoid content (364.30±56.398 mg CE/L) ($p<0.05$). In contrast, ceremonial grade matcha—the most expensive product group—showed the lowest TPC (550.58±136.48 mg GAE/L) and flavonoid levels (191.20±73.181 mg CE/L) among all tea types ($p<0.05$). Although culinary grade matcha contained higher bioactive compound levels than ceremonial grade, substantial variability was observed among brands. Overall, this study demonstrates that ceremonial grade matcha products sold in Türkiye do not exhibit the expected superiority in antioxidant capacity, flavonoid content, or phenolic composition despite their high cost. Economical loose-leaf green teas, when powdered and prepared similarly to matcha, were found to provide equal or even higher levels of bioactive compounds compared with many expensive matcha products.

Keywords: Green tea, catechins, flavonoids, healthy nutrition

1. GİRİŞ

Dünya genelinde en fazla tüketilen çaylardan birisi olan yeşil çay özellikle antioksidan, anikarsinojenik, antimutajenik ve antipertansif sağlık etkileri ile dikkat çekmektedir (Jakubczyk et al., 2020). Yeşil çayın bu sağlık etkileri ise bileşiminde bulunan fenolik bileşiklerle, özellikler de kateşinlerle (epikateşin (EC), epigallokateşin (EGC), epigallokateşin gallat (EGCG), epikateşin gallat (ECG)) ilişkilendirilmektedir. Japon yeşil çayının toz haline getirilmiş özel bir formu olan matcha çayı da bu potansiyel sağlık etkileri sebebiyle son yıllarda özellikle popülerlik kazanmıştır. Geleneksel çay seremonilerinde kullanılan matcha çayı, diğer yeşil çay türlerinden farklı yetiştirme koşullarına, hazırlama yöntemlerine ve kimyasal bileşime sahiptir (Sokary et al., 2023). Direkt güneş ışınları alacak şekilde yetiştirilen diğer yeşil çaylardan farklı olarak, gölge ortamda yetiştirilen ve bitkinin yalnızca en genç yapraklarının seramik değirmenlerde öğütülmesiyle üretilen matcha çayının theanin, klorofil, kafein gibi biyoaktif bileşik içeriğinin diğer yeşil çaylardan daha yüksek; kateşin içeriklerinin daha düşük olduğu belirtilmektedir (Jakubczyk et al., 2020; Meyer et al., 2023). Ancak matcha çayının hazırlama yönteminden kaynaklanan farklılıklar sebebiyle bileşiminde bulunan fenolik bileşiklerin kullanılabilirliğinin diğer yeşil çaylardan daha yüksek olduğu belirtilmektedir (Sokary et al., 2023). İnce toz formunda olan matcha çayı su içerisinde iyice karıştırılarak tüketilirken, diğer yeşil çaylar su içerisine atılan çay yapraklarının belirli sürelerde demlenmesiyle hazırlanmakta ve sonrasında yaprak içermeyen çay infüzyonları tüketilmektedir. Yapılan bir çalışmada yaprak çay kullanılarak hazırlanan çaylardan 34,7–120,1 mg EGCG ve 46,7–146,4 mg kafein alımı söz konusuyken toz formundaki yeşil çay kullanıldığında bu miktarların sırasıyla 126,1–369,1 mg ve 72,9–187,1 mg düzeylerine çıktığı tespit edilmiştir. Bu bulgular, öğütme işleminin EGCG ve kafein ekstraksiyonunu artırdığını göstermektedir (Fujioka et al., 2016).

Matcha çayları kalitelerine göre seremoni sınıfı ve mutfak sınıfı olmak üzere ikiye ayrılmaktadır. Seremoni sınıfı, matcha çayı içeceklerinin hazırlanmasında kullanılan en yüksek kalite ve en pahalı olan çay türüdür; mutfak sınıfı matcha ise daha ekonomiktir ve içeceklerde ya da atıştırmalık ve tatlılarda bir bileşen olarak kullanılabilmektedir. Seremoni sınıfı matcha; genellikle en genç yapraklardan hazırlanmaktadır. Mutfak sınıfı matcha ise daha ekonomiktir ve genellikle daha geç hasat edilen yapraklardan üretilmektedir (Meyer et al., 2023). Matcha türleri arasındaki bu kalite ve hasat zamanından kaynaklanan farklılıklar da çayların biyoaktif bileşik içeriğini (kateşinler, kafein, theanin, klorofil vb.) etkilemektedir (Meyer et al., 2023). Matcha çayının giderek artan popülaritesi beraberinde ürün çeşitliliğinin ve kalite farklılıklarının da belirginleşmesine neden olmuştur. Türkiye pazarında matcha adıyla satılan ürünlerin hammaddesi, üretim yöntemi, hasat zamanı, yaprak kalitesi ve öğütme tekniği açısından büyük değişkenlik gösterdiği tahmin edilmektedir. Bu durum, "seremoni sınıfı" ve "mutfak sınıfı" gibi kalite tanımlarının çoğu zaman yalnızca pazarlama stratejisi olarak kullanılmasına, ürün içeriklerinin ise yeterince şeffaf olmamasına yol açmaktadır. Nitekim literatürde matcha çaylarının fenolik bileşik ve antioksidan özelliklerinin, üretici firmaya, coğrafi bölgeye, hasat dönemine ve işleme yöntemlerine bağlı olarak oldukça geniş bir aralıkta değiştiği belirtilmektedir (Meyer et al., 2023; White et al., 2025). Buna rağmen ülkemizde piyasada satılan matcha çaylarının fenolik bileşik içeriği, antioksidan kapasitesi ve yeşil çayın diğer formlarıyla karşılaştırılması konusunda yapılmış bilimsel çalışma sayısı bildiğimiz kadarıyla bulunmamaktadır. Öte yandan tüketiciler arasında matchanın, özellikle de seremoni

sınıfının, "daha yüksek antioksidan kapasiteye sahip olduğu" yönünde yaygın bir kanı bulunmaktadır. Ancak bu iddiaların yerel ürünler üzerinden test edilmesi, ürünlerin kalite standartlarının belirlenmesi ve tüketici bilincinin artırılması açısından önem taşımaktadır. Matcha ile benzer kullanım alanlarına sahip olan poşet yeşil çayların, dökme yeşil çayların yaprak ve toz formlarının fenolik bileşik içeriği ile antioksidan kapasitesinin doğrudan karşılaştırılması ise literatürde eksik kalan bir başka husustur.
Bu nedenle bu çalışma, Türkiye'de satışta bulunan farklı matcha çayı türlerinin ve çeşitli yeşil çay formlarının toplam fenolik bileşik konsantrasyonu, antioksidan kapasitesi (CUPRAC), toplam flavonoid içeriği ve birim fiyat gibi temel parametreler açısından karşılaştırılmasını amaçlamaktadır. Böylece piyasadaki ürünlerin içerik farklılıklarının ortaya konulması ve tüketiciye sunulan matcha kategorilerinin kimyasal bileşimlerinin karşılaştırılması hedeflenmiştir. Çalışmadan elde edilecek sonuçlar özellikle tüketici tercihlerine rehberlik etmesi açısından büyük öneme sahiptir.

2. YÖNTEM

2. 1. Örneklerin temini ve hazırlanması

Piyasada satılan farklı markalara ait 19 adet matcha çayı (16 adet mutfak sınıfı matcha tozu, 3 adet seremoni sınıfı matcha tozu), 2 farklı markaya ait bardak poşet yeşil çay, 4 farklı markaya ait dökme yeşil çay ve bu dökme çayların blenderize edilmiş toz formları araştırmaya dahil edilmiştir. Örneklerin temini Mayıs 2025-Eylül 2025 tarihleri arasında online alışveriş sitelerinden sağlanmıştır. Örnek kodlarına göre çay türlerinin sınıflandırılması Tablo 1'de verilmiştir.

Tablo 1. Örnek kodlarına göre çay türleri

Örnek kodları	Çay türü
1-16	Mutfak sınıfı matcha tozu
17-19	Seremoni sınıfı matcha tozu
20-21	Poşet Yeşilçay
22-25	Dökme Yeşilçay (Yaprak)
26-29	Dökme Yeşilçay (Toz)

Bütün çaylar matcha çayı hazırlama seremonisinde önerilen şekilde; 2 gram çay örneği alınarak 100 mL ultra saf su (85°C) ile karıştırılarak hazırlanmıştır. Seremoniye uygun şekilde matcha hazırlanırken ayrıca 3 dakika boyunca bambu fırça (whisk) ile çırpma işlemi uygulanmaktadır. Bu işlemi laboratuvar koşullarında tüm örneklerde standart bir şekilde uygulayabilmek için ultrasonik su banyosunda 3 dakika sonikasyon yapılmıştır. Sonikasyon sonrasında örnekler 3000 rpm'de 5 dakika santrifüj edilmiştir. Santrifüj işlemi sonrasında örnekler hemen süzülerek bekletilmeden analiz edilmiştir (Sielicka-Różyńska et al., 2020; White et al., 2025).

2. 2. Toplam Fenolik Bileşik (TPC) Analizi

Çay örneklerinin toplam fenolik bileşik içeriği, Folin–Ciocalteu yöntemi kullanılarak belirlenmiştir (Singleton & Rossi, 1965). Sielicka-Różyńska et al. tarafından çay infüzyonlarında kullanılan yöntem uygulanmıştır (Sielicka-Różyńska et al., 2020). Çalışmada, 10 µL seyreltilmiş (1:1, v/v) çay infüzyonu; 50 µL Folin–Ciocalteu reaktifi ve 290 µL saf su ile karıştırılarak 3 dakika bekletildi. Ardından, 150 µL %20'lik Na_2CO_3 çözeltisi ve 500 µL su eklenip tekrar karıştırıldı. Reaksiyon karışımları ışık almayan koşullarda, 20°C'de 2 saat inkübe edildi. İnkübasyon süresinin sonunda absorbans değerleri 725 nm dalga boyunda UV-Vis spektrofotometre kullanılarak ölçüldü. TPC hesaplamasında, farklı derişimlerde hazırlanan galik asit standart eğrisi kullanıldı ve sonuçlar mg GAE/L olarak ifade edildi. Tüm ölçümler dublike şekilde gerçekleştirildi, dublike ölçümlerde tutarsızlık olması durumunda bu örnekler tekrar hazırlanarak analiz edildi.

2. 3. Toplam Antioksidan Aktivite (CUPRAC) Analizi

Örneklerin antioksidan kapasite analizinde Apak ve ark. Tarafından geliştirilen ve yeşil çay kateşinlerine yüksek duyarlılık gösterdiği belirtilen CUPRAC (antioksidanların Cu^{2+} (bakır(II)) iyonlarını indirgeme kapasitesi) yöntemi kullanılmıştır (Apak et al., 2004) . Bakır(II) klorür çözeltisi, 0.4262 g $CuCl_2 \cdot 2H_2O$ tartılarak su içinde çözülmüş ve hacim saf su ile 250 mL'ye tamamlanmıştır. pH 7.0 değerinde amonyum asetat (NH_4Ac)

tamponu, 19.27 g NH_4Ac'in suda çözülmesi ve hacmin 250 mL'ye tamamlanması ile hazırlanmıştır. 7.5×10^{-3} M derişimindeki neokuproin (Nc) çözeltisi ise 0.156 g Nc'in %96 EtOH içinde çözülmesi ve etanol ile 100 mL'ye tamamlanmasıyla hazırlanmıştır. Bir deney tüpüne sırasıyla 1 mL Cu (II), 1 mL Nc ve 1 mL NH_4Ac tampon çözeltisi eklenmiştir. Ardından her bir örnek çözeltisinden 0,1 mL ve karışıma son hacmi 4.1 mL olacak şekilde (1 mL) ultra saf su ilave edilmiştir. Tüpler kapatılarak oda koşullarında karanlık bir ortamda 30 dakika bekletildikten sonra 450 nm'de (A_{450}) absorbans değerleri reaktif körüne karşı uv- vis spektrofotometre ile ölçülmüştür. Antioksidan kapasite hesaplamalarında, altı farklı derişimde hazırlanan Trolox standart eğrisi kullanıldı ve sonuçlar mM TEAC (Trolox Equivalent Antioxidant Capacity) olarak ifade edildi.

2.4. Toplam Flavonoid Analizi

Örneklerin flavonoid içeriklerini belirlemek için Zhishen vd. (1999) ve Dewanto vd. (2002) yönteminin biraz değiştirilmiş bir versiyonu kullanıldı. 10 ml'lik bir hacimsel şişeye 1 ml ekstrakt konuldu ve 5 ml damıtılmış su ve 0,3 ml %5'lik NaNO2 eklendi ve karıştırıldı.
5 dakika sonra 0,6 ml %10'luk AlCl3.6H2O eklendi. 5 dakika sonra 2 ml 1 mol l-1NaOH eklendi ve ardından hacim damıtılmış su ile 10 ml'ye tamamlandı. Çözelti iyice karıştırıldı ve absorbans hemen 510 nm'de ölçüldü. Flavonoid içerikleri, (+) kateşinden hazırlanan standart bir kalibrasyon eğrisi kullanılarak hesaplandı.

2. 5. İstatistiksel Analizler

Araştırmadan elde edilen tüm veriler IBM SPSS Statistics paket programı kullanılarak analiz edilmiştir. Çalışmaya dahil edilen beş farklı çay türünün (mutfak sınıfı matcha, seremoni sınıfı matcha, poşet yeşil çay, dökme yeşil çay–yaprak, dökme yeşil çay–toz) CUPRAC antioksidan kapasitesi, TPC, toplam flavonoid ve birim fiyat (TL/kg) değerlerinin grup bazında karşılaştırılmasında tek yönlü varyans analizi (One-Way ANOVA) uygulanmıştır. Analizler öncesinde dağılımın normalliği Shapiro–Wilk testi ve histogram/grafik incelemeleri ile, varyans homojenliği ise Levene testi ile değerlendirilmiştir. Tüm değişkenlerde varyans homojenliği sağlandığı için parametrik testler tercih edilmiştir. Anlamlı farklılık saptanan değişkenlerde gruplar arası farklılığın kaynağını belirlemek amacıyla Bonferroni çoklu karşılaştırma testi uygulanmıştır. ANOVA analizlerinde ayrıca etki büyüklüğünü belirlemek için eta-squared (η^2) değerleri hesaplanmıştır. İstatistiksel anlamlılık düzeyi $p<0,05$ olarak kabul edilmiştir.

3. BULGULAR VE TARTIŞMA

Bu çalışmada piyasada satılan farklı matcha (seremoni ve mutfak sınıfı) ve yeşil çay türlerinin (poşet, dökme yaprak, dökme toz) toplam fenolik madde (TPC), toplam antioksidan kapasite, toplam flavonoid içeriği ve birim fiyat değerleri karşılaştırılmıştır. Elde edilen bulgular Tablo 2 ve Tablo 3'te sunulmuştur.
Çalışma kapsamında incelenen çay türlerinin toplam fenolik bileşik (TPC) düzeyleri istatistiksel olarak anlamlı şekilde farklılık göstermiştir ($p=0,022$; $F=3,121$; $\eta^2=0,191$). TPC bakımından en yüksek ortalamaya sahip olan grup dökme yeşil çay tozu örnekleri (1314±294,65 mg GAE/L) olarak bulunurken; bunu poşet yeşil çay (984,53±360,52 mg GAE/L), dökme yeşil çay-yaprak (972,09±253,14 mg GAE/L) ve mutfak sınıfı matcha (951,63±475,30 mg GAE/L) grupları takip etmiştir ($p>0,05$). Seremoni sınıfı matcha örneklerinin ise diğer gruplardan istatistiksel olarak anlamlı şekilde daha düşük TPC değerlerine (550,58±136,48 mg GAE/L) sahip olduğu tespit edilmiştir ($p<0,05$). Yeşil çay ile matcha çayının TPC içeriklerinin karşılaştırıldığı başka bir araştırmada da benzer şekilde yeşil çayın TPC değeri (1770 mg GAE/L), matcha çayından (1030 mg GAE/L) istatistiksel olarak anlamlı şekilde daha yüksek bulunmuştur (Meremäe et al., 2025). Yapılan başka bir araştırmada da poşet ve yaprak yeşil çayların TPC değerleri (178,40 GAE mg/g), hem mutfak sınıfı (142,49 GAE mg/g) hem de seremoni sınıfı (125,7 GAE mg/g) matchadan daha yüksek bulunmuştur (Meyer et al., 2023). Meyer ve ark. ayrıca çay formunun da önemli bir faktör olduğunu ve en yüksek TPC içeren çay türünün yaprak formundaki yeşil çay örneğine ait olduğunu ifade etmiştir (Meyer et al., 2023). Ancak çalışma kapsamında yalnızca 1 adet yaprak yeşil çay incelenmiştir. Bu çalışmada ise 4 farklı dökme yeşil çay hem yaprak hem de toz haline getirilerek analiz edilmiştir. En yüksek TPC değeri de toz haline getirilen örneklerde gözlemlenmiştir. Bu sonucun, çay yapraklarının yüzey alanının artmasına bağlı olarak suya geçen fenolik bileşik miktarının artmasından kaynaklanmış olabileceği düşünülmüştür. Bu çalışma sonuçları ayrıca, literatürde mutfak sınıfı matchaların seremoni sınıfı matchalardan daha yüksek fenolik içeriğe sahip olduğunu gösteren çalışmalarla tamamen örtüşmektedir. Meyer ve ark. (2023), aynı markaya ait mutfak sınıfı ve seremoni sınıfı matchaları karşılaştırmış, mutfak sınıfı matchaların (149.5 GAE mg/g), seremoni sınıfındakilerden (111.6 GAE mg/g) anlamlı şekilde daha yüksek TPC içerdiğini göstermiştir (Meyer et al., 2023). Benzer şekilde White

ve ark. (2025) de mutfak sınıfı matchaların ortalama TPC değerlerinin seremoni sınıfı matchalara göre anlamlı şekilde yüksek olduğunu belirtmiştir (81.21 mg/g vs. 62.95 mg/g GAE)(White et al., 2025). Pek çok fenolik bileşik çayda acı ve buruk tatla ilişkilendirilmektedir. Bu nedenle daha yumuşak tadıyla öne çıkan seremoni sınıfı matchaların TPC içeriğinin tutarlı şekilde mutfak sınıfı matchaya kıyasla daha düşük bulunması şaşırtıcı bir sonuç değildir (Meyer vd., 2023, p. 664). Seremoni sınıfı çaylarının, yeşil çayın aksine gölge bir ortamda yetişmesi, daha erken hasat edilmesinden kaynaklı farklılıklar da fenolik bileşik düzeylerini etkilemiş olabilir. Örnek sonuçları bireysel olarak incelendiğinde en yüksek TPC değerine sahip örnek mutfak sınıfı kategorisindeki 13 numaralı örnek (1913,15 mg GAE/L); en düşük değere sahip örneğin de yine aynı gruptan 3 numaralı örnek (100,85 mg GAE/L) olduğu görülmüştür (Tablo 2). Aynı gruptan örnekler arasındaki bu tutarsız sonuçların matcha çayı üretiminde kullanılan çayların kalitesi, matcha tozlarının öğütme düzeyleri ve yöntemleri arasındaki farklılıklardan kaynaklanmış olabileceği düşünülmüştür.

Çalışma kapsamında incelenen çay örneklerinin CUPRAC antioksidan kapasitelerinin 1,20 ile 9,37 mM TE arasında oldukça geniş bir değer aralığında değiştiği görülmüştür. En düşük CUPRAC değeri mutfak sınıfı matcha kategorisindeki 3 numaralı örnekte, en yüksek değer ise yine aynı kategorideki 8 numaralı örnekte ölçülmüştür. Bununla birlikte CUPRAC değerleri çay türleri arasında istatistiksel olarak anlamlı bir farklılık göstermemiştir ($p=0,723$; $F=0,518$; $\eta^2=0,038$). Bu konuda yapılan diğer araştırma sonuçları TPC sonuçlarına benzer şekilde yeşil çayların antioksidan kapasitelerinin (185,75 ± 10,26 TEAC mmol/100 g), mutfak sınıfı matchalardan (144,11 ± 3,20; $p<0,001$) ve seremoni sınıfı matchalardan (130,27±4,84; $p<0,001$) istatistiksel olarak anlamlı şekilde yüksek olduğunu göstermiştir (Meyer et al., 2023). White ve arkadaşlarının çalışmasında mutfak sınıfı matchaların seremoni sınıfı matchalardan daha yüksek CUPRAC kapasitesi gösterdiği belirlenmiştir (94.01 ± 2.14 vs. 75.67 ± 1.80 mmol TE /100 g, $p<0.001$) (White et al., 2025). Yapılan başka bir araştırmada ise yeşil çayın DPPH yöntemiyle analiz edilen antioksidan kapasitesi değeri 55,14 mM TE bulunurken matcha çayının 35,51 mM TE olarak bulunmuştur (Meremäe et al., 2025). White ve ark. çalışmasında matcha ürünlerinin genel olarak fenolik bileşikler, flavonoidler, kateşinler ve klorofiller açısından zengin olduğunu ancak matcha kalitesinin bu bileşenlerin seviyelerini belirgin şekilde etkilediğini vurgulamıştır (White et al., 2025). Bu çalışmada da Tablo 2'de de görüldüğü gibi aynı çay grubundan örneklerin bile (örnek 3 ile 14) antioksidan kapasite, TPC, flavonoid değerleri arasında oldukça değişken sonuçlar bulunmaktadır. Bu durumun da matcha tozu olarak satılan ürünlerin kaliteleri ve içerikleri arasındaki farklılıklardan kaynaklandığı düşünülmüştür. CUPRAC antioksidan kapasite sonuçlarının çay türlerine göre anlamlı farklılık göstermemesi de hem çay kaliteleri arasındaki farklılıklardan kaynaklanan tutarsız sonuçlardan hem de çay türlerine ait örnek sayılarının dengeli dağılım göstermemesinden kaynaklanmış olabilir. Ülkemiz piyasasında satılan matcha çaylarının çoğu mutfak sınıfı kategorisinde olduğu ve seremoni sınıfı çayların sayısı daha kısıtlı olduğu için çay türleri arasında böyle bir dağılım oluşmuştur. Seremoni sınıfı çay seçeneklerinin artması durumunda bu karşılaştırmaların tekrar yapılması daha ve güvenilir sonuçlar elde edilmesine imkân sağlayabilir.

Tablo 2. Çay örneklerinin CUPRAC, TPC, flavonoid ve birim fiyat değerlerinin karşılaştırılması

Örnek	CUPRAC (mM TE)	TPC (mg GAE/L)	Flavonoid (mg CE/L)	Birim Fiyat TL/Kg
1	8,67	954,95	339,45	7580,00
2	8,46	1018,70	356,02	7400,00
3	1,21	100,85	23,36	1200,00
4	5,58	359,80	165,55	678,00
5	6,50	493,30	326,32	2000,00
6	8,51	1227,40	324,71	3180,00
7	8,37	1328,10	312,79	9633,30
8	8,79	963,05	284,11	6780,00
9	8,44	1089,90	389,75	7140,00
10	8,41	1166,40	285,73	5400,00
11	7,27	395,40	106,97	36666,70
12	8,66	1035,50	361,07	8600,00
13	8,05	1913,15	371,57	7820,00
14	8,54	1528,00	419,24	8200,00
15	8,15	814,05	313,20	26160,00
16	7,81	837,55	296,84	12340,00
17	7,15	414,15	106,37	46666,70
18	7,92	657,70	269,57	14360,00
19	7,57	579,90	197,66	14600,00
20	8,04	1295,20	355,61	2000,00
21	7,43	673,85	288,35	2000,00
22	7,98	1194,50	348,14	1700,00
23	7,95	980,50	254,22	1030,00
24	8,15	1027,45	288,15	2000,00
25	8,05	685,90	276,84	650,00
26	8,61	1005,35	402,67	1700,00
27	8,41	1575,00	426,10	1030,00
28	8,15	1226,10	333,19	2000,00
29	8,17	1449,55	295,22	650,00

* Renklerin açıktan koyuya geçişi konsantrasyondaki artışı göstermektedir.

Bu çalışma kapsamında incelenen çay türlerinin toplam flavonoid içerikleri istatistiksel olarak anlamlı şekilde farklılık göstermiştir ($p=0,013$; $F=3,490$; $\eta^2=0,208$). Flavonoid düzeyleri açısından en yüksek ortalama dökme yeşil çay tozu örneklerinde (364,30±56,398 mg CE/L) bulunurken, bunu poşet yeşil çaylar (321,98±39,009 mg CE/L), mutfak sınıfı matcha (292,29±104,605 mg CE/L) ve dökme yeşil çay yaprak (291,84±38,552 mg CE/L) takip etmiştir. En düşük flavonoid içeriği seremoni sınıfı matcha grubunda (191,20±73,181 mg CE/L) ölçülmüştür. Bu sonuçlar, öğütülmüş yeşil çay tozlarının flavonoid düzeyinin yüksek olduğunu göstermektedir. Seremoni sınıfı ve mutfak sınıfı matchaların flavonoid içeriklerinin karşılaştırıldığı bir çalışmada; mutfak sınıfı matchaların belirgin biçimde daha yüksek flavonoid içerdiği rapor edilmiştir. Seremoni sınıfı matchalar ortalama 6,43±0,49 mg/g CE flavonoid içerirken, mutfak sınıfı matchalarda bu değer 12,39 ± 1,42 mg/g CE'ye ulaşmaktadır (White et al., 2025). Yeşil çayın en öne çıkan flavonoidlerinden olan EGCG düzeylerinin de matcha örnekleri arasında geniş bir aralık göstererek 4,36 mg/g ile 41,97 mg/g arasında değişmiştir (White et al., 2025). Matcha çaylarının gölgede yetişme gereksinimlerinin flavonoid sentezinde azalmaya neden olabileceği belirtilmektedir. Ayrıca seremoni sınıfı matchaların, mutfak sınıfı matchalara kıyasla daha erken hasat edilmesi flavonoid ve fenolik bileşik içeriklerinin daha düşük olmasıyla ilişkilendirilmiştir

Çalışmadaki dikkat çekici bulgulardan birisi de fiyat–içerik ilişkisidir. Birim fiyatlar açısından gruplar arasında belirgin ve istatistiksel olarak anlamlı bir farklılık gözlenmiştir ($p<0,001$; $F=8,894$; $\eta^2=0,402$). Seremoni sınıfı matcha örneklerinin birim fiyatının (25.208±16.621,49 TL/kg) diğer çay gruplarından istatistiksel olarak anlamlı şekilde daha yüksek olduğu tespit edilmiştir. İlginç bir şekilde bu grubun TPC ve flavonoid değerleri diğer gruplardan istatistiksel olarak anlamlı şekilde düşüktür ($p<0,001$). Bireysel olarak fiyatlar incelendiğinde de en yüksek fiyatlı iki çay örneğinin (birisi seremoni sınıfı, birisi mutfak sınıfı) de en düşük TPC ve flavonoid değerlerine sahip örnekler arasında yer aldığı göze çarpmaktadır. Yaprak formundaki ve toz formundaki dökme yeşil çay örnekleri birim fiyatlar açısından en ekonomik grubu oluşturmuştur (1.345±570,04 TL/kg). Özellikle dökme yeşil çay tozu örnekleri, yüksek TPC ve flavonoid içeriğine kıyasla düşük fiyatlarıyla öne çıkmıştır. Yapılan bir çalışmada mutfak sınıfı matchanın seremoni sınıfı matchaya kıyasla hem daha yüksek TPC ve flavonoid seviyelerine sahip olabildiği, hem de fiyatının anlamlı şekilde daha düşük olduğu rapor edilmiştir (0.31 USD/g vs. 0.88 USD/g) (White et al., 2025). Başka bir çalışmada da yaprak formundaki dökme yeşil çayın en düşük maliyetli ürünlerden (0,04 USD/g) birisi olmasına rağmen, en yüksek toplam fenolik içeriğe, CUPRAC antioksidan kapasitesine, EGCG düzeylerine ve E-CG konsantrasyonlarına sahip olduğu tespit edilmiştir. Yüksek maliyetli (ortalama 0,68 USD/g) matcha çayları (seremoni ve mutfak sınıfı) ise düşük toplam fenolik içerik ve CUPRAC antioksidan kapasiteleri ile karakterize edilmiştir (Meyer et al., 2023).

4. SONUÇ VE ÖNERİLER

Bu çalışmanın sonuçları toplam fenolik bileşik, flavonoid içeriği ve birim fiyat bakımından çay türleri arasında belirgin farklılıklar olduğunu göstermektedir. Özellikle dökme yeşil çay tozlarının fenolik bileşik ve flavonoid düzeylerinin birçok matcha örneğiyle aynı düzeyde veya daha yüksek olduğu görülmüştür. Buna karşılık ülkemiz piyasasında satılan seremoni sınıfı matchaların antioksidan kapasite, fenolik bileşik ve flavonoid içeriği açısından beklenen üstünlüğü göstermediği dikkat çekmiştir. Dahası seremoni sınıfı matchalara göre ekonomik açıdan daha uygun seçenekler olan mutfak sınıfı matcha ve dökme yeşil çay tozu örneklerinin birçok parametrede daha yüksek değerlere sahip olduğu ortaya koyulmuştur. Tüketicilerin, yüksek antioksidan içerikli ürün arayışında "seremoni sınıfı matcha"lara mucizevi bir ürün olarak yaklaşmaması, çalışmanın bulgularına göre daha doğru bir yaklaşım olacaktır. Matcha türleri arasında da "mutfak sınıfı" ürünler ise fiyat-fayda dengesi açısından daha avantajlı olarak değerlendirilebilir. Ancak bu ürünlerin bileşimlerinin ve kalitelerinin oldukça değişken olduğu ve belli bir standardın olmadığı görülmektedir. Düşük maliyetli dökme yeşil çaylar, özellikle de toz formları, birçok analiz parametresinde matcha çaylarıyla yarışan değerler sunmuştur.

Ancak matcha çayının biyoaktif bileşen profili yalnızca fenolik bileşikler ve flavonoidlerle sınırlı değildir. Theanin, kafein ve klorofil gibi bu çalışma kapsamında kantitatif olarak değerlendirilmemiş diğer önemli bileşiklerin matchanın bilişsel fonksiyonlar, stres yanıtı ve metabolik süreçler üzerindeki etkilerinde belirleyici rol oynadığı bilinmektedir. Bu nedenle elde edilen bulgular, yalnızca incelenen bileşik gruplarıyla sınırlı olup, çayların genel sağlık etkilerine yönelik kapsamlı ve kesin bir öneri niteliği taşımamaktadır. Çayların tüm biyoaktif bileşenlerini kapsayan daha geniş ölçekli, standardize edilmiş ve kantitatif analizlerin yapılacağı ileri çalışmalara ihtiyaç duyulmaktadır.

Tablo 3. Farklı matcha ve yeşil çay türlerinin CUPRAC, TPC, flavonoid ve birim fiyat değerlerinin karşılaştırılması

	n	CUPRAC (mM TE)				TPC (mg GAE/L)				Flavonoid (mg CE/L)				Birim Fiyat TL/Kg			
		x̄	ss	Min	Max	x̄	ss	Min	Max	x̄	ss	Min	Max	x̄	ss	Min	Max
Mutfak sınıfı matcha	16	7,59	1,90	1,20	9,37	951,63^{a,b}	475,30	62,60	2055,40	292,29a	104,605	22,55	419,64	9423,63^{a}	9192,15	678,00	36666,70
Seremoni sınıfı matcha	3	7,54	0,36	7,02	8,02	550,58^{a}	136,48	361,80	729,50	191,20^{a,b}	73,181	104,96	269,77	25208,90^{b}	16621,49	14360,00	46666,70
Dökme yeşilçay (yaprak)	4	8,03	0,31	7,64	8,51	972,09^{a,b}	253,14	598,00	1290,50	291,84^{a,b}	38,552	248,77	365,11	1345,00^{a}	570,04	650,00	2000,00
Poşet yeşilçay	2	7,74	0,37	7,39	8,19	984,53^{a,b}	360,52	630,20	1299,90	321,98^{a,b}	39,009	285,93	359,45	2000,00^{a}	0,00	2000,00	2000,00
Dökme yeşilçay (toz)	4	8,33	0,21	8,07	8,63	1314,00^{b}	294,65	747,00	1733,40	364,30^{b}	56,398	291,18	428,53	1345,00^{a}	570,04	650,00	2000,00
Total	29	7,76	1,44	1,20	9,37	965,22	430,32	62,60	2055,40	293,75	94,537	22,55	428,53	8316,02	10836,78	650,00	46666,70
İstatistiksel analiz		p=0,723 F=0,518 η^2 = 0,038				**p=0,022** F=3,121 η^2 = 0,191				**p=0,013** F=3,490 η^2 = 0,208				**p<0,001** F=8,894 η^2 = 0,402			

η^2 : Eta-squared etki büyüklüğü, TE: Troloks eş değeri, TPC: Toplam fenolik bileşik, CE: Kateşin eşdeğeri

ORAL PRESENTATION

Chick quality following in ovo feeding of *Viscum album* extract

Berk Can Kaplan[1*] (*ORCID: https://orcid.org/0009-0006-5345-389X*),
Canan Kop-Bozbay[1] (*ORCID: https://orcid.org/0000-0002-8071-5860*)

[*1]Department of Animal Science, Faculty of Agriculture, Eskişehir Osmangazi University, 26160, Eskişehir, Türkiye

*Corresponding author e-mail: berkkaplann11@gmail.com

Abstract

The growing search for alternatives to antibiotic growth promoters has led to increased use of phytobiotics during the embryonic period. This study investigated the effects of in ovo application of varying levels of mistletoe (*Viscum album*) extract (ME) on chick weight, Tona score, relative asymmetry, and chick length. A total of 300 fertile eggs were divided into five different treatment groups with six replicates of 10 eggs each. On day 18 of incubation, the negative control group (NC) received no injection. In contrast, the positive control (PC) group received 0.5 ml of physiological saline, and the ME100, ME200, and ME300 groups received 100 ppm, 200 ppm, and 300 ppm of ME, respectively, in 0.5 ml of physiological saline. The findings indicated that in ovo ME feeding had no significant effect on chick quality ($p > 0.05$). In conclusion, it was determined that in ovo ME feeding at doses up to 300 ppm during the embryonic period did not adversely affect chick quality. This finding provides a basis for the safe in ovo use of ME and necessitates future long-term studies on growth performance, organ development, and immune parameters.

Keywords: mistletoe, in ovo feeding, phytobiotics

INTRODUCTION

The limitations of using antibiotic growth promoters in poultry farming have accelerated research into alternative, safe additives and bioactive compounds of natural origin (Zaikina et al., 2022). Plant extracts, containing numerous bioactive compounds such as phenolic compounds, flavonoids, essential oils, and alkaloids, are attracting increasing attention for their antioxidant, antimicrobial, immunomodulatory, and intestinal development-supporting effects (Alghirani et al., 2021; Zaikina et al., 2022). In this context, phytobiotics have moved beyond dietary use and are now being investigated for hatchery applications (Ergün et al., 2023; Kop-Bozbay and Göneci, 2023).

In ovo feeding, also known as the embryonic nutrition approach, is a modern feeding strategy that aims to prepare the embryo for future environmental and metabolic stresses, accelerate the maturation of the intestinal and immune systems, and reduce variation in post-hatch growth performance (Akosile et al., 2023). In this method, the embryo gains a programmed advantage during critical stages of physiological development by directly supplementing it with targeted compounds at a specific developmental stage (Roto et al., 2016). The success of in ovo applications is evaluated on two basic criteria. These are being safe and tolerable during embryonic development and the potential to improve chick quality and performance indicators after hatching (Sözcü and İpek, 2013; Akosile et al., 2023). Therefore, chick quality is considered one of the most critical indicators of early physiological response in in ovo studies (Sözcü and İpek, 2013). Parameters such as Tona score, chick weight, chick length and leg asymmetry. It directly reflects the embryo's developmental level, yolk sac utilization efficiency, musculoskeletal system development, and post-hatch survival (Sözcü and İpek, 2013; Roto et al., 2016). Positive changes in these parameters indicate successful use of the additive by the embryo negative changes indicate the possibility of stress, toxicity, or metabolic disruption. Therefore, chick quality is considered the primary determinant of the safety and efficacy of in ovo applications (Roto et al., 2016; Akosile et al., 2023; Kop-Bozbay and Göneci, 2023).

Mistletoe (*Viscum album*) is a phytobiotic source with high antioxidant and immunomodulatory potential due to its bioactive components such as lectins, flavonoids, viscotoxins, polyphenols, and triterpenes (Ergun and Deliorman,

1995; Karasu and Öztürk, 2014). While there are limited studies on the dietary use of mistletoe in poultry (Ologhobo et al., 2017), data regarding its application during the embryonic period are very limited, and the dose-tolerance relationship is unclear. The potential effects, whether positive or negative, of in ovo administration of ME on embryonic growth and chick quality have not been scientifically elucidated. This lack of information creates a significant research need for both the development of phytobiotic strategies and the safety assessment of in ovo technologies (Roto et al., 2016; El-Kholy et al., 2021). Therefore, the present study aimed to evaluate the effects of ME administered at different levels in ovo on chick quality (chick weight, Tona score, chick length, and leg asymmetry).

MATERIALS AND METHODS

This study was conducted in a poultry house at the Poultry Unit of the Education, Research, and Application Farm of Eskişehir Osmangazi University's Faculty of Agriculture. 300 fertile Ross 308 broiler eggs purchased from a commercial enterprise (C.P.) were used in the study. The ME used for in ovo injection was purchased in liquid form from a commercial company (Çoruh Vital).

All eggs were individually weighed and recorded using a scale with a precision of 0.01 g. The average egg weight was 58.97 grams. The eggs were distributed into hatching trays according to a randomized plot design, with 10 eggs in 5 treatment groups with 6 replicates, and their average weights were similar (58.67-59.27). They were numbered.

The injection sites of the eggs, which were checked for fertility and ready for in ovo injection, were cleaned with ethyl alcohol. For each treatment group, three doses of mistletoe extract (100 ppm, 200 ppm, and 300 ppm) were prepared in advance, and 0.5 ml of physiological saline (0.9% saline) was prepared for the positive control group. The needle puncture sites of the eggs were cleaned with ethyl alcohol and sealed with liquid paraffin. Eggs that completed the in ovo injection process were placed individually on hatching trays that were numbered in the same way as their respective eggs. Negative control treatment groups were placed separately on hatching trays. They were kept in the in ovo environment throughout the in ovo period, and the time required for transportation from the setter to the hatcher was adjusted for each group.

As soon as hatching was complete, the chicks were individually weighed using a 0.01 g scale (Shimadzu ATX-224). The body length of each chick, from beak to toe, was measured using a digital caliper (Dasqua 2110-8105, 150 mm IP54). The chick quality score recommended by Tona et al. (2003) was used to determine chick quality. Leg relative asymmetry values were calculated as described by Yalçin et al. (2005).

Data obtained from analyses conducted within the scope of the study were analyzed using SPSS (version 21.0; Chicago, IL, USA). Data from the study were subjected to One-Way Analysis of Variance, and the Duncan test was used for multiple comparisons.

RESULTS and DISCUSSION

Chick weight is a composite parameter that reflects the overall outcome of embryonic growth at hatch. It is an indicator of numerous physiological processes, such as protein and energy metabolism and muscle tissue growth. In this study, chick weight did not differ between treatment groups (Figure 1, $p<0.05$), suggesting that the dose ranges applied during in ovo ME feeding did not elicit a physiological response sufficient to support or suppress growth metabolism.

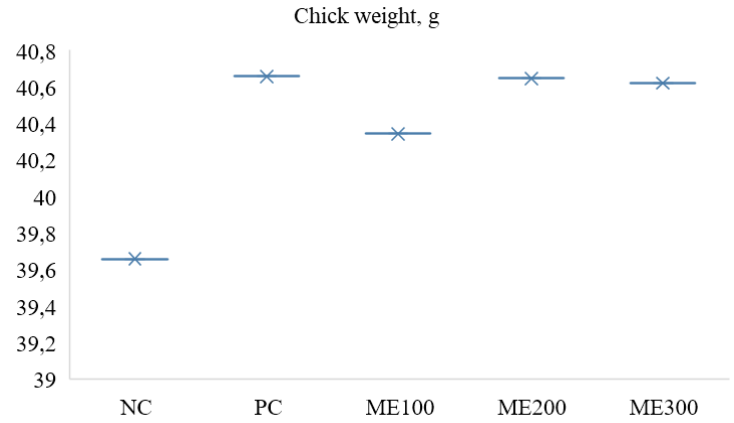


Figure 1. The influence of in ovo injection of mistletoe extract (ME) on chick weights

The fact that chick length did not change (Figure 2, $p<0.05$) supports a similar physiological perspective. The length parameter is highly sensitive, particularly because it reflects skeletal muscle, bone development, and cartilage mineralization. Therefore, the absence of a difference in length indicates that the supplement did not have an adverse or supportive effect on skeletal development and that embryonic growth maintained its naturalness. In conclusion, it is shown that in ovo phytobiotics may provide early physiological stability and metabolic/antioxidant support, but more targeted morphometric and long-term studies are required to prove their direct accelerating or suppressing effects on embryonic skeletal growth (Roto et al., 2016; Madkour et al., 2024).

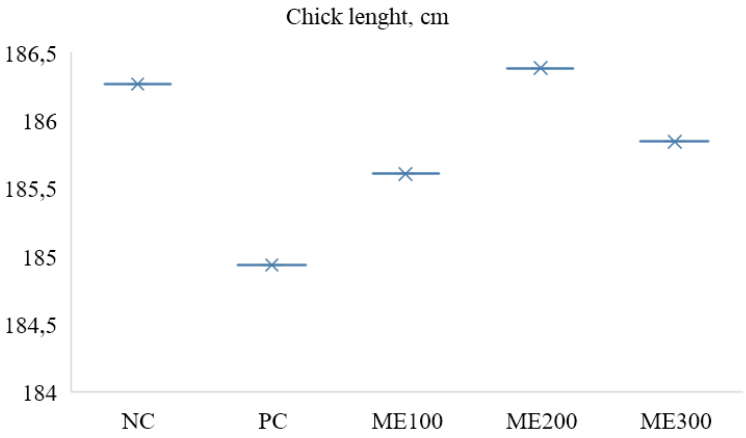


Figure 2. The influence of in ovo injection of mistletoe extract (ME) on chick lengths

The Tona score, one of the most comprehensive indicators used to assess chick quality, simultaneously reflects multiple physiological parameters, including behavioral reflexes, activity level, umbilical closure, yolk sac absorption, body condition, and general appearance (Tona et al., 2003; İpek and Sözcü, 2013). The lack of statistically significant differences in Tona scores across treatment groups (Figure 3, $p>0.05$) indicates that the in ovo applied extract did not negatively affect overall viability, metabolic stability, or post-hatch physiological integrity of the chicks during the embryonic period (Narinç, 2022). Given that even minimal stressors can be reflected in the Tona score, the lack of significant differences between groups indicates that the embryo safely tolerated the administered doses.

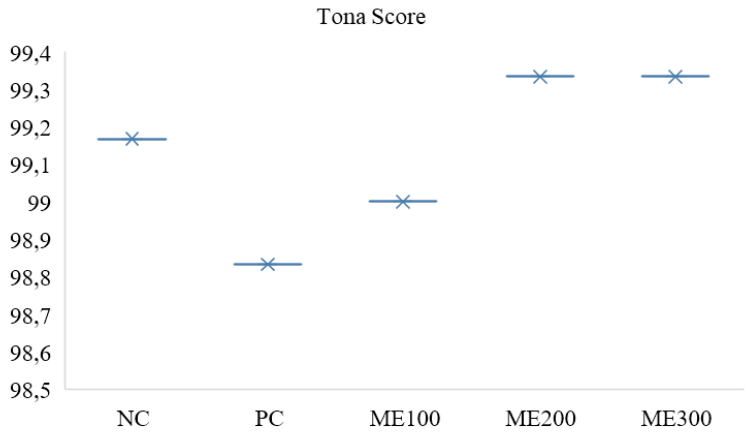


Figure 3. The influence of in ovo injection of mistletoe extract (ME) on Tona score

Leg asymmetry (relative asymmetry) was also found to be statistically insignificant between the groups in this study (Figure 4, $p>0.05$). Leg symmetry reflects multiple physiological processes, such as embryonic bone mineralization, cartilage development, embryo position, and mechanical stresses during hatching. Potential stress or toxicity during in ovo applications often manifests as limb imbalance (Ding et al., 2020). This study supports the finding that the applied extract did not have adverse effects on embryonic musculoskeletal development. Similarly, the literature reports that leg asymmetry was not altered by in ovo application of phytobiotics or natural extracts. Some studies have reported limb differences due to excessive dosage or the use of inappropriate solvents (Uni and Ferket, 2004; Madkour et al., 2024). Therefore, the dose, timing, and biological content of the supplement applied to the embryo are critical factors determining the results obtained.

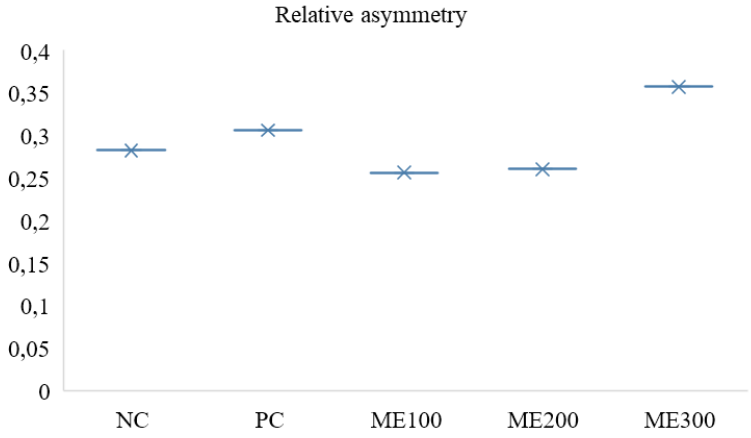


Figure 4. The influence of in ovo injection of mistletoe extract (ME) on relative asymmetry

CONCLUSION

In the current study, no statistically significant differences were observed between groups for chick weight, Tona score, relative asymmetry, or chick length, indicating that ME administration during the embryonic period did not adversely affect chick viability, physiological stability, or skeletal development. In conclusion, in ovo application of mistletoe (*Viscum album*) extract at doses up to 300 ppm during the embryonic period did not adversely affect chick quality, indicating that this extract has potential for safe embryonic applications in poultry.

ACKNOWLEDGEMENTS

This study, a part of M.Sc. thesis of the first author, was approved by the local Ethical Committee of Eskişehir Osmangazi University for Experimental Animals (Case no: 2025/1063). The authors are grateful for the support of the staff and facilities of Animal Science Department, Faculty of Agriculture, Eskişehir Osmangazi University.

REFERENCES

Akosile, O. A., Kehinde, F. O., Oni, A. I., & Oke, O. E. (2023). Potential implication of in ovo feeding of phytogenics in poultry production. Translational Animal Science, 7(1), txad094.

Alghirani, M. M., Chung, E. L. T., Jesse, F. F. A., Sazili, A. Q., & Loh, T. C. (2021). Could phytobiotics replace antibiotics as feed additives to stimulate production performance and health status in poultry? Journal of Advanced Veterinary Research, 11(4), 254–265.

Ding, Z., Zhou, H., McCauley, N., Ko, G., Zhang, K. K., & Xie, L. (2020). In ovo hyperglycemia causes congenital limb defects in chicken embryos via disruption of cell proliferation and apoptosis. Cell Death & Disease, 11, 1008.

Doğan Narinç, N. (2022). Effect of chick quality on viability, performance traits and meat quality characteristics of broiler chickens. Journal of Poultry Research, 19(2), 60–67.

El-Kholy, K. H., et al. (2021). Effect of in-ovo injection of herbal extracts on post-hatch performance, immunological and physiological responses of broiler chickens. Russian Journal of Poultry Science.

Ergun, F., & Deliorman, D. (1995). Chemical constituents of *Viscum album* L. Journal of Faculty of Pharmacy of Ankara University, 24(2), 95–107.

Henry, M. H., & Burke, W. H. (1998). Sexual dimorphism in broiler chick embryos and embryonic muscle development in late incubation. Poultry Science, 77(5), 728–736.

İpek, A., & Sözcü, A. (2013). Broiler chick quality and scoring methods. Uludağ Üniversitesi Ziraat Fakültesi Dergisi, 27(2), 131–137.

Karasu, K., & Öztürk, E. (2014). Tıbbi ve aromatik bitkilerin kanatlılarda antioksidan ve antimikrobiyal etkileri. Turkish Journal of Agricultural and Natural Sciences, 1(Özel Sayı 2), 1766–1772.

Kop Bozbay, C., & Göneci, B. (2023). Evaluation of in ovo cinnamon, ginger or anise extract injection on broiler hatching performance. Black Sea Journal of Agriculture, 6(3), 226–231.

Lilburn, M. S., Rilling, K., Mack, F., Mills, E. O., & Smith, J. H. (1986). Growth and development of broiler breeders. 1. Effect of early plane of nutrition and growth rate. Poultry Science, 65(6), 1070–1075.

Madkour, M., Abdel Fattah, S. A., Ali, S. I., Ali, N. G. M., Shourrap, M., Hosny, M., & Elolimy, A. A. (2024). Impact of in ovo feeding of grape pomace extract on the growth performance, antioxidant status, and immune response of hatched broilers. Poultry Science, 103(8), 103914.

Ologhobo, A. D., et al. (2017). Influence of mistletoe (*Viscum album*) leaf meal on growth performance, carcass characteristics and biochemical profile of broiler chickens. Food and Feed Research.

Roto, S. M., Kidd, M. T., & Peebles, E. D. (2016). Applications of in ovo technique for optimal development of the gastrointestinal tract and the potential for disease intervention in poultry. Frontiers in Veterinary Science, 3, 63.

Sözcü, A., & İpek, A. (2013). Broiler chick quality and scoring methods. Uludağ Üniversitesi Ziraat Fakültesi Dergisi, 27(2), 131–137.

Tona, K., Bamelis, F., De Ketelaere, B., Bruggeman, V., Moraes, V. M. B., Buyse, J., Onagbesan, O., & Decuypere, E. (2003). Effects of egg storage time on spread of hatch, chick quality and juvenile growth. Poultry Science, 82(5), 736–741.

Uni, Z., & Ferket, P. R. (2004). Methods for early nutrition and in ovo feeding in poultry. World's Poultry Science Journal, 60(1), 101–111.

Yalçin, S., Ozkan, S., Cabuk, M., Buyse, J., Decuypere, E., & Siegel, P. B. (2005). Pre– and postnatal conditioning induced thermotolerance on body weight, physiological responses and relative asymmetry of broilers originating from young and old breeder flocks. Poultry Science, 84, 967–975.

Zaikina, A. S., Buryakov, N. P., Buryakova, M. A., Zagarin, A. Y., Razhev, A. A., & Aleshin, D. E. (2022). Impact of supplementing phytobiotics as a substitute for antibiotics in broiler chicken feed on growth performance, nutrient digestibility, and biochemical parameters. Veterinary Sciences, 9(12), 672.

ORAL PRESENTATION

Optimization of malachite green photodegradation using quantum dots via response surface methodology

Zehra Gunaydin[1*] (*https://orcid.org/ 0009-0002-5621-8095*),
Pınar Sevim Elibol[1] (https://orcid.org/0000-0001-7758-4583)

[1]Duzce University, Faculty of Engineering, Environmental Engineering Department, Duzce, Turkiye.
[2] Duzce University University, Faculty, Department, City, Country.

*Corresponding author e-mail: zehragunaydinn81@gmail.com

Abstract

This study demonstrates the enhanced photocatalytic performance of novel quantum dots (QDs), specifically CdSeTe and Zn-doped CdSeTe, for the degradation of Malachite Green (MG) under visible light irradiation. The incorporation of Zn-doping was aimed at enhancing charge separation and overall photocatalytic efficiency. The CdSeTe and Zn-doped CdSeTe QDs were synthesized via an in-water synthesis method. The photocatalytic degradation process was systematically modeled and optimized using Response Surface Methodology (RSM) based on a Box-Behnken Design (BBD). Key operational parameters, including catalyst dosage, initial dye concentration, and pH, were investigated as independent variables to maximize MG removal efficiency. The results indicated that the Zn-doped CdSeTe QDs exhibited superior photocatalytic activity compared to the undoped CdSeTe QDs. The RSM model was found to be statistically significant and effectively predicted the optimal conditions for MG degradation. Under the optimized conditions (catalyst dosage = 2.97 mg/L, initial dye concentration = 20 mg/L, and pH = 7.8), a maximum MG removal efficiency of 99.99% was achieved. The study demonstrates the potential of Zn-doped CdSeTe QDs as a promising photocatalyst for the treatment of dye-contaminated wastewater.

Keywords: Quantum dots, Zn-doping, Malachite Green, Photocatalysis, Response Surface Methodology, Box-Behnken Design

INTRODUCTION

Water pollution, primarily driven by industrial effluents containing persistent organic pollutants, poses a significant threat to global ecosystems and human health. Among these pollutants, synthetic organic dyes, extensively used in industries such as textile, paper, plastic, and cosmetics, are particularly concerning due to their high visibility, toxicity, carcinogenicity, and resistance to conventional wastewater treatment methods (Chandrika et al., 2022; Thirugnanam et al., 2017). Malachite green (MG), a triphenylmethane dye, is a prominent example. It is widely employed as a colorant and antifungal agent but is known for its genotoxic and carcinogenic properties, necessitating efficient degradation strategies before discharge into aquatic environments (Molaei et al., 2022; Zahedi et al., 2025).

In response to these environmental challenges, advanced oxidation processes (AOPs), particularly photocatalysis, have emerged as highly promising and environmentally friendly technologies for the degradation of organic pollutants. Photocatalysis utilizes semiconductor materials as catalysts to generate reactive oxygen species (ROS) under light irradiation, which then mineralize organic contaminants into innocuous substances like carbon dioxide and water (Ahmed et al., 2022; Alasri et al., 2023). Traditional semiconductor photocatalysts, such as TiO2 and ZnO, have been widely studied; however, their large bandgaps often limit their efficiency to ultraviolet (UV) light absorption, which constitutes only a small fraction of the solar spectrum. This limitation drives the search for novel photocatalytic materials capable of harnessing visible light more effectively (Hemmateenejad et al., 2015).

Quantum dots (QDs), semiconductor nanocrystals exhibiting quantum confinement effects, have garnered considerable attention in photocatalysis due to their unique optical and electronic properties. These properties include size-dependent tunable bandgaps, high surface area-to-volume ratios, excellent light absorption capabilities across the visible spectrum, and efficient charge separation, all of which contribute to enhanced photocatalytic

activity (Wei et al., 2021; Xiang et al., 2022). Among various QDs, cadmium chalcogenide-based quantum dots, such as CdSe and CdTe, have shown significant potential. Ternary alloy quantum dots like CdSeTe offer further advantages by allowing precise tuning of their bandgap and electronic structure through compositional control, thereby optimizing their light absorption and charge carrier dynamics for specific photocatalytic applications (Jacob et al., 2019; Rajabi et al., 2018).

The photocatalytic efficiency of QDs can be further improved through doping with suitable metal ions. Doping introduces defects or alters the electronic band structure, which can enhance light absorption, promote charge separation, and increase the generation of reactive species. Zinc (Zn) doping in cadmium-based quantum dots has been explored to modify their optical and electronic properties, potentially leading to superior photocatalytic performance (Rajabi et al., 2013; Sharma et al., 2017). The incorporation of Zn into CdSeTe QDs is expected to create a more efficient photocatalyst for the degradation of malachite green by optimizing the electron-hole separation and reducing recombination rates, thus improving the overall quantum efficiency under visible light irradiation.

While several studies have reported Cd-based QDs for photocatalysis, the systematic optimization of Zn-doped CdSeTe QDs for MG degradation using RSM remains unexplored. Specifically, the synergistic effects of Zn-doping on charge separation efficiency in ternary QD systems have not been quantitatively investigated through statistical design approaches.

To systematically investigate and optimize the complex interplay of various experimental parameters affecting photocatalytic degradation, statistical experimental design methodologies are indispensable. Response Surface Methodology (RSM), particularly the Box-Behnken Design (BBD), is a powerful tool for this purpose. BBD is a three-level incomplete factorial design that allows for the evaluation of multiple factors and their interactions with a reduced number of experimental runs compared to full factorial designs, thereby saving time and resources (Amigun et al., 2022; Mbuyazi & Ajibade, 2025). This approach enables the identification of optimal operating conditions and provides a comprehensive understanding of the effects of independent variables, such as pH, catalyst dosage, and initial dye concentration, on the degradation efficiency of malachite green. Previous studies have successfully employed BBD to optimize the photocatalytic degradation of various dyes, demonstrating its effectiveness in achieving high degradation rates and understanding process mechanisms (Bendebane et al., 2024; Tolia et al., 2012)

This study focuses on the statistical optimization of malachite green photodegradation using CdSeTe and Zn-doped CdSeTe quantum dots through Response Surface Methodology. The research employs a Box-Behnken Design to: (1) systematically evaluate the individual and interactive effects of pH, catalyst dosage, and initial dye concentration on degradation efficiency; (2) quantitatively compare the photocatalytic performance of undoped and Zn-doped QDs under identical conditions; (3) establish statistically validated optimal parameters for maximum MG removal; and (4) demonstrate the enhancement achieved through Zn-doping in ternary quantum dot systems. The findings provide optimized operational conditions and fundamental insights into parameter interactions for efficient dye degradation applications.

MATERIALS AND METHODS

Preparation of Quantum Dots

The CdSeTe and Zn-doped CdSeTe quantum dots were prepared following previously optimized synthesis protocols. The as-synthesized catalysts were directly used without further modification for all photocatalytic experiments.

The synthesis of CdSeTe quantum dots (QDs) was performed following a modified literature procedure (Xiang et al., 2022). The process commenced with the preparation of precursor solutions.

First, the cadmium precursor was prepared by dissolving 0.4 mmol of cadmium chloride ($CdCl_2$) and 7.0 mmol of thioglycolic acid (TGA) as a stabilizer in 400 mL of ultrapure water. The pH of this solution was subsequently adjusted to 9 using a 1 M sodium hydroxide (NaOH) solution. For the selenium precursor, sodium hydroselenide (NaHSe) was freshly synthesized by reacting 0.4 mmol of selenium powder with 1.0 mmol of sodium borohydride ($NaBH_4$) in 20 mL of ultrapure water under stirring at 80°C for 20 minutes. The tellurium precursor, sodium

hydrotelluride (NaHTe), was prepared analogously using 0.4 mmol of tellurium powder and 1.0 mmol of $NaBH_4$ in 20 mL of ultrapure water, with stirring at 80°C for 30 minutes.

The core CdSeTe QDs were synthesized by initially adding 3.75 mL of the freshly prepared NaHSe solution to the cadmium precursor under vigorous stirring. This mixture was allowed to react at 10°C for 20 minutes. Subsequently, 1.25 mL of the NaHTe precursor was introduced. The reaction temperature was then raised to 100°C, and the solution was stirred for 9 hours to facilitate the growth and alloying of the nanocrystals.

For the deposition of a ZnS shell, a separate precursor solution containing 5.0 mmol of zinc chloride ($ZnCl_2$) and 5.0 mmol of sodium sulfide nonahydrate ($Na_2S{\cdot}9H_2O$) was prepared. Once the core QD reaction mixture reached a temperature of 90°C, the ZnS precursor solution was added dropwise. Following the complete addition, the temperature was maintained at 100°C for 40 minutes under continuous stirring to allow for shell growth.

Finally, the synthesized CdSeTe and CdSeTe/ZnS core–shell QDs were purified. The colloidal solutions were first concentrated using a rotary evaporator. The QDs were then precipitated by adding acetone at a volume ratio of 1:3 (QD solution:acetone). The precipitate was isolated via centrifugation, washed, and subsequently dried at 70°C to obtain the final product.

Photocatalytic Degradation Experiments

The photocatalytic performance of the synthesized CdSeTe and CdSeTe/ZnS quantum dots (QDs) was evaluated through the degradation of MGO under visible light irradiation. All batch experiments were conducted at ambient temperature (25 ± 2 °C) in 15-mL cylindrical glass reactors.

For a typical experiment, a specified mass (3–7 mg) of the QD photocatalyst was dispersed in 15 mL of an aqueous MGO solution. To investigate the effect of pollutant concentration, solutions with three different initial MGO concentrations—5, 12.5, and 20 ppm—were tested. Prior to irradiation, the suspension was stirred in complete darkness for 30 minutes to establish adsorption-desorption equilibrium between the dye molecules and the catalyst surface.

Following the dark adsorption period, the reaction mixture was exposed to visible light from a 60 W daylight LED lamp array. The irradiation was carried out under continuous shaking for a duration of 120 minutes. Aliquots were withdrawn at predetermined time intervals for subsequent analysis to monitor the degradation progress. Control experiments in the absence of either light or catalyst were performed in parallel to ascertain the photocatalytic nature of the degradation process.

Analytical Methods

Samples collected at the end of the photocatalysis experiments were first centrifuged at 10,000 rpm for 3 minutes to separate the catalyst. The absorbance of MGO was measured using a UV–Vis spectrophotometer (λmax = 617 nm). Peak areas were determined from the absorbance spectra. The percentage removal efficiency was calculated using the following formula:

$$Removal\ Efficiency\ (\%) = [(C_0 - Ce)/C_0] \times 100 \quad (1)$$

Where, C_0 and C_e are the initial and final concentrations of MG dye in the aqueous phase (Suganya Josephine et al., 2015).

Experimental Design and Statistical Analysis

The optimization of Malachite Green photodegradation was performed using Response Surface Methodology (RSM) with a Box-Behnken Design (BBD). This design was selected due to its efficiency in evaluating quadratic response surfaces with a reduced number of experimental runs compared to full factorial designs (Bendebane et al., 2024; Rajesh et al., 2023). Three independent variables were investigated at three levels, pH (5, 7, 9), catalyst dosage (3, 5, 7 mg) and initial MG concentration (5, 12.5, 20 ppm).

The experimental design comprised 30 randomized runs conducted with two replicates to enhance statistical reliability and estimate pure error. The design included 12 factorial points (each replicated once) and 6 center point replicates (at pH 7, catalyst 5 mg, concentration 12.5 ppm). The complete randomization of run order minimized the effects of extraneous variables and systematic errors.

A second-order polynomial model was fitted to the experimental data:

$$Y = \beta_0 + \sum_{i=1}^{3} \beta_i X_i + \sum_{i=1}^{3} \beta_i X_i^2 + \sum_{i<j} \beta_{ij} X_i X_j + \epsilon$$

(2)

where Y is predicted response, β_0 is constant, β_i are linear coefficients, β_{ii} are quadratic coefficients, β_{ij} are interaction coefficients, and ϵ is random error.

RESULTS and DISCUSSION

The photocatalytic degradation of Malachite Green (MG) was systematically investigated and optimized using Response Surface Methodology (RSM) based on a Box-Behnken Design (BBD). The experimental design, which included three independent variables—pH (A), catalyst dosage (B), and initial dye concentration (C)—was employed to model the removal efficiency of MG using both undoped CdSeTe and Zn-doped CdSeTe quantum dots (QDs) (Table 1). The statistical significance of the quadratic models for both catalysts was evaluated through the Analysis of Variance (ANOVA), as presented in Table 2 and Table 3.

Table 1. The RSM Box-Behnken Design Matrix

Variables	Symbol	Unit	Range and levels		
			− 1	**0**	**+ 1**
pH	A	-	5	7	9
Catalyst dosage	B	mg	3	5	7
Initial dye conc	C	mg/L	5	12.5	20

For the undoped CdSeTe QDs (Table 2), the model was highly significant ($p < 0.0001$), indicating that the chosen variables and their interactions effectively explain the variation in the MG removal efficiency. The high coefficient of determination ($R^2 = 95.94\%$) and the adjusted R^2 (93.91%) confirm the model's excellent fit to the experimental data and its strong predictive capability. The linear terms for pH (A), catalyst dosage (B), and initial dye concentration (C) were all highly significant ($p<0.0001$), demonstrating their critical individual influence on the degradation process. Furthermore, the two-way interaction terms AB, AC, and B*C were also statistically significant, highlighting the complex, synergistic effects between the operational parameters. The significant quadratic term for pH (A^2) suggests a non-linear relationship between pH and removal efficiency, which is a common observation in photocatalytic systems where surface charge and dye speciation are pH-dependent (Ma et al., 2018).

Table 2. ANOVA for Removal efficiency from RSM Box–Behnken Method for CdSeTe

Source	DF	Sum of squares	Mean square	F-Value	P-Value	
Model	**9**	4056.32	450.70	47.22	0.000	**Significant**
Linear	**3**	3105.83	1035.28	108.47	0.000	
A: pH	1	1788.13	1788.13	187.35	0.000	
B: Catalyst dosage	1	934.11	934.11	97.87	0.000	
C: Initial dye conc.	1	1060.22	1060.22	111.09	0.000	
Square	**3**	412.59	137.53	14.41	0.000	
A^2	1	400.31	400.31	41.94	0.000	
B^2	1	0.26	0.26	0.03	0.870	
C^2	1	9.20	9.20	0.96	0.339	
2-Way Interaction	**3**	452.48	150.83	15.80	0.000	
A*B	1	288.22	288.22	30.20	0.000	
A*C	1	91.54	91.54	9.59	0.006	
B*C	1	72.72	72.72	7.62	0.013	
$R^2 = 95.94\%$	Adjusted $R^2 = 93.91\%$		Predicted $R^2 = 89.45\%$			

Similarly, the ANOVA for the Zn-doped CdSeTe QDs (Table 3) also yielded a highly significant model ($p < 0.0001$), albeit with a slightly lower R^2 value (90.72%). The significance of the linear terms (A, B, C) and the interaction terms (AB, AC) again confirm the strong influence of the chosen variables. The statistical validation of both models provides a robust foundation for identifying the optimal operating conditions and for understanding the underlying mechanisms of the photocatalytic process (Rajesh et al., 2023)

Table 3. ANOVA for Removal efficiency from RSM Box–Behnken Method for Zn-Doped CdSeTe

Source	DF	Sum of squares	Mean square	F-Value	P-Value	
Model	**9**	21999.6	2444.4	20.64	0.000	**Significant**
Linear	**3**	14910.2	5342.5	45.11	0.000	
A: pH	1	8765.6	10383.8	87.67	0.000	
B: Catalyst dosage	1	2472.1	2472.1	20.87	0.000	
C: Initial dye conc.	1	3672.5	4270.4	36.06	0.000	
Square	**3**	4705.4	1631.1	13.77	0.000	
A^2	1	4406.8	4660.9	39.35	0.000	
B^2	1	293.5	216.2	1.83	0.193	
C^2	1	5.2	0.0	0.00	1.000	
2-Way Interaction	**3**	2383.9	794.6	6.71	0.003	
A*B	1	1665.8	1665.8	14.06	0.001	
A*C	1	699.0	699.0	5.90	0.025	
B*C	1	19.2	19.2	0.16	0.692	
R^2 = 90.72%	Adjusted R^2 =86.32%		Predicted R^2 =76.01%			

The successful application of the BBD model in this study is consistent with its proven efficacy in optimizing complex advanced oxidation processes (AOPs). For instance, a similar BBD-RSM approach was successfully employed to optimize the photocatalytic oxidation of Reactive Red 195 (RR195) dye, where the model effectively predicted the optimal conditions with high accuracy (Mollaie et al., 2025). This comparative success underscores the reliability of BBD for efficiently evaluating multiple factors and their interactions in dye degradation systems, thereby reducing the number of experimental runs required for optimization (Rajesh et al., 2023).

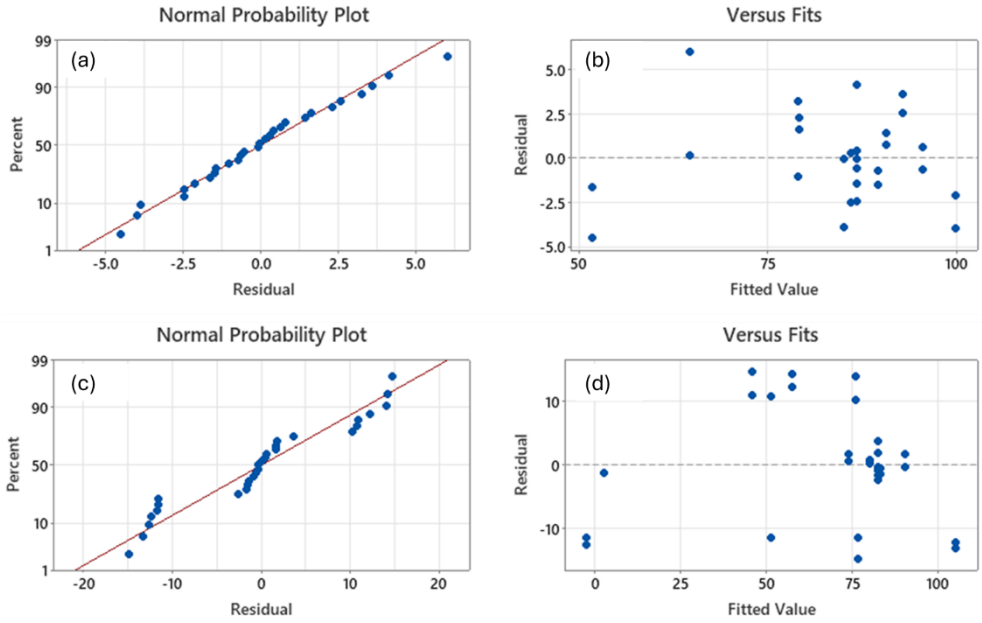


Figure 1. Residual plots for (a, c) CdSeTe and (b, d) Zn-doped CdSeTe

The analysis of the individual and interactive effects of the variables is crucial for process optimization. The contour plots (Figure 1 and Figure 2) visually represent the response surface, illustrating the combined effect of two variables while the third is held constant at its center point. The strong significance of the pH term in both models ($p< 0.0001$) underscores its role as a primary factor, a finding that is frequently reported across various photocatalytic systems (Ma et al., 2018). In photocatalysis, pH dictates the surface charge of the catalyst and the ionic state of the dye molecule. Since MG is a cationic dye, an increase in pH (moving towards the alkaline range) is expected to increase the negative charge on the QD surface, enhancing the electrostatic attraction between the catalyst and the dye, thereby promoting adsorption and subsequent degradation (Montazer et al., 2023). The optimization results (Table 4) confirm this, with the optimal pH for the Zn-doped CdSeTe system being 7.80, which is slightly higher than the optimal pH of 6.89 for the undoped system. This slight shift suggests that the Zn-doping may subtly alter the point of zero charge pH_{pzc} of the QD surface, favoring a slightly more alkaline environment for maximum electrostatic attraction with the cationic MG dye.

Catalyst dosage was also a highly significant factor. An increase in catalyst concentration provides more active sites for the reaction, leading to a higher degradation rate (Hasanpour et al., 2021). However, the quadratic term for catalyst dosage (B^2) was not significant in either model, suggesting that within the studied range (3 to 7 mg), the relationship is predominantly linear. The optimization found a low optimal dosage for both systems (3.00 mg for CdSeTe and 2.97 mg for Zn-doped CdSeTe), demonstrating the high efficiency of these QDs even at minimal concentrations.

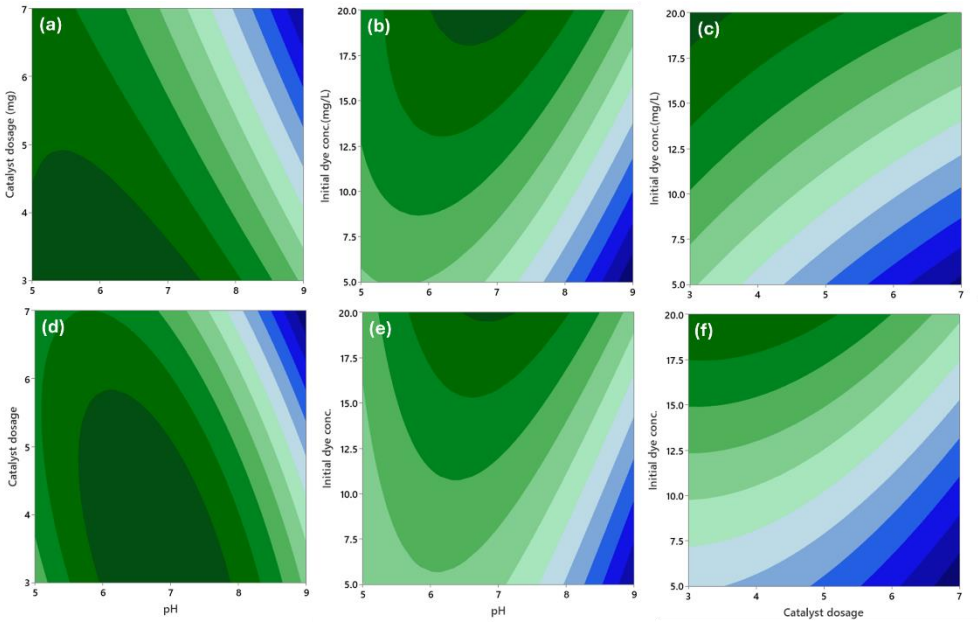


Figure 2. Contour Plots of Removal Efficiency (%) for CdSeTe (a, b, c) and Zn-doped CdSeTe (d, e, f)

The initial dye concentration was inversely related to the removal efficiency, as indicated by the negative coefficient (not explicitly shown but inferred from the significance and general photocatalytic principles). At higher concentrations, the dye molecules can act as an inner filter, reducing the light penetration to the catalyst surface, and also saturate the active sites, leading to a decrease in the overall degradation rate (Ma et al., 2018). Despite this, the optimized condition for both systems was the highest tested concentration (20 mg/L), which, combined with the near-perfect removal efficiency, highlights the exceptional performance of the QDs.

Table 4. Optimized conditions for maximum removal efficiency

Parameter	CdSeTe	Zn-doped CdSeTe
pH	6.89	7.80
Catalyst Dosage (mg)	3.00	2.97
Initial Concentration (mg/L)	20	20
Predicted Removal Efficiency (%)	99.97	99.99
Composite Desirability	1.0	1.0

The most significant finding of this study is the superior photocatalytic performance of the Zn-doped CdSeTe QDs compared to the undoped CdSeTe QDs. The optimization results (Table 4) show that both systems achieved a near-perfect predicted removal efficiency (99.97% for undoped and 99.99% for Zn-doped), but the underlying mechanism for this enhancement is critical.

The incorporation of Zn^{2+} ions into the CdSeTe lattice is a strategy for band-structure engineering and charge carrier dynamics modification (Han et al., 2020). Zinc doping is known to introduce defects or alter the electronic structure, which can serve two primary functions. First one is enhanced charge separation that occur when the presence of Zn^{2+} can create a localized electric field or form a type-II heterojunction-like structure within the QD, which effectively promotes the separation of photogenerated electron-hole pairs and suppresses their recombination (Montazer et al., 2023). This is a key bottleneck in the efficiency of many semiconductor photocatalysts.

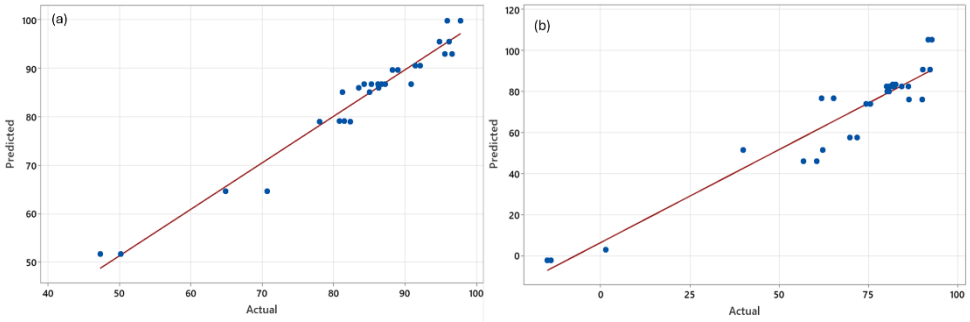


Figure 3. Contour Plots of Removal Efficiency (%) for CdSeTe (a) and Zn-doped CdSeTe (b)

Second is increased active Sites, doping can modify the surface chemistry, potentially create more surface-active sites or altering the adsorption properties, which is supported by the slight shift in optimal pH for the Zn-doped system.

The superior performance of the Zn-doped QDs, even under the statistically optimized conditions, aligns with recent literature demonstrating the effectiveness of metal-ion doping in enhancing the photocatalytic activity of quantum dots (Han et al., 2020). For instance, studies on Zn-doped CdSSe and InP QDs have confirmed that Zn doping reduces interface charge recombination and prolongs the lifetime of charge carriers, leading to a more efficient generation of reactive oxygen species (ROS) responsible for dye degradation (Amigun et al., 2022). The successful optimization via RSM, achieving a near-unity composite desirability, validates the potential of Zn-doped CdSeTe QDs as a highly efficient and promising photocatalyst for the treatment of dye-contaminated wastewater.

The high efficiency achieved under visible light irradiation is particularly noteworthy. While the comparative study on RR195 used a PCO system that included H_2O_2 as an oxidant and UV-A light [14], the current work demonstrates a near-complete degradation of MG using only the visible light-activated QDs. This highlights the intrinsic capability of the Zn-doped CdSeTe QDs to effectively utilize the visible spectrum for charge generation, making them a more sustainable and energy-efficient alternative compared to UV-dependent or H_2O_2-assisted AOPs. The remarkable 99.99% removal efficiency at the optimized conditions confirms the potential of these novel QDs for practical, real-world application in environmental remediation.

CONCLUSION

This study successfully demonstrated the enhanced photocatalytic degradation of Malachite Green (MG) using novel Zn-doped CdSeTe quantum dots (QDs) under visible light irradiation. The Response Surface Methodology (RSM) based on a Box-Behnken Design (BBD) proved to be a robust and effective statistical tool for modeling and optimizing the complex interplay of operational parameters, including pH, catalyst dosage, and initial dye concentration. The statistical models for both undoped and Zn-doped QDs were highly significant, confirming their strong predictive capability for the degradation process.

The key finding is the superior photocatalytic performance of the Zn-doped CdSeTe QDs, which achieved a remarkable maximum MG removal efficiency of 99.99% under the optimized conditions (catalyst dosage = 2.97 mg/L, initial dye concentration = 20 mg/L, and pH = 7.8). This enhancement is mechanistically attributed to the Zn-doping strategy, which acts to engineer the band structure and significantly suppress the recombination of photogenerated electron-hole pairs, thereby promoting the generation of reactive oxygen species.

In conclusion, the Zn-doped CdSeTe QDs represent a highly efficient, visible light-activated, and sustainable photocatalyst. Successful optimization via RSM validates the potential of this material for practical, low-cost, and energy-efficient treatment of dye-contaminated industrial wastewater, offering a promising alternative to UV-dependent or H_2O_2-assisted advanced oxidation processes. Further research should focus on the reusability and scale-up potential of these QDs for industrial application.

ACKNOWLEDGEMENTS

This work was financially supported by the Duzce University Scientific Research Projects (DUBAP) under the project number 2024.06.02.1539.

REFERENCES

Ahmed, M. K., Shalan, A. E., Afifi, M., El-Desoky, M. M., & Lanceros-Méndez, S. (2022). Correction: Silver-doped cadmium selenide/graphene oxide-filled cellulose acetate nanocomposites for photocatalytic degradation of malachite green toward wastewater treatment (ACS Omega (2021) 6:36 (23129-23138) DOI: 10.1021/acsomega.1c02667). In *ACS Omega* (Vol. 7, Issue 21, pp. 18190–18191). https://doi.org/10.1021/acsomega.2c02634

Alasri, T. M., Ali, S. L., Salama, R. S., & Alshorifi, F. T. (2023). Band-Structure Engineering of TiO2 Photocatalyst by AuSe Quantum Dots for Efficient Degradation of Malachite Green and Phenol. *Journal of Inorganic and Organometallic Polymers and Materials*, *33*(6), 1729–1740. https://doi.org/10.1007/s10904-023-02604-0

Amigun, A. T., Adekola, F. A., Tijani, J. O., & Mustapha, S. (2022). Photocatalytic degradation of malachite green dye using nitrogen/sodium/iron-TiO2 nanocatalysts. *Results in Chemistry*, *4*, 100480. https://doi.org/10.1016/J.RECHEM.2022.100480

Bendebane, S., Bendebane, H., Bendebane, F., & Ismail, F. (2024). Elimination of malachite green by modified Fenton like process. Application of Box Behnken design. *Global Nest Journal*, *26*(10). https://doi.org/10.30955/gnj.06822

Chandrika, K. C., Prabhu, T. N., Siva Kiran, R. R., & Krishna, R. H. (2022). Applications of artificial neural network and Box-Behnken Design for modelling malachite green dye degradation from textile effluents using TiO2 photocatalyst. *Environmental Engineering Research*, *27*(1). https://doi.org/10.4491/eer.2020.553

Han, C. Y., Kim, H. S., & Yang, H. (2020). Quantum dots and applications. *Materials*, *13*(4). https://doi.org/10.3390/ma13040897

Hasanpour, M., Motahari, S., Jing, D., & Hatami, M. (2021). Statistical analysis and optimization of photodegradation efficiency of methyl orange from aqueous solution using cellulose/zinc oxide hybrid aerogel by response surface methodology (RSM). *Arabian Journal of Chemistry*, *14*(11), 103401. https://doi.org/10.1016/j.arabjc.2021.103401

Hemmateenejad, B., Shadabipour, P., Khosousi, T., & Shamsipur, M. (2015). Chemometrics investigation of the light-free degradation of methyl green and malachite green by starch-coated CdSe quantum dots. *Journal of Industrial and Engineering Chemistry*, *27*, 384–390. https://doi.org/10.1016/J.JIEC.2015.01.018

Jacob, J. M., Rajan, R., Aji, M., Kurup, G. G., & Pugazhendhi, A. (2019). Bio-inspired ZnS quantum dots as efficient photo catalysts for the degradation of methylene blue in aqueous phase. *Ceramics International*, *45*(4), 4857–4862. https://doi.org/10.1016/J.CERAMINT.2018.11.182

Ma, Y., Ni, M., & Li, S. (2018). Optimization of malachite green removal from water by TiO2 nanoparticles under UV irradiation. *Nanomaterials*, *8*(6), 1–11. https://doi.org/10.3390/nano8060428

Mbuyazi, T. B., & Ajibade, P. A. (2025). Enhanced photocatalytic degradation of malachite green and trypan blue using 3-aminopropyl triethoxysilane (APTES) functionalized iron oxide nanocomposite. *RSC Advances*, *15*(8), 6400–6412. https://doi.org/10.1039/d4ra09025j

Molaei, M., Farahmandzadeh, F., Mousavi, T. S., & Karimipour, M. (2022). Photochemical synthesis, investigation of optical properties and photocatalytic activity of CdTe/CdSe core/shell quantum dots. *Materials Technology*, *37*(11). https://doi.org/10.1080/10667857.2021.1988040

Mollaie, F., Afroomand, M., Ahmadi, N., Mengelizadeh, N., & Balarak, D. (2025). Optimization of photodegradation of acid blue 1 dye on aluminosilicate supported Cu doped TiO2 magnetic nanocatalyst using response surface methodology. *Scientific Reports*, *15*(1), 1–18. https://doi.org/10.1038/s41598-025-89968-0

Montazer, M., Bagheri Pebdeni, A., Sheikholeslami, M. N., Dehghan Abkenar, S., Firoozbakhtian, A., Hosseini, M., & Dragoi, E. N. (2023). Synthesis of cuttlebone/ carbon quantum dots/nickel oxide nanocomposite for visible light photodegradation of malachite green used for environmental remediation. *Chemosphere*, *333*(January), 138880. https://doi.org/10.1016/j.chemosphere.2023.138880

Rajabi, H. R., Karimi, F., Kazemdehdashti, H., & Kavoshi, L. (2018). Fast sonochemically-assisted synthesis of pure and doped zinc sulfide quantum dots and their applicability in organic dye removal from aqueous media. *Journal of Photochemistry and Photobiology B: Biology*, *181*, 98–105. https://doi.org/10.1016/J.JPHOTOBIOL.2018.02.016

Rajabi, H. R., Khani, O., Shamsipur, M., & Vatanpour, V. (2013). High-performance pure and Fe3+-ion doped ZnS quantum dots as green nanophotocatalysts for the removal of malachite green under UV-light irradiation. *Journal of Hazardous Materials*, *250–251*. https://doi.org/10.1016/j.jhazmat.2013.02.007

Rajesh, C., Rajashekara, R., & Nagaraju, P. (2023). Response Surface Methodology (RSM) modelling for the photocatalytic optimization study of benzophenone removal using CuWO4/NiO nanocomposite. *Journal of Environmental Health Science and Engineering*, *21*(1), 187–199. https://doi.org/10.1007/s40201-023-00852-3

Sharma, S., Mehta, S. K., & Kansal, S. K. (2017). N doped ZnO/C-dots nanoflowers as visible light driven photocatalyst for the degradation of malachite green dye in aqueous phase. *Journal of Alloys and Compounds*, *699*. https://doi.org/10.1016/j.jallcom.2016.12.408

Suganya Josephine, G. A., Ramachandran, S., & Sivasamy, A. (2015). Nanocrystalline ZnO doped lanthanide oxide: An efficient photocatalyst for the degradation of malachite green dye under visible light irradiation. *Journal of Saudi Chemical Society*, *19*(5), 549–556. https://doi.org/10.1016/j.jscs.2015.05.011

Thirugnanam, N., Song, H., & Wu, Y. (2017). Photocatalytic degradation of Brilliant Green dye using CdSe quantum dots hybridized with graphene oxide under sunlight irradiation. *Cuihua Xuebao/Chinese Journal of Catalysis*, *38*(12). https://doi.org/10.1016/S1872-2067(17)62964-4

Tolia, J., Chakraborty, M., & Murthy, Z. (2012). Photocatalytic degradation of malachite green dye using doped and undoped ZnS nanoparticles. *Polish Journal of Chemical Technology*, *14*(2). https://doi.org/10.2478/v10026-012-0065-6

Wei, H., Wang, H., Xie, J., Qiu, P., Yan, K., Guo, P., He, Y., Song, Y., Peng, M., & Zheng, X. (2021). Photoexcited carrier dynamics within alloyed CdSeTe colloidal quantum dots and at the CdSeTe/TiO2 interface. *Ceramics International*, *47*(7), 9418–9423. https://doi.org/10.1016/J.CERAMINT.2020.12.074

Xiang, X., Wang, L., Zhang, J., Cheng, B., Yu, J., & Macyk, W. (2022). Cadmium Chalcogenide (CdS, CdSe, CdTe) Quantum Dots for Solar-to-Fuel Conversion. *Advanced Photonics Research*, *3*(11). https://doi.org/10.1002/adpr.202200065

Zahedi, M. M., Samarin, S. K., Abkenar, S. D., Pebdeni, A. B., Hosseini, M., Kalikeri, S., & Karimi-Maleh, H. (2025). Efficient visible light-driven Photodegradation of malachite green dye using carbon quantum dots-MXene nanocomposite: Synthesis, characterization, and performance evaluation. *Journal of the Taiwan Institute of Chemical Engineers*, *166*, 105521. https://doi.org/10.1016/J.JTICE.2024.105521

ORAL PRESENTATION

Trace elements essential for life in biological systems: Copper, zinc and selenium

Gulbin Erdogan (*https://orcid.org/0000-0002-6428-5899*)

Marmara University, Faculty of Pharmacy, Analytical Chemistry Department, Istanbul, Turkey.

Corresponding author e-mail: gerdogan@marmara.edu.tr

Abstract

Deficiencies or excesses of trace elements within these structures in biological systems can lead to numerous pathological disorders. The utility of metal-based compounds as pharmaceutical agents is based on their oxidation-reduction properties and their ability to form coordination complexes that play a critical role in various biochemical reactions. All heavy metals are inevitably toxic. In recent years, people have become aware of the widespread accumulation of heavy metals in the soil, air, and water of ecosystems. Heavy metals migrate from these environments to plants, and from plants to humans, creating significant problems in the human body. Numerous studies have been conducted on biological fluids to understand the toxic effects of trace elements such as copper, zinc, and selenium on the human body. This study highlights studies that illuminate the importance of copper, zinc, and selenium in biological systems for both therapeutic and diagnostic purposes.
Keywords: Copper, Zinc, Selenium, Biological Systems, Life.

INTRODUCTION

The human body is a complex biological system requiring numerous elements with diverse chemical properties to sustain biomolecular processes. These elements are classified as macro, micro, and ultra-trace elements based on their abundance and function, and they play a variety of vital roles, ranging from metabolic regulation and enzymatic catalysis to signal transduction and the formation of building blocks. While essential elements such as carbon, hydrogen, oxygen, and nitrogen ensure the structural integrity of the organism, metallic elements such as calcium, magnesium, iron, zinc, selenium, and copper are critical for maintaining cellular function and biological balance. Adequate levels of these elements are essential for maintaining homeostasis, and any deficiency or excess can lead to various pathophysiological disorders. The chemical properties of biological elements and their effects on metabolism and health constitute a fundamental area of research in biochemistry and medicine. (Amhare et al., 2025)

Minerals, similar to vitamins, are inorganic compounds that make up approximately 5% of the human body and are essential for life. These elements are found in the body mostly as salts, complex compounds, or ionic forms, and they play a role in many critical physiological processes, including regulating enzyme function, maintaining electrolyte balance, nerve conduction, muscle contraction, and maintaining skeletal structure. (Allaniyazova, and Tilewova, 2025). Minerals with a daily requirement above 100 mg are defined as macro minerals, while those with a requirement below this value are classified as micro minerals or trace elements. (Davison, 2017). Major micro minerals include iron, zinc, iodine, selenium, copper, manganese, fluorine, chromium and molybdenum; these elements play important roles in cellular metabolism, control of oxidative stress and hormone synthesis. (Zoroddu et al., 2019).

Trace element deficiencies most often occur in clinical situations such as malnutrition, increased metabolic demands, or long-term parenteral nutrition. The most common deficiencies are iron, iodine, and fluoride deficiencies, which can lead to iron deficiency anemia, thyroid dysfunction, and dental health problems. (Chapple et al., 2017) Deficiencies of other trace elements, particularly zinc, are of clinical importance in premature infants, individuals with protein-energy malnutrition, and patients with limited enteral intake. Therefore, understanding the physiological roles of minerals, their requirements, and the consequences of their deficiencies are of great importance for both clinical nutrition and public health. (Golden et al., 1978).

In recent years, heavy metals have begun to accumulate widely in ecosystems such as soil, water, and air, becoming an increasingly significant environmental problem for almost every organism, from plants to humans, requiring urgent action. Heavy metals accumulate in environmental media such as water, soil, and air, can have toxic effects, and can reach humans and other living organisms through the food chain. Therefore, numerous studies have been conducted on metal removal using natural products and nanotechnology-based methods. Nanomaterials, particularly graphene and its derivatives, magnetic and metal oxide nanoparticles, and carbon nanotubes, offer significant advantages in the effective analysis and removal of heavy metals from complex matrices. (Mitra et al., 2022)

Although heavy metals are trace elements that play a critical role in regulating certain biological processes, they exhibit serious toxic effects when consumed in excessive amounts. These metals lead to increased oxidative stress, particularly by increasing free radical production and suppressing endogenous antioxidant defense systems. Increased oxidative stress contributes to the deterioration of cellular functions and metabolic imbalances by causing structural damage to DNA, RNA, and proteins. Furthermore, heavy metals can disrupt biological functions by disrupting the proper folding of proteins and the normal structure of DNA (Chen et al., 2012; Sadiq, 2023). Chelation therapy is widely used in the treatment of heavy metal toxicity. Chelation is a chemical bonding process between metal ions and one or more ligands, forming complex ring-like structures. Recent studies have shown that the application of potent antioxidants in conjunction with chelation therapy significantly increases the effectiveness of the treatment in reducing cellular oxidative stress and preserving organ function. This approach is considered a promising strategy for improving therapeutic outcomes, especially in cases of toxicity due to chronic metal exposure. (Kim et al.,2019; Jomova et al., 2025)

The aim of this study is to evaluate the physiological roles of copper, zinc, and selenium, essential trace elements in biological systems, the pathophysiological consequences of deficiency or excess, and the oxidative stress mechanisms associated with heavy metal exposure, using a holistic perspective based on Web of Science and Scopus. Overall, the findings demonstrate that trace elements such as copper, zinc, and selenium are indispensable for cellular metabolism, antioxidant defense mechanisms, and the maintenance of enzymatic processes. Furthermore, the increasing accumulation of heavy metals in the environment triggers oxidative stress in ecosystems, leading to serious toxic effects in both plant and animal organisms. Therefore, maintaining trace element balance and preventing heavy metal toxicity are critical for both public health and environmental sustainability. Nanotechnology-based treatment methods and chelation-antioxidant combinations are anticipated to offer more effective and targeted detoxification strategies in the future. The results of this study serve as an important reference for future research in biochemistry and toxicology, as well as for environmental risk management.

MATERIALS AND METHODS

In this review, a study that can contribute to the literature consisting of data from recent years has been prepared by scanning the studies on "Trace Elements Necessary for Life in Biological Systems: Copper, Zinc and Selenium" from databases such as web of science and scopus.

Copper And Biological Systems

Copper is an element found in trace amounts in the body but is critical for biological functions, and its biological role has been recognized since the 19th century. The adult human body contains 70–80 mg of copper. Cu is a trace mineral essential for many important enzymes and proteins in living organisms. Cu homeostasis is generally well maintained by effective regulatory mechanisms, and Cu toxicity resulting from impaired homeostasis contributes significantly to a wide range of symptoms and disease states. Copper participates in the structure of many important enzymes and plays a role in the formation of blood, blood vessels, cartilage, and bone (Charkiewicz, 2024). Inadequate copper intake can lead to muscle weakness, fragility of blood vessels and bones, and impaired impulse transmission in the nervous system. Copper is also essential for hemoglobin synthesis. Excessive copper accumulation can have toxic effects (Maung et al., 2021). Copper is found in almost all foods and drinking water; its absorption and excretion are ensured by regular mechanisms. Daily copper intake is achieved by enterocytes by binding to either amino acids or metallothionein. Copper bound to amino acids is directly transferred to the circulation, while the remainder is bound to albumin and transported to the liver. Approximately 10% of copper is

excreted in the liver via bile, while the remainder is bound to ceruloplasmin synthesized in microsomes and hepatic metallothionein. Copper elimination occurs largely via bile and feces, as well as through mucosal shedding. These regular absorption and excretion mechanisms ensure that copper levels are maintained adequately and prevent potential toxicity (Brake, 2023).
Copper (Cu) is a trace element that plays a critical role in many cellular processes, such as energy metabolism, antioxidant defense, neurotransmitter production, and collagen synthesis. Copper-dependent enzymes such as cytochrome c oxidase (COX), NADH dehydrogenase-2 (ND2), and Cu/Zn-superoxide dismutase (SOD1) have been identified in prokaryotes, and their functions cannot be substituted by any other metal. Copper homeostasis in the human body is regulated by complex mechanisms, and its deficiency can lead to clinical symptoms such as anemia, leukopenia, neutropenia, and pancytopenia. On the other hand, high concentrations of copper can cause toxic effects; acute copper toxicity is characterized by nausea, vomiting, hemolytic anemia, and organ failure due to short-term high exposure, while chronic toxicity can lead to conditions such as Wilson's disease due to long-term low-dose exposure (Delik et al., 2024).

Zinc And Biological Systems

Zinc is one of the most abundant elements on Earth and, thanks to its chemical properties, has important and beneficial effects in biological systems (Brown et al., 2001). The importance of zinc, a trace element, in the growth of living organisms was reported in 1869. The human body contains between 1.4 and 2.3 g of zinc. While it is widespread in all cells, it is most abundant in the prostate, muscle, liver, kidneys, and bones. Zinc deficiency occurs more easily during pregnancy, breastfeeding, and growth. Growth failure, night blindness, and impaired sense of taste and smell are among the symptoms (Muhamed and Vadstrup, 2014).
Zinc deficiency is particularly prevalent in cirrhosis, pustular dermatitis, alopecia, weight loss, sickle cell disease, intestinal disease, hypogonadism, problems in ulcer healingand kidney failure. Zinc deficiency leads to decreased insulin production and storage, resulting in a diabetes-like condition (Gür et al. 1998; Muhamed and Vadstrup, 2014).
Because zinc is a component of many enzymes, it accelerates wound healing. It has been shown to be beneficial in decubitus ulcers and leg ulcers. It is used to reduce copper absorption in Wilson's disease (Di Dato and Hedera 2024). The normal daily zinc requirement for adults is 15 mg, and hazelnuts and walnuts, eggs, beef, and liver are rich sources of zinc. Zinc absorption occurs in the small intestine, but small amounts also occur in the stomach and colon. After absorption, it binds to a plasma protein and is transported to the liver. The primary route of excretion is via the stool, with some of this unabsorbed zinc and some excreted through the small intestinal mucosa (Hawrysz and Woźniacka 2023).

Selenium And Biological Systems

Selenium (Se) is a vital element that strengthens the immune system, provides resistance to disease, protects and supports cells by fighting free radicals, ensures the regular functioning of thyroid hormones, and has powerful antioxidant properties. Because it cannot be synthesized in the body, it must be obtained from foods. It supports cardiovascular health, reduces inflammation, and slows the aging process. Foods such as fish, eggs, walnuts, and whole grains are natural sources of selenium. Adequate intake through a balanced diet is crucial for overall health. Because inadequate Se intake can lead to various metabolic and physiological disorders, nutritional and agricultural strategies to increase Se intake are particularly important in regions with Se-poor soils. While the recommended daily Se intake for adults is generally between 40–70 µg, it is generally accepted that the total daily limit of 400 µg should not be exceeded to avoid the risk of potential toxicity (Ellis and Salt, 2003). The concentration of selenium in the blood is 60-100µg/L. It is found in all human tissues, especially the liver and kidneys (Hadrup and Ravn-Haren, 2020).

Selenium, an essential nutrient in trace amounts, is incorporated into the structure of the enzyme glutathione peroxidase, which protects the body against cancer by preventing the accumulation of hydrogen peroxide and organic peroxides in cells. High cobalt concentrations can increase the toxic effects of selenium and cause enlargement of the heart and liver. Many other human diseases are associated with selenium. These include arthritis, cataracts, cystic fibrosis, muscular dystrophy, phenylketonuria, Down syndrome, bronchopulmonary dysplasia, hemolytic anemia, multiple sclerosis, night blindness, defective immune response, malaria, kwashiorkor, and

sudden death syndrome in children (Manary et al., 1998). Selenium also prevents liver necrosis observed in vitamin E deficiency in rats. Selenium is an essential element required for growth in humans and animals at low concentrations, but it is toxic at high concentrations (Alahmadi et al., 2020). The most toxic compound of selenium is hydrogen selenide. Respiratory system irritation, a metallic taste in the mouth, pulmonary edema, garlic breath, and sweating are the primary signs of intoxication (Banerjee et al., 2022). Selenium is found in the structure of the antioxidant enzyme glutathione peroxidase (GSH-Px), which plays a role in the prevention of some metabolic diseases and cancer. Selenium's biological importance stems from its role as a cofactor in this enzyme. By interacting with vitamin E, selenium protects cell membranes from oxidative damage caused by peroxides formed during lipid metabolism (Memişoğulları et al., 2006; Erdoğan et al., 2025).

RESULTS and DISCUSSION

Studies with Copper in Biological Systems

Copper is a trace element that plays a critical role in redox balance and antioxidant defense systems and is transported in the blood primarily via the ferroxidase ceruloplasmin. Serum copper levels in SARS-CoV-2 infection are associated with immune and antioxidant system function, independent of a simple acute-phase response, and it has been suggested that adequate copper status may positively impact survival and health responses. However, there is no definitive evidence regarding the direct impact of copper status on the severity of COVID-19 or the need for treatment. Consequently, it is important to monitor reference values for trace elements such as copper and selenium, which are critical for both the immune and antioxidant systems in human health, and to supplement them if deficient; excessive levels may pose a risk of toxicity (Keskin et al., 2024).

This study aimed to evaluate the effects of serum copper, zinc, and the copper/zinc ratio on tumor staging in newly diagnosed head and neck (H&N) cancer patients and to compare them with healthy individuals. Serum copper and zinc levels were measured, and copper/zinc ratios were calculated. Findings showed that copper levels and the copper/zinc ratio were elevated in patients with H&N cancer, and these changes increased with tumor stage. Analyses revealed that zinc and copper are critical for cancer progression due to their roles in free radical formation and control. Furthermore, copper has been determined to support tumor nutrition and growth by promoting angiogenesis. The results indicate that high copper levels increase the risk of mortality, while adequate zinc levels are associated with better clinical outcomes (Kudva et al., 2022).

Copper is an element absorbed in the stomach and small intestine, and its deficiency can occur in cases of gastrointestinal anatomical changes and malabsorption. Copper deficiency can be associated with hematological and neurological disorders such as macrocytic anemia, neutropenia, and myelopathy. In one case of short bowel syndrome, progressive neurological symptoms due to severe hypocupria were partially resolved with intravenous copper replacement, highlighting the importance of timely diagnosis. Similar risks have been reported in other malabsorptive conditions such as celiac disease, chronic diarrhea, and inflammatory bowel disease. Furthermore, because copper is an acute-phase reactant, serum levels can be falsely elevated in the presence of inflammation. Therefore, routine copper assessment and, if necessary, early replacement therapy in patients with a history of gastrointestinal malabsorption or anatomical changes are clinically important to prevent potentially permanent neurological sequelae. (Moon et al., 2021).

A 68-year-old patient complained of unsteady gait for a year, prompting suspicion of Romberg's sign and mild hematological abnormalities. Tests revealed low serum copper and ceruloplasmin levels. Given the unavailability of copper-containing pharmaceutical products, the patient was advised to consume two to three cups of pure cocoa daily, which provides 0.4–0.6 mg of copper. Two months after treatment, serum copper levels returned to normal, and hematological parameters improved significantly. Neurological findings only partially resolved, but the subjective complaint of unsteadiness persisted. This case demonstrates that copper deficiency can be easily overlooked by physicians, that neurological symptoms can be irreversible if diagnosed late, and that oral cocoa consumption represents an option for copper replacement therapy (Fujikawa and Haruta, 2023).

Studies with Zinc in Biological Systems

To understand the toxic effects of zinc, many studies have examined zinc levels in biological fluids. The relationship between trace elements and oxidative damage was examined in beta-thalassemia minor patient groups. They found significantly lower Zn levels in patients compared to the control group. Their study concluded that trace element-

based antioxidative processes could increase scavenging enzyme activity and improve clinical symptoms (Kızıler et al., 2009). There is strong evidence that zinc deficiency delays wound healing after neurosurgery, highlighting the importance of preserving quality of life after surgery and assessing zinc levels before surgery. The literature demonstrates that zinc plays a critical role in wound healing through fundamental biological processes such as cell proliferation, immune function, membrane repair, and metalloenzyme activity. Because wound healing is a complex and coordinated process involving coagulation, inflammation, angiogenesis, and tissue remodeling, zinc's regulatory role in these stages is clinically relevant. Based on the current findings, neurosurgeons are encouraged to consider topical zinc applications more widely in appropriate patients to promote healing (Adjepong et al., 2020).

Genital warts are a common sexually transmitted disease, and there is no treatment that completely prevents them. Recent studies have shown promising results in the treatment of warts due to their immunomodulatory effects. In this case-control study, serum zinc levels were measured in patients and healthy volunteers and correlated with the clinical severity of the disease. Overall, the mean zinc level in the genital wart group was found to be lower than in the control group. Serum zinc levels were significantly lower in patients with multiple lesions and in patients with slightly more lesions. The findings suggest that severe genital warts may be associated with low serum zinc levels (Luong et al., 2022).

Febrile seizures are a significant complication in children with high fever, and this study compared serum selenium, zinc, vitamin D, vitamin B12, homocysteine, and magnesium levels in children aged 1-5 years who had and did not have febrile seizures. Selenium, zinc, vitamin D, and B12 levels were significantly lower in the study group compared to the control group, while no differences were observed in homocysteine and magnesium levels. No significant differences were found in these parameters between children with simple and complex febrile seizures. The findings suggest that high serum selenium, zinc, vitamin D, and B12 levels may help prevent febrile seizures and reduce the risk of seizures in children aged 1-5 years (Çığrı and İnan, 2023). This study examined the effects of zinc deficiency on angiogenesis and ischemia-induced revascularization in animal models and in patients with chronic limb-threatening ischemia (CLTI). Low serum zinc levels were independently associated with skin perfusion pressure and post-bypass wound healing in CLTI patients, and zinc supplementation in patients with low zinc levels may promote wound healing and reduce major limb adverse events (MALE). These findings suggest that monitoring zinc levels and, if necessary, supplementing may be an important clinical strategy in the management of ischemia-induced vascular diseases (Kodama et al., 2022).

This study evaluated the nutritional status, growth, and anthropometric and biochemical parameters (B12, folic acid, iron, ferritin, calcium, 25(OH)D3, zinc, plasma phenylalanine, and tyrosine levels) of children and adolescents with PKU aged 4 to 18 years in Tehran, Iran. The prevalence of overweight and obesity was high in PKU patients, and the use of specialized medical foods was recommended to address energy and nutrient deficiencies. Zinc levels were found to be subnormal in 37.5% of participants, and this was explained by dietary protein restriction, a vegetarian diet, and low bioavailability from phytates and fiber. Significant zinc deficiency was observed in 10% of patients, and it was emphasized that other micronutrient deficiencies (iron, vitamin D, B12, and folic acid) may increase the risk of neurological problems. In conclusion, balanced macro and micronutrient intake and the use of special medical foods are important to regulate phenylalanine levels of PKU patients and prevent possible neurological complications (Ahmadzadeh et al., 2022).

Studies with Selenium in Biological Systems

Selenium, previously known for its toxic and carcinogenic properties, has been evaluated as an important and beneficial element for biological systems through recent studies. Following the discovery in 1957 that selenium is an essential trace element for animals, it was determined that administering Se to experimentally induced liver tumors reduced cell death (Schrauzer, 2009). Furthermore, studies have linked the effects of metals such as Se and As on the human body to cancers in the liver, lung, kidney, prostate, and urinary tract (Genchi et al., 2023).

Another factor to consider is the decreased antioxidant activity of GPx and Tnx reductase that occurs with selenium deficiency. Selenium deficiency can therefore lead to ischemia-reperfusion injury, which can subsequently lead to acute myocardial infarction, coronary bypass surgery, heart transplantation, and coronary angioplasty. Similarly, selenium supplementation has been shown to be cardioprotective against ischemia-reperfusion injury. A small study of 46 patients demonstrated that selenium supplementation (400 µg/day for 7 days) reduced the need for cardiac surgery. Interestingly, this study also reported increased glutathione peroxidase mRNA expression in selenium-

supplemented patients (Tanguy et al., 2004). In addition to the pathologies observed in animals, a condition called Keshan disease, which develops due to selenium deficiency, has been encountered in humans. This juvenile cardiomyopathy, commonly seen in China, caused the death of many children and was completely treated with the administration of 0.5–1 mg of Se per week (Shi et al., 2021).

Selenium (Se) is an essential micronutrient for thyroid hormone synthesis and thyroid tissue maintenance. Antioxidant enzymes such as Se-dependent GPx and TRx protect thyroid cells from oxidative damage by detoxifying the high levels of hydrogen peroxide produced during hormone synthesis. In this study of patients with mildly to moderately active UC, Se supplementation (200 µg/day, 10 weeks) resulted in a significant reduction in serum Se levels, a higher rate of clinical improvement, and a higher rate of clinical remission compared to placebo. Data from thyroid disease indicate that even small increases in serum Se levels are associated with a greater normalization of TSH, T3, and T4 levels in individuals living in Se-deficient areas. The thyroid gland is a highly concentrated Se accumulator, which explains why Se elevations are so sensitive to thyroid function. The findings suggest that improving Se status in areas where Se deficiency is common may promote clinical improvement in both inflammatory bowel disease and thyroid dysfunction. (Duntas, 2006; Khazdouz et al., 2023).

CONCLUSION

Cu, Zn, and Se homeostasis is maintained in delicate balance in humans from infancy to old age; disruption of this balance can lead to a wide spectrum of clinical problems affecting all organs in the body, including neurodegenerative diseases, lung, liver, kidney, and systemic toxicity, thyroid, cardiovascular diseases, and cancer. Therefore, it appears that a balanced diet can always lead to a healthy life.

REFERENCES

Adjepong, D., Jahangir, S., & Malik, B. H. (2020). The effect of zinc on post-neurosurgical wound healing: A review. Cureus, 12(1).

Ahmadzadeh, M., Sohrab, G., Alaei, M., Eini-Zinab, H., Mohammadpour-Ahranjani, B., Rastgoo, S., & Namkhah, Z. (2022). Growth and nutritional status of phenylketonuric children and adolescents. BMC pediatrics, 22(1), 664.

Alahmadi, B. A., El-Alfy, S. H., Hemaid, A. M., & Abdel-Nabi, I. M. (2020). The protective effects of vitamin E against selenium-induced oxidative damage and hepatotoxicity in rats. Journal of Taibah University for Science, 14(1), 709-720.

Allaniyazova, M. Q., & Tilewova, G. B. (2025). Biogenic Elements And Their Importance In The Human Body. Recent scientific discoveries and methodological research, 2(5), 13-15.

Amhare, A. F., Liu, H., Qiao, L., Deng, H., & Han, J. (2025). Elemental Influence: The Emerging Role of Zinc, Copper, and Selenium in Osteoarthritis. Nutrients, 17(13), 2069.

Banerjee, M., Chakravarty, D., Kalwani, P., & Ballal, A. (2022). Voyage of selenium from environment to life: Beneficial or toxic?. Journal of Biochemical and Molecular Toxicology, 36(11), e23195.

Brake, J. (2023). Copper in Hepatocyte Functions and Fat Metabolism: Protection from Hepatic Lipid Toxicity by Copper Homeostasis (Doctoral dissertation, The University of Nebraska-Lincoln).

Brown, K.H., Wuehler, S.E., Peerson, J.M., 2001. The importance of zinc in human nutrition and estimation of the global prevalence of zinc deficiency. Food and Nutrition Bulletin 22: 113125.

Chapple, I. L., Bouchard, P., Cagetti, M. G., Campus, G., Carra, M. C., Cocco, F., ... & Schulte, A. G. (2017). Interaction of lifestyle, behaviour or systemic diseases with dental caries and periodontal diseases: consensus report of group 2 of the joint EFP/ORCA workshop on the boundaries between caries and periodontal diseases. Journal of clinical periodontology, 44, S39-S51.

Charkiewicz, A. E. (2024). Is copper still safe for us? What do we know and what are the latest literature statements?. Current Issues in Molecular Biology, 46(8), 8441-8463.

Chen, X., Guo, C., & Kong, J. (2012). Oxidative stress in neurodegenerative diseases☆. Neural regeneration research, 7(5), 376-385.

Çığrı, E., & İnan, F. Ç. (2023). Comparison of serum selenium, homocysteine, zinc, and vitamin D levels in febrile children with and without febrile seizures: a prospective single-center study. Children, 10(3), 528.

Davison, K. M. (2017). Mineral nutrients: from macro-level to ultra trace. In Nutrition guide for physicians and related healthcare professionals (pp. 261-272). Cham: Springer International Publishing.

Delik, E., Öztürk, B. E. T., & Kaya, B. (2024). Vitaminlerin ve Metallerin Çift Yönlü Etkileri: Sağlık, Mutajenite ve Antimutajenite Üzerine Bir İnceleme. Environmental Toxicology and Ecology, 4(2), 73-91.

Di Dato, F., & Hedera, P. (2024). Zinc for Wilson's Disease: What We Know and What We Don't Know. EMJ.

Duntas, L. H. (2006). The role of selenium in thyroid autoimmunity and cancer. Thyroid, 16(5), 455-460.

Ellis, D. R., & Salt, D. E. (2003). Plants, selenium and human health. Current opinion in plant biology, 6(3), 273-279.

Erdoğan, G. Ü. L. B. İ. N., Karadağ, S., Unay Demirel, Ö., Pelin, Z., Kuzu Okur, H., & Yüksel, M. E. R. A. L. (2025). Serum selenium and manganese levels in obstructive sleep apnea patients and their relationship with GPx and SOD enzyme activities. ACTA Pharmaceutica Sciencia, 63(2).

Genchi, G., Lauria, G., Catalano, A., Sinicropi, M. S., & Carocci, A. (2023). Biological activity of selenium and its impact on human health. International journal of molecular sciences, 24(3), 2633.

Golden, M. N., Harland, P. S. E. G., Golden, B., & Jackson, A. (1978). Zinc and immunocompetence in protein-energy malnutrition. The Lancet, 311(8076), 1226-1228.

Gür, G., Bayraktar, Y., Ozer, D., Ozdogan, M., & Kayhan, B. (1998). Determination of hepatic zinc content in chronic liver disease due to hepatitis B virus. Hepato-gastroenterology, 45(20), 472-476.

Hadrup, N., & Ravn-Haren, G. (2020). Acute human toxicity and mortality after selenium ingestion: A review. Journal of Trace Elements in Medicine and Biology, 58, 126435.

Hawrysz, Z., & Woźniacka, A. (2023). Zinc: an undervalued microelement in research and treatment. Advances in Dermatology and Allergology/Postępy Dermatologii i Alergologii, 40(2), 208-214.

Fujikawa, H., & Haruta, J. (2023). Copper deficiency: An overlooked diagnosis. Cureus, 15(11).

Jomova, K., Alomar, S. Y., Nepovimova, E., Kuca, K., & Valko, M. (2025). Heavy metals: toxicity and human health effects. Archives of toxicology, 99(1), 153-209.

Keskın, A., Acı, R., & Arı, M. (2024). Sars-Cov-2 Enfeksiyonu Patofizyolojisinde Çinko, Bakır Ve Selenyum Düzeylerinin Önemi Importance Of Zınc, Copper And Selenıum Levels In The Pathophysıology Of Sars-Cov-2 Infectıon. International Journal, 3(01), 27-03.

Khazdouz, M., Daryani, N. E., Cheraghpour, M., Alborzi, F., Hasani, M., Ghavami, S. B., & Shidfar, F. (2023). The effect of selenium supplementation on disease activity and immune-inflammatory biomarkers in patients with mild-to-moderate ulcerative colitis: a randomized, double-blind, placebo-controlled clinical trial. European Journal of Nutrition, 62(8), 3125-3134.

Kızıler, A. R., Aydemir, B., Kurtoğlu, E., & Uğur, A. (2009). Beta talasemi minörlü hastalarda eser element ve oksidatif hasar ilişkisi. Fırat Tıp Dergisi, 14(1), 28-32.

Kim, J. J., Kim, Y. S., & Kumar, V. (2019). Heavy metal toxicity: An update of chelating therapeutic strategies. Journal of Trace elements in Medicine and Biology, 54, 226-231.

Kodama, A., Komori, K., Koyama, A., Sato, T., Ikeda, S., Tsuruoka, T., ... & Nishida, K. (2022). Impact of serum zinc level and oral zinc supplementation on clinical outcomes in patients undergoing infrainguinal bypass for chronic limb-threatening ischemia. Circulation Journal, 86(6), 995-1006.

Kudva, A. K., Raghu, S. V., Achar, P. K., Rao, S., Suresh, S., & Shrinath Baliga, M. (2022). Study of serum zinc and copper levels and tumor pathology: a pilot study in people affected with head and neck cancers. Indian Journal of Otolaryngology and Head & Neck Surgery, 74(Suppl 3), 6007-6015.

Luong, T. N. D., Nguyen, C. T. H., Firas, A. N., & Van, T. T. (2022). Serum Zinc Level in Patients with Severe Genital Warts: A Case-Control Study in a Dermatology Hospital. Infectious Diseases in Obstetrics and Gynecology, 2022(1), 7616453.

Maung, M. T., Carlson, A., Olea-Flores, M., Elkhadragy, L., Schachtschneider, K. M., Navarro-Tito, N., & Padilla-Benavides, T. (2021). The molecular and cellular basis of copper dysregulation and its relationship with human pathologies. The FASEB Journal, 35(9), e21810.

Manary, M. J., Hart, C. A., & Whyte, M. P. (1998). Severe hypophosphatemia in children with kwashiorkor is associated with increased mortality. The Journal of pediatrics, 133(6), 789-791.

Memişoğullari, R., Gümüştekin, K., Dane, Ş., & Akçay, F. (2006). The effect of pre-injury supplementation with selenium or vitamin E on lipid peroxidation and antioxidant enzymes in burn injury. Turkish Journal of Medical Sciences, 36(3), 141-146.

Mitra, S., Chakraborty, A. J., Tareq, A. M., Emran, T. B., Nainu, F., Khusro, A., ... & Simal-Gandara, J. (2022). Impact of heavy metals on the environment and human health: Novel therapeutic insights to counter the toxicity. Journal of King Saud University–Science, 34.

Moon, N., Aryan, M., Westerveld, D., Nathoo, S., Glover, S., & Kamel, A. Y. (2021). Clinical manifestations of copper deficiency: a case report and review of the literature. Nutrition in Clinical Practice, 36(5), 1080-1085.

Muhamed, P. K., & Vadstrup, S. (2014). Zinc is the most important trace element. Ugeskrift for laeger, 176(5), V11120654-V11120654.

Sadiq, I. Z. (2023). Free radicals and oxidative stress: Signaling mechanisms, redox basis for human diseases, and cell cycle regulation. Current molecular medicine, 23(1), 13-35.

Shi, Y., Yang, W., Tang, X., Yan, Q., Cai, X., & Wu, F. (2021). Keshan disease: a potentially fatal endemic cardiomyopathy in remote mountains of China. Front Pediatr 9: 576916.

Tanguy, S., Morel, S., Berthonneche, C., Toufektsian, M. C., de Lorgeril, M., Ducros, V., ... & Boucher, F. (2004). Preischemic selenium status as a major determinant of myocardial infarct size in vivo in rats. Antioxidants and Redox Signaling, 6(4), 792-796.

Zoroddu, M. A., Aaseth, J., Crisponi, G., Medici, S., Peana, M., & Nurchi, V. M. (2019). The essential metals for humans: a brief overview. Journal of inorganic biochemistry, 195, 120-129.

ORAL PRESENTATION

Biochar production from spent coffee grounds by hydrothermal carbonization as a catalyst support material for hydrogen production by methanolysis of sodium borohydride

Asuman Kalkan[1] (*ORCID:0009-0001-6163-9997.*), Akın Sürücü[2] (*ORCID:0009-002-3469-084X*), Seda Hoşgün[3*] (*ORCID : 0000-0002-5884-9723*)

[1] Eskisehir Osmangazi University, Engineering and Architecture Faculty, Chemical Engineering Department, Eskisehir, Türkiye.
[2] Eskisehir Osmangazi University, Engineering and Architecture Faculty, Chemical Engineering Department, Eskisehir, Türkiye.
[3*] Eskisehir Osmangazi University, Engineering and Architecture Faculty, Chemical Engineering Department, Eskisehir, Türkiye.

*Corresponding author e-mail: serol@ogu.edu.tr

Abstract

Biomass-based Co catalysts were prepared using an impregnation–chemical reduction method and used to catalyze the methanolysis of sodium borohydride ($NaBH_4$) for hydrogen generation. The synthesized catalyst and pre-treated coffee samples were characterized by Fourier transform infrared (FTIR) spectroscopy and scanning electron microscopy (SEM) to determine the morphological and surface properties of the samples. At a solution temperature of 25 °C, the methanolysis reaction is effectively accelerated by the Co/HTCC catalyst, providing a desirable hydrogen generation rate, making it suitable for applications at low environmental temperatures. The catalytic activity of Co/HTCC toward NaBH4 methanolysis can be further improved by optimizing the solution conditions. The catalytic performance was rigorously evaluated for hydrogen generation via the methanolysis of sodium borohydride ($NaBH_4$). The Co/HTCC catalyst showed remarkable activity at an ambient temperature of 25 °C, with 10 mg of catalyst achieving the hydrogen generation rate as 8,882 mL $gcat^{-1}$ min^{-1}.

Keywords: Hydrothermal carbonization, catalyst synthesis, methanolysis, spent coffee grounds.

INTRODUCTION

The increasing global energy demand and the environmental issues caused by dependence on fossil fuels have highlighted the importance of scientific research on sustainable energy sources. Hydrogen is considered an energy carrier expected to play a significant role in the energy sector in the coming century because it produces no harmful emissions during combustion, has a high calorific value, is easily transportable, is simple to produce, and its cost is decreasing due to technological advancements [Hosgun S. (2018)]. Although hydrogen is abundant in nature, it does not exist as H_2 gas that can be directly used as a fuel [Akbar et al. (2024)].

The continuous rise in global energy demand drives the need for sustainable energy carriers that can serve as alternatives to conventional fossil fuels. In this context, hydrogen production from renewable resources is critically important for an environmentally friendly, low-carbon energy system. Given the high carbon emissions associated with conventional hydrogen production methods, environmentally compatible technologies such as biohydrogen are gaining increasing prominence [Jolly et al. (2025)]. Biohydrogen production stands out for its low energy requirements and its ability to valorize organic waste. In particular, coffee grounds, a waste product generated in large quantities by the coffee industry, serve as an ideal substrate for this process due to their high organic matter and carbon content. Effectively utilizing coffee grounds in microbial or dark fermentation processes not only provides environmental benefits by addressing a significant waste management issue but also offers an economical alternative for sustainable energy production. The fundamental scientific challenge is to develop efficient, low-cost, and environmentally compatible biotechnological systems that can convert this valuable waste into hydrogen with maximum yield.

According to research and survey results, coffee – one of the most consumed beverages worldwide and a product of substantial industrial importance – generated approximately 11 million tons of spent coffee grounds during the 2022–2023 coffee year [International Coffee Organization (2023)]. This represents a significant amount of biomass residue. Coffee by-products and wastes have considerable economic potential due to their composition, which includes valuable constituents such as fatty acids, polysaccharides, polyphenols, and minerals [Yusufoğlu et al. (2024)]. These materials can be repurposed across various industries, including pharmaceuticals, cosmetics, food, and energy. This supports a circular economy in which such by-products gain renewed value by being converted into biofuels, biopolymers, biofertilizers, food additives, or construction materials [Yusufoğlu et al. (2024); Chatzimitakos et al. (2023); Islam et al. (2024)]. Due to their lignocellulosic structure, high carbon content, and abundance of organic components, coffee grounds are considered a significant biomass feedstock suitable for energy conversion. However, most of this waste is disposed of by landfilling or incineration, practices that lead to environmental issues such as methane emissions and soil contamination. Although the literature includes studies on biogas and compost production from coffee waste, there is insufficient research on carbon synthesis via hydrothermal carbonization and on evaluating hydrolysis–methanolysis performance using such waste. This highlights a gap in the literature and underscores the originality of the present study.

Borohydride compounds such as $NaBH_4$ (sodium borohydride) and KBH_4 (potassium borohydride) offer significant advantages when reacted with alcoholic solvents such as methanol or ethanol (alcoholysis), compared to aqueous media. These alcohols can accelerate reaction kinetics and limit the formation of undesirable secondary products. However, despite these advantages, the reaction rate between $NaBH_4$ and ethanol remains notably low [Gurdal (2024)].

In this study, spent coffee grounds – an abundant waste material –are converted into activated carbon using the hydrothermal carbonization method to synthesize a cobalt (Co)-doped catalyst and comprehensively investigate the catalytic performance of this material in methanolysis reactions.

To incorporate coffee waste into an activated carbon structure via hydrothermal carbonization; to synthesize cobalt-loaded catalysts by impregnating and reducing the obtained hydrochar; to analyze the biochar and synthesized catalysts using SEM and FTIR characterization techniques to determine the pore structure of the synthesized catalysts. By integrating all experimental findings, the study aims to demonstrate the applicability of coffee-ground-supported Co–B catalysts as sustainable and efficient materials for hydrogen production.

MATERIALS AND METHODS

For the supported catalyst synthesis, spent coffee grounds collected from coffee shops were used and initially dried at 105°C for 24 hours to remove water content. Six grams of biomass and 24 mL of deionized water were mixed in a stainless-steel autoclave. The autoclave was placed in an oven for 90 minutes at 220°C. At the end of the carbonization period, the autoclave was immediately cooled, and the mixture was filtered. The hydrochar samples were dried in the oven at 105°C for 24 hours. The dry hydrochar samples were then mixed with KOH at a KOH/hydrochar ratio of 2. The samples were washed with 0.1 M HCl and deionized water until the pH of the filtrate reached 7. The samples were dried a second time in the oven at 105°C for 24 hours. The carbonized biomass was used as support material for the synthesis of Co catalysts using the impregnation and reduction method. The appropriate amount of $CoCl_2$ solution was prepared in a stoichiometric ratio with distilled water. The cobalt content in the supported catalysts was adjusted to 20% by weight. After impregnating the cobalt onto the supports at 75°C for one hour at 1000 rpm, $NaBH_4$ solution was added dropwise for the chemical reduction process to reduce Co^{2+}. An excess amount of borohydride was used to achieve complete reduction, with a molar ratio of $NaBH_4$:$CoCl_2$ of 3:1, and the reduced solution was stirred at 600 rpm for three hours at 25°C. The sample was then filtered and washed with an ethanol/water mixture (volume ratio 1:1) to remove insoluble inorganics from the catalyst. The sample was placed in the oven at 105°C for 24 hours. The resulting powder was stored for use in the methanolysis reaction.

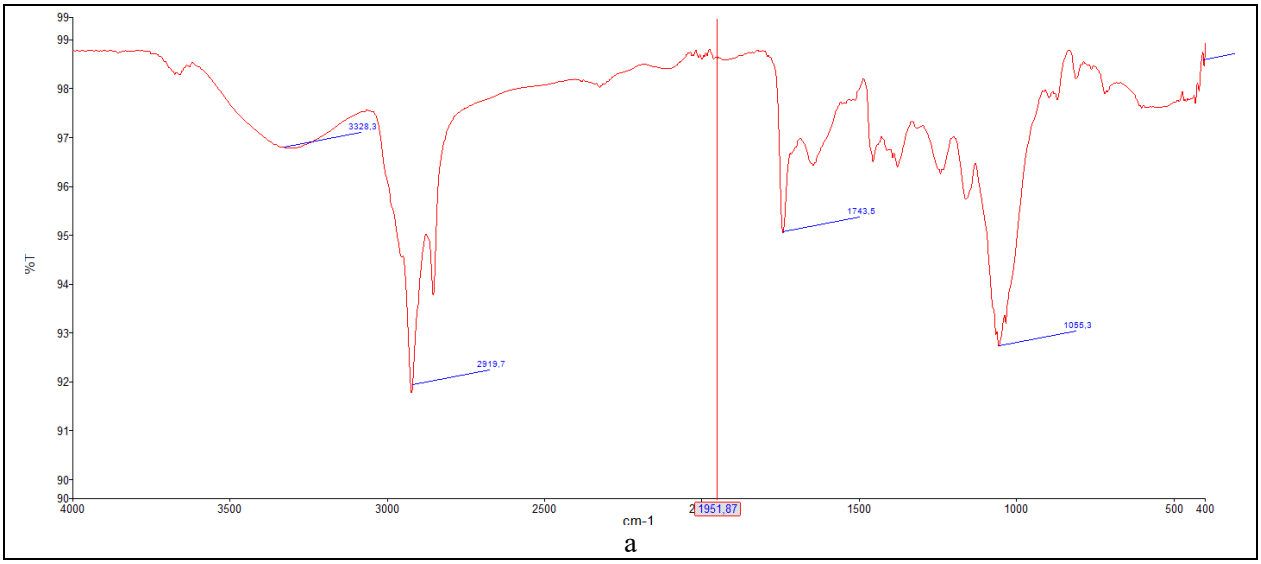
Scanning electron microscopy (SEM) was employed to examine the surface morphology of the manufactured catalyst. The chemical structure of the catalyst was analyzed using Fourier transform infrared (FTIR) spectroscopy (PerkinElmer) with a wavenumber range of 400–4000 cm^{-1}.

The methanolysis reactions were conducted in a 150 mL jacketed reactor. In a typical H_2 generation experiment, 0.05–0.1 g $NaBH_4$ and 10-30 mg catalyst was initially placed in the reactor. The methanolysis reaction was initiated by injecting 10 mL methanol into the reactor at 25ºC. The cumulative volume of generated hydrogen over time was measured using the water displacement method.

RESULTS and DISCUSSION

Characterization Results

In order to define the functional groups FT-IR analysis was undertaken for the SCG and Co/HTCC catalyst (Fig. 1). The FTIR spectra illustrating the transformation of spent coffee grounds (SCG) into the Co/HTCC catalyst reveal systematic changes in the material's functional group composition. The spectra for the raw biomass (SCG) (Fig.1a) and the post-hydrothermal carbonization (HTC) (Fig. 1b) product show a rich surface chemistry typical of a lignocellulosic matrix, with prominent absorption bands corresponding to hydroxyl (-OH) stretching vibrations in the 3300–3400 cm^{-1} region, aliphatic C–H stretching around 2920 cm^{-1}, and strong carbonyl (C=O) and C–O–C vibrations within the 1000–1750 cm^{-1} range. These features confirm the hydrophilic nature and the presence of oxygenated sites available for metal coordination. In contrast, the spectrum for the Co/HTCC catalyst (Fig 1c) shows a marked reduction in these band intensities and a flattened profile – most notably, the disappearance of hydroxyl and aliphatic functionalities – demonstrating that the material underwent extensive deoxygenation, dehydration, and decarboxylation during catalytic activation and thermal treatments. This process ultimately yields a highly stable, condensed carbonaceous framework with a dominant aromatic character.



a

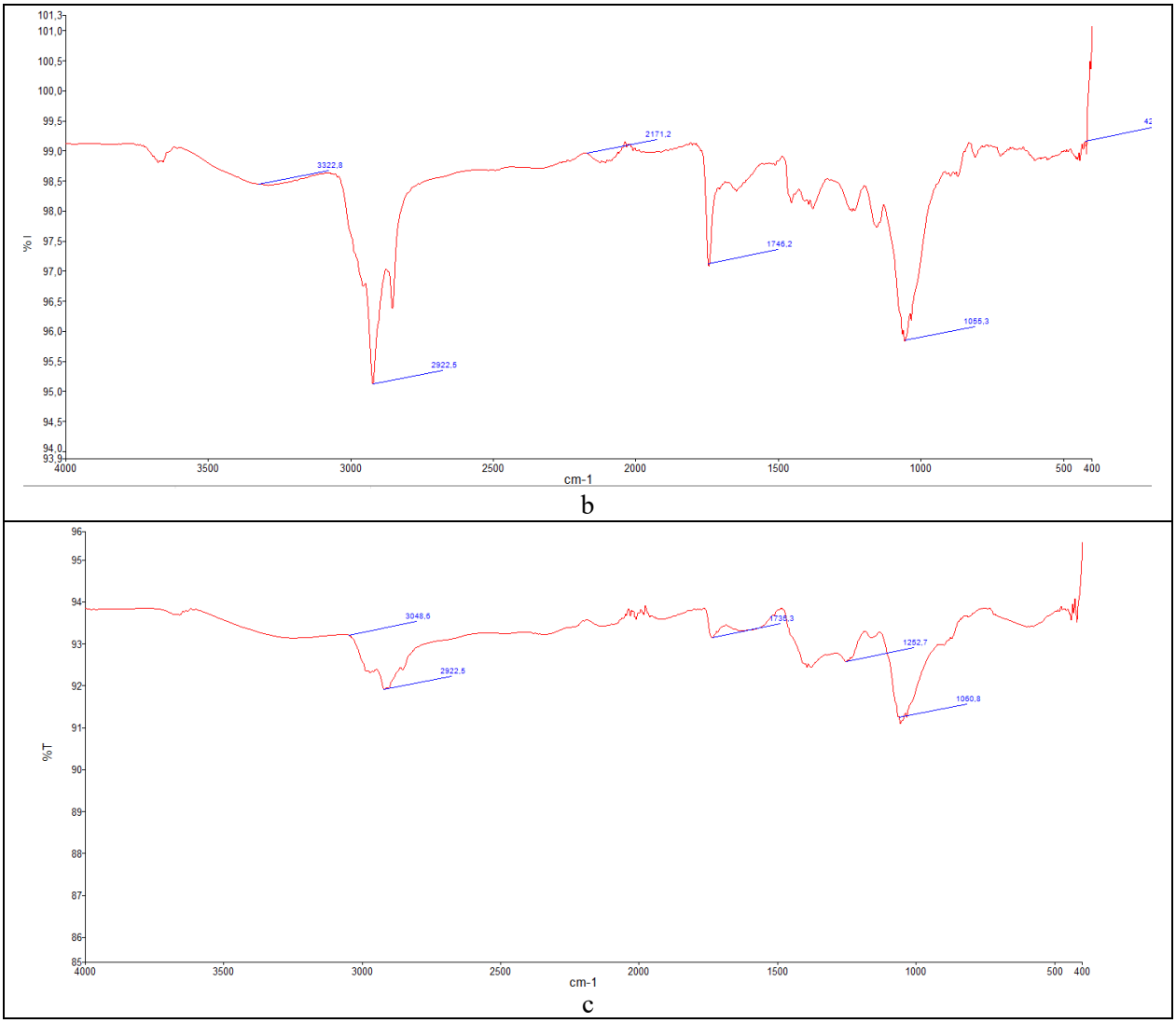


Figure 1. FTIR analysis of a) spent coffee ground, b) after hydrothermal carbonization c) Co/HTCC catalyst.

SEM-EDS and mapping images of coffee grounds and Co/HTCC catalyst were given in Table 1 and Fig. 2. The EDS results show that cobalt loading and methanolysis cause significant changes in the surface chemistry of HTCC. In the raw HTCC sample, the surface consists entirely of carbon (100% C), with no detectable oxygen or other elements. After cobalt is loaded onto the HTCC, the carbon content decreases to 82.31%, while the oxygen content increases to 17.69%, indicating the formation of new oxygen-containing functional groups on the surface due to the binding of cobalt salt or cobalt species. Following methanolysis, the carbon content further decreases to 77.81% and the oxygen content rises to 21.15%, suggesting that the surface has undergone additional oxygenation or that oxygenated species from methanol have bound to the surface. Additionally, the low concentration of Al (1.04%) detected on the surface after methanolysis indicates possible trace element contamination from equipment or chemicals used during the process. These findings suggest that the surface structure of HTCC is sensitive to both cobalt loading and methanolysis, and that its functional group structure changes significantly.

Table 1. EDS results of the samples HTCC, Co/HTCC and Co/HTCC (After Methanolysis).

Sample	C(Wt%)	O(Wt%)	Al (Wt%)
HTCC	100	-	-
Co/HTCC	82.31	17.69	-
Co/HTCC (After Methanolysis)	77.81	21.15	1.04

The Scanning Electron Microscopy (SEM) micrographs systematically illustrate the structural evolution and morphological stability of spent coffee grounds (SCG) from their raw state through the post-catalytic cycle. The untreated SCG sample (a) shows a heterogeneous morphology with compact, irregular block-like aggregates with limited porosity. After hydrothermal carbonization (b), the loss of cellular integrity due to hydrolytic degradation of the lignocellulosic matrix and removal of volatiles results in a rougher, sheet-like surface that promotes pore development. In the synthesized Co/HTCC catalyst (c), the incorporation of metal precursors onto the carbon skeleton, along with thermal activation, produces a more granular and complex surface topography that facilitates reactant diffusion. The micrograph after the methanolysis reaction (d) shows that, despite exposure to harsh reaction conditions – including solvent interaction and mechanical agitation – the catalyst largely maintains its macroscopic structural integrity. However, minor surface attrition, slight aggregation, or morphological deformations attributed to reaction dynamics are observed, providing important insights into the material's mechanical stability and potential for reuse.

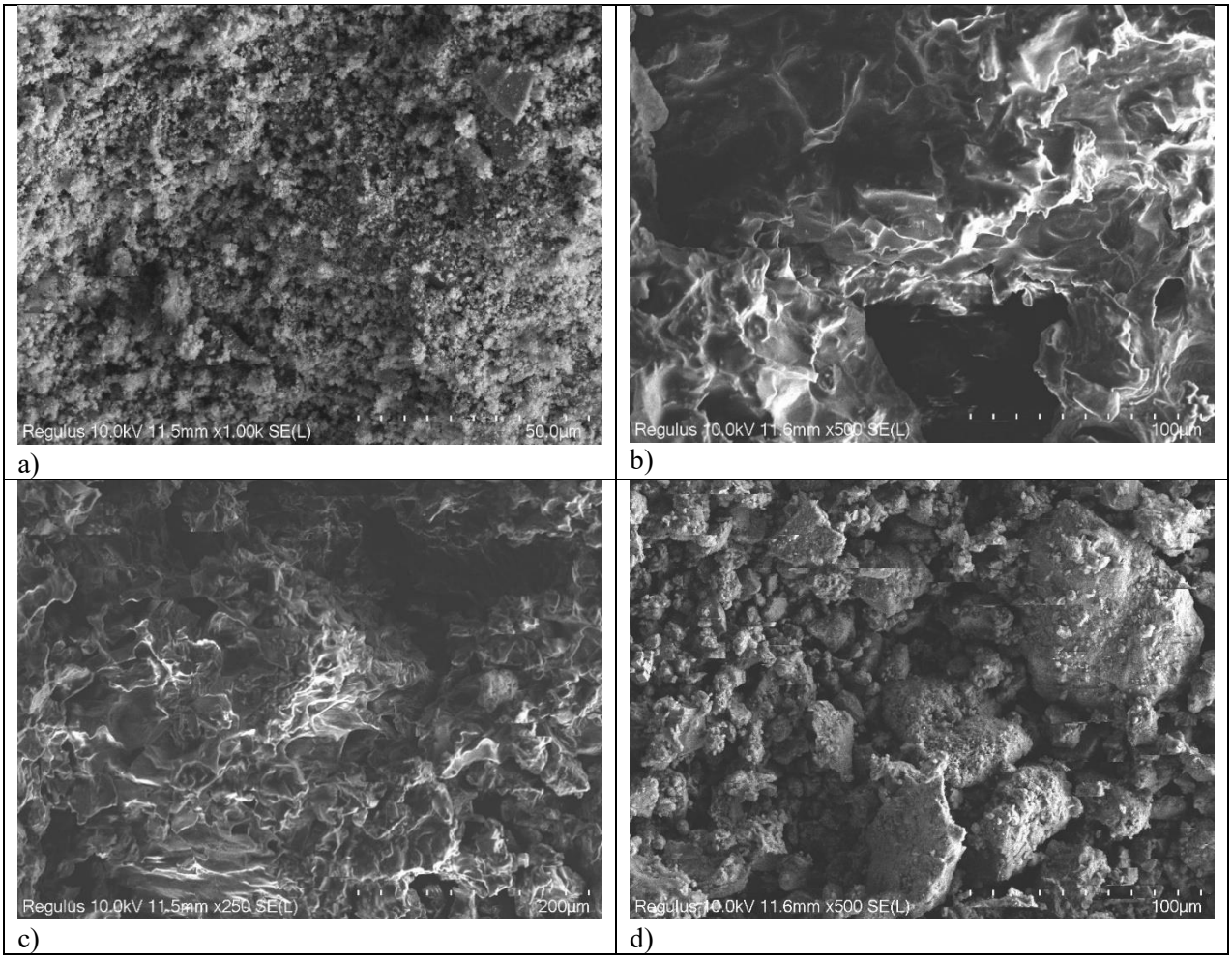


Figure 2. SEM analysis of a) spent coffee ground, b) after hydrothermal carbonization c) Co/HTCC catalyst d) Co/HTCC catalyst after methanolysis.

Catalytic Activity Results

The effect of catalyst amount and reactant concentration on hydrogen production performance in the catalytic hydrolysis of $NaBH_4$ is clearly shown in the Table 2. Data on the catalytic hydrolysis of $NaBH_4$ show that hydrogen production performance is significantly affected by both the catalyst amount and the $NaBH_4$ concentration. At a constant $NaBH_4$ concentration (0.27 M), increasing the catalyst amount significantly shortened the reaction time: the reaction, which was completed in 300 seconds with 10 mg of catalyst, was completed in 180 seconds with 30 mg of catalyst. However, the total hydrogen volume produced (285 mL) remained unchanged, while the hydrogen production rate per unit catalyst decreased, indicating that the mass yield decreased with increasing catalyst loading. On the other hand, increasing the $NaBH_4$ concentration directly increased hydrogen production; the hydrogen volume, which was 285 mL at 0.27 M, increased to 540 mL at 0.53 M and 830 mL at 0.79 M. The same trend was observed for the hydrogen production rate, with the highest value (8882 mL $g_{cat}.min^{-1}$) obtained at a 0.79 M $NaBH_4$ concentration and 10 mg catalyst. These findings suggest that the amount of catalyst has a limited effect on the reaction kinetics, while the $NaBH_4$ concentration is the main parameter determining hydrogen production capacity.

Table 2. Hydrogen generation rate of the methanolysis reaction via Co/HTCC at different reaction conditions.

Catalyst amount (mg)	$NaBH_4$ concentration (M)	Reaction Time (sec)	Generated Hydrogen Volume (mL)	Hydrogen Generated Rate (mL $g_{cat}.min^{-1}$)
10	0.27	300	285	5700
20	0.27	240	285	3562
30	0.27	180	285	3166
10	0.53	426	540	7605
10	0.79	560	830	8882

CONCLUSION

In this study, a cost-effective and sustainable cobalt-based catalyst supported on hydrothermally carbonized carbon (Co/HTCC) derived from spent coffee grounds was successfully synthesized using a simple impregnation–chemical reduction method. The catalytic performance was rigorously evaluated for hydrogen generation via the methanolysis of sodium borohydride (NaBH4). The Co/HTCC catalyst showed remarkable activity at an ambient temperature of 25 °C, demonstrating its viability for on-demand hydrogen production, particularly in low-temperature environments where energy efficiency is critical. The results show that the reaction kinetics in the catalytic hydrolysis of $NaBH_4$ are controlled by the $NaBH_4$ concentration rather than the catalyst dosage. Although increasing the catalyst amount at a constant $NaBH_4$ concentration (0.27 M) significantly decreased the reaction completion time (10 mg: 300 s; 30 mg: 180 s), the total hydrogen volume produced remained unchanged (285 mL), and the hydrogen production rate per unit mass decreased, indicating that the unit active surface efficiency decreased as the catalyst amount increased. In conclusion, the key parameter determining hydrogen production performance in the catalytic hydrolysis of $NaBH_4$ is the $NaBH_4$ concentration. While increasing the amount of catalyst shortens the reaction time, it has a limited effect on the yield per unit of catalyst. The highest hydrogen production rate was achieved with 0.79 M $NaBH_4$ and 10 mg of catalyst as 8882 mL $g_{cat}.min^{-1}$.

REFERENCES

Akbar, S., Qureshi, M., & Khan, S. (2024). Chitosan-supported copper nano catalyst fabrication for hydrogen. *International Journal of Hydrogen Energy, 101*, 313–322.

Chatzimitakos, T., Athanasiadis, V., Kotsou, K., Palaiogiannis, D., Bozinou, E., & Lalas, S. I. (2023). Optimized isolation procedure for the extraction of bioactive compounds from spent coffee grounds. *Applied Sciences, 13*(5), 2819.

Gurdal, S. (2024). Kinetic evaluation and catalytic efficiency of sebacic acid as a novel catalyst in hydrogen generation via $NaBH_4$ alcoholysis reactions. *Catalysts, 14*(9), 644. https://doi.org/10.3390/catal14090644

International Coffee Organization. (2023). *Coffee development report 2022–23*. https://www.icocoffee.org/documents/cy2024-25/coffee-development-report-2022-23.pdf

International Energy Agency. (2023). *World energy outlook 2023*. IEA.

Islam, K. M. O., Ahmad, N., Alboqami, F., Ahmed, U., Siddiqui, M. N., Ummer, A. C., & Jameel, A. G. A. (2024). Utilization of coffee waste for biofuel production through catalytic microwave-assisted pyrolysis approach. *Biomass Conversion and Biorefinery.* https://doi.org/10.1007/s13399

Jolly, S. S., Twinkle, A. R., Arun Sasi, B. S., & Reshma, R. (2025). Emerging paradigms in renewable hydrogen production: Technology, challenges, and global impact. *Next Energy, 8*, 100343. https://doi.org/10.1016/j.nxener.2025.100343

Hoşgün, S. (2018). *Kobalt ve nikel içerikli destekli katalizörlerin sentezi, karakterizasyonu ve sodyum borhidrürden hidroliz tepkimesi ile hidrojen üretiminde kullanılması* (Doktora tezi). Eskişehir Osmangazi Üniversitesi, Fen Bilimleri Enstitüsü, Eskişehir, Türkiye.

Yusufoğlu, B., Kezer, G., Wang, Y., Ziora, Z. M., & Esatbeyoglu, T. (2024). Bio-recycling of spent coffee grounds: Recent advances and potential applications. *Current Opinion in Food Science, 55*, 101111.

ORAL PRESENTATION

Fidelity of FDM-fabricated PLA bone scaffolds to CAD models: a comparative analysis of voronoi, TPMS, and lattice architectures

İzel Ekinci[1*] (*ORCID:0009-0006-9198-0324*), Daver Ali[1] (*ORCID:0000-0002-8500-7820*)

[1]Karabük University, Faculty of Engineering and Natural Sciences, Department of Biomedical Engineering, Karabük, Türkiye.

*Corresponding author e-mail: izelbagriyanik@gmail.com

Abstract

The success of scaffolds used in bone tissue engineering directly depends on how precisely the designed micro-architecture can be achieved after fabrication. Although Fused Deposition Modeling (FDM) technology stands out for its low cost and accessibility, it can lead to dimensional deviations in the production of complex geometries. This study aims to compare the manufacturability of different topological architectures produced by the FDM method. Scaffolds with irregular Voronoi, Schwarz (TPMS), and Diamond (Lattice) architectures were designed and fabricated using Polylactic Acid (PLA) material at four different porosity rates (50%, 60%, 70%, and 80%). Production quality was evaluated by deviation analysis between theoretical and fabricated models through mass measurements. The results showed that geometric architecture has a decisive effect on production accuracy. While regular Schwarz and Diamond structures exhibited high production stability (with a 0 deviation at Diamond and 70% porosity), Voronoi structures showed a mass increase of up to 10.05% due to their stochastic nature. This study demonstrates that TPMS and Lattice structures provide higher dimensional accuracy compared to Voronoi in FDM-based production, shedding light on geometric selection criteria for clinical applications.

Keywords: FDM, PLA, Manufacturability, Design fidelity.

1. INTRODUCTION

Bone tissue engineering offers a promising strategy for the repair of critical-sized bone defects, resulting from trauma, tumor resection, or congenital anomalies that are incapable of spontaneous healing (Tariverdian et al., 2019). Scaffolds utilized within this field are anticipated to mimic the natural extracellular matrix (ECM) to support cell adhesion, proliferation, and new tissue formation (Abbasi et al., 2020). An ideal bone scaffold must not only be biocompatible but also exhibit high porosity with an interconnected pore structure, facilitating the transport of nutrients and waste products (Lee et al., 2022). Fused Deposition Modeling (FDM) technology, paired with biocompatible Polylactic Acid (PLA), is a prevalent choice for fabricating patient-specific scaffolds due to its cost efficiency, accessibility, and geometric flexibility (Chalgham et al., 2021). Nevertheless, the clinical success of PLA scaffolds produced via FDM relies not solely on material characteristics, but fundamentally on the degree to which the designed geometric architecture is maintained under manufacturing constraints.

In recent years, scaffold design has undergone a transition from simple grid structures to advanced architectures that more closely replicate the complex morphology of natural bone. In this context, distinct architectures have emerged as prominent candidates: Voronoi structures, which biomimetically replicate trabecular bone through irregular pore distribution (Herath et al., 2021); Diamond lattice structures, composed of regular and repeating unit cells (Chen et al., 2021); and Schwarz Triply Periodic Minimal Surface (TPMS) structures, defined by their mathematically continuous curvature (Poltue et al., 2021). While Voronoi structures offer the potential to enhance nutrient transport and cell infiltration via heterogeneous porosity (Wang et al., 2018), Diamond lattice structures are noted for their superior load-bearing capacity, and Schwarz TPMS structures are distinguished by their high stiffness and extensive surface area (Guo et al., 2022). However, although existing literature has predominantly focused on the theoretical mechanical performance of these architectures, the impact of geometric constraints imposed by the manufacturing technique on the final scaffold quality is frequently overlooked.

Geometric discrepancies between idealized scaffold models generated in Computer-Aided Design (CAD) environments and the physical specimens obtained post-fabrication are unavoidable due to the inherent limitations of FDM technology. Parameters such as nozzle diameter, layer thickness, and temperature can adversely affect fabrication quality, particularly in complex structures with intricate details (Kuznetsov et al., 2018; Triyono et al., 2020). Specifically, the sharp angles and unsupported overhangs characteristic of stochastic structures, such as Voronoi, can induce sagging of the molten filament during cooling or result in unwanted material accumulation (stringing) during rapid nozzle transitions. These fabrication defects can lead to a reduction in designed porosity and pore occlusion, potentially impeding cellular migration. Conversely, although the continuous and self-supporting nature of TPMS and regular lattice structures offers an inherent advantage for additive manufacturing (Afshar et al., 2016), this potential benefit necessitates experimental validation regarding dimensional accuracy, specifically within the context of FDM.

The primary objective of this study is to compare the dimensional and mass deviations between idealized models generated in a CAD environment and the physical specimens obtained after fabrication. In this work, Voronoi, TPMS (Schwarz), and Lattice (Diamond) scaffolds manufactured from PLA via FDM were evaluated through mass measurements. By revealing which geometric architecture can be produced with the highest fidelity to the digital design (beyond mechanical strength), the findings aim to determine the most reliable design and fabrication strategy for clinical applications.

2. MATERIALS AND METHODS

In this study, bone scaffolds featuring irregular (Voronoi) and regular (TPMS: Schwarz; Lattice: Diamond) architectures were designed and subsequently fabricated from PLA material using FDM technology. The quality of the resulting production was evaluated through dimensional and morphological analyses.

2.1. Scaffold Design

Three distinct topological architectures were selected for bone substitution applications: Voronoi, Schwarz Primitive, and Diamond. Voronoi models were generated using the Grasshopper parametric design tool integrated within Rhinoceros 3D software, employing a cellular tessellation algorithm based on randomly distributed seed points. Conversely, the Schwarz models were developed based on Triply Periodic Minimal Surface (TPMS) functions, while the Diamond models were constructed to adhere to a regular lattice architecture using SolidWorks software. The CAD representations of these designed architectures and their corresponding unit cells are illustrated in Figure 1.

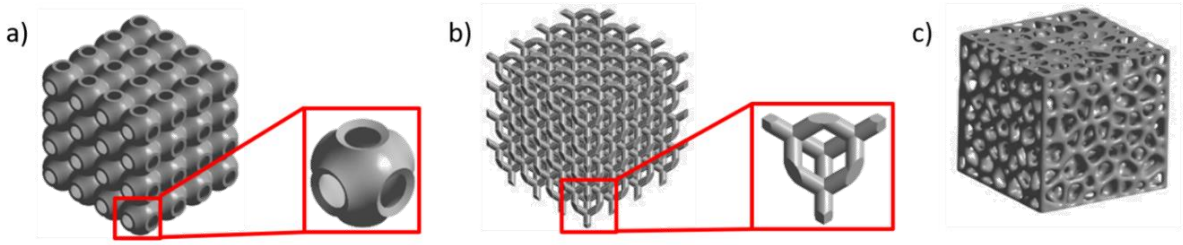


Figure 1. CAD model of three groups of scaffolds with related unit cells (60% porosity): a) Schwarz, b) Diamond, and c) Voronoi

To ensure comparability across all groups, each scaffold model was confined within a standard cubic volume measuring 15 mm × 15 mm × 15 mm. Four distinct theoretical porosity levels (50%, 60%, 70%, and 80%) were targeted for each architecture, achieved by parametrically adjusting the strut thickness. Surface optimization and pre-fabrication mesh refinement of the designed models were conducted using nTop and Meshmixer software, after which the files were exported in STL format.

2.2. Fabrication of the Scaffolds

The scaffolds were fabricated utilizing a FlashForge Creator 3 Pro (FlashForge, China) FDM 3D printer. Commercial FlashForge PLA filament, a biocompatible thermoplastic polymer, served as the feedstock material.

Throughout the manufacturing process, critical printing parameters influencing geometric accuracy were maintained constant across all experimental groups. The nozzle diameter, layer height, printing speed, and nozzle temperature were set to 0.4 mm, 0.18 mm, 60 mm/s, and 210°C, respectively. To preserve the intrinsic porosity of the scaffold architecture, the infill density was set to 100%; however, to evaluate the self-supporting capability of the structures, no additional support material was employed.

2.3. Dimensional Accuracy and Characterization

The 'design fidelity' of the fabricated scaffolds was assessed through mass measurements and microscopic imaging techniques.

• **Mass Deviation Analysis:** Theoretical mass values calculated in the CAD environment were compared with physical mass values measured post-production using a precision balance. This comparison was used to determine the printer's accuracy in reproducing the designed void volume and to identify potential issues with material over-extrusion or under-extrusion.

3. RESULTS and DISCUSSION

3.1. Macroscopic Observation and Fabrication Success

The Voronoi, Schwarz, and Diamond scaffold architectures designed for this study were successfully fabricated via the FDM method across four distinct porosity levels, ranging from 50% to 80%. The general appearance of the specimens is presented in Figure 2.

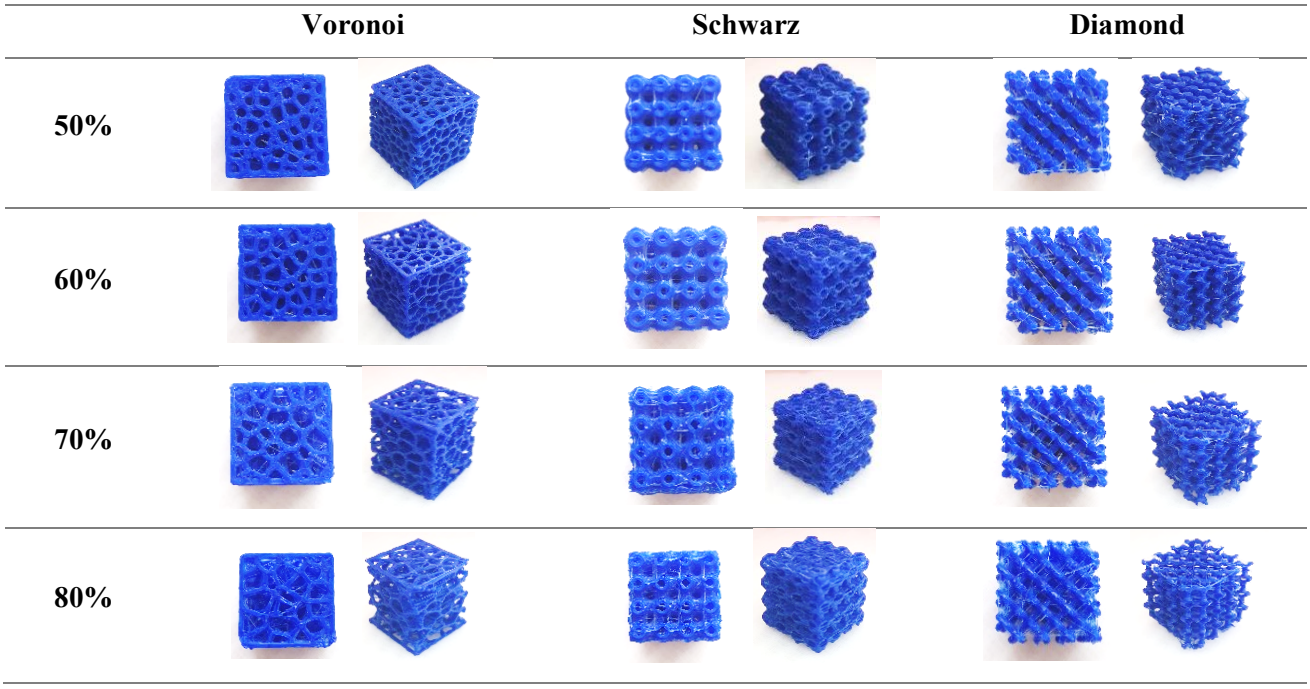


Figure 2. FDM fabricated PLA bone scaffold specimens.

Visual inspection of the specimens revealed that all models maintained their structural integrity and exhibited self-supporting characteristics. While the geometric regularity of the TPMS-based Schwarz and Lattice-based Diamond structures was clearly discernible to the naked eye, the stochastic and irregular nature of the Voronoi structures was distinctly prominent. Specifically, within the high-porosity Voronoi specimens, potential sagging issues associated with printing thin strut details were scrutinized at the macroscopic level; however, no major deformations compromising the integrity of the specimens were observed. Nevertheless, the dimensional accuracy underlying this apparent macroscopic success was subjected to a more detailed analysis through mass measurements.

3.2. Mass Deviation and Manufacturability Analysis

The manufacturability of the scaffolds was quantitatively assessed based on the percentage deviation between the theoretical mass calculated in the CAD environment and the actual mass measured after fabrication. While this difference is expected to be negligible in an ideal manufacturing scenario, deviations were observed due to the inherent nature of the FDM process. The obtained data are presented in Table 1.

Table 1. Comparison of theoretical and measured masses of the scaffolds showing deviation percentages

Geometry	Porosity (%)	Theoretical Mass (g)	Measured Mean Mass (g)	Difference (g)	Deviation (%)
Diamond	50	1,941	1,769	-0,172	-8,86
Diamond	60	1,553	1,596	0,043	2,77
Diamond	70	1,165	1,165	0	0
Diamond	80	0,776	0,779	0,003	0,39
Schwarz	50	1,941	1,7745	-0,1665	-8,58
Schwarz	60	1,553	1,5905	0,0375	2,41
Schwarz	70	1,165	1,1545	-0,0105	-0,9
Schwarz	80	0,776	0,827	0,051	6,57
Voronoi	50	1,941	2,022	0,081	4,17
Voronoi	60	1,553	1,5925	0,0395	2,54
Voronoi	70	1,165	1,2365	0,0715	6,14
Voronoi	80	0,776	0,854	0,078	10,05

Examination of Table 1 reveals that the geometric architecture has a decisive impact on fabrication accuracy:

Systematic Mass Increase in Voronoi Structures: All Voronoi scaffolds exhibited a measured mass exceeding the theoretical value (positive deviation). Notably, the deviation reached a critical level of 10.05% in the 80% porosity sample. This phenomenon can be attributed to the frequent retraction requirements of the printer nozzle, resulting from the stochastic and irregular nature of the Voronoi architecture. The oozing of residual molten PLA from the nozzle tip while traveling between irregular branches, or the formation of stringing, artificially increased the mass of the specimens.

Stability of TPMS and Lattice Structures: The regular Diamond (Lattice) and Schwarz (TPMS) architectures yielded more consistent results compared to Voronoi. A notable highlight is the Diamond structure at 70% porosity, which achieved perfect design fidelity with 0 deviation. The mathematically continuous and fluid surface nature of the Schwarz structure facilitated an uninterrupted toolpath (continuous path) for the nozzle, thereby stabilizing material extrusion and minimizing fabrication errors.

Negative Deviation at Low Porosity: Negative deviations (approximately 8.86% and -8.58%, respectively) were observed in the 50% porosity groups of the Diamond and Schwarz structures. This indicates a problem of incomplete filling of interlayer voids or under-extrusion associated with the increased material fill density in these denser structures.

4. CONCLUSION

This study comparatively investigated the manufacturability and dimensional fidelity of Voronoi (irregular), Schwarz (TPMS), and Diamond (Lattice) scaffold architectures designed for bone tissue engineering applications, fabricated using PLA via FDM technology. Deviations between the developed models and the physical specimens produced were evaluated through mass measurements and microscopic morphological analyses. In light of the findings, the following conclusions were drawn:

Design Fidelity: Thanks to their continuous and fluid geometric configurations, the TPMS-based Schwarz and Lattice-based Diamond architectures demonstrated superior compatibility with the FDM fabrication process, exhibiting significantly lower mass deviation rates compared to Voronoi structures. Notably, the Diamond structure achieved ideal manufacturing accuracy with a 0 deviation at 70% porosity.

Manufacturing Challenges of Voronoi: Despite their biomimetic advantages, Voronoi structures presented significant fabrication challenges due to their stochastic nature and inherent sharp directional changes. Mass increases reaching up to 10% and intense stringing defects.

Clinical Implication: In clinical scenarios where dimensional accuracy and pore patency are critical, prioritizing TPMS (specifically Schwarz) structures for FDM-based production represents a more reliable strategy to ensure the faithful translation of designed properties to the final product. For Voronoi architectures, alternative high-precision fabrication methods should be considered.

ACKNOWLEDGEMENTS

This research was funded by the Scientific and Technological Research Council of Turkey (TUBITAK) under project number 124M262.

REFERENCES

Abbasi, N., Hamlet, S., Love, R. M., and Nguyen, N.-T. (2020). Porous scaffolds for bone regeneration. Journal of Science: Advanced Materials and Devices, 5(1), 1-9.

Afshar, M., Anaraki, A. P., Montazerian, H., and Kadkhodapour, J. (2016). Additive manufacturing and mechanical characterization of graded porosity scaffolds designed based on triply periodic minimal surface architectures. Journal of the Mechanical Behavior of Biomedical Materials, 62, 481-494.

Brenne, F., Niendorf, T., and Maier, H. J. (2013). Additively manufactured cellular structures: Impact of microstructure and local strains on the monotonic and cyclic behavior under uniaxial and bending load. Journal of Materials Processing Technology, 213(9), 1558-1564.

Chalgham, A., Ehrmann, A., and Wickenkamp, I. (2021). Mechanical Properties of FDM Printed PLA Parts before and after Thermal Treatment. Polymers, 13(8), 1239.

Chen, Y., Liu, H., Shen, J., Gong, J., and Zhao, J. (2021). Compression Behavior of Diamond Lattice Structure and Its Hall-Petch Relationship. Advanced Engineering Materials, 23(3), 2001024.

Guo, X., Ding, J., Li, X., Qu, S., Song, X., Fuh, J. Y. H., Lu, W. F., and Zhai, W. (2022). Enhancement in the mechanical behaviour of a Schwarz Primitive periodic minimal surface lattice structure design. International Journal of Mechanical Sciences, 216, 106977.

Herath, B., Suresh, S., Downing, D., Cometta, S., Tino, R., Castro, N. J., Leary, M., Schmutz, B., Wille, M.-L., and Hutmacher, D. W. (2021). Mechanical and geometrical study of 3D printed Voronoi scaffold design for large bone defects. Materials & Design, 212, 110224.

Kuznetsov, V. E., Solonin, A. N., Urzhumtsev, O. D., Schilling, R., and Tavitov, A. G. (2018). Strength of PLA Components Fabricated with Fused Deposition Technology Using a Desktop 3D Printer as a Function of Geometrical Parameters of the Process. Polymers, 10(3), 313.

Lee, S. S., Du, X., Kim, I., and Ferguson, S. J. (2022). Scaffolds for bone-tissue engineering. Matter, 5(9), 2722-2759.

Poltue, T., Karuna, C., Khrueaduangkham, S., Seehanam, S., and Promoppatum, P. (2021). Design exploration of 3D-printed triply periodic minimal surface scaffolds for bone implants. International Journal of Mechanical Sciences, 211, 106762.

Tariverdian, T., Sefat, F., Gelinsky, M., and Mozafari, M. (2019). Scaffold for bone tissue engineering. In Handbook of Tissue Engineering Scaffolds: Volume One (pp. 189-209). Woodhead Publishing.

Triyono, J., Sukanto, H., Saputra, R. M., and Smaradhana, D. F. (2020). The effect of nozzle hole diameter of 3D printing on porosity and tensile strength parts using polylactic acid material. Open Engineering, 10(1), 762-768.

Wang, G., Shen, L., Zhao, J., Liang, H., Xie, D., Tian, Z., and Wang, C. (2018). Design and Compressive Behavior of Controllable Irregular Porous Scaffolds: Based on Voronoi-Tessellation and for Additive Manufacturing. ACS Biomaterials Science & Engineering, 4(2), 719-727.

ORAL PRESENTATION

Çiğ kıyma ve köfte kökenli *Klebsiella* spp. ve *Citrobacter* spp. izolatlarında antibiyotik direnç genleri ve biyofilm oluşumu

Emine Çelikoğlu[1,2*] (ORCID:https://orcid.org/0000-0002-5956-0008),
Ceren Başkan[3] (ORCID:https://orcid.org/0000-0001-7849-4459),
Önder İdil[2] (ORCID: https://orcid.org/0000-0003-1744-4006)

[1]Amasya Üniversitesi, Fen-Edebiyat Fakültesi, Biyoloji Bölümü, Amasya, Türkiye

[2]Amasya Üniversitesi, Eğitim Fakültesi, Matematik ve Fen Bilimleri Eğitimi Bölümü, Amasya, Türkiye

[3]Amasya Üniversitesi, Sağlık Hizmetleri Meslek Yüksekokulu, Amasya, Türkiye

[*]Sorumlu yazar e-mail: emine.turk@amasya.edu.tr

Özet

Et ve et ürünlerinin *Klebsiella* spp. ve *Citrobacter* spp. ile kontaminasyonu, bu bakterilerin antimikrobiyal direnç ve biyofilm oluşturma yetenekleri nedeniyle önemli bir halk sağlığı tehdidi oluşturmaktadır. Bu çalışmanın amacı, Amasya ilindeki market ve restoranlardan toplanan çiğ kıyma ve köfte örneklerinden izole edilen *Klebsiella* spp. ve *Citrobacter* spp. izolatlarının biyofilm oluşturma kapasiteleri ile β-laktamaz direnç genlerinin (*blaTEM*, *blaSHV*, *blaCTX-M*) varlığını araştırmaktır. Toplam 51 izolat (16 *Klebsiella* spp., 35 *Citrobacter* spp.) biyokimyasal testlerle identifiye edilmiştir. Biyofilm oluşumu, Kongo Kırmızı Agar (CRA) testi ve mikrotitrasyon yöntemi ile değerlendirilmiş; β-laktamaz genlerinin varlığı ise Polimeraz Zincir Reaksiyonu (PZR) ile tespit edilmiştir. Bulgulara göre, CRA testi *Klebsiella* spp. izolatlarının %75'inde pozitif sonuç verirken, *Citrobacter* spp. izolatlarının hiçbiri pozitif sonuç vermemiştir. Mikrotitrasyon yöntemi ise daha detaylı bir profil ortaya koymuştur. *Klebsiella* spp. izolatlarının %87.5'i (zayıf, orta, yüksek) biyofilm oluşturma kapasitesi sergilerken, bu oran *Citrobacter* spp. izolatlarında %100 olarak bulunmuştur. *Citrobacter* spp. izolatlarının %14.3'ü yüksek düzeyde biyofilm oluştururken, *Klebsiella* spp.'da bu oran %12.5 olarak tespit edilmiştir. Moleküler analizler, antibiyotik direnci açısından çarpıcı sonuçlar göstermiştir. İncelenen tüm izolatlarda (%100) *blaTEM* geni saptanmıştır. *blaSHV* geni *Klebsiella* spp. ve *Citrobacter* spp. izolatlarında sırasıyla %87.5 ve %94.3 gibi oldukça yüksek oranlarda tespit edilmiştir. *blaCTX-M* geni ise yalnızca *Citrobacter* spp. izolatlarının %11.4'ünde belirlenmiştir. Sonuç olarak, çalışılan et örneklerinden izole edilen *Klebsiella* spp. ve *Citrobacter* spp. suşlarının yüksek oranlarda biyofilm oluşturma yeteneğine ve yaygın β-laktamaz gen varlığına sahip olduğu ortaya konmuştur. Özellikle tüm izolatlarda *blaTEM* geninin bulunması, bu gıdaların halk sağlığı ve gıda güvenliği açısından potansiyel bir risk oluşturduğuna ve antimikrobiyal direnç yayılımında rezervuar görevi görebileceğine işaret etmektedir.

Anahtar Kelimeler: *Klebsiella* spp., *Citrobacter* spp., Biyofilm, β-Laktamaz Genleri

Antibiotic resistance genes and biofilm formation in *Klebsiella* spp. and *Citrobacter* spp. isolates from raw ground meat and meatballs

Abstract

The contamination of meat and meat products with *Klebsiella* spp. and *Citrobacter* spp. poses a significant public health threat due to their antimicrobial resistance and biofilm-forming abilities. This study aimed to investigate the biofilm formation capacity and the presence of β-lactamase resistance genes (*blaTEM, blaSHV, blaCTX-M*) in *Klebsiella* spp. and *Citrobacter* spp. isolates obtained from raw minced meat and meatball samples collected from markets and restaurants in Amasya province. A total of 51 isolates (16 *Klebsiella* spp., 35 *Citrobacter* spp.) were identified by biochemical tests. Biofilm formation was assessed using the Congo Red Agar (CRA) test and the microtiter plate method; the presence of β-lactamase genes was detected by Polymerase Chain Reaction (PCR). According to the findings, the CRA test yielded positive results for 75% of the *Klebsiella* spp. isolates, while none of the *Citrobacter* spp. isolates tested positive. The microtiter plate method revealed a more detailed profile. While 87.5% of the *Klebsiella* spp. isolates exhibited biofilm-forming capacity (weak, moderate, or strong), this rate was

100% for the *Citrobacter* spp. isolates. Among the *Citrobacter* spp. isolates, 14.3% were strong biofilm producers, whereas this rate was 12.5% for *Klebsiella* spp. Molecular analyses showed striking results regarding antibiotic resistance. The *blaTEM* gene was detected in all isolates (100%) examined. The *blaSHV* gene was found at very high rates in *Klebsiella* spp. and *Citrobacter* spp. isolates, at 87.5% and 94.3%, respectively. The *blaCTX-M* gene was identified only in 11.4% of the *Citrobacter* spp. isolates. In conclusion, it was demonstrated that the *Klebsiella* spp. and *Citrobacter* spp. strains isolated from the meat samples studied possessed a high capacity for biofilm formation and a high prevalence of β-lactamase genes. The detection of the *blaTEM* gene in all isolates, in particular, indicates that these foods pose a potential risk to public health and food safety and could act as a reservoir for the spread of antimicrobial resistance.

Keywords: *Klebsiella* spp., *Citrobacter* spp., Biofilm, β-Lactamase genes

GİRİŞ

Et ve et ürünlerinin *Klebsiella* spp. ve *Citrobacter* spp. ile kontaminasyonu, özellikle bu bakterilerin patojenitesi ve antimikrobiyal direnç özellikleri göz önüne alındığında, giderek artan bir halk sağlığı sorunu olarak değerlendirilmektedir. Her iki bakteri cinsi de gıda üretim ortamlarında yaygın biçimde bulunabilmekte ve antimikrobiyal direnç genlerini edinme, koruma ve yayma kapasiteleriyle öne çıkmaktadır. Bu durum, gıda güvenliği zincirinin bütün aşamalarında risklerin yeniden değerlendirilmesini gerekli kılmaktadır (Madhup ve ark., 2021; Enferad ve Mahdavi, 2021).

Özellikle *Klebsiella pneumoniae*, çeşitli gıda maddelerinde, işlenmiş et ürünleri dâhil olmak üzere, sık karşılaşılan bir kontaminanttır ve birçok çalışmada çok ilaca dirençli (MDR) suşların varlığı bildirilmiştir. Polonya'da yürütülen bir araştırmada, işlenmiş et örneklerinde *K. pneumoniae*'nin yüksek prevalansı belirlenmiş ve izole edilen suşların büyük bölümünün çoklu antibiyotik direnci gösterdiği ortaya konmuştur (Madhup ve ark., 2021). Benzer şekilde İran'da gerçekleştirilen çalışmalar, *K. pneumoniae*'nin çiğ süt ve süt ürünlerini de kontamine edebildiğini ve bu kontaminasyonun gıda kaynaklı hastalıklar üzerinde önemli etkiler oluşturduğunu göstermiştir (Enferad ve Mahdavi, 2021).

Citrobacter spp. türleri, özellikle *Citrobacter freundii*, son yıllarda önemli gıda kaynaklı fırsatçı patojenler olarak öne çıkmıştır. Et ve diğer gıda ürünlerinden düzenli olarak izole edilen bu bakteriler, çeşitli antibiyotiklere direnç kazandıran genetik belirteçleri taşıyabilmektedir (Witaningrum ve ark., 2022). Plazmid aracılı direnç faktörlerinin varlığı, bu bakterilerin farklı ortamlarda hızla yayılabilmesine ve direnç özelliklerini diğer Enterobacteriaceae üyelerine aktarabilmesine olanak sağlamaktadır (Husna ve ark., 2023; Cortés-Sánchez ve ark., 2023).

β-laktamaz genlerinin (ör. *blaSHV, blaTEM, blaCTX-M*) varlığı *Klebsiella* spp. ve *Citrobacter* spp. türlerinde antibiyotik direnç profilinin temel belirleyicileri arasında yer almaktadır. *K. pneumoniae* suşlarında genişlemiş spektrumlu β-laktamaz (GSBL) üretiminin yaygın olduğu, özellikle *blaSHV* ve *blaCTX-M* genlerinin et kaynaklı izolatlarda yüksek oranda tespit edildiği bildirilmektedir (Junaid ve ark., 2022; Silva ve ark., 2025). *Citrobacter* spp. türlerinde de GSBL üretiminin artmakta olduğu ve bu bakterilerin tarımsal üretimden tüketiciye kadar uzanan süreçte direnç genlerinin rezervuarı hâline gelebileceği ifade edilmektedir (Witaningrum ve ark., 2022; Husna ve ark., 2023). Gıda kaynaklı bu bakterilerin oluşturduğu risk, yalnızca kontaminasyonun yaygınlığından değil, aynı zamanda bu bakterilerin çok ilaca dirençli enfeksiyonlara neden olabilme potansiyelinden kaynaklanmaktadır. MDR fenotipine sahip suşların varlığı, özellikle gastrointestinal enfeksiyonların tedavisini zorlaştırmakta ve halk sağlığı açısından ek önlemleri gerekli kılmaktadır (Beamud ve ark., 2023). Bu nedenle, et ve et ürünlerinde *Klebsiella* spp. ve *Citrobacter* spp. türlerinin varlığını, biyofilm oluşum kapasitesini ve direnç mekanizmalarını izlemeye yönelik moleküler ve klasik yöntemleri kapsayan kapsamlı sürveyans programlarının geliştirilmesi büyük önem taşımaktadır (Bneed ve ark., 2025).

Türkiye'deki yerel gıda pazarlarında ve Amasya yöresinde, bu bakterilerin biyofilm oluşturma kapasiteleri ve direnç genleri konusunda daha fazla çalışmaya ihtiyaç duyulmaktadır. Bu çalışmanın amacı Amasya İli yerel market ve restoranlarında satışa sunulan çiğ kıyma ve köfte örneklerinden izole edilen *Klebsiella* spp. ve *Citrobacter* spp. izolatlarında biyofilm oluşumunun fenotipik olarak, β-laktamaz gen direnç genlerinin ise moleküler yöntemlerle değerlendirilmesidir.

MATERYAL VE METOT

2.1. Örnek Toplama ve Bakteriyel İzolasyon

Çalışmada kullanılan toplam 50 adet çiğ kıyma ve köfte örneği, Amasya ilindeki yerel market ve restoranlardan Eylül 2025 tarihinde temin edilmiştir. Her bir örnekten alınan 10 gram, 90 mL steril %0.1'lik tamponlanmış peptonlu su içinde homojenize edilerek 1:10'luk bir başlangıç dilüsyonu hazırlanmıştır. Hazırlanan bu süspansiyondan alınarak Chromocult Coliform Agar (Merck Milipore 110426) besiyerine yayma yöntemiyle ekim yapılmıştır. Plakalar 37°C'de 24 saat süreyle inkübe edilmiştir. İnkübasyon sonucunda, besiyerinin önerdiği şekilde kromojenik özelliklerine dayanarak; pembe renkli koloniler *Citrobacter* spp., mavi renkli koloniler ise *Klebsiella* spp. olarak ön tanı almış ve saf kültür elde etmek amacıyla Tryptic Soy Agar (TSA) besiyerine pasajlanmıştır.

2.2. Biyokimyasal İdentifikasyon

Saf kültürlerden elde edilen izolatların tanımlanması için bir dizi konvansiyonel biyokimyasal test gerçekleştirilmiştir. Testler, standart mikrobiyolojik prosedürlere uygun olarak yürütülmüştür. Kullanılan testler şunlardır; MacConkey Agar, Üre Agar, Triple Sugar Iron (TSI) Agar ve IMViC Testleri.

2.3. Biyofilm Oluşum Yeteneğinin Belirlenmesi

2.3.1. Kongo Kırmızısı Agar (CRA) Testi

İzolatların ekzopolisakkarit (slime) üretim yetenekleri, %0.08 Kongo kırmızısı ve %5 sükroz içeren Brain Heart Infusion (BHI) agar besiyeri kullanılarak değerlendirilmiştir. İnoküle edilen plakalar 37°C'de 24 saat inkübe edilmiştir. İnkübasyon sonunda siyahımsı, kuru ve kristalize koloni görünümü slime üretimi pozitif, pembe-beyaz renkli koloniler ise slime üretimi negatif olarak değerlendirilmiştir.

2.3.2. Mikrotitrasyon Plak Yöntemi ile Kantitatif Biyofilm Analizi

Biyofilm oluşumunun kantitatif olarak belirlenmesi için kristal viyole (KV) boyama yöntemi uygulanmıştır. Gece boyu (18-24 saat) besiyerinde geliştirilen bakteriyel kültürlerin optik dansiteleri (OD) 600 nm dalga boyunda ölçülerek OD600=0.1 olacak şekilde seyreltilmiştir. Hazırlanan bu süspansiyondan 96 kuyucuklu mikrotitrasyon plaklarına 20 µL eklenmiş ve üzerine 180 µL %1'lik glikozlu TSB ilave edilerek toplam 200 µL'lik hacim sağlanmıştır. Steril besiyeri içeren kuyucuklar negatif kontrol olarak kullanılmıştır. Plaklar 37°C'de 24 saat statik olarak inkübe edilmiştir. İnkübasyon sonunda, kuyucuklardaki süpernatantlar dikkatlice uzaklaştırılmış ve yapışmayan hücreleri temizlemek için kuyucuklar steril fizyolojik tuzlu su ile üç kez yıkanmıştır. Plaklar oda sıcaklığında 15 dakika kurumaya bırakılmıştır. Kuruyan biyofilmler 200 µL %99'luk metanol ile 15 dakika süreyle fikse edilmiştir. Metanol uzaklaştırıldıktan sonra plaklar tekrar kurutulmuş ve biyofilmler 200 µL %0.1'lik (a/h) kristal viyole çözeltisi ile 20 dakika boyanmıştır. Fazla boya, plaklar steril distile su ile yıkanarak uzaklaştırılmıştır. Bağlanan kristal viyole, 200 µL etanol:aseton (80:20) çözeltisi ile çözündürülmüştür. Çözeltinin optik dansitesi, mikroplaka okuyucu cihazı (Multiscan GO, Thermo Scientific) kullanılarak 570 nm dalga boyunda ölçülmüştür. Deney 3 tekrar şeklinde gerçekleştirilmiştir. Biyofilm üretimi, negatif kontrolün optik dansite (OD) ortalaması referans alınarak sınıflandırılmıştır. Eşik değer (ODc), negatif kontrollerin ortalama OD'sinin üç standart sapma üstü olarak tanımlanmıştır. İzolatlar, bu değere göre aşağıdaki şekilde kategorize edilmiştir: biyofilm üretmeyen ($OD \leq ODc$), zayıf biyofilm üreticisi ($ODc < OD \leq 2xODc$), orta derecede biyofilm üreticisi ($2xODc < OD \leq 4xODc$) ve kuvvetli biyofilm üreticisi ($4xODc < OD$).

2.4. Moleküler Analizler

2.4.1. Genomik DNA İzolasyonu

İzolatların genomik DNA'ları, modifiye edilmiş bir kaynatma yöntemi ile ekstrakte edilmiştir. TSA'da 24 saat boyunca üretilen taze bakteriyel kültürlerden bir öze dolusu, 100 µL nükleaz içermeyen steril distile su içine süspansiyon haline getirilmiştir. Süspansiyon, kuru blok ısıtıcıda 95°C'de 10 dakika boyunca inkübe edilerek hücre lizisi sağlanmıştır. Ardından, örnekler 12.000 xg'de 10 dakika santrifüjlenmiş ve süpernatant, polimeraz zincir reaksiyonu (PZR) için şablon DNA olarak kullanılmak üzere alınmıştır.

2.4.2. β-Laktamaz Genlerinin PZR ile Tespiti

blaTEM, *blaSHV* ve *blaCTX-M* gen varlığı, spesifik primerler kullanılarak polimeraz zincir reaksiyonu (PZR) ile araştırılmıştır (Tablo 1). PZR reaksiyonları, 25 µL'lik bir hacimde gerçekleştirilmiştir. Reaksiyon karışımı, 1X PZR tamponu, 2 mM dNTP karışımı, 3.4 pmol her bir primer, 2.5 mM $MgCl_2$, 1 U Taq DNA polimeraz ve 1 µL şablon DNA içermiştir. Amplifikasyon, bir termal döngür cihazında (TurboCycler Lite 9020, Blue-Ray, Biotech) aşağıdaki protokole uygun olarak yapılmıştır: 95°C'de 5 dakika ilk denatürasyon; ardından 94°C'de 1 dakika, 56°C'de 40 saniye (*blaTEM* ve *blaCTX-M*) veya 58°C'de (*blaSHV*) 40 saniye, 72°C'de 1 dakika olmak üzere 30 döngü; ve son olarak 72°C'de 10 dakika son uzatma. Amplifiye olan PZR ürünleri, %1'lik (a/h) agaroz jel elektroforezinde, 1X TAE tamponu içinde, 80 V sabit voltajda yaklaşık 1 saat süreyle yürütülmüştür. DNA bantları, jel redörü içerisine eklenen etidyum bromür ile boyanmış ve UV transillüminatör altında görüntülenmiştir. Bantların molekül ağırlıkları, 100 bp'lik DNA markır ile karşılaştırılarak doğrulanmıştır.

Tablo 1. *Klebsiella* spp. ve *Citrobacter* spp.'de β-laktamaz genlerinin tespiti için kullanılan primerler

Primer adı	Primer dizisi (5'-3')	Amplikon (bp)	Kaynak
blaCTX-M F	TTTGCGATGTGCAGTACCAGTAA	544	Edelstein ve ark., 2003
blaCTX-M R	CGATATCGTTGGTGGTGCCCATA		
blaTEM F	GAGTATTCAACATTTCCGTGTC	800	Edelstein ve ark., 2003
blaTEM R	TAATCAGTGAGGCACCTATCTC		
blaSHV F	AAGATCCACTATCGCCAGCAG	231	Edelstein ve ark., 2003
blaSHV R	ATTCAGTTCCGTTTCCCAGCGG		

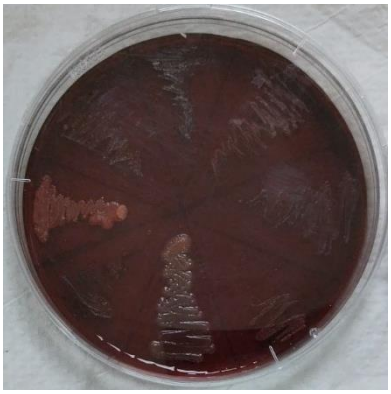
BULGULAR

İzolasyon ve Biyokimyasal İdentifikasyon

İzolasyon çalışması sonucunda, 16'sı *Klebsiella* spp. ve 35'i *Citrobacter* spp. olmak üzere toplam 51 izolat elde edilmiştir. Bu sonuçlara göre, izole edilen türlerin prevalansı %31.4 *Klebsiella* spp. ve %68.6 *Citrobacter* spp. olarak hesaplanmıştır. *Klebsiella* spp. izolatlarının (n=16) biyokimyasal karakterizasyonu, bu cins için beklenen tipik profille uyumlu sonuçlar vermiştir. Tüm izolatlar MacConkey Agar'da pembe koloniler oluşturmuş ve üre agarın rengini pembeye dönüştürerek pozitifleştirmiştir. IMViC test profili incelendiğinde, tüm *Klebsiella* spp. izolatlarının - + - + (İndol negatif, Metil Kırmızısı pozitif, Voges-Proskauer negatif, Sitrat pozitif) şeklinde sonuç verdiği belirlenmiştir. Triple Sugar Iron Agar'da izolatların 14'ü (%87.5) hem eğik yüzey hem de dip kısmında sarı renk oluşturarak glukoz, laktoz ve sükrozu tamamen fermente ettiğini göstermiş, iki izolatta (%12.5) ise glukoz fermentasyonuna bağlı dip kısmının sarı, laktoz/sükroz fermentasyonunun olmamasına bağlı eğik yüzeyin kırmızı kaldığı atipik bir reaksiyon gözlemlenmiştir. *Citrobacter* spp. izolatları (n=35) ise benzer bir biyokimyasal profil sergilemiştir. Tüm *Citrobacter* spp. izolatları MacConkey Agar'da pembe koloni oluşturmuş ve üre agarda pozitif reaksiyon vermiştir. IMViC test profili aynı şekilde - + - + olarak belirlenmiştir. Triple Sugar Iron Agar testinde ise tüm *Citrobacter* spp. izolatları (%100) hem eğik yüzey hem de dip kısmında sarı renk oluşturmuştur.

Biyofilm Oluşum Yeteneğinin Belirlenmesi

Bu çalışmada, izolatların slime oluşturma potansiyelini değerlendirmek için kullanılan CRA testi, *Klebsiella spp.* ve *Citrobacter spp.* cinsleri arasında farkı ortaya koymuştur. *Klebsiella* spp. izolatlarının 12'sinde (%75) CRA testi pozitif sonuç verirken, *Citrobacter* spp. izolatlarının tamamı (35/35, %100) negatif olarak değerlendirilmiştir (Şekil 1 A ve B).


A


B

Şekil 1. A. *Klebsiella spp.* izolatlarının CRA görüntüsü **B.** *Citrobacter* spp. izolatlarının CRA görüntüsü

Mikrobiyal yüzeylere tutunma ve biyofilm oluşturma yeteneği, patojen bakterilerin virülansında ve kronik enfeksiyonların gelişiminde kritik bir faktördür. Bu çalışmada, *Klebsiella* spp. ve *Citrobacter* spp. cinslerine ait izolatların biyofilm oluşturma kapasiteleri mikrotitrasyon yöntemi kullanılarak değerlendirilmiştir. Değerlendirme sonuçlarına göre, *Klebsiella* spp. izolatları arasında biyofilm oluşumu dağılımı heterojendir. İncelenen 16 *Klebsiella* spp. izolatından 2'si (%12.5) biyofilm oluşturamazken, 2 izolat (%12.5) zayıf, 10 izolat (%62.5) orta düzeyde ve 2 izolat (%12.5) ise yüksek düzeyde biyofilm oluşturma kapasitesi sergilemiştir. Bu veriler, *Klebsiella* spp. izolatlarının yaklaşık %85,5'inin (zayıf, orta ve yüksek düzeyde pozitiflik toplamı) biyofilm oluşturabildiğini ortaya koymaktadır. *Citrobacter* spp. izolatlarında ise daha yüksek bir biyofilm oluşturma eğilimi gözlemlenmiştir. Toplam 35 *Citrobacter* spp. izolatının 14'ü (%40) zayıf, 16'sı (%45.7) orta ve 5'i (%14.3) yüksek düzeyde biyofilm oluşturmuştur. Mikrotitrasyon testi, *Citrobacter* spp. izolatlarının %80'inden fazlasının biyofilm oluşturduğunu açıkça göstermektedir.

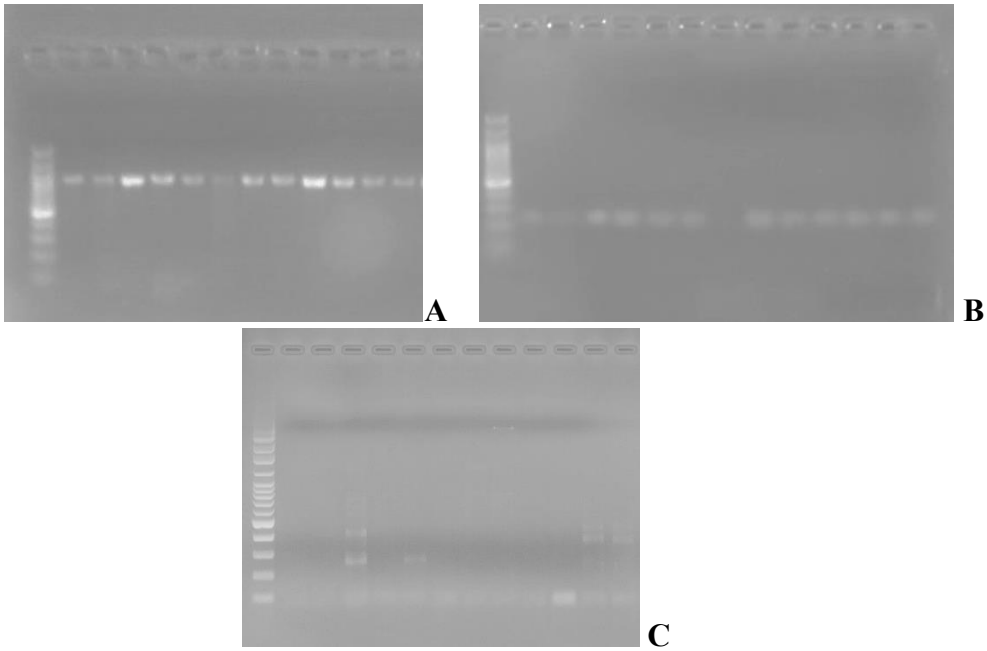
β-Laktamaz Genlerinin PZR ile Tespiti

PZR analizleri sonucunda, incelenen tüm bakteri izolatlarında (%100) *blaTEM* geni tespit edilmiştir. *Klebsiella* spp. izolatlarının %87.5'inde (14/16) ve *Citrobacter* spp. izolatlarının %94.3'ünde (33/35) *blaSHV* geni belirlenirken, *Citrobacter* spp. izolatlarının %11.4'ünde (4/35) *blaCTX-M* geni saptanmıştır. İzolatların β-laktamaz gen bölgelerine ait agaroz jel elektroforezi görüntüleri Şekil 2 (A-C) de gösterilmiştir.

TARTIŞMA

Bu çalışmada, Amasya ilinde satışa sunulan çiğ kıyma ve köfte örneklerinden izole edilen *Klebsiella* spp. ve *Citrobacter* spp. türlerinin biyofilm oluşturma kapasiteleri ile β-laktamaz direnç genleri sistematik biçimde değerlendirilmiştir. Elde edilen bulgular, her iki bakteri cinsinin de gıda zincirinde önemli bir kontaminasyon ve direnç rezervuarı olduğunu ortaya koymaktadır.

Literatürde çiğ etlerde β-laktamaz üreten Enterobacteriaceae üyelerinin yaygınlığı daha önce farklı çalışmalarla da ortaya konmuştur. Tekiner ve Özpınar (2016), çiğ et ürünlerinde GSBL üreten *Klebsiella* spp. türlerinin yüksek prevalans gösterdiğini ve diğer Enterobacteriaceae türleriyle birlikte *Citrobacter freundii* tespit edildiğini bildirmiştir. Bu bakterilerin gıda kaynaklı enfeksiyonlar için önemli bir tehdit oluşturduğu vurgulanmıştır. Türkiye'de, Tekirdağ köfte gibi geleneksel et ürünlerinin çeşitli patojen bakterilere ev sahipliği yaptığı bildirilmiş olup, sonuçlar bu ürünlerin gıda güvenliği mevzuatıyla belirlenen mikrobiyal limitleri aşabildiğini göstermektedir (Can ve ark., 2013). Polonya'da, Wasiński ve arkadaşları (2013) tarafından yapılan bir çalışma, mezbahalardan toplanan çiğ et örneklerinde GSBL üreten mikroorganizmaların varlığını bildirmiştir. Bu patojenlerin yaygınlığı, et tedarik zincirindeki uygun olmayan işleme, kesim uygulamaları ve hijyen koşulları ile ilişkilendirilebilir. Benzer şekilde Gwida ve ark. (2014), perakende çiğ etlerde *Klebsiella* spp. oranlarının yüksekliğini hijyenik olmayan kesim ve işlemeyle ilişkilendirmişlerdir. Ayrıca, Güney Çin'de yapılan çalışmalar, çiğ domuz etinden izole edilen genişlemiş spektrumlu β-laktamaz (GSBL) üreten *Klebsiella* spp. suşlarını karakterize etmiş ve etin antibiyotiğe dirençli bakteriler için bir rezervuar görevi gördüğünü doğrulamıştır (Li ve ark., 2016).



Şekil 2. A. Bazı izolatlara ait *blaTEM* PZR ürünlerinin agaroz jel elektroforezi görüntüsü. **B.** Bazı izolatlara ait *blaSHV* PZR ürünlerinin agaroz jel elektroforezi görüntüsü. **C.** Bazı izolatlara ait *blaCTX-M* PZR ürünlerinin agaroz jel elektroforezi görüntüsü.

Biyofilm oluşumu açısından elde edilen sonuçlar da hem gıda güvenliği hem de direnç ekolojisi bakımından kritik önemdedir. CRA testinde *Klebsiella* spp. izolatlarının %75'inin pozitif olmasına karşın *Citrobacter* spp. türlerinde hiçbir pozitifliğin görülmemesi, bu iki cinsin slime üretimi davranışlarında belirgin bir fark olduğunu göstermektedir. Ancak mikrotitrasyon testinde her iki cinste de %80–100 arasında biyofilm oluşturma kapasitesinin bulunması, CRA testinin biyofilm yeteneğini tek başına yansıtmakta yetersiz kalabileceğini göstermektedir. Özellikle *Citrobacter* spp. izolatlarının %14.3'ünde yüksek düzeyde biyofilm oluşturma yeteneği tespit edilmesi, bu türün gıda işleme yüzeylerinde uzun süre kalıcılık gösterebileceğini düşündürmektedir.

Biyofilm oluşumunun direnç gelişimiyle güçlü bir ilişkisi olduğu bilinmektedir. Biyofilm içindeki bakterilerde EPS matrisi nedeniyle antibiyotik penetrasyonu azalmakta, yatay gen transferi artmakta ve bu durum direnç genlerinin toplum içinde hızla yayılmasına yol açmaktadır (Poyrazoğlu ve Onur, 2023; Vuotto ve ark., 2017). Literatürde *K. pneumoniae*'nin tip 1 ve tip 3 fimbriyaları aracılığıyla yüzeylere güçlü adezyon sağladığı, bu nedenle dezenfektanlara ve antibiyotiklere karşı biyofilm modunda yüksek direnç gösterdiği belirtilmektedir (Schroll ve ark., 2010). *Citrobacter* spp. türlerinde de benzer şekilde curli lifleri ve selüloz içeren biyofilm matrisinin, mikroorganizmanın çevresel stres faktörlerine dayanımını artırdığı gösterilmiştir (Zogaj ve ark., 2003; Pereira ve ark., 2010). Çalışmamızdaki en güçlü bulgulardan biri, biyofilm oluşumu ile direnç genleri arasındaki paralelliktir. Hem *Klebsiella* spp. hem de *Citrobacter* spp. izolatlarında yüksek oranda biyofilm oluşumunun yanında *blaTEM* ve *blaSHV* genlerinin baskın şekilde bulunması, gıda zincirinde bu iki mekanizmanın birlikte hareket ettiğini düşündürmektedir. Bu durum, sadece et işleme ortamlarında değil, tüketici aşamasında da riskin devam ettiğini göstermektedir. Nitekim Manoharan ve ark. (2011), β-laktamaz genleri taşıyan Enterobacteriaceae suşlarının biyofilm içinde karbapenemlere dahi direnç gösterebildiğini bildirmiştir. Bizim çalışmamızda *Klebsiella* spp. izolatlarının %87.5'inde *blaSHV* geninin pozitif bulunması suşların genişlemiş spektrumlu direnç profili taşıyabileceğini göstermektedir. Özellikle incelenen tüm izolatlarda *blaTEM* geninin %100 oranında tespit edilmesi, çiğ et ürünlerinin antimikrobiyal direnç açısından kritik bir risk kaynağı olduğuna işaret etmektedir. *Citrobacter* spp. izolatlarının %94.3'ünde *blaSHV* ve %11.4'ünde *blaCTX-M* genlerinin saptanmış olması, bu türlerin de et ürünlerinde önemli bir direnç taşıyıcı olduğunu göstermektedir. Literatürde *Citrobacter freundii*'nin gıda kaynaklı antimikrobiyal direnç genlerini taşıdığı ve GSBL üretme kapasitesine sahip olduğu çeşitli çalışmalarla ortaya konmuştur (Shahid, 2010). Ayrıca Geser ve ark. (2012), gıda hayvanlarında *blaSHV* ve *blaTEM* genlerinin hızla yayılmasının, işlenmiş etlerin tüketiciye ulaşıncaya kadar dirençli bakteriler için bir rezervuar oluşturduğunu bildirmektedir.

Genel olarak değerlendirildiğinde, bu çalışma Amasya yöresindeki çiğ et ürünlerinde yüksek biyofilm potansiyeline sahip, direnç genleri taşıyan Enterobacteriaceae suşlarının varlığını net biçimde ortaya koymuştur. Bulgular hem yerel hem de ulusal düzeyde daha sıkı gıda güvenliği denetimlerine, moleküler sürveyans çalışmalarına ve et üretim işleme zincirinde hijyen protokollerinin güçlendirilmesine ihtiyaç olduğunu göstermektedir.

SONUÇ

Bu çalışmada, Amasya ilinde satışa sunulan çiğ kıyma ve köfte örneklerinden izole edilen *Klebsiella spp.* ve *Citrobacter spp.* türlerinin biyofilm oluşturma kapasiteleri ile β-laktamaz direnç gen profilleri ayrıntılı olarak değerlendirilmiştir. Elde edilen sonuçlar, her iki bakteri cinsinin de gıda güvenliği açısından yüksek risk taşıdığını ortaya koymaktadır. Özellikle tüm izolatlarda *blaTEM* geninin %100 oranında tespit edilmesi, bölgede satılan çiğ et ürünlerinin antimikrobiyal direnç açısından önemli bir rezervuar görevi gördüğünü göstermektedir. Buna ek olarak, *Klebsiella spp.* izolatlarında *blaSHV* geninin (%87.5) ve *Citrobacter spp.* izolatlarında hem *blaSHV* (%94.3) hem de *blaCTX-M* (%11.4) genlerinin bulunması, genişlemiş spektrumlu β-laktamaz üretimi açısından dikkate değer bir direnç yükünü işaret etmektedir.

Biyofilm oluşturma yeteneğinin hem *Klebsiella spp.* hem de *Citrobacter spp.* türlerinde yüksek oranlarda görülmesi, bu bakterilerin gıda işleme ekipmanlarında, tezgâhlarda ve dağıtım zinciri boyunca yüzeylerde uzun süre hayatta kalabilme potansiyeline sahip olduğunu göstermektedir. Özellikle mikrotitrasyon yöntemiyle elde edilen sonuçlara göre izolatların büyük bölümünün zayıf–orta–yüksek düzeyde biyofilm oluşturabilmesi, bu bakterilerin dezenfektanlara ve çevresel stres faktörlerine karşı direnç geliştirmesine katkıda bulunmakta ve kontaminasyonun süregen bir hale gelebileceğini düşündürmektedir.

Genel olarak değerlendirildiğinde, çiğ et ürünlerinde tespit edilen yüksek biyofilm potansiyeli ile β-laktamaz genlerinin yaygınlığı, tüketici sağlığı açısından ciddi bir risk oluşturmaktadır. Bu nedenle et üretim zincirinin tüm basamaklarında kesim, işleme, depolama ve satış aşamalarında hijyen uygulamalarının güçlendirilmesi, çapraz kontaminasyonun önlenmesine yönelik standartların sıkılaştırılması ve özellikle antimikrobiyal direnç açısından düzenli moleküler sürveyans çalışmalarının yürütülmesi büyük önem taşımaktadır. Ayrıca, gıda kaynaklı Enterobacteriaceae üyelerinde direnç genlerinin yayılımını sınırlamak için ulusal düzeyde kontrol stratejilerinin oluşturulması gerekmektedir.

Bu çalışma, Amasya yöresinde satılan çiğ et ürünlerinin direnç profili ve biyofilm potansiyeline ilişkin önemli bir veri seti sunmakta olup, ileride yapılacak daha geniş kapsamlı epidemiyolojik araştırmalar ve gıda güvenliği politikaları için temel oluşturmaktadır.

TEŞEKKÜR

Tekniker Melda Türk'e, çalışmanın veri toplama ve deneysel süreçlerindeki değerli katkıları için içten teşekkürlerimizi sunarız.

KAYNAKLAR

Beamud, B., Domínguez, M., Sevilla, J., Coque, T., García-González, N., Gónzález-Candelas, F., ... & Sánchez, V. (2023). Tracking the emergence and dissemination of a Klebsiella pneumoniae carbapenemase-producing K. pneumoniae ST307 clone in Spain: A nationwide surveillance study. The Lancet Microbe, 4(12), e1005-e1014. https://doi.org/10.1016/S2666-5247(23)00220-7

Bneed, Q., Abood, N., Faja, O., Alhasanawi, B., Sameer, Z., & Alzubaidy, M. (2025). Shared resistance and virulence of Klebsiella pneumoniae from human and meat sources: A one health perspective. Open Veterinary Journal, 15(9), 4162. https://doi.org/10.5455/ovj.2025.v15.i9.22

Can, Ö., Şahin, S., Erşan, M., & Harun, F. (2013). Sivas kofte and examination of microbiological quality. Biotechnology in Animal Husbandry, 29(1), 133-143. https://doi.org/10.2298/bah1301133c

Cortés-Sánchez, A., Salgado-Cruz, M., Díaz-Ramírez, M., Torres-Ochoa, E., & Espinosa-Chaurand, L. (2023). A review on food safety: The case of Citrobacter sp., fish and fish products. Applied Sciences, 13(12), 6907. https://doi.org/10.3390/app13126907

Edelstein, M., Pimkin, M., Palagin, I., Edelstein, I., & Stratchounski, L. (2003). Prevalence and molecular epidemiology of CTX-M extended-spectrum β-lactamase-producing Escherichia coli and Klebsiella pneumoniae in Russian hospitals. Antimicrobial agents and chemotherapy, 47(12), 3724-3732.

Enferad, E., & Mahdavi, S. (2021). Antibiotic resistance pattern and frequency of some beta lactamase genes in Klebsiella pneumoniae isolated from raw milk samples in Iran. Journal of the Hellenic Veterinary Medical Society, 71(4), 2455. https://doi.org/10.12681/jhvms.25925

Geser, N., Stephan, R., & Hächler, H. (2012). Occurrence and characteristics of extended-spectrum β-lactamase (ESBL) producing Enterobacteriaceae in food producing animals, minced meat and raw milk. BMC Veterinary Research, 8(1). https://doi.org/10.1186/1746-6148-8-21

Gwida, M., Hotzel, H., Geue, L., & Tomaso, H. (2014). Occurrence of Enterobacteriaceae in raw meat and in human samples from Egyptian retail sellers. International Scholarly Research Notices, 2014, 1-6. https://doi.org/10.1155/2014/565671

Husna, A., Rahman, M. M., Badruzzaman, A. T. M., Sikder, M. H., Islam, M. R., Rahman, M. T., ... & Ashour, H. M. (2023). Extended-spectrum β-lactamases (ESBL): challenges and opportunities. *Biomedicines*, *11*(11), 2937.

Junaid, K., Ejaz, H., Younas, S., Alanazi, A., Yasmeen, H., & Rehman, A. (2022). Detection of Klebsiella pneumoniae antibiotic-resistant genes: An impending source of multidrug resistance dissemination through raw food. Saudi Journal of Biological Sciences, 29(5), 3347-3353. https://doi.org/10.1016/j.sjbs.2022.02.020

Li, L., Ye, L., Yu, L., Zhou, C., & Meng, H. (2016). Characterization of Extended Spectrum B-Lactamase Producing Enterobacteria and Methicillin-Resistant Staphylococcus aureus Isolated from Raw Pork and Cooked Pork Products in South China. Journal of food science, 81(7), M1773-M1777.

Madhup, S., Shrestha, R., Panta, R., Chauguthi, L., Katuwal, N., & Shrestha, S. (2021). Prevalence of pathogenic bacteria in meat products and their antimicrobial resistance pattern. Annals of Clinical Chemistry and Laboratory Medicine, 4(1), 13-19. https://doi.org/10.3126/acclm.v4i1.42676

Manoharan, A., Premalatha, K., Chatterjee, S., & Mathai, D. (2011). Correlation of TEM, SHV and CTX-M extended-spectrum beta lactamases among Enterobacteriaceae with their in vitro antimicrobial susceptibility. Indian Journal of Medical Microbiology, 29(2), 161-164. https://doi.org/10.4103/0255-0857.81799

Pereira, A., Silva, T., Gomes, A., Araújo, A., & Giugliano, L. (2010). Diarrhea-associated biofilm formed by enteroaggregative Escherichia coli and aggregative Citrobacter freundii: A consortium mediated by putative F pili. BMC Microbiology, 10(1). https://doi.org/10.1186/1471-2180-10-57

Poyrazoğlu, E., & Onur, M. (2023). Isolation and identification of biofilm-forming bacteria in foods supplied for consumption in open-air market stalls: A case study in Aydin province. Trakya University Journal of Natural Sciences, 24(2), 77-84. https://doi.org/10.23902/trkjnat.1288588

Schroll, C., Barken, K., Krogfelt, K., & Struve, C. (2010). Role of type 1 and type 3 fimbriae in Klebsiella pneumoniae biofilm formation. BMC Microbiology, 10(1). https://doi.org/10.1186/1471-2180-10-179

Shahid, M. (2010). Citrobacter spp. simultaneously harboring bla CTX-M, bla TEM, bla SHV, bla ampC, and insertion sequences IS 26 and orf513: an evolutionary phenomenon of recent concern for antibiotic resistance. Journal of clinical microbiology, 48(5), 1833-1838.

Silva, V., Caniça, M., Rivière, R., Silva, A., Poeta, P., & Igrejas, G. (2025). Genomic characterization of multidrug-resistant and ESBL-producing Klebsiella pneumoniae isolated from healthy rabbits intended for human consumption. Microorganisms, 13(8), 1931. https://doi.org/10.3390/microorganisms13081931

Tekiner, İ., & Özpınar, H. (2016). Occurrence and characteristics of extended spectrum beta-lactamases-producing Enterobacteriaceae from foods of animal origin. Brazilian Journal of Microbiology, 47(2), 444-451. https://doi.org/10.1016/j.bjm.2015.11.034

Vuotto, C., Longo, F., Pascolini, C., Donelli, G., Balice, M., Libori, M., ... & Varaldo, P. (2017). Biofilm formation and antibiotic resistance in Klebsiella pneumoniae urinary strains. Journal of Applied Microbiology, 123(4), 1003-1018. https://doi.org/10.1111/jam.13533

Wasiński, B., Różańska, H., & Osek, J. (2013). Occurrence of extended spectrum β-lactamaseand ampc-producing escherichia coli in meat samples. Bulletin of the Veterinary Institute in Pulawy, 57(4), 513-517. https://doi.org/10.2478/bvip-2013-0089

Witaningrum, A., Wibisono, F., Permatasari, D., Effendi, M., & UGBO, E. (2022). Multidrug resistance-encoding gene in Citrobacter freundii isolated from healthy laying chicken in Blitar district, Indonesia. International Journal of One Health, 8(2), 161-166. https://doi.org/10.14202/ijoh.2022.161-166

Zogaj, X., Bokranz, W., Nimtz, M., & Römling, U. (2003). Production of cellulose and curli fimbriae by members of the family Enterobacteriaceae isolated from the human gastrointestinal tract. Infection and Immunity, 71(7), 4151-4158. https://doi.org/10.1128/iai.71.7.4151-4158.2003

ORAL PRESENTATION

Catalytic cottonization of hemp fibres at room temperature in the presence of a bimetallic iron oxide catalyst

Mustafa Yasin Aslan[1*] *(ORCID: https://orcid.org/0000-0002-4091-2114),*
Hatice Nur Kaya[1] (*ORCID: https://orcid.org/0009-0004-3963-6361*)

[1]Department of Chemical Engineering, Faculty of Engineering and Natural Sciences, Uşak University, 64200, Uşak, Türkiye

*Corresponding author email: mustafa.aslan@usak.edu.tr

Abstract

This study explores a low-energy way to prepare hemp fibres for textile use by bleaching them at room temperature with the help of a bimetallic iron oxide catalyst. Hemp normally requires strong chemicals and high energy because it contains large amounts of lignin and pectin. In this work, the fibres were first treated with a mild NaOH solution and then bleached with hydrogen peroxide, either with or without the catalyst. FT-IR results showed that the alkali step begins to remove unwanted plant materials, while the catalyst and hydrogen peroxide together remove much more lignin and expose the cellulose structure. Tests on hydrogen peroxide breakdown showed that it stays mostly unchanged without the catalyst but decomposes completely within a few hours when the catalyst is present. These results show that the catalyst makes it possible to bleach hemp fibres effectively at room temperature, offering a simpler and more environmentally friendly alternative to traditional high-temperature bleaching.

Keywords: Catalytic bleaching, hemp fiber, alkali treatment

INTRODUCTION

One of the major sustainability issues today is directly related to energy consumption across all manufacturing industries (Dursun and Yıldız, 2022; El-Kheir et al., 2014). The textile industry is no exception, as it is also highly energy intensive. One of the primary raw materials used in yarn production for clothing is natural fibres. To make natural fibres usable, they must undergo a bleaching process to remove unwanted compounds such as pectin, lignin, and other naturally occurring chemicals. In addition to significant energy consumption, bleaching also requires various chemicals to extract cellulose, which is the essential component of yarn. However, some of these bleaching agents are hazardous to the environment due to the harmful by-products they generate. Consequently, the high energy demand and extensive chemical use in bleaching natural fibres remain key challenges for the textile industry.

The bleaching process of some natural fibres, such as hemp, jute, and others from the bast fiber family, can be difficult in terms of obtaining cellulose because their lignin, pectin, and wax content is significantly higher than that of cotton. According to studies in the literature, the composition of a typical hemp plant includes approximately 60–80% cellulose, 7–15% hemicellulose, 1–9% pectin, and 1–10% lignin by mass (Tulaphol et al., 2021; Koohestani et al., 2019). The relatively high lignin content of hemp fibres causes difficulties in bleaching because it reduces the wettability of the structure, which plays a crucial role in the decomposition of lignin and pectin by bleaching agents. Due to that delignification of hemp fibres are difficult and costly, industrial application of hemp is restricted although its fibres are stronger than most of other natural fibres (Koohestani et al., 2019).

The traditional bleaching process is carried out at high temperatures (100–150 °C) and elevated pressures (3–4 bar) using oxidative chemicals such as hypochlorite, sodium sulfite, and hydrogen peroxide (Fattahi and Salehi, 2023; Dursun and Yıldız, 2022). These process conditions lead to significant energy consumption to obtain natural fibres primarily in cellulose form. Hypochlorite- and sulfite-based oxidants are major pollutants in industrial wastewater generated during bleaching. In contrast, hydrogen peroxide decomposes into water and oxygen, which are harmless

to downstream water systems (Farr et al.,2003). In addition, it seems that hydrogen peroxide prices can be comparable with the other bleaching agents as shown in Table 1.

Catalytic bleaching of natural fibres can be a good solution for yarn production with reduced energy consumption as the process is operated at room temperature and atmospheric pressure conditions. Some studies have shown that H_2O_2 can decompose, which is essential for the degradation of lignin and other materials in the structure of natural fibres- in the presence of catalytic materials such as transition metal oxides at lower temperatures (Pędziwiatr et al., 2018; Weiss, 1935; Lousada et al., 2013). The mechanism of the decomposition reaction occurs in a way that H_2O_2 molecules adsorb/interact with the metal oxides. As a result of interaction/surface reaction either ·OH or HO_2· radicals are produced according to the studies in the literature (Lin and Gurol, 1998). These types of reactions are known as Fenton-like reactions (Ensing et al., 2003; Andrade et al., 2009; Yang et al., 2016). The radicals that are produced through the catalytic decomposition of H_2O_2 directly attack the molecules in the structure of the natural fiber. As a result of the interaction, the degradation/oxidation of unwanted substances occurs. This characteristic of the H_2O_2 can offer an opportunity for carrying out the process with lower energy consumption.

Table 1. Price comparison of mostly used bleaching agents in textile industry

Chemical	Approx. Bulk Price (USD/MT)	References
Hydrogen Peroxide	$356 -797	İMARC Group, (2025)
Sodium Hypochlorite	$250–360	İNTRATEC, (2025)
Sodium Chlorite	$600–1,600	Made-in-China, (2025)
Sodium Sulfite	$2,000–4,600	Tridge, (2025)

In this study, the catalytic bleaching of hemp fibres and the decomposition behavior of H_2O_2 during the bleaching process were investigated. The influence of alkaline treatment and subsequent bleaching with H_2O_2 on lignin degradation, as well as on the structural and morphological changes of other fiber constituents such as cellulose, hemicellulose, and pectin, was examined using FT-IR spectroscopy. Additionally, the variation in H_2O_2 concentration throughout the bleaching process was monitored to assess the catalytic performance of the bimetallic oxide catalyst. The findings obtained under various experimental conditions are systematically presented and discussed in this contribution.

MATERIAL AND METHODS

Hemp was obtained from the producers. The hemp samples used in this study were subjected to mechanical opening after harvesting. H_2O_2 (Isolab, 35% w/w) was used as the bleaching agent. NaOH pellets (Merck, pure) were used as the pre-treatment (alkali) agent.

Bleaching without Catalyst

In order to obtain cellulose-based hemp fibres, two treatments were applied to the raw hemp materials. During the experiments, firstly alkali treatment was carried out inside NaOH baths. The alkali treatment bath was prepared with 300 mL of 0.2 M NaOH solution (Merck, pure). Prior to the alkali treatment, hemp fibres were cut to a length of 30 mm and weighed to 4-5 g. They were then treated in NaOH solution at 80 °C for 5 hours at a stirring speed of 300 rpm under atmospheric pressure. The temperature ramp from room temperature to 80 °C was determined as ca. 2 °C/min. After the pretreatment process, the fibres were washed several times with deionized water at room temperature.

After the alkali treatment, the bleaching of hemp fibres was carried out with H_2O_2 (Isolab, 35% w/w). The bleaching of hemp fibres in the presence of H_2O_2 at high temperature is considered as a reference treatment. The hemp fibres were bleached with 0.2 M 300 mL H_2O_2 at 80 °C, for one hour at a stirring rate of 300 rpm and under atmospheric pressure. The temperature ramp from room temperature to 80 °C was determined as ca. 2 °C/min. The bleached hemp fibres were washed with deionized water several times and dried overnight at room temperature.

Bleaching with Catalyst

To obtain cellulose by bleaching hemp fibres at room temperature and atmospheric pressure, a bimetallic catalyst was used. The other parameters of the experiments were the same as the experiments that were performed in the absence of a catalyst. Prior to catalytic bleaching, alkali treatment was performed with 0.2 M, 300 mL NaOH solution at 80 °C. After alkali treatment, hemp fibres were bleached in the presence 16 mg catalyst/L solution of 0.2 M H_2O_2. In addition, similar trials were performed to prove catalytic activity.

Kinetic Study

The decomposition of H_2O_2 with respect to time in the presence of bimetallic metal oxide catalyst were followed by titration of the bleaching solution with 0.03 M KMnO4 solution in acidic conditions at room temperature and under atmospheric pressure. Acidity of the titration solution was obtained with 2.5 M H_2SO_4. Titration was performed with 1 mL of bleaching solution, which contains H_2O_2, 25 mL of deionized water and 25 mL of 2.5 M H_2SO_4 solution.

Characterization

ATR-FTIR analyses were performed in a Perkin Elmer Spectrum Two spectrometer. 32 scans were recorded with 4 cm^{-1} resolution in the range of 4000–450 cm^{-1}. The change of amounts of components within the content of hemp fibres such as lignin, pectin, hemicellulose and cellulose compounds were detected by IR spectra of hemp fibres that were treated in different conditions.

RESULTS AND DISCUSSION

FT-IR Results

Comparison of untreated and NaOH & H_2O_2–treated hemp fibres reveals extensive chemical restructuring as shown in Figure 1. The treated fiber shows a broadened and slightly shifted O–H stretching band (3600–3200 cm^{-1}), consistent with increased hydrogen bonding due to removal of sterically hindering lignin and hemicellulose. The decline in C–H stretching at ~2920 and 2850 cm^{-1} suggests degradation of aliphatic lignin substituents. The 1730 cm^{-1} carbonyl band nearly disappears in the treated fiber, indicating efficient removal of hemicellulose acetyl groups and oxidation of lignin side-chain esters at high temperature. Aromatic skeletal vibrations at ~1600 and 1510 cm^{-1} are significantly reduced, confirming breakdown of lignin aromatic structures. The C–O–C asymmetric stretching at ~1160 cm^{-1} and the 1050–1030 cm^{-1} cellulose backbone peaks intensify and sharpen, while the peak centered at ~895 cm^{-1} becomes more prominent. Together, these changes point to high delignification and hemicellulose removal efficiencies and reveal a cellulose-enriched structure.

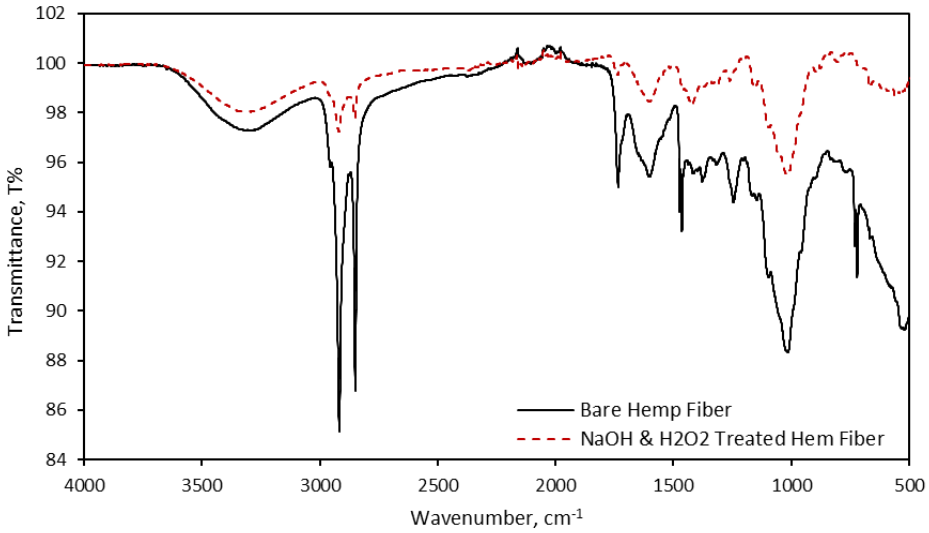


Figure 1. FT-IR spectra of bare (untreated) hemp fiber and hemp fiber after treatment with 0.2 M NaOH and 0.2 M H_2O_2 at 80 °C for 1 h.

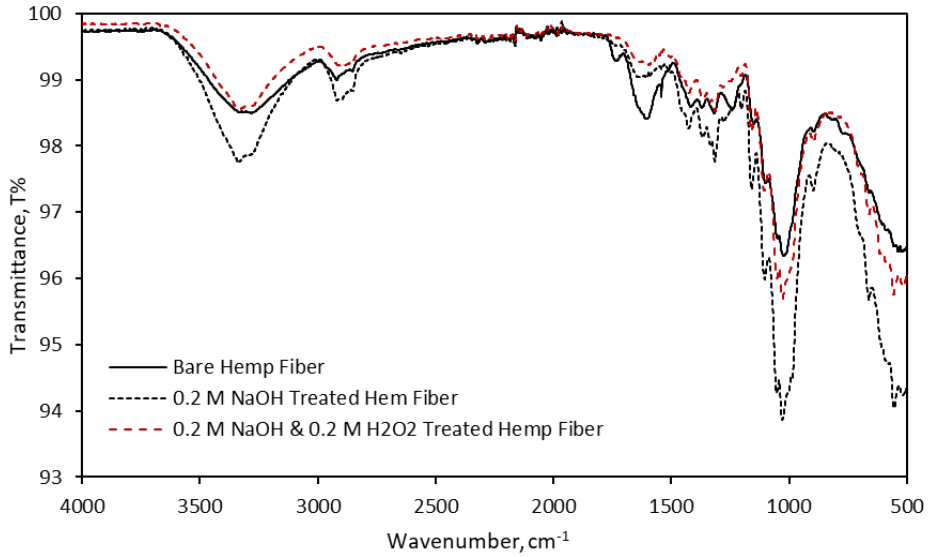


Figure 2. FT-IR spectra of bare hemp fiber (straight line), hemp fiber after treatment with 0.2 M NaOH at 80 °C (small gap - dashed line) and hemp fiber after consecutive treatments with 0.2 M NaOH at 80 °C and 0.2 M H_2O_2 at 25 °C in the presence of 16 mg bimetallic oxide catalyst (red-long gap dashed line).

The transition from bare fiber to NaOH-treated fiber to NaOH & H_2O_2-treated fiber shows a clear progression of lignocellulosic fraction removal as it can be seen clearly in Figure 2. NaOH treatment alone produces a moderate increase in the O–H stretching intensity and a noticeable decrease in the 1730 cm^{-1} carbonyl peak, indicating saponification of hemicellulose esters but limited oxidative lignin cleavage. Lignin aromatic peaks at ~1600 and ~1510 cm^{-1}, as well as the phenolic C–O band at ~1260 cm^{-1}, decrease but remain clearly visible after NaOH treatment. When H_2O_2 (with catalyst) is introduced after the NaOH step, these lignin-related bands undergo strong attenuation, demonstrating substantial aromatic ring disruption. The cellulose fingerprint peaks at 1160, 1100, and 1030 cm^{-1} become progressively sharper from NaOH to NaOH + H_2O_2, while the band at ~895 cm^{-1} intensifies, signaling improved cellulose accessibility and relative enrichment. The C–H stretching decrease and the overall flattening of the lignin-associated region in the H_2O_2 spectrum highlight the strong oxidative capability of the catalyst-assisted peroxide treatment

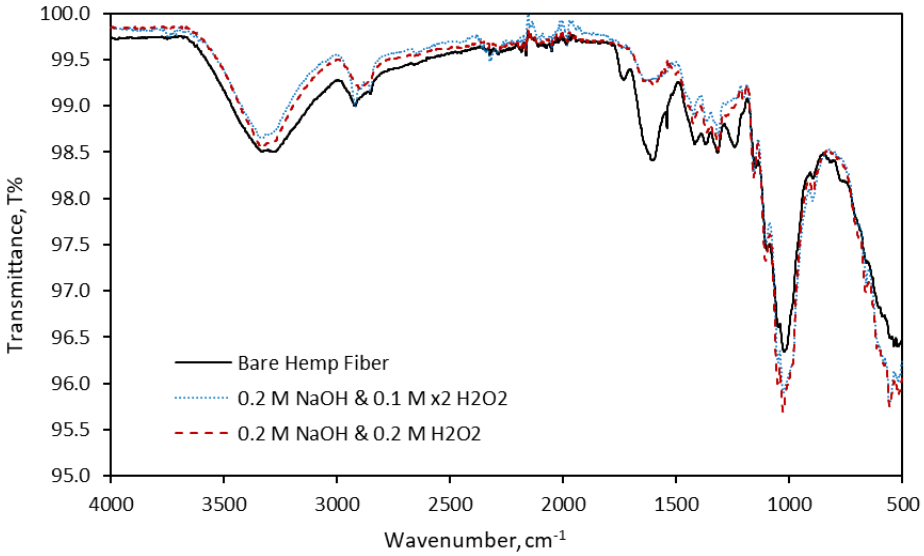


Figure 3. FT-IR spectra of: (i) untreated hemp fiber (solid line); (ii) hemp fiber treated sequentially with 0.2 M NaOH at 80 °C and 0.1 M H_2O_2 twice at 25 °C (short-dash line); and (iii) hemp fiber treated with 0.2 M NaOH at 80 °C followed by 0.2 M H_2O_2 at 25 °C (long-dash red line), all in the presence of 16 mg bimetallic oxide catalyst.

The FT-IR spectra, which is given in Figure 3, show consistent structural evolution of the hemp fiber after alkaline–peroxide treatments. Relative to the untreated fiber, both treated samples display an increase in the broad O–H stretching region at 3600–3200 cm^{-1}, indicating enhanced fiber swelling and greater exposure of cellulose hydroxyls following removal of matrix components. The C–H stretching bands at ~2920 and ~2850 cm^{-1} decrease in intensity for both peroxide-treated fibres, reflecting the loss of aliphatic side chains in lignin. The carbonyl peak at ~1730 cm^{-1}, arising from hemicellulose acetyl groups and lignin-bound esters, is strongly reduced in both treatments, with the most pronounced suppression observed in the 0.2 M H_2O_2 sample. Lignin aromatic ring vibrations at ~1510 cm^{-1} and C–O bands at ~1260 cm^{-1} also diminish progressively from the bare fiber to the two-step 0.1 M H_2O_2 treatment and most significantly in the 0.2 M H_2O_2 treatment. In the fingerprint region (1100–1000 cm^{-1}), cellulose-related C–O–C and C–O stretching bands become sharper and more intense with increasing oxidation strength, while the band at ~895 cm^{-1} becomes more distinct, confirming the increased exposure of the cellulose backbone. These observations indicate that NaOH initiates lignin and hemicellulose disruption, whereas the catalyst-assisted H_2O_2 steps produce deeper oxidative modification.

Across all three FT-IR comparisons, the combined results confirm that NaOH initiates structural loosening and partial removal of hemicellulose and lignin, while the catalyst-assisted H_2O_2 oxidation is responsible for most of the lignin degradation and deep purification of the hemp fiber. NaOH produces moderate reductions in the 1730 cm^{-1} carbonyl band and slight decreases in aromatic lignin signatures, consistent with ester cleavage and partial disruption of lignin–carbohydrate complexes. However, only upon introduction of H_2O_2 in the presence of the 16 mg catalyst do the spectra show strong suppression of the lignin aromatic bands (1600–1510 cm^{-1}), C–O–C lignin ether peaks (1270–1210 cm^{-1}), and aliphatic C–H bands (2920–2850 cm^{-1}), indicating oxidative scission of both aromatic rings and side chains. The broadening and strengthening of the O–H region across treatments suggests increasing exposure of cellulose hydroxyls as the matrix is removed. The fingerprint region further illustrates this trend: cellulose-associated peaks (1160–1030 cm^{-1}) sharpen progressively, and the band centered at 895 cm^{-1} becomes more defined, confirming enhanced cellulose accessibility. Notably, treatments with higher H_2O_2 concentration (0.2 M) consistently show the largest decreases in lignin-related peaks and the most pronounced cellulose band sharpening, demonstrating that oxidative delignification efficiency correlates directly with peroxide strength under catalytic conditions. Collectively, the three figures establish a clear mechanistic sequence: NaOH opens the structure and removes esters, while catalyst-assisted H_2O_2 drives deep lignin oxidation, resulting in a highly purified, cellulose-rich hemp fiber.



Figure 4. From left to right: untreated hemp fibres, hemp fibres treated with alkali, and hemp fibres treated with alkali followed by H_2O_2.

As seen in Figure 4 the evolution of bleaching states is in accordance with the found FT-IR results. The third picture from left shows that treating hemp fibres with alkali as well as H_2O_2 gives the best results in desired color and texture, while in the second picture from left it can be seen that while the results are better than untreated hemp fiber, they still lack the qualities of the two-times treated fiber.

Kinetic Results

The time-dependent decomposition of H_2O_2 under various conditions, both in the presence and absence of hemp fibres intended for bleaching, is presented in Figure 5. No significant change in H_2O_2 concentration was observed after approximately 4 hours, indicating that the solution reached a near-steady state. A similar experiment was also conducted using alkali-treated hemp fibres. Although a slightly greater decrease in H_2O_2 concentration was detected compared to the experiment performed without fibres, the extent of decomposition remained minimal overall.

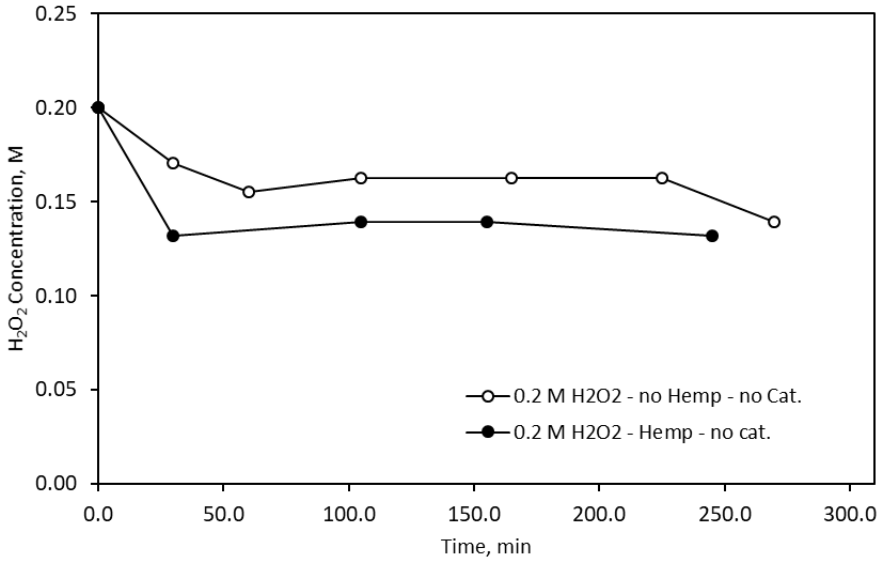


Figure 5. Variation of aqueous H_2O_2 concentration as a function of time, measured with and without hemp fibres at room temperature and atmospheric pressure

The change of concentration of H_2O_2 with time in bleaching solution was also followed in the presence of a bimetallic metal oxide catalyst as given in Figure 6. Two distinct experiments were performed which are decomposition of H_2O_2 in the presence and of absence of already alkali treated hemp fibres. It can be easily seen that the decomposition of H_2O_2 was completed in both experiments after almost 5 h. The experiment, which was performed in the absence of hemp fibres, was performed to check the influence of hemp fiber on the decomposition rate of H_2O_2. The results showed that decomposition rate was not a significant function of presence of hemp fibres.

To further examine the effect of initial H_2O_2 concentration on its decomposition rate, an experiment was conducted using a 1.0 M H_2O_2 solution in the presence of 40 mg of the bimetallic oxide catalyst. The time-dependent percentage decomposition of H_2O_2 is presented in Figure 7, along with results from analogous experiments performed with an initial concentration of 0.2 M H_2O_2 and 16 mg of catalyst. The findings indicate that, within the

experimental conditions employed, the initial concentration of H_2O_2 does not significantly influence its decomposition rate.

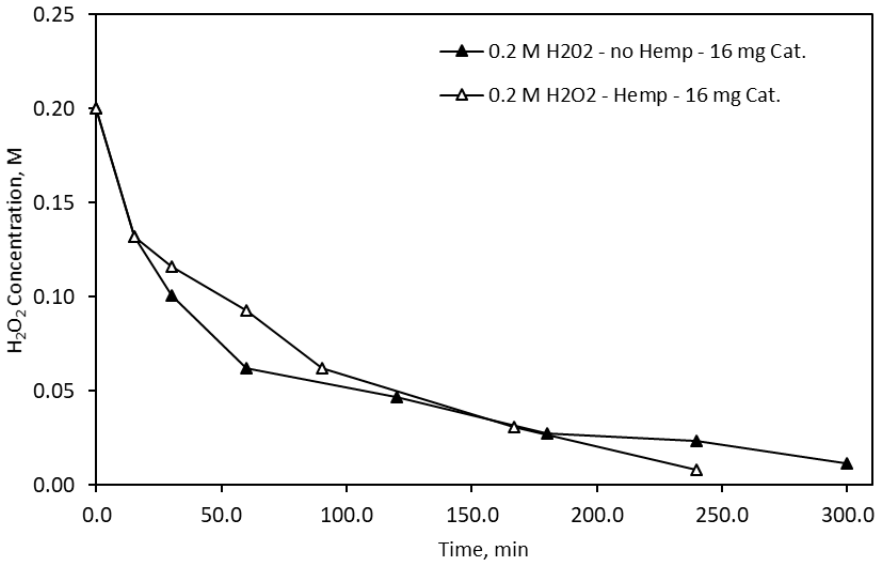


Figure 6. Variation of aqueous H_2O_2 concentration as a function of time, recorded both with and without hemp fibres, in the presence of 16 mg bimetallic oxide catalyst at room temperature and atmospheric pressure.

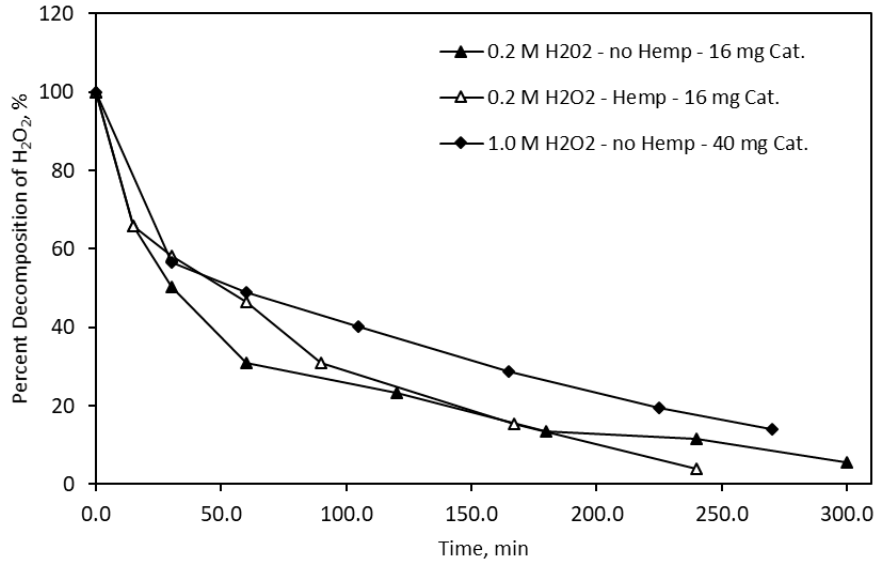


Figure 7. Percent decomposition of H_2O_2 with respect to initial concentration of H_2O_2 with respect to time in the presence of the bimetallic oxide catalyst at room temperature.

The decomposition behavior of H_2O_2 under the examined conditions provides insight into the dominant reaction pathways governing peroxide stability during hemp fiber bleaching. In the absence of the bimetallic oxide catalyst (Figure 5), Neither untreated nor alkali-treated hemp fibres produced a measurable catalytic effect, indicating that fiber components such as lignin fragments, phenolic groups, or trace metals do not significantly promote Fenton-like or peroxidase-type reactions (Wright et al., 2001). Upon addition of the bimetallic oxide catalyst (Figure 6), the decomposition of H_2O_2 accelerated markedly, reaching completion within 5 hours, demonstrating that heterogeneous catalysis dominates the reaction pathway. Such behavior is consistent with surface-mediated redox cycles in metal oxides, where adsorbed hydroperoxo and oxo intermediates undergo rapid electron-transfer-driven disproportionation (Lin and Gurol, 1998). The similar decomposition profiles in the presence and absence of alkali-treated fibres indicate that H_2O_2 consumption occurs primarily at the catalyst surface, with minimal contribution

from fiber-associated pathways (Plauck et al., 2016; Finocchiaro et al., 2023; Wang et al., 2018). Furthermore, varying the initial H_2O_2 concentration from 0.2 M to 1.0 M (Figure 7) did not significantly alter the decomposition kinetics, suggesting that the process proceeds under pseudo-first-order conditions and those catalyst surface sites remain far from saturation (Salem et al., 2000; Lousada et al., 2012). Collectively, these mechanistic insights confirm that the bimetallic oxide catalyst governs the decomposition of H_2O_2, while fiber-related reactions and solution-phase pathways play secondary roles under the bleaching conditions investigated.

CONCLUSION

The preliminary results of this study demonstrate that hemp fibres can be effectively bleached and prepared for textile applications using a catalyst-assisted hydrogen peroxide process operated entirely at room temperature. The FT-IR analyses clearly show that the alkali treatment loosens the fibre structure, removes some hemicellulose, and helps expose internal regions, but it does not remove enough lignin on its own. When hydrogen peroxide is added in the presence of the bimetallic iron oxide catalyst, far deeper changes occur. Lignin-related peaks decrease sharply, cellulose bands become sharper and more pronounced, and the overall fibre structure shifts toward a cleaner, cellulose-rich form suitable for cottonization.

Kinetic measurements support these findings. Without the catalyst, hydrogen peroxide remains largely stable and decomposes only slowly. With the catalyst, however, hydrogen peroxide breaks down in a moderate rate even at room temperature, showing that the reaction mainly occurs on the catalyst surface through a Fenton-like mechanism. The decomposition rate was not significantly influenced by the initial peroxide concentration or the presence of fibres, indicating that the catalyst controls the process and provides consistent performance.

Overall, this work shows that catalytic bleaching is a promising approach for producing cottonized hemp fibres in a more environmentally friendly and energy-efficient way. By allowing the process to occur at room temperature and atmospheric pressure, it has the potential to reduce production costs, decrease environmental impact, and encourage the broader use of hemp as a sustainable raw material in the textile industry. Future studies may further improve catalyst performance, optimise process times, or explore scaling strategies for industrial applications.

ACKNOWLEDGEMENTS

The authors would like to express their gratitude to Prof. Dr Serdar Akbayrak for providing bimetallic oxide catalysts, Doç. Dr. Eren Öner for providing hemp samples, Kübranur Ekin and Seher Kaya for contributing to the initial stages of the study for hemp bleaching.

REFERENCES

Abou El-Kheir, A., Haggag, K., Mowafi, S. I., & El-Sayed, H. (2014). Microwave-Assisted Bleaching of Wool Fabrics. Journal of Natural Fibres, 12(2), 97–107. https://doi.org/10.1080/15440478.2014.901202

Andrade, A. L., Souza, D. M., Pereira, M. C., Fabris, J. D., & Domingues, R. Z. (2009). Catalytic Effect of Magnetic Nanoparticles Over the H_2O_2 Decomposition Reaction. Journal of Nanoscience and Nanotechnology, 9: 3695–3699.

Dursun, S., & Yıldız, S. Z. (2022). Eco-Friendly Bleaching of Cotton Fabrics Without Heating Using Direct Process Water in the Presence of Sodium Chlorite and Phosphonate. Journal of Natural Fibres, 20(1). https://doi.org/10.1080/15440478.2022.2146248

Ensing, B., Buda, F., & Baerends, E. J. (2003). Fenton-like Chemistry in Water: Oxidation Catalysis by Fe(III) and H_2O_2 . J. Phys. Chem. A, 107: 5722-5731.

Farr, J.P., Smith, W. L. and Steichen, D.S. (2003). Bleaching Agents. In Kirk-Othmer Encyclopedia of Chemical Technology, (Ed.). https://doi.org/10.1002/0471238961.1921182206011818.a01.pub2

Fattahi, F. S., & Salehi, A.S. (2023). Environmentally Friendly Bleaching Process of Polyester Materials via Direct Process of Water without Heating System. Nanochem. Res., 8(4): 267-277.

Finocchiaro, G., Ju, X., Mezghrani, B., & Berret, J. (2024). Cerium Oxide Catalyzed Disproportionation of Hydrogen Peroxide: A Closer Look at the Reaction Intermediate. Chem. - Eur. J., 30(14).

İMARC Group, (2025). Hydrogen Peroxide Prices, Trend, Chart, Demand, Market Analysis, News, Historical and Forecast Data Report 2025 Edition. Available at: https://www.imarcgroup.com/hydrogen-peroxide-pricing-report [28.11.2025]

İNTRATEC, (2025). Sodium Hypochlorite Prices. Available at: Sodium Hypochlorite Price - Historical & Current | Intratec.us [28.11.2025]

Koohestani, B., Darban, A.K., Darezereshki, E., Mokhtari, P., & Yilmaz, E., (2019). Comparison of different natural fiber treatments: a literature review. Int. J. Environ. Sci. Technol., 16: 629–642. https://doi.org/10.1007/s13762-018-1890-9

Lin, S., & Gurol, M. D. (1998). Catalytic Decomposition of Hydrogen Peroxide on Iron Oxide: Kinetics, Mechanism, and Implications. Environ. Sci. Technol., 32(10): 1417-1423

Lousada, C. M., Brinck, T., & Jonsson, M. (2012). Mechanism of H2O2 Decomposition on Transition Metal Oxide Surfaces. The Journal of Physical Chemistry C, 116(17): 9533-9543

Lousada, C. M., Yang, M., Nilsson, K., & Jonsson, M. (2013). Catalytic decomposition of hydrogen peroxide on transition metal and lanthanide oxides. Journal of Molecular Catalysis A: Chemical, 379: 178-184.

Made-in-China, (2025). Sodium Chlorite, Hebei Fiza Technology Co., Ltd.. Available at: Sodium Chlorite Manufacturer, Strontium Carbonate, Potassium Nitrate Supplier - Hebei Fiza Technology Co., Ltd. [28.11.2025]

Pędziwiatr, P., Mikołajczyk, F., Zawadzki, D., Mikołajczyk, K., Bedka, A., & Oktan, K. N. (2018). Decomposition Of Hydrogen Perodixe - Kinetics And Review Of Chosen Catalysts. Acta Innovations, 26: 45-52.

Plauck, A., Stangland, E. E., Dumesic, J. A., & Mavrikakis, M. (2016). Active sites and mechanisms for H2O2 decomposition over Pd catalysts. Proc. Natl. Acad. Sci. U.S.A., 113(14):1973-1982.

Salem, I. A., El-Maazawi, M., & Zaki, A. B. (2000). Kinetics and mechanisms of decomposition reaction of hydrogen peroxide in presence of metal complexes. International Journal of Chemical Kinetics, 32(11): 643-666.

Tridge, (2025). Global Sodium Sulfite Price. Available at: Global Sodium sulfite Price. Tridge [28.11.2025]

Tuaphol, S., Sun, Z., & Sathitsuksanoh, N. (2021). Advances in Bioenergy. 6(1): 301-338.

Wang, G., Zhao, D., Kou, F., Ouyang, Q., Chen, J., & Fang, Z. (2018). Removal of norfloxacin by surface Fenton system ($MnFe_2O_4/H_2O_2$): Kinetics, mechanism and degradation pathway. Chemical Engineering Journal, 351: 747-755.

Weiss, J. (1935). The catalytic decomposition of hydrogen peroxide on different metals. Transactions of the Faraday Society, 67: 1-3681.

Wright, J. S., Johnson, E. R., DiLabio, G. A. (2001). Predicting the activity of phenolic antioxidants: theoretical method, analysis of substituent effects, and application to major families of antioxidants. J Am Chem Soc., 123(6):1173-83. doi: 10.1021/ja002455u. PMID: 11456671.

Yang, X., Tian, P., Wang, H., Xu, J., & Han, Y. (2016). Catalytic decomposition of H_2O_2 over a Au/carbon catalyst: A dual intermediate model for the generation of hydroxyl radicals. Journal of Catalysis, 336: 126-132.

ORAL PRESENTATION

Syringic acid mitigates chlorpyrifos-induced oxidative stress and DNA damage in HEK293 cells

Adem Güner

Department of Occupational Health and Safety, Faculty of Health Sciences, Sinop University, Sinop, Türkiye (Orcid: 0000-0003-3295-3538)

Corresponding author e-mail: ademeguner@gmail.com

Abstract

Chlorpyrifos (CPF), a widely used organophosphate pesticide, induces systemic toxicity through acetylcholinesterase inhibition and oxidative stress generation. Recent studies highlight its nephrotoxic potential via mitochondrial dysfunction, inflammation, and reactive oxygen species (ROS)-mediated injury. Syringic acid (SA), a naturally occurring phenolic acid abundant in fruits and medicinal plants, exhibits potent antioxidant, anti-inflammatory, and cytoprotective properties, including notable renoprotective effects in chemical-induced kidney injury models. This study investigated whether SA can mitigate CPF-mediated cytotoxicity in human embryonic kidney (HEK293) cells. Cells were exposed to CPF (400 µM) with or without SA (10, 25, 50 µM) for 24 h, and cell viability (MTT), cytotoxicity (LDH leakage), total antioxidant capacity (TAC), total oxidant status (TOS), and DNA fragmentation were evaluated. CPF significantly reduced cell viability and TAC while increasing LDH release, TOS, and DNA fragmentation ($p < 0.05$). SA co-treatment markedly alleviated these changes in a dose-dependent manner, restoring redox balance and reducing DNA damage. These findings suggest that syringic acid provides substantial protection against CPF-induced oxidative nephrotoxicity and may represent a promising therapeutic candidate for pesticide-associated renal injury.

Keywords: Chlorpyrifos, syringic acid, kidney, cytotoxicity

INTRODUCTION

Chlorpyrifos (CPF) is a broad-spectrum organophosphate pesticide extensively used in agriculture and household insect control. Although effective, CPF exhibits well-documented toxicity in humans and animals through inhibition of acetylcholinesterase (AChE), generation of reactive oxygen species (ROS), and induction of mitochondrial dysfunction. Beyond classical neurotoxicity, recent studies highlight its renal toxicity, characterized by increased oxidative stress, inflammatory signaling, and apoptosis in kidney tissues and renal-derived cell lines (Bai et al., 2023, Balakrishnan et al., 2025). Kidney cells are particularly susceptible to CPF due to high metabolic activity and abundant xenobiotic-metabolizing enzymes. CPF induces cellular injury through excessive ROS production, depletion of antioxidant defenses, lipid peroxidation, mitochondrial depolarization, and DNA fragmentation (Tanvir et al., 2016, Xu et al., 2018). These events contribute to nephrotoxicity and impair renal epithelial integrity, thereby increasing the risk of acute or chronic kidney damage.

Natural polyphenols have been widely studied for their capacity to attenuate xenobiotic-induced renal injury. Syringic acid (SA) is a methoxyphenolic acid naturally present in black currants, olives, dates, grapes, and several medicinal plants. SA exhibits potent free-radical scavenging, anti-inflammatory, anti-apoptotic, and mitochondrial protective effects (Sancak et al., 2016, Ogut et al., 2022;). Renal protection by SA has been reported in different chemical-induced nephrotoxicity models, where it reduces ROS, restores antioxidant enzymes, and inhibits DNA damage (Singh et al., 2021).

However, no study to date has evaluated whether SA can protect against chlorpyrifos-induced renal oxidative stress or DNA fragmentation. Therefore, the present study aimed to investigate the protective effects of SA in CPF-exposed HEK293 cells. We hypothesized that SA would ameliorate CPF-induced cytotoxicity, restore antioxidant balance, and reduce DNA fragmentation.

MATERIALS AND METHODS

2.1. Chemicals and reagents: Chlorpyrifos (≥98%) and syringic acid (≥98%) were purchased from Sigma-Aldrich (USA). MTT reagent, dimethyl sulfoxide (DMSO), and Triton X-100 were obtained from Merck (Germany). TAC and TOS kits were purchased from Rel Assay Diagnostics (Gaziantep, Turkey).

2.2. Cell culture: HEK293 cells were maintained in DMEM supplemented with 10% fetal bovine serum (FBS) and 1% penicillin–streptomycin at 37 °C in 5% CO_2. Cells between passages 5–15 were used.

2.3. Experimental design: Cells were seeded at densities of 1×10^5 cells/well (96-well plates) for MTT and LDH assays, and 2×10^5 cells/well (6-well plates) for oxidative and molecular analyses. After 24 h stabilization, the following groups were established: (1) Control (0.1% DMSO), 2) SA 10 µM 3) SA 25 µM 4) SA 50 µM 5) CPF 400 µM 6) CPF 400 µM + SA 10 µM 7) CPF 400 µM + SA 25 µM 8) CPF 400 µM + SA 50 µM

2.4. MTT Cell-Viability Assay

Cell viability was measured by the colorimetric MTT method. After exposure to treatments for 48 h, 10 µL of MTT solution (0.5 mg/mL) was added to each well of a 96-well plate and incubated for 3 h at 37 °C. Formazan crystals were dissolved in 100 µL DMSO and absorbance was read at 570 nm (reference 630 nm) using a microplate reader. Cell viability was expressed as % of control.

2.5. Lactate Dehydrogenase (LDH) Release Assay

LDH release was determined with a commercial kit (Abcam ab102526) following the supplier's protocol. Briefly, 100 µL of culture supernatant was mixed with 100 µL of LDH reaction solution in a new 96-well plate and incubated for 30 min at room temperature. Absorbance was recorded at 490 nm. Total LDH release was calculated relative to cells lysed with 2 % Triton X-100 (positive control) and expressed as % of control (n = 3 biological replicates with triplicates each).

2.6. Total Antioxidant Capacity (TAC) and Total Oxidant Status (TOS)

TAC and TOS were measured using Rel Assay Diagnostics kits (RL0017 and RL0024, Gaziantep, Turkey). For TAC, 30 µL of sample was added to 500 µL of Reagent 1, and absorbance was measured at 660 nm after 30 s. Then 75 µL of Reagent 2 was added and the absorbance was recorded again after 5 min. Values were calibrated with Trolox and expressed as mmol Trolox eq./L.

For TOS, 75 µL of sample was added to 500 µL of Reagent 1 and initial absorbance recorded at 530 nm; 15 µL of Reagent 2 was added and a second reading was taken after 5 min. Results were expressed as µmol H_2O_2 eq./L. All values were normalized to protein content and used to calculate the oxidative stress index.

2.7. DNA Fragmentation (DPA Colorimetric Assay)

DNA fragmentation was quantified by the diphenylamine (DPA) colorimetric assay (Burton method, modified). After treatments, cells were lysed in a hypotonic lysis buffer (10 mM Tris-HCl, 10 mM EDTA, 0.5 % Triton X-100, pH 7.4) and centrifuged at 13 000×g for 20 min at 4 °C to separate fragmented DNA (supernatant) from intact chromatin (pellet). Both fractions were precipitated overnight with 12.5 % TCA at 4 °C and hydrolyzed in 5 % TCA at 90 °C for 15 min. After cooling, 1 mL of fresh DPA reagent (150 mg DPA in 10 mL glacial acetic acid + 150 µL H_2SO_4 + 50 µL 1.6 % acetaldehyde) was added. Samples were incubated at 37 °C for 4 h and absorbance read at 600 nm.

2.9. Statistical analysis: Statistical analyses were conducted using IBM SPSS Statistics (Version 25.0, IBM Corp., Armonk, NY, USA). Differences among multiple groups were evaluated by one-way analysis of variance (ANOVA) followed by Tukey's post hoc test to determine pairwise significance. All experiments were performed in triplicate (n=3 per group), and the results were expressed as mean ± standard deviation (SD). A probability value of $p < 0.05$ was considered statistically significant.

RESULTS and DISCUSSION

The present study investigated the protective effects of SA, a naturally occurring phenolic compound, against CPF-induced cytotoxicity, oxidative stress, and DNA damage in HEK293 cells. CPF is known primarily for its neurotoxicity; however, emerging evidence highlights that the kidney is a major secondary target due to CPF accumulation, oxidative metabolism, and the kidney's high vulnerability to electrophilic xenobiotics. In this

context, HEK293 cells represent a suitable in vitro model for elucidating CPF-triggered nephrotoxic responses and evaluating potential renoprotective agents.

Exposure to CPF (50 µM, 48 h) significantly decreased cell viability, as shown by a reduction in MTT metabolic activity to 58.3 ± 3.1% compared to the control (100 ± 4.2%). The decline in mitochondrial metabolic capacity reflects CPF's known ability to inhibit mitochondrial respiratory complexes, impair ATP production, and generate excessive reactive oxygen species (ROS), all of which contribute to mitochondrial dysfunction and apoptotic signaling. A parallel increase in LDH release (199.6 ± 10.2%) further demonstrated that CPF caused substantial membrane damage, suggesting that both necrotic leakage and late-stage apoptotic processes were induced (Fig. 1).

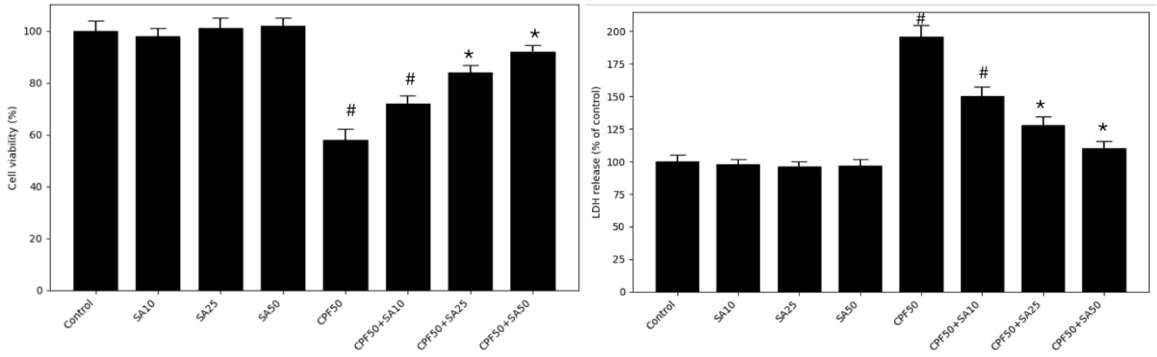


Figure 1. Effect of syringic acid on chlorpyrifos-induced cytotoxicity in HEK293 cells. Cell viability determined by the MTT assay and lactate dehydrogenase (LDH) release following 48 h exposure to chlorpyrifos (CPF, 400 µM) alone or in combination with SA (SA, 10–50 µM). CPF significantly decreased cell viability and increased LDH leakage compared with control ($p < 0.05$). Co-treatment with SA dose-dependently restored mitochondrial activity and reduced membrane damage, demonstrating its protective role against CPF-induced cytotoxicity. Data are expressed as mean ± SD (n = 3); *$p < 0.05$ versus control, # $p < 0.01$ versus control.

Co-treatment with SA significantly improved mitochondrial metabolic activity in a dose-dependent manner (from 72.4% at 10 µM to 92.3% at 50 µM) and markedly reduced LDH release (from 152.4% at 10 µM to 110.8% at 50 µM). These findings indicate that SA protects both mitochondrial and plasma membrane integrity. The improvements in MTT and LDH align with the well-documented antioxidant and cytoprotective actions of SA, which has been shown to stabilize lipid membranes, inhibit lipid peroxidation, and preserve mitochondrial function in toxin-exposed renal and hepatic cells (Sabahi et al., 2021, Mirza et al., 2022).

CPF treatment produced a pronounced oxidative shift characterized by a sharp decrease in total antioxidant capacity (TAC: 0.89 ± 0.05 mmol Trolox eq/L) and a more than twofold increase in total oxidant status (TOS: 18.7 ± 1.1 µmol H_2O_2 eq/L). This pattern is consistent with CPF's known ability to generate ROS through cytochrome P450 metabolism, mitochondrial complex inhibition, and oxidative biotransformation of chlorpyrifos-oxon. Oxidative stress is a key mechanism driving CPF-induced nephropathy, contributing to lipid peroxidation, protein oxidation, and DNA fragmentation (Fig. 2).

SA effectively counteracted CPF-induced redox imbalance. TAC increased progressively with SA concentration, reaching 1.92 ± 0.05 mmol Trolox eq/L at 50 µM, exceeding even the control mean value. This suggests not only restoration but enhancement of antioxidant defense, consistent with literature reporting SA's ability to modulate Nrf2 activation, upregulate antioxidant enzymes (SOD, CAT, GSH-Px), and regenerate redox cofactors (Ramachandran et al., 2012; Rashedinia et al., 2021; Demir et al., 2024). Correspondingly, TOS decreased dose-dependently to 10.3 ± 0.5 µmol H_2O_2 eq/L at the highest SA concentration, approaching near-control levels.

These results collectively indicate that SA efficiently suppresses CPF-generated ROS and restores intracellular redox equilibrium. Mechanistically, this effect may involve direct ROS scavenging, interruption of radical chain reactions, enhancement of endogenous antioxidants, and stabilization of mitochondrial redox centers.

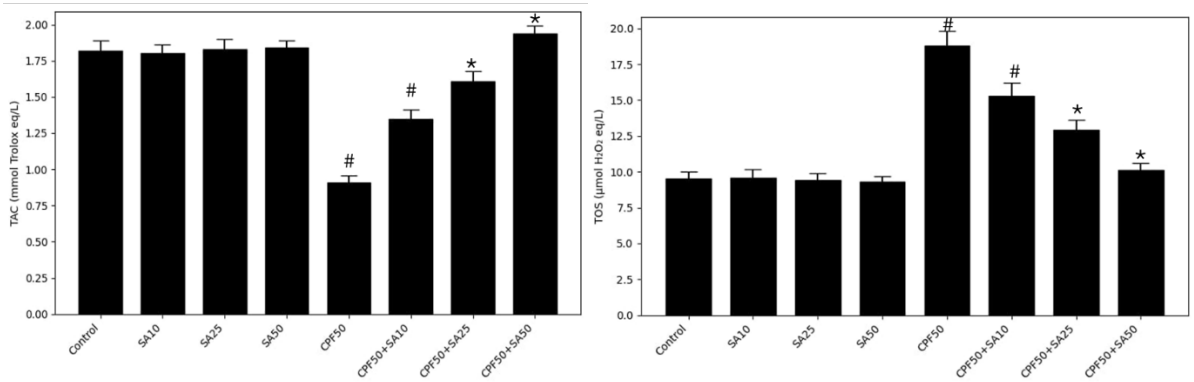


Figure 2. Effects of syringic acid on total antioxidant capacity (TAC) and total oxidant status (TOS) in CPF-treated HEK293 cells. SA co-treatment markedly reversed CPF-induced oxidative imbalance. TAC levels increased while TOS values decreased in a concentration-dependent manner, approaching control levels at 50 µM SA. These findings indicate that SA enhances the antioxidant defense system and mitigates CPF-triggered oxidative stress. Values are mean ± SD (n = 3); *p < 0.05 versus control, # p < 0.01 versus control.

CPF exposure resulted in a dramatic increase in DNA fragmentation (39.1 ± 2.8%) compared with the control (6.4 ± 0.6%), confirming that CPF induces substantial genomic instability. CPF-related DNA damage is attributed to ROS-induced strand breaks, oxidative modification of nucleotides, and activation of intrinsic apoptotic pathways, including cytochrome c release and caspase-dependent DNase activation. The magnitude of DNA fragmentation observed here is consistent with prior reports demonstrating CPF-induced genotoxicity in renal, hepatic, and neuronal cells (Fig. 3).

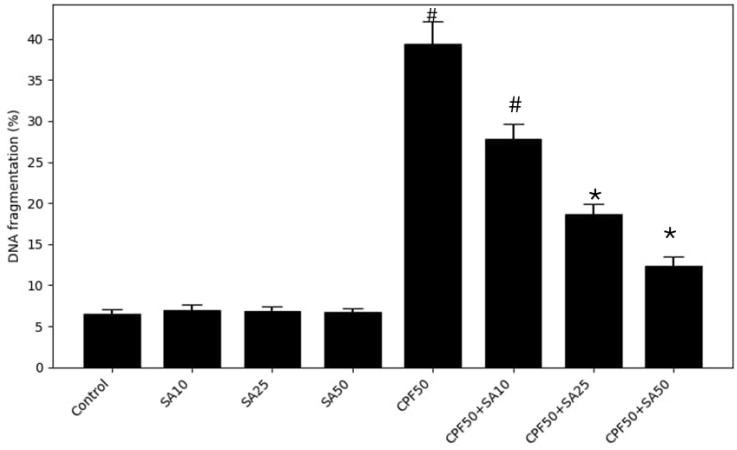


Figure 3. Effect of syringic acid on CPF-induced DNA fragmentation in HEK293 cells. CPF exposure significantly increased DNA fragmentation. SA markedly reduced DNA fragmentation in a dose-dependent manner. Data represent mean ± SD (n = 3); *p < 0.05 versus control # p < 0.01 versus control.

SA significantly reduced DNA fragmentation in a concentration-dependent manner. At 50 µM, fragmentation decreased to 12.2 ± 1.0%, representing nearly a 70% reduction in CPF-induced genomic damage. This effect may stem from SA's ability to inhibit ROS-driven DNA oxidation, protect nuclear chromatin, and prevent apoptotic nuclease activation. Moreover, the mitochondrial-protective action of SA likely prevents cytochrome c leakage and downstream caspase activation, thereby limiting apoptotic DNA cleavage (Mihanfar et al., 2021, Akarsu et al., 2024).

CONCLUSION

The integrated results strongly suggest that SA exerts potent protective effects against CPF-induced oxidative stress, cytotoxicity, and DNA damage in HEK293 cells. Through restoration of redox balance, stabilization of mitochondrial and plasma membranes, and suppression of genomic injury, SA emerges as a promising renoprotective agent. These findings warrant further mechanistic studies and in vivo evaluations to explore SA's therapeutic potential in environmental nephrotoxic exposures.

REFERENCES

Akarsu, S. A., Gür, C., Küçükler, S., Akaras, N., İleritürk, M., & Kandemir, F. M. (2024). Protective effects of syringic acid against oxidative damage, apoptosis, autophagy, inflammation, testicular histopathologic disorders, and impaired sperm quality in the testicular tissue of rats induced by mercuric chloride. *Environmental Toxicology, 39*(10), 4803–4814.

Bai, J., Deng, S., Fu, H., Yang, Q., Ren, F., Zeng, S., … & Wu, Z. (2023). Chlorpyrifos induces placental oxidative stress and barrier dysfunction by inducing mitochondrial apoptosis through the ERK/MAPK signaling pathway: In vitro and in vivo studies. *Science of the Total Environment, 903*, 166449.

Balakrishnan, P., Thirunavukarasu, K., Tamizhmani, P., Michael, A. A., & Velusamy, T. (2025). Toxicological impact of chronic chlorpyrifos exposure: DNA damage and epigenetic alterations induces neoplastic transformation of liver cells. *Biochemical and Biophysical Research Communications, 746*, 151287.

Demir, E. A. (2024). Syringic acid alleviates cisplatin-induced ovarian injury through modulating endoplasmic reticulum stress, inflammation and Nrf2 pathway. *Journal of Trace Elements in Medicine and Biology, 82*, 127356.

Mirza, A. C., Panchal, S. S., Allam, A. A., Othman, S. I., Satia, M., & Mandhane, S. N. (2022). Syringic acid ameliorates cardiac, hepatic, renal and neuronal damage induced by chronic hyperglycaemia in Wistar rats: A behavioural, biochemical and histological analysis. *Molecules, 27*(19), 6722.

Mihanfar, A., Darband, S. G., Sadighparvar, S., Kaviani, M., Mirza-Aghazadeh-Attari, M., Yousefi, B., & Majidinia, M. (2021). In vitro and in vivo anticancer effects of syringic acid on colorectal cancer: Possible mechanistic view. *Chemico-Biological Interactions, 337*, 109337.

Ogut, E., Armagan, K., & Gül, Z. (2022). The role of syringic acid as a neuroprotective agent for neurodegenerative disorders and future expectations. *Metabolic Brain Disease, 37*(4), 859–880.

Ramachandran, V., Saravanan, R., & Raja, B. (2012). Attenuation of oxidative stress by syringic acid on acetaminophen-induced nephrotoxic rats. *Comparative Clinical Pathology, 21*(6), 1559–1564.

Rashedinia, M., Khoshnoud, M. J., Fahlyan, B. K., Hashemi, S. S., Alimohammadi, M., & Sabahi, Z. (2021). Syringic acid: A potential natural compound for the management of renal oxidative stress and mitochondrial biogenesis in diabetic rats. *Current Drug Discovery Technologies, 18*(3), 405–413.

Sabahi, Z., Khoshnoud, M. J., Hosseini, S., Khoshraftar, F., & Rashedinia, M. (2021). Syringic acid attenuates cardiomyopathy in streptozotocin-induced diabetic rats. *Advances in Pharmacological and Pharmaceutical Sciences, 2021*(1), 5018092.

Sancak, E. B., Akbas, A., Silan, C., Cakir, D. U., Turkon, H., & Ozkanli, S. S. (2016). Protective effect of syringic acid on kidney ischemia-reperfusion injury. *Renal Failure, 38*(4), 629–635.

Singh, H. P., Singh, T. G., & Singh, R. (2021). Evaluation of the renoprotective effect of syringic acid against nephrotoxicity induced by cisplatin in rats. *Journal of Applied Pharmaceutical Science, 11*(1), 080–085.

Tanvir, E. M., Afroz, R., Chowdhury, M. A. Z., Gan, S. H., Karim, N., Islam, M. N., & Khalil, M. I. (2016). A model of chlorpyrifos distribution and its biochemical effects on the liver and kidneys of rats. *Human & Experimental Toxicology, 35*(9), 991–1004.

Xu, M. Y., Wang, P., Sun, Y. J., & Wu, Y. J. (2018). Disruption of kidney metabolism in rats after subchronic combined exposure to low-dose cadmium and chlorpyrifos. *Chemical Research in Toxicology, 32*(1), 122–129.

ORAL PRESENTATION

Neuroprotective effect of vanillic acid against paraquat-induced oxidative and cholinergic dysfunction

Adem Güner

Department of Occupational Health and Safety, Faculty of Health Sciences, Sinop University, Sinop, Türkiye
(Orcid: 0000-0003-3295-3538)

Corresponding author e-mail: ademeguner@gmail.com

Abstract

Paraquat (PQ) is a highly toxic bipyridyl herbicide known to induce dopaminergic neuronal degeneration primarily through excessive production of reactive oxygen species (ROS), mitochondrial dysfunction, and apoptotic DNA injury. Although its neurodegenerative effects are well documented, there is currently no effective therapeutic strategy for attenuating PQ-induced oxidative and cholinergic toxicity. Vanillic acid (VA), a naturally occurring phenolic acid abundant in edible plants, possesses potent antioxidant, anti-inflammatory, and mitochondrial protective properties, suggesting potential neuroprotective efficacy. This study investigated the protective effects of VA against PQ-induced cytotoxicity in human neuroblastoma SH-SY5Y cells. Cells were exposed to PQ (100 μM) alone or in combination with VA (10, 25, 50 μM) for 24 hours. Cell viability (MTT), cytotoxicity (LDH release), oxidative stress status (TAC, TOS), DNA fragmentation, and acetylcholinesterase (AChE) activity were assessed. PQ markedly reduced viability, TAC, and AChE activity while significantly elevating LDH release, TOS, and DNA fragmentation. VA co-treatment ameliorated all alterations in a dose-dependent manner, restoring redox balance, reducing apoptotic injury, and improving cholinergic enzyme function. These findings provide the first evidence that vanillic acid mitigates PQ-induced neurotoxicity via antioxidant and anti-apoptotic mechanisms, highlighting its potential as a natural neuroprotective candidate.

Keywords: Paraquat, vanilic acid, neurotoxic, protective effect

INTRODUCTION

Paraquat (PQ) is a widely used herbicide that remains a major public health concern due to its severe systemic and neurotoxic effects. PQ readily crosses neuronal membranes using the dopamine transporter (DAT) and accumulates in dopaminergic neurons, where it undergoes redox cycling and generates excessive superoxide radicals. This results in mitochondrial complex I inhibition, ATP depletion, lipid peroxidation, and oxidative DNA damage that mechanisms strongly associated with Parkinsonian neurodegeneration (Liu et al., 2022). Experimental studies have shown that PQ exposure induces ROS overproduction, mitochondrial membrane depolarization, and activation of intrinsic apoptotic pathways in models of dopaminergic toxicity. In addition to oxidative collapse, PQ disrupts cholinergic signaling through oxidative inhibition of acetylcholinesterase (AChE), further amplifying neuronal dysfunction. Despite extensive research, no clinically effective neuroprotective therapy exists for PQ-induced oxidative and apoptotic injury. Therefore, there is increasing interest in plant-derived phenolic compounds with strong antioxidant capacity that may counteract PQ-mediated toxicity (Colle et al., 2021, Xiao et al., 2022).

Vanillic acid (VA; 4-hydroxy-3-methoxybenzoic acid) is a naturally occurring phenolic acid found in numerous fruits, vegetables, and medicinal plants. VA exhibits potent antioxidant, free radical-scavenging, anti-inflammatory, and anti-apoptotic activities (Ingole et al., 2021). It has been shown to attenuate oxidative injury in models of renal, hepatic, and cardiovascular toxicity, and to prevent mitochondrial damage by suppressing lipid peroxidation and promoting endogenous antioxidant defense (Bains et al., 2022, Kaur et al., 2022). Although VA has demonstrated protective potential in several oxidative stress models, its effect on PQ-induced neuronal toxicity has not been previously investigated.

Given the strong mechanistic overlap between PQ-driven oxidative injury and the antioxidant properties of VA, we hypothesized that VA could mitigate PQ-induced cytotoxicity through restoration of redox homeostasis and attenuation of apoptotic DNA degradation. Therefore, this study was designed to evaluate the protective effects of

vanillic acid against PQ-induced neurotoxicity in SH-SY5Y cells using assays of viability (MTT), membrane damage (LDH), oxidative stress (TAC/TOS), DNA fragmentation, and AChE activity.

MATERIALS AND METHODS

2.1. Chemicals and reagents: Paraquat dichloride (≥98% purity) and vanillic acid (≥98%) were obtained from Sigma-Aldrich (USA). MTT (3-(4,5-dimethylthiazol-2-yl)-2,5-diphenyltetrazolium bromide), dimethyl sulfoxide (DMSO), and all analytical-grade salts and buffers were purchased from Merck (Germany). Total antioxidant capacity (TAC) and total oxidant status (TOS) assay kits were supplied by Rel Assay Diagnostics (Gaziantep, Türkiye). DNA fragmentation was quantified using the diphenylamine (DPA) colorimetric method. Acetylcholinesterase (AChE) activity was determined using Ellman's colorimetric assay.

2.2. Cell culture: SHSY-5Ycells were maintained in DMEM supplemented with 10% fetal bovine serum (FBS) and 1% penicillin–streptomycin at 37 °C in 5% CO_2. Cells between passages 5–15 were used.

2.3. Experimental design: Cells were seeded at densities of 1×10^5 cells/well (96-well plates) for MTT and LDH assays, and 2×10^5 cells/well (6-well plates) for oxidative and molecular analyses. After 24 h stabilization, the following groups were established: (1) Control (0.1% DMSO), 2) PQ 100 µM 3) PQ + VA 10 µM 4) PQ + VA 25 µM 5) PQ + VA 50 µM

2.4. MTT Cell-Viability Assay

Cell viability was measured by the colorimetric MTT method. After exposure to treatments for 48 h, 10 µL of MTT solution (0.5 mg/mL) was added to each well of a 96-well plate and incubated for 3 h at 37 °C. Formazan crystals were dissolved in 100 µL DMSO and absorbance was read at 570 nm (reference 630 nm) using a microplate reader. Cell viability was expressed as % of control.

2.5. Lactate Dehydrogenase (LDH) Release Assay

LDH release was determined with a commercial kit (Abcam ab102526) following the supplier's protocol. Briefly, 100 µL of culture supernatant was mixed with 100 µL of LDH reaction solution in a new 96-well plate and incubated for 30 min at room temperature. Absorbance was recorded at 490 nm. Total LDH release was calculated relative to cells lysed with 2 % Triton X-100 (positive control) and expressed as % of control (n = 3 biological replicates with triplicates each).

2.6. Total Antioxidant Capacity (TAC) and Total Oxidant Status (TOS)

TAC and TOS were measured using Rel Assay Diagnostics kits (RL0017 and RL0024, Gaziantep, Turkey). For TAC, 30 µL of sample was added to 500 µL of Reagent 1, and absorbance was measured at 660 nm after 30 s. Then 75 µL of Reagent 2 was added and the absorbance was recorded again after 5 min. Values were calibrated with Trolox and expressed as mmol Trolox eq./L.

For TOS, 75 µL of sample was added to 500 µL of Reagent 1 and initial absorbance recorded at 530 nm; 15 µL of Reagent 2 was added and a second reading was taken after 5 min. Results were expressed as µmol H_2O_2 eq./L. All values were normalized to protein content and used to calculate the oxidative stress index.

2.7. DNA Fragmentation (DPA Colorimetric Assay)

DNA fragmentation was quantified by the diphenylamine (DPA) colorimetric assay (Burton method, modified). After treatments, cells were lysed in a hypotonic lysis buffer (10 mM Tris-HCl, 10 mM EDTA, 0.5 % Triton X-100, pH 7.4) and centrifuged at 13 000×g for 20 min at 4 °C to separate fragmented DNA (supernatant) from intact chromatin (pellet). Both fractions were precipitated overnight with 12.5 % TCA at 4 °C and hydrolyzed in 5 % TCA at 90 °C for 15 min. After cooling, 1 mL of fresh DPA reagent (150 mg DPA in 10 mL glacial acetic acid + 150 µL H_2SO_4 + 50 µL 1.6 % acetaldehyde) was added. Samples were incubated at 37 °C for 4 h and absorbance read at 600 nm.

2.8. Acetylcholinesterase (AChE) activity: AChE activity was determined using Ellman's colorimetric assay. Briefly, cell lysates were incubated with acetylthiocholine iodide and DTNB (5,5′-dithiobis-2-nitrobenzoic acid), and absorbance was read at 412 nm. Activity was expressed as % of control.

2.9. Statistical analysis: Statistical analyses were conducted using IBM SPSS Statistics (Version 25.0, IBM Corp., Armonk, NY, USA). Differences among multiple groups were evaluated by one-way analysis of variance (ANOVA) followed by Tukey's post hoc test to determine pairwise significance. All experiments were performed in triplicate (n=3 per group), and the results were expressed as mean ± standard deviation (SD). A probability value of $p < 0.05$ was considered statistically significant.

RESULTS and DISCUSSION

As shown in Fig. 1, paraquat (PQ, 100 µM) exposure induced marked neurotoxic alterations in SH-SY5Y cells, consistent with its established role as a mitochondrial complex I inhibitor and ROS generator. PQ alone significantly reduced mitochondrial metabolic activity (MTT) to 52.8 ± 3.4% of the control ($p < 0.05$) and increased LDH release to 221.6 ± 11.2%, demonstrating severe impairment of membrane integrity. These findings align with earlier reports showing that PQ triggers oxidative collapse and apoptotic-necrotic hybrid cell death via ROS overload and mitochondrial dysfunction (Menchinskaya et al., 2021).

Co-treatment with vanillic acid (VA) produced a clear, dose-dependent cytoprotective improvement. VA at 10, 25, and 50 µM restored MTT viability to 67.4 ± 2.9%, 79.3 ± 3.1%, and 91.5 ± 2.4%, respectively, while reducing LDH release to 176.3 ± 8.2%, 139.7 ± 7.1%, and 118.2 ± 6.4% ($p < 0.05$ vs. PQ). These improvements strongly indicate that VA attenuates PQ-driven mitochondrial dysfunction and membrane destabilization, likely through its phenolic structure's ROS-scavenging ability (Ay 2022, Surya et al., 2023).

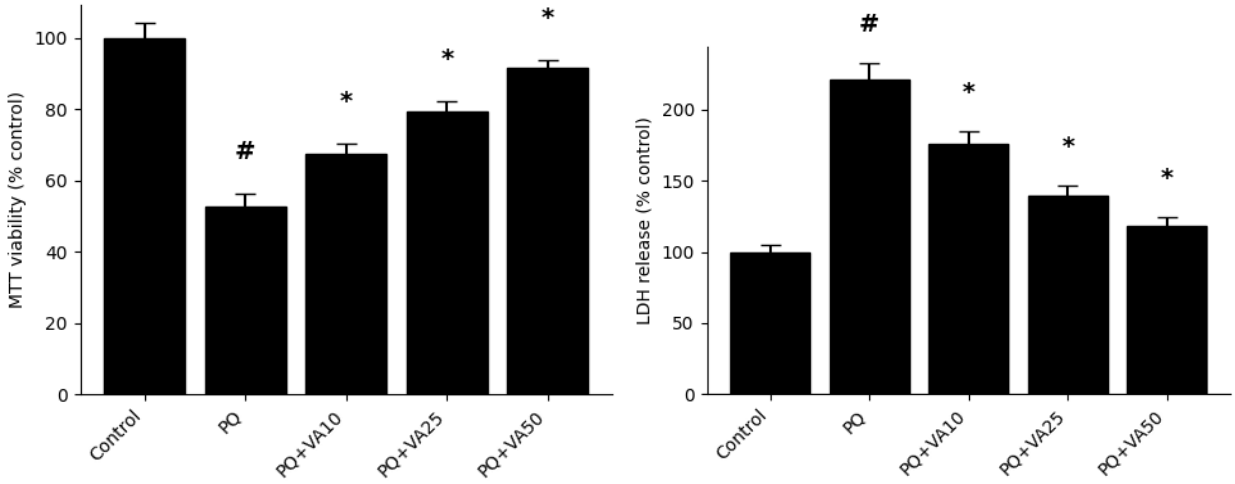


Figure 1. Effect of vanillic acid on paraquat-induced cytotoxicity in SH-SY5Y cells. Cell viability determined by the MTT assay and lactate dehydrogenase (LDH) release following 48 h exposure to paraquat alone or in combination with vanillic acid (10–50 µM). Data are expressed as mean ± SD (n = 3); *$p < 0.05$ versus PQ, # $p < 0.01$ versus control.

As shown Fig. 2, Oxidative stress markers further supported this protective mechanism. PQ significantly lowered total antioxidant capacity (TAC) from 1.48 ± 0.06 to 0.74 ± 0.04 mmol Trolox eq/L, while elevating total oxidant status (TOS) from 10.6 ± 0.7 to 21.8 ± 1.3 µmol H_2O_2 eq/L ($p < 0.05$). Co-administration of VA restored TAC values in a dose-dependent manner (10 µM: 1.12 ± 0.05, 25 µM: 1.34 ± 0.06, 50 µM: 1.56 ± 0.05) and simultaneously suppressed TOS (10 µM: 17.3 ± 0.9, 25 µM: 14.2 ± 0.8, 50 µM: 11.6 ± 0.7). These results confirm that VA effectively modulates PQ-induced oxidative imbalance by boosting endogenous antioxidant defenses and reducing ROS load (Colle and Farina, 2021, Alizadeh et al., 2022, Choi et al., 2024).

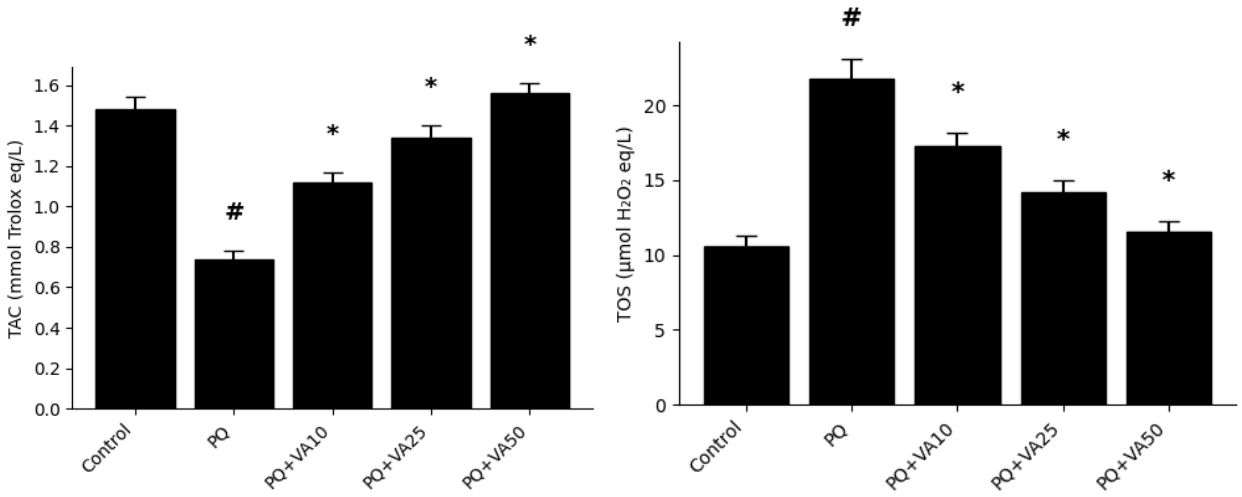


Figure 2. Effects of vanillic acid on total antioxidant capacity (TAC) and total oxidant status (TOS) in paraquat-exposed SH-SY5Y cells. Values are mean ± SD (n = 3); *p < 0.05 versus PQ, # p < 0.01 versus control.

PQ exposure also dramatically increased DNA fragmentation from 6.7 ± 0.6% to 44.1 ± 3.2%, reflecting extensive apoptotic DNA cleavage, which is consistent with PQ's known ability to generate hydroxyl radicals that directly damage DNA. VA significantly reduced fragmentation to 31.4 ± 2.2%, 21.7 ± 1.8%, and 13.9 ± 1.1% with 10, 25, and 50 μM treatments. This progressive attenuation suggests that VA suppresses mitochondrial-dependent apoptosis by stabilizing redox status and limiting ROS-mediated nuclear injury (Colle and Farina, 2021).

Finally, PQ caused substantial inhibition of acetylcholinesterase (AChE), lowering activity from 100 ± 4.5% to 47.2 ± 3.1% (p < 0.05), which may contribute to cholinergic dysfunction observed in PQ toxicity models (Fig. 3) (Ramalho et al., 2025). VA reversed this inhibition, restoring AChE activity to 59.8 ± 2.9%, 72.5 ± 2.6%, and 86.1 ± 2.4% across the three tested concentrations. This effect has not been previously documented and may involve VA's ability to reduce oxidative modification of AChE's catalytic residues.

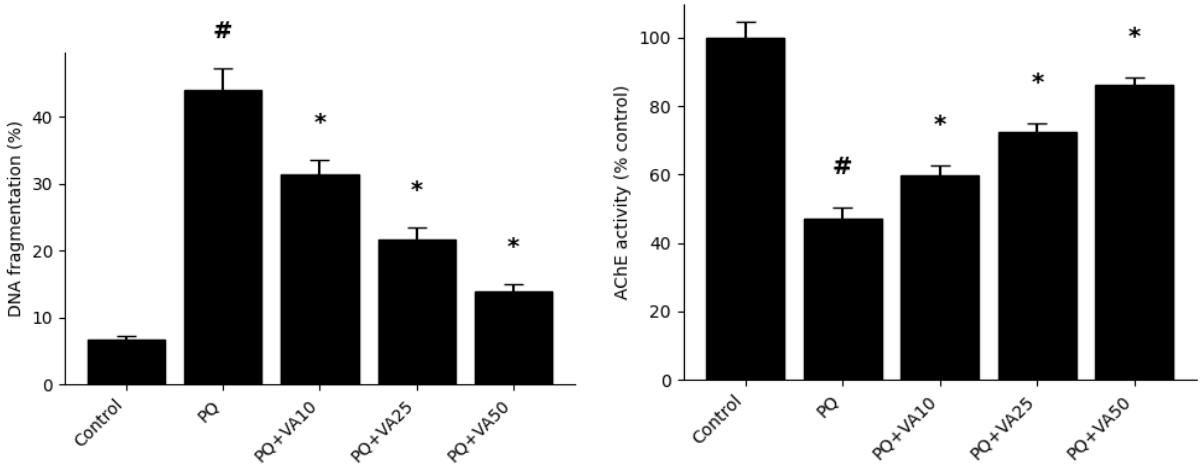


Figure 3. Effect of vanillic acid on DNA fragmentation and acetylcholinesterase (AChE) activity in paraquat-treated SH-SY5Y cells. Data represent mean ± SD (n = 3); *p < 0.05 versus PQ, # p < 0.01 versus control.

CONCLUSION

Collectively, these findings demonstrate that vanillic acid provides multi-level protection against paraquat-induced neurotoxicity by improving mitochondrial viability, reducing membrane leakage, restoring antioxidant status, inhibiting oxidative DNA fragmentation, and normalizing AChE function. Considering that no previous studies

have evaluated VA in PQ-induced neuronal injury, this work provides the first evidence supporting its therapeutic potential as a natural neuroprotective compound.

REFERENCES

Alizadeh, S., Anani-Sarab, G., Amiri, H., & Hashemi, M. (2022). Paraquat induced oxidative stress, DNA damage, and cytotoxicity in lymphocytes. *Heliyon, 8(7).*

Ay, M. (2022). Vanillic acid induces mitochondrial biogenesis in SH-SY5Y cells. *Molecular Biology Reports, 49(6), 4443–4449.*

Bains, M., Kaur, J., Akhtar, A., Kuhad, A., & Sah, S. P. (2022). Anti-inflammatory effects of ellagic acid and vanillic acid against quinolinic acid–induced rat model of Huntington's disease by targeting IKK–NF-κB pathway. *European Journal of Pharmacology, 934, 175316.*

Choi, G. Y., Lee, I. S., Moon, E., Choi, H., Je, A. R., Park, J. H., & Kweon, H. S. (2024). Ameliorative effect of vanillic acid against scopolamine-induced learning and memory impairment in rats via attenuation of oxidative stress and dysfunctional synaptic plasticity. *Biomedicine & Pharmacotherapy, 177, 117000.*

Colle, D., & Farina, M. (2021). Oxidative stress in paraquat-induced damage to nervous tissues. In *Toxicology* (pp. 69–78). Academic Press.

Ingole, A., Kadam, M. P., Dalu, A. P., Kute, S. M., Mange, P. R., Theng, V. D., ... & Patil, P. A. (2021). A review of the pharmacological characteristics of vanillic acid. *Journal of Drug Delivery and Therapeutics, 11(2-S), 200–204.*

Kaur, J., Gulati, M., Singh, S. K., Kuppusamy, G., Kapoor, B., Mishra, V., ... & Corrie, L. (2022). Discovering the multifaceted role of vanillic acid beyond flavours: Nutraceutical and therapeutic potential. *Trends in Food Science & Technology, 122, 187–200.*

Liu, X., Yang, H., & Liu, Z. (2022). Signaling pathways involved in paraquat-induced pulmonary toxicity: Molecular mechanisms and potential therapeutic drugs. *International Immunopharmacology, 113, 109301.*

Menchinskaya, E., Chingizova, E., Pislyagin, E., Likhatskaya, G., Sabutski, Y., Pelageev, D., ... & Aminin, D. (2021). Neuroprotective effect of 1,4-naphthoquinones in an in vitro model of paraquat and 6-OHDA-induced neurotoxicity. *International Journal of Molecular Sciences, 22(18), 9933.*

Ramalho, D. L., Silva, J. R., Monteiro Martins dos Santos, M. E., Soares, M. E. S., Jesus, A. A. T., Alves, T. H. O., ... & Souza, A. O. (2025). The neurotoxicity of paraquat and its degradation products on *Drosophila melanogaster*. *Scientific Reports, 15(1), 16447.*

Surya, S., Sampathkumar, P., Sivasankaran, S. M., Pethanasamy, M., Elanchezhiyan, C., Deepa, B., & Manoharan, S. (2023). Vanillic acid exhibits potent antiproliferative and free radical scavenging effects under in vitro conditions. *International Journal of Nutrition, Pharmacology, Neurological Diseases, 13(3), 188–198.*

Xiao, H. X., Song, B., Li, Q., Shao, Y. M., Zhang, Y. B., Chang, X. L., & Zhou, Z. J. (2022). Paraquat mediates BV-2 microglia activation by raising intracellular ROS and inhibiting Akt1 phosphorylation. *Toxicology Letters, 355, 116–126.*

ORAL PRESENTATION

Optimization and formulation of quetiapine bilosomes using a central composite design

Ayah Sawaie [1] (ORCID: https://orcid.org/0009-0000-0638-5464), Liban Barre[1*] (ORCID: https://orcid.org/0000-0001-8075-6622), Onur Pinarbasli[2] (ORCID: https://orcid.org/0000-0001-7091-683x), Mustafa Sinan Kaynak[3] (ORCID: https://orcid.org/0000-0003-2917-2407)

[1] Anadolu University, Graduate School, Department of Pharmaceutical Technology, Eskisehir, Turkey
[2] Ilko Pharmaceuticals, Research and Development Center, Ankara, Turkey
[3] Anadolu University, Faculty of Pharmacy, Department of Pharmaceutical Technology, Eskisehir, Turkey

*Corresponding author e-mail: liban72@anadolu.edu.tr

Abstract

Quetiapine is a poorly water-soluble atypical antipsychotic whose therapeutic performance is restricted by low dissolution rate, extensive hepatic first-pass metabolism, and variable oral bioavailability. These challenges contribute to fluctuating plasma concentrations and a narrow therapeutic window, necessitating advanced formulation strategies. Bilosomes—bile-salt-modified lipid vesicles—offer enhanced solubilization, permeability, and gastrointestinal stability for hydrophobic drugs. This study aimed to formulate quetiapine-loaded bilosomes and optimize their Critical quality attributes (CQAs) using a Central Composite Design (CCD) within a quality by design (QbD) framework. Sunflower phosphatidylcholine (SPC) and cholesterol were employed as lipid components, and STC as the bile salt modifier. Bilosomes were prepared using thin-film hydration followed by sonication. Amount of STC and sonication time served as independent variables, while particle size (PS), polydispersity index (PDI), Zeta potential (ZP), and Entrapment efficiency (EE%) were selected as CQAs. CCD revealed significant linear, quadratic, and interaction effects on all responses. Across the design space, PS ranged 148–340 nm, PDI 0.36–0.62, ZP −19.2 to −32.9 mV, and EE 61–84%. Optimal results were achieved with intermediate STC levels and moderate sonication times. Run 5 was identified as the optimal formulation, yielding PS 154.5 ± 9.2 nm, PDI 0.37 ± 0.02, ZP −28.2 ± 0.4 mV, and EE 83.0 ± 1.4%. These findings demonstrate the suitability of bilosomes as a robust nanocarrier platform for improving the oral delivery of quetiapine and similar poorly soluble drugs.

Keywords: Quetiapine; bilosomes; bile salts; QbD; CCD.

INTRODUCTION

Quetiapine is a widely prescribed atypical antipsychotic used for schizophrenia, bipolar disorder, and major depressive disorder, yet its clinical performance is restricted by major biopharmaceutical shortcomings. It exhibits extremely low aqueous solubility and undergoes extensive hepatic first-pass metabolism, resulting in oral bioavailability of only around 9% and substantial variability in systemic exposure (Narala & Veerabrahma, 2013). These characteristics place quetiapine within the Biopharmaceutics Classification System (BCS) Class II category, where absorption is primarily limited by dissolution rather than permeability. Additionally, rapid gastrointestinal absorption coupled with extensive metabolic conversion leads to low and unpredictable plasma levels, further contributing to highly variable therapeutic responses (Zubiaur et al., 2022). These limitations necessitate high oral doses to achieve effective plasma concentrations, increasing the likelihood of adverse effects such as sedation and metabolic disturbances. Collectively, these challenges highlight the urgent need for advanced drug delivery approaches capable of improving quetiapine's solubility, reducing first-pass metabolic loss, and ultimately enhancing its therapeutic effectiveness.

Lipid-based nanocarriers have become essential tools for improving the oral delivery of poorly soluble drugs, and among them, bilosomes have emerged as one of the most promising and advanced systems. Although structurally related to liposomes, bilosomes incorporate bile salts such as STC into the phospholipid bilayer, resulting in markedly enhanced membrane fluidity, elasticity, and stability under gastrointestinal conditions (Nayak et al., 2023). Unlike conventional liposomes—which rely primarily on cholesterol to reduce membrane permeability and

limit drug leakage (Torchilin, 2005)—bilosomes possess intrinsic resistance to bile salt exchange, enzymatic degradation, and pH fluctuations. Moreover, the presence of bile salts enhances mucosal penetration and facilitates lymphatic uptake, enabling drugs to partially bypass hepatic first-pass metabolism and significantly improve systemic exposure (Kaurav et al., 2024). While solid lipid nanoparticles (SLNs) also offer protection and controlled release, their relatively rigid and crystalline lipid matrices may limit adaptability in dynamic gastrointestinal environments (Müller et al., 2000). Taken together, these advantages position bilosomes as a superior oral nanocarrier platform, offering greater stability, enhanced permeability, and more efficient absorption compared with traditional liposomes and SLNs.

However, the fabrication of bilosomes is a complex process where the resulting physicochemical properties are highly sensitive to formulation composition and processing energy. To address this, the QbD approach offers a systematic framework for optimization. By utilizing statistical tools like the CCD, researchers can efficiently model the interactions between critical variables to ensure a robust final formulation (Chettupalli et al., 2025).

This study focuses on the formulation and optimization of Quetiapine-loaded bilosomes using SPC, cholesterol, and STC. Employing a CCD methodology, we investigated the influence of STC concentration and sonication time on CQAs, including PS, PDI, ZP, and EE. The primary objective of this work is to develop an optimized bilosome formulation that effectively mitigates the solubility and metabolic limitations of Quetiapine fumarate, thereby enhancing its oral bioavailability.

MATERIALS AND METHODS

Materials: SPC was obtained from Shankar (India). Cholesterol and STC were purchased from Sigma-Aldrich (St. Louis, MO, USA). Quetiapine was kindly provided by ILKO Pharmaceuticals (Ankara, Türkiye). All other reagents were of analytical grade.

Preparation Method for Quetiapine Bilosomes: Quetiapine bilosomes were prepared using a thin lipid film hydration method (Elkomy et al., 2022) followed by sonication. Briefly, 500 mg of SPC and 12 mg of cholesterol were dissolved in 20 mL of methanol in a round-bottom flask. Subsequently, 20 mg of quetiapine was added and stirred until fully dissolved. The organic solvent was evaporated under reduced pressure at 40°C using a rotary evaporator (IKA, RV 3 eco, Germany) to form a thin, uniform lipid film on the flask wall. The lipid film was hydrated with 30 mL of distilled water containing STC at amounts defined by the experimental design. The mixture was gently agitated to facilitate hydration. The hydrated lipid suspension was then sonicated in a bath sonicator (Ultrasonic Cleaner WUC-A, Germany) for specific times according to the DOE to produce a homogenous bilosomal dispersion. The bilosomal dispersions were stored at 4 °C until further characterization

Characterization of PS, PDI, ZP, and EE: PS, PDI, and ZP measurements were performed via dynamic light scattering (Aburahma, 2016) using a Zetasizer Nano ZS (Malvern Instruments Ltd., UK). Samples were diluted with distilled water and analyzed at room temperature. For the EE% calculation, 2 mL of bilosomal dispersion was centrifuged at 13,000 rpm for 1 hour. The supernatant containing free quetiapine was collected and analyzed by UV spectrophotometry at the drug's characteristic wavelength (254 nm). EE% was calculated using the equation (El Menshawe et al., 2020):

EE% = (Total amount of quetiapine – free quetiapine /Total amount of quetiapine used) x100

Experimental Design and Optimization: The formulation optimization was conducted using Design Expert® software (version 13, Stat-Ease Inc., Minneapolis, MN, USA) through a CCD approach. This systematic design evaluated the effects of the amount of STC (mg) and sonication time (minutes) on CQAs, including PS (nm), PDI, ZP (mV), and EE (%).

RESULTS and DISCUSSION

CCD provided a comprehensive understanding of how STC concentration and sonication time influence the CQAs of quetiapine-loaded bilosomes. Across the experimental design space, PS ranged from approximately 148 to 340 nm, PDI from 0.36 to 0.62, ZP from −19.2 to −32.9 mV, and EE from 61% to 84% as in table **1**. These broad response ranges clearly indicate that STC concentration and sonication time are genuinely critical formulation/process variables. The models confirmed statistically significant linear, quadratic, and interaction contributions for all CQAs, underscoring the suitability of QbD-based CCD for defining a scientifically justified design space. The observed behaviors can be interpreted in terms of phospholipid bilayer packing, bile-salt-induced membrane fluidity changes, cavitation-mediated fragmentation, and drug–bilayer interactions. These trends are

consistent with established findings in bilosomal (Zafar et al., 2022) and other lipid systems using QbD based optimized approaches (Cunha et al., 2020).

Table 1. CCD formulation runs and corresponding in vitro results of the responses (CQAs)

	Independent Variables		**Dependent variables (Responses)**			
Run	STC (mg)	Sonication time (minutes)	PS (nm)	PDI	ZP (mV)	EE (%)
1	20	10	175	0.48	-24.2	73
2	30	8	161	0.38	-27.9	82
3	20	5	243	0.46	-21.9	65
4	44	8	170	0.39	-32.9	78
5	30	8	148	0.36	-28.4	84
6	30	11	176	0.43	-29.4	79
7	40	5	288	0.55	-30.3	67
8	30	4	296	0.62	-27.0	61
9	16	8	340	0.53	-19.2	68
10	40	10	307	0.72	-27.1	80

Effects of independent variables on PS: The CCD revealed a distinct valley-shaped response surface for PS, wherein bilosomes produced under suboptimal conditions—particularly low STC concentrations and short sonication durations—were significantly larger, often approaching or exceeding 300 nm. This trend was evident in runs such as 8 and 9. At these conditions, the bilosomal bilayer is dominated by phosphatidylcholine and cholesterol, forming rigid, densely packed membranes with insufficient flexibility to form small vesicles upon hydration. As noted in lipid nanoparticle literature, rigid bilayers lacking adequate membrane-modifying agents tend to generate larger structures regardless of processing energy input (Cunha et al., 2020).

As STC concentrations increased into the intermediate range, PS decreased sharply due to reduced surface tension. This parallels that observed for bile-salt-modified bilosomes formulated with other drugs. Elkomy et al. (2022) demonstrated that the incorporation of sodium deoxycholate in soybean phosphatidylcholine bilosomes facilitated the formation of vesicles around 196.5 nm due to enhanced bilayer fluidization. Though the optimized quetiapine bilosomes in the present study achieved slightly smaller PS (~148–170 nm), the difference can reasonably be attributed to differences in phospholipid source (sunflower versus soybean), drug structure (quetiapine versus berberine), and bile-salt type (STC versus sodium deoxycholate). At the highest tested STC levels (near 44 mg), PS increased slightly relative to the optimum. This behavior can be explained by the classical bilayer solubilization model: once bile salts exceed a threshold concentration, they transition from acting as membrane-fluidizing amphiphiles to initiating bilayer solubilization and mixed micelle formation. This disrupts lamellar integrity, alters membrane curvature, and promotes the formation of larger or less stable vesicular structures. Similarly, the vesicle enlargement at excessive bile-salt concentrations has been attributed to the self-aggregation of bile salts (Elkomy et al. 2022).

Sonication time exhibited a clear nonlinear influence on bilosome formation. Short sonication durations (4–5 minutes) did not supply sufficient cavitational energy to fully disrupt multilamellar structures, resulting in larger and more heterogeneous vesicles. As sonication time increased toward an intermediate range (approximately 7–9 minutes), PS decreased markedly due to more efficient fragmentation and reorganization of the bilayers, consistent with the general pattern observed in lipid nanoparticle systems where extended sonication significantly reduces PS by enhancing cavitation-driven breakup of aggregates (Ali et al., 2010). However, when processing time exceeded the optimal window (beyond ~10–12 minutes), PS no longer decreased and PDI values began to widen, reflecting over-processing effects such as localized heating, membrane disruption, pore formation, and potential reaggregation of destabilized vesicles. Overall, these findings confirm that an intermediate sonication duration provides the optimal balance of mechanical energy to yield small, uniform, and physically stable bilosomes.

PDI values in the present study (0.36–0.62) reflected these structural and mechanical relationships. As STC concentration increased into the optimal region and sonication approached 8 minutes, PDI values decreased to ~0.36–0.39, indicative of more uniform nanoscale vesicles.

Effects of independent variables on ZP: ZP values ranged from −19.2 to −32.9 mV. Increasing STC concentration produced increasingly negative ZP values, reflecting the anionic nature of taurocholate and its sulfonate/carboxylate functional groups. Bile salts contribute directly to surface charge density and can dramatically improve electrostatic stabilization. The optimized quetiapine bilosomes in this study exhibited ZP around −28 to −29 mV, consistent with this stability threshold and comparable to the −30 mV reported for optimized berberine bilosomes in (Elkomy et al. 2022).

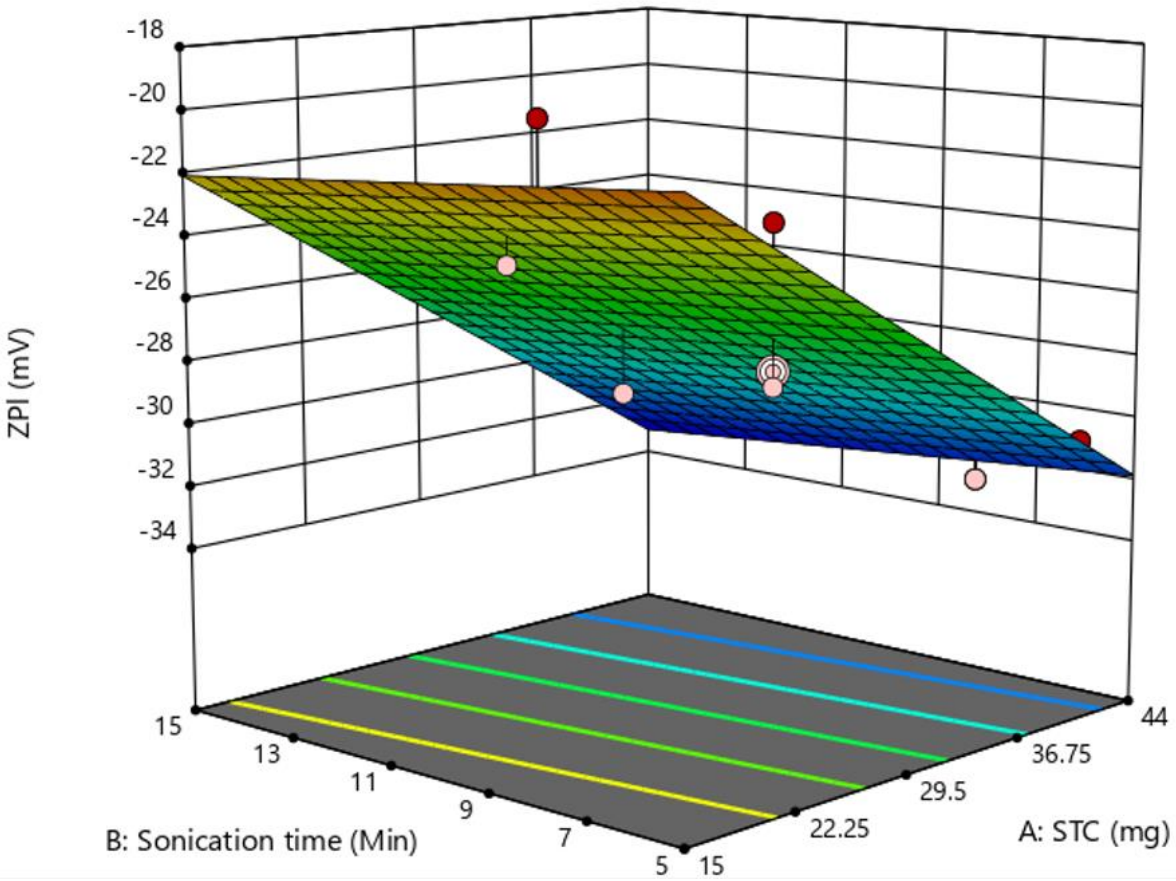


Figure 1. 3D response surface showing the effect of STC concentration and sonication time on ZP of bilosomes.

A clear trend is observed in Figure **1**, where increasing STC concentration and sonication time produces more negative ZP values, confirming that intermediate STC levels yield bilosomes with strong electrostatic stabilization capable of resisting aggregation during storage and gastrointestinal transit.

Effects of independent variables on Encapsulation Efficiency: EE% displayed a clear quadratic response to both STC concentration and sonication time, rising to an optimal region before declining when either factor exceeded its ideal range. Moderate levels of STC improved bilayer fluidity and drug accommodation, while intermediate sonication durations supported compact vesicle formation. However, excessive STC led to increased membrane permeability, and prolonged sonication caused structural disturbance—both resulting in reduced drug retention. This characteristic optimal window aligns with the established behavior of bile-salt-modified vesicular systems (Aburahma, 2016; Ahmed et al., 2020).

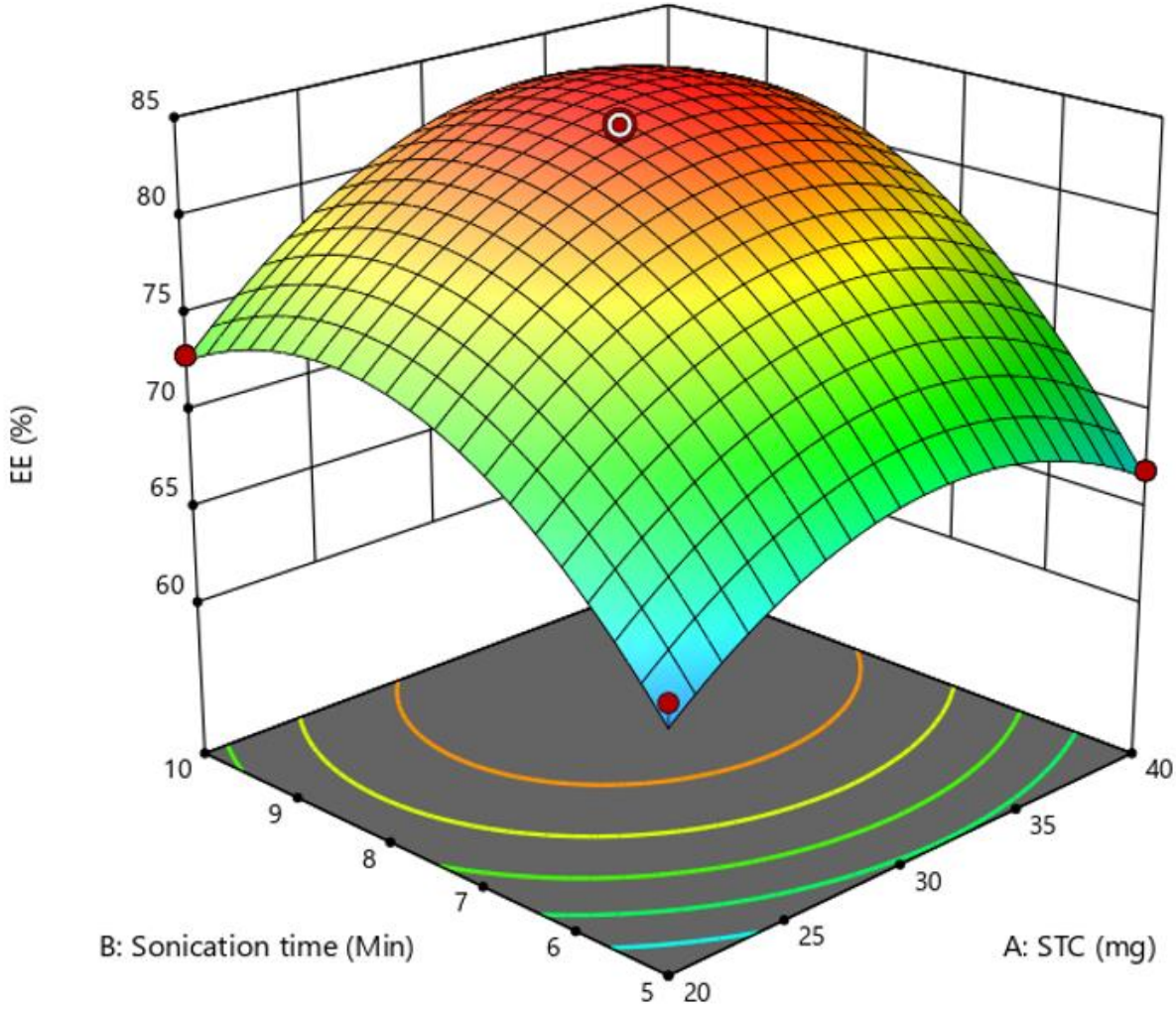


Figure 2. Response surface illustrating the combined effect of STC concentration and sonication time on EE% of quetiapine-loaded bilosomes.

Figure 2 shows a well-defined peak in EE% located at the center of the design space, confirming that the highest encapsulation is achieved only within a narrow combination of intermediate STC and sonication conditions. The curvature of the surface becomes steeper near the edges, indicating a rapid loss of EE as either variable moves away from the optimal range. The smooth gradient toward the apex reflects the strong synergistic contribution of both factors, while the lower regions demonstrate their destabilizing effect when present in excess.

Numerical Optimization and Experimental Validation of the Formulation:

Among all developed formulations, run 5 demonstrated the most optimal overall performance, combining the smallest PS with the highest encapsulation efficiency.

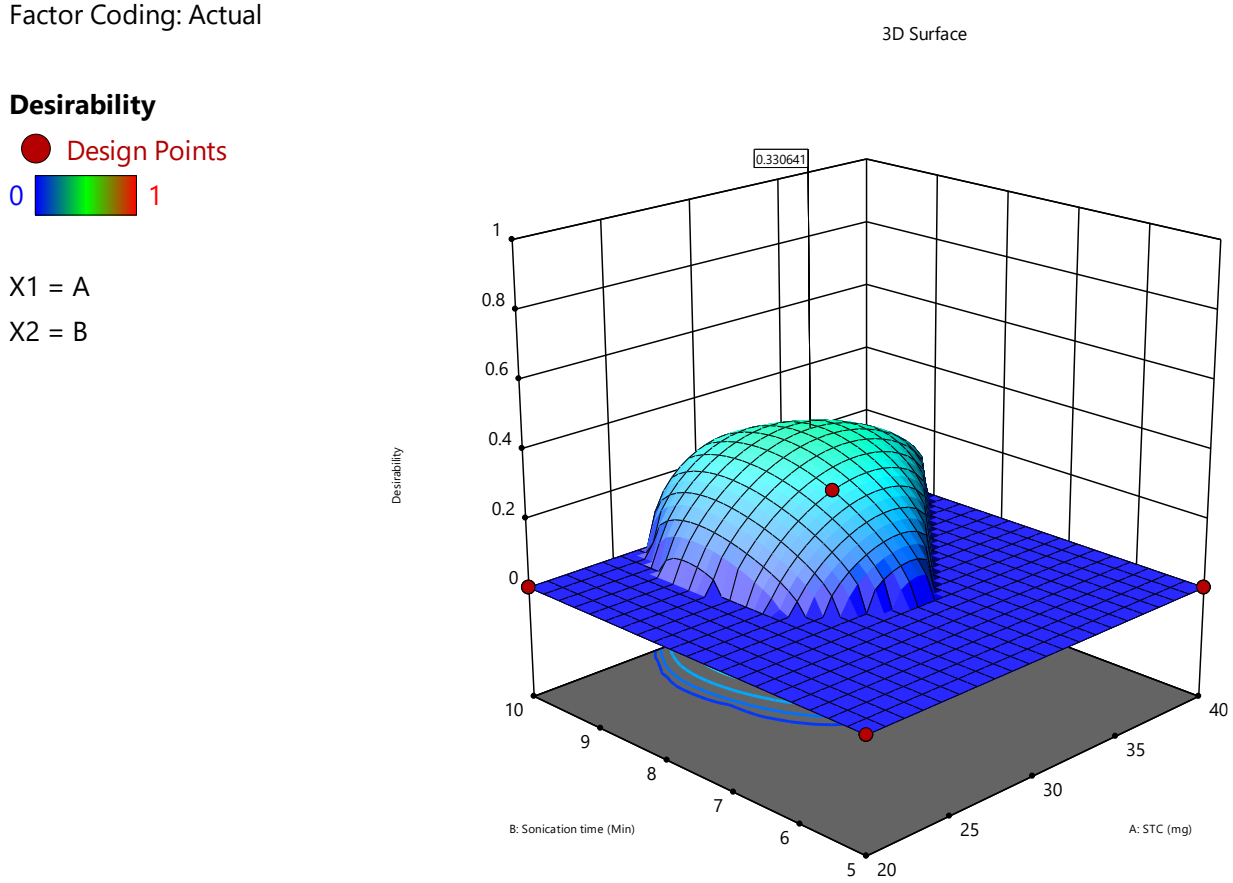


Figure 3. Numerical desirability plot showing the optimized combination of STC concentration and sonication time that provides the best overall PS, PDI, ZP, and encapsulation efficiency. The peak desirability value corresponds to the predicted optimal bilosome formulation.

Based on the desirability (Figure **3**) and point prediction method. The predicted and the observed values were very similar, and the target optimum was identified at an STC concentration of 32 mg and a sonication time of 9 minutes. This solution maximized overall desirability by simultaneously minimizing PS and PDI while maximizing ZP magnitude and EE. Optimum formulation yielded mean values of 154.5 ± 9.2 nm for PS, 0.37 ± 0.02 for PDI, −28.2 ± 0.4 mV for ZP, and 83.0 ± 1.4% for EE.

CONCLUSION

Quetiapine-loaded bilosomes were successfully formulated using SPC, cholesterol, and STC, and optimized systematically using a CCD. STC concentration and sonication time were shown to significantly affect PS, PDI, ZP, and EE, with both variables exhibiting pronounced nonlinear and interactive effects. Intermediate STC concentrations and moderate sonication times produced the most favorable bilosomal properties by balancing membrane fluidity, structural integrity, and energy input. The optimized bilosomes, with PS around 150–170 nm, PDI values below 0.4, ZP around −30 mV, and EE of approximately 80–84%, present a promising platform for enhancing the oral delivery of quetiapine. Future work should include comprehensive in vitro and permeability studies, as well as in vivo pharmacokinetic investigations to confirm the predicted improvements in bioavailability and therapeutic outcomes.

REFERENCES

Aburahma, M. H. (2016). Bile salts-containing vesicles: Promising pharmaceutical carriers for oral delivery of poorly water-soluble drugs and peptide/protein-based therapeutics or vaccines. Drug Delivery, 23(6), 1847–1867. https://doi.org/10.3109/10717544.2014.976892

Ahmed, S., Kassem, M. A., & Sayed, S. (2020). Bilosomes as promising nanovesicular carriers for improved transdermal delivery: Construction, in vitro optimization, ex vivo permeation and in vivo evaluation. International Journal of Nanomedicine, 15, 9783–9800. https://doi.org/10.2147/IJN.S278688

Ali, M. E., Lamprecht, A., & Rütten, S. (2010). Influence of process parameters on the particle size and zeta potential of polymeric nanoparticles. Colloids and Surfaces A: Physicochemical and Engineering Aspects, 372(1–3), 134–141. https://doi.org/10.1016/j.colsurfa.2010.09.020

Chettupalli, A. K., Kar, N. R., Iswariya, V. T., Panigrahy, U. P., Singh, L. P., Roy, H., Urs, D. V. M., Mandadi, S. R., Haque, M. A., Rana, R., & Emran, T. B. (2025). Development and optimization of dapagliflozin oral nano-bilosomes using response surface method: In vitro evaluation, in vivo evaluation. Nanotheranostics, 9(1), 1–19. https://doi.org/10.7150/ntno.99271

Cunha, S., Costa, C. P., Moreira, J. N., Sousa Lobo, J. M., & Silva, A. C. (2020). Using the quality by design (QbD) approach to optimize formulations of lipid nanoparticles and nanoemulsions: A review. Nanomedicine, 28, 102206. https://doi.org/10.1016/j.nano.2020.102206

Elkomy, M. H., Eid, H. M., Elmowafy, M., Shalaby, K., Zafar, A., Abdelgawad, M. A., Rateb, M. E., Ali, M. R. A., Alsalahat, I., & Abou-Taleb, H. A. (2022). Bilosomes as a promising nanoplatform for oral delivery of an alkaloid nutraceutical: Improved pharmacokinetic profile and snowballed hypoglycemic effect in diabetic rats. Drug Delivery, 29(1), 2694–2704. https://doi.org/10.1080/10717544.2022.2110997

Elkomy, M. H., Eid, H. M., El Menshawe, S. F., Ali, A. M. A., Morsy, M. A., & Alsaadi, M. (2022). Development and optimization of berberine-loaded bilosomes for improving its antidiabetic activity. Drug Delivery, 29(1), 1965–1978. https://doi.org/10.1080/10717544.2022.2092506

Kaurav, H., Tripathi, M., Kaur, S. D., Bansal, A., Kapoor, D. N., & Sheth, S. (2024). Emerging trends in bilosomes as therapeutic drug delivery systems. Pharmaceutics, 16(6), 697. https://doi.org/10.3390/pharmaceutics16060697

Müller, R. H., Mäder, K., & Gohla, S. (2000). Solid lipid nanoparticles (SLN) for controlled drug delivery – A review of the state of the art. European Journal of Pharmaceutics and Biopharmaceutics, 50(1), 161–177. https://doi.org/10.1016/S0939-6411(00)00087-4

Narala, A., & Veerabrahma, K. (2013). Preparation, characterization and evaluation of quetiapine fumarate solid lipid nanoparticles to improve the oral bioavailability. Journal of Pharmaceutics, 2013, 265741. https://doi.org/10.1155/2013/265741

Nayak, D., Rathnanand, M., & Tippavajhala, V. K. (2023). Unlocking the potential of bilosomes and modified bilosomes: A comprehensive journey into advanced drug delivery trends. AAPS PharmSciTech, 24, 238. https://doi.org/10.1208/s12249-023-02696-4

Torchilin, V. P. (2005). Recent advances with liposomes as pharmaceutical carriers. Nature Reviews Drug Discovery, 4(2), 145–160. https://doi.org/10.1038/nrd1632

Zafar, A., Alsaidan, O. A., Imam, S. S., Yasir, M., Alharbi, K. S., & Khalid, M. (2022). Formulation and evaluation of moxifloxacin-loaded bilosomes in-situ gel: Optimization to antibacterial evaluation. Gels, 8(7), 418. https://doi.org/10.3390/gels8070418

Zubiaur, P., Ortega-Ruiz, M., Soria-Chacartegui, P., Villapalos-García, G., & Abad-Santos, F. (2022). The pharmacogenetics of treatment with quetiapine. Future Pharmacology, 2(3), 18. https://doi.org/10.3390/futurepharmacol2030018

ORAL PRESENTATION

Kanatlılarda besleme ve DNA metilasyonu: Performans, hayvan sağlığı ve refahı üzerine etkiler

Helin Atan Çırpıcı[1*] (*https://orcid.org/0000-0003-3574-2891*),
Figen Kırkpınar[2] (*https://orcid.org/0000-0002-2018-755X*)

[1]Ege Üniversitesi, Ziraat Fakültesi, Zootekni Bölümü, İzmir, Türkiye
[2]Ege Üniversitesi, Ziraat Fakültesi, Zootekni Bölümü, İzmir, Türkiye

*Sorumlu yazar e-mail: helin.atan@ege.edu.tr

Özet

Son yıllarda genom teknolojilerindeki gelişmeler, epigenetik modifikasyonların kanatlılarda büyüme ve üretim performansı, bağışıklık fonksiyonu, hayvansal ürün kalitesi (et ve yumurta) gibi ekonomik açıdan önemli özellikler üzerinde kritik rol oynadığını göstermektedir. DNA metilasyonu, gen ekspresyonunu düzenleyen başlıca epigenetik mekanizmalar arasında yer almakta ve hem genetik hem de çevresel faktörlerden etkilenmektedir. Kanatlılarda DNA metilasyonu; büyüme, metabolik düzenleme, bağışıklık fonksiyonu ve çevresel adaptasyon gibi fizyolojik süreçlerin kontrolünde önemli bir mekanizma olarak bilinmektedir. DNA metilasyonu, sitozin bazlarına metil grubunun eklenmesiyle gerçekleşmekte ve tek karbon metabolizmasında yer alan metiyonin, kolin, betain, folat ve B vitaminleri gibi besin maddeleri tarafından etkilenmektedir. Bu besinler, hücresel metilasyon kapasitesini ve DNA metilasyon profillerini belirlemede kritik rol oynamaktadır. Ayrıca son çalışmalar, yem bileşimi, enerji ve protein düzeyleri, yağ asidi profilleri ile fitobiyotikler, antioksidanlar, probiyotikler ve prebiyotikler gibi fonksiyonel katkı maddelerinin epigenetik düzenlemeyi etkileyebileceğini ortaya koymaktadır. Özellikle embriyonik gelişim, yumurtadan çıkma öncesi ve sonrası ile karma yemlerdeki geçiş dönemleri gibi kritik gelişim aşamaları, epigenetik modülasyona karşı yüksek duyarlılık göstermektedir. Beslenme ile DNA metilasyonu arasındaki etkileşimlerin anlaşılması, kanatlılarda büyüme performansını, hayvan sağlığını ve refahını iyileştirmeye yönelik yeni bakış açısı sunmaktadır. Bu bildiride, kanatlılarda besleme uygulamalarının DNA metilasyonu üzerindeki güncel etkileri ele alınacak ve besin maddeleri, metabolik aktivite, epigenetik modifikasyonlar ile performans, hayvan sağlığı ve refahı arasındaki ilişkiler literatür ışığında incelenecektir. Elde edilen bilgiler, epigenetik temelli beslenme programlarının geliştirilmesi ve sürdürülebilir kümes hayvanı üretimi için potansiyel stratejiler sunmaktadır.

Anahtar Kelimeler: Besleme, DNA metilasyonu, epigenetik, kanatlı, performans.

Feeding and DNA methylation in poultry: Effects on performance, animal health, and welfare

Abstract

In recent years, advances in genomic technologies have shown that epigenetic modifications play a critical role in economically important traits in poultry, such as growth and production performance, immune function, and the quality of animal products (meat and eggs). DNA methylation is one of the main epigenetic mechanisms regulating gene expression and is influenced by both genetic and environmental factors. In poultry, DNA methylation is recognized as an important mechanism controlling physiological processes such as growth, metabolic regulation, immune function, and environmental adaptation. DNA methylation occurs through the addition of a methyl group to cytosine bases and is influenced by nutrients involved in one-carbon metabolism, including methionine, choline, betaine, folate, and B vitamins. These nutrients play a critical role in determining cellular methylation capacity and DNA methylation profiles. In addition, recent studies have shown that feed composition, dietary energy and protein levels, fatty acid profiles, and functional additives such as phytobiotics, antioxidants, probiotics, and prebiotics can affect epigenetic regulation. In particular, critical developmental stages such as embryonic development, the pre- and post-hatch periods, and transition phases in compound feeds exhibit high sensitivity to epigenetic modulation. Understanding the interactions between nutrition and DNA methylation provides a new perspective for improving

growth performance, animal health, and welfare in poultry. In this paper, the current effects of nutritional practices on DNA methylation in poultry are addressed, and the relationships among nutrients, metabolic activity, epigenetic modifications, and performance, animal health, and welfare are examined in light of the literature. The information obtained offers potential strategies for the development of epigenetic-based feeding programs and sustainable poultry production.

Keywords: Feeding, DNA methylation, epigenetics, poultry, performance.

Giriş

Hızla artan insan nüfusu ve küresel iklim değişikliğinin getirdiği zorluklar ile birlikte artan yüksek kaliteli hayvansal protein talebi sürdürülebilirliği elzem **hâle** getirmiştir. Bu nedenle hayvansal üretimde verimliliği artırmak, maliyeti düşürmek ve çevre dostu üretim sistemlerini geliştirmek amacıyla farklı yaklaşımlar geliştirmeye yönelik çalışmalara odaklanılmıştır (Capper ve Bauman, 2013; Scott, 2018; Wang ve Ibeagha-Awemu, 2021). Bu amaçla genotip analizler, genom dizilimleri ve haritası gibi ileri teknolojik uygulamalar kullanılmıştır. Bu da hayvancılıkta genetik iyileştirme programlarında önemli gelişmelere ve istenen hayvan özelliklerinin eldesine yol açmıştır (David ve ark., 2019; Soravia ve ark., 2021; Jianfang ve ark., 2025). Kanatlı yetiştiriciliğinde hızlı genetik ilerlemeler; yüksek büyüme hızı ve verim artışını mümkün kılmış olsa da, günümüz üretim modelleri hayvanların metabolik kapasitesi, bağışıklık sistemi ve stres yanıtı üzerinde önemli baskılar oluşturmaktadır. Bu nedenle, modern kanatlı üretiminde yalnızca klasik besleme stratejileri değil, aynı zamanda moleküler düzeyde besin–gen etkileşimlerini açıklayan **nutrigenomik** ve **epigenetik** yaklaşımlar giderek daha fazla önem kazanmaktadır (Zhang ve ark., 2015). Özellikle DNA metilasyonu, gen ekspresyonunu doğrudan etkileyen temel epigenetik mekanizmalardan biri olarak kabul edilmekte ve besin bileşenleri tarafından modüle edilebildiği bilinmektedir.

Metiyonin, kolin, betain, folik asit ve B_{12} vitamini gibi **metil vericiler**, kanatlılarda metilasyon döngüsünün temel bileşenlerini oluştururlar (Zhang ve ark., 2015). Bu bileşiklerin yetersizliği veya fazlalığı, büyüme ile üretim performansı, bağırsak sağlığı, lipit metabolizması ve stres yanıtı gibi fizyolojik süreçlerde önemli değişikliklere yol açabilmektedir. Dahası son çalışmalar, yem bileşimi, enerji ve protein düzeyleri, yağ asidi profilleri ile fitobiyotikler antioksidanlar, probiyotikler ve prebiyotikler gibi fonksiyonel katkı maddelerinin epigenetik düzenlemeyi etkileyebileceğini ortaya koymaktadır (Schreiber ve ark., 2025; Al Amaz ve ark., 2025). Ayrıca, epigenetik düzenlemelerin embriyonik gelişimden civciv çıkımına, bağışıklık sisteminin olgunlaşmasından yem değerlendirme kapasitesine kadar birçok fizyolojik aşamada kritik rol oynadığı bilinmektedir (Li ve ark., 2016; Zhu ve ark., 2020).

Son yıllarda yapılan çalışmalar, uygun besin bileşiminin yalnızca mevcut sürünün performansını değil, aynı zamanda **transgenerasyonel epigenetik aktarımla** gelecek nesillerin verim ve sağlık parametrelerini de etkileyebileceğini ortaya koymuştur (Yang ve ark., 2018; Ponsuksili ve ark., 2025). Bu bulgular, kanatlı besleme stratejilerinin artık sadece makro ve mikro besin gereksinimlerini karşılamanın ötesine geçerek, metabolik yolakları ve gen ekspresyon profillerini şekillendirecek biçimde tasarlanması gerektiğini göstermektedir. Bu bağlamda, DNA metilasyonunun kanatlı performansı, hayvan sağlığı ve refahı üzerindeki etkilerinin anlaşılması, hem bilimsel hem de sektörel açıdan önemli bir araştırma alanı haline gelmiştir. Epigenetik düzenlemelerin besleme ile modüle edilebilirliği, sürdürülebilir üretim modelleri ve refah odaklı yetiştiricilik açısından gelecek vaat eden bir yaklaşım sunmaktadır.

Bu bildiride, kanatlılarda besleme ve DNA metilasyonu: epigenetik, performans, hayvan sağlığı ve refahı üzerine etkilerine yönelik bilgilere ve önerilere yer verilmiştir.

Epigenetik

Epigenetik, ilk olarak Aristoteles yaklaşımı benimseyen Conrad Hal Waddington tarafından 1940'larda epigenez kelimesinden türetilmiş ve "DNA dizisinde değişiklik olmaksızın gen ifadesinde veya hücresel fenotipte meydana gelen değişiklikler" şeklinde tanımlamıştır (Zaccaria ve ark., 2025). Günümüzde ise epigenetik, "DNA dizisinde değişiklik olmaksızın bir kromozomdaki değişikliklerden kaynaklanan kararlı kalıtsal fenotip" ve "değişen aktivite durumlarını kaydetmek, sinyallemek veya sürdürmek için kromozomal bölgelerin yapısal adaptasyon" olarak ifade edilmektedir (Gibney ve Nolan, 2010; Schreiber ve ark., 2025). Epigenetik değişiklikler, genomun yapısal ve

fonksiyonel organizasyonunu etkileyerek hücrelerin hangi genleri ne zaman ve hangi düzeyde ifade edeceğini belirler.

Epigenetik süreçler; embriyonik gelişim, hücre farklılaşma, doku gelişim, metabolik süreçler, bağışıklık yanıtı ve çevresel uyaranlara adaptasyon gibi birçok biyolojik olayı yönlendiren temel mekanizmalardır (Carlberg ve Molnár, 2019). Son yıllarda hem insanlar hem de hayvanlar üzerine yapılan çalışmalarda, epigenetik süreçlerin canlı fizyolojisinde önemli roller üstlendiğini ifade etmişlerdir (Steffen ve Ringrose, 2014; Wang ve ark., 2022; Sindhu ve ark., 2024; Li ve ark., 2024). Çevresel koşullar, besleme stratejileri, stres faktörleri ve yetiştirme uygulamalarının epigenetik modifikasyonlar yoluyla gen ifadesini etkilemesi, hayvanların büyüme ve üretim performansı, ürün kalitesi, sağlık durumu ve refahı üzerinde belirleyici olabilmektedir (Ross ve ark., 2017; Zaccaria ve ark., 2025).

Epigenetik, birden fazla biyolojik mekanizma aracılığıyla gerçekleşmektedir. Bu mekanizmalardan histon modifikasyonları (PTM'ler), DNA metilasyonu (çoğunlukla CpG dinükleotidlerinde), kromatin değişiklikleri ve kodlamayan RNA **(miRNA, lncRNA vb.)** yaygın olarak kullanılmaktadırlar (Yakovlev, 2018; Wang ve Ibeagha-Awemu, 2021; Jianfang ve ark., 2025).

DNA metilasyonu

DNA metilasyonu en yaygın olarak kullanılan epigenetik mekanizmadır (Lindner ve ark., 2021; Garcia-Prieto ve ark., 2022; Ju ve ark., 2023). DNA metilasyonu, esas olarak sitozin kalıntılarının beşinci karbonunda bir metil (5mC) veya hidroksimetil (5hmC) grubunun eklenmesi ile gerçekleşir. Metilasyon çoğunlukla sitozin-fosfat-guanozin (CpG) dinükleotitlerinde görülse de, sitozin-fosfat-adenozin (CpA), sitozin-fosfat-timin (CpT) ve sitozin-fosfat-sitozin (CpC) dinükleotitlerinde de meydana gelebilir (Maiti ve Drohat, 2011). Bu süreç, DNA metiltransferazlar (DNMT'ler) olarak bilinen bir enzim sınıfının aktiviteleri tarafından katalize edilir. DNMT3A ve DNMT3B embriyonik gelişim sırasında veya çevresel uyaranlara yanıt olarak yeni metilasyon modellerinin kurulmasından sorumluyken, DNMT1 hücre bölünmesi sırasında mevcut metilasyon işaretlerini korur (Schmitz ve ark., 2019; Wang ve Ibeagha-Awemu, 2021). Kanatlı hayvanlarında DNA metilasyonu ile ilgili araştırmaların incelenmesi, üretimde bu mekanizmanın rolünü daha iyi anlamamıza ve belirli teorik temeller oluşturmamıza olanak tanımaktadır.

DNA metilasyonunu hayvanların çevresel faktörlere verilen biyolojik yanıtları şekillendirmede üstlendiği kritik rol göz önüne alındığında, özellikle besleme uygulamalarının bu epigenetik süreç üzerindeki etkilerini anlamak modern hayvancılık açısından büyük önem taşımaktadır. Bu mekanizmanın daha iyi anlaşılması; besleme stratejilerinin geliştirilmesi, büyüme ve üretim performansının artırılması, stresin azaltılması, hayvan sağlığının desteklenmesi ve hayvansal ürün kalitesinin iyileştirilmesi için yeni fırsatlar sunmaktadır. **Bu nedenle, beslemenin DNA metilasyonu üzerindeki etkisinin incelenmesi,** beslenme kaynaklı epigenetik düzenlemelerin hayvan performansı, sağlığı ve refahına nasıl yansıdığını anlamak açısından kritik rol oynamaktadır.

DNA metilasyonu üzerinde beslemenin rolü

Epigenom ile metabolom arasındaki yakın etkileşim, beslemenin bir hayvanın epigenetik düzenleme süreçlerinde belirleyici bir role sahip olduğunu göstermektedir (Gut ve Verdin, 2013; Carrillo ve ark., 2016). Bir organizmanın metabolomu, o organizmanın dokularında bulunan küçük moleküllü kimyasalları içerir ve temel besin maddelerinin yanı sıra temel olmayan bileşiklerin de dahil olduğu metabolizmanın ürünüdür; bu metabolizma, alınan besin maddelerini ve bileşikleri çok sayıda metabolitine dönüştürür (Schreiber ve ark., 2025). Bu metabolitlerin çoğu, epigenomu doğrudan veya dolaylı olarak etkileyebilir ve böylece gen ifadesini düzenleyebilir (Gut ve Verdin, 2013). Vücutta bulunan gerekli olan makro ve mikro besinlerin metabolizmasıyla ilişkili olan çeşitli metabolitler, aynı zamanda çeşitli epigenetik işlevler için ortak yardımcı faktörlerdir. Örnek olarak adenozin trifosfat (ATP), nikotinamid adenin dinükleotid (NAD^+), Asetil-CoA, S-Adenosilmetionin (SAM) ve α-ketoglutarat (αKG) verilebilir. Bu mekanizmalar, hayvanların çevresel koşullara yanıt verme kapasitesini belirleyen ve besleme-strateji-çevre etkileşimlerinin moleküler temelini oluşturan karmaşık bir düzenleme ağı ortaya çıkarır. Metiyonin, kolin, betain, folat ve B vitaminleri, yem bileşimi, enerji ve protein düzeyleri, yağ asidi profilleri ile fitobiyotikler,

antioksidanlar, probiyotikler ve prebiyotikler gibi fonksiyonel katkı maddelerinin epigenetik düzenlemeyi etkilemektedir.

Besleme DNA metilasyonunu üç şekilde etkilemektedir. Birincisi, uygun DNA metilasyonu için gerekli olan substratların sağlanması; ikincisi, DNMT'nin enzimatik aktivitesini düzenleyen kofaktörlerin sağlanması; üçüncüsü, tek karbon döngüsünü düzenleyen enzimlerin aktivitesinin değiştirilmesidir (Zhang ve ark., 2015). Önemli olan, bu üç mekanizmanın da birbirleriyle uyumlu olması ve zaman içinde birlikte çalışabilmesidir.

Metiyonin, kolin ve betain

Metiyonin, kolin ve betain gibi metil donörler, esas olarak tek karbon metabolizmasında görev alan ve biyokimyasal reaksiyonları, bağışıklık yanıtlarını, gen ekspresyonunu ve epigenetik olayları düzenleyen mikro besin maddeleridir (Kar ve ark., 2025). Esansiyel bir amino asit olan metiyonin, amino asitler arasında en iyi bilinen metil donörüdür. Metiyonin; DNA ve proteinler dâhil olmak üzere çeşitli moleküllere metil grubu aktararak temel biyolojik süreçlere katkı sağlar (Brosnan ve Brosnan, 2006). Betain (trimetilglisin), kolinden türeyen doğal bir bileşiktir ve üç metil grubu aktaran güçlü bir metil donörüdür. Betain; homosisteinin yeniden metiyonine dönüştürülmesi (remetilasyon) başta olmak üzere birçok metabolik reaksiyona katılır ve osmoregülasyon ile enerji metabolizmasında önemli bir rol oynar (Ducker ve Rabinowitz, 2017). Kanatlılarda karma yeme betain ilavesinin bağışıklık yanıtını güçlendirdiği de bilinmektedir (Yousefi ve ark., 2023). Kolin, betain sentezinin öncüsü olan, suda çözünebilen vitamin benzeri bir bileşiktir. Bir metil grubu aktarabilen kolin; DNA metilasyonu, lipid metabolizması ve nörotransmitter sentezinde görev alır (Kar ve ark., 2025). Bu metil donörleri bir metil grubunu diğer moleküllere aktararak gen ifadesini, lipit metabolizmasını, protein sentezini ve hücresel fonksiyonları etkilerler (Kar ve ark., 2025). Yapılan çalışmalarda kanatlı beslemede dengeli oranda metil donörlerinin bulunması, büyüme performansı, yem tüketimi, et kalitesi, bağışıklık fonksiyonlarını iyileştirirken sıcaklık stresinin olumsuz etkisini azalttığını belirtmişlerdir (Café, ve Waldroup, 2006; Su ve ark., 2009; Yang ve ark., 2017; Kar ve ark., 2025). Ayrıca yağlı karaciğer sendromunun oluşumunu önlediği ve yumurta tavuklarında sağlıklı tüylerin gelişimini ve yumurta üretimini teşvik ettikleri bildirmişlerdir (Zhang ve ark., 2022). Kanatlılarda üretim performansını, sağlığı ve refahı iyileştirmek için metil donörlerinin dikkate alınması ve dengelenmesi gerekecektir.

Folat, B_2, B_6 ve B_{12} vitaminleri

Folat B_2, B_6 ve B_{12} vitaminleri, folat döngüsündeki enzimlerin katalitik aktivitesinin düzenlenmesinde rol oynayan ve böylece SAM biyoyararlanımını belirleyen kofaktörlerdir. B_2 vitamini, 5,10-metilen THF'nin 5-metil THF'ye dönüşümünde metilentetrahidrofolat redüktazın (MTHFR) kofaktörü olan FAD'nin öncüsüdür. B_6 vitamini tetrahidrofolatın (THF) 5,10-metilen THF'ye dönüşümünde serin hidroksimetiltransferazın (SHMT) kofaktörüdür. Folat (B_9) ve kobalamin (B_{12}), sırasıyla DNA metilasyonu ve metiyonin sentezi için esansiyeldir (Kar ve ark., 2025). Folat, 5-metiltetrahidrofolat formunda bir metil grubunu homosisteine aktarır; bu reaksiyon vitamin B_{12}'nin kofaktör olarak görev yapmasını gerektirir ve

böylece metiyoninin yeniden oluşumunu sağlayarak tek-karbon metabolizmasını destekler. B_{12} vitamini, homosisteinin (Hcy) SAM'nin doğrudan öncüsü olan metiyonine dönüşümünü katalize eden 5-metiltetrahidrofolat-homosistein metiltransferazın (MTR) kofaktörüdür. Bu durumda, bu yardımcı faktörlerin biyoyararlanımı, tek karbon döngüsünün aktivitesini ve SAM üretimini değiştirerek DNA metilasyonunu etkileyebilir (Feil and Fraga, 2012; Zhang, 2015). Bu nedenle, karma yemlerin bu vitaminlerle desteklenmesin DNA metil işaretlerinin korunmasına veya yerleşmesine katkıda bulunacağı düşünülebilir (Farias ve ark., 2015).

Fonksiyonel katkı maddeleri

Bağırsak ortamındaki modülasyon epigenetik mekanizmaların düzenlenmesinde önemli bir rol oynamaktadır (Sharma ve ark., 2020). Bu nedenle mikrobiyom-konak etkileşimleri gen ifadesinin modülasyonunu etkilemektedir. Bağırsak mikrobiyotası metabolizma, immünomodülasyon ve nörolojik fonksiyonlar gibi hayati mekanizmalarda önemli rol oynamaktadır (Zheng ve ark., 2020). Fitobiyotikler, antioksidanlar, probiyotikler ve prebiyotikler gibi mikrobiyotayı düzenleme potansiyeline sahip yem katkı maddeleri kanatlılarda epigenetiği doğrudan veya dolaylı etkileyebilirler. Bu bileşiklerin bağırsak ortamında oluşturduğu değişiklikler, mikroorganizma metabolitlerinin

çeşitliliğini artırarak DNA metiltransferazların aktivitesi, metil donörlerinin biyoyararlanımı ve metilasyon kalıplarının yeniden düzenlenmesi üzerinde belirgin rol oynar. Özellikle kısa zincirli yağ asitleri gibi mikrobiyota kaynaklı metabolitler, gen promotör bölgelerindeki metilasyon düzeylerini etkileyerek hücresel farklılaşma, bağışıklık yanıtı ve metabolik fonksiyonlarla ilişkili genlerin ifade düzeylerinde değişikliklere yol açabilmektedir (Ponsuksili ve ark., 2025). Bu nedenle fonksiyonel katkı maddeleri, sadece besin öğesi olarak değil, aynı zamanda epigenetik birer düzenleyici olarak kanatlılarda büyüme performansı ve sağlık göstergeleri üzerinde önemli etkilere sahiptir (Dunislawska ve ark., 2020).

DNA metilasyonu ve Performans

DNA metilasyonu, gen ekspresyonunun çevresel ve beslenme faktörlerine yanıt olarak dinamik biçimde modüle edilmesini sağlayan önemli bir epigenetik mekanizmadır. Bu yaklaşım, kanatlılarda bir hayvanın gerçek fizyolojisini düzenleyen mekanizmaların daha iyi anlaşılmasını sağlar ve canlı ağırlık, canlı ağırlık artışı, yem tüketimi ve yemden yararlanma oranı gibi üretim performansına ilişkin karmaşık özelliklerin altında yatan biyolojik mekanizmaları yorumlamaya olanak tanır (Zaccaria ve ark., 2025).

Karma yemlerde metiyonin kısıtlaması büyüme performansını ve aminoasit metabolizmasını etkiler. Bu nedenle metil vericisi olarak bazı durumlarda betain ilavesi eklenir (Yang ve ark., 2017; Ju ve ark., 2023). Kazlarda yapılan bir çalışmada metiyonin ve betain kısıtlaması ile LOC106032502'nin karaciğer DNA metilasyonunu değiştirdiğini ve kazların transkripsiyonel düzenleyici ağını etkilediğini belirtmişlerdir (Yang ve ark., 2018).

Yapılan başka bir çalışmada ise yumurtacı tavuklarda embriyonik dönemin 11. gününde C vitaminin in ovo ile verilmesinin yumurtadan çıktıktan sonraki performansını ve bağışıklık durumunu iyileştirdiğini, antioksidan kapasitesini artırdığını bildirmişlerdir. Dahası enzimler ile ilgili DNA metilasyonu ve demetilasyonunun ekspresyon profili, dalak DNA metilasyon seviyesinin artmış olabileceğini düşündürmektedir, ancak anti-inflamatuar ve pro-inflamatuar sitokinlerde gözlenen ifade değişikliklerinin DNA metilasyonundaki değişikliklerle ilişkili olup olmadığı daha fazla araştırma gerektirmektedir (Zhu ve ark., 2020). Zhang ve ark. (2022) Jinghai Sarı tavuklarında ZP2 promotör metilasyonunun yumurta üretimi üzerindeki etkisi araştırılmıştır. ZP2 geninin eksik promotör vektörü oluşturularak, ZP2 geninin çekirdek bölgesinin -1.552 ile -1.348 arasında yer aldığı tahmin edilmiştir . *ZP2* gen promotör bölgesindeki mC-20 ve mC-21 bölgelerinin metilasyonu, mRNA ekspresyonu ile negatif korelasyon göstermiştir ($P < 0.05$). Her iki bölge de Sp1 transkripsiyon faktörü bağlanma bölgesinde yer almaktadır ve Sp1'in DNA'ya bağlanması engellenebilir, bu da ZP2 geninin transkripsiyonunu ve yumurta üretimini etkileyebilir (Zhang ve ark., 2022).

Kaz ciğeri, eşsiz aromasını veren çok sayıda doymamış yağ asidi içerir (Hermier et al., 2003; Dawail et al., 2003). Kazların karma yemine betain ilavesinin karaciğer ağırlığını artırdığı ve karaciğerindeki S14α mRNA ekspresyonun kontrol grubuna kıyasla yüksek olduğunu belirtmişlerdir. Bu bölgedeki tek bir alel (transkripsiyon başlangıç noktasına göre +374 ile -8 baz çifti arasında), 33 CpG dinükleotid içeren sodyum sülfit ile dizinlenmiştir. Yüksek düzeyde yem tüketen grupta daha yüksek S14α transkriptleri gözlenmesine rağmen, 33 CpG bölgesinin ortalama metilasyon oranı %87.9 olarak ölçülmüştür; kontrol grubunda bu oran %69.6 olup genin daha düşük ekspresyonunu olduğunu belirtmişlerdir ($P<0.01$). Bu sonuçlar, S14α geninin transkripsiyon başlangıç bölgesindeki DNA metilasyon modellerinin, betain ilavesinden sonra mRNA ekspresyon düzeylerinden bağımsız olabileceğini ifade etmişlerdir.

Sonuç olarak, belirli gen promotör bölgelerindeki metilasyon değişimleri, ilgili genlerin ekspresyonunu doğrudan baskılayabilir veya artırabilir; bu mekanizma özellikle büyüme ve üretim performansında kritik rol oynar. Bu bulgular, özellikle besleme ve mikrobiyota kaynaklı epigenetik modülasyonun, kanatlılarda performans özelliklerini optimize etmede potansiyel bir araç olduğunu göstermektedir.

DNA metilasyonu ile hayvan sağlığı ve refahı

Hayvansal üretim işletmelerinde, sağlık durumu kârlılık ve sürdürülebilirliği doğrudan etkilemektedir. Etlik piliçlerde yaygın olarak görülen bir beslenme ve metabolik bozukluk olan asit sendromu (AS), hayvan endüstrisinde önemli ekonomik kayıplara neden olmaktadır (Balog ve ark., 2003; Zhang ve ark., 2026). Zhang ve

ark. (2026) AS'li ve normal etlik piliçleri rutin hematolojik muayeneler ve kan parametrelerini karşılaştırmışlardır. Sonuç olarak, AS grubundaki etlik piliçlerde kalp doku hasarının artığı, kalp dokusundaki 891 ve akciğer dokusunda 1424 genin ekspresyon seviyelerinin promotör metilasyonu ile negatif korelasyon olduğunu tespit etmişlerdir. qPCR ve bisülfit sekanslama yoluyla yapılan doğrulama, HEMK1 ve PMEPA1'in ekspresyon seviyeleri ile promotör CpG adalarının metilasyon seviyeleri arasında anlamlı bir negatif korelasyon olduğunu doğrulayarak, bunların AS patogenezinde aday genler olarak rollerini desteklediğini ifade etmişlerdir.

Kuş lökoz virüsü alt grubu J (ALV-J) ve *Salmonella enterica serovar enteritidis* (SE), kanatlı üretimini etkileyerek endüstrisinde ciddi ekonomik kayıplara yol açabilecek ve halk sağlığı için tehdit oluşturabilecek potansiyele sahiptir (Wang et al., 2020; Ju ve ark., 2023). Yapılan çalışmalarda, hastalığın görülme sıklığındaki artış DNA metilasyonundaki değişikliklerle ilişkili olduğunu belirtmişlerdir (Bosilevac ve ark., 2009; Guibourdenche ve ark., 2010; Ju ve ark., 2023). Wang et al. (2020) tavuklarda SE reaksiyonunun tüm genom DNA metilasyon profilini analiz edilmiş ve SE aşılama kör bağırsak dokularında DNA metilasyonunu teşvik ederek bağışıklık ve metabolizma ile ilişkili genlerde metilasyon değişikliklerine yol açtığını bildirmişlerdir.

DNA metilasyonu, stresli koşullar sırasında aktive olan spesifik genlerin aktivitesini baskılayarak strese uyum sağlamak için potansiyel bir mekanizmadır (Mifsud ve ark., 2011; Al Amaz ve ark., 2025). Karaciğerde DNMT1, DNMT3A ve DNMT3B ekspresyonunun aşağı regülasyonu, tavuklarda beslenme stresi göstergesi olarak değerlendirilmektedir (Kang ve ark., 2017). Yüksek sıcaklık ortamında kuru erik takviyesi ile beslenen hayvanlarda DNMT1 ve DNMT3A'nın önemli ölçüde yukarı regülasyonu ($P<0.05$) gözlenmiş ve bu durum kuru erik ilavesi ile beslenmenin strese karşı koruyucu etkisi olabileceğini belirtmişlerdir. Aktif DNA demetilasyonun katalize eden evrimsel olarak korunduğu ve TET proteinleri (Tet1, Tet2 ve Tet3), 5-metilsitozin (5mC) üzerinde ardışık oksidasyonlar gerçekleştirerek 5-hidroksimetilsitozin (5hmC), 5-formilsitozin (5fC) ve 5-karboksilsitozin (5caC) oluşumunu sağladığını bildirmişlerdir. Sonuç olarak bu mekanizmalar, piliçlerde stres ve hastalık koşullarına yanıt olarak gen ekspresyonunun epigenetik olarak düzenlenmesinde merkezi bir rol oynadığını ifade etmişlerdir.

Sonuç

Kanatlılarda besleme-DNA metilasyonu arasındaki etkileşim performans, sağlık ve refahı doğrudan etkilemektedir. Özellikle metil donörleri (metiyonin, kolin, betain, folat ve B vitaminleri) ve mikrobiyotayı doğrudan etkileyen fonksiyonel katkı maddeleri (fitobiyotikler, probiyotikler ve prebiyotikler gibi) DNA metilasyonu etkileyerek büyüme, metabolizma, bağışıklık fonksiyonu ve stres yanıtı ile ilişkili genlerin ekspresyonunu modüle edebilmektedir. Bu nedenle; kanatlılarda karma yem hazırlanırken makro ve mikro besin madde ihtiyacını göz önünde bulundururken aynı zamanda epigenetik düzenlemeleri desteklemeyi de hedeflemek önerilmektedir. Metil donörlerinin dengeli ve yeterli düzeylerde karma yemlere dahil edilmesi, fonksiyonel yem katkı maddelerinin bağırsak mikrobiyotası ve epigenetik mekanizmalar üzerindeki etkilerinin dikkate alınması, hayvan performansı, sağlığı ve refahı iyileştirebilir. Ayrıca, farklı gelişim dönemlerine özgü epigenetik yanıtların ortaya konulması ve bu yanıtların gen–besin etkileşimleri temelinde değerlendirilmesi, daha hassas ve sürdürülebilir besleme stratejilerinin geliştirilmesine katkı sunacaktır. Gelecekte yapılacak çalışmaların, transgenerasyonel epigenetik etkiler ve uzun dönemli üretim sonuçları üzerine odaklanması, epigenetik temelli besleme yaklaşımlarının pratik uygulamalara aktarılmasını kolaylaştıracaktır.

KAYNAKLAR

Al Amaz, S., Wasti, S., Adnan, M. R., Chaudhary, A., Jha, R., & Mishra, B. (2025). Dried plum supplementation enhanced the expression of liver antioxidant capacity, metabolism, and epigenetic-related gene markers in broiler chickens under heat stress conditions: Dried plum increased liver metabolism in broiler. Poultry science, 104(4), 104911.

Balog, J. M., Kidd, B. D., Huff, W. E., Huff, G. R., Rath, N. C., & Anthony, N. B. (2003). Effect of cold stress on broilers selected for resistance or susceptibility to ascites syndrome. Poultry science, 82(9), 1383-1387.

Brosnan, J. T., & Brosnan, M. E. (2006). The sulfur-containing amino acids: an overview. *The Journal of nutrition*, *136*(6), 1636S-1640S.

Café, M. B., & Waldroup, P. W. (2006). Interactions between levels of methionine and lysine in broiler diets changed at typical industry intervals. *International journal of poultry science*, *5*(11), 1008-1015.

Capper, J. L., & Bauman, D. E. (2013). The role of productivity in improving the environmental sustainability of ruminant production systems. Annual Review of Animal Biosciences. 1(1), 469-489.

Carlberg, C., & Molnár, F. (2019). Human epigenetics: How science works (pp. 89-99). New York, NY, USA:: Springer.

Carrillo, J. A., He, Y., Li, Y., Liu, J., Erdman, R. A., Sonstegard, T. S., & Song, J. (2016). Integrated metabolomic and transcriptome analyses reveal finishing forage affects metabolic pathways related to beef quality and animal welfare. Scientific reports, 6(1), 25948.

Chamruspollert, M., Pesti, G. M., & Bakalli, R. I. (2002). Dietary interrelationships among arginine, methionine, and lysine in young broiler chicks. British journal of nutrition, 88(6), 655-660.

Davail, S., Rideau, N., Guy, G., André, J. M., Hermier, D., & Hoo-Paris, R. (2003). Hormonal and metabolic responses to overfeeding in three genotypes of ducks. *Comparative* biochemistry and physiology part a: molecular & integrative physiology, 134(4), 707-715.

David, S. A., Vitorino Carvalho, A., Gimonnet, C., Brionne, A., Hennequet-Antier, C., Piégu, B., Crochet, S., Courousse, N., Bordeau, T., Bigot, Y., Collin, A., & Coustham, V. (2019). Thermal manipulation during embryogenesis impacts H3K4me3 and H3K27me3 histone marks in chicken hypothalamus. Frontiers in genetics, 10, 1207.

Ducker, G. S., & Rabinowitz, J. D. (2017). One-carbon metabolism in health and disease. *Cell metabolism*, *25*(1), 27-42.

Dunislawska, A., Slawinska, A., & Siwek, M. (2020). Hepatic DNA methylation in response to early stimulation of microbiota with *Lactobacillus* synbiotics in broiler chickens. Genes, 11(5), 579.

Farias, N., Ho, N., Butler, S., Delaney, L., Morrison, J., Shahrzad, S., & Coomber, B. L. (2015). The effects of folic acid on global DNA methylation and colonosphere formation in colon cancer cell lines. The journal of nutritional biochemistry, 26(8), 818-826.

Feil, R., & Fraga, M. F. (2012). Epigenetics and the environment: emerging patterns and implications. Nature reviews genetics, 13(2), 97-109.

Garcia-Prieto, C. A., Álvarez-Errico, D., Musulen, E., Bueno-Costa, A., N. Vazquez, B., Vaquero, A., & Esteller, M. (2022). Validation of a DNA methylation microarray for 285,000 CpG sites in the mouse genome. Epigenetics, 17(12), 1677-1685.

Gibney, E. R., & Nolan, C. M. (2010). Epigenetics and gene expression. Heredity, 105(1), 4-13.

Gut, P., & Verdin, E. (2013). The nexus of chromatin regulation and intermediary metabolism. Nature, 502(7472), 489-498.

Hermier, D., Guy, G., Guillaumin, S., Davail, S., Andre, J. M., & Hoo-Paris, R. (2003). Differential channelling of liver lipids in relation to susceptibility to hepatic steatosis in two species of ducks. Comparative biochemistry and physiology part b: biochemistry and molecular biology, 135(4), 663-675.

Jianfang, W., Raza, S. H. A., Pant, S. D., Juan, Z., Prakash, A., Abdelnour, S. A., Aloufi, B. H., Mahasneh, Z. M. H., Amin, A. A., Şokrullahi, B., & Zan, L. (2025). Exploring epigenetic and genetic modulation in animal responses to thermal stress. Molecular biotechnology, 67(3), 942-956.

Kang, S. W., Madkour, M., & Kuenzel, W. J. (2017). Tissue-specific expression of DNA methyltransferases involved in early-life nutritional stress of chicken, Gallus gallus. *Frontiers in genetics*, *8*, 204.

Kar, I., Mukherjee, A., & Patra, A. K. (2025). Methyl donors and their roles in poultry nutrition. In organic feed additives for livestock (pp. 161-173). Academic Press.

Li, C. Z., Haghani, A., Yan, Q., Lu, A. T., Zhang, J., Fei, Z., Ernset, J., Yang, X. W., Gladyshev, V. N., Robeck, T. R., Chavez, A., S., Cook, J. A., Dunnum, J. L., Raj, K., Seluanov, A., Gorbunova, V., & Horvath, S. (2024). Epigenetic predictors of species maximum life span and other life-history traits in mammals. Science advances, 10(23), eadm7273.

Li, S., Zhi, L., Liu, Y., Shen, J., Liu, L., Yao, J., & Yang, X. (2016). Effect of in ovo feeding of folic acid on the folate metabolism, immune function and epigenetic modification of immune effector molecules of broiler. British journal of nutrition, 115(3), 411-421.

Lindner, M., Laine, V. N., Verhagen, I., Viitaniemi, H. M., Visser, M. E., van Oers, K., & Husby, A. (2021). Rapid changes in DNA methylation associated with the initiation of reproduction in a small songbird. Molecular ecology, 30(15), 3645-3659.

Maiti, A., & Drohat, A. C. (2011). Thymine DNA glycosylase can rapidly excise 5-formylcytosine and 5-carboxylcytosine: potential implications for active demethylation of CpG sites. Journal of biological chemistry, 286(41), 35334-35338.

Mifsud, K. R., Gutièrrez-Mecinas, M., Trollope, A. F., Collins, A., Saunderson, E. A., & Reul, J. M. (2011). Epigenetic mechanisms in stress and adaptation. Brain, behavior, and immunity, 25(7), 1305-1315.

Ponsuksili, S., Hadlich, F., Li, S., Trakooljul, N., Reyer, H., Oster, M., Abitew, Y. M., Sommerfeld, V., Rodehutscord, M., & Wimmers, K. (2025). DNA methylation dynamics in the small intestine of egg-selected laying hens along egg production stages. Physiological genomics, 57(3), 125-139.

Reik, W., W. Brown, K., E. Slatter, R., Sartor, P., Elliott, M., & R. Maher, E. (1994). Allelic methylation of H19 and IGF2 in the Beckwith—Wiedemann syndrome. Human molecular genetics, 3(8), 1297-1301.

Ross, J. W., Hale, B. J., Seibert, J. T., Romoser, M. R., Adur, M. K., Keating, A. F., & Baumgard, L. H. (2017). Physiological mechanisms through which heat stress compromises reproduction in pigs. Molecular reproduction and development, 84(9), 934-945.

Schmitz, R. J., Lewis, Z. A., & Goll, M. G. (2019). DNA methylation: shared and divergent features across eukaryotes. Trends in genetics, 35(11), 818-827.

Schreiber, S. P., Villalba, J., & Meyer-Ficca, M. L. (2025). Potential Epigenetic Impacts of Phytochemicals on Ruminant Health and Production: Connecting Lines of Evidence. Animals, 15(12), 1787.

Scott, C. (2018). Sustainably sourced junk food? Big food and the challenge of sustainable diets. *Global* environmental politics, 18(2), 93-113.

Sharma, M., Li, Y., Stoll, M. L., & Tollefsbol, T. O. (2020). The epigenetic connection between the gut microbiome in obesity and diabetes. Frontiers in genetics, 10, 1329.

Sindhu, P., Magotra, A., Sindhu, V., & Chaudhary, P. (2024). Unravelling the impact of epigenetic mechanisms on offspring growth, production, reproduction and disease susceptibility. Zygote, 32(3), 190-206.

Soravia, C., Ashton, B. J., Thornton, A., & Ridley, A. R. (2021). Investigating the relationship between heat stress and cognition in a wild animal. WIREs climate change, 12, e713.

Steffen, P. A., & Ringrose, L. (2014). What are memories made of? How Polycomb and Trithorax proteins mediate epigenetic memory. Nature reviews molecular cell biology, 15(5), 340-356.

Su, S. Y., Dodson, M. V., Li, X. B., Li, Q. F., Wang, H. W., & Xie, Z. (2009). The effects of dietary betaine supplementation on fatty liver performance, serum parameters, histological changes, methylation status and the mRNA expression level of Spot14α in Landes goose fatty liver. Comparative biochemistry and physiology part a: molecular & integrative physiology, 154(3), 308-314.

Wang, K., Liu, H., Hu, Q., Wang, L., Liu, J., Zheng, Z., Zhang, W., Ren, J., Zhu, F., & Liu, G. H. (2022). Epigenetic regulation of aging: implications for interventions of aging and diseases. Signal transduction and targeted therapy, 7(1), 374.

Wang, M., & Ibeagha-Awemu, E. M. (2021). Impacts of epigenetic processes on the health and productivity of livestock. Frontiers in genetics, 11, 613636.

Yakovlev, A. F. (2018). Epigenetic effects in livestock breeding. Russian journal of genetics, 4(8), 897-909.

Yang, Z., Wang, Z. Y., Yang, H. M., Xu, L., & Gong, D. Q. (2017). Effects of dietary methionine and betaine on slaughter performance, biochemical and enzymatic parameters in goose liver and hepatic composition. Animal feed science and technology, 228, 48-58.

Yang, Z., Yang, H. M., Gong, D. Q., Rose, S. P., Pirgozliev, V., Chen, X. S., & Wang, Z. Y. (2018). Transcriptome analysis of hepatic gene expression and DNA methylation in methionine-and betaine-supplemented geese (Anser cygnoides domesticus). Poultry science, 97(10), 3463-3477.

Yousefi, J., Taherpour, K., Ghasemi, H. A., Akbari Gharaei, M., Mohammadi, Y., & Rostami, F. (2023). Retracted Artıcle: Effects of emulsifier, betaine and l-carnitine on growth performance, immune response, gut morphology and nutrient digestibility in broiler chickens exposed to cyclic heat stress. *British poultry science*, *64*(4), iii-xvi.

Zaccaria, E., van der Valk, E., Kar, S. K., Rebel, J. M., & Schokker, D. (2025). Mini review: Studying epigenomic alteration can shed light on coping and adaptive abilities during heat stress in monogastric livestock. Frontiers in genetics, 16, 1561804.

Zhang, J., Zhang, X. Q., Ling, X. Z., Zhao, X. H., Zhou, K. Z., Wang, J. Y., & Zhang, G. X. (2022). Prediction of the effect of methylation in the promoter region of ZP2 gene on egg production in Jinghai yellow chickens. Veterinary sciences, 9(10), 570.

Zhang, N. (2015). Epigenetic modulation of DNA methylation by nutrition and its mechanisms in animals. Animal nutrition, 1(3), 144.

Zheng, D., Liwinski, T., & Elinav, E. (2020). Interaction between microbiota and immunity in health and disease. Cell research, 30(6), 492-506.

Zhu, Y., Li, S., Duan, Y., Ren, Z., Yang, X., & Yang, X. (2020). Effects of in ovo feeding of vitamin C on post-hatch performance, immune status and DNA methylation-related gene expression in broiler chickens. British journal of nutrition, 124(9), 903-911.

ORAL PRESENTATION

Effects of exogenous glucose on leaf color and biochemical–antioxidant properties of two purple basil (*Ocimum basilicum* L.) cultivars

Sercan Önder[1*] (Orcid: https://orcid.org/0000-0002-8065-288X),
Murat Mutlucan[2] (Orcid: https://orcid.org/0000-0002-6990-277X)

[*1]Isparta University of Applied Sciences, Faculty of Agriculture, Department of Agricultural Biotechnology, Isparta, Türkiye
[2]Isparta University of Applied Sciences, Rose and Aromatic Plants Application and Research Center, Isparta, Türkiye

*Corresponding author e-mail: sercanonder@isparta.edu.tr

Abstract

Basil (*Ocimum basilicum* L.) is an important aromatic herb rich in biologically active compounds, including pigments, phenolics, flavonoids, and antioxidants, and is widely recognized for its significant economic value in culinary and industrial applications. Glucose, a soluble sugar present in many plants, not only serves as a universal carbon source but also functions as a signaling molecule that regulates various metabolic processes in plants. This study investigated the effects of exogenous glucose treatment on color and pigment composition, primary and secondary metabolite accumulation, and antioxidant capacity in the leaves of two purple basil cultivars (Dark Opal and Red Boza). Following glucose treatment, L* and b* values decreased slightly, whereas a* values increased in both cultivars. Glucose also induced cultivar-specific metabolic responses: Dark Opal exhibited enhanced anthocyanin accumulation, resulting in more intense purple leaf coloration, while Red Boza showed increased chlorophyll and carotenoid accumulation, leading to darker green leaves. Although total phenolics content and CUPRAC activity were not significantly affected by glucose treatment, FIC capacity and starch accumulation increased significantly in both cultivars. These findings indicate that glucose acts not only as an energy source but also as a signaling molecule influencing pigment biosynthesis, antioxidant capacity, and carbohydrate metabolism in a genotype-dependent manner. The distinct metabolic responses observed between Dark Opal and Red Boza highlight the role of sugar signaling in regulating cultivar-specific physiological and biochemical processes.

Keywords: Anthocyanin, Antioxidant capacity, Chlorophyll, Leaf color, Starch content, Total phenolics

1. Introduction

Basil (*Ocimum basilicum* L.) belongs to the Lamiaceae family, which comprises annual and perennial herbs and shrubs native to tropical and subtropical regions. The basil is an aromatic plant and the market value of basil leaves is projected to increase from approximately US$ 1.5 million in 2024 to US$ 2.3 million by 2034 (FMI, 2025). Although basil has numerous varieties that do not differ markedly in morphology, they vary significantly in their chemical compositions. The leaves contain essential oils, flavonoids, phenolic acids, triterpenes, steroids, and other nutraceutical compounds, as well as abundance of vitamins and minerals (Cruz et al., 2020). In addition to being cultivated as a medicinal herb and as a vegetable, basil is widely used in both fresh and dried forms to enhance the flavor and aroma of food products, such as tomato paste, ketchup, sauces, and soups (Lupton et al., 2016). Furthermore, basil leaves have been reported to possess antidiabetic (Mousavi et al., 2018), antimicrobial (Stefan et al., 2013), antibacterial (Stanojevic et al., 2017), antioxidant, and anti-inflammatory properties (Dhama et al., 2023). Today, basil retains high commercial value due to its diverse applications in medicinal, nutritional, ornamental, cosmetic, religious, and insecticidal or insect-repellent uses.

Glucose serves as a primary precursor for many biomolecules in plants, including complex sugars, amino acids, and nucleic acids (Sami and Hayat, 2019). It plays a central role in regulating numerous physiological processes under both stress and normal conditions. In recent years, increasing attention has been given to the role of glucose as a major signaling molecule that promotes plant growth, including its involvement in photosynthesis (Jiang et al.,

2012), hypocotyl elongation (Gibson, 2005), seed germination (Price et al., 2004), flowering (Moghaddam and Ende, 2013), and the onset of senescence (Wingler et al., 2009). Previous studies on glucose-induced plant growth have demonstrated that exogenous glucose treatment increases plant height, root length, and root and shoot biomass under normal conditions (Gauchan, 2012; Singh et al., 2014). Moreover, sugar treatments have been shown to influence photosynthetic performance by enhancing chlorophyll biogenesis (Hill et al., 2011). A positive correlation has also been observed between exogenous glucose and carotenoid accumulation in tomato leaves (Mortain-Bertrand et al., 2008). Additionally, glucose is reported to improve photosynthesis under various abiotic stress conditions (MengYun et al., 2009; Jiang et al., 2012). Therefore, glucose treatment is considered an environmentally friendly and valuable approach to improve plant growth, pigment content, and bioactive compounds.

Foliar treatments offer a promising strategy to optimize crop performance, particularly in crops such as basil, where effective nutrient delivery is essential for vigorous growth and enhanced production of bioactive metabolites (Noroozlo et al., 2019). Foliar treatment of sugar-based biostimulants, including glucose, has attracted considerable attention due to their potential to improve plant growth, nutrient uptake, and overall productivity. Sugar molecules such as glucose can enhance both physiological and biochemical responses in plants.

Although glucose is recognized as a fundamental energy source supporting nearly all physiological processes in plants, information regarding the effects of exogenous glucose on basil growth, pigment content, and functional metabolites remains limited. Therefore, this study was designed to investigate the potential effects of foliar glucose treatment on the pigment composition, biochemical compounds, and antioxidant capacity of basil leaves.

2. Materials and Methods

2.1. Plant Materials and Treatments

This study was conducted in a greenhouse of the Rose and Aromatic Plants Application and Research Center of Isparta University of Applied Sciences (Isparta, Türkiye). Seeds of two purple basil (*Ocimum basilicum* L.) cultivars (Dark Opal and Red Boza) were purchased from commercial suppliers and sown to obtain seedlings. The seeds were sown in 1 L plastic pots filled with a perlite–peat mixture (1:1) on May 11, 2024. All plants were fertilized with an NPK solution (20-20-20) once during vegetative growth. Two treatments were applied twice with one-week intervals to plants before flowering. Before flowering, the control (distilled water) and 330 mM glucose (prepared with distilled water) solutions were applied by foliar spraying twice at 1-week intervals (10 mL per plant). Distilled water was sprayed to control plants under the same conditions. For each treatment, 15 plants (one plant per pot) were used, and each replication contained 5 plants. Plants were harvested on September 10, 2024 (Fig. 1). Leaf color parameters were measured immediately using fresh leaves, and the remaining samples were stored in deep-freeze conditions until further analyses.

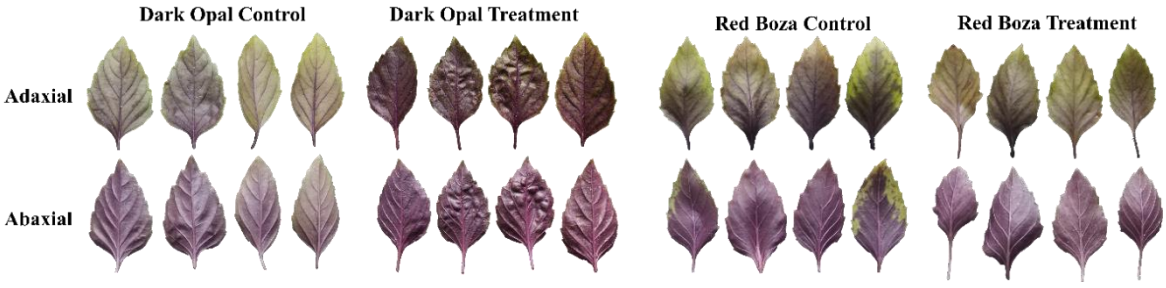


Fig. 1. Effect of glucose treatment on leaf color of Dark Opal and Red Boza cultivars.

2.2. Leaf Color Measurement

Color parameters of fresh basil leaves were determined using a portable colorimeter (Chroma Meter CR-400, Konica Minolta, Japan). Measurements were performed by placing leaf samples directly onto the measurement

port. Hunter's International Commission on Illumination color values (L^*, a^*, b^*) were recorded from three different points on the adaxial leaf surface.

2.3. Determination of Total Phenolic, Flavonoid and Antioxidant Capacity

Leaf samples (2 g) were extracted with 20 mL of 80% methanol in an ultrasonic bath at 40 °C for 30 min (Önder et al., 2023). The homogenate was centrifuged at 10.000 × g for 10 min, and aliquots of the supernatant were used to determine total phenolics, flavonoids, and antioxidant capacity. Total phenolics content was measured using the Folin-Ciocalteu method (Folin and Ciocalteu, 1927). To 100 µL of methanol extract, 2.5 mL of deionized water and 100 µL of Folin-Ciocalteu reagent (2 N) were added, and the mixture was incubated in the dark for 6 min. Then, 500 µL of 20% sodium carbonate was added, followed by a dark 30-min incubation. The color development in the samples was determined at a wavelength of 760 nm (Shimadzu UV-1280). Results were expressed as gallic acid equivalents (GAE) in mg g^{-1} fresh weight (FW).

Flavonoid content was determined using the aluminum chloride method (Sakanaka et al., 2005). To a 250 µL of methanolic extract, 1.25 mL of deionized water and 75 µL of 5% sodium nitrite were added and incubated for 6 min in the dark. Then, 150 µL of 10% aluminum chloride was added and incubated for 5 min, followed by the addition of 500 µL of 1 M NaOH and 275 µL of deionized water. After a 15-min incubation in the dark, absorbance was recorded at a wavelength of 510 nm. Results were expressed as (±)-catechin equivalent in mg g^{-1} FW.

Antioxidant capacity was measured by two different methods (CUPRAC and FIC). The CUPRAC assay was performed as described by Apak et al. (2006). A mixture of 1 mL of 10 mM Cu(II), 1 mL of 7.5 mM neocuproine, and 1 mL of 1 M ammonium acetate buffer (pH 7.0) was prepared. Then, 0.5 mL of diluted extract and 0.6 mL of distilled water were added to reach a final volume of 4.1 mL. After 30 min at room temperature, absorbance was measured at 450 nm. Results were expressed as Trolox equivalents (µmol Trolox g^{-1} FW).

Ferrous ion-chelating (FIC) ability was determined following Decker and Welch (1990). Sample extract (1 mL), 3.7 mL of distilled water, 100 µL of 2 mM iron (II) chloride, and 200 µL of 5 mM ferrozine was incubated for 20 min. Absorbance was measured at 562 nm against a blank, contained distilled water instead of methanolic extract and ferrozine solution. Results were expressed as EDTA equivalents (µmol EDTA g^{-1} FW).

2.4. Anthocyanin Content Measurement

Total anthocyanin content of leaves was determined using the pH differential method (Giusti and Wrolstad, 2001). Leaf samples (1 g) were homogenized in 10 mL ethanol containing 0.1% HCl in the dark. The homogenate was centrifuged at 10.000 × g for 20 min at 4 °C, and the supernatant was used for analysis. Two dilutions were prepared simultaneously: one adjusted to pH 1.0 with 0.025 M KCl and the other to pH 4.5 with 0.4 M sodium acetate. After 15 min of dark incubation, absorbance was recorded at 510 and 700 nm. Absorbance (A) of the samples was calculated as:

$$A = (A_{510} - A_{700})_{pH1.0} - (A_{510} - A_{700})_{pH4.5}$$

Monomeric anthocyanin concentration was calculated as cyanidin-3-glucoside equivalent using:

$$\text{Monomeric anthocyanin pigment (mg L}^{-1}) = \frac{A \times M_a \times DF \times 1000}{\varepsilon \times 1}$$

Where Ma =449.2, DF = dilution factor, and $\varepsilon = 26{,}900$

2.5. Total Chlorophyll and Carotenoid Content Measurement

Total chlorophyll (Zhang and Huang, 2013) and carotenoid (Torres et al., 2014) contents were determined spectrophotometrically. Leaf tissue (1 g) was homogenized with 10 mL dimethylformamide (100%). After centrifugation at 10.000 × g for 10 min at 4 °C, absorbance was recorded at 480, 647, and 664 nm wavelengths.

Chlorophyll and carotenoid contents were calculated using the following equations:

$$\text{Chlorophyll a } (\mu g\ mL^{-1}) = 12.7 \times A_{664} - 2.79 \times A_{647}$$

$$\text{Chlorophyll b } (\mu g\ mL^{-1}) = 20.7 \times A_{647} - 4.62 \times A_{664}$$

$$\text{Total Chlorophyll } (\mu g\ mL^{-1}) = 17.9 \times A_{647} + 8.08 \times A_{664}$$

$$\text{Total Carotenoids } (\mu g\ mL^{-1}) = (1000 \times A_{480} - 0.89 \times \text{Klorofil a}) / 245$$

2.6. Starch Content Measurement

Starch content was quantified using the Anthrone method (Sadasivam and Manickam, 1996). Leaf samples (0.5 g) were homogenized in 25 mL of 80% ethanol, boiled at 90 °C for 20 min, and centrifuged at 13,000 rpm for 10 min. The procedure was repeated three times. The pellet was washed, air-dried overnight, and then suspended in 5 mL deionized water and 6.5 mL of 52% cold perchloric acid. After incubation at 0 °C for 20 min, samples were centrifuged twice at 13,000 rpm for 10 min at 4 °C, and supernatants were combined and diluted to 100 mL with deionized water. After filtration (Whatman No. 42), 1 mL extract was mixed with 4 mL Anthrone reagent and heated in boiling water for 10 min. Absorbance was recorded at 630 nm. Results were expressed as glucose equivalents (mg g^{-1} FW).

2.7. Statistical analysis

Data were subjected to one-way analysis of variance (ANOVA) using SPSS Statistics 27 program (IBM, Armonk, NY, USA). Differences between the treatment means were separated using Tukey's test. Results are presented as mean ± standard deviation. Means sharing the same letter(s) are not significantly different at $P \leq 0.05$ significance level.

3. Results and Discussion

Color parameters measured from the adaxial surface are presented in Table 1. Following glucose treatment, the *L** value (brightness) decreased slightly in both cultivars; however, the reduction was not significant. The *a** value in Dark Opal significantly increased by 3.52-fold after glucose treatment, indicating a more intense red/purple coloration compared to the control. In Red Boza, the *a** value also increased by 2.21-fold, but the change was not statistically significant. The *b** value decreased in both cultivars; however, the decrease was significant only in Dark Opal. Comparison between the cultivars after glucose treatment showed that Dark Opal had lower *L** and *b** and higher *a** values, suggesting a stronger purple pigmentation.

Table 1. Effect of foliar treatment of 330 mM glucose on color parameters of Dark Opal and Red Boza (L*: black [−] with white [+]; a*: green [−] to red [+], b*: blue [−] to yellow [+])

		L*	***a****	***b****
Dark Opal	Control	32.71±5.27^{ab}	1.35±2.94^{b}	7.58±3.62^{a}
	Treatment	28.85±2.88^{b}	4.75±3.06^{a}	3.91±1.80^{b}
Red Boza	Control	32.77±7.13^{a}	1.55±5.59^{b}	7.45±5.69^{a}
	Treatment	31.44±4.55^{ab}	3.43±2.20^{ab}	5.60±3.09^{ab}

Basil is well known for its richness in bioactive compounds such as phytopigments, phenolics, flavonoids, and antioxidants. Glucose acts both as a key metabolite and as a signaling molecule in higher plants. Though total phenolics content increased in both cultivars following glucose treatment, the increases were not statistically significant (Fig. 2a). Total phenolics content increased from 6.41 (control) to 7.78 mg GAE g^{-1} in Dark Opal and from 7.79 (control) to 8.17 mg GAE g^{-1} in Red Boza. Consistent with our findings, glucose treatment increased total phenolics by 20% in Chinese cabbage sprouts and 25% in pak choi sprouts, whereas no effect was observed

in radish sprouts (Wei et al., 2011).

Total flavonoid content in the leaves ranged from 4.45 to 5.18 mg catechin g^{-1} (Fig. 2b). In Red Boza, any significant difference was not detected between the control (5.18 mg catechin g^{-1}) and glucose-treated plants (5.10 mg catechin g^{-1}). In Dark Opal, total flavonoid content decreased 1.16-fold following glucose treatment. Similarly, Hassanpouraghdam et al. (2022) reported that foliar application of 2 g L^{-1} D-glucose in *Tanacetum balsamita* did not alter flavonoid content under non-stress conditions.

The CUPRAC and FIC assays are widely used to evaluate antioxidant capacity. Glucose treatment did not significantly affect CUPRAC activity (Fig. 2c). While CUPRAC activity increased by 4.83% in Dark Opal relative to the control, it decreased by 4.79% in Red Boza. In contrast, glucose treatment significantly boosted FIC capacity in both cultivars (Fig. 2d). FIC capacity increased from 0.49 to 2.44 µmol EDTA g^{-1} (4.98-fold) in Dark Opal and from 1.42 to 3.09 µmol EDTA g^{-1} (2.18-fold) in Red Boza. These results suggest that basil cultivars differ in their response to sugar application and glucose appears to enhance total phenolic content, CUPRAC activity, and FIC capacity. Variations among antioxidant assays are common due to the involvement of diverse antioxidants compounds including tocopherols, polyphenols, sugars, and organic acids in overall antioxidant mechanisms (Cruz et al., 2020). Glucose has also been shown to enhance antioxidant content in *Brassica* sprouts (Wei et al., 2011).

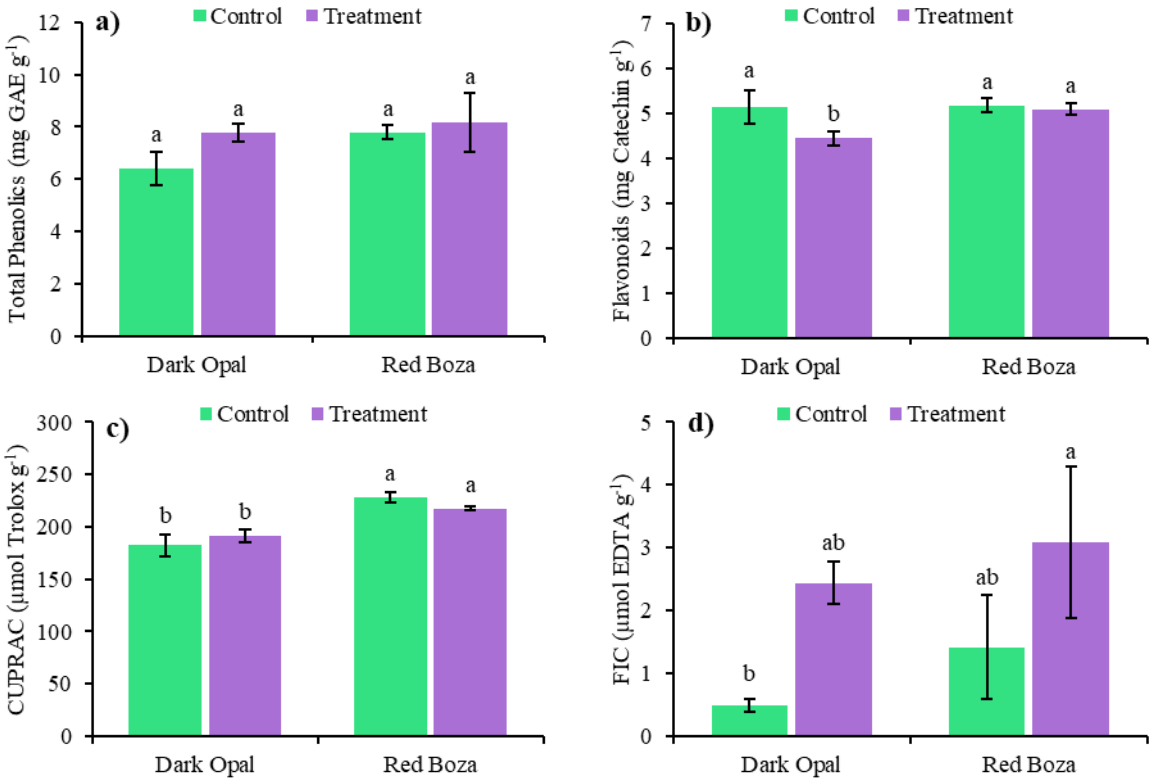


Fig 2. Effects of foliar treatment of 330 mM glucose to Dark Opal and Red Boza on a) total phenolic, b) flavonoid, c) CUPRAC and d) FIC. Vertical bars represent mean values ± SD.

Glucose treatment exerted genotype-dependent effects on total anthocyanin content (Fig. 3a). In Dark Opal, total anthocyanin content increased from 23.90 to 55.14 mg L^{-1}, whereas total anthocyanin content decreased from 14.76 to 9.21 mg L^{-1} in Red Boza. This demonstrates that sugar signaling operates differently between the genotypes. Glucose has been reported to significantly enhance anthocyanin biosynthesis in tree peony by activating the *PsMYB2* transcription factor (Zhang et al., 2022), supporting the idea that glucose acts not only as a carbon source but also as a signaling molecule.

Analysis of photosynthetic pigments revealed that total chlorophyll decreased significantly (18.08%) in Dark Opal

after 330 mM glucose treatment, whereas it increased significantly (39.40%) in Red Boza (Fig. 3b). Although glucose is a minor product of photosynthesis, its exogenous application can modify photosynthesis-related properties. For instance, glucose stimulated chlorophyll synthesis in dark-grown rice seedlings (Sheen, 1990), whereas 4 and 20 mM glucose significantly reduced chlorophyll levels in *Arabidopsis thaliana* (Stevenson and Harrington, 2009). High glucose concentrations can inhibit chloroplast development (To et al., 2003) and accumulation of non-structural carbohydrates can suppress photosynthesis (Araya et al., 2006). Reduced chlorophyll content may result from glucose- or sucrose-mediated repression of photosynthetic gene transcription (Sinha and Roitsch, 2002). Further investigation is required to determine whether the decline observed in this study is sufficient to impair photosynthetic efficiency.

A similar trend was observed for total carotenoid content. Carotenoid levels decreased from 8.07 to 7.36 μg L^{-1} in Dark Opal following glucose treatment but increased from 4.08 to 5.26 μg L^{-1} in Red Boza (Fig. 3c). Carotenoids, plant pigments with photoprotective functions and precursors of abscisic acid biosynthesis (Eldahshan and Singab, 2013) may be reduced under glucose treatment due to glucose-mediated repression of carotenoid pathway genes (Mortain-Bertrand et al., 2008). In contrast, β-carotene content can increase following glucose exposure (Prasanna et al., 2004). These findings further support the regulatory role of glucose in photosynthesis-associated processes.

No significant difference was detected between the control groups of Dark Opal (0.90 mg glucose g^{-1}) and Red Boza (0.53 mg glucose g^{-1}) with respect to total starch content (Fig. 3d). However, glucose treatment led to a marked increase in total starch levels in both basil cultivars. Following the treatment, total starch content increased 4.49-fold in Dark Opal, reaching 4.04 mg glucose g^{-1}, whereas Red Boza exhibited a 6.11-fold increase, reaching 3.24 mg glucose g^{-1}. After spraying 3% and 6% glucose solution to watermelon seedlings stored in the dark at low temperature for 6 days, starch content decreased continuously in control plants, while it increased significantly in glucose-treated seedlings on the 2nd and 4th days of storage (Jiang et al., 2012). This suggests that glucose can be effectively absorbed and stored and used as an alternative substrate for metabolism and energy expenditure. Exogenous carbon treatment can also lead to starch storage without photosynthetic carbon fixation. However, it is also known that high doses of sugar treatment can suppress photosynthetic pigments and change the resource distribution (carbon partitioning) between photosynthesis and storage (Lv et al., 2022). This may explain the decreased chlorophyll and carotenoid values alongside the increased starch in Dark Opal. The results obtained indicate that glucose is easily absorbed in leaves and may play a role in the coloration of basil plants.

Comparison of the two cultivars after glucose treatment revealed that total phenolics content and antioxidant capacity increased more prominently in Dark Opal. This may be attributed to its higher anthocyanin content, the key pigment responsible for purple, red, and blue hues. As shown in Fig. 1, control Dark Opal leaves appeared green, but turned purple following glucose application. This observation aligns with the steep increase in anthocyanins and reduction in chlorophyll and carotenoids levels. In contrast, Red Boza leaves, which were originally light green to reddish, turned dark green after glucose treatment, consistent with increased chlorophyll and carotenoid levels and reduced anthocyanins.

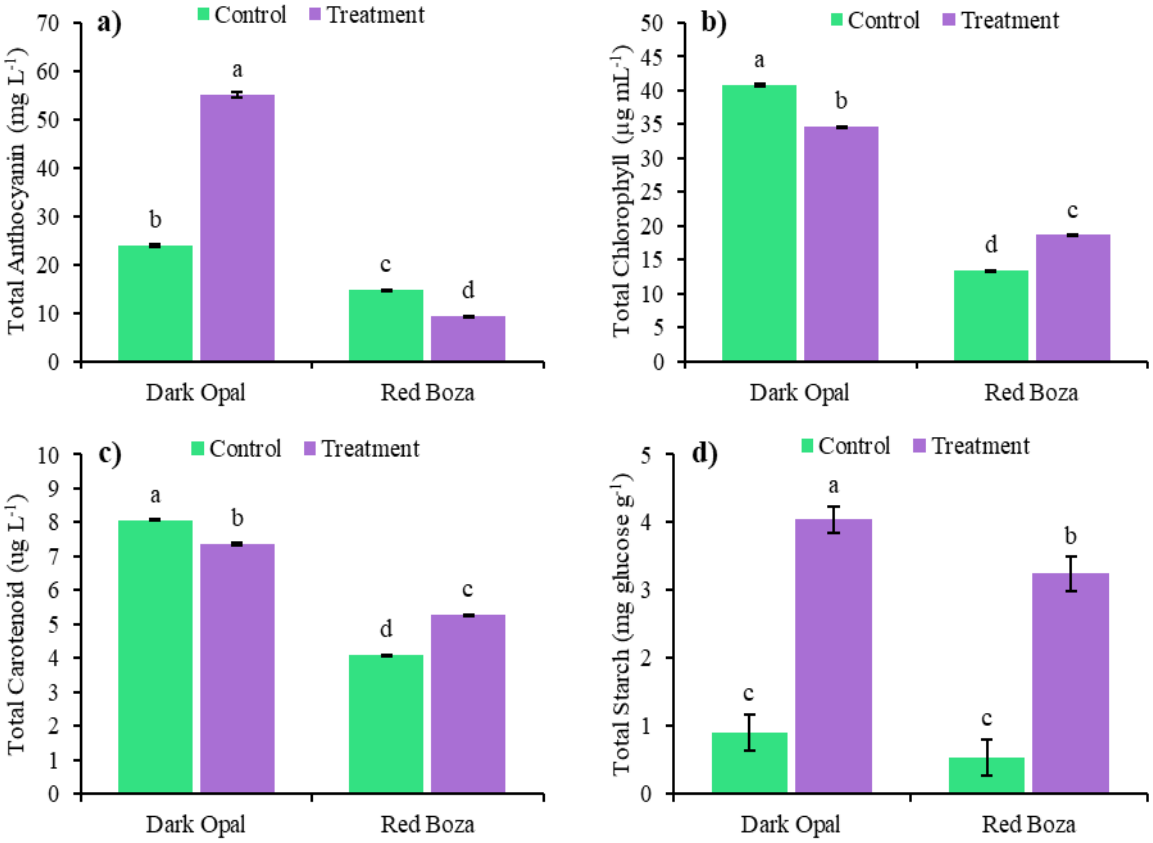


Fig 3. Effects of foliar treatment of 330 mM glucose to Dark Opal and Red Boza on a) total anthocyanin, b) total chlorophyll, c) total carotenoid, and d) total starch. Vertical bars represent mean values ± SD.

4. Conclusions

Sugars are key metabolic substrates that actively modulate various metabolic processes throughout different developmental stages in plants. Glucose treatment induced different metabolic responses in the two cultivars, indicating that sugar signaling operates in a genotype-specific manner. Anthocyanin accumulation increased in Dark Opal, resulting in more intense purple leaf coloration, whereas chlorophyll and carotenoid content increased in Red Boza, leading to cultivar-specific differences in pigment composition and leaf appearance. These findings highlight the significance of genetic background in glucose signal-metabolite interactions. Although total phenolic content and CUPRAC activity were not significantly affected, FIC capacity increased markedly in both cultivars, suggesting that glucose enhances specific components of antioxidant defense. Furthermore, glucose application significantly promoted starch accumulation in both cultivars, demonstrating that exogenously applied glucose can be efficiently absorbed and stored in leaf tissues. Overall, the results indicate that glucose functions not only as an energy source but also as a signaling molecule regulating pigment biosynthesis, antioxidant capacity, and carbohydrate metabolism. This study contributes to the development of sustainable cultivation practices and the production of high-quality basil. Additionally, it provides valuable insights for strategies aimed at improving leaf visual quality and enhancing bioactive compounds, with potential applications in the pharmaceutical, culinary, and industrial sectors. Future studies should explore a broader range of glucose concentrations and genotypic variation to further our understanding of the effects of glucose application on secondary metabolite accumulation.

References

Apak, R., Güçlü, K., Özyürek, M., Karademir, S. E., & Erçağ, E. (2006). The cupric ion reducing antioxidant capacity and polyphenolic content of some herbal teas. International Journal of Food Sciences and Nutrition, 57(5-6), 292-304.

Araya, T., Noguchi, K., & Terashima, I. (2006). Effects of carbohydrate accumulation on photosynthesis differ between sink and source leaves of *Phaseolus vulgaris* L. Plant and Cell Physiology, 47(5), 644-652.

Cruz, L. R., Polyzos, N., Fernandes, Â., Petropoulos, S. A., Gioia, F. D., Dias, M. I., Pinela, J., Kostić, M., Soković, M., Ferreira, I., & Barros, L. (2020). Effect of saline conditions on chemical profile and the bioactive properties of three red-colored basil cultivars. Agronomy, 10(11), 1824.

Decker, E. A., & Welch, B. (1990). Role of ferritin as a lipid oxidation catalyst in muscle food. Journal of Agricultural and Food Chemistry, 38(3), 674-677.

Dhama, K., Sharun, K., Gugjoo, M. B., Tiwari, R., Alagawany, M., Iqbal Yatoo, M., Thakur, P., Iqbal, H. M. N., Chaicumpa, W., Michalak, I., Elnesr, S. S., & Farag, M. R. (2023). A comprehensive review on chemical profile and pharmacological activities of *Ocimum basilicum*. Food Reviews International, 39(1), 119-147.

Eldahshan, O. A., & Singab, A. N. B. (2013). Carotenoids, Journal of Pharmacognosy and Phytochemistry, 2(1), 225-234.

FMI-Future Market Insights, (2025). Basil Leaves Market, Available at: https://www.futuremarketinsights.com/reports/basil-leaves-market [28.11.25]

Folin, O., & Ciocalteu, V. (1927). On tyrosine and tryptophane determinations in proteins. Journal of Biological Chemistry, 73, 627-650.

Gauchan, D. P. (2012). Effect of different sugars on shoot regeneration of maize (*Zea mays* L.). Kathmandu University Journal of Science Engineering and Technology, 8(1), 119-124.

Gibson, S. I. (2005). Control of plant development and gene expression by sugar signaling. Current Opinion in Plant Biology, 8(1), 93-102.

Giusti, M. M., & Wrolstad, R. E. (2001). Characterization and measurement of anthocyanins by UV-visible spectroscopy. Reid, D.S. Current Protocols in Food Analytical Chemistry (pp. F1.2..1-F1.2.13). United Kingdom; John Wiley & Sons Inc.

Hassanpouraghdam, M. B., Vojodi Mehrabani, L., Kheiri, M., Chrysargyris, A., & Tzortzakis, N. (2022). Physiological and biochemical responses of *Tanacetum balsamita* L. to the foliar application of Dobogen biostimulant, glucose and KNO_3 under salinity stress. Scientific reports, 12(1), 9320.

Hill, J. P., Germino, M. J., & Alongi, D. A. (2011). Carbon-use efficiency in green sinks is increased when a blend of apoplastic fructose and glucose is available for uptake. Journal of Experimental Botany, 62(6), 2013-2022.

Jiang, W., Ding, M., Duan, Q., Zhou, Q., & Huang, D. (2012). Exogenous glucose preserves the quality of watermelon (*Citrullus lanatus*) plug seedlings for low-temperature storage. Scientia Horticulturae, 148, 23-29.

Lupton, D., Mumtaz Khan, M., Al-Yahyai, R. A., Asif Hani, M. (2016). Basil. In leafy medicinal herbs: botany, chemistry, postharvest technology and uses (pp. 21-47). Wallingford, UK: CAB International.

Lv, Y. Q., Li, D., Wu, L. Y., Zhu, Y. M., Ye, Y., Zheng, X. Q., Lu, J. L., Liang, Y. R., Li, Q, S., & Ye, J. H. (2022). Sugar signal mediates flavonoid biosynthesis in tea leaves. Horticulture Research, 9, uhac049.

MengYun, H., Hui, L., YingJun, Z., & Qian, L. (2009). Photosynthesis and related physiological characteristics affected by exogenous glucose in wheat seedlings under water stress. Acta Agronomica Sinica, 35(4), 724-732.

Moghaddam, M. R. B., & Ende, W. V. D. (2013). Sugars, the clock and transition to flowering. Frontiers in Plant Science, 4, 22.

Mortain-Bertrand, A., Stammitti, L., Telef, N., Colardelle, P., Brouquisse, R., Rolin, D., & Gallusci, P. (2008). Effects of exogenous glucose on carotenoid accumulation in tomato leaves. Physiologia Plantarum, 134(2), 246-256.

Mortain-Bertrand, A., Stammitti, L., Telef, N., Colardelle, P., Brouquisse, R., Rolin, D., & Gallusci, P. (2008). Effects of exogenous glucose on carotenoid accumulation in tomato leaves. Physiologia Plantarum, 134(2), 246-256.

Mousavi, L., Salleh, R. M., & Murugaiyah, V. (2018). Phytochemical and bioactive compounds identification of

Ocimum tenuiflorum leaves of methanol extract and its fraction with an anti-diabetic potential. International Journal of Food Properties, 21(1), 2390-2399.

Noroozlo, Y. A., Souri, M. K., & Delshad, M. (2019). Effects of foliar application of glycine and glutamine amino acids on growth and quality of sweet basil. Advances in Horticultural Science, 33(4), 495-502.

Önder, D., Erdoğan, Ü., & Önder, S. (2023). Comparison of biochemical and antioxidantactivities of ultrasonic-assisted extraction with different solvents in olive leaf. BiotechStudies, 32, 31-40.

Prasanna, R., Pabby, A., & Singh, P. K. (2004). Effect of glucose and light-dark environment on pigmentation profiles in the cyanobacterium *Calothrix elenkenii*. Folia Microbiologica, 49(1), 26-30.

Price, J., Laxmi, A., Martin, S. K. S., & Jang, J. C. (2004). Global transcription profiling reveals multiple sugar signal transduction mechanisms in *Arabidopsis*. The Plant Cell, 16(8), 2128-2150.

Sadasivam, S., & Manickam, A. (1996). Biochemical Methods, Second Edition. Daryaganj, New Delhi: New Age International Publishers.

Sakanaka, S., Tachibana, Y., & Okada, Y. (2005). Preparation and antioxidant properties of extracts of Japanese persimmon leaf tea (kakinoha-cha). Food Chemistry, 89, 569-575.

Sami, F., & Hayat, S. (2019). Effect of glucose on the morpho-physiology, photosynthetic efficiency, antioxidant system, and carbohydrate metabolism in *Brassica juncea*. Protoplasma, 256(1), 213-226.

Sheen, J. (1990). Metabolic repression of transcription in higher plants. The Plant Cell, 2(10), 1027-1038.

Singh, M., Gupta, A., & Laxmi, A. (2014). Glucose and phytohormone interplay in controlling root directional growth in Arabidopsis. Plant Signaling & Behavior, 9(7), e29219.

Sinha, A. K., & Roitsch, T. (2001). Effect of different sugars on photosynthesis and chlorophyll fluorescence in photoautotrophic tomato suspension cell cultures. Photosynthetica, 39(4), 611-614.

Stanojevic, L. P., Marjanovic-Balaban, Z. R., Kalaba, V. D., Stanojevic, J. S., Cvetkovic, D. J., & Cakic, M. D. (2017). Chemical composition, antioxidant and antimicrobial activity of basil (*Ocimum basilicum* L.) essential oil. Journal of Essential Oil Bearing Plants, 20(6), 1557-1569.

Stefan, M., Zamfirache, M. M., Padurariu, C., Trută, E., & Gostin, I. (2013). The composition and antibacterial activity of essential oils in three *Ocimum* species growing in Romania. Central European Journal of Biology, 8(6), 600-608.

Stevenson, C. C., & Harrington, G. N. (2009). The impact of supplemental carbon sources on Arabidopsis thaliana growth, chlorophyll content and anthocyanin accumulation. Plant Growth Regulation, 59(3), 255-271.

To, J. P., Reiter, W. D., & Gibson, S. I. (2003). Chloroplast biogenesis by *Arabidopsis* seedlings is impaired in the presence of exogenous glucose. Physiologia Plantarum, 118(3), 456-463.

Torres, P. B., Chow, F., Furlan, C. M., Mandelli, F., Mercadante, A., & Santos, D. Y. A. C. (2014). Standardization of a protocol to extract and analyze chlorophyll a and carotenoids in *Gracilaria tenuistipitata* var. Liui. Zhang and Xia (Rhodophyta). Brazilian Journal of Oceanography, 62, 57-63.

Wei, J., Miao, H., & Wang, Q. (2011). Effect of glucose on glucosinolates, antioxidants and metabolic enzymes in *Brassica* sprouts. Scientia Horticulturae, 129(4), 535-540.

Wingler, A., Masclaux-Daubresse, C., & Fischer, A. M. (2009). Sugars, senescence, and ageing in plants and heterotrophic organisms. Journal of Experimental Botany, 60(4), 1063-1066.

Zhang, L., Yan, L., Zhang, C., Kong, X., Zheng, Y., & Dong, L. (2022). Glucose supply induces *PsMYB2*-mediated anthocyanin accumulation in *Paeonia suffruticosa* 'Tai Yang' cut flower. Frontiers in Plant Science, 13, 874526.

Zhang, Z., & Huang, R. (2013). Analysis of malondialdehyde, chlorophyll proline, soluble sugar, and glutathione content in *Arabidopsis* seedling. Bio-protocol, 3(14), e817.

ORAL PRESENTATION

Quality by design optimization of calcium phosphate nanocores for aquasomes: Role of precursor ratio and sonication time

Liban Barre[1*] (*ORCID: https://orcid.org/0000-0001-8075-6622*), Neslihan Avcı[1] (*ORCID: https://orcid.org/0000-0000-0000-0000*), Mustafa Sinan Kaynak[2] (*ORCID: https://orcid.org/0000-0003-2917-2407*)

[1] Anadolu University, Graduate School, Department of Pharmaceutical Technology, Eskisehir, Turkey
[2] Anadolu University, Faculty of Pharmacy, Department of Pharmaceutical Technology, Eskisehir, Turkey

*Corresponding author e-mail: liban72@anadolu.edu.tr

Abstract

Aquasomes are emerging as highly promising nanocarriers for delivering fragile and poorly soluble therapeutics, owing to their unique tri-layered architecture and exceptional structural stability. This study optimized the synthesis of calcium phosphate cores, the fundamental scaffold of aquasomes. Quality by Design (QbD) based Central Composite Design (CCD) was used in this study. By systematically varying diammonium hydrogen phosphate and calcium acetate concentrations along with sonication time, their influence on particle size, PDI, and zeta potential was evaluated. All parameters significantly shaped core formation, and the optimal conditions (279 nm, PDI 0.39, −15 mV) were achieved at 2 M phosphate, 3 M calcium acetate, and 30 minutes of sonication. These results provide a robust, reproducible pathway for engineering uniform and stable aquasome cores, strengthening their potential as advanced drug delivery systems.

Keywords: Aquasome, Calcium phosphate, CCD,QbD, Drug delivery

INTRODUCTION

Effective delivery of fragile and poorly water-soluble therapeutic molecules remains a significant challenge in pharmaceuticals. Nanoparticulate drug delivery systems offer promising solutions by enhancing drug stability, solubility, targeting, and controlled release (Bwalya et al., 2025). Due to their large surface area, high surface-to-mass ratio, and stable water-like core, aquasomes allow superior drug adsorption, deeper penetration into cells, and an extended drug release profile, making them an effective platform for delivering sensitive therapeutic molecules (Kulkarni et al., 2024). Aquasomes are nanosized, versatile drug delivery systems (60–300 nm) (Kossovsky et al., 1994) distinguished by a unique three-layered structure consisting of a solid crystalline core, a carbohydrate coating, and an outer layer of adsorbed therapeutic agents (Damera et al., 2019). A wide variety of core materials have been investigated for aquasome fabrication, including , and calcium phosphate, hydroxyapatite (HAP), ceramic nanocrystals, nanodiamonds, silica nanoparticles (Banerjee & Sen, 2018). Calcium phosphate due to its biocompatibility is fundamental to aquasome structure and dictates critical properties like particle size, entrapment efficiency, drug loading, and release kinetics. However, precise control over calcium phosphate core synthesis is complex, with input variables significantly impacting final core quality attributes. To ensure reproducible and efficient aquasome performance, this study employed a Quality by Design (QbD) approach. We systematically optimized key process parameters in the core synthesis, specifically reactant ratios and sonication time, to precisely control critical quality attributes including particle size, polydispersity index (PDI), and zeta potential, thereby enhancing the foundational basis for aquasome-based delivery systems (Shanmugam & Srinivasan, 2024).

MATERIALS AND METHODS

Materials

Diammonium hydrogen phosphate and calcium acetate were procured from Tekkim Kimya Sanayi ve Ticaret Ltd. Şti. (Turkey) and used as precursors for the calcium phosphate core synthesis. Distilled water served as the reaction medium. All procedures were performed using standard laboratory glassware, a bath sonicator, a centrifuge, a drying oven, and 0.2 µm cellulose acetate membrane filters.

Synthesis of Calcium Phosphate Core

Calcium phosphate cores were synthesized via a precipitation by sonication method (Dahir et al., 2020). Design-Expert version 13, a Central Composite Design (CCD) was employed to investigate experimental runs, varying the critical process parameters: the molar ratios of diammonium hydrogen phosphate and calcium acetate, and the sonication time during synthesis. Diammonium hydrogen phosphate and calcium acetate were separately dissolved in 20 mL of distilled water with continuous stirring. The calcium acetate solution was then subjected to sonication, maintaining the bath temperature with ice packs. The diammonium hydrogen phosphate solution was added dropwise under constant stirring to the sonicated calcium acetate solution, initiating the formation of calcium phosphate and ammonium acetate. Following the reaction, the resulting suspension underwent sonication for the specific duration defined by the experimental design. The suspension was then filtered through a 0.2 µm cellulose acetate membrane with triple washes of distilled water to remove unreacted species and residual ammonium acetate. The filtered product was centrifuged at 4000 rpm for 1 hour, and the precipitate was washed again with distilled water for further purification. Finally, the purified calcium phosphate cores were dried in an oven at 100°C for one day (Bwalya et al., 2025).

Characterization of Calcium Phosphate Cores

The dried cores were characterized for particle size, PDI, and zeta potential using a ZetaSizer (Malvern Instruments, UK). Samples were diluted with distilled water, placed in cuvettes, and analyzed in triplicate at room temperature. These parameters were used to evaluate the stability and uniformity of the synthesized cores (Makavana & Dudhat, 2025).

RESULTS and DISCUSSION

Twenty experimental runs were designed using a Central Composite Design to investigate the influence of Diammonium hydrogen phosphate (Factor A), Calcium acetate (Factor B), and Sonication time (Factor C) on the particle size, polydispersity index (PDI), and zeta potential of aqueousome core particles. Particle size ranged broadly, PDI varied from narrow to wide distributions, and zeta potential spanned from moderately to highly negative values, reflecting the sensitivity of the system to all three factors. Surface plots indicated that increasing A and B generally led to larger particle sizes, broader PDI, and less negative zeta potential (figure **1**-**3**), likely due to accelerated nucleation and ionic shielding effects. Despite the trend suggesting low A and B concentrations might favor better characteristics at a fixed sonication time, experimental findings revealed that Sonication time played a pivotal role. Its interaction with A and B significantly impacted nanoparticle properties by influencing nucleation, growth, and potential aggregation or breakdown. The optimum conditions were achieved at high concentrations of A (2 M) and B (3 M) with a sonication time of 30 minutes, yielding the smallest particle size (279 nm), lowest PDI (0.39), and most negative zeta potential (-15 mV). This highlights the necessity of optimizing all three factors simultaneously to produce uniform, stable, and nanosized aquasomes.

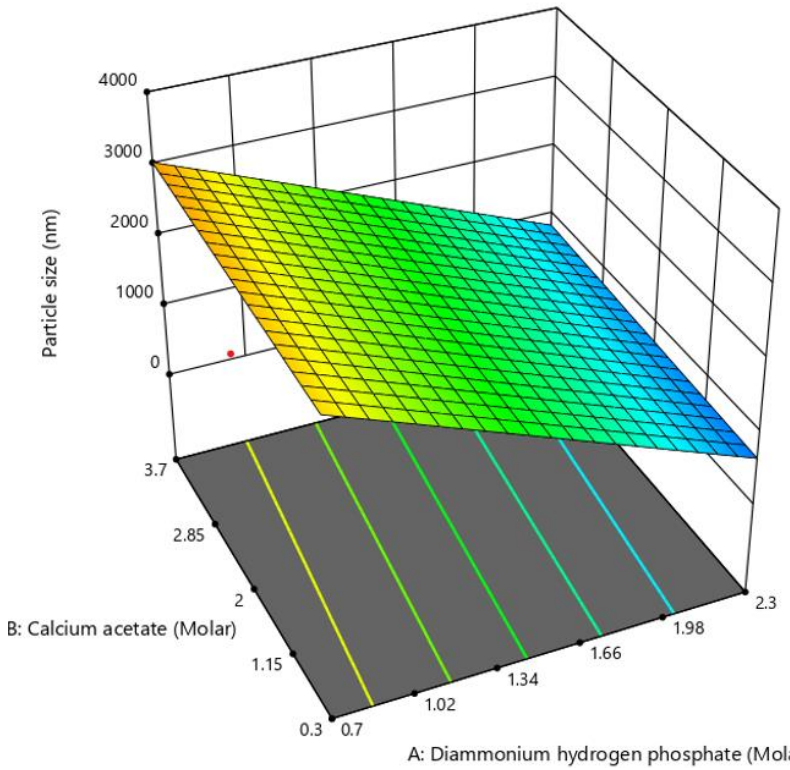


Figure 1. 3D Surface of Diammonium hydrogen phosphate and calcium acetate concentration on the particle size of calcium phosphate core

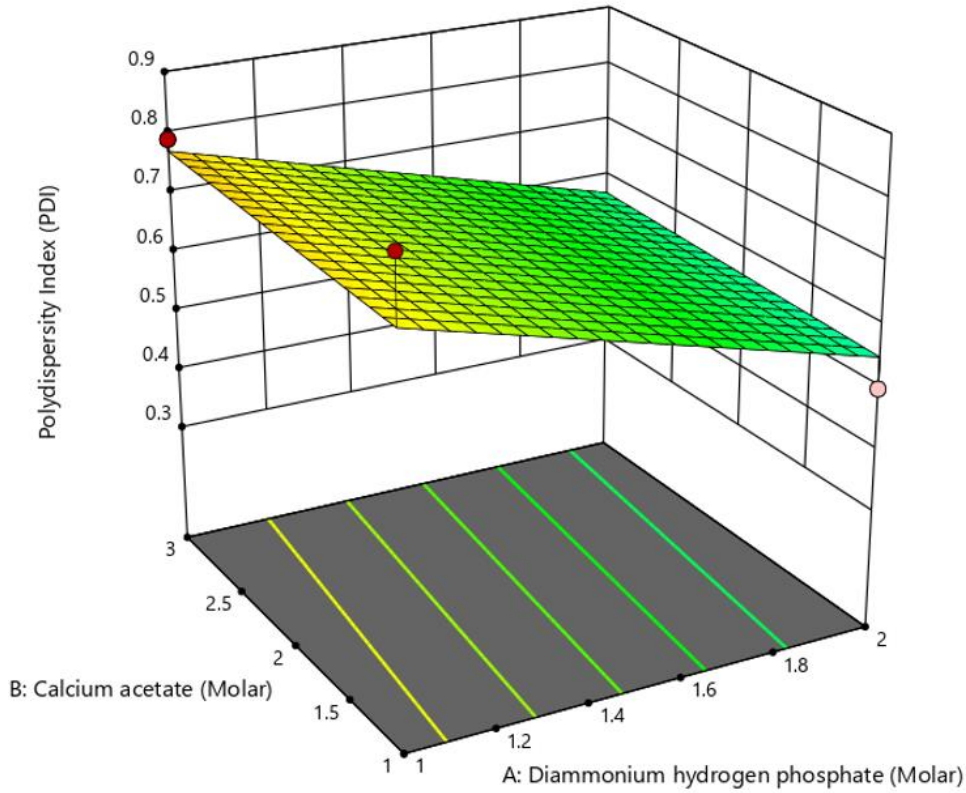


Figure 2. 3D Surface of Diammonium hydrogen phosphate and calcium acetate concentration PDI of calcium phosphate core

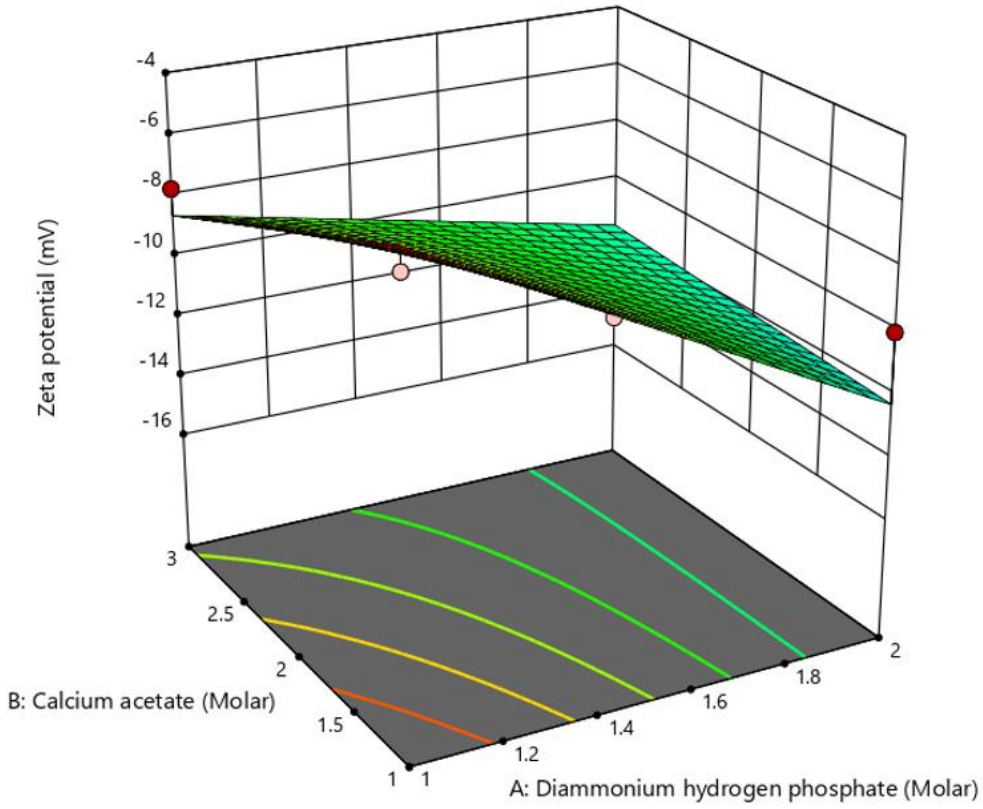


Figure 3. 3D Surface of Diammonium hydrogen phosphate and calcium acetate concentration on Zeta potential of calcium phosphate core

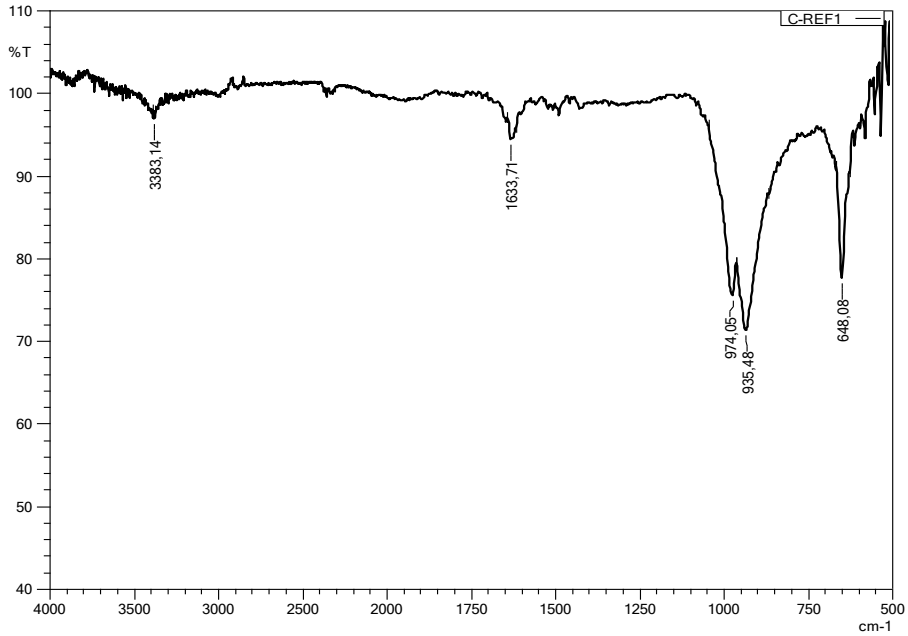


Figure 4. FTIR of optimum Calcium phosphate core

The FTIR spectrum of the optimized calcium phosphate core displays the characteristic vibrational signatures of phosphate-based nanocrystals (figure 4). The broad band at 3383 cm^{-1} corresponds to O–H stretching from surface-bound or lattice-associated water, while the peak at 1633 cm^{-1} represents H–O–H bending, confirming the hydrated nature commonly observed in calcium phosphate and hydroxyapatite structures. The prominent phosphate stretching band at 974 cm^{-1}, along with the secondary peak at 935 cm^{-1}, verifies the presence of PO_4^{3-} groups, and

the deformation band at 648 cm^{-1} reflects O–P–O bending vibrations. When compared to literature-reported hydroxyapatite (HA) spectra—characterized by PO_4^{3-} bands at 473, 564, 602, 962, 1033, and 1093 cm^{-1}, and an OH^- bending peak around 633 cm^{-1}—the observed peaks show clear correspondence, particularly the PO_4^{3-} stretching region near 974 cm^{-1}, which closely matches the HA band at 962 cm^{-1}. The bending vibration at 648 cm^{-1} is also consistent with the HA-associated OH^- deformation near 633 cm^{-1}, indicating partial structural similarity. Although the lower-wavenumber phosphate modes typical of highly crystalline HA are less pronounced, the overall spectral profile confirms the successful formation of a phosphate-rich, nanocrystalline calcium phosphate core, consistent with the broader and slightly shifted bands expected for nanoscale or less crystalline calcium phosphate materials (Goyal et al., 2008).

CONCLUSION

This study demonstrated that diammonium hydrogen phosphate concentration, calcium acetate concentration, and sonication time significantly influence the particle size, PDI, and zeta potential of aquasome core particles. Among the tested conditions, the precursor ratio of 2:3 (diammonium hydrogen phosphate: calcium acetate) combined with 30 minutes of sonication yielded the most optimal formulation, producing small, uniform, and stable nanoparticles. In addition to confirming the critical contribution of each parameter, this work highlights the strong interactive effects between precursor ratio and sonication energy, which collectively govern nucleation, growth behavior, and surface charge development. These findings underscore the importance of systematically optimizing formulation parameters to achieve desirable physicochemical characteristics.

REFERENCES

Banerjee, S., & Sen, K. K. (2018). Aquasomes: A novel nanoparticulate drug carrier. Journal of Drug Delivery Science and Technology, 43, 446–452. https://doi.org/10.1016/j.jddst.2017.11.011

Bwalya, F., Barre, L., Erdem, M., & Kaynak, M. S. (2025). Preparation and characterization of vitamin C aquasomes. Recent Advances in Drug Delivery and Formulation, 19(3), e26673878352032. https://doi.org/10.2174/0126673878352032250325002719

Bwalya, F., Erdem, M., & Kaynak, M. S. (2025). Formulation optimization, physicochemical characterization, and biocompatibility assessment of curcumin loaded aquasomes. Nano Select, 6, e202400162. https://doi.org/10.1002/nano.202400162

Damera, D. P., Prasad, E., & Ramakrishna, S. (2019). Synthesis, detailed characterization, and dual drug delivery application of BSA-loaded aquasomes. ACS Applied Bio Materials, 2(10), 4471–4484. https://doi.org/10.1021/acsabm.9b00635

Goyal, A. K., Khatri, K., Mishra, N., Mehta, A., Vaidya, B., Tiwari, S., & Vyas, S. P. (2008). Aquasomes: A nanoparticulate approach for the delivery of antigen. Drug Development and Industrial Pharmacy, 34(12), 1297–1305. https://doi.org/10.1080/03639040802071661

Kossovsky, N., Gelman, A., Sponsler, E. E., Hnatyszyn, H. J., Rajguru, S., Torres, M., Pham, M., Crowder, J., Zemanovich, J., Chung, A., & Shah, R. (1994). Surface modified nanocrystalline ceramics for drug delivery applications. Biomaterials, 15(15), 1201–1207. https://doi.org/10.1016/0142-9612(94)90270-4

Kulkarni, S., Prabhakar, B., & Shende, P. (2022). Aquasomes: Advanced vesicular based nanocarrier systems. Current Pharmaceutical Design, 28(29), 2404–2414. https://doi.org/10.2174/1381612828666220728112741

Kulkarni, S., Prabhakar, B., & Shende, P. (2024). Nanodiamond based berberine aquasomes for enhancing penetration across epidermis to treat psoriasis. International Journal of Pharmaceutics, 656, 124051. https://doi.org/10.1016/j.ijpharm.2024.124051

Liban, D., Kajol, K., Kaur, A., Manocha, A., Wadhwa, S., Mishra, V., Pandey, N., Kumar, R., Jain, S., & Charyulu, R. N. (2020). Aquasomes: Water like vesicular system for therapeutic molecules as a robust system for delivery. European Journal of Molecular and Clinical Medicine, 7(7), 2585–2607.

Makavana, A., & Dudhat, K. (2025). Aquasomes: Novel crystalline nanocarriers ensuring conformational integrity and high surface exposure for enhanced drug encapsulation and delivery. Journal of Nanoparticle Research, 27, 141. https://doi.org/10.1007/s11051-025-06336-9

Shanmugam, B., & Srinivasan, U. M. (2024). Formulation and characterization of antibiotic drug loaded aquasome for topical application. Future Science OA, 10(1), 2367849. https://doi.org/10.1080/20565623.2024.2367849

ORAL PRESENTATION

Molecular docking and DFT-based theoretical assessment of delpazolid's activity against *Mycobacterium tuberculosis*

Emel Ekinci[1] (ORCID: https://orcid.org/ 0000-0003-2323-2747), Özlem Gündoğdu Aytaç[2] (ORCID: https://orcid.org/0000-0002-6943-9674), Sertan Aytaç[2*] (ORCID: https://orcid.org/ 0000-0002-3196-4545)

[1] Çankırı Karatekin University, Central Research Laboratory, Application and Research Center, Çankırı, Türkiye.
[2] Kırşehir Ahi Evran University, Kaman Vocational School, Food Processing Department, Kaman-Kırşehir, Türkiye.

[*]Corresponding author e-mail: saytac@ahievran.edu.tr

Abstract

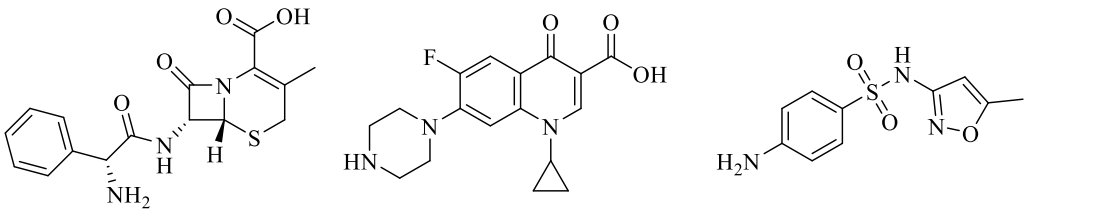
Oxazolidinone antibiotics, featuring five-membered heterocyclic rings, are effective against Gram-positive pathogens, including resistant strains like Methicillin-Resistant *Staphylococcus aureus* and Vancomycin-Resistant Enterococci. Delpazolid, a novel oxazolidinone, exhibits promising activity against resistant bacteria and *Mycobacterium tuberculosis* by inhibiting protein synthesis through binding to the 50S ribosomal subunit. This study explored Delpazolid's interactions with *Mycobacterium tuberculosis* shikimate kinase, an essential enzyme in the shikimate pathway absent in mammals, making it an attractive drug target. Density functional theory calculations assessed Delpazolid's electronic properties, revealing a small HOMO–LUMO gap, high chemical softness, and notable electrophilicity, indicating strong reactivity and potential for ligand–target interactions. In the comparative molecular docking analysis, Delpazolid was evaluated against the reference drug Teridizone. Delpazolid showed a binding energy of –5.60 kcal/mol, stabilized by hydrogen bonds, hydrophobic and π-interactions, and halogen bonding, while Teridizone exhibited slightly higher binding (–6.35 kcal/mol). Overall, results suggest Delpazolid has favorable structural and electronic features, supporting its potential as a candidate against drug-resistant *Mycobacterium tuberculosis* and Gram-positive pathogens.

Keywords: Oxazolidinones, Delpazolide, Tuberculosis, *Mycobacterium tuberculosis*, DFT, Molecular Docking

INTRODUCTION

Heterocyclic compounds are organic molecules that contain ring systems with heteroatoms such as nitrogen, oxygen, or sulfur in addition to carbon. These structures play a significant role in modern drug design due to the selectivity advantage they provide in interactions with biological targets (Jampilek, 2019). Their three-dimensional architectures facilitate more selective binding of molecules to specific biological targets (Aldeghi et al., 2014). Heteroatom-containing frameworks form the basis of many naturally occurring bioactive compounds and are frequently employed in the design of new drugs in medicinal chemistry (Heravi et al., 2020). Therefore, heterocyclic structures serve as guiding scaffolds in the development of numerous therapeutic molecules, including antibacterial agents (Mustafa, 2018).

Antibiotics are essential for treating bacterial infections (Ekinci et al., 2025a). The term "antibiotic" was first defined by Selman Waksman in 1941 (Davies & Davies, 2010). Antibiotics discovered between 1940 and 1960, such as penicillin, streptomycin, tetracycline, and chloramphenicol, were effective in treating infections, but emerging resistance has limited their efficacy (Foti et al., 2021). Many antibiotics owe their activity to the heterocyclic groups they contain (Shivaji & Kasabe, 2021). For example, β-lactams inhibit cell wall synthesis (Cho et al., 2014), Tetracyclines bind to the 30S ribosomal subunit, thereby inhibiting protein synthesis (Chukwudi, 2016), macrolides target the 50S subunit (Dinos, 2017), and aminoglycosides bind the 30S subunit for bactericidal effects (Krawczyk et al., 2024). Other classes include quinolones, which inhibit DNA replication (Drlica et al., 2009), glycopeptides targeting cell wall synthesis (Zeng et al., 2016), and sulfonamides with trimethoprim, which interfere with folate metabolism (Ovung & Bhattacharyya, 2021). Increasing antibiotic resistance drives the development of new classes, such as oxazolidinones, which are synthetic antibiotics effective against resistant pathogens (Foti et al., 2021). Some key antibiotic classes are illustrated in Figure 1.



Cephalexin
(Beta-Lactam-derived antibiotic)

Ciprofloxacin
Quinolone-derived antibiotic)

Sulfamethoxazole
(Sulfonamide-derived antibiotic)

Figure 1. Some important antibiotic derivatives

Oxazolidinone antibiotics are particularly effective against Gram-positive pathogens due to their five-membered heterocyclic rings and inhibit protein synthesis, making them clinically important for resistant bacteria such as Methicillin-Resistant *Staphylococcus aureus* (MRSA) and Vancomycin-Resistant Enterococci (VRE) (Bozdogan & Appelbaum, 2004; Aytaç et al., 2025). For instance, Tedizolid is effective against MRSA, VRE, and other Gram-positive pathogens and is used in the treatment of skin and soft tissue infections (Iqbal et al., 2022). Radezolid is FDA-approved due to its strong antibacterial activity (Wang et al., 2023). Posizolid is a promising candidate against *Staphylococcus*, *Enterococcus*, and *Streptococcus pneumoniae* (Almalki et al., 2022). Contezolid shows in vitro efficacy against MRSA and VRE by binding to 23S rRNA and inhibiting protein synthesis (Ekinci et al., 2025a). Sutezolid, a thio-morpholino derivative of linezolid, has shown high efficacy against *Mycobacterium tuberculosis* (MTB), (Kiran et al., 2025).

Tuberculosis (TB), caused by MTB, remains one of the deadliest infectious diseases globally (Tawfick et al., 2023). High mortality rates highlight the need for shorter, safe, and effective treatment regimens (Kou et al., 2025). Current TB treatments, particularly for drug-resistant strains, rely on drugs such as isoniazid, rifampin, pyrazinamide, and ethambutol (Lee et al., 2024). However, prolonged treatment protocols negatively affect both therapeutic efficacy and patient compliance (Kim et al., 2022; Minja et al., 2025). Therefore, developing new treatment candidates with lower toxicity and activity against resistant MTB strains is critical (Hoagland et al., 2016). The robustness of the MTB cell wall enables survival under harsh environmental conditions and exposure to chemotherapeutic agents (Xu et al., 2022), making essential structural and metabolic pathways such as cell wall biosynthesis and protein synthesis strategic therapeutic targets (Kuang et al., 2022).

In this context, the shikimate pathway is vital for MTB and represents an ideal target for TB therapy because it is absent in mammals (Ducati et al., 2007). This pathway, which extends from carbohydrate metabolism to the synthesis of aromatic compounds, plays a key role in producing metabolites essential for bacterial survival. One of the pathway's critical enzymes, shikimate kinase (SK), converts shikimate to shikimate-3-phosphate using ATP, and the MTB genome contains a single gene encoding this enzyme (Rajput et al., 2023). This makes SK both a selective and high-potential drug target.

Delpazolid (DPZ), a novel member of oxazolidinones gaining attention for its activity against Gram-positive pathogens, contains a cyclic amidrazone group and is a promising candidate against resistant pathogens such as MRSA, VRE, and MTB (Koh et al., 2024). DPZ's mechanism of action involves binding to the 50S ribosomal subunit, preventing the formation of the initiation complex where *N*-formylmethionyl-tRNA (fMet-tRNA) joins the 70S ribosome, thereby inhibiting protein synthesis (Lee et al., 2024). Its rapid elimination reduces toxicity risk, and preclinical and Phase 1 studies indicate safety and potential advantages in MDR-TB treatment with 14-day early bactericidal activity (Kim et al., 2022).

In this study, the interactions of DPZ with the bacterial enzyme SK were investigated in detail. Molecular docking analyses were performed to determine potential binding sites, binding energies, and interaction types, with Terizidone (TRD), a second-line drug recommended for drug-resistant TB, used as a reference compound (Mulubwa & Mugabo, 2019; Sahoo et al., 2022). Additionally, DPZ's electronic properties contributing to its antibacterial activity were examined using density functional theory (DFT) calculations, including HOMO-LUMO energy gaps, global reactivity parameters, and molecular electrostatic potential distribution. These analyses aim to comprehensively elucidate the mechanism of DPZ-SK interactions and their role in the antibacterial efficacy of DPZ against TB.

MATERIALS AND METHODS

Global reactivity descriptors

Molecular geometry was optimized, and harmonic vibrational frequencies were calculated using the B3LYP functional (Becke, 1993; Lee et al., 1988) with the 6-311++G(d,p) basis set (Frisch, 1984) with method DFT. Global reactivity parameters were analyzed to assess chemical reactivity and kinetic stability, providing insights into electronic properties and potential interactions with biological receptors. All calculations were performed using Gaussian 16.

Molecular docking analysis

Molecular docking studies play a crucial role in drug design and pharmacology. This technique is widely employed and recognized as a reliable method for rapidly identifying protein–ligand interactions and determining binding sites (Gündoğdu Aytaç et al., 2025). In this study, *Mycobacterium tuberculosis* Shikimate Kinase in complex with Shikimate (PDB ID: 1U8A) was selected for molecular docking, and TRD was used as the standard drug for comparison of docking results. Docking studies were performed using AutoDock Tools to evaluate the interactions of DPZ and TRD with the target protein. Steps including ligand and protein preparation, active site identification, and grid parameter selection were carried out according to the reference method (Gündoğdu Aytaç et al. 2025). Target protein were obtained from the Protein Data Bank (https://www.rcsb.org/). Grid parameters were set to 40 × 40 × 40 Å³ in x, y, z dimensions, with 0.353 Å spacing and centers at 36.677, –34.542, 31.093. The resulting molecular docking scores are presented in Figures 5-6.

RESULTS AND DISCUSSION

Molecular Geometry

Geometric optimization of the DPZ molecule was performed using the B3LYP functional and the 6-311++G(d,p) basis set within the scope of DFT (Figure 2). The optimization resulted in the lowest-energy stable conformation of the molecule. The absence of negative frequencies observed during frequency analysis confirmed that the optimized structure was located at a true energy minimum. This structure formed the basis for subsequent electronic property evaluations, molecular orbital analyses, and docking studies.

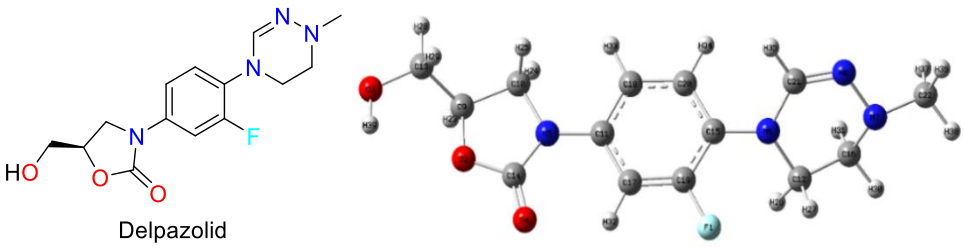


Figure 2. 2D and 3D structure of the DPZ molecule

Global reactivity descriptors

The electronic properties and chemical reactivity of DPZ were evaluated using calculated quantum chemical parameters, shown in Table 1.

Table 1. Global reactivity parameters in (eV) for DPZ

Parameters	Values
E_{HOMO} (eV)	-0.278
E_{LUMO} (eV)	-0.178
Energy gap $\|E_{HOMO}- E_{LUMO}\|$	0.100
Ionization potential ($I = -E_{HOMO}$)	0.278
Electron affinity ($A = -E_{LUMO}$)	0.178
Chemical hardness ($\eta = (I- A)/2$)	0.050
Chemical softness ($\sigma = 1/\eta$)	20.044
Electronegativity ($\chi = (I+A)/2$)	0.228
Chemical potential ($\mu = -(I+A)/2$)	-0.228
Electrophilicity ($\omega = \mu 2/2\eta$)	0.522

Based on the calculated quantum chemical parameters, the HOMO and LUMO energies of the DPZ molecule were –0.278 eV and –0.178 eV, respectively (Figure 3). The small energy gap (Egap = 0.100 eV) suggests high chemical reactivity and facile electronic transitions. Low ionization potential (I = 0.278 eV) and electron affinity (A = 0.178 eV) indicate strong electron-donating and -accepting abilities. The low chemical hardness (η = 0.050 eV) implies kinetic instability but high reactivity, while the high chemical softness (σ = 20.044 eV^{-1}) suggests adaptability with biological receptors (Ekinci et al., 2025b). Furthermore, the electronegativity (χ = 0.228 eV) and chemical potential (μ = –0.228 eV) values support the molecule's electron-attracting tendency and potential for electrophilic interactions. The notable electrophilicity index (ω = 0.522 eV) indicates that DPZ may strongly accept electrons and initiate interactions with target molecules in biological systems.

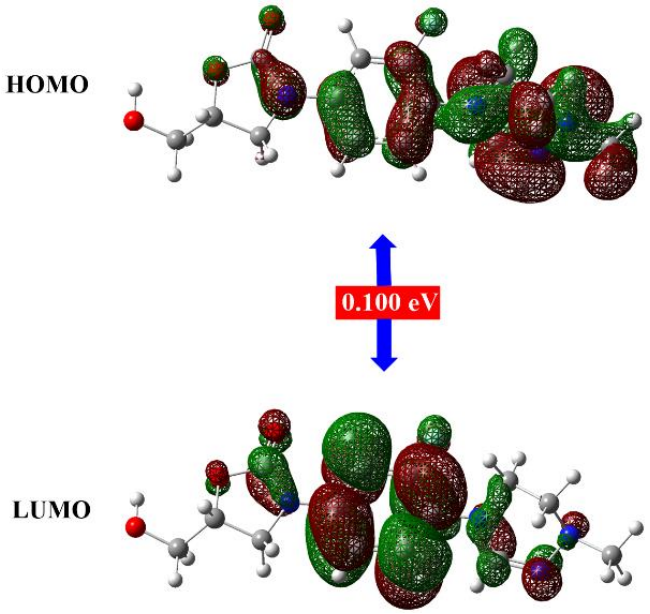


Figure 3. The frontier molecular orbitals of DPZ obtained at the B3LYP/6-311++(d,p) level.

Molecular Electrostatic Potential (MEP) Maps

The MEP map (Figure 4) illustrates the heterogeneous distribution of electrostatic potential on the DPZ molecule surface. The most negative regions (red) are around the ester carbonyl (C=O) on the left side and the carbonyl group of the oxazolidinone ring, representing the primary electrophilic centers that act as hydrogen bond acceptors and are critical for electron donation, ionic interactions, and hydrogen bonding with receptors. Slight blue regions around the oxazolidinone ring nitrogen and the secondary amine nitrogen in the side chain indicate hydrogen bond donors and protonatable sites. The central aromatic ring shows a generally neutral potential (greenish-turquoise),

while the slightly negative potential near the aromatic fluorine atom suggests its contribution to the molecule's electronic character. Overall, DPZ's electrostatic interactions are primarily mediated by electron acceptance via the carbonyl groups and proton donation and hydrogen bonding via the amine and ring nitrogens.

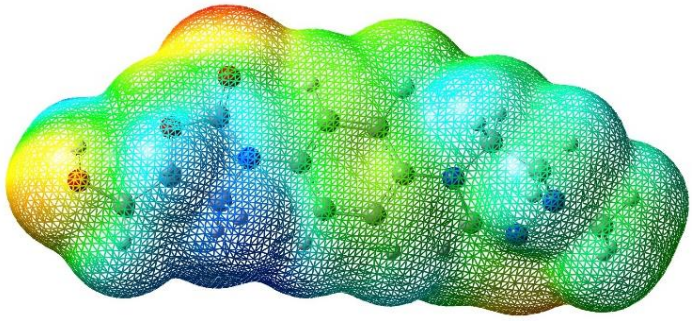


Figure 4. MEP map of DPZ obtained at the B3LYP/6-311++(d,p) level.

Molecular Docking Studies

In this study, a comparative molecular docking analysis was performed to evaluate the antibacterial properties of DPZ and the reference drug TRD. SK from MTB in complex with shikimate (PDB ID: 1U8A) was selected as the target protein. DPZ exhibited a total binding energy of –5.60 kcal/mol, indicating moderate affinity for the active site. The stability of the ligand–protein complex was primarily supported by hydrogen bonding and hydrophobic interactions. DPZ formed conventional hydrogen bonds with ARG117 (2.48 Å), GLY81 (2.11 Å), and ARG58 (2.64 and 2.13 Å), along with carbon–hydrogen bonds with GLU38 at distances of 2.92 and 3.24 Å. Non-polar interactions further stabilized the complex, including a π–anion interaction with ASP34 (3.14 Å), an alkyl contact with ILE45 (4.85 Å), and a π–alkyl interaction with ILE45 (4.82 Å). Additionally, halogen bonding between the fluorine atoms of DPZ and ARG117 (2.48 Å) and ASP34 (3.68 Å) contributed to overall stabilization. Van der Waals interactions were observed with PHE57, GLU61, GLY79, PHE49, GLY80, PRO11, ARG136, LEU132, LEU119, PRO118, and VAL35. These detailed interactions highlight the multifaceted binding mechanism of DPZ within the SK active site (Figure 5).

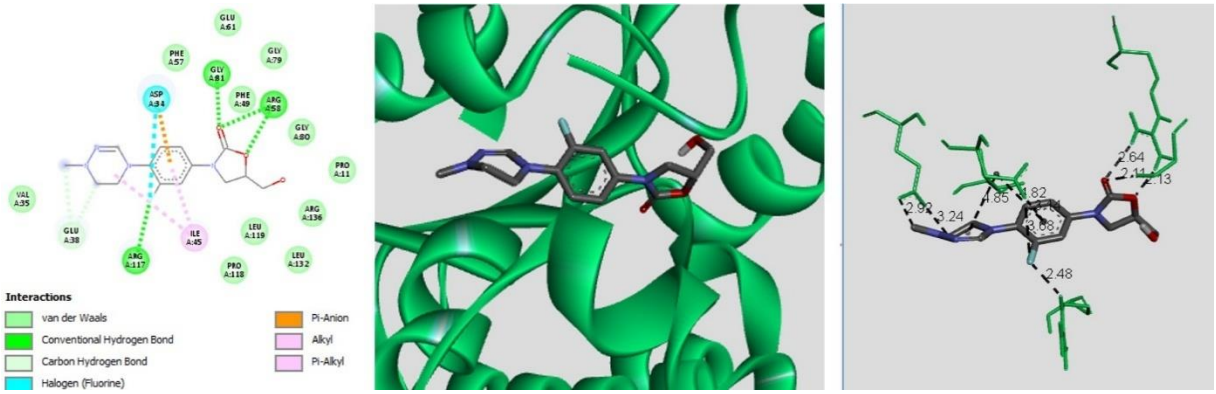


Figure 5. Docking interactions between the protein 1U8A and the DPZ

Analysis of TRD interactions within the active site of SK (PDB ID: 1U8A) revealed a total binding energy of –6.35 kcal/mol, indicating a slightly stronger affinity compared to DPZ. Conventional hydrogen bonds were observed with LEU120 (2.42 Å) and LEU119 (2.13 Å). Additionally, a π–sigma interaction was detected with ILE45 (3.57 Å), along with a π–alkyl interaction involving PRO118 (5.35 Å). Van der Waals interactions with PHE49, PHE59, ARG117, VAL35, GLU38, ASP34, VAL116, ARG58, ARG136, LEU132, and PRO11 further contributed to the stability of the protein–ligand complex. These interactions collectively provide a detailed insight into TRD's binding mechanism within the SK active site (Figure 6).

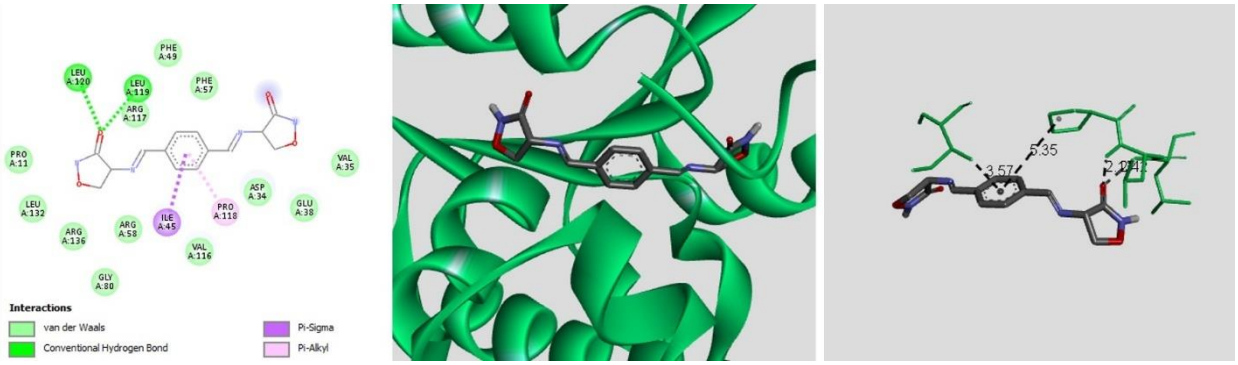


Figure 6. Docking interactions between the protein 1U8A and the TRD

CONCLUSION

This study investigated the structural and electronic properties of Delpazolid (DPZ), a novel oxazolidinone antibiotic, and its interactions with *Mycobacterium tuberculosis* shikimate kinase (SK) using computational methods. DFT analyses showed that DPZ adopts a stable, low-energy conformation, with a small HOMO–LUMO gap, high chemical softness, and significant electrophilicity, indicating strong chemical reactivity and suitability for binding interactions. Molecular electrostatic potential maps identified regions capable of hydrogen bonding and electrostatic interactions, supporting selective recognition by the target enzyme. Molecular docking results revealed that DPZ binds to the SK active site with a binding energy of –5.60 kcal/mol, stabilized by multiple hydrogen bonds, halogen bonds, hydrophobic contacts, π–anion, and Van der Waals interactions. Compared to the reference compound Terizidone (TRD), which exhibited a slightly higher binding energy of –6.35 kcal/mol, DPZ demonstrated a versatile interaction profile, suggesting its potential as an effective antibacterial agent. Overall, the findings highlight DPZ's favorable electronic and structural characteristics, as well as its ability to form stable and multifaceted interactions with SK, supporting its development as a candidate against drug-resistant *M. tuberculosis* and other Gram-positive pathogens.

REFERENCES

Aldeghi, M., Malhotra, S., Selwood, D. L., & Chan, A. W. E. (2014). Two- and three-dimensional rings in drugs. *Chemical Biology & Drug Design, 83*(4), 450–461.

Almalki, A. J., Ibrahim, T. S., Taher, E. S., Mohamed, M. F. A., Youns, M., Hegazy, W. A. H., & Al-Mahmoudy, A. M. M. (2022). Synthesis, antimicrobial, anti-virulence and anticancer evaluation of new 5(4H)-oxazolone-based sulfonamides. *Molecules, 27*(3), 671.

Aytaç, S., Gündoğdu Aytaç, Ö., & Ekinci, E. (2025). *Tedizolid fosfatın (TDZ-P) antibakteriyel özelliklerinin in-silico analizi*. In E. Bayram & H. Çiçek (Eds.), *Kimya alanında uluslararası araştırmalar ve değerlendirmeler* (pp. 117–140). Gece Kitaplığı: Çankaya/Ankara, Türkiye. ISBN 978-625-388-798-8

Becke, A. D. (1993). Density-functional thermochemistry. III. The role of exact exchange. *The Journal of Chemical Physics, 98*(7), 5648–5652.

Bozdogan, B., & Appelbaum, P. C. (2004). Oxazolidinones: Activity, mode of action, and mechanism of resistance. *International Journal of Antimicrobial Agents, 23*(2), 113–119.

Cho, H., Uehara, T., & Bernhardt, T. G. (2014). Beta-lactam antibiotics induce a lethal malfunctioning of the bacterial cell wall synthesis machinery. *Cell, 159*(6), 1300–1311.

Chukwudi, C. U. (2016). rRNA binding sites and the molecular mechanism of action of the tetracyclines. *Antimicrobial Agents and Chemotherapy, 60*(8), 4433–4441.

Davies, J., & Davies, D. (2010). Origins and evolution of antibiotic resistance. *Microbiology and Molecular Biology Reviews, 74*(3), 417–433.

Dinos, G. P. (2017). The macrolide antibiotic renaissance. *British Journal of Pharmacology, 174*, 2967–2983.

Drlica, K., Hiasa, H., Kerns, R., Malik, M., Mustaev, A., & Zhao, X. (2009). Quinolones: Action and resistance updated. *Current Topics in Medicinal Chemistry, 9*(11), 981–998.

Ducati, R. G., Basso, L. A., & Santos, D. S. (2007). Mycobacterial shikimate pathway enzymes as targets for drug design. *Current Drug Targets, 8*(4), 423–435.

Ekinci, E., Çiftçi, H., Adem, Ş., Gündoğdu Aytaç, Ö., & Eyüpoğlu, V. (2025b). A comprehensive investigation of Schiff bases and bis-α-aminophosphonates as potent agents against Alzheimer's disease by computer-aided drug discovery techniques and in vitro examinations. *Journal of Molecular Structure, 1333*, 141734.

Ekinci, E., Gündoğdu Aytaç, Ö., & Aytaç, S. (2025a). Investigation of the antibacterial activity of the contezolid molecule using in silico methods: DFT and molecular docking studies. In E. Bayram (Ed.), *International academic research and studies in chemistry* (pp. 25–43). Ankara, Turkey: Serüven Yayınevi.

Foti, C., Piperno, A., Scala, A., & Giuffrè, O. (2021). Oxazolidinone antibiotics: Chemical, biological and analytical aspects. *Molecules, 26*(14), 4280.

Frisch, M. J., Pople, J. A., & Binkley, J. S. (1984). Self-consistent molecular orbital methods. 25. Supplementary functions for Gaussian basis sets. *Journal of Chemical Physics, 80*, 3265–3269.

Frisch, M. J., Trucks, G. W., Schlegel, H. B., Scuseria, G. E., Robb, M. A., Cheeseman, J. R., … Fox, D. J. (2016). *Gaussian 16* (Revision C.01). Gaussian, Inc.

Gündoğdu Aytaç, Ö., Gündoğdu, H. B., Aytaç, S., Bingöl, Z., Gülçin, İ., & Kara, Y. (2025). Novel isoindole-1,3-dione-isoxazole hybrids: Synthesis, characterization, evaluation of their inhibitory activities on carbonic anhydrase and acetylcholinesterase. *Journal of Biochemical and Molecular Toxicology, 39*, e70550.

Heravi, M. M., & Zadsirjan, V. (2020). Prescribed drugs containing nitrogen heterocycles: An overview. *RSC Advances, 10*(72), 44247–44311.

Hoagland, D. T., Liu, J., Lee, R. B., & Lee, R. E. (2016). New agents for the treatment of drug resistant *Mycobacterium tuberculosis*. *Advanced Drug Delivery Reviews, 102*, 55–72.

Iqbal, K., Milioudi, A., & Wicha, S. G. (2022). Pharmacokinetics and pharmacodynamics of tedizolid. *Clinical Pharmacokinetics, 61*(5), 489–503.

Jampilek, J. (2019). Heterocycles in medicinal molecules. *Molecules, 24*(21), 3839.

Kim, J. S., Kim, Y. H., Lee, S. H., Kim, Y. H., Kim, J. W., Kang, J. Y., Kim, S. K., Kim, S. J., Kang, Y. S., Kim, T. H., Mok, J., Byun, M. K., Park, H. J., Joh, J. S., Park, Y. B., Lim, H. S., Choi, H., Lee, S. H., Kim, H., … Shim, T. S. (2022). Early bactericidal activity of delpazolid (LCB01 0371) in patients with pulmonary tuberculosis. *Antimicrobial Agents and Chemotherapy, 66*(2), e0168421.

Kiran, G. U., Kumar, L. P., Mahesh, M., Manikanta, K. U. S., Nehemiah, G., & Kumar, G. P. (2025). Sutezolid: A promising next generation tuberculosis agent. *World Journal of Biology Pharmacy and Health Sciences, 23*(2), 348–355.

Koh, J., Khwarg, J., Cho, Y. L., Yu, K.-S., & Chung, J.-Y. (2024). Comparative pharmacokinetics study of two tablet formulations of delpazolid, a novel oxazolidinone class antibiotic. *Translational and Clinical Pharmacology, 32*(4), 216–224.

Kou, Y., Wang, S., Shi, J., Tan, X., Zhang, R., Li, X., & Li, X. (2025). Analysis of the disease burden and attributable risk factors of tuberculosis in G20 countries from 1990 to 2021. *BMC Infectious Diseases, 25*, 1503.

Krawczyk, S. J., Leśniczak Staszak, M., Gowin, E., & Szaflarski, W. (2024). Mechanistic insights into clinically relevant ribosome targeting antibiotics. *Biomolecules, 14*(10), 1263.

Kuang, W., Zhang, H., Wang, X., & Yang, P. (2022). Overcoming Mycobacterium tuberculosis through small molecule inhibitors to break down cell wall synthesis. *Acta Pharmaceutica Sinica B, 12*(8), 3201–3214.

Lee, C., Yang, W., & Parr, R. G. (1988). Development of the Colle–Salvetti correlation-energy formula into a functional of the electron density. *Physical Review B, 37*(2), 785–789.

Lee, S. M., Choi, S. C., Mun, K. R., Seo, J. Y., Cho, Y. L., Shim, T. S., & Lim, H.-S. (2024). Pharmacokinetic and pharmacodynamic modeling analysis of delpazolid (LCB01-0371) in adult patients with pulmonary tuberculosis. *Journal of Clinical Pharmacy, 64*(6), 849–859.

Li, B., Liu, Y., Luo, J., Cai, Y., Chen, M., & Wang, T. (2023). Contezolid, a novel oxazolidinone antibiotic, may improve drug-related thrombocytopenia in clinical antibacterial treatment. *Frontiers in Pharmacology, 14*, 1157437.

Minja, L. T., van der Feltz, I., Manyama, C., Mpagama, S., Mhimbira, F., Noreña, I., Sebe, M., Rassool, M., Wallis, R. S., Ntinginya, N., Liyoyo, A., Mbeya, B., Wagnerberger, L., Zumba, T., Peter, D. D., Makkan, H., Sloan, D. J., te Brake, L., Schildkraut, J. A., Heinrich, N. (2025). Delpazolid in combination with bedaquiline, delamanid, and moxifloxacin for pulmonary tuberculosis (PanACEA-DECODE-01): A prospective, randomised, open-label, phase 2b, dose-finding trial. *Lancet Infectious Diseases, 25*, 1219–1229.

Mulubwa, M., & Mugabo, P. (2019). Steady-state population pharmacokinetics of terizidone and its metabolite cycloserine in patients with drug-resistant tuberculosis. *British Journal of Clinical Pharmacology, 85*(9), 1946–1956.

Mustafa, Y. F. (2018). Synthesis, characterization and antibacterial activity of novel heterocycle, coumacine, and two of its derivatives. *Saudi Pharmaceutical Journal, 26*(6), 870–875.

Ovung, A., & Bhattacharyya, J. (2021). Sulfonamide drugs: Structure, antibacterial property, toxicity, and biophysical interactions. *Biophysical Reviews, 13*(2), 259–272.

Rajput, V. S., Runthala, A., & Khan, I. A. (2023). Shikimate kinase inhibitors: An update on promising strategy against Mycobacterium tuberculosis. *Current Drug Targets, 24*, 388–405.

Shivaji, B. G., & Kasabe, A. J. (2021). A review of heterocyclic compound synthesis and antibacterial activity. *Journal of Pharmaceutical Negative Results, 12*(1), 98–102.

Tawfick, M. M., Badawy, M. S. E. M., Taleb, M. H., & El Menofy, N. G. (2023). Tuberculosis diagnosis and detection of drug resistance: A comprehensive updated review. *Journal of Pure and Applied Microbiology, 17*(4), 1978–2009.

Wang, C., Xiong, Y., Bao, C., Wei, Y., Wen, Z., Cao, X., Yu, Z., Deng, X., Li, G., & Deng, Q. (2023). Antibacterial and anti-biofilm activity of radezolid against *Staphylococcus aureus* clinical isolates from China. *Frontiers in Microbiology, 14*, 1131178.

Xu, X., Dong, B., Peng, L., Gao, C., He, Z., Wang, C., & Zeng, J. (2022). Antituberculosis drug development via targeting the cell envelope of *Mycobacterium tuberculosis*. *Frontiers in Microbiology, 13*, 1056608.

Zeng, D., Debabov, D., Hartsell, T. L., Cano, R. J., Adams, S., Schuyler, J. A., McMillan, R., & Pace, J. L. (2016). Approved glycopeptide antibacterial drugs: Mechanism of action and resistance. *Cold Spring Harbor Perspectives in Medicine, 6*(12), a026989.

ORAL PRESENTATION

Resveratrol'ün FOXP3 geni üzerindeki düzenleyici rolü

Tuğba Bayramoğlu[1*] (*https://orcid.org/0009-0006-7185-5753),*
Şevval Türk[1] (https://orcid.org/0009-0009-2983-263X),
Kader Başтepe[1] (*https://orcid.org/0009-0004-4600-0089)*,
Lutfiye Karcıoğlu Batur[1,2] (https://orcid.org/0000-0002-4803-9137) ,
Merve Yasemin Altintaş[3] (https://orcid.org/0000-0001-7733-4429).

[*1] Biruni Üniversitesi, Mühendislik ve Doğa Bilimleri Fakültesi, Moleküler Biyoloji ve Genetik Bölümü, İstanbul, Türkiye.
[2] Biruni Üniversitesi, Biruni Üniversitesi Araştırma Merkezi (B@MER), İstanbul, Türkiye.
[3] İstanbul Aydın Üniversitesi, Eczacılık Fakültesi, Farmakognozi Anabilim Dalı, İstanbul, Türkiye.

*Sorumlu yazar e-mail: byrmoglutugba@gmail.com

Özet

Bu çalışma, resveratrolün FOXP3 geni üzerindeki potansiyel etkilerini değerlendirmeyi amaçlamaktadır. FOXP3, düzenleyici T (Treg) hücre fonksiyonunun temel belirleyicisidir. Resveratrol (RSV), özellikle üzüm kabuğu, çekirdeği ve kırmızı meyveler gibi çeşitli bitkisel kaynaklarda bulunan doğal bir polifenoldür. Antioksidan, antikanser, antiinflamatuar ve immünomodülatör özellikleri sayesinde biyolojik olarak aktiftir. RSV, eikosanoid üretimi, oksidatif stres yanıtları ve mTOR, STAT3, AhR gibi sinyal yolaklarını modüle ederek bağışıklık sistemi üzerinde çok yönlü düzenleyici etkiler gösterir.

FOXP3, Treg hücrelerinin gelişimi ve immünosupresif fonksiyonu için kritik bir transkripsiyon faktörüdür. Çalışmalar, RSV'nin FOXP3 ekspresyonunu ve stabilitesini doğrudan veya dolaylı olarak etkileyebildiğini göstermektedir. Farklı deneysel modellerde resveratrol uygulamasının $FOXP3^+$ Treg hücre sayısını artırdığı, Treg/Th17 dengesini Treg lehine kaydırdığı, proinflamatuar sitokin seviyelerini azalttığı ve FOXP3 lokusundaki düzenleyici bölgeleri epigenetik olarak modüle ettiği bildirilmiştir. Obezite ve metabolik sendrom modellerinde RSV'nin SIRT1 aracılığıyla FOXP3 ekspresyonunu koruduğu ve inflamasyonu azalttığı gösterilmiştir. Astım ve otoimmün hastalık modellerinde ise RSV'nin miR-34a'yı baskılayarak FOXP3 aktivitesini artırdığı ve AhR/Notch1 aksını inhibe ederek Treg farklılaşmasını desteklediği bulunmuştur.

Kanser modellerinde RSV'nin etkileri daha karmaşıktır. Hepatoselüler karsinomda resveratrol, immünosupresif $CD8^+CD122^+$ Treg alt kümelerini azaltmış ve IFN-γ üreten $CD8^+$ T hücrelerini artırarak antitümör yanıtları güçlendirmiştir. Ayrıca TGF-β1 ve IL-10 gibi immünosupresif sitokinler azalırken, TNF-α ve IFN-γ gibi antitümör sitokinler artmıştır. Sınırlı klinik çalışmalar da resveratrolün Treg ve γδ T hücre popülasyonlarını artırdığını, proinflamatuar sitokinleri azalttığını ve antioksidan kapasiteyi yükselttiğini göstermektedir.

Sonuç olarak, resveratrol FOXP3 ve Treg fonksiyonlarını düzenleyerek otoimmün ve metabolik hastalıklarda immün dengenin korunmasına katkı sağlamakta, immünosupresif tümör mikroçevresini modüle ederek antitümör yanıtları güçlendirmektedir. Bu bulgular, resveratrolün FOXP3 ve Treg modülasyonu üzerinden potansiyel antikarsinojenik etkileri olan değerli bir molekül olduğunu göstermektedir. Ancak, uzun dönem etkileri ve optimal dozun belirlenmesi için daha kapsamlı preklinik ve klinik çalışmalara ihtiyaç vardır.

Anahtar Kelimeler: Resveratrol, FOXP3, Düzenleyici T hücreleri (Treg), İmmün modülasyon, Antikanser etkiler.

The regulatory role of resveratrol on the FOXP3 gene

Abstract

This study aims to evaluate the potential effects of resveratrol on the FOXP3 gene, a key determinant of regulatory T (Treg) cell function. Resveratrol (RSV) is a natural polyphenol found in various plant sources, particularly grape skins, seeds, and red fruits. It is biologically active due to its antioxidant, anticancer, anti-inflammatory, and immunomodulatory properties. RSV exerts multifaceted regulatory effects on the immune system by modulating eicosanoid production, oxidative stress responses, and signaling pathways such as mTOR, STAT3, and AhR.

FOXP3 is a critical transcription factor for the development and immunosuppressive function of Treg cells. Studies have shown that RSV can directly or indirectly influence FOXP3 expression and stability. In various experimental models, resveratrol treatment has been reported to increase the number of $FOXP3^+$ Treg cells, shift the Treg/Th17 balance toward Treg dominance, reduce proinflammatory cytokine levels, and modulate regulatory regions within the FOXP3 locus epigenetically. In obesity and metabolic syndrome models, RSV maintained FOXP3 expression via SIRT1 and reduced inflammation. In asthma and autoimmune models, RSV enhanced FOXP3 activity by downregulating miR-34a and promoted Treg differentiation by inhibiting the AhR/Notch1 axis.

In cancer models, RSV effects are more complex. In hepatocellular carcinoma, resveratrol reduced immunosuppressive $CD8^+CD122^+$ Treg subsets and increased IFN-γ–producing $CD8^+$ T cells, enhancing antitumor responses. Additionally, immunosuppressive cytokines such as TGF-β1 and IL-10 decreased, while antitumor cytokines TNF-α and IFN-γ increased. Limited clinical studies have also shown that resveratrol increases Treg and γδ T cell populations, reduces proinflammatory cytokines, and enhances antioxidant capacity.

In conclusion, resveratrol regulates FOXP3 and Treg functions, supporting immune balance in autoimmune and metabolic diseases and enhancing antitumor responses by modulating the immunosuppressive tumor microenvironment. These findings indicate that resveratrol is a valuable molecule with potential anticarcinogenic effects via FOXP3 and Treg modulation. However, more comprehensive preclinical and clinical studies are needed to determine its long-term effects and optimal dosing.

Keywords: Resveratrol, FOXP3, Regulatory T cells (Treg),Immune modulation, Anticancer effects.

GİRİŞ

Bağışıklık sistemi, etkili ve dinamik bir hücresel ağ olarak, canlıları patojenlere karşı koruma görevini üstlenmektedir. Bu nedenle, bağışıklık sistemi, gereksiz ve kendine zarar veren bağışıklık tepkilerini önlemek için kendi yapılarını yabancı yapılardan ayırmalı, ancak aynı zamanda zararlı olan ile zararsız olan yabancı antijenler (Ag'ler) arasında da ayrım yapabilmelidir (Jonuleit ve Schmitt,2003). Düzenleyici T hücreleri (Treg'ler), kendi antijenlerine (self-Ag'ler) karşı immünolojik tepkisizliği sürdürmede ve konağa zarar veren aşırı bağışıklık tepkilerini baskılamada vazgeçilmez bir rol oynayan benzersiz bir T hücresi soyudur (Sakaguchi ve ark., 2008). Treg hücrelerinin immün toleransın devamı için kritik rolleri nedeniyle, bu hücrelerin gelişimini ve fonksiyonunu kontrol eden moleküler mekanizmaların anlaşılması modern immünolojinin temel araştırma alanlarından biri hâline gelmiştir.FOXP3 geni, Forkhead/Winged-Helix (FOX) transkripsiyon faktörleri ailesine ait olup, düzenleyici T hücrelerin (Treg) gelişimi ve immün baskılayıcı fonksiyonlarını göstermeleri için temel bir gen olarak görev yapar. Treg hücrelerinin baskılayıcı işlevi için FOXP3'ün yapısal olarak ifade edilmesi gerekir; bu genin mutasyonu veya eksikliği otoimmün hastalıkların ortaya çıkmasına yol açar(Ziegler, 2006). T hücreleri, timusta $CD4^+CD25^+$ T hücrelerinin bir alt grubu olan doğal Treg'ler (nTreg'ler) olarak bilinen $Foxp3^+CD4^+$ T hücrelerine farklılaşır. Periferik lenfoid organlarda ise TGF-β, $CD4^+CD25^-$ T hücrelerinin adaptif veya indüklenmiş Treg'lere dönüşmesini sağlar (Fu ve ark., 2004). Ancak, nTreg'ler ile TGF-β ile indüklenen Treg'ler farklı işlevsel özellikler taşır (Tran ve ark., 2007). Bu ayrım, immün homeostazın farklı koşullara göre ince bir şekilde düzenlenmesini sağlar.FOXP3 geni, $CD4^+CD25^+$ Treg'lerin gelişimi, kimliği ve işlevi için merkezi bir role sahiptir(Floess ve ark., 2007; Lal ve ark., 2009; Lal ve Bromberg, 2009).FOXP3 ve Treg fonksiyonu, epigenetik ve post-translasyonel mekanizmalarla da düzenlenir; histon modifikasyonları, metilasyon/demetilasyon ve mikroRNA'lar Treg stabilitesi ve işlevi üzerinde etkili olur (Lal ve ark., 2009). FOXP3'ün sürekli ekspresyonu olmadan Treg hücreleri ya oluşamaz ya da baskılayıcı işlevlerini stabil şekilde sürdüremez. FOXP3 lokusunda, "Treg-specific demethylated region (TSDR)" adı verilen epigenetik olarak hassas bir bölge bulunur; bu bölgedeki CpG metilasyonu, FOXP3 ekspresyonunun kararlılığı ve Treg kimliğinin korunması açısından kritiktir (Floess ve ark., 2007; Lal ve ark., 2009; Lal ve Bromberg, 2009). Treg hücreleri, bağışıklık sisteminde fren rolü üstlenir; aşırı veya uygunsuz immün yanıtları baskılayarak, otoimmüniteyi engeller ve dokularda immün toleransın sürdürülmesine katkıda bulunur. FOXP3, Treg'lerde baskılayıcı genlerin (IL-10, TGF-β) aktivasyonunu sağlarken inflamatuvar genlerin (IL-2, IFN-γ) ifadesini azaltan bir transkripsiyon faktörüdür (Ohkura ve Sakaguchi, 2020). FOXP3 geninde meydana gelen mutasyon veya genin silinmesi, $CD4^+CD25^+$ Treg hücrelerinin oluşamamasına yol açarak hem farelerde hem de insanlarda ciddi otoimmün hastalıkların ortaya çıkmasına sebep olur (Bennett ve Ochs, 2001;

Fontenot, Gavin ve Rudensky, 2003). Bu nedenle FOXP3, immün toleransın sürdürülebilirliği açısından merkezi bir moleküler belirleyici olarak kabul edilmektedir. Bağışıklık sistemi üzerinde resveratrol, eikosanoid üretimi, oksidatif stres mekanizmaları ve çeşitli sinyal yolları (mTOR, STAT3, AhR gibi) aracılığıyla çok yönlü etkiler gösterir (Malaguarnera, 2019). Resveratrol (RSV) (3,4,5-trans-trihidroksi-stilben), başta üzüm kabuğu, çekirdeği, sapı ve posası olmak üzere kırmızı meyveler ile çeşitli meyvelerde bulunan doğal bir fenolik bileşiktir (Vincenzi ve ark., 2016). RSV; antioksidan, antikanser, antiinflamatuvar, nöroprotektif, kardiyoprotektif ve yaşlanma karşıtı etkiler gösteren biyolojik olarak aktif bir polifenoldür (Li ve ark., 2017; Cheng ve ark., 2020). Bu flavonoid, kemoradyoterapi kaynaklı toksisitelerin azaltılmasında etkili olabilir (Mortezaee ve ark., 2020). Terapötik açıdan önemli bir özelliği, hasarlı bölgelere hücre göçünü artırabilmesidir (Hajinejad ve ark., 2018). Ayrıca, tümör mikroçevresi üzerinde düzenleyici etkiler göstererek kanser hücrelerinin gelişimini etkileyebilir (Najafi ve ark., 2021). Bu polifenol, karaciğer metabolizmasının korunmasına katkı sağlar (Wang ve ark., 2020). Bağışıklık sistemiyle etkileşime girerek onun işlevini güçlendirir (Sebastiano ve ark., 2018). Son yıllarda resveratrolün bağışıklık sistemi üzerindeki düzenleyici mekanizmaları giderek daha fazla araştırılmakta, özellikle Treg hücreleri ve FOXP3 gen ekspresyonu üzerindeki etkileri bilimsel olarak dikkat çekmektedir. Resveratrolün FOXP3'ün epigenetik düzenleyicileri, sinyal yolları ve Treg stabilitesine katkıda bulunma potansiyeli, bu bileşiğin otoimmün hastalıklar, inflamatuvar patolojiler, metabolik bozukluklar ve kanser gibi geniş bir hastalık yelpazesinde terapötik hedef olarak değerlendirilmesini mümkün kılmaktadır. Bu bağlamda, resveratrolün FOXP3 üzerinden bağışıklık yanıtını nasıl modüle ettiği, farklı hastalık modellerinde ortaya çıkan sonuçların ortak biyolojik mekanizmalarını anlamak açısından önemli bir araştırma alanı oluşturmaktadır.

Bulgular ve Tartışma

Treg hücreleri bağlamında resveratrol kullanımını değerlendiren çalışmalar, bu molekülün immün sistemi çok yönlü olarak modüle edebildiğini göstermektedir. Düzenli resveratrol tüketen sağlıklı bireylerde "$CD3^+CD4^+CD25^+CD127^-$" Treg hücrelerinin anlamlı düzeyde arttığı, proinflamatuvar sitokin düzeylerinin (TNF-α, MCP-1) azaldığı ve antioksidan kapasitenin yükseldiği bildirilmiştir. İnflamasyona dayalı hastalık modellerinde, örneğin kolit gibi durumlarda resveratrol Treg/Th17 dengesini Treg yönüne kaydırarak Treg hücre popülasyonunu artırmış; IL-17/Th17 ekseninin ve proinflamatuvar sinyallerin aktivitesini azaltmıştır.
(Yao ve ark., 2015).Bu sonuçlar, resveratrolün mukozal inflamasyon süreçlerinde Treg aracılı immün düzenlemeyi desteklediğini göstermektedir.Astım modeli üzerinde yapılan deneysel çalışmalarda resveratrol uygulamasının miR-34a düzeylerini düşürdüğü ve buna bağlı olarak FOXP3 ekspresyonunun arttığı tespit edilmiştir. (Alharris ve ark., 2018). Bu durum RSV'nin mikroRNA aracılı düzenleme mekanizmaları yoluyla FOXP3 ekspresyonunu dolaylı olarak kontrol edebildiğini ortaya koymaktadır..Resveratrolün nanoemülsiyon formunun (Res-mNE) kullanıldığı bir otoimmün hastalık modelinde Th17/Treg dengesi ve FOXP3 ekspresyonu üzerinde önemli etkiler saptanmıştır. Res-mNE, aryl hydrocarbon receptor (AhR) ve Notch1 sinyal eksenlerini baskılayarak FOXP3 düzeyini artırmış ve Treg farklılaşmasını desteklemiştir. (Cheng ve ark., 2023). Bu bulgular, resveratrolün immün hücre farklılaşmasını düzenleyen sinyal yolları üzerinde hedefe yönelik etkiler oluşturabileceğini göstermektedir.Bu çalışmalara bakıldığında, FOXP3'ün epigenetik düzeyde düzenlenmesi açısından Treg hücre kimliğinin korunması için FOXP3 lokusundaki demetilasyon ve histon asetilasyonu gibi epigenetik değişikliklerin gerçekleşmesinin kritik olduğu görülmektedir. Literatürde, resveratrolün bu epigenetik süreçler üzerinde dolaylı etkiler gösterebileceği ileri sürülmektedir(Lal ve ark., 2009).Resveratrol (RSV) uygulamasının, $CD4^+$ hücreler arasında $CD4^+CD25^+$ hücre popülasyonunu baskılayabildiği, TGF-β üretimini azalttığı ve hem ex vivo hem de in vivo koşullarda $CD8^+$ T hücrelerinde IFN-γ düzeylerini artırarak immün yanıtı uyarabildiği bildirilmiştir.Ayrıca, resveratrolün otoimmün hastalık modellerinde T hücre aktivasyonunu baskılayabildiği; tümör modellerinde ise Treg hücrelerinin baskılayıcı kapasitesini sınırlayarak antitümör immün yanıtı güçlendirebildiği de rapor edilmiştir (Zunino ve Storms, 2009). Bu veriler, resveratrolün bağlam ve hastalık modeline bağlı olarak immün sistemi hem baskılayıcı hem de uyarıcı yönlerde modüle edebilen çift yönlü bir immünomodülatör olduğunu desteklemektedir.Obezite ve metabolik sendrom modellerinde resveratrol, bağışıklık sistemi üzerinde düzenleyici etkiler göstermektedir. Yüksek yağlı diyete maruz kalan farelerde yapılan çalışmalar, resveratrol uygulamasının $FOXP3^+$ Treg hücrelerinin sayısını artırdığını ve inflamasyonu azalttığını ortaya koymuştur (Shabani ve ark., 2020). Ayrıca, resveratrolün SIRT1 aracılığıyla Th17/Treg dengesini düzenlediği ve FOXP3 ekspresyonunu koruduğu, bunun sonucunda insülin direncinin azaldığı bildirilmiştir (Chen ve ark., 2025). Bu veriler, resveratrolün obeziteye bağlı metabolik bozukluklarda Treg aracılığıyla bağışıklık yanıtını düzenleyebileceğini göstermektedir

.Kanser modellerinde ise resveratrolün etkileri daha karmaşık bir yapı göstermektedir. Hepatoselüler karsinom fare modelinde yapılan çalışmalarda, resveratrol $CD8^+CD122^+$ Treg hücrelerini azaltmış ve IFN γ üreten $CD8^+$ T hücrelerini artırarak antitümör yanıtı güçlendirmiştir .Ayrıca immünsüpresif sitokinler (TGF β1, IL 10) azalırken, antitümör sitokinler (TNF α, IFN γ) artmış ve M2-benzeri makrofaj oranı düşmüştür. İn vitro olarak resveratrol, $CD8^+CD122^-$ hücrelerden Treg farklılaşmasını engellemiştir. (Zhang ve ark., 2020). Bu bulgular, resveratrolün tümör mikroçevresinde immünsüpresif ortamı tersine çevirebileceğini ve bağışıklık yanıtını güçlendirebileceğini göstermektedir.Klinik öncesi çalışmalar, resveratrolün otoimmün bozukluklar ve kanser üzerinde immünomodülatör etkiler gösterebileceğini ortaya koymuştur. Klinik öncesi veriler umut verici olmakla birlikte, insan çalışmaları sınırlıdır; sınırlı sayıda katılımcıyla yapılan bir klinik çalışmada, 28 gün boyunca resveratrol uygulanmış ve γδ T ile Treg hücrelerinde artış, proinflamatuvar sitokinler düzeylerinde azalma ve antioksidan aktivitesinde yükselme gözlemlenmiştir (Espinoza ve ark., 2017). Ancak katılımcı sayısının düşük olması, sonuçların genellenebilirliğini sınırlamaktadır. Bu bulgular, resveratrolün Treg ve γδ T hücrelerini artırarak bağışıklık yanıtını dengeleyebileceğini ve proinflamatuvar sitokinleri azaltarak inflamasyonu kontrol altına alabileceğini göstermektedir .Bütün bulgular bir arada değerlendirildiğinde, resveratrolün FOXP3 ve Treg hücreleri üzerinden immün tolerans, inflamasyon kontrolü ve antitümör yanıtlar üzerinde önemli rol oynadığı görülmektedir. Bununla birlikte mevcut çalışmaların çoğu hücre kültürü ve hayvan modeli düzeyinde olup, resveratrolün biyoyararlanımı, doza bağlı etkileri ve klinik karşılığı hâlen net değildir.

SONUÇ

Mevcut literatür, resveratrolün FOXP3 geni üzerinde bağlama duyarlı ve çok yönlü bir düzenleyici etkiye sahip olduğunu göstermektedir. Resveratrol, FOXP3 ekspresyonunu artırarak Treg hücrelerinin farklılaşmasını, stabilitesini ve immün baskılayıcı fonksiyonlarını desteklemekte; otoimmün hastalıklar, kronik inflamasyon ve metabolik bozukluklar gibi durumlarda immün homeostazın yeniden sağlanmasına katkı sunmaktadır. Metabolik sendrom modellerinde $FOXP3^+$ Treg hücrelerindeki artış, inflamasyonun azalması ve immün-metabolik eksende gözlenen iyileşme, resveratrolün terapötik potansiyelini güçlendirmektedir.

Kanser modellerinde ise resveratrolün etkisi farklılaşmakta; tümör mikroçevresindeki immünsüpresif Treg birikimini azaltarak $CD8^+$ T hücre aktivitesini güçlendirmekte, proinflamatuvar ve antitümör sitokin yanıtlarını artırarak tümör progresyonunu baskılamaktadır. Bu bağlamda resveratrol, tümör ortamında immün toleransı azaltan, sistemik inflamatuvar hastalıklarda ise toleransı artıran çift yönlü bir immünomodülatör olarak öne çıkmaktadır. Bununla birlikte, bu etkilerin doku tipi, hastalık bağlamı, doz ve uygulama süresine göre değişebileceği unutulmamalıdır.

Resveratrolün FOXP3 aracılı immün düzenleme üzerindeki etkilerinin; Treg/Th17 dengesinin yeniden kurulması, miRNA profillerinin değiştirilmesi, epigenetik düzenlemelerin (demetilasyon ve histon modifikasyonları gibi) yönlendirilmesi ve özellikle SIRT1 aracılı sinyal yolaklarının modülasyonu ile ilişkili olduğu bildirilmektedir. Bu veriler, resveratrolün FOXP3–Treg ekseninde hem doğuştan hem de edinilmiş bağışıklıkta anlamlı biyolojik etkiler oluşturabildiğini desteklemektedir.

Her ne kadar klinik öncesi bulgular güçlü ve tutarlı olsa da, mevcut insan çalışmalarının sayısı sınırlıdır ve uzun dönem etkiler, optimal doz aralıkları, biyoyararlanım profili ve güvenlilik gibi kritik parametreler net değildir. Bu nedenle, resveratrolün klinik bir immün düzenleyici ajan olarak değerlendirilebilmesi için daha geniş örneklemli, kontrollü, çok merkezli ve uzun süreli klinik çalışmalara ihtiyaç duyulmaktadır.

Genel olarak değerlendirildiğinde resveratrol, FOXP3 üzerinden bağışıklık sistemini modüle edebilen, hastalık bağlamına göre hem immün uyarıcı hem de immünsüpresif yanıtlar oluşturabilen, geniş bir hastalık yelpazesinde terapötik potansiyel taşıyan bir molekül olarak öne çıkmaktadır. FOXP3'ün Treg hücre stabilitesi ve immün tolerans açısından merkezi bir regülatör olduğu göz önüne alındığında, resveratrolün bu gen üzerindeki etkilerinin daha kapsamlı çalışmalarla desteklenmesi, gelecekteki klinik uygulamalar için önemli bir yol haritası oluşturacaktır.

KAYNAKLAR

Alharris, E., Alghetaa, H., Seth, R., Chatterjee, S., Singh, N. P., Nagarkatti, M., ve Nagarkatti, P. (2018). Resveratrol attenuates allergic asthma and associated inflammation in the lungs through regulation of MIRNA-34A that targets FOXP3 in mice. Frontiers in Immunology, 9.

Bennett, C. L., ve Ochs, H. D. (2001). IPEX is a unique X-linked syndrome characterized by immune dysfunction, polyendocrinopathy, enteropathy, and a variety of autoimmune phenomena. Current Opinion in Pediatrics, 13(6), 533–538.

Chen, Y., et al. (2025). Electroacupuncture regulates Th17/Treg cell balance through SIRT1 to ameliorate obesity induced insulin resistance. Diabetes, Metabolic Syndrome and Obesity, 18, 1123–1135.

Cheng, C. K., Luo, J. Y., Lau, C. W., Chen, Z. Y., Tian, X. Y., ve Huang, Y. (2020). Pharmacological basis and new insights of resveratrol action in the cardiovascular system. British Journal of Pharmacology, 177, 1258–1277.

Cheng, J., Wang, S., Lv, S. Q., Song, Y., ve Guo, N. H. (2023). Resveratrol inhibits AhR/Notch axis and reverses Th17/Treg imbalance in purpura by activating Foxp3. Toxicology Research, 12(3), 381–391.

Espinoza, J. L., Trung, L. Q., Inaoka, P. T., Yamada, K., An, D. T., Mizuno, S., Nakao, S., ve Takami, A. (2017). The repeated administration of resveratrol has measurable effects on circulating T-cell subsets in humans. Oxidative Medicine and Cellular Longevity, 2017, 6781872.

Floess, S., Freyer, J., Siewert, C., Baron, U., Olek, S., Polansky, J., Schlawe, K., Chang, H., Bopp, T., Schmitt, E., Klein Hessling, S., Serfling, E., Hamann, A., ve Huehn, J. (2007). Epigenetic control of the foxp3 locus in regulatory T cells. PLoS Biology, 5(2), e38.

Fontenot, J. D., Gavin, M. A., ve Rudensky, A. Y. (2003). Foxp3 programs the development and function of CD4+ CD25+ regulatory T cells. Nature Immunology, 4(4), 330–336.

Fu, S., Zhang, N., Yopp, A. C., et al. (2004). TGF-beta induces Foxp3+ T-regulatory cells from CD4+ CD25− precursors. American Journal of Transplantation, 4(10), 1614–1627.

Hajinejad, M., Pasbakhsh, P., Omidi, A., Mortezaee, K., Nekoonam, S., Mahmoudi, R., ve Kashani, I. R. (2018). Resveratrol pretreatment enhanced homing of SDF-1α-preconditioned bone marrow-derived mesenchymal stem cells in a rat model of liver cirrhosis. Journal of Cellular Biochemistry, 119, 2939–2950.

Jonuleit, H., ve Schmitt, E. (2003). The regulatory T cell family: distinct subsets and their interrelations. The Journal of Immunology, 171(12), 6323–6327.

Lal, G., ve Bromberg, J. S. (2009). Epigenetic mechanisms of regulation of Foxp3 expression. Blood, 114(18), 3727–3735.

Lal, G., Zhang, N., van der Touw, W., Ding, Y., Ju, W., Bottinger, E. P., Reid, S. P., Levy, D. E., ve Bromberg, J. S. (2009). Epigenetic regulation of Foxp3 expression in regulatory T cells by DNA methylation. Journal of Immunology, 182(1), 259–273.

Li, J., Zhang, C.-X., Liu, Y.-M., Chen, K.-L., ve Chen, G. (2017). A comparative study of anti-aging properties and mechanism: Resveratrol and caloric restriction. Oncotarget, 8, 65717–65729.

Malaguarnera, L. (2019). Influence of resveratrol on the immune response. Nutrients, 11(5), 946.

Mortezaee, K., Najafi, M., Farhood, B., Ahmadi, A., Shabeeb, D., ve Musa, A. E. (2020). Resveratrol as an adjuvant for normal tissues protection and tumor sensitization. Current Cancer Drug Targets, 20, 130–145.

Najafi, M., Majidpoor, J., Toolee, H., ve Mortezaee, K. (2021). The current knowledge concerning solid cancer and therapy. Journal of Biochemical and Molecular Toxicology, 35, e22900.

Ohkura, N., ve Sakaguchi, S. (2020). Transcriptional and epigenetic basis of Treg cell development and function: Its genetic anomalies or variations in autoimmune diseases. Cell Research, 30, 465–474.

Sakaguchi, S., Yamaguchi, T., Nomura, T., ve Ono, M. (2008). Regulatory T cells and immune tolerance. Cell, 133(5), 775–787.

Sebastiano, M., Eens, M., Messina, S., AbdElgawad, H., Pineau, K., Beemster, G. T. S., Chastel, O., ve Costantini, D. (2018). Resveratrol supplementation reduces oxidative stress and modulates the immune response in free-living animals during viral infection. Functional Ecology, 32, 2509–2519.

Shabani, M., et al. (2020). Resveratrol alleviates obesity induced skeletal muscle inflammation via Treg modulation. Scientific Reports, 10, 3791.

Tran, D. Q., Ramsey, H., ve Shevach, E. M. (2007). Induction of FOXP3 expression in naive human CD4+ FOXP3− T cells is transforming growth factor-beta-dependent but does not confer a regulatory phenotype. Blood, 110(8), 2983–2990.

Vignali, D. A., Collison, L. W., ve Workman, C. J. (2008). How regulatory T cells work. Nature Reviews Immunology, 8(7), 523–532.

Vincenzi, S., Tomasi, D., Gaiotti, F., Lovat, L., Giacosa, S., Torchio, F., Segade, S. R., ve Rolle, L. (2016). Comparative study of the resveratrol content of twenty-one Italian red grape varieties. South African Journal of Enology and Viticulture, 34, 30–35.

Wang, P., Wang, J., Li, D., Ke, W., Chen, F., ve Hu, X. (2020). Targeting the gut microbiota with resveratrol: Evidence for the management of hepatic steatosis. Journal of Nutritional Biochemistry, 81, 108363.

Yao, J., Wei, C., Wang, J. Y., Zhang, R., Li, Y. X., ve Wang, L. S. (2015). Effect of resveratrol on Treg/Th17 signaling and ulcerative colitis treatment in mice. World Journal of Gastroenterology, 21(21), 6572–6581.

Zhang, Q., Huang, H., Zheng, F., Liu, H., Qiu, F., Chen, Y., Liang, C. L., ve Dai, Z. (2020). Resveratrol exerts antitumor effects by downregulating CD8+CD122+ Tregs in murine hepatocellular carcinoma. Oncoimmunology, 9(1), 1829346.

Ziegler, S. F. (2006). FOXP3: Of mice and men. Annual Review of Immunology, 24, 209–226.

Zunino, S. J., ve Storms, D. H. (2009). Resveratrol alters proliferative responses and apoptosis in human activated B lymphocytes in vitro. Journal of Nutrition, 139, 1603–1608.

ORAL PRESENTATION

The acute gastrointestinal toxidrome: A triage algorithm distinguishing organophosphates, carbamates, and metal phosphides from foodborne illness

Elifnur Yıldırım[1*] (*ORCID: https://orcid.org/0009-0008-9103-8528*),
Mehtap Kara[1] (ORCID: https://orcid.org/0000-0001-7764-5593)

[*1] Istanbul University, Faculty of Pharmacy, Department of Pharmaceutical Toxicology, Istanbul, Turkey; Istanbul University, Institute of Graduate Studies in Health Sciences, Istanbul, Turkey.
[2] Istanbul University, Faculty of Pharmacy, Department of Pharmaceutical Toxicology, Istanbul, Turkey.

*Corresponding author e-mail: ecz.elifnur@hotmail.com

Abstract

Acute nausea and vomiting are among the most common non-specific clinical presentations in emergency settings, typically attributed to food poisoning or gastroenteritis. However, this clinical picture frequently mimics the early stages of pesticide intoxications, specifically cholinesterase inhibitors (organophosphates and carbamates) and metal phosphides (aluminum/zinc phosphide). The diagnostic gap is critical; epidemiological analysis indicates case fatality rates for aluminum phosphide (60%) and organophosphates (20%) are significantly higher than for other agents like pyrethroids (<3%), yet initial symptoms are frequently misinterpreted, leading to fatal premature discharge. This review aims to establish a clinical differential diagnosis algorithm to rapidly distinguish between foodborne illness, cholinergic intoxication, and phosphide poisoning in patients presenting with acute gastrointestinal symptoms, while ruling out common confounders like pyrethroid exposure. A review of current toxicological literature and case report series was conducted, focusing on the toxidrome triage markers: pupillary response, hemodynamic stability, respiratory secretions, and olfactory cues. The review identifies three distinct clinical pathways: the wet toxidrome of organophosphates and carbamates, characterized by miosis, bronchorrhea, and hypersecretion; for which the atropine challenge serves as a definitive physiological screen. The shock toxidrome of metal phosphides lacks a specific rapid assay and presents with a dry initial phase, but is characterized by early, refractory hypotension and metabolic acidosis; signs that are absent in typical food poisoning. Here, the silver nitrate test provides immediate chemical confirmation of phosphine gas. The irritant toxidrome of pyrethroids is identified primarily through paraesthesia and respiratory irritation rather than systemic shock. Reliance on patient history alone is insufficient. We propose a "Vomiting Triage Algorithm" that prioritizes hemodynamic assessment and pupillary examination, utilizing point-of-care testing with both chemical (silver nitrate) and physiological (atropine challenge) to rule out toxic pesticidal exposure. Implementation of this workflow can reduce the diagnostic gap responsible for iatrogenic errors regarding preventable mortality in pesticide poisoning.

Keywords: Differential Diagnosis, Toxidrome, Food Poisoning, Pesticide Exposure, Aluminum Phosphide, Organophosphates

INTRODUCTION

The catalyst for this review was the recent fatal incidents in the hospitality sector, specifically the tragic case of the Böcek family who were exposed to pesticide fumigants, namely aluminum phosphide in a hotel setting. In this and similar documented cases, patients presented to emergency departments with acute nausea, vomiting, and malaise—symptoms indistinguishable from common foodborne illness. Notably, the mother reported that her children were "lying motionless", a sign of profound lethargy and early central nervous system (CNS) depression distinct from the restlessness of simple gastroenteritis. Tragically, the absence of specific toxidrome recognition led to a diagnosis of food poisoning, resulting in premature discharge. This decision proved fatal, as the patients returned to the contaminated environment or succumbed to delayed systemic toxicity. These events underscore a critical failure in current triage protocols: the inability to rapidly distinguish between benign gastrointestinal illness and lethal chemical exposure in the absence of a clear history.

Beyond individual tragedies, pesticide poisoning remains a significant global public health challenge, accounting for approximately 150,000 deaths annually (Eddleston, 2024). While the majority of these fatalities occur in lower- and middle-income countries where agricultural chemicals are readily accessible, the clinical challenge of diagnosing acute intoxication is universal. Regulations aimed at restricting access to highly hazardous pesticides have reduced incidence in some regions (Gunnell et al., 2017), yet in the emergency setting, the "vomiting patient" remains a diagnostically ambiguous presentation. The overlap in symptoms between benign foodborne gastroenteritis and life-threatening pesticide exposure creates a dangerous "diagnostic gap". This gap is particularly evident in cases involving organophosphates (OPs), carbamates, and metal phosphides, which often present initially with non-specific gastrointestinal distress such as nausea, vomiting, and abdominal pain.

The consequences of misdiagnosis are severe. Epidemiological data indicates that case fatality rates vary drastically by chemical class. While pyrethroids have a low fatality rate of approximately 3.28% (Zheng et al., 2025), aluminum phosphide carries a catastrophic mortality rate often exceeding 60% due to the lack of a specific antidote (Mathai et al., 2010; Mew et al., 2017). Similarly, organophosphates remain highly lethal, with fatality rates around 17-20% depending on the agent (Zheng et al., 2025). In contrast to accidental poisoning, which often involves smaller doses via inhalation or dermal contact, intentional or incidental ingestion of these agents leads to rapid systemic toxicity.

Critically, initial symptoms are frequently misinterpreted, leading to premature discharge, delayed decontamination, and secondary complications such as aspiration pneumonia and multi-organ failure (Shi et al., 2023). A retrospective study of 553 poisoned patients revealed that delayed arrival at a toxicology center significantly impacts survival; patients arriving more than 8 hours post-exposure had 2.2 times higher odds of mortality compared to those arriving earlier (Kebede et al., 2025). Furthermore, survival in phosphide poisoning is entirely dependent on early recognition and aggressive supportive care, which is often delayed when symptoms are mistaken for common gastroenteritis. This review analyzes the pathophysiological distinctions between these toxidromes to propose a triage algorithm that moves beyond unreliable patient history and focuses on objective clinical phenotyping.

The Common Mimic: Bacterial and Viral Gastroenteritis

The primary diagnostic competitor in the "vomiting patient" is acute gastroenteritis caused by foodborne pathogens. In the emergency setting, this condition effectively acts as a diagnosis of exclusion for toxicology cases. The etiology is typically infectious, driven by viral agents (e.g., Norovirus, Rotavirus) or bacterial pathogens (e.g., *Salmonella*, *Escherichia coli*, *Campylobacter*). The pathophysiology involves either local mucosal invasion or the release of enterotoxins that disrupt the intestinal epithelial barrier, stimulating the enteric nervous system to trigger emesis and diarrhea as expulsion mechanisms (CDC, 2004). Unlike the systemic metabolic blockade seen in phosphide poisoning or the synaptic saturation of organophosphates, the pathology of foodborne illness is primarily localized to the gastrointestinal tract. Systemic symptoms, when present, are usually secondary consequences of volume depletion rather than direct cellular toxicity.

The clinical hallmark of uncomplicated gastroenteritis is hemodynamic stability relative to the severity of symptoms. While patients may present with profound misery, retching, and abdominal cramping, their cardiovascular reflexes typically remain intact. Unless dehydration is catastrophic, which may occur at late-stage, the patient maintains a normal blood pressure or exhibits a responsive tachycardia that resolves with fluid resuscitation. This stands in stark contrast to the "refractory hypotension" of metal phosphide poisoning, where the heart’s pumping function itself fails regardless of fluid volume (Shi et al., 2023).

Crucially, the patient with food poisoning remains alert and oriented (GCS 15). While they may appear lethargic due to exhaustion, they do not exhibit the rapid loss of consciousness, sudden coma, or fasciculations associated with toxic pesticidal exposures (Ntelios et al., 2013). The "Stable" phenotype is clinically "Dry." Mucous membranes are tacky or dry due to fluid loss, and the lungs are clear on auscultation. There is no evidence of the pathological hypersecretion (bronchorrhea, salivation) that defines the "Wet" organophosphate toxidrome.

Two specific features often serve as reliable differentiators between infectious and toxic etiologies: Pyrexia and event history.

Fever is a common systemic response to infection (e.g., Salmonellosis, Shigellosis) but is rare in the early stages of non-inflammatory pesticide poisoning. While aspiration pneumonia can cause delayed fever in poisoned patients, a patient presenting initially with high fever and vomiting is statistically more likely to have an infectious etiology than a toxic one (Shi et al., 2023).

Both food poisoning and pesticide exposure often present as cluster events (multiple people sick at once). However, the timeline differs. Foodborne outbreaks typically have an incubation period ranging from hours to days after a shared meal. In contrast, inhalational pesticide exposure (e.g., hotel fumigation) affects victims almost simultaneously or within minutes of entering the contaminated zone, without the delay unlike the incubation period in bacterial food poisonings (Eddleston, 2024). Clinicians must carefully interrogate the timeline of symptom onset so as to distinguish "shared meal" from "shared air."

The diagnosis of gastroenteritis should not be made solely on the presence of vomiting. It is a specific clinical entity characterized by hemodynamic stability (or fluid-responsive hypotension), normal pupillary function, clear lungs, and often pyrexia. Deviations from this "Stable" profile—specifically shock, miosis, or coma—must trigger an immediate search for toxicological causes.

The "Wet" Toxidrome: Organophosphates and Carbamates

Organophosphates (OPs) and Carbamates are potent insecticides widely utilized in commercial agriculture and, in some regions, for domestic pest control. Consequently, exposure most often results from occupational accidents or intentional ingestion of liquid concentrates. They represent the most significant class of pesticides requiring immediate differentiation from simple gastroenteritis. While both etiologies present with acute nausea, vomiting, and abdominal cramping, the underlying mechanism of OP toxicity creates a distinct "Wet" clinical phenotype characterized by hypersecretion and miosis (Eddleston, 2024). Unlike bacterial food poisoning, which acts through local mucosal irritation, both OPs and carbamates act systemically by inhibiting the enzyme acetylcholinesterase (AChE) (Lorke and Oz, 2025). This inhibition leads to an accumulation of acetylcholine (ACh) at the neuromuscular junctions and autonomic synapses, resulting in the overstimulation of muscarinic and nicotinic receptors (Zoofaghari et al., 2024). While the clinical presentation is nearly identical, the chemical bond formed by carbamates is transient and reversible, whereas OPs cause irreversible aging of the enzyme, often leading to more prolonged toxicity. Additionally, recent reviews suggest that oxidative stress and mitochondrial dysfunction play a significant role in the neurotoxicity of these agents, contributing to long-term sequelae. The pharmacokinetics of these compounds often involve rapid absorption and distribution, necessitating immediate recognition before the toxin binds to the enzyme.

The resulting "Cholinergic Crisis" is defined by a massive secretory response. Muscarinic overstimulation leads to the classic "SLUDGE" or "DUMBELS" symptoms: Salivation, lacrimation, urination, defecation, gastrointestinal distress, and emesis (Zoofaghari et al., 2024). While vomiting is the shared symptom with food poisoning, the accompanying signs are diametrically opposed. A patient with bacterial gastroenteritis is typically dehydrated with a dry mouth; conversely, patient poisoned by cholinesterase inhibitors presents with bronchorrhea, profound sweating, and hypersalivation (Eddleston, 2024). A case report by Bashyal et al. (2023) illustrates this distinction perfectly: a 39-year-old male presented with vomiting and epigastric pain but was noted to have a moist axilla and tongue and pinpoint pupils. This "moist axilla" sign is a critical triage marker, as patients with simple vomiting and dehydration should not be diaphoretic.

When clinical signs remain ambiguous, the "Atropine Challenge" serves as a definitive physiological bedside screen. The clinician administers a bolus of atropine IV (1 mg for adults). In a patient with benign gastroenteritis, this dose will block normal vagal tone, causing rapid tachycardia and a noticeably dry mouth. However, in a patient poisoned by cholinesterase inhibitors, the massive accumulation of acetylcholine at the synapses neutralizes the competitive antagonism of the atropine. Consequently, the patient will exhibit no significant change in heart rate or secretion status. This "negative response" confirms the toxic mechanism and justifies the immediate escalation to high-dose atropine therapy.

Once the toxidrome is identified, the immediate therapeutic goal is the reversal of muscarinic toxicity using aggressive atropine titration, followed by the administration of oximes (e.g., pralidoxime) to reactivate the phosphorylated enzyme before the chemical bond "ages" and becomes irreversible. While carbamate poisoning is generally reversible and may not strictly require oxime therapy, the initial emergency management—prioritizing

airway clearance and atropinization to dry secretions—remains identical to that of organophosphates (Eddlestone, 2024).

The "Shock" Toxidrome: Aluminum and Zinc Phosphides

Aluminum phosphide (AlP) and zinc phosphide are solid fumigants primarily used to protect stored grain from rodents and insects in silos, warehouses, and transport vessels. Unlike liquid insecticides, they are deployed as tablets or pellets that release lethal phosphine gas (PH_3) upon exposure to moisture in the air or stomach acid (Shi et al., 2023). While ingestion is a common method of self-harm, unintentional inhalation exposure represents a significant and insidious public health threat. Fatalities have been documented in families and hotel guests exposed to off-gassing from adjacent rooms or fumigated storage areas, often without their knowledge (Ntelios et al., 2013).

Unlike the "Wet" cholinergic crisis of organophosphates and carbamates, poisoning with aluminum phosphide (AlP) or zinc phosphide presents a distinct and arguably more deceptive clinical picture. Often referred to as the "Dry/Shock" toxidrome, this presentation is characterized by early gastrointestinal distress that rapidly progresses to refractory hypotension and cardiovascular collapse. The absence of dramatic initial signs like pinpoint pupils or hypersalivation makes this toxidrome particularly prone to being misdiagnosed as simple gastroenteritis, often with fatal consequences.

The toxicity of metal phosphides is driven by the liberation of phosphine gas (PH_3), a potent mitochondrial toxin. However, the pathway from exposure to systemic toxicity involves three distinct mechanisms that complicate the clinical presentation and contribute to the diagnostic confusion with gastrointestinal illness.

The first mechanism is "direct alveolar absorption". When phosphine gas is inhaled in confined spaces, it rapidly diffuses across the alveolar membrane into the bloodstream. Once systemic, the gas non-competitively inhibits cytochrome C oxidase in the mitochondrial electron transport chain (Singh et al., 2007). This blockade halts oxidative phosphorylation, creating a state of cellular suffocation and anaerobic metabolism that leads to severe metabolic acidosis and myocardial failure, even in the presence of adequate oxygen saturation. The heart muscle becomes inflamed and weak, leading to cardiovascular collapse. Since the heart and vessels are paralyzed, patients are unresponsive to treatment with fluids unlike in other hypovolemia inducing toxidromes such as food poisoning, pyrethroids and cholinergic crisis.

The second mechanism, often termed the "mucociliary escalator" effect, explains why patients with primarily respiratory exposure still present with severe vomiting. When phosphide dust or particles are inhaled, they may be trapped in the mucus of the respiratory tract. The body’s natural clearance mechanism moves this mucus up the trachea, where it is subsequently swallowed. Once these particles reach the stomach, they react with gastric acid (HCl) to release a secondary wave of phosphine gas directly into the gastrointestinal tract (Proudfoot, 2009). This effectively converts an inhalation exposure into a systemic ingestion toxicity, triggering the intense nausea and epigastric pain that mimics food poisoning.

The third and perhaps most insidious mechanism is the "absorption of intact phosphides". Contrary to the belief that the poison only acts as a gas, evidence suggests that metal phosphides can be absorbed largely intact from the gut before hydrolysis occurs. These solid phosphide particles travel through the portal circulation to the liver. Once inside the hepatic tissue, hydrolysis occurs, releasing high concentrations of phosphine gas locally (Anand et al., 2011). This mechanism accounts for the severe hepatic damage often observed in survivors and explains why gastric decontamination remains critical even hours after ingestion, as unreacted particles may act as a continuous reservoir for systemic toxicity.

These mechanisms create a "Double Hit" effect: the patient suffers immediate hypoxic stress from gas inhalation, followed by a delayed, secondary metabolic assault from swallowed or absorbed particles reacting in the stomach and liver. This complex pharmacokinetic profile underscores why simple supportive care for gastroenteritis fails; without specific intervention to neutralize gastric acid or remove the particulate reservoir, the internal production of gas continues building up.

The clinical differentiation of phosphide poisoning from food poisoning relies on two major deviations from the standard gastroenteritis profile: hemodynamic instability and rapid loss of consciousness. While severe dehydration from food poisoning can cause hypotension, it typically responds to fluid resuscitation. In contrast, phosphide poisoning causes primary cardiogenic shock due to direct myocardial toxicity. In a reported case of incidental

exposure, a 25-year-old male presented with a blood pressure of 83/51 mmHg despite no history of massive fluid loss (Çakın et al., 2018). This rapid onset of shock (typically within minutes to hours), characterized by profound hypotension (Systolic BP < 90 mmHg) that is refractory to standard fluid resuscitation, is the single most critical "Red Flag" differentiating toxic exposure from benign food poisoning. Furthermore, while patients with gastroenteritis typically remain alert, phosphine gas induces rapid CNS depression. In the case of the 25-year-old male reported by Çakın et al. (2018), the patient was found unresponsive with a Glasgow Coma Scale (GCS) of 3 shortly after exposure. Similarly, a 15-year-old male patient described by Shi et al. (2023) suddenly lost consciousness while working. This rapid progression to coma in a vomiting patient rules out benign gastroenteritis and necessitates immediate airway protection.

The peril of relying on non-specific symptoms is best illustrated by the case of a 15-year-old male who suffered fatal complications due to an initial misdiagnosis. The patient first presented to a local hospital with "nausea and chest tightness"—symptoms easily attributed to viral illness or food intolerance—and was sent home without toxicological screening (Shi et al., 2023). This discharge allowed for continued absorption of the toxin, leading to a sudden loss of consciousness and coma the following day. The rapid CNS depression resulted in the loss of airway protection and subsequent aspiration pneumonia, confirmed by the presence of *E. coli* in sputum cultures. This case underscores that history taking alone is insufficient; young patients presenting with nausea and chest tightness must be screened for hemodynamic instability to prevent fatal discharge errors. To bridge this diagnostic gap, the bedside silver nitrate test offers a rapid screening mechanism. The reaction relies on the reduction of silver ions to metallic silver ($PH_3 + 6AgNO_3 \rightarrow Ag_3P,3AgNO_3 + 3HNO_3$), forming a black precipitate. While not chemically specific—gases such as hydrogen sulfide can cause false positives (Demange et al., 2000)—a color change to black in a hypotensive patient provides a critical presumptive positive result indicating potential presence of phosphides, or sulfides. This justifies immediate aggressive resuscitation hours before definitive gas chromatography (GC-MS) is available.

Unlike organophosphates, there is currently no specific antidote for metal phosphide poisoning. Consequently, management relies entirely on early gastric lavage to interrupt the toxicokinetic process at its source. This procedure utilizes specific chemical interventions to reduce bioavailability. First, sodium bicarbonate ($NaHCO_3$) is administered to neutralize stomach acid; by elevating the gastric pH, this intervention inhibits the acid-catalyzed hydrolysis of phosphide pellets, thereby slowing the production of new gas. Second, potassium permanganate ($KMnO_4$) is utilized as a lavage fluid to chemically attack the poison; as a strong oxidizing agent, it converts the highly toxic phosphine gas (PH_3) into much less toxic phosphate (PO_4), effectively disabling the toxin before systemic absorption occurs. Following lavage, activated charcoal is administered to adsorb any remaining phosphine gas within the gastrointestinal tract, acting as a final barrier against systemic uptake.

Crucially, this decontamination protocol is not limited to cases of direct ingestion. As detailed in the previous section, the unique mucociliary clearance mechanism can transport inhaled phosphide dust from the respiratory tract to the stomach, where it reacts with gastric acid to release a secondary wave of gas. Therefore, gastric lavage is indicated even in suspected inhalation exposures to remove these swallowed particulates and prevent the "Double Hit" phenomenon. This absence of a systemic reversal agent makes the initial triage decision critical; if the window for this early chemical decontamination is missed due to a misdiagnosis of gastroenteritis, mortality rates rise sharply (Çakın et al., 2018).

The "Red Herring" Toxidrome: Synthetic Pyrethroids

Synthetic pyrethroids, such as permethrin, deltamethrin, and cypermethrin, represent the most widely used class of insecticides in modern hospitality and residential settings due to their favorable safety profile compared to older agrochemicals. Unlike the systemic acetylcholinesterase inhibition seen in organophosphates and carbamates, pyrethroids act primarily by delaying the closure of voltage-gated sodium channels in neuronal membranes. This mechanism results in a clinical toxidrome defined largely by hyperexcitability and local irritation rather than the systemic cholinergic crisis or metabolic blockade associated with more lethal agents. Consequently, the clinical presentation of pyrethroid exposure is distinct, typically manifesting as paresthesia—a subjective stinging or burning sensation of the skin without erythema—along with upper respiratory tract irritation, cough, and mild gastrointestinal distress if ingested.

The critical relevance of pyrethroids in the differential diagnosis of the "vomiting patient" lies in their role as a clinical distracter or "red herring." Because these agents are ubiquitous, patient history often reveals recent exposure. However, attributing severe systemic symptoms such as refractory hypotension or profound miosis to pyrethroid exposure is a significant diagnostic error. Clinical studies have demonstrated that while organophosphate-pyrethroid combinations are highly toxic, pure pyrethroid poisoning is associated with extremely low fatality and minimal systemic signs compared to organophosphates. Epidemiological data strongly supports this distinction in severity. While pyrethroids account for a significant portion of insecticide exposures, their case fatality rate is consistently reported as low (<3%) (Zheng et al., 2025). In stark contrast, aluminum phosphide poisoning carries a mortality rate of up to 60% (Mathai et al., 2010), and organophosphates around 20% (Mew et al., 2017).

This disparity in mortality underscores the necessity of a triage algorithm that prioritizes physiological signs over exposure history. While pyrethroids can cause nausea and vomiting, they rarely precipitate the immediate cardiovascular collapse seen in metal phosphide poisoning or the profound bronchorrhea of organophosphate intoxication. Eddleston (2024) notes that newer agents, including pyrethroids, result in far fewer deaths globally compared to the older classes of pesticides. Therefore, in the emergency setting, a patient presenting with acute vomiting accompanied by shock or "wet" cholinergic signs should not be diagnosed with pyrethroid toxicity solely based on the presence of a spray can in the vicinity. Instead, the algorithm proposes that pyrethroids be treated as a diagnosis of exclusion, to be considered only after the life-threatening "shock" and "wet" toxidromes have been clinically ruled out.

Management for these cases is primarily supportive, focusing on skin decontamination to alleviate paresthesia. Since there is no specific antidote and systemic toxicity is rare, aggressive resuscitation is seldom required, allowing clinical resources to be redirected toward patients presenting with the more lethal 'Wet' or 'Shock' toxidromes (Eddleston, 2024).

DISCUSSION

The central hypothesis of this review is that the standard "gastroenteritis" diagnosis in the emergency department acts as a cognitive bias, blinding clinicians to the early signs of fatal pesticide toxicity. This "Diagnostic Trap" leads to iatrogenic mortality—death caused not solely by the poison, but by the medical decision to discharge a chemically compromising patient. This error of omission is well-documented in the literature. Fang et al. (1995) described a cluster of patients presenting with vomiting and diarrhea who were initially managed for foodborne illness; the correct diagnosis of Coumaphos (organophosphate) intoxication was only made after the delayed appearance of miosis. Similarly, fatal cases of aluminum phosphide poisoning have been recorded where initial treatment was solely for "acute gastritis," resulting in premature discharge and subsequent death from cardiogenic shock at home (Zhang et al., 2018). These cases demonstrate that the high mortality of phosphide poisoning is exacerbated by missing the "Golden Hour" for decontamination. When a physician misdiagnoses a toxic exposure as viral gastroenteritis, they unwittingly commit two errors: delaying gastric decontamination, which allows the phosphide pellets to continue generating gas, and removing the patient from cardiac monitoring, meaning the onset of refractory shock occurs in an unmonitored setting.

To bridge this gap, we propose a physiological phenotype-based algorithm for the emergency department (Figure 1). This decision tree allows for rapid stratification of the "vomiting patient" without relying on often unreliable exposure histories. The first step in this algorithm is the hemodynamic and neurological screen, or the "shock" node. The clinician must ask if the vomiting patient is hypotensive (SBP < 90 mmHg), in shock, or exhibiting altered mental status (GCS<15). Bacterial gastroenteritis rarely causes immediate cardiogenic shock or sudden coma; patients typically remain alert despite dehydration. Zoofaghari et al. (2024) identified a low GCS as a key prognostic indicator for severe poisoning outcomes. Therefore, the combination of vomiting with either refractory hypotension or a precipitous drop in consciousness suggests metabolic blockade (phosphides) or severe CNS toxicity. If these signs are present, the clinician should immediately suspect metal phosphide toxicity, initiate resuscitation, and perform silver nitrate test.

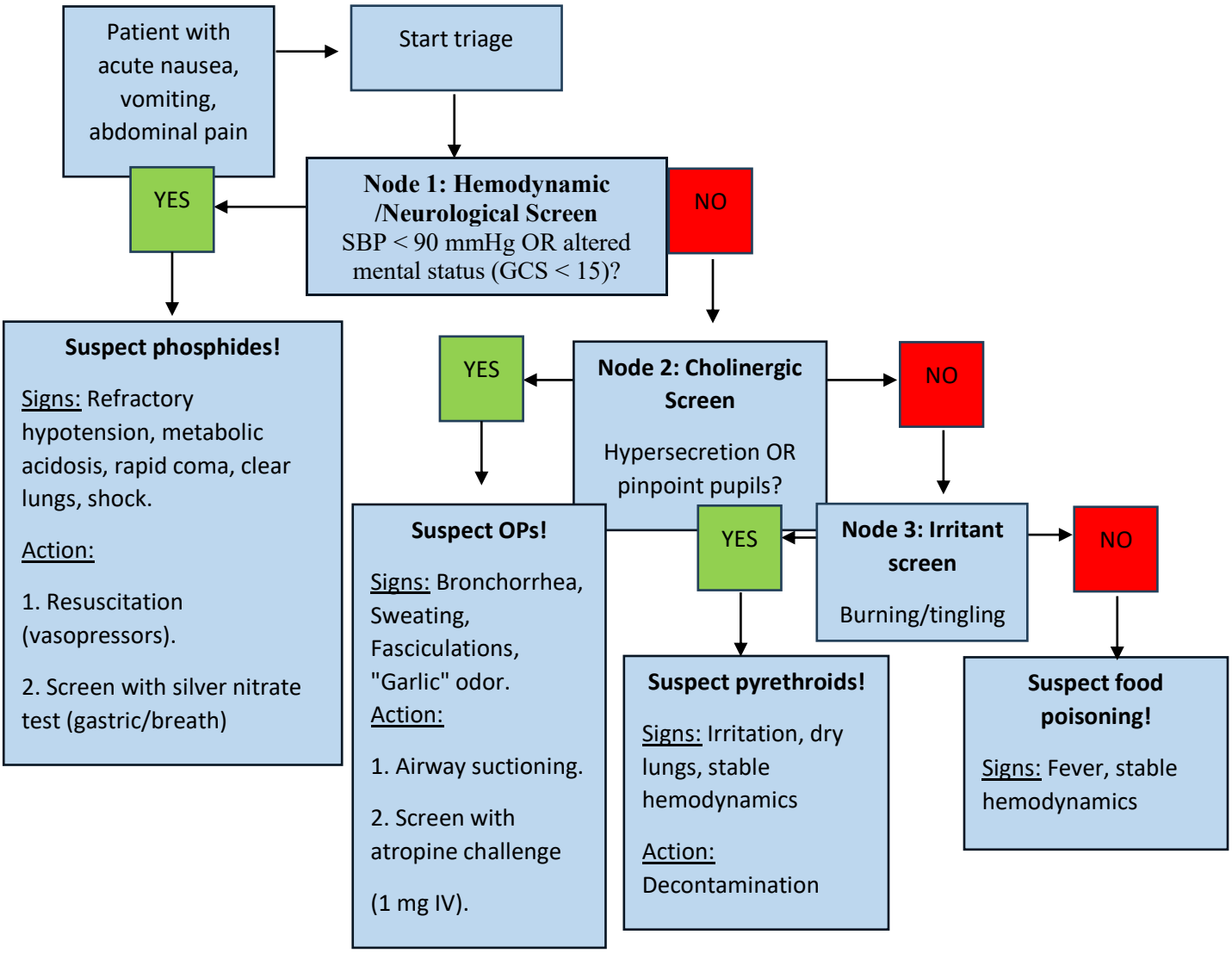


Figure 1. The Acute Gastrointestinal Toxidrome Triage Algorithm. This stepwise clinical decision tree facilitates the rapid differentiation of acute pesticide poisoning from benign gastroenteritis in the emergency department. Node 1 (Hemodynamic/Neurological Screen) prioritizes the identification of metal phosphide toxicity, defined by refractory hypotension (Systolic BP < 90 mmHg) or rapid central nervous system depression (GCS < 15), signs rarely seen in early foodborne illness. Node 2 (Cholinergic Screen) identifies organophosphate/carbamate poisoning through the "Wet" toxidrome of miosis and hypersecretion, confirmed via the physiological atropine challenge. Node 3 (Irritant Screen) classifies synthetic pyrethroids as a "Red Herring" or diagnosis of exclusion; despite their high prevalence, they are distinguished by cutaneous paresthesia and hemodynamic stability with a low fatality rate (~3.3%). Patients clearing all three nodes (stable, dry, alert) are triaged as presumptive gastroenteritis.

If the patient is hemodynamically stable, the algorithm moves to the cholinergic screen, or the "wet" node. The clinician checks for miosis (pinpoint pupils) or hypersecretion. Since food poisoning typically causes dehydration (dry mouth, tacky mucosa), the presence of "wet" signs such as sweating, salivation, or bronchorrhea alongside vomiting confirms a cholinergic crisis indicative of organophosphates or carbamates. In this scenario, the immediate action is to suspect OP toxicity and perform an atropine challenge (1mg IV) to confirm the diagnosis and begin aggressive atropinization.

If both shock and wet signs are absent, the algorithm proceeds to the irritant screen, or the "rule out" node. If the patient is stable, with normal pupils, but complains of skin burning or tingling (paresthesia), the clinician should suspect pyrethroid exposure. As these agents cause irritation and mild GI upset but rarely cause shock or cholinergic crisis, care is largely supportive. Finally, if the patient is hemodynamically stable, appears "dry" or dehydrated, has normal pupils, and presents with fever, the diagnosis of exclusion is likely foodborne illness or viral gastroenteritis, warranting standard rehydration protocols. It should be noted that this algorithm excludes organochlorines (e.g., Endosulfan) and anticoagulant rodenticides (e.g., Bromadiolone). Organochlorines were excluded because their primary presentation is typically neurological (seizures/status epilepticus) rather than the acute gastrointestinal/shock phenotype. Anticoagulants were excluded due to their delayed onset (3-5 days), which does not mimic the acute "vomiting patient" scenario in the ER. Future iterations of this algorithm could integrate these agents if rapid point-of-care coagulation testing becomes standard in low-resource settings.

CONCLUSION

The misdiagnosis of acute pesticide poisoning as benign gastroenteritis is a preventable cause of mortality in emergency medicine. By shifting the diagnostic focus from "history of exposure" to "clinical phenotyping", specifically through differentiating the "Wet" toxidrome of organophosphates and the "Shock" toxidrome of phosphides from the "Stable" profile of food poisoning, clinicians can identify intoxications early. Implementation of the proposed "Vomiting Triage Algorithm" and wider availability of point-of-care screening tools like the silver nitrate test are critical steps toward closing the diagnostic gap and preventing future fatalities in the hospitality and agricultural sectors.

REFERENCES

Anand, R., Binukumar, B. K., & Gill, K. D. (2011). Aluminium phosphide poisoning: An unsolved riddle. *Journal of Applied Toxicology*, *31*(6), 499–505.

Bashyal, B., Yadav, A., Deo, A. K., Kharel, K. K., Kharel, D., & Panthi, B. (2023). Severe acute organophosphate poisoning managed with 2-month prolonged atropine therapy: A case report. *Annals of Medicine and Surgery*, *85*(10), 5179–5182.

Bumbrah, G. S., Krishan, K., Kanchan, T., Sharma, M., & Sodhi, G. S. (2012). Phosphide poisoning: A review of literature. *Forensic Science International*, *214*(1-3), 1–6.

Centers for Disease Control and Prevention (CDC). (2004). Diagnosis and management of foodborne illnesses: A primer for physicians and other health care professionals. *MMWR. Recommendations and Reports*, *53*(RR-4), 1–33.

Chugh, S. N., Ram, S., Arora, B., & Malhotra, K. C. (1989). Spot diagnosis of aluminium phosphide ingestion: An application of a simple test. *Journal of the Association of Physicians of India*, *37*(3), 219–220.

Chugh, S. N., Arora, V., Sharma, A., & Chugh, K. (1996). Free radical scavengers and lipid peroxidation in acute aluminium phosphide poisoning. *Indian Journal of Medical Research*, *104*, 190–193.

Çakın, Ö., Tazegul, G., Gümüş, A., Cengiz, M., & Ramazanoğlu, A. (2018). Incidental aluminum phosphide poisoning: Case report and current management. *Folia Medica*, *60*(3), 464–467.

Demange, M., Elcabache, J. M., Grzebyk, M., Peltier, A., Proust, N., Thénot, D., Ducom, P., & Fritsch, J. (2000). Phosphine sampling and analysis using silver nitrate impregnated filters. *Journal of Environmental Monitoring*, *2*(5), 476–482.

Eddleston, M. (2000). Patterns and problems of deliberate self-poisoning in the developing world. *QJM: An International Journal of Medicine*, *93*(11), 715–731.

Eddleston, M. (2024). Poisoning by pesticides. *Medicine*, *52*(6), 390–393.

Fang, T. C., Chen, K. W., Wu, M. H., Sung, J. M., & Huang, J. J. (1995). Coumaphos intoxications mimic food poisoning. *Journal of Toxicology: Clinical Toxicology*, *33*(6), 699–703.

Gunnell, D., Knipe, D., Chang, S. S., Pearson, M., Konradsen, F., Lee, W. J., & Eddleston, M. (2017). Prevention of suicide with regulations aimed at restricting access to highly hazardous pesticides: A systematic review of the international evidence. *The Lancet Global Health*, *5*(10), e1026–e1037.

Iyyadurai, R., Peter, J. V., Immanuel, S., Begum, A., Zachariah, A., & Jasmine, S. (2014). Organophosphate-pyrethroid combination pesticides may be associated with increased toxicity in human poisoning compared to either pesticide alone. *Clinical Toxicology*, *52*(5), 538–541.

Kebede, Y. N., Mohammed, A. S., Menberu, C. S., & Mekete Diress, G. (2025). Pattern, severity, and treatment outcomes in acute poisoning patients admitted to the Saint Peter Specialized Hospital Toxicology Center in Addis Ababa, Ethiopia, 2023: A retrospective study. *Frontiers in Toxicology*, *7*, 1517970.

Konradsen, F., van der Hoek, W., Cole, D. C., Hutchinson, G., Daisley, H., Singh, S., & Eddleston, M. (2003). Reducing acute poisoning in developing countries—options for restricting the availability of pesticides. *Toxicology*, *192*(2-3), 249–261.

Lorke, D. E., & Oz, M. (2025). A review on oxidative stress in organophosphate-induced neurotoxicity. *The International Journal of Biochemistry & Cell Biology*, *180*, 106735.

Mathai, A., Bhanu, M. S., & Devi, P. (2010). Acute aluminium phosphide poisoning: Can we predict mortality?. *Indian Journal of Anaesthesia*, *54*(4), 302–307.

Mehrpour, O., Jafarzadeh, M., & Abdollahi, M. (2012). A systematic review of aluminium phosphide poisoning. *Arhiv za Higijenu Rada i Toksikologiju*, *63*(1), 61–73.

Mew, E. J., Padmanathan, P., Konradsen, F., Eddleston, M., Chang, S. S., Phillips, M. R., & Gunnell, D. (2017). The global burden of fatal self-poisoning with pesticides 2006-15: Systematic review. *Journal of Affective Disorders*, *219*, 93–104.

Ntelios, D., Mandros, C., Potolidis, E., & Fanourgiakis, P. (2013). Aluminium phosphide-induced leukopenia. *BMJ Case Reports*, *2013*, bcr2013201229.

Proudfoot, A. T. (2009). Aluminium and zinc phosphide poisoning. *Clinical Toxicology*, *47*(2), 89–100.

Roberts, D. M., & Buckley, N. A. (2007). Pharmacokinetic considerations in the clinical management of organophosphorus insecticide poisoning. *Clinical Pharmacokinetics*, *46*(5), 443–457.

Shi, L., Jian, T., Tao, Y., Li, Y., Yu, G., Zhao, L., Wen, Z., Kan, B., & Jian, X. (2023). Case Report: Acute intoxication from phosphine inhalation. *International Journal of Environmental Research and Public Health*, *20*(6), 5021.

Singh, S., Bhalla, A., Verma, S. K., Kaur, A., & Gill, K. (2007). Cytochrome-c oxidase inhibition in 26 aluminum phosphide poisoned patients. *Clinical Toxicology*, *45*(4), 355–358.

Zhang, Y., Liu, Y., Li, Y., Zhao, Y., & Liu, L. (2018). Phosphine analysis in postmortem specimens following inhalation of phosphine: Fatal aluminum phosphide poisoning in children. *Journal of Analytical Toxicology*, *42*(5), 330–336.

Zheng, X., Zheng, T., Wang, L., Jiao, S., Jiang, X., Lai, S., & Zhan, B. (2025). Epidemiological analysis of 2,368 pesticide poisoning patients in Quzhou City, China. *Frontiers in Public Health*, *13*, 1587271.

Zoofaghari, S., Maghami-Mehr, A., & Abdolrazaghnejad, A. (2024). Organophosphate poisoning: Review of prognosis and management. *Advanced Biomedical Research*, *13*(1), 82.

ORAL PRESENTATION

Influence of magnesium-doped zinc-tin-oxide nanoparticles on physiological and biochemical responses of tomato plants

Ahlem Sattuf[1*] (Orcid: https://orcid.org/0009-0003-5670-0436), Savaş Sönmezoğlu[2] (Orcid: https://orcid.org/0000-0002-6011-3504), Özlem Ateş Sönmezoğlu[1] (Orcı,id: https://orcid.org/0000-0002-3157-7895)

[1]Department of Bioengineering, Faculty of Engineering, Karamanoglu Mehmetbey University, Karaman/Türkiye
[2]Department of Metallurgical and Materials Engineering, Faculty of Engineering, Nanotechnology R&D Laboratory, Karamanoglu Mehmetbey University, Karaman/Türkiye

*Corresponding author e-mail: ahlem.st900@gmail.com

Abstract

Tomato (*Solanum lycopersicum* L.) is among the most widely cultivated vegetable crops worldwide, yet its productivity and physiological performance are often constrained by abiotic stresses, particularly drought. Essential mineral nutrients such as zinc (Zn) and magnesium (Mg) play critical roles in plant growth, photosynthesis, and metabolic regulation. Their deficiencies can limit yield, whereas excessive supplementation may disrupt plant homeostasis or lead to environmental risks. Therefore, identifying optimal application dosage of these nutrients is of increasing importance in sustainable agriculture. In this study, Magnesium-doped Zinc-Tin-Oxide (Mg-ZTO) nanoparticles were synthesized via a hydrothermal method and its benefits on biochemical and physiological effects of tomato seedlings were evaluated under in vivo conditions. Plants were foliar-treated with 1.5% Mg-ZTO at concentrations of 25-2000 $mg \cdot L^{-1}$, and subsequently analyzed for photosynthetic pigments. While low concentrations (25-100 $mg \cdot L^{-1}$) enhanced pigment levels, in contrast, higher concentrations (200-2000 $mg \cdot L^{-1}$) caused a pronounced reduction in pigment levels, reflecting activation of oxidative stress pathways. In brief, Mg-ZTO nanoparticles clearly caused dose-dependent biochemical changes in tomato seedlings, with lower concentrations yielding advantageous stimulatory effects, while higher concentrations triggered more pronounced defense responses. This highlights the necessity of optimizing nanoparticle dosage for safe and effective agricultural applications, providing valuable insights into nanomaterial-plant interactions.

Keywords: Photosynthetic pigments, Mg-ZTO nanoparticles, Oxidative stress, *Solanum lycopersicum*, Tomato

INTRODUCTION

Tomato (*Solanum lycopersicum* L.) is one of the most widely cultivated vegetable crops worldwide and plays a significant role in human nutrition due to its high content of vitamins, minerals, and antioxidants. Moreover, tomato production constitutes an important source of agricultural income in major producing countries such as Türkiye, China, and the United States (Arah, 2015). Despite its economic and nutritional importance, , tomato cultivation is frequently challenged by abiotic stress factors such as drought, salinity, and insufficient light, which negatively effect growth, yield, and fruit quality (Adrees et al., 2015). Abiotic stresses disrupt water and nutrient uptake, impair photosynthetic efficiency, and promote oxidative damage, thereby limiting plant performance under unfavourable environmental conditions (Subbaiah et al., 2016). In this context, nanotechnology has emerged as a promising and sustainable approach to mitigate stress-induced limitations in crop production (Wang et al., 2016).

Metal oxide nanoparticles, when applied as nanofertilizers, nanonutrients, or nanopesticides, can enhance plant growth by improving essential micronutrient delivery efficiency, stimulating photosynthetic performance, and increasing tolerance to environmental (De la Rosa et al., 2017; Kamo et al., 2024a). However their biological effects are strongly dependent on chemical composition, particle size, concentration, and application method. Therefore, appropriate doses may promote growth, excessive exposure can induce phytotoxic effects (Verma et al.,

2018; Aasim et al., 2023; Kamo et al., 2024b). The research in the literature generally reports that metal oxide nanoparticles positively influence fundamental growth parameters such as seed germination, root and shoot development, and simultaneously enhance plant defense capacity against environmental stress factors (Rastogi et al., 2017; Sönmezoğlu et al., 2024). Magnesium-based nanoparticles have been shown to enhance chlorophyll synthesis and photosynthetic capacity, particularly under low-light conditions (Lavanya & Namasivayam, 2025). Similarly, zinc-containing nanoparticles (e.g., ZnO) support enzymatic activity and nutrient uptake, thereby improving growth and stress tolerance (Pedruzzi et al., 2020). Beyond their nutritional role, such nanoparticles can act as elicitors, activating plant defense pathways through reactive oxygen species (ROS) signaling and hormone-mediated responses (Haq et al., 2024).

The present study aims to evaluate the physiological effects of magnesium-, zinc-, and tin-containing Mg-doped Zn_2SnO_4 (1.5% Mg-ZTO) nanoparticles on tomato plants. Suspensions of 1.5% Mg-ZTO prepared at seven different concentrations were applied foliarly, and their effects on photosynthetic pigment composition were systematically investigated. The results are expected to contribute to a better understanding of Mg-ZTO–plant interactions and to support the development of nanotechnology-based strategies for sustainable tomato production.

The present study aims to evaluate the physiological effects of magnesium-, zinc-, and tin- containing Mg-doped Zn_2SnO_4 (1.5% Mg-ZTO) nanoparticles on tomato plants (*Solanum lycopersicum* L.). Suspensions of 1.5% Mg-ZTO prepared at seven different concentrations were applied foliarly, and their effects on photosynthetic pigment composition were systematically investigated. The results are expected to contribute to a better understanding of Mg-ZTO–plant interactions and to support the development of nanotechnology-based strategies for sustainable tomato production.

MATERIALS AND METHODS

The 1.5% Mg-ZTO nanoparticles were synthesized using the hydrothermal method. For synthesis, solutions of magnesium nitrate hexahydrate, zinc acetate dihydrate, and tin(V) chloride pentahydrate were prepared with a Mg:Zn:Sn:OH molar ratio of 0.03:1.97:1:4. The prepared solutions were combined in a beaker and mixed thoroughly to obtain a homogeneous solution, after which NaOH solution was added to adjust the pH to 9. The mixture was then autoclaved in a hydrothermal unit at 180 °C for 24 h. After synthesis, the product was washed and dried to obtain Mg-ZTO nanoparticles.

The synthesized ZTO nanoparticles were dispersed in distilled water (ddH2O) to prepare suspensions at concentrations of 25, 50, 100, 200, 500, 1000, and 2000 $mg \cdot L^{-1}$. Each suspension was sonicated for 2 h to ensure homogeneous dispersion.
The required amounts of 1.5% Mg-ZTO powder were weighed and dispersed in distilled water (

Tomato seeds were sterilized by immersion in a 5% sodium hypochlorite solution for 15 min. After sterilization, the seeds were rinsed five times with distilled water (modified from Oyebanji et al., 2009) and soaked in water for approximately 30 min. Twelve seeds were placed in each Petri dish lined with sterile filter paper.

Following sowing, the Petri dishes were kept in darkness for three days to ensure proper germination. Subsequently, they were transferred to a growth chamber maintained at 25 °C, with a 16/8 h light–dark photoperiod and 40% relative humidity, and allowed to germinate for 20 days. After germination, healthy and well-developed seedlings were selected and transferred to jars. Hoagland nutrient solution was added to meet the nutritional requirements of the seedlings. After 10 days of growth in the jars, experimental treatments were initiated, and 1.5% Mg-ZTO nanoparticle suspensions prepared at concentrations of 0, 25, 50, 100, 200, 500, and 1000 mg/L were applied to the leaves by spray method at five-day intervals, for a total of three applications.
Photosynthetic pigment contents were determined according to the method described by Lichtenthaler (1987). Chlorophyll a, chlorophyll b, and carotenoid contents were extracted from leaf tissues using 80% (v/v) acetone. For this purpose, 0.2 g of fresh leaf tissue was homogenized in a porcelain mortar with 5 mL of 80% acetone, and the homogenate was transferred to 15 mL centrifuge tubes. Samples were centrifuged at 3000 g for 5 min, and the supernatant was collected.

Absorbance values of the supernatant were measured at 645, 663, and 450 nm using a spectrophotometer. Pigment contents were calculated using the following equations:

$$\text{chlorophyll a} = 12{,}7 \times A663 - 2{,}69 \times A645$$
$$\text{chlorophyll b} = 22{,}9 \times A645 - 4{,}68 \times A663$$
$$\text{Total chlorophyll} = 20{,}2 \times A645 + 8{,}02 \times A663$$
$$\text{Carotenoids} = 4.07 \times A_{450} - (0.0435 \times \text{chlorophyll a} + 0.3367 \times \text{chlorophyll b})$$

Calculated pigment values were expressed as pigment content per leaf.

DISCUSSION

In this study, the effects of 1.5% Mg-ZTO nanoparticles applied at different concentrations on the photosynthetic pigment contents of tomato plants were investigated. The present study demonstrates that 1.5% Mg-ZTO nanoparticles modulate photosynthetic pigment metabolism in tomato plants in a dose-dependent manner.. Chlorophyll *a*, chlorophyll *b*, and carotenoid contents significantly increased at low 1.5% Mg-ZTO concentrations (25–100 mg/L), whereas pronounced decreases were observed at higher concentrations (200–2000 mg/L). In particular, the 100 mg/L treatment resulted in the highest values for all pigment parameters, confirming that 1.5% Mg-ZTO enhances photosynthetic capacity at this concentration (Figure 1). These findings are consistent with literature reports indicating that elements such as Mg and Zn enhance chlorophyll biosynthesis and photosynthetic efficiency at low doses.

One-way ANOVA analyses demonstrated that the changes in pigment contents were statistically highly significant (Chl *a*: $F = 107.77$, $p < 0.0001$; Chl *b*: $F = 75.40$, $p < 0.0001$; Carotenoids: $F = 167.02$, $p < 0.0001$). This indicates that 1.5% Mg-ZTO nanoparticles elicit a strong biological response depending on the applied dose. The increase observed at low concentrations may be attributed to a mild priming effect of 1.5% Mg-ZTO in plant tissues, enhanced bioavailability of Mg and Zn ions required for chlorophyll synthesis, and stimulation of photosynthetic enzyme activities. In contrast, the reduction in pigment content at higher concentrations can be explained by mechanisms frequently reported in the literature, such as nanoparticle-induced oxidative stress, accumulation of reactive oxygen species (ROS), and damage to chloroplast structure. The sharp decline in pigment levels observed particularly at 1000 and 2000 mg/L suggests that Mg-ZTO may exert toxic effects at high doses (Table 1). In conclusion, photosynthetic pigment analyses indicate that the optimal concentration of Mg-ZTO for tomato seedlings is 100 mg/L, a dose that enhances photosynthetic performance while higher doses trigger stress responses. These findings demonstrate that 1.5% Mg-ZTO can be used as a growth-promoting agent in agricultural applications at appropriate concentrations, while emphasizing that dose optimization is of critical importance.

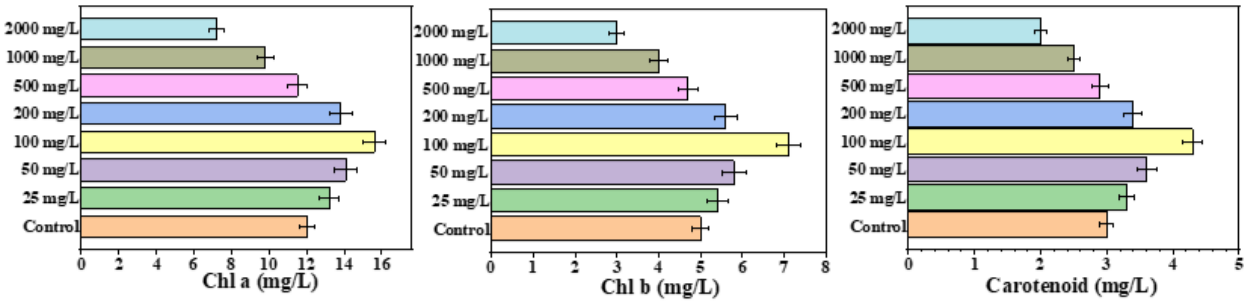


Figure 1. Effects of different Mg-ZTO concentrations on photosynthetic pigment contents in tomato seedlings: (a) chlorophyll a, (b) chlorophyll b, and (c) carotenoid levels (n = 5). All pigment parameters varied significantly depending on Mg-ZTO concentration (one-way ANOVA; Chl a: $F = 107.77$, $p \leq 0.0001$; Chl b: $F = 75.40$, $p \leq 0.0001$; carotenoids: $F = 167.02$, $p \leq 0.0001$). The highest pigment levels were consistently observed in the 100 mg/L 1.5% Mg-ZTO treatment.

Table 1. Effects of different 1.5% Mg-ZTO nanoparticle concentrations on chlorophyll *a*, chlorophyll *b*, and carotenoid contents in tomato seedlings (mean ± SD, $n = 5$). Different letters within the same column indicate significant differences according to one-way ANOVA followed by post hoc multiple comparison tests ($p < 0.05$).

1.5% Mg-ZTO	Chl a (mg/L)	Chl b (mg/L)	Carotenoids (mg/L)
0 mg/L	12.0 ± 0.4 d	5.0 ± 0.2 d	3.0 ± 0.1 d
25 mg/L	13.2 ± 0.5 c	5.4 ± 0.25 c	3.3 ± 0.12 c
50 mg/L	14.1 ± 0.6 ab	5.8 ± 0.28 ab	3.6 ± 0.15 ab
100 mg/L	14.6 ± 0.6 a	6.0 ± 0.3 a	3.7 ± 0.15 a
200 mg/L	13.8 ± 0.6 b	5.6 ± 0.27 b	3.4 ± 0.14 b
500 mg/L	11.5 ± 0.5 e	4.7 ± 0.23 e	2.9 ± 0.12 e
1000 mg/L	9.8 ± 0.43 f	4.0 ± 0.2 f	2.5 ± 0.1 f
2000 mg/L	7.2 ± 0.39 g	3.0 ± 0.13 g	2.0 ± 0.09 g

RESULTS

This study demonstrated that Mg-ZTO nanoparticles exert both beneficial and inhibitory effects on tomato physiology depending on the applied concentration. Increases in chlorophyll *a*, chlorophyll *b*, and carotenoid contents were observed at low concentrations (25–100 mg/L), with the highest values obtained at the 100 mg/L dose. In contrast, pigment levels decreased markedly at higher concentrations (200–2000 mg/L), indicating that excessive doses may adversely affect the photosynthetic apparatus. The ANOVA results confirmed that the differences among treatments were statistically significant ($p < 0.0001$). These findings underscore the importance of controlled application strategies for the safe integration of nanomaterials into sustainable agricultural practices.

REFERENCE

Aasim, M., Korkmaz, E., Culu, A., Kahveci, B. & Ates Sönmezoğlu, Ö. (2023). TiO2 nanoparticle synthesis, characterization and application to shoot regeneration of water hyssop (*Bacopa monnieri* L. pennel) in vitro. *Biotechnic & Histochemistry*, 98(1), 29-37.

Adrees, M., Ali, S., Rizwan, M., Ibrahim, M., Abbas, F., Farid, M., & Bharwana, S. A. (2015). The effect of excess copper on growth and physiology of important food crops: a review. *Environmental Science and Pollution Research*, 22(11), 8148-8162.

Arah, I. K. (2015). An overview of post-harvest challenges facing tomato production in Africa. In *Africa: diversity and development, 37th AFSAAP Conference Proceedings, AFSAAP* (pp. 1-21). The African Studies Association of Australasia and the Pacific.

De la Rosa, G., García-Castañeda, C., Vázquez-Núñez, E., Alonso-Castro, Á. J., Basurto-Islas, G., Mendoza, Á. & Molina, C. (2017). Physiological and biochemical response of plants to engineered NMs: Implications on future design. *Plant Physiology and Biochemistry*, 110, 226-235.

Haq, I. U., Cai, X., Ali, H., Akhtar, M. R., Ghafar, M. A., Hyder, M., & Hou, Y. (2024). Interactions between nanoparticles and tomato plants: influencing host physiology and the tomato leafminer's molecular response. *Nanomaterials*, 14(22), 1788.

Kamo, A., Ozcan, A., Ates Sonmezoglu, O., Sonmezoglu, S. (2024a). Nanocomposite and nanohybrid materials: Processing and applications. Book chapter 10: Understanding antibacterial disinfections mechanisms of oxide-based photocatalytic materials. De Gruyter Publisher. p. 195-220.

Kamo, A., Ates Sonmezoglu, O., Sonmezoglu, S. (2024b). Unraveling the Effects of strain-induced defect engineering on the visible-light-driven photodynamic performance of Zn_2SnO_4 nanoparticles modified by larger barium cations. *ACS Applied Bio Materials*, 7, 8656-8670

Lavanya, M., & Namasivayam, S. K. R. (2025). Eco-friendly Fabrication of Magnesium Oxide Nanoparticles from *Clitoria ternatea* and their influence on plant growth parameters of Vigna mungo, soil nutrient dynamics and computational analysis. *Plant Nano Biology*, 100200.

Pedruzzi, D.P.; Araujo, L.O.; Falco, W.F.; Machado, G.; Casagrande, G.A.; Colbeck, I.; Lawson, T.; Oliveira, S.L.; Caires, A.R. (2020). ZnO nanoparticles impact on the photosynthetic activity of Vicia faba: Effect of particle size and concentration. *Nano Impact*,19, 100246.

Rastogi, A., Zivcak, M., Sytar, O., Kalaji, H. M., He, X., Mbarki, S., & Brestic, M. (2017). Impact of metal and metal oxide nanoparticles on plant: A critical review. *Frontiers in Chemistry*, 5, 78.

Sonmezoglu, O. A., Kamo, A., Bozkaya, B., & Sonmezoglu, S. (2024). Assessing the impacts of titanium dioxide nanoparticles on seed germination and seedling growth in wheat. *Konya Journal of Engineering Sciences,* 12(2), 511-521.

Subbaiah, L. V., Prasad, T. N. V. K. V., Krishna, T. G., Sudhakar, P., Reddy, B. R., & Pradeep, T. (2016). Novel effects of nanoparticulate delivery of zinc on growth, productivity, and zinc biofortification in maize (*Zea mays* L.). *Journal of Agricultural and Food Chemistry*, 64(19), 3778-3788.

Verma, S.K., Das, A.K., Patel, M.K. et al. (2018). Engineered nanomaterials for plant growth and development: A perspective analysis. *Science of The Total Environment*, 630, 1413-1435.

Wang, P., Lombi, E., Zhao, F. J., & Kopittke, P. M. (2016). Nanotechnology: A new opportunity in plant sciences. *Trends in Plant Science*, 21(8), 699-712.

ORAL PRESENTATION

Ultrasound triggered piezocatalysis of organic pollutant degradation via Fe_3O_4 nanoparticles

Ahlem Sattuf[1*] (Orcid: https://orcid.org/0009-0003-5670-0436), Savaş Sönmezoğlu[2] (Orcid: https://orcid.org/0000-0002-6011-3504), Özlem Ateş Sönmezoğlu[1] (https://orcid.org/0000-0002-3157-7895)

[*1]Department of Bioengineering, Faculty of Engineering, Karamanoglu Mehmetbey University, Karaman/Türkiye
[2]Department of Metallurgical and Materials Engineering, Faculty of Engineering, Nanotechnology R&D Laboratory, Karamanoglu Mehmetbey University, Karaman/Türkiye

*Corresponding author e-mail: ahlem.st900@gmail.com

Abstract

Piezocatalysis provides a sustainable pathway for environmental remediation by converting ambient mechanical energy into reactive oxygen species that drives catalytic degradation processes. This approach is particularly useful for degrading persistent organic dyes such as Rhodamine B (RhB), which pose significant environmental risks. In this study, we synthesized iron oxide (Fe_3O_4) nanoparticles via hydrothermal method and evaluated as piezocatalyst for degradation of Rhodamine-B organic pollutant. Comprehensive characterization techniques were employed to investigate their crystal structure, surface morphology, and defect-related properties of magnetite nanoparticles, enabling relationships of their structure with piezocatalytic property. Under low ultrasonic vibration, Fe_3O_4 achieved 98.33% RhB degradation within 180 minutes, with a reaction rate constant of 0.023 min^{-1}. The excellent piezocatalytic performance arises from the intrinsic magnetic behavior of Fe_3O_4, together with its small particle size, high surface area, and efficient charge-transfer properties. The results provide an effective strategy for designing iron oxide based piezocatalysts and contribute to advancing sustainable approaches for environmental remediation.

Keywords: Fe_3O_4 magnetite nanoparticles, Piezocatalysis, Rhodamine B.

INTRODUCTION

The increasing accumulation of persistent pollutant compounds in water, soil, and air has become a major environmental concern due to their toxicity, stability, and adverse effects on ecosystems and human health (Kamo et al., 2025). Advanced oxidation processes (AOPs), particularly semiconductor-based photocatalysis, have been widely investigated as sustainable remediation strategies by utilizing solar energy (Yi et al., 2018; Tong et al., 2012; kamo et al., 2024). However, their practical application is severely constrained by low photocatalytic efficiency arising from poor charge separation and the rapid recombination of photoinduced electron–hole pairs (Grabowska, 2016; kamo et al., 2024). These limitations have motivated the exploration of alternative catalytic approaches capable of operating efficiently under non-illumination conditions.

Piezocatalysis, which exploits mechanical energy to drive redox reactions via piezoelectric polarization, has recently emerged as a promising alternative, particularly when coupled with ultrasonic sounds (Akhundi et al., 2019). Ultrasound-enhanced piezocatalytic systems benefit from the synergistic effects of mechanical vibration and acoustic cavitation, leading to improved charge separation and increased reactive oxygen species (ROS) generation (Xu et al., 2019). While various piezoelectric nanomaterials, including ZnO-, MoS_2-, and perovskite-based structures, have demonstrated enhanced piezocatalytic performance (Liang et al., 2019; Ning et al., 2020), the majority of studies have focused on classical piezoelectric semiconductors. In contrast, the piezocatalytic potential of non-traditional materials, particularly iron oxide–based systems, remains largely unexplored.

Magnetite (Fe_3O_4) nanoparticles are attractive candidates for advanced catalytic applications due to their mixed-valence electronic structure, size-dependent charge transport properties, chemical stability, and magnetic recoverability (Ali et al., 2017; Dos Santos-Durndell et al., 2018; Mohajerani et al., 2019; Bhole et al., 2023). Nevertheless, the role of Fe_3O_4 in ultrasound-triggered piezocatalytic systems, as well as the underlying mechanisms governing ultrasonic–piezocatalytic synergy, has not been systematically investigated. In this study, we report an ultrasound-driven piezocatalytic system based on hydrothermally synthesized Fe_3O_4 nanoparticles for the efficient degradation of Rhodamine B in aqueous media. The novelty of this work lies in elucidating the synergistic contribution of ultrasonic vibration and Fe_3O_4-induced piezocatalytic effects to charge transfer and ROS generation, while establishing structure–property–performance relationships. These findings demonstrate the potential of Fe_3O_4 nanoparticles as efficient, magnetically recoverable, and sustainable piezocatalysts for environmental remediation.

MATERIALS AND METHODS

Synthesis of Fe_3O_4 Nanoparticles

Fe_3O_4 nanoparticles were synthesized using by the hydrothermal method. A stoichiometric amount of ferric chloride hexahydrate ($FeCl_3 \cdot 6H_2O$) was dissolved in ethylene glycol. Sodium acetate was subsequently added to the solution, and the mixture was stirred at room temperature for a period using a magnetic stirrer. The resulting homogeneous solution was transferred into a Teflon-lined stainless-steel autoclave and subjected to hydrothermal treatment in a closed system at 180°C for 8h.

After the reaction, the black Fe_3O_4 precipitate was collected and washed several times with deionized water and ethanol. Following the washing steps, the product was dried in an oven at 80 °C to obtain Fe_3O_4 nanoparticles.

Characterization of Fe_3O_4 Nanoparticles

The crystal structures of the Fe_3O_4 nanoparticles were analyzed using X-ray powder diffraction (XRD, Bruker D8 Advanced).

The surface morphology of the samples were examined using scanning electron microscopy (SEM, HITACHI SU5000).

Piezocatalytic Activity of Fe_3O_4 Nanoparticles

Piezocatalytic activity experiments were carried out in a temperature-controlled ultrasonic system operating at a power of 150 W. The piezocatalytic performance of Fe_3O_4 nanoparticles was evaluated through the degradation of a 5 ppm Rhodamine B (RhB) dye solution. Prior to ultrasonic irradiation, the dye solution containing the catalyst was stirred for 30 min to establish adsorption–desorption equilibrium without exposure to any external triggering source. During the degradation process, 3 mL aliquots were collected at 20 min intervals. The collected samples were centrifuged and subsequently analyzed using a UV–vis spectrophotometer.

Based on the UV–vis absorbance data, the C/C_0 plots were constructed and the degradation efficiency was calculated using the following equation:

$$\text{Degradation efficiency (\%)} = \left(\frac{C_0 - C}{C_0}\right) X\ 100 \quad (1)$$

where C_0 and C, represent the dye concentrations at time $t = 0$ and time $t = t$ respectively. The apparent rate constant (k) was calculated from the slope of the linear fit of the $\ln\left(\frac{C_0 - C}{C_0}\right)$ plot.

The degradation of such dyes generally follows first-order kinetics, which can be expressed as:

$$-\frac{dC}{dt} = kC \quad (2)$$

Integration of this equation yields:

$$\ln\left(\frac{C_0 - C}{C_0}\right) \quad (3)$$

Kinetic analyses were performed using the above equations.

RESULTS

XRD Analysis

The crystal structure of the synthesized Fe_3O_4 nanoparticles was investigated using X-ray diffraction (XRD). As shown in Figure 1, all diffraction peaks can be unambiguously indexed to the cubic spinel structure of magnetite (Fe_3O_4), in good agreement with standard JCPDS data (e.g., JCPDS No. 19-0629). No additional diffraction peaks associated with impurity phases such as hematite (α-Fe_2O_3) or maghemite (γ-Fe_2O_3) were observed, confirming the high phase purity of the synthesized material. The absence of secondary phases is critical for ensuring stable electronic properties and consistent catalytic behavior, as impurity phases may act as recombination centers for charge carriers. Moreover, the sharp and well-defined diffraction peaks indicate a high degree of crystallinity in the Fe_3O_4 nanoparticles. High crystallinity is known to facilitate efficient charge transport by reducing lattice defects that can trap charge carriers, thereby enhancing catalytic and piezocatalytic performance (Ali et al., 2017; Bhole et al., 2023). In the context of ultrasound-triggered piezocatalysis, a well-crystallized spinel structure is particularly advantageous, as it supports effective charge migration under mechanical stimulation and promotes the generation of reactive oxygen species. These structural characteristics suggest that the synthesized Fe_3O_4 nanoparticles provide a suitable crystalline framework for efficient catalytic activity in environmental remediation applications.

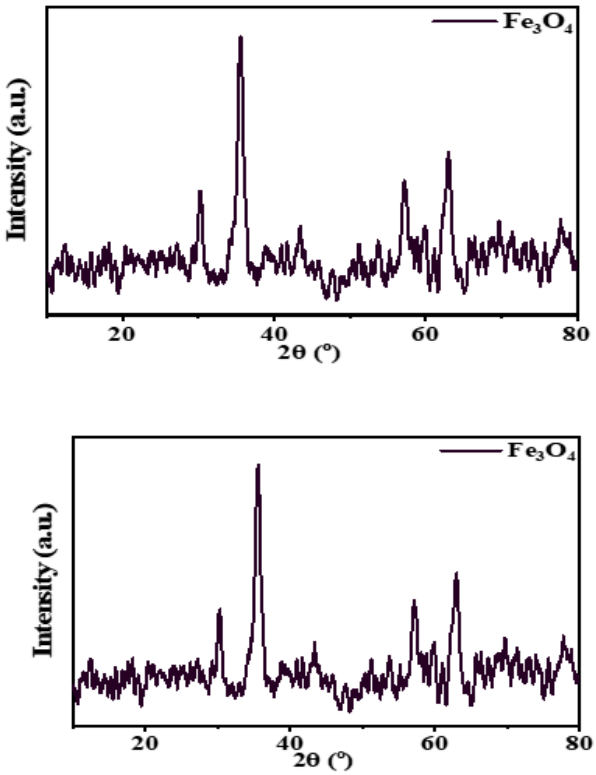


Figure 1. XRD pattern of synthesized Fe_3O_4 nanoparticles showing characteristic diffraction peaks of the spinel magnetite phase, indicating high crystallinity and phase purity.

SEM Analysis

The surface morphology and particle size of the synthesized Fe_3O_4 nanoparticles were investigated using scanning electron microscopy (SEM). As shown in Fig. 2, the nanoparticles predominantly exhibit a spherical to quasi-spherical morphology with nanoscale dimensions, accompanied by a moderate degree of agglomeration. This agglomeration behavior is commonly observed in magnetic nanoparticles and can be attributed to strong magnetic dipole–dipole interactions as well as the high surface energy inherent to nanosized Fe_3O_4 particles (Mohajerani et al., 2019; Dos Santos-Durndell et al., 2018). Despite partial agglomeration, the Fe_3O_4 nanoparticles remain relatively uniformly distributed, preserving their nanoscale features and providing a large effective surface area. Such morphological characteristics are advantageous for catalytic applications, as they increase the number of accessible active sites and promote interfacial reactions. Moreover, the nanoscale spherical morphology facilitates efficient coupling with ultrasonic waves, enabling effective transmission of mechanical vibrations to the catalyst surface. This enhanced mechanical energy transfer is expected to promote piezoelectric polarization and improve charge separation, thereby contributing to the generation of reactive oxygen species during ultrasound-assisted piezocatalytic processes (Xu et al., 2019; Liang et al., 2019).

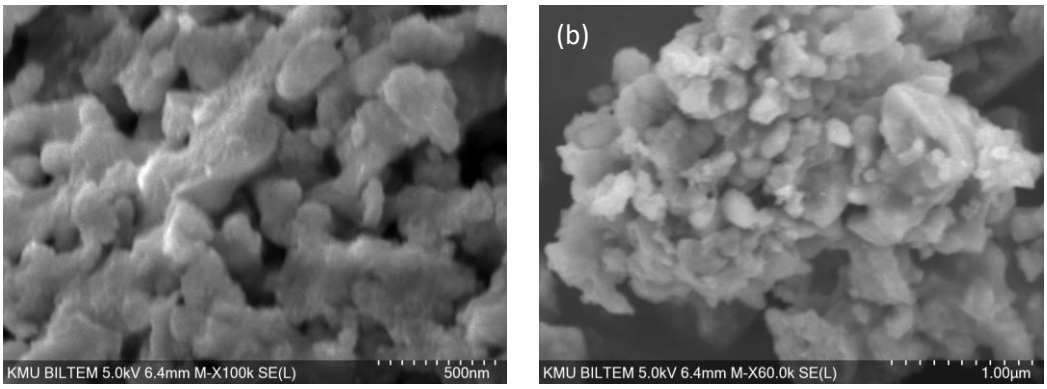


Figure 2. SEM images of Fe_3O_4 nanoparticles showing their surface morphology and particle aggregation behavior at different magnifications: (a) high-magnification image revealing quasi-spherical nanoparticles with nanoscale dimensions, and (b) low-magnification image illustrating agglomerated particle clusters resulting from magnetic interactions and high surface energy.

Piezocatalytic Activity

The piezocatalytic performance of the synthesized Fe_3O_4 nanoparticles was evaluated by monitoring the degradation of Rhodamine B (RhB) under low-intensity ultrasonic vibration. All experiments were conducted under dark conditions to eliminate any photocatalytic contribution and to isolate the ultrasound-induced piezocatalytic effect. RhB was selected as a representative organic pollutant due to its high chemical stability and widespread use as a model dye in catalytic degradation studies.

As shown in Fig. 3a, the RhB concentration decreased continuously with increasing reaction time in the presence of Fe_3O_4 nanoparticles, reaching a degradation efficiency of 98.33% after 180 min. In contrast, negligible RhB degradation was observed in control experiments performed without catalyst or with ultrasonic irradiation alone, confirming that dye removal predominantly resulted from the piezocatalytic activity of Fe_3O_4 rather than from sonolysis or adsorption effects. These results clearly demonstrate the ability of Fe_3O_4 nanoparticles to act as efficient piezocatalysts under ultrasonic excitation.

Kinetic analysis further revealed that RhB degradation followed a pseudo-first-order reaction model. As depicted in Fig. 3c, a linear relationship between $\ln(C_0/C)$ and reaction time was obtained, yielding an apparent rate constant (k) of 0.023 min^{-1}. This kinetic value is comparable to, or higher than, those reported for many Fe_3O_4-based catalytic systems, particularly considering the low ultrasonic energy input employed in this study. The enhanced piezocatalytic activity can be attributed to the transient polarization generated on the Fe_3O_4 nanoparticle surface

under mechanically induced stress from ultrasonic vibrations. This polarization promotes spatial separation of electrons and holes, suppresses their recombination, and facilitates the formation of reactive oxygen species such as •OH and $•O_2^-$, which are primarily responsible for RhB degradation (Xu et al.,

2019; Akhundi et al., 2019). Furthermore, acoustic cavitation associated with ultrasonic irradiation improves mass transfer and continuously refreshes surface-active sites, creating a synergistic effect that significantly enhances the overall catalytic performance.

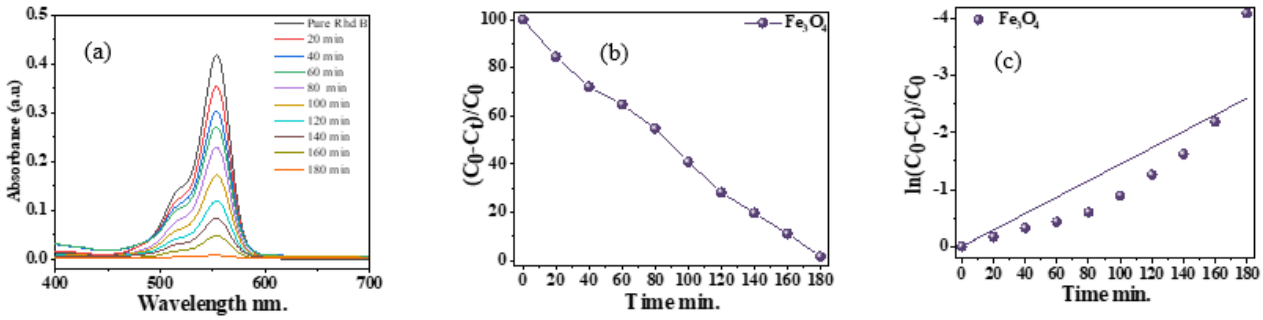


Figure 5. (a) Time-dependent UV–vis absorption spectra of Rhodamine B (RhB) during ultrasound-triggered piezocatalytic degradation in the presence of Fe_3O_4 nanoparticles, (b) variation of normalized concentration (C/C_0) as a function of irradiation time, and (c) pseudo-first-order kinetic plot of $\ln(C_0/C)$ versus time for RhB degradation under ultrasonic vibration.

CONCLUSION

In conclusion, Fe_3O_4 nanoparticles exhibited high piezocatalytic activity and favorable reaction kinetics under low-intensity ultrasonic vibration, achieving a RhB degradation efficiency of 98.33%. The combination of effective charge separation, ROS generation, and cavitation-assisted mass transfer highlights the strong potential of Fe_3O_4 nanoparticles as efficient and sustainable catalysts for ultrasound-triggered piezocatalytic environmental remediation.

REFERANCE

Akhundi, A., Habibi-Yangjeh, A., Abitorabi, M., & Rahim Pouran, S. (2019). Review on photocatalytic conversion of carbon dioxide to value-added compounds and renewable fuels by graphitic carbon nitride-based photocatalysts. Catalysis Reviews, 61(4), 595-628.

Ali, S. M., Galal, A., & Atta, N. F. (2017). Toxic heavy metal ions removal from wastewater by nano-magnetite: Case study Nile river water. Egyptian Journal of Chemistry, 60(4), 601-612.

Bhole, R., Gonsalves, D., Murugesan, G., Narasimhan, M. K., Srinivasan, N. R., Dave, N., ... & Selvaraj, R. (2023). Superparamagnetic spherical magnetite nanoparticles: synthesis, characterization and catalytic potential. Applied Nanoscience, 13(9), 6003-6014.

Chen, X., Shen, S., Guo, L., & Mao, S. S. (2010). Semiconductor-based photocatalytic hydrogen generation. Chemical reviews, 110(11), 6503-6570.

Dos Santos-Durndell, V. C., Machado Peruzzolo, T., Ucoski, G. M., Ramos, L. P., & Nakagaki, S. (2018). Magnetically recyclable nanocatalysts based on magnetite: an environmentally friendly and recyclable catalyst for esterification reactions. Biofuel Research Journal, 5(2), 806-812.

Grabowska, E. (2016). Selected perovskite oxides: Characterization, preparation and photocatalytic properties—A review. Applied Catalysis B: Environmental, 186, 97-126.

Kamo, A., Sonmezoglu, O. A., & Sonmezoglu, S. (2025). Highly efficient photocatalyst based on Zn2-xBaxSnO4 alloying nanoparticles with enhanced photocatalytic activity. Inorganic Chemistry Communications, 174, 114080.

Kamo, A., Ates Sonmezoglu, O., & Sonmezoglu, S. (2024). Unraveling the effects of strain-induced defect engineering on the visible-light-driven photodynamic performance of Zn2SnO4 nanoparticles modified by larger barium cations. ACS Applied Bio Materials, 7(12), 8656-8670.

Liang, Z., Yan, C. F., Rtimi, S., & Bandara, J. (2019). Piezoelectric materials for catalytic/photocatalytic removal of pollutants: Recent advances and outlook. Applied Catalysis B: Environmental, 241, 256-269.

Lin, J. H., Tsao, Y. H., Wu, M. H., Chou, T. M., Lin, Z. H., & Wu, J. M. (2017). Single-and few-layers MoS2 nanocomposite as piezo-catalyst in dark and self-powered active sensor. Nano Energy, 31, 575-581.

Mohajerani, A., Burnett, L., Smith, J. V., Kurmus, H., Milas, J., Arulrajah, A., ... & Abdul Kadir, A. (2019). Nanoparticles in construction materials and other applications, and implications of nanoparticle use. Materials, 12(19), 3052.

Ning, X., Hao, A., Cao, Y., Hu, J., Xie, J., & Jia, D. (2020). Effective promoting piezocatalytic property of zinc oxide for degradation of organic pollutants and insight into piezocatalytic mechanism. Journal of Colloid and Interface Science, 577, 290-299.

Tong, H., Ouyang, S., Bi, Y., Umezawa, N., Oshikiri, M., & Ye, J. (2012). Nano-photocatalytic materials: possibilities and challenges. Advanced materials, 24(2), 229-251.

Yi, H., Huang, D., Qin, L., Zeng, G., Lai, C., Cheng, M., ... & Guo, X. (2018). Selective prepared carbon nanomaterials for advanced photocatalytic application in environmental pollutant treatment and hydrogen production. Applied Catalysis B: Environmental, 239, 408-424.

You, H., Wu, Z., Zhang, L., Ying, Y., Liu, Y., Fei, L., ... & Huang, H. (2019). Harvesting the vibration energy of BiFeO3 nanosheets for hydrogen evolution. Angewandte Chemie, 131(34), 11905-11910.

Xu, X., Xiao, L., Jia, Y., Wu, Z., Wang, F., Wang, Y., ... & Huang, H. (2018). Pyro-catalytic hydrogen evolution by Ba 0.7 Sr 0.3 TiO 3 nanoparticles: harvesting cold–hot alternation energy near room-temperature. Energy & Environmental Science, 11(8), 2198-2207.

ORAL PRESENTATION

Arı ekmeği etanol ekstraktlarının HPLC tabanli bileşen analizi ve antioksidan potansiyeli

Fatma Ilgın Güller[1] (*ORCID: https://orcid.org/0009-0009-4102-2023*), Sibel Kaymak[1] (*ORCID: https://orcid.org/0000-0002-6523-7637*), Nilüfer Vural[1,2,*] (*ORCID: https://orcid.org/0000-0003-3047-3004*)

[*1]Ankara Yıldırım Beyazıt Üniversitesi, Halk Sağlığı Enstitüsü, Biyoterapötik Ürün Araştırma ve Geliştirme Programı, Ankara, Türkiye
[2]Ankara Yıldırım Beyazıt Üniversitesi, Sağlık Hizmetleri Meslek Yüksekokulu, Gıda Teknolojileri Programı, Ankara, Türkiye

*Sorumlu yazar e-mail: nilufervural@aybu.edu.tr

Özet

Arı ürünleri, içerdiği doğal biyoaktif bileşikler sayesinde sağlık alanında geniş bir kullanım potansiyeline sahiptir. Bal, propolis, polen, arı sütü ve arı zehri gibi ürünler uzun süredir geleneksel tıpta değerlendirilmektedir. Arı ekmeği ise son dönemde artan bilimsel araştırmalarla öne çıkan ve kovandaki polenlerin arı salgılarıyla fermantasyona uğraması sonucu oluşan değerli bir kovan ürünüdür. Genç arılar ve larvalar için temel bir besin kaynağı olmasının yanı sıra, kolay sindirilebilir yapısı ve yüksek besin içeriği ile dikkat çeker. Ürün bileşimi, polen kaynağı, mevsim ve bölgesel farklılıklara bağlı olarak değişiklik gösterebilmektedir. Arı ekmeği, proteinler, serbest amino asitler, karbonhidratlar ve yağ asitlerinin yanı sıra fenolik ve flavonoid bileşenler bakımından zengindir. Bu bileşenler, ürünün güçlü antioksidan kapasitesine katkı sağlar. Yapılan araştırmalar, arı ekmeğinin oksidatif stresin azaltılmasına, inflamasyonun kontrolüne ve mikroorganizmalara karşı korunmaya destek olabileceğini göstermektedir. Bunun yanında bağışıklık sistemi üzerindeki düzenleyici etkileri, metabolik sağlık ve doku yenilenmesi açısından da potansiyel faydalar sunmaktadır. Bütün bu özellikler, arı ekmeğini yalnızca besin değeri yüksek bir kovan ürünü olmaktan öteye taşıyarak fonksiyonel gıda ve doğal terapötik ajan olarak değerlendirilmesini sağlamaktadır. Arı ekmeği ekstrelerinin içerik profili ve biyolojik aktivitelerinin belirlenmesi, ürünün gelecekte sağlık destekleyici uygulamalarda kullanılabilirliğine dair önemli bilgiler sunmaktadır. Bu nedenle, arı ekmeği hem bilimsel araştırmaların hem de uygulamalı sağlık çalışmalarının ilgi odağı haline gelmektedir.

Anahtar Kelimeler: Arı ekmeği, antioksidan, HPLC analizi, polifenolik bileşenler

HPLC-based component analysis and antioxidant potential of bee bread ethanolic extracts

Abstract

Bee products possess a wide range of potential applications in health due to their natural bioactive compounds. Products such as honey, propolis, pollen, royal jelly, and bee venom have long been utilized in traditional medicine. Bee bread, however, has recently gained attention in scientific research and is produced through the fermentation of pollen with bee secretions within the hive. In addition to serving as a primary nutrient source for young bees and larvae, bee bread is notable for its high nutritional value and easily digestible composition. Its chemical profile can vary depending on the pollen source, season, and regional factors. Bee bread is rich in proteins, free amino acids, carbohydrates, and fatty acids, as well as phenolic and flavonoid compounds. These constituents contribute to its strong antioxidant capacity. Studies indicate that bee bread may help reduce oxidative stress, regulate inflammation, and provide protection against microbial agents. Additionally, it may exert modulatory effects on the immune system and offer potential benefits for metabolic health and tissue regeneration. Collectively, these properties position bee bread beyond a nutrient-rich hive product, highlighting its potential as a functional food and natural therapeutic agent. Characterizing the composition and biological activities of bee bread extracts provides valuable insights into their future applicability in health-supportive interventions. Consequently, bee bread has become a focus of both scientific research and applied health studies.

Keywords: Bee bread, antioxidant, HPLC analysis, polyphenolic compounds

GİRİŞ

Bal, propolis, polen, arı sütü ve arı zehri gibi arı ürünleri, güçlü terapötik özellikleri ve biyoaktif moleküller içermeleri nedeniyle halk hekimliğinde kullanılan en popüler doğal ürünler arasındadırlar (Mărgăoan ve ark., 2019). Arı ekmeği ise tüm bu kovan ürünleri arasında popülerliğini son dönemde kazanan ve bilimsel araştırma yayınlarına son yıllarda konu olmuş bir kovan ürünüdür. Arıların yaşamında, kolonilerin üreme dönemlerinde veya yüksek balmumu üretimi dönemlerinde olduğu gibi oldukça aktif oldukları zamanlar vardır. Bu dönemlerde polen talebi artar ve polen akışında bir azalma (sonbahar ve ilkbahar başı) veya besin değeri düşük polen varlığı, koloni için ciddi sonuçlar doğurur. Bu durum, arıları ihtiyaçları için arı ekmeği depolarına güvenmeye yönlendirir ki bu durumda kovanda arı ekmeğinin üretimi ile sonuçlanır (Bakour ve ark., 2022). Arı ekmeği kimyasal olarak, arılar tarafından bal bitkilerinin çiçeklerinden toplanan polenin laktik fermantasyon sonucu sindirim enzimleriyle karışması ve ardından kovana taşınarak ince bir bal ve balmumu tabakasıyla birlikte muhafaza edilmesiyle elde edilir. Arı ekmeği, özellikle arı sütü üreten larvalar ve genç arılar için kovandaki temel besindir (Kieliszek ve ark., 2018). Arı ekmeğinin kimyasal bileşimi üzerine yapılan çalışmalar, genellikle su, proteinler, serbest amino asitler, karbonhidratlar, yağ asitleri ve diğer biyoaktif moleküllerden oluştuğunu göstermiştir; bu bileşim, o bölgenin bal bitkilerine ve ayrıca iklim koşullarına ve mevsimsel değişime bağlı olarak bölgeden bölgeye değişmektedir. Bu ürün aynı zamanda fenolik bileşikler, α-tokoferol ve koenzim Q10 gibi antioksidan bileşiklerin de oldukça iyi bir kaynağı olarak değerlendirilmektedir (Urcan ve ark., 2017). Esasen arı ekmeğinin besin değeri arı poleninden daha yüksektir ve daha yüksek oranda serbest amino asit ve kolay sindirilebilen şekerler içerdiğinden daha kolay sindirilebilir (Kieliszek ve ark., 2018). Terapötik açıdan incelendiğinde arı ekmeği ve arı ekmeği ekstreleri çok yönlü bir biyofonksiyonel profil sergilemektedir. Bu kovan ürünü, antioksidan, antiinflamatuvar, antimikrobiyal ve immünomodülatör etkiler sergilemekte, özellikle metabolik sağlığın desteklenmesi, oksidatif stresin azaltılması ve doku yenilenmesinin hızlandırılması gibi alanlarda potansiyel uygulamalar sunmaktadır (Barta ve ark., 2022). Bu nedenle arı ekmeği, hem fonksiyonel gıda bileşeni hem de geleceğe dönük doğal bir terapötik ajan adayı olarak bilimsel ilgiyi giderek daha fazla üzerine çekmektedir. Bu çalışma da, arı ekmeği ekstrelerinin içerdiği biyoaktif bileşenlerin profilini, antioksidan potansiyelini ve olası kullanım alanlarına yönelik öngörüleri ortaya koymaktadır.

MATERYAL VE METOT

Arı Ekmeği Örneklerinin Elde Edilmesi

Arı ekmeği örnekleri, Ankara Yıldırım Beyazıt Üniversitesi Çubuk Kampüsü'nde yer alan Arılıkların Araştırma Kovanlarından elde edilmiştir. Örnekler ilkbahar mevsiminde arılıklardan taze olarak temin edilmiş ve analiz edilinceye kadar -18°C'de muhafaza edilmiştir.

Arı Ekmeği Ekstraktının Elde Edilmesi

Arı ekmeği etanol ekstraktının hazırlanması amacıyla öncelikle arı ekmekleri 5 gün süreyle liyofilize edilmiştir. Sonrasında liyofilize örnekler bir havan yardımıyla öğütülmüş ve elde edilen toz arı ekmeği örnekleri oda sıcaklığında bir su banyosunda ultrasonik güç uygulaması ile 30 dk boyunca %70'lik etanol ile muamele edilmiştir. Sonrasında Whatman No 1'den süzme işlemi gerçekleştirilerek ekstre amber renkli cam şişelerde +4°C'de saklanmıştır (Pérez-Pérez ve ark., 2018).

Arı Ekmeği Ekstraktının HPLC Analizi

Arı ekmeği ekstraktlarındaki polifenolik bileşenlerin analizi, Marhri ve ark. (2024) metodundan uyarlanarak geliştirilen laboratuvar içi bir ters faz HPLC yöntemi ile gerçekleştirildi. Analizler, Phenomenex Luna C18 (250 × 4.6 mm, 5 µm) kolon içeren bir HPLC sistemi (Shimadzu, Kyoto, Japonya) üzerinde, %0.2 asetik asit (A) ve asetonitrilden (B) oluşan gradyan mobil faz kullanılarak yürütüldü. Gradyan programı sırasıyla 0–15 dk %B 70→65, 15–20 dk 65→55, 20–30 dk 55→45, 30–35 dk %45, 35–45 dk 45→30 şeklinde uygulandı. Akış hızı 0.6 mL/dk, kolon sıcaklığı 40 °C olarak ayarlandı. Ekstraktlar ve standart çözeltiler 0.45 µm PTFE filtrelerden süzülerek 10 µL enjeksiyon hacmi ile sisteme verildi. PDA dedektörü ile 190–650 nm aralığında tarama yapıldı ve kantitatif analizler 280 nm'de gerçekleştirildi. Polifenollerin tanımlanması, referans standartlarla aynı koşullarda elde edilen alıkonma süreleri ve spektral özelliklerin karşılaştırılmasıyla doğrulandı. İstatistiksel değerlendirmeler Minitab 17 yazılımı ile yapılmıştır.

Antioksidan Aktivite Analizleri

2,2-Difenil-1-pikrilhidrazil (DPPH) radikali giderim aktivitesi ve Ferrik İndirgeme Antioksidan Gücü (FRAP) analizleri, arı ekmeği ekstrelerinin antioksidan kapasitesini belirlemek amacıyla gerçekleştirilmiştir. DPPH analizinde, metanollü DPPH çözeltisi ile ekstraktlar belirli oranlarda karıştırılmış, karışımlar karanlıkta inkübe edilmiş ve 517 nm'de absorbans ölçülmüştür. Radikal giderim yüzdesi, kontrol ve örnek absorbansları kullanılarak hesaplanmıştır. FRAP analizinde ise asetat tamponu, TPTZ (2,4,6-tripiridil-s-triazin) ve $FeCl_3$ çözeltilerinden hazırlanan FRAP reaktifi kullanılmış; ekstraktlarla karıştırılan reaktif 593 nm'de ölçülmüştür. Her iki analizde de kantitatif değerlendirme, ilgili standart kalibrasyon eğrileri üzerinden yapılmıştır (Rumpf ve Schulze, 2023).

Arı Ekmeği Biyoaktif Bileşenlerinin Farmakolojik Özellikleri

Arı ekmeğinde HPLC ile tanımlanan fenolik ve diğer biyoaktif bileşiklerin farmakolojik profilleri, güncel literatür verilerine dayanarak değerlendirilmiştir. Tanımlanan her bileşik için antioksidan, antienflamatuvar, antimikrobiyal ve potansiyel nöroprotektif etkiler gibi farmakolojik özellikler SCI indeksli çalışmalar ışığında taranmış ve özet bilgiler tabloya işlenmiştir. Değerlendirme, yalnızca benzer ekstraksiyon koşullarında incelenmiş, biyolojik olarak doğrulanmış çalışmalar dikkate alınarak yapılmıştır.

BULGULAR ve TARTIŞMA

Arı Ekmeği HPLC Analizi Sonuçları

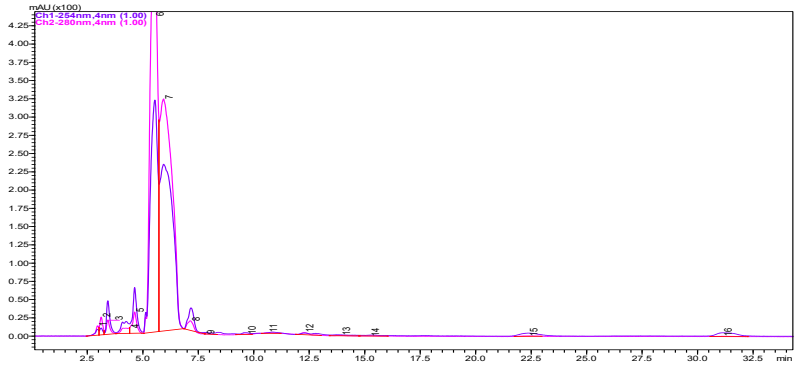
Arı ekmeği ekstresinden HPLC yöntemi ile belirlenen polifenolik bileşiklerin regresyon parametrelerini içeren veriler Tablo 1'de sunulmuştur.

Tablo 1. Regresyon parametreleri

	tR (dk)	Regresyon Denklemi y=m(x)+n	(r)	Çalışma Aralığı [a] (ug mL^{-1})	LOD[b] (ug mL^{-1})	LOQ[b] (ug mL^{-1})
ARI EKMEĞİ POLİFENOLİK BİLEŞİKLERİ						
Gallik asit	3.25	y = 54865.68 (x)+874.97	0.9998	0.5-200	0.010	0.300
Protokateşik asit	3.65	y = 2568 (x)+74.86	0.9996	0.1-200	0.013	0.040
Vanilik asit	4.00	y = 223871 (x)-46158.76	0.9998	2.0-250	0.350	1.550
Kafeik asit	4.55	y = 98.95 (x)+0.745	0.9995	0.1-250	0.485	1.250
trans 3-hidroksisinnamik asit	5.75	y = 678.98 (x)+11.659	0.9997	2.0-250	0.030	0.065
p-kumarik asit	6.25	y = 178.98 (x)+1.659	0.9998	0.1-250	0.255	0.765
Naringenin	7.00	y= 3498.65 (x)-27.16	0.9997	2.0-250	0.030	0.110
Kumarin	8.25	y = 87563.97 (x)+2564.98	0.9998	5.0-250	0.055	0.145
Krizin	9.75	y= 1.2417x-0.3396	0.9995	2.0-250	0.015	0.045
Kuersetin	11.00	y = 765.98 (x)+75.22	0.9969	0.2-150	0.072	0.245
Luteolin	12.45	y = 2134 (x)+165.12	0.9985	0.2-200	0.080	0.240
Hesperidin	14.00	y= 6249.11(x)-3.67	0.9989	0.1-250	0.110	0.350
Apigenin	15.50	y= 598.34(x)-11.87	0.9987	0.1-250	0.030	0.230
Akasetin	22.50	y= 32.78(x)-0.95	0.9994	0.1-250	0.050	0.150

[a]10 kalibrasyon noktası doğrusallık aralığı için incelendi (n=10), [b]Üç tekrar gerçekleştirildi (n=3), LOD (µg/mL) = 3,3 (yanıt/eğim standart sapması), LOQ (µg/mL) = 10 (yanıt/eğim standart sapması); tR: Alıkonma zamanı; r: Korelasyon Katsayısı

Tablo 2'de, etanol ekstresi alınmış olan arı ekmeğinde tespit edilen 16 adet polifenolik bileşiğin tR (dakika) değerleri ve µg/g kuru madde cinsinden kantitatif değerleri sunulmuştur (Şekil 1). Öne çıkan bulgu olarak, trans 3-hydroxycinnamik asit bileşiği en yüksek miktarda (965 ± 12,65 µg/g) saptanmış olup, bu değer diğer bileşiklerin miktarlarının oldukça üzerindedir. Bu durum, söz konusu bileşiğin arı ekmeği içerisindeki baskın fenolik bileşiklerden biri olabileceğini düşündürmektedir.



Şekil 1. Arı ekmeği ekstresinin HPLC kromatogramı

Tablo 2. Arı ekmeği HPLC analizi sonuçları

Pik No	Polifenolik Bileşenler	tR	Arı Ekmeği ekstresi
		(dk)	ug/g (KA)
1	**tanımlanamadı**	2.65	-
2	**Gallik asit**	3.25	48.96±1.06
3	**Protokateşik asit**	3.65	75.98±0.95
4	**Vanilik asit**	4.00	17.34±0.45
5	**Kafeik asit**	4.55	0.98±0.11
6	**trans 3-hidroksisinnamik asit**	5.75	965±12.65
7	**p-kumarik asit**	6.25	136.62±3.87
8	**Naringenin**	7.00	89.24±2.65
9	**Kumarin**	8.25	5.98±0.04
10	tanımlanamadı	9.75	-
11	tanımlanamadı	11.00	-
12	**Kuersetin**	12.45	115.32±2.98
13	**Luteolin**	14.00	1.69±0.03
14	**Hesperidin**	15.50	65.98±2.16
15	**Apigenin**	22.50	3.43±0.09
16	**Akasetin**	31.50	2.65±0.04

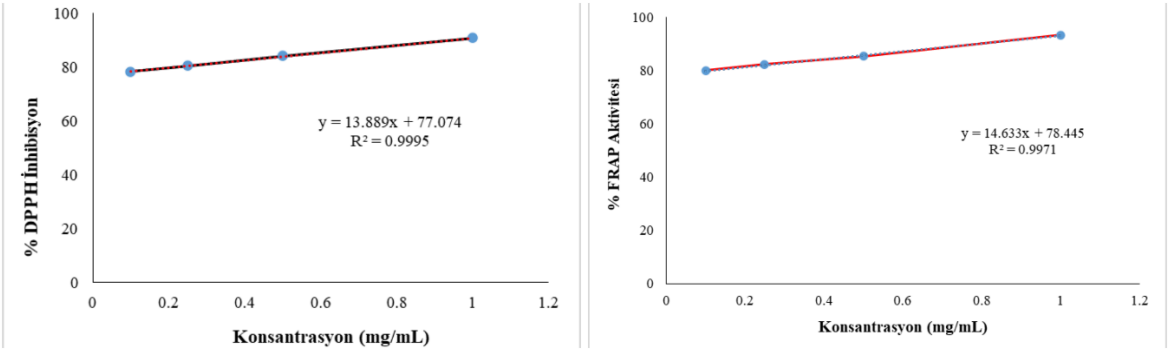
KA: kuru ağırlık , tR:Alıkonma zamanı

Bununla birlikte, protocateşik asit (75,98 ± 0,95 µg/g) ve p-kumarik asit (136,62 ± 3,87 µg/g) da görece yüksek düzeylerde bulunmuştur. Öte yandan, klasik olarak fenolik profil çalışmaları içinde sıkça rapor edilen kafeik asit yalnızca 0,98 ± 0,11 µg/g düzeyinde saptanmış; bu sonuç, arı ekmeğinin kaynağına, ekstraksiyon yöntemine ve analitik koşullara bağlı olarak kafeik asit miktarının oldukça düşük olabileceğini göstermektedir. Ayrıca kuersetin (115,32 ± 2,98 µg/g) düzeyi dikkat çekici olup, flavonoid sınıfında önemli bir yer tutmaktadır. Elde edilen bu veriler, literatürde bildirilenlerle uyumlu olduğu kadar farklılıklar da göstermektedir. Örneğin, arı ekmeği ürünlerinde fenolik bileşenlerin çeşitliliğinin ve miktarlarının coğrafi kaynak, botanik köken, ekstraksiyon yöntemi gibi değişkenlere bağlı olarak değişkenlik gösterdiği daha önce bildirilmiştir (Aksoy ve ark., 2024). Bu çalışmada da yüksek düzeyde trans 3-hidroksisinnamik asit saptanması, arı ekmeği örneklerinin muhtemelen sinnamik asit türevleri açısından zengin olduğunu ve bu yönüyle fonksiyonel gıda ya da nutrasötik materyal potansiyeli taşıdığını göstermektedir (Sawicki ve ark., 2024). Flavonoid sınıfındaki bileşiklerden naringenin (89,24 ± 2,65 µg/g) ve

hesperidin (65,98 ± 2,16 µg/g) de makul miktarlarda gözlenmiştir. Bu bulgu, arı ekmeğinin sadece fenolik asitler değil aynı zamanda flavonoid yönünden de zengin olduğunu desteklemektedir. Literatürde arı ekmeğinin antioksidan, anti-inflamatuar, antimikrobiyal ve hücre koruyucu etkilerinin bu tip bileşenlerin varlığıyla ilişkilendirildiği de bildirilmiştir (Khalifa ve ark., 2020). Bu nedenle, kampüsümüzde yer alan arı ekmeklerinden elde ettiğimiz bu bulgular, arı ekmeği ekstraktlarının biyolojik aktiviteler yönünden incelenmesi için sağlam bir bileşen profili ve potansiyel sunmaktadır.

Antioksidan Aktivite Sonuçları

Çalışmanın bu kısmında, arı ekmeği etanol ekstresinin antioksidan kapasitesi, DPPH radikal giderme aktivitesi ve FRAP aktivite değerleri üzerinden değerlendirilmiştir. Elde edilen sonuçlar, numune konsantrasyonundaki artışa paralel olarak hem DPPH inhibisyon yüzdesinin hem de FRAP aktivitesinin belirgin şekilde yükseldiğini göstermektedir. DPPH analizinde en düşük konsantrasyon olan 0,1 mg/mL'de %78,4 inhibisyon görülürken, bu değer 1 mg/mL'de %90,89'a ulaşmıştır. Benzer şekilde, FRAP değerleri de 0,1 mg/mL'de %80 iken; en yüksek konsantrasyonda %93,25'e yükselmiştir (Şekil 2).



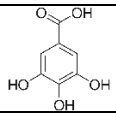
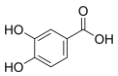
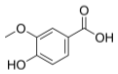
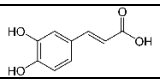
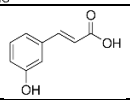
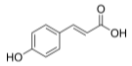
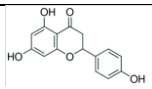
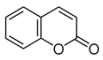
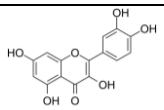
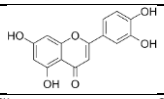
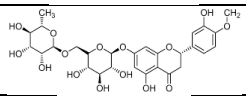
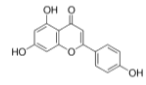
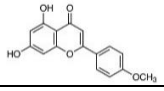
Şekil 2. Arı ekmeği antioksidan aktivite sonuç grafikleri

Bu bulgular, arı ekmeği ekstraktının güçlü bir elektron ve hidrojen donörü olduğunu ve konsantrasyon bağımlı bir antioksidan mekanizma sergilediğini göstermektedir. Literatürde arı ekmeği ve arı ürünlerinin yüksek polifenolik içerik nedeniyle güçlü radikal süpürücü özelliklere sahip olduğu daha önce vurgulanmıştır. Çalışmamızdan elde edilen veriler, özellikle yüksek DPPH inhibisyon oranları ile bu bulgularla uyumluluk göstermektedir (Mayda ve ark., 2020). Bazı çalışmalarda 80–85% aralığında bildirilen maksimum DPPH inhibisyon oranlarının aksine, bizim çalışmamızda >90% düzeyine ulaşılmış olması, ekstraksiyon yöntemimizin (etanolik ekstraksiyon) polifenolik bileşiklerin daha yüksek verimle kazanılmasını sağlamış olabileceğini düşündürmektedir (Bakour ve ark., 2019). FRAP sonuçları da benzer şekilde arı ekmeği ekstraktının güçlü indirgeme kapasitesine sahip olduğunu ortaya koymuştur. FRAP aktivitesinin %93,25 gibi yüksek bir değere ulaşması, ekstrakta bulunan sinnamik asit türevleri, flavonoidler (kuersetin, naringenin, hesperidin) ve fenolik asitlerin ferrik iyonları indirgeme potansiyelinin yüksek olduğuna işaret etmektedir. Bu yüksek antioksidan kapasite, HPLC analizinde belirlenen zengin polifenolik profile paralellik göstermektedir ve özellikle trans 3-hidroksisinnamik asit, p-kumarik asit ve kuersetin gibi bileşiklerin bu aktiviteye önemli katkıda bulunduğu değerlendirilebilir.

Arı Ekmeği Biyoaktif Bileşenlerinin Farmakolojik Özellikleri

HPLC sonuçlarının ışığında arı ekmeğinde yer alan biyoaktif bileşenlerin farmakolojik etkileri ve diğer terapötik özellikleri Tablo 3'te sunulmuştur. Elde edilen veriler arı ekmeğinin çok yönlü terapötik etkiler gösterebileceğini ve yalnızca bir fonksiyonel gıda değil aynı zamanda terapötik açıdan değerlendirilebileceğini de ortaya koymaktadır.

Tablo 3. Bileşenlerin terapötik özellikleri

Bileşik	Kimyasal Yapısı	Başlıca Farmakolojik Özellikler	Referanslar
Gallik asit		Güçlü antioksidan, antiinflamatuar, antimikrobiyal, antiproliferatif ve gastrointestinal koruyucu	(Kahkeshani ve ark., 2019)
Protokateşik asit		Antioksidan, hepatoprotektif, antiinflamatuar, antikanser	(Semaming ve ark., 2015)
Vanilik asit		Antidepresan, tansiyon düzenleyici, yara iyileştirme, anti-fungal aktivite	(Ingole ve ark., 2021)
Kafeik asit		Antiviral, antiinflamatuar, anti-tümör	(Lv ve ark., 2021)
trans 3-hidroksisinnamik asit		Antikanser, antioksidan, Antityrosinase	(Medini ve ark., 2015)
p-kumarik asit		Antioksidan, UV-koruyucu, antimikrobiyal, antikanser	(Ferreira ve ark., 2019)
Naringenin		Antidiyabetik, antiviral, kardiyovasküler ve nörolojik koruyucu etkiler	(Patel ve ark., 2018)
Kumarin		Antikoagülan, antimikrobiyal, antispazmodik	(Venugopala ve ark., 2013)
Kuersetin		Antialerjik, antiviral, kardiyoprotektif, nöroprotektif	(Wang ve ark., 2022)
Luteolin		Nöroprotektif, antioksidan, antikanser	(Nabavi ve ark., 2015)
Hesperidin		Venoprotektif, antihipertansif	(Li ve Schluesener, 2017)
Apigenin		Antiinflamatuvar, anksiyolitik	(Li ve ark., 2023)
Akasetin		Kardiyoprotektif, antikanser, antioksidan	(Li ve ark., 2023)

SONUÇ

Arı ekmeği, zengin besin içeriği ve çok yönlü biyofonksiyonel profili sayesinde hem kovandaki temel bir besin kaynağı hem de sağlık destekleyici potansiyele sahip fonksiyonel bir ürün olarak öne çıkmaktadır. Proteinler ve serbest amino asitlerin yanında fenolik ve flavonoid bileşenler de arı ekmeğinin biyolojik aktivitelerinde kritik rol oynamaktadır. Elde edilen veriler, arı ekmeği ve ekstrelerinin oksidatif stresin azaltılması, inflamasyonun kontrolü, immünomodülasyon ve metabolik sağlık gibi alanlarda potansiyel faydalar sunabileceğini göstermektedir. Bu nedenle, arı ekmeği hem bilimsel araştırmaların hem de fonksiyonel gıda ve doğal terapötik uygulamaların ilgi odağı haline gelmektedir. Gelecekte yapılacak çalışmalar, içerik profili ve biyolojik aktivitelerin daha ayrıntılı incelenmesi yoluyla, arı ekmeğinin sağlık destekleyici uygulamalarda etkin kullanımını daha iyi anlamamıza katkı sağlayacaktır.

TEŞEKKÜR

Bu çalışma Doç. Dr. Nilüfer Vural danışmanlığında yürütülen Fatma Ilgın Güller'in Yüksek Lisans tezindeki verilerden üretilmiştir.

KAYNAKLAR

Aksoy, A., Altunatmaz, S. S., Aksu, F., Tokatlı Demirok, N., Yazıcı, K., & Yıkmış, S. (2024). Bee bread as a functional product: phenolic compounds, amino acid, sugar, and organic acid profiles. Foods, *13*(5), 795.

Bakour, M., Fernandes, Â., Barros, L., Sokovic, M., & Ferreira, I. C. (2019). Bee bread as a functional product: Chemical composition and bioactive properties. Lwt, *109*, 276-282.

Bakour, M., Laaroussi, H., Ousaaid, D., El Ghouizi, A., Es-Safi, I., Mechchate, H., & Lyoussi, B. (2022). Bee bread as a promising source of bioactive molecules and functional properties: an up-to-date review. Antibiotics, 11(2), 203.

Barta, D. G., Cornea-Cipcigan, M., Margaoan, R., & Vodnar, D. C. (2022). Biotechnological processes simulating the natural fermentation process of bee bread and therapeutic properties—an overview. Frontiers in Nutrition, 9, 871896.

Ferreira, P. S., Victorelli, F. D., Fonseca-Santos, B., & Chorilli, M. (2019). A review of analytical methods for p-coumaric acid in plant-based products, beverages, and biological matrices. Critical reviews in analytical chemistry, *49*(1), 21-31.

Ingole, A., Kadam, M. P., Dalu, A. P., Kute, S. M., Mange, P. R., Theng, V. D., ... & Patil, P. A. (2021). A review of the pharmacological characteristics of vanillic acid. J. Drug Deliv. Ther, 11(2-S), 200-204.

Kahkeshani, N., Farzaei, F., Fotouhi, M., Alavi, S. S., Bahramsoltani, R., Naseri, R., ... & Bishayee, A. (2019). Pharmacological effects of gallic acid in health and diseases: A mechanistic review. Iranian journal of basic medical sciences, *22*(3), 225.

Khalifa, S. A., Elashal, M., Kieliszek, M., Ghazala, N. E., Farag, M. A., Saeed, A., ... & El-Seedi, H. R. (2020). Recent insights into chemical and pharmacological studies of bee bread. Trends in Food Science & Technology, 97, 300-316.

Kieliszek, M., Piwowarek, K., Kot, A. M., Błażejak, S., Chlebowska-Śmigiel, A., & Wolska, I. (2018). Pollen and bee bread as new health-oriented products: A review. *Trends in Food Science & Technology*, *71*, 170-180.

Li, C., & Schluesener, H. (2017). Health-promoting effects of the citrus flavanone hesperidin. Critical reviews in food science and nutrition, 57(3), 613-631.

Li, Z., Zhou, J., Ji, L., Liang, Y., & Xie, S. (2023). Recent advances in the pharmacological actions of apigenin, its complexes, and its derivatives. Food Reviews International, 39(9), 6568-6601.

Lv, L., Cui, H., Ma, Z., Liu, X., & Yang, L. (2021). Recent progresses in the pharmacological activities of caffeic acid phenethyl ester. Naunyn-Schmiedeberg's Archives of Pharmacology, *394*(7), 1327-1339.

Marhri, A., Rbah, Y., Allay, A., Boumediene, M., Tikent, A., Benmoumen, A., ... & Addi, M. (2024). Comparative Analysis of Antioxidant Potency and Phenolic Compounds in Fruit Peel of Opuntia robusta, Opuntia dillenii, and Opuntia ficus-indica Using HPLC-DAD Profiling. Journal of Food Quality, 2024(1), 2742606.

Mărgăoan, R., Stranț, M., Varadi, A., Topal, E., Yücel, B., Cornea-Cipcigan, M., ... & Vodnar, D. C. (2019). Bee collected pollen and bee bread: Bioactive constituents and health benefits. Antioxidants, 8(12), 568.

Mayda, N., Özkök, A., Ecem Bayram, N., Gerçek, Y. C., & Sorkun, K. (2020). Bee bread and bee pollen of different plant sources: Determination of phenolic content, antioxidant activity, fatty acid and element profiles. Journal of Food Measurement and Characterization, 14(4), 1795-1809.

Medini, F., Bourgou, S., Lalancette, K., Snoussi, M., Mkadmini, K., Coté, I., ... & Ksouri, R. (2015). Phytochemical analysis, antioxidant, anti-inflammatory, and anticancer activities of the halophyte Limonium densiflorum extracts on human cell lines and murine macrophages. South African Journal of Botany, *99*, 158-164.

Nabavi, S. F., Braidy, N., Gortzi, O., Sobarzo-Sanchez, E., Daglia, M., Skalicka-Woźniak, K., & Nabavi, S. M. (2015). Luteolin as an anti-inflammatory and neuroprotective agent: A brief review. Brain research bulletin, *119*, 1-11.

Patel, K., Singh, G. K., & Patel, D. K. (2018). A review on pharmacological and analytical aspects of naringenin. Chinese journal of integrative medicine, *24*(7), 551-560.

Pérez-Pérez, E., Sulbarán-Mora, M., Barth, O. M., Flavia Massaro, C., & Vit, P. (2018). Bioactivity and botanical origin of Austroplebeia and Tetragonula Australian pot-pollen. In Pot-Pollen in Stingless Bee Melittology (pp. 377-390). Cham: Springer International Publishing.

Rumpf, J., Burger, R., & Schulze, M. (2023). Statistical evaluation of DPPH, ABTS, FRAP, and Folin-Ciocalteu assays to assess the antioxidant capacity of lignins. International Journal of Biological Macromolecules, 233, 123470.

Sawicki, T., Jabłońska, M., Danielewicz, A., & Przybyłowicz, K. E. (2024). Phenolic compounds profile and antioxidant capacity of plant-based protein supplements. Molecules, 29(9), 2101.

Semaming, Y., Pannengpetch, P., Chattipakorn, S. C., & Chattipakorn, N. (2015). Pharmacological properties of protocatechuic acid and its potential roles as complementary medicine. Evidence-Based Complementary and Alternative Medicine, 2015(1), 593902.

Urcan, A., Marghıtaş, L. A., Dezmirean, D. S., Bobış, O., Bonta, V., Mureşan, C. I., & Margaoan, R. (2017). Chemical Composition and Biological Activities of Beebread-Review. Bulletin of the university of agricultural sciences & veterinary medicine Cluj-Napoca. Animal Science & Biotechnologies, 74(1).

Venugopala, K. N., Rashmi, V., & Odhav, B. (2013). Review on natural coumarin lead compounds for their pharmacological activity. BioMed research international, *2013*(1), 963248.

Wang, G., Wang, Y., Yao, L., Gu, W., Zhao, S., Shen, Z., ... & Yan, T. (2022). Pharmacological activity of quercetin: an updated review. Evidence-Based Complementary and Alternative Medicine, *2022*(1), 3997190.

ORAL PRESENTATION

Production of biochar from hazelnut shells by hydrothermal carbonization and determination of its effect as a catalyst support in hydrogen production

Seda Hoşgün (Orcid : 0000-0002-5884-9723)

Eskisehir Osmangazi University, Engineering and Architecture Faculty, Chemical Engineering Department, Eskisehir, Türkiye.

Corresponding author e-mail: serol@ogu.edu.tr

Abstract

In this study, three different catalyst supports were synthesized by the hydrothermal method using hazelnut shell–derived biochar, and their potential as support materials for the hydrolysis reaction of $NaBH_4$ was investigated. The effects of catalyst structure and composition were thoroughly examined to design suitable supports for heterogeneous catalyst synthesis. The highest hydrogen production rate was achieved at 30 °C with 30 mg of catalyst, using the hazelnut shell–based CoB catalyst supported on ACFK_1:1 (CoB/ACFK_1:1), reaching 3148.2 $mL \cdot g_{cat}^{-1} \cdot min^{-1}$. The activation energy for the hydrolysis reaction was calculated as 54.65 $kJ \cdot mol^{-1}$. Furthermore, the catalyst showed good reusability, retaining 90.14 % of its activity. Overall, these findings emphasize the importance of rational catalyst design and highlight the potential of agricultural residues, such as hazelnut shells, as efficient and sustainable catalyst support materials for $NaBH_4$ hydrolysis–based hydrogen generation.

Keywords: Hydrothermal carbonization, Hazelnut shell, Hydrolysis, CoB catalyst.

INTRODUCTION

Hydrogen is the most abundant gas in the universe and is classified by the World Energy Organization as the cleanest fuel in the world compared to other energy products. Therefore, it is considered essential for achieving the zero-fuel emissions strategy adopted by the largest countries. It is also projected that by 2050, hydrogen consumption will account for 24% of the global energy sector, with investments estimated at 2.5 trillion dollars, compared to only 139 billion dollars at present (Yousef 2021). For hydrogen to be used as an energy carrier, it must be produced from sources such as water (H_2O), fossil fuels (such as methane and coal), or biomass, and separated from these sources by suitable chemical or electrochemical processes (Levin and Chahine 2010). Thanks to these production processes, hydrogen can be considered a clean and sustainable energy source (Midilli et al., 2005). Once produced, hydrogen must be transported to the desired locations, used, and stored when demand decreases. Hydrogen can be stored in pure form in tanks as a liquid or gas, physically in nanotubes, or chemically as a hydride. Sodium borohydride ($NaBH_4$), one of the chemical hydride storage methods, is an excellent hydrogen storage material due to its stability in dry air, high hydrogen content, light weight, ability to produce hydrogen when reacting with alcohol, water, or an alcohol-water mixture at room temperature, and its non-toxic and non-flammable nature (Zhong 2025).

The hydrolysis of $NaBH_4$ was proposed by Schlesinger in the 1950s for hydrogen production under suitable conditions, and it was found that 90% of the stoichiometric hydrogen content was obtained. Sodium borohydride hydrolyzes with water in the presence of a suitable catalyst in an alkaline environment according to the reaction given in equation (i) (Hoşgün and Hoşgün,2024).

$$2H_2O + NaBH_4 \rightarrow 4H_2 + NaBO_2 \quad \text{(i)}$$

To increase the rate of hydrolysis of $NaBH_4$, suitable catalysts must be added to the reaction medium. It has been found that platinum, ruthenium, and other precious metal catalysts with various loading ratios and carrier forms significantly increase the hydrolysis and methanolysis rates of $NaBH_4$. However, the high cost and limited supply of these precious metals restrict their use. Various studies have been conducted and are ongoing to develop catalysts based on non-precious metals, which are more abundant on earth and have similar efficiencies, to replace these

precious metals. In these studies, cobalt-containing catalysts have been synthesized specifically for the use of $NaBH_4$ in hydrogen production reactions due to their low cost and high activity. Heterogeneous solid catalysts lose some catalytic activity because of metal agglomeration. To address this problem, the metals are deposited on a suitable support material. Carrier materials provide a larger, more accessible surface area for the active metals, thereby increasing catalytic activity. The most commonly used carrier materials are metal oxides, clay minerals, silica (SiO_2), aluminum oxide (Al_2O_3), and activated carbon. Most carrier materials have low surface energy and are hydrophobic, which makes it difficult for them to adhere to other materials (Wei et., 2017).

The potential of natural materials to enhance catalyst performance and promote environmental sustainability has been frequently highlighted, especially in studies on materials such as clay minerals. These materials can increase catalytic activity and support the development of sustainable chemical processes. In this context, biochar, produced by the thermochemical conversion of biomass through pyrolysis, gasification, or hydrothermal carbonization, has recently become an important research focus as a catalyst support material. Biochar is a carbon-rich material obtained by the controlled thermal degradation of biomass and is characterized by high porosity, large surface area, and chemical stability (Liu et al. 2015). These properties make biochar an ideal material for catalytic applications. Additionally, biochar produced from biomass conversion is considered an economical and environmentally friendly alternative. Biochar also provides environmental benefits such as waste management and carbon sequestration (Luo et al., 2023).

The surface chemistry of biochar, its functional groups, and its ability to bind metal ions can be optimized to increase catalytic activity. The oxygen-containing functional groups (e.g., carboxyl, hydroxyl) on the surface of biochar play an important role in binding metal ions and enhancing catalytic activity. These properties make biochar attractive as a carrier material in heterogeneous catalysts (Sun et al., 2016). Such applications increase the sustainability of energy production and minimize environmental impact (Li et al., 2021). These properties enable the effective use of biochar in catalytic applications and contribute significantly to the development of renewable energy systems. Biochar has a wide range of applications, especially in hydrogen production, chemical synthesis, and wastewater treatment.

Hydrothermal carbonization (HTC), the process of producing biochar from green biomass using pressure and heat, is an increasingly widespread and proven method. It is an environmentally friendly and cost-effective thermochemical conversion process used to convert green biomass and wastewater. Amongst emerging biomass conversion technologies, hydrothermal carbonization (HTC) stands out for its unique ability to process wet biomass without the need for energy-intensive drying. HTC operates at moderate temperatures (180–280 °C) and utilizes water, which is non-toxic, eco-friendly, and cost-effective, as a reaction medium. While HTC is widely known for producing energy-dense hydrochar, it also generates a liquid by-product known as process water, which contains large amounts of soluble organic and inorganic compounds (Boamah and Salaudeen 2025).

This study investigates the influence of hydrothermally produced biochar, derived from agricultural residues, as a catalyst support material on the catalytic performance of sodium borohydride ($NaBH_4$) hydrolysis. By examining how the structural and physicochemical properties of biochar affect hydrogen generation efficiency, the research aims to identify a sustainable and effective support medium capable of enhancing catalyst stability, activity, and reusability during the $NaBH_4$ hydrolysis reaction.

MATERIALS AND METHODS

The hazelnut shell residues used in the study were crushed, ground, and sieved to determine size distribution. Samples dried in an oven at 105°C for 6 hours and stored. 3 g of sample were mixed with 30 ml of pure water and Hydrothermal carbonization (HTC) was carried out in a pressurized reactor at 180°C for 6 hours. The samples were removed stirred with NaOH solution for 4 hours using the chemical activation method with a magnetic stirrer. After mixing, the solid was filtered, dried, and activated at 80°C for 24 hours with NaOH mass ratios of 1:1, 2:1, and 1:2. The samples were filtered and washed with distilled water until neutralized. The activated samples (ACFK) were separated from the NaOH solution, and the pH was adjusted. After the prepared biochars were dried and crushed, used as catalyst support material.

For the synthesis of ACFK-supported Co metal catalysts, $CoCl_2 \cdot 6H_2O$ solution was impregnated onto the support material and reduced with sodium borohydride. Metal impregnation was performed by dissolving 5 g of $CoCl_2 \cdot 6H_2O$, weighed according to the desired metal loading ratios, in 100 ml of water and adding it to the support

material. The mixture was stirred at 75°C and 400 rpm on a magnetic stirrer for 1 hour. After cooling to 25°C, $NaBH_4$ solution was added dropwise at the appropriate concentration with a molar ratio of 3:1 BH_4/Co. The temperature was maintained between 25°C and 30°C during the reduction process. After gas evolution, indicated by the formation of black precipitates, was complete, stirring continued at 400 rpm for 1 hour. The precipitates were filtered under vacuum through suitable filter paper and washed 2–3 times with a mixture of pure water and ethanol. After drying at 100°C for 24 hours, the material was ground and used for the hydrolysis reaction. The aim was to load 10–15% Co metal by weight onto the ACFK.

Experiments on the catalytic activity for hydrogen production by hydrolysis of sodium borohydride were conducted in a glass reactor equipped with a circulating water bath. Before each experiment, a measured amount of catalyst was added to the jacketed glass reactor designated for the NaBH4 hydrolysis reaction. Once the desired temperature was reached using the circulating water bath, a sodium borohydride solution of specified concentration was introduced into the reactor. The reactor was sealed, and the reaction was initiated by stirring with a magnetic stirrer at 400 rpm. The amount of hydrogen produced by catalytic hydrolysis was determined by the weight of water collected, as the released hydrogen displaced water from the gas wash bottle into a flask placed on a balance, due to the closed system of the apparatus. The volume of water collected in the flask was recorded at specific time intervals. Hydrogen volumes were calculated based on the density values measured at the beginning of the experiment according to ambient conditions. All experiments were performed in duplicate to verify the repeatability and accuracy of the data.

RESULTS AND DISCUSSION

Table 1 shows the hydrogen generation rate of the hydrolysis reaction in the presence of different Co/ACFK catalysts, with a catalyst amount of 30 mg, NaBH4 concentration of 0.79 M, and reaction temperature of 30°C. The hydrolysis experiments with Co/ACFK catalysts showed clear differences in catalytic performance depending on the Co/ACFK support materials NaOH ratio. Among the tested materials, the Co/ACFK_1:1 catalyst exhibited the highest hydrogen generation activity, achieving a 98% hydrogen yield, the fastest reaction completion time (540 min), and the highest hydrogen generation rate (3148.2 mL gcat·min^{-1}). In particular, Co/ACFK_1:2 showed the lowest performance, with a prolonged reaction time and a reduction in hydrogen generation rate to 2209.9 mL gcat·min^{-1}. These results indicate that an optimal NaOH: support ratio is crucial for maximizing hydrogen production efficiency. Overall, the findings suggest that Co/ACFK_1:1 provides the most favorable balance of catalytic activity and stability under identical reaction conditions, highlighting its potential as an effective catalyst for $NaBH_4$ hydrolysis–based hydrogen generation systems.

Table 1. Hydrogen generation rate of the hydrolysis reaction in the presence of different Co/ACFK catalysts (Catalyst amount 30 mg; $NaBH_4$ concentration 0.79 M; Reaction temperature 30°C).

Catalyst	Reaction Time (min)	Generated Hydrogen Volume (mL)	Hydrogen Generation Yield (%)	Hydrogen Generated Rate (mL g_{cat}.min^{-1})
Co/ACFK_1:1	540	850	98	3148.2
Co/ACFK_2:1	612	830	95.6	2712.4
Co/ACFK_1:2	724	800	92.5	2209.9

The cyclic activity results show that the catalyst maintains robust and stable performance over multiple consecutive runs (Fig .1). Although a gradual decline in activity is observed from the first to the fifth cycle, the decrease is controlled and predictable, indicating only minor deactivation during repeated hydrolysis reactions. The activity decreases slightly from 3148.20 mL·gcat^{-1}·min^{-1} in the first cycle to 3031.67 mL·gcat^{-1}·min^{-1} in the second cycle, and continues to decline progressively in subsequent cycles, stabilizing at 2837.89 mL·gcat^{-1}·min^{-1} in the fifth cycle. This corresponds to a retention of approximately 90% of the initial catalytic performance. The primary causes of activity loss may be partial surface blockage, slight structural changes, or limited leaching of active metal species. However, the absence of sharp or abrupt decreases between cycles confirms that the catalyst preserves its

structural integrity and retains a significant portion of its active sites even after multiple uses. Overall, the cyclic performance evaluation strongly supports the catalyst's reusability and highlights its potential for long-term operation in $NaBH_4$ hydrolysis–based hydrogen production systems. The catalyst's ability to sustain high activity over five consecutive cycles demonstrates its practicality and reliability, making it a promising candidate for sustainable and efficient hydrogen generation applications.

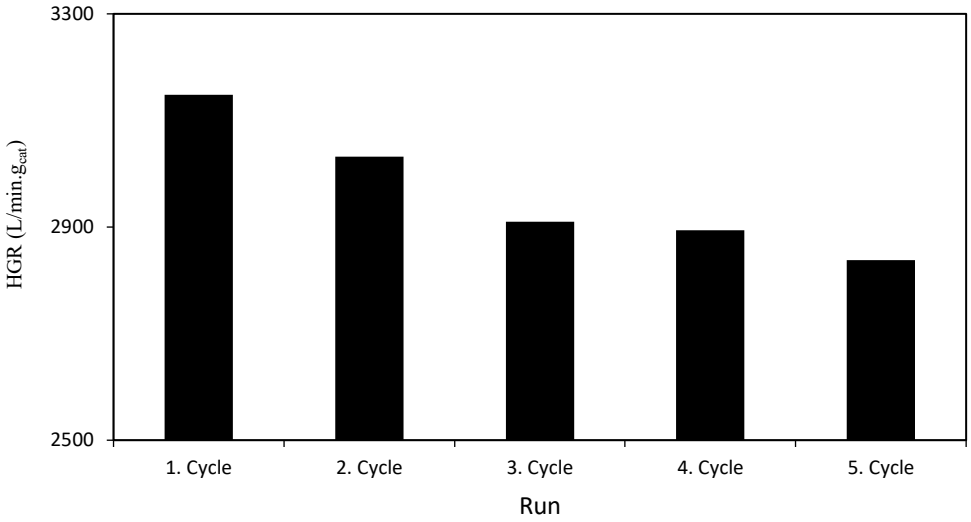


Fig 1. Reusability performance of Co/ACFK_1:1 catalyst (Catalyst amount 30 mg; $NaBH_4$ concentration 0.79 M; Reaction temperature 30°C).

CONCLUSION

The findings from this study show that hazelnut shell–derived biochar can be effectively used as a sustainable and functional support material for Co-based catalysts in the hydrolysis of $NaBH_4$. Among the synthesized supports, the ACFK_1:1 structure provided the most favorable catalytic environment, allowing the CoB/ACFK_1:1 catalyst to achieve the highest hydrogen production rate (3148.2 $mL \cdot g_{cat}^{-1} \cdot min^{-1}$) at 30 °C with 30 mg of catalyst. The activation energy of 54.65 $kJ \cdot mol^{-1}$ and the retention of 90.14 % catalytic activity upon reuse further confirm the efficiency and stability of this system. Additionally, the comparative evaluation of different Co/ACFK catalysts showed that deviations from the optimal support ratio led to reduced hydrogen yield, lower rate performance, and longer reaction times. The importance of optimizing both support material and catalyst composition, demonstrating that biomass-derived residues such as hazelnut shells offer a promising, renewable, and highly effective platform for designing next-generation catalysts for $NaBH_4$ hydrolysis–based hydrogen production technologies.

REFERENCES

Boamah, N. N., & Salaudeen, S. A. (2025). Process water from the hydrothermal carbonization of biomass: A review on the characterization, applications, and potential for future work. Journal of Water Process Engineering, 77, 108531.

Hoşgün, S., & Hoşgün, E. Z. (2024). Optimization of hydrogen generation rate with Co/MMT catalyst from NaBH4 using Box-Behnken method. Pamukkale Üniversitesi Mühendislik Bilimleri Dergisi, 30(1), 87-94.

Levin, D. B., & Chahine, R. (2010). Challenges for renewable hydrogen production from biomass. International journal of hydrogen energy, 35(10), 4962-4969.

Li, W., Dan, Q., Chi, M., & Wang, W. (2021). Influence of price level and perceived price dispersion on consumer information search behaviour: moderating effect of durables and consumables. Sustainability, 13(4), 2105.

Liu, W. J., Jiang, H., & Yu, H. Q. (2015). Development of biochar-based functional materials: toward a sustainable platform carbon material. Chemical reviews, 115(22), 12251-12285.

Luo, L., Wang, J., Lv, J., Liu, Z., Sun, T., Yang, Y., & Zhu, Y. G. (2023). Carbon sequestration strategies in soil using biochar: advances, challenges, and opportunities. Environmental Science & Technology, 57(31), 11357-11372.

Midilli, A., Ay, M., Dincer, I., & Rosen, M. A. (2005). On hydrogen and hydrogen energy strategies: I: current status and needs. Renewable and sustainable energy reviews, 9(3), 255-271.

Sun, D., Lan, Y., Xu, E. G., Meng, J., & Chen, W. (2016). Biochar as a novel niche for culturing microbial communities in composting. Waste Management, 54, 93-100.

Wei, Y., Wang, R., Meng, L., Wang, Y., Li, G., Xin, S., ... & Zhang, K. (2017). Hydrogen generation from alkaline NaBH4 solution using a dandelion-like Co–Mo–B catalyst supported on carbon cloth. international journal of hydrogen energy, 42(15), 9945-9951.

Yousef, S. (2021). Hydrogen as a clean and sustainable energy for green future. Sustainable technologies for green economy., 1(1), 8-13.

Zhong, Y. (2025). Hydrogen release in composite complex hydride systems (Doctoral dissertation, University of Glasgow).

ORAL PRESENTATION

İksut otu *(Cuscuta europaea* L.) kullanılarak sentezlenen çinko oksit nanopartiküllerin antimikrobiyal ve küf (ekmek küfü) üzerine etkisinin belirlenmesi

Nisa Altıöz[1*] (Orcid: *https://orcid.org/* 0009-0007-0825-4653),
Cemile Günbegi Çalışkan[2] (Orcid: *https://orcid.org/*0000-0002-6640-4927)

[1] Mardin Artuklu Üniversitesi, Sağlık Hizmetleri Meslek Yüksekokulu, Tıbbi Tanıtım ve Pazarlama, Mardin, Türkiye
[2] Mardin Artuklu Üniversitesi, Sağlık Hizmetleri Meslek Yüksekokulu, Tıbbi Hizmetler ve Teknikler Bölümü, Mardin, Türkiye

*Sorumlu yazar e-mail: nisaaltioz@gmail.com

Özet

Küsküt bitkisi (*Cuscuta europaea* L.) ülkemizde ‘’Cinsaçı’’olarak da bilinir. Mardin yöresinde ise İksut otu olarak adı anılmaktadır. Geleneksel olarak mide ve bağırsak rahatsızlıklarında kullanılan bu bitkinin biyoteknolojik açıdan kullanıma yönelik çalışmalar bulunmamaktadır. Bitkiler son yıllarda gıdadan sağlığa pek çok alanda kullanım alanı bulunan nanopartiküllerin yeşil sentezinde yaygın şekilde kullanılmaktadır. Bu nanopartiküllerden metalik nanopartiküller stabilitesi, iletkenliği, antimikrobiyal özelliği, antikanserojen etkinliği gibi özellikleri nedeniyle sağlığa yönelik uygulamaların yanı sıra antioksidan özelliği nedeniyle gıda koruyucu ya da gıda endüstrisinde gibi çeşitli alanlarda da uygulama alanı bulabilmektedir. Metalik nanopartiküllerden olan çinko oksit nanopartiküller antimikrobiyal oluşları, UV koruma özelliği nedeniyle kozmetik sanayide, tekstilde kullanılmaya aday olmalarının yanı sıra gıda araştırmalarında da güvenilir gıda katkı maddesi olarak kabul edilebilmektedir. Bu çalışma da Küsküt (*Cuscuta europaea* L.) bitkisinden sentezlenen çinko oksit nanopartiküllerinin çeşitli patojenler üzerine etkisi araştırılacak ve aynı zamanda gıda üzerindeki etkisini belirlemek için ekmek küfü üzerine inhibisyon etkisi araştırılacaktır. Bu amaçla yeşil sentezle sentezlenen çinko oksit nanopartiküllerinin SEM, EDX, FTIR analizleri yapılarak bu nanopartiküllerin karakterizasyon analizi yapılacak ardından well difüzyon yöntemi ile patojenler üzerine inhibisyon etkisi ve çinko oksit kullanılarak hazırlanmış buğday ekmeklerinin küf değerlendirme yapılacaktır. Böylece Küsküt (*Cuscuta europaea* L.) bitkisinden hem sağlığa yararlı etkileri olan hem de funguslar üzerine etki araştırılmak istenmektedir.

Anahtar Kelimeler: *Cuscuta europaea* L., Çinko oksit nanopartikül, Antimikrobiyal, Antifungal, Ekmek raf ömrü

Determination of antimicrobial and mold (bread mold) effects of zinc oxide nanoparticles synthesized using ichthyosaur (*Cuscuta europaea* L.)

Abstract

The dodder plant (*Cuscuta europaea* L.) is also known as "Cinsaçı" (Cinsaçı) in Turkey. In the Mardin region, it is known as İksut herb. Traditionally used for stomach and intestinal disorders, there are no biotechnological studies on the use of this plant. In recent years, the plants have been widely used in the green synthesis of nanoparticles, which have applications in many areas from food to health. Among these nanoparticles, metallic nanoparticles, due to their stability, conductivity, antimicrobial properties, and anticarcinogenic activity, have found applications in various fields such as food preservatives and the food industry, as well as antioxidant properties. Zinc oxide nanoparticles, a type of metallic nanoparticles, are candidates for use in the cosmetics and textile industries due to their antimicrobial and UV-protective properties, and can be considered a reliable food additive in food research. This study will investigate the effects of zinc oxide nanoparticles synthesized from *Cuscuta europaea* L. on various pathogens and will also investigate their inhibitory effect on bread mold to determine their impact on food. For this purpose, characterization will be carried out using SEM, EDX, and FTIR analyses of zinc oxide nanoparticles synthesized through green synthesis. Following this, the inhibitory effect on pathogens and mold assessment of

wheat breads prepared using zinc oxide will be conducted using the well diffusion method. This study aims to investigate both the health benefits of *Cuscuta europaea* L. and its effects on fungi.

Keywords: *Cuscuta europaea L*, Zinc oxide nanoparticle, Antimicrobial, Antifungal, Bread shelf life

GİRİŞ

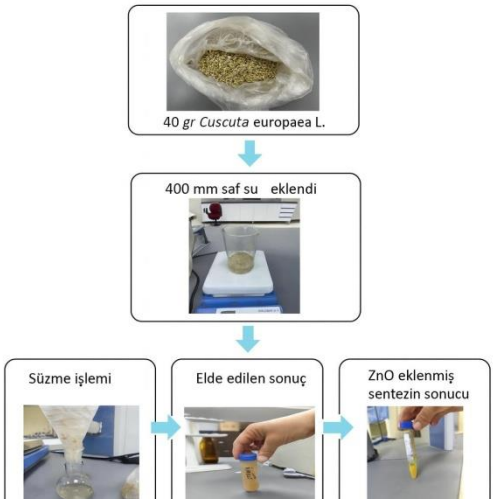
Nano, gözle görülemeyecek boyutlarda yapılan teknolojik çalışmaları kapsayan ve metrenin milyarda birine karşılık gelen bir ölçü birimidir (V. Yadav, 2013). Nanobilim kavramı ilk kez 1959 yılında Nobel Fizik Ödülü sahibi Richard Feyman tarafından bilim felsefesiyle ilgili bir sohbeti sırasında dile getirilmiştir (RP. Feyman, 1999) .“Nanoteknoloji” kavramı; nano ve teknoloji kelimelerinin birleşmesinden oluşmuştur. Teknoloji, yararlı ürünler üretmeye ve yeni ürünler tasarlamaya yarayan bilgilerin bütününe denir (Ayhan, A. 2002). Nanoteknoloji, maddenin atomik-moleküler boyutta mühendisliğinin yapılarak yepyeni özelliklerinin açığa çıkarılması; nanometre ölçeğindeki fiziksel, kimyasal ve biyolojik olayların anlaşılması, kontrolü ve üretimi amacıyla, fonksiyonel materyallerin, cihazların ve sistemlerin geliştirilmesine denir. Bir başka deyişle araçların, malzemelerin ve yapıların moleküler düzeyde işlenmesi, oluşturulması ve manipüle edilmesi olarak tanımlanmaktadır (Kut, D., Güneşoğlu, C. 2005). Nanoteknolojinin kullanım alanları başlıca ilaç sanayi, tekstil, sağlık, gıda, otomotiv, boya gibi farklı alanlardan örnek verilebilir (D. Şanoğlu, 2019). Günlük hayatta nanoteknolojinin öneminin artması ve sıkça kullanılmasından dolayı nanoteknoloji hızla gelişmiştir. Nanoteknolojinin hızla gelişmesi bu alanın özünü oluşturan nanopartikülleri dikkat çekici bir konu haline getirmiştir. Nanopartiküller sahip oldukları bu üstün özellikleri sayesinde enerji, fizik, kimya, biyoloji, biyoteknoloji, tıp, sanayi, teknoloji ve endüstri gibi çeşitli alanlarda kullanılır (A. Aygün, 2019). Nanopartiküllerin eldesinde fiziksel, kimyasal ve biyolojik metotlar kullanılmaktadır. Nanopartiküllerin sentez işlemlerinde fiziksel metotlar kullanılırken yüksek sıcaklık ve basıncın yanı sıra pahalı ekipmanlar gerektirmekte olup, kimyasal metotlar tercih edildiğinde ise, toksik kimyasallar kullanılmakta bunun sonucu olarak da doğaya kalıcı zararlar vermektedir (J. Singh ve ark ., 2018). Endüstriyel alanlarda toplu formlarından farklı olarak belirli elektriksel ve optik özelliklere sahip oldukları için nanopartiküller tarımsal, çevresel ve biyomedikal gibi farklı alanlarda faydalıdır (Nayak, V ve ark ., 2021). Dünya çapındaki bilimsel topluluk, olağanüstü katalitik etkinlikleri, yarı iletken yapıları ve ultraviyole filtrasyon yetenekleri sebebiyle çinko oksit nanopartiküllerine hayran kalmıştır (Nagajyothi, P. C. ve ark. 2013). Ayrıca, raporlar bu nanopartiküllerin biyolojik olarak uyumlu, toksik olmayan ve biyolojik sistemler için güvenli olduğunu göstermektedir (Anjum ve ark.,2021; Agarwal & Shanmugam., 2020; Bhuyan ve ark ., 2015). Çinko oksit nanopartikülleri UV-A ve UV-B gibi tehlikeli radyasyonu içine çekebildiği için güneş kremlerinde ve kozmetiklerde de kullanılır (Ramesh, P., ve ark. 2014). ABD Gıda ve İlaç Dairesi'ne göre çinko oksit güvenli olduğundan ilaç olarak kullanılabilir (Lopez De Romaña, D., ve ark. 2002). Bulaşıcı mikroorganizmaları ortadan kaldırmak için çinko oksit nanopartikülleri antibakteriyel bir madde olarak işlev görebilir. Şekil, partikül boyutu, konsantrasyon ve bakteri hücresiyle temas halinde olma süresi , hücre duvarına nasıl zarar verdiklerini, içeriye nasıl sızdıklarını, hücre zarında nasıl biriktiklerini ve sonunda metabolik aktivitelere müdahale ederek nasıl ölüme neden olduklarını etkiler (Siddiqi, K. S., ve ark., 2018). Canlılardaki önemli eser elementler olan çinko ve selenyum, insanlarda bağışıklık sistemi işlevi, antioksidan savunma ve antitümör aktivitesi için hayati önem taşır. Biyosentezlenen çinko ve selenyum nanopartikülleri daha biyolojik olarak parçalanabilir, daha az toksik ve vücuttan kolayca atılım sağlandığından çok avantajlıdırlar ((Zhuang ve ark ., 2007; Schomburg, 2017). Bitkiler, sadece doğayı güzelleştiren özelliklerinin yanı sıra doğanın en önemli ve en estetik öğelerinden biridir. Yaşamın temel taşlarını oluşturan oksijen üretimi, besin zinciri ve ekosistem dengesine sağladığı katkılarla dünyamızın vazgeçilmez birer parçaları haline gelmişlerdir. Ayrıca bitkiler birçok çeşitli alanlarda kullanılmaktadır. Bitkiler; tıbbi kullanım, gıda üretimi, sanayi, tekstil, süs bitkileri, inşaat, çevre düzenlemesi, kimya, kozmetik, biyoyakıt ve enerji gibi pek çok alanlarda kullanılmaktadır. Küsküt, Cuscutacea e familyasının tek üyesi olan Cuscuta cinsindendir. Güneydoğu Anadolu bölgesinde kullanımı yaygın bir öneme sahip olan iksut otu (*Cuscuta europaea L.*) yoğun aroması, hoş tadı ile ilgi çekmektedir (Nemli,1982). İpliksi gövdeli ve pullu yapraklı bir yapıya sahip olan küsküt, klorofilsiz tam parazit bir bitki olarak yeşil bitkilerin iletim demetlerine emeçlerini göndererek beslenir ve tırmanıcı bir yaşam sürer.(Zeybek ve Zeybek, 1994).Türkiye'de tarımsal üretim ve geleneksel halk hekimliği için mühim parazitik bitkiler olan Cuscuta türleri, Mardin bölgesinde ‘İksut’ olarak bilinir ve diğer bölgelerde ‘bostanbozan, canavar otu, bağbozan, cinsaçı, eftimon, gelin saçı, kızıl sarmaşık ve şeytansaçı’ gibi isimlerle adlandırılırlar (Baytop, 1997).Bitkinin gelişme dönemi yetiştiği bölgenin iklim şartlarına bağlı olarak Mayıs ile Ekim ayları arasıdır (Jamshid ve Esther 2011). Küsküt bitkisi (*Cuscuta europaea L.*)’nin çiçekli dallarının idrar

söktürücü, mushil, gaz ve safra söktürücü etkilere sahip olduğu bildirilmektedir.*Cuscuta chinensis Lam.*'ın tohumları karaciğer ve böbrek rahatsızlıklarında, cinsel fonksiyonları iyileştirmek için, bulanık görme, yorgunluk gibi göz şikayetlerini gidermek için, ve klinik olarak yaşlanmayı geciktirmek için kullanılmıştır. Yapılan in vitro ve in vivo çalışmalar Cuscuta türlerinin farklı farmakolojik etkilere sahip olduğunu ortaya koymuştur. Araştırmalara göre *C. chinensis* antikanser (Nisa ve ark. 1986; Umehara ve ark., 2004), immunostimulation, ve antioksidan etkilere sahip olduğu ortaya çıkmıştır. (Bao ve ark. 2002). *C. chinensis* glikozidlerinin yaşlanmaya karşı etkiler gösterdiği ve PC12 hücre farklılaşmasını uyararak hafızayı güçlendirdiği gösterilmiştir (Liu ve ark. 2003). İlerleyen çalışmalarda ise *C. reflexa* gövdelerinin metanol ekstresinin antibakteriyel (Pal ve ark. 2006) ve *C. chinensis* etil asetat ve metanol ekstresinin antioksidan (Yen ve ark. 2008); *C. japonya*'nın major bileşenlerinin antihipertansif (Oh ve ark., 2002) etkileri olduğu keşfedilmiştir. Ayrıca Cuscuta türlerinin flavonoidler, glikozitler ve alkaloidler, tanenler, ligninler ve diğer organik maddelerde dahil olmak üzere çeşitli fitokonsitüentler içerdiği bildirilmiştir.Bunların yanı sıra uçucu yağ ve eser elementler içermektedir (D.Garvey ve ark., 2010).*Cuscuta europaea L.* bitkisinde yapılan araştırmada bu türlerin metanol özütlerinin fenolik bileşenleri keşfedilmiştir. Diğer cuscuta türlerinin yanı sıra, özütlerde kafeik asit, p-kumarik asit, isorhamnetin ve isorhamnetin 3-0 glikozit tespit edilmiştir (P.Hrıbova ve ark. 2009).*Cuscuta europaea L.* bitkisinin içerdiği bileşenlerinin nanopartikül sentezinde indükleyici bir özellik gösterebileceği düşünülüyor.Gıda paketlemenin ana işlevi,ürünü mikrobiyal bozulmalarla kimyasal kirleticilerle, nem ve oksijen gibi olumsuz çevresel etkilere karşı korumaktır. Ekmek bozulmalarının temel sebepleri mikroorganizmaların yol açtığı bozulmalar ile kimyasal ve fiziksel değişikliklerdir. Ekmek taze olarak tüketilen bir ürün olmasına rağmen ne yazık ki piştikten sonra sadece birkaç saat taze kalabilmektedir (Alhendi ve Choudhary, 2013). Ekmekler için küf sayısının büyüklüğü ile nem absorbsiyonu veya desorpsiyonu raf ömrünü ve kalite özelliklerini belirleyen temel kriterlerdir. Ekmeğin bayatlamasında etken olan nişasta retrogradasyonunun temel sebebide nem kaybıdır. Bu yüzden ekmekler yüksek su bariyeri özelliğine sahip materyallerle paketlenmelidir (Petersen ve ark., 1999).Ekmeğin Bayatlaması mikrobiyolojik olmayan fiziksel ve kimyasal değişiklikler nedeniyle kabul edilebilirliğinin azalması olarak tanımlanır. Bu durumdan dolayı çok büyük ekonomik kayıplara neden olmaktadır (Ronda ve ark., 2011). Mikrobiyal bulaşı kaynakları ekmeklere üretim öncesinde, üretim sırasında ve depolama esnasında kontamine olmaktadırlar (Değirmencioğlu ve ark., 2011). Ekmeklerde bozulmaya neden olan üç çeşit mikroorganizma grubu vardır. Bunların birincisi küfler olup ekmekteki bozulmaların temel sebebidir.Küfler fırın ısısında inaktif olduklarından, pişirme işleminden sonraki dilimleme ve paketleme gibi aşamalarda kontamine olmaktadırlar (Alhendi ve Choudhary, 2013). Küfler ekmeklerde aroma kayıplarına, mikotoksin oluşumuna ve alerjik bileşiklerin oluşumuna sebep olmaktadırlar (Değirmencioğlu ve ark., 2011). Literatürde *Cuscuta europaea L.*bitkisinden çinko oksit nanopartikül sentezi bulunmamaktadır. Yapılan çalışmada iksut bitkisi (*Cuscuta europaea L.*) bitkisinden sentezlenen çinko oksit nanopartiküllerin çeşitli patojenler üzerine etkisi araştırılmıştır.Aynı zamanda gıda üzerine etkisini araştırmak için ekmek küfü üzerinde çalışma yapıldı.Bu amaçla yeşil sentezle sentezlenen çinko oksit nanopartiküllerinin SEM, EDX, FTIR analizleri yapılarak bu nanopartiküllerin karakterizasyon analizi yapıldı ardından well difüzyon yöntemi ile patojenler üzerine inhibisyon etkisi incelendi.

MATERYAL VE METOT:

Deneyde kullanılan bitki Mardin'de aktardan kurutulmuş örneği alınan iksut otudur.

Cuscuta Europaea L.Ekstraktının Hazırlanması: iksut otu örneğin 40 gr alınarak 400 milimetre su ilave edildi. Özüt elde etmek için manyetik karıştırıcıda 70°C'de 3 saat karıştırıldı. Sıvı faz süzgeç kâğıdı vasıtasıyla ayrıldıktan sonra 300 milimetrelik ekstrakta 200 mililitre 0.1 Molar çinko asetat dihidrat çözeltisi eklenerek 3 saat 60°C'de karıştırma işlemi yapıldı. Reaksiyon sonucunda özütün renginde bir açılma (açık sarı) gözlemlendi.



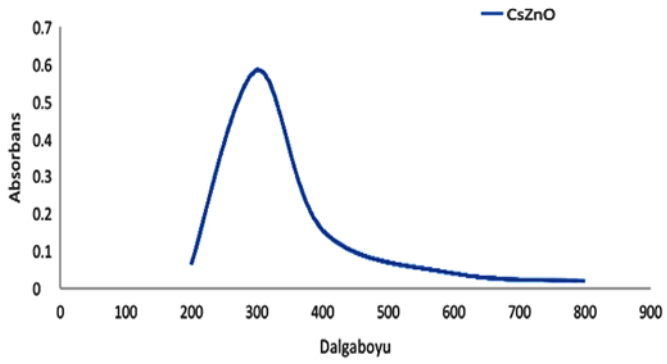
Şekil1: *Cuscuta Europaea* L. Ekstraktının Hazırlanması

T80+ UV/VIS spektrofotometre de 200 ve 800 nm dalga boyları arasında absorbansın tranmasıyla çinko oksit nanopartiküllerin karakteristik zirvesi belirlendi. Elde edilen ürün 5000 rpm 10 dk santrifüj edilerek dibinde oluşan çökelek kısmı ayrıt dilerek 100 °C 4 saat boyunca etüvde inkübe edildi. Üretilen nanopartiküllerin SEM, SEM-EDX ve FTIR analizleri gerçekleştirildi . Üretilen nanopartikülün 100 mg/ml'lik çözeltileri antimikrobiyal analiz için hazırlandı. Testlerde kullanılan bakteri suşları Staphylococcus aureus ATCC 25923, Escherichia coli ATCC 11229 .Antimikrobiyal aktivite testi S. Aureus ve E. Coli üzerinde well difüzyon yöntemi kullanılarak gerçekleştirildi [O. Erdoğan ve ark., 2019)

BULGULAR VE TARTIŞMA

UV/VIS Spektrofotometre

Şekil 2, C.sZnO UV-VIS spektrofotometresinde 200-800 nm arasında absorbans taramalarını göstermektedir.

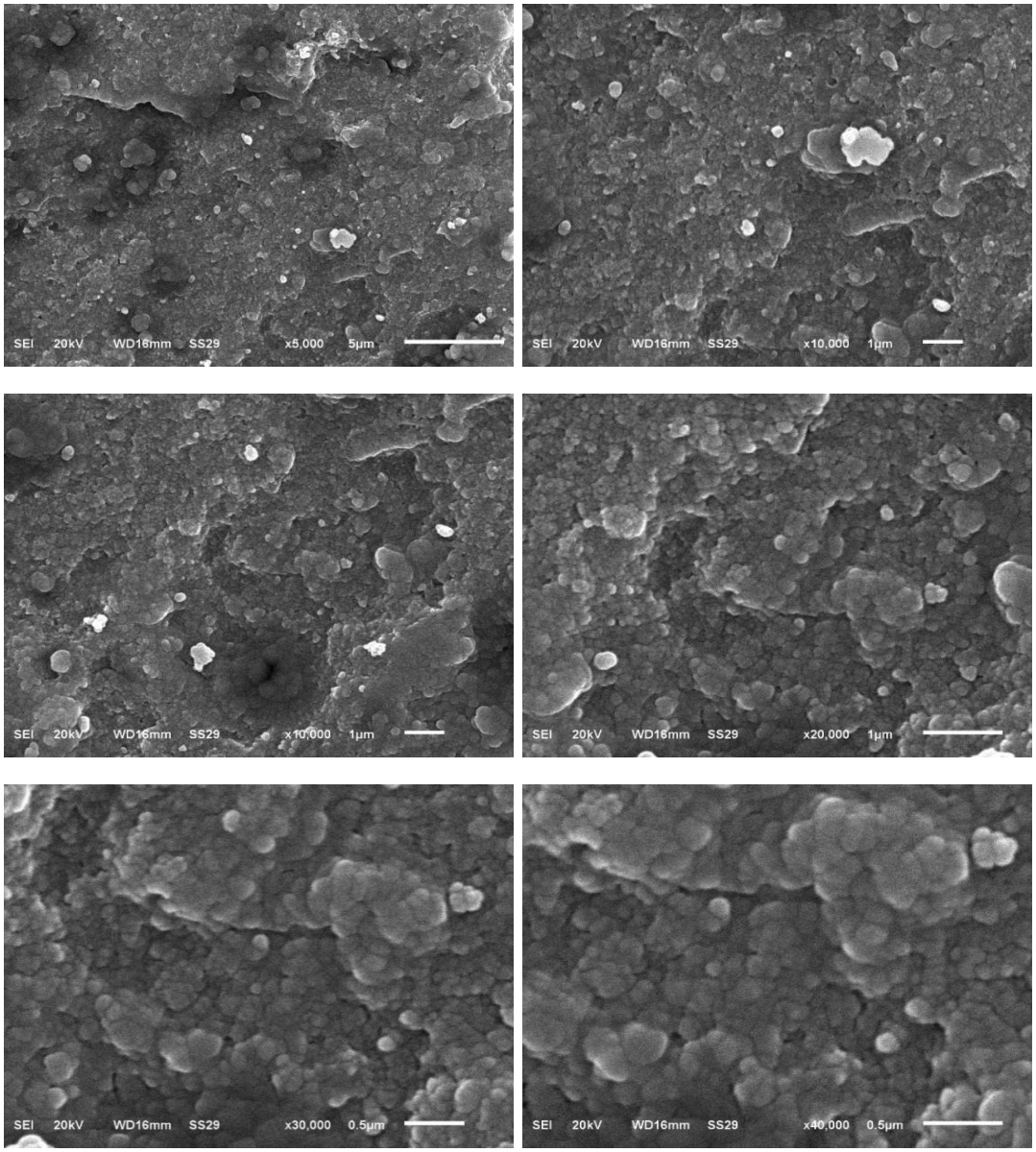


Şekil2: C.sZnO UV-VIS Grafiği

CsZnO için SPR 350 nm'de kaydedildi (E. Darvishi ve ark., 2019).

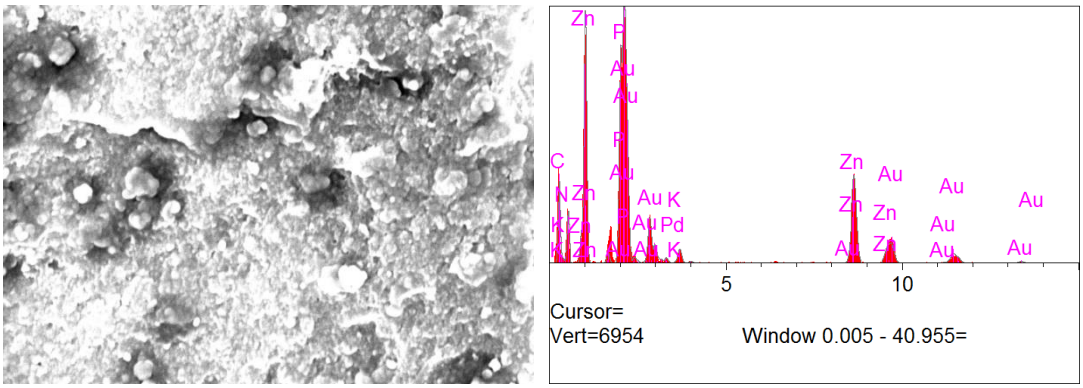
SEM ve EDX ANALİZİ:

Cuscuta Europaea L. ekstraktı kullanılarak yeşil sentezlenen ZnO NP'lerin taramalı elektron mikroskobu (SEM) görüntüleri Şekil 3'te görülmektedir. SEM görüntüleri, *Cuscuta Europaea* L. ekstraktının çinkonun farklı tuzları kullanılarak sentezlenen ZnO NP'nin şekil ve boyutlarında farklılıklar meydana getirdiğini göstermektedir.



Şekil 3:SEM Görüntüleri

SEM fotoğraflarında görüldüğü gibi Çinko Oksit nanopartikülleri sentezlenmiştir. Şekil 3'deki görüntüler stafilokoklara benzemektedir. Sentezlenen Çinko Oksit nanopartiküllerinin SEM-EDX sonuçları Şekil 4'te verilmiştir.



Elt.	Line	Intensity (c/s)	Error 2-sig	Conc	Units
C	Ka	324.86	5.144	21.066	wt.%
N	Ka	15.62	1.932	1.824	wt.%
O	Ka	191.23	4.266	8.330	wt.%
P	Ka	978.03	9.218	8.428	wt.%
K	Ka	20.92	3.872	0.208	wt.%
Ca	Ka	80.19	4.063	0.826	wt.%
Zn	Ka	692.41	7.206	21.876	wt.%
Pd	La	227.85	5.605	7.840	wt.%
Au	La	151.33	3.935	29.602	wt.%
			Total	100.000	wt.%

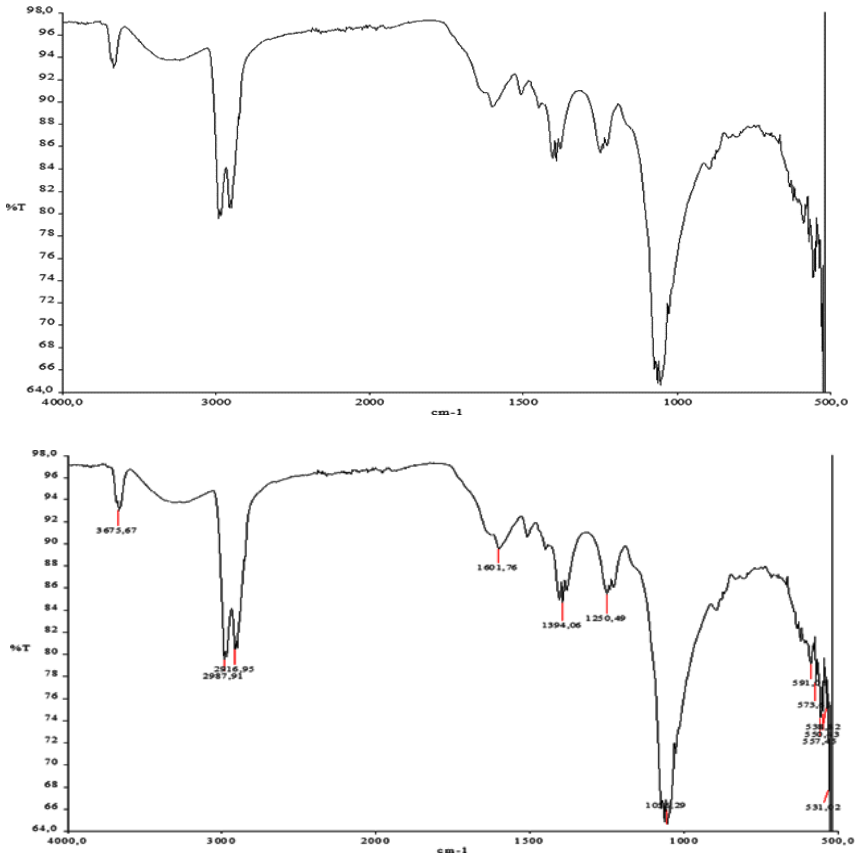
Şekil 4: SEM-EDX sonuçları

EDX analizi, *Cuscuta europaea L.*'nın elementel bileşimini başarıyla belirlemiştir; bu bileşimde karbon, çinko ve fosfor elementleri en yüksek oranlarda yer almaktadır. Elde edilen veriler, bitkinin tam parazit yaşam tarzının, mineral madde akümülasyonunu önemli ölçüde etkilediğini ortaya koymaktadır.

FTIR ANALİZİ

3400–3200 cm^{-1} (O–H gerilme) bu aralıktaki geniş absorpsiyon bandı, fenolik bileşikler ve polisakkaritler gibi moleküllerin karakteristik O–H gerilmelerinden kaynaklanır ve *Cuscuta europaea L.*'nın önemli bir polifenol ve karbonhidrat kaynağı olduğunu ortaya koyar. 2920–2850 cm^{-1} (C–H alifatik gerilme) gözlenen alifatik C–H gerilme titreşimleri, örneğin bitki lipitlerinin, selüloz/hemiselüloz yapılarını oluşturan metil ve metilen gruplarının varlığını gösterir ve bu da bitkinin temel hücre duvarı yapısıyla uyumludur. 1650–1600 cm^{-1} (C=O ve C=C titreşimleri) Spektrumun bu kısmında görülen güçlü pikler, aromatik $\mathrm{C=C}$ titreşimleri (özellikle flavonoidler ve fenolik bileşikler) ve Amid I ($\mathrm{C=O}$) bandından (proteinler) kaynaklanır. Bu yoğun absorpsiyon, *C. europaea L.*'nın sekonder metabolitler açısından zenginliğini güçlü bir şekilde desteklemektedir. 1400–1250 cm^{-1} (C–H bükülme, C–O gerilme) Bu bölge, fenolik bileşiklerin aromatik halka iskelet titreşimlerini, karboksilat iyonlarının simetrik/asimetrik titreşimlerini ve lignin/polisakkaritlerin çeşitli C–O gerilmelerini içerir. Bu pikler, bitki örneğinin yapısal çeşitliliğini yansıtır. 1150–1000 cm^{-1} (C–O–C polisakkarit titreşimleri) spektrumun bu kısmındaki yoğun pikler, karbonhidrat iskeletinin karakteristik $\mathrm{C–O}$ gerilmelerini ve $\mathrm{C–O–C}$ bağlarını yansıtır; böylece selüloz ve hemiselülozun temel bileşimde bulunduğunu doğrular. 600–500 cm^{-1} (aromatik halka dışı titreşimler) bu düşük dalga sayısı aralığı, molekülün bütünündeki yapısal ayrıntıları yansıtan, aromatik yapıların ve diğer karmaşık organik bileşiklerin özel titreşimlerini barındırır.

FTIR analizindeki pik değerleri Şekil 5'te verilmiştir.



Şekil 5: FTIR analizi

WELL DİFÜZYON YÖNTEMİ

Yapılan testler neticesinde, *Cuscuta europaea* ekstraktının ne *Staphylococcus aureus* ne de *Escherichia coli* üzerinde belirgin bir antibakteriyel etki göstermediği (inhibisyon zonu oluşturmadığı) tespit edilmiştir. Ancak, pozitif kontrol antibiyotikleri, deneyin geçerliliğini doğrulayacak şekilde, beklenen çaplarda inhibisyon zonları oluşturmuştur.

SONUÇ

CsZnO'da 350 nm çevresinde karakteristik absorpsiyon / SPR benzeri tepe bulunur. (AlHamoud ve ark., 2021 ; Saeed ve ark.,2019) Yüzey boyunca gözlenen büyük ve parlak yapılar, yüksek elektron yoğunluğuna sahip ve muhtemelen çinko oksit gibi metal oksit nanopartiküllerine işaret etmektedir. Bu parlak alanların EDX doğrulaması yapıldığında metal oksit olduğunu destekleyen sonuçlar elde edilmesi beklenir. Bu yapı, bitkisel ekstre ile sentezlenen nanopartiküllere özgü bir görünüm olup literatürde fitosentezlenmiş nanopartiküllerin SEM görüntülerinde sıklıkla bildirilen morfoloji özellikleriyle uyumludur. (Ahmed, S ve ark ., 2016) EDX analizi, *Cuscuta europaea L.*'nın elementel bileşimini başarıyla belirlemiştir; bu bileşimde karbon, çinko ve fosfor elementleri en yüksek oranlarda yer almaktadır. Elde edilen veriler, bitkinin tam parazit yaşam tarzının, mineral madde akümülasyonunu önemli ölçüde etkilediğini ortaya koymaktadır. (Koo, B. J., Li, Y., ve Miyasaka, S. C. 2018). *Cuscuta europaea L*'nın FTIR spektral analizi, bitki bileşiminin fenolik bileşikler, karbonhidratlar ve diğer doğal organik moleküller açısından zengin olduğunu ortaya koymuştur. Bu analiz, biyolojik aktivite için temel teşkil eden fonksiyonel grupların varlığını teyit ederek, türün tıbbi değerlendirilmesine önemli bir katkı sağlamaktadır. Mevcut well difüzyon çalışmasının bulguları, *C. Europaea* L. ekstraktının test edilen S. aureus ve E. coli üzerinde antimikrobiyal bir etki oluşturmadığını göstermiştir. Bitkinin taşıdığı biyoaktif potansiyelin

derinlemesine anlaşılması için, çeşitli ekstraksiyon prosedürlerini içeren ileri araştırmaların yapılması önerilmektedir. (Afifi, F. U., ve Al-Khalil, S. 2020). (Kokoska, L., ve ark. 2002 ; Sharma, R. , ve Gupta, R. 2020).

TEŞEKKÜR

Bu çalışma, TÜBİTAK tarafından desteklenen 2209-A [Proje No: 1919B012470578] numaralı proje kapsamında gerçekleştirilmiştir. Araştırmanın yürütülmesi sürecinde sağlanan finansal destek için TÜBİTAK'a teşekkür ederiz. Proje araştırmacılarına, laboratuvar altyapısını sağlayan [Mardin Artuklu Üniversitesine], Kimyager Dr. Leyla ERCAN'a ve Proje Danışmanı Öğretim Görevlisi Cemile GÜNBEGİ ÇALIŞKAN'a teşekkür ederim.

KAYNAKLAR

1. Afifi, F. U., & Al-Khalil, S. (2020). Phytochemical and Biological Analysis of *Cuscuta* Species: A Review. *Journal of Ethnopharmacology*, 249, 112–256.
2. Agarwal, H., & Shanmugam, V. (2020). A review on anti-inflammatory activity of green synthesized zinc oxide nanoparticle. *Bioorganic Chemistry*, 94, 103423.
3. Ahmed, S., Saifullah, Ahmad, M., Swami, B. L., & Ikram, S. (2016). Green synthesis of silver nanoparticles… *Journal of Radiation Research and Applied Sciences*, 9(1), 1–7.
4. Aygün, A. (2019). Yeni nesil nanokompozitler… Yüksek lisans tezi, Dumlupınar Üniversitesi.
5. Ayhan, A. (2002). Dünden Bugüne Türkiye'de Bilim-Teknoloji… Beta Basım Yayım.
6. Bao, X., Wang, Z., Fang, J., & Li, X. (2002). Polysaccharide of *Cuscuta chinensis*. *Planta Medica*, 68, 237–243.
7. Baytop, T. (1997). *Turkish Plant Names Dictionary*. TDK Yayınları.
8. Bhuyan, T., Mishra, K., Khanuja, M., Prasad, R., & Varma, A. (2015). Biosynthesis of zinc oxide nanoparticles. *Mater. Sci. Semicond. Process.*, 32, 55–61.
9. Çınar Avar, E., Türkmen, K. E., Loğoğlu, E., & Katırcıoğlu, H. (2022). *Juglans regia* ekstraktı ile ZnO NP biyosentezi. *Mater. Technol.*, 37, 3194–3204.
10. Darvishi, E., Kahrizi, D., & Arkan, E. (2019). *Juglans regia* ile sentezlenen ZnO NP karşılaştırılması. *J. Mol. Sıvı.*, 286, 110831.
11. Değirmencioğlu, N., Göçmen, D., İnkaya, A. N., Aydın, E., Güldaş, M., & Gönenç, S. (2011). MA paketleme etkisi. *Journal of Food Science and Technology*, 48(2), 236–241.
12. D. Garvey, A. Dorsey, L. Brown, E. Rampersad, & H. Forbes (2010). Multicomponent ethnomedical preparations. Pacifichem Congress.
13. Erdoğan, O., Birtekocak, F., Oryaşin, E., Abbak, M., Demirbolat, G. M., Paşa, S., & Çevik, Ö. (2019). ZnO NP yeşil sentezi—enginar yaprağı. *Düzce Tıp Dergisi*, 21, 19–26.
14. Feyman, R. P. (1999). *The pleasure of finding things out*. Helix Books.
15. Gour, A., & Jain, N. K. (2019). Advances in green synthesis of nanoparticles. *Artificial Cells, Nanomedicine and Biotechnology*, 47, 844–851.
16. Günay, K., Leblebici, Z., & Koca, F. D. (2021). ZnO NP biyosentezi… *Nevşehir Bilim ve Teknoloji Dergisi*, 10, 56–66.
17. Hırbova, P., Zemlicka, M., Bartl, T., & Švajdlenka, E. (2009). *Chem Listy*, 103, 243–245.
18. Jamshid, A., & Esther, E. M. (2011). *Dodder (Cuscuta spp.) Biology and Management*. A-615.
19. J. Singh, Dutta, T., Kim, K., Rawat, M., Samddar, P., & Kumar, P. (2018). Green synthesis of metal nanoparticles. *Journal of Nanobiotechnology*, 16(84).
20. Koo, B. J., Li, Y., & Miyasaka, S. C. (2018). EDX temel kaynak. In: *X-ray Spectroscopy* (pp. 45–60). Springer.
21. Kut, D., & Güneşoğlu, C. (2005). Nanoteknoloji ve tekstil uygulamaları. *Tekstil&Teknik*, 224–230.
22. Liu, J. H., Jiang, B., Bao, Y. M., & An, L. J. (2003). *Cuscuta chinensis* glikozid etkisi. *Int. J. Dev. Neurosci.*, 21, 277–281.
23. Lopez De Romaña, D., Brown, K. H., & Guinard, J. X. (2002). Zinc fortification sensory trial. *Journal of Food Science*, 67, 461–465.
24. Nagajyothi, P. C., Minh An, T. N., Sreekanth, T. V. M., Lee, J. I., Joo, D. L., & Lee, K. D. (2013). ZnO NP synthesis. *Materials Letters*, 108, 160–163.
25. Nemli, Y. (1982). Anadolu'da yetişen *Cuscuta* türleri anatomisi. *Doğa Bilim Dergisi*, 6, 35–41.

26. Nayak, V., Singh, K. R., Singh, A. K., & Singh, R. P. (2021). Selenium nanoparticles. *New Journal of Chemistry*, 45(6), 2849–2878.
27. Oh, H., Kang, D. G., Lee, S., & Lee, H. S. (2002). *Cuscuta japonica* ACE inhibitörleri. *Journal of Ethnopharmacology*, 83, 105–108.
28. Pal, D. K., Mandal, M., Senthilkumar, G. P., & Padhiari, A. (2006). Antibacterial activity of *Cuscuta reflexa*. *Fitoterapia*, 77, 589–591.
29. Petersen, K., Nielsen, P. V., Bertelsen, G., Lawther, M., Olsen, M. B., Nilsson, N. H., & Mortensen, G. (1999). Biobased materials in food packaging. *Trends in Food Science & Technology*, 10(2), 52–68.
30. Ramesh, P., Rajendran, A., & Sundaram, M. (2014). Green synthesis of ZnO NP with *Cassia auriculata*. *Nanotechnology*, 2, 41–45.
31. Ronda, F., Caballero, P. A., Quilez, J., & Roos, Y. H. (2011). Bread staling mechanisms. *Journal of Cereal Science*, 53, 97–103.
32. Saeed, D. A., et al. (2019). Cesium incorporated ZnO nanostructures. *Applied Surface Science*, 489, 232–241.
33. Schomburg, L. (2017). Dietary selenium and human health. *Nutrients*, 9, 22.
34. Şanoğlu, D. (2019). Alev sprey pirolizi ile alümina nano toz sentezi. Yüksek lisans tezi, Eskişehir Teknik Üniversitesi.
35. Siddiqi, K. S., Rahman, A., Tajuddin, & Husen, A. (2018). ZnO NP properties. *Nanoscale Research Letters*, 13, 141.
36. Sharma, R., & Gupta, R. (2020). *Cuscuta europaea* phytochemical profile. *Plant Science Letters*.
37. Şekeroğlu, N., Meraler, S. A., & Koca, U. (2011). Mardin'in şifalı bitkileri. *Mardin Haber*.
38. Umehara, K., Nemoto, K., Ohkubo, T., Miyase, T., Degawa, M., & Noguchi, H. (2004). Cuscutic resinoside A izolasyonu. *Planta Medica*, 70, 299–304.
39. V. Yadav (2013). Nanotechnology review. *Research India Publications*, 3(6), 771–778.
40. Yen, F. L., Wu, T. H., Lin, L. T., Cham, T. M., & Lin, C. C. (2008). Antioxidant activity in *Cuscuta chinensis*. *Food Chemistry*, 108, 455–462.
41. Zeybek, N., & Zeybek, V. (1994). *Kapalı Tohumlu Bitkiler Sistematiği*. EÜ Eczacılık Fakültesi Yayınları.
42. Zhuang, C., Yao, D., Li, F., Zhang, K., Feng, Q., & Gan, Z. (2007). MgB2 films. *Superconductor Science and Technology*, 20, 291.

ORAL PRESENTATION

İğde meyvesinden sentezlenen çinkooksit nanopartiküllerin antimikrobiyal etkinliği ve akciğer ve kolon kanseri üzerine sitotoksik etkisi

Leyla Ercan[1] *(https://orcid.org/ 0000-0002-6570-8128)*, Cemile Günbegi Çalışkan[2] *(https://orcid.org/0000-0001-8129-4394)*, Serap Toprak Döşlü[3] *(https://orcid.org/0000-0002-5455-8179)*

[1]Mardin Artuklu Üniversitesi, Sağlık, Kültür ve Spor Daire Başkanlığı, Mardin, Türkiye
[2]Mardin Artuklu Üniversitesi, Sağlık Hizmetleri Meslek Yüksekokulu, Tıbbi Hizmetler ve Teknikler Bölümü, Mardin, Türkiye
[3]Mardin Artuklu Üniversitesi, Sağlık Bilimleri Fakültesi, Beslenme ve Diyetetik Bölümü, Mardin, Türkiye

Sorumlu yazar e-mail: seraptoprak@artuklu.edu.tr

Özet

İğde ağacı hoş kokulu çiçekleri ve tatlı ve küçük partiküllü meyveleri ile dikkat çeken bir bitkidir. Çinko oksit nanopartiküller kararlı oluşları ve antioksidan, antimikrobiyal özellikler sergilemeleri nedeniyle son yıllarda pek çok çalışmada araştırma konusu olmaktadır. Bu çalışmada iğde meyvesinden çinko oksit nanopartiküller sentezlenerek bu nanopartikülün antimikrobiyal, antikanserojen özellikleri araştırılmıştır. Bu amaçla sentezlenen nanopartiküllerin SEM, EDX, SEM MAP, FTIR analizleri yapılmıştır. Ayrıca çinko oksit nanopartikülün disk difüzyon yöntemi ile antimikrobiyal özelliğinin yanısıra WST testi ile A549 ve HT29 hücre hatları üzerine sitotoksik etkileri incelenmiştir. Sonuç olarak EaZnO nanopartikülleri *K. pneumoniae, P. aeruginosa* üzerinde antimikrobiyal özellikler sergilemiştir. Ayrıca bu nanopartiküller HT29 hücre hattı üzerinde A549 hücre hattına nazaran daha etkili sonuçlar vermiştir. Bu sonuçlara göre iğde meyvesinden sentezlenen bu nanopartiküller antimikrobiyal etkinliğinin yanısıra antikanserojen özelliği ile adjuvan, nutrasötik ya da fitofarmasötik olarak kullanıma aday olabilir.

Anahtar Kelimeler: Antimikrobiyal aktivite, Antikanserojen, İğde meyvesi

Antimicrobial activity of zinc oxide nanoparticles synthesised from *Elaeagnus angustifolia* fruit and their cytotoxic effect on lung and colon cancer

Abstract

The *Elaeagnus angustifolia* tree is a plant that attracts attention with its sweet-smelling flowers and sweet, small-grained fruits. Zinc oxide nanoparticles have been the subjects of numerous studies in recent years because of their stable structure and their antioxidant and antimicrobial properties. In this study, zinc oxide nanoparticles were obtained from *Elaeagnus angustifolia* fruits, and the antimicrobial and anticarcinogenic effects of these nanoparticles were evaluated. For this purpose, SEM, EDX, SEM MAP, and FTIR analyses were conducted on the produced nanoparticles. In addition to the antimicrobial properties of zinc oxide nanoparticles by the disc diffusion method, their cytotoxic effects on A549 (lung cancer) and HT29 (colorectal adenocarcinoma) cell lines by the WST method were investigated. As a result, EaZnO displayed antimicrobial activity against *K. pneumoniae* and *P. aeruginosa*. EaZnO nanoparticles have given more efficient results on the HT29 cell line than the A549 cell line. These synthesised nanoparticles, in addition to their antimicrobial activity, may be candidates for application as adjuvants, nutraceuticals, or phytopharmaceuticals thanks to their anticarcinogenic properties.

Keywords: Antimicrobial activity, Anticarcinogenic, *Elaeagnus angustifolia* fruit

GİRİŞ

Son yıllarda nanoteknoloji, kanser tedavisi de dahil olmak üzere tıp alanında çeşitli uygulamalara sahip, umut vadeden bir alan olarak ortaya çıkmıştır. Bitkilerin meyve yaprak kök gibi farklı kısımlarından sentezlenen nanopartiküllerin antioksidan, antimikrobiyal, antikanserojen ve antiinflamatuar etki gibi sağlığa faydalı yönlerinin

yanı sıra gıda koruyucu olarak kullanımı da araştırılmaktadır. Dikkat çeken nanomalzemelerden biri, çok yönlü özellikleri ve biyomedikal uygulamalarda kullanım potansiyeli nedeniyle ilgi gören çinko oksit nanopartikülleridir (Günay vd., 2021; Singh vd., 2017; Koçak ve Meydan, 2023). Yeşil sentez olarak bilinen bitki kaynaklı malzemeler kullanılarak çinko oksit nanopartiküllerinin sentezlenmesi, sürdürülebilir ve çevre dostu bir yaklaşım sunduğu için özellikle ilgi görmüştür (Günay vd., 2021).

Araştırmacılar, elde edilen nanopartiküllerin antimikrobiyal etkinliğini artırdığı gösterilen bitki özleri kullanan yeşil sentez yaklaşımları da dahil olmak üzere çinko oksit nanopartiküllerini sentezlemek için çeşitli yöntemler araştırdılar (Koçak ve Meydan, 2023). Nanopartiküllerin boyutu ve dağılımının antimikrobiyal etkinliklerinde önemli bir rol oynadığı, daha küçük ve iyi dağılmış nanopartiküllerin genellikle daha güçlü antibakteriyel etkiler gösterdiği bildirilmiştir (Zakharova vd., 2019). Çinko oksit nanopartiküllerinin antibakteriyel aktivitesi, Gram pozitif ve Gram negatif bakteriler de dahil olmak üzere çok çeşitli bakteri türlerine karşı gösterilmiştir (Hameed vd., 2023).

Ayrıca bir meta-analiz, çinko oksit nanopartiküllerinin tek başına veya fotokatalitik terapi veya doksorubisin gibi antikanser ilaçlar gibi diğer terapilerle birlikte güçlü antitümör aktiviteleri sergilediğini ortaya koymuştur (Vinardell ve Mitjans, 2015). Bu antikanser etkisinin altında yatan mekanizmaların, reaktif oksijen türlerinin üretilmesi ve kanser hücrelerinde apoptoz ve nekrozun indüklenmesini içerdiğine inanılmaktadır. (Premanathan vd., 2010) Özellikle, çalışmalar çinko oksit nanopartiküllerinin kanser hücrelerinde apoptozu seçici olarak hedef aldığını ve indüklediğini, normal hücreler üzerinde nispeten daha düşük bir sitotoksik etkiye sahip olduğunu ve bu durumun kullanımları için potansiyel bir terapötik pencere olduğunu göstermiştir (Premanathan vd., 2010).

Bu çalışmada çeşitli çevre koşullarında yetişebilen ve Elaeagnaceae familyasına ait bir bitki olan, hoş kokulu sarı çiçekleri, gümüş grisi pullarla kaplı yaprakları, nitrojen fiksasyonu yapan kökleri (Khamzina vd., 2009; Guo ve Wang; 2021) ve tek çekirdekli yenebilen tatlı meyvesi ile bilinen *Elaeagnus angustifolia* L. meyvesinin özütü kullanılmıştır (Shafroth vd., 1995; Pan vd., 2011; Guo ve Wang; 2021).

E. angustifolia L. meyvesi insan sağlığı için önemli olan pek çok flavonoid ve terpenoid bileşikleri, glikoz, fruktoz, saponinler, fenolik asit, tanenler, kafeik asit, amino asitler, karotenoidler ve vitaminleri; potasyum, magnezyum, sodyum, demir, kalsiyum, çinko gibi mineralleri ve linoleik asit, palmitoleik asit, palmitik asit, fosfolipidler, glikolipidler ve beta-sitostrol gibi yağ asitlerini içerir (Ayaz ve Bertoft, 2001; Hassanzadeh ve Hassanpour, 2018; Okmen ve Türkcan, 2013; Hamidpour vd., 2017).

Bu çalışma, yaygın olarak Rus zeytini olarakta bilinen *Elaeagnus angustifolia* L. meyvesinden sentezlenen çinko oksit nanopartiküllerinin antibakteriyal etkisi ile akciğer ve kolon kanserinin tedavisi için potansiyelini incelemektedir.

2. MATERYAL VE METOD

2.1. Nanopartikül Sentezi ve Karekterizasyonu

Marketten alınan iğde meyvelerinin çekirdekleri çıkarıldı ve 50 gram kuru iğde örneğine 1000 mL saf su eklenerek 700 rpmd 85 °C'de 4 saat manyetik karıştırıcıda karıştırıldı. Daha sonra ekstrakt süzgeç kağıdından süzülerek alındı. İğde ekstresinin 500 mL'sine 100 mL 0,1 M $ZnCH_3COOH$ eklendi ve bir gün boyunca oda sıcaklığında inkübasyona bırakıldı. ZnO nanopartikül sentezi hem renk değişiminden hemde UV-VIS spektrofotometre ölçümü ile gözlendi. Ardından 5000 rpm'de 25 °C'de soğutmalı santrifüj ile santrifüjlenerek çökelek alındı ve 100 °C de etüvde 4 saat bekletilerek dekarboksile edildi. Ardından nanopartikülün SEM, EDX, FTIR anaizleri yapıldı.

2.2. Antimikrobiyal Etkinlik Testi

EaZnO nanopartiküllerinin antimikrobiyal etkinliği disk difüzyon yöntemi uygulanarak tespit edildi. Taze kültürden alınarak çoğaltılan mikroorganizmalar ağarlı petrilere yayma ile ekildi. Ardından petrilere yerleştirilen steril disklere numune emdirilerek 24 saat 30°C de inkübasyona bırakıldıktan sonra inhibisyon çapları ölçüldü (Kirby-Bauer, 2009).

2.3. Sitotoksisite Testleri

2.3.1. A549 ve HT29 Hücre Hattı Çoğaltımı : A549 hücre hattının % 10 FBS (Pan Biotech P30-1301) içeren RPMI1640 içerisinde 25T Flaskta günde 2 defa kontrol edilerek % 70 ve üzerinde konfluensiye gelmesi beklendi. (Doubling Time: 20-24 saat) (A549 Hücre hattı ATCC CCL-185 kökenlidir)

HT29 hücre hattının % 10 FBS (Pan Biotech P30-1301) içeren DMEM-High Glucose içerisinde 25T Flaskta günde 2 defa kontrol edilerek % 70 ve üzerinde konfluensiye gelmesi beklendi. (Doubling Time: 40-60 saat) (HT29 Hücre hattı DSMZ ACC 299 kökenlidir).

2.3.2. Pozitif, Negatif ve Blank Kuyucukların Hazırlanması: Pozitif kontrol test kuyucuğu hücresel ölümün gösterildiği test kuyucuğu olup hücre içeren kuyucuklara materyal uygulanması ile aynı zamanda %2 H_2O_2 eklenerek yapıldı. Negatif Kontrol %100 hücresel büyümenin olduğu kuyucuk olup herhangi bir madde uygulanması yapılmadı.

2.3.3. Numunelerin Hazırlanması: Nanopartiküller 1 mg / mL konsantrasyonda hazırlandı. 30 dakika UV ışığına maruz bırakıldıktan sonra, en yüksek güçte ultrasonik banyoda 30 dakika bekletilerek homojenizasyon sağlandı. Bu işlem sonrasında kullanılacak konsantrasyonlar tam besiyeri ile seyreltilerek kullanıldı.

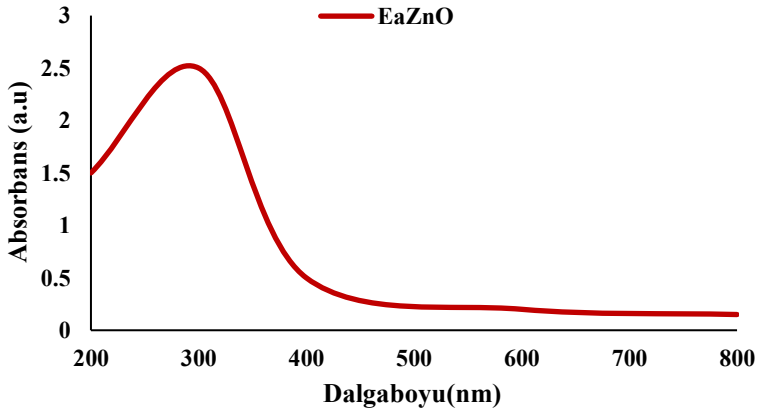
2.3.4. Hücrelerin 96 Kuyucuklu Kaplara Ekilmesi: 25T flask içerisinde %70 ve üzerinde konfluensiye ulaşan hücrelere 500 µL Tripsin-EDTA (Gibco, 15400054) eklendi ve 37°C'de %5 CO2 ortamında 3-5 dakika bekletildi. İnverted mikroskop (Zeiss Primovert, Almanya) altında hücrelerin dissosiye oldukları gözlemlendiği anda %10 FBS içeren besiyeri eklenir. 300xg'de 5 dakika santrifüj edilip besiyeri atıldı ve üzerine 1 mL DMEM-High Glucose besiyeri eklendi. Trypan mavisi (Gibco, 1525061) kullanılarak Logos Luna II cihazında sayım yapıldı. Kuyucuk başına 10^4 hücre gelecek şekilde %10 FBS'li besiyeri eklendi.

2.3.5. Sitotoksite Testinin Uygulanması: Her kuyucukta % 70 konfluensi yakalandığında kültür kabındaki besiyeri çekildi. Taze besiyeri eklendikten sonra numuneler hücre kabına eklendi. Her grup en az 3 tekrar kuyucuğu şeklinde yapılarak tekrarlı analiz yapıldı. Materyal uygulaması yapıldıktan sonra 22 saat hücreler inkübatörden hiç çıkarılmadan beklendi. 22 saat sonunda kuyucuk hacminin % 10'u kadar WST-1 solusyonu eklendi. Hücre kültür kabı alüminyum folyo ile sarılarak 2 saat daha inkübatörde bekletildi. 2 saat sonunda hücre kültür kabında 450 nm ve 630 nm dalga boylarında okuma yapılarak çıkan sonuçlardan % canlılık hesaplandı.

3. SONUÇLAR VE TARTIŞMA

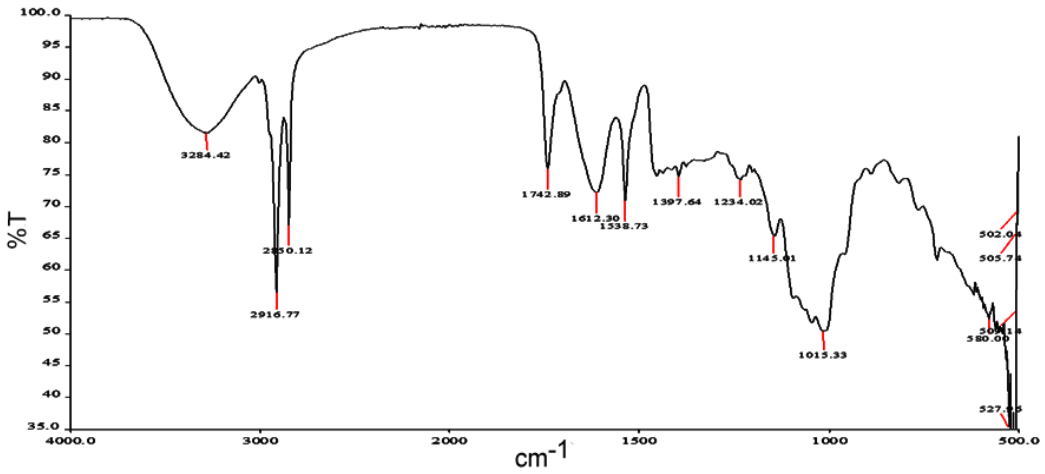
3.1. Nanopartiküllerin Karekterizasyonu

EaZnO nin UV-VIS Spektrofotometrede 200 - 800 nm aralığındaki analiz sonucu Şekil 1'de verilmiştir.



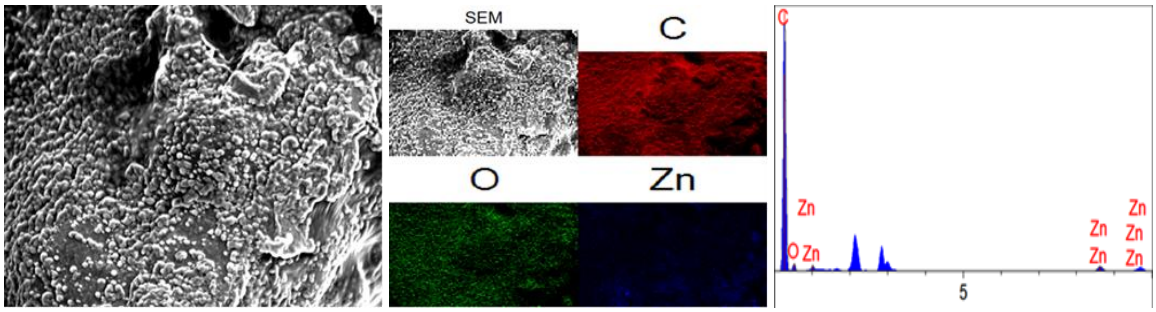
Şekil 1. EaZnO nanopartiküllerinin UV-VIS spektrofotometre analiz sonucu

Şekil 1'de görüldüğü gibi EaZnO literatürle uyumlu olarak 300 nm'de maksimum pik vermiştir. EaZnO'nun FTIR analiz sonuçları Şekil 2'de verilmiştir (Manojkumar, U. vd.,2023).



Şekil 2. EaZnO nanopartiküllerinin FTIR sonuçları

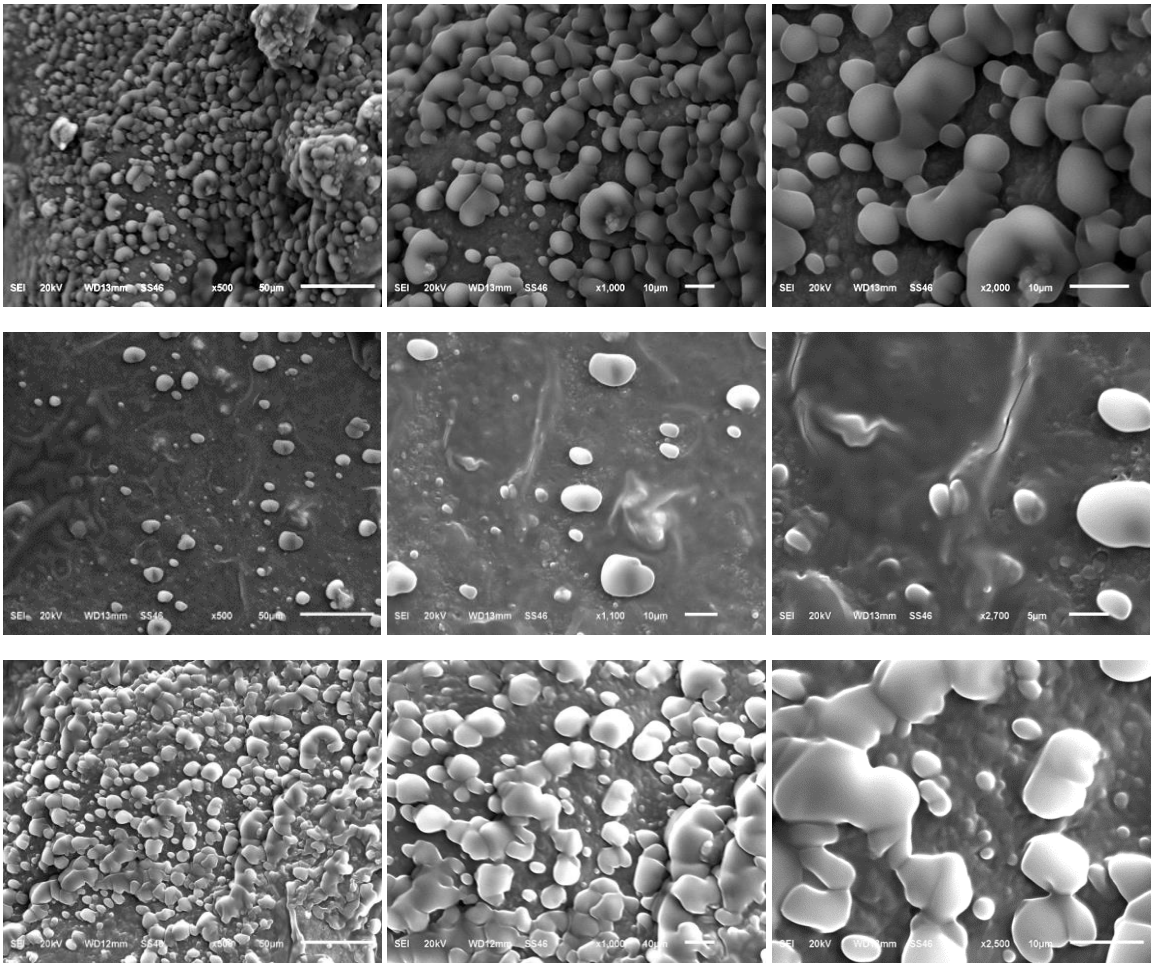
EaZnO nanopartikülleri iğde meyvesinin yapısında bulunan çok sayıda bileşik ile stabilize edilmiştir. EaZnO nanopartiküllerinin EDX sonuçları Şekil 3'te sunulmuştur.



Elt.	Line	Intensity (c/s)	Error 2-sig	Conc	Units
C	Ka	1,621.55	3.699	53.287	wt.%
O	Ka	48.36	0.821	30.910	wt.%
Zn	Ka	68.10	0.998	15.803	wt.%
			Total	100.000	wt.%

Şekil 3. EaZnO nanopartiküllerinin SEM map, EDX sonuçları

EaZnO nanopartiküllerinin sentezinin gerçekleştiği EDX spektrumundan da görülebilmektedir. EaZnO nanopartiküllerinin SEM görüntüleri Şekil 4'te verilmiştir.



Şekil 4. EaZnO nanopartiküllerinin SEM görüntüleri

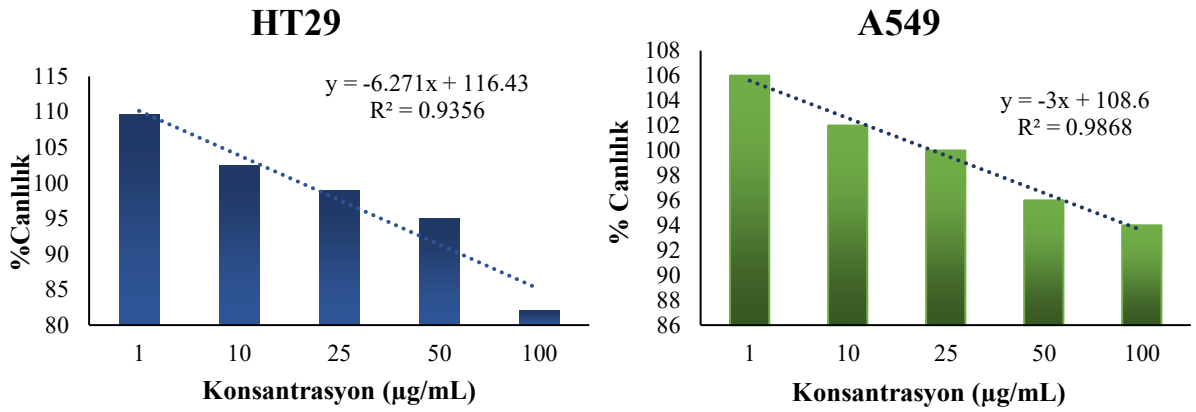
SEM görüntülerine göre EaZnO nanopartiküllerinin küçük kabarcıklar ve küreler şeklinde oluştuğu belirlenmiştir. EaZnO nanopartiküllerinin antimikrobiyal analiz sonuçları Tablo 1'de sunulmuştur.

Tablo 1. Antimikrobiyal Analiz sonuçları (inhibisyon bölgesi çapları (mm))

Mikroorganizmalar	Eritromisin (15µg/mL)	EaZnO (40mg/mL)
P. aeruginosa	8.0	8.0
K. pneumoniae	10.0	8.0
E. coli	14.0	
S. aureus	19.5	

EaZnO nanopartikülleri sadece *P. aeruginosa* ve *K. pneumoniae* üzerinde etkinlik göstermiştir. Antimikrobiyal analizlerde Eritromisin antibiyotiği pozitif kontrol olarak kullanılmıştır. EaZnO nanopartikülleri *P. aeruginosa* üzerinde eritromisin kadar etkinlik sergilerken *K. pneumoniae* üzerinde eritromisinden daha düşük bir inhibisyon etkinliği göstermiştir.

Hücre kültürü ve sitotoksisite analiz sonuçlarında EaZnO'nun IC_{50} değerleri A549 hücreleri için 484 µg/mL, HT 29 hücreleri için 225 µg/mLolarak tespit edilmiştir. EaZnO nanopartikülleri A549 ve HT29 hücrelerine uygulandıktan sonra hücrelerin göstermiş olduğu doza bağlı canlılık grafiği Şekil 5'te sunulmuştur.



Şekil 5. Doza bağlı % canlılık grafiği

Doza bağlı olarak hücrelerin canlılığı azalmıştır. EaZnO nanopartikülleri HT29 hücre hattı üzerinde A549 hücrelerine nazaran daha fazla sitotoksik etki sergilemiştir.

Sentezlenen nanopartiküller *P. aeruginosa* ve *K. pneumoniae* baklerileri üzerindeki etkinliğinin yanı sıra kanser hücreleri üzerinde gösterdiği sitotoksik etkiyle tamamlayıcı olarak kullanılmaya aday ajanlardır. Bu özellikleri ile özellikle gıda endüstrisi, kozmetik ve tıbbi uygulamalar için önemli potansiyel taşımaktadır.

References

1- Shafroth, P. B., Auble, G. T., Scott, M. L., (1995). Germination and establishment of the native plains cottonwood (*Populus deltoides* Marshall subsp. monilifera) and the exotic Russian-olive (*Elaeagnus angustifolia* L.). Conserv. Biol. 9 (5), 1169–1175. doi: 10.1046/j.1523-1739.1995.9051159.x-i1

2- Pan, C., Zhao, H., Zhao, X., Liu, J., Liu, L., Hou, Y., Zhang, L., (2011). Pollination ecology and breeding system of *Elaeagnus angustifolia*. International Conference on Multimed Technol. 4507–4509. doi: 10.1109/ICMT.2011.6003345

3- Khamzina, A., Lamers, J. P. A., Vlek, P. L. G., 2009. Nitrogen fixation by *Elaeagnus angustifolia* in the reclamation of degraded croplands of Central Asia. Tree Physiol. 29(6), 799–808. doi: 10.1093/treephys/tpp017

4- Guo, J., Wang, B., (2021). Blocked pollen release prevents fruit formation in the halophyte *Elaeagnus angustifolia* in non-saline habitats. Environmental and Experimental Botany, 189, 104566. https://doi.org/10.1016/j.envexpbot.2021.104566

5- Ayaz, F. A., Bertoft, E., (2001). Sugar and phenolic acid composition of stored commercial oleaster fruits. J. Food Comp. Anal. 14, 505–511. https://doi.org/10.1006/jfca.2001.1004

6- Okmen, G., Turkcan, O., (2013). A study on antimicrobial, antioxidant and antimutagenic activities of *Elaeagnus angustifolia* L. leaves. Afr. J. Tradit. Complement. Altern. Med. 11, 116–120. doi: 10.4314/ajtcam.v11i1.17

7- Hamidpour, R., Hamidpour, S., Hamidpour, M., Shahlari, M., Sohraby, M., Shahlari, N., Hamidpour, R., (2017). Russian olive (*Elaeagnus angustifolia* L.): From a variety of traditional medicinal applications to its novel roles as active antioxidant, anti-infl ammatory, anti-mutagenic and analgesic agent. J. Tradit Complement. Med. 7 (1), 24–29. doi: 10.1016/j.jtcme.2015.09.004

8- Hassanzadeh, Z., Hassanpour, H., (2018). Evaluation of physicochemical characteristics and antioxidant properties of *Elaeagnus angustifolia* L Scientia Horticulturae, 238, 83–90. https://doi.org/10.1016/j.scienta.2018.04.041

9- Günay, K., Leblebici, Z., & Koca, F. D. (2021). Çinko Nanopartiküllerinin (ZnO NP) Biyosentezi, Karakterizasyonu ve Anti- Bakteriyel Etkisinin İncelenmesi. Nevşehir Bilim ve Teknoloji Dergisi, 10(1), 56-66. https://doi.org/10.17100/nevbiltek.917256.

10- Singh, A., Singh, N. B., Afzal, S., Singh, T., & Hussain, I. (2017). Zinc oxide nanoparticles: a review of their biological synthesis, antimicrobial activity, uptake, translocation and biotransformation in plants. Journal of Materials Science, 53(1), 185-201. https://doi.org/10.1007/s10853-017-1544-1
11- Koçak, Y., & Meydan, İ. (2023). Assessment of the Bioactivity of Zinc Nanoparticles Synthesized Using *Erica arborea* Plant. Journal of Anatolian Environmental and Animal Sciences, 8(3), 361-366. https://doi.org/10.35229/jaes.1301513
12- Hameed, H., Waheed, A., Sharif, M. S., Saleem, M., Afreen, A., Tariq, M., Kamal, A., Al-onazi, W. A., Farraj, D. A. A., Ahmad, S., & Mahmoud, R. M. (2023). Green Synthesis of Zinc Oxide (ZnO) Nanoparticles from Green Algae and Their Assessment in Various Biological Applications. In Micromachines 14(5), 928. https://doi.org/10.3390/mi14050928
13- Zakharova, O. V., Kolesnikov, E., Vishnyakova, E., Strekalova, N., & Gusev, A. (2019). Antibacterial activity of ZnO nanoparticles: dependence on particle size, dispersion media and storage time. In IOP Conference Series Earth and Environmental Science, 226, 12062. https://doi.org/10.1088/1755-1315/226/1/012062
14- Vinardell, M. P., & Mitjans, M. (2015). Antitumor Activities of Metal Oxide Nanoparticles. Nanomaterials, 5(2), 1004-1021. https://doi.org/10.3390/nano5021004
15- Premanathan, M., Krishnamoorthy, K., Jeyasubramanian, K., & Manivannan, G. (2010). Selective toxicity of ZnO nanoparticles toward Gram-positive bacteria and cancer cells by apoptosis through lipid peroxidation. In Nanomedicine Nanotechnology Biology and Medicine 7(2), 184. https://doi.org/10.1016/j.nano.2010.10.001
16- Kirby-Bauer Disk Diffusion Susceptibility Test Protocol, (2009). American Society for Microbiology © 2016
17- Manojkumar, U., Kaliannan, D., Venkatesan, S., Balasubramanian, B., Kamyab, H., Mussa, Z., Jayanthi, P., Mesbah, M., Chelliapan, S., & Palaninaicker, S. (2023). Green synthesis of zinc oxide nanoparticles using *Brassica oleracea* var. botrytis leaf extract: Photocatalytic, antimicrobial and larvicidal activity. Chemosphere, 138263. https://doi.org/10.1016/j.chemosphere.2023.138263.

ORAL PRESENTATION

Evaluation of the effect of postbiotics on common food pathogens

Gülçin Alp Avcı[1*] (*Orcid: https://orcid.org/0000-0003-4049-0756*),
Emre Avcı[2] (*Orcid:https://orcid.org/0000-0003-1046-8208)*

[*1]University of Health Sciences, Gulhane Faculty of Dentistry, Department of Basic Medical Sciences, Ankara, Türkiye

[2]University of Health Sciences, Gulhane Faculty of Pharmacy, Department of Biochemistry, Ankara, Türkiye

*Corresponding author e-mail:alp.gulcin@yahoo.com

Abstract

This study aimed to evaluate the antimicrobial effects of postbiotics derived from *Lactobacillus reuteri* ENA31 and *Lactobacillus rhamnosus* GAA6 against common foodborne pathogens. Postbiotics were obtained by culturing the probiotic strains in MRS broth, followed by centrifugation and membrane filtration of the supernatants. Antimicrobial activity was assessed using the disk diffusion method against *Salmonella typhi* ATCC 19430, *Staphylococcus aureus* ATCC 25923, and *Bacillus cereus* ATCC 11778. The results revealed that postbiotics from *L. reuteri* ENA31 exhibited significant inhibitory activity against *S. typhi*, while those from *L. rhamnosus* GAA6 demonstrated strong antimicrobial effects against *S. aureus* and *B. cereus*. These findings suggest that postbiotics may serve as promising bioprotective agents for controlling foodborne pathogens and enhancing food safety.

Keywords: Postbiotics; Probiotics; Antimicrobial activity; *Lactobacillus reuteri*; *Lactobacillus rhamnosus*; Food safety.

INTRODUCTION

Postbiotics are metabolites released by probiotic microorganisms during fermentation and are described in the literature as inactivated microbial cell components (1). These substances may consist of a mixture of bioactive end-products released into the culture medium, including secreted proteins, short-chain fatty acids, organic acids, peptides, vitamins, enzymes, biosurfactants, and amino acids (2). Although the mechanisms of action of postbiotics are not yet fully understood, studies have demonstrated that they can modulate the host's immune response.

Postbiotics have gained attention due to their potential to alter enzyme structure and activity, disrupt the electron transport chain, damage pathogen cell membranes, inhibit macromolecule synthesis, and reduce pH, thereby creating unfavorable conditions for the survival of pathogenic microorganisms (3,4). Owing to these advantages, research on the use of postbiotics against foodborne pathogens has intensified (5). Furthermore, many in vitro and in vivo studies indicate that postbiotics exhibit antimicrobial activity against various pathogenic organisms.

In recent years, the increasing incidence of foodborne illnesses in our country has highlighted the need to explore this topic further. Therefore, the aim of this study was to evaluate the effects of postbiotics on commonly encountered foodborne pathogens.

MATERIALS AND METHODS

Materials

In this study, postbiotics obtained from *Lactobacillus reuteri* ENA31 and *Lactobacillus rhamnosus* GAA6 strains were used. As foodborne pathogens, *Salmonella typhi* ATCC 19430—commonly found in eggs, poultry, and nuts; *Staphylococcus aureus* ATCC 25923—frequently present in meat and sandwiches; and *Bacillus cereus* ATCC 11778—often detected in rice, sauces, and foods stored at room temperature—were selected.

Postbiotic Preparation

L. reuteri ENA31 and *L. rhamnosus* GAA6 strains were activated in Man Rogosa Sharp (MRS) broth at 37°C for 16–18 hours. Following incubation, cultures were centrifuged at 14,000 g for 15 minutes. The resulting supernatants were collected and filtered through 0.45 µm membrane filters to obtain sterile postbiotic preparations.

Pathogen Cultivation

Specific broths were used for the growth of each pathogen:
Tryptic Soy Broth for *S. typhi*
Brain Heart Infusion Broth for *S. aureus*
Nutrient Broth for *B. cereus*

Antimicrobial Activity Assessment

The antimicrobial activity of the postbiotics was evaluated using the disk diffusion method on Mueller-Hinton Agar (MHA). Inhibition zones were measured in millimeters (mm±sd).

RESULTS

Postbiotics derived from *L. reuteri* ENA31 exhibited significant antimicrobial activity against *S. typhi*. In contrast, postbiotics obtained from *L. rhamnosus* GAA6 demonstrated strong inhibitory effects on *S. aureus* and *B. cereus*. The results are presented in Table 1.

Table 1. Inhibition Zones (mm)

	S.typhi ATCC 19430	*S.aureus* ATCC 25923	*B.cereus* ATCC 11778
L.reuteri ENA31 postbiyotiği	18.5±1.5	16.0±1.5	11.0±2.0
L.rhamnosus GAA6 postbiyotiği	12.0±1.0	23.7±1.3	24.0±1.5

DISCUSSION

Postbiotics produced by lactic acid bacteria, particularly probiotics, are known to contain substantial amounts of organic acids (6). These acids—including lactic acid, acetic acid, CO_2, diacetyl, and ethanol—create unfavorable growth conditions for pathogens (6,7). Postbiotic preparations also contain high concentrations of bacteriocins, peptides, and proteins, which contribute to their stability under heat and variable pH conditions. Several studies support that these molecules are responsible for the antimicrobial activities of postbiotics (2,8).

In the present study, postbiotics derived from *L. reuteri* ENA31 exhibited notable inhibitory activity against *S. typhi*, whereas postbiotics from *L. rhamnosus* GAA6 were highly effective against *S. aureus* and *B. cereus*. The number of studies examining the effects of postbiotics on foodborne pathogens is limited. In a previous study, postbiotics obtained from *L. plantarum* strains showed minimal antimicrobial activity against *E. coli* O157:H7, *S. enteritidis*, and *S. aureus* (9).

The findings of this study suggest that postbiotics derived from selective probiotic strains may serve as effective agents in controlling pathogenic microorganisms in foods. Considering their known contribution to extending shelf life, postbiotics hold promise as important bioprotective components in combating foodborne pathogens. Moreover, future studies focusing on the combined use of organic acids with other antimicrobial components present in postbiotics may provide valuable strategies for preventing foodborne intoxication.

REFERENCES

Arena, M. P., Silvain, A., Normanno, G., Grieco, F., Drider, D., Spano, G., & Fiocco, D. (2016). Use of *Lactobacillus plantarum* strains as a bio-control strategy against food-borne pathogenic microorganisms. *Frontiers in Microbiology, 7*, 464. https://doi.org/10.3389/fmicb.2016.00464

Babu, A. S., Guruprasath, N., Adeyeye, S. A. O., Sankarganesh, P., Kumar, A. G., & Sivapriya, T. (2023). A critical analysis of postbiotics: Exploring their potential impact on the health and food industries. *Journal of Pure and Applied Microbiology, 17*(4), 2041–2059. https://doi.org/10.22207/JPAM.17.4.18

Du, W., Di Martino, L., & Li, J. (2024). Natural polysaccharides-based postbiotics and their potential applications. *Exploration of Medicine, 5*, 444–458. https://doi.org/10.37349/emed.2024.00230

Hijová, E. (2024). Postbiotics as metabolites and their biotherapeutic potential. *International Journal of Molecular Sciences, 25*(10), 5441. https://doi.org/10.3390/ijms25105441

Ibrahim, S. A., Ayivi, R. D., Zimmerman, T., Siddiqui, S. A., Altemimi, A. B., Fidan, H., Esatbeyoglu, T., & Bakhshayesh, R. V. (2021). Lactic acid bacteria as antimicrobial agents: Food safety and microbial food spoilage prevention. *Foods, 10*(12), 3131.

Isaac-Bamgboye, F. J., Mgbechidinma, C. L., Onyeaka, H., Isaac-Bamgboye, I. T., & Chukwugozie, D. C. (2024). Exploring the potential of postbiotics for food safety and human health improvement. *Journal of Nutrition and Metabolism, 2024*, 1868161. https://doi.org/10.1155/2024/1868161

Mishra, B., Mishra, A. K., Mohanta, Y. K., & colleagues. (2024). Postbiotics: The new horizons of microbial functional bioactive compounds in food preservation and security. *Food Production, Processing and Nutrition, 6*, 28. https://doi.org/10.1186/s43014-023-00200-w

Moradi, M., Kousheh, S. A., Almasi, H., Alizadeh, A., Guimarães, J. T., Yılmaz, N., & Lotfi, A. (2020). Postbiotics produced by lactic acid bacteria: The next frontier in food safety. *Comprehensive Reviews in Food Science and Food Safety, 19*(6), 3390–3415. https://doi.org/10.1111/1541-4337.12613

Pramanik, P. (2023). Anti-microbial and anticarcinogenic activity of postbiotics: A review. *Sayam*. https://doi.org/10.1002/pro.3714

ORAL PRESENTATION

Türkiye'de yetişen *Salvia* taksonlarına ve halk tıbbında kullanımına genel bir bakış

Hatice Tosyagülü Çelik[1-2*] (*Orcid: https://orcid.org/0000-0003-2739-7047*), Sibel Kaymak[3] (*Orcid: https://orcid.org/0000-0002-6523-7637*), Nilüfer Vural[3-4](*Orcid: https://orcid.org/0000-0003-3047-3004*)

[*1]Ankara Yıldırım Beyazıt Üniversitesi, Sağlık Hizmetleri MYO, Bitkisel ve HAyvansal Üretim Bölümü, Ankara, Türkiye.
[2] Ankara Yıldırım Beyazıt Üniversitesi, Geleneksel ve Tamamlayıcı Tıp Uygulama ve Araştırma Merkezi, Ankara, Türkiye.
[3] Ankara Yıldırım Beyazıt Üniversitesi, Halk Sağlığı Enstitüsü, Biyoterapötik Ürünler Araştırma ve Geliştirme Programı, Ankara, Türkiye.
[4] Ankara Yıldırım Beyazıt Üniversitesi, Sağlık Hizmetleri MYO, Gıda İşleme Bölümü, Ankara, Türkiye.

*Sorumlu yazar e-mail: htosyagulu@aybu.edu.tr

Özet

Son zamanlarda yapılan çalışmalarda, özellikle *Salvia* türlerinin potansiyel biyolojik aktivitelerine odaklanıldığı görülmektedir. Antioksidan, antimikrobiyal, antidiabetik, antikanser ve nöroprotektif özelliklerin yanında, bu türlerin fitoterapi, fonksiyonel gıda ve ilaç bitkisi olarak ilgi çekici hâle geldiği belirtilmektedir. *Salvia* türlerinin çok geniş ekolojik aralıklarda, farklı iklim, yükselti, toprak ve substrat koşullarında bulunması, bu taksonlar üzerine daha ayrıntılı çalışmalara ihtiyaç olduğunu göstermektedir. Özellikle endemik türlerin ekolojik nişleri, adaptasyon mekanizmaları ve iklim değişikliği ile habitat bozunumu gibi değişimleri tolere etme durumları üzerine yapılan araştırmaların yetersiz olduğu anlaşılmaktadır. Son yıllarda yeni tür tayinlerinin devam ediyor olması, *Salvia* cinsinin aktif bir taksonomik çalışma alanı olduğunu göstermektedir. Bazı türlerin uçucu yağ kompozisyonu ve biyolojik aktiviteleri incelenmeye başlanmış olsa da, Türkiye'deki çeşitliliğin ancak küçük bir kısmının değerlendirildiği anlaşılmaktadır. Nadir, dar yayılışlı ve endemik türler üzerine daha fazla araştırma yapılması gerekliliği ortaya çıkmaktadır. Sonuç olarak, Türkiye'de *Salvia* türleri tıbbi ve kültürel açıdan önemli olup, yüksek endemizm, geniş ekolojik çeşitlilik, etnobotanik kullanım ve farmakolojik potansiyel ile dikkat çekmektedir.

Anahtar Kelimeler: *Salvia*, endemizm, etnobotanik kullanım, geleneksel tıp

An overview of *Salvia* taxa in Turkey and their use in traditional medicine

Abnstract

Recent studies indicate that research has increasingly focused on the potential biological activities of *Salvia* species. In addition to antioxidant, antimicrobial, antidiabetic, anticancer, and neuroprotective properties, these species have become attractive as phytotherapeutic agents, functional foods, and medicinal plants. The presence of *Salvia* species across a wide ecological range—different climate, altitude, soil, and substrate conditions—demonstrates the need for more detailed studies on these taxa. Research on the ecological niches of endemic species, their adaptation mechanisms, and their ability to tolerate changes such as climate change and habitat degradation remains insufficient. The continued description of new species in recent years shows that the genus *Salvia* represents an active area of taxonomic research. Although the essential oil composition and biological activities of some species have begun to be examined, only a small portion of the diversity present in Türkiye has been evaluated. Consequently, there is a growing need for further studies on rare, narrowly distributed, and endemic species. In conclusion, *Salvia* species in Türkiye are of great medicinal and cultural importance and stand out due to their high endemism, wide ecological diversity, ethnobotanical uses, and pharmacological potential.

Keywords: *Salvia*, *Salvia*, endemism, ethnobotanical use, traditional medicine

GİRİŞ

Angiospermler arasında altıncı en büyük familya olan Lamiaceae (Ballıbabagiller), hem beslenme hem de hastalık tedavisi için kullanılan çok sayıda tıbbi ve aromatik bitki türü kapsayan kutup bölgeleri hariç, deniz seviyesinden yüksek dağlık bölgelere kadar çeşitli rakımlarda ve habitatlarda yetişen, dünya genelinde ekonomik ve tıbbi önemi olan çok sayıda türü kapsayan yaklaşık 230 – 250 cins ve 7000-8000'den fazla türden oluşan büyük bir familyadır (Zhao ve ark., 2021; Kılıç Mungan, 2022; Dirmenci, 2024; Çalış, 2025). Taksonomi üzerine yapılan son çalışmalar, Lamiaceae familyasını on iki alt familyaya ayırmıştır. Bunlar: Ajugoideae, Lamioideae, Nepetoideae, Prostantheroideae, Scutellarioideae, Symphorematoideae, Viticoideae, Cymarioideae, Peronematoideae, Premnoideae, Callicarpoideae ve Tectonoideae'dir (Zhao ve ark., 2021; Cole ve ark., 2021; Çalış, 2025). Özellikle son yıllarda gerçekleştirilen moleküler filogenetik çalışmalar ve morfolojik değerlendirmeler sonucu Türkiye'deki Lamiaceae türlerinin yedi klad tarafından temsil edildiği belirlenmiştir. Bunlar: *Zhumeria*, *Salvia*, *Sclarea*, *Glutinaria*, *Heterosphace*, *Dorystaechas* ve *Rosmarinus*'dur (Celep ve Doğan, 2023).

Bitki familyaları arasında tıbbi kullanım açısından en önemli familyalardan biri olan Lamiaceae familyasının taksonları, güçlü aromatik bitkilerden oluşur. Bu bitkilerin farklı organları (yapraklar, rizomlar, gövdeler) gıda amaçlı, boya ekstraksiyonu, çeşitli hastalıkların tedavisi (sinir, dolaşım, solunum, üreme sistemleri), böcek kovucu, süs amaçlı, gıda katkı maddesi ve koruyucu olarak uçucu yağlar, parfüm ve kozmetik endüstrisinde kullanılmaktadır ve bu nedenle geniş bir uygulama alanına sahiptir. İnsanlık tarihi boyunca bu amaçlarla kullanıldıklarına dair kanıtlar arkeolojik kazılarda ve eski yazıtlarda bulunmuştur (Celep ve Doğan, 2023; Ghoran ve ark., 2023; Dirmenci, 2024).

Son zamanlarda yapılan çalışmalar, Lamiaceae familyasının birçok üyesinin yüksek düzeyde antioksidan, antikolinesteraz, antifungal, antimikrobiyal ve diğer etkilere sahip olduğunu da ortaya koymuştur (Yumrutas ve ark., 2023). Bu çalışmalardan elde edilen sonuçlar da Lamiaceae türlerinin, bitki kimyası, bitki taksonomisi ve doğal kaynaklardan yeni ilaç adayı molekül araştırmaları, etnofarmakolojik ve etnobotanik çalışmalar gibi farklı alanlarda planlanan bilimsel araştırmalar için her açıdan zengin çeşitliliğe sahip kaynaklar olduğunu kanıtlamaktadır.

Küresel olarak Lamiaceae familyasında en fazla tür sayısına sahip cinsler arasında *Salvia* yaklaşık 1.000 türle başı çekmekte, onu *Scutellaria* (480 tür), *Stachys* (370 tür), *Nepeta* (300 tür), *Teucrium* (300 tür), *Thymus* (270 tür) ve *Vitex* (210 tür) izlemektedir. Türkiye'de Lamiaceae, 45 cins ve 614 tür (yaklaşık 800 takson) ile temsil edilmektedir. Türkiye'de en fazla tür sayısına sahip cinsler arasında *Salvia*, *Stachys*, *Sideritis*, *Thymus*, *Nepeta* ve *Teucrium* bulunmaktadır.

MATERYAL METOD

Bu çalışma, Türkiye florasında yer alan *Salvia* türleri ve halk tıbbında kullanımını kapsamlı bir şekilde değerlendirmek amacıyla literatür taraması yöntemiyle hazırlanmıştır. Çalışmada hem ulusal hem de uluslararası akademik kaynaklar taranmıştır. Toplanan veriler, türlerin taksonomik çeşitliliği, ekolojik dağılımı ve etnobotanik kullanım özellikleri açısından sınıflandırılmış ve yorumlanmıştır. Bu yöntem sayesinde, Türkiye'de yetişen *Salvia* türlerinin hem biyolojik çeşitlilik hem de geleneksel kullanım açısından güncel bir değerlendirmesi sunulmuştur.

BULGULAR

Salvia'nın Dünya ve Türkiye'deki Durumu

Genellikle adaçayı olarak bilinen *Salvia* L. cinsi, dünya çapında şu ana kadar kabul edilen 1000'den fazla tür ile çiçekli bitkiler arasında tür açısından en zengin cinslerden biridir. Başlıca çeşitlilik merkezleri Akdeniz bölgesi, Güneybatı Asya, Meksika ve Orta/Güney Amerika ile Doğu Asya'dır. Amerika, Akdeniz, Orta Doğu, Pasifik Adaları ve tropikal Afrika'da yetişen *Salvia*'nın Meksika'da yaklaşık 3000 türü kaydedilmiştir. Bu nedenle Meksika, *Salvia* cinsi açısından en büyük çeşitliliğe sahip ülke olarak kabul edilir. Meksika'dan sonra Türkiye, 1000'den fazla türü ile *Salvia* bitkilerinin çeşitliliğinin yüksek olduğu ikinci sıradaki ülke olarak karşımıza çıkar. Türkiye'yi Çin (yaklaşık 840) ve İran (yaklaşık 620) izlemektedir. *Salvia* türleri çoğunlukla çalımsı ve aromatik çok yıllık bitkilerdir. Farklı boya, farklı çiçek tipi ve renge sahiptirler.

Türkiye florası'nda *Salvia* cinsine ait 97 tür, 4 alttür ve 8 varyete bulunmaktadır. Bu türlerden 51 tanesinin endemik olduğu ve 58 tanesinin İran-Turan, 27 tanesinin Akdeniz, 5 tanesinin Avrupa-Sibirya fitocoğrafik bölgesine, diğer kalan 7 tanesinin de birden fazla fitocoğrafik bölgede yayılış gösterdiği belirtilmiştir (İpek ve Gürbüz, 2010).

Ancak Türkiye Florası 7. Cildin yayınlanmasının ardından geçen özellikle son 20 yıllık sürede bir dizi yeni takson, yeni kayıt ve taksonomik değişiklik yayınlanmıştır. Moleküler filogenetik sonuçlar ve morfolojik incelemelerin

sonucu doğrultusunda Türkiye'de *Salvia* cinsine ait 116 takson bulunduğu tespit edilmiş olup bunların 64'ünün endemik olduğu belirlenmiştir. Bu da %55'lik bir endemiz oranına işaret etmektedir. 116 taksonun, 58 tanesi İran-Turan elementi, 31'inin Akdeniz elementi, 6'sının Avrupa-Sibirya elementi ve 21 tanesinin de çoklu bölgeli element olduğu tespit edilmiştir (Güner ve ark., 2012; Eminagaoglu ve ark., 2022; Celep ve Doğan, 2023; İlçim ve ark., 2023).

Tablo 1. Türkiye'de yetişen Salvia taksonları (* endemik)

Takson	Yerel isim	Element	Takson	Yerel isim	Hayat Formu
**Salvia absconditiflora* (Montbret & Aucher ex Benth.) Greuter & Burdet	kara şalba	Ir-Tur	**Salvia heldreichiana* Boiss. ex Benth.	ayaklı şalba	Akd
**Salvia adenocaulon* P.H.Davis	Kızlar yülmesi	Akd	**Salvia huberi* Hedge	meryemiye	Ir-Tur
**Salvia adenophylla* Hedge & Hub.-Mor.	poruk	Akd	*Salvia hydrangea* DC. ex Benth.	koç şalba	Ir-Tur
Salvia aethiopis L.	habeş adaçayı	Çok.Böl.	**Salvia hypargeia* Fisch. & C.A.Mey.	siyahot	Çok.Böl.
**Salvia albimaculata* Hedge & Hub.-Mor.	hoşdudak	Akd	*Salvia indica* L.	sultan şalba	Çok.Böl.
Salvia amplexicaulis Lam.	ekin şalbası	Av-Sib	**Salvia kronenburgii* Rech.f.	van şalbası	Ir-Tur
**Salvia anatolica* Hamzaoğlu & A.Duran	ana şalba	Ir-Tur	*Salvia kurdica* Boiss. & Hohen. ex Benth.	kürt şalbası	Ir-Tur
Salvia aramiensis Rech.f.	pohur	Akd.	*Salvia limbata* C.A.Mey.	maldili	Ir-Tur
Salvia argentea L.	gümüş şalba	Çok.Böl.	**Salvia longipedicellata* Hedge	duvaklı şalba	Ir-Tur
Salvia aristata Aucher ex Benth.	bayır şalbası	Ir-Tur	*Salvia macrochlamys* Boiss. & Kotschy	gevrek şalba	Ir-Tur
Salvia atropatana Bunge	çayır şalbası	Ir-Tur	*Salvia macrosiphon* Boiss.	çöl şalbası	Ir-Tur
**Salvia aucheri* subsp. *canescens* × *Salvia heldreichiana*	mavi şalba	Akd	**Salvia marashica* İlçim, Celep & Doğan	maraş adaçayı	Akd
**Salvia aucheri* subsp. *aucheri* Benth.	mavi şalba	Akd.	*Salvia microstegia* Boiss. & Balansa	yağlambaç	Çok.Böl.
**Salvia aucheri* subsp. *canescens* (Boiss. & Heldr.) Celep, Kahraman & Doğan	koramaz	Akd.	**Salvia modesta* Boiss.	yoksul şalba	Ir-Tur
**Salvia aytachii* Vural & Adıgüzel	ay şalbası	Ir-Tur	*Salvia montbretii* Benth.	kaba şalba	Ir-Tur
**Salvia ballsiana* (Rech.f.) Hedge	gerger şalbası	Ir-Tur	*Salvia multicaulis* Vahl	kürtreyhanı	Ir-Tur
**Salvia blepharochlaena* Hedge & Hub.-Mor.	hoş şalba	Ir-Tur	*Salvia napifolia* Jacq.	ters şalba	Akd
**Salvia adiyamanensis* İlçim & Tel		Ir-Tur	*Salvia nemorosa* L.	gehareş	Çok.Böl.
Salvia brachyantha subsp. *brachyantha* (Bordz.) Pobed	kazan şalbası	Ir-Tur	*Salvia nutans* L.	müsellim	Av-Sib

**Salvia brachyantha* subsp. *tankutiana* Bagherpour, Celep, Kahraman & Doğan	gönül şalbası	Ir-Tur	**Salvia nydeggeri* Hub.-Mor.	sarıelmacık	Akd
Salvia bracteata Banks & Sol.	çoban şalbası	Ir-Tur	**Salvia odontochalmys* Hedge	kulaklı şalba	Ir-Tur
**Salvia dorystaechas* B.T.Drew	Devren kekiği	Akd	*Salvia pachystachys* Trautv.	yedi şalba	Ir-Tur
**Salvia cadmica* var. *bozkiriensis* Celep, Kahraman & Doğan	Kaya şalbası	Ir-Tur	*Salvia palaestina* Benth.	sürmeli şalba	Ir-Tur
**Salvia cadmica* var. *cadmica* Boiss.	kaya şalbası	Ir-Tur	**Salvia pilifera* Montbret & Aucher ex Benth.	etekli şalba	Akd
**Salvia caespitosa* Montbret & Aucher ex Benth.	kırk şalba	Ir-Tur	*Salvia pinnata* L.	çanak şalbası	Akd
**Salvia cyanescens* × S. *vermifolia*		Ir-Tur	**Salvia pisidica* Boiss. & Heldr. ex Benth.	benli şalba	Akd
Salvia candidissima subsp. *candidissima* Vahl	galabor	Çok.Böl.	*Salvia poculata* Náb.	küllü şalba	Ir-Tur
Salvia candidissima subsp. *occidentalis* Hedge	ak galabor	Çok.Böl.	*Salvia pomifera* L.	acıelmaotu	Akd
Salvia cassia Samuelss. ex Rech.f.	kel şalba	Akd	**Salvia potentillifolia* Boiss. & Heldr. ex Benth.	sarıporuk	Akd
**Salvia cedronella* Boiss.	sarı şalba	Akd	**Salvia pseudeuphratica* Rech.f.	keban adaçayı	Ir-Tur
Salvia ceratophylla L.	tarak şalba	Çok.Böl.	**Salvia quezelii* Hedge & Afzal-Rafii	limon adaçayı	Akd
**Salvia cerino-pruinosa* Rech.f.	çıplak şalba	Ir-Tur	**Salvia recognita* Fisch. & C.A.Mey.	puslu şalba	Ir-Tur
**Salvia chionantha* Boiss.	kılıç şalba	Akd	**Salvia reeseana* Hedge & Hub.-Mor.	kır şalbası	Ir-Tur
**Salvia chrysophylla* Stapf	boz şalba	Akd	**Salvia rosifolia* Sm.	gülmeryemiye	Ir-Tur
**Salvia cilicica* Boiss. & Kotschy	narin galabor	Akd	*Salvia russellii* Benth.	kurdeşk	Çok.Böl.
**Salvia cyanescens* Boiss. & Balansa	mor galabor	Çok.Böl.	*Salvia sclarea* L.	paskulak	Çok.Böl.
**Salvia dichroantha* Stapf	kutnu	Çok.Böl.	*Salvia pratensis* L.	Çayır otu	Av-Sib
**Salvia divaricata* Montbret & Aucher ex Benth.	saplı şalba	Ir-Tur	**Salvia sericeotomentosa* var. *hatayica* Celep & Doğan	Nur şalbası	Akd
**Salvia divaricata* Montbret & Aucher ex Benth. subsp. *artvinense* Eminagaoglu, Ozcan & Akyıldırım		Ir-Tur	**Salvia sericeotomentosa* var. *sericeotomentosa* Rech.f.	nur şalbaşı	Akd
**Salvia ekimiana* Celep & Doğan	bey şalbası	Ir-Tur	**Salvia siirtica* Kahraman, Celep & Doğan	siirt adaçayı	İr-Tur

*_Salvia eriophora_ Boiss. & Kotschy	yünlü şalba	Ir-Tur	*_Salvia smyrnaea_ Boiss.	nif şalbası	Akd
*_Salvia ertekinii_ Yıld.	er şalba	Ir-Tur	_Salvia spinosa_ L.	yabani adaçayı	Ir-Tur
*_Salvia euphratica_ var. _euphratica_ Montbret & Aucher.	fırat şalbası	Ir-Tur	_Salvia staminea_ Montbret & Aucher ex Benth.	erkek şalba	Ir-Tur
*_Salvia euphratica_ var. _leiocalycina_ (Rech.f.) Hedge	Fırat şalbası	Ir-Tur	_Salvia suffruticosa_ Montbret & Aucher ex Benth.	kalın şalba	Ir-Tur
Salvia forskahlei L.	dolmayaprağı	Av-Sib	_Salvia syriaca_ L.	çevlikotu	Çok.Böl.
*_Salvia freyniana_ Bornm. ex Freyn	göl şalba	Ir-Tur	_Salvia rosmarinus_ Spenn.	biberiye	Akd
Salvia frigida Boiss.	sağır şalba	Çok.Böl.	_Salvia reuteriana_ Boiss.		Ir-Tur
Salvia fruticosa Mill.	adaçayı	Akd.	*_Salvia suffruticosa_ x _Salvia bracteata_		Ir-Tur
Salvia glutinosa L.	oklu şalba	Av-Sib	*_Salvia tchihatcheffii_ (Fisch. & C.A.Mey.) Boiss.	kekik şalbası	Ir-Tur
*_Salvia halophila_ Hedge	tuz şalbası	Ir-Tur	*_Salvia tigrina_ Hedge & Hub.-Mor.	musa adaçayı	Akd
Salvia hasankeyfensis		Ir-Tur	*_Salvia tobeyi_ Hedge	yayla şalbası	Av-Sib
*_Salvia haussknechtii_ Boiss.	öksüz şalba	Akd	_Salvia tomentosa_ Mill.	şalba	Çok.Böl.
*_Salvia hedgeana_ Dönmez	bodur şalba	Ir-Tur	_Salvia trichoclada_ Benth.	meşe şalbası	Ir-Tur
Salvia verticillata subsp. _amasiaca_ (Freyn & Bornm.) Bornm.	hart şalbası	Çok.Böl.	_Salvia verbenaca_ L.	elmakekiği	Çok.Böl.
Salvia verticillata subsp. _verticillata_ L.	dadırak	Çok.Böl.	*_Salvia vermifolia_ Hedge & Hub.-Mor.	ince şalba	Ir-Tur
Salvia virgata Jacq.	fatmanaotu	Çok.Böl.	_Salvia viscosa_ Jacq.	kızıllık	Akd
Salvia viridis L.	zarif şalba	Çok.Böl.	_Salvia xanthocheila_ Boiss. ex Benth.	dağ şalbası	Ir-Tur
*_Salvia wiedemannii_ Boiss.	sultantacı	Ir-Tur	*_Salvia yosgadensis_ Freyn & Bornm.	bozok şalbası	Ir-Tur

Ir-Tur: İran-Turan, Akd: Akdeniz, Av-Sib: Avrupa-Sibirya, Çok.Böl.: Çoklu bölge

Salvia'nın ülkemizde halk tıbbında kullanımı

Salvia'nın iyileştirici özellikleri, eski Mısır'da ve Anglosaksonlar, Yunanlılar ve Romalılar tarafından çok eski zamanlardan beri bilinmektedir (Eksi ve Yılmaz 2021, Yılmaz ve ark., 2023). Son yıllarda, *Salvia* ile ilgili, sayısız yeni taksonomik, mikromorfolojik, moleküler filogenetik, karyolojik, anatomik ve tozlaşma ekolojisi çalışması yayınlanmıştır. Özellikle *Salvia* türlerinin, parfümeri ve kozmetik endüstrisinde, süs bitkileri endüstrisinde, tıpta, bitkisel ilaçlarda ve gıda katkı maddelerinde çok çeşitli kullanım alanlarına sahip, yine antioksidan, antimikrobiyal, Alzheimer önleyici, kanser önleyici ve hatta böcek öldürücü özelliklere sahip ikincil metabolitler, özellikle de uçucu yağlar içerdiği pek çok çalışma ile gösterilmiştir (Pavlidou ve ark., 2004; Bahadırlı ve Ayanoğlu, 2020).

Salvia türleri, bazı kanserler, bronşit, ishal, astım, romatizma, soğuk algınlığı, grip, baş ağrısı, bazı kalp hastalıkları, hafıza güçlendirme, menopoz, kas ağrısı, gece terlemesi, farenjit, cilt enfeksiyonları, mide ağrısı, stomatit, boğaz ağrısı, diş ağrısı, tüberküloz ve yaraların tedavisinde kullanılmaktadır (Paksoy ve ark., 2016; Abak ve ark., 2018; Şenkal ve ark., 2019; Bakir ve ark., 2020; Selvi ve ark., 2022; Yılmaz ve ark., 2023). *Salvia* türleri, steroller, flavonoidler, seskiterpenoidler, sesterpenoidler, diterpenoidler, triterpenoidler, uçucu yağlar ve flavonoidler gibi çeşitli ikincil metabolitler içerir ve bu metabolitler antioksidan, antimikrobiyal, antialzheimer, antikanser, antidiyabetik, antitümör, antiplazmodiyal, antiinflamatuar, antinörodejeneratif, antienzimatik (antikolinesteraz, antiüreaz, antitirozinaz, antielastaz), antipiretik, analjezik, hepatotoksik, sitotoksik, insektisidal aktiviteler gibi

çeşitli biyolojik ve farmakolojik aktivitelere sahiptir (Abak ve ark., 2018; Karik ve ark., 2018; Tulukcu ve ark., 2019; Bakir ve ark., 2020; Eksi ve Yılmaz, 2021; Yılmaz ve ark., 2023).

Zengin geleneksel kültürü nedeniyle, ülkemizde *Salvia*'nın farklı kısımları sıklıkla kullanılmaktadır. Mesela, Türkiye'nin batı Akdeniz bölgesinde, *Salvia viridis*, *Salvia sclarea* ve *Salvia tomentosa* sürgünleri, çiçekleri ve yaprakları gibi toprak üstü kısımlarının infüzyonu, boğaz ağrısı, boğaz iltihabı, bronşit, astım, öksürük kesici, ülser, bağırsak spazmları, jinekolojik rahatsızlıklar ve solunum yolu hastalıklarının tedavisi için halk hekimliğinde yaygın olarak tüketilmektedir. Örneğin, *Salvia wiedemannii* Boiss. peptik ülserlerin tedavisi ve ağrının giderilmesi için; *Salvia cryptantha* Montbert & Aucher ex Benthan ve *Salvia triloba* L. mide semptomlarının tedavisi, yara dezenfektanı, öksürük ve soğuk algınlığı için; *Salvia tomentosa* ve *Salvia chrysophylla* Stapf karın ve romatizmal ağrıları hafifletmek ve dişleri güçlendirmek için; *Salvia aethiopis* ve *Salvia nemorosa* yara iyileşmesi ve kanama için, Karadeniz Bölgesi'nde, *Abies bornmülleriana* Mattf. reçinesinin *Salvia aethiopsis* L. kökü, sabun, balmumu ve tereyağı ile kaynatılarak hazırlanan merhemlerin yara iyileşmesi için kullanımı oldukça dikkat çekicidir (Günbatan ve ark., 2023).

Ege bölgesinde de *Salvia fruticosa* Miller gibi aromatik bir bitkinin ağırlıklı olarak halk ilacı olarak kullanıldığı ve hazırlanan halk ilaçlarının sıklıkla gastrointestinal, solunum sistemi ve dermatolojik hastalıkların tedavisinde kullanıldığı tespit edilmiştir (Honda ve ark, 1996; Kargıoğlu ve ark., 2010; Güler ve ark., 2020; Günbatan ve ark., 2023). *Salvia adenophylla* Hedge et Hub. ve *Salvia tomentosa* Miller türlerinin de karın ağrısı, mide ağrısı ve solunum yolu hastalıklarının tedavisinde kullanıldığı tespit edilmiştir (Bulut ve Tuzlacı, 2015).

Marmara Bölgesinde'de *Salvia* türlerinin karın ağrısı, mide ağrısı ve solunum yolu hastalıklarının tedavisinde sıklıkla kullanıldığı tespit edilmiştir (Uzun ve ark., 2004; Koçyiğit ve Özhatay, 2006; Yeşilyurt ve ark., 2017; Günbatan ve ark., 2023).

Özellikle son zamanlarda diabetes mellitus tedavisi için de pek çok bitkinin kullanıldığı tespiti yapılmıştır. Ülkemizde de diabetes mellitus için kullanılan *Salvia* türleri şu şekilde sıralanmaktadır: *Salvia cyanescens* (Han ve Bulut, 2015), *Salvia fruticosa* (Öztürk ve ark., 2018), *Salvia hydrangea* (Altundag ve Ozturk, 2011), *Salvia multicaulis* (Çakilcioglu ve Türkoğlu, 2010), *Salvia officinalis* (Öztürk ve ark., 2018), *Salvia virgata* (Ahiskalı ve ark., 2012).

Ülkemizde 50'ye yakın *Salvia* türünün etnobotanik kullanımı tespit edilmiş olup (Tablo 2) geri kalan taksonların da kullanımı olduğu tahmin edilmektedir. Bu sebeple arazi çalışmalarının arttırılması etnobotanik kullanımın tespitine imkan sağlaması açısından önemlidir.

Tablo 2 Türkiye'de geleneksel tıpta kullanımı tespit edilmiş *Salvia* taksonları ve kullanıldıkları hastalık çeşitleri

Takson	Kullanılan kısım	Hastalık	Kullanım yöntemi	Kaynak
Salvia absconditiflora (Montbret & Aucher ex Benth.) Greuter & Burdet*	TÜK, çiçek	Astım, bronşit, soğuk algınlığı ve grip, idrar söktürücü, balgam söktürücü, böbrek taşı, mide ağrısı, üretrit, kalp hastalıkları, hemoroid	Lapa, inf. yaprağı çiğtüketme	Özdemir ve Alpınar, 2015; Sargın ve ark., 2015; Doğan ve Bağcı, 2011
Salvia adenophylla Hedge & Hub.- Mor.	TÜK, çiçek	Karın ağrısı	İnf	Bulut ve ark., 2017
Salvia aethiopis L.	TÜK, çiçek, kök	Soğuk algınlığı ve grip, gastrit, yara iyileşmesi, kanama	İnf	Doğan ve Bağcı, 2011; Günbatan ve ark., 2023
Salvia aramiensis Rech.f.	TÜK	Bronşit	İnf	Altayve Karahan 2012
Salvia argentea L.	TÜK	Soğuk algınlığı ve grip	İnf	Koyuncu ve ark., 2010
Salvia bracteata Banks & Sol.	TÜK	Soğuk algınlığı ve grip	İnf	Koyuncu ve ark., 2010
Salvia cadmica Boiss. var. *cadmica*	TÜK	Karın ağrısı, kanama, soğuk algınlığı ve grip	İnf	Bulut ve ark., 2017; Özdemir ve Alpınar, 2015
Salvia candidissima Vahl subsp. *candidissima*	TÜK	Anjina, bronşit, soğuk algınlığı ve grip, böbrek taşı	İnf, grg	Altundag ve Ozturk, 2011; Korkmaz ve Karakurt, 2015

Salvia cryptantha Montbert & Aucher ex Benthan	TÜK	Yara dezenfektanı, öksürük ve soğuk algınlığı	Kyn.	Ghoran ve ark., 2023
Salvia dichroantha Stapf	TÜK	Soğuk algınlığı, Mide ağrısı	İnf	Sezik ve ark., 2001; Üstün ve Sezik, 2011, Ghoran ve ark., 2023
Salvia forskahlei L.	TÜK	Sakinleştirici, mide ağrısı, kabızlık	İnf	Akbulut ve Bayramoğlu., 2014; Karaköse, 2022
Salvia fruticosa Mill.	TÜK,yaprak, çiçek	Karın ağrısı, antiseptik, gaz giderici, soğuk algınlığı ve grip, dispepsi, baş ağrısı, prostat, yatıştırıcı, mide rahatsızlıkları, bademcik iltihabı	İnf	Uysal ve ark., 2012;; Bulut, 2011; Emre ve ark., 2021; Akbaş ve ark., 2024
Salvia glutinosa L.	TÜK	Yanık yaraları	İnf	Saraç ve ark., 2013; Demirci Kayıran ve ark., 2023
Salvia huberi Hedge	TÜK	Sakinleştirici, mide ağrısı, kabızlık	İnf	Toksoy ve ark., 2010
Salvia hydrangea DC. ex Benth.	TÜK	Ateş düşürücü, soğuk algınlığı ve grip, diyabet, adet söktürücü, mide rahatsızlıkları	İnf	Altundag ve Ozturk, 2011
Salvia hypargeia Fisch. & C.A.Mey.	TÜK	Soğuk algınlığı ve grip	İnf	Özdemir ve Alpınar, 2015
Salvia limbata C.A.Mey.	TÜK	Diyabet, diş ağrısı	İnf, grg	Özgen ve ark., 2012; Dalar, 2018
Salvia macrochlamys Boiss. & Kotschy	TÜK	Diyabet	İnf	Dalar, 2018
Salvia multicaulis Vahl	TÜK, çiçek, meyve	İştah açıcı, astım, diyabet, soğuk algınlığı ve grip, sindirim, migren, bademcik iltihabı, solunum ve idrar yolu rahatsızlıkları, karın ve menstrual ağrısı, siğil, yara	İnf, kyn	Güneş ve ark., 2017; Nadiroğlu ve ark., 2019; Cakilcioglu ve Turkoglu, 2010; Yeşil ve İnal, 2021; Demirci ve Kayıran, 2023
Salvia nemorosa L.	TÜK	Nezle, soğuk algınlığı, kanama durdurucu, yara iyileşmesi	İnf, kyn	Altundag ve Ozturk, 2011
Salvia officinalis L.	Yaprak	Soğuk algınlığı ve grip, böbrek rahatsızlıkları	İnf	Gürbüz ve ark., 2019; Cakilcioglu ve ark., 2011
Salvia palaestina Bentham	TÜK	Soğuk algınlığı ve grip, diyabet, balgam söktürücü, karın ve menstrual ağrısı, yara	İnf	Bulut ve ark., 2019; Yeşil ve İnan, 2021; Demirci Kayıran ve ark., 2023
Salvia pinnata L.	TÜK	Soğuk algınlığı ve grip	İnf	Koyuncu ve ark., 2010
Salvia poculata Náb	TÜK	Diyabet	İnf	Dalar, 2018
Salvia rosifolia Sm.	TÜK	Gaz giderici, kabızlık, böbrek taşı, mide ağrısı	İnf	Korkmaz ve Karakurt, 2015
Salvia russellii Benth.	TÜK	Karın ağrısı, soğuk algınlığı	Kyn	Sezik ve ark., 2001; Üstün ve Sezik, 2011, Ghoran ve ark., 2023
Salvia sclarea L.	TÜK,çiçek, taze (çiğ), yaprak	Soğuk algınlığı ve grip, sindirim sistemi, solunum sistemi hastalıkları, ağız ve boğaz ağrısı, yatıştırıcı	İnf, grg	Fakir ve ark., 2016; Akbulut ve Zengin, 2023; Demirci Kayıran ve ark., 2023
Salvia staminea Montbret & Aucher ex Benth.	TÜK	Yara iyileşmesi	Lapa	Güneş ve Özhatay, 2011
Salvia syriaca L.	TÜK, çiçek yaprak	Apse, anti-asit, soğuk algınlığı ve grip	Taze (çiğ), inf	Behçet ve Arık, 2013; Tetik ve ark., 2013; Demirci Kayıran ve ark., 2023

Salvia tomentosa Mill.	Yaprak, TÜK	Karın ağrısı, soğuk algınlığı ve grip, böbrek taşı, farenjit, yara	İnf	Fakir ve ark., 2016; Karaköse, 2022; Akbulut ve Zengin, 2023
Salvia triloba L.	TÜK	Yara dezenfektanı, öksürük ve soğuk algınlığı	Kyn	Ghoran ve ark., 2023
Salvia trichoclada Benth.	TÜK	Diyabet	İnf	Dalar, 2018
Salvia verticillata L. subsp. *amasiaca* (Freyn & Bornm.) Bornm.	TÜK	Karın ağrısı, soğuk algınlığı, müshil, mide bulantısı, diş ağrısı	Kyn	Altundag ve Ozturk,2011; Karakaya ve ark., 2020
Salvia verticillata L. subsp. verticillata	TÜK	Nezle, soğuk algınlığı ve grip, diyabet, mide ağrısı, müshil, yara iyileşmesi	Kyn, inf	Altundag ve Ozturk, 2011; Koyuncu ve ark., 2010; Dalar, 2018;
Salvia virgata Jacq.		Soğuk algınlığı ve grip, kas ağrısı	İnf	Nadiroğlu ve ark., 2019; Koyuncu ve ark.,2010;Akbulut ve Zengin, 2023
Salvia viridis L.	TÜK, çiçek	Soğuk algınlığı ve grip, mide ağrısı	Kyn, inf, taze (çiğ)	Güneş ve ark., 2017; Koyuncu ve ark., 2010
Salvia wiedemannii Boiss.	TÜK	Soğuk algınlığı ve grip, ülser, mide ağrısı	İnf	Koyuncu ve ark., 2010; Üstün ve Sezik, 2011
Salvia verbenaca L.	TÜK	Antiseptik, diüretik, mide ağrısı	İnf	Ertuğ ve ark., 2004

Kısaltmalar: TÜK: toprak üstü kısımlar, İnf: infüzyon; grg: gargara; kyn: kaynatma

TARTIŞMA

Son zamanlar da yapılan çalışmalara bakıldığında özellikle *Salvia* türlerinin, potansiyel biyolojik aktivitelerine odaklanıldığı (antioksidan, antimikrobiyal, antidiabetik, antikanser, nöroprotektif (örneğin Alzheimer'a karşı), antidiyabetik), bu yüzden *Salvia* türlerine halkın ilgisinin fitoterapi veya fonksiyonel gıda / ilaç bitkisi olarak cazip hale geldiği görülmektedir (Karadeniz Pekgöz ve ark., 2024).

Salvia türleri çok geniş ekolojik aralıklarda (iklim, yükselti, toprak, substrat) bulunduğundan dolayı bunlar üzerine daha ayrıntılı çalışmalara ihtiyaç vardır. Özellikle endemik türlerin ekolojik nişleri, adaptasyon mekanizmaları, tolere edebilecekleri değişimler (iklim değişikliği, habitat bozunumu vb.) yapılan çalışmalara bakıldığında yetersiz görünmektedir. Özellikle son yıllarda halen yeni tür tayinlerinin yapılıyor olmasıyla, aktif bir taksonomik çalışma alanı olduğu daha net görülmektedir. Bazı türlerin uçucu yağ kompozisyonu ve biyolojik aktiviteleri incelenmeye başlanmış olsa da, ülke genelindeki çeşitliliğin ancak küçük bir kısmı değerlendirilmiş durumdadır ve özellikle nadir, dar yayılışlı, endemik türlerin üzerine daha fazla araştırma yapılabilir.

SONUÇ

Sonuç olarak, Türkiye'de *Salvia* türleri hem tıbbi hem de kültürel anlamda büyük önem taşıyan yüksek endemizm, geniş ekolojik çeşitlilik, zengin etnobotanik kullanım, farmakolojik potansiyel ile öne çıkan bir taksondur. Buna karşın, pek çok türün varlığı habitat baskısı ve yanlış kullanım nedeniyle tehlikededir. Hem bilimsel araştırmalar (etnobotani, kimya, moleküler ekoloji, farmakoloji) hem de toplum temelli koruma programları gereklidir.

KAYNAKÇA

Abak, F., Yıldız, G., Atamov, V., & Kürkçüoğlu, M. (2018). Composition of the essential oil of Salvia montbretii Benth. from Turkey. Rec. Nat. Prod. 12:5 (2018) 426-431.

Ahiskalı, M., Arı, Ç., Selvi, S. (2012). Edible wild plants and their consumption during winter in a rural village on Kazdağı (Mount Ida). Bocconea 24:195–198.

Akbaş, K., Çıtakoğlu, M., Davran, S. (2024). Natural plants of the Sandras Mountain (Köyceğiz-Muğla) traditionally employed for therapeutic purposes. Turkish Journal of Forestry, 25(1), 32-40.

Akbulut, S., & Zengin Z. (2023). Ethnobotanical survey of wild plants used in Gümüşhane province (Turkey) Bol Latinoam Caribe Plant Med Aromat 22(2):237-254. https://doi.org/10.37360/blacpma.23.22.2.18

Akbulut, S., & Bayramoğlu, M. M. (2014). Reflections of socio-economic and demographic structure of urban and rural on the use of medicinal and aromatic plants: the sample of Trabzon Province. Studies Ethno Medicines 8(1): 89-100. doi: 10.1080/09735070.2014.11886477

Altay, V., & Karahan, F. (2012). Tayfur Sökmen Kampüsü (Antakya-Hatay) ve çevresinde bulunan bitkiler üzerine etnobotanik bir araştırma. Karadeniz Fen Bilimleri Dergisi, 3(2), 13-28.

Altundag, E. & Ozturk, M. (2011). Ethnomedicinal studies on the plant resources of east Anatolia,

Turkey. Proc Soc Behav Sci 19:756–777.

Bahadırlı, N. P., Ayanoglu, F. (2020). Genetic diversity of Salvia species from Turkey assessed by microsatellite markers, Journal of Applied Research on Medicinal and Aromatic Plants. doi: https://doi.org/10.1016/j.jarmap.2020.100281.

Bakir, D., Akdeniz, M., Ertas, A., Yılmaz, M. A., Yener, I., Fırat, M., Kolak, U. (2020). A GC–MS method validation for quantitative investigation of some chemical markers in *Salvia hypargeia* Fisch. & C.A. Mey. of Turkey: Enzyme inhibitory potential of ferruginol. J Food Biochem. 2020; 44:e13350. https://doi.org/10.1111/jfbc.13350.

Behçet, L., Arık, M. (2013). An ethnobotanical investigation in East Anatolia Turkey. Turkish Journal of Nature and Science 2: 1-15

Bulut, G. (2011). Folk medicinal plants of Silivri (İstanbul- Turkey). Marmara Pharmaceutical Journal 15: 25-29. doi:10.12991/201115441

Bulut, G., Tuzlacı, E. (2015). An ethnobotanical study of medicinal plants in Bayramiç. Marmara Pharm J 19(3):268–282.

Bulut, G., Haznedaroğlu, M. Z., Doğan, A., Koyu, H., Tuzlacı, E. (2017). An ethnobotanical study of medicinal plants in Acipayam (Denizli-Turkey). Journal of Herbal Medicine 10: 64-81. doi: 10.1016/j.hermed.2017.08.001

Bulut, G., Doğan, A., Şenkardeş, İ., Avcı, R., Tuzlacı, E. (2019). The medicinal and wild food plants of Batman City and Kozluk District (Batman-Turkey). Agriculturae Conspectus Scientificus 84 (1): 29-36

Celep, F., & Doğan, M. (2023). The genus Salvia in Turkey: morphology, ecology, phytogeograpy, endemism and threat categories. In: Medicinal and Aromatic Plants of Turkey (pp. 107-120). Cham: Springer International Publishing.

Cole, T. C. H., Li, B., Xiang, C-L., & Olmstead, R. G. (2021). Lamiaceae: Subfamilies (LamSubfam).

Çakilcioglu, U., & Turkoglu, I. (2010) An ethnobotanical survey of medicinal plants in Sivrice (Elazıg-Turkey). J Ethnopharmacol 132:165–175.

Cakilcioglu, U., Khatun, S., Turkoglu, I., Hayta, S. (2011). Ethnopharmacological survey of medicinal plants in Maden (Elazığ-Turkey). Journal of Ethnopharmacology 137 (1): 469- 486. doi:10.1016/j.jep.2011.05.046

Çalış, İ. (2025). A Mini Review on the Chemodiversity of Lamiaceae plants That Are Native to Türkiye and Turkish Republic of Northern Cyprus. Records of Natural Products, 19 (SI): 350-374.

Dalar, A. (2018). Plant taxa used in the treatment of diabetes in Van Province, Turkey. International Journal of Secondary Metabolite, 5(3), 171-185.

Demirci Kayıran, S., Parlak, M., Yılmaz Oral, D. (2023). Ethnobotany of medicinal plants used in dermatology in Türkiye: a review. Turkish Journal of Botany 47 (6): 408-463. https://doi.org/10.55730/1300-008X.2779

Dirmenci, T. (2024). The Lamiaceae Family: Biodiversity and Uses. Rec. Agric. Food. Chem. 3rd Food Chemıstry Congress Abstract. 4:SI (2024) OP:5-5.

Doğan, G.& Bağcı, E. (2011). Elazığ'ın bazı yerleşim alanlarında (Cip Baraj Gölü ve Arındık Köyü civarı) halkın geleneksel ekolojik bilgisine dayanarak kullandığı bitkiler ve etnobotanik özellikleri. Fırat Üniversitesi Fen Bilimleri Dergisi 23 (2): 77- 86.

Eksi, G., & Yılmaz, G. (2021). The Leaf and Stem Anatomy of Two Endemic Salvia (Section Salvia, Lamiaceae) from Turkey: S. aucheri subsp. canascens and S. heldrichiana. Sakarya University Journal of Science, *25*(6), 1352-1365.

Eminagaoglu, Ö., Ozcan, M., & Akyıldırım Beğen, H. (2022). A New Taxon of Salvia (Lamiaceae) From Türkiye. Bangladesh Journal of Plant Taxonomy, 29(2):167–181. https://doi.org/10.3329/bjpt.v29i2.63524

Emre, G., Dogan, A., Haznedaroglu, M. Z., Senkardes, I., Ulger, M., Satiroglu, A., Emmez, B. C., Tugay, O. (2021). An ethnobotanical study of medicinal plants in Mersin (Turkey). Frontiers in Pharmacology, 12, 664500. https://doi.org/10.3389/fphar.2021.664500

Ertuğ, F., Tümen, G., Çelik, A., Dirmenci, T. (2004). Buldan Denizli Etnobotanik Alan Araştırması 2003. TÜBA-KED Türkiye Bilimler Akademisi Kültür Envanteri Dergisi (2), 187-218.

Fakir, H., Korkmaz, M., Icel, B. (2016). Medicinal plants traditionally used for pain alleviation in Antalya Province, Turkey. Studies on Ethno-Medicine 10 (3): 314-324. doi:10.1080/09735070.20 16.11905503

Ghoran, S. H., Taktaz, F., Mozafari, A. A., Saed-Moucheshi, A., & Hosseini, A. (2023). Sage plants (Salvia sp.; Lamiaceae) in the Middle East: phytochemistry, ethnopharmacology, and traditional use. In: Ancient and Traditional Foods, Plants, Herbs and Spices used in the Middle East (pp. 263-277). CRC Press.

Güler, B., Erkan, Y., Uğurlu, E. (2020). Traditional uses and ecological resemblance of medicinal plants in two districts of the Western Aegean Region (Turkey). Environ Dev Sustain 22(3):2099–2120.

Günbatan, T., Gürbüz, İ., Gençler Özkan,, A. M. (2023). Ethnobotany in Turkey: Retrospect and Prospect. In: Medicinal and Aromatic Plants of Turkey (pp 31-55). Springer Nature Switzerland AG, Cham, Switzerland.

Güner, A., Aslan, S., Ekim, T., Vural, M., Babaç, M. T. (eds). 2012.Türkiye Bitkileri Listesi (Damarlı Bitkiler). Nezahat Gökyiğit Botanik Bahçesi ve Flora Araştırmaları Derneği Yayını. İstanbul.

Han, M. I., Bulut, G. (2015). The folk-medicinal plants of Kadişehri (Yozgat-Turkey). Acta Soc Bot
Pol 84(2):237–248.

Güneş, S., Savran, A., Paksoy, M.Y., Koşar, M., Çakılcıoğlu, U. (2017). Ethnopharmacological survey of medicinal plants in Karaisalı and its surrounding (Adana-Turkey). Journal of Herbal Medicine 8: 68-75. doi: 10.1016/j.hermed.2017.04.002

Güneş, F., & Özhatay, N. (2011). An ethnobotanical study from Kars (Eastern) Turkey. Biological Diversity and Conservation 4: 30-41

Gürbüz, İ., Özkan, A.M.G, Akaydın, G., Salihoğlu, E., Günbatan, T., Demirci, F., Yeşilada, E. (2019). Folk medicine in Düzce Province (Turkey). Turkish Journal of Botany 43: 769-784. doi:10.3906/bot-1905-13

Honda, G., Yeşilada, E., Tabata, M., Sezik, E., Fujita, T., Takeda, Y., Takaishi, Y., Tanaka, T. (1996). Traditional medicine in Turkey VI. Folk medicine in West Anatolia: Afyon, Kütahya, Denizli, Muğla, Aydin provinces. J Ethnopharmacol 53(2):75–87.

İlçim A., Tel, A. Z. & Kocabaş, Y. Z. (2023). *Salvia adiyamanensis* (Lamiaceae), a new species from South East Anatolia, Turkey. Phytotaxa 592 (1): 49–58. https://doi.org/10.11646/phytotaxa.592.1.4

İpek, A., & Gürbüz, B. (2010). Türkiye florasında bulunan Salvia türleri ve tehlike durumları. Tarla Bitkileri Merkez Araştırma Enstitüsü Dergisi, 19(1-2), 30-35.

Karadeniz-Pekgöz, A., Turgut, A.C., Çinbilgel, İ. *ve ark.* Phytochemical contents and bioactivity of four endemic *Salvia* seeds from Turkey: a comparative study to chia seed. *Food Measure* **18**, 5638–5645 (2024). https://doi.org/10.1007/s11694-024-02594-8

Karakaya, S., Polat, A., Aksakal, Ö., Sümbüllü, Y. Z., & İncekara, Ü. (2020). Ethnobotanical study of medicinal plants in Aziziye district (Erzurum, Turkey). Turkish Journal of Pharmaceutical Sciences, 17(2), 211.

Karaköse, M. (2022). An ethnobotanical study of medicinal plants in Güce district, north-eastern Turkey. Plant Diversity, 44(6), 577-597.

Kargıoğlu, M., Cenkci, S., Serteser, A., Konuk, M., Vural, G. (2010). Traditional uses of wild plants in the middle Aegean region of Turkey. Hum Ecol 38(3):429–450

Karik, U., Çinar, O., Tuncturk, M., Sekeroglu, N., & Gezici, S. (2018). Essential oil composition of some sage (Salvia spp.) species cultivated in İzmir (Turkey) ecological conditions. Indian Journal of Pharmaceutical Education and Research, 52(4), 102-107.

Kılıç, Ö., Bağcı, E. (2013). An ethnobotanical survey of some medicinal plants in Keban (Elazığ-Turkey). J. Med. Plants Res. 7(23): 1675-1684. http://www.academicjournals.org/JMPR

Kılıç Mungan, F. (2022). Mardin İlinde Yayılış Gösteren Salvia L. Taksonları Üzerine Bir Araştırma. MAS Journal of Applied Sciences, 7(1), 169-186.

Koçyiğit, M., Özhatay, N. (2006). Wild plants used as medicinal purpose in Yalova (Northwest Turkey). Turk J Pharm Sci 3(2):91–103.

Korkmaz, M., & Karakurt, E. (2015). An ethnobotanical ınvestigation to determine plants used as folk medicine in Kelkit Gümüşhane/Turkey district. Biological Diversity and Conservation, 8(3), 290-303.

Koyuncu, O., Yaylacı, Ö.K., Öztürk, D., Erkara, İ.P., Savaroğlu, F., Akcoşkun, Ö., Ardıç, M. (2010). Risk categories and ethnobotanical features of the Lamiaceae taxa growing naturally in Osmaneli (Bilecik/ Turkey) and environs. Biological Diversity and Conservation 3 (3): 31-45

Nadiroğlu, M., Behçet, L., Çakılcıoğlu, U. (2019). An ethnobotanical survey of medicinal plants in Karlıova (Bingöl-Turkey). Indian Journal of Traditional Knowledge 18 (1): 76-87.

Özdemir, E. & Alpınar, K. (2015). An ethnobotanical survey of medicinal plants in western part of central Taurus Mountains: Aladaglar (Nigde - Turkey). Journal of Ethnopharmacology 166: 53-65. doi: 10.1016/j.jep.2015.02.052

Özgen, U., Kaya, Y., Houghton, P. (2012). Folk medicines in the villages of Ilıca District (Erzurum, Turkey). Turkish Journal of Biology 36: 93-106. doi:10.3906/biy-1009-124

Öztürk, M., Altay, V., Latiff, A., Ziaee, M. A., Choudhry, M. I., Shaheen, F., and Durmuşkahya, C. (2018). A Comparative Analysis of the Medicinal Plants Used for Diabetes Mellitus in the Traditional Medicine in Turkey, Pakistan, and Malaysia. In: Plant and Human Health, Volume 1.Ethnobotany and Physiology (pp 409-461). Springer, Cham, Switzerland.

Paksoy, M. Y., Selvi, S., & Savran, A. (2016). Ethnopharmacological survey of medicinal plants in Ulukışla (Niğde-Turkey). Journal of Herbal Medicine, *6*(1), 42-48.

Pavlidou, V., Karpouhtsis, I., Franzios, G., Zambetaki, A., Scouras, Z., Mavragani Tsipidou, P. (2004). Insecticidal and genotoxic effects of essential oils of Greek sage, Salvia fruticosa, and Mint, Mentha pulegium, on Drosophila melanogaster and Bactrocera oleae (Diptera: Tephritidae) J Agric Urban Entomol 21(1):39–49.

Saraç, D.U., Özkan, Z.C., Akbulut, S. (2013). Ethnobotanic features of Rize/Turkey province. Biological Diversity and Conservation 6 (3): 57-66

Sargın, S.A., Selvi, S., López, V. (2015). Ethnomedicinal plants of Sarigöl district (Manisa), Turkey. Journal of Ethnopharmacology 171: 64-84. doi:10.1016/j.jep.2015.05.031

Selvi, S, Polat, R, Çakılcıoğlu, U, Celep, F, Dirmenci, T, & Ertuğ, Z. F. (2022). An ethnobotanical review on medicinal plants of the Lamiaceae family in Turkey. Turkish Journal of Botany 46 (4): 283-332. https://doi.org/10.55730/1300-008X.2712.

Sezik, E., E. Yeşilada, G. Honda, Y. Takaishi, Y. Takeda, and T. Tanaka. (2001). Traditional medicine in Turkey X. Folk medicine in central Anatolia. Journal of Ethnopharmacology 75:95–115.

Şenkal, B. C., Uskutoğlu, T., Cesur, C., Özavcı, V., & Doğan, H. (2019). Determination of essential oil components, mineral matter, and heavy metal content of *Salvia virgata* Jacq. grown in culture conditions. Turkish Journal of Agriculture and Forestry, 43(4), 395-404.

Tetik, F., Civelek, S., Cakilcioglu, U. (2013). Traditional uses of some medicinal plants in Malatya (Turkey). Journal of Ethnopharmacology 146 (1): 331-346. doi: 10.1016/j. jep.2012.12.054

Toksoy, D., Bayramoglu, M., Hacisalihoglu, S. (2010). Usage and the economic potential of the medicinal plants in Eastern Black Sea Region of Turkey. Journal of Environmental Biology 31: 623-628

Tulukcu, E., Cebi, N., & Sagdic, O. (2019). Chemical Fingerprinting of Seeds of Some *Salvia* Species in Turkey by Using GC-MS and FTIR. Foods, 8(4), 118. https://doi.org/10.3390/foods8040118

Turdiboev, O. A., Shormanova, A. A., Sheludyakova, M. B., Akbarov, F., Drew, B. T., & Celep, F. (2022). Synopsis of the Central Asian Salvia species with identification key. *Phytotaxa*, *543*(1): 001-020.

Uysal, İ., Gücel, S., Tütenocaklı, T., Öztürk, M. (2012). Studies on the medicinal plants of Ayvacık-Çanakkale in Turkey. Pakistan Journal of Botany 44: 239-244

Uzun, E., Sarıyar, G., Adsersen, A., Karakoç, B., Ötük, G., Oktayoğlu, E., Pirildar,S. (2004). Traditional medicine in Sakarya province (Turkey) and antimicrobial activities of selected species. J Ethnopharmacol 95(2–3): 287–296.

Üstün, O., & E. Sezik. (2011). Analgesic activity of *Salvia wiedemannii* Boiss. used in Turkish folk medicine. Records of Natural Products, 5:328–331.

Yeşil, Y., & Inal, I. (2021). Ethnomedicinal plants of Hasankeyf (Batman-Turkey). Frontiers in Pharmacology, 11, 624710.

Yeşilyurt, E. B., Şimşek, I., Tuncel, T., Akaydın, G., Yeşilada, E. (2017) Marmara Bölgesi'nin bazı yerleşim merkezlerinde halk ilacı olarak kullanılan bitkiler. Marmara Pharm J 21(1):132–148

Yılmaz, G., Eruygur, N., Bona, G. E., Bona, M., Akdeniz, M., Yilmaz, M. A., & Ertas, A. (2023). Phytochemical analysis, antioxidant, and enzyme inhibition activity of five Salvia taxa from Turkey. South African Journal of Botany, 152, 212-221.

Yumrutaş, O., Martinez, J. L., Parlar, A., Morales, B., Yumrutas, P., & Jaimes, L. (2023). Genus Salvia: Its Secondary Metabolites and Roles in the Treatment of Common Cancer Types in Men and Women. In *Ethnobotany* (pp. 191-215). CRC Press.

Zhao, F., Chen, Y.P., Salmaki, Y., Drew, B.T., Wilson, T.C., Scheen, A.-C., Celep, F., Bräuchler, C., Bendiksby, M., Wang, Q., Min, D.-Z., Peng, H., Olmstead, R.G., Li, B. & Xiang, C.-L. (2021). An updated tribal classification of Lamiaceae based on plastome Phylogenomics. BMC Biol

ORAL PRESENTATION

Mixed-ligand thiosemicarbazone Ni(II) complex with 2,6-dimethylpyridine: Characterization and cytotoxicity studies

Elif Avcu Altiparmak[1*] (*Orcid: https://orcid.org/0000-0002-5491-8445*), Güneş Özen Eroğlu[2] (*Orcid: https://orcid.org/0000-0003-3681-9336*), Namık Özdemir[3] (*Orcid: https://orcid.org/0000-0003-3371-9874*), Tülay Bal Demirci[1] (*Orcid: https://orcid.org/0000-0003-4663-2209*)

[*1]Istanbul University-Cerrahpaşa, Faculty of Engineering, Department of Chemistry, Istanbul, Türkiye.
[2]Istanbul University, Department of Molecular Medicine, Aziz Sancar Institute of Experimental Medicine, Istanbul, Türkiye.
[3]Ondokuz Mayıs University, Faculty of Art and Science, Department of Physics, Istanbul, Türkiye.

*Corresponding author e-mail: avcuelif@iuc.edu.tr

Abstract

In this work, a novel mixed-ligand nickel(II) complex based on S-methyl isothiosemicarbazone ligand was synthesized using 3-bromo-5-chlorosalicylaldehyde-S-methylisothiosemicarbazone as the primary ligand in the presence of 2,6-dimethylpyridine as the co-ligand. The structure of the synthesized complex was characterized by elemental analysis, FT-IR, UV–Visible spectroscopy, and ^{1}H-NMR spectroscopic techniques. In addition, detailed crystallographic analysis via single-crystal X-ray diffraction elucidated the molecular structure and confirmed the mixed-ligand coordination environment of the complex. To assess its biological potential, the cytotoxic activity of the complex was evaluated on the MCF-7 breast cancer cell line, K562 human chronic myelogenous leukemia cell line and HUVEC human healty endothelial cell line by using the MTT assay. The results demonstrate that the complex exhibits measurable cytotoxic effects, highlighting its potential as a bioactive nickel-based coordination compound.

Keywords: Thiosemicarbazone, Mixed-ligand complexes, Nickel(II) ion, MTT assay, X-ray diffraction.

INTRODUCTION

The success of cisplatin as a chemotherapeutic agent has markedly increased the trend toward the use of metal complexes in cancer treatment, as well as the discovery of new metal-based active pharmaceutical ingredients (Jung and Lippard, 2007). In this context, the metal complexes of Schiff bases are particularly among the most frequently investigated classes of compounds (Ali et al., 1997; Arafath, 2023; Kaya, 2023; Morgan et al., 2017).
Thiosemicarbazones are a class of ligands that have attracted significant attention in bioinorganic chemistry owing to their multifunctional metal-chelating properties, broad-spectrum biological activities, and structural flexibility (Khan et al., 2022; Ramanchandran et al., 2012; Pelosi et al., 2010; Atasever et al., 2010; The metal complexes of these ligands have been the subject of numerous biological activity studies, including antidiabetic, antimicrobial, anticancer, antioxidant, antiviral, and antifungal activities, as well as enzyme inhibition and DNA-binding investigations (Palanumithu et al., 2013; Yousef and Abu El-Reash, 2020; Karpagam et al., 2021; Malarz et al., 2018; Avcu Altıparmak et al., 2021; Yanardağ et al., Zhang et al., 2015; Rzycka-Korzec et al., 2021) Studies focusing on the anticancer activities of these compounds have gained substantial popularity, particularly after the approval of Triapine as an anticancer agent (Ma et al., 2008).
In a similar vein, the metal complexes of nickel–thiosemicarbazone ligands have also gained strong visibility in the literature, highlighting their growing importance as bioinorganic therapeutic candidates (Jakupec et al., 2008; Rupam et al., 2013). In this study, a novel mixed-ligand nickel(II) thiosemicarbazone complex incorporating 2,6-dimethylpyridine as a co-ligand has been synthesized. The molecular structure of the synthesized compound has been characterized using elemental analysis, UV–visible spectroscopy, FT-IR, and ^{1}H-NMR techniques, while its solid-state structure has been elucidated through single-crystal X-ray diffraction. The cytotoxic activities of both the free ligand and its nickel(II) complex were evaluated by the MTT assay on cancerous cell models including

K562 (chronic myelogenous leukemia), MCF-7 (breast adenocarcinoma), and healty cell line HUVEC (human umbilical vein endothelial cells).

MATERIALS AND METHODS

Preparation of the Thiosemicarbazone Ligand: The 3-bromo-5-chlorosalicylaldehyde-S-methyl thiosemicarbazone ligand was prepared using a literature-reported method for nickel(II) complex synthesis (Avcu Altıparmak et al., 2021). The formation of the ligand was confirmed using melting point determination and spectroscopic techniques.

Synthesis of the Ni(II) Complex: Equimolar amounts of the thiosemicarbazone ligand (1 mmol, 0.32 g) and $NiCl_2.6H_2O$ (1 mmol, 0.24 g) salt were refluxed in ethanol for 30 min. The resulting green solution was treated with 2,6-dimethylpyridine as a secondary ligand (1 mmol, 0.11 g), and refluxed for an additional 1 h. Upon complex formation, the reaction mixture turned red. The red solution was filtered while hot, and the filtrate was allowed to slowly crystallize at room temperature for 3 days, yielding red single crystals. The isolated crystals were dried for further characterization.

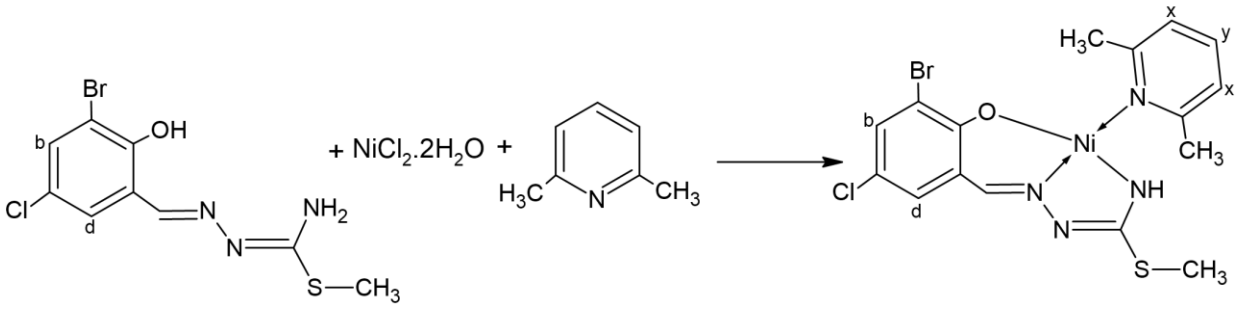
Characterization Details of the Thiosemicarbazone Ligand: Yellow, *Molecular Formula:* $C_9H_9BrClN_3OS$; *Formula Weight:* 322.6 $g.mol^{-1}$. *Elemental Analysis (Calculation% (Found %)):* C (33.51 (33.52)), H (2.81 (2.84)), N (13.03 (13.05)), S (9.94 (9.91)). *FT-IR:* 3480 ν(-OH); 3269, 3231 ν(-NH_2); 1632 σ(-NH); 1600, 1573 ν(C=N); 707 ν(C-S). *UV-Vis (5.10^{-5} M, $CHCl_3$, λ (nm) (ε ($M^{-1}.cm^{-1}$)):* 239.5 (16260); 304.5 (19540); 316.5 (18400); 345.5 (15480). *^{1}H-NMR (DMSO-d_6, (δ, ppm)):* 11.61, 10.64 (*cis*/*trans* ratio: 3/2, s, 1H, OH); 8.42, 8.32 (*syn*/*anti* ratio: 1/2, s, 1H, CH=N[1]), 7.76 (d, 1H, *J* = 2,45, *d*), 7.50 (d, *J* = 2.44, 1H, *b*), 6.99 (s, broad, 2H, NH_2), 2.43, 2.37 (*cis*/*trans* ratio: 1/2, s, 3H, S-CH_3).

Characterization Details of the Complex: Red, *Molecular Formula:* $C_{16}H_{16}BrClN_4NiOS$; *Formula Weight:* 486.44 $g.mol^{-1}$. Melting Point: 288 ºC. *Elemental Analysis (Calculation% (Found %)):* C (39.51 (39.54)), H (3.32 (3.30)), N (11.52 (11.56)), S (6.59 (6.52)). *FT-IR:* 3368 ν(-NH); 3052, 3034, 2971, 2958, 2922 ν(C-H); 1623 σ(-NH); 1603, 1580 ν(C=N); 699 ν(C-S). *UV-Vis (5.10^{-5} M, $CHCl_3$, λ (nm) (ε ($M^{-1}.cm^{-1}$)):* 246.5 (21620); 310 (4840); 386.5 (9100). *^{1}H-NMR (DMSO-d_6, (δ, ppm)):* 7.77 (t, 1H, *y*); 7.53 (m, 2H, *x,x*); 7.40 (s,1H, *CH=N*); 7.33 (d, 1H, *d*); 7.02 (d, 1H, *b*); 4.53 (s, 1H, *-NH*); 2.37 (s, 3H, *S-CH_3*); 2.39 (s, 6H, *-CH_{3Py}*).

X-ray Analysis: Crystal data of Ni(II) complex were collected with a STOE IPDS II diffractometer at room temperature using graphite-monochromated Mo Kα radiation by applying the ω-scan method. Data collection and cell refinement were carried out using X-AREA while data reduction was applied using X-RED32 (Stoe and Cie, 2002). The structure was solved using SHELXT 2018/2 (Sheldrick, 2015) and refined by using SHELXL2019/3 (Sheldrick, 2015). Molecular graphics were generated using OLEX2 (Dolomanov et al., 2009) and PLATON (Spek, 2009).

MTT Assay: The cytotoxic activity of complex and ligand was evaluated using MTT (3-(4,5-dimethylthiazol-2-yl)-2,5-diphenyl-2H-tetrazoliumbromide) assay (Mosmann, 1983). The MCF-7 human breast cancer cell line, K562 human chronic myelogenous leukemia cell line and HUVEC human umbilical vein endothelial cell line were obtained from the American Type Culture Collection (ATCC) (VA, U.S.A.). Cells were cultured according to the standard procedure and maintained in Dulbecco's modified Eagle's medium (DMEM, Sigma, Chemical Co., St Louis, MO) and RPMI-1640 (Sigma, Chemical Co., St Louis, MO) medium. Medium solutions were supplemented with 10% FBS and 1% penicillin/streptomycin. The cells were cultured in a standard humidified incubator at 5% CO_2 at 37 °C. The number of viable cells was calculated using the trypan blue dye exclusion test. Cells were grown in 96-multiwell flat bottom microtiter plates with 10000 cells/100 µL of complete medium per well. Thiosemicarbazone ligand and complex stock solutions (5 mg mL^{-1}) were prepared in DMSO and diluted with culture medium to obtain final test concentrations of 1–50 µM per well in 96-well plates. The solvent percentage was 0.1% (v/v). 10 µl was added to wells, each one in triplicate. The plates were incubated for 72 hours, and evaluation of cell viability was performed by using the MTT colorimetric assay. Optical density was measured by using a Biotek microplate reader at 560 nm with a reference wavelength of 620 nm. In each experiment, 5 different concentrations were analyzed with 3 replicate microplate wells for each concentration. The IC50 values of all compounds tested in the cell lines were calculated using GraphPad Prism 9 software. Statistical analyses were performed nonparametrically with Student's t-test.

Tables and Figures



Scheme 1. Formation of the Mixed-ligand Ni(II) Complex.

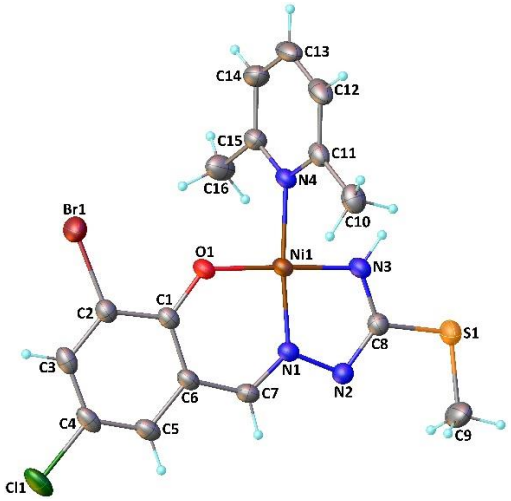


Figure 1. Ortep Diagram of Ni(II) Complex.

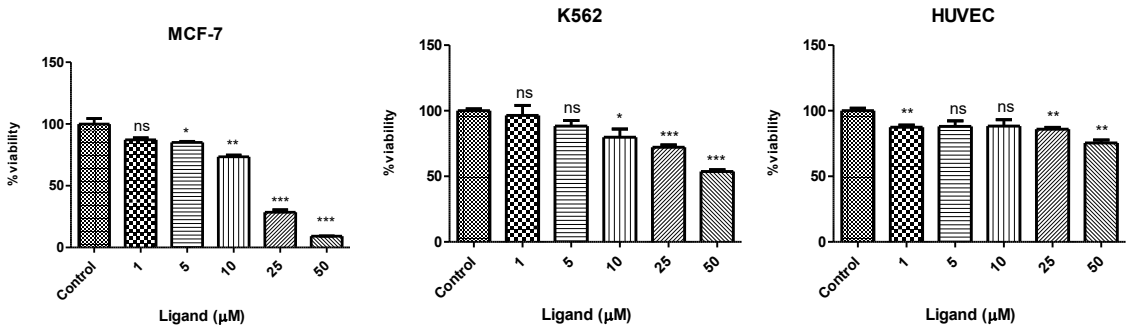


Figure 2. Graphs showing the cell viability% compared to control in MCF-7, K562 and HUVEC cells treated with different concentrations of ligand according to MTT assay.

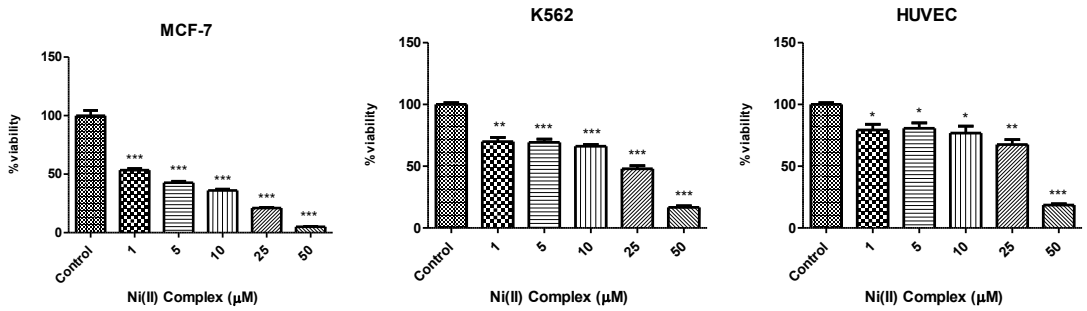


Figure 3. Graphs showing the cell viability% compared to control in MCF-7, K562 and HUVEC cells treated with different concentrations of Ni(II) complex according to MTT assay.

Table 1. Crystal data and structure refinement for Ni(II) Complex.

Empirical formula	$C_{16}H_{16}BrClN_4NiOS$	
Formula weight	486.46	
Temperature	296(2) K	
Wavelength	0.71073 Å	
Crystal system	Triclinic	
Space group	P -1	
Unit cell dimensions	a = 9.4077(5) Å	α= 65.301(4)°.
	b = 10.8744(6) Å	β= 66.177(4)°.
	c = 11.1901(6) Å	γ = 89.258(4)°.
Volume	934.56(10) $Å^3$	
Z	2	
Density (calculated)	1.729 Mg/m^3	
Absorption coefficient	3.442 mm^{-1}	
F(000)	488	
Crystal size	0.680 x 0.670 x 0.240 mm^3	
Theta range for data collection	2.409 to 27.716°.	
Index ranges	-12<=h<=12, -14<=k<=14, -14<=l<=14	
Reflections collected	17130	
Independent reflections	4366 [R(int) = 0.0600]	
Completeness to theta = 25.242°	99.9 %	
Absorption correction	Integration	
Max. and min. transmission	0.4947 and 0.1556	
Refinement method	Full-matrix least-squares on F^2	
Data / restraints / parameters	4366 / 0 / 229	
Goodness-of-fit on F^2	1.123	
Final R indices [I>2sigma(I)]	R_1 = 0.0397, wR_2 = 0.0914	
R indices (all data)	R_1 = 0.0491, wR_2 = 0.0952	
Extinction coefficient	n/a	
Largest diff. peak and hole	0.431 and -0.643 e.$Å^{-3}$	

Table 2. IC_{50} values of the Ni(II) complex and ligand in HUVEC, MCF-7 and K562 cell lines determined by the MTT assay after 72 h.

Compounds / Cell Lines	K562	MCF-7	HUVEC
TSC Ligand	>50 µM	16 µM	>50 µM
Ni(II) Complex	10.6 µM	2.6 µM	32.2 µM
Cisplatin	6.7 µM	7.4 µM	5.95 µM

RESULTS and DISCUSSION

The condensation reaction between S-methyl-isothiosemicarbazide and 3-bromo-5-chloro-salicylaldehyde produced the isothiosemicarbazone ligand, comparable to related thiosemicarbazone systems reported in the literature (Avcu Altıparmak et al., 2025). The ligand formation was confirmed through spectroscopic techniques and melting point determination.

The mixed ligand Ni(II) complex was synthesized by the reaction of equimolar amounts (1:1:1) of the ligand, $NiCl_2.6H_2O$ and 2,6-dimethylpyridine. The red crystal product showed good solubility in dichloromethane, diethyl ether, chloroform, DMF and alcohols. It was characterized by elemental analysis, FT-IR, UV-Vis and ^{1}H-NMR spectroscopic methods and the structure of crystal was determined by X-ray diffraction (Scheme 1).

The UV-Vis spectra of the starting material and complex were measured in $CHCl_3$. In the UV-Vis spectrum of the ligand, the bands located at 239.5, 304.5, 316.5 and 345.5 nm can be attributed the π–π* transitions of the aromatic ring, n–π* transition of azomethine and π–π* transition of the thioamide group on thiosemicarbazone. The electronic spectrum of the Ni(II) complex exhibited three bands, with the band at 246.5 nm corresponding to the π–π* transition of the aromatic ring, 310 and 386.5 nm attributed to the π → π* and n → π*, charge transfer transitions, respectively.

The formation of the ligand and Ni(II) were confirmed through characteristic infrared spectral bands. Ligand condensation was demonstrated by the presence of a phenolic O–H band at 3480 cm^{-1}, primary amine (NH_2) stretching bands at 3269 and 3231 cm^{-1}, and azomethine (C=N) vibrations at 1600 and 1573 cm^{-1}, respectively. In the complex FT-IR spectrum, a coordinated N–H stretching band appears at 3368 cm^{-1}. The C=N stretching bands at 1603 and 1580 cm^{-1} indicate the Schiff base unit is preserved upon metal coordination. Aromatic C–H stretches assigned to the coordinated pyridine ring are observed in the 3052–2922 cm^{-1} range. These key features confirm formation of the metal–thiosemicarbazone–pyridine coordination complex.

Ligand formation was supported by ^{1}H-NMR data showing O–H signals at 12.57 and 11.78 ppm arising from cis/trans isomers. The imine (CH=N) protons were recorded at 8.43 and 8.36 ppm, consistent with syn/anti conformers. Aromatic protons appeared at 7.55 and 7.53 ppm, while the NH_2 resonance was observed as a broad peak at 7.19 ppm. S-methyl protons were detected at 2.49 and 2.36 ppm, corresponding to cis/trans isomers, confirming successful condensation into the S-methyl thiosemicarbazone ligand. In the NMR spectrum of the complex, the imine (CH=N) proton was observed at 7.40 ppm. All aromatic protons from the phenolate and coordinated pyridine ring appeared in the 7.77–7.02 ppm range. The NH proton was recorded at 4.53 ppm. The S-methyl group gave a 3H singlet at 2.37 ppm, and the two methyl substituents on coordinated pyridine showed a 6H signal at 2.39 ppm, confirming formation of the Ni(II) mixed-ligand complex.

The structure of the Ni(II) complex was elucidated by single-crystal X-ray diffraction. The complex crystallizes in the triclinic P-1 space group. Structural analysis confirmed that the thiosemicarbazone ligand coordinates to the Ni(II) center through the phenolic oxygen, azomethine nitrogen, and the terminal amine nitrogen, while pyridine acts as a co-ligand via its ring nitrogen, forming an N,O,N,N donor set. The coordination environment generates a slightly distorted square-planar geometry (Figure 1). The key bond lengths are Ni1—O1: 1.8388(19) Å, Ni1—N4: 1.932(2) Å, Ni1—N1: 1.849(2) Å, and Ni1—N3: 1.829(2) Å, supporting strong O/N-based binding with thiolate contribution. Selected bond angles (°) include O1—Ni1—N1: 95.90(9), O1—Ni1—N3: 177.23(10), N1—Ni1—N4: 174.15(9), N1—Ni1—N3: 82.08(10), confirming deviation from ideal planarity. The structural distortion parameter was determined as τ = 0.06, indicating moderate square-planar distortion consistent with analogous heteroaromatic co-ligated Ni(II) thiosemicarbazone complexes reported in the literature (Bal-Demirci et al., 2020; Avcu Altıparmak et al., 2025).

The cytotoxic profile of the Ni(II) complex and its ligand was further benchmarked against the standard chemotherapeutic agent, Cisplatin (Figure 2 and 3). In complexation studies, the Ni(II) complex demonstrated significantly improved potency relative to the ligand and showed competitive activity when compared to Cisplatin, with IC_{50} values of 2.6 µM for MCF-7 breast cancer cells (vs 7.4 µM for Cisplatin), 10.6 µM for K562 leukemia cells (vs 6.7 µM for Cisplatin), and 32.2 µM for HUVEC non-tumorigenic endothelial control cells (vs 5.95 µM for Cisplatin). Although Cisplatin exhibits strong cytotoxicity across all tested lines, the Ni(II) complex achieves markedly lower IC_{50} values in cancer lines—especially in MCF-7—and shows reduced potency in healthy endothelial cells compared to malignant cells, where its IC_{50} (32.2 µM) remains substantially higher than that of Cisplatin. This comparison supports that complexation enhances cytotoxic activity in malignant cell lines and reveals a favorable, measurable shift in selectivity, with the Ni(II) complex exerting a stronger cytotoxic effect on cancer cells than on healthy endothelial cells (Table 2).

CONCLUSION

A novel mixed-ligand Ni(II) complex incorporating the S-methyl-isothiosemicarbazone ligand and 2,6-dimethylpyridine co-ligand has been successfully synthesized and characterized. Spectroscopic (FT-IR, UV-Vis, ^{1}H-NMR) analyses together with melting point and elemental data conclusively verified ligand formation and metal complexation. X-ray diffraction clearly revealed a slightly distorted square-planar coordination environment involving an *N,O,N,N* donor set. The calculated distortion index ($\tau = 0.061$) and key bond metrics align well with analogous structural motifs reported for heteroaromatic co-ligated Ni(II) thiosemicarbazone complexes.

Biological evaluation demonstrated that Ni(II) complexation leads to a clear and measurable increase in cytotoxic activity compared to the free ligand, particularly against malignant cells. The complex exhibited substantially improved IC_{50} values in MCF-7 and K562, indicating that coordination chemistry directly enhances anticancer potency. Importantly, cytotoxicity in the non-tumorigenic HUVEC line remained significantly weaker, reinforcing the notion of a stronger biological effect in cancer-derived models than in healthy controls. These data supporting Ni(II) thiosemicarbazone complexes as promising candidates for further development of selective anticancer agents.

ACKNOWLEDGEMENTS

This work was supported by the Scientific Research Projects Coordination Unit of Istanbul University-Cerrahpaşa (Project number: FBA-2025-38160).

REFERENCES

Ali, M.A., Majumder, S.M.U.H., Butcher, R.J., Jasinski, J.P., Jasinski, J.M. (1997). The preparation and characterization of bis-chelated nickel (II) complexes of the 6-methylpyridine-2-carboxaldehyde Schiff bases of S-alkyldithiocarbazates and the X-ray crystal structure of the bis {S-methyl-β-N-(6-methylpyrid-2-yl)-methylenedithiocarbazato} nickel (II) complex. Polyhedron, 16(16), 2749-2754.

Arafath, A. (2023). Thiosemicarbazone Schiff base ligands and their complexes with nickel, palladium and platinum show anticancer and antibacterial activities. Journal of Sulfur Chemistry, 45(1), 138–171.

Atasever, B., Ülküseven, B., Bal-Demirci, T., Erdem Kuruca, S., Solakoğlu, Z. (2010). Cytotoxic activities of new iron(III) and nickel(II) chelates of some S-methyl-thiosemicarbazones on K562 and ECV304 cells. Investigational New Drugs, 28, 421–432.

Avcu Altiparmak, E., Yazar, S., Özdemir, N., Bal-Demirci, T., Ülküseven, B. (2021). Supramolecular Ni(II) complex aggregates with a circular linkage of intermolecular multi-hydrogen bonding frameworks based on thiosemicarbazone, and a Cu(II) complex: Synthesis, structural, DFT, electrochemical and antioxidant studies. Polyhedron, 209, 115457.

Avcu Altiparmak, E., Özen Eroğlu, G., Özdemir, N., Erdem Kuruca, S., Bal Demirci, T. (2025). Synthesis, cytotoxicities, structural properties and comparison of dihalogeno-substituted-thiosemicarbazone ligands and mixed-ligand Ni(ii) complexes. Dalton Transactions, 54, 1454-1467.

Bal-Demirci, T., Güveli, Ş., Yeşilyurt, S., Özdemir, N., Ülküseven, B. (2020). Thiosemicarbazone ligand, nickel(II) and ruthenium(II) complexes based on vitamin B6 vitamer: The synthesis, different coordination behaviors and antioxidant activities. Inorganica Chimica Acta, 502, 119335.

Bal, T., Atasever, B., Solakoğlu, Z., Erdem-Kuruca, S., Ülküseven, B. (2007). Synthesis, characterisation and cytotoxic properties of the N1,N4-diarylidene-S-methyl-thiosemicarbazone chelates with Fe(III) and Ni(II). European Journal of Medicinal Chemistry, 42 (2), 161-167,

de Araújo Neto, L.N., de Lima, M.C.A., de Oliveira, J.F., de Souza, E.R., Buonafina, M.D.S., Anjos, M.N.V., Brayner, F.A., Alves, L.C., Neves, R.P., Mendonça-Junior, F.J.B. (2017). Synthesis, cytotoxicity and antifungal activity of 5-nitro-thiophene-thiosemicarbazones derivatives. Chemico-Biological Interactions, 272, 172-181.

Jakupec, M.A., Galanski, M.S., Arion, V.B., Hartingera, C.G., Keppler, B.K. (2008). Antitumour metal compounds: more than theme and variations. Dalton Transactions, 183-194.

Jung, Y., Lippard, S.J. (2007). Direct cellular responses to platinum-induced DNA damage. Chemical Reviews, 107, 1387– 1407.

Karpagam, B., Sankarganesh, M., Ravi, L., Kesavan, M.P., Kumar, G.G.V., Rajagopal, G., Rajesh, J. (2021). Synthesis, spectroscopic and crystal structure of nickel(II) complex of thiosemicarbazone basedSchiff base: Antimicrobial, anticancer and molecular docking studies, Inorganic Chemistry Communications, 132, 108850.

Kaya, Y. (2023). Synthesis, Spectral Characterization, Crystal Structure, and Antioxidant Properties of novel Palladium(II) Complex from ONS Donor 1,5-bis(2-hydroxybenzylidene)thiocarbohydrazone. JOTCSA, 10(1), 129-38.

Khan, T., Raza, S., Lawrence, A.J. (2022) Medicinal Utility of Thiosemicarbazones with Special Reference to Mixed Ligand and Mixed Metal Complexes: A Review. Russian Journal of Coordination Chemistry, 48, 877–895.

Ma, B., Goh, B.C., Tan, E.H., Lam, K.C., Soo, R., Leong, S.S., Wang, L.Z., Mo, F., Chan, A.T.C., Zee, B., Mok, T. (2008). A multicenter phase II trial of 3-aminopyridine-2-carboxaldehyde thiosemicarbazone (3-AP, Triapine®) and gemcitabine in advanced non-small-cell lung cancer with pharmacokinetic evaluation using peripheral blood mononuclear cells. Investigational New Drugs, 26, 169–173.

Malarz, K., Mrozek-Wilczkiewicz, A., Serda, M., Rejmund, M., Polanski, J., Musiol, R. (2018) The role of oxidative stress in activity of anticancer thiosemicarbazones. Oncotarget, 9(25), 17689-17710.

Morgan, S.M., El-Sonbati, A.Z., Eissa, H.R. (2017). Geometrical structures, thermal properties and spectroscopic studies of Schiff base complexes: Correlation between ionic radius of metal complexes and DNA binding. Journal of Molecular Liquids, 240, 752-776.

Mosmann, T. (1983). Rapid colorimetric assay for cellular growth and survival: application to proliferation and cytotoxicity assays, Journal of Immunological Methods, 65, 55-63.

Palanimuthu, D., Shinde, S.V., Somasundaram, K., Samuelson, A.G. (2013). In Vitro and in Vivo Anticancer Activity of Copper Bis(thiosemicarbazone) Complexes. Journal of Medicinal Chemistry, 56 (3), 722-734.

Pelosi, G., Bisceglie, F., Bignami, F., Ronzi, P., Schiavone, P., Re, M.C., Casoli, C., Pilotti, E. (2010). Antiretroviral Activity of Thiosemicarbazone Metal Complexes. Journal of Medicinal Chemistry, 53 (24), 8765-8769.

Ramachandran, E., Kalaivani, P., Prabhakaran, R., Rath, N.P., Brinda, S., Poornima, P., Padma, V.V., Natarajan, K. (2012). Synthesis, X-ray crystal structure, DNA binding, antioxidant and cytotoxicity studies of Ni(II) and Pd(II) thiosemicarbazone complexes, Metallomics, 4, 218–227,

Rupam, D., Schmiesing, C.S., Sinn, E., Patil, Y.P., Nethaji, M., Stoeckli-Evans, H., Acharyya, R. (2013). Mixed-ligand nickel (II) thiosemicarbazone complexes: Synthesis, characterization and biological evaluation. Polyhedron, 50, 354-363.

Rzycka-Korzec, R., Malarz, K., Gawecki, R., Mrozek-Wilczkiewicz, A., Małecki, J.G., Schab-Balcerzak, E., Korzec, M., Polanski, J. (2021). Effect of the complex-formation ability of thiosemicarbazones containing (aza)benzene or 3-nitro-1,8-naphthalimide unit towards Cu(II) and Fe(III) ions on their anticancer activity. Journal of Photochemistry and Photobiology A: Chemistry, 415, 113314.

Sheldrick, G.M. (2015). Crystal structure solution with ShelXT. Acta Crystallographica A, 71, 3-8.

Stoe & Cie, (2002). X-AREA Version 1.18 and X-RED32 Version 1.04, Stoe & Cie, Darmstadt, Germany.

Yanardag, R., Bal Demirci, T., Ülküseven, B., Bolkent, S., Tunali, S., Bolkent, S. (2009). Synthesis, characterization and antidiabetic properties of N1-2,4-dihydroxybenzylidene-N4-2-hydroxybenzylidene-S-methyl-thiosemicarbazidato-oxovanadium(IV). European Journal of Medicinal Chemistry, 44, 818-826.

Yousef, T.A., Abu El-Reash, G.M. (2020). Synthesis, and biological evaluation of complexes based on thiosemicarbazone ligand, Journal of Molecular Structure, 1201, 127180.

Zhang, X.M., Guo, H., Li, Z.S., Song, F.H., Wang, W.M., Dai, H.Q., Zhang, L.X., Wang, J.G. (2015). Synthesis and evaluation of isatin-β-thiosemicarbazones as novel agents against antibiotic-resistant Gram-positive bacterial species. European Journal of Medicinal Chemistry, 101, 419-430.

ORAL PRESENTATION

Fast and complete destruction of acid fuchsin dye from water by electro-Fenton based processes

Elif Nesli Yanık[1] (*ORCID: https://orcid.org/0009-0001-1722-5383*), Şule Camcıoğlu[1] (*ORCID: https://orcid.org/0000-0002-8983-3193*), Baran Özyurt[1*] (*ORCID: https://orcid.org/0000-0003-0011-8351*), Eren Yağız Tumbul[1] (*ORCID: https://orcid.org/0009-0002-5033-9646*), Yıldız Kayacı[1] (*ORCID: https://orcid.org/0009-0004-1687-0593*), Yaren Babadağ[1] (*ORCID: https://orcid.org/0009-0005-8454-6354*), Rümeysa Sarıtaş[1] (*ORCID: https://orcid.org/0009-0002-5935-0315*),

[*1]Ankara University, Faculty of Engineering, Department of Chemical Engineering, Ankara, Türkiye.

*Corresponding author e-mail: bozyurt@ankara.edu.tr

Abstract

Dyes discharged from industrial activities pose a major threat to the environment due to their high solubility, chemical stability, and resistance to biodegradation. Commonly used in textile, paper, leather, food, and cosmetic industries, these pollutants accumulate in aquatic ecosystems, causing toxicity, bioaccumulation, and risks to human health. Conventional treatment methods such as filtration, sedimentation, and biological processes are often ineffective for dye removal because they cannot break down recalcitrant dye structures. Advanced oxidation processes (AOPs) have therefore emerged as effective technologies capable of degrading and mineralizing persistent organic contaminants. These processes rely on the in-situ generation of highly reactive hydroxyl radicals (•OH), typically produced through iron-catalyzed decomposition of hydrogen peroxide (H_2O_2). In the electro-Fenton (EF) process, hydrogen peroxide (H_2O_2) is electrogenerated at the cathode while Fe^{2+} is continuously regenerated, sustaining radical formation. Photoelectro-Fenton (PEF) further improves EF performance by applying UV irradiation, which accelerates $Fe^{3+} \rightarrow Fe^{2+}$ cycling and enhances •OH production. The heterogeneous electro-Fenton (HEF) approach uses solid iron-based catalysts instead of soluble iron, enabling operation over a wider pH range and facilitating catalyst recovery. The heterogeneous photoelectro-Fenton (HPEF) process combines solid catalysts with electrochemical and photonic activation, providing higher stability and increased degradation efficiency. In this study, the effects of current intensity on the degradation and mineralization of Acid Fuchsin dye in aqueous media were examined using EF, PEF, HEF, and HPEF processes with a boron-doped diamond (BDD) anode and carbon felt (CF) cathode at pH 3. Under 100 mA and 0.1 mM Fe^{2+}, EF achieved complete color removal in 18 min and full COD removal in 36 min. PEF achieved complete color removal in 18 min and full COD removal in 60 min under 100 mA and 0.1 mM Fe^{2+}. HEF, using 0.1 $g \cdot L^{-1}$ Fe_3O_4, provided complete color removal in 24 min and total COD removal in 90 min. The HPEF process, performed with 0.1 $g \cdot L^{-1}$ Fe_3O_4 and 100 mA, achieved identical color removal (18 min) and COD removal (60 min). These findings demonstrate the high efficiency of electrochemical and photoelectrochemical AOPs for rapid and complete dye degradation.

Keywords: Electro-Fenton, Photoelectro-Fenton, Heterogeneous catalysts, Advanced oxidation processes, Dye degradation, Magnetic nanoparticles

INTRODUCTION

Dyes are complex organic compounds widely used in textile, paper, leather, food, and cosmetic industries, and their release into wastewater significantly alters the physical and chemical characteristics of aquatic environments (Liu et al., 2023). Industrial wastewater is one of the major contributors to environmental pollution, as it contains diverse toxic compounds originating from washing, extraction, heating, cooling, separation, and various production steps (Khan et al., 2022). Within this context, the textile industry represents one of the largest global consumers of dyes, generating wastewater enriched with recalcitrant and persistent colorants (Mahroudi et al., 2022). Worldwide synthetic dye production is estimated at nearly 70 million tons per year, with approximately 10% discharged directly into the environment (Góralczyk-Bińkowska et al., 2021). Growing concerns over diminishing freshwater resources and increasing pollution have intensified the need for sustainable wastewater treatment and reuse (Özyurt

& Camcıoğlu, 2018). Industrial effluents often contain high levels of harmful chemicals such as dyes, arising from processes including equipment cleaning, mixing, packaging, and floor washing (Camcıoğlu, 2016). Once discharged, these dyes reduce light penetration, inhibit aquatic photosynthesis, increase COD and BOD levels, and exert toxic, mutagenic, and carcinogenic effects on living organisms (Fungaro et al., 2011; Kuczyński et al., 2021). Typical dye concentrations in textile wastewater range between 5–30 mg L^{-1} and may exceed the acute toxicity limits reported for aquatic organisms, typically 0.16–0.43 ppm (Liu et al., 2022). Acid Fuchsin, selected as the model contaminant in this study, is a water-soluble, violet-colored acidic dye used in textile dyeing, corrosion inhibition, and laboratory staining (Xing et al., 2019). Due to its aromatic and sulfonated structure, it is resistant to biodegradation, capable of spreading over wide areas, and poses risks including irritation, respiratory effects, and long-term carcinogenicity (Carmen & Daniela, 2012). Therefore, efficient removal of Acid Fuchsin and similar dyes from wastewater is essential for protecting both environment and human health.

As these micro-pollutants continue to be detected and accumulate in surface and groundwater resources, the implementation of effective treatment technologies has become increasingly important (McBeath et al., 2019). Among the available options, advanced oxidation processes (AOPs) have gained prominence due to their ability to generate highly reactive hydroxyl radicals (•OH) that can non-selectively oxidize a broad range of organic pollutants in water; the overall process efficiency is closely related to the rate and extent of •OH generation (Oturan & Aaron, 2014). Depending on the mode of radical formation, AOPs can be classified as chemical, photochemical, sonochemical, or electrochemical (Rodrigo et al., 2014). Electrochemical advanced oxidation processes (EAOPs) have emerged as efficient, environmentally compatible, and easily automated technologies for the removal of recalcitrant pollutants (Sirés et al., 2014; Nidheesh et al., 2018). Among EAOPs, the electro-Fenton (EF) process is one of the most widely applied. EF relies on the in-situ electrogeneration of hydrogen peroxide (H_2O_2) from the two-electron reduction of dissolved oxygen at the cathode and the continuous regeneration of Fe^{2+}, which catalyzes H_2O_2 decomposition into •OH in acidic medium, typically around pH 3 (Oturan, 2000; Oturan & Pinson, 1995). In parallel, the use of anodes with high oxygen-evolution overpotential, such as boron-doped diamond (BDD), enables additional •OH formation via water oxidation, further enhancing oxidation capacity (Oturan, 2021). The efficiency of EF strongly depends on H_2O_2 production at the cathode, and numerous carbon-based materials—including activated carbon, carbon fiber, graphite, carbon felt (CF), carbon black, carbon nanotubes, and graphene—have been investigated to improve oxygen reduction and H_2O_2 yield (Wang et al., 2018; Trellu et al., 2018; Nidheesh & Gandhimathi, 2014; El-Ghenymy et al., 2014; Sopaj et al., 2020; Liu et al., 2013; Khataee et al., 2014; Yang et al., 2017; Wang et al., 2023). EF has been successfully applied to the degradation of various organic contaminants, including pesticides, pharmaceuticals, and dyes, achieving fast and often complete mineralization (Barhoumi et al., 2017; Camcioglu et al., 2022; Martínez-Huitle et al., 2023; Nidheesh et al., 2022). The homogeneous photoelectro-Fenton (PEF) process couples EF with UV or solar irradiation. In PEF, UVA or UVB radiation accelerates Fe^{3+}/Fe^{2+} cycling via photoreduction of $Fe(OH)^{2+}$ and Fe(III)–carboxylate complexes and promotes additional •OH generation through photolysis of H_2O_2 and organic intermediates, leading to higher mineralization rates than conventional EF (Garcia-Segura & Brillas, 2014; Ye et al., 2020; Brillas, 2020). However, the need to operate at acidic pH and the requirement for post-treatment removal and disposal of soluble iron species limit the large-scale application of homogeneous PEF systems (Brillas, 2020).

To overcome these drawbacks, research has increasingly focused on heterogeneous Fenton and photo-Fenton systems employing insoluble iron-based catalysts such as Fe_3O_4, γ-Fe_2O_3, and Fe-modified semiconductor oxides (Ganiyu et al., 2018; Wang et al., 2020; Thomas et al., 2021). These heterogeneous systems offer important advantages, including operation over a wider pH range, easy separation and reuse of the catalyst, and mitigation of iron sludge production (Poza-Nogueiras et al., 2018). In heterogeneous photo-Fenton processes, irradiation plays a key role in enhancing interfacial $\equiv Fe^{3+}/\equiv Fe^{2+}$ cycling, promoting charge separation, and boosting H_2O_2 activation at the catalyst surface (Banerjee et al., 2018; Khalid et al., 2012; Sun et al., 2018). Magnetite (Fe_3O_4), in particular, is an attractive catalyst owing to its mixed-valence Fe^{2+}/Fe^{3+} structure, good magnetic separability, and ability to efficiently activate H_2O_2 for •OH production (Banerjee et al., 2018; Camcıoğlu et al., 2023).

The integration of heterogeneous catalysts into electro-Fenton and photoelectro-Fenton configurations has led to the development of heterogeneous electro-Fenton (HEF) and heterogeneous photoelectro-Fenton (HPEF) processes, which combine the benefits of EF, photo-Fenton, and heterogeneous Fenton chemistries (Ganiyu et al., 2018; Poza-Nogueiras et al., 2018). In these systems, the electrochemical generation of H_2O_2, the regeneration of surface $\equiv Fe^{2+}$ sites, and the photonic activation under UV or solar irradiation act synergistically, enabling high •OH

fluxes and improved degradation of persistent organic pollutants (Brillas, 2020; Camcıoğlu et al., 2023). Within this framework, the present study comparatively evaluates EF, PEF, HEF, and HPEF processes for the degradation and mineralization of Acid Fuchsin dye using a BDD anode and a CF cathode, with particular emphasis on the influence of current intensity on treatment performance.

MATERIALS AND METHODS

Experiments were conducted in a 250 mL glass reactor with 200 mL of a 0.05 mM Acid Fuchsin solution and 50 mM Na_2SO_4 as the supporting electrolyte. A BDD anode (16 cm^2) and CF cathode (16 cm^2) were used and connected to a DC power supply. Compressed air was introduced five minutes prior to the experiment and maintained throughout the experimental period to promote the in-situ generation of H_2O_2 at the cathode. The experiments were carried out under constant current conditions, with the applied current ranging from 100 to 500 mA. For homogeneous Fenton-based experiments (EF and PEF) 0.1 mM $FeSO_4 \cdot 7H_2O$ was introduced as the catalyst prior to initiating the experiments, whereas for heterogeneous Fenton-based experiments (HEF and HPEF) 0.1 $g \cdot L^{-1}$ Fe_3O_4 was used. Fe_3O_4 was synthesized via the co-precipitation method. For photoelectrochemical degradation studies (PEF and HPEF), UVA (365 nm) and UVC (254nm) light sources were utilized. Initial pH was adjusted using acid (0.2 M H_2SO_4) or base (0.1 M NaOH) solutions. Solution homogeneity was ensured through magnetic stirring. Samples were periodically collected throughout the experiment for color and COD analyses to evaluate treatment efficiency and monitor dye removal and COD reduction. Dye removal was quantified by measuring the solution absorbance at 546 nm using a UV-VIS spectrophotometer, while COD removal was assessed following Standard Methods for COD analysis. In this study, the effects of current intensity on dye and COD removal were investigated for EF, PEF, HEF, and HPEF processes.

RESULTS and DISCUSSION

The results of studies conducted to determine the effect of current intensity for the treatment of Acid Fuchsin solution using the EF method under pH 3 and 0.1 mM Fe^{2+} catalyst concentration conditions are presented in Figure 1. The complete degradation of 0.05 mM Acid Fuchsin was quickly achieved in all cases, verifying that the dye was efficiently oxidized by •OH both in the bulk solution and at the surface of the anode. The decay of Acid Fuchsin concentration was improved by the increase in current value up to 100 mA for which complete degradation was achieved in 18 min. Further increase in current value did not enhance the degradation efficiency. The decrease in the degradation kinetics at higher current intensities may be related to the enhancement of the rate of the side reactions that inhibit the formation or promote the consumption of •OH. The most important of these side reactions are evolution of H_2 at the cathode which competes with the formation of H_2O_2 and the evolution of O_2 on the anode surface.

The mineralization of Acid Fuchsin solution was performed at different current values with regard to COD removal efficiency. COD removal rate increased with the increments of current from 50 to 500 mA, as expected from the enhanced production of •OH. This fact can be explained by the high oxygen evolution overpotential of the BDD anode allowing the formation of high amounts of heterogeneously formed •OH as well as homogeneously formed •OH in the bulk, due to the increased rate of electrogenerated H_2O_2 and fast electro-regeneration of Fe^{2+} promoting Fenton's reaction. The fastest and complete COD removal was achieved within 36 min under 100 mA current intensity, showing acceleration of parasitic non-oxidative reactions of the •OH at higher current values, mainly heterogeneously formed •OH oxidation to O_2 and the recombination of homogeneously formed •OH to H_2O_2.

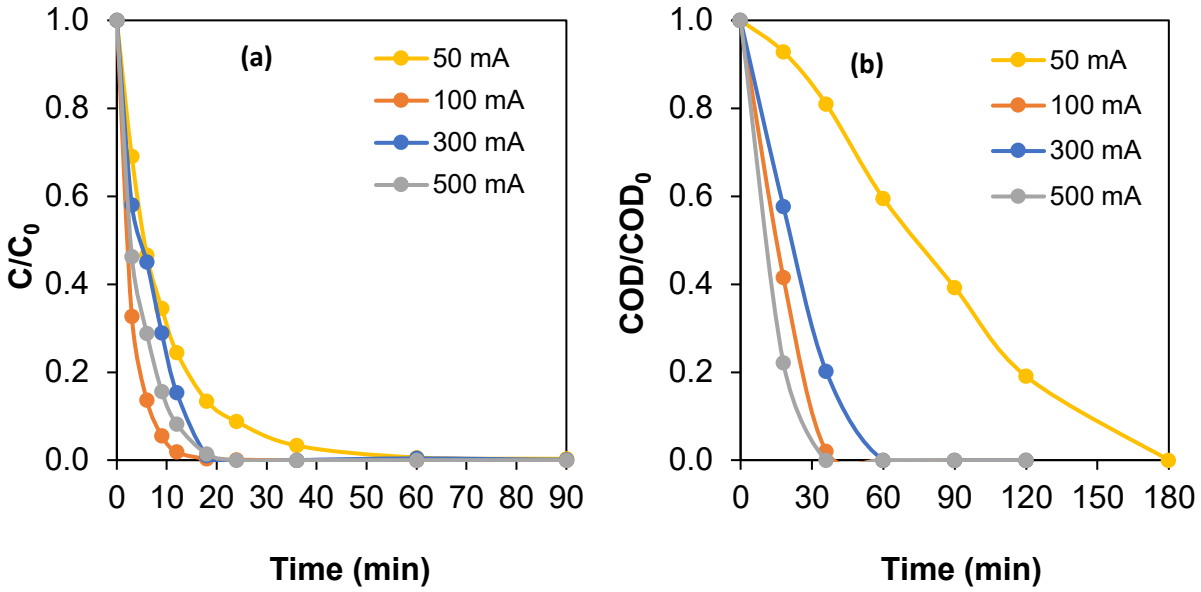


Figure 1. The effect of current intensity on color (a) and COD (b) removal using the EF method

The influence of current intensity on the performance of the PEF process in degrading and mineralizing Acid Fuchsin under pH 3 and 0.1 mM Fe^{2+} catalyst concentration conditions is presented in Figure 2. The process exhibits higher efficiency with complete degradation and mineralization at 18 min and 60 min under applied current of 100 mA compared to 300 mA and 500 mA. Increasing the applied current appears to promote side reactions that either inhibit the formation of •OH or enhance their consumption. The most significant of these side reactions is the evolution of O_2 at the anode and H_2 generation at the cathode. These competing reactions adversely affect the overall process efficiency, explaining the reason that lower currents yield better performance than higher currents. Based on these observations, 100 mA was selected as the optimum current intensity for PEF process.

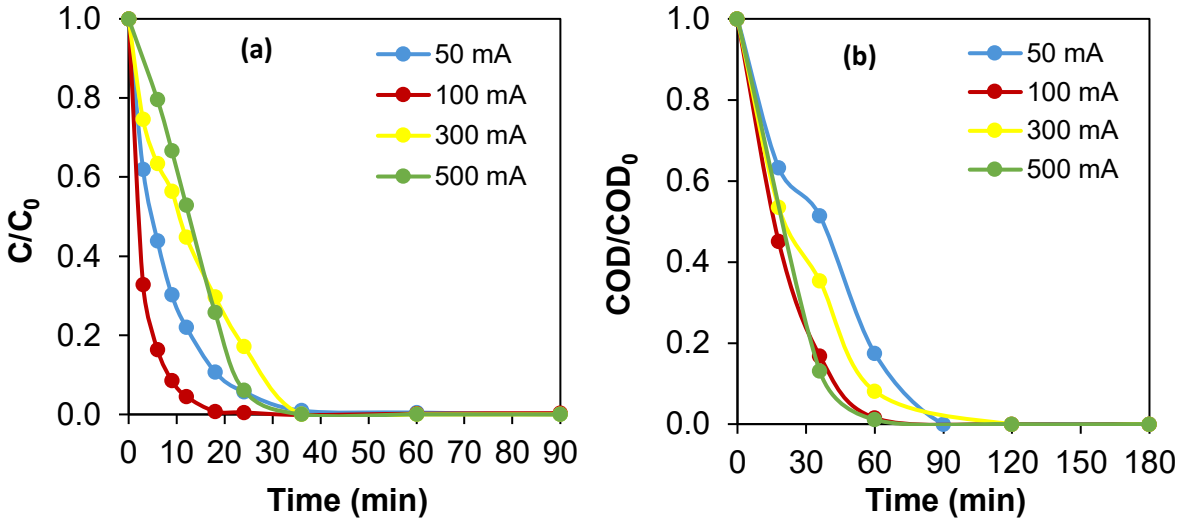


Figure 2. The effect of current intensity on color (a) and COD (b) removal using the PEF method

The results of studies conducted to determine the optimum current intensity for the treatment of Acid Fuchsin dye using the HEF method under pH 3 and 0.1 $g.L^{-1}$ Fe_3O_4 catalyst concentration conditions are presented in Figure 3 demonstrates that complete degradation of Acid Fuchsin was achieved within 24 min at the current intensity of 100 mA. The acceleration of the Acid Fuchsin decay kinetics with increasing applied current intensity up to 100 mA can be attributed to the enhancement of H_2O_2 electro-generation and regeneration of heterogeneous catalyst $\equiv Fe^{II}$, resulting in a higher production rate of •OH. However, further increases in current from 100 to 500 mA did not enhance degradation. This can be associated with an increase in the rate of side reactions that either inhibit the

generation of •OH or accelerate its consumption. The most notable side reactions are cathodic H_2 formation, which competes with the production of H_2O_2, reduction of H_2O_2 to H_2O at the cathode, O_2 evolution reaction in the bulk and at the anode.

Mineralization efficiency increased regularly with increasing applied current density up to 500 mA owing to the promotion of HEF in three ways. First, the electro-regeneration of the $\equiv Fe^{II}$ catalyst increases at high currents due to the cathodic reduction of $\equiv Fe^{III}$, resulting in an increase in the reaction rate. Secondly, anodic oxidation (AO) increases with applied current and creates a synergy with the catalyst regeneration at the cathode enhancing EF mineralization of organics in water. Finally, the in situ electro-generation of H_2O_2 by the cathodic reduction of oxygen is dependent on the applied current.

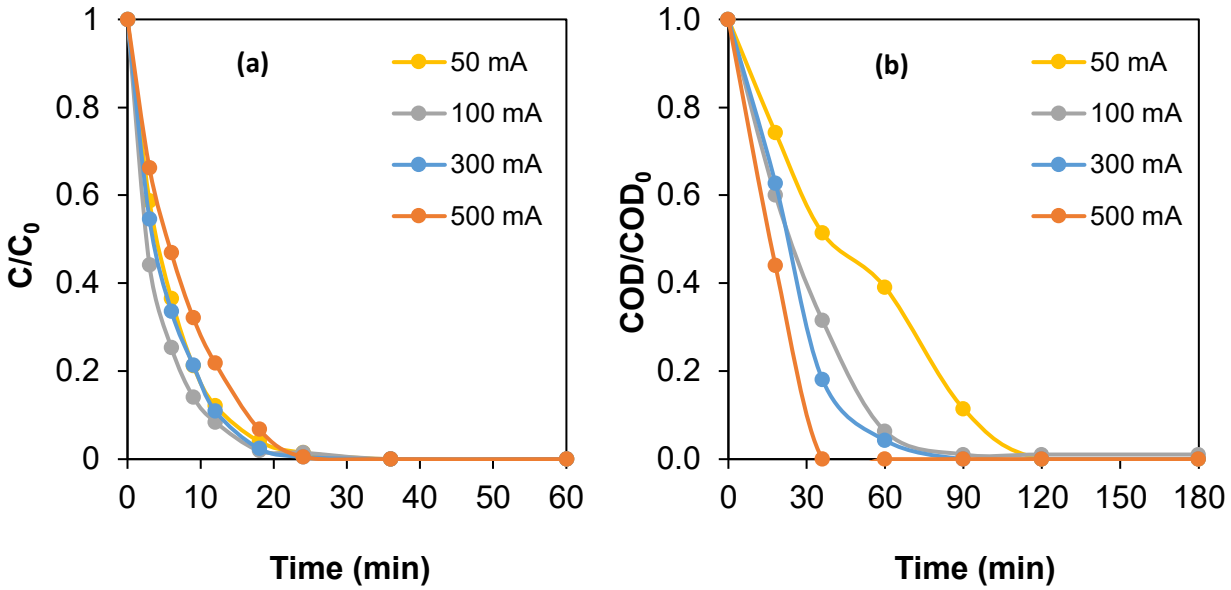


Figure 3. The effect of current intensity on color (a) and COD (b) removal using the HEF method

The effect of applied current intensity on the degradation and mineralization of Acid Fuchsin was investigated utilizing HPEF method under pH 3 and 0.1 $g.L^{-1}$ Fe_3O_4 catalyst concentration conditions by varying the applied current from 50 mA to 500 mA and the results are illustrated in Figure 4. The results indicate that COD removal efficiencies improve progressively with an increase in current intensity up to 500 mA. This enhancement is attributed to the facilitation of AO and HPEF mechanisms. Higher currents favor the electro-regeneration of catalyst via the cathodic reduction of $\equiv Fe^{III}$, leading to increased •OH generation. Furthermore, an increase in applied current enhances anodic oxidation, synergizing with the EF process to boost the mineralization of the target molecule in water. The in-situ electro-generation of H_2O_2 through the cathodic reduction of oxygen is notably affected by the applied current. Nevertheless, elevating the applied current to 500 mA does not yield significant enhancements in degradation, attributable to an escalation in side reactions that either impede •OH formation or augment its consumption. Prominent among these side reactions are the evolution of O_2 at the anode surface and within the bulk solution, which decelerates the rate of AO. Additionally, the production of H_2 at the cathode, resulting from H_2O reduction, competes with the oxygen reduction reaction, thus limiting H_2O_2 production.

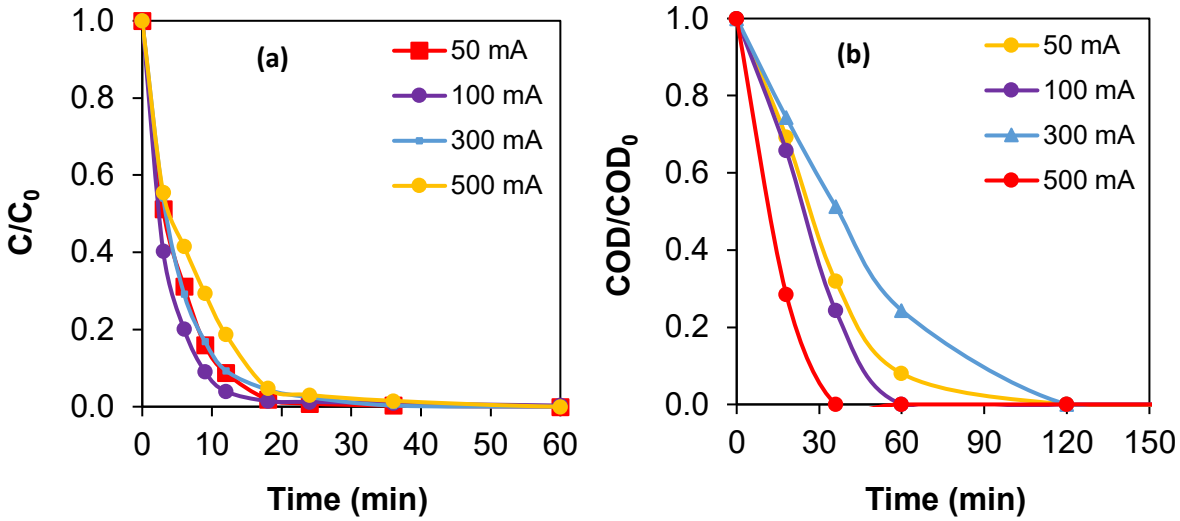


Figure 4. The effect of current intensity on color (a) and COD (b) removal using the HPEF method

CONCLUSION

In this study, the degradation and mineralization of Acid Fuchsin dye were systematically evaluated using four electrochemical advanced oxidation processes—EF, PEF, HEF, and HPEF—employing a BDD anode and CF cathode at pH 3. For all processes, color removal was very fast, confirming that the investigated systems can efficiently oxidize the chromophoric groups of the dye. Under the optimum operating conditions, complete discoloration was achieved within 18–24 min for all methods, demonstrating the strong oxidative capacity of both homogeneous and heterogeneous Fenton-based routes. Current intensity was found to be a key parameter controlling process performance. For EF and PEF, increasing the current up to 100 mA enhanced both decolorization and mineralization, but further increases led to lower efficiency due to competing side reactions, such as O_2 evolution at the anode and H_2 formation or H_2O_2 reduction at the cathode. Under 100 mA and 0.1 mM Fe^{2+}, EF provided the fastest mineralization, achieving complete COD removal in 36 min, whereas PEF required 60 min for full COD removal at the same current and catalyst concentration. In the heterogeneous systems, the use of magnetite (0.1 $g \cdot L^{-1}$ Fe_3O_4) enabled efficient treatment while offering the additional advantages of solid catalyst recovery and the potential for operation over a wider pH range. In HEF, complete color removal was obtained in 24 min and full COD removal in 90 min, with mineralization efficiency increasing with current due to enhanced H_2O_2 electrogeneration and $\equiv Fe^{2+}$ regeneration. The HPEF process further improved performance, reaching complete discoloration in 18 min and full COD removal in 60 min at 100 mA, owing to the synergistic action of electrochemical H_2O_2 production, interfacial Fenton reactions, and UV-driven radical generation.

Overall, the results confirm that electrochemical and photoelectrochemical AOPs are highly effective for the rapid and complete removal of Acid Fuchsin from water. EF offers the highest mineralization rate under optimized current density, whereas HEF and HPEF provide attractive, magnetically recoverable catalytic systems, with HPEF combining high efficiency with the practical advantages of a heterogeneous catalyst. These findings highlight the strong potential of Fenton-based EAOPs, particularly EF and HPEF, as advanced treatment options for dye-laden industrial wastewaters and motivate further studies on energy consumption optimization, catalyst stability, and application to real effluents.

ACKNOWLEDGEMENTS

The authors acknowledge TUBITAK (The Scientific and Technological Research Council of Turkey) for providing financial support through 2209-A Research Project Support Programme for Undergraduate Students under grant number 1919B012417289.

REFERENCES

Banerjee, S., Benjwal, P., Singh, M., & Kar, K. K. (2018). Graphene oxide (rGO)-metal oxide (TiO_2/Fe_3O_4) based nanocomposites for the removal of methylene blue. *Applied Surface Science, 439*, 560–568.

Barhoumi, N., Olvera-Vargas, H., Oturan, N., Huguenot, D., Gadri, A., Ammar, S., Brillas, E., & Oturan, M. A. (2017). Kinetics of oxidative degradation/mineralization pathways of the antibiotic tetracycline by the novel

heterogeneous electro-Fenton process with solid catalyst chalcopyrite. *Applied Catalysis B: Environmental, 209*, 637–647.

Brillas, E. (2020). A review on the photoelectro-Fenton process as efficient electrochemical advanced oxidation for wastewater remediation. Treatment with UV light, sunlight, and coupling with conventional and other photo-assisted advanced technologies. *Chemosphere, 250*, 126198.

Camcıoğlu, Ş. (2016). *Kâğıt endüstrisi atıksularının elektrokimyasal yöntemle arıtılması* (Doctoral dissertation, Ankara University).

Camcioglu, S., Özyurt, B., Oturan, N., Trellu, C., & Oturan, M. A. (2022). Fast and complete destruction of the anti-cancer drug cytarabine from water by electrocatalytic oxidation using electro-Fenton process. *Catalysts, 12*(12), 1598.

Camcıoğlu, Ş., Özyurt, B., Oturan, N., Portehault, D., Trellu, C., & Oturan, M. A. (2023). Heterogeneous electro-Fenton treatment of chemotherapeutic drug busulfan using magnetic nanocomposites as catalyst. *Chemosphere, 341*, 140129.

Carmen, Z., & Daniela, S. (2012). Textile organic dyes—characteristics, polluting effects and separation/elimination procedures from industrial effluents—A critical overview. In *Textile Organic Dyes* (Vol. 3, pp. 55–86). Rijeka: IntechOpen.

El-Ghenymy, A., Rodríguez, R. M., Brillas, E., Oturan, N., & Oturan, M. A. (2014). Electro-Fenton degradation of the antibiotic sulfanilamide with Pt/carbon-felt and BDD/carbon-felt cells. Kinetics, reaction intermediates, and toxicity assessment. *Environmental Science and Pollution Research, 21*, 8368–8378.

Fungaro, D. A., Yamaura, M., & Carvalho, T. E. M. (2011). Adsorption of anionic dyes from aqueous solution on zeolite from fly ash–iron oxide magnetic nanocomposite. *Journal of Atomic and Molecular Sciences, 2*(4), 305–316.

Garcia-Segura, S., & Brillas, E. (2014). Advances in solar photoelectro-Fenton: Decolorization and mineralization of the Direct Yellow 4 diazo dye using an autonomous solar pre-pilot plant. *Electrochimica Acta, 140*, 384–395.

Ganiyu, S. O., Zhou, M., & Martínez-Huitle, C. A. (2018). Heterogeneous electro-Fenton and photoelectro-Fenton processes: A critical review of fundamental principles and application for water/wastewater treatment. *Applied Catalysis B: Environmental, 235*, 103–129.

Góralczyk-Bińkowska, A., Długoński, A., Bernat, P., Długoński, J., & Jasińska, A. (2021). Environmental and molecular approach to dye industry waste degradation by the ascomycete fungus *Nectriella pironii*. *Scientific Reports, 11*(1), 23829.

Khalid, N. R., Hong, Z., Ahmed, E., Zhang, Y., Chan, H., & Ahmad, M. (2012). Synergistic effects of Fe and graphene on photocatalytic activity enhancement of TiO_2 under visible light. *Applied Surface Science, 258*, 5827–5834.

Khan, S., Malik, A., & Zhao, X. (2022). A critical review on the treatment of dye-containing wastewater. *Journal of Hazardous Materials, 436*, 127545.

Khataee, A., Akbarpour, A., & Vahid, B. (2014). Photoassisted electrochemical degradation of an azo dye using Ti/RuO_2 anode and carbon nanotubes containing gas-diffusion cathode. *Journal of the Taiwan Institute of Chemical Engineers, 45*, 930–936.

Kuczyński, M., Łuba, M., Mikołajczyk, T., Pierożyński, B., Jasiecka-Mikołajczyk, A., Smoczyński, L., Sołowiej, P., & Wojtacha, P. (2021). Electrodegradation of Acid Mixture Dye through the employment of Cu/Fe macro-corrosion galvanic cell in Na_2SO_4 synthetic wastewater. *Molecules, 26*(15), 4580.

Liu, Z., Zhang, Y., & Wang, X. (2023). Recent advances in the remediation of textile-dye-containing wastewater. *Sustainability, 16*(2), 495.

Liu, J., Wei, S., Zhang, H., Deng, Y., Baeyens, J., Dewil, R., Sweygers, N., & Appels, L. (2022). Adsorption of Acid Fuchsine dye from wastewater by Mg-ferrite particles. *Journal of Environmental Management, 318*, 115427.

Liu, J., Sun, X., Song, P., Zhang, Y., Xing, W., & Xu, W. (2013). High-performance oxygen reduction electrocatalysts based on cheap carbon black, nitrogen, and trace iron. *Advanced Materials, 25*, 6879–6883.

Mahroudi, A., Aghasi, M., Dolatabadi, M., & Ahmadzadeh, S. (2022). Removal of reactive blue 171 dye from aqueous solution and textile industrial wastewater using peroxi-electrocoagulation process by iron electrode: Application of response surface methodology. *Desalination and Water Treatment, 272*, 266–276.

Martínez-Huitle, C. A., Rodrigo, M. A., Sirés, I., & Scialdone, O. (2023). A critical review on latest innovations and future challenges of electrochemical technology for the abatement of organics in water. *Applied Catalysis B: Environmental, 328*, 122430.

McBeath, S. T., Wilkinson, D. P., & Graham, N. J. D. (2019). Application of boron-doped diamond electrodes for the anodic oxidation of pesticide micropollutants in a water treatment process: A critical review. *Environmental Science: Water Research & Technology, 5*, 2090–2107.

Nidheesh, P. V., & Gandhimathi, R. (2014). Removal of Rhodamine B from aqueous solution using graphite–graphite electro-Fenton system. *Desalination and Water Treatment, 52*, 1872–1877.

Nidheesh, P. V., Zhou, M., & Oturan, M. A. (2018). An overview on the removal of synthetic dyes from water by electrochemical advanced oxidation processes. *Chemosphere, 197*, 210–227.

Nidheesh, P. V., Ganiyu, S. O., Martínez-Huitle, C. A., Mousset, E., Olvera-Vargas, H., Trellu, C., Zhou, M., & Oturan, M. A. (2022). Recent advances in electro-Fenton process and its emerging applications. *Critical Reviews in Environmental Science and Technology*, 1–27.

Oturan, M. A. (2000). An ecologically effective water treatment technique using electrochemically generated hydroxyl radicals for in situ destruction of organic pollutants: Application to herbicide 2,4-D. *Journal of Applied Electrochemistry, 30*, 475–482.

Oturan, M. A. (2021). Outstanding performances of the BDD film anode in electro-Fenton process: Applications and comparative performance. *Current Opinion in Solid State and Materials Science, 25*, 100925.

Oturan, M. A., & Aaron, J.-J. (2014). Advanced oxidation processes in water/wastewater treatment: Principles and applications. *Critical Reviews in Environmental Science and Technology, 44*, 2577–2641.

Oturan, M. A., & Pinson, J. (1995). Hydroxylation by electrochemically generated OH• radicals. Mono- and polyhydroxylation of benzoic acid: Products and isomer distribution. *Journal of Physical Chemistry, 99*, 13948–13954.

Özyurt, B., & Camcıoğlu, Ş. (2018). Applications of combined electrocoagulation and electrooxidation treatment to industrial wastewaters. *Wastewater and Water Quality, 56*(1), 71–89.

Poza-Nogueiras, V., Rosales, E., Pazos, M., & Sanromán, M. A. (2018). Current advances and trends in electro-Fenton process using heterogeneous catalysts – A review. *Chemosphere, 201*, 399–416.

Rodrigo, M. A., Oturan, N., & Oturan, M. A. (2014). Electrochemically assisted remediation of pesticides in soils and water: A review. *Chemical Reviews, 114*, 8720–8745.

Sirés, I., Brillas, E., Oturan, M. A., Rodrigo, M. A., & Panizza, M. (2014). Electrochemical advanced oxidation processes: Today and tomorrow. *Environmental Science and Pollution Research, 21*, 8336–8367.

Sopaj, F., Oturan, N., Pinson, J., Podvorica, F. I., & Oturan, M. A. (2020). Effect of cathode material on electro-Fenton process efficiency for electrocatalytic mineralization of the antibiotic sulfamethazine. *Chemical Engineering Journal, 384*, 123249.

Sun, Q., Hong, Y., Liu, Q., & Dong, L. (2018). Synergistic operation of photocatalytic degradation and Fenton process by magnetic Fe_3O_4 loaded TiO_2. *Applied Surface Science, 430*, 399–406.

Trellu, C., Oturan, N., Keita, F. K., Fourdrin, C., Pechaud, Y., & Oturan, M. A. (2018). Regeneration of activated carbon fiber by the electro-Fenton process. *Environmental Science & Technology, 52*, 7450–7457.

Wang, X., Zhu, K., Ma, X., Sun, Z., & Hu, X. (2018). Degradation of diuron by heterogeneous electro-Fenton using modified magnetic activated carbon as the catalyst. *RSC Advances, 8*, 19971–19978.

Wang, Z., Olvera-Vargas, H., Martins, M. V. S., Garcia-Rodriguez, O., Garaj, S., & Lefebvre, O. (2023). High performance and durable graphene-grafted cathode for electro-Fenton degradation of tetramethyldecynediol. *Chemical Engineering Journal, 455*, 140643.

Wang, F., Yu, X., Ge, M., & Wu, S. (2020). One-step synthesis of TiO_2/γ-Fe_2O_3/GO nanocomposites for visible light-driven degradation of ciprofloxacin. *Chemical Engineering Journal, 384*, 123381.

Xing, J., Yang, B., Shen, Y., Wang, Z., Wang, F., Shi, X., & Zhang, Z. (2019). Selective removal of Acid Fuchsin from aqueous solutions by rapid adsorption onto polypyrrole crosslinked cellulose/gelatin hydrogels. *Journal of Dispersion Science and Technology*.

Ye, Z., Schukraft, G. E. M., L'Hermitte, A., Xiong, Y., Brillas, E., Petit, C., & Sirés, I. (2020). Mechanism and stability of an Fe-based 2D MOF during the photoelectro-Fenton treatment of organic micropollutants under UVA and visible light irradiation. *Water Research, 184*, 115986.

ORAL PRESENTATION

Extraction of bioactive components from black elderberry (*Sambucus nigra* L.) with deep eutectic solvents and characterization of the components

Rüveyda Alptekin[1] Seda Özgen[1*] (*https://orcid.org/0000-0001-9952-5015)*

[*1] Çankırı Karatekin University, Faculty of Engineering, Department of Food Engineering, Çankırı, Türkiye.

*Corresponding author e-mail: sozgen@karatekin.edu.tr

Abstract

This research utilized dried elderberry fruits (*Sambucus nigra* L.). an edible and medicinal plant. in conjunction with ultrasound-assisted extraction (UAE) and deep eutectic solvents (DESs) to produce elderberry extracts by environmentally friendly extraction methods. Six varieties of DESs were made with choline chloride as Hydrogen bond acceptors (HBAs) and 6 distinct Hydrogen bond donors (HBDs) (citric acid. L-ascorbic acid. fructose. sucrose. ethylene glycol. glycerol) and compared with extracts derived from ethanol and methanol solutions of standard organic solvents. Antioxidant activities (DPPH and ABTS). total monomeric anthocyanin content (pH differential technique) and total phenolic content (Folin-Ciocalteu) were examined. The LC-MS/MS method was used to assess the quantities of phenolic compounds. The results indicate that the glycerol-based deep eutectic solvent. ChCl:GLY:Water (1:1:2). exhibits superior efficiency compared to ethanol solvent in assessing antioxidant activity. anthocyanin content. and phenolic content. In the assessment of total phenolic content (Folin-Ciocalteu). the ChCl:GLY:Water (1:1:2) deep eutectic solvent yielded 4.216 mg GAE/g dry matter. whereas the 50% ethanol-water solution produced 3.635 mg GAE/g dry matter. and the methanol solution resulted in 5.014 mg GAE/g dry matter. In the examination of phenolics using LC-MS/MS. it was noted that glycerol-based deep eutectic solvents (14 phenolics) extracted a greater quantity of phenolic compounds and exhibited superior performance compared to methanol (8 phenolics). Elderberry extracts made with DES were rich in anthocyanins (cyanidin-3-rutinoside chloride and cyanidin-3-o-glucoside). flavonoids (hesperidin). and phenolic acids (fumaric acid and chlorogenic acid). Specifically. glycerol-based DES has demonstrated that deep eutectic solvents derived from green solvents can be a good substitute for conventional solvents like ethanol and methanol. which are detrimental to both human health and the environment.

Keywords: *Sambucus nigra* L., Green Extraction, Green Solvents, Deep Eutectic Solvents

INTRODUCTION

Green technology is actively researching new solvents to replace common organic solvents, which exhibit high volatility and inherent toxicity, leading to the evaporation of volatile organic compounds into the atmosphere (Paiva et al., 2014). Green technologies aim to reduce the production and consumption of hazardous substances, reduce the amount of energy consumed in the production of hazardous chemicals, and increase the use of renewable resources (Kantar et al., 2021).

Extraction of phenolic compounds is generally based on solid-liquid extraction with water/organic solvent mixtures and organic solvents (methanol, ethanol, acetone, chloroform, ethyl acetate, etc.). However, organic solvents have been noted to have some disadvantages, such as toxicity, volatility, non-degradability, flammability, and high cost (Clarke et al., 2018). Extraction solvents are known to be primarily derived from non-renewable resources, particularly petroleum-based volatile organic compounds, which are suspected of being harmful to both human health and the environment (Chemat et al., 2019). Furthermore, increasing awareness of human impact on the environment has brought the concept of green extraction to the forefront of interest within the scientific and industrial communities. Green extraction is generally based on the discovery and design of extraction methods that will provide safe and high-quality extracts/products, allowing the use of renewable natural products and alternative solvents that will reduce energy consumption (Chemat et al., 2012).

In recent years, there has been a growing concern about environmental issues worldwide, and people must be more aware of and responsible about the environmental impact of their activities (Armenta et al., 2019). Therefore, it is important to investigate alternative solvents that are inexpensive, readily available, safe to use, and compatible with the idea of "green chemistry" (Kowalska et al., 2021). Ideal candidates are those with high solubilizing capacity and low toxicity for specific target molecules; They must be readily biodegradable and recyclable without any harmful environmental impacts (Chemat et al., 2019).

Deep eutectic solvents (DESs) are green alternatives to traditional organic solvents with unique physicochemical properties that offer the opportunity to be designed for specific purposes. In many cases, they have achieved higher extraction efficiencies compared to traditional organic solvents (Mišan et al., 2020). DESs are generally defined as mixtures of binary or more compounds that can be solid or liquid and can combine primarily through hydrogen bonds. Combining these compounds in specific proportions results in eutectic mixtures with lower melting points than their individual components (Paiva et al., 2014). Hydrogen bond acceptors (HBAs) in the formation of DESs primarily include quaternary ammonium or phosphonium salts, while amides, alcohols, and carboxylic acids have been used as the most common HBAs. Compounds such as sugars, sugar alcohols, and amino acids are also considered in the preparation of DESs (Dai et al., 2013). The most common DESs, or DESs, are formed using choline chloride (ChCl) as a hydrogen bond acceptor (HBA) and carboxylic acids and other HCAs, such as citric acid, glycerol, and succinic acid, as hydrogen bond donors (HBDs) (Mbous et al., 2017; Paiva et al., 2014).

Recently, a combination of DESs and new green extraction techniques, such as ultrasound-assisted extraction (UAE), has been proposed to increase the extraction efficiency of DESs in the extraction of phenolic compounds (Patil et al., 2021; Wu et al., 2020). UDE; It is considered a green technology due to its advantages of high extraction efficiency, low solvent consumption, low energy consumption and short-term consumption (Kumar et al., 2021; Wu et al., 2020).

Elderberry (Sambucus nigra L.), belonging to the family Adoxaceae, is a highly accessible and abundant plant native to the Northern Hemisphere and is now found in diverse habitats such as the subtropical regions of Asia, North Africa, and North America (Finn et al., 2008; Młynarczyk et al., 2018). The content of primary metabolites (sugars and organic acids) gives elderberry its typical sweet and tart taste, while its characteristic aroma is attributed to the presence of various volatile and phenolic compounds (Ferreira et al., 2020). Elderberry is rich in nutrients such as carbohydrates, proteins, fats, fatty acids, organic acids, minerals, vitamins, and essential oils, but also contains potentially toxic cyanogenic glycosides (Młynarczyk et al., 2018). While the use of elderberries is sometimes restricted due to the presence of cyanogenic glycosides, ripe elderberries are reportedly safe for consumption and processing, as increasing fruit ripeness leads to a decrease in the content of these compounds (Ferreira et al., 2020).

In this study extracts were obtained from the dried fruits of the black elderberry (Sambucus Nigra), an edible and medicinal plant, using ultrasound-assisted extraction (UAE) combined with DESs, which are less toxic, environmentally friendly, and have higher solubility than organic solvents. They were compared with extracts obtained using two conventional organic solvents. The aim was to produce products with less costly and environmentally friendly extraction processes that are harmless to human health and to promote the use of green solvents. Today, it is necessary to increase the use of environmentally friendly products for climate change, environmental pollution and sustainable living, which are considered as important problems internationally.

MATERIALS AND METHODS

In this study. dried black elderberries with organic certification code TR-OT-014-127/05R were used as raw materials. All other chemicals were supplied by Sigma Aldrich.

Preparation of Deep Eutectic Solvents

In the presented study. solvents were prepared by calculating their molar ratios based on information obtained from the literature. First. the prepared DES were heated in a water bath at the specified temperatures for 6 hours until they liquefied. They were then stirred on a magnetic stirrer for 1 hour until they became a clear liquid. The resulting liquefied. clear DES were then incubated in an ultrasonic water bath at 100 Hertz and 60°C for 30 minutes. A literature search (Popovic et al., 2022; Vladimir-Knežević et al., 2022) found that the water content in DES should

be between 0-70%. In this study. it was decided to work at a 50% water ratio (15 mL water - 15 mL DW). 0.5 g of black elderberry powder was placed in 50 mL tubes. For the six DES solutions. it was decided to use 50% ethanol and 100% methanol with 1% HCl as two control groups. The molar ratios of HBD and HBA used in the preparation of DESs are given in Table1.

Table 1. Components and molar ratios used in the preparation of DESs (Mišan et al., 2020)

Solvent	Components	Molar Ratio
1	ChCl: Citric Acid: Water	1:1:2
2	ChCl: L-Ascorbic Acid: Water	1:1:2
3	ChCl: Fructose: Water	5:2:5
4	ChCl: Sucrose: Water	4:1:4
5	ChCl: Ethylene Glycol: Water	1:1:2
6	ChCl: Glycerol: Water	1:1:2
7	50% Ethanol-Purified Water Solution (1% acidified)	
8	100% Methanol (1% acidified)	

Ultrasound-Assisted Deep Eutectic Solvent Extraction from Black Elderberry

Extraction was performed by adding 25 mL of DOS solution to 0.5 g of dry powdered sample. The extract was shaken by hand for approximately 10-15 seconds to mix the extract and solution. then left at room temperature for 30 minutes. Ultrasound-assisted extraction was then applied for 10 minutes at 20 kHz. 500 watts. and 40% amplitude. Finally. the extract was centrifuged at 5000 rpm for 10 minutes. filtered through filter paper. and then passed through a 0.45-micron syringe filter. The resulting extracts were stored in a +4°C refrigerator until bioactive analyses were performed.

Bioactive Analyses

Determination of Total Monomeric Anthocyanin Content (pH Differential Method)

The pH differential method described by Fuleki and Francis (1968) was used to determine total anthocyanin content. This method is based on the color change of anthocyanin pigments depending on the pH of the medium. The difference between measurements at different pH values at the wavelengths where the samples exhibit maximum absorbance is directly proportional to the anthocyanin content of the sample. In this context. pH 1.0 and pH 4.5 buffers prepared with 0.02 M Na_2HPO_4 and 0.02 M NaH_2PO_4 were added simultaneously to 1 ml of each extract and incubated for 30 minutes in the dark at room temperature. In the study. each sample. prepared for pH 1.0 and pH 4.5 and diluted to yield absorbance in the 0.4-0.8 range. was measured at 516 nm (maximum wavelength) and 700 nm to detect turbidity (Agilent-Cary 60. USA). Results are given in mg of cyanidin 3-O-glucoside per gram of sample. Experiments were performed in two replicates and five replicates. The total anthocyanin content was calculated using the formula below.

$$Anthocyanin\,(mg/L) = (\Delta A/\mathcal{E} * L)10\text{^}3 * MW * SF \quad (1)$$

ΔA: Absorbance difference (A= ((A516nm- A700nm) pH 1.0) – ((A516nm- A700nm) pH 4.5))
Ɛ: Molar absorbance
L: Optical path of the absorbance measurement cuvette (=1)
MW: Molecular weight
SF: Dilution factor

Determination of DPPH Radical Scavenging Activity

The antiradical activity of the samples was determined using the method recommended by Faller and Fialho. 2010 with some modifications. For this purpose. 100 µL of the prepared extract solutions were mixed with 3.9 ml of DPPH (Sigma. USA) solution (0.1 mM and prepared in methanol) and then allowed to stand in the dark for 30 minutes. At the end of this period. the absorbance values of the test tubes were determined at 517 nm using a UV-Vis spectrophotometer (Agilent-Cary 60. USA) zeroed with methanol. Experiments were performed in two replicates and five parallels. The DPPH radical scavenging activity of the samples was calculated as % inhibition using the formula below.

$$A\%\ Inhibition = [(Abs\ Control - Abs\ Extract)/Abs\ Control] \quad (2)$$

Determination of Total Phenolic Content

100 µL of black elderberry extracts were diluted at specific ratios. 2.9 ml of 0.2 N Folin-Ciocalteu reagent was added and vortexed for 2 minutes. 2 ml of 7.5% sodium carbonate was added. After 2 hours in the dark. 5 ml of distilled water was added and centrifuged at 5000 rpm for 5 minutes. The absorbance of each sample was measured at 765 nm using a spectrophotometer (Agilent-Cary 60. USA). Total phenolic content was expressed as gallic acid equivalents (GAE) in mg GAE/g dry matter.

ABTS Method

ABTS Scavenging Activity was determined by making some modifications to the method established by Almajano et al., (2007). In this method. 2.45 mM K2S2O8 and 7 mM ABTS (2.2'-azino-bis (3-ethylbenzthioazoline-6-sulfonic acid)) solutions were mixed at a 1:1 ratio and incubated for 16 hours at room temperature in the dark. The absorbance of this prepared ABTS radical solution was measured at 734 nm and diluted with ethyl alcohol until an absorbance of 1.850±0.05 was achieved. This absorbance was used as the control absorbance (Agilent. Carry 60 UV-Vis. USA). 4 mL of this radical solution was then added to test tubes. 100 µL of plant extracts were added to these tubes and incubated for 2 hours at room temperature in the dark. At the end of this period. the absorbance of the samples was recorded at 734 nm against a blank composed of PBS (Phosphate Buffer. pH = 7.4) (Wu et al., 2009). The decreased absorbance indicates the amount of ABTS radicals scavenged from the medium (Keser et al., 2013). The amount of ABTS radicals scavenged by the extracts in the medium was calculated using the following formula:

$$ABTS\ \%\ Inhibition = [\,[(A_0 - A_1)/A_0]\ x\ 100\,] \quad (3)$$

A_0 was taken as the absorbance of the control and A_1 was taken as the absorbance of the samples.

Determination of Phenolic Content by LC-MS/MS

LC-MS/MS (Agilent 6460 Triple Quadrapole) High-Performance Liquid Chromatography/Sequential Mass Chromatography was used in the study. Samples obtained from the phenolic extraction were vortex-mixed and injected onto the LC-MS/MS column. All analyses were run in two parallel runs.
LC-MS/MS operating conditions for the phenolic content determination of black elderberry samples are carried with Zorbax SB18 C18 (1.8 µm x 2.1 x 50 mm), 0.3mL/min flow rate, 40°C oven temperature,1 µL injection volume and gradient flow profile. The mobile phase consisted of A (0.1% of formic acid aqueous solution) and B (acetonitrile) phases at 0.1 mL/min and 35 °C. The LC gradient was operated as follows 0–5 min (%7 B); 5–8 min (%30 B); 8–35 min (%50 B); and 35–50 min (%7 B).

RESULTS and DISCUSSION

Table 3 shows the antioxidant activities (DPPH and ABTS). Total phenolic amounts (Folin-Ciocalteu) and total anthocyanin amounts (pH differential method) of black elderberry extracts obtained with 6 DES (Choline chloride: Citric Acid (1). Choline chloride: L-Ascorbic Acid (2). Choline chloride: Fructose (3). Choline chloride: Sucrose

(4). Choline chloride: Ethylene Glycol (5). Choline chloride: Glycerol (6)). Ethanol: Distilled Water Solution (7) and 100% Methanol Solution (8) solutions.

Table 3. Bioactive Analysis Results of Samples

	DPPH (% Inh.)	Total Anthocyanin (mg C_3G /g)	Total Phenolic (mg GAE /g dry matter)	ABTS (µmol trolox/g)
1	14.67±1.21	1.02±0.08	1.48±0.03	12.16±0.94
2	19.61±2.04	0.81±0.04	1.18±0.02	11.43±1.12
3	34.98±0.97	1.34±0.05	1.95±0.03	13.74±1.78
4	35.07±2.71	1.58±0.06	2.31±0.04	15.17±0.83
5	35.91±1.05	1.97±0.13	2.79±0.03	15.84±1.31
6	49.07±2.65	2.88±0.09	4.22±0.14	19.35±1.25
7	47.94±1.75	2.49±0.07	3.64±0.16	18.58±0.96
8	63.14±2.12	3.13±0.17	5.01±0.41	20.06±1.07

In the antioxidant activity analysis with DPPH. the values ranged between 14.67% inhibition and 49.074% inhibition. Although ChCl:Citric Acid (14.67% inhibition) and ChCl:L-Ascorbic Acid (19.6% inhibition) DESs number 1 showed lower performance than the other DESs (34.982%-49.074% inhibition). similar results were obtained in other analyses. Methanol solution showed the highest performance in antioxidant activities (DPPH and ABTS). total phenolic amount (Folin-Ciocalteu) and total anthocyanin amounts (pH differential method) analyses. However. ChCl:GLY DES number 6 (49.074% inhibition) was observed to be better than 50% ethanol-water solution number 7 (47.942% inhibition).

There are very few studies in the literature on the extraction of black elderberry with DES. In one study. Vladimir-Knežević et al., (2022) compared the extraction efficiencies of DES based on water. 70% ethanol. and a 1:3 molar ratio of choline chloride (ChCl) and ethylene glycol (EG). and the same molar ratio of choline chloride and glycerol (GLY) using dried black elderflower (Sambucus nigra L.) and rosemary (Rosmarinus officinalis L.) plants. They reported that high levels of phenolic acids were found in elderflower leaves (3.64±0.13%). Regarding the extraction of total phenolic acids. it was found that ChCl:EG and ChCl:GLY were almost as effective as 70% ethanol solutions with a 1:3 molar ratio of 50% water by volume. They reported that 50% ChCl:GLY gave slightly better results than the other two. A similar result was obtained in this thesis. In the analysis of total phenolic content. DES formed with ChCl:EG (2.785 mg GAE/g dry matter). 50% ethanol-water solution (3.635 mg GAE/g dry matter). and ChCl:GLY yielded the best results with a dry matter value of 4.216 mg GAE/g.

In another study. DES formed with different molar ratios of L-lactic acid (HBD) and glycine (HBA) and extracts obtained using water. a 60% methanol aqueous solution. and a 60% ethanol aqueous solution were compared after ultrasonication pretreatment of black elderberry flowers. They reported that the DES formed with L-Lactic Acid: Glycine (5:1) was the highest-performing system (Kaltsa et al., 2020).

Another study evaluated the possibility of using water-glycerol systems to obtain anthocyanin extracts from black aronia and black elderberry berries. The highest anthocyanin concentrations were obtained from the 50% water-glycerol system at extraction temperatures of 20°C and 50°C (Kowalska et al., 2021). The study concluded that glycerol could be an alternative solvent to ethanol for the extraction of anthocyanins. A similar result was obtained in this thesis. with the ChCl:Glycerol-based DES-containing extract yielding better results than ethanol.

The composition and amounts of phenolic compounds in black elderberry are given in Table 4. In one of the two studies in the literature on the extraction of elderberry using DES, Vladimir-Knežević et al., (2022) investigated elderberry flowers and rosemary leaves for their polyphenolic content and composition. The presence of flavonoids

and phenolic acids in the plant extracts was proven by thin-layer chromatography. Among the phenolic acids, chlorogenic acid was the most abundant in dried elderberry flowers, followed by rutin and isoquercetin. In another study, Kaltsa et al., (2020) reported that rutin, di-p-coumaroylquerciic acid, and chlorogenic acid were predominant in the richest elderberry flower extract obtained by LC-DAD-MS analysis.

Table 4. Composition and amounts of phenolic compounds in samples (ng/mL)

	(1) ChCl: Citric Acid	(2) ChCl: L-Ascorbic Acid	(3) ChCl: Fructose	(4) ChCl: Sucrose	(5) ChCl: Ethylene Glycol	(6) ChCl: Glycerol	(7) Et-OH	(8) Me-OH
Quinic Acid	-	-	-	-	-	-	3693.384	21.0580
Fumaric Acid	115.495	48.337	1136.355	999.998	1512.488	668.522	1634.477	-
Gallic Acid	-	-	57.4757	-	123.932	276.6473	50.308	-
Cyanidin-3-Rutinoside Chloride	1005.711	1884.195	2213.972	2615.010	2348.815	3226.328	3785.298	1618.120
Cyanidin-3-O-Glucoside	1360.884	1.202	899.885	1071.093	2246.913	3486.664	2008.594	6366.665
Chlorogenic Acid	2245.225	3203.494	6655.810	5838.168	4529.798	5041.925	7802.790	8.414
4-OH-Benzoic Acid	119.625	125.784	148.539	196.662	233.251	384.267	270.202	-
Caffeic Acid	-	-	37.076	79.161	301.826	3419.369	-	-
Vanillic Acid	28.794	-	47.905	-	-	121.096	-	-
Hesperidin	2276.262	4531.547	5919.334	6615.910	6563.851	7697.769	8814.598	2705.401
P-Coumaric Acid	89.239	56.718	125.965	149.041	212.700	693.062	150.364	-
Ferulic Acid	9.183	-	-	3.766	93.847	553.140	23.310	-
Vanillin	5.258	0.877	1.817	3.879	1.983	6.442	2.028	5.087
Rosmarinic Acid	3.641	2.339	7.248	8.0710	4.276	5.313	0.317	1.238
Quercetin	177.186	79.384	72.480	161.176	21.015	176.543	257.122	21955.16
Quinic Acid	-	-	-	-	-	-	3693.384	21.0580

Similar to two studies in the literature on elderberry extracts obtained using DES, this thesis also found abundant chlorogenic acid, a phenolic acid, in the extracts obtained using DES. LC-MS/MS analysis revealed that elderberry extracts contained abundant chlorogenic acid. Domínguez et al., (2020), using ethanol as a solvent, aimed to characterize the potential use and nutritional value of elderberry as a source of antioxidant compounds. Optimization of extraction parameters was designed using a Box-Behnken design combined with response surface methodology and desirability function analysis. Finally, numerical optimization revealed that the optimal extraction parameters were a temperature of 60°C, a 50% ethanol solution, and a pH of 2. LC-MS/MS analysis revealed abundant flavonoids (rutin and quercetin) and phenolic acids (gallic acid and gentisic acid) in elderberries. In this

thesis, because of LC-MS/MS analysis performed with the extracts obtained using DES, hesperidin and quercetin were detected in the highest amounts among the flavonoids.

CONCLUSION

Although other studies in the literature used different raw materials and methods, analysis results generally yielded advantages for green solvents. Furthermore, most studies indicate that deep eutectic solvents can be an alternative to traditional solvents, but further research is needed on this topic. Green solvents, which offer significant advantages such as biodegradability, recyclability, non-toxicity, sustainability, low cost, and ease of preparation, have been shown to be an alternative to traditional organic solvents commonly used in extraction processes, such as ethanol and methanol, which are volatile, non-degradable, flammable, costly, and harmful to human health and the environment.

REFERENCES

Almajano, M. P., Delgado, M. E., & Gordon, M. H. (2007). Changes in the antioxidant properties of protein solutions in the presence of epigallocatechin gallate. *Food Chemistry*, *101*(1), 126-130.

Armenta, S., Garrigues, S., Esteve-Turrillas, F. A., & de la Guardia, M. (2019). Green extraction techniques in green analytical chemistry. TrAC Trends in Analytical Chemistry, 116: 248-253.

Chemat, F., Abert Vian, M., Ravi, H. K., Khadhraoui, B., Hilali, S., Perino, S. and Fabiano Tixier, A. S. (2019). Review of alternative solvents for green extraction of food and natural products: Panorama, principles, applications and prospects. Molecules, 24(16): 3007.

Chemat, F., Vian, M. A. and Cravotto, G. (2012). Green extraction of natural products: Concept and principles. International journal of molecular sciences, 13(7): 8615-8627.

Clarke, C. J., Tu, W. C., Levers, O., Brohl, A. and Hallett, J. P. (2018). Green and sustainable solvents in chemical processes. Chemical Reviews, 118(2): 747-800.

Dai, Y., van Spronsen, J., Witkamp, G. J., Verpoorte, R., & Choi, Y. H. (2013). Natural deep eutectic solvents as new potential media for green technology. Analytica chimica acta, 766: 61-68.

Domínguez, R., Zhang, L., Rocchetti, G., Lucini, L., Pateiro, M., Munekata, P. E. and Lorenzo, J. M. (2020). Elderberry (Sambucus nigra L.) as potential source of antioxidants. Characterization, optimization of extraction parameters and bioactive properties. Food chemistry, 330: 127266.

Faller, A. L. K., & Fialho, E. F. N. U. (2010). Polyphenol content and antioxidant capacity in organic and conventional plant foods. *Journal of Food Composition and Analysis*, *23*(6), 561-568.

Ferreira, S. S., Silva, P., Silva, A. M., & Nunes, F. M. (2020). Effect of harvesting year and elderberry cultivar on the chemical composition and potential bioactivity: A three-year study. Food Chemistry, 302: 125366.

Finn, C. E., Thomas, A. L., Byers, P. L., and Serçe, S. (2008). Evaluation of American (Sambucus canadensis) and European (S. nigra) elderberry genotypes grown in diverse environments and implications for cultivar development. HortScience, 43(5): 1385-1391.

Fuleki, T., & Francis, F. J. (1968). Quantitative methods for anthocyanins. 2. Determination of total anthocyanin and degradation index for cranberry juice. *Journal of food science*, *33*(1), 78-83.

Kaltsa, O., Lakka, A., Grigorakis, S., Karageorgou, I., Batra, G., Bozinou, E., Lalas, S. and Makris, D. P. (2020). A green extraction process for polyphenols from elderberry (Sambucus nigra) flowers using deep eutectic solvent and ultrasound-assisted pretreatment. Molecules, 25(4): 921.

Kantar, N. K., Yılmaz, M. S., Yakan, A. İ. ve Demirkol, Ö. Ş. (2021). Gıdalardan biyoaktif bileşiklerin ekstraksiyonunda derin ötektik çözücülerin kullanımı. Niğde Ömer Halisdemir Üniversitesi Mühendislik Bilimleri Dergisi, 10(2): 591-597.

Kowalska, G., Wyrostek, J., Kowalski, R., & Pankiewicz, U. (2021). Evaluation of glycerol usage for the extraction of anthocyanins from black chokeberry and elderberry fruits. Journal of Applied Research on Medicinal and Aromatic Plants, 22: 100296.

Kowalska, G., Wyrostek, J., Kowalski, R., & Pankiewicz, U. (2021). Evaluation of glycerol usage for the extraction of anthocyanins from black chokeberry and elderberry fruits. Journal of Applied Research on Medicinal and Aromatic Plants, 22: 100296.

Kumar, K., Srivastav, S., and Sharanagat, V. S. (2021). Ultrasound assisted extraction (UAE) of bioactive compounds from fruit and vegetable processing by-products: A review. Ultrasonics Sonochemistry, 70: 105325.

Mbous, Y. P., Hayyan, M., Hayyan, A., Wong, W. F., Hashim, M. A., and Looi, C. Y. (2017). Applications of deep eutectic solvents in biotechnology and bioengineering. Promises and challenges. Biotechnology advances, 35(2): 105-134.

Mišan, A., Nađpal, J., Stupar, A., Pojić, M., Mandić, A., Verpoorte, R., and Choi, Y. H. (2020). The perspectives of natural deep eutectic solvents in agri-food sector. Critical reviews in food science and nutrition, 60(15): 2564-2592.

Młynarczyk, K., Walkowiak-Tomczak, D. and Łysiak, G. P. (2018). Bioactive properties of Sambucus nigra L. as a functional ingredient for food and pharmaceutical industry. Journal of Functional Foods, 40: 377-390.

Paiva, A., Craveiro, R., Aroso, I., Martins, M., Reis, R. L. and Duarte, A. R. C. (2014). Natural deep eutectic solvents–solvents for the 21st century. ACS Sustainable Chemistry & Engineering, 2(5): 1063-1071.

Paiva, A., Craveiro, R., Aroso, I., Martins, M., Reis, R. L. and Duarte, A. R. C. (2014). Natural deep eutectic solvents–solvents for the 21st century. ACS Sustainable Chemistry & Engineering, 2(5): 1063-1071.

Patil, S. S., Pathak, A., and Rathod, V. K. (2021). Optimization and kinetic study of ultrasound assisted deep eutectic solvent based extraction: A greener route for extraction of curcuminoids from Curcuma longa. Ultrasonics sonochemistry, 70: 105267.

Vladimir-Knežević, S., Perković, M., Zagajski Kučan, K., Mervić, M. and Rogošić, M. (2022). Green extraction of flavonoids and phenolic acids from elderberry (Sambucus nigra L.) and rosemary (Rosmarinus officinalis L.) using deep eutectic solvents. Chemical Papers, 76(1): 341-349.

Wu, L., Li, L., Chen, S., Wang, L., and Lin, X. (2020). Deep eutectic solvent-based ultrasonic-assisted extraction of phenolic compounds from Moringa oleifera L. leaves: Optimization, comparison and antioxidant activity. Separation and Purification Technology, 247: 117014.

ORAL PRESENTATION

Investigation of the use of colorimetric films containing cranberry extract as ph indicators

Abukar Mohamud Omar[1], Zehra Özbaş[1*] (*https://orcid.org/0000-0001-9729-4938*)

[1] Çankırı Karatekin University, Faculty of Engineering, Department of Chemical Engineering, Çankırı, Türkiye.

*Corresponding author e-mail: zehraozbas@karatekin.edu.tr

Abstract

The smart packaging system for real-time visual monitoring of food freshness plays a significant role in food safety. The use of biopolymer as a matrix and natural anthocyanin as a pH indicator has led to increased interest in freshness detection in recent years. However, anthocyanin migration and the relatively weak mechanical strength of the film limit the applicability of biopolymer based smart packaging systems. Techniques such as blending two or more biopolymers, adding reinforcing agents, and crosslinking have been developed to improve mechanical properties. The aim of this study is to determine the pH-dependent color change in cross-linked films prepared with biopolymer blends by adding cranberry extract to monitor food freshness, and thus to develop colorimetric films that can be used for smart packaging. The effect of the extract on the film properties including structural characterization, color parameters, bioactivity, and pH-dependent color changes was investigated.

Keywords: Colorimetric film, Cranberry, Anthocyanin, pH indicator.

INTRODUCTION

With the emergence of impressive healthy nutrition management, smart packaging systems have gained significant attention due to their ability to quickly and easily visually detect food quality during storage and transportation. In practice, volatile alkaline substances are released during the decomposition of protein-rich or fatty products, causing pH changes as well as an alkaline state. Colorimetric films, which operate on the principle of color changes caused by pH, are the preferred films for accurately assessing food freshness. Today, anthocyanins, natural substances that can be obtained from fruits, vegetables, flowers, and even food waste, are widely added to film compositions as pH-sensitive dyes for detecting food freshness (Liu et al., 2017; Shaik et al., 2022). The use of synthetic dyes such as methyl orange and bromocresol green/blue as pH indicators is limited due to their high toxicity and genotoxicity.

The cranberry (CR) used in the study is a small red fruit grown in the cooler climates of the Northeastern United States, Canada, and Chile (Philip and Walsh, 2019). Cranberries are rich in many bioactive compounds with nutritional components and antioxidant properties. Both American (Vaccinium macrocarpon) and European (Vaccinium oxycoccus) cranberry species are rich in polyphenols such as phenolic acids, anthocyanins, and flavonoids (Nemzer et al., 2022). For this reason, cranberries were used as an anthocyanin source in the study.

Polymer-based indicators preserve and even improve the performance of pH-sensitive molecules, and in some cases, the polymer matrix increases their stability by protecting them from oxidation or other environmental factors (Kossyvaki et al., 2022). However, the hydrophilic and water-soluble nature of biopolymer films results in weak mechanical and physical properties, making them unsuitable for application in the food industry. These weak mechanical properties can be improved by adding crosslinkers, bioactive compounds, nanoparticles, etc. (Özgen and Özbaş, 2025).

Starch, carboxymethyl cellulose, sodium alginate, and other biopolymers are widely used in food packaging due to their low toxicity, biocompatibility, and biodegradability. Carboxymethyl cellulose (CMC) is a cellulose derivative obtained by the carboxymethylation process of cellulose. It is non-toxic, safe, renewable, biocompatible, biodegradable, and has excellent film-forming ability. It can also be used to carry pH dye indicators in colorimetric films (Kaewprachu et al., 2024). Sodium alginate (SA) is a natural biopolymer obtained from brown seaweed that is water-soluble, biocompatible, and has film-forming properties (Yang et al., 2022). Starch (ST) is widely used in

food packaging due to its stability against heat, acid, and base conditions, low cost, and good film-forming properties (Liu et al., 2017; Zhai et al., 2017). Polymer blends are often used to improve the water resistance and thermal stability of polymeric films. Additionally, calcium chloride ($CaCl_2$), an excellent crosslinking agent, is preferred to enhance the mechanical properties of biopolymer based packaging films (Yang et al., 2021).

Numerous investigations on visual and intelligent pH indicator films with various biodegradable matrixes made by adding anthocyanins have been conducted in recent years to investigate food spoilage. The following are some studies using biopolymers used in the study to assess food freshness: ST/polyvinyl alcohol incorporated with roselle anthocyanins (Zhai et al., 2017), pectin/SA/xanthan gum incorporated with raspberry pomace extract (Yang et al., 2021), polyvinyl alcohol/CMC incorporated with red cabbage anthocyanins, SA/CMC incorporated with rose anthocyanins (Yang et al., 2022), and gellan gum/ST/xanthan gum with aronia extract (Eker et al., 2025).

In this study, crosslinked colorimetric films were prepared from CMC, SA, and ST polymers containing CR extract, a polyphenolic compound rich in anthocyanins, to monitor the freshness of foods. The potential of these films for use in smart packaging was investigated based on the color change they exhibit in response to pH changes.

MATERIALS AND METHODS

Chemicals

CR extract was obtained from Pharmatoka (Rueil-Malmaison, France) and used as received. The CMC and SA biopolymers used to prepare the films were Sigma-Aldrich products, and ST was ISOLAB product. The crosslinking agent ($CaCl_2$), glycerin, Na_2CO_3, Folin-Ciocalteu phenol reagent, 2,2-Diphenyl-1-picrylhydrazil (DPPH), HCl-KCl buffer (pH 1.0), and CH_3COONa buffer (pH 4.5) were Sigma-Aldrich products. Merck buffer solutions ranging from pH 2.0 to 13.0 were used to monitor the color change of the films.

Film Preparation

The solvent casting method was used to obtain colorimetric films. First, 0.27 g of CMC, 0.27 g of SA, and 0.06 g of ST were dissolved in distilled water at ~80°C with continuous stirring for 3 hours using a magnetic stirrer. Then, glycerol (500 µL) was added to the solution as a plasticizer. After cooling to 50°C, different amounts of powdered CR extract (CR: 0; 0.03 g, 0.06 g, and 0.09 g) were added to the film solution. Finally, 0.15% $CaCl_2$ was added to the solution as the crosslinker. The final volume of the solutions was adjusted to 30 mL, poured into petri dishes, and allowed to dry at 40°C. The prepared films were named CSS-CR0, CSS-CR1, CSS-CR2, and CSS-CR3 according to the amount of extract they contained.

Film Characterization

Film thickness and color: A digital micrometer was used to measure the thickness of each film, and the average values were reported. A portable Konica Minolta CR-400 chroma meter was used to record the color parameters (L, a, and b) of the films. The total color difference (ΔE) was calculated using the Equation (1) (L*: 92.60, a*: -0.92, b*: -2.24):

$$\Delta E = \sqrt{(L^* - L)^2 + (a^* - a)^2 + (b^* - b)^2} \quad (1)$$

Fourier transform infrared (FTIR) analysis: Structural analysis of the biopolymers and the resulting films was recorded with an FTIR spectroscopy (Bruker Tensor II) equipped with attenuated total reflection (ATR) accessory in the range of 4000-500 cm^{-1}.

Bioactivity analysis: Bioactive characterization of the films was evaluated by total antioxidant capacity (TAC) and total monomeric anthocyanin content (TMAC).

100 mg of film was extracted with 15 ml of 80% ethanolic solution (acidified with HCl). This extract was used in all bioactivity analyses. DPPH radical scavenging activity (Kan et al., 2019) and ABTS radical scavenging activity (Almajano et al., 2007) tests were used to evaluate the TAC of the film.

30 µL of each sample was mixed with 2970 µL of 0.1 mM DPPH methanol solution in a test tube and allowed to react for one hour in the dark. The absorbance of the reaction solution at 517 nm was measured with an Agilent Cary 60 UV-Vis spectrophotometer.

The ABTS+ cation radical was obtained by the reaction between 7 mM ABTS and 2.45 mM potassium persulfate (1:1) and was stored in the dark at room temperature for 12-16 hours before use. The absorbance of the ABTS radical solution at 734 nm was adjusted with ethyl alcohol to 1.850±0.05. 25 µL of film extract was mixed with 2975 µL of ABTS solution and stored in the dark at room temperature for 2 hours. The absorbance at 734 nm was then measured using an Agilent Cary 60 UV-Vis spectrophotometer. The TAC of the samples was determined by the Equation (2):

$$TAC\ (\%) = \left({}^{A_0 - A_1}/_{A_0}\right) * 100 \quad (2)$$

where A_0 and A_1 are the absorbance of the control and sample, respectively.

TMAC determination of the samples was carried out according to the pH differential method (Giusti and Wrolstad, 2001). The total amount of anthocyanin present in the sample was determined based on measuring the absorbance difference between pH 4.5 and pH 1.5. The results were presented as cyanidin-3-glucoside (cyd-3-glc) equivalents according to the Equation (3):

$$TMAC = {}^{(A * MW * DF * 1 * d)}/_{\varepsilon M} \quad (3)$$

where A is the absorbance, MW is the molecular weight of cyd-3-glc (449.2 g/mol), d is the path length of the cuvette (1.0 cm), DF is the dilution factor, and ε is the molar extinction coefficient (26 900 L/cm.mol^{-1}).

Determination of pH sensitivity of films: The film samples were immersed in different buffer solutions (pH 2-13) for 5 minutes at ambient temperature. A portable Konica Minolta CR-400 chroma meter was used to record ΔE of the films at different pHs.

All experiments in the study were performed in triplicate, averaged, and standard deviations were calculated.

RESULTS and DISCUSSION

Thickness and Color Parameters of Films

The thickness, color parameters, ΔE values, and appearance of the prepared films were given in Table 1. The film without extract (CSS-CR0) was thinner than the films containing extract, and the thickness increased with increasing extract amount. The CSS-CR0 film was transparent, and the color parameters were L= 91.49, a= -0.37, and b= 1.29. Increasing the CR concentration decreased the L value while increasing the a and b values. Furthermore, increasing the CR amount resulted in increased ΔE values.

Table 1. Thickness, color parameters, ΔE values and appearance of films

Films	Thickness (µm)	L	a	b	ΔE	Appereance
CSS-CR0	93.47±0.68	91.49±0.29	0.37± 0.03	1.29±0.11	4.15±0.06	
CSS-CR1	96.43±0.74	81.10±0.79	3.31± 0.20	8.68±0.62	16.41±1.01	
CSS-CR2	98.40±0.66	72.50±0.42	8.87±0.28	14.01±0.63	27.64±0.74	
CSS-CR3	100.53±1.02	60.90±2.47	17.54±1.79	17.27±1.16	42.47±1.63	

FTIR Analysis

The pure biopolymers, films containing/not containing CR, and CR extract were structurally characterized by FTIR. The FTIR spectra of the biopolymers and the film without CR (CSS-CR0) were given in Figure 1 (A), while the FTIR spectra of the films with CR extract and CR were presented in Figure 1 (B). In the FTIR spectrum of CMC, the peak at 3234 cm^{-1} was attributed to the stretching vibration of the –OH group, the strong peak at 1591 cm^{-1} was attributed to the stretching vibration of the COO– group, the peak around 1414 cm^{-1} was assosiated with the CH_2 shearing vibration, and the peak around 1025 cm^{-1} was attributed to the CHO–CH_2 stretching vibration (Acar et al., 2023). In the FTIR spectrum of SA, the peak at 3241 cm^{-1} was attributed to the stretching vibration of the hydroxyl group (O-H), the strong peaks at 1595 and 1406 cm^{-1} were related to the asymmetric and symmetric stretching vibrations of the carboxylate group (COO−), and the peak at 1026 cm^{-1} was attributed to the stretching vibration of the C-O group (Bekin et al., 2014). In the FTIR spectrum of ST, the peak at 3289 cm^{-1} was attributed to the stretching vibration originating from hydrogen-bonded O-H groups, and the strong band with three peaks seen between 980 and 1200 cm^{-1} was relatedto the C-O stretching vibrations characteristic of polysaccharides (Zarski et al., 2016).

The shifts in the wave numbers of the vibrations were observed in the FTIR spectrum of CSS-CR0 film containing CMC, SA and ST. This situation showed that there were strong interactions in terms of hydrogen bonding, electrostatic forces and van der Waals forces between CMC, SA and ST molecules, and good compatibility was found between the polymers.

The FTIR spectrum of pure CR showed typical absorption peaks indicating the presence of rich polyphenolic contents. The broad peak around 3276 cm^{-1} was attributed to the symmetric and asymmetric stretching of the polymeric O–H group, while the peak at ~2936 cm^{-1} was related with the stretching vibrations of -CH, -CH_2, and -CH_3 derived from carbohydrates and sugars in the CR structure. On the other hand, the peak at ~1708 cm^{-1} was attributed to the carbonyl groups (C=O) of aldehydes and sugar derivatives. In addition, the stretching vibration of C=C–C and C–H of aromatic bonds, the stretching vibration of C=C aromatic rings, and the phenolic C-O stretching peak were observed at 1605 cm^{-1}, 1515 cm^{-1}, and 1274 cm^{-1}, respectively (Zepon et al., 2019; Rizwana et al., 2023).

The characteristic peaks of biopolymers were observed in the FTIR spectra of films containing CR. With the incorporation of CR into the structure, shifts and slight increases in peak intensities were observed in the stretching vibration peaks of O-H and C-O groups. The absence of a new peak indicated that there was no chemical interaction between CR and the polymers.

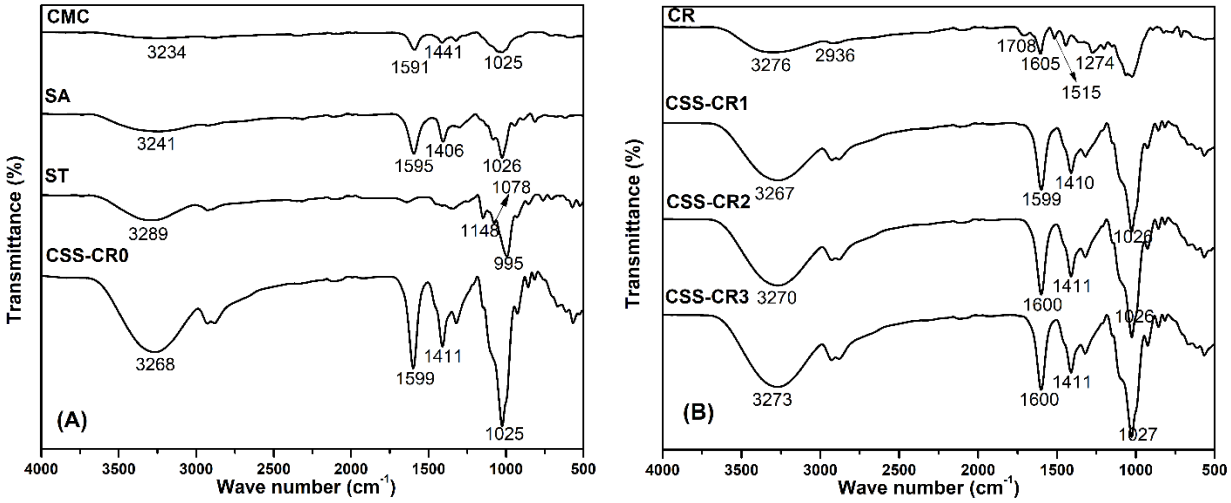


Figure 1. (A) FTIR spectra of biopolymers (CMC, SA, ST) and CR-free film (CSS-CR0), (B) FTIR spectra of CR extract and CR containing films

Bioactivity Analyses

Antioxidant activity results were determined as the percentage of DPPH and ABTS radical scavenging activities, and the total anthocyanin amount was determined as cyd-3-glc equivalents (Table 2). As CR amounts increased, TMAC, DPPH radical scavenging activity, and ABTS radical scavenging activity values increased as expected.

Table 2. TMAC and antioxidant activity (as a percentage of DPPH and ABTS radical scavenging activities) results of the films

Films	TMAC (µg/g)	TAC–DPPH (%)	TAC–ABTS (%)
CSS-CR0	0±0	0.86±0.13	1.53±0.52
CSS-CR1	0.526±0.03	7.48±0.45	8.11±1.34
CSS-CR2	1.034±0.14	25.93±0.21	36.41±1.41
CSS-CR3	1.518±0.23	40.57±1.04	53.02±1.95

pH Sensitivity of Films

Since food spoilage can typically be monitored by pH changes, the pH sensitivity of packaging films can be used to track food freshness. The pH-sensitive color changes of the prepared films were evaluated using buffer solutions with pH values ranging from 2 to 13.

The ΔE values and appearances of films containing/not containing CR after immersion in buffer solutions were listed in Table 3. As shown in the tables, the prepared films exhibited visible color changes after immersion in buffer solutions. The fact that color changes can be observed with the naked eye indicated that the films were suitable for detecting food spoilage.

Table 3. ΔE values and appearances of the films after 5 minutes of exposure to different buffer solutions

	CSS-CR0		CSS-CR1		CSS-CR2		CSS-CR3	
pH	**ΔE**	**Film**	**ΔE**	**Film**	**ΔE**	**Film**	**ΔE**	**Film**
2	4.37±0.05		20.07±0.38		34.81±1.37		49.34±1.06	
3	4.53±0.05		23.22±0.28		34.37±1.68		44.06±1.55	
4	4.61±0.09		22.25±0.46		36.33±1.62		46.69±1.95	
5	5.12±0.11		21.55±0.55		32.18±2.12		47.14±1.34	
6	4.82±0.11		21.05±0.55		29.80±1.18		52.45±1.78	
7	4.69±0.07		19.66±0.52		33.93±1.53		52.92±1.86	
8	4.89±0.08		20.80±0.55		41.27±1.68		62.74±2.42	
9	5.13±0.09		26.99±0.96		49.09±1.25		63.80±2.53	
10	5.35±0.13		34.78±1.03		47.45±1.61		69.36±2.26	
11	5.45±0.06		32.09±1.16		51.85±2.41		66.97±2.58	

12	5.95±0.10		31.36±1.29		50.56±2.44		60.27±1.42	
13	6.45±0.19		34.82±1.23		66.77±2.16		73.84±3.04	

CONCLUSION

The findings revealed that the crosslinked films prepared from CMC, SA, and ST polymers containing CR extract, a polyphenolic compound rich in anthocyanins, were synthesized to monitor the freshness of foods, and that these films exhibited color changes depending on pH. Thus, the potential of the developed films to be used as colorimetric films for smart packaging is demonstrated.

ACKNOWLEDGEMENTS

This study was supported by the Scientific and Technological Research Council of Türkiye (TUBITAK) within the scope of 2209-Research Project Support Programme for Undergraduate Students with project number 1919B012318928.

REFERENCES

Acar, G., Özkahraman, B., & Özbaş, Z. (2023). Thymol incorporated gellan gum/carboxymethyl cellulose/hyaluronic acid films for wound dressings applications. Cellulose, 30(15), 9517-9528.

Almajano, M. P., Delgado, M. E., & Gordon, M. H. (2007). Changes in the antioxidant properties of protein solutions in the presence of epigallocatechin gallate. Food Chemistry, 101(1), 126-130.

Bekin, S., Sarmad, S., Gürkan, K., Keçeli, G., & Gürdağ, G. (2014). Synthesis, characterization and bending behavior of electroresponsive sodium alginate/poly (acrylic acid) interpenetrating network films under an electric field stimulus. Sensors and Actuators B: Chemical, 202, 878-892.

Eker, T. Y., Özgen, S., & Özbaş, Z. (2025). Smart pH-Sensitive indicator films based on gellan gum/starch/xanthan gum with aronia extract: Real-time tracking of chicken freshness. Packaging Technology and Science, 38(12), 937-952.

Giusti, M. M., & Wrolstad, R. E. (2001). Characterization and measurement of anthocyanins by UV-visible spectroscopy. Current Protocols in Food Analytical Chemistry, (1), F1-2.

Kaewprachu, P., Romruen, O., Jaisan, C., Rawdkuen, S., & Klunklin, W. (2024). Smart colorimetric sensing films based on carboxymethyl cellulose incorporated with a natural pH indicator. International Journal of Biological Macromolecules, 259, 129156.

Kan, J., Liu, J., Yong, H., Liu, Y., Qin, Y., & Liu, J. (2019). Development of active packaging based on chitosan-gelatin blend films functionalized with Chinese hawthorn (Crataegus pinnatifida) fruit extract. International Journal of Biological Macromolecules, 140, 384-392.

Kossyvaki, D., Contardi, M., Athanassiou, A., & Fragouli, D. (2022). Colorimetric indicators based on anthocyanin polymer composites: A review. Polymers, 14(19), 4129.

Liu, B., Xu, H., Zhao, H., Liu, W., Zhao, L., & Li, Y. (2017). Preparation and characterization of intelligent starch/PVA films for simultaneous colorimetric indication and antimicrobial activity for food packaging applications. Carbohydrate Polymers, 157, 842-849.

Nemzer, B. V., Al-Taher, F., Yashin, A., Revelsky, I., & Yashin, Y. (2022). Cranberry: Chemical composition, antioxidant activity and impact on human health: Overview. Molecules, 27(5), 1503.

Özgen, S., & Özbaş, Z. (2025). Multifunctional intelligent packaging films incorporated with elderberry anthocyanin for monitoring milk freshness. Polymer Bulletin, 82, 837-859.

Philip, N., & Walsh, L. J. (2019). Cranberry polyphenols: Natural weapons against dental caries. Dentistry Journal, 7(1), 20.

Rizwana, H., Khan, M., Aldehaish, H. A., Adil, S. F., Shaik, M. R., Assal, M. E., Hatshan, M. R., & Siddiqui, M. R. H. (2023). Green biosynthesis of silver nanoparticles using Vaccinium oxycoccos (Cranberry) extract and evaluation of their biomedical potential. Crystals, 13(2), 294.

Shaik, M. I., Azhari, M. F., & Sarbon, N. M. (2022). Gelatin-based film as a color indicator in food-spoilage observation: A review. Foods, 11(23), 3797.

Yang, J., Fan, Y., Cui, J., Yang, L., Su, H., Yang, P., & Pan, J. (2021). Colorimetric films based on pectin/sodium alginate/xanthan gum incorporated with raspberry pomace extract for monitoring protein-rich food freshness. International Journal of Biological Macromolecules, 185, 959-965.

Yang, Y., Yu, X., Zhu, Y., Zeng, Y., Fang, C., Liu, Y., Hu, S., Ge, Y., & Jiang, W. (2022). Preparation and application of a colorimetric film based on sodium alginate/sodium carboxymethyl cellulose incorporated with rose anthocyanins. Food Chemistry, 393, 133342.

Zarski, A., Ptak, S., Siemion, P., & Kapusniak, J. (2016). Esterification of potato starch by a biocatalysed reaction in an ionic liquid. Carbohydrate Polymers, 137, 657-663.

Zepon, K. M., Martins, M. M., Marques, M. S., Heckler, J. M., Morisso, F. D. P., Moreira, M. G., Ziulkoski, A. L., & Kanis, L. A. (2019). Smart wound dressing based on κ–carrageenan/locust bean gum/cranberry extract for monitoring bacterial infections. Carbohydrate polymers, 206, 362-370.

Zhai, X., Shi, J., Zou, X., Wang, S., Jiang, C., Zhang, J., Huang, X., Zhang, W., & Holmes, M. (2017). Novel colorimetric films based on starch/polyvinyl alcohol incorporated with roselle anthocyanins for fish freshness monitoring. Food Hydrocolloids, 69, 308-317.

ORAL PRESENTATION

Bioactive potential of *Raphanus sativus* L. var. *longipinnatus* (Daikon): Cytotoxicity and antioxidant activity

Simge Helvacılar[1] (*ORCID: https://orcid.org/0009-0007-9779-0270*), Furkan Ozan Çöven[1] (*ORCID: https://orcid.org/0000-0001-7696-3418*), Tülay Öncü-Öner[1] (*ORCID: https://orcid.org/0000-0001-6180-5409*)

[1]Manisa Celal Bayar University, Faculty of Engineering and Natural Sciences, Department of Bioengineering, Manisa, Türkiye

*Corresponding author e-mail: tulay.oncu@cbu.edu.tr

Abstract

Raphanus sativus L. var. *longipinnatus* (daikon) is a Brassicaceae plant rich in glucosinolates, isothiocyanates, and flavonoids, compounds known for their antioxidant and anticancer activities. Although several studies have documented cytotoxic effects of *R. sativus* extracts in various cancer models, their activity against the human pancreas adenocarcinoma cell line (MiaPaCa-2), human urinary bladder carcinoma cell line (T24, ATCC, HTB-4), and human umbilical cord epithelial cell line (HUVEC, ATCC, HTB-4) remains underexplored. Cytotoxicity was assessed using the MTT assay at concentrations ranging from 62.5–4000 µg/mL for 24, 48, and 72 hours, and IC_{50} values were calculated by nonlinear regression. Total phenolic content was determined using the Folin–Ciocalteu method, while total flavonoid content was determined using the aluminum chloride method. The DPPH antioxidant activity test assessed antioxidant capacity. The extract produced a clear time and dose-dependent reduction in cell viability, with T24 cells exhibiting the most incredible sensitivity, followed by MiaPaCa-2 and HUVEC cells. The moderate antioxidant activity (13.14% inhibition) together with measurable phenolic (1.326 mg GAE/g) and flavonoid levels (0.727 mg CE/g) supports the presence of bioactive phenolic compounds. Collectively, these results indicate that *R. sativus* var. *longipinnatus* exhibits selective cytotoxicity and measurable antioxidant activity, supporting its relevance as a natural candidate for anticancer research.

Keywords: *Raphanus sativus* var. *longipinnatus,* ethanol extract, cytotoxicity, antioxidant activity

INTRODUCTION

Raphanus sativus, is a member of the Brassicaceae family, has been used in traditional medicine for centuries, especially for respiratory and liver-related disorders (Perez-Gutierrez et al., 2004). Several recent studies have shown that aqueous, methanolic, and hydrophobic *R. sativus* extracts exhibit biological activities such as antioxidant, antiproliferative, and antimutagenic effects. These effects are attributed to secondary metabolites such as phenolic acids and anthocyanins contained in *R. sativus*. Modern studies support these traditional uses (Hanlon & Barnes, 2011). Radish juice shows antimicrobial activity against *Bacillus subtilis*, *Pseudomonas aeruginosa* and *Salmonella typhosa*. Ethanol and water extracts inhibit *Streptococcus mutans* and *Candida albicans*, leaf extracts display antiviral properties, and the roots show antimutagenic effects in *Salmonella typhimurium* assays (Perez-Gutierrez et al., 2004).

Raphanus sativus L., commonly known as Japanese radish or daikon, is a widely used vegetable in the Brassicaceae family. The plant grows naturally across Europe and Asia, typically reaching 30–90 cm in height, and its roots vary in size, shape and colour (Perez-Gutierrez et al., 2004). *R. sativus* var. *longipinnatus* contains high levels of phenolic compounds and isothiocyanates, which contribute to its biological activity (Zappia et al., 2023). The breakdown of glucosinolates forms isothiocyanates, molecules known to trigger cell death pathways and exert protective effects against cancer (Barillari et al., 2008; Egner et al., 2011). The plant is also rich in flavonoids, which act as strong antioxidants that neutralise free radicals and help reduce oxidative stress (Wang & Zhang, 2011).

Although extracts of *R. sativus* have shown cytotoxic effects in various cancer cell lines (Umamaheswari et al., 2021), their impact on pancreatic cancer cell line (MiaPaCa-2), bladder cancer cell line (T24), and endothelial cell line (HUVEC) remains poorly understood. This study aims to investigate the cytotoxic activity of *R. sativus* var.

longipinnatus ethanol extract in these three cell lines using the MTT assay, and to measure its total flavonoid content and antioxidant capacity using the DPPH method. These findings will help deepen our understanding of the biological effects of *R. sativus* var. *longipinnatus* and support future efforts to develop plant-derived anticancer agents.

MATERIALS AND METHODS

Extract preparation

Fresh *Raphanus sativus* var. *longipinnatus* was purchased from a local market in Türkiye. The plant was sliced, frozen at –80°C, and then lyophilised. Dried samples were ground to a fine powder and extracted with 70% ethanol (1:10 w/v) in an ultrasonic bath at 40°C for 5 hours. After centrifugation (4000 rpm, 15 min), the supernatant was collected, and ethanol was removed under reduced pressure using a rotary evaporator. Extracts were stored at –20°C until further experiments.

Total phenolic content

The total phenolic content was determined using the Folin–Ciocalteu method. Briefly, 200 µL of 0.2 N Folin–Ciocalteu reagent was added to 100 µL of extract and mixed thoroughly. Subsequently, 2 mL of distilled water and 1 mL of 6% sodium carbonate (Na_2CO_3) solution were added, the mixture was vortexed, and then incubated at room temperature in the dark for 2 hours. After incubation, the absorbance was measured at 765 nm using a spectrophotometer. Total phenolic content was expressed as gallic acid equivalents (mg GAE/g).

Total flavonoid content

Total flavonoid content was measured using a modified aluminum chloride method (Saeed et al., 2012). To perform this test, 25 µL of the extract and 100 µL distilled water were mixed in microplate. Then, seven µL of 5% $NaNO_2$ was added and microplate was kept at room temperature for 5 minutes. After incubation, seven µL of 10% $AlCl_3$ was added to the mixture, and further incubated for 5 minutes. After adding 50 µL of 1M NaOH and 60 µL of distilled water, absorbance was measured at 490 nm in a microplate reader. Total flavonoid content was expressed in terms of catechin equivalent (mg CE/g).

Antioxidant activity assay

Antioxidant activity was analysed using the DPPH radical-scavenging activity method (Mathangi & Prabhakaran, 2013). 50 µL of *R. sativus* var. *longipinnatus* ethanol extract was mixed with 150 µL of methanol, and 3.8 mL of DPPH solution was then added to the mixture, which was incubated in the dark for 30 minutes. Absorbance was measured at 515 nm with the help of a spectrophotometer. The following formula calculated percentage inhibition:

$$\text{Inhibition } \% = \left(\frac{Abs_{control} - Abs_{sample}}{Abs_{control}}\right) \times 100$$

In vitro cytotoxicity assay

MTT [3-(4,5-dimethylthiazol-2-yl)-2,5-dipenyltetrazolium bromide] method was used to determine the cytotoxic activity of *R. sativus* var. *longipinnatus* ethanol extract on human pancreas adenocarcinoma cell line (MiaPaCa-2, ATCC, CRL-1420), human urinary bladder carcinoma cell line (T24, ATCC, HTB-4), and human umbilical cord epithelial cell line (HUVEC, ATCC, HTB-4). The cells were grown in Dulbecco's modified Eagle's medium (DMEM) supplemented with 10% FBS, 1% L-glutamine, and 1% penicillin/streptomycin in a humidified environment with 5% CO_2 at 37°C in a incubator.

Cells were seeded at 1×10^4 cells per well in 96-well plates and incubated overnight. Then, different extract concentrations prepared as 2-fold dilutions from 62.5 to 4000 µg/mL were treated with cells in triplicate. After 24, 48, and 72 hours of exposure, 10 µL of MTT solution (5 mg/mL) was added, and the mixture was incubated for 4 hours. Formazan crystals formed by adding MTT solution were dissolved in 200 µL DMSO, and absorbance was measured at 570 nm. Cell viability was calculated using the following formula, and IC_{50} values were determined from the cell viabilities at different extract concentrations.

$$\text{Viability \%} = \left(\frac{Abs_{test\ well}}{Abs_{control\ well}}\right) \times 100$$

Statistical Analysis

All experiments were performed in triplicate (n=3). Results are expressed as the mean ± standard deviation (SD). Statistical evaluations were performed using one-way analysis of variance (ANOVA) via the GraphPad Prism software. A p value of <0.05 was considered statistically significant.

RESULTS

In this study, the antioxidant activity value of ethanol extracts obtained from *R. sativus* var. *longipinnatus* was calculated according to the DPPH method, and the results are expressed as a percentage inhibition compared to the control group (Table 1).

Table 1. Antioxidant activity results of *Raphanus sativus* var. *longipinnatus* ethanol extract.

Sample	Antioxidant activities (%Inhibition)
Raphanus sativus var. longipinnatus ethanol extract	13.14
Butylated hydroxyanisole (BHA)	97.09

The antioxidant activity test revealed that the inhibition value of *R. sativus* var. *longipinnatus* ethanol extract was 13.14%. The antioxidant activity value of BHA, a standard antioxidant, was found to be 97.09%.

Herein, total phenolic content was calculated as 1.326 mg GAE/g; while total flavonoid content was determined as 0.727 mg CE/g (Table 2).

Table 2. Total phenolic and flavonoid content results of *Raphanus sativus* var. *longipinnatus* ethanol extract.

Assay	Extract
Total phenolic content	1.326 mg GAE/g
Total flavonoid content	0.727 mg CE/g

The cytotoxic effect of *R. sativus* var. *longipinnatus* ethanol extract was determined using the MTT assay after 24, 48, and 72 hours of incubation on MiaPaCa-2 (Figure 1), T24 (Figure 2), and HUVEC (Figure 3) cell lines, and the percentage viability values were calculated. The percentage viability values obtained from the applied concentrations in the MTT assay were statistically analyzed relative to the control group.

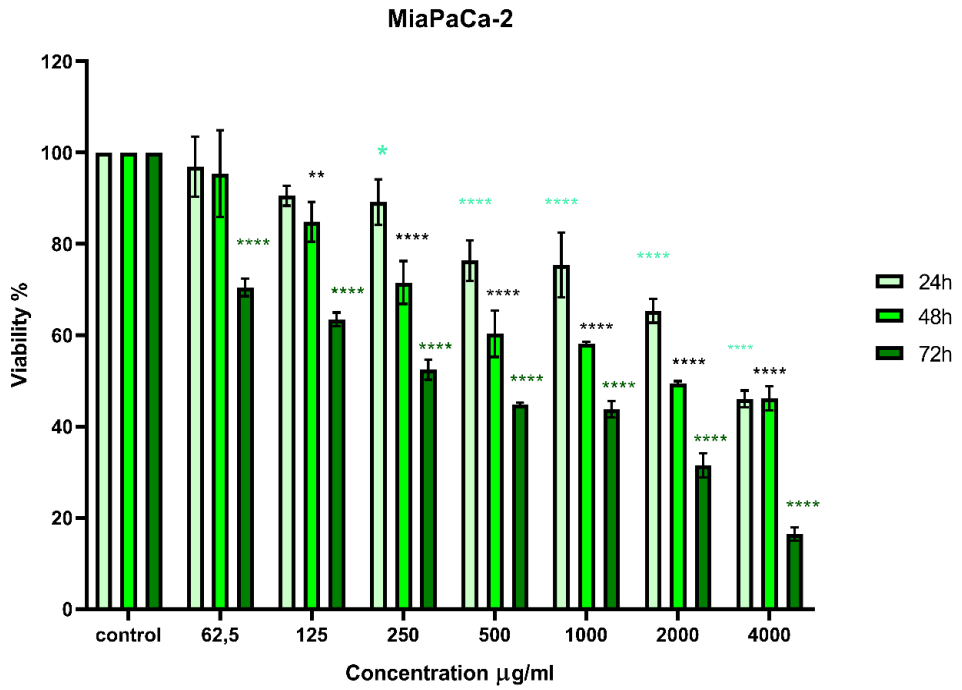


Figure 1. Cell viability values of different concentrations of *Raphanus sativus* var. *longipinnatus* extract on MiaPaCa-2 cell line (*: p<0.05, **: p<0.01, ***: p<0.001, ****: p<0.0001)

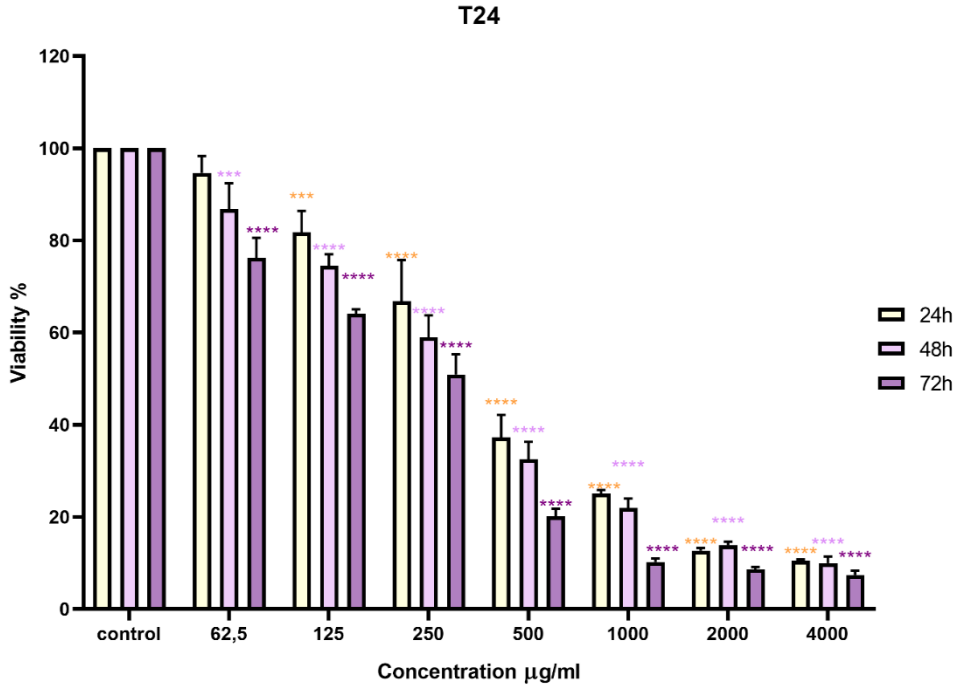


Figure 2. Cell viability values of different concentrations of *Raphanus sativus* var. *longipinnatus* extract on T24 cell line (*: p<0.05, **: p<0.01, ***: p<0.001, ****: p<0.0001)

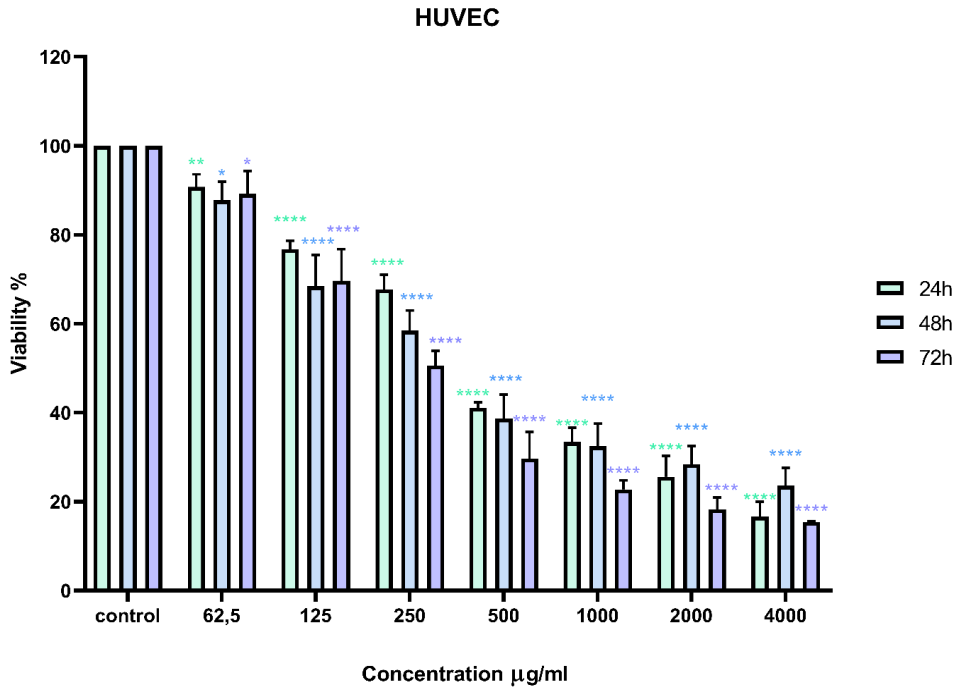


Figure 3. Cell viability values of different concentrations of *Raphanus sativus* var. *longipinnatus* extract on HUVEC cell line (*: p<0.05, **: p<0.01, ***: p<0.001, ****: p<0.0001)

The IC_{50} values were calculated using GraphPad software (GraphPad, Version 8.4.2, San Diego, CA, USA) based on the cell viability values obtained after 24, 48, and 72 hours of treatment (Table 3).

Table 3. IC_{50} values of *Raphanus sativus* var. *longipinnatus* ethanol extract on MiaPaCa-2, T24, and HUVEC cell lines.

Cell lines	IC_{50} (µg/ml)		
	24h	48h	72h
MiaPaCa-2	3110.00±250.46	1490.33± 92.19	389.63±5.22
T24	404.26±33.45	318.06±13.55	197.43±15.64
HUVEC	481.06±13.87	404.36±24.73	287.3±13.07

*: p<0.05, **: p<0.01, ***: p<0.001, ****: p<0.0001

The experimental results demonstrated that the *R. sativus* var. *longipinnatus* ethanol extract exerted a time and dose-dependent cytotoxic effect on all tested cell lines (MiaPaCa-2, T24, and HUVEC). As shown in Table 3, the IC_{50} values summarize the cytotoxic potential of the extract and the relative sensitivity of each cell line.

The extract demonstrated a time-dependent decrease in IC_{50} values across all tested cell lines. In MiaPaCa-2 cells, IC_{50} values reduced from 3110 ± 250 µg/mL (24 h) to 1490 ± 92 µg/mL (48 h) and 389 ± 5 µg/mL (72 h), indicating a progressive increase in sensitivity over time. T24 bladder cancer cell line exhibited the highest level of sensitivity, with IC_{50} values dropping from 404 ± 33 µg/mL (24 h) to 197 ± 15 µg/mL (72 h). This range is consistent with moderate-to-strong cytotoxicity reported in the literature for plant-derived extracts, suggesting active constituents compatible with anti-proliferative mechanisms.In contrast, HUVEC endothelial cells displayed higher IC_{50} values compared with both cancer cell lines (481 ± 13 µg/mL at 24 h; 287 ± 13 µg/mL at 72 h), indicating that the extract was less toxic to normal cells. These values collectively demonstrate that the extract is more potent against cancer

cells, particularly T24 and MiaPaCa-2, than against HUVEC cells. The cytotoxic activity follows a clear time-dependent pattern, implying that more prolonged exposure enhances the biological effect.

In the MiaPaCa-2 cell line, the IC_{50} value at 48 and 72 hours was found to be significantly higher than at 24 hours ($p<0.0001$), while the significance between 48 and 72 hours was lower ($p<0.001$). In the T24 cell line, the IC_{50} value between 24 and 72 hours had a higher statistical significance ($p<0.0001$) compared to the IC_{50} values between 24 and 48 hours and between 48 and 72 hours ($p<0.01$). The HUVEC cell line, similar to the T24 cell line, showed a high statistical significance for the IC_{50} value between 24 and 72 hours ($p<0.0001$); however, the IC_{50} values between 48 and 72 hours ($p<0.001$) and between 24 and 48 hours ($p<0.01$) had lower significance.

DISCUSSION

The findings of this study demonstrate that *Raphanus sativus* var. *longipinnatus* ethanol extract exerts a concentration and time dependent cytotoxic effect on MiaPaCa-2, T24, and HUVEC cells. Among the tested cell lines, T24 bladder cancer cells were the most sensitive, while normal HUVEC endothelial cells showed comparatively higher IC_{50} values, indicating reduced susceptibility. This trend aligns with earlier researchs suggesting that radish-derived glucosinolate metabolites particularly isothiocyanates preferentially target malignant cells by inducing apoptosis, modulating detoxification enzymes, and disrupting mitochondrial signaling pathways (Barillari et al., 2008; Egner et al., 2011; Umamaheswari et al., 2021).

The moderate antioxidant capacity observed in the present study contrasts with higher scavenging activities reported for radish extracts obtained using other solvents or extraction conditions (Zappia et al., 2023). Methodological differences including solvent polarity, extraction duration, plant part used, and harvest maturity strongly influence the yield of phenolic compounds and may account for the lower DPPH inhibition obtained (Perez-Gutiérrez & Pérez, 2004; Zappia et al., 2023).

When compared with previous cytotoxicity studies, the IC_{50} values obtained for MiaPaCa-2 and T24 cells fall within the range reported for radish and related Brassicaceae extracts tested against breast, colon, and liver cancer cell lines (Umamaheswari et al., 2021). However, little is documented regarding the effects of radish extracts on pancreatic and bladder cancer cells, making the present findings a valuable contribution to the broader understanding of the plant's anticancer potential. The observed progressive decline in IC_{50} values over time suggests that the extract's active compounds may accumulate intracellularly or initiate delayed apoptotic signaling, a pattern similarly reported for other isothiocyanate-rich species (Barillari et al., 2008).

A study used the above-ground parts of *R. sativus* and analyzed ethanol-extracted samples in MDA-MB-231 human breast cancer cells. A dose-dependent decrease in cell viability was observed in cells treated with the extract at concentrations of 100-300 µg/mL for 48 hours (Kim et al., 2011). In another study, red radish tubers were extracted using Soxhlet extraction with water, ethanol, and methanol, and were found to exhibit cytotoxic effects at high doses (Kaya, 2023). In a study in which silver-nanoparticles (NPs) were synthesized via the aqueous extraction of *Raphanus sativus* leaves, cytotoxic activity was evaluated in human dermal fibroblasts (HDF) and SK-OV-3, CaCo-2, and U118 cancer cell lines. NPs applied to cells at a concentration of 25 µg/mL reduced viability by 76.97% in the HDF cell line compared to the control group. This value was found to be 68.44%, 87.37%, and 89.10% in the SK-OV-3, CaCo-2, and U118 cancer cell lines, respectively (Hatipoğlu et al., 2023).

Altogether, the current study results are consistent with the existing literature on the biological activities of *R. sativus* var. *longipinnatus* while expanding current knowledge by providing new evidence of its effects on specific cancer models. The combination of cytotoxic activity, total phenolic and flavonoid contents, and antioxidant potential underscores the promise of *R. sativus* var. *longipinnatus* as a natural source of bioactive compounds.

CONCLUSION

This study demonstrates that *Raphanus sativus* var. *longipinnatus* ethanol extract exhibits selective cytotoxic activity against MiaPaCa-2 and T24 cancer cells, with reduced toxicity toward HUVEC endothelial cells. The extract also displayed moderate antioxidant capacity and measurable levels of phenolics and flavonoids, confirming the presence of bioactive phytochemicals associated with anticancer and antioxidant effects. When compared with

literature, the results align with well-established properties of *R. sativus* var. *longipinnatus* while contributing new data regarding its impact on pancreatic and bladder cancer cell lines. These findings suggest that *Raphanus sativus* var. *longipinnatus* ethanol extract may serve as a promising natural candidate for further development in anticancer research. Future studies should focus on identifying the specific active compounds, elucidating their molecular mechanisms, and evaluating their effects in *in vivo* models.

ACKNOWLEDGEMENTS

The authors thanks to Dr. Ayşegül İnam for her support.

REFERENCES

Barillari, J., Iori, R., Papi, A., Orlandi, M., Bartolini, G., Gabbanini, S., … & Valgimigli, L. (2008). Kaiware daikon (*Raphanus sativus* L.) extract: a naturally multipotent chemopreventive agent. Journal of Agricultural and Food Chemistry, 56(17), 7823–7830. https://doi.org/10.1021/jf8011213

Cannavacciuolo, C., Cerulli, A., Dirsch, V., Heiß, E., Masullo, M., & Piacente, S. (2023). LC-MS- and 1H NMR-based metabolomics to highlight the impact of extraction solvents on chemical profile and antioxidant activity of daikon sprouts (*Raphanus sativus* L.). Antioxidants, 12(8), 1542. https://doi.org/10.3390/antiox12081542

Cannavacciuolo, C., Cerulli, A., Dirsch, V., Heiß, E., Masullo, M., & Piacente, S. (2023). LC-MS- and 1H NMR-based metabolomics to highlight the impact of extraction solvents on chemical profile and antioxidant activity of daikon sprouts (*Raphanus sativus* L.). Antioxidants, 12(8), 1542. https://doi.org/10.3390/antiox12081542

Choi, H., Kim, H., Han, S., Park, H., Ha, I., Kim, J., … & Lee, S. (2023). Antioxidant and anti-inflammatory activities of high-glucosinolate-synthesis lines of Brassica rapa. Antioxidants, 12(9), 1693. https://doi.org/10.3390/antiox12091693

Egner, P., Chen, J., Wang, J., Wu, Y., Sun, Y., Lu, J., … & Kensler, T. (2011). Bioavailability of sulforaphane from two broccoli sprout beverages: results of a short-term, cross-over clinical trial in Qidong, China. Cancer Prevention Research, 4(3), 384–395. https://doi.org/10.1158/1940-6207.capr-10-0296

Egner, P., Chen, J., Zarth, A., Ng, D., Wang, J., Kensler, K., … & Kensler, T. (2014). Rapid and sustainable detoxication of airborne pollutants by broccoli sprout beverage: results of a randomized clinical trial in China. Cancer Prevention Research, 7(8), 813–823. https://doi.org/10.1158/1940-6207.capr-14-0103

Hanlon, P. R., & Barnes, D. M. (2011). Phytochemical composition and biological activity of 8 varieties of radish (*Raphanus sativus* L.) sprouts and mature taproots. Journal of Food Science, 76(1), C185-C192. https://doi.org/10.1111/j.1750-3841.2010.01972.x

Hatipoğlu, A., Baran, A., Keskin, C., Baran, M. F., Eftekhari, A., Omarova, S., ... & Kandemir, S. İ. (2023). Green synthesis of silver nanoparticles based on the *Raphanus sativus* leaf aqueous extract and their toxicological/microbiological activities. Environmental Science and Pollution Research, 1-13. https://doi.org/10.1007/s11356-023-26499-z

Kaya, N. (2023). Evaluation of anti-cytotoxicity and anti-genotoxicity of *Raphanus sativus* L. tuber on *Allium cepa* L. root tips. Biology Bulletin, 50(3), 293-299. https://doi.org/10.1134/S1062359022601690

Khan, R., Khan, S., & Siddique, R. (2022). Radish (*Raphanus sativus*): potential antioxidant role of bioactive compounds extracted from radish leaves – a review. PJMHS, 16(9), 2–4. https://doi.org/10.53350/pjmhs221692

Kim, W. K., Kim, J. H., Jeong, D. H., Chun, Y. H., Kim, S. H., Cho, K. J., & Chang, M. J. (2011). Radish (Raphanus sativus L. leaf) ethanol extract inhibits protein and mRNA expression of ErbB2 and ErbB3 in MDA-MB-231 human breast cancer cells. Nutrition research and practice, 5(4), 288-293. https://doi.org/10.4162/nrp.2011.5.4.288

Mathangi, T., & Prabhakaran, P. (2013). DPPH free radical scavenging activity of the extracts of the aquatic fern *Marsilea quadrifolia* Linn. Original Research Article, Department of Microbiology, PRIST University, Thanjavur, India; Shrimad Aandavar College, Thiruchirappalli, India.

Ward, P. C., & Mawdsley, W. (2000). Fire management in the boreal forests of Canada. In Fire, climate change, and carbon cycling in the boreal forest (pp. 66-84). New York, NY: Springer New York.

Papi, A., Orlandi, M., Bartolini, G., Barillari, J., Iori, R., Paolini, M., … & Valgimigli, L. (2008). Cytotoxic and antioxidant activity of 4-methylthio-3-butenyl isothiocyanate from Raphanus sativus L. (Kaiware Daikon) sprouts. Journal of Agricultural and Food Chemistry, 56(3), 875–883. https://doi.org/10.1021/jf073123c

Pérez Gutiérrez, R. M., & Pérez, R. L. (2004). *Raphanus sativus* (Radish): their chemistry and biology. The Scientific World Journal, 4, 811–837. https://doi.org/10.1100/tsw.2004.131

Saeed, N., Khan, M.R. & Shabbir, M. Antioxidant activity, total phenolic and total flavonoid contents of whole plant extracts *Torilis leptophylla* L. BMC Complement Altern Med 12, 221 (2012). https://doi.org/10.1186/1472-6882-12-221

Shoaib, S., Tufail, S., Sherwani, M., Yusuf, N., & Islam, N. (2021). Phenethyl isothiocyanate induces apoptosis through ROS generation and caspase-3 activation in cervical cancer cells. Frontiers in Pharmacology, 12. https://doi.org/10.3389/fphar.2021.673103

Umamaheswari, A., Prabu, S., John, S., & Puratchikody, A. (2021). Green synthesis of zinc oxide nanoparticles using leaf extracts of *Raphanus sativus* var. *longipinnatus* and evaluation of their anticancer property in A549 cell lines. Biotechnology Reports, 29, e00595. https://doi.org/10.1016/j.btre.2021.e00595

Wang, B., & Zhang, X. (2011). Inhibitory effects of Broccolini leaf flavonoids on human cancer cells. Scanning, 34(1), 1–5. https://doi.org/10.1002/sca.20278

Zappia, A., Spanti, A., Princi, R., Imeneo, V., & Piscopo, A. (2023). Evaluation of the efficacy of antioxidant extract from lemon by-products on preservation of quality attributes of minimally processed radish (*Raphanus sativus* L.). Antioxidants, 12(2), 235. https://doi.org/10.3390/antiox12020235

ORAL PRESENTATION

Potential of two *Sideritis* species against EMS-induced DNA damage in *Drosophila melanogaster*

Neva Çelik[1] (*ORCID: https://orcid.org/ 0000-0002-5954-5051*),
Deniz Altun Çolak[2*] (*ORCID: https://orcid.org/ 0000-0002-3576-0355*)

[1]Erzincan Binali Yıldırım University, Institute of Natural and Applied Science, Erzincan, Türkiye.
[*2]Erzincan Binali Yıldırım University, Faculty of Arts and Sciences, Department of Biology, Erzincan, Türkiye.

*Corresponding author e-mail: daltun@erzincan.edu.tr

Abstract

This study investigated the potential antigenotoxic effects of methanol extracts obtained from the aerial parts of *Sideritis brevidens* and *Sideritis libanotica* subsp. *violascens*, traditionally used in folk medicine for its antioxidant properties. Plants were collected from the Mersin region of Turkey, and four extract concentrations (1.25, 2.5, 5, and 10 mg/mL) were tested against genotoxicity induced by ethyl methanesulfonate (EMS), an alkylating agent. The Somatic Mutation and Recombination Test (SMART; wing-spot test) was performed using two *Drosophila melanogaster* strains carrying the recessive markers *flare-3* (*flr*^{3}) and *multiple wing hairs* (*mwh*). Transheterozygous larvae (72±4 hours old) obtained from crosses between these strains were chronically fed with plant extracts, EMS, and their combinations. Wings of emerged adults were microscopically examined for spot formation. The extracts showed no genotoxic effects at any concentration. However, co-treatment with EMS significantly reduced the frequency of somatic mutations and recombinations, particularly at 5 and 10 mg/mL ($p<0.05$). These results indicate that the tested *Sideritis* extracts possess notable antigenotoxic activity and may serve as natural agents for reducing DNA damage, warranting further pharmacological evaluation.

Keywords: Antigenotoxicity, *Sideritis brevidens*, *Sideritis libanotica*, SMART assay

INTRODUCTION

Throughout human history, plants have been regarded as one of the most valuable natural resources in traditional medicine (Atanasov et al., 2015; Çarıkçı et al., 2023). Many species have been utilized for their therapeutic potential, particularly due to their rich content of bioactive compounds (Eruygur et al., 2024). Among these, antioxidant-rich plants are notable for their ability to scavenge free radicals and mitigate oxidative stress- a major contributor to cellular damage and various diseases, including cancer (Lobo et al., 2010; Valko et al., 2006). In this context, the exploration of the protective roles of plant-derived compounds against DNA damage has garnered significant scientific attention.

The genus *Sideritis*, part of the Lamiaceae family, is traditionally used as a herbal tea and is common in Mediterranean regions (Selvi et al., 2022). Several species of *Sideritis* have demonstrated antioxidant, anti-inflammatory, antimicrobial, and even anticancer potential in prior phytochemical and pharmacological studies (González-Burgos et al., 2011; Elbouny et al., 2022; Chrysargyris et al., 2023; Walasek-Janusz et al., 2025). Despite these findings, data regarding the antigenotoxic capacity of *Sideritis* species remain scarce, especially in the context of in vivo genotoxic assays.

In this study, methanol extracts obtained from the aerial parts of *Sideritis brevidens* and *Sideritis libanotica* subsp. *violascens,* collected from the Mersin region of Turkey, were evaluated for their potential protective effects against ethyl methanesulfonate (EMS)- induced genetic damage. EMS is a well-known alkylating agent that generates point mutations and chromosomal aberrations by modifying DNA structure, and it is frequently used as a standard genotoxin in experimental systems (Ansari et al., 2025).

To assess the potential antigenotoxic effects of these plant extracts, the *Drosophila melanogaster* wing somatic mutation and recombination test (SMART) was employed. This in vivo assay allows the detection of somatic

mutation and recombination events through phenotypic markers (Frölich and Würgler, 1990; Graf et al., 1998). *Drosophila*, as a model organism, offers various advantages for toxicological and genetic research due to its short life cycle, well-characterized genome, and conserved cellular mechanisms related to DNA repair and oxidative stress response (Rand et al., 2023).

By investigating whether the selected *Sideritis* species can reduce EMS-induced genetic alterations in *Drosophila*, this research aims to provide new insight into the protective potential of plant-derived natural products. The results may contribute to the identification of novel candidates for developing protective agents against genotoxicity and may support the ethnopharmacological use of *Sideritis* in preventive medicine.

MATERIALS AND METHODS

***Drosophila* Strains:** In this study, two distinct *Drosophila melanogaster* strains were utilized: *multiple-wing hair* (*mwh/mwh*) males and *flare-3* (*flr*^{3}/*In*(*3LR*) TM3, *ri p*^{p} *sep I*(*3*)*89Aabx*^{34e}) females. Both strains were obtained from the Laboratories of Basic Sciences Application and Research Center at Erzincan Binali Yıldırım University. The *multiple-wing hair* (*mwh*) gene is located on chromosome 3 and is characterized by a unique phenotype in which homozygous individuals exhibit multiple trichomes per epithelial cell. The *flare-3* (*flr*^{3}) gene, also mapped to chromosome 3, is recessive and results in the development of abnormal point-like trichomes on the wing surface. The genetic markers and associated phenotypes have been previously described in detail in earlier studies (Graf et al., 1984; Lindsley and Zimm, 1987).

Chemical: Ethyl methanesulfonate (EMS, 62-50-0) was obtained from Sigma Aldrich.

Plant Material Collection and Extract Preparation: The plant samples used in this study were collected at their maturation stage from the Anamur district of Mersin province by Dr. Emre SEVİNDİK, who also carried out the botanical identification. The aerial parts of the air-dried plants were treated with liquid nitrogen and homogenized to obtain material suitable for extraction. From the powdered plant material, 50 g was accurately weighed for each extract using an analytical balance, and the volume was brought to 250 mL with methanol. Extraction was carried out accordingly. The methanolic extracts were then concentrated by removing most of the solvent under reduced pressure at 40°C using a rotary evaporator (Kotan et al., 2010). Stock solutions were prepared from the obtained *Sideritis brevidens* (SB) and *Sideritis libanotica* subsp. *violascens* (SL) extracts and applied to the experimental groups at final concentrations of 1.25, 2.5, 5, and 10 mg/mL. The stock solutions were stored at +4°C until further use.

Survival Rate (Larval Mortality) Assay: To evaluate the potential toxic effects of SB and SL plant extracts, survival rate assays were conducted using transheterozygous (*mwh/flr*^{3}) *Drosophila melanogaster* larvae. A total of 100 larvae aged 72±4 hours were transferred into food media supplemented with different concentrations (1.25, 2.5, 5, and 10 mg/mL) of SB and SL extracts. Each treatment group was tested in triplicate, and the number of larvae that successfully developed into adult flies was recorded for each replicate. Survival rates were then calculated to evaluate the potential toxicity of the extracts. EMS was used as the positive control, while the negative control group consisted of larvae reared on standard medium without any extract. The survival percentages were calculated based on the number of emerged adults, and the data were comparatively evaluated to determine the potential toxic or protective effects of the plant extracts.

Somatic Mutation and Recombination Test (SMART) Assay: The wing SMART assay was employed to evaluate the genotoxic effects of test compounds in *D. melanogaster* by assessing loss of heterozygosity (LOH) at two recessive loci: *multiple-wing hair* (*mwh*, 3-0.3) and *flare-3* (*flr*^{3}, 3-38.8) (Graf et al., 1984). This assay allows for the detection of various genetic alterations, including point mutations, deletions, chromosomal loss, nondisjunction, and mitotic recombination (Würgler and Vogel, 1986). The trans-heterozygous larvae were obtained by crossing virgin *flr*^{3} females with *mwh* males. Eggs were collected over 8 hours, and third instar larvae (72±4 hours old) were harvested and rinsed with tap water. Subsequently, 100 larvae were transferred into plastic vials containing 1.5 g of dry *Drosophila* Instant Medium (Carolina Biological Supply Company, Burlington, NC) rehydrated with 9 mL of the respective treatment solutions. Test groups consisted of various concentrations (1.25, 2.5, 5, and 10 mg/mL) of plant extracts (SB and SL). The positive control group was exposed to EMS (1mM),

while the negative control group received only distilled water. All treatments were administered via larval feeding until pupation. Experiments were conducted at 25±1°C and ~65% relative humidity.

Following adult emergence, trans-heterozygous flies were collected and preserved in 70% ethanol at 14°C. Wings were dissected and mounted in Faure's solution (50 g chloral hydrate, 30 mL glycerol, 30 g of gum arabic, and 50 mL distilled water). Slides were examined under a light microscope at 400x magnification. Wings were analyzed for mutant spots categorized as:

(1) small single spots (1-2 mutant cells) and

(2) large single spots (>2 mutant cells), both showing either the *mwh* or *flr*^{3} phenotype, and

(3) twin spots, characterized by adjacent clones both *mwh* or *flr*^{3} phenotype (Graf et al., 1984).

While single spots may arise from point mutations, deletions, or chromosomal events (e.g., nondisjunction or recombination), twin spots are specifically indicative of reciprocal mitotic recombination events. Genotoxicity modulation was evaluated by comparing total spot frequencies. The inhibitory effect of plant extracts was calculated using the following formula (Abraham, 1994):

$$Inhibition = (a - b/a)x100$$

Where a represents the mean total spot frequency induced by EMS alone, and b represents the frequency observed in the presence of both EMS and the test extract.

Statistical Analysis: Statistical analyses for survival rate were performed using SPSS version 22.0 (IBM Corp., Armonk, NY, USA). For normally distributed data, comparisons between groups were made using one-way analysis of variance (One-Way ANOVA). Results were expressed as mean ± standard error of mean (SEM), and a p-value of <0.05 was considered statistically significant. The genotoxic potential in the Somatic Mutation and Recombination test was performed using a two-tailed χ^2 test for proportions ($\alpha = \beta = 0.05$) following the method described by Frei and Würgler (Frei and Würgler, 1995).

RESULTS

In this study, the effects of *Sideritis brevidens* (SB) and *Sideritis libanotica* subsp. *violascens* (SL) extracts on larval mortality and genotoxicity in *Drosophila melanogaster* were evaluated, and the results were compared in terms of both parameters.

Survival rate determination: Survival rate findings (Figure 1) demonstrated that EMS, used as a positive control, exerted significant toxicity by reducing larval viability in *D. melanogaster* larvae (n = 100, 72 ± 4 h trans-heterozygous larvae). In contrast, SB and SL extracts at concentrations of 5 and 10 mg/mL significantly increased survival rates compared to the negative control group ($p<0.05$).

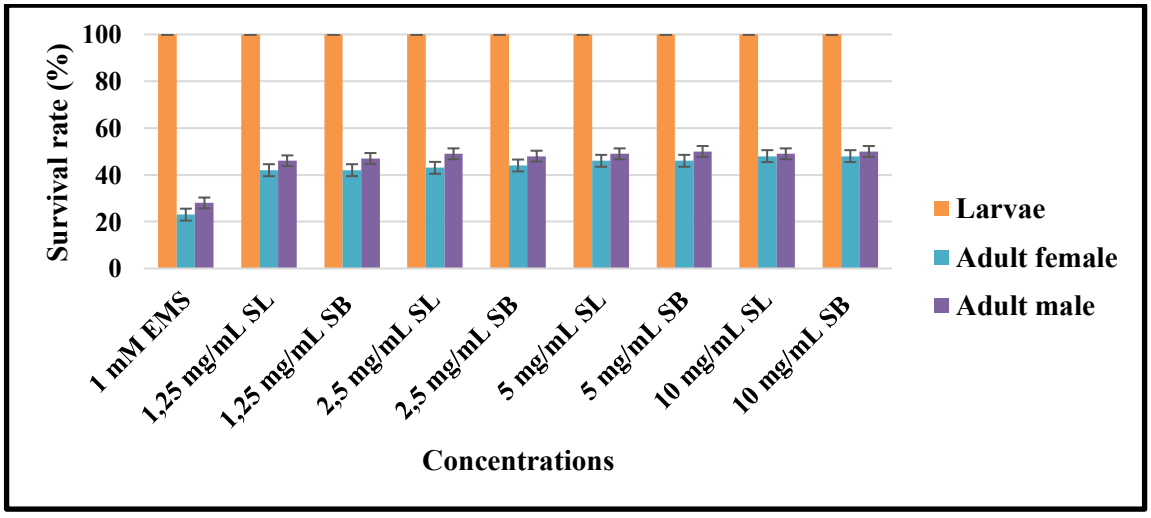


Figure1. Larval survival of *D. melanogaster* exposed to SB and SL extracts

Genotoxicity assay: After treating trans-heterozygous larvae with EMS and changing concentrations of plant extracts, administered both alone and together, the emerging adult flies were classified based on their phenotypes as either normal (*mwh/flr³*) or serrated (*mwh/TM3)*.

According to data in Table 1, EMS (1 mM) treatment in the *mwh/flr³* and *mwh/TM3* genotypes induced significant increases in small, large, and twin spots compared to the distilled water control, indicating a pronounced mutagenic effect. Individually applied *Sideritis brevidens* (SB) and *Sideritis libanotica* subsp. *violascens* (SL) extracts at low and medium concentrations did not elicit mutagenicity, while high concentrations generated limited positive responses. Co-treatment with EMS and plant extracts, particularly at concentrations of 5 mg/mL and above, markedly reduced the total spot frequency. Inhibition rates reached up to 54.81% for SB and 50.62% for SL, demonstrating that both extracts possess antimutagenic properties. The efficacy of these extracts varied depending on concentration and genotype. Overall, SL exhibited slightly lower or comparable protective effects concerning SB at certain concentrations.

Table 1. Wing spot test analysis of *Sideritis brevidens* and *Sideritis libanotica* subsp. *violascens* extracts in *Drosophila melanogaster*: results for *mwh/flr³* and *mwh/TM³* genotypes

	Experimental groups	N	Small single spots (1–2 cells) (m = 2)			Large single spots (>2 cells) (m = 5)			Twin spots (m = 5)			Total mwh spots (m = 2)			Total spots (m = 2)			CIF	% Inhibition
			No	Fr.	D	No	Fr.	D	No	Fr.	D	No	Fr.	D	No	Fr.	D		
mwh/flr³	Distilled water	80	26	(0.33)		3	(0.04)		2	(0.03)		30	(0.38)		31	(0.39)		1.54	
	EMS (1mM)	80	176	(2.20)	+	111	(1.39)	+	29	(0.36)	+	271	(3.39)	+	316	(3.95)	+	13.88	
	1.25 mg/mL SB	80	14	(0,18)	-	4	(0,05)	i	1	(0,01)	-	16	(0,20)	-	19	(0,24)	-	0,82	
	1.25 mg/mL SL	80	13	(0,16)	-	3	(0,04)	i	2	(0,03)	i	14	(0,18)	-	18	(0,23)	-	0,72	
	EMS+1.25 mg/mL SB	80	146	(1.82)	-	100	(1.25)	-	22	(0.28)	-	115	(1.44)	-	268	(3.35)	-	5.89	15,19↓
	EMS+1.25 mg/mL SL	80	151	(1.88)	-	97	(1.21)	-	20	(0.25)	-	122	(1.53)	-	268	(3.35)	-	6.25	15,19↓
	2.5 mg/mL SB	80	12	(0,15)	-	2	(0,03)	i	2	(0,03)	i	13	(0,16)	-	16	(0,20)	-	0,67	
	2.5 mg/mL SL	80	14	(0,18)	-	2	(0,03)	i	0	(0,00)	-	15	(0,19)	-	16	(0,20)	-	0,76	
	EMS+2.5 mg/mL SB	80	139	(1.74)	-	90	(1.13)	-	19	(0.24)	-	93	(1.16)	-	248	(3.10)	-	4.76	21,52↓
	EMS+2.5 mg/mL SL	80	130	(1.63)	-	93	(1.16)	-	22	(0.28)	-	89	(1.11)	-	245	(3.06)	-	4.56	22,53↓
	5 mg/mL SB	80	13	(0,16)	-	2	(0,03)	i	1	(0,01)	-	14	(0,18)	-	16	(0,20)	-	0,72	80
	5 mg/mL SL	80	11	(0,14)	-	1	(0,01)	-	2	(0,03)	i	12	(0,15)	-	14	(0,18)	-	0,61	80
	EMS+5 mg/mL SB	80	121	(1.51)	-	88	(1.10)	-	17	(0.21)	-	77	(0.96)	-	226	(2.83)	-	3.94	28,36↓
	EMS+5 mg/mL SL	80	114	(1.43)	-	81	(1.01)	-	16	(0.20)	-	73	(0.91)	-	211	(2.64)	-	3.74	33,17↓
	10 mg/mL SB	80	10	(0,13)	-	1	(0,01)	-	0	(0,00)	-	11	(0,14)	-	11	(0,14)	-	0,56	
	10 mg/mL SL	80	8	(0,10)	-	3	(0,04)	i	1	(0,01)	-	8	(0,10)	-	12	(0,15)	-	0,41	
	EMS+10 mg/mL SB	80	71	(0,89)	-	71	(0,89)	-	11	(0,14)	-	68	(0,85)	-	153	(1,91)	-	3,48	51,65↓
	EMS+10 mg/mL SL	80	69	(0,86)	-	67	(0,84)	-	9	(0,11)	-	65	(0,81)	-	145	(1,81)	-	3,33	54,18↓
mwh/TM3	Distilled water	80	17	(0.21)		2	(0.03)					21	(0.26)		19	(0.24)		1.08	
	EMS (1mM)	80	157	(1.96)	+	107	(1.34)	+				232	(2.90)	+	264	(3.30)	+	11.88	
	1.25 mg/mL SB	80	13	(0,16)	-	4	(0,05)	i				21	(0,26)	i	17	(0,21)	-	1,08	
	1.25 mg/mL SL	80	14	(0,18)	-	4	(0,05)	i				19	(0,24)	-	18	(0,23)	i	0,97	
	EMS+1.25 mg/mL SB	80	142	(1,78)	-	101	(1,26)	-				101	(1,26)	-	243	(3,04)	-	5,17	7,88↓
	EMS+1.25 mg/mL SL	80	140	(1,75)	-	98	(1,23)	-				97	(0,21)	-	238	(2,98)	-	4,97	9,70↓
	2.5 mg/mL SB	80	13	(0,16)	-	2	(0,03)	i				20	(0,25)	i	15	(0,19)	-	1,02	
	2.5 mg/mL SL	80	13	(0,16)	-	1	(0,01)	-				19	(0,24)	-	14	(0,18)	-	0,97	
	EMS+2.5 mg/mL SB	80	130	(1,63)	-	94	(1,18)	-				89	(0,11)	-	224	(2,80)	-	4,56	15,15↓
	EMS+2.5 mg/mL SL	80	133	(1,66)	-	91	(1,14)	-	*			83	(1,04)	-	224	(2,80)	-	4,25	15,15↓
	5 mg/mL SB	80	12	(0,15)	-	3	(0,04)	i				19	(0,24)	-	15	(0,19)	-	0,97	
	5 mg/mL SL	80	10	(0,13)	-	1	(0,01)	-				17	(0,21)	-	11	(0,14)	-	0,87	
	EMS+5 mg/mL SB	80	125	(1,56)	-	83	(1,04)	-				71	(0,89)	-	208	(2,60)	-	3,64	21,21↓
	EMS+5 mg/mL SL	80	110	(1,38)	-	81	(1,01)	-				73	(0,91)	-	191	(2,39)	-	3,74	27,57↓
	10 mg/mL SB	80	9	(0,11)	-	2	(0,03)	i				16	(0,20)	-	11	(0,14)	-	0,82	
	10 mg/mL SL	80	8	(0,10)	-	0	(0,00)	-				15	(0,19)	-	8	(0,10)	-	0,76	
	EMS+10 mg/mL SB	80	67	(0,84)	-	70	(0,86)	-				56	(0,70)	-	137	(1,71)	-	2,87	48,18↓
	EMS+10 mg/mL SL	80	64	(0,80)	-	66	(0,83)	-				50	(0,63)	-	130	(1,63)	-	2,56	50,60↓

N: Number of wings, No: number of clones, Fr.: frequency, D: statistical diagnosis according to Frei and Würgler (1985), CIF: Frequency of clone formation per 10^5 cells, *: balancer chromosome *TM3* does not carry the *flr³* mutation.+: positive, -: negative, i: inconclusive, m: multiplication factor, probability levels α=β=0.05.

DISCUSSION

In vivo toxicity assay using *Drosophila* larvae indicated that *Sideritis* extracts are non-toxic. Moreover, these extracts improved survival, pupation, and eclosion rates in flies exposed to oxidative stress, suggesting a protective effect (Diken and Yilmaz, 2022). *Sideritis* essential oils are rich in monoterpenes, such as carvacrol and thymol, which are associated with their biological activities (Sevindik et al., 2021; Chrysargyris et al., 2023). *S. scardina* hot water extract treatment significantly prolonged both average and maximum lifespan of wild-type *C. elegans* in a dose-dependent manner, indicating its potential to promote longevity (Nishioka et al., 2020). *S. scardina* extracts demonstrated notable antiaging effects in yeast models by enhancing survival rates and improving stress responses in premature aging mutants, underscoring their potential role in modulating cellular longevity mechanisms (Vasileva et al., 2022).

Plant extracts have been shown to modulate EMS-induced genotoxicity in *Drosophila,* although their effects vary considerably depending on factors such as plant species, extraction method, and dosage. Certain extracts, such as those derived from *Rosa canina* and *Echium amoenum*, have demonstrated significant antigenotoxic activity by reducing DNA damage, whereas others may exert minimal effects or even enhance genotoxicity. Therefore, careful selection of plant species, standardized extraction procedures, and rigorous evaluation are essential to establish plant extracts as effective antigenotoxic agents (Jacociunas et al., 2013; Kızılet et al., 2013; Uysal et al., 2015; Çetinkaya and Yurtsever, 2021; Okorie et al., 2021).

The genotoxic and antigenotoxic potentials of *Sideritis* species have attracted growing attention due to their well-documented antioxidant and anti-inflammatory properties (Oalđe et al., 2021). However, no studies to date have directly evaluated *Sideritis* extracts using the *Drosophila* wing spot test (SMART), a widely accepted in vivo model for assessing genotoxicity and antigenotoxicity of various substances, including plant-derived compounds. The SMART assay has been effectively applied to different herbal extracts, revealing their ability to inhibit mutagen-induced wing spot formation and indicating protective effects against DNA damage (Pitchakarn et al., 2021; Çarıkçı et al., 2023). Despite the promising bioactivities of *Sideritis,* its potential to modulate EMS-induced genotoxicity in *Drosophila melanogaster* remains unexplored. This study addresses this gap by providing the first evidence of the antigenotoxic effects of two *Sideritis* species against EMS-induced DNA damage in *Drosophila*, thereby contributing valuable insights into the safety and therapeutic potential of these medicinal plants. Future research should focus on elucidating the molecular mechanisms underlying these protective effects and further evaluating the potential of *Sideritis* in reducing genotoxicity.

CONCLUSION

The findings of this research demonstrate that *Sideritis brevidens* and *Sideritis libanotica* subsp. *violascens* can effectively counteract EMS-induced genetic damage in *Drosophila melanogaster*, as evidenced by reductions in wing spot formation. The observed protective effects, particularly at higher extract concentrations, suggest that these species may serve as valuable natural candidates for developing agents that aim to minimize DNA damage. Beyond expanding the biological profile of *Sideritis* species, the present results provide a foundation for future work exploring their bioactive components, underlying mechanisms, and broader applications in genotoxicity prevention.

ACKNOWLEDGEMENTS

We thank Dr. Emre SEVİNDİK for providing support in the field collection and taxonomic identification of the studied *Sideritis* species.

REFERENCES

Abraham, S. K. (1994). Antigenotoxicity of coffee in the *Drosophila* assay for somatic mutation and recombination. Mutagenesis, 9(4), 383-386.

Ansari, S. Z., Varshney, H., Gaur, K., Subhan, I., Fatima, J., Ara, G., & Siddique, Y. H. (2025). Effect of *Azadirachta indica* Leaf Extract on the Toxicity Induced by Ethyl Methanesulphonate (EMS) in the Third Instar Larvae of Transgenic *Drosophila melanogaster* (hsp70-lacZ) Bg9. Current Nutraceuticals, 6(1), E26659786331452.

Atanasov, A. G., Waltenberger, B., Pferschy-Wenzig, E. M., Linder, T., Wawrosch, C., Uhrin, P., & Stuppner, H. (2015). Discovery and resupply of pharmacologically active plant-derived natural products: A review. Biotechnology Advances, 33(8), 1582-1614.

Chrysargyris, A., Tomou, E. M., Goula, K., Dimakopoulou, K., Tzortzakis, N., & Skaltsa, H. (2023). *Sideritis* L. essential oils: A systematic review. Phytochemistry, 209, 113607.

Çarıkçı, S., Kılıç, T., Gören, A. C., Dirmenci, T., Alim Toraman, G. Ö., & Topçu, G. (2023). Chemical profile of the Anatolian *Sideritis* species with bioactivity studies. Pharmaceutical Biology, 61(1), 1484-1511.

Çetinkaya, A. Y,, & Yurtsever, S. (2021). Investigation of the genotoxicity of tatrazine and anti-genotoxicity of some plants extracts in *Drosophila melanogaster* using the smart test. Journal of Health, Medicine and Nursing, 89, 20-29.

Diken, M. E., & Yılmaz, B. (2022). Inhibitory effect on acetylcholinesterase and toxicity analysis of some medicinal plants. International Journal of Secondary Metabolite, 9(1), 27-42.

Elbouny, H., Ouahzizi, B., Bakali, A., Sellam, K., & Alem, C. (2022). Phytochemical study and antioxidant activity of two Moroccan Lamiaceae species: *Nepeta nepetella* subsp. *amethystina* and *Sideritis arborescens* Salzm. ex Benth. Journal of Analytical Sciences and Applied Biotechnology, 4, 15-21.

Eruygur, N., Kırcı, D., Ayaz, F., Bağcı, Y., Doğu, S., & Yılmaz, M. A. (2024). Biological activities and phytochemical investigation of some *Sideritis* species. Indian Journal of Traditional Knowledge (IJTK), 23(10), 988-998.

Frölich, A., & Würgler, F. E. (1990). *Drosophila* wing-spot test: improved detectability of genotoxicity of polycyclic aromatic hydrocarbons. Mutation Research/Environmental Mutagenesis and Related Subjects, 234(2), 71-80.

Frei, H., & Würgler, F. E. (1995). Optimal experimental design and sample size for the statistical evaluation of data from somatic mutation and recombination tests (SMART) in *Drosophila*. Mutation Research/Environmental Mutagenesis and Related Subjects, 334(2), 247-258.

González-Burgos, E., Carretero, M. E., & Gómez-Serranillos, M. P. (2011). *Sideritis* spp.: Uses, chemical composition and pharmacological activities—A review. *Journal of Ethnopharmacology, 135(2), 209-225.*

Graf, U., Abraham, S. K., Guzmán-Rincón, J., & Würgler, F. E. (1998). Antigenotoxicity studies in *Drosophila melanogaster.* Mutation Research/Fundamental and Molecular Mechanisms of Mutagenesis, 402(1-2), 203-209.

Graf, U., Würgler, F. E., Katz, A. J., Frei, H., Juon, H., Hall, C. B., & Kale, P. G. (1984). Somatic mutation and recombination test in *Drosophila melanogaster*. Environmental Mutagenesis, 6(2), 153-188.

Jacociunas, L. V., Dihl, R. R., Lehmann, M., Ferraz, A. D. B. F., Richter, M. F., Silva, J. D., & Andrade, H. H. R. D. (2014). Effects of artichoke (*Cynara scolymus*) leaf and bloom head extracts on chemically induced DNA lesions in *Drosophila melanogaster*. Genetics and Molecular Biology, 37, 93-104.

Kızılet, H., Kasımoğlu, C., & Uysal, H. (2013). Can the *Rosa canina* plant be used against alkylating agents as a radical scavenger. Polish Journal of Environmental Studies, 22(4), 1263-1267.

Kotan, R., Cakir, A., Dadasoglu, F., Aydin, T., Cakmakci, R., Ozer, H., Kordali, S., Mete, E., & Dikbas, N. (2010). Antibacterial activities of essential oils and extracts of Turkish *Achillea*, *Satureja* and *Thymus* species against plant pathogenic bacteria. *Journal of the Science of Food and Agriculture, 90(1), 145-160.*

Lindsley DL, Zimm GG. The genome of *Drosophila melanogaster*. Academic Press. San Diego, CA; 1987.

Lobo, V., Patil, A., Phatak, A., & Chandra, N. (2010). Free radicals, antioxidants and functional foods: Impact on human health. *Pharmacognosy Reviews, 4(8), 118.*

Nishioka, Y., Nishikawa, S., & Shibata, T. (2020). A hot water extract of *Sideritis scardica* prolongs life span and enhances heat shock resistance in *Caenorhabditis elegans*. Natural Product Communications, 15(4), 1934578X20917283.

Oalđe, M., Kolarević, S., Živković, J., Aradski, A. A., Marić, J. J., Kolarević, M. K., Đorđević, J., Marin, P., Šavikin, K., Vuković-Gačić, B., & Duletić-Laušević, S. (2021). A comprehensive assessment of the chemical composition, antioxidant, genoprotective and antigenotoxic activities of Lamiaceae species using different experimental models in vitro. Food & Function, 12(7), 3233-3245.

Okorie, A., & Magama, S. (2021). Evaluation of leaf extracts of *Artemisia afra* Jacq. ex Willd. and *Leucosidea sericea* Eckl. Zeyh. for genotoxicity and the modulation of EMS-induced genotoxicity. Journal of Medicinal Plants Research, 15(6), 269-282.

Pitchakarn, P., Inthachat, W., Karinchai, J., & Temviriyanukul, P. (2021). Human hazard assessment using *Drosophila* wing spot test as an alternative in vivo model for genotoxicity testing—A review. International Journal of Molecular Sciences, 22(18), 9932.

Rand, M. D., Tennessen, J. M., Mackay, T. F., & Anholt, R. R. (2023). Perspectives on the *Drosophila melanogaster* model for advances in toxicological science. Current Protocols, 3(8), e870.

Selvi, S., Polat, R., Çakilcioğlu, U., Celep, F., Dirmenci, T., & Ertuğ, Z. F. (2022). An ethnobotanical review on medicinal plants of the Lamiaceae family in Turkey. Turkish Journal of Botany, 46(4), 283-332.

Sevindik, E., Gübeş, İ., Murathan, Z. T., & Tümen, G. (2021). Determination of total phenolic content, total flavonoid content and total antioxidant capacity in some endemic *Sideritis* L. (Lamiaceae) species grown in Turkey. European Journal of Biological Research, 11(2), 260-266.

Uysal, H., Kızılet, H., Ayar, A., & Taheri, A. (2015). The use of endemic Iranian plant, *Echium amoenum*, against the ethyl methanesulfonate and the recovery of mutagenic effects. Toxicology and Industrial Health, 31(1), 44-51.

Walasek-Janusz, M., Papliński, R., Mysiak, B., & Nurzyńska-Wierdak, R. (2025). Phenolic Profile and Antioxidant Activity of Extracts from Aerial Parts of *Thymus vulgaris* L. and *Sideritis scardica* Griseb. Applied Sciences, 15(7), 3842.

Würgler FE, Vogel EW. In vivo mutagenicity testing using somatic cells of *Drosophila melanogaster*. In: de Serres FJ, editor. Chemical Mutagens: Principles and Methods for their Detection. New York: Plenum Press. pp 1-72; 1986.

Valko, M., Rhodes, C. J. B., Moncol, J., Izakovic, M. M., & Mazur, M. (2006). Free radicals, metals and antioxidants in oxidative stress-induced cancer. Chemico-Biological Interactions, 160(1), 1-40.

Vasileva, B., Staneva, D., Grozdanova, T., Petkov, H., Trusheva, B., Alipieva, K., Popova, M., Miloshev, G., Bankova, V., & Georgieva, M. (2022). Natural deep eutectic extracts of propolis, *Sideritis scardica,* and *Plantago major* reveal potential antiageing activity during yeast chronological lifespan. Oxidative Medicine and Cellular Longevity, 2022(1), 8368717.

ORAL PRESENTATION

Seedlessness genes and molecular identification studies in grapevines (*Vitis vinifera* L.)

Abdullah Ozdemir [1] (*ORCID: https://orcid.org/0009-0007-9137-5199*),
Emine Orhan [2*] (*ORCID: https://orcid.org/0000-0002-5503-6081*)

[1]Ministry of Agriculture and Forestry, Erzincan Horticulture Research Institute, Erzincan, Türkiye.
[*2]University of Ataturk, Faculty of Agriculture, Department of Agricultural Biotechnology, Erzurum, Türkiye

*Corresponding author e-mail: eorhan@atauni.edu.tr

Abstract

Seedlessness is a preferred trait for many plant species, including grapevines. Consumer demand for seedless table grape cultivars, both fresh and dried, has increased globally. Furthermore, almost all dried grape consumed in global markets are seedless. For this reason, breeding studies have focused on the development of seedless varieties for many years. The aim of this study is to share some information about the seedlessness-associated genes and the mechanism of seedlessness in grapevines. For this purpose, firstly, the flower structure and flower types of grapevines have been introduced and the concepts of flowering and pollination have been explained. Then, some molecular mechanisms related to seedlessness have been explained, including information on seedlessness-associated genes in grapevines. Additionally, some research examples on the effective use of both classical and modern breeding methods for seedlessness have been included. There are numerous studies on seedlessness in *Vitis vinifera* L. species, including the identification of quantitative loci, gene identification, gene expression studies, molecular marker development, and characterization using markers in hybridization and selection breeding studies. Studies on these topics have been identified as being both illustrative and complementary. As a result of these studies, it appears that the single-gene effect approach is now being replaced by a multi-gene effect approach. Within the scope of the information given in this study, it is anticipated that future studies on alternative seedless grape breeding will be more effective.

Keywords: *Vitis vinifera* L., Seedlessness-associated genes, Molecular identification

INTRODUCTION

The grapevine known as *Vitis vinifera* L. belongs to the genus *Vitis*. The genus *Vitis* is divided into two sections, *Muscadinia* (2n=2x=40) and *Euvitis* (2n=2x=38), due to differences in some morphological features and chromosome numbers. There are approximately sixty known *Vitis* species worldwide. The most commonly grown grapevine species is known as *Vitis vinifera* L. (native to Europe, North Africa and the Near East) (Owens, 2008). The total world grape production amount has been reported as approximately 72.5 million tons (FAOSTAT, 2023). Türkiye's grapevine production amount has been recorded as 3.4 million tons (approximately 5% of world production) (TUIK, 2023; OIV, 2023). Emphasizing the importance of seedlessness, this study aims to share the functions of genes associated with seedlessness in grapes. Some molecular mechanisms involved in seedlessness in grapes have been explained. Examples of classical and modern seedlessness breeding studies have been also included.

FLOWER TYPES AND FLOWER STRUCTURE IN GRAPEVINES

Three flower types have been identified in grapevines: (i) Functional hermaphrodite flower (both male and female organs are functional), (ii) Functional female flower (non-functional male organs are present) and (iii) Functional male flower (female organ is not fully developed and is not functional) (Oberle et al., 1938). *Vitis vinifera* L. grapevine varieties of European origin have hermaphrodite flowers, while American grapevine varieties have male and female flowers. (Snyder et al., 1937; Olmo et al., 1943). UPOV (The International Union for the Protection of New Varieties of Plants) criteria mention four flower types for the *Vitis vinifera* grapevines. These are: (i) fully developed stamens and absence of gynoecium, (ii) fully developed stamens and presence of reduced gynoecium,

(iii) fully developed stamens and fully developed gynoecium, and (iv) reflexed stamens and fully developed gynoecium (Figure 1a).

The pistil of hermaphrodite flowers is surrounded by five stamens. However, individual flowers of the same inflorescence may have more than five stamens. Fused petals (corolla) surround the flower parts mentioned above. During flower development, these petals loosen from the base, forming a cap-like structure (calyptra) (Snyder et al., 1937) (Figure 1b, Alfrey et al., 2019).

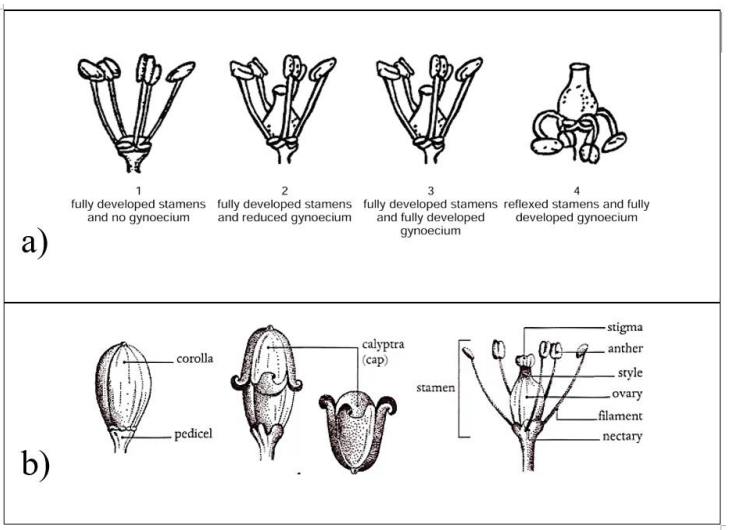


Figure 1. a) Grapevine flower types (UPOV, 2023), **b)** Flower appearances with and without calyptra in grapevine and parts of the hermaphrodite flower (Alfrey et al., 2019).

FLOWERING AND POLLINATION IN GRAPEVINES

The period during which the flowers are open is called anthesis. Flowering can last from one to three weeks, depending on weather conditions. Not all flowers on a cluster open at the same time. Cleistogamy is observed in some varieties. That is, self-pollination occurs before the flowers open. The number of flowers in which cleistogamy, a genetic trait, occurs varies greatly among varieties (Barbagallo et al., 1988; Staudt, 1999). In their study on the onset time of pollination of grapevine flowers under calyptras, Wang et al. (2023a) have been able to determine the flowering process before the flower opened in the cultivar 'Shine muscat'. The separated floral buds stage has been identified as the initial stage of cleistogamy. According to these researchers, this situation will reduce labor and time and provide a theoretical basis for hybridization breeding.

Pollination of grapevine flowers generally occurs with their own pollen. Wind, honeybees, and other insects assist in pollination as active pollinators (Olmo, 1943; Bronner and Wagner, 1997; Kimura et al., 1998). Pollination is affected by temperature, relative humidity, and the pollen acceptance status of the stigma (Bronner and Wagner, 1997). On the other hand, it is reported that pollen is alive in flowers before the cap falls and that the pollen can survive for several days after the cap falls (Heazlewood and Wilson, 2004).

SEEDLESSNESS AND SEEDLESSNESS-RELATED GENES IN GRAPEVINES

Seedlessness is one of the most valuable quality characteristics of grapevines, whether for consumption as fresh fruit or dried fruit (Ledbetter and Ramming, 1989). In seeded grape varieties, the ovary develops after fertilization. However, in most seedless grape varieties, the seed does not develop fully (Burger and Goussard, 1996). "Seedlessness" occurs by two mechanisms: parthenocarpy and stenospermocarpy (Değirmenci and Marasalı, 2007). Parthenocarpic seedless fruits occur without pollination and fertilization (Perl et al., 2000). For the formation of stenospermocarpic seedless fruit, pollination and fertilization initially occur normally. However, after pollination, integument development in the ovaries is prevented by genetic mechanisms. Degeneration of the embryo and endosperm occurs. As a result, seed development is impossible. Only partially formed seeds are seen

with development in the form of seed scars (Costantini et al., 2008). When parthenocarpic grapevine cultivars were used as pollinators for seeded grapevine cultivars, new seedless generations could not be obtained (Stout, 1937). However, when stenospermocarpic grapevine cultivars were used to pollinate seeded grapevine cultivars, it was possible to obtain seedless individuals (Stout, 1937; Weinberger and Harmon, 1964). For this reason, plant breeders have focused on stenospermocarpic cultivars (Burger and Goussard, 1996). Although seeds do not form in parthenocarpic grapevine cultivars such as Black Corinth, rudimentary seeds containing living embryos can develop (Kunter and Sehit, 2019). On the other hand, it has been determined that there is no development or maturation of the embryo and/or endosperm in stenospermocarpic grapevine cultivars such as seedless 'Sultani' (also known as 'Thompson Seedless') (Ledbetter and Burgos, 1994; Mejia et al., 2011).

There are two methods used to obtain seedless grapes: (i) applications of cytokinin (CK) and gibberellic acid (GA) before full flowering stage, (ii) genetic breeding of seedless grapevine cultivars. In an example study for the first of these methods, it was stated that plant hormones can effectively trigger seed degeneration in seeded grapevines (Reynolds et al., 1992). However, although this method has become a common practice in seedless grapevine production, it has been emphasized that it may raise concerns about labor costs and food safety (Park et al., 2022). Correa et al. (2015) investigated the response of fruit size and seed mass to gibberellic acid (GA) applications and quantitative trait loci in table grapes. As a result of gibberellic acid applications tested for 'Ruby seedless' × 'Sultanina' hybrid individuals, an increase in fruit size and a decrease in seed dry mass during ripening were observed. The response to GA3 has been found to have a significant genetic basis associated with QTLs localized in linkage group 2 and linkage group 18. According to the 19 gene clusters covered by these QTLs, fruit size was associated with the response to GA3. Despite the masking effect, the VvAGL11 gene (AGL, AGAMOUS-LIKE) was associated with the response to GA3. According to the second main method used to obtain seedless grapes, plant breeders have been utilized triploid and diploid breeding approaches and embryo rescue techniques to obtain new seedless cultivars (Park et al., 1999; di Rienzo et al., 2021). For example, Roytchev (2007) has been used agronomic characters to determine the genetic variation among F1 individuals obtained by crossing seeded and seedless grapevine varieties ('Super early bolgar' × 'Ruby seedless'), to explain the reasons for clustering and to select elite hybrid individuals. The fact that seeded and seedless individuals were collected into two different groups has been revealed that clustering and principal component analysis could be used effectively. In Roychev (2011) path analysis was carried out on the variability of yield and quantitative traits in hybridization between seeded and seedless grapevine cultivars ('Armira' × 'Russalka-1') based on some agronomic characters. Parent cultivars have been found to specifically affect the phenotype of hybrid plants. In a study conducted by Roychev and Keranova (2023), cluster analysis has been performed to determine phenotypic similarity/dissimilarity based on ampelographic characteristics of seedless grapevine varieties. Based on the groupings obtained for all individuals, the level of stenospermocarpy in the cultivars could also be determined.

Seedlessness is an important quality trait in table grape (*Vitis vinifera* L.) breeding. However, seed development involves a complex mechanism (Wang et al., 2024). During fruit formation in grapevines, some genes associated with the development of different tissues such as integument (seed coat), endosperm, embryo and ovule (Ehlers et al., 2016) have been summarized in Table 1.

Seedlessness in grapevines is associated with mutation (missense mutation) in the VviAGL11 gene (Royo et al., 2018). Mejia et al. (2011) have stated the VvAGL11 gene as a gene belonging to the D lineage of MADS-box genes that control ovule identity. It has stated that this gene could be effectively used for the early detection of stenospermocarpic seedlessness. According to Bolander (2004), MADS is an abbreviation derived from the first letter of four transcription factors defined by the motif MCM1, AG, DEFA and SRF. In Moniruzzaman et al. (2023), who created a schematic model of the hormonal regulation of seedless fruit set in grapevine, the formation of stenospermocarpy due to embryo abortion during the seed coat development stage heve mentioned. Here, there is an explanation that embryo abortion occurs as a result of the effect of CKX7 (cytokinin oxidase-7), one of the CK-degrading enzymes. According to information provided by Mejía et al. (2007 and 2011), Bergamini et al. (2013), and Amato et al. (2022), VviAGL11 likely directly affects seed development by regulating, auxin, MeJA and isoflavonoid synthesis. The VviAGL11 expression level has been found and confirmed to depend on the promoter coding sequence allelic combination. This gene has been identified as activating key triggers of seed coat development. The effect of mutated VviAGL11 was confirmed at the molecular level. A novel mechanism linking

VviAGL11 haplotype diversity and seedlessness class has been described. The p3-VvAGL11 marker has been identified in the promoter region of the VviAGL11 gene. A tight link between this gene the and seedlessness trait has been demonstrated (Table 1).

An interesting example of seedless fruit production has been described in the spontaneous mutant 'Thai seedless' of the species sugar apple (*Annona squamosa*) (Lora et al., 2011). This mutant produces normal-sized fruits that are completely seedless following pollination. The authors have been suggested that the failure to set seeds was due to a deficiency in the outer of the two normal seed coats. They have beeen suggested that this was due to a defect in the ovule, similar to the *Arabidopsis* "inner no outer" (INO-1) mutant (Villanueva et al., 1999). This gene encodes a transcription factor belonging to the YABBY family, which plays a role in determining abaxial identity in various organs. This gene has been expressed in *Arabidopsis thaliana*, where it is required for the formation of the outer shell and asymmetric growth of the egg cell. This mutation has been reported to cause a phenotypic defect in ovules, negatively affecting seed formation (Lora et al., 2011; di Rienzo et al., 2021). According to di Rienzo et al. (2021), the VviINO gene in grapevine has an activity similar to the gene in *Arabidopsis* (Table 1).

According to Zhang et al. (2021), NAC TFs have numerous irreplaceable biological functions in plants, such as ovule development, seed coat formation, fruit ripening, leaf fall, and response to various environmental stresses. In addition to these functions, they have been associated with the early development of flowers and fruits (Tello et al., 2015). The absence of VviAGL11 expression has been found to activate the overexpression of WRKY, Homeobox and NAC, transcription factors. Seed coat differentiation is inhibited, endosperm degeneration occurs, and embryonic development is inhibited (Malabarba et al., 2017; Royo et al., 2018) (Table 1).

In Tang et al. (2016), caspase-1 like activities of VPEs (vacuolar processing enzymes) and their importance in the development of stenospermocarpic seedless grapevine ovules were mentioned. To characterize the relationship between the VPE gene family and stenospermocarpic grapevines, these researchers have been identified three *Vitis vinifera* VPE genes (VvβVPE, VvγVPE, and VvδVPE from the PN40024 grapevine genome). According to phylogenetic analysis of four *Arabidopsis thaliana* and six *Vitis vinifera* VPEs, ten VPEs form three main branches. While six grapevine VPEs have been identified in a similar gene structure containing eight introns and nine exons, six grapevine VPEs have been found on three different chromosomes. According to tissue-specific expression analysis, VvδVPE has expressed in ovules, flowers and buds. While VvγVPE has expressed in various tissues, VvβVPE has expressed in roots, flowers, buds and ovules. However, a study by Gong et al. (2019) determined that the *Vitis vinifera* (Vv) βVPE gene processes seed proteins during seed development and exhibits seed-specific expression. However, it has been stated that this was not yet fully understood. The researchers have been characterized the pVvβVPE (VvβVPE promoter) in seeded and seedless grape genotypes. According to the GUS staining results performed on different tissues and organs, VvβVPE was expressed in the embryo, hypocotyl, cotyledon and suspensor (Table 1).

As a result of transcriptomic and genomic analyses, HB-KNOX members, which are among the Homeobox (HB) transcription factors, play a role in the development of grape fruit and seed. The VvHB63 gene in grapes has been functionally characterized. Although no differences heve been observed in the sequences of seeded and seedless grapevines, higher expression levels of the VvHB63 gene have been observed in integument and chalaza of ovules in seedless grapevines compared to seeded grapevines. In situ hybridization analysis showed that the VvHB63 gene was expressed in ovules and episperm cells of "Thompson Seedless" cultivar (Li et al., 2017; Yao et al., 2023) (Table 1).

Different stages of the flowering plant life cycle are primarily controlled by different classes of MADS-box genes (type-I or SRF-like and type-II or MEF2-like: M group for plants in type-I/MIKCC group and MIKC* group for plants in type-II). It is stated that the development of the female gametophyte (embryo sac), embryo and seed is controlled by type I genes. Most stages of diploid sporophyte development involve the activity of the MIKCC group of type II genes, while male gametophyte (pollen) development is controlled by the activity of the MIKC* group of genes (Gramzow and Theissen, 2010). According to this study; AG (AGAMOUS) and SEP (SEPALLATA) promoters included in the MIKCC group whave been found to be determinants of carpel development. In addition, AG and SEP dimer and AP3 (AP, APETALA) and PI (PISTILLATA) dimer together have been expressed as

determinants of stamen development. While AP1 and SEP dimer and AP3 and PI dimer together have been expressed as determinants of petal development, AP1 and SEP double dimer have been expressed as determinants of sepal development.

According to a study conducted using the SRAP-cDNA analysis system, the VviABCG20 gene was identified as a gene differentially expressed during ovule development between the stenospermocarpic the seeded cultivar 'Pinot noir' and seedless cultivar 'Youngle' (*A. thaliana*, ATP-binding cassette G transporter 20, also known as the ABC-2 type transporter gene family protein) (Wang et al., 2016). According to the expression analysis of VviABCG20 during seed development or fertilization in seeded and seedless cultivars, the VviABCG20 gene has been found to have a role in seed development. According to the results of a study conducted by Wang et al. (2023a), the VviABCG20 gene has been strongly expressed in the seeds of seeded grapes and silencing of the homolog of the same gene in tomato has been resulted in a decrease in the number of seeds. VviABCG20 gene expression was shown to be higher in the seeds of seeded grapes than in seedless grapes. Furthermore, VviABCG20 gene expression was significantly higher in the seed coat than in the ovules and endosperm. According to the intracellular localization analysis performed as a result of induction of grape leaves by exogenous hormones, especially MeJA; the protein product of the VviABCG20 gene is a membrane protein. According to the study results, the VviABCG20 gene may function in seed development in grapevine, partly by participating in suberin biosynthesis in the seed coat. (Tang et al., 2020; Wang et al., 2022a) (Table 1). According to Tang et al. (2020), the ABCG20 model provides a new insight and the expression of single and combined transcription factors in grapevines is effective in flower identity development.

In a study by Palumbo et al. (2019), have been based on 18 representative grapevine "ABCDE genes" encoding MADS-box transcription factors. Transcript levels and biological consistencies obtained in a developmental process, from pre-flowering to post-fertilization stage and in different floral organs (embryos, ovary, filaments, anthers, calyx and calyptra), have been compared with the model proposed for *Arabidopsis*. With a few exceptions, the results have been confirmed the expected expression pattern based on the *Arabidopsis* data. According to this ABCDE model, based on their expression for organ identity determination for *Vitis vinifera* L., there are five classes of flower homeotic genes (Class A, Class B, Class C, Class D, and Class E). A+E genes (VviFUL1, VviFUL2, VviAP1 + VviSEP1, VviSEP2, VviSEP3, VviSEP4) in sepals (FUL, FRUITFULL), A+B+E genes (VviFUL1, VviFUL2, VviAP1 + VviAP3a, VviAP3b, VviPI + VviSEP1, VviSEP2, VviSEP3) in petals, B+C+E genes (VviAP3a, VviAP3b, VviPI + VviAG1, VviAG2, VviAGL6a, VviAGL6b + VviSEP1, VviSEP2, VviSEP3, VviSEP4) in stamens, C+E genes (VviAG1, VviAG2 + VviSEP1, VviSEP3, VviSEP4 + ABS1, ABS2) in carpels (ABS, *Arabidopsis* B sister) and C+D+E genes (VviAG1, VviAG2 + VviAG3 + VviSEP1, VviSEP2, VviSEP3) in ovules have been expressed determinantly according to the ABCDE model (Table 1). The above mentioned VvPI gene has been studied for the *Malus domestica* species (Md-PISTILLATA) by Yao et al. (2001) and has been expressed as a MADS-box TF. According to Pelaz et al. (2000), all the floral whorls of the SEP1, SEP2, and SEP3 triple mutant develop into sepals and flowers that become indeterminate. On the other hand, according to Ditta et al. (2004), vegetative leaves are formed instead of sepals in the SEP1, SEP2, SEP3, and SEP4 quadruple mutant. According to Grimplet et al. (2016), SEP1, SEP2, and SEP3 were stated to be associated with the E class group.

MADS-box genes encode a large family of transcription factors in higher plants and have diverse developmental roles, including flower, fruit and seed development (Sun et al., 2020). These researchers have been stated that there was very little information about the function of these genes in grapevine, especially regarding seed development. In tomato, heterologous expression of VvMADS45 (VvMADS45-OE) has been resulted in larger flowers, fruits, and seeds. However, disruption of a tomato homolog of VvMADS45 (SlAGL104-KO) has been resulted in smaller seeds, fruits and flowers. Both SlAGL104-KO and VvMADS45-OE lines have been produced fewer seeds than the control. It has been emphasized that VvMADS45 plays a role particularly in seed development (Table 1). However, in the study on seedlessness in *Vitis vinifera* L. by Zhang et al. (2022), VvMADS39, which is orthologous to *Arabidopsis* SEP2 and has an E MADS-box gene, was characterized. It has been hypothesized that active VvMADS39 expression in the cultivar ‘Thompson seedless’ may restrict cellular expansion, resulting in the development of smaller fruits and seeds. It has been stated that this gene may play a role in the regulation of ovule development in ‘Thompson seedless’ and contribute to the formation of seedless fruit. In contrast, suppression of the VvMADS39 gene in the ‘Red Globe’ cultivar has been associated with increased histone H3 lysine 27 trimethylation in the promoter region of VvMADS39, resulting in normal ovule formation (Table 1). On the other hand, Zhang et al. (2023) conducted a study on the regulatory mechanisms of ovule and seed development has been

associated with VvMADS28. VvMADS28 has been expressed as a seed development regulatory gene that is positively regulated by the VvERF98 gene. The relatively low expression level of the VvMADS28 gene in the 'Thompson seedless' seedless grapevine cultivar has been associated with increased H3K27me3 repressive marks in the promoter region. It has been stated that the VvMADS28 protein interacts with the VvMADS5 (TypeI/Mβ MADS-domain protein) gene to repress this gene by specifically binding to the VvWUS (WUSCHEL) promoter. Seed development is affected by maintaining VvMADS28 and VvWUS expression homeostasis (Table 1).

In a study conducted by Wang et al. (2022b), according to the results of real-time PCR analysis, VviASN1, VviASN2, VviGS1.1, VviGS1.2 and VviGS2b transcript levels were higher in seedless cultivars than in seeded cultivars during ovule development. It has been stated that asparagine content is higher in the seeds of seedless grapes than in seeded varieties, while glutamine content is higher in seeded varieties. Levels of both amino acids has increased during early seed development and then has decreased as development progressed. VviASN1 is expressed in flowers, while VviASN2 is expressed in leaves. VviGS2a, VviGS2b, and VviGS1.1 are expressed in leaves. VviGS1.2 is expressed in roots (Table 1).

The FUS3 gene has been implicated as a regulator of seed development. It has been well studied in *Arabidopsi*s due to its role in embryo and seed development. In a study conducted by Ahmad et al. (2022), information was shared that the VvFUS3 gene significantly reduces seed number and weight by affecting multiple hormonal signaling pathways (Table 1).

MOLECULAR STUDIES ON SEEDLESSNESS IN GRAPEVINES

Over the last three decades, numerous molecular studies on seedlessness have been conducted for *Vitis vinifera* L.. These studies generally have been covered topics such as identifying quantitative loci, developing molecular markers, performing characterization with the help of markers in hybridization and selection breeding studies, identifying genes, and performing genomic and transcriptomic studies.

Table 1. Some seedlessness-related genes responsible for the development of different flower tissues in the grapevines

Seedlessness-Related Genes	Different Flower Tissues	References
AGL11	ovule, integument	*Mejía et al. (2007)* *Mejía et al. (2011)* *Bergamini et al. (2013)* *Royo et al. (2018)* *Amato et al. (2022)* *Moniruzzamanet al. (2023)*
INO	outer integument ('inner no outer')	*Villanueva et al. (1999)* *Lora et al. (2011)* *di Rienzo et al. (2021)*
NAC26	ovule, integument	*Tello et al. (2015)* *Malabarba et al. (2017)* *Royo et al. (2018)* *Zhang et al. (2021)*
bVPE	ovule, embryo	*Tang et al. (2016)* *Gong et al. (2019)*
HB63	ovule, integument	*Li et al. (2017)* *Yao et al. (2023)*
Type I and Type II MADS-box (Type I or SRF-like and Type II or MEF2-like: M group for plants in type I/MIKC^{C}	sepal, petal, stamen, polen, carpel, embryo, embryo sac	*Gramzow ve Theissen 2010*

group and MIKC* group for plants in type II)		
Type I MADS-box, MIKC* group	central cell, endosperm, embryo	*Grimplet et al (2016*)
ABCG20	ovule, integument, endosperm	*Wang et al. (2016)* *Tang et al. (2020)* *Wang et al. (2022a)* *Wang et al. (2023b)*
SEP1, SEP2, SEP3, SEP4	sepal, petal, anther, flament, carpel	*Pelaz vd. (2000)* *Ditta vd. (2004)* *Grimplet vd. (2016)*
FUL1, FUL2 AP1 SEP1, SEP2, SEP3, SEP4	sepal	*Palumbo et al. (2019)*
FUL1, FUL2 AP1, AP3a, AP3b PI SEP1, SEP2, SEP3	petal	*Palumbo et al. (2019)*
AP3a, AP3b, AG1, AG2 AGL6a, AGL6b SEP1, SEP2, SEP3, SEP4	stamen	*Palumbo et al. (2019)*
PI	stamen	*Palumbo et al. (2019)* *Yao et al. (2001)*
AG1, AG2 SEP1, SEP3, SEP4 ABS1, ABS2	carpel	*Palumbo et al. (2019)*
AG1, AG2, AG3 SEP1, SEP2, SEP3	ovule	*Palumbo et al. (2019)*
MADS45	ovule	*Sun et al. (2020)*
MADS39	ovule	*Zhang et al. (2022)*
MADS28	ovule	*Zhang et al. (2023)*
ASN1, ASN2, GS1.1, GS1.2, GS2b	ovule	*Wang et al. (2022b)*
FUS3	embryo	*Ahmad et al. (2022)*

Striem et al. (1994 and 1996) has been reported RAPD markers associated with seedlessness. The SDI (seed development inhibitor) gene, a seed development inhibitor associated with seedlessness, has been mentioned in sources such as Bouquet and Danglot (1996), Lahogue et al. (1998), Adam-Blondon et al. (2001) ve Doligez et al. (2002). Lahogue et al. (1998) have been analyzed with RAPD markers and have been developed a SCAR marker (sequence characterized amplified region) linked to the SDI gene. The marker SCC8 was found to explain a large portion of the phenotypic variation in seedless component traits. Similarly, Meija and Hinrichsen (2003) have been developed the SCAR marker to determine seedlessness in grapevines. Among the individuals obtained from the 'Ruby' × 'Sultanina' cross, RAPD primers associated with seedlessness have been used in individuals selected for different stenospermocarpy subtraits. The RAPD fragment, named WF27-2000, was cloned, sequenced, and converted into a SCAR marker named SCF27, which produced a specific amplicon of 2.0 kb. The utility of SCAR markers for marker-assisted selection of seedless grapevine cultivars have been investigated. Specific SCAR markers SCP18 and SCC8, developed from the RAPD marker, heve been used for 43 seedless and 38 seeded grape genotypes. Unlike SCP18, SSC8 has been reported to be a useful marker, at least in seedless × seedless offspring (Adam-Blondon et al., 2001). In a study conducted in the Czech Republic (Korpas et al., 2009), twenty-four seedless grape genotypes, one endosperm-free genotype with a hard seed scar, nine seeded grape genotypes and

three hybrid lines showing segregation according to seedlessness have been examined. For the characterization of seedlessness, SCAR markers named SCC8 and SCF27 linked to the SDI locus have been used. However, it has been stated that this locus is necessary but does not provide sufficient information for the seedless phenotype. The possibility of other loci coexisting with this locus has been considered. However, in a study by Li et al. (2010), the sequence accuracy of the SCAR marker associated with seedlessness was determined by comparative sequence analysis. Based on PCR and DNA sequencing results, both the seeded and seedless phenotypes of *Vitis* species have been found to have highly homologous sequences within an EcoRI-restricted region of up to 5 kbp surrounding the SCAR marker. No linkage haas been found between the marker and the seedless trait. On the other hand, Amca (2011) has preferred SCF27 and SCC8 markers to detect seedlessness in hybrid combinations ('Cınarlı karası' × 'Tekirdag cekirdeksizi', 'Italia' × 'Barıs', 'Italia × Perlette', 'Gri kara' × 'Tekirdag cekirdeksizi') where seeded grape varieties were used as female parents and seedless grape varieties were used as male parents. The SCC8 marker has been reported as a successful DNA marker for detecting seedlessness. However, the SCF27 marker, despite giving distinct bands, has not been found to be useful in distinguishing homozygous and heterozygous genotypes.

There are also molecular characterization studies in which different markers for the determination of seedlessness in grapes have been preferred in the same study. For example, Akkurt et al. (2012), have been used SCAR markers (SCC8, SCF27) and SSR marker (VMC7f2) for the detection of seedlessness in hybrid products (372 F1 individuals) of seeded variety 'Alphonse Lavallée' and seedless variety 'Sultanina'. Homozygous alleles have been detected at the seed development inhibitor locus in 40 F1 individuals. Bands with SCF27 marker have been obtained in 80 F1 individuals. The 198 bp allele of the VMC7f2 marker associated with seedlessness has been identified in 174 F1 individuals. In the second year, 183 F1 individuals heve been positive for at least one marker and seedless grape candidate individuals could have been identified. As a result, a total of twenty individuals providing information on seedlessness for three markers have been identified, and the VMC7f2 SSR marker has been stated to be the marker most associated with seedlessness. On the other hand, Bennici et al. (2019) has been evaluated the effectiveness of four seedlessness-related markers (SCF27, p3-VvAGL11, VMC7f2 and VVIn16) in 97 F1 genotypes obtained from sixteen hybrid combinations. p3-VvAGL11 and VMC7f2 have been determined to be the most effective markers.

In a study conducted by Royo et al. (2018) for *Vitis vinifera*, molecular characterization has been performed based on the TF gene named AGAMOUS-Like 11 (MADS-box gene) and it has been confirmed that the markers of this gene can be used to detect seedlessness. Boztepe et al. (2023) has used the VvAGL11 marker (Forward: CTCCCTTTCCCTCTCCCTCT and Reverse: AAACGCGTATCCCAATGAAG) for F1 genotypes obtained from 'Yalova Seedless' × 'Glenora' and 'Yalova seedless' × 'Philipp' hybrid combinations. Seedless individuals have been successfully detected.

In a study conducted by Xi et al. (2023) to develop a KASP (competitive allele-specific PCR) marker for stenospermocarpic seedlessness in grapevine, a total of 83 grape cultivars with various genetic backgrounds (32 seeded and 51 seedless), 113 F1 hybrid individuals (53 seeded and 60 seedless) and two populations have been used. The KASP marker developed in association with the validated SNP locus for the VviAGL11 gene hes been found to successfully distinguish between seedless and seeded genotypes with high sensitivity and efficiency.

To date, in addition to studies on the development of molecular markers related to seedlessness in grapes, studies on the preparation of quantitative trait loci maps and the identification of linkage groups have also been carried out (Doligez et al., 2002; Fanizza et al., 2005; Cabezas et al., 2006; Costantini et al., 2007 and 2008; Mejía et al., 2007). The aim of a study conducted by Dalbo et al. (2000) has to create a linkage map of genes controlling sex in grapevine, with emphasis on linkage group-2. Cabezas et al. (2006) have developed a QTL map from the hybrid F1 products obtained from a crossbreeding program using the seeded variety 'Dominga' and the seedless variety 'Autumn seedless'. An SSR marker named VMC7F2, closely related to the seedless trait in linkage group-18, has been reported and it has been stated that this marker could be used for early detection in breeding of seedless individuals. Costantini et al. (2008) have been confirmed this finding after analyzing QTL associated with berry size and ripening time in grapes and have been identified the VMC7F2 marker as the marker most closely associated with the SDI locus. Linkage group-18 and linkage group-4 have been defined in Dai et al. (2011). Akkurt

et al. (2013) have detected seedlessness in 314 F1 individuals obtained from the cross of 'Hamburg Muscat' (seeded) × 'Sultani' (seedless) using VMC7f2, SCF27 and SCC8 markers. They have reported that the 198 bp allele identified with the VMC7F2 marker was closely associated with seedlessness in the F1 generation and could have been used in early selection. Karaagac et al. (2012) also have reported that the VMC7F2 SSR marker can be used successfully in the selection of seedless individuals.

p3-VvAGL11 (a sequence-tagged region marker) has been developed to detect the dominant allele controlling seedlessness (stenospermocarpic) in grapevine. This marker has been designed to perform genetic analysis of INDELs in the regulatory region of VviAGL11. Bergamini et al. (2013) have conducted a study to validate the p3-VvAGL11 marker. Only eight of 475 individuals have been found to be seedless. Conner et al. (2018) has performed a characterization of stenospermocarpic seedlessness in *Euvitis* × *Muscadinia* grapevine hybrid progenies using the p3-VvAGL11 marker. They have used the VvAGL11 marker in F1 lines (seeded and seedless hybrid individuals). They have found that this marker (214 bp) gave successful results in all seedless phenotypes. The p3-VvAGL11 marker has useful in identifying seedless offspring at the seedling stage. Early detection of stenospermocarpic seedlessness has possible.

Costenaro-da-Silva et al. (2011) carried out a study on the identification of genes associated with early fruit development in a seedless cultivar (Sultanina). The RDA (Representative Difference Analysis) strategy was developed in the study. A total of 2.400 transcript derivative fragments (TDFs) have been identified and have been cloned via RDA according to three specific developmental fruiting stages. Nine candidate genes have been selected from cDNAs and quantitative PCR analysis has been performed with two reference genes. Seven of the nine genes have been demonstrated consistent stage-specific expression, allowing their isolation by RDA.

The genetics of seedlessness in grapevines were investigated using specific locus amplified fragment sequencing and genome-wide association mapping, which are considered to be strongly complementary approaches. Genome sequences were compared with the reference genome. Single nucleotide polymorphisms were identified (a total of 414.223 SNPs). 294 SNPs have been identified that showed significant correlation with seedlessness. In adddition, candidate genes related to seed development were identified at loci close to significant SNPs. (Zhang et al., 2017).

In recent years, studies on genomic prediction using various programs using artificial intelligence-assisted machine learning (AI-ML) have attracted attention. For example, Wang et al. (2024) utilized the "machine learning-based genomic selection" method to create predictive models for seedlessness in grapes. Using the seedless grapevine varieties 'Black Monukka' and 'Thompson Seedless' they achieved a prediction accuracy of approximately 97%. The study was based on genome-wide association analyses in mapping populations obtained using whole-genome sequencing data. In grapevines, two loci affecting seedlessness were identified from a total of 110 loci, including additional loci identified for the mapping populations.

CONCLUSION

Seedlessness in grapes is a trait highly preferred by consumers due to its ease of eating and improved flavor. Therefore, numerous examples of classical and modern breeding efforts exist to achieve seedlessness in both table and dried grape varieties. In terms of commercial production and consumption, stenospermocarpic seedless grape varieties are in greater demand due to their quality as both table and dried grapes.

This study covers the functions of genes associated with seedlessness and the functioning of some molecular mechanisms related to seedlessness in grapevines. Studies on these topics have been identified as being both illustrative and complementary. As a result of these studies, it appears that the single-gene effect approach is now being replaced by a multi-gene effect approach. Within the scope of the information given in this study, it is anticipated that future studies on alternative seedless grape breeding will be more effective.

AUTHOR CONTRIBUTIONS

All authors reviewed and approved final version of the manuscript.

CONFLICT OF INTEREST

The authors declare no conflict of interest.

REFERENCES

Adam-Blondon AF, Lahogue F, Bouquet A, Boursiquot JM, This P. 2001. Usefulness of two SCAR markers for marker-assisted selection of seedless grapevine cultivars. Vitis, 40(3), 147-155.

Ahmad B, Zhang S, Yao J, Chai S, Yadav V, Athar HR, Rahman, MU, Wang L, Wang X. 2022. Ectopic expression of VvFUS3, B3- domain transcription factor, in tomato influences seed development via affecting endoreduplication and hormones. Hortic Plant J, 8, 351-360.

Akkurt M, Çakır A, Shidfar M, Çelikkol BP, Söylemezoğlu G. 2012. Using SCC8, SCF27 and VMC7f2 markers in grapevine breeding for seedlessness via marker assisted selection. Genetics and Molecular Research, 11(3), 2288-2294.

Akkurt M, Çakır A, Shidfar M, Mutaf F, Söylemezoğlu G. 2013. Using seedlessness-related molecular markers in grapevine breeding for seedlessness via marker-assisted selection (MAS) into Muscat of Hamburg × Sultani Progeny. Turk J Biol, 37, 101-105.

Alfrey P, 2019. The Very Fine Grapevine: The Essential Guide to Everything you Need to Know about Growing Grapes.

Amato A, Cardone MF, Ocarez N, Alagna F, Ruperti, B, Fattorini, C, Velasco R, Mejı´a N, Zenoni S, Bergamini C. 2022. VviAGL11 self-regulates and targets hormone-and secondary metabolism-related genes during seed development. Hortic Res, 9, uhac133.

Amca SD. 2011. Using DNA markers for pre-selection of seedlessness in grapes, MSc thesis, Akdeniz University, Institute of Science, Antalya, pp.67.

Bennici S, Di Guardo M, Distefano G, La Malfa S, Puglisi D, Arcidiacono F, Ferlito F, Deng Z, Gentile A, Nicolosi E. 2019. Influence of the genetic back ground on the performance of molecular markers linked to seedlessness in table grapes. Scientia Horticulturae, 252, 316-323.

Barbagallo MG, Crescimanno FG, De Michele A, Di Lorenzo R, Sottile I. 1988. Osservazioni sulla cleistogamia nella vite (Vitis vinifera L.). Vignevini, Bologna 15, 51-54 (Eng. abstr.).

Bergamini C, Cardone MF, Anaclerio A, Perniola R, Pichierri A, Genghi R, Alba V, Forleo LR, Caputo AR, Montemurro C, Blanco A, Antonacci D. 2013. Validation assay of p3_VvAGL11 marker in a wide range of genetic background for early selection of stenospermocarpy in Vitis vinifera L.. Mol Biotechnol, 54(3), 1021-1030.

Bolander JrFF. 2004. CHAPTER 13 - Hormonally Regulated Transcription Factors. Third Edition. Molecular Endocrinology, pp.387-44.

Bouquet A, Danglot Y. 1996. Inheritance of Seedlessness in Grapevine (Vitis vinifera L.). Vitis, (35), 35-42.

Bronner A, Wagner R. 1997. Pollen et floraison chez Vitis vinifera L. Techniques de controle ˆ du pouvoir germinatif du pollen (Eng. abstr.). Progr Agric Vitic, 114, 130-139.

Burger P, Goussard PG. 1996. In vitro culture of ovules and embryos from seedless grapes (Vitis vinifera L.). S Afr J Enol Vitic, 17, 31-37.

Cabezas JA, Cervera MT, Ruiz-Garcia L, Carreno J, Martinez-Zapater JM. 2006. A genetic analysis of seed and berry weight in grapevine. Genome, 49(12), 1572-1585.

Conner PJ, Gunawan G, Clark JR. 2018. Characterization of the p3-VvAGL11 Marker for Stenospermocarpic Seedlessness in Euvitis x Muscadinia Grape Hybrid Progenies. J. Amer Soc Hort Sci, 143(3), 167-172.

Correa J, Ravest G, Laborie D, Mamani M, Torres E, Muñoz C, Pinto M, Hinrichsen P. 2015. Quantitative trait loci for the response to gibberellic acid of berry size and seed mass in tablegrape (Vitis vinifera L.). Australian Journal of Grape and Wine Research, 21, 496-507.

Costantini L, Grando MS, Feingold S, Ulanovsky S, Mejía N, Hinrichsen P, Doligez A, This P, Cabezas JA, Martinez-Zapater JM. 2007. Generation of a common set of mapping markers to assist table grape breeding. Am J Enol Viticult, 58(1), 102-111.

Costantini L, Battilana J, Lamaj F, Fanizza G, Grando MS. 2008. Berry and phenology-related traits in grapevine (Vitis vinifera L.): From quantitative trait loci to underlying genes. BMC Plant Biol, 8:38.

Costenaro-da-Silva D, Passaia G, Henriques JAP, Margis R, Pasquali G, Revers LF. 2010. Identification and expression analysis of genes associated with the early berry development in the seedless grapevine (Vitis vinifera L.) cultivar Sultanine. Plant Science, 179, 510-519.

Dai ZW, Ollat N, Gomès E, Decroocq S, Tandonnet JP, Bordenave L, Pieri P, Hilbert G, Kappel C, Van Leeuwen C, Vivin P, Delrot S. 2011. Ecophysiological, genetic, and molecular causes of variation in grape berry weight and composition: A review. Am J Enol Viticult, 62(4), 413-425.

Dalbó MA, Ye, GN, Weeden NF, Steinkellner H, Sefc KM, Reisch BI. 2000. A gene controlling sex in grapevines placed on a molecular marker-based genetic map. Genome, 43(2), 333-340.

Değirmenci D, Marasalı KB. 2007. Üzümlerde çekirdeksizlik ve ıslah amaçlı kullanımı. Alatarım, 6(1), 10-17.

di Rienzo V, Imanifard Z, Mascio I, Gasser CS, Skinner DJ, Pierri CL, Marini M, Fanelli V, Sabetta W, Montemurro C, Bellin D. 2021. Functional conservation of the grapevine candidate gene INNER NO OUTER for ovule development and seed formation. Hortic Res, 8:29.

Ditta G, Pinyopich A, Robles P, Pelaz S, Yanofsky MF. 2004. The SEP4 gene of Arabidopsis thaliana functions in floral organ and meristem identity. Curr Biol, 14(21), 1935-1940.

Doligez A, Bouquet A, Danglot Y, Lahogue F, Riaz S, Meredith CP, Edwards KJ, This P. 2002. Genetic mapping of grapevine (Vitis vinifera L.) applied to the detection of QTLs for seedlessness and berry weight. Theor Appl Genet, 105, 780-795.

Ehlers K, Bhide AS, Tekleyohans DG, Wittkop B, Snowdon RJ, Becker A. 2016. The MADS box genes ABS, SHP1, and SHP2 are essential for the coordination of cell divisions in ovule and seed coat development and for endosperm formation in Arabidopsis thaliana. PLoS One, 11, e0165075.

Fanizza G, Lamaj F, Costantini L, Chaabane R, Grando MS. 2005. QTL analysis for fruit yield components in table grapes (Vitis vinifera). Theor Appl Genet, 111(4), 658-664.

FAOSTAT 2023. Crops and Livestock Products. Production Quantity: Grapes.

Grimplet J, Martínez-Zapater, JM, Carmona MJ. 2016. Structural and functional annotation of the MADS-box transcription factor family in grapevine. BMC Genomics, 17, 80.

Gramzow L, Theissen G. 2010. A hitchhiker's guide to the MADS world of plants. Genome Biology, 11, 214.

Gong P, Wei R, Li Y, Wang R, Tang Y, Wang L, Zhu H, Wang Y, Zhang C. 2019. Molecular cloning and functional characterization of a seed-specific VvbVPE gene promoter from Vitis vinifera. Planta, 250, 657-665.

Heazlewood JE, Wilson S. 2004. Anthesis, pollination and fruit set in Pinot Noir. Vitis, 43(2), 65-68.

Karaagac E, Vargas AM, De Andrés MT, Carreño I, Ibáñez J, Carreño J, Cabezas JA. 2012. Marker assisted selection for seedlessness in table grape breeding. Tree Genet and Geno, 8(5), 1003-1015.

Kimura, P.H., Okamoto, G. & Hirano, K. 1998. The mode of pollination and stigma receptivity in Vitis coignetiae Pulliat. Am J Enology Viticulture, 49, 1-5.

Korpás A, Baránek M, Pıdra M, Hradılík J. 2009. Behaviour of two SCAR markers for seedlessness within Central European varieties of grapevine. Vitis, 48(1), 33-42.

Kunter B, Sehit A. 2019. Çekirdekli Üzüm Çeşitlerinde Salkım Morfolojisini Etkileyen Tane Tutum Sorunları. Current Research and Assesments For Agricultural Sciences, (Editors: Birhan Kunter, Nurhan Keskin), ISBN:978-9940-540-95-1, p.9.

Lahogue F, This P, Bouquet A. 1998. Identification of a codominant scar marker linked to the seedlessness character in grapevine. Theor Appl Genet, 97(5), 950-959.

Ledbetter CA, Ramming DW. 1989. Seedlessness in grapes. Horticultural Reviews (Ed: Jules Janick), 11, 159-184.

Ledbetter CA, Burgos L. 1994. Inheritance of stenospermocarpic seedlessness in Vitis vinifera L. Journal of Heredity, 85(2), 157-160

Li Y, Zhu Y, Yao J, Zhang S, Wang L, Guo C, Van Nocker S, Wang X. 2017. Genome-wide identification and expression analyses of the homeobox transcr ption factor family during ovule development in seedless and seeded grapes. Sci Rep, 7, 12638.

Li ZT, Dhekney SA, Gray DJ. 2010. Molecular characterization of a SCAR marker purportedly linked to seedlessness in grapevine (Vitis). Mol Breeding, 25, 637-644.

Lora J, Hormaza JI, Herrero M, Gasser CS. 2011. Seedless fruits and the disruption of a conserved genetic pathway in angiosperm ovule development. PNAS, 108(13), 5461-5465.

Malabarba J, Buffon V, Mariath JEA, Gaeta ML, Dornelas MC, Margis- Pinheiro M, Pasquali, G, Revers LF. 2017. The MADS-box gene Agamous-like 11 is essential for seed morphogenesis in grapevine. J Exp Bot, 68(7), 1493-1506.

Mejía, N. & Hinrichsen, P. 2003. A new, highly assertive scar marker potentially useful to assist selection for seedlessness in table grape breeding. VIII International Conference on Grape Genetics and Breeding. Acta Horticulturae, 603.

Mejía N, Gebauer M, Munoz L, Hewstone N, Munoz C, Hinrichsen P. 2007. Identification of QTLs for seedlessness, berry size, and ripening date in a seedless x seedless table grape progeny. Am J Enol Vitic, 58(4), 499-507.

Mejía N, Soto B, Guerrero M, Casanueva X, Houel C, de los Ángeles Miccono M, Ramos R, Le Cunff L, Boursiquot JM, Hinrichsen P, Adam Blondon AF. 2011. Molecular, genetic and transcriptional evidence for a role of VvAGL11 in stenospermocarpic seedlessness in grapevine. BMC Plant Biology, 11(57), 1-19.

Moniruzzaman M, Darwish AG, Ismai A, El-kereamy A, Tsolova V, El-Sharkawy I. 2023. Seedlessness Trait and Genome Editing-A Review. Int. J. Mol. Sci, 24, 5660.

Oberle GD. 1938. A genetic study of variations in floral morphology and function in cultivated forms of Vitis. Bull NY St Agric Exp Stn, No:250, 63 pp. https://www.cabidigitallibrary.org/doi/full/10.5555/19391600862.

Olm H.P. 1943. Pollination of the Almeria Grape. Proc Amer Soc Hort Sci, 42, 401-406.

OIV 2023. Database: Grape production. International Organisation of Vine and Wine.

Owens CL. 2008. Grapes (Chapter 7) In: Hancock, J.F. (ed.), Temperate Fruit Crop Breeding, Germplasm to Genomics. pp.197-234. Springer, ISBN:978-1-4020-6906-2, eISBN:978-1-4020-6907-9.

Palumbo F, Vannozzi A, Magon G, Lucchin M, Barcaccia G. 2019. Genomics of Flower Identity in Grapevine (Vitis vinifera L.). Frontiers in Plant Science, 10, Article 3016.

Park SM, Hiramatsu M, Wakana A. 1999. Aneuploid plants derived from crosses with triploid grapes through immature seed culture and subsequent embryo culture. Plant Cell Tissue Organ Cult, 59, 125-133.

Park YS, Lee JC, Jeong HN, Um, NY, Heo JY. 2022. A red triploid seedless grape 'Red Dream'. Hortscience, 57, 741-742.

Pelaz S, Ditta GS, Baumann E, Wisman E, Yanofsky MF. 2000. B and C floral organidentity functions require SEPALLATAMADS-boxgenes. Nature, 405, 9-12.

Perl A, Sahar N, Spiegel-Roy P, Gavish S, Elyasi R, Orr E, Bazak H. 2000. Conventional And Biotechnological Approaches In Breeding Seedless Table Grapes. Acta Hortic, 528, 613-618.

Reynolds AG, Wardle DA, Zurowski C, Looney NE. 1992. Phenylureas CPPU and thidiazuron affect yield components, fruit composition, and storage potential of four seedless grape selections. J Am Soc Hortic Sci, 117, 85-89.

Roytchev V. 2007. Application of Cluster Analysis and Principal Component Analysis in the Development of Table Seeded and Seedless Vine Cultivars (Vitis vinifera L.). Bulgarian Journal of Agricultural Science, 13, 409-421.

Roychev V. 2011. Yield structure and variability of quantitative traits in a cross between a seeded and seedless vine cultivar (Vitis vinifera L.). Vitis, 50(1), 17-19.

Roychev V, Keranova N. 2023. Phenotypic proximity and remoteness of seedless vine varieties depending on their ampelographic characteristics. Horticultural Science, 50(1), 72-89.

Royo C, Rafael TP, Nuria M, Nieves D, Antonio CJ, C´ecile M, Thierry L, Javier IE, Manuel T, Juan CO. 2018. The major origin of seedless grapes is associated with a missense mutation in the MADS-box gene VviAGL11. Plant Physiol, 177(3), 1234-1253.

Snyder E. 1937. Grape Development And Improvement. US Dept Agr Yearbook, 1937, 631-655.

Staudt G. 1999. Opening of flowers and time of anthesis in grapevines, Vitis vinifera L.. Vitis, 38, 15-20.

Stout AP. 1937. Solitary cutaneous and subcutaneous leiomyoma. The American Journal of Cancer, 29(3), 435-469.

Striem MJ, Ben-Hayyim G, Spiegel-Roy P. 1994. Developing molecular markers for grape breeding, using polymerase chain reaction procedures. Vitis, 33, 53-54.

Striem MJ, Ben-Hayyim G, Spiegel-Roy P. 1996. Identifying molecular genetic markers associated with seedlessness in grape. Journal of the American Society for Horticultural Science, 121(5), 758-763.

Sun X, Zhang S, Li X, Zhang X, Wang X, Wang L, Li Z, Wang X. 2020. A MADS-box transcription factor from grapevine, VvMADS45, influences seed development. Plant Cell Tissue Organ Cult. PCTOC, 141, 105-118.

Tang Y, Wang R, Gong P, Li S, Wang Y, Zhang C. 2016. Gene cloning, expression and enzyme activity of Vitis vinifera vacuolar processing enzymes (VvVPEs). PLoS One, 11, e0160945.

Tang Y, Liu B, Li Y, Van Nocker S, Wang Y, Zhang C. 2020. Differential expression of the seed-specific gene ABCG20 between seedless and seeded grapes and its roles in tomato seed development. S Afr J Bot, 131, 428-436.

Tello J, Torres-P´erez R, Grimplet J, Carbonell-Bejerano P, Martínez-Zapater JM, Ib´a˜nez J. 2015. Polymorphisms and minihaplotypes in the VvNAC26 gene associate with berry size variation in grapevine. BMC Plant Biol, 15, 253.

TUIK 2023. Bitkisel Üretim İstatistikleri: Üzüm. Türkiye İstatistik Kurumu.

UPOV 2023. Grapevine (Vitis L.). International Union For The Protection of New Varieties of Plants.

Villanueva JM, Broadhvest J, Hauser BA, Meister RJ, Schneitz K, Gasser CS. 1999. INNER NO OUTER regulates abaxial- adaxial patterning in Arabidopsis ovules. Genes Dev, 13, 3160-3169.

Wang YQ, Li SX, Zhang XT, Wang YJ, Zhang CH. 2016. Isolation and analysis of differentially expressed genes during ovule abortion in the seedless grape. Scientia Horticult, 211, 376-383.

Wang L, Dai W, Shi Y, Wang Y, Zhang C. 2022a. Cloning and activity analysis of the highly expressed gene VviABCG20 promoter in seed and its activity is negatively regulated by the transcription factor VviDof14. Plant Sci, 315, 111152.

Wang L, Yan J, Zhang X, Qu Z, Yao W, Tang Y, Wang R, Van Nocker S, Wang Y, Li Y, Zhang C. 2022b. Genome-wide identification and comprehensive expression analysis of VviASN and VviGS gene families during seed development/abortion in grapevine. Sci Hortic, 292, 110625.

Wang Y, Li X, Wu Y, Cai Z, Li B, Xie Z. 2023a. Observation of Flowering Process of Grape (Vitis vinifera L.): Insight in to the Starting of Pollination of Flower Hiding in Calyptras (Cap). Phyton, International Journal of Experimental Botany, 92(6), 1859-1871.

Wang L, Yao W, Zhang X, Tang Y, Van Nocker S, Wang Y, Zhang C. 2023b. The putative ABCG transporter VviABCG20 from grapevine (Vitis vinifera) is strongly expressed in the seed coat of developing seeds and may participate in suberin biosynthesis. Physiol Mol Biol Plants, 29, 23-34.

Wang X, Liu Z, Zhang F, Xiao H, Cao S, Xue H, Liu W, Su Y, Liu Z, Zhong H, Zhang F, Ahmad B, Long Q, Zhang Y, Liu Y, Gan Y, Hou T, Jin Z, Wu X, Liu G, Wang Y, Peng Y, Zhou Y. 2024. Integrative genomics reveals the polygenic basis of seedlessness in grapevine. Current Biology, 34(16), 3763-3777 (In: In-ovulo embryo culture in seedless grapes (Vitis vinifera L.) Chapter, pp.249-254).

Weinberger JH, Harmon FN. 1964. Seedlessness in vinifera grapes. Proc Amer Soc Hort Sci, 85, 270-274.

Xi X, Gutierrez B, Zha Q, Yin X, Sun P, Jiang A. 2023. Optimization of In Vitro Embryo Rescue and Development of a Kompetitive Allele-Specific PCR (KASP) Marker Related to Stenospermocarpic Seedlessness in Grape (Vitis vinifera L.). Int J Mol Sci, 24:Article number 17350.

Yao J, Zhang S, Wu N, Li X, Ahmad B, Wu J, Guo R, Wang X. 2023. KNOX transcription factor VvHB63 affects grape seed development by interacting with protein VvHB06. Plant Science, 330, 111665.

Yao J, Dong Y, Morris BA. 2001. Parthenocarpic apple fruit production conferred by transposon insertion mutations in a MADS-box transcription factor. Proc Natl Acad Sci 98(3),1306-1311.

Zhang H, Fan X, Zhang Y, Jiang J, Liu C. 2017. Identification of favorable SNP alleles and candidate genes for seedlessness in Vitis vinifera L. using genome-wide association mapping. Euphtyica, 213(7), Article number 136.

Zhang S, Dong R, Wang Y, Li X, Ji M, Wang X. 2021. NAC domain gene VvNAC26 interacts with VvMADS9 and influences seed and fruit development. Plant Physiol Biochem, 164, 63-72.

Zhang S, Yao J, Wang L, Wu N, van Nocker S, Li Z, Gao M, Wang X. 2022. Role of grapevine SEPALLATA-related MADS-box gene VvMADS39 in flower and ovule development. Plant J, 111:1565-1579.

Zhang S, Wang L, Yao J, Wu N, Ahmad B, Nocker S, Wu J, Abudureheman R, Li Z, Wang X. 2023. Control of ovule development in Vitis vinifera by VvMADS28 and interacting genes. Hortic Res, 10(6):uhad070.

ORAL PRESENTATION

Effect Of tinkal added cement on neutron rays absorption capacity

Hayrettin Eroğlu*[1], İhsan İş[1], Mahmut Engin Kocadağistan[2], Ali Gürol[3]

*[1]Erzurum Technical University, Faculty of Engineering and Architecture, Department of Chemical Engineering
[2]Ataturk University, Faculty of Engineering, Department of Metallurgical and Materials Engineering
[3]Ataturk University, Faculty of Science, Department of Physics

*Corresponding author e-mail: hayrettin.eroglu@erzurum.edu.tr

Abstract

With the recent proliferation of nuclear technology, the importance of radiation protection has increased. For this purpose, experiments were conducted on samples obtained by mixing certain proportions of calcined and dewatered tincal ore obtained from the Balıkesir/Bigadiç region with cement to investigate the neutron absorption capacity of these mixtures. Neutron absorption experiments and XRD analyses were conducted under various parameters within the scope of the research. Evaluating the data from the samples, it was concluded that tincal has potential in nuclear safety, radiation protection, and building materials. It could contribute to economic sustainability and strategies for reducing external dependency by enabling the conversion of domestic mineral resources in the Bigadiç region, one of Türkiye's significant boron reserves, into value-added products. Furthermore, it is envisioned that radiation-attenuating composites developed with natural minerals could contribute to the dissemination of environmentally friendly material technologies aimed at minimizing toxic waste production.

Keywords: Cement, Tincal, Boron, Radiation, Neutron Absorption

1. INTRODUCTION

In daily life, we are constantly exposed to radiation due to both natural resources and technological advances. The construction materials chosen, especially in living spaces, are crucial for protection against this condition. The type, thickness, and density of the material are among the determining factors in radiation absorption (Yılmaz 2011).

Radiation can be defined as the process resulting from the energy dissipation of atoms and the transport of this energy through space via electromagnetic waves, or particles. This type of energy can occur in both particle and electromagnetic waves, and its spectrum spans a wide range, from long radio waves to cosmic rays. Initially used extensively in medical and industrial applications, radiation has now expanded its scope and is being utilized extensively in various environments and sectors (Sehhatigdiri 2014).

Just as no cell in nature is resistant to radiation, it's also difficult to claim that a place or region in nature is completely free of radiation. This is because everyone living on Earth is exposed to radiation as a part of life, from cosmic rays, from ground-based sources derived from radioactivity, and from artificial sources. While it varies from place to place, 78% of the total public dose comes from natural sources, 20.7% from medical exposure, and the remainder from occupational exposure and artificial sources (Berk, 2003).

Radiation protection has three fundamental elements: necessity, optimization, and personal dose limitations. The goal of radiation protection is to prevent deterministic effects by keeping doses below threshold values and to ensure that the probability of harmful effects remains at acceptable levels. Practically, important measures can be taken to protect against radiation. These are duration, distance, and shielding (Berk, 2003).

The dose of radiation received is inversely proportional to the square of the distance between the radiation source and the worker. Furthermore, the most important and effective way to prevent external radiation hazards is shielding. Shielding involves placing a barrier between the radiation source and the worker, absorbing all or a large portion of the radiation, thus reducing its intensity. This process utilizes the radiation attenuation properties of materials, thus extending the time spent working close to the source. Shielding can be of various shapes and thicknesses, depending on the type and energy of the radiation. α rays can be stopped by a sheet of paper or body skin, β rays by a 2.5 cm thick layer, and ϒ rays are only stopped by large amounts of lead or concrete (Berk, 2003).

To protect the outside world from the harmful effects of radiation, shielding is particularly crucial in units operating under radiation, and the radioactive area is surrounded by lead bricks or concrete. These shielding methods are both costly and cumbersome.

In recent years, a great deal of research has been conducted in the field of building materials, particularly cement-based materials. Nanostructured materials, with their diverse properties such as self-cleaning, dirt-repellent, flame-retardant, sound-insulating, and light-control films, offer a different perspective on conventional building materials (Parhizgar and Ghasemi, 2009).

Concrete, used as a building material, is a multicomponent material obtained by mixing cement, water, sand, and various mineral additives such as silica fume, fly ash, and blast furnace slag in specific proportions. Cement is one of the highest-cost components in concrete production, and Portland cement is widely preferred. Today, mineral additives are often included in concrete mixtures, and these additives are used to improve the performance of concrete in both its fresh and hardened states (Yılmaz 2011).

Boron is not found free in nature. It is generally found in crystalline or amorphous compounds. Boron is present in the Earth's crust at an average level of 10 ppm in environments such as soil, rocks, and water. Natural boron exists as a mixture of two stable isotopes, with mass numbers of 10 (19.8%) and 11 (80.2%), respectively. Boron occurs in varying proportions in the structure of more than 150 minerals in nature, generally as boron oxide (B_2O_3). Economically important boron minerals occur as hydrate compounds with elements such as calcium, sodium, and magnesium and are classified according to these elements. Among the primary boron minerals with industrial value are tincal, colemanite, ulexite, probertite, boracite, pandemite, szaybelite, hydroboracite, and kernite. After mining, these minerals are generally washed and ground to make them suitable for use (TMMOB Chamber of Metallurgical Engineers 2003).

Tincal, also known as borax, a boron mineral, appears colorless and transparent in its pure form. However, in areas where it is layered with clay and in fine-grained form, it can turn pale pink, yellowish-orange, and gray under the influence of external substances (Dırak 2011). A review of scientific literature suggests that boron oxide may have radiation shielding properties. Studies have shown that:

Experiments were conducted on concrete samples containing boron oxide, colemanite, and boron, and the radiation shielding capacity of the concrete's chemical components was analyzed. The study demonstrated that boron-added heavyweight concretes offered advantages not only in terms of effective shielding performance but also in terms of cost (Henrie 1962a).

In a study conducted by Sychev, the shielding performance of concrete samples prepared using hematite minerals against neutrons emitted from a beryllium source was investigated. In this context, evaluations were made considering five different neutron energy levels ranging from 170 MeV to 660 MeV (Sychev 1967).

In their study, Erdoğan et al. (2000) produced different types of cement by adding ground boron minerals to cement and examined their physical and mechanical properties. They also evaluated the shielding capacity of boron minerals against neutron rays in concrete using theoretical approaches. Based on their findings, they concluded that boron mineral addition positively affected shielding performance (Erdoğan et al. 2000).

Erdoğmuş and colleagues (2011) investigated the effects of adding different mixtures of colemanite concentrator waste and Karabük slag to Portland cement on the mechanical properties of the cement. Additionally, the effect of adding different ratios of Na_2CO_3 to Portland cement on the mechanical properties of the cement was investigated. The colemanite concentrator waste, slag, gypsum, and clinker used in the experiments were chemically analyzed using XRF. The mechanical properties examined in the study included compressive strength, setting time, volumetric expansion, and normal consistency water. The findings were compared with Turkish Standards (TS), and the research concluded that colemanite concentrator waste and Karabük slag can be utilized appropriately in cement production (Erdoğmuş et al. 2011).

Uğurlu and colleagues (2004) investigated the usability of solid waste, called "clay paste," generated during the concentration of borax mineral during tincal production, in cement. For the cement study, ground clay paste waste was added to Portland cement mortar at different ratios, and fresh and hardened concrete tests were conducted on the resulting mortar samples. These tests investigated the behavior of clay paste in cement and its effect on cement mortar samples. The results were compared with reference samples and Turkish Standards (TS). The results

indicate that borax-containing clay paste waste can be used as a retarder in mortar or concrete, and that low percentages of clay paste waste can increase the impermeability of concrete (Uğurlu et al. 2004).

In 2010, Akkurt and his colleagues conducted a study using heavy concretes produced using barite and lead. They measured linear absorption coefficients using radioactive sources with energies of 0.662 MeV, 1.173 MeV, and 1.332 MeV using a NaI(Tl) detector. The results were compared with XCOM data. The results revealed that barite and barite-added heavy concretes are good gamma-ray absorbers, but their shielding properties are lower than those of lead (Akkurt et al. 2010).

In another study conducted by Korkut and colleagues in 2011, the shielding properties of amethyst ore were investigated using the FLUKA Monte Carlo code and linear attenuation coefficients were calculated. These calculations concluded that amethyst ore has potential as a material for shielding against radiation (Korkut et al. 2011).

2. MATERIALS and METHODS

2.1. Materials

2.1.1. Materials used in experiments

In this study, tincal, a primary boron mineral, was used to investigate its neutron beam absorption properties. The cement used in the experiments was Portland cement (CEM I 42.5 R) supplied by the Aşkale Cement Factory.

Tincal, a natural borate mineral with a high boron content, was obtained from the Balıkesir-Bigadiç/Türkiye region. Before being used in experimental studies, it underwent preliminary preparation processes such as grinding, drying, and sieve analysis. Following these processes, the samples were reduced to micron size and finally heat-treated at 650°C to remove the crystal water, resulting in anhydrous boron.

2.2. Method

2.2.1. Production of Concrete

The concretes examined in this study were produced at the Civil Engineering Department Laboratory of Erzurum Technical University. Three types of concrete were produced in this study: standard concrete and tincal-added concrete. First, cement-only samples were prepared for comparison. Then, 1%, 5%, and 10% tincal were added to each cement sample, sequentially and separately. The water/binder ratio was set at 0.20 in the experiments. The temperature of the sample was measured with a digital thermometer, and the mixing water temperature was determined to be between 25-30°C. The prepared samples were placed in 5x5x5cm cube sample molds. The samples were kept in their molds for 24 hours and then removed from the molds. During the curing process, the samples were maintained in a constant temperature environment (24°C), and the ambient temperature and relative humidity were regularly monitored with a digital thermometer.

2.2.2. Neutron Absorption

The experimental measurements undertaken in relation to the attenuation coefficient of the concrete produced as part of the study were conducted at the High Energy Spectroscopy Laboratory, which is housed within the Department of Atomic and Molecular Physics at Atatürk University's Faculty of Science.

The measurement of the neutron absorbed dose rate was conducted using a ^{241}Am/Be fast neutron source, which emits 2–11 MeV neutron particles. The Canberra NP100B-BF_3 gaseous neutron detector and the Canberra ADM606 series of digital rate meters were utilized in this process. The experimental neutron dose rate measurement system is illustrated in Figure 1.

The intensity of a photon flux with intensity I_0 decreases when it passes through an absorbing material of thickness t. If the transmitted intensity is I, this decrease in intensity is described by the Lambert-Beer law (Yılmaz 2011) as the linear attenuation coefficient (MM),

$$\mu = -\frac{1}{t}\, ln\, ln\left(\frac{I}{I_0}\right) \text{ (cm}^{-1}\text{)}$$

However, the mass attenuation coefficient (μ/ρ), defined as the ratio of the linear attenuation coefficient (μ) to the sample density (ρ) and does not change depending on the phase of the material, is more commonly used.

The values in the Table 1. were calculated using the equation below.

$$\frac{\mu}{\rho} = -\frac{1}{\rho t} ln \ln\left(\frac{I}{I_0}\right)$$

where ρt is called the mass thickness. The unit of the mass attenuation coefficients is cm^2/g.

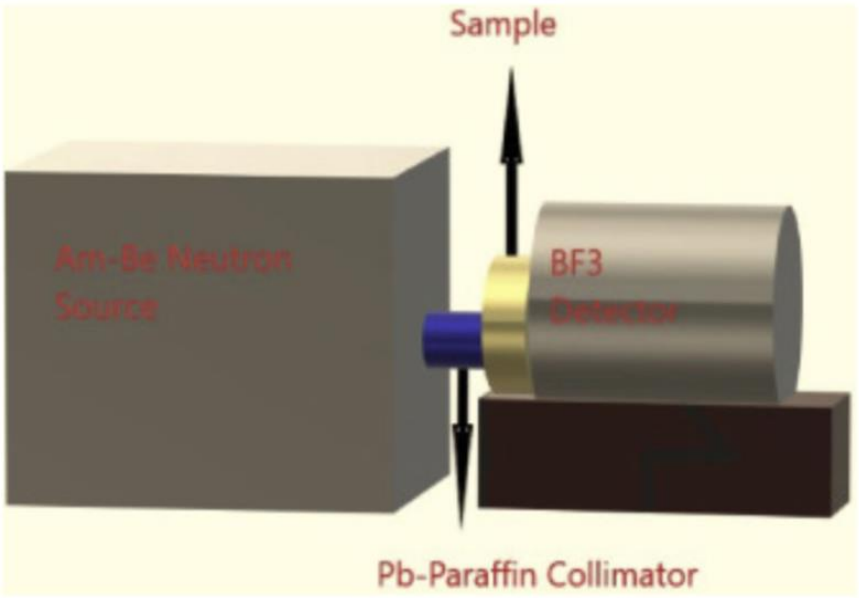


Figure 1. Experimental setup for neutron absorption experiments.

2.2.3. X-ray diffraction (XRD)

XRD analysis of the concretes produced within the scope of this study was measured at Erzurum Technical University's High Technology Application and Research Center (YUTAM).

Calculating compound or phase compositions from oxide components can be accomplished using both theoretical and experimental methods. X-ray diffraction (XRD) has been successfully used for many years to determine mineral concentrations. Since 1958, various studies have been conducted on the use of XRD analysis in determining cement compositions (Winter 2012).

Concrete, a composite material, exhibits complex behavior due to its high cement content. Microstructural differences from the cement paste have been observed, particularly at the cement-aggregate interface. The formation of new compounds as a result of exposure to various aggressive environmental conditions and the formation of characteristic structures during the natural deterioration processes of concrete have made X-ray diffraction (XRD) analysis an important and essential method for investigating service life, durability, and related product performance (Ramachandran et al. 2000).

2.2.4. Heat treatment

The use of boron in the cement sector has become widespread, but boron ores are suitable for use up to a maximum water content of 2% (Kocadağistan and Arslan, 2024). Tincal was dewatered in a muffle furnace at 650°C for 6 hours. Following the heat treatment, the chemically bound water removal rate was calculated by taking the weight differences of tincal and ulexite ores. According to the calculations, 98% water removal was achieved in the ore (Ataç 2024).

According to XPS and chemical analysis results, tincal was determined to contain 47.2% H_2O. Based on the weight difference calculations, the H_2O content was reduced to 1% after heat treatment and used in the experiments.

3. RESEARCH FINDINGS AND DISCUSSION

Cement, mixtures of cement and dewatered tincal at 1%, 5%, and 10% were examined, and their neutron absorption values are given below. These values revealed that 5% tincal was the best. XRD analyses were conducted based on these values. Furthermore, the samples with the best absorption values were subjected to unconfined compression tests, and their suitability as a building material was evaluated.

3.1. XRD Analysis Evaluation (5% Tincal Added Sample)

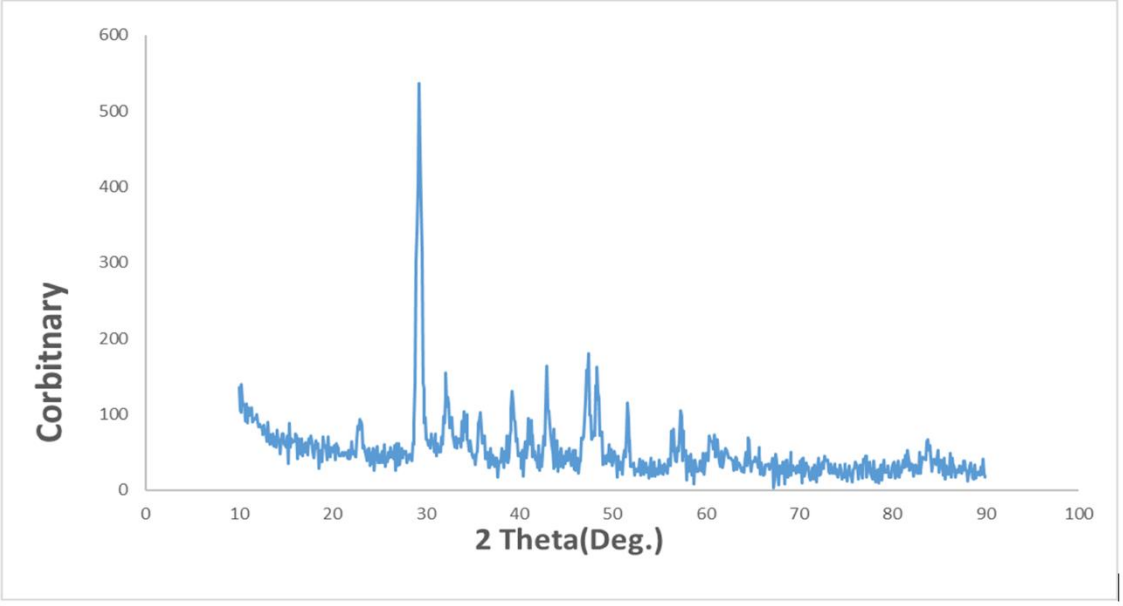


Figure 2. XRD analysis of the 5% Tincal added sample (Tincal:)) %5

The X-ray diffraction (XRD) pattern of a tincal-added cement sample allows the determination of its crystal structure and mineralogical composition. The graph presents intensity values corresponding to the 2θ angle, and these data are used to identify the crystalline phases within the sample.

Tincal, dolomite, smectite, and calcite are observed in the planes corresponding to the prominent peaks in the XRD spectrum of tincal ore. The high-intensity peak observed at approximately 29° 2θ in the obtained diffractogram reveals the dominant presence of tincal ($Na_2B_4O_7.10H_2O$) and calcite ($CaCO_3$) phases in the sample. Calcite is a common component in the cement matrix, and its presence may be due to either the clinker structure or the carbonation process of the cement matrix. In addition, other intense pixels observed in the 32–34° 2θ range indicate the presence of calcium silicate hydrate (C-S-H) and ettringite phases, which are cement hydration products.

Some pixels detected in the graph with low intensity but distinct levels can be associated with X-ray reflections of the crystal structure of the mineral tincal ($Na_2B_4O_7 \cdot 10H_2O$), which is used as an additive. This suggests that the additive is preserved in physical or chemical form within the cement matrix and integrated into the structure. However, diffraction pixels appearing between 40° and 50° 2θ suggest that tincal may have interacted with cement hydration products, triggering the formation of new mineral phases.

These data indicate that a 5% tincal addition can lead to the formation of specific crystalline phases in the cement matrix, thereby inducing structural changes in the cement microstructure. Such structural changes have the potential to directly affect the mechanical and physical properties (e.g., compressive strength, durability, and impermeability) of cement-based composites.

3.2. Neutron Absorption Experiments of Tincal Added Cement

The values of the Neutron absorption test results of the samples of the mixtures are given in Table 1. and Figure 3.

Table 1. Tincal neutron absorption experiment values

Sample	Transmitted Ray Intensity (I)	Relative Beam Intensity (I/I₀)	Thickness (t, cm)	Mass (M, g)	Intensity (ρ, g/cm³)	Linear Attenuation Coefficient Sigma (cm⁻¹)	Mass Attenuation Coefficient (Sigma/Rho) cm²/g
Control	0,886	0,875	0,540	9,9676	1,8245	0,248	0,136
Control + Tincal 1%	0,856	0,845	0,540	9,8815	1,8087	0,313	0,173
Control + Tincal 5%	0,846	0,839	0,540	9,9705	2,1424	0,381	0,178
Control + Tincal %10	0,839	0,830	0,540	9,3464	1,8476	0,373	0,202

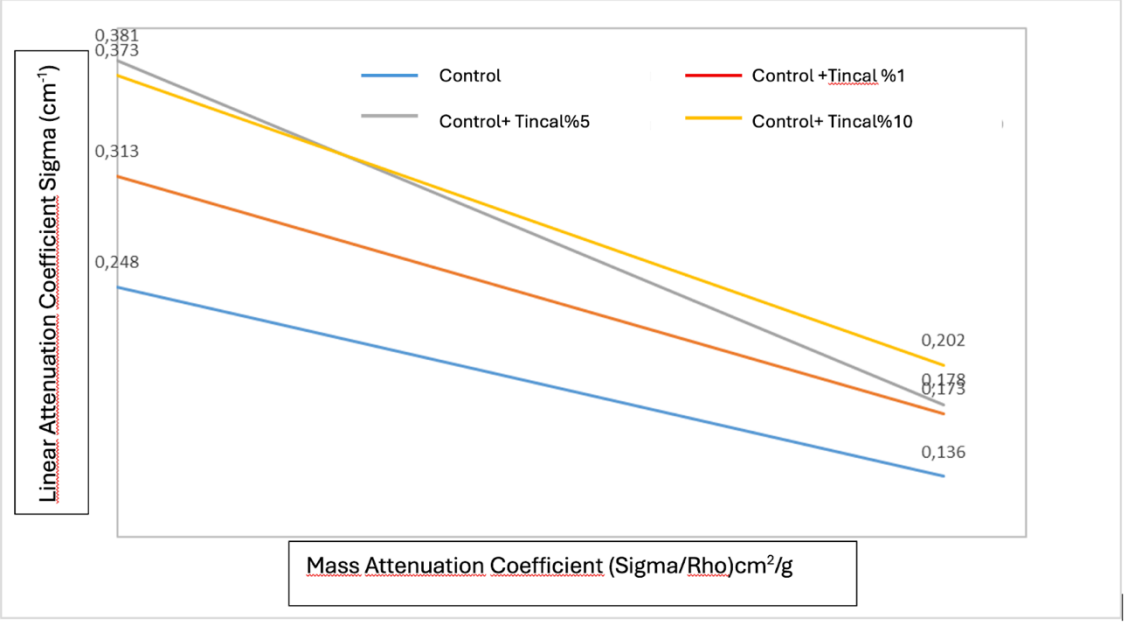


Figure 3. Tincal neutron absorption experiment values

The data in Table 1. demonstrate the effects of tincal addition on the neutron attenuation behavior of cement-based samples. As tincal addition increases, a decrease in transmitted light intensity is observed, indicating that the material becomes more effective attenuator against neutrons. Particularly with 5% and 10% tincal additions, the relative radiation intensity reaches lower values, and the linear attenuation coefficient increases significantly. This indicates that neutron interactions within the material increase, increasing the attenuation capacity. The change in density values fluctuates depending on the doping ratio, with the highest density value recorded at 5% tincal. This increase may contribute to attenuation performance in terms of neutron scattering and absorption. The increase in the mass attenuation coefficient also supports this finding. Consequently, tincal addition has the potential to improve the attenuation performance of cement-based composites against neutron radiation.

4. CONCLUSION AND RECOMMENDATIONS

In this study, various experimental methods were applied to tincal ores obtained from the Balıkesir-Bigadiç region to investigate their neutron absorption capacity. These experimental studies included neutron absorption experiments under various parameters, and X-ray diffraction (XRD) analyses. Following these analyses, the neutron absorption properties of tincal ores were evaluated in detail, and the findings are presented below.

The neutron absorption capacities of composite samples formed by adding tincal ore at different rates were experimentally investigated. It was observed that as the tincal addition rate increased, the transmitted radiation intensity decreased, while at the same time, the attenuation properties became more effective against neutrons. Particularly at 5% and 10% tincal additions, the relative radiation intensity reached lower values, and the linear attenuation coefficient increased significantly. This indicated that the interactions between neutrons within the material increased, increasing the attenuation capacity. Consequently, tincal addition has the potential to improve the attenuation performance of cement-based composites against neutron radiation.

Demonstrating the attenuation performance of tincal ore against neutron radiation with varying amounts of additives suggests that these natural minerals can be considered alternative shielding materials in radiation protection applications. This finding contributes to the development of environmentally friendly solutions that can reduce reliance on toxic and environmentally hazardous materials, particularly lead.

The utilization of tincal ore from the Bigadiç region, one of Turkey's significant boron reserves, allows for the transformation of domestic mineral resources into value-added products. This supports both economic sustainability and offers a strategic contribution to reducing external dependency.

The attenuation coefficients obtained over a wide energy range constitute a valuable database that can be used in the design and development of next-generation radiation shielding materials. These data serve as a reference for the scientific literature, providing the basis for further research.

Slimming composites developed using natural minerals minimize toxic waste production, contributing to the dissemination of environmentally friendly material technologies. In this respect, the study can be considered within the scope of sustainable engineering practices.

REFERENCES

Akkurt, I. Akyildirim, H., Mavi, B., Kilincarslan, S., Basyigit, C., 2010d. Radiation shielding of concrete containing zeolite. Radiation Measurements, 45, 827– 830.

Ataç,E.2024.Isıtma Hızının Tinkal Cevherinin Bozunma Sıcaklığına Etkisi ve Kalsinayonu, Yüksek Lisans Tezi, Atatürk Üniversitesi Fen Bilimleri Enstitüsü, Metalurji ve Malzeme Bilimi Mühendisliği Anabilim Dalı,92,Erzurum

Berk, F., 2002. Tek kullanımlık tıbbi malzemelerin gama radyasyonu ile sterilizasyonu ve diğer yöntemlerle karşılaştırılması. Hacettepe Üniversitesi Sağlık Bilimleri Enstitüsü, yüksek lisans tezi.

Dırak, S., 2011,Eti Maden Müdürlüğü Kırka Bor İşletmesi Bor Endüstri Atıklarında Eser Elementlerin Tayini ve Lityumun Kazanılması, Kütahya: Dumlupınar Üniversitesi Fen Bilimleri Enstitüsü, 83 s.

Erdoğan, Y., Zeybek, M. S. ve Demirbaş, A. (2000). Cement mixes containing colemanite from concentrator wastes. Cement and Concrete Research, 28, 605-609

Erdoğmuş, E., Erdoğan, Y., Gencel, O., Targan, S. ve Avcıata, U. (2011). Influence of colemanite admixture on Portland cement durability. Advances in Cement Research, 24, 155-164.

Henrie, J.O., 1962a. Concrete for radiation shielding. Concrete For Radiation Shielding. (American Concrete Institute, 2nd Ed., s., 31-40, American Concrete Institute, U.S.A.).

Kocadağistan, M.E., Arslan, H. (2024). Advantageous approach for boron ores used in cement production: optimization of dehydration. Challenge Journal of Concrete Research Letters 15 (1)(2024) 7–19.

Korkut, T., Korkut, H., Karabulut, A. and Budak, G. (2011), A New Radiation Shielding Material: Amethyst ore. Annals of Nuclear Energy, 38: 56-59.BERK

Parhizgar and Gasemi. (2009), İran inşaat araştırma merkezi, Tahran.

Ramachandran, V.S.,Beaudoin, J. J., 1999. Handbook of Analytical Techniques in Concrete Scienceand Technology. Noyes Publications / William Andrew Publishing, 964 s, New York.

Sehhatigdiri,A.2014.Farklı Killerin Radyoaktif Maddelere Karşı Zırhlama Özelliklerinin Deneysel Olarak Araştırılması.Yüksek Lisans Tezi,Atatürk Üniversitesi Fen Bilimleri Enstitüsü, İnşaat Mühendisliği Anabilim Dalı, 53 ,Erzurum

Sychev, B.S., Mal'kov, V.V., Komochkov, M.M., Zaitsev, L.I., 1967. Penetration of heavy concrete shields by high-energy neutrons. Journal Of Nuclear Energy, 21(3), 315-317.

TMMOB Metalurji Mühendisleri Odası, 2003, Bor Raporu, Ankara.

Uğurlu, A., Özdemir, M., Topçu, İ., 2004. Bor İçeren Kil Atıkların Çimento İçerisinde Değerlendirilmesi Evaluation of Boron Containing Clay Wastes in Cement. 2.Uluslararası Bor Sempozyumu, 23-25 Eylül, Eskişehir, Türkiye, 405-411.

Winter, N.B., 2012. Scanning Electron Microscopy of Cementand Concrete. WHD Microanalysis Consultants Ltd, 192 p, United Kingdom.

Yılmaz, E. 2011.Bazı İnşaat Malzemelerinde Gama Işını Soğurma Katsayısı Ve Nötron Soğurma Katsayısı Tesir Kesitinin Belirlenmesi. Yüksek Lisans Tezi, Rize Üniversitesi, Fen Bilimleri Enstitüsü, Fizik Anabilim Dalı, 81,Rize

ORAL PRESENTATION

Beyin hasarı ve kuersetin: Deneysel bulgular ve klinik potansiyel

Mücahit Börekçi[1*] (*ORCID: https://orcid.org/0009-0008-1134-8922*),
Ali Şenol[2] (*ORCID: https://orcid.org/0000-0003-4080-7776)*

[*1]Kırıkkale Üniversitesi, Sağlık Bilimleri Enstitüsü, Veterinerlik Biyokimyası AD, Kırıkkale, Türkiye
[2]Kırıkkale Üniversitesi, Veteriner Fakültesi, Biyokimya AD, Kırıkkale, Türkiye

*Sorumlu yazar e-mail: mchtbrkci@gmail.com

Özet

Beyin hasarı; travmatik beyin hasarı, iskemi-reperfizyon, intrakraniyal hemoraji veya nörotoksik maddelere bağlı olarak ortaya çıkar ve yüksek morbidite ile mortaliteye sahiptir. Bu süreçte oksidatif stres, inflamasyon, mitokondriyal disfonksiyon ve apoptoz gibi karmaşık biyokimyasal ve moleküler mekanizmalar etkin rol oynar. Kuersetin, doğal bir flavonoid olup güçlü antioksidan, antiinflamatuar, antiapoptotik ve mitokondri stabilizan özelliklere sahiptir. Deneysel modellerde kuersetin; oksidatif stres göstergelerini azaltma, inflamatuar sitokinleri düşürme, kan-beyin bariyerini koruma, mitokondriyal fonksiyonu iyileştirme ve nöronal apoptozu sınırlama gibi çok yönlü nöroprotektif etki gösterdiği ifade edilmiştir. Ancak kuersetinin zayıf suda çözünürlüğü ve düşük biyoyararlanımı, klinik uygulamadaki potansiyelini sınırlamaktadır. Bu derleme mevcut deneysel kanıtları ve geleceğe dönük araştırma ihtiyaçlarına dikkat çekerek kuersetinin beyin hasarındaki rolünü ele almaktadır.

Anahtar Kelimeler: kuersetin, antioksidan ajan, beyin hasarı, nöroinflamasyon

Quercetin and brain ınjury: Experimental findings and clinical potential

Abstract

Brain injury may result from traumatic brain injury, ischemia–reperfusion, intracranial hemorrhage, or exposure to neurotoxic agents, and is associated with high morbidity and mortality. In this process, complex biochemical and molecular mechanisms including oxidative stress, inflammation, mitochondrial dysfunction, and apoptosis play critical roles. Quercetin, a natural flavonoid, possesses potent antioxidant, anti-inflammatory, anti-apoptotic, and mitochondrial-stabilizing properties. Experimental models have demonstrated that quercetin exerts multifaceted neuroprotective effects by reducing oxidative stress markers, suppressing inflammatory cytokines, preserving the blood–brain barrier, improving mitochondrial function, and limiting neuronal apoptosis. However, the poor water solubility and low bioavailability of quercetin restrict its potential clinical application. This review addresses the role of quercetin in brain injury by highlighting current experimental evidence and future research needs.

Keywords: quercetin, antioxidant agent, brain injury, neuroinflammation

GİRİŞ

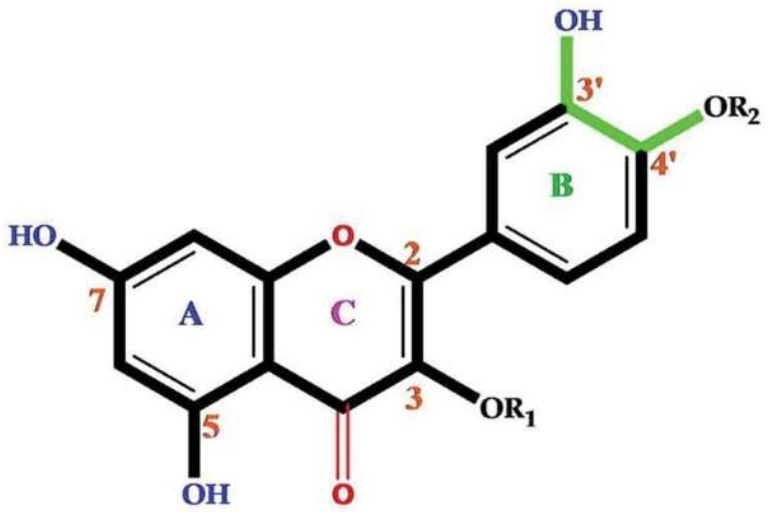
Beyin hasarı, hem insanlarda hem de hayvan modellerinde önemli mortalite ve morbidite nedenlerinden biri olmakla birlikte travma kökenli ya da sekonder kaynaklı olarak ortaya çıkabilmektedir. Travmatik beyin hasarı, serebral iskemi-reperfüzyon, intrakraniyal hemoraji veya toksik etkenlere bağlı nöronal yıkım, kompleks biyokimyasal ve moleküler mekanizmaların etkileşimiyle gelişir (Yan ve ark., 2024). Sekonder beyin hasarı, oksidatif stres, inflamasyon ve apoptoz gibi moleküler olaylar aracılığıyla nöronal dejenerasyonu derinleştirir (Aronowski ve Zhao, 2011; Shao ve ark., 2022). Bu süreçte reaktif oksijen türleri (ROS) ve proinflamatuar sitokinlerin artışı, lipid peroksidasyonu ve mitokondriyal disfonksiyon ile birleşerek beyin dokusunun yapısal ve fonksiyonel bütünlüğünü bozar. Bu nedenle, sekonder hasarı hedefleyen terapötik ajanlar, hem nöronal korunma hem de klinik iyileşme açısından kritik öneme sahiptir (Davis ve Vemuganti, 2022).

Beyin hastalıklarında oksidatif stres, nöronal ölümle sonuçlanan tanımlanmış patolojik mekanizmaların birçoğunda rol oynar. Reaktif oksijen ve azot türlerinin (ROS ve NOS) aşırı üretimi, nörodejeneratif hastalıkların başlangıcında, devamında ve ilerlemesinde kritik olarak kabul edilmiştir (Uttara ve ark., 2009; Gandhi ve Abramov, 2012; Dajas ve ark., 2015). Ortaya çıkan oksidatif hasarın önlenebilmesi adına birçok çalışmada çeşitli antioksidan ajanlardan yararlanılmıştır. Önemli flavonoid türevlerinden biri olan kuersetin'de bunlardan biridir.

Kuersetin (3,3′,4′,5,7-pentahidroksiflavon), ilk olarak meşe ağacından izole edilen bitkisel kökenli güçlü bir antioksidan olarak dikkat çekmektedir. Soğan, elma, üzüm, karadut, yaban mersini, kırmızı kiraz ve yeşil çay gibi birçok gıdada doğal olarak bulunur (Rasouli ve ark., 2017). Kuersetin, insanlar için önemli bir diyet besin maddesi, antioksidan ve potansiyel terapötik ajan olmakla birlikte (Lawson, 2023) metabolik ve inflamatuvar bozuklukların tedavisi için en yaygın kullanılan biyoflavonoidlerden biridir (Anand ve ark., 2016). Fizyopatolojik süreçlerde gösterdiği antioksidan etki, kuersetinin en önemli özelliğidir. Kuersetinin, vücuttaki bir antioksidan olan glutatyon seviyesini artırarak oksidatif stresin neden olduğu birçok hastalığı ve vücuttaki proinflamatuvar maddelerin salınmasını önlemek/tedavi etmek için önemli bir terapötik ajan olduğu (Imran ve ark., 2022), oksidatif stres ile ilişkili hücre hasarı durumlarında koruyucu etkisinin olabileceği düşünülmektedir (Becerra-Torres ve ark., 2009; Özçiflikçi, 2023). Bu bilgiler ışığında çalışmanın yapılmasındaki temel amaç; çeşitli biyoaktif özellikleri ile öne çıkan kuersetin kullanımına ve beyin hasarına karşı olası protektif etkilerine dikkat çekmektir.

KUERSETİN

Kuersetin, sarımsı kristal yapıda bulunan ve yüksek erime noktasına sahip (316.5 °C) hidrofobik bir bileşikdir (Lawson, 2023). Uluslararası Saf ve Uygulamalı Kimya Birliği (IUPAC) terminolojisinde 3, 3', 4', 5, 7 pentahidroksiflvanon olarak tanımlanan bu molekülün kimyasal formülü C15H10O7'dir (Li ve ark., 2016; Nguyen ve Bhattacharya, 2022). Kuersetin, diğer flavonoidlerle kıyasla en az lipofilik olan flavonoiddir (Lawson, 2023). Kuersetinin biyolojik aktivitesi, içerisinde yer alan aktif fenolik hidroksil gruplarına ve çift bağlara atfedilmektedir (Wang G ve ark., 2022). Bu yapısal özellikler, kuersetine antioksidan, antiinflamatuvar, antimikrobiyal, antiviral, antikanser, antiobezite kardiyovasküler ve nöroproteksiyon gibi birçok farmakolojik etkiler kazandırmaktadır (Nguyen ve Bhattacharya, 2022). Kuersetin'in kimyasal yapısı Şekil 1'de, içerisinde yoğun olarak bulunan gıdalar ise Şekil 2'de verilmiştir.



Şekil 1. Kuersetin kimyasal yapısı (Rasouli ve ark., 2017).



Şekil 2. Kuersetin içeren besin kaynakları (Rasouli ve ark., 2017).

Diyetle alınan kuersetin hızlı bir metabolik dönüşüme uğrar ve gastrointestinal sistemin farklı bölgelerinde değişen oranlarda emilir: midede %24–53, ince bağırsakta %5–10 ve kolonda %90–95 (Li ve ark., 2016; Deepika ve Maurya, 2022). Duodenumda emilen kuersetin glikozitleri, daha sonra ince bağırsakta ve karaciğerde enzimler aracılığı ile metillenerek metabolitlere ayrılmaya başlar (Li ve ark., 2016). Özellikle karaciğerde oluşturulan kuersetin metabolitleri emilir, daha sonra sistemik dolaşıma katılır, dokulara dağılır, dönüştürülür veya atılır. Kuersetin, lipofilik olması nedeniyle plazma zarından kolayca geçer (Deepika ve Maurya, 2022) ve plazmada albümine güçlü bir şekilde bağlanır. Kuersetinin eliminasyonu, yağlı beslenme sonrası gecikmesiyle beraber eliminasyon yarı ömrü yaklaşık olarak 25 saattir (Lakhanpal, 2007).

Kuersetin, serbest radikallerle reaksiyona girerek hidrojen atomu bağışlayabilme ve ROS'u söndürebilme kapasitesi nedeniyle güçlü bir antioksidan olarak tanımlanır (Deepika ve Maurya, 2022). Aktif oksijen radikallerinin parçalanması; hidrojen atomu nakli (HAT), basit elektron nakli ve ardından proton aktarımı (SET-PT), proton kaybıyla sıralı elektron aktarımı (SPLET) ve geçiş metallerinin şelasyonu (TMC) mekanizmaları ile sağlanabilir (Michala ve Pritsa, 2022). Ayrıca kuersetinin metal iyonlarına bağlanmada etkin bir iyonofor olduğu da vurgulanmaktadır (Imran ve ark., 2022). Bunun yanında, glutatyon (GSH) düzeylerini artırarak endojen antioksidan kapasitenin güçlenmesine katkı sağlar (Imran ve ark., 2022). Kuersetin, hücresel düzeyde oksidatif hasarı azaltma, inflamatuar sinyal yollarını baskılama, mitokondri fonksiyonlarını koruma ve apoptozu önleme gibi çok yönlü etkiler gösterir. Bu nedenle kuersetin, beyin hasarının biyokimyasal ve moleküler sonuçlarını hafifletmede potansiyel bir nöroprotektif ajan olarak değerlendirilmektedir.

Literatürde, kuersetinin AMPK aktivasyonunu uyararak hücresel enerji metabolizmasını iyileştirdiği, oksidatif stresi azalttığı ve proinflamatuvar sitokin üretimini baskıladığı gösterilmiştir. Bu etkiler hem antiinflamatuvar hem de nöroprotektif özelliklerinin temel mekanizmalarından biri olarak değerlendirilmektedir. Deneysel çalışmalarda kuersetin; orta serebral arter oklüzyonu ve travmatik beyin hasarı modellerinde davranışsal ve biyokimyasal parametrelerde belirgin iyileşmeler sağlamıştır. Bu modellerde SOD, CAT ve GSH gibi antioksidan enzim aktivitelerinin artması; MDA düzeylerinin azalması ve nörolojik skorların iyileşmesi, kuersetinin çok yönlü koruyucu etkilerini açıkça ortaya koymakta ve desteklemektedir (Li ve ark., 2021). Kuersetinin nöroprotektif etkilerinin önemli bir boyutu, kan–beyin bariyeri (KBB) bütünlüğü üzerindeki koruyucu rolüdür. Beyin hasarı sonrası KBB'nin yapısal bütünlüğünün bozulması periferal inflamatuvar hücrelerin beyin dokusuna geçişini

kolaylaştırarak ödem ve ikincil hasara yol açar. Kuersetin, bariyer bütünlüğünün korunmasına katkı sağlayarak inflamasyonun ve doku yıkımının ilerlemesini sınırlayabilmektedir (Dong ve ark., 2014; Chiang ve ark., 2023).

Moleküler düzeyde ise kuersetinin Nrf2'nin nükleusa translokasyonunu artırdığı, NF-κB'nin fosforilasyonunu engellediği ve bu sayede oksidatif stres–inflamasyon eksenindeki etkileşimi dengelediği bildirilmektedir. Mitokondriyal membran potansiyelinin korunması ve ATP düzeylerinin artışı da kuersetinin enerji metabolizması üzerindeki olumlu etkilerini desteklemektedir (Li X ve ark., 2016). Sonuç olarak, kuersetinin AMPK aktivasyonu, oksidatif stres modülasyonu, inflamasyonun baskılanması ve KBB bütünlüğünün korunması gibi çok yönlü mekanizmalar aracılığıyla nöroprotektif potansiyel taşıdığı açıkça ortaya konulmaktadır. Bununla birlikte, kuersetinin optimal doz aralığı, uygulama şekli ve uzun dönem etkilerini netleştirmek amacıyla daha kapsamlı çalışmalara ihtiyaç duyulmaktadır.

DENEYSEL BULGULAR VE KLİNİK POTANSİYEL

Oksidatif stres, hücrelerde ve dokularda reaktif oksijen türleri (ROS) ve reaktif azot türlerinin (RNS) üretimi ve birikimi ile endojen savunma sistemlerinin bu yan ürünleri ortadan kaldırma yeteneği arasındaki dengesizlikten kaynaklanan bir durumdur. Temelde antioksidan dengede yer alan homeostatik mekanizmalardaki bozulmalardan kaynaklanmakta olup, yüksek lipid içeriği, yoğun oksijen tüketimi ve sınırlı antioksidan savunma kapasitesi nedeniyle beyin dokusunun oksidatif strese karşı son derece hassas olduğu bilinmektedir (Olufunmilayo ve ark., 2023). Beyin hasarına eşlik eden oksidatif stresin, enerji üretiminde eksiklik, lipid peroksidasyonu, nöroinflamasyon, metal homeostazında değişiklik ve nöronal apoptoz gibi patofizyolojik mekanizmalar ile birçok nörodejeneratif bozukluğun tipik özelliği olan toksik protein agregatlarının birikmesine yol açan mitokondriyal işlev bozukluklarında kritik rol oynamaktadır (Olufunmilayo ve ark., 2023). Bu nedenle, antioksidan bileşiklerin beyin hasarına karşı etkili bir tedavi seçeneği olabileceği düşünülmekte ve çok yönlü biyolojik aktiviteye sahip doğal moleküllerin nöroprotektif stratejiler açısından giderek daha fazla dikkat çektiği görülmektedir. Flavonoid yapısındaki güçlü antioksidanlardan biri olan kuersetin, serbest radikalleri temizleme kapasitesi/antioksidayon (Costa ve ark., 2016), inflamatuvar yolakları baskılama etkisi/antiinflamatuar (Li ve ark., 2016), nöroprotektif aktivite (Barreca ve ark., 2016) ve mitokondriyal stabiliteyi artırıcı fonksiyonları nedeniyle beyin hasarı modellerinde umut vadeden bir ajan olarak öne çıkmaktadır (Dajas ve ark., 2015; Chiang ve ark., 2023).

Lin ve ark., (2021) tarafından yapılan bir çalışmada 250–300 g ağırlığındaki 40 adet erkek Sprague–Dawley sıçan, çevresel koşullara adapte edildikten sonra rastgele dört gruba ayrılmıştır: sham, ligasyon, kuersetin ve önleyici grup. Kuersetin gruplarına, fizyolojik salin içinde çözülmüş 20 mg/kg dozunda kuersetin intraperitoneal olarak günde bir kez 10 gün süreyle uygulanmıştır. İskemik model oluşturmak için sağ orta serebral arter (MCA) ve sağ ortak karotid arter (CCA) 60 dakika süreyle bağlanmıştır. Operasyon sonunda hayvanlar anestezi altında dekapite edilerek ipsilateral beyin korteksi alınmış, homojenize edilip süpernatantları biyokimyasal analizler için kullanılmıştır. Doku örneklerinde malondialdehit (MDA) düzeyi tiobarbitürik asit reaktif madde (TBARS) yöntemiyle, Mg, Zn, Se, Fe ve Cu konsantrasyonları atomik absorpsiyon spektrofotometresiyle, SOD ve CAT aktiviteleri ticari kitlerle spektrofotometrik olarak belirlenmiştir Kuersetin uygulamasının serebral iskemiye karşı belirgin nöroprotektif etki gösterdiği belirlenmiştir. Kuersetin ön tedavisi, ligasyon grubuna kıyasla beyin korteksinde MDA, Fe, Cu düzeyleri ve Cu/Zn oranını anlamlı biçimde azaltırken; Mg, Zn, Se elementleri ile SOD ve CAT aktivitelerini artırmıştır. Bu bulgular, kuersetinin antioksidan savunma sistemini güçlendirerek ve esansiyel element dengesini düzenleyerek oksidatif stres kaynaklı lipid peroksidasyonunu azalttığını göstermektedir.

Wang ve ark., (2020), kuersetinin oksidatif stresi ve inflamasyonu azaltarak sıçan hipokampal nöronlarında serebral iskemi/reperfüzyon hasarına ve oksijen-glikoz yoksunluğu/reoksijenasyon nörotoksisitesine karşı koruduğunu bulmuştur. Li ve ark., (2021), kuersetinin hipoksi ve reoksijenasyon nedeniyle hasar gören endotel hücreleri üzerindeki koruyucu etkisini araştırmıştır. Araştırmacılar, kuersetinin insan göbek kordonu endotel hücrelerinde hücre apoptozunu ve oksidatif stresi azalttığını buldular. Bu çalışmalar, kuersetinin inflamasyonu ve oksidatif stresi azaltarak farklı serebral iskemi ve hipoksik-iskemik beyin hasarı modellerinde nöroprotektif etkilere sahip olduğunu ileri sürmektedir.

Kuersetinin subaraknoid kanama (SAK) sonrası beyin hasarı üzerindeki etkilerinin araştırıldığı bir çalışmada (Dong ve ark., 2014) deneysel olarak indüklenen SAK modelinde 10 mg/kg ve 50 mg/kg dozunda kuersetin etkinliği inclenmiş ve özellikle 50mg dozunda kuersetin alan grupta SOD ve GPx aktivitelerini belirgin şekilde artırdığı, MDA düzeylerini ise azalttığı belirlenmiştir. Ayrıca beyin ödeminin ve nörodavranışsal eksikliklerin düzeldiğini belirten çalışma ekibi, optimal dozda kuersetin uygulamasının endojen antioksidan enzimlerin aktivitesini artırarak ve serbest radikal oluşumunu engelleyerek SAK modelinde beyin hasarını iyileştirebileceğini ve nöroproteksiyon sağlayabileceğini vurgulamışlardır.

Robinson ve ark., (2025) tarafından yapılan bir çalışmada in vitro ve in vivo modellemeler ile travmatik beyin hasarı üzerinde durulmuş ve kuersetin kullanımının; serebral endotel hücrelerinde ROS'u azaltmada etkili olduğu, beyin endotel hücrelerinde sıkı bağlantıları, yapışık bağlantı proteinlerini ve aktin sitoskeletal düzeneğini koruyarak KBB sıkı bağlantı bütünlüğünün kaybına karşı koruma sağladığı; oksidatif strese maruz kaldığında endotel hücrelerinin kritik bariyer fonksiyonunu koruduğu ve intravenöz uygulamasının, orta şiddette travmatik beyin hasarlı bir fare modelinde KBB bozulmasına ve hiperpermeabiliteye karşı terapötik potansiyeline sahip olduğunu vurgulamışlardır.

Kuersetinin Alzheimer hastalığı (AD) patofizyolojisine yönelik çok yönlü koruyucu etkileri çeşitli moleküler mekanizmalarla ilişkilendirilmektedir. Kuersetinin amiloid-beta (Aβ) agregasyonunu inhibe ettiği ve Aβ plak oluşumunu azalttığı gösterilmiş olup, bu etkiler hastalığın ilerlemesini yavaşlatmada önemli bir rol oynayabileceği ifade edilmiştir (Alghamdi ve ark., 2022). Ayrıca kuersetinin, proinflamatuvar sitokinlerin ve diğer inflamatuvar mediyatörlerin üretimini baskılayarak belirgin antiinflamatuvar özellikler sergilediği de bildirilmiştir (Wang L ve ark., 2022). Kuersetinin nöroprotektif etkilerinin bir diğer önemli boyutu, gen ekspresyonunun düzenlenmesine yönelik etkileridir. Özellikle nöronal sağkalım ve sinaptik plastisite ile ilişkili genlerin ekspresyonunu modüle ettiği; böylece nöronal hasara karşı koruma sağladığı ve bilişsel fonksiyonların sürdürülmesine katkıda bulunduğu belirtilmektedir (Thiruvengadam ve ark., 2021). Bunun yanı sıra kuersetinin, beyinde kritik sinyal yolakları arasında yer alan PI3K/Akt ve MAPK/ERK sinyol yollarını modüle ettiği bildirilmiştir (Ghafouri-Fard ve ark., 2021). Bu yolaklar, nöronal hayatta kalma, sinaptik plastisite ve hafıza oluşumunun düzenlenmesinde temel öneme sahiptir. Genel olarak kuersetinin AD'de gösterdiği moleküler etkiler kompleks ve çok faktörlü olup, mevcut kanıtlar bu flavonoidin hastalığın önlenmesi ve tedavisi açısından umut vadettiğini göstermektedir. Bu kapsamda Cheng ve ark., (2024) tarafından yürütülen deneysel AD modelinde kuersetinin; öğrenme ve hafıza bozukluklarını iyileştirdiği, amiloidojenik süreci baskıladığı, oksidatif stresi azalttığı ve Keap1/Nrf2/HO-1 yolu üzerinden asetilkolinesteraz (AChE) aktivitesini düzenlediği rapor edilmiştir. Ayrıca, APP/PS1 transgenik farelerde hücre apoptozunu önlediği gösterilmiştir. Bu bulgular, kuersetinin AD tedavisinde klinik değerlendirmeler için güçlü bir moleküler temel sağlayabileceğini ortaya koymaktadır.

Kuersetinin, proinflamatuar sitokinlerin ve diğer inflamatuar mediyatörlerin üretimini inhibe ederek anlamlı düzeyde anti-inflamatuar etki gösterdiği bildirilmektedir. Beyinde ortaya çıkan kronik inflamasyonun Parkinson hastalığının (PD) gelişimi ve ilerlemesinde merkezi bir rol oynadığı bilindiğinden, inflamatuar yanıtın baskılanmasının hastalığın seyrini yavaşlatabileceği düşünülmektedir (Chiang ve ark., 2023). Kuersetinin PD ile ilişkili önemli moleküler süreçlerden biri olan alfa-sinüklein agregasyonunu inhibe ettiği ve bu protein birikimlerinin oluşumunu azalttığı gösterilmiştir (Zhu ve ark., 2013). Alfa-sinüklein agregasyonunun azalması, nöronal hasarın sınırlanmasına ve hastalığın progresyonunun yavaşlatılmasına katkı sağlayabilir. Ek olarak kuersetin, nöronal hücre ölümünü azaltarak dopaminerjik nöronların korunmasına yardımcı olmakta ve böylelikle PD'ye özgü motor fonksiyon bozukluklarının hafifletilmesine katkıda bulunmaktadır. Parkinson hastalığına yönelik deneysel modellerde kuersetinin nöroprotektif etkilerini değerlendiren çeşitli çalışmalar bulunmaktadır. Yapılan çalışmalarda kuersetinin, rotenon kaynaklı nöroinflamasyon, oksidatif stres ve davranış değişiklikleri üzerindeki düzenleyici etkileri (Sharma ve ark., 2020; Jain ve ark., 2022), dopamin metabolizması ve gen ekspresyonu üzerindeki etkileri (Josiah ve ark., 2022), hücre kültürü ve MitoPark transgenik fare modellerinde kuersetinin mitokondriyal disfonksiyon ve dopaminerjik nörodejenerasyona karşı koruyucu mekanizmaları (Ay ve ark., 2017) incelenmiştir. Bu çalışmalar, kuersetinin oksidatif stres, inflamasyon, mitokondriyal bozulma ve toksik ajanlara maruziyet gibi PD patogeneziyle ilişkili süreçler üzerinde belirgin düzenleyici etkilere sahip olduğunu ortaya koymaktadır. Ayrıca dopamin metabolizmasının modülasyonu ve inflamasyonun baskılanması gibi etkiler, kuersetinin nöroprotektif potansiyelinin temel mekanizmaları arasında yer almaktadır. Genel olarak mevcut

bulgular, kuersetinin Parkinson hastalığında tedavi edici potansiyele sahip doğal bir aday bileşik olabileceğini düşündürmekte; ancak klinik kullanımın netleştirilmesi için daha kapsamlı çalışmalara ihtiyaç duyulduğunu göstermektedir (Chiang ve ark., 2023).

SONUÇ

Kuersetin, antioksidan, antiinflamatuar, antiapoptotik ve mitokondri koruyucu özellikleri sayesinde beyin hasarının sekonder biyokimyasal süreçlerine karşı potansiyel bir nöroprotektif ajan olarak öne çıkmaktadır. Hücresel düzeyde AMPK aktivasyonu ile enerji metabolizmasını dengeleyebilmesi, NF-κB ve NLRP3 inflamazom yollarını inhibe ederek pro-inflamatuar sitokin üretimini azaltması, kuersetinin nöroinflamatuar hasara karşı etkili olmasını sağlamaktadır. Bununla birlikte, kuersetinin düşük suda çözünürlüğü, sınırlı oral biyoyararlanımı ve kısa plazma yarı ömrü, klinik uygulamalarını kısıtlamaktadır. Gelecekteki araştırmaların, kuersetinin biyoyararlanımını artırmaya yönelik stratejileri, optimal doz-zaman ilişkilerini ve kombinasyon tedavilerini incelemesi, ayrıca biyokimyasal ve moleküler biyobelirteçlerle korelasyonlarını değerlendirmesi, kuersetinin translasyonel değerini yükseltecek ve beyin hasarı tedavisinde tamamlayıcı bir yaklaşım olarak kullanımını destekleyecektir.

KAYNAKLAR

Alghamdi, A., Birch, D.J.S., Vyshemirsky, V., & Rolinski, O.J. (2022). Impact of the flavonoid quercetin on beta-Amyloid aggregation revealed by intrinsic fluorescence. J. Phys. Chem. 126, 7229–7237.

Anand David, A.V., Arulmoli, R., & Parasuraman, S. (2016). Overviews of biological ımportance of quercetin: a bioactive flavonoid. Pharmacognosy Reviews, 10(20), 84-89.

Aronowski, J., & Zhao, X. (2011). Molecular pathophysiology of cerebral hemorrhage: secondary brain injury. Stroke. 42, 1781–1786.

Ay, M., Luo, J., Langley, M., Jin, H., Anantharam, V., Kanthasamy, A., & Kanthasamy, A.G. (2017). Molecular mechanisms underlying protective effects of quercetin against mitochondrial dysfunction and progressive dopaminergic neurodegeneration in cell culture and MitoPark transgenic mouse models of Parkinson's Disease. J. Neurochem, 141, 766–782.

Barreca, D., Bellocco, E., DOnofrio, G., Fazel Nabavi, S., Daglia, M., Rastrelli, L., & Mohammad Nabavi, S. (2016). Neuroprotective effects of quercetin: from chemistry to medicine. CNS & Neurological Disorders-Drug Targets-CNS & Neurological Disorders), 15(8), 964-975.

Becerra-Torres, S.L., Rodríguez-Vázquez, M.L., Medina-Ramírez, I.E., & Jaramillo-Juárez, F. (2009). The flavonoid quercetin protects and prevents against potassium dichromate-induced systemic peroxidation of lipids and diminution in renal clearance of para-aminohippuric acid and inulin in the rat. Drug and Chemical Toxicology, 32(1), 88-91.

Cheng, M., Yuan, C., Ju, Y., Liu, Y., Shi, B., Yang, Y., Jin, S., He, X., Zhang, L., & Min, D. (2024). Quercetin attenuates oxidative stress and apoptosis in brain tissue of APP/PS1 double transgenic AD mice by regulating Keap1/Nrf2/HO-1 pathway to improve cognitive impairment. Behavioural NeurologyVolume, Article ID 5698119,

Chiang, M.C., Tsai, T.Y., & Wang, C.J. (2023). The potential benefits of quercetin for brain health: a review of anti-ınflammatory and neuroprotective mechanisms. Int. J. Mol. Sci. 24, 6328.

Costa, L.G., Garrick, J.M., Roquè P.J., & Pellacani C. (2016). Mechanisms of neuroprotection by quercetin: counteracting oxidative stress and more. Oxidative Medicine and Cellular Longevity. 2016:10.

Dajas, F., Abin-Carriquiry, J.A., Arredondo, F., Blasina, F., Echeverry, C., Martinez, M., Rivera, F., & Vaamonde, L. (2015). Quercetin in brain diseases: Potential and limits. Neurochemistry International 89(2015): 140-148.

Davis, C.K., & Vemuganti, R. (2022). Antioxidant therapies in traumatic brain injury. Neurochem Int., 152: 105255.

Deepika, & Maurya, P.K. (2022). Health benefits of quercetin in age-related diseases. Molecules, 27(8), Article 8. https://doi.org/10.3390/molecules27082498.

Dong, Y.S., Wang, J.L., Feng, D.Y., Qin, H.Z., Wen, H., Yin, Z.M., Gao, G.D., & Li, C. (2014). Protective effect of quercetin against oxidative stress and brain edema in an experimental rat model of subarachnoid hemorrhage. Int. J. Med. Sci., 11(3):282-290. doi: 10.7150/ijms.7634.

Gandhi, S., & Abramov, A.Y. (2012). Mechanism of oxidative stress in neuro degeneration. Oxid. Med. Cell. Longev. 2012, 428010.

Ghafouri-Fard, S., Shoorei, H., Khanbabapour Sasi, A., Taheri, M., & Ayatollahi, S.A. (2021). The impact of the phytotherapeutic agent quercetin on expression of genes and activity of signaling pathways. Biomed. Pharmacother, 141, 111847.

Imran, M., Thabet, H.K., Alaqel, S. I., Alzahrani, A.R., Abida, A., & Alshehri, S. (2022). The therapeutic and prophylactic potential of quercetin against COVID-19: An outlook on the clinical studies, inventive compositions, and patent literature. Antioxidants, 11(5), 876.

Jain, J., Hasan, W., Biswas, P., Yadav, R.S., & Jat, D. (2022). Neuroprotective effect of quercetin against rotenone-induced neuroinflammation and alterations in mice behavior. J. Biochem. Mol. Toxicol, 36, e23165.

Josiah, S.S., Famusiwa, C.D., Crown, O.O., Lawal, A.O., Olaleye, M.T., Akindahunsi, A.A., & Akinmoladun, A.C. (2022). Neuroprotective effects of catechin and quercetin in experimental Parkinsonism through modulation of dopamine metabolism and expression of IL-1beta, TNF-alpha, NF-kappaB, IkappaKB, and p53 genes in male Wistar rats. Neurotoxicology, 90, 158–171.

Lakhanpal, P. (2007). Quercetin: A versatile flavonoid. Internet Journal of Medical Update, 2. https://doi.org/10.4314/ijmu.v2i2.39851.

Lawson, M.K. (2023). Improvement of therapeutic value of quercetin with chitosan nanoparticle delivery systems and potential applications. International Journal of Molecular Sciences, 24(4), 3293.

Li, M.T., Ke, J., Guo, S.F., Wu, Y., Bian, Y.F., Shan, L.L., Liu, Q.Y., Huo, Y.J., Guo, C., & Liu, M.Y. (2021). The Protective effect of quercetin on endothelial cells Injured by hypoxia and reoxygenation. Front. Pharmacol. 12, 732874.

Li, X., Wang, H., Gao, Y., Li, L., Tang, C., Wen, G., Zhou, Y., Zhou, M., Mao, L., & Fan, Y. (2016). Protective effects of quercetin on mitochondrial biogenesis in experimental traumatic brain ınjury via the NRF2 signaling pathway. PLoS One, 25;11(10):e0164237. doi: 10.1371/journal.pone.0164237.

Li, Y., Yao, J., Han, C., Yang, J., Chaudhry, M. T., Wang, S., Liu, H., & Yin, Y. (2016). Inflammation and immunity. Nutrients, 8(3), 167.

Lin, M.C., Liu, C.C., Liao, C.S., Ro, J.H. (2021). Neuroprotective effect of quercetin during cerebral ischemic injury involves regulation of essential elements, transition metals, Cu/Zn ratio, and antioxidant activity. Molecules, 26, 6128.

Michala, A.S., & Pritsa, A. (2022). Quercetin: A molecule of great biochemical and clinical value and its beneficial effect on diabetes and cancer. Diseases, 10(3), 37.

Nguyen, T.L.A., & Bhattacharya, D. (2022). Antimicrobial activity of quercetin: An approach to its mechanistic principle. Molecules, 27(8), Article 8. https://doi.org/10.3390/molecules27082494.

Olufunmilayo, E.O., Gerke-Duncan, M.B., & Holsinger, R.D. (2023). Oxidative stress and antioxidants in neurodegenerative disorders. Antioxidants, 12(2), 517.

Özçiflikçi, H. (2023). Potasyum dikromat verilen ratlarda oksidatif stres ve inflamatuvar cevap üzerine kuersetinin etkisi. Kırıkkale Üniversitesi Sağlık Bilimleri Enstitüsü Yüksek Lisans Tezi, Kırıkkale.

Rasouli, H., Farzaei, M. H., & Khodarahmi, R. (2017). Polyphenols and their benefits: A review. International Journal of Food Properties, 20. https://doi.org/10.1080/10942912.2017.1354017

Robinson, B.D., Yeager, A., Lomas, A., Seplovich, G., Shaji, C.A., Wiggins-Dohlvik, K., Huang, J.H., Isbell, C.L., & Tharakan, B. (2025). Quercetin protects blood–brain barrier integrity and maintains Microvascular Permeability Following Traumatic Brain Injury. Neurocrit Care, 43:947–959

Shao, L., Chen, S., & Ma, L. (2022). Secondary brain ınjury by oxidative stress after cerebral hemorrhage: recent advances. Front. Cell. Neurosci. 16:853589. doi: 10.3389/fncel.2022.853589

Sharma, S., Raj, K., & Singh, S. (2020). Neuroprotective effect of quercetin in combination with piperine against rotenone- and iron supplement-induced parkinson's disease in experimental rats. Neurotox. Res., 37, 198–209.

Thiruvengadam, M., Venkidasamy, B., Subramanian, U., Samynathan, R., Ali Shariati, M., Rebezov, M., Girish, S., Thangavel, S., Dhanapal, A.R., & Fedoseeva, N. (2021). Bioactive compounds in oxidative stress-mediated diseases: Targeting the NRF2/ARE signaling pathway and epigenetic regulation. Antioxidants, 10, 1859.

Uttara, B., Singh, A.V., Zamboni, P., & Mahajan, R.T. (2009). Oxidative stress and neurodegenerative diseases: a review of upstream and downstream antioxidant therapeutic options. Curr. Neuropharmacol. 7, 65e74.

Wang, G., Wang, Y., Yao, L., Gu, W., Zhao, S., & Yan, T. (2022). Pharmacological activity of quercetin: an updated review. Evidence-Based Complementary and Alternative Medicine, 2022, e3997190.

Wang, L., Sun, J., Miao, Z., Jiang, X., Zheng, Y., & Yang, G. (2022). Quercitrin improved cognitive impairment through inhibiting inflammation induced by microglia in Alzheimer's disease mice. NeuroReport, 33, 327–335.

Wang, Y.Y., Chang, C.Y., Lin, S.Y., Wang, J.D., Wu, C.C., Chen, W.Y., Kuan, Y.H., Liao, S.L., Wang, W.Y., & Chen, C.J. (2020). Quercetin protects against cerebral ischemia/reperfusion and oxygen glucose deprivation/reoxygenation neurotoxicity. J. Nutr. Biochem. 83, 108436.

Yan, A., Torpey, A., Morrisroe, E., Andraous, W., Costa, A., & Bergese, S. (2024). Clinical management in traumatic brain injury. Biomedicines, 12, 781. https://doi.org/ 10.3390/biomedicines12040781.

Zhu, M., Han, S., & Fink, A.L. (2013). Oxidized quercetin inhibits alpha-synuclein fibrillization. Biochim. Biophys. Acta, 1830, 2872–2881.

ORAL PRESENTATION

Periodontal destruction, periodontal regeneration and considerations in endo-perio lesions

Akif Nalbant[1*] (*Orcıd: https://orcid.org/0009-0007-4123-5008.*), Gamze Ebrar Nalbant[2] (*Orcıd: https://orcid.org/0009-0000-0783-9069*), Hatice Ebru Olgun[1] (*Orcıd: https://orcid.org/0000-0001-7298-8589*)

[*1] Kırıkkale University, Faculty of Dentistry, Department of Periodontology, Kırıkkale, Türkiye.

[*2] Kırıkkale University, Faculty of Dentistry, Department of Endodontics, Kırıkkale, Türkiye.

*Corresponding author e-mail: nalbant1020@gmail.com

Abstract

Due to their anatomical relationships and shared microbial environments, pulpal and periodontal tissues interact bidirectionally during inflammatory processes. Endo-perio lesions can occur when pulpal and periodontal inflammatory conditions occur sequentially in the same tooth, but they can also occur simultaneously. Disease progression results from a disruption of the microbial balance in both tissues, leading to an excessive host response. Disease progression exceeds the physiological limits of the host defense system, leading to the emergence of a chronic inflammatory response. Although the results of regenerative periodontal treatment were reported as unpredictable in the past, advances in technology and a better understanding of periodontal tissue biology have improved its success. Today, the success of periodontal regenerative treatments is evaluated based on objective clinical and radiographic parameters, such as increases in radiographic bone density and volume, decreases in probing depth, and clinical attachment gain. Regenerative surgical procedures are classified into three main categories: graft-based, graft-free, and biologically based. In the treatment of endo-perio lesions, accurate diagnosis is crucial for treatment planning. Vitality testing is one of the key clinical data used for accurate diagnosis. In periodontal lesions, as long as the pulp is not secondarily affected, the tooth is vital, and periodontal treatment is sufficient. For lesions resulting from pulpal inflammation, endodontic treatment is essential. For complete healing of endo-perio lesions, both periodontal and endodontic treatments, whether independent or combined, are indicated. Periodontal defects are treated after successful endodontic treatment. In combined endo-perio lesions, both pulp and periodontal tissues are affected. Due to the presence of endotoxins and biofilm on the root surface, adhesion of periodontal ligament cells is limited. Additionally, periodontal regeneration treatments can also be applied to endo-perio lesions.

Keywords: Periodontal regeneration, Regenerative endodontic treatment, Endo-perio lesions, Guided periodontal tissue regeneration

INTRODUCTION

The periodontal disease process begins with the formation of a subgingival biofilm. Over time, as bacteria proliferate, plaque matures. As bacteria proliferate, they produce specific chemical compounds that damage the periodontium, such as hydrogen sulfide, proteases, and ammonia, and stimulate the immune system (Socransky et al., 1998). Periodontal microbial agents trigger periodontitis. The severity of periodontitis is primarily determined by interactions between bacterial factors and the host response (Song et al., 2017). Both the innate and adaptive immune systems are involved in defense against microbial agents. The role of these systems is to eliminate the causative agents of periodontal disease and maintain periodontal health (Genco & Slots, 1984). The balance between neutrophils, the complement system, and antibodies constitutes the first line of defense for periodontal tissues. Microorganism-derived toxins, lipopolysaccharides, and enzymes activate the immune system by stimulating tissue destruction (Darveau, 2009). After neutrophil chemotaxis, various products are released from neutrophils that reach tissues, causing local tissue destruction (Kantarci, Oyaizu, and Van Dyke, 2003).

Periodontal inflammation progresses from an initial neutrophil-dominant lesion to an early lesion containing a high number of macrophages and T lymphocytes. The established lesion and advanced lesion progress in complexity, with B lymphocyte and plasma cell dominance (Hajishengallis, Chavakis, & Lambris, 2020). Treatment of chronic periodontal disease involves a combination of different therapeutic steps (Rojas et al., 2019). Conventional

periodontal therapy does not promote tissue regeneration, but instead aims to halt the existing disease (Sculean, Chapple, & Giannobile, 2015).

Due to their anatomical relationships and shared microbial environments, pulpal and periodontal tissues interact bidirectionally during inflammatory processes. Endo-periolesions are lesions that occur when pulpal and periodontal inflammatory conditions occur sequentially or simultaneously in the same tooth. Endo-perioles are considered to result from polymicrobial dysbiosis. The disease progresses due to the disruption of the microbial balance in both tissues and the resulting excessive host response. Disease progression exceeds the physiological limits of the host defense system, leading to the emergence of a chronic inflammatory response (Kinane, Stathopoulou, and Papapanou, 2017; Adam, 2021).

Various pro-inflammatory mediators such as cytokines, chemokines, prostaglandins, and matrix metalloproteinases accelerate extracellular matrix degradation and cause progressive tissue destruction in periodontal tissues (Graves, 2008). As in periodontal inflammation, increased vascular pressure, immune cell infiltration, and rapid extracellular matrix degradation disrupt tissue integrity in pulp inflammation (Cooper & Smith, 2013). Therefore, the tissue damage seen in endo-perio lesions is often the result of a shared biological integrity rather than two separate systems (Rotstein & Simon, 2006a).

Wound healing is essentially a natural mechanism involving various cell types and biological mediators. In periodontal wound healing, various cell populations migrate, differentiate, and proliferate. Epithelial and connective tissue interact with each other. Cytokines and extracellular matrix molecules are organized in intertwined phases (Cho et al., 2021).

The epithelium and surrounding connective tissue transform into non-functional scar tissue during the healing process following traditional periodontal treatment. These effects of traditional periodontal treatment can be prevented by applying regenerative procedures to correct periodontal tissue loss (Nyman et al., 1982). In recent years, many periodontal regeneration treatments, regenerative endodontic treatments, and multifaceted biological treatments that reorganize root development, promote new connective tissue formation, and stimulate cementum and bone formation have been offered (Duarte et al., 2025). Regenerative treatment has been developed to restore lost portions of tooth support structures. The literature shows that regenerative periodontal treatments yield more favorable outcomes compared to traditional periodontal treatments (Eickholz et al., 2007).

Achieving regeneration in endo-periodontal lesions, where two different tissue types heal simultaneously, is a biologically challenging clinical application (Rotstein & Simon, 2006a). This review aims to summarize the biology of periodontal tissue destruction and current regenerative approaches. Furthermore, considering the biological limitations and specific challenges of periodontal regeneration in endo-perio lesions, the potential for regenerative treatment in these complex lesions will be discussed.

PERIODONTAL TISSUE DESTRUCTION

Periodontal inflammation and the subsequent tissue loss are complex processes initiated by the interaction between gram-negative anaerobic bacteria and the host response, and developed through various cytokines and mediators (Lindhe, Lang, and Karring, 2009). Some of the molecules that cause inflammation and tissue destruction are of bacterial origin, while others are endogenous (Kinane et al., 2011).

The natural and acquired immune responses play an important role in the periodontal disease process. The natural immune response represents the first line of defense against infectious agents (Kinane et al., 2001). Periodontal tissues attempt to counteract bacteria and bacterial products found in the biofilm through various mechanisms. Epithelial cell turnover; antimicrobial peptides and cytokines secreted by epithelial cells; the barrier function of the junctional epithelium; the washing effect of saliva and DOS; and various antibodies and proteases found in DOS and saliva are among the many mechanisms that contribute to the defense of periodontal tissues. However, the insufficiency of these mechanisms and the disruption of physiological balance can lead to gingivitis and subsequently periodontitis (Lindhe, Lang, and Karring, 2009).

The pathogenesis of periodontitis was first defined histopathologically by Page & Schroeder (1976) as the Initial lesion, Early lesion, established lesion (Gingivitis), and Advanced lesion (Periodontitis). In 1997, Kornman, Page,

and Tonetti explained the pathogenesis of periodontal disease at the genetic and molecular levels, proposing new definitions: 1. Acute bacterial attack phase, 2. Acute inflammatory response phase 3. Immune response phase 4. Regulation and resolution phase. The pathways activated by bacteria that cause tissue destruction in host cells through various antigens and virulence factors have been clarified. The effects of genetic, environmental, and acquired risk factors on the periodontal disease chain have been emphasized (Page & Kornman, 1997).

During the acute bacterial attack phase, the epithelium is exposed to various bacteria. Following bacterial plaque formation, fatty acids, peptides, and bacterial metabolites are secreted and can diffuse from the plaque into the junctional epithelium. Various cytokines and MMPs produced by the junctional epithelium cross the epithelial tissue and reach the connective tissue. Neutrophils are recruited in response to bacterial stimulation. Interleukin-8 is expressed in the junctional epithelial cells. Neutrophils migrate from the junctional epithelium to the gingival crevice. During the acute inflammatory response phase, as is the case with all epithelial surfaces, the epithelial turnover rate increases with the increasing bacterial load in the gingival crevice. The amount of interstitial fluid increases due to mild inflammation. The expansion of the intercellular space facilitates the migration of neutrophils from the connective tissue to the gingival crevice.

Among the migrating cells are macrophages, antigen-presenting cells, and lymphocytes. Collagen destruction and tissue damage begin due to migrating cells and the cytokines they release. Macrophages determine the immune response. They secrete cytokines that stimulate the recruitment of new macrophages and lymphocytes. Macrophages, under the influence of lipopolysaccharides, produce interleukin, MMP, and prostaglandin E2. MMPs lead to increased collagen degradation. Activation of B lymphocytes leads to the transformation into plasma cells. In the gingival sulcus, accessory elements begin to come into play. Plasma cells still predominate during the assembly and resolution phase. Mediators that cause tissue destruction increase. If the local immune response cannot limit the bacterial attack, the environment is ripe for the development of periodontitis and bone resorption (Kornman, Page, and Tonetti, 1997).

WOUND HEALING AND PERIODONTAL REGENERATION

Periodontal regeneration is defined as the reconstruction or rebuilding of lost or damaged periodontal tissue. Periodontal regeneration requires the regeneration of the cementum that forms the root surface, the alveolar bone, the periodontal ligament that connects them, and the gingiva. However, regeneration of the periodontium is a complex process. Although the complete chain of events during regeneration and healing is not fully understood, first, cells must migrate and attach to the affected root surface. This process is controlled by extracellular matrix elements and other cells (Lindhe, Lang, and Karring, 2009). Wound healing, similar to that in other parts of the body, proceeds through a series of distinct processes, beginning with the formation of a blood clot. Clot formation, followed by the absorption and adhesion of plasma proteins to the root surface, is the first stage of healing (Wikesjö, Nilvéus, and Selvig, 1992). An early inflammatory phase, involving neutrophils and monocytes, occurs within a few hours. Within three days, macrophages migrate to the area and form granulation tissue. By the seventh day, connective tissue attachment, along with collagen fibers, may form. By the fourteenth day, new collagen fibers may form an arrangement that allows for physical binding to dentin (Selvig, Bogle, and Claffey, 1988). It may take 3–5 weeks for these fibers to become functional and mature. As the healing process progresses, increasing mechanical stimulation promotes the formation of an organized extracellular matrix. Alveolar bone and cementum maturation are also promoted (Lindhe, Lang, and Karring, 2009). New bone formation begins from days 10–21 (Wilderman, 1964). In the apical region, a thin layer of cementum is observed along the connective tissue attachment, whereas in the coronal region, it is absent (King et al., 1997). After the formation of mineralized tissues, the microenvironment between cementum and alveolar bone is regulated by the placement and orientation of periodontal ligament fibers (Mine et al., 2005).

Although the outcomes of regenerative periodontal treatment were previously reported to be unpredictable, studies have shown that advances in technology and a better understanding of periodontal tissue biology have improved its success. Today, the success of periodontal regenerative treatments is evaluated using various criteria. Examples of these criteria include a reduction in probing depth, radiographic monitoring of bone density, and clinical attachment gain (Aichelmann-Reidy et al., 2015; Lee & Kim, 2025).

Regenerative surgical procedures are primarily classified into three main categories: graft-based, graft-free, and biologically based procedures. The bone graft materials used in these applications are classified according to their osteogenic, osteoinductive, and osteoconductive potentials based on bone regeneration mechanisms, while they are classified as autografts, allografts, xenografts, and synthetic grafts according to the source of the material (Newman et al., 2023).

Directed tissue regeneration is based on the concept of preventing epithelial migration into the defect, thereby allowing space and time for the healing of other tissues, such as the periodontal ligament and bone. This concept can stimulate the formation of new cementum, connective tissue, and bone in conjunction with growth and differentiation factors secreted by stem cells. The three fundamental structures necessary for guided tissue regeneration are scaffold material for tissue regeneration, cell signaling for stem cell migration and differentiation, and stem cells (Lang et al., 1995; Prabhakaran, Venugopal, and Ramakrishna, 2009). While graft materials are not used in traditional directed tissue regeneration, directed tissue regeneration is combined with bone grafts in the United States.

With increased research in tissue engineering, biologically derived products for regenerative therapies have been developed. Examples of biological products used in regeneration include platelet-derived growth factor, platelet-rich plasma, platelet-rich fibrin, dentin matrix derivatives, recombinant fibroblast growth factor, and recombinant bone morphogenetic protein (Newman et al., 2023). With advances in tissue engineering, studies on the use of autologous blood products in medicine and dentistry have increased, offering hope for future treatments. By varying the centrifugation times and speeds of platelet-rich fibrin, PRF derivatives with more advanced properties, such as advanced platelet-rich fibrin and advanced platelet-rich fibrin plus, have been developed. There are also studies on the use of PRF derivatives in regenerative applications such as periodontal regeneration and regenerative endodontic treatment (Simões-Pedro et al., 2022; Ashour et al., 2023; Bains et al., 2023).

REGENERATIVE ENDODONTIC TREATMENT

Regenerative endodontic treatment is a biologically based treatment method applied to support continued root development, achieve apical closure, and promote thickening of the dentin walls in teeth with immature necrotic pulp (Murray, 2023). This procedure involves disinfecting the root canal system, then inducing apical bleeding with a file and forming a blood clot in the root canal (Kahler, Lu, and Taha, 2024). Regenerative endodontic treatment began to be applied in the 2000s and was first referred to as revascularization in 2001, then as revitalization in 2010 (Iwaya, Ikawa, and Kubota, 2001; Huang et al., 2010). In 2007, the American Association of Endodontists began using the term “regenerative endodontic treatment,” stating that the treatment extends beyond simply restoring blood circulation and encompasses tissue-engineering principles (Murray, Garcia-Godoy, and Hargreaves, 2007). While regenerative endodontic treatment was initially applied only to immature teeth, it is now also used for mature teeth with closed apices and for teeth that have previously undergone root canal treatment (He et al., 2017; Barbosa-Ribeiro et al., 2021).

ENDODONTIC-PERIODONTAL LESIONS

Pulp and periodontal tissues are connected through physiological and iatrogenic pathways. Dentin tubules, furcation canals, apical foramina, and exposed dentin tubules are physiological communication pathways between the pulp and periodontium. Conditions such as dentin cracks, root damage, palatogingival grooves, perforations, and vertical root fractures can also cause transmission between the pulp and periodontium. Endo-perio lesions occur in conjunction with bidirectional communication between the pulp and periodontium via various pathways, including anatomical and pathological ones (Lisican, 2024).

Endodontic-periodontal lesions have been classified in various ways. According to the classification made by Simon et al. in 1972, they are divided into five groups: 1. Primary Endodontic Lesions, 2. Primary Endodontic Lesions with Secondary Periodontal Involvement, 3. Primary Periodontal Lesions, 4. Primary Periodontal Lesions with Secondary Endodontic Involvement, 5. True Combined Lesions (Simon, Glick, and Frank, 1972). According to another classification made in 2022, endodontic-periodontal lesions are divided into three classes. Class 1 – Crown-down Plaque-induced Periodontal Lesions start at the crown and progress apically toward deep periodontal tissues. Although clinically mimicking pulp pathologies, there is no initial pulp involvement. Periodontal treatment alone is sufficient. As the condition worsens, the pulp may be affected via lateral canals and other transmission pathways. At this stage, root canal treatment and periodontal treatment are necessary. Class 2 – Down-crown

Periodontal Lesions of Endodontic Origin start in the apico-coronal direction; the periodontium is healthy as long as the periodontal ligament is not affected by lateral canals and other transmission pathways. Class 3 – Combined Endodontic-periodontal lesions. An endodontic lesion formed at the tooth apex is connected to a periodontal pocket formed due to plaque (Cerutti, 2024).

Accurate diagnosis is crucial for treatment planning in endo-periodontal lesions. The vitality test is an important clinical test that can aid accurate diagnosis. In periodontal lesions, the tooth is vital as long as the pulp is not secondarily affected, and periodontal treatment is sufficient. However, endodontic treatment is essential for lesions caused by pulp inflammation. Both periodontal and endodontic treatments are indicated for the complete healing of endo-periodontal lesions, whether independent or combined. Periodontal defects are treated after successful endodontic treatment (Rotstein & Simon, 2006b; Newman et al., 2023). In combined endo-perio lesions, both the pulp and periodontal tissues are affected. Due to the presence of endotoxins and biofilm on the root surface, the adhesion of periodontal ligament cells is limited (Farag et al., 2025). In addition, periodontal regeneration treatments can also be applied in endo-perio lesions. Alquthami et al. achieved successful results by applying routine root canal treatment and regenerative periodontal treatment in the treatment of a tooth with endo-perio lesions (Alquthami et al., 2018).

Guided tissue regeneration has been used in several studies to treat teeth with endo-perio lesions (AlJasser et al., 2021). Numerous in vitro and clinical studies demonstrate that guided tissue regeneration, enamel matrix derivative, and cell-based approaches promote healing in periodontal tissue. Similar principles apply to endo-perio lesions (Rosen et al., 2023; Tietmann et al., 2024). A review of the current literature reveals insufficient data on cases where both regenerative endodontic treatment and periodontal regeneration were combined in teeth with endo-perio lesions.

CONCLUSION AND FUTURE DIRECTIONS

The pathophysiology of periodontal and combined endo-periodontal lesions is characterized by complex interactions between inflammatory responses and extracellular matrix degradation, leading to tissue loss. Although periodontal tissue reconstruction is possible with treatments using various biomaterials, such as guided tissue regeneration and enamel matrix derivatives, the simultaneous regeneration of pulp and periodontal tissues in endo-perio lesions remains a significant clinical challenge. Due to limited strong clinical evidence in these complex cases, the success of regenerative strategies largely depends on meticulous multidisciplinary case management, including accurate case selection, effective disinfection of the root canal system, and root surface debridement. In the future, the integration of innovative tissue engineering applications such as extracellular matrix-based scaffolds, controlled growth factor release systems, exosomes, and three-dimensional bioprinting aims to increase the clinical predictability of both periodontal and endodontic regeneration.

REFERENCES

Adam, M. (2021) "'Combined endo-perio lesions' - what is the best treatment?," *Evidence-Based Dentistry*, 22(4), pp. 158–159. Available at: https://doi.org/10.1038/s41432-021-0230-y.

Aichelmann-Reidy, M.E., Perry R. Klokkevold, Kevin G. Murphy, Paul S. Rosen, Robert G. Schallhorn, Anton Sculean, Hom-Lay Wang, Michael S. Reddy and Gustavo Avila-Ortiz (2015) "Periodontal Regeneration — Furcation Defects: Practical Applications From the AAP Regeneration Workshop." Available at: https://aap.onlinelibrary.wiley.com/doi/full/10.1902/cap.2015.140068

AlJasser, R. *et al.* (2021) "Regenerative Therapy Modality for Treatment of True Combined Endodontic-Periodontal Lesions: A Randomized Controlled Clinical Trial," *International Journal of Environmental Research and Public Health*, 18(12), p. 6220. Available at: https://doi.org/10.3390/ijerph18126220.

Alquthami, H. *et al.* (2018) "Successful Management of Teeth with Different Types of Endodontic-Periodontal Lesions," *Case Reports in Dentistry*, 2018(1), p. 7084245. Available at: https://doi.org/10.1155/2018/7084245.

Ashour, S.H. *et al.* (2023) "The Effects of Injectable Platelet-Rich Fibrin and Advanced-Platelet Rich Fibrin on Gingival Fibroblast Cell Vitality, Proliferation, Differentiation," *Tissue Engineering and Regenerative Medicine*, 20(7), pp. 1161–1172. Available at: https://doi.org/10.1007/s13770-023-00586-1.

Bains, V.K. *et al.* (2023) "Technical considerations in obtaining platelet rich fibrin for clinical and periodontal research," *Journal of Oral Biology and Craniofacial Research*, 13(6), pp. 714–719. Available at: https://doi.org/10.1016/j.jobcr.2023.09.003.

Barbosa-Ribeiro, M. *et al.* (2021) "Microbiological analysis of endodontically treated teeth with apical periodontitis before and after endodontic retreatment," *Clinical Oral Investigations*, 25(4), pp. 2017–2027. Available at: https://doi.org/10.1007/s00784-020-03510-2.

Cerutti, F. (2024) "ENDO-PERIO LESIONS: SIMPLIFIED CLASSIFICATION," *Style Italiano Endodontics*, 1 November. Available at: https://endodontics.styleitaliano.org/endo-perio-lesions-simplified-classification/ (Accessed: December 6, 2025).

Cho, Y.-D. *et al.* (2021) "Periodontal Wound Healing and Tissue Regeneration: A Narrative Review," *Pharmaceuticals*, 14(5), p. 456. Available at: https://doi.org/10.3390/ph14050456.

Cooper, P.R. and Smith, A.J. (2013) "Molecular mediators of pulp inflammation and regeneration," *Endodontic Topics*, 28(1), pp. 90–105. Available at: https://doi.org/10.1111/etp.12036.

Darveau, R.P. (2009) "The oral microbial consortium's interaction with the periodontal innate defense system," *DNA and cell biology*, 28(8), pp. 389–395. Available at: https://doi.org/10.1089/dna.2009.0864.

Duarte, N.D. *et al.* (2025) "Biomaterials for Guided Tissue Regeneration and Guided Bone Regeneration: A Review," *Dentistry Journal*, 13(4), p. 179. Available at: https://doi.org/10.3390/dj13040179.

Eickholz, P. *et al.* (2007) "Stability of clinical and radiographic results after guided tissue regeneration in infrabony defects," *Journal of Periodontology*, 78(1), pp. 37–46. Available at: https://doi.org/10.1902/jop.2007.060097.

Farag, A.F. *et al.* (2025) "Effects of different curcumin concentrations on human periodontal ligament fibroblast adhesion and proliferation on periodontally involved root surfaces: In-vitro study," *Journal of Oral Biology and Craniofacial Research*, 15(4), pp. 729–736. Available at: https://doi.org/10.1016/j.jobcr.2025.04.006.

Genco, R.J. and Slots, J. (1984) "Host responses in periodontal diseases," *Journal of Dental Research*, 63(3), pp. 441–451. Available at: https://doi.org/10.1177/00220345840630031601.

Graves, D. (2008) "Cytokines that promote periodontal tissue destruction," *Journal of Periodontology*, 79(8 Suppl), pp. 1585–1591. Available at: https://doi.org/10.1902/jop.2008.080183.

Hajishengallis, G., Chavakis, T. and Lambris, J.D. (2020) "Current understanding of periodontal disease pathogenesis and targets for host-modulation therapy," *Periodontology 2000*, 84(1), pp. 14–34. Available at: https://doi.org/10.1111/prd.12331.

He, L. *et al.* (2017) "Regenerative Endodontics for Adult Patients," *Journal of Endodontics*, 43(9, Supplement), pp. S57–S64. Available at: https://doi.org/10.1016/j.joen.2017.06.012.

Huang, G.T.-J. *et al.* (2010) "Stem/progenitor cell-mediated de novo regeneration of dental pulp with newly deposited continuous layer of dentin in an in vivo model," *Tissue Engineering. Part A*, 16(2), pp. 605–615. Available at: https://doi.org/10.1089/ten.TEA.2009.0518.

Iwaya, S.I., Ikawa, M. and Kubota, M. (2001) "Revascularization of an immature permanent tooth with apical periodontitis and sinus tract," *Dental Traumatology: Official Publication of International Association for Dental Traumatology*, 17(4), pp. 185–187. Available at: https://doi.org/10.1034/j.1600-9657.2001.017004185.x.

Kahler, B., Lu, J. and Taha, N.A. (2024) "Regenerative endodontic treatment and traumatic dental injuries," *Dental Traumatology: Official Publication of International Association for Dental Traumatology*, 40(6), pp. 618–635. Available at: https://doi.org/10.1111/edt.12979.

Kantarci, A., Oyaizu, K. and Van Dyke, T.E. (2003) "Neutrophil-mediated tissue injury in periodontal disease pathogenesis: findings from localized aggressive periodontitis," *Journal of Periodontology*, 74(1), pp. 66–75. Available at: https://doi.org/10.1902/jop.2003.74.1.66.

Kinane, D.F. *et al.* (2001) "Etiopathogenesis of periodontitis in children and adolescents," *Periodontology 2000*, 26, pp. 54–91. Available at: https://doi.org/10.1034/j.1600-0757.2001.2260104.x.

Kinane, D.F. *et al.* (2011) "Host-response: understanding the cellular and molecular mechanisms of host-microbial interactions--consensus of the Seventh European Workshop on Periodontology," *Journal of Clinical Periodontology*, 38 Suppl 11, pp. 44–48. Available at: https://doi.org/10.1111/j.1600-051X.2010.01682.x.

Kinane, D.F., Stathopoulou, P.G. and Papapanou, P.N. (2017) "Periodontal diseases," *Nature Reviews. Disease Primers*, 3, p. 17038. Available at: https://doi.org/10.1038/nrdp.2017.38.

King, G.N. *et al.* (1997) "Recombinant human bone morphogenetic protein-2 promotes wound healing in rat periodontal fenestration defects," *Journal of Dental Research*, 76(8), pp. 1460–1470. Available at: https://doi.org/10.1177/00220345970760080801.

Kornman, K.S., Page, R.C. and Tonetti, M.S. (1997) "The host response to the microbial challenge in periodontitis: assembling the players," *Periodontology 2000*, 14, pp. 33–53. Available at: https://doi.org/10.1111/j.1600-0757.1997.tb00191.x.

Lang, H. *et al.* (1995) "Formation of differentiated tissues in vivo by periodontal cell populations cultured in vitro," *Journal of Dental Research*, 74(5), pp. 1219–1225. Available at: https://doi.org/10.1177/00220345950740051201.

Lee, J.-H. and Kim, Y.-T. (2025) "Comparative long-term augmentation stability of L- and I-shaped guided bone regeneration techniques for maxillary anterior region," *Journal of Periodontology*, n/a(n/a). Available at: https://doi.org/10.1002/JPER.24-0867.

Lindhe, J., Lang, N.P. and Karring, T. (2009) *Clinical Periodontology and Implant Dentistry*. Wiley.

Lisican, E. (2024) "Endodontic Periodontic Lesions," *American Association of Endodontists*, 1 November. Available at: https://www.aae.org/specialty/endodontic-periodontic-lesions/ (Accessed: December 6, 2025).

Microbial Modulation of Stem Cells and Future Directions in Regenerative Endodontics - Journal of Endodontics (no date). Available at: https://www.jendodon.com/article/S0099-2399(17)30871-3/abstract (Accessed: December 5, 2025).

Mine, K. *et al.* (2005) "Occlusal forces promote periodontal healing of transplanted teeth and prevent dentoalveolar ankylosis: an experimental study in rats," *The Angle Orthodontist*, 75(4), pp. 637–644. Available at: https://doi.org/10.1043/0003-3219(2005)75%255B637:OFPPHO%255D2.0.CO;2.

Murray, P.E. (2023) "Review of guidance for the selection of regenerative endodontics, apexogenesis, apexification, pulpotomy, and other endodontic treatments for immature permanent teeth," *International Endodontic Journal*, 56 Suppl 2, pp. 188–199. Available at: https://doi.org/10.1111/iej.13809.

Murray, P.E., Garcia-Godoy, F. and Hargreaves, K.M. (2007) "Regenerative endodontics: a review of current status and a call for action," *Journal of Endodontics*, 33(4), pp. 377–390. Available at: https://doi.org/10.1016/j.joen.2006.09.013.

Newman, M.G. *et al.* (2023) *Newman and Carranza's Clinical Periodontology and Implantology E-Book: Newman and Carranza's Clinical Periodontology and Implantology E-Book*. Saunders.

Nyman, S. *et al.* (1982) "New attachment following surgical treatment of human periodontal disease," *Journal of Clinical Periodontology*, 9(4), pp. 290–296. Available at: https://doi.org/10.1111/j.1600-051x.1982.tb02095.x.

Page, R.C. and Kornman, K.S. (1997) "The pathogenesis of human periodontitis: an introduction," *Periodontology 2000*, 14, pp. 9–11. Available at: https://doi.org/10.1111/j.1600-0757.1997.tb00189.x.

Page, R.C. and Schroeder, H.E. (1976) "Pathogenesis of inflammatory periodontal disease. A summary of current work," *Laboratory Investigation; a Journal of Technical Methods and Pathology*, 34(3), pp. 235–249.

Prabhakaran, M.P., Venugopal, J. and Ramakrishna, S. (2009) "Electrospun nanostructured scaffolds for bone tissue engineering," *Acta Biomaterialia*, 5(8), pp. 2884–2893. Available at: https://doi.org/10.1016/j.actbio.2009.05.007.

Rojas, M.A. *et al.* (2019) "Early wound healing outcomes after regenerative periodontal surgery with enamel matrix derivatives or guided tissue regeneration: a systematic review," *BMC oral health*, 19(1), p. 76. Available at: https://doi.org/10.1186/s12903-019-0766-9.

Rosen, E. *et al.* (2023) "Effect of guided tissue regeneration on the success of surgical endodontic treatment of teeth with endodontic-periodontal lesions: A systematic review," *International Endodontic Journal*, 56(8), pp. 910–921. Available at: https://doi.org/10.1111/iej.13936.

Rotstein, I. and Simon, J.H. (2006a) "The endo-perio lesion: a critical appraisal of the disease condition," *Endodontic Topics*, 13(1), pp. 34–56. Available at: https://doi.org/10.1111/j.1601-1546.2006.00211.x.

Rotstein, I. and Simon, J.H. (2006b) "The endo-perio lesion: a critical appraisal of the disease condition," *Endodontic Topics*, 13(1), pp. 34–56. Available at: https://doi.org/10.1111/j.1601-1546.2006.00211.x.

Sculean, A., Chapple, I.L.C. and Giannobile, W.V. (2015) "Wound models for periodontal and bone regeneration: the role of biologic research," *Periodontology 2000*, 68(1), pp. 7–20. Available at: https://doi.org/10.1111/prd.12091.

Selvig, K.A., Bogle, G. and Claffey, N.M. (1988) "Collagen linkage in periodontal connective tissue reattachment. An ultrastructural study in beagle dogs," *Journal of Periodontology*, 59(11), pp. 758–768. Available at: https://doi.org/10.1902/jop.1988.59.11.758.

Simões-Pedro, M. *et al.* (2022) "Tensile Strength Essay Comparing Three Different Platelet-Rich Fibrin Membranes (L-PRF, A-PRF, and A-PRF+): A Mechanical and Structural In Vitro Evaluation," *Polymers*, 14(7), p. 1392. Available at: https://doi.org/10.3390/polym14071392.

Simon, J.H., Glick, D.H. and Frank, A.L. (1972) "The relationship of endodontic-periodontic lesions," *Journal of Periodontology*, 43(4), pp. 202–208. Available at: https://doi.org/10.1902/jop.1972.43.4.202.

Socransky, S.S. *et al.* (1998) "Microbial complexes in subgingival plaque," *Journal of Clinical Periodontology*, 25(2), pp. 134–144. Available at: https://doi.org/10.1111/j.1600-051x.1998.tb02419.x.

Song, B. *et al.* (2017) "The role of Toll-like receptors in periodontitis," *Oral Diseases*, 23(2), pp. 168–180. Available at: https://doi.org/10.1111/odi.12468.

Tietmann, C. *et al.* (2024) "Management of Teeth with Grade 3 Endo-Periodontal Lesions by Combined Endodontic and Regenerative Periodontal Therapy," *Journal of Clinical Medicine*, 13(1), p. 93. Available at: https://doi.org/10.3390/jcm13010093.

Wikesjö, U.M., Nilvéus, R.E. and Selvig, K.A. (1992) "Significance of early healing events on periodontal repair: a review," *Journal of Periodontology*, 63(3), pp. 158–165. Available at: https://doi.org/10.1902/jop.1992.63.3.158.

Wilderman, M.N. (1964) "Exposure of Bone in Periodontal Surgery," *Dental Clinics of North America*, 8(1), pp. 23–36. Available at: https://doi.org/10.1016/S0011-8532(22)01997-8.

ORAL PRESENTATION

Nar atıklarından yarı katı kültür fermantasyonuyla sitrik asit üretiminin incelenmesi

Onur Kozan[1] (ORCID: https://orcid.org/0009-0005-6760-6837), Ayşe Sude Güven[1] (ORCID: https://orcid.org/0009-0002-7820-4110), *Işık Çoban[1]

[1]İstanbul Medeniyet Üniversitesi, Mühendislik ve Doğa Bilimleri Fakültesi, Biyomühendislik Bölümü, İstanbul, Türkiye

*Sorumlu yazar e-mail: isik.coban@medeniyet.edu.tr

Özet

Gıda endüstrisi ve biyoteknoloji alanlarında önemli bir organik asit olan sitrik asit, yüksek talep gören bir metabolittir. Günümüzde sitrik asit üretimi genellikle karbonhidrat kaynaklı substratlarla gerçekleştirilmektedir. Ancak endüstriyel üretimde maliyetlerin düşürülmesi ve çevresel sürdürülebilirliğin sağlanması amacıyla tarımsal atıkların değerlendirilmesi önem kazanışmıştır. Bu çalışmada, nar üretiminde ortaya çıkan atık kabukların, *Aspergillus niger* kullanılarak yarı katı kültür fermantasyonu yöntemiyle sitrik asit üretiminde substrat olarak kullanılabilirliği araştırılmıştır. Deneylerde farklı nar atığı miktarları (3–25 g), sıvı besi yeri hacimleri (25–35 mL) ve metanol konsantrasyonları (%0–3 v/v) kullanılmıştır. Optimum koşulların belirlenmesi amacıyla pH, sıcaklık ve iz element etkileri incelenmiştir. Elde edilen sonuçlara göre, 10 g nar atığı, 25 mL sıvı besi yeri ve %3 metanol içeren ortamda en yüksek sitrik asit üretimi (15,43 g/kg) elde edilmiştir. Ayrıca, $CuSO_4$ ilavesi fermantasyon verimini anlamlı ölçüede artırmıştır. Bu sonuçlar, nar atıklarının sitrik asit üretiminde sürdürülebilir, ekonomik ve çevre dostu bir alternatif substrat olabileceğini göstermektedir.

Anahtar Kelimeler: Sitrik asit, nar atığı, *Aspergillus niger*, yarı katı kültür, fermantasyon

Investigation of citric acid production from pomegranate waste by semi solid-state fermentation

Abstract

Citric acid, a tricarboxylic organic acid, is widely used in the food, pharmaceutical, and detergent industries. To reduce production costs and promote sustainability, this study investigated the potential use of pomegranate waste as a substrate for citric acid production via semi solid-state fermentation using *Aspergillus niger*. Various parameters such as substrate mass (3–25 g), liquid medium volume (25–35 mL), and methanol concentration (0–3% v/v) were optimized. The effect of trace elements and pH were also evaluated. The optimum citric acid yield (15.43 g/kg) was achieved at 10 g pomegranate peel, 25 mL medium, and 3% methanol. The addition of 0.0078 g/L $CuSO_4$ significantly enhanced production efficiency. Results demonstrate that pomegranate waste can serve as a low-cost and eco-friendly substrate for citric acid fermentation.

Keywords: Citric acid, pomegranate waste, *Aspergillus niger*, semi solid-state, fermentation

GİRİŞ

Nar üretimi Türkiye'de önemli bir tarımsal faaliyettir. İzmir Ticaret Borsası'nın 2024 verilerine göre 2023 yılında yaklaşık 638 kiloton nar üretilmiş olup, bunun %54'ü atık olarak değerlendirilemeden çevreye atılmaktadır (Cano-Lamadrid ve diğ., 2022). Nar kabuğu, yüksek şeker (%31,38) ve protein (%8,7) içeriği nedeniyle biyoteknolojik üretimlerde potansiyel karbon kaynağıdır (Naseem Ullah ve diğ., 2012). Sitrik asit ($C_6H_8O_7$), gıda, ilaç ve kimya sektörlerinde çok yönlü kullanım alanına sahip bir organik asittir (Sinko ve diğ., 2006). Endüstriyel ölçekte sitrik asit üretimi genellikle *Aspergillus niger* kullanılarak fermantasyon yoluyla yapılmaktadır (Behera, 2020). Bu çalışmanın amacı, nar atıklarının yarı katı kültür fermantasyonu yöntemiyle değerlendirilmesi ve sitrik asit üretimi için uygun koşulların belirlenmesidir.

MATERYAL VE METOT

Kullanılan Mikroorganizma:
Aspergillus niger, patates dekstroz agar (PDA, 42 g/L) üzerinde 30 °C'de 7 gün inkübe edilmiştir.

Katı Besi Yeri:
Nar kabukları 40 °C'de kurutulmuş, öğütülerek toz haline getirilmiştir.

Sıvı Besi Yeri Kompozisyonu:
(NH_4Cl 0.25 % w/v, K_2HPO_4 0.1 %, $MgSO_4 \cdot 7H_2O$ 0.02 %, $MnSO_4 \cdot 4H_2O$ 0.001 %, $CuSO_4 \cdot 5H_2O$ 0.078 %) (Vandenberghe & R. Soccol, 1999).

Yarı Katı Fermantasyon:
Nar kabuğu tozu belirlenen miktarlarda (3–25 g) erlenlere eklenmiş, sıvı besi yeri hacimleri (25–35 mL) ve pH = 5 olacak şekilde ayarlanmıştır. 121 °C'de 15 dk otoklavlanarak sterilizasyon sağlanmıştır. Metanol konsantrasyonları %0–3 (v/v) olarak değişmiştir.

Sitrik Asit Tayini:
Numuneler 4100 rpm'de 10 dk santrifüyj edilerek süpematant alınmış, 0.1 N NaOH ile titre edilmiştir (Kareem ve diğ., 2010). Ayrıca spektrofotometrik analizde Cu–Amonyak kompleksi yöntemi kullanılmış, absorbans 750 nm'de ölçülmüştür (Farajzadeh & Nagizadeh, 2002). Kareem et al., 2010'da verilem formüle göre titrasyon hesapları yapılmıştır.

Parametreler:

Tablo 1: Deneyin Parametreleri

Parametreler	Değişkenler
Nar Atığı Miktarı	3, 5, 10, 15, 20, 25 (g)
Sıvı Besi Yeri Miktarı	25, 30, 35 (mL)
Metanol Miktarı	%0, %1, %2, %3 (v/v)
Sıvı Besi Yeri Türü	Sıvı Besi Yeri, 0,0078 (%w/v) $CuSO_4$.5H2O, Distile Su
Fermantasyon Süresi	7 gün

BULGULAR ("BULGULAR ve TARTIŞMA" şeklinde tek başlıkta da verilebilir.)

Nar atığı miktarı 10 g olduğunda en yüksek sitrik asit verimi (12.78 g/kg) elde edilmiştir. Daha düşük miktarlarda yüzey alanı yetersiz kalmış, yüksek miktarlarda ise miselyum yayılımı sınırlanmıştır. Sıvı besi yeri hacmi arttıkça sitrik asit üretimi azalmış; optimum değer 25 mL olarak belirlenmiştir. Metanol miktarı arttıkça üretim verimi %3'e kadar artmış ve 15.43 g/kg sitrik asit üretimi elde edilmiştir. Metanolün hücre zar geçirgenliğini artırması, sitrik asidin dışarı difüyonunu kolaylaştırmıştır. Ayrıca, $CuSO_4$ ilavesi fermantasyon verimini artırmış; optimum Cu^{2+} konsantrasyonu 0.0078 g/L olarak tespit edilmiştir. Fermantasyon süreci 7 gün boyunca izlenmiş, 4. günde maksimum üretim, 6. günde pH 2.35'e düşmesiyle üretim azalmıştır. *Aspergillus niger*'in optimum pH aralığı pH = 5 civarında olup, aşırı asidik koşullar üretimi sınırlandırmıştır (Andersen ve diğ., 2009).

Tablo 2. Değişkenin Nar Atığı Miktarı ile Yapılan Deneylerin Sonuçları

Nar Kabuğu Miktarı (g)	Sıvı Besi Yeri Miktarı (mL)	Metanol Miktarı (mL)	Ortalama g/Kg Sitrik Asit	Sıvı Besi Yeri Tipi
3	25	0,5	9,606 ± 0,896	Sıvı Besi Yeri
5	25	0,5	11,669 ± 0,499	Sıvı Besi Yeri
10	25	0,5	12,789 ± 0,194	Sıvı Besi Yeri
15	40	0,8	7,160 ± 0,296	Sıvı Besi Yeri
20	40	0,8	6,079 ± 0,729	Sıvı Besi Yeri
25	40	0,8	6,789 ± 0,194	Sıvı Besi Yeri

Tablo 3: Değişkenin Sıvı Besi Yeri Miktarı ile Yapılan Deneylerin Sonuçları

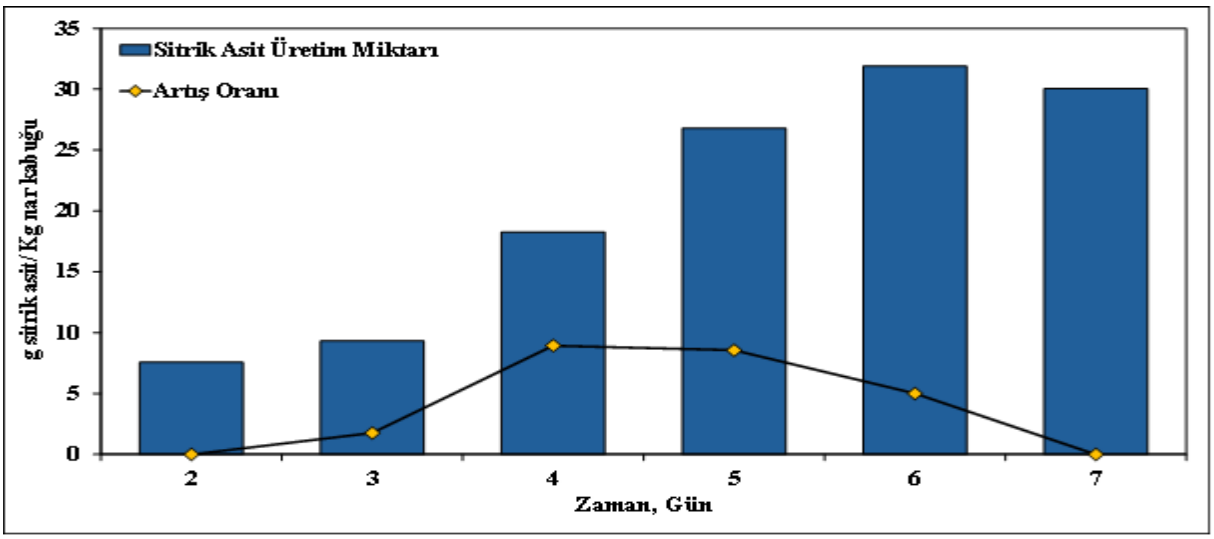
Nar Kabuğu Miktarı (g)	Sıvı Besi Yeri Miktarı (mL)	Metanol Miktarı (mL)	Ortalama g/Kg Sitrik Asit	Sıvı Besi Yeri Tipi
10	25	0,5	12,789 ± 0,194	Sıvı Besi Yeri
10	30	0,5	8,453 ± 0,512	Sıvı Besi Yeri
10	35	0,5	7,745 ± 0,3202	Sıvı Besi Yeri

Tablo 4: Değişkenin Metanol Miktarı ile Yapılan Deneylerin Sonuçları

Nar Kabuğu Miktarı (g)	Sıvı Besi Yeri Miktarı (mL)	Metanol Miktarı (mL)	Ortalama g/Kg Sitrik Asit	Sıvı Besi Yeri Tipi
10	25	0	7,621 ± 0,704	Sıvı Besi Yeri
10	25	0,25	8,517 ± 0,192	Sıvı Besi Yeri
10	25	0,5	12,789 ± 0,194	Sıvı Besi Yeri
10	25	0,75	15,433 ± 0,6203	Sıvı Besi Yeri

Tablo 5: Değişkenin Metanol Miktarı ile Yapılan Deneylerin Sonuçları

Nar Kabuğu Miktarı (g)	Sıvı Besi Yeri Miktarı (mL)	Metanol Miktarı (mL)	Ortalama g/Kg Sitrik Asit	Sıvı Besi Yeri Tipi
10	25	0,75	15,433 ± 0,6203	Sıvı Besi Yeri
10	25	0,75	8,517 ± 0,192	Distile Su
10	25	0,75	18,445 ± 1,009	0,0078 g/L Bakır Çözeltisi



Şekil 1. Sitrik asit üretim miktarı ve üretimin artış miktarının zamana bağlı değişim grafiği

SONUÇ

Elde edilen bulgular, nar atıklarının yarı katı kültür fermantasyonu ile sitrik asit üretiminde etkili bir substrat olduğunu göstermiştir. 10 g nar kabuğu, 25 mL sıvı besi yeri, %3 metanol ve 0.0078 g/L $CuSO_4$ koşulları optimum olarak belirlenmiştir. Bu yöntem, hem tarımsal atıkların yeniden değerlendirilmesini sağlamakta hem de ekonomik ve çevreci bir üretim yaklaşımı sunmaktadır.

TEŞEKKÜR

Bu çalışma, İstanbul Medeniyet Üniversitesi Biyomühendislik Bölümü bünyesinde gerçekleştirilmiştir. Araştırma süresince desteklerinden dolayı Biyomühendislik Bölümü Lisans Öğrencisi Ayceren KIYAK'a teşekkür ederiz.

KAYNAKLAR

Andersen, M. R. et al. (2009). Systemic analysis of the response of Aspergillus niger to ambient pH. Genome Biology, 10, 1–14.
Apelblat, A. (2014). Properties of citric acid and its solutions. Citric Acid, 13–141.
Ayeni, A. et al. (2019). Production of citric acid from pineapple waste fermentation. The Open Chemical Engineering Journal, 13(1).
Behera, B. C. (2020). Citric acid from Aspergillus niger: a comprehensive overview. Critical Reviews in Microbiology, 46(6), 727–749.
Cano-Lamadrid, M. et al. (2022). From pomegranate byproducts waste to worth: a review of extraction techniques. Foods, 11(17), 2596.
Farajzadeh, M. A., & Nagizadeh, S. (2002). Citric acid determination by dual wavelength spectrophotometry. J. Chinese Chem. Soc., 49(4), 619–624.
Kareem, S. O. et al. (2010). Production of citric acid by Aspergillus niger using pineapple waste. Malaysian J. Microbiology, 6(2), 161–165.
Machado, I., Teixeira, J., & Rodriguez-Couto, S. (2013). Semi-solid state fermentation: a promising alternative for neomycin production.
Naseem Ullah, N. U. et al. (2012). Proximate composition and mineral content of pomegranate peels.
Soccol, C. R. et al. (2006). New perspectives for citric acid production and application. Food Technol. Biotechnol., 44(2), 141–159.
Vandenberghe, L. P., & R. Soccol, C. (1999). Solid-state fermentation for the synthesis of citric acid by Aspergillus niger. *Bioresource Technology*, *74*, 175–178.

ORAL PRESENTATION

Biopreservation with postbiotics: The Potential of microbial metabolites to enhance food safety and extend shelf life

Sarhan Mohammed (*https://orcid.org/0000-0003-2450-7191)* ,
Nilgün Özdemir* (*ORCID: https://orcid.org/0000-0002-4517-9214*)

Ondokuz Mayis University, Engineering Faculty, Food engineering Department, Samsun, Turkey.

*Corresponding author e-mail: nilgun.ozdemir@omu.edu.tr

Abstract

This study was designed to investigate the role of postbiotics—non-viable microbial cells, their components, and metabolites produced during fermentation—in food bio preservation. The aim was to evaluate current findings on the antimicrobial and antioxidant effects of postbiotics and their practical application in extending the shelf life of perishable foods. Researchers typically make postbiotics by cultivating probiotic strains such as Lactobacillus plantarum, L. acidophilus, and Bifidobacterium bifidum in a special broth, followed by treatments such as centrifugation, filtration, and heat to remove viable cells. Cell-free supernatants containing organic acids, bacteriocins, peptides, and enzymes have been applied to a variety of food models, including milk, meat, and plant-based products. In reviewing numerous studies, postbiotics have consistently been shown to reduce microbial spoilage and inhibit common pathogens such as Listeria monocytogenes, Escherichia coli, and Salmonella spp. They also contributed to lipid stability and maintained sensory quality during storage. While the results suggest that postbiotics offer promising natural preservation benefits, their effectiveness depends on the microbial strain, extraction conditions, and food matrix. Overall, postbiotics represent a viable alternative to traditional preservatives, but further research is needed to address their regulatory status and scalability for industrial use

Keywords: postbiotics, lactic acid bacteria, antimicrobial activity, fermentation metabolites, natural preservatives

INTRODUCTION

Microbial biopreservation strategies represent one of the most rapidly evolving fields within modern food safety science. Although traditional food-processing techniques—such as thermal treatment, dehydration, salting, and the use of chemical preservatives—are effective in ensuring microbial stability, they involve considerable limitations regarding sensory quality, nutrient retention, consumer perception, and sustainability. In contrast, the controlled application of microbial cellular components or metabolic products to food matrices, without the presence of viable cells, has gained considerable attention due to its potential to enhance food safety through a “natural, clean-label, thermally stable, and toxicologically safe” approach. This next-generation biopreservation strategy has recently been associated with postbiotics, defined as microbially derived, non-viable molecules that nevertheless exhibit physiological and functional activity (Collins & Stanton, 2021).

Postbiotics comprise a wide range of bioactive compounds, including organic acids, short-chain fatty acids (SCFAs), antimicrobial peptides and bacteriocins, hydrogen peroxide, reactive oxygen species, surface proteins, cell wall fragments, exoenzymes, and exopolysaccharides (EPS). These molecules exert multifaceted functions, ranging from pathogen inhibition and suppression of quorum sensing mechanisms to biofilm disruption and enhancement of oxidative stability. Compared with probiotics, postbiotics possess superior environmental stability, thermal tolerance, longer shelf-life, functional durability during food processing, and lower regulatory risk due to the absence of viable microorganisms (Aguilar-Toalá et al., 2018). Collectively, these attributes position postbiotics as a strategic tool for mitigating food safety risks, controlling spoilage microorganisms, and extending shelf life.

The use of postbiotics in biopreservation is primarily rooted in metabolites produced by lactic acid bacteria (LAB). LAB species are particularly well-suited for postbiotic production due to their natural presence in food ecosystems, GRAS/QPS status, tolerance to low pH, homo- and heterofermentative metabolic flexibility, and high capacity to

produce antimicrobial compounds. Species belonging to the genera Lactobacillus, Leuconostoc, Pediococcus, Lactococcus, and Streptococcus are widely utilized at industrial scale. Bacteriocins synthesized by these microorganisms—such as nisin, pediocin, and plantaricin—display inhibitory activity against both Gram-positive and Gram-negative bacteria, offering effective protection against foodborne and opportunistic pathogens (Silva et al., 2022).

The significance of postbiotic-based biopreservation strategies extends beyond their contribution to microbial safety; they also exert minimal impact on the sensory and technological properties of foods, align with the "chemical preservative-free" product development trend, and meet consumer demand for clean-label ingredients. Consequently, postbiotics are increasingly recognized as effective biopreservatives across a wide range of food categories, including meat products, dairy products, fermented fruits and vegetables, cereal-based foods, and plant-based alternatives. Moreover, integrating postbiotic components into edible films and coatings, active packaging systems, and controlled-release technologies further strengthens their industrial applicability. This multi-layered approach enables the sustained antimicrobial activity of postbiotics over time, supporting shelf-life extension and minimizing food safety hazards.

In summary, the use of postbiotics in biopurification offers a potent biological functionality independent of microbial viability, providing an innovative solution to critical challenges faced by the food industry, such as pathogen control, spoilage management, consumer expectations, and sustainability concerns. This review aims to comprehensively examine the role of postbiotics in enhancing food safety and extending shelf life, their mechanisms of action, application areas, technological integration strategies, regulatory considerations, and future research perspectives.

DEFINITION, CLASSIFICATION AND CHARACTERISTICS OF POSTBIOTICS

The concept of postbiotics is defined as a new generation of terminology that refers to bioactive components of microbial origin that exhibit health or technological functions without the involvement of living microorganisms. The International Scientific Association of Probiotics and Prebiotics (ISAPP) defines postbiotics as "prepared microbially derived biological products that do not contain living cells but are produced by microorganisms or their metabolites and that confer a health benefit on the host" (Salminen et al., 2021). This definition significantly broadens the functional scope of postbiotics, encompassing both physical and morphological cellular components and the end products of microbial metabolism.

Postbiotics are classified into various categories based on structural properties, mode of production, molecular nature, and biological activity. The general classification is as follows: (i) metabolic products, (ii) cellular components, (iii) secreted macromolecules, and (iv) inactive microbial cell preparations (paraprobiotics).

Metabolic Products (Organic and Metabolic Fractions)

The largest group of postbiotics consists of the end products of microbial metabolism. These components are:

- *Organic Acids (lactic acid, acetic acid, propionic acid, etc.):* Lactic acid, synthesized by lactic acid bacteria (LAB), is a powerful bioprotective agent with its ability to lower pH, disrupt membrane potential, and inhibit pathogen growth. Acetic acid, on the other hand, has a strong effect on Gram-negative bacteria by disrupting membrane permeability (Prajapati et al., 2023).

- *Short-Chain Fatty Acids (SCFAs):* SCFAs such as acetate, propionate, and butyrate are important postbiotic molecules that possess both antimicrobial potential and influence redox balance. SCFA production in functional food products is also associated with supporting intestinal health (Mousavi Ghahfarrokhi et al., 2024).

- *Bacteriocins and Antimicrobial Peptides:* Ribosomal protein/peptide-based antibacterial molecules such as nisin, pediocin, plantaricin, and enterocin exhibit high inhibitory capacity, particularly against Gram-positive pathogens such as *Listeria monocytogenes*. Their heat resistance and narrow/targeted spectrum of activity constitute an important subclass of postbiotics. Nisin (*Lactococcus lactis*) is a heat-stable lantibiotic approved by the FDA and EFSA as a food preservative. Pediocin PA-1 (Pediococcus acidilactici) exhibits superior inhibition against *Listeria* spp (Zhao et al., 2025).

- *Hydrogen Peroxide and Reactive Oxygen Species (ROS):* H_2O_2, synthesized by LAB during oxidative metabolism, is a broad-spectrum antimicrobial agent. It is particularly effective in inhibiting yeast and mold (Guerrero-Encinas et al., 2021).

Cellular Components

The second largest group of postbiotics consists of the structural components of the non-viable cells of microorganisms:

- *Peptidoglycan and Cell Wall Fragments:* Peptidoglycan fragments derived from LAB play a role in immune modulation, anti-inflammatory activity, and antimicrobial mechanisms of action Tao et al., (2024).

- *Lipopeptides and Lipoteichoic Acids:* These components are cell membrane components, particularly of Gram-positive species, and support antimicrobial activity in foods. They also contribute to the regulation of the immune response (Balaguer et al., 2022).

- *Surface Proteins and S-Layer Proteins:* S-layers are protein layers that form a crystalline structure on the cell surface. They are effective in adhesion, biofilm interaction, and pathogen exclusion mechanisms.

Exo-Secreted Molecules and Macromolecules

- *Exopolysaccharides (EPS; especially dextran, levan, etc.):* EPSs both improve food technological properties (viscosity, water-holding capacity, gel structure) and provide bioprotection by forming a protective barrier against pathogens.

- *Enzymes and Proteases:* Microbial proteases, lipases, and glycosidases support bioprotection mechanisms and can also affect the textural properties of the food matrix.

- *Heat-Inactivated Microorganism Preparations (Paraprobiotics):* This group consists of microbial fractions that are not alive but exhibit cellular activity. They are increasingly used in industry due to their stability advantage (Danladi et al., 2022).

Key Properties of Postbiotics

The functional properties of postbiotics differ significantly from those of classical probiotics (Thirumdas et al., 2025):

- *Heat and Processing Stability:* Unlike live microorganisms, postbiotics do not lose activity during processes such as pasteurization, UHT, drying, or freezing. Therefore, they are more flexible in industrial applications.

- *Functional Stability Throughout Shelf Life:* Molecules can remain active for extended periods and are resistant to oxidative and mechanical stresses.

- *Safety Profile (GRAS, QPS):* The absence of living cells eliminates risks such as the transmission of antibiotic resistance genes.

- *Mechanism-Specific Activity:* Postbiotics possess versatile mechanisms such as cell membrane damage, inhibition of metabolic pathways, disruption of signaling, and suppression of biofilm formation.

- *Clean-Label Compliance:* This directly aligns with positive consumer perceptions such as "natural preservative" and "microbial-derived."

FOOD SAFETY PRACTICES

The primary advantage of postbiotic ingredients in food safety is their stable and predictable antimicrobial activity, independent of the variable factors of living microorganisms such as survival, proliferation, or susceptibility to environmental stresses. This property is particularly critical for thermally processed, cold-chain-stored, packaged, or minimally processed products. Postbiotics offer a multifaceted contribution to food safety by inactivating foodborne pathogens, suppressing spoilage microorganisms, and preventing toxin formation. In this context, the protection provided by postbiotics occurs through both direct antimicrobial effects and modulation of microbial behavior (Moradi et al., 2020).

Patojen İnhibisyonu

The effectiveness of postbiotics in pathogen control relies on the synergistic effects of different molecular mechanisms. One of the most studied and widely used compounds in industry is nisin, a lantibiotic produced by *Lactococcus lactis*. Nisin inhibits cell wall synthesis by binding to the lipid II molecule in the cell membrane and causes pore formation in the membrane, leading to leakage of cell contents. Thanks to this bidirectional mechanism, nisin exhibits high inhibitory activity against *Listeria monocytogenes*, *Bacillus cereus, Clostridium botulinum* spores, and some Gram-negative bacteria (under conditions with weakened outer membranes). Nisin's stability between 50 and 120°C makes it an ideal postbiotic for pasteurized, UHT, or sterilized products. Therefore, nisin is widely used in liquid eggs, cheese, pasteurized meat products, shelf-stable dairy products, and canned goods.

Control of Spoilage Microorganisms

Postbiotics effectively suppress not only pathogens but also spoilage microorganisms that shorten shelf life. This effect is mediated primarily by organic acids, hydrogen peroxide, SCFAs, and exopolysaccharides (Nikravan et al., 2024). Firstly, the role of organic acids; lactic acid, acetic acid, and other organic acids produced by lactic acid bacteria: (I) limit the reproductive capacity of microorganisms by lowering pH; (II) diffuse into cells in protonated form, disrupting internal pH and leading to metabolic collapse; and (III) suppress yeast and mold growth. Through these mechanisms, postbiotics delay spoilage and increase shelf life in products such as fermented dairy products (ayran, kefir, and plant-fermented beverages), bread, and bakery products (fruit juice and fruit-based beverages). Secondly, the contribution of propionic acid bacteria; propionic acid, produced by Propionibacterium freudenreichii, is one of the most effective natural compounds, particularly in mold inhibition. Therefore, it is frequently used to extend the shelf life of products such as bread and cheese (especially Swiss cheese). Finally, the hydrogen peroxide and ROS effect; LAB-derived H_2O_2 destroys the cell walls of yeast and molds through oxidative damage. This mechanism is particularly effective in products stored at low temperatures.

Suppression of Toxin Production

One of the most critical effects of postbiotic ingredients is the prevention of toxin formation. This effect is mostly mediated through: (I) inhibition of quorum sensing (QS) mechanisms, (II) suppression of virulence gene expression, and (III) modulation of stress response pathways. Quorum Sensing Inhibition: Some small peptides and metabolites contained in postbiotics bind to autoinducer (AHL, AI-2) signals, interrupt signal transmission, prevent the activation of virulence genes, and reduce toxin synthesis. This provides a critical safety advantage, particularly for ready-made meals, protein-based foods, low-acid products, and cold-stored foods (Tomar et al., 2015).

EFFECTS ON SHELF LIFE

The effect of postbiotics on shelf life is not limited to microbial stability; they also play a significant role in improving oxidative stability, tissue preservation, water activity, color stability, and flavor integrity. Some postbiotics play a role in improving oxidative stability. In this mechanism, antioxidant peptides derived from LAB and yeast delay lipid oxidation. This provides a significant shelf life extension, especially in products containing vegetable oils, nut/cereal-based beverages, and products high in polyunsaturated fats. On the other hand, some postbiotics are effective in preserving sensory properties. EPS reduces synergistic liquid separation in yogurt, plant-based yogurts, and fermented beverages by improving texture and viscosity. This ensures a stable product appearance throughout shelf life. As for the other, some postbiotics also contribute to improving microbial stability. Organic acids, bacteriocins, EPS, and lipopeptides contribute to shelf life extension by reducing the microbial load of the product. For example: Nisin and natamycin applications can extend shelf life by up to 40%, especially in fresh meat and meat products.

POSTBIOTIC–PACKAGING TECHNOLOGIES

The integration of postbiotics into active packaging systems is one of the most researched areas of modern biopreservation strategies. The thermal stability, non-volatile nature, and toxicological reliability of postbiotics make them ideal components for active packaging systems (Awad et al., 2025). For example, the use of postbiotics in the production of antimicrobial films and coatings; nisin, pediocin, and organic acids are integrated into biopolymer films (chitosan, gelatin, pectin) to inhibit surface-borne pathogens, maintain their activity at low water activity, and provide long-term microbial stability through controlled release. Furthermore, incorporating

postbiotics into packaging materials via nanoencapsulation or microencapsulation allows the release rate to be adjusted according to ambient humidity or temperature (Gökçe et al., 2024).

TECHNOLOGICAL AND SENSORY IMPACTS

Postbiotics play a critical role in enhancing the technological functionality of food. The key components of this effect are: First, the textural effect; this effect occurs when EPS-producing LAB species (especially *Leuconostoc, L. kefiranofaciens*, and *S. thermophilus*) provide significant advantages in plant-based dairy products by increasing the creaminess and viscosity of the product. Second, the aroma and flavor development effect; this effect occurs when organic acids, esters, and metabolites such as diacetyl create a yogurt-like flavor profile, fermented fruit aroma, and complex volatile compound profiles. Third, the emulsion and gel structure development effect occurs when EPSs increase emulsion stability in oil-water systems.

CONCLUSION

Postbiotics are highly promising ingredients for improving food safety, extending shelf life, maintaining sensory quality, and developing sustainable production strategies. Their lack of viable microorganisms, toxicological safety, thermal stability, and industrial applicability make them superior to traditional preservatives. Their compatibility with clean label practices in the food industry suggests that postbiotics will have widespread use in the future.

REFERENCES

Aguilar-Toalá, J. E., Garcia-Varela, R., Garcia, H. S., Mata-Haro, V., González-Córdova, A. F., Vallejo-Cordoba, B., & Hernández-Mendoza, A. (2018). Postbiotics: An evolving term within the functional foods field. Trends in Food Science & Technology, 75, 1–12.

Awad, N. M., Capozzi, V., Guillard, V., & Goksen, G. (2025). An innovative approach for probiotics and postbiotics-based antimicrobial packaging systems: Design, characterization, and benefit for food application. Current Opinion in Food Science, 101315.

Balaguer, F., Enrique, M., Llopis, S., Barrena, M., Navarro, V., Álvarez, B., ... & Martorell, P. (2022). Lipoteichoic acid from Bifidobacterium animalis subsp. lactis BPL1: a novel postbiotic that reduces fat deposition via IGF-1 pathway. Microbial biotechnology, 15(3), 805-816.

Collins, F., & Stanton, C. (2021). The emergence of postbiotics as functional ingredients: Evidence and applications. Current Opinion in Biotechnology, 70, 1–7.

Danladi, Y., Loh, T. C., Foo, H. L., Akit, H., Md Tamrin, N. A., & Mohammad Naeem, A. (2022). Impact of feeding postbiotics and paraprobiotics produced from Lactiplantibacillus plantarum on colon mucosa microbiota in broiler chickens. Frontiers in veterinary science, 9, 859284.

Gökçe, H. B., & Aslan, İ. (2024). Novel Liposome–Gel Formulations Containing a Next Generation Postbiotic: Characterization, Rheological, Stability, Release Kinetic, and In Vitro Antimicrobial Activity Studies. Gels, 10(11), 746.

Guerrero-Encinas, I., González-González, J. N., Santiago-López, L., Muhlia-Almazán, A., Garcia, H. S., Mazorra-Manzano, M. A., ... & Hernández-Mendoza, A. (2021). Protective effect of Lacticaseibacillus casei CRL 431 postbiotics on mitochondrial function and oxidative status in rats with aflatoxin b1–induced oxidative stress. Probiotics and Antimicrobial Proteins, 13(4), 1033-1043.

Moradi, M., Kousheh, S. A., Almasi, H., Alizadeh, A., Guimarães, J. T., Yılmaz, N., & Lotfi, A. (2020). Postbiotics produced by lactic acid bacteria: The next frontier in food safety. Comprehensive reviews in food science and food safety, 19(6), 3390-3415.

Mousavi Ghahfarrokhi, S. S., Mohamadzadeh, M., Samadi, N., Fazeli, M. R., Khaki, S., Khameneh, B., & Khameneh Bagheri, R. (2024). Management of cardiovascular diseases by short-chain fatty acid postbiotics. Current Nutrition Reports, 13(2), 294-313.

Nikravan, L., Zamanpour, S., & Noori, S. M. A. (2024). Postbiotics: an innovative approach to increase shelf life and quality of foods. Nutrition & Food Science, 54(1), 192-206.

Prajapati, N., Patel, J., Singh, S., Yadav, V. K., Joshi, C., Patani, A., ... & Patel, A. (2023). Postbiotic production: harnessing the power of microbial metabolites for health applications. Frontiers in Microbiology, 14, 1306192.

Tao, B., Li, X., Li, X., Lu, K., Song, K., Mohsen, M., ... & Zhang, C. (2024). Derivatives of postbiotics (cell wall constituents) from Bacillus subtilis (LCBS1) relieve soybean meal-induced enteritis in bullfrog (Aquarana catesbeianus). International Journal of Biological Macromolecules, 279, 135359.

Thirumdas, R., & Mudgil, P. (2025). Emerging Nonthermal Technologies for the Production of Postbiotics. Comprehensive Reviews in Food Science and Food Safety, 24(6), e70335.

Tomar, S. K., Anand, S., Sharma, P., Sangwan, V., & Mandal, S. (2015). Role of probiotics, prebiotics, synbiotics and postbiotics in inhibition of pathogens. The Battle against Microbial Pathogens: Basic Science, Technological Advances and Educational Programs; Méndez-Vilas, A., Ed, 717-732.

Zhao, Y., Yang, B., Xing, G., Wu, Z., Chen, Z., Li, T., & Wu, J. (2025). Antibacterial and Antibiofilm Activities of Postbiotics Produced by Lactobacillus Rhamnosus KC3 Isolated from Camel Milk Against CR-APEC and MRSA, and Their Synergistic Effects with β-Lactam Antibiotics. Probiotics and Antimicrobial Proteins, 1-15.

ORAL PRESENTATION

Effects of different nitrogen sources and potassium doses on plant growth and some quality characteristics in lettuce

Adnan Uğur[1] (*Orcid: https://orcid.org/0000-0001-6015-3146*),
Andaç Kutay Saka[1*] (*Orcid: https://orcid.org/0000-0001-5550-1978*)

[1]Ordu University, Faculty of Agriculture, Department of Horticulture, Ordu, Türkiye.

*Corresponding author e-mail: andacsaka@gmail.com

Abstract

This study examined the effects of different nitrogen resources and potasium doses on growth performance and quality characteristics in greenhouse lettuce cultivation. The study was conducted in a high plastic tunnel belonging to the Horticulture Department at the research and application field of the Faculty of Agriculture, Ordu University. The Toscanas lettuce variety was used in the study. In the study, different nitrogen sources were ammonium sulfate (AS), calcium ammonium nitrate (CAN), and calcium nitrate (CN) and different potassium doses are 0, 2.5, 5, 7.5 and 10 kg/da. Plant height, plant width, SPAD, leaf color characteristics, total water-soluble dry matter content, pH, dry matter content, plant head weight and total yield were determined in the study. Plant heights in the study ranged from 10.0 to 11.5 cm, and it was observed that the highest plant height in CAN nitrogen source and 2.5 kg/da potassium dose. Plant widths in the study ranged from 18.3 to 21.83 cm. The highest head weight of 504.6 g was obtained with CAN nitrogen application at a potassium dose of 7.5 kg/da. The SPAD values in the study ranged from 32.6 to 40.9 cci, the dry matter content ranged from 2.80 to 3.78, and the soluble solid content values ranged from 0.8 to 1.86. The combined application of nitrogen resources and potasium doses was found to be statistically significant ($p < 0.01$) for the characteristics of pH, soluble solid content and colour characteristics (a,b and chroma) examined in lettuce. The study aimed to determine the optimal nitrogen resources and potasium fertilizer doses for lettuce cultivation and to identify effective nitrogen-potasium dose combinations.

Keywords:, Fertilization, lettuce, nitrogen, SPAD, yield

Özet

Bu çalışmada, farklı azot kaynakları ve potasyum dozlarının serada marul yetiştiriciliğinde büyüme performansı ve kalite özellikleri üzerindeki etkileri incelenmiştir. Çalışma, Ordu Üniversitesi Ziraat Fakültesi araştırma ve uygulama sahasındaki Bahçe Bitkileri Bölümü'ne ait yüksek plastik tünelde gerçekleştirilmiştir. Çalışmada Toscanas marul çeşidi kullanılmıştır. Çalışmada farklı azot kaynakları olarak amonyum sülfat (AS), kalsiyum amonyum nitrat (CAN) ve kalsiyum nitrat (CN) ve farklı potasyum dozları olarak 0, 2,5, 5, 7,5 ve 10 kg/da kullanılmıştır. Çalışmada bitki boyu, bitki genişliği, SPAD, yaprak rengi özellikleri, toplam suda çözünür kuru madde içeriği, pH, kuru madde içeriği, bitki baş ağırlığı ve toplam verim belirlenmiştir. Çalışmada bitki boyları 10,0 ile 11,5 cm arasında değişmiş ve en yüksek bitki boyunun CAN azot kaynağı ve 2,5 kg/da potasyum dozunda olduğu gözlemlenmiştir. Çalışmada bitki genişlikleri 18,3 ile 21,83 cm arasında değişmiştir. En yüksek baş ağırlığı 504,6 g, 7,5 kg/da potasyum dozunda CAN azot uygulamasıyla elde edilmiştir. Çalışmada SPAD değerleri 32,6 ile 40,9 cci arasında değişirken, kuru madde içeriği 2,80 ile 3,78 arasında, çözünür katı madde içeriği değerleri ise 0,8 ile 1,86 arasında değişmiştir. Azot kaynakları ve potasyum dozlarının birlikte uygulanmasının, marulda incelenen pH, çözünür katı madde içeriği ve renk özellikleri (a, b ve kroma) için istatistiksel olarak anlamlı olduğu ($p < 0,01$) bulunmuştur. Çalışma, marul yetiştiriciliği için optimal azot kaynakları ve potasyum gübre dozlarını belirlemeyi ve etkili azot-potasyum doz kombinasyonlarını tanımlamayı amaçlamıştır.

Anahtar kelimeler: Azot, gübreleme, marul, SPAD, verim

INTRODUCTION

Lettuce (*Lactuca sativa* L.) is a high-value leafy vegetable belonging to the Asteraceae family and widely consumed worldwide. Due to its low calorie content, high water content, and rich nutritional value, lettuce is particularly preferred for fresh consumption and is an important source of vitamins, minerals, and fiber in human nutrition (Kim et al., 2016). Approximately 28.1 million tons of lettuce are produced annually worldwide, with a significant portion of this production taking place in countries such as China, the United States, and India (FAO, 2023). In Türkiye, lettuce production occupies a strategic position in terms of both domestic consumption and exports. Plant nutrition is one of the most critical factors affecting yield and quality in lettuce cultivation. Nitrogen and potassium are essential macronutrients for lettuce plant development (Hong et al., 2022). Nitrogen, a fundamental component of proteins, chlorophyll, nucleic acids, and many enzymatic structures, plays a role in key metabolic processes that determine plant growth and yield, such as chlorophyll synthesis, protein formation, cell division, and directly affecting photosynthetic capacity. Potassium, on the other hand, is involved in physiological functions such as enzyme activation, osmotic regulation, and photosynthesis (Marschner, 2012; Sublett et al., 2018). Yield and quality parameters in lettuce cultivation are influenced by various environmental and cultural factors. Among these factors, fertilization practices, particularly the balanced use of macro and micro nutrients, are of critical importance. In modern agriculture, optimal nutrient management for sustainable production is essential for both economic efficiency and environmental sustainability. Nitrogen nutrition plays an even more critical role in leafy vegetables, especially lettuce, because the economic product is directly the leaf tissue, and leaf development is highly sensitive to nitrogen levels. The most commonly used nitrogen sources are nitrate (NO_3^-), ammonium (NH_4^+), and urea forms. When plants are fed with a mixture of ammonium and nitrate, they grow better than when fed with either form alone. However, plants generally fail to show optimal growth at high ammonium concentrations or when ammonium is used as the sole nitrogen source (Song et al., 2021). A recent study reported that a 20% ammonium and 80% nitrate ratio (20:80 NH_4^+:NO_3^-) increased lettuce biomass by 138% and provided the highest nitrogen and phosphorus recovery efficiency (Xu et al., 2025). Ammonium toxicity alters various physiological characteristics and biochemical parameters in plants; it causes a decrease in plant growth, yield, and root/shoot ratio, as well as chlorosis in leaves and stunted root development (Song et al., 2021). When ammonium constitutes more than 50% of total nitrogen nutrition, growth and calcium and potassium accumulation are significantly reduced in both lettuce varieties (Weil et al., 2021). Nitrate accumulation is a major food safety issue in leafy vegetables. As the amount of nitrogen fertilizer increases, the total nitrogen concentration in the soil and the nitrate concentration in lettuce increase (Liu et al., 2014). It has been determined that an increase in the NH_4^+ ratio reduces nitrate accumulation in all growing environments, and therefore, adding ammonium to the nutrient solution is recommended to reduce nitrate accumulation (Söylemez, 2021). A significant decrease in nitrate concentrations has been observed as ammonium concentrations increase, especially in the fall (Urlic et al., 2017). Potassium fertilization is of great importance in lettuce cultivation. Within a specific nutrient application range, plant height, stem diameter, yield, vitamin C, and water-soluble sugar concentrations were found to be higher than in unfertilized conditions. Compared to unfertilized conditions, it has been reported that increasing nitrogen, phosphorus, and potassium applications can increase yield by up to 40% (Hong et al., 2022). Furthermore, it has been reported that potassium application in fresh-cut lettuce grown under a 14-hour photoperiod increases water content and soluble solid accumulation, supports antioxidant enzyme activity stability, and reduces decay rates during storage (Wang et al., 2025). The balanced application of nitrogen, phosphorus, and potassium to plants during the cultivation period ensures the highest yield and best post-harvest quality in lettuce. Significant relationships have been observed between lettuce yield and fertilizer application rates, as well as between quality characteristics. While nitrate concentration is directly proportional to the nitrogen fertilization rate, soluble sugar and vitamin C concentrations show a positive correlation with nitrogen and phosphorus application rates (Hong et al., 2022). Yield increased with increasing nitrogen application rate, but post-harvest quality decreased at high nitrogen and phosphorus levels (Hoque et al., 2010). These findings emphasize the importance of balanced fertilization programs. Recent studies have revealed significant interactions between nitrogen and potassium, and that optimizing these two elements together can create synergistic effects on yield and quality. Particularly in greenhouse cultivation and hydroponic systems, where nutrient solutions can be precisely adjusted, researching the effects of different combinations of nitrogen sources and potassium doses has become highly important. The aim of this study is to investigate the effects of different nitrogen sources (nitrate, ammonium, urea) and different potassium doses on yield, plant growth characteristics, and certain quality parameters in lettuce. The results of the study are expected to contribute to the development of sustainable and efficient fertilization strategies in lettuce cultivation. Furthermore, the data

obtained will provide practical recommendations for producers and form a scientific basis for the development of fertilization programs suitable for regional conditions.

MATERIALS AND METHODS

Material

This study was conducted between September 15 and November 25, 2020, in an unheated greenhouse belonging to the Horticulture Department at the Research and Application Field of the Faculty of Agriculture, Ordu University. The Toscanas variety was used as the lettuce variety in the study. The Toscanas lettuce variety is an ideal iceberg lettuce variety for processing and fresh consumption, with slow bolting characteristics in hot weather conditions and a large, uniform head structure. In the study, the plants were grown in balcony-type plastic pots measuring 50x16x18 cm. The seedlings were planted in pots containing garden soil as the growing medium.

Method

After planting the lettuce seedlings, basic fertilization was carried out. N-P-K basic fertilization was applied to the plants in 4 different periods at a rate of 2-4-K kg/da. Triple superphosphate (P_2O_5) was used as the phosphorus source and potassium sulfate (K_2O) fertilizer as the potassium source in basic fertilization. During the four fertilization periods, nitrogen and phosphorus were applied to the plants, and potasium (K_2O) fertilizer was also applied during the first and second fertilization periods. Ammonium sulfate (AS), calcium ammonium nitrate (CAN), and calcium nitrate (CN) fertilizers were used as nitrogen sources in the nitrogen fertilization in the study. Potassium fertilization was also applied to the plants during the basic fertilization periods (1st and 2nd fertilization periods) at doses determined for the experiment (0, 2.5, 5, 7.5, and 10 kg/da). All maintenance procedures from seedling planting to harvest were carried out without exception in the study. The experimental applications in question are presented in Table 1. Seventy days after planting the seedlings, harvesting was performed at soil level using a sickle (Figure 1).

Table 1. Nitrogen sources and potassium doses used in the research

Nitrogen (N) resources	Potasium (K) doses (kg da^{-1})
AS- %21 N CAN- %26 N CN- %15.5 N	0
	2.5
	5.0
	7.5
	10.0



Figure 1. View of lettuce plants ready for harvest

Traits examined in the research

Plant head weight: Harvested lettuce plants were weighed using a scale with a sensitivity of 0.01 g (Radwag, PS600, Poland) and expressed in grams.

Plant height: Plant height was determined in cm by measuring the plants from ground level to the highest point of the plant using a steel tape measure.

Plant width: Plant width was determined by measuring the widest part of the plants from above using a steel ruler in cm.

Chlorophyll index (SPAD): The chlorophyll content index (cci) of lettuce leaves was measured using a SPAD meter (Konica Minolta SPAD-502, Japan) in the early morning hours (Li et al., 2023; Saka, 2023).

Soluble solid content: To determine the soluble solid content, 5 g of homogeneously selected leaf samples were crushed in a hand blender with 10 mL of distilled water, then filtered through a fine sieve and measured with a digital refractometer (Atago PAL-1, USA) and expressed as Brix %. (Demir et al., 2024).

pH: After passing the lettuce leaves through a hand blender and filtering the water, the leaf juice obtained was analyzed using a pH meter (WTW 3110 Set 2 pH Meter, Germany) (Karaçalı, 2009).

% Dry matter content: The intact leaves of the harvested lettuce plants were placed in weighed paper bags, weighed, and their fresh weights were recorded. The same samples were dried in an oven at 72°C for 48 hours. The final dry weights of the completely dried lettuce leaves were weighed, and the % dry matter was calculated based on the fresh weight values, and the % dry weight ratios were determined (Uğur and Saka, 2022).

Color characteristics: For leaf color, the hue° angle value [°h= $\tan^{-1}$ (b/a)] and chroma [C*=[(a^2+b^2)]1/2] were determined using the L* a* b* values obtained by taking 5 measurements each with Konica-Minolta, CR-400 in the CIE system (McGuire, 1992).

Total yield: Yield per decare was expressed in tons based on plant head weight.

Data Evaluation: The study was set up in a randomized block design with three replications. Each pot was considered a replication. The LSD multiple comparison test was used to determine the difference between the averages of nitrogen sources, potassium doses, and nitrogen source*potassium dose interactions. Significant differences between means were determined at the $P<0.05$ significance level. Statistical analyses were performed using JMP software (JMP 13.2, USA).

RESULTS and DISCUSSION

Plant Growth and Yield Parameters

Results regarding plant width, plant height, plant head weight, and total yield are presented in Table 2. Statistical analyses showed that nitrogen sources had a significant effect ($P<0.05$) on plant width, plant head weight, and total yield; however, potassium doses and nitrogen*potassium interaction were found to be statistically insignificant on these parameters. Among nitrogen sources, CAN application generally showed higher values for plant width and created a statistical difference. In terms of plant height, no application factor created a statistically significant difference. CAN application produced the widest plants (20.67-22.17 cm), while AS and CN applications resulted in narrower plants. It has been reported that plant growth is significantly reduced when ammonium sulfate constitutes more than 50% of total nitrogen nutrition (Santos et al., 2013). When total yield and plant head weight were examined, the effect of nitrogen sources on these traits was evident, as in previous studies (Kavak et al., 2003; Çakmak, 2011; Gün, 2019; Uğur et al., 2022). In plots where CAN fertilizer was applied, the highest yield value of 5.05 t ha^{-1} was achieved, especially at a dose of 7.5 kg ha^{-1}, while yield values were observed to be lower (in the range of 3.33-3.98 t ha^{-1}) in AS application. The findings of our study showed that calcium nitrate (CAN) application provided significantly higher head weight and yield compared to ammonium sulfate (AS) and calcium nitrate + ammonium nitrate mixture (CN). In the CAN application, head weights of 502.67 g and 504.67 g were obtained at potassium doses of 5 and 7.5 kg/da, respectively, while the highest value recorded in the AS application was 398.00 g (Table 2). These findings are consistent with studies reporting that calcium nitrate application at a dose of 470 kg/ha provides the best yield in American lettuce (Li et al., 2014; Xu et al., 2025). It has been reported that the percentage of dry matter in leaves decreased with increasing ammonium sulfate rates, with the lowest values occurring in 100% ammonium sulfate applications (Santos et al., 2013). In our study, head weight reached 474.0 g in the CAN application compared to the control group where no fertilizer was applied. In our study, potassium doses did not show significant effects on yield, but the interaction between nitrogen source and potassium dose was found to be particularly decisive on head weight. Similarly, it has been reported that lettuce yield increased by approximately 13.56-22.03%, 15.15-42.42%, and 7.14-10.32%, respectively, with increased nitrogen, phosphorus, and potassium applications compared to unfertilized conditions. Significant quadratic parabolic relationships were observed between lettuce yield and fertilizer application rates, and it was determined that plant height, stem diameter, yield, and quality parameters were higher than under unfertilized conditions within a specific nutrient element application range (Wang et al., 2025). In our study, potassium doses of 5 and 7.5 kg da^{-1} in the CAN source were also found to yield optimal results.

Table 2. Effects of different nitrogen sources and potassium doses on plant width, plant height, plant head weight, and yield

Nitrogen resources	Potasium Doses (kg da^{-1})	Plant width (cm)	Plant height (cm)	Plant head weight (g)	Total yield (t da^{-1})
AS	0	20.17	10.67	332.67	3.33
AS	2.5	21.17	10.00	370.00	3.70
AS	5	19.50	10.50	398.00	3.98
AS	7.5	19.00	10.67	378.67	3.79
AS	10	18.33	10.17	340.67	3.41
CAN	0	21.83	10.50	474.00	4.74
CAN	2.5	22.17	11.50	377.67	3.78
CAN	5	20.67	11.17	502.67	5.03
CAN	7.5	21.83	10.17	504.67	5.05
CAN	10	22.00	10.00	334.00	3.34
CN	0	18.67	10.17	382.67	3.83
CN	2.5	19.33	10.33	463.33	4.63
CN	5	18.33	10.83	432.00	4.32
CN	7.5	19.00	11.17	425.67	4.26
CN	10	19.17	10.83	365.67	3.66
		$LSD_{nitrogen}$: 1.47 $LSD_{potasium}$: n.s. $LSD_{nitrogen*potasium}$: n.s.	$LSD_{nitrogen}$: n.s. $LSD_{potasium}$: n.s. $LSD_{nitrogen*potasium}$: n.s.	$LSD_{nitrogen}$: 55.93 $LSD_{potasium}$: n.s. $LSD_{nitrogen*potasium}$: n.s.	$LSD_{nitrogen}$: 0.559 $LSD_{potasium}$: n.s. $LSD_{nitrogen*potasium}$: n.s.

n.s. :not significant

Quality Traits

The effects of different nitrogen sources and potassium doses on plant quality parameters in lettuce are presented in Table 3. The main effects of both nitrogen sources and potassium doses on SPAD values, which are an indicator of leaf chlorophyll content, were found to be significant. However, the interaction was insignificant. The highest SPAD value was measured at a CAN application rate of 7.5 kg da^{-1}. SPAD values were found to be statistically different among nitrogen sources. SPAD values ranged from 35.83 to 40.9 in CAN application, from 32.60 to 36.87 in AS application, and from 33.47 to 38.93 in CN application. SPAD measurements showed high, positive, and significant linear correlations with leaf nitrogen concentration (R^2=0.90) and chlorophyll concentration (R^2=0.97) (Hong et al., 2022). High SPAD values indicate that CAN application increases nitrogen use efficiency. pH values showed significant differences among nitrogen sources. In the CAN application, pH values were higher, ranging between 5.84 and 5.95. It has been reported that ammonium uptake combined with proton release from the root zone and millimolar ammonium additions cause rapid pH decreases (Liu et al., 2014). Both nitrogen sources and potassium doses affected the soluble solid content.

In the AS application, the soluble solid content increased from 0.87 to 1.87 with increasing potassium doses. A study reported that soluble sugar values showed a positive correlation with nitrogen and phosphorus application rates (Wang et al., 2025). The nitrogen source and nitrogen*potassium interaction were found to have a significant effect on the pH value determined in leaves obtained from lettuce plants. Similarly, nitrogen sources, potassium doses, and their interaction also have statistically significant effects on the soluble solid content.

Table 3. Effects of different nitrogen sources and potassium doses on chlorophyll index, dry matter content, pH, and water-soluble dry matter content

Nitrogen resources	Potasium doses (kg da^{-1})	SPAD (cci)	Dry Matter (%)	pH	Soluble solid content (Brix, %)
AS	0	36.87	3.26	5.73	0.87
AS	2.5	32.93	3.62	5.71	1.53
AS	5	32.60	3.39	5.83	**1.87**
AS	7.5	33.63	3.49	5.82	1.67
AS	10	36.17	3.60	5.84	1.73
CAN	0	40.13	2.93	**5.95**	1.53
CAN	2.5	35.83	3.78	**5.87**	**1.70**
CAN	5	37.10	2.82	5.84	1.63
CAN	7.5	**40.90**	3.02	5.84	1.57
CAN	10	37.70	2.81	5.86	1.67
CN	0	37.33	3.04	5.88	1.53
CN	2.5	33.47	3.03	5.90	1.47
CN	5	38.93	3.39	5.80	1.37
CN	7.5	38.27	2.99	**5.92**	1.60
CN	10	35.33	3.01	5.88	1.47
		$LSD_{nitrogen}$: 1.71 $LSD_{potasium}$: 2.21 $LSD_{nitrogen*potasium}$: n.s.	$LSD_{nitrogen}$: n.s. $LSD_{potasium}$: n.s. $LSD_{nitrogen*potasium}$: n.s.	$LSD_{nitrogen}$: 0.02 $LSD_{potasium}$: n.s. $LSD_{nitrogen*potasium}$: 0.066	$LSD_{nitrogen}$: 0.08 $LSD_{potasium}$: 0.103 $LSD_{nitrogen*potasium}$: 0.179

n.s. :not significant

In particular, the SÇKM value reached high levels of 1.87 at a dose of 5 kg da-1 of AS application. No application was found to have a statistically significant effect on the plant dry matter percentage (%).

Color Characteristics

Findings regarding the effects of different nitrogen sources and potassium doses on color values in lettuce leaves are presented in Table 4.

The effects of potassium doses and nitrogen*potassium interaction on the Chroma value, which indicates color saturation through redness-greenness and yellowness-blueness values, are statistically significant. This highlights the importance of fertilization balance in color formation. The differences created by the applications on the L value, which expresses leaf brightness, and the Hue angle, which expresses color tone, were found to be statistically insignificant. In all applications, Hue values showed a narrow variation between 162.40 and 163.46. It has been reported that green lettuce varieties show higher L* and Chroma values than red lettuce, and that outer leaves have lower (more negative) a* values than inner leaves due to their higher chlorophyll content (Hong et al., 2025).

In our study, a* values were negative, ranging from -14.11 to -16.41 in all applications, indicating that green is the dominant color. It has been stated that hue angle values are related to chlorophyll and anthocyanin levels, and that hue values decrease as anthocyanin levels increase (Hong et al., 2025). In our study, hue angle values ranged between 162.40 and 163.46, and no significant difference was observed between nitrogen sources and potassium doses.

Table 4. Effects of different nitrogen sources and potassium doses on leaf color characteristics

Nitrogen resources	Potasium doses (kg da^{-1})	L	a	b	Chroma	Hue
AS	0	48.67	-16.41	28.27	**32.69**	163.26
AS	2.5	49.11	-14.77	24.79	28.86	162.90
AS	5	47.79	-15.47	26.04	30.29	162.91
AS	7.5	47.72	-15.66	26.22	30.54	162.86
AS	10	45.43	-14.47	25.23	29.08	163.41
CAN	0	48.38	-15.07	25.25	29.41	162.88
CAN	2.5	49.27	-14.86	25.03	29.12	162.93
CAN	5	50.29	-16.31	27.80	32.23	163.10
CAN	7.5	50.06	-15.29	25.72	29.93	162.92
CAN	10	47.55	**-14.11**	23.50	27.42	162.79
CN	0	49.66	-15.53	26.47	30.69	163.11
CN	2.5	49.51	-14.91	25.48	29.53	163.15
CN	5	47.24	-14.66	23.98	28.10	162.54
CN	7.5	47.93	-15.19	24.65	28.96	162.40
CN	10	50.21	-15.14	26.50	30.52	163.46
		$LSD_{nitrogen}$: n.s. $LSD_{potasium}$: n.s. $LSD_{nitrogen*potasium}$: n.s.	$LSD_{nitrogen}$: n.s. $LSD_{potasium}$: 0.48 $LSD_{nitrogen*potasium}$: 0.83	$LSD_{nitrogen}$: n.s. $LSD_{potasium}$: 1.15 $LSD_{nitrogen*potasium}$: 1.99	$LSD_{nitrogen}$: n.s. $LSD_{potasium}$: 1.17 $LSD_{nitrogen*potasium}$: 2.03	$LSD_{nitrogen}$: n.s. $LSD_{potasium}$: n.s. $LSD_{nitrogen*potasium}$: n.s.

n.s. :not significant

CONCLUSION

The findings from the study revealed that nitrogen source is a critical factor in lettuce cultivation and that its combination with potassium doses creates significant interactions. As a result of the study, it was determined that calcium nitrate application combined with medium potassium doses provided the highest lettuce yields. In terms of yield, these findings are consistent with the literature reporting that calcium nitrate application provides optimal yields in lettuce cultivation. It is known from previous studies that plants generally fail to show optimal growth when high ammonium concentrations are used or when ammonium is used as the sole nitrogen source. These findings indicate that calcium nitrate-based nitrogen fertilization is more suitable than ammonium sulfate in lettuce cultivation and that medium potassium doses are necessary for optimal yield. This study aimed to provide practical information to lettuce growers on topics such as selecting the right nitrogen source, optimal potassium dose, balanced plant nutrition, and soil pH management. This research has revealed that combining nitrogen fertilizers in the form of calcium nitrate with potassium doses of 5-7.5 kg da^{-1} is the most suitable strategy for optimal yield and quality in lettuce cultivation. The application of ammonium sulfate is not recommended in terms of yield, quality, and plant development. The findings are consistent with the scientific literature and provide practical applications for producers. For sustainable and efficient lettuce production, it is necessary to develop and disseminate optimized fertilization programs based on scientific data. Furthermore, future studies should investigate nitrate accumulation, the responses of different lettuce varieties to nitrogen sources and potassium doses, the effects of different nitrogen forms on calcium and magnesium uptake, and the cost-benefit analyses of different fertilizer sources. -benefit analyses of different fertilizer sources, the impact of different nitrogen sources on soil and water resources, and the effects of different fertilization practices on post-harvest quality, storage life, and shelf life should be investigated.

REFERENCES

Çakmak, P. 2011. Farklı dikim zamanları ve organik gübrelerin topraksız tarım koşullarında kıvırcık yapraklı salata (*Lactuca sativa* L. var. crispa) yetiştiriciliğinde verim ve kalite özelliklerine etkisi (Yüksek Lisans Tezi). Gaziosmanpaşa Üniversitesi Fen Bilimleri Enstitüsü Bahçe Bitkileri Anabilim Dalı, Tokat, 65s.

Demir, H., Saka, A. K., Uçan, U., Akgün, İ. H., & Yalçı, H. K. (2024). Impact of effective micro-organisms (EM) on the yield, growth and bio-chemical properties of lettuce when applied to soil and leaves. BMC Plant Biology, 24(1), 1189.

FAO, (2023). FAOSTAT statistical database. https://www.fao.org/faostat/en/#data/QCL [28.11.2025]

Gün, A. 2019. Marulda (*Lactuca sativa* L. var. crispa) organik gübrelerin verim ve kaliteye etkisi (Yüksek Lisans Tezi). Ordu Üniversitesi Fen Bilimleri Enstitüsü Bahçe Bitkileri Anabilim Dalı Ordu, 78s.

Hong, J., Xu, F., Chen, G., Huang, X., Wang, S., Du, L., & Ding, G. (2022). Evaluation of the effects of nitrogen, phosphorus, and potassium applications on the growth, yield, and quality of lettuce (Lactuca sativa L.). Agronomy, 12(10), 2477.

Hoque, M. M., Ajwa, H., Othman, M., Smith, R., & Cahn, M. (2010). Yield and postharvest quality of lettuce in response to nitrogen, phosphorus, and potassium fertilizers. HortScience, *45*(10), 1539-1544.

Karaçalı, İ. (2009). Bahçe Ürünlerinin Muhafaza ve Pazarlanması. Ege Üniversitesi, Ziraat Fakültesi Yayınları No: 494, Bornova-İzmir, 502s.

Kavak, S., Bozokalfa, M.K., Uğur, A., Yağmur, B., Eşiyok, D., 2003. Farklı azot kaynaklarının baş salatada (*Lactuca sativa* L. var. *capitata*) verim, kalite ve mineral madde miktarı üzerine etkisi. Ege Üniv Ziraat Fakültesi Dergisi 40(3):33-40.

Kim, M. J., Moon, Y., Tou, J. C., Mou, B., & Waterland, N. L. (2016). Nutritional value, bioactive compounds and health benefits of lettuce (*Lactuca sativa* L.). Journal of Food Composition and Analysis, *49*, 19-34. https://doi.org/10.1016/j.jfca.2016.03.004

Li, F., Yuan, Y., Gong, P., Imazumi, Y., Na, R. & Shimizu, N. (2023). Comparative effects of mineral fertilizer and digestate on growth, antioxidant system, and physiology of lettuce under salt stress. Horticulture, Environment, and Biotechnology, 64(3), 379-391.

Liu, C. W., Sung, Y., Chen, B. C., & Lai, H. Y. (2014). Effects of nitrogen fertilizers on the growth and nitrate content of lettuce (Lactuca sativa L.). *International journal of environmental research and public health*, *11*(4), 4427-4440.

Marschner, P. (2012). Marschner's mineral nutrition of higher plants (3rd ed.). Academic Press.

McGuire, R.G., 1992. Reporting of objective color measurements. Scientia Horrticulturae, 27(12), 1254-1255.

Saka, A.K. (2023). Orta ve Doğu Karadeniz Bölgesinden Toplanan Bazı Yerel Domates Popülasyonlarının Karakterizasyonu ve Biyokimyasal İçeriklerinin Belirlenmesi. Doktora Tezi, Ordu Üniversitesi, Fen Bilimleri Enstitüsü, Ordu, 186 s.

Santos, L., Wright, A. L., Luo, Y., Lu, H., & Odero, D. C. (2013). Nitrogen Cycling and Management for Romaine and Crisphead Lettuce Grown on Organic Soils: SL386/SS588, 9/2013. EDIS, 2013(8).

Song, J., Yang, J., & Jeong, B. R. (2021). Growth, quality, and nitrogen assimilation in response to high ammonium or nitrate supply in cabbage (Brassica campestris L.) and lettuce (Lactuca sativa L.). *Agronomy*, *11*(12), 2556.

Söylemez, S. (2021). The impact of different growth media and ammonium-nitrate ratio on yield and nitrate accumulation in lettuce (Lactuca sativa var. longifolia). *Notulae Botanicae Horti Agrobotanici Cluj-Napoca*, *49*(4), 12540-12540.

Sublett, W. L., Barickman, T. C., & Sams, C. E. (2018). Effects of elevated temperature and potassium on biomass and quality of dark red 'Lollo Rosso'lettuce. Horticulturae, 4(2), 11.

Uğur, A., & Saka, A. K. (2022). Bor ve salisilik asit uygulamalarinin aci ve tatli kil biberde verim, meyve kalitesi ve biyokimyasal içerikler üzerine etkileri. Bahçe, 51(Özel Sayı 1), 286-293.

Uğur, A., Saka, A. K., & Uçan, U. (2022). Marulda Farklı Azot ve Çinko Dozlarının Verim ve Kaliteye Etkileri. Bahçe, 51(Özel Sayı 1), 300-309.

Urlić, B., Jukić Špika, M., Becker, C., Kläring, H. P., Krumbein, A., Goreta Ban, S., & Schwarz, D. (2017). Effect of NO3 and NH4 concentrations in nutrient solution on yield and nitrate concentration in seasonally grown leaf lettuce. *Acta agriculturae scandinavica, section b—soil & plant Science*, *67*(8), 748-757.

Wang, W., Muhmood, M. U. R., Jizhan, L., Wu, S., & Zhao, S. (2025). Synergistic effects of foliar potassium supplementation with photoperiod on storage tolerance and taste of fresh cut lettuce. Frontiers in Plant Science, 16, 1627792.

Weil, S., Barker, A. V., Zandvakili, O. R., & Etemadi, F. (2021). Plant growth and calcium and potassium accumulation in lettuce under different nitrogen regimes of ammonium and nitrate nutrition. *Journal of Plant Nutrition*, *44*(2), 270-281.

Xu, J., Che, G., Yan, J., Luo, Y., Good, A., Yuan, T., ... & Shizumi, K. (2025). Optimizing nitrogen form ratio for enhanced nutrient uptake and lettuce performance in hydroponic systems. *Bioresource Technology Reports*, 102384.

ORAL PRESENTATION

Obtaining free amino acids from raw sheep wool by solvothermal acid hydrolysis in a hydrothermal reactor

Şükrü Acar (*0000-0002-9817-1419)*

SelcukUniversity, Sarayönü Vocational School, Department of Food Technology Sarayönü, Konya, Türkiye

Corresponding author e-mail: sukruacar@gmail.com

Abstract

Sheep wool is a keratin-rich biopolymer that exhibits strong resistance to biochemical degradation due to its high mechanical strength and extensive disulfide crosslinking. In this study, free amino acid recovery from raw sheep wool was systematically investigated via solvothermal acid hydrolysis performed in a hydrothermal reactor. Hydrothermal carbonization was not employed; instead, the reactor was used exclusively as a sealed pressure-resistant vessel to enable acid-mediated hydrolysis under elevated temperature and pressure conditions, used the optimum point of the temperature was also determined. Reaction temperature (140–180 °C), reaction time (120–200 min), acid concentration (3.0–6.0 M), and solid-to-liquid ratio were evaluated as key process parameters. The results revealed that increasing temperature and acid concentration significantly enhanced amino acid yield, whereas excessive reaction severity resulted in partial amino acid degradation. The maximum free amino acid yield was achieved at 160 °C for 180 min using 6.0 M acid concentration and a moderate solid-to-liquid ratio. Overall, the findings demonstrate that solvothermal acid hydrolysis in hydrothermal reactors is an effective and scalable strategy for the valorization of keratin-based waste into high value-added products.

Keywords: Keratin; Sheep wool; Solvothermal hydrolysis; Hydrothermal reactor; Amino acids; Biomass valorization

1. Introduction

The increasing global demand for sustainable chemicals and bio-based building blocks has intensified interest in the valorization of protein-rich agro-industrial wastes within the framework of circular economy and green chemistry principles (Clark & Deswarte, 2015; Sheldon, 2019). Among such wastes, raw sheep wool constitutes a largely underutilized biomass resource, generated in significant quantities by the livestock and textile industries. Despite its high nitrogen content and rich amino acid composition, a substantial fraction of low-grade wool is discarded or incinerated, causing both environmental and economic concerns (Zoccola et al., 2013; Tesfaye et al., 2017).

Sheep wool is primarily composed of keratin, a fibrous structural protein characterized by a highly ordered hierarchical structure stabilized by extensive disulfide cross-links, hydrogen bonds, and hydrophobic interactions (Fraser et al., 1972). These features impart exceptional mechanical strength and chemical resistance to keratin, rendering wool highly recalcitrant to biodegradation and conventional chemical processing (Wang et al., 2016). Consequently, the efficient conversion of native wool keratin into value-added products remains a significant technical challenge.

Free amino acids derived from protein hydrolysis are widely used in food supplements, pharmaceuticals, cosmetics, agriculture (as biostimulants or chelated fertilizers), and fermentation-based industries due to their high bioavailability and functional properties (Kristinsson & Rasco, 2000; Chalamaiah et al., 2018). Conventional amino acid production relies predominantly on microbial fermentation or extraction from edible protein sources, both of which involve high costs, long processing times, and competition with food resources (Ikeda, 2003). Therefore, the recovery of free amino acids from non-food, protein-rich biomass such as waste wool presents an attractive and sustainable alternative.

Several strategies have been investigated for keratin decomposition, including enzymatic hydrolysis, alkaline treatment, oxidative cleavage, and sulfidolysis (Gupta et al., 2012; Yamamoto et al., 2016). Enzymatic methods, although selective, are limited by high enzyme costs, long reaction times, and incomplete hydrolysis due to limited

accessibility of keratin's crystalline regions (Brandelli et al., 2015). Alkaline hydrolysis, on the other hand, often leads to racemization, amino acid degradation (notably cysteine, serine, and threonine), and excessive salt formation, which negatively affects downstream applications (Zhang et al., 2014).

Acid hydrolysis remains one of the most effective approaches for complete protein depolymerization and free amino acid recovery. However, conventional atmospheric acid hydrolysis requires harsh conditions, prolonged reaction times, and substantial acid consumption, raising concerns regarding process efficiency and sustainability (Linder et al., 2018). In recent years, solvothermal and hydrothermal technologies have emerged as powerful tools for biomass conversion, offering enhanced reaction rates, improved mass transfer, and reduced processing times by operating at elevated temperatures and autogenous pressures in closed reactor systems (Titirici et al., 2012; Kruse & Dinjus, 2007).

Hydrothermal reactors enable precise control of temperature, pressure, and reaction media, facilitating the cleavage of peptide bonds and disulfide linkages in keratin under relatively milder chemical conditions compared to traditional methods (Zhang et al., 2020). When combined with acid catalysis, solvothermal hydrolysis can significantly enhance amino acid release while limiting excessive degradation, thus improving overall yield and product quality (Luque et al., 2014). Nevertheless, systematic studies focusing on the direct production of free amino acids from *raw sheep wool*using solvothermal acid hydrolysis remain scarce in the literature.

In this context, the present study aims to investigate the efficient recovery of free amino acids from untreated sheep wool through solvothermal acid hydrolysis conducted in a hydrothermal reactor. The effects of key process parameters, including acid concentration, reaction temperature, and residence time, are systematically evaluated to elucidate their influence on hydrolysis efficiency and amino acid profile. By providing insight into the controlled depolymerization of keratin-rich waste under solvothermal conditions, this work contributes to the development of sustainable protein valorization pathways and supports the transformation of wool waste into high-value biochemical products.

2. Materials and Methods

2.1. Materials

Raw sheep wool was obtained from a local sheep farm (Türkiye) and used as the sole protein source. Prior to hydrolysis, the wool was manually cleaned to remove visible contaminants such as dust and plant residues, followed by washing with deionized water to eliminate surface impurities. The cleaned wool was air-dried at ambient conditions and stored in sealed polyethylene bags until use.

Hydrochloric acid (HCl, 37 wt%) was used as the hydrolyzing agent and obtained from Merck (analytical grade). Deionized water was used for all dilutions and washing steps.

2.1.1. Pretreatment of Raw Wool

To improve the accessibility of keratin fibers and ensure homogeneous hydrolysis, the raw wool was subjected to a physical size reduction step. The dried wool was cut into fibers of approximately 1–3 mm length using stainless-steel scissors (Fig. 1.). No chemical or enzymatic pretreatment was applied in order to evaluate the direct conversion potential of raw wool under solvothermal acid hydrolysis conditions.



Figure 1. Weighing

2.2. Methods

2.2.1. Solvothermal acid hydrolysis procedure

2.2.1.1. Preliminary preparation and cleaning purpose

To remove impurities (dust, sweat, oil, fertilizer residues) from wool (Fig. 2.). Unclean wool reduces productivity and causes undesirable reactions (Fig. 1.).
Entries: Raw, wool, hot water.
Detergent Process: The wool is washed by mixing it with warm water and detergent. Detergent residues are removed by rinsing. The wool is wrung out or centrifuged to dry as much as possible.



Figure 2. Shredded wool

2.2.1.2. Acidic hydrolysis step

Solvothermal acid hydrolysis experiments were conducted in a laboratory-scale Teflon-lined stainless-steel hydrothermal reactor (Fig. 3.) with a total volume of 250 mL. In a typical experiment, 10.0 g of pretreated raw

sheep wool was placed into the reactor vessel, followed by the addition of 100 mL of aqueous hydrochloric acid solution, corresponding to a solid-to-liquid ratio of 1:10 (w/v) (Fig. 5).

The acid solutions were freshly prepared at different molar concentrations (typically 3–6 M HCl) depending on the experimental design (Fig. 6). The reactor was tightly sealed and placed in a temperature-controlled electric oven. Hydrolysis was carried out at temperatures ranging from 140 to 180 °C, under autogenous pressure generated within the closed system. The residence time was varied between 2 and 6 h to evaluate the effect of reaction duration on amino acid release (Fig. 4.).



Figure 3. Reactor



Figure 4. Reactor components

After completion of the reaction, the reactor was allowed to cool naturally to room temperature before opening. The resulting hydrolysate consisted of a dark-colored liquid phase (Fig. 7). containing dissolved amino acids and a minor amount of insoluble residue.



Figure 5. Blend



Figure 6. Hydrolysis

2.2.1.3. Separation and neutralization of hydrolysate

The solid residue was separated from the liquid hydrolysate by vacuum filtration. The filtrate was subsequently neutralized to pH 6.5–7.0 using 1.0 M KOH solution under continuous stirring to prevent localized precipitation or excessive thermal degradation (Fig. 7).
Following neutralization, the solution was centrifuged at 5000 rpm for 10 min to remove any precipitated salts or fine particulates. The clarified, containing free amino acids, was collected and stored at 4 °C prior to further analyses.



Figure 7. Amino acid extract

2.2.1.4. Experimental Design and Process Parameters

To systematically evaluate the efficiency of solvothermal acid hydrolysis, the effects of three main parameters were investigated:

Acid concentration: 3, 4, 5, and 6 M HCl

Reaction temperature: 140, 160, and 180 °C

Reaction time: 2, 3,4, and 6 h

All experiments were performed in duplicate, and the average values are reported to ensure reproducibility.

2.2.1.5. Determination of Free Amino Acids

The total free amino acid content of the hydrolysates was quantified using standard analytical techniques (ör. ninhydrin-based colorimetric assay or HPLC after appropriate derivatization). Prior to analysis, samples were appropriately diluted with deionized water.

2.2.1.6. Calculation of Hydrolysis Yield

The amino acid yield was calculated based on the initial dry mass of wool using the following expression (1):

Amino Acid Yield (%) = Mass of free amino acids obtained x Initial wool mass (g)\times 100 (1)

2.3. HPLC amino acid profile analysis

2.3.1. HPLC analytical conditions

Free amino acid profiles of the hydrolysates were determined using high-performance liquid chromatography (HPLC) following pre-column derivatization with o-phthalaldehyde (OPA), which enables sensitive detection of primary amino acids (Lindroth & Mopper, 1979; Henderson et al., 2000).

Table 1. Chromatographic conditions (HPLC system)

Parameter	Specification
Column	4.6 × 150 mm, 5 µm
Column temperature	40 °C
Mobile phase A	40 mM Na_2HPO_4 buffer, pH 7.8
Mobile phase B	Acetonitrile: Methanol: Water (45:45:10, v/v/v)
Flow rate	1.0 mL·min^{-1}
Injection volume	10 µL
Detector	Fluorescence detector
Excitation / Emission	340 nm / 450 nm

Table 2. Gradient Program

Time (min)	B (%)
0	0
10	20
20	45
30	70
35	100
40	0

This method provides effective separation of keratin-derived amino acids, including sulfur-containing species, with high resolution and reproducibility.

3. Results and discussion

3.1. Amino acid composition of wool hydrolysate

Table 3 presents amino acid profile obtained under optimum hydrolysis conditions (6 M HCl, 160 °C, 4 h).

Table 3. Free amino acid composition of sheep wool hydrolysate

Amino acid	Content (g / 100 g wool)
Glutamic acid	8.4
Aspartic acid	5.1
Glycine	4.8
Proline	3.9
Alanine	3.6
Serine	2.9
Leucine	2.2
Valine	1.8
Tyrosine	1.4
Cysteine	1.1
Total free amino acids	**35.2**

3.2. Effect of process parameters on amino acid yield (HCl/temperature)

The influence of temperature on total amino acid yield (6 M HCl, 3 h) is summarized in Table 4.

Table 4. Effect of temperature on amino acid yield

Temperature (°C)	Yield (%)
140	21.6
160	35.2
180	33.1

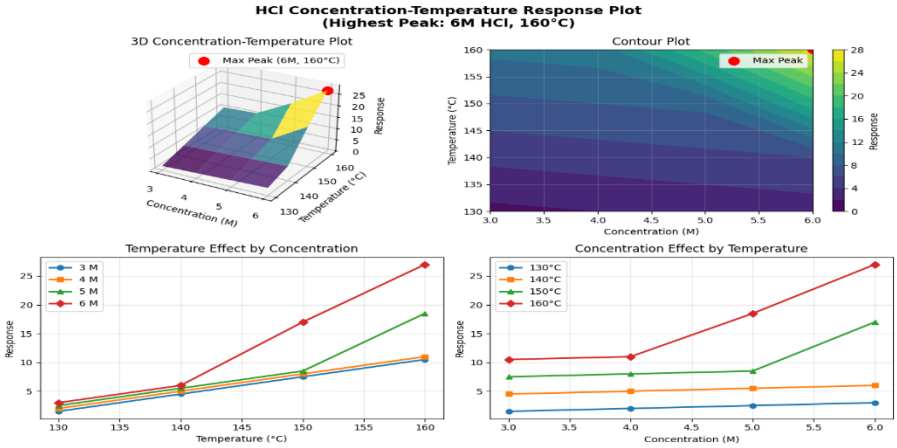


Figure 8: HCl/temperature diagram

4. Discussion:

The predominance of glutamic and aspartic acids is consistent with the known amino acid composition of wool keratin (Fraser et al., 1972). The preservation of cysteine indicates partial survival of sulfur-containing amino acids despite acidic solvothermal conditions, which is notable given their known susceptibility to degradation (Zhang et al., 2014).

A significant increase in yield is observed up to 160 °C due to accelerated peptide bond cleavage. At 180 °C, a slight decrease occurs, attributed to secondary degradation reactions (deamination, decarboxylation).

References

Brandelli, A., Daroit, D. J., & Riffel, A. (2015). Biochemical features of microbial keratinases and their production and applications. *Applied Microbiology and Biotechnology, 99*, 8301– 8317.

Chalamaiah, M., Kumar, B. D., Hemalatha, R., & Jyothirmayi, T. (2018). Fish protein hydrolysates: Proximate composition, amino acid profile, antioxidant properties. *Food Chemistry, 135*, 3020 –3038.

Clark, J. H., & Deswarte, F. E. I. (2015). *Introduction to Chemicals from Biomass* (2nd ed.). Wiley-VCH. Fraser, R. D. B., MacRae, T. P., & Rogers, G. E. (1972). *Keratins: Their Composition, Structure and Biosynthesis*. Charles C. Thomas Publisher.

Gupta, R., Rajput, R., Sharma, R., & Gupta, N. (2012). Biotechnological applications of keratinase enzymes for sustainable development. *Journal of Environmental Management, 93*(1), 48–54.

Henderson, J. W., Ricker, R. D., Bidlingmeyer, B. A., & Woodward, C. (2000). *Rapid, Accurate, Sensitive, and Reproducible HPLC Analysis of Amino Acids*. Agilent Technologies Technical Note.

Ikeda, M. (2003). Amino acid production processes. *Advances in Biochemical Engineering/Biotechnology 79*, 1–35.

Kristinsson, H. G., & Rasco, B. A. (2000). Fish protein hydrolysates: Production, biochemical and functional properties. *Critical Reviews in Food Science and Nutrition, 40*(1), 43–81.

Kruse, A., & Dinjus, E. (2007). Hot compressed water as reaction medium and reactant. *Journal of Supercritical Fluids, 39*(3), 362–380.

Linder, M., Fanni, J., & Parmentier, M. (2018). Protein hydrolysis: Scale-up and optimization challenges. *Biotechnology Advances, 36*(3), 870–882.

Lindroth, P., & Mopper, K. (1979). High performance liquid chromatographic determination of amino acids by precolumn derivatization with OPA. *Analytical Chem., 51*(11), 1667–1674.

Luque, R., Herrero-Davila, L., Campelo, J. M., Clark, J. H., Hidalgo, J. M., Luna, D., & Romero, A. A.(2014). Biofuels: A technological perspective. *Energy & Environ. Sci., 7*, 386401.

Lynam, J. G., Coronella, C. J., Yan, W., Reza, M. T., & Vasquez, V. R. (2015). Humin formation during thermal processing of biomass. *Bioresource Technology, 182*, 301–307.

Sheldon, R. A. (2019). The road to biorenewables: Carbohydrates to commodity chemicals. *ACS Sustainable Chemistry & Engineering, 7*(1), 176–188.

Tesfaye, T., Sithole, B., Ramjugernath, D., & Chunilall, V. (2017). Valorisation of sheep wool as a source of keratin for textile and biomaterial applications. *Waste Management, 68*, 626–635.

Titirici, M. M., White, R. J., Falco, C., & Sevilla, M. (2012). Black perspectives for a green future: Hydrothermal carbons. *Energy & Environmental Science, 5*, 6796–6822.

Wang, K., Wang, B., & Ma, J. (2016). Keratin degradation and extraction from wool: A review. *Waste and Biomass Valorization, 7*, 157–171.

Yamamoto, K., Arai, T., & Kume, S. (2016). Chemical conversion of keratin fibers by alkaline and reductive treatments. *Journal of Applied Polymer Science, 133*(11), 43120.

Zhang, Y., Zhao, W., Yang, R., & Wang, Z. (2014). Effects of acid and alkali hydrolysis on amino acid composition of wool keratin. *Journal of Cleaner Production, 66*, 229–235.

Zhang, B., Fan, T., Liu, C., & Chen, X. (2020). Hydrothermal processing of protein-rich biomass for amino acid recovery. *Bioresource Technology, 307*, 123224.

Zoccola, M., Aluigi, A., & Tonin, C. (2013). Characterisation of keratin biomass from wool and its exploitation in sustainable materials. *Industrial Crops and Products, 44*, 236–245.

ORAL PRESENTATION

Evaluation of antioxidant capacity of *Morus indica* L. leaf extract by DPPH method

Yeşim Özkan[1*] (*Orcid: https://orcid.org/ 0000-0001-8740-1162*)

[*1]Ordu University, Faculty of Arts and Sciences, Molecular Biology and Genetics Department, Ordu, Türkiye.

*Corresponding author e-mail: yozkan52@gmail.com

Abstract

Morus indica L. leaves are rich in phenolic compounds and have been traditionally used as an antioxidant herb. Mulberry leaves are rich in flavonoids, phenolic acids, and especially potent antioxidant compounds such as quercetin, rutin, and chlorogenic acid. These phenolic compounds have important biological effects, such as neutralizing free radicals, chelating metals, and reducing cellular damage caused by oxidative stress. The high phenolic content of mulberry leaf extracts constitutes the fundamental chemical building block supporting the plant's use in traditional medicine for anti-inflammatory and protective purposes. The DPPH method is a common colorimetric antioxidant activity test that rapidly and reliably assesses the free radical scavenging capacity of plant extracts. The DPPH molecule used in the test is a stable, purple-colored free radical. Its color brightens when it reacts with an antioxidant substance, and inhibitory activity is calculated by measuring the decrease in absorbance. This method is considered an important indicator of the antioxidant power of plant extracts because it reflects the ability of phenolic compounds to donate electrons or hydrogen atoms. In this study, the antioxidant capacity of Morus indica L. leaf extract was evaluated at seven different concentrations (0.1-2.0 mg/mL) using the DPPH radical scavenging assay. Compared to the standard antioxidant (ascorbic acid), the IC_{50} value was measured as 0.90 mg/mL. Inhibition ranged from ~52–55% at low concentrations, reaching 67.1% at 1 mg/mL and 75.7% at 2 mg/mL. The positive control achieved 68.9% inhibition, indicating that the antioxidant activity of mulberry leaf was similar to that of the positive control, but its free radical scavenging capacity was moderate. In conclusion, *Morus indica* L. leaf extract demonstrated significant antioxidant activity in vitro, supporting its potential for nutraceutical applications.

Keywords: Antioxidant activity, DPPH, *Morus indica,* mulberry.

INTRODUCTION

Antioxidants are compounds that prevent or reduce cellular and tissue damage caused by oxidative stress resulting from free radicals. They are found both endogenously (glutathione, superoxide dismutase, catalase, etc.) and exogenously (plant-derived phenolics, flavonoids, vitamins) (Teixeira et al., 2005). Plant-based antioxidants hold a significant place in functional food and nutraceutical research due to their natural and safe nature (Rice-Evans et al., 1997). Oxidative stress is an imbalance caused by the accumulation of reactive oxygen species (ROS) and free radicals in cells and tissues (Halliwell & Gutteridge, 2015). This situation leads to damage in DNA, lipids, and proteins, playing a critical role in the aging process and the development of various chronic diseases (cancer, cardiovascular diseases, neurodegenerative diseases) (Pham-Huy et al., 2008). Therefore, the discovery and evaluation of antioxidants derived from natural sources are of great importance, especially in the nutritional, nutraceutical, and pharmaceutical fields. Mulberry a plant species belonging to the Moraceae family, has had its leaves used throughout history as a source of antioxidants in both traditional medicine and functional foods and supplements. Mulberry leaves are rich in flavonoids, phenolic acids, and powerful antioxidant components such as chlorogenic acid, quercetin, rutin, and gallic acid (Polumackanycz et al., 2021). These compounds exhibit biological effects such as neutralizing free radicals, chelating metal ions, and reducing cellular oxidative damage. In particular, phenolic compounds are key determinants of the antioxidant activity of plant extracts due to their capacity to stabilize free radicals by donating electrons or hydrogen atoms (Asif, 2015).

The content of phenolic compounds and flavonoids varies depending on the plant species, growing conditions, harvest time, and extraction method. Because phenolic compounds reflect the ability to neutralize radicals by donating electrons or hydrogen atoms, they are widely used in evaluating the biological potential of plant extracts

(Brand-Williams et al., 1995; Blois, 1958). The DPPH (2,2-diphenyl-1-picrylhydrazyl) radical scavenging test, one of the methods used in measuring antioxidant activities, is a color spectrophotometric method that quickly and reliably evaluates the capacity of plant extracts to neutralize free radicals (Brand-Williams et al., 1995; Blois, 1958). The DPPH radical is a stable, purple-colored free radical that lightens in color upon reaction with antioxidant compounds, and the percentage of inhibition is calculated by measuring the change in absorbance. This method is widely used in determining the antioxidant capacity of plant extracts, particularly because it reflects the ability of phenolic and flavonoid components to stabilize free radicals by donating electrons or hydrogen atoms. In this context, evaluating the antioxidant capacity of mulberry leaf extract using the DPPH method is important both for confirming the results reported in the literature regarding phenolic richness and for identifying the plant as a potential natural antioxidant source. Previous studies have shown that Morus leaves can exhibit strong radical scavenging activity even at low concentrations, depending on their phenolic content and flavonoid diversity, and that the extracts may have significant biological potential even when compared to pure antioxidants (Guo et al., 2023; Cao et al., 2020; Polumackanycz et al., 2021). Therefore, systematically evaluating the DPPH free radical scavenging activity of mulberry leaf extract at different concentrations was determined as a fundamental objective of our study, both to contribute to the literature and to reveal its natural antioxidant potential.

MATERIALS AND METHODS

Preparation of *Morus indica* L. Leaf Extract

Mulberry leaves were obtained fresh from a local herbalist in Ordu province. After the plant material was brought to the laboratory, it was gently washed first with tap water and then with distilled water to remove dust and foreign particles from the leaf surface. The cleaned leaves were dried in the shade at room temperature (22–25°C) for 36 hours, protected from direct sunlight. After the drying process was completed, the leaves were ground in a laboratory-type grinder to obtain a homogeneous powder and stored in airtight containers. For extraction, 2 g of the prepared dried mulberry leaf powder was weighed and added to 20 mL of 80% methanol at a ratio of 1:10 (w/v). The mixture was transferred to an amber-colored glass bottle that did not allow light to pass through and was left to stand at room temperature for approximately 36 hours using the maceration method. During this time, the bottle was shaken manually every 2–3 hours to ensure more effective penetration of the solvent into the plant tissue. At the end of the extraction period, the mixture was first coarsely filtered through cheesecloth to remove solid plant residues, and then passed through Whatman No. 1 filter paper to obtain a clear filtrate. The filtrate was concentrated in a rotary evaporator operating at 40°C under low pressure to remove the solvent. After complete removal of methanol, the resulting crude extract is a viscous solution. This extract was transferred to amber-colored screw-cap tubes and stored at -20°C until use in analyses. The prepared extract was diluted to the target concentration in a suitable solvent (e.g., DMSO or methanol) before use in subsequent biochemical and biological tests.

DPPH Method

The antioxidant capacity of mulberry leaf extract obtained with methanol was evaluated using the 2,2-diphenyl-1-picrylhydrazyl (DPPH) radical scavenging test. The method was optimized with minor modifications based on protocols described by Brand-Williams et al. (1995) and Blois (1958). DPPH radical (Sigma-Aldrich, ≥95% purity) was used. A 0.1 mM DPPH solution was freshly prepared in cold methanol and left in the dark for 30 minutes. The absorbance of the solution was measured at 517 nm in a spectrophotometer. As a positive control, a 1 mg/mL stock solution of ascorbic Acid (L-AA) was prepared in methanol. On the same day as the experiment, the extract was diluted to 7 different concentrations (10, 20, 40, 60, 80, 100, 200 µg/mL). Seven different concentrations (0.1, 0.2, 0.3, 0.4, 0.5, 1, and 2 mg/L) were prepared from the methanol-based extract stock solution. All solutions were prepared in light-proof amber tubes and stored at room temperature throughout the experiment. For each extract or control concentration, 1 mL of extract solution was mixed with 1 mL of DPPH (0.1 mM) solution in amber glass tubes. A negative control (1 mL methanol + 1 mL DPPH) and a blank (1 mL sample solution + 1 mL methanol) solution were prepared. All tubes were incubated in the dark at room temperature (22–25°C) for 30 minutes. This waiting time is considered optimal in the literature in terms of the stability of the DPPH radical and reaction kinetics (Brand-Williams et al., 1995). At the end of the waiting time, the absorbance of all samples was measured at a wavelength of 517 nm using a UV–Vis spectrophotometer. Each measurement was performed in triplicate (n = 3).

Free radical scavenging activity was calculated using the following formula:

$$\text{DPPH Removal Activity (\%)} = \left(\frac{A_{\text{control}} - A_{sample}}{A_{\text{sample}}}\right) \times 100$$

A_"control" = absorbance of the solution containing only DPPH
A_"sample" = absorbance of the extract + DPPH mixture (sample color corrected)

Determination of IC_{50} Value

The obtained percentage radical scavenging values were plotted against concentration. The point at which the concentration corresponds to 50% inhibition was determined as IC_{50}. IC_{50} calculation was performed using linear regression from the dose-response curve. The antioxidant power of Morus indica leaf was evaluated by comparing the IC_{50} value with the positive control (ascorbic acid).

RESULTS and DISCUSSION

In figure 1, The DPPH free radical scavenging capacities of mulberry leaf extract and ascorbic acid were evaluated in the concentration range of 0.1–2 µg/mL. Both samples showed increasing radical scavenging activity with increasing concentration. At the lowest concentration of 0.1 µg/mL, ascorbic acid showed 49% inhibition, while the extract showed 52% inhibition. It is noteworthy that the extract showed higher activity than ascorbic acid at a lower concentration. This suggests that different phenolic or flavonoid components in the extract may be more effective at lower concentrations. When the concentration was increased to 0.2 µg/mL, the inhibition of ascorbic acid reached 52%, and the inhibition of the extract reached 54%, showing a similar increase. At 0.3 µg/mL, ascorbic acid increased to 57%, while the extract showed 59% inhibition. The fact that the extract exhibited slightly higher activity than ascorbic acid in the low concentration range suggests that the extract contains compounds that can be effective independently of concentration. At higher concentrations (0.4–2 µg/mL), the difference between ascorbic acid and the extract became more pronounced. Ascorbic acid achieved 66% inhibition at 0.4 µg/mL, 70% at 0.5 µg/mL, 81% at 1 µg/mL, and 94% at 2 µg/mL. In contrast, mulberry extract showed inhibition of 61%, 63%, 68%, and 77%, respectively. Although both test substances showed a linear increase trend as the concentration increased, ascorbic acid showed stronger antioxidant activity at all high concentrations. Nevertheless, the 77% inhibition capacity of the extract indicates that the leaf extract has a strong radical scavenging potential. Overall, the data indicate that the antioxidant activity of mulberry extract increases in a concentration-dependent manner, showing activity close to or slightly higher than ascorbic acid at low concentrations, while at high concentrations, as expected, ascorbic acid exhibits stronger activity. These findings demonstrate that the extract possesses a distinct antioxidant profile.

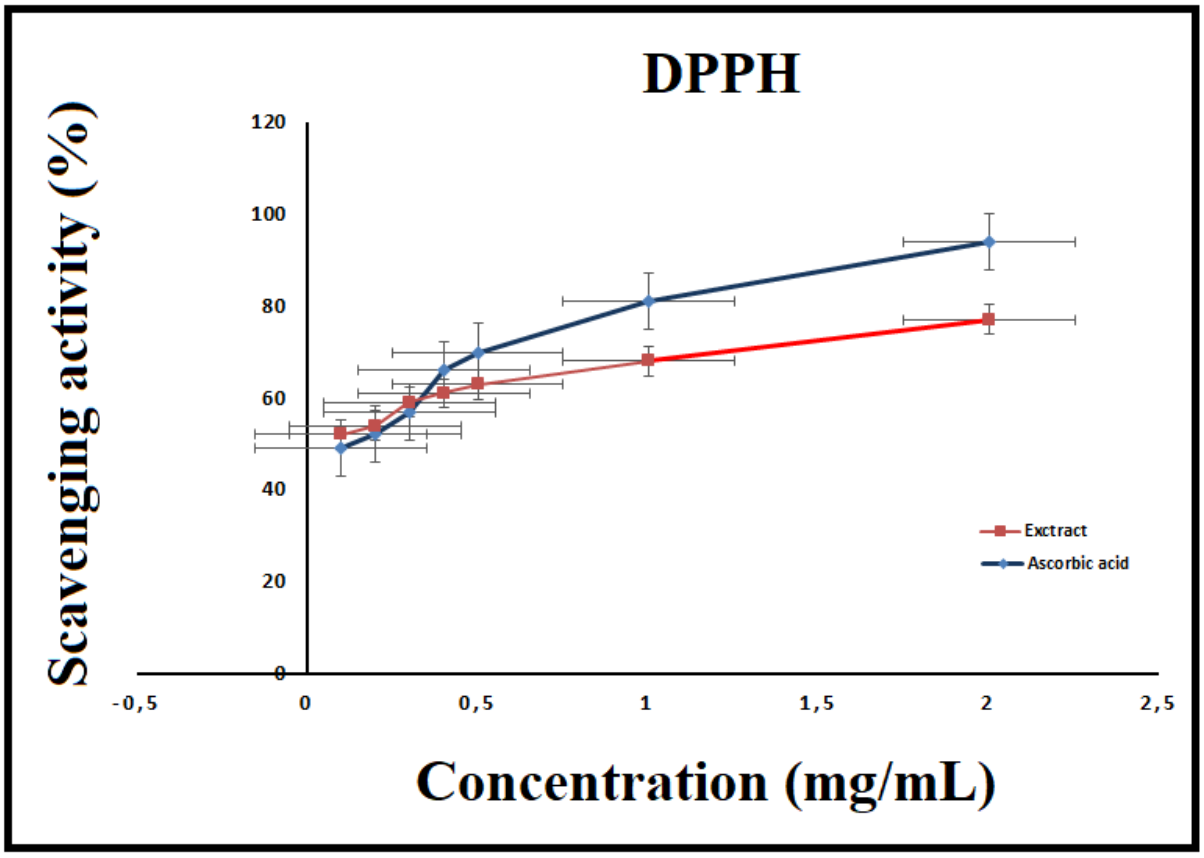


Figure 1. DPPH free radical scavenging activity of *Morus indica* L. Leaf extract and of ascorbic acid. Values are the average of triplicate experiments.

In this study, the DPPH free radical scavenging activity of mulberry leaf extract was evaluated, and the results revealed a strong natural antioxidant potential. The data show that the extract exhibited significant and concentration-dependent inhibition in the concentration range of 0.1–2 µg/mL, reaching 77% at the highest concentration. These findings are consistent with previous studies reporting that Morus species have high antioxidant capacity due to phenolic compounds. Guo et al. (2023) reported significant antioxidant activity and high inhibition values in DPPH in Morus leaves obtained from different harvest periods, depending on the diversity of phenolic compounds. The high activity in our study supports the idea that Morus indica leaves possess similar phytochemical richness.

It is noteworthy that the extract showed higher inhibition than ascorbic acid in the low concentration range (0.1–0.3 µg/mL). Similarly, another study reported that *Morus alba* leaf extract showed comparable or higher activity than standard antioxidants at some low concentrations (Margaria et al., 2013). This suggests that the leaf extract contains components such as flavonoids, anthocyanins, rutin, catechins, and phenolic acids, which may be more effective at low concentrations. There is evidence that these compounds in plant extracts increase radical scavenging capacity through synergistic interaction (Cao et al., 2020). This synergistic effect explains why extracts with a multi-component structure, unlike pure ascorbic acid, can generate a strong antioxidant response even at low concentrations.

The fact that ascorbic acid (94%) showed stronger activity than the extract (77%) at high concentrations confirms the relationship between antioxidant power and molecular structure. Ascorbic acid is a single-molecule, pure, and potent reducing agent. However, mulberry leaf extracts consist of a complex phenolic/flavonoid mixture, and therefore their maximum activity values may not be as high as those of pure antioxidants. Nevertheless, the literature has extensively shown that mulberry leaves have high potential in terms of phenolic compounds,

flavonoids, and antioxidant activity. For example, *Morus nigra* and *Morus alba* leaves have been reported to contain significant amounts of chlorogenic acid, quercetin, rutin, and gallic acid, and these compounds have shown high activity in DPPH, ABTS, and FRAP tests (Polumackanycz et al., 2021). Therefore, the strong inhibition rates in our study demonstrate that leaf phenolics make a significant contribution to antioxidant activity.

Furthermore, it is known that antioxidant capacity can vary significantly depending on the plant species, growing conditions, and extraction method. Guo et al. (2023) emphasized that environmental factors affect the phenolic profile in Morus species, while Cao et al. showed in their study that bioactive compounds in the leaf extract are one of the key factors driving antioxidant capacity (Cao et al., 2020). In this context, the concentration-dependent increase observed in our study is thought to be due to the unique phytochemical composition of mulberry leaf. Overall, the obtained data show that mulberry leaf extract, especially with its strong radical scavenging capacity in the medium-high concentration range, can be evaluated as a natural antioxidant source in food, cosmetic, and pharmaceutical applications. Similar to the literature on the antioxidant activities of Morus species, the results of this study provide an important basis for suggesting that the leaf extract may exhibit a protective effect against oxidative stress in biological systems. However, confirmation of the chemical profiling of phenolic and flavonoid components using LC-MS/MS or HPLC techniques, as well as determination of the biological effect through cell culture and in vivo experiments, should be the focus of future studies.

CONCLUSION

This study revealed that mulberry (*Morus indica* L.) leaf extract exhibits a significant level of antioxidant capacity, evaluated using the DPPH free radical scavenging method. Within the concentration range used in the study (0.1–2 mg/mL), the radical scavenging activity of the extract increased significantly with increasing concentration, and at certain concentrations, it showed values close to or exceeding those of ascorbic acid. The fact that the extract exhibited higher inhibition than ascorbic acid, particularly at low concentrations, suggests that the leaf extract is rich in phenolic compounds and potentially contains powerful bioactive substances. While ascorbic acid showed a stronger radical scavenging effect at high concentrations, as expected, the inhibition capacity of Morus indica L. extract, reaching 77%, indicates that it could be a significant natural antioxidant source. This performance is consistent with findings presented in the literature regarding the breadth of phenolic profiles of mulberry leaves and fruits. Therefore, mulberry leaf extract stands out as both a potential alternative to synthetic antioxidants and a complementary antioxidant candidate of natural origin. These results provide important preliminary data on the usability of mulberry leaves as a natural antioxidant component in the food, cosmetic, nutraceutical, and pharmaceutical sectors. However, further advanced chemical characterization studies, such as total phenolic content, flavonoid profile, and HPLC or LC-MS/MS analyses, are needed to gain a more detailed understanding of the extract's antioxidant mechanism. Furthermore, investigating the effects of the extract on oxidative stress in *in vitro* cellular models and in vivo biological systems will be an important step in confirming its biological activity. Overall, this study has shown that mulberry leaf extract is a potent and viable natural antioxidant candidate, and it is believed that this potential will be further revealed through comprehensive phytochemical and biological evaluations in the future.

ACKNOWLEDGEMENTS

I wish to express my deepest and sincere gratitude to my late father, Murat ÖZKAN, for his unwavering dedication, guidance, and support to his children. His encouragement has profoundly influenced my personal and professional journey and continues to serve as a lasting inspiration. May he rest in peace.

REFERENCES

Asif, M. (2015). Chemistry and antioxidant activity of plants containing some phenolic compounds. Chemistry international, 1(1), 35-52.

Blois, M. S. (1958). Antioxidant determinations by the use of a stable free radical. Nature, 181(4617), 1199-1200.

Brand-Williams, W. (1999). Use of a free radical method to evaluate antioxidant activity. Food Sci. Technol., *28*, 1231-1237.

Brand-Williams, W., Cuvelier, M. E., & Berset, C. (1995). *Use of a free radical method to evaluate antioxidant activity.* LWT - Food Science and Technology, 28(1), 25–30. https://doi.org/10.1016/S0023-6438(95)80008-5

Cao, X., Yang, L., Xue, Q., Yao, F., Sun, J., Yang, F., & Liu, Y. (2020). Antioxidant evaluation-guided chemical profiling and structure-activity analysis of leaf extracts from five trees in Broussonetia and Morus (Moraceae). Scientific reports, *10*(1), 4808.

Guo, Z., Lai, J., Wu, Y., Fang, S., & Liang, X. (2023). Investigation on antioxidant activity and different metabolites of mulberry (Morus spp.) leaves depending on the harvest months by UPLC–Q-TOF-MS with multivariate tools. Molecules, 28(4), 1947.

Halliwell, B., ve Gutteridge, J. M. C. (2015). Free radicals in biology and medicine (5th ed.). Oxford University Press.

Ham-huy L.A., He H., Pham-huy C., 2008 - Free radicals, antioxidants in disease and health. International Journal of Biomedical Science 4(2), 89-96.

Margaria, P., Abbà, S., & Palmano, S. (2013). Novel aspects of grapevine response to phytoplasma infection investigated by a proteomic and phospho-proteomic approach with data integration into functional networks. BMC genomics, 14(1), 38.

Polumackanycz, M., Wesolowski, M., & Viapiana, A. (2021). *Morus alba* L. and *Morus nigra* L. leaves as a promising food source of phenolic compounds with antioxidant activity. Plant Foods for Human Nutrition, 76(4), 458-465.

Rice-Evans, C., Miller, N., & Paganga, G. (1997). Antioxidant properties of phenolic compounds. Trends in plant science, 2(4), 152-159.

Teixeira, S., Siquet, C., Alves, C., Boal, I., Marques, M. P., Borges, F., ... & Reis, S. (2005). Structure–property studies on the antioxidant activity of flavonoids present in diet. Free Radical Biology and Medicine, 39(8), 1099-1108.

ORAL PRESENTATION

Effect of artichoke (*Cynara scolymus* L.) leaf extract on *Caenorhabditis elegans* population growth

Yeşim Özkan[1*] (*ORCID: https://orcid.org/0000-0001-8740-1162*),
Ayşenur Çelik[2] (*ORCID: https://orcid.org/ 0000-0001-8533-7101*)

[1]Ordu University, Faculty of Arts and Sciences, Molecular Biology and Genetics Department, Ordu, Türkiye.

*Corresponding author e-mail: yozkan52@gmail.com

Abstract

Artichoke (*Cynara scolymus* L.) leaves are rich in flavonoids, phenolic acids, lignans, and other polyphenolic compounds, and numerous *in vitro* studies have demonstrated potent antioxidant and free radical scavenging properties. This study was conducted to evaluate the effects of *Cynara scolymus* leaf extract on population growth and life performance in *Caenorhabditis elegans* (*C. elegans*). Extract groups exposed at different concentrations (0.5, 1, and 2 mg/mL) were compared with the control group. A population increase of 1900% was calculated in the control group. A population increase of 1500% was determined in the low-dose extract group (0.5 mg/mL); this result indicated that the low dose partially reduced reproduction but did not significantly affect life performance. At the medium dose (1 mg/mL), population growth decreased by 900%. The highest dose (2 mg/mL) showed a significant toxic effect, with population growth decreasing by 100%. These findings suggest that artichoke leaf extract is relatively well tolerated at low doses, but higher concentrations produce strong growth suppressive and toxic effects on *C. elegans*. The results indicated that the biological activity of phenolic compounds in artichoke leaves varies dose-dependently and at high levels may negatively affect reproductive capacity and population dynamics.

Keywords: Artichoke, *Caenorhabditis elegans*, *Cynara scolymus*.

INTRODUCTION

Cynara scolymus L. (artichoke) is a perennial plant belonging to the Asteraceae family and has long been widely used in traditional medicine, especially in the Mediterranean basin, for its liver-protective, digestive-regulating, and bile-flow-enhancing properties. The increasing interest in the biological activity of artichoke leaf extracts in recent years stems from the plant's rich phytochemical secondary metabolite content. Artichoke leaves are particularly rich in phenolic acids, flavonoids, secoiterpene lactones, inulin, and various volatile compounds. Among these compounds, chlorogenic acid, cynarin (1,5-dicapheoylquinic acid), luteolin, and apigenin derivatives are considered key determinants of the pharmacological effects of artichoke leaves (Lattanzio et al., 2009; Gonçalves, 2018).

Phenolic compounds and flavonoids stand out with their strong antioxidant and free radical scavenging properties; thus, they exhibit a potential protective effect against oxidative stress-based diseases. Artichoke leaf extracts have been shown in various *in vitro* and *in vivo* studies to suppress lipid peroxidation, increase glutathione levels, and protect liver cells against toxic agents (El Morsy & Kamel, 2015; Zapolska-Downar et al., 2002). In addition, the choleretic and hepatoprotective properties of cynarin and its derivatives are consistent with the traditional use of the plant and are among the main reasons why artichoke leaf is preferred in herbal medicine as a regulator of liver function (Wagner et al., 1982).

Artichoke leaves are also increasingly being studied in scientific research due to their significant anti-inflammatory, hypolipidemic, antimicrobial, and anticancer effects. Flavonoids such as luteolin and apigenin reduce pro-inflammatory cytokine production by suppressing inflammation-related cellular signaling pathways like NF-κB, thus contributing to the anti-inflammatory effect of artichoke (Park & Song, 2013). In addition, artichoke leaf extracts have been reported to reduce LDL oxidation and exhibit an inhibitory effect on the HMG-CoA reductase

enzyme involved in cholesterol biosynthesis (Gonçalves, 2018). These findings make artichoke leaves an important natural agent in terms of metabolic diseases and cardiovascular risk factors. In recent years, the effects of artichoke leaf components on aging biology, oxidative stress resistance, mitochondrial function, and cellular protection mechanisms have also begun to be investigated in model organisms (e.g., *Caenorhabditis elegans*). Polyphenolic fractions have been shown to enhance stress tolerance, particularly by regulating antioxidant defense genes (sod-3, gst-4, etc.) (Kittimongkolsuk, 2020).

In this context, artichoke leaf has gained a significant place in modern pharmacology, natural product research, and functional food development studies due to its rich phytochemical content and multifaceted biological activities. Increasing evidence in the literature shows that artichoke leaf extracts have broad therapeutic potential through antioxidant and cell-protective mechanisms.

C. elegans is considered an ideal model organism for the rapid and reliable study of *in vivo* biological effects due to its short life cycle (approximately 2-3 weeks), genetically well-characterized structure, transparent body, and high reproductive capacity (Brenner, 1974; Kim et al., 2017). Evaluating the effect of herbal extracts or natural products on population growth allows for holistic observation of the organism's potential effects on overall health, reproductive capacity, and lifespan. Population growth experiments are critical in determining the effects of sublethal or low-dose herbal extracts on toxicity, fertility, and embryonic development (Ha et al., 2016). Reproductive and population dynamics in *C. elegans* are closely related to nutrient intake, metabolic status, and cellular stress responses. Therefore, the antioxidant, adaptogenic, or cellular protective properties of an extract can indirectly demonstrate biological benefit by positively influencing population growth (Lithgow & Walker, 2002). Furthermore, since the cellular and molecular response mechanisms of *C. elegans* are largely conserved with human homologs, observations on population growth are also valuable in predicting the potential effects of herbal extracts on human health (Kaletta & Hengartner, 2006). This approach allows for the systematic and rapid assessment of biological effects, particularly antioxidant capacities, potential to slow aging processes, and increased stress tolerance (Jeon & Cha, 2016). In conclusion, *C. elegans* population growth assays offer a robust, low-cost, and ethically sound method for comprehensively evaluating both the biosafety and pharmacological efficacy of plant extracts.

MATERIALS AND METHODS

Preparation of *Cynara scolymus* L. Leaf Extract

Artichoke leaves (*Cynara scolymus* L.) were obtained fresh from a local herbalist in Ordu province. After the plant material was brought to the laboratory, it was gently washed first with tap water and then with distilled water to remove dust and foreign particles from the leaf surface. The cleaned leaves were dried in the shade at room temperature (22–25°C) for 36 h, protected from direct sunlight. After the drying process was completed, the leaves were ground in a laboratory-type grinder to obtain a homogeneous powder and stored in airtight containers. For extraction, 2.5 g of the prepared artichoke leaf powder was weighed and added to 25 mL of 80% methanol at a ratio of 1:10 (w/v). The mixture was transferred to an amber-colored glass bottle that did not allow light to pass through and left to macerate at room temperature for approximately 36 hours. During this period, the bottle was manually shaken every 2–3 hours to ensure more effective penetration of the solvent into the plant tissue. At the end of the extraction period, the mixture was first coarsely filtered through cheesecloth to remove solid plant residues, and then passed through Whatman No. 1 filter paper to obtain a clear filtrate. The filtrate was concentrated in a rotary evaporator operating at 40°C under low pressure to remove the solvent. After complete removal of methanol, the resulting crude extract is a viscous solution. This extract was transferred to amber-colored screw-cap tubes and stored at -20°C until use in analyses. The prepared extract was diluted to the target concentration in a suitable solvent (e.g., DMSO or methanol) before being used in subsequent biochemical and biological tests.

C. elegans culture

In this study, the N2 wild-type strain of *C. elegans* was used. Nematodes were maintained on Nematode Growth Medium (NGM) and fed with *Escherichia coli* OP50 under standard culture conditions at a constant temperature of 20 °C. Synchronized populations were generated by washing NGM plates containing predominantly gravid adults. To obtain synchronized nematodes, adult worms were treated with a bleaching solution (1 N NaOH and 5% sodium hypochlorite) and gently vortexed every 2 minutes over a total period of 10 minutes. The solution was then centrifuged, and the supernatant containing lysed worm debris was removed, leaving behind an egg pellet. The egg

pellet was washed three times and resuspended in M9 buffer. Eggs were incubated with gentle agitation for approximately 12 hours to hatch and establish a synchronized population. Larvae at the L3–L4 stage were subsequently used for all experimental assays.

Acute Toxicity / LC_{50} Determination

The acute toxicity test was performed to determine sublethal concentrations. For the population growth experiment, the acute toxicity of artichoke leaf extract was first determined by exposure for 24, 48, and 72 hours. Synchronized L4 larvae were incubated at different concentrations for 24–72 hours. Three replicates were performed for each concentration. 80% methanol was used as the solvent control, and only M9 buffer + OP50 was used as the negative control. Live/dead nematode counts were performed at the end of the exposure time. LC_{50} was calculated by probit analysis. For sublethal concentrations, concentrations of LC_{10}–LC_{20} (0–10%) that cause mortality without significant non-mortality side effects on reproduction and growth were preferred.

Population growth assay

To evaluate the effect of artichoke leaf extract after exposure at sublethal concentration, the growth of *C. elegans* population was assessed (Dhawan et al., 1999). Age-synchronized L4 stage nematodes were transferred to 24-well NGM (Nematode Growth Medium) plates at a density of 20 nematodes per well (Corsi et al., 2015). *E. coli* OP50 was used as the food source. All plates containing the experimental and control groups were incubated at 20 ± 1°C for 5 days. On day 5, the total number of live individuals in each well, including parent nematodes, larvae, and offspring, was counted under a stereomicroscope. Nematodes from each well were collected into 2 mL of M9 buffer, homogenized carefully, and 5 µL aliquots were taken for counting under a stereomicroscope. Counts were performed separately for each group, and the average across three replicates was calculated. All measurements were conducted on the same day by the same investigator to minimize variability. Population growth was expressed relative to the initial number of nematodes using the following formula (Zhang et al., 2018):

$$\text{Population Increase (\%)} = \frac{\text{Observed live nematodes} - \text{Initial nematodes}}{\text{Initial nematodes}} \times 100$$

RESULTS AND DISCUSSION

Caenorhabditis elegans, with its short life cycle and high reproductive capacity, is an ideal model organism for evaluating the biological effects of plant extracts (Brenner, 1974; Kim et al., 2017). The effects of plant extracts on the growth rate of nematode populations are important in revealing both the overall health status of the organism and the potential biological activities of the extracts (Hu et al., 2016). *Cynara scolymus* L. leaves exhibit antioxidant, hepatoprotective, and metabolic regulatory effects thanks to their rich phenolic and flavonoid content (Lattanzio et al., 2009; Olas 2024). It has been reported in the literature that artichoke leaf extracts can positively affect the growth and reproductive capacity of organisms by combating oxidative stress at the cellular level (El-Boshy et al., 2017; Zapolska-Downar et al., 2002). In this context, our study investigated the effects of artichoke leaf extract on *C. elegans* population growth (Fig.1).

In our study, the effect of different sublethal concentrations of artichoke leaf extracts on the population growth of C. elegans was evaluated. While population growth was observed to be 1900% in the control group, a significant decrease in population growth was recorded with increasing concentration in the extract-treated groups. Growth was measured as 1500% in the group treated with 0.5 mg/ml, 900% in the 1 mg/ml group, and 100% in the 2 mg/ml group. The data obtained show that artichoke leaf extract can inhibit *C. elegans* reproduction and population growth depending on the concentration.

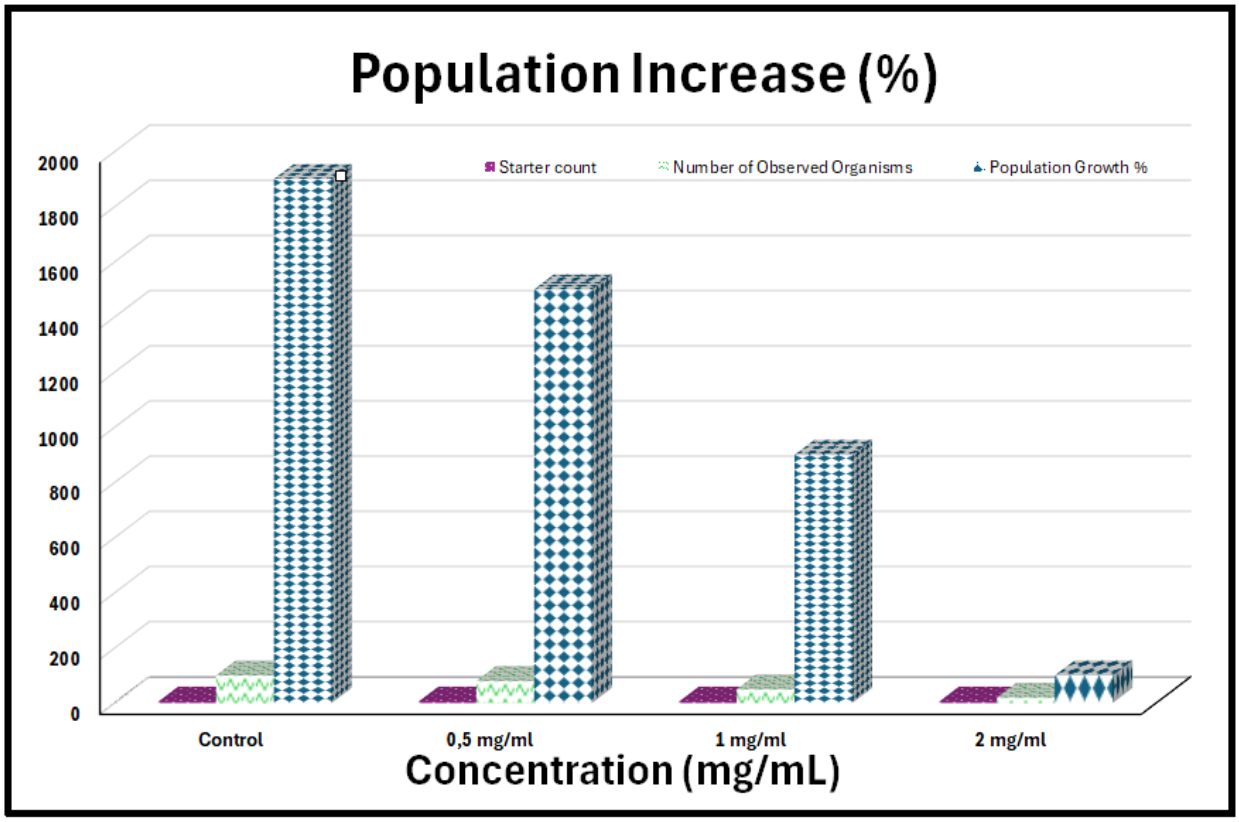


Figure 1. Effects of sublethal concentrations of *Cynara scolymus* leaf extract on the growth of *C. elegans* populations.

This findings suggests that the biological activity of artichoke leaf extract is related to its phenolic and flavonoid compounds. Literature reports that artichoke leaf extracts contain components such as chlorogenic acid, cynarin, and luteolin, and that these components can exhibit antioxidant, antiproliferative, and metabolic regulatory effects. These compounds can affect the growth and reproductive capacity of organisms by modulating the oxidative stress response at the cellular level (Gebhardt & Fausel, 1997.; Lattanzio et al., 2009). The population growth inhibition observed, particularly at high concentrations (100% growth, 2 mg/ml), is likely related to sublethal stress and cellular metabolic repression mechanisms. Similarly, the inhibitory effects of plant extracts on *C. elegans* reproduction have been supported by previous studies. For example, Ha et al. (2022) reported that sublethal concentrations of different plant extracts showed a significant suppressive effect on the *C. elegans* life cycle; This effect was particularly observed in larval development and reproductive capacity. Similarly, Jeon and Cha (2016) showed that certain pharmacological compounds can negatively affect the reproduction and generation time of *C. elegans*. These findings reveal that various natural and synthetic compounds have the potential to inhibit population growth in nematodes, and the observed mechanism of action may occur through both developmental and reproductive processes. The partial population increase observed in the 0.5 mg/ml and 1 mg/ml groups suggests that low-dose artichoke extract may reflect adaptogen-like effects that increase the organism's stress tolerance. In the literatures, it has been reported that low-dose phenolic compounds support reproduction and growth in *C. elegans* by increasing antioxidant gene expression (Vasconcellos et al., 2024). However, as the concentration increases, a significant decrease in population growth is observed as a result of the suppression of cellular metabolism by the extract components. This situation reveals the dose-dependent biphasic effect of artichoke leaf extract. Studies in the literature on the effects of phenolic compounds on *C. elegans* demonstrate the existence of dose-dependent responses. Many plant polyphenols, at low doses, promote stress resistance, reproduction, and growth by increasing antioxidant gene expression, while at high doses they can have negative effects by suppressing cell metabolism. This type of biphasic behavior is described as similar to hormesis interactions, where stimulatory effects are observed at low doses and inhibitory effects at high doses. For example, a recent study reported that plant polyphenols showed dose-dependent effects on *C. elegans* at different concentrations, and that nematode

survival decreased at high doses. In this study, increasing plant extract concentrations were shown to decrease the survival rate and the adult rate, which is consistent with dose-dependent toxicity (Hu et al., 2025). Similarly, studies with a potent polyphenol like epigallocatechin 3-gallate (EGCG) have reported that low to moderate doses prolong the lifespan of *C. elegans* and activate antioxidant mechanisms, but high doses reverse the positive effects and lead to harmful consequences. These findings suggest that phenolic compounds may exhibit a hormetic effect (Peng et al., 2021). Furthermore, numerous studies have shown that polyphenols can exhibit antioxidant, anti-aging, or stress response gene expression-enhancing effects in the C. elegans model, but these effects vary significantly depending on concentration and composition (Ha et al., 2022). In light of this general view, the bidirectional effect of phenolic-containing plant extracts such as artichoke leaf in *C. elegans* (benefit at low doses, suppression at high doses) has been similarly reported in other herbal polyphenol studies in the literature. In this context: Substances with a rich phenolic profile, such as artichoke extract, can support energy and reproductive processes by activating antioxidant defense systems at low concentrations, which is associated with increased antioxidant gene expression and oxidative stress tolerance. However, high doses of phenolics can trigger reactive species that can suppress metabolic pathways, thus reducing population growth, survival, and reproductive output. The unique phenolic composition of artichoke leaf extract (chlorogenic acid, flavonoids, etc.) has been confirmed in the literature to enhance its antioxidant capacity, which is consistent with other herbal examples where these compounds both regulate stress response genes and exhibit dose-related inhibitory effects depending on different doses. Overall, the findings suggest that artichoke leaf extract modulates *C. elegans* population growth in a concentration-dependent manner, and particularly at high doses.

CONCLUSION

In this study, the effects of artichoke leaf (*Cynara scolymus* L.) extract on the population growth of *Caenorhabditis elegans* were evaluated. The findings reveal that artichoke leaf extract exhibits a dose-dependent biphasic effect. At low concentrations, the extract was observed to positively influence reproductive and developmental processes by promoting *C. elegans* population growth; this is consistent with the low-dose phenolic compounds reported in the literature to enhance stress resistance by increasing antioxidant gene expression. On the other hand, at high concentrations, the extract significantly reduced population growth, an effect likely related to the suppression of cellular metabolism and the inhibitory effects of high-dose phenolic compounds. In conclusion, it was determined that artichoke leaf extract can exhibit both stimulatory and inhibitory effects on *C. elegans*, and this effect varies in a dose-dependent manner. These findings provide an important basis for evaluating the potential biological activities of artichoke leaf phenolic compounds and the balance between toxicity and biological benefit through a nematode model; Furthermore, it has been shown that dose optimization of natural phenolic compounds is critical to maximizing their biological effects.

ACKNOWLEDGEMENTS

I wish to express my deepest and sincere gratitude to my late father, Murat ÖZKAN, for his unwavering dedication, guidance, and support to his children. His encouragement has profoundly influenced my personal and professional journey and continues to serve as a lasting inspiration. May he rest in peace.

REFERENCES

Brenner, S. (1974). The genetics of *Caenorhabditis elegans*. Genetics, 77(1), 71-94.

Corsi, A. K., Wightman, B., & Chalfie, M. (2015). A transparent window into biology: a primer on *Caenorhabditis elegans*. Genetics, 200(2), 387-407.

Dhawan, K., Dhawan, S., & Sharma, A. (2004). Passiflora: a review update. *Journal of ethnopharmacology*, *94*(1), 1-23.

El Morsy, E. M., & Kamel, R. (2015). Protective effect of artichoke leaf extract against paracetamol-induced hepatotoxicity in rats. Pharmaceutical biology, 53(2), 167-173.

El-Boshy, M., Ashshi, A., Gaith, M., Qusty, N., Bokhary, T., AlTaweel, N., & Abdelhady, M. (2017). Studies on the protective effect of the artichoke (*Cynara scolymus*) leaf extract against cadmium toxicity-induced

oxidative stress, hepatorenal damage, and immunosuppressive and hematological disorders in rats. Environmental Science and Pollution Research, 24(13), 12372-12383.

Gebhardt, R., & Fausel, M. (1997). Antioxidant and hepatoprotective effects of artichoke extracts and constituents in cultured rat hepatocytes. Toxicology in vitro, 11(5), 669-672.

Gonçalves, A. I. P. (2018). Analysis of antioxidant and antigenotoxic activities of artichoke (*C. cardunculus* L.) natural leaves extracts (Master's thesis, Universidade do Minho (Portugal)).

Ha, N. M., Tran, S. H., Shim, Y. H., & Kang, K. (2022). *Caenorhabditis elegans* as a powerful tool in natural product bioactivity research. Applied biological chemistry, 65(1), 18.

Hu, A., Meng, Q., Liu, Z., Wu, Y., Borris, R. P., & Kim, H. M. (2025). ROS-Mediated Nematocidal Activity and Reproductive Toxicity of Herbal Extracts in *Caenorhabditis elegans*. Nutrients, 17(21), 3337.

Jeon, H., & Cha, D. S. (2016). Anti-aging properties of *Ribes fasciculatum* in *Caenorhabditis elegans*. Chinese Journal of Natural Medicines, 14(5), 335-342.

Kaletta, T., & Hengartner, M. O. (2006). Finding function in novel targets: *C. elegans* as a model organism. Nature reviews Drug discovery, 5(5), 387-399.

Kim, W., Hendricks, G. L., Lee, K., & Mylonakis, E. (2017). An update on the use of *C. elegans* for preclinical drug discovery: screening and identifying anti-infective drugs. Expert Opinion on Drug Discovery, 12(6), 625-633.

Kittimongkolsuk, P. (2020). Protective effects of tiger milk mushroom (*lignosus rhinocerus*) extracts on oxidative stress-induced neurotoxicity and aging in HT22 cells and *C. elegans*.

Lattanzio, V., Kroon, P. A., Linsalata, V., & Cardinali, A. (2009). Globe artichoke: A functional food and source of nutraceutical ingredients. Journal of functional foods, 1(2), 131-144.

Lithgow, G. J., & Walker, G. A. (2002). Stress resistance as a determinate of C. elegans lifespan. Mechanisms of ageing and development, 123(7), 765-771.

Olas, B. (2024). An overview of the versatility of the parts of the globe artichoke (Cynara scolymus L.), its by-products and dietary supplements. Nutrients, 16(5), 599.

Park, C. M., & Song, Y. S. (2013). Luteolin and luteolin-7-O-glucoside inhibit lipopolysaccharide-induced inflammatory responses through modulation of NF-κB/AP-1/PI3K-Akt signaling cascades in RAW 264.7 cells. Nutrition Research and Practice, *7*(6), 423-429.

Peng, Y., Dai, S., Lu, Y., Xiong, L., Huang, J., Liu, Z., & Gong, Y. (2021). Theanine improves high-dose epigallocatechin-3-gallate-induced lifespan reduction in *Caenorhabditis elegans*. Foods, 10(6), 1404.

Vasconcellos, M. C., Bezerra, I. C., dos Santos Macedo, D. C., Fernandes, B. L., & Gubert, P. (2024). *Caenorhabditis elegans* as an Outstanding Model to Explore Flavonoids Under Stress Conditions. The Natural Products Journal, *14*(8), 72-85.

Wagner, H. (1979). Phenolic compounds in plants of pharmaceutical interest. In *Biochemistry of Plant Phenolics* (pp. 589-616). Boston, MA: Springer US.

Zapolska-Downar, D., Zapolski-Downar, A., Naruszewicz, M., Siennicka, A., Krasnodębska, B., & Kołodziej, B. (2002). Protective properties of artichoke (*Cynara scolymus*) against oxidative stress induced in cultured endothelial cells and monocytes. Life sciences, 71(24), 2897-2908.

Zhang, Y., et al. (2018). Natural product-mediated modulation of *C. elegans* population growth under oxidative stress. Frontiers in Aging, 10, 123–135.

ORAL PRESENTATION

Evaluation of antioxidant activity of artichoke leaves with DPPH radical scavenging assay

Ayşenur Çelik[1 *] (*ORCID: https://orcid.org/0000-0001-8740-1162*),
Yeşim Özkan[2] (*ORCID: https://orcid.org/ 0000-0001-8533-7101*)

[1]Ordu University, Faculty of Arts and Sciences, Molecular Biology and Genetics Department, Ordu, Türkiye.

*Corresponding author e-mail: nur.armagan70@gmail.com

Abstract

Artichoke leaves are a rich plant source of flavonoids, phenolic compounds, caffeol derivatives, and other polyphenols. These compounds have the capacity to neutralize free radicals and reduce oxidative stress. Antioxidant capacity plays a critical role in protecting cells and tissues from oxidative damage and is important for assessing the biological value of natural products. The antioxidant potential of artichoke leaf extract is being investigated to determine its potential use as both a food additive and a functional food. The DPPH (2,2-diphenyl-1-picrylhydrazyl) test is a widely used, rapid, and reliable spectrophotometric method for measuring free radicals. In this test, the DPPH radical is purple and loses its color when neutralized by antioxidants by donating electrons or hydrogen. The radical scavenging capacity (% inhibition) of the extract is calculated by measuring the absorbance change with a spectrophotometer. The DPPH test allows quantitative determination of the antioxidant potency of extracts at different concentrations, and comparative assessments can be made using the IC_{50} value. Therefore, the DPPH test is the standard and preferred method for determining the antioxidant potential of natural products such as artichoke leaves. The IC_{50} value represents the concentration at which the extract reaches 50% radical scavenging capacity and is a widely used parameter for determining the comparable antioxidant potential of natural products. In this study, the antioxidant capacity of artichoke leaf extract was evaluated by the DPPH radical screening method. Spectrophotometric measurements were taken at different concentrations (0.1–2.0 mg/mL), and the radical scavenging activity IC_{50} value was estimated to be approximately 0.81 mg/mL. The results indicate that artichoke leaf extract has a strong antioxidant potential and can be used in functional food or nutraceutical applications. The DPPH test reveals the antioxidant potential of the extract based on its ability to neutralize free radicals. The study results showed that artichoke leaf extract increased its radical scavenging capacity in a concentration-dependent manner. The radical scavenging rate increased at higher concentrations and reached a level comparable to the positive control. The results support the potential of artichoke leaf as a natural antioxidant source and constitute an important reference in the fields of functional food and nutraceuticals.

Keywords: Antioxidant, artichoke, *Cynara scolymus,* DPPH.

INTRODUCTION

Oxidative stress is an imbalance resulting from the overwhelm of antioxidant defense systems by intracellular reactive oxygen species (ROS) and free radicals. This damages essential biomolecules such as DNA, proteins, and lipids, leading to cellular dysfunction and playing a critical role in the pathogenesis of chronic diseases. Elevated ROS levels cause DNA strand breaks, protein oxidation, and lipid peroxidation, contributing to genomic instability, enzyme dysfunction, and membrane integrity disruption. These mechanisms have significant implications in many chronic pathologies, including cancer, cardiovascular diseases, neurodegenerative disorders (such as Alzheimer's and Parkinson's), and metabolic diseases (Jomova et al., 2023). Antioxidants are compounds that neutralize these molecules, limiting oxidative damage, maintaining cellular homeostasis, and helping to reduce disease risk. Endogenous enzymatic antioxidants (e.g., superoxide dismutase, catalase, glutathione peroxidase) and exogenously derived antioxidants (such as vitamin C, vitamin E, flavonoids) prevent biomolecular damage by scavenging reactive species. Antioxidant activity refers to the capacity of a compound or extract to neutralize free radicals or oxidative agents. This activity is a key parameter in evaluating the health benefits of herbal extracts because it is

associated with the presence of phenolic compounds, flavonoids, and similar phytochemicals (Kähkönen et al., 1999; Subedi et al., 2014; Muflihah et al., 2021).

The DPPH (1,1-diphenyl-2-picrylhydrazyl) radical scavenging assay is a commonly used spectrophotometric method to measure antioxidant capacity. DPPH exists as a stable free radical in solution and exhibits a characteristic absorbance in a purplish-red solution. When an antioxidant substance reacts with DPPH, the DPPH radical accepts hydrogen or electrons, causing the color to fade and absorbance values to decrease. This change reflects an increase in antioxidant activity and is measured by quantitative parameters such as IC_{50}: a lower IC_{50} value indicates a stronger radical scavenging capacity (Gulcin & Alwasel, 2023). The main reasons for preferring the DPPH test are: Simplicity, sensitivity, and reproducibility: The method is a fast, easy-to-apply, and cost-effective test. Suitability for plant extracts: It reliably measures the effectiveness of hydrogen-donating antioxidant components such as phenolics and flavonoids (Gulcin & Alwasel, 2023). High literature support: It is used as a standardized test in numerous plant antioxidant studies worldwide (Kedare & Singh, 2011). Therefore, the DPPH test has gained widespread acceptance as a first-stage bioactivity assessment method, especially in plant extracts, for in vitro antioxidant screening (Kedare & Singh, 2011).

Plants are rich sources of powerful antioxidants such as phenolic acids, flavonoids, tannins, and other phytoactive compounds. These biomolecules can react with free radicals, reducing oxidative damage and consequently maintaining cellular homeostasis. When evaluating the antioxidant efficacy of plant extracts, radical scavenging tests such as DPPH provide valuable preliminary information about the bioactive compound profile and pharmacological potential of the extracts (Mustafa et al., 2010; Chew et al., 2011; Formagio et al., 2014; Yu et al., 2021). *Cynara scolymus* L. (artichoke), a plant native to the Mediterranean region, is widely used both as food and in traditional medicine. Its leaves are particularly rich in phenolic compounds and flavonoids, and have many biological effects associated with antioxidant activity (Salekzamani et al., 2019). Systematic reviews and in vitro studies have revealed that artichoke exhibits antioxidant effects as well as anti-tumor, hepatoprotective, and lipid metabolism regulating effects (Salekzamani et al., 2019). Artichoke leaves stand out with their phenolic profile (e.g., luteolin, apigenin, chlorogenic acid derivatives), and these compounds play an active role in combating oxidative stress. Therefore, artichoke leaf extracts are considered natural antioxidant sources and were investigated in this study due to their potential value in herbal medicine development, functional food production, and nutritional supplements.

MATERIALS AND METHODS

Preparation of *Cynara scolymus* L. Leaf Extract

Artichoke leaves (*Cynara scolymus* L.) were obtained fresh from a local herbalist in Ordu province. After the plant material was brought to the laboratory, it was gently washed first with tap water and then with distilled water to remove dust and foreign particles from the leaf surface. The cleaned leaves were dried in the shade at room temperature (22–25°C) for 36 hours, protected from direct sunlight. After the drying process was completed, the leaves were ground in a laboratory-type grinder to obtain a homogeneous powder and stored in airtight containers. For extraction, 50 g of the prepared artichoke leaf powder was weighed and added to 500 mL of 80% methanol at a ratio of 1:10 (w/v). The mixture was transferred to an amber-colored glass bottle that did not allow light to pass through and was left to macerate at room temperature for approximately 36 hours. During this time, the bottle was shaken manually every 2–3 hours to ensure more effective penetration of the solvent into the plant tissue. At the end of the extraction period, the mixture was first coarsely filtered through cheesecloth to remove solid plant residues, and then passed through Whatman No. 1 filter paper to obtain a clear filtrate. The filtrate was concentrated in a rotary evaporator operating at 40°C under low pressure to remove the solvent. After complete removal of methanol, the resulting crude extract is a viscous solution. This extract was transferred to amber-colored screw-cap tubes and stored at -20°C until use in analyses. The prepared extract was diluted to the target concentration in a suitable solvent (e.g., DMSO or methanol) before use in subsequent biochemical and biological tests.

DPPH Method

The antioxidant capacity of artichoke leaf extract obtained with methanol was evaluated using the 2,2-diphenyl-1-picrylhydrazyl (DPPH) radical scavenging test. The method was optimized with minor modifications based on protocols described by Brand-Williams et al. (1995) and Blois (1958). DPPH radical (Sigma-Aldrich, ≥95% purity) was used. A 0.1 mM DPPH solution was freshly prepared in cold methanol and left in the dark for 30 minutes. The

absorbance of the solution was measured at 517 nm in a spectrophotometer. As a positive control, a 1 mg/mL stock solution of Ascorbic Acid (L-AA) was prepared in methanol. On the same day as the experiment, the extract was diluted to 7 different concentrations (e.g., 10, 20, 40, 60, 80, 100, 200 µg/mL). Seven different concentrations (0.1, 0.2, 0.3, 0.4, 0.5, 1, and 2 mg/L) were prepared from the methanol-based extract stock solution. All solutions were prepared in light-proof amber tubes and stored at room temperature throughout the experiment. For each extract or control concentration, 1 mL of extract solution was mixed with 1 mL of DPPH (0.1 mM) solution in amber glass tubes. A negative control (1 mL methanol + 1 mL DPPH) and a blank (1 mL sample solution + 1 mL methanol) solution were prepared. All tubes were incubated in the dark at room temperature (22–25°C) for 30 minutes. This waiting time is considered optimal in the literature in terms of the stability of the DPPH radical and reaction kinetics (Brand-Williams, 1995). At the end of the waiting time, the absorbance of all samples was measured at a wavelength of 517 nm using a UV–Vis spectrophotometer. Each measurement was performed in triplicate (n = 3).

Free radical scavenging activity was calculated using the following formula:

$$\text{DPPH Removal Activity (\%)} = \left(\frac{A_{\text{control}} - A_{sample}}{A_{\text{sample}}}\right) \times 100$$

A_"control" = absorbance of the solution containing only DPPH
A_"sample" = absorbance of the extract + DPPH mixture (sample color corrected)

Determination of IC_{50} Value

The obtained percentage radical scavenging values were plotted against concentration. The point where the concentration corresponds to 50% inhibition was determined as IC_{50}. IC_{50} calculation was performed using linear regression from the dose-response curve. The antioxidant power of artichoke leaf was evaluated by comparing the IC_{50} value with the positive control (ascorbic acid).

RESULTS and DISCUSSION

The DPPH radical scavenging capacity of artichoke leaf extract was evaluated at concentrations ranging from 0.1–2 mg/mL, and the results were compared with ascorbic acid (Figure 1). The data clearly show that the antioxidant capacity of the extract exhibits a dose-dependent increase. At the lowest concentration (0.1 mg/mL), the DPPH inhibition percentage of artichoke leaf extract was determined to be 51%, and this value reached 66% when the concentration was increased to 2 mg/mL. This linear trend can be attributed to the increasing radical neutralization capacity of phenolic acids, flavonoids, and especially chlorogenic acid derivatives present in the extract as their concentration increases. Ascorbic acid, as a positive control, showed higher radical scavenging activity at all concentrations (49%–94%). However, artichoke extract yielded results quite close to ascorbic acid, especially in the low and medium concentration ranges. For example, at a concentration of 0.3 mg/mL, the inhibition of ascorbic acid was measured at 57%, while the inhibitory activity of the extract was 56%; this indicates that artichoke has a biologically significant antioxidant capacity. Similarly, at 0.5 mg/mL, ascorbic acid offered 70% inhibition, while the extract reached 59%; this shows that the difference between the artichoke extract and ascorbic acid becomes more pronounced as the concentration increases, but its activity remains at a strong level. These findings show that the radical scavenging activity of artichoke leaf extract increases with concentration, but even at high doses, the activity is not as strong as ascorbic acid. However, the performance close to that of ascorbic acid exhibited at low concentrations supports the high biological activity of the polyphenolic components in the artichoke extract. When the known chemical profile of artichoke leaves is examined, it is reported that chlorogenic acid, luteolin derivatives, and caffeoylquinic acid, in particular, play an active role in free radical neutralization. Therefore, the obtained antioxidant capacity is consistent with the phenolic richness of the plant. In addition, the fact that the inhibition curve of the extract shows a regular increase throughout the concentration range suggests that the capacity of the extract to chemically interact with DPPH radicals can be explained by a linear kinetic model. This indicates that the antioxidant components of the extract may have a synergistic effect on each other, and that the radical

scavenging efficiency becomes more pronounced as the concentration increases. Thus, artichoke leaf extract is considered a strong antioxidant candidate consistent with its phenolic profile, and the results are also consistent with the DPPH inhibition trends in other artichoke studies reported in the literature.

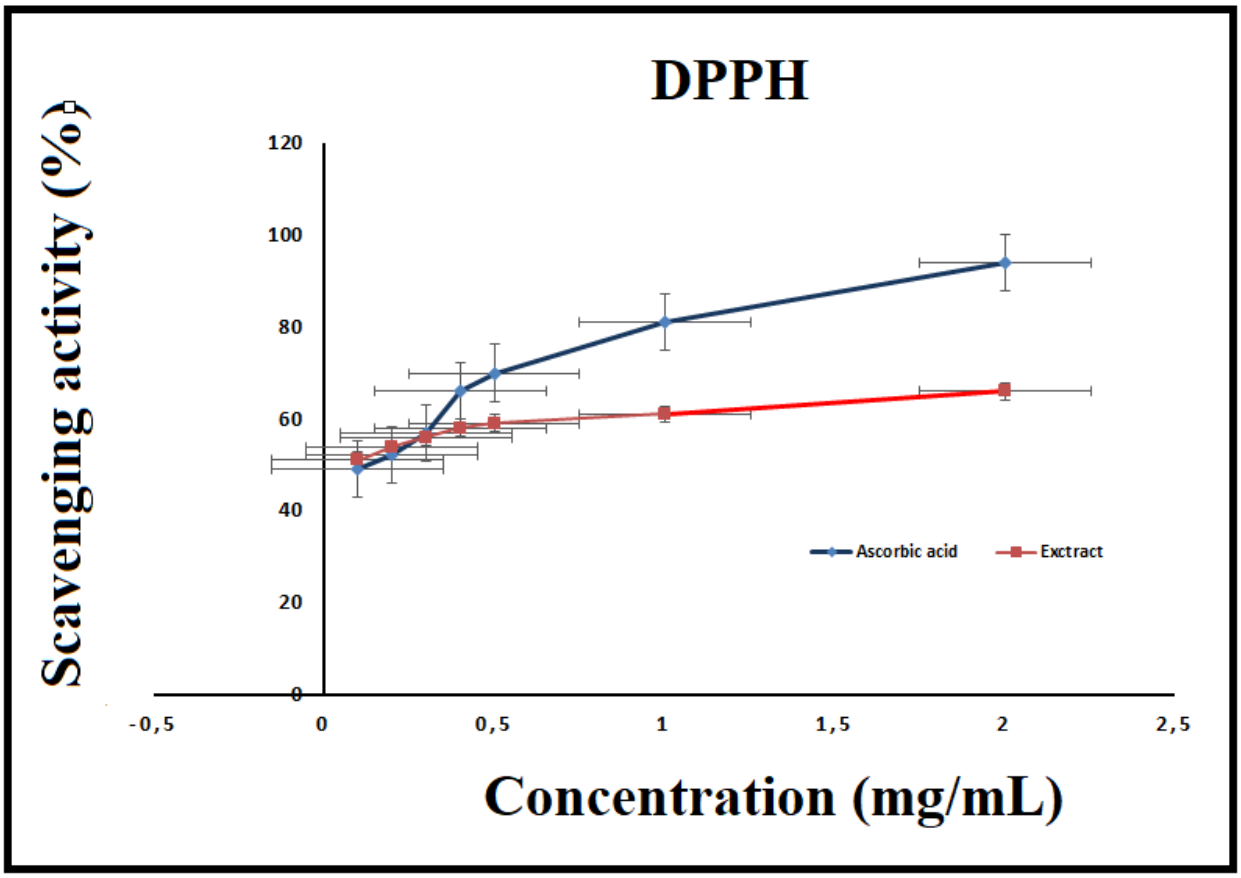


Figure 1. DPPH free radical scavenging activity of *Cynara scolymus* L. Leaf extract and of ascorbic acid. Values are the average of triplicate experiments.

According to DPPH data, a remarkable difference in profile was observed between artichoke leaf extract and ascorbic acid. Linear interpolation for quantitative assessment of dose-response behavior showed that the IC_{50} value of the extract was approximately 0.098, while the IC_{50} value of ascorbic acid was approximately 0.133. This theoretically suggests that the extract has a higher radical scavenging potential than ascorbic acid at lower doses. However, the reliability of this result is limited because the 50% inhibition point for the extract is just below the lowest measured concentration (~0–0.1 range); therefore, additional low-dose measurements for the extract IC_{50} are recommended. Nevertheless, the two substances clearly differ in terms of maximum effect. Ascorbic acid showed a very high radical scavenging capacity of 94% at a concentration of 2 mg/mL; the maximum observed inhibition for the extract was 66%. This indicates that ascorbic acid offers a higher efficacy against DPPH over a wider concentration range, while the extract has a relative advantage in the initial/intermediate ranges. In other words, the extract is potent (effective at low concentrations), while ascorbic acid has a more effective maximum scavenging capacity.

In our study, artichoke leaf extract showed a dose-dependent increase in the DPPH radical scavenging test, exhibiting inhibition values ranging from 51% to 66% in the 0.1-2 concentration range; ascorbic acid, used as a positive control, yielded results between 49% and 94% in the same range, demonstrating both a higher maximum efficacy and a wider dynamic range of efficacy. When the dose-response relationship and the calculated IC_{50} values (extract ≈ 0.098; ascorbic acid ≈ 0.133 by linear interpolation) are evaluated together, the available data highlight two important points: (1) artichoke extract shows a relatively high potency (low IC_{50}) at low concentrations; (2) ascorbic acid can reach a much higher maximum radical scavenging capacity (Emax) at high concentrations. These

two properties reflect the classic potency-efficacy distinction between potent single-molecule antioxidants and complex phytochemical mixtures (Ucar Turker et al., 224). When we compare the obtained results with the literature, it is seen that the antioxidant capacity of artichoke extract is comparable to that of similar medicinal plant extracts. For example, Saeed et al., who examined the relationship between the phenolic richness of medicinal plants and their antioxidant activity, (2012) reported that high phenolic content leads to a significant increase in DPPH inhibition (Saeed et al., 2012). The dose-dependent increase in our study is consistent with this mechanism. Furthermore, the medicinal importance of artichoke is not limited solely to antioxidant activity. The literature reports that artichoke leaf extract has hepatoprotective, anti-inflammatory, and lipid-lowering effects, and most of these functional activities are associated with its high polyphenol content (Liao et al., 2021). In this context, our study confirms that artichoke leaf extract has strong potential as a natural antioxidant source and provides a scientific basis for its use, especially in the fields of food supplementation, functional foods, and phytotherapy.

CONCLUSION

his study revealed the biological potential of artichoke (*Cynara scolymus* L.) leaf extract by evaluating its antioxidant capacity at different concentration ranges using the DPPH radical scavenging method. The findings showed that the extract exhibited a linearly increasing radical inhibition activity with increasing concentration, reaching 66% inhibition at the maximum dose of 2 mg/mL. Although ascorbic acid showed higher activity at each dose, the fact that artichoke extract produced values close to ascorbic acid, especially at low and medium concentrations, confirms the strong natural antioxidant capacity of the plant. These results support the literature reporting that the rich composition of artichoke leaves in phenolic compounds, especially flavonoids such as caffeoylquinic acid derivatives, luteolin, and apigenin, significantly contributes to antioxidant activity. Therefore, artichoke leaf extract is an important natural antioxidant source that can be evaluated in pharmacological and nutraceutical applications in reducing oxidative stress caused by free radicals. Overall, the study findings reveal that artichoke leaf extract is a reliable herbal agent with high antioxidant activity, and its dose-dependent effect supports its usability in functional foods, phytotherapy, and pharmaceutical formulations. Future studies are recommended to focus on verifying the IC_{50} value of the extract, detailing the phenolic compound profile by HPLC or LC-MS, and investigating its in vivo antioxidant effect in biological systems.

ACKNOWLEDGEMENTS

I wish to express my deepest and sincere gratitude to my late father, Murat ÖZKAN, for his unwavering dedication, guidance, and support to his children. His encouragement has profoundly influenced my personal and professional journey and continues to serve as a lasting inspiration. May he rest in peace.

REFERENCES

Blois, M. S. (1958). Antioxidant determinations by the use of a stable free radical. *Nature*, *181*(4617), 1199-1200.

Brand-Williams, W. (1999). Use of a free radical method to evaluate antioxidant activity. Food Sci. Technol., 28, 1231-1237.

Chew, Y. L., Ling Chan, E. W., Tan, P. L., Lim, Y. Y., Stanslas, J., & Goh, J. K. (2011). Assessment of phytochemical content, polyphenolic composition, antioxidant and antibacterial activities of Leguminosae medicinal plants in Peninsular Malaysia. BMC complementary and alternative medicine, 11(1), 12.

Formagio, A. S. N., Volobuff, C. R. F., Santiago, M., Cardoso, C. A. L., Vieira, M. D. C., & Pereira, Z. V. (2014). Evaluation of antioxidant activity, total flavonoids, tannins and phenolic compounds in Psychotria leaf extracts. Antioxidants, 3(4), 745-757.

Gulcin, İ., & Alwasel, S. H. (2023). DPPH radical scavenging assay. Processes, 11(8), 2248.

Jomova, K., Raptova, R., Alomar, S. Y., Alwasel, S. H., Nepovimova, E., Kuca, K., & Valko, M. (2023). Reactive oxygen species, toxicity, oxidative stress, and antioxidants: chronic diseases and aging. Archives of toxicology, 97(10), 2499-2574.

Kähkönen, M. P., Hopia, A. I., Vuorela, H. J., Rauha, J. P., Pihlaja, K., Kujala, T. S., & Heinonen, M. (1999). Antioxidant activity of plant extracts containing phenolic compounds. Journal of agricultural and food chemistry, 47(10), 3954-3962.

Kedare, S. B., & Singh, R. P. (2011). Genesis and development of DPPH method of antioxidant assay. Journal of food science and technology, 48(4), 412-422.

Liao, G. C., Jhuang, J. H., & Yao, H. T. (2021). Artichoke leaf extract supplementation lowers hepatic oxidative stress and inflammation and increases multidrug resistance-associated protein 2 in mice fed a high-fat and high-cholesterol diet. Food & Function, 12(16), 7239-7249.

Muflihah, Y. M., Gollavelli, G., & Ling, Y. C. (2021). Correlation study of antioxidant activity with phenolic and flavonoid compounds in 12 Indonesian indigenous herbs. Antioxidants, 10(10), 1530.

Mustafa, R. A., Hamid, A. A., Mohamed, S., & Bakar, F. A. (2010). Total phenolic compounds, flavonoids, and radical scavenging activity of 21 selected tropical plants. Journal of food science, 75(1), C28-C35.

Saeed, N., Khan, M. R., & Shabbir, M. (2012). Antioxidant activity, total phenolic and total flavonoid contents of whole plant extracts Torilis leptophylla L. BMC complementary and alternative medicine, 12(1), 221.

Salekzamani, S., Ebrahimi-Mameghani, M., & Rezazadeh, K. (2019). The antioxidant activity of artichoke (Cynara scolymus): A systematic review and meta-analysis of animal studies. Phytotherapy research, 33(1), 55-71.

Subedi, L., Timalsena, S., Duwadi, P., Thapa, R., Paudel, A., & Parajuli, K. (2014). Antioxidant activity and phenol and flavonoid contents of eight medicinal plants from Western Nepal. Journal of Traditional Chinese Medicine, 34(5), 584-590.

Ucar Turker, A., Basay, S., Cimen, A., Baba, Y., & Birinci Yildirim, A. (2024). Evaluation of the phenolic content and the nutraceutical potential of ancestor and cultivated artichokes. Chemistry & Biodiversity, 21(4), e202400203.

Yu, M., Gouvinhas, I., Rocha, J., & Barros, A. I. (2021). Phytochemical and antioxidant analysis of medicinal and food plants towards bioactive food and pharmaceutical resources. Scientific reports, 11(1), 10041.

ORAL PRESENTATION

Investigation of the effect of mulberry leaf extract on population growth of *Caenorhabditis elegans*

Ayşenur Çelik[1 *] (*ORCID: https://orcid.org/0000-0001-8740-1162*),
Yeşim Özkan[2] (*ORCID: https://orcid.org/ 0000-0001-8533-7101*)

[1]Ordu University, Faculty of Arts and Sciences, Molecular Biology and Genetics Department, Ordu, Türkiye.

*Corresponding author e-mail: nur.armagan70@gmail.com

Abstract

Mulberry (*Morus indica* L.) leaves are a natural source of biologically active compounds used in traditional medicine and modern research. Mulberry also holds potential as a biological agent, particularly in pest and nematode control studies using natural products. *C. elegans* is a widely used model organism in biological and toxicological research. The effect of mulberry leaf extract on *C. elegans* populations is important both for understanding potential biological effects on reproduction and survival and for assessing the potential use of natural products as biological control agents. Population growth measurements directly indicate the inhibitory or stimulatory effects of the extract on reproduction and survival, depending on its concentration. In this study, the effect of mulberry leaf extract on *C. elegans* population growth was investigated. Mulberry leaf extract was applied at different concentrations (0.5-2 mg/ml) and the results were observed over a 5–7 day period. A visibly decreased population growth was observed in the group treated with mulberry leaf extract at a low concentration of 0.5 mg/ml. This indicates that the low concentration affected the growth and reproduction of *C. elegans* to a limited extent, but did not suppress them completely. Mulberry leaf extract significantly reduced the *C. elegans* des population in the group treated with the medium concentration of 1 mg/ml, and its inhibitory effect on reproduction increased. A negative increase of 50% was observed in the group treated with the highest concentration of 2 mg/ml. This result indicates that high concentrations negatively affect the survival of nematodes and increase mortality. The obtained data reveal that mulberry leaf extract has a significant inhibitory effect on nematodes population growth, depending on the concentration. Low concentrations exert mild suppression and have limited effects on nematode reproduction, while medium and high concentrations significantly inhibit reproduction and, at high doses, increase mortality.

Keywords: *Caenorhabditis elegans*, *Morus indica,* mulberry, population growth

INTRODUCTION

investigation of the effects of plant-derived bioactive compounds on biological systems has become a subject of increasing interest in pharmacology and nutritional sciences in recent years. These compounds include various chemical groups such as phenols, flavonoids, alkaloids, terpenoids, and glycosides, and can exhibit a wide range of biological effects in the organism, including antioxidant, anti-inflammatory, antimicrobial, hepatoprotective, and cardioprotective properties (Mickymaray, 2019; Ding et al., 2017). The role of herbal extracts, particularly in the prevention and treatment of chronic diseases, is increasingly being evaluated by modern medicine. Medicinal plants, used for many years in traditional medicine, have become the focus of modern pharmacological studies due to their low toxicity profile and versatile biological activities stemming from their natural content.

Morus species, especially *Morus alba* and *Morus nigra*, have a long history in folk medicine in different regions of Asia and Europe. These species are used in the management of diabetes, hypertension, hyperlipidemia, inflammatory conditions, and age-related diseases (Hussain et al., 2017). The phenolic compounds and flavonoids contained in Morus leaves, with their strong antioxidant activity, scavenge free radicals and reduce cellular damage caused by oxidative stress. In addition, leaf extracts can contribute to blood sugar control by regulating glucose metabolism and help balance serum cholesterol and triglyceride levels by improving lipid metabolism (Wang et al., 2023). Furthermore, according to some studies, Morus leaf extracts also exhibit hepatoprotective effects; this protects liver cells against toxic effects, reducing oxidative damage and inflammation (Hussain et al., 2017). Moreover, their antimicrobial properties increase the potential use of Morus leaf extracts in the food and

pharmaceutical industries (Wang et al., 2023). All these biological effects indicate that Morus leaf should be investigated not only in traditional medicine but also in modern pharmacological and nutritional studies.

Mulberry leaf (*Morus indica* L.) extracts have a rich content of phenolic compounds, flavonoids, and other phytochemicals. Numerous studies exist in the literature investigating the antioxidant activities of mulberry leaf extracts, as well as their effects on diabetes management, cholesterol regulation, and anti-aging (Song et al., 2009; He et al., 2022). In particular, its antioxidant capacity is important in modeling aging and neurodegenerative diseases due to its ability to reduce cellular oxidative stress by scavenging free radicals (Sies, 2015). However, reliable and rapid model systems are needed to determine the systematic biological effects of plant extracts. At this point, *Caenorhabditis elegans* (*C. elegans*) stands out as an ideal model organism for studying the biological activities of plant extracts. *C. elegans* is a transparent, approximately 1 mm long model organism known as a soil nematode. Its short life cycle (~3 days), simple anatomy, and ease of manipulation with complete genetic mapping and molecular tools make it widely used in toxicity, senescence, and pharmacological efficacy studies (Brenner, 1974; Kaletta & Hengartner, 2006). Furthermore, the transparent structure of *C. elegans* allows for direct observation of cellular changes in living individuals, providing a significant advantage, particularly in antioxidant and gene expression studies (Aranaz et al., 2020; Liu et al., 2021). Another reason for preferring *C. elegans* in toxicity testing is its ability to quickly and efficiently examine a large number of individuals. This feature provides a reliable system for determining the sublethal and lethal effects of plant extracts. Furthermore, the conserved nature of certain metabolic and genetic pathways in humans and other mammals increases the translational value of the findings (Long et al., 2023). In recent years, the evaluation of plant extracts with antioxidant and anti-aging potential in *C. elegans* models has allowed for the mechanistic investigation of biological activities (Aranaz et al., 2020; Liu et al., 2021).

Investigating the effects of mulberry leaf extract on the *C. elegans* population is important both for understanding the biological potential of the plant and for determining the safe dosage. This study aims to determine the effects of mulberry leaf extract on *C. elegans* population growth and to provide a scientific basis for the applications of mulberry leaf in traditional and modern medicine.

MATERIALS AND METHODS

Preparation of Artichoke. Leaf Extract

Artichoke leaves (*Morus indica*) were obtained fresh from a local herbalist in Ordu province. After the plant material was brought to the laboratory, it was gently washed first with tap water and then with distilled water to remove dust and foreign particles from the leaf surface. The cleaned leaves were dried in the shade at room temperature (22–25°C) for 36 hours, protected from direct sunlight. After the drying process was completed, the leaves were ground in a laboratory-type grinder to obtain a homogeneous powder and stored in airtight containers.

For extraction, 3.5 g of the prepared artichoke leaf powder was weighed and added to 65 mL of 80% methanol at a ratio of 1:10 (w/v). The mixture was transferred to an amber-colored glass bottle that did not allow light to pass through and left to stand at room temperature for approximately 36 hours using the maceration method. During this time, the bottle was shaken manually every 2–3 hours to ensure more effective penetration of the solvent into the plant tissue. At the end of the extraction period, the mixture was first coarsely filtered through cheesecloth to remove solid plant residues, and then passed through Whatman No. 1 filter paper to obtain a clear filtrate. The filtrate was concentrated in a rotary evaporator operating at 40°C under low pressure to remove the solvent. After complete removal of methanol, the resulting crude extract is a viscous solution. This extract was transferred to amber-colored screw-cap tubes and stored at -20°C until use in analyses. The prepared extract was diluted to the target concentration in a suitable solvent before use in subsequent biochemical and biological tests.

C. elegans culture

In this study, the N2 wild-type strain of *C. elegans* was used. Nematodes were maintained on Nematode Growth Medium (NGM) and fed with *Escherichia coli* OP50 under standard culture conditions at a constant temperature of 20 °C. Synchronized populations were generated by washing NGM plates containing predominantly gravid adults. To obtain synchronized nematodes, adult worms were treated with a bleaching solution (1 N NaOH and 5% sodium hypochlorite) and gently vortexed every 2 minutes over a total period of 10 minutes. The solution was then

centrifuged, and the supernatant containing lysed worm debris was removed, leaving behind an egg pellet. The egg pellet was washed three times and resuspended in M9 buffer. Eggs were incubated with gentle agitation for approximately 12 hours to hatch and establish a synchronized population. Larvae at the L3–L4 stage were subsequently used for all experimental assays.

Acute Toxicity / LC_{50} Determination

The acute toxicity test was performed to determine sublethal concentrations. For the population growth experiment, the acute toxicity of *Cynara scolymus* L. leaf extract was first determined by exposure for 24, 48, and 72 hours. Synchronized L4 larvae were incubated at different concentrations for 24–72 hours. Three replicates were performed for each concentration. 80% methanol was used as the solvent control, and M9 buffer + OP50 alone was used as the negative control. Live/dead counts were performed at the end of the exposure time. LC_{50} was calculated by probit analysis. For sublethal concentrations, concentrations of LC_{10}–LC_{20} (0–10%) that did not have significant non-mortality side effects on reproduction and growth were preferred.

Population growth assay

To evaluate the effect of *Morus indica* leaf extract after exposure at sublethal concentration, the growth of *C. elegans* population was assessed (Dhawan et al., 1999). Age-synchronized L4 stage nematodes were transferred to 24-well NGM (Nematode Growth Medium) plates at a density of 20 nematodes per well (Corsi et al., 2015). *Escherichia coli* OP50 was used as the food source. All plates containing the experimental and control groups were incubated at 20 ± 1°C for 5 days. On day 5, the total number of live individuals in each well, including parent nematodes, larvae, and offspring, was counted under a stereomicroscope. Nematodes from each well were collected into 2 mL of M9 buffer, homogenized carefully, and 5 µL aliquots were taken for counting under a stereomicroscope. Counts were performed separately for each group, and the average across three replicates was calculated. All measurements were conducted on the same day by the same investigator to minimize variability. Population growth was expressed relative to the initial number of nematodes using the following formula (Zhang et al., 2018):

$$\text{Population Increase (\%)} = \frac{\text{Observed live nematodes} - \text{Initial nematodes}}{\text{Initial nematodes}} \times 100$$

RESULTS

Figure 1 below evaluates the effect of different concentrations (0.5; 1; 2 mg/mL) of Mulberry (*Morus indica* L.) leaf extract on *C.elegans* population growth. Initially, 20 individuals were placed in each group, and the population growth rate was calculated based on the number of viable individuals observed at the end of the experiment. In the control group, the initial 20 individuals reached 400 viable individuals at the end of the experiment. This represents a 1900% population increase. This high growth rate indicates that the experimental conditions used (*C. elegans* culture medium, nutrient amount, temperature, and plate quality) were optimal for reproduction and development. Since the control group was used as a reference in the experiment, decreases or increases in other groups were interpreted based on this value. In the concentration group where 0.5 mg/mL extract was applied, the number of viable individuals was measured as 320. This corresponds to a 1500% population increase. Although the growth rate was lower compared to the control group, the population still multiplied at a high level. This result suggests that the 0.5 mg/mL concentration caused mild inhibition; However, it shows that it does not completely suppress *C. elegans* reproduction. In the group treated with 1 mg/mL extract, the number of live individuals decreased significantly, and 50 individuals were observed. This value represents a 150% population increase. This result shows that mulberry leaf extract at the 1 mg/mL level causes significant reproductive inhibition. The dramatic decrease in population growth may be related to developmental delay, larval losses, or suppression of reproductive capacity. In the group treated with the highest concentration of 2 mg/mL, the number of live individuals was measured as 10, falling below the initial number. This was calculated as a -50% population increase. In other words, the population decreased. This finding shows that the 2 mg/mL concentration has a toxic effect on nematodes, causing loss of adults or complete cessation of larval development. When evaluated in terms of dose-response relationship, the data obtained clearly show that mulberry leaf extract has a concentration-dependent suppressive effect on *C. elegans* population growth: Low concentration (0.5 mg/mL) slightly reduced the population. Medium

concentration (1 mg/mL) severely reduced population growth. High concentration (2 mg/mL) caused population decline and possible toxicity (Figure 1).

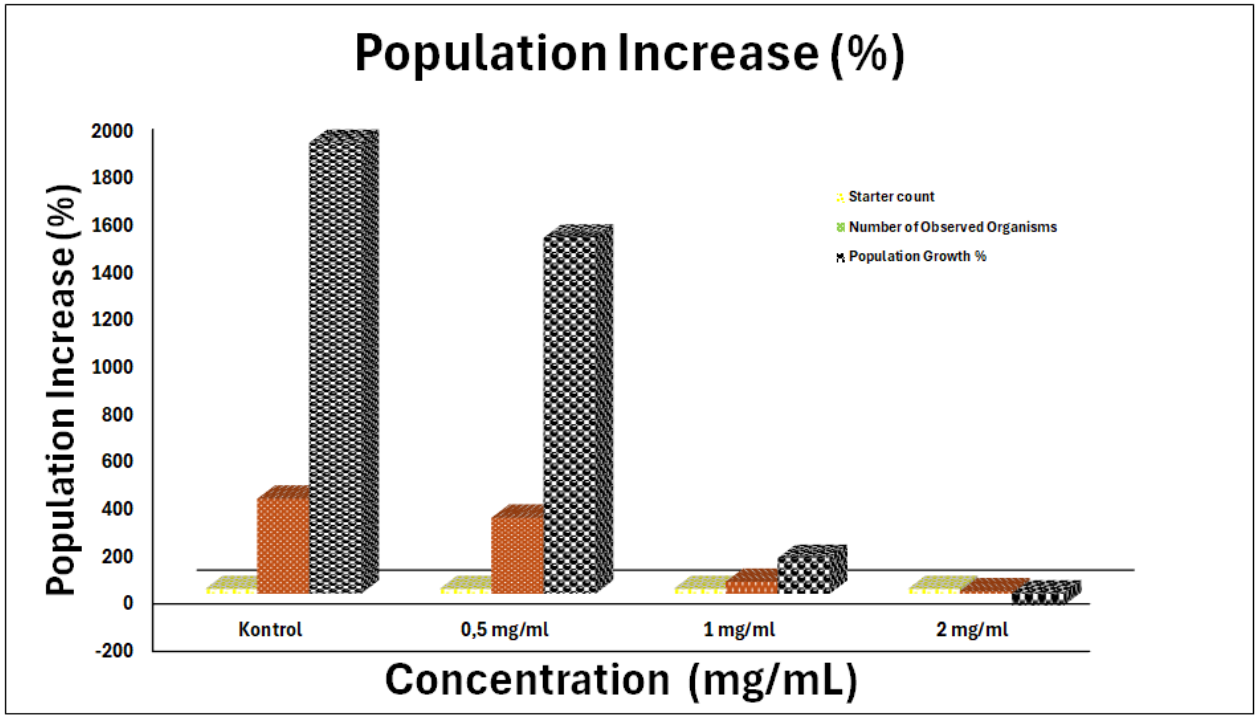


Figure 1. Effects of sublethal concentrations of *Cynara scolymus* leaf extract on the growth of *C. elegans* populations.

This trend suggests that the phenolic compounds and flavonoids in the extract may damage nematode physiology at high concentrations; and may show milder effects at low concentrations. In particular, the negative growth at 2 mg/mL indicates that mortality may occur as a result of developmental arrest, cellular stress, or oxidative damage.

DISCUSSION

Morus indica possesses high antioxidant capacity due to its numerous bioactive molecules, including phenolic compounds, flavonoids, alkaloids, anthocyanins, stilbene derivatives, and ascorbic acid (Mahesh et al., 2017; Memete et al., 2022). Polyphenols, particularly quercetin, rutin, morin, and chlorogenic acid, enhance the plant's pharmaceutical importance. Various studies have shown that *Morus indica* leaf and fruit extracts exhibit high antioxidant activity using methods such as DPPH, ABTS, and FRAP (Yang et al., 2016; Wang et al., 2021; Li et al., 2023; Kumari, 2025).

This study demonstrates that mulberry leaf extract has a concentration-dependent effect on *C. elegans* population growth. At low concentrations, a slight decrease in population growth was observed, at moderate concentrations a significant suppression, and at high concentrations a net population reduction (mortality/sterility). These results are consistent with the literature reporting that plant polyphenols and flavonoids can have both protective and toxic effects on *C. elegans*. For example, in a study by Grünz et al., the lifespan of *C. elegans* was analyzed using flavonols (e.g., quercetin, myricetin, naringenin); the results showed that all of these flavonols extended the lifespan of wild-type worms, but that "structural characteristics" (e.g., number of hydroxyl groups) were important along with the antioxidant effect (Grünz et al., 2012). In another study, the effects of six different flavonoids (baicalein, chrysin, etc.) on lifespan, stress resistance, fat accumulation, and gene expression in *C. elegans* were investigated. Some flavonoids (e.g., baicalein, chrysin) have been shown to prolong lifespan in worms, providing higher stress tolerance under oxidative stress and less fat accumulation; these effects have been reported to occur via signaling pathways (Guerrero-Rubio et al., 2021). In another study, the effects of four different plant polyphenols (tannic acid, gallic acid, ellagic acid, catechin) on *C. elegans* were compared. While all extended lifespan, different and complex effects were found on other parameters such as stress protection, growth, and reproduction. The

researchers observed a combination of "life-extending" and "toxic/negative" effects even with a single polyphenol. They noted that the mechanisms of these polyphenols are not solely dependent on antioxidant capacity; they can also be shaped through different pathways such as hormetic effects, calorie restriction-like effects, or antimicrobial activity (Saul et al., 2011). Previous studies have shown that polyphenols obtained from mulberry (Morus alba) leaves prolong the lifespan and increase oxidative stress resistance in *C. elegans*; however, these positive effects mostly occur in low-to-medium concentration ranges and vary depending on the dose. For example, mulberry leaf polyphenols have been reported to delay aging in *C. elegans*, a short-lived nematode model. These studies suggest that the antioxidant activity of leaf extracts and their effect on pathways regulating cellular stress response may have a positive impact on aging/functional resistance (Zheng et al., 2014).

In our findings, the observation of a still high reproduction rate (1500%) at 0.5 mg/mL suggests that the extract is not entirely harmful at low doses; in fact, some phenolic compounds may stimulate cellular defense mechanisms through a hormetic effect. Numerous studies in the literature on polyphenols report that in *C. elegans*, low/optimal concentrations enhance antioxidant defense and stress response (e.g., gst-4, sod-3 expression), leading to longevity and increased resistance; while higher concentrations conversely lead to oxidative stress, mitochondrial dysfunction, and mortality. This "hormesis" phenotype has been replicated for many plant compounds and is biologically consistent with the sharp decreases in the 1–2 mg/mL range in our findings (Ayuda-Durán et al., 2022). The dramatic population decrease at 1 mg/mL (regression to 150% increase) and the net population decrease at 2 mg/mL (−50%) in our study are likely the result of one or more mechanisms: (i) suppression of reproductive capacity (low egg yield or reproductive organ damage), (ii) larval developmental blockade (arrest at L1–L4 stages), (iii) adult mortality and/or (iv) nutritional deficiency due to inhibition of nutrient intake/interaction with green food (E. coli OP50). Separation of these mechanisms is common in the literature; for example, different polyphenols have been reported to have disparate effects on both growth and aging parameters in C. elegans. Therefore, relying solely on lifespan measurements can be misleading, and most reliable studies report multiple endpoints together, such as lifespan and reproduction/brood size, developmental time, and stress response (Saul et al., 2011). In terms of molecular mechanisms, flavonoids and other polyphenols are frequently associated with insulin/insulin-related processes.

CONCLUSION

This study demonstrates that mulberry leaf extract affects *C. elegans* population growth in a concentration-dependent manner. Low concentrations showed a mild suppressive effect on reproduction, while moderate and high concentrations resulted in significant reproductive inhibition and mortality. The findings reveal the potential biological activities and dose-dependent toxic effects of mulberry leaf extract, and provide a basis for future mechanistic and molecular-level studies.

ACKNOWLEDGEMENTS

I wish to express my deepest and sincere gratitude to my late father, Murat ÖZKAN, for his unwavering dedication, guidance, and support to his children. His encouragement has profoundly influenced my personal and professional journey and continues to serve as a lasting inspiration. May he rest in peace.

REFERENCES

Aranaz, P., Navarro-Herrera, D., Zabala, M., Romo-Hualde, A., López-Yoldi, M., Vizmanos, J. L., ... & González-Navarro, C. J. (2020). Phenolic compounds reduce the fat content in *Caenorhabditis elegans* by affecting lipogenesis, lipolysis, and different stress responses. Pharmaceuticals, 13(11), 355.

Ayuda-Durán, B., Sánchez-Hernández, E., González-Manzano, S., Santos-Buelga, C., & González Paramás, A. M. (2022). The effects of polyphenols against oxidative stress in *Caenorhabditis elegans* are determined by coexisting bacteria. Frontiers in Nutrition, 9, 989427.

Corsi, A. K., Wightman, B., & Chalfie, M. (2015). A transparent window into biology: a primer on *Caenorhabditis elegans*. Genetics, 200(2), 387-407.

Dhawan, K., Dhawan, S., & Sharma, A. (2004). Passiflora: a review update. Journal of ethnopharmacology, 94(1), 1-23.

Ding, A. J., Zheng, S. Q., Huang, X. B., Xing, T. K., Wu, G. S., Sun, H. Y., ... & Luo, H. R. (2017). Current perspective in the discovery of anti-aging agents from natural products. Natural products and bioprospecting, 7(5), 335-404.

Grünz, G., Haas, K., Soukup, S., Klingenspor, M., Kulling, S. E., Daniel, H., & Spanier, B. (2012). Structural features and bioavailability of four flavonoids and their implications for lifespan-extending and antioxidant actions in *C. elegans*. Mechanisms of Ageing and Development, 133(1), 1-10.

Guerrero-Rubio, M. A., Hernández-García, S., García-Carmona, F., & Gandía-Herrero, F. (2021). Flavonoids' effects on *Caenorhabditis elegans'* longevity, fat accumulation, stress resistance and gene modulation involve mTOR, SKN-1 and DAF-16. Antioxidants, 10(3), 438.

He, L., Xing, Y., Ren, X., Zheng, M., Yu, S., Wang, Y., ... & Dong, Y. (2022). Mulberry leaf extract improves metabolic syndrome by alleviating lipid accumulation *in vitro* and *in vivo*. Molecules, 27(16), 5111.

Hussain, F., Rana, Z., Shafique, H., Malik, A., & Hussain, Z. (2017). Phytopharmacological potential of different species of *Morus alba* and their bioactive phytochemicals: A review. Asian Pacific journal of tropical biomedicine, 7(10), 950-956.

Kaletta, T., & Hengartner, M. O. (2006). Finding function in novel targets: C. elegans as a model organism. Nature reviews Drug discovery, 5(5), 387-399.

Kumari, P. (2025). Phytochemical composition and antioxidant activity of mulberry (Moru s spp.) fruit extracts: a comparative analysis. J food Biotech, *6*(1), 11-14.

Li, Z., Liu, Y., Xiang, J., Wang, C., Johnson, J. B., & Beta, T. (2023). Diverse polyphenol components contribute to antioxidant activity and hypoglycemic potential of mulberry varieties. *LWT*, *173*, 114308.

Liu, L., Guo, P., Wang, P., Zheng, S., Qu, Z., & Liu, N. (2021). The review of anti-aging mechanism of polyphenols on Caenorhabditis elegans. *Frontiers in bioengineering and biotechnology*, *9*, 635768.

Long, N. P., Kang, J. S., & Kim, H. M. (2023). Caenorhabditis elegans: a model organism in the toxicity assessment of environmental pollutants. Environmental Science and Pollution Research, 30(14), 39273-39287.

Mahesh, D. S., Vidhathri, B. S., Vidyashree, D. N., Narayanaswamy, T. K., Subbarayappa, C. T., & Muthuraju, R. (2017). Biochemical composition and pharmacological properties of mulberry (Morus spp.)-a review. International Journal of Current Microbiology and Applied Sciences, 6(7), 2207-2217.

Memete, A. R., Timar, A. V., Vuscan, A. N., Miere, F., Venter, A. C., & Vicas, S. I. (2022). Phytochemical composition of different botanical parts of Morus species, health benefits and application in food industry. *Plants*, *11*(2), 152.

Mickymaray, S. (2019). Efficacy and mechanism of traditional medicinal plants and bioactive compounds against clinically important pathogens. Antibiotics, 8(4), 257.

Saul, N., Pietsch, K., Stürzenbaum, S. R., Menzel, R., & Steinberg, C. E. (2011). Diversity of polyphenol action in Caenorhabditis elegans: between toxicity and longevity. Journal of natural products, 74(8), 1713-1720.

Sies, H. (2015). Oxidative stress: a concept in redox biology and medicine. Redox biology, 4, 180-183.

Song, W., Wang, H. J., Bucheli, P., Zhang, P. F., Wei, D. Z., & Lu, Y. H. (2009). Phytochemical profiles of different mulberry (Morus sp.) species from China. Journal of agricultural and food chemistry, 57(19), 9133-9140.

Wang, Y. A., Liu, C., Guo, X., Zhang, M. Q., Sun, S., Sun, J. Y., ... & Chen, Y. Y. (2023). Natural Products and Biological Activities of Plants from Genus Morus: 2011-2023. Current Topics in Medicinal Chemistry, 23(28), 2640-2698.

Wang, Z., Tang, C., Xiao, G., Dai, F., Lin, S., Li, Z., & Luo, G. (2021). Comparison of free and bound phenolic compositions and antioxidant activities of leaves from different mulberry varieties. BMC chemistry, 15(1), 21.

Wanyu, L. (2025). Advancements in research on the anti-aging effects and mechanisms of flavonoids in natural products. Frontiers in Medicine, 12, 1637992.

Yang, J., Liu, X., Zhang, X., Jin, Q., & Li, J. (2016). Phenolic profiles, antioxidant activities, and neuroprotective properties of mulberry (Morus atropurpurea Roxb.) fruit extracts from different ripening stages. Journal of Food Science, 81(10), C2439-C2446.

Zhang, Y., et al. (2018). Natural product-mediated modulation of *C. elegans* population growth under oxidative stress. Frontiers in Aging, 10, 123–135.

Zheng, S., Liao, S., Zou, Y., Qu, Z., Shen, W., & Shi, Y. (2014). Mulberry leaf polyphenols delay aging and regulate fat metabolism via the germline signaling pathway in Caenorhabditis elegans. Age, 36(6), 9719.

ORAL PRESENTATION

Alüminyum fosfit zehirlenmesinde klinik yaklaşımlar ve gelecek perspektifleri

Gökçe Durmuş[1,2*] (*Orcid: https://orcid.org/0000-0001-9998-0499*),
Tülay Çoban[3] (*Orcid: https://orcid.org/0000-0002-9696-6613*)

[*1]Ankara Üniversitesi, Sağlık Bilimleri Enstitüsü, Farmasötik Toksikoloji Anabilim Dalı, Ankara, Türkiye
[2]Kastamonu Üniversitesi, İnebolu Meslek Yüksekokulu, Eczane Hizmetleri Bölümü, Kastamonu, Türkiye
[3]Ankara Üniversitesi, Eczacılık Fakültesi, Farmasötik Toksikoloji Anabilim Dalı, Ankara, Türkiye

*Sorumlu yazar e-mail: gdurmus@kastamonu.edu.tr

Özet

Alüminyum fosfit (ALP) zehirlenmesi, özellikle gelişmekte olan ülkelerde yüksek mortalite oranları ile seyreden kritik bir halk sağlığı sorunudur. Kolay erişilebilirliği ve spesifik bir antidotunun bulunmaması, bu zehirlenmeyi küresel bir toksikolojik acil durum haline getirmektedir. ALP'nin toksisitesi, mide asidi veya nem ile temas ettiğinde açığa çıkan fosfin (PH_3) gazından kaynaklanır. Fosfin gazının temel toksik mekanizması, mitokondriyal elektron taşıma zincirini, özellikle sitokrom c oksidazı (Kompleks IV) non-kompetitif olarak inhibe ederek hücresel solunumu bloke etmesidir. Bu durum, ATP üretiminin azalmasına, belirgin bir enerji krizine ve yoğun oksidatif strese yol açar. Klinik tabloya, en sık ölüm nedeni olan tedaviye dirençli (refrakter) kardiyojenik şok, derin metabolik asidoz ve çoklu organ yetmezliği hakimdir. Spesifik bir antidotun yokluğunda, tedavi yoğun bakım koşullarında yürütülen agresif destekleyici bakıma dayanmaktadır. Bu yaklaşım, hemodinamik ve solunumsal fonksiyonların sürdürülmesini hedefler ancak mortaliteyi düşürmede genellikle yetersiz kalır. Son yıllarda, zehirlenmenin temel patofizyolojisini hedef alan adjuvan tedaviler üzerine yapılan araştırmalar umut verici sonuçlar sunmaktadır. Özellikle, güçlü bir antioksidan olan N-asetilsistein (NAC) ve miyokardiyal enerji metabolizmasını destekleyen Glikoz-İnsülin-Potasyum (GIK) veya yüksek doz insülin tedavilerinin, yapılan meta-analizler ve klinik çalışmalarda mortaliteyi istatistiksel olarak anlamlı düzeyde azalttığı gösterilmiştir. Hindistancevizi yağı ile yapılan gastrik lavaj ve Koenzim Q10 gibi diğer antioksidanlar da klinik sonuçları iyileştirme potansiyeli taşımaktadır. Ayrıca, metabolomik yaklaşımlar ile alüminyum fosfit maruziyeti sonrası hücresel düzeyde gelişen biyokimyasal değişikliklerin sistematik olarak incelenmesi, erken risk tayini ve tedavi yanıtının değerlendirilmesi açısından tamamlayıcı bir perspektif sunabilir. Bu bilgiler, ALP zehirlenmesi için kanıta dayalı, standart bir tedavi protokolü oluşturma yolunda önemli bir temel oluşturmaktadır.
Anahtar Kelimeler: Alüminyum fosfit, fosfin, mitokondriyal disfonksiyon, oksidatif stres, antioksidan tedaviler, metabolomiks

Clinical approaches and future perspectives in aluminum phosphide poisoning

Abstract

Aluminum phosphide (ALP) poisoning is a critical public health problem, particularly in developing countries, characterized by high mortality rates. Its easy accessibility and the lack of a specific antidote make it a global toxicological emergency. The toxicity of ALP stems from phosphine (PH_3) gas, which is released upon contact with stomach acid or moisture. The primary toxic mechanism of phosphine gas is its non-competitive inhibition of the mitochondrial electron transport chain, particularly cytochrome c oxidase (Complex IV), thereby blocking cellular respiration. This leads to decreased ATP production, a significant energy crisis, and intense oxidative stress. The clinical picture is dominated by refractory cardiogenic shock, profound metabolic acidosis, and multiple organ failure, which is the most frequent cause of death. In the absence of a specific antidote, treatment relies on aggressive supportive care in intensive care settings. This approach aims to maintain hemodynamic and respiratory function but is generally insufficient to reduce mortality. In recent years, research on adjuvant therapies targeting the underlying pathophysiology of poisoning has yielded promising results. In particular, N-acetylcysteine (NAC), a potent antioxidant, and Glucose-Insulin-Potassium (GIK) or high-dose insulin therapy, which supports

myocardial energy metabolism, have been shown to statistically significantly reduce mortality in meta-analyses and clinical trials. Gastric lavage with coconut oil and other antioxidants such as Coenzyme Q10 also have the potential to improve clinical outcomes. Furthermore, systematically examining the biochemical changes at the cellular level following aluminum phosphide exposure using metabolomic approaches can offer a complementary perspective for early risk assessment and evaluation of treatment response. This information forms an important foundation for establishing an evidence-based, standardized treatment protocol for ALP poisoning.
Keywords: Aluminum phosphide, phosphine, mitochondrial dysfunction, oxidative stress, antioxidant therapies, metabolomics

GİRİŞ

Alüminyum fosfit (ALP) zehirlenmesi, özellikle gelişmekte olan ülkelerde, yüksek toksisitesi, tarımsal amaçlarla yaygın kullanılması ve kolay erişilebilir olması ve en önemlisi spesifik bir antidotunun bulunmaması nedeniyle son derece yüksek mortalite oranlarına sahip, kritik bir halk sağlığı sorunudur. Pestisitler dünya genelinde yılda yaklaşık 300.000 ölüme neden olmakta ve ALP, bu vakalar arasında %30-80 arasında değişen ölüm oranlarıyla en ölümcül ajanlardan biri olarak öne çıkmaktadır (Ullah ve ark., 2024; Hooshangi Shayesteh ve ark., 2024; Hájek ve ark., 2024; Sedaghattalab, 2022; Khodavysi ve ark., 2023).

Halk arasında "pirinç tableti" olarak da bilinen ALP, tahıl ve diğer depolanmış ürünleri zararlılardan korumak amacıyla yaygın olarak kullanılan katı formda bir fumigant, insektisit ve rodentisittir (Ullah ve ark., 2024; Hooshangi Shayesteh ve ark., 2024). Zehirlenme vakalarının artmasının ardındaki temel nedenler, ALP'nin kasıtlı (intihar amaçlı) kullanım için kolayca satın alınabilmesi ve bu ölümcül zehirlenmeyi geri döndürebilecek etkili ve spesifik bir antidot tedavisinin bulunmamasıdır (Ullah ve ark., 2024; Hooshangi Shayesteh ve ark., 2024; Salimi ve ark., 2022). Bu zehirlenmenin karmaşık patofizyolojisini ve yönetimindeki zorlukları anlamak, daha etkili tedavi stratejileri geliştirmek için elzemdir. Bu bağlamda, ALP'nin kullanım alanları, maruziyet yolları, toksik etki mekanizmaları ve güncel tedavi yaklaşımlarının ayrıntılı olarak ele alınması amaçlanmıştır.

Kullanım Alanları ve Maruziyet Yolları

ALP'nin tarımsal ve endüstriyel alandaki yaygın kullanımı, insan maruziyeti için önemli bir zemin hazırlamaktadır. Bu kullanım alanlarının ve maruziyet yollarının anlaşılması, zehirlenme risklerini belirleme ve önleme stratejileri geliştirme açısından stratejik bir öneme sahiptir.

ALP'nin birincil kullanım alanları şu şekilde özetlenebilir:

Tarım ve Depolama: Tahıl ve diğer gıda ürünlerinin depolanması sırasında zararlı böceklerden ve kemirgenlerden korunması amacıyla kullanılan katı bir fumiganttır (Ullah ve ark., 2024; Rahimi Kakavandi, 2022).

Endüstriyel Kullanım: Genel amaçlı bir insektisit (böcek ilacı) ve rodentisit (kemirgen ilacı) olarak da kullanılmaktadır (Ullah ve ark., 2024).

İnsanların ALP'ye maruz kalma yolları ise üç ana başlık altında incelenebilir:

Kasıtlı Maruziyet: Özellikle kolay erişilebilirliği ve yüksek toksisitesi nedeniyle, intihar amaçlı oral yolla alım, en yaygın ve en ölümcül maruziyet şeklidir (Ullah ve ark., 2024; Hooshangi Shayesteh ve ark., 2024).

Kazara Maruziyet: Çocuklarda tabletlerin kazara yutulması ve çiftçiler arasında güvenli olmayan depolama veya uygulama pratikleri sonucu mesleki maruziyetler de sıkça rapor edilmektedir (Elsharkawy ve ark., 2023).

İnhalasyon Yoluyla Maruziyet: Fumigasyon işlemi yapılan gemi konteynerleri, silolar veya bu alanlara bitişik binalar gibi kapalı mekanlarda, ortama salınan toksik fosfin gazının solunması yoluyla da ciddi zehirlenmeler meydana gelebilmektedir (Hájek ve ark., 2024; Sedaghattalab, 2022).

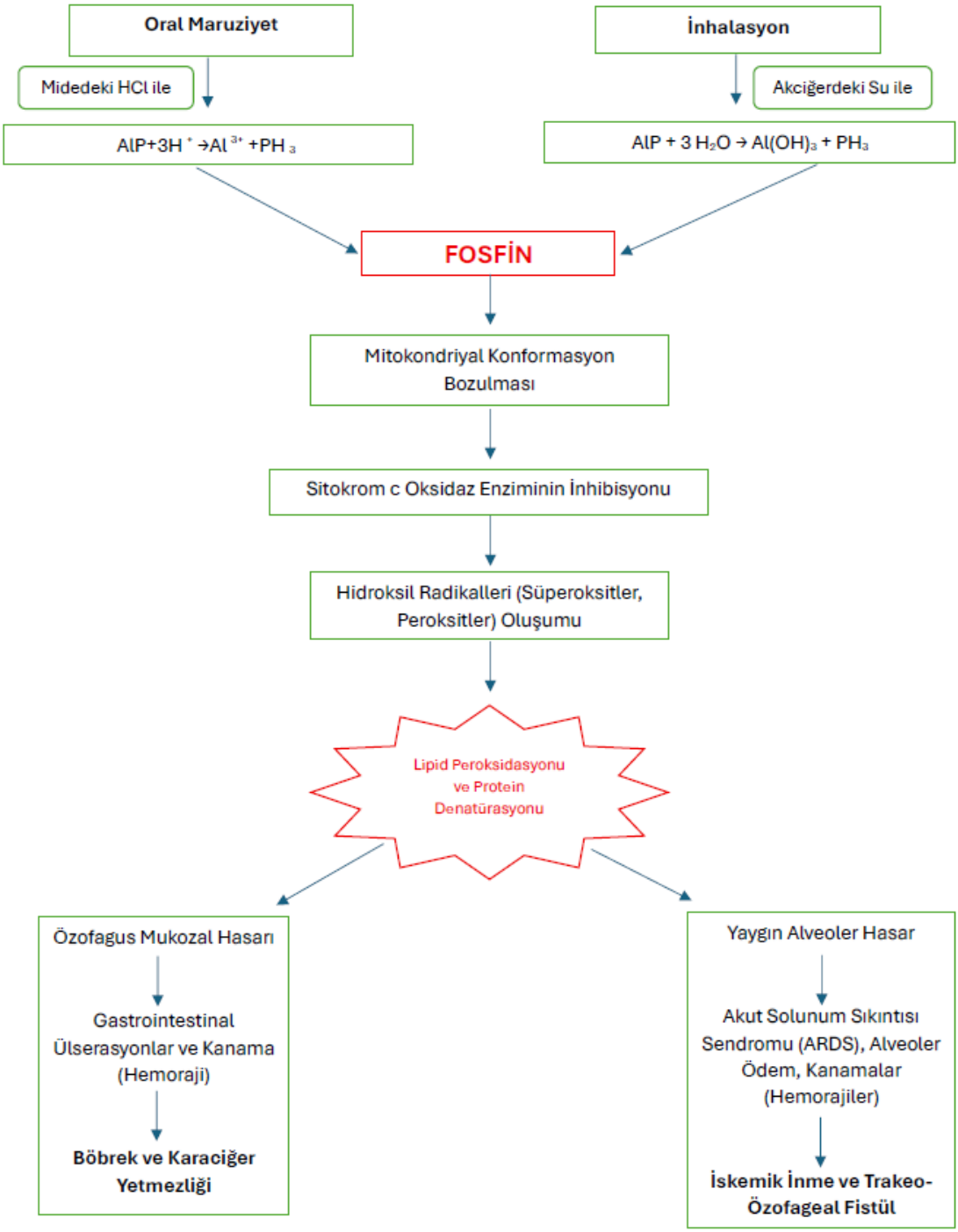
Bu maruziyet yollarının her biri, zehirlenmenin altında yatan ölümcül toksisite mekanizmalarını tetiklemektedir.

Toksisite Mekanizması

Alüminyum fosfit zehirlenmesinin yıkıcı etkileri, hücresel düzeyde başlayan karmaşık bir patofizyolojik süreçten kaynaklanır. Bu mekanizmayı anlamak, potansiyel tedavi hedeflerini belirlemede temel bir stratejik rol oynamaktadır. Toksik etkinin başlangıç adımı, katı haldeki ALP tabletlerinin mide asidi veya ortamdaki nem ile temas etmesi sonucu son derece toksik olan **fosfin gazını (PH_3)** açığa çıkarmasıdır (Ullah ve ark., 2024; Hooshangi Shayesteh ve ark., 2024; Khodavysi ve ark., 2023; Salimi ve ark., 2022). Bu gazın sistemik dolaşıma katılmasıyla hücresel hasara yol açan iki ana mekanizma devreye girer:

Mitokondriyal İnhibisyon ve Enerji Krizi: Fosfin, hücrenin enerji santralleri olan mitokondrilerde, elektron taşıma zincirinin son halkası olan **sitokrom c oksidazı (Kompleks IV)** başta olmak üzere diğer kompleksleri de (Kompleks I, II) non-kompetitif olarak inhibe eder. Bu inhibisyon, oksidatif fosforilasyonu, yani oksijen kullanarak ATP (hücresel enerji) üretme sürecini tamamen bloke eder. Sonuç olarak hücrede şiddetli bir enerji krizi başlar (Ullah ve ark., 2024; Hooshangi Shayesteh ve ark., 2024; Hájek ve ark., 2024; Rahimi Kakavandi ve ark., 2022; Abdelhamid ve ark., 2023). Kalp gibi metabolik aktivitesi ve enerji ihtiyacı çok yüksek olan organlar, bu enerji krizinden en ağır şekilde etkilenir ve bu durum, zehirlenmenin klinik seyrindeki kardiyovasküler kollapsın temelini oluşturur (Hooshangi Shayesteh ve ark., 2024; Rahimi Kakavandi ve ark., 2022).
Oksidatif Stres ve Hücresel Hasar: Mitokondriyal fonksiyonların bozulması, bir yan ürün olarak reaktif oksijen türlerinin (ROS) aşırı üretilmesine neden olur. Aynı zamanda fosfin, vücudun doğal antioksidan savunma sistemlerini oluşturan katalaz (CAT) ve süperoksit dismutaz (SOD) gibi enzimleri de baskılar. Bu iki etkinin birleşmesiyle hücrede kontrolsüz bir oksidatif stres tablosu ortaya çıkar. Aşırı ROS, hücre zarlarında lipid peroksidasyonuna, proteinlerin yapısının bozulmasına (denatürasyon), DNA hasarına ve nihayetinde apoptoz (programlanmış hücre ölümü) yoluyla hücre ölümüne yol açar (Salimi ve ark., 2022; Mahlooji ve ark., 2022; Parvizrad ve ark., 2022; Shaker ve ark., 2023; Zaare Nahandi ve ark., 2023).
Hücresel düzeyde yaşanan bu yıkım, çoklu organ sistemlerini etkileyen ciddi klinik bulgulara dönüşür.

Klinik Bulgular ve Toksisite Belirtileri
Alüminyum fosfit zehirlenmesinin klinik tablosu, altta yatan hücresel enerji krizi ve oksidatif stresin sistemik bir yansımasıdır. Bu bulguların erken dönemde tanınması, hayat kurtarıcı acil müdahalenin zamanında başlatılabilmesi açısından büyük önem taşımaktadır. Zehirlenmeye bağlı klinik belirti ve bulgular, etkilenen organ sistemlerine göre değerlendirilmektedir.
Kardiyovasküler Sistem: Kardiyovasküler sistem, alüminyum fosfit zehirlenmesinde en erken ve en ciddi şekilde etkilenen sistem olup, mortalitenin başlıca nedenini oluşturmaktadır. Klinik tabloda tedaviye dirençli (refrakter) hipotansiyon, kardiyojenik şok ve dolaşım kollapsı ön plandadır. Sinüs taşikardisi, atriyal fibrilasyon ve ventriküler aritmiler gibi ciddi ritim bozukluklarının sık görüldüğü bildirilmiştir. Miyokardiyal hasarı yansıtan ST segment elevasyonu veya depresyonu gibi elektrokardiyografik değişiklikler rapor edilmiş olup, fosfinin miyokard hücreleri üzerindeki doğrudan toksik etkisine bağlı olarak miyokardit ve perikardit gelişebileceği belirtilmektedir (Rahimi Kakavandi ve ark., 2022; Elsharkawy ve ark., 2023; Shaker ve ark., 2023).
Metabolik Bulgular: Dokuların yetersiz oksijenlenmesi (hipoperfüzyon) ve mitokondriyal solunum zincirinin bloke olması sonucu gelişen şiddetli metabolik asidoz ve laktik asidoz, alüminyum fosfit zehirlenmesinin en karakteristik laboratuvar bulguları arasında yer almaktadır (Ullah ve ark., 2024; Hooshangi Shayesteh ve ark., 2024; Hájek ve ark., 2024; Sedaghattalab, 2022; Khodavysi ve ark., 2023; Elsharkawy ve ark., 2023).
Solunum Sistemi: Solunum sistemi tutulumunda öksürük ve nefes darlığı (dispne) ile başlayan klinik tablo, hızla toksik akciğer ödemine ve akut solunum sıkıntısı sendromuna (ARDS) ilerleyebilmektedir. Bu durumda olguların önemli bir kısmında mekanik ventilasyon desteği gereksinimi ortaya çıkmaktadır (Abdelhamid ve ark., 2023; Shukla ve ark., 2024).
Gastrointestinal Sistem: Oral alımı takiben ilk klinik belirtiler genellikle gastrointestinal sistemde ortaya çıkmaktadır. Bulantı, kusma, ishal ve şiddetli karın ağrısı sık bildirilen bulgular arasında yer almaktadır (Sedaghattalab, 2022; Khodavysi ve ark., 2023; Abdelhamid ve ark., 2023; Shukla ve ark., 2024).
Nörolojik Sistem: Nörolojik bulgular baş dönmesi, baş ağrısı ve yorgunluk gibi hafif semptomlardan ataksi (denge bozukluğu), parestezi (uyuşma/karıncalanma) ve letarjiden komaya kadar ilerleyebilen bilinç bozukluklarına kadar geniş bir klinik spektrumda görülebilmektedir (Ullah ve ark., 2024; Shaker ve ark., 2023).
Diğer Organ Etkileri: Sistemik hipoperfüzyon ve fosfinin doğrudan toksik etkileri sonucunda akut karaciğer ve böbrek yetmezliği gelişiminin de klinik tabloya eşlik edebileceği bildirilmektedir (Ullah ve ark., 2024; Hooshangi Shayesteh ve ark., 2024; Shaker ve ark., 2023).
Bu ağır klinik tablonun ciddiyeti, mevcut tedavi yaklaşımlarının neden büyük ölçüde destekleyici nitelikte olduğunu ve özgül, geri döndürücü tedavilere duyulan gereksinimi açık bir biçimde ortaya koymaktadır.



Şekil 1: Alüminyum fosfitin toksik etki mekanizması.

MATERYAL VE METOT

Mevcut Tedavi Yaklaşımları

Alüminyum fosfit zehirlenmesi yönetimindeki en büyük zorluk, toksinin etkilerini doğrudan geri çevirecek, kanıta dayalı ve onaylanmış spesifik bir antidotun bulunmamasıdır. Bu nedenle tedavinin temelini, toksin vücuttan atılana kadar hayati organ fonksiyonlarının sürdürülmesini amaçlayan agresif destekleyici bakım oluşturmaktadır. Bu

özellikleri nedeniyle, alüminyum fosfit zehirlenmesi tanısı alan hastaların yönetimi tercihen 3. basamak yoğun bakım ünitelerinde yürütülmelidir (Rahimi Kakavandi ve ark., 2022; Parvizrad ve ark., 2022; Zaare Nahandi ve ark., 2023).

Tedavi planlamasında kabul edilmesi gereken ilk ve en temel gerçek, bu zehirlenme için spesifik bir antidotun mevcut olmamasıdır. Bu durum, tedavi yaklaşımının semptomlara ve gelişen komplikasyonlara yönelik olarak şekillendirilmesini zorunlu kılmaktadır. Oral alımı takiben özellikle ilk saatlerde, midede kalan tabletlerden fosfin gazı salınımını önlemek veya azaltmak amacıyla mide dekontaminasyonu uygulanabilmektedir. Su bazlı solüsyonların fosfin salınımını artırabileceğine dair endişeler nedeniyle, mide lavajında potasyum permanganat, sodyum bikarbonat ve fosfin salınımını azaltabileceği ve lokal antioksidan etki gösterebileceği düşünülen hindistancevizi yağı gibi yağ bazlı solüsyonların tercih edildiği bildirilmektedir (Ullah ve ark., 2024; Elsharkawy ve ark., 2023; Abdelhamid ve ark., 2023; Zaare Nahandi ve ark., 2023; Aghebat-Bekheir ve ark., 2024). Emilimi azaltmaya yönelik olarak aktif kömür uygulaması da tedavi seçenekleri arasında yer almaktadır (Elsharkawy ve ark., 2023; Shaker ve ark., 2023).

Hastanın hayatta kalması büyük ölçüde yoğun bakım koşullarında sağlanan destekleyici tedavilere bağlıdır. Özellikle dolaşım kollapsı, alüminyum fosfit zehirlenmesinin en sık mortal seyreden komplikasyonlarından biri olduğundan, agresif intravenöz sıvı resüsitasyonu ve kan basıncının sürdürülmesi amacıyla norepinefrin gibi vazopresör ajanların kullanımı kritik önem taşımaktadır (Elsharkawy ve ark., 2023; Aghebat-Bekheir ve ark., 2024). Dokularda gelişen hipoksi ve mitokondriyal fonksiyon bozukluğuna bağlı olarak ortaya çıkan şiddetli metabolik asidozun düzeltilmesi amacıyla intravenöz sodyum bikarbonat infüzyonu uygulanabilmektedir (Ullah ve ark., 2024; Sedaghattalab, 2022; Elsharkawy ve ark., 2023; Shaker ve ark., 2023).

Solunum sistemi tutulumu olan hastalarda hipoksinin düzeltilmesi için oksijen tedavisi temel yaklaşımlardan biridir. Akut solunum sıkıntısı sendromu (ARDS) gelişen olgularda ise erken entübasyon ve mekanik ventilasyon desteği hayat kurtarıcı olmaktadır (Hájek ve ark., 2024; Elsharkawy ve ark., 2023; Sobh ve ark., 2023).

Mevcut destekleyici tedavi yaklaşımlarının, özellikle ağır vakalarda, yüksek mortalite oranlarını anlamlı düzeyde düşürmedeki yetersizliği; alüminyum fosfit zehirlenmesinin temel patofizyolojik mekanizmalarını hedef alan yeni ve deneysel tedavi yöntemlerine yönelik araştırmaların artmasına neden olmuştur.

Araştırılan ve Mevcut Deneysel Tedavi Yöntemleri

Mevcut standart tedavilerin sınırlılıkları ve yüksek mortalite oranları göz önüne alındığında, ALP'nin temel toksik mekanizmaları olan oksidatif stresi ve mitokondriyal enerji krizini hedef alan deneysel ve adjuvan (destekleyici) tedavilerin araştırılması büyük bir stratejik önem taşımaktadır. Bu yaklaşımlar, zehirlenmenin temel patofizyolojisine müdahale ederek klinik sonuçları iyileştirme potansiyeli sunmaktadır.

Antioksidan Tedaviler

Bu tedaviler, fosfin gazının neden olduğu yoğun hücresel oksidatif stresi nötralize etmeyi veya azaltmayı hedefler. Bu gruptaki ajanlar arasında, N-asetilsistein (NAC) meta-analiz düzeyinde güçlü kanıtlarla desteklenirken, diğer antioksidanlar için kanıtlar daha çok tekil klinik çalışmalar veya hayvan modellerine dayanmaktadır (Sobh ve ark., 2023).

N-Asetilsistein (NAC): Güçlü bir antioksidan ve vücudun en önemli endojen antioksidanı olan glutatyonun öncül maddesidir. Yapılan çok sayıda klinik çalışmayı bir araya getiren meta-analizler, standart tedaviye eklenen NAC'nin mortaliteyi istatistiksel olarak anlamlı ölçüde azalttığını göstermiştir; bir meta-analiz bu azalmayı yaklaşık üç kat olarak, bir diğeri ise risk oranını yaklaşık 0.5 olarak belirlemiştir (Parvizrad ve ark., 2022; Shaker ve ark., 2023; Sobh ve ark., 2023).

Koenzim Q10 (CoQ10): Mitokondriyal elektron taşıma zincirinde rol alan ve aynı zamanda güçlü bir lipofilik antioksidan olan CoQ10, klinik çalışmalarda hemodinamik parametreleri (kan basıncı) ve vücudun toplam antioksidan kapasitesini iyileştirmiştir. Hayvan deneylerinde ise karaciğer koruyucu (hepatoprotektif) etkileri olduğu gösterilmiştir. Bununla birlikte, mevcut klinik çalışmaları birleştiren bir meta-analizde, CoQ10'un mortalite üzerinde istatistiksel olarak anlamlı bir etki göstermediği bulunmuştur (Hooshangi Shayesteh ve ark., 2024; Elsharkawy ve ark., 2023; Sobh ve ark., 2023).

Diğer Antioksidanlar: Bir meta-analizde, **Vitamin E**'nin mortaliteyi anlamlı ölçüde azalttığı bulunmuş, ancak bu bulgunun tek bir çalışmaya dayanması ve sonucun istatistiksel güven aralığının çok geniş olması nedeniyle güvenilirliğinin düşük olduğu ve daha fazla çalışmaya ihtiyaç duyulduğu vurgulanmıştır (Sobh ve ark., 2023). Hayvan modellerinde, **nanokurkuminin** karaciğer ve akciğer koruyucu etkileri gösterilmiştir (Khodavysi ve ark., 2023; Salimi ve ark., 2022; Mahlooji ve ark., 2022). **Melatonin** ve **L-karnitin** gibi diğer antioksidan ajanlar da

hem hayvan deneylerinde hem de klinik çalışmalarda araştırılmış ve potansiyel faydaları bildirilmiştir (Abdelhamid ve ark., 2023; Parvizrad ve ark., 2022; Zaare Nahandi ve ark., 2023).

Metabolik Destek Tedavileri

Bu yaklaşımlar, özellikle fosfinin neden olduğu enerji krizinden en çok etkilenen kalp kasının (miyokard) enerji metabolizmasını desteklemeyi amaçlar.

Glikoz-İnsülin-Potasyum (GIK) / Yüksek Doz İnsülin Tedavisi: Stres altındaki miyokardın birincil yakıtı olan glikozun hücre içine alımını ve kullanımını artırarak pozitif inotropik (kalp kasılma gücünü artırıcı) etki gösterir. Yapılan klinik çalışmalar ve bu çalışmaları özetleyen sistematik derlemeler, yüksek doz insülin içeren GIK tedavilerinin mortaliteyi anlamlı derecede düşürdüğünü ortaya koymuştur; örneğin, bir çalışmada GIK tedavisi almayan gruptaki %73'lük mortalite oranını %20'ye düşürdüğü bildirilmiştir (Ullah ve ark., 2024; Sedaghattalab, 2022; Shukla ve ark., 2024).

İleri Yaşam Desteği ve Diğer Yaklaşımlar

Yağ Bazlı Gastrik Lavaj: Özellikle **hindistancevizi yağı** gibi yağların, fosfin salınımını azaltma ve lokal antioksidan etki gösterme potansiyeli ile klinik çalışmalarda sonuçları iyileştirdiği raporlanmıştır (Elsharkawy ve ark., 2023).

Ekstrakorporeal Membran Oksijenasyonu (ECMO): Tedaviye dirençli şiddetli kardiyojenik şok ve/veya solunum yetmezliği olan seçilmiş vakalarda, kalp ve akciğer fonksiyonlarını geçici olarak devralan bir kurtarma tedavisi olarak kullanılmıştır (Hájek ve ark., 2024; Shukla ve ark., 2024).

Hiperbarik Oksijen Tedavisi (HBOT): Bir olgu sunumunda başarılı bir şekilde kullanıldığı ve bir hayvan çalışmasında sağkalım süresini uzattığı gösterilmiştir. Ancak bu alanda daha fazla araştırmaya ihtiyaç duyulmaktadır (Hájek ve ark., 2024).

Magnezyum Sülfat: Anti-aritmik ve membran stabilize edici özellikleri nedeniyle birçok merkezde destekleyici tedavi protokollerinin bir parçası olarak kullanılmaktadır (Ullah ve ark., 2024; Elsharkawy ve ark., 2023).

Sevelamer: Bir in vivo çalışmada, ALP zehirlenmesine karşı yeni bir antidot olarak araştırıldığı belirtilmiştir (Heidari ve ark., 2023).

Bu umut vaat eden yaklaşımların varlığına rağmen, her birinin kendi sınırlılıkları bulunmaktadır ve zehirlenme yönetimindeki genel zorluklar devam etmektedir.

Gelecek Perspektifleri

Alüminyum fosfit zehirlenmesinde klasik klinik parametreler ve biyobelirteçler, prognoz tayininde çoğu zaman yetersiz kalmaktadır. Bu sınırlılık, maruziyet sonrası erken dönemde hücresel düzeyde gelişen metabolik ve biyokimyasal değişikliklerin daha bütüncül yaklaşımlarla incelenmesini gündeme getirmektedir. Metabolomik analizler, hücrelerdeki enerji metabolizması bozuklukları, oksidatif stres yanıtları ve diğer biyokimyasal değişimleri sistematik olarak değerlendirme olanağı sunar. Bu tür biyoteknolojik yaklaşımlar, henüz klinik pratiğe doğrudan yansımamış olsa da, ileride erken risk sınıflaması, hastalık şiddetinin öngörülmesi ve tedavi yanıtının izlenmesi açısından önemli bir tamamlayıcı perspektif sağlayabilir (Wishart, 2022).

BULGULAR ve TARTIŞMA

Alüminyum fosfit zehirlenmesinde bildirilen son derece yüksek mortalite oranları, hem altta yatan patofizyolojik mekanizmaların ağırlığını hem de mevcut tedavi yaklaşımlarının sınırlılıklarını açıkça yansıtmaktadır. Fosfin gazının mitokondriyal solunumu hızlı ve büyük ölçüde geri döndürülemez biçimde inhibe etmesi, özellikle yüksek enerji gereksinimi olan kalp gibi organlarda hücresel enerji üretiminin durmasına yol açmaktadır. Bu süreç, standart tedavilere yanıt vermeyen refrakter kardiyojenik şok ve derin metabolik asidoz gelişimiyle sonuçlanmakta ve çoğu vakada ölümle sonlanan ortak patofizyolojik yol olarak karşımıza çıkmaktadır.

Tedavideki en temel ve kritik sınırlılık, bu yıkıcı süreci doğrudan hedefleyerek geri çevirebilecek spesifik bir antidotun bulunmamasıdır. Bu durum, alüminyum fosfit zehirlenmesinin yönetimini büyük ölçüde semptom kontrolü ve hayati organ fonksiyonlarının desteklenmesine dayalı bir yaklaşımla sınırlandırmaktadır.

Son yıllarda araştırılan N-asetilsistein, GIK/yüksek doz insülin tedavisi ve diğer antioksidan ajanlar, zehirlenmenin temel patofizyolojik mekanizmalarına yönelik müdahale potansiyelleri nedeniyle dikkat çekmektedir. Bu yaklaşımların öne çıkması rastlantısal değildir; N-asetilsistein oksidatif stresi doğrudan hedeflerken, insülin temelli

tedaviler fosfin toksisitesinin en belirgin etkilerinin görüldüğü miyokardda hücresel enerji üretimini destekleyen alternatif bir metabolik yol sunmaktadır. Bununla birlikte, bu tedavilere ilişkin mevcut kanıtların önemli bir bölümü küçük örneklemli klinik çalışmalara, hayvan deneylerine veya sınırlı sayıda olgu sunumuna dayanmaktadır. Bu nedenle elde edilen sonuçların geniş hasta popülasyonlarına doğrudan genellenmesi güçtür.
Özellikle N-asetilsistein ve yüksek doz insülin tedavisi gibi mortalite üzerine olumlu etkiler bildiren yaklaşımlar için, bu bulguların doğrulanması ve standart tedavi protokollerine entegrasyonu amacıyla daha geniş örneklemli, çok merkezli ve randomize kontrollü klinik çalışmalara ihtiyaç olduğu açıktır.

SONUÇ

Alüminyum fosfit zehirlenmesi, spesifik bir antidotunun bulunmaması ve yol açtığı yüksek mortalite oranları nedeniyle küresel ölçekte önemli bir toksikolojik acil durum olmaya devam etmektedir. Zehirlenmenin temel toksik mekanizması, fosfin gazına bağlı mitokondriyal solunum inhibisyonu ve bunun sonucunda gelişen şiddetli oksidatif stres ile hücresel enerji krizidir.
Güncel tedavi yaklaşımı, yoğun bakım koşullarında uygulanan agresif destekleyici tedavi ile sınırlı olup, özellikle ağır vakalarda sıklıkla yetersiz kalmaktadır. Bu nedenle, zehirlenmenin patofizyolojisini hedef alan adjuvan tedaviler giderek daha fazla önem kazanmaktadır. Mevcut literatür ışığında, N-asetilsistein gibi antioksidan yaklaşımlar ile GIK/yüksek doz insülin gibi metabolik destek tedavileri mortaliteyi azaltma potansiyeli açısından öne çıkan seçenekler arasında yer almaktadır. Bununla birlikte, bu tedavilerin etkinliğini ve güvenliğini kesin olarak ortaya koyacak, kanıta dayalı ve standartlaştırılmış bir tedavi protokolü oluşturabilmek için daha fazla yüksek kaliteli, çok merkezli klinik araştırmaya ihtiyaç bulunmaktadır.

KAYNAKLAR

Abdelhamid, W. G., Sakr, M. L., Mostafa, O. E., Zaafar, D., & Abdelwahab, H. M. (2023). Comparing the effectiveness of L-carnitine and paraffin oil in acute aluminum phosphide poisoning using predictive biomarkers and scores: a randomized controlled clinical trial. *Human & Experimental Toxicology, 42*, 09603271221149650.

Aghebat-Bekheir, S., & Abdollahi, M. (2024). Discovering the most impactful treatments for aluminum phosphide cardiotoxicity gleaned from systematic review of animal studies. *Human & Experimental Toxicology, 43*, 09603271241290922.

Elsharkawy, R. E., Ghonem, M. M., El-Sarnagawy, G. N., Nagy, A. A., & Heshmat, M. M. (2023). Cardioprotective role of the coenzyme Q10 and coconut oil in acute aluminum phosphide poisoning: a randomized controlled clinical trial. *Toxicology Research, 12*(3), 507–519.

Hájek, M., Chmelař, D., Tlapák, J., Rybárová, V., Ondra, P., & Halouzka, V. (2024). Accidental aluminum phosphide intoxication successfully treated with hyperbaric oxygen therapy: a case report. *Toxics, 12*(4), 272.

Heidari, R., Mohammadi, H. R., Goudarzi, F., & Farjadian, F. (2023). Repurposing of sevelamer as a novel antidote against aluminum phosphide poisoning: an in vivo evaluation. *Heliyon, 9*(4).

Hooshangi Shayesteh, M. R., Hami, Z., Chamanara, M., Parvizi, M. R., Golaghaei, A., & Nassireslami, E. (2024). Evaluation of the protective effect of coenzyme Q10 on hepatotoxicity caused by acute phosphine poisoning. *International Journal of Immunopathology and Pharmacology, 38*, 03946320241250286.

Khodavysi, M., Kheiripour, N., Ghasemi, H., Soleimani-Asl, S., Jouzdani, A. F., Sabahi, M., … & Ranjbar, A. (2023). How can nanomicelle-curcumin modulate aluminum phosphide-induced neurotoxicity?: Role of SIRT1/FOXO3 signaling pathway. *AIMS Neuroscience, 10*(1), 56.

Mahlooji, M. A., Heshmati, A., Kheiripour, N., Ghasemi, H., Asl, S. S., Solgi, G., … & Hosseini, A. (2022). Evaluation of protective effects of curcumin and nanocurcumin on aluminium phosphide induced subacute lung injury in rats: modulation of oxidative stress through SIRT1/FOXO3 signalling pathway. *Drug Research, 72*(02), 100–108.

Parvizrad, R., Marghamlki, E. G., Nikfar, S., & Dermani, S. K. (2022). Effects of melatonin and N-acetylcysteine on aluminum phosphide poisoning in rats. *Journal of Family Medicine and Primary Care, 11*(8), 4500–4504.

Rahimi Kakavandi, N., Asadi, T., Hooshangi Shayesteh, M. R., Baeeri, M., Rahimifard, M., Baghaei, A., … & Abdollahi, M. (2022). The electrocardiographic, hemodynamic, echocardiographic, and biochemical

evaluation of treatment with edaravone on acute cardiac toxicity of aluminum phosphide. *Frontiers in Pharmacology, 13*, 1032941.

Salimi, A., Kheiripour, N., Fathi Jouzdani, A., Ghasemi, H., Soleimani Asl, S., Ghafouri-Khosrowshahi, A., & Ranjbar, A. (2022). Nanocurcumin improves lipid status, oxidative stress, and function of the liver in aluminium phosphide-induced toxicity: cellular and molecular mechanisms. *BioMed Research International, 2022*(1), 7659765.

Sedaghattalab, M. (2022). Treatment of critical aluminum phosphide (rice tablet) poisoning with high-dose insulin: a case report. *Journal of Medical Case Reports, 16*(1), 192.

Shaker, H. O., Rageh, O. E. S., Alnajar, M., Alshamaly, N. F., Abdelmaged, W. A., & Abd-ElGawad, M. (2023). Efficacy of intravenous N-acetylcysteine as an adjuvant therapy in the treatment of acute aluminum phosphide poisoning: a systematic review and meta-analysis. *BMC Pharmacology and Toxicology, 24*(1), 59.

Shukla, R., Lamichhane, K., Pandey, D., Gupta, C. K., & Shukla, S. (2024). Insulin in aluminum phosphide poisoning: a systematic review of the current literature. *Medicine, 103*(42), e40066.

Sobh, Z. K., & Abd-Elhameed, A. (2023). The therapeutic benefit of antioxidants on the outcome of acute aluminum phosphide poisoning: a systemic review and meta-analysis. *Toxicology Research, 12*(3), 345–354.

Ullah, A., Jan, S., Shahzad, H., Dar, M. R., Khan, S., Ahmad, K., … & Dar, M. (2024). Therapeutic effect of glucose-insulin-potassium (GIK) infusion therapy in the treatment of acute aluminum phosphide poisoning: an institutional study. *Cureus, 16*(12).

Wishart, D. (2022). Metabolomics and the multi-omics view of cancer. *Metabolites, 12*(2), 154.

Zaare Nahandi, M., & Banagozar Mohammadi, A. (2023). Problems with the effectiveness of L-carnitine and paraffin oil in acute aluminum phosphide poisoning. *Human & Experimental Toxicology, 42*, 09603271231210974.

ORAL PRESENTATION

Enhancement of diagnostic power of miR-126-3p and inflammatory clinical markers in COPD with random forest machine learning

Sumeyye Yildirim[1*] (*ORCID: https://orcid.org/0009-0008-5402-3140*),
Nevin Karakus[1] (*ORCID: https://orcid.org/0000-0002-1916-7471*)

[*1] Tokat Gaziosmanpasa University, Faculty of Medicine, Department of Medical Biology, Tokat, Turkey.

*Corresponding author e-mail: sumeyyeyldrm997@gmail.com

Abstract

Chronic obstructive pulmonary disease (COPD) is a common pulmonary disease characterized by airway inflammations, associated with high morbidity and mortality, and increasing in prevalence with age. MicroRNAs (miRNAs) play critical regulatory roles in COPD pathogenesis. This study aimed to determine the diagnostic potential obtained by combining miR-126-3p and inflammatory clinical markers (CRP, WBC, etc.) using Machine Learning (ML) algorithms. To assess the limitations of traditional approaches, the Logistic Regression classification model (Traditional ML) was used as a reference for single miR-126-3p analysis. For the primary analysis, a powerful ensemble algorithm (Random Forest) classifier model was employed to model the non-linear complex interactions of the entire biomarker panel (miR-126-3p + 4 clinical parameters). Data were scaled with StandardScaler and split into Training/Test sets (%80/%20). Diagnostic performance was evaluated using Area Under the Curve (AUC), Accuracy, and the Confusion Matrix. The Logistic Regression model using single miR-126-3p exhibited limited performance in COPD diagnosis (AUC=0.58). The performance of the multi-parameter panel created with Random Forest combining miR-126-3p and clinical parameters increased substantially. The model achieved 100.00% accuracy and an AUC value of 1.0000 on the test data. Confusion Matrix analysis confirmed that the model recorded no False Positive or False Negative errors, thereby confirming its perfect (optimum) discriminatory power. Feature Importance analysis showed that miR-126-3p provided a significant independent contribution to the model's final decision alongside clinical markers. Our study proves that traditional statistical methods must be transcended to reveal the true clinical value of potential biomarkers. The resulting AUC 1.0000 demonstrates that combining miR-126-3p with clinical parameters via ML establishes a strong foundation for developing next-generation diagnostic tools with impeccable reliability in COPD diagnosis.

Keywords: COPD, miR-126-3p, Machine Learning, Random Forest

KOAH tanısında miR-126-3p ve inflamatuar klinik belirteçlerin tanısal gücünün random forest (RF) makine öğrenimi ile artırılması

Özet

Kronik obstrüktif akciğer hastalığı (KOAH), solunum yolu inflamasyonları ile karakterize edilen, yüksek morbidite ve mortaliteye sahip, yaygın bir akciğer hastalığıdır. MikroRNA (miRNA)'lar, KOAH patogenezinde kritik düzenleyici roller üstlenir. Bu çalışma, miR-126-3p'nin ve inflamatuar klinik belirteçlerin (CRP, WBC vb.) Makine Öğrenimi (ML) ile birleştirilmesi sonucu elde edilen tanısal potansiyeli belirlemeyi amaçlamıştır. Geleneksel yaklaşımların sınırlılıklarını değerlendirmek üzere, tekli miR-126-3p analizinde Lojistik Regresyon sınıflandırma modeli (Geleneksel ML) referans olarak kullanılmıştır. Birincil analiz olarak, tüm biyobelirteç panelinin (miR-126-3p + 4 klinik parametre) doğrusal olmayan karmaşık etkileşimlerini modellemek amacıyla güçlü bir ensemble (topluluk) algoritması olan Rastgele Orman (Random Forest) sınıflandırıcı modeli kullanılmıştır. Veriler StandardScaler ile ölçeklenmiş ve Eğitim/Test (%80/%20) olarak ayrılmıştır. Tanısal performans Eğri Altındaki Alan (AUC), Doğruluk ve Hata Matrisi ile değerlendirilmiştir. Tek başına miR-126-3p'yi kullanan Lojistik

Regresyon modeli, KOAH tanısında sınırlı performans göstermiştir (AUC=0.58). Random Forest ile oluşturulan multi-parametre panelinin performansı önemli ölçüde artmıştır. Model, test verisi üzerinde %100.00 doğruluk ve 1.0000 AUC değeri elde etmiştir. Hata Matrisi analizi, modelin hiçbir Yalancı Pozitif (False Positive) veya Yalancı Negatif (False Negative) hata kaydetmediğini, ayırma gücünün mükemmel (optimum) olduğunu teyit etmiştir. Özellik Önem Düzeyi analizi, miR-126-3p'nin klinik belirteçlere önemli bir bağımsız katkı sunduğunu göstermiştir. Çalışmamız, potansiyel biyobelirteçlerin klinik tanıdaki gerçek değerini ortaya çıkarmak için geleneksel istatistiksel yöntemlerin ötesine geçilmesi gerektiğini kanıtlamaktadır. Elde edilen AUC 1.0000 sonucu, miR-126-3p'nin klinik parametrelerle ML ile birleştirilmesinin, KOAH tanısında kusursuz güvenilirliğe sahip yeni nesil tanısal araçlar geliştirmek için güçlü bir zemin hazırladığını göstermektedir.

Anahtar Kelimeler: KOAH, miR-126-3p, Makine Öğrenimi, Random Forest

1. GİRİŞ

Kronik obstrüktif akciğer hastalığı (KOAH), kalıcı hava akımı kısıtlılığı ve kronik solunum yolu inflamasyonu ile karakterize olup dünya genelinde yüksek morbidite ve mortaliteye yol açan bir akciğer hastalığıdır. 2025 GOLD raporunda vurgulandığı üzere, hastalığın erken dönemde tanımlanması ve klinik seyrinin doğru öngörülmesi, hem kişiselleştirilmiş tedavi yaklaşımları hem de hastalık yükünün azaltılması açısından kritik önem taşımaktadır (GOLD, 2025).

Son yıllarda mikroRNA'lar (miRNA'lar), KOAH patogenezi ve klinik uygulamalar açısından önemli bir araştırma alanı hâline gelmişir. Bu küçük, kodlamayan RNA'lar inflamasyon, oksidatif stres, hücresel yaşlanma ve doku yeniden yapılanması gibi KOAH ile ilişkili temel biyolojik süreçleri düzenlemektedir. Kan ve doku örneklerinde değerlendirilen miRNA ekspresyon düzeyleri, hem stabil hastalık döneminde hem de alevlenme süreçlerinde potansiyel tanısal ve prognostik belirteçler olarak incelenmiştir. Meta-analiz ve sistematik çalışmalar, dolaşımdaki miRNA'ların KOAH'ın tanısal doğruluğunu artırma potansiyeline sahip olduğunu göstermektedir (Li ve ark., 2024; Zhu ve ark., 2023).

KOAH'ta miR-126-3p gibi miRNA'ların inflamasyon ve vasküler yapıdaki değişikliklerle ilişkili olduğu, bazı çalışmalarda bu molekülün hastalarda azalmış düzeylerde bulunduğu bildirilmiştir (Peng ve ark., 2022). Bununla birlikte, tek bir biyobelirtece veya CRP gibi klasik inflamatuar parametrelere dayalı tanısal yaklaşımların gücü, hastalığın biyolojik heterojenliği ve değişken inflamatuar yanıt nedeniyle çoğu zaman sınırlı kalmaktadır. Bu sınırlılıklar, çoklu biyobelirteç panelleri ve gelişmiş analiz yöntemlerinin kullanımını giderek daha gerekli hâle getirmektedir (Li ve ark., 2024).

Makine Öğrenimi (ML) yöntemleri, çoklu klinik ve moleküler değişkenler arasındaki doğrusal olmayan ilişkileri modelleyebilme, değişken önemini değerlendirebilme ve yüksek sınıflandırma doğruluğu sağlayabilme özellikleri sayesinde tıp alanında giderek daha yaygın kullanılmaktadır. KOAH özelinde yapılan derleme ve karşılaştırmalı çalışmalar, ensemble yöntemlerin ve özellikle Random Forest (RF) algoritmasının sınıflandırma performansı, değişken seçimi ve aşırı uyumu azaltmadaki başarısı nedeniyle biyobelirteç temelli tanısal modellerde öne çıktığını göstermektedir (Topalovic ve ark., 2019; Esteban ve ark., 2021).

Bu çalışmanın amacı, miR-126-3p ekspresyon düzeylerini CRP, WBC, NEU ve LYM gibi inflamatuar belirteçlerle birlikte değerlendirerek, Random Forest tabanlı makine öğrenimi modeli aracılığıyla bu biyobelirteç panelinin KOAH tanısındaki ayırt edici potansiyelini ortaya koymaktır.

2. MATERYAL VE METOD

Çalışmamız, miR-126-3p ekspresyon düzeyleri ile dört rutin klinik belirtecin (CRP, WBC, NEU, LYM) kombine edilerek KOAH tanısındaki ayırt edici gücünü ML algoritmaları aracılığıyla inceleyen ikincil (sekonder) ve hesaplamalı bir analizdir.

2.1 Çalışma Grubu

Bu analiz için kullanılan biyolojik ve klinik veriler, daha önce yayınlanmış olan bir prospektif çalışmadan elde edilmiştir (Yıldırım ve ark., 2026). Orijinal çalışma, toplam 53 KOAH tanılı hasta ile 52 sağlıklı bireyden oluşan kontrol grubunun verilerini içermektedir.

Orijinal veri toplama süreci, Tokat Gaziosmanpaşa Üniversitesi Tıp Fakültesi Dekanlığı Etik Kurulunun onayıyla gerçekleştirilmiş olup, tüm katılımcılardan Bilgilendirilmiş Onam Formu alınmıştır. Bu retrospektif ML analizi, mevcut veriler üzerinde yeni bir hesaplamalı yöntem uyguladığı için ayrıca bir etik onayı gerektirmemektedir.

2.2 Biyobelirteç Ölçümleri

2.2.1 Klinik Veriler

Çalışma grubuna ait CRP, WBC, NEU ve LYM düzeyleri, hastaların tanı anındaki rutin klinik laboratuvar kayıtlarından elde edilmiştir. Bu dört klinik parametre, miR-126-3p ile birlikte tanı panelini oluşturmuştur.

2.2.2 miR-126-3p Ekspresyon Analizi

miR-126-3p ekspresyon düzeyleri, hasta ve kontrol gruplarından toplanan kan örneklerinden izole edilen RNA'lar kullanılarak Gerçek Zamanlı Polimeraz Zincir Reaksiyonu (qRT-PCR) yöntemiyle ölçülmüştür. miR-126-3p için log2-delta delta CT ($2^{-\Delta\Delta Ct}$) yöntemiyle ekspresyon değerleri, bağımsız değişken olarak ML analizine dahil edilmiştir.

2.3 İstatistiksel ve Makine Öğrenimi Değerlendirmesi

2.3.1 Veri Ön İşleme ve Ayrımı

Makine öğrenimi modellemesinden önce, farklı ölçüm ölçeklerine sahip değişkenlerin model üzerindeki etkilerini eşitlemek amacıyla tüm sayısal veriler StandardScaler yöntemi ile normalize edilmiş ve ölçeklendirilmiştir. Veri seti, modelin genelleme yeteneğini ve test verisi üzerindeki performansını değerlendirmek için Eğitim (%80) ve Test (%20**)** veri setleri olarak rastgele ikiye ayrılmıştır.

2.3.2 Makine Öğrenimi Modelleri

Karşılaştırma Modeli (Lojistik Regresyon): Tek başına miR-126-3p'nin tanısal gücünü standart bir ML yöntemiyle değerlendirmek için Lojistik Regresyon sınıflandırma modeli kullanılmıştır.

Birincil Model (Random Forest): Esas analiz, tüm biyobelirteç panelinin (miR-126-3p + 4 klinik parametre) doğrusal olmayan ve karmaşık etkileşimlerini modellemek amacıyla güçlü bir topluluk (ensemble) algoritması olan Random Forest (RF) Sınıflandırıcısı ile gerçekleştirilmiştir.

2.3.3 Performans Değerlendirmesi Metrikleri

Modellerin tanısal performansı, test veri seti üzerinde aşağıdaki metrikler kullanılarak değerlendirilmiştir:

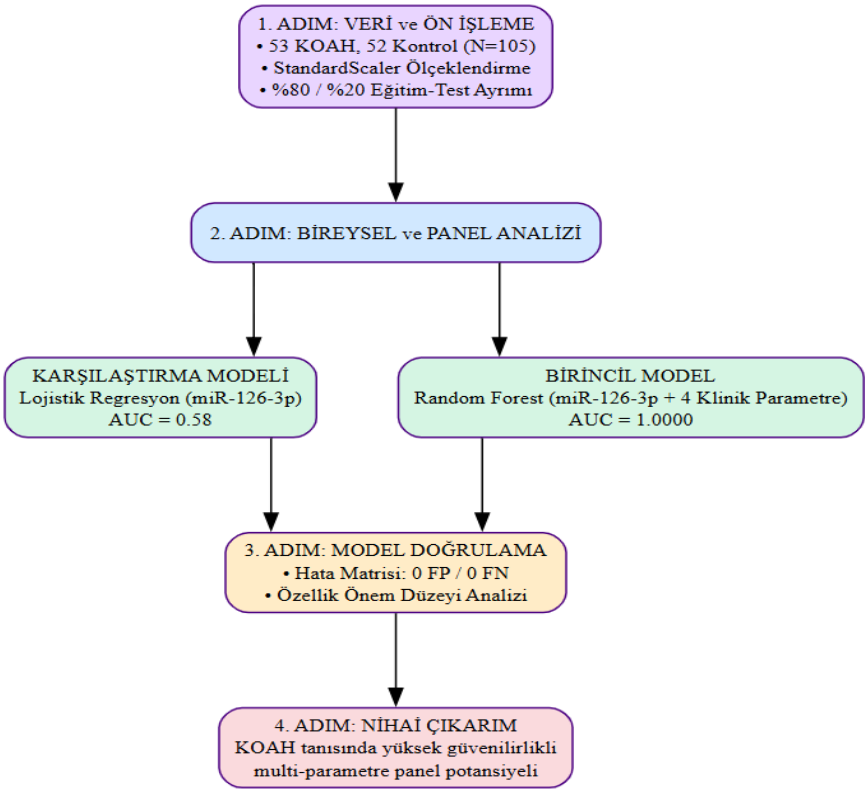
Eğri Altındaki Alan (AUC): Modelin ayırma gücünün temel ölçütü olarak.

Doğruluk (Accuracy): Genel doğru sınıflandırma oranını temsil etmek üzere.

Hata Matrisi (Confusion Matrix): Yalancı Pozitif ve Yalancı Negatif hata sayılarını somutlaştırarak klinik güvenilirliği değerlendirmek için.

Özellik Önem Düzeyi (Feature Importance): Paneldeki her bir belirtecin (miR-126-3p, CRP, WBC vb.) nihai tanı kararına olan katkısını belirlemek için.

3. BULGULAR



Şekil 1. miR-126-3p ve Klinik Parametreler Panelinin KOAH Tanısındaki Geleneksel ve Random Forest Makine Öğrenimi Yaklaşımlarıyla Karşılaştırmalı Çalışma Akış Şeması.

Çalışmamız, miR-126-3p ekspresyon düzeylerinin tek başına tanısal gücünü geleneksel bir yaklaşımla değerlendirmiş ve klinik parametrelerle birleştirilerek Random Forest algoritması ile tanısal potansiyelini artırmıştır. Çalışmamızın tüm metodolojik akışı, kullanılan modeller ve ana sonuç karşılaştırması Şekil 1'de özetlenmiştir.

3.1. Çalışma Grubu Özellikleri ve İstatistiksel Analiz

Çalışmaya dahil edilen 53 KOAH hastası ve 52 sağlıklı kontrolden oluşan grubun demografik ve klinik özellikleri Tablo 1'de gösterilmiştir. Gruplar arasında yaş ve cinsiyet açısından istatistiksel olarak anlamlı bir farklılık saptanmamıştır ($p>0.05$), CRP, WBC, NEU ve LYM gibi tüm inflamatuar belirteçler ile miR-126-3p ekspresyon düzeyleri KOAH grubunda istatistiksel olarak anlamlı farklılık göstermiştir ($p<0.05$). Özellikle, miR-126-3p düzeyleri KOAH hastalarında kontrol grubuna göre anlamlı derecede yüksektir ($p=0.034$).

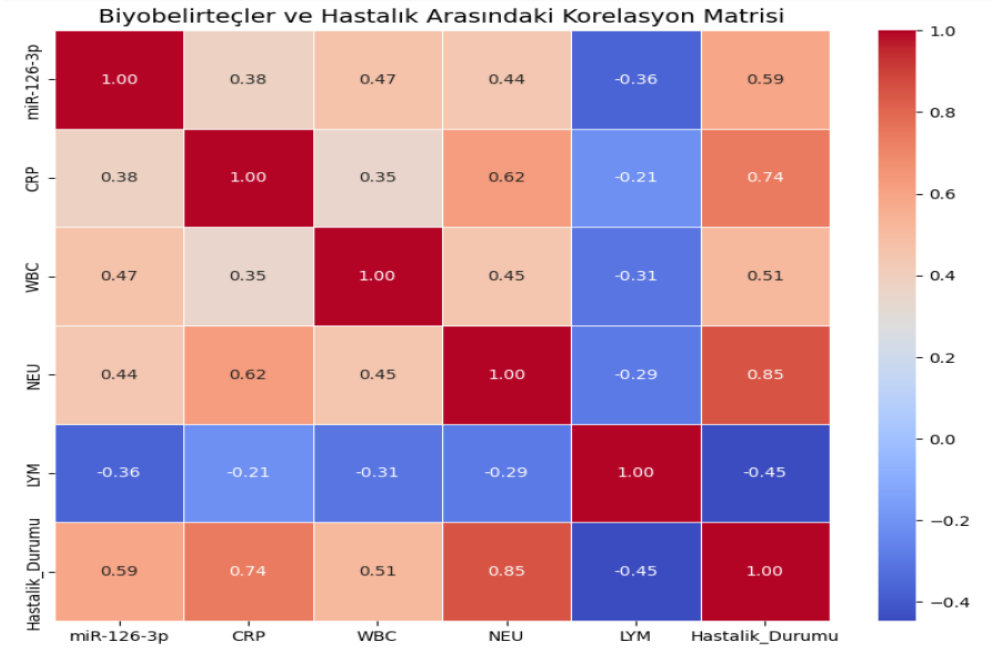
Tablo 1. Çalışmaya dahil edilen KOAH hastaları ve kontrol grubunun demografik ve klinik özelliklerine ilişkin istatistiksel bulgular

Değişkenler	KOAH Hastaları (n=53) Medyan [IQR]	Kontrol (n=52) Medyan [IQR]	p değeri
Cinsiyet, n(%)			
Kadın	10 (%18.9)	4 (%7.7)	0.150
Erkek	43 (%81.1)	48 (%92.3)	
Yaş (yıl)	72 [63–77]	66 [60–72.5]	0.075
CRP (mg/L)	16 [4.7–66]	1.88 [0.97–8.9]	**<0.001**
WBC (×10³/µL)	9010 [8220–10290]	7510 [6325–8605]	**<0.001**
NEU (×10³/µL)	6772 [5240–7800]	4060 [3350–5430]	**<0.001**
LYM (×10³/µL)	1580 [1060–2220]	1980 [1645–2520]	**0.023**
miR-126-3p ($2^{-\Delta\Delta Ct}$)	9.51 (3.61–53.02)	0.83 (0.17–8.40)	**0.034**

Cinsiyet verilerinin analizi için $\chi 2$ (Ki-Kare) testi kullanılmıştır. Nicel değişkenlerin normal dağılım göstermemesi nedeniyle (Shapiro–Wilk, $p<0.05$), Yaş, CRP, WBC, NEU, LYM ve miR-126-3p değerlerinin gruplar arası karşılaştırmaları Mann–Whitney U testi kullanılarak yapılmıştır. Sürekli değişkenler Medyan (Çeyrekler Arası Aralık, IQR) olarak, kategorik değişkenler ise sayı (yüzde) biçiminde sunulmuştur. KOAH hastaları ve kontrol grubu arasındaki karşılaştırmalar Mann–Whitney U testi ile değerlendirilmiş olup istatistiksel olarak anlamlı bulgular koyu olarak gösterilmiştir. Kısaltmalar: CRP, C-reaktif protein; WBC, beyaz kan hücresi; NEU, nötrofil; LYM, lenfosit.

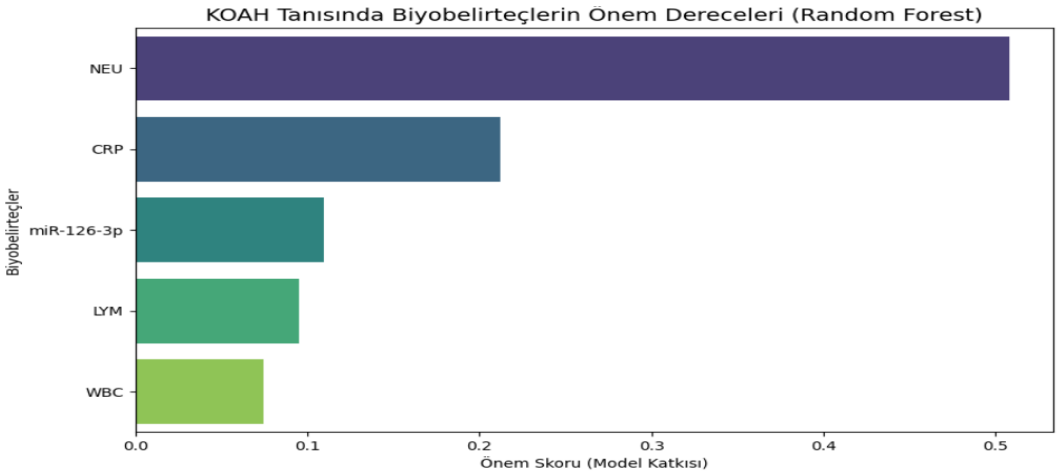
Tek başına miR-126-3p'nin tanısal gücünü değerlendirmek amacıyla kurulan Lojistik Regresyon sınıflandırma modeli kullanılarak KOAH tanısındaki ayırt edici gücü açısından değerlendirilmiştir. Bu geleneksel modelleme sonucunda, miR-126-3p'nin tanısal performansı AUC=0.58 olarak belirlenmiştir. Bu değer, tek değişkenli belirteçlerin KOAH gibi heterojen bir hastalıkta sınırlı ayırma gücüne sahip olduğunu göstermektedir.

İkinci aşamada, miR-126-3p ekspresyonu ile dört klinik parametrenin (CRP, WBC, NEU, LYM) birleştirildiği multi-parametre paneli, Random Forest (RF) sınıflandırıcısı kullanılarak analiz edilmiştir. Bu ensemble yaklaşımı, tanısal performansı belirgin şekilde artırmış ve test veri setinde %100.00 doğruluk ile AUC = 1.0000 değerine ulaşmıştır. Bu sonuç, modelin hasta ve kontrol gruplarını hatasız biçimde ayırt edebildiğini göstermektedir (Şekil 2).

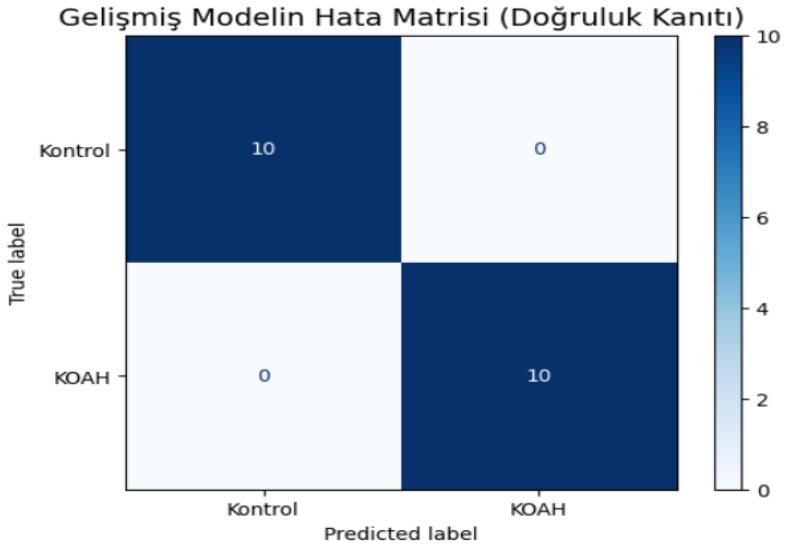


Şekil 2. Biyobelirteçler ile Klinik Parametrelerin KOAH Hastalık Durumu ile İlişkisinin Korelasyon Matrisi

Modelin klinik güvenilirliğini test veri setinde değerlendirmek amacıyla gerçekleştirilen Hata Matrisi (Confusion Matrix) analizi, bu hatasız sınıflandırma performansı doğrulamıştır. Şekil 3'te gösterildiği üzere, model sıfır (0) yalancı pozitif ve sıfır (0) yalancı negatif hata ile sınıflandırma yapmıştır. Ayrıca, Özellik Önem Düzeyi analizi, miR-126-3p'nin rutin klinik belirteçlerin yanı sıra yüksek ve bağımsız bir katkı sağladığını, böylece panelin tanısal gücünü belirgin şekilde artırdığını göstermiştir (Şekil 4).



Şekil 3. Random Forest Modelinde Biyobelirteçlerin Göreceli Önem Düzeyleri



Şekil 4. Test Veri Setinde Modelin Sınıflandırma Performansını Gösteren Hata Matrisi

4. TARTIŞMA

Bu çalışmanın temel amacı, miR-126-3p ekspresyon düzeylerinin hem tek başına hem de yaygın inflamatuar klinik belirteçlerle (CRP, WBC, NEU, LYM) oluşturulan bir panel içerisinde KOAH tanısındaki potansiyelini Makine Öğrenimi (ML) yaklaşımlarıyla değerlendirmektir. Elde edilen bulgular, miR-126-3p'nin klinik anlamı ve ML entegrasyonunun tanısal gücü artırmadaki kritik rolüne dair önemli çıkarımlar sağlamaktadır.

Karşılaştırmalı analizlerimiz, miR-126-3p ekspresyon düzeylerinin KOAH hastalarında kontrol grubuna kıyasla istatistiksel olarak anlamlı derecede farklı olduğunu göstermiştir ($p = 0.034$). Bu sonuç, miR-126-3p'nin KOAH ile ilişkili inflamasyon veya vasküler disfonksiyon süreçlerinde biyolojik bir role sahip olduğunu desteklemektedir. Bununla birlikte, KOAH'ın heterojen fenotiplere ve multifaktöriyel bir patogenezine sahip bir hastalık olması, tek bir moleküler belirteçle yüksek doğrulukta sınıflandırma yapılmasını güçleştirmektedir. Nitekim yalnızca miR-126-3p kullanılarak oluşturulan Lojistik Regresyon modelinin AUC=0.58 düzeyinde kalması, etkili tanısal modellerin birden fazla klinik ve biyolojik parametreyi entegre etmesi gerektiğini göstermiştir.

Tek başına miR-126-3p kullanılarak oluşturulan Lojistik Regresyon modelinin AUC = 0.58 gibi sınırlı bir performans göstermesi, KOAH'ın heterojen fenotiplere ve multifaktöriyel bir patogenezine sahip bir hastalık olmasıyla uyumludur ve yüksek doğrulukta sınıflandırma için birden fazla belirtecin entegrasyonunun gerekliliğini ortaya koymaktadır. Bu nedenle çalışmada, miR-126-3p'nin klinik belirteçlerle bir arada değerlendirildiği multi-parametre bir panel oluşturulmuştur.

Analizlerimizin ortaya koyduğu önemli sonuçlardan biri, miR-126-3p'nin dört inflamatuar belirteçle birlikte kullanılmasıyla oluşturulan panelin Random Forest algoritmasıyla değerlendirildiğinde AUC = 1.0000 ve %100.00 doğruluk değerlerine ulaşmış olmasıdır. Bu yüksek performans, RF algoritmasının ensemble yapısının belirteçler arasındaki doğrusal olmayan ilişkileri ve karmaşık etkileşimleri etkili biçimde modelleyebilme kapasitesiyle açıklanabilir. Bunun yanında, miR-126-3p'nin moleküler düzeydeki etkilerinin sistemik inflamasyon belirteçlerinin klinik yansımalarıyla birlikte değerlendirilmesi, panelin ayırt edicilik performansını artıran bir katkı sağlamıştır.

Modelin klinik uygulanabilirliği, test veri setinde elde edilen Hata Matrisi sonuçlarıyla da doğrulanmıştır. Model, sıfır Yalancı Pozitif (FP) ve sıfır Yalancı Negatif (FN) hata ile çalışarak hastalığın tespit edilememesi veya sağlıklı bireylerin yanlış sınıflandırılması gibi kritik klinik hataları tamamen ortadan kaldırmıştır. Ek olarak, Özellik Önem Düzeyi analizi, miR-126-3p'nin panelde bağımsız ve güçlü bir karar katkısı sağladığını göstermiştir.

Elde ettiğimiz sonuçlar, miR-126-3p gibi moleküler belirteçlerin rutin klinik parametrelerle birlikte kullanıldığında KOAH tanısal doğruluğunu artırma potansiyeli taşıdığını ortaya koymaktadır. Bununla birlikte, KOAH'ın heterojen fenotipleri ve multifaktöriyel patogenezi göz önünde bulundurulduğunda, bu bulguların doğruluğunu değerlendirmek için daha geniş örneklemli, çok merkezli ve bağımsız kohortlarda harici doğrulama (external validation) çalışmalarına ihtiyaç duyulmaktadır.

5. SONUÇ

Çalışmamızın bulguları, miR-126-3p gibi moleküler belirteçlerin rutin klinik parametrelerle birlikte Random Forest tabanlı bir makine öğrenimi (ML) modeli kapsamında değerlendirildiğinde KOAH tanısında son derece yüksek bir ayırt edicilik ortaya koyduğunu göstermektedir. Tek başına kullanıldığında sınırlı tanısal performans sunan miR-126-3p (AUC = 0.58), dört klinik parametre ile birlikte değerlendirildiğinde AUC = 1.0000 düzeyine ulaşmış ve modelin tanısal doğruluğunu kayda değer biçimde artırmıştır. Buna ek olarak, Hata Matrisi analizinde 0 yalancı pozitif (FP) ve 0 yalancı negatif (FN) değerin elde edilmesi, oluşturulan panelin klinik açıdan kritik yanlış sınıflandırmaları önleme potansiyeline işaret etmektedir. Bununla birlikte, KOAH'ın heterojen fenotipleri ve multifaktöriyel patogenezi dikkate alındığında, bu güçlü sonuçların klinik uygulamaya uyarlanabilmesi için daha geniş örneklemli ve çok merkezli harici doğrulama çalışmalarının yanı sıra panelin farklı KOAH fenotipleri üzerinde test edilmesine yönelik ileri araştırmalara ihtiyaç duyulmaktadır.

6. KAYNAKLAR

Esteban, C., Arostegui, I., Aburto, M., Moraza, J., Quintana, J. M., Aizpiri, S., & diğerleri. (2021). Development of mortality prediction index for COPD patients using machine learning techniques. *Journal of Clinical Medicine*, 10(3), 1–14.

GOLD. (2025). Global Strategy for the Diagnosis, Management, and Prevention of COPD. *Global Initiative for Chronic Obstructive Lung Disease (GOLD) Report*.

Li, X., Zhang, Y., Wang, Y., Chen, L., & Liu, H. (2024). Circulating microRNAs as diagnostic biomarkers in chronic obstructive pulmonary disease: A systematic review and meta-analysis. *Respiratory Research*, 25(1), 1–15.

Peng, Y., Zhou, L., Chen, M., & Zhang, H. (2022). Dysregulated miR-126-3p expression and its association with inflammatory and vascular remodeling pathways in COPD. *International Journal of Chronic Obstructive Pulmonary Disease*, 17, 1123–1134.

Topalovic, M., Das, N., Burghuber, O., Daenen, M., Derom, E., Haenebalcke, C., & diğerleri. (2019). Artificial intelligence outperforms pulmonologists in the interpretation of pulmonary function tests. *European Respiratory Journal*, 53(4), 1–13.

Yıldırım, S., Karakuş, N., & Yılmaz, E. (2026). Evaluation of miR-126-3p expression in COPD patients and its association with inflammatory parameters. *Journal of Medical Biology*, 14(2), 85–94.

Zhu, X., Liu, J., Wang, H., & Wu, F. (2023). Diagnostic and prognostic roles of circulating microRNAs in COPD: A systematic review. *BMC Pulmonary Medicine*, 23(1), 1–10.

ORAL PRESENTATION

Use of metal-organic frameworks in enzyme immobilization

Elif Toku[1*](*ORCID: https://orcid.org/0009-0006-4836-9888*),
Özlem Alptekin[2] (*ORCID: https://orcid.org/0000-0002-0458-7609*)

[*1]Mersin University, Faculty of Pharmacy, Department of Biochemistry, Mersin, Türkiye.
[2]Çukurova University, Faculty of Pharmacy, Department of Biochemistry, Adana, Türkiye.

*Corresponding author e-mail: eliftoku01@gmail.com

Abstract

Metal–organic frameworks (MOFs) are crystalline porous materials with exceptionally tunable structural architecture, pore geometry, chemical functionality, and stability. Enzymes are biocatalysts that exhibit high selectivity and activity; however, they are highly sensitive to environmental changes such as temperature, pH, organic solvents, or ionic strength. Consequently, their in-use stability is limited, limiting their applicability in industrial bioprocesses, environmental applications, biosensor technologies, and biocatalyst synthesis. In recent years, research on the use of MOFs for enzyme immobilization has accelerated. The aim of this study is to systematically classify metal–ligand–enzyme combinations, perform a comparative evaluation of MOF structures, and investigate the influence of cage structure, pore size, and ligand functionality on enzyme behavior. In this context, a bibliometric analysis was conducted based on 4,180 articles published in the Web of Science database between 2015 and 2025. Current development trends and future directions were identified through literature-based analyses. Future work may focus on developing scalable methods for MOF synthesis, expanding computational modeling for enzyme-MOF conformation, designing new functional ligands that control enzyme orientation, synthesizing mesoporous MOFs for larger enzymes, implementing MOF-enzyme hybrids at the reactor scale, and optimizing suitable structures for multi-enzyme cascade systems.

Keywords: Enzyme, immobilization, metal organic framework

INTRODUCTION

Enzymes are biocatalysts, mostly protein in structure, that enable reactions in biological systems to occur under mild conditions (pH 7.0, body temperature). The ability to exert their effects outside their natural environment, provided adequate conditions are met, allows enzymes to be utilized in many areas. Enzymes find wide applications for industrial, analytical, medical diagnostic, therapeutic, and drug design purposes (Wiseman, 1986). The enzyme market value was US$15.4 billion in 2025 and is expected to reach US$29.7 billion in 2035 (FutureMarketInsights, 2025). The raw material problem in enzyme production appears to have been largely solved via microbial sources. However, purifying enzymes from microbial sources is a very costly endeavor. In industrial applications, it is very difficult to recover the free enzyme without losing its activity. Because the free enzyme cannot be removed from the reaction medium at the desired time, the reaction is very difficult to control. Since it is impossible to remove the free enzyme used as a catalyst from the reaction medium without losing its activity, reuse of the enzyme is not possible. This is a significant cost factor due to the specific but expensive nature of enzymes. Furthermore, free enzymes are not suitable for continuous production systems. In addition to the laborious and expensive nature of enzyme purification processes, various immobilization techniques have been developed to overcome certain challenges encountered in industrial applications. Enzymes are immobilized by physical or chemical binding to a water-insoluble carrier, by incorporating the enzyme molecule as a monomer in a copolymerization process that yields an insoluble product, and by entrapping them in water-insoluble microcapsules (Klibanov, 1983).

Metal–organic frameworks (MOFs) are crystalline porous materials with exceptionally tunable structural architectures, pore geometries, chemical functionality, and stability. Since the late 1990s, thousands of different MOF structures have been developed. These structures are formed by arranging inorganic metal cations with organic ligands in specific coordination geometries. The ultra-high surface area, adjustable internal surface

chemistry, and amenability to post-synthetic modification of MOFs have increased their use in materials science, catalysis, adsorption processes, and biotechnological applications (Furukawa et al., 2013). Their ability to synthesize with a wide variety of ligand and metal sources allows them to be designed to meet diverse industrial needs. MOFs are used for various purposes in the food, chemical, environmental, and pharmaceutical industries. These applications include the retention of toxic chemicals, gas storage, catalysis, and drug delivery systems (Rogacka et al., 2025). Among these application areas, research on the use of MOFs in enzyme immobilization has gained significant momentum. Due to their rigid and porous structure, MOFs provide a protective and customizable microenvironment, preserving the enzyme's three-dimensional structure, increasing reusability, and reducing denaturation, thus providing solutions to the problems encountered in the use of free enzymes (Li et al., 2023; Pang et al., 2016). Studies have shown that a wide variety of metal cations are used. Examples of these metal cations include Zn^{2+}, Cu^{2+}, Zr^{4+}, Co^{2+}, Ni^{2+}, Ca^{2+}, Mg^{2+}, and Fe^{3+} ions, while molecules such as imidazole, 2-methylimidazole (Hmim), fumaric acid, p-aminobenzoate (PABA), terephthalic acid (BDC), and amino-terephthalic acid (NH_2-BDC) serve as ligands (**Figure 1**). These different combinations allow for the formation of a wide variety of MOF structures that are ideal for enzyme immobilization (Li et al., 2023).

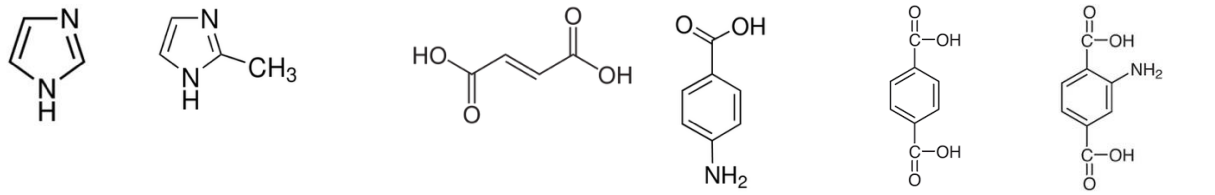


Figure 1. Commonly preferred ligands in MOF synthesis in enzyme immobilization.

MOFs have properties such as very high surface areas (most >1000 m^2/g) providing high enzyme loading capacity, coordination geometry that can be controlled at the atomic scale, tunable pore sizes that allow cage selection according to enzyme size, the ability to arrange hydrophilic or hydrophobic internal cavities, the ability to synthesize enzymes under mild conditions and in aqueous media, high chemical and thermal stability, suitability for surface functionalization with covalent or coordinate covalent bonds (with groups such as $–NH_2$, –OH, –COOH, imidazole, and sulfonate), and the potential to form hydrophobic/hydrophilic gradients. Due to these properties, they exhibit high performance that classical carriers (silica, alumina, chitin) cannot provide (Furukawa et al., 2013). Four basic methods are used for enzyme immobilization on MOFs: surface adsorption, covalent bonding, encapsulation, and co-precipitation (**Figure 2**).

Adsorption: The physical binding of the enzyme to the MOF surface. The main forces are: electrostatic attraction, hydrogen bonds, van der Waals interactions, and π–π interactions. Its advantages include mild conditions that do not damage the enzyme, suitability for immobilization of large enzymes, simple and rapid application, and high surface activity. While this method is suitable for large enzymes under mild conditions, its biggest drawback is the possibility of desorption.

Covalent attachment to the surface: The enzyme is covalently bonded via functional groups on the MOF surface. In some cases, silanization followed by activation processes such as glutaraldehyde binding are used to make the surface suitable for binding. In this method, the enzyme is not easily removed from the support, however, in some cases, a significant decrease in enzyme activity can occur (Zhang et al., 2022).

Pore encapsulation: The enzyme diffuses into the MOF pores and is retained there. Microporous structures are suitable for small enzymes, while mesoporous MOFs are suitable for larger enzymes. While enzymes exhibit high stability after immobilization, their biggest drawback is the diffusion limitations that may occur during immobilization (Weng et al., 2024).

Co-precipitation: The enzyme plays an active role during synthesis and crystallizes simultaneously with the MOF. This method provides the highest stability and maximizes MOF-enzyme compatibility. It is the most preferred method in the literature.

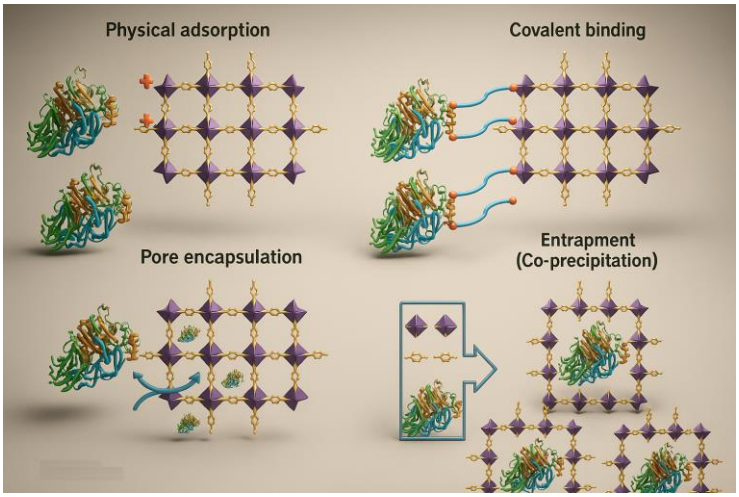


Figure 2. Enzymes to MOF immobilization used methods. The figure was re-illustrated using AI-assisted graphic tools based on the concepts described in Huang et al. (2022).

Enzyme leaching is a primary problem in preparing MOF-enzyme systems. Especially in studies where enzymes are immobilized onto MOFs by adsorption, enzymes can detach under conditions such as high ionic strength or low pH. This leads to a loss of catalytic efficiency, limits the reuse of the immobilized enzyme, and poses various challenges in reactor applications. High enzyme loading rates can block MOF pores, reducing substrate and product diffusion. This is a significant performance limiter, especially in small-pore MOFs and high-molecular-weight enzymes. Even when using the same metal-ligand system, minor changes such as solvent type, stirring speed, ligand/metal molar ratio, and synthesis time can lead to significant differences in the MOF crystalline phase. This makes comparative studies difficult. Some buffers (especially phosphate buffers) can bind metals, such as Zr-MOFs, by breaking coordinate covalent bonds, weakening MOF integrity, and reducing enzyme loading capacity. Most studies have been conducted on milligram-gram scales, under laboratory conditions, with purified substrates. Data on the long-term stability of MOF-enzymes in real wastewater streams or industrial bioreactors are scarce.

Today, various databases are available for bibliometric analysis. This study used the Web of Science (WoS) database. A bibliometric analysis of research and review articles on enzyme immobilization with MOFs published between 2015 and 2025 was conducted. Among these articles, traditional medicine studies were identified and analyzed from a bibliometric perspective.

MATERIALS AND METHODS

A search was performed using the SCI-EXPANDED index in the WoS database on 04.12.2025 with the keywords ((“enzyme immobiliz*” OR “immobilized enzyme” OR “enzyme encapsulat*” OR “enzyme load*” OR (“enzyme” AND (“incorporat*” OR “attach*” OR “fix*” OR “support*”))) AND (“MOF*” OR “metal organic framework*” OR “ZIF*” OR “UiO*” OR “MIL*” OR “HKUST*”)) in studies written in English. This search was conducted by searching titles, and the “Article and Review” option was used to retrieve data from original research articles and reviews. A total of 4,180 studies published between 2015 and 2025, the first publication date of which was determined in the WoS database on “enzyme immobilization with MOF” were retrieved. The obtained data were analyzed between December 1 and 7, 2025, for the number of citations, publication year, authors, countries, institutions and funding organizations and publishers. VOSviewer 1.6.20 and Bibliometrix was used in the bibliometric analyses (van Eck & Waltman, 2010; Aria & Cuccurullo, 2017). Tables and graphs were created from the database and the analyses, and these were used in the bibliometric evaluation. Used key with words unreachable and WoS data at the base unscanned publications This of the study limitation constitutes the word subject of the study realization for ethic board approval is not required.

RESULTS and DISCUSSION

The visualization of the co-word analysis (COA) performed on MOFs using the keywords given in the method section of WOS, regarding enzyme immobilization, in VOSviewer is given in **Figure 3**. As seen in the figure,

biosensors, lipase immobilization, ZIF-8, enzymes in the oxidoreductase and hydrolase classes, and cascade catalysis come to the fore.

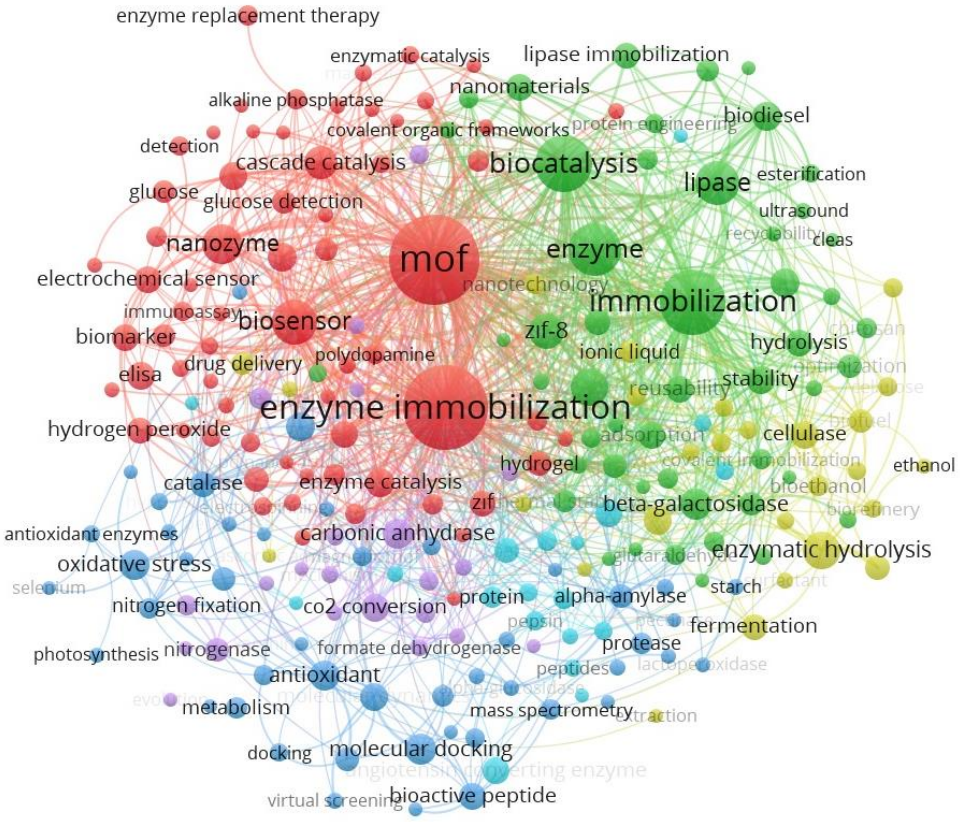


Figure 3. Keyword co-occurrence network generated using VOSviewer (version 1.6.20) based on the Web of Science Core Collection dataset (TS = ((“enzyme immobiliz*” OR “immobilized enzyme” OR “enzyme encapsulat*” OR “enzyme load*” OR (“enzyme” AND (“incorporat*” OR “attach*” OR “fix*” OR “support*”))) AND (“MOF*” OR “metal organic framework*” OR “ZIF*” OR “UiO*” OR “MIL*” OR “HKUST*”)); accessed on 4 December 2025).

The initial search of the WoS database on “enzyme immobilization with MOF” identified a total of 7.989 studies. A search for data from research and review articles yielded a total of 4.180 studis. It was determined that the largest number of research and review articles in the last decade was published in 2021 (n=995, 10.930%) (**Table 1**). Studies conducted in the last decade account for more than 60% of all research.

Table 1. Numerical and proportional distribution of studies on “enzyme immobilization with MOF” in the last decade

Publication Year	Publication Number	The rate
2025	631	15.085%
2024	506	12.097%
2023	440	10.519%
2022	447	10.686%
2021	434	10.375%
2020	394	9.419%

2019	306	7.315%
2018	309	7.387%
2017	208	4.973%
2016	228	5.451%
2015	205	4.901%

When the citation numbers were examined by years, it was observed that both the citation numbers and the number of studies increased (**Figure 4**).

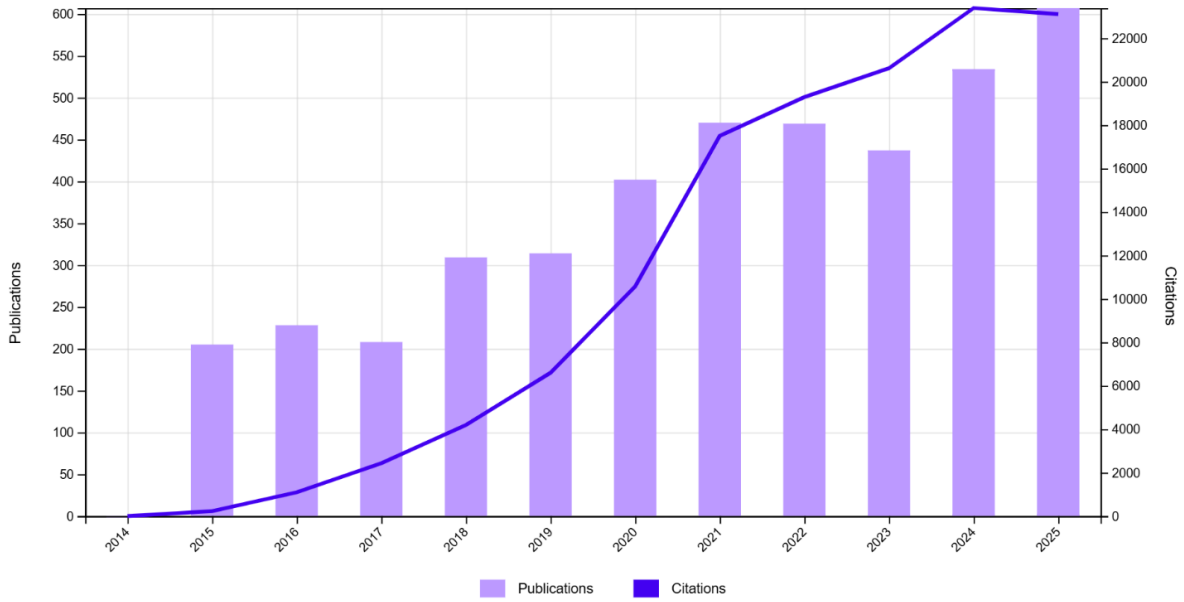


Figure 4. Number of publications and citations by year

The 10 authors with the most studies on "enzyme immobilization with MOF" are shown in **Table 2**. Elif Özyılmaz, who published the most articles on the subject in Turkey, has conducted the most research.

Table 2. The top 10 authors who published most on " enzyme immobilization with MOF", the number of publications, and the ratio of these publications to the total

Author	Publication Number	Rate (%)
Wang Y	47	1.124
Zhang Y	42	1.004
Liu Y	42	1.004
Zhang X	39	0.932
Chen Y	38	0.908
Li Y	37	0.885
Wang L	35	0.837
Li H	32	0.765
Wang J	31	0.741
Bilal M	29	0.693

The temporal distribution of publications produced by the most prolific authors over the last decade is shown in **Figure 5**. Overall, author productivity remained relatively low and scattered during 2015–2017, followed by a

gradual rise beginning in 2018. A marked increase is observed after 2020, where almost all leading researchers demonstrate both higher publication frequency and larger contribution magnitude, indicating intensified research activity in the field. Notably, Zhang X, Chen Y, and Zhang Y exhibit consistently high output, with pronounced peaks between 2019 and 2023, suggesting their central role in driving advancements in the topic. The continued presence of substantial publication activity in 2024–2025 further indicates that the field remains dynamic and rapidly evolving.

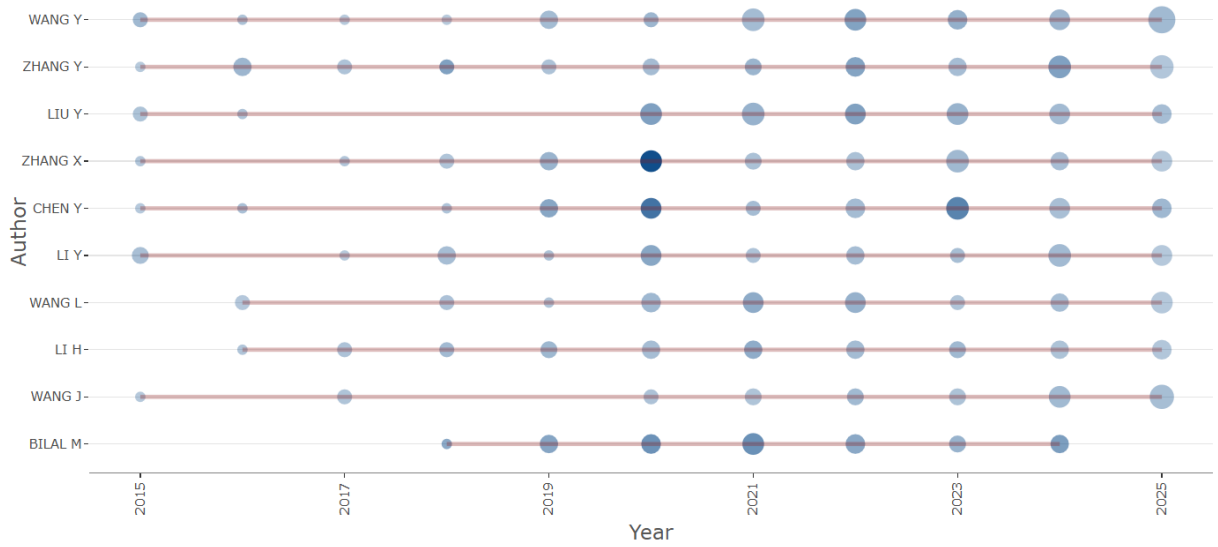


Figure 5. Annual scientific productivity of the top contributing authors in the field between 2015 and 2025.

The top 10 most cited articles are listed in **Table 3**. As a result of the evaluation conducted across Turkey, the study ranked first, receiving 124 citations (Atacan et al., 2016).

Table 3. The top 10 articles with the highest number of citations

Author	Publication Year	Citation Number of
Folegatti , PM (Folegatti et al., 2020)	2020	1.713
Foster, S.L. (Foster et al., 2018)	2018	1.379
Lian, XZ (Lian et al., 2017)	2017	1.165
Grasselli, G (Grasselli et al., 2020)	2020	1.129
Li, W (Li et al., 2021)	2021	777
Brown, K.A. (Brown et al., 2016)	2016	739
Chen, L (Chen et al., 2017)	2017	614
Krishnan, SK (Krishnan et al., 2019)	2019	589
Feng, D. (Feng et al., 2015)	2015	575
Mohamad, NR (Mohamad et al., 2015)	2015	565

According to the WoS category, the largest number of studies were conducted in the field of Chemistry Multidisciplinary (n=676, 16.161%). This was followed by Biochemistry Molecular Biology (n=567, 13.555%), Biotechnology Applied Microbiology (n=409, 9.778%), Materials Science Multidisciplinary (n=375, 8.965%), and Chemistry Physical (n=371, 8.869%).

Data analysis reveals that China (n=1.542) has the most published studies. This is followed by the US (n=777), India (n=337), and Germany (n=205) (**Figure 6**). Turkey ranks 16th out of 143 countries with 77 studies (1.841%).

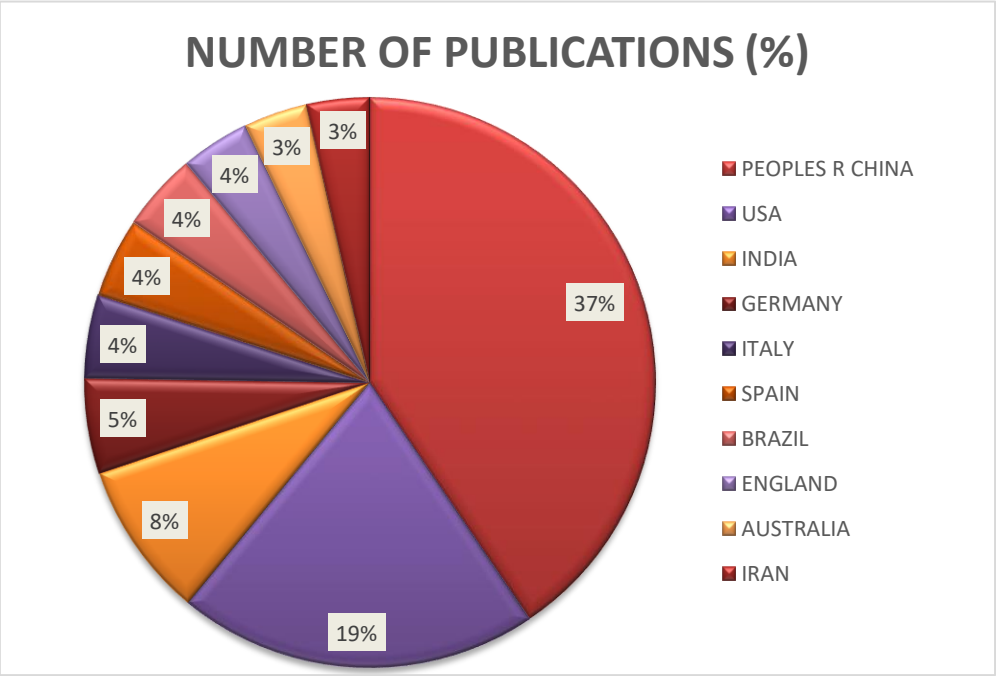


Figure 6. Proportional distribution of the number of publications by country.

Over 100 articles on " enzyme immobilization with MOF " have been published by 200 institutions from different countries. The top 10 leading institutions, their publication numbers, and their relative values are shown in **Table 4**.

Table 4. Top 10 institutions with the highest number of publications

Organisation	Publication Number	Rate (%)
Chinese Academy of Sciences	129	3.084
University of California System	98	2.343
Consejo Superior De Investigaciones Cientificas Csic	62	1.482
Center National De La Recherche Scientifique Cnrs	54	1.291
Egyptian Knowledge Bank Ekb	54	1.291
Beijing University of Chemical Technology	52	1.243
University Of Chinese Academy of Sciences Cas	52	1.243
Sun Yat Sen University	46	1.100
Tianjin University	46	1.100
United States Department of Energy Doe	46	1.100

The top three organizations providing the most financial support for the "enzyme immobilization with MOF" studies were NSFC from China (n=977, 23.356%), HHS (n=269, 6.431%), and NIH (n=264, 6.311%) from the USA. The most supported studies from Turkey were from TÜBİTAK (n=1, 14.286%). The publishers with the most studies were Springer Nature (n=1.739, 19.104%), Elsevier (n=1.722, 18.917%), and Wiley (n=860, 9.447%).

Successful MOF–enzyme coupling depends on four key parameters: the compatibility of the enzyme size with the MOF pore size, the MOF internal surface chemistry, the chemical nature of the metal cations, and compatibility with enzyme cofactors. MOFs with small pores, such as ZIF-8, are suitable for small enzymes. Mesoporous Cu-MOFs can accommodate large enzymes. Amine-functionalized MOFs exhibit high compatibility with polar

enzymes, while hydrophobic MOF–carbons increase the stability of enzymes such as lipases. The Cu^{2+} cation exhibits synergistic interactions with laccase, the Zr^{4+} cation provides stability in environmental applications due to its chemical resistance, and the Co^{2+} cation exhibits strong compatibility with aminotransferases. Redox enzymes are more stable in electron-dense MOF environments. Conformational protection is more critical for hydrolases.

Metal–organic frameworks (MOFs) are crystalline, three-dimensional structures formed by the coordination of metal cations or metal clusters with organic linkers. The inorganic metal cations that form the basis of these structures can be mononuclear metal ions or polynuclear clusters. Organic ligands are the fundamental elements that determine the MOF's topology, pore size, chemical functionality, and intrapore polarity (Furukawa et al., 2013).

Cu^{2+}–fumarate MOFs, Zr^{4+}–BDC (UiO-66**)** and amino-terephthalate (UiO-66-NH_2) MOFs, Zn^{2+}–imidazolate (ZIF-8) structures, Co^{2+}–aminoterephthalate MOFs, and ZIF-derived carbon materials are available in the literature (Li et al., 2023). The end groups of the ligands (NH_2, OH, COOH) can be easily modified for enzyme binding.

Zn^{2+} ions form tetrahedrally bonded imidazolate ligands to form ZIF (zeolitic imidazolate cage) structures. These structures have high chemical stability, hydrophobic interior surfaces, high surface area, and are suitable for room-temperature synthesis (Li et al., 2023). The hydrophobic structure of Zn-MOFs is particularly suitable for lipase and oxidoreductase enzymes.

Cu-MOFs are quite superior in terms of both coordination geometry and redox capacity. Their properties include square-planar or octahedral coordination, structures suitable for electron transfer, and electrostatic interactions between positively charged ionic centers and negative regions on the enzyme surface. These properties are particularly well-suited to multi-copper oxidases such as laccase. The literature reports that the Cu -MOF/laccase system exhibits high activity even at 95 °C. Mesoporous Cu-MOFs have reached very high enzyme loading capacities of 502 mg/g. Cu-BDC has been found to be effective in EE2 and dye removal. Therefore, Cu-MOFs play an important role in environmental bioremediation (Zhong et al. 2017).

Zr-MOFs (especially UiO-66 and UiO-67) are the most stable structures of the MOF family. This is due to the high bond energy of the Zr–O bonds and the resistance of the $Zr_6O_4(OH)_4$ clusters to hydrolysis and thermal degradation. Their advantages include high mechanical stability, durability over a wide pH range, and ease of operation in real wastewater environments. UiO-66-NH_2(30)/laccase degraded almost all antibiotics such as rifampicin and lincomycin. MMU-Zr-MOFs have demonstrated success in environmental catalysis with their very high loading capacity (Liu et al. 2023). Therefore, Zr-MOFs are one of the best options for enzymes that must operate under harsh chemical conditions.

Co^{2+} MOFs show very high activity recovery (up to 108%) in aminotransferases (Wang et al. 2023). Ni^{2+} MOFs are compatible with hydrolases, but few studies have been conducted. Mg/Ca MOFs have the advantage of biocompatibility. These metals enable targeted MOF design for specific enzyme classes.

The ligands of MOFs play a decisive role in enzyme immobilization. Imidazole ligands (e.g., ZIF-8, ZIF-67), hydrophobic interior cavities, and defined pore windows (~3.4 Å) provide high compatibility with lipases and redox enzymes. Carboxylate ligands (BDC, NH_2-BDC, fumarate) have the potential for hydrogen bonding, a polar interior, strong binding with metal clusters, and NH_2 functionality, facilitating loading, particularly in polar enzymes such as laccase. Aromatic amino ligands (PABA, aminoterephthalate) provide π–π interactions, high compatibility with specific enzyme surfaces, and an ideal environment for aminotransferases. MOF-derived carbon ligands, graphitic layers, and high surface area provide superior performance for hydrophobic enzymes (e.g., lipases).

CONCLUSION

MOFs are widely studied materials for enzyme immobilization, and studies are ongoing to obtain enzyme preparations with high catalytic activity and stability. A total of 4,180 studies published between 2015 and 2025, the first publication date of which was determined in the WoS database on “enzyme immobilization with MOF,” were retrieved. Biosensors, lipase immobilization, ZIF-8, enzymes in the oxidoreductase and hydrolase classes, and cascade catalysis come forward in the co-word analysis. Chinese Academy of Sciences is a leader institution. Future work may focus on developing scalable methods for MOF synthesis, expanding computational modeling for enzyme-MOF conformation, designing new functional ligands that control enzyme orientation, synthesizing

mesoporous MOFs for larger enzymes, implementing MOF-enzyme hybrids at the reactor scale, and optimizing suitable structures for multi-enzyme cascade systems.

ACKNOWLEDGEMENTS

We would like to acknowledge Research Assistant Fırat Çınar for his methodological evaluations and insightful comments that contributed to this study.

REFERENCES

Aria, M., & Cuccurullo, C. (2017). bibliometrix: An R-tool for comprehensive science mapping analysis. *Journal of Informetrics* , 11(4), 959-975.

Atacan, K., Çakıroğlu, B., & Özacar, M. (2016). Improvement of the stability and activity of immobilized trypsin on modified Fe_3O_4 magnetic nanoparticles for hydrolysis of bovine serum albumin and its application in bovine milk. *Food Chemistry, 212*, 460–468. https://doi.org/10.1016/j.foodchem.2016.06.011

Brown, K. A., Chambers, M. B., Guo, J., Gudmundsson, M., Warren, J. J., Hamby, H., ... King, P. W. (2016). Light-driven dinitrogen reduction catalyzed by a CdS:nitrogenase MoFe protein biohybrid. *Science, 352*(6284), 448–450. https://doi.org/10.1126/science.aaf2091

Chen, L., Luque, R., & Li, Y. (2017). Controllable design of tunable nanostructures inside metal–organic frameworks. *Chemical Society Reviews, 46*(15), 4614–4630. https://doi.org/10.1039/C6CS00537C

Feng, D., Liu, TF., Su, J. *et al.* Stable metal-organic frameworks containing single-molecule traps for enzyme encapsulation. *Nat Commun* 6, 5979 (2015). https://doi.org/10.1038/ncomms6979

Folegatti, P. M., Ewer, K. J., Aley, P. K., Angus, B., Becker, S., Belij-Rammerstorfer, S., Bellamy, D., Bibi, S., Bittaye, M., Clutterbuck, E. A., Dold, C., Faust, S. N., Finn, A., Flaxman, A. L., Hallis, B., Heath, P., Jenkin, D., Lazarus, R., Makinson, R., ... Pollard, A. J. (2020). Safety and immunogenicity of the ChAdOx1 nCoV-19 vaccine against SARS-CoV-2: A preliminary report of a phase 1/2, single-blind, randomised controlled trial. *The Lancet, 396*(10249), 467–478. https://doi.org/10.1016/S0140-6736(20)31604-4

Foster, S. L., Bakovic, S. I. P., Duda, R. D., Mahoney, M. R., Greenlee, L. F., Hsu, J. T., et al. (2018). *Catalysts for nitrogen reduction to ammonia*. Nature Catalysis, 1, 490–500. https://doi.org/10.1038/s41929-018-0092-7

Furukawa, H., Cordova, K. E., O'Keeffe, M., & Yaghi, O. M. (2013). The chemistry and applications of metal–organic frameworks. *Science, 341*, 1230444. https://doi.org/10.1126/science.1230444

FutureMarketInsights. (2025, September 29). *Enzymes market: Size and share forecast outlook 2025 to 2035*. Retrieved December 1, 2025, from https://www.futuremarketinsights.com/reports/enzymes-market

Grasselli, G., Greco, M., Zanella, A., Albano, G., Antonelli, M., Bellani, G., Bonanomi, E., Cabrini, L., Carlesso, E., Castelli, G., Cattaneo, S., Cereda, D., Colombo, S., Coluccello, A., Crescini, G., Forastieri Molinari, A., Foti, G., Fumagalli, R., ... Pesenti, A. (2020). Risk factors associated with mortality among patients with COVID-19 in intensive care units in Lombardy, Italy. *JAMA Internal Medicine, 180*(10), 1345–1355. https://doi.org/10.1001/jamainternmed.2020.3539

Klibanov, A. M. (1983). Immobilized enzymes and cells as practical catalysts. *Science, 219*(4585), 722–727.

Krishnan, S. K., Singh, E., Singh, P., Meyyappan, M., & Nalwa, H. S. (2019). *A review on graphene-based nanocomposites for electrochemical and fluorescent biosensors*. *RSC Advances, 9*(16), 8778–8881. https://doi.org/10.1039/C8RA09577A

Li, W., O'Neill, K. R., Haft, D. H., DiCuccio, M., Chetvernin, V., Badretdin, A., Coulouris, G., Chitsaz, F., Derbyshire, M. K., Durkin, A. S., Gonzales, N. R., Gwadz, M., Lanczycki, C. J., Song, J. S., Thanki, N., Wang, J., Yamashita, R. A., Yang, M., Zheng, C., Marchler-Bauer, A., & Thibaud-Nissen, F. (2021). *RefSeq: expanding the Prokaryotic Genome Annotation Pipeline reach with protein family model curation. Nucleic Acids Research, 49*(D1), D1020–D1028. https://doi.org/10.1093/nar/gkaa1105

Li, Y., Wang, R., Liu, X., Li, K., & Xu, Q. (2023). Recent advances in MOF–bio-interface: A review. *Nanotechnology, 34*(20). https://doi.org/10.1088/1361-6528/acbc81

Lian, X., Fang, Y., Joseph, E., Wang, Q., Li, J., Banerjee, S., Lollar, C., Wang, X., & Zhou, H.-C. (2017). *Enzyme–MOF (metal–organic framework) composites*. *Chemical Society Reviews, 46*(11), 3386–3401. https://doi.org/10.1039/C7CS00058H

Liu, H., Zhang, X., Zhou, Y., Zhu, L., Zhang, C., Yan, X., You, S., Qi, W., & Su, R. (2023). A reusable and leakage-proof immobilized laccase@UiO-66-NH_2(30) for the efficient biodegradation of rifampicin and lincomycin. *Biochemical Engineering Journal, 194*, 108897. https://doi.org/10.1016/j.bej.2023.108897

Mohamad, N. R., Marzuki, N. H. C., Buang, N. A., Huyop, F., & Wahab, R. A. (2015). *An overview of technologies for immobilization of enzymes and surface analysis techniques for immobilized enzymes*. *Biotechnology & Biotechnological Equipment, 29*(2), 205–220. https://doi.org/10.1080/13102818.2015.1008192

Pang, S., Wu, Y., Zhang, X., Li, B., Ouyang, J., & Ding, M. (2016). Immobilization of laccase via adsorption onto bimodal mesoporous Zr-MOF. *Process Biochemistry, 51*(2), 229–239.

Rogacka, J., & Labus, K. (2025). Metal–organic frameworks as highly effective platforms for enzyme immobilization – current developments and future perspectives. *Brazilian Journal of Chemical Engineering, 42*, 1273–1301. https://doi.org/10.1007/s43153-024-00513-4

Van Eck, N. J., & Waltman, L. (2010). *Software survey: VOSviewer, a computer program for bibliometric mapping*. Scientometrics, 84(2), 523–538. https://doi.org/10.1007/s11192-009-0146-3

Wang, H., Wang, J., Yao, Y., Liu, J.-Y., Gao, Y., Hua, Q., Jiao, Q., Liu, J., Jin, Y., Zhang, H., & Chen, L. (2023). A mild one-pot self-assembly approach to encapsulating enzymes into metal-organic framework with Asp-boosted enzymatic performance for clean production. *Journal of Cleaner Production, 401*, 136710. https://doi.org/10.1016/j.jclepro.2023.136710

Weng, Y., Chen, R., Hui, Y., Chen, D., & Zhao, C.-X. (2024). *Boosting enzyme activity in enzyme metal–organic framework composites*. Chem & Bio Engineering, 1(2), 99–112. https://doi.org/10.1021/cbe.3c00091

Wiseman, A. (1986). *Handbook of enzyme biotechnology* (2nd ed.). John Wiley & Sons.

Zhang, W., Taheri-Ledari, R., Saeidirad, M., Qazi, F. S., Kashtiaray, A., Ganjali, F., Tian, Y., & Maleki, A. (2022). Regulation of porosity in MOFs: A review on tunable scaffolds and related effects and advances in different applications. *Journal of Environmental Chemical Engineering, 10*(6), 108836. https://doi.org/10.1016/j.jece.2022.108836

Zhong, Z., Pang, S., Wu, Y., Jiang, S., & Ouyang, J. (2017). Synthesis and characterization of mesoporous Cu–MOF for laccase immobilization. *Journal of Chemical Technology & Biotechnology, 92*(8), 1841–1847. https://doi.org/10.1002/jctb.5189

ORAL PRESENTATION

Probiotic extracellular vesicles as postbiotic therapeutics in precision medicine

Rafig Gurbanov[1,2*] (*ORCID: https://orcid.org/0000-0002-5293-6447)*

[*1]Bilecik Şeyh Edebali University, Faculty of Engineering, Department of Bioengineering, Bilecik, Türkiye.
[2]Bilecik Şeyh Edebali University, Central Research Laboratory Application and Research Center (BARUM), Bilecik, Türkiye

*Corresponding author e-mail: rafig.gurbanov@bilecik.edu.tr

Abstract

Probiotic-derived extracellular vesicles (PEVs) are nanoscale lipid bilayer particles approximately 20 to 400 nm that package bacterial proteins, lipids, enzymes, metabolites, and nucleic acids, including small RNAs. With low immunogenicity, high physicochemical stability, and capacity to cross biological barriers, PEVs function as postbiotic effectors that deliver bioactive cargo to specific tissues without the viability and safety constraints of live probiotics. This review synthesizes preclinical evidence on mechanisms and applications across the gut, bone, skin, and nervous system. Mechanistically, PEVs engage pattern-recognition receptors, especially TLR2, to reprogram innate immunity. Across models, they promote anti-inflammatory M2 macrophage polarization, increase IL-10, and reduce pro-inflammatory mediators such as IL-1β and IL-6, while strengthening epithelial barrier function. In toxin-induced intestinal injury, *Lactobacillus murinus* PEVs mitigate deoxynivalenol-driven barrier disruption through TLR2 activation and M2 polarization, and *Lactobacillus johnsonii* PEVs similarly support mucosal homeostasis. Beyond the gut, PEVs from *Lactobacillus reuteri* and *Lactobacillus paracasei* accumulate in bone, enhance osteogenic differentiation, and attenuate osteoporosis-like phenotypes in vivo. In the nervous system, *Lactobacillus plantarum* PEVs increase brain-derived neurotrophic factor signaling and alleviate depression-like and Alzheimer's disease-like features in rodents, consistent with neuromodulatory cargo actions. In dermatology, PEVs from *Lactobacillus paracasei* and *Lactobacillus brevis* reduce TNF-α-driven inflammation, upregulate barrier-related proteins, including filaggrin, claudin-1, loricrin, and aquaporin-3, and protect against mechanical and UVB injury. *Lactobacillus plantarum* PEVs also show promise in atopic dermatitis and skin aging models. Antimicrobial effects and use as nanocarriers for small molecules or nucleic acids further broaden their scope. Key challenges include standardized high yield and high purity isolation, rigorous in vivo cargo to target mapping, long-term safety evaluation, and strain-specific potency metrics. Progress on these fronts, together with scalable bioprocessing, robust analytics, and pharmacokinetic and pharmacodynamic guided dosing, will be essential for clinical translation.

Keywords: Anti-inflammatory, Probiotic extracellular vesicles, Postbiotics, Pattern-recognition receptors, M2 macrophage polarization, *Lactobacillus* spp.

INTRODUCTION

Probiotics are widely recognized for their capacity to promote human health, yet the molecular vehicles by which they communicate with the host have only recently come into focus. Among these, extracellular vesicles (EVs) released by probiotic bacteria have emerged as pivotal mediators of cross-kingdom signaling (Yadav et al., 2025). These nanoscale, lipid-bilayer–bounded particles (typically ~20–400 nm in diameter) encapsulate proteins, nucleic acids, lipids, and small metabolites, enabling the protected transfer of bioactive cargo across biological barriers and into target cells (Hao et al., 2021). Functionally, they parallel many aspects of eukaryotic exosomes, orchestrating changes in host cell signaling, metabolism, and immunity without requiring direct cell to cell contact (Di Naro et al., 2025).

Within this broader landscape, *Lactobacillus*-derived extracellular vesicles (LDEVs) have attracted particular attention. Produced by Gram-positive bacteria, LDEVs are increasingly linked to immunomodulation, reinforcement of epithelial barrier integrity, maintenance of gut homeostasis, and modulation of neuroimmune pathways along the gut-brain axis. Proposed mechanisms include delivery of microbial enzymes, peptides, and small RNAs. Despite the thickness of the Gram-positive cell wall, accumulating evidence suggests that membrane blebbing and cell-wall remodeling can generate EVs with distinct molecular signatures and biological activities (Hao et al., 2021; Li et al., 2024; Yadav et al., 2025).

At the same time, methodological advances are rapidly maturing this field (Di et al., 2024; Gurunathan et al., 2019). Differential and density-gradient ultracentrifugation, size-exclusion chromatography (SEC), and emerging microfluidic strategies are being refined for EV isolation from complex probiotic cultures, while electron microscopy, nanoparticle tracking analysis (NTA), dynamic light scattering (DLS), and omics-level profiling, provides increasingly granular views of vesicle composition and heterogeneity (Caruana et al., 2021; Dean et al., 2019; Lazarus et al., 2023; Martora et al., 2019). Parallel progress in engineering approaches (e.g., surface functionalization, cargo loading, and strain-level tailoring) is opening the door to purpose-built EVs designed for precise therapeutic tasks (X. Liu et al., 2023; Ou et al., 2023; Sun et al., 2023).

This review study synthesizes current knowledge on probiotic-derived extracellular vesicles (PEVs) with an emphasis on LDEVs, focusing on three interlocking themes. First, we outline biogenesis and molecular composition, highlighting how vesicle origin and cargo determine biological function. Second, we survey methodological pipelines for isolation, characterization, and engineering. Third, we examine mechanistic pathways and biomedical applications, with dedicated sections on cancer therapy, immunomodulation, and gut-brain axis modulation. By integrating mechanistic insights with emerging preclinical data, our goal is to provide a coherent framework for understanding how probiotic EVs can be harnessed as stable, programmable, and biologically compatible nanosystems for next-generation therapeutics.

MATERIALS AND METHODS

Biogenesis and Characteristics

Bacterial EVs are produced by both Gram-negative and Gram-positive bacteria, albeit via somewhat different mechanisms. Gram-negative bacteria constitutively shed vesicles (often termed outer membrane vesicles, OMVs) by blebbing of the outer membrane, naturally enclosing periplasmic content and lipopolysaccharide (LPS) in the vesicle (Haas-neill and Forsythe, 2020). Gram-positive bacteria, once thought incapable of vesicle production due to their thick peptidoglycan cell wall (Y. Liu et al., 2018), are now known to also release EVs (Lee et al., 2009). In Gram-positives, vesicles form by protrusion of the cytoplasmic membrane through the cell wall, possibly aided by localized cell wall remodeling or membrane turgor stress. These vesicles lack LPS (since Gram+ have none) but often carry lipoteichoic acids (LTA) and peptidoglycan fragments on their surface, which can act as immune-active ligands (Haas-neill and Forsythe, 2020).

Proteomic analyses reveal that probiotic EVs contain a broad repertoire of bacterial proteins and enzymes. For example, EVs from *Lactobacillus plantarum* BGAN8 (a dairy isolate) were found to encapsulate over a thousand proteins, with enrichment in metabolic enzymes (e.g. glycolysis pathway) and membrane transport proteins (notably subunits of amino acid/peptide ABC transporters) (Bajic et al., 2020). These vesicles also carry nucleic acids (DNA and various RNAs) and small metabolites. In one striking example, EVs from the gut commensal *Bacteroides fragilis* were shown to contain the neurotransmitter γ-aminobutyric acid (GABA) along with its metabolic precursors (glutamate and α- ketoglutarate) (Zakharzhevskaya et al., 2017). This suggests probiotic EVs can ferry not only macromolecules but also small bioactive compounds. Their surface components also differ by species. Gram-negative probiotic EVs (e.g. from *Escherichia coli* Nissle 1917) will display LPS and outer membrane proteins, whereas Gram-positive probiotic EVs have components like LTA, peptidoglycan fragments, or polysaccharides that can interact with host pattern-recognition receptors. These molecular traits enable EVs to engage in host signaling, for instance, LTA on LDEVs can activate Toll-like receptor 2 (TLR2) on immune cells, modulating cytokine responses (Yadav et al., 2025).

Isolation and Purification

PEVs are isolated from clarified culture supernatants using a staged workflow that balances yield with purity (Yang et al., 2024). Probiotic strains (e.g., *Lacticaseibacillus/Lactobacillus* spp.) are typically cultivated in an appropriate medium (such as De Man-Rogosa-Sharpe, MRS) to late-log or stationary phase, when vesiculation is maximal. Whole cells are removed by low-speed centrifugation (~5,000–10,000 ×g) and 0.22 μm microfiltration to generate a cell-free supernatant. EVs are then concentrated and purified by ultrafiltration and high-speed ultracentrifugation (>100,000 ×g), with optional SEC or precipitation steps. Density-gradient ultracentrifugation (e.g., iodixanol/OptiPrep) further resolves vesicles from protein aggregates and similarly sized contaminants. Yields from batch cultures are modest (often in the ~μg mL^{-1} protein range over 24 h), but process optimization, medium formulation, harvest timing, bioreactor operation, and tangential-flow filtration can improve recovery and batch-to-batch consistency (W. Kim et al., 2020; Lei et al., 2024; Yang et al., 2024).

Characterization

Physicochemical and imaging assays are combined to confirm vesicle identity and quality. NTA or tunable resistive pulse sensing (TRPS) provide size distributions and particle counts, where LDEVs commonly span ~70–400 nm with modes near ~140 nm (Yang et al., 2024). Transmission electron microscopy (TEM) or cryo-EM visualizes lipid-bilayer-bound, roughly spherical particles and can reveal single or occasional double membranes (W. Kim et al., 2020). Bulk cargo is quantified by protein assays (e.g., bicinchoninic acid assay, BCA), while targeted immunoassays (e.g., LTA detection) help verify Gram-positive vesicle features and exclude lysis artifacts (Yang et al., 2024). Shotgun proteomics (LC–MS/MS) and complementary lipidomic/transcriptomic readouts profile cargo, noting that, unlike mammalian exosomes, no universal bacterial EV markers exist; thus, orthogonal criteria (size, morphology, density, and cargo) are recommended (Bajic et al., 2020).

Functional Validation

Cellular uptake and entry routes are assessed using fluorescently labeled EVs (e.g., PKH dyes) and confocal microscopy. LDEVs are readily internalized by mammalian cells including microglia within ~12 h of co-culture and pharmacological inhibition in epithelial models supports a predominantly clathrin-mediated endocytic pathway. Continued methodological advances, simplified, scalable isolation pipelines and engineered secretion systems are accelerating the production of well-defined, functional probiotic EV preparations suitable for downstream mechanistic and translational studies (Bajic et al., 2020; Lei et al., 2024; Sawant et al., 2025).

RESULTS and DISCUSSION

Immunomodulatory Effects

PEVs exert broad immunomodulatory effects across innate immune compartments. In vitro and in vivo studies consistently show that LDEVs rebalance cytokine milieus by elevating anti-inflammatory IL-10 while constraining pro-inflammatory mediators such as TNF-α, IL-6, and IL-1β under endotoxin (LPS) challenge (Hao et al., 2021; Yang et al., 2024). A prominent mechanism involves macrophage reprogramming, in which LDEVs shift THP-1–derived macrophages toward an M2-like, resolution-oriented state, downregulating M1 surface cues and promoting IL-10 production (W. Kim et al., 2020). EVs from other beneficial bacteria attenuate NF-κB signaling, supporting M1→M2 repolarization and reduced inflammatory tissue damage (Rodovalho et al., 2020). Similar anti-inflammatory signatures are observed in microglia, where LDEVs suppress IL-1β/IL-6 and increase IL-10, suggesting potential to temper neuroinflammation (Yang et al., 2024). Beyond macrophages, PEVs modulate antigen-presenting cells and mucosal adaptive responses. Evidence indicates effects on dendritic-cell maturation and mast-cell activity, as well as reinforcement of gut immune tolerance through enhanced IgA production, potentially via LTA-TLR2 signaling in gut-associated lymphoid tissue. In gastrointestinal models, including LPS-challenged poultry and murine colitis, EV administration preserves mucosal integrity and curbs excessive cytokine responses, thereby maintaining intestinal immune homeostasis (Yadav et al., 2025; Yang et al., 2024). Collectively,

these findings position PEVs as natural, cell-free immunotherapeutics that quell pathological inflammation while promoting disease resolution and barrier protection.

Gut Microbiome and Intestinal Health

PEVs shape intestinal ecology by acting as interkingdom messengers that influence both microbial communities and host epithelial physiology. In dextran sodium sulfate (DSS)-induced colitis, *L. plantarum* Q7 EVs restored microbial diversity, reduced Proteobacteria, and enriched beneficial taxa such as *Bifidobacterium* and *Muribaculaceae*, changes that coincided with clinical improvement (Hao et al., 2021). Mechanistically, EV cargo may include bacteriocins and signaling molecules that suppress pathobionts and favor commensals. At the same time, parallel effects on the epithelium, including upregulation of tight junction proteins, preservation of mucosal architecture, and possible stimulation of mucus production, reinforce the barrier and limit the translocation of luminal toxins (Melo-Marques et al., 2024). These ecosystem-level effects translate into suppressed mucosal inflammation across experimental inflammatory bowel disease (IBD) models. EV administration has been associated with longer colon length, reduced bleeding and weight loss, and lower tissue levels of IL-6, IL-1β, IL-2, and TNF-α, alongside increased regulatory pathways consistent with the broader immunomodulatory profile of probiotic EVs (Hao et al., 2021). Beyond IBD, EV-mediated pathogen antagonism (e.g., plantaricin-bearing vesicles) and barrier fortification suggest benefits for metabolic endotoxemia and, indirectly, colorectal cancer risk mitigation by reducing chronic inflammation and dysbiosis (Keyhani et al., 2022; Li et al., 2017). As cell-free "postbiotics" that cannot colonize or cause infection, probiotic EVs offer a scalable, potentially safer avenue for maintaining gut homeostasis and treating inflammatory disorders.

Gut-Brain Axis and Neurological Impacts

PEVs influence the gut-brain axis by curbing neuroinflammation and directly modulating central immune cells. By reducing intestinal inflammation, they indirectly lower inflammatory signaling to the brain. They also act within the central nervous system. In a murine perioperative neurocognitive disorder model, LDEVs crossed the blood-brain barrier, shifted microglia from an M1 to an M2 phenotype, decreased *iNOS*, increased *Arg1*, and rebalanced cytokines by lowering IL-1β and IL-6 while elevating IL-10. These changes dampened neuroinflammation and protected cognition (Yang et al., 2024). EVs can enhance neurotrophic support and stress resilience. In neuronal culture, *L. plantarum* EVs reversed corticosterone-induced suppression of BDNF, restoring *Bdnf* and *Sirt1* expression via pathways consistent with *Sirt1-Creb* signaling (Choi et al., 2019). In vivo, EV administration during chronic restraint stress preserved hippocampal BDNF and prevented depressive-like behaviors, indicating that EV cargo can engage intracellular programs that sustain plasticity (Choi et al., 2019). Given that *L. plantarum* produces neuromodulators such as GABA (Haas-neill and Forsythe, 2020), EV-borne small RNAs or metabolites may contribute to these antidepressant- and anxiolytic-like effects. A complementary mechanism is direct neurochemical signaling (Hermann et al., 2025). EVs carrying neurotransmitters or their precursors can enter circulation from the gut via epithelial transcytosis or immune-cell trafficking, cross the blood–brain barrier or access fenestrated regions, and potentially signal through the vagus. Once in the brain, they may release GABA or serotonin precursors or induce neurons and glia to upregulate neuroactive factors, including BDNF and NT-4/5 (Choi et al., 2019). Together, these pathways position probiotic EVs as candidate "psychobiotics" for conditions driven by dysbiosis, peripheral inflammation, or impaired neurotrophic signaling, with early preclinical data supporting applications in depression, anxiety, and neuroinflammatory disorders (Wu et al., 2022).

Anticancer Potential

PEVs display direct antitumor activity in preclinical models. EVs from *L. rhamnosus* GG (LGG) reduce viability of HepG2 hepatocellular carcinoma cells and shift the *Bax/Bcl-2* ratio toward apoptosis at 50–100 μg mL^{-1}, consistent with activation of intrinsic death pathways (Behzadi et al., 2017). Related work in colorectal cancer models reports LGG EV–mediated downregulation of carcinoembryonic antigen (CEA), pointing to additional marker-level antitumor effects (Keyhani et al., 2022). These findings suggest that EV cargo, such as cytotoxic peptides, enzymes, or regulatory RNAs can engage tumor-cell stress and death programs. EVs may also overcome chemoresistance by rewiring tumor metabolism. In 5-fluorouracil (5-FU)-resistant HCT116 cells, *L. plantarum*

EVs restored drug sensitivity by suppressing pyruvate dehydrogenase kinase-2 (PDK2) through a p53/p21-dependent pathway, thereby reversing glycolytic reprogramming and re-enabling apoptosis under 5-FU treatment (An and Ha, 2022). Because metabolic plasticity underlies many resistance phenotypes, this mechanism highlights EVs as rational adjuvants to standard chemotherapy. A third axis of activity is immune modulation within the tumor microenvironment. Probiotic EVs can act as natural adjuvants, increasing dendritic-cell recruitment and $CD8^+$ T-cell infiltration and potentially synergizing with direct tumor apoptosis to slow growth (Lu et al., 2023). EVs may also carry enzymes that activate prodrugs in situ or deliver beneficial metabolites and regulatory RNAs that tune oncogenic pathways. Looking ahead, engineered probiotic EVs-loaded with small interfering RNAs against oncogenes or pro-apoptotic proteins offer a biocompatible alternative to synthetic nanocarriers for targeted anticancer therapy (Lu et al., 2023).

Other Biomedical Applications

PEVs are being investigated across diverse indications beyond the gut and brain. In dermatology, LDEVs show anti-inflammatory activity in human skin culture and may benefit disorders marked by barrier disruption and hyperinflammation, such as atopic dermatitis (M. H. Kim et al., 2018). Early translational signals include improved collagen output in dermal fibroblasts and small clinical gains in skin elasticity and hydration (Jo et al., 2022; Krzyżek et al., 2023). Wound-healing applications are also emerging (Han et al., 2023). EVs from LGG accelerated re-epithelialization and angiogenesis by delivering miR-21-5p, suggesting utility for chronic wounds and diabetic ulcers (Wang et al., 2024). EVs may promote immune tolerance and antimicrobial defense at mucosal surfaces. *Bifidobacterium longum* EVs reduced food-allergy responses in mice by suppressing mast-cell degranulation, pointing to oral or intranasal "vaccines" that train tolerance or bolster mucosal immunity (J. H. Kim et al., 2016). Vaginal LDEV, specifically from *L. crispatus* BC3 and *L. gasseri* BC12, protected human T cells and ex vivo cervico-vaginal and tonsillar tissues from HIV-1 infection, with activity linked to EV cargo enriched in lactic acid and amino acids (Ñahui Palomino et al., 2019). Separately, EVs from the probiotic *E. coli* Nissle 1917 enhanced macrophage inhibition of *E. coli*, *Salmonella typhimurium*, and *Staphylococcus aureus* (Hu et al., 2020). Looking forward, probiotic EVs are attractive drug and gene-delivery vehicles due to their biocompatibility (H. Liu et al., 2022). Recent reviews highlight engineered EVs loaded with antimicrobial peptides or nucleic-acid cargos (e.g., siRNA) to silence inflammatory genes or enhance tumor targeting. Analogous strategies could encapsulate chemotherapeutics for site-directed delivery. Strain engineering to overproduce specific vesicles, together with surface functionalization using homing peptides, may improve targeting to tumors or inflamed tissue (J. H. Kim et al., 2016; Wei et al., 2025).

CONCLUSION

PEVs emerge as versatile, cell-free modalities that recapitulate many benefits traditionally attributed to live microbes, across preclinical models. These position PEVs as programmable "postbiotics" with relevance to many different indications. Clinical translation depends on identifying causal EV cargo and their host receptors, standardizing isolation, purity, and potency assays for EVs, and establishing scalable bioprocesses supported by rigorous quality control. Essential prerequisites include detailed pharmacokinetic and biodistribution analyses, along with comprehensive immunogenicity and safety assessments. With advances in vesicle engineering such as cargo loading and surface targeting, and rational combinations with existing therapies, probiotic EVs could mature from compelling preclinical tools into clinically actionable nanotherapeutics.

REFERENCES

An, J. J., & Ha, E. M. (2022). Extracellular vesicles derived from Lactobacillus plantarum restore chemosensitivity through the PDK2-mediated glucose metabolic pathway in 5-FU-resistant colorectal cancer cells. Journal of Microbiology, 60(7).

Bajic, S. S., Cañas, M. A., Tolinacki, M., Badia, J., Sánchez, B., Golic, N., Margolles, A., Baldomá, L., & Ruas-Madiedo, P. (2020). Proteomic profile of extracellular vesicles released by Lactiplantibacillus plantarum BGAN8 and their internalization by non-polarized HT29 cell line. Scientific Reports, 10(1).

Behzadi, E., Mahmoodzadeh Hosseini, H., & Imani Fooladi, A. A. (2017). The inhibitory impacts of Lactobacillus rhamnosus GG-derived extracellular vesicles on the growth of hepatic cancer cells. Microbial Pathogenesis, 110.

Caruana, J. C., Dean, S. N., & Walper, S. A. (2021). Isolation and characterization of membrane vesicles from lactobacillus species. Bio-Protocol, 11(17).

Choi, J., Kim, Y. K., & Han, P. L. (2019). Extracellular vesicles derived from Lactobacillus plantarum increase BDNF expression in cultured hippocampal neurons and produce antidepressant-like effects in mice. Experimental Neurobiology, 28(2).

Dean, S. N., Leary, D. H., Sullivan, C. J., Oh, E., & Walper, S. A. (2019). Isolation and characterization of Lactobacillus-derived membrane vesicles. Scientific Reports, 9(1).

Di Naro, M., Petronio Petronio, G., Mukhtar, F., Cutuli, M. A., Magnifico, I., Falcone, M., Brancazio, N., Guarnieri, A., Di Marco, R., & Nicolosi, D. (2025). Extracellular Vesicles in Bacteria, Archaea, and Eukaryotes: Mechanisms of Inter-Kingdom Communication and Clinical Implications. In *Microorganisms* (Vol. 13, Issue 3). Multidisciplinary Digital Publishing Institute (MDPI).

Di, S., Huang, Y., Qiao, W., Zhang, X., Wang, Y., Zhang, M., Fu, J., Zhao, J., & Chen, L. (2024). Advances in the isolation and characterization of milk-derived extracellular vesicles and their functions. In Frontiers in Nutrition (Vol. 11). Frontiers Media SA.

Gurunathan, S., Kang, M. H., Jeyaraj, M., Qasim, M., & Kim, J. H. (2019). Review of the isolation, characterization, biological function, and multifarious therapeutic approaches of exosomes. In Cells (Vol. 8, Issue 4).

Haas-neill, S., & Forsythe, P. (2020). A budding relationship: Bacterial extracellular vesicles in the microbiota–Gut–brain axis. In International Journal of Molecular Sciences (Vol. 21, Issue 23).

Han, F., Wang, K., Shen, K., Wang, J., Han, S., Hu, D., & Wu, G. (2023). Extracellular vesicles from Lactobacillus druckerii inhibit hypertrophic scar fibrosis. Journal of Nanobiotechnology, 21(1).

Hao, H., Zhang, X., Tong, L., Liu, Q., Liang, X., Bu, Y., Gong, P., Liu, T., Zhang, L., Xia, Y., Ai, L., & Yi, H. (2021). Effect of Extracellular Vesicles Derived From Lactobacillus plantarum Q7 on Gut Microbiota and Ulcerative Colitis in Mice. Frontiers in Immunology, 12.

Hermann, D. M., Wang, C., Mohamud Yusuf, A., Herz, J., Doeppner, T. R., & Giebel, B. (2025). Extracellular vesicles lay the ground for neuronal plasticity by restoring mitochondrial function, cell metabolism and immune balance. In Journal of Cerebral Blood Flow and Metabolism. SAGE Publications Ltd.

Hu, R., Lin, H., Li, J., Zhao, Y., Wang, M., Sun, X., Min, Y., Gao, Y., & Yang, M. (2020). Probiotic Escherichia coli Nissle 1917-derived outer membrane vesicles enhance immunomodulation and antimicrobial activity in RAW264.7 macrophages. BMC Microbiology, 20(1).

Jo, C. S., Myung, C. H., Yoon, Y. C., Ahn, B. H., Min, J. W., Seo, W. S., Lee, D. H., Kang, H. C., Heo, Y. H., Choi, H., Hong, I. K., & Hwang, J. S. (2022). The Effect of Lactobacillus plantarum Extracellular Vesicles from Korean Women in Their 20s on Skin Aging. Current Issues in Molecular Biology, 44(2).

Keyhani, G., Hosseini, H. M., & Salimi, A. (2022). Effect of extracellular vesicles of Lactobacillus rhamnosus GG on the expression of CEA gene and protein released by colorectal cancer cells. Iranian Journal of Microbiology, 14(1).

Kim, J. H., Jeun, E. J., Hong, C. P., Kim, S. H., Jang, M. S., Lee, E. J., Moon, S. J., Yun, C. H., Im, S. H., Jeong, S. G., Park, B. Y., Kim, K. T., Seoh, J. Y., Kim, Y. K., Oh, S. J., Ham, J. S., Yang, B. G., & Jang, M. H. (2016). Extracellular vesicle-derived protein from Bifidobacterium longum alleviates food allergy through mast cell suppression. Journal of Allergy and Clinical Immunology, 137(2), 507-516.e8.

Kim, M. H., Choi, S. J., Choi, H. Il, Choi, J. P., Park, H. K., Kim, E. K., Kim, M. J., Moon, B. S., Min, T. K., Rho, M., Cho, Y. J., Yang, S., Kim, Y. K., Kim, Y. Y., & Pyun, B. Y. (2018). Lactobacillus plantarum-derived extracellular vesicles protect atopic dermatitis induced by Staphylococcus aureus-derived Extracellular Vesicles. Allergy, Asthma and Immunology Research, 10(5).

Kim, W., Lee, E. J., Bae, I. H., Myoung, K., Kim, S. T., Park, P. J., Lee, K. H., Pham, A. V. Q., Ko, J., Oh, S. H., & Cho, E. G. (2020). Lactobacillus plantarum-derived extracellular vesicles induce anti-inflammatory M2 macrophage polarization in vitro. Journal of Extracellular Vesicles, 9(1).

Krzyżek, P., Marinacci, B., Vitale, I., & Grande, R. (2023). Extracellular Vesicles of Probiotics: Shedding Light on the Biological Activity and Future Applications. In Pharmaceutics (Vol. 15, Issue 2). MDPI.

Lazarus, H., Vasudevan, S., Farooque, N., & Easwaran, N. (2023). Isolation and characterization of Gram-positive and Gram-negative Bacterial Membrane Vesicles using Poly Ethylene Glycol Method. Current Trends in Biotechnology and Pharmacy, 17(3).

Lee, E. Y., Choi, D. Y., Kim, D. K., Kim, J. W., Park, J. O., Kim, S., Kim, S. H., Desiderio, D. M., Kim, Y. K., Kim, K. P., & Gho, Y. S. (2009). Gram-positive bacteria produce membrane vesicles: Proteomics-based characterization of Staphylococcus aureus-derived membrane vesicles. Proteomics, 9(24).

Lei, Q., Divakarla, S. K., Winsley, T., Roux, S., & Chrzanowski, W. (2024). Bioprocessing strategies for enhanced probiotic extracellular vesicle production: culture condition modulation. Frontiers in Bioengineering and Biotechnology, 12.

Li, M., Lee, K., Hsu, M., Nau, G., Mylonakis, E., & Ramratnam, B. (2017). Lactobacillus-derived extracellular vesicles enhance host immune responses against vancomycin-resistant enterococci. BMC Microbiology, 17(1).

Li, M., Mao, B., Tang, X., Zhang, Q., Zhao, J., Chen, W., & Cui, S. (2024). Lactic acid bacteria derived extracellular vesicles: emerging bioactive nanoparticles in modulating host health. In Gut Microbes (Vol. 16, Issue 1). Taylor and Francis Ltd.

Liu, H., Geng, Z., & Su, J. (2022). Engineered mammalian and bacterial extracellular vesicles as promising nanocarriers for targeted therapy. In Extracellular Vesicles and Circulating Nucleic Acids (Vol. 3, Issue 2, pp. 63–86). OAE Publishing Inc.

Liu, X., Xiao, C., & Xiao, K. (2023). Engineered extracellular vesicles-like biomimetic nanoparticles as an emerging platform for targeted cancer therapy. In Journal of Nanobiotechnology (Vol. 21, Issue 1).

Liu, Y., Alexeeva, S., Defourny, K. A., Smid, E. J., & Abee, T. (2018). Tiny but mighty: bacterial membrane vesicles in food biotechnological applications. In Current Opinion in Biotechnology (Vol. 49).

Lu, S., Xu, J., Zhao, Z., Guo, Y., Zhang, H., Jurutka, P. W., Huang, D., Cao, C., & Cheng, S. (2023). Dietary Lactobacillus rhamnosus GG extracellular vesicles enhance antiprogrammed cell death 1 (anti-PD-1) immunotherapy efficacy against colorectal cancer. Food and Function, 14(23).

Martora, F., Pinto, F., Folliero, V., Cammarota, M., Dell'Annunziata, F., Squillaci, G., Galdiero, M., Morana, A., Schiraldi, C., Giovane, A., Galdiero, M., & Franci, G. (2019). Isolation, characterization and analysis of pro-inflammatory potential of Klebsiella pneumoniae outer membrane vesicles. Microbial Pathogenesis, 136.

Melo-Marques, I., Cardoso, S. M., & Empadinhas, N. (2024). Bacterial extracellular vesicles at the interface of gut microbiota and immunity. In Gut Microbes (Vol. 16, Issue 1). Taylor and Francis Ltd.

Ñahui Palomino, R. A., Vanpouille, C., Laghi, L., Parolin, C., Melikov, K., Backlund, P., Vitali, B., & Margolis, L. (2019). Extracellular vesicles from symbiotic vaginal lactobacilli inhibit HIV-1 infection of human tissues. Nature Communications, 10(1), 5656.

Ou, Z., Situ, B., Huang, X., Xue, Y., He, X., Li, Q., Ou, D., He, B., Chen, J., Huang, Y., Deng, L., Zhang, M., Wang, Q., & Zheng, L. (2023). Single-particle analysis of circulating bacterial extracellular vesicles reveals their biogenesis, changes in blood and links to intestinal barrier. Journal of Extracellular Vesicles, 12(12).

Rodovalho, V. de R., Luz, B. S. R. da, Rabah, H., do Carmo, F. L. R., Folador, E. L., Nicolas, A., Jardin, J., Briard-Bion, V., Blottière, H., Lapaque, N., Jan, G., Le Loir, Y., de Carvalho Azevedo, V. A., & Guédon, E. (2020). Extracellular Vesicles Produced by the Probiotic Propionibacterium freudenreichii CIRM-BIA 129 Mitigate Inflammation by Modulating the NF-κB Pathway. Frontiers in Microbiology, 11.

Sawant, H., Bihl, J., & Borthakur, A. (2025). A Simplified Method for the Isolation of Extracellular Vesicles from Probiotic Bacteria and Their Characterization. International Journal of Molecular Sciences, 26(3).

Sun, Y., Sun, F., Xu, W., & Qian, H. (2023). Engineered Extracellular Vesicles as a Targeted Delivery Platform for Precision Therapy. In *Tissue Engineering and Regenerative Medicine* (Vol. 20, Issue 2).

Wang, J., Li, X., Zhao, X., Yuan, S., Dou, H., Cheng, T., Huang, T., Lv, Z., Tu, Y., Shi, Y., & Ding, X. (2024). Lactobacillus rhamnosus GG-derived extracellular vesicles promote wound healing via miR-21-5p-mediated re-epithelization and angiogenesis. Journal of Nanobiotechnology, 22(1).

Wei, J., Ding, W., Song, K., Zhang, Y., Luo, Q., & Qi, C. (2025). Next-generation probiotics and engineered BEVs for precision therapeutics in osteoporosis. In Frontiers in Nutrition (Vol. 12). Frontiers Media SA.

Wu, Q., Duan, W. Z., Chen, J. B., Zhao, X. P., Li, X. J., Liu, Y. Y., Ma, Q. Y., Xue, Z., & Chen, J. X. (2022). Extracellular Vesicles: Emerging Roles in Developing Therapeutic Approach and Delivery Tool of Chinese Herbal Medicine for the Treatment of Depressive Disorder. In Frontiers in Pharmacology (Vol. 13).

Yadav, P., Debnath, N., Pradhan, D., Mehta, P. K., Kumar, A., Yadav, M. L., & Yadav, A. K. (2025). Probiotic Lactobacillus-Derived Extracellular Vesicles: Insights Into Disease Prevention and Management. Molecular Nutrition & Food Research, n/a(n/a), e70013.

Yang, Y., Li, N., Gao, Y., Xu, F., Chen, H., Zhang, C., & Ni, X. (2024). The activation impact of lactobacillus-derived extracellular vesicles on lipopolysaccharide-induced microglial cell. *BMC* Microbiology, 24(1).

Zakharzhevskaya, N. B., Vanyushkina, A. A., Altukhov, I. A., Shavarda, A. L., Butenko, I. O., Rakitina, D. V., Nikitina, A. S., Manolov, A. I., Egorova, A. N., Kulikov, E. E., Vishnyakov, I. E., Fisunov, G. Y., & Govorun, V. M. (2017). Outer membrane vesicles secreted by pathogenic and nonpathogenic Bacteroides fragilis represent different metabolic activities. Scientific Reports, 7(1).

ORAL PRESENTATION

Ferroptosis and kidney injury: Therapeutic perspectives in diabetic nephropathy

Muhammed Taha Kaya[*1] (*Orcid: 0000-0003-2744-4763*)

[*1]Yozgat Bozok University, Faculty of Veterinary Medicine, Department of Pathology, Yozgat, TURKIYE

*Corresponding author e-mail: m.taha.kaya@bozok.edu.tr

Abstract

Diabetic nephropathy (DN) is a major microvascular complication of diabetes mellitus and a leading cause of end-stage renal disease. Chronic hyperglycemia induces oxidative stress, lipid peroxidation, and iron dysregulation in renal cells, ultimately promoting ferroptosis, a regulated form of cell death distinct from apoptosis and necrosis. Ferroptosis is characterized by iron-dependent lipid peroxidation, accumulation of reactive oxygen species (ROS), mitochondrial shrinkage, and glutathione peroxidase 4 (GPX4) inactivation. These molecular events lead to podocyte injury, tubular dysfunction, and glomerular damage, contributing to the progression of DN.Diabetic nephropathy (DN) is a major microvascular complication of diabetes mellitus and a leading cause of end-stage renal disease. Chronic hyperglycemia induces oxidative stress, lipid peroxidation, and iron dysregulation in renal cells, ultimately promoting ferroptosis, a regulated form of cell death distinct from apoptosis and necrosis. Ferroptosis is characterized by iron-dependent lipid peroxidation, accumulation of reactive oxygen species (ROS), mitochondrial shrinkage, and glutathione peroxidase 4 (GPX4) inactivation. These molecular events lead to podocyte injury, tubular dysfunction, and glomerular damage, contributing to the progression of DN.Recent studies have highlighted the potential of natural compounds in counteracting ferroptosis and protecting renal function. Bioactive molecules such as glabridin, calycosin, mangiferin, glycyrrhizic acid, ginkgolide B, sennoside A, and umbelliferone have demonstrated renoprotective effects in both in vitro and in vivo diabetic models.Collectively, these findings indicate that ferroptosis is a central mechanism in DN progression and that targeting ferroptotic pathways may provide a promising therapeutic strategy. Natural compounds with anti-ferroptotic activity hold potential as adjunctive treatments to slow or prevent DN development. Further research, including clinical studies, is needed to validate efficacy, optimize dosing, and explore their translational potential in patients with diabetic nephropathy.

Keywords: Diabetic Nephropathy, Ferroptosis, Phytotherapy

INTRODUCTION

Diabetes mellitus (DM) is defined as a metabolic disease characterized by chronic hyperglycemia resulting from impaired insulin secretion, impaired insulin action, or both (Poznyak et al., 2020). According to 2025 data, 589 million adults are living with diabetes, and this number is estimated to reach 853 million by 2050 (Duncan et al., 2025). In diabetes, prolonged hyperglycemia affects various organs and tissues, leading to macrovascular and microvascular complications (Morrish et al., 2001). Damage caused by hyperglycemia affects the coronary and cerebrovascular arteries—known as macrovascular complications—as well as organs such as the kidneys, eyes, and nerves—referred to as microvascular complications—resulting in mortality among diabetic patients (Deshpande et al., 2008). Diabetic nephropathy (DN) is a complication that leads to end-stage renal disease and can ultimately result in death. Chronic hyperglycemia is considered one of the main causes of DN. According to data from the Centers for Disease Control and Prevention in the United States, 14% of individuals aged 20 years and older are affected by chronic kidney disease, and 30% of these individuals are diabetic (Lin et al., 2024). Approximately 30–40% of diabetic patients develop diabetic nephropathy (Umanath and Lewis, 2018; Qu et al., 2023). With the expected increase in diabetes incidence in the coming years, mortality related to diabetic complications is also anticipated to rise (Yang and Liu, 2022; Qu et al., 2023). Hyperglycemia triggers the production of reactive oxygen species (ROS), leading to the activation of various molecular pathways and causing kidney damage (Tonneijck et al., 2017). Factors involved in the development of kidney injury include the formation of advanced glycation end products, increased oxidative stress, activation of nuclear factor kappa B (NF-κB) and protein kinase C, upregulation of transforming growth factor-beta (TGF-β)/SMAD signaling, and increased lipotoxicity (Rout and Jialal, 2025). ROS, which play a major role in the progression of DN, not only cause

endothelial damage but also induce injury and apoptosis in podocytes—one of the key components of the glomerular filtration barrier—resulting in proteinuria and podocyte loss (Rayego-Mateos et al., 2020). While blockade of the renin–angiotensin–aldosterone system (RAAS) has been shown to reduce apoptosis in tubular epithelial cells, increased RAAS activation in diabetic kidneys is suggested to enhance tubular apoptosis (Satou et al., 2020). Additionally, in the polyol pathway, the accumulation of glucose by-products such as fructose and sorbitol increases intracellular osmotic pressure, leading to edema and subsequent membrane rupture, ultimately contributing to kidney injury. Moreover, urate—a by-product of fructose—further exacerbates insulin resistance, endothelial dysfunction, and tubular damage (Yang and Liu, 2022).

Ferroptosis is defined as a regulated cell death mechanism that is distinct from other forms of cell death such as apoptosis, autophagy, pyroptosis, and necrosis, and is characterized by iron dependence and lipid peroxidation (Stockwell et al., 2017; Mou et al., 2019). Iron accumulation leads to the generation of reactive oxygen species (ROS) through the Fenton reaction, causing oxidative stress, which in turn triggers lipid peroxidation—a key event in ferroptosis (Li et al., 2022). Recent studies have shown that hyperglycemia in diabetes leads to excessive ROS production, thereby promoting ferroptosis, particularly in diabetic nephropathy (DN), one of the major diabetes-related complications (Kang et al., 2014; Coughlan and Sharma, 2016; Park et al., 2020). For this reason, ferropto-reducing/inhibiting treatments are expected to be applied in the coming years. In recent years, the use of phytotherapeutic substances has been increasing and plays an important role in preventing the progression of DN (Liu et al., 2022; Zhao et al., 2022b; Yan et al., 2023). While the roles of programmed cell death mechanisms such as apoptosis, autophagy, and necroptosis in the pathogenesis of diabetic nephropathy are well established, the significance of ferroptosis has not been fully elucidated (Erekat, 2022). This review aims to provide insights into the potential mechanisms of ferroptosis, its role in diabetic nephropathy, and the effects of various phytotherapeutic interventions on DN (Anandhan et al., 2020).

MECHANISM OF FERROPTOSIS

Cells undergoing ferroptosis display distinct biochemical and morphological features, including mitochondrial shrinkage, increased mitochondrial membrane density, excessive accumulation of lipid peroxides and ROS, and a decreased antioxidant capacity (Zhao et al., 2020). Iron accumulation and excessive lipid peroxides are key factors triggering ferroptotic cell death by depleting or reducing glutathione peroxidase 4 (GPx4), the main enzyme regulating the antioxidant system (Sharma and Flora, 2021).Mitochondrial acetyl coactivators are involved in the production of polyunsaturated fatty acids (PUFAs) catalyzed by acetyl-CoA carboxylase (ACC) (Barrow et al., 2018). PUFAs are components of cell membranes and regulate various biological functions, including inflammation, immunity, synaptic plasticity, and cellular growth (Gill and Valivety, 1997). However, peroxidation of PUFAs can cause cellular damage. The mere presence of PUFAs in the environment does not directly induce ferroptosis. Studies have shown that ACSL4 plays a critical role as a biomarker in the execution of ferroptosis by influencing the catalysis of PUFAs (Doll et al., 2017). Circulating ferric iron (Fe^{3+}) binds to transferrin and is transported into cells via the membrane protein transferrin receptor-1 (TfR1). Once inside the cell, Fe^{3+} is reduced to ferrous iron (Fe^{2+}) by six-transmembrane epithelial antigen of prostate 3 (STEAP3) and stored in the labile iron pool (LIP) by binding to ferritin. Ferritin also prevents reactive Fe^{2+} from reacting with H_2O_2 (Harrison and Arosio, 1996; Xie et al., 2016). Excess accumulation of Fe^{3+} inside the cell or reduced Fe^{3+} export leads to elevated levels of free Fe^{2+}. Reactive Fe^{2+} reacts with H_2O_2 via the Fenton reaction, increasing the production of reactive oxygen species (ROS). ROS induce lipid peroxidation within cell membranes (Valko et al., 2005; Latunde-Dada, 2017). PUFAs are particularly susceptible to lipid peroxidation due to their unstable carbon–carbon double bonds. Free PUFAs are esterified by activated ACSL4 and incorporated into membrane phospholipids by lysophosphatidylcholine acyltransferase 3 (LPCAT3). They are then oxidized by lipoxygenases (LOXs) into toxic lipid peroxides. These peroxidized lipids and their byproducts, such as malondialdehyde (MDA) and 4-hydroxynonenal (4-HNE), damage mitochondrial and cellular membranes, initiating ferroptosis (Kagan et al., 2017) .

GPX4 is a selenoenzyme that serves as a central regulator and primary defense enzyme in ferroptosis by detoxifying small-molecule peroxides as well as more complex lipid peroxides (Yang et al., 2022). GPX4 binds to lipid peroxides and reduces ROS, thereby mitigating ROS-induced cellular damage. The intracellular antioxidant

system, System Xc^-, plays a key role in GSH synthesis. GSH serves as the main substrate for GPX4, which exerts protective effects on cells. Various diseases or external factors can lead to intracellular cysteine depletion or inhibition of System Xc^-. This reduces GSH production and consequently decreases GPX4 activity, resulting in increased ROS and lipid peroxidation, membrane damage, and ultimately the induction of ferroptosis (Jiang et al., 2021; Feng et al., 2022b). Cysteine is a critical component required for GSH biosynthesis, catalyzed by glutamate-cysteine ligase and glutathione synthase, and its depletion leads to a reduction in cellular antioxidant capacity (XL et al., 2022). Glutathione (GSH) is an essential cofactor for the proper functioning of GPXs. During glutamate-induced excitotoxic cell death, glutamate initiates ferroptosis through two main pathways: one via calcium influx and the other via inhibition of cystine uptake through System Xc^- (Dixon et al., 2012). While calcium chelators do not inhibit Erastin-induced ferroptosis, elevated glutamate levels suppress System Xc^- function and trigger ferroptosis. Reduced System Xc^- activity decreases cystine uptake, which in turn lowers GSH levels and indirectly decreases GPX4 activity. This leads to diminished cellular resistance to peroxidation, accumulation of lipid reactive oxygen species, and oxidative cell death (Kinowaki et al., 2021).

THE EFFECT OF PHYTOTHERAPEUTIC SUBSTANCES ON DIABETIC NEPHROPATHY

Glabridin

Glabridin is a prenylated isoflavone derived from the roots and rhizomes of *Glycyrrhiza glabra* L. Previous studies have demonstrated its hepatoprotective, neuroprotective, antidiabetic, and antioxidant effects in diabetic animal models (Hasanein, 2011; Wu et al., 2013; Komolkriengkrai et al., 2019; Yoshioka et al., 2019). Tan et al. (2022) reported that glabridin increased the activities of SOD, GSH, and catalase (CAT) in diabetic rats; upregulated GPX4, SLC7A11, and SLC3A2 expression; and downregulated TfR1, vascular endothelial growth factor (VEGF), p-AKT, and p-ERK1/2 expression, thereby reducing MDA levels and iron accumulation both in vitro and in vivo. Collectively, these findings indicate that glabridin suppresses ferroptosis by mitigating oxidative stress and delays the progression of diabetic nephropathy by inhibiting the VEGF/Akt/ERK signaling pathway.

Calycosin

Calycosin is an isoflavone phytoestrogen derived from *Astragalus membranaceus* and exhibits a broad range of pharmacological activities, including anti-inflammatory, antioxidant, antidiabetic, anti-osteoporotic, antitumor, hepatoprotective, neuroprotective, and cardioprotective effects (Deng et al., 2021). Huang et al. (2022) reported that calycosin improved kidney function in diabetic mice, alleviated tubular injury, and enhanced the viability of HK-2 cells exposed to high glucose. They further demonstrated that calycosin exerts its protective effects in diabetic nephropathy by suppressing ferroptosis, as evidenced by reduced levels of lactate dehydrogenase (LDH), MDA, and lipid ROS, alongside a significant increase in GPX4 expression driven by elevated GSH activity.

Mangiferin

Mangiferin is a natural flavonoid that is derived from mango (Sha et al., 2019). It has a wide range of pharmacological activities, including antioxidant, anti-inflammatory, antidiabetic, and nephroprotective (Akter et al., 2022; Feng et al., 2022a; Wang et al., 2022a). It has been demonstrated that mangiferin enhances the mevalonate-mediated antioxidant defense (through the FSP1/CoQ10 axis and GPX4) in DN rats, thereby reducing ACSL4-mediated lipid peroxidation and preventing ferroptotic cell death in the kidney (Zhao et al., 2022a).

Glycyrrhizic acid

Glycyrrhizic acid is a triterpene isolated from the medicinal plant *Glycyrrhiza glabra* and exhibits diverse pharmacological activities, including anti-inflammatory, antioxidant, antiviral, antidiabetic, anticancer, and organ-protective effects (Cao et al., 2020; Rehman et al., 2020). Recent studies have shown that glycyrrhizic acid upregulates GPX4 expression and reduces ROS production in mouse glomerular podocytes exposed to high glucose. These findings indicate that glycyrrhizic acid alleviates high glucose-induced podocyte injury, likely through the inhibition of ferroptosis (Wang et al., 2022b).

Ginkgolide B

Ginkgolide B is a diterpenoid isolated from Ginkgo biloba leaves and exhibits multiple pharmacological properties, including anti-inflammatory, antioxidant, anti-apoptotic, and anti-ferroptotic effects (Hu et al., 2018; Liu et al., 2020; Yang et al., 2020; Lin et al., 2021). Recently, Chen et al. (2022) reported that ginkgolide B upregulates the

ferroptosis-related proteins ferritin heavy chain 1 (FTH1) and GPX4, while downregulating TfR1, thereby reducing ROS levels and intracellular iron accumulation. They further demonstrated that ginkgolide B inhibits ferroptosis by preventing the ubiquitin-mediated degradation of GPX4 and sustaining GPX4 protein levels.

Anthraquinones

Rhubarb and senna are plants commonly used to treat constipation. Sennoside A, a bioactive compound derived from these plants, exhibits various pharmacological activities, including laxative, antidiabetic, antitumor, and hepatoprotective effects (Cao et al., 2018; Ma et al., 2020; Le et al., 2021; Zhu et al., 2021). In DN mice, Sennoside A has been shown to suppress ferroptotic cell death by reducing PTGS2 protein expression and MDA levels, enhancing GSH activity and GPx4 expression, and modulating the Nrf2/HO-1 signaling pathway (Ding and Wang, 2021)

Umbelliferone

Umbelliferone is a natural coumarin compound derived from *Eucommiae Cortex*, *Prunellae Spica*, and *Angelica dahurica*. It has been reported to exhibit diverse biological activities, including antidiabetic, antihyperlipidemic, antitumor, neuroprotective, cardioprotective, hepatoprotective, and renoprotective effects (Ramesh and Pugalendi, 2005; Yu et al., 2015; Hindam et al., 2020; Hassanein et al., 2021; Althunibat et al., 2022; Khadrawy and El Sayed, 2023). Umbelliferone increases GSH activity by inhibiting ROS production in diabetic mice and high glucose–induced HK-2 cells, while reducing MDA levels and iron accumulation, upregulating GPX4, Nrf2, and HO-1 expression, and downregulating ACSL4. These findings indicate that umbelliferone exerts inhibitory effects on oxidative stress and ferroptosis both in vitro and in vivo (Jin and Chen, 2022).

CONCLUSION

Increasing evidence indicates that ferroptosis plays a critical role in the pathogenesis and progression of diabetic nephropathy (DN). Hyperglycemia-induced oxidative stress, iron overload, and excessive lipid peroxidation contribute to GPX4 inactivation and glutathione depletion, ultimately triggering ferroptotic cell death in renal cells. These processes promote podocyte injury, tubular dysfunction, and glomerular damage, all of which are hallmarks of DN.Although no clinically approved therapies currently target ferroptosis directly, recent studies highlight the therapeutic potential of various natural compounds. Phytochemicals such as glabridin, calycosin, mangiferin, glycyrrhizic acid, ginkgolide B, sennoside A, and umbelliferone have been shown to modulate ferroptosis-related pathways by enhancing GPX4 activity, restoring GSH levels, reducing ROS and lipid peroxidation, regulating iron homeostasis, and influencing key signaling pathways including ACSL4, TfR1, and Nrf2/HO-1. These renoprotective effects suggest that targeting ferroptosis may offer a promising new direction for DN management.Further experimental and clinical studies are needed to validate these findings, determine optimal dosing strategies, and assess long-term safety and efficacy. Overall, ferroptosis represents an emerging therapeutic target, and natural compounds with anti-ferroptotic properties may provide valuable adjunctive strategies for slowing or preventing the progression of diabetic nephropathy.

REFERENCES

Akter, S., Moni, A., Faisal, G. M., Uddin, M. R., Jahan, N., Hannan, M. A., et al. (2022). Renoprotective effects of mangiferin: pharmacological advances and future perspectives. *International Journal of Environmental Research and Public Health, 19*(3), 1864.

Althunibat, O. Y., Abduh, M. S., Abukhalil, M. H., Aladaileh, S. H., Hanieh, H., & Mahmoud, A. M. (2022). Umbelliferone prevents isoproterenol-induced myocardial injury by upregulating Nrf2/HO-1 signaling, and attenuating oxidative stress, inflammation, and cell death in rats. *Biomedicine & Pharmacotherapy, 149*, 112900.

Anandhan, A., Dodson, M., Schmidlin, C. J., Liu, P., & Zhang, D. D. (2020). Breakdown of an Ironclad Defense System: The Critical Role of NRF2 in Mediating Ferroptosis. *Cell Chem Biol, 27*(4), 436-447. doi:10.1016/j.chembiol.2020.03.011

Barrow, A. D., Edeling, M. A., Trifonov, V., Luo, J., Goyal, P., Bohl, B., et al. (2018). Natural Killer Cells Control Tumor Growth by Sensing a Growth Factor. *Cell, 172*(3), 534-548.e519. doi:10.1016/j.cell.2017.11.037

Cao, Y., He, Y., Wei, C., Li, J., Qu, L., Zhang, H., et al. (2018). Aquaporins alteration profiles revealed different actions of senna, sennosides, and sennoside a in diarrhea-rats. *International journal of molecular sciences, 19*(10), 3210.

Cao, Z.-Y., Liu, Y.-Z., Li, J.-M., Ruan, Y.-M., Yan, W.-J., Zhong, S.-Y., et al. (2020). Glycyrrhizic acid as an adjunctive treatment for depression through anti-inflammation: A randomized placebo-controlled clinical trial. *Journal of Affective Disorders, 265*, 247-254.

Chen, J., Ou, Z., Gao, T., Yang, Y., Shu, A., Xu, H., et al. (2022). Ginkgolide B alleviates oxidative stress and ferroptosis by inhibiting GPX4 ubiquitination to improve diabetic nephropathy. *Biomedicine & Pharmacotherapy, 156*, 113953.

Coughlan, M. T., & Sharma, K. (2016). Challenging the dogma of mitochondrial reactive oxygen species overproduction in diabetic kidney disease. *Kidney international, 90*(2), 272-279.

Deng, M., Chen, H., Long, J., Song, J., Xie, L., & Li, X. (2021). Calycosin: a review of its pharmacological effects and application prospects. *Expert review of anti-infective therapy, 19*(7), 911-925.

Deshpande, A. D., Harris-Hayes, M., & Schootman, M. (2008). Epidemiology of Diabetes and Diabetes-Related Complications. *Physical Therapy, 88*(11), 1254-1264. doi:10.2522/ptj.20080020

Ding, Y., & Wang, L. (2021). Mechanism exploration of sennoside a in treating DN based on Nrf2/HMOX-1 ferroptosis signaling pathway. *Info Traditional Chine Med, 38*(07), 36-39.

Dixon, S. J., Lemberg, K. M., Lamprecht, M. R., Skouta, R., Zaitsev, E. M., Gleason, C. E., et al. (2012). Ferroptosis: an iron-dependent form of nonapoptotic cell death. *Cell, 149*(5), 1060-1072. doi:10.1016/j.cell.2012.03.042

Doll, S., Proneth, B., Tyurina, Y. Y., Panzilius, E., Kobayashi, S., Ingold, I., et al. (2017). ACSL4 dictates ferroptosis sensitivity by shaping cellular lipid composition. *Nature Chemical Biology, 13*(1), 91-98.

Duncan, B. B., Magliano, D. J., & Boyko, E. J. (2025). IDF diabetes atlas 11th edition 2025: global prevalence and projections for 2050. In (pp. gfaf177): Oxford University Press.

Feng, M., Wei, S., Zhang, S., & Yang, Y. (2022a). Anti-inflammation and anti-pyroptosis activities of mangiferin via suppressing NF-κB/NLRP3/GSDMD signaling cascades. *International journal of molecular sciences, 23*(17), 10124.

Feng, Q., Yu, X., Qiao, Y., Pan, S., Wang, R., Zheng, B., et al. (2022b). Ferroptosis and acute kidney injury (AKI): molecular mechanisms and therapeutic potentials. *Frontiers in Pharmacology, 13*, 858676.

Gill, I., & Valivety, R. (1997). Polyunsaturated fatty acids, Part 1: Occurrence, biological activities and applications. *Trends Biotechnol, 15*(10), 401-409. doi:10.1016/s0167-7799(97)01076-7

Harrison, P. M., & Arosio, P. (1996). The ferritins: molecular properties, iron storage function and cellular regulation. *Biochim Biophys Acta, 1275*(3), 161-203. doi:10.1016/0005-2728(96)00022-9

Hasanein, P. (2011). Glabridin as a major active isoflavan from Glycyrrhiza glabra (licorice) reverses learning and memory deficits in diabetic rats. *Acta Physiologica Hungarica, 98*(2), 221-230.

Hassanein, E. H., Ali, F. E., Kozman, M. R., & Abd El-Ghafar, O. A. (2021). Umbelliferone attenuates gentamicin-induced renal toxicity by suppression of TLR-4/NF-κB-p65/NLRP-3 and JAK1/STAT-3 signaling pathways. *Environmental Science and Pollution Research, 28*(9), 11558-11571.

Hindam, M. O., Sayed, R. H., Skalicka-Woźniak, K., Budzyńska, B., & El Sayed, N. S. (2020). Xanthotoxin and umbelliferone attenuate cognitive dysfunction in a streptozotocin-induced rat model of sporadic Alzheimer's disease: The role of JAK2/STAT3 and Nrf2/HO-1 signalling pathway modulation. *Phytotherapy Research, 34*(9), 2351-2365.

Hu, H., Li, Y., Xin, Z., & Zhanga, X. (2018). Ginkgolide B exerts anti-inflammatory and chondroprotective activity in LPS-induced chondrocytes. *Advances in Clinical and Experimental Medicine, 27*(7), 913-920.

Huang, D., Shen, P., Wang, C., Gao, J., Ye, C., & Wu, F. (2022). Calycosin plays a protective role in diabetic kidney disease through the regulation of ferroptosis. *Pharmaceutical biology, 60*(1), 990-996.

Jiang, X., Stockwell, B. R., & Conrad, M. (2021). Ferroptosis: mechanisms, biology and role in disease. *Nat Rev Mol Cell Biol, 22*(4), 266-282. doi:10.1038/s41580-020-00324-8

Jin, T., & Chen, C. (2022). Umbelliferone delays the progression of diabetic nephropathy by inhibiting ferroptosis through activation of the Nrf-2/HO-1 pathway. *Food and Chemical Toxicology, 163*, 112892.

Kagan, V. E., Mao, G., Qu, F., Angeli, J. P. F., Doll, S., Croix, C. S., et al. (2017). Oxidized arachidonic and adrenic PEs navigate cells to ferroptosis. *Nature Chemical Biology, 13*(1), 81-90. doi:10.1038/nchembio.2238

Kang, H. S., Yang, H., Ahn, C., Kang, H. Y., Hong, E. J., & Jaung, E. B. (2014). Effects of xenoestrogens on streptozotocin-induced diabetic mice. *J Physiol Pharmacol, 65*(2), 273-282.

Khadrawy, S. M., & El Sayed, R. A. (2023). Umbelliferone attenuates diabetic cardiomyopathy by suppression of JAK/STAT signaling pathway through amelioration of oxidative stress and inflammation in rats. *Journal of Biochemical and Molecular Toxicology, 37*(4), e23296.

Kinowaki, Y., Taguchi, T., Onishi, I., Kirimura, S., Kitagawa, M., & Yamamoto, K. (2021). Overview of Ferroptosis and Synthetic Lethality Strategies. *Int J Mol Sci, 22*(17). doi:10.3390/ijms22179271

Komolkriengkrai, M., Nopparat, J., Vongvatcharanon, U., Anupunpisit, V., & Khimmaktong, W. (2019). Effect of glabridin on collagen deposition in liver and amelioration of hepatocyte destruction in diabetes rats. *Experimental and therapeutic medicine, 18*(2), 1164-1174.

Latunde-Dada, G. O. (2017). Ferroptosis: Role of lipid peroxidation, iron and ferritinophagy. *Biochim Biophys Acta Gen Subj, 1861*(8), 1893-1900. doi:10.1016/j.bbagen.2017.05.019

Le, J., Fu, Y., Han, Q., Ma, Y., Ji, H., Wei, X., et al. (2021). Transcriptome analysis of the inhibitory effect of sennoside A on the metastasis of hepatocellular carcinoma cells. *Frontiers in Pharmacology, 11*, 566099.

Li, Y., Sun, M., Cao, F., Chen, Y., Zhang, L., Li, H., et al. (2022). The ferroptosis inhibitor liproxstatin-1 ameliorates LPS-induced cognitive impairment in mice. *Nutrients, 14*(21), 4599.

Lin, D., Wu, H., Zhou, Z., Tao, Z., Jia, T., & Gao, W. (2021). Ginkgolide B improves multiterritory perforator flap survival by inhibiting endoplasmic reticulum stress and oxidative stress. *Journal of Investigative Surgery, 34*(6), 610-616.

Liu, J., Gao, L.-d., Fu, B., Yang, H.-t., Zhang, L., Che, S.-q., et al. (2022). Efficacy and safety of Zicuiyin decoction on diabetic kidney disease: a multicenter, randomized controlled trial. *Phytomedicine, 100*, 154079.

Liu, J., Wu, P., Xu, Z., Zhang, J., Liu, J., & Yang, Z. (2020). Ginkgolide B inhibits hydrogen peroxide-induced apoptosis and attenuates cytotoxicity via activating the PI3K/Akt/mTOR signaling pathway in H9c2 cells. *Molecular Medicine Reports, 22*(1), 310-316.

Ma, L., Cao, X., Ye, X., Ye, J., & Sun, Y. (2020). Sennoside a induces GLP-1 secretion through activation of the ERK1/2 pathway in l-cells. *Diabetes, Metabolic Syndrome and Obesity*, 1407-1415.

Morrish, N., Wang, S.-L., Stevens, L., Fuller, J., Keen, H., & Group, W. M. S. (2001). Mortality and causes of death in the WHO Multinational Study of Vascular Disease in Diabetes. *Diabetologia, 44*(Suppl 2), S14.

Mou, Y., Wang, J., Wu, J., He, D., Zhang, C., Duan, C., et al. (2019). Ferroptosis, a new form of cell death: opportunities and challenges in cancer. *Journal of hematology & oncology, 12*(1), 34.

Park, J. E., Lee, H., Kim, S. Y., & Lim, Y. (2020). Lespedeza bicolor extract ameliorated renal inflammation by regulation of NLRP3 inflammasome-associated hyperinflammation in type 2 diabetic mice. *Antioxidants, 9*(2), 148.

Poznyak, A., Grechko, A. V., Poggio, P., Myasoedova, V. A., Alfieri, V., & Orekhov, A. N. (2020). The diabetes mellitus–atherosclerosis connection: The role of lipid and glucose metabolism and chronic inflammation. *International journal of molecular sciences, 21*(5), 1835.

Qu, Z., Wang, B., Jin, Y., Xiao, Q., Zhao, Y., Zhao, D., et al. (2023). Shenkang protects renal function in diabetic rats by preserving nephrin expression. *BMC Complement Med Ther, 23*(1), 244. doi:10.1186/s12906-023-04078-6

Ramesh, B., & Pugalendi, K. (2005). Antihyperlipidemic and antidiabetic effects of umbelliferone in streptozotocin diabetic rats. *The Yale journal of biology and medicine, 78*(4), 189.

Rayego-Mateos, S., Morgado-Pascual, J. L., Opazo-Ríos, L., Guerrero-Hue, M., García-Caballero, C., Vázquez-Carballo, C., et al. (2020). Pathogenic Pathways and Therapeutic Approaches Targeting Inflammation in Diabetic Nephropathy. *Int J Mol Sci, 21*(11). doi:10.3390/ijms21113798

Rehman, M. U., Farooq, A., Ali, R., Bashir, S., Bashir, N., Majeed, S., et al. (2020). Preclinical evidence for the pharmacological actions of glycyrrhizic acid: a comprehensive review. *Current drug metabolism, 21*(6), 436-465.

Rout, P., & Jialal, I. (2025). Diabetic nephropathy. StatPearls-NCBI Bookshelf. 2025. In.

Satou, R., Cypress, M. W., Woods, T. C., Katsurada, A., Dugas, C. M., Fonseca, V. A., et al. (2020). Blockade of sodium-glucose cotransporter 2 suppresses high glucose-induced angiotensinogen augmentation in renal proximal tubular cells. *American Journal of Physiology-Renal Physiology, 318*(1), F67-F75.

Sha, H., Zeng, H., Zhao, J., & Jin, H. (2019). Mangiferin ameliorates gestational diabetes mellitus-induced placental oxidative stress, inflammation and endoplasmic reticulum stress and improves fetal outcomes in mice. *European Journal of Pharmacology, 859*, 172522.

Sharma, A., & Flora, S. J. S. (2021). Positive and Negative Regulation of Ferroptosis and Its Role in Maintaining Metabolic and Redox Homeostasis. *Oxid Med Cell Longev, 2021*, 9074206. doi:10.1155/2021/9074206

Stockwell, B. R., Angeli, J. P. F., Bayir, H., Bush, A. I., Conrad, M., Dixon, S. J., et al. (2017). Ferroptosis: a regulated cell death nexus linking metabolism, redox biology, and disease. *Cell, 171*(2), 273-285.

Tan, H., Chen, J., Li, Y., Li, Y., Zhong, Y., Li, G., et al. (2022). Glabridin, a bioactive component of licorice, ameliorates diabetic nephropathy by regulating ferroptosis and the VEGF/Akt/ERK pathways. *Molecular Medicine, 28*(1), 58.

Tonneijck, L., Muskiet, M. H., Smits, M. M., Van Bommel, E. J., Heerspink, H. J., Van Raalte, D. H., et al. (2017). Glomerular hyperfiltration in diabetes: mechanisms, clinical significance, and treatment. *Journal of the American Society of Nephrology, 28*(4), 1023-1039.

Umanath, K., & Lewis, J. B. (2018). Update on Diabetic Nephropathy: Core Curriculum 2018. *Am J Kidney Dis, 71*(6), 884-895. doi:10.1053/j.ajkd.2017.10.026

Valko, M., Morris, H., & Cronin, M. T. (2005). Metals, toxicity and oxidative stress. *Curr Med Chem, 12*(10), 1161-1208. doi:10.2174/0929867053764635

Wang, M., Liang, Y., Chen, K., Wang, M., Long, X., Liu, H., et al. (2022a). The management of diabetes mellitus by mangiferin: advances and prospects. *Nanoscale, 14*(6), 2119-2135.

Wang, Y., Wang, Z., Zhao, T., & Hou, S. (2022b). Effect of glycyrrhizic acid on high glucose induced podocyte injury in mice. *J Ningxia Med Univ, 44*(3), 267-271.

Wu, F., Jin, Z., & Jin, J. (2013). Hypoglycemic effects of glabridin, a polyphenolic flavonoid from licorice, in an animal model of diabetes mellitus. *Molecular Medicine Reports, 7*(4), 1278-1282.

Xie, Y., Hou, W., Song, X., Yu, Y., Huang, J., Sun, X., et al. (2016). Ferroptosis: process and function. *Cell Death Differ, 23*(3), 369-379. doi:10.1038/cdd.2015.158

XL, L., GY, Z., R, G., & N, C. (2022). Ferroptosis in sepsis: The mechanism, the role and the therapeutic potential. *Frontiers in immunology, Volume 13 - 2022*. doi:10.3389/fimmu.2022.956361

Yan, G., Chang, T., Zhao, Y., Yu, M., Mi, J., Wang, G., et al. (2023). The effects of Ophiocordyceps sinensis combined with ACEI/ARB on diabetic kidney disease: A systematic review and meta-analysis. *Phytomedicine, 108*, 154531.

Yang, J., & Liu, Z. (2022). Mechanistic Pathogenesis of Endothelial Dysfunction in Diabetic Nephropathy and Retinopathy. *Front Endocrinol (Lausanne), 13*, 816400. doi:10.3389/fendo.2022.816400

Yang, S., Xie, Z., Pei, T., Zeng, Y., Xiong, Q., Wei, H., et al. (2022). Salidroside attenuates neuronal ferroptosis by activating the Nrf2/HO1 signaling pathway in Aβ1-42-induced Alzheimer's disease mice and glutamate-injured HT22 cells. *Chinese Medicine, 17*(1), 82.

Yang, Y., Chen, J., Gao, Q., Shan, X., Wang, J., & Lv, Z. (2020). Study on the attenuated effect of Ginkgolide B on ferroptosis in high fat diet induced nonalcoholic fatty liver disease. *Toxicology, 445*, 152599.

Yoshioka, Y., Kubota, Y., Samukawa, Y., Yamashita, Y., & Ashida, H. (2019). Glabridin inhibits dexamethasone-induced muscle atrophy. *Archives of Biochemistry and Biophysics, 664*, 157-166.

Yu, S. M., Hu, D. H., & Zhang, J. J. (2015). Umbelliferone exhibits anticancer activity via the induction of apoptosis and cell cycle arrest in HepG2 hepatocellular carcinoma cells. *Molecular Medicine Reports, 12*(3), 3869-3873.

Zhao, C., Pu, Z., Gao, J., Liu, C., Xing, J., Lang, W., et al. (2022a). "Multiomics" Analyses combined with systems pharmacology reveal the renoprotection of mangiferin monosodium salt in rats with diabetic nephropathy: focus on improvements in renal ferroptosis, renal inflammation, and podocyte insulin resistance. *Journal of Agricultural and Food Chemistry, 71*(1), 358-381.

Zhao, J., Tostivint, I., Xu, L., Huang, J., Gambotti, L., Boffa, J.-J., et al. (2022b). Efficacy of combined abelmoschus manihot and irbesartan for reduction of albuminuria in patients with type 2 diabetes and diabetic kidney disease: a multicenter randomized double-blind parallel controlled clinical trial. *Diabetes care, 45*(7), e113-e115.

Zhao, Y., Li, Y., Zhang, R., Wang, F., Wang, T., & Jiao, Y. (2020). The Role of Erastin in Ferroptosis and Its Prospects in Cancer Therapy. *Onco Targets Ther, 13*, 5429-5441. doi:10.2147/ott.S254995

Zhu, H., Zhao, H., Xu, S., Zhang, Y., Ding, Y., Li, J., et al. (2021). Sennoside A alleviates inflammatory responses by inhibiting the hypermethylation of SOCS1 in CCl4-induced liver fibrosis. *Pharmacological Research, 174*, 105926.

ORAL PRESENTATION

Removable prosthetic rehabilitation with the third impression of a completely edentulous patient with temporomandibular disorders: A case report.

Neada Hysenaj[1,2] (*https://orcid.org/0000-0001-7785-4563*), Endrit Paparisto[1], Edit Xhajanka[1], Tedi Verçani[1], Edlira Mulo[1], Alketa Qafmolla[1], Blerta Lila[1], Belisa Kaleci[2]

[1]Faculty of Dental Medicine, University of Medicine, Tirana
[2]University Dental Clinic, Tirana, Albania

Abstract

Background: Edentulism is an oral health condition that is associated with reduced ability of mastication, phonetic issues, esthetic issues, and reduced quality of life.
Case Presentation: A 68-year-old completely edentulous patient had intermittent right pre-auricular pain and muscle soreness on the right side of the face, which worsened by mastication. The patient had worn the same complete dentures for eight years, which had unilateral occlusion. Occlusal wear of the artificial teeth was observed. During the clinical examination, normal mandibular movements with mild discomfort on maximum opening were observed. During the palpation of the right temporomandibular joint, this caused a familiar pain. Palpation of the right masseter muscles also caused familiar pain that remained localized. Based on DC/TMD Axis I criteria, the diagnoses were right TMJ arthralgia and local myalgia. New dentures with adjusted vertical dimension, bilateral balanced occlusion, and with the third impression were constructed.
Results: A marked improvement in the oral health quality of life of the patient was noticed after 1 month and after one year of denture insertion. In clinical examination, there was significant improvement in the denture parameters; also, there was a lack of pain reported by the patient and confirmed clinically on palpation of the right TMJ and right masseter muscle.
Conclusion: The construction of the new dentures with bilateral balanced occlusion, adjusted vertical dimension, and through the piezography technique contributed to improved denture parameters, patient comfort, relief of the TMD symptoms, and also to an improvement in the patient's quality of life.

Keywords: Edentulism; Temporomandibular Disorders; Neutral Zone; Piezography; Complete Denture.

INTRODUCTION

Edentulism is still a major challenge worldwide, particularly among older populations. It is associated with functional limitations such as reduced masticatory efficiency, altered phonetics, and esthetic issues. All these factors influence in a negative way the oral health–related quality of life. Despite these consequences, the absence of natural dentition has important implications for temporomandibular joint (TMJ) health. Tooth loss might be the cause of several changes in the temporomandibular joint, such as condylar displacement, disc malposition, and flattening of the articular eminence.
Prosthodontic rehabilitation plays an important role not only in restoring esthetics and function but also in re-establishing neuromuscular balance and reducing TMJ overload. Bilateral balanced occlusion is particularly recommended in complete denture construction, as it ensures equal distribution of functional forces and reduces the destabilizing effects that the unilateral contacts cause.
The piezography impression can be registered during the final impression, centric occlusion record, and try-in stage. In our case, we made the registration in the try-in stage, recording the periprosthetic muscles' impression during function and phonetics.
With the aging of the population and the high prevalence of edentulism in many countries, the proper construction of total removable prosthetic restorations has high relevance.
This case report presents the prosthetic rehabilitation of a completely edentulous patient with TMD symptoms, treated through a combination of correctly constructed total removable dentures with a restored vertical dimension, bilateral balanced occlusion, and through the neutral zone technique.



Fig.1. Previous dentures



Fig. 2 The edentulous mandible

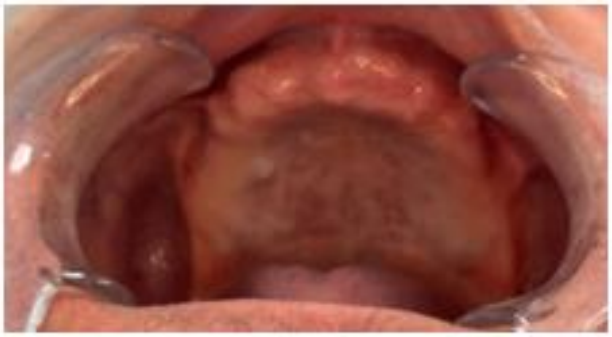


Fig.3 The edentulous maxilla



Fig.4 Facebow transfer registration

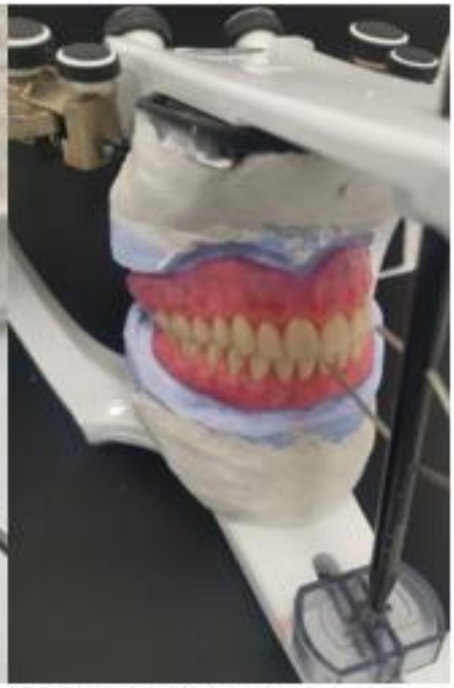


Fig. 5 Mounted dentures on articulator



Fig.6 Bilateral balanced occlusion



Fig. 7 Try in stage



Fig.8 Piezographic Impression



Fig.9 Denture Insertion Phase

CASE PRESENTATION

A completely edentulous 68-year-old patient came to the University Dental Clinic. He had worn the same dentures for 8 years (Fig.1). The patient referred about masticating mainly on the right side. The previous old dentures had unilateral occlusion, and the artificial teeth were worn. The patient described intermittent pain in the right pre-auricular area, which worsens when the patient chews harder foods. He also refers about muscle soreness in the right cheek region, particularly after prolonged mastication. He did not report joint noises, locking, or limitations in mouth opening.

During the clinical examination, mandibular movements were within normal limits, although the patient reported slight discomfort when he maximally opened the mouth. The palpation on the right TMJ caused the same pain the patient usually feels, and found it familiar. During the palpation of the right masseter muscle, that caused pain which was localized. No joint crepitus or clicking was found, excluding in this way degenerative joint disease and disc displacement with reduction.

Based on the DC/TMD Axis I, the following clinical diagnoses were made: local myalgia of the right masseter muscle and arthralgia of the right TMJ.

On intraoral examination, the following were observed: in the lower jaw, severe resorption of the residual ridge (Fig.2), and in the upper jaw, non-uniform resorption of the residual ridge was observed, especially in the posterior areas (Fig.3).

After careful examination of old dentures, the need to increase the vertical dimension was confirmed. New complete dentures with bilateral occlusion, adjusted vertical dimension and through the piezography technique were decided to be constructed. The goal was not only to restore function and esthetics but also to relieve the

temporomandibular disorder symptoms. Advice was also given to the patient, like the application of moist heat, gentle mandibular exercises, and also to avoid excessive parafunctional habits.

Primary impressions were made with alginate with stock trays. The definitive impressions were made with the addition silicone, light body (PVS) through individual trays made with photo-polymerizing resin, to ensure accurate registration of the resorbed ridges. Through the maxilla-mandibular records, the following were determined: the occlusal plane, vertical dimension, and centric relation. We used the facebow to register the position of the maxilla toward the intercondylar transverse hinge axis. The recording was then transferred to the semi-adjustable BioArt articulator (Fig. 4,5).

The vertical dimension of occlusion was increased by 3 mm compared with the old dentures, correcting the previous loss of support and allowing a more physiologic jaw relation. This was decided after several measurements were made to determine the correct vertical dimension. The measurements were based on phonetics, esthetics, and the measurement of the interocclusal rest space.

The artificial teeth were arranged in order to establish bilateral balanced occlusion (Fig. 6), eliminating in this way the unilateral contacts.

In the try-in stage (Fig.7), the centric occlusion, phonetic, and aesthetics were checked.

At the try-in stage, a third impression was performed using the piezography technique (Fig.8)**.** The patient was instructed to make functional movements such as smiling, whistling, swallowing, and pronouncing phonemes (oo, ee, m, p, b, s), which allowed the registration of the polished surfaces in harmony with the surrounding structures such as lips, cheeks, and tongue. This functional registration was particularly important given the severe mandibular ridge resorption, ensuring in this case, increased stability and reducing the destabilizing influence of muscular forces.

After the try-in procedure, the traditional cycle of flasking and polymerization was followed.

At the delivery stage, the centric occlusion was again checked (Fig.9). The patient was informed about instructions on adaptation and denture, and oral hygiene. The follow-up appointments were planned after 24 hours, one week, one month, three months, six months, and twelve months. The patient fulfilled the OHIP EDENT questionnaire at the beginning, after 1 month and after 1 year.

At the beginning, the patient reported moderate preauricular pain (VAS 6/10), familiar pain on palpation of the right TMJ and masseter, and also a negative impact on the oral health–related quality of life (OHIP-EDENT score 32). After the patient received the new dentures, significant improvements were noted after one month and also after one year. After 1 month, the patient reported a lack of pain, and both joint and muscle pain were absent. OHIP-EDENT score improved to 10, reflecting better function, stability, and comfort. At the 1-year follow-up, outcomes remained stable, with no recurrence of TMD symptoms and sustained improvement in quality of life (OHIP-EDENT score 6), Table 1.

Table 1. *Results of Complete Removable Denture Treatment*

Parameter	**Baseline (old dentures)**	**1-month follow-up (new dentures)**	**1-year follow-up (new dentures)**
TMJ arthralgia (VAS 0–10 & palpation)	VAS 6; familiar pain present on right TMJ palpation	VAS 0; no familiar pain on palpation	VAS 0; no familiar pain on palpation
Masseter muscle pain (patient report & palpation)	Patient reported right cheek soreness; familiar localized pain on palpation	Patient reported no muscle pain; palpation negative	Patient reported no muscle pain; palpation negative
OHIP-EDENT (0–56)	32	10	6
Denture stability/retention	Poor	Good	Good

DISCUSSION

Several radiographic and clinical studies have shown that edentulism is associated with reduced joint spaces, posterior displacement of the condyles, and flattening of the articular eminence, contributing in this way to functional overload and also TMJ discomfort (Zheng et al., 2023; Tabatabaei et al., 2024).
In the study of Diernberger et al. (2008), the authors found a strong association between unilateral chewing activity and asymmetric occlusion with temporomandibular symptoms.
In the study of Jouhadi et al. (2025), nearly one-third of the 130 completely edentulous patients included in their study had TMD symptoms. In the review of Nguyen et al. (2021), it was concluded that the lack of occlusal units has been linked to a higher risk for TMD, while balanced support helps in preventing TMD. In our case, the patient's previous dentures were constructed with unilateral occlusion, which likely contributed to muscular and preauricular pain. The construction of new dentures with bilateral balanced occlusion redistributed the occlusal forces evenly in both sides, minimizing lateral stresses and improving so stability. Balanced occlusion in the removable complete dentures is a key component as it reduces tipping forces during the process of mastication and also ensures smoother mandibular movements.

Another important clinical point is that, in edentulous patients, well-constructed dentures can act as functional appliances. In completely edentulous patients, however, the complete denture itself must serve both functional and therapeutic roles. Several authors have reported that complete denture therapy can alleviate mild functional TMD (Nimonkar et al., 2025; Abdelnabi & Swelem, 2015; Vasavi et al., 2023).

Nimonkar et al. (2025) included 110 edentulous patients with temporomandibular disorders, treated with new complete dentures. Using the Craniomandibular Index, mean scores significantly dropped after three months, showing a significant reduction in TMD symptoms. Abdelnabi and Swelem (2015) showed that replacing the old defective complete dentures significantly improved TMD symptoms in edentulous patients. In a two-year follow-up, clinical signs such as pain and joint noises showed improvement, also better disc positioning and reduced joint effusion were detected, though disc morphology remained unchanged. Vasavi et al. (2023) analyzed the effect that new complete dentures have on temporomandibular joint function using a Joint Vibration Analyzer, where they found significant reductions in vibration parameters, showing so smoother and more stable condylar movement.

The Diagnostic Criteria for Temporomandibular Disorders (DC/TMD) were used to determine the clinical diagnosis (Schiffman et al., 2014).

The use of the neutral zone (piezography) technique was an important step of the total removable denture construction. This technique records the functional dynamics of the organs that sound the periprosthetic zone: muscles of the lips, cheeks, and tongue leave their impression, by constructing so dentures in harmony with the neuromuscular environment. In clinical cases where there is a high resorption of the residual ridge, such as in our patient, the neutral zone technique is highly recommended, as it minimizes the tendency of dislodgment that the muscles have. Several studies have demonstrated that dentures that have been constructed using the neutral zone technique provide improved retention, improved phonetics, and higher patient satisfaction compared to dentures constructed with the conventional technique (Limpuangthip et al., 2024).

The follow-up is an important step for these cases. Advice on chewing bilaterally, having a soft diet during the phase of adoption, also advice on how to keep dentures and oral hygiene were given. In the check-up visits, pre-contacts, and minor occlusal adjustments should be considered to maintain a balanced occlusal support. The OHIP EDENT questionnaire (Allen & Locker, 2002) was used to analyze patients' perception of stability, comfort, social, and psychological aspects, etc, after treatment.

CONCLUSIONS

This case report highlights the importance of proper removable prosthetic rehabilitation in the management of completely edentulous patients with mild temporomandibular disorders. In edentulous patients with mild TMD, carefully constructed complete dentures, restoring vertical dimension, balancing occlusal contacts, and shaping polished surfaces via the piezography technique, can improve denture outcomes, relieve TMD symptoms, and improve oral health-related quality of life of the patients.

Anyway, further research is suggested to analyze the effect of total removable prosthetic rehabilitation in completely edentulous patients with temporomandibular disorders.

FUNDING AND ACKNOWLEDGMENT. We would like to express our appreciation to the National Agency for Scientific Research and Innovation (NASRI), Albania, for the financial support.
PATIENT CONSENT. The patient's written consent was taken.
ETHICS STATEMENT: This case report is part of a larger project, which has been approved by the Ethical Board of the University of Medicine, Tirana, Nr. 28, date 29.08.2024.
CONFLICT OF INTEREST: None.
DATA AVAILABILITY: Not applicable.

REFERENCES

Abdelnabi, M. H., & Swelem, A. A. (2015). Influence of defective complete dentures renewal on TMD; An MRI and clinical controlled prospective study. *Gerodontology, 32*(3), 211–221. https://doi.org/10.1111/ger.12102

Allen, F., & Locker, D. (2002). A modified short version of the Oral Health Impact Profile for assessing health-related quality of life in edentulous adults. *International Journal of Prosthodontics, 15*(5), 446–450.

Diernberger, S., Bernhardt, O., Schwahn, C., & Kordass, B. (2008). Self-reported chewing side preference and its associations with occlusal, temporomandibular and prosthodontic factors: Results from the population-based Study of Health in Pomerania (SHIP-0). *Journal of Oral Rehabilitation, 35*(8), 613–620. https://doi.org/10.1111/j.1365-2842.2007.01790.x

Jouhadi, E. M., Benazouz, I., Nabli, M., Hamza, M., Al Jalil, Z., & El Boussiri, K. (2025). Prevalence of temporomandibular disorders in completely edentulous patients attending the Dental Consultation and Treatment Center in Casablanca: A descriptive cross-sectional study. *Cureus, 17*(5), e83398. https://doi.org/10.7759/cureus.83398

Limpuangthip, N., Techapiroontong, S., & Prawatvatchara, W. (2024). A systematic review of patient-oriented outcomes following complete denture treatment: A comparison between the neutral zone technique and conventional approach. *BDJ Open, 10*(1), 37. https://doi.org/10.1038/s41405-024-00222-7

Nguyen, M. S., Saag, M., Jagomägi, T., Nguyen, Q. H., & Voog-Oras, Ü. (2021). The impact of occlusal support on temporomandibular disorders: A literature review. *Proceedings of Singapore Healthcare, 31*(2), 109–117. https://doi.org/10.1177/20101058211023779

Nimonkar, S., Godbole, S., Belkhode, V., Nimonkar, P., Khubchandani, S., & Zilpilwar, N. (2025). Assessing, categorizing and proposing the therapeutic effect of complete dentures on temporomandibular disorders analyzed by craniomandibular index: A prospective interventional study. *BMC Oral Health, 25*(1), 580. https://doi.org/10.1186/s12903-025-05979-3

Schiffman, E., Ohrbach, R., Truelove, E., Look, J., Anderson, G., Goulet, J. P., List, T., Svensson, P., Gonzalez, Y., Lobbezoo, F., Michelotti, A., Brooks, S. L., Ceusters, W., Drangsholt, M., Ettlin, D., Gaul, C., Goldberg, L. J., Haythornthwaite, J. A., Hollender, L., Jensen, R., et al. (2014). Diagnostic Criteria for Temporomandibular Disorders (DC/TMD) for clinical and research applications: Recommendations of the International RDC/TMD Consortium Network and Orofacial Pain Special Interest Group. *Journal of Oral & Facial Pain and Headache, 28*(1), 6–27. https://doi.org/10.11607/jop.1151

Tabatabaei, S., Paknahad, M., & Poostforoosh, M. (2024). The effect of tooth loss on the temporomandibular joint space: A CBCT study. *Clinical and Experimental Dental Research, 10*(1), e845. https://doi.org/10.1002/cre2.845

Vasavi, M., Ramaraju, A. V., Sajjan, M. C. S., Rao, D. B., Manikyamba, Y. J. B., & Thorreti, V. S. L. (2023). An evaluation of the effect of wearing complete dentures on temporomandibular joint vibrations over time using the joint vibration analyzer. *Journal of the Indian Prosthodontic Society, 23*(1), 30–37. https://doi.org/10.4103/jips.jips_215_22

Zheng, H., Shi, L., Lu, H., Liu, Z., Yu, M., Wang, Y., & Wang, H. (2023). Influence of edentulism on the structure and function of temporomandibular joint. *Heliyon, 9*(10), e20307. https://doi.org/10.1016/j.heliyon.2023.e20307

ORAL PRESENTATION

Balık hastalıklarına yanıtta moleküler mekanizmalar

Naime Filiz Karadaş (Orcid: 0000_0003-3488-3481)

Atatürk Üniversitesi. Su Ürünleri Fakültesi. Erzurum. Türkiye

Corresponding author e-mail: filizkaradas66@gmail.com

Özet

Balık hastalıkları, küresel ölçekte akuakültür sektörünün en önemli kısıtlayıcı faktörlerinden biri olarak öne çıkmaktadır. Artan üretim kapasitesi ve yoğun yetiştiricilik uygulamaları, enfeksiyöz ajanların yayılımını hızlandırarak ekonomik kayıplara yol açmaktadır. Bu bağlamda, balıklarda hastalık direncini şekillendiren moleküler mekanizmaların anlaşılması, hem seçici ıslah hem de hastalık kontrol stratejileri için kritik öneme sahiptir. Son yıllarda moleküler biyoloji alanındaki gelişmeler, bakteriyel, viral ve paraziter balık hastalıklarının tanısı ve epidemiyolojisinin araştırılmasında yeni ufuklar açmıştır. Özellikle polimeraz zincir reaksiyonu (PCR) ve türevleri, restriksiyon fragment uzunluk polimorfizmi (RFLP), in situ hibridizasyon, DNA mikroarrayleri ve multipleks PCR gibi yöntemler; yüksek duyarlılık ve özgüllükleri sayesinde asemptomatik bireylerde dahi patojenlerin tespitini mümkün kılmaktadır. Bu teknikler, klasik yöntemlere kıyasla daha hızlı ve güvenilir sonuçlar sunmakta, antibiyotik kullanımını azaltarak dirençli bakteri gelişiminin önlenmesine katkı sağlamaktadır. Bununla birlikte, kontaminasyon ve hatalı negatif veriler gibi olası sorunların önüne geçilebilmesi için laboratuvar uygulamalarında titiz önlemler alınması gerekmektedir. Sonuç olarak, moleküler biyolojik yaklaşımlar balık hastalıklarının erken teşhisi ve kontrolünde modern akuakültür için vazgeçilmez araçlar haline gelmiştir.

Anahtar kelimeler: PCR, DNA, Moleküler Mekanizma, Balık Hastalık Kontrolü

Molecular mechanisms in the response to fish diseases

Abstract

Fish diseases stand out as one of the most significant limiting factors in the aquaculture sector worldwide. Increasing production capacity and intensive farming practices accelerate the spread of infectious agents, leading to substantial economic losses. In this context, understanding the molecular mechanisms shaping disease resistance in fish is of critical importance for both selective breeding and disease control strategies. In recent years, advances in molecular biology have opened new horizons in the diagnosis and epidemiological investigation of bacterial, viral, and parasitic fish diseases. In particular, methods such as polymerase chain reaction (PCR) and its derivatives, restriction fragment length polymorphism (RFLP), in situ hybridization, DNA microarrays, and multiplex PCR enable the detection of pathogens even in asymptomatic individuals due to their high sensitivity and specificity. Compared to classical approaches, these techniques provide faster and more reliable results, while contributing to the prevention of resistant bacterial development by reducing antibiotic usage. However, meticulous precautions in laboratory practices are required to prevent potential problems such as contamination and false negative results. In conclusion, molecular biological approaches have become indispensable tools for modern aquaculture in the early diagnosis and control of fish diseases.

Keywords: PCR, DNA, Molecular Mechanism, Fish Disease Control

1.Giriş

Dünya genelinde gıda üretimi ve güvenliği artan baskılarla karşı karşıyadır. Bu bağlamda akuakültür, insan beslenmesi ve sürdürülebilir gıda arzında kritik bir rol üstlenmektedir. Ancak bulaşıcı hastalıklar, balık ölümlerinin başlıca nedeni olup su ürünleri yetiştiriciliğinin verimliliği için küresel ölçekte ciddi bir tehdit oluşturmaktadır

(Robinson, 2017). Balıklarda hastalıklara karşı direnç geliştirmeyi amaçlayan genetik ıslah, hastalık kaynaklı kayıpları kalıcı ve etkili biçimde azaltma potansiyeli nedeniyle uzun süredir önceliklidir. Bununla birlikte, seçici ıslah ve hastalık kontrol programlarının başarısı, konak–patojen etkileşimlerini ve dayanıklılığı belirleyen moleküler süreçlerin ayrıntılı biçimde anlaşılmasına bağlıdır (Zhou et al., 2022). Öte yandan, doğal sucul ekosistemlerin insan faaliyetleri ve iklim değişikliği nedeniyle bozulması, yabani balık popülasyonlarında salgın riskini artırarak yönetim ve koruma çabalarını daha da güçleştirmektedir.

Hastalık direnci kavramı, konağın patojenlerin hedef dokulara girişini ve çoğalmalarını sınırlandırma kapasitesini tanımlar. Balıklarda bu direnç; epitel tabakalarının ve mukus örtüsünün bütünlüğünün korunması, makrofaj ve nötrofillerin fagositoz aktivitesi gibi özgül olmayan hücresel savunma unsurları, lizozim, kompleman sistemi ve transferrin gibi özgül olmayan humoral bileşenler ile özgül humoral ve hücresel bağışıklık yanıtlarını içermektedir (Blazer, 1992). Nicel özellik lokusu (QTL) haritalama ve genom çapında ilişkilendirme çalışmaları (GWAS), balıklarda hastalık direnci ile bağlantılı tek nükleotid polimorfizmleri (SNP'ler) ve genlerin belirlenmesine olanak sağlamıştır. Bu tür araştırmalar özellikle Atlantik somonu, gökkuşağı alabalığı ve Çin dilbalığında yürütülmüştür. Ayrıca, dirençli ve duyarlı bireylerin patojen enfeksiyonlarına karşı verdiği transkripsiyonel tepkilerin karşılaştırıldığı çalışmalar, farklı patojenler tarafından uyarılan gen yanıtlarının genellikle ortak bağışıklık mekanizmalarını içerdiğini ortaya koymuştur. Bu mekanizmalar arasında kompleman sistemi, bağışıklık sinyal iletim yolları, bazı enzimler ve kemokinler yer almakta olup, söz konusu bulgular Atlantik somonu, gökkuşağı alabalığı, sazan ve Çin dilbalığında da rapor edilmiştir. Sonuç olarak, yapılan araştırmalar dirençli ve duyarlı balıkların, geçici enfeksiyonlara maruz kaldıktan sonra farklı genetik özellikler ve moleküler yanıtlar sergilediklerini göstermektedir (Zhou et al., 2022).

Son yıllarda, balık patojenleri ve konaklarının moleküler biyolojisinin anlaşılmasında önemli gelişmeler kaydedilmiş ve moleküler biyoloji, balık hastalıklarının tanısı, kontrolü ve bakteriyel, viral ile paraziter hastalıkların epidemiyolojisinin araştırılmasında rutin bir araç haline gelmiştir. Nükleik asitlerin tespiti, zor ya da hiç kültüre edilemeyen ve hatta ölü mikroorganizmaların belirlenmesinde yararlı olmuş, böylece yeni ve alternatif tanı teknolojilerinin geliştirilmesine olanak sağlamıştır. Moleküler yöntemler, bu tür sorunların çözümünde kullanılabilmekte ve patojen tespitinde duyarlılığı ile özgüllüğü artırmaktadır. Bu teknikler arasında polimeraz zincir reaksiyonu (PCR), restriksiyon enzimi kesimi, prob hibridizasyonu, in situ hibridizasyon ve mikroarray sistemleri yer almaktadır. Konvansiyonel yöntemlere kıyasla daha hızlı ve hassas olan bu tanı teknikleri, asemptomatik balıklarda dahi patojenlerin saptanmasına imkân tanır. Böylece olası salgınların önüne geçilebilir, antibiyotik kullanımına duyulan ihtiyaç azalır ve antibiyotik dirençli bakteri oluşumunun önlenmesine katkı sağlanır (Altınok ve Kurt 2003).

2. Balık Hastalıklarının Saptanmasında Moleküler Teknolojiler

Ticari akuakültür işletmeleri için balıklarda hastalıkların yönetimi ve izlenmesi büyük önem taşımaktadır. Patojenlerin balıklarda bulunup bulunmadığının hızlı bir şekilde tespit edilmesi, ciddi ekonomik avantajlar sağlayabilir. Bunun yanında, enfeksiyöz organizmaların balıkta veya çevredeki yoğunluğunun belirlenebilmesi, popülasyondaki değişimlerin izlenmesine imkân tanır. Ayrıca, hastalık etkeninin bulunduğu bölgelerde balıkların taşıyıcılık durumunu doğru şekilde değerlendirebilecek bir sistemin geliştirilmesi, etkili hastalık yönetim programlarının oluşturulmasına katkı sunar.

Son yıllarda bakteriyel, viral ve paraziter balık hastalıklarının tanısında duyarlılık ve özgüllüğün artırılmasına yönelik önemli ilerlemeler kaydedilmiştir. Moleküler tanı tekniklerinde genellikle örneklerden DNA izolasyonu yapılır. Bu DNA, DNA hibridizasyonu veya restriksiyon parça uzunluk polimorfizmi (RFLP) ile analiz edilebilmektedir. Daha yaygın kullanılan yöntem ise özgül primerler aracılığıyla polimeraz zincir reaksiyonu (PCR) ile DNA'nın çoğaltılmasıdır. PCR uygulamasını, RFLP analizi, spesifik oligoprob hibridizasyonu ile ilişkili PCR teknikleri veya rastgele çoğaltılmış polimorfik DNA (RAPD) üretimine dayalı yöntemler takip edebilmektedir (McKeand, 1998).

2.1. Polimeraz zincirleme reaksiyonu

Polimeraz Zincir Reaksiyonu (PCR), karmaşık bir DNA havuzundan belirli bir DNA parçasının çoğaltılmasına olanak sağlayan basit fakat etkili bir enzimatik tekniktir. Bu yöntemi geliştiren Dr. Kary Mullis, PCR'ı "ilgilendiğiniz DNA bölümünü seçmenizi ve ondan sınırsız miktarda elde etmenizi mümkün kılar" sözleriyle tanımlamıştır (Mullis, 1990). PCR, periferik kan, deri, saç, tükürük ve mikroorganizmalar gibi çok çeşitli doku ve organizmalardan elde edilen DNA örnekleri üzerinde uygulanabilir. Sadece çok küçük miktarda DNA, PCR ile analiz için yeterli sayıda kopya üretmek açısından yeterlidir. Bu özelliği nedeniyle PCR oldukça duyarlı bir yöntem olarak kabul edilmektedir (Garibyan and Avashia, 2013).

Duyarlılık ve özgüllük açısından primer tasarımı kritik öneme sahiptir. Primerler yüksek bağlanma sıcaklığı sağlayacak kadar uzun olmalı, ancak aşırı uzun primerler yanlış bağlanmalara yol açabilir. PCR reaksiyon karışımı; şablon DNA (doku lizatı veya saf DNA), primerler, polimeraz enzimi ve nükleotidleri içerir. Termal döngü sürecinde DNA denatüre edilir, primerler tamamlayıcı dizilere bağlanır ve polimeraz enzimi yeni zincirlerin sentezini gerçekleştirir. Her döngüde ürün miktarı katlanarak artar. **Ters transkriptaz PCR (RT-PCR)**, mRNA düzeylerini tespit etmek ve gen ekspresyonunu ölçmek için yaygın olarak kullanılır (Koo ve Jaykus, 2000). Northern blot ve RNase koruma testi gibi yöntemlere kıyasla çok daha küçük örneklerden analiz yapılabilmesi ve tek bir hücreden RNA miktarının ölçülebilmesi en büyük avantajlarıdır. Son yıllarda geliştirilen yeni sistemler, PCR ürünlerinin gerçek zamanlı izlenmesine olanak tanımış ve **gerçek zamanlı RT-PCR**'yi gen ekspresyon değişimlerinin ölçümünde tercih edilen yöntem haline getirmiştir. Ayrıca, gen ekspresyonunu küresel ölçekte inceleyen yöntemlerden elde edilen bulguların doğrulanmasında da sıkça kullanılmaktadır. Yüksek özgüllük ve duyarlılık sağlaması, RT-PCR'yi gizli enfeksiyonların izlenmesi için de uygun kılar (Altinok ve Kurt 2003)

Ökaryotlarda olduğu gibi prokaryotların rRNA genlerinde de korunmuş bölgeler bulunur. Bu bölgeler tanımlama ve çoğaltma amacıyla kullanılabilirken, değişken bölgeler kültürü zor ya da imkânsız bakterilerin tespitinde yararlanılır (Barry ve ark., 1990). rRNA genleri, **Renibacterium salmoninarum** (Rhodes ve ark., 1998), **Aeromonas salmonicida** (Høie ve ark., 1999) ve **Yersinia ruckeri** (Altinok ve ark., 2000) için PCR testlerinde başarıyla uygulanmıştır. Benzer yöntemler ayrıca **Vibrio anguillarum**, **Lactococcus garvieae**, **Piscirickettsia salmonis**, **Flexibacter**, **Flavobacterium**, **Photobacterium** ve **Mycobacterium** gibi Avrupa Birliği mevzuatına dahil edilmeyen ancak önemli balık patojenlerinin tanısında da kullanılmaktadır.

2.2. Multipleks PCR

Aynı anda birden fazla patojeni belirlemeye yönelik multipleks PCR, zaman ve maliyet açısından önemli avantajlar sağlamaktadır (Williams ve ark., 1999). Bu yöntemde, birden fazla hedef diziyi çoğaltmak için farklı primer çiftleri aynı reaksiyonda kullanılabilir. Böylece testin güvenilirliği korunurken laboratuvarda ciddi ölçüde zaman ve emek tasarrufu elde edilir. Multipleks PCR; gen delesyonu analizi (Chamberlain ve ark., 1988, 1989), kantitatif analiz (Zimmermann ve ark., 1996; Rithidech ve ark., 1997), RNA tespiti (Zou, 1997) ve virüs, bakteri, mantar ile parazitlerin tanımlanmasında başarıyla uygulanmıştır.

2.3. Nükleik Asitlerin İşaretlenmesi ve Tespiti

Nükleik asit probları için farklı işaretleme ve tespit sistemleri geliştirilmiştir (Tijssen, 1993). Eskiden yaygın kullanılan radyoizotoplar güvenlik nedeniyle yerini biyotin veya digoksigenin gibi haptenlere bırakmıştır. Bu işaretler, antikor bağlanmasıyla floresan, kemilüminesans veya kolorimetrik yöntemlerle saptanabilmektedir (Tyagi ve Kramer, 1996; Gonzalez ve ark., 1997).

2.4. Restriksiyon Enzimleri ile Sindirim

Restriksiyon enzimleri (endonükleazlar), DNA'yı belirli dizilerden kesen özel enzimlerdir. Tip II restriksiyon enzimleri, genetik analiz ve mühendislikte en çok kullanılanlardır ve genellikle altı baz çifti uzunluğunda palindromik dizileri tanır, ancak dört ya da sekiz bazlık dizileri hedefleyenler de vardır. Bu enzimlerle DNA parçalanarak jel elektroforeziyle ayrıştırılır ve her DNA'ya özgü bir "parmak izi" deseni elde edilir. Ayrıca kesim

bölgeleri belirlenerek restriksiyon haritaları oluşturulabilir ve plazmid ya da DNA bölgelerinin tanımlanmasında kullanılabilir (Grizzle ve ark., 2002).

Tek baz değişiklikleri, restriksiyon bölgesinin oluşmasına veya kaybolmasına yol açabilir. Bu durum DNA parçalarının sayısını değiştirir ve RFLP (Restriction Fragment Length Polymorphism) adı verilen farklılıkları ortaya çıkarır. RFLP profilleri, adli incelemeler, babalık testleri, populasyon genetiği ve çeşitli hastalıkların tanısında önemli bir araç haline gelmiştir.

2.5. İn Situ Hibridizasyon

İn situ PCR, hem araştırma hem de klinik alanda enfeksiyon ve tümörlerin anlaşılması ve tanısında önemli bir araçtır. İn situ RT-PCR, düşük seviyedeki gen ekspresyonunu yüksek hassasiyetle saptayarak anatomik bilgi sağlar. Ancak düşük duyarlılık, tekrarlanabilirlik sorunları ve yüksek arka plan sinyali gibi kısıtlamaları vardır. Floresan işaretli in situ RT-PCR yöntemleri bu sınırlamaları azaltarak daha net sonuçlar sunar. Uygulama alanları arasında enfeksiyon etkenlerinin ve tümör hücrelerinin tanısı, genetik mutasyonların tespiti ve gen ekspresyonunun incelenmesi bulunur. Floresan in situ hibridizasyon (FISH) ise hücre veya kromozomları nükleik asit dizilerine göre işaretler. Yaklaşık 20 nükleotitlik floresan problar hedef RNA veya DNA dizilerine bağlanır. Bu şekilde işaretlenen hücreler, floresan mikroskopi ya da akış sitometrisiyle görüntülenebilir (Long, 1998; Nuovo, 1996).

2.6. DNA Mikroarrayler

DNA mikroarrayler, özgül DNA veya RNA dizilerini belirlemede kullanılan modern bir tekniktir. Test örneği floresanla işaretlenir ve çip üzerindeki uygun oligonükleotidlere bağlanan diziler özel dedektörlerle saptanır. Rekabetçi hibridizasyon yönteminde ise test DNA'sı, floresan işaretli rakip oligonükleotidlerle yarışarak çipe bağlanır. Uyumlu diziler hedefe tutunurken, uyumsuz olanlar yerini floresan işaretliye bırakır. Böylece tür veya suş spesifik diziler kolayca tespit edilir.

Mikroarrayler, klasik hibridizasyon yöntemlerine göre daha hızlı, hassas, düşük maliyetli ve otomasyona uygun sonuçlar verir (Shalon ve ark., 1996). GenBank'taki mevcut veriler sayesinde pek çok patojene özgü problar tek bir çipte toplanabilir ve aynı anda çok sayıda etken belirlenebilir (Southern, 1996; Mir, 2000). Bu teknoloji, özellikle balıklarda asemptomatik dönemdeki hastalıkların erken teşhisi için büyük potansiyel taşır (Zhou ve Dorothea, 2004).

Ayrıca mikroarrayler, gen ekspresyonunu incelemede de etkilidir. Belirli genlerin varlığı veya yokluğu, bir patojenin hastalık yapıcı olup olmadığını gösterebilir. Yüksek kurulum maliyetine rağmen, hazır sistemlerde test başına düşen maliyet düşük, analiz süresi ise oldukça kısadır.

3. Olası Sorunlar ve Kontaminasyonun Önlenmesi

PCR sonuçları, kullanılan dokuya ve örnekteki inhibitörlere bağlı olarak değişebilir. Hemoglobin, bakteriyel bileşenler veya konak DNA'sının fazlalığı çoğaltmayı engelleyebilir (Wilson, 1997; Høie ve ark., 1997). Bu nedenle yüksek kaliteli nükleik asit ekstraksiyon sistemleri tercih edilmelidir.

Kontaminasyonu önlemek için her balıkta tek kullanımlık aletler kullanılmalı veya ekipman çamaşır suyu ile temizlenip bol suyla durulanmalıdır. Alkol ve alev güvenilir değildir. Örnek homojenizasyonunda bulaşmayı önlemek için stomacher tercih edilmelidir. Ayrıca nekropsi, DNA ekstraksiyonu, PCR hazırlığı ve elektroforez işlemleri için ayrı odalar kullanılmalı; laboratuvar malzemeleri odalar arasında taşınmamalıdır. PCR ürünleriyle kontaminasyonu engellemek için dUTP ile birlikte UNG kullanılabilir. Yalancı negatif sonuçların önüne geçmek için β-aktin gibi iç kontroller önerilir; bu, amplifikasyonu engelleyen örneklerin kolayca belirlenmesini sağlar (Grizzle ve ark., 2003).

Sonuç

Balık sağlığında immünolojik ve moleküler tanı yaklaşımları, son dönemde önemli bir ivme kazanmış; PCR ve türevleri, multipleks PCR, restriksiyon temelli analizler, in situ hibridizasyon ve DNA mikroarrayleri gibi araçlar sayesinde patojenlerin yüksek duyarlılık ve özgüllükle, hatta asemptomatik evrede bile saptanması mümkün hale gelmiştir. Bu kazanımlar, salgınların erken bastırılmasına, tedavinin hedefe yönelik planlanmasına, antibiyotik kullanımının azaltılmasına ve direnç gelişiminin sınırlandırılmasına somut katkı sağlar. Bununla birlikte yöntemlerin güvenilirliği; kontaminasyon, inhibitör varlığı ve yalancı negatifler gibi teknik sınırlılıkların titizlikle yönetilmesine bağlıdır. Standartlaştırılmış protokoller, kaliteli nükleik asit ekstraksiyonu, uygun iç kontroller ve ayrık çalışma alanları zorunludur. Bu gereksinimler karşılandıkça, söz konusu teknolojilerin rutin izleme ve tanıda daha geniş yer bulacağı; karar süreçlerini güçlendirerek akuakültürde verimliliği artıracağı ve ekonomik kayıpları azaltırken sürdürülebilirliği destekleyeceği öngörülmektedir.

Kaynaklar

Altinok, I., Grizzle, J.M. and Liu, Z. (2000). Detection of Yersinia ruckeri in rainbow trout blood by use of polymerase chain reaction. *Dis. Aquat. Org*., 44: 29- 34.

Altinok, İ., & Kurt, İ. (2003). Molecular diagnosis of fish diseases: a review. *Turkish Journal of Fisheries and Aquatic Sciences*, 3(2).

Blazer, V. S. (1992). Nutrition and disease resistance in fish. *Annual Review of Fish Diseases*, *2*, 309-323.

Barry, T., Powell, R. and Gannon, F. (1990). A general method to generate DNA probes for microorganisms. *Bio/Tech*., 8: 233–236.

Chamberlain, J.S., Gibbs, R.A., Ranier, J.E., Nguyen, P.N. and Caskey, C.T. (1988). Deletion screening of the Duchenne muscular dystrophy locus via multiplex DNA amplification. *Nucleic Acids Res*., 16: 11141-11156.

Chamberlain, J.S., Gibbs, R.A., Ranier, J.E., Nguyen, P.N. and Caskey, C.T. (1989). Multiplex PCR for the diagnosis of Duchenne muscular dystrophy, D.H. Gelfand, M.A. Innis, J.J. Shinsky, and T.J. White (Eds.), PCR protocols: a guide to methods and applications. *Academic Press, San Diego, California*: 272-281

Deering, R.E., Arakawa, C.K., Oshima, K.H., O'Hara, P.J., Landolt, M.L. and Winton, J.R. (1991). Development of a biotinylated DNA probe for detection and identification of infectious hematopoietic necrosis virus. *Dis. Aquat. Org*., 11: 57–65

Gabriyan, L., & Avashia, N. (2013). Research techniques made simple: polymerase chain reaction (PCR). *J Invest Dermatol*, *133*(3), e6.

Gonzalez, M.P., Sanchez, X., Ganga, M.A., Lopez-Lastra, M., Jashes, M. and Sandino, A.M. (1997). Detection of the infectious hematopoietic necrosis virus directly from infected fish tissues by dot blot hybridisation with a non-radioactive probe. *J. Virol. Methods*, 65: 273–279.

Grizzle, J.M., Altinok, I., Fraser, W.A. and Francis-Floyd, R. (2002). First isolation of largemouth bass virus. *Dis. Aquat. Org*., 50: 233-235.

Grizzle, J.M., Altinok, I. and Noyes, A.D. (2003). PCR method for detection of largemouth bass virus. *Dis. Aquat. Org*., 54: 29-33.

Høie, S., Heum, M., Thoresen, O.F. (1997). Evaluation of a polymerase chain reaction-based assay for the detection of Aeromonas salmonicida salmonicida in Atlantic salmon Salmo salar. *Dis. Aquat. Org*., 30: 27–35.

Høie, S., Dalsgaard, I., Aase, I.L., Heum, M., Thornton, J.M., Powell, R. (1999). Polymerase chain reaction (PCR)-based typing analysis of atypical isolates of the fish pathogen Aeromonas salmonicida. *Syst. Appl. Microbiol*., 22: 403–411.

Koo, K., Jaykus, L.A. (2000). Selective amplification of bacterial RNA: use of a DNA primer containing mismatched bases near its 3' terminus to reduce falsepositive signals. *Lettters App. Microbiol*., 31: 187- 192.

Long, A. A. (1998). In-situ polymerase chain reaction: Foundation of the technology and today's options. *European Journal of Histochemistry, 42*(2), 101–109.

McKeand, J.B. (1998). Molecular diagnosis of parasitic nematodes. *Parasitology*, 117: 87–96.

Mullis, K. B. (1990). The unusual origin of the polymerase chain reaction. *Scientific American, 262*(4), 56–61, 64–65.

Mir, K.U. (2000). The hypothesis is there is no hypothesis. *Trends Genet*. 16(2): 63–64.

Nuovo, G. J. (1996). The foundation of successful RT in situ PCR. *Frontiers in Bioscience, 1*.

Robinson, N. A., Gjedrem, T., & Quillet, E. (2017). Improvement of disease resistance by genetic methods. In *Fish diseases* (pp. 21-50). Academic Press.

Rhodes, L. D., Nilsson, W. B., & Strom, M. S. (1998). Sensitive detection of Renibacterium salmoninarum in whole fry, blood, and other tissues of Pacific salmon by reverse transcription-polymerase chain reaction. *Molecular Marine Biology and Biotechnology*, *7*(4), 270-279.

Rithidech, K. N., Dunn, J. J., & Gordon, C. R. (1997). Combining multiplex and touchdown PCR to screen murine microsatellite polymorphisms. *Biotechniques*, *23*(1), 36-44.

Shalon, D., Smith, S. J., & Brown, P. O. (1996). A DNA microarray system for analyzing complex DNA samples using two-color fluorescent probe hybridization. *Genome research*, *6*(7), 639-645.

Southern, E. M. (1996). DNA chips: analysing sequence by hybridization to oligonucleotides on a large scale. *Trends in Genetics*, *12*(3), 110-115.

Tijssen, P. (1993). *Hybridization with Nucleic Acid Probes, Part II: Part II. Probe Labeling and Hybridization Techniques* (Vol. 24). Elsevier.

Tyagi, S., & Kramer, F. R. (1996). Molecular beacons: probes that fluoresce upon hybridization. *Nature biotechnology*, *14*(3), 303-308.

Williams, K., Blake, S., Sweeney, A., Singer, J. T., & Nicholson, B. L. (1999). Multiplex reverse transcriptase PCR assay for simultaneous detection of three fish viruses. *Journal of Clinical Microbiology*, *37*(12), 4139-4141.

Wilson, I. G. (1997). Inhibition and facilitation of nucleic acid amplification. *Applied and environmental microbiology*, *63*(10), 3741-3751.

Zhou, Q., Chen, Y., Chen, Z., Wang, L., Ma, X., Wang, J., ... & Chen, S. (2022). Genomics and transcriptomics reveal new molecular mechanism of vibriosis resistance in fish. *Frontiers in immunology*, *13*, 974604.

Zimmermann, K., Schögl, D., Plaimauer, B., & Mannhalter, J. W. (1996). Quantitative multiple competitive PCR of HIV-1 DNA in a single reaction tube. *BioTechniques*, *21*(3), 480-484.

Zou, S. (1997). A practical approach to genetic screening for influenza virus variants. *Journal of Clinical Microbiology*, *35*(10), 2623-2627.

Zhou, J., & Thompson, D. K. (2004). Microarray technology and applications in environmental microbiology. *Advances in Agronomy*, *82*(10.1016), S0065-2113.

ORAL PRESENTATION

Zebra balığı embriyolarında imidakloprid ve bisfenol E'nin kombine maruziyetine bağlı morfolojik anomaliler ve apoptoz yanıtı

Hüseyin Demirci[1*] (*https://orcid.org/0009-0000-0141-5572)*
Cansu Akbulut [2] (*https://orcid.org/0000-0003-4333-7669)*

[*1]Sakarya Üniversitesi, Fen Fakültesi, Biyoloji Bölümü, Serdivan, Sakarya, Turkiye

*Sorumlu yazar e-mail: huseyin.demirci8@ogr.sakarya.edu.tr

Özet

Pestisitler, modern tarım uygulamalarında zararlı organizmaların kontrolünde yaygın olarak kullanılmakta ve tarımsal verimliliğin artırılmasında önemli rol oynamaktadır. Neonikotinoid grubuna ait imidakloprid (IMI), böceklerle mücadelede sıkça tercih edilen bir insektisittir. Diğer yandan, endüstriyel bir kimyasal olan ve plastik üretiminde kullanılan bisfenol A (BPA)'nın toksisitesi belirlenmiş ve endüstriyel uygulamalarda plastikleştirici ajan olarak BPA'nın diğer türevleri olan bisfenol E (BPE) gibi alternatifleri kullanılmaya başlanmıştır. Bu iki kimyasal, sıklıkla kullanıldığı için sucul ekosisteme karışmakta olup birlikte etki gösterme potansiyeline sahiptir. Zebra balığı, genomunun iyi bilinmesi, insan ile ilgili ortak genlere sahip olması, hızlı üreme döngüsü, çevresel toksisite çalışmalarında duyarlılığı ve şeffaf yumurtalara sahip olması nedeniyle en çok tercih edilen model organizmalardan biridir. Bu projede, IMI ve BPE'nin zebra balığı embriyoları üzerindeki tekil ve kombine toksik etkileri gelişimin ilk 120 saatinde değerlendirilmiştir. Çalışma kapsamında kontrol, çözücü kontrol (% 0,1 DMSO), 12,16 mg/L IMI (%10 LC_{50}), 24,32 mg/L IMI (%20 LC_{50}), 1,36 mg/L BPE (%10 LC_{50}), 2,72 mg/L BPE (%20 LC_{50}), 12,16 mg/L IMI+ 1,36 mg/L BPE (Kombine %10), 24,32 mg/L IMI + 2,72 mg/L BPE (Kombine %20) olmak üzere 8 grup oluşturulmuştur. Morfolojik özellikler, gelişimsel anomaliler, koryondan çıkış süreleri, kalp atım hızı ve embriyo boy uzunluğu gibi gelişim parametreleri gözlemlenerek istatistiksel analizler yapılmıştır. BPE %10, BPE %20, IMI %10, IMI %20, kombine %10 ve kombine %20 konsantrasyon gruplarında; perikardiyal ödem, vitellus kesesi ödemi, omurga eğriliği ve çeşitli morfolojik bozukluklar gözlemlenmiştir. Ayrıca, BPE içeren tüm gruplarda embriyoların koryondan çıkışında gecikme tespit edilmiştir. Hücre ölümüne olan etkiler whole mount TUNEL yöntemi kullanılarak değerlendirilmiştir. Kontrol grubuna kıyasla 1,36 mg/L BPE grubunda anlamlı bir değişiklik gözlenmezken, 2,72 mg/L BPE ve her iki IMI grubunda apoptotik hücre sayısında belirgin artışlar kaydedilmiştir. Kombine maruziyet gruplarında ise, tekil maruziyetlere kıyasla daha belirgin bir artış izlenmiş ve sinerjistik toksik etkiler tespit edilmiştir.

Anahtar Kelimeler: İmidakloprid, Bisfenol E, Kombine toksisite, Zebra balığı, apoptoz

Morphological anomalies and apoptotic response induced by combined exposure to imidacloprid and bisphenol E in zebrafish embryos

Abstract

Pesticides are widely used in modern agriculture to control harmful organisms and play a crucial role in enhancing crop productivity. Imidacloprid (IMI), a neonicotinoid insecticide, is among the most commonly used agents for pest control. Meanwhile, the toxicity of bisphenol A (BPA), an industrial chemical used in plastic production, has been well documented, leading to the increased use of alternative derivatives such as bisphenol E (BPE). Due to their frequent use, IMI and BPE are prone to entering aquatic environments, where they may exert combined effects on non-target organisms. Zebrafish (*Danio rerio*) is a widely preferred model organism in ecotoxicological research owing to its well-characterized genome, genetic similarity to humans, rapid reproductive cycle, high sensitivity to pollutants, and transparent embryos.This study aimed to evaluate the individual and combined toxic effects of IMI and BPE on zebrafish embryos during the first 120 hours of development. Eight experimental groups were established: control, solvent control (0.1% DMSO), 12.16 mg/L IMI (10% LC_{50}), 24.32 mg/L IMI (20% LC_{50}),

1.36 mg/L BPE (10% LC_{50}), 2.72 mg/L BPE (20% LC_{50}), 12.16 mg/L IMI + 1.36 mg/L BPE (combined 10%), and 24.32 mg/L IMI + 2.72 mg/L BPE (combined 20%).

Developmental parameters, including morphological abnormalities, pericardial and yolk sac edema, spinal deformities, hatching time, heart rate, and body length, were assessed and statistically analyzed. Pericardial edema, yolk sac edema, spinal curvature, and various morphological defects were observed in the BPE 10%, BPE 20%, IMI 10%, IMI 20%, combined 10%, and combined 20% groups. Delayed hatching was detected in all BPE-treated groups. Whole-mount TUNEL analysis revealed no significant change in apoptotic cell counts at 1.36 mg/L BPE, whereas significant increases were observed at 2.72 mg/L BPE and in both IMI groups. Combined exposure groups showed a more pronounced increase than single exposures, indicating synergistic toxic effects.

Keywords: Imidacloprid, Bisphenol E, Combined toxicity Zebrafish, Apoptosis

GİRİŞ

Pestisitler, zararlıları önlemek, yok etmek, uzaklaştırmak veya azaltmak için kullanılan kimyasal maddelerdir. Genelde, hedef aldıkları zararlı grubuna göre insektisitler, fungisitler, herbisitler, rodentisitler, molluskisitler, nematisitler gibi benzer kimyasalları ifade eder (Eldridge., 2008 ; Tiryaki ve ark., 2010). Neonikotinoid grubu insektisit pestisitlerinden olan IMI, böceklerin nikotinik asetilkolin reseptörlerine (nAChR) bağlanarak nörotoksik bir etki oluşturarak felç ve ölüme sebep olur (Tomizawa ve Casida, 2003 ; Yadav ve ark., 2020). Yaygın olarak kullanılan IMI toprakta 3000 güne kadar kalıntısı bulunabilmekteyken sucul ekosistemdeki etkisini anlamak büyük önem taşımaktadır (Bhende ve Dafale, 2023).

BPA, gıda ambalajları, içecek şişeleri, oyuncaklar vb. gibi plastik ürünlerde ve plastik malzemelerin sertleştirilmesinde yaygın olarak kullanılmaktadır. BPA östrojen hormonunu taklit edici özelliği olduğu, dolayısıyla endokrin bozucu etki göstererek potansiyel sağlık riski taşıdığı bilinmektedir (Moreman ve ark., 2017). BPA kullanımına yönelik kısıtlamaların artmasıyla birlikte, endüstride alternatif bisfenol türevlerinin kullanımına yönelim olmuştur. Bu alternatiflerden biri olan BPE, kimyasal yapısal benzerliği nedeniyle BPA yerine polimer ve plastik üretiminde giderek daha yaygın kullanılmaktadır (Czarny-Krzymińska ve ark., 2024). BPE'nin, artan kullanımına bağlı olarak sucul ekosistemde IMI gibi diğer kirleticilerle birlikte bulunma ve etkileşime girme olasılığı yüksektir.

Zebra balığı (*Danio rerio*), omurgalı model organizma olarak, birçok kimyasalın ekosistem üzerindeki olumsuz etkilerinin araştırılmasında önemli rol oynar. Hızlı gelişim döngüsü, şeffaf embriyo yapısı ve genetik manipülasyona uygunluğu sebebiyle gelişimsel toksisite, nörotoksisite, endokrin bozucu ve genotoksik etkilerini incelemek için idealdir (Stegeman ve ark., 2010). Bu çalışmada, BPE ve IMI tekil ve kombine toksisitesinin araştırılması amaçlanmıştır.

MATERYAL VE METOT

Embriyo Eldesi

Çalışma kapsamında, Sakarya Üniversitesi Fen Fakültesi Biyoloji Bölümü Balık Yetiştirme Laboratuvarı bünyesinde akvaryumlara kloru uzaklaştırılmış musluk suyu ile doldurulmuştur. Su sıcaklığı 28 ± 1 °C düzeyinde ve 12 saat aydınlık – 12 saat karanlık olacak şekilde sirkadiyen ışık döngüsü sağlanmıştır.

Toksisite Testleri

Tüm toksisite testleri OECD FET Test (2013)'e uygun olarak yapılmıştır. Deneyler 3 tekrarlı olarak gerçekleştirilmiştir. Toksisite testlerinde 24 kuyucuklu plakalar kullanılmıştır. Her kuyucuğa 1 embriyo ve 2 ml E3 ortamı eklenmiştir. Kontrol ve deney grupları aşağıdaki şekilde oluşturulmuştur.

Kontrol: Hiçbir uygulama yapılmamıştır.
Çözücü Kontrol: % 0.1 DMSO
Bisfenol E %10: 1.36 mg/L (%10 LC_{50})

Bisfenol E %20: 2.72 mg/L (%20 LC_{50})
İmidakloprid %10: 12.16 mg/L (%10 LC_{50})
İmidakloprid %20: 24.32 mg/L (%20 LC_{50})
Kombine %10: 1.36 mg/L BPE (%10 LC_{50}) + 12.16 mg/L IMI (%10 LC_{50})
Kombine %20: 2.72 mg/L BPE (%20 LC_{50}) + 24.32 mg/L IMI (%20 LC_{50}) uygulanmıştır.

Gelişim anomalileri 24, 48, 72, 96 ve 120. saatlerde mikroskop altında gözlenmiştir.

Whole-Mount TUNEL

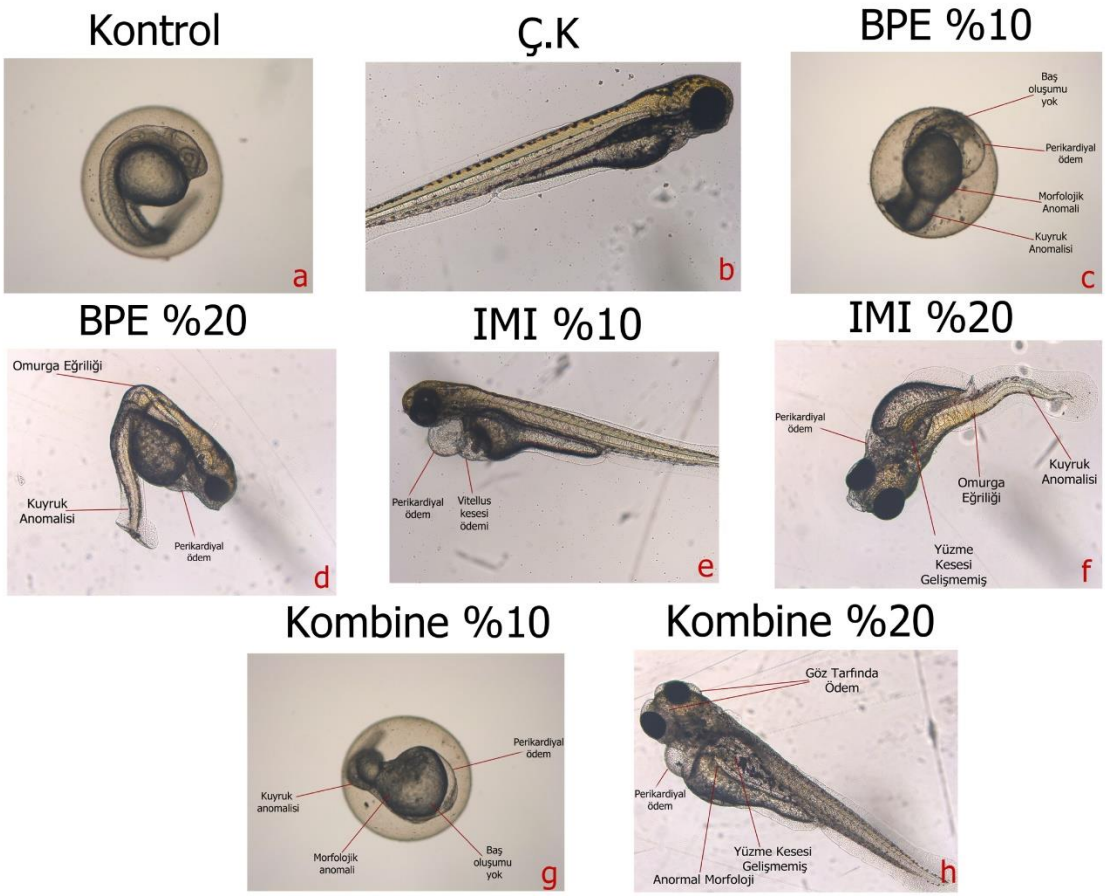
Whole-mount TUNEL analizi ticari kit kullanılarak yapılmıştır. Kontrol ve deney gruplarına ait dekoryonize edilmiş 24 saatlik embriyolar, %4'lük paraformaldehit içerisinde 24 saat boyunca fikse edilmiştir. Uygulamadan sonra örnekler boyanarak ve kahverengi renkteki apoptotik hücreler ışık mikroskobu altında gözlenmiştir.

İstatistiksel Analizler
Tüm istatistiksel analizlerde SPSS 25.0 programı kullanılmıştır. Tüm analizlerde istatistiksel anlamlılık ANOVA testi kullanılarak belirlenmiştir. ANOVA Post Hoc testlerinden Tukey HSD testi kullanılarak araştırılmıştır. İstatistiksel anlamlılık düzeyi $p<0,05$ olarak kabul edilmiştir (Bertoni ve ark., 2024).

BULGULAR

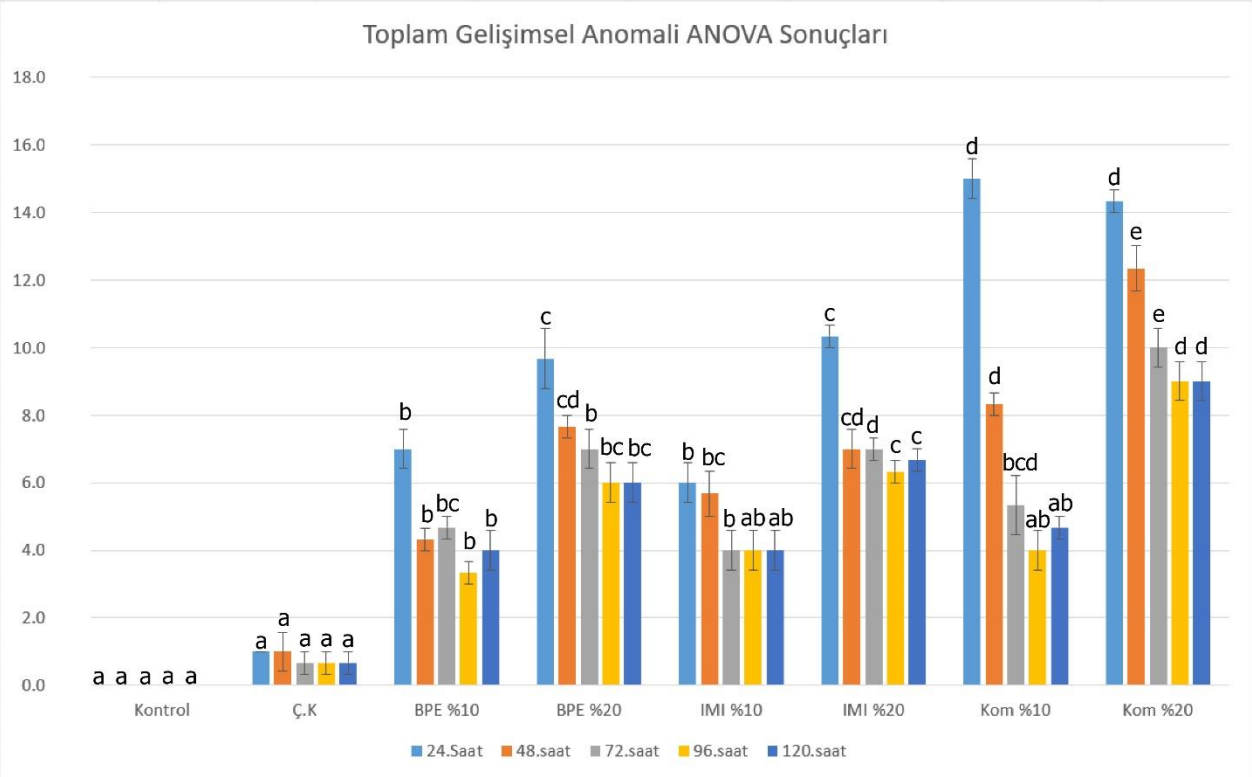
Gelişimsel Morfolojik Bulgular

Gelişimsel morfolojik bulgular incelendiğinde gruplarda farklı zamanlarda birçok anomali gözlenmiştir. Kontrol ve çözücü kontrol grupları süreç boyunca normal gelişim göstermiştir. %10 BPE uygulanan grupta asefali, perikardiyal ödem, kuyruk deformitesi ve morfolojik olarak anormal bir görünüm gözlemlenmiştir. BPE %20 uygulanan deney grubunda, omurga eğriliği, perikardiyal ödem ve kuyruk yamukluğu tespit edilmiştir. %10 IMI grubunda perikardiyal ödem ve vitellus kesesi ödemi görülmüştür. IMI %20'de ise perikardiyal ödem, yüzme kesesi gelişiminde gecikme, kuyruk deformitesi ve omurga eğriliği görülmektedir. Kombine %10 grubunda morfolojik bozukluk olarak, perikardiyal ödem, kuyruk malformasyonu, ve asefali görülen tespit edilmiştir. Kombine %20 uygulanan grupta ise göz çevresinde ödem, perikardiyal ödem ve yüzme kesesi gelişiminde gecikme gözlemlenmiştir. Kontrol, çözücü kontrol, BPE ve IMI gruplarında 24. saatten 120.saate kadar olan gelişimsel anomaliler aşağıda Şekil 1'de verilmiştir.



Şekil 1. BPE ve IMI uygulaması sonucu zebra balığında gözlenen gelişim anomalileri (a) kontrol, (b) çözücü kontrol, (c) BPE %10, (d) BPE %20, (e) IMI %10, (f) IMI %20, (g) kombine %10, (h) kombine %20 grubu

Gelişimsel anomalilere bakıldığında kontrol gruplarına kıyasla önemli ölçüde teratojenik etki gösterdiğini ve kombine maruziyet durumunda bu etkilerin sinerjistik şekilde arttığını göstermektedir. Kontrol grubunda anomali gözlemlenmezken, çözücü kontrol grubunda minimum düzeyde anomali gözlenmiştir. Fakat, istatistiksel olarak kontrol ve çözücü kontrol grupları arasında anlamlı bir fark tespit edilmemiştir. BPE ve IMI uygulamalarında anomali sıklığının konsantrasyon artışına paralel olarak arttığı görülmüştür. Kombine gruplarda ise özellikle erken gelişim evresinde (24. saat) yüksek düzeyde anomaliler tespit edilmiş, bu değerlerin tekil maruziyet gruplarına kıyasla belirgin şekilde daha yüksek olduğu görülmüştür (Şekil 2). Sonuç olarak, IMI ve BPE'nin birlikte maruziyeti, tekil uygulamalara göre daha şiddetli gelişimsel bozukluklara yol açmakta ve kimyasalların birlikte bulunması durumunda toksik etkilerinin güçlendiğini ortaya koymaktadır.



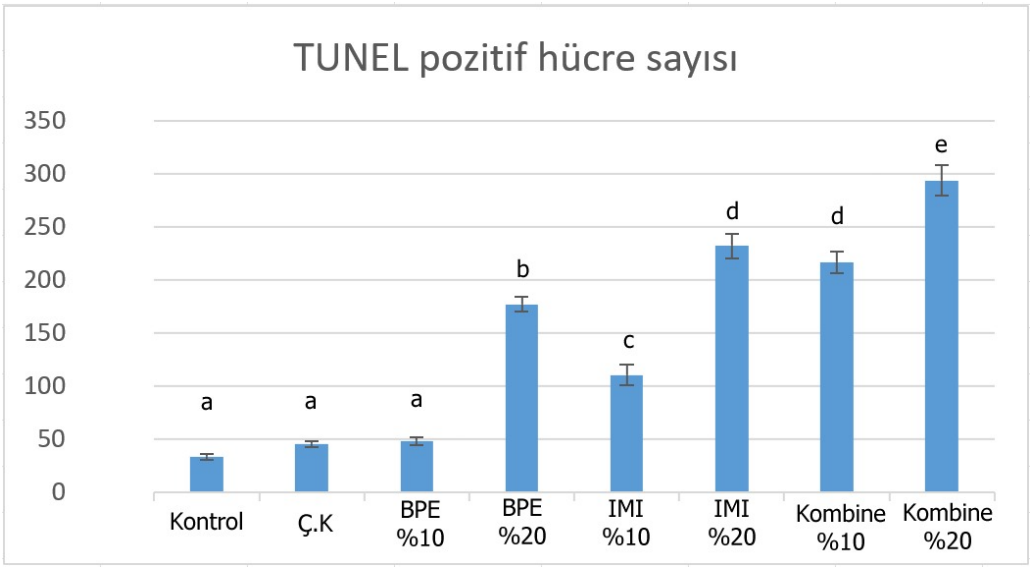
Şekil 2: Zebra balığı embriyolarında farklı gruplara (Kontrol, Çözücü Kontrol, BPE %10, BPE %20, IMI %10, IMI %20, Kombine %10, Kombine %20) ve zaman noktalarına ait toplam gelişimsel anomali sayıları

Whole mount TUNEL ile Apoptotik Hücrelerin Tayini

Çalışmada, 24 saatlik embriyolar üzerinde TUNEL analizi, zebra balığı embriyolarında hem tekil hem de kombine maruziyetlerin apoptoz üzerine etkilerini ortaya koymuştur. Her bir grupta mikroskop altında kahverengi renkte gözlenen TUNEL pozitif hücre sayımları yapılmış (Şekil 3) ve istatistiksel analizler gerçekleştirilmiştir (Şekil 4). Kontrol ve çözücü kontrol gruplarında apoptotik hücre sayısı düşük seviyede kalmış, aralarında istatistiksel olarak anlamlı bir fark bulunmamıştır. Bu durum çözücünün apoptoz süreci üzerinde herhangi bir etkisinin olmadığını göstermektedir. BPE gruplarında ise doza bağımlı bir artış gözlenmiştir. %10 BPE grubunda kontrol ile benzer sonuçlar elde edilirken, %20 BPE grubunda apoptotik hücre sayısı anlamlı biçimde yükselmiştir. Bu bulgu, BPE'nin yüksek konsantrasyonlarda apoptotik hücre ölümünü tetikleyebildiğini göstermektedir. IMI gruplarında (%10 ve %20) apoptotik hücre sayısı kontrol grubuna kıyasla belirgin biçimde artmıştır. Bu durum, IMI'nin tek başına dahi güçlü bir apoptotik etki ortaya çıkardığını ve hücresel düzeyde toksisiteye yol açtığını göstermektedir. Kombine gruplarda (özellikle %20'de), apoptotik hücre sayısındaki artış tekil maruziyetlere kıyasla daha da belirgindir. Özellikle kombine %20 grubunda apoptotik aktivitenin en üst düzeye ulaştığı tespit edilmiştir. Bu bulgu, IMI ve BPE'nin birlikte maruz kalındığında sinerjistik bir etki yaratarak apoptotik hücre ölümünü şiddetlendirdiğini düşündürmektedir.



Şekil 3. 24 saatlik zebra balığı embriyolarında gerçekleştirilen TUNEL analizi bulguları. TUNEL pozitif hücreler kahverengi renkte gözlenmektedir. (a) kontrol, (b) çözücü kontrol, (c) BPE %10, (d) BPE %20, (e) IMI %10, (f) IMI %20, (g) kombine %10, (h) kombine %20 grubu



Şekil 4. Zebra balığı embriyolarında 24. saatte TUNEL yöntemi ile belirlenen apoptotik hücre sayıları ($p<0,05$).

TARTIŞMA

Bu çalışmada IMI ve BPE'nin tekil ve kombine uygulamalarının zebra balığı embriyolarında belirgin gelişimsel anomalilere ve apoptoza yol açtığı ortaya konmuştur. Özellikle kombine maruziyetlerde gözlenen sonuçlar, bu iki kimyasalın birlikte bulunduğunda sinerjistik etki yaratarak toksisiteyi artırdığını göstermektedir.

Gelişimsel parametrelerde, perikardiyal ödem, vitellus kesesi ödemi, omurga eğriliği ve kuyruk malformasyonu gibi anomaliler tekil uygulamalarda da gözlenmiş, ancak kombine gruplarda bu anomalilerin daha yüksek oranda ve daha erken dönemde görüldüğü tespit edilmiştir. Bu durum, IMI ve BPE'nin embriyonik gelişim üzerinde güçlü bir teratojenik potansiyele sahip olduğunu göstermektedir.

TUNEL analizi bulguları da bu değerlendirmeleri desteklemektedir. BPE %20 grubunda apoptoz belirgin şekilde artarken, IMI gruplarında kontrolle kıyaslandığında apoptotik hücre sayısının anlamlı düzeyde yükseldiği görülmüştür. Özellikle kombine %20 grubunda apoptotik hücre sayısının en yüksek seviyeye ulaşması, iki kimyasalın birlikte maruziyetinde apoptozun sinerjistik biçimde şiddetlendiğini ortaya koymuştur. Bu sonuç, IMI ve BPE'nin benzer veya farklı toksikolojik mekanizmaları aynı anda tetikleyerek hücresel ölümü artırdığını düşündürmektedir.

Literatür bulguları da çalışmamızı desteklemektedir. IMI'nin düşük konsantrasyonlarda dahi zebra balığı embriyolarında gelişimsel anomalilere yol açtığı daha önce rapor edilmiştir (Santiago ve ark., 2023). Bizim çalışmamız da benzer şekilde IMI'nin tek başına bile güçlü bir apoptozu tetikleyici olduğunu ortaya koymuştur. Benzer şekilde, Gao ve ark. (2022), BPE maruziyetinin vitellus kesesi ödemi ve omurga deformasyonuna sebep olduğunu bildirmiştir. Çalışmamızda kombine gruplarda apoptozun en üst düzeye ulaşması, çevresel risk değerlendirmelerinde kimyasalların birlikte etkilerinin göz ardı edilmemesi gerektiğini göstermektedir.

Sonuç olarak, bu çalışma IMI ve BPE'nin zebra balığı embriyolarında yalnızca tekil toksisiteye yol açmadığını, aynı zamanda birlikte maruziyet koşullarında sinerjistik toksik etki oluşturduğunu ortaya koymuştur. Bu bulgular, endüstriyel kimyasalların çevredeki kombinasyonlarının potansiyel risklerini anlamak açısından önem taşımakta ve çevresel risk değerlendirmelerinde kombine toksisite parametresinin mutlaka dikkate alınması gerektiğini vurgulamaktadır.

KAYNAKLAR

Bertoni, Í., Sales, B. C. P., Viriato, C., Peixoto, P. V. L., & Pereira, L. C. (2024). Embryotoxicity induced by Triclopyr in zebrafish (Danio rerio) early life stage. Toxics, *12*(4), 255. https://doi.org/10.3390/toxics12040255

Bhardwaj, J. K., Kamboj, H., & Tyor, A. K. (2022). The toxicity of imidacloprid on early embryonic stages and growth rate of hatchlings of common carp, Cyprinus carpio. Toxicology International, *29*(1), 105-115. https://doi.org/10.18311/ti/2022/v29i1/28317

Bhende, R. S., & Dafale, N. A. (2023). Insights into the ubiquity, persistence and microbial intervention of imidacloprid. Archives of Microbiology, *205*(5), 215. https://doi.org/10.1007/s00203-023-03553-5

Eldridge, B. F. (2008). Pesticide application and safety training for applicators of public health pesticides. California Department of Public Health.

Erhunmwunse, N. O., Tongo, I., & Omigie, K. (2023). Embryonic toxicity of Imidacloprid: Impact on hatchability, survivability, swimming speed and cardiac function of catfish, Clarias gariepinus. Ecotoxicology, *32*(1), 127-134. https://doi.org/10.1007/s10646-023-02628-9

Gao, Y., Li, A., Zhang, W., Pang, S., Liang, Y., & Song, M. (2022). Assessing the toxicity of bisphenol A and its six alternatives on zebrafish embryo/larvae. Aquatic Toxicology, *246*, 106154. https://doi.org/10.1016/j.aquatox.2022.106154

OECD. (2013). Test No. 236: Fish embryo acute toxicity (FET) test. OECD Guidelines for the Testing of Chemicals, Section 2. OECD Publishing. https://doi.org/10.1787/9789264203709-en

Santiago, M. R., Salvo, L. M., Badaró-Pedroso, C., & Costa, E. M. F. (2023). Single and mixed

exposure to distinct groups of pesticides suggests endocrine disrupting properties of imidacloprid in zebrafish embryos. Journal of Environmental Science and Health, Part B, *58*(3), 217-228. https://doi.org/10.1080/03601234.2023.2184158

Stegeman, J. J., Goldstone, J. V., & Hahn, M. E. (2010). Perspectives on zebrafish as a model in environmental toxicology. In A. P. Farrell (Ed.), Fish physiology: Zebrafish (Vol. 29, pp. 367-439). Academic Press.

Tiryaki, O., & Temur, C. (2010). The fate of pesticide in the environment. Journal of Biological and Environmental Sciences, *4*(10), 29-38.

Tomizawa, M., & Casida, J. E. (2003). Selective toxicity of neonicotinoids attributable to specificity of insect and mammalian nicotinic receptors. Annual Review of Entomology, *48*, 339-364. https://doi.org/10.1146/annurev.ento.48.091801.112731

Yadav, V., Ahmad, S., & Zahra, K. (2020). Imidacloprid toxicity and its attenuation by aqueous extract of Moringa oleifera leaf in zebra fish, Danio rerio. International Journal of Current Pharmaceutical Research, *12*(2), 1-6. https://doi.org/10.22159/ijcpr.2020v12i2.37483

ORAL PRESENTATION

Extract to protect: Redefining betalain stability in natural colorant research

Ayşenur Acar[1] (ORCID: https://orcid.org/0000-0003-1081-4166)
Vildan Eyiz[2*] ORCID: https://orcid.org/0000-0002-2086-7109)

[1] Selçuk University, Faculty of Agriculture, Department of Food Engineering, Konya, Turkey

[2*]Necmettin Erbakan University, Faculty of Engineering, Department of Food Engineering, Konya, Turkey

*Corresponding author e-mail: vtop@erbakan.edu.tr

Abstract

Betalains are water-soluble nitrogenous pigments found mainly in plants of the *Caryophyllales* order. They are widely appreciated for their bright coloration and biological properties, including antioxidant and anti-inflammatory activities. Due to these dual functions, betalains are considered promising alternatives to synthetic dyes in food, nutraceutical, and pharmaceutical applications. Nevertheless, their use remains limited because they are highly sensitive to heat, light, pH changes, and oxygen, which results in rapid degradation and loss of color intensity. This review examines the relationship between extraction methods and betalain stability. Solvent choice is a crucial factor: while water and ethanol mixtures are commonly used, glycerol and natural deep eutectic solvents (NADES) have emerged as protective media that reduce degradation and improve bioaccessibility. In addition, novel technologies such as ultrasound- and microwave-assisted extraction have demonstrated the ability to accelerate pigment recovery under milder conditions, limiting exposure to factors that trigger instability. Pressurized hot water extraction also shows potential when carefully optimized to balance efficiency with pigment preservation. A further step forward is the development of integrated "extract-and-protect" strategies, where stabilization occurs simultaneously with pigment recovery. By embedding protective conditions directly in the extraction medium—such as antioxidant-rich solvents or oxygen-limiting systems—betalains can be better preserved for downstream applications. İn conclusion, the evidence suggests that extraction should not be regarded solely as a recovery process but as a decisive stage influencing the stability and usability of betalains. A deeper understanding of solvent–pigment interactions and optimized processing conditions will facilitate the transition from laboratory-scale studies to industrial applications, enabling betalains to become sustainable, safe, and functional natural colorants.

Keywords: Betalains, deep eutectic solvents, extraction, ultrasound, microwave, stability

INTRODUCTION

Natural pigments are gaining increasing relevance in food, cosmetic, and pharmaceutical applications, driven by consumer preference for "clean label" products and health-promoting ingredients. Within this context, betalains—classified into red-violet betacyanins and yellow-orange betaxanthins—stand out because they provide intense and appealing coloration while simultaneously exhibiting biological activities, such as antioxidant, anti-inflammatory, and antimicrobial effects (Sadowska-Bartosz & Bartosz, 2021). These characteristics have encouraged their exploration in nutraceuticals and functional food formulations, positioning betalains as versatile compounds of dual functional and aesthetic value.

Betalains are water-soluble nitrogenous pigments found in members of the botanical order *Caryophyllales*, including *Beta vulgaris*, *Amaranthus*, and *Opuntia*, as well as in certain fungi (Leal-Alcázar et al., 2025). Their structural uniqueness, compared to anthocyanins or carotenoids, provides specific advantages but also presents considerable challenges. Despite their promising application potential, betalains remain limited in large-scale use because of their inherent instability. After extraction, they are particularly prone to degradation when exposed to

heat, light, extreme pH, oxygen, and catalytic factors such as enzymes or metal ions (Kumorkiewicz-Jamro et al., 2021; Eyshi et al., 2024).

Thermal stress accelerates betalain breakdown, typically through decarboxylation, dehydrogenation, or isomerization reactions, which can occur even at moderate processing temperatures above 50–70 °C (Martinez et al., 2024). pH also exerts a decisive role: betalains are most stable within a moderately acidic range, whereas highly acidic or alkaline conditions promote hydrolysis and pigment discoloration (Eyshi et al., 2024). Light and oxygen exposure further aggravate instability, initiating photooxidation and radical-mediated degradation, thereby reducing both chromatic intensity and bioactive function (Leal-Alcázar et al., 2025). In addition, co-extracted matrix components, such as sugars, phenolics, or proteins, may interact synergistically or antagonistically with betalains, further influencing their degradation kinetics (Kumorkiewicz-Jamro et al., 2021).

Given these multiple destabilizing factors, it has become increasingly clear that not only extraction yield but also the *mode of extraction* significantly determines betalain integrity. Recent advances emphasize that solvent choice, extraction conditions, and the presence of protective agents can dictate the extent of pigment preservation. Mild and emerging extraction techniques—such as ultrasound, microwave, or pressurized hot water—are particularly attractive, as they can both enhance yield and mitigate degradation compared to harsher methods (Eyshi et al., 2024). Moreover, integrated "extract-and-protect" strategies are gaining attention, where the extraction medium itself functions as a stabilizing environment, for example by limiting oxygen exposure, lowering water activity, or simultaneously incorporating natural antioxidants (Leal-Alcázar et al., 2025).

In this context, the present review first outlines the structural features, classification, and instability mechanisms of betalains, and subsequently provides a critical discussion of how different extraction techniques, particularly mild or green approaches, affect pigment stability. Special emphasis is placed on solvent systems (water, ethanol, glycerol, and natural deep eutectic solvents), innovative energy-assisted techniques, and emerging integrated approaches that combine extraction and stabilization in a single step.

Betalain Structure, Classification, and Instability Mechanisms

Betalains are a unique class of water-soluble pigments derived from the amino acid L-tyrosine through a biosynthetic pathway distinct from that of anthocyanins. Structurally, they are immonium derivatives of betalamic acid, which serves as the chromophore backbone (Kumorkiewicz-Jamro et al., 2021). Based on their conjugation partners, betalains are divided into two main groups: betacyanins, which impart red to violet colors (e.g., betanin in beetroot), and betaxanthins, which produce yellow to orange hues by forming Schiff base conjugates with amino acids or amines (Wybraniec & Stintzing, 2020). The balance of these two subgroups determines the final hue in plant tissues, and their relative ratios are influenced by both genetics and environmental conditions (Leal-Alcázar et al., 2025).

Despite their structural attractiveness and high molar extinction coefficients, betalains are chemically labile. Their instability arises from a series of degradation pathways triggered by external stress factors. Thermal degradation is among the most critical, where elevated temperatures lead to decarboxylation, dehydrogenation, and hydrolytic cleavage of glycosidic bonds, resulting in discoloration and loss of bioactivity (Esatbeyoglu & Rohn, 2021). pH sensitivity is another determinant; betalains are most stable under mildly acidic conditions (pH 4–6), but instability increases under strongly acidic or alkaline environments, causing hydrolytic and oxidative breakdown (Eyshi et al., 2024).

Light and oxygen also play major roles in betalain instability. Photooxidation induced by UV or visible light exposure leads to bleaching and pigment fragmentation, while oxygen accelerates radical-mediated degradation (Leal-Alcázar et al., 2025). In addition, metal ions such as Cu^{2+} or Fe^{3+} can catalyze oxidation, further exacerbating color loss (Sadowska-Bartosz & Bartosz, 2021). Matrix components co-extracted with betalains—such as sugars, organic acids, or phenolic compounds—may either protect pigments through copigmentation or contribute to instability through pro-oxidant reactions (Wybraniec & Stintzing, 2020).

Recent analytical studies have provided insights into these mechanisms at the molecular level. High-resolution mass spectrometry and nuclear magnetic resonance have revealed intermediate products such as neobetanin (an oxidized derivative of betanin), which is often used as a marker of degradation (Kumorkiewicz-Jamro et al., 2021). Similarly, kinetic modeling approaches demonstrate that betalain degradation follows first-order or pseudo-first-order kinetics, with activation energies dependent on both matrix and environmental conditions (Martinez et al., 2024).

In summary, betalains present a delicate balance between vivid chromatic properties and high susceptibility to degradation. Understanding their structural classification and instability mechanisms is essential for designing effective extraction and stabilization strategies, which is the focus of the subsequent sections.

Relationship Between Extraction Techniques and Betalain Stability

Effect of solvents (water, ethanol, glycerol, NADES) on stability

Solvent selection determines not only yield but also the microenvironment that governs betalain oxidation, hydrolysis, and isomerization after extraction. Hydroalcoholic media (water–ethanol) typically maximize recovery while keeping pH in a range (≈3–6) compatible with pigment integrity; however, high ethanol fractions can dehydrate the chromophore and accelerate color loss if temperature rises or oxygen is not controlled (Eyshi et al., 2024).

Designing the solvent to "protect while extracting" is increasingly effective. Deep eutectic solvents (DES/NADES) can hydrogen-bond with the iminium and phenolic sites of betalains, reduce dissolved oxygen, and suppress photooxidation. In beetroot waste, a $MgCl_2 \cdot 6H_2O$–urea DES preserved ~75% of initial betalain content after 340 days in amber storage and 150 days under visible light—far exceeding aqueous extracts (Hernández-Aguirre et al., 2021).

Glycerol deserves special mention as a benign, food-grade polyol that both extracts and stabilizes. Ultrasound extraction of prickly-pear betalains in ~23% glycerol followed by in-situ encapsulation delivered high encapsulation efficiency (≈94%) and markedly extended shelf-life (e.g., modeled ~404 days at 4 °C in amber), with improved bioaccessibility versus conventional extracts (Mehta et al., 2024).

Beyond beets, DES built from choline chloride with organic acids/sugars have extracted betalains from red beet and cactus/pitaya matrices with superior pigment retention and in vitro bioaccessibility compared with conventional solvents, underscoring the stabilizing role of eutectic H-bond networks (Kaba et al., 2024; Liu et al., 2025).

Mild extraction (ultrasound, microwave, PHWE) as a means to reduce degradation

Lower-energy, short-time processes limit thermal and oxidative stress during cell disruption. Optimized ultrasound-assisted extraction (UAE) from beet matrices increases betalain yield at modest temperatures and short times, preserving color attributes relative to long conventional macerations (Tabio-García et al., 2021; Eyshi et al., 2024).

Microwave-assisted extraction (MAE) can be protective when pulse-programmed and time-limited: pulsed microwave regimes (controlling power, duty cycle, seconds-scale exposure) enhanced beet betalain recovery while minimizing thermal decomposition compared with continuous heating (Hazervazifeh et al., 2023). Mechanistically, fast volumetric heating expedites mass transfer, allowing extraction at lower overall thermal load if exposure is tightly bounded (Hazervazifeh et al., 2023; Eyshi et al., 2024).

Pressurized hot-water (subcritical water; PHWE/SWE) is attractive because water's dielectric constant drops with temperature, increasing solvating power for moderately polar pigments. Recent work on beet leaves/stems showed that carefully optimized 150–170 °C, short-time SWE can extract betalains alongside phenolics for active packaging, although excessive time/temperature risks pigment breakdown—therefore time–temperature–pH windows must be narrow (de Carvalho et al., 2025).

Integrated "extract-and-protect" approaches

A converging trend is to engineer the extraction medium and unit operation so the pigment exits the plant matrix already protected against light, oxygen, metals, and pH drift. Two practical archetypes are evident:

Solvent-stabilization: DES/NADES and glycerol create low-oxygen, H-bond-rich matrices that slow chromophore degradation; the $MgCl_2$–urea DES case above demonstrates multi-month stability at room conditions, while glycerol-based UAE plus encapsulation boosts shelf-life and bioaccessibility (Hernández-Aguirre et al., 2021; Mehta et al., 2024). **Process-integration:** Combine rapid cell disruption (UAE/MAE) with immediate phase management or separation to remove pro-oxidants. Examples include pulsed-MAE to minimize heat load (Hazervazifeh et al., 2023) and one-step, thermoreversible aqueous biphasic systems that extract/separate betalains

from chlorophyll-rich beet by-products—reducing downstream exposure to degradative cofactors (Rosa et al., 2023).

Across techniques, the design principle is consistent: keep temperature-time integrals low, exclude oxygen/light/transition metals, and embed the pigment in protective hydrogen-bonding or encapsulating networks as early as possible—ideally during extraction—to conserve the native chromophore state for downstream formulation (Eyshi et al., 2024; Hernández-Aguirre et al., 2021).

CONCLUSION

Betalains are valuable natural pigments with strong potential as food colorants and bioactive ingredients, yet their practical application is restricted by their chemical fragility. The present review highlights that extraction is not a neutral step but rather a decisive factor influencing pigment integrity. The choice of solvent, the intensity of applied processing, and the design of the extraction medium all contribute to the stability of these compounds.

Studies demonstrate that hydroalcoholic mixtures, glycerol, and especially deep eutectic solvents not only enhance pigment yield but also create protective environments that limit degradation. Likewise, techniques such as ultrasound- and microwave-assisted extraction allow shorter processing times and milder conditions, reducing exposure to heat and oxygen. Pressurized hot water extraction can be effective when carefully optimized, while integrated approaches that combine extraction and stabilization simultaneously appear particularly promising.

Looking ahead, there is a need to refine these methods across different plant sources and to establish protocols that maintain pigment integrity throughout industrial processing and storage. A deeper understanding of solvent–pigment interactions, combined with scalable process optimization, will support the wider use of betalains as safe, sustainable, and functional alternatives to synthetic dyes in the food sector.

REFERENCES

de Carvalho, M. C., Nunes, R. A., Brígida, A. I. S., & Pastrana, L. (2025). Valorization of beetroot waste via subcritical water extraction: Active extracts rich in betalains and phenolics for antioxidant films. Molecules, 30(9), 1928. https://doi.org/10.3390/molecules30091928

Esatbeyoglu, T., & Rohn, S. (2021). Betalains: Occurrence, chemistry, and biological activities. Trends in Food Science & Technology, 109, 594–606. https://doi.org/10.1016/j.tifs.2021.01.039

Eyshi, S., Mohebbi, M., Amiryousefi, M. R., & Ghorbani, M. (2024). Red beet betalains extraction process: A comprehensive review. Food Science & Nutrition, 12(5), 2675–2692. https://doi.org/10.1002/fsn3.4458

Eyshi, S., Mohebbi, M., Amiryousefi, M. R., & Ghorbani, M. (2024). Red beet betalains extraction process: A comprehensive review. Food Science & Nutrition, 12(5), 2675–2692. https://doi.org/10.1002/fsn3.4458

Eyshi, S., Mohebbi, M., Amiryousefi, M. R., & Ghorbani, M. (2024). Red beet betalains extraction process: A comprehensive review. Food Science & Nutrition, 12(5), 2675–2692. https://doi.org/10.1002/fsn3.4458

Hazervazifeh, A., Rezazadeh, A., Banihashemi, A., Ghasempour, Z., & Moghaddas Kia, E. (2023). Pulsed microwave radiation for extraction of betalains from red beetroot: Engineering and technological aspects. Process Biochemistry, 134, 121–130. https://doi.org/10.1016/j.procbio.2023.09.018

Hernández-Aguirre, O. A., Muro, C., Hernández-Acosta, E., Alvarado, Y., & Díaz-Nava, M. d. C. (2021). Extraction and stabilization of betalains from beetroot (Beta vulgaris) wastes using deep eutectic solvents. Molecules, 26(21), 6342. https://doi.org/10.3390/molecules26216342

Kaba, B., Asci, A., Koç, M., & Yılmaz, V. A. (2024). Enhancing extraction of betalains from beetroot (Beta vulgaris L.) using deep eutectic solvents: Optimization, bioaccessibility and stability. Food Production, Processing and Nutrition, 6, 12. https://doi.org/10.1186/s43014-023-00208-2

Khan, M. I. (2016). Stabilization of betalains: A review. Food Chemistry, 197, 1280–1285. https://doi.org/10.1016/j.foodchem.2015.11.043

Kumorkiewicz-Jamro, A., Świergosz, T., Sutor, K., Spórna-Kucab, A., & Wybraniec, S. (2021). Multi-colored shades of betalains: Recent advances in betacyanin chemistry. Natural Product Reports, 38(10), 2011–2042. https://doi.org/10.1039/D1NP00018G

Leal-Alcázar, M. C., Rocha-Pizaña, M. del R., & Luna-Vital, D. A. (2025). Extraction, stabilization, and health application of betalains: An update. Food Chemistry, 437, 137262. https://doi.org/10.1016/j.foodchem.2024.137262

Liu, Y., Zhang, S., Zhao, W., & Wang, H. (2025). Extraction of betalain from red pitaya peel using deep eutectic solvents (DES) composed of choline chloride and citric acid. Food Chemistry, 446, 138934. https://doi.org/10.1016/j.foodchem.2024.138934

Martinez, R. M., Vargas-Mendoza, N., Morales-González, A., & Morales-González, J. A. (2024). Betalains: A narrative review on pharmacological and safety aspects. Nutrients, 16(3), 512. https://doi.org/10.3390/nu16030512

Mehta, D., Kuksal, K., Yadav, K., Yadav, S. K., Zhang, Y., & Nile, S. H. (2024). Ultrasound-assisted extraction and encapsulation of betalain from prickly pear: Process optimization, in-vitro digestive stability, and development of functional gummies. Ultrasonics Sonochemistry, 108, 106975. https://doi.org/10.1016/j.ultsonch.2024.106975

Sadowska-Bartosz, I., & Bartosz, G. (2021). Biological properties and applications of betalains. Molecules, 26(8), 2520. https://doi.org/10.3390/molecules26082520

Tabio-García, D., Radzki, W., & Zieliński, H. (2021). Optimisation of the ultrasound-assisted extraction of betalains from beetroot by-products. International Journal of Food Science & Technology, 56(8), 4049–4061. https://doi.org/10.1111/ijfs.14929

Wybraniec, S., & Stintzing, F. C. (2020). Betalains: Properties, sources, applications, and stability – A review. Food Research International, 132, 109046. https://doi.org/10.1016/j.foodres.2020.109046 Carrera de Rosa, M. E., Ferreira, A. M., Neves, C. M. S. S., Almeida, M. R., Barros, R., Cristovão, A. C., … Freire, M. G. (2023). Valorisation of red beet waste: One-step extraction and separation of betalains and chlorophylls using thermoreversible aqueous biphasic systems. Green Chemistry, 25(5), 1852–1865. https://doi.org/10.1039/D2GC04480C

ORAL PRESENTATION

Production and characterization af aldehyde fractionated regenerated cellulose-chitosan based bioaerogel

Onur Şenol[1], Orçun Çağlar Kurtuluş[2*] (*ORCID: https://orcid.org/0000-0002-3233-7279*)

[1] Kastamonu University, Tosya Vocational School, Department of Biomedical Device Technology, Kastamonu, Türkiye.
[2*] Kastamonu University, Tosya Vocational School, Department of Materials and Material Processing Technology, Kastamonu, Türkiye.

*Corresponding author e-mail: ckurtulus@kastamonu.edu.tr

Abstract

In this study, regenerated cellulose-chitosan based bioaregels were produced by the simple lyophilisation method. Cellulose was dissolved using the LiCl/DMAc (lithium chloride-N,N-dimethyl acetamide) solvent system, and after the regeneration process, regenerated cellulose (RC) was obtained by incorporating aldehyde groups into its structure. Bioaerogels were produced by mixing RC with chitosan (CH) biopolymer at different mixing ratios (70-30, 50-50, and 30-70). Porosity-density, BET surface area, liquid absorption performance (water, NaCl, $MgCl_2$), water vapor transmission (WVTR), crystallinity index (CI), and antibacterial activity of the produced bioaerogels were determined, and their micro morphological structures were imaged using SEM to determine general characterization properties. In addition to the 100% polymer (RC and CH)-based sample, bioaerogels produced at 70-30, 50-50, and 30-70 mixing ratios showed low density (0.0166-0.0198 g/cm³) and, in contrast, almost high porosity values. The high porosity values obtained by all samples were in the range of 96.77%-99.02%; however, the maximum value was obtained by the 100% RC-based sample. Both liquid absorption performance and WVTR results were decreased by the addition of CH into RC composition. The specific surface area values of the samples were tested, revealing high levels ranging from 279.631 m²/g to 386.221 m²/g, with pure CH exhibiting the greatest value. Antibacterial performance versus *S. aureus* and *E. coli* results revealed that all aerogels both pure polymers (100% RC and 100% CH) and compositions with different mixing ratios (70-30, 50-50, and 30-70) showed antibacterial performances with different efficiencies. As a being known as one of the most popular antibacterial polymers, CH and higher levels of CH in RC compositions performed better antibacterial performances, and the inhibition zone measured higher for *E. coli* compared to *S. aureus*.

Keywords: Cellulose, Bioaerogel, Regenerated Cellulose, Chitosan

INTRODUCTION

RC is a cellulose precursor characterized by a cellulose II crystal structure, obtained by dissolving natural cellulose polymer in polar solvents and subsequently recrystallizing. This structure, identified as its crystalline form of cellulose II, has superior strength qualities compared to natural cellulose (cellulose I) owing to its negligible structural abnormalities (Eichorn et al., 2001; Shafizadeh et al., 1985). The initial endeavors to generate RC occurred 150 years ago, aimed at dissolving cellulose-rich substances like cotton and inner bark. Advancements in technology have led to the testing and development of several solvents and chemical methods for cellulose dissolving. A prevalent technique employed in RC manufacturing is the NMMO (N-methyl morpholine-N-oxide) procedure. The technique of dissolving cellulose in an NMMO solution is commercially referred to as the "Lyocell" approach. Subsequent to dissolution, the cellulose is extruded and then subjected to a washing procedure to eliminate the NMMO liquid from the cellulose fibers. The primary benefit of this procedure is the recovery of over 99% of the solvent. The cellulosic fibers generated by this process exhibit exceptional strength characteristics in both dry and wet conditions, enabling the use of these materials in the fabrication of thin, lightweight structures (Woodings, 2001). Numerous researchers, including Krysztof et al., (2018), Peng et al., (2021), Makarov et al., (2022), and Zhang et al., (2022), have conducted studies on the utilization of NMMO for cellulose solubilization. Another production technique used in RC production is the NaOH/Urea solubilizer system. During this manufacturing method, the NaOH/Urea combination is pre-cooled to -12 °C, cellulose is incorporated into the

mixture, and the dissolving process transpires within a brief duration of two minutes (Liebert et al., 2010). Recent research by Wei et al., (2020), and Armir et al., (2022) have investigated the efficacy of the NaOH/Urea system in solubilizing cellulose. The LiCl/DMAc binary process was initially discovered and utilized by DuPont for the dissolving and spinning of synthetic fibers, then adapted to cellulose-based polymers. This solvent system is reported to be highly effective, with no undesirable side reactions occurring in cellulose during the reaction, and it can solubilize even very high molecular weight (10^6) celluloses under ambient conditions (Matsumoto et al., 2002; Ishii and Isogai, 2008). Ionic liquids are molten organic salts composed of cationic and anionic species, with a melting point below 100 °C. Asymmetric organic cation structures engage with organic or inorganic anions, undermining the stability of the crystal lattice system and rendering it unstable. The most notable characteristic of these liquids is that their chemical and physical properties, including viscosity, conductivity, hydrophilic-hydrophobic nature, polarity, and hydrogen bonding capacity, can be altered by choosing the appropriate cation or anion or by incorporating specific functional groups into the structure (Rabideau et al., 2020; Azimi et al., 2022). Owing to these characteristics, these liquids are distinguished as a simple and eco-friendly method in RC manufacturing (Huang et al., 2022).

CH is a natural polymer derived from the partial or complete deacetylation of chitin, characterized by a primary chain of 1-4 linked 2-amino-deoxy-β-D-glucopyranose units. Its polycationic structure in acidic conditions, attributed to the presence of amino groups, facilitates gelation properties (Yang et al., 2007). The inherent chemical characteristics of this polymer varies mostly based on the degree of deacetylation (DAD) and the molecular weight (MA) of the polymer (Roberts, 1992; Bodek, 2006). This polymer has been utilized for numerous years in sectors including water treatment, papermaking, medicinal and pharmaceutical applications, agriculture, biotechnology, food additives, textiles, and membrane manufacture (Struszczyk, 2002).

This study involved the production of bioaerogel through the dissolution of cellulose using a LiCl/DMAc solvent system. Aldehyde groups were subsequently introduced into the structure following the regeneration process. The resultant RC and CH biopolymer were mixed in varying ratios, and the overall characterization of the final products was assessed through measurements of porosity-density, BET surface area, liquid absorption performance, WVTR, XRD, antibacterial activity, and micromorphological imaging via SEM.

MATERIALS AND METHODS

MATERIALS

The cellulose constituting the basic structure of the bioaerogels developed in this study was sourced from bleached magnesium bisulfite soluble pulp (MBP) and provided in sheet form by Solucell Lenzing AG (Austria). CH, LiCl, DMAc, $NH_2OH.HCl$, NaOH, NaCl, MgCl, and $NaIO_4$ utilized in the experiment were procured from Merck Sigma Aldrich, whereas acetone, as a technical chemical, was purchased from the appropriate industrial supplier.

METHODS

Aldehyde Process with LiCl/DMAc (N-N-Dimethylacetamide)

RC was obtained by the LiCl/DMAc method as described by Ishii and Isogai (2008). To expedite the reaction of cellulose with DMAc and reduce the reaction duration, the pulp was initially maintained in a vacuum oven at 60 °C for 24 hours, followed by immersion in water for 24 hours prior to extraction in acetone. Subsequent to substituting the water in the structure with acetone, the cellulose underwent treatment with the LiCl/DMAc combination. The cellulose was solubilized in an 8% LiCl/DMAc solution (3:97 by weight) at ambient temperature, and the resultant cellulosic gel was precipitated in acetone. RC, synthesized at a 4% concentration, was oxidized to an aldehyde structure at pH 4.5 and 45 °C for 4 hours in darkness, utilizing an RC/$NaIO_4$ ratio of 0.6. Subsequent to the procedure, the resultant RC containing the aldehyde portion was thoroughly rinsed with copious amounts of water and preserved at +4 °C for utilization in aerogel fabrication (Sun et al., 2015).

Determination of Aldehyde Content of RC

The aldehyde concentration of RC was measured using the methodology of Sirvio et al., (2011). To achieve this, 0.1 g of thoroughly desiccated RC was combined with 30 ml of water. The pH was modified to 4.5 using HCl, and 0.43 g of $NH_2OH.HCl$ was incorporated into 20 ml at pH 4.5. The suspension was agitated at 200 rpm for 24 hours prior to titration with 0.1 N NaOH, and the quantity of aldehyde groups was ascertained based on the volume of NaOH utilized.

$$\text{Aldehyde Amount}\left(\frac{\text{mmol}}{\text{g}}\right)=\frac{V * N}{W} \quad (1)$$

Where:
V: Amount of NaOH consumed in the titration (ml)
N: Normality of NaOH used in the titration (mol/L)
W: Amount of completely dry aldehyde fractionated RC used in the titration (g)

Production of RC-CH-Based Bioaerogels

Composite manufacturing was accomplished by a straightforward lyophilization method. To do this, an RC suspension and CH solution, both produced at a 1% polymer concentration, were combined at polymer ratios of 100%, 70%-30%, 50%-50%, and 30%-70% using a homogenizer at 10.000 rpm for 3 minutes. The solution was transferred onto glass Petri plates and subjected to pre-freezing at -86°C for 24 hours. The samples were thereafter positioned in a lyophilizer and subjected to lyophilization at -55°C and a vacuum of -50 mbar for 48 hours. The specimens were thereafter kept in sealed polyethylene bags for analysis.

Determination of Density and Porosity Values of Bioaerogels

The density of composites was determined by weight/volume measurements, and porosity was determined using a helium pycnometer (Quantachrome Ultrapyc 1200 E) using the formula below.

$$\text{Porosity}\ (\%) = \frac{[V1 - V2]}{V2} \text{x}\ 100 \quad (2)$$

Where:
V1: Measured volume of bioaerogels (cm^3)
V2: Volume measured by pycnometer (cm^3)

Liquid Absorption Performance

Liquid absorption (water, NaCl, MgCl) performances of bioaerogels were determined by placing approximately 0.005 g of sample in 50 ml of liquid and waiting for 24 hours, then weighing the bioaerogel at the end of the period. The liquid absorption value was determined as a percentage using the formula below.

$$\text{Liquid Absorption}\ (\%) = \frac{[Mt - Mo]}{Mo} \text{x}\ 100 \quad (3)$$

Where:
Mt: Sample weight measured after 24 hours (g)
Mo: Initial weight of sample (g)

WVTR

The WVTR of the samples was determined in accordance with ASTM E96-90 (Procedure D). The samples were positioned in a desiccator with 6 ml of deionized water, measuring 8.5 cm in length, 1.2 cm in breadth, and 0.6 cm in mouth diameter, under a 40% humidity environment created by a saturated solution of $MgCl_2 \cdot 6H_2O$. The samples were maintained at 37 °C for 24 hours, and the WVTR was determined using the formula below.

$$\text{WVTR} = \frac{(G/t)}{A} \quad (4)$$

Where:
G/t: The gradient of the weight variation in relation to time (g/h)
A: Test area (m^2)

BET Surface Area

A Quantachrome Nova Touch LX4 instrument used to determine the specific surface areas of the bioaerogels. A vacuum treatment was employed to remove any water from the samples initially. Nitrogen adsorption-desorption

isotherms were employed to determine specific surface areas using the methodology established by Brunauer, Emmett, and Teller (1938).

CI

The CI variations in the compositions of bioaerogels, derived from pure polymers (RC, CH) and their combinations at various ratios were assessed utilizing a Bruker D8 Advance X-ray powder diffractometer (Billerica/Massachusetts, U.S.A.). Sample measurements were conducted using a radiation source (Cu Kα) with a wavelength of λ = 0.154 nm, a scanning range of 3°≤2Θ≤90°, and a scanning speed of 2°/min. The index values were computed using the formula provided by Segal et al., (1959).

$$CI = \frac{[I002 - Iam]}{I002} x\ 100 \qquad (5)$$

Where:
I002: Cellulose crystalline region peak (2Θ=21.5°-22.9°)
Iam: Cellulose amorphous region peak (2Θ=16.9°-18.2°)

Antibacterial Performance

The antibacterial efficacy of the composite materials was evaluated using the usual disk diffusion method. Bacteria cultured in SS (*E. coli*) and BHA (*S. aureus*) enriched media were inoculated onto agar media using the swab method. Subsequently, samples with a diameter of 1 cm were placed in contact with the bacterial medium. The medium was incubated at 28 °C for 24 hours. At the conclusion of this period, inhibitory zones on the agar medium were assessed at many sites, and averages were calculated.

Micromorphological Views

The material's micromorphology was examined using a scanning electron microscope (FEI Quanta FEG 250, 11 kV). Prior to imaging, samples were sectioned with a scalpel and coated with gold-palladium at 40 mA and 50 mbar pressure.

RESULTS and DISCUSSION

Density and Porosity

The density and porosity metrics of RC/CH-based bioaerogels are presented in Table 1. Bioaerogels have elevated porosity levels. The analysis of porosity data reveals that the maximum porosity, recorded at 99.02%, was found in pure RC samples. Bioaerogels based on 100% pure CH had a porosity of 96.77%, whereas RC/CH-based samples demonstrated porosity values of 98.28%, 98.01%, and 97.29% for mixture ratios of 70-30, 50-50, and 30-70, respectively. The reduced porosity of materials fabricated with CH polymers, in contrast to pure RC polymers, influenced the compositions, resulting in porosity values of RC/CH-based composites aligning with those of pure polymers. The density values of bioaerogels were determined to be in the range of 0.01 g/cm³. The addition of CH to the RC structure resulted in lower density and porosity values. The aldehyde group generated in the RC structure (0.613 mmol/g) by $NaIO_4$ oxidation likely interacted with the amine groups in the CH structure, resulting in the proximity of molecular chains and the formation of bigger cluster structures, which consequently reduced porosity values.

Table 1. Density and porosity values of bioaerogels

Bioaerogel	Density (g/cm³)	Porosity (%)
RC	0.0198	99.02
CH	0.0166	96.77
RC/CH 70-30	0.0186	98.28
RC/CH 50-50	0.0176	98.01
RC/CH 30-70	0.0168	97.29

Liquid Absorption Performance

Figure 1 illustrates the absorption values of water, NaCl, and $MgCl_2$ in the composites. The examination of water absorption values in bioaerogels revealed that the maximum absorption value was 1813.56% in 100% RC bioaerogels, whilst the minimum absorption rate was 1102.36% in composites created with a 30-70 mixing ratio. Nonetheless, water absorption values could not be ascertained in 100% CH-based composites owing to their very hydrophilic nature. Variations in porosity levels corresponded with alterations in water absorption performance. The values of water absorption diminished as porosity decreased. As the concentration of CH inside the structure increased, porosity values diminished, leading to a corresponding influence on water absorption. Besides porosity, the reduction in absorption attributed to the increased quantity of CH can be elucidated by the highly hydrophilic nature of CH, which induces progressive structural degradation in water and the disintegration of the aerogels' surface structure due to the gelation effect occurring at the surface.

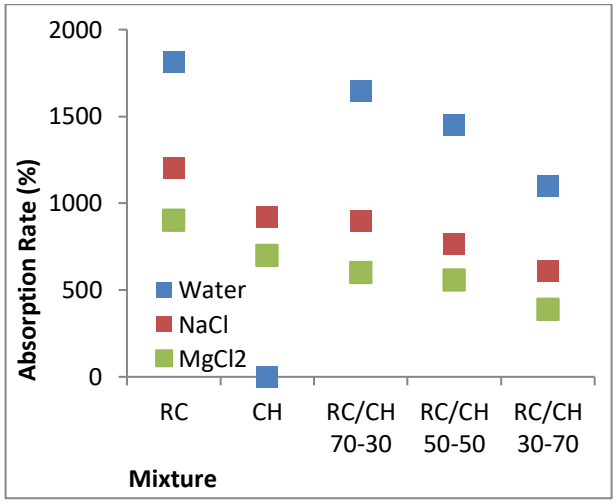


Figure 1. Liquid absorption performances of bioaerogels

Figure 1 also presents the NaCl and $MgCl_2$ absorption findings of the bioaerogels, alongside the water absorption data. The trend in salt absorption performance followed that of water absorption. NaCl, due to its reduced molecular size, diffused more readily into the bioaerogel matrix than $MgCl_2$, leading to elevated absorption levels.

WVTR Results of Bioaerogels

The WVTR of bioaerogels derived from RC/CH-based and pure polymers are presented in Figure 2. The figure illustrates that the maximum value for RC-based bioaerogels was 203.66 g/h m^2, but the minimum value for pure CH-based bioaerogels was 121.58 g/h m^2. Water vapor transpires when water vapor diffuses vertically through the medium. The transfer of water vapor through the composite structures operates via pores, with the size of these holes and the resultant porosity directly influencing the transfer rate, leading to variations in water vapor transfer that correspond with changes in porosity. The graph clearly illustrates that the incorporation of CH into the RC structure resulted in a reduction in the WVTR corresponding with the porosity data.

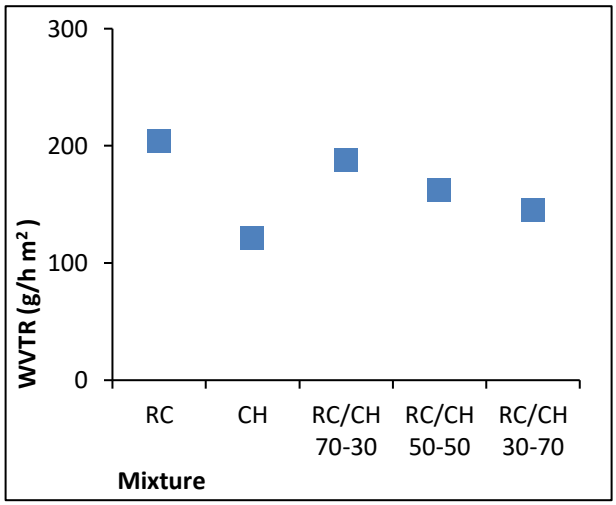


Figure 2. WVTR of bioaerogels

BET Surface Area

Table 2 presents the BET surface area measurements of bioaerogels. Upon examination of the table, the specific surface area values were determined to vary from 279.631 to 386.221 m^2/g. The maximum specific surface area, 386.221 m^2/g, was seen in pure CH-based samples, whilst the minimum surface area, 276.631 m^2/g, was recorded in pure RC-based composites. Although the specific surface area values of materials generated with CH incorporation into the RC structure were inferior to those of pure CH, a higher CH concentration in the structure enhanced the specific surface area values of the samples. These composites, characterized by elevated porosity and specific surface area, are thought to be appropriate for diverse applications including liquid-gas absorption, sound insulation, and thermal insulation.

Table 2. Surface area values of bioaerogels

Bioaerogel	Surface Area (m^2/g)
RC	279.631
CH	386.221
RC/CH 70-30	291.256
RC/CH 50-50	328.256
RC/CH 30-70	351.042

CI

The CI values of bioaerogels are provided in Table 3. The CI value for MBP was established at 74.55%, while the CI value for RC was determined to be 48.22%. However, the CI value of 100% CH-based bioaerogel could not be ascertained due to the predominantly amorphous nature of its structure. Dissolving cellulose using the LiCl/DMAc solvent system induces a transformation of the cellulose I crystal structure into the cellulose II crystalline form, resulting in a subsequent decrease in the crystallinity index values (Eichorn et al., 2001; Shafizadeh et al., 1985). With the incorporation of amorphous CH polymer into the RC structure and the progressive increase in its quantity, the crystallinity index values were observed to be lower.

Table 3 . CI values of bioaerogels

Bioaerogel	CI (%)
MBP	74.55
RC	48.22
CH	-
RC/CH 70-30	21.02
RC/CH 50-50	19.33
RC/CH 30-70	17.06

Bacterial Resistance

The findings of the inhibition zone measurements for the antibacterial efficacy of bioaerogels are displayed in Table 3. An analysis of the table indicates that all bioaerogel structures exhibit resistance to both bacterial species, hence reducing bacterial proliferation. Bioaerogels demonstrate superior resistance to the gram-negative bacteria *E. coli*. The positively charged amine groups $(NH_2)^+$ in the CH polymer structure compromise the integrity of bacterial cell walls, inhibiting adhesion to the material and so providing antibacterial resistance. The same is true for RC, where the aldehyde fractions in the structure likely interact with bacterial cell wall components, inhibiting bacterial adhesion to the matrix and proliferation.

Table 4 . Inhibition zone measurements of bioaerogels

Bioaerogel	Inhibition Zone (*S. aureus*)	Inhibition Zone (*E. coli*)
RC	0.25	0.33
CH	0.58	0.64
RC/CH 70-30	0.33	0.41
RC/CH 50-50	0.42	0.53
RC/CH 30-70	0.49	0.58

Macro and Micro Views of Bioaerogels

Figure 3 shows the macro surface and micro SEM images of bioaerogels produced with RC and RC/CH 50-50 compositions. As seen in both figures, the bioaerogels have a homogeneous macro surface structure, and with the addition of CH, the structure becomes more yellow due to CH. The micro-surface morphology of the RC structure without CH addition exhibits denser and tighter pore walls, but the pore structures in the RC/CH 50-50 configuration are broader, corroborated by the porosity and specific surface area findings. SEM images of bioaerogels demonstrate elevated liquid absorption, significant specific surface area, and WVTR values that correlate directly with porosity.

a

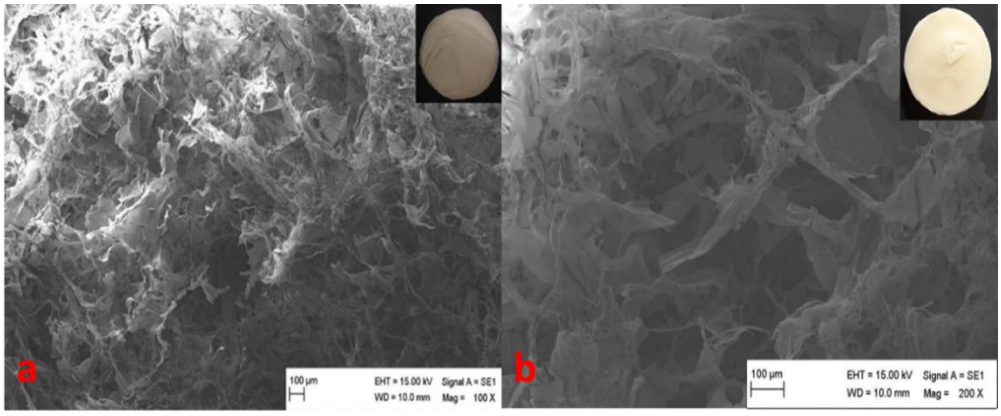


Figure 3. Macro and micro images of pure RC (a) and RC/CH 50-50 based bioaerogels

CONCLUSION

In this study, bioaerogel production was accomplished by dissolving cellulose using the LiCl/DMAc solvent system, introducing aldehyde groups into the structure following the regeneration process, and mixing the resulting RC and CH biopolymers at various ratios. The general characterization properties of the bioaerogels were assessed through measurements of porosity and density, BET surface area analysis, liquid absorption performance (water, NaCl, and MgCl2), WVTR, CI, antibacterial activity, and the examination of their micromorphological structures via SEM. The density of the produced bioaerogels was found to range from 0.0168 to 0.0198 g/cm³, while their porosity values ranged from 96.77% to 99.02%. Furthermore, although all bioaerogels demonstrated high liquid absorption capacity, the incorporation of CH into the RC structure adversely impacted their liquid absorption

performance. The WVTR values of the bioaerogels were determined to vary from 121.58 g/h·m² to 203.66 g/h·m², while the surface area measurements were notably high, corresponding to their porous structures. However, both the WVTR and surface area measurements tended to decline with the incorporation of CH into the RC structure. In addition to these properties, it is believed that RC/CH-based bioaerogels, which exhibit resistance to *S. aureus* and *E. coli* bacteria, can be assessed for application in various fields.

ACKNOWLEDGEMENTS

The authors wish to acknowledge TÜRİTAK, the Scientific and Technological Research Council of Turkey, for the financial support they provided.

REFERENCES

Armir, N. A. Z., Salleh, K. M., Zulkifli, A., & Zakaria, S. (2022). pH-responsive ampholytic regenerated cellulose hydrogel integrated with carrageenan and chitosan. Industrial Crops and Products, 178, 114588.

ASTM E 96/96 M. (2002). Standard Test Methods for Water Vapor Transmission of Materials. ASTM International.

Azimi, B., Maleki, H., Gigante, V., Bagherzadeh, R., Mezzetta, A., Milazzo, M., ... & Danti, S. (2022). Cellulose-based fiber spinning processes using ionic liquids, Cellulose, 1-51.

Bodek, K. H. (2006). MICROCRYSTALLINE CHITOSAN AS PHARMACEUTICAL PREPARATION. Polish Chitin Society, Monograph XI, 85-94.

Brunauer, S., Emmett, P. H. & Teller, E. (1938). Adsorption of Gases in Multimolecular Layers. Journal of the American Chemical Society, 60(2), 309-319.

Eichorn, S. J., Young, R. J., & Yeh, W. Y. (2001). Deformation processes in regenerated cellulose fibers. Textile research journal, 71(2), 121-129.

Huang, X., Ji, Y., Guo, L., Xu, Q., Jin, L., Fu, Y., & Wang, Y. (2022). Incorporating tannin onto regenerated cellulose film towards sustainable active packaging. Industrial Crops and Products, 180, 114710.

Ishii, D., & Isogai, A. (2008). The residual amide content of cellulose sequentially solvent-exchanged and then vacuum-dried. Cellulose, 15(4), 547-553.

Krysztof, M., Olejnik, K., Kulpinski, P., Stanislawska, A., & Khadzhynova, S. (2018). Regenerated cellulose from N-methylmorpholine N-oxide solutions as a coating agent for paper materials. Cellulose, 25(6), 3595-3607.

Liebert, T. F., Heinze, T. J., Edgar, K. J. (2010). Cellulose Solvents: For Analysis, Shaping and Chemical Modification. Washington-United States: ACS Symposium Series.

Makarov, I. S., Golova, L. K., Smyslov, A. G., Vinogradov, M. I., Palchikova, E. E., & Legkov, S. A. (2022). Flax Noils as a Source of Cellulose for the Production of Lyocell Fibers. Fibers, 10(5), 45.

Matsumoto, T., Tatsumi, D., Tamai, N., Takaki, T. (2002). Solution properties of celluloses from different biological origins in LiCl.DMAc. Cellulose, 00, 1-8.

Peng, J., Li, Y., Liu, X., Ke, G., Song, D., Wu, S., ... & Zhu, K. (2021). Cellulose film with air barrier and moisture-conducting character fabricated by NMMO. Journal of Materials Science, 56(32), 18313-18326.

Rabideau, B. D., Soltani, M., Parker, R. A., Siu, B., Salter, E. A., Wierzbicki, A., ... & Davis, J. H. (2020). Tuning the melting point of selected ionic liquids through adjustment of the cation's dipole moment. Physical Chemistry Chemical Physics, 22(21), 12301-12311.

Roberts, G. A. F. (1992). Chitin Chemistry. London-United Kingdom: Macmillan Education.

Segal, L., Creely, J. J., Martin Jr, A. E. & Conrad, C. M. (1959). An Empirical Method for Estimating the Degree of Crystallinity of Native Cellulose Using the X-Ray Diffractometer. Textile Research Journal, 29(10), 786-794.

Shafizadeh, F., Newell, T. P., & Zeronian, S. H. (1985). Cellulose chemistry and its applications. Halsted Press, John Wiley, New York.

Sirvio, J., Hyvakko, U., Liimatainen, H., Niinimaki, J., & Hormi, O. (2011). Periodate Oxidation of Cellulose at Elevated Temperatures Using Metal Salts as Cellulose Activators. Carbohydrate Polymers, 83(3), 1293–1297.

Struszczyk, M. H. (2002). Chitin and Chitosan, Part II. Application of Chitosan. Polimery, 47, 396-403.

Sun, B., Hou, Q., Liu, Z., & Ni, Y. (2015). Sodium periodate oxidation of cellulose nanocrystal and its application as a paper wet strength additive. Cellulose, 22(2), 1135-1146.

Wei, Q. Y., Lin, H., Yang, B., Li, L., Zhang, L. Q., Huang, H. D., ... & Li, Z. M. (2020). Structure and properties of all-cellulose composites prepared by controlling the dissolution temperature of a NaOH/Urea solvent. Industrial & Engineering Chemistry Research, 59(22), 10428-10435.

Woodings, C. (2001). Regenerated Cellulose Fibres. Cambridge-England: Woodhead Publishing Limited.

Yang, J., Tian, F., Wang, Z., Wang, Q., Zeng, Y.J., Chen, S.Q. (2007). Effect of Chitosan Molecular Weight and Deacetylation Degree on Hemostasis. Journal of Biomedical Materials Research Part B: Applied Biomaterials, 84B(1), 131-137.

Zhang, C., Liu, R., Xiang, J., Hongliang, K., Liu, Z., Huang, Y. (2014). Dissolution Mechanism of Cellulose in N,N-Dimethylacetamide/Lithium Chloride: Revisiting through Molecular Interactions. The Journal of Physical Chemistry B, 118, 9507-9514.

ORAL PRESENTATION

Synthesis of novel benzothiazole/thiazole hybrids and *in silico* investigations via SwissADME and BioFinder programs

Aybüke Züleyha Kaya[1,2,*](Orcid: https://orcid.org/0009-0002-1614-2380)

[1] Anadolu University, Faculty of Pharmacy, Department of Pharmaceutical Chemistry, Eskisehir, Türkiye.
[2] Institute of Graduate Education, Anadolu University, Eskisehir, Türkiye.

*Corresponding author e-mail: aybukezuleyhakaya@anadolu.edu.tr

Abstract

In this work, synthesis of novel 2-((5-chlorobenzothiazol-2-yl)thio)-*N*-(4-(2-(substituted)thiazol-4-yl)phenyl)acetamide (**4a-4c**) derivatives and physicochemical properties investigation were aimed. Synthesis of the compounds is carried out with according to the synthesis scheme. Pathway of synthesis had two simple and affordable steps. The structures of final compounds were proven with hydrogen and carbon nuclear magnetic resonance (NMR) spectral analysis. Physicochemical and toxicity properties were investigated via SwissADME and Deep-PK software. Further investigation was evaluated via SwissTarget and BioFinder prediction software. Kinase and family AG coupled receptors were main targets of the compounds.

Keywords: Benzothiazole, *In silico* studies, Pharmacokinetic properties, Thiazole, Toxicity profile.

INTRODUCTION

Human health takes place as biggest cause of concern of people from the past to the present. All fields of science make effort to understand and solve the mystery of human body. While some diseases heal via hydration and rest, some other diseases need complicated treatment. These treatments can include chemotherapy, radiotherapy, hormone replacement therapy, immunotherapy, bone marrow replacement, targeted therapy and drug therapy (Kaur et al., 2023; Wargo et al., 2015; Zafar et al., 2025). Among given therapies chemotherapy with various types of drugs is preferred to treat common diseases (Mathan et al., 2022). Sometimes drugs lose effectiveness against pathogens because of incorrect use of dosage, unrelated disease-medication combination, unnecessary usage. Therefore, synthesizing new compounds and investigating their activities is highly important. Today, thanks to computational chemist predictions can be made about compounds before synthesizing (Engkvist et al., 2018; Goh et al., 2017; Keith et al., 2021). Various software provides H-bond acceptor (HBA), H-bond acceptor (HBD), topologic polar surface area (TPSA), solubility class (water) (SC), gastrointestinal absorption (GIA), skin permeation (Log K_p), rule of five (violation number), Ghose filter, leadlikeness information (Bakchi et al., 2022; Daina et al., 2017; Yurttaş et al., 2022). Predictions provide an opportunity to make modifications on compounds. Thus, finalize compounds investigate to find their possible targets such as enzymes, receptors, nucleic acids (Sanad et al., 2023; Tshiluka et al., 2025). Before expensive and tedious *in vitro* and *in vivo* studies, compounds investigate via *in silico* studies. *In silico* studies are planned according to the results of the target predictions. If the obtained results are found to be reasonable, the next step is to plan the synthesis and activity studies of the molecules.

Thiazole and benzothiazole rings frequently are seen in drugs and drug candidates (Cheekatla, 2025; Rouf & Tanyeli, 2015; Yadav et al., 2023). Thiazole is found in structures of sulphathiazole (antibiotic) (Meşeli et al., 2021), fanetizole (anti-inflammatory) (Potewar et al., 2007), combendazole (antifungal) (Desai et al., 2012), niridazole (schistozomicidal) (Moczon & Swiderski, 1983), meloxicam (NSAID) (Luger et al., 1996), thiamine (vitamin B1) (Tylicki et al., 2018), dasatinib (anticancer) (Das et al., 2006), and ritonavir (antiviral) (Samuels & Sevrioukova, 2019). On the other hand, benzothiazole is found in structures of riluzole (treatment of ALS) (Hollingworth et al., 2024), ethoxzolamide (carbonic anhydrase inhibitor) (Johnson et al., 2015), zopolrestat (antidiabetic) (Yahya et al., 2022), thioflavin T (diagnostic agent) (Khurana et al., 2005), frentizole (immunosuppressant) (Chrienova et al., 2023). Researchers investigated the combination of these two rings on

various activities (Irfan et al., 2020; Meltzer-Mats et al., 2013; Radwan et al., 2022). We have synthesized seven molecules containing both thiazole and benzothiazole rings and investigated their possible activities via *in silico* studies.

RESULTS and DISCUSSION

Chemistry

Chemical synthesis part of this study started with acetylation of 4-aminoacetophenone. Then, 2-mercapto-5-chlorobenzothiazole and *N*-(4-acetylphenyl)2-chloroacetamide (**1**) in equal molars as shown in **Scheme 2**. Obtained mid-product (**2**) used to synthesis of final products. Next step is bromination of the intermediate product, followed by reaction of the resulting product with thiobenzamide/4-methoxythiobenzamide/thiourea (**4a-4c**). Total three novel final compounds (**Table 5**) and investigated. Structural analyses of the compounds evaluated with hydrogen and carbon nuclear magnetic resonance spectroscopic (NMR) techniques. In ^{1}H-NMR spectra aliphatic peaks were observed between 3.84-4.44 ppm range. Hydrogen peaks belonging to -CH_2 group were seen as singlet at 4.43-4.44 ppm range, protons of -OCH_3 group were detected as singlet peaks at 3.84 ppm. And also -NH hydrogens can be clearly seen at the spectra of compounds. -NH hydrogen was observed at 10.58-10.62 ppm range. The other aromatic hydrogen was observed between 7.06-8.08 ppm as expected. ^{13}C-NMR spectra also indicated specified peaks. Aliphatic -CH_2 carbon peak was observed at 33.87-38.34 ppm. The carbon peak observed at 83.66 ppm is considered to belong to the -OCH_3 group. Carbon peaks at 160.60-171.94 ppm proved that there were carbonyl peaks in our structure.

2-((5-Chlorobenzothiazol-2-yl)thio)-N-(4-(2-phenylthiazol-4-yl)phenyl)acetamide (4a)

$C_{24}H_{16}ClN_3OS_3$, yield 60%, M.P.: 206°C. ^{1}H-NMR (300 MHz, DMSO-d_6, ppm) δ 4.44 (s, 2H, C$\underline{H}_2$), 7.43 (dd, 1H, J_1: 2.07 Hz, J_2: 8.58 Hz, Ar-C$\underline{H}$), 7.51-7.56 (m, 3H, Ar-C$\underline{H}$), 7.71 (d, 2H, *J*: 8.70 Hz, Ar-C$\underline{H}$), 7.90 (d, 1H, *J*: 2.01 Hz, Ar-C$\underline{H}$), 8.01-8.04 (m, 4H, Ar-C$\underline{H}$), 8.08 (m, 2H, Ar-C$\underline{H}$), 10.60 (s, 1H, N$\underline{H}$). ^{13}C-NMR (75 MHz, DMSO-d_6, ppm) δ 38.20, 114.17, 119.80, 120.95, 121.04, 123.87, 125.06, 126.66, 127.20, 129.75, 129.91, 131.73, 134.08, 139.22, 155.33, 165.57, 171.94.

2-((5-Chlorobenzothiazol-2-yl)thio)-N-(4-(2-(4-methoxyphenyl)thiazol-4-yl)phenyl)acetamide (4b)

$C_{25}H_{18}ClN_3O_2S_3$, yield 65%, M.P.: 198°C. ^{1}H-NMR (300 MHz, DMSO-d_6, ppm) δ 3.84 (s, 3H, OC$\underline{H}_3$), 4.44 (s, 2H, C$\underline{H}_2$), 7.08 (dd, 2H, J_1: 2.07 Hz, J_2: 6.80 Hz, Ar-C$\underline{H}$), 7.43 (dd, 1H, J_1: 2.07 Hz, J_2: 8.58 Hz, Ar-C$\underline{H}$), 7.70 (d, 2H, *J*: 8.76 Hz, Ar-C$\underline{H}$), 7.90-8.02 (m, 6H, Ar-C$\underline{H}$), 8.08 (d, 1H, *J*: 8.61 Hz, Ar-C$\underline{H}$), 10.58 (s, 1H, N$\underline{H}$). ^{13}C-NMR (75 MHz, DMSO-d_6, ppm) δ 33.87, 83.66, 95.05, 113.00, 115.07, 119.75, 127.16, 128.26, 129.85, 131.88, 146.55, 148.11, 156.85, 160.60, 161.38, 165.59.

N-(4-(2-Aminothiazol-4-yl)phenyl)-2-((5-chlorobenzothiazol-2-yl)thio)acetamide (4c)

$C_{18}H_{13}ClN_4OS_3$, yield 68%, M.P.: 165°C. ^{1}H-NMR (300 MHz, DMSO-d_6, ppm) δ 4.43 (s, 2H, C$\underline{H}_2$), 7.06 (s, 1H, Ar-C$\underline{H}$), 7.43 (dd, 1H, J_1: 2.04 Hz, J_2: 8.58 Hz, Ar-C$\underline{H}$), 7.65-7.72 (m, 4H, Ar-C$\underline{H}$), 7.88 (d, 1H, *J*: 1.98 Hz, Ar-C$\underline{H}$), 8.07 (d, 1H, *J*: 8.58 Hz, Ar-C$\underline{H}$), 10.62 (s, 1H, N$\underline{H}$). ^{13}C-NMR (75 MHz, DMSO-d_6, ppm) δ 38.34, 102.06, 102.45, 104.53, 115.69, 116.88, 118.82, 119.67, 123.84, 125.04, 126.90, 131.16, 131.85, 135.72, 136.85, 139.51, 139.73, 155.28, 156.06, 159.34, 165.78.

In Silico Studies

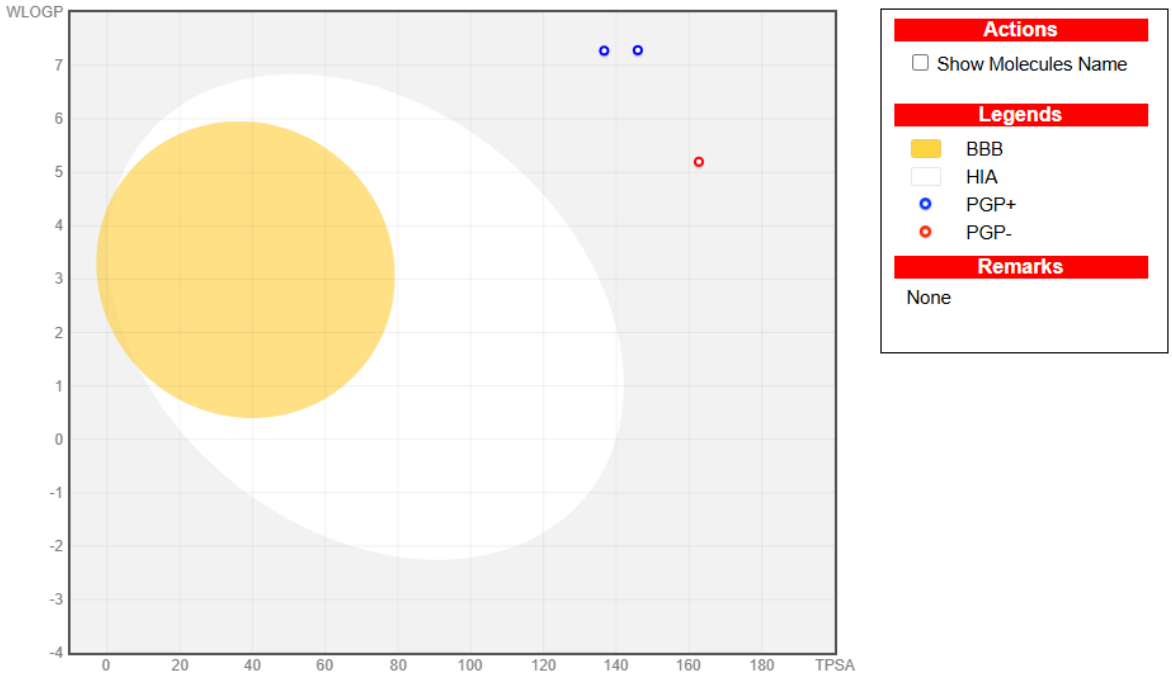
The use of computational software allows for the prediction of compounds' physicochemical properties, pharmacokinetic properties, and lead-likeness properties. The predictions obtained from SwissADME (SwissADME, 2021) are listed in **Table 1**. ADME parameters such as H-bond acceptor, H-bond acceptor, topological polar surface area, Log Po/w, aqueous solubility, skin permeability, gastrointestinal absorption, Lipinski's rule of five were calculated and has been converted into a table. When we investigated the results of the study, all of our compounds have low gastrointestinal absorption and also, they did not dissolve in water sufficiently. Our compounds structure is highly lipophilic, so this finding was found accurate. According to Lipinski's rule of five, compounds **4a** and **4c** fit the criteria for druglikeness. Compound **4b** only violated one criterion. None of our compounds passed the leadlikeness property described by Teague and team. SwissADME software also predicted blood-brain barrier (BBB) transition states of molecules between WLOGP and TPSA. This

prediction is displayed in **Scheme 1** illustrated as the boiled egg. None of the compounds penetrate BBB and also did not show gastrointestinal absorption.

Table 1. Physicochemical and pharmacokinetic properties of synthesized compounds from SwissADME.

	HBA	HBD	TPSA	Log $P_{o/w}$	SC	Log K_p	GIA	RoF (V)	Leadlikeness (V)
4a	3	1	136.66	6.03	Poorly	-4.27	Low	0	No (2)
4b	4	1	145.89	6.11	Poorly	-4.47	Low	1	No (3)
4c	3	2	162.68	4.37	Moderately	-5.32	Low	0	No (2)

HBA: H-bond acceptor, **HBD**: H-bond acceptor, **TPSA**: Topological polar surface area, **Log $P_{o/w}$:** Log Po/w (-6.5 / 0.5), **SC:** Aqueous solubility, **Log K_p:** skin permeability (cm/hr), **GIA**: Gastrointestinal absorption, **RoF (V):** Rule of Five (violation number).



Scheme 1. The boiled egg illustration of blood-brain barrier penetration.

With SwissTargetPrediction (SwissTargetPrediction, 2021) and BioFinder (BioFinder, 2025) software before *in vitro* and *in vivo* studies target enzyme, receptor, or nucleic acids can be predicted. This prediction can save time, money, and unnecessary use of biological substances. Possible targets of our compounds identified with SwissTarget software. First fifteen targets were selected and investigated. Targets above 10% probability rate are listed in **Table 2**. Compounds **4a**, **4b** and **4c** were determined to target kinase with 40.0-80.0 percentage rate. Compound **4b** were also found to target the AG protein-coupled receptor family in second place. The potential targets of oxidoreductase are **4a**, and **4c**, with a percentage of 6.7. Further, **4c** can target the enzyme over with ratio of 26.7%. Only compound that targets the eraser (histone deacetylase, NAD-dependent deacetylase sirtuin) is **4b** with 13.3%. By blocking the histone deacetylase enzyme, molecule can induce apoptosis, and this way shows anticancer activity. However, BioFinder predictions suggest that among the synthesized compounds, **4b** is predicted to target the most and various proteins and receptors. Only compound that targets both glycogen synthase kinase-3 alpha and beta is **4b** despite the substituent position and groups being different. Unlike other compounds, **4a** and **4b** might target the vasopressin V2 receptor, replicase polyprotein 1ab, and the nicotinamide phosphoribosyltransferase enzyme.

SwissADME and BioFinder software gave different enzymes, protein, and receptors with each other. Biofinder software gave more specified targets, while SwissADME gave more general targets such as enzyme family. It is

believed that BioFinder software will be more useful and convenient before detection of in vitro study aspect. Difference of predicted targets may have result of the unvalidated software.

Table 2. SwissTarget prediction of synthesized compounds (**4a-4c**) (%).

	Kinase	Family AG protein-coupled receptor	Protease	Eraser	Enzyme	Oxidoreductase	Phosphodiesterase
4a	46.7	13.3	6.7	-	13.3	6.7	-
4b	40.0	26.7	6.7	13.3	6.7	-	6.7
4c	40.0	-	-	-	26.7	6.7	6.7

Table 3. BioFinder prediction of synthesized compounds (**4a-4c**).

	4a	4b	4c
Neuropeptide Y receptor type 2	x	x	x
Transient receptor potential cation channel subfamily A member 1			x
Calcium-activated potassium channel subunit alpha-1			x
Neuropeptide Y receptor type 5	x	x	
Glycogen synthase kinase-3 alpha		x	
Glycogen synthase kinase-3 beta		x	
Vasopressin V1a receptor	x	x	
Carbonic anhydrase 1		x	x
Carbonic anhydrase 2	x	x	x
Alkaline phosphatase, tissue-nonspecific isozyme			
Adenosine receptor A2b			
Kallikrein-1			
Vasopressin V2 receptor	x	x	
Replicase polyprotein 1ab	x	x	
Nicotinamide phosphoribosyltransferase	x	x	

Toxicicity profile of the compounds predicted via Deep-PK (DeepPK, 2024) software and results displayed in **Table 4**. This website makes predictions on Ames toxicity, maximum tolerated dose, hERG blockers, oral rat acute toxicity, oral rat chronic toxicity, hepatoxicity, respiratory diseases, skin sensitization, eye irritation, carcinogenesis, biodegradation etc. Ames toxicity indication of mutagenicity of chemicals by various mechanisms. While **4a**, and **4b** predicted to be not show Ames toxicity, predictions on compound **4c** indicated otherwise. Maximum tolerated dosage of the compounds predicted to be between 0.44-1.05 log mg/kg/day. It has been detected that **4c** is the least tolerated one, while **4a** is the most tolerated one. Compound **4a** has been estimated that they are toxic to the hERG blockers. Oral rat acute toxicity detected range of 2.41-2.71 log[1/(mol/kg)], oral rat chronic toxicity detected range of 0.61-0.89 log(mg/kg_bw/day). Hepatotoxic effects are expected to occur in all compounds. None of the compounds have been expected to show respiratory diseases, skin or eye irritation, carcinogenic effects. Biodegradation of compounds is not anticipated.

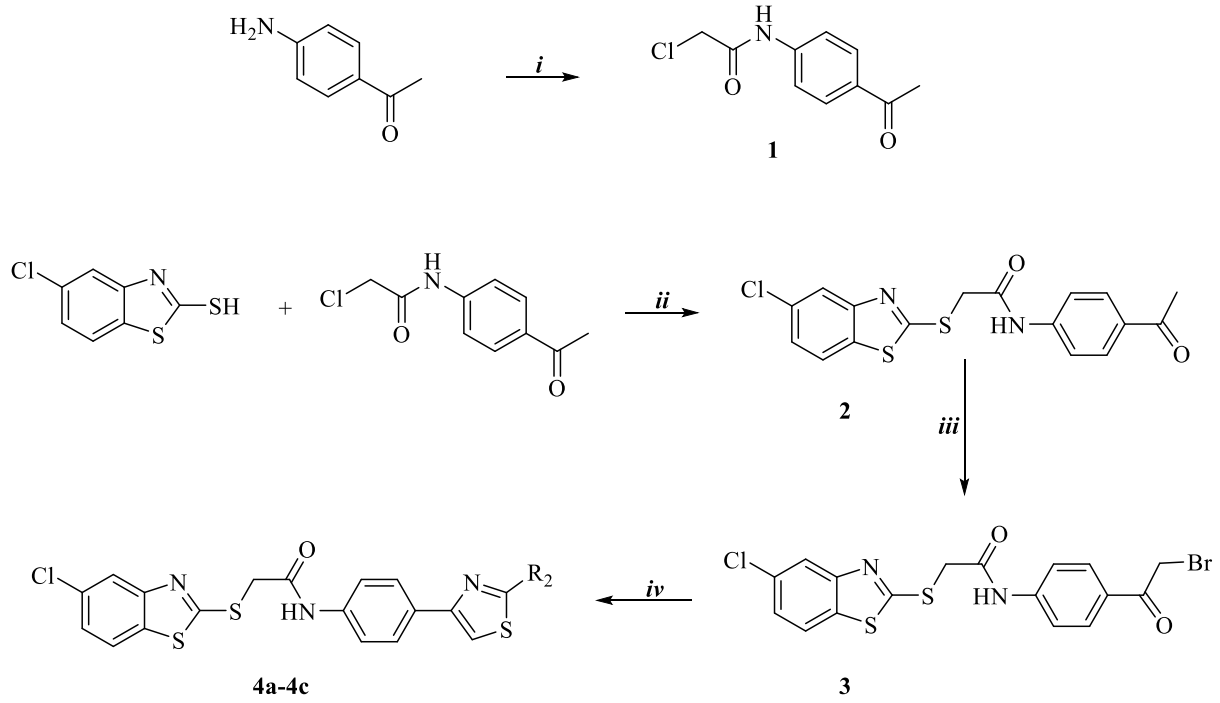
Table 4. Toxicity profiles of the compounds (**4a-4c**) predicted using Deep-PK software.

	4a	4b	4c
Ames toxicity	No	No	Yes
Max. tolerated dose (log mg/kg/day)	0.70	0.69	0.44
hERG blockers	Yes	No	No
Oral Rat Acute Toxicity (log[1/(mol/kg)])	2.41	2.71	2.71
Oral Rat Chronic Toxicity [log(mg/kg_bw/day)]	0.80	0.61	0.89
Hepatoxicity	Yes	Yes	Yes
Respiratory diseases	Yes	No	No
Skin sensitization	No	No	No
Eye irritation	No	No	No
Carcinogenesis	No	No	No
Biodegradation	No	No	No

MATERIAL METHODS

Chemistry

All the chemicals used to synthesize final compounds provided from Merck Co (Darmstadt, Germany). Reactions in the procedure monitored by thin layer chromatography (TLC) analysis. Melting points of final molecules detected by Electrothermal 9300 digital melting point apparatus (Essex, UK). Structural analysis of the compounds made by nuclear magnetic resonance spectrometry (^{1}H and ^{13}C spectrometer, Bruker Bioscience, USA).



Scheme 2. Synthetic scheme. *Reaction conditions:* **i)** THF, TEA, Chloracetyl chloride, 0°C, **ii)** Acetone, K_2CO_3, 1 hour, rt, **iii)** Bromine, HBr, AcOH, 1 hour, rt, **iv)** Thiobenzamide/4-methoxythiobenzamide/thiourea, EtOH, 1 hour, rt.

Table 5. Synthesized compounds and substituents.

Compounds	R_2
4a	Phenyl
4b	4-OCH_3 Phenyl
4c	NH_2

N-(4-acetylphenyl)-2-chloroacetamide (1)

4-Aminoacetophenone (1 eq) dissolved in tetrahydrofuran (THF). Reaction cooled to 0°C to slowed down the reaction. 1.5 eq dimethyl formamide added to reaction mixture as a catalyst. Acetylation agent chloracetyl chloride diluted with THF and added dropwise to the reaction. After chloracetyl chloride addition completed TLC analysis conducted, according to the result reaction finalized by evaporating the solvent. Dried content washed with water, filtered and dried.

N-(4-Acetylphenyl)-2-((5-chlorobenzothiazol-2-yl)thio)acetamide (2)

2-Mercapto-5-chlorobenzothiazole (1 eq) and *N*-(4-acetylphenyl)2-chloroacetamide (1eq) dissolved in acetone. Then potassium carbonate (1.5 eq) added to the flask and stirred for 1 hour at room temperature. After TLC analysis reaction condition determined and finalized. All solvent evaporated obtained crude washed with water and filtered. Finally recrystallized from ethanol.

N-(4-(2-bromoacetyl)phenyl)-2-((5-chlorobenzothiazol-2-yl)thio)acetamide (3)

N-(4-Acetylphenyl)-2-((5-chlorobenzothiazol-2-yl)thio)acetamide (**2,** 1 eq) dissolved in acetic acid. Reaction flask placed in ice-cold bath. Hydrogen bromide (HBr) added at catalytic amount approximately 5-6 drops. For bromination, first bromine (1.2 eq) diluted in acetic acid, then added dropwise to the reaction. After bromine addition was done, reaction checked with TLC. Reaction mixture was poured into ice-cold water, formed solid product filtered and dried.

2-((5-Chlorobenzothiazol-2-yl)thio)-N-(4-(2-(substituted)thiazol-4-yl)phenyl)acetamide (4a-4c)

N-(4-(2-Bromoacetyl)phenyl)-2-((5-chlorobenzothiazol-2-yl)thio)acetamide (**3**, 1 eq) and thiobenzamide/4-methoxythiobenzamide/thiourea (1 eq) dissolved in ethanol and stirred for 1 hour at room temperature. Reaction checked via TLC analysis. Formed final compound filtered and dried. Compounds are recrystallized from ethanol.

In Silico Studies

SwissADME and CAS BioFinder software programs calculated the physicochemical parameters of the compounds. Compounds have been launched to the program with their Smile codes. SwissADME program also provided BBB penetration rates as boiled egg illustration. The prediction of potential activity and toxicity profiles was performed using SwissTarget Prediction and Deep-PK software programs.

CONCLUSION

Novel seven benzothiazole/thiazole based compounds (**4a-4c**) were synthesized according to the procedure and structural analyses were evaluated via spectral analysis. Physicochemical, pharmacokinetic and toxicity profile of the compounds were estimated via various software. Kinase and family AG protein-coupled receptors were main targets of the most compounds results of the SwissADME prediction. More distinguished targets were predicted by BioFinder. The carbonic anhydrase enzyme was the most widely targeted compound. By validating these software programs, more accurate results can be obtained, and further research can be planned based on the data obtained. According to the results obtained, **4b** is the most promising compound to investigate for further investigations. To advance the work to the next level, it is necessary to derivatize the compounds. *In vitro* studies must be supported by molecular docking and dynamics simulation, according to the findings.

Author Information

Corresponding Author

A.Z. Kaya: https://orcid.org/0009-0002-1614-2380

Acknowledgements

We would like to thank the DOPNA-LAB of Anadolu University for their support in our study by performing spectroscopic analyses of our compounds.

I'm grateful to Prof. Dr. Leyla YURTTAŞ, Assoc. Prof. Dr. Asaf Evrim EVREN for their support and help during the study.

Declaration of interest

The author declares that they have no conflicts of interest.

REFERENCES

Bakchi, B., Krishna, A. D., Sreecharan, E., Ganesh, V. B. J., Niharika, M., Maharshi, S.,…Shaik, A. B. (2022). An overview on applications of SwissADME web tool in the design and development of anticancer, antitubercular and antimicrobial agents: A medicinal chemist's perspective. *Journal of Molecular Structure*, *1259*, 132712.

BioFinder. American Chemical Society. (2025). Retrieved 20 September, 2025 from https://biofinder.cas.org/.

Cheekatla, S. R. (2025). Benzothiazole-Based Therapeutics: FDA Insights and Clinical Advances. *Chemistry*, *7*(4), 118.

Chrienova, Z., Rysanek, D., Novak, J., Vasicova, P., Oleksak, P., Andrys, R.,…Nepovimova, E. (2023). Frentizole derivatives with mTOR inhibiting and senomorphic properties. *Biomed Pharmacother*, *167*, 115600.

Daina, A., Michielin, O., & Zoete, V. (2017). SwissADME: a free web tool to evaluate pharmacokinetics, drug-likeness and medicinal chemistry friendliness of small molecules. *Sci Rep*, *7*, 42717.

Das, J., Chen, P., Norris, D., Padmanabha, R., Lin, J., Moquin, R. V.,…Barrish, J. C. (2006). 2-aminothiazole as a novel kinase inhibitor template. Structure-activity relationship studies toward the discovery of N-(2-chloro-6-methylphenyl)-2-[[6-[4-(2-hydroxyethyl)-1- piperazinyl)]-2-methyl-4-pyrimidinyl]amino)]-1,3-thiazole-5-carboxamide (dasatinib, BMS-354825) as a potent pan-Src kinase inhibitor. *J Med Chem*, *49*(23), 6819-6832.

DeepPK. Biosig Lab. (2024). Retrieved 20 September, 2025 from https://biosig.lab.uq.edu.au/deeppk/.

Desai, N. C., Joshi, V. V., Rajpara, K. M., Vaghani, H. V., & Satodiya, H. M. (2012). Facile synthesis of novel fluorine containing pyrazole based thiazole derivatives and evaluation of antimicrobial activity. *Journal of Fluorine Chemistry*, *142*, 67-78.

Engkvist, O., Norrby, P. O., Selmi, N., Lam, Y. H., Peng, Z., Sherer, E. C.,…Smyth, L. A. (2018). Computational prediction of chemical reactions: current status and outlook. *Drug Discov Today*, *23*(6), 1203-1218.

Goh, G. B., Hodas, N. O., & Vishnu, A. (2017). Deep learning for computational chemistry. *J Comput Chem*, *38*(16), 1291-1307.

Hollingworth, D., Thomas, F., Page, D. A., Fouda, M. A., De Castro, R. L., Sula, A.,…Wallace, B. A. (2024). Structural basis for the rescue of hyperexcitable cells by the amyotrophic lateral sclerosis drug Riluzole. *Nat Commun*, *15*(1), 8426.

Irfan, A., Batool, F., Zahra Naqvi, S. A., Islam, A., Osman, S. M., Nocentini, A.,…Supuran, C. T. (2020). Benzothiazole derivatives as anticancer agents. *J Enzyme Inhib Med Chem*, *35*(1), 265-279.

Johnson, B. K., Colvin, C. J., Needle, D. B., Mba Medie, F., Champion, P. A., & Abramovitch, R. B. (2015). The Carbonic Anhydrase Inhibitor Ethoxzolamide Inhibits the Mycobacterium tuberculosis PhoPR Regulon and Esx-1 Secretion and Attenuates Virulence. *Antimicrob Agents Chemother*, *59*(8), 4436-4445.

Kaur, R., Bhardwaj, A., & Gupta, S. (2023). Cancer treatment therapies: traditional to modern approaches to combat cancers. *Mol Biol Rep*, *50*(11), 9663-9676.

Keith, J. A., Vassilev-Galindo, V., Cheng, B., Chmiela, S., Gastegger, M., Muller, K. R., & Tkatchenko, A. (2021). Combining Machine Learning and Computational Chemistry for Predictive Insights Into Chemical Systems. *Chem Rev*, *121*(16), 9816-9872.

Khurana, R., Coleman, C., Ionescu-Zanetti, C., Carter, S. A., Krishna, V., Grover, R. K.,…Singh, S. (2005). Mechanism of thioflavin T binding to amyloid fibrils. *J Struct Biol*, *151*(3), 229-238.

Luger, P., Daneck, K., Engel, W., Trummlitz, G., & Wagner, K. (1996). Structure and physicochemical properties of meloxicam, a new NSAID. *European Journal of Pharmaceutical Sciences*, *4*(3), 175-187.

Mathan, S. V., Rajput, M., & Singh, R. P. (2022). Chemotherapy and radiation therapy for cancer. 217-236.

Meltzer-Mats, E., Babai-Shani, G., Pasternak, L., Uritsky, N., Getter, T., Viskind, O.,…Gruzman, A. (2013). Synthesis and mechanism of hypoglycemic activity of benzothiazole derivatives. *J Med Chem*, *56*(13), 5335-5350.

Meşeli, T., Doğan, Ş. D., Gündüz, M. G., Kökbudak, Z., Skaro Bogojevic, S., Noonan, T.,…Nikodinovic-Runic, J. (2021). Design, synthesis, antibacterial activity evaluation and molecular modeling studies of new sulfonamides containing a sulfathiazole moiety. *New Journal of Chemistry*, *45*(18), 8166-8177.

Moczon, T., & Swiderski, Z. (1983). Schistosoma haematobium: oxidoreductase histochemistry and ultrastructure of niridazole-treated females. *Int J Parasitol*, *13*(2), 225-232.

Potewar, T. M., Ingale, S. A., & Srinivasan, K. V. (2007). Efficient synthesis of 2,4-disubstituted thiazoles using ionic liquid under ambient conditions: a practical approach towards the synthesis of Fanetizole. *Tetrahedron*, *63*(45), 11066-11069.

Radwan, I. T., Elwahy, A. H. M., Darweesh, A. F., Sharaky, M., Bagato, N., Khater, H. F., & Salem, M. E. (2022). Design, synthesis, docking study, and anticancer evaluation of novel bis-thiazole derivatives linked to benzofuran or benzothiazole moieties as PI3k inhibitors and apoptosis inducers. *Journal of Molecular Structure*, *1265*, 133454.

Rouf, A., & Tanyeli, C. (2015). Bioactive thiazole and benzothiazole derivatives. *Eur J Med Chem*, *97*, 911-927.

Samuels, E. R., & Sevrioukova, I. (2019). Structure-Activity Relationships of Rationally Designed Ritonavir Analogues: Impact of Side-Group Stereochemistry, Headgroup Spacing, and Backbone Composition on the Interaction with CYP3A4. *Biochemistry*, *58*(15), 2077-2087.

Sanad, S. M. H., Mekky, A. E. M., & Ahmed, A. A. M. (2023). Pyrazolo[5,1-b]quinazolines and Their Bis-analogues Linked to Different Spacers: Regioselective Synthesis, Antibacterial Screening and SwissADME Prediction Study. *ChemistrySelect*, *8*(22).

SwissADME. Swiss Institute of Bioinformatics. (2021). Retrieved 20 September, 2025 from https://www.swissadme.ch/index.php.

SwissTargetPrediction. Swiss Institute of Bioinformatics. (2021). Retrieved 20 September, 2025 from https://www.swisstargetprediction.ch/.

Tshiluka, N. R., Mbedzi, D. T., Bvumbi, M. V., & Mnyakeni-Moleele, S. S. (2025). In vitro alpha-Glucosidase Inhibition, Cytotoxicity, SAR, Swiss ADME Prediction and Molecular Docking Study of New N-Substituted Hydantoin Derivatives. *ChemistryOpen*, *14*(4), e202400119.

Tylicki, A., Lotowski, Z., Siemieniuk, M., & Ratkiewicz, A. (2018). Thiamine and selected thiamine antivitamins - biological activity and methods of synthesis. *Biosci Rep*, *38*(1).

Wargo, J. A., Reuben, A., Cooper, Z. A., Oh, K. S., & Sullivan, R. J. (2015). Immune Effects of Chemotherapy, Radiation, and Targeted Therapy and Opportunities for Combination With Immunotherapy. *Semin Oncol*, *42*(4), 601-616.

Yadav, K. P., Rahman, M. A., Nishad, S., Maurya, S. K., Anas, M., & Mujahid, M. (2023). Synthesis and biological activities of benzothiazole derivatives: A review. *Intelligent Pharmacy*, *1*(3), 122-132.

Yahya, S., Haider, K., Pathak, A., Choudhary, A., Hooda, P., Shafeeq, M., & Shahar Yar, M. (2022). Strategies in synthetic design and structure-activity relationship studies of novel heterocyclic scaffolds as aldose reductase-2 inhibitors. *Arch Pharm (Weinheim)*, *355*(12), e2200167.

Yurttaş, L., Evren, A. E., & Özkay, Y. (2022). Synthesis and In Silico Evaluation of Some New 2,4-Disubstituted Thiazole Derivatives. *European Journal of Life Sciences*, *1*(1), 8-19.

Zafar, A., Khatoon, S., Khan, M. J., Abu, J., & Naeem, A. (2025). Advancements and limitations in traditional anti-cancer therapies: a comprehensive review of surgery, chemotherapy, radiation therapy, and hormonal therapy. *Discov Oncol*, *16*(1), 607.

ORAL PRESENTATION

The impact of academic stress on eating behaviors, lifestyle and weight among University students.

Enkelejda Trebicka

Aldent University, Faculty of Medical Thecnical Sciences, Tirana, Albania.

Abstract

University students often experience elevated stress levels, particularly during exams and assignment deadlines, which may lead to unhealthy lifestyle habits. This study aimed to assess the relationship between perceived stress and eating behaviors among University students. A cross-sectional descriptive study was conducted among 400 students, from Aldent University of whom 85% were female and 15% male, mostly aged 18–20 years (69.5%). Data were collected through a structured online questionnaire and analyzed using descriptive statistics. Questionnaires were distributed among the students as an electronic form. They were encouraged to answer honestly. Findings revealed that 39% of students reported high stress levels. The main sources of stress were exams, tight deadlines, and academic overload. Regarding sleep, 50% reported sleeping 5–6 hours per night. Stress significantly influenced eating patterns: 59.3% experienced loss of appetite. 35.5% consumed more sweets and fast food under stress. Caffeine and energy drink consumption increased in 16.5% of respondents, while 35.3% consumed them daily. Fast food was consumed two to three times weekly by 36.5% of participants. Nearly half of the students (47.7%) reported irregular meals, and 48.5% did not engage in any physical activity. Over half (56.5%) believed that stress affects their body weight, while 38% acknowledged insufficient nutritional knowledge. Encouragingly, 61.3% expressed interest in training programs on stress management and healthy nutrition. High academic stress among university students is closely linked to irregular eating habits, reduced sleep duration, and low physical activity. Interventions focusing on stress management and nutritional education are essential to promote healthier coping behaviors and overall student well-being.

Keywords: Academic stress, eating habits, nutritional education

INTRODUCTION

University students represent a population particularly vulnerable to stress due to academic pressures, lifestyle changes, and the transition toward independent living. Academic stress, which arises from exams, tight deadlines, and heavy coursework, can significantly influence both mental and physical health outcomes. According to the **World Health Organization (WHO, 2023)**, stress-related disorders are among the most common psychological challenges affecting young adults, with direct implications for their eating behavior and general well-being.

Previous research has shown that elevated stress levels are often linked to **emotional eating, increased consumption of high-calorie or sugary foods**, and decreased physical activity. Studies conducted by **Harvard Health (2023) and Elsevier (2022)** emphasize that students under stress tend to consume more caffeine, snacks, and fast food, while neglecting balanced meals. Such behaviors not only contribute to weight changes but also to nutrient imbalances, sleep disturbances, and long-term metabolic issues. In addition, university life often introduces irregular daily routines, limited time for meal preparation, and social or emotional triggers that further alter eating patterns. Evidence from **Oxford Academic (2021)** indicates that stress-related eating habits during university years may persist into adulthood, increasing the risk of obesity, hypertension, and cardiovascular diseases.

In Albania, little is known about how academic stress affects students' dietary patterns and physical activity. This study, conducted at **Aldent University**, aims to explore the relationship between stress, eating behaviors, and perceived weight changes among students from different study programs. Understanding these associations is crucial for designing effective health promotion strategies and educational interventions targeting young adults in academic environments.

MATERIALS AND METHODS

Study design and participants

A cross-sectional descriptive study was conducted among students of Aldent University, a private higher education institution in Tirana, Albania. The research aimed to evaluate the relationship between academic stress, eating habits, and weight-related behaviors. A total of 400 students participated in the study, recruited voluntarily through an online questionnaire distributed via Google Forms. Participation was anonymous and confidential. The inclusion criteria required students to be enrolled in undergraduate health programs, including Nursing, Pharmacy, Dentistry, Physiotherapy, Laboratory Technology, and Imaging Technology.

2.2 Research instrument

Data were collected using a structured, self-administered questionnaire designed specifically for this study. The instrument consisted of four main sections:

Demographic information (gender, age, and study program),

Academic stress (frequency, intensity, and sources of stress such as exams, deadlines, and workload),

Eating habits and nutritional behaviors (meal frequency, food type preferences, caffeine and fastfood consumption, appetite changes under stress),

Physical activity and lifestyle factors (exercise frequency, sleep patterns, and self-perception of weight).The questionnaire was validated by a panel of academic experts from the Faculty of Health Sciences, and a **pilot test** was conducted with 20 students to ensure clarity and reliability. Cronbach's alpha coefficient was calculated at **0.87**, indicating good internal consistency.

Data collection procedure

Data collection took place over a two-week period in 2025. Participants completed the questionnaire electronically, requiring approximately **10–15 minutes**. Prior to participation, students were informed about the purpose of the research and provided digital consent.

Data analysis

Data were entered and analyzed using **Microsoft Excel and IBM SPSS Statistics (version 26.0)**. Descriptive statistics (frequencies, means, and percentages) were used to summarize categorical variables. **Pearson's correlation coefficient (r)** was applied to examine the relationship between stress levels and dietary behaviors, physical activity, and nutrition knowledge. Statistical significance was set at $\mathbf{p < 0.05}$.

2.5 Ethical considerations

The study was approved by the **Ethics Committee of Aldent University**. Participation was voluntary, and no personal identifying information was collected. All responses were treated with strict confidentiality and used

exclusively for academic and research purposes.

Tables and Figures

Demographic characteristics of participants

Table 1. Gender distribution of participants (N = 400)

Gender	Frequency (n)	Percentage (%)
Male	60	15.0
Female	340	85.0
Total	**400**	**100.0**

The study population was predominantly female, representing 85% of participants.

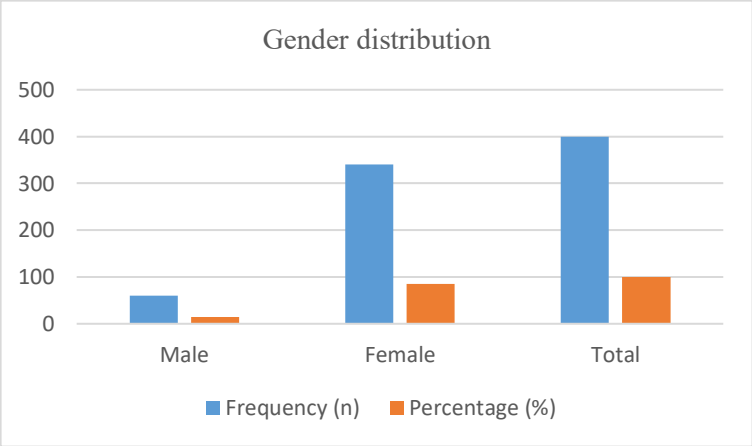


Figure.1 Gender distribution of participants.

Table 2. Age distribution of participants (N = 400)

Age group (years)	Frequency (n)	Percentage (%)
18–20	278	69.5
21–23	109	27.3
24–26	8	2.0
Above 26	5	1.2
Total	**400**	**100.0**

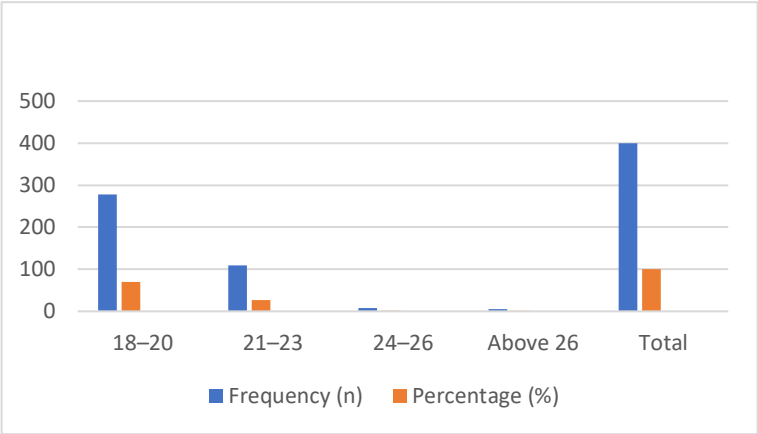


Figure 2. Age distribution of participants (N = 400)

Most respondents were aged between 18–20 years, consistent with typical undergraduate demographics.

Table 3. Distribution of students by field of study (N = 400)

Study program	Frequency (n)	Percentage (%)
Nursing	175	43.8
Pharmacy	59	14.8
Dentistry	58	14.5
Laboratory technology	51	12.8
Physiotherapy	16	4.0
Imaging technology	38	9.5
Total	**400**	**100.0**

Nursing students constituted the largest group, followed by Pharmacy and Dentistry students.

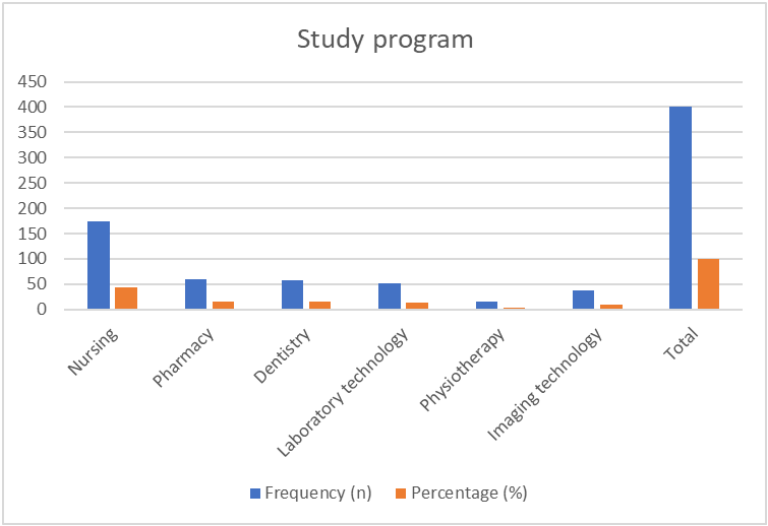


Figure 3. Distribution of students by field of study (N = 400)

Table 4. Housing status among students (N = 400

Housing status	Frequency (n)	Percentage (%)
Living with parents	172	43.0
Living independently	228	57.0
Total	**400**	**100.0**

More than half of students (57%) reported living independently. The results indicate that a slight majority of students (57%) live independently, while 43% continue to live with their parents. Living independently may influence lifestyle behaviors, including eating habits, stress levels, and time management. Students living on their own may face additional pressures related to academic workload, financial responsibilities, and household tasks, potentially contributing to less structured meal patterns and higher stress levels. Conversely, students living with parents may benefit from greater emotional, financial, and nutritional support, which can positively influence their overall well-being.

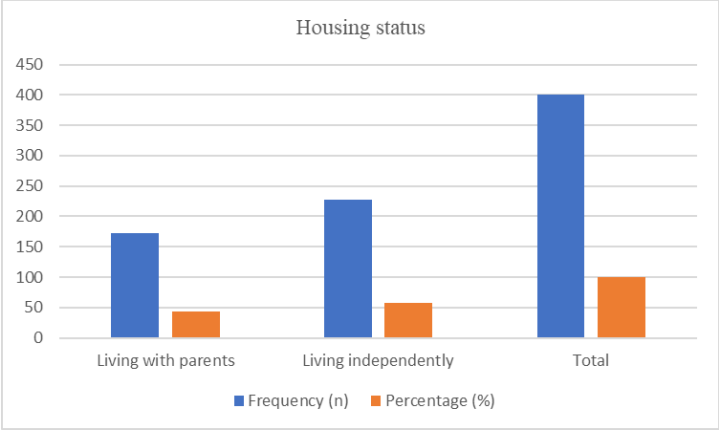


Figure 4. Housing status among students (N = 400)

Table 5. Frequency of stress during exams (N = 400)

Response	Frequency (n)	Percentage (%)
Always	158	39.5
Often	157	39.3
Sometimes	70	17.5
Rarely	10	2.5
Never	5	1.2
Total	**400**	**100.0**

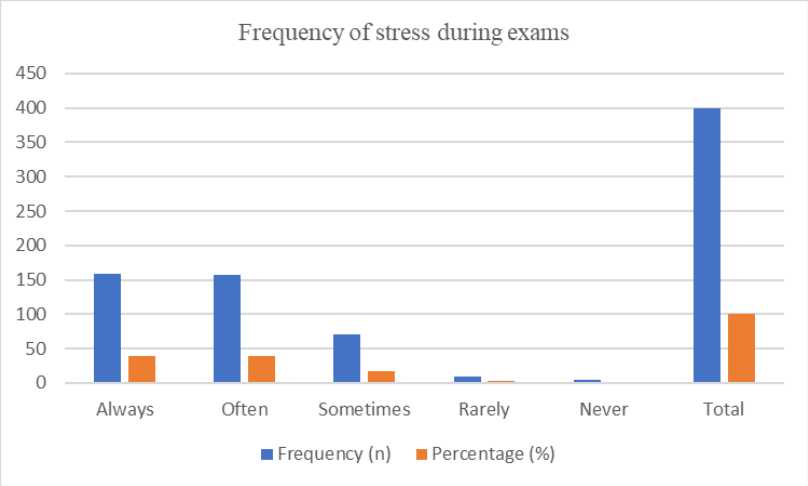


Figure 5. Frequency of stress during exams (N = 400)

The results show that stress during exams is highly prevalent among university students, with the majority reporting frequent stress. Specifically, 39.5% of students indicated that they always feel stressed during exam periods, and an additional 39.3% reported feeling stressed often. Together, this accounts for nearly 79% of the total sample, demonstrating that exam-related stress is a widespread and persistent issue.

A smaller proportion of students (17.5%) reported experiencing stress only sometimes, suggesting that while they may not experience constant pressure, exam periods still trigger significant emotional tension. Very few students reported rarely (2.5%) or never (1.2%) experiencing stress, indicating that minimal stress during exams is uncommon.

Table 6. Perceived overall level of stress during studies (N = 400)

Stress level	Frequency (n)	Percentage (%)
Very high	60	15.0
High	156	39.0
Moderate	169	42.3
Low	8	2.0
Very low	7	1.7
Total	**400**	**100.0**

A total of 81.3% of students reported moderate to high stress levels during their studies.

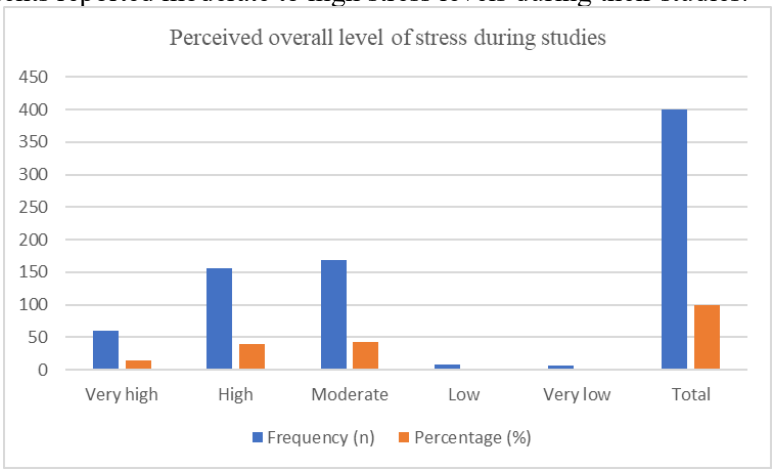


Figure. 6 Perceived overall level of stress during studies (N = 400)

Table 7. Average hours of sleep per night (N = 400)

Sleep duration	Frequency (n)	Percentage (%)
Less than 5 hours	38	9.5
5–6 hours	200	50.0
7–8 hours	152	38.0
More than 8 hours	10	2.5
Total	**400**	**100.0**

Half of the students reported sleeping only 5–6 hours per night, indicating reduced rest likely associated with academic stress.

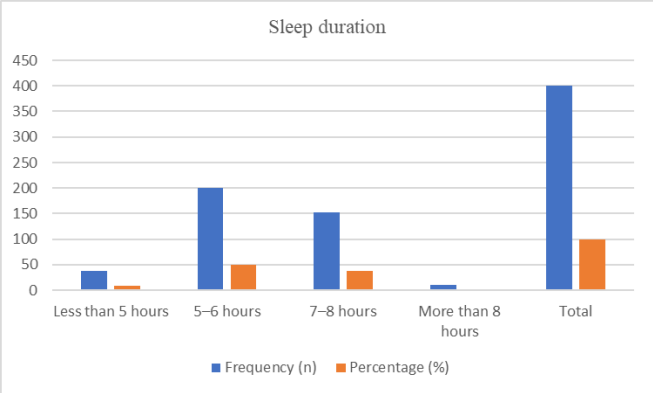


Figure 7. Average hours of sleep per night among students (N = 400)

Half of the participants (50%) reported sleeping 5–6 hours per night, which is below the commonly recommended 7–9 hours for young adults. Additionally, 9.5% sleep less than 5 hours, indicating a concerning level of sleep deprivation within a segment of the student population. Only 38% of students reported sleeping 7–8 hours, falling within the optimal range for healthy cognitive and physiological functioning. A very small proportion (2.5%) reported sleeping more than 8 hours, which may reflect individual variation or compensatory sleep patterns following periods of sleep deficit.

These findings suggest that inadequate sleep is prevalent among university students. Insufficient sleep has been widely documented in the literature as a significant contributing factor to stress, impaired concentration, decreased academic performance, emotional instability, and unhealthy eating behaviors. The high percentage of students sleeping fewer than 6 hours per night may help explain the elevated levels of stress and irregular dietary patterns observed in this study.

Eating habits under stress

Table 8. Changes in eating behavior when stressed (N = 400)

Behavioral change	Frequency (n)	Percentage (%)
Eat less than usual	92	23.0
Eat more than usual	70	17.5
Consume more sweets / fast food	53	13.3
Increase caffeine / energy drinks	66	16.5
No change	119	29.7
Total	**400**	**100.0**

The most common coping behavior under stress was eating less (23%) or consuming more caffeine and energy drinks (16.5%).

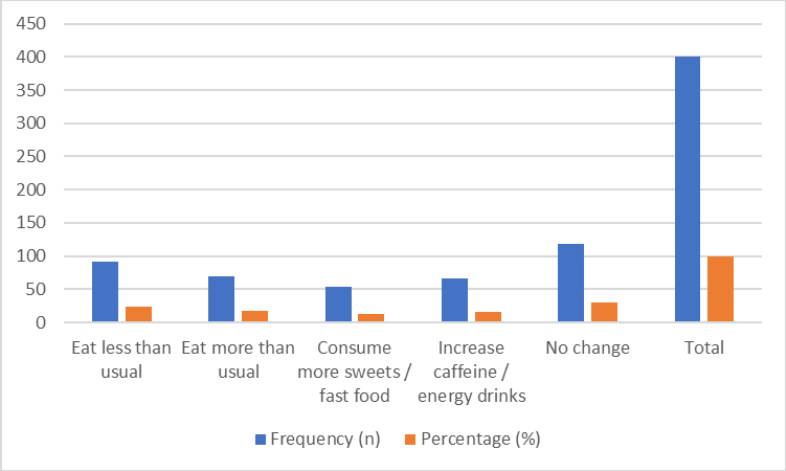


Figure 8. Stress-related changes in eating habits (N = 400)

This figure demonstrates the variations in eating habits during stressful periods. Reduced appetite and increased caffeine consumption were the most reported responses.

Table 9. Frequency of physical activity among students (N = 400)

Frequency	**Frequency (n)**	**Percentage (%)**
Daily	26	6.5
3–4 times per week	41	10.0
1–2 times per week	140	35.0
Rarely	99	24.5
Never	94	24.0
Total	**400**	**100.0**

Almost half of the participants (48.5%) reported engaging in physical activity rarely or never, reflecting sedentary tendencies.

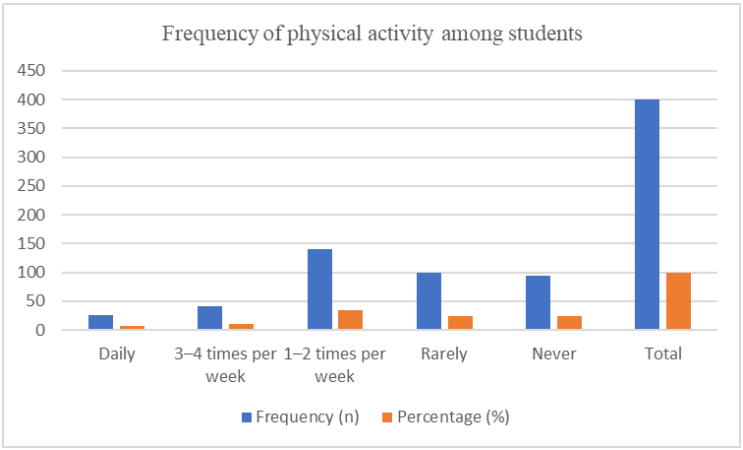


Figure 9. Frequency of physical activity among students (N = 400)

This figure illustrates the physical activity distribution. Only a small portion of students (6.5%) exercise daily.

Table 10. Students' perception of whether nutrition affects stress-coping (N = 400)

Response	Frequency (n)	Percentage (%)
Yes, it affects positively	144	36.0%
Yes, it affects negatively	108	27.0%
Not much	148	37.0%
Total	**400**	**100.0%**

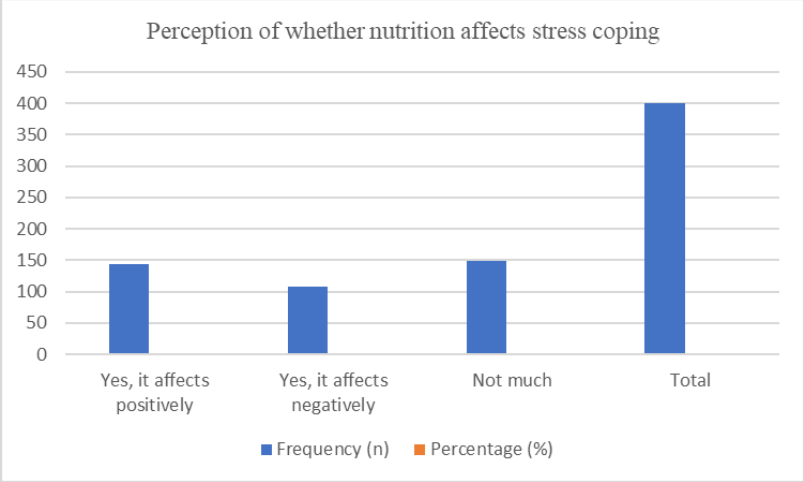


Figure.10 Students' perception of whether nutrition affects stress-coping (N = 400)

Specifically, 36% of respondents believe that nutrition has a positive impact on how they manage stress. This suggests that more than one-third of students perceive healthy eating habits as supportive in enhancing resilience, mood stability, and overall stress management.

Meanwhile, 27% of students report that nutrition affects their stress-coping ability negatively. This group may associate poor dietary patterns—such as increased consumption of fast food, sweets, or caffeine—with heightened stress levels or reduced emotional stability. This aligns with existing literature showing that unhealthy eating behaviors can exacerbate stress responses and decrease cognitive functioning. Interestingly, the largest group, 37%, stated that nutrition does not significantly influence how they cope with stress. This indicates that a substantial proportion of students may not fully understand or acknowledge the role that diet plays in psychological well-being, or they may prioritize other factors such as sleep, social support, or physical activity.

Overall, the results highlight a diversity of perceptions among students. However, the combined 63% who believe nutrition has either a positive or negative effect suggests a general awareness that dietary behaviors are intertwined with stress experiences. This underscores the importance of educational interventions that emphasize the role of nutrition in mental health and stress regulation.

Table 11. Students' Perception of Having Sufficient Information on Healthy Nutrition (N = 400)

Response	Frequency (n)	Percentage (%)
Yes	106	26.5%
No	152	38.0%
Not sure	142	35.5%
Total	**400**	**100.0%**

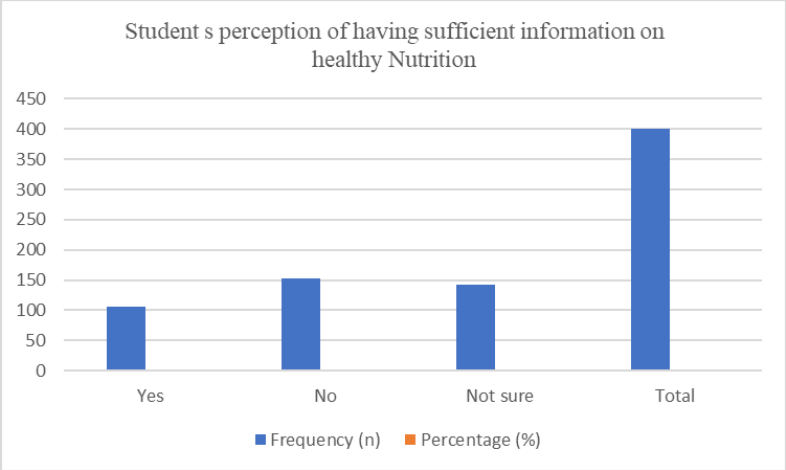


Figure 11. Students' Perception of Having Sufficient Information on Healthy Nutrition

The results indicate that a considerable proportion of students feel uncertain or uninformed about healthy nutrition. Specifically, 38% of respondents believe that students do not have sufficient information on healthy eating, making this the largest response group. This finding suggests significant gaps in nutritional knowledge among the student population. Additionally, 35.5% of students report being unsure whether they have adequate information on healthy nutrition. This high level of uncertainty highlights a lack of confidence in their nutrition-related understanding and may reflect inconsistent exposure to reliable dietary education or unclear sources of nutritional guidance.

Table 12. Interest in Seminars or Training on Stress Management and Healthy Nutrition (N = 400)

Response	**Frequency (n)**	**Percentage (%)**
Yes	245	61.3%
No	61	15.2%
Maybe	94	23.5%
Total	**400**	**100.0%**

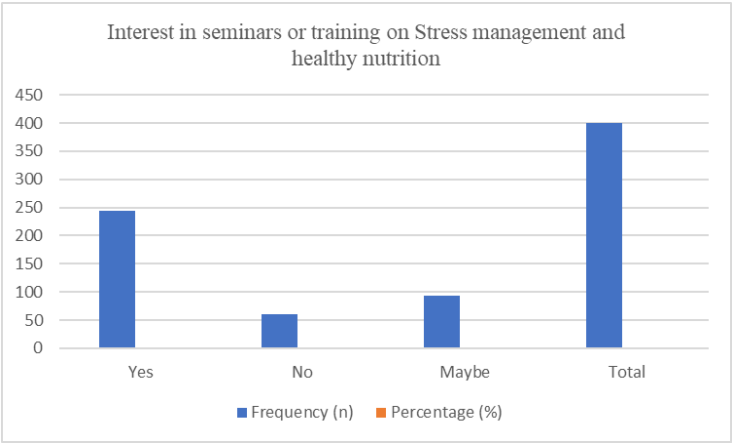


Figure 12. Interest in Seminars or Training on Stress Management and Healthy Nutrition (N = 400)

The findings show a strong level of interest among students in receiving additional education on stress management and healthy nutrition. Specifically, 61.3% of respondents indicated that they would be interested in seminars or training on these topics. This majority response suggests that students recognize the value of such educational initiatives and may be actively seeking strategies to better manage stress and improve their dietary habits.

Table 13. Students' perception of whether stress has influenced their weight (N = 400)

Response	Frequency (n)	Percentage (%)
Yes, a lot	226	56.5%
Sometimes	144	36.0%
Not at all	30	7.5%
Total	**400**	**100.0%**

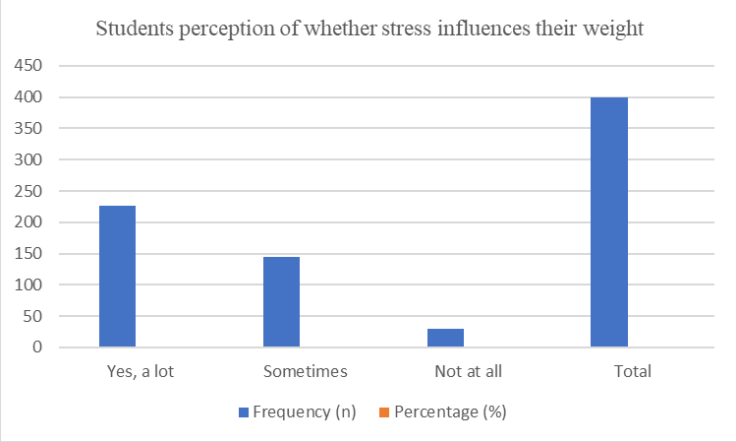


Figure 13. Students' perception of whether stress has influenced their weight

The results show that more than half of the students (56.5%) believe that stress has significantly contributed to either weight gain or weight loss. This indicates that stress is perceived as a major factor affecting body weight among university students. Another 36% reported that stress has influenced their weight sometimes, suggesting that even for students who do not consistently experience stress-related weight changes, stress still plays a noticeable role in their physical well-bein

Correlation analysis

Table 14. Correlation between stress level and selected variables (N = 400

Variables	r-value	p-value	Interpretation
Stress ↔ Fast food consumption	0.42	< 0.01	Moderate positive correlation
Stress ↔ Sweet food preference	0.36	< 0.01	Positive correlation
Stress ↔ Caffeine intake	0.33	< 0.01	Positive correlation
Stress ↔ Physical activity	–0.38	< 0.01	Moderate negative correlation
Field of study ↔ Nutrition knowledge	0.29	< 0.05	Weak positive correlation
Stress ↔ Weight change	0.41	< 0.01	Moderate positive correlation

Significant correlations were observed between higher stress levels and increased consumption of fast food, sweets, and caffeine, as well as reduced physical activity.

The correlation analysis provides important insights into the relationship between academic stress and key lifestyle behaviors among university students. First, a moderate positive correlation was found between stress level and fast-food consumption ($r = 0.42$, $p < 0.01$). This indicates that students experiencing higher stress are more likely to consume fast food more frequently. This trend aligns with well-documented evidence showing that students often rely on convenience foods when under pressure due to time constraints, emotional burden, and reduced motivation for healthy meal preparation.

Similarly, stress showed a positive correlation with sweet food preference ($r = 0.36$, $p < 0.01$). This suggests that as stress increases, students are more likely to crave or consume sugary snacks, consistent with research linking stress to emotional eating and increased preference for high-sugar, high-fat foods as short-term coping mechanisms. A positive correlation between stress and caffeine intake was also observed ($r = 0.33$, $p < 0.01$). This means that students with higher stress levels tend to consume more caffeinated beverages such as coffee and energy drinks, likely as an attempt to maintain alertness during academic overload. This behavior is frequently reported among university populations facing tight deadlines and exam-related pressure.

In contrast, stress was moderately and negatively correlated with physical activity ($r = –0.38$, $p < 0.01$). This demonstrates that students who experience higher stress levels are less likely to engage in regular exercise. High stress may reduce motivation, energy, or available time for physical activity, which could further exacerbate stress and negatively impact overall well-being.

Finally, the correlation between field of study and nutrition knowledge was weak but positive ($r = 0.29$, $p < 0.05$). This suggests that students in health-related programs (e.g., Nursing, Physiotherapy, Dentistry, Pharmacy) tend to have slightly better nutrition knowledge compared to those in non-nutrition-focused fields. However, the weakness of this correlation indicates that nutrition knowledge is not exclusively determined by program of study and may depend on personal interest, exposure to health topics, or prior education.

The correlation between stress and weight change ($r = 0.41$, $p < 0.01$) indicates a moderate positive relationship, meaning that as stress levels increase, students are more likely to experience fluctuations in weight—either weight gain or weight loss. This aligns with the descriptive data, where 56.5% of participants reported that stress affected their weight “a lot,” and another 36% said it affected their weight “sometimes.”

This positive correlation supports existing evidence that high stress disrupts eating patterns, appetite regulation, and metabolic balance, contributing to both overeating or appetite suppression depending on the individual.

Collectively, these correlations underscore a pattern where higher academic stress is associated with unhealthy eating behaviors, higher caffeine use, and reduced physical activity—factors that can further undermine mental and physical health. The findings highlight the urgent need for university-based interventions that integrate stress management, nutrition education, and physical activity promotion to support healthier coping mechanisms among students.

The scatter plot illustrates positive relationships between stress and unhealthy eating behaviors and a negative relationship between stress and physical activity.

RESULTS

The findings of this study revealed that the majority of participants were young female students, primarily enrolled in Nursing and Pharmacy programs. Most students reported experiencing frequent or constant stress during exams, with perceived stress levels categorized as moderate to high in over 80% of cases. Sleep deprivation was common, with half of the respondents sleeping only 5–6 hours per night.

Stress significantly influenced students’ eating habits: nearly one in four students ate less under stress, while others increased their consumption of fast food, sweets, and caffeine. Physical activity levels were generally low, with almost half of participants reporting no regular exercise.

Correlation analysis demonstrated a positive association between stress and unhealthy eating behaviors (fast food, sweets, and caffeine intake) and a negative correlation between stress and physical activity. Additionally, students from health-related programs exhibited higher nutrition awareness, indicating the importance of educational background in promoting healthier coping mechanisms.

Overall, these findings emphasize the need for targeted interventions within universities to reduce academic stress, promote mental well-being, and encourage balanced nutrition and physical activity among students.

DISCUSSION

The findings of this study demonstrate a significant relationship between academic stress, eating behaviors, and physical activity among university students. The high prevalence of stress reported (nearly 80% experiencing

frequent or constant stress) aligns with evidence from international studies published in **PubMed** and **Elsevier**, which indicate that academic pressure is one of the most consistent predictors of poor mental well-being among young adults (Lee et al., 2022; Shankar & Park, 2023).

Consistent with the results of the current research, studies have shown that psychological stress often triggers **emotional or compensatory eating behaviors**, leading to the consumption of **high-calorie, sugar-rich, or processed foods** (Adam & Epel, 2021; Torres & Nowson, 2022, *PubMed Central*). In this study, 36.5% of participants reported eating fast food 2–3 times per week, and 35.3% consumed caffeine daily—habits that mirror global trends among university students (Harvard Health Publishing, 2023). Such stress-induced dietary choices are associated with transient relief of anxiety but may result in metabolic dysfunction, including weight gain and sleep disturbances.

The study also identified that **stress negatively affects physical activity**, with almost half of the students (48.5%) reporting a sedentary lifestyle. This observation is supported by findings from **WHO (2023)** and **Oxford Academic (2021)**, which emphasize that chronic academic stress contributes to fatigue, low motivation, and reduced engagement in exercise, further increasing the risk of obesity and cardiovascular disorders.

An encouraging observation is that students from health-related disciplines demonstrated higher levels of nutritional knowledge ($r = 0.29$, $p < 0.05$). Similar associations were observed in research indexed on **PubMed** (Al-Rethaiaa et al., 2021; Musaiger et al., 2020), suggesting that health sciences curricula can promote awareness and preventive behaviors related to diet and stress management.

Overall, the results reinforce the growing concern that **academic stress significantly alters health-related behaviors**, increasing the likelihood of unhealthy dietary intake, irregular meal patterns, and reduced physical activity. These findings highlight the urgent need for university-based interventions focused on **mental health support, nutritional education, and lifestyle counseling**, as recommended by **WHO's Global Strategy on Health Promotion (2023)**.

CONCLUSION

This study highlights the strong relationship between academic stress and lifestyle behaviors among university students, revealing significant implications for their mental and physical health. The findings showed that 39.5% of students experienced constant stress during examinations, and an additional 39.3% frequently felt stressed. Nearly half of the participants (39%) rated their stress as high, and 15% as very high, confirming that academic stress is a widespread issue in higher education (Solomou & Constantinidou, 2023; Choi et al., 2020).

Consistent with previous evidence, students under higher stress reported poor dietary patterns and reduced physical activity (El-Zayat et al., 2025; Mitri et al., 2025). In this study, 23% reported eating less when stressed, while 17.5% consumed more food than usual, often favoring sugary and high-calorie foods. Approximately 36.5% consumed fast food two to three times per week, and 35.3% reported daily intake of caffeine or energy drinks. These results align with prior research linking academic stress to emotional or disordered eating (Adam & Epel, 2007; Caso et al., 2020; Shatwan et al., 2024). Moreover, 56.5% of respondents believed that stress directly influences their body weight, reflecting findings by Nowson and Torres (2007) on stress-related metabolic changes.

Sleep deprivation emerged as a major concern, with 50% of students sleeping only 5–6 hours per night and nearly 10% reporting fewer than 5 hours of sleep. Prior studies confirm that stress and irregular sleep significantly impair cognitive function and increase vulnerability to anxiety and depression (Huang et al., 2024; Vega-Martínez et al., 2023). Likewise, 48.5% of participants reported never engaging in physical activity, underscoring the sedentary habits typical of stressed students (Teuber et al., 2024; White et al., 2024).

Encouragingly, 61.3% of students expressed interest in educational programs focused on stress management and healthy nutrition. This suggests a readiness among young adults to adopt healthier coping mechanisms if supported institutionally. Such findings reinforce global recommendations emphasizing early preventive strategies for student mental health and lifestyle improvement (WHO, 2023; Vasconcelos et al., 2025). Additionally, many students lack sufficient knowledge about healthy nutrition, and more than half show strong interest in attending training or seminars on stress management and healthy eating. This indicates a significant educational gap and a clear opportunity for universities to develop evidence-based health promotion programs.

Overall, the findings highlight the need for targeted interventions that address both academic stress and nutritional education. Universities should consider integrating workshops, counseling services, and structured wellbeing programs aimed at fostering healthier coping strategies, improving dietary behaviors, and reducing the negative impact of stress on students' physical and mental health.

RECOMMENDATIONS

Based on the findings of this study, several recommendations can be made to support student well-being, promote healthier lifestyle behaviors, and reduce the negative effects of academic stress:

Implement university-based stress management programs

Given that more than 80% of students reported moderate to high stress levels, universities should establish structured stress management initiatives. These may include mindfulness training, time-management workshops, mental health counseling, and peer-support systems. Consistent exposure to evidence-based stress-reduction techniques can improve students' emotional resilience and academic performance.

Integrate nutrition education into university curricula

With only 26.5% of students believing they possess sufficient nutrition knowledge, there is a clear need for comprehensive dietary education. Universities should incorporate optional or mandatory modules, guest lectures, or seminars focused on healthy eating, dietary planning, and understanding stress-related eating patterns.

Promote healthier food environments on campus

Since stress was positively correlated with fast-food and sweet consumption, educational institutions should ensure the availability of affordable, nutritious food options on campus. Introducing healthier cafeteria menus, vending-machine alternatives, and awareness campaigns can help shift student choices toward balanced nutrition.

Encourage regular physical activity through accessible programs

The strong negative correlation between stress and physical activity suggests that exercise is an underused coping mechanism. Institutions should promote physical activity by offering free or low-cost gym access, organizing sports clubs, and integrating short physical-activity breaks into academic schedules.

Develop targeted interventions for high-risk groups

Students with higher stress levels and irregular eating patterns should be prioritized for early intervention. Counseling services, nutritional coaching, or personalized support programs can help them build healthier behaviors and reduce long-term health risks.

Utilize digital platforms for health promotion

Given that university students are highly engaged with technology, mobile apps, online webinars, and virtual coaching programs can effectively deliver nutrition education, stress-coping strategies, and motivational tools for healthier behaviors.

Strengthen collaboration between academic departments and student wellness offices

Interdisciplinary cooperation—between health sciences, psychology, nursing, and nutrition units—can lead to comprehensive wellness initiatives and improve the reach and effectiveness of health promotion activities.

Conduct periodic monitoring and follow-up studies

Universities should regularly assess students' stress levels and lifestyle habits to identify emerging trends and evaluate the effectiveness of interventions. Longitudinal research is recommended to explore how academic stress impacts long-term physical and mental health outcomes.

Universities should integrate structured, multidisciplinary programs that promote stress management, balanced nutrition, adequate sleep, and physical activity. Collaborative interventions involving healthcare professionals, educators, and psychologists can mitigate the adverse health impacts of chronic academic stress and foster resilience among students. Future longitudinal and intervention-based studies are recommended to further explore causal pathways between academic stress, eating behaviors, and metabolic health (Donnelly et al., 2024; Jurado-Gonzalez et al., 2025).

REFERENCES

Adam, T. C., & Epel, E. S. (2007). Stress, eating and the reward system. Physiology & Behavior, 91(4), 449–458.

AlHamlan, A. W., AlRashed, A. A., & AlOtaibi, A. A. (2025). The impact of academic stress on the lifestyle of university students in Kuwait. BMC Public Health, 25(1), 122.

Almogbel, E., Alsharif, M., & Alshehri, F. (2019). Stress associated alterations in dietary behaviours of undergraduate students. Public Health Nutrition, 22(12), 2260–2267.

Avram, C., Petrescu, L., & Popa, D. (2024). Food behavior and lifestyle among students: The influence of academic pressure. BMC Public Health, 24(1), 2413.

Bui, C., Lin, J., & Tran, H. (2021). Association between emotional eating and consumption of fast food and snacks among young adults. Appetite, 160, 105120.

Caso, G., Rossi, L., & Marino, F. (2020). Stress and unhealthy eating among undergraduate students: A cross-sectional study. Health Psychology, 39(6), 543–551.

Choi, J., Park, S. Y., & Kim, H. J. (2020). Impact of stress levels on eating behaviors among college students. Nutrients, 12(8), 2435.

Donnelly, S., O'Brien, M., & Byrne, D. (2024). Effectiveness of physical activity interventions in higher education students: A systematic review. Journal of American College Health, 72(2), 174–183.

ElBarazi, A., Al-Houqani, M., & Al Maskari, F. (2024). Association between university student junk food consumption and mental health. Public Health Nutrition, 27(3), 423–430.

El-Zayat, A., El-Gamal, S., & Hussein, N. (2025). Perceived stress and emotional eating among university students: A cross-sectional study. Journal of Affective Disorders, 358, 212–219.

Huang, Y., Li, R., & Chen, T. (2024). Effects of perceived stress on sleep quality of college students. BMC Psychology, 12(1), 88.

Jurado-Gonzalez, P., Fernández, R., & López, A. (2025). Barriers and enablers of healthy eating among university students: A mixed-methods study. Nutrients, 17(3), 512.

Kosecka, O., Nowak, J., & Michalski, M. (2025). Caffeine intake mediates the relationship between study overload and perceived stress. Nutrients, 17(2), 390.

Lee, J., Kang, E., & Song, H. (2022). Academic pressure and mental health in young adults: A systematic review. Psychiatry Research, 315, 114717.

Mitri, R., Fares, A., & El-Masri, D. (2025). Emotional eating and mental health among Lebanese university students. BMC Psychiatry, 25(1), 110.

Nowson, C. A., & Torres, S. J. (2007). Relationship between stress, eating behaviour and obesity. Nutrition Research Reviews, 20(1), 1–17.

Pe, F. A. S., & Luo, X. (2025). Positive emotional eating among college students: A narrative review. Appetite, 195, 107561.

Qin, T., Zhang, J., & Li, H. (2024). Impact of physical activity on anxiety among university students. Frontiers in Psychology, 15, 1362428.

Shatwan, I. M., Aljefree, N. M., & Almoraie, N. M. (2024). Association between perceived stress, emotional eating, and food consumption patterns among university students. Frontiers in Nutrition, 11, 1312415.

Solomou, I., & Constantinidou, F. (2023). Diet quality and stress in students: A systematic review. Nutrients, 15(3), 411.

Teuber, M., Schwarz, M., & Pohl, D. (2024). Physical activity improves stress recovery and academic outcomes: A multi-country study. BMC Public Health, 24(1), 1743.

Torres, S. J., & Nowson, C. A. (2007). Stress, diet and obesity: Mechanisms and implications for treatment. Nutrition Reviews, 65(2), 68–74.

Vasconcelos, J. D. V., Silva, L. R., & Furtado, M. (2025). Nutrition and physical activity in university populations: Review and perspectives. Sports, 13(1), 34.

Vega-Martínez, M., García, M. E., & Pérez, R. (2023). Sleep deprivation and dietary changes during exam periods: An observational study. Sleep Health, 9(4), 369–377.

White, R. L., Babic, M. J., & Parker, P. D. (2024). Physical activity and mental health: Systematic review of mediators and moderators. Frontiers in Psychology, 15, 1302310.

World Health Organization (WHO). (2023). Mental health of adolescents and young people: Global report. Geneva: World Health Organization.

ORAL PRESENTATION

Fitoterapötik bir umut: Silimarinin hayvan sağlığı üzerindeki etkilerine ilişkin klinik ve deneysel kanıtlar

Cansu Çelik[1*] (*ORCID: https://orcid.org/0000-0002-4682-4617*), Gül Fatma Yarım[2] (*ORCID: https://orcid.org/0000-0003-4050-429X*), Murat Yarım[3] (*ORCID: https://orcid.org/0000-0002-0636-4214*)

[1*]Gaziantep Üniversitesi, Araban Meslek Yüksekokulu, Veterinerlik Bölümü, Gaziantep, Türkiye
[2]Ondokuz Mayıs Üniversitesi, Veteriner Fakültesi, Biyokimya Anabilim Dalı, Samsun, Türkiye
[3]Ondokuz Mayıs Üniversitesi, Veteriner Fakültesi, Patoloji Anabilim Dalı, Samsun, Türkiye

*Sorumlu yazar e-mail: cansud@gantep.edu.tr

Özet
Silimarin, süt devedikeni (*Silybum marianum*) bitkisinin tohumlarında bulunan bir flavonolignan kompleksidir. Geleneksel tıpta uzun zamandır bitkisel bir takviye olarak kullanılmaktadır ve modern bilimsel çalışmalar da potansiyel sağlık yararlarını desteklemektedir. Bu kompleks silibin, izosilibin, silikristin ve silidianin içermektedir. Silimarin, günümüzde hem insan hem de hayvan sağlığında tamamlayıcı ve destekleyici bir tedavi seçeneği olarak bilimsel çalışmaların konusudur. Hayvan sağlığı ile ilgili deneysel ve klinik çalışmalarda, silimarinin birçok sistem üzerinde önemli faydalı etkilere sahip olduğu bildirilmiştir. Silimarin, karaciğer hücre yenilenmesini destekleyerek, inflamasyonu baskılayarak, toksinlerin hücrelere girmesini ve fibrozu önleyerek karaciğer hastalıklarında koruyucu ve tedavi edici bir destek olarak başarıyla kullanılmaktadır. Güçlü antioksidan özellikleri sayesinde silimarin, serbest radikallerin neden olduğu oksidatif hücre hasarını önleyerek çeşitli organların, özellikle de karaciğerin işlevsel bütünlüğünün korunmasında önemli bir rol oynamaktadır. Antiinflamatuar etkisi inflamasyonu azaltmaya yardımcı olmakta, bağışıklık sistemini desteklemekte ve inflamatuar hastalıklar için diğer tedavilerle birlikte kullanılmaktadır. Silimarinin deneysel modellerde insülin direncini azalttığı, diyabet gelişimini önlediği, glukoz metabolizmasını artırdığı ve diyabetle ilişkili komplikasyonları önlediği gösterilmiştir. Silimarinin nöronları oksidatif strese karşı koruduğu ve merkezi sinir sistemindeki inflamasyonu baskılayarak nörodejeneratif süreçlere karşı potansiyel nöroprotektif etkiler gösterdiği gözlemlenmiştir. Klinik ve deneysel çalışmalar silimarinin, tümör hücrelerinin çoğalmasını engellediğini göstermiştir. Silimarin metabolik bozukluklar, karaciğer hastalıkları, nörodejeneratif hastalıklar, oksidatif stres ve inflamasyon ile kanserle ilişkili birçok sağlık sorununda tamamlayıcı tedavi seçeneği olarak başarıyla kullanılmaktadır. Ancak silimarinin biyoyararlanımı, etkinliği ve güvenlik profili türler arasında değiştiğinden doz-cevap ilişkileri ve emilimi, dağılımı, metabolizması ve atılımı ile ilgili süreçler hakkında daha kapsamlı araştırmalara ihtiyaç duyulduğu düşünülmektedir.

Anahtar kelimeler: Hayvan sağlığı, fitoterapötik, silimarin.

A phytotherapeutic hope: Clinical and experimental evidence on the effects of silymarin in animal health

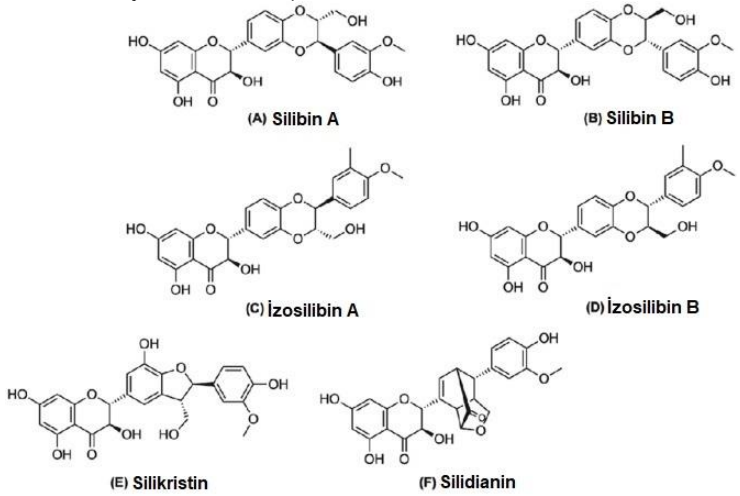
Abstract
Silymarin is a flavonolignan complex found in the seeds of the milk thistle (*Silybum marianum*) plant. Traditional medicine has long used it as an herbal supplement, and modern scientific studies also support its potential health benefits. This complex contains silybin, isosilybin, silicristin, and silidianin. Silymarin is currently the subject of scientific studies as a complementary and supportive treatment option in both human and animal health. In experimental and clinical studies related to animal health, silymarin has been reported to have significant beneficial effects on many systems. Silymarin is successfully used as a protective and therapeutic support in liver diseases by supporting liver cell regeneration, suppressing inflammation, preventing toxins from entering cells, and preventing fibrosis. Owing to its potent antioxidant properties, silymarin plays a significant role in protecting the functional integrity of various organs, particularly the liver, by preventing oxidative cell damage caused by free radicals. Its anti-inflammatory effect helps reduce inflammation, supports the immune system, and is used alongside other treatments for inflammatory diseases. Silymarin has been shown to reduce insulin resistance, prevent the development of diabetes, enhance glucose metabolism, and prevent diabetes-related complications in experimental models. Silymarin has been observed to protect neurons against oxidative stress and exhibit potential neuroprotective effects against neurodegenerative processes by suppressing inflammation in the central nervous

system. Clinical and experimental studies have shown that silymarin inhibits the proliferation of tumor cells. Silymarin has been successfully used as a complementary treatment option in many health problems associated with metabolic disorders, liver diseases, neurodegenerative diseases, oxidative stress, and inflammation, as well as in cancer. However, since the bioavailability, efficacy, and safety profile of silymarin vary between species, it is thought that more comprehensive research is needed on dose-response relationships and the processes related to its absorption, distribution, metabolism, and excretion.

Keywords: Animal health, phytotherapeutic, silymarin.

1. GİRİŞ

Silimarin, Asteraceae familyasına ait deve dikeni (*Silybum marianum*) tohumlarında ve meyvesinde bulunan silibin, izosilibin, silikristin ve silidianini içeren biyoaktif polifenolik maddeler ailesidir (Dixit ve ark., 2007; Akhtar ve ark., 2023) (Şekil 1). Bitkinin tohumlarından ve meyvelerinden elde edilen silimarin kompleksi, flavonolignanlar, flavonoidler ve polifenoller bakımından oldukça zengin olup bu kompleksin yaklaşık %50-60'ını oluşturan silibinin, diğer flavonolignan izomerleriyle birlikte yaklaşık %35'ini oluşturmakta ve silimarinin terapötik potansiyelinin temelini oluşturmaktadır (Kren ve ark., 2013; Jaffar ve ark., 2024).



Şekil 1. Silimarinin kimyasal yapı formülü (Kesharwani ve ark., 2020).

Geleneksel tıpta uzun süredir kullanılan silimarinin hepatoprotektif, antiinflamatuar, immünomodülatör, antioksidan, antiviral ve antikanser etkiler sergilediği bilimsel olarak kanıtlanmıştır (Bahmani ve ark., 2015; Surai, 2015; Zhao ve Li, 2015; Ahmad ve ark., 2018; Cui ve ark., 2018; Liu ve ark., 2019). Silimarin, oksidatif strese ve hücre hasarına yol açabilen hücresel metabolizmanın zararlı yan ürünleri olan reaktif oksijen türlerinin güçlü bir temizleyicisidir. Serbest radikalleri nötralize eden silimarin karaciğer hücrelerini oksidatif hasardan korumakta ve karaciğer fonksiyonlarını desteklemektedir (Jaffar ve ark., 2024). Silimarin, serbest radikalleri doğrudan temizlemenin yanı sıra, süperoksit dismutaz (SOD), katalaz ve glutasyon peroksidaz (GPX) gibi endojen antioksidan enzimlerin aktivitesini de artırmaktadır. Bunun yanında, hücresel faaliyetler sonucunda oluşan maddelerin detoksifiye edilmesinde görev alan hücre içi bir antioksidan olan glutasyon seviyelerini de artırmaktadır (Taleb ve ark.,2018). Silimarin, proinflamatuar gen ekspresyonuna aracılık eden bir transkripsiyon faktörü olan nükleer faktör kappa B (NF-κB) aktivasyonunu baskılayarak çeşitli inflamatuar yolları düzenlemektedir (Karimi ve ark., 2011). Silimarin proinflamatuar sitokinler olan tümör nekroz faktörü-alfa (TNF-α) ve interlökin-6 (IL-6) salınımın baskılamaktadır (Jaffar ve ark., 2024). Karaciğer fibrozu ve hücresel apoptoz süreçlerinde silimarinin hücre sağkalım yollarını desteklemek suretiyle koruyucu etkileri gözlemlenmiştir (Gillessen ve Schmidt, 2020). Klinik çalışmalar, silimarin takviyesinin karaciğer fonksiyonlarının önemli belirteci olan alanin aminotransferaz (ALT) ve aspartat aminotransferaz (AST) aktivitelerinin referans aralıkta tutulmasını sağladığını ve karaciğer fonksiyonunun desteklediğini göstermiştir (Malik ve ark., 2024).

2. SİLİMARİNİN HAYVAN SAĞLIĞI ÜZERİNDEKİ ETKİLERİNE İLİŞKİN KLİNİK VE DENEYSEL KANITLAR

2.1. SİLİMARİNİN ATLARIN SAĞLIĞINA ETKİLERİ

Silimarinin atlarda antiinflamatuar, antioksidan, hepatoprotektif ve nöroprotektif etkileri sayesinde enerji metabolizması ve genel sağlık üzerinde faydaları olduğu bildirilmiştir (Dockalova ve ark., 2021b). Atlarda silimarin biyoyararlanımının düşük olduğu, oral yolla uygulanan silibinin-fosfolipit formunun biyoyararlanımının %0,6 düzeyinde olduğu gözlemlenirken nazogastrik uygulamada %2,9'a yükseldiği rapor edilmiştir (Hackett ve ark., 2013). Silibininin, atların periferik kan mononükleer hücrelerinde (PBMC) lipopolisakkarit (LPS) kaynaklı inflamatuar yanıt üzerindeki etkisinin değerlendirildiği in vitro bir çalışmada, 10 μM ve 50 μM silibininin koruyucu etkileri olduğu ve LPS'nin neden olduğu TNF-α, IL-1β, IL-6 ve IL-8 düzeylerindeki artışı önlediği bildirilmiştir. LPS ile uyarılmış at PBMC'leri üzerinde yapılan bu çalışmanın sonucunda araştırmacılar, silibininin atlarda çeşitli inflamatuar durumların tedavisi veya önlenmesinde yararlı bir farmakolojik yaklaşım olabileceğini ifade etmişlerdir (Gugliandolo ve ark., 2020).

Atlarda sindirilebilirlik açısından en uygun silimarin dozunun 400 g/gün olabileceği belirtilirken (Dockalova ve ark., 2021a), en uygun doz ve uygulama aralığını doğrulamak için karaciğer hastalığı olan atlarda farmakokinetik ve güvenlik değerlendirmesi gerekliliği vurgulanmıştır (Hackett ve ark., 2013).

2.2. SİLİMARİNİN RUMİNANTLARIN SAĞLIĞINA ETKİLERİ

Ruminantlarda özellikle geçiş döneminde silimarinin hepatoprotektif etkilerinin ve bazı biyokimyasal parametrelerin araştırıldığı çalışmalara rastlanmaktadır (Tedesco ve ark., 2004; Garavaglia ve ark., 2015; Onmaz ve ark., 2017). Onmaz ve ark. (2017), doğum öncesi ve doğum sonrası dönemde Holstein ineklerin rasyonlarına 20 g/hayvan/gün silimarin takviyesinin laktasyonun başlangıcında süt ineklerinin metabolik adaptasyon sürecini hızlandırdığını, pik süt verimine daha erken sürede ulaşılmasını sağladığını belirlemişler ve geçiş döneminde silimarin kullanılmasını tavsiye etmişlerdir. Benzer şekilde geçiş döneminde süt ineklerine uygulanan silimarinin laktasyon performansını ve vücut kondisyonunu olumlu yönde etkilediği ortaya konulmuştur (Tedesco ve ark., 2004). Doğal bir hepatoprotektif olan silimarin, subklinik yağlı karaciğer hastalığına maruz kaldıkları peripartum döneminde süt ineklerine buzağılama tarihinden 10 gün önce buzağılama sonrası 15. güne kadar 10 g/gün dozda oral yolla uygulanmıştır. Silimarin takviyesi alan ineklerin almayanlara kıyasla süt üretiminlerinin daha yüksek olduğu belirlenmiştir (Tedesco ve ark., 2004). Doğum öncesi ve doğum sonrası erken dönemde doğal bir hepatoprotektif madde olan silimarin ile güçlü bir antioksidan olan likopenin birlikte kullanılması, süt verimini artırmış, ayrıca somatik hücre sayısı ve oksidatif stres belirteçlerinde olumlu etkiler rapor edilmiştir (Garavaglia ve ark., 2015). Sığırlarda fasioliazise bağlı gelişen karaciğer hasarında, antihelmintik tedaviye ek olarak silimarinin, hepatoprotektif etkileriyle iyileşme sürecine katkı sağladığı rapor edilmiştir (Alabbody, 2025). Ketotik süt ineklerinde yürütülmüş bir çalışmada % 2,34 silibin ve silidianin içeren süt devedikeni tohumlarının rasyona ilavesi ile kandaki aseton, asetoasetik asit ve β-hidroksibutirik asit düzeylerinde azalma, ketonüri derecesinde düşüş ve daha yüksek süt verimi gözlemlenmiştir (Vojtísek ve ark., 1991). Besi sığırlarında % 0,50 silimarin içeren rasyonla yürütülen 6 aylık bir besleme denemesi, kas kütlesi, mermerleşme puanı ve kalite derecesinde artış, düşük ALT aktivitesi ile sonuçlanmıştır. Bu bulgulara göre araştırmacılar, silimarinin etkili bir besin takviyesi olarak kullanılabileceğini ve besi dönemi sonunda sentetik bileşiklere göre daha güvenli ve tüketiciler tarafından daha kabul edilebilir bir alternatif olabileceğini ifade etmişlerdir (Kim ve ark., 2013).

Silimarin doğal bir hepatoprotektör olarak koyun ve keçi gibi küçük ruminantlarda da kullanım potansiyeli göstermektedir. Koyunlarda postpartum dönemde rasyona silimarin ilavesinin, hepatoprotektif ve antioksidan fonksiyonları yoluyla süt kalitesini iyileştirmek için etkili bir strateji olduğu ileri sürülmüştür (Khamisabadi, 2020). Sanjabi koyunlarının rasyonuna postpartum 15 gün boyunca 2000 mg/kg silimarin takviyesinin; doğum sonrası canlı ağırlık kaybını azalttığı, yem tüketimini artırdığı ve süt veriminde pik seviyeye ulaşma süresini komtrol grubuna göre anlamlı derecede kısalttığı bildirilmiştir. Buna ek olarak silimarin takviyesinin kan serumunda HSP70 geninin ekspresyonunu azalttığı; ayrıca, reaktif oksijen türleri ve malondialdehit (MDA) düzeyini kontrol grubuna göre anlamlı derecede düşürdüğü; glutasyon peroksidaz, süperoksit dismutaz ve katalaz aktivitelerini ise artırdığı rapor edilmiştir (Khamisabadi, 2020)

Günde üç kez 80 mg'lık dozda silymarin, koyunlarda gentamisin tarafından indüklenen nefrotoksisitenin patogenezini hafifletmiş, böbreği antimikrobiyal toksik etkilerden koruyan böbrek hasarı belirteçlerini azaltmıştır. Bu çalışma, silimarinin koyunlarda gentamisin kaynaklı nefrotoksisiteye karşı koruma potansiyelini göstermektedir

(Mashayekhi, 2012). Yapılan literatür taramaları, keçi rasyonlarına silimarin ilavesinin süt verimi, süt bileşimi ve süt yağ asidi profilini olumlu yönde etkilediğini göstermektedir. Dört ay süreyle yürütülen ve farklı seviyelerde silimarin açısından zengin özütlerin (10 g, 20 g veya 30 g) kullanıldığı bir besleme denemesi sonucunda, protein ve yağ konsantrasyonlarının artarak süt bileşiminin ve kalitesinin iyileştiği, süt veriminin arttığı; ayrıca doymamış yağ asitleri oranı artarken doymuş yağ asitlerinin azaldığı bildirilmiştir (Shedeed ve ark., 2023). Isı stresi altındaki Barbari keçilerinde 90 günlük periyot boyunca bazal rasyona ilave edilen 600 mg/kg/gün silimarinin oksidatif ve metabolik stresi, lipit peroksidasyonunu azalttığı ve antioksidan kapasiteyi iyileştirdiği rapor edilmiştir (Maurya ve ark., 2025). Genel olarak ruminantlarda peripartum dönemde silimarin uygulamasının, laktasyon döneminin metabolik adaptasyonunu teşvik edebileceği sonucuna varılabilir (Tedesco ve Guerrini, 2023).

2.3. SİLİMARİNİN KEDİ VE KÖPEKLERİN SAĞLIĞINA ETKİLERİ

Kedi ve köpeklerde silimarinin hepatotoksisiteye karşı koruyucu ve iyileştirici etkisi olduğu bildirilmiştir (Avizeh ve ark., 2010; Sgorlon ve ark., 2016; Gogulski ve ark., 2020; Gogulski ve ark., 2021). Hepatopatili hayvanlar için silimarin takviyesinin potansiyel bir terapötik seçenek olabileceği ifade edilmiştir (Tedesco ve Guerrini, 2023). Kedilerde mebendazol kaynaklı hepatotoksisiteye karşı silimarinin güçlü hepatoprotektif etkisi gözlemlenmiştir (Mosallanejad ve ark., 2012). Bu konuda yapılan bir çalışmada, kedilerde silimarinin özellikle mebendazol uygulamasından sonraki ilk iki saat içinde verildiğinde, oksidatif strese bağlı karaciğeri koruduğunu göstermiştir (Mosallanejad ve ark., 2012). 30 mg/kg-BW dozunda silimarinin, kedilerde asetaminofen zehirlenmesinden kaynaklanan karaciğer hasarının tedavisinde N-asetilsistein ile aynı etkiye sahip olduğu ve karaciğer dokusunu oksidatif hasara karşı koruyabileceği ileri sürülmüştür (Avizeh ve ark., 2010). Sağlıklı kedilere 5 gün boyunca oral yolla 10 mg/kg/gün silibinin-fosfatidilkolin kompleksi (SPC; %31 silibin içeren) uygulanmasının ardından granülositlerde glutasyon düzeylerinin anlamlı olarak arttığı, *Escherichia coli* ile gerçekleştirilen *in vitro* fagositoz testinde fagositik hücre oranı ve antioksidatif yanıtın uyarıldığı bildirilmiştir. Araştırmacılar, bu bulgulardan yola çıkarak silimarinin oksidatif stresle ilişkili hastalıklarda potansiyel fayda sağlayabileceğini vurgulamışlardır (Webb ve ark., 2009). Köpekler için de benzer şekilde nutrasötik uygulamalar, genel sağlık durumunun iyileştirilmesi ve bağışıklık yanıtının modülasyonu amacıyla yaygın olarak kullanılmaktadır (Sgorlon ve ark., 2016). Silimarinin, köpekler için % 50 öldürücü dozunun (LD_{50}) 140 mg/kg damar içi ve 10 g/kg ağızdan maksimum tolere edilebilir dozun ise 300 mg/kg olduğu; ayrıca embriyonik gelişim üzerinde herhangi bir etkisinin görülmediği, dolayısıyla silimarinin akut, subakut ve kronik toksisitesinin çok düşük olduğu ve güvenli bir nutrasötik olarak değerlendirilebileceği ileri sürülmektedir (Fraschini ve ark., 2002; Gogulski ve ark., 2020). Genel olarak, silibin takviyesinin, hepatopatiye sahip köpekler için etkili bir terapötik seçeneği olabileceği belirtilmiştir (Gogulski ve ark., 2020; Gogulski ve ark., 2021). Ayrıca köpeklerde sepsis tedavisinde silimarinin rutin kortikosteroid tedavisinden daha etkili olduğu bildirilmiştir (Soltanian ve ark., 2020). Köpeklerde prolipozom ile kapsüllenmiş silimarinin oral uygulanmasının, saf silimarin veya silibin uygulamasına göre daha yüksek biyoyararlanıma sahip olduğu saptanmıştır (Yan-yu ve ark., 2006). Diyetlerine günlük 10 mg/kg dozunda silimarin eklendiğinde, deneyin başlangıcında yüksek ALT aktivitelerine sahip olan köpeklerde, 60 gün sonunda bu enzim aktivitelerinde azalma gözlendiği bildirilmiştir (Sgorlon ve ark., 2016). Köpeklerde silimarin ve E vitamininin birlikte uygulanmasının, gentamisin kaynaklı nefrotoksisiteyi hafiflettiği rapor edilmiştir. Silimarinin bu koruyucu etkisinin, antioksidan aktivitesinden kaynaklandığı ifade edilmiştir (Varzi ve ark., 2007).

2.4. SİLİMARİNİN KÜMES HAYVANLARININ SAĞLIĞINA ETKİLERİ

Kümes hayvanlarında silimarin uygulamalarına yönelik araştırmalar; büyüme performansı, yemden yararlanma, bağışıklık yanıtı ve antioksidan kapasite gibi çok yönlü parametreler üzerinde olumlu etkiler gösterdiğini ortaya koymaktadır (Armanini ve ark., 2021; Shanmugam ve ark., 2022). Özellikle yumurtacı tavuklar üzerinde yürütülen çalışmalar, silimarin takviyesinin yumurta kalitesiyle ilişkili parametrelerde genel bir iyileşme sağladığını göstermektedir (Guo ve ark., 2024; Khan ve ark., 2024). Yirmi sekiz haftalık Hy-Line Brown yumurtacı tavuklarda yapılan 12 haftalık bir besleme denemesinde rasyonlarına % 0,02, % 0,04 ve % 0,06 düzeylerinde misel silmarin ilave edilmiş ve yumurta üretim yüzdesi, yumurta ağırlığı, kabuk kalınlığı, kabuk dayanıklılığı gibi kalite parametrelerinde iyileşme gözlemlenmiştir (Khan ve ark., 2024). Başka bir çalışmada, yumurtacı tavuk rasyonuna 12 hafta boyunca 250 mg/kg, 500 mg/kg, 750 mg/kg, 1000 mg/kg silimarin takviyesi ile; yumurta ağırlığı, yumurta üretim oranı, yem-yumurta verim oranı gibi performans parametrelerinde iyileşme kaydedilmiş ve bu etki, karaciğer lipit metabolizması ve çekum mikrobiyota fonksiyonunun iyileşmesiyle ilişkilendirilmiştir. Genel olarak en olumlu etkilerin, rasyona 500 mg/kg silimarin katkısıyla görüldüğü bildirilmiştir (Guo ve ark., 2024).

Ross 308 broiler civcivlerinde yürütülen bir yedirme denemesinde, % 0,06 silimarin ilavesi ile, büyüme performansı, besin sindirilebilirliği, bağırsak Lactobacillus sayısının arttığı, kan profili ve et kalitesi özelliklerinin iyileştiği anlaşılmıştır (Shanmugam ve ark., 2022). Ross broiler civcivlerinde, 0,5 ppm ve 2 ppm aflatoksine maruziyette 500 ppm ve 1000 ppm silimarin takviyesinin, ortalama günlük yem tüketiminde ve ağırlık kazancında belirgin bir artışla ve yemden yararlanma oranı değerlerinde iyileşmeyle sonuçlandığı saptanmıştır. Yüksek aflatoksin düzeyleri ileal bölgede *Escherichia coli*, *Salmonella* ve *Klebsiella* gibi bakterilerin popülasyonlarını artırırken, silimarin takviyesi bu bakteriyel yükü baskılamıştır (Jahanian ve ark., 2017). Piliç yemine silimarin eklenmesinin, mikotoksinin büyüme performansı, sağlık durumu, karaciğer oksidatif stresi ve et yağ asidi profilleri üzerindeki olumsuz etkilerini azaltıp azaltamayacağını değerlendiren bir çalışmanın bulguları, silimarinin üretim döngüsünün sonunda büyüme performansındaki bozulmayı azalttığını, oksidatif stresi önlediğini, et kalitesini iyileştirdiğini ve çoklu doymamış yağ asitleri düzeyini artırdığını göstermiştir (Armanini ve ark., 2021).
Broilerlerde kurşun kaynaklı oksidatif stres üzerine yapılan bir çalışmada, 200 mg/kg düzeyinde silimarin takviyesinin süperoksit dismutaz aktivitesini anlamlı düzeyde artırdığı, buna karşılık malondialdehit konsantrasyonu ile heterofil/lenfosit oranını azalttığı bildirilmiştir. Araştırmacılar, elde edilen bulgular doğrultusunda silimarin takviyesinin kurşunla indüklenen oksidatif strese karşı koruyucu etki gösterdiğini ve antioksidan savunma sistemini güçlendirdiğini ifade etmişleridir (Ebrahimi ve ark.,2014).

2.5. SİLİMARİNİN DENEYSEL MODELLERDE KANITLANMIŞ ETKİLERİ

Karbon tetraklorür indüklü karaciğer hasarı rat modelinde ağız yoluyla 3 hafta boyunca haftada dört kez oral olarak 200 mg/kg silimarin uygulamasının serum AST, ALT ve alkalen fosfataz (ALP) aktivitelerinin yükselmesini önemli ölçüde azalttığı ve karaciğer dokusunda alfa-düz kas aktinin değişmiş ifadelerini tersine çevirmek suretiyle hepatoprotektif etkiler sergilediği rapor edilmiştir (Tsai ve ark., 2008). Karbon tetraklorürle oluşturulan karaciğer fibrozu rat modelinde haftada beş kez oral gavajla 50 mg/kg ve 200 mg/kg dozlarında silimarin uygulamasının hepato-sitolizi, oksidatif stresi, fibrozu, hepato-sitolizi, Kupffer hücrelerinin aktivasyonunu, α-SMA ve TGF-β1 ekspresyonunu azalttığı, 50 mg/kg doz uygulamasının daha etkin olduğu saptanmıştr. Araştırmacılar, fibrotik değişikliklerin erken evrelerinde uygulanan silimarinin fibrogenetik mekanizmayı ve karaciğer fibrozisinin ilerlemesini inhibe ettiğini vurgulamışlardır (Clichici ve ark., 2015). Ratlarda iskemik reperfüzyon ile oluşturulan akut karaciğer hasarında reperfüzyondan hemen önce 5 mg/kg silibinin intravenöz uygulamasının pro-inflamatuar sitokinler TNF-α, IL-6, kemokin monosit kemotaktik protein-1 (MCP-1) ve matriks metalloproteinaz (MMP) ekspresyonunu azalttığını, aynı zamanda doku inhibitörü (TIMP-2) düzeylerini artırdığı ve bu sayede karaciğeri koruduğu rapor edilmiştir (Betsou ve ark., 2021). Farelerde yüksek yağlı diyetle tetiklenen non-alkolik yağlı karaciğer hastalığını iyileştirmek amacıyla silimarinin tek başına veya salvianolik asit B ve puerarin ile kombinasyonunun 16 hafta boyunca diyetle takviyesinin karaciğer fonksiyonlarını iyileştirdiği, bağırsak mikrobiyotasını ve metabolizmasını düzenlediği gözlemlenmiştir (Wang ve ark., 2024). Silibininin MPTP ile indüklenen Parkinson hastalığı fare modelinde, MPTP'nin neden olduğu dopaminerjik nöron kaybını etkin şekilde azalttığı, bu etkisini antioksidan veya antiinflamatuar etkilerden ziyade mitokondriyal membran potansiyelinin stabilizasyonu yoluyla nöroprotektif etki göstererek sergilediği bildirilmiştir. Araştırmacılar,
Silibininin mitokondriyi koruduğunu ve Parkinson hastalığının semptomlarının iyileştirilmesinde ve tedavilerin geliştirilmesinde silibinin potansiyel olduğunu ifade etmişlerdir (Lee ve ark., 2015). On iki hafta boyunca yüksek yağlı diyetle beslenen C57BL/6 farelere 1 ay boyunca günde 30 mg/kg oral silimarin uygulamasının hepatik SIRT1 yolunu aktive ederek diyet kaynaklı obezitede bozulmuş glukoz metabolizmasını iyileştirdiği saptanmıştır (Feng ve ark., 2021). Silimarinin, reaktif oksijen türlerinin aracılık ettiği bir deri inflamasyonu fare modelinde kulak ödemini %74'e kadar azalttığı ve histopatolojik lezyonları hafifletiği bildirilmiştir (Mota ve ark., 2025). Deneysel otoimmün ensefalomiyelit C57BL/6 fare modelinde, silimarin takviyesinin klinik semptomlarını vönemli ölçüde azalttığı, inflamasyonu hafiflettiği, demiyelinasyonu önlediği, beyin kolesterol metabolizmasında rol oynayan genlerin ekspresyonunu düzenlediği belirlenmiştir. Araştırma ekibi, silimarinin kolesterol takviyeli bir diyetle birlikte kullanımının, multipl skleroz için potansiyel koruyucu bir strateji olarak klinik çalışmalarla desteklenmesi gerekliliğini vurgulamışlardır (Mosaddeghi ve ark., 2025). Silimarinin, septik farelerde, sağkalımı belirgin şekilde iyileştirdiği, sepsis skorlarını ve dolaşımdaki proinflamatuar sitokin düzeylerini düşürdüğü ve inflamatuar hastalıklar için bir ilaç olma potansiyeli olabileceği ileri sürülmüştür (Lim ve Yi, 2025).

3. SONUÇ

Silimarin, içeriğindeki silibin başta gelmek flavonolignan kompleksi ile hayvansal organizma için önemli biyolojik etkilere sergilemektedir. Geleneksel tıpta daha çok hepatoprotektif etkilerinden yararlanılmış olan silimarin günümüzde antioksidan, antiinflamatuar, antifibrotik, immumodülatör, nefroprotektif etkinliği sayesinde önemli bir fitoterapötik konumundadır. Silimarinin terapötik etkinliği bitkisel ekstraksiyonun standardizasyonu, biyoyararlanım profili, kullanılan doz ve süreye göre değişkenlik göstermektedir. Hayvanlarda karaciğer hastalıklarının tedavisinde, mikotoksin maruziyetinin olumsuz etkilerinin giderilmesinde, metabolik bozuklukların hafifletilmesinde silimarin takviyeleri umut vaad etmektedir. Silimarin, atlarda enerji metabolizmasını regüle etmekte, geviş getiren hayvanlarda rumen fermentasyonunu desteklemekte, kümes hayvanlarında büyüme performansını artırmakta, koyun, kedi ve köpeklerde karaciğer enzim aktivitelerini normalize etmektedir. Bilimsel çalışmalar, silimarinin veteriner hekimlikte tamamlayıcı ve destekleyici tedavide önemli bir potansiyele sahip olduğuna işaret etmektedir.

KAYNAKLAR

Ahmad, U., Akhtar, J., Singh, S. P., Badruddeen, Ahmad, F. J., Siddiqui, S., & Wahajuddin. (2018). Silymarin nanoemulsion against human hepatocellular carcinoma: development and optimization. Artificial Cells, Nanomedicine, and Biotechnology, 46(2), 231-241.

Akhtar, M. N., Saeed, R., Saeed, F., Asghar, A., Ghani, S., Ateeq, H., ... & Asif Shah, M. (2023). Silymarin: a review on paving the way towards promising pharmacological agent. International Journal of Food Properties, 26(1), 2256-2272.

Alabbody HHK (2025). Silymarin and its effect on improving the health of cattle infected with liver flukes, a clinical and pathological study. International Journal of Environmental Sciences, 11(1s), 630-637.

Armanini, E. H., Boiago, M. M., Cécere, B. G. D. O., Oliveira, P. V., Teixeira, C. J., Strapazzon, J. V., ... & Da Silva, A. S. (2021). Protective effects of silymarin in broiler feed contaminated by mycotoxins: growth performance, meat antioxidant status, and fatty acid profiles. Tropical Animal Health and Production, 53(4), 442.

Avizeh, R., Najafzadeh, H., Jalali, M. R., & Shirali, S. (2010). Evaluation of prophylactic and therapeutic effects of silymarin and N-acetylcysteine in acetaminophen-induced hepatotoxicity in cats. Journal of Veterinary Pharmacology and Therapeutics, 33(1), 95-99.

Bahmani, M., Shirzad, H., Rafieian, S., & Rafieian-Kopaei, M. (2015). Silybum marianum: beyond hepatoprotection. Journal of Evidence-Based Complementary & Alternative Medicine, 20(4), 292-301.

Betsou, A., Lambropoulou, M., Georgakopoulou, A. E., Kostomitsopoulos, N., Konstandi, O., Anagnostopoulos, K., ... & Tsaroucha, A. K. (2021). The hepatoprotective effect of silibinin after hepatic ischemia/reperfusion in a rat model is confirmed by immunohistochemistry and qRT-PCR. Journal of Pharmacy and Pharmacology, 73(9), 1274-1284.

Clichici, S., Olteanu, D., Nagy, A. L., Oros, A., Filip, A., & Mircea, P. A. (2015). Silymarin inhibits the progression of fibrosis in the early stages of liver injury in CCl4-treated rats. Journal of medicinal food, 18(3), 290-298.

Cui, H., Li, T. L., Guo, H. F., Wang, J. L., Xue, P., Zhang, Y., ... & Gao, Y. J. (2018). Silymarin-mediated regulation of the cell cycle and DNA damage response exerts antitumor activity in human hepatocellular carcinoma. Oncology Letters, 15(1), 885-892.

Dixit, N., Baboota, S., Kohli, K., Ahmad, S., & Ali, J. (2007). Silymarin: A review of pharmacological aspects and bioavailability enhancement approaches. Indian Journal of Pharmacology, 39(4), 172-179.

Dockalova H, Zeman L, Baholet D, Batik A, Skalickova S, Horky P. (2021a). Dose effect of milk thistle (Silybum marianum) seed cakes on the digestibility of nutrients, flavonolignans and the individual components of the silymarin complex in horses. Animals (Basel). 11(6):1687.

Dockalova, H., Zeman, L., & Horky, P. (2021b). Influence of milk thistle (*Silybum marianum*) seed cakes on biochemical values of equine plasma subjected to physical exertion. Animals, 11(1), 210.

Ebrahimi, R., Mohammadabadi, T., Sari, M., Sallari, S., Zamiri, M. J., & Beygi, N. M. (2014). Effect of silymarin against lead induced oxidative stress in broiler chicken. Iranıan Journal of Animal Science Research, 5(4), 302-312.

Feng, B., Huang, B., Jing, Y., Shen, S., Feng, W., Wang, W., ... & Zhu, D. (2021). Silymarin ameliorates the disordered glucose metabolism of mice with diet-induced obesity by activating the hepatic SIRT1 pathway. Cellular Signalling, 84, 110023.

Fraschini, F., Demartini, G., & Esposti, D. (2002). Pharmacology of silymarin. Clinical Drug Investigation, 22(1), 51-65.

Garavaglia, L., Galletti, S., & Tedesco, D. (2015). Silymarin and lycopene administration in periparturient dairy cows: effects on milk production and oxidative status. New Zealand Veterinary Journal, 63(6), 313-318.
Gillessen, A., & Schmidt, H. H. J. (2020). Silymarin as supportive treatment in liver diseases: A narrative review. Advances in Therapy, 37(4), 1279-1301.
Gogulski, M., Ardois, M., Grabska, J., Libera, K., Szumacher-Strabel, M., Cieślak, A. D. A. M., & Strompfova, V. (2020). Dietary supplements containing silymarin as a supportive factor in the treatment of canine hepatopathies. Medycyna Weterynaryjna, 76(12), 700-708.
Gogulski, M., Cieślak, A., Grabska, J., Ardois, M., Pomorska-Mól, M., Kołodziejski, P. A., ... & Szumacher-Strabel, M. (2021). Effects of silybin supplementation on nutrient digestibility, hematological parameters, liver function indices, and liver-specific mi-RNA concentration in dogs. BMC Veterinary Research, 17(1), 228.
Gugliandolo, E., Crupi, R., Biondi, V., Licata, P., Cuzzocrea, S., & Passantino, A. (2020). Protective effect of silibinin on lipopolysaccharide-induced inflammatory responses in equine peripheral blood mononuclear cells, an in vitro study. Animals, 10(11), 2022.
Guo, Y., Xu, Y., Wang, D., Yang, S., Song, Z., Li, R., & He, X. (2024). Dietary silymarin improves performance by altering hepatic lipid metabolism and cecal microbiota function and its metabolites in late laying hens. Journal of Animal Science and Biotechnology, 15(1), 100.
Hackett, E. S., Mama, K. R., Twedt, D. C., & Gustafson, D. L. (2013). Pharmacokinetics and safety of silibinin in horses. American Journal of Veterinary Research, 74(10), 1327-1332.
Jaffar, H. M., Al-Asmari, F., Khan, F. A., Rahim, M. A., & Zongo, E. (2024). Silymarin: Unveiling its pharmacological spectrum and therapeutic potential in liver diseases—A comprehensive narrative review. Food Science & Nutrition, 12(5), 3097-3111.
Jahanian, E., Mahdavi, A. H., Asgary, S., & Jahanian, R. (2017). Effects of dietary inclusion of silymarin on performance, intestinal morphology and ileal bacterial count in aflatoxin-challenged broiler chicks. Journal of Animal Physiology and Animal Nutrition, 101(5), e43-e54.
Karimi, G., Vahabzadeh, M., Lari, P., Rashedinia, M., & Moshiri, M. (2011). "Silymarin", a promising pharmacological agent for treatment of diseases. Iranian journal of Basic Medical Sciences, 14(4), 308.
Kesharwani, S. S., Jain, V., Dey, S., Sharma, S., Mallya, P., & Kumar, V. A. (2020). An overview of advanced formulation and nanotechnology-based approaches for solubility and bioavailability enhancement of silymarin. Journal of Drug Delivery Science and Technology, 60, 102021.
Khamisabadi, H. (2020). Effects of Silymarin on milk production, liver enzymes, oxidative status and HSP70 gene expression in postparturient Sanjabi ewes. Cellular and Molecular Biology, 66(1), 76-81.
Khan, S. U., Jeon, Y. H., & Kim, I. H. (2024). Dietary inclusion of micelle silymarin enhances egg production, quality, and lowers blood cholesterol in Hy-line brown laying hens. Journal of Animal Physiology and Animal Nutrition, 108(4), 1038-1045.
Kim, D. H., Kim, K. H., Nam, I. S., Lee, S. S., Choi, C. W., Kim, W. Y., ... & Oh, Y. K. (2013). Effect of indigenous herbs on growth, blood metabolites and carcass characteristics in the late fattening period of Hanwoo steers. Asian-Australasian journal of animal sciences, 26(11), 1562.
Kren, V., Marhol, P., Purchartova, K., Gabrielova, E., & Modriansky, M. (2013). Biotransformation of silybin and its congeners. Current Drug Metabolism, 14(10), 1009-1021.
Lee, Y., Park, H. R., Chun, H. J., & Lee, J. (2015). Silibinin prevents dopaminergic neuronal loss in a mouse model of Parkinson's disease via mitochondrial stabilization. Journal of Neuroscience Research, 93(5), 755-765.
Lim, H. R., Yi, Y. S. (2025). Silymarin in *Silybum marianum* ameliorated acute lethal sepsis in mice by targeting caspase-11 noncanonical inflammasome in macrophages. Journal of Ethnopharmacology, 355(Pt B):120742.
Liu, C. H., Jassey, A., Hsu, H. Y., & Lin, L. T. (2019). Antiviral activities of silymarin and derivatives. Molecules, 24(8), 1552.
Malik, A., Malik, M., & Qureshi, S. (2024). Effects of silymarin use on liver enzymes and metabolic factors in metabolic dysfunction-associated steatotic liver disease: a systematic review and meta-analysis. Canadian Liver Journal, 7(1), 40-53.
Mashayekhi, M. (2012). Renoprotective effect of silymarin on gentamicin-induced nephropathy. Afr J Pharm Pharmacol, 6(29), 2241-2246.
Maurya, P. K., Singh, R. K., Chandra, G., Ranjan, K., Roy, D., Kumar, P., ... & Sejian, V. (2025). The effect of silymarin and selenium-yeast supplementation on antioxidant status, lipid peroxidation and metabolic hormones in heat-stressed Barbari goats. International Journal of Biometeorology, 69(9), 2313-2323.

Mosaddeghi, P., Mesbah-Namin, S. A., & Javan, M. (2025). Evaluating the Protective Effects of Silymarin Along with a Cholesterol-Supplemented Diet Against Demyelination in an EAE Mouse Model of Multiple Sclerosis: Lipidomic and Inflammatory Aspects. Molecular Neurobiology, 1-19.

Mosallanejad, B., Avizeh, R., Najafzadeh Varzi, H., & Pourmehdi, M. (2012). Evaluation of prophylactic and therapeutic effects of silymarin on mebendazole-induced hepatotoxicity in cats. Comparative Clinical Pathology, 21(5), 681-685.

Mota, J., Faria-Silva, C., Resendes, A., Santos, M. I., Carvalheiro, M. C., Lima, A., & Simões, S. (2025). Silymarin inhibits dermal gelatinolytic activity and reduces cutaneous inflammation. Natural Product Research, 39(16), 4718-4729.

Onmaz, A., Ulger, I., & Ayaşan, T. (2017). Effects of silymarin (Silybum marianum) supplementation on milk and blood parameters of dairy cattle. South African Journal of Animal Science, 47(6), 758-765.

Sgorlon, S., Stefanon, B., Sandri, M., & Colitti, M. (2016). Nutrigenomic activity of plant derived compounds in health and disease: Results of a dietary intervention study in dog. Research in Veterinary Science, 109, 142-148.

Shanmugam, S., Park, J. H., Cho, S., & Kim, I. H. (2022). Silymarin seed extract supplementation enhances the growth performance, meat quality, and nutrients digestibility, and reduces gas emission in broilers. Animal Bioscience, 35(8), 1215.

Shedeed, S. M., ElSabaawy, E. H., Mohamed, M. I., Mabrok, H. B., & Abd El-Wahab, W. M. (2023). Impact of feeding ration supplemented with silymarin-rich extract on milk quality of goat and utilization of milk in producing functional soft-cheese. Egyptian Journal of Chemistry, 66(1), 205-215.

Soltanian, A., Mosallanejad, B., Jalali, M. R., Varzi, H. N., & Ghorbanpour, M. (2020, September). Comparative evaluation of therapeutic effects of silymarin and hydrocortisone on clinical and hematological alterations, and organ injury (liver and heart) in a low-dose canine lipopolysaccharide-induced sepsis model. Veterinary Research Forum 11(3), 235-241.

Surai, P. F. (2015). Silymarin as a natural antioxidant: an overview of the current evidence and perspectives. Antioxidants, 4(1), 204-247.

Taleb, A., Ahmad, K. A., Ihsan, A. U., Qu, J., Lin, N. A., Hezam, K., ... & Qilong, D. (2018). Antioxidant effects and mechanism of silymarin in oxidative stressinduced cardiovascular diseases. Biomedicine & Pharmacotherapy, 102, 689-698.

Tedesco, D., Tava, A., Galletti, S., Tameni, M., Varisco, G., Costa, A., & Steidler, S. (2004). Effects of silymarin, a natural hepatoprotector, in periparturient dairy cows. Journal of Dairy Science, 87(7), 2239-2247.

Tedesco, D. E. A., & Guerrini, A. (2023). Use of milk thistle in farm and companion animals: a review. Planta Medica, 89(06), 584-607.

Tsai, J. H., Liu, J. Y., Wu, T. T., Ho, P. C., Huang, C. Y., Shyu, J. C., ... & Liu, Y. C. (2008). Effects of silymarin on the resolution of liver fibrosis induced by carbon tetrachloride in rats. Journal of Viral Hepatitis, 15(7), 508-514.

Varzi, H. N., Esmailzadeh, S., Morovvati, H., Avizeh, R., Shahriari, A., & Givi, M. E. (2007). Effect of silymarin and vitamin E on gentamicin-induced nephrotoxicity in dogs. Journal of Veterinary Pharmacology and Therapeutics, 30(5), 477-481.

Vojtisek, B., Hronová, B., Hamrik, J., & Janková, B. (1991). Milk thistle (Silybum marianum, L., Gaertn.) in the feed of ketotic cows. Veterinarni Medicina, 36(6), 321-330.

Wang, X., Jin, Y., & Di, C. (2024). Supplementation of silymarin alone or in combination with salvianolic acids B and puerarin regulates gut microbiota and its metabolism to improve high-fat diet-induced NAFLD in mice. Nutrients, 16 (8), 1169.

Webb, C. B., McCord, K. W., & Twedt, D. C. (2009). Assessment of oxidative stress in leukocytes and granulocyte function following oral administration of a silibinin-phosphatidylcholine complex in cats. American Journal of Veterinary Research, 70(1), 57-62.

Yan-yu, X., Yun-mei, S., Zhi-peng, C., & Qi-neng, P. (2006). Preparation of silymarin proliposome: a new way to increase oral bioavailability of silymarin in beagle dogs. International Journal of Pharmaceutics, 319(1-2), 162-168.

Zhao, F., & Li, X. (2015). Research Article Evaluation of Immunomodulatory Activity of Silymarin Extract from Silybum Marianum in Mice of Health Food. Advance Journal of Food Science and Technology, 8(4), 278-282.

ORAL PRESENTATION

QTL analysis in plum (*Prunus* spp.)

Ödül Efsane Ayçiçek[1*] (*ORCID: https://orcid.org/0009-0000-0091-6156*), Hayat Topçu[2] (*ORCID: https://orcid.org/0000-0003-3108-4393*), Behiye Banu Bilgen[2] (*ORCID: https://orcid.org/0000-0001-8323-2509*)

[*1]Tekirdağ Namık Kemal University, Faculty of Agriculture, Agricultural Biotechnology, Tekirdağ, Türkiye.
[2]Tekirdağ Namık Kemal University, Faculty of Agriculture, Agricultural Biotechnology, Tekirdağ, Türkiye.

*Corresponding author e-mail: 1228131154@nku.edu.tr

Abstract

The genus *Prunus* comprises numerous fruit species of significant economic importance worldwide, including peach, apricot, cherry, and plum. Among these, plum (*Prunus* spp.) stands out due to its cultural and economic value, with Japanese plum (*Prunus salicina*) and European plum (*Prunus domestica*) being the most widely cultivated forms. Quantitative trait locus (QTL) analysis is an important tool for elucidating the genetic basis of complexly inherited quantitative traits, and it has been applied to plum species since the 2010s. Although studies conducted to date remain limited, Japanese plum has been the most extensively investigated species in QTL mapping research. In several studies, molecular markers such as SNPs, SSRs, and EST-SSRs have been used to construct high-density linkage maps, leading to the identification of major loci associated with quality parameters including fruit ripening time, fruit weight, skin and flesh color, sugar and acid content, flesh firmness, and phenolic compounds. These findings provide a valuable basis for marker-assisted selection (MAS) and genomic breeding strategies. In contrast, QTL analyses in polyploid species such as European plum remain scarce, and their application to wild genotypes is nearly absent. In conclusion, the current state of research highlights the need for more comprehensive QTL mapping studies encompassing different species and their wild relatives in order to fully elucidate the genetic diversity of plum species.

Keywords: Molecular markers, *Prunus* spp., Plum, QTL analysis

INTRODUCTION

Within the Rosaceae family, the genus Prunus, belonging to the subfamily Prunoideae and the subgenus Prunophora, comprises approximately 200-230 species. This genus encompasses agriculturally significant stone fruit species, including peach, apricot, cherry, Japanese plum, myrobalan plum, and European plum. A substantial proportion of these species is widely cultivated worldwide due to their high nutritional value and considerable economic importance, serving both the fresh fruit market and various processing industries. Among them, plum (Prunus spp.) is particularly prominent owing to its broad genetic diversity and adaptability to diverse ecological conditions. In particular, Japanese plums (*Prunus salicina*) and European plums (*Prunus domestica*) are extensively cultivated throughout Asia, Europe, and the Americas, contributing significantly to both fresh fruit production and processed commodities such as dried plums, jams, and juices. Their capacity to thrive under a wide range of climatic and soil environments has positioned plums among the globally important fruit species in terms of production volume. Moreover, the extensive genetic resources of plum species make them a valuable asset for breeding programs, contributing strategically to the improvement of traits such as yield, fruit quality, and resistance to diseases and pests. According to FAO (2025) statistics, the global average yield of plum and sloe production was 4,763.7 kg per hectare (approximately 4.76 t/ha). The Japanese plum (*P. salicina*), which possesses a diploid chromosome complement (2n = 2x = 16), is self-incompatible and has been cultivated for nearly 4,000 years for both fruit production and ornamental purposes. In contrast, the European plum (*P. domestica* L.) exhibits marked genetic differentiation due to its hexaploid genome structure (6n = 2x = 48) (Salazar et al., 2014; Carrasco et al., 2018; Salazar et al., 2017; Okie and Hancock, 2008; Hartmann and Neumüller, 2009; Faust and Surányi, 1999; Boonprakob et al., 2011; FAO, 2023).

In recent years, molecular research has gained increasing prominence as a means to elucidate the extensive genetic diversity present in plums and to harness this variability more efficiently in breeding programs. Because

morphological and physiological traits are highly influenced by environmental conditions, classical selection approaches often fail to yield reliable, stable differentiation (Hartmann and Neumüller, 2009). Consequently, molecular markers have emerged as powerful analytical tools for assessing genetic diversity, clarifying interspecific relationships, and monitoring target traits within breeding schemes (Kumar et al., 2018; Vieira et al., 2005). Although marker-assisted selection (MAS) provides substantial advantages-particularly in improving complex traits such as yield, fruit quality, and tolerance to biotic and abiotic stresses-it is well established that these traits are typically governed by multiple genes (Salazar et al., 2020). Therefore, MAS alone is insufficient, and identifying quantitative trait loci (QTLs) is essential for deciphering the genetic architecture underlying such traits (Zhang et al., 2020; Battistoni et al., 2022).

Quantitative trait loci (QTLs) are chromosomal regions that underlie continuously varying phenotypes and are influenced by multiple genetic factors. These loci are identified through statistical associations between genotypic data (molecular markers) and phenotypic measurements of the target traits. During QTL mapping, genetic linkage maps are integrated with phenotypic datasets to identify the specific genomic regions that govern trait variation (Miles and Wayne, 2008; Kushanov et al., 2021). The most commonly employed molecular markers in QTL analyses include simple sequence repeats (SSRs) and single nucleotide polymorphisms (SNPs). SNPs can be detected with high resolution using advanced high-throughput sequencing platforms (Mammadov et al., 2012). In contrast, SSRs remain valuable due to their co-dominant inheritance, high allelic variability, and practical applicability (Kumar, 2024). Localizing QTLs on genetic linkage maps enables the precise implementation of marker-assisted selection strategies. It facilitates the identification and isolation of potential candidate genes underlying the quantitative traits of interest (Collard et al., 2005).

Molecular markers, such as SSRs and SNPs, are widely used in QTL mapping studies across Prunus species. For instance, QTLs associated with fruit quality and chilling requirement in peach have been identified using SSRs and high-density SNP arrays (Martínez-García et al., 2013). In contrast, GBS-derived SNPs and SSR markers were used to detect QTLs linked to fruit quality and postharvest traits in the F1 population derived from Japanese plum (98-99) × 'Angeleno' (Salazar et al., 2017, 2020). These investigations clarify the genetic architecture underlying traits such as fruit quality, phenology, and disease resistance, and facilitate the development of robust markers to support MAS applications (Valderrama-Soto et al., 2021). Consequently, QTL mapping not only elucidates the genetic determinants of complex traits but also enhances the precision and efficiency of MAS-based breeding strategies (Collard et al., 2005). Moreover, the notable ecological adaptability of plums and the availability of cultivars with high commercial value further underscore the importance of QTL research in this genus; such studies provide a strategic framework for improving key attributes including fruit quality, yield potential, and biotic/abiotic stress resistance (Battistoni et al., 2022; Valderrama-Soto et al., 2021).

QUANTITATIVE TRAIT LOCI (QTLs) ON PLUM

Genetic linkage maps for the Japanese plum (*P. salicina*) cultivars 'Chatard' and 'Santa Rosa' were constructed by Vieira et al. (2005) using a pseudo-testcross strategy and AFLP markers. The mapping population consisted of 88 individuals derived from a cross between these two cultivars. They differ in several ways, including how easily they develop plum leaf blight. The linkage map generated for the 'Chatard' cultivar comprised 56 markers distributed across 11 linkage groups, spanning a total length of 905.5 cM with an average intermarker distance of 16.2 cM. In contrast, the 'Santa Rosa' map contained 84 markers across 14 linkage groups, covering 1349.6 cM with a mean intermarker interval of 16.1 cM. The authors emphasized that these maps represent a foundational framework for genetic and breeding studies in Japanese plum; however, they also noted that further marker enrichment is needed to improve their resolution and applicability for broader breeding objectives.

Milošević and Milošević (2011) established a trial orchard in Prislonica in 2000, planting seven F_1 genotypes and control cultivars derived from three hybrid combinations of *P. domestica* L. ('Čačanska Lepotica' × 'Stanley', 'Čačanska Najbolja' × 'Stanley', and 'Stanley' × 'Stanley'). Biological and fruit quality traits were assessed between 2005 and 2007. The results revealed substantial variation among genotypes. All F_1 progenies exhibited later flowering times compared with their parental cultivars; the earliest harvest occurred in genotype 'P4,' whereas genotype 'P7' reached maturity the latest. The highest yield was recorded in genotype 'P5,' while genotype 'P4' was superior in fruit weight, flesh proportion, fruit size, soluble solids, fructose content, and total sugar levels.

Overall, the authors reported that the cross 'Čačanska Lepotica' × 'Stanley' produced the most biologically and qualitatively promising genotypes.

Salazar et al. (2017) conducted a genotyping-by-sequencing (GBS) study based on SNP markers to identify QTLs associated with fruit quality in Japanese plum. The primary objective of the study was to improve the implementation of marker-assisted selection (MAS) for complex fruit-quality traits under the influence of numerous genes. For this purpose, 272 seedlings derived from crosses involving the cultivars 'Angeleno,' 'September King,' and 'September Queen,' using '98-99' as the female parent, were genotyped, resulting in the detection of 42,909 SNPs. In addition, a high-resolution genetic linkage map containing 981 SNPs was constructed for the '98-99' × 'Angeleno' population. Across two consecutive years, 55 seedlings were phenotypically evaluated for fruit-quality parameters, including fruit weight, skin and flesh color, firmness, soluble solids content, and ripening time. QTL analysis revealed several genomic regions associated with these traits. The findings demonstrated that GBS is a highly effective approach for identifying genetic variants underlying fruit-quality traits in Japanese plum and holds considerable promise for integration into MAS-oriented breeding programs.

Zhang et al. (2020) constructed a high-density genetic linkage map using Specific-Locus Amplified Fragment (SLAF) sequencing technology in an F_1 population derived from the Japanese plum cross '09-16' × 'Fortune'. The resulting map comprised 3,341 SLAF markers and 720 loci distributed across eight linkage groups, spanning a total genetic distance of 869.9 cM with an average inter-marker interval of 1.21 cM. The map showed strong collinearity with the peach (*Prunus persica*) reference genome. The authors noted that this work represents one of the most comprehensive linkage maps developed for Japanese plum to date and provides a valuable foundation for both marker-assisted selection (MAS) and future reference genome assembly studies.

Salazar et al. (2020) developed a genetic linkage map integrating SNP and SSR markers using 151 individuals derived from the '98-99' × 'Angeleno' F1 population and evaluated phenological, fruit quality, and postharvest traits over three years. QTL analyses demonstrated that fruit development duration was strongly associated with loci on LG4, whereas fruit weight was predominantly associated with regions on LG2. Although the QTLs detected for postharvest characteristics exhibited comparatively lower statistical significance, minor-effect QTLs influencing fruit firmness were consistently identified on LG4 and LG5. The authors emphasized that these results provide important insights into the genetic regulation of fruit development, quality, and postharvest performance in Japanese plum, and that they represent a valuable resource for advancing marker-assisted breeding strategies in this species.

Valderrama-Soto et al. (2021) employed the same F1 population ("98-99" × "Angeleno") used in previous studies to characterize quantitative trait loci (QTLs) governing phenolic compound accumulation in both the fruit peel and flesh. Phenotypic data collected over two consecutive years were integrated with high-resolution genetic linkage maps, resulting in the identification of 21 QTLs-13 contributed by the "98-99" parent and eight by "Angeleno." These loci accounted for 12-27% of the observed phenotypic variation and were predominantly associated with cyanidin-3-glucoside and cyanidin-3-rutinoside (LG4), total flavonoids and procyanidins (LG5, LG8), and reduced concentrations of certain anthocyanin compounds (LG3, LG4). The authors emphasized that these findings provide a robust foundation for improving the precision and efficiency of marker-assisted breeding strategies to develop new plum cultivars with elevated phenolic compound content.

Almansa et al. (2021) examined the inheritance patterns and interrelationships of 15 agronomic traits-including phenological characteristics (onset of flowering, full bloom time, flowering intensity, and ripening date) and pomological attributes (yield, fruit weight, diameter, shape, skin and flesh coloration, firmness, soluble solids, and acidity)-in Japanese plum (*P. salicina* Lindl.) across two years and three distinct hybrid populations. The results demonstrated substantial phenotypic variation and pronounced segregation, particularly within the 'Black Splendor' × 'Pioneer' progeny. The distribution patterns for skin and flesh color indicated that a limited number of significant genes likely govern these traits. In contrast, the near-normal distribution observed for the remaining characteristics suggested polygenic control influenced by multiple loci. Moreover, strong correlations were detected among several phenological and fruit-quality traits. The authors emphasized that these findings markedly enhance the efficiency of Japanese plum breeding programs and provide a robust foundation for future QTL mapping and marker-assisted selection initiatives.

Battistoni et al. (2022) examined the genetic regulation of flavan-3-ol compounds in Japanese plum by evaluating the '98-99' × 'Angeleno' F1 population across two growing seasons. The concentrations of these compounds in both peel and flesh were quantified and integrated with linkage maps constructed using the reference genome of *P. salicina* cv. 'Sanyueli'. The analyses revealed that QTL clusters governing flavan-3-ol composition-particularly in individuals inheriting alleles from 'Angeleno'-accounted for much of the variation in the catechin/epicatechin (C/EC) ratio. Moreover, a novel major genomic region on LG1 was identified as a key determinant directing the biosynthesis toward either catechin or epicatechin. This study provides valuable insights into the metabolic pathways underlying fruit quality and nutritionally important traits; however, the authors highlight that further validation across diverse genotypes and incorporation into breeding programs are essential for practical application.

The study conducted by Lili et al. (2022) sought to construct a genetic linkage map for Japanese plum (*P. salicina* L.) using ISSR and SRAP molecular markers. To support the development of new cultivars of this economically significant species in northeastern China, the cultivars 'Jilin 6' and 'Longyuan Qiuli' were selected as parental lines, and the authenticity of the resulting F1 progeny was verified using SSR primers. Marker data derived from ISSR and SRAP analyses were subsequently processed with JoinMap 4.0 employing the double-pseudotestcross strategy. The study identified 120 marker loci from 72 validated F1 individuals, ultimately generating a genetic map comprising 16 linkage groups with a total length of 528.5 cM. The authors emphasized that this linkage map provides a valuable framework for QTL detection, marker-assisted selection, and gene mapping in plums and represents an important foundational resource for breeding programs in cold-climate regions.

Lili et al. (2023) conducted genetic mapping studies on six fruit-related traits-including fruit weight, transverse and longitudinal diameters, shape index, flesh thickness, and total sugar content-using F1 populations derived from the Japanese plum cultivars Jilin 6 and Longyuanqiuli grown in northeastern China. The analyses revealed strong positive correlations between fruit weight and both diameter measurements, whereas total sugar content exhibited a negative correlation with the remaining traits. QTL mapping identified 11 loci distributed across linkage groups LG2, LG3, LG8, and LG15, explaining approximately 10-14% of the phenotypic variation. The researchers emphasized that these findings provide a valuable scientific foundation for implementing molecular-assisted breeding strategies in plum, particularly for programs targeting cultivar improvement in cold-climate regions.

Osorio et al. (2025) established a core collection to more effectively harness the genetic diversity of Japanese plums and facilitate the identification of quantitative trait loci (QTLs). In their study, a large population of 1,062 individuals, genetically characterized through sequencing data, was evaluated, and several core collection alternatives were generated based on genetic distance metrics and allelic representation. Comparative assessments led to the selection of a set of 108 individuals that maintained the highest level of genetic diversity while accurately reflecting the overall population structure. The robustness of this selection was validated through linkage disequilibrium and population structure analyses. Moreover, the practical utility of the core collection was demonstrated by the successful mapping of QTLs for flowering time and fruit ripening. The authors emphasized that this core collection constitutes a valuable resource not only for elucidating phenological traits but also for improving the understanding of fruit quality attributes and plant responses to biotic and abiotic stresses, thereby providing a strong foundation for marker-assisted breeding programs.

CONCLUSION

QTL-based genetic improvement studies in plums remain relatively scarce, with most existing research concentrated on Japanese plum (*P. salicina*). Several major factors underlying this limitation have been highlighted in the literature. Foremost, QTL mapping resolution in Prunus species has generally been constrained by the small size of mapping populations; many studies do not meet the recommended range of 50-250 individuals, and such limited populations tend to detect only large-effect QTLs. Moreover, the diploid genome structure of Japanese plum, its amenability to controlled hybridization, and the availability of broad genetic resources make this species particularly well-suited for QTL analyses. The existence of a high-quality reference genome for Japanese plum ('Sanyueli') has further facilitated GBS-based SNP discovery and the development of high-density linkage maps, thereby accelerating QTL research in this species. In contrast, the absence of fully assembled and annotated reference genomes for other plum species substantially impedes progress in their QTL mapping studies. Finally, the high commercial relevance of Japanese plum cultivars and their adaptability across diverse ecological regions

have increased scientific and economic interest in this species, resulting in a disproportionate focus on *P. salicina* within QTL research efforts.

Consequently, the scarcity of QTL studies in plums can largely be attributed to constraints related to mapping population size, limited genomic resources, and species-specific genetic advantages. To overcome these limitations, future QTL research should be expanded to encompass additional species such as the European plum (*P. domestica*), *Prunus cerasifera*, and wild taxa, including *Prunus spinosa*. The development of high-quality reference genomes, the use of larger and genetically diverse populations, and the application of multi-population high-resolution analyses are essential. Such efforts will enable the field to transcend the current knowledge base, which is predominantly centered on Japanese plum, and will generate novel insights from a broader spectrum of plum species. Ultimately, this comprehensive approach will enhance the effectiveness of breeding programs and substantially bridge the existing knowledge gap in plum genomics.

REFERENCES

Almansa, M. N., Salazar, J. A., Rubio, M., Guevara, A., Carrillo, A., & Ruiz, D. (2021). Inheritance and correlation of main phenological and pomological traits in Japanese plum (Prunus salicina Lindl.). Acta Horticulturae, 1322(9), 61-68.

Battistoni, B., Salazar, J., Vega, W., Valderrama-Soto, D., Jiménez-Muñoz, P., Sepúlveda-González, A., ..., & Pacheco, I. (2022). An upgraded, highly saturated linkage map of Japanese plum (Prunus salicina Lindl.), and identification of a new major locus controlling the flavan-3-ol composition in fruits. Frontiers in Plant Science, 13, 805744.

Boonprakob, U., Byrne, D. H., & Ramming, D. W. (2011). Genetic improvement of Japanese plum for adaptation, fruit quality, and disease resistance. Acta Horticulturae, 901, 95-100.

Carrasco, B., González, M., Gebauer, M., García-González, R., Maldonado, J., & Silva, H. (2018). Construction of a highly saturated linkage map in Japanese plum (Prunus salicina L.) using GBS for SNP marker calling. PloS one, 13(12), e0208032.

Collard, B. C. Y., Jahufer, M. Z. Z., Brouwer, J. B., & Pang, E. C. K. (2005). An introduction to markers, quantitative trait loci (QTL) mapping and marker-assisted selection for crop improvement: The basic concepts. Euphytica, 142(1-2), 169-196.

Decroocq, V., Hagen, L. S., Favery, B., Eyquard, J. P., Barres, B., Renaud, C., ..., & Dondini, L. (2014). The determinant of resistance to Plum pox virus (PPV) in apricot (Prunus armeniaca L.) is located within a major QTL (PPVres) on linkage group 1. Molecular Breeding, 34, 691-705.

FAO. (2025). Production/Yield quantities of Plums and sloes, World, Yield, 2023. FAOSTAT.

Faust, M., & Surányi, D. (1999). Origin and dissemination of plums. Horticultural Reviews, 23, 179-231.

Hartmann, W., & Neumüller, M. (2009). Plum breeding. In M. L. Badenes and D. H. Byrne (Eds.), Fruit Breeding (pp. 161-231). Springer.

Kumar, S., Bink, M. C. A. M., Volz, R. K., Bus, V. G. M., & Chagné, D. (2018). Towards genomic selection in apple (Malus × domestica Borkh.) breeding programmes: Prospects, challenges and strategies. Tree Genetics & Genomes, 8, 1-14.

Kushanov, F. N., Turaev, O. S., Ernazarova, D. K., Gapparov, B. M., Oripova, B. B., Kudratova, M. K., ..., & Abdurakhmonov, I. Y. (2021). Genetic diversity, QTL mapping, and marker-assisted selection technology in cotton (Gossypium spp.). Frontiers in plant science, 12, 779386.

Lili, S. U. N., Lina, P. E. N. G., Yunhui, M. U., & Wanjun, Y. E. (2023). Correlation analysis and primary QTL mapping of fruit traits in plum. Guangdong nongye kexue, 50(5), 39-45.

Lili, S. U. N., Lina, P. E. N. G., Zheng, L. I., Ruining, H. O. U., & Yunhui, M. O. U. (2022). Construction of genetic linkage map of plum (Prunus salicina L.) with ISSR and SRAP markers. Guangdong nongye kexue, 49(3), 40-48.

Martínez-García, P. J., Parfitt, D. E., Becerra, V., & Arús, P. (2013). Genetic and QTL analysis of phenology and fruit quality traits in peach (Prunus persica L. Batsch). Tree Genetics & Genomes, 9, 541-555.

Miles, C. M., & Wayne, M. L. (2008). Quantitative trait locus (QTL) analysis. Nature Education, 1(1), 208.

Milošević, T. and Milošević, N. (2011). Quantitative analysis of the main biological and fruit quality traits of F1 plum genotypes (Prunus domestica L.). Acta Scientiarum Polonorum Hortorum Cultus, 10(2), 95-107.

Okie, W. R., & Hancock, J. F. (2008). Plums. In J. F. Hancock (Ed.), Temperate fruit crop breeding (pp. 337-357). Springer.

Osorio, M., Ahumada, S., Infante, R., Pacheco, I., Fiol, A., & Ballesta, P. (2025). A Japanese plum breeding core collection capturing and exploiting genetic variation. Agriculture, 15(13), 1369.

Salazar, J. A., Pacheco, I., Shinya, P., Zapata, P., Silva, C., Aradhya, M., ..., & Infante, R. (2017). Genotyping by sequencing for SNP-based linkage analysis and identification of QTLs linked to fruit quality traits in Japanese plum (Prunus salicina Lindl.). Frontiers in Plant Science, 8, 476.

Salazar, J. A., Pacheco, I., Zapata, P., Shinya, P., Ruiz, D., Martínez-Gómez, P., & Infante, R. (2020). Identification of loci controlling phenology, fruit quality and post-harvest quantitative parameters in Japanese plum (Prunus salicina Lindl.). Postharvest Biology and Technology, 169, 111292.

Salazar, J. A., Ruiz, D., Campoy, J. A., Sánchez-Pérez, R., Crisosto, C. H., Martínez-García, P. J., ..., & Rubio, M. (2014). Quantitative trait loci (QTL) and Mendelian trait loci (MTL) analysis in Prunus: a breeding perspective and beyond. Plant Molecular Biology Reporter, 32(1), 1-18.

Salazar, J. A., Ruiz, D., Tartarini, S., Dondini, L., Arús, P., Cipriani, G., & Rubio, M. (2020). Genotyping by sequencing for SNP-based linkage analysis and identification of QTLs linked to fruit quality traits in Japanese plum (Prunus salicina Lindl.). Frontiers in Plant Science, 11, 955.

Valderrama-Soto, D., Salazar, J., Sepúlveda-González, A., Silva-Andrade, C., Gardana, C., Morales, H., ..., & Pacheco, I. (2021). Detection of quantitative trait loci controlling the content of phenolic compounds in an Asian plum (Prunus salicina L.) F1 population. Frontiers in Plant Science, 12, 679059.

Vieira, E. A., Nodari, R. O., de Mesquita Dantas, A. C., Ducroquet, J. P. H. J., Dalbó, M., & Borges, C. V. (2005). Genetic mapping of Japanese plum. Crop Breeding and Applied Biotechnology, 5(1), 29-37.

Zhang, Q. P., Wei, X., Liu, N., Zhang, Y. P., Xu, M., Zhang, Y. J., ..., & Liu, W. S. (2020). Construction of an SNP-based high-density genetic map for Japanese plum in a Chinese population using specific length fragment sequencing. Tree Genetics & Genomes, 16(1), 18.

ORAL PRESENTATION

Abiotic stress factors and molecular approaches in grapevine

Seçil Ayaz[1*] (*ORCID: https://orcid.org/0009-0000-0759-6730*), Hayat Topçu[2] (*ORCID: https://orcid.org/0000-0003-3108-4393*), Behiye Banu Bilgen[2] (*ORCID: https://orcid.org/0000-0001-8323-2509*)

[*1]Tekirdağ Namık Kemal University, Faculty of Agriculture, Agricultural Biotechnology, Tekirdağ, Türkiye.
[2]Tekirdağ Namık Kemal University, Faculty of Agriculture, Agricultural Biotechnology, Tekirdağ, Türkiye.

*Corresponding author e-mail: secilayz@gmail.com

Abstract

Among berry-like fruits, grapevine (*Vitis vinifera* L.) is one of the leading species both worldwide and Turkey in terms of production volume and economic value. However, viticulture is increasingly affected by abiotic stress factors such as drought, high temperature, salinity and frost, which are exacerbated by climate change. These conditions significantly limit plant growth and lead to considerable reductions in yield and fruit quality. In particular, cluster and berry development, as well as quality parameters such as sugar, acidity, and aroma compounds, are directly influenced by these stresses. In recent years, molecular-level studies have come to the forefront in order to better understand the effects of these stress factors on grapevine. Research conducted in Turkey has mainly focused on cultivar identification through molecular markers, with special emphasis on resolving homonym and synonym confusions. Moreover, the identification of genomic regions associated with tolerance to abiotic stresses and their examination through linkage analyses has also emerged as an important research area. The combined use of different marker systems provides a more comprehensive evaluation of genetic diversity in grapevine and contributes to a deeper understanding of stress tolerance. In conclusion, the molecular investigation of abiotic stress factors in grapevine represents a strategic field of research for both the development of stress-tolerant cultivars and the sustainability of viticulture.

Keywords: Abiotic stress, Grape (*Vitis vinifera* L.), Molecular characterization, Viticulture

INTRODUCTION

Fruits constitute a critical component of human nutrition, serving as rich sources of vitamins, minerals, and antioxidant compounds. Nevertheless, the growth and productivity of fruit crops are highly dependent on prevailing environmental conditions. Climate change–associated factors such as elevated temperatures, water scarcity, and soil salinity adversely affect both yield and fruit quality. Grapevines (*Vitis vinifera* L.) are particularly vulnerable to extended periods of heat stress, drought, and salinization, all of which impair vegetative development, berry enlargement, and overall fruit quality (Ren et al., 2025).

Stress in plants arises from both biotic (viruses, bacteria, fungi, insects) and abiotic factors (drought, salinity, extreme temperatures, waterlogging, radiation, chemical exposure, and nutrient deficiencies), all of which can cause substantial reductions in yield (Odabaşıoğlu et al., 2018). In recent years, the impact of global warming on agricultural productivity has intensified, making it increasingly critical to increase yields from the limited arable land available. Consequently, there has been a growing emphasis on breeding and selecting cultivars and rootstocks that can adapt to adverse abiotic stress conditions. (Küskü and Söylemezoğlu, 2022).

Turkey possesses a long-standing viticultural tradition and harbors extensive grapevine genetic diversity owing to its favorable climatic conditions and its position at the crossroads of major Vitis gene centers. However, global warming, natural disasters, unplanned urban expansion, and biotic stresses such as phylloxera have reduced vineyard areas, thereby heightening the risk of losing uncharacterized or unprotected genetic resources. Safeguarding this genetic diversity is essential for ensuring food security and for enabling the development of stress-resilient cultivars. Moreover, because most current conservation initiatives focus on only a limited subset of

species, integrating wild relatives into the genetic pool is crucial for sustaining long-term breeding and conservation success (Baykul, 2022; Marwah and Jamwal, 2024).

In viticultural research conducted in Turkey, molecular marker technologies have thus far been employed predominantly for genotype identification. However, the persistent confusion caused by the use of homonyms and synonyms in grapevine cultivars necessitates further clarification, and studies focusing on stress tolerance must be broadened. Employing multiple marker systems in combination can yield more comprehensive and robust results (Sabır et al., 2008; Bozkuş and Bozkuş, 2024). The rich diversity of cultivated varieties and wild grapevine genotypes present in Turkey provides valuable genetic resources for introgressing resistance traits into commercial cultivars, thereby supporting the development of new grape varieties capable of withstanding environmental stresses while also meeting market expectations (Arslan, 2023).

In this context, the conservation of grapevine genetic resources and the elucidation of molecular-level stress-tolerance mechanisms are critical for ensuring the long-term sustainability of viticulture and facilitating the development of novel cultivars that can adapt to changing climatic conditions.

Grape (*Vitis Vinifera* L.)

Grapevines belong to the order Rhamnales, and among the three families represented within this order, only the Vitaceae (also referred to as Vitidaceae, Ampelidaceae, or Ampelidae) include true grapevine species. This family comprises approximately 12 genera and 700 species, with the genus Vitis being the most prominent (Şahin, 2009). The genus Vitis contains nearly 60 species, among which *Vitis vinifera* L. is the most extensively cultivated due to its broad climatic adaptability. Nevertheless, the high sensitivity of this species to various stress factors has underscored the importance of wild grapevine relatives as valuable reservoirs of adaptive genetic variation. North American species such as *Vitis riparia, Vitis rupestris*, and *Vitis berlandieri* are widely employed in the development of rootstocks with enhanced resistance to abiotic stresses. Traditional grapevine breeding predominantly relies on hybridization and subsequent selection; however, the inherently long juvenile phase of grapevines significantly prolongs the breeding cycle (Bozkuş and Bozkuş, 2024).

Turkey has a long-standing tradition of viticulture owing to its favorable climatic conditions, its position within the grapevine gene centers, and its location at the crossroads of ancient trade routes (Baykul, 2022). This placement at the intersection of grapevine gene pools has endowed the country with vibrant grape genetic diversity. To conserve and evaluate this diversity, the National Collection Vineyard Project was initiated in 1965 (Candar et al., 2020). Grapes (*Vitis vinifera* L.) represent the most economically significant berry crop both globally and within Turkey. According to data from TÜİK (2025), Turkey produces 3.47 million tons of grapes across 3.72 million decares of cultivated land, with 1.82 million tons designated for table consumption, 1.26 million tons for drying, and 380,000 tons allocated for winemaking. This production volume highlights the strategic agricultural and economic importance of grape cultivation in the country.

Abiotic stress

Biotic and abiotic stress factors can induce substantial morphological, physiological, and biochemical alterations in plants, thereby disrupting their normal growth and development. Abiotic stress manifests through diverse symptoms triggered by unfavorable environmental conditions; however, these effects often remain imperceptible during the early stages. Consequently, early and accurate diagnosis is essential for minimizing stress-related yield and quality losses. Although traditional diagnostic approaches primarily rely on visible symptoms-such as leaf discoloration, necrotic lesions, or wilting-these indicators are frequently insufficient for precise identification of the underlying stressor. Thus, more systematic and integrative diagnostic strategies are required to reliably detect and characterize stress conditions before irreversible damage occurs (Gao, 2020).

Plants' responses to stress depend on their genetic makeup. When stress is detected, signal transduction processes are initiated, and transcriptional regulators activate target genes, generating physiological and metabolic adaptation responses (Ors and Ekinci, 2015). The duration and recurrence of stress, the plant's developmental stage, and its genetic characteristics determine the level of these responses (Bahar et al., 2024). Furthermore, applying exogenous substances to plants under stress conditions, particularly with plant growth regulators, can increase resistance to abiotic stresses such as drought and metal toxicity (Nasircılar et al., 2019)

Salinity represents one of the foremost abiotic constraints limiting agricultural productivity, affecting nearly 20% of irrigated lands worldwide. Elevated salt concentrations impede water absorption and disrupt cellular osmotic equilibrium, while excessive ion accumulation can induce toxicity. Consequently, plants experience a range of detrimental effects, including growth inhibition, impaired root system development, chlorosis, necrosis, and significant yield reduction (Dölarslan and Gül, 2012). Grapevine (*Vitis vinifera* L.), in particular, exhibits low tolerance to salinity owing to its glycophytic nature and is considered more susceptible to salt-induced stress compared with many other cultivated species (Odabaşıoğlu et al., 2018).

Drought constitutes a major abiotic stress factor in plants, and conventionally, drought-resistant cultivars have been developed through selection and hybridization based on naturally occurring variation. However, these breeding approaches are inherently slow and resource-intensive. Marker-assisted selection (MAS) markedly accelerates improvement efforts by enabling the identification and introgression of genomic regions associated with drought tolerance into breeding populations. In particular, the characterization of stress-responsive genes-most notably members of the DREB (Dehydration Responsive Element Binding) transcription factor family-has significantly advanced the development of new grapevine genotypes capable of adapting to water-limited conditions (Çirka, 2024).

Wild grapevines constitute a crucial genetic reservoir for both rootstock development and hybridization in viticulture, owing to their broad resistance to diverse biotic and abiotic stresses. While American species provide strong resistance to salinity, drought, and major grapevine diseases, Asian species are notable for their high tolerance to low temperatures. Molecular approaches such as marker-assisted selection (MAS), together with genetic analyses employing SNP and SSR markers, play a pivotal role in identifying resistance-associated genomic regions within these taxa. Moreover, introgressive hybridization between wild grapevines and cultivated *Vitis vinifera* genotypes represents a key strategy for transferring these resistance traits into elite cultivars (Şehit, 2024).

Other applications for abiotic stress tolerance

The role of salicylic acid (SA) in mediating defense responses and stress tolerance in grapevines has been extensively investigated. Nasircılar et al. (2019). Demonstrated that SA enhances photosynthetic activity, strengthens defense pathways, and mitigates oxidative damage under various abiotic stresses, including drought, salinity, elevated temperatures, and heavy metal toxicity; however, its effectiveness varies depending on species and application conditions. In another study, Altıncı et al. (2020). Reported that exogenous SA application in the 'Narince' grapevine cultivar improved growth parameters such as shoot length and root biomass, thereby enhancing tolerance to heat stress. Similarly, Rahman et al. (2022). Showed that *Vitis davidii* exhibits natural resistance to white rot (*Coniella diplodiella*), with higher endogenous SA levels recorded in resistant genotypes. Transcriptome (RNA-seq) analyses conducted following SA treatment in susceptible *V. vinifera* cultivars revealed differential expression of 511 genes, notably the induction of key defense regulators such as VvWRKY1/2, VvNPR1, VvTGA2, and VvPR1. Additionally, SA-responsive cis-regulatory elements were identified in the promoter region of the VvPR1 gene, further highlighting SA's central role in grapevine immunity.

Various approaches beyond salicylic acid have also been shown to enhance abiotic stress tolerance in grapevines. Salicylic acid (SA) is well known for its ability to enhance plant resilience to heat, drought, and other environmental stresses. Similarly, methyl jasmonate (MeJA) plays a key regulatory role in plant defense and stress signaling. Hakeem et al. (2025). Demonstrated that MeJA strengthened antioxidant defense systems, safeguarded photosynthetic performance, and activated stress-responsive gene expression in grapevines subjected to salinity, drought, and cold stress. These findings indicate that MeJA, much like SA, functions as a critical modulator of abiotic stress tolerance in grapes. Moreover, Meng et al. (2014). Examined the effects of melatonin application on wine grape seedlings exposed to PEG-induced water deficit. Melatonin alleviated PEG-induced growth inhibition and oxidative damage while helping preserve Photosystem II efficiency, chlorophyll content, and structural integrity. Collectively, these results suggest that melatonin confers protective effects against drought stress in grapevines.

Molecular studies on abiotic stress resistance

In recent years, molecular approaches have advanced substantially in elucidating genetic diversity in plants. Traits such as extended life cycles, long generation intervals, and widespread vegetative propagation increase the relevance and utility of these techniques in fruit crops (Marwah and Jamwal, 2024). Genome-wide association

studies (GWAS) and genomic selection (GS) in grapevine play a pivotal role in improving stress tolerance by uncovering associations between genetic markers and key agronomic traits. Nevertheless, overcoming challenges posed by large datasets and computational complexity will further enhance the effectiveness of these approaches in advancing agricultural productivity (Huang, 2024).

Wang et al. (2023). Conducted whole-genome sequencing of 77 widely used grape rootstock genotypes and identified more than 2.8 million SNPs. Based on their genetic composition, the rootstocks were classified into ten groups derived from five ancestral components. The study demonstrated that the Chinese species *Vitis amurensis* and *Vitis davidii* possess markedly high resistance to both biotic and abiotic stresses, and it revealed numerous candidate genomic regions associated with tolerance to phylloxera, root-knot nematodes, salinity, drought, cold, and waterlogging. In addition, Motha et al. (2018). Evaluated the genetic diversity of grape rootstocks tolerant to abiotic stress using ISSR and SSR markers, reporting 88% polymorphism and PIC values ranging from 0.66 to 0.86 for ISSRs and 24 alleles with PIC values between 0.43 and 0.78 for SSRs. Both marker systems grouped genotypes into two major clusters, and PCA results were highly consistent with the dendrogram analyses.

High temperatures associated with global warming exert markedly detrimental impacts on grapevine development and fruit quality. Zhang et al. (2023) reported that elevated temperatures cause substantial reductions in both yield and quality and analyzed miRNA-derived SSR polymorphisms to identify molecular markers linked to heat tolerance. Their study identified eight SSR markers capable of discriminating heat-tolerant and heat-sensitive cultivars, among which the VMIRSSR167c3 marker exhibited particularly high accuracy in differentiating thermotolerant from thermosensitive genotypes.

Zhang et al. (2024) investigated the molecular responses of 38 grapevine germplasm accessions to high-temperature stress and identified 177 previously characterized and 20 novel miRNAs using next-generation sequencing. Their analyses revealed that 65 miRNAs exhibited differential expression under heat stress. Vvi-miR3633a was significantly downregulated at elevated temperatures, and heterologous expression assays in Arabidopsis confirmed that this miRNA functions as a regulator of thermotolerance. These findings underscore the pivotal role of miRNAs in the adaptive heat-stress response to grapevine. Cold-stress tolerance in grapevines is similarly governed by key physiological and molecular regulatory mechanisms, with C-repeat binding factor (CBF) genes representing central components of the cold-response network. Aazami and Mahna (2017) reported that exogenous application of salicylic acid (SA) in the Iranian *Vitis vinifera* cultivar ‘Sultanina’ markedly enhanced VvCBF4 expression, with the highest transcriptional activation observed when SA was applied six hours before cold exposure.

Shi et al. (2024) conducted another genome-wide investigation, comprehensively characterizing the CBS gene family in grapevine and identifying 32 VvCBS genes distributed across 15 chromosomes. Phylogenetic and structural analyses showed that these genes clustered into three major subgroups. Expression profiling demonstrated that many family members exhibited high transcript abundance across multiple tissues and showed differential regulation in response to cold, drought, and salinity stress. Moreover, the cloning of VvCBS27 and its localization to the plasma membrane, cytoplasm, and nucleus suggest multifaceted functional roles of CBS proteins in abiotic stress responses in grapevine. This work provides a valuable foundation for elucidating the biological functions of the CBS gene family in Vitis species. In another study, Wang et al. (2024) developed robust SSR markers (e.g., OMT2.1-211, SIRT276) capable of discriminating cold tolerance across eight hybrid grape populations. Collectively, these findings highlight that both transcription factors and molecular markers are essential tools for deciphering cold-tolerance mechanisms in grapevine and for advancing the development of stress-resilient cultivars.

Drought and salinity represent major abiotic constraints that substantially reduce productivity in grapevine cultivation. To identify genes associated with tolerance to these stresses, Hanana et al. (2014) isolated the dehydrin gene VvDhn from the Cabernet, Sauvignon cultivar and demonstrated that its expression is markedly elevated, particularly during the late stages of seed embryogenesis. VvDhn expression was strongly induced by salt and drought stress and ABA treatment. Under salinity stress, transcript levels were significantly higher in the tolerant cultivar Razegui, whereas no detectable change was observed in the sensitive cultivar Syrah. Although both cultivars exhibited increased expression under drought stress, the magnitude of induction was greater in the tolerant genotype. Collectively, these findings indicate that VvDhn constitutes a vital candidate gene involved in abiotic stress tolerance mechanisms in grapevine.

CONCLUSION

This review highlights the vital roles of both physiological and molecular mechanisms in governing grapevine responses to major abiotic stresses-including drought, salinity, heat, and cold-in sustaining viticultural productivity. Previous studies have demonstrated that signaling molecules such as salicylic acid, methyl jasmonate, and melatonin enhance stress resilience by augmenting antioxidant defense pathways and modulating the expression of stress-responsive genes. Moreover, integrative analyses based on GWAS, SSR and SNP markers, miRNA profiling, and transcriptomics have identified key stress-associated loci-including VvPR1, VvWRKY transcription factors, the CBF gene family, Dhn genes, and members of the CBS gene family-which collectively provide a strong genomic foundation for targeted breeding strategies. The substantial genetic variability within wild Vitis species represents a critical resource for developing stress-tolerant cultivars. In this context, it is essential to integrate physiological datasets with molecular evidence and incorporate this information into modern breeding programs to ensure the long-term sustainability and adaptability of viticulture under changing environmental conditions.

REFERENCES

Aazami, M. A., & Mahna, N. (2017). Salicylic acid affects the expression of VvCBF4 gene in grapes subjected to low temperature. Journal of Genetic Engineering and Biotechnology, 15(1), 257-261.

Altıncı, N. T., Cangi, R., & Üstün, D. (2020). Determining the effects of salicylic acid applications on high temperature stress in Narince grape variety. Turkish Journal of Agriculture-Food Science and Technology, 8(5), 1227-1231.

Arslan, T. (2023). Üzümün atası yabani asma. In M. Ayçiçek & S. S. Bal (Eds.), Tarımda iyileştirmeler (ss. 101–120). Iksad Publications..

Bahar, E., Korkutal, İ., & Abay, C. (2024). Salkım Özelliklerine Bazı Abiyotik Streslerin Etkisi: Cabernet-Sauvignon (*Vitis vinifera* L.) Üzüm Çeşidi Örneği. ÇOMÜ Ziraat Fakültesi Dergisi, 12(1), 32-42.

Baykul, A. (2022). Eskişehir ilinde yetiştirilen üzüm çeşitlerinin ampelografik özelliklerinin belirlenmesi ve SSR markörler ile tanımlanması. (Doktora tezi), Ankara Üniversitesi Fen Bilimleri Enstitüsü. Ankara.

Bozkuş, Ş., & Bozkuş, M. (2024). Asma ıslahında son gelişmeler ve güncel metotlar. Bahçe, 53(2), 127-135.

Candar, S., Alço, T., Ekiz, M., Korkutal, İ., & Bahar, E. (2020). Milli koleksiyon bağından seçilen bazı yöresel şaraplık üzüm çeşitlerinde budama şekli ve abiyotik etmenlerin fizyolojik aktiviteler üzerine etkileri. Ege Üniversitesi Ziraat Fakültesi Dergisi, 57(2), 173-183.

Çirka, M. (2024). Kuraklığın tarım ve ürün kalitesi üzerindeki etkileri. In M. Yaşar & D. Katar (Eds.), Ziraat, Orman ve Su Ürünleri Alanında Akademik Çalışmalar II (ss. 141–160). İksad Yayınevi.

Dölarslan, M., & Gül, E. (2012). Toprak bitki ilişkileri açısından tuzluluk. Türk Bilimsel Derlemeler Dergisi, (2), 56-59.

Gao, Z. (2020). Spectral imaging based non-contact detection of biotic and abiotic stress in berry crops. (Doctoral dissertation), Washington State University.

Hakeem, A., Li, S., Nasiru, M. M., Mustafa, G., Elatafi, E., Shangguan, L., & Fang, J. (2025). Methyl jasmonate acts as a crucial player in abiotic stress responses in grape. Stresses, 5(2), 40.

Hanana, M., Daldoul, S., Fouquet, R., Deluc, L., Leon, C., Hoefer, M., ... & Ghorbel, A. (2014). Identification and characterization of a seed-specific grapevine dehydrin involved in abiotic stress response within tolerant varieties. Turkish Journal of Botany, 38(6), 1157-1168.

Huang, W. (2024). The current situation and future of using GWAS strategies to accelerate the improvement of crop stress resistance traits. Molecular Plant Breeding, 15.

Küskü, D. Y., & Söylemezoğlu, G. (2022). Kuraklık ve tuz stresinin *V. vinifera* x *V. rupestris* melezlerinin toplam fenolik bileşik ve antioksidan kapasiteleri üzerine etkileri. Harran Tarım ve Gıda Bilimleri Dergisi, 26(1), 72-81.

Marwah, A., & Jamwal, N. (2024). Adoption of molecular markers for analysis of genetic diversity in fruit tree crops. *Agri Roots e-Magazine, 2*(9), 33-36.

Meng, J. F., Xu, T. F., Wang, Z. Z., Fang, Y. L., Xi, Z. M., & Zhang, Z. W. (2014). The ameliorative effects of exogenous melatonin on grape cuttings under water-deficient stress: antioxidant metabolites, leaf anatomy and chloroplast morphology. Journal of Pineal Research, 57(2), 200-212.

Motha, K., Singh, S. K., Singh, A. K., Singh, R., Srivastav, M., Verma, M. K., & Bhardwaj, C. (2018). Molecular characterization and genetic relationships of some stress-tolerant grape rootstock genotypes as revealed by ISSR and SSR markers. Plant Tissue Culture and Biotechnology, 28(1), 77-90.

Nasircılar, A. G., Ulukapı, K., & Şener, S. (2019). Exogenous salicylic acid applications as an example of molecules effective in abiotic stress tolerance in plants. *Turkish Journal of Agriculture - Food Science and Technology, 7*(sp3), 5-10.

Odabaşıoğlu, M. İ., Demirtaş, G., Yıldırım, K., & Gürsöz, S. (2018). Salt stress on grapes (*Vitis* spp.). In Proceedings of the 1st International GAP Agriculture and Livestock Congress (pp. 10–17). Harran University.

Ors, S., & Ekinci, M. (2015). Kuraklık stresi ve bitki fizyolojisi. Derim, 32(2), 237-250.

Rahman, F. U., Khan, I. A., Aslam, A., Liu, R., Sun, L., Wu, Y., ... & Zhang, Y. (2022). Transcriptome analysis reveals pathogenesis-related gene 1 pathway against salicylic acid treatment in grapevine (*Vitis vinifera* L). Frontiers in Genetics, 13, 1033288.

Ren, C., Aini, N., Kuang, Y., Lin, Y., & Liang, Z. (2025). Sensing, adapting and thriving: How fruit crops combat abiotic stresses. Plant, Cell and Environment, 48, 5584–5603.

Sabır, A., Tangolar, S., & Büyükalaca, S. (2008). Moleküler markör tekniklerinin bağcılıkta kullanımı. Alatarım, 26.

Shi, X., Xu, S., Li, Y., & Yin, Y. (2024). Expression of Cystathionine-β-Synthase (CBS) Genes in grape under various abiotic stresses and subcellular localization of VvCBS27. Horticulturae, 10(9), 1009.

Şahin, Ö. (2009). Farklı asma anaçları üzerine aşılı sultani çekirdeksiz *(Vitis Vinifera L.)* üzüm çeşidinin bor ve tuz stresine tolerans mekanizmalarının stresle ilgili fizyolojik parametreler ve antioksidan enzimlerle belirlenmesi, (Yüksek Lisans Tezi), Ankara Üniversitesi Fen Bilimleri Enstitüsü Toprak Anabilim, Ankara.

Şehit, A. (2024, October). The importance of wild grapevines in viticulture and the conservation of genetic resources. In 13th International İstanbul Scientific Research Congress Proceedings Book and Mathematics (pp. 696–707). Iksad Publishing.

TÜİK (Türkiye İstatistik Kurumu). (2025). Bitkisel üretim istatistikleri - 2024 [Veri seti]. https://data.tuik.gov.tr/Bulten/Index?p=Bitkisel-Uretim-Istatistikleri-2024-53447

Wang, P., Zhao, F., Zheng, T., Liu, Z., Ji, X., Zhang, Z., ... & Fang, J. (2023). Whole-genome re-sequencing, diversity analysis, and stress-resistance analysis of 77 grape rootstock genotypes. Frontiers in Plant Science, 14, 1102695.

Wang, Z. L., Han, X., Ma, W. L., Xu, G. Q., & Xue, T. T. (2024). Mining, screening, and validation of cold-resistance molecular markers in *Vitis vinifera* L. Euphytica, 220(6), 81.

Zhang, L., Song, Y., Li, J., Liu, J., Zhang, Z., Xu, Y., ... & Ma, C. (2023). Development, identification and validation of a novel SSR molecular marker for heat resistance of grapes based on miRNA. Horticulturae, 9(8), 931.

Zhang, L., Teng, Y., Song, Y., Li, J., Zhang, Z., Xu, Y., ... & Ma, C. (2024). Assessment of heat tolerance and identification of miRNAs during high-temperature response in grapevine. Frontiers in Plant Science, 15, 1484892.

ORAL PRESENTATION

Deronectes hakkariensis Wewalka, 1989b türünün (Coleoptera, Dytiscidae, Hydroporinae) dişisinin ilk tanımı, Elâzığ, Türkiye

Medeni Aykut[1*] (*ORCID: https://orcid.org/0000-0001-6824-1394*)
Sadreddin Tusun[2] (*ORCID: https://orcid.org/0000-0002-0696-4244*)

[*1]Dicle Üniversitesi, Ziya Gökalp Eğitim Fakültesi, Matematik ve Fen Bilimleri Eğitimi Bölümü, Diyarbakır, Türkiye.
[2]Dicle Üniversitesi, Ziya Gökalp Eğitim Fakültesi, Matematik ve Fen Bilimleri Eğitimi Bölümü, Diyarbakır, Türkiye

*Sorumlu yazar e-mail: medeniaykut@hotmail.com

Özet

Deronectes hakkariensis türü ilk kez Wewalka (1989) tarafından Türkiye'nin Güneydoğu Anadolu Bölgesi'nde yer alan Şırnak ilinin Uludere ilçesinden toplanan tek bir erkek örneğe dayanarak tanımlanmıştır. Daha sonraki arazi çalışmalarında bu tür Türkiye'nin kuzeydoğusundaki yer alan Erzurum İl'inde de kaydedilmiştir. Her iki çalışmada da yalnızca bu türe ait erkek örnekler ayrıntılı olarak tanımlanmış, dişi örnekler tanımlanmamıştır. Çalışmamızda *Deronectes hakkariensis* türüne ait örnekler Türkiye'nin Doğu Anadolu Bölgesi'nde yer alan Elâzığ ili Arıcak ilçesi Akdağlar Yaylası'ndan toplanmıştır. *D. hakkariensis*'in vücut yapısı ve genel görünümü ile dişi genital organları ilk kez çizilmiş ve şekillerle ayrıntılı bir şekilde gösterilmiştir. Elâzığ ilinden toplanan örneklerimiz daha önce tanımlamaları yapılan orijinal örneklere ile uyumluluk göstermektedir ve incelenen dişiler erkeklere dış morfolojik açıdan benzerlikler göstermektedir.

Anahtar Kelimeler: Yırtıcı dalgıç böcekleri, Kın kanatlılar, Dalgıç böcekleri, Elâzığ, Türkiye

First description of the female of *Deronectes hakkariensis* Wewalka, 1989b from Elazığ province, Türkiye (Coleoptera, Dytiscidae, Hydroporinae)

Abstract

Deronectes hakkariensis was firstly described by Wewalka (1989) based on a single male specimen collected from the Uludere district of Şırnak Province, located in Southeastern Anatolian region of Türkiye. Subsequent field studies have also recorded this species in Erzurum Province northeastern of Türkiye. In both of these studies, only male specimens were described in detail, while female specimens remained undescribed. In our study, the specimens belong to *Deronectes hakkariensis* were collected from the Akdağlar Plateau of Arıcak district in Elazıg province located in Eastern Anatolian Region of Türkiye. The habitus and the female genitalia of *D. hakkariensis* are illustrated and figures for the first time. The specimens collected from Elazığ Province are consistent with the original description and the examined females exhibit external similarities to males.

Key words: Predaceous diving beetles, Coleoptera, Dytiscidae, Elâzığ, Türkiye

GİRİŞ

Sucul habitatların biyotasında önemli bir yere sahip olan Dytiscidae familyasının üyeleri, yırtıcı dalgıç böcekleri olarak da bilinmektedir. Bu familyaya ait böceklere genellikle bütün tatlı su habitatlarında rastlamak mümkündür. Dytiscidae familyası günümüzde 182 cinse ait 4600 civarında tür ile temsil edilmektedir (Nilsson ve Hájek, 2025). Dytiscidae familyasına ait *Deronectes* Sharp, 1882 cinsi, yeryüzünde 61 tür ile temsil edilmektedir. Deronectes cinsinin üyeleri tamamen Palearktik bölgeye ait olup, ağırlıklı olarak batıda Fas'tan başlayarak Avrupa'nın büyük bir bölümünde ve Orta Asya'da Batı Çin'e kadar dağlık alanlarda görülür (Fery ve Brancucci, 1997; Fery ve Hosseinie, 1998; Fery, 2003; Aykut ve Ark., 2018; 2019). *Deronectes* cinsine ait türler genellikle akan sularda

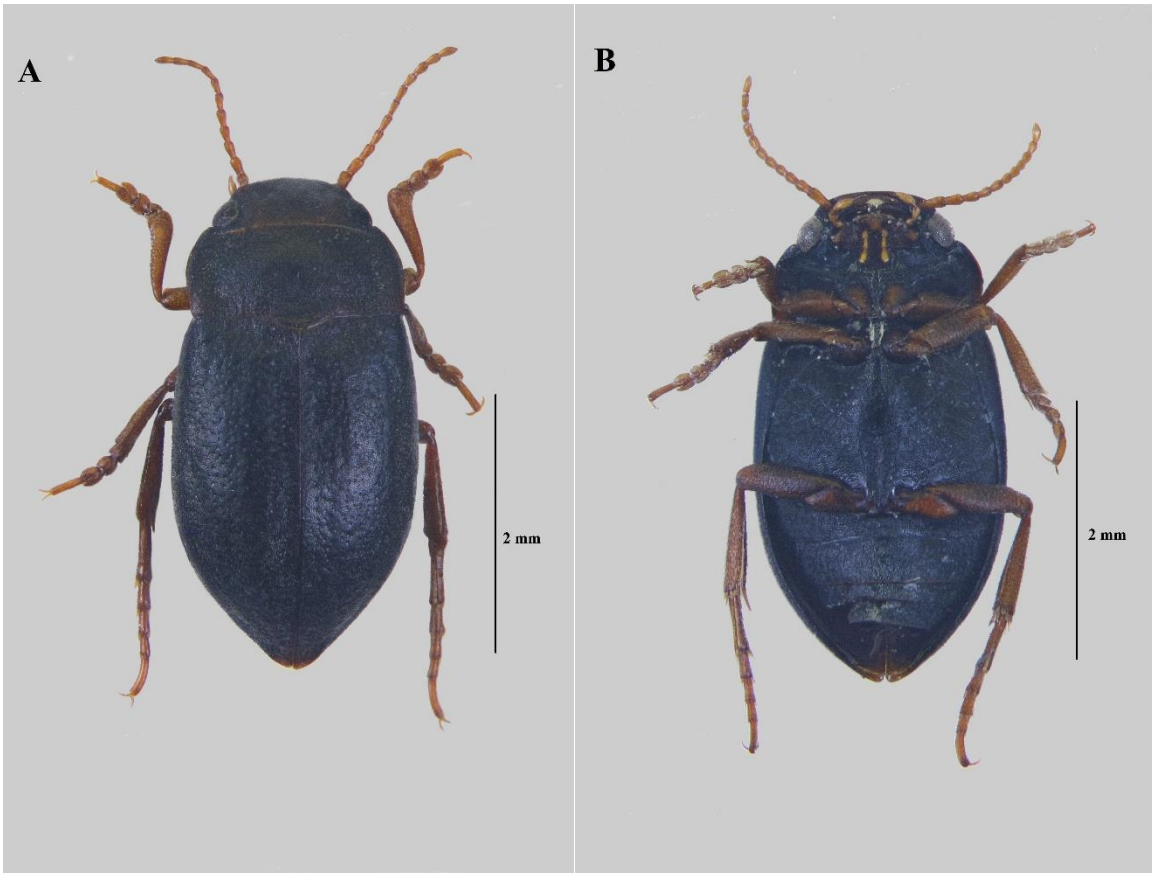
yaşar istinai olarak durgun sularda ve göletlerde bulunanları da mevcuttur (Fery, 2003). Bu cinse ait Türkiye'den şu ana kadar 15 endemik türün varlığı bildirilmiştir (Aykut ve Ark., 2018; 2019). Ayrıca Son 10 yıl içerisinde bölgede yapılan çalışmalar ile Türkiye'nin Doğu ve Güneydoğu'sundan Dytiscidae familyasına ait beş yeni tür ve bir alt tür bilime eklenmiştir: *Hydroporus karabegan* (Aykut ve ark., 2025), *Bidessus anatolicus adiyaman* (Aykut ve ark., 2021*). Deronectes kabilcevz* ve *D. propedoriae* (Aykut ve ark., 2019), *Deronectes taron* (Aykut ve ark., 2018), *Scarodytes costatus* (Aykut ve Fery, 2017). Ayrıca, *Hydaticus (Prodaticus) histrio* Clark, 1864 (Erman ve ark., 2018) ve *Hydroporus inscitus* (Sharp, 1882) (Aykut, 2018) Türkiye için ilk kez kaydedilmiştir. Bu çalışmalar ile Türkiye'den bilinen Dytiscidae tür ve alt tür sayısı 178'e ulaşmış olup, bunların 40'ı ülkemiz için endemiktir. Bu durum Dytiscidae familyasının çeşitliliğinin Türkiye'de yüksek olduğunu göstermektedir. Bu çalışmanın amacı Türkiye için endemik olan ve henüz dişi örnekleri tanımlanmamış olan *Deronectes hakkariensis* türünün dişisinin ayrıntılı tanımlanmasını yapmaktır.

MATERYAL VE METOT

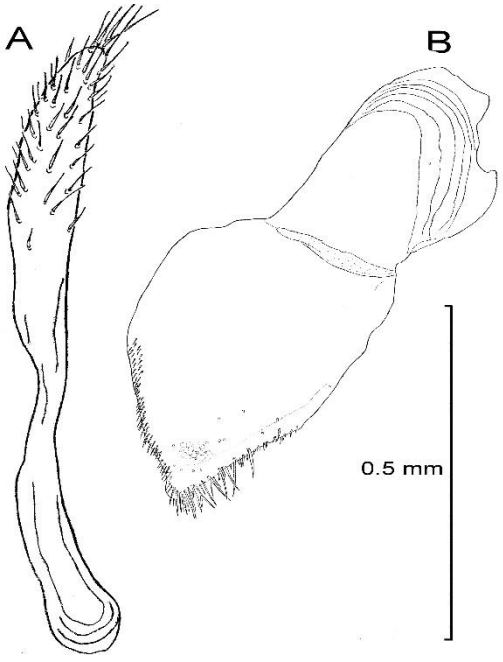
Çalışmaya konu olan böcek örnekleri 4 Haziran 2024 tarihinde Elâzığ İli, Arıcak İlçesi Akdağlar Yaylası'ndan (Şekil 1) gözenek çapı 0,5 ile 1mm arasında değişen elek, süzgeç ve sucul ağ kullanılarak toplanmıştır. Çalışma yapılan ve böcek örneği alınan istasyonun koordinat ve yükselti bilgileri el GPS'i (Global Position System; Küresel Konumlama Sistemi) kullanılarak (Magellan Explorist 610) kayıt altına alınmıştır. Arazi çalışmalarında toplanan böcek örnekleri çalışma alanında %70'lik etil alkole alınıp etiketlenerek laboratuvara getirilmiştir. Laboratuvara getirilen böcek örnekleri teşhis işlemi için ince fırçalar ve ultrasonik aletler ile temizlenmiştir. Örnekler temizlendikten sonra teşhisleri yapılmıştır. Teşhisi yapılan örnekler etiketlenerek, muhafaza edilmek üzere, birinci yazarın Dicle Üniversitesi Ziya Gökalp Eğitim Fakültesinde bulunan kişisel koleksiyonunda depolanmaktadır.



Şekil 1. *Deronectes hakkariensis* örneklerinin toplandığı istasyon



Şekil 2. *Deronectes hakkariensis* (dişi) genel görünüşü: **(A)** sırttan; **(B)** karından



Şekil 3. *Deronectes hakkariensis*, dişi: gonocoxae (A) ve gonocoxosternum (B).

BULGULAR

Taksonomi

Tür lokalitesi: Elâzığ İli, Arıcak İlçesi, Akdağlar Yaylası, Türkiye. 38^{0}07'23"K, 40^{0}10'32"D, Rakım: 2086 m. Küçük, çamurlu kaynak suyu.

Genel tanım: Vücut genel görünümü dar, uzun ve oval, elitra kenarları ilk iki üçte birlik kısımda yuvarlak omuzların arkasında zayıf ve aşağı yukarı eşit şekilde yuvarlak, daha arkada ise daha belirgin bir şekilde kavislidir (Şekil 2). Maksimum genişlik, uzunluğun ortasından hemen öncedir. Pronotum gövdeden belirgin şekilde daha dardır ve omuzlardaki vücut hatlarının sürekliliği belirgindir. Baş hariç sırt yüzeyi ipeksi parlaklıktadır ve kısa, şeffaf kıllarla kaplıdır, ancak bazı kısımlarda kıl yoktur.

Renk: Sırt yüzeylerinin rengi siyah; sadece başın tepe noktası ve pronotumun arka kenarı kahverengimsi, dar bir şekilde parlıyor. Alt yüzey baskın olarak siyah; ağız parçaları ile üçüncü ila beşinci abdominal ventrillerin arka kenarları kahverengimsi. Bacaklar genellikle koyu kahverengi. Antenler ve palpler kahverengimsi, IV ila X anten segmentleri uca doğru giderek koyulaşmış.

Baş: Tüm yüzey belirgin şekilde ağsı, gözenekler küçük, çokgen. Noktalama seyrek, düzensiz, bazen çift. Gözenekler arası mesafe klipeusta yaklaşık dört nokta, alında yaklaşık beş nokta kadar. Klipeustaki büyük deliklerin çapı, küçük olanların yaklaşık iki katı, alında ise daha da büyük; küçük delikler arasında düzensiz olarak serpiştirilmiş. Klipeus olukları büyük, uzun ve noktalama belirgin şekilde daha yoğun. Gözlerin iç kenarı boyunca, birkaç büyük delik de dahil olmak üzere, derin ve keskin bir şekilde sınırlanmış bir oluk bulunur. Başın ön kenarı çok zayıf bir şekilde girintili çıkıntılıdır. Klipeus oluklarında çok az kıl, diğer yerlerde kıl yoktur.

Pronotum: Kenarlar büyük kısımda neredeyse eşit şekilde kavisli, ön açılardan kısa, biraz daha düz, arka açılardan kısa içbükey, kıvrımlı, arka açılar az çok dikdörtgen. Arka üçte birlik kısımda dar bir baskıyla yan kenara paralel, özellikle arka açılara yakın derin baskı. Orta kısmın sağ ve solunda ön kenarın arkasında zayıf baskı, arka kenardan önce daha güçlü baskı; bu nedenle pronotum diski şişkin görünüyor. Yan kenarlar parlak kenarlı, ön açılardan kısa kenar oldukça inceliyor. Tüm yüzey ağsı, poligonal ağlar baştakinden biraz daha küçük. Noktalama düzgün, delikler baştaki daha küçük delikler kadar küçük, delikler arasındaki mesafe aşağı yukarı iki veya üç ağ kadar. Diskin merkezinde derin baskı, büyük delik; Ön kenarın arkasında ve arka kenarın önünde çok düzensiz düzenlenmiş büyük delikler mevcut. Tüm yüzeyde kıllar mevcut, diskte daha seyrek, yanlarda daha yoğun.

Elitra: Yuvarlak, omuzlar belirgin; omuzların arkasındaki yanlar uç hizasından hemen öncesine kadar eşit şekilde kavisli; burada çok belirsiz bir şekilde kıvrımlı ve sonra uca doğru daha güçlü bir şekilde kavisli; elitra uzunlamasına şişkinliklere sahip değil, uç hizasından önce çok belirgin ve büyük bir izlenime sahip. Üst yüzeyde dik görünümde, yan görünümde, yan kenar omuzlara doğru güçlü bir şekilde yükseliyor; epipleuron omuzlara kadar görülebilir. Yüzeyin büyük kısımları ağ şeklinde değil, sadece kenarlara yakın ve arka üçte birlik kısımda bazı ağ çizgileri algılanabilir. Yüzey az çok eşit şekilde küçük deliklerle kaplı; delikler pronotumun merkezinden daha küçük; delikler arasındaki mesafe yaklaşık olarak çapları kadar veya biraz daha fazla. Tüm yüzey, bazı kısımlar hariç, oldukça uzun kıllarla az çok eşit şekilde kaplıdır.

Alt yüzey: Vücudun alt yüzeyi neredeyse tamamen yoğun noktacıklı olduğundan genellikle mattır; büyük delikler yoktur (Şekil 2). Başın alt kısmı ağsı değildir, ince deliklerle yoğun bir şekilde kaplıdır, ön kenarın arkasında uzunlamasına birkaç belirgin kırışıklık vardır; daha ortada, daha büyük deliklerin enine düzensiz çizgisi vardır, arkasında ağsıdır. Gözlerin yanında üçgen düz bir alan mevcuttur. Prosternal çıkıntı prosternal kolona hafifçe eğimlidir, çıkıntının ucu biraz yukarı kıvrıktır. Prosternal kolon dardır; prosternal çıkıntı mızrak şeklindedir, ucu genişçe yuvarlaktır; çıkıntı belirgin şekilde tonozludur, yanal olarak, yan kenara paralel delik çizgileriyle; kenar kenarlı değildir.

Bacaklar: Femur ve tibiaların şekli normaldir. Ön protarsal pençe biraz kalınlaşmış, tabana yakın kavisli, sonra neredeyse düz, uçta tekrar kavisli. Ön mezotarsal pençe de biraz kalınlaşmış, aşağı yukarı eşit şekilde kavisli. Metafemurun tepesi arkaya doğru lobludur.

♀**: Dişi eşey yapılar:** Gonocoxae ve gonocoxosterna Şekil 3'te verilmiştir.

Vücut Ölçümleri: Toplam uzunluk: 3.95- 4.30 mm (4.05 mm), Maksimum genişlik: 2.05- 2.15 mm (2.06 mm), Toplam uzunluk / Maksimum genişlik: 1.93- 2.00 (1.97).

Yayılış: 2 ♂♂, 1989; Şırnak Uludere, 2 ♂♂, 2 ♀♀, 27.7.1999 Erzurum ili, Demir döven Barajı; 3 ♂♂, 3 ♀♀, 7.9.2000 Erzurum ili, Serdarlı köyü ve 7 ♂♂, 2 ♀♀, 18.9.2000 Erzurum ili, Yedigöller; 7 ♀♀, 4.6.2024 Elâzığ İli, Arıcak İlçesi, Akdağlar Yaylası.

TARTIŞMA

Deronectes hakkariensis türü ilk kez Wewalka tarafından 1989 yılında Hakkari ilinin Uludere ilçesinden toplanan tek bir erkek örneğe dayanarak tanımlanmıştır. 18 Mayıs 1990 tarihinde Şırnak'ın il olması ile Şırnak'a bağlandı. Örnek teşhis edildiğinde Uludere ilçesi Hakakri İli'ne bağlı olduğu için örneğe *Deronectes hakkariensis* ismi verilmiştir. Daha sonraki arazi çalışmalarında bu tür Türkiye'nin kuzeydoğusundaki yer alan Erzurum İl'inde de kaydedilmiştir. Her iki çalışmada da yalnızca bu türe ait erkek örnekler ayrıntılı olarak tanımlanmış, dişi örnekler tanımlanmamıştır. Bu çalışma ile *Deronectes hakkariensis* türünün dişi bireyleri ilk kez tanımlanmış oldu. Elâzığ ilinden toplanan örneklerimiz daha önce tanımlamaları yapılan orijinal örneklere ile uyumluluk göstermektedir ve incelenen dişiler erkeklere dış morfolojik açıdan benzerlikler göstermektedir.

SONUÇ

Ülkemiz için endemik bir tür olan *Deronectes hakkariensis*'in dişi bireyleri ilk olarak bu çalışma ile ayrıntılı bir şekilde tanımlanmıştır. Gelecekteki ayrıntılı ve kapsamlı saha faaliyetlerinin Türkiye'deki Dytiscidae türlerinin sayısını daha da artırması oldukça muhtemeldir.

TEŞEKKÜR

Bu çalışma, Dicle Üniversitesi Bilimsel Araştırma Projeleri Koordinatörlüğü (DÜBAP) tarafından ZGEF. 23.018 proje numarasıyla desteklenmiştir. DÜBAP yönetimine destekleri için teşekkür ederiz.

KAYNAKLAR

Aykut, M., Tusun, S., & Fery, H. (2025). *Hydroporus karabegan* sp. nov. from eastern Türkiye (Coleoptera, Dytiscidae, Hydroporini). *Zootaxa*, *5609*(1), 125-131.

Aykut, M., Taşar, G.E. & Fery, H. (2021) *Bidessus anatolicus adiyaman* ssp. n. from Adyaman province, southern Turkey (Coleoptera, Dytiscidae, Bidessini). *Zootaxa*, 5027 (4), 563–575. https://doi.org/10.11646/zootaxa.5027.4.5

Aykut, M., Yıldırım, İ.H., Tusun, S. & Fery, H. (2019) *Deronectes kabilcevz* sp. n. and *D. propedoriae* sp. n. from south-eastern Anatolia (Turkey) (Coleoptera, Dytiscidae, Hydroporinae). *Zootaxa*, 4691 (1), 5–10. https://doi.org/10.11646/zootaxa.4691.5.10

Aykut, M., Taşar, G.E. & Fery, H. (2018) *Deronectes taron* sp. n. from the eastern Anatolian region of Turkey (Coleoptera, Dytiscidae, Hydroporinae). *Zootaxa*, 4422 (2), 403–410. https://doi.org/10.11646/zootaxa.4422.3.6

Erman, Ö.K., Taşar, G.E., Aykut, M. & Kurt, K. (2018) First record of *Hydaticus histrio* Clark, 1864 (Coleoptera, Dytiscidae) from Turkey. *Acta Biologica Turcica*, 31 (4), 174–177.

Aykut, M. (2018). The Diving Beetle Fauna of Diyarbakır and Bingöl Provinces, Turkey (Coleoptera: Dytiscidae) with a New Record. Pakistan Journal of Zoology, 50(1), 65-74.

Aykut, M. & Fery, H. (2017) *Scarodytes costatus* nov. sp. from the Bingöl Province in Turkey, the first species of the genus with costate elytra (Insecta: Coleoptera: Dytiscidae: Deronectina). *Linzer Biologische Beiträge*, 49, 395–414.

Fery, H. & Brancucci, M. (1997) A taxonomic revision of *Deronectes* Sharp, 1882 (Insecta: Coleoptera: Dytiscidae) (part I). *Annalen des Naturhistorischen Museums in Wien*, 99 B, 217–302.

Fery, H. & Hosseinie, S.O. (1998) A taxonomic revision of *Deronectes* Sharp, 1882 (Insecta: Coleoptera: Dytiscidae) (part II). *Annalen des Naturhistorischen Museums in Wien*, 100 B, 219–290.

Fery, H. (2003) Dytiscidae: IV. The Central Asian and Chinese species of *Deronectes* Sharp (Coleoptera). *In*: Jäch, M.A. & Ji, L. (Eds.), *Water Beetles of China. Vol. III.* Zoologisch-Botanische Gesellschaft in Österreich and Wiener Coleopterologenverein, Wien, pp. 125–131.

Nilsson, A.N. & Hájek, J. (2025) A world catalogue of the family Dytiscidae, or the diving beetles (Coleoptera, Adephaga). Version 1 January 2025, 329 pp. Update distributed as a PDF file via Internet. Available from: http://www.waterbeetles.eu (accessed 5 February 2025)

ORAL PRESENTATION

The future of eggs: The functional food market and consumer trends

Muhammed Yüceer[1*] (*ORCID: https://orcid.org/ 0000-0001-6709-1347*),
Meltem Aşık[2] (*ORCID: https://orcid.org 0009-0000-4727-2781*)

[*1]Çanakkale Onsekiz Mart University, Çanakkale Vocational School of Technical Sciences (CTBMYO) Department of Food Processing, Çanakkale, Türkiye.
[2] Çanakkale Onsekiz Mart University, Graduate School, Department of Food Safety and Quality, Çanakkale, Türkiye.

*Corresponding author e-mail: myuceer@comu.edu.tr and 25424826002@ogr.comu.edu.tr

Abstract

The concept of functional foods first emerged in Japan in the 1980s and gained legal status under the term "FOSHU" (Foods for Specified Health Use). These foods aim to improve overall health by supporting physiological functions beyond basic nutrition, particularly enhancing immune, cardiovascular, digestive, skeletal, and nervous system health. They also contribute to reducing the risk of chronic diseases through their antioxidant and metabolic regulatory effects. Eggs are considered an important animal-derived functional food due to their high-quality protein content and natural bioavailability. In addition to their nutritional value, eggs contain biologically active compounds such as phosvitin, ovalbumin, lysozyme, ovotransferrin, and lutein, which exhibit antioxidant, antimicrobial, immunomodulatory, and cholesterol-regulating properties. Furthermore, with the development of food processing technologies, eggs enriched with omega-3 fatty acids, vitamin D, selenium, probiotics, or lutein have become functional egg products designed to provide specific health benefits. This review summarizes the current literature on functional egg production techniques, market trends, and consumer perceptions. It also discusses the growth potential of the functional egg market and future research directions. Findings indicate that consumer preferences are increasingly shaped by health, naturalness, and ethical production, positioning functional eggs as a strategic product within these dynamics.

Keywords: Functional food, egg, consumer trends, bioactive compounds, food market, functional egg

INTRODUCTION

In recent years, the understanding of food science has gone beyond meeting basic nutritional needs and focused on developing foods that protect health and help prevent disease. The concept of "functional food," which has gained importance with this approach, defines products that offer additional health benefits to the body in addition to their basic nutritional value (Hardy, 2000; Kwak & Jukes, 2001). In this context, eggs attract attention as an ideal functional food due to both their valuable components in their natural structure and their suitability for fortification applications. Although eggs are an important source of animal protein, they have faced negative perceptions for many years due to debates about their cholesterol content. However, current scientific data shows that dietary cholesterol has no direct effect on blood cholesterol levels in healthy individuals (Rehault-Godbert, et al., 2019). These developments have increased confidence in the nutritional value of eggs and paved the way for the development of "functional eggs" enriched with omega-3 fatty acids or various vitamins (Surai & Sparks, 2001). However, a product's scientific superiority does not guarantee its success in the market. Consumer perceptions and preferences regarding health, price, and reliability play a critical role in the acceptance of functional foods. The burgeoning global population necessitates a substantial increase in egg production, concurrently driving a demand for diverse, high-quality, and sustainably produced egg options (El-Sabrout, et al., 2022; Rondoni, et al., 2020). This escalating demand, coupled with increased consumer awareness regarding nutrition and ethical production practices, has propelled the egg industry into a transformative era, moving beyond basic commodity production towards value-added differentiation (Zollman Thomas, et al., 2023). This paradigm shift focuses on developing novel egg products that offer enhanced nutritional profiles, improved functional properties, and cater to specific

dietary needs and ethical considerations (Miranda, et al., 2015; Vlaicu, et al., 2023). This evolution encompasses advancements in conventional egg production, such as enriched eggs and those derived from insects, as well as the emergence of innovative alternatives like plant-based and precision fermentation-derived egg products (Rondoni, et al., 2020; Rondoni, et al., 2021). The increasing prevalence of egg allergies, coupled with a growing consumer shift towards vegan diets and heightened environmental sustainability awareness, further accentuates the market demand for these innovative alternatives (Boukid & Gagaoua, 2022).

Consumer habits, attitudes toward sustainability, health, and animal welfare significantly influence purchasing decisions for eggs (Rondoni, et al., 2020). A substantial proportion of consumers in various countries, such as China, Malaysia, the Philippines, and Thailand, express a willingness to pay more for cage-free eggs, indicating a growing preference for products aligned with higher animal welfare standards (Sinclair, et al., 2022). This willingness to pay a premium extends to other animal welfare considerations, such as the removal of beak trimming practices or the provision of enriched environments with perches and nesting areas for hens (Rondoni, et al., 2020). This shift towards ethical sourcing is further evidenced by consumer preferences in regions where cage-free options are not yet widely available, indicating a clear market opportunity for producers to diversify into higher-welfare systems (Sinclair, et al., 2022). Moreover, a deeper understanding of the influence of demographics, dietary identity, and consumption habits on the acceptance of novel egg products, particularly through direct exposure in retail or food service environments, is crucial for market penetration and sustained growth (Zollman Thomas, et al., 2023). Furthermore, exploring how consumer perceptions of product quality, safety, and sensory attributes, such as taste and texture, contribute to the acceptance of value-added eggs is essential for developing successful marketing strategies and product formulations (Harju, C., et al., 2023; Rondoni, et al., 2020). Conversely, a lack of comprehensive understanding regarding the nuanced differences between terms like 'cage-free' and 'free-range' can inadvertently influence consumer preferences, sometimes favoring caged eggs due to misconceptions about outdoor exposure and predation risks (Sinclair, et al., 2022). Therefore, clear and transparent labeling, coupled with consumer education initiatives, is paramount to fostering informed purchasing decisions that align with ethical production practices.

The aim of the study is to bring together the existing scientific literature on functional eggs and consumer perceptions to provide a comprehensive overview of the subject. In this context, a comprehensive search was conducted in international academic databases such as Web of Science and ScienceDirect using the keywords “functional egg,” “designer egg,” “functional food,” “consumer perception,” and “consumer perception.” Accordingly, the data were examined under the headings of “functional properties of eggs,” “fortification methods,” and “consumer perception.”

This review synthesizes current literature on consumer behavior, perceptions, and preferences concerning value-added eggs and egg products, highlighting key drivers and barriers to adoption (Rondoni, et al., 2020). It also examines how socio-economic factors, cultural backgrounds, and geographical locations impact the adoption rates of these specialized products (Ajetunmobi & Laobangdisa, 2024). Moreover, it explores the impact of increasing consumer awareness regarding health, sustainability, and animal welfare on the market for conventional, enriched, and alternative egg products. This review further investigates the influence of labeling, certifications, and marketing strategies on consumer trust and purchasing decisions for these diverse egg offerings (Harju, C., et al., 2023; Rondoni, et al., 2020) Finally, it assesses the potential future trajectories for the value-added egg market, considering emerging technologies and evolving consumer expectations. This comprehensive analysis aims to bridge existing research gaps by identifying areas where consumer understanding is limited, particularly regarding the benefits of omega-3-enriched eggs, which may lead to an unwillingness to pay a premium (Rondoni, et al., 2020). Such hesitancy often stems from insufficient clear communication regarding the specific health advantages and production methods associated with these specialized products (Harju, C., et al., 2023). Consequently, effective communication strategies that delineate the specific health benefits and the rigorous production standards of omega-3-enriched eggs are vital to enhancing consumer willingness to invest in such premium products (Usturoi, et al., 2025). This is further complicated by consumer misconceptions, such as associating brighter yolk color with enhanced health benefits, irrespective of actual nutritional content, or believing brown eggs are inherently healthier than white eggs. Moreover, preferences for specific sensory attributes, like yolk color and egg size, along with the perceived freshness and safety associated with them, significantly influence purchasing decisions across diverse consumer segments. For instance, consumers from various countries, including Malaysia, Ghana, and Spain, often exhibit a preference for larger eggs, driven by perceptions of greater healthfulness and suitability for common recipes. Similarly, preferences for bright yellow yolk color are common, stemming from an association with

freshness, healthfulness, and safety, although surprisingly, caged eggs have shown higher yolk color acceptance in some comparative studies. Beyond visual appeal, the production method itself significantly influences consumer preferences, with studies indicating a complex perceived interaction between farming practices and attributes like healthfulness, food safety, and sensory qualities (Rondoni, et al., 2020). This complexity highlights the need for transparent communication strategies that educate consumers about the true benefits of various egg types, moving beyond superficial indicators like yolk color or size. To address this, future research should delve into measuring consumers' perceptions and investigating how sociodemographic backgrounds, personal values, beliefs, and knowledge influence purchasing preferences for egg products related to sustainability aspects. Such research could illuminate the factors driving willingness to pay for attributes like local origin and animal welfare, which have been shown to influence consumer choices in other functional food categories (Harju, C., et al., 2023; Migliore, et al., 2022). Furthermore, understanding the interplay between extrinsic cues, such as labeling and certifications, and intrinsic attributes like taste and texture, is crucial for developing effective marketing strategies that resonate with diverse consumer segments (Merlino, et al., 2025). For instance, some consumers show preferences for brown eggs over white eggs, while others prioritize specific yolk colors or reject eggs with visible shell imperfections, all of which influence their purchasing decisions. This underscores the necessity for comprehensive consumer education campaigns that clarify the actual benefits and production methodologies behind different egg types, thereby dispelling common misconceptions and fostering informed purchasing behaviors (Rondoni, et al., 2020). Such campaigns could leverage insights from studies indicating that younger, well-educated females tend to value sustainable product properties more, thereby allowing for targeted messaging to key demographics. Consequently, understanding these demographic nuances and tailoring communication strategies to emphasize environmental impact and ethical production practices can significantly enhance market penetration for sustainably produced eggs. Conversely, a disconnect often exists between consumers' stated preferences for sustainability and their actual purchasing behavior, necessitating a deeper examination of the factors that bridge this attitude-behavior gap (Harju, C., et al., 2023; Li, et al., 2024). This gap is particularly evident in the market for higher quality products, where despite expressed preferences for sustainable and ethically produced options, actual purchasing decisions may still be heavily influenced by price considerations (Bosseaux, et al., 2024). This attitudinal-behavioral disparity highlights the critical role of economic accessibility and perceived value in the adoption of premium egg products (Schaufele & Janssen, 2021). Therefore, future research should explore the efficacy of price signaling mechanisms and their interaction with consumer trust to bridge this gap and encourage greater adoption of sustainably produced eggs. This includes analyzing the influence of regulatory frameworks and public policy interventions, such as eco-labeling and certification systems, which could mitigate the cost sensitivity of consumers and foster broader market acceptance for sustainable egg production (Bosseaux, et al., 2024).

MATERIALS AND METHODS

This study is a qualitative review based on an analysis of current literature published between 2015 and 2025. Data were obtained by searching the Scopus, Web of Science, and Google Scholar databases using the keywords functional food, egg, consumer trends, bioactive compounds, food market and functional egg. In addition, European Union, TÜBİTAK, and KOSGEB reports were also examined in detail to assess the current market dynamics of the sector. Finally, all data obtained were systematically analyzed, taking into account the future of egg industry, the functional food market and consumer trends. Thus, the study provides a comprehensive assessment based on both academic literature and sectoral reports. The literature review identified three main themes that reveal the value of eggs as a functional food and how this value is perceived by consumers.

1. Natural Functional Properties of Eggs

Even without any fortification, eggs naturally contain numerous bioactive compounds that are beneficial to health. These properties make eggs a functional food in their own right.

Lysozyme and Ovotransferrin: These proteins, found particularly in egg whites, exhibit strong antimicrobial properties (Abdou & Awad, 2024; Yüceer, 2022; Yüceer, et al., 2023).

Lutein and Zeaxanthin: These carotenoids, which give egg yolks their color, are antioxidants that play a role in protecting eye health and may reduce the risk of age-related macular degeneration.

Phosphovitins and Bioactive Peptides: Phosphovitins in egg yolk are powerful antioxidants. In addition, peptides produced by the digestion of egg proteins may have blood pressure-regulating and immune system-supporting effects (Yüceer, 2019).

Table 1: Natural Bioactive Components of Eggs and Their Functions (Yüceer, 2019)

Bioactive Component	Location	Potential Functional Effect
Lysozyme	Egg White	Exhibits antimicrobial and antiviral properties.
Ovotransferrin	Egg White	Has antimicrobial and antiviral effects; inhibits bacterial growth by binding iron ions.
Phosvitin	Egg Yolk	Strong antioxidant; has mineral-binding properties.
Lutein and Zeaxanthin	Egg Yolk	Protects eye health; strong antioxidants that help reduce the risk of age-related macular degeneration.
Bioactive Peptides	Egg Proteins (Post-Digestion)	May show antihypertensive (blood pressure regulating) and immunomodulatory (immune-regulating) effects.

2. Enrichment Methods

The nutritional value of eggs can be enhanced to target specific health benefits by adjusting the chickens' feed. These products, called "designer eggs," aim to meet specific consumer needs (Lesnierowski & Stangierski, 2018; Surai & Sparks, 2001).

Omega-3 Fatty Acids: The omega-3 content of eggs is increased by adding flaxseed or fish oil to feed. These eggs are often marketed with the claim of supporting cardiovascular health (Abdel-Nour & Ngadi, 2011; Açıkgöz & Önenç, 2006)

Vitamins (especially vitamin D): Supplements added to feed increase the vitamin D content of eggs, aiming to contribute to bone health and the immune system.

Selenium: Eggs are produced with the aim of strengthening the body's defense system by adding selenium, a powerful antioxidant, to feed.

3. Factors Shaping Consumer Perception

The scientific properties of a product alone do not guarantee its success in the market. Consumer perception and preferences are decisive at this point.

The Importance of Production Methods: Despite the rich nutrient content mentioned above, some of the factors are limits egg consumption and therefore affects consumer preferences (age, lifestyle, income level, education level, animal welfare, price, health concerns, etc.). Consumers view labels such as "organic" and "free-range" not only as a production standard but also as an indicator of health, naturalness, and animal welfare (Rondoni, et al., 2020). Therefore, clear and transparent labeling, along with consumer education initiatives, are crucial for encouraging informed purchasing decisions that align with ethical production practices. This educational requirement is further complicated by regional variations in consumer awareness, such as in Australia and the UK, where consumers still exhibit uncertainty about predominant egg production systems despite the prevalence of cage-free egg production. This highlights the need for clearer communication strategies to accurately convey the welfare standards associated with different production systems to the general public (Rondoni, et al., 2020). This underscores the need for targeted, region-specific information campaigns to enable consumers to make informed choices that reflect their ethical and sustainability values (Sinclair, et al., 2022).

Price Sensitivity and Lack of Information: One of the most significant barriers to functional eggs is price. Consumers are reluctant to pay higher prices because they do not fully understand the health effects of supplements such as omega-3. This highlights the importance of effective and understandable labeling. This situation is further complicated by consumer misconceptions, such as associating a brighter yellow color with enhanced health benefits regardless of actual nutritional content or believing that brown eggs are naturally healthier than white eggs Understanding the interaction between external cues such as labeling and certifications and internal characteristics such as taste and texture is crucial for developing effective marketing strategies that resonate with various consumer segments (Rondoni, et al., 2020).

Market Potential: Although per capita egg consumption in Turkey is increasing, it remains below recommended levels, indicating room for growth with the right market management strategies. Furthermore, researching the role of government incentives and industry collaborations in promoting the production and consumption of these products is essential for developing a more sustainable and economically viable egg market.

It is important to analyze whether consumers in different regions place more value on external sustainability cues, such as organic or free-range chicken certifications, when making purchasing decisions, rather than internal product characteristics, such as perceived freshness or nutritional content (Harju et al., 2023) (Piras et al., 2023).

RESULTS and DISCUSSION

Overcoming Barriers in Consumer Perception: Communication and Marketing Strategies

The functional egg market can be expanded by developing niche products tailored to the needs of specific demographic groups, rather than adopting a "one-size-fits-all" approach.

1. Target Audience-Focused Product Development

Consumer demand for functional foods is not homogeneous. Market success depends on developing products that meet the needs of specific demographic and lifestyle groups, rather than a "one size fits all" approach. In this context, four main target audiences stand out for the functional egg market:

- **Athletes and Active Individuals:** With its high bioavailable protein structure, eggs are a natural choice for muscle repair and development. For this audience, eggs with an optimized amino acid profile or anti-inflammatory properties hold strategic value.
- **Elderly Population:** Functional eggs can play an important protective role against the increased risk of chronic diseases associated with aging. Eggs enriched with lutein and zeaxanthin for eye health, vitamin D for bone health, and choline and DHA for cognitive function and memory directly address the specific needs of this group.
- **Children and Pregnant Women:** Choline, critical for brain and nervous system development in early life, and DHA content, which can be increased through feed manipulation, can be marketed to this target audience with the "smart egg" concept.
- **Health-Conscious Millennials and Generation Z:** For these generations, the product's story is as important as its health benefits. Ethical production conditions, animal welfare, and environmental sustainability are decisive factors in this segment's purchasing decisions.

2. Sustainability, Ethics, and Legal Frameworks

Modern consumers care not only about their own health but also about the health of the planet. The future of functional eggs depends on the ability to minimize the environmental footprint of production processes. The transition from traditional cage systems to alternative systems (cage-free, free-range) following animal welfare regulations introduced in the European Union in 2012 is the most concrete manifestation of this trend. Consumers believe that eggs produced under higher animal welfare standards are safer and healthier and are willing to pay a higher price for these products. The sustainability of feed sources also plays a critical role at this point. For example, using innovative feed additives such as microalgae, which have a lower environmental impact, instead of unsustainable fish oil sources for omega-3 enrichment will strengthen the product's sustainability claim. Eggshell, the industry's largest by-product, is a valuable source of calcium, while eggshell membrane is a source of collagen and other bioactive components that can be utilized in the nutraceutical industry. Marketing a product as "functional" is subject to strict legal frameworks. Both international authorities (e.g., EFSA in Europe) and Turkey's Turkish Food Codex Nutrition and Health Claims Regulation require that any health claim on a food package, such as "strengthens immunity," be supported by scientific evidence. These legal controls play a fundamental role in protecting consumers from false claims and establishing trust in products on the market (Leinonen, et al., 2012; Rondoni, et al., 2020).

3. Competitor Products and Market Positioning

Functional eggs are not alone in the market. Consumers can also meet their omega-3 needs from fish oil capsules, flaxseed, or other enriched foods such as plant-based milks. The rapid increase in the consumption of plant-based milk, meat, and egg alternatives in recent years has created a new competitive environment for animal products. In this competitive environment, the biggest advantage of functional eggs is that they are a "natural whole food." Therefore, the marketing strategy should emphasize that eggs are not just a single enriched ingredient; rather, they are a holistic food source that provides valuable nutrients such as protein, vitamins, and bioactive peptides. The increasing prevalence of egg allergies, the growing consumer shift towards vegan diets, and rising environmental sustainability awareness further emphasize the market demand for innovative alternatives (Boukid & Gagaoua, 2022). This significant market growth underscores a major shift in consumer preferences driven by factors such as

allergen reduction, improved food safety, healthier nutritional profiles, and environmental sustainability growing awareness is significantly influencing market dynamics and product development (Bianchi & Simonato, 2025).
Furthermore, a deeper understanding of the impact of demographic characteristics, dietary identity, and consumption habits on the acceptance of new egg products, particularly through direct exposure in retail or food service settings, is crucial for market penetration and sustainable growth. Additionally, investigating how consumer perceptions of product quality, safety, and sensory attributes such as taste and texture contribute to the acceptance of value-added eggs is essential for developing successful marketing strategies and product formulations (Harju, A., et al., 2023; Zollman Thomas, et al., 2023).

Conclusion and Future Perspectives

Eggs hold a strategic position in the functional food market due to both their naturally occurring bioactive components (lysozyme, phosvitin, lutein, etc.) and their potential to be enriched with valuable components such as omega-3, selenium, and vitamin D. As one of the world's largest egg producers, Turkey has the opportunity to transform this potential into value-added products both in the domestic market and for export. However, fully realizing this potential requires reshaping technology and marketing strategies with a consumer-centric approach.
Ultimately, the future of functional eggs depends on addressing information gaps through transparent labeling, building trust with science-based health claims, and meeting modern consumers' ethical expectations through sustainable production practices.

• **Transparent Communication:** Developing labeling and marketing strategies that clearly explain the product's added functional components, natural composition, and production methods to address consumer information gaps.
• **Scientific Credibility:** Supporting health claims with scientific evidence and presenting them to consumers with approval from credible authorities.
• **Holistic Approach:** Develop products that meet consumer expectations for health, naturalness, and ethical production as a whole.

Future research should examine in more detail the market acceptance of new functional eggs developed for the specific needs of different consumer segments (athletes, seniors, etc.) and the potential impact of the growing plant-based egg alternatives on this market. Eliminating the risk of these scientifically superior products failing to pass the consumer's perception filter on the market shelf will only be possible with this multifaceted approach.

CONCLUSION

In conclusion, the trajectory of value-added egg products is heavily influenced by the evolving interplay between consumer perceptions, technological advancements, and sustainable production practices, requiring a dynamic approach to product development and market positioning. This entails a continuous effort to align product innovation with consumer expectations, particularly regarding health, ethical considerations, and environmental impact, while simultaneously addressing existing knowledge gaps through transparent communication. For instance, emphasizing the superior nutritional profiles of certain value-added eggs, such as those enriched with omega-3 fatty acids or vitamins, could appeal to health-conscious consumers. Moreover, future research should investigate the impact of emerging trends like insect-fed eggs on both nutritional properties and consumer preferences, alongside exploring the market potential and consumer acceptance of plant-based egg alternatives. These studies should also consider the potential for precision fermentation-derived egg proteins to disrupt traditional egg markets, examining consumer attitudes towards such novel food technologies and their willingness to integrate them into their diets. Finally, understanding consumer behavior, perceptions, and preferences towards eggs and egg products is crucial for producers to develop appropriate strategies and policies that can satisfy the complex and diverse demands of consumers.

REFERENCES

Abdel-Nour, N., & Ngadi, M. (2011). Detection of omega-3 fatty acid in designer eggs using hyperspectral imaging. *Int J Food Sci Nutr, 62*, 418-422.

Abdou, A. M., & Awad, D. A. B. (2024). Lysozyme Peptides as a Novel Nutra-Preservative to Control Some Food Poisoning and Food Spoilage Microorganisms. *Probiotics Antimicrob Proteins*.

Açıkgöz, Z., & Önenç, S. S. (2006). Fonksiyonel Yumurta Üretimi. *Hay. Üret., 47*, 36-46.

Ajetunmobi, O. A., & Laobangdisa, S. (2024). The Effect of Cultural and Socio-economics Factors on Consumer Perception. In D. Bogueva (Ed.), *Consumer Perceptions and Food* (pp. 23-44). Singapore: Springer Nature Singapore.

Bianchi, F., & Simonato, B. (2025). Pulses Protein Concentrates and Isolates as Stand-Alone Plant-Based Egg Replacers: An Explorative Study of Their Functional Properties and Technological Effect in Pancakes. *Food and Bioprocess Technology*.

Bosseaux, J., Balcombe, K., & Aurier, P. (2024). Impact of European egg marking system in France: empirical time series analysis between 2017 and 2022. *Review of Agricultural, Food and Environmental Studies, 105*, 229-250.

Boukid, F., & Gagaoua, M. (2022). Vegan Egg: A Future-Proof Food Ingredient? *Foods, 11*.

El-Sabrout, K., Aggag, S., & Mishra, B. (2022). Advanced Practical Strategies to Enhance Table Egg Production. *Scientifica (Cairo), 2022*, 1393392.

Hardy, G. (2000). Nutraceuticals and functional foods: introduction and meaning. *Nutrition, 16*, 688-689.

Harju, A., Hallikas, J., Immonen, M., & Lintukangas, K. (2023). The impact of procurement digitalization on supply chain resilience: empirical evidence from Finland. *Supply Chain Management: An International Journal, 28*, 62-76.

Harju, C., Lähtinen, K., Heinola, K., Väre, M., Bonnefous, C., Collin, A., Cozma, V., Kliphuis, S., Parrott, P. A., Rodenburg, T. B., Spinu, M., & Niemi, J. (2023). Consumers' views on egg quality and preferences for responsible production – results from nine European countries. *British Food Journal, 126*, 623-644.

Kwak, N.-S., & Jukes, D. J. (2001). Functional foods. Part 1: the development of a regulatory concept. *Food Control, 12*, 99-107.

Leinonen, I., Williams, A. G., Wiseman, J., Guy, J., & Kyriazakis, I. (2012). Predicting the environmental impacts of chicken systems in the United Kingdom through a life cycle assessment: egg production systems. *Poult Sci, 91*, 26-40.

Lesnierowski, G., & Stangierski, J. (2018). What's new in chicken egg research and technology for human health promotion? - A review. *Trends in Food Science & Technology, 71*, 46-51.

Li, P., Lin, I. K., & Chen, H. S. (2024). Low Carbon Sustainable Diet Choices-An Analysis of the Driving Factors behind Plant-Based Egg Purchasing Behavior. *Nutrients, 16*.

Merlino, V. M., Sciullo, A., Mastromonaco, G., Sparacino, A., Costamagna, C., & Mosca, O. (2025). The role of sustainable production attributes and certification in determining consumer choices. In *The Sustainable Food Choice* (pp. 321-334).

Migliore, G., Rizzo, G., Bonanno, A., Dudinskaya, E. C., Tóth, J., & Schifani, G. (2022). Functional food characteristics in organic food products—the perspectives of Italian consumers on organic eggs enriched with omega-3 polyunsaturated fatty acids. *Organic Agriculture, 12*, 149-161.

Miranda, J. M., Anton, X., Redondo-Valbuena, C., Roca-Saavedra, P., Rodriguez, J. A., Lamas, A., Franco, C. M., & Cepeda, A. (2015). Egg and egg-derived foods: effects on human health and use as functional foods. *Nutrients, 7*, 706-729.

Rehault-Godbert, S., Guyot, N., & Nys, Y. (2019). The Golden Egg: Nutritional Value, Bioactivities, and Emerging Benefits for Human Health. *Nutrients, 11*.

Rondoni, A., Asioli, D., & Millan, E. (2020). Consumer behaviour, perceptions, and preferences towards eggs: A review of the literature and discussion of industry implications. *Trends in Food Science & Technology, 106*, 391-401.

Rondoni, A., Millan, E., & Asioli, D. (2021). Plant-based Eggs: Views of Industry Practitioners and Experts. *Journal of International Food & Agribusiness Marketing*, 1-24.

Schaufele, I., & Janssen, M. (2021). How and Why Does the Attitude-Behavior Gap Differ Between Product Categories of Sustainable Food? Analysis of Organic Food Purchases Based on Household Panel Data. *Front Psychol, 12*, 595636.

Sinclair, M., Lee, N. Y. P., Hötzel, M. J., de Luna, M. C. T., Sharma, A., Idris, M., Islam, M. A., Iyasere, O. S., Navarro, G., Ahmed, A. A., Curry, M., Burns, G. L., & Marchant, J. N. (2022). Consumer attitudes towards egg production systems and hen welfare across the world. *Frontiers in Animal Science, 3*.

Surai, P., & Sparks, N. (2001). Designer eggs: from improvement of egg composition to functional food. *Trends in Food Sci. & Tech., 12*, 7-16.

Usturoi, M. G., Rațu, R. N., Crivei, I. C., Veleșcu, I. D., Usturoi, A., Stoica, F., & Radu Rusu, R.-M. (2025). Unlocking the Power of Eggs: Nutritional Insights, Bioactive Compounds, and the Advantages of Omega-3 and Omega-6 Enriched Varieties. *Agriculture, 15*.

Vlaicu, P. A., Untea, A. E., Varzaru, I., Saracila, M., & Oancea, A. G. (2023). Designing Nutrition for Health-Incorporating Dietary By-Products into Poultry Feeds to Create Functional Foods with Insights into Health Benefits, Risks, Bioactive Compounds, Food Component Functionality and Safety Regulations. *Foods, 12*.

Yüceer, M. (2019). *Yumurta ve Yumurta Ürünleri İşleme Teknolojisi ve Uygulamaları* Sidas Medya Ltd.Şti. İzmir, Turkiye.

Yüceer, M. (2022). Yumurta Biyoaktif Bileşenleri (2): Lizozim. *Yumurta Üreticileri Merkez Birliği Dergisi, 58*, 30-33.

Yüceer, M., Çelikten, C., Mavuş, R., Dişli, E., Ağıral Akgün, Ş., & Sarı, E. (2023). Yumurta Akından Lizozim Ekstraksiyonu, Saflaştırılması ve Kurutulması: Güncel Gelişmeler ve Uygulamaları. *International Journal of Life Sciences and Biotechnology, 6*, 245-261.

Zollman Thomas, O., Chong, M., Leung, A., Fernandez, T. M., & Ng, S. T. (2023). Not getting laid: consumer acceptance of precision fermentation made egg. *Frontiers in Sustainable Food Systems, 7*.

ORAL PRESENTATION

DPP4 (CD26) geninin akut myeloid lösemi patogenezindeki rolünün değerlendirilmesi

Deniz Aşlar Öner (*Orcid: https://orcid.org/ 0000-0002-9515-0073*)

Afyonkarahisar Sağlık Bilimleri Üniversitesi, Atatürk Sağlık Hizmetleri Meslek Yüksekokulu, Afyonkarahisar, Türkiye

*Sorumlu yazar e-mail: deniz.oner@afsu.edu.tr

Özet

Bu çalışma, in silico yaklaşımlar kullanılarak *DPP4* (dipeptidil peptidaz-4/CD26) geninin Akut Miyeloid Lösemi (AML) patogenezindeki olası rolünü ekspresyon, mutasyon ve protein stabilitesi düzeyinde kapsamlı biçimde değerlendirmeyi amaçlamıştır. AML, genetik ve epigenetik değişimlerin etkisiyle hematopoietik kök hücrelerin farklılaşma yeteneğini kaybettiği, yüksek mortalite oranına sahip bir malignitedir. Bu nedenle, hücre yüzeyinde yer alan ve sinyal iletiminde rol oynayan DPP4 gibi genlerin moleküler etkilerinin anlaşılması, hastalığın biyolojik temellerinin aydınlatılmasında kritik önem taşımaktadır. AML hastalarına ait transkriptom verileri The Cancer Genome Atlas (TCGA-LAML) veri tabanından, normal kemik iliği örnekleri ise GTEx veri tabanından alınmıştır. GEPIA aracıyla yapılan analizlerde, DPP4 ekspresyonunun AML örneklerinde normal kontrollere göre anlamlı şekilde arttığı belirlenmiştir ($p<0.05$). Mutasyon analizinde PolyPhen-2 aracı kullanılmış; G633E mutasyonu "probably damaging", I107L mutasyonu ise "benign" olarak tanımlanmıştır. I-Mutant 2.0 ve DynaMut2 sonuçları, G633E mutasyonunun DPP4 proteininin termodinamik kararlılığını azalttığını ($\Delta\Delta G$ = -1.05 kcal/mol) ve yapısal bütünlüğü zayıflattığını göstermiştir. HOPE analizi, glisin yerine geçen glutamik asidin daha büyük ve negatif yüklü olması nedeniyle lokal elektrostatik dengeyi bozabileceğini ve hidrofobik çekirdek stabilitesini zayıflatabileceğini ortaya koymuştur. Sonuç olarak, bu çalışma *DPP4'ün* AML'deki rolünün yalnızca ekspresyon artışıyla sınırlı olmadığını, aynı zamanda yapısal varyasyonların da genin biyolojik işlevlerini etkileyebileceğini göstermektedir. Ancak bu öngörülerin kesinleştirilmesi için deneysel doğrulama ve fonksiyonel analiz çalışmalarına ihtiyaç vardır. DPP4, mevcut veriler ışığında, AML'nin moleküler patogenezinin anlaşılmasına katkı sağlayabilecek potansiyel bir biyobelirteç olarak değerlendirilebilir.

Anahtar Kelimeler Akut Myeloid Lösemi, DPP4, CD26, mutasyon

Evaluation of the role of the DPP4 (CD26) gene in the pathogenesis of acute myeloid leukemia

Abstract

This study aimed to comprehensively evaluate the potential role of the *DPP4* (dipeptidyl peptidase-4/CD26) gene in the pathogenesis of Acute Myeloid Leukemia (AML) using in silico approaches at the expression, mutation, and protein stability levels. AML is a malignancy with a high mortality rate, where hematopoietic stem cells lose their ability to differentiate due to genetic and epigenetic alterations. Therefore, understanding the molecular effects of genes such as DPP4, which are located on the cell surface and play a role in signal transduction, is critical for elucidating the biological basis of the disease. Transcriptome data from AML patients were obtained from The Cancer Genome Atlas (TCGA-LAML) database, and normal bone marrow samples were obtained from the Genotype-Tissue Expression (GTEx) database. Analysis using the GEPIA (Gene Expression Profiling Interactive Analysis) tool revealed that DPP4 expression was significantly increased in AML samples compared to normal controls ($p<0.05$). The PolyPhen-2 tool was used for mutation analysis; the G633E mutation was identified as "probably damaging" and the I107L mutation as "benign". I-Mutant 2.0 and DynaMut2 results showed that the G633E mutation reduces the thermodynamic stability of the DPP4 protein ($\Delta\Delta G$ = -1.05 kcal/mol) and weakens its structural integrity. HOPE (Have (y)Our Protein Explained) analysis revealed that the larger and more negatively charged glutamic acid replacing glycine may disrupt local electrostatic equilibrium and weaken the stability of the

hydrophobic core. In conclusion, this study demonstrates that the role of DPP4 in AML is not limited to increased expression; structural variations can also affect the biological functions of the gene. However, experimental validation and functional analysis are needed to confirm these predictions. In light of the available data, DPP4 can be considered as a potential biomarker that can contribute to the understanding of the molecular pathogenesis of AML.

Keywords: Acute Myeloid Leukemia, DPP4, CD26, mutation

GİRİŞ

Akut myeloid lösemi (AML), erişkinlerde en sık görülen akut lösemi türü olup, lösemiler arasında en yüksek yıllık mortalite oranına sahiptir. Son yıllarda hedefe yönelik tedaviler ve düşük yoğunluklu tedavi rejimleri özellikle mutasyon pozitif AML alt tiplerinde ve 65 yaş üzeri hastalarda kullanılmaya başlanmıştır (Tallman ve ark., 2019). Bu gelişmeler bazı hasta alt gruplarında klinik sonuçları iyileştirse de, genel olarak AML prognozu halen kötüdür ve beş yıllık sağkalım oranı yalnızca %29'dur. AML tedavisinde en önemli zorluklardan biri, lösemik hücrelerde sınırlı sayıda özgül terapötik hedefin tanımlanabilmiş olmasıdır. Ayrıca mevcut tedavi yaklaşımları çoğunlukla normal hematopoietik hücreleri de etkileyerek ciddi yan etkilere yol açmaktadır (Kumar, 2011). Bu bağlamda, klasik kemoterapi rejimleri veya kök hücre nakli yüksek morbidite ve mortalite oranları ile ilişkilidir (Sanford ve Ravandi, 2015). Bu nedenle AML için etkili ancak tolere edilebilir yeni tedavi stratejilerine ihtiyaç duyulmaktadır.

Hücre yüzey proteinleri, hem hücresel belirteç olarak rolleri hem de ekstrasellüler erişilebilirlikleri nedeniyle önemli terapötik hedeflerdir. Bununla birlikte, bu yüzey proteinlerinin ekspresyonu ve fonksiyonu, lösemik hücreler ile normal hematopoietik hücreler arasında belirgin farklılıklar gösterebilmektedir (Wang ve ark., 2023). Bu farklılıkları temel alan bir tarama çalışmasında, insan ve fare AML hücrelerinde eksprese edilen hücre yüzey proteinlerini hedefleyen bileşikler incelenmiş ve bu analiz sonucunda *DPP4/CD26*, AML tedavisinde potansiyel bir hedef olarak tanımlanmıştır. DPP4 pek çok hücre tipinde ve farklı organ sistemlerinde, hematopoietik sistem dahil olmak üzere, eksprese edilmektedir (Nistala ve Savin, 2017). Ayrıca *DPP4*, hem kronik myeloid lösemi (CML) hem de akut lenfoblastik lösemi (ALL) kök hücreleri için bir biyobelirteç ve terapötik hedef olarak tanımlanmıştır (Herrmann ve ark., 2014; Castillo ve ark., 2012; Blatt ve ark., 2018). Ancak *DPP4'ün* AML hücrelerindeki kesin fonksiyonu ve AML gelişimindeki rolü tam olarak aydınlatılamamıştır.

Bu çalışmada, *DPP4* geninin AML patogenezindeki olası rolünü değerlendirmek amacıyla in silico yaklaşımlar kullanılarak genin ekspresyon düzeyleri ve mutasyon profillerinin belirlenmesi hedeflenmiştir. Bu kapsamda elde edilecek bulguların, *DPP4'ün* AML ile ilişkili moleküler mekanizmalarının anlaşılmasına katkı sağlaması ve gelecekteki deneysel doğrulama çalışmalarına temel oluşturması amaçlanmıştır.

MATERYAL VE METOT

Bu çalışmada AML hastalarına ait gen ekspresyon verileri The Cancer Genome Atlas (TCGA-LAML) veri tabanından elde edilmiştir. Toplam 200 AML hastasına ait transkriptom verileri indirilmiş, karşılaştırmalı analizlerde ise normal kemik iliği örnekleri Genotype-Tissue Expression (GTEx) veri tabanından alınmıştır. AML ve normal örneklerde gen ekspresyon farklılıklarını değerlendirmek amacıyla GEPIA (Gene Expression Profiling Interactive Analysis) web aracı kullanılmıştır. Ekspresyon düzeyleri $\log_2$ (TPM + 1) dönüşümü sonrası normalizasyonla elde edilmiş, $p < 0.05$ anlamlılık sınırı olarak kabul edilmiştir.

AML hasta verilerinde *DPP4* genine ait potansiyel varyantların fonksiyonel etkilerini değerlendirmek için PolyPhen-2 (Polymorphism Phenotyping v2) aracı kullanılmıştır (Adzhubei ve ark., 2013). Bu analiz, aminoasit değişimlerinin proteinin yapısal bütünlüğü ve fonksiyonu üzerindeki olası etkilerini "benign", "possibly damaging" veya "probably damaging" olarak sınıflandırmıştır. Çalışmada mutasyon ve ekspresyon profillerinin yanı sıra *DPP4* geninin sağkalım üzerine olan etkisi de %95 güven aralığı ile belirlenmiştir

DPP4 proteininde gözlenen varyantların termodinamik kararlılık değişimi, I-Mutant 2.0 yazılımı kullanılarak analiz edilmiştir. Ayrıca, aynı varyantın yapısal stabilite değişimleri DynaMut2 aracı kullanılarak değerlendirilmiştir (Rodrigues ve ark., 2018). DynaMut2, wild-type ve mutant protein modelleri arasında serbest enerji farkını ($\Delta\Delta G$) hesaplayarak mutasyonun proteinin konformasyonel kararlılığı üzerindeki etkisini öngörmüştür.

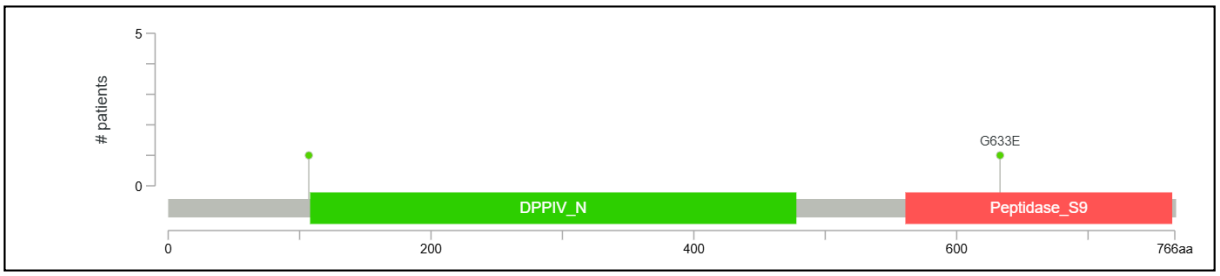
Ayrıca, *DPP4* geninde tanımlanan aminoasit değişimlerinin olası yapısal ve fonksiyonel etkilerini değerlendirmek amacıyla HOPE yazılımı kullanılmıştır. Bu analiz, mutasyonun proteinin üç boyutlu yapısındaki konumu, aminoasit özelliklerindeki değişiklikler ve olası yapısal bozunumlar açısından değerlendirilmesini sağlamıştır (Venselaar ve ark., 2010).

BULGULAR ve TARTIŞMA

Bu çalışmada, *DPP4* geninin AML patogenezindeki olası rolünü değerlendirmek amacıyla in silico yaklaşımlar kullanılarak genin ekspresyon düzeyleri ve mutasyon profilleri belirlenmiştir. Ayrıca, saptanan varyantların proteinin yapısal kararlılığı ve biyolojik fonksiyonu üzerindeki olası etkileri hesaplamalı yöntemlerle analiz edilmiştir.

Analiz sonuçlarına göre *DPP4* geninde iki missense mutasyon tanımlanmıştır (Şekil 1).

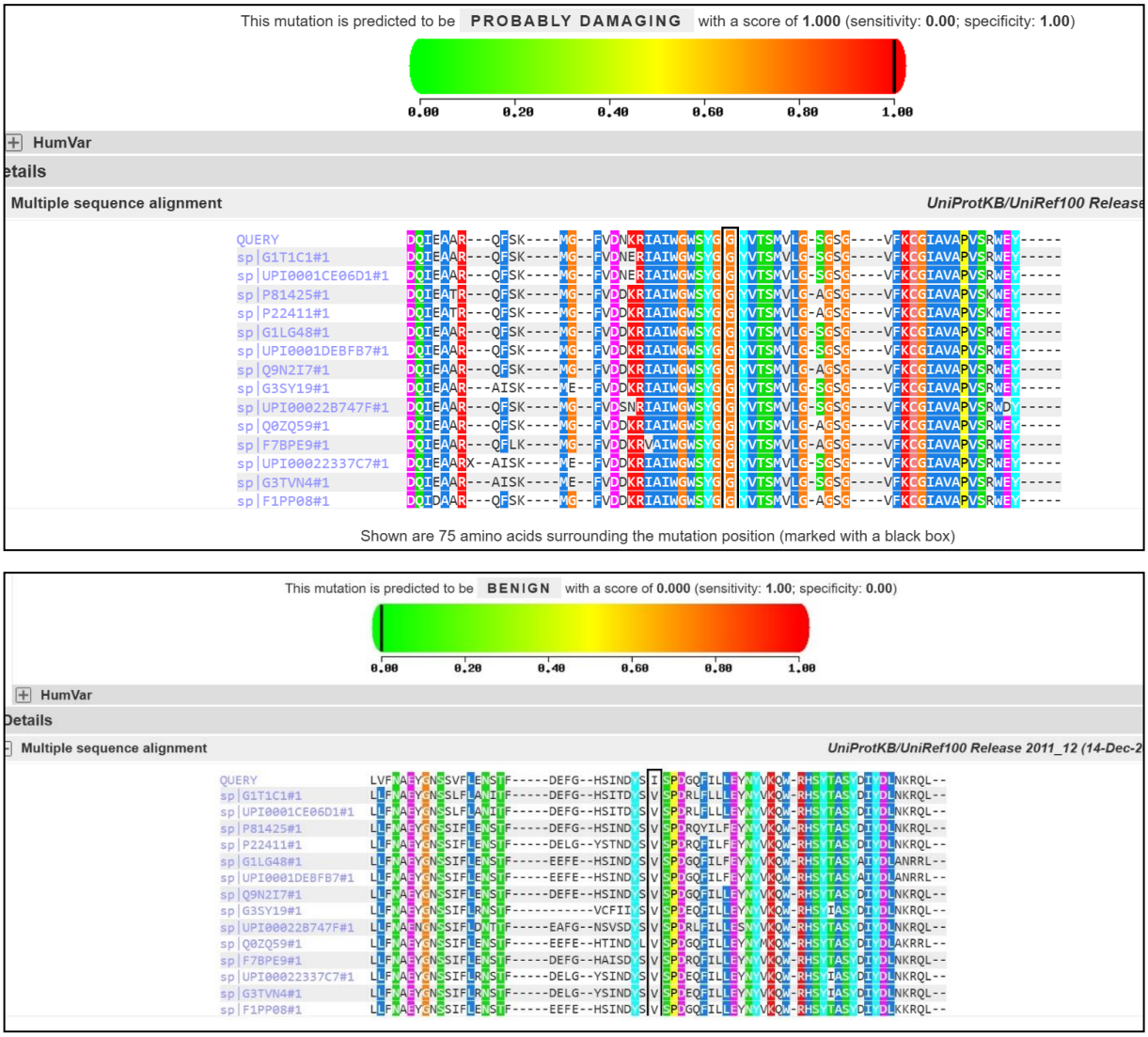
Sample ID	Protein Change	Annotation	Mutation Type	Copy #	Allele Freq (T)	# Mut in Sample
TCGA-AB-2808-03	*G633E*		Missense	Diploid	0.08	782
TCGA-AB-2828-03	*I107L*		Missense	Diploid	0.08	753



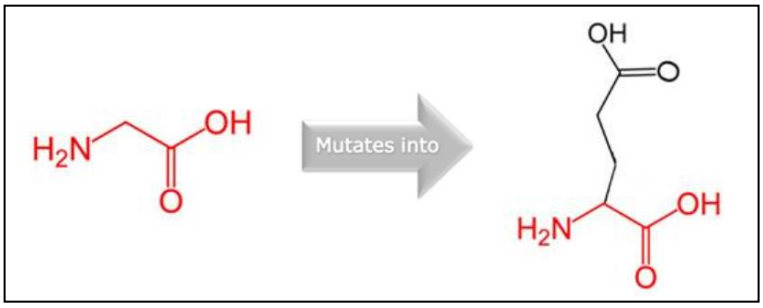
Şekil 1. DPP4'ün domain yapısının şematik gösterimi

G633E mutasyonu, PolyPhen-2 analizi sonucunda "probably damaging" olarak değerlendirilmiş olup, proteinin yapısal stabilitesi ve fonksiyonel bütünlüğü üzerinde olumsuz etki potansiyeline sahip olduğu öngörülmüştür. Buna karşın, I107L mutasyonu "benign" olarak sınıflandırılmış ve proteinin yapısal veya fonksiyonel özelliklerini anlamlı düzeyde etkilemediği tahmin edilmiştir. (Şekil 2).

I-Mutant analizi, G633E mutasyonunun DPP4 proteininin termodinamik stabilitesini azalttığını ortaya koymuştur. Bu bulgu, DynaMut2 analizinden elde edilen sonuçlarla da desteklenmiş olup, söz konusu mutasyonun *DPP4'ün* kararlılığında belirgin bir azalmaya yol açtığı doğrulanmıştır ($\Delta\Delta G$ = -1.05 kcal/mol; destabilizing). HOPE analizine göre *DPP4* genindeki G633E (Glycine→Glutamic acid) mutasyonu, proteinin yapısal ve biyokimyasal özelliklerini olumsuz etkilemektedir (Şekil 3). Küçük ve nötr bir amino asit olan glisinin yerine daha büyük ve negatif yüklü bir glutamik asidin geçmesi, sterik engellere ve elektrostatik dengenin bozulmasına yol açmaktadır. Ayrıca, mutasyon sonrası artan hidrofiliklik, hidrofobik çekirdek stabilitesini zayıflatabilir. Bu değişiklikler, DPP4 proteininin konformasyonel kararlılığında azalmaya neden olabileceğini göstermektedir. Bulgular, DynaMut2 ve I-Mutant analizlerinde gözlenen destabilizasyon eğilimi ile uyumludur.



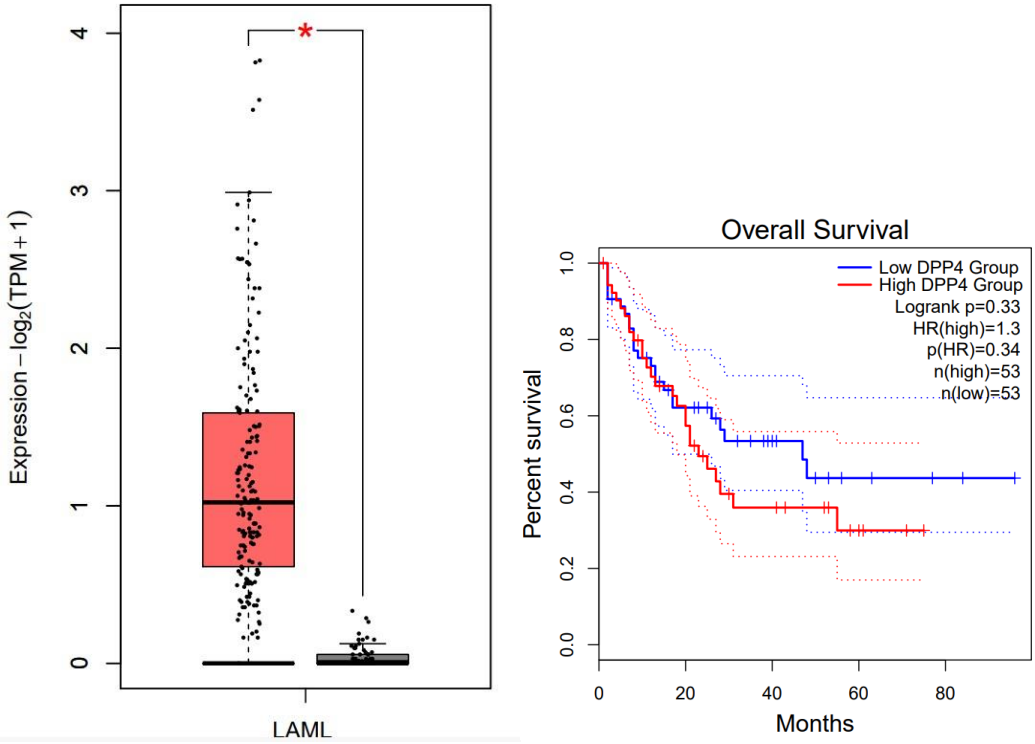
Şekil 2. DPP4 genindeki missense mutasyonların olası fonksiyonel etkilerinin PolyPhen-2 programı ile tahmin edilmesi



Şekil 3. G633E missense mutasyon için wild-type (sol) ve mutant (sağ) amino asit modellemesi

GEPIA analizi sonuçlarına göre, *DPP4* geninin ekspresyon düzeyi, LAML örneklerinde normal kontrollere kıyasla anlamlı düzeyde artış göstermiştir ($p < 0.05$). Bu bulgu, *DPP4* geninin AML patogenezinde önemli bir biyolojik role sahip olabileceğini ve hastalığa özgü potansiyel bir terapötik hedef olarak değerlendirilebileceğini göstermektedir. Yapılan sağkalım analizinde, *DPP4* gen ekspresyon düzeyleri ile AML hastalarının genel sağkalım süreleri arasında belirgin bir ilişki eğilimi gözlenmiştir. Ancak bu farklılık istatistiksel olarak anlamlı düzeyde

bulunmamıştır (p = 0.33). Bu bulgu, *DPP4* ekspresyonunun hastalık seyrine olası etkilerinin daha geniş örneklemlerle desteklenmesi gerektiğini düşündürmektedir (Şekil 4).



Şekil 4. AML hastalarında DPP4 ekspresyon düzeyi ile sağkalım analizi

TARTIŞMA

Bu çalışmada, *DPP4* geninin AML patogenezindeki potansiyel rolü in silico yaklaşımlar ile değerlendirilmiştir. GEPIA verileri, *DPP4* ekspresyonunun AML örneklerinde normal kemik iliği dokularına kıyasla anlamlı biçimde artmış olduğunu göstermiştir. Bu durum, DPP4'ün AML hücrelerinde biyolojik olarak aktif olabileceğini ve lösemik hücre davranışlarını etkileyebileceğini düşündürmektedir. Nitekim, Wang ve ark. (2023) tarafından yürütülen çalışmada da *DPP4'ün*, AML kök hücrelerinin yaşamı ve kök hücre benzeri özelliklerinin sürdürülmesinde kritik bir rol oynadığı bildirilmiştir. DPP4'ün Src kinaz ile etkileşerek NF-κB sinyal yolunu aktive ettiği, bu yolla AML kök hücrelerinin anti-apoptotik ve self-renewal kapasitesini koruduğu gösterilmiştir. Ayrıca, DPP4 inhibitörlerinin hem insan hem de fare AML modellerinde lösemik hücre proliferasyonunu baskıladığı ve apoptozu artırdığı rapor edilmiştir. Bu bulgular, DPP4'ün hedeflenmesinin AML tedavisinde yeniden konumlandırılabilecek farmakolojik bir strateji olabileceğini desteklemektedir.

Moleküler düzeyde yapılan varyant analizleri, *DPP4* genindeki G633E mutasyonunun PolyPhen-2 tarafından "probably damaging" olarak, I107L mutasyonunun ise "benign" olarak sınıflandırıldığını ortaya koymuştur. I-Mutant ve DynaMut2 analizleri, G633E değişiminin DPP4 proteininin termodinamik kararlılığını azalttığını (ΔΔG = −1.05 kcal/mol) göstermiştir. HOPE analizi ise Glisin'den Glutamik asit'e geçişin, artan yan zincir hacmi ve negatif yük nedeniyle lokal elektrostatik etkileşimleri ve çekirdek paketlenmesini bozabileceğini göstermiştir. Bu bulgular bir arada değerlendirildiğinde, G633E mutasyonunun DPP4'ün yapısal bütünlüğü üzerinde bozucu etkiler oluşturabileceği ve proteinin fonksiyonel stabilitesini zayıflatabileceği anlaşılmaktadır. Bu sonuçlar, Wei ve ark. (2021) tarafından bildirilen verilerle de paralellik göstermektedir. Söz konusu çalışmada, ferroptozisle ilişkili genlerden oluşan çalışmanın (*DPP4, GPX4, LPCAT3, SLC7A11 ve TFRC*) AML prognozunu anlamlı biçimde öngördüğü; özellikle *DPP4'ün* tanısal ve prognostik biyobelirteçler olarak klinik öneme sahip olduğu vurgulanmıştır.

SONUÇ

Bu çalışma, in silico analizler aracılığıyla *DPP4* geninin AML patogenezindeki olası rolünü kapsamlı biçimde ortaya koymuştur. Elde edilen bulgular, *DPP4* ekspresyonunun AML örneklerinde anlamlı düzeyde arttığını ve genin hastalığın biyolojik süreçlerinde potansiyel bir düzenleyici rol üstlenebileceğini göstermektedir. Ayrıca, G633E missense mutasyonunun proteinin yapısal stabilitesini ve fonksiyonel bütünlüğünü olumsuz etkilediği, buna karşın I107L mutasyonunun nötr bir etkiye sahip olduğu belirlenmiştir. Bu sonuçlar, *DPP4'ün* AML'de hem moleküler patogenezde hem de terapötik hedefleme stratejilerinde dikkate alınması gereken önemli bir biyobelirteç olabileceğini düşündürmektedir. Bulguların, gelecekte gerçekleştirilecek deneysel ve klinik doğrulama çalışmaları için bilimsel temel oluşturacağı öngörülmektedir.

KAYNAKLAR

Adzhubei, I., Jordan, D. M., & Sunyaev, S. R. (2013). Predicting functional effect of human missense mutations using PolyPhen-2. Current Protocols in Human Genetics, 76(1), Unit 7.20.

Blatt, K., Menzl, I., Eisenwort, G., Cerny-Reiterer, S., Herrmann, H., Herndlhofer, S., Stefanzl, G., Sadovnik, I., Berger, D., Keller, A., et al. (2018). Phenotyping and target expression profiling of CD34(+)/CD38(−) and CD34(+)/CD38(+) stem- and progenitor cells in acute lymphoblastic leukemia. Neoplasia, 20(7), 632–642.

Castillo, J. J., Mull, N., Reagan, J. L., Nemr, S., & Mitri, J. (2012). Increased incidence of non-Hodgkin lymphoma, leukemia, and myeloma in patients with diabetes mellitus type 2: A meta-analysis of observational studies. Blood, 119(21), 4845–4850.

Herrmann, H., Sadovnik, I., Cerny-Reiterer, S., Rülicke, T., Stefanzl, G., Willmann, M., Hoermann, G., Bilban, M., Blatt, K., Herndlhofer, S., et al. (2014). Dipeptidylpeptidase IV (CD26) defines leukemic stem cells (LSC) in chronic myeloid leukemia. Blood, 123(24), 3951–3962.

Kumar, C. C. (2011). Genetic abnormalities and challenges in the treatment of acute myeloid leukemia. Genes & Cancer, 2(1), 95–107.

Nistala, R., & Savin, V. (2017). Diabetes, hypertension, and chronic kidney disease progression: Role of DPP4. American Journal of Physiology-Renal Physiology, 312(4), F661–F670. https://doi.org/10.1152/ajprenal.00316.201

Rodrigues, C. H., Pires, D. E., & Ascher, D. B. (2018). DynaMut: Predicting the impact of mutations on protein conformation, flexibility and stability. Nucleic Acids Research, 46(W1), W350–W355.

Sanford, D., & Ravandi, F. (2015). Management of newly diagnosed acute myeloid leukemia in the elderly: Current strategies and future directions. Drugs & Aging, 32(12), 983–997.

Tallman, M. S., Wang, E. S., Altman, J. K., Appelbaum, F. R., Bhatt, V. R., Bixby, D., Coutre, S. E., De Lima, M., Fathi, A. T., Fiorella, M., et al. (2019). Acute myeloid leukemia, version 3.2019, NCCN clinical practice guidelines in oncology. Journal of the National Comprehensive Cancer Network, 17(6), 721–749.

Venselaar, H., te Beek, T. A. H., Kuipers, R. K. P., Hekkelman, M. L., & Vriend, G. (2010). Protein structure analysis of mutations causing inheritable diseases: An e-Science approach with life scientist friendly interfaces. BMC Bioinformatics, 11, 548.

Wang, C., Nistala, R., Cao, M., Pan, Y., Behrens, M., Doll, D., Hammer, R. D., Nistala, P., Chang, H. M., Yeh, E. T. H., & Kang, X. (2023). Dipeptidylpeptidase 4 promotes survival and stemness of acute myeloid leukemia stem cells. Cell Reports, 42(2), 112105.

Wei, J., Nai, G. Y., Dai, Y., Huang, X. J., Xiong, M. Y., Yao, X. Y., Huang, Z. N., Li, S. N., Zhou, W. J., Huang, Y., Cheng, P., & Deng, D. H. (2021). Dipeptidyl peptidase-4 and transferrin receptor serve as prognostic biomarkers for acute myeloid leukemia. Annals of Translational Medicine, 9(17), 1381.

ORAL PRESENTATION

Dysregulated lipid metabolism in colon tissue: The impact of *SCD* and *ACSL1* on tumor progression

Tugba AGBEKTAS[1]* (*ORCID ID: https://orcid.org/0009-0004-4533-0019*), Husnu Cagri GENC[2] (*ORCID ID: https://orcid.org/0000-0001-6963-2805*), Yavuz SILIG[3] (*ORCID ID: https://orcid.org/0000-0002-0562-7457*)

[*1]Sivas Cumhuriyet University, Yıldızeli Vocational School, Department of Food Processing Technologies Services, Sivas, Türkiye

[2]Sivas Cumhuriyet University, Faculty of Medicine, Department of General Surgery, Sivas, Türkiye

[3]Sivas Cumhuriyet University, Faculty of Medicine, Department of Biochemistry, Sivas, Türkiye

*Corresponding author e-mail: tubaagbektas@cumhuriyet.edu.tr

Abstract

Alterations in lipid metabolism are closely associated with tumorigenesis and cancer progression. This study aimed to investigate the expression levels of *Stearoyl-CoA Desaturase 2 (SCD2*) and *Acyl-CoA Synthetase Long Chain Family Member 1 (ACSL1)* in colon tissue to elucidate their potential involvement in cancer progression. Quantitative PCR analysis (qPCR) revealed that *SCD2* expression decreased to approximately 0.6-fold, whereas ACSL1 expression increased to nearly 1.8-fold in tumor tissues compared with matched adjacent normal tissues, while GAPDH remained stable across both groups. However, paired-samples statistical analysis demonstrated that these expression differences were not statistically significant ($p>0.05$). Taken together, these findings suggest that SCD2 and ACSL1 may play distinct yet complementary roles in the metabolic reprogramming of colon tumor cells. Increased ACSL1 expression suggests enhanced fatty-acid activation and lipid accumulation, potentially promoting tumor cell proliferation, whereas decreased *SCD2* activity may indicate reduced desaturation capacity, affecting membrane fluidity and oncogenic signaling pathways.

Keywords: Colon Cancer, *SCD2*, *ACSL1*, Lipid Metabolism, Gene Expression, Tumor Progression

INTRODUCTION

Colon cancer (CC) is defined as a malignant tumour that occurs in the colon (large exit), which represents the final segment of the human digestive system. While it is more prevalent among the elderly, the risk of developing it at any age is present. The initial stage in the pathogenesis of CC is the formation of diminutive, initially benign polyps in the colonic mucosa. These polyps have the potential to become proliferative, resulting in growth and subsequent clinical manifestations. Consequently, the implementation of regular screening programmes is imperative for individuals deemed to be at risk. The implementation of a screening programme with the objective of detecting and removing polyps in the premalignant stage has been shown to be an effective method of preventing the development of CC. Surgery constitutes the primary treatment option, and, depending on the tumour stage, can be supported by pharmacological and oncological treatments such as radiotherapy and immunotherapy. The term “colorectal cancer” is employed when the disease has spread to the rectum, and in such cases, the probability of metastatic propagation is elevated (Ferlay et al., 2013; Aoki et al., 2017). *ACSL1* is a critical enzyme that catalyses the conversion of long-chain fatty acids to acyl-CoA derivatives (Coleman et al., 2002) and plays a role in metabolic processes associated with carcinogenesis (Mashima et al., 2009; Gaisa et al., 2013). *SCD*, a rate-limiting enzyme in the biosynthesis of monounsaturated fatty acids (FA), has been found to be associated with malignant cellular transformation, proliferation, and maintenance of tumour cell survival (Roongta et al., 2011; Mason et al., 2012; Von Roemeling et al., 2013). The lipid metabolism network, which is regulated by *ACSL* and *SCD*, has been demonstrated to enhance the migration and invasion capacity of tumour cells by inducing epithelial-mesenchymal transition (EMT). Furthermore, this network has been associated with an increased risk of recurrence in colorectal

cancer patients (Sánchez-Martínez et al., 2015). Gene expression also plays a crucial role in colorectal carcinogenesis by enhancing the expression of associated oncogenic proteins. β-catenin–mediated signalling contributes to the upregulation of oncogenes, and elevated levels of nuclear β-catenin have been widely observed in colorectal cancer cells, indicating its involvement in tumour progression (Igarashi and Guarente, 2016). Studies have demonstrated that obesity constitutes a significant risk factor for multiple malignancies at least 13 cancer types including CC. Tumour cells frequently exploit lipid metabolism to satisfy their increased energy demand required for rapid proliferation (German et al., 2016; Patel et al., 2023). Lipid biology encompasses FA metabolism as well as fat and cholesterol homeostasis, which are fundamental processes contributing to tumour progression and metastasis (Lee et al., 2019). Notably, FA accumulation is more pronounced in metastatic tumours compared to primary lesions. In lipid-rich environments such as lymph nodes, metastatic cancer cells preferentially utilize FAs as their main energy source (Ell and Kang, 2013). In ovarian cancer, adipocytes facilitate tumour development by supplying FAs to malignant cells, thereby enhancing their metastatic potential (Nieman et al., 2011). Collectively, these findings support the energy storage/production hypothesis as a critical mechanism underlying tumour metastasis.

Therefore, this study aimed to investigate the expression levels of *SCD2* and *ACSL1* in colon tissue, with the goal of elucidating their potential roles in colorectal tumour progression and their relevance as metabolic biomarkers.

MATERIALS AND METHODS

Study Population

This study included 30 patients who were diagnosed with CC at the Department of General Surgery, Sivas Cumhuriyet University Faculty of Medicine. Written informed consent was obtained from all participants prior to surgical intervention. Tumor tissues excised during surgery, along with histologically normal adjacent colon tissues serving as controls, were collected in accordance with the recommendations of the attending pathologist. Patients were enrolled only after histopathological confirmation of tumor subtype by the Department of Pathology. The study protocol was approved by the Clinical Research Ethics Committee of Sivas Cumhuriyet University (Decision No: 2025-06/64, Date: 12.06.2025) and conducted in accordance with the principles of the Declaration of Helsinki.

RNA Isolation and cDNA Synthesis

Total RNA was isolated from colon tissue samples of all patients using the RNeasy Plus Mini Kit (Qiagen), following the manufacturer's protocol. RNA concentration and purity were assessed using a NanoDrop spectrophotometer, and samples with an A260/A280 ratio between 1.8 and 2.0 were considered acceptable for downstream applications. Subsequently, complementary DNA (cDNA) was synthesized from the purified RNA using the A.B.T.™ cDNA Synthesis Kit (Cat. No: C03-01-20) according to the manufacturer's instructions.

qPCR Analysis

The transcriptional profiles of *SCD2* and *ACSL1* genes were evaluated using qPCR. Reactions were carried out with EvaGreen® qPCR Master Mix and primers designed specifically for each gene. The cDNA synthesized from previously isolated RNA served as the amplification template. For each well, a final reaction volume of 20–25 µL was prepared, consisting of Master Mix, gene-specific primers, nuclease-free water, and cDNA. To correct for potential variations in sample loading and amplification efficiency, GAPDH was employed as an internal reference gene. The amplification was initiated with a denaturation phase at 95°C, followed by 40 cycles of denaturation and annealing/extension steps, with cycling conditions optimized according to primer melting temperatures. Each biological sample was analyzed in triplicate to ensure consistency and technical reliability. After amplification, melting curve analysis was performed, and reactions displaying a single specific peak were accepted as valid. Quantification of relative gene expression was calculated based on $\Delta\Delta_{CT}$ values, comparing tumor tissues with matched adjacent non-tumorous tissues.

RESULTS

The study cohort consisted of 30 CC patients. For each participant, paired samples were obtained, including the primary tumor tissue and the matched adjacent healthy colon tissue, yielding a total of 60 biological specimens for comparative gene expression analysis. Of them, 56.7% were male and 43.3% were female. Smoking was reported in 33.3%, while only 3.3% consumed alcohol. The prevalence of comorbidities included hypertension (30.0%), diabetes mellitus (16.7%), hyperlipidemia (6.7%), and heart disease (23.3%). A family history of cancer was present in 43.3% of the participants. Nutritional habits varied, with 36.7% consuming fruit/vegetable-based diets, followed by 26.7% meat-based diets. The mean age of male participants was higher than females (63.2 vs. 57.2 years). BMI values indicated that females had a higher average BMI (28.9 vs. 25.3 kg/m²) (Table 1). Expression analysis demonstrated gene-specific regulatory alterations between colon tumor tissues and matched adjacent normal tissues. Compared to the control, *SCD2* expression decreased to approximately 0.6-fold, indicating a downward trend in its transcriptional activity. Conversely, *ACSL1* expression showed a strong upregulation to nearly 1.8-fold, while *GAPDH* remained stable across both groups (Table 2, Figure 1). However, paired-samples analysis revealed that neither *SCD2* nor *ACSL1* expression change reached statistical significance (*SCD2: $p = 0.396$*; *ACSL1: $p = 0.196$*) (Table 3, Figure 2).

Table 1. Sociodemographic and clinical characteristics of CC patients

Variable	Category / Statistics	Total (n = 30)
Gender	Female, Male	13 (43.3%), 17 (56.7%)
Age (years)	Mean ± SD Range	60.57 ± 10.70 (38–79)
Height (cm)	Mean ± SD Range	166.03 ± 10.04 (150–195)
Weight (kg)	Mean ± SD Range	74.23 ± 15.89 (40–103)
BMI (kg/m²)	Mean ± SD Range	26.91 ± 5.41 (15.63–37.83)
Alcohol consumption	Yes, No	1 (3.3%), 29 (96.7%)
Smoking status	Yes, No	10 (34.5%), 19 (65.5%)*
Hypertension	Yes, No	9 (30.0%), 21 (70.0%)
Diabetes Mellitus	Yes, No	5 (16.7%), 25 (83.3%)
Hyperlipidemia	Yes, No	2 (6.7%), 28 (93.3%)
Heart disease history	Yes, No	7 (23.3%), 23 (76.7%)
Cancer family history	Yes, No	13 (43.3%), 17 (56.7%)
Dietary habits	Balanced diet, Meat-based diet, High-pastry diet, Fruit & vegetable-based diet	4 (13.3%), 8 (26.7%), 7 (23.3%) 11 (36.7%)

Table 2. qPCR analysis of CT values, fold regulation, and statistical differences in CC patient samples

Genes	Groups	Mean CT	Fold Change	*p-value*
SCD2	Group 1	10.02	0.60	*0.44*[a]
	Control	9.29		
ACSL1	Group 1	7.23	1.88	*0.31*[a]
	Control	8.15		
GAPDH	Group 1	0	1.00	N/A
	Control	0		

Significant indicates $p>0.05$
[a]Student's t-test
GAPDH: Glyceraldehyde 3-phosphate dehydrogenase, CT: Cycle threshold.

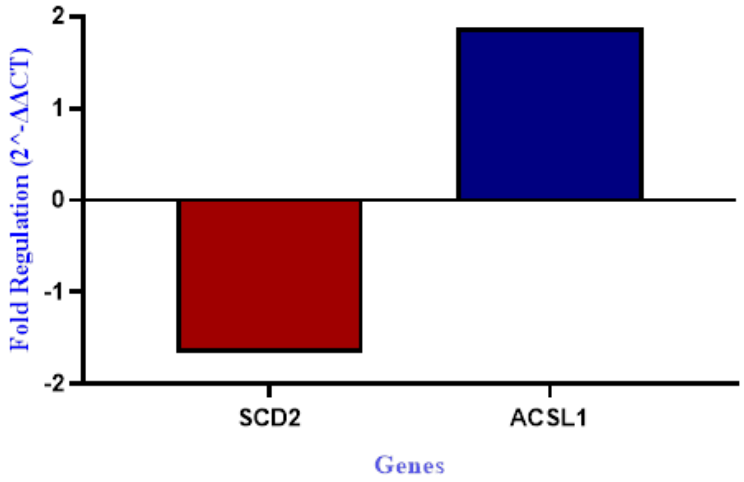


Figure 1. Differential fold regulation of *SCD2* and *ACSL1* in CC patients based on qPCR analysis.

Table 3. Paired samples t-test analysis for SCD2 and ACSL1 between CC patient conditions

Paired Comparison	Mean Difference	95% CI of Difference (Lower–Upper)	t	*p-value*
SCD2/SCD2-CT	0.606	−0.854 to 2.066	0.869	*0.396*
ACSL1/ACSL1-CT	−1.043	−2.672 to 0.587	−1.339	*0.196*

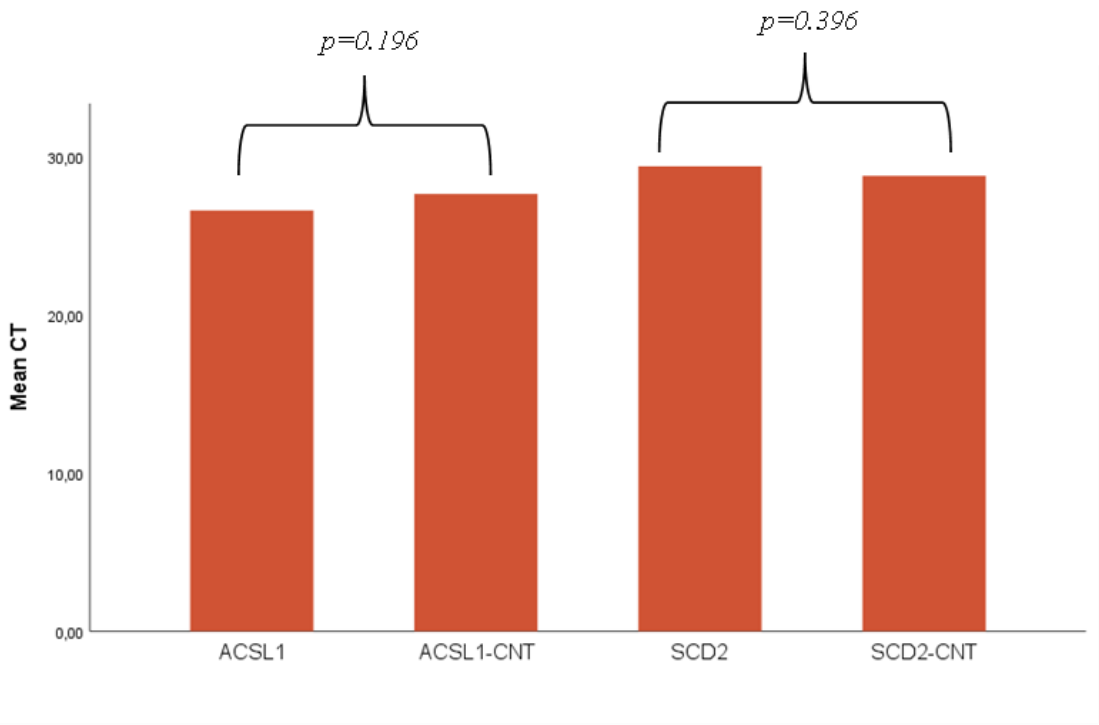


Figure 2. Paired comparison of mean CT values of ACSL1 and SCD2 between CC tissues and their matched control samples.

DISCUSSION

Colorectal tumors demonstrate profound metabolic reprogramming to sustain uncontrolled proliferation, adapt to hypoxic niches, and promote metastatic dissemination. Among these metabolic alterations, dysregulated lipid homeostasis has emerged as a critical hallmark of cancer progression. In the present study, we investigated transcriptional changes in two key lipid-regulating enzymes, *SCD2* and *ACSL1*, in matched tumor and adjacent normal colon tissues from CC patients. Although *SCD2* expression exhibited a downward trend and *ACSL1* showed an upward trend, these changes did not reach statistical significance, suggesting moderate but biologically relevant alterations. *ACSL1* functions at the intersection of lipid activation and storage, converting long-chain fatty acids into acyl-CoA derivatives that feed into lipogenesis, β-oxidation, and membrane synthesis pathways (Shen et al., 2022). Its upregulation has been linked to enhanced tumor cell proliferation, epithelial mesenchymal transition (EMT), and increased metastatic potential in multiple cancers (Chen et al., 2025). Consistent with these reports, the elevated *ACSL1* levels observed in our cohort support the hypothesis that fatty acid activation and accumulation contribute to the energetic and biosynthetic demands of colorectal tumor cells. Conversely, *SCD* family enzymes participate in monounsaturated fatty acid biosynthesis and influence membrane fluidity, signal transduction, and oncogenic survival pathways (Ascenzi et al., 2021). Unlike previous studies reporting *SCD* overexpression in aggressive cancers, our findings demonstrated a slight reduction in *SCD2* expression in tumor tissues. One possible explanation is isoform-specific compensation, where *SCD1*, a more extensively studied homolog, may remain highly active in colon tumors, masking *SCD2* downregulation. Additionally, reduced desaturation may alter membrane lipid composition, modulating stress tolerance in early-stage tumors rather than driving proliferation (Tracz-Gaszewska and Dobrzyn, 2019). Several clinical characteristics of our patient cohort, including obesity associated metrics such as BMI, strengthen mechanistic relevance. Previous studies have established obesity and excess adiposity as prevalent risk contributors for colorectal cancer, primarily through lipid driven metabolic rewiring (Ungvari et al., 2025). Although the observed changes in *SCD2* and *ACSL1* did not reach statistical significance, their expression trends indicate a potential shift in lipid metabolism in colon cancer. These findings suggest that metabolic regulation may contribute to tumor progression, even when transcript level alterations are modest.

CONCLUSION

This study demonstrated modest but biologically relevant alterations in *SCD2* and *ACSL1* expression in colon cancer tissues compared with adjacent normal tissues. The observed trends suggest a potential involvement of lipid metabolism in colorectal tumor progression. Future studies with larger cohorts and complementary functional analyses are needed to clarify the clinical relevance of these genes and to assess their utility as metabolic biomarkers or therapeutic targets in CC.

REFERENCES

Aoki, T., Narumiya, S. J. I., & Regeneration. (2017). Prostaglandin E2-EP2 signaling as a node of chronic inflammation in the colon tumor microenvironment. International Immunology and Regeneration, 37(1), 4.

Ascenzi, F., De Vitis, C., Maugeri-Saccà, M., Napoli, C., Ciliberto, G., Mancini, R. J. J. o. E., & Cancer Research. (2021). SCD1, autophagy and cancer: Implications for therapy. Journal of Experimental & Clinical Cancer Research, 40(1), 265.

Chen, I.-S., Hsieh, C.-C., Li, C.-C., Wei, Y.-L., Cheng, C.-C., Feng, S.-W., Lee, H.-L., Chiang, N.-J., Shen, C.-H., & Hsu, H.-P. (2025). ACSL6 modulates docosahexaenoic acid-induced cytotoxicity to potentiate chemotherapy response in colorectal and breast cancer. Oncology, 14(1), 45.

Coleman, R. A., Lewin, T. M., Van Horn, C. G., & Gonzalez-Baró, M. R. (2002). Do long-chain acyl-CoA synthetases regulate fatty acid entry into synthetic versus degradative pathways? The Journal of Nutrition, 132(8), 2123–2126.

Ell, B., & Kang, Y. J. T. i. c. b. (2013). Transcriptional control of cancer metastasis. Trends in Cell Biology, 23(12), 603–611.

Ferlay, J., Steliarova-Foucher, E., Lortet-Tieulent, J., Rosso, S., Coebergh, J.-W. W., Comber, H., Forman, D., & Bray, F. (2013). Cancer incidence and mortality patterns in Europe: Estimates for 40 countries in 2012. European Journal of Cancer, 49(6), 1374–1403.

Gaisa, N. T., Reinartz, A., Schneider, U., Klaus, C., Heidenreich, A., Jakse, G., Kaemmerer, E., Klinkhammer, B. M., Knuechel, R., & Gassler, N. (2013). Levels of acyl-coenzyme A synthetase 5 in urothelial cells and corresponding neoplasias reflect cellular differentiation.

German, N. J., Yoon, H., Yusuf, R. Z., Murphy, J. P., Finley, L. W., Laurent, G., Haas, W., Satterstrom, F. K., Guarnerio, J., & Zaganjor, E. J. M. C. (2016). PHD3 loss in cancer enables metabolic reliance on fatty acid oxidation via deactivation of ACC2. Molecular Cell, 63(6), 1006–1020.

Igarashi, M., & Guarente, L. (2016). mTORC1 and SIRT1 cooperate to foster expansion of gut adult stem cells during calorie restriction. Cell, 166(2), 436–450.

Lee, C.-K., Jeong, S.-H., Jang, C., Bae, H., Kim, Y. H., Park, I., Kim, S. K., & Koh, G. Y. (2019). Tumor metastasis to lymph nodes requires YAP-dependent metabolic adaptation. Science, 363(6427), 644–649.

Mashima, T., Seimiya, H., & Tsuruo, T. (2009). De novo fatty-acid synthesis and related pathways as molecular targets for cancer therapy. British Journal of Cancer, 100(9), 1369–1372.

Mason, P., Liang, B., Li, L., Fremgen, T., Murphy, E., Quinn, A., Madden, S. L., Biemann, H.-P., Wang, B., & Cohen, A. J. P. O. (2012). SCD1 inhibition causes cancer cell death by depleting mono-unsaturated fatty acids. PLoS ONE, 7(3), e33823.

Nieman, K. M., Kenny, H. A., Penicka, C. V., Ladanyi, A., Buell-Gutbrod, R., Zillhardt, M. R., Romero, I. L., Carey, M. S., Mills, G. B., & Hotamisligil, G. S. (2011). Adipocytes promote ovarian cancer metastasis and provide energy for rapid tumor growth. Nature Medicine, 17(11), 1498–1503.

Patel, A. V., Patel, K. S., Teras, L. R., & Scient. for Obesity and Related Diseases. (2023). Excess body fatness and cancer risk: A summary of the epidemiologic evidence. Science for Obesity and Related Diseases, 19(7), 742–745.

Roongta, U. V., Pabalan, J. G., Wang, X., Ryseck, R.-P., Fargnoli, J., Henley, B. J., Yang, W.-P., Zhu, J., Madireddi, M. T., & Lawrence, R. M. J. M. C. R. (2011). Cancer cell dependence on unsaturated fatty acids implicates stearoyl-CoA desaturase as a target for cancer therapy. Molecular Cancer Research, 9(11), 1551–1561.

Sánchez-Martínez, R., Cruz-Gil, S., de Cedrón, M. G., Álvarez-Fernández, M., Vargas, T., Molina, S., García, B., Herranz, J., Moreno-Rubio, J., & Reglero, G. J. O. (2015). A link between lipid metabolism and epithelial-mesenchymal transition provides a target for colon cancer therapy. Oncotarget, 6(36), 38719.

Shen, Z., Li, Z., Liu, Y., Li, Y., Feng, X., Zhan, Y., Lin, M., Fang, C., Fang, Y., & Deng, H. J. C. L. (2022). GLUT5-KHK axis-mediated fructose metabolism drives proliferation and chemotherapy resistance of colorectal cancer. Cancer Letters, 534, 215617.

Tracz-Gaszewska, Z., & Dobrzyn, P. J. C. (2019). Stearoyl-CoA desaturase 1 as a therapeutic target for the treatment of cancer. Cancers, 11(7), 948.

Ungvari, Z., Fekete, M., Varga, P., Lehoczki, A., Fekete, J. T., Ungvari, A., & Győrffy, B. J. G. (2025). Overweight and obesity significantly increase colorectal cancer risk: A meta-analysis of 66 studies revealing a 25–57% elevation in risk. Genes, 47(3), 3343–3364.

Von Roemeling, C. A., Marlow, L. A., Wei, J. J., Cooper, S. J., Caulfield, T. R., Wu, K., Tan, W. W., Tun, H. W., & Copland, J. A. J. C. C. R. (2013). Stearoyl-CoA desaturase 1 is a novel molecular therapeutic target for clear cell renal cell carcinoma. Cancer Cell Research, 19(9), 2368–2380.

ORAL PRESENTATION

Exosomes as extracellular vesicles: Clinical and experimental perspectives

Damla Terzi[1*] (*ORCID: https://orcid.org/0009-0001-2387-2018*), Gül Fatma Yarım[2] (*ORCID: https://orcid.org/0000-0003-4050-429X*), Murat Yarım[3] (*ORCID: https://orcid.org/0000-0002-0636-4214*)

[1]Ondokuz Mayis University, Faculty of Veterinary Medicine, Department of Biochemistry, Samsun, Turkey.
[2]Ondokuz Mayis University, Faculty of Veterinary Medicine, Department of Biochemistry, Samsun, Turkey.
[3]Ondokuz Mayis University, Faculty of Veterinary Medicine, Department of Pathology, Samsun, Turkey.

*Corresponding author e-mail: damlabukulmezer2616@gmail.com

Abstract

Exosomes are nanovesicles secreted outside the cell and containing biomolecules such as proteins, lipids, mRNA, and miRNA. These vesicles reorganize cellular communication during normal physiological processes and various disease states. First observed in the 1980s during the removal of unnecessary membrane proteins during the maturation of reticulocytes, exosomes were initially considered "waste products." However, studies in the following years have demonstrated that these vesicles are part of a complex communication system within the body. Exosomes are known to play important roles in a wide variety of processes, including immune response regulation, tumour microenvironment formation, neuronal signaling, cardiovascular function, and infection. Exosomes hold great potential not only in basic biology but also in medicine, biotechnology, and the pharmaceutical industry. They are particularly used as biomarkers and therapeutic tools in cancer, neurodegenerative diseases, cardiovascular disorders, autoimmune diseases, and viral infections. Thanks to their unique biomolecular potential, exosomes can be used as biomarkers in early diagnosis and as drug carriers in targeted therapy applications. Mesenchymal stem cell-derived exosomes, in particular, offer promising results in regenerative medicine by increasing cell proliferation, suppressing apoptosis, and supporting angiogenesis and collagen synthesis. Exosomes affect synaptic plasticity by transporting proteins and RNA between brain cells. The detection of brain-derived exosomes in peripheral blood has the potential to revolutionize the early diagnosis of neurodegenerative diseases. Standardizing exosome research processes is critical for both diagnostic and therapeutic applications. New technologies and modification methods enable more effective and safe use of exosomes. In conclusion, as important components of cellular communication, exosomes are promising tools in translational medicine. Although there are currently intensive scientific studies and reports on exosomes, it is understood that further experimental and clinical research is needed on the bioactive roles of exosomes.

Keywords: Clinical trial, exosomes, experimental study, extracellular vesicles.

1. INTRODUCTION

Cell communication in living organisms is vital for sustaining life. Traditionally, it was thought that this communication was achieved through direct cell contact, secreted soluble molecules, or electrical signals. However, recently, the discovery of exosomes, a much more complex pathway for intercellular information transfer, has brought a new perspective to this field. Exosomes are nanovesicles secreted outside the cell that contain biomolecules, including micro ribonucleic acid (miRNA) and messenger RNA (mRNA), proteins, and lipids. These small vesicles reorganise cellular communication in normal physiological processes and various disease states. Exosomes were first observed in the 1980s during the process of reticulocyte maturation, when unnecessary membrane proteins were removed. Initially, they were considered 'waste products'. However, detailed studies conducted in subsequent years have revealed that these vesicles are part of a complex communication system within the organism. Exosomes play crucial roles in various molecular processes by regulating immune responses, establishing the tumor microenvironment, facilitating neuronal signaling, supporting cardiovascular function, and protecting cells against infectious agents and diseases. Exosomes have great potential not only in terms of basic biology but also in terms of medicine, biotechnology, and the pharmaceutical industry. Intense research is being conducted on their use as biomarkers and biomedical therapeutic strategies, particularly in cancer,

neurodegenerative diseases, viral infections, and tissue engineering. Their unique biomolecular properties give exosomes the ability to be used as biomarkers in early-stage disease diagnosis and as drug carriers in targeted therapy applications.

2. THE STRUCTURE OF EXOSOMES

Exosomes are small, spherical particles derived from endosomes, approximately 30-100 nm in size. These vesicles are surrounded by a double-layered phospholipid membrane, and intercellular communication is facilitated by means of the macromolecules that are contained within them, such as ribonucleic acid, deoxyribonucleic acid (DNA), proteins, and lipids. Many cell types in the organism secrete exosomes, which consist of numerous vesicles and are formed by integration with the plasma membrane. They arise as a product of the intracellular endosomal system. Almost any cell type can secrete exosomes, including epithelial/mesenchymal stem cells, neurons, tumour and immune cells (Raposo and Stoorvogel, 2013). These small vesicles exhibit important effects in cell-to-cell communication by mediating the delivery of important biomolecules in cellular activities, particularly lipids, nucleic acids, and proteins to intended cells. The release of the vesicles they contain is triggered by their fusion with the plasma membrane, a process called biogenesis (Armstrong et al., 2017).

The structure of exosomes contains cell-specific proteins and genetic material. The molecules present in the structure of exosomes are listed below.

A. Protein Content:

Tetraspanins: CD9, CD63, CD81 (exosome markers),
Tumor susceptibility gene 101 protein (TSG101), ALG-2-interacting protein X (ALIX),
HSP70, HSP90 (chaperone proteins),
MHC I and II (immune-related molecules).

B. Lipid Content:

Sphingomyelin, cholesterol, phosphatidylserine.

C. Genetic Material:

mRNA, miRNA, long non-coding RNA (lncRNA), and trace amounts of DNA.

The biogenesis of exosomes occurs in three main stages listed below (Théry et al., 2009; Yáñez-Mó et al., 2015).

A. Endocytosis: The plasmalemma invaginates to form endosomes. Subsequently, these early endosomes collect intracellular materials and signals.

B. Multivesicular Body Formation: After early endosomes complete their maturation, late endosomes are formed, resulting in the development of numerous small intraluminal vesicles.

C. Exocytosis (Secretion): Degradation by fusion with lysosomes or transport to the plasma membrane.

Exosomes are divided into different subtypes based on the cell type and the molecules they contain (Barile and Vassalli, 2017). These subtypes are listed below.

Immune system exosomes: They exhibit antigenic effects.
Tumor-derived exosomes: They influence metastasis and tumor progression.
Mesenchymal stem cell-derived exosomes: They are used in regenerative interventions

3. FUNCTIONS OF EXOSOMES

Beyond facilitating cell-to-cell interaction and participating in various cellular and molecular processes, exosomes are vital for transferring biological information and maintaining cellular homeostasis. In-depth scientific research has revealed that exosomes play pivotal roles in many processes such as immune function, inflammation, infections, and tumor growth. Both healthy individuals and patients with various diseases release exosome particles containing distinct RNA and protein profiles into the bloodstream, which could be exploited as a predictive marker (Barile and Vassalli, 2017).

3.1. Intercellular Communication

One of the primary functions of exosomes is to contribute to intercellular information transfer. They transport genetic material (mRNA, miRNA), proteins, and signaling molecules from cell to cell. This transport occurs through three different pathways, listed below (Théry et al., 2009).

1. Direct membrane fusion with the target cell.
2. Binding of ligands to receptors on the cell surface.
3. Internalization via endocytosis.

3.2. Immune System Regulation
Exosomes significantly impact both the adaptive and innate immunological responses. The T cells can be activated by antigen-presenting cells (APCs), including dendritic cells, via the secretion of exosome molecules that carry MHC-I and MHC-II. Exosomes secreted by tumor cells can cause immune suppression (Robbins and Morelli, 2014).

3.3. Tissue Regeneration and Repair
In particular, the use of mesenchymal stem cell-generated exosomes has shown great promise in the domain of regenerative medicine. The results have included increased cell proliferation, suppressed apoptosis, and supported angiogenesis and collagen synthesis (Barile & Vassalli, 2017).

4. BIOMEDICAL APPLICATIONS OF EXOSOMES
Exosomes are used in medicine for diagnostic and therapeutic approaches. In particular, the use of exosomes as biomarkers and therapeutics is relevant in neurodegenerative and cardiovascular diseases, as well as cancer. Additionally, exosomes hold potential significance in therapeutic strategies such as gene therapy and drug delivery (Barile and Vassalli, 2017). Severe acute respiratory syndrome coronavirus-2 (SARS-CoV-2) and human immunodeficiency virus (HIV) have been shown to mimic exosome-like structures to facilitate intercellular spread. Exosomes released from immune cells support host defense by carrying antiviral miRNAs (Kalluri and LeBleu, 2020). Both glial cells and neurons secrete exosomes into the central nervous system regularly. An important role is played by these vesicles in both physiological and pathological processes. Exosomes affect synaptic plasticity by transporting proteins and RNA between brain cells (Chivet et al., 2013; Kumari and Anji, 2022). Exosomes released after myocardial ischemia reduce cell death in heart muscle cells (Liu et al., 2017; Cheng et al., 2020).

The level and miRNA load of exosomes in milk samples milked for three days from cows with subclinical mastitis changed in relation to certain physiological processes, and the bta-miR-223-3p exosome expression increased and could be used as a detection marker for subclinical mastitis (Saenz-de-Juano et al., 2022). Researchers have demonstrated that mastitis modifies the composition and biological activities of exosomes present in milk. The microRNA and protein profiles of the exosomes derived from mammary alveolar cells and T cells were found to be consistent with the profiles of the exosomes found in milk. The authors emphasized the potential use of mammary alveolar cell-T cells in studies focusing on milk exosomes (Ogunnaike et al., 2021). Findings of a study examining the expression of miRNA in mastitic bovine milk exosomes caused by *Staphylococcus aureus* reported that Bta-miR-142-5p and bta-miR-223 could serve as potential biomarkers for the early detection of mastitis (Sun et al., 2015; Cai et al., 2018). A study showed that 37 miRNAs within exosomes in milk from *Staphylococcus aureus*-infected cows significantly differed from those in milk from control cows (Ma et al., 2019).

Exosomes are used as non-invasive diagnostic tools because they contain nucleic acids and cell-specific proteins, including miRNA and mRNA. Exosome content varies based on the cell type from which it is secreted, and also varies based on the pathophysiological status of the cell. Measuring exosomes secreted from brain tissue cells in peripheral blood has the promise for improving the early diagnosis of neurodegenerative disorders (Kim et al., 2021). In Alzheimer's disease, neuronal exosomes carrying tau and beta-amyloid are used as biomarkers, as are exosomes containing alpha-synuclein in Parkinson's disease. Exosomes secreted by cancer cells carry the genetic profile of the tumor and can be visualized by liquid biopsy (Kalluri, 2016). The types of cancer in which exosomes are used as biomarkers are listed below. In prostate cancer, exosomes carrying prostate-specific antigen can be detected in urine (Wei et al., 2023). For breast cancer patients, analysing cancer-derived extracellular vesicles is important for diagnosis and personalised treatment (Wilhelm et al., 2025). In brain tumors, EGFRvIII-positive exosomes can be detected in plasma (Skog et al., 2008; Ciregia et al., 2017; Gilazieva et al., 2024).

In recent years, scientists have been excited by studies and developments in the study of exosomes, which are small vesicles playing a key role in communication between cells and the transfer of biological molecules and have

beneficial effects on health, especially in the diagnosis and treatment of various diseases and disorders. Studies conducted at clinical and preclinical levels suggest that exosomes could be used to treat various diseases. The unique biological structures of exosomes and their lack of recognition by the immune system allow them to be used as drug and gene carriers or immunotherapeutic agents (El Andaloussi et al., 2013). They offer the advantages of low toxicity and targeted distribution. Doxorubicin-loaded exosomes have been shown to reduce chemotherapy side effects by providing tumor-specific targeting (Gomari et al., 2019; Wei et al., 2022). These small vesicles generated from mesenchymal stem cells have been used successfully in muscle ischemia, kidney damage, and liver cirrhosis, and accelerate tissue repair (Barile and Vassalli, 2017). The use of exosome-derived mesenchymal stem cells has been investigated as an effective treatment for liver fibrosis, with promising results. A meta-analysis has shown that mesenchymal stem cell-derived exosomes can improve liver function and aid the repair of damaged liver tissue. Furthermore, mesenchymal stem cell-exosomes combined with drugs are more effective than mesenchymal stem cell-exosomes alone (Zhou et al., 2024). Researchers reported that exosomes secreted from mesenchymal stem cells suppressed experimental fibrosis and thus improved kidney function in a mouse model of chronic kidney disease. These findings indicate that mesenchymal stem cell exosomes could be used to regenerate the kidneys (Li et al., 2025; Lv et al., 2025; Pandey et al., 2025).

Exosomes effectively cross the blood-brain barrier, slow disease progression, and clear Aβ or tau, which play key roles in Alzheimer's disease pathogenesis, and can also serve as biomarkers for early diagnosis (Gao et al., 2021; Duan et al., 2024). Exosomes generated from neural stem cells prevent abnormal protein distribution in the APP/PS1 mouse model (Li et al., 2024). It has been reported that phosphatase and tensin homolog (PTEN)-targeted miR-223-loaded mesenchymal stem cell exosomes inhibit apoptosis by activating the PI3K/Akt pathway, and may be a potential alternative therapeutic intervention for Alzheimer's disease (Wei et al., 2020). Exosome-enriched extracellular vesicles isolated from the brain tissue of tau transgenic rTg4510 mice have been shown to carry tau in different phosphorylation states, suggesting that extracellular vesicles contribute to the spread of tau pathology (Polanco et al., 2016). The exosomes derived from human adipose mesenchymal stem cells have been postulated as a potential treatment option for the treatment of Alzheimer's disease (Lee et al., 2018). Additionally, the administration of exosomes derived from iPS cells as intranasal drops has been successful in the treatment of refractory focal epilepsy (Gotoh et al., 2024). Exosomes generated from mesenchymal stem cells have improved motor function in acute spinal cord injury. Significant improvements were observed in rats treated within the first four weeks (Mou et al., 2025).

Tumor-derived exosomes are both potential biomarkers that can be targeted and therapeutic agents that can be used. Immunotherapy can be performed using exosomes carrying tumor-specific antigens (Hoshino et al., 2015). Exosomes secreted in large amounts from cancer cells are involved in reshaping the tumor microenvironment. They do this by carrying signals that facilitate metastasis, increase angiogenesis, and support the escape of immune cells (Liu et al., 2021). Exosomes generated from dendritic cells and enriched with tumour-associated peptides have been used to treat metastatic melanoma and stages III and IV non-small cell lung cancer. This treatment is safe, and tumor responses have been observed in some patients (Escudier et al., 2005; Van Delen et al., 2024). Potential applications of exosomes in areas such as gene therapy, immunotherapies, and tissue engineering are being investigated. The use of exosomes within the context of a targeted delivery system has the potential to revolutionize the development of specific therapeutic approaches (Kučuk et al., 2021).

5. CONCLUSION

In recent years, in-depth molecular studies indicate that exosomes are being used successfully in biotechnology and clinical research. New technologies and modification methods ensure that exosomes can be used more effectively and safely. Scientists predict that in the future, exosomes will be successfully used in the early diagnosis and treatment of metabolic, infectious, and cancer-related diseases, and their mechanisms will be elucidated.
Small vesicles called exosomes play a key role in intercellular communication and perform diverse biological functions, driven both by their structure and the lipids, proteins, and nucleic acids they transport. These functions range from the maintenance of physiological processes to the development of pathological events. Exosomes are not merely cellular debris, but rather highly complex and functional structures. These vesicles, which are part of a broad biological system from their formation processes to their molecular content, play a key role in understanding

and treating diseases. Their characterization and isolation are an important part of studies focusing on exosomes. These small vesicles can be isolated using techniques such as ultrasonic centrifugation, ultrasonication, and immunological methods. Characterization of these vesicles is achieved by sensitive and advanced techniques such as Western blotting, electron microscopy, and nanoparticle tracking. These techniques help in understanding the biological properties and potential applications of exosomes. Exosomes are not only involved in cellular communication but have also become promising biological tools in many areas of modern medicine. Their potential, particularly in diagnosis, treatment, and disease monitoring, takes them beyond classical biomarkers and drug delivery systems. Exosomes have significant potential in delivering drugs to target cells thanks to their natural carrier properties. Exosomes can be equipped with desired properties using methods such as genetic engineering and metabolic labeling. These modifications can increase the drug delivery capacity of exosomes and increase treatment efficacy. While there is currently a wealth of scientific research and reports on exosomes, it is clear that more experimental and clinical research is needed on the bioactive roles of exosomes.

REFERENCES

Barile, L., & Vassalli, G. (2017). Exosomes: Therapy delivery tools and biomarkers of diseases. Pharmacology & Therapeutics, 174, 63-78.

Cai, M., He, H., Jia, X., Chen, S., Wang, J., Shi, Y., ... & Lai, S. (2018). Genome-wide microRNA profiling of bovine milk-derived exosomes infected with Staphylococcus aureus. Cell Stress and Chaperones, 23(4), 663-672.

Cheng, H., Chang, S., Xu, R., Chen, L., Song, X., Wu, J., ... & Ma, J. (2020). Hypoxia-challenged MSC-derived exosomes deliver miR-210 to attenuate post-infarction cardiac apoptosis. Stem Cell Research & Therapy, 11, 1-14.

Chivet, M., Javalet, C., Hemming, F., Pernet-Gallay, K., Laulagnier, K., Fraboulet, S., & Sadoul, R. (2013). Exosomes as a novel way of interneuronal communication. Biochemical Society Transactions, 41(1), 241-244.

Ciregia, F., Urbani, A., & Palmisano, G. (2017). Extracellular vesicles in brain tumors and neurodegenerative diseases. Frontiers in molecular neuroscience, 10, 276.

Duan, X., Zheng, Q., Liang, L., & Zhou, L. (2024). Serum exosomal miRNA-125b and miRNA-451a are potential diagnostic biomarker for Alzheimer's diseases. Degenerative Neurological and Neuromuscular Disease, 21-31.

El-Andaloussi, S., Lee, Y., Lakhal-Littleton, S., Li, J., Seow, Y., Gardiner, C., ... & Wood, M. J. (2012). Exosome-mediated delivery of siRNA in vitro and in vivo. Nature protocols, 7(12), 2112-2126.

Escudier, B., Dorval, T., Chaput, N., André, F., Caby, M. P., Novault, S., ... & Zitvogel, L. (2005). Vaccination of metastatic melanoma patients with autologous dendritic cell (DC) derived-exosomes: results of thefirst phase I clinical trial. Journal of Translational Medicine, 3, 1-13.

Gao, P., Li, X., Du, X., Liu, S., & Xu, Y. (2021). Diagnostic and therapeutic potential of exosomes in neurodegenerative diseases. Frontiers in Aging Neuroscience, 13, 790863.

Gilazieva, Z., Moldavskii, D., Luzina, E., Kadyrova, A., Shaimardanova, A., Issa, S., ... & Solovyeva, V. (2024). Extracellular vesicles as brain tumor biomarkers. Biocell, 48(12), 1667.

Gomari, H., Forouzandeh Moghadam, M., Soleimani, M., Ghavami, M., & Khodashenas, S. (2019). Targeted delivery of doxorubicin to HER2 positive tumor models. International journal of nanomedicine, 5679-5690.

Gotoh, S., Kawabori, M., & Fujimura, M. (2024). Intranasal administration of stem cell-derived exosomes for central nervous system diseases. Neural Regeneration Research, 19(6), 1249-1255.

Hoshino, A., Costa-Silva, B., Shen, T. L., Rodrigues, G., Hashimoto, A., Tesic Mark, M., ... & Lyden, D. (2015). Tumour exosome integrins determine organotropic metastasis. Nature, 527(7578), 329-335.

Kalluri, R., & LeBleu, V. S. (2020). The biology, function, and biomedical applications of exosomes. science, 367(6478), eaau6977.

Kim, K. Y., Shin, K. Y., & Chang, K. A. (2021). Brain-derived Exosomal proteins as effective biomarkers for Alzheimer's disease: a systematic review and Meta-analysis. Biomolecules, 11(7), 980.

Kučuk, N., Primožič, M., Knez, Ž., & Leitgeb, M. (2021). Exosomes engineering and their roles as therapy delivery tools, therapeutic targets, and biomarkers. International Journal of Molecular Sciences, 22(17), 9543.

Kumari, M., & Anji, A. (2022). Small but mighty—exosomes, novel intercellular messengers in neurodegeneration. Biology, 11(3), 413.

Lee, M., Ban, J. J., Yang, S., Im, W., & Kim, M. (2018). The exosome of adipose-derived stem cells reduces β-amyloid pathology and apoptosis of neuronal cells derived from the transgenic mouse model of Alzheimer's disease. Brain research, 1691, 87-93.

Li, B., Chen, Y., Zhou, Y., Feng, X., Gu, G., Han, S., ... & Liu, J. (2024). Neural stem cell-derived exosomes promote mitochondrial biogenesis and restore abnormal protein distribution in a mouse model of Alzheimer's disease. Neural Regeneration Research, 19(7), 1593-1601.

Li, R., Tao, H., Pan, K., Li, R., Guo, Z., Chen, X., & Li, Z. (2025). Extracellular vesicles derived from mesenchymal stem cells alleviate renal fibrosis via the miR-99b-5p/mTOR/autophagy axis in diabetic kidney disease. Stem Cell Research & Therapy, 16(1), 142.

Liu, L., Jin, X., Hu, C. F., Li, R., Zhou, Z. E., & Shen, C. X. (2017). Exosomes derived from mesenchymal stem cells rescue myocardial ischaemia/reperfusion injury by inducing cardiomyocyte autophagy via AMPK and Akt pathways. Cellular Physiology and Biochemistry, 43(1), 52-68.

Liu, Y., Shi, K., Chen, Y., Wu, X., Chen, Z., Cao, K., ... & Zhou, J. (2021). Exosomes and their role in cancer progression. Frontiers in oncology, 11, 639159.

Lv, Y., Hua, Z., & Lu, X. (2025). Protective effects and possible mechanisms of mesenchymal stem cells and mesenchymal stem cell-derived extracellular vesicles against kidney fibrosis in animal models: a systematic review and meta-analysis. Frontiers in Pharmacology, 15, 1511525.

Ma, S., Tong, C., Ibeagha-Awemu, E. M., & Zhao, X. (2019). Identification and characterization of differentially expressed exosomal microRNAs in bovine milk infected with Staphylococcus aureus. BMC genomics, 20(1), 934.

Mou, C., Xia, Z., Wang, X., Dai, X., Wang, J., Zhang, C., & Xu, Y. (2025). Stem cell-derived exosome treatment for acute spinal cord injury: a systematic review and meta-analysis based on preclinical evidence. Frontiers in Neurology, 16, 1447414.

Ogunnaike, M., Wang, H., & Zempleni, J. (2021). Bovine mammary alveolar MAC-T cells afford a tool for studies of bovine milk exosomes in drug delivery. International journal of pharmaceutics, 610, 121263.

Pandey, R. P., Mukherjee, R., & Chang, C. M. (2025). Meta-analysis study of the therapeutic impact of Mesenchymal stem cells derived exosomes for chronic kidney diseases. Biochemistry and Biophysics Reports, 43, 102072.

Polanco, J. C., Scicluna, B. J., Hill, A. F., & Götz, J. (2016). Extracellular vesicles isolated from the brains of rTg4510 mice seed tau protein aggregation in a threshold-dependent manner. Journal of Biological Chemistry, 291(24), 12445-12466.

Saenz-de-Juano, M. D., Silvestrelli, G., Weber, A., Röhrig, C., Schmelcher, M., & Ulbrich, S. E. (2022). Inflammatory response of primary cultured bovine mammary epithelial cells to Staphylococcus aureus extracellular vesicles. Biology, 11(3), 415.

Skog, J., Würdinger, T., Van Rijn, S., Meijer, D. H., Gainche, L., Curry Jr, W. T., ... & Breakefield, X. O. (2008). Glioblastoma microvesicles transport RNA and proteins that promote tumour growth and provide diagnostic biomarkers. Nature Cell Biology, 10(12), 1470-1476.

Sun, J., Aswath, K., Schroeder, S. G., Lippolis, J. D., Reinhardt, T. A., & Sonstegard, T. S. (2015). MicroRNA expression profiles of bovine milk exosomes in response to Staphylococcus aureus infection. BMC genomics, 16(1), 806.

Théry, C., Ostrowski, M., & Segura, E. (2009). Membrane vesicles as conveyors of immune responses. Nature Reviews Immunology, 9(8), 581–593.

Van Delen, M., Derdelinckx, J., Wouters, K., Nelissen, I., & Cools, N. (2024). A systematic review and meta-analysis of clinical trials assessing safety and efficacy of human extracellular vesicle-based therapy. Journal of Extracellular Vesicles, 13(7), e12458.

Wei, C., Chen, X., Ji, J., Xu, Y., He, X., Zhang, H., ... & Wang, F. (2023). Urinary exosomal prostate-specific antigen is a noninvasive biomarker to detect prostate cancer: Not only old wine in new bottles. International Journal of Cancer, 152(8), 1719-1727.

Wei, H., Chen, F., Chen, J., Lin, H., Wang, S., Wang, Y., ... & Zhong, G. (2022). Mesenchymal stem cell derived exosomes as nanodrug carrier of doxorubicin for targeted osteosarcoma therapy via SDF1-CXCR4 axis. International journal of nanomedicine, 17, 3483.

Wei, H., Xu, Y., Chen, Q., Chen, H., Zhu, X., & Li, Y. (2020). Mesenchymal stem cell-derived exosomal miR-223 regulates neuronal cell apoptosis. Cell death & disease, 11(4), 290.

Wilhelm, A., Flynn, C., Hammer, E., Roessler, J., Haller, B., Napieralski, R., ... & Höchst, B. (2025). Two-dimensional analysis of plasma-derived extracellular vesicles to determine the HER2 status in breast cancer patients. Breast Cancer Research, 27(1), 107.

Zhou, X., Xu, Y., Wang, X., Lu, W., Tang, X., Jin, Y., & Ye, J. (2024). Single and combined strategies for mesenchymal stem cell exosomes alleviate liver fibrosis: a systematic review and meta-analysis of preclinical animal models. Frontiers in pharmacology, 15, 1432683.

ORAL PRESENTATION

Nörodejenerasyonda laktoferrinin koruyucu rolü: Klinik ve deneysel perspektifler

Ezel Hür Doğan Acar[1*] (*ORCID: https://orcid.org/0009-0007-2105-0436*), Gül Fatma Yarım[2] (*ORCID: https://orcid.org/0000-0003-4050-429X*), Murat Yarım[3] (*ORCID: https://orcid.org/0000-0002-0636-4214*)

[1] Ondokuz Mayıs Üniversitesi, Veteriner Fakültesi, Biyokimya Anabilim Dalı, Samsun, Türkiye
[2]Ondokuz Mayıs Üniversitesi, Veteriner Fakültesi, Biyokimya Anabilim Dalı, Samsun, Türkiye
[3]Ondokuz Mayıs Üniversitesi, Veteriner Fakültesi, Patoloji Anabilim Dalı, Samsun, Türkiye

*Sorumlu yazar e-mail: ezelhur@hotmail.com

Özet

Laktoferrin, transferrin ailesine ait çok işlevli bir demir bağlayıcı glikoproteindir ve özellikle süt olmak üzere birçok vücut sıvısında bulunmaktadır. Laktoferrin, karaciğer, böbrekler, pankreas, akciğerler, bağırsaklar, safra kesesi, prostat, sinovyal sıvı, beyin omurilik sıvısı, tükürük, bronşiyal salgılar, gözyaşı, idrar, göbek kordonu kanı, sperm, kan plazması ve bağışıklık sistemi hücreleri dahil olmak üzere çeşitli organ ve vücut sıvılarında tanımlanmıştır. Laktoferrin, nöroprotektif, antienflamatuar, antibakteriyel, antiviral ve antitümör etkilere sahiptir. Laktoferrin, kan-beyin bariyerini geçerek nöronlar, mikrogliyalar ve astrositler üzerinde önemli etkiler göstermektedir. Klinik öncesi kanıtlar, laktoferrinin gelişmekte olan beyni nöronal hasardan koruduğunu, nörotrofin üretimini artırdığını, mikrogliyal aktivasyonu baskıladığını, sinaptik plastisiteyi desteklediğini ve neonatal hipoksi-iskemi modellerinde enflamasyonu azalttığını göstermektedir. Laktoferrin, beyin gelişimi ve bilişi desteklemenin yanı sıra yaşamın ilerleyen dönemlerinde nörodejeneratif hastalıkların başlamasını önleme potansiyeline bulunmaktadır. Laktoferrin üzerine gerçekleştirilen araştırmaların büyük çoğunluğu anne sütünde laktoferrin bulunması nedeniyle yenidoğan dönemine odaklanmış olsa da yeni kanıtlar nörodejeneratif hastalıklarda faydalarını göstermektedir. Çalışmalar, laktoferrin ekspresyonunun çeşitli nörodejeneratif hastalıklarda değiştiğini göstermiştir. Laktoferrinin nörogelişimi ve nöroproteksiyonu uyardığı ve hem aktif bir terapötik ajan hem de bir ilaç nanotaşıyıcısı olarak kullanım potansiyeline sahip olduğu bildirilmiştir. Bununla birlikte, laktoferrin proteinlerinin merkezi sinir sistemi hastalıklarının başlaması, ilerlemesi ve nörogenezindeki rolleri henüz açıklığa kavuşturulamamıştır. Laktoferrinin nörodejeneratif hastalıkları önlemek için bir tedavi seçeneği olarak kullanılabilmesi için, merkezi sinir sistemindeki dağılımının, biyoyararlanımının ve moleküler hedeflerinin açıklığa kavuşturulması önem arz etmektedir. Nöro-redoks düzenleyicisi olarak mikrogliyal laktoferrinin nöronları koruma ve onarma ve sağlıklı beyin fonksiyonunu sürdürmedeki rolü kritik öneme sahiptir. Laktoferrinin, iskemik beyin hasarı, Alzheimer hastalığı ve Parkinson hastalığının deneysel modellerinde inflamasyonu hafiflettiği, oksidatif stresi engellediği ve nöronları apoptozdan koruduğu gösterilmiştir. Yenilikçi laktoferrin bazlı nanoterapiler, nörodejeneratif hastalıkların tedavisi için umut verici ve hedefli ilaç iletim stratejileri olarak araştırılmaktadır. Nöroprotektif etkileri iyi belgelenmiş çok işlevli bir glikoprotein olan laktoferrin, son yıllarda nörodejeneratif süreçlerin potansiyel bir düzenleyicisi olarak giderek artan bir ilgi görmektedir.

Anahtar Kelimeler: Deneysel model, klinik araştırma, laktoferrin, nörodejenerasyon.

Protective role of lactoferrin in neurodegeneration: Clinical and experimental perspectives

Abstract

Lactoferrin, a multifunctional iron-binding glycoprotein of the transferrin family, is present in numerous bodily fluids, with notably high levels in milk. Lactoferrin has been identified in various organs and bodily fluids, including the liver, kidneys, pancreas, lungs, intestines, gallbladder, prostate, synovial fluid, cerebrospinal fluid, saliva, bronchial secretions, tears, urine, umbilical cord blood, sperm, blood plasma, and immune system cells. Lactoferrin has neuroprotective, anti-inflammatory, antibacterial, antiviral, and antitumor effects. Lactoferrin

crosses the blood-brain barrier and exerts significant effects on neurons, microglia, and astrocytes. Preclinical evidence suggests that lactoferrin protects the developing brain from neuronal damage, increases neurotrophin production, suppresses microglial activation, promotes synaptic plasticity, and reduces inflammation in neonatal hypoxia-ischemia models. Lactoferrin has the potential to support cognitive development and offer neuroprotective effects that reduce the risk of neurodegenerative diseases in later stages of life. Although most studies on lactoferrin have traditionally centered on its role during the neonatal stage due to its abundance in breast milk, emerging research highlights its potential therapeutic effects in neurodegenerative disorders. Studies have demonstrated that lactoferrin expression is altered in various neurodegenerative diseases. Lactoferrin has been reported to stimulate neurodevelopment and neuroprotection, with potential for use as both an active therapeutic agent and a drug nanocarrier. However, the roles of lactoferrin proteins in the initiation, progression, and neurogenesis of central nervous system diseases remain unclear. Before lactoferrin can be used as a therapeutic option to prevent neurodegenerative diseases, it is crucial to elucidate its distribution, bioavailability, and molecular targets in the central nervous system. As a neuro-redox regulator, the role of microglial lactoferrin in protecting and repairing neurons and in maintaining healthy brain function is critical. Lactoferrin has been shown to alleviate inflammation, inhibit oxidative stress, and protect neurons from apoptosis in experimental models of ischemic cerebral damage, Alzheimer's disease, and Parkinson's disease. Innovative lactoferrin-based nanotherapies are under investigation as promising and targeted drug delivery strategies for neurodegenerative disease treatment. Lactoferrin, a multifunctional glycoprotein with well-documented neuroprotective effects, has garnered increasing interest in recent years as a potential modulator of neurodegenerative processes.

Keywords: Clinical research, experimental model, lactoferrin, neurodegeneration.

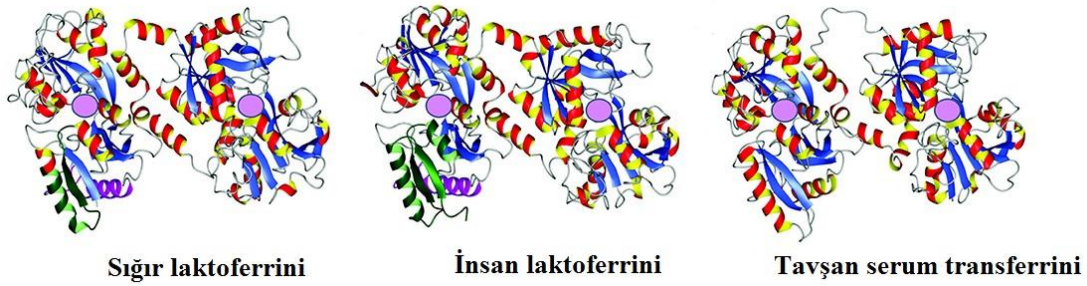
GİRİŞ

Laktoferrin, çoğu memelinin sütündeki peynir altı suyu proteininin bir bileşenidir. Sütteki laktoferrin konsantrasyonu laktasyon evresine bağlı olup kolostrumun olgun sütten yedi kat daha fazla laktoferrin içerdiği bulunmuştur. Çoğu memelinin birçok organında ve hücresinde laktoferrin bulunmaktadır. Böbreklerde, akciğerlerde, safra kesesinde, pankreasta, bağırsakta, karaciğerde, prostatta, tükürükte, sinovyal sıvıda, beyin omurilik sıvısında, bronşiyal sekresyonlarda, gözyaşında, idrarda, göbek kordon kanında, spermde, kan plazmasında ve bağışıklık sistemi hücrelerinde laktoferrin varlığı doğrulanmıştır. (Legrand ve ark., 2008; Baker ve Baker, 2012; McCarthy ve ark., 2014; Ponzini ve ark., 2020). Merkezi sinir sistemi hastalıkları dünyadaki en büyük sağlık sorunlarından biri olmaya devam etmektedir. Çoğu merkezi sinir sistemi hastalığı, yüksek oksidatif stres seviyeleri ve etkilenen dokularda yoğun inflamatuar yanıtlarla karakterizedir. Çok işlevli bir demir bağlayıcı glikoprotein olan laktoferrin antiinflamatuar, antibakteriyel, antiviral, antitümör etkiler sergilemektedir. Laktoferrinin çeşitli nörodejeneratif hastalıklarda anormal şekilde eksprese edildiği gösterilmiştir. Güncel çalışmalarda laktoferrin tarafından nörogelişimin ve nöroproteksiyonun teşviki kanıtlanmış ve laktoferrinin hem aktif bir terapötik ajan hem de ilaç nanotaşıyıcısı olarak kullanılabileceği ortaya konulmuştur (Li ve ark., 2023; Reddy ve ark., 2025). Ancak, laktoferrin proteinlerinin merkezi sinir sistemi hastalıklarının başlatılması veya ilerlemesindeki rollerine ilişkin çalışmaların, özellikle laktoferrinin nörogenezi düzenlemedeki rolüne ilişkin bilimsel kanıtların oldukça sınırlı olduğu anlaşılmaktadır.

LAKTOFERRİNİN YAPISI VE BİYOLOJİK FONKSİYONLARI

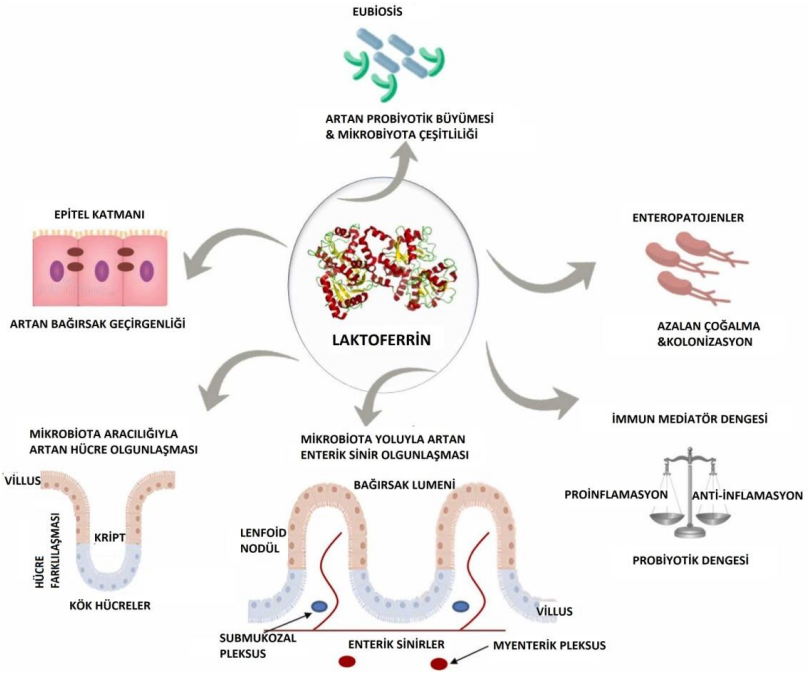
Laktoferrin, ilk kez 1939 yılında sığır sütünden demir içeren bir protein olarak izole edilmiştir (Sorensen, 1939). 1960 yılında yayınlanan bir çalışmada yapısı ve kimyasal özellikleri detaylandırılmıştır (Groves, 1960). Laktoferrinin demir bağlayan glikoproteinlerin süper ailesi olan transferrinler ile ilişkili ve serum transferrin ile % 60 amino asit sekansı özdeşliğine sahip olduğu rapor edilmiştir (Baker ve Lindley, 1992; Karav ve ark., 2017). Laktoferrin, ~80 kDa'lık büyük molekül boyutuna sahip somon pembesi renkte peynir altı suyu proteinidir. Sütte, daha küçük düzeylerde ise böbreklerde, akciğerlerde, safra kesesinde, pankreasta, bağırsakta, karaciğerde, prostatta, tükürükte, sinovyal sıvıda, beyin omurilik sıvısında, bronşiyal sekresyonlarda, gözyaşında, idrarda, göbek kordon kanında, spermde, kan plazmasında ve bağışıklık sistemi hücrelerinde bulunmaktadır (Legrand ve ark., 2008; Baker ve Baker, 2012; McCarthy ve ark., 2014). İzoelektrik noktası (pI) 8,0-8,5'tir, dolayısıyla fizyolojik pH 7,4'te pozitif yüklüdür (González-Chávez ve ark., 2009). İnsan laktoferrini bir alfa-sarmal ile

bağlanan iki küresel lob (80 kDa bi-lobal glikoprotein) halinde katlanmış 691 amino asitten oluşan katyonik glikosile edilmiş bir proteindir (Andersen ve ark., 1990; Vogel, 2012; Karav ve ark., 2017; 2018). Sığır laktoferrini 689 amino asit içermektedir (Moore ve ark., 1997). Laktoferrin ve transferrin benzer amino asit bileşimlerine, ikincil yapılara (disülfit bağlantıları dahil) ve üçüncül yapılara sahiptir, ancak biyolojik işlevler açısından farklılıklar göstermektedirler. Sığır laktoferrininin, insan laktoferrininin ve tavşan serum transferrininin kristal yapıları Şekil 1'de sunuldu.



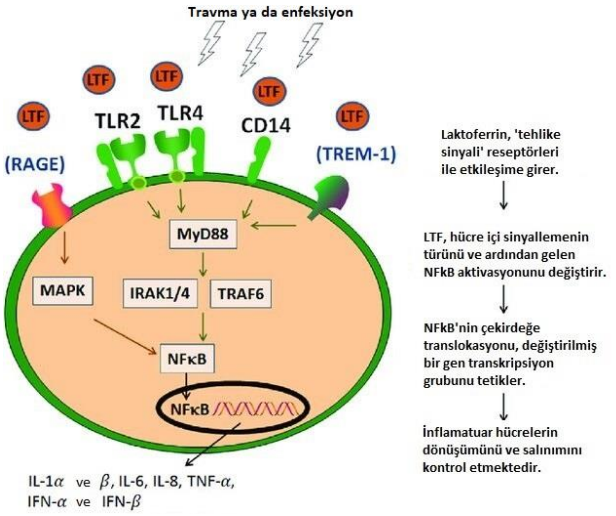
Şekil 1. Sığır laktoferrininin, insan laktoferrininin ve tavşan serum transferrininin kristal yapıları. Pembe küreler ferrik demir (Fe^{+3}) bağlanma bölgelerini temsil etmektedir (Kell ve ark., 2020).

İnsan ve sığır laktoferrinleri yüksek sekans homolojisine sahip olup çok benzer antibakteriyel, antifungal, antiviral, antiparaziter, antiinflamatuar ve immünomodülatör aktiviteler sergilemektedirler (Togawa ve ark., 2002, Teraguchi ve ark., 2004; Rosa ve ark., 2017). Takviye olarak rekombinant insan formunu ifade etmek yerine sığır formunu sunmak daha yaygın görülmektedir. Sığır laktoferrini ayrıca Gıda ve İlaç İdaresi (FDA, ABD) tarafından "genel olarak güvenli olarak kabul edilen" bir madde olarak kabul edilmektedir ve ticari olarak büyük miktarlarda mevcuttur (Rosa ve ark., 2017). Sığır laktoferrininin oral alımından sonra pepsin ile hidrolizine ek olarak, laktoferrininin yapısını tutmaktan sorumlu amino asitlerin iyonizasyonu midenin düşük pH'sı tarafından değiştirilerek ikincil ve üçüncül yapısında değişikliklere yol açmaktadır. Daha sonra laktoferrin, ince bağırsak proteazları olan tripsin, kimotripsin, amino ve karboksil peptidaz etkisiyle tamamen parçalanmaktadır (Takeuchi ve ark., 2006; Yao, 2015). Buna karşılık, laktoferrinin yetişkin ratların ince bağırsağında bulunan enzimlere rağmen parçalanmadan kaldığı saptanmıştır (Takeuchi ve ark., 2006). Laktoferrinin bağırsaklarda yararlı bakterilerin çoğalmasını artırdığı, bağırsak geçirgenliğini güçlendirebileceği, bağışıklık medyatörlerini dengeleyebileceği ve patojenik bakterilerin çoğalmasını ve kolonizasyonunu azaltabileceği ifade edilmiştir (Abd El-Hack ve ark., 2023). Laktoferrinin bağırsak mikrobiyotasının büyümesini ve çeşitliliğini desteklemedeki etkisi Şekil 2'de sunulmuştur.



Şekil 2. Laktoferrinin bağırsak mikrobiyotasının büyümesini ve çeşitliliğini desteklemedeki etkisi (Abd El-Hack ve ark., 2023).

Laktoferrinin bilinen en iyi etkilerinin antibakteriyel (Pogoutse ve Moraes, 2017; Rosa ve ark., 2017), antiviral (Chen ve ark., 2017), antifungal (Liao ve ark., 2019), antiinflamatuar (Nakamura ve ark., 2022) ve antikanserojenik (Wang ve ark., 2019; Zhang ve ark., 2019; Li ve ark., 2023; Rodriguez-Ochoa ve ark., 2023; Kholerdi ve ark., 2024) olduğu bilinmektedir. Laktoferrin, hücre içi sinyallemenin türünü ve ardından NF-κB aktivasyonunu tanımlanmış sinyal reseptörleri [toll benzeri reseptör (TLR)2, TLR4 ve CD14] aracılığıyla değiştirmektedir. Laktoferrin ayrıca NF-κB aktivasyon yollarını kullanan RAGE veya TREM-1 gibi diğer ek sinyalleme reseptörleri aracılığıyla da etkilerini sergilemektedir (Kruzel ve ark., 2017). Laktoferrinin sinyal reseptörlerine afinitesi Şekil 3'te şematize edilmiştir (Kruzel ve ark., 2017).



Şekil 3. Laktoferrinin sinyal reseptörlerine afinitesi (Kruzel ve ark., 2017).

LAKTOFERRİNİN NÖROPROTEKTİF ETKİLERİ

Laktoferrin kolostrumda bulunan önemli bir protein olup gerek insanların gerekse hayvanların doğum sonrası gelişimi sırasında önemli bir rol oynamaktadır. Klinik öncesi kanıtlar, laktoferrinin gelişmekte olan beyni nöronal hasardan koruduğunu, nörotrofin üretimini artırdığını ve neonatal hipoksi-iskemi modellerinde inflamasyonu azalttığını göstermektedir. Bu bağlamda, laktoferrinin beyin gelişimi ve biliş için besin desteği sağlayabilme ve yaşamın ilerleyen dönemlerinde nörodejeneratif hastalıkların ortaya çıkmasını önleyebilme potansiyeli bulunmaktadır. Laktoferrin üzerine gerçekleştirilen araştırmaların büyük çoğunluğu anne sütünde laktoferrin bulunması nedeniyle yenidoğan dönemine odaklanmış olsa da yeni kanıtlar laktoferrinin nörodejeneratif hastalıklarda faydalarını ortaya koymaktadır. Laktoferrin nörodejenerasyonun potansiyel bir biyolojik belirteci olarak kabul edilmekte ve nörodejeneratif hastalıkların önlenmesi için test edilmek üzere iyi bir aday haline getirmektedir. Laktoferrin merkezi sinir sisteminde mevcuttur ve LRP1 gibi laktoferrin reseptörlerinin bir kısmı beyin endotelinde bulunduğundan periferik dolaşımdan kan-beyin bariyerini kolayca geçebilmektedir (Huang ve ark., 2010; Zhao ve ark., 2021). Bu nedenle, ilaçların hedeflenen merkezi sinir sistemine verilmesi için lipozomlarda uygulanmak üzere laktoferrinin yapısal motifleri üzerinde çalışılmaktadır ve bu reseptörler, laktoferrine bağlı ilaçların merkezi sinir sistemine girişine aracılık etmek için kullanılabilmektedir (Agrawal ve ark., 2017).

Laktoferrinin nörodejenerasyondaki rolüyle ilgili olarak, Alzheimer hastalığının başlangıcıyla güçlü bir şekilde ilişkili olan APOE ε4 aleli beyindeki demir homeostazisindeki anormallikler ve ferroptozun indüksiyonu ile ilişkilendirilmiştir (Belaidi ve ark., 2022; Stockwell, 2022). Laktoferrinin intranazal uygulanmasının nöroprotektif etkileri, Alzheimer hastalığının APPswe/PS1DE9 transgenik fare modelinde test edilmiştir. Alzheimer hastalığı modeli oluşturulmuş hayvanlarında intranazal yolla insan laktoferrini uygulaması, ERK1/2-CREB ve HIF-1α sinyal yollarının aktivasyonu ve bunun sonucunda ADAM10 ekspresyonu yoluyla beta-amiloid birikimini azaltmış ve bilişsel gerilemeyi iyileştirmiştir (Guo ve ark., 2017). Laktoferrin nörodejeneratif hastalıkların erken teşhisi için varsayılan bir biyobelirteç olarak kabul görmeye başlamıştır. Amiloidin PET görüntülenmesiyle doğrulandığı Alzheimer ve hafif bilişsel bozukluk hastalarında tükürük laktoferrin düzeyinin azaldığı ve amiloid yükü ile negatif bir ilişki gösterdiği saptanmıştır (Carro ve ark., 2017; Bermejo-Pareja ve ark., 2020; Antequera ve ark., 2021; Reseco ve ark., 2021). Tükürükteki laktoferrin ile Alzheimer hastalığı arasındaki nedensel ilişki hala bilinmemektedir; ancak, azalmış tükürük laktoferrin düzeyinin Alzheimer hastalarında yaygın olarak gözlenen bağışıklık sistemi anormalliklerini yansıtabileceği hipotezi öne sürülmüştür (Bermejo-Pareja ve ark., 2020). Azalmış tükürük laktoferrin düzeyinin Alzheimer patolojisine özgü olduğu ileri sürülmektedir (González-Sánchez ve ark., 2020). Parkinson hastalığı modellerinde MPTP uygulamasından sonra rat beyinlerinde laktoferrin düzeyindeki artışın bu hastalıkta gözlenen demir düzensizliğine karşı koruyucu bir doku tepkisi olduğu ileri sürülmüştür (Jiang ve ark., 2017). Oral insan laktoferrini uygulamasının, Parkinson hastalığı MPTP indüklü *in vivo* ve *in vitro* modellerinde nöroprotektif etkili olduğu gösterilmiştir (Xu ve ark., 2019; Liu ve ark., 2020).

Mikroglia, yüksek proinflamatuar sitokin seviyelerinde, oksidatif streste ve demir birikiminde demir şelatör molekülü laktoferrini sentezlemek üzere uyarılmaktadır. Bu bulgu laktoferrinin nöroprotektif bir ajan olarak kullanılabileceğini göstermektedir (Fillebeen ve ark., 2001). Ratlarda lipopolisakkarit indüklü hafıza bozukluğunda laktoferrin tedavisinin inflamatuar sitokin seviyelerini önemli ölçüde azalttığı ve nörotrofik faktör seviyesini normale döndürerek nöroprotektif etkili olduğu rapor edilmiştir (Madi ve El-Saka, 2018). Deferoksamin kaynaklı hipoksi oluşturulmuş farelerde insan laktoferrini apo formunun kullanımının beyin dahil çoklu organ korumasını sağladığı gözlemlenmiştir (Zakharova ve ark., 2012). Farelerde laktoferrin uygulamasının mikroglial aktivasyonu ve nöroinflamasyonu mikrobiyom-bağırsak-beyin ekseni yoluyla inhibe ederek bilişsel bozulmayı hafiflettiği saptanmıştır (He ve ark., 2023). Hipoksik iskemik beyin hasarı oluşturulan yenidoğan rat yavrularına emzirme yoluyla verilen laktoferrinin beyin metabolizması ve serebral gri ve beyaz cevher iyileşmesi üzerinde nöroprotektif etkiler gösterdiği ve bu beslenme müdahalesinin prematüre beyin nöroproteksiyonunun klinik alanı için önemli olabileceği ifade edilmiştir (Van De Looij ve ark., 2014). İntraserebroventriküler lipopolisakkarit enjekte edilen rat yavrularında emzirme süresince laktoferrin takviyesinin ventriküler dilatasyonu, hipomiyelinasyonu azaltarak ve aksonların çapını artırarak beyin hasarını hafiflettiği rapor edilmiştir (Ginet ve ark., 2016). Doğum öncesi hipoksiye maruz bırakılan rat yavrularına rekombinant insan laktoferrin uygulamasının bilişsel işlevler üzerinde koruyucu etki sergilediği saptanmıştır (Sokolov ve ark., 2022). Yenidoğan domuz yavrularında laktoferrin uygulamasının

mekansal görevlerde daha iyi performans gösterilmesini sağladığı ve bilişle ilişkili beyin kaynaklı nörotrofik faktör genlerinin ve proteinlerinin ekspresyonunu modüle ettiği bildirilmiştir (Chen ve ark., 2021).

SONUÇ

Demir bağlayıcı çok işlevli bir glikoprotein olan laktoferrinin antiinflamatuar, antibakteriyel, antiviral, antitümör etkilere sahip olduğu iyi bilinmektedir. Laktoferrinin bu önemli biyolojik etkilerinin yanında nöroprotektif etkileri de bulunmaktadır. Nörodejeneratif hastalıklarda laktoferrin ekspresyonlarının arttığı gösterilmiştir. Laktoferrinin nörogelişimi ve nöroproteksiyonu uyardığı hem aktif bir terapötik ajan hem de ilaç nanotaşıyıcısı olarak kullanım potansiyeli olduğu rapor edilmiştir. Bununla birlikte laktoferrin proteinlerinin merkezi sinir sistemi hastalıklarının başlamasında, ilerlemesinde ve nörogenezde olası katkıları henüz tam olarak açıklığa kavuşturulamamıştır. Laktoferrinin nörodejeneratif hastalıkların önlenmesinde bir tedavi seçeneği olarak kullanılmasından önce merkezi sinir sistemindeki dağılımının, biyoyararlanımının ve moleküler hedeflerinin açıklığa kavuşturulması önem arz etmektedir. Tükürük laktoferrinini bir biyobelirteç olarak değerlendiren bilimsel çalışmaların, özellikle nörodejenerasyonun bilinen biyobelirteçleri ile birlikte çalışıldığında, Alzheimer hastalığı ve diğer demanslarda laktoferrinin rolünün aydınlatılmasına yardımcı olabileceği anlaşılmaktadır. Nöro-redoks düzenleyicisi olarak mikroglial laktoferrin, nöronların korunması/onarımı ve sağlıklı beyin fonksiyonu için kritik öneme sahiptir. Demir dengesizliği ve oksidatif stres, Parkinson hastalığı, Alzheimer hastalığı, bunama, depresyon ve multipl skleroz gibi nörodejeneratif bozuklukları olan hastalarda yaygın olarak görülmektedir. Yeni laktoferrin bazlı nano-terapötikler, nörodejeneratif bozuklukların klinik yönetimi için etkili ilaç iletim sistemleri olarak geliştirilmektedir. Laktoferrinin beyinde çeşitli nöroprotektif faydalarla tanınan bir molekül olması özellikle nörodejenerasyon konusunda çalışan bilim insanlarını heyecanlandırmaktadır.

KAYNAKLAR

Abd El-Hack, M. E., Abdelnour, S. A., Kamal, M., Khafaga, A. F., Shakoori, A. M., Bagadood, R. M., ... & Świątkiewicz, S. (2023). Lactoferrin: Antimicrobial impacts, genomic guardian, therapeutic uses and clinical significance for humans and animals. Biomedicine & Pharmacotherapy, 164, 114967.

Agrawal, M., Tripathi, D. K., Saraf, S., Saraf, S., Antimisiaris, S. G., Mourtas, S., ... & Alexander, A. (2017). Recent advancements in liposomes targeting strategies to cross blood-brain barrier (BBB) for the treatment of Alzheimer's disease. Journal of Controlled Release, 260, 61-77.

Andersen, B. F., Baker, H. M., Morris, G. E., Rumball, S. V., & Baker, E. N. (1990). Apolactoferrin structure demonstrates ligand-induced conformational change in transferrins. Nature, 344(6268), 784-787.

Antequera, D., Moneo, D., Carrero, L., Bartolome, F., Ferrer, I., Proctor, G., & Carro, E. (2021). Salivary lactoferrin expression in a mouse model of Alzheimer's disease. Frontiers in Immunology, 12, 749468.

Baker, E. N., & Lindley, P. F. (1992). New perspectives on the structure and function of transferrins. Journal of Inorganic Biochemistry, 47(1), 147-160.

Baker, H. M., & Baker, E. N. (2012). A structural perspective on lactoferrin function. Biochemistry and Cell Biology, 90(3), 320-328.

Belaidi, A. A., Masaldan, S., Southon, A., Kalinowski, P., Acevedo, K., Appukuttan, A. T., ... & Ayton, S. (2022). Apolipoprotein E potently inhibits ferroptosis by blocking ferritinophagy. Molecular Psychiatry, 1-10.

Bermejo-Pareja, F., Del Ser, T., Valentí, M., de la Fuente, M., Bartolome, F., & Carro, E. (2020). Salivary lactoferrin as biomarker for Alzheimer's disease: Brain-immunity interactions. Alzheimer's & Dementia, 16(8), 1196-1204.

Carro, E., Bartolomé, F., Bermejo-Pareja, F., Villarejo-Galende, A., Molina, J. A., Ortiz, P., ... & Orive, G. (2017). Early diagnosis of mild cognitive impairment and Alzheimer's disease based on salivary lactoferrin. Alzheimer's & Dementia: Diagnosis, Assessment & Disease Monitoring, 8, 131-138.

Chen, J. M., Fan, Y. C., Lin, J. W., Chen, Y. Y., Hsu, W. L., & Chiou, S. S. (2017). Bovine lactoferrin inhibits dengue virus infectivity by interacting with heparan sulfate, low-density lipoprotein receptor, and DC-SIGN. International Journal of Molecular Sciences, 18(9), 1957.

Chen, Y., Wang, B., Yang, C., Shi, Y., Dong, Z., & Troy, F. A. (2021). Functional correlates and impact of dietary lactoferrin intervention and its concentration-dependence on neurodevelopment and cognition in neonatal piglets. Molecular Nutrition & Food Research, 65(8), 2001099.

Fillebeen, C., Ruchoux, M. M., Mitchell, V., Vincent, S., Benaïssa, M., & Pierce, A. (2001). Lactoferrin is synthesized by activated microglia in the human substantia nigra and its synthesis by the human microglial CHME cell line is upregulated by tumor necrosis factor α or 1-methyl-4-phenylpyridinium treatment. Molecular brain research, 96(1-2), 103-113.

Ginet, V., van de Looij, Y., Petrenko, V., Toulotte, A., Kiss, J., Hüppi, P. S., & Sizonenko, S. V. (2016). Lactoferrin during lactation reduces lipopolysaccharide-induced brain injury. Biofactors, 42(3), 323-336.

González-Chávez, S. A., Arévalo-Gallegos, S., & Rascón-Cruz, Q (2009). Lactoferrin: structure, function and applications. International Journal of Antimicrobial Agents, 33(4), 301-e1.

González-Sánchez, M., Bartolome, F., Antequera, D., Puertas-Martín, V., González, P., Gómez-Grande, A., ... & Carro, E. (2020). Decreased salivary lactoferrin levels are specific to Alzheimer's disease. EBioMedicine, 57:102834.

Groves, M. L. (1960). The isolation of a red protein from Milk2. Journal of the American Chemical Society, 82(13), 3345-3350.

Guo, C., Yang, Z. H., Zhang, S., Chai, R., Xue, H., Zhang, Y. H., ... & Wang, Z. Y. (2017). Intranasal lactoferrin enhances α-secretase-dependent amyloid precursor protein processing via the ERK1/2-CREB and HIF-1α pathways in an Alzheimer's disease mouse model. Neuropsychopharmacology, 42(13), 2504-2515.

He, Q., Zhang, L. L., Li, D., Wu, J., Guo, Y. X., Fan, J., ... & Qin, L. Q. (2023). Lactoferrin alleviates Western diet-induced cognitive impairment through the microbiome-gut-brain axis. Current Research in Food Science, 7, 100533.

Huang, R., Ke, W., Han, L., Liu, Y., Shao, K., Jiang, C., & Pei, Y. (2010). Lactoferrin-modified nanoparticles could mediate efficient gene delivery to the brain in vivo. Brain Research Bulletin, 81(6), 600-604.

Jiang, H., Wang, J., Rogers, J., & Xie, J. (2017). Brain iron metabolism dysfunction in Parkinson's disease. Molecular Neurobiology, 54, 3078-3101.

Karav, S. (2018). Selective deglycosylation of lactoferrin to understand glycans' contribution to antimicrobial activity of lactoferrin. Cellular and Molecular Biology, 64(9), 52-57.

Karav, S., German, J. B., Rouquié, C., Le Parc, A., & Barile, D. (2017). Studying lactoferrin N-glycosylation. International Journal of Molecular Sciences, 18(4), 870.

Kell, D. B., Heyden, E. L., & Pretorius, E. (2020). The biology of lactoferrin, an iron-binding protein that can help defend against viruses and bacteria. Frontiers in immunology, 11, 550441.

Kholerdi, A., Moradian, F., & Mehralitabar, H. (2024). In vitro study of the expression of autophagy genes ATG101, mTOR and AMPK in breast cancer with treatment of lactoferrin and in silico study of their communication networks and protein interactions. Progress in Biophysics and Molecular Biology, S0079-6107(24)00054-3.

Legrand, D., Pierce, A., Elass, E., Carpentier, M., Mariller, C., & Mazurier, J. (2008). Lactoferrin structure and functions. Bioactive components of milk, 163-194.

Li, H., Li, C., Zhang, B., & Jiang, H. (2023). Lactoferrin suppresses the progression of colon cancer under hyperglycemia by targeting WTAP/m6A/NT5DC3/HKDC1 axis. Journal of Translational Medicine, 21(1), 156.

Li, L., Tan, L., Zhang, Q., Cheng, Y., Liu, Y., Li, R., & Hou, S. (2023). Nose-to-brain delivery of self-assembled curcumin-lactoferrin nanoparticles: Characterization, neuroprotective effect and in vivo pharmacokinetic study. Frontiers in Bioengineering and Biotechnology, 11, 1168408.

Liao, H., Liu, S., Wang, H., Su, H., & Liu, Z. (2019). Enhanced antifungal activity of bovine lactoferrin-producing probiotic *Lactobacillus casei* in the murine model of vulvovaginal candidiasis. BMC Microbiology, 19, 1-13.

Liu, H., Wu, H., Zhu, N., Xu, Z., Wang, Y., Qu, Y., & Wang, J. (2020). Lactoferrin protects against iron dysregulation, oxidative stress, and apoptosis in 1-methyl-4-phenyl-1, 2, 3, 6-tetrahydropyridine (MPTP)-induced Parkinson's disease in mice. Journal of neurochemistry, 152(3), 397-415.

Madi, N. M., & El-Saka, M. H. (2018). The possible protective effect of lactoferrin on lipopolysaccharide-induced memory impairment in albino rats. Alexandria Journal of Medicine, 54(4), 295-298.

McCarthy, N. A., Kelly, A. L., O'Mahony, J. A., & Fenelon, M. A. (2014). Sensitivity of emulsions stabilised by bovine β-casein and lactoferrin to heat and CaCl2. Food Hydrocolloids, 35, 420-428.

Moore, S. A., Anderson, B. F., Groom, C. R., Haridas, M., & Baker, E. N. (1997). Three-dimensional structure of diferric bovine lactoferrin at 2.8 Å resolution. Journal of Molecular Biology, 274(2), 222-236.

Nakamura, A., Kimura, F., Tsuji, S., Hanada, T., Takebayashi, A., Takahashi, A., ... & Murakami, T. (2022). Bovine lactoferrin suppresses inflammatory cytokine expression in endometrial stromal cells in chronic endometritis. Journal of Reproductive Immunology, 154, 103761.

Pogoutse, A. K., & Moraes, T. F. (2017). Iron acquisition through the bacterial transferrin receptor. Critical Reviews in Biochemistry and Molecular Biology, 52(3), 314-326.

Ponzini, E., Scotti, L., Grandori, R., Tavazzi, S., & Zambon, A. (2020). Lactoferrin concentration in human tears and ocular diseases: A meta-analysis. Investigative Ophthalmology & Visual Science, 61(12), 9-9.

Reddy, P. N., Kaur, J., & Naqvi, S. (2025). Lactoferrin-conjugated quercetin-loaded organically modified silica nanocargoes ameliorate cognitive impairment in a rat model of amnesia. RSC Pharmaceutics, 2(6), 1545-1557.

Reseco, L., Atienza, M., Fernandez-Alvarez, M., Carro, E., & Cantero, J. L. (2021). Salivary lactoferrin is associated with cortical amyloid-beta load, cortical integrity, and memory in aging. Alzheimer's Research & Therapy, 13, 1-12.

Rosa, L., Cutone, A., Lepanto, M. S., Paesano, R., & Valenti, P. (2017). Lactoferrin: a natural glycoprotein involved in iron and inflammatory homeostasis. International Journal of Molecular Sciences, 18(9), 1985.

Sokolov, A. V., Dubrovskaya, N. M., Kostevich, V. A., Vasilev, D. S., Voynova, I. V., Zakharova, E. T., ... & Vasilyev, V. B. (2022). Lactoferrin induces erythropoietin synthesis and rescues cognitive functions in the offspring of rats subjected to prenatal hypoxia. Nutrients, 14(7), 1399.

Sorensen M.S. The Proteins in Whey, Whey. Compte rendu des Travaux du Laboratoire de Carlsberg Ser. Chim. 1939;23:55-99.

Stockwell, B. R. (2022). Ferroptosis turns 10: Emerging mechanisms, physiological functions, and therapeutic applications. Cell, 185(14), 2401-2421.

Takeuchi, T., Jyonotsuka, T., Kamemori, N., Kawano, G., Shimizu, H., Ando, K., Harada, E. (2006). Enteric-formulated lactoferrin was more effectively transported into blood circulation from gastrointestinal tract in adult rats. Experimental Physiology, 91(6), 1033-1040.

Teraguchi, S., Wakabayashi, H., Kuwata, H., Yamauchi, K., & Tamura, Y. (2004). Protection against infections by oral lactoferrin: evaluation in animal models. Biometals, 17, 231-234.

Togawa, J. I., Nagase, H., Tanaka, K., Inamori, M., Umezawa, T., Nakajima, A., ... & Sekihara, H. (2002). Lactoferrin reduces colitis in rats via modulation of the immune system and correction of cytokine imbalance. American Journal of Physiology-Gastrointestinal and Liver Physiology, 283(1), G187-G195.

Van De Looij, Y., Ginet, V., Chatagner, A., Toulotte, A., Somm, E., Hüppi, P. S., & Sizonenko, S. V. (2014). Lactoferrin during lactation protects the immature hypoxic-ischemic rat brain. Annals of Clinical and Translational Neurology, 1(12), 955-967.

Vogel, H. J. (2012). Lactoferrin, a bird's eye view. Biochemistry and Cell Biology, 90(3), 233-244.

Xu, S. F., Zhang, Y. H., Wang, S., Pang, Z. Q., Fan, Y. G., Li, J. Y., ... & Guo, C. (2019). Lactoferrin ameliorates dopaminergic neurodegeneration and motor deficits in MPTP-treated mice. Redox Biology, 21, 101090.

Yao, X. (2015). Development of a novel drug delivery system to enhance the oral bioavailability of lactoferrin (Doctoral dissertation, ResearchSpace@ Auckland).

Zakharova, E. T., Kostevich, V. A., Sokolov, A. V., & Vasilyev, V. B. (2012). Human apo-lactoferrin as a physiological mimetic of hypoxia stabilizes hypoxia-inducible factor-1 alpha. Biometals, 25(6), 1247-1259.

Zhao, X., Kruzel, M., & Aronowski, J. (2021). Lactoferrin and hematoma detoxification after intracerebral hemorrhage. Biochemistry and Cell Biology, 99(1), 97-101.

ORAL PRESENTATION

Effects of paclobutrazol on basil (*Ocimum basilicum* L.) during germination

Asena Aslan [1] (https://orcid.org/0009-0006-6401-3670),
Hande Otu Borlu [1] *(*https://orcid.org/0000-0002-0381-7345)*

*[1]Çukurova University, Faculty of Science and Letters, Department of Biology, Sarıçam, Adana, Türkiye

*Corresponding author e-mail: hotu@cu.edu.tr

Abstract

Basil (*Ocimum basilicum* L.) is an annual medicinal and aromatic plant belonging to the Lamiaceae family. Owing to its pleasant fragrance, essential oil content, nutritional value, and distinctive flavor, it is widely utilized in various aspects of daily life. Paclobutrazol (PBZ) is an organic compound known to suppress vegetative growth while enhancing reproductive development.

This study aimed to investigate the effects of different paclobutrazol concentrations on basil (O. basilicum L.) seedlings during the vegetative stage. For this purpose, PBZ solutions at concentrations of 0 (control), 10, 20, 30, 40, and 50 ppm were applied to basil seeds sown in Petri dishes through irrigation under controlled conditions to ensure germination. At the end of the experiment, germination percentage was calculated, while root and shoot lengths as well as fresh and dry weights were measured. According to statistical analyses (ANOVA, $p<0.05$), all PBZ concentrations significantly reduced both germination percentage and -germination index compared to the control. Similarly, all concentrations markedly decreased radicle and plumule lengths along with shoot fresh weight. In contrast, shoot dry weight together with root fresh and dry weights were significantly reduced only by higher PBZ concentrations. Except for the 30 ppm treatment, no decline was observed in root and shoot water content.

Considering the protective role of paclobutrazol against stress factors, studies of this nature are expected to help determine the concentration at which plants are least affected, thereby minimizing agricultural yield losses by through its potential ameliorative effects against biotic and abiotic stresses.

Keywords: Basil, Paclobutrazol, Germination, Growth.

INTRODUCTION

Chemical growth inhibitors have been used densely in seedling cultivation, especially in fruit growing and ornamental plants recently. The reason of this choice is that they have high chemical activity and are more practical in terms of applicability. Akdemir, 2018). Although there are many advantages to using growth inhibitory chemicals, some problems can arise if not used correctly. They may cause chlorosis, disruption in growth mechanism, delay on harvest time and environmental pollution (Uslu and Özgüri 2002; Ergun et al., 2007). Although the two most well-known of these are abscisic acid (ABA) and jasmonic acid (JA), most of the studies conducted to date to provide height control by suppressing plant growth are onis Paclobutrazol (PBZ), which used as treatment agent in the present study (Rademacher, 2000; Özgül, 2021).

Paclobutrazol is one of the plant growth inhibitory chemicals used to suppress stem length in the seedling industry. It retards seedling development by showing antagonistic effect against gibberellins which take part tiller elongation without leave chemical residue or without affect harvest yield. It provides seedling length control by slowing down cell division that causes shoot elongation (Rademacher, 2000; Özgül, 2021).

Paclobutrazol [(2RS,3RS)-1-(4-chlorophenyl)-4,4-dimethyl-2-(1,2,4-triazol-1-yl)pentan-3-ol], is a gibberellin inhibitor that belongs to triazole family (Davis and Curry,1991: Baninasab, 2009Kaynak and Ersoy 1997, Kumlay et al. 2011). It is absorbed by plants from the roots and the shoots (Hazar and Bora 2018). It was discovered that PBZ protects lots of crops from the abiotic stress factors like cold, heat and UV radiation Orabi et al., 2010; Duman and Nas, 2024).

The plant material of the present research, Ocimum basilicum L. is a member of Lamiaceae family and it has for about 65 species from annual and perennial (Ekren et al.,2009; Paton et al., 1999; Karaca, 2017). Its seeds are

generally small and black coloured. The basil flowers are clustered, white, purple, lilac or dark green coloured. Although its tolerance to cold weather is low, the heat tolerance is quiet high (Arabacı ve Bayram, 2004; Baydar, 2013).

Basil is pretty liked and used in a lot of areas in Turkey, which is highly rich about medicinal and aromatic plants. Its production and consumptions are also common in worldwide (Dumanoğlu ve Mokhtarzadeh, 2021),, according to the researches its homeland is South Asia, India and Iran as well(Razavi et al., 2009). In some regions especially east provinces of Turkey, purple coloured species are more common and named 'reyhan' (Telci et al., 2005).

The basil essential oils are used in different areas like perfumery, cosmetic, medicine, hygiene, food and drink industries (Javanmardi et al, 2003; Oxenham et al., 2005; Hussain et al., 2008; Bassolé et al., 2010; Günay and Telci, 2017; Poonkodi, 2016). The extracts that obtained from basil contain amounts of phenolics, caffeic, p-coumaric, ferulic, camphor and some acids (Marki and Kinitzios, 2008; Baydar, 2013). In addition to these, it is used in traditional medicine as carminative, urinary tract antiseptic, analgesic, expectorant, antitussive, diarrhea and chronic dysentery, cardiovascular diseases, Alzheimer's and various cancers treatment (Baytop, 1999).

The wide area of use that mentioned above requires more researches about basil. So, the scope of the present study is to research the effects of the PBZ applications on basil seeds' germination stage.

MATERIALS AND METHODS

Plant Material an Laboratory Conditions

Ocimum basilicum L. seeds were obtained from a commercial firm and used as plant material .The study was conducted in Cukurova University Biology Department Plant Physiology Labaratory. The laboratory's controllled conditions were provided with Arçelik marked air conditioner and fluorescent lambs.

Chemicals and Treatment

Paclobutrazol, active ingredient of the study was obtained from Sigma firm. The PBZ concentrations were 0-(only distilled water as control)-10-20-30-40 and 50 ppm, prepared by diluting 50 ppm PBZ solution.

The basil seeds were disinfected with %5 commercial sodium hypochloride. They put in Petri dishes between the filter papers and watered with PBZ solutions. Each petri had 20 seeds (Figure 1) and each application had five replicates. The Petri dishes were put in controlled climate room for germination (24/18±2 ^{0}C, firstly dark but 16/8 light/dark photoperiod after plumule emergence, and 350 µmol/m^2 s light intensity,%60±5 humidity) completely randomise design. The Petri dishes were watered with PBZ solutions as needed until the end of the experiment. The germinated seeds were counted for seven days. At least 2 mm radicle emergence was accepted as the germination criterion (Scott et al., 1984; Soltani et al., 2012; Özyazıcı, 2023).

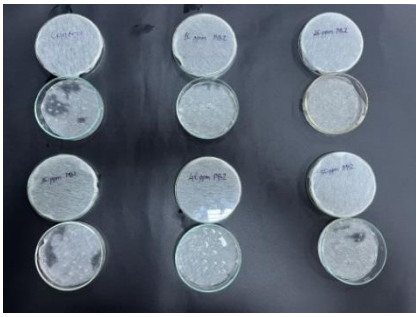


Figure 1. The first day of the basil seeds that applicated with increasing PBZ solutions

Measurements and Statistics

At the end of the experiment, random five germinated plantlet were selected from each Petri dish and their radicle-plumul lengths and fresh weights were recordedi and dried dried at 65 °C in an oven to record dry weights.Germination rate, germination index and water contents were calculated according to following formulas.

Germination percentage = (number of germinated seeds on the final day/number of tested seeds) × 100 (Ikić et al., 2012)

Germination indeks= ∑Germination seeds at a given day/Day number (Wang et al.,2004)

Water content=[(Fresh weight-dry weight)/Fresh Weight]*100

To determine the effects of PBZ treatments on basil, statistical analyses were performed using IBM SPSS Statistics 22 (ANOVA, $p<0.05$). The significant differences ($p < 0.05$).with between control and PBZ applications were shown with * in the tables.

RESULTS and DISCUSSION

The Effects of the Paclobutrazol Applications on Basil Germination Parameters

Table 1 shows the effects of the paclobutrazol applications on basil germination parameters**.** Paclobutrazol had negative effect on the Basil seeds'germination significantly($p < 0.05$). Increasing PBZ concentrations caused the germination index and germination rate of the Basil seeds. The highest germination rate and index values were recorded at Control application, while the lowest values measured at the highest PBZ concentration.

Table 1. The effects of Paclobutrazol applications on Basil seedlings' germination parameters

PBZ Concentration (ppm)	Germination Index (%)		Germination Rate (%)	
	Mean	Std. Deviation	Mean	Std. Deviation
Control (0)	53,29	± 1,53	100,00	± 0,00
10	*21,71	± 7,10	*50,00	± 17,32
20	*16,02	± 4,76	*39,00	± 13,42
30	*16,86	± 4,54	*41,00	± 8,94
40	*15,92	± 4,13	*44,00	± 8,22
50	*12,46	± 4,71	*38,00	± 9,75
LSD	6,91		15,96	

Gibberellin is known to stimulate germination in plants, such as quinoa (Altuner et al.,2020). Triazols, inhibits gibberellin synthesis by inhibiting monooxygenases that oxidize ent-kauren to ent-kaurenoic acid in the pathway's first steps (Hedden and Kamiya, 1997, Shahrohki et al., 2011). This explanation may be a comment to decline in germination parameter of basil against increasing PBZ applications.

The Effects of the Paclobutrazol Applications on Basil seedlings' Growth at Germination Period

Table 2 states the effects of the paclobutrazol applications on basil seedlings' radicle and plumule lengths. All PBZ applications affected Basil elongation negatively ($p < 0.05$). The highest length values were measured at Control application, too.

Table 2. The effects of Paclobutrazol applications on Basil seedlings' radicle and plumule lengths

PBZ Concentration (ppm)	Radicle Length (mm)		Plumule Length (mm)	
	Mean	Std. Deviation	Mean	Std. Deviation
Control (0)	50,00	± 12,69	27,67	± 4,220
10	*28,93	± 9,26	*4,07	± ,704
20	*18,13	± 4,10	*3,40	± ,737
30	*13,93	± 2,89	*2,40	± ,910
40	*14,8	± 3,93	*3,13	± ,834
50	*11,73	± 2,25	*3,47	± ,743
LSD	5,23		1,40	

The effects of the paclobutrazol applications on basil seedlings' radicle and plumule weights are shown in Table 3. All PBZ applications decreased plumule fresh weight negatively ($p < 0.05$). At the highest PBZ concentration, radicle-plumule fresh and dry weights' declines were found significantly.

Table 3. The effects of Paclobutrazol applicaTions on Basil seedlings' radicle and plumule weights

PBZ Concentration (ppm)	Radicle fresh weight (mg)		Radicle dry weight (mg)		Plumule fresh weight (mg)		Plumule dry weight (mg)	
	Mean	Std. Deviation	Mean	Std. Deviation	Mean	Std. Deviation	Mean	Std. Deviation
Control (0)	4,67	± 0,38	0,34	± 0,12	14,77	± 1,63	0,82	± 0,18
10	*5,99	± 0,95	0,34	± 0,02	*6,67	± 0,78	0,57	± 0,10
20	5,06	± 0,80	*0,53	± 0,13	*6,24	± 0,41	0,81	± 0,07
30	4,47	± 0,73	*0,55	± 0,09	*5,96	± 0,73	1,19	± 0,65
40	*3,69	± 0,55	0,38	± 0,11	*6,01	± 1,09	0,68	± 0,21
50	*2,81	± 0,11	*0,06	± 0,06	*6,10	± 0,63	*0,23	± 0,10
LSD	0,95		0,15		1,40		0,43	

Paclobutrazol organized the plant growth by arranging the regulators that contains gibberellin, abscisic acid and cytokinins (Fletcher and Hofstra, 1990). It repressed growth elongation by blocking cell division and enlargement mechanism because of its antigibberellin activity (Grossman,1988, Soumya et al.,2017). As a result of these mechanisms, the decreases in radicle-plumule length and weight in the present study may be associated with.

The Effects of the Paclobutrazol Applications on Basil seedlings' Water Contents

The effects of the paclobutrazol applications on basil seedlings' radicle and plumule water contents are presented in Table 4. While 30 ppm PBZ decreased the water contents of two diferent tisues ($p < 0.05$), the highest PBZ concentration, increased radicle and plumule water content.

Table 4. The effects of Paclobutrazol applications on Basil seedlings' radicle and plumule water contents

PBZ Concentration (ppm)	Radicle water content (%)		Plumule water content (%)	
	Mean	Std. Deviation	Mean	Std. Deviation
Control (0)	92,75	± 2,43	94,35	± 1,59
10	95,14	± 2,57	91,42	± 1,00
20	89,58	± 2,01	86,90	± 1,75
30	*87,54	± 1,55	*79,73	± 11,54
40	89,28	± 4,21	88,36	± 4,34
50	*97,84	± 2,20	96,28	± 1,72
LSD	3,82		7,55	

Paclobutrazol was stated to ameliorate leaf water potential (Watson, 2001) and decrease transpiration under drought stress (Still and Pill, 2004), induce stomatal closure (Srethar, 1991) and increase water use efficiency (Driessche, 1996; Soumya et al.,2017). In the present study, the highest water content in radicle and plumule against the highest PBZ concentration may be clarified with these.

CONCLUSION

Paclobutrazol, which is a synthetic plant growth regulator from the triazole family, decreased germination rate and index, radicle and plumule weights and lengths, but increased water content in basil plantlets. This pret-reatment may be developed to the generative stages to understand the other effects of triazole on basil.
Afterwards PBZ may be used to ameliorate stress factors or control plant growth to obtain a higher herb yield.

REFERENCES

Akdemir, S. (2018).Marul (*Lactuca sativa* L.) fide kalitesi ve bitki gelişimi üzerinepaclobutrazol ve prohexadione-calciumuygulamalarının etkileri(Master's thesis, Kirsehir Ahi Evran University (Turkey)).

Altuner, F., Oral, E., Tunctürk, R., & Baran, İ. (2020). Giberellik asit (GA3) ön uygulamasına tabi tutulmuş kinoa (*Chenopodium quinoa* Willd.) tohumunda tuz (NaCl) stresinin çimlenme özellikleri üzerine etkisi. Kahramanmaraş Sütçü İmam Üniversitesi Tarım ve Doğa Dergisi, 23(2), 350-357.

Arabaci, O., & Bayram, E. (2004). The effect of nitrogen fertilization and different plant densities on some agronomic and technologic characteristic of *Ocimum basilicum* L.(Basil).

Baninasab, B., 2009. Ameliorationof chilling stress by paclobutrazol in watermelon seedlings. Scientia Horticulture. 121:144-148.

Bassolé, I. H. N., Lamien-Meda, A., Bayala, B., Tirogo, S., Franz, C., Novak, J., ... & Dicko, M. H. (2010). Composition and antimicrobial activities of *Lippia multiflora* Moldenke, *Mentha x piperit*a L. and *Ocimum basilicum* L. essential oils and their major monoterpene alcohols alone and in combination. Molecules, 15(11), 7825-7839.

Baydar, H. (2009). Tıbbi ve aromatik bitkiler bilimi ve teknolojisi. Nobel Akademik Yayıncılık.

Baytop, T. (1999). Türkiye'de Bitkiler ile Tedavi, Geçmişte ve Bugün. Nobel Tıp Kitabevleri, İstanbul.

Davis, T.D., Curry, E.A., 1991. Chemical regulation of vegetative growth. Crit. Rev.Plant Sci. 10:151–188.

Duman, İ., & Nas, Y., (2024). Biber (*Capsicum annuum* L.), Domates (*Solanum lycopersicum* L.) ve Patlıcan (*Solanum melongena* L.) Fide Kalitesi Üzerine Paclobutrazol, Prohexadione Calcium ve Chlormequat Chloride Uygulamalarının Etkileri. ISPEC Journal of Agricultural Sciences, 8(3), 621-637.

Dumanoğlu, Z., & Mokhtarzadeh, S. (2021). Farklı fesleğen (*Ocimum basilicum* L.) populasyonlarına ait tohumların bazı karakteristik özelliklerinin belirlenmesi üzerine bir araştırma. Akademik Ziraat Dergisi, 10(1), 97-104.

Ekren, S., Sönmez, Ç., Sancaktaroğlu, S., & Bayram, E. (2009). Farklı dikim sıklıklarının fesleğen (*Ocimum basilicum* L.) bitkisinin verim ve kalite özellikleri üzerine etkisi. Journal of Ege University Faculty of Agriculture (Turkey), 46(3).

Ergun, N., Çağlar, G., Özbay, N., & Ergun, M. (2007). Effects of prohexadione-calcium applications on cucumber seedlings quality and plant growth.

Fletcher, R. A., & Hofstra, G. (1990). Improvement of uniconazole-induced protection in wheat seedlings. Journal of Plant Growth Regulation, 9, 207–212.

Grossman, K. (1988). Plant cell suspensions for screening and studying the mode of action of plant growth retardants. In K. Maramorosch & G. Sato (Eds.), Advances in cell culture (pp. 89–136). San Diego: Academic Press.

Günay, E., & Telci, İ. (2017). Isparta ekolojik koşullarında bazı reyhan (*Ocimum basilicum* L.) genotiplerinin verim ve kalite özelliklerinin belirlenmesi. Ziraat Fakültesi Dergisi, 12(2), 100-109.

Hazar, D., & Bora, Ö. F. (2018). Küpe çiçeğinde (*Fuchsia* spp.) paclobutrazol uygulamalarının bitki gelişimi üzerine etkileri. Ziraat Fakültesi Dergisi, 528-538.

Hedden, P. and Kamiya, Y., (1997). Gibberellin biosynthesis: enzymes, genes and their regulation. Ann. Rev. Plant Physiology. Plant Molec. Biol. 48:431-460.

Hussain, A. I., Anwar, F., Sherazi, S. T. H., & Przybylski, R. (2008). Chemical composition, antioxidant and antimicrobial activities of basil (*Ocimum basilicum)* essential oils depends on seasonal variations. Food chemistry, 108(3), 986-995.

Ikić, I., Maričević, M., Tomasović, S., Gunjača, J., Šatović, Z., Šarčević, H. (2012): The effect of germination temperature on seed dormancy in Croatian-grown winter wheats. Euphytica 188(1): 25–34. https://doi.org/10.1007/s10681-012-0735-8

Javanmardi, J., Stushnoff, C., Locke, E., & Vivanco, J. M. (2003). Antioxidant activity and total phenolic content of Iranian Ocimum accessions. Food chemistry, 83(4), 547-550.

Karaca, M. (2017). Bazı fesleğen (*Ocimum basilicum* L.) populasyonlarının herba verimi ve uçucu yağ oranının belirlenmesi (Master's thesis, Ordu Üniversitesi Fen Bilimleri Enstitüsü).

Kaynak, L., & Ersoy, N. (1997). Bitki büyüme düzenleyicilerinin genel özellikleri ve kullanım alanları. Akdeniz University Journal of the Faculty of Agriculture, 10(1), 223-236.

Kumlay, A. M., & Eryiğit, T. (2011). Bitkilerde büyüme ve gelişmeyi düzenleyici maddeler: bitki hormonları. Journal of the Institute of Science and Technology, 1(2), 47-56.

Makri, O., & Kintzios, S. (2008). *Ocimum* sp.(basil): Botany, cultivation, pharmaceutical properties, and biotechnology. Journal of herbs, spices & medicinal plants, 13(3), 123-150.

Orabi, S. A., Salman, S. R., & Shalaby, M. A. (2010). Increasing resistance to oxidative damage in cucumber (*Cucumis sativus* L.) plants by exogenous application of salicylic acid and paclobutrazol. World Journal of Agricultural Sciences, 6(3), 252-259.

Oxenham, S. K., Svoboda, K. P., & Walters, D. R. (2005). Antifungal activity of the essential oil of basil (*Ocimum basilicum*). Journal of phytopathology, 153(3), 174-180.

Özgül, Y. (2021). Büyümesi baskılanmış karnabahar fidelerinde perlan ticari preparat etkisinin araştırılması (Master's thesis, Bursa Uludag University (Turkey)).

Özyazici, G. Fesleğen (*Ocimum Basilicum* L.)'De Çimlenme Parametrelerine Borikasit Uygulamalarinin Etkisi.

Paton, A., Harley, R. M., & Harley, M. M. (1999). Ocimum-an overview of relationships and classification. Medicinal and Aromatic Plants-Industrial Profiles, 1(8).

Poonkodi, K. (2016). Chemical composition of essential oil of *Ocimum basilicum* L.(Basil) and its biological activities-an overview. J. Crit. Rev, 3(3), 56-62.

Rademacher, W. (2000). Growth retardants: effects on gibberellin biosynthesis and other metabolic pathways. Annual review of plant biology, 51(1), 501-531.

Razavi, S. M., Mortazavi, S. A., Matia-Merino, L., Hosseini-Parvar, S. H., Motamedzadegan, A., & Khanipour, E. (2009). Optimisation study of gum extraction from Basil seeds (*Ocimum basilicum* L.). International Journal of Food Science and Technology, 44(9), 1755-1762.

Scott, S. J., Jones, R. A., & Williams, W. (1984). Review of data analysis methods for seed germination 1. Crop science, 24(6), 1192-1199.

Shahrokhi, M., Tehranifar, A., Hadizadeh, H. and Selahvarzi, Y., 2011. Effect of Drought Stress and Paclobutrazol Treated Seeds on Physiological Response of *Festuca arundinacea* L. Master and *Lolium perene* L. Barrage. J. Biol. Environ. Sci. 5(14): 77-85.

Soltani, A., Khodarahmpour, Z., Jafari, A. A., & Nakhjavan, S. (2012). Selection of alfalfa (*Medicago sativa* L.) cultivars for salt stress tolerance using germination indices. African Journal of Biotechnology, 11(31), 7899-7905.

Soumya, P. R., Kumar, P., & Pal, M. (2017). Paclobutrazol: a novel plant growth regulator and multi-stress ameliorant. Indian Journal of Plant Physiology, 22(3), 267-278.

Sreethar, V. M. (1991). Proline accumulation and reduced transpiration in the leaves of triazole treated mulberry plant. Indian Botanical Reporter, 101, 1–5.

Still, J. R., & Pill, W. G. (2004). Growth and stress tolerance of tomato seedlings (*Lycopersicon esculentum* Mill) in response to seed treatment with paclobutrazol. Journal of Horticultural Science and Biotchnology, 79, 197–200.

Telci, İ., Bayram, E., Yılmaz, G., & Avcı, A. B. (2005). Türkiye'de kültürü yapılan yerel fesleğen (*Ocimum* spp) genotiplerinin morfolojik, agronomik ve teknolojik özelliklerinin karakterizasyonu ve üstün bitkilerin seleksiyonu (Sonuç Raporu). TOGTAG-3102 No'lu Proje, TÜBİTAK.

Uslu, A. (2002). Aşılı hıyar fidesi yetiştiriciliğinde, farklı aşı yöntemlerinin karşılaştırılması üzerine bir araştırma.

Van den Driessche, R. (1996). Drought resistance and water use efficiency of conifer seedlings treated with paclobutrazol. New Forests, 11, 65–83.

Wang, Y. R., Yu, L., Nan, Z. B., Liu, Y. L. (2004): Vigor tests used to rank seed lot quality and predict field emergence in four forage species. Crop Science 44(2): 535–541. https://doi.org/10.2135/cropsci2004.5350

Watson, G. (2001). Soil applied paclobutrazol affects root growth, shoot growth, and water potential of american elm seedlings. Journal of Environmental Horticulture, 19, 119–122.

ORAL PRESENTATION

Schiff baz ve 1,10-fenantrolinden türeyen karışık ligand Cu(II) ve Fe(II) komplekslerinin sentez ve karakterizasyonu

Hatice Gamze Sogukomerogullari[1*] (*ORCID: https://orcid.org/0000-0002-0575-8131*),
Ahmet Oral Sarıoğlu[2,3] (*ORCID: https://orcid.org0000-0001-7787-7968*)

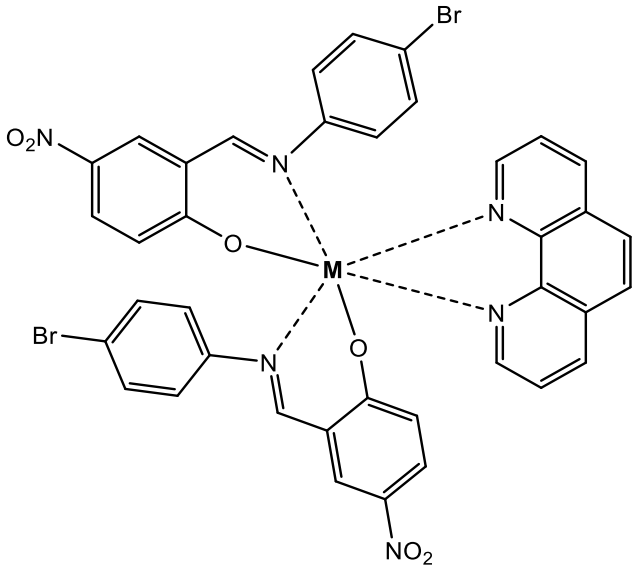
*[1] Gaziantep Üniversitesi, Sağlık Hizmetleri Meslek Yüksekokulu, Tıbbi Hizmetler ve Teknikler Bölümü, 27310, Gaziantep, Türkiye
[2] Gaziantep Üniversitesi, Naci Topçuoğlu Meslek Yüksekokulu, Kimya ve Kimyasal İşleme Teknolojileri Bölümü, 27310, Gaziantep, Türkiye
[3] Gaziantep Üniversitesi, Uluğ Bey Yüksek Teknoloji Uygulama ve Araştırma Merkezi (ULUTEM), 27310, Gaziantep, Türkiye

*Sorumlu yazar e-mail: hgcelikel@gantep.edu.tr

Özet

Hugo Schiff, 150 yılı aşkın bir süredir kapsamlı araştırmaların konusu olan ve inorganik bilimcileri büyülemeye devam eden Schiff bazının mucididir. Schiff bazları, birincil aminlerin karbonil bileşikleri ile yoğunlaşmasıyla oluşur. Çeşitli metal iyonları ile kararlı metal kompleksleri oluşturabilirler ve bu en önemli özelliklerinden biridir. Schiff bazları ve komplekslerinin birçok kullanım alanından bazıları elektrokimya, ilaç, sensör, mantar ilacı, zirai kimya, katalitik, boya ve analitik reaktif endüstrileridir. Son yıllarda, karışık ligand komplekslerine olan ilgi önemli ölçüde artmıştır. Bunun nedeni, çoğunlukla sentezlerinin basit olması, işleme tekniklerinin temel düzeyde olması, yüksek verim sağlamaları ve geniş bir uygulama alanına sahip olmalarıdır.
Bu çalışmada, 2-hidroksi-5-nitrobenzaldehit ve 4-bromoanilinin kondenzasyonundan türeyen Schiff baz ligandı sentezlenmiştir. Elde edilen Schiff bazı ve 1,10-fenantrolin ligandı ile Fe(II) ve Cu(II) metal tuzlarından karışık ligand kompleks bileşikleri sentezlenmiştir. Sentezlenen karışık ligand metal kompleks bileşiklerinin yapıları NMR (ligand için), UV-Vis ve FT-IR gibi spektroskopik yöntemlerin yanı sıra elementel analiz ve elektrolitik iletkenlik gibi ölçümlerle aydınlatılmıştır.

Anahtar Kelimeler: Schiff baz, karışık ligand metal kompleks, sentez, karakterizasyon



M=Cu, Fe

Şekil 1. Sentezlenen kompleks bileşiklerin yapısı

Synthesis and characterization of Schiff base and 1,10-phenanthroline derived mixed-ligand Cu(II) and Fe(II) complexes

Abstract

The Schiff base, which has been the focus of intensive research for more than 150 years and continues to amaze inorganic scientists, was first conceived of and developed by Hugo Schiff. Schiff bases are generated by the condensation of primary amines with carbonyl compounds. They may form stable metal complexes with various metal ions, which is among their most significant characteristics.Some of the many uses for Schiff bases and complexes include those in the electrochemical, pharmaceutical, sensor, fungicidal, agrochemical, catalytic, dye, and analytical reagent industries. In recent years, there has been a significant increase in interest in mixed ligand complexes. This is mostly due to the fact that they are simple to synthesize, their work-up technique is basic, they give a high yield, and they have a wide range of applications.
In this study, a Schiff base ligand derived from the condensation of 2-hydroxy-5-nitrobenzaldehyde and 4-bromoaniline was synthesised. Mixed ligand complex compounds were synthesised from Fe(II) and Cu(II) metal salts using the obtained Schiff base and 1,10-phenanthroline ligand. The structures of the synthesised mixed-ligand metal complex compounds were elucidated using spectroscopic methods such as NMR (for the ligand), UV-Vis and FT-IR, as well as measurements such as elemental analysis and electrolytic conductivity.

Keywords: Schiff base, mixed ligand metal complex, synthesis, characterization

GİRİŞ

Organik bileşik sınıflarından biri olan Schiff bazları, birçok uygulama alanına sahip oldukları için halen incelenmeye devam edilmektedir (Goswami ve ark., 2024). Schiff bazları yapısındaki azometin grubu sayesinde Lewis bazı olarak hareket edip ligand görevini üstlenirler(Thakur ve ark., 2024). Schiff bazları yapılarında oksijen, azot, fosfor ve kükürt gibi çeşitli donör atomlarını içerebilir ve çeşitli metal iyonlarıyla kararlı koordinasyon bileşiklerini oluşturabilir (Sogukomerogullari ve ark., 2026). Yaklaşık 150 yıl boyunca araştırılan Schiff baz ligandları ve metal komplekslerinin sentez ve karakterizasyonu günümüzde de büyük ilgi görmektedir .(Schiff, 1864; Shah ve ark., 2024). Öyle ki Schiff bazları çok işlevli moleküler platformların stratejik tasarımını ve sentezini oluşturur ve tek bir kimyasal ile sinerjik faydalar sunar. Dahası Schiff baz ligandlarının kolay sentezlenebilir olması, elektronik özelliklerinin ayarlanabilir olması ve yapısal çok yönlülükleri nedeniyle bir çok alanda işlevsellik sağlar. (Ceramella ve ark., 2022)Schiff bazlarının geçiş metal kompleksleri biyolojik açıdan önem arz etmekte ve hem terapötik hem de farmasötik olarak incelenmektedir. Schiff baz metal komplekslerinin biyolojik uygulamaları arasında antibakteriyel, antiviral, antioksidan, antikanser ve antifungal çalışmalar yer almaktadır(Goswami ve Barman, 2026; Sagunthala Devi ve ark., 2025; Sogukomerogullari ve ark., 2025; Sogukomerogullari, ve ark., 2025; Sogukomerogullari ve ark., 2026) Schiff baz metal komplekslerinin, kolay sentezlenebilir olması, yapı ve elektronik özelliklerinin ayarlanabilmesi ve ekonomik olması katalitik ve fotokatalitik çalışmalarda da etkili rol oynamasını sağlamaktadır. (Juyal ve ark., 2023; Kiruthika, 2012; Wise ve ark., 2015)
Schiff bazları koordinasyon kimyasında önemli bir sınıfı oluşturmakta ve yaygın kullanımı, biyolojik ve katalitik alanlardaki kayda değer sonuçların olması nedeniyle yeni kompleksler tasarlanmaya devam etmektedir. Birinci sıra geçiş metalleri arasında bulunan Cu(II) ve Fe(II) metallerinin, biyolojik öneme sahip oldukları ve koordinasyon yoluyla ligand aktivitesini yönlendirdikleri bilinmektedir. (Elaaraj ve ark., 2026; Sogukomerogullari ve ark., 2025). Buna ilaveten en az iki farklı ligandın yapıya girerek oluşturdukları karışık ligand kompleksleri ise son zamanlarda dikkatleri üzerine çekmektedir. Bunun nedeni bu komplekslerin kolay sentezlenmeleri, basit işleme tekniklerinin olması, yüksek verimleri ve çeşitli uygulama alanlarının olması olarak görülmektedir (Sogukomerogullari, ve ark., 2025). Schiff bazları, piridin, fosfin, etilendiamin, bipiridin ve 1,10-fenantrolin içeren Fe (II) ve Cu (II) kompleksleri, antifungal, antibakteriyel, kimyasal algılama, antiviral ve katalitik gibi alanlarda sayısız uygulamaları nedeniyle dikkat çekmektedir (Abdelgawad ve ark., 2016; Gómez-Coca ve ark., 2001; Loginova ve ark., 2008; Sogukomerogullari, ve ark., 2025; Valentini ve ark., 2007).
Bu çalışmada 4-bromoanilin ve 2-hidroksi-5-nitrobenzaldehitten türeyen Schiff baz ligandı (L_1) sentezlenmiştir. Karışık ligand metal kompleksleri hazırlamak için co-ligand olarak 1,10-fenantrolin (L) kullanılmıştır. Bu

ligandların varlığında Fe(II) ve Cu(II) karışık ligand metal komplesleri sentezlenmiş ve FT-IR, UV-Vis, kütle, elemental analiz, manyetik duyarlılık gibi yöntemlerle karakterize edilmiştir.

2. MATERYAL ve METOT

2.1. Schiff Baz Ligandının Sentezi (L_1)

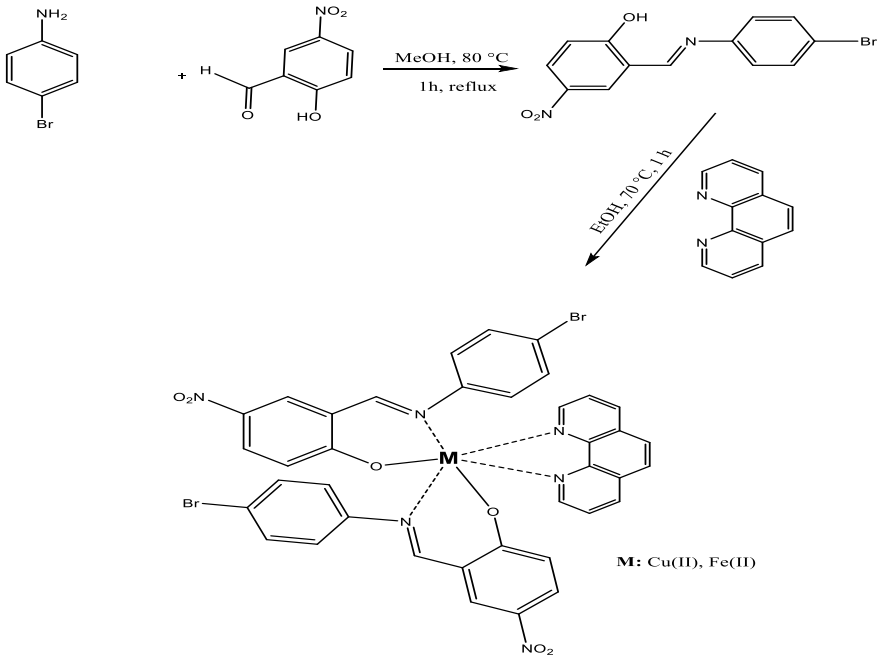
Bu çalışmada 2-hidroksi-5-nitrobenzaldehit ve 4-bromoanilin bileşiklerinden Schiff bazı ligandı (L_1) 2-(((4-bromofenil)imino)metil)-4-nitrofenol sentezlendi(van Dyk ve ark., 2023). Verim = 76 %, E.N. = 181–183 °C. UV–Vis (DMF) λmax (Abs): 430 (1.101), 370 (0.822), 310 (0.386); IR ν ATR (cm^{-1}): ν(Ar-CH) 3084, ν(N–O) 1330 & 1298, ν(C=N) 1618. ^{1}H NMR (400 MHz, aseton-d_6): δ 14.22 (s, 1H, OH), 9.19 (s, 1H, HC=N), 8.63 (s, 1H, Ar), 8.32 (s, 1H, Ar), 7.70 (s, 2H, Ar), 7.52 (s, 2H, Ar), 7.17 (s, 1H, Ar). ^{13}C NMR (600 MHz, aseton-d_6): δ 167.54, 164.32, 147.45, 133.62, 129.95, 129.35, 124.56, 121.84, 119.52, 119.01. Kapalı Formül: $C_{13}H_9BrN_2O_3$; Ma: 321,13 g/mol; Teorik $C_{13}H_9BrN_2O_3$ (%): Hesaplanan: C: %48.62, H: %2.83, N: %8.72 Bulunan: C: %48.61, H: %2. 66, N: %8.36.

2.2. Karışık Ligand Metal Komplekslerinin Sentezi

Schiff baz ligand (L_1) (1 mmol) ve 1,10-fenantrolin (0.5 mmol) ligandları 25 mL etanolde çözüldü üzerine metal tuzlarından (Cu(II) ve Fe(II)) (0.5 mmol) eklenerek 70 ºC de 1 saat karıştırıldı. Çöken madde süzüldü, dietileter ve saf su ile yıkandı. Elde edilen ürün desikatörde kurutuldu.

$[Cu(L_1)_2L].5H_2O$: Verim = 75 %, E.N. = 300 °C dekompoze. UV–Vis (DMF) λmax (Abs): 468 (0.202), 438 (0.740), 380 (1.789), 356 (1.555); IR (ATR, cm^{-1}): ν(O-H) 3406, ν(Ar-CH) 3074, ν(N–O) 1338 & 1253, ν(C=N) 1612. Ma: 974 LC-MS/MS(m/z): 884 $[M(L_1)_2(L)–5H_2O]^+$. Hesaplanan: C:%46.86, H: %3.52, N: %8.63 Bulunan: C: %46.75, H: %3.29, N: %8.55

$[Fe(L_1)_2L].5H_2O$: Verim = 67 %, E.N. = 315 °C dekompoze. UV–Vis (DMF) λmax (Abs): 534 (0.078), 434 (1.481), 374 (1.004), 356 (0.864); IR ν ATR (cm^{-1}): ν(O-H) 3367, ν(Ar-CH) 3086, ν(N–O) 1330 & 1226, ν(C=N) 1616; Ma: 966, LC-MS/MS(m/z): 876 $[M(L_1)_2(L)–5H_2O]^+$. Hesaplanan: C: %47.23, H: %3.55, N: %8.70 Bulunan: C: %47.29, H: %3.52, N: %8.64.

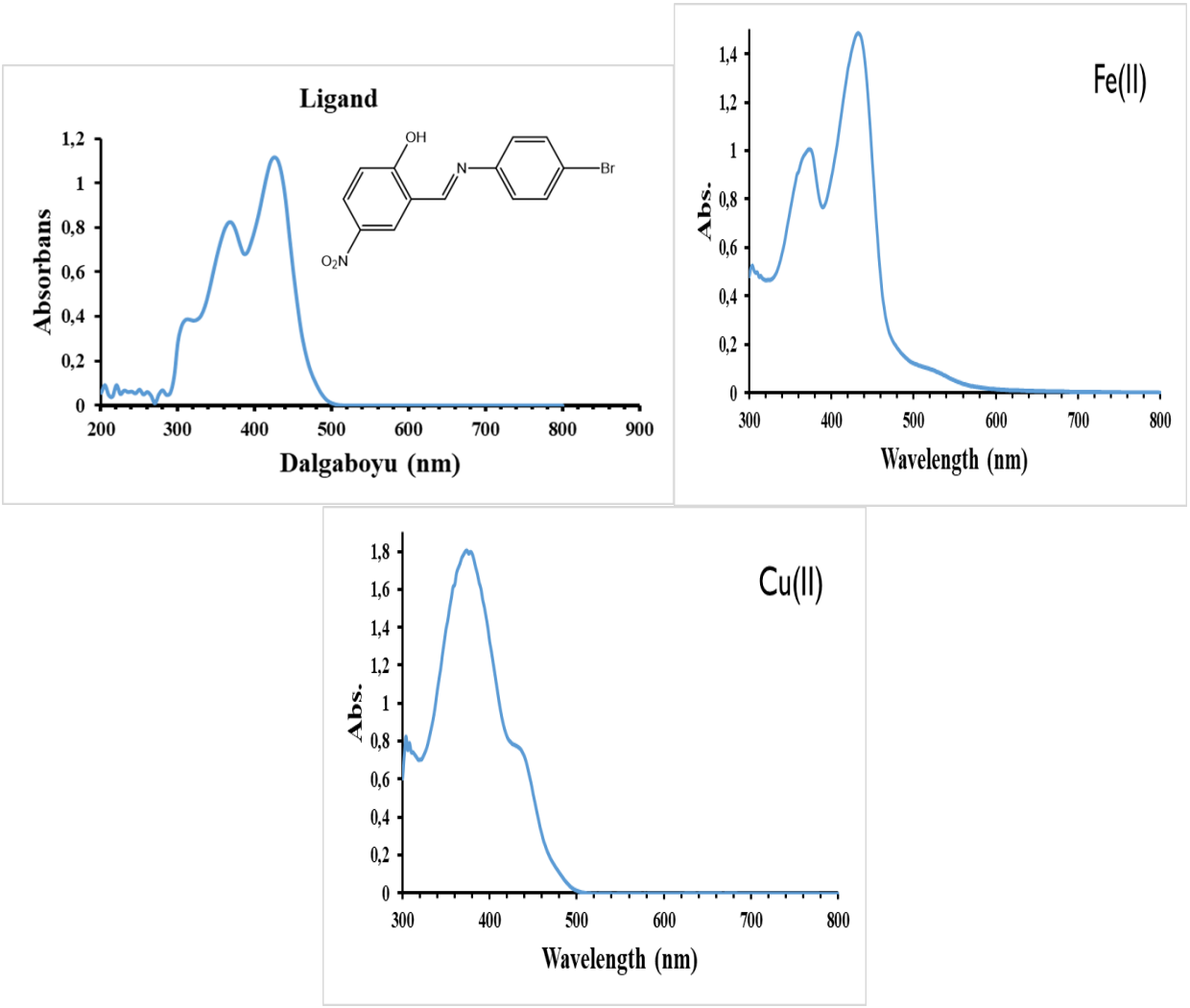


Şekil 2. Sentez şeması

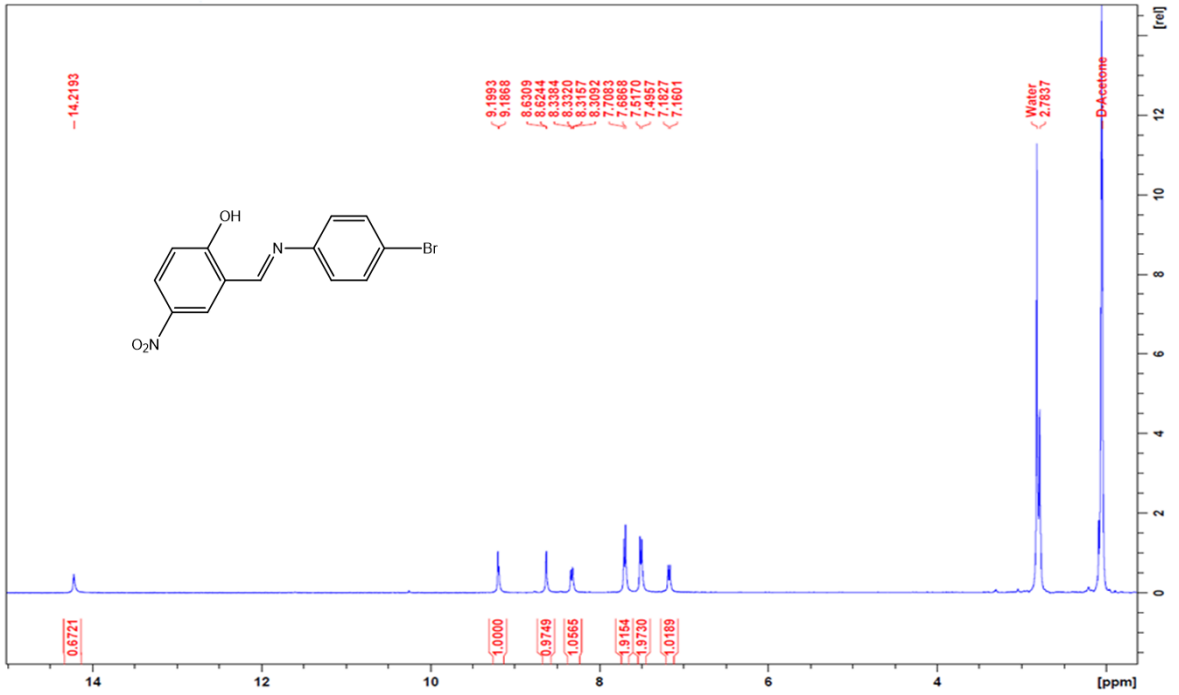
BULGULAR ve TARTIŞMA

Bu çalışmada sentezlenmiş olan Schiff baz ligand ve karışık ligand komplekslerinin tümünün UV-Vis spektrumlarına ait veriler; bu bileşiklerin DMF içerisinde çözünmesi gerçekleşerek 190-800 nm aralığında spekturumu incelenmiştir. 310, 370 ve 430 nm'deki ligandın en yüksek pikleri, sırasıyla π-π* ve n-π* geçişlerine karşılık gelmektedir. $[Cu(L_1)_2L].5H_2O$ ve $[Fe(L_1)_2L].5H_2O$ için en büyük pikler sırasıyla 356, 380, 438, 468 ve

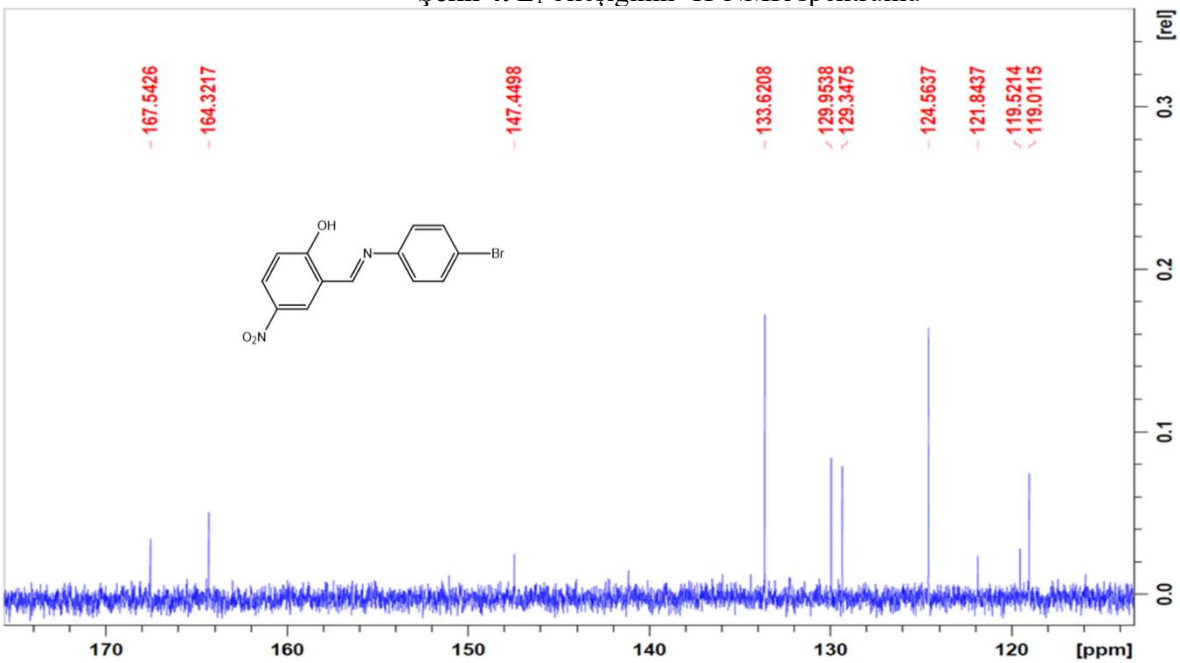
356, 374, 434, 534 nm'de kaydedilmiştir. π-π* ve n-π* geçişlerinin varlığı nedeniyle, $[Cu(L_1)_2L].5H_2O$ ve $[Fe(L_1)_2L].5H_2O$ kompleksinin absorbansının küçük bir kırmızıya kayma sergilediği keşfedilmiştir (Şekil 3). Ayrıca 468 ve 534 nm'deki piklerin yük transfer ve d-d geçişlerine ait olduğu düşünülmektedir. Bu da kompleksleşmenin olduğunu göstermektedir. Ligandın (L_1) ^{1}H-NMR ve ^{13}C-NMR spektrumları, döterolanmış bir çözücü olan aseton içinde kaydedilmiştir. L_1 'ın ^{1}H-NMR spektrumu, δ 14.22 ppm (1H) değerinde bir singlet fenolik proton, δ 9,19 ppm (1H) değerinde bir singlet azometin grubu (CH=N) protonu, δ 8.63–7.17 ppm (7H) değerinde bir çoklu aromatik proton sinyallerini göstermektedir. L_1'nin ^{13}C-NMR spektrumları, 167.54 ppm'de C-O karbon, 164.32 ppm'de azometin karbon (CH=N), 147.45–119.52 ppm'de aromatik karbonlara ait sinyaller sergilemektedir (Şekil 4 ve 5).



Şekil 3. Bileşiklerin UV-Vis spektrumları

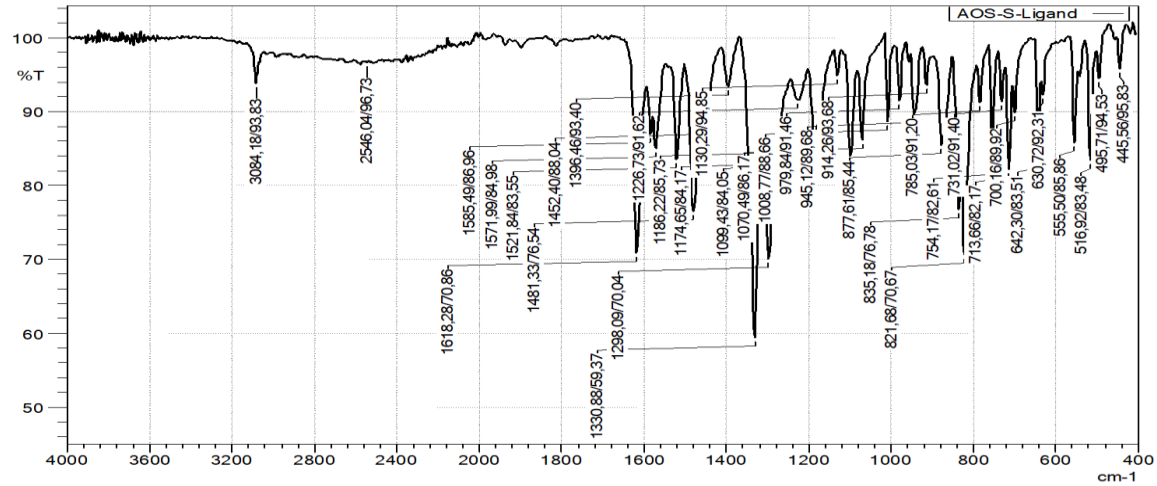


Şekil 4. L_1 bileşiğinin ^{1}H-NMR spektrumu

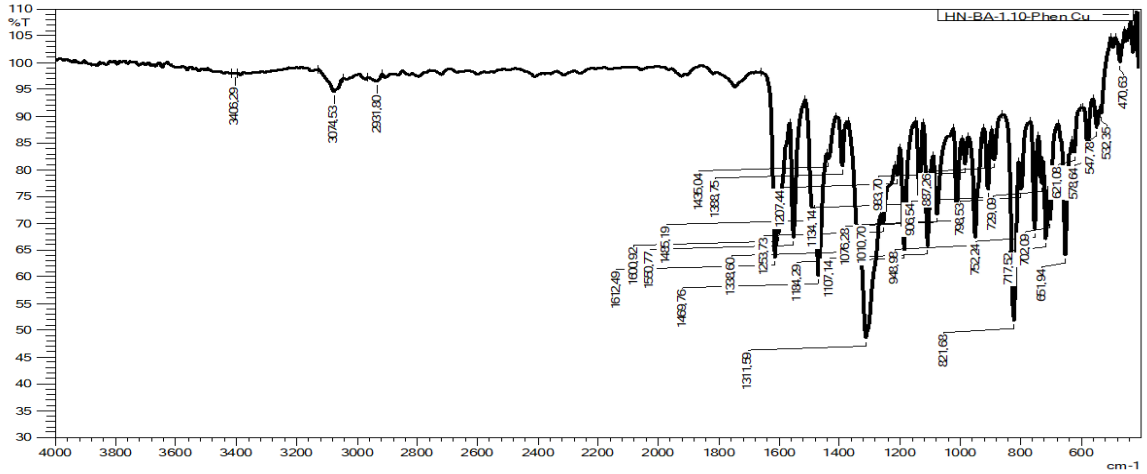


Şekil 5. L_1 bileşiğinin ^{13}C-NMR spektrumu

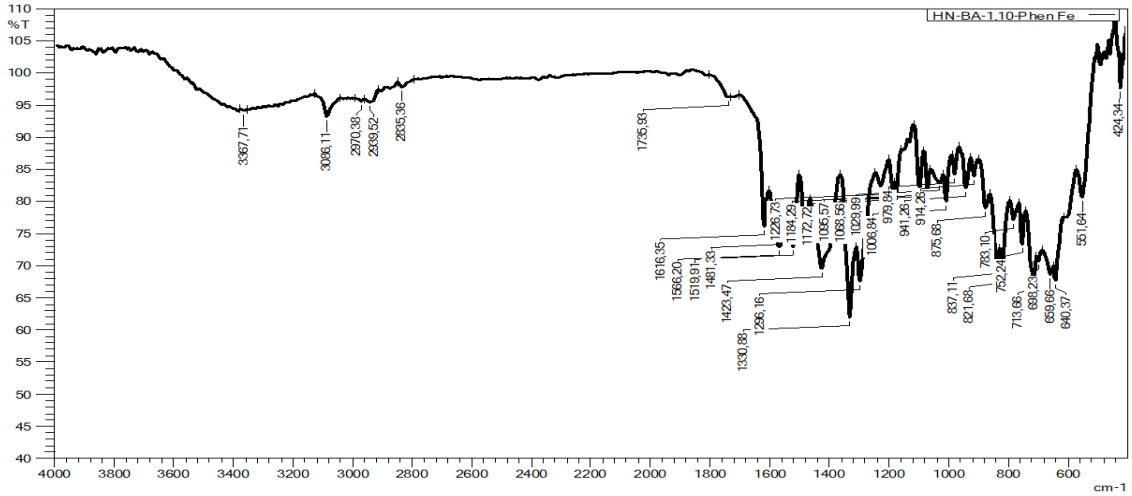
Ligandın (L_1) ve $[Cu(L_1)_2L].5H_2O$ ve $[Fe(L_1)_2L].5H_2O$ metal kompleksleri, FT-IR spektrumları karşılaştırılarak incelenmiştir. Ligand ve karışık ligand Cu(II) ve Fe(II) kompleksleri için sırasıyla 3084, 3074, ve 3086 cm^{-1} frekanslarında aromatik karbon ν(C-H) adsorpsiyonu için bir bant görülmüştür. Ligand ve komplekslerin azometin ν(C=N) gerilme bandı sırasıyla 1618, 1612, ve 1616 cm^{-1} frekanslarında tanımlanmıştır. (Şekil 6-8)



Şekil 6. L_1 bileşiğinin FT-IR spektrumu

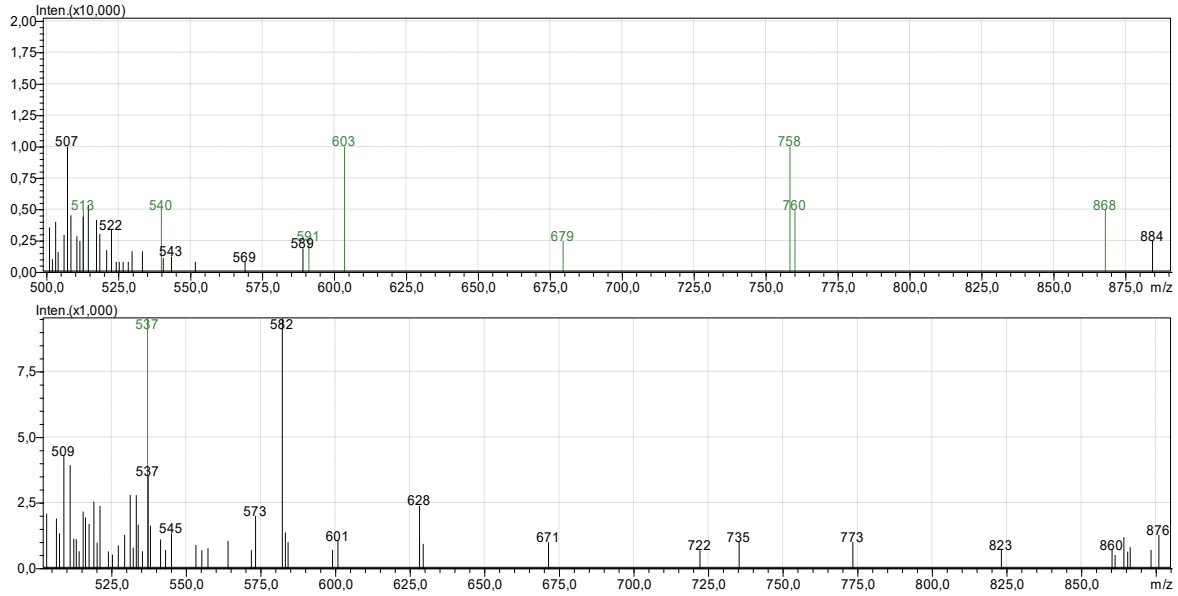


Şekil 7. $[Cu(L_1)_2L_2].5H_2O$ bileşiğinin FT-IR spektrumu



Şekil 8. $[Fe(L_1)_2L_2].5H_2O$ bileşiğinin FT-IR spektrumu

Schiff baz karışık ligand metal komplekslerinin kütle spektrumları incelendiğinde, moleküler iyon pikinin (m/z): 884 $[Cu(L_1)_2L–5H_2O]^+$ ve (m/z): 876 $[Fe(L_1)_2L–5H_2O]^+$ olduğu görülmektedir. Bu formül ağırlığıyla uyumludur ve yapının kimliğini desteklemektedir. (Şekil 9)



Şekil 9. Sentezlenen bileşiklerin kütle spektrumu

4. SONUÇ

Bu çalışmada elde edilen sonuçlar 'N' ve 'O' tipi donör atom taşıyan ligandlara ait karışık ligand metal kompleksleri ile ilgili literatüre katkı sağlamıştır. Bu çalışmada 4-bromoanilin ve 2-hidroksi-5-nitrobenzaldehitin reaksiyonundan Schiff baz ligand olan 2-(((4-bromofenil)imino)metil)-4-nitrofenol (L_1) elde edildi (van Dyk ve ark., 2023). Sentezlenen ligand (L_1) ve 1,10-fenantrolin (L) ile Cu(II) ve Fe(II) asetat tuzları ile (L_1:L:M) 2:1:1 stokiyometrik oranda karışık ligand metal kompleksleri sentezlendi. Bu kompleksler oksijen ve azot atomlarının metal merkezine koordine olmasıyla oluşmuşlardır.

Sentezlenen ligand (L_1) literatürdeki verilere göre elde edilmiştir. Sentezlenen karışık ligand metal komplekslerinin orijinal ve literatür çalışmaları ile uyumlu olduğu görülmüştür. Ayrıca sentezlenen karışık ligand komplekslerin elektrolitik iletkenlik özelliği bulunmamaktadır. Sentezlenen metal komplekslerin manyetik duyarlılık değerleri $[Cu(L_1)_2L].5H_2O$ 1.98 B.M. ve $[Fe(L_1)_2L].5H_2O$ 5.32 B.M olarak bulunmuştur. Manyetik duyarlılık sonuçlarına göre kompleksler oktahedral geometriye sahiptir. Literatür çalışmaları incelendiğinde Schiff baz ile 1,10-fenantrolin ligandlarından elde edilen karışık ligand komplekslerinin biyolojik olarak aktif olması beklenmektedir.

KAYNAKLAR

Abdelgawad, M. A., Bakr, R. B., Alkhoja, O. A., & Mohamed, W. R. (2016). Design, synthesis and antitumor activity of novel pyrazolo[3,4-d]pyrimidine derivatives as EGFR-TK inhibitors. *Bioorganic Chemistry*, *66*, 88–96.

Ceramella, J., Iacopetta, D., Catalano, A., Cirillo, F., Lappano, R., & Sinicropi, M. S. (2022). A Review on the Antimicrobial Activity of Schiff Bases: Data Collection and Recent Studies. *Antibiotics*, *11*(2), 191.

Elaaraj, I., Oulidi, O., Nakkabi, A., Nalbone, L., Sorrentino, G., Giarratana, F., Moualij, N. El, & Fahim, M. (2026). Synthesis, characterization, and evaluation of biological activities of M(II) metal complexes (M=Co, Zn and Cu) based on a bidentate Schiff base ligand 2-((4-nitrobenzylidene)amino)phenol. *Journal of Molecular Structure*, *1351*, 144362.

Gómez-Coca, R. B., Kapinos, L. E., Holý, A., Vilaplana, R. A., González-Vílchez, F., & Sigel, H. (2001). Intramolecular stacking interactions in ternary copper(II) complexes formed with 2,2′-bipyridine or 1,10-phenanthroline and 9-(4-phosphonobutyl)adenine (dPMEA), the carba relative of the antiviral nucleotide analogue 9-[2-(phosphonomethoxy)ethyl]adenine (PMEA). *Journal of Inorganic Biochemistry*, *84*(1–2), 39–46.

Goswami, N., & Barman, P. (2026). Schiff base metal complexes as alternative heterocatalysts in water remediation: Photocatalytic degradation of toxic organic pollutants. *Journal of Molecular Structure*, *1349*, 143925.

Goswami, N., Priya Gogoi, H., & Barman, P. (2024). A hydrazine-based unsymmetrical bis-imine-Schiff base as a chemosensor for turn-off fluorescence and naked-eye detection of Cu2+ ion: Application in aqueous media using test strips. *Journal of Photochemistry and Photobiology A: Chemistry*, *446*, 115106.

Juyal, V. K., Pathak, A., Panwar, M., Thakuri, S. C., Prakash, O., Agrwal, A., & Nand, V. (2023). Schiff base metal complexes as a versatile catalyst: A review. *Journal of Organometallic Chemistry*, *999*, 122825.

Kiruthika, M. , E. R. , & V. T. (2012). Synthesis and antifungal potential of a ruthenium (II) complex. . *Der Chemica Sinica*, *3*(5), 1175–1180.

Loginova, N. V., Koval'chuk, T. V., Polozov, G. I., Osipovich, N. P., Rytik, P. G., Kucherov, I. I., Chernyavskaya, A. A., Sorokin, V. L., & Shadyro, O. I. (2008). Synthesis, characterization, antifungal and anti-HIV activities of metal(II) complexes of 4,6-di-tert-butyl-3-[(2-hydroxyethyl)thio]benzene-1,2-diol. *European Journal of Medicinal Chemistry*, *43*(7), 1536–1542.

Sagunthala Devi, P. R., David, S. T., Joel, C., Bennie, R. B., & Abraham, S. D. (2025). Studies on corrosion inhibition efficiencies of new mixed ligand complexes of SNSN donor Schiff base and NN donor 2-2′-bipyridine with 3d metal ions. *Materials Chemistry and Physics*, *332*, 130279.

Schiff, H. (1864). Communications from the University laboratory in Pisa: a new range of organic bases. . *Annal Chem*, *131*(1), 118–119.

Shah, T. A., Alam, A., Zainab, Assad, M., Parveen, Z., Rafiq, H., Ayaz, M., Shah, S. A. A., Latif, A., Ali, M., & Ahmad, M. (2024). Synthesis and Molecular Docking Study of Hydrazone Schiff Bases of α-Naphthalene-Containing Alkyl Phenyl Ether Fragment as Potent α-Amylase and α-Glucosidase Inhibitors. *ChemistrySelect*, *9*(42).

Sogukomerogullari, H. G., Aytar, E., Çakmak, R., & Başaran, E. (2025). Synthesis and catalytic application to form cyclic carbonates of novel Pd(II) Cu(II), and Fe(II) benzoate-based Schiff base metal complexes. *Journal of Organometallic Chemistry*, *1023*, 123424.

Sogukomerogullari, H. G., Başaran, E., Kepekçi, R. A., Türkmenoğlu, B., Sarıoğlu, A. O., & Köse, M. (2025). Novel europium(III), terbium(III), and gadolinium(III) Schiff base complexes: Synthesis, structural, photoluminescence, antimicrobial, antioxidant, and molecular docking studies. *Polyhedron*, *265*, 117275.

Sogukomerogullari, H. G., Dede, B., Sahin, D., & Akkoç, S. (2025). Comprehensive Study on Synthesis, Quantum Chemical Calculations, Molecular Modeling Studies, and Cytotoxic Activities of Metal(II) Schiff Base Complexes. *Applied Organometallic Chemistry*, *39*(3).

Sogukomerogullari, H. G., Sarıoğlu, A. O., Demir Kanmazalp, S., & Akkoç, S. (2026). Novel mixed ligand Cu(II), Co(II), and Fe(II) metal complexes: Synthesis, characterization, anticancer, and molecular docking studies. *Journal of Molecular Structure*, *1351*, 144158.

Sogukomerogullari, H. G., Sarıoğlu, A. O., Kepekçi, R. A., Türkmenoğlu, B., & Morcali, M. H. (2025). Copper(II), cobalt(II), nickel(II), and iron(II) mixed complexes formed by Schiff base and 1,10-phenanthroline as secondary chelates: Preparation, characterization, antimicrobial, antioxidant, and molecular docking studies. *Inorganica Chimica Acta*, *583*, 122692.

Thakur, S., Jaryal, A., & Bhalla, A. (2024). Recent advances in biological and medicinal profile of schiff bases and their metal complexes: An updated version (2018–2023). *Results in Chemistry*, *7*, 101350.

Valentini, F., Biagiotti, V., Lete, C., Palleschi, G., & Wang, J. (2007). The electrochemical detection of ammonia in drinking water based on multi-walled carbon nanotube/copper nanoparticle composite paste electrodes. *Sensors and Actuators B: Chemical*, *128*(1), 326–333.

van Dyk, H., Jacobs, F. J. F., Kroon, R. E., Makhafola, T. J., & Brink, A. (2023). Characterisation, structural investigations and biological activity of substituted salicylidene-based compounds. *Journal of Molecular Structure*, *1276*, 134737.

Wise, C. F., Liu, D., Mayer, K. J., Crossland, P. M., Hartley, C. L., & McNamara, W. R. (2015). A nickel complex of a conjugated bis-dithiocarbazate Schiff base for the photocatalytic production of hydrogen. *Dalton Transactions*, *44*(32), 14265–14271.

ORAL PRESENTATION

Flor sübstitüe Schiff baz ve 1,10-fenantrolinden türeyen karışık ligand Fe(II) ve Cu(II) komplekslerinin sentez ve karakterizasyonu

Hatice Gamze Sogukomerogullari[1*] (*ORCID: https://orcid.org/0000-0002-0575-8131*),
Ahmet Oral Sarıoğlu[2,3] (*ORCID: https://orcid.org0000-0001-7787-7968*)

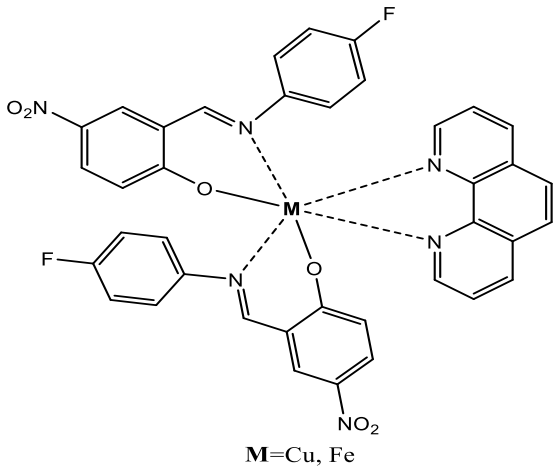
*[1] Gaziantep Üniversitesi, Sağlık Hizmetleri Meslek Yüksekokulu, Tıbbi Hizmetler ve Teknikler Bölümü, 27310, Gaziantep, Türkiye
[2] Gaziantep Üniversitesi, Naci Topçuoğlu Meslek Yüksekokulu, Kimya ve Kimyasal İşleme Teknolojileri Bölümü, 27310, Gaziantep, Türkiye
[3] Gaziantep Üniversitesi, Uluğ Bey Yüksek Teknoloji Uygulama ve Araştırma Merkezi (ULUTEM), 27310, Gaziantep, Türkiye

*Sorumlu yazar e-mail: hgcelikel@gantep.edu.tr

Özet

Biyoinorganik kimya, biyolojik, tıbbi ve çevresel bilimlerde çeşitli uygulamalar için geçiş metali komplekslerini kullanan, yeni gelişen disiplinlerarası bir bilim dalıdır. Biyoinorganik kimya alanındaki gelişmeler, biyolojik açıdan önemli bileşikler için model görevi görebilen Schiff baz komplekslerine olan ilgiyi artırmıştır. Schiff bazları, azot, oksijen ve kükürt gibi çeşitli donör atomları içerdikleri ve metal iyonlarıyla kararlı koordinasyon bağları oluşturabilecekleri için çok ilginç bir ligand sınıfını temsil ederler. Son yıllarda, araştırmacılar Schiff baz ligandlarının ve bunların metal komplekslerinin sentezi ve karakterizasyonuna büyük önem vermişlerdir. Bu kimyasal bileşik sınıfı, kataliz, elektrokataliz, sıvı-sıvı ekstraksiyonu ve korozyon gibi birçok yaşam alanında ve ayrıca biyolojik sistemlerde, bakterisit, fungisit, antikanser, antitüberküloz, antienflamatuar, antiviral ve anti-HIV ajanları olarak kullanıldıkları ve birçok tedavi edilemez hastalığın tedavisinde geniş bir potansiyel uygulama alanına sahiptir. Son yıllarda, karışık ligand komplekslerine olan ilgi önemli ölçüde artmıştır. Bu durum, öncelikle bunların sentez kolaylığı, basit işleme prosedürleri, yüksek verim ve geniş uygulama alanlarına bağlanabilir. Bu çalışmada, 2-hidroksi-5-nitrobenzaldehit ve 4-floroanilinin kondenzasyonundan türeyen Schiff baz ligandı sentezlenmiştir. Elde edilen Schiff bazı ve 1,10-fenantrolin ligandı ile Fe(II) ve Cu(II) metal tuzlarından karışık ligand kompleks bileşikleri sentezlenmiştir. Sentezlenen karışık ligand metal kompleks bileşiklerinin yapıları NMR (ligand için), UV-Vis ve FT-IR gibi spektroskopik yöntemlerin yanı sıra elementel analiz ve elektrolitik iletkenlik gibi ölçümlerle aydınlatılmıştır.

Anahtar Kelimeler: Schiff baz, karışık ligand, metal kompleks, sentez, karakterizasyon



M=Cu, Fe

Şekil 1. Sentezlenen kompleks bileşiklerin yapısı

Synthesis and characterization of mixed-ligand Fe(II) and Cu(II) complexes derived from flor substitute Schiff base and 1,10-phenanthroline

Abstract

The developing discipline of bioinorganic chemistry is an interdisciplinary scientific field that makes use of transition metal complexes for a wide range of applications in the fields of biology, medicine, and environmental research. There has been a rise in interest in Schiff base complexes as a result of the emergence of the discipline of bioinorganic chemistry. Schiff base complexes have the potential to act as models for biologically significant compounds. Schiff bases are a fascinating category of ligands, as they can establish stable coordination bonds with metal ions and contain a diverse array of donor elements, including nitrogen, oxygen, and sulfur. The synthesis and characterization of Schiff base ligands and their metal complexes have been of significant importance to researchers in recent years. This category of chemical compounds possesses extensive potential applications across various domains, including catalysis, electrocatalysis, liquid-liquid extraction, and corrosion, as well as in biological systems, where they serve as bactericides, fungicides, anticancer, antituberculosis, anti-inflammatory, antiviral, and anti-HIV agents, and in the management of numerous incurable diseases. In recent years, there has been a notable rise in interest about mixed ligand complexes. This is primarily attributable to their ease of synthesis, straightforward work-up procedures, high yield, and extensive applicability. In this study, a Schiff base ligand derived from the condensation of 2-hydroxy-5-nitrobenzaldehyde and 4-floroaniline was synthesised. Mixed ligand complex compounds were synthesised from Fe(II) and Cu(II) metal salts using the obtained Schiff base and 1,10-phenanthroline ligand. The structures of the synthesised mixed-ligand metal complex compounds were elucidated using spectroscopic methods such as NMR (for the ligand), UV-Vis and FT-IR, as well as measurements such as elemental analysis and electrolytic conductivity.

Keywords: Schiff base, mixed ligand, metal complex, synthesis, characterization

GİRİŞ

Schiff bazları, sentetik erişilebilirlikleri ve esnek koordinasyon özellikleri nedeniyle bilim camiasında büyük ilgi görmüştür. Bunlar, birincil aminlerin karbonil bileşikleri ile yoğunlaşmasıyla sentezlenen azometin (C=N) gruplarına sahip kimyasal bileşiklerdir. Bu bileşikler, oksijen, nitrojen veya kükürt gibi hetero donör atomlar aracılığıyla koordinasyon sağlayan çok dişli ligandlar olarak işlev görür ve geçiş metalleri için olağanüstü bir afiniteye sahiptir (Raj ve ark., 2013). Schiff bazları birçok farklı kimyasal sentezlerde önemli ara maddeler olarak işlev görürler ve çok sayıda uygulamalarıyla tanınırlar. Bu maddelerin biyolojik etkileri arasında antitümör, antikanser, antitüberkülar, antibakteriyel, antifungal, antifertilite, antioksidan, herbisidal, antiproliferatif ve antifungal özellikler bulunur (Divya Mohan ve ark., 2026; Elaaraj ve ark., 2026; Sogukomerogullari ve ark., 2023, 2025, 2026).

Schiff baz ligandlarına metallerin dahil edilerek komplekslerinin oluşturulması, Schiff bazlarının biyolojik uygulamalarını da geliştirir (Shahraki ve Heydari, 2017). Schiff bazlarının çeşitli metallerle koordinasyon kurma konusundaki geniş kapsamlı yeteneği, onları daha da çekici hale getirmektedir (Abu-Dief ve Mohamed, 2015). Schiff baz ligandları, çeşitli donör atomları (O, N, S) ve dişlilikleri (monodentat, bidentat, tridentat vb.) ile uyarlanabilir, bu da çok çeşitli komplekslerin sentezine olanak tanır (Shah ve ark., 2024). Örneğin, multidentat ligandlar, metal etrafında belirli geometrileri uygulayan şelatlar oluşturur. Bu yapısal esneklik, kompleksin redoks davranışının ve stabilitesinin ince ayarını mümkün kılar, bu da biyolojik aktiviteyi etkiler. Basit aromatik aldehitlerden makrosikliklere ve polimerik çerçevelere kadar çok çeşitli Schiff baz ligantları araştırılmıştır. Her ligant sistemi, metal merkezinin etrafında farklı elektron bağışlayıcı özellikler ve sterik ortamlar sağlayarak, kompleksin serbest radikalleri ne kadar etkili bir şekilde nötralize edebileceğini veya oksidanları ne kadar etkili bir şekilde azaltabileceğini etkiler (Divya Mohan ve ark., 2026). Schiff bazları metal iyonlarına karşı güçlü bir kenetleme özelliği gösterir, bu da metal toksisitesini azaltmakla kalmaz, aynı zamanda metal komplekslerinde ligand olarak koordine edildiğinde işlevselliklerini de artırır (Fahmi ve ark., 2021). Schiff bazları, bir veya daha fazla donör atomla birleştiğinde makrosikller oluşturan kararlı metal kompleksleme ajanlarıdır ve metallerin yüksek oksidasyon durumlarını stabilize etmede çok önemlidir (Nworie ve ark., 2016). Bu bileşikler kolay ve ekonomik bir şekilde sentezlenebilir ve endüstriyel açıdan büyük öneme sahiptir. Ayrıca, bazı metaller için birkaç bağlanma bölgesi boş olduğundan çok dişlidirler ve boş bölgeler olası enzimatik reaksiyonlar için cazip yerlerdir

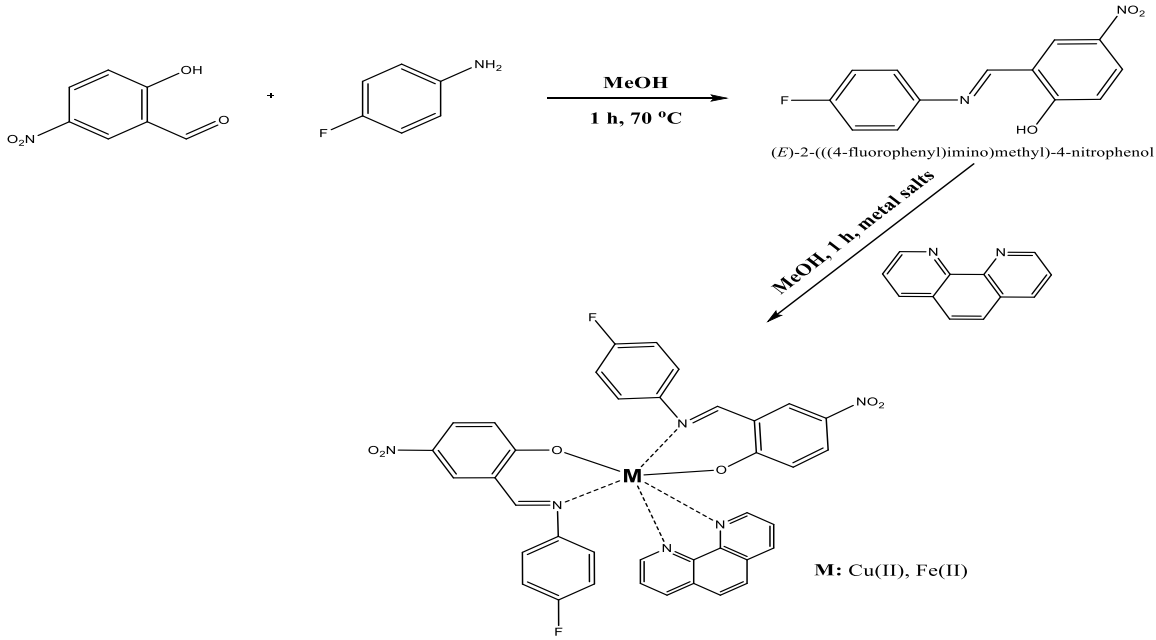
(Rohmawati ve ark., 2026; Sogukomerogullari ve ark., 2026). Modern inorganik kimyanın temel bir alanı olan koordinasyon kimyası, geçiş metali iyonları ve ligandlar arasında oluşan kompleksleri inceler. Bu komplekslerde, kısmen dolu d-orbitalleri çeşitli bağlar, karmaşık geometriler ve benzersiz elektronik özellikler sağlar. Koordinasyon sayısı, ligand türü ve uzamsal düzenleme, fizikokimyasal ve biyolojik davranışı belirler ve kataliz, malzeme bilimi ve tıbbi kimya alanlarında uygulamaları vardır (Kolhe ve ark., 2026).

Bu çalışmada 4-floroanilin ve 2-hidroksi-5-nitrobenzaldehitten türeyen Schiff baz ligandı (L_1) sentezlenmiştir. Karışık ligand metal kompleksleri hazırlamak için co-ligand olarak 1,10-fenantrolin (L) kullanılmıştır. Bu ligandların varlığında Fe(II) ve Cu(II) karışık ligand metal komplesleri sentezlenmiş ve FT-IR, UV-Vis, kütle, elemental analiz, manyetik duyarlılık gibi yöntemlerle karakterize edilmiştir.

2. MATERYAL ve METOT

2.1. Schiff Baz Ligandının Sentezi (L_1)

2-hidroksi-5-nitrobenzaldehit (167.2 mg, 1 mmol) ve 4-floroanilin (94.8 µL, 1 mmol) 25 mL metanol içinde 70 °C'de bir saat geri soğutucu altında karıştırıldı (Qiu ve ark., 2019; van Dyk ve ark., 2023). Sarı renkli ligand çöktükten sonra süzüldü, metanol ve dietileter ile yıkandı ve tam bir gün boyunca vakumda kurumaya bırakıldı. M.A.: 260.22 g/mol; Verim = 69 %, E. N. = 173-175 °C. Elementel Analiz, $C_{13}H_9FN_2O_3$(%); Hesaplanan: C, 60.00; H, 3.49; F, 7.30; N, 10.77 Bulunan (%): C, 59.73; H, 3.30; N, 10.29. IR ν ATR (cm^{-1}): 3066 (C-H), 2924 $(C\text{-}H)_{alf.}$, 1620 (C=N), 1521 $(NO_2)_{asim}$, 1336 $(NO_2)_{sim}$. ^{1}H-NMR (400 MHz, DMSO-d_6) δ: 14.15 (s, 1H, –OH), 9.14 (s, 1H, –CH=N), 8.67 (s, 1H, H-7), 8.27 (dd, 1H, H-5, 4, 8 Hz), 7.14 (d, 1H, H-4, 8 Hz), 7.57-7.54 (m, 2H, H-9), 7.37-7.32 (m, 2H, H-10); ^{13}C-NMR (400 MHz, DMSO-d_6) δ: 166.74, 163.04, 161.80, 160.61, 143.68, 139.71, 128.78, 28.61, 123.96, 119.20,118.57, 116.90, 116.68; UV–Vis λmax (nm) in DMF: 430 (1.882), 370 (1.174), 340 (0.597), 310 (0.438).



Şekil 2. Sentez şeması

2.2. Karışık Ligand Metal Komplekslerinin Sentezi

Schiff baz ligand (L_1) (1 mmol) ve 1,10-fenantrolin (0.5 mmol) ligandları 25 mL metanolde çözüldü üzerine metal tuzlarından (Cu(II) ve Fe(II)) (0.5 mmol) eklenerek 70 ºC de 1 saat karıştırıldı. Çöken madde süzüldü, dietileter ve saf su ile yıkandı. Elde edilen ürün desikatörde kurutuldu.

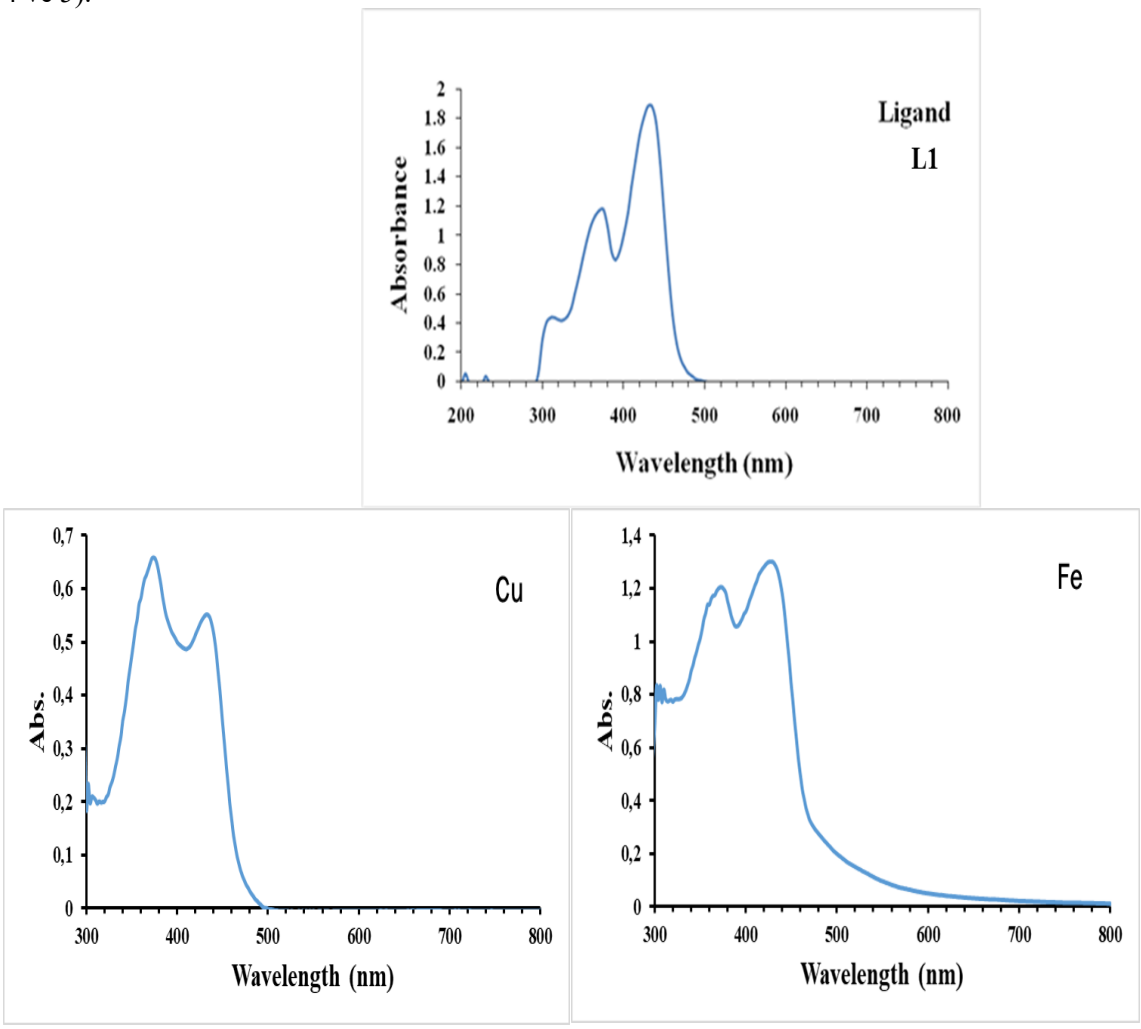
$[Cu(L_1)_2L].H_2O$: Verim = 82 %, E.N. = 312 °C dekompoze. UV–Vis (DMF) λmax (Abs): 470 (0.07), 436 (0.546), 374 (0.659), 340 (0.352); IR (ATR, cm^{-1}): ν(O-H) 3116, ν(Ar-CH) 3074, ν(N–O) 1338 & 1234, ν(C=N) 1604. Ma: 780.2, LC-MS/MS(m/z): 763 $[Cu(L_1)_2L+H\text{-}H_2O]^+$. Hesaplanan (%): C, 58.50; H, 3.36; N, 10.77. Bulunan (%): C: 58.49, H: 3.10, N: 10.30.

$[Fe(L_1)_2L].2H_2O$: Verim = 73 %, E.N. = 329 °C dekompoze. UV–Vis (DMF) λmax (Abs): 476 (0.29), 432 (1.288), 376 (1.195), 338 (0.855); IR ν ATR (cm^{-1}): ν(O-H) 3387, ν(Ar-CH) 3066, ν(N–O) 1338 & 1226, ν(C=N) 1620;

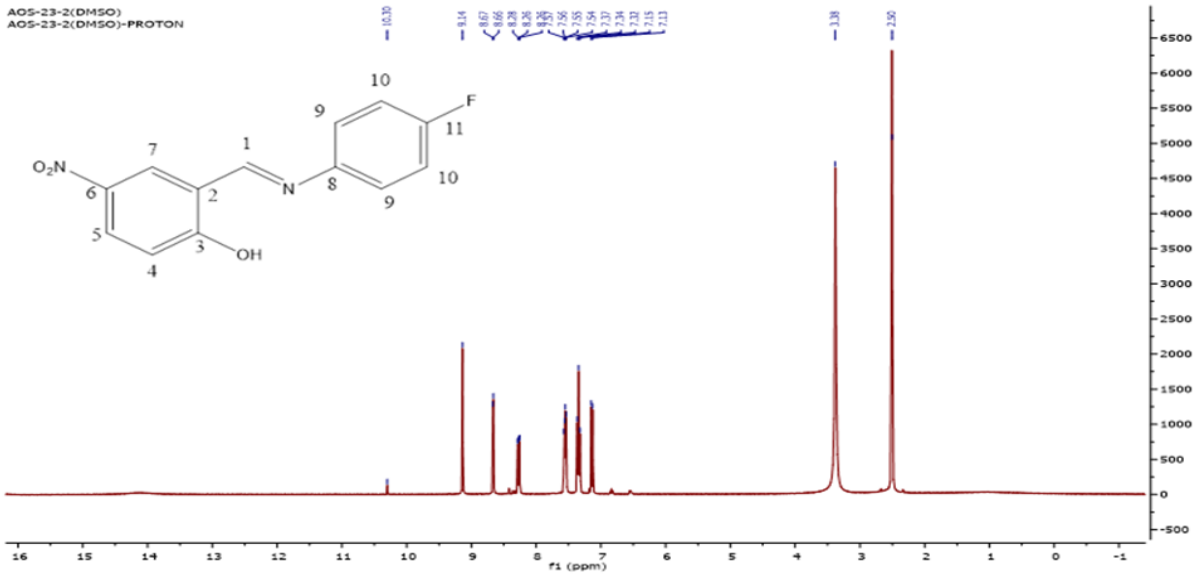
Ma: 790.52, LC-MS/MS(m/z): 813 $[Fe(L_1)_2L+2H_2O+Na]^+$. Hesaplanan: C: %57.74, H: %3.57, N: %10.63. Bulunan: C: %57.60, H: %3.66, N: %10.51.

3.BULGULAR ve TARTIŞMA

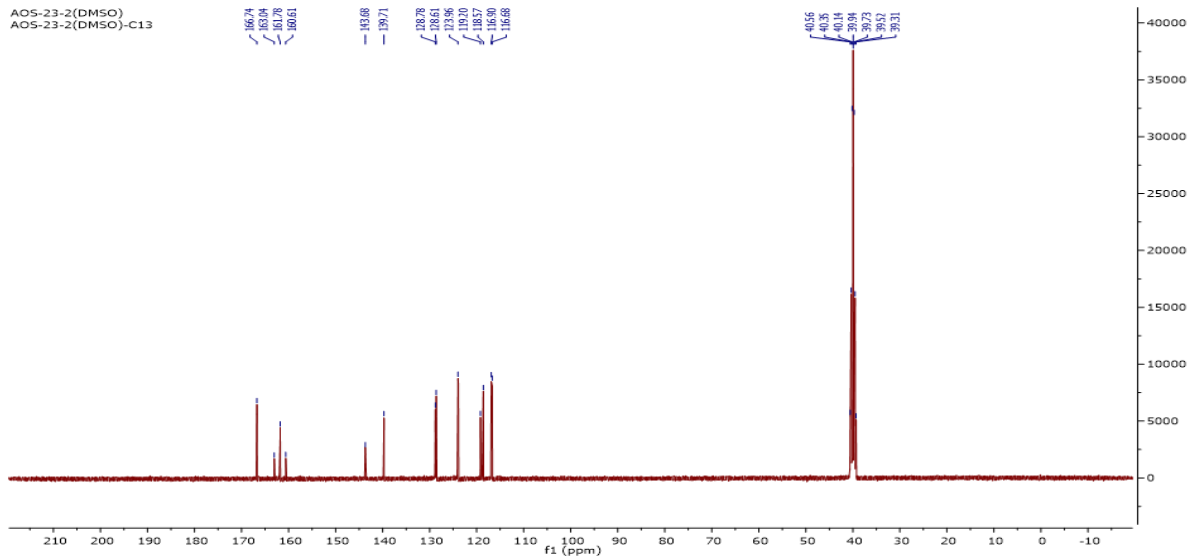
Bu çalışmada sentezlenmiş olan Schiff baz ligand ve karışık ligand komplekslerinin tümünün UV-Vis spektrumlarına ait veriler; bu bileşiklerin DMF içerisinde çözünmesi gerçekleşerek 190-800 nm aralığında spekturumu incelenmiştir. 310, 340, 370 ve 430 nm'deki ligandın en yüksek pikleri, sırasıyla π-π* ve n-π* geçişlerine karşılık gelmektedir. $[Cu(L_1)_2L].H_2O$ ve $[Fe(L_1)_2L].2H_2O$ için en büyük pikler sırasıyla 340, 374, 436, 470 ve 338, 376, 432, 476 nm'de kaydedilmiştir. π-π* ve n-π* geçişlerinin varlığı nedeniyle, $[Cu(L_1)_2L].H_2O$ ve $[Fe(L_1)_2L].2H_2O$ kompleksinin absorbansının küçük bir kırmızıya kayma sergilediği keşfedilmiştir (Şekil 3). Ayrıca 470 ve 476 nm'deki piklerin yük transfer geçişlerine ait olduğu düşünülmektedir. Bu da kompleksleşmenin olduğunu göstermektedir. Ligandın (L_1) ^{1}H-NMR ve ^{13}C-NMR spektrumları, döterolanmış bir çözücü olan aseton içinde kaydedilmiştir. L_1 'ın ^{1}H-NMR spektrumu, δ 14.15 ppm (1H) değerinde bir singlet fenolik proton, δ 9.14 ppm (1H) değerinde bir singlet azometin grubu (CH=N) protonu, δ 8.67–7.32 ppm (7H) değerinde bir çoklu aromatik proton sinyallerini göstermektedir. L_1'nin ^{13}C-NMR spektrumları, 166.74 ppm'de C-O karbon, 163.04 ppm'de azometin karbon (CH=N), 161.80–116.68 ppm'de aromatik karbonlara ait sinyaller sergilemektedir (Şekil 4 ve 5).



Şekil 3. Bileşiklerin UV-Vis spektrumları

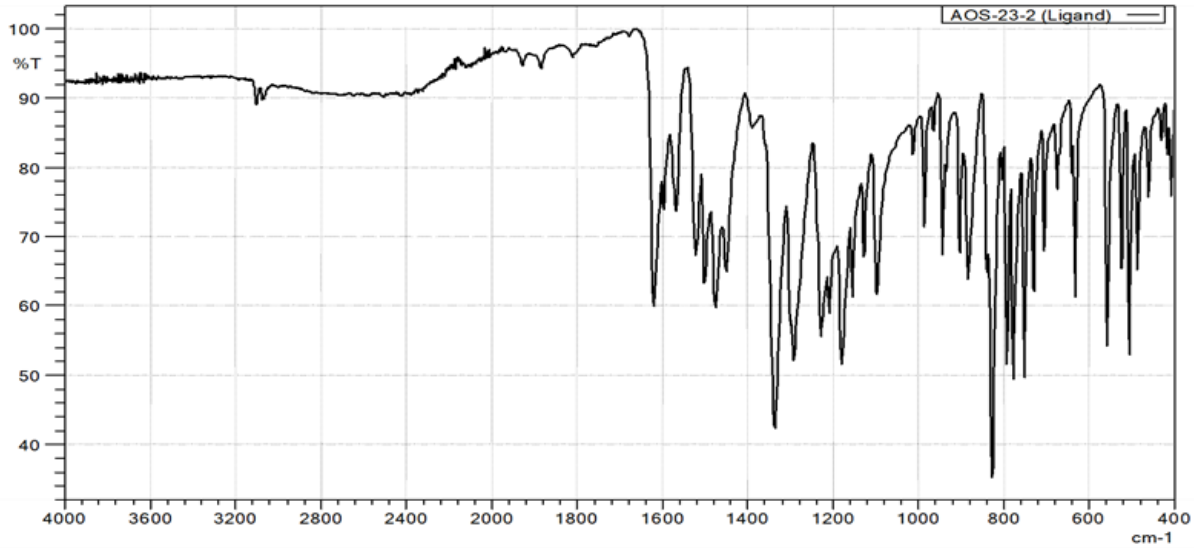


Şekil 4. L_1 bileşiğinin ^{1}H-NMR spektrumu

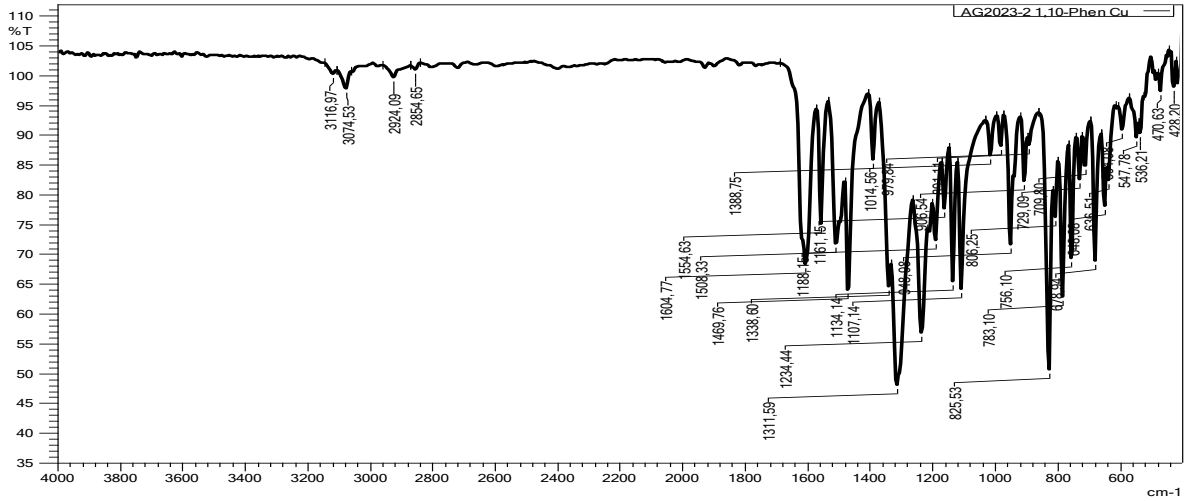


Şekil 5. L_1 bileşiğinin ^{13}C-NMR spektrumu

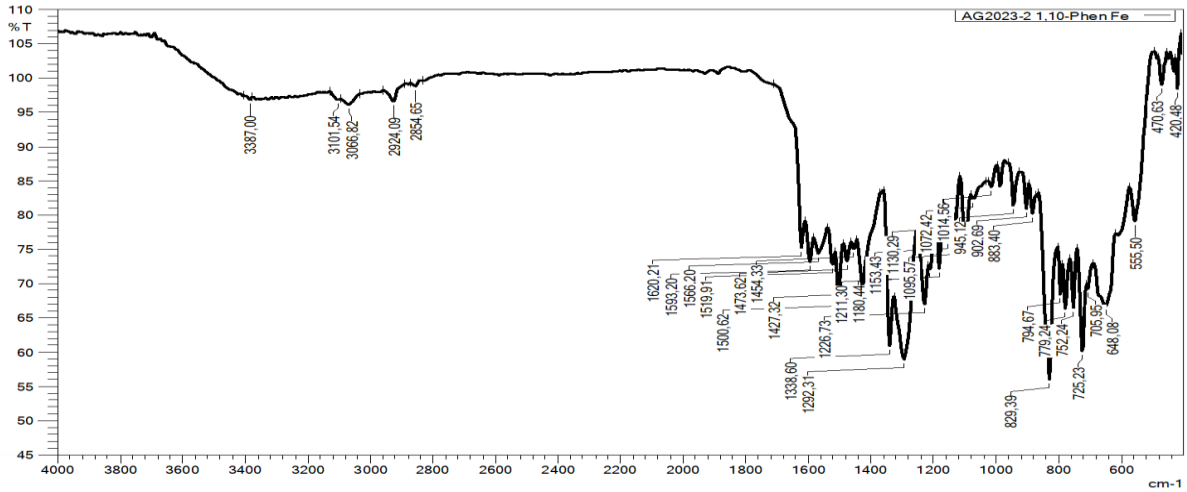
Ligandın (L_1) ve $[Cu(L_1)_2L].H_2O$ ve $[Fe(L_1)_2L].2H_2O$ metal kompleksleri, FT-IR spektrumları karşılaştırılarak incelenmiştir. Ligand ve karışık ligand Cu(II) ve Fe(II) kompleksleri için sırasıyla 3066, 3074, ve 3066 cm^{-1} frekanslarında aromatik karbon ν(C-H) adsorpsiyonu için bir bant görülmüştür. Ligand ve komplekslerin azometin ν(C=N) gerilme bandı sırasıyla 1620, 1604, ve 1620 cm^{-1} frekanslarında tanımlanmıştır. (Şekil 6-8)



Şekil 6. L_1 bileşiğinin FT-IR spektrumu

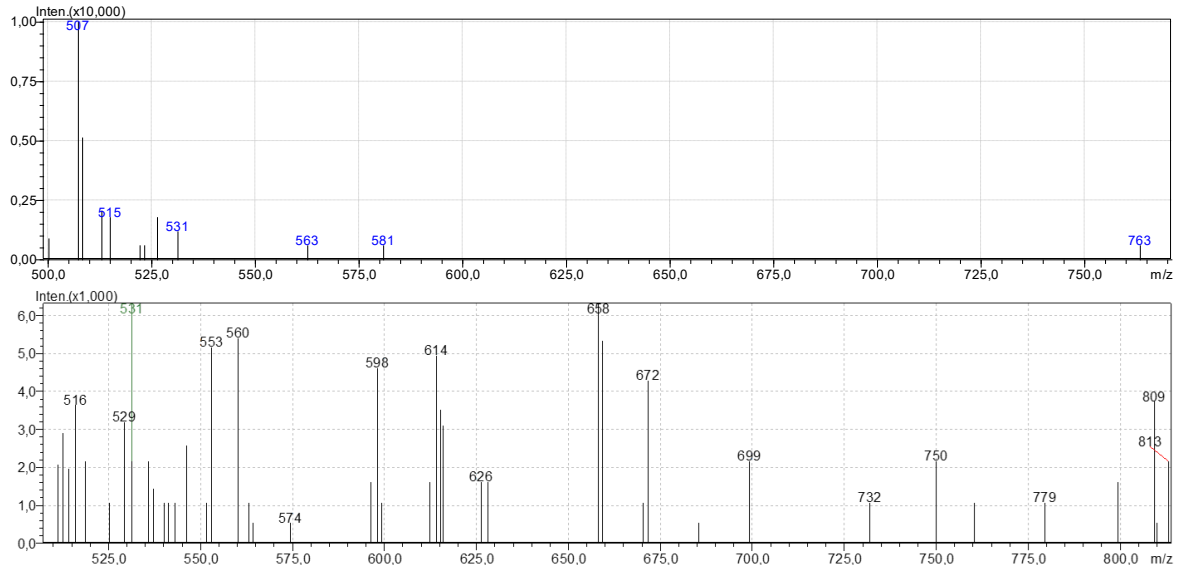


Şekil 7. $[Cu(L_1)_2L].H_2O$ bileşiğinin FT-IR spektrumu



Şekil 8. $[Fe(L_1)_2L].2H_2O$ bileşiğinin FT-IR spektrumu

Schiff baz karışık ligand metal komplekslerinin kütle spektrumları incelendiğinde, moleküler iyon pikinin (m/z): 763 $[Cu(L_1)_2L+H-H_2O]^+$ ve (m/z): 813 $[Fe(L_1)_2L+2H_2O+Na]^+$ olduğu görülmektedir. Bu formül ağırlığıyla uyumludur ve yapının kimliğini desteklemektedir. (Şekil 9)



Şekil 9. Sentezlenen bileşiklerin kütle spektrumu

4. SONUÇ

Bu çalışmada elde edilen sonuçlar 'N' ve 'O' tipi donör atom taşıyan ligandlara ait karışık ligand metal kompleksleri ile ilgili literatüre katkı sağlamıştır. Bu çalışmada 4-floroanilin ve 2-hidroksi-5-nitrobenzaldehitin reaksiyonundan Schiff baz ligand olan 2-(((4-florofenil)imino)metil)-4-nitrofenol (L_1) elde edildi. Sentezlenen ligand (L_1) ve 1,10-fenantrolin (L) ile Cu(II) ve Fe(II) asetat tuzları ile (L_1:L:M) 2:1:1 stokiyometrik oranda karışık ligand metal kompleksleri sentezlendi. Bu kompleksler oksijen ve azot atomlarının metal merkezine koordine olmasıyla oluşmuşlardır.

Sentezlenen ligand (L_1) literatürdeki verilere göre elde edilmiştir. Sentezlenen karışık ligand metal komplekslerinin orijinal ve literatür çalışmaları ile uyumlu olduğu görülmüştür. Ayrıca sentezlenen karışık ligand komplekslerin elektrolitik iletkenlik özelliği bulunmamaktadır. Sentezlenen metal komplekslerin manyetik duyarlılık değerleri $[Cu(L_1)_2L].H_2O$ 1.86 B.M. ve $[Fe(L_1)_2L].2H_2O$ 5.03 B.M olarak bulunmuştur. Manyetik duyarlılık sonuçlarına göre kompleksler oktahedral geometriye sahiptir. Literatür çalışmaları incelendiğinde Schiff baz ile 1,10-fenantrolin ligandlarından elde edilen karışık ligand komplekslerinin biyolojik olarak aktif olması beklenmektedir.

KAYNAKLAR

Abu-Dief, A. M., & Mohamed, I. M. A. (2015). A review on versatile applications of transition metal complexes incorporating Schiff bases. *Beni-Suef University Journal of Basic and Applied Sciences*, *4*(2), 119–133. https://doi.org/10.1016/j.bjbas.2015.05.004

Divya Mohan, R., Sarukrishna, S., Babu, A. S., Santhosh, D., Ahsana Fathima, S., & Parvathy, B. (2026a). A review of ligand denticity in copper–Schiff Base complexes: Structural tuning toward enhanced antioxidant activity. *Inorganica Chimica Acta*, *590*, 122980. https://doi.org/10.1016/j.ica.2025.122980

Elaaraj, I., Oulidi, O., Nakkabi, A., Nalbone, L., Sorrentino, G., Giarratana, F., Moualij, N. El, & Fahim, M. (2026). Synthesis, characterization, and evaluation of biological activities of M(II) metal complexes (M=Co, Zn and Cu) based on a bidentate Schiff base ligand 2-((4-nitrobenzylidene)amino)phenol. *Journal of Molecular Structure*, *1351*, 144362. https://doi.org/10.1016/j.molstruc.2025.144362

Nworie, F., Nwabue, F., Elom, N., Eluu, S. (2016). Schiff bases and schiff base metal complexes: from syntheses to applications. *J. Basic Appl. Res.* , 295–305.

Fahmi, N., Kumari. A., Meena. R., Singh. R. V. (2021). Synthesis, characterization, antimicrobial and DNA cleavage study of organoantimony(III) and organoarsenic(III) complexes with monofunctional bidentate Schiff base. *Indian Journal of Chemistry -Section A*, *60*(3). https://doi.org/10.56042/ijca.v60i3.31459

Kolhe, N. H., Tamboli, Y., Bawazir, H. A., & Parihar, V. S. (2026). Advances in mixed ligand transition metal complexes: Chromone derivatives and N, O donor ligands – a comprehensive review. *Polyhedron*, *284*, 117900. https://doi.org/10.1016/j.poly.2025.117900

Qiu, Y., Chan, S. T., Lin, L., Shek, T. L., Tsang, T. F., Zhang, Y., Ip, M., Chan, P. K., Blanchard, N., Hanquet, G., Zuo, Z., Yang, X., & Ma, C. (2019). Nusbiarylins, a new class of antimicrobial agents: Rational design of bacterial transcription inhibitors targeting the interaction between the NusB and NusE proteins. *Bioorganic Chemistry*, *92*, 103203. https://doi.org/10.1016/j.bioorg.2019.103203

Raj, A., Sheena Mary, Y., Yohannan Panicker, C., Varghese, H. T., & Raju, K. (2013). IR, Raman, SERS and computational study of 2-(benzylsulfanyl)-3,5-dinitrobenzoic acid. *Spectrochimica Acta Part A: Molecular and Biomolecular Spectroscopy*, *113*, 28–36. https://doi.org/10.1016/j.saa.2013.04.096

Rohmawati, S., Salim, F., Damanhuri, H. A., Hassan, W. R. M., Nasaruddin, N. H., Bakar, S. I. A., & Ahmad, S. N. (2026). Therapeutic potential of Ni(II), Pd(II), and Pt(II) coumarin Schiff base complexes for acetylcholinesterase and butyrylcholinesterase inhibition. *Journal of Molecular Structure*, *1354*, 144869. https://doi.org/10.1016/j.molstruc.2025.144869

Shah, T. A., Alam, A., Zainab, Assad, M., Parveen, Z., Rafiq, H., Ayaz, M., Shah, S. A. A., Latif, A., Ali, M., & Ahmad, M. (2024). Synthesis and Molecular Docking Study of Hydrazone Schiff Bases of α-Naphthalene-Containing Alkyl Phenyl Ether Fragment as Potent α-Amylase and α-Glucosidase Inhibitors. *ChemistrySelect*, *9*(42). https://doi.org/10.1002/slct.202402297

Shahraki, S., & Heydari, A. (2017). New zinc(II) N4 tetradentate Schiff base complex: A potential cytotoxic metallodrug and simple precursor for the preparation of ZnO nanoparticles. *Colloids and Surfaces B: Biointerfaces*, *160*, 564–571. https://doi.org/10.1016/j.colsurfb.2017.10.026

Sogukomerogullari, H. G., Başaran, E., Sarıoğlu, A. O., Köse, A., & Akkoç, S. (2023). Synthesis, Characterization, Photoluminescence Properties and Antiproliferative Activity of New Pd(II), Ni(II) and Cu(II) Mixed Complexes Bearing Schiff Base Ligand and 1,10-phenanthroline. *ChemistrySelect*, *8*(24). https://doi.org/10.1002/slct.202301014

Sogukomerogullari, H. G., Sarıoğlu, A. O., Demir Kanmazalp, S., & Akkoç, S. (2026). Novel mixed ligand Cu(II), Co(II), and Fe(II) metal complexes: Synthesis, characterization, anticancer, and molecular docking studies. *Journal of Molecular Structure*, *1351*, 144158. https://doi.org/10.1016/j.molstruc.2025.144158

Sogukomerogullari, H. G., Sarıoğlu, A. O., Kepekçi, R. A., Türkmenoğlu, B., & Morcali, M. H. (2025). Copper(II), cobalt(II), nickel(II), and iron(II) mixed complexes formed by Schiff base and 1,10-phenanthroline as secondary chelates: Preparation, characterization, antimicrobial, antioxidant, and molecular docking studies. *Inorganica Chimica Acta*, *583*, 122692. https://doi.org/10.1016/j.ica.2025.122692

van Dyk, H., Jacobs, F. J. F., Kroon, R. E., Makhafola, T. J., & Brink, A. (2023). Characterisation, structural investigations and biological activity of substituted salicylidene-based compounds. *Journal of Molecular Structure*, *1276*, 134737. https://doi.org/10.1016/j.molstruc.2022.134737

ORAL PRESENTATION

Mardin ili Diplura (Hexapod) faunasınası için yeni kayıt

Sadreddin Tusun[1] (*ORCID: https://orcid.org/0000-0002-0696-4244*)
Medeni Aykut[2*] (*ORCID: https://orcid.org/0000-0001-6824-1394*)

[*1]Dicle Üniversitesi, Ziya Gökalp Eğitim Fakültesi, Matematik ve Fen Bilimleri Eğitimi Bölümü, Diyarbakır, Türkiye.
[2]Dicle Üniversitesi, Ziya Gökalp Eğitim Fakültesi, Matematik ve Fen Bilimleri Eğitimi Bölümü, Diyarbakır, Türkiye

*Sorumlu yazar e-mail: medeniaykut@hotmail.com

Özet

Bu çalışma Nisan 2023 ile Ekim 2024 tarihleri arasında Türkiye'nin Güneydoğu Anadolu Bölgesi'nde yer alan Mardin ilinde gerçekleştirilmiştir. Daha önce yapılan araştırmalar incelendiğinde Mardin ilinde Diplura'nın tespiti ile ilgili olarak sadece üç çalışma yapıldığı anlaşılmaktadır. Yapılan bu araştırma sonucunda Mardin merkeze bağlı üç farklı lokaliteden toplam 20 örnek toplanmış ve tanımlanmıştır. Teşhisi yapılan örneklerden *Campodea (Dicampa) sprovierii* (Silvestri, 1933) Mardin ili için yeni kayıttır. Çalışmanın amacı ülkemiz (Türkiye) ve özellikle Mardin ili Diplura faunasına katkıda bulunmaktır.

Anahtar Kelimeler: Diplura, Hexapoda, Fauna, Mardin, Türkiye.

New record for the Diplura (Hexapod) fauna of Mardin province

Abstract

This study was carried out between April 2023 and October 2024 in Mardin province, located in the Southeastern Anatolian Region of Türkiye. A review of previous studies reveals that only three studies have been conducted with regard of identification of Diplura in Mardin province. As a result of this research, a total of 20 specimens were collected and identified from three different localities within the central Mardin district. Of the identified specimens, *Campodea (Dicampa) sprovierii* (Silvestri, 1933) is a new record for Mardin province. The aim of the study is to contribute to the Diplura fauna of our country (Türkiye) and especially Mardin province.

Key words: Diplura, Hexapoda, Fauna, Mardin, Türkiye.

GİRİŞ

Diplura (Çatal Kuyruklular), Apterygota (Kanatsız) sınıfına ait, yüzeysel olarak böceklere benzeyen fakat gerçek böcek olmayan, genellikle nemli ortamlarda yaşayan ilkel eklembacaklılardır (Allen, 1994). Bu canlılar; toprakta, kaya ve taşların alt yüzeyinde, ağaçların gevşek kabuklarının altında veya gevşek organik maddelerde yaşayabilen eski böceklerdir. Takımın çeşitli üyeleri, Antarktika ve birçok okyanus adası hariç, neredeyse tüm kara kütlelerinde bulunur. Vücut segmentleri değişken sayıda farklı türde kıl veya pul taşır.On abdominal segment, bileşik gözlerinin olmaması, lateral stiluslar ve kaudal cercis ile karakterize edilirler (Allen, 2002). Türkiye'de Diplura üzerine yapılan çalışmalar; Paclt, 1976; Sendra ve ark., 2006, 2010 ve 2022; Tusun, 2006, 2011; Tusun ve Satar, 2020 ye ait olup, çok az sayıdadır. Bölgemizdeki ve Ülkemizdeki Diplura tür sayısını artırmak için yeni ve kapsamlı faunistik çalışmalara ihtiyaç duyulmaktadır.

MATERYAL VE METOT

Çalışmaya konu olan böcek örnekleri Nisan 2023 ile Ekim 2024 tarihleri arasında Mardin Artuklu merkez ilçesinin üç farklı lokalitesinden toplanmıştır (Şekil 1). Çalışma yapılan ve böcek örneği alınan istasyonun koordinat ve yükselti bilgileri el GPS'i (Global Position System; Küresel Konumlama Sistemi) kullanılarak (Magellan Explorist 610) kayıt altına alınmıştır. Yumuşak fırça ile toplanan böcek örnekleri çalışma alanında %70'lik etil alkole alınıp etiketlenerek laboratuvara getirilmiştir. Laboratuvara getirilen böcek örnekleri teşhis işlemi için ince fırçalar ve ultrasonik aletler ile temizlenmiştir. Örnekler temizlendikten sonra teşhisleri yapılmıştır. Teşhisi yapılan örnekler etiketlenerek, muhafaza edilmek üzere, birinci yazarın Dicle Üniversitesi Ziya Gökalp Eğitim Fakültesinde bulunan kişisel koleksiyonunda muhafaza edilmektedir.



Şekil 1. *Campodea (Dicampa) sprovierii* örneklerinin toplandığı istasyon

BULGULAR

Tür lokalitesi: Mardin ili, Artuklu İlçesi,Türkiye. 37^{0}23'08"K, 40^{0}41'34"D, Rakım:1130 m.

Taksonomi

Sınıf (Class): Diplura Börner, 1904
Takım (Order): Rhadura Cook, 1896
Aile (Family): Campodeidae Meinert, 1865
Alt aile (Subfamily): Campodeinae Condé, 1956
Cins (Genus): C*ampodea* Westwood, 1842
Alt cins (Subgenus): Dicampa, Silvestri, 1932
Tür (species): *Campodea (Dicampa) sprovierii* Silvestri, 1933

Yayılış: Artvin: Karkal dağları, 11.06.1986, 1 ♀ leg. C. Besuchet, I. Löbl &D.H. Burckhardt (Sendra ve ark., 2006); **Bitlis:** Adilcevaz, Göldüzü köyü, 29. 05.2008, 1 ♂, 2 ♀; Hizan, Süttaşı köyü, 29.04.2010, 3 ♂, 3 ♀; Mutki, Dereyolu köyü, 29.04.2010, 4 ♂, 3 ♀ leg. S. Tusun (Tusun, 2011); **Diyarbakır:** Dicle nehri, 09.04.2006, 1 ♂, 2 ♀ leg. S. Tusun; Dicle Üniversitesi, Sera, 08.04.2006, 5 ♂, 4 ♀, 3 juv., leg. A. Satar (Tusun, 2006; Sendra ve ark., 2010); **Düzce:** Yığılca köyü, 13.08.2005, 4 ♂, 2 ♀, 10 juv., leg. S. Truel; **Gümüşhane:** Zigana Pass, 18.VIII.2005, 3 ♂, 4 ♀, 4 juv.; Zigana tüneli, Değirmendere köyüne 22 km mesafede, 18.08.2005, 4 ♂, 5 ♀, 7 juv., leg. A. Sendra; Çayra, 19. 08.2005, 5 ♂, 4 ♀; Skilope, 19. 08.2005, 1 ♂, 3 ♀, 1 juv., leg A. Moreno; Kurtün, Harşit vadisi, 19.08.2005, 2 ♀ leg. S. Truel & A. Sendra (Sendra ve ark., 2010); **Hakkâri:** Şemdinli, Günyazı köyü, 29.05.2009, 1 ♂, 3 ♀; Yüksekova, Altınoluk köyü, 30.05.2009, 2 ♂, 1 ♀ leg. S. Tusun (Tusun, 2011); **İstanbul:** Belgrad, 04.06.1967, 1 ♂, 1 ♀, 50 juv.; **Kırklareli:** Yeniceköy ve Demirköy arası, Demirköy'e 15 km mesafede, 31.07.1969, 3 juv., leg. C. Besuchet (Sendra ve ark., 2006); **Samsun:** Çakallı, Kavac, 20.07.2005, 1 ♂, 1 juv., leg. A. Moreno (Sendra ve ark., 2010); **Siirt:** Kurtalan, Çayırlı köyü, 05.04.2008, 2 ♂, 4 ♀; Şirvan, Demirkapı köyü, 05.04.2008–23.04.2010, 6 ♀ leg. S. Tusun (Tusun, 2011); **Zonguldak:** Çaycuma, Öngüldak köyü, 23.05.1976, 5 juv., leg. C. Besuchet & I. Löbl; İnağzı mağarası, 07.07.2004, 1 ♂, 1 ♀, 1 juv.; Yenimestanoğlu, Mengen'e 25 km mesafede 1 ♂, 2 ♀, 1 juv., (Sendra ve ark., 2006); Mengen Zonguldak yolu 15. km, 14.08.2005, 2 ♂, 3 ♀, 12 juv., (Sendra ve ark., 2010).

TARTIŞMA

Campodea (Dicampa) sprovierii Silvestri, 1933, türü Türkiye faunası için ilk kez 1967 yılında İstanbul Belgrad Ormanı'nda toplanmış, ancak ilgili kayıt 2006 yılında Sendra ve arkadaşları tarafından yayımlanmıştır. Bunu izleyen dönemlerde farklı bölgelerde yürütülen faunistik çalışmalar sonucunda türün Kırklareli, Zonguldak ve Artvin illerinde de bulunduğu ortaya konmuştur. Daha sonraki kapsamlı araştırmalarla türün varlığı yedi ilde daha doğrulanmış ve Türkiye içindeki dağılımı giderek daha iyi anlaşılmıştır. Mardin'den elde edilen yeni kayıt, *C. (D.) sprovierii*'nin yalnızca Karadeniz ve Trakya bölgeleriyle sınırlı olmadığını, aynı zamanda Güneydoğu Anadolu Bölgesi'nde de uygun habitatlar bulunabildiğini göstermektedir.

SONUÇ

Mardin kaydı ile birlikte *C. (D.) sprovierii*'nin Türkiye'de bilinen il sayısı on ikiye yükselmiştir. Bu bulgu, türün ulusal ölçekteki dağılımının hâlâ tam olarak ortaya konulamadığını ve gelecekte yürütülecek detaylı arazi çalışmalarının yeni kayıtlar sağlamaya devam edebileceğini göstermektedir.

TEŞEKKÜR

Bu çalışma, Dicle Üniversitesi Bilimsel Araştırma Projeleri Koordinatörlüğü (DÜBAP) tarafından ZGEF. 25.004 proje numarasıyla desteklenmiştir. DÜBAP yönetimine destekleri için teşekkür ederiz.

KAYNAKLAR

Allen, R. T. (1994). An annotated checklist and distribution records of the subfamily Campodeiinae in North America (Insecta: Diplura: Rhabdura: Campodeidae). *Transactions of the American Entomological Society*, 181-208.

Allen, R. T. (2002). A synopsis of the Diplura of North America: Keys to higher taxa, systematics, distributions and descriptions of new taxa (Arthropoda: Insecta). *Transactions of the American Entomological Society, 128*(4), 403–466.

Paclt, J. (1976). New contributions to the knowledge of the Apterygota collection of the Zoological Institute and Zoological Museum of the University of Hamburg. V. Further materials from Turkey (Diplura, Thysanura). *Entomologische Mitteilungen aus dem Zoologischen Museum Hamburg, 5*(94), 111–113.

Sendra, A., Satar, A., & Montague, S. (2006). First contribution to the campodeid fauna of the Anatolian Peninsula, Turkey (Diplura: Campodeidae). *Revue Suisse de Zoologie, 113*(3), 693–709.

Sendra, A., Teruel, S., Satar, A., Tusun, S., & Özbay, C. (2010). New species, new records, and distribution of Campodeidae (Diplura) in Anatolia. *Zootaxa, 2639*(1), 40–52.

Sendra, A., Palero, F., Sánchez-García, A., Selfa, J., Tusun, S., & Satar, A. (2022). New evidence for an Anatolian bridge: Colonization of Euromediterranean lands by cave-adapted Plusiocampinae (Diplura, Campodeidae), with establishment of a new genus. *Zoologischer Anzeiger, 301*, 205–214.

Tusun, S. (2006). *Determination of Diplura (Insecta) fauna of Batman, Diyarbakır, Mardin and Şanlıurfa province* (Master's thesis). Dicle University, Science Institute.

Tusun, S. (2011). *Determination of Diplura (Insecta) fauna of Bitlis, Hakkâri, Siirt and Şırnak province* (Doctoral dissertation). Dicle University, Science Institute.

Tusun, S., & Satar, A. (2020). First annotated checklist of the Diplura (Insecta) of Turkey. *Zootaxa, 4821*(2), 353–362.

ORAL PRESENTATION

Innovative use of hydroxyapatite-based structures in bone tissue regeneration

Tuğçe Küçükali[1*] (ORCID: *https://orcid.org/0009-0000-6348-5031*), Dilek Bilgiç Alkaya[2,3] (ORCID: *https://orcid.org/0000-0002-7837-0250),* Serap Ayaz Seyhan[2,3] (ORCID: *https://orcid.org/0000-0001-5908-2766*)
[1]Department of Analytical Chemistry, Faculty of Pharmacy, Marmara University, Istanbul, Turkey
[2]Center for Nanotechnology & Biomaterials Application and Research (NBUAM), Marmara University, Istanbul, Turkey
[3] Department of Metallurgical and Materials Engineering, Faculty of Technology, Marmara University, Turkey

Abstract

Bone tissue is vital for providing mechanical support, mineral storage, and maintaining biological functions in the body. The treatment of bone defects resulting from trauma, tumors, or degenerative diseases continues to pose a significant clinical challenge. Therefore, hydroxyapatite (HA, $Ca_{10}(PO_4)_6(OH)_2$), which is highly similar to bone tissue in terms of chemical and structural properties, has emerged as an important ceramic phase in tissue engineering and biomaterials research. Thanks to its high biocompatibility, bioactivity, and osteoconductive properties, HA is one of the most suitable materials to support bone regeneration. Hydroxyapatite can be obtained synthetically, and studies have demonstrated that HA derived from natural sources exhibits biological performance similar to or even superior to synthetic elastics. However, the brittle nature and low mechanical strength of pure HA limit its use on its own. Therefore, in recent years, composite systems composed of natural (gelatin, chitosan, alginate, etc.) and synthetic (PLGA, PCL, PLLA, etc.) polymers have been developed. These structures have been shown to yield successful results in terms of cell adhesion, tissue integration, and controlled drug release. Furthermore, ion-doped or surface-modified HA structures are reported to enhance antibacterial, osteogenic, and piezoelectric properties. Current studies reveal the versatile potential of HA-based nanocomposites in bone tissue engineering and drug delivery systems. However, long-term biosafety, biodegradability, and performance evaluations are needed to translate the obtained preclinical findings into clinical applications.

Keywords: Hydroxyapatite, biomaterial, composite scaffold, biocompatibility

1. Introduction

Bone tissue is vital for providing mechanical support, mineral storage, and maintaining biological functions in the body. The treatment of bone defects resulting from trauma, tumors, or degenerative diseases continues to pose a significant clinical challenge. Therefore, hydroxyapatite $Ca_{10}(PO_4)_6(OH)_2$ which is highly similar to bone tissue in terms of chemical and structural properties, has emerged as an important ceramic phase in tissue engineering.

Bone consists of organic and inorganic phases, a nanocomposite structure where the organic phase is largely composed of collagen and the inorganic phase is largely composed of hydroxyapatite. Bone is a mineralized tissue strengthened by the accumulation of calcium and phosphate crystals; in other words, it is a natural composite material. As with other organs and structures, bone tissue also has a hierarchical order ranging from macro to nano scales.

1.1. Hydroxyapatite: Synthesis and Composites

HA is one of the most suitable materials to support bone regeneration due to its high biocompatibility, bioactivity, and osteoconductive properties.

1.1.1. Synthesis Methods

HA can be obtained synthetically or from natural sources. The choice of method depends on the intended application and desired properties.

- Chemical precipitation: A commonly used method where calcium and phosphate ions are mixed in an aqueous solution.
- Sol-gel synthesis: Utilizes a precursor solution that forms a gel through hydrolysis and condensation.

- Hydrothermal synthesis: Uses high pressure and temperature to produce a crystalline material.
- Natural Sources: These include animal bones (chicken/beef), fish scales, eggshells, and plant extracts. Natural HA exhibits biological performance similar to or even superior to synthetic versions.

2.1.2. HA-Polymer Composites

The brittle nature and low mechanical strength of pure HA limit its use on its own. Therefore, composite systems composed of natural and synthetic polymers have been developed.

- Synthetic Polymers: PLA, PCL, PLGA, PEEK, and PMMA are used. PLA/PCL + nano HA combinations show osteogenic properties.
- Natural Polymers: Chitosan, collagen, alginate, and gelatin are advantageous in terms of biological solubility and cell interaction. Composites such as chitosan-HA and collagen-HA enhance cellular adhesion.

2.1.3. Characterization Techniques

Many methods are used in the characterization of hydroxyapatite to determine its structural and chemical properties.

- X-ray Diffraction (XRD): Provides information about the crystal structure, phase purity, and crystal size. Crystal size is often calculated using the Scherrer Equation.
- Fourier Transform Infrared Spectroscopy (FTIR): Determines the chemical structure by examining the interaction of infrared radiation with the substance. It detects characteristic vibrations of phosphate (PO_4^{3-}) and hydroxyl (OH^-) groups.
- Scanning Electron Microscopy (SEM): Surface morphology is imaged at high resolution to determine grain size, porosity, and surface regularity.
- Thermal Analysis (TGA/DSC): Examines the mass changes with temperature to investigate thermal stability and organic component content.

3. Hydroxyapatite Applications

3.1. Synthesis, Characterization and Material Development Studies

Synthesis methods and material characterization are key factors determining the performance of HA-based structures. Daldiken (2024) demonstrated increased crystallinity by synthesizing clinoptilolite-reinforced HA compounds using the sol-gel method. Toktaş et al. (2022) revealed an inverse relationship between porosity and mechanical strength by producing microporous HAp beads. Jaiswal et al. (2020) found that Mg addition increased hardness and corrosion resistance. Dokgöz (2019) synthesized dexamethasone-loaded GELMA/nanosilica nanocomposites and demonstrated that these structures offered successful mechanical strength and drug delivery.

Bang et al. (2014) reported that carbonate-modified HA was absorbed more quickly by osteoclasts, thus accelerating bone growth. Metin (2013) showed that bovine bone-derived HA powders yielded high-quality products under appropriate particle size and sintering conditions. Lee et al. (2008) reported that carbonate addition increased the solubility of HA and decreased its crystallinity, while Cengiz (2007) optimized the production of biocompatible nHA by investigating the effect of different synthesis parameters on nanoparticle morphology. This group generally emphasizes the decisive effect of synthesis parameters and additives on the structural properties of HA.

3.2.Natural and Biopolymer-Based Composites

HA structures supported by natural polymers have great potential in terms of biocompatibility and biodegradability. Alpan et al. (2022) showed that bacterial cellulose–HA nanocomposite supported new bone formation in rats. Souto Lopes et al. (2024) reported that chitosan-based nHA bioaerogel increased both in vitro cell proliferation and in vivo bone regeneration. Özcan (2017) accelerated mineralization by functionalizing fibroin and PLLA mixed scaffolds with OSN peptide. In addition, gelatin–PVA–alginate-based structures of Bahrawy et al. (2025) and gelatin/chitosan-reinforced composites of Aydın (2018) also belong to this group, demonstrating that natural polymers offer ideal matrices that combine mechanical flexibility with biocompatibility.

3.3. Drug Delivery and Delivery Systems

Hydroxyapatite (HA)-based structures stand out as highly effective carrier systems in drug delivery and bone tissue repair. Han et al. (2025) developed a nanocomposite with a core-shell structure coated with cationic starch and HA and zirconia cores to reduce the side effects of zoledronic acid and showed that this structure provides controlled release with high drug loading capacity. Similarly, Bahrawy et al. (2025) prepared multifunctional bone scaffolds loaded with ceftazidim and 5-fluorouracil by adding hydroxyapatite nanoparticles to a gelatin-PVA-alginate matrix; it was determined that these structures released drugs for up to 28 days and enhanced bone regeneration. Aydın (2018) reported that by loading 5-fluorouracil onto HA-gelatin and HA-chitosan composites, the cross-linking ratio determined the release rate, and controlled release was obtained at higher GA ratios. In his study, Öztürk (2018) combined boron-doped nHA with PLGA nanoparticles loaded with the anticancer drug salinomycin; in this hybrid system, release lasting up to 59 days and synergistic antibacterial effect were observed. Kahraman (2016) also investigated the release of 5-fluorouracil in HA-gelatin composites and emphasized that a lower gelatin ratio provided more controlled release. Overall, these studies demonstrate that HA-based systems offer promising carrier structures for both bone regeneration and targeted drug delivery.

3.4. Structures Produced with 3D Printing and Their Mechanical Properties

Three-dimensional printing technology is frequently preferred in the production of biomimetic scaffolds in bone tissue engineering. Chen et al. (2025) developed a ceramic scaffold system with antibacterial and piezoelectric properties and produced it using DLP 3D printing technique; they reported that ZnO addition increased the antibacterial effect. Yan et al. (2025) showed that integrating adipose tissue-derived mesenchymal stem cells (ADMSC) into 3D-printed PLGA/nHA scaffolds increased osteogenic differentiation in both in vitro and in vivo environments. Eldokmak et al. (2025) significantly increased cell adhesion, biocompatibility, and mechanical strength of 3D-printed PLA scaffolds by coating them with nano-HA and polydopamine. Similarly, Tut et al. (2022) and Gündüz et al. (2022) produced 3D-printed scaffolds containing PVA/WPI/HA/GEN and reported that gentamicin addition reduced pore size but maintained biocompatibility. The common conclusion of these studies is that 3D printing technology offers significant advantages in bone engineering in terms of controlled pore structure, mechanical stability, and biocompatibility.

3.5. Coating and Surface Modification Works

Vangölü et al. (2025) conducted 18-week implantation tests in New Zealand rabbits by coating Ti6Al4V screws with HA and Ca-P layers, and stated that HA-coated samples showed the best performance in terms of osteogenesis and biocompatibility. Eldokmak et al. (2025) found that polydopamine/nano-HA coatings increased cell adhesion in PLA scaffolds. Koç (2019), on the other hand, modified the surface of PRP-supported HAp/PLLA nanofiber grafts with NaOH and showed that this process accelerated osteogenic differentiation through PRP activation. These studies demonstrate that coating and surface modification methods strengthen biomaterial-cell interaction and increase implant success.

3.6. Studies Focusing on Antibacterial and Osteogenic Effects

Many studies have aimed to enhance the antibacterial and osteogenic effects of HA through modification. Li et al. (2025) reported that linezolid-loaded mHAP composites enriched with Sr were effective against MRSA and increased osteogenic potential. Zhao et al. (2024) synthesized micro/nano HA bioceramics functionalized with tea polyphenols, showing that these structures suppress osteoclast activity while supporting osteogenic differentiation. Shaikh et al. (2024) produced nHA without chemical additives using laser energy and reported that these structures increased bone formation when supported by collagen and gelatin. Santos et al. (2025), in a literature review, emphasized that HA is the most frequently preferred calcium-based material in tooth and bone regeneration. These findings highlight the importance of HA-based materials as both biocompatible and antimicrobial tissue regeneration agents.

4. Conclusion and Discussion

This study examines research on hydroxyapatite (HA), a biomaterial notable for its high degree of similarity to bone tissue, in bone tissue therapy. HA has been shown to be an important biomaterial in terms of biocompatibility and supporting bone regeneration due to its structure similar to natural bone. To overcome its brittle structure and mechanical limitations, HA has been enriched with various inorganic, polymeric, and biological additives.

The studies examined showed that nanotechnology-supported research was particularly prominent. Controlled release of potent drugs like zoledronic acid via HA-zirconia core and cationic starch-coated nanocomposite carriers increased osteogenic differentiation in bone cells and also allowed for a reduction in side effects. These types of core-shell structured systems have been shown to offer significant advantages in chemotherapy, osteoporosis, and local drug applications.

Skeletal systems containing HA, barium titanate, and ZnO, produced using DLP 3D printing technology, have offered significant approaches in the treatment of infected bone defects by combining antibacterial and osteogenic properties. 3D-printed biomaterials have shown significant advancements in skeletal technology.

In conclusion, hydroxyapatite and its derivatives are among the most powerful and promising materials in bone tissue engineering due to their structure mimicking natural bone tissue, high integration capability with functional additives, and multifaceted biological effects. When combined with evolving production techniques, next-generation modification strategies, and multidisciplinary approaches, it is predicted that HA-based systems will be used more widely in clinical applications in the future. However, it should be noted that more systematic clinical-level validations, biosafety analyses, and long-term performance tests are needed to fully realize this potential.

REFERENCES

Agbeboh, N. I., Oladele, I. O., Daramola, O. O., Adediran, A. A., Olasukanmi, O. O., & Tanimola, M. O. (2020). Environmentally sustainable processes for the synthesis of hydroxyapatite. *Heliyon*, *6*(4).

Ahmed, I., Lewis, M. P., & Knowles, J. C. (2005). Phosphate-based glasses for soft tissue engineering. *Journal of Materials Science: Materials in Medicine*, 16(11), 1047–1056.

Akpan, E. S., Dauda, M., Kuburi, L. S., & Obada, D. O. (2021). Box-Behnken experimental design for the process optimization of catfish bones derived hydroxyapatite: A pedagogical approach. *Materials Chemistry and Physics*, *272*, 124916.

Alpan, A. L., Dogan, N., Denizli, T. H., & Özmen, Ö. (2022). Ratlarda Oluşturulan Kritik Boyutlu Kalvaryal Defektlerde Bakteriyel Selüloz Temelli Hidroksiapatit (BS-HAp) Nanokompozitinin Kemik Oluşumu Üzerine Etkisi. Karaelmas Fen ve Mühendislik Dergisi, 12(2), 242-250.

Aydın, N. E. (2018). Hidroksiapatit-Jelatin ve Hidroksiapatit-Kitosan Biyokompozitlerin Yapay Vücut Sıvısı Ortamında Üretimi Sırasında 5-FU İlacının Yüklenmesi ve İlaç Salım Çalışmaları. Erzincan University Journal of Science and Technology, 11(3), 587-605.

Bang, L. T., Ramesh, S., Purbolaksono, J., Long, B. D., Chandran, H., & Othman, R. (2015). Development of a bone substitute material based on alpha-tricalcium phosphate scaffold coated with carbonate apatite/poly-epsilon-caprolactone. Biomedical Materials, 10(4), 045011.

Barrère, F., van Blitterswijk, C. A., & de Groot, K. (2006). Bone regeneration: molecular and cellular interactions with calcium phosphate ceramics. International journal of nanomedicine, 1(3), 317-332.

Boutinguiza, M., Pou, J., Comesaña, R., Lusquiños, F., de Carlos, A. and León, B., "Biological hydroxyapatite obtained from fish bones", Mater. Sci. Eng. C, 32(3), 478–486, (2012).

Cengiz, B. (2007). Hidroksiapatit nanoparçacıklarının sentezi. Fen Bilimleri Enstitüsü, Kimya Mühendisliği Ana Bilim Dalı, Yüksek Lisans Tezi, Ankara Üniversitesi, Ankara.

Chen, K., Wang, F., Sun, X., Ge, W., Zhang, M., Wang, L., ... & Wu, G. (2025). 3D-printed zinc oxide nanoparticles modified barium titanate/hydroxyapatite ultrasound-responsive piezoelectric ceramic composite scaffold for treating infected bone defects. Bioactive Materials, 45, 479-495.

Codescu, M. M., Vladescu, A., Geanta, V., Voiculescu, I., Pana, I., Dinu, M., ... & Iordoc, M. (2022). Zn based hydroxyapatite based coatings deposited on a novel FeMoTaTiZr high entropy alloy used for bone implants. Surfaces and Interfaces, 28, 101591.

Cullity, B. D., & Stock, S. R. (2001). *Elements of X-ray Diffraction* (3rd ed.). Prentice Hall.

Daldiken, E., Koçak, F. Z., & Küçükdeveci, N. (2024). Synthesis and characterisations of clinoptilolite enriched hydroxyapatite nanoceramics by sol-gel route for bone regeneration. Ceramics International, 50(11), 19650-19659.

Dokgöz, A. B. (2019). Kemik hasarlarının onarımı için deksametazon yüklü nanokompozit doku iskelelerinin geliştirilmesi ve in vitro karekterizasyonu (Master's thesis, Marmara Universitesi (Turkey)).

Dos Santos, C. P. C., Cruel, P. T. E., Buchaim, D. V., da Cunha, M. R., Ervolino, E., Issa, J. P. M., ... & Buchaim, R. L. (2025). Calcium hydroxyapatite combined with photobiomodulation for bone tissue repair: a systematic review. Materials, 18(5), 1120.

Durukan Gül, C. (2024). Dondurarak kurutma ve çözücü döküm-parçacık uzaklaştırma tekniği ile PCL bazlı doku iskelesinin karakterizasyonu= Characterization of PCL-based tissue scaffold using freeze drying and solvent casting-particulate leaching(Master's thesis, Sakarya Üniversitesi).

El-Bahrawy, N. R., Hafez, A. A. A. E., Elmekawy, A., Salem, M., Sarhan, N., & Morsy, R. (2025). Development and characterization of nano-hydroxyapatite/gelatin/PVA/alginate-based multifunctional active scaffolds for bone regeneration: An in vitro and in vivo study. International Journal of Biological Macromolecules, 307, 141160.

Eldokmak, M. M., Essawy, M. M., Abdelkader, S., & Abolgheit, S. (2025). Bioinspired poly-dopamine/nano-hydroxyapatite: an upgrading biocompatible coat for 3D-printed polylactic acid scaffold for bone regeneration. Odontology, 113(1), 89-100.

Fu, Z., Cui, J., Zhao, B., Shen, S. G., & Lin, K. (2021). An overview of polyester/hydroxyapatite composites for bone tissue repairing. Journal of Orthopaedic Translation, 28, 118-130.

Goldstein, J. I., Newbury, D. E., Joy, D. C., Lyman, C. E., Echlin, P., Lifshin, E., Sawyer, L., & Michael, J. R. (2018). Scanning Electron Microscopy and X-ray Microanalysis (4th ed.). Springer.

Gündüz, O., & Cesur, S. (2022). Production and characterisation of pva/whey protein/hydroxyapatite/gentamicin loaded scaffolds for bone tissue engineering applications.

Güner, A. T., & Meran, C. (2020). Ortopedik implantlarda kullanılan biyomalzemeler. Pamukkale Üniversitesi Mühendislik Bilimleri Dergisi, 26(1), 54-67.

Güven, Ş. (2014). Biyouyumluluk ve biyomalzemelerin seçimi. Mühendislik Bilimleri ve Tasarım Dergisi, 2(3), 303-311.

Haider, A., Haider, S., Han, S. S., & Kang, I. K. (2017). Recent advances in the synthesis, functionalization and biomedical applications of hydroxyapatite: A Review. RSC Advances, 7(13), 7442–7458.

Han, K., Sathiyaseelan, A., & Srinivas, B. (2025). Fabrication and evaluation of the zoledronic acid loaded cationic starch-hydroxyapatite-ZrO2 nanocomposites for bone disease treatment. Journal of Molecular Liquids, 128049.

International Centre for Diffraction Data (ICDD). PDF-2 Database. https://www.icdd.com.

Jaiswal, S., Dubey, A., & Lahiri, D. (2020). The influence of bioactive hydroxyapatite shape and size on the mechanical and biodegradation behaviour of magnesium based composite. Ceramics International, 46(17), 27205-27218.

Jenkins, R., & Snyder, R. L. (1996). Introduction to X-ray Powder Diffractometry. Wiley-Interscience.

Jouda, N. S., & Essa, A. F. (2021). Preparation and study of the structural, physical and mechanical properties of hydroxyapatite nanocomposite. Materials Today: Proceedings, 47, 5999-6005.

Kahraman, E. (2017). SBF ortamında üretilen hidroksiapatit-jelatin kompozit malzemelerin ilaç salım performansının incelenmesi.

Koç, S. (2019). Trombositten Zengin Plazma Destekli Sıkıştırılabilir Kemik Greftleri.

Koutsopoulos, S. (2002). Synthesis and characterization of hydroxyapatite crystals: A review study on the analytical methods. Journal of Biomedical Materials Research, 62(4), 600–612.

Küçük, A., & Evcin, A. (2014). Elektroeğirme yöntemiyle bor katkılı hidroksiapatit nanoliflerin üretimi ve karakterizasyonu. Afyon Kocatepe Üniversitesi Fen Ve Mühendislik Bilimleri Dergisi, 14(3), 319-324.

Lee, K. W., Wang, S., Yaszemski, M. J., & Lu, L. (2008). Physical properties and cellular responses to crosslinkable poly (propylene fumarate)/hydroxyapatite nanocomposites. Biomaterials, 29(19), 2839-2848.

Li, H., Du, Q., Guo, P. Y., Yi, Y. T., Mickymaray, S., Balu, A., ... & Li, X. (2025). Linezolid-Loaded Strontium-Substituted Hydroxyapatite-Biopolymeric Composite for Enhanced Bone Regeneration in Osteomyelitis Treatment. Journal of Inorganic and Organometallic Polymers and Materials, 1-17.

McMahon, R. E., Wang, L., Skoracki, R., & Mathur, A. B. (2013). Development of nanomaterials for bone repair and regeneration. Journal of Biomedical Materials Research Part B: Applied Biomaterials, 101(2), 387-397.

Metin, N. (2013). Organik hidroksiapatit tozlarının sinterlenmesi ve karakterizasyonu.

Özcan, İ. (2016). Biyomineralizasyonu tetikleyen, fonksiyonel ve biyobozunur bir kemik doku mühendisliği iskelesi yapımı.

Öztürk, M. G. (2018). Salinomisin ve BnHAp Yüklü Doku İskelelerinin Antikanserojen ve Antibakteriyel Etkinliğinin Araştırılması.

Prakash, V. C. A., Venda, I., & Thamizharasi, V. J. M. T. P. (2022). Synthesis and characterization of surfactant assisted hydroxyapatite powder using microemulsion method. Materials Today: Proceedings, 51, 1788-1792.

Pu'ad, N. M., Haq, R. A., Noh, H. M., Abdullah, H. Z., Idris, M. I., & Lee, T. C. (2020). Synthesis method of hydroxyapatite: A review. Materials Today: Proceedings, 29, 233-239.

Ramesh, S., Tan, C. Y., Bhaduri, S. B., & Teng, W. D. (2007). Synthesis and characterization of nano-hydroxyapatite obtained by precipitation method. Ceramics International, 33(7), 1419–1423.

Shaikh, S., Gupta, S., Mishra, A., Sheikh, P. A., Singh, P., & Kumar, A. (2024). Laser-assisted synthesis of nano-hydroxyapatite and functionalization with bone active molecules for bone regeneration. Colloids and Surfaces B: Biointerfaces, 237, 113859.

Souto-Lopes, M., Grenho, L., Manrique, Y., Dias, M. M., Lopes, J. C. B., Fernandes, M. H., ... & Salgado, C. L. (2024). Bone regeneration driven by a nano-hydroxyapatite/chitosan composite bioaerogel for periodontal regeneration. Frontiers in Bioengineering and Biotechnology, 12, 1355950.

Sepantafar, M., Mohammadi, H., Maheronnaghsh, R., Tayebi, L. and Baharvand, H., "Single phased silicate-containing calcium phosphate bioceramics: Promising biomaterials for periodontal repair", Ceram., 44(10), 11003–11012, (2018).

Smith, B. C. (2011). Infrared Spectral Interpretation: A Systematic Approach. CRC Press.

Toktaş, A. G., Mert, G. Ü. L., Nusret, K. Ö. S. E., & Doğan, A. (2022). Farklı Gözenek Boyutuna ve Miktarına Sahip Hidroksiapatit Kemik Greftlerinin Mekanik Özelliklerinin İncelenmesi. OMÜ Mühendislik Bilimleri ve Teknolojisi Dergisi, 2(1), 15-23.

Tunçay, Ö. E. (2013). Biyomimetik yöntemle bor katkılı doku iskelelerinin geliştirilmesi ve kemik doku mühendisliğindeki etkinliklerinin araştırılması.

Turnbull, G., Clarke, J., Picard, F., Riches, P., Jia, L., Han, F. And Shu, W., "3D bioactive composite scaffolds for bone tissue engineering", Bioactive Materials, 3(3), 278–314, (2018).

Tut, T. A., Cesur, S., Ilhan, E., Sahin, A., Yildirim, O. S., & Gunduz, O. (2022). Gentamicin-loaded polyvinyl alcohol/whey protein isolate/hydroxyapatite 3D composite scaffolds with drug delivery capability for bone tissue engineering applications. European Polymer Journal, 179, 111580.

Uysal, I., & Evis, Z. (2014). Co-doping of hydroxyapatite with zinc and fluoride improves mechanical and biological properties. Progress in Natural Science: Materials International, 24(5), 530–538.

ORAL PRESENTATION

Efficient multiple testing procedure for belief propagation on biological network with conformal prediction

Mehmet Ali Kaygusuz[1], Vilda Purutçuoğlu[2]

[1]Department of Economics, Anadolu University, Türkiye
[2]Department of Statistics, Middle East Technical University, Türkiye

*Corresponding author e-mail : makaygusuz1988@gmail.com, vpurutcu@metu.edu.tr

Abstract

Belief propagation (BP) is a message-passing algorithm commonly used for inference in graphical models, particularly, probabilistic graphical models such as Bayesian networks and Markov random fields. It works by passing messages between nodes in a graph to estimate the probability of variables given evidence, efficiently handling uncertainty in complex systems. Belief propagation (BP) is a term with meanings in different fields, but it most commonly refers to an algorithm in computer science and machine learning. Furthermore, BP has been successfully applied to a range of machine learning tasks, including clustering, classification, and probabilistic inference in Bayesian network models, thereby, facilitating efficient learning and decision-making in complex systems. "Biological networks" is a broad term that can refer to various interconnected systems in biology, often modeled as graphs or networks to understand complex interactions.These networks provide a valuable framework for understanding the complex processes that underlie biological functions and systems. However, inference in high-dimensional biological networks is often computationally demanding. To address this difficulties, we propose integrating conformal prediction with belief propagation for biological network analysis. In addition, alternative multiple testing procedures for high-throughput biological data have gained increasing attention in recent years. As a complementary approach, we introduce the use of *e-value* within belief propagation for biological networks, especially, in scenarios where the number of parameters exceeds the number of observations.

Keywords: 3-6 words. (Use commas to separate words.)

INTRODUCTION

Graphical models have been extensively studied in the literature, with important contributions by Jordan (2003), Wainwright and Jordan (2008), and Koller (2009). The message-passing algorithm, central to inference in these models, was proposed by Donoho (2008) and further developed by Fan (2022). Moreover, comprehensive overview of message passing algorithm is provided by Fang et al. (2022). Applications of message passing to biological networks were highlighted by Newman (2023). Message passing in the context of Wigner matrices has been investigated by Çakmak et al. (2014), Deshpande and Montanari (2014), Wein et al. (2019), and Stephan (2021). Furthermore, message passing alorithm with biological networks is studied by Bayati et al. (2013) and Chang et al. (2013). Graphical belief propogation and wavelet on graphs are suggested by Jia et al. (2021) and Hy and Kondor (2022), respectively. El-Hay et al. (2010) have proposed continuous belief propagation. Moreover, graphical learning for long run dependencies in protein structures is proposed by Hariri and Vandergheynst (2024). More specifically, message-passing algorithms for protein–protein interaction networks were proposed by Iqbal et al. (2008), Weigt et al. (2009), and Bailly-Bechet et al. (2011). In the area of machine learning, message passing and neural networks were studied by Gilmer et al. (2020), while the integration of belief propagation with deep neural networks was discussed by Lucibello et al. (2022).

In parallel, conformal prediction was originally introduced by Shafer and Vovk (2008). It has since been applied in various contexts, including outlier detection by Kaygusuz and Purutçuoğlu (2025), and message-passing frameworks by Clarte and Zdeberova (2024) and Wen et al. (2025). Conformal prediction with clusetring is proposed by Jung et al. (2021). For instance, one of initial study for multiple testing procedure for wavalet is studied by Abramovich and Benjamini (1996). On the other hand, Kunisky et al. (2019) have showed computational

difficulties of hypotheses testing with likelihood ratio test. More reently, Danadel et al. (2024) have proposed knockoff multiple testing procedure to avoid over clustering for single cell data. Furthermore, e-value for multiple testing was proposed by Vovk and Wang (2020), with subsequent detailed investigations by Wang and Ramdas (2022) and Xu and Ramdas (2024).

Building on these foundations, we focus on belief propagation, a message-passing algorithm commonly used for inference in probabilistic graphical models such as Bayesian networks and Markov random fields. BP provides an elegant and efficient framework for computing marginal distributions and making predictions from observed data, and it has been successfully applied in machine learning tasks such as clustering, classification, and probabilistic inference in Bayesian networks, enabling efficient learning and decision-making in complex systems.

Biological networks, which represent the interactions among genes, proteins, and cells, provide a powerful framework for understanding the intricate processes underlying biological functions. However, performing inference in high-dimensional biological networks remains computationally demanding. To address these challenges, we propose the integration of conformal prediction with belief propagation for the analysis of biological networks with clustered data, offering assumption-free prediction in such settings. Moreover, in light of recent interest in alternative multiple testing procedures for high-throughput biological data, we introduce the use of e-value within belief propagation, particularly, in scenarios where the number of parameters exceeds the number of observations.

MATERIALS AND METHODS

THEORY AND METHOD

Belief propagation on biological networks

Traditionally, belief propagation (BP) is an algorithm used to perform inference on graphical models, particularly probabilistic graphical models such as Bayesian networks and Markov random fields. BP is a message-passing algorithm that enables the computation of marginal distributions of random variables in a network.

Graphical models represent the relationships between random variables using graphs. More specifically, nodes correspond to random variables, and edges represent dependencies between them. There are two main types of graphical models:

Directed acyclic graphs (Bayesian networks): edges represent conditional dependencies.

Markov random fields (undirected graphs): edges represent direct dependencies.

In belief propagation, nodes iteratively exchange messages with their neighbors. A message from node A to node B encodes information about the probability distribution of A as it relates to B. These messages are computed using both local evidence and the messages received from neighboring nodes. The belief of a node is the current estimate of the probability distribution of the variable which it represents, given the incoming messages. Beliefs are updated iteratively until convergence.

The BP algorithm can be summarized in the following steps:

Initialization: Assign initial beliefs for each node, typically based on prior or uniform distributions.

Message passing: Iteratively pass messages between neighboring nodes until convergence or until a maximum number of iterations is reached.

Belief update: Update each node's belief based on the messages which it has received.

Marginal computation: After convergence, compute the marginal distributions for the desired nodes.

For a better representation, we can consider a simple Bayesian network with three variables A, B, and C, where A influences both B and C. To compute the marginal distribution of B, belief propagation would proceed as follows: We initialize beliefs for B based on prior knowledge. Then, the messages are passed from A to B and from C to B. Later, we update the belief for B using the received messages. Finally, we repeat the process until the belief for B stabilizes.

As a results, belief propagation is a powerful and efficient algorithm for inference in graphical models. Its ability to capture complex dependencies and provide approximate solutions even in loopy graphs makes it a valuable tool across a wide range of applications and domains.

Conformal prediction for belief propagation

Conformal prediction is a statistical methodology designed to quantify the uncertainty of predictions generated by machine learning models. Instead of providing a single point estimate, it produces prediction sets or intervals that contain the true outcome with a specified probability, under certain assumptions. For example, a conformal predictor may output a set of possible values that includes the true outcome with 95% confidence.

A central concept in conformal prediction is the ***nonconformity measure***, which evaluates how "strange" or "nonconforming" a new observation is relative to the training data. This measure determines whether a particular prediction should be included in the prediction set. To ensure statistical validity, conformal prediction relies on a ***calibration set***, a subset of the training data used to assess nonconformity and maintain the desired coverage probability.

One of the main advantages of conformal prediction is that it provides valid prediction sets under minimal assumptions. The coverage probability, which refers to the proportion of times the true outcome is contained within the prediction set, is guaranteed to meet or exceed the specified level (e.g., 95%) as long as the data points are exchangeable. Because of this, conformal prediction has been successfully applied across diverse fields such as bioinformatics, machine learning, and other domains where uncertainty quantification is critical.

More recently, conformal prediction has been integrated with ***message passing algorithms***. In this context, conformal prediction enhances the efficiency of computing prediction intervals while ensuring that true outcomes are captured within the specified confidence levels. When applied to clustered data, however, the integration of conformal prediction with message passing presents additional challenges. Nevertheless, in settings where models must aggregate information from neighboring nodes, this combination accelerates the computation of prediction sets and improves overall predictive performance.

Belief propagation with conformal prediction for Wigner matrix

In the 1950s, Wigner introduced a simple model of random matrices to approximate generic self-adjoint operators. Hereby, consider a family of independent, zero-mean, real or complex-valued random variables $\{Z_{i,j}\}_{\{1 \le i < j\}}$ independent from a family of i.i.d. centered real-valued random variables $\{Y_i\}_{\{1 \le i\}}$. Then, we define the (N × N)-dimensioanl real-symmetric or Hermitian random matrix X_N with entries:

$$X_{\{N(i,j)\}} = Z_{\{i,j\}},\ i < j;\ \{Z_{\{j,i\}}\}, i > j;\ Y_i;\ i = j. \quad (1)$$

Such a matrix is called a Wigner matrix. If the random variables $Z_{\{i,j\}}$ and Y_i are Gaussian, then X_N is referred to as a Gaussian Wigner matrix. A particularly important case arises when $E[Y_1^2] = 2\ and\ E[|Z_{\{1,2\}}^2|] = 1$. In this setting, the law of X_N is invariant under the action of the orthogonal group (when entries are real).

On the other hand, the basic goal of conformal prediction is to construct valid predictive sets with guaranteed coverage. Hence, let $(X_i, Y_i) \sim P,\ i = 1, \ldots, n$ be i.i.d. feature–response pairs from some distribution P on (X × Y). For concreteness, we may take X = R^d and Y = R, though more general cases are possible. Also, let α ∈ (0,1) be a nominal error level. Accordingly, the goal is to construct a prediction set $\hat{C}_n: X \to \{subsets\ of\ Y\}$ such that for a new i.i.d. pair $(X_{n+1}, Y_{n+1}) \sim P$.

$$P(Y_{n+1} \in \hat{C}_n(X_{n+1})) \geq 1 - \alpha. \quad (2)$$

At first glance, achieving Equation 1 without assumptions on P and without asymptotics seems difficult. Yet a trivial construction works as

$$\hat{C}_n(X_{n+1}) = \{Y\ with\ prob\ 1 - \alpha;\ \emptyset\ with\ prob\ \alpha\}. \quad (3)$$

Equation 3 guarantees exact coverage at level (1-α), thereby, satisfying Equation 2. However, this solution is not informative. The real question is whether we can construct nontrivial sets that also achieve Equation 2 in finite

samples without assumptions on P. Ideally, our strategy is to adapt to the difficulty of prediction: the more predictable Y_{n+1} is from X_{n+1}, the smaller we want $\widehat{C}_n(X_{n+1})$ to be.

On conclusion, although Wigner matrices and conformal prediction arise from very different traditions from random matrix theory in mathematical physics and distribution-free predictive inference in statistics, there is a conceptual link. Both frameworks deal with uncertainty in high-dimensional systems. But Wigner matrices provide tractable models for understanding the spectral behavior of large random operators, while conformal prediction offers rigorous ways to quantify predictive uncertainty in complex data. In modern applications, particularly in high-dimensional biological or network models, insights from random matrix theory can inform the stability and calibration of conformal prediction methods. More details about random matrix theory can be found on the book of Tao (2012).

E-value multiple testing procedure for belief propagation on biological networks

E-value, introduced by Vovk in 2019, provides an alternative to p-values in multiple testing scenarios. It is nonnegative test statistics that quantifies evidence against the null hypothesis and is closely related to betting scores and likelihood ratios. Unlike p-value, e-value allows for inference by making it especially powerful in sequential or adaptive experimental settings.

Accordingly, one of the key advantages of e-value is its ability to handle optional continuation. Specifically, e-value from subsequent experiments can simply be multiplied, producing a new "product e-value" that represents the combined evidence across all experiments. This property holds even when later experiments are decided adaptively by depending in unknown ways on earlier results or when the total number of trials is not predetermined. Importantly, the resulting product e-value continues to control Type-I error by ensuring valid inference. This property motivates the notion of the *e-process*, the sequential extension of e-value, which serves as a fundamental building block for anytime-valid statistical methods.

Another strength of e-value is its robustness under dependence. Any weighted average of e-value remains an e-value, even if the individual components are arbitrarily dependent. This flexibility makes them useful for combining evidence across diverse sources.

E-value admits several complementary interpretations as listed below.

Rescaling of tests**:** It can be seen as presenting evidence on a scale that naturally facilitates aggregation.

Relationship to p-value: The reciprocal of an e-value corresponds to a special p-value that retains a generalized Type-I error guarantee.

Connection to likelihood ratios: E-value generalizes likelihood ratios and, while related to Bayes factors, remains conceptually distinct.

Betting scores**:** It can be viewed as bets in a sequential gambling framework.

Supermartingale increments**:** In sequential contexts, it corresponds to increments of nonnegative supermartingales.

Since 2019, interest in e-value has grown rapidly, with several research groups producing breakthrough results. Formally, an e-variable is a nonnegative random variable whose expectation under the null hypothesis is at most one, and an e-value is a realized outcome of such a variable. Whereas p-value is defined in terms of probabilities, e-value is defined in terms of expectations.

Finally, under the assumption of independence, the product of e-value is itself an e-value, yielding a particularly rich domination structure. Even without full independence, this assumption can often be relaxed to the weaker condition of sequentiality, preserving the validity of e-values in adaptive settings.

Numerical examples

We began by generating data from a Wigner matrix with 1,000 observations. Following this, we applied conformal prediction based on belief propagation to identify the strongest clustered signal within the data.

Next, four Erdos–Rényi graphs were generated and assembled into a block-diagonal matrix, representing a modular network with four clusters. As expected, the nearest-neighbor spacing distribution (NNSD, shown at left side of Figure 1) is exponential, reflecting the modular structure of the matrix. Using the clusters command of the *igraph* package, we were able to clearly reveal this clustered structure.

When validating the new noisy matrix, we found that it behaves like a completely random matrix: its NNSD is Wigner-like (shown at right side of Figure 1). The modular structure disappears, and the entire matrix appears as a single large cluster. However, spurious matrix elements emerge, artificially connecting the true clusters.

Gaussian density of the eigenvalue spectrum; another method is based on fitting spline function to the cumulative empirical eigenvalue distribution. The latter is determined by the parameter unfold method. For each threshold, a distance between the empirical eigenvalue spacing distribution (NNSD) and both limiting distributions (Wigner-Dyson distribution and Exponential distribution, respectively) are estimated. Threshold and loglikelihood values per eigenvalue with exponential and Wigner distribution are obtained in Figure 1. In this figure, it is seen that exponential fits better than Wigner since the spacing decreases monotonically which may imply uncorrelated levels. On the other side, the Wigner distribution rises to a peak near spacing equal to 1, but, it has a Gaussian tail which may represent correlated levels. Hereby, the former indicates that there is a strong localization which is built from many independent spacing. The latter presents strong short-range correlations.

For conformal prediction with belief propagation on biological networks, we again used 1,000 observations. In the case without outliers, conformal prediction revealed two clusters, with 356 and 644 observations, respectively. When outliers were present, three clusters were detected, containing 198, 701, and 101 observations.

Finally, under the same setting of 1,000 observations, we applied a log-likelihood ratio e-value multiple testing procedure. This method selected five variables, with corresponding values (interpretable as transformed test statistics) of **2.969, 3.7010, 3.923, 4.551, and 5.975.**

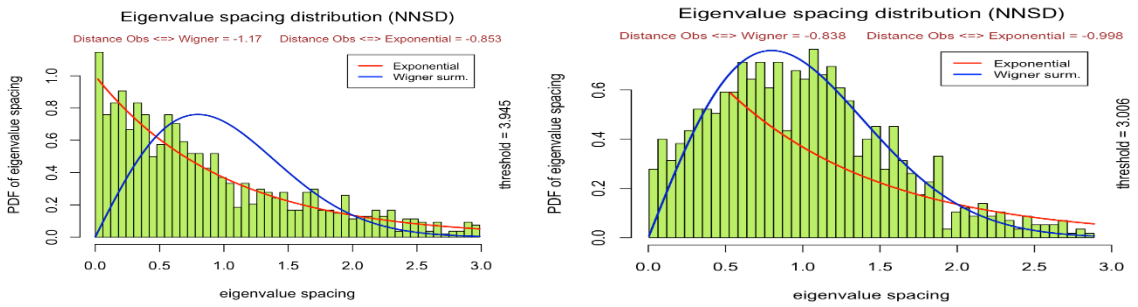


Fig.1. Eigenvalue spacing distributions (Exponential and Wigner) for biological networks (Erdös-Renyi) with different Wigner matrix parameter

CONCLUSIONS

In this study, we applied belief propagation to biological networks using Wigner matrices. However, this approach can be computationally demanding. As an alternative, we employed conformal prediction combined with belief propagation to analyze clustered biological network data.

In recent years, e-value–based multiple testing procedures have gained popularity for model selection in high-dimensional settings. Motivated by this, we proposed a framework that integrates belief propagation on biological networks with conformal prediction.

Future studies may extend this work by applying the method to other types of data, such as protein–protein interaction networks, or by incorporating spline functions with the Kullback–Leibler information criterion for model evaluation.

REFERENCES

Abramovich, F., & Benjamini, Y. (1996). Adaptive thresholding of wavelet coefficients. *Computational Statistics & Data Analysis*, *22*(4), 351-361.

Bailly-Bechet, M., Borgs, C., Braunstein, A., Chayes, J., Dagkessamanskaia, A., François, J. M., & Zecchina, R. (2011). Finding undetected protein associations in cell signaling by belief propagation. *Proceedings of the National Academy of Sciences*, *108*(2), 882-887.

Bayati, M., Gleich, D. F., Saberi, A., & Wang, Y. (2013). Message-passing algorithms for sparse network alignment. *ACM Transactions on Knowledge Discovery from Data (TKDD)*, *7*(1), 1-31.

Braunstein, A., Pagnani, A., Weigt, M., & Zecchina, R. (2008). Gene-network inference by message passing. In *Journal of Physics: Conference Series* (Vol. 95, No. 1, p. 012016). IOP Publish

Clarté, L., & Zdeborová, L. (2024). Building Conformal Prediction Intervals with Approximate Message Passing. *arXiv preprint arXiv:2410.16493*.

Chang, R., Karr, J. R., & Schadt, E. E. (2014). Causal inference in biology networks with integrated belief propagation. In *Pacific Symposium on Biocomputing Co-Chairs* (pp. 359-370).

Deshpande, Y., & Montanari, A. (2014). Information-theoretically optimal sparse PCA. In *2014 IEEE International Symposium on Information Theory* (pp. 2197-2201). IEEE

Cakmak, B., Winther, O., & Fleury, B. H. (2014). S-AMP: Approximate message passing for general matrix ensembles. In *2014 IEEE Information Theory Workshop (ITW 2014)* (pp. 192-196). IEEE

Donoho, D. L., Maleki, A., & Montanari, A. (2009). Message-passing algorithms for compressed sensing. *Proceedings of the National Academy of Sciences*, *106*(45), 18914-18919.

DenAdel, A., Ramseier, M. L., Navia, A. W., Shalek, A. K., Raghavan, S., Winter, P. S., ... & Crawford, L. (2024). A knockoff calibration method to avoid over-clustering in single-cell RNA-sequencing. *bioRxiv*, 2024-03.

Fan, Z. (2022). Approximate message passing algorithms for rotationally invariant matrices. *The Annals of Statistics*, *50*(1), 197-224.

Hy, T. S., & Kondor, R. (2022) Multiresolution matrix factorization and wavelet networks on graphs. In *Topological, Algebraic and Geometric Learning Workshops 2022* (pp. 172-182). PMLR.

El-Hay, T., Cohn, I., Friedman, N. and Kupferman, R., 2010, June. Continuous-Time Belief Propagation. In *ICML* (pp. 343-350).

Hariri, A. and Vandergheynst, P., (2024), November. Graph learning for capturing long-range dependencies in protein structures. In *Mach*

Gilmer, J., Schoenholz, S. S., Riley, P. F., Vinyals, O., & Dahl, G. E. (2020). Message passing neural networks. *Machine learning meets quantum physics*, 199-214.

Feng, O. Y., Venkataramanan, R., Rush, C., & Samworth, R. J. (2022). A unifying tutorial on approximate message passing. *Foundations and Trends® in Machine Learning*, *15*(4), 335-536.

Jordan, M. I. (2003). *An introduction to probabilistic graphical models*.

Jia, J., Baykal, C., Potluru, V. K., & Benson, A. R. (2021). Graph belief propagation networks. *arXiv preprint arXiv:2106.03033*

Jung, S., Park, K., & Kim, B. (2021). Clustering on the torus by conformal prediction. *The Annals of Applied Statistics*, *15*(4), 1583-1603.

Kaygusuz, M. A., & Purutçuoğlu, V. (2023) Conditional independence testing for conformal robust neural networks in outlier detection. Proceeding of International Young Statistician Conference.

Kunisky, D., Wein, A. S., & Bandeira, A. S. (2019). Notes on computational hardness of hypothesis testing: Predictions using the low-degree likelihood ratio. In *ISAAC Congress (International Society for Analysis, its Applications and Computation)* (pp. 1-50). Cham: Springer International Publishing.

Iqbal, M., Freitas, A. A., Johnson, C. G., & Vergassola, M. (2008). Message-passing algorithms for the prediction of protein domain interactions from protein–protein interaction data. *Bioinformatics*, *24*(18), 2064-2070.

Lucibello, C., Pittorino, F., Perugini, G., & Zecchina, R. (2022). Deep learning via message passing algorithms based on belief propagation. *Machine Learning: Science and Technology*, *3*(3), 035005.

Newman, M. E. J. (2023). Message passing methods on complex networks. *Proceedings of the Royal Society A*, *479*(2270), 20220774.

Koller, D. (2009). *Probabilistic Graphical Models: Principles and Techniques*. The MIT Press.

Tao, T. (2012). *Topics in random matrix theory* (Vol. 132). American Mathematical Society, Rhode Island, USA.

Stephan, L. (2021). *Inference problems in large random graphs* (Doctoral dissertation, Sorbonne Université

Yanover, C., & Weiss, Y. (2002). Approximate inference and protein-folding. *Advances in neural information processing systems*, *15*.

Xu, Z., & Ramdas, A. (2024) Online multiple testing with e-values. In *International Conference on Artificial Intelligence and Statistics* (pp. 3997-4005). PMLR.

Vovk, V., & Wang, R. (2021). E-values: Calibration, combination and applications. *The Annals of Statistics*, *49*(3), 1736-1754.

Wein, A. S., El Alaoui, A., & Moore, C. (2019, November). The Kikuchi hierarchy and tensor PCA. In *2019 IEEE 60th Annual Symposium on Foundations of Computer Science (FOCS)* (pp. 1446-1468). IEEE.

Wen, H., Xing, H., & Simeone, O. (2025). Distributed Conformal Prediction via Message Passing. *arXiv preprint arXiv:2501.14544*.

Wang, R., & Ramdas, A. (2022). False discovery rate control with e-values. *Journal of the Royal Statistical Society Series B: Statistical Methodology*, *84*(3), 822-852.

Wainwright, M. J., & Jordan, M. I. (2008). Graphical models, exponential families, and variational inference. *Foundations and Trends® in Machine Learning*, *1*(1–2), 1-305.

Weigt, M., White, R. A., Szurmant, H., Hoch, J. A., & Hwa, T. (2009). Identification of direct residue contacts in protein–protein interaction by message passing. *Proceedings of the National Academy of Sciences*, *106*(1), 67-72.

ORAL PRESENTATION

Optimal multiple testing procedure for double machine learning with clustering data

Mehmet Ali Kaygusuz[1], Vilda Purutçuoğlu[2]

[1]Department of Economics, Anadolu University, Türkiye.
[2]Department of Statistics, Middle East Technical University, Türkiye.

*Corresponding author e-mail: makaygusuz1988@gmail.com, vpurutcu@metu.edu.tr

Abstract

Double machine learning (DML) is a statistical framework designed to estimate causal effects while effectively controlling for confounding variables. By integrating machine learning techniques with principles of causal inference, DML yields unbiased treatment effect estimates and supports robust analysis across disciplines such as economics, epidemiology, and statistical machine learning. Its utility becomes particularly evident in high-dimensional settings, where traditional estimation methods often fail due to complex interdependencies among variables. DML leverages cross-fitting procedures to mitigate overfitting, thereby, enhancing generalizability. Beyond causal inference, DML can be extended to unsupervised learning tasks such as clustering, where it facilitates the identification of meaningful data groupings while adjusting for potential confounders. In this context, we propose an innovative methodology that incorporates e-value, which is a nonnegative test statistics from likelihood ratio-based multiple testing frameworks, as a means of quantifying statistical evidence and controlling false discoveries. This approach is especially pertinent when the number of parameters exceeds the number of observations, a common scenario in modern high-dimensional data analysis. Furthermore, recent developments in multiple testing procedures for graphical models have highlighted the need for more flexible and interpretable tools. In response, we introduce a novel framework that integrates e-value within the DML paradigm to improve inference and clustering accuracy in structured, high-dimensional datasets. Our method provides a promising direction for future research in both causal inference and high-dimensional unsupervised learning.

Keywords: double machine learning, clustered data, multiway clustering, multiple testing procedure.

INTRODUCTION

Traditionally, double machine learning (DML) is a statistical methodology which is designed for causal inference that improves the estimation of the effect of a treatment or intervention while controlling for confounding variables. It combines machine learning models with a technique called orthogonalization to remove biases from regularization and overfitting, enabling unbiased and efficient estimation of causal effects even in complex, high-dimensional settings. Furthermore, the key idea is to use two separate machine learning models: one to predict the treatment and another to predict the outcome, then combine these predictions in a way that "orthogonalizes" the estimation of the treatment effect, making it robust to errors in the nuisance parameter estimation. Cross-fitting, where data is splitted and models are trained on different folds, further reduces overfitting bias. This approach provides for reliable inference about causal relationships by using flexible machine learning tools without sacrificing statistical validity.

Beyond causal inference, DML can be extended to unsupervised learning tasks such as clustering, where it facilitates the identification of meaningful data groupings while adjusting for potential confounders. clustering for instrumental variables (IV) refers to adjusting the standard errors of IV estimators to account for correlation in the error terms along multiple clustering dimensions simultaneously. In instrumental variable regression, we use instruments to address endogeneity in explanatory variables. Like in ordinary least squares (OLS), valid inference requires correctly estimating the variance-covariance matrix of the IV estimator. If the error terms are correlated within clusters (e.g., firms, regions, time periods), failing to account for this clustering can lead to underestimated standard errors and invalid inference. IV regressions often use panel or grouped data where errors may be

correlated within multiple dimensions. For example, in a dataset of firms observed over time and across regions, errors might be correlated within firms and within regions. Moreover, ignoring one or more clustering dimensions can bias standard errors downward, increasing the risk of false positives. It adjusts the variance-covariance matrix of the IV estimator to reflect clustering along all relevant dimensions simultaneously. The multiway clustered variance estimator for IV is conceptually similar to that in OLS.

In the literature, instrumental variable based on correlated with error term is introduced by Wright (1928) and Imbens (2014) has provided econometrician perspective for instrumental variables. More specifically, instrumental variables estimation for nonparametric models is proposed by Newey and Powell (2003). Hansen et al. (2008) have studied estimation procedure with many instrumantal variable. Furthermore, nonparametric additive instrumental variable estimator is proposed by Fan and Zhang (2018). Alternatively, instrumental variable in survival context is studied by Tchetgen et al. (2015). Also, instrumental variables estimation for additive hazard models is suggested by Brueckner et al. (2019). For example, insturmental variables to estimate a Cox's proportional hazards regression subject provided by Li et al. (2015).

On the other hand, double machine learning is suggested by Chernuzkov (2016,2018). R package for double machine learning is provided by Bach et al. (2024). Angrist and Pische (2009) have investigated identification properties of causal effects by using instrumental variables. More recently, double machine learning algorithm for cluster data is proposed by Chiang et al. (2022). Fingerhut et al. (2022) have proposed coordinated double machine learnig methedology. Moreover, Klyne and Shah (2023) have suggested average partial estimation with double machine learning methods. Furthermore, Duan et al. (2024) and Niu et al. (2024) have studied conditional indepedence testing procedure for double machine learning data.

Finally, e-value is introduced by Vovk and Wang (2021). Later, Xu and Ramdas (2024) an Xu et al. (2025) have proposed e-value multiple testing procedure for different models. Wang et al. Ramdas (2024) and Geoman et al. (2025) have combined false discovery rate control and e-value multiple testing procedure.

As a result, in this context, we have suggested an novel and popular methodology that incorporates e-value, which is a nonnegative test statistics from likelihood ratio-based multiple testing frameworks, as a means of quantifying statistical evidence and controlling false discoveries. This approach is especially pertinent when the number of parameters exceeds the number of observations, a common scenario in modern high-dimensional data analysis. Furthermore, recent developments in multiple testing procedures for graphical models have highlighted the need for more flexible and interpretable tools. In response, we introduce a novel framework that integrates e-values within the DML paradigm to improve inference and clustering accuracy in structured, high-dimensional datasets.

THEORY and METHOD

Double Machine Learning for Estimation of a Causal Parameter

A key element of double machine learning (DML) models is the score functions identifying the estimates for the target parameter. These functions play an essential role for valid inference with machine learning methods because of the fact that they have to satisfy a property, called Neyman orthogonality. With the score functions as key elements, we implements DML in a very general way by using object orientation.

With more mathematical details, let we assume that we have a sample $(W_{ij}; i = 1,..,N; j = 1,...,M)$ which has a double indexed of observation size as NM and modeled as i.i.d. copies of W = (Y, D, Z, X). Let P denote the probability law of $\{W_{ij}\}_{ij}$ and let E_p be the expectation of P via

$$E_p\left[\psi(W_{11;}\theta_{0,}\eta_{0})\right] = 0. \quad (1)$$

where we call ψ the score function, W = (Y, D, X, Z), $\theta_{0,}$is the parameter of interest, and η denotes nuisance functions with population value η_{0}. Therefore, we define a probability measure P and assume that N is divisible by K in order to simplify the notation.

On the other side, linear IV model can be used for multiway cluster sample. For instance, we consider a practical example of the partially linear IV model adapted to the multiway cluster sample data as below.

$$Y_{ij} = D_{ij}\theta_0 + g(X_{ij}) + q_{ij} \text{ while } E(q_{ij}|X_{ij}, Z_{ij}) = 0 \quad (2)$$
$$Z_{ij} = m(X_{ij}) + v_{ij} \text{ while } E(v_{ij}|X_{ij}) = 0$$

where Y_{ij} is the outcome variable and Z_{ij} is the policy variable of interest. The high-dimensional vector X_{ij} = ($X_{1j}, \ldots, X_{ij}$) consists of other confounding covariates, and ζ and V are stochastic errors. Equation 2 is our major expression and θ_0 is the main regression coefficient that we would like to infer. Moreover, if Z_{ij} is conditionally exogenous, θ_0 has the interpretation of a structural or causal parameter. The second equation represents confounding variable, more specfically, the dependence of Z_{ij} on covariates. The characteristics X affect the policy variable Z_{ij} via the function $m(X_{ij})$ and the outcome variable via the function $g(X_{ij})$.

One may want to observe the random variables Y_{ij}, D_{ij}, X_{ij}, and Z_{ij}, which are typically interpreted as the outcome, endogenous regressor, exogenous regressors, and instrumental variable, respectively. Moreover, the low-dimensional parameter vector θ_0 refers to an object of interest. Accordingly, a Neyman orthogonal score ψ for such model is given by

$$\psi(w;\theta, \eta) = (y - g_1(x) - \theta (d - g_2(x)))(z - m(x)) \quad (3)$$

while w = (y, d, x, z), η = (g_1, g_2, m) and g_1, g_2, m ∈ L_2 (P). Furthermore, it is straightforward to verify that this score satisfies both the moment restriction in equation (3), EP [ψ(w_{11} ; θ_0, η_0)] = 0, and the Neyman orthogonality condition (1), ∂_ηEP ψ(w_{11} ; θ_0, η_0)[η − η_0] = 0 for all η ∈ T_n)[at η_0 = (g_{10}, g_{20}, m_0), where g_{10} (X) = EP [Y |X], g_{20} (X) = EP [D|X], and m_0 (X) = EP [Z|X].

Multiway clustering for double machine learning data

Here, we suggested a novel K^2-fold multiway cross fitting procedure for estimation of θ_0. For any r ∈ N, we use the notation [r] = {1, ..., r}. With a fixed positive integer K, randomly partition [N] into K parts $\{I_1, \ldots, I_K\}$ and [M] into K parts $\{J_1, \ldots, J_K\}$. Thus, for each (k, l) ∈ [K] we obtain an estimate. Accordingly, we provided the partially linear IV model formula which is introduced in Section 2.1. Therefore, we would like to express in more details on the following high-dimensional linear representations for multiway clustering data,

$$Y_{ij} = D_{ij}\theta_0 + X_{ij}(\zeta_0) + q_{ij},$$
$$D_{ij} = Z_{ij}\pi_{10} + X_{ij}(\pi_{20}) + v_{ij},$$
$$Z_{ij} = X_{ij}(\xi_0) + V_{ij},$$

where the parameter values are set to $\theta_0 = \pi_{10} = 1.0$ and $\zeta_0 = \pi_{20} = \xi_0 = (0.5, 0.5^2, \ldots, 0.5^{\dim(X)})$ for some large dim(X). Also, the primitive random vector $(X_{ij}, q_{ij}, v_{ij}, V_{ij})'$ is constructed by

$$X_{ij} = (1 - w_1^X - w_2^X)\alpha X_{ij} + w_1^X \text{ Xα} + w_2^X \text{ Xj},$$
$$q_{ij} = (1 - w_1^q - w_2^q)\alpha q_{ij} + w_1^q q_i + w_2^q q_{ij},$$
$$v_{ij} = (1 - w_1^v - w_2^v)\alpha v_{ij} + w_1^v v_i + w_2^v v_j,$$

and

$$V_{ij} = (1 - w_1^v - w_2^v)\alpha V_{ij} + w_1^v V_i + w_2^v V_j$$

with two-way clustering weights (w_1^X, w_2^X), (w_1^q, w_2^q), (w_1^v, w_2^v), and (w_1^v, w_2^v), where α_{ij}^X, α_i^X and α_j^X are independently generated and $(\alpha_{ij}^\varepsilon, \alpha_{ij}^v)'$, $(\alpha_i^\varepsilon, \alpha_i^v)'$, $(\alpha_j^\varepsilon, \alpha_j^v)'$ are independently generated by,

$$\begin{pmatrix}\alpha_{ij}^q \\ \alpha_{ij}^v\end{pmatrix}, \begin{pmatrix}\alpha_i^q \\ \alpha_i^v\end{pmatrix}, \begin{pmatrix}\alpha_j^q \\ \alpha_j^v\end{pmatrix} \sim N\left(0, \begin{pmatrix}1 & s_{qv} \\ s_{qv} & 1\end{pmatrix}\right) \quad (5)$$

and α_{ij}^V, α_i^V, *and* α_j^V are independently generated via

$$\alpha_{ij}^V, \alpha_i^V, \text{and } \alpha_j^V \sim N(0,1). \quad (6)$$

Therefore, the weights (w_1^X, w_2^X), (w_1^q, w_2^q), (w_1^v, w_2^v), and (w_1^v, w_2^v), specify the extent of dependence in two-way clustering in $X_{ij}, q_{ij}, v_{ij}, V_{ij}$, respectively. The parameter s_X specifies the extent of collinearity among the high-dimensional regressors X_{ij}. The parameter s_{qv} specifies the extent of endogeneity. Finally, it is taken the values of these parameters (due to we have four specific points therefore, 1/4=0.25) to (w_1^X, w_2^X), (w_1^q, w_2^q), (w_1^v, w_2^v), and (w_1^v, w_2^v), =(0.25,0.25) and $s_X = s_{qv} = 0.25$ as we have four specific points.

E-value multiple testing procedure for double machine learning with clustered data

E-value, introduced by Vovk in 2019, serves as an alternative to p-value in multiple testing scenarios. It is a nonnegative test statistics that provides evidence against the null hypothesis, closely related to concepts like betting scores and likelihood ratios, allowing for more flexible statistical inference with the property that under the null hypothesis its expected value is at most 1.
This contrasts with p-value, which represents tail probabilities under the null. Traditional multiple testing procedures (like Bonferroni or Benjamini-Hochberg) control error rates based on p-value. Hence, e-value provides an alternative framework that can be more flexible and robust, especially in sequential or adaptive testing. It allows for combining evidence across tests and can be used to control error rates such as the family-wise error rate (FWER) or false discovery rate (FDR). So, we can compute e-value for each hypothesis test. Then, we can combine or adjust these e-values by using specific rules or algorithms designed to control the desired error rate. We can also reject hypotheses where the combined or adjusted e-value exceeds a certain threshold. Lastly, the e-value multiple testing procedure is a framework for controlling error rates in multiple hypothesis testing by using e-values by random variables with expected value ≤ 1 under the null, instead of p-values. As a result, this approach offers flexibility, robustness, and potential advantages in sequential and adaptive testing scenarios.

On the other hand, the e-value log-likelihood multiple testing procedure, as an extention of the above e-value testing procedure, is a method in statistical hypothesis testing that uses e-value derived from likelihood ratios (or log-likelihood ratios) to perform multiple hypothesis tests while controlling error rates. This spefic extention is called *e-value from Log-Likelihood ratio.* In this approach, an e-value can be constructed from the likelihood ratio statistic, which compares the likelihood of the observed data under the alternative hypothesis and under the null hypothesis. In the decision part, if the likelihood ratio has an expected value under the null hypothesis less than or equal to 1, it can qualify as an e-value. Furthermore, similar to above explanation, multiple testing with e-value when testing multiple hypotheses simultaneously, we can compute an e-value for each test based on the log-likelihood ratio. These e-values serve as the evidence measures against each null hypothesis. Lastly, to control error rates (like family-wise error rate or false discovery rate) across multiple tests, e-value can be combined or adjusted by using procedures analogous to those for p-value, but tailored for e-values.

As the advantages of using log-likelihood e-values is presented as follows. It is naturally interpretable as evidence ratios. It allows for anytime-valid inference, meaning that we can stop testing at any point without inflating error rates. Moreover, it can be more powerful and flexible than traditional p-value based methods, especially, in

sequential and adaptive testing contexts. Consequently, the e-value log-likelihood multiple testing procedure uses e-value derived from likelihood ratio as measure of evidence against null hypotheses in multiple testing scenarios. By leveraging the properties of e-value, this procedure controls error rates while allowing flexible, robust, and potentially more powerful inference compared to classical p-value based methods.

Numerical examples

We have conducted Monte Carlo simulations to examine proposed double machine learning methedology with 1000 iterations for each clustered data set. Table 1 indicates simulation and covariate dimension dim(X). The next column in the same table shows the integer K for K^2-fold cross fitting method. For this reason, we have proposed K = 2 and 3 in the simulations for the following results in Table 1, since 2^2 (≈ 5) and 3^2 (≈ 10) are close to the common numbers of folds used in cross fitting. The next column indicates the machine learning method for estimation of η where η shows nuisance parameter. Moreover, we have used the ridge methedology for double machine learning with clustered data. The other three columns of the table indicate Monte Carlo simulation statistics, involves the bias, standard deviation and root mean square error. For the purpose of the underlying effect of clustering assumptions. Furthermore, the number $K^2 = 4$ of folds of cross fitting is used for the zero- and one-way cluster robust DML, while the number $K^2 = 4$ of folds of two-way cross fitting is used for the two-way cluster robust DML. For each covariate dimension dim(X) ∈ {100,200}, for each choice K ∈ {2,3} for the number K^2 of multiway cross fitting, and for each of the three machine learning methods. According to simulation analysis when sample size increases, bias approximates to zero and standard deviation has the lowest value at optimal sample size where n=50 and p=100.

	Dim(X)	**Bias**	**Deviation**	**RMSE**	**Selected number of parameters by FDR**	**Selected number of variables by e-value**
n=50, p=50	100	0.0810	0.0800	0.0810	2	2
n=100, p=50	100	0.0970	0.0820	0.0780	3	3
n=50, p=100	100	0.0780	0.0580	0.0680	3	4
n=100, p=100	200	0.0912	0.0610	0.0510	3	4

Table 1: The bias, standard deviation and root means square error (RMSE) for double machine learning with multiway clustering with different number of observations (N) and the number of parameters (p) with ridge regression methodology under dimension of X (Dim(X)) to 100 and 200.

On the other side in Table 2 we have presented changes in bias standard deviation,RMSE under different N and p while ridge regression and lasso methedolody are implemented for double machine learning with clustered data.Hence,from compertaive analyses it is seen that the proposal strategy via DML with lasso methodology reduce standard error more than ridge models.

	Dim(X)	Bias	Deviation	RMSE	Selected number of parameters by FDR	Selected number of variables by e-value
n=50, p=50	100	0.0410	0.0400	0.0710	2	2
n=100, p=50	100	0.0570	0.0420	0.0680	2	3
n=50, p=100	100	0.0680	0.0380	0.0480	3	3
n=100, p=100	200	0.0812	0.0410	0.0410	3	4

Table 2: The bias, standard deviation and root means square error (RMSE) for double machine learning with multiway clustering with different number of observations (N) and the number of parameters (p) with lasso methodology under dimension of X (Dim(X)) to 100 and 200.

Hereby, we have applied e-value loglikelihood multiple testing procedure for double machine learning with multiway clustering. In the interpretation of Table 1, for illustration, it is seen that when the number of parameter is 50 and the number of observation is 50, e-value multiple testing procedure has selected two variables with associated e-values 1.89 and 3.78. Furthermore, when the number of parameters is 50 and the number of observations is 100, e-value multiple testing procedure has selected three variables with the following e-values: 1.66, 3.76 and 5.56. when the number of parameters is 100 and the number of observations is 50, e-value multiple testing procedure has selected three variables with the following e-values: 1.89, 2.79 and 4.34. Moreover, while the number of observations is 100 and the number of parameters is 100, e-value multiple testing procedure has selected four variables with the e-values 1.89, 2.56, 3.78 and 4.67.

CONCLUSION

In this work, we have suggested double machine learning procedure based on clustered data. Originally, this task can be computationally difficult. As an alternatibe solution of this problem, we have used double machine learning procedure with multiway clustering in the presence of multiway cluster sampled data, which is commonly used with real data sets. According to our small simulation analysis, we have seen that the proposed procedure has promising results to reduce standard error for finite sample performance under various multiway cluster sampling particularly for lasso methedology. Therefore, we have proposed e-value loglihood multiple testing procedure as alternative model selection procedure for double machine learning with clustered data while we have different number of obervations and number of parameters. The results have shown reduced standard error and reduced root mean square error, resulting in promising solution for the underlying challenge.

REFERENCES

Angrist, J. D., & Pischke, J. S. (2009). *Mostly harmless econometrics: An empiricist's companion*. Princeton university press.

Bach, P., Chernozhukov, V., Kurz, M. S., & Spindler, M. (2021). DoubleML--An Object-Oriented Implementation of Double Machine Learning in R. *arXiv preprint arXiv:2103.09603*.

Brueckner, M., Titman, A., & Jaki, T. (2019). Instrumental variable estimation in semi-parametric additive hazards models. *Biometrics*, *75*(1), 110-120.

Chernozhukov, V., Chetverikov, D., Demirer, M., Duflo, E., Hansen, C., Newey, W., & Robins, J. (2018). Double/debiased machine learning for treatment and structural parameters.

Chernozhukov, V., Hansen, C., Kallus, N., Spindler, M., & Syrgkanis, V. (2024). Applied causal inference powered by ML and AI. *arXiv preprint arXiv:2403.02467*.

Chiang, H. D., Kato, K., Ma, Y., & Sasaki, Y. (2022). Multiway cluster robust double/debiased machine learning. *Journal of Business & Economic Statistics*, *40*(3), 1046-1056.

Duan, B., Wasserman, L., & Ramdas, A. (2024). Interactive identification of individuals with positive treatment effect while controlling false discoveries. *Journal of Causal Inference*, *12*(1), 20230059.

Dukes, O., Vansteelandt, S., & Whitney, D. (2021). On doubly robust inference for double machine learning. *arXiv preprint arXiv:2107.06124*.

Fan, Q., & Zhong, W. (2018). Nonparametric additive instrumental variable estimator: A group shrinkage estimation perspective. *Journal of Business & Economic Statistics*, *36*(3), 388-399.

Fingerhut, N., Sesia, M., & Romano, Y. (2022). Coordinated Double Machine Learning. In *International Conference on Machine Learning* (pp. 6499-6513). PMLR.

Imbens, G. (2014). *Instrumental variables: an econometrician's perspective* (No. w19983). National Bureau of Economic Research.

Hansen, C., Hausman, J., & Newey, W. (2008). Estimation with many instrumental variables. *Journal of Business & Economic Statistics*, *26*(4), 398-422.

Kaygusuz, M. A., & Purutçuoğlu, V. (2023). Efficient multiple testing procedure for heterogeneous effect with survival forest. *ICFAS 2023 proceeding, Istanbul*.

Kaygusuz, M. A., & Purtutçuoğlu, V. Conditional randomization test of heterogeneus effect on biological networks with conformal inference.

Klyne, H., & Shah, R. D. (2023). Average partial effect estimation using double machine learning. *arXiv preprint arXiv:2308.09207*.

Li, J., Fine, J., & Brookhart, A. (2015). Instrumental variable additive hazards models. *Biometrics*, *71*(1), 122-130.

Newey, W. K., & Powell, J. L. (2003). Instrumental variable estimation of nonparametric models. *Econometrica*, *71*(5), 1565-1578.

Niu, Z., Chakraborty, A., Dukes, O., & Katsevich, E. (2024). Reconciling model-X and doubly robust approaches to conditional independence testing. *The Annals of Statistics*, *52*(3), 895-921.

Tchetgen, E. J. T., Walter, S., Vansteelandt, S., Martinussen, T., & Glymour, M. (2015). Instrumental variable estimation in a survival context. *Epidemiology (Cambridge, Mass.)*, *26*(3), 402.

Goeman, J., de Heide, R., & Solari, A. (2025). The e-Partitioning Principle of False Discovery Rate Control. *arXiv preprint arXiv:2504.15946*.

Xu, Z., & Ramdas, A. (2024, April). Online multiple testing with e-values. In *International Conference on Artificial Intelligence and Statistics* (pp. 3997-4005). PMLR.

Xu, Z., Wang, C., Wasserman, L., Roeder, K., & Ramdas, A. (2025). Active multiple testing with proxy p-values and e-values. *arXiv preprint arXiv:2502.05715*.

Vovk, V., & Wang, R. (2021). E-values: Calibration, combination and applications. *The Annals of Statistics*, *49*(3), 1736-1754.

Wang, R., & Ramdas, A. (2022). False discovery rate control with e-values. *Journal of the Royal Statistical Society Series B: Statistical Methodology*, *84*(3), 822-852.

Wang, L., Lin, Y., & Zhao, H. (2024). False Discovery Rate Control via Data Splitting for Testing-after-Clustering. *arXiv preprint arXiv:2410.06451*.

Wooldridge, J. M. (2016). *Introductory econometrics a modern approach*. South-Western cengage learning.

Wright PG (1928). *Tariff on Animal and Vegetable Oils*. Macmillan Company, New York.

ORAL PRESENTATION

STAT4 genindeki missense varyantların romatoid artrit üzerine olası etkilerinin biyoinformatik analizi

Deniz Aşlar Öner (*Orcid: https://orcid.org/ 0000-0002-9515-0073*)

Afyonkarahisar Sağlık Bilimleri Üniversitesi, Atatürk Sağlık Hizmetleri Meslek Yüksekokulu, Afyonkarahisar, Türkiye

*Sorumlu yazar e-mail: deniz.oner@afsu.edu.tr

Özet

Romatoid artrit (RA) patogenezinde kilit rol üstlenen *STAT4* geni, bağışıklık hücrelerinin aktivasyonu ve diferansiyasyonunda görev yapan temel bir transkripsiyon faktörüdür. Bu çalışma, *STAT4* geninde missense varyantların olası yapısal ve fonksiyonel sonuçlarını hesaplamalı biyoinformatik yöntemlerle değerlendirmeyi amaçlamıştır. *NCBI dbSNP* veritabanından elde edilen varyantlar, *SIFT, PolyPhen-2, I-Mutant, Project HOPE* ve *ConSurf* yazılımlarıyla analiz edilmiştir. Analizlerde altı missense varyantın (Ile115Val, Glu128Val, Thr446Ile, Ile244Met, Gln282His ve Ile80Met) zararlı etki potansiyeli taşıdığı öngörülmüştür. Evrimsel korunum analizine göre özellikle Ile115Val ve Thr446Ile değişimlerinin yüksek derecede korunmuş bölgelerde yer aldığı ve bu değişimlerin STAT4 proteininin stabilitesini olumsuz yönde etkileyebilecek yapısal değişikliklere neden olabileceği tahmin edilmiştir. Aynı zamanda GeneMANIA analizi, *STAT4*'ün *STAT1, STAT3, IL12RB2* ve *IFNGR1* genleriyle güçlü etkileşimler sergilediğini ve bu genlerin *JAK-STAT* sinyal yoluna bağlı biyolojik süreçlerde birlikte görev aldığını ortaya koymuştur. Elde edilen bulgular, *STAT4* varyantlarının protein fonksiyonu ve bağışıklık yanıtı üzerinde etkili olabileceğini göstermekte olup, gelecekteki deneysel araştırmalar için önemli ön bilgiler sunmaktadır.

Anahtar Kelimeler *STAT4*, Romatoid artrit, Tek nükleotid polimorfizmi, Biyoinformatik analiz

Bioinformatic analysis of the potential effects of missense variants in the *STAT4* gene on rheumatoid arthritis

Abstract

The *STAT4* gene, which plays a key role in the pathogenesis of rheumatoid arthritis (RA), is a key transcription factor involved in the activation and differentiation of immune cells. This study aimed to evaluate the potential structural and functional consequences of missense variants in *STAT4* using computational bioinformatics methods. Variants obtained from the *NCBI dbSNP* database were analyzed using *SIFT, PolyPhen-2, I-Mutant, Project HOPE,* and *ConSurf* software. Six missense variants (Ile115Val, Glu128Val, Thr446Ile, Ile244Met, Gln282His, and Ile80Met) were predicted to have deleterious effects. Evolutionary conservation analysis revealed that the Ile115Val and Thr446Ile substitutions, in particular, are located in highly conserved regions and are predicted to cause structural changes that could negatively affect the stability of the STAT4 protein. GeneMANIA analysis also revealed that *STAT4* exhibits strong interactions with *STAT1, STAT3, IL12RB2*, and *IFNGR1* genes, and that these genes are involved in biological processes related to the *JAK-STAT* signaling pathway. These findings suggest that *STAT4* variants may impact protein function and immune responses, providing important preliminary information for future experimental studies.

Keywords *STAT4*, Rheumatoid arthritis, Single nucleotide polymorphism, Bioinformatic analysis

GİRİŞ

Romatoid artrit (RA), ilerleyici sinovit ile karakterize olan otoimmün kökenli, kronik inflamatuvar bir eklem hastalığıdır. Bu süreç zamanla geri dönüşü olmayan kıkırdak ve kemik erozyonuna yol açarak eklem deformiteleri

ve fonksiyonel kayıplarla sonuçlanır (Jahid ve ark., 2023). Hastalığın gelişiminde genetik yatkınlık (özellikle *HLA-DRB1*) ve çevresel faktörlerin etkileşimi belirleyicidir. Genom çapında ilişkilendirme çalışmaları, RA patogenezinde *JAK/STAT*, NF-κB ve *MAPK* yollarının kritik rollerini ortaya koymuştur (Okada ve ark., 2014; Smolen ve ark., 2018).

RA patogenezinin temel özelliği, sinovyal hücreler tarafından TNF, IL-1 ve IL-6 gibi proinflamatuvar sitokinlerin aşırı üretimidir. Birçok çalışma, bu sitokinlerin *JAK-STAT* sinyal yolunu aktive ederek hastalığın sürekliliğini ve kronik inflamasyonu sürdürdüğünü göstermiştir (Xue ve ark., 2023). Bu sinyal yolunun önemli üyelerinden biri olan Signal Transducer and Activator of Transcription 4 (*STAT4),* özellikle *IL-12-STAT4* ekseni üzerinden bağışıklık yanıtının düzenlenmesinde kritik rol oynar. STAT4 aktivasyonu, Th1 ve Th17 hücre polarizasyonu, IFN-γ üretimi ve immün yanıtın amplifikasyonu süreçlerini destekler. Bu nedenle STAT4, RA patogenezinde inflamatuvar sitokin dengesizliğinin ve otoimmün yanıtın moleküler merkezinde yer almaktadır (Xia ve ark., 2024).

RA'da *STAT4* gen varyantlarının, özellikle IL-12 aracılı *JAK/STAT* sinyallemesinde rol oynayan mekanizmalar üzerindeki etkilerinin daha iyi anlaşılması, hastalığın genetik temellerinin aydınlatılmasına katkı sağlayabilir. Bu bağlamda, bu çalışmada *STAT4* genindeki amino asit değişimine yol açan tek nükleotid polimorfizm (SNP)'lerin, proteinin yapısal stabilitesi ve fonksiyonel bütünlüğü üzerindeki potansiyel etkilerinin biyoinformatik analizlerle değerlendirilmesi ve elde edilen bulguların romatoid artrit patogeneziyle olası ilişkilerinin incelenmesi amaçlanmıştır.

MATERYAL VE METOT

Bu çalışmada *STAT4* genine ait SNP, *NCBI dbSNP* (National Center for Biotechnology Information Single Nucleotide Polymorphism Database) veritabanından elde edilmiştir. Her bir varyanta ait amino asit değişimi, genetik konum ve mutasyon tipi kaydedilmiştir. İn silico analizlerin yürütülmesi için insan STAT4 proteininin FASTA formatındaki amino asit dizisi ve UniProtKB erişim numarası, ilgili UniProt veritabanından temin edilmiştir.

SNP'lerin proteinin yapısı ve işlevi üzerindeki olası etkilerini değerlendirmek için, açık erişimli biyoinformatik analiz platformları kullanılmıştır. *SIFT* ve *PolyPhen-2* programları, amino asit değişimlerinin proteinin fonksiyonel bütünlüğü üzerindeki olası etkilerini tahmin etmek için kullanılmıştır (Ng ve ark., 2003; Adzhubei ve ark., 2013). *I-Mutant* yazılımı, mutasyonların protein stabilitesi üzerindeki artırıcı veya azaltıcı etkilerini değerlendirmek üzere uygulanmıştır. Ayrıca, elde edilen varyantların üç boyutlu yapısal etkilerinin yorumlanması için *Project HOPE* aracı kullanılmış (Venselaar ve ark., 2010) ve mutasyon bölgelerinin evrimsel korunma düzeyleri *ConSurf web* sunucusu aracılığıyla analiz edilmiştir (Ashkenazy ve ark., 2016). Bunun yanı sıra, *STAT4* geninin diğer genlerle olan etkileşim ağlarını belirlemek amacıyla *GeneMANIA* yazılım aracı kullanılmıştır (Warde-Farley ve ark., 2010).

BULGULAR VE TARTIŞMA

STAT4 proteininin (UniProtKB: Q14765) kodlandığı *STAT4* geni (Gene ID: 6775) üzerinde yapılan veri tabanı taramalarında, toplam 82.160 varyant bulunduğu belirlenmiştir. Bu varyantların 742 tanesi amino asit değişimine neden olan missense tiptedir.

Bu varyantların protein yapısı ve fonksiyonu üzerindeki olası etkilerini değerlendirmek amacıyla *SIFT, PolyPhen-2, I-Mutant, Project HOPE* ve *ConSurf* yazılım araçları kullanılmıştır. Analizler sonucunda, tüm araçlar tarafından zararlı olarak tahmin edilen altı missense SNP belirlenmiştir: rs3024839 (Ile115Val), rs140675301 (Glu128Val), rs141331848 (Thr446Ile), rs557179689 (Ile244Met), rs755772067 (Gln282His) ve rs957846209 (Ile80Met) (Tablo 1).

Tablo 1. *STAT4* genindeki missense varyantların olası zararlı etkilerinin biyoinformatik analiz sonuçları

SNP ID	Amino Asit Değişimi	SIFT	PolyPhen-2	I-Mutant	RI
rs3024839	Ile115Val	Deleterious	Possibly damaging	Decrease	8
rs140675301	Glu128Val	Deleterious	Possibly damaging	Decrease	4
rs141331848	Thr446Ile	Deleterious	Probably damaging	Decrease	9
rs557179689	Ile244Met	Deleterious	Probably damaging	Decrease	5
rs755772067	Gln282His	Deleterious	Possibly damaging	Decrease	8
rs957846209	Ile80Met	Deleterious	Possibly damaging	Decrease	6

HOPE analizi sonucunda incelenen altı missense varyantın proteininin lokal konformasyonu, hidrofobik etkileşimleri ve domain yapısı üzerinde farklı düzeylerde değişimlere yol açtığı belirlenmiştir. Değişimlerin büyük kısmı, amino asit yan zincir hacmi ve polarite farklılıklarına bağlı olarak lokal stabilite azalması, hidrojen bağı bozulması veya dimerizasyon yüzeyinde yapısal uyumsuzluk ile ilişkilendirilmiştir (Tablo 2).

Tablo 2. *Project HOPE* analiziyle amino asit değişimlerinin değerlendirilmesi

SNP	Amino Asit Değişimi	Domain	Analiz Sonucu
rs3024839	Ile115Val	coiled-coil	Mutant kalıntı, orijinal kalıntıdan daha küçük olup proteinin hidrofobik çekirdeğinde boşluk oluşumuna neden olabilir. Bu kalıntı, protein aktivitesi açısından önemli bir domain içerisinde yer almaktadır.
rs140675301	Glu128Val	N-terminal coiled-coil	Glutamatın valin ile yer değiştirmesi negatif yük kaybına ve hidrofobikliğin artmasına yol açmaktadır. Bu değişim, çevredeki elektrostatik etkileşimleri etkileyebilir. Kalıntı, fonksiyonel öneme sahip bir domain içerisinde bulunmaktadır.
rs141331848	Thr446Ile	SH2 geçiş bölgesi	Treoninin izolösin ile yer değiştirmesi sonucu polar grubun kaybı meydana gelmiştir. Mutant kalıntı daha büyük ve hidrofobik olup, yakın temaslardaki etkileşimleri bozma potansiyeli taşımaktadır.
rs557179689	Ile244Met	DNA bağlanma domaini	İzolösin yerine daha büyük metiyonin kalıntısının geçmesi, yerel paketlenme yoğunluğunu etkileyebilir. Bu kalıntı, protein fonksiyonu açısından kritik bir bölge içerisinde yer almaktadır.
rs755772067	Gln282His	Linker domaini	Nötr bir kalıntı olan glutaminin, zayıf bazik özellikteki histidin ile değişimi yük dağılımında değişikliğe neden olmaktadır. İlgili kalıntı, diğer domainlerle temas hâlinde bulunan bir bölgededir.
rs957846209	Ile80Met	N-terminal	Metiyonin kalıntısı izolösinden daha büyük olup, yan zincir hacmindeki artış lokal esnekliği etkileyebilir. Bu kalıntı, aktiviteyle ilişkili bir domain içerisinde yer almaktadır.

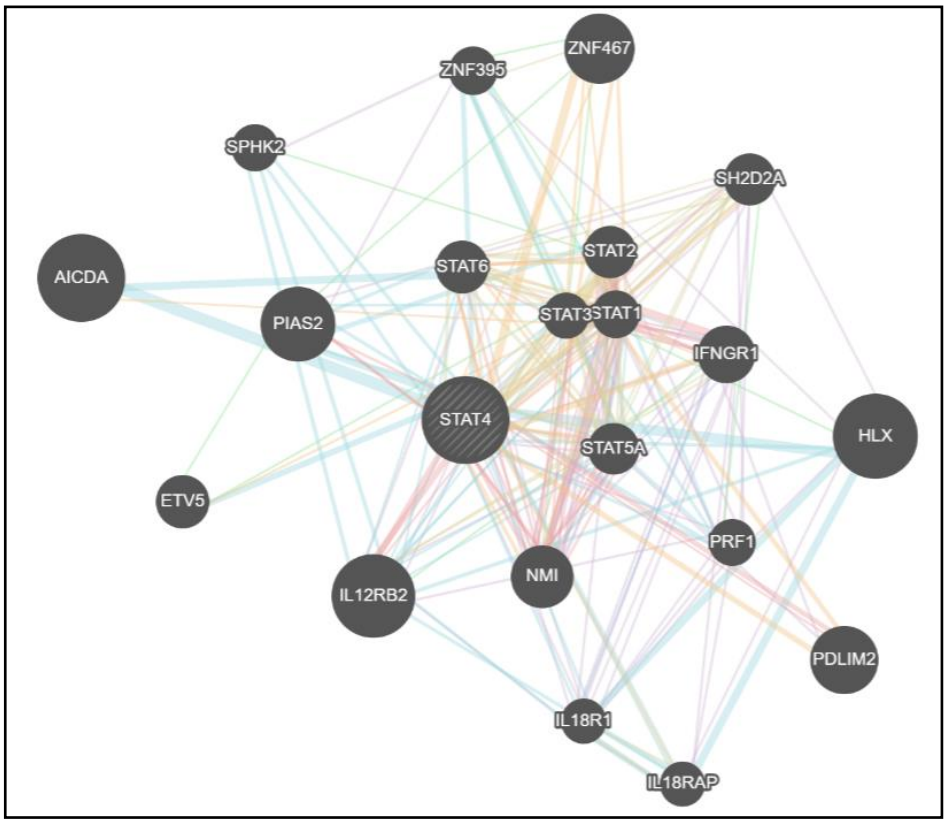
ConSurf analizine göre STAT4 proteininin Ile115Val ve Thr446Ile varyantları yüksek derecede korunum gösteren bölgelerde yer almaktadır. Bu bölgelerde meydana gelen amino asit değişimleri, proteinin yapısal ve fonksiyonel bütünlüğü açısından kritik öneme sahiptir. Ile115Val mutasyonu, coiled-coil domaininde yer alan hidrofobik çekirdek yapısında izolösinin daha küçük hacimli valinle yer değiştirmesi sonucu lokal hidrofobik etkileşimlerin zayıflamasına ve protein stabilitesinde azalmaya yol açabilir. Thr446Ile değişimi ise SH2 domainine yakın bölgede

gerçekleşmekte olup, treoninin hidroksil grubunun kaybı hidrojen bağı ağını zayıflatabilir ve bölgesel konformasyonel uyumsuzluklara neden olabilir. Bu nedenle her iki varyantın da STAT4 proteininin stabilitesi ve sinyal iletim etkinliği üzerinde olumsuz etkiler oluşturma potansiyeline sahip olduğu düşünülmektedir.



Şekil 1. STAT4 proteininin amino asit düzeyinde evrimsel korunum haritası

GeneMANIA yazılım aracı kullanılarak *STAT4* geninin fonksiyonel etkileşim ağı oluşturulmuştur. Analiz sonucunda *STAT4* geninin 20 farklı genle etkileşim içinde olduğu ve ağda toplam 21 gen ile 278 bağlantı bulunduğu belirlenmiştir. Bu ilişkilerin büyük çoğunluğunu fiziksel etkileşimler ve ko-ekspresyon temelli bağlantılar oluşturmaktadır. Ağın merkezinde *STAT4* yer almakta olup, *STAT1, STAT3, STAT5A, IL12RB2, IFNGR1, SH2D2A, PIAS2, HLX, IL18R1, IL18RAP, STAT2, STAT6, NMI, PRF1, AICDA, PDLIM2, ETV5, SPHK2, ZNF395* ve *ZNF467* genleriyle güçlü bağlantılar göstermektedir. Bu etkileşimler, *STAT4*'ün bağışıklık yanıtı ve sitokin aracılı sinyal süreçlerinde düzenleyici rol üstlenebileceğini düşündürmektedir.



Şekil 2. *GeneMANIA* tarafından oluşturulan *STAT4* gen-gen etkileşim ağı

SONUÇ

Bu çalışma, *STAT4* geninde amino asit değişimine yol açan varyantların proteinin yapısal stabilitesi ve fonksiyonel bütünlüğü üzerindeki potansiyel etkilerini hesaplamalı biyoinformatik yaklaşımlar kullanarak değerlendirmiştir. Yapılan analizler sonucunda, altı missense varyantın (rs3024839, rs140675301, rs141331848, rs557179689, rs755772067 ve rs957846209) STAT4 proteininin lokal konformasyonu, hidrofobik etkileşimleri ve domain organizasyonunu farklı düzeylerde etkileyebileceği öngörülmüştür. Özellikle yüksek korunum gösteren bölgelerde bulunan Ile115Val ve Thr446Ile değişimlerinin, protein stabilitesinde azalmaya ve sinyal iletim etkinliğinde zayıflamaya neden olabileceği tahmin edilmiştir.

GeneMANIA analizi, *STAT4*'ün *STAT1, STAT3, STAT5A, IL12RB2* ve *IFNGR1* genleriyle güçlü etkileşimler sergilediğini göstermiştir. Bu etkileşimler, *IL-12/IL-23/IFN-γ* aracılı *JAK-STAT* sinyal ağında *STAT4*'ün merkezi bir düzenleyici rol oynadığını desteklemektedir.

Elde edilen bulgular, *STAT4* genindeki yapısal varyasyonların bağışıklık yanıtının düzenlenmesi ve romatoid artrit patogenezinde rol oynayabilecek moleküler mekanizmalar hakkında ön bilgi sağlamaktadır. Bu sonuçlar, gelecekte yapılacak deneysel ve klinik doğrulama çalışmalarına yön verebilecek niteliktedir.

KAYNAKLAR

Adzhubei, I., Jordan, D. M., & Sunyaev, S. R. (2013). Predicting functional effect of human missense mutations using PolyPhen-2. Current Protocols in Human Genetics, 76(1), Unit 7.20.

Ashkenazy, H., Abadi, S., Martz, E., Chay, O., Mayrose, I., Pupko, T. & Ben-Tal, N. (2016). ConSurf 2016: an improved methodology to estimate and visualize evolutionary conservation in macromolecules. Nucleic Acids Research, 44(W1), W344–W350.

Jahid, M., Khan, K. U., Rehan-Ul-Haq, & Ahmed, R. S. (2023). Overview of Rheumatoid Arthritis and Scientific Understanding of the Disease. Mediterranean journal of rheumatology, 34(3), 284-291.

Ng, P.C., & Henikoff, S. (2003). SIFT: Predicting amino acid changes that affect protein function. Nucleic Acids Res, 31(13):3812-3814.

Okada, Y., Wu, D., Trynka, G., Raj, T., Terao, C., Ikari, K., Kochi, Y., Ohmura, K., Suzuki, A., Yoshida, S., & et al. (2014). Genetics of rheumatoid arthritis contributes to biology and drug discovery. Nature, 506(7488):376-81.

Smolen, J.S., Aletaha, D., Barton, A., Burmester, G.R., Emery, P., Firestein, G.S., Kavanaugh, A., McInnes, I.B., Solomon, D.H., Strand, V., & Yamamoto, K. (2018). Rheumatoid arthritis. Nat Rev Dis Primers, 4:18001.

Venselaar, H., te Beek, T.A.H., Kuipers, R.K.R., Hekkelman, M.L., & Vriend, G. (2010). Protein structure analysis of mutations causing inheritable diseases. An e-Science approach with life scientist friendly interfaces. BMC Bioinformatics, 11:548.

Warde-Farley, D., Donaldson, S.L., Comes, O., Zuberi, K., Badrawi, R., Chao, P., Franz, M., Grouios, C., Kazi, F., Lopes, C.T., Maitland, A., Mostafavi, S., Montojo, J., Shao, Q., Wright, G., Bader, G.D., & Morris, Q. (2010). The GeneMANIA prediction server: biological network integration for gene prioritization and predicting gene function. Nucleic Acids Res, 8(Web Server issue):W214-20.

Xia, Y., Xie, Y., Zhang, H. & Liu, L. (2024). STAT4 gene polymorphisms in human diseases. Front Immunol, 15:1479418.

Xue, C., Yao, Q., Gu, X., Shi, Q., Yuan, X., Chu, Q., Bao, Z., Lu, J., & Li, L. (2023). Evolving cognition of the JAK-STAT signaling pathway: autoimmune disorders and cancer. Signal transduction and targeted therapy, 8(1), 204.

ORAL PRESENTATION

Farklı gıdalardan elde edilen *A. flavus* izolatlarının genetik ve toksijenik profilinin incelenmesi

Berfin Sucu[1] (*ORCID: https://orcid.org/0000-0002-7500-903X*), Işıl Var[2*] (*ORCID: https://orcid.org/*0000-0002-0421-6330), Seda Yılmaz[3] (*ORCID: https://orcid.org/*0000-0002-5833-3639)

[1]Çukurova Üniversitesi, Fen Bilimleri Enstitüsü, Biyoteknoloji Anabilim Dalı, Adana, Türkiye
[*2]Çukurova Üniversitesi, Mühendislik Fakültesi, Gıda Mühendisliği Bölümü, Adana, Türkiye
[3]Çukurova Üniversitesi, Fen Bilimleri Enstitüsü, Biyoteknoloji Anabilim Dalı, Adana, Türkiye

*Sorumlu yazar e-mail: ivar@cu.edu.tr

Özet

Aspergillus flavus, gıda ve yemlerde aflatoksin kontaminasyonuna yol açan başlıca mikotoksijenik türlerden biridir. Geniş ekolojik adaptasyon kapasitesi ve yüksek toksijenik potansiyeli nedeniyle tropikal ve subtropikal bölgelerde halk sağlığı ve ekonomi açısından önemli bir risk oluşturmaktadır. Bu çalışmada, çeşitli gıda ürünlerinden izole edilen *A. flavus* suşlarının morfolojik ve moleküler karakterizasyonu ile aflatoksin üretim potansiyelleri değerlendirilmiştir. Toplam 100 gıda örneği beş farklı seçici besiyerinde [Potato Dextrose Agar (PDA), Chloramphenicol Glucose Agar (CGA), Dichloran Rose Bengal Chloramphenicol Agar (DRBC), Dichloran Glycerol Agar (DG18) ve Symphony Agar] kültüre edilmiştir. Bu besiyerlerinin birlikte kullanımı, türün morfolojik varyasyonlarını, sporulasyon yoğunluğu ve pigmentasyon gibi karakteristik özelliklerini gözlemleyerek izolasyon başarısını artırmayı hedeflemiştir. Çalışılan gıda örneklerinden (tahin helvası, kuru hurma, nohut unu ve mısır) izole edilen şüpheli beş *A. flavus* izolatının tür tayini ve filogenetik analizi için ITS ve β-tubulin gen bölgeleri amplifiye edilmiştir. Şüpheli *A. flavus* izolatlarının tür doğrulaması, ITS bölgesinin PCR ile çoğaltılmasının ardından *HhaI* restriksiyon enzimi kullanılarak gerçekleştirilen RFLP analiziyle desteklenmiştir. *A. flavus* izolatlarının ITS ve β-tubulin gen dizileri sekanslanmış, elde edilen diziler BLAST analiziyle GenBank veri tabanındaki referans *A. flavus* suşlarıyla karşılaştırılmış ve %99-100 oranında nükleotid benzerliği göstermiştir. Filogenetik ilişkiler, MEGA 12 yazılımı kullanılarak Maximum Likelihood yöntemi (1000 bootstrap) ile değerlendirilmiştir. Toksijenik potansiyelin belirlenmesi amacıyla *aflR*, *aflQ*, *aflO*, *aflP* ve *aflD* aflatoksin biyosentez genlerinin varlığı multiplex-PCR ile analiz edilmiştir. Tahin helvasından izole edilen *A. flavus*'ta düzenleyici gen olan *aflR* geni, kuru hurma ve nohut unundan izole edilen izolatlarda ise geç yol geni olan *aflQ* geni saptanmamıştır. Mısırdan izole edilen *A. flavus* izolatı ise tüm genler bakımından pozitif bulunmuş ve ELISA analizinde yalnızca bu izolatın aflatoksin B_1 (62,05 ppb) ürettiği tespit edilmiştir. Bulgular, farklı gıdalardan elde edilen *A. flavus* izolatlarının genetik ve toksijenik çeşitlilik gösterdiğini ve bölgesel gıda zincirlerinde aflatoksin riski açısından heterojen bir dağılım sergilediğini ortaya koymaktadır.

Anahtar Kelimeler: *Aspergillus flavus*, aflatoksin, PCR, ELISA, gıda güvenliği

Genetic and Toxigenic Profiling of *A. flavus* Isolates Obtained from Different Food Sources

Abstract

Aspergillus flavus is one of the major mycotoxigenic species responsible for aflatoxin contamination in food and feed. Due to its wide ecological adaptability and high toxigenic potential, it poses a significant risk to public health and the economy, particularly in tropical and subtropical regions. In this study, the morphological and molecular characterization of *A. flavus* strains isolated from various food products, as well as their aflatoxin production potentials, were evaluated. A total of 100 food samples were cultured on five different selective media [Potato Dextrose Agar (PDA), Chloramphenicol Glucose Agar (CGA), Dichloran Rose Bengal Chloramphenicol Agar (DRBC), Dichloran Glycerol Agar (DG18), and Symphony Agar]. The use of multiple culture media aimed to enhance isolation efficiency by observing morphological variations, sporulation density, and pigmentation

characteristics of the species. From the analyzed samples (tahin halva, dried date, chickpea flour, and maize), five presumptive *A. flavus* isolates were obtained. For species identification and phylogenetic analysis, the ITS and β-tubulin gene regions were amplified. The identification of *A. flavus* isolates was further confirmed by RFLP analysis, performed on the ITS region amplified by PCR using the *HhaI* restriction enzyme. The ITS and β-tubulin gene sequences of the isolates were sequenced, and BLAST analysis revealed 99-100% nucleotide similarity with reference *A. flavus* strains in the GenBank database. Phylogenetic relationships were evaluated using the Maximum Likelihood method (1000 bootstrap) implemented in the MEGA 12 software. To determine the toxigenic potential, the presence of the *aflR*, *aflQ*, *aflO*, *aflP*, and *aflD* genes involved in aflatoxin biosynthesis was analyzed by multiplex PCR. The regulatory gene *aflR* was not detected in the isolate obtained from tahin halva, while the late-pathway gene *aflQ* was absent in isolates from dried date and chickpea flour. The maize-derived isolate was positive for all targeted genes and was the only one found to produce aflatoxin B_1 (62,05 ppb) according to ELISA results. The findings indicate that *A. flavus* isolates obtained from different food sources exhibit genetic and toxigenic diversity, highlighting a heterogeneous distribution of aflatoxin risk across regional food chains.

Keywords: *Aspergillus flavus*, aflatoxin, PCR, ELISA, food safety

GİRİŞ

Funguslar doğada yaygın olarak bulunmakla birlikte, gıda üretim zincirinde kontaminant hâline geldiklerinde ciddi kalite ve güvenlik sorunlarına yol açmaktadır. Uygun koşullarda hızla çoğalarak gıdanın duyusal ve besinsel özelliklerini bozmakta ve mikotoksin oluşumuna neden olabilmektedirler (Maggon vd., 1977; Var ve Kabak, 2004). *Aspergillus* section *Flavi* üyelerinin (*A. flavus*, *A. parasiticus*, *A. nomius*, *A. niger*) trofofazdan idiyofaza geçişte üretilen ikincil metabolitler olup yüksek sıcaklık ve düşük su aktivitesine karşı dirençleri nedeniyle gıda güvenliği açısından büyük risk taşımaktadır (Bordin vd., 2014; Kale ve Bennet, 1992). Bu grup içerisinde yer alan aflatoksinler, *A. flavus*, *A. parasiticus* ve *A. nomius* gibi türler tarafından üretilen poliketid türevi toksinlerdir ve hepatokarsinojenik etkileri nedeniyle en tehlikeli mikotoksin gruplarından biri kabul edilmektedir (Benkerroum, 2019). Bu toksinlerin en bilinen analogları AFB_1, AFB_2, AFG_1 ve AFG_2'dir; bunlar arasında AFB_1, Uluslararası Kanser Araştırmaları Ajansı (IARC) tarafından Grup 1 karsinojen olarak sınıflandırılmıştır (IARC, 1993). Aflatoksin oluşumu, özellikle mısır, yer fıstığı, antepfıstığı, ayçiçeği, badem gibi yüksek yağ içeren ürünlerde daha sık gözlenmektedir (Bordin vd., 2014).

Aflatoksin üretimi, substrat bileşimi, sıcaklık, pH ve su aktivitesi gibi çevresel faktörlerden önemli ölçüde etkilenmektedir. *A. flavus*'un optimum gelişme sıcaklığının 28-30 °C, toksin üretim aralığının ise 24-35 °C arasında olduğu; ayrıca minimum su aktivitesi gereksiniminin 0.71-0.74, optimumun ise 0.98 a_w olduğu bildirilmektedir (Milani, 2013; Sanchis ve Magan, 2004). Türkiye'nin Akdeniz Bölgesi sıcak ve nemli iklimi, *Aspergillus* türlerinin gelişimi ve aflatoksin üretimi için elverişlidir. Adana ve çevresinde mısır, buğday ve yer fıstığı yoğun yetiştirilmektedir ve tahin helvası gibi yağlı tohum ürünlerinde *A. flavus* ve AFB_1 kontaminasyonu rapor edilmiştir (Var vd., 2007; Var vd., 2020).

Küf-maya sayımı ve izolasyonu, bakteriyel analizlere kıyasla daha uzun inkübasyon süreleri gerektirdiğinden gıda endüstrisinde hızlı ve güvenilir yöntemlere ihtiyaç duyulmaktadır (Taniwaki vd., 2001). *Aspergillus* türleri morfolojik özellikleriyle tanımlanabilse de (Klich, 2002), birçok türün fenotipik olarak birbirine son derece benzer olması tanımlamayı güçleştirmekte ve bu nedenle farklı besiyerlerinde izolasyon ve alt-kültürleme yapılması önerilmektedir. Literatürde *Aspergillus* ve diğer gıda kaynaklı küflerin ayrıntılı morfolojik tanımlamasında Czapek Yeast Extract Agar (CYA), Malt Extract Agar (MEA), Yeast Extract Sucrose (YES) Agar, Oatmeal Agar (OA), Potato Dextrose Agar (PDA) ve Dichloran Glycerol Agar (DG18) gibi birden fazla besiyerinin eş zamanlı kullanılmasının önerildiği birçok çalışma bulunmaktadır (Samson vd., 2005; Pitt ve Hocking, 2009; Samson vd., 2014). Farklı besiyerlerinin kullanılmasının bilimsel temeli, ortamların karbon/nitrojen oranı, su aktivitesi, ozmotik basınç, mineral bileşimi ve inhibitör maddeler açısından farklılık göstermesidir. Bu değişkenler, koloni rengi, doku yapısı, konidiasyon paterni, pigment oluşumu ve büyüme hızı gibi ayırt edici fenomenlerin her ortamda farklı şekillerde ortaya çıkmasına neden olmaktadır (Frisvad vd., 2007). Bu çok boyutlu yaklaşım, gıda matrislerinden izole edilen küflerin doğru şekilde tanımlanmasını sağlamakta; aynı zamanda potansiyel mikotoksijenik risklerin daha güvenilir biçimde değerlendirilmesine katkıda bulunmaktadır. Ayrıca uluslararası bir mikrobiyolojik standart olan ISO 21527-1:2008 ve ISO 21527-2:2008, gıdalarda küf-maya izolasyonunda ürünün su aktivitesine bağlı

olarak farklı besiyerlerinin kullanılmasını metodolojik bir gereklilik olarak tanımlamakta; bu yönüyle çoklu besiyeri yaklaşımının uygulamada da desteklendiğini göstermektedir (Anonim, 2008a; Anonim, 2008b).

Aspergillus'ların tür düzeyinde doğru tanımlamaları için moleküler DNA analizleri yaygın olarak kullanılmaktadır (Godet ve Munaut, 2010). Bu analizlerde; *Aspergillus* türlerinin Polimoreraz Zincir Reaksiyonu (PCR) ve Restriksiyon Parça Uzunluğu Polimorfizmi (RFLP) tabanlı tanımlamaları genellikle ITS, β-tubulin, 18S rDNA veya mitokondriyal DNA gibi bölgeler üzerine kuruludur (Rodrigues vd., 2007). Aflatoksin biyosentezi, *A. flavus* genomunda yaklaşık 75 kb'lik bir gen kümesi tarafından kodlanmaktadır ve bu kümede erken, orta ve geç yol genleri (örneğin *aflD*, *aflM*, *aflP*, *aflR*, *aflS*) yer almaktadır (Yu vd., 2004; Zeng vd., 2020). Aflatoksin biyosentez genlerini hedefleyen PCR yaklaşımları, özellikle toksijenik ve atoksijenik suşların ayrımında etkin bir strateji sunmaktadır (Somashekar vd., 2004; González-Salgado vd., 2008).

Bu çalışmada, Adana ve çevresinden temin edilen çeşitli gıda örnekleri küf izolasyonu için kullanılması önerilen beş farklı besiyeri (Potato Dextrose Agar, Sypmhony Agar, Dichloran Rose Bengal Chloramphenicol Glucose Agar, Dichloran Glycerol %18 Agar ve Chloramphenicol Glucose Agar) kullanılarak izolasyon performansları, izolat sayısı ve izolasyon süresi bakımından değerlendirilmiştir. Ardından PDA besiyerine ekilen gıdalardan izole edilen *Aspergillus flavus* üyelerinin morfolojik ve moleküler tanımlamaları yapılmış; ayrıca aflatoksin biyosentez genlerinin varlığı ve AFB_1 üretimi incelenmiştir. Böylece, bölgesel gıda ürünlerinde *A. flavus* kaynaklı aflatoksin kontaminasyon potansiyeli ortaya konulmuş ve aflatoksijenik-apatojenik izolat ayrımında genetik ve immünokimyasal düzeyde bir değerlendirme yapılmıştır.

MATERYAL VE YÖNTEM

MATERYAL

Bu çalışmada, Adana ve çevresinden rastgele örnekleme yöntemiyle temin edilen çeşitli gıda ürünleri (mısır, nohut unu, tahin helvası, kuru hurma, buğday unu, arpa, yulaf, çavdar, irmik, pirinç ve mısır gevreği) materyal olarak kullanılmıştır. Bu ürünlerden *Aspergillus flavus* izolatlarının elde edilmesi, moleküler karakterizasyonlarının yapılması ve izolatların aflatoksin üretim potansiyellerinin değerlendirilmesi amaçlanmıştır.

YÖNTEM

Gıdalardan Küf İzolasyonu

Küf izolasyonu için ISO 21527-1:2008 standardı temel alınmış ve özellikle düşük su aktivitesine sahip gıdalarda kullanılmaya uygun yöntemler tercih edilmiştir. Analize alınan her örnekten 10 g alınarak 90 ml steril peptonlu fizyolojik tuz çözeltisi (%0,1 pepton + %0,85 NaCl) ile karıştırılmış ve stomacher cihazında 2 dakika boyunca homojenize edilmiştir. Hazırlanan süspansiyondan uygun seri dilüsyonlar yapılarak, her dilüsyondan 0,1 ml örnek aşağıdaki beş farklı besiyerine (Dichloran Rose Bengal Chloramphenicol Agar (DRBC), Dichloran Glycerol 18% Agar (DG18), Potato Dextrose Agar (PDA), Chloramphenicol Glucose Agar (CGA), Symphony Agar (SA) yayma yöntemiyle ekilmiştir. Besiyerleri 25 ± 1 °C'de 5-7 gün inkübe edilmiştir. İnkübasyon süresi sonunda oluşan koloniler, koloni ve hücre morfolojisine göre tanımlanmıştır (Anonim, 2008a; Anonim, 2008b).

Küf İzolatlarının Morfolojik Olarak Tanımlanması

Küf izolasyonu yapılan örneklerden elde edilen izolatların tanımlanmasında kültürel ve morfolojik özellikler dikkate alınmıştır. Bu amaçla izolatlar Czapek Agar ve Malt Ekstrakt Agar (MEA) besiyerlerinde geliştirilmiş, koloni rengi, yapısı ve çapı, kolonin ters yüzeyindeki renk, konidiyal başlığın şekli, çapı ve rengi, konidyofor yapısı ile sterigmanın uniseriate veya biseriate dizilişi ve sklerot varlığı değerlendirilmiştir. İzolatlar, steril petrilere dökülen 15-20 ml Czapek Agar üzerinde tek spor izolasyonu şeklinde ekilmiş ve 25 °C'de 10-12 gün süreyle inkübe edilmiştir. Koloni büyüme hızı, 4. günden başlayarak 12. güne kadar ölçülmüştür. Miselyumun rengi ve yapısı ile kolonin ters yüzeyinde oluşan renk kaydedilmiş; konidiyal başlık, konidyofor ve sterigmanın morfolojisi mikroskobik inceleme ile değerlendirilmiştir. Ayrıca, sklerot varlığı veya yokluğu not edilmiştir. Tür tanımlamalarında Raper ve Fennell (1977), Samson ve Pitt (1990), Ruiqian vd. (2004), Rodrigues vd. (2007) ile Varga vd. (2011) tarafından önerilen tanı anahtarları esas alınmıştır.

Aspergillus İzolatlarının Moleküler Olarak Tanımlanması

Şüpheli beş *A. flavus* suşunun moleküler tanımlaması için ilk olarak, Fungi/Yeast Genomic DNA Isolation Kit (Norgen Biotek Corp.) kullanılarak DNA izolasyonu gerçekleştirilmiştir. Öncelikle, tek spor izolasyonu yapılarak her izolat PDA (Potato Dextrose Agar) besiyerine ekilmiş ve 25 °C'de 7 gün inkübe edilmiştir. Küf kolonisinden elde edilen miselyum ve sporlar steril şartlarda 1,5 mL eppendorf tüplerine aktarılmıştır. Pellet, kitin sağladığı liziz buffer ile çözündürülmüş ve boncuklar içeren filtre tüplerine aktarılmıştır. Örnekler maksimum hızda vortekslenip 65 °C'de ısıtıcı blokta inkübe edilerek hücre duvarının parçalanması sağlanmıştır. Boncuklar kısa bir spin ile dibe çöktürülmüş ve üstteki süpernatant yeni bir mikrosantrifüj tüpüne aktarılmıştır. Üst faza eş hacimde %96-100 etanol eklenip vortekslenmiş, ardından kitin bağlanma ve yıkama solüsyonlarıyla (wash solution A ve solution BX) işlem tekrarlanmıştır. Son aşamada DNA, elution buffer B kullanılarak filtre tüplerinden elüsyonla elde edilmiş ve -20 °C'de saklanmıştır. İzole edilen DNA, konsantrasyon ve saflık açısından NanoDrop spektrofotometre ile doğrulanmıştır.

PCR ile Şüpheli A. flavus Suşlarının Hedef Gen Bölgelerinin Çoğaltılması

Tür tanımlaması amacıyla ITS ve β-tubulin gen bölgeleri PCR ile çoğaltılmıştır. ITS bölgesi için ITS1/ITS4 (600 bp) (White vd., 1990), β-tubulin bölgesi için Tub-F/R (340 bp) (El Khoury vd., 2011) primerleri kullanılmıştır. Ayrıca aflatoksijenik özelliklerin değerlendirilmesi amacıyla *aflR* (999 bp), *aflQ* (1088 bp), *aflO* (1333 bp), *aflP* (1490 bp) ve *aflD* (990 bp) aflatoksin biyosentez genleri (Scherm vd., 2005) multiplex-PCR yöntemiyle incelenmiştir. Her PCR reaksiyonu 25 µL hacimde hazırlanmış, 1 µL genomik DNA, 12,5 µL Master Mix, 1 µL forward ve 1 µL reverse primer ile 9,5 µL ddH_2O içermiştir. PCR cihazında literatüre göre belirlenen döngü programları uygulanmış ve ürünler %1,5 agaroz jel elektroforezi ile doğrulanmıştır. Agaroz jel hazırlanırken 1,5 g agar 100 mL TBE tamponunda çözülmüş, 60 °C'ye soğutulduktan sonra 5 µL DNA boyası eklenmiştir. PCR ürünleri jele yüklenmiş ve 90 voltta 60 dakika elektroforez uygulanmıştır.

Şüpheli A. flavus Suşlarının RFLP Yöntemiyle Tanımlanması

Tür doğrulamasını desteklemek amacıyla ITS PCR ürünleri *HhaI* restriksiyon enzimi ile kesilmiştir (Krulj vd., 2020). Kesim reaksiyonu, 10 µL PCR ürünü, 2 µL 10x Fast Digest tampon, 2 µL Fast Digest enzimi ve 16 µL nuclease-free su ile hazırlanmış ve 37 °C'de 10 dakika inkübe edilmiştir. Oluşan restriksiyon fragmanları %2 agaroz jel elektroforezi ile görselleştirilmiştir.

Şüpheli A. flavus Hedef Gen Bölgelerinin Doğrulanması ve Filogenetik Çalışmalar

ITS ve β-tubulin PCR ürünleri Sanger sekanslama yöntemi ile özel bir firma tarafından dizilenmiştir. Her örnek için ileri ve geri yönlü diziler elde edilmiş, düşük kaliteli uç bölgeler manuel olarak çıkarılmış ve konsensüs diziler oluşturulmuştur. Konsensüs diziler CLUSTAL X (Chenna vd., 2003) programı ile çoklu hizalamaya tabi tutulmuş ve GenBank referans dizileriyle BLAST algoritması aracılığıyla karşılaştırılmıştır. Tür tanımlaması, %100 nükleotid benzerliğine sahip referans dizilere dayanarak yapılmıştır. *A. flavus* olarak tanımlanan izolatların β-tubulin ve ITS bölgesine ait DNA dizileri CLUSTAL X programı (Chenna vd., 2003) kullanılarak hizalanmış, ardından NCBI veri tabanından yüksek benzerlik gösteren beş *A. flavus*'un DNA dizileri ile Kimura 2-parameter (K2P) modeli kullanarak 1000 bootstrap tekrarıyla Maximum Likelihood yöntemi (Felsenstein, 1981) uygulanarak MEGA 12 yazılımı aracılığıyla filogenetik ağaçlar oluşturulmuştur.

Aflatoksin B_1 Üretiminin ELISA ile Değerlendirilmesi

Aflatoksijenik potansiyelin belirlenmesi amacıyla izolatlar MEA+S besiyerinde kültüre alınmıştır (Abbas vd., 2011). Katı besiyeri 22,5 g Malt Ekstrakt Agar ve %15 D-sükroz ile hazırlanmış, 121 °C'de sterilize edildikten sonra 50 mg/L kanamisin eklenmiştir. Ön kültür için izolatlar 3 mL MEA+S sıvı besiyerinde 25 °C'de bir gece inkübe edilmiş, ardından yaklaşık 15 mL katı besiyerine yayma yöntemiyle ekilmiş ve 25 °C'de 10 gün inkübe edilmiştir. Gelişen misel yapıları toplanıp tartılmış, biyokütleye orantılı olarak %70 metanol eklenmiş ve 4000 rpm'de 10 dakika santrifüj edilmiştir. Üst faz homojenize edilip Elabscience® Aflatoxin B_1 (AFB_1) ELISA kitine uygun şekilde analiz edilmiştir.

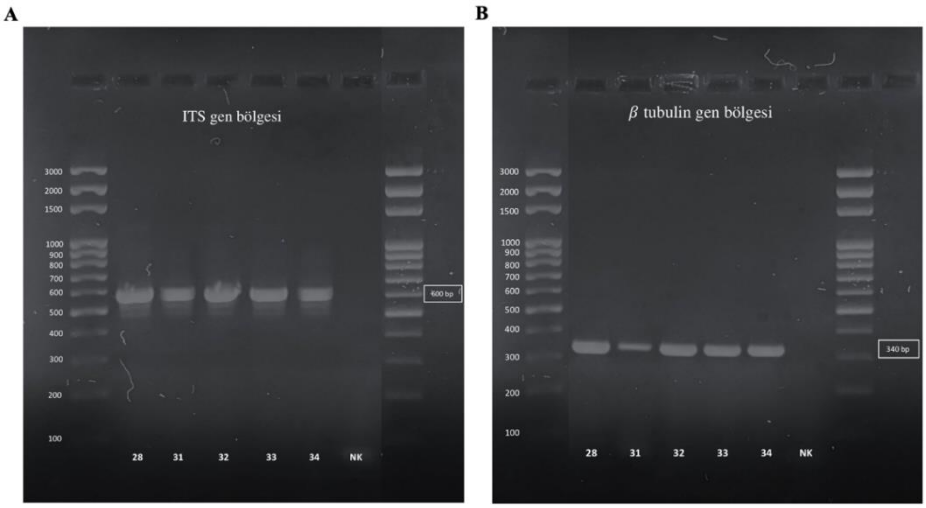
BULGULAR ve TARTIŞMA

Morfolojik Bulgular

Mısır, nohut unu, tahin helvası ve kuru hurma örneklerinden izole edilen *Aspergillus* izolatları, kültürel ve morfolojik özellikleri dikkate alınarak tür spesifik tanımlama anahtarları kullanılmış ve değerlendirilmiştir. Konidiyal başlık yapılarının, sterigma diziliminin, konidiyofor özelliklerinin ve sklerot varlığının tüm izolatlarda *A. flavus*'a özgü karakteristiklerle yüksek oranda örtüşmesi ile bu izolatlar *A. flavus* olarak tanımlanmıştır. *A. flavus* türü; genellikle yeşilimsi tonlarda, küresel veya yarı küresel yapıda konidiyal başlıklara (20-50 µm), biseriate (çift sıra) sterigma dizilimine, pürüzlü yüzeyli konidiyoforlara ve koyu renkli düzensiz sklerotlara sahip olmasıyla karakterize edilmektedir (Klich, 2002; Samson vd., 2014). Çalışmada incelenen beş izolatta bu özelliklerin tamamı tutarlı biçimde gözlenmiş ve izolatların koloni rengi, doku yapısı ve hava hifi oluşumu gibi kültürel özelliklerinin kullanılan besiyerine bağlı olarak değişiklik gösterdiği belirlenmiştir. Farklı besiyerlerinde (PDA, DRBC, DG18, CGA ve SA) gözlenen bu varyasyonlar, *A. flavus*'un besiyeri bileşimine duyarlı fenotipik çeşitliliğiyle uyumludur. Çalışma sonucunda, PDA ve CGA'da kahverengi-zeytin yeşili merkez ve çevresinde yoğun hava hifi oluşumu gözlenirken, DG18'de daha sarımsı bir merkez rengi dikkat çekmiştir.

Moleküler Bulgular

Bu çalışmada, şüpheli *A. flavus* izolatlarının tür düzeyinde tanımlanması amacıyla ITS ve β-tubulin gen bölgeleri PCR yöntemiyle çoğaltılmıştır. ITS (600 bp) bölgesi, fungus türlerinin moleküler tanımlamasında yaygın olarak kullanılan, evrimsel olarak korunmuş bir bölge olup (White vd., 1990); çalışmadaki 5 izolatın tamamında tek bir bant amplifiye edilmiştir. Tub gen bölgesi (340 bp), türler arası varyasyonu yansıttığı için filogenetik analizlerde önemli bir belirteç olarak değerlendirilmektedir (Glass ve Donaldson, 1995); bu çalışmada tüm izolatlarda başarılı amplifikasyon elde edilmiştir (Şekil 1).



Şekil 1. DNA izolasyonları yapılan 5 şüpheli *A. flavus* izolatının hedeflenen genleri olan A) ITS (600 bp), B) β-tubulin (340 bp) gen bölgelerinin PCR ürünlerinin DNA jel elektroforezi sonuçları (NK: negatif kontrol).

Toplamda beş *Aspergillus flavus* izolatı için hem ITS hem de β-tubulin gen bölgelerine ait yaklaşık 600 bp ve 340 bp uzunluğunda bantlar gözlemlenmiştir. Bu sonuçlar, amplifikasyon işleminin başarıyla gerçekleştiğini ve her iki gen bölgesinin tüm izolatlarda korunduğunu göstermektedir. Elde edilen bu veriler, mısır, nohut unu, kuru hurma ve tahin helvası örneklerinden izole edilen bu izolatların tür düzeyinde doğru şekilde tanımlandığını ve genetik olarak *A. flavus* ile yüksek oranda benzerlik gösterdiğini desteklemektedir. Ayrıca bu durum, kullanılan primer çiftlerinin *A. flavus* türünün spesifik bölgelerini hedeflemede etkin olduğunu ve ilerleyen filogenetik analizler için uygun bir temel oluşturduğunu ortaya koymaktadır. Samson vd. (2007) da ITS dizilerinin *Aspergillus* türlerinin hızlı ve doğru tanımlanmasında temel belirteç olarak kullanılabileceğini bildirmiştir.

A. flavus izolatlarının aflatoksijenik potansiyelini belirlemek amacıyla gerçekleştirilen multiplex-PCR analizlerinde *aflR*, *aflQ*, *aflO*, *aflP* ve *aflD* genlerinin varlığı izolatlara göre değişiklik göstermiştir (Tablo 1). Tahin helvası örneğinden elde edilen İzolat 28'de *aflR* geni saptanmamış olup diğer dört gen pozitif bulunmuştur. Kuru

hurmadan elde edilen İzolat 31 ile nohut unu kaynaklı İzolat 32 ve İzolat 33'te *aflQ* geni dışındaki tüm genler amplifiye edilmiştir. Mısır örneğinden izole edilen İzolat 34 ise beş genin tamamının pozitifliği ile dikkat çekmiş ve genetik olarak tam aflatoksijenik profil göstermiştir. Bu sonuçlar, çalışmada yer alan izolatların büyük çoğunluğunun aflatoksin biyosentez yolunda yer alan temel genleri taşıdığını ve potansiyel olarak AFB_1 üretme kapasitesine sahip olabileceğini göstermektedir.

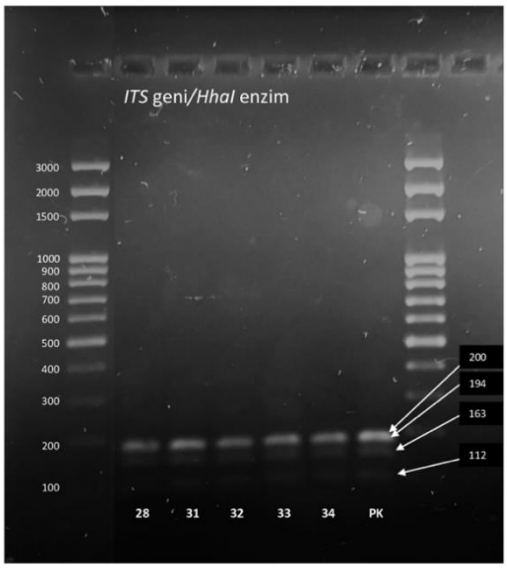
Tablo 1. *A. flavus* izolatlarının kaynak/bölge bilgileri ve bu izolatların aflatoksin biyosentez genlerinin (*aflR*, *aflD*, *aflP*, *aflO*, *aflQ*) klasik PCR sonuçları

***A. flavus* İzolatı**	**Kaynak/Ülke-Şehir**	***aflR***	***aflQ***	***aflO***	***aflP***	***aflD***
28	Tahin Helvası/Adana	-	+	+	+	+
31	Kuru Hurma/Mersin	+	-	+	+	+
32	Nohut unu/Mersin	+	-	+	+	+
33	Nohut unu/Mersin	+	-	+	+	+
34	Mısır/Adana	+	+	+	+	+

+: Gen varlığı pozitif (amplifikasyon gözlendi)
–: Gen varlığı negatif (amplifikasyon gözlenmedi)

Şüpheli A. flavus İzolatlarının RFLP Analiziyle Tanımlanması

ITS1/ITS4 primerleriyle çoğaltılan beş PCR ürününe *HhaI* restriksiyon enzimiyle PCR ürünlerinin belirli bölgelerinden kesim işlemi gerçekleştirilmiştir. ITS1/ITS4 primerleri ile çoğaltılan beş PCR ürününe uygulanan *HhaI* restriksiyon enzimi kesimi sonrası elde edilen DNA fragmanlarının %2'lik agaroz jel elektroforez görüntüleri Şekil 2'de gösterilmiştir.



Şekil 2. ITS1/ITS4 primerleri ile çoğaltılan beş PCR ürününe *HhaI* restriksiyon enzimiyle kesim sonuçlarının %2 agaroz jel elektroforez görüntüsü (PK: pozitif kontrol).

ITS gen bölgesinin *HhaI* restriksiyon endonükleazı ile kesilmesi, *Aspergillus* türleri arasında tür düzeyinde ayırt edici fragman desenlerinin oluşmasına olanak sağlamaktadır. Literatürde, *A. flavus* izolatlarının *ITS* bölgesinin *HhaI* enzimiyle sindirimi sonucunda yaklaşık 200 bp, 194 bp, 163 bp ve 112 bp uzunluklarında dört fragman elde edildiği bildirilmektedir (Krulj vd., 2020). Bu çalışmada da *ITS1/ITS4* primerleriyle çoğaltılan beş PCR ürününün *HhaI* enzimiyle kesimi sonucu benzer fragmentasyon profilleri gözlenmiştir (Şekil 2). Elde edilen bu bant desenleri, kesimin hedeflenen bölgelerde başarıyla gerçekleştiğini ve izolatların *A. flavus* türüne özgü karakteristik bir restriksiyon paterni sergilediğini göstermektedir. Bu bulgu, PCR-RFLP yönteminin morfolojik tanımlamayı destekleyen güvenilir bir moleküler doğrulama aracı olduğunu ortaya koymaktadır.

Literatürde yer alan verilerle karşılaştırıldığında, bu tez kapsamında elde edilen sonuçlar Krulj vd. (2020) tarafından bildirilen bulgularla yüksek oranda uyumluluk göstermiştir. Söz konusu çalışmada, farklı gıda kaynaklarından izole edilen *A. flavus* suşlarının *ITS* bölgesi PCR-RFLP yöntemiyle analiz edilmiş ve *HhaI* enzimiyle yapılan kesim sonrasında yaklaşık 200 bp, 194 bp, 163 bp ve 112 bp uzunluklarında dört belirgin fragmanın oluştuğu belirtilmiştir. Araştırmacılar, bu fragmentasyon modelinin *A. flavus* için karakteristik olduğunu ve yöntemin tür düzeyinde güvenilir bir şekilde ayırt edici olduğunu vurgulamıştır.

A. flavus İzolatlarının ITS ve β-tubulin Gen Bölgelerine Ait Dizileme ve Filogenetik Analiz Sonuçları

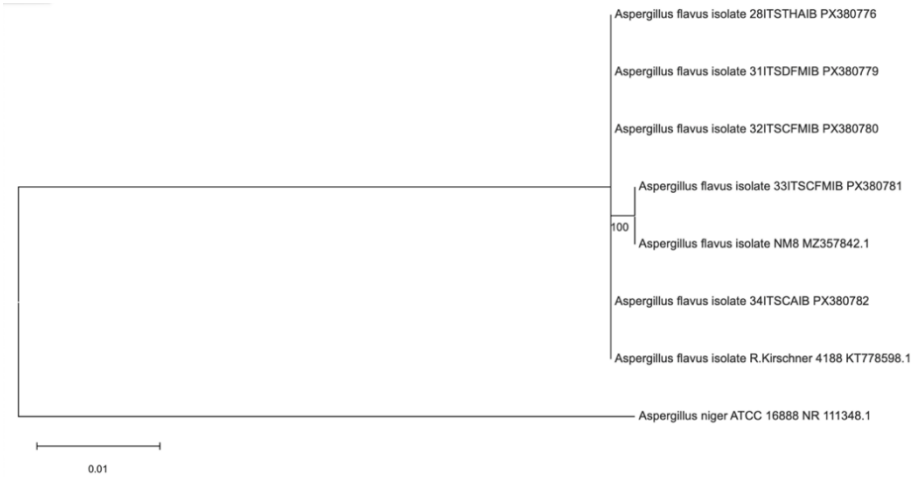
ITS ve β-tubulin gen bölgelerinde amplifikasyon gösteren beş *A. flavus* izolatı üzerinde özel bir firma tarafından dizileme analizleri gerçekleştirilmiştir. Hedeflenen gen bölgelerinin dizilenmesi, her bölgeye özgü ileri (forward) ve geri (reverse) primerler kullanılarak Sanger sekanslama yöntemiyle yapılmıştır. Elde edilen diziler Chromas yazılımı ile kontrol edilerek düşük kaliteli uç kısımlar temizlenmiş ve FASTA formatında kaydedilmiştir. Her örnek için elde edilen ileri ve geri yönlü diziler NCBI BLASTn aracı kullanılarak hizalanmış ve bu hizalamalardan konsensüs diziler oluşturulmuştur. Konsensüs diziler daha sonra CLUSTAL X (Chenna vd., 2003) programı kullanılarak çoklu hizalamaya tabi tutulmuş ve GenBank veri tabanındaki referans dizilerle karşılaştırılmıştır. Karşılaştırmalar sonucunda, izolatların tamamının %100 oranında benzerlik gösterdiği belirlenmiş ve bu değerler tür düzeyinde tanımlamada referans alınmıştır. Elde edilen sonuçlara göre, tüm diziler NCBI GenBank veri tabanına kaydedilerek erişim numaraları alınmıştır. BLAST analizinden elde edilen benzerlik oranları Tablo 2'de verilmiştir.

Tablo 2. *A. flavus* izolatlarına ait ITS gen bölgelerinin GenBank veri tabanında çıkan benzerlik oranları.

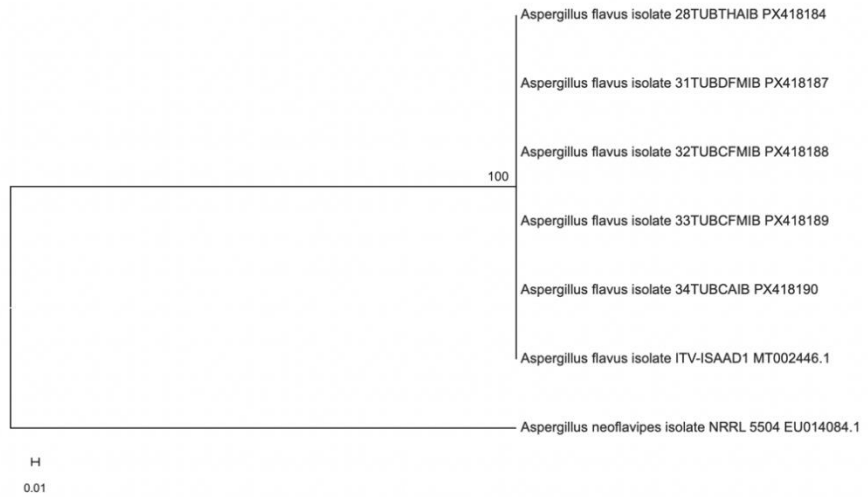
***A. flavus* İzolat No**	**Gen Bölgesi**	**İzolat Erişim Numarası**	**GenBank Referans İzolat**	**Benzerlik Oranı**	**Erişim Numarası**
28ITSTHAIB	ITS	PX380776	*Aspergillus flavus* isolate R. Kirschner 4188 18S ribosomal RNA gene, partial sequence…	100	KT778598.1
31ITSDFMIB	ITS	PX380779	*Aspergillus flavus* isolate R. Kirschner 4188 18S ribosomal RNA gene, partial sequence…	100	KT778598.1
32ITSCFMIB	ITS	PX380780	*Aspergillus flavus* isolate R. Kirschner 4188 18S ribosomal RNA gene, partial sequence…	100	KT778598.1
33ITSCFMIB	ITS	PX380781	*Aspergillus flavus* isolate NM8 small subunit ribosomal RNA gene, partial sequence…	100	MZ357842.1
34ITSCAIB	ITS	PX380782	*Aspergillus flavus* isolate R. Kirschner 4188 18S ribosomal RNA gene, partial sequence…	100	KT778598.1
28TUBTHAIB	β-tubulin	PX418184	*A.flavus* beta-tubulin gene, complete cds	100	M38265.1
31TUBDFMIB	β-tubulin	PX418187	*A.flavus* beta-tubulin gene, complete cds	100	M38265.1
32TUBCFMIB	β-tubulin	PX418188	*A.flavus* beta-tubulin gene, complete cds	100	M38265.1
33TUBCFMIB	β-tubulin	PX418189	*A.flavus* beta-tubulin gene, complete cds	100	M38265.1
34TUBCAIB	β-tubulin	PX418190	*A.flavus* beta-tubulin gene, complete cds	100	M38265.1

Bu çalışmada, beş *A. flavus* izolatın moleküler tanımlanmasında, ITS ve β-tubulin gen bölgelerine yönelik dizileme yapılmış ve bu izolatlar NCBI veri tabanındaki referans dizileriyle karşılaştırılmıştır. Yapılan dizileme analizleri sonucunda *A. flavus* benzerlik oranının %100 aralığında olduğu görülmüştür. Lavkor (2019) tarafından yapılan bir

çalışmada, Adana ve Osmaniye illerinden toplanan yerfıstığı örneklerinden izole edilen *A.* section *Flavi* üyeleri üzerinde yapılan moleküler tanımlamalar, β-tubulin gen bölgesi PCR ürünlerinin BLAST analizi yapılarak GenBank veri tabanıyla karşılaştırılması sonucunda, *A. flavus* ve *A. parasiticus* türlerine ait izolatların sırasıyla %89-100 ve %96-100 oranında benzerlik gösterdiğini bildirmiştir. Bu da β-tubulin gen bölgesinin *Aspergillus* türlerinin tanımlanmasında oldukça güvenilir bir genetik işaretleyici olduğunu ortaya koymaktadır. Bu tez çalışmasında *A. flavus* türünün GenBank veri tabanıyla karşılaştırılması sonucunda %100 benzerlik göstermesi, tür içi varyasyonun sınırlı olabileceğini düşündürmektedir. Lavkor (2019) çalışmasında, *A.* section *Flavi* üyesi izolatlar arasında *A. flavus* türünün en sık tespit edilen tür olduğunu belirtmiştir ve benzer şekilde bu tez çalışmasında da yoğun olarak *A. flavus* türü tespit edilmiştir. Sonuç olarak, bu çalışma, *A. flavus* türünün moleküler tanımlamasında ITS ve β-tubulin gen bölgeleri kullanılarak elde edilen dizileme sonuçlarının güvenilir olduğunu ortaya koymaktadır. Filogenetik ağaç oluşturulurken dış grup (outgroup) olarak, ITS bölgesine dayalı analizde *Aspergillus niger* ATCC 16888 (Şekil 3), β-tubulin bölgesine dayalı analizde ise *Aspergillus neoflavipes* isolate NRRL 5504 (EU014084.1) kullanılmıştır (Şekil 4).



Şekil 3. *A. flavus* izolatlarının genetik ilişkilerini ITS dizilerine dayanarak gösteren Maximum Likelihood filogenetik ağacı.



Şekil 4. *A. flavus* izolatlarının akrabalık derecelerini β-tubulin dizileri üzerinden Maximum Likelihood analizi ile ortaya koyan filogenetik ağaç.

A. flavus İzolatlarının Aflatoksin B_1 Üretiminin ELISA Yöntemi ile Değerlendirilmesi

Beş *A. flavus* izolatında aflatoksin üretim potansiyelinin belirlenmesi amacıyla gerçekleştirilen ELISA analizleri sonucunda, yalnızca mısır kaynaklı İzolat 34'te tespit limiti olan 0,15 ppb'nin üzerinde AFB_1 üretimi gözlenmiş

ve konsantrasyonun 62,05 ppb olduğu belirlenmiştir. Diğer dört izolatta ise aflatoksin miktarı tespit limitinin altında kalmıştır. Klasik PCR sonuçlarıyla birlikte değerlendirildiğinde, İzolat 34'ün *aflR*, *aflQ*, *aflO*, *aflP* ve *aflD* genlerinin tamamını taşıdığı ve yüksek aflatoksijenik potansiyel gösterdiği görülmüştür. Buna karşılık, bir veya birden fazla aflatoksin biyosentez geninde eksiklik bulunan İzolat 28, 31, 32 ve 33'ün AFB_1 üretmediği tespit edilmiştir. Bu bulgular, çalışmadaki *A. flavus* izolatlarının genetik olarak aflatoksijenik olsalar bile toksin üretim kapasitelerinin izolata özgü değişiklik gösterebildiğini ortaya koymaktadır.

SONUÇ

Bu çalışmada, farklı gıda ürünlerinden izole edilen *A. flavus* suşlarının morfolojik ve moleküler tanımlamaları ve toksijenik özellikleri değerlendirilmiştir. Farklı besiyerlerinde gözlenen fenotipik varyasyonlara rağmen konidiyal yapı, sterigma dizilimi ve sklerot oluşumu gibi ayırt edici özelliklerin tüm izolatlarda tutarlı biçimde görülmesi, bu izolatların *A. flavus* olarak sınıflandırılmasını güçlü biçimde desteklemektedir. Ayrıca birden fazla besiyerinin kullanılması, koloni rengi, doku yapısı ve hava hifi oluşumu gibi kültürel özelliklerin daha net ortaya çıkmasını sağlayarak tür tanımlamasında önemli bir avantaj sağlamıştır. Moleküler tanımlamada ITS ve β-tubulin gen bölgelerinin dizilenmesi sonucunda tüm izolatların *A. flavus* türüyle yüksek düzeyde (%100) benzerlik gösterdiği doğrulanmıştır. Filogenetik analizler, izolatların birbirleriyle yakın akrabalık ilişkileri olmakla birlikte, farklı gıdalardan elde edilen suşlar arasında belirgin genetik çeşitlilik olabileceğini göstermiştir. Multiplex-PCR ile gerçekleştirilen aflatoksin biyosentez gen analizi, çalışılan izolatların büyük bölümünde *aflR*, *aflO*, *aflP* ve *aflD* genlerinin varlığını ortaya koymuş, ancak bazı izolatlarda düzenleyici gen (*aflR*) veya geç yol genlerinden biri (*aflQ*) bulunmamıştır. Bu durum, gıda kaynaklı *A. flavus* popülasyonlarında aflatoksijenik kapasitenin genetik düzeyde heterojen olduğunu göstermektedir.

Toksijenik özelliklerin ELISA ile değerlendirilmesi, yalnızca mısırdan izole edilen suşun tespit limiti üzerinde (62,05 ppb) aflatoksin B_1 ürettiğini ortaya koymuştur. Diğer izolatlarda ise, aflatoksin biyosentez genlerinin çoğunun pozitif olmasına rağmen toksin üretimi tespit edilememiştir. Bu durum, aflatoksin üretim kapasitesinin yalnızca gen varlığına değil, aynı zamanda çevresel koşullara, suşların fizyolojik durumuna ve olası epigenetik düzenlemelere bağlı olarak değişebileceğini göstermektedir. Genel olarak, farklı gıda ürünlerinden elde edilen *A. flavus* izolatlarının hem genetik özellikleri hem de toksin üretim profilleri arasında önemli düzeyde çeşitlilik bulunduğu belirlenmiştir. Bu çeşitlilik, bölgesel gıda zincirlerinde aflatoksin riskinin tahmin edilmesi ve kontrol stratejilerinin geliştirilmesi açısından kritik bir öneme sahiptir.

TEŞEKKÜR

Bu çalışma Çukurova Üniversitesi Bilimsel Araştırma Projeleri Birimi (BAP) tarafından FDK-2023-16038 nolu proje kapsamında desteklenmektedir.

KAYNAKLAR

Anonim (2008a). ISO 21527-1:2008 Microbiology of food and animal feeding stuffs - Horizontal method for the enumeration of yeasts and moulds Part 1: Colony count technique in products with water activity greater than 0,95. s.8

Anonim (2008b) ISO 21527-2:2008 Microbiology of food and animal feeding stuffs - Horizontal method for the enumeration of yeasts and moulds Part 2: Colony count technique in products with water activity less than or equal to 0,95. s.8

Abbas, H. K., Zablotowicz, R. M., Horn, B. W., Phillips, N. A., Johnson, B. J., Jin, X., Abel, C. A. (2011). Comparison of major biocontrol strains of non-aflatoxigenic *Aspergillus flavus* for the reduction of aflatoxins and cyclopiazonic acid in maize. *Food Additives and Contaminants - Part A*, *28*(2), 198-208. https://doi.org/10.1080/19440049.2010.544680

Benkerroum, N. (2019). Retrospective and prospective look at aflatoxin research and development from a practical standpoint. *International Journal of Environmental Research and Public Health*, *16*(19), 3633. https://doi.org/10.3390/ijerph16193633

Bordin, K., Sawada, M. M., Rodrigues, C. E. da C., da Fonseca, C. R., Oliveira, C. A. F. (2014). Incidence of Aflatoxins in Oil Seeds and Possible Transfer to Oil: A Review. Içinde *Food Engineering Reviews* (C. 6, Sayı 1-2, ss. 20-28). Springer New York LLC. https://doi.org/10.1007/s12393-014-9076-9

Chenna, R., Sugawara, H., Koike, T., Lopez, R., Gibson, T. J., Higgins, D. G., Thompson, J. D. (2003). Multiple sequence alignment with the Clustal series of programs. *Nucleic Acids Research*, *31*(13), 3497-3500. https://doi.org/10.1093/nar/gkg500

El Khoury, A., Atoui, A., Rizk, T., Lteif, R., Kallassy, M., Lebrihi, A. (2011). Differentiation between *Aspergillus flavus* and *Aspergillus parasiticus* from Pure Culture and Aflatoxin-Contaminated Grapes Using PCR-RFLP Analysis of aflR-aflJ Intergenic Spacer. *Journal of Food Science*, *76*(4), M247-M253. https://doi.org/10.1111/J.1750-3841.2011.02153.X

Felsenstein, J. (1981). Evolutionary trees from DNA sequences: A maximum likelihood approach. *Journal of Molecular Evolution*, *17*(6), 368-376. https://doi.org/10.1007/BF01734359/METRICS

Frisvad, J. C., Larsen, T. O., De Vries, R., Meijer, M., Houbraken, J., Cabañes, F. J., Ehrlich, K., Samson, R. A. (2007). Secondary metabolite profiling, growth profiles and other tools for species recognition and important *Aspergillus* mycotoxins. *Studies in mycology*, *59*, 31-37. https://doi.org/10.3114/SIM.2007.59.04

Glass, N. L., Donaldson, G. C. (1995). Development of primer sets designed for use with the PCR to amplify conserved genes from filamentous ascomycetes. *Applied and Environmental Microbiology*, *61*(4), 1323-1330. https://doi.org/10.1128/AEM.61.4.1323-1330.1995,

Godet, M., Munaut, F. (2010). Molecular strategy for identification in *Aspergillus* section *Flavi*. *FEMS Microbiology Letters*, *304*(2), 157-168. https://doi.org/10.1111/j.1574-6968.2009.01890.x

González-Salgado, A., González-Jaén, T., Vázquez, C., Patiño, B. (2008). Highly sensitive pcr-based detection method specific for *Aspergillus flavus* in wheat flour. *Food Additives and Contaminants - Part A Chemistry, Analysis, Control, Exposure and Risk Assessment*, *25*(6), 758-764. https://doi.org/10.1080/02652030701765715

Hocking, A. D., Pitt, J. I. (1980). Dichloran-glycerol medium for enumeration of xerophilic fungi from low-moisture foods. *Applied and environmental microbiology*, *39*(3), 488-492. https://doi.org/10.1128/AEM.39.3.488-492.1980

IARC. (1993). *Some Naturally Occurring Substances: Food Items and Constituents, Heterocyclic Aromatic Amines and Mycotoxins.* (C. 56).

Kale, S. P., Bennet, J. W. (1992). Strain instability in filamentous fungi. *Mycotoxins in Ecological Systems*, *5*, 311-331.

Klich, M. A. (2002). *Indentification of common Aspergillus species*.

Krulj, J., Ćurčić, N., Bočarov Stančić, A., Kojić, J., Pezo, L., Peić Tukuljac, L., Bodroža Solarov, M. (2020). Molecular identification and characterisation of *Aspergillus flavus* isolates originating from serbian wheat grains. *Acta Alimentaria*, *49*(4), 382-389. https://doi.org/10.1556/066.2020.49.4.3

Lavkor, I. (2019). Yerfıstığından İzole Edilen *Aspergillus* section *Flavi* Türlerinin Tanımlanması ve Mikotoksijenik Özelliklerinin Belirlenmesi. *Akademik Gıda*, *17*(4), 450-457. https://doi.org/10.24323/akademik-gida.667256

Maggon, K. K., Gupta, S. K., Venkitasubramanian, T. A. (1977). Biosynthesis of Aflatoxmns. Içinde *BACTERIOLOGICAL REVIEWS* (C. 41, Sayı 4). https://journals.asm.org/journal/br

Milani, J. M. (2013). Ecological conditions affecting mycotoxin production in cereals: a review. *Veterinární medicína*, *58*(8), 405-411. https://doi.org/10.17221/6979-VETMED

Pitt, J. I., Hocking, A. D. (2009). Fungi and food spoilage. *Fungi and Food Spoilage*, 1-519. https://doi.org/10.1007/978-0-387-92207-2/COVER

Raper, K. B., Fennell, D. (1977). *The Genus Aspergillus.* Robert E. Krieger Publishing Company. https://www.scirp.org/reference/referencespapers?referenceid=3976442

Rodrigues, P., Soares, C., Kozakiewicz, Z. (2007). Identification and characterization of *Aspergillus flavus* and aflatoxins. Içinde A. Méndez-Vilas (Ed.), *Communicating Current Research and Educational Topics and Trends in Applied Microbiology* (ss. 527-534). Formatex Research Center. https://repositorium.sdum.uminho.pt/handle/1822/7565

Ruiqian, L., Qian, Y., Thanaboripat, D., Thansukon, P. (2004). Biocontrol of *Aspergillus flavus* and Aflatoxin Production. *Kmitl Science Journal*, *4*(1), 238-250.

Samson, R. A., Hoekstra, E. S., Frisvad, J. C. (2005). *Introduction to food- and airborne fungi.* (R. A. Samson, E. S. Hoekstra, J. C. Frisvad, Ed.; 7. bs). Centraalbureau voor Schimmelcultures (CBS).

Samson, R. A., Pitt, J. I. (1990). *Modern Concepts in Penicillium and Aspergillus Classification*. Springer US. https://doi.org/10.1007/978-1-4899-3579-3

Samson, R. A., Visagie, C. M., Houbraken, J., Hong, S. B., Hubka, V., Klaassen, C. H. W., Perrone, G., Seifert, K. A., Susca, A., Tanney, J. B., Varga, J., Kocsubé, S., Szigeti, G., Yaguchi, T., Frisvad, J. C. (2014). Phylogeny, identification and nomenclature of the genus *Aspergillus*. *Studies in mycology*, *78*(1), 141-173. https://doi.org/10.1016/J.SIMYCO.2014.07.004

Sanchis, V., Magan, N. (2004). Environmental conditions affecting mycotoxins. Içinde *Mycotoxins in Food* (ss. 174-189). Elsevier. https://doi.org/10.1533/9781855739086.2.174

Scherm, B., Palomba, M., Serra, D., Marcello, A., Migheli, Q. (2005). Detection of transcripts of the aflatoxin genes *aflD*, *aflO*, and *aflP* by reverse transcription-polymerase chain reaction allows differentiation of aflatoxin-producing and non-producing isolates of *Aspergillus flavus* and *Aspergillus parasiticus*. *International Journal of Food Microbiology*, *98*(2), 201-210. https://doi.org/10.1016/j.ijfoodmicro.2004.06.004

Somashekar, D., Rati, E. R., Chandrashekar, A. (2004). PCR-restriction fragment length analysis of *aflR* gene for differentiation and detection of *Aspergillus flavus* and *Aspergillus parasiticus* in maize. *International Journal of Food Microbiology*, *93*(1), 101-107. https://doi.org/10.1016/j.ijfoodmicro.2003.10.011

Taniwaki, M. H., Da Silva, N., Banhe, A. A., Iamanaka, B. T. (2001). Comparison of Culture Media, Simplate, and Petrifilm for Enumeration of Yeasts and Molds in Food. *Journal of Food Protection*, *64*(10), 1592-1596. https://doi.org/10.4315/0362-028X-64.10.1592

Var, I.,Kabak, B. (2004). Removal of aflatoxins by viable and heat-killed lactic acid bacteria and bifidobacteria. *ARCHIV FUR LEBENSMITTELHYGIENE*, *55*(5), 106-109.

Var, I., Kabak, B., Gök, F. (2007). Survey of aflatoxin B1 in helva, a traditional Turkish food, by TLC. *Food Control*, *18*(1), 59-62. https://doi.org/10.1016/J.FOODCONT.2005.08.008

Var, I., Uzunlu, S., Maviş, F. G. (2020). Microbial quality of a confection (Tahini Halva) manufactured in Turkey. *Journal of Food Safety and Food Quality-Archiv für Lebensmittelhygiene 2020, 71(5), 124-128*, *71*(5), 124-128. https://doi.org/10.2376/0003-925X-71-124

Varga, J., Frisvad, J. C., Samson, R. A. (2011). Two new aflatoxin producing species, and an overview of *Aspergillus* section *Flavi*. *Studies in Mycology*, *69*, 57-80. https://doi.org/10.3114/sim.2011.69.05

White, T. J., Bruns, T., Lee, S., Taylor, J. (1990). Amplification and Direct Sequencing of Fungal Ribosomal RNA Genes for Phylogenetics. Içinde *PCR Protocols* (ss. 315-322). Elsevier. https://doi.org/10.1016/b978-0-12-372180-8.50042-1

Yu, J., Chang, P. K., Ehrlich, K. C., Cary, J. W., Bhatnagar, D., Cleveland, T. E., Payne, G. A., Linz, J. E., Woloshuk, C. P., Bennett, J. W. (2004). Clustered Pathway Genes in Aflatoxin Biosynthesis. Içinde *Applied and Environmental Microbiology* (C. 70, Sayı 3, ss. 1253-1262). https://doi.org/10.1128/AEM.70.3.1253-1262.2004

Zeng, H., Cai, J., Hatabayashi, H., Nakagawa, H., Nakajima, H., Yabe, K. (2020). Vera gene is involved in the step to make the xanthone structure of demethylsterigmatocystin in aflatoxin biosynthesis. *International Journal of Molecular Sciences*, *21*(17), 1-23. https://doi.org/10.3390/ijms21176389

ORAL PRESENTATION

*Capnodis tenebricosa'*nın (Olivier, 1790) (Coleoptera: Buprestidae) biyolojik mücadele ajanı olarak değerlendirilmesi

Üzeyir Çağlar[1*] (*Orcid: https://orcid.org/0000-0002-8401-0155*)

[*1] Gazi Üniversitesi Sağlık Hizmetleri Meslek Yüksekokulu, Ankara, Türkiye

*Sorumlu yazar e-mail: ucaglar@gazi.edu.tr

Özet

Buprestidae familyasına ait *Capnodis* cinsinin bazı türlerinin larvaları canlı dokularda gelişerek kültürü yapılan pek çok ağaçta, orman ve süs bitkisi ağaç ve ağaççıklarında önemli zararlar yapmaktadırlar. *Capnodis* türleri meyve ve bağ zararlısı olarak bilinir.

Tarımsal üretim alanlarında kültür bitkilerinin dışında doğal olarak kendiliğinden yetişen tüm bitkilere tarla yabancı otları adı verilmektedir. Bu bitkiler, tarımı yapılan bitkilerin, kalitesine ve ürün miktarına olumsuz etki eden en önemli faktörlerden biri olarak kabul edilir. Yabancı otlar, tarım bitkilerinin ekolojik gereksinimleri olan ışığına, besin elementlerine ve suyuna ortak olmaktadır. Bu durum tarımı yapılan bitkilerin gelişimi olumsuz etkiler ve ürünün kalitesi ile ürün miktarı düşer.

Durum biyoçeşitlilik açısından ele alındığında ise tarla yabancı otları ülkelerin biyolojik zenginlikleridir. Bu bitkilerden gereğince yararlanılması ve zararlarından korunabilmesi için bunların her türlü sistematik, morfolojik ve üreme özellikleri gibi biyolojik özelliklerinin bilinmesi gereklidir.

Biyolojik mücadelenin amacı, yabancı otların eradikasyonu değil, ancak populasyon ekolojisi prensiplerine dayanarak, yabancı ot yoğunluğunu hoşgörü eşiği altında tutmaktır.

Yabancı otların kontrolünde son yıllarda yaşanan direnç problemleri, araştırmacıların doğal ve sürdürülebilirliği olan biyolojik mücadele gibi alternatif yöntemlere olan ilgisini artırmıştır.

Rumex crispus L. (Kıvırcık kuzukulağı) (Polygonaceae), tohum ve kazık kökün en üst kısmındaki tomurcuklardan gelişen sürgünlerle çoğalan çok yıllık bir bitkidir; Ülkemizde şeker pancarı ve ayçiçeği de dahil olmak üzere birçok ürünü istila eder. Hasat sırasında tohumları buğday tohumlarını kirleterek tane kalitesini düşürür.

Avrupa ülkeleri ve İtalya'da yapılan çalışmalarda *Rumex* bitkisi üzerinde yaklaşık 200 böcek türü gözlenmiştir. Gözlenen bazı böcek türlerinin *Rumex*'in biyolojik kontrolünde kullanılabilme potansiyeline sahip oldukları belirlenmiştir.

2025 yılında arazi çalışmalarında Buprestidae familyasından *Capnodis* cinsine ait *Capnodis tenebricosa* türünün ergin bireyleri *Rumex crispus* L. (Kıvırcık kuzukulağı) bitkisi üzerinde dinlenme ve beslenme faaliyetlerini yaparken gözlenmiştir. *Rumex crispus* bitkisinin gövdesi içinde yaprak sürgününün olduğu kısımda *Capnodis tenebricosa* larvalarına rastlanmıştır.

Capnodis türleri; ormancılık ve zirai açıdan ağaçlarda zararlı türler olarak kabul edilmektedir. Yapılmış olan çok sayıdaki bilimsel çalışmalarda bu durum açıkça ifade edilmektedir. Bu durumun aksine Buprestidae familyasından bazı türler biyolojik mücadelede ajan olarak kullanılmaktadır. Bu çalışmada *Capnodis tenebricosa* türü tarımsal alanlarda istilacı tür olarak bilinen *Rumex crispus* için Biyolojik mücadele ajanı olarak düşünülmektedir.

Keywords: Buprestidae, *Capnodis tenebricosa,* biyolojik kontrol ajanı, *Rumex crispus*

GİRİŞ

Türkiye, bulunduğu konumu ve farklı ekosistemlere sahip olması nedeniyle biyolojik çeşitlilik açısından son derece zengindir (Önen & Özcan, 2010). Buprestidae familyası tür sayısı bakımından Coleoptera takımının en büyük 8 familyasından birisidir ve Dünya'da 15 000 civarında türü bilinmektedir (Muskovits ve Hegyessy, 2002; Booth ve ark., 1990). *Capnodis* cinsinin Dünyada 18 türü, (Obenberger, 1926), Palearktik bölgede 15 türü vardır (Löbl ve Smetana, 2006). Türkiye'de ise bu cinsin 10 türü bulunmaktadır (Lodos ve Tezcan, 1992; Löbl ve Smetana, 2006).

Capnodis türleri genellikle 20 °C'nin altındaki ve 40 °C'nin üzerindeki sıcaklıklarda hareketsiz ya da çok az hareketlidirler (Akman ve San, 1975; Erdem ve Çanakçıoğlu, 1977; Bily, 1982; Donald ve ark., 1989; Booth ve ark., 1990; Lodos ve Tezcan, 1995; Kaya, 1999; Muskovits ve Hegyessy, 2002; Kaygın, 2007).

Buprestidae familyasına ait *Capnodis* cinsinin bazı türlerinin larvaları canlı dokularda gelişerek kültürü yapılan pek çok ağaçta, orman ve süs bitkisi ağaç ve ağaççıklarında önemli zararlar yapmaktadırlar (Tezcan, 1990; Lodos ve Tezcan, 1995). *Capnodis* türleri meyve ve bağ zararlısı olarak bilinir (Yaşar 1996).

Capnodis miliaris türü çeşitli kavak ve söğüt türlerinde zararlıdır (Kaygın, 2007). Kiraz yetiştirilen alanlarda ise *Capnodis tenebrionis* ve *Capnodis carbonaria* türlerinin zararlarından bahsedilmektedir (Tezcan, 1990).

Capnodis tenebrionis türü taş çekirdekli meyve bahçelerinde önemli bir zararlıdır. Bu türün erginleri yumurtalarını ağacın çeşitli bölgelerine bırakır. Yumurtadan çıkan larvalar özellikle köklerde ve ağaç gövdelerinde galeriler oluşturarak ağaçların ölümüne ve verim kaybına neden olabilir. Bu zararlının İspanya, İtalya, Türkiye, İran, Suriye, Kuzey Afrika, İsrail, Fransa ve Filistin'de görüldüğü bildirilmiştir (David'yan, 2003; Abu Jbara, 2005; Booth ve ark., 1990; Bonsignore ve ark., 2008; Şahin ve Gözel, 2017; Tüzün, 1975; Grasselly ve Crossa-Rayaud, 1980; Zobar ve ark., 2019; Marannino ve de Lillo, 2005).

Tarımsal üretim alanlarında kültür bitkilerinin dışında doğal olarak kendiliğinden yetişen tüm bitkilere tarla yabancı otları adı verilmektedir (Türe ve Köse, 2000). Yabancı otlar tarımı yapılan bitkilerin kalitesine ve ürün miktarına olumsuz etki eden en önemli faktörlerden biri olarak kabul edilir (Türe ve Köse, 2000).

Yabancı otlar, tarım bitkilerinin ekolojik gereksinimleri olan ışığına, besin elementlerine ve suyuna ortak olmaktadır. Bu durum tarımı yapılan bitkilerin gelişimi olumsuz etkiler ve ürünün kalitesi ile ürün miktarı düşer. (Türe ve Köse, 2000; Uluğ ve ark., 1993; Özer, 1993). Türkiye'de yabancı otlardan meydana gelen verim kaybı %20 ile %50 arasında değişmektedir (Uluğ ve ark., 1993; Özer, 1993).

Durum biyoçeşitlilik açısından ele alındığında ise tarla yabancı otları ülkelerin biyolojik zenginlikleridir (Söker ve ark., 2012). Ülkemiz sahip olduğu coğrafik konum ve elverişli iklim sayesinde biyololik çeşitlilik açısından çok zengin bir flora ve faunaya sahiptir. Bu çeşitlilik bitkisel üretim alanlarında önemli bir sorun olan yabancı otları da kapsamaktadır (Uygur ve Uygur, 2010). Bu bitkilerden gereğince yararlanılması ve zararlarından korunabilmesi için bunların her türlü sistematik, morfolojik ve üreme özellikleri gibi biyolojik özelliklerinin bilinmesi gereklidir (Söker ve ark., 2012).

Yabancı otların kontrolünde son yıllarda yaşanan problemler, araştırmacıların doğal ve sürdürülebilir olan biyolojik mücadele gibi alternatif yöntemlere olan ilgisini artırmıştır (Sırrı ve Özaslan, 2024). Yabancı otlarla biyolojik mücadele; genellikle potansiyel doğal düşman olabilen eklem bacaklılar (böcekler ve akarlar), bitki patojenleri (mantarlar, bakteriler, virüsler ve nematodlar), balıklar, kuşlar ve diğer hayvan türleri kullanılarak, yabancı ot popülasyon ve yoğunluğunu kontrol altına alınması veya baskılanması şeklinde tanımlanmaktadır (Uygur ve Uygur, 2010).

Rumex crispus L. (Kıvırcık kuzukulağı) (Polygonaceae) tohum ve kazık kökün en üst kısmındaki tomurcuklardan gelişen sürgünlerle çoğalan çok yıllık bir bitkidir. Türkiye'de, Erzurum'da şeker pancarı ve ayçiçeği de dahil olmak üzere birçok ürünü istila eder (Zengin,1996; Tozlu ve Zengin, 1997). Hasat sırasında tohumları buğday tohumlarını kirleterek tane kalitesini düşürür. Bu saf olmayan tohum partileri, ekim sırasında yabancı otun diğer tarlalara yayılmasını kolaylaştırır (Zengin, 1999).

Ülkemizde Bayburt, Erzurum ve Kars illerinde *Rumex crispus* L. bitkisi üzerinde tespit edilen *Lixus bardanae* (F.) (Coleoptera: Curculionidae)'nin biyolojisi üzerine yapılan çalışmada bitkinin yaprakları ile beslendiği, dişi böceklerin yumurtalarını bitki gövdesine bıraktığı ve yumurtadan çıkan larvaların bitki gövdesinde galeriler açtığı gözlenmiştir. Pupadan çıkan ergin böceklerin Eylül ayı sonlarında toprağa geçip bitki kökü etrafında dik pozisyonda kış mevsimini geçirdikleri tespit edilmiştir. Bu çalışma kapsamında *Lixus bardanae* böcek türünün tarla bitkileri için istilacı ve kaliteyi düşürücü rolü olan *Rumex crispus* (kıvırcık kuzukulağı) türü için popülasyonunu kontrol altında tutacak biyolojik ajan olduğu kanısına varılmıştır (Gültekin ve ark., 2004)

Avrupa ülkeleri ve İtalya'da yapılan çalışmalarda *Rumex* türleri üzerinde yaklaşık 200 böcek türü gözlenmiştir. Curculionidae familyasına ait 3 böcek türünün *Rumex*'in biyolojik kontrolünde kullanılabilme potansiyeline sahip

oldukları belirlenmiştir. Aynı çalışma kapsamında *Capnodis tenebricosa* larvalarının *Rumex crispus* köklerinde oldukça yaygın olduğu ve fide köklerini tamamen öldürebildiği gözlenmiştir (Spencer ve Hostettler, 1979).

MATERYAL VE METOT

Bu çalışma 2025 yılı, Temmuz ayında gerçekleştirilen entomofaunistik çalışmalarında elde edilen verilere dayanmaktadır. Arazi çalışmaları, Eskişehir ili, Mihallıççık ilçesinde gerçekleştirilmiştir. Bölgede yapılan arazi çalışmaları esnasında Buprestidae familyasından *Capnodis* cinsine ait *Capnodis tenebricosa* türüne ait ergin bireyler *Rumex crispus* L. (Kıvırcık kuzukulağı) bitkisi üzerinde dinlenme ve beslenme faaliyetlerini yaparken gözlenmiştir.

Ergin böcek bireyleri bir süre gözlendikten sonra *Rumex crispus* bitkisinin gövdesi bir çakı ile boyuna olarak iki bölüme ayrılmıştır. Bitki gövdesi içinde yaprak sürgününün olduğu kısımlarda *Capnodis tenebricosa* larvalarına rastlanmıştır.

Arazi çalışması esnasında gözlenen ergin böceklerden birkaç tanesi tür teşhislerinin doğrulanması amacıyla % 70'lik etil alkol kavanozlarına konulmuştur. Böceklerin toplandığı bölgenin lokalite bilgileri kaydedilmiştir. Laboratuvara getirilen böcekler müze materyali haline getirildikten sonra teşhis işlemleri yapılmış ve böcek kasalarına yerleştirilmiştir.

SONUÇLAR VE TARTIŞMA

Bu çalışmadaki veriler 2025 yılı, Temmuz ayında Eskişehir ili Mihallıççık ilçesinde yapılan arazi çalışmaları sonucunda elde edilmiştir. Arazi çalışmaları esnasında Buprestidae familyasından *Capnodis* cinsine ait *Capnodis tenebricosa* türünün ergin bireyleri *Rumex crispus* L. (Kıvırcık kuzukulağı) bitkisi üzerinde dinlenme ve beslenme faaliyetlerini yaparken gözlenmiştir.

Ergin *Capnodis tenebricosa* bireylerinin bitki üzerinde görülmesinin ardından tarımsal açıdan zararlı olarak bilinen *Rumex crispus* bitkisinin gövdesi çakı yardımıyla boyuna iki parçaya ayrılmıştır. Bitki gövdesi içerisinde ise *Capnodis tenebricosa* türünün larvalarına rastlanmıştır.

Yabancı otların tarımsal açıdan parazit etkileri, toprağı işlemede ve hasat yapmada sebep oldukları zorluklar, zehirli ve zararlı yönleri ele alıdığında yabancı ot mücadelesi kaçınılmazdır. (Önen, 2020). Bu mücadele başarılı bir şekilde yapılmazsa tarımsal üretimin sürdürülebilirliği mümkün değildir (Önen, 2021).

Yabancı otların mücadelesinde herbisitlerin (kimyasallar) çevreyi kirletmesi ve insan sağlığına olumsuz etkisi, yabancı otlarda dayanıklılığın ortaya çıkması gibi olumsuz etkilerinden dolayı günümüzde yabancı otlarla biyolojik kontrol yöntemi oldukça önem kazanmıştır (Zengin, 2013).

Yabancı ot kontrolünde biyolojik ajan olarak fitofag veya fitopatojenik doğal düşmanlar kullanılmaktadır (DeBach, 1964). Biyolojik ajanların yabancı ot kontrolünde kullanılmasındaki amaç, popülasyon ekolojisi prensiplerine dayanarak, yabancı ot yoğunluğunu hoşgörü eşiği altında tutmaktır. Pratikte biyolojik kontrol, faydalı bitki türlerine zarar vermeden, üzerinde bulunduğu konukçu bitkilerine direkt veya indirekt olarak zarar veren ya da zayıflatan doğal düşmanların kullanılması ile gerçekleşir (Zengin, 2013).

Yabancı otların biyolojik mücadelesinde potansiyel öneme sahip bazı böcek türlerinin yapılan gözlemlerde konukçu yabancı otlar üzerinde yoğun şekilde beslendiği, biyolojik dönemlerini geçirdiği ve konukçularının yaprak/sürgünlerinde deformasyona ve kurumalara yol açabildikleri görülmüştür (Sırrı ve Özaslan, 2024).

Bu böceklerin konukçu yabancı otların tohum tablası, gövde ve yan dallara yumurta bırakmak için delikler açtıkları ve çıkan genç bireylerin beslenme sonucu bitkinin iletim demetlerinde/çiçek tablalarında hasar oluşturarak kurumalara neden olabildikleri saptanmıştır. Özellikle yumurta bırakılan bölgelerde (gövde, yan dal, tohum tablası) çıkan larvaların beslenmesi sonucu konukçu bitkinin gövdesi neredeyse tamamen deforme olabilmekte, gövde, dal ve çiçek tablaları kırılabilmekte, larvaların tohumlarla beslenmesi sonucu konukçu yabancı otun tohum miktarı azalabilmektedir (Sırrı ve Özaslan, 2024).

Dolayısıyla bazı böcek türlerinin konukçu yabancı ot türlerinin popülasyon yoğunluğunun azalmasında (bitkinin büyümesi, gelişimi, tohum oluşması) oldukça etkili olabildiği gözlemlenmiştir (Sırrı ve Özaslan, 2024).

Capnodis türleri; ormancılık ve zirai açıdan ağaçlarda zararlı türler olarak kabul edilmektedir. Yapılmış olan çok sayıdaki bilimsel çalışmalarda bu durum açıkça ifade edilmektedir. Ancak Buprestidae familyasından bazı türler biyolojik mücadelede ajan olarak kullanılmaktadır. Bu çalışmada *Capnodis tenebricosa* türü tarımsal alanlarda istilacı tür olarak bilinen *Rumex crispus* için Biyolojik mücadele ajanı olarak düşünülmektedir.

KAYNAKLAR

Abu Jbara, A. (2005). "Identification and Bioecology of Capnodis spp. (Coleoptera: Buprestidae) in Irbid Governate, Jordan". University of Jordan, (Unpublished) M.Sc. Thesis, Amman, Jordan, 81 pp.

Akman, K., San, S. (1975). "Ege Bölgesinde Zarar Yapan Capnodis Türleri Üzerinde Araştırmalar", Zirai Mücadele Araştırma Yıllığı, 9: 21-23.

Bily, S. (1982). "The Buprestidae (Coleoptera) of Fennoscandia and Denmark", Fauna Entomologica Scandinavica, 10: 1-109.

Bonsignore, C.P., Van Achterberg, C. and Vacante, V. (2008). "First record of Braconidae as parasitoids of Capnodis tenebrionis (Linnaeus) (Coleoptera: Buprestidae), with notes on the ecology of Spathius erythrocephalus Wesmael (Hymenoptera: Braconidae)". Zool. Med. Leiden, 82 (44): 489-498.

Booth, R. G., Cox, M. L. & Madge, R. B. (1990). "Iie Guides to Insects of Importance to Man, 3. Coleoptera", Printed in the UK at the University Pres, Cambridge, 1-384.

David'yan, G. E. (2003). Capnodis tenebrionis (L.). Peach flatheaded rootborer. (Web page: http://www.agroatlas.ru/en/ content/pests/Capnodis tenebrionis/index.html)

DeBach, P. (1964). "Successes, trends and future possibilities. In Biological Control of Insect Pests and Weeds" (Eds. P. DeBach and E.I. Schlinger), 673-713.

Donald J. B., Charles A. T., Norman F. J. (1989). "Introduction to the Study of Insects, 6th Edition" Saunders College Pub., 370-478.

Erdem, R., Çanakçıoğlu, H. (1977). "Türkiye Odun Zararlıları", İstanbul Üniversitesi Orman Fakültesi Yayınları, İ. Ü. Yayın No: 2336, O. F. Yayın No: 241, 91-104.

Grasselly, C. & Crossa-Rayaud, P. (1980). L'Amandier, Moisonneuve, Paris, 446 pp

Gültekin, L., Zengin, H. & Hayat, R. (2004). "Note: Life history of *Lixus bardanae* on curly dock (*Rumex crispus*) in Turkey". Phytoparasitica 32, 97–99.

Kaya, M. (1999). "Bursa İlinde Ahududu Zararlılarının Tespit Edilmesi ve Bunlardan Böğürtlen süslü böceği, Coroebus rubi (L.) (Coleoptera: Buprestidae)'nin Morfolojisi, Biyolojisi ve Ekolojisi Üzerinde Araştırmalar", Doktora Tezi, Uludağ Üniversitesi, Fen Bil. Enst. Bit. Kor. Anabilim Dalı, Bursa, 76-118.

Kaygın, A. T. (2007). "Endüstriyel Odun Zararlıları", Nobel Yayınları, 1-224.

Lodos, N., Tezcan, S. (1992). "Türkiye Buprestidae (Coleoptera) faunasının genel görünümü ve zoocoğrafik yönden değerlendirilmesi", Ege Üniv. Ziraat Fak. Dergisi, 29(1): 15-22.

Lodos, N. Tezcan, S. (1995). "Türkiye Entomolojisi V: Buprestidae" Entomoloji Derneği Yay., 8:1-138.

Löbl, I. & A. Smetana. (2006). "Catalogue of Palaearctic Coleoptera. Volume 3. Scarabaeoidea - Scirtoidea - Dascilloidea - Buprestoidea – Byrrhoidea". Apollo Books. Stenstrup, Denmark. 690 pp.

Marannıno, P. & De Lillo E. (2005): "Nemici naturali di Capnodis tenebrionis (L.) (Coleoptera: Buprestidae) ed effetto dell'u miditàdel suolo sulla schiusura delle uova". XX Congresso Nazionale Italiano di Entomologia, Assisi, 13–18 Giugno. 233 pp.

Muskovits J., Hegyessy G. (2002). "Magyarország díszbogarai. Jewel beetles of Hungary (Coleoptera: Buprestidae)", Grafon Kıado Nagykovacsı, 1-404.

Obenberger, J. (1926). "Buprestidae I", Coleopterum Catalogus, Vol: 12, Pars: 84, , Eds. W. Junk and S. Schenkling, Berlin, 1-212.

Önen, H. (2020). "Endüstriyel kenevirde hastalık, zararlı ve yabancı ot mücadelesi". Harf Yayınları, Büyük Reşitpaşa Cad. Yümni İşmerkezi No: 22/2, Fatih/İstanbul, 92s.

Önen, H. (2021). Yabancı otlar ve herboloji (Yabancı Ot Bilimi), 2. Bölüm. "Herboloji (Yabancı Ot Bilimi): İlkeler, Kavramlar ve Uygulamalar / Weed Science: Theory and Practice" içinde Adana, 8-27.

Önen, H. & Özcan, S. (2010). "İklim değişikliğine bağlı olarak yabancı ot mücadelesi. Ed. SAYILI, M. 2010. İklim Değişikliğinin Tarıma Etkileri ve Alınabilecek Önlemler". T.C. Kayseri Valiliği İl Tarım Müdürlüğü Yayın No:2, Fidan Ofset, Kayseri, 336-357.

Özer, Z. (1993). "Niçin yabancı ot bilimi (Herboloji)?" Türkiye I. Herboloji Kongresi Bildirileri, Zirai mücadele araştırma enstitüsü yayınları, Adana, s. 1-7

Sırrı, M., & Özaslan, C. (2024). Hakkari/Yüksekova Havzasında Yabancı Otlar Üzerinde Saptanan Coleoptera Türleri. KSÜ Tarım ve Doğa Derg 27 (3), 610-622.

Söker, A., Koyuncu O., Yaylacı Ö.K, Tokur S., (2012) "Eskişehir ve Çevresindeki Bazı Tarım Alanlarındaki Tarla Yabancı Otlarının Florası" Artvin Çoruh Üniversitesi Orman Fakültesi Dergisi 13(1):100-127.

Spencer, N. R., N. Hostettler. (1979). "Annual Report. Biological Control of Weeds Laboratory Europe", USDA ARS, Roma, 5-30.

Şahin, Ç. & U. Gözel, 2017. "Preliminary studies on distribution and biology of Capnodis tenebrionis L. (Coleoptera: Buprestidae) in Çanakkale Province, 348". VIII. International Symposium on Ecology and Environmental Problems (4-7 October 2017, Çanakkale, Turkey), 388 pp.

Tezcan, S. (1990). "İzmir İlinde Bulunan Sphenopterini, Buprestini ve Psiloterini (Coleoptera: Buprestidae: Buprestinae) tribus'larına bağlı türler üzerinde sistematik araştırmalar", Doktora tezi, E. Ü. Fen Bil. Enst. Bit. Kor. Anabilim Dalı, Bornova, İzmir, 1- 162.

Tozlu, E. and Zengin, H. (1997) Studies on the species, density, frequency and association in sugar beet weeds in Erzurum province. J. Fac. Agric. Atat¨urk ¨Univ. 28:625-636.

Türe C, Köse YB (2000) An investigation on the weed distribution in some agricultural fields of Eskisehir and Environs. Turkish Journal of Agriculture and Forestry 24: 327-331

Tüzün, S. (1975). "Marmara Bölgesindeki Taş Çekirdekli Meyve Ağaçlarında Zararlı Olan Önemli Coleoptera Türleri, Tanınmaları, Zararları ve Oranları Üzerinde Araştırmalar", İhtisas Tezi, İstanbul Üniversitesi, Ziraat Fakültesi, Bitki Koruma Bölümü, İstanbul, 20- 24.

Uluğ E, Kadıoğlu İ, Üremiş İ (1993) Türkiye'nin yabancı otları ve bazı özellikleri. T.C. Tarım Orman ve Köyişleri Bakanlığı, Zirai Mücadele Araştırma Enstitüsü Müd., Yay. No: 78, Adana.

Uygur, S. & Uygur, F.N. (2010). Yabancı otların biyolojik mücadelesi. Türkiye Biyolojik Mücadele Dergisi, 1(1), 79-95.

Yaşar, B. (1996). "Meyve Ve Bağ Zararlıları", Yüzüncü Yıl Üniv. Ziraat Fak., Bitki Koruma Böl., Ziraat Fakültesi Yayın ve Basım Bürosu, Van, No: 11: 1-30.

Zengin, H. (1996) Studies on weed seeds and their intensity in winter wheat production in Erzurum and its provinces. Turk. J. Agric. For. 20: 207-213.

Zengin, H. (1999) Studies on the species, density, frequency and sociability of sunflower weeds in Erzurum. Turk. J. Agric. For. 23: 39-44.

Zengin, H. (2013). YABANCI OTLARLA BİYOLOJİK MÜCADELE YÖNTEMLERİ. Atatürk Üniversitesi Ziraat Fakültesi Dergisi, 28(3) 496-514.

Zobar, D, Kıvan, M, Candar, S, Yaşasın, A. (2019). Tekirdağ ili sert çekirdekli meyve ağaçlarında bulunan Bup restidae (Coleoptera) türleri, Bitki Koruma Bülteni, 59-4.

ORAL PRESENTATION

Fitoterapötik ajanlar olarak *Melissa officinalis* ve *Thymbra spicata:* Antibakteriyel ve antikanser aktivite üzerine bir araştırma

Melisa Gireksan[1] (*https://orcid.org/0009-0005-9810-336X*), Yusuf Ceylan[1*](*https://orcid.org/0000-0001-8186-7252)*, Kübra Sena Baş Topçu[1] (*https://orcid.org/0000-0003-3161-1042*)

[1]Bartın Üniversitesi, Fen Fakültesi, Moleküler Biyoloji ve Genetik, Bartın, Türkiye

*Sorumlu yazar e-mail: yceylan@bartin.edu.tr

Özet

Melissa officinalis ve *Thymbra spicata,* içeriklerindeki fenolik bileşikler, uçucu yağlar ve çeşitli fitokimyasallar nedeniyle antibakteriyel ve antikanser etkilere sahip tıbbi ve aromatik bitkilerdir. Bu bitkilerden elde edilen ekstraktların biyolojik aktiviteleri, kullanılan çözücü türüne göre değişiklik gösterebilmektedir. Bu nedenle çalışmada, bitkilerin etanol, kloroform ve bu çözücülerin karışımı kullanılarak hazırlanan ekstraktlarının antibakteriyel ve antikanser özellikleri değerlendirilmiştir. Bitkilerin özütlerinin *Staphylococcus aureus* ve *Escherichia coli* suşları üzerine antibakteriyel etkileri incelenmiştir. Elde edilen bulgular, hem *M. officinalis* hem de *T. spicata* ekstraktlarının farklı çözücülerde değişen düzeylerde antibakteriyel aktivite gösterdiğini ortaya koymuştur. *T. spicata'*nın en iyi antibakteriyel aktivitesi etanol ekstraktında görülmüş olup, her iki bakteri için MİK 15.625 µg/mL ve MBK 31.25 µg/mL değerleriyle çalışmadaki en düşük konsantrasyonları vermiştir. *M. officinalis'*in en etkili sonucu ise kloroform ekstraktında elde edilmiş ve her iki bakteri için MİK 93.75 µg/mL ile MBK 187.5 µg/mL değerleri kaydedilmiştir. Çalışmanın bir diğer aşamasında, elde edilen ekstraktların HeLa serviks kanseri hücre hattı üzerindeki sitotoksik etkileri değerlendirilmiştir. Uygulanan bitki özütlerinin, doza bağlı olarak hücre canlılığını azalttığı ve özellikle kloroform ekstraktlarının daha belirgin antiproliferatif etki gösterdiği gözlenmiştir. Bu çalışmada en etkili sitotoksik sonuçlar *T. spicata*'nın kloroform ekstraktında (IC_{50} = 52,59 µg/mL) elde edilirken, *M. officinalis*'te en iyi etki kloroform ekstraktında (IC_{50} = 69,24 µg/mL) görülmüş ve genel olarak *T. spicata*'nın *M. officinalis*'e kıyasla daha güçlü antiproliferatif aktivite gösterdiği belirlenmiştir. Sonuçlar, *M. officinalis* ve *T. spicata* bitkilerinin doğal antimikrobiyal ve antikanser ajanlar olarak potansiyel taşıdığını ve biyolojik etkinin kullanılan çözücü türüne göre önemli ölçüde farklılaştığını ortaya koymuştur.

Anahtar Kelimeler: Antibakteriyel, Antikanser, *Melissa officinalis*, *Thymbra spicata*

Melissa officinalis and *Thymbra spicata* as phytotherapeutic agents: An investigation of their antibacterial and anticancer activities

Abstract

Melissa officinalis and *Thymbra spicata* are medicinal and aromatic plants with antibacterial and anticancer properties owing to their phenolic compounds, essential oils, and various phytochemicals. The biological activities of the extracts obtained from these plants may vary depending on the type of used solvent. Therefore, the antibacterial and anticancer properties of extracts prepared using ethanol, chloroform, and a mixture of these solvents were evaluated in this paper. The antibacterial effects of the plant extracts were investigated against *Staphylococcus aureus* and *Escherichia coli* strains. The findings revealed that both *M. officinalis* and *T. spicata* extracts exhibited varying levels of antibacterial activity depending on the solvent type. The highest antibacterial activity of *T. spicata* was observed in the ethanol extract, which exhibited the lowest concentrations in the study with MIC and MBC values of 15.625 µg/mL and 31.25 µg/mL, respectively, for both bacterial strains. The most effective result for *M. officinalis* was obtained from the chloroform extract, recording MIC and MBC values of 93.75 µg/mL and 187.5 µg/mL, respectively, against both bacteria.

The cytotoxic effects of the obtained extracts were evaluated on the HeLa cervical cancer cell line in another part of the study. The applied plant extracts decreased cell viability in a dose-dependent manner, and particularly the

chloroform extracts exhibited a more pronounced antiproliferative effect. The most potent cytotoxic result in this study was obtained from the chloroform extract of *T. spicata* (IC_{50} = 52.59 µg/mL), while in *M. officinalis*, the best effect was also observed in the chloroform extract (IC_{50} = 69.24 µg/mL). Overall, *T. spicata* demonstrated stronger antiproliferative activity compared to *M. officinalis*. The results indicate that *M. officinalis* and *T. spicata* possess potential as natural antimicrobial and anticancer agents and that the biological efficacy varies significantly depending on the used solvent type.

Keywords: Antibacterial, Anticancer, *Melissa officinalis*, *Thymbra spicata*

GİRİŞ

Bitkilerin tedavide kullanımları insanlık tarihiyle birlikte başlamıştır. Binlerce yıl önce insan, bitkilerin tedavi edici gücünü tanımış ve sağlıklı yaşayabilmek için ondan yararlanmıştır (Faydaoğlu ve Sürücüoğlu, 2011). Tıbbi ve aromatik bitkiler, hastalıkları önlemek, sağlığı sürdürmek veya hastalıkları iyileştirmek için ilaç olarak kullanılan bitkilerdir (Kızıloğlu ve ark., 2017). Ülkemiz zengin florasıyla çok sayıda tıbbi ve aromatik bitkiyi bünyesinde bulundurmaktadır. Ayrıca Anadolu, tedavi gücü yüksek aromatik bitkilerin varlığı konusunda çok önemli bir potansiyele sahiptir (Dönmez, 2016). Araştırmamız da yer alan, tıbbi ve aromatik bitkilerden olan zahter (*Thymbra spicata)* acımsı tadı ve keskin kokusuyla bilinen *Lamiaceae* (Ballıbabagiller) familyasına ait bir bitkidir (Çınar ve ark., 2018). Türkiye'de özellikle Akdeniz ve Güneydoğu Anadolu bölgelerinde yaygın olarak bulunmaktadır. Zahter, başta Hatay olmak üzere, Gaziantep, Kilis ve ülkemizin Akdeniz iklim kuşağında doğal olarak yetişmekte ve genellikle baharat olarak kullanılmaktadır (Koçer, 2021). Zahter bitkisinden elde edilen ana bileşenler, simen (%7.17), c-terpinen (%12.30), o-simen (%10.05), ve karvakrol (%65.15) olarak tespit edilmiştir (Koçer, 2021). Karvakrolun analjezik, antiinflamatuvar, antikanserojen, antibakteriyel, antifungal, yara iyileşmesini ve hücre çoğalmasını hızlandırıcı etkileri olduğunu gösteren birçok çalışma bulunmaktadır (Canbek, 2008). Bunların yanı sıra bitkinin özünde fenolik bileşikler ağır basarken öne çıkan rosmarinik asittir. Biberiye, kekik, gibi bitkilerde bulunan, doğal antioksidan olan rosmarinik asit (RA) antimikrobiyal etkiye sahiptir (Önal ve Erden, 2011). Rosmarinik asitin *in vitro* çalışmalarda anti-HIV-1, antibakteriyel, antioksidan, anti-kanserojen ve anti-alerjik aktiviteler, antiviral özellikler gibi bazı biyolojik faaliyetleri olduğu bildirilmiştir. *In vivo* çalışmalar da rosmarinik asitin antikanserojenik özellikler sergilediğini göstermiştir (Bulduk ve Gökçe, 2017). Benzen halkası içeren organik maddeler genel olarak fenolik bileşikler olarak adlandırılmakta olup bunlar bitkiler aleminde bulunan ikincil metabolitlerdir (Uylaşer ve İnce, 2008). Bu bilgiler kapsamında, fenololik bileşiklerin antikarsinojen, antimutajen ve antimikrobiyal aktivite göstermeleri bakımından insan sağlığı üzerinde olumlu etkileri olduğuna ulaşılmıştır. (Korcan ve ark., 2018).

Zahterle ortak kimyasal bileşenlere sahip bitkiler arasında yer alan *Melissa officinalis* (limon otu) zengin kimyasal bileşimi ve biyolojik olarak aktif bileşenleri sayesinde tanınmış olan tıbbi bir bitkidir (Düvenci, 2024). *M. officinalis* , son on yılda araştırmaların odak noktası olmuştur (Draginic ve ark., 2022). *M. officinalis'*in başlıca aktif bileşenleri uçucu bileşikler (geranial, neral, sitronelal ve geraniol), triterpenler (ursolik asit ve oleanolik asit), fenolik asitler (rosmarinik asit, kafeik asit ve klorojenik asit) ve flavonoidlerdir (kuersetin, ramnositrin ve luteolin) (Petrisor ve ark., 2022). Bu bileşenler, bitkinin antioksidan, antimikrobiyal ve anti-inflamatuar özellikler sağlayıp; bitkiyi modern bitkisel tıpta değerli bir kaynak haline getirmektedir (Düvenci, 2024). Biyolojik çalışmalara göre, *Melissa officinalis'in* uçucu yağı ve özleri , potansiyel tıbbi kullanımları olan birçok farmakolojik etkiyi belirleyen aktif bileşiklere sahiptir (Petrisor ve ark., 2022). *M. officinalis* ülkemizde Akdeniz Bölgesi'nde yetişmektedir. *M. officinalis* arı otu, bal otu olarak da bilinen çok yıllık bir bitkidir ve Lamiaceae (nane) familyasının bir üyesidir (Miraj ve ark., 2016). *M. officinalis* bitkisinin en bilinen özellikleri; antiviral, antifungal, antikanser, antibakteriyel ve antioksidan etkiler göstermesidir. *M. officinalis* eczacılık, parfümeri, kozmetik ve gıda sanayinde çok sayıda kullanım alanına sahiptir (Topdemir, 2018). Köklü bir geçmişe sahip olan, tıbbi özellikleri ile insanoğlunun hayatında yer tutmuş ve tarih boyunca önemini korumuş olan *M. officinalis* günümüzde de birçok hastalığın tedavisinde fitoterapik amaçlar ile kullanılmaktadır (Başkal ve ark., 2017). Gastrointestinal sistem rahatsızlıklarından sinir sistemi rahatsızlıklarına, kalp ve damar hastalıklarından astıma kadar birçok hastalığın tedavisinde kullanılan *M. officinalis* gerek modern tıpta standardize ekstreleri şeklinde gerekse halk hekimliğinde yaygın olarak kullanıla gelen bir bitkidir (Başkal ve ark., 2017). Çalışmalar kapsamında *M. officinalis* ekstraktlarının patojenlere karşı önemli derecede antibakteriyel ve antifungal etkinlik gösterdiğini ortaya koymuştur (Düvenci, 2024).

Kanser büyüme özellikleri bozulmuş hücrelerin klonal yayılımıdır ve somatik genetik hastalıkların en sık, en yaygın ve aynı zamanda en komplike olanıdır (Yokuş ve Çakır, 2012). Tek bir organı etkileyebildiği gibi uzaktaki organlara da yayılarak etkisini gösterebilmektedir. Her ne kadar bazı standartlar belirlenmiş olsa da her kanser türüne özgü olarak farklı yaklaşımlar ve tedaviler uygulanmaktadır (Baykara, 2016). Günümüzde bitki ekstraktlarının antikanserojenik etkileri bulunmuş ve antikanserojenik ilaçların %63'ünün bitkilerden elde edildiği, ayrıca bu ilaçların yan etkilerinin az olduğu ve tedavide başarı oranının yüksek olduğu tespit edilmiştir (Saraç ve ark., 2018). Kanser tedavisinde bitkisel kaynaklı ürünlerin kullanımı nispeten oluşabilecek sağlık sorunlarının önüne geçebilir. Bu yüzden son yıllarda antikanser ajan olarak kullanılan çeşitli bitki kaynaklarının kimyasal bileşenleriyle ilgili çalışmalar artmıştır (Desai ve ark., 2008). Meme ve serviks kanseri kadınlarda en çok görülen iki kanser türü olarak tanımlanmıştır (Maraşlı ve Öztürk, 2021). Serviks kanseri, dünyada her iki dakikada bir kadın ölümüne neden olan ve kadınlarda meme kanserinden sonra en sık görülen ikinci kanserdir (Aydoğdu ve Özsoy, 2018). Araştırmada, HeLa hücre hattı olan rahim ağzı kanseri (serviks adinokarsinom) üzerinde durulmuştur.Bitki ekstrelerinin antikanser özellikleri üzerinde çalışmalar yapılmakta olup, *M. officinalis* ve *T. spicata* bitkileri de meme kanseri başta olmak üzere rahim ağzı (HeLa) kanserine de antikanser etki göstermektedirler.

Akne vulgaris, halk arasında bilinenin aksine, kıl folikülü, kıl şaftı ve yağ bezinden oluşan pilosebase ünitenin kronik inflamatuar bir hastalığıdır ve dünya çapında en sık görülen dermatolojik rahatsızlıklar arasındadır (Tuchayi ve ark., 2015). Bakteriler, toprak ve suda yaygın olarak bulunan ve diğer organizmaların simbiyontları olarak yaşayan prokaryotlara ait tek hücreli canlı organizmaların önemli bir grubudur (Vijayaraghavan ve Yun, 2008). Akneye sebep olan bakteri çeşitleri arasında *Propionibacterium acnes* bakterisinin yanı sıra *Escherichia coli*, *Staphylococcus aureus* bakterileri de bulunmaktadır. Araştırma da kullanılan bakteriler; gram negatif özellikte olan *Escherichia coli* ve gram pozitif özelliğe sahip olan *Staphylococcus aureus* bakterileridir.

Araştırmamızın içeriklerinden olan *M. officinalis* ve *T. spicata* bitkilerinin antibakteriyel ve antikanser etkilerine değinilmiştir. Araştırma da temelini *M. officinalis* ve *T. spicata* bitkilerinin oluşturduğu, akne üzerindeki antibakteriyel etkileri ve HeLa hücre hattı üzerindeki antikanser etkilerinin incelenmesi amaçlanmış ve hangi oranlarda etki ettiğine bakılmıştır.

MATERYAL VE METOT

1.Bitki Materyali ve Ekstrakt Hazırlanması

Çalışmada kullanılan *M. officinalis* ve *T. spicata* bitkileri gölgede kurutulduktan sonra elektrikli değirmende öğütülerek toz haline getirilmiştir. Her iki bitki grubu hem etanol hem de klorofom çözücülerinde ekstre edilmiştir. Ekstraksiyon işlemi sonrasında karışımlar filtre kâğıdı yardımıyla süzülmüş, ardından çözücüler evaporatör cihazı kullanılarak uzaklaştırılmıştır. Elde edilen özütler 37°C'de 24 saat inkübe edilmiştir. Son olarak özütler +4°C'de analiz aşamasına kadar muhafaza edilmiştir.

2.Antibakteriyel Aktivite Testi

Bitki ekstraktlarının ekstraksiyon işlemi sonrasında elde edilerek hazırlanmasının ardından antibakteriyel aktivitelerinin araştırılması amacıyla, *Staphylococcus aureus* (Gram pozitif) ve *Escherichia coli* (Gram negatif) kullanılmış ve stok olan suşlar Luria-Bertani (LB) sıvı besiyerinde aktive edilmiştir. Tüm bakteriler Mueller Hinton sıvı besiyerine inoküle edilmiş ve bakteri büyümeleri 0,5 McFarland standardı bulanıklığına ($1,5\times10^8$ CFU/mL) göre standardize edilmiştir. Aynı hacimde büyüme ortamı ve çözeltisi, 96 kuyucuklu mikroplaka sisteminin ilk kuyucuğuna eklenmiş ve karışım 37 °C'de inkübe edilmiştir. Bakteri suşlarının gelişimi ve minimum bakterisidal konsantrasyon (MBC) tayini için Nutrient Agar (NA) ortamı kullanılmıştır.

3. Antikanser Özelliklerinin Belirlenmesi

3.1. Hücre Kültürü

İnsan serviks karsinomu hücreleri (HeLa hücre hattı) Amerikan Tip Kültür Koleksiyonu'ndan (ATCC, Manassas, VA, ABD) temin edildi. HeLa hücre hattı, %10 fetal sığır serumu (FBS) ve %1 penisilin-streptomisin ile takviye edilmiş yüksek glikoz içeren Dulbecco's Modified Eagle Medium (DMEM) besiyerinde, %5 CO_2 içeren nemli ortamda ve 37 °C sıcaklıkta inkübatörde kültüre edilmiştir. Hücreler %80 doluluğa ulaştıktan sonra deneysel uygulamalara geçilmiştir.

3.2. Hücre sitotoksisite analizi (MTT analizi)

Bitki ekstraktlarının HeLa hücre hattı üzerindeki sitotoksisite düzeyinin belirlenmesi için MTT (3-(4,5-dimetiltiazol-2-il)-2,5-difenil tetrazolyum bromür) analizi yapılmıştır. 96 kuyucuklu plakaya her bir kuyucukta yaklaşık 7500 hücre olacak şekilde hücre ekimi yapılmış ve bir gece 5 CO_2 içeren nemli ortamda ve 37 °C sıcaklıkta inkübe edilmiştir. Süre sonunda besiyeri çekilmiştir ve taze besiyeri içerisinde bitki ekstraktları 5-1000 ug/mL konsantrasyon aralığında hücrelere 48 saat boyunca uygulanmıştır. Bitki ekstraktları hazırlanırken kullanılan kloroform ve etil alkol çözücüleri, hücre canlılığına toksik etki oluşturmamak amacıyla seyreltilmiş ve nihai uygulamalarda çözücü konsantrasyonu %0.1'i geçmeyecek biçimde ayarlanmıştır. Pozitif kontrol olarak 200 uM 5-Florourasil kullanılmıştır. Süre sonunda tüm besiyeri uzaklaştırılmış, ardından PBS içerisinde hazırlanmış 0.5 mg/mL MTT çözeltisinden 20 µL her bir kuyucuğa eklenmiştir. Hücreler 3 saat süreyle inkübatörde bekletildikten sonra, MTT içeren ortam uzaklaştırılmış ve her kuyucuğa 100 µL DMSO eklenmiştir. Oluşan formazan kristallerinin çözünmesi için 30 dakika beklenmiş, ardından absorbans değerleri 570 nm dalga boyunda mikroplaka okuyucu (Thermo Scientific Multiscan GO, ABD) ile ölçülmüştür. Elde edilen absorbans değerleri kontrol grubuna göre normalize edilerek hücre canlılığı (%) hesaplanmış, IC_{50} değerleri GraphPad Prism 10.3.1 yazılımı kullanılarak grafikler çizilmiştir. Deneyler üç tekrarlı olarak yürütülmüştür. Hücre hatlarındaki IC_{50} değerleri https://www.aatbio.com/tools/ic50-calculator çevrim içi aracı kullanılarak hesaplanmıştır.

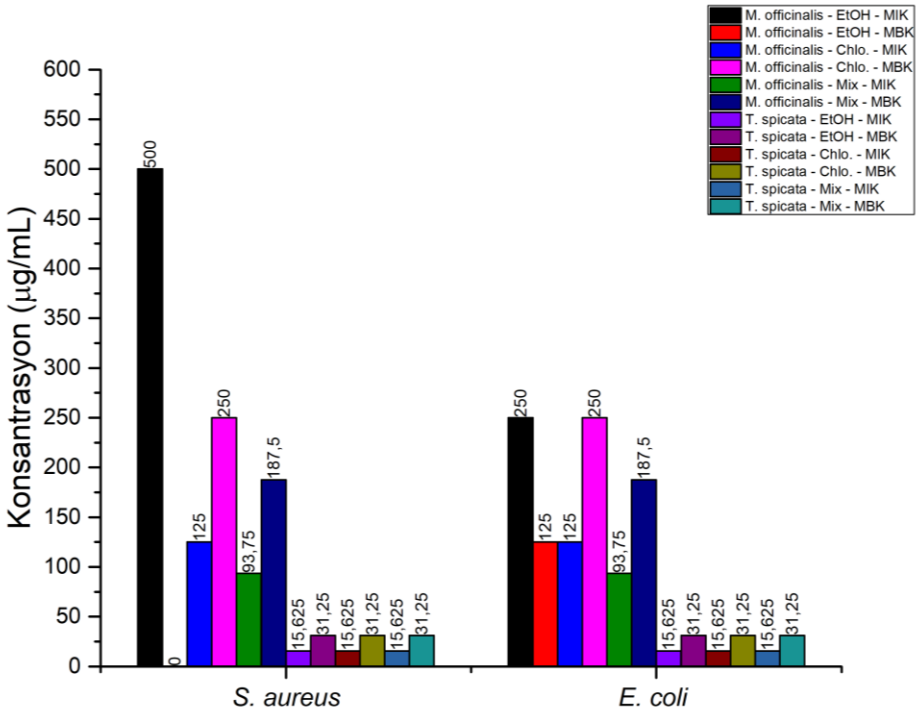
BULGULAR ve TARTIŞMA

Yapılan MİK (Minimum inhibitör konsantrasyon) ve MBK (Minimum bakterisidal konsantrasyon) testleri sonucunda, *M. officinalis* ve *T. spicata* ekstraktlarının hem *S. aureus* hem de *E. coli* bakterileri üzerinde farklı düzeylerde antibakteriyel aktivite gösterdiği belirlenmiştir (Şekil 1). *T. spicata* ekstraktları, etanol, kloroform ve etanol-kloroform karışımı çözücülerde en düşük MİK değerlerine sahiptir, bu da en yüksek antibakteriyel etkiyi göstermektedir. Örneğin, *T. spicata* ekstraktlarının MİK değeri 15,625 µg/mL olarak ölçülmüştür. Bu sonuç, *T. spicata* bitkisinin içerdiği karvakrol ve timol gibi fenolik bileşiklerin bakteriyel üremeyi güçlü bir şekilde inhibe ettiğini ve bakterisidal etki sağladığını göstermektedir. *M. officinalis* ekstraktları, *E. coli* üzerinde orta düzeyde inhibitör etki göstermişlerdir. *T. spicata* da etanol-kloroform çözücüleri birlikte kullanıldığında, ayrı ayrı çözücülerde ekstre edildiklerindeki gibi yüksek etkinlik göstermeye devam etmiş, aynı şekilde *M. officinalis* de etanol-kloroform çözücüleri birlikte kullanıldığında ise ayrı ayrı çözücülerde ekstre edildiklerinde çıkan sonuçlardan daha iyidir. Her iki bitki ekstraktı da Gram pozitif (*S. aureus*) ve Gram negatif (*E. coli*) bakterilere karşı etkili olmuştur, bu durum ekstraktların geniş spektrumlu antimikrobiyal potansiyele sahip olduğunu ortaya koymaktadır. *M. officinalis* bitkisinin orta düzeyde etkisi ise, rosmarinik asit ve flavonoid içerikleriyle açıklanabilir.

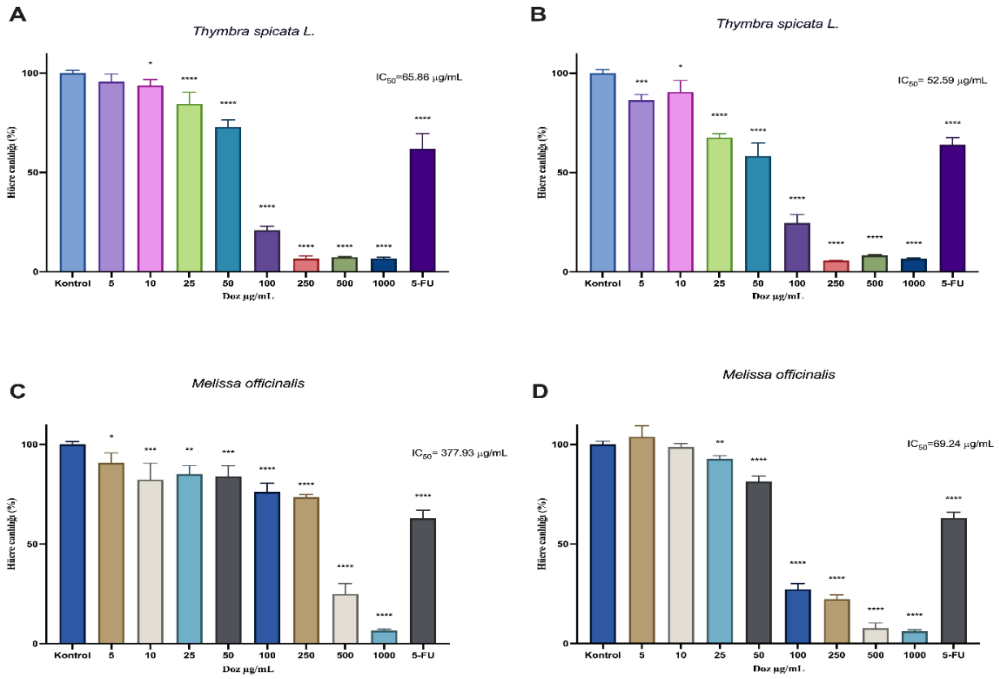
Çalışma kapsamında *T. spicata* ve *M. officinalis* bitkilerinden elde edilen kloroform ve etil alkol ekstraktlarının HeLa hücre hattı üzerindeki sitotoksik etkileri değerlendirilmiştir (Şekil 2). Elde edilen sonuçlar, her iki bitkinin de özellikle kloroform çözücüsü ile hazırlanan ekstraktının hücre canlılığını anlamlı düzeyde azalttığı tespit edilmiştir. Pozitif kontrol olarak HeLa hücre hattına uygulanan 5-fluorourasil (5-FU), 200 µM konsantrasyonda hücre canlılığını yaklaşık %65 seviyesine düşürmüştür. Daha önceden yapılmış bir çalışmada *M. officinalis* bitkisinin sudaki ekstraktının 48 saat boyunca kolon kanseri hücrelerine uygulanmasının IC_{50} değeri 264,4 µg/mL olarak tespit edilmiştir. Buna ek olarak *M. officinalis* özütünün hücre döngüsünü G2/M fazında durdurulmasını indüklediği, apoptozu tetiklediği ve hücre göçünü baskıladığı belirlenmiştir (Kuo ve ark., 2020). Bir başka çalışmada ise *M. officinalis*'in etanol kullanılarak elde edilen ekstraktın akciğer, meme, prostat ve yumurtalık kanseri hücre hatlarında 72 saat boyunca uygulanmasının tüm hücre hatlarında yüksek antiproliferetif etki gösterdiği belirlenmiştir (Jahanban-Esfahlan ve ark., 2015). 2018 yılında yapılan bir çalışmada, *M. officinalis* bitkisinin etanolik ekstraktının akciğer kanseri hücrelerine 48 saat uygulanması sonucunda IC_{50} değeri 100,9 µg/mL olarak belirlenmiştir (Magalhães ve ark., 2018). Yaptığımız çalışmada *M. officinalis* bitkisinin insan serviks karsinomu hücre hattında (HeLa) özellikle kloroformdaki ekstraktının 48 saat boyunca uygulanması sonucunda IC_{50} değeri 69,24 µg/mL olarak tespit edilmiştir. Bu bulgular, *M. officinalis bitkisinin* antiproliferatif aktivitesinin çözücü tipine bağlı olarak değişkenlik gösterebildiğini ancak genel olarak bitkinin içeriğindeki polifenolik bileşenler sayesinde farklı kanser türlerinde güçlü bir fitoterapötik potansiyele sahip olabileceğini desteklemektedir. *T. spicata'*nın farklı kanser türleri üzerindeki antiproliferatif etkileri daha önce çeşitli çalışmalarda araştırılmıştır. *T. spicata'*nın sulu ve etil alkollü ekstraktlarının kolon, meme ve melanoma üzerindeki anti proliferatif etkilerinin değerlendirilmesi için yapılan bir çalışmada sulu ekstraktta önemli bir sitotoksik etki

gözlenmezken, etil alkoldeki ekstraktlarında konsantrasyona bağlı olarak hücre canlılığının azaldığı gözlemlenmiştir. *T. spicata'*nın etil alkol ekstraktının IC_{50} değerleri meme kanseri, kolon kanseri ve melanoma hücre hatlarında sırasıyla 58,447, 110,238, 31,443 µg/mL olarak tespit edilmiştir (Diab ve ark., 2022). Yaptığımız çalışmada ise *T. spicata* bitkisinin insan serviks karsinomunda etil alkol ekstraktının 48 saat boyunca uygulanması sonucunda IC_{50} değeri 65,86 µg/mL,kloroform ekstraktı içinse 52,59 µg/mL olarak hesaplanmıştır. Bu bulgular *M. officinalis* ve *T. spicata* bitkilerinin içerdiği bileşikler ile kanser tedavisinde destekleyici ajanlar olarak kullanılabileceğini göstermektedir. Gelecekteki çalışmalarda bu bitkilerin aktif bileşenlerinin moleküler etki mekanizmalarının, hücre ölüm yolakları üzerindeki rollerinin ve potansiyel terapötik etkilerinin araştırılması, kanser tedavisi için yeni stratejilerin geliştirilmesine önemli katkı sunabilir.

Bitki içerikli ilaçların kanser tedavisinde kullanıldığı bilinmektedir. Daha önce yapılan araştırmalarda MCF-7 hücreleri üzerinde *M. officinalis* ekstraktlarının antikanser özelliklere bakılmıştır ve araştırma sonucu ekstraktların sitotoksik etki (hücreyi öldüren) gösterdiği görülmüştür (Öğüt ve ark., 2022). Elde edilen bulgular daha önce yapılan bu araştırmaları desteklemekte olup, *M. offcinalis* bitkisinin kanserin çoğalmasını engelleyen nitelikte olduğu kanısına varılmıştır. *T. spicata* bitkisinde yoğun oranda bulunan karvakrolun antikansarojen etkileri bulunmaktadır. Son yıllarda akciğer kanseri içindeki oranı artan adenokarsinomda karvakrolun, kanserli hücrelerin sayısını azalttığı, hücrelerin morfolojisini bozduğu ve total protein oranını azalttığı gösterilmiştir (Koparal ve Zeytinoğlu, 2003). Yapılan çalışmada elde edilen sonuca göre de, zahterin HeLa kanser hattı üzerinde antikanser etkisinin oranının yüksek olduğu görülmektedir.



Şekil 1. *M. officinalis* ve *T. spicata* bitkilerinin MİK ve MBK sonuçları (X: özütler) µg/mL



Şekil 2. *Thymbra spicata* (A) etil alkol (B) kloroform ve *Melissa officinalis* (C) etil alkol (D) kloroformda çözünen bitki ekstraktlarının HeLa hücre hattı üzerindeki 48 saatlik sitotoksik etkileri (****: $p < 0.0001$; ***: $p < 0.001$; **: $p < 0.01$; *: $p < 0.05$)

SONUÇ

Çalışmada *M. officinalis* ve *T. spicata* bitkilerinin farklı çözücülerle hazırlanan ekstraktlarının *S. aureus* ve *E. coli* bakterileri üzerinde antimikrobiyal etkinlikleri, Minimum İnhibitör Konsantrasyon (MİK) ve Minimum Bakterisidal Konsantrasyon (MBK) testleriyle değerlendirildiğinde, elde edilen sonuçlar, zahter ekstraktlarının, özellikle etanol, kloroform ve karışım çözücüleri ile hazırlanmış olanlarının, her iki bakteri türüne karşı *M. officinalis* ekstraktlarına kıyasla daha düşük MİK ve MBK değerleri sergileyerek daha yüksek antimikrobiyal potansiyele sahip olduğunu göstermiştir. Buna karşılık, *M. officinalis* ekstraktlarının kloroform ve karışım çözücü ile hazırlanan formları etanol ekstraktına göre daha etkili bulunmakla birlikte, bu ekstraktların MİK ve MBK değerleri *T. spicata* ekstraktlarına göre yüksek olup, dolayısıyla antibakteriyel etkinlikleri daha sınırlı kalmıştır. Bu bulgular doğrultusunda, *T. spicata* ekstraktlarının hem Gram (+) hem de Gram(-) bakterilere karşı güçlü bir antimikrobiyal ajan olarak potansiyel taşıdığı, *M. officinalis* ekstraktlarının ise özellikle kloroform ve karışım ekstraktifleri aracılığıyla destekleyici antibakteriyel rol üstlenebileceği söylenebilir.

T. spicata ve *M. officinalis* rahim ağzı kanseri hücrelerinin çoğalmasını baskılar. Bu çalışmada *T. spicata.* ve *M. officinalis* bitkilerinden elde edilen etanol ve kloroform ekstraktlarının HeLa hücre hattı üzerindeki sitotoksik etkileri MTT analizi ile değerlendirilmiştir. *T. spicata* ve *M. officinalis* bitki özütlerinin 48 saatlik HeLa hücre hatlarına uygulanması, kanser hücrelerin canlılığında doza bağlı bir azalmaya neden olmuştur. Etanol ekstraktı için IC_{50} değeri 65,86 µg/mL,kloroform ekstraktı için 52,59 µg/mL olarak belirlenmiştir. Bitki özütünün kloroform içerisinde çözünmesinin etanol çözeltisine göre daha yüksek sitotoksik etki gösterdiği saptanmıştır. Etanol ekstraktı için IC_{50} değeri 377,93 µg/mL, kloroform ekstraktı için 69,24 µg/mL olarak hesaplanmıştır. Etanol ekstraktı daha düşük toksisiteye sahipken, kloroform ekstraktı belirgin antiproliferatif etki oluşturmuştur. Elde edilen veriler, *T. spicata* ekstraktlarının *M. officinalis* ekstraktlarına kıyasla daha güçlü antiproliferatif etki gösterdiğini ortaya koymuştur.

Teşekkür

Bu proje TÜBİTAK 2209-A kapsamında desteklenmiştir (1919B012332249).

KAYNAKLAR

Aydoğdu, S. G. M., & Özsoy, Ü. (2018). Serviks Kanseri ve Hpv. 20 : 25-29.

Başkal, G., Köngül, E., & Karatoprak, G. Ş. (2017). Melissa Officinalis(Oğul otu)'in Geleneksel Kullanımı. Sağlık Bilimleri Dergisi, 26(3), 267-269.

Baykara, O. (2016). Kanser Tedavisinde Güncel Yaklaşımlar. Balıkesir Sağlık Bilimleri Dergisi, 5(3), 154-165.

Bulduk, İ., & Gökçe, S. (2017). Yüzey Yanıt Metodolojisi ile Biberiye Yapraklarından Rosmarinik Asit Ekstraksiyonunun Optimizasyonu. Düzce Üniversitesi Bilim ve Teknoloji Dergisi, 5(2) ,441-454.

Canbek, M. (2008). Sıçan Karaciğerinde İskemi-Reperfüzyon Bozuklukları Üzerine Karvakrolün Etkileri. Bitki İlacı Dergisi, 15(6-7), 447-452.

Çınar, G., & Yaman, N., & Aydın, M. (2018). Antibacterial Effects of Thymbra spicata L. Extracts on Escherichia coli O157:H7, Salmonella enterica subsp. enterica serovar Typhimurium, and Campylobacter jejuni. Commagene Journal of Biology, 2(1), 21-24.

Desai, A., Qazi,G., Ganju, R. , Mahmoud, T., Singh, J., Saxena, A., Bedi,Y., Taneja,S., & Bhat, H. (2008). Medicinal Plants and Cancer Chemoprevention, 9(7), 581-591.

Diab, F., Khalil, M., Lupidi, G., Zbeeb, H., Salis, A., Damonte, G., Bramucci, M., Portincasa, P., & Vergani, L. (2022). Influence of Simulated In Vitro Gastrointestinal Digestion on the Phenolic Profile, Antioxidant, and Biological Activity of Thymbra spicata L. Extracts. Antioxidants (Basel, Switzerland), 11(9), 1778.

Dönmez, Ş. (2016). Bartın'da Yetişen Bazı Tıbbi ve Aromatik Bitkilerin Peyzaj Mimarlığında Kullanımı. Journal of Architectural Sciences and Applications, 1(2), 1-8.

Draginic, N., Andjic, M., Jeremic,J., Zivkovic, V., Kocovic, A., Tomovic, M., Bozin, B., Kladar, N., Bolevich, S., Jakovljevic, V., & Milosavljevic, I. (2022). Anti-inflammatory and Antioxidant Effects of Melissa officinalis Extracts: A Comparative Study. Iran J Pharm Res, 21(1).

Düvenci, E. S. (2024). Tıbbi ve Aromatik Bir Bitki Olarak Melissa officinalis'in Geçmişten Geleceğe Yolculuğu. Düzce Üniversitesi Süs ve Tıbbi Bitkiler Botanik Bahçesi Dergisi, 3(2), 13-22.

Faydaoğlu, E., & Sürücüoğlu, M. S. (2011). Geçmişten günümüze tıbbi ve aromatik bitkilerin kullanılması ve ekonomik önemi. Kastamonu Ünversitesi Orman Fakültesi Dergisi, 11(1), 52-67.

Jahanban-Esfahlan, A., Modaeinama, S., Abasi, M., Abbasi, M. M., & Jahanban-Esfahlan, R. (2015). Anti Proliferative Properties of Melissa officinalis in Different Human Cancer Cells. Asian Pacific journal of cancer prevention : APJCP, 16(14), 5703–5707.

Kızıloğlu, R., Kızılarslan, H., & Eren, H. Z. (2017). Tıbbi ve Aromatik Amaçlı Kullanılan Bitkilerde Tüketici Davranışlarının İncelenmesi (Kahramanmaraş İli Örneği). Gaziosmanpaşa Üniversitesi Ziraat Fakültesi Dergisi, 34(3), 27-35.

Koçer, O. (2021). Hatay Yöresinde Yetişen Thymbra Spicata L.(Zahter&Karabaş Kekiği) Bitkisinin Uçucu Yağ Oran ve Bileşenlerinin Belirlenmesi. Avrupa Bilim ve Teknoloji Dergisi, (27), 446-449.

Koparal, T., & Zeytinoğlu, M. (2003). Effects of carvacrol on a human non-small cell lung cancer (NSCLC) cell line, A549. CYTOTECHNOLOGY, 43,149-154.

Korcan, S. E., Bulduk, İ., Kahraman, T., Kayhan, R., Çitekçi, K., Kömelek, H., & Öztürk, M. (2018). Narcissus papyraceus Soğanlarında Toplam Fenolik Bileşikler, Toplam Antioksidan Kapasite, Toplam Flavonoid Maddelerin ve Antimikrobiyal Aktivitenin Belirlenmesi. Uşak Üniversitesi Fen ve Doğa Bilimleri Dergisi, 10-17.

Kuo, T. T., Chang, H. Y., Chen, T. Y., Liu, B. C., Chen, H. Y., Hsiung, Y. C., Hsia, S. M., Chang, C. J., & Huang, T. C. (2020). Melissa officinalis Extract Induces Apoptosis and Inhibits Migration in Human Colorectal Cancer Cells. ACS omega, 5(49), 31792–31800.

Magalhães, D. B., Castro, I., Lopes-Rodrigues, V., Pereira, J. M., , Barros, L., Ferreira, I. C. F. R., Xavier, C. P. R., , & Vasconcelos, M. H., (2018). Melissa officinalis L. ethanolic extract inhibits the growth of a lung cancer cell line by interfering with the cell cycle and inducing apoptosis. Food & function, 9(6), 3134–3142.

Maraşlı, Ç., & Öztürk, A. (2021). The Role of Oxidative Stress in the Anticancer Activity of Tannic Acid on the Cervical Cancer (HeLa) Cell Line. Health Sciences Student Journal, 1(3), 86-92.

Miraj, S., Kopaei, R., & Kirani, S. (2016). Melissa officinalis L: A Review Study With an Antioxidant Prospective. J Evid Based Complementary Altern Med, 22(3), 385-394.

Öğüt, S., Erdoğan, Ö., & Karul, A. (2023). Meme Kanseri Hücre Dizisi Üzerinde (MCF-7) Oğulotu (Melissa Officinalis) Bitki Ekstresinin Antiproliferatif , Apoptotik ve Antioksidan Etkilerinin Araştırılması. Adnan Menderes Üniversitesi Sağlık Bilimleri Fakültesi Dergisi, 7(1), 136-144.

Önal, Ö., & Erden, A. (2011). Karvakrol'un oleik asitle oluşturulan akut akciğer hasarına etkisi. Anestezi Dergisi,19(2), 90-98.

Petrisor, G., Motelica, L., Craciun, LN, Oprea, OC, Ficai, D., & Ficai, A. (2022). Melissa officinalis : Kompozisyon, Farmakolojik Etkiler ve Türetilmiş Salım Sistemleri - Bir İnceleme. Uluslararası Moleküler Bilimler Dergisi , 23 (7), 3591.

Saraç, H., Daştan, T., Demirbaş, A., Daştan, S., Karaköy, T., & Durukan, H. (2018). Madımak (Polygonum cognatum Meissn.) Bitki Özütlerinin Besin Elementleri ve In Vitro Antikanserojen Aktiviteleri Yönünden Değerlendirilmesi. Süleyman Demirel Üniversitesi Ziraat Fakültesi Dergisi, 340-347.

Topdemir, A. (2018). Melissa officinalis L. kallus kültürlerinin antoksidan özellikleri. Avrasya Biyolojik ve Kimyasal Bilimler Dergisi, 1(1), 12-15.

Tuchayi, S., Makrantonaki, E., Ganceviciene, R. Dessinioti, C., Feldman, S. & Zouboulis, C. (2015). Akne vulgaris, Nat Rev Dis Primerleri, 15029.

Uylaşer, V., & İnce, K. (2008). Şaraptaki Antioksidanlar ve Fenolik Bileşikler. Uludağ Üniversitesi Ziraat Fakültesi Gıda Mühendisliği Bölümü.

Vijayaraghavan, K., & Yun, Y. (2008). Bacterial biosorbents and biosorption. Biotechnol Adv, 26(3), 266-91.

Yokuş, B., & Çakır, D. Ü. (2012). Kanser Biyokimyası, Dicle Üniversitesi Veteriner Fakültesi Dergisi, 1(2), 7-18.

ORAL PRESENTATION

Evaluation of the cytotoxic effects of Hydroxy Methyl Butyrate (HMB) used as an ergogenic Aid

S. Kara-Ertekin,[1*] (*https://orcid.org/0000-0002-7976-7057*)

[*1]Ülke 1Istanbul Yeni Yuzyil University, Faculty of Pharmacy, Department of Pharmaceutical Toxicology, Istanbul, Turkey

*Corresponding author e-mail: simge.karaertekin@yeniyuzyil.edu.tr

Abstract

Hydroxy Methyl Butyrate (HMB), a leucine-derived metabolite, is widely used as an ergogenic aid to support and increase muscle mass. While its performance-enhancing effects have been demonstrated, data on its toxicological profile at the cellular level remain limited. This study aimed to evaluate the cytotoxic effects of HMB on various normal and cancerous cell lines to assess its tissue-specific toxicity. Cytotoxicity was assessed in seven cell lines, including normal (L929, HOB, HEK) and cancerous (MCF-7, A549, U87MG, Ishikawa) cells. Cells were exposed to HMB concentrations ranging from 10 µM to 2000 µM for 24 hours. Cell viability was measured using the MTT assay. HMB did not show significant cytotoxic effects on HEK and HOB cells at any concentration. However, L929 cells exhibited a substantial decrease in viability (up to 80%) at higher concentrations. Among the cancer cell lines, MCF-7 and U87MG were sensitive to HMB, showing a 75–80% reduction in viability at concentrations ≥1000 µM, while A549 and Ishikawa cells showed minimal response. Cytotoxic effects were primarily observed at concentrations exceeding typical plasma levels achieved through oral supplementation. HMB demonstrated selective cytotoxicity depending on cell type and concentration. Although HMB appears to be safe at recommended doses, tissue-specific adverse effects may occur if exposure levels exceed physiological norms. These findings provide baseline data to support future molecular studies on the safety profile of HMB.

Keywords: Ergogenic aid, Hydroxy Methyl Butyrate, cytotoxicity, sports supplement

INTRODUCTION

In sports science, dietary ergogenic aids are defined as substances or procedures used to enhance performance and accelerate recovery processes. Although the term 'ergogenic aids' is the most common in the scientific literature for performance-enhancing substances, these products are also known as nutritional or sports supplements. The use of ergogenic aids for both professional and recreational purposes is becoming increasingly common (Lopez-Samanes et al., 2015). Substances used as ergogenic aids include anabolic-androgenic steroids, protein powders, branched-chain amino acids (BCAAs), hydroxy methyl butyrate (HMB), colostrum, glutamine, creatine, carnitine, ginseng, taurine, caffeine, chitosan, and ephedrine (Bayram & Öztürkcan, 2020; Dhar et al., 2005).

Beta-hydroxy beta-methylbutyrate (HMB) is a naturally occurring metabolite of leucine, a well-known anticatabolic amino acid, and it can be produced endogenously in humans and animals. Leucine is a crucial amino acid that plays a regulatory role in muscle metabolism. It acts as a precursor for protein synthesis and energy metabolism. The first step in leucine metabolism is its transformation into α-ketoisocaproate (KIC) through transamination. HMB can then be produced from KIC with the help of a cytosolic enzyme called KIC-dioxygenase. Most of the KIC is broken down by KIC-dehydrogenase, an enzyme found only in mitochondria. Roughly 80% of leucine is typically used for protein synthesis, with the remaining portion being converted to α-KIC. Only a small percentage (about 5%) of leucine is changed into HMB (Baxter et al., 2005; Molfino et al., 2013; Pitchford et al., 2018). The formation of HMB through this pathway relies heavily on hepatic KIC dioxygenase. Following this

pathway, cytosolic HMB is initially converted to cytosolic β-hydroxy-β-methylglutaryl-CoA (HMG-CoA), which can then be directed towards cholesterol synthesis. Another pathway involves the production of isovaleryl-CoA by the enzymatic action of branched-chain ketoacid dehydrogenase (BCKD) on α-KIC in the liver after transamination, followed by the production of HMG-CoA via the HMG-CoA synthase enzyme (Zanchi et al., 2011). Numerous biochemical studies have provided evidence that HMB is primarily converted to HMG-CoA, a cholesterol precursor, in the liver and muscles. Therefore, HMB may serve as a precursor for cellular cholesterol synthesis, particularly in tissues like muscle that rely on de novo cholesterol synthesis (Nissen et al., 2000). The possible role of HMB in protecting against muscle damage caused by contraction activity may be related to increased stability of the muscle plasma membrane and enhanced metabolic efficiency. HMB, converted to hydroxy methylglutaryl-CoA (HMG-CoA) for cholesterol synthesis, affects the electrical properties of the skeletal muscle fiber membrane Additionally, Nissen et al. (Nissen et al., 2000) suggested that HMB might act as a precursor to the structural components of cell membranes by enhancing the repair of the sarcolemma after contraction activity. The effect of HMB supplementation on acute muscle fatigue may also involve an increase in acetyl-CoA content, likely through the conversion of HMG-CoA to acetoacetyl-CoA by HMG-CoA synthase within mitochondria. It has also been shown that HMB supplementation leads to increased ATP and glycogen content in the gastrocnemius muscle. HMB may enhance the tricarboxylic acid (TCA) cycle, increase ATP content, activate the malate-aspartate shuttle, and provide a carbon skeleton for glycogen synthesis. In vitro data also suggest that HMB may support an increase in the oxidation of free fatty acids (FFA) in skeletal muscle. Additionally, HMB supplementation may support an increase in lipid availability due to the enhanced lipolysis. Studies have shown that HMB supplementation for 28 days in rats results in decreased epididymal fat tissue content and is also associated with increased plasma FFA concentrations and enhanced gene and protein expression of hormone-sensitive lipase (HSL) in white adipose tissue. This effect may be attributed to an increase in growth hormone (GH) in response to HMB supplementation, as GH stimulates lipolytic enzymes such as HSL (Pinheiro et al., 2013).

Pharmacokinetic data for HMB indicate that its plasma half-life is approximately 2.5 hours. Around 9 hours after intake, HMB levels in the plasma return to baseline. While some HMB is excreted in the urine, 70-85% is retained in the body for further metabolic processes (Pinheiro et al., 2013). The concentration of HMB in the blood following oral administration depends on the dose and whether it is consumed with other foods (Wilson et al., 2013). The pharmacokinetic data for HMB are provided in Table 1.

Table 1. Pharmacokinetic data of HMB (Pinheiro et al., 2013).

Parameter	1g HMB	3g HMB	3g HMB+ 75 g Glucose
Peak plasma concentration	115nmol/L	~480 nmol/L	~350 nmol/L
Time to peak plasma concentration	2.0 h	1.0 h	1.9 h
Plasma half-time	2.37 h	2.38 h	2.69 h
Accumulation in urine	14 %	29%	27%

Given that the endogenous production of HMB is minimal, a 70 kg individual synthesizes only about 0.2 to 0.4 grams of HMB daily from dietary leucine. HMB is found in foods such as citrus fruits, some fish, and breast milk. However, it is very difficult and impractical to obtain the quantities of HMB used in studies that inhibit proteolysis and promote muscle mass gains through diet alone. Although the liver is the primary site of HMB production and shows high dioxygenase activity, studies have shown that muscles and other tissues also produce small amounts of HMB (Pinheiro et al., 2013). It is thought that stressed or damaged muscle cells may not produce sufficient HMG-CoA to support the cholesterol synthesis needed. Supplemented HMB could serve as an adequate source of HMG-CoA production in such muscle cells to maintain proper cholesterol synthesis and support membrane function and structural integrity. As evidenced by a reduction in the leakage of creatine phosphokinase (CK) from muscle cells after intense exercise, it has been observed that supplemented HMB can significantly reduce muscle damage (Baxter et al., 2005). This feature is an option that can be used not only in athletes but also in pathological conditions where muscle loss occurs. It has been adopted as an alternative supplement by individuals under extreme muscle stress, elderly individuals and patients with diseases associated with muscle loss syndromes such as cachexia

(Pinheiro et al., 2013; Zanchi et al., 2011). The mechanisms by which HMB promotes increases in strength and muscle hypertrophy are thought to include the upregulation of IGF-I gene expression in skeletal muscles, stimulation of protein synthesis via the mTOR signaling pathway, and suppression of proteolysis through inhibition of the ubiquitin-proteasome system (Zanchi et al., 2011). This supplement suppresses protein breakdown during the post-workout recovery phase, allowing only carbohydrates and fats to be burned for energy, which results in an increase in lean body mass (Tokish et al., 2004). Additionally, a critical analysis of HMB conducted by the International Society of Sports Nutrition concluded that chronic HMB consumption is safe for both young and elderly populations (Wilson et al., 2013). Studies support that taking 3g of HMB daily as an ergogenic aid is effective in enhancing recovery, lean body mass, strength, power, and aerobic performance (Pinheiro et al., 2013; Wilson et al., 2013). In a study conducted in accordance with FDA Good Laboratory Practices, rats consuming a diet containing up to 5% HMB-CA for 91 days showed no adverse effects in clinical observations, hematology, clinical chemistry, or organ weights. The study reported observed no-adverse-effect levels (NOAEL) of 3.49 g/kg for male rats and 4.16 g/kg for female rats (Baxter et al., 2005; Wilson et al., 2013). Based on the body surface area correction factors recommended by the United States Food and Drug Administration, these levels correspond to approximately 0.5 g/kg in humans. For a 70 kg individual, this equates to more than 30 g/day, which is over 10 times the recommended dose (Pitchford et al., 2018). In humans, consuming up to 6 g of CaHMB per day has not caused any changes in kidney function, liver function, or hematology. Although these data are compelling and support the safe use of HMB, some aspects of HMB's safety profile have not been published to date (Pitchford et al., 2018). However, there has been very little research on the hematologic, hepatic, renal, or cardiac side effects of HMB. This lack of research raises discussions about the safety of HMB use (Dhar et al., 2005).
This study aims to determine the cytotoxic effects of HMB, an ergogenic aid, on various cell lines including L929 (mouse fibroblast cell line), HOB (human osteoblast cell line), HEK (human embryonic kidney cell line), MCF-7 (human breast cancer cell line), A549 (human lung adenocarcinoma cell line), U87MG (human glioblastoma cell line), and Ishikawa (human endometrial cancer cell line). The data obtained will provide a basis for future molecular studies and help in dose selection related to HMB use.

MATERİALS AND METHODS

Chemicals

3-Hydroxy-3-methylbutyric acid (Cas no. 625-08-1) were purchased from Alfa Aesar (Thermo Scientific). Phosphate-buffered saline (PBS), cell culture medium, and all other supplements were obtained from Multicell Wisent Bio Products (Saint-Bruno, Quebec, Canada) and sterile plastic materials were purchased from NEST (Science Co., Ltd., China).

Cell culture and treatment

To determine the cytotoxic effects of HMB, cell lines L929 (mouse fibroblast), HOB (human osteoblast), HEK (human embryonic kidney cell line), MCF-7 (human breast cancer), A549 (human lung adenocarcinoma), U87MG (human glioblastoma), and Ishikawa (human endometrial cancer) were used, and the cells were obtained from ATCC (American Type Culture Collection, Rockville, MD, USA). The cells were incubated in DMEM containing 10% fetal bovine serum and 1% penicillin-streptomycin, with 5% CO2 at 37°C. Stock solutions of 3-Hydroxy-3-methylbutyric acid (HMB) were prepared in PBS at a concentration of 10 mM, and the cells were exposed to concentrations of 10, 100, 200, 400, 600, 1000, and 2000 µM for 24 hours. The solutions were filtered through 0.22 µm filters.
In pharmacokinetic studies, it was reported that the peak plasma concentration of HMB in its free acid form was approximately 487 µM after a 3 g intake, with 28% of this concentration excreted in the urine. Additionally, plasma concentrations may vary depending on whether it is taken with glucose (Vukovich et al., 2001; Wilson et al., 2013). Based on this, and considering that the recommended daily intake is 1, 3, or 6 g, the dose range used in this study was selected to be between 10 µM and 2000 µM.

Cell viability assay

For the MTT (3- (4,5-dimethylthiazol-2-yl)-2,5-diphenyltetrazolium bromide) assay, cells were seeded at a density of 5 × 104 cells per well in 96-well plates and allowed to adhere overnight. The cells were then exposed to six different concentrations of HMB (10-2000 µM). At the end of the exposure period, 10 µl of MTT solution (5 mg/ml in PBS) was added to each well and incubated in the dark for 4 hours. After the formazan crystals formed by viable

cells were dissolved in DMSO, their absorbance was measured at 570 nm using ELISA multi-well plate reader (Thermo Scientific Multiskan GO), and cell viability was calculated relative to the control.

Statistical analysis

Data from the experimental groups and standard errors of the means (SEM) were evaluated using GraphPad Prism 9.5.1 software (StatSoft Inc.). For statistical analysis, One-Way ANOVA was performed followed by Dunnett's multiple comparisons test. A significance level of $p<0.01$ and $p<0.05$ was used for the evaluation of results.

RESULTS

Effects of HMB on cytotoxicity

The effect of different concentrations of HMB on the survival of three normal cells and four cancer cell measured via MTT assay is shown in Figure 2 and 3. After a 24-hour incubation with six different concentrations of HMB (10-2000 µM), cell viability in normal cells did not exhibit a significant difference in HEK and HOB cell lines compared to untreated cells. However, in L929 cells, there was a significant decrease in cell viability, with a reduction of up to approximately 80% (Figure 2).

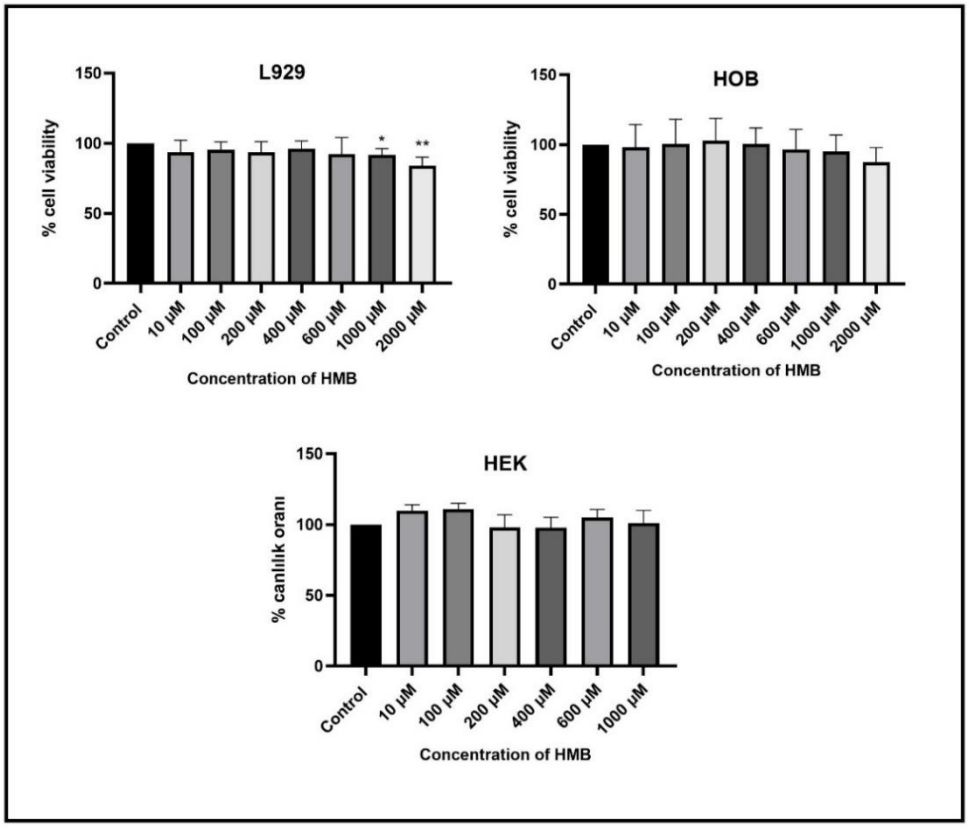


Figure 2. The cytotoxic effect of HMB on L929 (mouse fibroblast), HOB (human osteoblast) and HEK (human embryonic kidney) cells. Each bar denotes the mean (±SEM). HMB indicates β-hydroxy-β-methylbutyrate. Significance at *$p<0.05$, **$p<0.01$, compared with control.

Similarly, the effect of HMB on cell viability in cancer cells was assessed after 24 hours of exposure. A significant decrease in viability, around 75-80%, was observed at 1000 µM concentrations in MCF-7 breast cancer cells and U87MG glioblastoma cells. However, no significant difference was observed in the other investigated cells, including A549 lung adenocarcinoma cells and Ishikawa endometrial adenocarcinoma cells (Figure 3).

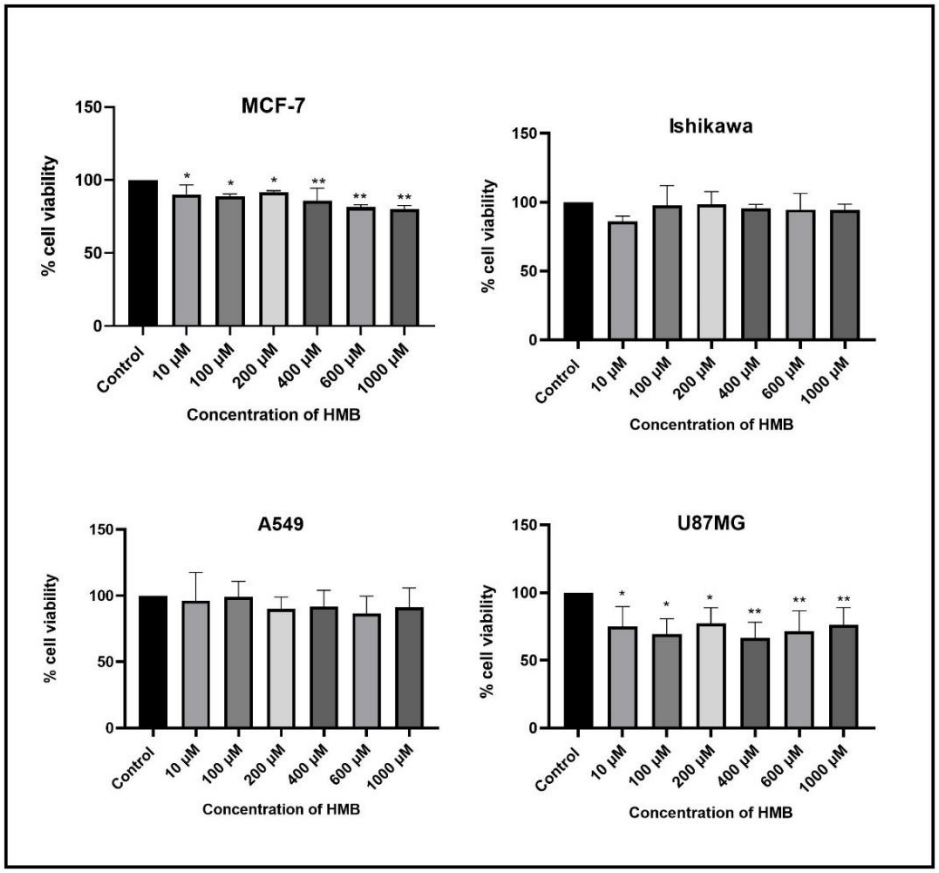


Figure 3. The cancer cells cytotoxicity of HMB. MCF-7 (human breast cancer), A549 (human lung adenocarcinoma), U87MG (human glioblastoma), and Ishikawa (human endometrial cancer) cells were treated with HMB for 24 h. Each bar denotes the mean (±SEM). HMB indicates β-hydroxy-β-methylbutyrate. Significance at *p<0.05, **p<0.01, compared with control.

DISCUSSION

In this study, the cytotoxic effects of Hydroxy Methyl Butyrate (HMB), a widely used ergogenic aid, were evaluated in normal and cancer cell lines using the MTT assay. The data obtained revealed that HMB caused dose-dependent and cell type-specific cytotoxicity, especially at high concentrations. In normal cell lines, HEK (human embryonic kidney) and HOB (human osteoblast) cells maintained high viability at all concentrations after HMB exposure, suggesting that HMB did not cause significant toxicity in these epithelial and bone-derived cells. In contrast, L929 cells (mouse connective tissue cells) showed significant sensitivity with a decrease in viability of up to 80% at higher doses. This discrepancy may be due to both species differences between cells and the higher proliferative activity or metabolic sensitivity of fibroblasts compared to more specialized cells such as osteoblasts (Xia et al., 2008). In the cancer cell group, MCF-7 (breast epithelial adenocarcinoma) and U87MG (glioblastoma) cells were sensitive to HMB and showed a decrease in viability up to 75-80%, while A549 (lung adenocarcinoma) and Ishikawa (endometrial adenocarcinoma) cells showed more resistance. When the results were evaluated according to the tissue origin of the cells; cells of mesenchymal origin (L929) and some epithelial cancer cells (MCF-7) and U87MG cells of nervous system origin appeared to be more sensitive to HMB-induced cytotoxicity. In contrast, cells of renal, pulmonary and osteoblastic origin were found to be relatively resistant.

These findings suggest that tissue-specific metabolic features, such as differences in mitochondrial activity or membrane composition, may influence the cellular response to HMB. The observed sensitivity of U87MG and MCF-7 cells may reflect their higher metabolic demands or unregulated proliferation, making them more vulnerable to metabolic modulators such as HMB.

Importantly, cytotoxic effects were observed at concentrations of 1000 µM and above, while the typical oral dose of HMB of 3 grams per day resulted in the highest plasma concentrations (~487 µM) that were not cytotoxic in any of the human cell lines tested. This finding supports the idea that recommended daily doses of HMB are within safe physiological limits, especially for healthy individuals or athletes using supplements (Vukovich et al., 2001; Wilson et al., 2013). In terms of sports health, the data support the idea that HMB is unlikely to pose a cytotoxic risk at standard supplementation levels, particularly to tissues of kidney, bone, or lung origin. However, the effects observed in certain cancer lines highlight the potential for selective cytotoxicity that could be investigated in future therapeutic repurposing studies.

In conclusion, this study provides a detailed view of the cytotoxic profile of HMB by including a variety of cell types from different tissue origins and highlights the importance of both dose and cellular context in assessing the safety and potential applications of ergogenic supplements.

Conflict of interest statement

The authors declare that there are no conflicts of interest.

Data Availability Statement

The data supporting the findings of this study are available from the corresponding author upon reasonable request.

REFERENCE

Baxter, J. H., Carlos, J. L., Thurmond, J., Rehani, R. N., Bultman, J., & Frost, D. (2005). Dietary toxicity of calcium beta-hydroxy-beta-methyl butyrate (CaHMB). *Food Chem Toxicol*, *43*(12), 1731-1741. https://doi.org/10.1016/j.fct.2005.05.016

Bayram, H. M., & Öztürkcan, S. A. (2020). Sporcularda ergojenik destekler. *Türkiye Klinikleri Sağlık Bilimleri Dergisi*.

Dhar, R., Stout, C. W., Link, M. S., Homoud, M. K., Weinstock, J., & Estes III, N. M. (2005). Cardiovascular toxicities of performance-enhancing substances in sports. (Ed.),^(Eds.). Mayo Clinic Proceedings.

Lopez-Samanes, A., Fonseca, J. F. O., Elías, V. E. F., Borreani, S., Maté-Muñoz, J. L., & Kovacs, M. S. (2015). Nutritional ergogenic aids in tennis: A brief review. *Strength & Conditioning Journal*, *37*(3), 1-11.

Molfino, A., Gioia, G., Rossi Fanelli, F., & Muscaritoli, M. (2013). Beta-hydroxy-beta-methylbutyrate supplementation in health and disease: a systematic review of randomized trials. *Amino Acids*, *45*, 1273-1292.

Nissen, S., Sharp, R., Panton, L., Vukovich, M., Trappe, S., & Fuller Jr, J. (2000). β-Hydroxy-β-methylbutyrate (HMB) supplementation in humans is safe and may decrease cardiovascular risk factors. *The Journal of nutrition*, *130*(8), 1937-1945.

Pinheiro, C. H. J., Guimaraes-Ferreira, L., Gerlinger-Romero, F., & Curi, R. (2013). An overview on beta-hydroxy-beta-methylbutyrate (HMB) supplementation in skeletal muscle function and sports performance. *Nutrition and Enhanced Sports Performance*, 455-463.

Pitchford, L. M., Fuller, J. C., Jr., & Rathmacher, J. A. (2018). Genotoxicity assessment of calcium beta-hydroxy-beta-methylbutyrate. *Regul Toxicol Pharmacol*, *100*, 68-71. https://doi.org/10.1016/j.yrtph.2018.10.016

Tokish, J. M., Kocher, M. S., & Hawkins, R. J. (2004). Ergogenic aids: a review of basic science, performance, side effects, and status in sports. *Am J Sports Med*, *32*(6), 1543-1553. https://doi.org/10.1177/0363546504268041

Vukovich, M. D., Slater, G., Macchi, M. B., Turner, M. J., Fallon, K., Boston, T., & Rathmacher, J. (2001). β-hydroxy-β-methylbutyrate (HMB) kinetics and the influence of glucose ingestion in humans. *The Journal of nutritional biochemistry*, *12*(11), 631-639.

Wilson, J. M., Fitschen, P. J., Campbell, B., Wilson, G. J., Zanchi, N., Taylor, L., Wilborn, C., Kalman, D. S., Stout, J. R., & Hoffman, J. R. (2013). International society of sports nutrition position stand: beta-hydroxy-beta-methylbutyrate (HMB). *Journal of the International Society of Sports Nutrition*, *10*, 1-14.

Xia, M., Huang, R., Witt, K. L., Southall, N., Fostel, J., Cho, M.-H., Jadhav, A., Smith, C. S., Inglese, J., & Portier, C. J. (2008). Compound cytotoxicity profiling using quantitative high-throughput screening. *Environmental health perspectives*, *116*(3), 284-291.

Zanchi, N. E., Gerlinger-Romero, F., Guimaraes-Ferreira, L., de Siqueira Filho, M. A., Felitti, V., Lira, F. S., Seelaender, M., & Lancha, A. H. (2011). HMB supplementation: clinical and athletic performance-related effects and mechanisms of action. *Amino Acids*, *40*, 1015-1025.

ORAL PRESENTATION

Health emergency management in a regional coastal hospital during the tourist season

Mirva Hoxha* (ORCID: https://orcid.org/0009-0004-2757-3340)
Arber Hoxha* (ORCID: https://orcid.org/0009-0003-4715-7582)

Aldent University, Faculty of Medical Tecnical Sciences, Department of Nursing, Tirana, Albania.

*Corresponding author e-mail: mirva.hoxha@ual.edu.al

Abstract

The World Health Organization defines health emergencies as medical events requiring immediate intervention. Hospitals located in tourist areas face increased workload during the tourist season due to the influx of domestic and foreign visitors. This study focuses on the management of health emergencies during the tourist season in a Regional Hospital in Albania, which experiences exceptionally high patient inflows every summer. The aim of the study is to identify effective management challenges, assess existing capacities, and propose improvements in organizational and nursing services during peak tourist periods (Alsomali et al. 2024). The research question guiding this study is: How does the high patient influx affect the quality and effectiveness of health emergency management during the tourist season? A qualitative methodological approach was applied, using a structured questionnaire administered to emergency department staff to collect data on their experiences, perceptions, and needs. The results suggest the necessity for concrete measures, including mandatory staff training, enhanced inter-institutional cooperation, improved emergency protocols, and investments in infrastructure. These actions are essential to ensure a rapid, safe, and efficient response to emergencies during periods of high patient load. In conclusion, the study highlights the urgent need for a clear emergency management strategy during the tourist season, increased staffing levels, improved infrastructure, and the development of specialized protocols. The findings aim to contribute to the improvement of health emergency management in tourist cities and serve as a basis for strategic health policy planning at both local and national levels.

Keywords: emergency management, tourist season, nursing care, patient influx, healthcare system

INTRODUCTION

Coastal and tourist areas face unique challenges in managing health emergencies. Although these regions attract a large number of visitors during the tourist season, they often operate with limited healthcare resources and infrastructure. Consequently, hospitals in such areas are frequently required to handle a sudden and significant increase in emergency cases, including trauma, infectious diseases, cardiac events, gastrointestinal disorders, and incidents related to environmental or weather conditions. (Turcato et al. 2023)

Regional coastal hospitals, situated in high-tourism zones, experience a notable rise in emergency admissions during the summer months. This seasonal surge affects resource management, staff organization, and the ability to deliver timely and effective patient care. In this context, the present study seeks to examine and analyze the existing practices of health emergency management (HEM) in a regional coastal hospital and to identify opportunities for improvement. The primary aim of this study is to assess how health emergencies are managed during the tourist season and to identify methods and practices that can enhance the efficiency and quality of emergency medical services. It further evaluates the challenges

faced by nurses and physicians, with the goal of developing recommendations that can strengthen emergency management and optimize healthcare delivery during peak tourist periods.
The study focuses on three main objectives: (1) to analyze the impact of the tourist season on the management of health emergencies; (2) to identify strategies for improving emergency management during the tourist season; and (3) to review current policies and practices related to emergency care. (Hitzek et al. 2022)
This research is significant for several reasons. First, it provides an opportunity to evaluate and improve how health emergencies are managed in coastal hospitals where patient influx is highly seasonal. Second, it offers practical insights for healthcare professionals—particularly nurses and physicians—by identifying the main challenges they encounter and proposing ways to enhance their working conditions and reduce occupational stress. Finally, the findings of this study have implications for local and national health policy, as they can inform the development of more effective emergency management strategies and resource allocation plans. Ultimately, this research aims to contribute to improving the quality and responsiveness of healthcare services for both local communities and tourists during high-demand periods

MATERIALS AND METHODS:

Methodological Approach

This research employs a mixed-method approach, combining both quantitative and qualitative data collection and analysis. Such a design enables a comprehensive understanding of the factors influencing emergency management and allows for triangulation between statistical evidence and staff perceptions. (Lewis et al. 2023)
The study is empirical, descriptive, and comparative in nature, grounded in both theoretical frameworks of health management and practical data collected from hospital records and staff surveys. The analysis focuses on identifying trends in emergency case frequency, workload variation, and service organization during the tourist season compared to other period*s.*

Study Setting and Period

The research was conducted at a Regional Hospital located in a coastal area of Albania, chosen intentionally for its distinct seasonal fluctuations in patient volume. This hospital serves as a regional referral center, providing emergency services not only to the local urban population but also to surrounding rural communities and a large number of domestic and international tourists during summer. Data collection took place between March and May 2025, using structured questionnaires distributed electronically to the hospital's medical and nursing staff.

Data Collection Instrument

The main research instrument was a structured questionnaire, specifically designed for this study and divided into two sections.
The first section (Questions 1–4) collected demographic data about participants.
The second section (Questions 5–12) focused on issues related to emergency management, including patient waiting times, infrastructure adequacy, workload, and operational challenges during the tourist season.
All questions were closed-ended, using a five-point Likert scale (1–5) to measure participants' perceptions and experiences. The questionnaire was distributed electronically to ensure accessibility, data accuracy, and participant anonymity. This digital approach also facilitated efficient data collection and real-time monitoring of responses.

Data Analysis

Data obtained from the questionnaires were analyzed using descriptive statistical methods with Microsoft Excel. The analysis included calculations of frequencies, percentages, and mean scores, and the results were presented through tables and charts. This allowed for a clear interpretation of the staff's perceptions regarding waiting times, workload intensity, and the overall effectiveness of institutional and organizational management during the tourist season.

Ethics and Confidentiality

In accordance with ethical standards for scientific research, special attention was given to protecting participants' rights and ensuring the confidentiality of collected data. All participating physicians and nurses were clearly informed about the study's purpose, significance, and the use of their responses. Participation was voluntary, and informed consent was obtained electronically from each respondent. No personally identifiable information was collected, ensuring full anonymity and privacy. All responses were used solely for research purposes and analyzed in aggregate form to maintain confidentiality

RESULTS

Table 1: Dermografic datas, age and gender of nursing and medical staff

Age Group	Female (n, %)	Male (n, %)	Total (n, %)
Under 25 years	1 (3.6%)	0 (0%)	1 (3.6%)
25–35 years	6 (21.4%)	5 (17.9%)	11 (39.3%)
36–45 years	6 (21.4%)	5 (17.9%)	11 (39.3%)
46–55 years	2 (7.1%)	2 (7.1%)	4 (14.3%)
Over 55 years	0 (0%)	1 (3.6%)	1 (3.6%)
Total	15 (53.5%)	13 (46.5%)	28 (100%)

Table 2: Profession of healthcare staff

Profession	Number	Percentage (%)
Doctor	5	18
Nurse	23	82
Total	28	100

Table 3 Experience of healthcare staff in the hospital emergency department

Experience in the Healthcare System	Number	Percentage(%)
Less than 1 year	1	3.6
1–5 years	7	25
6–10 years	10	35.7
More than 10 years	10	35.7
Total	28	100

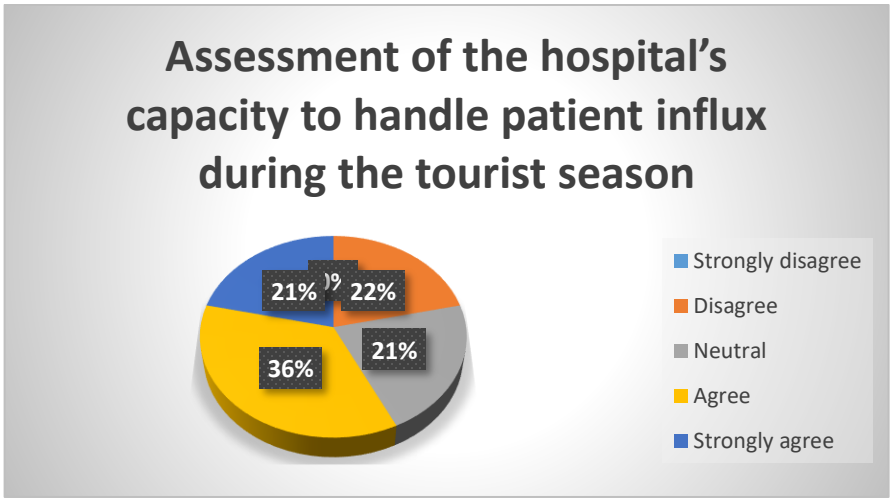


Figure 1: Assessment of the hospital's capacity to handle patient influx during the tourist season

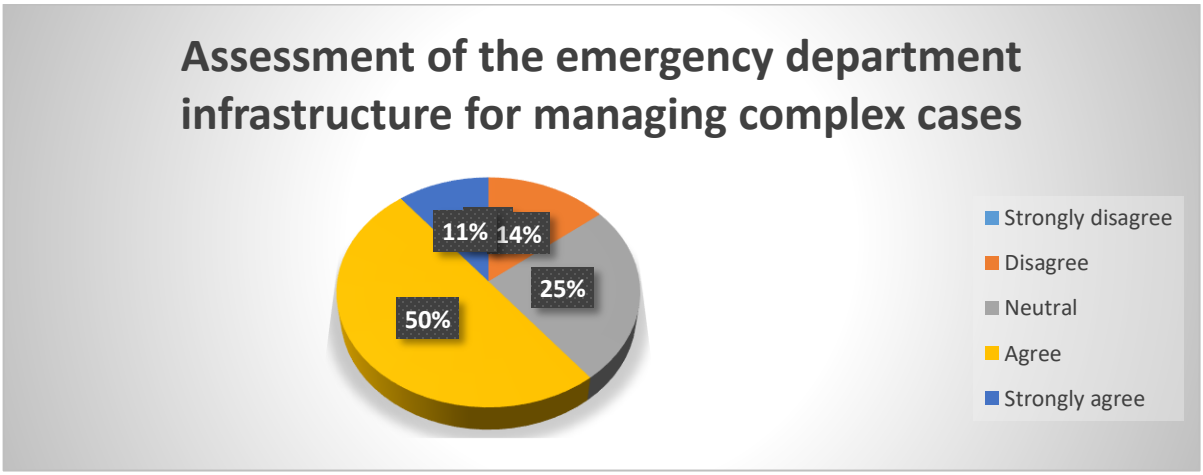


Figure 2: **Assessment of the emergency department infrastructure for managing complex cases**

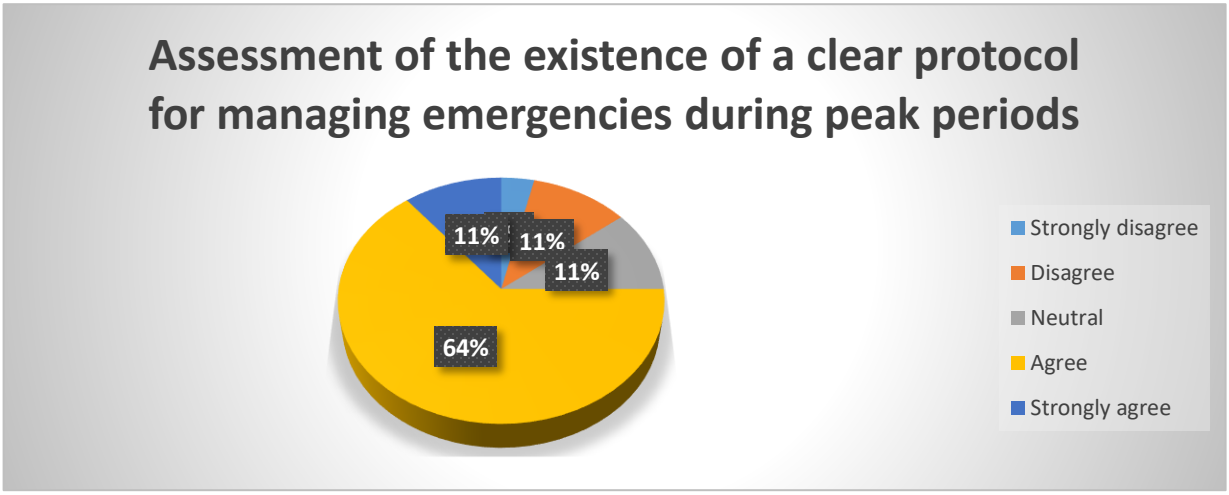


Figure 3: Assessment of the existence of a clear protocol for managing emergencies during peak periods

Tabela 4. **Assessment of the impact of patient influx on response time and quality of healthcare**

Patient influx affects response time and quality of care provided	**Number**	**Percentage (%)**
Strongly disagree	13	46.4
Disagree	7	25
Neutral	1	3.6
Agree	6	21.4
Strongly agree	1	3.6
Total	28	100

Tabela 5. **Assessment of patient waiting time in the emergency department during the tourist season**

How do you evaluate the patient waiting time from arrival at the emergency department to receiving medical care during the tourist season?	**Number**	**Percentage (%)**
Very long	0	0
Long	1	3.6
Acceptable	15	53.6
Short	9	32.1
Very short	3	10.7
Total	28	100

Tabela 6. Hospital Preparedness and Challenges in Managing High Patient Load and Foreign Patients

Statement	**Strongly Disagree**	**Disagree**	**Neutral**	**Agree**	**Strongly Agree**	**Total**
The hospital provides training for managing emergencies during high patient load periods	1 (3.6%)	2 (7.1%)	12 (42.9%)	13 (46.4%)	0 (0%)	28 (100%)
There are procedures for managing non-resident or foreign patients	2 (7.1%)	1 (3.6%)	3 (10.7%)	20 (71.4%)	2 (7.1%)	28 (100%)
The increase in tourists creates challenges in communication and rapid diagnosis	1 (3.6%)	5 (17.9%)	4 (14.3%)	9 (32.1%)	9 (32.1%)	28 (100%)

CONCLUSIONS AND RECOMMENDATIONS

The study shows that the Regional Hospital effectively maintains the quality of emergency services despite a substantial increase in patient flow during the tourist season. The majority of staff positively evaluated the department's infrastructure, the existence of protocols, and response times, indicating a well-organized and functional system. Nevertheless, certain gaps were identified, particularly the lack of structured training programs for managing high patient volumes and challenges in communication and rapid diagnosis with non-resident and foreign patients. These findings highlight that while the hospital operates reliably under peak conditions, targeted improvements in technical resources, staff training, and patient communication strategies are essential to enhance overall emergency care performance during periods of high tourist activity.

The study recommends developing a seasonal operational plan to ensure adequate staffing, equipment, and flexible shifts during peak tourist months, complemented by regular training for managing high patient volumes and high-risk emergencies. (Walker et al. 2016) Strengthening triage systems, providing multilingual support for foreign patients, and investing in medical infrastructure are essential. Enhancing inter-institutional coordination, promoting community awareness, supporting staff wellbeing, and conducting post-season evaluations will further improve the quality and efficiency of emergency care during the tourist season.

REFERENCES

Alsomali, M. S., et al. (2024). "Improving Quality of Care for Vacation-Related Emergency Department Visits." *Journal of Emergency Medicine*, 67(3), 123-130. https://pmc.ncbi.nlm.nih.gov/articles/PMC11677494/

Turcato, G., et al. (2023). "Impact of Tourists on Emergency Department in a High-Tourism Region." *European Journal of Emergency Medicine*, 30(2), 85-92. https://www.sciencedirect.com/science/article/pii/S147789392200237X

Hitzek, J., et al. (2022). "Influence of Weekday and Seasonal Trends on Urgency and Hospital Mortality in Emergency Departments." *BMC Emergency Medicine*, 22(1), 45. https://pmc.ncbi.nlm.nih.gov/articles/PMC9068998/

Lewis, J., et al. (2023). "Understanding Seasonal Demand for Emergency Care." *Emergency Medicine Journal*, 40(12), 883-889. https://emj.bmj.com/content/40/12/883

Walker, N. J., et al. (2016). "Identifying Seasonal and Temporal Trends in Pressures Experienced by Hospitals in Relation to Unscheduled Care." *BMC Health Services Research*, 16, 555. https://bmchealthservres.biomedcentral.com/articles/10.1186/s12913-016-1555-7

ORAL PRESENTATION

Koç testislerinin 3B modellenmesinde doku matlaştırma işleminin model parametrelerine etkisi

Alper Koçyiğit[1*] (*ORCID: https://orcid.org/0000-0001-9639-5497)*

[*1]Ondokuz Mayıs Üniversitesi, Veteriner Fakültesi, Dölerme ve Suni Tohumlama ABD, Samsun, Türkiye

*Sorumlu yazar e-mail: alper.kocyigit@omu.edu.tr

Özet

Bu çalışma, koç testislerinin üç boyutlu (3B) modellenmesinde yüzey matlaştırma işleminin model kalitesi üzerindeki etkisini değerlendirmek amacıyla yürütülmüştür. Mezbahadan temin edilen altı çift testis laboratuvara getirilmiş, serum fizyolojik ile temizlenmiş ve morfometrik ölçümleri yapılmıştır. Örnekler rastgele iki gruba ayrılmıştır: Grup 1'deki testisler herhangi bir yüzey işlemi uygulanmadan, Grup 2'deki testisler ise tüm yüzeylerine matlaştırıcı sprey (3D Mat) uygulanarak taranmıştır. Tüm örnekler optik tarayıcı (Structure Sensor, Occipital Inc.) kullanılarak 0,5 mm çözünürlükte 360° taranmış ve elde edilen .obj dosyaları 3D Builder yazılımında işlenmiştir. Modeller Autodesk Meshmixer yazılımında poligon sayısı, yüzey hatası ve artefakt varlığı açısından analiz edilmiştir. Sonuçlar her iki grup arasında morfometrik ölçümler açısından anlamlı fark olmadığını ($p>0.05$) göstermiştir. Hata sayısı matlaştırıcı uygulanan grupta (6.5 ± 0.2), doğal yüzeyli gruba (7.1 ± 0.7) göre düşük olmakla birlikte fark istatistiksel olarak anlamlı bulunmamıştır ($p>0.05$). Görsel değerlendirmede matlaştırılmış modellerin yüzey yansımalarının azaldığı ve tarama bütünlüğünün daha kararlı olduğu gözlenmiştir. Elde edilen bulgular, yüzey matlaştırma uygulamasının organların 3B modellenmesinde optik yansıma kaynaklı hataları azaltma potansiyeline sahip olduğunu, ancak etkinin istatistiksel olarak anlamlı düzeyde olmadığını göstermektedir. Bu durum, yüzey işlemlerinin karmaşık dokularda daha belirgin fayda sağlayabileceğini düşündürmektedir.

Anahtar Kelimeler: Veteriner hekimliği eğitimi, testis biyomodelleri, 3B modelleme, optik tarama, matlaştırma

The effect of surface matting on model parameters in 3D modelling of ram testes

Abstract

This study was conducted to evaluate the effect of surface matting on the quality of three-dimensional (3D) models of ram testes. Six pairs of testes obtained from a slaughterhouse were brought to the laboratory, cleaned with physiological saline, and subjected to morphometric measurements. The samples were randomly divided into two groups: Group 1 testes were scanned without any surface treatment, while Group 2 testes were coated with a matte spray (3D Mat) covering the entire surface before scanning. All samples were scanned using an optical scanner (Structure Sensor, Occipital Inc.) at 0.5 mm resolution with 360° rotation, and the obtained .obj files were processed using 3D Builder software. The models were analysed in Autodesk Meshmixer software in terms of polygon count, surface errors, and artifact presence. The results showed no significant difference between the groups in morphometric measurements ($p > 0.05$). The number of surface errors was lower in the matte-coated group (6.5 ± 0.2) compared to the untreated group (7.1 ± 0.7), but the difference was not statistically significant ($p > 0.05$). Visual assessment revealed that the matte-coated models exhibited reduced surface reflections and more stable scanning integrity. These findings indicate that surface matting has the potential to reduce optical reflection-related

errors in the 3D modelling of biological organs, although the effect was not statistically significant. This suggests that surface treatment may provide more evident benefits when applied to complex tissues.
Keywords: Veterinary medical education, testis biomodels, 3D modelling, optical scanning, matting

GİRİŞ

Veteriner hekimliği eğitimi, öğrencilerin karmaşık anatomik yapıları üç boyutlu (3B) olarak kavrayabilmelerini gerektiren uygulamalı bir disiplindir. Ancak, geleneksel kadavra temelli eğitim materyalleri; etik kaygılar, biyogüvenlik gereksinimleri, sınırlı örnek erişimi ve uzun vadede doku bozulması gibi çeşitli kısıtlarla karşı karşıyadır (McMenamin ve ark., 2018). Bu nedenlerle son yıllarda, sanal anatomi uygulamaları, 3B biyomodeller gibi alternatif eğitim araçları giderek önem kazanmıştır (Kocyigit ve ark., 2023a). Bu araçlar hem öğrencilerin öğrenme deneyimlerini zenginleştirmekte hem de sürdürülebilir ve etik açıdan uygun eğitim materyalleri sağlamaktadır (Seymour ve ark., 2020; Kocyigit ve ark., 2023b).

Veteriner anatomi eğitiminde testis biyomodelleri, erkek üreme sisteminin morfolojik özelliklerinin anlaşılmasında önemli bir rol oynamaktadır. Gerçek dokuya morfolojik olarak yüksek benzerlik gösteren modeller, testis-epididimis ayrımı, epididimisin kısımları, spermin izlediği yol gibi karmaşık anatomik detayların öğretiminde yüksek görsel doğruluk sağlamaktadır (Kocyigit ve ark., 2021; ve ark., 2013). Bu doğruluk, öğrencilerin topografik anatomi kavrayışını güçlendirerek klinik uygulamalarda palpasyon ve cerrahi beceri gelişimini desteklemektedir.

Organların 3B modellenmesinde çeşitli yöntemler kullanılmaktadır. Bunlar arasında bilgisayarlı tomografi (BT), manyetik rezonans görüntüleme (MRG), optik ve lazer temelli tarama sistemleri öne çıkmaktadır (Li ve ark., 2021). Her yöntemin uzamsal çözünürlük, renk doğruluğu, maliyet ve işlem süresi açısından avantaj ve sınırlılıkları vardır. Özellikle optik tarama yöntemleri, organların dış yüzey morfolojisini yüksek detayda yakalayabilme potansiyeli nedeniyle anatomik modellemelerde yaygınlaşmaktadır. Ancak, bu yöntemlerde parlak veya ıslak yüzeylerin yüksek yansıtıcılığı, sensörlerin doğru derinlik algısını bozarak geometri hatalarına neden olmaktadır (Zheng ve ark., 2022).

Bu sorunun giderilmesi için son dönemde yüzey matlaştırma teknikleri geliştirilmiştir. Organ yüzeylerine uygulanan matlaştırıcı sprey veya pudra tabakaları, yansıma kaynaklı optik hataları azaltmakta ve tarayıcının ışık geri yansımasını homojenleştirerek nokta bulutu kalitesini artırmaktadır (Rebner ve ark., 2020). Bu yaklaşım, özellikle nemli ve düzensiz yüzeyli biyolojik dokuların taranmasında model bütünlüğünü koruma açısından kritik öneme sahiptir.

Bu çalışmanın amacı, koç testis dokularının 3B modellenmesinde yüzey matlaştırma işleminin model kalitesi üzerindeki etkisini değerlendirmektir. Çalışmanın hipotezi, organ yüzeylerine uygulanan 3D Mat gibi matlaştırıcı ajanların, ıslak doku yüzeylerine kıyasla yansımaları azaltarak optik tarama kalitesini ve buna bağlı olarak elde edilen 3B modelin geometrik doğruluğunu artırdığı yönündedir. Bu hipotezin test edilmesi, veteriner anatomi eğitiminde kullanılacak biyomodellerin üretiminde standartlaştırılmış tarama protokollerinin geliştirilmesine katkı sağlayacaktır.

MATERYAL VE METOT

Testislerin Hazırlanması ve Deneme Gruplarına Ayrılması

Bu çalışmada, toplam altı çift koç (Ovis aries) testisi, mezbahada kesim sonrasında elde edilmiştir. Testisler, kesimi takiben en fazla 30 dakika içinde laboratuvara getirilmiştir. Numuneler oda sıcaklığında tutulmuş, serum fizyolojik (0,9% NaCl) ile nazikçe yıkanarak yüzeydeki kan, pıhtı ve sekresyon kalıntılarından arındırılmıştır. Daha sonra, testisi çevreleyen tunika vajinalis tabakası makas yardımıyla uzaklaştırılmıştır. Her testis için morfometrik ölçümler (uzunluk, genişlik ve çevre) dijital kumpas (±0,01 mm hassasiyet) kullanılarak gerçekleştirilmiştir.

Morfometrik ölçümlerin ardından testisler rastgele yöntemle iki deneme grubuna ayrılmıştır. Birinci grupta yer alan testislere (n = 6) modelleme öncesinde herhangi bir yüzey işlemi uygulanmamış, doğrudan tarama sehpasına yerleştirilmiştir. İkinci grup testislere (n = 6) ise optik tarama öncesinde, organın tüm yüzeyini eşit şekilde kaplayacak biçimde matlaştırıcı sprey (3D Mat, Aesub®) uygulanmıştır. Uygulama, homojen kaplama sağlamak amacıyla 20–25 cm mesafeden, 10 saniyelik püskürtme aralıklarıyla gerçekleştirilmiştir.

Testislerin 3B Modellenmesi

Her bir testisin üç boyutlu (3B) hacimsel verileri optik tarayıcı (Structure Sensor; Occipital Inc., San Francisco, ABD) kullanılarak elde edilmiştir. Tarama işlemleri, sabit bir platform üzerinde 360° döndürme yöntemiyle yapılmış; 0,5 mm çözünürlükte veri setleri elde edilmiştir. Elde edilen yüzey verileri, Object dosya formatında (.obj) kaydedilerek bilgisayar ortamına aktarılmıştır.

Model Verilerinin Analizi

Her iki grupta elde edilen 3B modeller, Autodesk Meshmixer yazılımı (Autodesk Inc., ABD) aracılığıyla analiz edilmiştir. Modeller, referans organlarla morfometrik ölçüler bakımından karşılaştırılmıştır. Ayrıca her iki gruba ait 3B modeller yüzey kalitesi, poligon sayısı ve artefakt (bozulmuş veya hatalı yüzey alanı) varlığı açısından birbirleriyle karşılaştırılmıştır. Yüzey düzgünlüğü görsel olarak incelenmiş, poligon sayısı otomatik olarak yazılım tarafından raporlanmıştır. Artefakt sayısı manuel inceleme ile belirlenmiştir.

İstatistiksel Analiz

Her iki gruba ait sayısal veriler için ortalama ve standart sapma değerleri hesaplanmıştır. Gruplar arasındaki farkın istatistiksel anlamlılığı Student t testi ile değerlendirilmiştir. İstatistiksel analizler IBM SPSS Statistics (v.25.0; IBM Corp., Armonk, NY, ABD) yazılımı kullanılarak gerçekleştirilmiş ve anlamlılık düzeyi $p < 0,05$ olarak kabul edilmiştir.

BULGULAR

Referans testislerin ortalama uzunluğu 81.37 ± 5.4 mm, genişliği ise 22.07 ± 2.8 mm olarak ölçülmüştür. Üç boyutlu modellemeye tabi tutulan gruplar arasında morfometrik ölçümler açısından anlamlı fark saptanmamıştır ($p > 0.05$). Doğal yüzeyli (matlaştırılmamış) testis modellerinde ortalama uzunluk 79.23 ± 4.4 mm, genişlik 20.12 ± 1.7 mm; matlaştırıcı uygulanan testis modellerinde ise uzunluk 80.92 ± 3.5 mm ve genişlik 21.61 ± 3.5 mm olarak belirlenmiştir.

Model kalitesi açısından değerlendirildiğinde, optik tarama sonrasında elde edilen 3B verilerde her iki grup arasında yüzey bütünlüğü bakımından sayısal fark gözlenmiş olsa da bu fark istatistiksel olarak anlamlı bulunmamıştır ($p > 0.05$). Doğal yüzeyli grupta ortalama hata (artefakt) sayısı 7.1 ± 0.7 iken, matlaştırıcı uygulanan grupta bu değer 6.5 ± 0.2 olarak kaydedilmiştir.

Tablo 1. Testis modellerinin morfometrik verileri ve hata sayıları

	nn	**Uzunluk mm**	**Genişlik mm**	
Referans testisler	112	81.37 ± 5.4	22.07 ± 2.8	Hata sayısı
Grup 1 (Natural) testis modelleri	66	79.23 ± 4.4	20.12 ± 1.7	7.1 ± 0.7
Grup 2 (Matlaştırılan) testis modelleri	6	80.92 ± 3.5	21.61 ± 3.5	6.5 ± 0.2

$p>0.05$

TARTIŞMA

Bu çalışmada, koç testislerinin üç boyutlu (3B) modellenmesinde yüzey matlaştırma işleminin tarama kalitesi üzerindeki etkisi değerlendirilmiştir. Optik tarama yöntemi, referans dokuların morfolojik özelliklerinin yüksek çözünürlükte dijitalleştirilmesine olanak tanıyan, invaziv olmayan bir tekniktir. Ancak ıslak ve parlak organ yüzeyleri, tarayıcı sensörlerde aşırı yansımalara ve buna bağlı olarak tarama eksikliklerine neden olmaktadır (Zheng ve ark., 2022). Bu nedenle yüzey matlaştırma uygulamaları, yansımayı azaltmak ve model geometrisinin bütünlüğünü korumak amacıyla önerilmektedir (Rebner ve ark., 2020).

Elde edilen sonuçlar, matlaştırıcı uygulanan testis modellerinde hata (artefakt) sayısının sayısal olarak daha düşük olduğunu, ancak bu farkın istatistiksel olarak anlamlı olmadığını göstermiştir ($p>0.05$). Bu bulgu, yüzey matlaştırma işleminin tarama sürecinde bir miktar iyileşme sağladığını ancak örnek sayısının sınırlı olması nedeniyle anlamlı düzeyde farklılık oluşturmadığını düşündürmektedir. Benzer biçimde, Furtner (2020) ve Li ve ark., (2021) tarafından yapılan çalışmalar da yüzey optik özelliklerinin tarama kalitesini etkilediğini, fakat nem oranı, doku homojenliği ve ışık açısının da sonucu önemli ölçüde belirlediğini bildirmiştir. Morfometrik ölçümler, referans testislerle modellenmiş testisler arasında anlamlı fark göstermemiştir. Bu durum, 3B tarama sisteminin temel geometrik doğruluğunu koruduğunu ve organ boyutlarının dijital modele doğru biçimde aktarıldığını ortaya koymaktadır. Diğer yandan testis dokusunun parlak yapısına rağmen 3B tarayıcı ile 0,5 mm çözünürlükte kabul edilebilir düzeyde modelleme yapılabilmiştir. Bu durum, uygun tarama mesafesi ve sabit ışık koşullarının doğru şekilde ayarlanmasının, matlaştırma uygulaması kadar belirleyici olduğunu göstermektedir. Ayrıca, matlaştırıcı ajanların doku yüzeyinde kalın tabaka oluşturması olası mikro-doku detaylarının kaybına neden olabileceğinden, uygulama miktarının standardize edilmesi önemlidir.

Elde edilen bulgular matlaştırıcı sprey kullanımının 3B modelleme sürecinde optik hataları azaltabileceğini, ancak bu etkinin belirgin düzeyde istatistiksel fark yaratmadığını ortaya koymaktadır. Bu durum, yüzey işlemlerinin özellikle karmaşık organlarda daha belirgin fayda sağlayabileceği hipotezini destekler niteliktedir.

Koç testislerinin 3B modellenmesinde yüzey matlaştırma işlemi, optik tarama sürecinde yansıma kaynaklı veri kayıplarını azaltma eğilimi göstermiştir. Matlaştırıcı uygulanan grupta hata sayısı daha düşük olmasına rağmen fark istatistiksel olarak anlamlı bulunmamıştır ($p > 0.05$). Bu bulgu, tarama kalitesinin yalnızca yüzey optik özelliklerinden değil, tarayıcı çözünürlüğü, örnek konumlandırması ve çevresel ışık koşullarından da etkilendiğini göstermektedir. Veteriner hekimliği eğitiminde kullanılacak biyomodellerin geliştirilmesinde, yüzey matlaştırma uygulamalarının organlarda tarama kalitesini artırabileceğini değerlendirmekteyiz.

KAYNAKLAR

Braid, H. R., Premkumar, K., & Clarke, A. F. (2022). The use of simulators for teaching practical clinical skills: A review in the context of veterinary education. Journal of Veterinary Medical Education, 49(4), 562–570. https://doi.org/10.3138/jvme-2021-0123

Díaz Martínez, E., Zarzosa, G. J. R., Arencibia Espinosa, A., Soler Laguía, M., Rojo Ríos, D., Lorente, A. O., & Gil Cano, F. (2025). Veterinary students' assessment of 3D anatomical prints as new teaching material in practical veterinary anatomy classes. Education Sciences, 15(3), 355. https://doi.org/10.3390/educsci15030355

Furtner, M. J. (2020). Comparing the accuracy of close-range photogrammetry to micro-CT scanning via surface deviation analysis of 3D digital models (Master's thesis). Louisiana State University. https://repository.lsu.edu/gradschool_theses/5099

Kocyigit, A., & Narlicay, S. (2021). The production of testis biomodels using three-dimensional (3D) technologies. Andrologia, 53(9), e14171.

Kocyigit, A., Yuksel, E., & Yuksel, O. (2023a). Assessing the Effectiveness of 3D-Printed Testes and Ovary Biomodels in Veterinary Reproduction Education: Student-Centered Approach. Journal of Veterinary Medical Education, 51(6), 722-729.

Koçyiğit, A., ARI, H., & USLU, B. (2023b). An Insight Into Veterinary Students' Perceptions on the use of 3D-Printed Bone Biomodels in Anatomy Learning Vpogled v mnenje študentov veterine o uporabi 3D-tiskanih bioloških modelov kosti pri učenju anatomije. Slovenian Veterinary Research, 60(3).

Li, X., Zhang, Y., & Zhao, W. (2021). Accuracy evaluation of structured-light 3D scanning for biological surface modeling. Journal of Imaging, 7(9), 185. https://doi.org/10.3390/jimaging7090185

McMenamin, P. G., Quayle, M. R., McHenry, C. R., & Adams, J. W. (2014). The production of anatomical teaching resources using three-dimensional (3D) printing technology. Anatomical Sciences Education, 7(6), 479-486. https://doi.org/10.1002/ase.1475

Preece, D., Williams, S. B., Lam, R., & Weller, R. (2013). "Let's get physical": Advantages of a physical model over 3D computer models and textbooks in learning imaging anatomy. Anatomical Sciences Education, 6(4), 216–224. https://doi.org/10.1002/ase.1345

Rebner, M., Henn, S., & Fischer, A. (2020). Effect of matte coating on optical 3D scanning accuracy for reflective surfaces. Procedia CIRP, 95, 763–768. https://doi.org/10.1016/j.procir.2020.01.178

Seymour, K., Haden, C., & Campbell, R. (2020). The impact of digital anatomy tools on student learning in veterinary education. Animals, 10(12), 2265. https://doi.org/10.3390/ani10122265

Zheng, Q., Wu, L., & Li, D. (2022). Optical reflection effects on structured-light scanning of moist biological tissues. Optics and Lasers in Engineering, 152, 106923. https://doi.org/10.1016/j.optlaseng.2021.106923

ORAL PRESENTATION

Sütçü sığırlarda süt verimi ile suni tohumlama sonrası gebelik oranı ilişkisinin araştırılması

Alper Koçyiğit[1*] (ORCID: https://orcid.org/0000-0001-9639-5497),
Hüseyin Ün[1] (ORCID: https://orcid.org/0009-0008-6620-6825)

[*1]Ondokuz Mayıs Üniversitesi, Veteriner Fakültesi, Dölerme ve Suni Tohumlama ABD, Samsun, Türkiye

*Sorumlu yazar e-mail: alper.kocyigit@omu.edu.tr

Özet

Bu çalışma, Amasya ili Suluova ilçesinde 109 sütçü sığırda süt verimi ile suni tohumlama sonrası gebelik oranı arasındaki ilişkiyi incelemiştir. Gebe ineklerin süt verimi 17.9 ± 4.6 L/gün, gebe kalmayanların ise 20.3 ± 5.2 L/gün olarak bulunmuştur. Gruplar arası fark anlamlıdır ($p < 0.05$). Süt verimi ile gebelik durumu arasında negatif bir korelasyon ($r = -0.28$) saptanmıştır. Bulgular, yüksek süt veriminin döl verimini olumsuz etkileyebileceğini göstermektedir.

Anahtar Kelimeler: Süt sığırcılığı, süt verimi, suni tohumlama, gebelik

The Relationship Between Milk Yield and Post-Insemination Pregnancy Rate in Dairy Cows

Abstract

This study investigated the relationship between milk yield and post-insemination pregnancy rate in 109 dairy cows in Suluova, Amasya. Pregnant cows produced 17.9 ± 4.6 L/day of milk, while non-pregnant cows produced 20.3 ± 5.2 L/day. The difference was significant ($p < 0.05$). A negative correlation ($r = -0.28$) was found between milk yield and pregnancy status, indicating that higher milk production may adversely affect fertility.

Keywords: Dairy, milk yield, artificial insemination, pregnancy

GİRİŞ

Süt sığırcılığı, hayvancılık sektörünün ekonomik sürdürülebilirliği ve verimliliği açısından temel üretim dallarından biridir. Başarılı bir süt sığırcılığı işletmesinde hem yüksek süt verimi hem de yeterli dölverimi elde edilmesi gerekmektedir. Süt verimi, genetik potansiyel, beslenme, çevresel koşullar ve yönetim uygulamalarıyla belirlenirken; döl verimi, ineklerin yeniden gebe kalma yeteneği, buzağılama aralığı ve hizmet başına gebelik oranı gibi parametrelerle değerlendirilir (LeBlanc, 2010). Bu iki üretim parametresinin birlikte optimize edilmesi hem ekonomik hem de biyolojik açıdan büyük önem taşımaktadır.

Bununla birlikte, çok sayıda araştırma süt verimi ile döl verimi arasında genetik ve metabolik düzeyde negatif bir ilişki bulunduğunu ortaya koymuştur (Walsh ve ark., 2010; Bello ve ark., 2012). Yüksek süt verimli ineklerde laktasyonun erken döneminde belirginleşen negatif enerji dengesi, ovaryum aktivitesinin gecikmesine, östrus belirtilerinin zayıflamasına ve gebelik oranlarının azalmasına neden olmaktadır (Nebel ve ark., 1993). Bu durum, enerji dengesi bozukluğu ile ilişkili hormonal düzensizliklerin (örneğin insülin, IGF-1, LH dalgalanmaları) üreme fizyolojisini baskılamasıyla açıklanmaktadır (Walsh ve ark., 2010). Ancak bazı araştırmacılar bu ilişkinin yalnızca fizyolojik değil, aynı zamanda yönetimsel faktörlerden de etkilendiğini, özellikle yüksek verimli sürülerde östrus tespit hataları ve besleme dengesizliklerinin rol oynadığını bildirmiştir (LeBlanc, 2013).

Suni tohumlama (ST), modern süt sığırcılığı işletmelerinde genetik ilerlemeyi hızlandıran, bulaşıcı hastalık riskini azaltan ve sürü yönetimini kolaylaştıran bir üreme teknolojisidir (Cardoso Consentini ve ark., 2021). Ancak ST'nin başarısı, yalnızca sperma kalitesi veya uygulama tekniğine değil; aynı zamanda ineğin fizyolojik durumu, metabolik dengesi ve süt verim düzeyine de bağlıdır (Hamid ve ark., 2021). Özellikle yüksek süt verimli ineklerde ovulasyon zamanlamasında kaymalar, uterus ortamında pH değişimleri ve implantasyon başarısında azalmalar görülebilmektedir (Inchaisri ve ark., 2010; Rutten ve ark., 2016). Bu faktörler, hayvan başına gebelik oranlarını düşürerek suni tohumlamanın etkinliğini sınırlayabilir.

Bu nedenle saha koşullarında süt verimi ile suni tohumlama sonrası gebelik oranı arasındaki ilişkinin incelenmesi hem fizyolojik hem de yönetimsel düzeyde üretim stratejilerinin geliştirilmesi açısından önem taşımaktadır. Bu çalışmanın amacı, farklı süt verim düzeylerine sahip ineklerde suni tohumlama sonrası gebelik oranlarını karşılaştırarak, süt üretimi ile döl verimi arasındaki ilişkinin saha koşullarındaki pratik yansımalarını değerlendirmektir.

MATERYAL VE METOT

Bu araştırmada materyali, Amasya ili Suluova ilçesinde faaliyet gösteren 18 işletmede kayıtları düzenli tutulan toplam 109 baş sütçü sığıra ait suni tohumlama (ST) ve süt verimi verileri oluşturmuştur. Çalışmaya dahil edilen hayvanlar, benzer bakım, besleme ve barınak koşullarında yetiştirilmiş olup, veriler 2024 yılı üretim dönemine aittir. Araştırmada incelenen veriler Amasya Damızlık Sığır Yetiştiricileri Birliğinden temin edilmiştir.

Suni tohumlama uygulamaları, işletmede görevli veteriner hekim tarafından rektovajinal yöntemle gerçekleştirilmiş; tohumlama tarihleri, kullanılan sperma bilgileri ve gebelik sonuçları kayıt altına alınmıştır. Gebelik durumu, tohumlamadan yaklaşık 60 gün sonra yapılan rektal muayene ile belirlenmiştir. Süt verimi verileri ise günlük kayıtlar temel alınarak bireysel ortalama süt üretimi litre cinsinden hesaplanmıştır.

Elde edilen verilerin istatistiksel değerlendirmesinde parametrik test yöntemleri kullanılmıştır. Gebelik durumu (1 = gebe, 0 = boş) ile süt verimi arasındaki farkın belirlenmesinde bağımsız iki örneklem t-testi uygulanmıştır. Bu analiz, gebelik elde eden ve etmeyen gruplar arasındaki ortalama süt verimlerinin istatistiksel olarak farklı olup olmadığını belirlemek amacıyla yapılmıştır. Gruplar arası süt verimi değerleri ortalama ± standart sapma biçiminde ifade edilmiştir.

Ayrıca, gebelik durumu ile süt verimi arasındaki ilişkinin yönü ve gücünü ortaya koymak için Pearson korelasyon analizi kullanılmış, buna göre korelasyon katsayısı (r) hesaplanmıştır. Analizlerde anlamlılık düzeyi $p < 0.05$ olarak kabul edilmiştir.

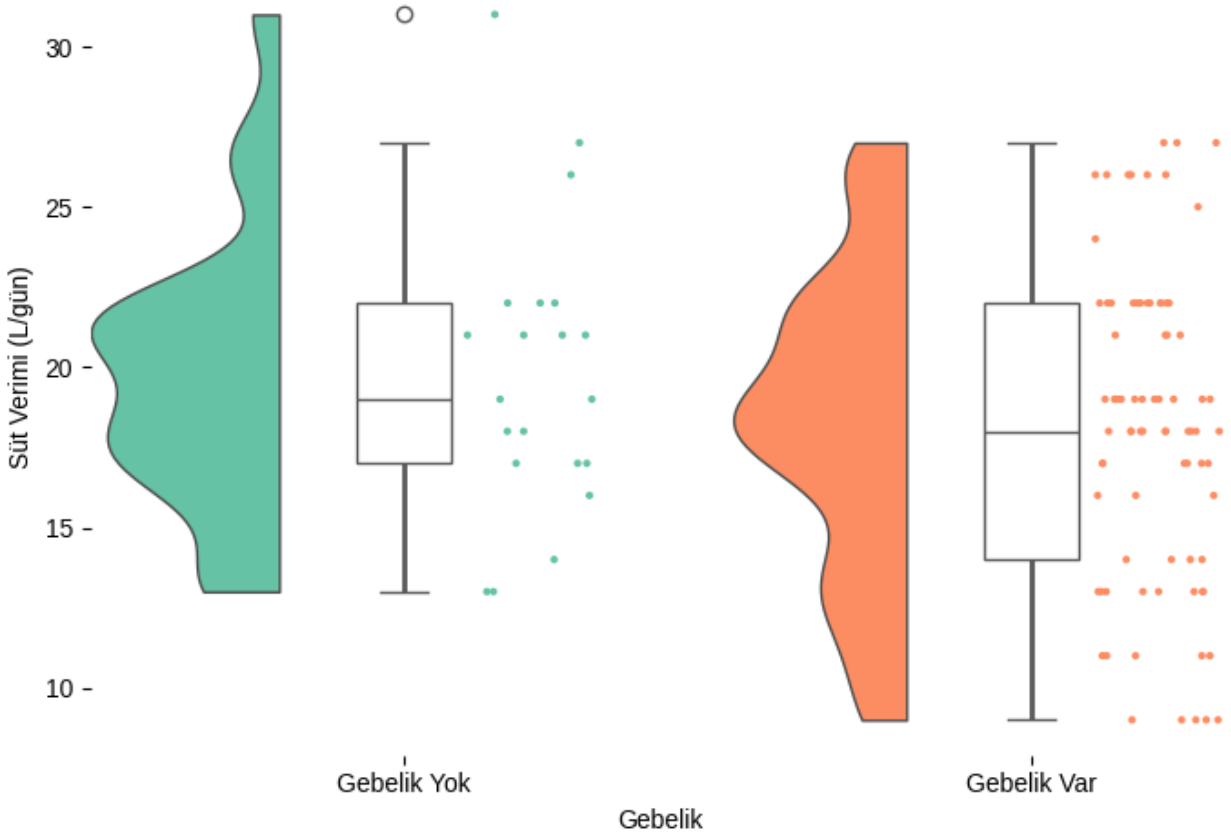
Tüm istatistiksel hesaplamalar IBM SPSS Statistics 22.0 paket programı kullanılarak gerçekleştirilmiştir. Verilerin normal dağılım varsayımı Kolmogorov–Smirnov testi ile doğrulanmış, varyans homojenliği ise Levene testi ile kontrol edilmiştir.

BULGULAR

Araştırmada incelenen toplam 109 sütçü sığıra ait suni tohumlama ve süt verimi verilerinin değerlendirilmesi sonucunda, 86 hayvanda suni tohumlama sonrası gebelik tespit edilmiştir. Gebe ineklerin günlük ortalama süt verimi 17.9 ± 4.6 L/gün, gebe kalmayan ineklerin ise 20.3 ± 5.2 L/gün olarak belirlenmiştir. Genel ortalama süt verimi tüm popülasyon için 18.4 ± 4.8 L/gün olarak hesaplanmıştır.

Gruplar arası farkın istatistiksel olarak anlamlı olup olmadığını belirlemek amacıyla yapılan bağımsız iki örneklem t-testi sonucunda, süt verimi ile gebelik durumu arasında anlamlı bir fark saptanmıştır ($p < 0.05$). Buna göre, gebelik elde edemeyen ineklerin süt verimi ortalaması, gebe kalanlara göre anlamlı derecede daha yüksek bulunmuştur.

Süt verimi (sürekli değişken) ile gebelik durumu (ikili değişken) arasındaki ilişkiyi belirlemek için yapılan Pearson korelasyon analizi sonucunda r = –0.28 değeri elde edilmiştir.



Şekil 1. Sığırlarda gebelik durumu ile süt verimi arasındaki ilişki

TARTIŞMA

Bu çalışmada, Amasya ili Suluova ilçesinde bulunan sığırcılığı işletmelerinde 109 inekten elde edilen suni tohumlama ve süt verimi verileri incelenmiş, süt verimi ile gebelik oranı arasındaki ilişki değerlendirilmiştir. Bulgular, süt verimi yüksek olan ineklerde suni tohumlama sonrası gebelik oranının anlamlı derecede düşük olduğunu göstermiştir. Gebe ineklerin ortalama süt verimi (17.9 ± 4.6 L/gün), gebe kalmayanlara (20.3 ± 5.2 L/gün) kıyasla istatistiksel olarak daha düşük bulunmuş ($p = 0.0035$). Ayrıca, süt verimi ile gebelik durumu arasında negatif yönlü, zayıf düzeyde bir korelasyon ($r = –0.28$) belirlenmiştir. Bu bulgu, literatürde bildirilen süt verimi ile döl verimi arasındaki antagonistik ilişkinin saha koşullarında da gözlendiğini doğrulamaktadır.

Süt verimi ve döl verimi arasındaki negatif ilişki, uzun yıllardır süt sığırcılığı genetiği ve fizyolojisi alanında tartışılan temel bir konudur. Bu ilişkinin kökeninde çoğunlukla negatif enerji dengesi (NED), metabolik stres ve hormonal bozukluklar yer almaktadır. Laktasyonun erken döneminde, yüksek süt verimi potansiyeline sahip ineklerde enerji gereksinimi alım kapasitesini aşmakta, bu durum vücut yağ rezervlerinin mobilizasyonuna yol açmaktadır. Yüksek süt veriminde plazmada yağ asitleri (NEFA) ve β-hidroksibutirat (BHBA) düzeyleri yükselirken, insülin ve IGF-1 düzeyleri azalmakta; bu biyokimyasal

değişiklikler ovaryum fonksiyonlarını olumsuz etkilemektedir (Walsh ve ark., 2010; Bello ve ark., 2012). Özellikle folikül gelişimi ve ovulasyon süreci, negatif enerji dengesi koşullarında baskılanmakta, luteal fonksiyon zayıflamakta ve embriyonik kayıplar artmaktadır (LeBlanc, 2010).

Bulgularımız, yüksek süt veriminin üreme performansını olumsuz etkilediğini bildiren önceki araştırmalarla büyük ölçüde paralellik göstermektedir. Nebel ve ark. (1993), yüksek süt verimli Holstein ineklerde gebelik oranlarının düşük süt verimli akranlarına göre belirgin şekilde azaldığını; bununla birlikte bu ilişkinin sadece fizyolojik değil, yönetimsel etkenlerle de pekiştiğini bildirmiştir. Benzer şekilde, Inchaisri ve ark. (2010) yüksek süt veriminin ilk tohumlamada gebelik olasılığını azalttığını ve enerji dengesiyle ilişkili metabolik belirteçlerin bu süreçte önemli rol oynadığını vurgulamıştır. Rutten ve ark. (2016) ise süt verimi ile suni tohumlama başarısı arasında istatistiksel olarak anlamlı negatif korelasyon tespit etmiş, bu ilişkinin doğrusal bir modelle öngörülebilir olduğunu belirtmiştir. Bu çalışmalarla uyumlu olarak, mevcut çalışmada da yüksek süt verimi grubundaki ineklerin gebelik oranı anlamlı biçimde daha düşük bulunmuştur.

Yüksek süt verimi düzeyinin döl verimi üzerindeki olumsuz etkilerinin bir diğer açıklaması, östrus davranışlarının bastırılması ve tespit güçlüğüdür. Yüksek süt üretimi, artan metabolik hız nedeniyle steroid hormonlarının (özellikle östradiol ve progesteron) dolaşımdan daha hızlı uzaklaştırılmasına neden olur (Walsh ve ark., 2010). Bu durum östrus süresinin kısalmasına, belirti şiddetinin azalmasına ve sonuç olarak östrus tespit oranlarının düşmesine yol açar. Yanlış zamanlamayla yapılan suni tohumlamalar ise fertilizasyon başarısını düşürür (Cardoso Consentini ve ark., 2021). Çalışmamızda da gebelik oranı düşük bulunan ineklerin süt verim ortalamasının yüksek olması, bu mekanizmayı destekler niteliktedir.

Bununla birlikte, süt verimi ile üreme performansı arasındaki bu olumsuz ilişkinin mutlak olmadığı, yönetimsel faktörlerle hafifletilebileceği literatürde vurgulanmıştır. LeBlanc (2013), yüksek verimli sürülerde uygun vücut kondisyon skoru yönetimi, enerji yoğunluğu yüksek rasyonlar ve metabolik sağlık izleme protokollerinin uygulanmasının üreme verimliliğini koruyabildiğini belirtmiştir. Aynı şekilde Hamid ve ark. (2021), besleme yönetimi, tohumlama zamanı optimizasyonu ve stres faktörlerinin azaltılmasının yüksek süt verimi koşullarında döl verimini desteklediğini bildirmiştir. Bu bağlamda, mevcut çalışmanın saha koşullarında yapılmış olması, elde edilen bulguların pratik geçerliliğini artırmaktadır.

Korelasyon analizinde elde edilen r = –0.28 değeri, ilişkinin yönünün negatif, ancak gücünün zayıf düzeyde olduğunu göstermektedir. Bu durum, süt verimi tek başına gebelik başarısını belirleyen bir faktör olmadığını; enerji dengesi, hormonal profil, tohumlama zamanı, sperma kalitesi, çevresel stres ve yönetim uygulamaları gibi çok sayıda faktörün üreme başarısına katkıda bulunduğunu düşündürmektedir (Bello ve ark., 2012; Rutten ve ark., 2016). Bu nedenle, yüksek süt verimli sürülerde döl verimi düşüşünü önlemek için çok boyutlu bir yönetim stratejisinin benimsenmesi gereklidir.

Sonuç olarak, bu çalışma yüksek süt verimi ile suni tohumlama sonrası gebelik oranı arasında anlamlı düzeyde negatif bir ilişki bulunduğunu göstermektedir. Bulgular, süt verimi arttıkça üreme performansının belirli bir sınırda gerileyebileceğini, ancak bu etkinin uygun sürü yönetimiyle azaltılabileceğini ortaya koymaktadır. Enerji dengesi yönetimi, östrus tespiti doğruluğunun artırılması ve besleme stratejilerinin optimize edilmesi hem üretim hem de üreme verimliliğini birlikte koruyabilmek açısından kritik önem taşımaktadır.

TEŞEKKÜR

Araştırma verilerine sorunsuz ulaşmamıza sağlayan Amasya Damızlık Sığır Yetiştiricileri Birliği'ne ve veteriner hekim Cem Çağdaş ARKÖSE'ye teşekkür ederiz.

KAYNAKLAR

Bello, N. M., & Steibel, J. P. (2012). Invited review: Milk production and reproductive performance. Journal of Dairy Science, 95(12), 7399–7410. https://doi.org/10.3168/jds.2012-5740

Cardoso Consentini, C. E., Filho, M. F. S., & Santos, J. E. P. (2021). Factors that optimize reproductive efficiency in dairy cattle. Animals, 11(2), 301. https://doi.org/10.3390/ani11020301

Hamid, M., Li, Y., & Zhang, Y. (2021). Risk factors for the efficiency of artificial insemination in dairy cows: A review. Frontiers in Veterinary Science, 8, 716352. https://doi.org/10.3389/fvets.2021.716352

Inchaisri, C., Jorritsma, R., Vos, P. L. A. M., & Hogeveen, H. (2010). Effect of milk yield characteristics, breed, and parity on the success of the first insemination in dairy cows. Journal of Dairy Science, 93(11), 4888–4896. https://doi.org/10.3168/jds.2010-3280

LeBlanc, S. J. (2010). Assessing the association of the level of milk production with reproductive performance in dairy cattle. Journal of Reproduction and Development, 56(1), S1–S7. https://doi.org/10.1262/jrd.1056S1

LeBlanc, S. J. (2013). Is a high level of milk production compatible with good fertility? Animal Frontiers, 3(4), 84–91. https://doi.org/10.2527/af.2013-0032

Nebel, R. L., McGilliard, M. L., & Cassell, B. G. (1993). Interactions of high milk yield and reproductive performance in dairy cows. Journal of Dairy Science, 76(10), 3257–3268. https://doi.org/10.3168/jds.S0022-0302(93)77662-6

Rutten, C. J., Velthuis, A. G. J., Steeneveld, W., & Hogeveen, H. (2016). A prognostic model to predict the success of artificial insemination in dairy cows. Journal of Dairy Science, 99(12), 9770–9781. https://doi.org/10.3168/jds.2016-11616

Walsh, S. W., Williams, E. J., & Evans, A. C. O. (2010). A review of the causes of poor fertility in high milk producing dairy cows. Animal Reproduction Science, 123(3–4), 127–138. https://doi.org/10.1016/j.anireprosci.2010.02.001

ORAL PRESENTATION

Sürdürülebilir Boyamacılıkta *Juglans regia* L. Yaprağı Kaynaklı Biyomordanın Kullanımı

Mehmet Kılınç[1*] (*ORCID: 0000-0001-9129-5251*), Nur Kilinç[2] (*ORCID: 0000-0003-4494-5084*)

[*1] Giresun Üniversitesi, Şebinkarahisar Uygulamalı Bilimler Yüksek Okulu, Tekstil ve Moda Tasarımı Bölümü, Giresun, Türkiye.
[2] Giresun Üniversitesi, Şebinkarahisar Meslek Yüksek Okulu, Moda Tasarımı Bölümü, Giresun, Türkiye.

*Sorumlu yazar e-mail: m.kilinc@giresun.edu.tr

Özet

Doğal boyalar, tekstil endüstrisinde yenilikçi ve sürdürülebilir kaynaklar olarak giderek daha fazla önem kazanmaktadır. Bu çalışmada, Giresun Şebinkarahisar yöresinden temin edilen ceviz (*Juglans regia* L.) yaprakları, pamuklu kumaşların boyanmasında biyomordan olarak farklı konsantrasyonlarda (%5, %10 ve %20) kullanılmıştır. Boyama işlemleri, doğal boya kaynağı *Rubia tinctorium* ile üç farklı konsantrasyonda (%10, %20 ve %30) gerçekleştirilmiştir. Biyomordan ve boya konsantrasyonlarındaki değişimlerin kumaşların renk özellikleri üzerindeki etkileri sistematik olarak incelenmiştir. Numunelerin renk ölçümleri CIELAB renk uzayı (L*, a*, b*), renk doygunluğu (C*), renk tonu açısı (h°) ve renk derinliği (K/S) değerleri üzerinden değerlendirilmiştir. Ayrıca, sürtme haslığı testleri uygulanmış ve sonuçlar ISO 105-X12 standardı kapsamında değerlendirilmiştir. Elde edilen sonuçlar, hem boya hem de biyomordan konsantrasyonlarındaki değişimin renk derinliği ve ton üzerinde belirgin etkiler yarattığını göstermiştir. Artan *Rubia tinctorium* konsantrasyonu ile birlikte K/S ve C* değerlerinde artış gözlenmiş; renkler daha koyu ve doygun hale gelmiştir. Tüm numunelerde elde edilen haslık değerleri kabul edilebilir düzeydedir. Bu bulgular, ceviz yaprağı ekstraktının çevre dostu ve sürdürülebilir bir biyomordan olarak pamuklu kumaşların doğal boyanmasında etkin biçimde kullanılabileceğini ortaya koymaktadır.

Anahtar Kelimeler: Doğal Boyama, Biyomordan, sürdürülebilir tekstiller

The Use of Biomordant from *Juglans regia* L. Leaves in Sustainable Dyeing

Abstract

Natural dyes are becoming increasingly important as innovative and sustainable resources in the textile industry. In this study, walnut (Juglans regia L.) leaves sourced from the Giresun Şebinkarahisar region were used as a biomordant at different concentrations (5%, 10%, and 20%) for dyeing cotton fabrics. Dyeing processes were carried out with the natural dye source Rubia tinctorium at three concentrations (10%, 20%, and 30%). The effects of varying biomordant and dye concentrations on the colour properties of the fabrics were systematically investigated. Colour measurements of the samples were evaluated based on the CIELAB colour space (L*, a*, b*), colour saturation (C*), hue angle (h°), and colour depth (K/S) values. In addition, rubbing fastness tests were conducted, and the results were evaluated according to the ISO 105-X12 standard. The results showed that changes in both dye and biomordant concentrations had significant effects on colour depth and hue. An increase in Rubia tinctorium concentration was accompanied by an increase in K/S and C* values; the colours became darker and more saturated. The fastness values obtained for all samples were acceptable. These findings demonstrate that walnut leaf extract can be effectively used as an environmentally friendly and sustainable biomordant for the natural dyeing of cotton fabrics.

Keywords: Natural Dyeing, Biomordant, Sustainable Textiles

Introduction

The Industrial Revolution has made people's lives and livelihoods more appealing worldwide through the adoption of sustainability and the use of advanced technologies and products. Among these advanced technologies and products, textiles play an important role in national economies. People have used natural dyes in textiles since prehistoric times. Natural dyes can be obtained from the roots, stems, and leaves of plants, from insects, or from minerals. Synthetic dyes were discovered in 1856. Synthetic dyes have significant potential for industrial applications due to their ease of application and cost-effectiveness. With the increased use of synthetic dyes across various sectors, people gained easier access to products with a wide variety of colour options. However, many researchers have observed that the wastewater released during the preparation and finishing stages negatively affects water quality and soil fertility. Furthermore, a World Bank study reports that the textile dyeing industry is responsible for up to 20% of global water pollution, as 13–45% of all dyes used in dyeing or printing are released into the environment through wastewater. It has been observed that people have contracted various diseases such as cancer and asthma due to this wastewater, which contains many chemicals. In recent years, due to growing environmental awareness and increasing interest in sustainable products, the toxicity of synthetic dyes, their non-biodegradability, and the serious health risks they pose have become a global concern. In addition, the fact that natural dyes are obtained from sustainable sources, have a low chemical reaction effect, and are environmentally friendly has encouraged people to use textile products dyed with natural dyes again (Prabhu et al., 2012; Korkmaz et al., 2023; Ibrahim et al., 2025; Khatun et al., 2025).

Today, mordants are used to ensure that natural dyes bind more permanently and to enhance the colour tone. Metal salts are generally preferred as mordants. However, the use of these mordants can also pose environmental hazards. Therefore, the use of biomordants as an alternative to traditional metal mordants is increasingly popular (Kılınç et al., 2025).

Juglans regia leaves, which have a high tannin content, phenolic compounds, and antioxidant properties, are a suitable alternative for use as a biomordant. The phenolic compounds in walnut leaves interact with the hydroxyl groups on the fibre surface, facilitating easier binding of natural dyes. Therefore, it is known that walnut derivatives have the potential to be used as biomordants due to their rich tannin content (İşmal, 2017; Kılınç et al., 2025).

In this study, cotton/polyester fabrics mordanted with Juglans regia at different concentrations were dyed with Rubia tinctorium (root dye) at various concentrations, and their colour characteristics and fastness values were examined. It is thought that the use of *Juglans regia* and *Rubia tinctorium* for sustainable green technologies could be a high-potential alternative in the textile industry.

MATERIAL and METHOD

Cotton/polyester (75/25) twill woven fabric was used in the studies. Table 1 shows that the fabric properties.

Table 1. Fabric properties

Properties	Cotton/Polyester(75/25%)
Fabric construction	Plain weave 1/1
GSM (g/m²)	110
Ends per inch (cm⁻¹)	24
Picks per inch (cm⁻¹)	16
Warp count (Nm)	30
Weft count (Nm)	60

Mordanting Process

As part of the study, a pre-mordanting process was applied to woven fabrics. For the mordanting process, three concentrations of walnut leaf (*Juglans regia*) biomordant were used: 5%, 10%, and 20%. The amount of mordant was determined according to the fabric weights. The flotte ratio in the mordanting process was 1:100.

Dyeıng Process

Dye (*Rubia tinctorium*) concentrations were calculated based on fabric weight and applied at three levels during the dyeing process: 10%, 20%, and 30%. The fabrics were dyed at 100°C for 30 minutes. The dyeing was performed using pure water at a 1:30 flotte ratio. After dyeing, the fabrics were washed sequentially in cold water, boiling water, and cold water to remove any undyed dye.

Colour Measurement

Colour measurements of painted fabric samples were performed using the LS175 colorimeter. Measurements were taken under a D65 light source and 10° standard observer conditions.

The % reflectance (R) values in the visible range (400–700 nm) were obtained and converted to colour strength (K/S) values using the Kubelka–Munk equation (Equation 1).

$$K/S = (1-R)^2 / 2R \quad (1)$$

In addition to colour intensity measurements, the CIELAB colour coordinates of the samples have been determined. In this context, L* (lightness: 0 = black, 100 = white), a* (positive = red, negative = green), and b* (positive = yellow, negative = blue) values were measured; additionally, the C* (chroma, 0 = dull, 100 = vivid) parameter was used to evaluate colour saturation.

Fastness Tests

Rubbing fastness tests were performed on dyed fabrics. Fastness tests were conducted in accordance with ISO 105-X12 standards.

RESULTS and DISCUSSION

The colour values of the samples are presented in Table 2. Examination of the L* values shows that the dyeing process reduces this value. Regarding lightness, the use of mordant generally does not cause a change, except in samples containing 30% dye, where mordant reduces lightness values. The a* values indicate that the red hue in the samples increases compared to the standard fabric. The use of mordant in the sample containing 30% dye also results in an increased red hue. This value is similar at other concentrations. The b* values show an increase in the yellow hue compared to the raw fabric, and mordanting does not significantly affect the yellow hue overall. Chroma values increase compared to the raw fabric, and the use of mordant slightly increases these values in some samples, but no significant difference is observed.

Table 2. Colour values of the samples

	L*	a*	b*	C*	h°	λ	K/S
Standart	84,0361	1,8552	12,2294	12,3694	81,3739	360	0,77168
%5 JG+%10 RB	66,2455	19,7812	16,0150	25,4514	38,9938	360	1,72658
%5 JG+% 20RB	65,1269	19,8797	19,5211	27,8618	44,4785	360	1,91181
%5 JG+%30 RB	61,2370	22,0849	21,9499	31,1374	44,8243	360	2,37608
%10 JG+%10 RB	66,0699	18,7727	18,8863	26,6291	45,1728	360	1,73327
%10 JG+%20 RB	64,3862	20,3586	20,2747	28,7322	44,8817	360	1,95099
%10 JG+%30 RB	59,7420	22,1869	22,7218	31,7575	45,6824	360	2,62897
%20 JG+%10 RB	67,2045	16,2884	19,8786	25,6996	50,6690	360	1,72791
%20 JG+%20 RB	64,4341	18,8411	20,8896	28,1312	47,9516	360	2,02618
%20 JG+%30 RB	61,2011	21,4290	20,9091	29,9399	44,2965	360	2,32375
%10 RB	66,7995	18,0948	17,0365	24,8529	43,2744	360	1,59163
%20 RB	63,9868	18,7215	21,3140	28,3686	48,7050	360	2,08976
%30 RB	63,1855	19,4165	22,2510	29,5314	48,8916	360	2,25729

L * Lightness (0 = black, 100 = white), ; a* ± Red/green, ; b* ± Yellow/blue, C * To vividness-dullness (100 = vivid, 0 = dull) JG: *Juglans regia,* RB*: Rubia tinctorium.*

Looking at the colour wheel in Figure 1, it can be seen that the raw fabric is in region 3 (orange-yellow), while the dyed samples are in region 2 (red-orange).

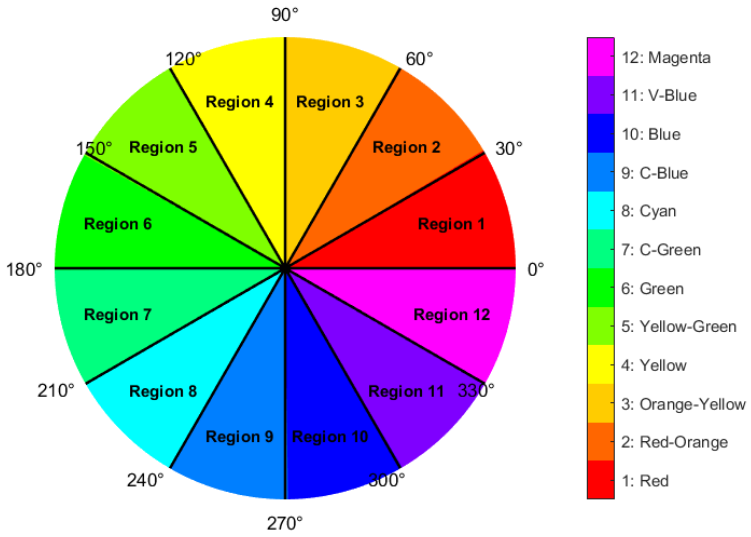


Figure 1. Colour Wheel

An increase in the K/S values of the samples is observed after dyeing. The use of mordant does not cause much change in the K/S values in general, except for samples with 30% dye used, as seen in Table 2 and Figure 2.

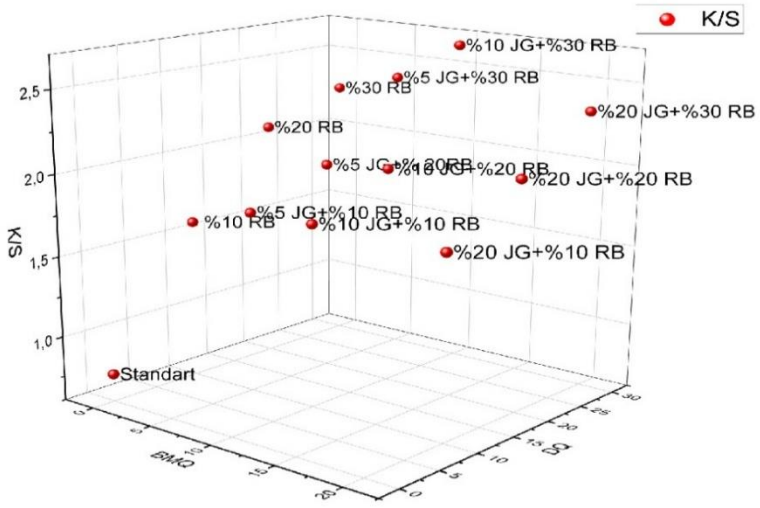


Figure 2. Relationship between K/S, biomordant quantity (BMQ) and dye quantity (DQ)

The fastness values of the samples are given in Table 3. When examining the dry rubbing fastness, it is seen that the values range between 4 and 4-5. In general, the dry rubbing fastness of the samples is similar. The wet rubbing fastness values are 1 degree lower than the dry fastness values. Wet rubbing fastness values range between 3 and 3-4. Wet rubbing fastness values also show similarity in general terms.

Table 3. Rubbing fastness values

Rubbing Fastness		
	Wet	Dry
%5 JG+%10 RB	3--4	4--5
%5 JG+% 20RB	4	4--5
%5 JG+%30 RB	3	4
%10 JG+%10 RB	4	4--5
%10 JG+%20 RB	3--4	4--5
%10 JG+%30 RB	3	4
%20 JG+%10 RB	4	4--5
%20 JG+%20 RB	3--4	4--5
%20 JG+%30 RB	3	4
%10 RB	3--4	4--5
%20 RB	3	4
%30 RB	3	4

CONCLUSION

In sustainable textile dyeing, colouring fabrics using entirely natural resources is highly important. In this study, the positive effects of using Juglans regia as a biomordant, notable for its rich tannin and phenolic compound content, have been observed. As the concentration of *Rubia tinctorium* dye increased, colour yield and saturation also increased. The use of the biomordant contributed positively to colour depth, especially at high dye concentrations. Rubbing fastness results are acceptable. Overall, this study indicates that using *Juglans regia* as a biomordant produces successful results and that an effective natural dyeing process is achieved when combined with *Rubia tinctorium*. This study may provide scientific guidance for future research on sustainable textile dyeing using waste-based natural resources.

REFERENCES

Ibrahim, M., Adeel, S., Mehrizi, M. K., Imran, M., Tahir, M. A., & Mia, R. (2025). Dyeing of silk with isolated bixin based orange yellow natural dye: kinetic, thermodynamic and colorimetric aspects. Results in Engineering, 25, 103794.

İşmal, Ö. E. (2017). Greener natural dyeing pathway using a by-product of olive oil; prina and biomordants. *Fibers and Polymers*, *18*(4), 773-785.

Khatun, M. H., Rabbi, M. A., Ahmed, F., Kadri, H. J., Maitra, B., Al-Amin, M., ... & Akter, R. (2025). Transforming waste into eco-friendly dye: A study of silk dyeing with Terminalia catappa using metal mordants and bio-mordants. *Sustainable Chemistry One World*, 100143.

Kılınç, M., Cüce, M., Kılınç, N., Tiritoğlu, M., & Kut, D. (2025). Comparison of Biomordant and Chemical Mordant on the Color, Fastness, and Antimicrobial Properties of Wool Fabrics Dyed with Juglans regia Waste Product. Fibers and Polymers, 1-17.

Korkmaz, G., Kılınç, M., Kılınç, N., & Kut, Y. D. (2023). The role of surface modification methods for sustainable textiles. In *Roadmap to Sustainable Textiles*. IntechOpen.

Prabhu, K. H., & Bhute, A. S. (2012). Plant based natural dyes and mordants: A Review. J. Nat. Prod. Plant Resour, 2(6), 649-664.

ORAL PRESENTATION

Preparation of tin (ii) sulfide photoelectrodes for photocapacitor applications

Özlem Budak Doğramacı[1,2*] (*ORCID: https://orcid.org/0000-0002-0240-8320*), Jose Francisco Serrano Claumarchirant[2] (*ORCID:* https://orcid.org/0000-0002-4894-4399), Muhammet S. Toprak[2] (*ORCID: https://orcid.org/0000-0001-5678-5298*)

[1]Marmara University, Faculty of Engineering, Department of Chemical Engineering, Istanbul,Turkey.
[2]KTH Royal Institute of Technology, Department of Applied Physics, SE10691, Stockholm, Sweden.

*Corresponding author e-mail: ozlem.budak@marmara.edu.tr

Abstract

Photocapacitors integrate solar energy yield and storage processes into single device, which offers a promising option for efficient and sustainable solar energy utilization. In this study, tin (II) sulfide (SnS) was synthesized via facile co-precipitation method and used as the photoelectrode active material for photoacapacitor applications. The crystal structure and surface morphology of the synthesized samples were examined by X-ray Diffraction (XRD) and scanning electron microscopy (SEM) analysis, respectively. The electrochemical energy storage performance of the photoelectrodes was then investigated both in the dark and under solar light irradiation. Photoelectrochemical measurements revealed that light irradiation provided noticeable enhancement in the specific capacitance of ITO/SnS photoelectrode. The ITO/SnS photoelectrode exhibited the specific capacitance of 10.4 mF cm^{-2} at the current density of 0.03 mA cm^{-2} under light illumination. As a result, this study presents a novel perspective for highly effective photo-responsive active materials for photocapacitors.

Keywords: tin (II) sulfide, photoelectrodes, photocapacitors, energy storage.

INTRODUCTION

The excessive fossil fuel consumption driven by rapid population growth and the requirement for worldwide economic progress has resulted in the scarcity of traditional energy sources, global warming and a great deal of crucial environmental and health problems (Kansal et al., 2023). As a vital sustainable technology, solar energy can be converted into electricity through solar cells; however, variability in solar intensity limits a consistent supply, thereby decreasing reliability. Thus, to overcome this limitation, the combination of solar cells and energy storage systems has been regarded as a practical approach that provides to enhance their effectiveness for commercial applications. Photocapacitors are newly developed devices capable of directly harvesting and storing solar energy directly (Kajana et al., 2022, Sangaraju et al., 2023). Among several metal chalcogenide materials, tin (II) sulfide (SnS) is particularly remarkable because it is composed of earth-abundant elements, is eco-friendly and offers efficient light absorption with suitable optical energy band gap (E_g) of 1.3 eV (Caoet al., 2021). Furthermore, SnS displays outstanding pseudocapacitive behavior due to the high redox activity and higher conductivity (Dar et al., 2023). Tariq et al. synthesized Cu-doped SnS thin films to evaluate their potential as solar cell materials for photovoltaic applications (Tariq et al., 2023). In the study of Thong Ho et al., the SnS thin films were prepared by the vapor transport deposition technique and they reported increase in solar cell power conversion efficiency from 0.11% to 2% (Ho et al., 2022). In addition, Dar et al. synthesized SnS structures with hydrothermal method and achieved noticeable specific capacitance (Dar et al., 2022). In another work, Ni-doped SnS electrodes were fabricated for supercapacitor applications. The achieved specific capacitance of the electrode was 47 F g^{-1} at the scan rate of 10 mV s^{-1}, indicating the superior charge storage capability (Dar et al., 2023). Considering these findings, the present study aims to

investigate the synthesis of SnS structures and examine the charge storage capacity under solar light irradiation for photocapacitor applications.

MATERIALS AND METHODS

Synthesis of SnS powder and preparation of ITO/SnS photoelectrodes

To synthesize SnS via simple precipitation method, tin (II) chloride ($SnCl_2$) and sodium sulfide nonahydrate ($Na_2S.9H_2O$) were used as tin and sulfur sources, respectively. First, 0.32 g of $SnCl_2$ was dissolved in deionized (DI) water, and the pH was adjusted to 2.5. Separately, 0.81 g of $Na_2S.9H_2O$ was dissolved in DI water, and both solutions were stirred for 30 min. After that, the $Na_2S.9H_2O$ solution was mixed with $SnCl_2$ solution and heated to 80 °C under stirring for 1h. Then, the mixture was cooled down, and the precipitate was washed with DI water and ethanol, followed by vacuum drying at 40 °C for 12 h. Prior to the drop-casting process, indium tin oxide (ITO) substrates were ultrasonically cleaned with acetone, ethanol and DI water. The synthesized SnS powder was dispersed in DI water to prepare a suspension, which was used for photoelectrode preparation. For the drop-casting method, a five-cycle deposition process was carried out. After each cycle, the photoelectrodes were dried. Finally, the fabricated photoelectrodes were annealed at 250 °C for 1 h.

Material characterization and electrochemical/photoelectrochemical measurements

X-ray diffraction (XRD) analysis of the as-fabricated samples was employed using a Siemens D5000 (2θ range from 10° to 80°). Morphology of the sample was studied using scanning electron microscopy (SEM, FEI Nova 200, 10 kV).

Electrochemical experiments were conducted in a three-electrode-cell system by Metrohm Autolab. The electrochemical cell composed of an ITO (1x1 cm^2) working electrode, a Pt counter electrode and an Ag/AgCl reference electrode. All electrodes were immersed in a 1.0 M Sodium sulfate (Na_2SO_4) aqueous electrolyte. Cyclic voltammetry (CV) tests were applied to study the reversibility of the fabricated electrodes while galvanostatic charge–discharge (GCD) analyses were employed to determine their specific capacitance (C_s). For photoelectrochemical experiments, the CV and GCD tests were further performed in the presence of solar light illumination using an Ossila Solar Simulator (1000 W m^{-2}).

The C_s of the electrode was calculated using the following equation (Budaket al., 2022):

$$C_s = \frac{(I \times \Delta t)}{(\Delta V \times A)} \quad (1)$$

where C_s states the specific capacitance (F cm^{-2}), I is the discharge current (A), Δt is the discharge time (s) and A is the area of ITO (cm^2).

RESULTS and DISCUSSION

Phase composition and morphology of as-synthesized SnS structures were characterized by XRD and SEM analyses, respectively. As presented in Fig. 1a, the XRD pattern of SnS displayed characteristic diffraction peaks corresponding to the (201), (111), (410), (511) and (512) planes, observed at 2θ values of 26.3, 31.5, 39.2, 51.2, and 64.9°, respectively. All the diffraction peaks are in good agreement with the standard JCPDS card No. 01–073-1859 (Khademalrasool et al., 2023) corresponding to orthorhombic phase of SnS. Fig. 1b illustrates a typical SEM image of the as-prepared SnS powder, which shows primary particles in the order of <100 nm, forming larger secondary particles involving plenty of interconnected nanoparticles. Agglomeration of this type is commonly observed in aqueous synthesis, where no specific surface passivating molecules, or surfactants have been used, as in this case.

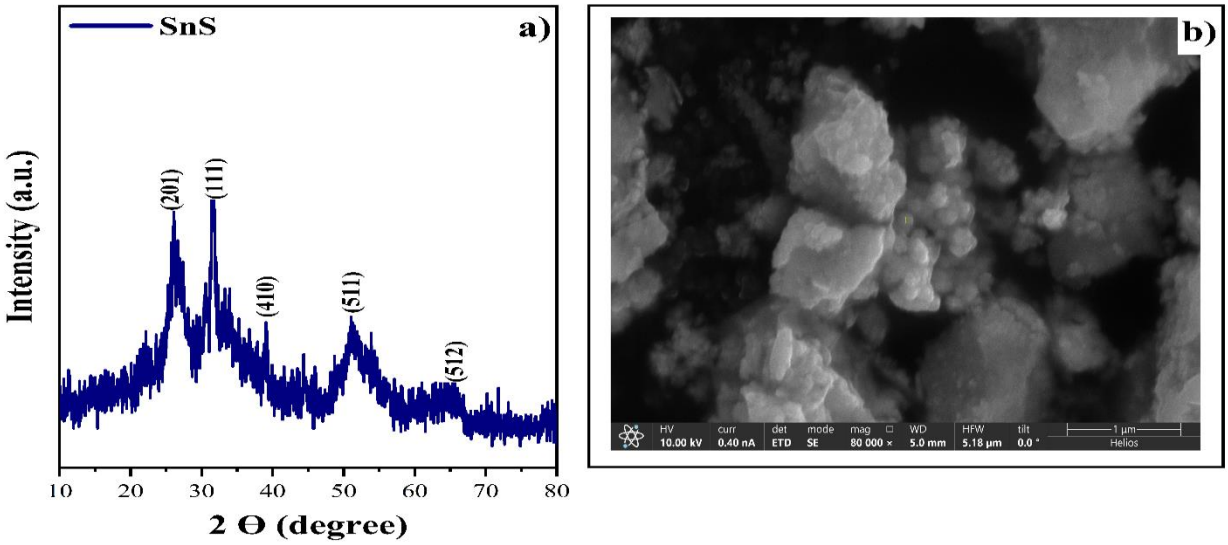


Figure 1. Characterization of as-synthesized SnS nanopowder: **a)** powder XRD pattern, and **b)** SEM micrograph.

Cyclic voltammetry (CV) and galvanostatic charge/discharge (GCD) measurements were both performed under both solar light irradiation and dark conditions in a standard three-electrode system to clarify the effect of light on capacitive behavior. The three-electrode system was constructed of an ITO/SnS working electrode, a Pt wire counter electrode and Ag/AgCl reference electrode. Photoelectrochemical properties and charge storage efficiency of the ITO/SnS photoelectrode are presented in Fig. 2. The enclosed CV area of the ITO/SnS was larger under light illumination than that of dark conditions, implying a higher specific capacitance (Fig. 2a). Under exposure to light, higher peak currents were recorded, and a more reversible redox response was clearly noticed. These results could be attributed to increased electroactivity arising from high-energy photoelectrons generated under light illumination (Huang et al., 2022). Fig. 2b depicts the CV profiles of the ITO/SnS photoelectrode at several scan rates changing from 10 to 150 mV s^{-1} within the potential window of -0.2 to 0.2 V vs. Ag/AgCl under light irradiation. As the scan rates increased, no distinct change was observed in the CV curves, suggesting good reversibility. As shown in Fig. 2c, a longer discharge time was detected under light irradiation compared to dark conditions, which supports the CV findings. The specific capacitance of the ITO/SnS reached 10.4 mF cm^{-2} at a current density of 0.03 mA cm^{-2} in the presence of light, whereas it was estimated 4.1 mF cm^{-2} in the dark. Thus, the capacitive performance was enhanced by 2.5-fold under light irradiation. In Fig. 2d, all GCD curves displayed a comparable triangular shape with increasing current density, demonstrating the characteristic capacitive charge storage mechanism. Furthermore, almost symmetric GCD plots at various current densities revealed that the ITO/SnS photoelectrode possessed favorable rate capability (Momeni et al., 2022).

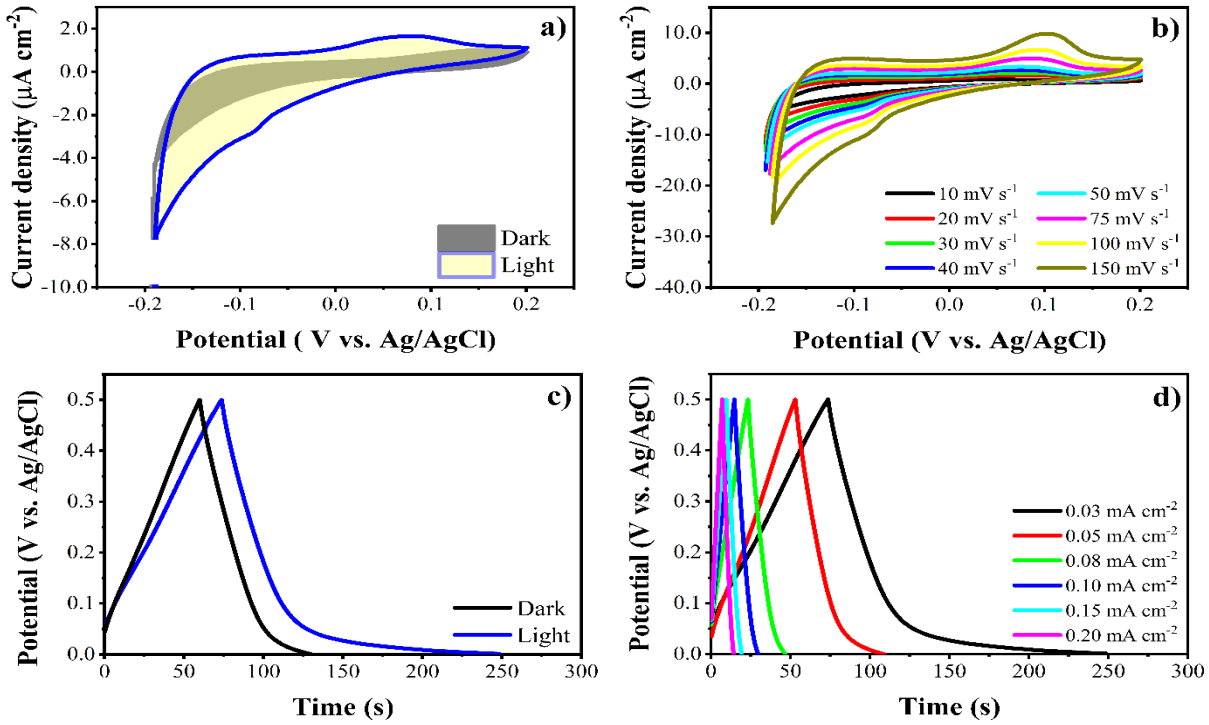


Figure 2. a) CV curves at a scan rate of 20 mV s^{-1}, **b)** CV profiles at various scan rates ranging 10 to 150 mV s^{-1} in the presence of light, **c)** GCD curves at a current density of 0.03 mA cm^{-2}, d) GCD profiles at different current densities ranging 10 to 150 mV s^{-1} in the presence of light.

CONCLUSION

In summary, SnS particles were successfully synthesized and deposited on the ITO surface using a drop casting technique followed by annealing for novel photocapacitor applications. The crystal structure and morphological properties of the synthesized SnS powder were characterized by XRD and SEM, respectively. Photoelectrochemical performance tests were conducted in 1.0 M Na_2SO_4 electrolyte solution under solar light illumination. This facilitated ion diffusion and charge transfer, leading to an increase in the photoactive behavior of the ITO/SnS photelectrode. The recorded CV profile at various scan rates showed that the SnS films exhibited redox charge storage mechanism. According to GCD tests, the ITO/SnS photoelectrode delivered an improved specific capacitance of 10.4 F g^{-1} at a current density of 0.03 mA cm^{-2} under light irradiation compared to its performance in the dark. In conclusion, this work highlights the potential of SnS as a photoactive material for future photocapacitor applications.

ACKNOWLEDGEMENTS

This work was supported by the Scientific and Technological Research Council of Turkey (TUBITAK) through 2219 International Postdoctoral Research Fellowship Program (Grant Number:1059B192402262).

REFERENCES

Budak, Ö., Uğuz, Ö., and Koca, A. (2022). Simultaneous electrochemical deposition of nickel cobalt oxide-reduced graphene oxide composites for high performance asymmetric supercapacitors. Journal of Energy Storage, 47: 103538.

Cao, M., Guan, Y., Bie, J., Zhang, X., Gong, H., Tao, J., Sun, Y., Sun, C., Zhang, S., and Jiang, Y. (2021). Synthesis of SnS: Ag nanosheets for solar energy water splitting. Materials Letters, 300: 130158.

Dar, M.A., Dinagaran, S., Batoo, K.M., Ahamed, S.R., Hussain, S., Ahmad, Z., and Shim, J.-J. (2023). Morphological nanoflowers of Ni-doped SnS for high-performance electrode materials for supercapacitors. Journal of Energy Storage, 68: 107717.

Dar, M.A., Govindarajan, D., Batoo, K.M., and Siva, C. (2022). Supercapacitor and magnetic properties of Fe doped SnS nanoparticles synthesized through solvothermal method. Journal of Energy Storage, 52: 105034.

Ho, T.-T., Jokar, E., Quadir, S., Chen, R.-S., Liu, F.-C., Chen, C.-Y., Chen, K.-H., and Chen, L.-C. (2022). Enhancing the photovoltaic properties of SnS-Based solar cells by crystallographic orientation engineering. Solar Energy Materials and Solar Cells, 236: 111499.

Huang, R., Zhang, J., Dong, Z., Lin, H., and Han, S. (2022). Reticulated TiO_2-modified carbon fiber enabling as a supercapacitor electrode material for photoelectric synergistic charge storage. Energy & Fuels, 36(16): 9261-9271.

Kajana, T., Pirashanthan, A., Yuvapragasam, A., Velauthapillai, D., Ravirajan, P., and Senthilnanthanan, M. (2022). Bimetallic AC/Ag_2CrO_4/SnS heterostructure photoanode for energy conversion and storage: A self-powered Photocapacitor. Journal of Power Sources, 520: 230883.

Kansal, S., Priya, S., Porwal, S., Chandra, A., and Singh, T. (2023). Integrated energy generation and storage systems for low-power device applications. Energy Storage, 5(6): e413.

Khademalrasool, M. and Kharatzadeh, E. (2023). SnS-rGO heterojunction: fabrication, characterization, and visible light-induced optoelectronic performance analysis. Journal of Photochemistry and Photobiology A: Chemistry, 443: 114878.

Momeni, M.M., Aydisheh, H.M., and Lee, B.-K. (2022). Effectiveness of MnO_2 and V_2O_5 deposition on light fostered supercapacitor performance of $WTiO_2$ nanotube: novel electrodes for photo-assisted supercapacitors. Chemical Engineering Journal, 450: 137941.

Sangaraju, S., Kabeer, S., and Nallabala, N.K.R. Flexible Photocapacitor Device Using Reduced Graphene Oxide@MoS_2 Nano Sheets for Future Flexible and Wearable Electronic and IoT Devices. in 2023 IEEE 22nd International Conference on Micro and Nanotechnology for Power Generation and Energy Conversion Applications (PowerMEMS). 2023. IEEE.

Tariq, G.H., Asghar, G., Shifa, M.S., Anis-Ur-Rehman, M., Ullah, S., Shah, Z.A., Ziani, I., Tawfeek, A.M., and Sher, F. (2023). Effect of copper doping on plasmonic nanofilms for high performance photovoltaic energy applications. Physical Chemistry Chemical Physics, 25(46): 31726-31740.

ORAL PRESENTATION

Gene-level modulation of stress response by karrikin in tomato under heat and drought stress

Zeynep Özmen[1] (ORCID: 0009-0002-2831-336X), Pınar Büyük[1] (ORCID: 0009-0000-2858-734X), Havin Doğan[1] (ORCID: 0009-0003-4604-2310), Dilan Yıldız[1] (ORCID: 0009-0006-1525-7003), Zelal Erdoğan[1] (ORCID: 0009-0008-5045-0073), Yasemin Kemeç Hürkan[2] (ORCID: 0000-0003-4089-2683), Kaan Hürkan[3*] (ORCID: 0000-0001-5330-7442)

[1] Department of Plant Protection, Faculty of Agriculture, Iğdır University, 76000, Iğdır, Türkiye.
[2] Department of Biology, Faculty of Science, Çanakkale Onsekiz Mart University, 17000, Çanakkale, Türkiye.
[3*] Department of Agricultural Biotechnology, Faculty of Agriculture, Iğdır University, 76000, Iğdır, Türkiye.

*Corresponding author e-mail: kaanhurkan@hotmail.com

Abstract

Abiotic stress factors such as heat and drought are among the most detrimental environmental challenges affecting global tomato (*Solanum lycopersicum*) production. These stressors disrupt cellular homeostasis, trigger oxidative stress, and inhibit metabolic processes critical for early development. This study investigates the modulatory role of smoke-derived compound karrikin 1 (KAR1) on gene expression patterns in tomato seedlings subjected to simultaneous heat and drought stress. Four experimental treatments were applied: control (G1), KAR1 pre-treatment (G2), stress (G3), and KAR1 + stress (G4). While germination data were excluded from this version, molecular analysis revealed substantial transcriptional activation of *CAT*, *SOD*, *SlWRKY31*, *ERF84*, and *NHX1* genes under stress. KAR1 pre-treatment under stress attenuated these upregulations, suggesting a regulatory priming effect that enhances adaptability without excessive energy demand. These findings position KAR1 as a natural signaling molecule capable of fine-tuning stress responses and promoting sustainable approaches to crop resilience.

Keywords: Karrikin, abiotic stress, Solanum lycopersicum, gene expression, antioxidant response.

INTRODUCTION

Abiotic stresses such as high temperature and drought are key constraints limiting crop productivity, especially in arid and semi-arid regions. In tomato (*S. lycopersicum* L.), these stressors impair germination, root elongation, photosynthesis, and reproductive processes. The dual impact of heat and drought creates a synergistic stress condition that disrupts the antioxidant defense system and alters gene expression networks controlling stress perception and tolerance.

The increasing frequency of heat waves and prolonged droughts caused by global climate change has prompted research into environmentally friendly plant bioregulators that can enhance resilience. Karrikins (KARs) are butenolide compounds released from burning plant material that have drawn attention for their dual roles in seed germination and stress adaptation (Flematti et al., 2004; Nelson et al., 2012). KAR1, the most potent member of this family, interacts with the *KARRIKIN INSENSITIVE2* (KAI2) receptor and F-box protein MAX2, initiating a signaling cascade that overlaps with strigolactone and abscisic acid (ABA) pathways (Waters et al., 2017). These interactions result in transcriptional modulation of stress-responsive genes and improved oxidative stress management.

Recent studies demonstrate that KAR1 enhances plant tolerance to drought by increasing enzymatic antioxidant activity (e.g., superoxide dismutase, catalase, peroxidase) and osmolyte accumulation (Sun et al., 2020). Similarly, *Arabidopsis thaliana* exposed to KAR1 exhibits controlled activation of drought-inducible genes, preventing excessive metabolic cost under mild stress (Li et al., 2017). However, research focusing on combined heat and drought stress remains scarce, especially in tomato cultivars known for stress sensitivity. This study provides the first gene-level assessment of KAR1-induced modulation under simultaneous abiotic stresses, offering mechanistic insight into molecular priming effects.

MATERIALS AND METHODS

Tomato cultivar 'Celebrity' was used for its well-characterized heat and drought sensitivity. Four experimental groups were established: G1 (Control), G2 (KAR1, 10 µM), G3 (Heat + Drought Stress), and G4 (KAR1 + Stress). KAR1 was applied by soaking seeds in 10 µM solution for 12 hours before planting. Seedlings were grown in peat:vermiculitesubstrate (3:2, w/w) under 23°C/18°C (day/night), 16-hour photoperiod, and 70% relative humidity. Stress was applied at 38°C/26°C with 30% humidity for 72 hours, combined with irrigation withholding to simulate drought (Table 1).

Table 1. Experimental design of treatment groups for germination analysis

Groups	**Karrikin**	**Distilled Water**	**Heat+Drought Stress**
G1 – Control	-	5 mL	-
G2 – Karrikin	+		-
G3 – Stress	-	2,5 mL	+
G4 – Karrikin + Stress	+		+

Leaf samples were flash-frozen in liquid nitrogen and homogenized for total RNA extraction using TriZol reagent (Invitrogen, USA) and purified with Direct-zol RNA MiniPrep Kit (Zymo Research, USA). RNA integrity was confirmed by agarose gel electrophoresis and A260/A280 ratios (1.9–2.1). cDNA synthesis was performed using the High-Capacity cDNA Reverse Transcription Kit (Applied Biosystems, USA) following manufacturer's instructions.

qRT-PCR analyses targeted five genes: *CAT*, *SOD*, *SlWRKY31*, *ERF84*, and *NHX1*, with *Actin* as reference. Reactions were run in triplicate using RealQ SYBR Green Master Mix (Ampliqon, Denmark) on a Bio-Rad CFX96 system. Thermal cycling conditions were 95°C for 15 min, followed by 40 cycles at 95°C (20 s), 60°C (20 s), and 72°C (20 s). Melting curves confirmed amplicon specificity. Relative expression was calculated using the $2^{-\Delta\Delta Ct}$ method (Livak & Schmittgen, 2001). Data were analyzed by one-way ANOVA ($p < 0.05$) using Python libraries *numpy*, *scipy*, and *statsmodels*.

RESULTS and DISCUSSION

Heat and drought stress caused pronounced transcriptional activation of oxidative stress-related and regulatory genes in tomato seedlings. In the stress-only group (G3), *CAT* and *SOD* expression increased nearly 16-fold, confirming the central role of reactive oxygen species (ROS) scavenging enzymes in early stress response. *SlWRKY31* and *ERF84* were also highly upregulated, indicating strong activation of transcriptional networks involved in osmotic and heat shock signaling. Similarly, *NHX1*, responsible for vacuolar Na+/H+ antiport, exhibited a 10-fold induction, suggesting enhanced ion homeostasis and osmoprotection (Table 2).

Table 2. Relative expression levels ($2^{-\Delta\Delta Ct}$ ± SD) of selected stress-related genes in tomato seedlings under different treatment conditions. Expression was normalized to the *actin* reference gene and calculated using the ΔΔCt method, with the control group (G1) as the calibrator (relative expression = 1.00). Values represent mean ±standard deviation of three biological replicates. Treatments include control (G1), KAR1 pre-treatment without stress (G2), stress without KAR1 (G3), and KAR1 pre-treatment under stress (G4).

Gene	G1	G2	G3	G4
CAT	1.0 ± 0.1	1.23 ± 0.1	16.0 ± 0.82	4.0 ± 0.22
SOD	1.0 ± 0.09	1.15 ± 0.13	16.0 ± 1.34	4.59 ± 0.45
SlWRKY31	1.0 ± 0.07	1.15 ± 0.12	16.0 ± 1.15	4.0 ± 0.28
ERF84	1.0 ± 0.07	1.15 ± 0.1	11.31 ± 1.05	2.83 ± 0.28
NHX1	1.0 ± 0.06	1.23 ± 0.12	9.85 ± 0.76	2.46 ± 0.26

In contrast, the KAR1 + stress group (G4) exhibited moderated expression for all genes: *CAT* (4.0-fold), *SOD* (4.6-fold), *SlWRKY31* (4.0-fold), *ERF84* (2.8-fold), and *NHX1* (2.5-fold) (Fig 1). This controlled induction reflects KAR1's priming capacity—preparing cellular defense without overstimulation. KAR1 likely facilitates ROS detoxification and membrane stabilization by modulating signal transduction through the KAI2-MAX2 axis, which regulates hormonal crosstalk between ABA and gibberellin pathways (Nelson et al., 2016).

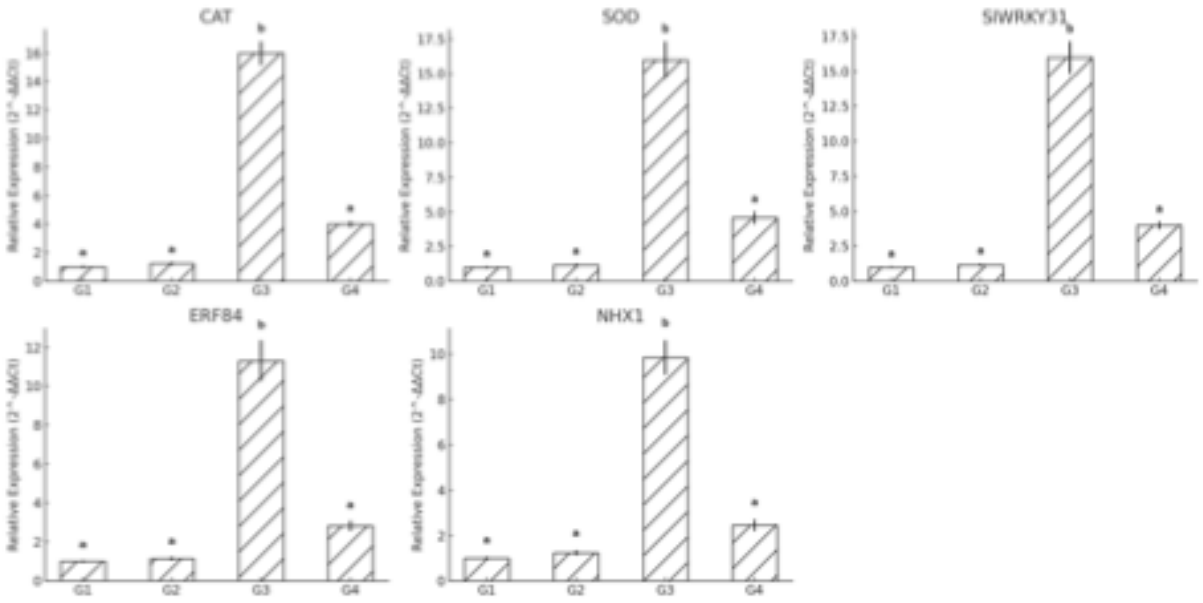


Figure 1. Relative expression levels ($2^{-\Delta\Delta Ct}$ ± SD) of selected stress-responsive genes in tomato seedlings under different treatments. The expression of five genes CAT, SOD, SlWRKY31, ERF84, and NHX1 was measured via qPCR using Actin as the reference gene and the control group (G1) as the calibrator. Treatments include G1 (control), G2 (KAR1-only), G3 (stress-only), and G4 (KAR1 + stress). Values are means ±standard deviation (n = 3). Different letters above bars indicate significant differences among treatments for each gene ($p < 0.05$, one-way ANOVA with Tukey's post hoc test). The data show strong induction under combined stress (G3), and moderated expression in KAR1-treated stressed seedlings (G4), highlighting the regulatory effect of KAR1

Comparable studies in *Avena fatua*, *Arabidopsis*, and wheat confirm that KAR1-treated plants display enhanced antioxidant enzyme activity and improved tolerance to dehydration and high temperature (Gupta et al., 2022; Saini et al., 2023). The ability of KAR1 to regulate *WRKY* and *ERF* transcription factors highlights its role in modulating stress memory and adaptive plasticity—traits critical for climate-resilient agriculture.

CONCLUSION

This study demonstrated that KAR1 acts as an effective molecular modulator of stress-responsive gene expression in tomato under combined heat and drought stress. KAR1 pre-treatment mitigated excessive gene activation, maintaining metabolic stability and promoting efficient oxidative stress management. These findings suggest that KAR1 can be developed as a sustainable biostimulant for enhancing plant resilience under multifactorial environmental stresses.

Future research should focus on identifying downstream transcriptional regulators of the KAR1 signaling cascade, exploring interactions with phytohormones such as ABA and ethylene, and evaluating field-level effects of KAR1-based treatments for tomato and other economically important crops.

ACKNOWLEDGEMENTS

This study was supported by the Iğdır University Scientific Research Projects Unit (Project No: YİP0723İ04). The authors thank the AgriQueens undergraduate research team for their contributions to laboratory work and data collection.

REFERENCES

Flematti, G. R., Ghisalberti, E. L., Dixon, K. W., & Trengove, R. D. (2004). A compound from smoke that promotes seed germination. *Science*, **305**, 977. https://doi.org/10.1126/science.1099944

Gupta, A., Choudhary, R., & Chauhan, D. (2022). Karrikins: New molecular players in plant abiotic stress tolerance. *Plant Stress*, **4**, 100070. https://doi.org/10.1016/j.stress.2022.100070

Li, W., Nguyen, K. H., Chu, H. D., Ha, C. V., Watanabe, Y., & Osakabe, Y. (2017). The karrikin receptor KAI2 promotes drought resistance in *Arabidopsis thaliana*. *PLoS Genetics*, **13**, e1007076. https://doi.org/10.1371/journal.pgen.1007076

Li, W., Nguyen, K. H., Chu, H. D., & Ha, C. V. (2024). Karrikins, redox, and plant abiotic stress tolerance: A focal review. *Metabolites*, **14**, 213. https://doi.org/10.3390/metabo14040213

Nelson, D. C., Flematti, G. R., Ghisalberti, E. L., Dixon, K. W., & Smith, S. M. (2012). Regulation of seed germination and seedling growth by chemical signals from burning vegetation. *Annual Review of Plant Biology*, **63**, 107–130. https://doi.org/10.1146/annurev-arplant-042811-105545

Nelson, D. C., Guo, H., & Flematti, G. R. (2016). Smoke- and hormone-mirrors: Action and evolution of karrikin and strigolactone signaling. *Trends in Genetics*, **32**, 176–186. https://doi.org/10.1016/j.tig.2016.01.002

Saini, D., Singh, A., & Prasad, R. (2023). Smoke-derived karrikins modulate stress-responsive gene networks and boost drought resilience in wheat. *Plant Physiology Reports*, **28**, 412–423. https://doi.org/10.1007/s40502-023-00693-1

Sun, Y., Guo, J., Yang, Z., & Han, L. (2020). Exogenous karrikin enhances drought tolerance of wheat seedlings through regulation of antioxidant enzyme activities and osmolyte accumulation. *Plant Physiology and Biochemistry*, **151**, 727–736. https://doi.org/10.1016/j.plaphy.2020.03.056

Waters, M. T., Scaffidi, A., Flematti, G. R., Smith, S. M., & Nelson, D. C. (2017). The karrikin signal transduction pathway. *The Plant Journal*, **89**, 627–640

ORAL PRESENTATION

Supercritical extraction of clove (*Syzygium aromaticum*) and investigation of essential oil components by GC-MS

Fatih DURMAZ* (https://orcid.org/0000-0001-9878-7961)

*Selçuk University, Faculty of Science, Department of Chemistry, Konya, Türkiye.

*e-mail: fdurmaz@selcuk.edu.tr:

Abstract

In recent years, interest in the use of naturally occurring bioactive compounds as alternatives to synthetic additives and chemical drugs has increased. Clove oil is considered a natural option in the food preservative, pharmaceutical, and cosmetic industries. GC-MS analyses have revealed the presence of various phenolic and terpenic compounds that support the therapeutic potential of clove oil. The positive effects of these compounds on human health have made clove oil an important tool for food supplements and natural therapeutic methods. In this study, Clove (Syzygium Aromaticum) was extracted using a Supercritical Extraction System (SFE). The products obtained from this SFE extraction were analyzed for their essential oil components using Gas Chromatography-Mass Spectrometry (GC-MS). Clove oil (Syzygium aromaticum) is a valuable herbal product known for its rich phenolic compound content and widely used in traditional medicine. Studies using Gas Chromatography-Mass Spectrometry (GC-MS) analyses have shown that eugenol, the primary component of clove oil, is present in high concentrations (70-90%). In addition, other bioactive compounds such as β-caryophyllene, acetyl eugenol, and humulene also contribute to the pharmacological effects of clove oil

Keywords: Supercritical Extraction System (SFE), Clove (Syzygium Aromaticum), Gas Chromatography-Mass Spectrometry (GC-MS)

INTRODUCTION

Clove (Syzygium aromaticum) is a versatile plant known as both a spice and a flower. Clove buds (Syzygium aromaticum), used as a spice, originated in Indonesia and are widely used in cuisines around the world for their strong aroma. They offer numerous health benefits. They aid digestion, alter the structure of the digestive system, have analgesic effects, and may help regulate blood sugar. The buds of Syzygium aromaticum, commonly known as cloves, have been used in traditional medicine for various purposes for many years (Khader et al., 2014). Beyond modern medical science, certain symbols and services have been maintained in traditional medicine in Far and Middle Eastern countries for many years. These include gum disease, oral diseases, digestive disorders, moderate well-being, respiratory diseases, inflammatory diseases, rheumatic pain, initiation, blood problems, and skin diseases (Arunava et al., 2018). Tincture obtained from clove buds is reported to be used in the treatment of toothaches, mouth sores, digestive problems, and generally respiratory diseases and rheumatic pain. A few drops of clove oil mixed with honey is taken internally for vomiting and indigestion, and the oil is used externally as an antiseptic and painkiller for skin diseases and wounds (Cortés-Rojas et al., 2014). Usage in Dentistry: Thanks to its eugenol content, clove oil is used to quickly relieve toothaches. Studies have shown that gels containing 20-30% clove oil relieve dental pain intermittently within 15 minutes (Markowitz et al., 1992). Regular use has been observed to reduce swelling and pain (Kim et al., 2013). Bacterial and Fungal Infections: Eugenol is effective against bacteria such as S. Aureus and E. Coli. It also prevents the dissolution of fungi such as Candida albicans (Chaieb et al., 2007). Oral Health: As a gargle, it constricts the mouth (Pinto et al., 2009). Blood Sugar Regulation: It has been observed that it lowers fasting blood sugar in patients with type 2 diabetes (Selles et al., 2020). Fights Free Radicals: It has a high ORAC value (10,700 µmol TE/g) and is effective in preventing heart damage (Prasad et al., 2005). Asthma and Bronchitis: They breathe by dilating the bronchi (Pandey et al., 2024). Stomach Ulcer and Indigestion: It balances stomach acids and prevents the proliferation of H. Pylori bacteria (Maggini et al. 2024). Effects on Alzheimer's and Memory: Clove oil has protective properties for the nerves. It can be used as a treatment in many centers as a natural healing source (Zhang et al., 2017).

MATERIALS AND METHODS

A supercritical fluid is the physical state of a substance at or above its critical temperature and pressure. In this state, the fluid combines the diffusion properties of a gas with the solvent properties of a liquid. The most commonly used supercritical fluid is carbon dioxide (CO_2) (because it is environmentally friendly, non-toxic, and inexpensive). As shown in Figure. 1, Clove (Syzygium Aromaticum) was extracted using a supercritical fluid extraction system, and an extract was obtained for analysis.

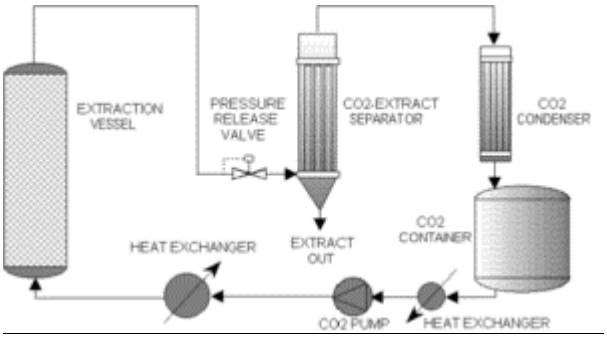


Figure1. Supercritical Fluid Extraction System

Gas Chromatography-Mass Spectrometry (GC-MS), especially for essential oils. In this method, clove oil is dissolved in acetone and injected into the gas chromatograph. Gas chromatography separates the components, while mass spectrometry determines their identity. Eugenol, the main component of clove oil, exhibits a distinct peak in this analysis. Other phenolic compounds and terpenoids present in the oil can also be detected. 0.02 g of clove oil extracted using the SFE method was placed in a tube. 2 mL of acetone was added and dissolved to create a homogeneous solution. The liquid phase of this solution was filtered through a 0.45 µm PTFE filter to remove particles, and the cleaned sample was transferred to a GC-MS vial. Finally, this sample was injected into the GC-MS instrument for chemical component analysis. For the GC-MS analysis of clove oil, the analysis conditions were prepared as shown in Table. 1; an HP-5 MS column (5% phenylmethylpolysiloxane) was used to separate volatile components. 1 µL was injected in Pulsed Split (50:1) mode, and helium (0.7 mL/min flow rate) was used as the carrier gas. The column oven temperature program was gradually increased from 50°C to 280°C, while the ion source temperature was set at 230°C and the quadrupole temperature was set at 150°C. These conditions were optimized for optimal determination of components specific to clove oil, such as eugenol.

Table 1. Gas Chromatography Mass Spectrometry Detector (GC-MS) Method Conditions

injector		carrier gas		column furnace			MS temperature	
mode	temperature	type	flow rate	°C/min	°C	minute	source	Quadro pole
1µL pulsed split(50:1)	180 °C	He	0,7 mL/min	10 20	50 200 280	2 10 7	230°C	150°C
stationary phase (column)	HP-5 MS column(5%-Phenyl methylpolysiloxan)							

The analysis results obtained from the GC-MS analysis of Clove (Syzygium Aromaticum) oil are given in Figure 2.

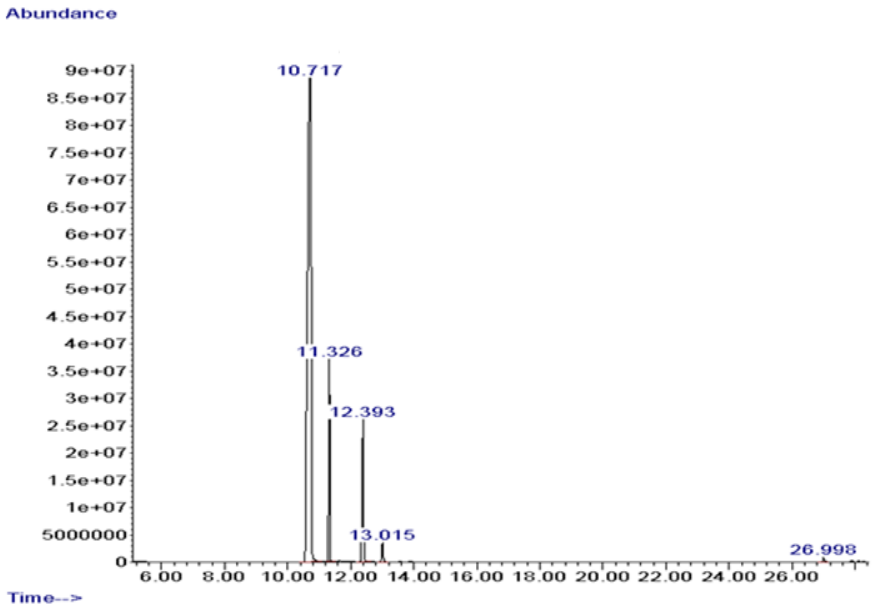


Figure 2. GC-MS Analysis Spectrum of Clove (Syzygium Aromaticum) Oil

The analysis results obtained from the GC-MS analysis of Clove (Syzygium Aromaticum) oil are given in Table 2.

Table 2. GC-MS Analysis Result of Clove (Syzygium Aromaticum) Oil

Retention time	% amount	Component Name
11,326 min	%79,170	Eugenol
12,394 min	%10,876	Caryophyllene
13,015 min	%8,636	Aceteugenol
14,012 min	%1,015	Caryophyllene oxide
15,27 min	%0,300	Phenol Derivative (Phenol, 2,2'-methylenebis[6-(1,1-dimethylethyl)-4-methyl-)

RESULTS and DISCUSSION

Clove (Syzygium Aromaticum) oil, extracted using SFE systems, is a valuable herbal product known for its rich phenolic compound content and widely used in traditional medicine. Studies using GC-MS analyses have identified a high concentration of eugenol (79.170%), the primary component of clove oil. In addition, other bioactive compounds such as β-caryophyllene (10.876%), acetyl eugenol (8.636%), and humulene also contribute to the pharmacological effects of clove oil. The high 79% eugenol content of clove (Syzygium Aromaticum) oil explains why cloves have been used as a painkiller for centuries. The presence of over 10% caryophyllene demonstrates that this oil not only relieves pain but also has anti-inflammatory properties. The approximately 8% acetyl eugenol content, responsible for the oil's milder effects, contributes to the effectiveness of clove oil.

CONCLUSION

The SFE system, unlike traditional solvent extraction, does not require heating or steaming. It is environmentally friendly, consumes little energy, is fast, does not require post-extraction purification, and requires very little time to prepare the product for extraction. The SFE extraction system has become a widely used technique for extracting certain plants with pharmacological properties. It has become a modern and powerful extraction system preferred for obtaining active ingredients. Therefore, the study has become a modern and preferred technique that not only maximizes extraction efficiency but also provides accurate results for active ingredient analysis.

REFERENCES

Arunava,D., Harshadha, K., Dhinesh Kannan, S K., Hari, R.K., Bindhu, J., (2018). Evaluation of Therapeutic Potential of Eugenol-A Natural Derivative of Syzygium aromaticum on Cervical Cancer. Asian Pac J Cancer Prev, 19(7), 1977-1985.

Chaieb, K., Hajlaoui, H., Zmantar, T., Kahla-Nakbi, A. B., Rouabhia, M., Mahdouani, K., & Bakhrouf, A. (2007). The chemical composition and biological activity of clove essential oil, Eugenia caryophyllata (Syzygium aromaticum L. Myrtaceae): A short review. Phytotherapy Research Journal, 21(6), 501-506.

Cortés-Rojas, D. F., de Souza, C. R. F., & Oliveira, W. P. (2014). Clove (Syzygium aromaticum): A precious spice. Asian Pacific Journal of Tropical Biomedicine, 4(2), 90-96.

Khader, M., Bresgen, N., Eckl, P. M. (2014). Antimutagenic effects of ethanolic etrafta from selected Palestinian medicinal plants. Journal of Ethnopharmacology, 154(1), 192-197.

Kim, H.-M., Lee, E.-H., Hong, S.-H., Song, H.-J., Shin, M.-K., Kim, S.-H., & Shin, T.-Y. (2013). Effect of Syzygium aromaticum extract on immediate hypersensitivity in rats. Journal of Ethnopharmacology, 120(1), 51-56.

Maggini, V., Semenzato, G., Gallo, E., Nunziata, A., Fani, R., Firenzuoli, F. (2024). Antimicrobial Activity of Syzygium aromaticum Essential Oil in Human Health Treatment. Molecules, 29(5), 999-1-13.

Markowitz, K., Moynihan, M., Liu, M., & Kim, S. (1992). Biologic properties of eugenol and zinc oxide-eugenol. Oral Surgery, Oral Medicine, Oral Pathology, 73(6), 729-737.

Pandey, V.K., Srivastava, S.A., Dash, K.K., Singh, R., Dar, A.H., Singh, T., Farooqui, A., Shaikh, A.M., Kovacs, B. (2024). Bioactive properties of clove (Syzygium aromaticum) essential oil nanoemulsion: A comprehensive review. Heliyon Journal, 10(1), e22437.

Pinto, E., Vale-Silva, L., Cavaleiro, C., & Salgueiro, L. (2009). Antifungal activity of the clove essential oil from Syzygium aromaticum on Candida, Aspergillus and dermatophyte species. Journal of Medical Microbiology, 58(11), 1454-1462.

Prasad, R. C., Herzog, B., Boone, B., Sims, L., & Waltner-Law, M. (2005). An extract of Syzygium aromaticum represses genes encoding hepatic gluconeogenic enzymes. Journal of Ethnopharmacology, 96(1-2), 295-301.

Selles, S.M.A., Kouidri, M., Belhamiti B.T., Amrane, A.A. (2020). Chemical composition, in-vitro antibacterial and antioxidant activities of Syzygium aromaticum essential oil. Journal of Food Measurement and Characterization, 14(4), 2352–2358.

Zhang, Y., Wang, Y., Zhu, X., Cao, P., Wei, S., Lu, Y. (2017). Antibacterial and Antibiofilm Activities of Eugenol from Essential Oil of Syzygium aromaticum (L.) Merr. & L. M. Perry (Clove) Leaf against Periodontal Pathogen Porphyromonas gingivalis. Microb. Pathog, 113, 396–402.

ORAL PRESENTATION

Kinetic, thermodynamic and isothermal study of mechanically activated seashells at different durations

Mervenur Genç[1] (*ORCID:https://orcid.org/0009-0003-7475-7524*), Aybuke Şirin[1] (*ORCID: https://orcid.org/0009-0007-2325-0239*), Seda Karayünlü Bozbaş[1] (*ORCID: https://orcid.org/0000-0002-5177-3826*)

[1] Kocaeli University, Faculty of Arts and Sciences, Department of Chemistry, Kocaeli, Türkiye

*Corresponding author e-mail: sedak@kocaeli.edt.tr

Abstract

In this study, the biosorption performance of mechanically activated seashells (MAS) prepared at three different activation times (1, 2, and 3 hours) was evaluated for the removal of Methyl Violet 6B (MV6B) dye. The experiments revealed that the highest adsorption efficiency was achieved under the same conditions for all MAS samples, regardless of the activation time. These optimal conditions were found to be pH 6, 30 minutes contact time, 100 mg/L MV6B concentration, and 30°C temperature. Equilibrium biosorption data were applied to Langmuir, Freundlich, and Temkin isotherm models, and the Freundlich isotherm was determined to be the most suitable model for all MAS (1h, 2h and 3h) samples, showing heterogeneous multilayer adsorption behavior. Kinetic analyses using pseudo-first-order, pseudo-second-order, and Elovich kinetic models showed that the pseudo-second-order model best fit the biosorption process for MAS (1h, 2h and 3h). The negative values of Gibbs free energy (ΔG°), enthalpy (ΔH°), and entropy (ΔS°) in the thermodynamic parameters calculated for MAS samples confirmed that the biosorption of MV6B onto MAS is spontaneous and exothermic, and also that disorder at the solid–solution interface decreases. It was observed that MAS samples exhibit similar adsorption properties even when the activation time varies and possess strong potential as an effective biosorbent for MV6B removal.

Keywords: mechanical activation, isotherm, kinetics, thermodynamics, seashell, methyl violet 6B

INTRODUCTION

With the development of industry, there has been a significant increase in the amount of dye waste entering water sources. Cationic triphenylmethane dyes used in the textile and similar industries pose an environmental risk. One such dye, Methyl Violet 6B (MV6B), is a difficult pollutant to treat due to its high solubility and stability, and is also harmful to health (Rai et al., 2005). Therefore, effective removal of dye waste is important. While existing methods are often costly and inadequate, adsorption stands out as a low-cost and highly efficient alternative (Kausar et al., 2023).

Systems in which biomass is used as an adsorbent in the adsorption process are defined as bioadsorption. Due to their low cost, biodegradability, and easy accessibility, marine product wastes such as oyster, snail, and shrimp shells have emerged as effective bioadsorbents in recent years (Su et al., 2022; Hossain et al., 2024). Seashells, which contain approximately 95% $CaCO_3$, were preferred in this study because they exhibit strong adsorbent properties due to their porous structure and high binding capacity when properly prepared and ground (He et al., 2015; Wang, 2021).

Mechanical activation is typically achieved by high-energy ball milling of a powdered material (Baláž et al., 2003). The primary purpose of mechanical activation is to increase the surface area, thereby providing energy input to the system and increasing the reaction rate for subsequent processes (Alex et al., 2016).

In this study, the removal of the cationic dye MV6B from aqueous solutions was investigated using mechanically activated sea shells for different durations. The aim was to improve the surface properties of shell powder without chemical treatment and to increase its adsorption capacity through mechanical activation. The isothermal, kinetic, and thermodynamic behavior of the system was evaluated using the adsorbents obtained.

MATERIALS AND METHODS

Materials

In the bioadsorption study, Methyl Violet 6B (MV6B) (molecular weight: 393.96 g/mol) was used as the dye (Figure 1). The required amount of powdered dye was dissolved in deionized water to prepare a stock solution (1000 mg/L). All working solutions at the desired concentrations were prepared by diluting the stock solution. The pH of the solution was adjusted using 0.1 mol/L HCl or 0.1 mol/L NaOH solution with a HANNA/pH 211 model pH meter.

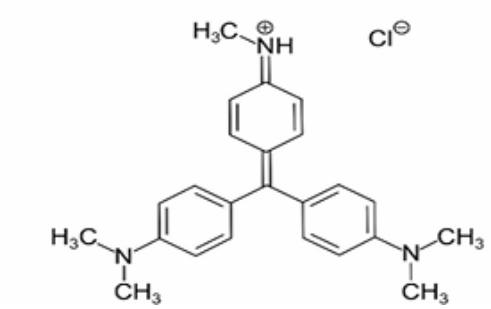


Figure 1. Methyl Violet 6B chemical structure

Preparation of seashells

The seashells were obtained from the Karabiga coast in the district of Biga (Çanakkale, Turkey). The seashells were washed with tap water and then with pure water to remove coarse dirt. The seashells washed in pure water were dried in an oven at 80 °C for 12 hours. The dried seashells were crushed with a hammer and then ground into powder using an IKA A11 mill. The mechanical activation process of the seashells was carried out in a planetary ball mill (Fritsch pulverisette) at 600 rpm for 1.2 and 3 hours.

Adsorption experiments

The bioadsorption performance of seashells (MAS) activated at different times was evaluated for the removal of MV6B from aqueous solutions. MV6B bioadsorption experiments were conducted using 50 mL falcon tubes with the batch bioadsorption method. The solutions were shaken using a Biosan Multi Rotator at 100 rpm. For bioadsorption optimization, the initial dye concentration (10-125 mg/L), adsorbent amount (0.1-0.5 g), temperature (25°C-60°C), adsorption contact time (5-60 min), and pH 2-8 conditions were investigated. The MV6B concentration in the solution was measured at the maximum dye wavelength (λ = 580 nm) using a spectrophotometer (UV-Vis) (T80 + PG device LTD).

The bioadsorption efficiency (% R) and capacity (qe) of MV6B dye on MAS were calculated according to Equations (1) and (2):

$$R\% = \frac{C_0 - C_e}{C_0} x\ 100 \quad (1)$$

$$q_e = \frac{(C_0 - C_e)}{W} xV \quad (2)$$

Here, in the %R and qe formulas, C_0 represents the initial MV6B concentration (mg/L), C_e represents the MV6B concentration at equilibrium (mg/L), q_e represents the adsorption capacity (mg/g), W represents the adsorbent amount (g), and V represents the solution volume (L).

Isotherm studies

Adsorption isotherm studies are an important factor in explaining the fundamental interaction between adsorbent and adsorbate substances and the adsorption mechanism. In this study, the Langmuir, Freundlich, and Temkin models, which are common isotherms, were used to define the adsorption equilibrium.

The Langmuir isotherm model is expressed by Equation 3:

$$\frac{C_e}{q_e} = \frac{1}{q_{max} K_L} + \frac{C_e}{q_{max}} \quad (3)$$

where q_e is the amount of dye adsorbed per unit mass of adsorbent at equilibrium (mg/g), C_e is the equilibrium concentration of the dye in solution (mg/L), qmax is the maximum monolayer adsorption capacity (mg/g), and K_L is the Langmuir adsorption constant (L/mg).

The Freundlich isotherm model is expressed by Equation 4:

$$\ln q_e = ln K_F + \frac{1}{n} ln\, C_e \quad (4)$$

where K_F is the Freundlich constant related to adsorption capacity (mg/g) and n is the heterogeneity factor. The value of 1/n indicates the adsorption intensity or surface heterogeneity.

The Temkin isotherm model is expressed by Equation 5:

$$q_e = B ln K_T + B ln C_e \quad (5)$$

where K_T is the Temkin isotherm equilibrium binding constant (L/g) and B is a constant related to the heat of sorption (J/mol).

Kinetic studies

Adsorption kinetics is described by pseudo-first-order (equation 6), pseudo-second-order (equation 7) and Elovich (equation 8) models.

$$\ln(q_e - q_t) = \ln q_e - k_1 t \quad (6)$$

Here, q_e (mg/g) and q_t (mg/g) are the amount of dye adsorbed at time t, and k_1 (min^{-1}) is the first-order adsorption rate constant.

$$\frac{t}{q_t} = \frac{1}{k_2 q_e^2} + \frac{1}{q_e} t \quad (7)$$

where k_2 is the pseudo-second-order equation constant (g/mg min^{-1}); t is the specified time constant (min); q_t is the amount of adsorbed material at the end of the t period (mg/g); q_e is the amount of adsorbed material in equilibrium (mg/g).

$$q_t = \frac{1}{\beta}\ln(\alpha\beta) + \frac{1}{\beta}\ln t \quad (8)$$

Here, q_t represents the amount of adsorbate adsorbed at time t. In this equation, α is the initial adsorption rate, reflecting how quickly adsorption begins; β is related to the activation energy for surface coverage and chemisorption, and shows how the adsorption rate decreases as the surface fills up.

Thermodynamic studies

The thermodynamic analyses were performed using the following Equations (9), (10), and (11):

$$K_D = \frac{q_e}{C_e} \quad (9)$$

$$\Delta G° = -RTlnK_D \quad (10)$$

$$\Delta G° = \Delta H° - T\Delta S° \quad (11)$$

In the equations, ΔG° is the Gibbs free energy change, ΔH° is the adsorption enthalpy change, ΔS° is the entropy change, and T is the absolute temperature; R is the gas constant (8.314 joules.mol/K).

RESULTS and DISCUSSION

Adsorption parameters effects

In this study, various optimization parameters were investigated to evaluate the bioadsorption performance of MAS samples (1 h, 2 h, and 3 h) on MV6B dye. In this context, the effects of pH (2–8), initial dye concentration (20–125 ppm), contact time (5–60 min), adsorbent amount (0.1–0.5 g), and temperature (25–60 °C) were investigated.The results obtained showed that the optimal conditions for all MAS samples were pH 6, 30 min

contact time, 100 mg/L MV6B concentration, and 30 °C temperature. Under these optimal conditions, the MV6B removal efficiency was calculated as 94.13% for 1 hour MAS, 93.09% for 2 hours MAS, and 98.55% for 3 hours MAS, demonstrating that MAS samples have a high bioadsorption capacity.

Bioadsorption Isotherms

It is a parameter that describes how adsorbate molecules are distributed between the liquid and solid phases when the adsorption process reaches equilibrium. The isotherm model results for 1, 2, and 3-hour mechanical activation times (MAS) are given in Table 1.

Table 1. Isothermal model results for 1h (a), 2h (b), and 3h (c) MAS

a)

Isotherm Model	Parameter	Value
Langmuir	R^2	0,4607
	q_{max}(mg/g)	-8,0645
	K_L(L/mg)	-0,0720
	R_L	-0,1611
Freundlich	R^2	0,9596
	K_F (mg/g)	0,3304
	1/n	1,7249
Temkin	R^2	0,9503
	K_t (L/g)	0,3995
	B	10,694

b)

Isotherm Model	Parameter	Value
Langmuir	R^2	0,4686
	q_{max}(mg/g)	-11,7233
	K_L(L/mg)	-0,0738
	R_L	-0,1566
Freundlich	R^2	0,9337
	K_F (mg/g)	0,6455
	1/n	1,565
Temkin	R^2	0,923
	K_t (L/g)	0,5362
	B	10,19

c)

Isotherm Model	Parameter	Value
Langmuir	R^2	0,4977
	q_{max}(mg/g)	-13,8504
	K_L(L/mg)	-0,0815
	R_L	-0,1398
Freundlich	R^2	0,956
	K_F (mg/g)	0,9559
	1/n	1,504
Temkin	R^2	0,934
	K_t (L/g)	0,6694
	B	9,9357

Among the applied models, the Freundlich isotherm has the highest correlation coefficient for all MAS samples. This supports the idea that the adsorbent surface has a heterogeneous structure and that adsorption occurs through a multi-layer mechanism (Sultana et al., 2022). The negative q_{max} values obtained in the Langmuir model indicate that the assumption of single-layer adsorption is not valid in the process and that this model is insufficient to explain the system. Similarly, there are studies in the literature that report negative values (Lu et al., 2018; Esfandiar et al., 2021; Ščasná et al., 2025). These findings support the notion that the applicability of the Langmuir model may be limited in some adsorption systems. The Temkin model parameters reveal that the adsorbate–adsorbent interactions change throughout the process and that the adsorption heat decreases regularly as the surface coverage increases (Kanwal et al., 2024). These findings indicate that the adsorption mechanism occurs on heterogeneous surfaces with variable energy distribution rather than on a homogeneous monolayer structure.

Bioadsorption Kinetics

Adsorption kinetics is used to determine the mechanisms by which adsorbed species attach to the adsorbent surface and the rate of these processes (Khandaker et al., 2020). The kinetic model results for 1, 2, and 3 hours of mechanical activation time (MAS) are presented in Table 2.

Table 2. Kinetic model results of 1h (a), 2h (b) and 3h (c) MAS

a)

Kinetic Model	Parameter	Value
Pseudo-first-order	R^2	0,7200
	k1 (1/min)	0,0193
	qe,cal (mg/g)	2,5609
Pseudo-second-order	R^2	0,9996
	k2 (g/mg.min)	0,0667
	$q_{e,cal}$ (mg/g)	13,6612
Elovich	R^2	0,8180
	β (g/mg)	1,2294
	α (mg/g.min)	247274,0

b)

Kinetic Model	Parameter	Value
Pseudo-first-order	R^2	0,7705
	k1 (1/min)	0,0184
	qe,cal (mg/g)	1,9169
Pseudo-second-order	R^2	0,9998
	k2 (g/mg.min)	22,2474
	$q_{e,cal}$ (mg/g)	13,6425
Elovich	R^2	0,8842
	β (g/mg)	1,8494
	α (mg/g.min)	703000751,3

c)

Kinetic Model	Parameter	Value
Pseudo-first-order	R^2	0,7142
	k1 (1/min)	0,0186
	qe,cal (mg/g)	2,2049
Pseudo-second-order	R^2	0,9995
	k2 (g/mg.min)	0,0724
	$q_{e,cal}$ (mg/g)	13,9082
Elovich	R^2	0,7310
	β (g/mg)	1,7102
	α (mg/g.min)	153784651,5

According to the table results, the pseudo-second-order (PSO) model showed the best fit among the adsorption kinetics data. This finding indicates that chemical interactions are dominant in the adsorption process and that the adsorption capacity of the adsorbate is a rate-determining factor (Singh et al., 2024). The pseudo-first-order and Elovich models provided lower fit in explaining the process, and the PSO model was seen to represent the kinetic behavior more accurately. This situation indicates that adsorption occurring on the adsorbent surface is largely carried out by chemical binding mechanisms.

Bioadsorption Thermodynamics

The primary reason for performing a thermodynamic evaluation is to determine the appropriate nature and spontaneity of this process (Balji et al., 2023). The thermodynamic model results for 1, 2, and 3-hour mechanical activation times (MAS) are presented in Table 3.

Table 3. Thermodynamic model results of 1h (a), 2h (b) and 3h (c) MAS

a)

T (°C)	ΔG°(kJ/mol)	ΔH° (kJ/mol)	ΔS° (J/(mol.K))
25	-3,028		
30	-2,211		
40	-2,212	-8,553	-19,791
50	-2,113		
60	-2,129		

b)

T (°C)	ΔG°(kJ/mol)	ΔH° (kJ/mol)	ΔS° (J/(mol.K))
25	-0,954		
30	-1,774		
40	-0,902	-12,132	-36,036
50	-0,276		
60	-0,174		

c)

T (°C)	ΔG°(kJ/mol)	ΔH° (kJ/mol)	ΔS° (J/(mol.K))
25	-4,593		
30	-5,859		
40	-4,382	-19,964	-49,554
50	-3,501		
60	-3,689		

The results of the thermodynamic analysis indicate that the values of ΔG°, ΔH°, and ΔS° are negative. A negative ΔG° value indicates that the adsorption process occurs spontaneously, while a negative ΔH° value indicates that the process is exothermic. Furthermore, the negative ΔS° value indicates that the system acquires a more ordered structure during adsorption and that entropy decreases. These results demonstrate that adsorption is thermodynamically favorable and that the process occurs exothermically.

CONCLUSION

The adsorption data showed the best fit to the Freundlich isotherm model, indicating that the adsorbent surface is heterogeneous and that adsorption occurs via a multistage mechanism. In contrast, the Langmuir isotherm proved insufficient in explaining the process due to its assumption of monolayer adsorption. Kinetic analyses showed that adsorption best fits the pseudo-second-order (PSO) model, thus indicating that the process is controlled by chemical interactions. The negative values of the thermodynamic parameters (ΔG°, ΔH°, ΔS°) indicate that adsorption occurs spontaneously, exothermically, and through a mechanism that leads to a more ordered state of the system.

Additionally, the optimal conditions for all MAS samples have been determined as pH 6, 30 minutes contact time, 100 mg/L MV6B concentration, and 30 °C. Under these conditions, the MV6B removal efficiency was calculated as 94.13% for 1-hour MAS, 93.09% for 2-hour MAS, and 98.55% for 3-hour MAS. These results demonstrate that mechanically activated seashell powders with different durations are effective biosorbents with high bioadsorption capacity and can be successfully used in MV6B removal.

ACKNOWLEDGEMENTS

The authors would like to thank Kocaeli University for providing laboratory facilities and technical support for this research.

This work was supported by TÜBİTAK 2209-A. The authors sincerely thank TÜBİTAK for funding this project and making this research possible.

REFERENCES

Rai, H. S., Bhattacharyya, M. S., Singh, J., Bansal, T. K., Vats, P. & Banerjee, U. C. (2005). *Removal of dyes from the effluent of textile and dyestuff manufacturing industry: A review of emerging techniques with reference to biological treatment.* Critical Reviews in Environmental Science and Technology, 35(3), 219–238.

Kausar, A., Zohra, S. T., Ijaz, S., Iqbal, M., Iqbal, J., Bibi, I., Nouren, S., El Messaoudi, N., & Nazir, A. (2023). Cellulose-based materials and their adsorptive removal efficiency for dyes: A review. International Journal of Biological Macromolecules, https://doi.org/10.1016/j.ijbiomac.2022.10.220

Su, H., Guo, X., Zhang, X., Zhang, Q., Huang, D., Lin, L., & Qiang, X. (2022). Ultrafine biosorbent from waste oyster shell: A comparative study of Congo red and methylene blue adsorption. Bioresource Technology Reports, 19, 101124. https://doi.org/10.1016/j.biteb.2022.101124

Hossain, M. S., Hossain, M. S., Ahmed, S., & Bin Mobarak, M. (2024). Characterization and adsorption performance of nano-hydroxyapatite synthesized from Conus litteratus waste seashells for Congo red dye removal. RSC Advances, 14, 38560–38577. https://doi.org/10.1039/d4ra07733d

He, P., Chen, J., Su, M., Han, J., & Cheng, K. (2015). Chemical composition and structural characteristics of seashells. CIESC Journal, 66, 450–454.

Wang, H. (2021). Status quo and research progress of waste seashell resource utilization. Aquaculture, 42(5).

Baláž, P., Takacs, L., Boldižárová, E., & Godočı́ková, E. (2003). Mechanochemical transformations and reactivity in copper sulphides. Journal of Physics and Chemistry of Solids, 64(11), 1413–1417.

Alex, T. C., Kumar, R., Roy, S. K., & Mehrotra, S. P. (2016). Mechanical activation of Al-oxyhydroxide minerals: A review. Minerals Processing and Extractive Metallurgy Review, 37(1), 1–26.

Sultana, S., Deb, A., Islam, K., Al Raihan, M., Hasan, M. A., Khan, H. M. J., & Rahman, M. W. (2022). *Adsorption of crystal violet dye by coconut husk powder: Isotherm, kinetics and thermodynamics perspectives*. Environmental Nanotechnology, Monitoring & Management, Article 100651. https://doi.org/10.1016/j.enmm.2022.100651

Lu, X., Tang, B., Zhang, Q., Liu, L., Fan, R., & Zhang, Z. (2018). The Presence of Cu Facilitates Adsorption of Tetracycline (TC) onto Water Hyacinth Roots. International Journal of Environmental Research and Public Health, 15(9), 1982. https://doi.org/10.3390/ijerph15091982

Esfandiar, N., Suri, R., & McKenzie, E. R. (2021). Simultaneous removal of multiple polycyclic aromatic hydrocarbons (PAHs) from urban stormwater using low-cost agricultural/industrial byproducts as sorbents. *Chemosphere, 281*, 129812. https://doi.org/10.1016/j.chemosphere.2021.129812

Ščasná, M., Kucmanová, A., Sirotiak, M., Blinová, L., Soldán, M., Hajzler, J., Ďuriška, L., & Palcut, M. (2025). Chlorella vulgaris-Derived Biochars for Metribuzin Removal: Influence of Thermal Processing Pathways on Sorption Properties. Materials, 18(14), 3374. https://doi.org/10.3390/ma18143374

Kanwal, S., Devi, P., Ahmed, Z., & Qambrani, N. A. (2024). *Adsorption isotherm, kinetic and thermodynamic studies for adsorption of fluoride on waste marble powder*. Desalination and Water Treatment, Article 100441. https://doi.org/10.1016/j.dwt.2024.100441

Khandaker, S., Toyohara, Y., Saha, G. C., Awual, M. R., & Kuba, T. (2020). *Development of synthetic zeolites from bio-slag for cesium adsorption: Kinetic, isotherm and thermodynamic studies*. Journal of Water Process Engineering, Article 101055. https://doi.org/10.1016/j.jwpe.2019.101055

Singh, V., Ahmed, G., Vedika, S., Kumar, P., Chaturvedi, S. K., Rai, S. N., Vamanu, E., & Kumar, A. (2024). *Toxic heavy metal ions contamination in water and their sustainable reduction by eco-friendly methods: Isotherms, thermodynamics and kinetics study*. Scientific Reports. https://doi.org/10.1038/s41598-024-58061-3

Balji, G. B., & Kumar, P. S. (2023). Sulphuric acid-modified coal fly ash for the removal of Rhodamine B dye from water environment: Isotherm, kinetics, and thermodynamic studies. *Adsorption Science & Technology, 2023*, 1-15. https://doi.org/10.1155/2023/2808794

ORAL PRESENTATION

CZTSe Nanokristallerin Sentezi ve Karakterizasyonu

Faysal Selimoğlu[1*] (https://orcid.org/0000-0003-3798-9054) ve İlker AKIN[1] (https://orcid.org/0000-0002-8683-0210)
[*1]Necmettin Erbakan Üniversitesi, Fen Fakültesi, Biyoteknoloji Bölümü, Konya,Türkiye

* Sorumlu yazar e-mail:faysalselimoglu@gmail.com

Özet

$Cu_2ZnSnSe_4$ (CZTSe), güneş hücrelerinin soğurucu katmanlarının kullanımında umut vadeden malzemelerden biridir. Dünya çapında bol miktarda bulunan çinko ve kalay elementleri, yaklaşık 1,5 eV'lik optimuma yakın bir doğrudan bant aralığı ve yaklaşık 10^4 cm^{-1} gibi yüksek bir soğurma katsayısı içerir. Oleylamin (OLA) içindeki CZTSe nanokristalleri, sıcak enjeksiyon yöntemiyle başarıyla hazırlanmıştır. Yapısının, bileşiminin ve morfolojisinin karakterizasyonu taramalı elektron mikroskobu (SEM) ve parçacık boyut analizörü kullanılarak yapılmıştır. Sonuçlar, monodispers nanokristallerin 9 nm aralığında tek fazlı polikristalin olduğunu ortaya koymuştur.

Anahtar Kelimeler: CZTSe, Nanokristal, Yarı iletken

Synthesis and characterization of CZTSe nanocrystals

Abstract

$Cu_2ZnSnSe_4$ (CZTSe) is one of promising materials in the use of absorber layers of solar cells. It contains earth-abundant elements of zinc and tin, a near-optimal direct band gap of ~1.5 eV, as well as a large absorption coefficient ~10^4 cm^{-1}. The CZTSe nanocrystals in oleylamine (OLA) was successfully prepared via hot-injection method. The characterization of its structure, composition and morphology were done using scanning electron microscope (SEM), and particle size analyzer. The results revealed that the monodispersed nanocrystals were single phase polycrystalline within the range of 9 nm.

Keywords: CZTSe, Nanocrystal, Semiconductor

GİRİŞ

Son zamanlarda güneş hücrelerinde etkili ışık emici malzemeler olarak $Cu_2ZnSnSe_4$ (CZTSe), Cu2ZnSnS4 (CZTS) ve $Cu_2ZnGeSe_4$ gibi Cu_2-II–IV–VI4 kuaterner yarı iletkenler, kapsamlı bir şekilde araştırılmıştır. Bu sistemlerden biri olan CZTSe, 1,4–1,56 eV optik bant aralığı ve 10^4 cm^{-1}'in üzerindeki yüksek emilim katsayısı sayesinde güneş hücrelerinde uygulama için en ilgi çekici malzemelerden biri olduğunu kanıtlanmıştır (Babu ve ark. 2011; Wibowo ve ark. 2007-a). Pahalı indiyum (In) ve galyum (Ga) kullanan CdTe ve $Cu_2InGaSe_4$ (CIGS) gibi iyi bilinen güneş hücresi malzemelerinin aksine, CZTSe'deki bileşen elementler Zn ve Sn nispeten bol ve ucuzdur (Zoppi ve ark. 2009). Maliyetli, yüksek sıcaklık ve düşük verimli üretim teknikleri kullanılarak püskürtme ve termal buharlaştırma teknikleri kullanılarak CZTSe soğurucu malzemenin hazırlanmasına ilişkin birkaç rapor bulunmaktadır (Babu ve ark. 2008-2011; Long ve ark. 2009; Zoppi ve ark. 2009; Wibowo ve ark. 2007-a). Kalkopirit bazlı ince film güneş hücrelerinde kullanılan indiyumun bulunabilirliği ve pahalılığı, mevcut büyük ölçekli ince film güneş hücrelerinin yüksek üretim maliyetlerine yol açmaktadır. Bu nedenle, güneş hücresi cihazlarının üretim maliyetini düşürmek amacıyla CZTSe, yeni bir soğurucu malzeme olarak incelenmiştir. Mellikov ve ark. (2009), bir CZTSe güneş hücresinde CZTSe mono tanecikleri kullanarak %2,14'lük bir verim elde etmişlerdir. Çoğunlukla vakum biriktirme (Wibowo ve ark. (2007-b); Friedlmeier ve ark. 1997) ve selenizasyon kullanılarak yapılan çeşitli CZTSe bileşik preparatları, CZTSe filmleri için başarıyla gösterilmiştir (Babu ve ark. 2008; Volobujeva ve ark. 2009). İnce film güneş hücrelerinin düşük sıcaklıkta biriktirme tekniklerinin

geliştirilmesine yönelik büyük bir talep vardır. Yüksek sıcaklık ve basınç gerektirmeyen CZTSe güneş hücreleri için yeni bir hazırlama yöntemi, kontrollü stokiyometri ile CZTSe nanokristallerini kimyasal olarak sentezlemek ve bunları bir "mürekkep" içinde dağıtmaktır. Bu çözeltiye dayalı yaklaşım, selenyum kaybına neden olabilen selenyum atmosferinde yüksek sıcaklıkta tavlama ihtiyacını ortadan kaldıracaktır. Özellikle, $CuInS_2$, $CuInSe_2$, CIGS ve CZTS dahil olmak üzere nanokristal mürekkebe dayalı fotovoltaik cihazlar yakın zamanda bildirilmiştir (Altosaar ve ark. 2006; Guo ve ark. 2009; Steinhagen ve ark. 2009). Burada, oleylamin (OLA) içinde CZTSe nanokristallerinin sentezlenerek SEM ve DLS ile karakterizasunu gerçekleştirilmiştir.

MATERYAL VE METOT

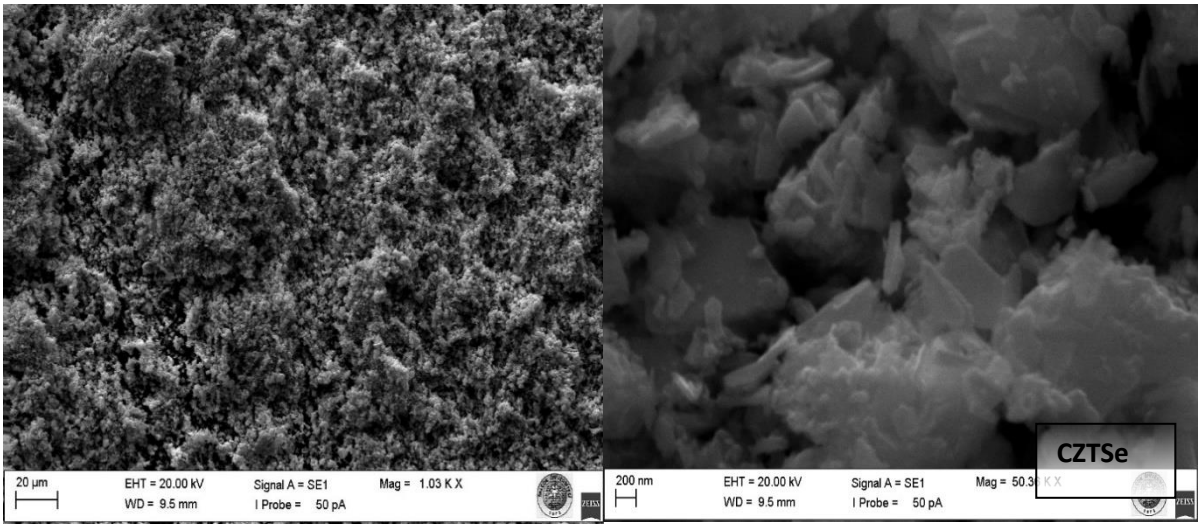
Tüm kimyasal reaktifler ve çözücüler daha fazla saflaştırma yapılmaksızın kullanıldı. CZTSe nanokristalleri sıcak enjeksiyon yöntemiyle sentezlendi. Sentez süreci aşağıdaki gibidir:

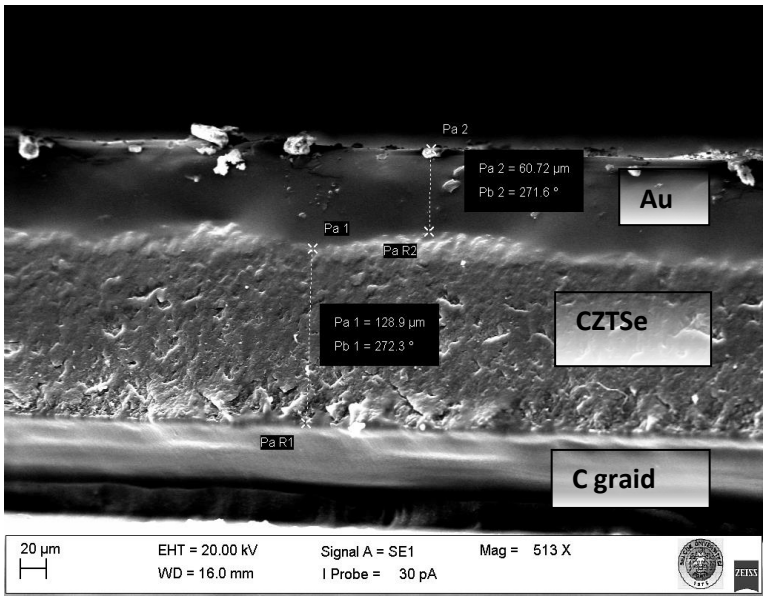
$$2CuCl_2.2H_2O + ZnCl_2 + SnCl_2 \cdot 2H_2O + 4Se \xrightarrow{OLA-\ 230°C} Cu_2ZnSnSe_4\ nanokristaller$$

12 mmol selenyum (Se, %99,98) ve 10 mL OLA (> %70 saflıkta), 100 mL üç boyunlu bir balona eklendi ve ardından N_2 atmosferi oluşturuldu. Karışım 1 saat bekletildi; 6 mmol bakır klorür dihidrat ($CuCl_2.2H_2O$, analitik saflıkta), 3 mmol çinko klorür ($ZnCl_2$, analitik saflıkta), 3 mmol kalay (II) klorür dihidrat ($SnCl_2 \cdot 2H_2O$, analitik saflıkta) ve 10 mL OLA, başka bir 100 mL başka üç boyunlu balonda karıştırıldı ve argon altında 150 °C'ye ısıtıldı. Isıtma sırasında çözelti koyu maviden kahverengi-yeşil renge döndü ve bu, Cu-, Zn- ve Sn-oleylamin komplekslerinin oluşumunu gösterdi. Karışım 100 °C'ye ısıtıldığında, hızla selenyum çözeltisine enjekte edildi. Sıcaklık 230 °C'ye çıkarıldı ve kuvvetlice karıştırılarak 2 saat tutuldu. Karışım oda sıcaklığına soğutulduktan sonra, balona 20 mL etanol eklendi, 30 dakika boyunca ultrasonik dispersiyonla işlendi ve ardından 7000 rpm'de 10 dakika santrifüj edildi. Üst faz, 1 mL OLA ve 10 mL etanol ile karıştırıldıktan sonra 8000 rpm'de 10 dakika santrifüj edildi. Çökelti, 10 mL etanolde yeniden dağıtıldı ve yüksek saflıkta CZTSe nanokristalleri elde etmek için tekrar santrifüj edildi. CZTSe nanokristalleri, kloroform ve toluen dahil olmak üzere polar olmayan organik çözücülerde dağıtılabildi gözlemlendi.

BULGULAR ve TARTIŞMA

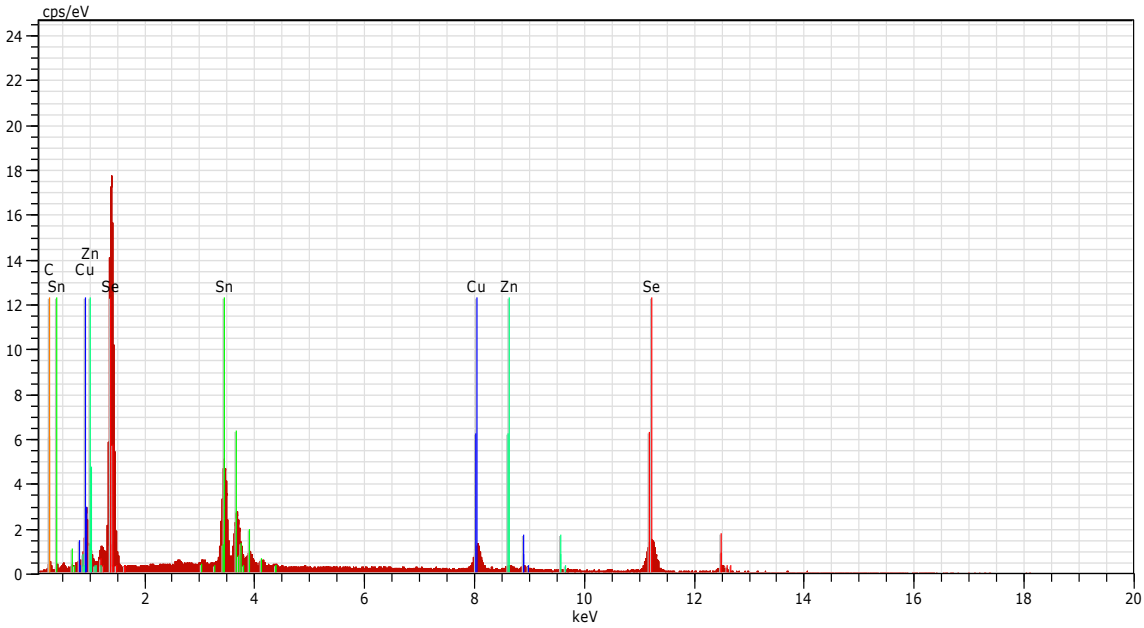
Elde edilen CZTSe nanokristallerin karakterizasyon işlemleri SEM-EDX, Numunelerin yüzey morfolojisi ve EDX analizleri SEM (ZEISS, EVO LS10) ile incelendi ve Şekil 1'de gösterilmiştir.





Şekil 1. Karbon SEM ızgarası üzerinde desteklenen altın kaplı CZTSe nanoparçacıklarının SEM görüntüleri

Şekil 2'de görüldüğü gibi EDX analizini gerçekleştirmiş ve aşağıdaki tabloda gösterilen sonuçlar elde edilmiştir:



Şekil 2. Karbon SEM ızgarasında desteklenen CZTSe nanoparçacıklarının EDX spektrumu

Tablo 1. CZTSe nanokristallerin EDX değerleri

	EDX
Cu	8.8 %
Sn	30.2 %
Zn	2.1 %
Se	58.6 %

Böylece başlangıçta katılan Zn'nin yaklaşık %2'si ve katılan Sn'nin yaklaşık %30'u CZTSe yapısının içine girer.

Partikül boyutu tespiti analizi sonucu elde edilen sonuçlarda CZTSe ortalama 9.7 nm civarında olduğu tespit edilmiş ve Şekil 3.' de gösterilmiştir.

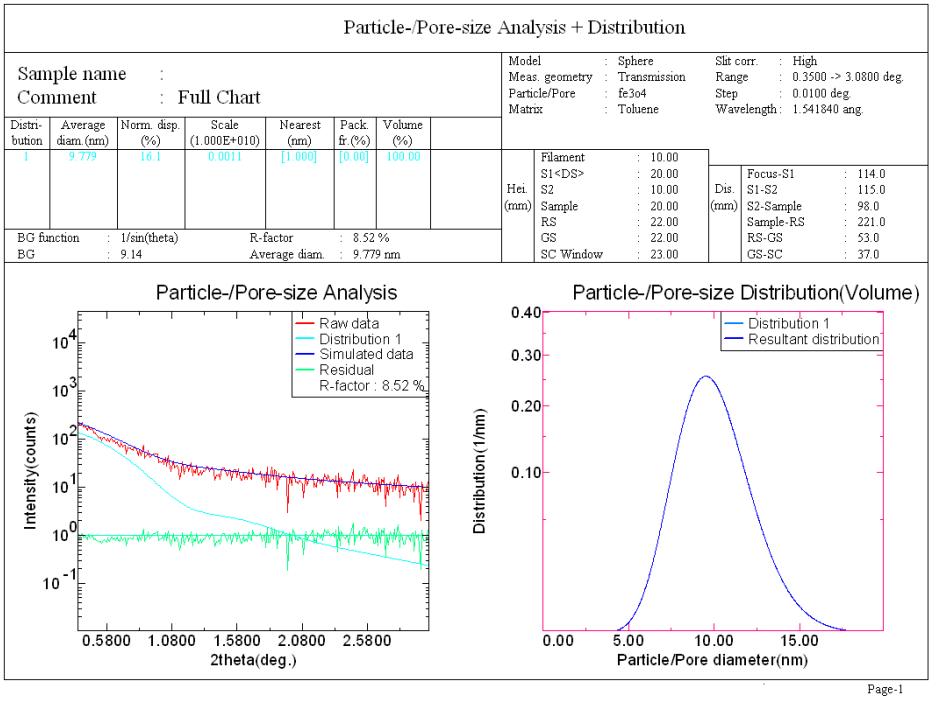


Fig. 3 Partikül boyutu analizi

SONUÇ

Yüksek emilim katsayısı sayesinde güneş hücrelerinde uygulama için en ilgi çekici malzemelerden biri olan ortalama 9 nm boyutunda CZTSe nanokristalleri oleyamin içerisinde başarılı bir şekilde sentezlenmiş ve güneş hücreleri için yüzey karakterizasyonları ve kompozisyonu SEM-EDX ile gerçekleştirilmiştir. Farklı metaller yapıya doplanarak da optik bant genişliği yükseltilerek güneş hücrelerinde daha etkin bir yapı ortaya çıkarabileceği literatüre yeni katkılar sunacağı aşikardır.

KAYNAKLAR

Altosaar, M., Raudoja, J., Timmo, K., Danilson, M., Grossberg, M., Krunks, M., Varema, T. (2006). Proceedings of the Fourth IEEE World Conference on Photovoltaic Energy Conversion, 468–470.

Babu, G.S., Kumar, Y.B.K., Bhaskar, P.U., Raja, V.S. (2011). Investigations on co-evaporated Cu_2SnSe_3 and Cu_2SnSe_3–ZnSe thin films. Semiconductor Science and Technology 251(20), 8529-8534.

Babu, G.S., Kumar, Y.B.K., Bhaskar, P.U., Raja, V.S. (2008). Growth and characterization of co-evaporated $Cu_2ZnSnSe_4$ thin films for photovoltaic applications. Journal of Physics D: Applied Physics 41 (21), 205305.

Friedlmeier, T.M., Dittrich, H., Schock, H. W. (1997). Institute of Physics Conferance Seriesno. 152, Section B, 11th International Conferance on Ternaryand Multinary Compound, ICTMC-11 Salford, 8–12 September 1997.

Guo, Q., Hillhouse, H.W., Agrawal, R. J. (2009). Synthesis of Cu2ZnSnS4 Nanocrystal Ink and Its Use for Solar Cells. Journal of the American Chemical Society 131(33),11672-11673.

Long, F., Wang, W.M., Tao, H.C., Jia, T.K., Li, X.M., Zou, Z.G., Fu, Z.Y. (2010). Solvothermal synthesis, nanocrystal print and photoelectrochemical properties of CuInS2 thin film. Materials Letter 64(2), 195.

Mellikov, E., Meissner, D., Varema, T., Altosaar, M., Kauk, M., Volobujeva, O., Raudoja, J., Timmo, K., Danilson, M. (2009). Monograin materials for solar cells. Solar Energy Materials & Solar Cells 93, 65–68.

Steinhagen, C., Panthani, M.G., Akhavan, V., Goodfellow, B., Koo, B., Korgel, B.A.(2009). Synthesis of Cu2ZnSnS4 Nanocrystals for Use in Low-Cost Photovoltaics. Journal of the American Chemical Society 131(35),12554-12555

Volobujeva, O., Raudoja, J., Mellikov, E., Grossberg, M., Bereznev, S., Traksmaa, R. (2009). Cu2ZnSnSe4 films by selenization of Sn–Zn–Cu sequential films. Journal of Physics and Chemistry of Solids 70(3-4), 567–570.

Zoppi, G., Forbes, I., Miles, R.W., Dale, P.J., Scragg, J.J., Peter, L.M. (2009). Cu2ZnSnSe4 thin film solar cells produced by selenisation of magnetron sputtered precursors. Progress in Photovoltaics: Research and Applications 17(5), 315-319.

Wibowo, R.A., Lee, E.S., Munir, B., Kim, K.H. (2007-a). Pulsed laser deposition of quaternary Cu2ZnSnSe4 thin films. Physica Status Solidi A 204(10), 3373-3379.

Wibowo, R.A., Kim, W.S., Lee, E.S., Munir, B., Kim, K.H. (2007-b). Single step preparation of quaternary Cu2ZnSnSe4 thin films by RF magnetron sputtering from binary chalcogenide targets. Journal of Physics and Chemistry of Solids 68(10), 1908–1913.

ORAL PRESENTATION

Effect of post-mating administration of different doses of TAK-683 on luteal function and pregnancy-associated glycoprotein (PAG) levels during early pregnancy in Aleppo goats

Gökhan Uyanık[1*] (ORCID: https://orcid.org/0000-0003-4488-3055)

[*1] Hatay Mustafa Kemal University, Faculty of Veterinary Medicine, Department of Obstetrics and Gynaecology, Antakya, Türkiye.

[*]Corresponding author e-mail: gokhan.uyanik@mku.edu.tr

Abstract

This study evaluated the effects of post-mating administration of the kisspeptin analog TAK-683 on luteal function and pregnancy-associated glycoprotein (PAG) levels during early pregnancy in Aleppo goats. A total of 45 lactating does synchronize during the non-breeding season were mated and randomly assigned on day 4 post-mating to receive either 1 mL saline (Control), 5 µg TAK-683 (TAK-5), or 25 µg TAK-683 (TAK-25) subcutaneously. Pregnancy diagnosis was performed on day 35, after which luteal ultrasonography and blood sampling were carried out only in the goats confirmed pregnant. Serum progesterone (P_4) and PAG concentrations were then determined from these samples using chemiluminescence immunoassay (CLIA) and enzyme-linked immunosorbent assay (ELISA), respectively. Both TAK-683 treatments significantly increased corpus luteum (CL) diameter compared with controls (Control: 7.68 ± 0.30 mm; TAK-5: 11.88 ± 0.67 mm; TAK-25: 11.56 ± 1.10 mm; P=0.023). The CL Doppler area tended to be higher in the TAK-25 group (45.55 ± 4.33 mm²) compared with the TAK-5 (33.61 ± 4.97 mm²) and Control (26.37 ± 4.90 mm²) groups (P=0.092). Endocrinologically, P4 concentrations were significantly elevated in TAK-5 and TAK-25 groups (Control: 4.63 ± 0.74 ng/mL; TAK-5: 7.73 ± 0.93 ng/mL; TAK-25: 10.08 ± 1.57 ng/mL; P = 0.022). Similarly, PAG levels were significantly higher following TAK-683 treatment (Control: 1.57 ± 0.07 O.D; TAK-5: 2.00 ± 0.07 O.D; TAK-25: 2.24 ± 0.13 O.D; P=0.015). A strong positive correlation was observed between P_4 and PAG values (r = 0.855; P<0.001). The findings demonstrate that TAK-683 exerts a dose-dependent luteotropic effect, improving early placental biochemical indicators through enhanced maternal progesterone secretion. These results suggest that TAK-683 may serve as a promising post-mating hormonal support strategy in goats, strengthening luteal-placental interaction during early gestation.

Keywords: Corpus luteum, goat, kisspeptin analog, pregnancy-associated glycoprotein, progesterone, TAK-683

INTRODUCTION

Progesterone (P_4) is a fundamental hormone that plays a critical role in maintaining pregnancy by regulating the production of various endometrial secretions required for embryonic growth (Spencer et al., 2007). Insufficient exposure of the uterus to P_4 during early gestation may lead to small and poorly developed embryos that fail to produce adequate interferon-tau (IFN-τ) during the period of maternal recognition, resulting in increased pregnancy losses (Antoniazzi et al., 2013). Therefore, decreased circulating P_4 associated with luteal insufficiency has been reported as one of the major causes of early embryonic mortality in ruminants (Diskin & Morris, 2008). One of the most common strategies to prevent reproductive losses due to luteal insufficiency is to increase endogenous P_4 levels through gonadotropin administration (Uyanık et al., 2024). In goats, treatments acting through luteinizing hormone (LH), such as gonadotropin-releasing hormone (GnRH) agonists and human chorionic gonadotropin (hCG), administered during or shortly after mating, have been reported to increase maternal P_4 concentrations, support corpus luteum (CL) function, improve pregnancy rates, and positively influence embryonic-fetal development (Çam et al., 2004; Lashari and Tasawar, 2010; Çetin et al., 2024).

In recent years, newly developed kisspeptin analogs have attracted attention as strong alternatives to gonadotropins (Beltramo and Decourt, 2018; Uyanık et al., 2024). The discovery that kisspeptins act through a central neuroendocrine mechanism regulating GnRH secretion has led to the development of new therapeutic approaches in reproduction (Roa and Tena-Sempere, 2007). Because kisspeptins strongly stimulate the release of LH and follicle-stimulating hormone (FSH) (Smith, 2009; Clarke, 2011), they have been reported to be potentially useful

in ovulation synchronization, puberty management, and anestrus treatment (Caraty and Franceschini, 2008; Okamura et al., 2013). Among these new long-acting kisspeptin analogs, TAK-683 is a potent KISS1 receptor (KISS1R) agonist with enhanced metabolic stability (Nishizawa et al., 2016; Uyanık et al., 2024). It has been demonstrated that bolus administration of TAK-683 stimulates GnRH and LH secretion in ovariectomized goats (Tanaka et al., 2013). In addition, TAK-683 induces ovulation and accelerates luteal formation when administered during the follicular phase in goats (Goto et al., 2014). Furthermore, subcutaneous administration of 5 µg TAK-683 has been shown to induce ovulation through a sustained 10-hour LH release, thereby accelerating CL formation in synchronized cyclic goats (Kanai et al., 2017). Parallel to these luteotropic effects observed in goats, post-mating administration of TAK-683 in ewes outside the breeding season has also been shown to strengthen luteal function, elevate maternal P_4 concentrations, and reduce pregnancy losses, similar to the action of GnRH agonists (Uyanık et al., 2024).

Although TAK-683 has been shown to strengthen luteal function and increase maternal P_4 levels, the biochemical reflection of this hormonal response in embryo-uterus interaction and placentation has not yet been fully clarified. Understanding these physiological processes requires not only hormonal evaluation but also the assessment of specific biomarkers that reflect embryonic development and trophoblastic activity. In this context, pregnancy-associated glycoproteins (PAGs) are highlighted as specific and early indicators of placentation in ruminants (Sousa et al., 2006). PAGs are glycosylated aspartic proteinases synthesized by binucleate trophoblast cells, which are unique to pregnancy (Wallace et al., 2015). They reflect biochemical communication between the embryo and the uterine environment, as well as the degree of trophoblastic invasion (Wooding, 2022). PAG concentrations increase in parallel with the progression of implantation, strengthening of placental maturation, and increased trophoblast proliferation (Szafranska et al., 2004; Wallace et al., 2015). Therefore, high PAG concentrations are associated with effective embryo-maternal signaling, an advanced placentation process, and healthy embryonic development (Sousa et al., 2006). Considering that maternal P_4 has an indirect regulatory role on uterine secretions and placental maturation, how luteotropic agents modulate the PAG response is an important clinical research question. Accordingly, although TAK-683 is known to increase P_4, its effect on PAG concentrations, which are biochemical indicators of embryonic-placental development, has not been investigated to date.

Based on the current literature, the present study hypothesizes that TAK-683 administration on day 4 after mating will dose-dependently (5 µg vs. 25 µg) strengthen luteal function, increase maternal P_4 secretion, support embryonic development and placentation, and consequently elevate PAG concentrations. Therefore, this study aimed to evaluate the effects of two different doses of TAK-683 administered on day four after mating in Aleppo goats synchronized during the non-breeding season with a short-term progesterone-based protocol on luteal function and serum PAG concentrations during early pregnancy.

MATERIALS AND METHODS

The experiment was conducted in the Reyhanlı district of Hatay, located in southeastern Türkiye (36°15′12.2″N, 36°32′02.6″E), during the non-breeding season (March-May). All procedures involving animals were performed in accordance with ethical standards and were approved by the Hatay Mustafa Kemal University Local Ethics Committee for Animal Experiments (Approval No: 2024/11-06).

Animal Material

A total of 45 clinically healthy, aged 3-5 years, weighing 40-50 kg, with a body condition score (BCS) ≥ 2.5, lactating and multiparous Aleppo goats were included in the study. Goats were housed in semi-open barns and grazed on natural pasture for approximately 12 hours per day. No additional concentrate or roughage was provided beyond grazing, and no flushing diet was applied. However, all goats had ad libitum access to fresh water.

Experimental Procedure

For estrus induction, intravaginal sponges containing 60 mg medroxyprogesterone acetate (MAP) (Esponjavet®, Hipra, Spain) were inserted into all goats (n = 45) for 7 days. At sponge removal, each doe received an intramuscular injection of 75 µg *d*-cloprostenol (Senkrodin®, Vetaş, Türkiye) and 500 IU equine chorionic gonadotropin (eCG) (Oviser®, Hipra Spain). Between 24 and 72 hours after sponge removal, fertile bucks were introduced to the herd twice daily for 2-hour mating sessions. Goats that accepted mating were marked and separated, and the day of mating was designated as Day 0.

Goats that mated within 24-72 hours after sponge removal were randomly assigned to one of three treatment groups on day 4 post-mating. The control group received a subcutaneous injection of 1 mL sterile physiological saline (0.9% NaCl, Polifleks®, Türkiye), while the experimental groups were administered either 5 µg (TAK-5) or 25 µg

(TAK-25) of TAK-683 acetate (TAK-683 acetate, MedChemExpress, USA, Cat. No: HY-P2161B) subcutaneously (Figure 1). TAK-683 was prepared following the manufacturer's instructions and previously reported methods (Uyanık et al., 2024), resulting in a final injectable solution containing 10 µg/mL (7.361 µM) of the compound.

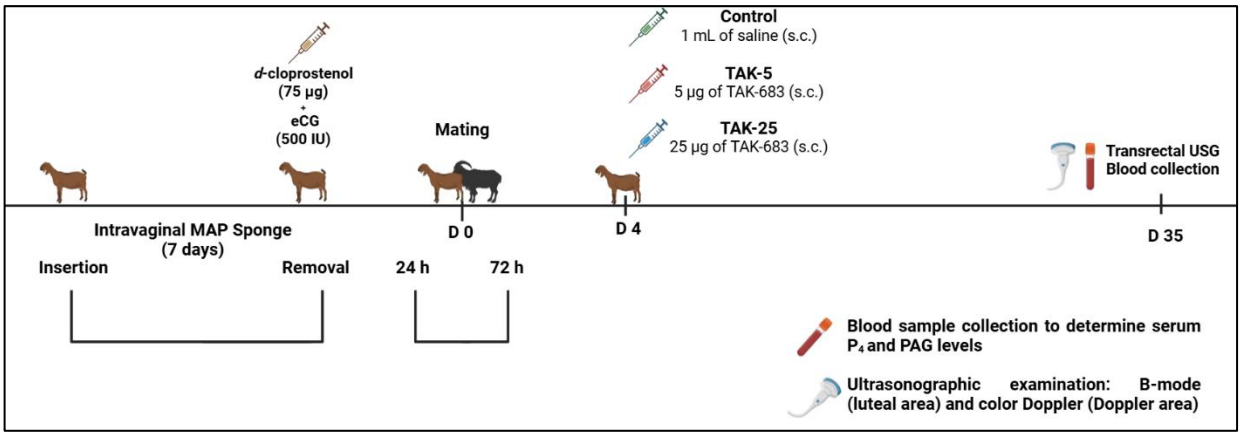


Figure 1. Experimental design and timeline of the study in goats.

Ultrasonographic Examination

Ultrasonographic examinations were performed transrectally on day 35 post-mating using a portable real-time B-mode ultrasound device equipped with a 5-10 MHz linear probe and color Doppler mode (SonoSite M-Turbo®, Fujifilm, USA). Both B-mode and color Doppler modes were used in all sequential examinations (Figure 1). Pregnancy diagnosis was based on the ultrasonographic visualization of the CL, embryonic vesicle, amniotic fluid, embryo, and embryonic heartbeat. Luteal assessments were conducted only in pregnant goats from the Control (n = 4), TAK-5 (n = 4), and TAK-25 (n = 4) groups. B-mode images were used to measure the luteal area (LA; mm²), defined as the sum of the maximum cross-sectional areas of all detected luteal structures. Color Doppler images corresponding to the same maximum cross-sectional plane were used to measure the Doppler area (DA; mm²), representing the total area of color Doppler signals within the defined LA. For each CL, a 30-second color Doppler video clip was recorded, and an image with the highest vascular signal was selected by frame-by-frame screening (Figure 2). All images were analyzed using ImageJ software (version 1.54d, National Institutes of Health, Bethesda, MD, USA). The mean DA value was calculated from the selected frames for each CL. The percentage of vascularization area was calculated by the following equation: percentage of vascularization area (%) = (DA/LA) × 100.

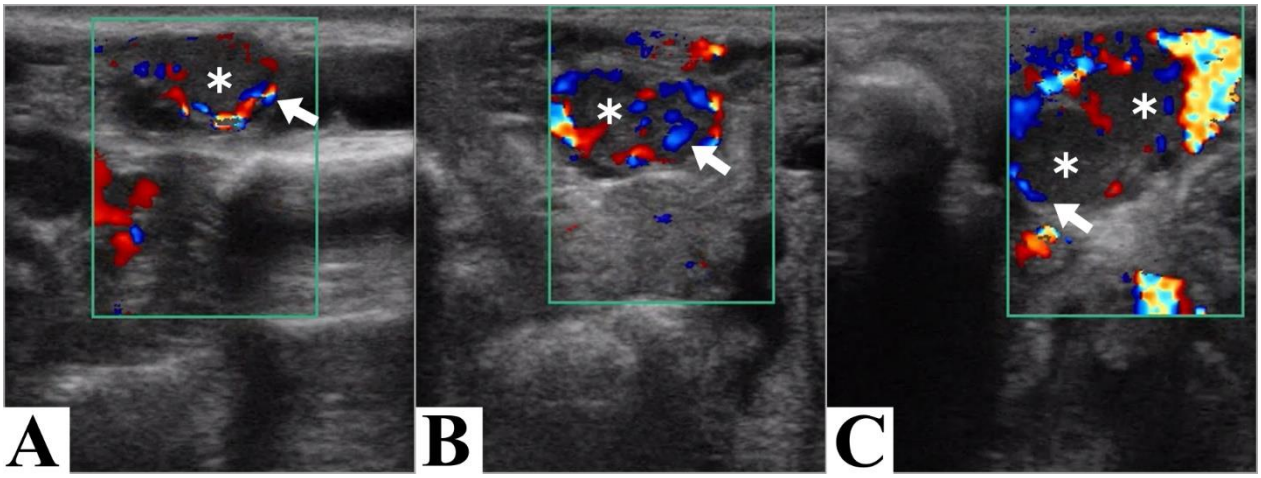


Figure 2. Color Doppler ultrasonographic images of the corpus luteum (CL) on day 35 of gestation in goats. Representative B-mode and color Doppler views of luteal tissue in (A) Control, (B) TAK-5 (5 µg TAK-683), and (C) TAK-25 (25 µg TAK-683) groups. *The asterisk (*) indicates the corpus luteum, and arrows (→) denote Doppler vascular areas within the luteal parenchyma.*

Determination of Serum P_4 (ng/mL) and PAG (O.D.) Levels

Approximately 8 mL of blood was collected from the jugular vein into dry serum tubes containing a clot activator gel (Vacusera®, Disera, Türkiye) for the determination of serum P_4 (ng/mL) and PAG (O.D.) concentrations (Figure 1). The collected samples were centrifuged at 3000 rpm for 10 minutes, and the obtained serum was stored at -20°C until analysis. Serum P_4 concentrations were measured using a chemiluminescence immunoassay (CLIA) analyzer (MAGLUMI-X8, Snibe Diagnostic, China). Serum PAG levels were assessed using a commercial Enzyme-Linked Immunosorbent Assay (ELISA) kit (Alertys Ruminant Pregnancy Test Kit, IDEXX Laboratories, Westbrook, ME, USA, Cat. No. 99-41169). Absorbance values were read at 450 nm using a microplate reader (Erba Mannheim, Lisascan EM, Czech Republic). The optical density (OD) value of each sample was calculated by subtracting the mean OD value of the negative control group from the sample OD value (S-N method). Since the intensity of the color reaction was directly proportional to the PAG concentration, OD values were used as indicators of serum PAG levels.

Statistically Analysis

Descriptive statistics for quantitative variables were expressed as mean ± standard error (Mean ± SEM), whereas categorical variables were presented as percentages. Due to the non-parametric distribution of the data, differences among treatment groups were analyzed using the Kruskal-Wallis test. When significant effects were detected, Dunn's post-hoc multiple comparison test was applied to determine pairwise differences. The relationship between serum P_4 and PAG concentrations was evaluated using Spearman's rank correlation coefficient. A significance level of $P<0.05$ was adopted for all analyses, and values between 0.05 and 0.10 were interpreted as a tendency. All statistical procedures were conducted using IBM SPSS Statistics software (Version 23.0, IBM Corp., Armonk, NY, USA).

RESULTS

On day 35 of gestation, CL diameter differed significantly among treatments, and both TAK-683 doses resulted in larger luteal diameters than the control group (Control: 7.68 ± 0.30 mm; TAK-5: 11.88 ± 0.67 mm; TAK-25: 11.56 ± 1.10 mm; P=0.023). In addition, color Doppler measurements tended to be higher in TAK-683-treated goats, indicating a numerical increase in luteal vascularization, with the greatest value observed in the TAK-25 group (Control: 26.37 ± 4.90 mm²; TAK-5: 33.61 ± 4.97 mm²; TAK-25: 45.55 ± 4.33 mm²; P=0.092). However, the number of CL, luteal area, and the DA/LA ratio did not differ among groups, despite numerically higher values in TAK-683-treated goats, particularly in the TAK-25 group (P>0.05) (Table 1).

Table 1. Luteal ultrasonographic parameters in pregnant goats treated with a single dose of TAK-683 (5 µg; TAK-5 or 25 µg; TAK-25) on Day 4 after mating or receiving no treatment (Control).

Parameters	Groups			P-value
	Control *(n=4)*	TAK-5 *(n=4)*	TAK-25 *(n=4)*	
CL number	1.50 ± 0.29	1.50 ± 0.29	1.75 ± 0.25	0.730
CL diameter (mm)	**7.68 ± 0.30 [b]**	**11.88 ± 0.67 [a]**	**11.56 ± 1.10 [a]**	**0.023***
CL area (LA) (mm²)	77.16 ± 15.06	97.43 ± 10.70	136.36 ± 22.05	0.118
CL Doppler area (DA) (mm²)	**26.37 ± 4.90 [d]**	**33.61 ± 4.97 [d]**	**45.55 ± 4.33 [c]**	**0.092****
CL DA/LA (%)	34.36 ± 1.81	34.32 ± 2.70	35.19 ± 3.71	0.668

**Different superscripts (a, b) in the same row indicate significant differences among the groups (P<0.05).*
***Different superscripts (c, d) in the same row indicate tendency differences (0.05 ≤ P ≤ 0.1) among the groups.*

Endocrine evaluation revealed a significant increase in serum P_4 concentrations in both TAK-683 treatment groups compared with the control (Control: 4.63 ± 0.74 ng/mL; TAK-5: 7.73 ± 0.93 ng/mL; TAK-25: 10.08 ± 1.57 ng/mL; P=0.022). A similar pattern was observed for PAG, with higher levels detected in TAK-683-treated goats (Control: 1.57 ± 0.07 O.D; TAK-5: 2.00 ± 0.07 O.D; TAK-25: 2.24 ± 0.13 O.D; P=0.015) (Table 2). Additionally, correlation analysis revealed that serum P_4 and PAG concentrations were strongly and positively associated on day 35 of gestation (r=0.855; P<0.001).

Table 2. Serum progesterone (P_4, ng/mL) and pregnancy-associated glycoprotein (PAG, O.D.) concentrations on Day 35 of gestation in goats that were pregnant following treatment with TAK-683 at 5 µg (TAK-5) or 25 µg (TAK-25) on Day 4 post-mating or following no treatment (Control).

Parameters	Groups			P-value
	Control *(n=4)*	TAK-5 *(n=4)*	TAK-25 *(n=4)*	
Serum P_4 level (ng/mL)	**4.63 ± 0.74 [b]**	**7.73 ± 0.93 [a]**	**10.08 ± 1.57 [a]**	**0.022***
Serum PAG level (O.D.)	**1.57 ± 0.07 [b]**	**2.00 ± 0.07 [a]**	**2.24 ± 0.13 [a]**	**0.015***

**Different superscripts (a, b) in the same row indicate significant differences among the groups ($P<0.05$).*

DISCUSSION

Our findings demonstrate that administration of the kisspeptin analogue TAK-683 on day 4 post-mating exerts a clear luteotropic effect in goats. Both doses significantly increased CL diameter and area compared with the Control group, which is consistent with previous studies reporting that TAK-683 stimulate LH release and strengthen luteal function (Goto et al., 2014; Kanai et al., 2017; Rahayu et al., 2017; Uyanık et al., 2024). The dose-dependent response suggests that luteotropic efficacy increases with higher TAK-683 doses, consistent with studies showing weaker effects at lower doses (Kanai et al., 2017). Although luteal blood flow ratios were numerically higher in TAK-683-treated goats, the difference was not statistically significant (Table 1), which may be related to the limited sample size. Biologically, however, this increase is relevant, since luteal perfusion is a major determinant of P_4 synthesis by enabling the transport of cholesterol substrates and LH to luteal cells (Kanazawa et al., 2025). In accordance, serum P_4 concentrations were significantly higher on day 35 of pregnancy in goats treated with TAK-683, confirming that this biological effect translated into an endocrine response (Table 2).

Pregnancy-associated glycoproteins are unique glycoproteins secreted by trophoblastic binucleate cells of the ruminant placenta and are important biomarkers of trophoblast activity and embryo-maternal interaction (Lear, 2020). In goats, PAGs become detectable in maternal circulation during approximately the third week of pregnancy, become more prominent on days 25-28, and increase sharply with progressive placental attachment (Singh et al., 2019). In dairy goats, PAG profiles gradually increase from day 26 to around day 50 (Singh et al., 2019), which corresponds to a period of accelerated placental growth and functional maturation. In the present study, PAG concentrations were significantly higher in TAK-683-treated goats, indicating stronger early placental development. This is likely associated with increased P_4 concentrations, since P_4 supports uterine secretions and conceptus development (Simintiras et al., 2019). Particularly during the early luteal phase, high P_4 accelerates embryo growth and elongation and has been linked to more advanced embryos in cattle (Simintiras et al., 2019). Similarly, Lashari and Tasawar (2010) reported that post-mating hCG administration in goats increased maternal P_4, improved placentation, enhanced placentome number, and consequently supported fetal development. Therefore, improved placentation potentially induced by TAK-683 through increased P_4 secretion may have accelerated trophoblastic development, leading to higher PAG production on day 35.

The strongest evidence supporting this interpretation is the highly positive correlation observed between serum P_4 and PAG levels ($r=0.855$; $P<0.001$). The fact that the highest P_4 levels coincided with the highest PAG levels indicates that strong luteal support positively influences placental growth. Previous studies also reported that goats carrying multiple fetuses exhibit higher P_4 concentrations and elevated PAG levels due to larger placental area (Singh et al., 2019). Adequate P_4 is crucial for preparing the uterus for placental attachment and maintaining functional placental development (Simintiras et al., 2019; Lonergan and Sánchez, 2020). Accordingly, the strong P_4-PAG association observed following TAK-683 administration provides important biochemical evidence that this treatment strengthens the luteal-placental unit as a whole.

CONCLUSION

In conclusion, our findings reveal that TAK-683 exerts a dose-dependent and pronounced luteotropic effect during early pregnancy in goats, indirectly supporting early placental development through increased P_4 secretion. Thus, TAK-683 may serve as a potential reproductive management tool by supporting the conceptus via both its direct effect on the CL and improvement of the uterine environment. The strong relationship between P_4 and PAG levels confirms enhanced luteal-placental interaction. Kisspeptin analogues appear promising for post-mating hormonal support strategies in ruminants; however, further field studies are required to evaluate the long-term impacts of TAK-683 on pregnancy maintenance, parturition, and offspring development.

Acknowledgements
The study was funded by the Scientific Research Projects Coordination Unit of Hatay Mustafa Kemal University (Grant No. 25.GAP.007).

REFERENCES

Antoniazzi, A.Q., Webb, B.T., Romero, J.J., Ashley R.L., Smirnova, N.P., Henkes, L.E., Bott, R.C., Oliveira, J.F., Niswender, G.D., Blazer, F.W., ansen, T.R. (2013). Endocrine delivery of interferon tau protects the corpus luteum from prostaglandin F2 alpha-induced luteolysis in ewes. Biology of Reproduction, 88, 1-12.

Beltramo, M., & Decourt, C. (2018). Towards new strategies to manage livestock reproduction using kisspeptin analogs. Theriogenology, 112, 2-10.

Cam, M. A., & Kuran, M. (2004). GnRH agonist treatment on day 12 post-mating to improve reproductive performance in goats. Small ruminant research, 52(1-2), 169-172.

Caraty A, Franceschını I. (2008). Basic aspects of the control of GnRH and LH secretions by kisspeptin: potential applications for better control of fertility in females. Reproduction Domestic Animals, 43(2), 172-178.

Cetin, N., Kosal, V., Kuru, M., Oner, A. C., & Eski, F. (2024). The effect of hCG administration on reproductive performance in undernourished lactating hair goats synchronized during non-breeding season. Acta Veterinaria Brno, 93(3), 339-345.

Clarke IJ. (2011). Control of GnRH secretion: One step back. Frontiers in Neuroendocrinology, 32(3), 367-375.

Diskin M.G., Morris D. (2008). Embryonic and early foetal losses in cattle and other ruminants. Reproduction in Domestic Animals, 43, 261-268.

Goto, Y., Endo, N., Nagai, K., Ohkura, S., Wakabayashi, Y., Tanaka, A., Tanaka, T. (2014). Ovarian and Hormonal Responses to Follicular Phase Administration of Investigational Metastin/Kisspeptin Analog, TAK-683, in Goats. Reproduction in Domestic Animals, 49(2), 338-342.

Kanai, N., Endo, N., Ohkura, S., Wakabayashi, Y., Matsui, H., Matsumoto, H., Tanaka, T. (2017). An administration of TAK-683 at a minimally effective dose for luteinizing hormone stimulation under the absence of the ovary induces luteinizing hormone surge in ovary-intact goats. Journal of Reproduction and Development, 63(3), 305-310.

Kanazawa, T., Seki, M., Iga, K., & Kizaki, K. (2025). Effects of luteal blood flow on endometrial progesterone concentrations and gene expression in Japanese Black cows. Journal of Reproduction and Development, 71(5), 272-281.

Lashari, M. H., & Tasawar, Z. (2010). The effect of hCG given on day 12 post-mating on ovarian function and embryo survival in Beetal goats in southern Punjab, Pakistan. Turkish Journal of Veterinary & Animal Sciences, 34(6), 513-517.

Lear, A. S. (2020, September). Determination of fetal viability. In American Association of Bovine Practitioners Conference Proceedings (pp. 342-343).

Lonergan, P., & Sánchez, J. M. (2020). Symposium review: Progesterone effects on early embryo development in cattle. Journal of Dairy Science, 103(9), 8698-8707.

Nishizawa, N., Takatsu, Y., Kumano, S., Kiba, A., Ban, J., Tsutsumi, S., Asami, T. (2016). Design and synthesis of an investigational nonapeptide KISS1 receptor (KISS1R) agonist, Ac-d-Tyr-hydroxyproline (Hyp)-Asn-Thr-Phe-azaGly-Leu-Arg (Me)-Trp-NH2 (TAK-448), with highly potent testosterone-suppressive activity and excellent water solubility. Journal of Medicinal Chemistry, 59(19), 8804-8811.

Okamura H, Yamamura T, Wakabayashi Y. (2013). Kisspeptin as a master player in the central control of reproduction in mammals: An overview of kisspeptin research in domestic animals. Animal Science Journal, 84(5), 369-381.

Roa J, Tena-Sempere M. (2007). KiSS-1 system and reproduction: comparative aspects and roles in the control of female gonadotropic axis in mammals. General and Comparative Endocrinology, 153(1-3), 132-140

Simintiras, C. A., Sánchez, J. M., McDonald, M., Lonergan, P. (2019). The influence of progesterone on bovine uterine fluid energy, nucleotide, vitamin, cofactor, peptide, and xenobiotic composition during the conceptus elongation-initiation window. Scientific Reports, 9(1), 7716.

Singh, S. P., Ramachandran, N., Sharma, N., Goel, A. K., Gururaj, K., & Kharche, S. D. (2019). Temporal changes in plasma profile of pregnancy-associated glycoprotein, progesterone and estrone sulfate associated with fetal number during early-and mid-pregnancy in goats. Animal Reproduction Science,

205, 115-125.

Smith JT. (2009). Sex steroid control of hypothalamic Kiss1 expression in sheep and rodents: comparative aspects. Peptides, 30(1), 94-102.

Sousa, N. M., Ayad, A., Beckers, J. F., Gajewski, Z. (2006). Pregnancy-associated glycoproteins (PAG) as pregnancy markers in the ruminants. Journal of Physiology and Pharmacology, 57(8), 153-171.

Spencer, T.E., Johnson, G.A., Bazer, F.W., Burghardt, R.C., Palmarini, M. (2007). Pregnancy recognition and conceptus implantation in domestic ruminants: roles of progesterone, interferons and endogenous retroviruses. Reproduction, Fertility and Development, 19, 65-78.

Szafranska, B., Majewska, M., & Panasiewicz, G. (2004). N-glycodiversity of the Pregnancy-Associated Glycoprotein family (PAG) produced in vitro by trophoblast and trophectoderm explants during implantation, placentation and advanced pregnancy in the pig. Reproductive Biology, 4(1), 67-89.

Tanaka, T., Ohkura, S., Wakabayashi, Y., Kuroiwa, T., Nagai, K., Endo, N., Okamura, H. (2013). Differential effects of continuous exposure to the investigational metastin/kisspeptin analog TAK-683 on pulsatile and surge mode secretion of luteinizing hormone in ovariectomized goats. Journal of Reproduction and Development, 59(6), 563-568.

Uyanık, G., Abay, M., & Demiral, Ö. O. (2024). Effect of post-mating GnRH or TAK-683 (Kisspeptin analog) treatment on the reproductive performance and serum progesterone concentration in ewes during the non-breeding season. Small Ruminant Research, 238, 107331.

Wallace, R. M., Pohler, K. G., Smith, M. F., Green, J. A. (2015). Placental PAGs: gene origins, expression patterns, and use as markers of pregnancy. Reproduction, 149(3), 115-126.

Wooding, F. B. P. (2022). The ruminant placental trophoblast binucleate cell: an evolutionary breakthrough. Biology of Reproduction, 107(3), 705-716.

ORAL PRESENTATION

Acyclic and cyclic Schiff base–modified cyclophosphazenes

Yasemin Tümer[1*] (*ORCID: https://orcid.org/0000-0002-2460-9414*)

[*1]Karabük Üniversitesi, Mühendislik ve Doğa Bilimleri Fakültesi, Kimya Bölümü, Karabük, Türkiye

*Corresponding author e-mail: yasemintumer@karabuk.edu.tr

Abstract

Cyclophosphazenes, an important class of inorganic ring compounds, possess a robust framework composed of phosphorus and nitrogen atoms, along with easily substitutable phosphorus–chlorine bonds. This structure provides an excellent core for the synthesis of organophosphazene derivatives, dendrimers, and polymers. Through the substitution of phosphorus–chlorine bonds with various nucleophiles, numerous derivatives with different physical and chemical properties can be obtained, many of which find applications in technology, medicine, and pharmacology. Schiff bases, which contain a carbon–nitrogen double bond (C=N, imine group), can be used in technology as catalysts, OLED (organic light-emitting diode) materials, and sensors (pH, metal-ion, and gas sensors). Furthermore, their strong activity against bacteria and fungi, their effectiveness against *Mycobacterium tuberculosis*, and their ability to scavenge free radicals and exhibit antioxidant properties make them noteworthy in medical applications.Owing to this broad functional profile, Acyclic and Cyclic Schiff base–modified cyclophosphazenes continue to attract increasing interest for the development of advanced materials, biologically active agents, and supramolecular architectures.

Keywords: Cyclophosphazene, Schiff base, Inorganic cyclic compounds

INTRODUCTION

Halocyclophosphazenes, among the most well-known members of inorganic heterocyclic rings, possess a backbone composed of repeating (-N=PX_2; X: Cl or F) units, in which each phosphorus atom is covalently bonded to two halogen atoms. Hexachlorocyclotriphosphazene ($N_3P_3Cl_6$, HCCP) and octachlorocyclotetraphosphazene ($N_4P_4Cl_8$, OCCP), possessing six and eight chemically reactive P–Cl bonds, respectively, act as key precursor molecules for the synthesis of cyclophosphazene derivatives (Chakraborty et al., 2021; Lee et al., 2024). Through nucleophilic substitution reactions with a variety of nucleophiles—such as amines, alcohols, aryloxides, and alkoxides—functionalized phosphazene derivatives can be readily obtained. Partially or fully substituted cyclophosphazene derivatives are obtained from the reactions of HCCP and OCCP with monofunctional nucleophiles, whereas their reactions with difunctional nucleophiles yield spiro-, ansa-, or bino-type derivatives (Tümer et al., 2008; Türe et al., 2020; Tümer 2022; Mutlu et al., 2022). Moreover, the reactions of HCCP and OCCP with tri- or tetrafunctional nucleophiles afford spiro-bino-spiro and spiro-ansa-spiro phosphazene derivatives (Kocak et al., 2013; Cemaloğlu et al., 2025). Therefore, the number of functional groups present in the nucleophile, as well as the stoichiometric ratio, plays a critical role in the synthesis of new compounds with structurally and functionally distinct properties. Moreover, the physical and chemical behaviors of these compounds vary depending on the nature of the nucleophiles attached to the cyclophosphazene framework. Such hybrid inorganic/organic heterocyclic cyclophosphazene derivatives exhibit a structural diversity that enables specialized applications in the fields of pharmacology, medicine, and technology (Usri et al., 2021; Casella et al., 2022; Dagdag and Kim, 2023).

Schiff bases are synthesized through the condensation reaction of aldehydes or ketones with primary amines, resulting in the formation of a characteristic azomethine (C=N) functional group (Raczuk et al., 2022). Their structural diversity and ease of modification make Schiff bases valuable intermediates in coordination chemistry

(Abd-El-Aziz et al., 2025; Rana et al., 2025), catalysis (Juyal et al., 2023), and the design of functional materials. They are also widely used in technology as OLED (organic light-emitting diode) materials (Kagatikar and Sunil, 2021; Nayak et al., 20221), and pH-, metal-ion-, and gas-responsive sensors (Goshisht et al., 2022; Alam et al., 2023; Azhar et al., 2025). Furthermore, their strong antibacterial and antifungal activities, as well as their ability to scavenge free radicals and exhibit antioxidant properties, make them noteworthy in medical applications (Abdel et al., 2023; Kumar et al., 2024; Marinova and Tamahkyarova, 2025).

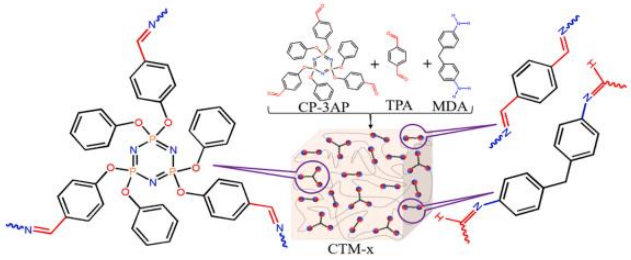
The multi-armed architecture of HCCP and OCCP enables the attachment of numerous and diverse Schiff base ligands. The incorporation of Schiff base ligands into an inorganic phosphazene framework enhances their robustness and thermal stability, while reducing their sensitivity to solvent effects, pH variations, and light exposure. In conclusion, the synthesis of novel cyclophosphazene–Schiff base derivatives and the investigation of their potential applications are becoming increasingly important areas of research.

SCHIFF BASE–MODIFIED CYCLOPHOSPHAZENES

Acyclic Schiff base–modified cyclophosphazenes

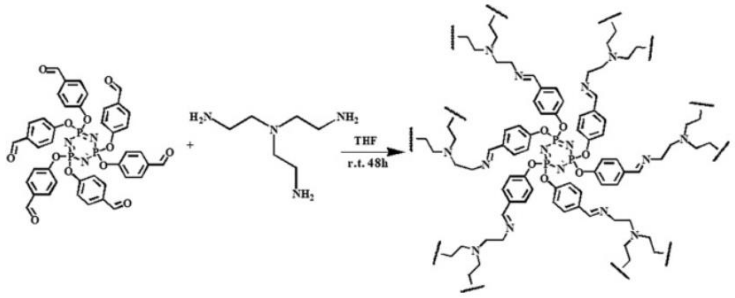
Acyclic Schiff base–modified cyclophosphazene derivatives represent a notable class due to their versatile structural features and functional properties (Bertani et al., 1989; Khatri and Jain, 2012; El Brahmi et al., 2015; Katir et al., 2015; Jamain et al., 2020). They are typically obtained either by the reaction of halocyclophosphazene precursors with aldehyde-derived nucleophiles followed by condensation with primary amines to form the Schiff base (Tümer et al., 2010), or via the initial formation of the Schiff base through the reaction of primary amines with aldehydes or ketones, which is subsequently substituted onto the halocyclophosphazene framework (Odabaşoğlu and Turgut, 1999).

A novel Schiff base-derived polyimine vitrimer (CTM-x) was synthesized via the reaction of a cyclophosphazene bearing three aldehyde groups (CP-3AP) with terephthalaldehyde (TPA) and methylenediphenylamine (MDA) (Scheme 1). The resulting phosphazene-centered vitrimer exhibits outstanding flame retardancy and thermal stability due to the incorporation of cyclic phosphazene units, highlighting its potential for the development of high-performance vitrimers (Zhang et al., 2022).



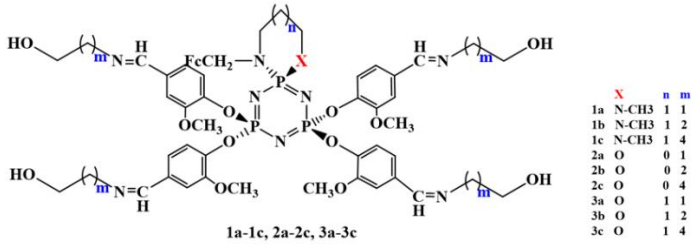
Scheme 1. Preparation of CTM-x Vitrimers (Zhang et al., 2022)

A cyclophosphazene-centered hybrid porous polymer (PHPP) was successfully synthesized via a Schiff base reaction between hexakis(4-formylphenoxy)cyclophosphazene and 4-(2-aminoethyl)diethylenetriamine (Scheme 2). Despite its relatively low porosity, PHPP demonstrated high adsorption capacities for iodine vapor, Hg^{2+} ions, and Congo Red (CR), with values of 4.6 g g^{-1}, 435 mg g^{-1}, and 440 mg g^{-1}, respectively. The mesoporous structure and heteroatom-enriched framework of PHPP significantly enhanced host-guest interactions, thereby compensating for the limited surface area and pore volume and ensuring excellent recyclability. These findings highlight the potential of PHPP as an effective material for pollutant adsorption, environmental remediation, and the design of functional porous materials.



Scheme 2. Synthesis of a hybrid porous polymer via cross-linking of HAPCP with N,N-bis(2-aminoethyl)-1,2-ethanediamine (Wang et al., 2022).

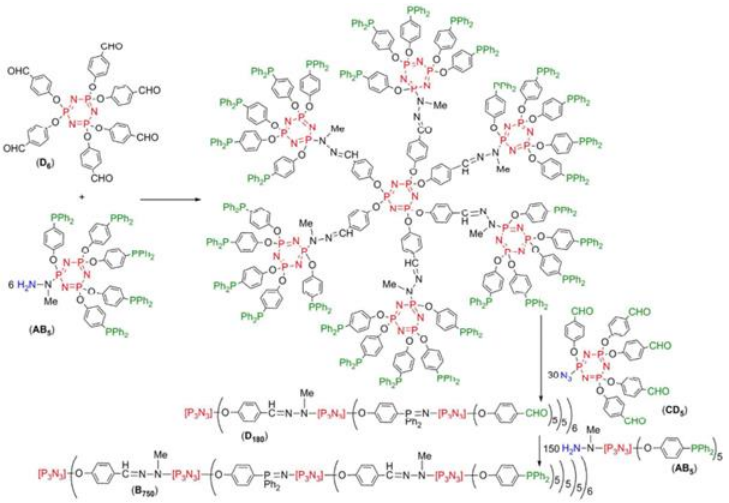
As a result of the substitution of monospiroferrocenylphosphazene compounds with vanillin, three different compounds bearing four active aldehyde groups were synthesized. Subsequent reactions of these compounds with aliphatic amino-alcohol derivatives afforded nine Schiff base derivatives (Scheme 3). These newly synthesized Schiff base–modified compounds possess active hydroxyl groups at their terminal positions (Örgüler, 2025).



	X	n	m
1a	N-CH3	1	1
1b	N-CH3	1	2
1c	N-CH3	1	4
2a	O	0	1
2b	O	0	2
2c	O	0	4
3a	O	1	1
3b	O	1	2
3c	O	1	4

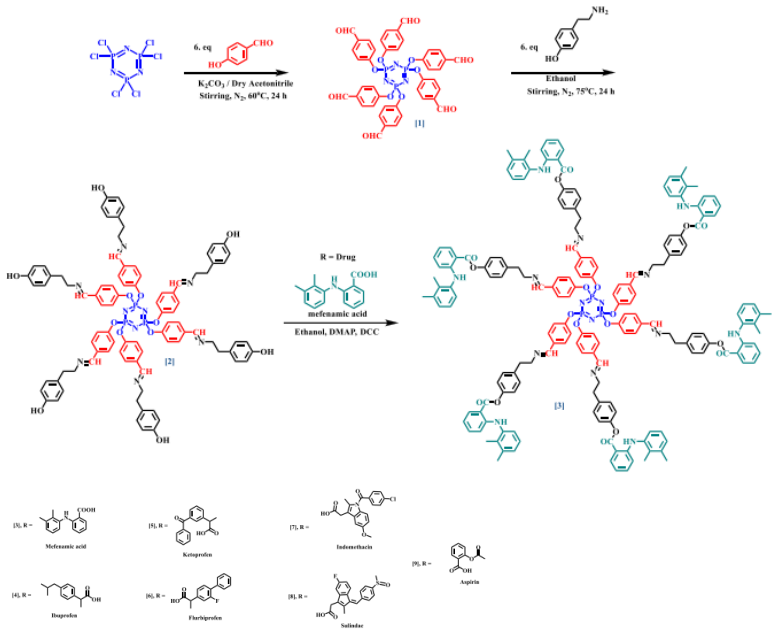
Scheme 3. Synthesis of Ferrocenylphosphazene-Schiff Base Compounds (Örgüler, 2025)

HCCP, due to its rich reactivity, continues to inspire researchers in the design and development of sophisticated dendrimer architectures. It enables the synthesis and functionalization of highly dense dendrimers bearing numerous terminal groups through only a few synthetic steps (Scheme 4). Acyclic Schiff base–modified cyclophosphazenes offer promising opportunities as next-generation smart dendrimers (Caminade et al., 2016).



Scheme 4. Three-step synthesis of a third-generation dendrimer, a Schiff base derivative based on a cyclotriphosphazene core (Caminade et al., 2016).

As reported in a study by Meenink (2025), nine first-generation dendrimers were synthesized, seven of which were functionalized at their terminal ends with drugs to enhance anti-inflammatory activity (Scheme 5). Cytotoxicity assays using the RAW-264.7 macrophage cell line indicated that all dendrimers were non-toxic. ELISA analysis demonstrated that the dendrimer-drug conjugates significantly reduced TNF-α secretion compared to free NSAIDs, with the D4 dendrimer, bearing terminal ibuprofen groups, showing the highest anti-inflammatory efficacy. These results underscore the potential of dendrimer-based drug conjugates as a novel approach to improving the effectiveness of anti-inflammatory therapies (Meenink 2025).

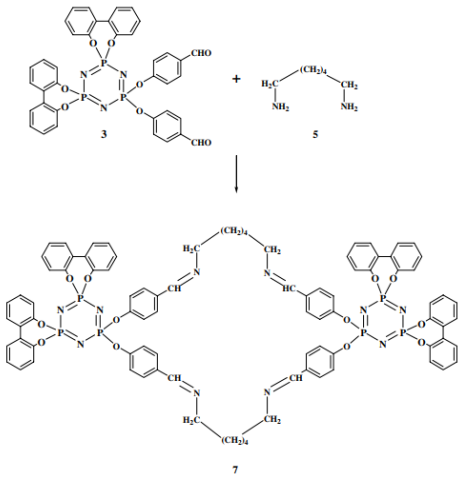


Scheme 5. Synthesis of cyclophosphazene-centered dendrimers bearing Schiff bases (Meenink 2025).

Cyclic Schiff base–modified cyclophosphazenes

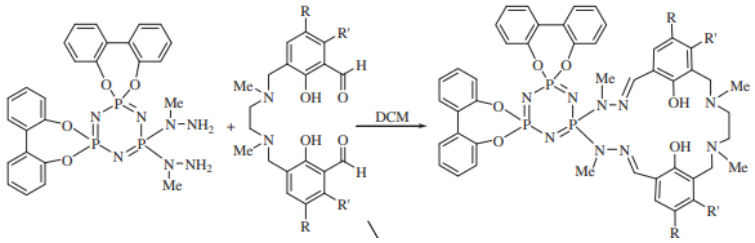
Few studies have reported the synthesis of large macrocyclic Schiff bases attached on the cyclotriphosphazene framework. The imino nitrogen atoms within the macrocyclic cavity are capable of coordinating with metal ions, highlighting their potential for further applications.

$N_3P_3Cl_2(O_2C_{12}H_8)_2$ is an ideal precursor for advanced syntheses due to the presence of two reactive P–Cl bonds. Reaction with the sodium salt of 4-hydroxybenzaldehyde yielded $N_3P_3(O_2C_{12}H_8)_2[–O–C_6H_4–p\text{-}CHO]_2$ (3). Compound 3 is a notable scaffold, as it possesses two reactive CHO groups that allow for the facile formation of Schiff bases. Reaction of compound 3 with hexamethylenediamine led to the formation of a 42-membered macrocyclic structure (Scheme 6) (Chandrasekhar et al., 2006).



Scheme 6. Synthesis of macrocyclic Schiff bases centered on cyclophosphazene (Chandrasekhar et al., 2006)

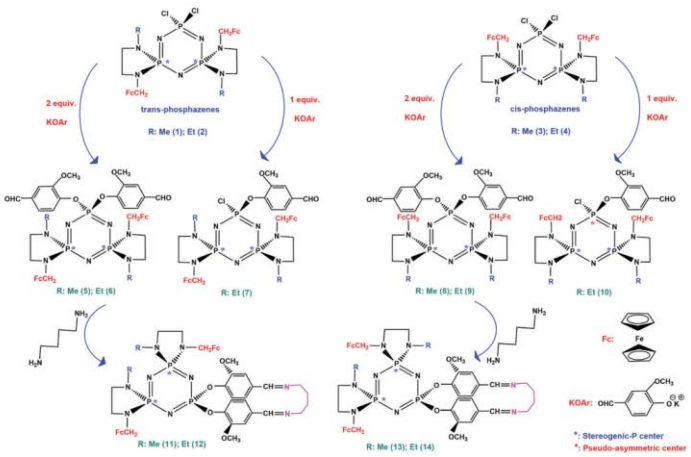
The precursor $N_3P_3Cl_2(O_2C_{12}H_8)_2$ was reacted with $MeNH–NH_2$ to afford a fully substituted cyclic phosphazene derivative bearing two reactive amino groups. Subsequent reaction with dialdehyde compounds (3–6) led to the synthesis of 18-membered cyclotriphosphazene-containing macrocycles (7–10) containing two Schiff base units. These compounds are also structurally noteworthy, as they represent macrocycles with a high number of strong donors, such as phenolate oxygens and nitrogens, which can coordinate incoming metal atoms very effectively (Thilagar et al., 2012).



Scheme 7. Synthesis of macrocyclic Schiff bases (Thilagar et al., 2012)

In a study carried out by our research group in 2022, compounds (5, 6, 8, 9) were synthesized via the reaction of trans/cis-dispiroferrocenylphosphazene derivatives with vanillin. Subsequent reaction of these compounds with 1,4-diaminobutane gave rise to novel macrocyclic phosphazene Schiff bases (11–14) (Scheme 8) (Tümer et al., 2022).

The introduction of an imine functionality into ferrocenyldispirocyclotriphosphazenes is particularly noteworthy, as it has the potential to enhance both the biological activity and the complexation properties of these compounds. Moreover, the two imino nitrogen atoms within the macrocyclic cavity provide additional coordination sites, facilitating the development of novel coordination compounds with transition metal cations.



Scheme 8. Synthesis of bis-vanillinato bisferrocenyl dispiro-(N/N)cyclotriphosphazenes and their macrocyclic Schiff bases (Tümer et al., 2022)

CONCLUSIONS

Halocyclophosphazenes, particularly HCCP, play a central role in the synthesis of functionalized derivatives capable of forming both linear and macrocyclic architectures due to their versatile reactivity. Modification with Schiff bases enhances structural diversity and offers significant potential in areas such as coordination chemistry, catalysis, electronic materials, and sensor applications. Moreover, these compounds expand strategies for the design of phosphazene-based dendrimers and hybrid polymers, providing new opportunities for functional materials, drug design, and environmental applications. In the future, these systems are expected to be the focus of further studies in comprehensive biological and materials science applications.

REFERANCES

Abd-El-Aziz, A., Li, Z., Zhang, X., Elnagdy, S., Mansour, M. S., ElSherif, A., ... & Abd-El-Aziz, A. S. (2025). Advances in coordination chemistry of Schiff base complexes: A journey from nanoarchitectonic design to biomedical applications. Topics in Current Chemistry, 383(1), 8.

Abdel Aziz, A. A., Ramadan, R. M., Sidqi, M. E., & Sayed, M. A. (2023). Structural characterisation of novel mononuclear Schiff base metal complexes, DFT calculations, molecular docking studies, free radical scavenging, DNA binding evaluation and cytotoxic activity. Applied Organometallic Chemistry, 37(2), e6954.

Alam, M. Z., Alimuddin, & Khan, S. A. (2023). A review on Schiff base as a versatile fluorescent chemo-sensors tool for detection of Cu2+ and Fe3+ metal ion. Journal of Fluorescence, 33(4), 1241-1272.

Azhar, S., Alam, M. Z., & Khan, S. A. (2025). Advances in coumarin-linked Schiff base for fluorometric and colorimetric sensing of toxic metal ions (Hg2+, Pb2+, Cd2+): a critical review. Inorganica Chimica Acta, 122875.

Bertani, R., Facchin, G., & Gleria, M. (1989). Organometallic and coordination chemistry on phosphazenes Part I. Zn (II), Pd (II) and Pt (II) complexes on Schiff base-containing cyclophosphazenes. Inorganica chimica acta, 165(1), 73-82.

Caminade, A. M., Hameau, A., & Majoral, J. P. (2016). The specific functionalization of cyclotriphosphazene for the synthesis of smart dendrimers. Dalton Transactions, 45(5), 1810-1822.

Casella, G., Carlotto, S., Lanero, F., Mozzon, M., Sgarbossa, P., & Bertani, R. (2022). Cyclo-and polyphosphazenes for biomedical applications. Molecules, 27(23), 8117.

Cemaloğlu, R., Asmafiliz, N., Hökelek, T., Kılıç, Z., Açık, L., Sabah, B. N., ... & Özbük, M. (2025). Phosphorus-nitrogen compounds: Part 79. Design and synthesis of spiro-bino-spiro (sbs)-bis (tetraalkylaminocyclotriphosphazenes) and novel twenty-membered bis (dichlorocyclotriphos-phaza) macrocycles: Structural analysis, chirality and bioactivity studies. *Journal of Molecular Structure*, *1335*, 141926.

Chakraborty, A., Ahmed, N., & Chandrasekhar, V. (2021). Phosphazenes.

Chandrasekhar, V., Andavan, G. T. S., Azhakar, R., & Pandian, B. M. (2006). 36-and 42-Membered cyclophosphazene-containing macrocycles. *Tetrahedron letters*, *47*(47), 8365-8368.

Dagdag, O., & Kim, H. (2023). Progress in the field of cyclophosphazenes: Preparation, properties, and applications. *Polymers*, *16*(1), 122.

El Brahmi, N., Mignani, S. M., Caron, J., El Kazzouli, S., Bousmina, M. M., Caminade, A. M., ... & Majoral, J. P. (2015). Investigations on dendrimer space reveal solid and liquid tumor growth-inhibition by original phosphorus-based dendrimers and the corresponding monomers and dendrons with ethacrynic acid motifs. Nanoscale, 7(9), 3915-3922.

Goshisht, M. K., Patra, G. K., & Tripathi, N. (2022). Fluorescent Schiff base sensors as a versatile tool for metal ion detection: strategies, mechanistic insights, and applications. *Materials Advances*, *3*(6), 2612-2669.

Jamain, Z., Khairuddean, M., & Guan-Seng, T. (2020). Synthesis of novel liquid crystalline and fire retardant molecules based on six-armed cyclotriphosphazene core containing Schiff base and amide linking units. RSC advances, 10(48), 28918-28934.

Juyal, V. K., Pathak, A., Panwar, M., Thakuri, S. C., Prakash, O., Agrwal, A., & Nand, V. (2023). Schiff base metal complexes as a versatile catalyst: A review. *Journal of organometallic chemistry*, *999*, 122825.

Kagatikar, S., & Sunil, D. (2021). Schiff bases and their complexes in organic light emitting diode application. *Journal of Electronic Materials*, *50*(12), 6708-6723.

Katir, N., El Brahmi, N., El Kadib, A., Mignani, S., Caminade, A. M., Bousmina, M., & Majoral, J. P. (2015). Synthesis of onion-peel nanodendritic structures with sequential functional phosphorus diversity. Chemistry–A European Journal, 21(17), 6400-6408.

Khatri, P. K., & Jain, S. L. (2012). Multiple oxo-vanadium Schiff base containing cyclotriphosphazene as a robust heterogeneous catalyst for regioselective oxidation of naphthols and phenols to quinones. Catalysis letters, 142(8), 1020-1025.

Kocak, S. B., Koçoğlu, S., Okumuş, A., Kılıç, Z., Öztürk, A., Hökelek, T., ... & Açık, L. (2013). Syntheses, spectroscopic properties, crystal structures, biological activities, and DNA interactions of heterocyclic amine substituted spiro-ansa-spiro-and spiro-bino-spiro-phosphazenes. Inorganica Chimica Acta, 406, 160-170.

Kumar, S., Arora, A., Maikhuri, V. K., Chaudhary, A., Kumar, R., Parmar, V. S., ... & Mathur, D. (2024). Advances in chromone-based copper (ii) Schiff base complexes: synthesis, characterization, and versatile applications in pharmacology and biomimetic catalysis. RSC advances, 14(24), 17102-17139.

Lee, J. J. C., Chua, M. H., Wang, S., Qu, Z., Zhu, Q., & Xu, J. (2024). Cyclotriphosphazene: A versatile building block for diverse functional materials. *Chemistry–An Asian Journal*, *19*(17), e202400357.

Marinova, P. E., & Tamahkyarova, K. D. (2025). Synthesis, Investigation, Biological Evaluation, and Application of Coordination Compounds with Schiff Base—A Review. Compounds, 5(2).

Meenink, E. (2025). The synthesis of first-generation anti-inflammatory Schiff base Cyclotriphosphazene dendrimer-based NSAIDs (Doctoral dissertation, University of Prince Edward Island).

Mutlu, G., Okumuş, A., Elmas, G., Kılıç, Z., Güzel, R., Sabah, B. N., ... & Hökelek, T. (2022). Phosphorus–nitrogen compounds. Part 65. Novel diansa-spiro-cyclotetraphosphazenes: synthesis, characterization, bioactivity and electrochemical properties, and dye-sensitized solar cell fabrication studies. *New Journal of Chemistry*, *46*(38), 18384-18401.

Nayak, P. A., Naik, H. B., Viswanath, R., & Kirthan, B. R. (2021). Green light emitting fluorescent [Zn (II)(Schiff base)] complexes as electroluminescent material in organic light emitting diodes. *Journal of Physics and Chemistry of Solids*, *159*, 110288.

Odabaşoğlu, M., Turgut, G., & Karaer, H. (1999). Preparation and characterization of chromophor group containing cyclotriphosphazenes: I imino chromophor carrying some cyclotriphosphazenes. Phosphorus, Sulfur, and Silicon and the Related Elements, 152(1), 9-25.

Örgüler, G. (2025). Monospirohalkalifosfazen-Schiff Bazi Türevlerinin Sentezi Ve Karakterizasyonu, Yüksek Lisans Tezi

Raczuk, E., Dmochowska, B., Samaszko-Fiertek, J., & Madaj, J. (2022). Different Schiff bases—structure, importance and classification. *Molecules*, *27*(3), 787.

Rana, M. S., Rayhan, N. M. A., Emad, A. H., Hossain, M. I., Shah, M. M., Kudrat–E-Zahan, M., ... & Asraf, M. A. (2025). Salicylaldehyde-based Schiff bases and their transition metal complexes: an overview on synthesis and biological activities. *Journal of Coordination Chemistry*, *78*(9), 937-1006.

Thilagar, P., Sudhakar, P., Swamy, P. C. A., & Mukherjee, S. (2012). Synthesis and spectral characterization of cyclotriphosphazene based 18-membered macrocycles. Inorganica Chimica Acta, 390, 163-166.

Tümer, Y., Bati, H., Çalişkan, N., Yüksektepe, Ç. D., & Büyükgüngör, O. (2008). Synthesis, Crystal Structure and Characterization of Hexakis [2-methoxy-4-formylphenoxy] cyclotriphosphazene. *Zeitschrift für anorganische und allgemeine Chemie*, *634*(3), 597-599.

Tümer, Y. (2022). Synthesis, structural, and stereogenic characterizations of new trispirocyclotriphosphazenes. *Journal of the Chinese Chemical Society*, *69*(11), 1897-1907.

Tümer, Y., Asmafiliz, N., Kılıç, Z., & Hökelek, T. (2022). Phosphorus–nitrogen compounds: part 63. Mono-and bis-vanillinatobisferrocenyldispiro (N/N) cyclotriphosphazenes and their macrocyclic Schiff-bases: synthesis, structural characterization and isomerism. New Journal of Chemistry, 46(21), 10368-10378.

Türe, S., Silah, H., & Tuna, M. (2020). Reinvestigations of the reactions of hexachlorocyclotriphosphazene with difunctional primary amines leading to novel dangler, ansa and bridged derivatives. Spectroscopic studies of the derived products. Journal of Molecular Structure, 1202, 127232.

Usri, S. N. K., Jamain, Z., & Makmud, M. Z. H. (2021). A review on synthesis, structural, flame retardancy and dielectric properties of hexasubstituted cyclotriphosphazene. Polymers, 13(17), 2916.

Wang, Y., Yang, N., Soldatov, M., & Liu, H. (2022). A novel phosphazene-based amine-functionalized porous polymer with high adsorption ability for I2, dyes and heavy metal ions. Reactive and Functional Polymers, 173, 105235.

Zhang, X., Eichen, Y., Miao, Z., Zhang, S., Cai, Q., Liu, W., ... & Wu, Z. (2022). Novel Phosphazene-Based flame retardant polyimine vitrimers with Monomer-Recovery and high performances. Chemical Engineering Journal, 440, 135806.

ORAL PRESENTATION

Mayaların tanımlanmasında kullanılan yöntemler

Mustafa Evren[1] (*Orcid: https://orcid.org/0000-0002-3815-1184*),
Mustafa Apan[2*] (*Orcid: https://orcid.org/0000-0002-1842-7358*)

[1.] Ondokuz Mayıs Üniversitesi, Mühendislik Fakültesi, Gıda Mühendisliği Bölümü, Gıda Bilimleri Anabilim Dalı. Samsun, Türkiye
[2*.]Ondokuz Mayıs Üniversitesi, Terme Meslek Yüksekokulu, Gıda İşleme Bölümü, Samsun, Türkiye

*Sorumlu yazar e-mail: m.apan@omu.edu.tr

Özet

Yıllardır mayaların, fermentasyon teknolojisinde ve biyoteknolojisinde; sirke, organik asit, etil alkol, enzim, protein, yağ ve vitamin, sucuk, kımız, kefir, yoğurt, peynir, ekmek, pasta vb. gıdaların ve gıda bileşimlerin üretiminde önemli rol oynamaları nedeniyle endüstriyel gıda üretiminde vazgeçilmez bir yerleri bulunmaktadır. Mayaların bu faydalarının yanında, hatalı üretim, uygun olmayan koşullarda depolama ve taşıma koşullarının yanında, tüketicilerin bu ürünleri tüketim aşamasına kadar geçen süreçte yanlış muhafaza etmelerinden dolayı gıdanın bozulmasına neden olmaktadır. Mayalar, fungusların *Ascomycetes* ve *Basidiomycetes* sınıfına ait ökaryotik, heterotrof, tek hücreli mikroorganizmalardır. Hücre büyüklüğü, hücre yapısı ve metabolik aktiviteleri yönünden diğer mikroorganizmalardan önemli farklılıklar göstermektedirler. Genellikle yuvarlak, silindirik, oval ya da limon şeklinde kendilerine özgü hücre yapısına sahiptirler. Mayalar çeşitli morfolojik ve biyokimyasal özellikleriyle birbirlerinden ayrılırlar. Mayaların bu özelliklerinden yararlanılarak tanımlamaları yapılmaktadır. Bu tanımlama işlemi için biyokimyasal (şeker asimilasyonu, üre hidrolizi, fermentasyonu vb), ve morfolojik (sıvı ve katı besiyerlerindeki görünüşleri, hücre bölünmesi, spor yapıları vb.) testlere dayanan geleneksel tanımlama yöntemleri geliştirilmiştir. Ancak bu yöntemler fazla işgücü ve zaman harcanmasının yanında bazı durumlarda yetersiz kalmaktadır. Bu nedenle API 20 C, API 20 C AUX ve API ID 32 C, Vitek gibi alternatif yöntemler geliştirilmiştir. Bu geleneksel yöntemlere paralel olarak, son yıllarda, moleküler biyolojinin gelişmesiyle birlikte mayaların tespit ve tanımlamasında Polimeraz Zincir Reaksiyonuna (PZR; Polymerase Chain Reaction-PCR) dayalı moleküler yöntemler oldukça önem kazanmıştır. PZR yöntemi; klasik belirleme ve tanımlama yöntemlerine alternatif olarak geliştirilen ve hızlı olduğu kadar yüksek seçicilik ve duyarlılığa sahip bir yöntem olarak, gıdalardaki kaliteyi bozan mayaların tanımlanmasında günümüzde kullanımı en çok tercih edilen yöntem olarak karşımıza çıkmaktadır. Hem faydalı hem de zararlı yönleri ile mayalar da gıda endüstrisinde önemli bir yer tutmaktadır. Bu nedenle tanımlamaları çok önemlidir. Bu derlemede mayaların tanımlanmasında kullanılan yöntemler açıklanacaktır.

Anahtar Kelimeler: PZR, Maya, API

Methods used in ıdentifying yeasts

Abstract

For years, yeasts have played an indispensable role in industrial food production due to their significant contribution to fermentation technology and biotechnology in the production of vinegar, organic acids, ethyl alcohol, enzymes, proteins, fats, vitamins, sausages, kumis, kefir, yogurt, cheese, bread, pastries, and other food products and food compounds. In addition to these benefits of yeast, food spoilage can occur due to faulty production, improper storage and transportation conditions, and incorrect preservation by consumers throughout the process leading up to consumption. Yeasts are eukaryotic, heterotrophic, single-celled microorganisms belonging to the *Ascomycetes* and *Basidiomycetes* classes of fungi. They differ significantly from other microorganisms in terms of cell size, cell structure, and metabolic activities. They generally have a unique cell structure that is round, cylindrical, oval, or lemon-shaped. Yeasts differ from one another in various morphological and biochemical characteristics. Yeasts are described using these characteristics. Traditional identification methods have been developed for this process, based on biochemical (sugar assimilation, urea hydrolysis, fermentation, etc.) and morphological (appearance in liquid and solid media, cell division, spore structures, etc.) tests. However, these methods require a lot of labor and time, and are insufficient in some cases. Therefore, alternative methods such as API 20 C, API 20 C AUX, API ID

32 C, and Vitek have been developed. In parallel with these traditional methods, molecular methods based on Polymerase Chain Reaction (PCR) have gained considerable importance in the detection and identification of yeasts in recent years, with the development of molecular biology. PCR, developed as an alternative to classical detection and identification methods, is a fast method with high selectivity and sensitivity, and is currently the most preferred method for identifying yeasts that spoil the quality of food. With both beneficial and harmful aspects, yeasts also hold an important place in the food industry. Therefore, their definitions are very important. This review will describe the methods used to identify yeasts.

Keywords: PCR, Yeast, API

GİRİŞ

Mayalar organik asitleri kullanabilme, laktozu fermente edebilme proteolitik ve lipolitik aktiviteye sahip olmalarından dolayı, fermentasyon teknolojisinde ve biyoteknolojide; çeşitli gıdaların ve gıda bileşimlerin üretiminde önemli rol oynamaktadır (Biberoğlu, 2012).

Mayaların bu faydalarının yanında, hatalı üretim, uygun olmayan koşullarda depolama ve taşıma koşullarının yanında, tüketicilerin bu ürünleri tüketim aşamasına kadar geçen süreçte yanlış muhafaza etmelerinden dolayı gıdanın bozulmasına neden olmaktadır. Bu nedenlerle gıdalarda şişmeye, lezzet kaybına ve tekstür kalitesinde azalmaya neden olmaktadır. Ayrıca bazı mayalar, insan sağlığını olumsuz etkilemektedir (Anğ, 2014)

Bu nedenlerle, mayaların çeşitli kaynaklardan aranması ve tanımlanması çok önemlidir.

MAYALARIN TANIMLANMASINDA KULLANILAN YÖNTEMLER

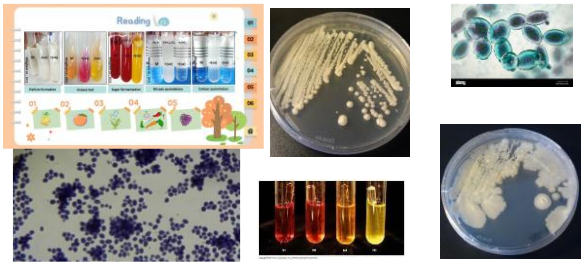
Tanımlama işlemi yapılmadan önce elde edilen izolatların maya olup olmadığı mikroskobik olarak belirlendikten sonra saflığının kontrolü yapılması gerekmektedir. Ayrıca analize alınan mikroorganizmaların genç kültür olması tavsiye edilmektedir. Mayaların tanımlanmasında en çok kullanılan yöntemler;

Ticari kitler

Moleküler Teknikler şeklinde sıralanmaktadır.

Mayaların Tanımlanmasında Kullanılan Konvansiyonel Yöntemler

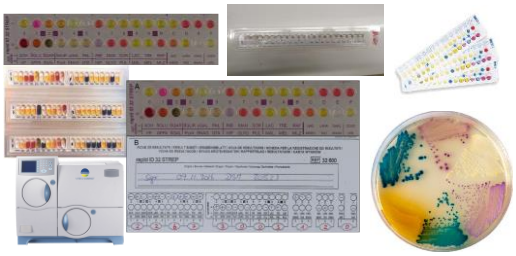
Bu tanımlama yöntemleri mayaların morfolojik (makroskobik ve mikroskobik) ve biyokimyasal profillerinin incelenmesine dayanan Wickerham ve Auxanographic metotlarıdır. Konvansiyonel tanımlama yöntemleri şeker asimilasyonu-fermentasyon, azot asimilasyonu, Arbutini asimilasyonu, Diazonyum Blue B (DBB) testi, çeşitli ortamlarda gelişme (sıcaklık, çeşitli tuz ve şeker oranında gelişme) testi, üre hidrolizi, askospor oluşumu gibi analizleri içermektedir (Barnett ve ark., 1990); (Deak ve Beuchat, 1996); (Kreger–Van Rij,1987); (Kurtzman ve Fell, 2000). Bu testlerin örnekleri şekil 1’ de verilmiştir.



Şekil 1 Mayaların tanımlanmasında kullanılan konvansiyonel yöntemler (Hartline, 2025)

Mayaların Tanımlanmasında Kullanılan Ticari Kitler

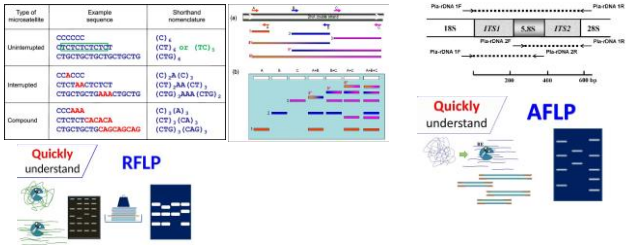
Konvansiyonel tanımlama yöntemlerinin yanında, CHROMagar, API 20 C, API 20 C AUX ve API ID 32 C, Vitek gibi alternatif yöntemler geliştirilmiştir. Bu tanımlama yöntemlerinde spesifik besiyerleri ve çeşitli karbonhidrat kaynakları kullanılmaktadır. Ticari kitler konvansiyonel tanımlama yöntemlerinin minyatürize yapılmış şeklidir. Bu testlerin örnekleri şekil 2’ de verilmiştir (İnci ve ark., 2012); (Morovati ve ark., 2023); (Pincus ve ark., 2007).



Şekil 2 Mayaların tanımlanmasında kullanılan ticari kitler (Morovati ve ark., 2023)

Mayaların Tanımlanmasında Kullanılan Moleküler Teknikler

Mayaların belirli gen bölgelerinin ITS, IGS, (CGT) gibi çeşitli primerler kullanılarak çoğaltılması ve elektroforez ile gösterilmesine dayanan parmak izi (fingerprint) analizleri şeklinde sıralanmaktadır. Bu yöntemler PZR-RAPD, PZR-RFLP, PZR-AFLP ve Microsatellite analizleri şeklinde sıralana bilmektedir. Bu analiz yöntemleri şekil 3' te verilmiştir (Yalçın ve ark., 2010); (Pincus ve ark., 2007).



Şekil 3 PZR-RAPD, PZR-RFLP, PZR-AFLP ve Microsatellite analizleri (Anonymous, 2020a); (Anonymous, 2020b);

Mayaların tanımlanmasında kullanılan diğer moleküler teknikler;

Real-Time PZR; Herhangi bir çift sarmallı DNA ile araya giren spesifik olmayan flüoresan boyalar boyanması ve probun tamamlayıcı dizisi ile hibridizasyonununa dayanan bir yöntemdir. Bu analizde PZR aşamasında mikroorganizma moleküler olarak tanımlanmaktadır (Mackay, 2002).

MALDI-TOF MS; Bu yöntemde mikroorganizmalara ait biyomeküllerin (protein, peptid, şeker) ve büyük organik moleküllerin (polimer, dendrimer, makromolekül) iyonize edildikten sonra elektrik ve/veya manyetik alandan geçirilerek protein profilleri çıkarılmasıyla, bu profilin spektrumlarına ait grafiksel görüntüler, sistemin veri tabanındaki referans mikroorganizmaların uyumuna göre yapılmaktadır (Eren ve ark., 2021).

DNA SEKANS ANALİZİ; Genetik materyaldeki baz çiftlerinin (A, T, C, G) tam sırasını belirlenmesiyle genlerin yapısını, mutasyonları ve varyasyonları tespit etmeyi sağlayan bir yöntemdir. Bu yöntemde elde edile veriler çeşitli programlarla analize tabi tutulmaktadır (Behjati ve Tarpey, 2013).

Bu tanımlama yöntemlerin yanında Antijen ve antikor temelli, 1,3-beta-D-glukan, Galaktomannan, Koenzim Q10 gibi analizler de yapılmaktadır (Gülmez ve Alp, 2021); (Kurtzman ve Fell, 2000).

SONUÇ

Mayaların tanımlanmasında hızın yanında doğruluğun da çok fazla önemi vardır. Bu nedenle günümüzde konvansiyonel tanımlama yöntemlerini doğrulayıcı çeşitli (ticari ve genetik) yöntemler kullanılmaktadır.

Böylelikle hakim maya florasının belirlemesinin yanında, bu floranın teknolojik açıdan araştırılmasına imkan sağlamaktadır.

Teknolojinin ve genetik biliminin gelişmesiyle birlikte maya tanımlama yöntemlerinin gelişmesine ve optimizasyonuna imkan sağlamaktadır.

KAYNAKLAR

Anğ, Ö. (2014). Hastalık etkeni mayalarda patojenliğin evrimi. Türk mikrobiyoloji cemiyeti dergisi, 44 (1), 1-9.

Anonymous, (2020a). Restriction fragment length polymorphism. https://www.youtube.com/watch?v=swQ_pm4cR5o. (09.12.2025).

Anonymous, (2020b). Random amplification of polymorphic DNA, https://www.youtube.com/ watch?v=i5_ecgyY3dY. (09.12.2025).

Barnett, J. A., Payne, R. W. & Yarrow, D., (1990). Yeasts: characteristics and ıdentification. Cambridge University Press, Cambridge, 1002s.

Behjati, S., & Tarpey, P. S. (2013). What is next generation sequencing?. Archives of disease in childhood. Education and practice edition, 98 (6), 236–238. https://doi.org/10.1136/archdischild-2013-304340.

Biberoğlu, Ö. (2012). Geleneksel olarak üretilen yoğurtlardan mayaların izolasyonu ve identifikasyonu. Atatürk Üniversitesi Sağlık Bilimleri Enstitüsü Besin Hijyeni ve Teknolojisi Ana Bilim Dalı Doktora Tezi, 93. Erzurum.

Deak, T. & Beuchat, L. R., (1996). Handbook of spoilage yeasts, CRC Press, Boca Raton, New York. 210s.

Eren, S., Metin, D. Y. & Polat, S. H. (2021). Maya mantarlarının hızlı tanımlanmasında lizis filtrasyon sonrası MALDI TOF-MS yönteminin kullanımı. Türk Mikrobiyoloji Cemiyeti Dergisi, 51(4), 421 - 427. doi.org/10.5222/TMCD.2021.04909.

İnci, M., Atalay, M. A., Koç, A. N. & Özer, B. (2012). Comparison of VITEK 2 YST Card and API 20C AUX system in identification of non- albicans Candida species. Dicle Medical Journal, 39(1), 80-82. https://doi.org/10.5798/diclemedj.0921.2012.01.0099.

Hartline, R. (2025). Fermentation. https://bio.libretexts.org/Bookshelves/Microbiology/Microbiology_Laboratory_Manual_ %28Hartline%29/01%3A_Labs/1.22%3A_Fermentation. (09.12.2025).

Gülmez, D. & Alp, S. (2021). Mantar infeksiyonlarının laboratuvar tanısında klasik yöntemler ve yeni gelişmeler. Flora İnfeksiyon Hastalıkları ve Klinik Mikrobiyoloji Dergisi, 26 (1), 34-49. doi.org/10.5578/flora.20219904.

Kreger–Van Rij N. J. W., 1987. The Yests, a taxonomic study, Elsevier Science Publishers B.U., Amsterdam, 1082s.

Kurtzman, C.P. & Fell, J.W., 2000. The Yeast, A Taxonometric Study.Third impression, Elsevier Science B.V.The Nederlands., 1055s.

Mackay I. M. (2004). Real-time PCR in the microbiology laboratory. Clinical microbiology and infection : the official publication of the European Society of Clinical Microbiology and Infectious Diseases, 10(3), 190–212. https://doi.org/10.1111/j.1198-743x.2004.00722.x.

Morovati, H., Kord, M., Ahmadikia, K., Eslami, S., Hemmatzadeh, M., Kurdestani, K. M., Khademi,

M., & Darabian, S. (2023). A Comprehensive Review of Identification Methods for Pathogenic Yeasts: Challenges and Approaches. Advanced biomedical research, 12, 187. https://doi.org/10.4103/abr.abr_375_22.

Pincus, D. H., Orenga, S., & Chatellier, S. (2007). Yeast identification--past, present, and future methods. Medical mycology, 45(2), 97–121. https://doi.org/10.1080/13693780601059936.

Yalçın, S. K., Ergül, Ş. Ş., & Özbaş, Z. Y. (2010). Moleküler esaslı yöntemlerin gıda kaynaklı mayaların tanımlanmalarında kullanılmaları. Gıda, 35(5), 379-386.

ORAL PRESENTATION

Mikroorganizmaların DNA izolasyon ve saflaştırma yöntemleri

Mustafa Evren[1] (Orcıd: https://orcid.org/0000-0002-3815-1184),
Mustafa Apan[2*] (Orcıd: https://orcid.org/0000-0002-1842-7358)

[1.] Ondokuz Mayıs Üniversitesi, Mühendislik Fakültesi, Gıda Mühendisliği Bölümü, Gıda Bilimleri Bölümü.
[2.] Ondokuz Mayıs Üniversitesi, Terme Meslek Yüksekokulu, Gıda İşleme Bölümü,

*Sorumlu yazar e-mail: m.apan@omu.edu.tr

Özet

Gıdaların üretimden tüketiciye ulaşıncaya kadar yapılan işlemler sırasında çeşitli kaynaklardan bulaşan mikroorganizmalar, uygun koşullarda hızla çoğalarak fiziksel ve kimyasal kalitenin bozulmasına, bunun sonucunda çeşitli ekonomik kayıplara ve insan sağlığının bozulmasına neden olmaktadır. Mikroorganizmalar, bu zararlarının yanında, tıp, gıda, tarım gibi çeşitli alanlarda kullanılmaktadır. Bu organizmaların tespiti ve tanımlamaları çok önemlidir. Bu yöntemler arasında klasik (biyokimyasal ve morfolojik özelliklere dayanan) ve test kiti (enzim aktivitelerine dayanan) ile yapılan yöntemler gelmektedir. Günümüz de ise bu yöntemlerin yanında daha hızlı ve güvenilir DNA esaslı mikroorganizma tespit ve tanımlama yöntemleri geliştirilmiş ve yaygın bir şekilde kullanılmaya başlanmıştır. Bu yöntemin doğruluğunu artıran en önemli faktörlerden biri tespit edilecek veya tanımlanacak mikroorganizmanın DNA'sının olabildiğince saf olmasıdır. Bu nedenle çeşitli yöntemler geliştirilmiştir. Çeşitli araştırıcılarla ilk olarak tavsiye edilen tespit edilecek veya tanımlanacak mikroorganizmaların saf olarak elde edilmesidir. Bu yöntemler: mikroorganizma hücre duvarını mekanik (cam boncuk, mikro-akışkanlaştırıcı, sıcaklığın değiştirilmesi), fiziksel (yüksek basınçlı homojenizatör) ve kimyasal (Lizis) yöntemlerle parçalayıp, çeşitli kimyasallar (fenol, chloroform, proteinaz K) kullanılarak genetik materyalin saflaştırmasına dayanmaktadır. Hazır kitler, klasik saflaştırma yönteminin hızlı versiyonu olarak görülmektedir. Bu izolasyon ve saflaştırma yöntemlerinde çeşitli steril filtreler de kullanılmaktadır. Bu sektörün gelişmesiyle bazı firmalar DNA izolasyonunu otomatik olarak yapan aletler de geliştirilmiştir. Bu yöntemde analizi yapan kişi hücre parçalamasını yaptıktan sonra, saflaştırıcı solüsyonları içeren mikropleyt kutularını ve pipetleri alete yerleştirmesinden sorumludur. Bazı araştırıcılar mikroorganizmaları hücre parçalamayı ve analizi birlikte yaparak zamandan tasarruf etmeye çalışmaktadırlar.

Bu derlemede mikroorganizmaların DNA izolasyon ve saflaştırma yöntemlerinin çeşitlerine, işlem basamaklarına avantaj ve dezavantajlarına değinilecektir.

Anahtar Kelimeler: DNA, Saflaştırma, İzolasyon

DNA Isolation And Purification Methods Of Microorganisms

Abstract

During the processing of food from production to consumption, microorganisms from various sources can multiply rapidly under suitable conditions, leading to a deterioration in physical and chemical quality, resulting in various economic losses and harming human health. Despite their harmful effects, microorganisms are used in various fields such as medicine, food, and agriculture. Identifying and describing these organisms is crucial. Today, alongside these methods, faster and more reliable DNA-based microorganism detection and identification methods have been developed and are widely used. These methods include classical methods (based on biochemical and morphological characteristics) and test kit methods (based on enzyme activities). One of the most important factors in increasing the accuracy of this method is ensuring that the DNA of the microorganism to be detected or identified is as pure as possible. Therefore, various methods have been developed. The initial recommendation from various researchers is to obtain the microorganisms to be detected or identified in pure form. These methods are based on breaking down the microorganism cell wall using mechanical (glass beads, microfluidizer, temperature modification), physical (high-pressure homogenizer), and chemical (lysis) methods, and purifying the genetic

material using various chemicals (phenol, chloroform, proteinase K). Ready-made kits are considered a faster version of the classic purification method. Various sterile filters are also used in these isolation and purification methods. With the development of this sector, some companies have also developed devices that automate DNA isolation. With the development of this sector, some companies have also developed devices that automate DNA isolation. In this method, after performing the cell lysis, the analyst is responsible for placing the microplate boxes containing the purifying solutions and the pipettes into the instrument. Some researchers are trying to save time by performing cell lysis and analysis of microorganisms simultaneously. This review will discuss the various methods for DNA isolation and purification from microorganisms, their procedural steps, advantages, and disadvantages.

Keywords: DNA, Purification, Isolation

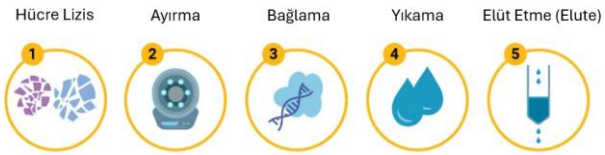
GİRİŞ

1983 yılından günümüzde, moleküler biyoloji ve genetik bilimlerinin gelişmesiyle birlikte gıdaları bozan ve patojen mikroorganizmaların tanımlanmasında ve aranmasında kolaylıklar sağlanmaktadır. Ayrıca, gıdalardan izole edilen mikroorganizmaların probiyotik ve starter kültür özelliklerinin araştırılmasına olanak sağlamaktadır. Moleküler çalışmaların, temeli DNA, RNA gibi genetik materyaller üzerinde yapılan analizlere dayanmaktadır (Anonymous, 2025; Sambrook ve ark., 1989).

Genotipik olarak tanımlamanın doğruluğu başta çalışan kişilerin profesyonelliği, optimum DNA izolasyon yöntemlerinin ve ideal malzemelerinin (kimyasal ve alet-ekipman) kullanılması gelmektedir. Özellikle DNA izolasyon yöntemleri mikroorganizmaların hücre yapılarına (hücre zarı, spor, endospor, hif vd.) göre değişiklik göstermektedir. Mikroorganizmaların DNA izolasyonu yapılmadan önce genç ve saf kültür olması önerilmektedir. Böylelikle daha sağlıklı sonuçlar çıktığı bildirilmektedir (Yıldırım vd., 2011).

MİKROORGANİZMALARIN DNA İZOLASYON VE SAFLAŞTIRMA YÖNTEMLERİ

DNA izolasyonunu genel prensibi hücre zarının parçalanması, DNA dışında kalan materyallerin uzaklaştırmasına (inaktivasyonu) ve DNA' nın elde edilip, saflaştırılmasına dayanmaktadır. Yöntem prensibi şekil 1' de verilmiştir. 1) Hücre yapısının bozulması, 2) Çözünür DNA'nın hücre kalıntılarından ve diğer çözünmeyen maddelerden ayrılması, 3) istenen DNA'yı saflaştırma matrisine bağlanması, 4) Protein ve diğer materyallerin saflaştırma matrisinden ayrılması, 5) İstenen DNA' nın eldesi (elüsyon oluşturma). Mikroorganizmaların DNA izolasyon ve saflaştırma yöntemleri aşağıda verildiği gibidir (Shetty ve Dairawan, 2020).



Şekil 1 DNA izolasyon ve saflaştırılma yöntemlerinin prensibi (Anonymous, 2025a).

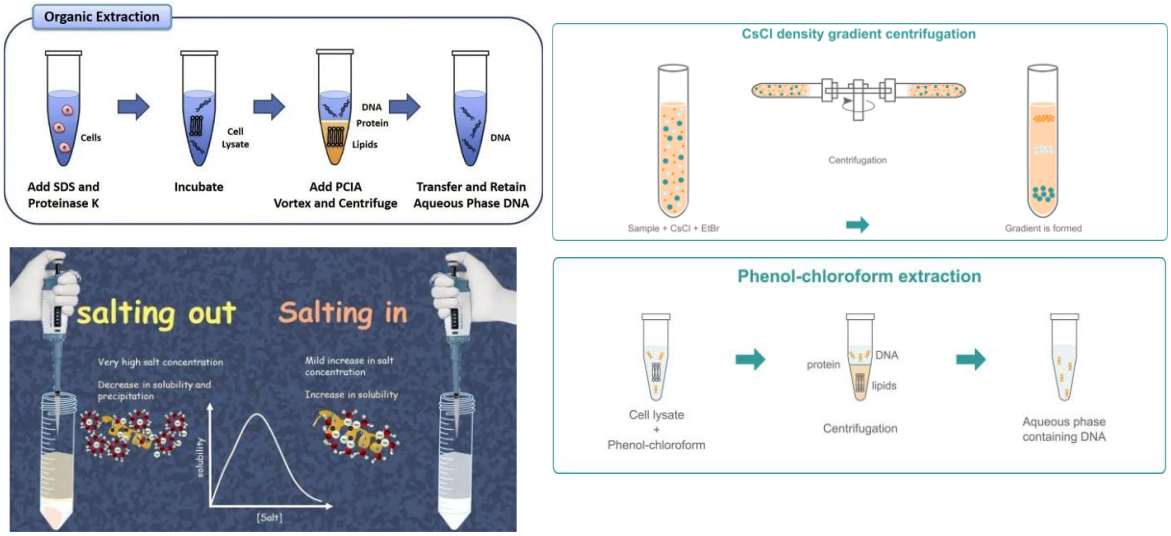
A- Kromatografi Temelli DNA İzolasyon Yöntemi:

Kolon, poliakrilamid, dekstran veya agarozdan oluşan gözenekli boncuklar içerir. Örnek üst kısma uygulanıp kolondan geçirildiğinde, mRNA ve proteinler gibi daha küçük moleküller boncukların küçük gözeneklerinden ve kanallarından içeri girmektedir. DNA molekülü geçememektedir. Sonuç olarak, DNA, daha küçük moleküllere kıyasla kolondan daha hızlı ayrılır.

Bu yöntemler arasında mikroorganizmaların DNA' sının izolasyonunda en çok kullanılan yöntemler Setiltrimetilamonyum Bromür (CTAB) ve Fenol-Kloroform yöntemleridir. Ayrıca bu iki yöntemlerde Proteinaz K kullanılabilmektedir. Bu yöntemler konvensiyonel DNA izolasyon metotları olarak geçmektedir.

Kromatografi temelli DNA izolasyon yöntemlerinde hazırlanan çözeltilerin pH, iyon dengesi, sıcaklık, analizi yapan kişinin profesyonelliği ve kullanılan alet-ekipmanlar çok önemlidir. Bu yöntemlerin prensipleri şekil 2' de görülmektedir (Ausubel, 1988); (Chacon-Cortes ve Griffiths, 2014); (Ghaheri ve ark., 2016); (Prins ve ark.,2024); (Ranjan ve Mahato, 2024); (Wydro, 2022); (Shetty ve Dairawan, 2020).

- EtBr-CsCl Gradyan Santrifüjleme Yöntemi:
- Alkali Ekstraksiyon Yöntemi:
- Silika Matrisler Yöntemi:
- Tuzlama (Salting-out) Yöntemi:
- Setiltrimetilamonyum Bromür (CTAB) Ekstraksiyon Yöntemi:
- Fenol-Kloroform Yöntemi:
- SDS-Proteinaz K Yöntemi:

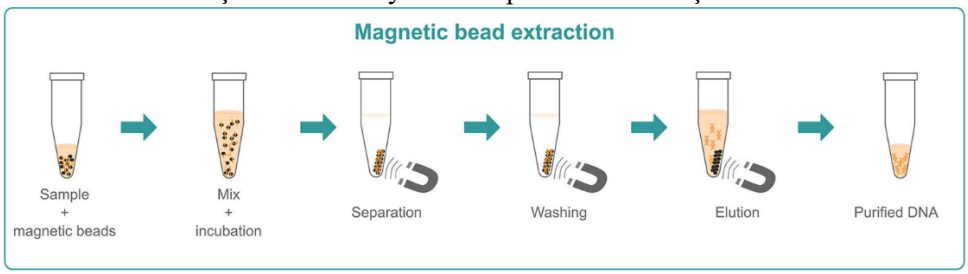


Şekil 2 Bazı Kromatografi temelli DNA izolasyon yöntemi (Elmesery, 2025); (Mészáros, 2024)

B- Silika Kolon Temelli DNA Ekstraksiyon Yöntemi:

Bu yöntemde, hücre içerisinde bulunan protein, inorganik ve organik materyaller silika kolonunun altında hapsederken, DNA içeren sulu fazın jel polimer tabakasının üzerinde kalmasını sağlanmaktadır. Bu yöntemle yüksek yoğunlukta DNA elde edilebilir (Chacon-Cortes ve Griffiths, 2014); (Prins ve ark.,2024); (Ranjan ve Mahato, 2024); (Shetty ve Dairawan, 2020); (Wydro, 2022); (Topçu ve ark., 2016).

- Manyetik Boncuk Yöntemi: Şekil 3' de bu yöntemin prensibi verilmiştir.

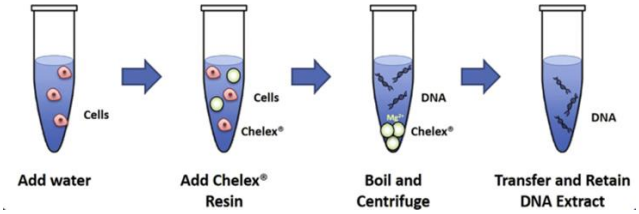


Şekil 3 Manyetik boncuk yöntem prensibi (Mészáros, 2024)

C- Selüloz Temelli Kağıt Yöntemi:

Selüloz, DNA'ya yüksek bağlanma eğilimine sahip, yoğun şekilde hidroksillenmiş bir polimerdir. Whatman FTA™ kaplamalı selüloz filtrelerin DNA' yı bağlama özelliği kullanılmaktadır (Chacon-Cortes ve Griffiths, 2014); (Prins ve ark.,2024); (Ranjan ve Mahato, 2024); (Wydro, 2022); (Shetty ve Dairawan, 2020).

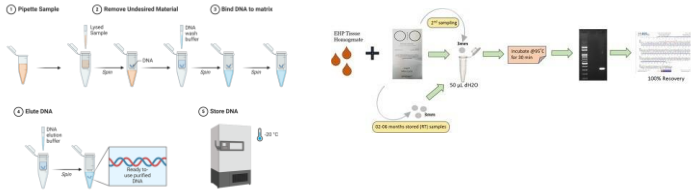
-Chelex-100 Ekstraksiyon Yöntemi: Şekil 4' te bu yöntemin prensibi verilmiştir.



Şekil 4 Chelex-100 Ekstraksiyon yöntem prensibi

D- Filtre Kâğıt Temelli DNA Ekstraksiyon Yöntemi:

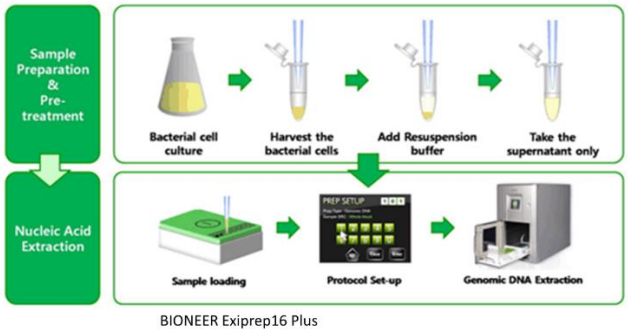
Çeşitli kaynaklardan DNA izole etmek için kullanılan, filtre kâğıdı kullanılan bir DNA ekstraksiyon yöntemidir. Ticari kit olarak kullanılır. Kullanılan kimyasal maddeler hazır halde gelmektedir. Şekil 5' de bu yöntemin prensibi verilmiştir (Chacon-Cortes ve Griffiths, 2014); (Çöl ve Karaali, 2016); (Dashti ve ark., 2009); (Prins ve ark.,2024); (Ranjan ve Mahato, 2024); (Wydro, 2022); (Shetty ve Dairawan, 2020).



Şekil 5 Filtre kâğıt temelli DNA ekstraksiyon yöntem prensibi (Mészáros, 2024)

E- Alet Temelli DNA Ekstraksiyon Yöntemi:

DNA izolasyon sektörünün gelişmesiyle bazı firmalar DNA izolasyonunu otomatik olarak yapan aletler de geliştirilmiştir. Bu yöntemde analizi yapan kişi hücre parçalamasını yaptıktan sonra, saflaştırıcı solüsyonları içeren mikropleyt kutularını ve pipetleri alete yerleştirmesinden sorumludur. Şekil 6' da bu yöntemin prensibi verilmiştir (Anonymous, 2025b); (Anonymous, 2025c).

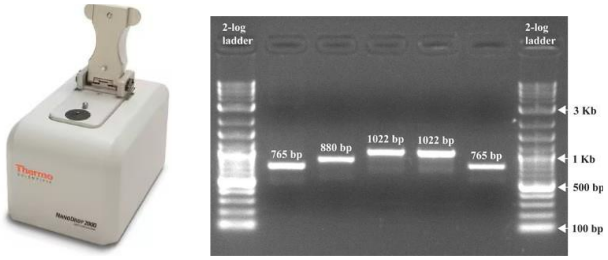


Şekil 6 Alet temelli DNA ekstraksiyon yöntem prensibi (Anonymous, 2025b)

Ayrıca DNA izolasyon yöntemlerde hücre parçalama ve ekstraksiyon aşamalarında yüksek ısı ve düşük sıcaklıklar kullanılabilir. Bu yöntemlerin yanında, bazı araştırıcılar mikroorganizmaları hücre parçalamayı ve analizi birlikte yaparak zamandan tasarruf etmeye çalışmaktadırlar.

DNA İzolatlarının Saflık ve Büyüklük Kontrolü

İzole edilen ve saflaştırılan mikroorganizma DNA' larının saflık ve büyüklük kontrolü yapılması gerekmektedir. Bu amaçla, agaroz jel elektroforezi ve spektrofotometri (nanodrop) kullanılmaktadır. Nu yöntemler şekil 7' de verilmiştir (Lee ve ark., 2012).



Şekil 7 DNA izolatlarının saflık ve büyüklük kontrolü (Anonymous, 2025d); (Lee ve ark., 2012)

SONUÇ

DNA izolasyon ve saflaştırma yöntemleri moleküler analizlerin en önemli adımlarından biridir. Bu analizlerin doğruluğu için DNA izolasyonun ve saflaştırmasının doğru şekilde yapılması gerekmektedir. Bu nedenlerle birçok yöntem geliştirilmiştir.

DNA izolasyonun ve saflaştırmasında konvansiyonel yöntemler en çok kullanılan yöntemlerdir. Ancak bu yöntemlerin dezavantajı hazırlanan çözeltilerin pH, iyon dengesi, sıcaklık, analizi yapan kişinin profesyonelliği ve kullanılan alet-ekipmanlara dikkat edilmez ise DNA izolasyonu düzgün yapılamamaktadır. Avantajı ise maliyeti daha düşük ve çok fazla mikroorganizmanın DNA izolasyonu mümkündür. Diğer yöntemlerde (kit ve alet temelli DNA izolasyon yöntemlerinde) ise maliye yüksek ve mikroorganizmanın DNA izolasyon sayısı kısıtlıdır. Ancak kullanılan kimyasallar daha güvenilirdir.

Teknolojinin gelişmesi ve moleküler analiz tekniklerinin kullanımı arttıkça DNA izolasyon ve saflaştırma yöntemlerinin çeşitliği artmaktadır.

KAYNAKLAR

Anonymous, (2004). Polymerase Chain Reaction (PCR). https://en.wikipedia.org/wiki/ Polymerase_chain _reaction. (09.12.2025).

Anonymous, (2025a). DNA purification. https://worldwide.promega.com/resources/guides/nucleic-acid-analysis/dna-purification/. (09.12.2025).

Anonymous, (2025b). ExiPrep™ 16 plus. https://eng.bioneer.com/20-a-5030.html. (09.12.2025).

Anonymous, (2025c). ExiPrep16 plus user guide. https://www.schaefer-tec.it/sites/default/files/PM-451-ExiPrep16_Plus_User_Guide_EN%28V1.2%29_140117.pdf. (09.12.2025).

Anonymous, (2025d). Thermo scientific™ nanodrop™ 2000/2000c spectrophotometers. https://www.thermofisher.com/order/catalog/product/ND-2000. (09.12.2025).

Ausubel, F. M. (1988). Current protocols in molecular biology. Greene Pub. Associates ; Wiley-Interscience. http://onlinelibrary.wiley.com/book/10.1002/0471142727. (09.12.2025).

Chacon-Cortes D & Griffiths L. (2014). Methods for extracting genomic DNA from whole blood samples: current perspectives. Journal of biorepository science for applied medicine. 2:1-9. https://doi.org/10.2147/BSAM.S46573.

Çöl, B. & Karaali, M. (2016). Evaluatıon of dıfferent dna ısolatıon methods from pıne honey. mugla journal of science and technology, 2 (2), 152-155. https://doi.org/10.22531/muglajsci.283638.

Dashti, A.A., Jadaon, M.M., Abdulsamad, A.M., & Dashti, H.M. (2009). Heat Treatment of Bacteria: A Simple method of dna extraction for molecular techniques. Kuwait medical journal; 41 (2): 117-122.

Elmesery, M. (2025). 7 Different DNA extraction methods. https://praxilabs.com/en/blog/2022/08/24/7-different-dna-extraction-methods/.(09.12.2025).

Lee, P.Y., Costumbrado, J., Hsu, C.Y. & Kim, Y.H. (2012).Agarose gel electrophoresis for the separation of DNA fragments. J. Vis. Exp. (62), e3923, 1-5. doi:10.3791/3923.

Ghaheri, M., Kahrizi, D., Yari, K., Babaie, A., Suthar, R. S., & Kazemi, E. (2016). A comparative evaluation of four DNA extraction protocols from whole blood sample. Cellular and molecular biology (Noisy-le-Grand, France), 62 (3), 120–124.

Mészáros, E. (2024). Comprehensive introduction to DNA extraction. https://www.integra-biosciences.com/global/en/blog/article/comprehensive-introduction-dna-extraction. (09.12.2025).

Ranjan, R. & Mahato, K., K. (2024). A Review on DNA isolation method. International journal of emerging technologies and ınnovative research, 11 (5). 368-370. http://www.jetir.org/papers/JETIR2405F39.pdf.

Prins, T.W., Broothaerts, W., Burns, M., Demšar, T., Edelmann, S., Papazova, N., Peterseil, V. & Taverniers, I., (2024). Guidance on the selection and use of DNA extraction methods, publications office of the european union, luxembourg, doi:10.2760/76162, JRC134298.

Wydro, U. (2022). Soil microbiome study based on DNA extraction: a review. water, 14 (24), 3999. https://doi.org/10.3390/w14243999.

Sambrook, J., Fritsch, E.F., & Maniatis, T., 1989. Molecular Cloning, A Laboratory manual. cold spring harbor laboratory press, New York.

Shetty, P., J. & Dairawan, M., (2020). The Evolution of DNA extraction methods. american journal of biomedical science & research, 8 (1), 39–45. https://doi.org/10.34297/ajbsr.2020.08.001234.

Topçu, A. A., Aşır, S., & Türkmen, D. (2016). Katı faz ayırma yöntemiyle DNA saflaştırılması. Hacettepe journal of biology and chemistry, 44 (3), 259-266.

Yıldırım, A., Kandemir, N., Sönmezoğlu, Ö. A., & Güleç, T. (2011). Buğdayda polimeraz zincir reaksiyonu ve olası sorunların optimizasyonu. Anadolu tarım bilimleri dergisi, 26 (1), 36-39.

ORAL PRESENTATION

Investigation of the antioxidant and anticholinesterase activities of methanol extracts of *Thymus sipyleus* Boiss. and *T. zygıoides* Griseb.

Züleyha Özer (ORCID: *https://orcid.org/0000-0003-4957-5756*)

Balıkesir University, Altınoluk Vocational School, Department of Chemistry and Chemical Processing Technologies, Balıkesir, Türkiye

*Corresponding author e-mail: zuleyhaozer@balikesir.edu.tr

Abstract

Lamiaceae family has 300-400 endemic species that are widely distributed worldwide in particularly in the Mediterranean. One of the most used Lamiaceae members is *Thymus* L. The genus *Thymus* comprises 39 species in Türkiye. This species is named ‘‘kekik’’ in Turkish and used as tea and traditional medicine. In this study, the antioxidant and anticholinesterase activity of methanol extracts of *Thymus sipyleus* Boiss. (sipil kekiği) and *T. zygioides* Griseb. (bodur kekiği) were investigated. The species were collected in the region of Balıkesir. The antioxidant activities were analyzed based on DPPH free radical scavenging activity, *β*-carotene linoleic acid and cupric ion reducing antioxidant capacity (CUPRAC) assays.

Keywords: Lamiaceae, *Thymus,* antioxidant, anticholinesterase, DPPH

INTRODUCTION

The genus *Thymus* is a large genus belonging to the Lamiaceae (Labiatae) family (Touaibia, 2025). In Turkey, these species are described by 39 species with 64 taxa, of which 27 are endemic and are widely used as spices or drugs (Başer et al., 1995; Başer et al., 1997; Davis, 1988; Jalas, 1982). These species are well-known for their various biological activity, like antioxidant, antimicrobial, antifungal, antiviral, antitumor, anti-inflammatory, anticancer, and antihypertensive (Anwar et al., 2024; Nickavar and Esbati 2012).These species are native to the Marmara, Aegean, and Black Sea regions of Turkey and are used as traditional medicine because of their biological properties.

Thymus species are known as a source of phenolic compounds, which have strong antioxidant activity. Antioxidant compounds are polyphenolic structures and present in almost all plants, fruits, vegetables, microorganisms, fungi, and animal tissues. Antioxidants neutralize active oxygen formation or keep the active oxygen that can damage the body. Phenolic compounds act as antioxidants and inhibit various diseases such as cancer, cardiovascular, and neurodegenerative diseases (Safaei-Ghomi et al., 2009; Rice-Evans et al., 1996). Oxidative stress, as an instability in the manufacture and removal of free radicals and another reactive species, is well known to reason that the oxidation of major biomolecules leads to cellular damage and death (Kindl et al., 2015).

In the literature, research on the phenolic components in plant extracts and their bioactivities (antioxidant, antibacterial, and antifungal) has been conducted using various solvents (Asres et al., 2025; El-Bouzidi et al., 2025; Kaska et al., 2018; Polat et al., 2007; Rosenova et al., 2025). There are a few studies evaluating the phenolic profiles of methanol extracts of *T. sipyleus* and *T. zygioides* species and their contribution to their bioactivities (Llorent-Martínez et al., 2022; Gökbulut, 2015).

This study involved the definition of the antioxidant and anticholinesterase activities of *T. sipyleus* and *T. zygioides* through standard techniques: DPPH free radical scavenging activity, *β*-carotene linoleic acid assays and cupric ion reducing antioxidant capacity (CUPRAC). Additionally, the anticholinesterase activity of the samples was evaluated by AChE and BChE inhibitions. No prior research has been conducted to compare and analyze the antioxidant and anticholinesterase properties of *T. sipyleus* and *T. zygioides* collected from the Balıkesir region.

MATERIALS AND METHODS

Plant Material

The aerial parts of *T. sipyleus* collected from Balıkesir (Kazdağları, Edremit, rocky slopes), 913 m altitude in July 2016, and *T. zygioides* collected from Balikesir (Edremit, Kazdağları, Ortaoba village, rocky slopes), 355 m altitude in July 2016. The species were identified by Dr Selami Selvi of Balikesir University. The voucher sample is stored at the Altınoluk Vocational School, Balıkesir University, Balıkesir, Türkiye as SV 850 and SV 121, respectively. The plant samples were dried in the shade at room temperature for 15 days.

Preparation of Extracts

100 g of aerial parts of air-dried species were extracted with methanol (1 L) for 15 days. After filtration and evaporation, it was coded as TS (11.45 g) and TZ (13.23 g). All the extracts were kept at -20 °C until they were used for experimental studies.

Antioxidant activity

DPPH (1,1-diphenyl-2- picrylhydrazyl) free radical scavenging method

The free radical scavenging activity of *T. sipyleus* and *T. zygioides* essential oil and extracts was determined by the DPPH assay (Blois, 1958; Köksal et al., 2017; Miller, 1971; Ozer, 2018). Butylated hydroxyanisole (BHA) and butylated hydroxytoluene (BHT) were used as standard compounds. DPPH absorbs at 517 nm in its radical form, but upon reduction by an antioxidant or a radical species, its absorption decreases. A 0.1 mM solution of DPPH in methanol was prepared and 160 µL of this solution was added to 40 µL of the sample solutions in methanol at 10, 25, 50 and 100 µg/mL concentrations. The mixtures were kept in the dark for 30 min. The absorbance was measured at 517 nm.

β-carotene bleaching method

The antioxidant activity of *T. sipyleus* and *T. zygioides* was evaluated using *β*-carotene linoleic acid model system (Miller, 1971; Yılmaz et al., 2017). BHA and BHT were used as standard compounds. 0.5 mg *β* -carotene in 1 mL of chloroform was added to 25 µL of linoleic acid, and 200 mg of Tween 40 emulsifier mixture. After evaporation of chloroform under vacuum, 100 mL of distilled water saturated with oxygen, was through vigorous shaking. A mixture of four thousand microlitres was transferred into different test tubes containing different concentrations of the sample (10, 25, 50 and 100 µg/mL). As soon as the emulsion was added to each tube, the zero time absorbance was measured at 470 nm using a spectrophotometer. The emulsion system was incubated for 2 h at 50 °C. A blank, devoid of *β* -carotene, was prepared for background subtraction.

The CUPRAC method

The reducing capacity of *T. sipyleus* and *T. zygioides* was evaluated using the CUPRAC method (Apak et al., 2004; Bener et al., 2016; Ozer, 2018). EtOH was used as a negative control and curcumin as a positive control. Briefly, solution (1 mM DMF, 10 mM $CuCl_2$, 7.5 mM neocuproine, 1 M NH_4-CH_3COO pH 7.0), and distilled water were mixed in a 1:1:1:0.6 volume ratio. Afterward, 180 µl of the mixture was added into the wells, followed by 25 µL diluted compounds (1:20) in ethanol. The samples were held for 30 min at 25 °C. The absorbance was measured at 450 nm against a reagent blank.

Determination of the anticholinesterase activity

Determination of the anticholinesterase activity in vitro inhibition of AChE and BChE of the *T. sipyleus* and *T. zygioides* MeOH extracts were assessed by the spectrophotometric method developed by Ellman, Courtney, Andres and Featherston (Ellman et al., 1961; Reddy et al., 2015; Yılmaz et al., 2016). Galanthamine was used as a positive control. All tests were conducted in triplicate.

RESULTS and DISCUSSION

The antioxidant activities were mainly evaluated using three methods: DPPH free radical scavenging activity, *β*-carotene linoleic acid, and CUPRAC assays. In the DPPH and *β*-carotene linoleic acid assays, activities were measured at four concentrations: 10, 25, 50, and 100 µg/mL. BHA and BHT served as standards. The results are given in Table 1. In the CUPRAC, $TEAC_{CUPRAC}$ values of the extracts were calculated by using curcumin as a reference. $TEAC_{CUPRAC}$ of curcumin was found as 0.9 mmol TR g^{-1}.

To evaluate the free radical scavenging effectiveness of *T. sipyleus* and *T. zygioides* species, DPPH method was used. Methanol extracts of both sections have good antioxidant activity for all tested methods. As shown in Table 1, among the studied species, all of the extracts of *T. sipyleus* and *T. zygioides* exhibited a significant activity for *β*-carotene and DPPH methods when compared to those of BHA and BHT. In particular, *T. sipyleus* methanol extract exhibited a remarkable DPPH free radical scavenging activity with 100 µg/mL concentration. Inhibition value for the radical scavenging activity of the *T. sipyleus* methanol extract was found to be 78.79%. Also, the free radical scavenging activity of *T. sipyleus* extract was compared to that of BHA and BHT. On the other hand, inhibition values for BHA and BHT were found to be 72,74% and 81,05 %, respectively. These results indicated that the free radical scavenging effect of *T. sipyleus* methanol extract was higher than BHA. It could be concluded that the strong activity observed in that species is associated with a high amount of phenolic compounds. *T. sipyleus* methanol extract showed significant inhibition of lipid peroxidation in the *β*-carotene-linoleic acid system (72.92% inhibition at 100 µg/mL). Inhibition values of BHA and BHT were 71.99% and 81.63%, respectively.

Cu^{2+} reducing ability (CUPRAC method) is frequently used to determine the reducing powers of curcumin and methanol extracts of *T. sipyleus* and *T. zygioides* species (Figure 1). In CUPRAC method, *T. zygioides* methanol extract have better activity than the methanol extract of *T. sipyleus.*

Table 1. DPPH free radical scavenging activity and lipid peroxidation of the extracts, BHA and BHT (%inhibition)

DPPH				
Samples	**10 µg/mL**	**25 µg/mL**	**50 µg/mL**	**100 µg/mL**
TZ	24,39±9,47	26,35±11,6	65,23±3,31	70,09±4,18
TS	32,08±5,09	42,31±1,45	52,94±5,43	78,79±7,94
BHA	54,86±1,67	69,19±5,53	78,82±8,93	72,74±2,35
BHT	62,13±3,32	43,49±9,18	75,44±5,29	81,05±5,34
***β*-carotene**				
TZ	60,80±1,28	65,04±2,51	63,40±1,36	69,96±5,65
TS	67,71±1,33	66,28±8,30	66,43±1,06	72,92±2,56
BHA	55,06±1,23	62,70±7,33	71,35±3,65	71,99±6,19
BHT	55,25±14,74	56,17±10,47	59,39±5,04	81,63±16,79

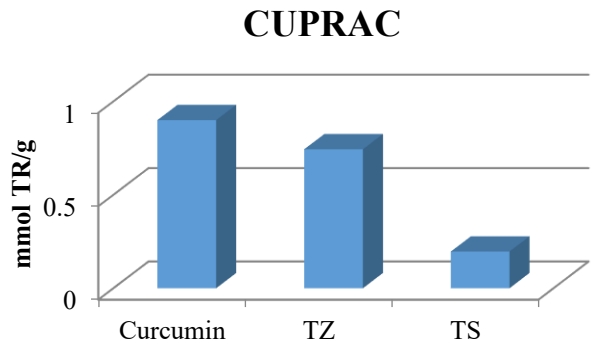


Figure 1. Cu^{2+} ion reducing power (CUPRAC) assay of the extracts and curcumin.

Acetylcholinesterase (AChE) is a crucial enzyme in the cholinergic system within both the central and peripheral nervous systems. Studies have shown that decreased levels of acetylcholine and butyrylcholine in the brain are among the most significant biochemical alterations observed in patients with Alzheimer's Disease. Consequently, one of the therapeutic strategies for Alzheimer's Disease involves the inhibition of AChE and BChE enzymes, which are responsible for the degradation of Acetylcholine and butyrylcholine (Özer et al., 2020).

Anticholinesterase activities of extracts from the species were assessed at a concentration of 200 mg/mL, with galanthamine serving as the standard compound. The results are presented in Table 2. The methanol extracts of *T. zygioides* and *T. sipyleus* showed moderate AChE (33,40 ± 3,59 and 32,19 ± 0,93%, respectively) and BChE (38,03 ± 1,94% and 47,89 ± 0,08 %, respectively) inhibitory activity.

Table 2. Anticholinesterase activity of the the extracts.

	AChE % Inhibition (200 mg/mL)	**BChE % Inhibition (200 mg/mL)**
TZ	33,4±3,59	38,03±1,94
TS	32,19±0,93	47,89±0,08
Galanthamine*	80,24 ± 0,28	80,78 ± 1,22
*Positive control		

CONCLUSION

In this study, *T. sipyleus* and *T. zygioides* methanol extracts were determined antioxidant activities and anticholinesterase properties. It was defined that the methanol extracts of these species had considerable effects in terms of the signified parameters. The fact that bioactivities such as free radical scavenging activity, *β*-carotene bleaching and anticholinesterase activities in the *T. sipyleus* extract were found to be higher than those in the *T. zygioides* extract. The data acquired in this work revealed that *T. sipyleus* and *T. zygioides* methanol extracts can be used in the food, cosmetic and pharmaceutical industries as natural antioxidants. In addition, the findings indicated that these two species were rich sources of natural AChE and BChE inhibitors. They can be used for the treatment of Alzheimer's Disease for their AChE and BChE inhibition effects.

REFERENCES

Anwar, F., Mahrye, Khan, R., Qadir, R., Saadi, S., Gruczynska-Sekowska, E., ... & Hossain Brishti, F. (2024). Exploring the biochemical and nutra-pharmaceutical prospects of some *Thymus* species–A review. Chemistry & Biodiversity, 21(7), e202400500.

Apak, R., Güçlü, K., Özyürek, M., Karademir, S. E. (2004). Novel total antioxidant capacity index for dietary polyphenols and vitamins C and E, using their cupric ion reducing capability in the presence of neocuproine: CUPRAC method. Journal of Agricultural and Food Chemistry, 52(26), 7970-7981.

Asres, Y., Hymete, A., Admassu, H., Ayalew, A., & Ayalneh, S. (2025). Optimization of supercritical fluid extraction and characterization of essential oil from Ethiopian thymus species. Journal of Food Measurement and Characterization, 1-18.

Başer, K. H. C., Özek, T., Kürkçüoğlu, M., & Duman, H. (1997). Composition of the essential oil of *Thymus subcollinus* Klokov from Turkey. Journal of Essential Oil Research, 9, 105-106.

Başer KHC, Vural M, Tümen, G., Akyalçın, F., & Satıl, F. (1995). Two new records for the flora of Turkey, Turkish Journal of Botany, 19, 489-490.

Bener, M., Shen, Y., Xu, Z., & Apak, R. (2016). Changes of the anthocyanins and antioxidant properties of concord Grape (*Vitis labrusca*) pomace after acid hydrolysis. Records of Natural Products 10(6), 794-799

Blois, M. S. (1958). Antioxidant determinations by the use of a stable free radical. Nature, 181, 1199–2000.

Davis, P. H., Mill, R. R., & Tan, K. (1988). Flora of Turkey and the Aegean Islands, Edinburgh Univ. Press.

El-Bouzidi, L., Ouchtiti, H., Ben-Bakrim, W., Benbnidak, K., Mounir, A., Khadra, A., ... & Bekkouche, K. (2025). Cytogenotoxicity assessment of the essential oils from aerial parts of *Thymus pallidus* Batt, *Thymus satureioides* Cosson, and *Thymus broussonnetii* Boiss. Journal of Essential Oil Bearing Plants, 28(3), 579-590.

Ellman, G. L., Courtney, K. D., Andres, V., & Featherston, R. M. (1961). A new and rapid colorimetric determination of acetylcholinesterase activity. Biochem Pharma, 7, 88–95.

Gökbulut, A. (2015). Validated RP-HPLC method for quantification of phenolic compounds in methanol extracts of aerial parts and roots of *Thymus sipyleus* and evaluation of antioxidant potential. Tropical Journal of Pharmaceutical Research, 14(10), 1871-1877.

Jalas, J. (1982). *Thymus*, Flora of Turkey and the East Aegean Islands, Ed. P.H.Davis, Edinburgh Univ. Press, Edinburgh.

Kaska, A., Çiçek, M., Deniz, N. & Mammadov, R. (2018). Investigation of phenolic content, antioxidant capacities, anthelmintic and cytotoxic activities of *Thymus zygioides* Griseb. Journal of Pharmaceutical Research International, 21(1), 1-13

Kindl, M., Blažeković, B., Bucar, F., & Vladimir-Knežević, S. (2015). Antioxidant and anticholinesterase potential of six *Thymus* species. Evidence-Based Complementary and Alternative Medicine, 2015(1), 403950.

Köksal, E., Bursal, E., Gülçin, İ., Korkmaz, M., Çağlayan, C., & Gören A. C. (2017). Antioxidant activity and polyphenol content of Turkish thyme (*Thymus vulgaris*) monitored by liquid chromatography and tandem mass spectrometry. International Journal of Food Properties, 20, 514–525

Llorent-Martínez, E. J., Ruiz-Medina, A., Zengin, G., Ak, G., Jugreet, S., Mahomoodally, M. F., ... & Chiavaroli, A. (2022). New biological and chemical evidences of two Lamiaceae species (*Thymbra capitata* and *Thymus sipyleus* subsp. *rosulan*s): in vitro, in silico and ex vivo approaches. Molecules, 27(24), 9029.

Miller, H. E. (1971). A simplified method for the evaluation of antioxidants. Journal of the American Oil Chemists' Society, 48, 91.

Nickavar, B., & Esbati, N. (2012). Evaluation of the antioxidant capacity and phenolic content of three *Thymus* species. Journal of Acupuncture and Meridian Studies, 5(3), 119-125.

Ozer, Z. (2018). Investigation of phenolic compounds and antioxidant activity of *Mentha spicata* subsp. *spicata* and *M. longifolia* subsp. *typhoides* (Briq.) Harley decoction and infusion. Journal of the Turkish Chemical Society, Section A: Chemistry, 5, 445-456

Özer, Z., Gören, A. C., Kılıc, T., Öncü, M., Çarıkçı, S., & Dirmenci, T. (2020). The phenolic contents, antioxidant and anticholinesterase activity of section Amaracus (Gled.) Vogel and Anatolicon Ietsw. of *Origanum* L. species. Arabian Journal of Chemistry, 13(4), 5027-5039.

Polat, Z. A., Tepe, B., & Vural, A. (2007). In vitro effectiveness of *Thymus sipyleus* subsp. *sipyleus* var. *sipyleus* on Acanthamoeba castellanii and its cytotoxic potential on corneal cells. Parasitology Research, 101(6), 1551- 1555

Reddy, N. B., Sundar, C. S., Jayaprakash, S. H., Mohan, G., Reddy, P. V., & Reddy, C. S. (2015). Synthesis and antioxidant activity of dioxazaphosphinin-2-ones. Organic Communications, 8, 17–23.

Rice-Evans, C. A., Miller, N. J., & Paganga, G. (1996). Structure-antioxidant activity relationships of flavonoids and phenolic acids. Free Radical Biology and Medicine, 20, 933-956.

Rosenova, Y., Boycheva, P., Dyankov, S., Dzhakova, Z., Dzhoglova, V., Todorova, S., ... & Slavov, I. (2025). Chemical composition of *Thymus* species from Bulgarian Flora. Diversity, 17(9), 596.

Safaei-Ghomi, J., Ebrahimabadi, A. H., Djafari-Bidgoli, Z., & Batooli, H. (2009). GC/MS analysis and in vitro antioxidant activity of essential oil and methanol extracts of *Thymus caramanicus* Jalas and its main constituent carvacrol. Food Chemistry, 115, 1524-1528.

Touaibia, M. (2025). In vitro antioxidant and anti-inflammatory properties of *Thymus algeriensis* and *Thymus dreatensis* essential oils from Algeria. Journal of Essential Oil Bearing Plants, 1-14.

Yilmaz, A., Boga, M., & Topçu, G. (2016). Novel terpenoids with potential anti-alzheimer activity from Nepeta obtusicrena. Records of Natural Products, 10(5), 530–541.

Yılmaz, H., Çarıkçı, S., Kılıc¸ T., Dirmenci, T., Arabacı, T., & Goren, A. C. (2017). Screening of chemical composition, antioxidant and anticholinesterase activity of section Brevifilamentum of *Origanum* (L.) species. Records of Natural Products, 11(5), 439–455.

2. POSTER PRESENTATIONS
2.1. ABSTRACTS

POSTER PRESENTATION

Anti-ulcer activity of pumpkin (*Cucurbita moschata* & *Cucurbita maxima*) pulp and seed extracts in rats

Djahida Hadj Merabet [1*] (Orcid: 0009-0007-7561-6159) , Meriem Saker [1] , Malika Hamiani [2], Djihene Bali[3], Salim Habi[1]

[*1] Laboratory of Physiology, Physiopathology and Biochemistry of Nutrition, University Abou Bekr BELKAID , Faculty of Natural sciences and life, earth and universe , Department of Biology , Tlemcen, Algeria
[2]University Abou Bekr BELKAID , Faculty of Natural sciences and life, earth and universe , Department of Agronomy , Tlemcen, Algeria
[3]Laboratory of Natural Products, University Abou Bekr BELKAID , Faculty of Natural sciences and life, earth and universe , Department of Biology , Tlemcen, Algeria

*Corresponding author e-mail: hadjmerabetd@gmail.com

Abstract

This study aimed to evaluate the gastroprotective and therapeutic effects of ethanolic and methanolic extracts from the pulp and seeds of two pumpkin species, *Cucurbita moschata* and *Cucurbita maxima*, against gastric ulcers induced in rats. Thirty-six rats were used to assess the impact of methanolic and ethanolic extracts administered orally at two doses (100 and 200 mg/kg) on gastric lesions provoked by ethanol and aspirin. The anti-ulcer efficacy was compared to the standard drug omeprazole. Parameters measured included the ulcer index, gastric fluid volume, pH, and total acidity. Pretreatment with all pumpkin extracts resulted in a significant and dose-dependent reduction in the ulcer index compared to the negative control group. The extracts also significantly modulated acid secretion parameters, notably reducing gastric fluid volume and total acidity while increasing pH. The ethanolic extracts from both species demonstrated superior efficacy, showing the most potent anti-ulcer activity. Qualitative phytochemical analysis revealed that these potent ethanolic extracts were rich in polyphenols and flavonoids, correlating with a high in vitro antioxidant power. The findings provide preliminary scientific evidence that *C. moschata* and *C. maxima* extracts possess significant anti-ulcer properties, attributed to their antioxidant phytoconstituents and ability to suppress gastric acid secretion. This supports the potential of pumpkin as a valuable dietary supplement or natural therapeutic agent for managing gastric ulcers.

Keywords: Pumpkin; Dietary Supplement; Gastric ulcer; Antiulcer activity; Plant Extracts; Rats

POSTER PRESENTATION

From waste to nanofibers: Pullulan-assisted electrospinning of keratin

Havva Baskan-Bayrak[1,*] (Orcid: 0000-0002-8635-666X)

[1]Sabanci University Integrated Manufacturing Technologies Research and Application Center & Composite Technologies Center of Excellence, Manufacturing Technologies, Istanbul, 34906, Turkiye

*Corresponding author e-mail: havva.baskan@sabanciuniv.edu

Abstract

Electrospinning of biopolymer-based nanofibers provides opportunities for developing sustainable and functional materials. Keratin, from abundant agricultural waste such as poultry feathers, represents a renewable and eco-friendly resource that contributes to circular economy strategies and waste valorization. Its biocompatibility and biodegradability make it highly attractive for sustainable applications; however, the relatively low molecular weight, limited solubility, and viscosity-related challenges complicate its electrospinning. Pullulan, on the other hand, is a natural polysaccharide with excellent film-forming ability, and biodegradability, making it a suitable carrier matrix for fiber formation. Therefore, in this study, to overcome with the drawbacks of keratin and enable the formation of continuous nanofibers, keratin derived from poultry feathers was blended with aqueous pullulan solutions to produce pullulan/keratin nanofibers by electrospinning. Separate pullulan and keratin solutions were prepared and blended at various volume ratios (90/10, 80/20, 70/30, 60/40, and 50/50), and the resulting mixtures were electrospun at a tip-to-collector distance of 15 cm, an applied voltage of 20–25 kV, and a flow rate of 1 mL/h. Based on the morphological characterization, SEM analysis demonstrated the formation of uniform nanofibers, with fiber diameters progressively decreasing as the keratin content increased from 728 ± 96 nm for pure pullulan to 309 ± 48 nm for the 50/50 blend. The chemical structure of the nanofibers was also examined, and FTIR-ATR analysis confirmed the incorporation of keratin through the characteristic amide II peak at 1544 cm^{-1}. Furthermore, the nanofibers were subjected to heat treatment at different temperatures and subsequently tested for water solubility, revealing that all samples rapidly dissolved upon contact with water droplets, indicating limited resistance to aqueous environments. Overall, this study demonstrates the feasibility of producing pullulan/keratin nanofibers by electrospinning, highlights the processing limitations associated with keratin content, and suggests modification strategies to enhance water resistance and functionality of such biopolymer-based nanofibers.

Keywords: Electrospinning, keratin, pullulan, waste valorization, sustainable nanofibers.

POSTER PRESENTATION

From resistance profiles to novel therapies: A systems approach to combat *Pseudomonas aeruginosa*

İrem Erguven[1*] (ORCID: https://orcid.org/0009-0002-9572-6762), Mehmet Mucahit Guncu[2] (ORCID: https://orcid.org/0000-0003-2004-8477), Kazim Yalcin Arga[1] (ORCID: https://orcid.org/0000-0002-6036-1348), Mehmet Burak Aksu[2] (ORCID: https://orcid.org/0000-0002-3439-9158), Ceyda Kula[1] (ORCID: https://orcid.org/0000-0001-7240-407X)

[*1]Marmara University, Faculty of Engineering, Department of Bioengineering, İstanbul, Türkiye.
[2]Marmara University, School of Medicine, Medical Microbiology, İstanbul, Türkiye.

*Corresponding author e-mail: iremerguven@marun.edu.tr

Abstract

Antimicrobial resistance (AMR) represents a growing global health crisis, particularly with opportunistic pathogens such as *Pseudomonas aeruginosa*. This study aims to identify novel drug candidates against antimicrobial-resistant *P. aeruginosa* strains using a molecular profiling-based approach and to evaluate their efficacy in clinical isolates with distinct genotypes and phenotypes. The project was designed within a holistic framework encompassing: (i) determination of resistance profiles of clinical isolates to selected antibiotics, (ii) transcriptome-level analysis of genome reprogramming at sub-MIC and supra-MIC doses in strains resistant to piperacillin-tazobactam, imipenem, amikacin, and levofloxacin, (iii) identification of new therapeutic targets and drug candidates, (iv) evaluation of drug susceptibility in diverse genotypic and phenotypic backgrounds, and (v) assessment of candidate effects on biofilm formation and motility. From an extensive clinical strain library, 10 isolates were initially selected via disc diffusion method. DNA isolation, ERIC and RAPD-PCR, and agarose gel electrophoresis were employed to assess clonal relationships between the selected strains. Similarity analysis was accomplished by using the algorithm Paired group and similarity measure Dice coefficient. Analysis results were visualized with a dendrogram graph and identified eight distinct strains. Their biofilm formation and eradication abilities were characterized, and minimum inhibitory concentrations (MICs) for the selected antibiotics were determined. Subsequently, strains were cultivated under sub-MIC and supra-MIC conditions, RNA was extracted, and RNA-seq–based transcriptomic profiling was initiated. This study uniquely investigates transcriptomic responses of genetically diverse *P. aeruginosa* isolates to different antibiotic concentrations, enabling the identification of both concentration-dependent and concentration-independent regulatory patterns. Unlike conventional designs, our approach integrates antibiotic exposure and dose-dependent transcriptomic profiling, providing an unprecedented opportunity to reveal drug candidates that can inhibit or eradicate biofilm production. Ultimately, this work is expected to expand the therapeutic landscape against *P. aeruginosa* by guiding the repurposing or discovery of compounds effective in overcoming resistance.

Keywords: Antimicrobial resistance, *Pseudomonas aeruginosa*, Biofilm, Transcriptome, Systems Biology

POSTER PRESENTATION

Carbon dots synthesized using eutectic solvents and tangerine peels as a sustainable carbon source

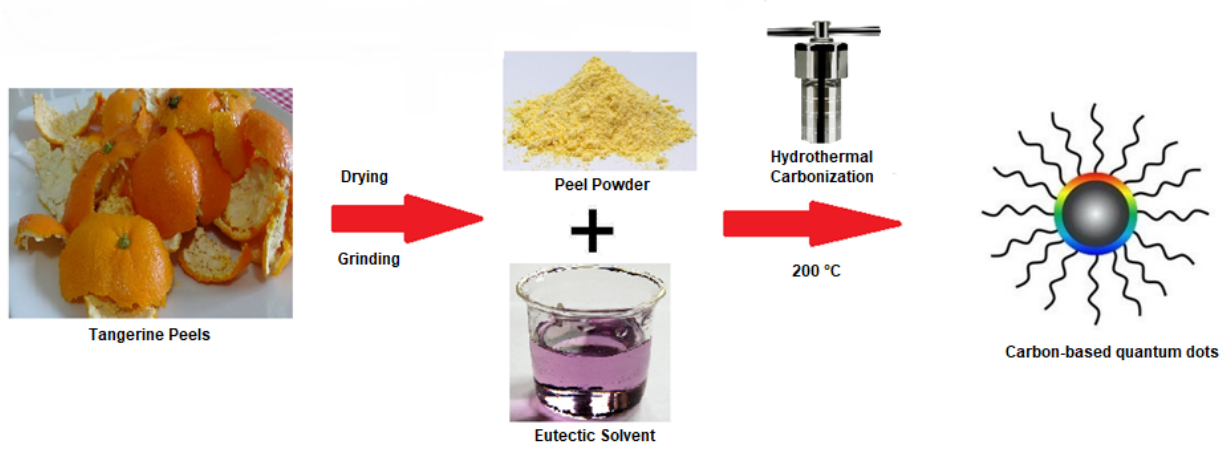
Fatma Bal[1*] (Orcid: https://orcid.org/0009-0004-9786-829.), N.Didem Kahya[2] (Orcid: https://orcid.org/0000-0001-9255-0867.)

[*1]Ankara University, Faculty of Science, Department of Chemistry, Ankara, Türkiye.
[2]Ankara University, Faculty of Science, Department of Chemistry, Ankara, Türkiye.

*Corresponding author e-mail: ftmbal@ankara.edu.tr

Abstract

Carbon dots have attracted the attention of researchers in recent years due to their various properties, which make them usable in many application areas. In this study, we investigated the use of basic waste such as tangerine peels and the effect of various eutectic solvents on the synthesis of carbon dots. The role of different synthesis conditions in the synthesis of carbon dots has been studied. Eutectic solvents played a very effective role in the carbon dots synthesis, yielding successful results. In this study, hydrothermal synthesis approach, which is a common method for the preparation of carbon dots, was preferred. The synthesized carbon dots showed a strong luminescence ability because of their prominent fluorescence under UV light. In addition, the functional groups detected on the surfaces of the synthesized carbon dots were identical those in their overall structure.



Keywords: Carbon dots, eutectic solvents, hydrothermal synthesis.

Acknowledgement: This study was supported by TÜBİTAK 2209-A [grant-number: 1919B012310746]. Fatma Bal is supported by TÜBİTAK/BİDEB 2210/A National Master Scholarship Programs.

References:

Cui, L.; Ren, X.; Sun, M.;Liu, H.; Xia, L. Carbon Dots:Synthesis, Properties and Applications. Nanomaterials 2021, 11, 3419.
Manju Kuriana, Anju Paul, 2021. Recent trends in the use of green sources for carbon dot synthesis–A short review. Carbon Trends Vol. 3. 100032.
Selda Doğan Çalhan, Melis Özge Alaş, et al., 2018. One-pot synthesis of hydrophilic and hydrophobic fluorescent carbon dots using deep eutectic solvents as designer reaction media. J Mater Sci (2018) 53:15362–15375.

POSTER PRESENTATION

Evaluation of the *in vitro* genotoxicity of potassium acetate using single-cell gel electrophoresis

Merve Yıldız[1*] (ORCID: https://orcid.org/0009-0007-5023-0532) Deniz Yüzbaşıoğlu[2] (ORCID: https://orcid.org/0000-0003-2756-7712) Fatma Ünal[2] (ORCID: https://orcid.org/0000-0002-7468-6186)

[1]Gazi University, Graduate School of Natural and Applied Sciences, Ankara, Turkey.
[2]Gazi University, Science Faculty, Department of Biology, Ankara, Turkey.

*Corresponding author e-mail: yildizmerve@gazi.edu.tr

Abstract

Acetic acid and its salts are a group used in many foods such as sweets, food supplements, yeast and yeast products, processed meat products, and sauces. Potassium acetate (PA) is a food preservative that is one of the salts of acetic acid. Genotoxicity tests help determine the genotoxic or antigenotoxic effects of various physical, chemical, and biological agents on genetic material. The single-cell gel electrophoresis assay, also known as the comet assay, can be applied to tissues that can be converted into a single-cell suspension, allowing for the detection of single and double-strand breaks in DNA, alkali-labile regions, apoptotic, and necrotic nuclei. In this study, human peripheral blood lymphocytes were treated with five doses of PA (12.5, 25, 50, 100, and 200 µg/mL) for 1 hour. Distilled water served as the negative control, and hydrogen peroxide as the positive control, in the study. Statistical analysis was performed using One-Way ANOVA. Upon examination of the results, a significant increase in comet tail length was observed with increasing concentration, except at the lowest concentration. A significant increase in comet tail intensity was observed at each concentration compared to the negative control group with increasing concentration. PA significantly increased the comet tail moment compared to the negative control at all concentrations except 12.5 and 100 µg/mL. It was concluded that PA causes genotoxic effects, especially at high doses. To draw conclusions regarding its use in foods, these findings need to be supported by other genotoxicity studies.

Keywords: Comet Assay, Food additives, Food Preservatives, Genotoxicity, Potassium acetate.

Acknowledgments: This study was financially supported by Gazi University Scientific Research Projects Coordination Unit under project number FYL-2025-10168.

POSTER PRESENTATION

Development and characterization of carbon-based flexible electrodes for electrochemical technology applications

Kaan Umut Yıldırım[1] (ORCID: https://orcid.org/0009-0006-0385-5428), Erhan Şükrü Cengiz[1] (ORCID: https://orcid.org/0009-0001-8889-0196), Ali Rıza Özkaya[1*] (ORCID: https://orcid.org/0000-0001-9863-4543)

[*1] Department of Chemistry, Marmara University, Faculty of Science,34722, Göztepe, Istanbul, Turkey

*Corresponding author e-mail: aliozkaya@marmara.edu.tr

Abstract

The rapidly increasing global energy demand and excessive consumption of fossil fuels have resulted in severe CO_2 emissions and environmental pollution. This situation has intensified the need for sustainable and clean energy production technologies. Among these, the electrochemical splitting of water into hydrogen (HER) and oxygen (OER) evolution reactions has emerged as one of the most promising carbon-free energy conversion strategies. However, the high cost and scarcity of noble-metal-based catalysts such as platinum (Pt) and iridium oxide (IrO_2) limit their large-scale application. Therefore, developing low-cost, earth-abundant, and highly active electrocatalysts has become a major focus in energy conversion research. Carbon-based composite materials have attracted great attention due to their high electrical conductivity, large surface area, and chemical stability. These materials are widely employed in energy storage, electrocatalysis, and electrochemical sensing. In particular, graphene oxide (GO) and reduced graphene oxide (rGO) can form strong interactions with nanomaterials such as metal nanoparticles and carbon dots through their surface functional groups and flexible structures. Such interactions enhance electron transfer and reduce overpotential, improving overall electrocatalytic efficiency. Electrochemical modification is an effective approach to further enhance the performance of carbon-based materials. Electrodeposition offers advantages including controllable metal loading, short processing time, and simple operation. In this study, GO was transformed into flexible rGO films through chemical reduction, followed by electrochemical activation to increase their active surface area and improve charge transfer kinetics. Subsequently, rGO films were modified in a carbon dot–metal ion bath via electrochemical deposition. The resulting composite electrodes were systematically investigated to evaluate their electrocatalytic and energy storage properties.

Keywords: Graphene Oxide, Water-Splitting, Electrodeposition

POSTER PRESENTATION

Synthesis of methylsulfonylmethane-doped hydroxyapatite for drug delivery

Tuğçe Küçükali[1*] (ORCID: https://orcid.org/0009-0000-6348-5031), Dilek Bilgiç Alkaya[2,3] (ORCID: https://orcid.org/0000-0002-7837-0250), Serap Ayaz Seyhan[2,3] (ORCID: https://orcid.org/0000-0001-5908-2766) Serap Karaderi[2](ORCID: https://orcid.org/0000-0001-7998-5065), Sümeyye Cesur Satıç[3,4] (ORCID: https://orcid.org/0000-0001-5050-1303), Oğuzhan Gündüz[3,4] (ORCID: https://orcid.org/0000-0002-9427-7574)

[1*] Marmara University,Institute of Health Sciences , Department of Analytical Chemistry, Istanbul, Turkey
[2] Marmara University, Faculty of Pharmacy, Department of Analytical Chemistry, Istanbul, Turkey
[3] Marmara University, Center for Nanotechnology & Biomaterials Application and Research (NBUAM), Istanbul, Turkey
[4] Marmara University, Faculty of Technology, Department of Metallurgical and Materials Engineering, Istanbul, Turkey

*Corresponding author e-mail: kucukalitugce@gmail.com

Abstract

Osteoarthritis is the most prevalent form of arthritis in middle-aged and elderly populations and represents a serious degenerative joint condition. Methylsulfonylmethane MSM is a widely used dietary supplement, either alone or in combination with other nutrients, and has been reported to exhibit therapeutic benefits in the management of arthritis. Bioactive materials such as hydroxyapatite HAp and other calcium phosphates have gained significant attention as advanced pharmaceutical carriers due to their combined drug delivery potential and enhanced osteoconductivity. In this study, MSM doped HAp nanoparticles were successfully synthesized via the cost-effective and controllable wet precipitation method. Structural characterization utilizing XRD and FTIR confirmed the nanometer size of the material and the successful incorporation of MSM into the HAp matrix while maintaining the core crystal structure.

Keywods: methylsulfonylmethane, hydroxyapatite, drug delivery

POSTER PRESENTATION

Identification of candidate genes associated with cold tolerance in sitka spruce (*Picea sitchensis*)

Tuğçe Önbaş[1], Katherine Steele[2]

[*1]General Directorate of Forestry, Ankara, Türkiye
[2]Bangor University, Bangor, England

* Corresponding author e-mail: tuceonbs@gmail.com

Abstract

Sitka spruce (*Picea sitchensis*), a conifer species of both economic and ecological importance, is a vital candidate for genetic selection and breeding programs due to its broad genetic diversity. However, spruce species face increasing threats from environmental changes, particularly cold stress, which significantly impairs growth and productivity by inducing mechanical and physiological damage. Plants have developed adaptive responses such as cold acclimation to mitigate these effects, yet considerable variation in cold tolerance exists among individuals, driven by underlying genetic mechanisms. This study aimed to identify gene sequences associated with cold tolerance in Sitka spruce and to determine which candidate genes warrant further investigation. Cold-responsive genes from *Arabidopsis thaliana* were used in BLAST analyses against *Picea* genomic databases to identify homologous sequences. Phylogenetic relationships were assessed using BioEdit and MEGA, while conserved motif analyses were conducted via MEME and GOMo to infer functional significance and gene ontology. Results revealed that the GIGANTEA (GI) gene showed a high level of amino acid sequence homology. Phylogenetic analyses indicated close relationships between *Picea glauca* sequences and the *A. thaliana* genes CBF1, COR314-TM2, COR6.6, and COR15A. The genes GI, GRP7, and ERD10 were found to possess highly conserved motifs specific to each gene. Notably, all three genes were associated with chloroplast-related gene ontology terms, suggesting a shared functional role in cold stress response. These findings highlight ERD10, GI, and GRP7 homologs in *P. sitchensis* as promising candidates for further research.

Keywords: Sitka spruce, cold tolerance, *Arabidopsis thaliana*, gene ontology, next-generation sequencing

POSTER PRESENTATION

Comparative analysis of EPS biosynthesis-related genes expression in *Ligilactobacillus salivarius* KC27L and *Limosilactobacillus reuteri* KC21L

Aysegül Aybüke Bayburt[1] (ORCID: https://orcid.org/0000-0002-0985-039X), Zehranur Yüksekdağ[2*] (ORCID: https://orcid.org/0000-0002-0381-5876) Berat Çınar Acar[2] (ORCID: https://orcid.org/0000-0003-4662-0865)

[1] Gazi University, Graduate School of Natural and Applied Sciences, Ankara, Türkiye.
[*2] Gazi University, Faculty of Science, Department of Biology, Ankara, Türkiye.

*Corresponding author e-mail: zehranur@gazi.edu.tr

Abstract

Exopolysaccharide (EPS) production is a key feature that enhances the probiotic potential and biotechnological value of lactic acid bacteria (LAB). EPS biosynthesis largely depends on the expression of genes such as *glycosyltransferase, epsA, epsC, epsD, flippase*, and *sugar transferase*. In this study, the expression levels of genes involved in EPS production were comparatively analyzed under standard medium (MRS, control) and optimized culture conditions that provided the highest EPS yield (for *L. salivarius* KC27L: 2% sucrose, 2% beef extract, incubation at 35°C for 18 h, pH 4.5; for *L. reuteri* KC21L: 2% sucrose, 2% peptone, incubation at 35°C for 18 h, pH 4.5). RT-PCR analyses (validated by melt curve) revealed that in *L. salivarius* KC27L, expression of *epsC* and *oligosaccharide* genes increased, whereas expression of *glycosyltransferase, epsA, epsD*, and *flippase* decreased. In *L. reuteri* KC21L, expression of *glycosyltransferase, epsA, epsC, epsD, flippase*, and *oligosaccharide flippase* genes showed an overall decrease. These findings indicate that EPS production capacity depends not only on culture conditions but also on the regulation of the corresponding biosynthetic genes. In particular, the increased expression of *epsC* and *oligosaccharide* genes suggests that they may serve as critical genetic determinants of EPS biosynthesis under optimized conditions. Overall, the results highlight that gene expression analysis is an important tool for understanding metabolic capacity and improving EPS production in LAB.

Keywords: Exopolysaccharide (EPS), *Ligilactobacillus salivarius*, *Limosilactobacillus reuteri*, EPS biosynthesis, Gene expression, qRT-PCR

Acknowledgements: This study was supported by Gazi University Scientific Research Projects Unit with the code FYL-2022-7846.
This study is a part of Ayşegül Aybüke BAYBURT's master thesis accepted by *Ligilactobacillus salivarius* KC27L ve *Limosilactobacillus reuteri* KC21L Bakterilerinde Farkli Ortam Koşullarinin Ekzopolisakkarit (EPS) Üretiminden Sorumlu Genlerin Ekspresyon Düzeylerine Etkisinin Belirlenmesi

POSTER PRESENTATION

$[Zn(Hssal)(o\text{-}bix)]_n$ kompleksinin sentezi ve X-işını tek kristal çalışması

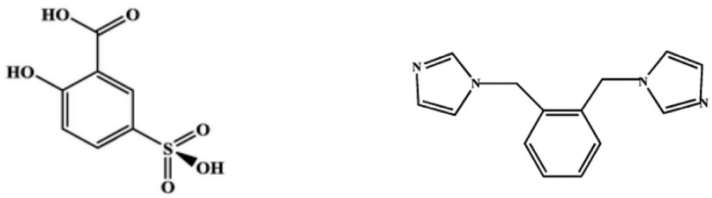
Ahmed Jamal Abbas Hajı[1*], Figen Arslan Biçer[1], Ceren Koşansu[2], Okan Zafer Yeşilel[2]

[*1]Karabük Üniversitesi, Mühendislik ve Doğa Bilimleri Fakültesi, Kimya Bölümü, Karabük, Türkiye
[2]Eskişehir Osmangazi Üniversitesi, Fen Fakültesi, Kimya Bölümü, Eskişehir, Türkiye

*Sorumlu yazar e-mail: 2328125507@ogrenci.karabuk.edu.tr

Özet

3-karboksi-4-hidroksibenzen sülfonik asit (5-sülfosalisilik asit, H_3ssal), sülfonik asit, karboksilik asit ve fenolik gruplarındaki altı potansiyel verici bölge sayesinde metal iyonlarına farklı biçimlerde koordine olabilen çok fonksiyonlu bir aromatik sülfonik asittir [1]. H_3ssal, üç farklı anyonik ligand tipi (H_2ssal^-, $Hssal^{2-}$, $ssal^{3-}$) oluşturabilir ve floresans ile proton iletkenliği gibi fiziksel özellikler sergiler [2-3]. Metal kompleksleri, serbest H_3ssal'a göre daha yüksek antimikrobiyal aktivite göstermektedir. Asimetrik yapısı nedeniyle ikinci dereceden doğrusal olmayan optik malzeme adayı olan H_3ssal, çok sayıdaki oksijen alıcısı sayesinde hidrojen bağları ve su molekülleri aracılığıyla kendi kendine düzenlenen kristal yapılar oluşturur [4]. İkincil N-verici bis(imidazol) ligandlar, $–CH_2–$ grupları sayesinde yarı rijit yapıda olup düşük boyutlu ağları daha karmaşık supramoleküler yapılara bağlamada etkilidir. Ayrıca, o-, m-, p- konumsal izomerizmleri koordinasyon polimerlerinin nihai yapısını ve özelliklerini belirgin biçimde etkiler [5].



(b)

Şekil1. 5-sülfosalisilik asit (a) ve 1,2-bis((imidazol-1-yl)metil)benzen (b) yapısı

Bu çalışmada, Zn(II) metal iyonu ile 5-sülfosalisilik asit ve 1,2-bis((imidazol-1-yl)metil)benzen kullanılarak hidrotermal olarak $[Zn(Hssal)(o\text{-}bix)]_n$ koordinasyon polimeri sentezlenmiş ve yapısı X-ışını tek kristal çalışmaları ile karakterize edilmiştir.

Anahtar Kelimeler: 5-sülfosalisilat, bis(imidazole) complexes, koordinasyon polimerleri, hidrotermal sentez, 1,2-bis((imidazol-1-yl)metil)benzen

Teşekkür: Bu çalışma Karabük Üniversitesi Bilimsel Araştırma Projeleri Koordinatörlğü tarafından KBÜBAP-25-YL-122 numaralı Yüksek Lisans Projesi kapsamında desteklenmiştir.

Kaynaklar:

1. Song, J. F., Chen, Y., Li, Z. G., Zhou, R. S., Xu, X. Y., Xu, J. Q., & Wang, T. G. (2007) *Polyhedron*, *26*(15), 4397-4410.
2. Lavrik, N. L., & Mulloev, N. U. (2010) *High energy chemistry*, *44*, 139-142.
3. Chatterjee, K., Mitra, M., Ganguly, S., Kargupta, K., & Banerjee, D. (2014) *Journal of Applied Polymer Science*, *131*(4).
4. Sun, D., Cao, R., Sun, Y., Bi, W., Li, X., Wang, Y., ... & Li, X. (2003) *Inorganic chemistry*, *42*(23), 7512-7518.
5. Biçer, F. A., Arıcı, M., & Yeşilel, O. Z. (2023) *Journal of Molecular Structure*, *1284*, 135444.

POSTER PRESENTATION

{[Cd(DTPA)(bpy)]H_2O}$_n$ kompleksinin sentezi ve X-Işını tek kristal çalışması

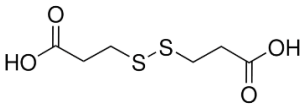
Maryam Jamal Abbas Hajı[1*], Figen Arslan Biçer[1], Ceren Koşansu[2], Okan Zafer Yeşilel[2]

[*1]Karabük Üniversitesi, Mühendislik ve Doğa Bilimleri Fakültesi, Kimya Bölümü, Karabük, Türkiye
[2]Eskişehir Osmangazi Üniversitesi, Fen Fakültesi, Kimya Bölümü, Eskişehir, Türkiye

*Sorumlu yazar e-mail: 2328125506@ogrenci.karabuk.edu.tr

Özet:

3,3-Ditiyodipropiyonik asit (DTDP) (Şekil 1), biyoteknolojik açıdan mikrobiyal olarak sentezlenen politiyoesterlerin (PTE'lerin) üretiminde öncü substrat olarak kullanılmasından dolayı önem taşımaktadır. DTDP, elektrokimyasal ve termodinamik araştırmalarda, ikincil pillerin geliştirilmesinde, amino asit analizlerinde kullanılmanın yanısıra kendiliğinden düzenlenen yapıların oluşturulmasında da tercih edilmektedir [1]. Bu ligant, hem şelatlayıcı hem de köprüleyici modlarda davranarak farklı anyonik türler oluşturabilir ve metal komplekslerinin kararlılığını arttırabilir. Öte yandan, 4,4′-bipiridin (bpy) sert N-verici merkezleri ile yarı rijit lineer yapısı, düşük boyutlu birimlerin zincir benzeri koordinasyon polimerlerine dönüşmesini kolaylaştırır [2-3].



Şekil 1. 3,3′-ditiyodipropiyonik asit ligantının yapısı

Bu çalışmada, Cd(II) metal iyonu ile 3,3′-ditiyodipropiyonik asit ve 4,4′-bipiridin ligandları kullanılarak {[Cd(DTPA)(bpy)]H_2O}$_n$ koordinasyon polimeri sentezlenmiştir. Elde edilen kompleksin kristal yapısı X-ışını tek kristal difraksiyon yöntemiyle aydınlatılmış ve Cd(II) iyonunun bozulmuş oktahedral geometriye sahip olduğu belirlenmiştir. DTPA ligantı karboksil oksijenleri üzerinden üç dişli köprü ligant olarak davranırken bpy ligantı aksiyel koordinasyondadır. Hidrat su molekülleriyle kurulan hidrojen bağları, supramoleküler yapıyı ek olarak stabilize etmektedir. Bu sonuçlar, Cd(II) iyonlarının karışık O- ve N-verici ligantların karışık ligantlı koordinasyon çeşitliliğine yeni bir örnek sunmaktadır.

Anahtar kelimeler: 3,3′-ditiyodipropiyonik asit**,** Cd(II) kompleksleri, bipiridin türevleri, koordinasyon polimerleri, tek kristal X-ışını analizi.

Teşekkür: Bu çalışma Karabük Üniversitesi Bilimsel Araştırma Projeleri Koordinatörlğü tarafından KBÜBAP-25-YL-126 numaralı Yüksek Lisans Projesi kapsamında desteklenmiştir.

Kaynaklar:
1. Wübbeler, J. H., Bruland, N., Kretschmer, K., & Steinbüchel, A. (2008). *Applied and environmental microbiology*, *74*(13), 4028-4035.
2. Zhu, Y., Wang, L., Li, J., Shi, X., Deng, Z., and Zhang, H., (2025), *Journal Of Molecular Structure*, 1320: 139719.
3. Su, X., Zhang, Y., Yin, H., Liu, L., Zhang, Y., Wu, L., Zhang, Q., Wang, C., Zhang, L., and Zhang, Y. (2019) *Journal Of Molecular Structure*, 1177: 107-116.

POSTER PRESENTATION

The effect of orlistat on nitric oxide levels in LPS+IFN-ɣ-stimulated RAW 264.7 macrophage cells

Büşra Altay[1*](*Orcıd:https://orcid.org/0009-0009-1077-7909*),
Aslı Koç[2] (*Orcid*:*https://orcid.org/0000-0002-4679-9079)*

[1*]Ankara University, Faculty of Pharmacy, Department of Biochemistry, Ankara, Turkey
[1*]Ankara University, Institute of Health Sciences, Ankara, Turkey
[2*]Ankara University, Faculty of Pharmacy, Department of Biochemistry, Ankara, Turkey

*Corresponding author e-mail: busrafirat02@gmail.com

Abstract

Excessive nitric oxide (NO) production upon macrophage activation plays a critical role in the pathophysiology of inflammatory processes. This study aimed to investigate the potential anti-inflammatory effects of Orlistat, a lipase inhibitor, on NO synthesis in LPS/IFN-ɣ-stimulated RAW 264.7 macrophages. An inflammation model was established by stimulating the cells for 20 hours with a combination of 100 ng/mL LPS and 2.5 ng/mL IFN-ɣ per well. The efficacy of Orlistat (0.625 µM and 1.25 µM) was evaluated at four different time points: two protective protocols (1-hour and 20-hour pre-incubation with Orlistat) and two therapeutic protocols (1-hour and 20-hour Orlistat application after LPS/IFN-ɣ stimulation). Nitrite levels in cell culture supernatants, an indicator of NO production, were measured spectrophotometrically using Griess reagent. Our findings confirmed that LPS/IFN-ɣ stimulation triggered a statistically significant ($p < 0.05$) increase in nitrite levels compared to the unstimulated control group. However, in all tested application protocols and at both Orlistat doses (0.625 µM and 1.25 µM), no statistically significant inhibition of this high NO production was observed. These results indicate that the low-dose Orlistat used was unable to exert sufficient suppressive effects on inducible nitric oxide synthase (iNOS) expression or activity. In conclusion, further *in vitro* studies using formulations with optimized solubility across a wider dose range (especially at higher concentrations) are needed to clearly assess the anti-inflammatory potential of Orlistat.

Keywords: Orlistat, Nitric Oxide, LPS/IFN-ɣ, RAW 264.7

Acknowledgment: This study was supported by the Scientific and Technological Research Council of Turkey (TÜBİTAK 2211-A General National PhD Scholarship Program). This work was also supported by Ankara University Scientific Research Projects Coordination Unit under project number TDK-2024-3444.

POSTER PRESENTATION

Antileukemic potential of *Nerium oleander* L. extract: Cytotoxic and apoptotic effects on leukemia cells

Belgin Sever [1,2,*] (ORCID: https://orcid.org/0000-0003-4847-9711), Ayben Erkan [3] (ORCID: https://orcid.org/0009-0006-3981-9971), Bahar Ozer [3] (ORCID: https://orcid.org/0009-0006-9965-3547), Nermin Sarıgül [3] (ORCID: https://orcid.org/0000-0001-9526-3310), Damla Bayana [4] (ORCID: https://orcid.org/0000-0003-0466-7470), Selinay Başak Erdemli Köse [5] (ORCID: https://orcid.org/0000-0001-8986-585X), Tulay Tutenocakli [6] (ORCID: https://orcid.org/0000-0002-9795-1034), Yalcin Coskun [6] (ORCID: https://orcid.org/0000-0002-1764-1731), Ayhan Oral [7] (ORCID: https://orcid.org/0000-0003-4965-8754), Masami Otsuka [2,8] (ORCID: https://orcid.org/0000-0002-2968-3939), Mikako Fujita [2] (ORCID: https://orcid.org/0000-0001-6705-4052), Halilibrahim Ciftci [2,3,8] (ORCID: https://orcid.org/0000-0002-9796-7669)

[*1] Anadolu University, Faculty of Pharmacy, Department of Pharmaceutical Chemistry, Eskisehir 26470, Türkiye
[2] Kumamoto University, Faculty of Life Sciences, Medicinal and Biological Chemistry Science Farm Joint Research Laboratory, Kumamoto 862-0973, Japan
[3] Burdur Mehmet Akif Ersoy University, Department of Molecular Biology and Genetics, Burdur 15200, Türkiye
[4] Burdur Mehmet Akif Ersoy University, Research and Development Coordination Office, Burdur 15200, Türkiye
[5] Burdur Mehmet Akif Ersoy University, Faculty of Arts and Science, Department of Chemistry, Burdur 15200, Türkiye
[6] Canakkale Onsekiz Mart University, Lapseki Vocational School, Department of Plant Production and Animal Production Programs, Canakkale 17800, Türkiye
[7] Canakkale Onsekiz Mart University, Faculty of Science, Department of Chemistry, Canakkale 17800, Türkiye
[8] Department of Drug Discovery, Science Farm Ltd., Kumamoto 862-0976, Japan

*Corresponding author e-mail: belginsever@anadolu.edu.tr

Abstract

Chronic myeloid leukemia (CML) is marked by the excessive growth of myeloid granulocytic cells in the bone marrow. The driving force behind this disease is the Bcr-Abl fusion protein, formed through a reciprocal translocation between the Abl gene on chromosome 9 and the Bcr gene on chromosome 22. This resulting Bcr-Abl1 oncoprotein exhibits continuously active tyrosine kinase activity, triggering cancer-promoting signaling pathways that enhance cell growth and suppress apoptosis. Tyrosine kinase inhibitors (TKIs) remain the cornerstone of CML treatment, providing improved survival and fewer side effects. However, resistance, often driven by mutations in the Bcr-Abl kinase domain, continues to pose a major clinical challenge. This underscores the urgent need for novel therapies that enhance treatment response, prevent resistance, and minimize toxicity. Consequently, there is growing interest in developing safer, natural-origin compounds as promising alternatives in anticancer therapy. *Nerium oleander*, a plant from the Apocynaceae family, is rich in various phytochemicals with broad therapeutic and pharmacological properties, including notable anticancer potential. In this study, *Nerium oleander* L. (MP-15) was collected from Burdur, Türkiye, and extracted with 70% ethanol. The extract's cytotoxic effects were assessed in vitro using the MTT assay on K562 and HL-60 leukemia cell lines, as well as on healthy peripheral blood mononuclear cells (PBMCs). According to the results, MP-15 demonstrated strong cytotoxic activity against K562 CML cells, with an IC_{50} value of 1.10 ± 0.42 µg/mL, outperforming imatinib ($IC_{50} = 3.84 \pm 1.04$ µg/mL), while showing less toxicity toward healthy PBMCs ($IC_{50} = 28.20 \pm 4.41$ µg/mL; Selectivity Index = 25.6). MP-15 also exhibited cytotoxic effects on HL-60 cells, with an IC_{50} of 8.53 ± 1.46 µg/mL. The apoptotic effects of MP-15 on K562 cells were further assessed using Annexin V/ethidium homodimer-III staining. After 24 hours of treatment, fluorescence microscopy of Annexin V-positive cells revealed that MP-15 induced strong apoptosis in K562 cells.

Keywords: CML, Bcr-Abl, Natural Product, Plant Extract, Apoptosis, Drug development

POSTER PRESENTATION

Yeni benzaldehit türevi Schiff bazı sentezi ve yapılarının spektroskopik yöntemlerle karakterizasyonu

Gözde Bulut[1*] (Orcid: https://orcid.org/0009-0004-9323-8989)
Seyhan Öztürk[2] (Orcid: https://orcid.org/0000-0003-4638-5578)

[*1]Ondokuz Mayıs Üniversitesi, Fen Fakültesi, Kimya Bölümü, Samsun, Türkiye
[2]Ondokuz Mayıs Üniversitesi, Fen Fakültesi, Kimya Bölümü, Samsun, Türkiye

*Sorumlu yazar e-mail: 55gzdbulut@gmail.com

Özet

Schiff bazları, imin (C=N) fonksiyonel grubunu içeren ve geçiş metalleriyle kararlı kompleksler oluşturabilen önemli organik ligandlardır. Geniş biyolojik ve katalitik uygulama alanları nedeniyle yeni Schiff bazı türevlerinin sentezi ve karakterizasyonu literatürde önemli bir araştırma alanı oluşturmaktadır. Bu çalışma, benzaldehit türevlerinden 3 yeni Schiff bazı ligandının sentezlenmesini ve spektroskopik yöntemlerle karakterize edilmesini amaçlamaktadır. Sentezlerde; (1) 2-brombenzaldehit + 2-amino-4-nitrofenol, (2) 2-brom-5-metoksibenzaldehit + 2-amino-4-nitrofenol ve (3) 2-brom-5-metoksibenzaldehit + 2-aminofenol reaksiyonları kullanılmıştır. Bileşikler etanol çözeltisi içerisinde geri soğutucu altında 80 °C'de 6 saat kaynatılarak hazırlanmış, süzülüp kurutularak kristal formda izole edilmiştir. Sentezlenen Schiff bazlarının yapısal karakterizasyonu erime noktası tayini, FT-IR ve UV-Vis spektroskopisi ile gerçekleştirilmiştir. FT-IR analizlerinde karakteristik C=N gerilme bandı gözlenmiş; UV-Vis verileri bileşiklerin konjuge sistemlerine bağlı elektronik geçişleri doğrulamıştır. Çalışmanın ileri aşamasında, elde edilen bu yeni ligandların çeşitli geçiş metalleriyle kompleks reaksiyonları gerçekleştirilerek ilgili metal komplekslerinin sentezi ve karakterizasyonunun yapılması planlanmaktadır. Elde edilen sonuçların yeni ligand tasarımlarına ve potansiyel uygulama alanlarına katkı sağlaması beklenmektedir.

Anahtar kelimeler: Schiff bazı, Benzaldehit türevleri, Spektroskopik karakterizasyon

POSTER PRESENTATION

Literature-based analysis of cytotoxic and genotoxic effects of microplastic exposure

Derya Binay[1*] (Orcıd: https://orcid.org/0000-0002-0277-761X), Fatma Ünal[2] (Orcıd: https://orcid.org/0000-0001-7648-9584), Deniz Yüzbaşıoğlu[2] (Orcıd: https://orcid.org/0000-0003-2756-7712)

[1] Gazi University, Graduate School of Natural and Applied Sciences, Department of Biology, Ankara, Türkiye.
[2]Gazi University, Science Faculty, Department of Biology, Ankara, Türkiye.

*Corresponding author e-mail: deryabinay.53@gmail.com

Abstract

Due to the rapid increase in global population, industrialization, and fast-paced consumption patterns, plastic use has become an integral component of modern life. Plastics are widely employed in various sectors, including packaging, cosmetics, medical devices, and electronics, due to their lightweight nature, durability, low cost, and ease of production. Microplastics (MP), defined as particles ≤5 mm, are categorized as primary and secondary. Primary MPs are intentionally manufactured in small sizes for use in cosmetics, cleaning products, and industrial applications. Secondary MPs emerge from the environmental degradation of larger plastic materials through sunlight, mechanical abrasion, and other external factors. These particles vary in size, shape, and chemical composition, enabling their widespread distribution across ecological systems. Humans and other organisms are exposed to MPs through inhalation, ingestion, dermal contact, and various environmental pathways. Once internalized, MPs may accumulate in tissues, inducing cellular, biochemical, and genetic alterations. This study aims to systematically evaluate research conducted between 2019 and 2025 that investigated the genotoxic potential of MP using chromosome aberration (CA), cytokinesis-block micronucleus (CBMN), and comet assays. The reviewed literature consistently demonstrates that MP exposure poses notable genotoxic hazards, either through direct interactions with DNA or indirectly by triggering oxidative stress. MPs can disrupt redox homeostasis by increasing the production of reactive oxygen and nitrogen species (ROS/RNS), leading to lipid peroxidation, protein oxidation, and DNA base modifications or strand breaks. Inadequate DNA repair further contributes to genomic instability, chromosome aberrations, micronucleus formation, and potentially carcinogenesis, as well as neurotoxic, immunotoxic, and hepatotoxic outcomes. Overall, the findings indicate that MPs may pose significant cytotoxic and genotoxic risks to environmental and human health, with toxicity influenced by particle size, shape, surface characteristics, and chemical composition. More comprehensive and mechanistic studies are required to elucidate better the genotoxic pathways and long-term biological consequences associated with MP exposure.

Keywords: Microplastic, cytotoxicity, genotoxicity, chromosome abnormality, micronucleus, DNA damage

POSTER PRESENTATION

Effect of PLGA–PEG–based *Hypericum perforatum* extract nanoparticles targeted with panitumumab in colorectal cancer cells

Sude Uveyik[1] (https://orcid.org/0009-0002-4726-0873), Fatma YURT [1,2*] (https://orcid.org/0000-0002-9394-6908)

[1]Ege University, Institute of Natural and Applied Sciences, Department of Biotechnology, 35100, Izmir, Turkey.
[*2]Ege University, Institute of Nuclear Science, Department of Nuclear Applications, Bornova, 35100, Izmir, Turkey

*Corresponding author e-mail: fatma.yurt.lambrecht@ege.edu.tr

Abstract

Colorectal cancer is among the most prevalent malignancies worldwide and is particularly notable for its limited therapeutic response in advanced stages. In this study, Hypericum perforatum (HP) extract, possessing potential for photodynamic therapy (PDT), together with the EGFR-targeting monoclonal antibody Panitumumab within the same nanosystem, was aimed to evaluate for the treatment of colorectal cancer. Accordingly, PLGA–PEG–based nanoparticles were prepared for HP loading using a double emulsion (W/O/W) technique, while Panitumumab was conjugated onto the nanoparticle surface through EDC/NHS-mediated covalent coupling. Dynamic light scattering measurements revealed that the PLGA–HP nanoparticles exhibited an average hydrodynamic diameter of 158 ± 5 nm, a main peak size of 187 ± 3 nm, and a PDI value of 0.218 ± 0.02, confirming a monodisperse distribution profile. The zeta potential of the Panitumumab-modified nanosystem was approximately –30 mV, indicating a surface charge consistent with electrostatic colloidal stability. FTIR analysis demonstrated characteristic changes in the 1650 cm^{-1} (Amide I) and 1540 cm^{-1} (Amide II) regions, along with a detectable shift in the ester C=O band at 1750 cm^{-1}, collectively confirming the successful covalent bound of the antibody onto the polymeric matrix. According to the BCA protein assay, the average conjugation efficiency was 27.29%, corresponding to 32.97 µg of Panitumumab per 1 mg of nanoparticles. HP release studies indicated higher cumulative release values under acidic conditions (pH 5.5) than at physiological pH (7.4), demonstrating a time-dependent and controlled release behavior. Overall, the findings show that HP and Panitumumab can be co-delivered effectively within a single polymeric nanosystem, and in vitro studies on the HT-29 colorectal cancer cell line are currently underway

Keywords: PLGA–PEG, Panitumumab, *Hypericum perforatum*, colorectal cancer, nanoparticles

Acknowledgment:
This work was supported by the Scientific Research Projects Commission of Ege University (BAP, Grant No. 35057).

POSTER PRESENTATION

Investigating the role of *COL1A1* and *FN1* gene expression in cisplatin-resistant ovarian cancer

Dayana Muaaz[1] (https://orcid.org/0009-0004-7307-7604), Yalda Hekmatshoar[2*] (https://orcid.org/0000-0003-4683-074X)

[1]Altinbas University, Institute of Graduate Studies, Biomedical Science Department, Istanbul, Türkiye.
[*2]Altinbas University, School of Medicine, Medical biology Department, Istanbul, Türkiye.

* Corresponding author e-mail: yalda.hekmatshoar@altinbas.edu.tr:

Abstract

Ovarian cancer is considered one of the most common gynaecological cancers with a high mortality rate that is developed across the world after cervical cancer and uterine cancer. One of the main causes of failure in the ovarian cancer therapy is the development of chemoresistance. Cisplatin, a widely used chemotherapeutic agent for multiple human cancers, acts primarily by forming DNA cross-links that generate DNA adducts and ultimately block DNA repair in cancer cells. Although cisplatin is a first-line treatment, one of the biggest clinical issues is its resistance. This study investigated the involvement of two extracellular matrix (ECM) genes, *COL1A1* and *FN1*, in ovarian cancer that is resistant to cisplatin (A2780). A2780 cell lines were cultured in in RPMI-1640 medium. Moreover, RNA isolation, cDNA synthesis, qRT- PCR were performed respectively. Using quantitative real-time PCR (qRT-PCR), we investigated *FN1* and *COL1A1* genes expression levels in the human ovarian cancer cell line A2780 and its cisplatin-resistant variant A2780-R. The decreased *FN1* and *COL1A1* expression observed in cisplatin-resistant ovarian cells may reflect a cell-specific adaptive response, potentially influenced by differences in cisplatin dosing or exposure conditions that alter extracellular-matrix–related gene regulation. Cisplatin dose and the pattern of its administration can influence how cancer cells respond different dosing regimes may affect development of cisplatin resistance and therapeutic outcomes

Keywords: Ovarian Cancer, Cisplatin Resistance, *COL1A1*, *FN1*, Gene Expression, A2780 Cell Line.

POSTER PRESENTATION

Examination of the capacitive properties of reduced graphene oxide based electrodes functionalized with isonitrosoacetophenone derivatives

Ömer Yıldız[1*] (*ORCID: https://orcid.org/0009-0008-7545-74310009-0008-7545-7431*), Tolga Göktürk[2] (*ORCID: https://orcid.org/0000-0002-7234-8079*), Tuğba Ören Varol[1] (*ORCID: https://orcid.org/0000-0003-3680-5743*)

[*1]Muğla Sıtkı Koçman University, Faculty of Science, Chemistry Department, Kötekli/Muğla, Türkiye.

*Corresponding author e-mail: yildizomer235@gmail.com

Abstract

Nowadays, increasing energy demand and environmental challenges require the development of sustainable, clean, and high-performance energy storage systems. In this context, owing to their high power density, long cycle life, and rapid charge-discharge capabilities, supercapacitors stand out as promising energy storage devices and the development of new materials with increased power density, cycle life, and charge-discharge capabilities is crucial in this area. Graphene and graphene oxide have been extensively used for energy storage devices due to their improved mechanical properties, large surface area and electrical conductivity. However, charge storage mechanism of these nanomaterials may be affected by the lack of a redox site, exhibiting lower capacitance values in comparison with active carbon. In order to solve the mentioned issue, several techniques such as doping, modification and functionalization have been highly encouraged [1]. Within this motivation, in this study*, firstly, graphene oxide was synthesized by Hummer's method and then a chemical reduction method with hydrazine monohydrate was used to obtain reduced graphene oxide (rGO). In order to prepare functionalized rGO structures, two types of pre-synthesized isonitrosoacetophenone derivative (INAP and Me-INAP) were separately interacted with RGO by applying ultrasonication through a non-covalent functionalization strategy [2]. After the examination of the structural and morphological properties of the prepared materials, drop-casting technique was applied for the preparation of the modified carbon paste electrodes. Capacitive properties of INAP and Me-INAP functionalized rGO based electrodes were investigated by cyclic voltammetry in 2M H_2SO_4, 2M KOH and 2M Na_2SO_4 and specific capacitance values were calculated for acidic, alkaline and neutral medium. The obtained results revealed the efficiency of INAP and Me-INAP functionalized RGO as a promising alternative material in the field of energy storage for future applications.

Keywords: Reduced graphene oxide, non-covalent functionalization, energy storage, supercapacitor.

(*) This study has been produced from Master's Thesis of Ömer Yıldız.

References

1. Srinivasan, S., Kittappa, G., Sundramoorthy, A. K., Rajendran, G. K., Nesakumar, N., & Gunasekaran, B. M. (2025). Covalently linked 4-Aminopyridine on reduced graphene oxide for high performance electrochemical supercapacitor electrode material. Journal of Molecular Structure, 1321, 140225.

2. Göktürk, T., Hökelek, T., Karaman, S. G., Ağar, H., Aksu, E. N., Çetin, E. S., Canlı, E. & Güp, R. (2025). Syntheses of novel 1, 2, 3-triazole-based Schiff base ligands and their Co (II) complexes: DNA/BSA binding, DNA cleavage, topoisomerase IIα inhibition and cytotoxicity studies. Inorganic Chemistry Communications, 115544.

POSTER PRESENTATION

Expression analysis of PCBB and IVD genes in metastatic prostate cancer

Safa Ahmed A Abudaya[1] (https://orcid.org/0009-0004-6798-0151), Yalda Hekmatshoar [2*] (https://orcid.org/0000-0003-4683-074X)

[1]Altinbas University, Institute of Graduate Studies, Biomedical Science Department, Istanbul, Türkiye.
[2] Altinbas University, School of Medicine, Medical Biology Department, Istanbul, Türkiye.

*Corresponding author e-mail: yalda.hekmatshoar@altinbas.edu.tr

Abstract

Prostate cancer remains a leading cause of cancer-related mortality in men worldwide, exhibiting heterogeneous biological behavior from indolent to highly metastatic forms. Metastasis is the critical event determining prostate cancer prognosis and is responsible for the majority of prostate cancer–related deaths worldwide. While localized tumors are often manageable, metastatic spread renders the disease largely incurable. Understanding the molecular mechanisms driving this progression is essential for improving diagnostic and therapeutic strategies. This study investigated the expression profiles of the PCBB and IVD genes in prostate cancer cell lines representing distinct disease stages: PC3 and LNCaP. Following total RNA isolation, cDNA synthesis, and quantitative real-time PCR analysis, PCBB expression was significantly reduced in PC3 cells compared to LNCaP cells, suggesting a potential association between PCBB downregulation and metastatic phenotype. In contrast, IVD expression showed no statistically significant difference between the cell lines, indicating stable transcription across disease stages. These findings highlight the possible involvement of PCBB in molecular alterations linked to prostate cancer metastasis and underscore its potential value for future diagnostic or prognostic research.

Keywords: Prostate Cancer; PCBB; IVD; Metastasis; Gene Expression; RT-qPCR.

POSTER PRESENTATION

Efficacy of rosmarinic acid in reducing symptoms of acne vulgaris: Case study

Wioleta Faruga-Lewicka[1], Oliwia Kaczmarczyk[2], Wiktoria Kapica[2], Paulina Frątczak[2], Kamila Dutkiewicz[2], Julia Skwara[2], Jonatan Filarowicz[2], Julia Kościołek[2], Marek Kardas[1]

Zakład Technologii i Oceny Jakości Żywności w Zabrzu, Śląski Uniwersytet Medyczny
Śląska Wyższa Szkoła Medyczna w Katowicach, Koło Naukowe Skóra holistycznie

Abstract

Rosmarinic acid is becoming increasingly popular in cosmetology. It has been shown to inhibit elastase activity, thus preventing the degradation of elastin fibres. In addition, it has a purifying effect, reduces sebum secretion and inhibits excessive bacterial activity, so it appears to be an ingredient with beneficial effects in the treatment of acne vulgaris. The study involved evaluating the efficacy of rosmarinic acid 5% in reducing symptoms of acne vulgaris. Five women between the ages of 18 and 25 were enrolled in the study. Each had a diagnosis of acne vulgaris by a dermatologist and was not currently undergoing dermatological or any cosmetic treatment. The GEA (Global Acne Severity) and GAGS (Global Acne Grading System) scales were used to assess the severity of acne. The probands underwent 4 treatments at 2-week intervals. After a series of 4 treatments with 5% rosmarinic acid, improvements were observed in each proband. This was a reduction in inflammation, papules, pimples and blackheads. The clients' mean GAGS score before therapy was 23.8± 6.4, while after therapy it was 15.8± 7.03. On the GEA scale, the mean score before therapy was 2.8±0.75, while after therapy it was 2.0±0.63. These differences were statistically significant. Rosmarinic acid at a concentration of 5% showed high efficacy in reducing symptoms of acne vulgaris, as indicated by the results obtained in the GEA and GAGS scales. No irritant or other side effects were observed. More studies are needed to confirm its effectiveness.

Keywords: acne vulgaris; rosmarinic acid; GAGS; GEA;

POSTER PRESENTATION

Bazı N-(4-sübstitüearil) maleimit bileşiklerinin sentezi ve asit katalizli hidroliz reaksiyon mekanizmasının araştırılması

Emre Hasten* (Orcid: https://orcid.org/0009-0009-0280-5412),
Halil Kütük (Orcid: https://orcid.org/0000-0002-8135-7874)

Ondokuz Mayıs Üniversitesi, Fen Fakültesi, Kimya Bölümü, Samsun, Türkiye

*Sorumlu yazar e-mail: emrehasten518@gmail.com

Özet

Bu çalışmada N-(Fenil)maleimit, N-(4-Klorofenil)maleimit ve N-(4-Metilfenil)maleimit bileşikleri sentez edildi ve kinetik çalışma için asetonitrilde stok çözeltileri hazırlandı. Sentezlenen bileşiklerin asit katalizli hidrolizleri H_2SO_4, $HClO_4$ ve HCl çözeltilerinde 35.0±0.1°C' de incelendi. Elde edilen verilere Aşırı Asitlik metodu, aktivasyon entropisi ve sübstitüent etkisi uygulandığında farklı asit konsantrasyonlarında A-2 mekanizması ile uyumlu olduğu görüldü. Çalışılan bileşiklerin asit katalizli hidrolizlerinde kullanılan asitlerin katalitik etkileri farklı asit konsantrasyonlarında $HCl > H_2SO_4 > HClO_4$ sırasındadır. Bu sıralama A-2 mekanizması için karakteristiktir.

Anahtar Kelimeler: Aşırı Asitlik, Hidroliz, Asit kataliz, Aktivasyon entropisi, Sübstitüent etki.

POSTER PRESENTATION

Cloning and expression of the *Ananas comosus Bromelain* gene in *Escherichia coli*

Burcu Arıkan[1*](https://orcid.org/0000-0002-8973-0813), Çağla Akman[1](https://orcid.org/0009-0008-6085-9147), Ezgi Nur Çatı[1](https://orcid.org/0009-0005-1875-2088)

[*1]Istanbul University, Faculty of Science, Department of Molecular Biology and Genetics, Istanbul, Türkiye.

[*]Corresponding author e-mail: burcuarikan@istanbul.edu.tr

Abstract

Plants serve as valuable sources of raw materials and enzymes, and have been explored for these purposes for decades. However, challenges associated with plant cultivation, labor-intensive extraction processes, and contamination risks have driven a shift toward microbial production systems. Advances in biotechnology, especially gene cloning, that allowed the transfer and overexpression of target protein-coding regions in bacterial hosts have enabled the efficient microbial production of enzymes of plant origin. Plant-derived enzymes have been gaining industrial importance due to ethical, religious, and cultural preferences, their potentially lower allergenicity compared to animal-based proteins, and their wide range of applications. Bromelain, a cysteine protease with significant industrial and biomedical importance, is increasingly in demand. It possesses a broad range of therapeutic applications due to its fibrinolytic, anti-inflammatory, anticoagulant, analgesic, immunomodulatory, anticancer, and wound-healing properties and finds wide applications in food-processing, including meat tenderization and gluten-free flour production, textile, and cosmetic industries. Previous studies have shown that pineapple (*Ananas comosus*) fruit and stem tissues contain high bromelain activity. In contrast, crown leaves, typically considered agricultural waste, represent an underutilized biomass source, and their biotechnological valorization for enzyme production offers both economic and environmental advantages. This study aimed to clone the *Bromelain* gene, isolated from the *Ananas comosus* crown leaf into *E. coli* using recombinant DNA technology, and to confirm recombinant protein expression via SDS-PAGE analysis. The findings are expected to support optimization efforts in industrial bromelain production and to contribute to the expanding body of literature in plant-based enzyme biotechnology.

Keywords: Bromelain, *Ananas comosus*, gene cloning, enzyme production, biotechnology.

POSTER PRESENTATION

Development of clay-based kserogel structures for thermal energy storage systems

[1] Yaren İlayda Gürkan (*Orcid: https://orcid.org/0009-0006-5617-5143.*)
[1–2]Bilge Coşkuner Filiz (https://orcid.org/0000-0002-2737-119X),

[1] Yıldız Technical University, Clean Energy Institute, Advanced Energy Technologies, İstanbul, Turkiye
[2] Yıldız Technical University, Metallurgical and Materials Engineering, İstanbul, Turkiye

Corresponding author e-mail: ilayda.gurkan@std.yildiz.edu.tr
coskuner@yildiz.edu.tr

Abstract

Effective Thermal Energy Storage (TES) solutions are crucial for increasing energy efficiency and integrating renewable energy sources into thermal systems. Phase Change Materials (PCMs), with their high energy storage density, are promising candidates in this context. However, drawbacks such as leakage in the liquid phase and low thermal conductivity restrict their widespread commercial application. The objective of this study is to develop a porous hybrid supporting matrix utilizing the synergy of organic (PVA) and inorganic (Diatomite and Kaolin) components, capable of encapsulating PCMs without leakage. Mixtures prepared with varying ratios of Diatomite, Kaolin, and Polyvinyl Alcohol (PVA) were processed using the lyophilization (freeze-drying) technique. This method employs ice crystals as porogens, resulting in highly porous, open-celled scaffolds (matrices) with high surface area. A systematic optimization approach, featuring 12 different blend compositions, has been undertaken to study the effect of the Diatomite/Kaolin/PVA ratio. This systematic ratio analysis is critical for determining the optimal hybrid composition that maximizes the mechanical and morphological (SEM) properties and thermal stability (TGA) of the supporting scaffold. This work demonstrates the potential for developing high-performance composite FSPCMs, addressing the critical leakage problem in TES systems by utilizing the synergy of environmentally friendly and cost-effective clay-based materials.

Keywords: Thermal Energy Storage; Phase Change Material (PCM); Diatomite; Kaolin; Polyvinyl Alcohol; Lyophilization; Form-Stable Composites.

POSTER PRESENTATION

The effectiveness of cavitation liposuction and radiofrequency in reducing excess abdominal fat. A pilot study

Weronika Seroka[1], Wiola Faruga-Lewicka [1], Estera Wajdzik[1], A. Żoń-Biedroń[1]

[1]Śląska Wyższa Szkoła Medyczna w Katowicach, ul. Mickiewicza 29, 40-085 Katowice, Polska

*Correspondence e-mail : seroka.weronika@wp.pl

Abstract

Overweight and obesity are health disorders that can lead to serious non-communicable diseases. Non-invasive treatments that support fat reduction are increasingly used in cosmetology and aesthetic medicine. The study aimed to evaluate the effectiveness of a combination therapy involving ultrasonic lipocavitation and radiofrequency treatments in patients with excess abdominal fat. The treatments proved to be ineffective when not accompanied by lifestyle changes. Further studies are recommended in which participants will additionally follow a low-calorie diet and engage in regular physical activity.

Keywords: cavitation liposuction, radiofrequency, fat eduction, excess weight.

POSTER PRESENTATION

In silico screening and selection of the optimal asparaginase gene for cloning from *Tetrahymena thermophila*

İrem Zafnaki[1*] (https://orcid.org/0009-0008-0583-2021), Nurçin Küçükoğlu[2] (http://orcid.org/0000-0001-5309-4416), Handan Açelya Kapkaç[2] (http://orcid.org/0000-0002-2812-1686)

[1]Eskişehir Technical University, Institute of Graduate Programs, Department of Molecular Biology, Eskisehir, Turkey.
[2]Eskişehir Technical University, Faculty of Science, Department of Biology, Eskisehir, Turkey.

* Corresponding author e-mail: izafnaki@gmail.com

Abstract

L-asparaginases (L-ASNases) are hydrolase enzymes of critical clinical and industrial importance, widely utilized in pharmaceutical, food, and biotechnological sectors. They play a key role in acrylamide detoxification in the food industry and are effectively employed as antiproliferative biotherapeutics, particularly in the treatment of Acute Lymphoblastic Leukemia (ALL). Although the enzymes currently used in food applications are functional, there remains a need for variants that exhibit stability at higher temperatures and across broader salt ranges. Clinically used L-asparaginase preparations, primarily derived from *Escherichia coli* and *Erwinia chrysanthemi*, present major limitations such as immunogenicity, short serum half-life, and undesired glutaminase activity. Therefore, identifying alternative L-asparaginase sources with higher substrate specificity, lower toxicity, and improved stability has become increasingly important. In this context, the unicellular eukaryotic model organism *Tetrahymena thermophila* stands out as a promising source of novel enzymes and therapeutic proteins due to its broad physiological tolerance, glycosylation capacity, and suitability for recombinant protein production. Genomic data reveal two potential asparaginase variants with the annotations TTHERM_00042680 and TTHERM_00483700. Studies on the closely related species Tetrahymena pyriformis have highlighted a membrane-associated L-asparaginase that exhibits antiproliferative activity, lacks glutaminase function, and possesses a unique protein kinase-like feature. However, the actual biochemical activities of the asparaginase-like genes encoded in the *T. thermophila* genome have not yet been experimentally validated. In this study, we aimed to identify the most suitable *T. thermophila* enzyme for industrial and clinical applications by performing an in-depth bioinformatic analysis of the TTHERM_00042680 and TTHERM_00483700 genes. Accordingly, phylogenetic analyses, similarity matrices, and AlphaFold-based structural models were generated for the candidate sequences and compared with commercially known enzymes, leading to the identification of the optimal candidate.

Keywords: L-asparaginase, *Tetrahymena thermophila*, bioinformatics, phylogenetics, 3D modeling

POSTER PRESENTATION

Elucidation of the anatomy, ecology, and micromorphology of three *Glaucium* species in the Aegean Region

Şerife Zeynep Dinler[1*] (https://orcid.org/0009-0009-6738-9579), Ahmet Kahraman[1] (https://orcid.org/0000-0002-9344-1993)

[*1]Uşak University, Faculty of Engineering and Natural Sciences, Molecular Biology and Genetics, Uşak, Turkey

* Corresponding author e-mail: zeynebdinler@gmail.com

Abstract

This study aimed to conduct the first comprehensive investigation into the anatomical, micromorphological, and ecological characters of the *Glaucium flavum*, *G. corniculatum*, and *G. leiocarpum* species belonging to the genus *Glaucium* Mill. (Papaveraceae), in order to contribute to their taxonomic distinction. Analyses of stem, sepal, and petal samples collected from the three species in the Aegean Region were conducted by sectioning using the paraffin embedding method, followed by staining with Safranin O and Fast Green FCF for anatomical examination. Scanning Electron Microscopy (SEM) was used to detect distinguishing structures on the epidermal surfaces of the petals and ovaries. Furthermore, soil samples were collected to determine the ecological variation of each species' habitat; their pH, salinity, organic matter, and various macro/micro element contents were analyzed. The findings allow for the determination of interspecific boundaries: Anatomically, calcium oxalate druse crystals were detected only in the leaf mesophyll of *G. corniculatum*. In terms of ovary epidermal micromorphology, dense, appressed trichomes were found in *G. corniculatum*, while distinct tubercles were observed in *G. leiocarpum*, and indistinct tubercles in *G. flavum*. Ecological analyses showed that the species are adapted to different soil chemistries. These new, measurable, and visually supported character sets make significant contributions to strengthening the systematic position of these taxa by being included in the identification keys for *Glaucium* species

Keywords: *Glaucium*, petal, ovary, micromorphology, anatomy, Aegean Region

Acknowledgements: This study was supported by the Scientific and Technological Research Council of Türkiye (TÜBİTAK) as a part of 2209-A University Undergraduate Students Research Projects (project number: 1919B012335072) and Uşak University Scientific Research Projects Unit (project number: FBA-2025-580).

POSTER PRESENTATION

Development and characterization of nanocomposites for high-performance supercapacitors

Ramin Jahangirov[1*] (ORCID: https://orcid.org/0000-0002-9063-7931), Sema Aslan[2] (ORCID https://orcid.org/0000-0001-9796-7311), Derya Bal Altuntaş[3](ORCID https://orcid.org/0000-0001-6544-6271)

[*1]Mugla Sitki Kocman University, Institute of Science, Department of Renewable Energy Resources and Technologies, Muğla, Turkey
[2]Mugla Sitki Kocman University, Faculty of Science, Department of Chemistry, Muğla, Turkey
[3]Recep Tayyip Erdoğan University, Faculty of Engineering and Architecture, Department of Bioengineering, Rize, Turkey

*Corresponding author e-mail: ramin.cahangir2@gmail.com

Abstract

Supercapacitors are attractive energy storage devices due to their high-power density (10 kW kg^{-1}) and long cycling stability (>10,000 cycles). However, conventional carbon materials such as rGO typically deliver only 120–200 F g^{-1}, while MoS_2 suffers from limited conductivity, resulting in capacitance values of ≈150–350 F g^{-1} [1]. Even MoS_2/rGO hybrids rarely exceed 600 F g^{-1}, highlighting the need to design advanced composite electrodes that combine EDLC and pseudocapacitive properties to achieve higher specific capacitance [2]. In this study, a ternary hybrid electrode was prepared by integrating MoS_2, rGO, and NiMn-LDH via a hydrothermal method. The synthesis ratios were fixed as MoS_2:rGO = 9:1, Ni:Mn = 3:1, and MoS_2/rGO:LDH-NiMn = 1:1, with urea used in a 1:5 ratio relative to the total metal cations. The structural properties of the prepared materials were characterized by XRD (2°/min). XRD analysis showed rGO's broad (002) peak (25–26°), MoS_2 sharp peaks of the 2H hexagonal phase ($P6_3/mmc$), and in the hybrid, additional peaks at 11.58°, 23.5°, and 34.4° corresponding to NiMn-LDH (003)/(006)/(009), confirming successful LDH formation.

Keywords: Supercapacitors, Pseudocapacitive Materials, Hydrothermal Synthesis, XRD Characterization.

* This study is derived from the PhD thesis work of Ramin Jahangirov.

References:

[1] Ma, Y.; Liu, J.; Lin, Y.; Jia, Y. Recent Advances in Hierarchical MoS_2/Graphene-Based Materials for Supercapacitor Applications. Phys. Chem. Chem. Phys. 2023, *25*, 8263–8280.
[2] Zhang, Y.; Xu, J.; Lu, S.; et al. Engineering Few-Layer MoS_2 and rGO Heterostructure Composites for High-Performance Supercapacitors. Adv. Compos. Hybrid Mater. 2025, 8, 108.

POSTER PRESENTATION

CID-1067700 treatment differentially modulates lysosomal acidification in bortezomib-sensitive and -resistant myeloma cells

Gülüzar Günur İtez[1*] (Orcid: 0009-0007-5367-6687), Nazila Farhangzad[2] (ORCID: 0009-0002-3150-6103), Doğa Tezal Altındağ[2] (ORCID: 0009-0005-5003-4852), Kübra Gayret[2] (ORCID: 0009-0006-4758-6741), Tülin Özkan[3] (0000-0002-1431-2385), Asuman Sunguroğlu[3] (ORCID: 0000-0001-7693-0958)

[*1]Ankara University, Institute of Health Sciences, Stem Cell Institute, Ankara, TURKEY.
[2]Ankara University,Institute of Health Sciences, Department of Medical Biology, Ankara, TURKEY.
[3]Ankara University, Medical Faculty, Department of Medical Biology, Ankara, TURKEY

*Corresponding author e-mail: gulnuritez@gmail.com

Abstract

Multiple myeloma (MM) is characterized by excessive immunoglobulin production, leading to constant proteostasis stress. When proteasomal capacity becomes limited, cells rely on lysosomal-autophagic pathways to maintain protein homeostasis. Rab7 is a key regulator of late endosome-lysosome trafficking, autophagosome-lysosome fusion, lysosomal positioning, and vesicular dynamics. However, the pharmacological inhibition of Rab7 has not previously been investigated in MM or other cancers. To evaluate the effects of CID-1067700 (known as Rab7 inhibitor) on lysosomal acidification in bortezomib-resistant (RPMI 8226 7B) and bortezomib-sensitive (RPMI-8226) myeloma cell lines. Parental RPMI-8226 (S) and long-term bortezomib-exposed resistant RPMI-8226-7B (R) cells were treated with CID-1067700. Cell viability was assessed by MTT assay (48-hour IC_{50}), while lysosomal acidification was evaluated through a single-run preliminary flow cytometry analysis using BioTracker NIR 633 across 6, 18, 24, and 48-hour time points. Rab7 inhibition reduced cell viability in a dose-dependent manner in both cell lines (48 h IC_{50}: Sen 50 µM; Res 55 µM). Lysosomal acidification increased over time in both lines; however, CID-1067700 produced minimal additional effect in sensitive cells. In contrast, resistant cells displayed a marked and exaggerated lysosomal acidification response at 48 hours following CID treatment, indicating a heightened stress-induced lysosomal activation capacity. These findings suggest that resistant cells are not characterized by elevated basal lysosomal activity, but rather by a stronger inducible lysosomal response under stress conditions. This study provides the first preliminary insight into Rab7 pharmacological inhibition in MM. Resistant cells exhibited a pronounced lysosomal acidification response to CID-1067700, whereas sensitive cells showed minimal changes. Further confirmation through additional experimental replicates is needed to substantiate these observations.

Keywords: Multiple myeloma, Rab7 inhibition, lysosomal acidification, drug resistance

POSTER PRESENTATION

Enhanced topical efficacy of ketoprofen: Development of beta-cyclodextrin-based inclusion complexes and biopharmaceutical performance analysis

Betul Ayil (0009-0004-7907-3540)[1] Irem COKSU (0000-0003-4597-4872)[2] Serap Acar (0000-0002-6662-6642)[2]

[1]Yıldız Technical University, Graduate School of Science and Engineering, Department of Biotechnology, 34210 Esenler, Istanbul, Türkiye
[2]Yıldız Technical University, Faculty of Chemical and Metallurgical Engineering, Department of Bioengineering, 34210 Esenler, Istanbul, Türkiye

* Corresponding author e-mail: betulayil_@hotmail.com

Abstract

Ketoprofen (KTP), a potent analgesic and anti-inflammatory non-steroidal anti-inflammatory drug (NSAID), exhibits limited bioavailability in topical applications due to its low aqueous solubility. The restricted solubility decreases the drug's dissolution rate, thereby negatively affecting dermal permeability[1]. Cyclodextrins are effective carrier systems capable of forming inclusion complexes with lipophilic drugs through their hydrophobic inner cavities, thereby enhancing solubility, dissolution rate, and stability. In this context, β-cyclodextrin (β-CD) can form effective and stable inclusion complexes with hydrophobic drugs such as KTP due to its structurally compatible internal cavity, and it is widely preferred in formulation studies owing to its well-established safety profile in the pharmaceutical field. This study aims to prepare β-CD inclusion complexes of KTP to enhance its solubility and dissolution rate and to evaluate the performance of these complexes in topical formulations[2-3]. KTP/β-CD inclusion complexes were prepared in a 1:1 molar ratio using the solvent evaporation method, and the KTP content in the complexes was quantified by UV–Vis spectrophotometry. A phase solubility study was conducted to investigate the solubility of KTP in the β-CD environment. The prepared complexes were comprehensively characterized using Fourier Transform Infrared Spectroscopy (FT-IR), X-ray Diffraction (XRD), Scanning Electron Microscopy (SEM), and Derivative Thermogravimetry/ Differential Scanning Calorimetry (DTG/DSC) analyses. Following characterization, two topical formulations were designed: a control formulation containing only KTP and a test formulation containing the KTP/β-CD complex. The *in vitro* release profiles of these formulations will be evaluated using Franz diffusion cells, and the collected samples will be quantitatively analyzed by a validated HPLC method. Comparative release data will reveal the effects of β-CD complexation on the release kinetics and potential topical bioavailability of KTP. This study aims to investigate the potential of β-CD complexation to improve the solubility and topical release behavior of KTP through comprehensive physicochemical and *in vitro* evaluations.

Keywords: Franz diffusion cell, inclusion complex, ketoprofen, topical formulation, β-cyclodextrin,

References:

[1] Stamate Cretan, M., Ochiuz, L., Ghizdovat, V., Molcalut, M., Agop, M., Gafițanu, C. A., Barsan, A., Sha'at, M., & Stamate, C. (2025). *Formulation and in vitro evaluation of matrix tablets containing ketoprofen–beta cyclodextrin complex for enhanced rheumatoid arthritis therapy: Experimental and computational insights.* Pharmaceutics, 17(4), 474.
[2] Rajamohan, R., Kamaraj, E., Muthuraja, P., Murugavel, K., Govindasamy, C., Prabakaran, D. S., Malik, T., & Lee, Y. R. (2024). *Enhancing ketoprofen's solubility and anti-inflammatory efficacy with safe methyl-β-cyclodextrin complexation. Scientific Reports, 14*, 21516.
[3] Betlejewska-Kielak, K., Bednarek, E., Budzianowski, A., Michalska, K., & Maurin, J. K. (2021). *Comprehensive characterisation of the ketoprofen-β-cyclodextrin inclusion complex using X-ray techniques and NMR spectroscopy*. Molecules, 26(13), 4089.

POSTER PRESENTATION

Production of a chitosan-based hydrogel packaging film to extend the shelf life of packaged foods

Doruk Nil[1*] (ORCID: https://orcid.org/0009-0008-6650-4515), Nuse Sendogan[2] (ORCID: https://orcid.org/0009-0000-7724-7368), Muhammet Yigit Cucen[3] (ORCID https://orcid.org/0009-0008-6213-1707)

[*1]Yeditepe University, Computer Engineering, Student, Istanbul, Turkey.
[2] Modern Bilimler Akademisi School Of Science Camlica Campus, Student, Istanbul, Turkey.
3 Modern Bilimler Akademisi School Of Science Camlica Campus, Student, Istanbul, Turkey.

*Corresponding author e-mail: doruknil79@gmail.com

Abstract

Since the Industrial Revolution, the widespread expansion of urban life has necessitated the emergence of packaged foods, significantly increasing consumer demand. While packaged foods are favored today for their ease of use, accessibility, and cost-effectiveness, their ready availability often leads to unconscious consumer behavior. Consequently, consumers frequently purchase more than needed, resulting in spoilage and increased food waste. This constitutes a serious global problem regarding economic loss and food accessibility; therefore, studies focused on extending shelf life are crucial. Accordingly, this study investigates the usability of chitosan-based hydrogel films to increase the shelf life of packaged foods. Chitosan is a biopolymer obtained through the deacetylation of chitin, a natural polysaccharide derived from marine crustaceans like shrimp and crabs. Chitosan hydrogel was selected due to its antimicrobial, antifungal, and biodegradable properties, as extensive literature reviews suggest it effectively reduces microbial contamination. Unlike synthetic preservatives posing toxic risks or plastic packaging causing environmental damage, chitosan hydrogel offers an eco-friendly, biotechnological solution. In the experimental phase, chitosan powder will be dissolved in a 1% acetic acid solution at 25°C to obtain a homogeneous mixture, with glycerol added as a plasticizer. The mixture will be cast onto sterile surfaces and dried to produce a transparent hydrogel film. To test efficacy, perishable foods (e.g., sliced apples, tomatoes, or cheese) will be packaged using both chitosan hydrogel and standard synthetic plastic materials. Samples will be observed at specific intervals (Days 1, 3, 5, and 7) to record parameters including color change, odor, surface deformation, pH, mold growth, and weight. Additionally, vacuum packaging applications will be evaluated. It is expected that chitosan packaging will delay spoilage. Physical properties such as film thickness, permeability, and biodegradability will be analyzed to evaluate the material's durability and potential as an additive-free shelf-life extender.

Keywords: Chitosan, hydrogel, packaged, food, shelf-life

POSTER PRESENTATION

The use of lithium obtained from the recycling of lithium-ion batteries as a raw material in lithium-carbonate-based mental health medications

Doruk Nil (Orcid: https://orcid.org/0009-0008-6650-4515)

Yeditepe University, Computer Engineering, Student, Istanbul, Turkey.

Corresponding author e-mail: doruknil79@gmail.com

Abstract

Rechargeable electronic devices, such as electric cars, mobile phones, and laptops, widely use mineral-rich lithium-ion batteries. These batteries have a limited lifespan and, when disposed of improperly, can cause significant environmental pollution. Recycling lithium from waste batteries offers a sustainable solution, reducing environmental impact while providing valuable raw materials for the pharmaceutical sector. This project focuses on obtaining lithium carbonate from waste lithium-ion batteries to be used as a raw material in lithium-based mental health medications. Lithium metal in waste batteries was precipitated using the ethanol sulfate technique, and the resulting lithium sulfate was converted into lithium carbonate by washing with sodium carbonate. The process achieved a 98% recovery rate for lithium. In parallel, cobalt from the batteries was separated as cobalt sulfate and cobalt hydroxide with high efficiency. The obtained lithium carbonate is suitable for use in psychiatric drugs addressing bipolar disorder and depression. By recycling lithium, this study simultaneously contributes to environmental sustainability and helps mitigate raw material shortages in the pharmaceutical sector, which have intensified after the Covid-19 pandemic. The project also demonstrates a practical roadmap for post-recycling utilization of lithium and highlights the potential of converting hazardous electronic waste into valuable resources. This approach may inspire future studies to explore the recycling and repurposing of other battery components or alternative battery technologies. Overall, the findings show that lithium from waste lithium-ion batteries can be efficiently recovered and transformed into pharmaceutical-grade lithium carbonate, bridging the gap between environmental management and pharmaceutical raw material supply.

Keywords: Lithium, battery, pharmacology, environment, recycle, medication

POSTER PRESENTATION

Morphological and phylogenetic analyses of species belonging to the Lamiaceae family at Uşak University Campus

Tevfik İlker Demir[1*] (Orcid: https://orcid.org/0009-0000-1485-8049), Ahmet Ganci[2] (Orcid: https://orcid.org/0009-0004-2877-1066), Ahmet Kahraman[3] (Orcid: https://orcid.org/0000-0002-9344-1993)

[*1] Uşak University, Faculty of Engineering and Natural Sciences, Department of Molecular Biology and Genetics, Uşak, TÜRKİYE
[2] Uşak University, Faculty of Engineering and Natural Sciences, Department of Molecular Biology and Genetics, Uşak, TÜRKİYE
[3] Uşak University, Faculty of Engineering and Natural Sciences, Department of Molecular Biology and Genetics, Uşak, TÜRKİYE

*Corresponding author e-mail: tevfikilker.064@gmail.com

Abstract

The Lamiaceae family is one of the richest families, containing over 7,000 species. Members of this family are distributed across various ecological environments in different regions of Turkey. The primary objective of this current study is to examine the morphological and phylogenetic aspects of Lamiaceae species identified in the Uşak University Campus and its surroundings. At the same time, the aim is to reveal the Lamiaceae biodiversity in the study area. First, the collected plant specimens were identified. After completing the identification of Lamiaceae species, morphological images of their flower structures were taken. Furthermore, phylogenetic trees were constructed using the sequences of the ITS gene region registered on the NCBI platform for each species, and their phylogenetic relationships were examined. Consequently, phylogenetic relationships were compared based on both morphological characteristics and the phylogenetic analyses obtained. The results of the study showed that the morphological and phylogenetic analyses supported each other, and the species generally clustered within their own genera. As seen in the tree and morphological images, Uşak University Campus is home to various genera, primarily the genus Salvia.

Keywords: Lamiaceae, Phylogenetics, Morphology, Uşak, Türkiye

Acknowledgments: This study was financially supported by the Scientific Research Projects Coordination Unit of Uşak University (FBA-2025-685) and the Scientific and Technological Research Council of Turkey (TÜBİTAK) under the 2209-A University Student Research Projects programme (project no: 1919B012471389).

POSTER PRESENTATION

Effects of human osteoblast-derived exosomes on the osteogenic commitment of multipotent and pluripotent stem cells

Vildan Torun Baltacıoglu[1]* (ORCID: https://orcid.org/0000-0003-2851-2019),
Burak Derkuş[1] (ORCID: https://orcid.org/0000-0001-5558-0995)

[1]Ankara University, Faculty of Science, Department of Chemistry, Stem Cell Research Laboratory, Ankara, Türkiye

*Corresponding author e-mail: vtorun@ankara.edu.tr

Abstract

Exosomes have emerged as promising biological tools in regenerative medicine due to their ability to transfer bioactive molecules and influence cell fate decisions. Human mesenchymal stem cells (hMSCs) and induced pluripotent stem cells (iPSCs) are widely used in tissue engineering owing to their multilineage differentiation capacity; however, directing their differentiation in a controlled and efficient manner remains a major challenge. In this study, exosomes derived from human osteoblast (hFOB) cells (Osteo-Exo) were investigated for their potential to induce osteogenic commitment in hMSCs and iPSCs. Exosomes were isolated using serial centrifugation and ultracentrifugation protocols, and their physicochemical properties were characterized by bicinchoninic acid (BCA) protein quantification and nanoparticle tracking analysis (NTA). Osteo-Exo were administered to hMSC and iPSC cultures at defined loading intervals. Morphological alterations associated with osteogenesis were monitored by inverted phase-contrast microscopy, while osteogenic differentiation was validated by immunofluorescence staining of RUNX2, osteopontin (OPN), and type I collagen (COL1A1). Furthermore, quantitative real-time PCR analyses were performed to assess the expression of osteogenic markers (Runx2, ALP, OPN) and pluripotency markers (OCT4, NANOG). Both hMSCs and iPSCs demonstrated early osteogenic commitment following the first exposure to Osteo-Exo, showing strong RUNX2, OPN, and COL1A1 signals, while untreated control cells remained negative for these markers. Gene expression analysis confirmed significant upregulation of osteogenic genes and downregulation of pluripotency markers, supporting the osteo-inductive effect of Osteo-Exo. These findings indicate that human osteoblast-derived exosomes promote osteogenic differentiation in both multipotent and pluripotent stem cells. Osteo-Exo represent a promising, cell-free biomimetic strategy that may contribute to future regenerative medicine and bone tissue engineering applications.

Keywords: Exosomes, Osteogenesis, hMSC, iPSC, Osteoblast, Regenerative medicine.

POSTER PRESENTATION

Synthesis and characterization of new liquid crystalline polyurethane copolymer

Sermin Hız[a], Yeşim Gürsel[b]

[a,b] Istanbul Technical University, Faculty of Science and Letters
Polymer Science and Technology Program, Istanbul, Turkey

Corresponding author e-mail: hizs@itu.edu.tr

Abstract

Polyurethanes (PU) are polymers synthesized by the reaction of polyols with isocyanates, producing materials that range from soft and flexible to highly rigid depending on their chemical structure. Their physical properties, such as heat resistance, hardness, and flexibility, are strongly influenced by the type of monomers used, while the (-NH-CO-O-) bonds in their backbone provide chemical stability and mechanical strength. Liquid crystal (LC) compounds exhibit an intermediate state of matter, combining the fluidity of liquids with the long-range molecular order of crystalline solids. This unique dual nature allows LC materials to form highly ordered structures while maintaining mobility, making them attractive for advanced functional applications. When incorporated into polymer backbones, LC monomers can significantly enhance thermal, mechanical, and morphological properties. The incorporation of mesogenic groups into polymer structures is intended to improve molecular order and introduce liquid crystalline behavior, while long alkyl chains are often employed to lower the glass transition temperature (Tg), enhancing flexibility and processability. In this study, a side-chain liquid crystal polyurethane copolymer was synthesized. For this purpose, two different monomers, M1-diol (0.5 mmol, octadecyl-2,2-bis(hydroxymethyl)propionate) and M2-diol (0.5 mmol, 8-(4-cyanobiphenyl-4′-oxy) octyl-2,2-bis(hydroxymethyl)propionate) with HMDI (1 mmol, hexamethylene diisocyanate) in the presence of dibutyltin dilaurate as the catalyst. This study, conducted in our research group, was designed by taking as a reference our earlier study on PU synthesis with M2-diol. The objective was to improve the liquid crystalline properties of PU by incorporating long alkyl chains into its structure. Characterization results confirmed that long alkyl chains reduce crystallization and improve liquid crystalline behavior in the polyurethane copolymer. The chemical structure characterization was carried out using FTIR and HNMR spectroscopy, while the thermal properties were examined by differential scanning calorimetry (DSC), and the identification of liquid crystal mesophase structures and transition temperatures were performed using polarized optical microscopy (POM) and DSC, respectively.

Keywords: Polyurethane, Liquid Crystal,Liquid Crytal Polyurethane Copolymer

POSTER PRESENTATION

Biyokatalizör kullanılarak $NaBH_4$ 'den hidrojen üretiminin araştırılması

Barış Postallıkara[1], Songül Kaskun Ergani[2]

[1*]Karabük Üniversitesi, Mühendislik ve Doğa Bilimleri Fakültesi, Çevre Mühendisliği, Karabük, Türkiye
[2]Karabük Üniversitesi, Mühendislik ve Doğa Bilimleri Fakültesi, Çevre Mühendisliği, Karabük, Türkiye

[*] Sorumlu yazar e-mail: barispostallikara@karabuk.edu.tr

Özet

Bu çalışmada, potansiyel bir hidrojen depolama bileşiği olan Sodyum bor hidrür'ün ($NaBH_4$) sulu faz hidroliz reaksiyonunda, bir biyo-atık olan pirinanın (zeytin posası) piroliz ve asitle fonksiyonelleştirilmesi yoluyla hazırlanan heterojen bir katalizörün performansı incelenmiştir. Araştırma, katalizörün hidrojen üretim hızı, reaksiyon kinetiği ve aktivasyon enerjisi üzerindeki etkilerini belirlemeye odaklanmıştır. Katalitik dehidrojenlenme reaksiyonu, karıştırmalı kesikli reaktör içerisinde gerçekleştirilmiştir. Üretilen hidrojen miktarı volumetrik olarak yüksek hassasiyetle belirlenmiştir. Deneysel koşullar 25 °C, 30 °C ve 35 °C olmak üzere farklı sıcaklıklarda standardize edilmiştir. Bulgular, reaksiyon sıcaklığındaki her 5°C'lik artışın (30 dakikalık zaman aralığında) Hidrojen verimini yaklaşık %15 oranında yükselttiğini göstermektedir. Esas olarak, pirina bazlı katalizörün kullanımı, self-hidroliz (katalizörsüz) reaksiyonlarına kıyasla aynı koşullar altında hidrojen verimini %27 oranında artırarak reaksiyon hızını önemli ölçüde katalize ettiğini kanıtlamıştır. Katalizörün yüzey morfolojisi ve kristal yapısı sırasıyla Taramalı Elektron Mikroskobu (SEM) ve X-Işını Kırınımı (XRD) analizleri ile karakterize edilmiştir. Sonuçlar, pirinanın ucuz ve çevresel açıdan sürdürülebilir bir kaynak olarak, $NaBH_4$ hidrolizi için yüksek performanslı katalizörlerin geliştirilmesinde önemli bir potansiyel taşıdığını doğrulamaktadır.

Anahtar Kelimeler: Hidrojen Üretimi, NaBH4, Hidroliz, biyokatalizör

POSTER PRESENTATION

Hybrid renewable mobile energy station for off-grid molecular diagnostics and cold-chain healthcare

Tormi Lillerand[1*] (ORCID: https://orcid.org/0000-0002-1095-7485),
Indrek Virro[1] (ORCID: https://orcid.org/0000-0001-6166-7376)

[*1]Estonian University of Life Sciences, Institute of Forestry and Engineering, Biosystems Engineering, Tartu, Estonia.

*Corresponding author e-mail: tormi.lillerand@emu.ee

Abstract

Reliable electricity is a prerequisite for almost all contemporary biological and chemical workflows, from PCR-based diagnostics to vaccine cold-chain logistics. However, mobile laboratories and outreach clinics in rural or disaster-affected regions still depend largely on diesel generators, which are noisy, carbon-intensive and commercially unattractive due to fuel and maintenance costs. We present a trailer-mounted, renewably powered mobile energy station engineered to support three-phase biomedical and analytical instrumentation in off-grid contexts. The system integrates 22 photovoltaic modules with a LiFePO4 storage pack, three single-phase 48/8000 inverters configured for three-phase output, and an LPG backup generator. A layered automation scheme (Siemens S7-1200 PLC with distributed modules and Victron Cerbo GX telemetry) enables safe power management, alarm handling and remote supervision of critical loads such as −20 °C freezers, incubators and PCR thermocyclers. Proof-of-concept field tests used electric-vehicle charging as a proxy for peak laboratory demand: under overcast conditions, the station delivered 13.9 kWh over 75 minutes to an 11 kW load while maintaining system stability, revealing storage sizing and thermal management as key design levers. As a case application, we outline powering a 20–30 sample/day field PCR unit for zoonotic disease surveillance in remote agricultural communities, including continuous operation of biosafety cabinets, cold storage and data communication equipment. Target users are ministries of health, NGOs and commercial providers of mobile molecular diagnostics and vaccination campaigns who currently “buy power” piecemeal through diesel solutions. We identify a commercialization gap for standardized, field-tested power platforms tailored to biological and clinical equipment, bridging engineering suppliers and mobile health operators. By packaging renewable generation, storage, control and remote monitoring into a certified product that can be leased or sold as enabling infrastructure for mobile laboratories, the proposed architecture lowers operational costs, reduces emissions and de-risks deployment of off-grid biomedical services.

Keywords: autonomous instrumentation support, field PCR laboratory support, remote clinical outreach services, NGO-focused technology commercialization

2.2. FULL-TEXTS

POSTER PRESENTATION

Influence of different Albanian freshwater sources on pale ale beer quality

Fatbardha Lamce*[1] (orcid.org/0000-0002-8517-512X), Mamica Ruci[1](https://orcid.org/0000-0002-8151-6142), Julian Karaulli[1] (https://orcid.org/0000-0003-0693-3592), Nertil Xhaferaj[2] (https://orcid.org/0000-0001-7420-8902), Albert Kopali[3] https://orcid.org/0009-0008-4059-0259**)** and Onejda Kycyk[1] (orcid.org/0000-0001-9361-042X)

[1]Agricultural University of Tirana, Faculty of Biotechnology and Food, Food Research Center, Tirana, Albania
[2]Agricultural University of Tirana, Faculty of Biotechnology and Food, Department of Agri-Food Technology, Tirana, Albania
[3]Agricultural University of Tirana, Faculty of Agriculture and Environment, Department of Environmental and Natural Resources, Tirana, Albania

Abstract
Water represents the main raw material in beer production, typically accounting for over 90% of the final product. Albania is characterized by abundant natural freshwater resources, originating from mountainous terrains with minimal anthropogenic impact. Despite this, limited scientific data exist regarding the suitability of different Albanian natural water sources in brewing technology. This study investigates the influence of water composition on the physicochemical characteristics of a Pale Ale beer style. Four natural spring waters sourced from distinct Albanian regions such as Selita, Lajthiza, Bogova, and Germenj were used in same brewing conditions. The purpose of this study is to assess how variations in mineral content and water profile may affect the final attributes of beer. Preliminary analytical results revealed minor variations across pH values, ethanol concentration, and total acidity among the samples. A more pronounced difference was observed in beer produced with Selita water, with the highest color intensity at 19.5 EBC. Although differences were limited at this stage, the findings suggest a measurable impact of water origin on brewing performance and final beer characteristics. These preliminary data support the suitability of Albanian natural water resources for application in the craft brewing industry.

Keywords: Water brewing, Albanian spring water, Pale ale beer, beer color, craft beer

INTRODUCTION

Albania is rich in water resources and hosts significant biodiversity, which represents an important natural asset for agro-industrial applications (Cullaj *et al.,* 2005). Despite this abundance, Albanian water resources remain largely under-investigated in relation to their technological suitability for food and beverage production, particularly in the brewing sector. Beer is one of the oldest alcoholic beverages and the most widely produced worldwide in terms of volume (Buiatti, 2009; Briggs *et al.,* 2004). Given that water constitutes more than 90% of beer, it should be considered a primary raw material whose characteristics can significantly influence the brewing process and the quality of the final product (Eumann, 2006; Comrie, 1967; Kunze, 2014). Discussions of brewing water composition commonly focus on total hardness, defined as the sum of alkaline-earth metal ions, primarily calcium and magnesium, with minor contributions from strontium and barium (Kadlec, 2002; Palmer & Kaminski, 2013). From this perspective, water chemistry plays a crucial role in determining beer style and ensuring the physicochemical stability of the final product (Punčochářová *et al.,* 2019; Briggs *et al.,* 2004). The mineral composition of brewing water is particularly critical because dissolved ions directly influence mash chemistry, enzymatic activity, yeast metabolism, and sensory attributes of beer (Kunze, 2014; De Clerck, 1957). Among these minerals, calcium (Ca^{2+}) is especially important, as it lowers mash pH through reactions with malt phosphates, enhances enzymatic efficiency during starch conversion, improves protein coagulation and beer clarity, and supports yeast flocculation and metabolic activity (Briggs *et al.,* 2004; Kunze, 2014). Magnesium (Mg^{2+}) contributes to water hardness and serves as a cofactor for yeast enzymes, thereby supporting fermentation performance (Walker, 1998; Stewart, 2017). Sulfate (SO_4^{2-}) accentuates hop bitterness and promotes a drier mouthfeel, whereas chloride (Cl^-) enhances perceived malt sweetness and fullness; the balance between these ions is a key determinant of beer flavor profile (Palmer & Kaminski, 2013; Bamforth, 2009). Because water chemistry affects mash pH, fermentability, and the extraction of bitter and aromatic compounds, brewers frequently adjust

mineral concentrations to optimize process conditions and achieve desired stylistic characteristics (Palmer, 2006; Kunze, 2014). Numerous scientific studies have demonstrated that variations in water mineral composition significantly influence both the technological aspects of brewing and the chemical composition of wort and beer (Punčochářová *et al.,* 2019; Barth, 2013; Montinari *et al.,* 2009; Briggs *et al.,* 2004). For these reasons, the present study aims to evaluate beers of the same style produced using different water sources from Albania, in order to assess the impact of water mineral composition on brewing performance and final beer quality.

MATERIAL AND METHODS

Yeast strains and growth condition

For this study 4 different spring water were used for the production of same style beer, respectively Germenj, Bogova, Selita and Lajthiza water. For the preliminary characterization and for the brewing trials, the commercial *S. cerevisiae* US-05 (SafeAle, Fermentis, Belgium) strain was used. For the beer fermentation, the yeasts were cultured aerobically at 28 °C in YEPD broth (Merck Millipore, Darmstadt, Germany) and after 48 hours the broth cultures were centrifuged at 8,000 rpm for 10 min at 4 °C. Finally, the cell pellet was washed twice with saline solution (0.9% w/v NaCl) and used as a starter. Cell density of inoculum was assessed using Thoma Counting Chamber (Thermo-Fisher Scientific) (Karaulli *et al.,* 2024).

Beer production

Saccharomyces cerevisiae US-05 commercial yeast strain was choose as starter for the production of a Pale Ale beer top fermentation style using a Brewzilla belonging to Pan's Microbrewery in Albania. Fermentation experiments were conducted at 20 °C ± 1 °C. In detail, 3 tests for each scheme were performed. For beer production, was used 90% Pale Ale malt and 10% Wienna malt (Château Pale ale, Castle Malting, Lambermont, Belgium) purchased by local distributors Albania. Hallertauer hop (Barth-Hass, Nürnberg, Germany) was added during the boiling and dry hopping phase. The main analytical characteristics of beer are shown on Table 1.

Table 1. Key parameters of the wort used for Pale Ale beer production.

	Unit	Germenj	Bogova	Selita	Lajthiza
pH	-	5.92 ± 0.03[a]	5.87 ± 0.03	5.86 ± 0.08	5.70 ± 0.05
Extract content	°Plato	13.80 ± 0.24	13.57 ± 0.21	13.73 ± 0.167	13.57 ± 0.21
Color (Wort)	EBC	20.27 ± 0.17	20.63 ± 0.12	20.83 ± 0.12	20.23 ± 0.33
Density	g/cm^3	1.055 ± 0.002	1.054 ± 0.001	1.055 ± 0.001	1.054 ± 0.001

a – Mean ± Stdev

Fermentation experiments were carried out at 20°C ± 1°C using thermoregulated stainless steel tanks (capacity 30 L), containing 20 L of wort. The starter cultures were inoculated at an initial concentration around 10^6 CFU/mL. At the end of the primary fermentation 5 g/L of sucrose was added as a primer for the secondary fermentation which took place in 330 mL dark brown glass bottles. After 40 days of maturation at 20 °C, the beers were subjected to chemical analysis.

Beer Chemical Analysis

A pH meter (Crison basic 20, Barcelona, Spain) was used to measure the pH. The density (g/cm3), alcohol content(%v/v) and color were determined according to the analytical procedures described by the European Brewery Convention (EBC). Titratable acidity (g/L) and volatile acidity (g/L) were determined according to Baiano *et al.,* (2023).

RESULTS

Beer is composed of approximately 90% water, making water an essential ingredient (Comrie, 1967). Water has a significant effect on the chemical and organoleptic characteristics of beer (Punčochářová *et al.,* 2019).

Fermentation Kinetics

In this study, four different natural freshwater sources (Bogova, Germenj, Selita, and Lajthiza) were used for the production of Pale Ale beer. The experiments were conducted to evaluate the suitability of these water sources for beer production. Figure 1 illustrates the density trends observed during alcoholic fermentation across the four experimental trials.

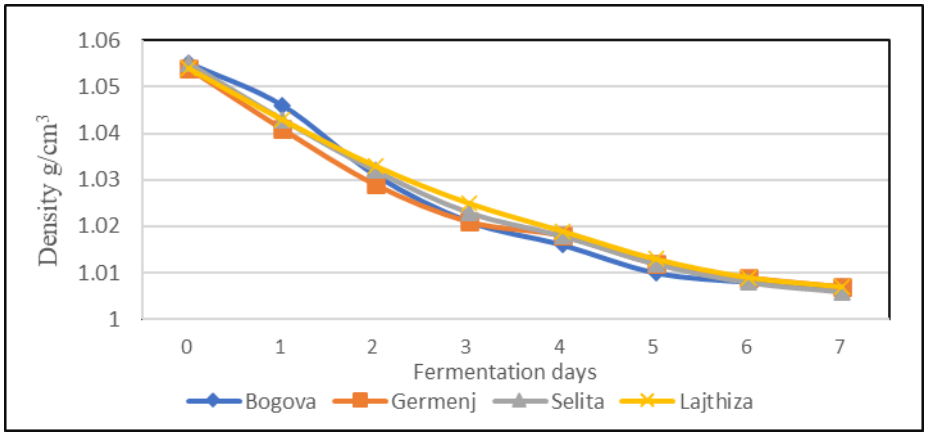


Figure 1. Density trends in Pale Ale beer produced from the four water sources studied.

As shown in Figure 1, the density decreased gradually in all four experiments, indicating active and stable fermentation. Fermentation lasted seven days for each experiment, and in all cases the final density reached 1.007 g/cm³, confirming the completion of the fermentation process and the utilization of fermentable sugars by the yeast. The progressive decrease in density is a typical indicator of fermentable sugar metabolism into ethanol and carbon dioxide, as widely described in the brewing literature (Briggs *et al.,* 2004; Kunze, 2014).

During the fermentation period, beer produced from the Bogova water source showed a slight slowdown in the first two days, reflected by a smaller decrease in density. This phenomenon may be related to the yeast adaptation phase (lag phase), during which the cells adjust to the new environment and activate metabolic mechanisms for fermentation. According to Palmer and Kaminski (2013), the physicochemical characteristics of water, particularly pH and mineral content (Ca^{2+}, Mg^{2+}), directly influence yeast metabolic activity and can cause variations in the initial fermentation kinetics. However, after this initial period, fermentation proceeded steadily and was completed within seven days, with the density decreasing from 1.055 g/cm³ to 1.007 g/cm³, indicating a complete and efficient fermentation.

Similarly, beer produced from the Germenj water source exhibited a slight slowdown in the middle of fermentation (days 3–4). This minor delay may be related to temporary changes in the rate of sugar consumption, as well as the influence of the water's ionic composition on yeast enzymatic and cellular stability. Several studies have reported that high or low concentrations of certain ions, such as bicarbonates or sulfates, can affect wort pH and fermentation efficiency (Bamforth, 2023; Kunze, 2014). Indeed, preliminary analyses of Germenj water (unpublished data) revealed high levels of Ca^{2+} and Mg^{2+} ions, which may explain the observed fermentation fluctuations. Despite this temporary slowdown, fermentation was completed within seven days, with the density decreasing from 1.054 g/cm³ to 1.007 g/cm³, indicating that the yeast successfully metabolized the available substrates.

Another important parameter indicating the progress of fermentation in the experiments conducted in this study is pH. Figure 2 shows the pH trends in beers produced from the water sources included in this study.

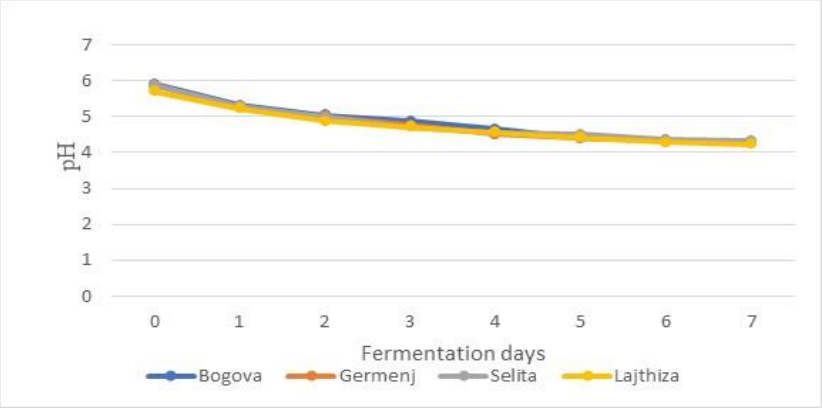


Figure 2. pH trends during fermentation in beers produced from the studied water sources.

As observed in the graph (Figure 2), the decrease in pH occurred gradually. The pH values during fermentation show expected changes corresponding to yeast metabolic activity. Beers produced from the water sources included in this study exhibited very similar initial pH values, while at the end of fermentation, the pH decreased to a range of 4.22–4.32 for all experiments. These values are consistent with the typical pH range of traditionally fermented beers and indicate complete and stable fermentation. According to the literature, the final pH of beer usually ranges from 4.0 to 4.5, depending on the beer style, yeast strain, and fermentation conditions (Kunze, 2014).
The slight differences in initial pH values among the experiments may be related to the physicochemical characteristics of the water used, particularly its bicarbonate content. Waters with higher HCO_3^- levels tend to produce a higher initial pH in the wort and, consequently, in the beer during the early stages of fermentation. Nevertheless, yeast metabolic activity during fermentation was strong, resulting in similar acidification across all experiments and achieving comparable final pH values.

Chemical parameters of beers.
The values of the main physicochemical parameters of the beers in this study are presented in Figure 3 and Table 2.

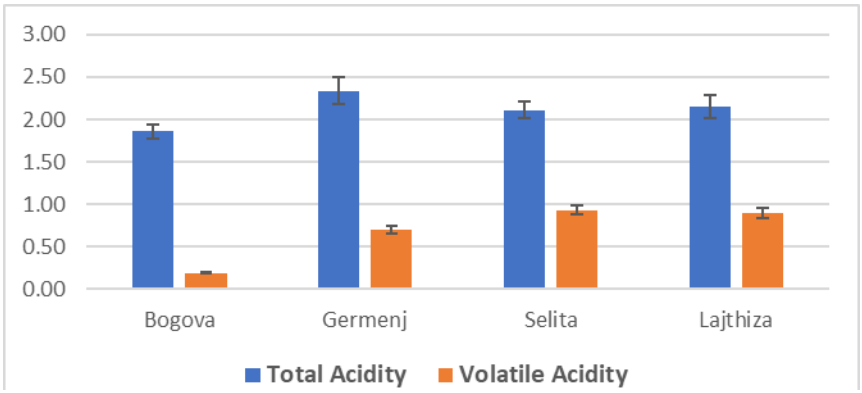


Figure 3. Total and volatile acidity values in the studied beers.

Figure 3 shows the total and volatile acidity values of the beers studied during fermentation. Total acidity values were higher in all four experiments, likely due to the production of organic acids resulting from yeast metabolic activity, including lactic, acetic, and succinic acids. (Briggs *et al.,* 2004; Bamforth, 2023).

Some studies suggest that certain yeast strains used in fermentation can produce high amounts of acetic acid in the presence of oxygen, particularly during wine fermentation (Comitini *et al.,* 2011). Volatile acidity, expressed as acetic acid, showed significant differences among the experiments. Beer produced from the Bogova water source exhibited the lowest value, approximately 0.19 g/L, while beer from the Selita water source showed the highest value, around 0.93 g/L.

Table 2. Alcohol content and color evaluation in the studied beers.

	Bogova	Germenj	Selita	Lajthiza
Alcohol (% v/v)	5.56 ± 0.04[a]	5.66 ± 0.03	5.63 ± 0.10	5.70 ± 0.09
Color (EBC)	17.67 ± 0.09	16.83 ± 0.29	19.50 ± 0.16	17.23 ± 0.42

a – Mean ± Stdev

Table 2, shows the alcohol content (% v/v) and color values (EBC) of the beers produced from the four studied water sources.

The alcohol content was relatively consistent across all beers, ranging from 5.56% (Bogova) to 5.70% (Lajthiza). This indicates that, despite minor differences in the mineral composition of the water, fermentation proceeded fully, and the yeast efficiently metabolized the available sugars. The alcohol values fall within the typical range for Pale Ale beers (4.5–6.0% v/v) (Briggs *et al.,* 2004; Kunze, 2014).

Regarding color, the measured EBC values ranged from 16.83 (Germenj) to 19.50 (Selita). This indicates that the beers produced fall within the typical Pale Ale color range (12–20 EBC), reflecting the controlled use of roasted malt. Minor differences in color between the water sources may be related to interactions between water minerals and malt components, as well as the formation of melanoidins during heating and mashing. However, the primary influence on color is attributed to the malt and thermal treatment (Bamforth, 2023; Palmer & Kaminski, 2017).

CONCLUSIONS

The water source influenced the initial fermentation kinetics, pH and volatile acidity of the beers, while the final alcohol content and color remained within the typical Pale Ale ranges. The beer from the Bogova spring water showed a higher initial pH (≈5.91) and slower early fermentation, with lower volatile acidity (0.19 g/L) and final alcohol of 5.56% v/v. Germenj beer reached 5.66% v/v alcohol at pH 4.22, Selita had the highest color (19.50 EBC) and volatile acidity (0.93 g/L), and Lajthiza beer fermented faster, reaching 5.70% v/v alcohol.

These results indicate that water composition affects fermentation and delicate chemical parameters, but controlled yeast activity ensures consistent final beer quality. Proper water selection is essential to optimize fermentation and maintain desired chemical and sensory characteristics.

ACKNOWLEDGEMENTS

The authors express their sincere gratitude to the staff of the Food Research Center at the Agricultural University of Tirana for their assistance with the chemical analyses performed for this study. We gratefully acknowledge the National Agency for Scientific Research and Innovation (AKKSHI) for funding this research project and for its continued institutional support in promoting applied scientific research and innovation in Albania.

REFERENCE

Baiano, A., Fiore, A., la Gatta, B., Tufariello, M., Gerardi, C., Savino, M., & Grieco, F. (2023). Single and Interactive Effects of Unmalted Cereals, Hops, and Yeasts on Quality of White-Inspired Craft Beers. Beverages, 9(1), 9. https://doi.org/10.3390/beverages9010009

Bamforth, C. W. (2009). *Beer: Tap into the Art and Science of Brewing*. Oxford University Press.

Bamforth, Charles. (2023). Beer: Tap Into the Art and Science of Brewing. https://doi.org/10.1093/oso/9780199996742.001.0001

Briggs, D. E., Boulton, C. A., Brookes, P. A., & Stevens, R. (2004). Brewing: Science and practice. Woodhead Publishing. https://doi.org/10.1201/9780203024195

Briggs, D. E., Boulton, C. A., Brookes, P. A., & Stevens, R. (2004). *Brewing: Science and Practice*. Woodhead Publishing.

Comitini, F.; Gobbi, M.; Domizio, P.; Romani, C.; Lencioni, L.; Mannazzu, I.; Ciani, M. " Selected non-Saccharomyces wine yeasts in controlled multistarter fermentations with Saccharomyces cerevisiae", Food Microbiology, Volume 8, Issue 5, August 2011, Pages 873-882. DOI: 10.1016/j.fm.2010.12.001

Comrie, A. A. D. 1967. Brewing liquor. Journal of the institute of brewing, vol. 73, no. 4, p. 335-346. https://doi.org/10.1002/j.2050-0416.1967.tb03050.x)

Comrie, A. A. D. 1967. Brewing liquor. Journal of theinstitute of brewing, vol. 73, no. 4, p. 335-346. https://doi.org/10.1002/j.2050-0416.1967.tb03050.x

Cullaj, H. ; Hasko, A.; Miho, A.; Schanz, F.; Brandl, H.; Bachhofen, R.; "The quality of Albanian natural waters and the human impact" Environment International, Volume 31, Issue 1, January 2005, Pages 133-146)

De Clerck, J. (1957). *A Textbook of Brewing*. Chapman & Hall.

Kadlec, P. 2002. Technologie potravin II (Food Technology II), Praha : Vydavatelství VŠCHT, 236 p. (In Czech). ISBN: 80-7080-510-2

Karaulli, J.; Xhaferaj, N.; Coppola, F.; Testa, B.; Letizia, F.; Kyçyk, O.; Kongoli, R.; Ruci, M.; Lamçe, F.; Sulaj, K.; Iorizzo, M. "Bioprospecting of Metschnikowia pulcherrima Strains, Isolated from a Vineyard Ecosystem, as Novel Starter Cultures for Craft Beer Production" MDPI Journal, Fermentation 2024, 10(10), 513; https://doi.org/10.3390/fermentation10100513

Kunze, W. (2014). Technology brewing and malting (5th ed.). VLB Berlin.

Kunze, W. (2014). *Technology Brewing and Malting*. VLB Berlin.

M. Eumann 9 – "Water in brewing" Woodhead Publishing Series in Food Science, Technology and Nutrition 2006, Pages 183-207

Montinari , L.; Meyer, H. ; Marconi, O.; Fantozzi, P. "Minerals in Beer" , Academic Press - Beer in Health and Disease Prevention, 2009, Pages 359-365

Palmer, J. (2006). *How to Brew*. Brewers Publications.

Palmer, J., & Kaminski, C. (2013). Water: A comprehensive guide for brewers. Brewers Publications.

Palmer, J., & Kaminski, C. (2013). *Water: A Comprehensive Guide for Brewers*. Brewers Publications.

Punčochářová L, Pořízka J, Diviš P, Štursa V. Study of the influence of brewing water on selected analytes in beer. Slovak J Food Sci/Potravinarstvo.2019;13(1). https://doi.org/10.5219/1046

Punčochářová, L., Pořízka, J., Diviš, P., & Štursa, V. (2019). Study of the influence of brewing water on selected analytes in beer. Potravinarstvo: Slovak Journal of Food Sciences. DOI:10.5219/1046.)

Roger Barth, "The Chemistry of Beer" ASC Publication, May 17, 2013 DOI: 10.1021/bk-2013-1130.ch004

Stefano Buiatti ' Beer composition: An overview", Academic Press, Beer in Health and Disease Prevention, 2009, Pages 213-225

Stewart, G. G. (2017). *Brewing and Distilling Yeasts*. Springer.

Walker, G. M. (1998). *Yeast Physiology and Biotechnology*. Wiley.

POSTER PRESENTATION

Evaluating the relationship between chronological age and ATR-FTIR spectral ratios in thai dental samples

Pohnnapha Khakradook[1](*ORCID*: *https://orcid.org/0009-0002-0582-8280*), Giatgong Konguthaithip[2](*ORCID*: *https://orcid.org/ 0000-0002-0076-249X*), Tawachai Monum[2](*ORCID*: *https://orcid.org/0000-0001-6621-9150*), Yutti Amornlertwatana[2] *(ORCID*: *https://orcid.org/0000-0002-0619-1333)*, Churdsak Jaikang[2,*](*ORCID*: *https://orcid.org/0000-0002-9262-0404*)

[1] Chiang Mai University, Multidisciplinary and Interdisciplinary School, Master's Degree Program in Forensic Science, Chiang Mai, 50200 Thailand.
[2] Department of Forensic medicine, Faculty of Medicine, Chiang Mai University, Chiang Mai 50200 Thailand

Abstract

Age estimation constitutes a critical aspect of the autopsy process, particularly in the context of forensic identification. Due to their exceptional resistance to postmortem degradation, teeth are considered highly reliable indicators for age determination. Fourier Transform Infrared Spectroscopy (FT-IR) offers a non-destructive and efficient analytical technique for evaluating age-associated changes in the chemical composition of dental tissues. Diet, environmental exposures, and geological conditions are influential factors affecting the chemical composition of teeth and should be investigated within specific population contexts. The present study aimed to explore the association between chronological age and FT-IR spectral parameters in a Thai population, with the objective of contributing to the development of population-specific age estimation models. A total of 95 second molars (46 males and 49 females) were sectioned transversely and ground into fine powder prior to analysis using Attenuated Total Reflectance Fourier Transform Infrared Spectroscopy (ATR-FTIR). The carbonate-to-phosphate ratio was found to be correlated with age at death ($\rho = 0.184$), as was the amide-to-phosphate ratio ($\rho = 0.186$, $p < 0.05$). Additionally, a negative correlation with age was observed for ν_1PO_4/Amide I ($\rho = -0.178$, $p < 0.05$). Although further validation with larger and more diverse sample populations is required, these findings underscore the potential of ATR-FTIR spectral analysis for developing reliable and non-destructive age estimation models for forensic applications in Thailand.

Keywords: Age estimation, ATR-FTIR spectroscopy, Forensic Science

INTRODUCTION

Personal identification is a fundamental aspect of forensic investigations, with age estimation being essential information alongside sex, height, and ancestry. In living individuals, age can be determined through dental development examinations, official documents, and physical characteristics, whereas in deceased individuals, age estimation relies on cranial suture analysis, rib cartilage examination, and long bone measurements. However, post-mortem decomposition and thermal damage significantly reduce the accuracy of these methods, making precise age determination challenging in forensic cases.

Dental tissues are highly valuable forensic evidence due to their resistance to decomposition and unique individual characteristics. As the most mineralized structures in the human body, teeth remain intact long after other tissues have degraded, making them ideal specimens for victim identification in mass disasters, accidents, and criminal cases. The chemical composition of dental tissues comprises both organic and inorganic components. Enamel contains approximately 96% inorganic material (w/w), with proteins (mainly amelogenin at approximately 90%), collagen, lipids, and water constituting about 4% (w/w). Dentine has a composition similar to bone, consisting of approximately 70% inorganic material (w/w), 20% organic material, and 10% water.

Fourier Transform Infrared Spectroscopy with Attenuated Total Reflectance (FTIR-ATR) is a sensitive, non-destructive technique that requires minimal sample size and few chemicals. This method has gained increasing recognition in forensic investigations because it can identify the molecular-level chemical properties of various types of evidence. FTIR-ATR allows detailed analysis of both the organic and inorganic components of dentine,

enabling the correlation of spectral features with chronological age, and making it a potentially powerful tool in forensic dentistry.

However, dentine composition varies significantly between populations due to environmental factors, dietary habits, and genetic differences, making it inappropriate to directly apply international standards to Thai populations. Given the limited research on age estimation using dentine with FT-IR spectroscopy, the present study aimed to investigate the relationship between chronological age and FT-IR spectral characteristics in a Thai population, with the objective of developing population-specific forensic age estimation models.

MATERIALS AND METHODS

2.1 Dentine sample collection

Ninety-five non-carious permanent second molar samples (46 males and 49 females), with ages ranging from 20 to 85 years, were obtained from the Department of Forensic Medicine, Faculty of Medicine, Chiang Mai University, Thailand. This study was approved by the Ethics Committee of the Faculty of Medicine, Chiang Mai University (FOR-2565-09049). The teeth samples were cleaned with 0.9% normal saline solution followed by distilled water to remove any remaining blood, according to the method of Manuela et al. The dried samples were then stored in plastic bags at -20 °C until analysis.

2.2 Dentine preparation

Dentine samples were isolated by transverse sectioning (1 mm) using a low-speed cross-sectional saw, and the enamel surface was subsequently removed with a high-speed diamond bur. Both preparation steps were performed under continuous cooling with water to prevent heat-induced damage.

2.3 Fourier-Transform Infrared Spectroscopy - Attenuated Total Reflection (FTIR-ATR)

Dentine samples were pulverized using a freezing mill (SPEX CertiPrep 6750 Freezer/Mill) for 15 minutes. Ten milligrams of the dentine powder were analyzed using a Bruker INVENIO S FT-IR spectrometer equipped with a Specac Golden Gate™ single-reflection diamond ATR accessory (Specac Ltd., UK). Spectra were collected over the range of 4000–400 cm^{-1}, with a spectral resolution of 4 cm^{-1} and 32 scans per sample using OPUS software. An air background spectrum was recorded prior to each measurement, and the diamond crystal was cleaned between runs. Band intensities were quantified as absorbance peak heights after baseline correction and spectral normalization.

2.4 Spectra analysis

The spectra were acquired over the full mid-IR range (4000–400 cm^{-1}) using OPUS software. In order to evaluate the chemical composition of the samples several indices, summarized in Table 1 were calculated.

Table 1. Description of the indices used to evaluate the chemical composition of human dentine sample.

Index	Spectral relationship	Reference
Crystallinity index (CI)	$\frac{Abs(602\ cm^{-1})+Abs(562\ cm^{-1})}{Abs(590\ cm^{-1})}$	Weiner and Bar-Yosef, 1990
Carbonate to Phosphate (C/P)	$\frac{Abs(1415\ cm^{-1})}{Abs(1035\ cm^{-1})}$	Thompson et al., 2009
Carbonate to Phosphate (2) (C/P)	$\frac{Abs(1540\ cm^{-1})}{Abs(1035\ cm^{-1})}$	France et al., 2020
Type A Carbonate (API)	$\frac{Abs(1540\ cm^{-1})}{Abs(603\ cm^{-1})}$	Snoeck et al., 2014 Sponheimer and Lee-Thorp, 1999
Type B Carbonate (BPI)	$\frac{Abs(1415\ cm^{-1})}{Abs(603\ cm^{-1})}$	Snoeck et al., 2014 Sponheimer and Lee-Thorp, 1999
Carbonate (A+B) to Carbonate B (C/C)	$\frac{Abs(1450\ cm^{-1})}{Abs(1415\ cm^{-1})}$	Snoeck et al., 2014 and Thompson et al., 2009
Amide to Phosphate (Am/P)	$\frac{Abs(1650\ cm^{-1})}{Abs(1035\ cm^{-1})}$	Thompson et al., 2009
ν_1Phosphate to Amide I (ν_1PO_4/Amide I)	$\frac{Abs(960\ cm^{-1})}{Abs(1640\ cm^{-1})}$	France et al., 2014

2.5 Data analysis

Principal Component Analysis (PCA) is an unsupervised chemometric method used to reduce the dimensionality of multivariate data into a smaller number of variables called principal components (PCs). The PCs capture most of the information from the original dataset, with the information content decreasing in subsequent components; thus, the first PC contains the majority of information from the total dataset.

In this study, PCA was performed to analyze spectral data from human dentine samples. The dataset consisted of intensity values at various wavenumbers corresponding to different functional groups present in dentine. Samples were classified into two groups based on sex: male (group 1) and female (group 2). PCA was used to provide an overview of the multivariate data and to identify trends or patterns within the dataset. Score plots were generated to visualize the clustering of samples with similar characteristics and to highlight differences between sex groups.

Subsequent statistical analyses focused on chemometric indices to identify those showing the strongest associations with age at death or sex. Analyses were performed using IBM SPSS Statistics Base version 22. Pearson and Spearman correlation coefficients were used to assess associations. Indices exhibiting significant associations with age at death were subsequently modeled using linear regression to derive equations relating them to age at death. A significance level of 0.05 (95%) was adopted for all tests.

RESULTS and DISCUSSION

Figure 1 illustrates the ATR-FTIR spectral patterns of dentine from male and female samples. All spectra across different ages and sexes were visually inspected by examining the peaks present. No differences in the observed functional groups were detected between male and female samples.

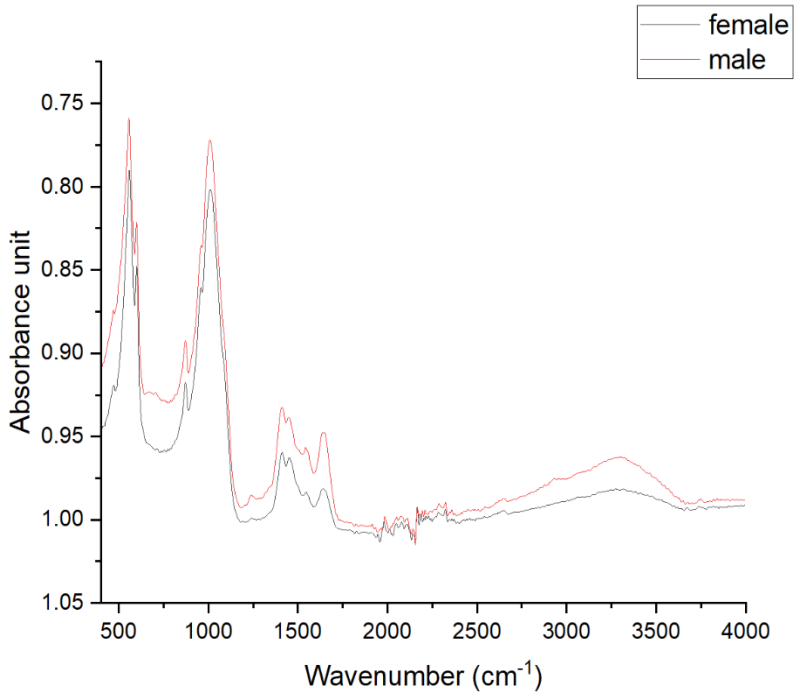


Fig.1 FT-IR spectrum of male and female dentine sample

Table 2. Absorption bands and/or range of chemical components present in human dentine.

Components	Absorption (cm^{-1})
PO_4^{3-} ν_2	464-476
PO_4^{3-} ν_4	553-561
PO_4^{3-} ν_1	958
	960
	961
PO_4^{3-} ν_3	1010
	1014
	1000-11 00
CO_3^{2-} ν_2	871
	873
CO_3^{2-} ν_3 overlapped with collagen	1409
	1411
	1425-1450
C-N stretching	1236
	1240
	1244
Scissoring CH_2	1450
Carbonate + Amide II	1541
C = O stretching	1633
	1652
Amide I	1641
Amide A and amine N-H	3257; 3313
B-type carbonate	872

male

As shown in Figure 1, ATR-FTIR analysis of human dentine revealed signals corresponding to the main functional groups within the tooth samples, as summarized in Table 2. Signals in the 460–470 cm^{-1} and 553–561 cm^{-1} ranges correspond to bending vibrations of phosphate groups, while those in the 958–961 cm^{-1} and 1000–1100 cm^{-1} ranges correspond to stretching vibrations of phosphate groups, reflecting the hydroxyapatite structure in dentine. Carbonate vibrations at 871 cm^{-1} indicate the substitution of phosphate positions in the mineral hydroxyapatite structure. Additionally, overlapping peaks associated with collagen were observed at 1409–1450 cm^{-1}, with amide III at 1240 cm^{-1}, amide II at 1541 cm^{-1}, and amide I at 1641 cm^{-1}.

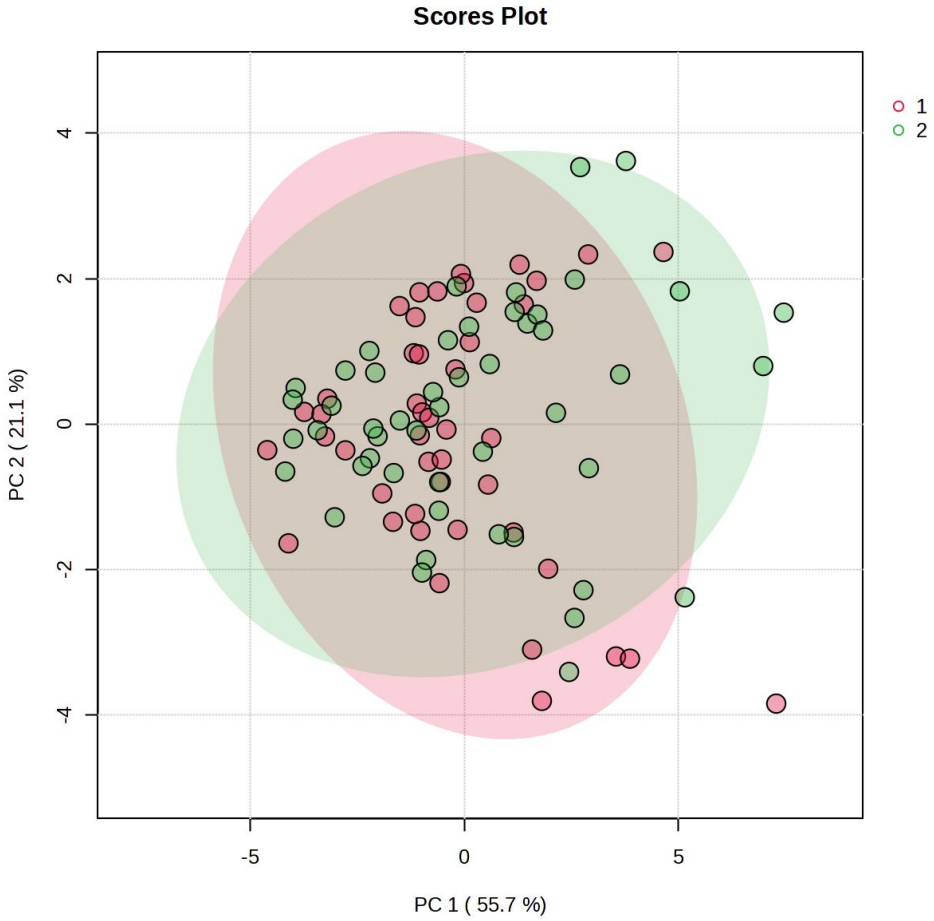


Fig.2 PCA score plot of functional groups found in human dentine

The PCA plot for sex classification showed that PC-1 (55.7%) and PC-2 (21.1%) accounted for the largest variation in the dataset. A total of 76.8% of the variation was captured by the first six PCs of the PCA model. However, as shown in Figure 2, PCA was unable to differentiate between male and female samples.

Statistical analysis revealed that the CI, API, BPI, and C/C indices showed no significant association with age at death (Table 3). In contrast, the carbonate-to-phosphate ratio was significantly correlated with age at death (Spearman's $\rho = 0.180$ and 0.184, $p < 0.05$), as was the amide-to-phosphate ratio (Spearman's $\rho = 0.186$, $p < 0.05$) and ν_1PO_4/Amide I (Spearman's $\rho = -0.178$, $p < 0.05$).

This study found that the carbonate-to-phosphate and amide-to-phosphate ratios in dentine spectra were significantly correlated with age at death, reflecting age-related changes in the chemical composition and structure of bioapatite and proteins in dental tissue. The use of FTIR-ATR for dentine analysis in this study aligns with previous research employing FTIR-ATR and chemometrics to estimate age at death from human bone, which

demonstrated statistical relationships between phosphate and carbonate indices and age, successfully developing accurate age prediction models (Pedrosa et al., 2020).

Furthermore, these findings highlight the potential application of FTIR-ATR spectroscopy for forensic age estimation from dental tissues. However, the observed statistically significant correlations in this study were of small to moderate magnitude. A larger sample size and a more balanced distribution of age groups are required to validate and strengthen the observed trends.

Table 3. Results of Spearman's correlation coefficients between CI, C/P, C/P(2), API, BPI, C/C, Am/P, and ν_1PO_4/Amide I chemometric indices and age-at-death.

	n	ρ	*p* value
CI	95	0.079	0.222
C/P	95	0.180*	0.041
C/P(2)	95	0.184*	0.037
API	95	0.054	0.303
BPI	95	0.012	0.453
C/C	95	0.122	0.119
Am/P	95	0.186*	0.036
ν_1PO_4/Amide I	95	-0.178*	0.043

*Significant for $\alpha = 0.05$

CONCLUSION

The application of the FTIR-ATR technique, combined with chemometric indices such as CI, C/P, API, BPI, C/C, Am/P, and ν_1PO_4/Amide I, was used to analyse human dentine. The study found that the carbonate-to-phosphate and amide-to-phosphate ratios increased with age, whereas the ν_1PO_4/Amide I ratio decreased, suggesting promising potential for estimating age at death. However, a larger sample size is needed to more accurately characterize changes in these indices, and this method should be applied in conjunction with other approaches to enhance reliability.

ACKNOWLEDGEMENTS

This work was supported by the Teaching Assistant/Research Assistant Scholarship from Chiang Mai University. We are also grateful to Miss Wirintra Watcharanone, Miss Kanjana Inthong, Miss Atchara Pothinkunapat, and Miss Preeyajak Chinwaraphat for their assistance in collecting the teeth samples.

REFERENCES

Diez, C., Rojo, M. Á., Martín-Gil, J., Martín-Ramos, P., Garrosa, M., & Córdoba-Diaz, D. (2022). Infrared Spectroscopic Analysis of the Inorganic Components from Teeth Exposed to Psychotherapeutic Drugs. *Minerals*, *12*(1), 28.

Fernández-Escudero, A. C., Legaz, I., Prieto-Bonete, G., López-Nicolás, M., Maurandi-López, A., & Pérez-Cárceles, M. D. (2020). Aging and trace elements in human coronal tooth dentine. *Scientific Reports*, *10*(1), 9964.

France, C. A. M., Sugiyama, N., & Aguayo, E. (2020). Establishing a preservation index for bone, dentin, and enamel bioapatite mineral using ATR-FTIR. *Journal of Archaeological Science: Reports*, *33*, 102551.

France, C. A. M., Thomas, D. B., Doney, C. R., & Madden, O. (2014). FT-Raman spectroscopy as a method for screening collagen diagenesis in bone. *Journal of Archaeological Science*, *42*, 346-355.

Karuna, K., Rao, R., Sarode, S., Sarode, G., & Patil, S. (2017). Raman Microspectrometry: An Alternative Method of Age Estimation from Dentin and Cementum. *Journal of Clinical and Diagnostic Research*, *11*, ZC11-ZC16.

Krishan, K., Kanchan, T., & Garg, A. K. (2015). Dental Evidence in Forensic Identification - An Overview, Methodology and Present Status. *The Open Dentistry Journal, 9*, 250-256.

Lopes, C. d. C. A., Limirio, P. H. J. O., Novais, V. R., & Dechichi, P. (2018). Fourier transform infrared spectroscopy (FTIR) application chemical characterization of enamel, dentin and bone. *Applied Spectroscopy Reviews*, *53*(9), 747-769.

Mistek-Morabito, E., & Lednev, I. (2018). FT-IR spectroscopy for identification of biological stains for forensic purposes. *Spectroscopy (Santa Monica)*, *33*, 8-19.

Pedrosa, M., Curate, F., Batista de Carvalho, L. A. E., Marques, M. P. M., & Ferreira, M. T. (2020). Beyond metrics and morphology: the potential of FTIR-ATR and chemometrics to estimate age-at-death in human bone. *International Journal of Legal Medicine, 134*(5), 1905-1914.

Pretty, I. A., & Sweet, D. (2001). A look at forensic dentistry – Part 1: The role of teeth in the determination of human identity. *British Dental Journal*, *190*(7), 359-366.

Thompson, T. J. U., Gauthier, M., & Islam, M. (2009). The application of a new method of Fourier Transform Infrared Spectroscopy to the analysis of burned bone. *Journal of Archaeological Science*, *36*(3), 910-914.

Thompson, W. (2018). How should forensic scientists present source conclusions? *Seton Hall Law Review, 48*(3), Article 9.

Snoeck, C., Lee-Thorp, J. A., & Schulting, R. J. (2014). From bone to ash: Compositional and structural changes in burned modern and archaeological bone. *Palaeogeography, Palaeoclimatology, Palaeoecology*, *416*, 55-68.

Weiner, S., & Bar-Yosef, O. (1990). States of preservation of bones from prehistoric sites in the Near East: A survey. *Journal of Archaeological Science*, *17*(2), 187-196.

Yadav, A., Nimi, C., Bhatia, D., Rani, N., & Singh, R. (2024). Estimation of age and sex from fingernail clippings by using ATR-FTIR spectroscopy coupled with chemometric interpretation. *International Journal of Legal Medicine*, *138*(6), 2401-2410.

Yu, K., Xiong, H., Wei, X., Wu, H., Zhang, B., Wang, G., Yang, X., & Wang, Z. (2022). Chronological Age Estimation of Male Occipital Bone Based on FTIR and Raman Microspectroscopy. *Bioinorganic Chemistry and Applications, 2022*, 1729131.

POSTER PRESENTATION

Van Gölü alkalifilik fungusları üzerine ön çalışma

Nilgün Poyraz[1*] (https://orcid.org/0000-0002-5861-7922),
Suat Sezen[2] (https://orcid.org/0000-0002-5901-5747)

[*1]Kütahya Dumlupınar Üniversitesi, Fen Edebiyat Fakültesi, Biyoloji Bölümü, Kütahya,Türkiye
[2]Eskişehir Osmangazi Üniversitesi, Fen Fakültesi, Biyoloji Bölümü, Eskişehir Türkiye

*Sorumlu yazar e-mail: nilgun.kavak@dpu.edu.tr

Özet

Funguslar, doğada en yaygın olarak bulunan mikroorganizmalardan biridir. Bu canlılar, organik maddelerin ayrıştırılmasında önemli rol oynar ve endüstri ile gıda sektörlerinde çeşitli biyoaktif bileşiklerin ve katma değerli ürünlerin üretiminde yaygın biçimde kullanılmaktadır. Ayrıca, funguslar bitki, hayvan ve insan sağlığı üzerinde doğrudan ya da dolaylı etkiler yaratarak önemli ekonomik ve sağlık sorunlarına neden olabilmektedir. Yaşam alanlarının çeşitliliği, fizyolojik, biyolojik ve biyoteknolojik özelliklerinin geniş spektrumu nedeniyle, fungusların biyolojik çeşitliliğinin belirlenmesine yönelik çalışmalar hem ekolojik hem de endüstriyel açıdan büyük önem taşımaktadır. Bu çalışmanın amacı, Van Gölü'nde bulunan fungusların biyolojik çeşitliliğini araştırmak ve bu ekstrem ekosistemdeki fungal topluluğun yapısını ortaya koymaktır. Bu kapsamda, Van Gölü'nden su örnekleri alınmış ve örnekler pH ve tuzluluk değerleri açısından analiz edilmiştir. Fungus türlerinin sudan izolasyonu için membran filtrasyon yöntemi uygulanmış ve Malt Extract Agar (MEA) besiyeri kullanılmıştır. Saflaştırma işlemleri sonucunda toplam 10 izolat elde edilmiştir. Elde edilen izolatlar, geleneksel morfolojik incelemeler ve moleküler tanımlama yöntemleri ile karakterize edilmiştir. Çalışma sonuçları, Van Gölü'nde alkalifilik ve alkalitolerant özellik gösteren mikrofungus türlerinin bulunduğunu ve bu türlerin ağırlıklı olarak *Aspergillus, Penicillium*, *Alternaria* ve *Fusarium* cinslerine ait olduğunu ortaya koymuştur. Bu bulgular, yüksek pH ve tuzluluk içeren ekstrem ortamların sahip olduğu özgün mikrobiyal çeşitliliğin anlaşılmasına katkı sağlamaktadır.

Anahtar kelimeler: Van Gölü, biyolojik çeşitlilik, alkalifilik funguslar, izolasyon

A preliminary study on alkaliphilic fungi from Lake Van

Abstract

Fungi represent one of the most ubiquitous groups of microorganisms in the environment. They play a vital role in the decomposition of organic matter and are extensively utilized in the industrial and food sectors for the production of various bioactive compounds and value-added products. Furthermore, fungi exert considerable economic and health impacts through their diverse interactions with plants, animals, and humans. Given the diversity of their habitats and the breadth of their physiological, biological, and biotechnological characteristics, studies aimed at elucidating fungal biodiversity are of significant scientific importance. The present study aimed to investigate the biological diversity of fungi inhabiting Lake Van. For this purpose, water samples were collected and analyzed for pH and salinity parameters. Fungal species were isolated using the membrane filtration technique in conjunction with Malt Extract Agar (MEA) medium. Following purification procedures, a total of ten isolates were obtained. These isolates were subsequently identified through a combination of conventional morphological characterization and molecular analyses. The findings revealed that alkaliphilic and alkalitolerant fungal species are present in Lake Van, predominantly belonging to the genera Aspergillus, Penicillium, Alternaria, and Fusarium. These results contribute to the understanding of extremophilic fungal diversity in hypersaline and alkaline aquatic ecosystems.

Keywords: Lake Van, biodiversity, alkaliphilic fungi, isolation

GİRİŞ

Ekstremofiller, yüksek ve düşük sıcaklıklar, aşırı pH veya tuzluluk, radyasyon varlığı, aşırı basınç veya çok yüksek hidrokarbon konsantrasyonu gibi aşırı fiziksel veya jeokimyasal koşullarda gelişebilen mikroorganizmalardır. Fungusların genel olarak nötr veya hafif asidik pH'ta büyümeyi tercih etmelerine rağmen, bazılarının yüksek pH'ta da gelişebildiği belirlenmiştir. Bu ortamlarda gelişebilen organizmalar, yüksek pH'a dayanıklı olan amilaz, lipaz ve proteaz gibi alkali enzimler üretir ve bu enzimler biyoteknolojik olarak tekstil, gıda, ilaç endüstrisi vb. alanlarda kullanılabilir (Fernández-López ve ark.,2023).

Sodalı (veya alkali) topraklar ve göller, Dünya'daki en alkali doğal yaşam alanlarıdır. pH değerleri genellikle 9 ila 11 arasında değişen bu ortamlar, aynı zamanda genellikle yüksek Na+ konsantrasyonlarına sahip çok tuzlu ortamlardır. Sodalı göller ve toprakların önemli bir rezervuarı Batı Sibirya, Altay, Trans-Baykal bölgeleri (Rusya), Moğolistan ve Afrika'da bulunur. Bu bölgelerdeki Magadi ve Natron Gölleri'nin pH değerleri 12'ye yaklaşır (Grum-Grzhimaylo ve ark.,2018). Ayrıca çimento üretimi, çivit boyası üretimi, madencilik faaliyetleri, kağıt ve kağıt hamuru üretimi ve gıda işleme atık suları gibi çeşitli endüstriyel faaliyetler sonucu da alkali ortamlar meydana gelebilir (Fernández-López ve ark.,2023).

Yüksek pH değerlerinde (pH: 8-11) gelişebilen fungusların türleri ve çeşitliliği geniş çapta ve yeterince incelenmemiştir (Grum-Grzhimaylo ve ark.,2016). Funguslar ile çalışılırken alkalifilik ve alkaliye toleranslı suşları izole etmek zordur çünkü alkalin ortamların fungus çeşitliliğini incelemek için nötr veya asidik izolasyon ortamları kullanılmaktadır ve bu da alkalifilik suşların tanımlanma ve izole edilme olasılığını azaltmaktadır (Fernández-López ve ark.,2023).

Ülkemizde de Doğu Anadolu Bölgesi'nde yer alan ve tuzlu bir soda gölü özelliği taşıyan Van Gölü bulunmaktadır. Van Gölü sadece ülkemizde değil, Dünyada da en büyük soda göllerinden biridir ve Dünya'nın en büyük 3. kapalı havza gölüdür (Poyraz ve Mutlu,2017). Son yıllarda, soda göllerinin alkalifilik mikroorganizmaları üzerine yapılan çalışmalar artış göstermiştir. Mikrobiyal çeşitliliği araştırmak için kültüre bağımlı yöntemleri, kültür bağımsız yöntemleri ve modern yöntemler kullanmışlardır (Paquette ve ark.,2024; Kaale ve ark.,2025; Jeilu ve ark.,2025). Bunlara ek olarak, çeşitli mikrobiyal toplulukların yapısını ve çeşitliliğini incelemek için amplikon dizilemeler ve yüksek verimli dizilemelerden yararlanılmıştır (Jeilu ve ark.,2022). Ancak Van Gölü üzerine yapılan çalışmalar sınırlıdır (Poyraz ve Mutlu,2017; Ersoy Omeroglu ve ark.,2021) ve funguslar üzerine çalışmalar üzerine yeterince odaklanılmamıştır. Bu sebeple çalışmada Van Gölü'nden alınan su örneklerinden fungal cinslerin ve türlerin izolasyonu üzerine ön deneme yapılması amaçlanmıştır.

MATERYAL METOD

Örnekleme ve İzolasyon

Su örnekleri üç farklı lokasyondan alınmıştır. Örnekleme lokasyonu olarak kullanılan bu kıyıların isimleri Merkez (yaklaşık 38,6ºK, 43,3ºD), Tatvan (yaklaşık 38,5ºK, 42,3ºD) ve Ahlat'tır (yaklaşık 38,8ºK, 42,6ºD). Su örnekleri kıyıdan yaklaşık 1-2 m uzaklıktan ve 1 m derinlikten alınmıştır. Örnekler steril şişelere konularak hemen taşınmış ve oda sıcaklığında saklanmıştır. Örneklerin tuzluluğu (Eclipse El Refraktometresi), ve pH'ı (Mettler Toledo) belirlenmiştir.

Alkalitolerant/alkalifilik suşların ilk izolasyonu için Malt Extract Agar kullanılmıştır. Ortaya çıkan fungal izolatlar saflaştırılmış ve morfolojik karakterizasyonu yapılmıştır. İzolasyon için 100'er ml su örneği steril 0,45 µm 'lik membran filtrelerden filtrasyon yöntemi ile filtre edilmiştir ve filtreler besiyerine alınarak 25°C'de 7-10 gün boyunca inkübe edilmiştir.

Morfolojik ve Genetik Karakterizasyon

Filtrasyon petrileri 25°C'de 7-10 gün boyunca inkübe edildikten oluşan küf kolonileri incelenmiş ve farklı morfolojide olduğu düşünülen küf kolonileri Malt Ekstrakt Agar'a 3 nokta yöntemiyle inoküle edilmiş ve 25°C'de 7 gün inkübe edilmiştir. İnkübasyon sonucu gelişen fungal izolatların morfolojik tanımlaması, kültürel özelliklerine göre yapılmıştır. Koloni çapları, renkleri ve dokuları, misel ve spor yapıları stereomikroskop ve ışık mikroskobu ile incelenmiştir. İzolatlar morfolojik ve mikroskobik özelliklerine göre cins düzeyinde ayırt edilmiştir.

Tüm izolatlar, DNA ekstraksiyonu için 25 °C'de 7 gün geliştirilmiştir. Mantar genomik DNA'sı, üreticinin talimatlarına göre "Zymo Fungal/Bacterial DNA İzolasyon Kiti" kullanılarak ekstrakte edilmiştir. Elde edilen DNA, ITS (Internal Transcribed Spacer) bölgelerinin PCR amplifikasyonu için kullanılmıştır. Bu primerler ribozomal DNA (rDNA) dizisinin 18S – 5.8S – 28S bölgeleri arasındaki ITS1 ve ITS2 bölgelerini çoğaltır. Tür tanımlamada en yaygın kullanılan genetik markerdir. Elde edilen DNA'nın kalitesi ve miktarı NanoDrop ile ölçülmüştür (Esen ve Turgay,2022; Seri,2022)

DNA Dizi Analizi

PCR örnekleri agaroz jelde yürütülerek yaklaşık 500-600 bç ürün verip vermediğine bakılmıştır. Ardından ITS PCR örnekleri sekansa gönderilerek dizi analizi yaptırılmıştır. Analiz ve verilerden elde edilen diziler BLAST ile NCBI veri tabanında bulunan dizilerle karşılaştırma yapılarak küf cinsleri tanımlanmıştır.

BULGULAR

Örnekleme ve İzolasyon

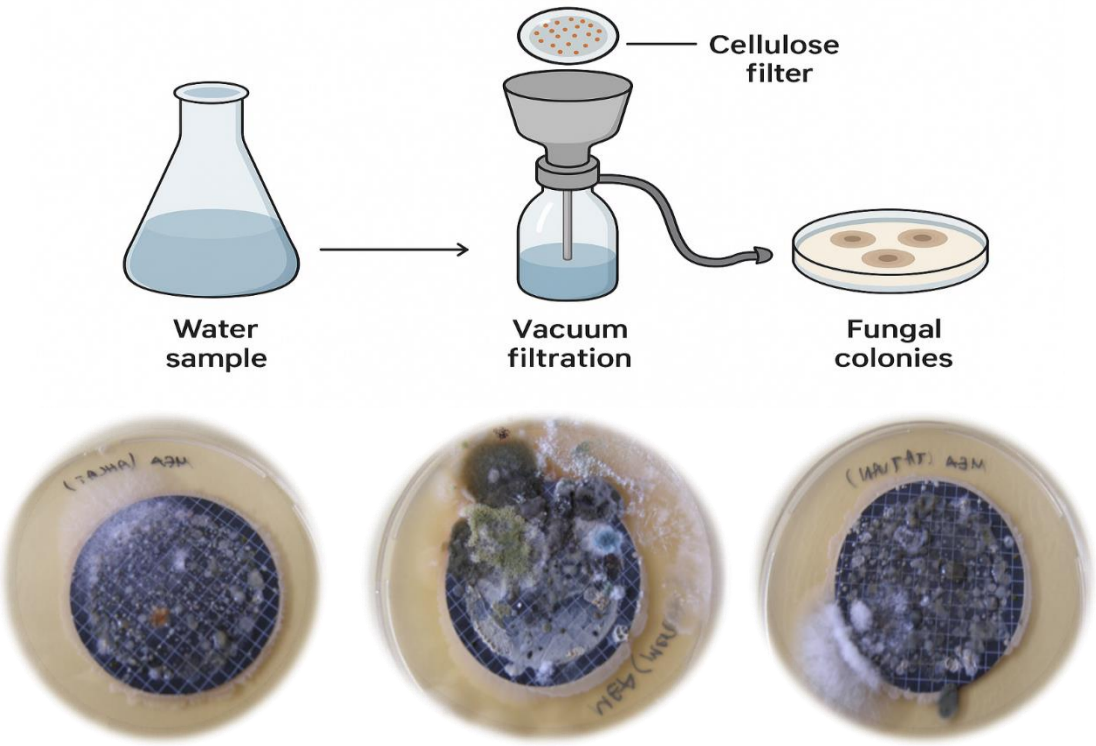
Su örneklerinin tuzluluk ve pH sonuçları çizelgede verilmiştir.

Tablo 1: Örneklerin tuzluluk ve pH değerleri

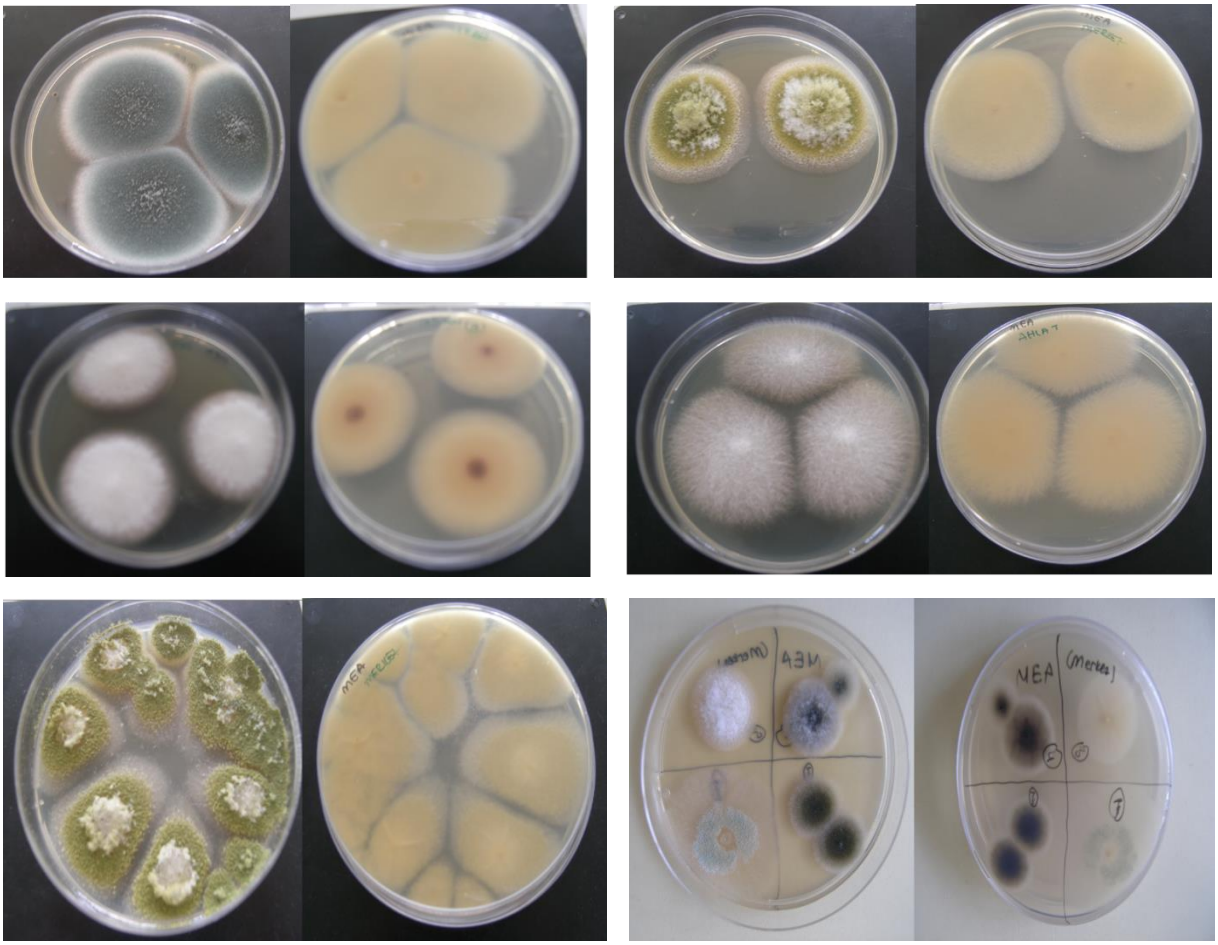
ÖRNEK	TUZLULUK (%)	pH
Merkez	%1.7	9.5
Tatvan	%1.8	9.8
Ahlat	%1.8	9.6

Küf izolatlarının makroskobik ve mikroskobik analizleri

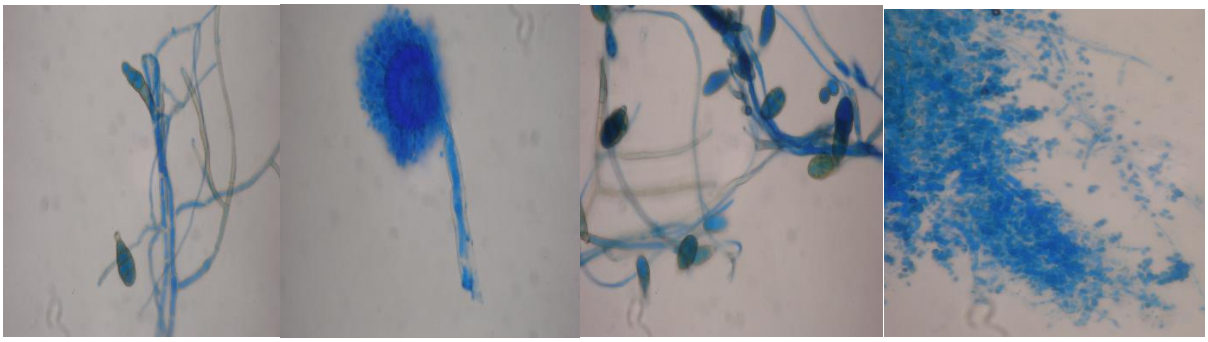
Su örnekleri membran filtreden geçirildikten sonra farklı olduğu düşünülen toplamda 9-10 küf kolonisi saflaştırılmıştır.



Şekil 1: Memran filtrasyon ve inkübasyon sonrası filtrelerde gelişen koloniler



Şekil 2: MEA besiyerlerindeki koloni morfolojileri (25°C'de 5 gün)



Şekil 3: Kolonilerin mikroskopik görüntüleri

Yapılan morfolojik incelemelerde koyu yeşil/siyah renkte, tozlu-kadifemsi yüzeyi bulunan kolonilerin *Aspergillus* cinsine ait olabileceği (*Aspergillus niger*), mavi-yeşil, kadifemsi koloni morfolojisine sahip kolonilerin *Penicillum* cinsi, gri-yeşil merkez ve pamuksu beyaz kenarı olan kolonilerin *Cladosporium,* sarı-yeşil spor tabakası oluşturabilen, ortası beyaz, kenarları yeşilimsi-sarı renk tipik özellik gösteren kolonilerin *Aspergillus flavus* olabileceği belirlenmiştir. Kolonileri kadifemsi, yoğun ve dairesel ortada koyu mavi-yeşil, kenarlara doğru daha açık yeşil, arka yüz renksizden sarımsı-beje kadar olan koloniler *Penicillium'un* tipik özelliğidir ve muhtemelen *P. chrysogenum* olabileceği sonucuna varılmıştır. *Alternaria spp.* Kültürde genellikle orta koyu, kenar açık dairesel koloniler oluşturur. Mikroskop altında tipik olarak zincir halinde, bölmeli görülür. Koloniler yoğun, pamuksu (cotton-like), beyaz-krem renkte ve merkezde hafif sarımsı/bej tonlamalar görülüyorsa ve kolonilerin arkadan görünümü pembe-kahverengi ise bu görünüm *Fusarium*'un tipik özelliğidir ve koloni morfolojisi ile örtüşmektedir.

Diğer petrilerde de koloniler gençken beyaz/krem, olgunlaştığında siyah renkli ve yoğun, tozlu ve siyah renkte koloniler olduğundan *Aspergillus niger* olarak tanımlanmıştşr.

Moleküler Karakterizasyon

Yapılan DNA Ekstraksiyonu sonrası 9 adet ekstraksiyon başarı ile yapılmıştır. PCR işlemi ve DNA dizi analizi sonrası ise 4 adet dizi verisi analiz edilmiştir.

Tablo 2: Dizilenen İzolatlar ve Benzerlik Gösterdiği Türler

ÖRNEK	Benzerlik Gösterdiği Tür	Numarası	Baz Eşleşme Oranı
V1	*Aspergillus flavus* isolate AF-36	PQ422926.1	527/529(99%)
V2	*Penicillium* sp. G418	KJ443251.1	506/511(99%)
V3	*Alternaria* sp. CBS 127959	KY940806.1	559/560(99%)
V4	*Penicillium chrysogenum* isolate 5a-6	PV612027.1	557/560(99%)

TARTIŞMA ve SONUÇ

Çalışmada analizler sonucu *Aspergillus*, *Penicillium* ve *Alternaria* cinslerine ait fungus cinsleri belirlenmiştir. Alkalifilik funguslar üzerine yapılan çalışmalar incelendiğinde Steiman ve ark. (2004) Mono Gölü'nden (ABD) elde edilen, pH'ı 8 ila 9,2 arasında değişen toprak ve tortu örneklerinden çok çeşitli funguslar izole etmiştir. İzolasyon için çalışmamıza benzer şekilde pH = 8 olan Malt Extract Agar kullanmışlardır. Elde edilen izolatların çoğu alkaliye toleranslıdır.

Farklı çalışmalarda *Acremonium* ve *Sodiomyces* türleri farklı alkali ortamlardan izole edilmiştir. Bu türlerden bazıları 10 ve 11 pH aralığında gelişebilir. Diğer izole edilmiş türler arasında elde edilen *Fusarium* ve *Penicillium* cinslerine ait türler bulunmaktadır. Bu iki cinsin bazı suşları hafif ile orta alkali toleranslı bir profil sergilemiştir (Fernández-López ve ark.,2023).

Asya ve Afrika'daki soda göllerinin etrafındaki topraklardan alınan 100 alkalitolerant ve alkalifilik izolat tanımlandığında ise Emericellopsis(Hypocreales, Hypocreomycetidae), Plectosphaerellaceae (Hypocreomycetidae), Pleosporaceae (Dothideomycetes), Chaetomiaceae (Sordariomycetidae) belirlenmiştir. Özellikle Sodiomyces türleri *Acrostalagmus luteoalbus Emericellopsis alkalina*, ve Alternaria yüksek ortam pH'ında en iyi şekilde gelişmiştir. Orta alkalitolerantlar arasında Scopulariopsis üyeleri, Fusarium, Cladosporium türleri belirlenmiştir. Zayıf alkalitolerantlar, nötr veya asidik pH'ta büyüme optimumuyla *Penicillium* sp, *Purpureocillium lilacinum* ve *Alternaria alternata* türleri olarak belirlenmiştir (Grum-Grzhimaylo ve ark.,2016).

KAYNAKÇA

Ersoy Omeroglu, E., Sudagidan, M., Yurt, M. N. Z., Tasbasi, B. B., Acar, E. E., & Ozalp, V. C. (2021). Microbial community of soda Lake Van as obtained from direct and enriched water, sediment and fish samples. Scientific Reports, 11(1), 18364.

Esen, Y., & Turgay, Ö. (2022). Sürk Peynirinden İzole Edilen Küflerin Pcr Yöntemiyle Tanımlanması. Gıda, 47(1), 136-146.,

Fernández-López, M. G., Batista-García, R. A., & Aréchiga-Carvajal, E. T. (2023). Alkaliphilic/alkali-tolerant fungi: molecular, biochemical, and biotechnological aspects. Journal of Fungi, 9(6), 652.

Grum-Grzhimaylo, A. A., Falkoski, D. L., van den Heuvel, J., Valero-Jiménez, C. A., Min, B., Choi, I. G., ... & Debets, A. J. (2018). The obligate alkalophilic soda-lake fungus Sodiomyces alkalinus has shifted to a protein diet. Molecular ecology, 27(23), 4808-4819.

Grum-Grzhimaylo, A. A., Georgieva, M. L., Bondarenko, S. A., Debets, A. J., & Bilanenko, E. N. (2016). On the diversity of fungi from soda soils. Fungal diversity, 76(1), 27-74.

Jeilu, O., Gessesse, A., Simachew, A., Johansson, E., & Alexandersson, E. (2022). Prokaryotic and eukaryotic microbial diversity from three soda lakes in the East African Rift Valley determined by amplicon sequencing. Frontiers in Microbiology, 13, 999876.

Jeilu, O., Simachew, A., Hartmann, E. M., Alexandersson, E., & Johansson, E. (2025). Comparative Metagenomics of Soda Lakes and the Rumen Reveals Novel Microbial Lineages and Carbohydrate-active Enzyme Diversity. bioRxiv, 2025-06.

Kaale, S. E., Machang'u, R. S., & Lyimo, T. J. (2025). Taxonomic diversity of bacterial communities in the sediments of a soda lake in Arusha, Tanzania. Journal of Great Lakes Research, 102649.

Paquette, A. J., Bhatnagar, S., Vadlamani, A., Gillis, T., Khot, V., Novotnik, B., ... & Rattray, J. E. (2024). Ecology and biogeochemistry of the microbial underworld in two sister soda lakes. Environmental Microbiome, 19(1), 98.

Poyraz, N., & Mutlu, M. B. (2017). Van Gölü'nün alkalifilik bakteriyel çeşitliliği. Biological Diversity and Conservation, 10(1), 92-103.

Seri, M. (2020). Konya küflü peynirinden izole edilen küflerin moleküler identifikasyonu ve Penicillium roqueforti izolatlarının morfolojik karakterizasyonu (Master's thesis, Istanbul Sabahattin Zaim University (Turkey)).

POSTER PRESENTATION

The importance of sampling in the statistical study of STR markers

Ela Zaimi[1](https://orcid.org/0009-0001-2898-1408),
Merita Xhetani[2,3](https://orcid.org/0000-0001-6982-5489)

[1]Albanian University, Faculty of Medical Science, Department of Dentistry, Tirana, Albania.
[*2] University of Tirana, Faculty of Natural Sciences, Department of Biology, Tirana, Albania.
[3]Center of Molecular Diagnostics and Genetic Research, University Hospital Obstetric and Gynecologic (Queen Geraldine), Tirana, Albania

Abstract

The genetic composition of a population is crucial for understanding its evolutionary history, genetic diversity and for applications in forensic science and medicine. Short Tandem Repeats (STRs) are powerful molecular markers used in genetic studies due to their high variability and widespread distribution in the genome.The number of repeats varies from one individual to another, making these sequences suitable for identification purposes due to their high discriminatory power. DNA analysis for this purpose in Albania began in 2009, using a technique that studies 17 STR markers. For the purposes of this study, allelic data from STR markers were processed in three sample sets of different sizes—specifically 200, 1000, and 2000 unrelated individuals from the Albanian population.Differences were observed in some of the allelic frequency values when comparing data from the three samples. Forensic population parameters for the Albanian population were analysed using the STRAF program version 2.1.5. The results showed that the first sample, consisting of 200 individuals, was insufficient for assessing Hardy-Weinberg equilibrium. For the other two samples, the processing results confirmed equilibrium conditions.These experiments with different size of the sample emphasize the fact that in statistical study of STR markers, the sampling of data to be analysed is of great importance.

Keywords:STR, sampling, STRAF, Hardy-Weinberg.

INTRODUCTION

Genetic studies have emerged as a cornerstone in the fields of biology and medicine, offering essential insights into human evolution, health, and population diversity. Over the last decades, advances in molecular biology have enabled researchers to analyze genetic variation with unprecedented precision, allowing for more accurate reconstructions of population history, improved understanding of hereditary diseases, and the development of powerful forensic identification tools (Jobling and Gill, 2004). One of the most significant areas of focus within modern genetic research is the study of Short Tandem Repeats (STRs)**.** STRs consist of short DNA sequences, typically between two and six base pairs that are repeated consecutively at specific loci throughout the genome. First introduced into forensic applications in the early 1990s, STRs quickly became central markers due to their abundance, stability, and ease of amplification through polymerase chain reaction (PCR) techniques (Jeffreys et al., 1985; Butler, 2012). These markers are exceptionally valuable because of their high degree of polymorphism**.** The number of repeated units at an STR locus varies widely among individuals, which results in a high level of allelic diversity within populations (Butler, 2015). This variation makes STRs particularly powerful for distinguishing between individuals, supporting their widespread use in human identification, kinship testing, and population genetic studies (Gill et al., 2006). Beyond forensic applications, STRs also contribute to broader biological research. Population geneticists use them to investigate gene flow, migration patterns, and demographic events such as bottlenecks or expansions (Holsinger and Weir, 2009). In medical genetics, STR instability has been linked to certain hereditary disorders, highlighting their relevance not only as neutral markers but also as elements with potential functional significance (Pearson et al., 2005). In Albania the analysis of STRs for identification purposes started in 2009, in the beginning with few biological samples which grow up year after year. In this paper we will discuss about the sample size and its implications in allele frequencies and other parameters studied. The size of the sample plays a critical role in the accuracy and reliability of studies involving Short Tandem Repeat

(STR) markers. Adequate sampling ensures that observed allele frequencies reliably reflect the true genetic diversity of the target population, reducing the risk of sampling error and frequency distortion (Weir, 2005). When sample sizes are too small, rare alleles may be missed, allele frequency estimates become unstable, and key statistical parameters such as heterozygosity or F-statistics can be significantly biased (Balding & Nichols, 1997). Such limitations may lead to incorrect interpretations of population structure, genetic differentiation, or the forensic informativeness of specific loci. Conversely, sufficiently large samples improve statistical power, increase the precision of allele frequency estimation, and enhance the reliability of population comparisons, kinship calculations, and forensic match probabilities (Butler, 2015). Therefore, careful selection of an adequate sample size is essential for producing robust and interpretable results in STR-based genetic research.

MATERIALS AND METHODS

Biological sample used for this study was saliva in buccal swabs, from unrelated anonymized albanian individuals. The ratio between number of samples representing 12 administrative divisions in which is organized Albania is saved in three sample sets of different sizes - specifically 200, 1000 and 2000 individuals.

DNA extraction, STR typing and fragment analysis

Extraction was performed using QIAamp DNA Investigator Kit with a final volume of DNA extract of 50µl. The commercial STR kit for amplification is NGM SelectTM kit (Thermo Fisher) a five dyes kit which simultaneously amplifies 16 separate STRs: D3S1358, VWA, D16S539, D2S1338, D8S1179, D21S11, D18S51, D19S433, THO1, FGA, D10S1248, D22S1045, D2S441, D1S1656, D12S391 and SE33 and the sex determining marker Amelogenin. Volumes for PCR reactions were halved resulting in the final volume of 12.5 µl. Fragment separation was performed using ABI PRISM® 3500 Genetic Analyzer (Applied Biosystems) using POP-4 polymer and the collection software Data Collection, version 2.0. Data was sized using GeneMapperTMID-X Software version 1.5. All laboratory procedures were conducted in accordance with rigorous internal control standards, including the use of controls supplied within the kits, to ensure quality control.

Data analysis

Forensic parameters such as Hardy-Weinberg equilibrium, match probability, power of discrimination, and other statistical analyses of STR data were conducted using STRAF version 2.1.5. Allele frequencies were studied in three samples

RESULTS AND DISCUSSION

The comparison between samples resulted in the expected changes in allele frequency values, reflecting the natural variability that arises from differences in sample size, composition and population representation. Such fluctuations are common when analyzing STR markers, as allele frequencies are sensitive to factors such as sample size, population substructure, and the presence of rare alleles. In some cases, even slight variations in the demographic or geographic characteristics of the sampled individuals can lead to measurable shifts in the distribution of alleles across loci. These differences do not necessarily indicate methodological inconsistencies; rather, they highlight the dynamic nature of genetic diversity and the importance of carefully selecting representative samples to ensure accurate population-level inferences. In the third sample there are 39 more alleles present than in the first sample. Results of these findings are presented in the table 1.

Table 1. The diferences in the number of alleles

Locus	Number of alleles in sample 1 (200 individuals)	Number of Alleles in sample 3 (2000 individuals)	Difference between sample 1 and sample 3
D1S1656	15	17	2
D16S539	7	8	1
vWA	7	10	3
D2S441	9	10	1
D12S391	17	19	2
D18S51	13	15	2
D19S433	14	15	1
D21S11	13	15	2
FGA	14	19	5
SE33	33	48	15

The differences between the second and the third sample in terms of number of alleles resulted in smaller changes such as in locus SE33 there were detected 45 alleles in second sample (1000 individuals analysed) versus 48 alleles in the third sample (2000 samples analysed) but comparing with the first sample (200 individuals analysed) there were detectes 13 alleles more. There were identified respecively these number of alleles in sample 1 – 194 alleles; in sample 2 – 228 alleles; in sample 3 – 252 alleles.
Distribution of alleles for 16 STRs studied in the third sample is presented in figure 1.

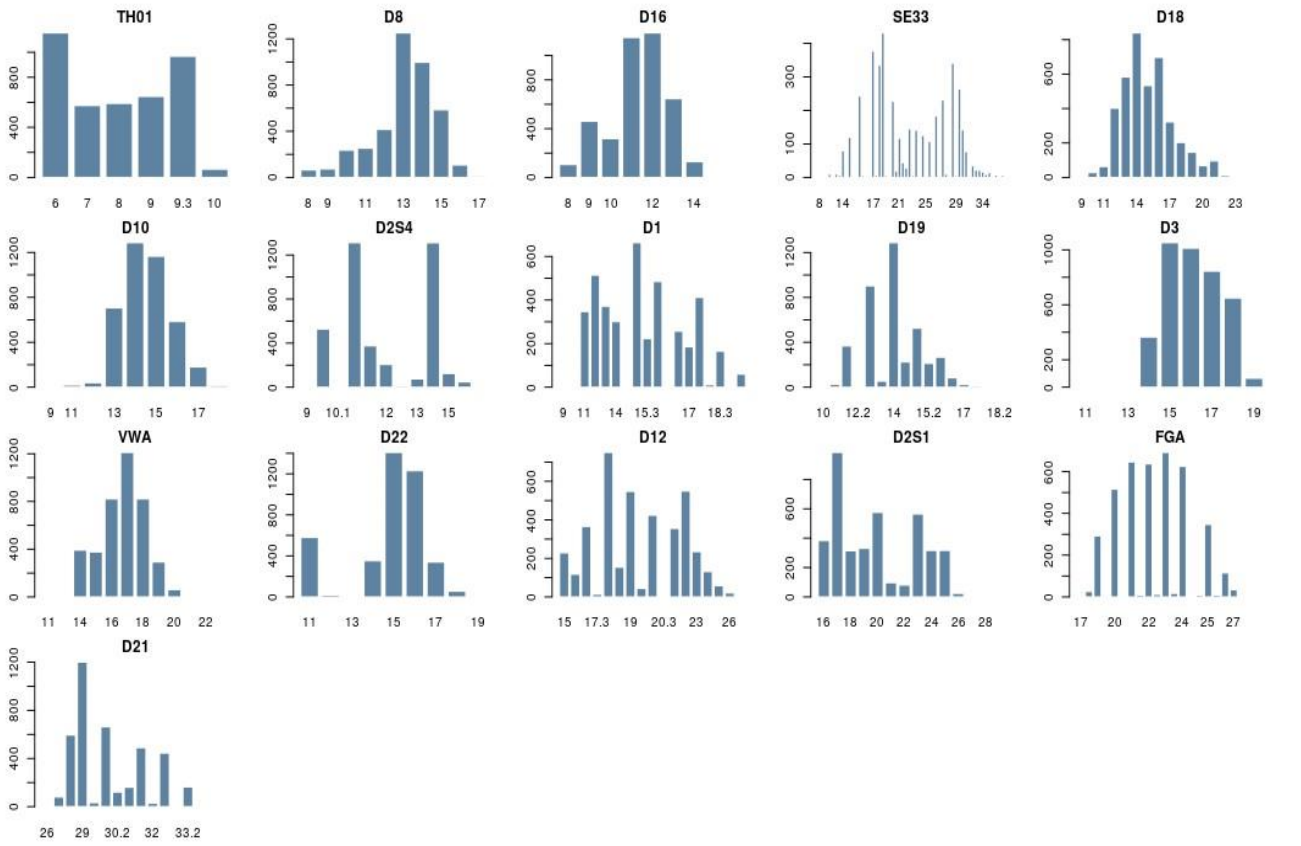


Figure 1. Distribution of alleles for 16 STR

There were no significant changes in forensic parameters analyzed by STRAF, statistical tests for sample 1 resulted in insufficient data for Hardy- Weinberg equilibrium meanwhile for the second and third sample showed no significant deviance from Hardy- Weinberg equilibrium (P-value > 0.05).

SE33 locus resulted in the highest levels of both expected and observed heterozygosity(Hexp and Hobs), reflecting significant genetic diversity at this locus within the population (Zaimi et al., 2025).
Across comparative studies, locus SE33 consistently emerges as one of the most polymorphic and forensically informative autosomal STR markers. In the Albanian population, SE33 exhibits very high variability, with 48 detected alleles, observed heterozygosity around 0.93, and a powerof discrimination (PD) of 0.9928**.**These values closely align with findings from other European populations. For example, studies from Slovenia report similarly high heterozygosity (≈0.93–0.97) and extremely high PD values, confirming SE33's exceptional discriminatory capacity across the region(Zupanič et al., 2014).Similarly, a study in a Western Sicilian population (n = 120) found that SE33 had a PIC of 0.9705 and an astounding PD of 0.99999, together with a high power of exclusion (PE = 0.9001) (Ventura Spagnolo et al., 2017).

CONCLUSION

In the statistical study of STR markers, the size of the sample represents one of the most critical determinants of analytical reliability. A sufficiently large sample is essential for capturing the true distribution of alleles within a population, minimizing the effects of random genetic drift and sampling error (Kalinowski, 2012). Small or inadequate sample sizes can lead to underrepresentation of rare alleles, unstable allele frequency estimates, and inflated measures of genetic diversity, which compromise the accuracy of key forensic parameters (such as heterozygosity, power of discrimination, or match probability) (Josse et al.,, 2001). Moreover, small samples limit the statistical power of tests for Hardy–Weinberg equilibrium and population differentiation, increasing the likelihood of false positives or negatives in genetic inference (BMC Genomics, 2016).

Recent work re-evaluating guidance on population sampling for highly polymorphic STR loci has shown that as sample size increases, the probability of capturing rare or previously unobserved alleles improves markedly, and the benefit of further sampling eventually plateaus. (Hares, 2025). These findings reinforce that robust sample sizes ensure greater precision, narrower confidence intervals, and more dependable interpretations of population structure. In forensic applications, where allele frequency data directly inform match probabilities and likelihood ratios, such reliability is indispensable. Careful attention to sample size is fundamental for producing valid, reproducible, and forensically meaningful results in STR-based genetic research.

REFERENCES

Balding, D. J., & Nichols, R. A. (1997). Significant genetic differentiation among subpopulations in the UK population of *Helix aspersa* revealed by microsatellite markers. *Molecular Ecology, 6*(4), 351–365. https://doi.org/10.1046/j.1365-294X.1997.00188.x

Butler, J. M. (2012). *Advanced topics in forensic DNA typing: Methodology*. Academic Press.

Butler, J. M. (2015). *Forensic DNA typing: Biology, technology, and genetics of STR markers* (2nd ed.). Academic Press.

Gill, P., Fereday, L., Morling, N., & Schneider, P. M. (2006). The evolution of DNA databases—Recommendations for new European STR loci. *Forensic Science International, 156*(2–3), 242–244. https://doi.org/10.1016/j.forsciint.2005.12.009

Hares, D. R. (2025). Revisiting guidance on population sampling for highly polymorphic STR loci. [Journal Name]. https://pubmed.ncbi.nlm.nih.gov

Holsinger, K. E., & Weir, B. S. (2009). Genetics in geographically structured populations: Defining, estimating and interpreting FST. *Nature Reviews Genetics, 10*(9), 639–650. https://doi.org/10.1038/nrg2611

Jeffreys, A. J., Brookfield, J. F. Y., &Semeonoff, R. (1985). Positive identification of an immigration test-case using human DNA fingerprints. *Nature, 317*, 818–819. https://doi.org/10.1038/317818a0

Jobling, M. A., & Gill, P. (2004). Encoded evidence: DNA in forensic analysis. *Nature Reviews Genetics, 5*(10), 739–751. https://doi.org/10.1038/nrg1455

Josse, L., & others. Sample size considerations in genetic polymorphism studies. [Journal].

Kalinowski, S. T. (2005). Sampling for microsatellite-based population genetic studies: 25 to 30 individuals per population is enough to accurately estimate allele frequencies. *Molecular Ecology, 14*(5), 1335–1340. https://pubmed.ncbi.nlm.nih.gov

Pearson, C. E., Nichol Edsall, L., & Cleary, J. D. (2005). Repeat instability: Mechanisms of dynamic mutations. *Nature Reviews Genetics, 6*(10), 729–742. https://doi.org/10.1038/nrg1689

Weir, B. S. (2005). *Genetic data analysis III: Methods for discrete population genetic data*. Sinauer Associates.

Ventura Spagnolo, E., Mondello, C., Procaccianti, S., et al. (2017). Allele frequencies distribution of 16 forensic STR loci in a Western Sicilian population sample. *Egyptian Journal of Forensic Sciences, 7*, Article 13. https://ejfs.springeropen.com/articles/10.1186/s41935-017-0013-y

Zaimi, E., Xhetani, M., & Haxhia, A. (2025). Genetic variation for 16 autosomal STR loci in a population sample from Albania. *International Journal of Ecosystems and Ecology Science, 15*(1), 231–238. https://doi.org/10.31407/ijees15.1

Zupanič Pajnič, I., Podovšovnik Axelsson, E., & Balažic, J. (2014). Slovenian population data for five new European Standard Set short tandem repeat loci and SE33 locus. *Croatian Medical Journal, 55*(1), 14–18. https://www.ncbi.nlm.nih.gov/pmc/articles/PMC3944414/

POSTER PRESENTATION

Sığır ve insanlarda bruselloz kontrol ve kontrol stratejileri

Sercan Geçici[1],* (0009-0006-5858-6923), Evrim Genç[1] (0000-0002-6405-6076), Oktay Genç[1] (0000-0003-0777-6824)

[1]Ondokuz Mayıs Üniversitesi, Veteriner Fakültesi, Mikrobiyoloji Anabilim Dalı, Samsun, Türkiye

*Sorumlu yazar e-mail:gecicisercan@gmail.com

Özet

Bruselloz, dünyanın çeşitli bölgelerinde çok sayıda insan ve hayvan türünü etkileyen, hayvancılık, halk sağlığı ve ekonomi üzerinde etkisi olan önemli zoonotik bir hastalıktır. Brusellozun kontrolü, üreticiler arasındaki farklı düzeyde çiftçilik uygulamaları ve hastalık hakkında algı farklılıkları, sürü sağlığı politikasının eksikliği, bruselloz prevalansının belirli zaman aralıklarıyla yapılmaması, aşılama eksikliği, hayvan hareketliliğinin takibindeki aksaklıklar, mesleki riskler nedeniyle veterinerlik uygulamalarında hala büyük bir sorun olmaya devam etmektedir. Birçok ülke, bruselloz kontrolünde farklı kontrol yöntemleri seçse de çoğu, var olan prevalansa bağlı olarak ilk seçeneği aşılama yönünde kullanarak sürü bağışıklığını artırmayı hedeflemektedir. Sonrasında sürveyans çalışmaları ve screening testler ile oluşan bağışıklık ve prevalans/insidans oranına göre mevcut stratejiler değerlendirilerek faz-kontrol programları yürütülmektedir. Dünyada hastalığı eradike edebilen çok az ülke mevcut ise de WOAH, FAO ve WHO gibi uluslararası organizasyonlar ile ortak yürütülen projeler sayesinde 30'dan fazla ülkede hastalık kontrol altına alınabilmiştir. Bruselloz, ruminantlar başta olmak üzere çok sayıda hayvan ve insan türünü etkilese de bu sunuda, brusellozun kontrol ve eradikasyonu amacıyla temel olarak sığırlarda ve insanlarda uygulanan yaklaşımlar anlatılmaktadır.

Anahtar Kelimeler: Bruselloz, Eradikasyon, Kontrol Stratejileri

Brucellosis control and control strategies in cattle and humans

Abstract

Brucellosis is a significant zoonotic disease affecting numerous human and animal species worldwide, impacting livestock production, public health, and the economy. Control of brucellosis remains a significant challenge in veterinary practice due to inconsistent farming practices and perceptions about the disease among producers, inadequacy of herd health policy, lack of regular brucellosis monitoring, inadequate vaccination and monitoring of animal movements, and occupational risks. While many countries employ different methods for brucellosis control, most aim to increase herd immunity by using vaccination as the first step depending on the existing prevalence. Subsequently, existing strategies are evaluated based on the immunity generated by surveillance and screening tests, and the prevalence/incidence ratio, and phase-control programs are implemented. While only a few countries have eradicated the disease globally, the disease has been brought under control in more than 30 countries thanks to joint projects with international organizations such as WOAH, FAO and WHO. Although brucellosis affects numerous animal and human species, particularly ruminants, this presentation primarily describes approaches used in cattle and humans to control and eradicate brucellosis.

Keywords: Brucellosis, Control Strategies, Eradication

GİRİŞ

Bruselloz kontrol programlarının amacı hastalığın insan sağlığı üzerine ve ekonomik sonuçlara etkilerini azaltmaktır. Hastalığın popülasyondan eliminasyonu kontrol programının tek amacı değildir. Enfeksiyonun popülasyondaki kontrol edilebilir bir seviyede kalması kabul edilebilir. Kontrol programının süresi belirsizdir ve hastalık yeniden çıkmasın diye kabul edilebilir seviyeye indirildikten sonra bile gözden geçirilmelidir. Çoğu ülkede bruselloz kontrol yöntemleri hükümet mevzuat düzenlemeleri ile desteklenir. Desteklerin olmadığı diğer ülkelerde otorite yoktur. Bu sebeple enfekte sürülere uygulanan yöntemler değişkenlik gösterebilir. Bu işlemler test ve izolasyon/kesim, hijyen, hayvan hareketlerinin kontrolü ve aşılama genel kategorileri altında sınıflandırılır (Corbel MJ, 2006).

Brusellozun önlenmesi ve kontrolü, sürveyans ve risk faktörlerinin önlenmesinden geçer. En etkili önleme stratejisi enfekte hayvanların eliminasyonu ile mümkündür. Yüksek prevalansa sahip bölgelerde hayvanların aşılanması öncelikli kılınmıştır. Düşük prevalanslı bölgelerde ise masraf-fayda analizi hesabına göre strateji düşünülmelidir. Aşılama ve uzaklaştırmanın uygulanmadığı ülkelerde korunma, hayvanların itlafı ile birlikte insanlardaki enfeksiyona farkındalık oluşturmak, gıda güvenlik önlemleri, mesleki hijyen ve laboratuvar güvenliği gibi biyogüvenlik uygulamalarına bağlıdır. Diğer koruma stratejileri pastörize süt ürünleri kullanımı ve bu konuda eğitim kampanyaları, tarım ve et işleme, koruyucu bariyerler ve doğumdan sonra enfekte materyallerin uygun şekilde imhasıdır (Wasif M ve ark., 2024).

Uluslararası çeşitli kamu kuruluşları brusellozun önlenmesi ve kontrolü amacıyla birlikte çalışmalar yürütmektedir. Bu kuruluşlardan WHO, bruselloz uygulamalarında standartları sağlamada teknik tavsiye ve destek sağlar. İnsan ve hayvan sağlığı sektörleri arasında bilgi paylaşımını ve koordinasyonu sağlar. FAO, OIE, MZCP (Akdeniz Zoonoz Kontrol Programı), majör hayvan hastalıkları için global bir erken uyarı sistemi (Global Early Warning System for Major Animal Disease-GLEWS) ile ülkeleri hastalıkların önlenmesi ve yönetimi konusunda destekler. Bruselloz kontrol programlarının hazırlanmasından evvel; genel tanımlamalar ve ölçüm sistematiği için veri sağlanması gerekliğidir. İzleme (monitoring), Gözetim ve Tarama (screening) (MOSS) ile aşağıda belirtilen maddeler kontrol programı öncesi belirlenir (Corbel MJ, 2006 - Zhanga N ve ark., 2018).

Hayvanlarda bruselloz sürveyansı ile aşağıda belirtilen çeşitli etiyolojik, epidemiyolojik, klinik durum, koruma ve kontrol stratejilerine ait veri setleri oluşturulur. Bunlar; Hayvanlarda bruselloza neden olan majör türlerin tespiti, Primer rezervuarlarda temel seviyede enfeksiyon seviyesinin tespiti, Evcil hayvan yetiştirme türü, pazarlama ve kesim sistemleri, Mevcut hayvan sayıları ile köy/sürü deki tanımlamalar (kayıtlar), Sürveyans için veri kayıt sistemleri ile mevcut veri kaynakları, Sürveyans belirleyicileri, Sürveyans verisinin epidemiyolojik analizi, Sürveyansdaki politik ve yasal durumlar, Sürveyansda finansal ve yönetim faktörleri, Sürveyansda kültür, motivasyon ve eğitim faktörleri, Laboratuvar desteği ve test stratejileri, Bruselloz kontrol stratejileri ve uygunluğu (Fizibilite, etkinliği, kabul edilebilirliği)

Yukarıda belirtilen veriler doğrultusunda bulaş yollarının belirlenmesi veya mevcut durumun ortaya konulması amacıyla; prevalans, insidans, letalite gibi tanımlanmış hedeflerin ortaya konulması, laboratuvar teşhisleri için bakteriyolojik, serolojik (+,-, şüpheli), klinik (belirsizlik süresi) gibi tanımlamaların yapılması, özel vaka tanımları geliştirilmesi, akış şeması oluşturulması, yeni veri toplama sistemleri oluşturulması, öngörülmeyen problemler için pilot test belirlenmesi, laboratuvarların rolünün yeniden gözden geçirilmesi, hatalar olduğunda sistemin kontrolü amacıyla izleme ve müdahale seçeneklerinin oluşturulması, sürveyans analizi sonrası, sürveyans yaygınlaştırma yöntemleri geliştirilmesi, biyogüvenlik başlığı altında ifade edilen kategoriler (a. Hayvan hareketlerinin kontrolü, b. Suni tohumlama, c. Ziyaretçi girişi, d. Hijyenik uygulamalar, e. Karkas, fetüs, plasentanın imhası, f. Ortak meralar, g. Halk sağlığı eğitimi) ile pastörizasyon kontrol stratejileri birlikte değerlendirilerek aşağıda belirtilen kontrol stratejileri ve uygunluğu (Fizibilite, etkinliği, kabul edilebilirliği) belirlenir. Stratejilerinin ekonomik, etkinlik ve sürdürülebilirlik analizleri yapılarak en uygun olanı belirlenir (Corbel MJ, 2006 - Zhanga N ve ark., 2018- Roy S ve ark., 2011).

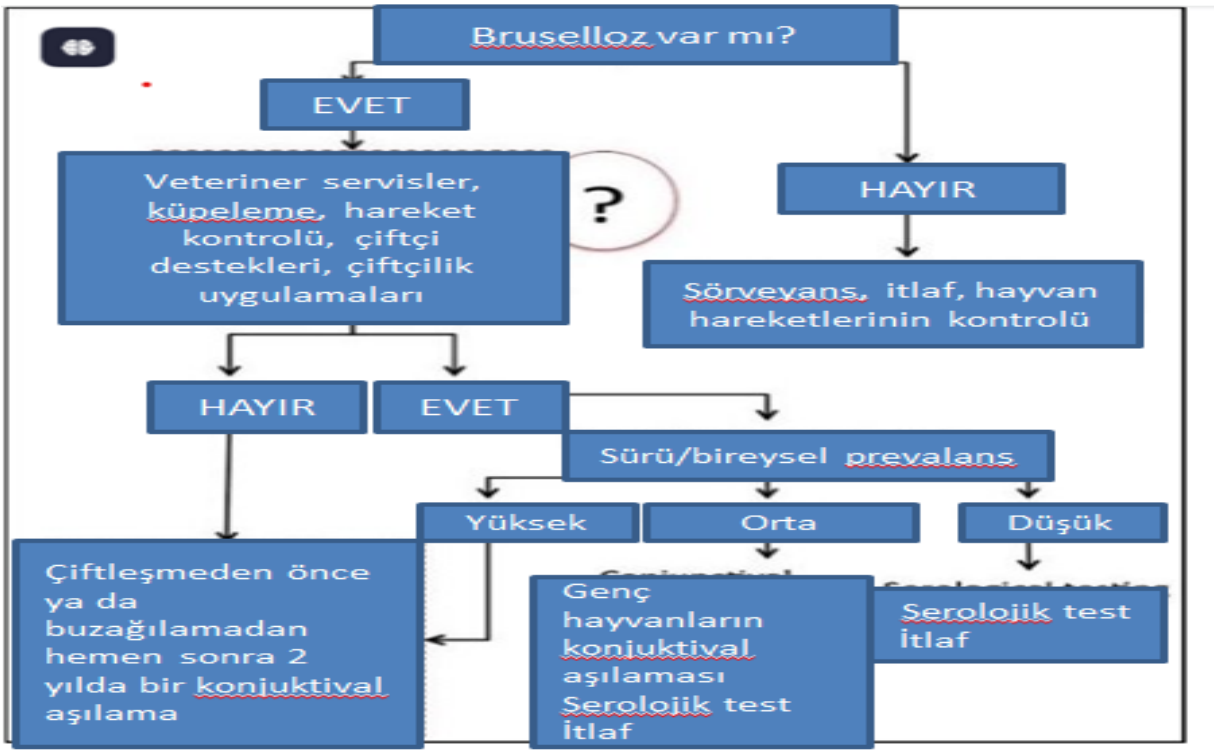
Stratejilerin oluşturulması ile ilgili bilgiler coğrafik dağılım ve uygulanan yöntemler, mevcut altyapı, mevcut kanun ve yönetmelikler, ekonomi, başarı oranları, sürdürülebilirlik gibi çok çeşitli faktörlerin değerlendirilmesi ile elde edilir. Tablo-1 (Zhanga N ve ark., 2018) de bu faktörlerin bazılarının değerlendirilmesi gösterilmiştir. Bu stratejiler Şekil 2 (Corbel MJ, 2006). de belirtildiği gibi kontrol fazının dönemine bağlı olarak genellikle aşağıda belirtildiği üzere birden fazla stratejik yaklaşımın kombinasyonu ile elde edilmektedir.

Aşılama stratejisi
Test ve itlaf/tazminat stratejisi
Test ve ayırım stratejisi
Test ve kesim stratejileri

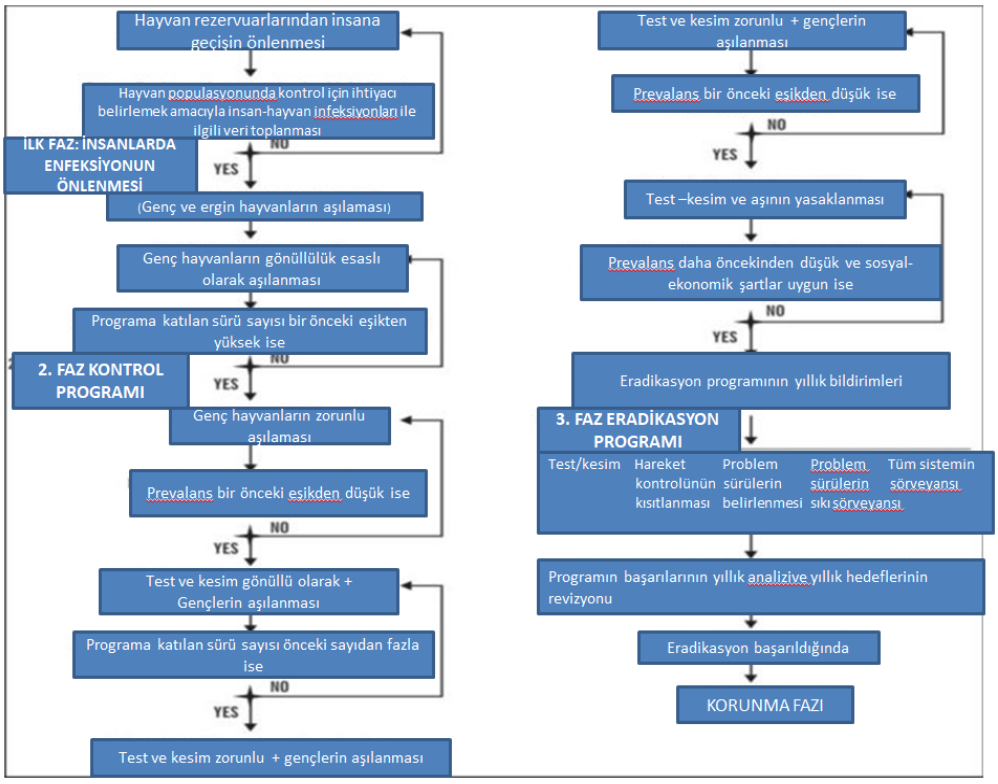
Tablo-1. Aşılama, test ve kesim özelliklerine göre bruselloz stratejileri (Zhanga vd 2018)

Ülke	Süre	Test ve Kesim				Aşılama		
		Süt	Screen Test	Konfirm Test	Kesim	Aşı	Hayvanlar	Başlama Zamanı
Yunanistan	1975-2004	-	-	-	-	Rev.1	Genç ve Erişgin	1998
		-	-	-	-	S19	Süt sığırları	1987
Kuveyt	1985-1988	-	-	-	-	Rev.1	3-8 aylık dişi koyun-keçi	
		-	-	-	-	Rev.1	8 aylık dişi koyun-keçi	
Tacikistan	2004-2009	-	-	-	-	Rev.1	Ergin dişi ve erkek	2004
Fiji	2009-2013	MRT	RBT	ELİSA, CFT	Evet			2009
İrlanda	1998-2005	MRT	SAT	CFT	Evet			1998
Malta	1987-1996	MRT	RBT/SAT	CFT	14 Gün İçinde			1987
Malezya	1979-2016	-	RBPT	CFT	Evet			2016
Makedonya	2004 - 2006	-	RBT	CFT/ELİSA	1 ay içinde	S19	3-9 aylık ve ergin	2008
Avustralya	1970 - 1989	MRT	RBT	CFT	Evet	S19	3-9 aylık ve ergin	1970-1985
						S19	3-8 aylık ve ergin	1999
Arjantin	1999 - 2002	MRT	BPAT/2-ME	CFT	Evet	RB51	10 aylıktan büyük gebeliğin 3. Ayından önce	
Brezilya	2001 - 2002	-	RBT	2-ME, CFT	Evet	S19	3-8 aylık buzağı	2001
						RB51	Ergin dişiler	
İngiltere	1967 - 1976	-	SAT/CFT			S19	3-6 aylık buzağı	1967
Yeni Zelanda	1966 - 1989	MRT	Card Test	CFT	Evet	S19	3-6 aylık buzağı	1969-1975
ABD	1934 - 2001	MRT	SAT	CFT/RIVT	Evet	RB51	4-12 aylık buzağı	1997
						S19- RB51	3-8 aylık buzağı	2002

MRT: milk Ring Test, SAT: Serum Aglütinasyon Testi, CFT: Komplement Fikzasyon Test, RBT: Roz Bengal Test, ELISA: Enzyme Linked Immunosorbent Assay



Şekil 1. Bruselloz varlığına dayalı kontrol yaklaşımları (Corbel JM 2006).



Şekil 2. İnsanlarda ve hayvanlarda bruselloz kontrol ve eradikasyon programları (Corbel JM 2006)

İnsanlarda Brusellozun Kontrolü

Bruselloz, insanlarda kronik seyirli rekurrent zoonotik bir hastalıktır. Hayvanlardan insanlara bulaş başlıca üç şekilde önlenebilmektedir: 1) süt ürünlerinin pastörizasyonu ve et ürünlerinin uygun şekilde hazırlanması; 2) bruselloz gözetimi ve kontrol programları; ve 3) hayvancılık ürünlerini işleyenlere bulaşın önlenmesi, iyileştirilmiş sanitasyon ve hayvancılık ürünlerinin güvenli bir şekilde işlenmesi konusunda eğitim. Bu kontrol yöntemleri temel olarak, hayvan sürülerinin bazılarından (veya muhtemelen hepsinden) insan popülasyonuna bulaş oranlarını azaltmayı sağlar (Roy S ve ark., 2011). Aşı eksikliği ve insanda hastalık yönetimiyle ilişkili zorluklara rağmen, gerçek zorluk hayvan brusellozunu ortadan kaldırmaktan geçer (Ko J ve ark., 2003). Brusellozun kontrolünde başarılı olan programların çoğu gelişmiş ülkelerde gerçekleşmiş ancak gelişmekte olan ülkeler bu hastalığın yükünü taşımaya devam etmektedir. Özellikle, endemik olmayan gelişmiş ülkelerdeki insan bruselloz vakalarının çoğu, endemik bölgelerden ithal edilen süt ürünlerinden (Al Dahouk S ve ark., 2003) veya hastalığı ithal eden hastalardan (Luzzi GA ve ark., 1993) kaynaklanmaktadır. Sığırlar (S19), koyun ve keçiler (Rev 1) etkili aşılarına rağmen, ekonomik olarak zayıf endemik bölgelerdeki kontrol çabaları, yetersiz altyapı ve fon eksikliği nedeniyle başarısız olmuştur. Önemli bir sorun, kontrol önlemlerinin uzun bir süre devam etmesi gerekliliği ve vaka sayısı azalmaya başladığında sürdürülmesi zor olabilecek bir izleme sistemiyle tamamlanması gerektiğidir (Şekil 1 ve 2). Buna örnek, eski Sovyet Cumhuriyetinin mevcut durumu verilebilir; burada SSCB'nin; idari, ekonomik ve kamu sağlığı altyapısının çöküşü, brusellozun yeniden ortaya çıkmasına yol açmıştır (Lundervold M ve ark., 2004). Gelişmekte olan dünyada, özellikle Afrika'da, hayvancılıkla ilişkili brusellozun yıllık ekonomik etkisine ilişkin verilerin değerlendirilmesi genellikle zor olmuştur (McDermott JJ ve ark., 2002). Hem iç hem de uluslararası pazarlar için hayvancılık ürünleri satışının önemli olduğu Arjantin ve Meksika gibi ülkelerde, yıllık korunma maliyetlerin sırasıyla 60 milyon ABD doları ve 200 milyon ABD doları olduğu tahmin edilmektedir. Kullanılan önlemlere bakılmaksızın, endemik bölgelerde insan brusellozunun ekonomik yükü yüksektir ve yaygın ve sürdürülebilir kontrol çabalarını haklı çıkarır (Kahl-McDonagh MM ve ark., 20007). Göçebe ve göçmen popülasyonlarında hastalık kontrolünün zor olduğu kanıtlanmıştır. İnsanlar için kullanılan bir bruselloz aşısı yoktur ve brusellozun ortaya çıkması doğrudan bir bölgedeki hayvan brusellozunun varlığıyla bağlantılıdır. Bu bağlamda, Dünya Sağlık Örgütü, hayvanlarda kontrol ve eradikasyon programlarının uygulanmasının yanı sıra insan aşısının geliştirilmesini yüksek bir öncelik olarak tanımlamıştır. Aşı uygulaması, yalnızca eski Sovyetler Birliği ülkelerinde kullanılan bir korunma yöntemidir. Sovyet bilim insanları aşı uygulama yöntemlerini deri altı, deri içi, kas içi ve damar içi (Franco MP ve ark., 2007) olarak farklı şekillerde denemişlerdir. Gürcistan'da aşının intravenöz kullanımı yapılmıştır. Aşı uygulamasında humoral bağışıklığın aktivasyonu ile sağlanan antikorların aglütinasyon yeteneğinin korunmada etkili olduğu bildirilmiştir.

Şu anda, aşı etkinliği ile ilgili belirsizlikler, hastada oluşturduğu olumsuz etkiler ve antibiyotiklerin daha etkili bir tedavi seçeneği olması nedeniyle kullanılmamaktadır. Son olarak, aşı tedavisinin gözden geçirilmesi, Brusella aşısının geliştirilmesi için yararlı bilgiler sağlar. İnsan Brusella aşı adaylarının, aşının serolojik ölçümlerde artışa neden olması ancak etkisiz olduğu gözlemlenmesi nedeniyle hücre aracılı bağışıklık tepkisine dayanan koruma korelasyonlarını kullanmaları gerektiği öne sürülmüştür (Akhvlediani T ve ark., 2010). Güvenli ve etkili bir insan bruselloz aşısının geliştirilmesi, halk sağlığı üzerinde geniş bir etkiye sahip olacaktır. Endemik bölgelerdeki insan aşıları, kontamine gıda ürünlerinin tüketiminden kaynaklanan hastalık bulaşını ve potansiyel biyoterörizm veya biyolojik savaş ajanlarını önleyebilir ve aerosol tehdidine karşı koruma sağlayabilir (Bossi P ve ark., 2004 - , Bossi P ve ark., 2004). S19'un canlı zayıflatılmış aşı modeli olarak tanınması, SSCB'de 3 milyondan fazla insanın aşılanması da dahil olmak üzere insan kullanımına yönelik girişimde bulunulmasına yol açmıştır (Vershilova PA ve ark., 1961).

İnsanlarda brusellozun önlenmesi hala hayvan konaklarında hastalığın ortadan kaldırılmasına veya kontrol altına alınmasına, mesleki faaliyetler yoluyla enfeksiyona maruziyeti sınırlamak için hijyenik önlemlerin alınmasına ve süt ürünlerinin ve diğer potansiyel olarak enfekte olmuş gıdaların etkili bir şekilde ısıtılmasına bağlıdır. Aşılamanın insan hastalıklarının önlenmesinde artık sadece küçük bir rolü vardır, ancak geçmişte canlı zayıflatılmış *B. abortus* suşları 19-BA ve 104M (esas olarak eski Sovyetler Birliği ve Çin'de kullanılmıştır), fenol-çözünmeyen peptidoglikan aşısı (önceden Fransa'da mevcuttu) ve polisakkarit protein aşısı (Rusya'da kullanılmıştır) dahil olmak üzere çeşitli preparatlar kullanılmıştır. Hepsinin etkinliği sınırlı bulunmuş ve canlı aşılar söz konusu olduğunda potansiyel olarak ciddi reaktojenite ile ilişkilendirilmiştir. Şu anda, böyle bir gelişmenin aşılama ve bağışıklama konusunda DSÖ küresel programı kapsamında bir öncelik olması gerektiği yönündeki önerilere rağmen, görünürde

insan aşısı olmamasına rağmen, insan brusellozunun kontrolü hayvan hastalıklarının kontrolüne ve uygun gıda güvenliği düzenlemelerinin yürürlükte olmasına bağlı olmaya devam etmektedir. Sütün pastörizasyonunun veya kaynatılmasının insanlarda brusellozun en temel kontrolü olduğu öne sürülmüştür (Makita K ve ark., 2010).

Brusellozun bir sürü problemi olması ve uzun süre antibiyotik kullanımı gerektirmesi sebebi ile hayvanlarda antibiyotik kullanımı yapılmamaktadır. Ancak etkenin zoonotik yapısı ve insanlarda kullanılan bir aşısının olmaması sebebi ile antibiyotiklerle tedavi edilmektedir (Solera J, 2010). Tedavide kullanılan antibiyotik tercihleri açısından bir direnç gelişimi yoktur. Ancak koyun suşu *B. melitensis* için intermedier bir durumun varlığı belirlenmiştir (Wareth G ve ark., 2021).

Eradikasyon

Eradikasyon, patojenik ajanı bir ülkeden ya da bir bölgeden yok etmek demektir. Bir alandan veya bir popülasyondan eradikasyon için oldukça organize çabalar gerekir. Eradikasyon kavramsal olarak kontrolden çok farklıdır. Kontrol ne kadar iyi uygulanırsa uygulansın ne geçici ne de otomatik bir sonucudur. Kontrol programı için uygulamadan tamamen farklı bir organizasyon ve saniter önlemlere bağlıdır. Eradikasyon programının başarısı için hayati faktörler yeterli laboratuar desteği alınan bir sürveyans sistemi ile çiftçiler, karar vericiler ve tüm paydaşlar tarafından eradikasyonun anlaşılması ve amaçlarının paylaşılması gerekir. Popülasyonu enfeksiyondan etkilenmeden tutabilmek için önleyici tedbirler alınmalıdır (Corbel MJ, 2006 - Zhanga N ve ark., 2018).

Lokal insan ve hayvan popülasyonu ve bölge ile ilgili yeterli bilgi gereklidir. Yukarıda önleme ve kontrol için tanımlanan stratejiler eradikasyon içinde kullanılabilir. Ancak birbirini kapsayacak şekilde olmalıdır. Yapılacak işlemler uygun stratejinin belirlenmesi sonrası Şekil 1 ve 2 de gösterildiği gibidir.

Uzun süreçte, eradikasyon programları kontrol programları ile kıyaslansa da ekonomik olarak daha avantajlıdır. Ancak bu avantaj daima pratiğe aktarılmaz. Aslında eradikasyon programı var olmayan kaynakların mobilizasyonunu ya da karar vericilerin destekleyebileceğinden daha uzun zaman gerektiren yatırımları gerekli kılar. Kontrol stratejilerinde kararları desteklemek için cost-benefit ve cost-etkinlik analizleri kullanılır. Ancak epidemiyolojik analiz yokluğunda derinliğine bir analiz bulunmamaktadır (Corbel MJ, 2006 - Zhanga N ve ark., 2018- Roy S ve ark., 2011).

SONUÇ

Sonuçlar, brusellozun eradikasyonunun sistematik ve karmaşık bir program olduğunu ve kısa sürede tamamlanamayacağını göstermiştir. Başarı veya iyimser beklentiler elde edilse bile, projeler her zaman sürdürülmelidir. Avustralya ve Yeni Zelanda, ari duruma ulaşmak için 20 yıldan fazla zaman harcanmış ve programlar ariliğin sürdürülmesi için devam etmektedir. Amerika Birleşik Devletleri ise 1934 ile 2000 yılları arasında ari sürü bildirimine ulaşmak için 64 yıl harcamıştır. Hastalığın kontrol programlarına dahil edilen diğer ülkeler ve bölgeler de onlarca yıldır bruselloz kontrol programları uygulanmasına rağmen çok sınırlı sayıda ülke hastalığın bulaşını kontrol altına alabilmiştir (Corbel MJ, 2006 - Wasif M ve ark., 2024 - Zhanga N ve ark., 2018).. Bu nedenle daha fazla zamana ve çabaya ihtiyaç duyulmaktadır. Başarısız uygulama ve kampanyaların sonuçları, İrlanda ve Yunanistan'ın deneyimleri ile ortaya konulmuştur (Minas A ve ark., 2004- Sheahan M ve ark., 2006).

Aşılama, test-kesim ve itlaf uygulamaları tek başına sığırlarda eradikasyon için yeterli olmamaktadır. Hayvan hareketlerinin kontrolü, sürveyans sistemlerinin kullanımı ve yeterli laboratuvar desteği programın başarısına katkı sunan yardımcı önlemlerdir. İnsan ve hayvan bruselloz sürveyansında rol oynayan birçok faktör tüm ülkelere veya bölgelere uymayacağından, yukarıda tartışılan tüm faktörler tasarım veya değerlendirme aşamasında dikkatlice düşünülmelidir. Ayrıca, kontrol veya eradikasyon başarılı bir şekilde ilerledikçe, bir sürveyans programı, azalan insidans oranlarını hesaba katmak ve tanımlanması daha zor olabilecek yeni veya yeniden enfeksiyonları değerlendirmek için gerekecektir. Eradikasyon sağlandıktan sonra gözetimi sürdürmek problemin sürüden-bölgeden ariliğinin sürdürülmesi için zorunludur. Arilik döneminin konfirmasyonu için eradikasyon sonrası hastalık ajanının populasyondaki varlığı en az 5 yıl takip edilmelidir. Eradikasyon başarıldığında prevalans 5 yıl boyunca <%0.2 ve son 3 yılda abort bildirimi olmamalıdır.

REFERANSLAR

Akhvlediani T, Clark DV, Chubabria G, Zenaishvili O, Hepburn MJ. The changing pattern of human brucellosis: clinical manifestations, epidemiology, and treatment outcomes over three decades in Georgia. BMC Infect Dis. 2010; 9:10:346.

Al Dahouk S, Nöckler K, Hensel A, Tomaso H, Scholz HC, Hagen RM, Neubauer H. Human brucellosis in a nonendemic country: a report from Germany, 2002 and 2003. Eur J Clin Microbiol Infect Dis. 2005; 24: 450–56.

Bossi P, Tegnell A, Baka A, Van Loock F, Hendriks J, Werner A, Maidhof H, Gouvras G. Bichat guidelines for the clinical management of brucellosis and bioterrorism-related brucellosis. Euro Surveill. 2004; 15;9(12):E15-6.

Corbel MJ. Brucellosis in humans and animals. WHO/CDS/EPR/2006.7. World Health Organization 2006 ISBN 978 92 4 154713 0

Franco MP, Mulder M, Gilman RH, Smits HL. Human brucellosis. Lancet Infect Dis. 2007; 7(12):775-786.

Kahl-McDonagh MM, ArenasGamboa AM, Ficht TA. Aerosol infection of BALB/c mice with Brucella melitensisand Brucella abortus and protective efficacy against aerosol challenge. Infect Immun. 2007; 75(10):4923–4932.

Ko J, Splitter GA. Molecular hostpathogen interaction in brucellosis: current understanding and future approaches to vaccine development for mice and humans. Clin Microbiol Rev. 2003; 16: 65–78.

Lundervold M, Milner-Gulland EJ, O'Callaghan CJ, Hamblin C, Corteyn A, Macmillan AP. A serological survey of ruminant livestock in Kazakhstan during post- Soviet transitions in farming and disease control. Acta Vet Scand. 2004; 45: 211–24.

Luzzi GA, Brindle R, Sockett PN, Solera J, Klenerman P, Warrell DA. Brucellosis: imported and laboratory acquired cases, and an overview of treatment trials. Trans R Soc Trop Med Hyg.1993; 87: 138–141.

Makita K, Fèvre EM, Waiswa C, Eisler MC, Welburn SC. How human brucellosis incidence in urban Kampala can be reduced most efficiently? A stochastic risk assessment of informally-marketed milk. PLoS One. 2010; 1;5(12):e14188.

McDermott JJ, Arimi SM. Brucellosis in sub-Saharan Africa: epidemiology, control and impact. Vet Microbiol. 2002; 90(1-4):111-34.111.

Minas A, Minas M, Stournara A, Tselepidi S. The “effects” of Rev-1 vaccination of sheep and goats on human brucellosis in Greece. Preventive Veterinary Medicine. 2004; 464 1, 10: 41-47.

Roy S, McElwain TF, Wan Y. A network control theory approach to modeling and optimal control of zoonoses: case study of brucellosis transmission in 29 Journal of Zoonoses 2014;1(1)sub-Saharan Africa. PLoS Negl Trop Dis.2011; 5(10):e1259

Sheahan M, O'Hagan G, Power S, Kenny K. Brucellosis in cattle in Ireland 1998-2005: Progress towards eradication continues. Irish Veterinary Journal. 2006; 59(4):217-221.

Solera J. Update on brucellosis: therapeutic challenges. Intl J Antimicrob Agent. 2010; 36S, S18–S20. http://www.ncbi.nlm.nih.gov/pubmed/20692127

Vershilova PA. The use of live vaccine for vaccination of human beings against brucellosis in the USSR. Bull World Health Organ. 1961; 24:85–89.

Wareth G, El-Diasty M, Abdel-Hamid N-H, Holzer K,. Hamdy MER, Moustafa S, Shahein M, Melzer F, Beyer W, Pletz MW, Neubauer H. Molecular characterization and antimicrobial susceptibility testing of clinical and non-clinical *Brucella melitensis* and *Brucella abortus* isolates from Egypt. One Health. 2021; 13, 100255, 1-6.

Wasif M, Mushtaq MH, Chaudhry M , Nazeer MA, Raza SM. Strategies for Combatting Brucellosis: A Review on Control and Prevention in Bovines. Science Letters 2024; 12(2):50-57.

Zhanga N, Huanga D, Wua W, Liua J, Lianga F, Zhoua B, Guana P. Animal brucellosis control or eradication programs worldwide: A systematic review of experiences and lessons learned. Preventive Veterinary Medicine. 2018; 160 105–115.

POSTER PRESENTATION

Academic stress and exam-period nutrition: Implications for student well-being and academic performance

Gerta Kupi [1] * (ORCID: https://orcid.org/0009-0004-3527-9520), Arjana Mucaj[2]

[*1]. Aldent University, Faculty of Medical Sciences, Health Promotion Center, Tirana, Albania.
[2]. Tirana University, Faculty of Social Science, Departament of Psychology, Tirana, Albania.

Abstract

The examination period represents one of the most demanding phases in university life, characterized by increased academic pressure, elevated stress levels, and substantial changes in students' daily routines. Academic stress is widely recognized as a significant predictor of students' psychological well-being and academic performance. At the same time, nutritional habits tend to deteriorate during exams, often leading to insufficient energy intake, irregular meals, or increased consumption of fast food and stimulants. This study explores the interaction between academic stress and exam-period dietary patterns, and their combined influence on students' physical, mental, and academic functioning.
A cross-sectional descriptive study was conducted with university students from various public and private institutions in Tirana, Albania. Data were collected through a structured questionnaire evaluating stress levels, dietary habits, sleep patterns, concentration difficulties, and perceived academic performance. Findings indicate that 62.8% of students rely on fast food and energy drinks during examinations, while 74% report changes in appetite and eating patterns. High stress levels were associated with insomnia (79%), concentration difficulties (82%), increased fatigue (68%), and self-reported reductions in academic performance.The results highlight the importance of addressing academic stress as a core factor influencing student functioning, while also recognizing nutrition as a mediating component that may exacerbate or alleviate stress-related outcomes. Strengthening awareness and promoting healthier lifestyle strategies during examination periods may contribute to improved well-being and better academic results among university students. Insights from this study align with the doctoral research focus on academic stress and performance, offering practical implications for student support services in higher education.

Keywords: exam stress, nutrition, university students, dietary habits, mental health

INTRODUCTION

The examination period often represents a phase of increased psychological pressure, strict deadlines, and high cognitive demand for university students. During this time, maintaining balanced nutrition plays a crucial role not only in academic performance but also in overall physical, emotional, and psychosocial well-being. The relationship between stress and nutrition is bidirectional: academic stress influences eating behaviors, while inadequate nutrition can further exacerbate stress, anxiety, and cognitive impairment.

Unhealthy dietary choices during exam periods, such as skipping meals or consuming energy-dense, nutrient-poor foods, may result in fatigue, impaired concentration, emotional instability, and weakened immune function. Previous studies have shown that students experiencing high academic stress tend to consume fewer fruits and vegetables, skip breakfast more frequently, and increase their intake of fast food, sugary snacks, and energy drinks. These behaviors are consistently associated with poorer mental health outcomes and reduced academic performance.

Despite growing international evidence on the relationship between diet, stress, and student well-being, data from Albania remain limited. Therefore, this study aims to assess dietary habits during exam periods and their impact

on the physical, mental, and emotional health of students at Aldent University, contributing valuable evidence to the national literature.

MATERIALS AND METHODS

Study Design and Setting

A descriptive cross-sectional study was conducted at Aldent University following the February 2025 examination period. Data collection took place in March 2025 to capture students' recent experiences related to diet, stress, and well-being during exams.

Participants

The study population consisted of Bachelor and Master students enrolled at Aldent University. A total of 448 students voluntarily participated by completing an anonymous online questionnaire. Doctoral students were excluded due to differences in academic workload and stress patterns.

Data Collection Instrument

Data were collected using a structured online questionnaire designed to assess: - Socio-demographic characteristics (gender, age, residence, level of study) - Dietary habits during the examination period - Physical activity frequency - Sleep quality and concentration difficulties - Perceived impact of nutrition on physical, mental, and emotional health

Statistical Analysis

Data were analyzed using Google Forms and Microsoft Excel. Descriptive statistics were applied, and results were presented as frequencies and percentages. Data visualization included bar charts, histograms, and pie charts.

Ethical Considerations

Participation was voluntary, and informed consent was obtained prior to questionnaire completion. The survey was anonymous, and all data were treated confidentially and used exclusively for research purposes.

RESULTS

Table 1. Socio-demographic Characteristics of Participants (n = 448)

Variable	Category	Percentage (%)
Gender	Female	92.0
	Male	8.0
Residence	Urban	86.6
	Rural	13.4
Age group	18–21 years	78.6
	22–24 years	20.3
	>25 years	1.1
Level of study	Bachelor Year I	45.5
	Bachelor Year II	27.5
	Bachelor Year III	4.9
	Master Year I (Scientific)	8.0
	Master Year II (Scientific)	10.7
	Professional Master	3.3

Table 3. Meal Frequency During Examination Period

Meals per day	Percentage (%)
1 meal	13.2
2 meals	40.8
3 meals	28.8
4 meals	13.4
>4 meals	3.8

Table 4. Food Categories Consumed During Examinations

Food category	Percentage (%)
Fast food	65.2
Energy drinks	56.0
Sweets	49.3
Coffee/Tea	39.3
Fruits	27.0
Vegetables	20.5
Dairy products	15.2
Nuts	11.2
Grains	10.9
Alcohol	2.7

Table 5. Lifestyle and Well-being Indicators During Examinations

Variable	Category	Percentage (%)
Dietary imbalance	Yes	71.0
	No	29.0
Weight changes	Yes	76.0
	No	24.0
Weight change type	Weight loss	66.0
	Weight gain	34.0
Physical activity	None	69.6
	1–2 times/week	20.8
	3–5 times/week	6.7
	Daily	2.9
Sleep disturbances	Yes	80.0
	No	20.0
Concentration difficulties	Yes	90.0
	No	10.0

DISCUSSION

The findings of this study confirm that the examination period is a critical phase for university students, during which dietary habits, physical activity, and sleep patterns are significantly disrupted. In line with the study hypothesis, changes in diet quality and meal frequency were associated with negative physical, mental, and emotional outcomes.

The high prevalence of fast food, energy drink, and sugary food consumption reflects coping behaviors linked to academic stress and time constraints. Similar patterns have been reported in previous studies, which demonstrated that poor diet quality is associated with reduced academic performance and poorer mental health outcomes. The predominance of female and first-year Bachelor students may reflect greater health awareness and increased vulnerability to academic stress during early university years.

The majority of students reported sleep disturbances, concentration difficulties, and lack of physical activity, all of which are known to exacerbate stress and impair cognitive functioning. Weight fluctuations observed during the examination period further indicate metabolic and behavioral disruptions associated with stress and unhealthy eating habits.

Overall, the results highlight the need for targeted interventions aimed at promoting healthy eating, regular physical activity, and stress management strategies during examination periods. Universities should consider implementing nutrition education programs, accessible healthy food options, and initiatives encouraging physical activity to support student well-being and academic success.

CONCLUSIONS

This study demonstrates that examination periods significantly affect dietary habits, physical activity, and overall well-being of university students. Unhealthy eating patterns, combined with high stress levels and physical inactivity, negatively impact physical, mental, and emotional health. Implementing structured nutritional education programs, promoting regular meal planning, and encouraging physical activity during exam periods may help improve student well-being and academic performance.

REFERENCES

Oliver G, Wardle J (1999). Efektet e përceptuara të stresit në zgjedhjen e ushqimit. Fiziologjia & Sjellja 66:511-515.

Wardle J, et al. (2000). Stresi, kufizimi në dietë dhe marrja e ushqimit. Journal of Psychosomatic Research 48:195-202.

Reuter, P., Forster, B. L., & Brister, S. (2020). The influence of eating habits on the academic performance of university students. Journal of American College Health, 69(8), 921–927. https://doi.org/10.1080/07448481.2020.1715986

Wengreen H, Moncur C. (2009). Change in Diet, Physical Activity, and Body Weight among Young-Adults during the Transition from High School to College. Nutr J. 8(1):32. doi:10.1186/1475-2891-8-32

Grace T. (1997). Health Problems of College Students. J Am Coll Health, 45(6), 243–251. doi:10.1080/07448481.1997.9936894

Kobayashi F. (2009). Academic Achievement, BMI, and Fast Food Intake of American and Japanese College Students. Nutr Food Sci. 39(5):555–556. doi:10.1108/00346650910992213

Food for thought: is poor diet affecting students' stress levels? Sanitarium Health Food Company. https://www.sanitarium.com/au/health-nutrition/mind/how-diet-impacts-university-students

World Health Organization. (2006). Constitution of the World Health Organization – Basic Documents, Forty-fifth edition, Supplement, October 2006.

World Health Organization. The determinants of health, Geneva. Accessed 12 May 2011.

POSTER PRESENTATION

Preparation of chalcone modified polyHIPE for removal of aluminum ions from water

Ebru Tekneci Akgül, Büşra Akın Özmen, Erdem Yavuz, Berkay Sütay, Bahire Filiz Senkal*

* Istanbul Technical University, Department of Chemistry, 34469 Maslak, Istanbul, Turkey

*Corresponding author e-mail: bsenkal@itu.edu.tr

Abstract

In this study, a novel chalcone-modified sulfonamide-based polymeric sorbent was successfully synthesized, starting from a cross-linked polystyrene high internal phase emulsion (PS-HIPE). The synthesis involved sequential chlorosulfonation of PS-HIPE, followed by sulfonamidation with aminoacetophenone, and subsequent reaction with salicylaldehyde via a Claisen–Schmidt reaction to incorporate the chalcone functional group. The resulting polymeric sorbent was comprehensively characterized using various analytical techniques, including scanning electron microscopy with energy-dispersive X-ray spectroscopy (SEM-EDX), Fourier-transform infrared spectroscopy (FTIR), X-ray photoelectron spectroscopy (XPS), Brunauer–Emmett–Teller (BET) analysis, and classical analytical methods. Also, the molecular structure of the resulting aluminum complex was also predicted using density functional theory. Batch adsorption studies were performed to evaluate the sorbent's efficiency for aluminum Al^{3+} removal from aqueous solutions, investigating the effects of adsorbent dosage, pH, initial Al^{3+} concentration (5–500 ppm), and contact time. The optimal adsorbent dosage was determined to be 25 mg. The maximum aluminum sorption capacity of the adsorbent was found to be 56.84 mg g^{-1}. Analysis of the equilibrium data using Langmuir and Freundlich isotherm models demonstrated that the experimental results fitted the Langmuir isotherm model best, suggesting a monolayer adsorption mechanism. The kinetic study indicated that the adsorption process followed the pseudo-second-order kinetic model. These findings suggest that the chalcone-modified polyHIPE is a highly effective sorbent for aluminum removal from water.

Keywords: Aluminum Removal, PolyHIPE, Chalcone, Sulfonamide, Adsorption.

INTRODUCTION

There is growing concern regarding contamination of drinking water sources with metals due to their potential acute and chronic adverse effects on humans. Aluminum (Al) is the most prevalent metallic element in Earth's outer crust, accounting for 8% of its mass. It is released from both natural and anthropogenic sources. Due to anthropogenic impacts that encourage aluminum release into aquatic environments, many natural water bodies are affected by acidification (Lydersen et al., 2002). Over recent decades, significant research has focused on removing toxic metals from natural water bodies and wastewater. Electrodialysis, adsorption, chemical precipitation, membrane filtration, and cation exchange are methods suggested for Al removal from aqueous solutions (Al-Muhtaseb et al., 2008; Aly et al., 2014; WANG et al., 2007). Among available water treatment technologies, adsorption is considered reliable for metal removal due to its low cost, efficiency, and diverse adsorbent selection. Polymeric adsorbents have been extensively used for effective heavy metal removal through physical mechanisms. This method has advantages including simplicity, scalability, recyclability, and ease of functionalization. These materials can be prepared with high porosity and substantial surface areas, making them effective adsorbents for heavy metal removal from wastewater.

High internal phase emulsion (HIPE) methods are templates with an internal phase volume ratio of 0.74 or greater. In water-in-oil emulsions, curing the external phase forms highly porous polymers called polyHIPEs (Barbetta & Cameron, 2004; Cameron, 2005; Silverstein, 2014; Yavuz et al., 2019). PolyHIPEs have hierarchical porosity, with properties including ease of preparation and tunable porosity. Removing the water phase creates voids, while surfactant ratio calibration enables void interconnections through polymer wall thinning.

The interconnected macroporous structure of open-cell PolyHIPE reduces diffusional paths and improves mass transport. This makes it widely used in applications like adsorption, separation, tissue engineering, and loading materials (Aldemir Dikici et al., 2022; Lima et al., 2023; Zhao et al., 2021).

This porous material suits adsorption applications due to its surface area, functional groups, and mass transfer properties. MS Silverstein [24] showed improved adsorption of polar VOCs and CO2 through polyHIPE hypercrosslinking (Castaldo et al., 2023).
PolyHIPE with epoxy groups was prepared by emulsion polymerization, followed by hyper-crosslinking and functionalization to create adsorbents with porous structures and dithiocarbamate groups for Pb^{2+} extraction (Yin et al., 2025).
Chalcone consists of aromatic rings connected by an α, β-unsaturated carbonyl system (Menezes et al., 2025). Chalcone products occur in plants, spices, fruits, and vegetables (Orlikova et al., 2011). Their structure allows metal ion coordination, as studied in 2'-hydroxychalcone-aluminium systems (Debattista & Pappano, 1997).
We report a chalcone-modified polystyrene PolyHIPE for aluminum ion removal from aqueous solutions. Chalcone was introduced via chlorosulfonation/sulfonamidation/Claisen-Schmidt reaction. The sorbent was characterized and its Al3+ adsorption studied through batch experiments examining parameters like dosage, concentration, pH, and kinetics. Maximum capacity was determined and mechanisms evaluated using isotherm and kinetic models.

MATERIALS AND METHODS

Chemicals and Materials

Styrene (Sigma Aldrich), Divinyl benzene (Sigma Aldrich), sorbitan monooleate (Sigma Aldrich), $K_2S_2O_8$ ((Sigma Aldrich) , $CaCl_2$ (Sigma Aldrich), isopropyl alcohol (Sigma Aldrich), chlorosulfonic acid (Fluka), acetone (Sigma Aldrich) p-aminoacetophenone (Sigma Aldrich), salicyl aldehyde (Sigma Aldrich), 1-methyl-2-pyrrolidone (Sigma Aldrich), trimethylamine (Fluka), ether (Sigma Aldrich), ethanol, sodium hydroxide, $NaNO_3$, HCl , phenol-phthalein and other chemicals were supplied commercially.

Preparation of PolyHIPE

The organic phase, which contained styrene (8 mL, 69.7 mmol), divinylbenzene (DVB) (2 mL, 7.1 mmol), and sorbitan monooleate (Span 80) (2.05 g, 4.7 mmol), was added to a 250 mL round-bottom reaction flask equipped with a mechanical stirrer. Nitrogen gas was passed through the mixture for 15 min to remove ambient oxygen. The aqueous phase was prepared separately by dissolving potassium persulfate (0.2 g, 0.74 mmol) and calcium chloride (1 g, 6.80 mmol) in distilled water (90 mL) and passed through nitrogen gas for 15 min. Under nitrogen gas flow, the organic phase in the reaction flask was stirred at a constant stirring speed of 300 rpm while the water phase was added dropwise through a dropping funnel for 30 minutes. After the addition of the entire water phase, stirring was continued at 300 rpm for 1 hour to obtain a homogeneous emulsion. The mixture was stirred at room temperature at 50 rpm for 20 minutes to remove any air bubbles that might remain in the emulsion. The resulting emulsion was placed in a 50 ml centrifuge tube for polymerization and left in an oven at 60°C for 48 hours. The resulting PolyHIPE was washed first with water and then with isopropyl alcohol by Soxhlet extraction for 24h to remove purities and then left to dry in a vacuum oven at 40°C for 24 hours.

Chlorosulfonation of the PolyHIPE (CS-polyHIPE)

The polyHIPE obtained was subsequently reacted with an excess of chlorosulfonic acid, utilized as a solvent, for a duration of 24 hours at ambient temperature. This reaction resulted in the formation of chlorosulfonated polyHIPE (Bicak & Senkal, 1997). The obtained CS-polyHIPE was washed successively with acetone, ice water, and acetone in order to remove soluble impurities. Subsequently, CS-polyHIPE was dried in a vacuum oven for 24 hours at room temperature.

Sulfonamidation of the CS-polyHIPE with 4-aminoacetophenone

A quantity of 4 g of p-aminoacetophenone (0.030 mol) was dissolved in 20 mL of 1-methyl-2-pyrrolidone (NMP). Then, 4 mL of (0.030 mol) trimethylamine was added as an acid scavenger. CS-polyHIPE (5 g) was added to this solution in portions at 0 °C. The reaction mixture was stirred with a magnetic stirrer at ambient temperature for 24 hours and at 60°C for 2 hours. Following the completion of the reaction, the sulfonamidated polyhipe was washed with excess water, ethanol, and ether, respectively, to remove soluble impurities. The sulfonamidated polyhipe obtained was then dried under vacuum at room temperature for 24 hours.

Preparation of the Chalcone modified PolyHIPE

The synthesis of chalcone-modified polyHIPE was performed through a Claisen-Schmidt reaction. For this purpose, 25 mL ethanol was added to 2.40 grams of sulfonamide modified polyHIPE. A base solution was prepared by dissolving 0.5 grams of sodium hydroxide in 5 milliliters of water. This base solution was then slowly added to the reaction medium. Subsequently, 1.10 milliliters of salicylaldehyde (0.010 moles) were added dropwise, and the reaction was carried out at 25°C for 24 hours. The resultant product was then subjected to a thorough wash with water and filtration. The product was purified by Soxhlet extraction with acetone for 2 days and then dried in a vacuum oven for 1 day.

Characterization of the Chalcone modified polyHIPE

The synthesized materials were characterized using Fourier-Transform Infrared Spectroscopy (FTIR-ATR) (Perkin Elmer Spectrum 100), SEM FEI-Philips XL30 environmental scanning electron microscope with a field emission gun equipped with an energy-dispersive X-ray analysis unit operating at 10.0 kV was used to analyze the surface morphology. Thermo Scientific K-Alpha X-ray Photoelectron Spectrometer was used to identify the elemental composition of the polymer surfaces operated in the range between 100 and 4000 eV.

Adsorption Experiment

Batch adsorption experiments were conducted by mixing a known amount of the adsorbent with Al(III) solutions of various concentrations. The effects of pH (2.0–5.0), initial concentration (5–500 mg/L), and contact time (5–120 min) were studied. The residual Al(III) concentration in the solution was determined using an UV-spektrophotometry). The amount of Al(III) adsorbed and the removal efficiency were calculated.

RESULTS

In this study, chlorosulfonated poly (styrene-DVB)-based PolyHIPE was interacted with 4-aminoacetophenone to obtained sulfonamidated PolyHIPE. After that, this product was reacted with salicyl aldehyde in the presence base catalyst using Claissen-Schmidt reaction for 24 h at room temperature (Scheme 1).

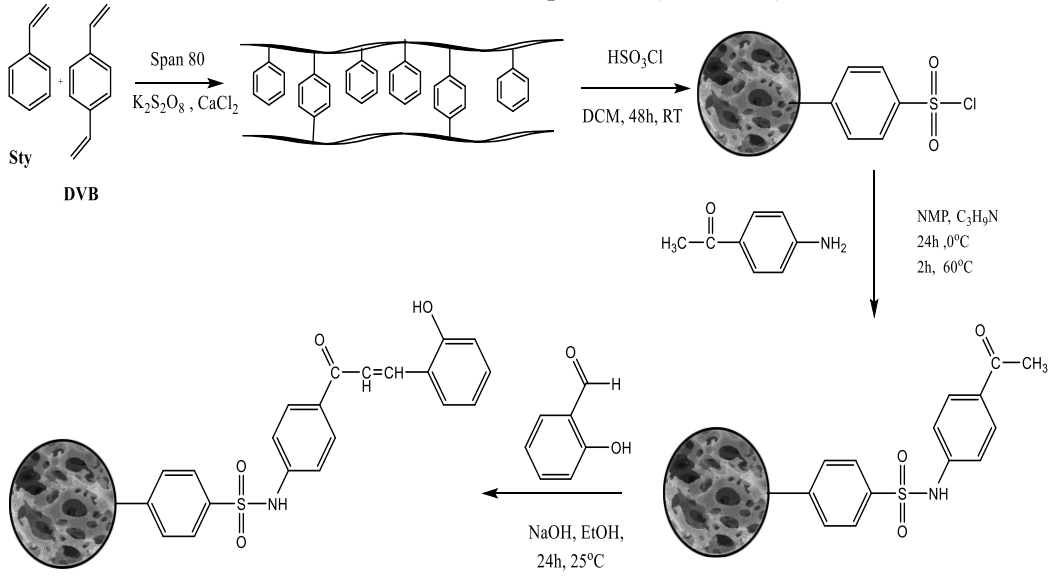


Figure 1. Chalcone modified PolyHIPE

The molecular structure of aluminum complex was predicted using M06-2X density functional in 6-31+G(d,p) basis, in Gaussian suite(Frisch et al., 2009) . The chalcone group chelated with aluminum ion and the remaining positions were saturated with water, Figure 1. The average Al-O bond distances were predicted to be 1.9 Å.

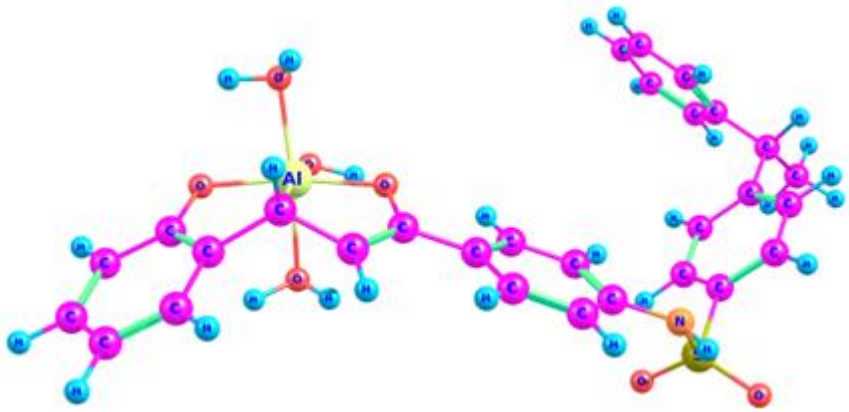


Figure 2. The structure of the aluminum complex of chalcone-modified polyHIPE.

The adsorbents were characterized using FTIR spectra. According to the Figure 3, S=O stretching vibration occurs at 1124-1161 cm^{-1} in the sulfonamide modified polyHIPE. The stretching vibration bands in the chalcone modified polyHIPE were observed at 1640 cm^{-1} is attributed to the C= O group. Also, the stretching vibration band at about 1598 cm^{-1} belongs to olefinic C=C conjugated to the chalcone group. Subsequent to the adsorption process, a decline in the peak intensity of the carbonyl group (1640 cm^{-1}) and the C=C (1598 cm^{-1}) double bond is observed. This is attributable to the formation of a complex Al^{3+} with the chalcone group.

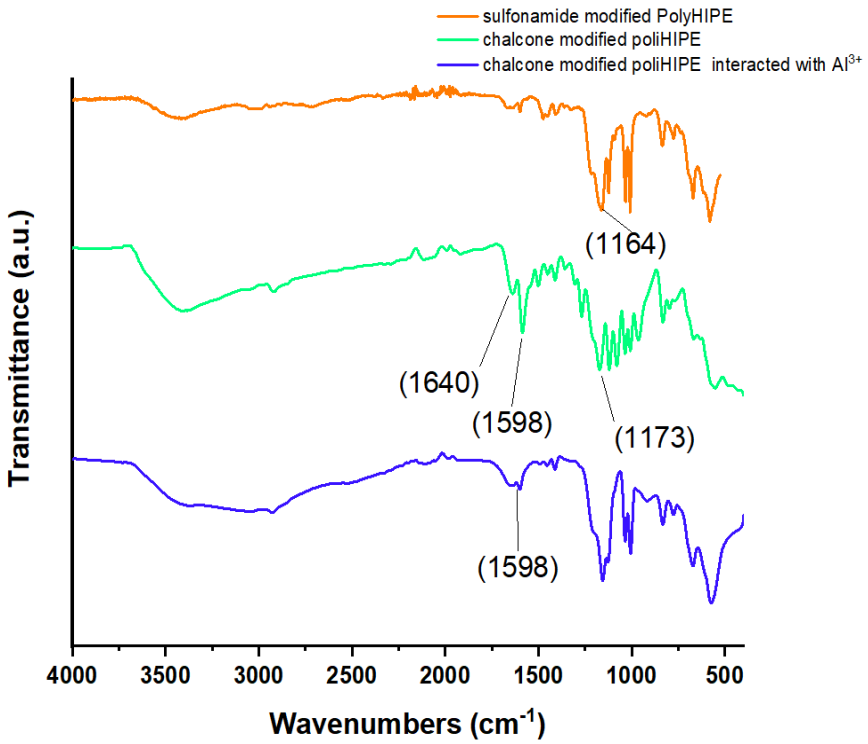


Figure 3. The FTIR spectra of sulfonamide modified polyHIPE, chalcone modified polyHIPE and chalcone modified polyHIPE interacted with Al^{3+}

In order to ascertain the effect of aluminum concentration on adsorption capacity, 0.025 g of polyHIPE was utilized in an interaction with 10 mL of an Al^{3+} solution, with initial concentrations ranging from 5 to 500 ppm. Following the filtration of the samples, the resin's sorption capacities were examined colorimetrically, as previously described, and calculations were performed in accordance with equation 1. According to the Figure 9, the data indicate a positive correlation between the initial Al^{3+} concentration and the Al^{3+} sorption capacity. The maximum capacity for Al^{3+} was determined to be 56.84 mg/g adsorbent in a solution with a concentration of 500 ppm.

Table 1: Aluminum Adsorption Capacity

Concentration (mg/L)	Capacity
5	0.15
10	1.52
25	4.05
50	15.25
65	18.25
125	40.04
250	51.02
350	56.56
500	56.84

CONCLUSION

In this study, a chalcone-modified polystyrene-based PolyHIPE was successfully synthesized and fully characterized using morphological (SEM), spectrophotometric (FTIR, XPS), and analytical methods. The characterization results indicated that the chalcone functional group was successfully incorporated and that an ionic interaction occurred between the chalcone group and the Al^{3+} ion upon adsorption. The molecular structure of the resulting aluminum complex was also predicted using density functional theory and the complexation via chalcone group was also verified.

Following the determination of the optimal adsorbent dosage, comprehensive batch sorption experiments were conducted, varying key parameters such as initial aluminum concentration and pH. The maximum aluminum sorption capacity of the synthesized sorbent was determined to be 56.84 mg g^{-1}. The adsorption equilibrium data were found to be best described by the Langmuir isotherm model (R^2=0.993), which suggests a favorable, monolayer adsorption process on a uniform surface. Furthermore, kinetic studies demonstrated that the adsorption process closely followed the pseudo-second-order kinetic model (R^2=0.999), indicating that chemisorption, likely involving the formation of a covalent bond between the adsorbent and aluminum, is the primary rate-limiting step.In conclusion, the findings of this research highlight the potential efficacy and superior performance of the chalcone-modified polyHIPE adsorbent for the efficient removal of aluminum ions from contaminated wastewater.

ACKNOWLEDGEMENTS

This work is supported by the Scientific Research Project Center of the Istanbul Technical University (Project number: TDK-2023-45107). Additional support was provided by TÜBİTAK through the 2211-A National PhD Scholarship Program.

REFERENCES

Aldemir Dikici, B., Malayeri, A., Sherborne, C., Dikici, S., Paterson, T., Dew, L., Hatton, P., Ortega Asencio, I., MacNeil, S., Langford, C., Cameron, N. R., & Claeyssens, F. (2022). Thiolene- and Polycaprolactone Methacrylate-Based Polymerized High Internal Phase Emulsion (PolyHIPE) Scaffolds for Tissue Engineering. *Biomacromolecules*, *23*(3), 720–730. https://doi.org/10.1021/ACS.BIOMAC.1C01129

Al-Muhtaseb, S. A., El-Naas, M. H., & Abdallah, S. (2008). Removal of aluminum from aqueous solutions by adsorption on date-pit and BDH activated carbons. *Journal of Hazardous Materials*, *158*(2), 300–307. https://doi.org/https://doi.org/10.1016/j.jhazmat.2008.01.080

Aly, Z., Graulet, A., Scales, N., & Hanley, T. (2014). Removal of aluminium from aqueous solutions using PAN-based adsorbents: characterisation, kinetics, equilibrium and thermodynamic studies. *Environmental Science and Pollution Research*, *21*(5), 3972–3986. https://doi.org/10.1007/s11356-013-2305-6

Barbetta, A., & Cameron, N. R. (2004). Morphology and Surface Area of Emulsion-Derived (PolyHIPE) Solid Foams Prepared with Oil-Phase Soluble Porogenic Solvents: Span 80 as Surfactant. *Macromolecules*, *37*(9), 3188–3201. https://doi.org/10.1021/ma0359436

Bicak, N., & Senkal, B. F. (1997). Aldehyde separation by polymer-supported oligo(ethyleneimines). *Journal of Polymer Science, Part A: Polymer Chemistry*, *35*(14), 2857–2864. https://doi.org/10.1002/(SICI)1099-0518(199710)35:14<2857::AID-POLA6>3.0.CO;2-N

Cameron, N. R. (2005). High internal phase emulsion templating as a route to well-defined porous polymers. *Polymer*, *46*(5), 1439–1449. https://doi.org/https://doi.org/10.1016/j.polymer.2004.11.097

Castaldo, R., Berezovska, I., Silverstein, M. S., & Gentile, G. (2023). PolyHIPEs Containing Hyper-Cross-Linked Resins: Hierarchical Porosity with Broad and Versatile Sorption Properties. *ACS Applied Polymer Materials*, *5*(9), 6920–6931. https://doi.org/10.1021/ACSAPM.3C00974/SUPPL_FILE/AP3C00974_SI_003.MP4

Debattista, N. B., & Pappano, N. B. (1997). Complexant efficiency of 2'-hydroxy-4-R-chalcones for Aluminium (III) and substituent's effect. In *Talanta* (Vol. 44).

Frisch, M., Trucks, G., Schlegel, H., Scuseria, G., Robb, M., Cheeseman, J., Scalmani, G., Barone, V., Mennucci, B., Petersson, G., Nakatsuji, H., Caricato, M., Li, X., Hratchian, H., Izmaylov, A., Bloino, J., Zheng, G., Sonnenberg, J., Hada, M., & Fox, D. (2009). Gaussian 09 (Revision A02). *Gaussian Inc. Wallingford CT*.

Lima, I. de P., Valle, S. P., Oliveira, M. A. L. de, Marques, F. F. de C., & Vaz, F. A. S. (2023). Monolithic stationary phases preparation for use in chromatographic and electromigration techniques: The state-of-the-art. *Microchemical Journal*, *190*, 108598. https://doi.org/10.1016/J.MICROC.2023.108598

Lydersen, E., Löfgren, S., & Arnesen, R. T. (2002). Metals in Scandinavian Surface Waters: Effects of Acidification, Liming, and Potential Reacidification. *Critical Reviews in Environmental Science and Technology*, *32*(2–3), 73–295. https://doi.org/10.1080/10643380290813453

Menezes, R. A., Bhuvaneshwari, C. N., Venkatachalam, H., & Bhat, K. S. (2025). Focused review on applications of chalcone based compounds in material science. *Discover Applied Sciences*, *7*(8), 814. https://doi.org/10.1007/s42452-025-07478-0

Orlikova, B., Tasdemir, D., Golais, F., Dicato, M., & Diederich, M. (2011). Dietary chalcones with chemopreventive and chemotherapeutic potential. *Genes & Nutrition*, *6*(2), 125–147. https://doi.org/10.1007/s12263-011-0210-5

Silverstein, M. S. (2014). Emulsion-templated porous polymers: A retrospective perspective. *Polymer*, *55*(1), 304–320. https://doi.org/https://doi.org/10.1016/j.polymer.2013.08.068

WANG, W., YANG, H., ZHAO, H., & JIANG, Z. (2007). Transfer and transport of aluminum in filtration unit. *Journal of Environmental Sciences*, *19*(8), 897–901. https://doi.org/https://doi.org/10.1016/S1001-0742(07)60149-1

Yavuz, E., Cherkasov, N., & Degirmenci, V. (2019). Acid and base catalysed reactions in one pot with site-isolated polyHIPE catalysts. *RSC Advances*, *9*(15), 8175–8183. https://doi.org/10.1039/C9RA01053J

Yin, Z., Chen, J., Zhang, Y., Li, S., & Yin, D. (2025). Dithiocarbamate-decorated adsorbent based on hyper-crosslinked PolyHIPE for Pb2+ removal from aqueous solution. *Journal of Polymer Research*, *32*(6), 1–9. https://doi.org/10.1007/S10965-025-04412-1/FIGURES/9

Zhao, J., Zhang, W., Gao, C., & Yin, D. (2021). Shape stabilization of phase change material by polymerized high internal phase emulsion for thermal energy storage. *International Journal of Energy Research*, *45*(4), 5263–5271. https://doi.org/10.1002/ER.6143

POSTER PRESENTATION

Design of a ZIF-8 functionalized glassy carbon electrode-based electrochemical sensor for high-sensitivity TBHQ determination

Emaduldeen J. M. Alisawi [1*] *https://orcid.org/0000-0001-9280-5874*
Zuhair Nazar Mohammed[2] *https://orcid.org/0009-0000-9467-2729*
Bakr Aldoori[3] *https://orcid.org/0000-0002-8663-2986*
Sema Gokdemir[1] *https://orcid.org/0009-0007-0421-4785*
Semahat Kucukkolbasi[1] *https://orcid.org/0000-0002-5129-5385*

[*1] Selçuk University, Faculty of Science, Department of Chemistry, Konya, Türkiye.
[2] Northern Technical University, College of Health and Medical Techniques, Department of Medical Laboratory Techniques, Kirkuk, Iraq.
[3] Samarra University, College of education for pure science, Department of Chemistry - Samarra - Iraq

Abstract

tert-Butylhydroquinone (TBHQ) is one of the synthetic phenolic antioxidants widely used in edible oils due to its strong antioxidant properties, low cost, chemical stability, and availability (Yue et al., 2016). TBHQ has become attractive in the field of food technology due to its superior shelf-life extension, particularly in snack foods with high surface area and oil absorption(Asap & Augustin, 1986). Considered one of the most effective synthetic antioxidants, TBHQ is widely used in the food industry to delay oxidative spoilage and maintain quality of food products. TBHQ is a critical food additive with the ability to stabilize free radicals by interrupting oxidation chain reactions; it remains on the product, maintaining its protective properties even after high heat treatments during production, making it essential for post-packaging stability (Warner & Gupta, 2005). zeolitic imidazolate frameworks (ZIF-8) is a porous structure belonging to the MOF class, formed by the coordination of zinc ions with imidazole-derived ligands. Its unique structure makes it widely used in gas storage, catalysis, drug delivery, and, especially, electrochemical sensing. In recent years, hybrid structures obtained by modifying ZIF-8 have shown higher electrochemical performance (Lu et al., 2020). The most important properties of ZIF-8 are chemical stability, high surface area, biocompatibility, and the presence of various chemical groups. Thanks to these properties, ZIF-8 is an excellent adsorbent for biomaterials. This composite material combines the unique properties of its components, improving the properties of each in various applications, especially in electrochemical sensing, drug delivery, catalysis, and biotechnology (Jiang et al., 2019; Khezerlou et al., 2022; Paul et al., 2022). Although traditional instrumental methods such as high-performance liquid chromatography (HPLC)(Amlashi et al., 2014), gas chromatography-mass spectrometry (GC-MS) (Guo et al., 2006), and UV-visible spectrophotometry (Capitán-Vallvey et al., 2001) have been used for the detection of antioxidants, these have always been quite laborious and time-consuming techniques. Electrochemical sensors offer a timely alternative for the detection of TBHQ due to their simplicity, amenability to miniaturization, rapid and sensitive quantitative analysis (Tormin et al., 2012), (Ziyatdinova et al., 2014). In the first part of the study, the synthesis and characterization of novel ZIF-8 were performed. In the second part, ZIF-8 was used alone and in combination with AuNPs to modify the GCE surface and investigate its electrochemical properties.

Keywords: Electrochemical Sensor, ZIF-8, Biocompatibility, AuNPs, TBHQ

INTRODUCTION

Substances used for purposes such as preservation, preservation, flavor deterioration, and inhibition of microorganism growth during the production, processing, packaging, and storage stages of foods are called "food additives" (Ayper & Binokay, 2010). Approved by the European Union and classified with the "E" code, these substances can cause various health problems, ranging from allergic reactions to cancer, when consumed above the acceptable daily limits set by international commissions (Karatepe & Ekerbiçer, 2017). Antioxidants, which hold a significant place among these additives, are widely used to extend the shelf life of foods by preventing oxidative spoilage. In addition to natural antioxidants, synthetic antioxidants are more frequently preferred in the industry

due to their low cost, high stability, and easy availability (Thomas et al., 2015). However, it has been reported that excessive use of synthetic antioxidants can cause nutrient losses and toxic effects (Liu et al., 2020; Prabakar & Narayanan, 2006).

TBHQ, a synthetic phenolic antioxidant, is frequently added to food products to prevent oxidative deterioration of fats and oils (Fan et al., 2018). While not causing changes in the color, taste, or odor of foods is a significant advantage of TBHQ, excessive use is known to carry serious health risks such as liver damage and carcinogenic effects (Lu et al., 2020). Therefore, the use of TBHQ is strictly regulated in many countries, and the Acceptable Daily Intake (ADI) has been determined as 0−0.7 mg kg^{-1} by the JECFA (JECFA, 2011). These potential effects of TBHQ on food quality and public health necessitate the determination of its amount in foods using sensitive, rapid, and cost-effective methods. Although chromatographic methods such as spectrophotometry, HPLC, and GC-MS have been reported in the literature for the determination of TBHQ, the expensive equipment and time-consuming nature of these techniques have increased the need for more practical alternatives. In this context, electrochemical sensors, with their simple instrumentation, high sensitivity, and fast response time, offer a significant advantage over traditional methods (Paul et al., 2022).

In recent years, metal-organic frameworks (MOFs) have attracted considerable attention in the development of electrochemical sensors due to their large surface areas and tunable pore structures (Yuan et al., 2020). ZIF-8, a subclass of ZIFs, are particularly notable for its excellent thermal and chemical stability (Assfour et al., 2010). However, like most MOF structures, ZIF-8's insulating properties and low electrical conductivity limit its performance in electrochemical applications(Song et al., 2012). To overcome this limitation, integrating highly conductive metal nanoparticles into MOF structures has emerged as an effective strategy. The high catalytic activity and electron transfer rate enhancement of gold nanoparticles (AuNPs) significantly improve the sensor performance of MOF-based composites (Wang et al., 2018).

In this study, AuNPs@ZIF-8 nanocomposites functionalized with Au nanoparticles were synthesized and modified onto a glassy carbon electrode (GCE) for the electrochemical determination of TBHQ. This developed sensor platform aims to offer high sensitivity, low limit of detection (LOD), and superior selectivity for TBHQ analysis, thanks to the synergistic effect created by the high conductivity of Au nanoparticles and the large surface area of ZIF-8.

MATERIALS AND METHODS

Materials and reagents

2-methylimidazole (2-MeIm), KOH, $Zn(NO_3)_2.6H_2O$, disodium monohydrogen phosphate, sodium dihydrogen phosphate, TBHQ, sodium sulfate, chitosan, potassium ferricyanide ($K_3[Fe(CN)_6]$), potassium chloride KCl, and potassium ferrocyanide ($K_4[Fe(CN)_6]$) were purchased from Sigma-Aldrich and used as received. Butylated hydroxyanisole and phosphate-buffered saline buffer solution were prepared fresh before each measurement. Double distilled water (DDW) was used throughout the experiments. All chemicals were of analytical grade and were used without any purification process, and distilled water and methanol were used in the preparation of the solutions.

Preparation of ZIF-8

ZIF-8 was synthesized using the following procedure (Yang et al., 2018). First, 10 mmol of $Zn(NO_3)_2.6H_2O$ was dissolved in 100 mL of methyl alcohol and stirred for 10 min. Then, 100 mL of methyl alcohol containing 40 mmol of 2-MeIm was slowly added and stirring continued for 24 h at room temperature. The resultant ZIF-8 was isolated by centrifugation, washed thoroughly with methanol, and dried at 70°C, yielding 77 % as a brown solid compound.

Preparation of ZIF-8 sensor and the electrodeposition of ZIF-8/Au-NPs

During the cleaning process of the electrode surfaces, a 0.05 µM alumina solution was dropped onto the cleaning pad, and the surface was cleaned with circular movements. Then, the electrode surface was cleaned with ultrapure water and ethyl alcohol in an ultrasonic bath for 2 minutes for each solution to remove any impurities that might remain on the surface. The working electrode (GCE) surface was prepared using a simple and rapid technique called "drop-casting" to obtain ZIF-8 using 6 µL with micropipette, and the electrode was dried at room

temperature. After obtaining ZIF-8/GCE, the electrode deposed with AuNPs using CV electrodeposition method, for electrodeposition of Au NPs, by cyclic voltammetry, a potential window of 0.5 to 1 V and a scan rate of 100 mV s^{-1} for 20 cycles was applied into the 5 mM solution of chloroauric acid. And the modified electrode was obtained with AuNPs@ZIF-8/GCE.(Saeb & Asadpour-Zeynali, 2022)

Electrochemical characterization

Computer controlled IVIUM electrochemical analyzer and BASi brand cell stand (C3) were used for electrochemical measurements. In the experiments, glassy carbon electrode (GCE) was used as the working electrode, Ag/AgCl electrode as the reference electrode, and platinum wire electrode as the counter electrode. Electrochemical characterization of sensors made using Cyclic Voltammetry (CV) and Electrochemical Impedance Spectroscopy (EIS) methods using a 5.0 mM $Fe(CN)_6^{3-/4}$ solution containing 100 mM KCl. The Nyquist plots of EIS were used to follow the impedance changes of the electrode surface after the modification.

RESULTS AND DISCUSSION

FT-IR Spectroscopy

Fourier transform infrared spectroscopy (FT-IR) (λ = 400–4000 cm^{-1}) was performed to identify the functional groups of 2-MeIm and the synthesized ZIF-8 shown in Fig. 1A. In both spectra, the stretching vibrations of the ring v(C–H) appear around ~2925 cm^{-1}, indicating the presence of the imidazole heterocycle. The characteristic ring vibrations v(C=N) in 2-MeIm and ZIF-8 at showed at 1043 cm^{-1}, 1060 cm^{-1} respectively, while the v(C=C) group are observed in the region 1450–1600 cm^{-1} in both 2-MeIm and ZIF-8, indicating that the heterocycle remains intact. Bands in the 1300–1100 cm^{-1} region are assigned to v(C–N) stretching within the imidazole ring, demonstrating that the organic linker structure is conserved upon framework formation. Additionally, a band in the low-frequency region at 421 cm^{-1} is attributed to the v(Zn–N) stretching bond, providing direct evidence for coordination between Zn^{2+} ions and the nitrogen atoms of deprotonated 2-MeIm, thus confirming the successful construction of the ZIF-8 framework (Attwa et al., 2024; Rahim & Majid, 2023).

SEM-EDS

The Scanning Electron Microscope (SEM) analysis of the synthesized ZIF-8 Fig. 1C illustrates an aggregated microstructure composed of closely packed, irregularly shaped particles with rough surfaces, characteristic of polycrystalline framework materials. The wide particle size distribution and pronounced surface corrugation are expected to increase the accessible surface area and create a large number of potential active sites, which can facilitate mass transport and enhance interfacial interactions in adsorption or sensing processes. The formation of these dense agglomerates with nanoscale texturing (around 150-205nm) suggests a reproducible synthesis route.

The elemental composition of the synthesized ZIF-8 was evaluated by Energy Dispersive X-ray Spectroscopy (EDS), as shown in the elemental mapping and corresponding spectrum. The EDS map as shown in Fig. 1C reveals a homogeneous spatial distribution of zinc (Zn), carbon (C), and nitrogen (N) over the examined area, indicating that the inorganic nodes and organic imidazolate linkers are uniformly dispersed within the framework. The EDS spectrum Fig. 1C, exhibits intense peaks in the low-energy region (0–3 keV) associated with light elements such as nitrogen, which is characteristic of the 2-MeIm linker that contain the light elements such as carbon (C), nitrogen (N) and oxygen (O), with pronounced Zn peaks at higher energies, confirming the presence of Zn^{2+} centers in the structure. The table of elemental composition also provides the ration of the element in the framework of ZIF-8.

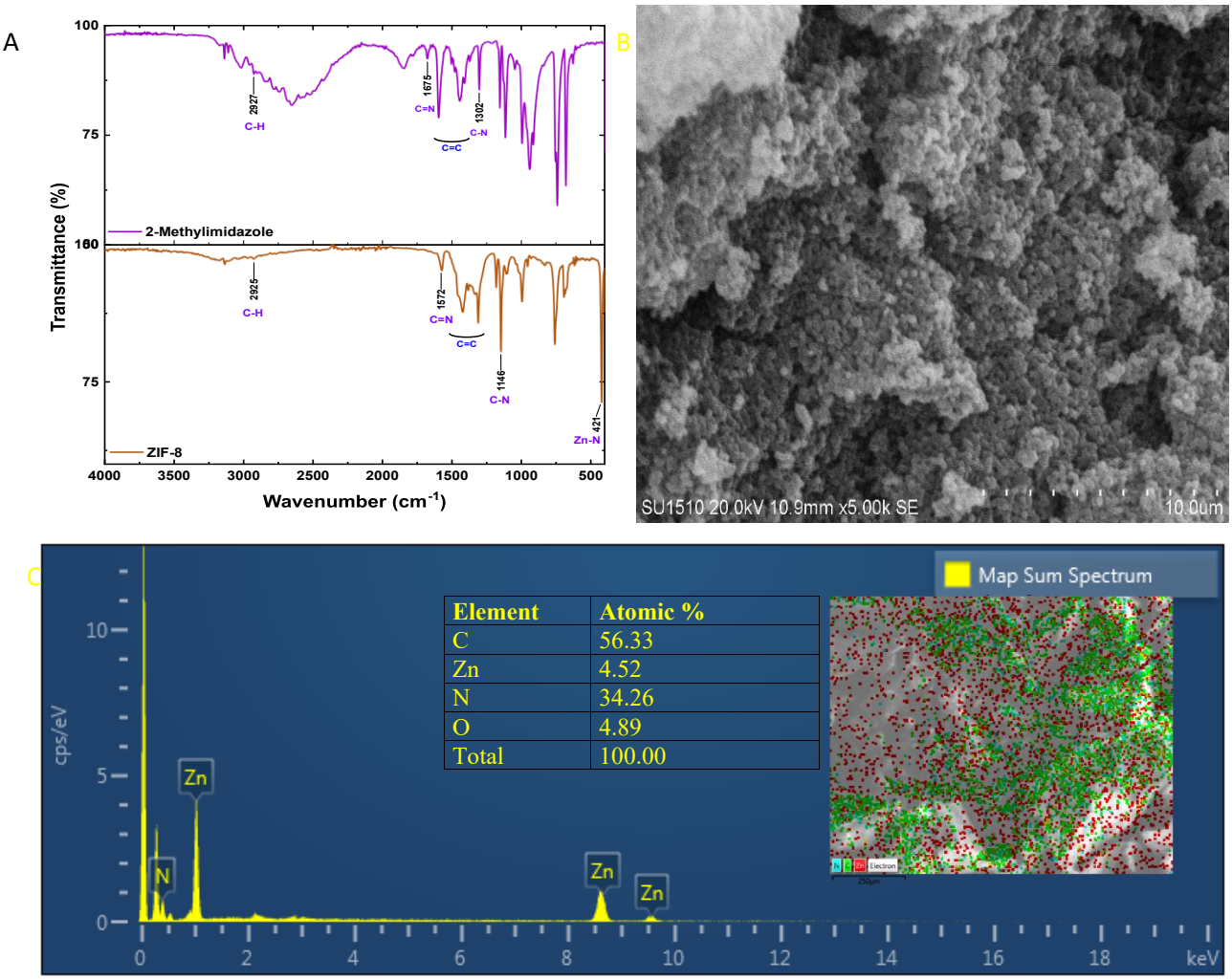


Figure 1. (A) FTIR spectroscopy of 2-MeIm and the synthesized ZIF-8. **(B)** SEM images of ZIF-8**. (C)** EDS spectrum and elemental composition of ZIF-8 powder.

Voltammetric Study

In order to examine electrochemical characterization of the modified electrodes with ZIF-8/GCE and Fe-AuNPs@ZIF-8/GCE, Cyclic voltammetry was tested in a redox probe containing 0.1 M KCl. High peak current was observed in the GC electrode modified with ZIF-8/GCE but voltammograms showed the highest peak current of GC electrode modified with AuNPs@ZIF-8/GCE. Additionally, the potential difference between the oxidation peak and reduction peak of the AuNPs@ZIF-8/GCE electrode in $[Fe(CN)_6]^{3-/4-}$ redox probe decreased because of the good electron transfer capability.

In this study, EIS, a common electrochemical characterization method was also used to further investigate the electron transfer kinetics of the different electrodes, According to the results of Impedance Spectroscopy, it can be said that ZIF-8 and Au nanoparticles increase the electrode surface conductivity and improve the electrochemical properties. These results are in consistent with those obtained using CV and show that the best conductivity is observed in ZIF-8/Au-NPs modified electrode.

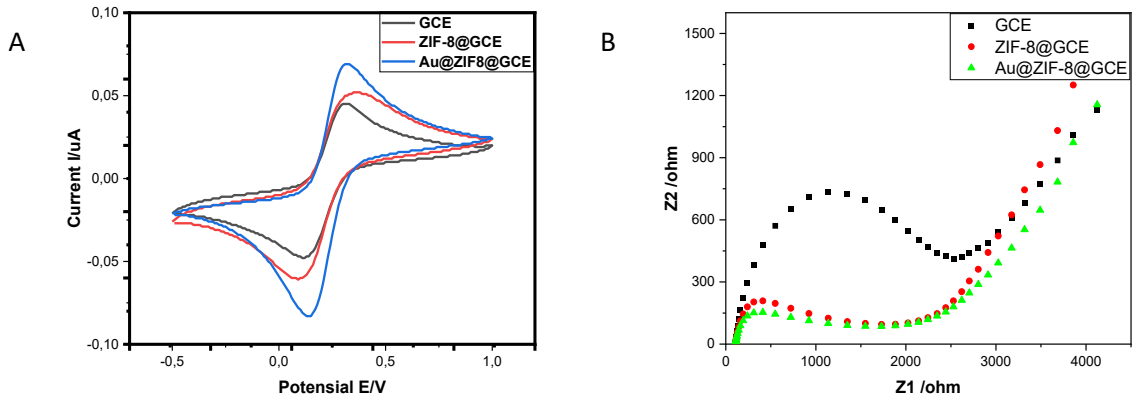


Figure 2. **(A)** CV voltammograms of Bare GC electrode (black), ZIF-8/GCE (red) and AuNPs@ZIF-8/GCE (blue). **(B)** EIS voltammograms of Bare GC electrode (black), ZIF-8/GCE (red) and 2-MeIm AuNPs@ZIF-8/GCE (green).

Optimization of Experimental Conditions

In this study, the amount of ZIF-8 and pH value were investigated to determine the optimal experimental conditions for AuNPs@ZIF-8/GCE that result in the highest detection sensitivity of TBHQ. the results shown in Fig. 3.

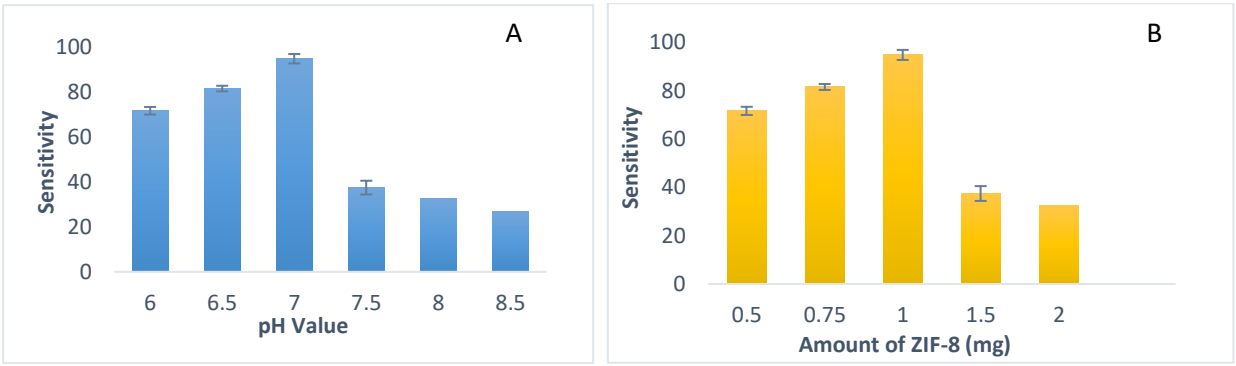


Figure 3. The optimum conditions of AuNPs@ZIF-8/GCE for TBHQ in PBS solution.

Calibration Curve plotting

DPV measurements were taken in 5 mL of 0.1 M PBS (pH 7) at constant temperature (vs. Ag/AgCl) under optimum experimental conditions. The typical current-potential response of ZIF-8/GCE for TBHQ measurements and the DPV curve depending on the TBHQ concentration. The current response increased linearly as the TBHQ concentration increased from 1.96×10^{-5} M to 1.67×10^{-4} M, the correlation value was 0.999 and the sensitivity was found to be 5.943±0.063 $\mu A.\mu M^{-1}$, shown in Figure 4 A, B. The typical current-potential response of AuNPs@ZIF-8/GCE and the DPV curve depending on the TBHQ concentration. The current response increased linearly as the TBHQ concentration increased from 1.96×10^{-5} M to 1.67×10^{-4} M, the correlation value was 0.998 and the sensitivity was 13.844±0.1 $\mu A.\mu M^{-1}$. shown in Figure 4 C, D.

The limit of detection (LOD) of the AuNPs@ZIF-8/GCE sensor was estimated to be as 5.52×10^{-6} M, and the limit of quantification (LOQ) was estimated to be as $1.84x10^{-5}$ M.

The repeatability and reproducibility of AuNPs@ZIF-8/GCE for TBHQ has been studied the response current of 5.0×10^{-5} M DA in PBS buffer by using five paralleled modified electrodes prepared under the same conditions. The relative standard deviation (RSD) of measurements is calculated to be 4.7%, and 2.8% for repeatability and reproducibility, respectively.

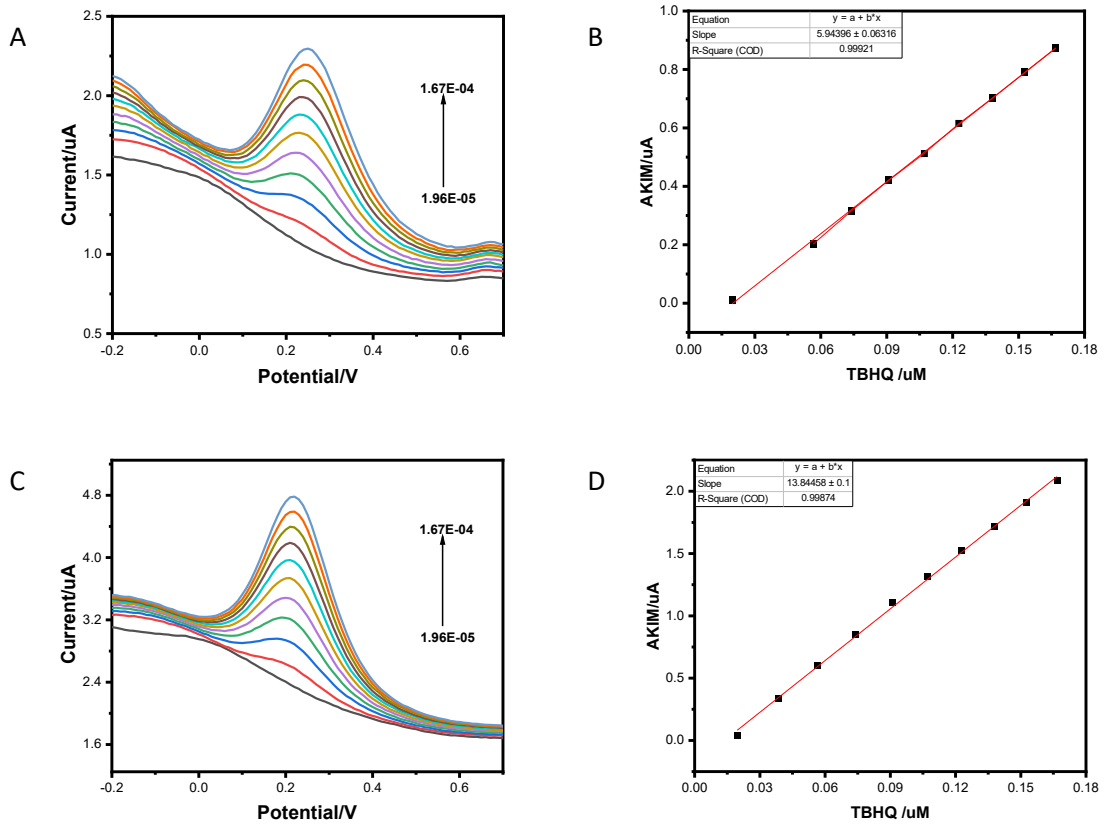


Figure 4. (A) Calibration curves **(B)** Plots of peak currents vs. the concentration by successive additions of TBHQ for ZIF-8/GCE in optimum conditions. **(C)** Calibration curves **(D)** Plots of peak currents vs. the concentration by successive additions of TBHQ for AuNPs@ZIF-8/GCE in optimum conditions.

CONCLUSION

In this study, ZIF-8 was synthesized via hydrothermal technique using $Zn(NO)_3.6H_2O$ and 2-methylimidazole for chemical sensing and TBHQ detection. The ZIF-8/Au-NP combination exhibits high conductivity when tested in electrochemical voltammetry and can be tested on a variety of biological analytes. These ZIF-8/Au-NPs exhibit activity and very high sensitivity, serving as a superior sensor for TBHQ detection at pH 7. Our work develops a promising, low-cost, and stable electrochemical sensor for TBHQ detection.

ACKNOWLEDGEMENTS

The authors would like to thank Selçuk University, College of Science, Department of Chemistry for their infrastructural work.

REFERENCES

Amlashi, N. E., Hadjmohammadi, M. R., & Nazari, S. S. S. J. (2014). Water-contained surfactant-based vortex-assisted microextraction method combined with liquid chromatography for determination of synthetic antioxidants from edible oil. *Journal of Chromatography A*, *1361*, 9–15.

Asap, T., & Augustin, M. A. (1986). Effect of frying oil quality and TBHQ on the shelf-life of potato crisps. *Journal of the Science of Food and Agriculture*, *37*(10), 1045–1051.

Assfour, B., Leoni, S., & Seifert, G. (2010). Hydrogen adsorption sites in zeolite imidazolate frameworks ZIF-8 and ZIF-11. *The Journal of Physical Chemistry C*, *114*(31), 13381–13384.

Attwa, M., Said, A., ElGamal, M., El-Shaer, Y., & Elbasuney, S. (2024). Bespoke energetic zeolite imidazolate frameworks-8 (ZIF-8)/ammonium perchlorate nanocomposite: a novel reactive catalyzed high energy dense

material with superior decomposition kinetics. *Journal of Inorganic and Organometallic Polymers and Materials*, *34*(1), 387–400.

Ayper, B., & Binokay, S. (2010). Gıda katkı maddeleri ve sağlığımıza etkileri. *Arşiv Kaynak Tarama Dergisi*, *19*(3), 141–154.

Capitán-Vallvey, L., Valencia, M., & Nicolás, E. A. (2001). Monoparameter sensors for the determination of the antioxidants butylated hydroxyanisole and n-propyl gallate in foods and cosmetics by flow injection spectrophotometry. *Analyst*, *126*(6), 897–902.

Fan, L., Hao, Q., & Kan, X. (2018). Three-dimensional graphite paper based imprinted electrochemical sensor for tertiary butylhydroquinone selective recognition and sensitive detection. *Sensors and Actuators B: Chemical*, *256*, 520–527.

Guo, L., Xie, M.-Y., Yan, A.-P., Wan, Y.-Q., & Wu, Y.-M. (2006). Simultaneous determination of five synthetic antioxidants in edible vegetable oil by GC–MS. *Analytical and bioanalytical chemistry*, *386*(6), 1881–1887.

JECFA. (2011). Evaluations of the Joint FAO/WHO Expert Committee on Food Additives. In (pp. 960): WHO Technical Report Series.

Jiang, P., Hu, Y., & Li, G. (2019). Biocompatible Au@ Ag nanorod@ ZIF-8 core-shell nanoparticles for surface-enhanced Raman scattering imaging and drug delivery. *Talanta*, *200*, 212–217.

Karatepe, T. U., & Ekerbiçer, H. Ç. (2017). Gıda katkı maddeleri. *Sakarya Tıp Dergisi*, *7*(4), 164–167.

Khezerlou, A., pouya Akhlaghi, A., Alizadeh, A. M., Dehghan, P., & Maleki, P. (2022). Alarming impact of the excessive use of tert-butylhydroquinone in food products: A narrative review. *Toxicology reports*, *9*, 1066–1075.

Liu, X., Zhang, X., Li, R., Du, L., Feng, X., & Ding, Y. (2020). A highly sensitive and selective "turn off-on" fluorescent sensor based on Sm-MOF for the detection of tertiary butylhydroquinone. *Dyes and Pigments*, *178*, 108347.

Lu, S., Hummel, M., Chen, K., Zhou, Y., Kang, S., & Gu, Z. (2020). Synthesis of Au@ ZIF-8 nanocomposites for enhanced electrochemical detection of dopamine. *Electrochemistry Communications*, *114*, 106715.

Paul, A., Banga, I. K., Muthukumar, S., & Prasad, S. (2022). Engineering the ZIF-8 pore for electrochemical sensor applications─ a mini review. *ACS omega*, *7*(31), 26993–27003.

Prabakar, S. R., & Narayanan, S. S. (2006). Surface modification of amine-functionalised graphite for preparation of cobalt hexacyanoferrate (CoHCF)-modified electrode: an amperometric sensor for determination of butylated hydroxyanisole (BHA). *Analytical and bioanalytical chemistry*, *386*(7), 2107–2115.

Rahim, A., & Majid, S. (2023). Ni/Co-based zeolitic-imidazolate framework pseudocapacitance in asymmetrical cells. *Journal of Applied Electrochemistry*, *53*(9), 1727–1737.

Saeb, E., & Asadpour-Zeynali, K. (2022). A novel ZIF-8@ ZIF-67/Au core–shell metal organic framework nanocomposite as a highly sensitive electrochemical sensor for nitrite determination. *Electrochimica Acta*, *417*, 140278.

Song, Q., Nataraj, S., Roussenova, M. V., Tan, J. C., Hughes, D. J., Li, W., Bourgoin, P., Alam, M. A., Cheetham, A. K., & Al-Muhtaseb, S. A. (2012). Zeolitic imidazolate framework (ZIF-8) based polymer nanocomposite membranes for gas separation. *Energy & Environmental Science*, *5*(8), 8359–8369.

Thomas, D., Rasheed, Z., Jagan, J. S., & Kumar, K. G. (2015). Study of kinetic parameters and development of a voltammetric sensor for the determination of butylated hydroxyanisole (BHA) in oil samples. *Journal of food science and technology*, *52*(10), 6719–6726.

Tormin, T. F., Cunha, R. R., Richter, E. M., & Munoz, R. A. (2012). Fast simultaneous determination of BHA and TBHQ antioxidants in biodiesel by batch injection analysis using pulsed-amperometric detection. *Talanta*, *99*, 527–531.

Wang, H., Zhang, S., Li, S., & Qu, J. (2018). Electrochemical sensor based on palladium-reduced graphene oxide modified with gold nanoparticles for simultaneous determination of acetaminophen and 4-aminophenol. *Talanta*, *178*, 188–194.

Warner, K., & Gupta, M. (2005). Potato chip quality and frying oil stability of high oleic acid soybean oil. *Journal of food science*, *70*(6), s395–s400.

Yang, X., Wen, Z., Wu, Z., & Luo, X. (2018). Synthesis of ZnO/ZIF-8 hybrid photocatalysts derived from ZIF-8 with enhanced photocatalytic activity. *Inorganic Chemistry Frontiers*, *5*(3), 687–693.

Yuan, N., Zhang, X., & Wang, L. (2020). The marriage of metal–organic frameworks and silica materials for advanced applications. *Coordination Chemistry Reviews*, *421*, 213442.

Yue, X., Zhu, W., Ma, S., Yu, S., Zhang, Y., Wang, J., Wang, Y., Zhang, D., & Wang, J. (2016). Highly sensitive and selective determination of tertiary butylhydroquinone in edible oils by competitive reaction induced "on–off–on" fluorescent switch. *Journal of Agricultural and Food Chemistry*, *64*(3), 706–713.

Ziyatdinova, G., Saveliev, A., Evtugyn, G., & Budnikov, H. (2014). Simultaneous voltammetric determination of phenolic antioxidants with chemometric approaches. *Electrochimica Acta*, *137*, 114–120.

POSTER PRESENTATION

Preparation of liquid crystalline poly (vinyl tetrazole) based cholesteryl modified polymer

Eda Küçük Aydın[1*] (*ORCID: https://orcid.org/0000-0002-3340-375X*), Yeşim Gürsel[1] (*ORCID: https://orcid.org/0000-0003-4523-345X*), Bahire Filiz Şenkal[1] (*ORCID*:https://orcid.org/0000-0002-1616-6828)

[*1]Istanbul Technical University, Faculty of Science and Letters, Chemical Department, Istanbul, Turkey.

*Corresponding author e-mail: bsenkal@itu.edu.tr

Abstract

Liquid crystals (LCs) occupy an intermediate state between crystalline solids and isotropic liquids, exhibiting partial molecular order and temperature-dependent anisotropy. These properties allow the modulation of optical and mechanical behavior, which underpins their use in displays, sensors and other photonic devices. The integration of heterocyclic rings into LC structures is crucial for tailoring molecular polarity, geometry, mesophase stability and luminescence. In particular, five-membered heterocycles can generate significant dipole moments, enabling thermotropic liquid crystals with desirable alignment characteristics for applications such as spatial light modulation, optical data storage, thin-film transistors, ferroelectric switching and fluorescent bioanalytical probes.

Nitrogen-rich heterocycles have gained increasing interest due to their technological and biological versatility. Compounds like 1,2,3-triazoles show notable biological activity and are used in dyes, corrosion inhibitors and photostabilisers, with several derivatives also exhibiting fluorescence. Tetrazoles constitute another important class, widely employed in pharmaceuticals, energetic materials, coordination cheff **Computational approach to evaluating** mistry and sensor technologies. Their role as bioisosteres of carboxylic acids, owing to comparable pKa values, further enhances their relevance in drug design. Efficient syntheses based on azide addition to activated nitriles allow high-yield formation of aryl tetrazoles under mild conditions.

In this study, poly (vinyl tetrazole) (PVT) was prepared starting from poly(acrylonitrile) (PAN). Obtained PVT was modified with cholesteryl chloroformate for preparation of the liquid crystalline polymer.

Keywords: Liquid crystals, Tetrazoles, Thermotropic mesophases, Nitrogen-rich heterocycles, Polyacrylonitrile.

INTRODUCTION

Liquid crystals (LCs) represent a unique class of materials that cannot be fully categorized as solids or liquids, as they exhibit intermediate ordering and anisotropic behavior within specific temperature ranges. While solids possess a well-defined lattice structure with ordered molecular arrangement, liquids display disordered molecular motion; LCs lie between these two states, maintaining partial molecular orientation despite(Collings & Hird, 2017; Dierking, 2003). This molecular tunability enables significant changes in optical and mechanical properties, forming the basis of LC-based technologies such as displays, thermometers, and various optoelectronic devices.

The incorporation of heterocyclic rings into LC structures has become strategically important for designing advanced functional materials due to their influence on phase behavior, polarity, molecular geometry, and luminescence (Seed, 2007). Five-membered heterocycles, in particular, introduce longitudinal and lateral dipoles that support applications including spatial light modulators (Sandman, 2000), optical data storage (H. Zhang et al., n.d.), thin-film transistors (Dimitrakopoulos et al., 2006; O'Neill & Kelly, 2003), ferroelectric materials (Geelhaar & Merck, 1988), and fluorescent probes (Barbarella et al., 2001). Luminescent LCs are especially valuable because their self-organizing ability enhances optical performance, including polarized light emission (Tariq et al., 2013).

Nitrogen-rich heterocycles, such as 1,2,3-triazoles, are widely studied for their biological activity (Calderone, 2002) and utility in dyes, inhibitors, photostabilizers, and imaging applications (Padwa & Pearson, 2003; Sivakumar et al., 2004). Similarly, tetrazole derivatives have gained major importance across pharmaceuticals, coordination chemistry, energetic materials, and sensor technologies due to their stability and versatile functionality (Benson, 2002; Cui et al., 2012; Fischer et al., 2016; Frija et al., 2010; Göbel et al., 2010; Kumar et al., 2016; Liu et al., 2014; Roh et al., 2012; Sarvary & Maleki, 2015; Wang et al., 2007; Wittenberger, 1994; Z. Bin Zhang et al., 2016). Tetrazoles also act as bioisosteres of carboxylic acids owing to their comparable pKa values (Herr, 2002). Their synthesis commonly proceeds via azide addition to activated nitriles, followed by cyclization into the tetrazole ring, producing yields of 63–97% (Sarngadharan et al., 2022).

Recent developments highlight tetrazoles as efficient ligands in coordination chemistry and as essential components in applications ranging from explosives to agrichemicals. Their chemical stability and metabolic resistance further support their use as carboxylate substitutes in drug design, reinforcing their significance in modern material and pharmaceutical research (Du et al., 2012; Gallardo et al., 2000; Meyer et al., 1998).

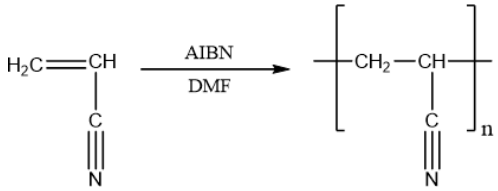
Cholesteryl functional tetrazole based polymer was synthesized and characterized spectrophotometrically. After that, phase transition temperatures were determined by differential scanning calorimetry (DSC) measurement. The phase exhibiting the nematic (N) phase was determined by polarizing optical microscope (POM) and DSC.

MATERIALS AND METHODS

Acrylonitrile (Sigma Aldrich), cholesteryl chloroformate (Sigma Aldrich), AIBN (Fluka) and other chemicals are commercially available and were used as received.

Polymerization of ACN

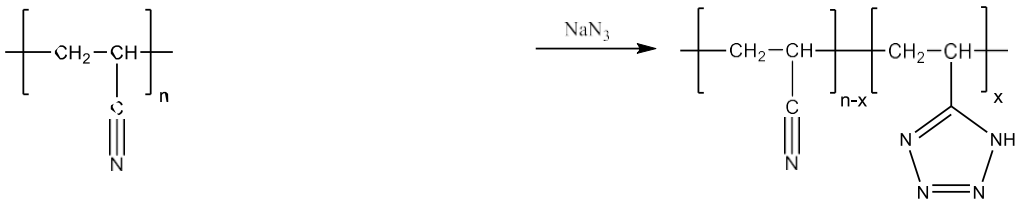
10 mL of ACN was placed into a 250 mL two-necked flask. Subsequently, 0.334 g AIBN and 35 mL DMF were added and dissolved. The polymerization reaction was carried out in an oil bath at 65 °C under nitrogen for 4 hours. Upon achieving room temperature, the viscous reaction mixture was added to into 250 mL of water for precipitation of the polyacrylonitrile (PAN). Following filtration, the obtained PAN was washed with excess of ethanol. After that, PAN was dried under vacuum (Scheme 1).



Scheme 1. Polymeryzation of acrylonitrile

Modification of PAN with sodium azide and click reaction

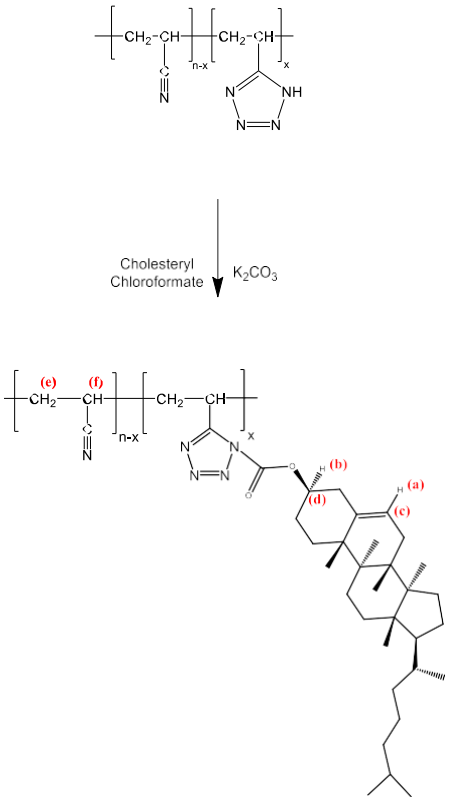
The tetrazole-cyclization reaction of PAN with sodium azide and ammonium chloride was carried out in a conical bottle equipped with a stirrer and a reflux condenser. Approximately 2.65 g of PAN powder and 100 mL of DMF were added to a 250 mL conical bottle, with stirring conducted at ambient temperature. Subsequently, 3.25 g of NaN_3 and 2.675 g of NH_4Cl were added into the PAN solution with constant stirring at room temperature. The bottle was promptly transferred into a water or oil bath and heated to 120 °C, with constant stirring for a duration of 18 hours. The intermediate product underwent spontaneous and gradual precipitation from the reaction mixture over the course of the reaction. The final reaction mixture was added to distilled water, resulting in the formation of a complete precipitate and the elimination of DMF. The products obtained were treated in 150 mL of 0.5 M HCl for the formation of the PVT and repeatedly washed with distilled water for a complete removal of Cl^-, Na^+, and H^+. The desired polymer was then left to dry in air for several days to constant weight. The following is a description of the nominal tetrazole-cyclization reaction (Scheme 2):



Scheme 2. Preparation of PVT

Cholesteryl functional tetrazole based polymer

A quantity of 0.60 g of PVT was dissolved in 28 mL of dimethylformamide (DMF) in the presence of 3.65 mL of triethylamine (TEA). 2.80 g of cholesteryl chloroformate was dissolved in 15 mL of THF. The solution was added dropwise to the reaction mixture and was stirred at room temperature for a period of 24 h. The reaction mixture was subjected to a process of precipitation on ice, followed by the addition of a small quantity of distilled water to ensure thorough precipitation. The mixture was stirred at room temperature using magnetic stirring and the filtrate was decanted. The residue was filtered through filter paper and washed with distilled water. The drying process was conducted within a vacuum oven. Scheme 3 also shows the synthesis of cholesteryl functional tetrazole based polymer.



Scheme 4. Preparation of cholesteryl functional tetrazole based polymer

RESULTS and DISCUSSION

PVT was prepared starting from PAN. For this purpose, PAN was obtained radical polymerization of acrylonitrile monomer using AIBN at 65 °C under nitrogen for 4 hours. The tetrazole-cyclization reaction of PAN with sodium azide and ammonium chloride were performed to obtain PVT.

Amine content of the PVT was found using titrimetric method and amine content of the polymer was calculated as 12.5 mmol amine per gram polymer.

According to the FT-IR spectra (Figure 1), the bands between 3200 and 3700 cm^{-1} were observed due to NH stretching vibration. Strong absorption peaks at 2242 cm^{-1} and 1632 cm^{-1} belong PAN C≡N and C=C stretching vibrations respectively. Also, the peak at 1357 cm^{-1} belongs to C-H and N-H bending.

In the spectra of PVT, a strong absorption was observed at 2930 cm^{-1} due to asymmetric CH_2 stretching vibration. The bands between at 2868–2612 cm^{-1} suggests the presence of tetrazole groups. A much stronger peak at 2240 cm^{-1} is belong PAN C≡N stretching vibration. After tetrazole formation, this band becomes weaker and disappears. Also, four PVTs all exhibit medium bands at 1551, 1416 and 1384, 1046 cm^{-1}, which are due to the C≡N stretching and bending vibrations of the characteristic tetrazole ring, respectively.

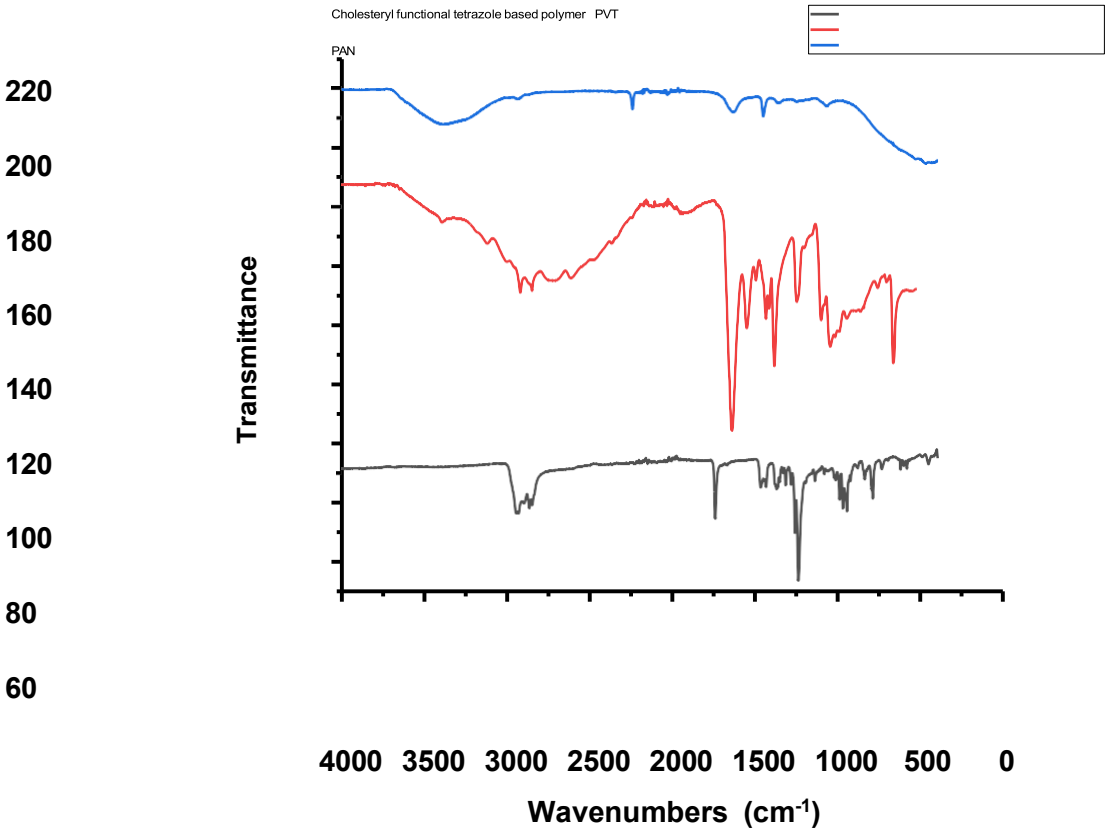


Figure 1. FT-IR spectra of PAN, PVT and cholesteryl functional tetrazole based polymer

Cholesteryl functional tetrazole based polymer was characterized by using FT-IR (Figure 1), ^{1}H-NMR ($CDCl_3$) (Figure 2) and ^{13}C-NMR ($CDCl_3$) (Figure 3).
According to Figure 1, aliphatic C–H stretching peaks of cholesterol were observed at between 2845-2863 cm^{-1} and 2928 cm^{-1}. The peak at 1742 cm^{-1} belongs to C=O stretching vibration.

^{1}H -NMR (Figure 2) ($CDCl_3$, d): 0.70–2.04 (m, 41H, cholesteryl protons), 2.50–2.51 (d, 2H, CH_2), 4.80–4.87 (m, 1H, oxycyclohexyl) (b), 5.45 (1H, s, alkenyl) (a), 2.0-2.10 (e) (CH_2), 3.0-3.5 (f) (CH).

A different method of characterization, ^{13}C-NMR (Figure 3), is said to produce prominent peaks at 123 and 80 ppm, thus confirming the existence of =C-H bond (c) and -CHO functional group (d), respectively.

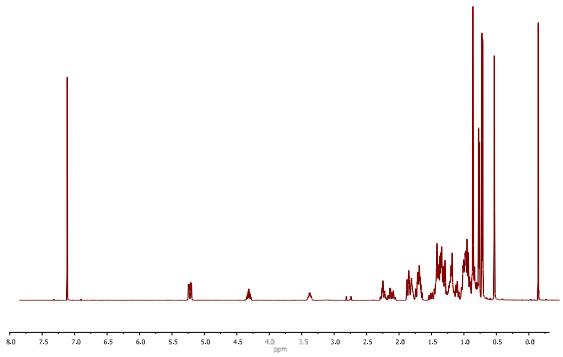


Figure 2. ^{1}H-NMR spectrum of modification of cholesteryl functional tetrazole based polymer

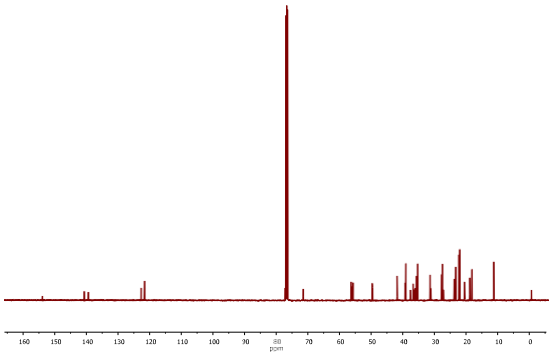


Figure 3. ^{13}C-NMR spectrum of cholesteryl functional tetrazole based polymer

The mesophase properties of the cholesteryl functional tetrazole based polymer were determined using DSC and POM.

In the DSC thermogram (Figure 4), an endothermic melting peak was recorded at 128.2 °C during the heating cycle, corresponding to the formation of the mesophase. In the cooling cycle, an exothermic crystallization peak was observed at around 105 °C.

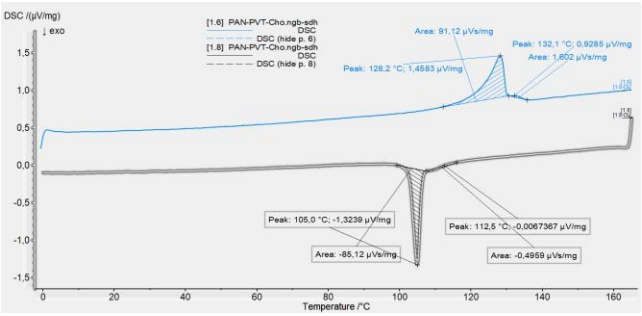


Figure 4. DSC thermogram of the cholesteryl functional tetrazole based polymer

During the POM analysis (Figure 5), a monotropic nematic liquid-crystalline phase was observed at 134 °C in the cooling cycle. At this temperature, a narrow temperature interval of nematic texture appeared, indicating a transition from the isotropic phase to the nematic phase. As cooling continued, a transition from the nematic phase to the crystalline phase was detected at approximately 130 °C. These observations are in good agreement with the thermal data obtained from the DSC measurements.

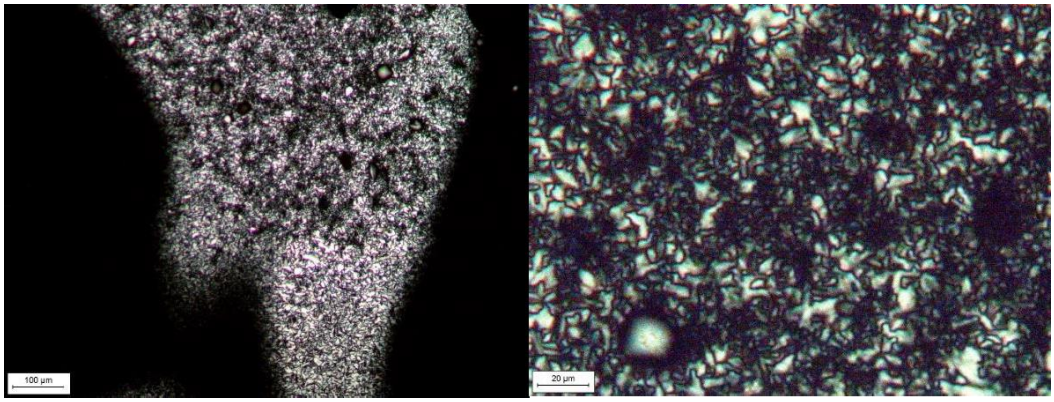


Figure 1. Snapshot pictures of mesophases of the cholesteryl functional tetrazole based polymer observed by POM

When evaluated together, the POM and DSC results clearly confirm the presence of a monotropic nematic phase in the compound.

CONCLUSION

Liquid crystals occupy a unique state of matter, combining fluidity with partial molecular order, and their properties can be finely tuned through structural modifications. Incorporating heterocyclic units-especially nitrogen-rich five-membered rings-significantly enhances the functional capabilities of LC materials by influencing polarity, geometry, phase behavior, and optical performance. Among these, triazole and tetrazole derivatives stand out for their structural versatility, stability, and wide applicability across optoelectronics, sensing, coordination chemistry, and pharmaceutical design. Their ability to act as bio isosteres and form robust intermolecular interactions further strengthens their role in developing next- generation functional materials. Overall, heterocycle-modified liquid crystals represent a powerful platform for advancing modern technological and biomedical applications.

ACKNOWLEDGEMENTS

This work is supported by the Scientific Research Project Center of the Istanbul Technical University (Research Universities Project) (Project number: TGA-2025-46664). Additional support was provided by TÜBİTAK through the 2211-A National PhD Scholarship Program.

REFERENCES

Barbarella, G., Zambianchi, M., Pudova, O., Paladini, V., Ventola, A., Cipriani, F., Gigli, G., Cingolani, R., & Citro, G. (2001). Oligothiophene isothiocyanates as a new class of fluorescent markers for biopolymers. *Journal of the American Chemical Society*, *123*(47), 11600–11607. https://doi.org/10.1021/JA011209V

Benson, F. R. (2002). The Chemistry of the Tetrazoles. *Chemical Reviews*, *41*(1), 1–61. https://doi.org/10.1021/CR60128A001

Calderone, V. (2002). Large-conductance, ca(2+)-activated k(+) channels: function, pharmacology and drugs. *Current Medicinal Chemistry*, *9*(14), 1385–1395. https://doi.org/10.2174/0929867023369871

Collings, P. J., & Hird, M. (2017). Introduction to liquid crystals: Chemistry and physics. *Introduction to Liquid Crystals: Chemistry and Physics*, 1–298. https://doi.org/10.1201/9781315272801/INTRODUCTION-LIQUID-CRYSTALS-PETER-COLLINGS-GEORGE-GRAY-JOHN-GOODBY-MICHAEL-HIRD/RIGHTS-AND- PERMISSIONS

Cui, P., Ma, Y. G., Li, H. H., Zhao, B., Li, J. R., Cheng, P., Balbuena, P. B., & Zhou, H. C. (2012). Multipoint interactions enhanced CO2 uptake: A zeolite-like zinc-tetrazole framework with 24-nuclear zinc cages. *Journal of the American Chemical Society*, *134*(46), 18892–18895. https://doi.org/10.1021/JA3063138

Dierking, Ingo. (2003). *Textures of liquid crystals*. 218.

Dimitrakopoulos, C. D., Malenfant, P. R. L., Garnier, F., Horowitz, G., Katz, H. E., Funahashi, M., & Hanna, J.-I. (2006). Donor−Acceptor−Donor-Type Liquid Crystal with a Pyridazine Core. *Organic Letters*,

8(21), 4699–4702. https://doi.org/10.1021/OL061711Q

Du, Z., Si, C., Li, Y., Wang, Y., & Lu, J. (2012). Improved Synthesis of 5-Substituted 1H-Tetrazoles via the [3+2] Cycloaddition of Nitriles and Sodium Azide Catalyzed by Silica Sulfuric Acid. *International Journal of Molecular Sciences 2012, Vol. 13, Pages 4696-4703*, *13*(4), 4696–4703. https://doi.org/10.3390/IJMS13044696

Fischer, D., Klapötke, T. M., Stierstorfer, J., & Szimhardt, N. (2016). 1,1′-Nitramino-5,5′-bitetrazoles.

Chemistry – A European Journal, *22*(14), 4966–4970. https://doi.org/10.1002/CHEM.201600177 Frija, L. M. T., Ismael, A., & Cristiano, M. L. S. (2010). Photochemical Transformations of Tetrazole

Derivatives: Applications in Organic Synthesis. *Molecules 2010, Vol. 15, Pages 3757-3774*, *15*(5),

3757–3774. https://doi.org/10.3390/MOLECULES15053757

Gallardo, H., Begnini, I. M., Neves, A., & Vencato, I. (2000). Synthesis, Characterization and Thermal Properties of Palladium(II) Complexes Containing Phenyltetrazole. Crystal Structure of trans-[C40H64N8O2PdCl2]. *Journal of the Brazilian Chemical Society*, *11*(3), 274–280. https://doi.org/10.1590/S0103-50532000000300013

Geelhaar, T., & Merck, E. (1988). Ferroelectric mixtures and their physico-chemical properties. *Ferroelectrics*, *85*(1), 329–349. https://doi.org/10.1080/00150198808007667;PAGE:STRING:ARTICLE/CHAPTER

Göbel, M., Karaghiosoff, K., Klapötke, T. M., Piercey, D. G., & Stierstorfer, J. (2010). Nitrotetrazolate-2N-oxides and the strategy of N-oxide introduction. *Journal of the American Chemical Society*, *132*(48), 17216–17226. https://doi.org/10.1021/JA106892A

Herr, R. J. (2002). 5-Substituted-1H-tetrazoles as carboxylic acid isosteres: medicinal chemistry and synthetic methods. *Bioorganic & Medicinal Chemistry*, *10*(11), 3379–3393. https://doi.org/10.1016/S0968-0896(02)00239-0

Kumar, A., Kumar, S., Khajuria, Y., & Awasthi, S. K. (2016). A comparative study between heterogeneous stannous chloride loaded silica nanoparticles and a homogeneous stannous chloride catalyst in the synthesis of 5-substituted 1H-tetrazole. *RSC Advances*, *6*(79), 75227–75233. https://doi.org/10.1039/C6RA14352K

Liu, K., Peng, Y., Yang, F., Ma, D., Li, G., Shi, Z., & Feng, S. (2014). Three metal–organic frameworks based on the semirigid V-shaped 5-(3-amino-tetrazole-5-phenoxy)-isophthalic acid ligand: syntheses, topological structures and properties. *CrystEngComm*, *16*(21), 4382–4389. https://doi.org/10.1039/C4CE00105B

Meyer, E., Zucco, C., & Gallardo, H. (1998). Metallomesogens: synthesis and properties. *Journal of Materials Chemistry*, *8*(6), 1351–1354. https://doi.org/10.1039/A801159A

O'Neill, M., & Kelly, S. M. (2003). Liquid crystals for charge transport, luminescence, and photonics. *Advanced Materials*, *15*(14), 1135–1146. https://doi.org/10.1002/ADMA.200300009;PAGE:STRING:ARTICLE/CHAPTER

Padwa, Alber., & Pearson, W. H. . (2003). *Synthetic Applications of 1,3-Dipolar Cycloaddition Chemistry Toward Heterocycles and Natural Products, Volume 59*.

Roh, J., Vávrová, K., & Hrabálek, A. (2012). Synthesis and functionalization of 5-substituted tetrazoles. *European Journal of Organic Chemistry*, *2012*(31), 6101–6118. https://doi.org/10.1002/EJOC.201200469;WGROUP:STRING:PUBLICATION

Sandman, D. J. (2000). A review of: "Electronic Materials: The Oligomer Approach", edited by K. Müllen and G. Wegner, Wiley-VCH, Weinheim, 1998; ISBN 3-527-29438-4; xxvii +599 pages; DM 398.00;,

sFr 354.00. *Molecular Crystals and Liquid Crystals Science and Technology. Section A. Molecular Crystals and Liquid Crystals*, *338*(1), 277–278. https://doi.org/10.1080/10587250008024438

Sarngadharan, S. C., Aronson, J., Gelbaum, C., Griffith, K., Faris, J., Moihdeen, A. B., Patel, M., Malone, M., Richman, K., Eckert, C. A., Liotta, C. L., & Pollet, P. (2022). *Synthesis of 5-Substituted Tetrazoles: Reaction of Azide Salts with Organonitriles Catalyzed by Trialkylammonium Salts in Non-polar Media*. https://doi.org/10.1021/ACS.OPRD.2C00032.S001

Sarvary, A., & Maleki, A. (2015). A review of syntheses of 1,5-disubstituted tetrazole derivatives.

Molecular Diversity, *19*(1), 189–212. https://doi.org/10.1007/S11030-014-9553-3

Seed, A. (2007). Synthesis of self-organizing mesogenic materials containing a sulfur-based five-membered heterocyclic core. *Chemical Society Reviews*, *36*(12), 2046–2069. https://doi.org/10.1039/B612666A

Sivakumar, K., Xie, F., Cash, B. M., Long, S., Barnhill, H. N., & Wang, Q. (2004). A Fluorogenic 1,3-

Dipolar Cycloaddition Reaction of 3-Azidocoumarins and Acetylenes†. *Organic Letters*, *6*(24), 4603–4606. https://doi.org/10.1021/OL047955X

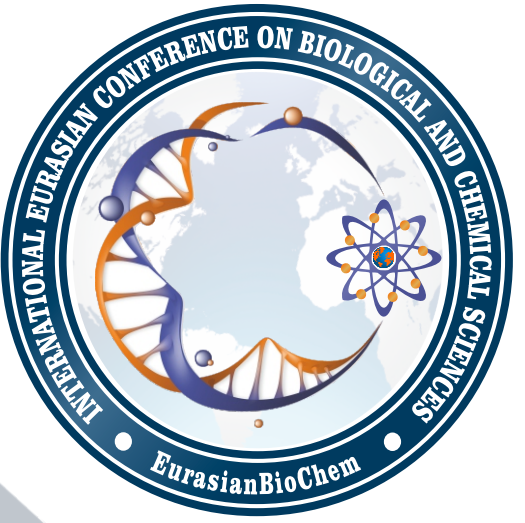
Tariq, M., Hameed, S., Bechtold, I. H., Bortoluzzi, A. J., & Merlo, A. A. (2013). Synthesis and characterization of some novel tetrazole liquid crystals. *Journal of Materials Chemistry C*, *1*(35), 5583–5593. https://doi.org/10.1039/C3TC30966E

Wang, X. W., Chen, J. Z., & Liu, J. H. (2007). Photoluminescent Zn(II) metal-organic frameworks built from tetrazole ligand: 2D four-connected regular honeycomb (4363)-net. *Crystal Growth and Design*, *7*(7), 1227–1229. https://doi.org/10.1021/CG070330W

Wittenberger, S. J. (1994). Recent developments in tetrazole chemistry. A review. *Organic Preparations and Procedures International*, *26*(5),499–531. https://doi.org/10.1080/00304949409458050;SUBPAGE:STRING:ABSTRACT;JOURNAL:JOURNAL:UOPP19;ISSUE:ISSUE:DOI

Zhang, Z. Bin, Xu, C. X., Yin, L., Wang, Z., Yin, X., & Zhang, J. G. (2016). Synthesis, crystal structure and properties of a new 1D polymeric nitrogen-rich energetic complex {TAG[Li(BTO)(H2O)]}n based on 1H,1′H-5,5′-bitetrazole-1,1′-diolate. *RSC Advances*, *6*(77), 73551–73559. https://doi.org/10.1039/C6RA12649A

Zhang, H., Shiino, S., Shishido, A., Kanazawa, A., Tsutsumi, O., Shiono, T., & Ikeda, T. (n.d.). *A Thiophene Liquid Crystal as a Novel p-Conjugated Dye for Photo-Manipulation of Molecular Alignment*. https://doi.org/10.1002/1521-4095(200009)12:18



EJBCS
Eurasian Journal of Biological and Chemical Sciences
www.dergipark.org.tr/ejbcs